INTERNATIONAL MINERALOGICAL ASSOCIATION

16*th* General Meeting

4-9 September 1994 *Pisa, Italy*

ABSTRACTS

Organizing Committee

General Chairman: S. Merlino
Vice–Chairman: M. Franzini
Secretary: F. Sartori
Field Trips: R. Santacroce (*chairman*), A. Boriani, G. Ferrara, C.A. Ricci, A. Sbrana
Registration: S. Merlino (*chairman*), M. Franzini, M. Pasero
Finance: M. Franzini (*chairman*), P. Armienti, C. Cipriani, P. Manetti, R. Mazzuoli
Grants: G. Ferraris (*chairman*), S. Merlino, F.P. Sassi
Publications: F. Innocenti (*chairman*), M. Pasero, S. Rocchi, G. Serri
Local Arrangements: G. Cortecci (*chairman*), L. Leoni, P. Orlandi, N. Perchiazzi

Program Committee

F. Barberi (*chairman*), M. Mellini (*secretary*), A. Baronnet, E. Bonatti, C. Chopin, G. Ferrara, G. Ferraris, S. Hafner, S. Merlino, G. Ottonello, C.T. Prewitt, G.D. Price, F.P. Sassi, W. Schreyer, N.V. Sobolev, V. Trommsdorff, L. Ungaretti

For additional copies of this volume, contact:

SOCIETA' ITALIANA DI MINERALOGIA E PETROLOGIA
Dipartimento di Scienze della Terra dell'Università
Via S. Maria 53
I–56126 Pisa

phone: +39 50 568204 fax: +39 50 40976

TEXTURAL AND CHEMICAL RELATIONSHIPS BETWEEN CHLORITE AND BERTHIERINE IN METAMORPHIC NODULES ENCLOSED IN GRANITIC PEGMATITES OF SIERRA ALBARRANA (SW. SPAIN)

Abad-Ortega, M.M. and Nieto, F. *(Dpto. de Mineralogía y Petrología & Instituto Andaluz de Geología Mediterránea, Univ. de Granada - C.S.I.C., Granada, Spain).*

Chlorite and berthierine occur through alteration of cordierite within nodules that are enclaves of metamorphic rocks texturally and mineralogically transformed by the Sierra Albarrana pegmatites during their emplacement (Abad-Ortega, 1993). The coexistence of both phyllosilicates, in some cases at lattice level, allows us to study their stability relationships and to compare their chemical compositions by means of powder X-ray difraction, electron microprobe and analytical high resolution transmission electron microscopy.

Three different types of samples were defined according to their textural characteristics. Type I are samples showing incipient replacement of cordierite by small cryptocrystalline aggregates, that can be identified by XRD as berthierine with small quantities of chlorite. EMPA analyses give mixed compositions of berthierine and cordierite. Type II are samples with extensive replacement of cordierite by aggregates showing similar characteristics as those described for type I, but some small crystals are present, showing optical properties of chlorite and EMPA composition coherent with chlorite or berthierine. Type III samples show complete replacement of cordierite by crystals with similar characteristics as those described for Type II. Their XRD diffractogram corresponds to chlorite.

HRTEM images of these crystals only show perfect sequences of 14Å lattice fringes. Nevertheless, the cryptocrystalline aggregates of type II and III samples present coexistent areas of 14 and 7Å lattice fringes that are intergrown at different levels: (1) large areas (> 1 mμ) of 7Å layers, (2) packets of 7Å layers between 14Å layer areas, with visible 7 to 14 Å lateral changes, and (3) random mixed-layers of 7 and 14 Å. Although identification of chlorite and berthierine in lattice fringe images is complicated by dynamical effects and 2-layer polytype berthierine (Amouric *et al.*, 1988), XRD diffractograms allow the identification of berthierine as the major phyllosilicate in the type I and II samples. EDS microanalyses of 14Å, 7Å and (14+7)Å areas show lack of systematic differences in chemical compositions.

We conclude that chlorite is the final stable product of alteration of cordierite + magnetite + quartz + melt, with berthierine as an intermedium metastable phase. When both phyllosilicates coexist in the same sample, no chemical differences are present between them and they may be considered as true polymorphs.

References:
Abad-Ortega, M.M. (1993). *Tesis Doctoral Univ. Granada*, 294 pp.
Amouric, M., Gianetto, I., Proust, D. (1988). *Bull. Mineral.*, **111**, 29-37.

CALCIUM PHOSPHATE MINERALS GROWN FROM VERY DILUTED SOLUTIONS

Abbona F.*, Franchini-Angela M.** and Didoli P.F.**
* Dip. di Scienze della Terra, Univ. della Calabria - 87036 Arcavacata di Rende (CS)
** Dip. di Scienze Mineralogiche e Petrologiche, Via Valperga Caluso 37 - 10125 Torino

Systematic researches have been carried out on the crystallyzation at room temperature of calcium phosphates from solutions of very low concentration (1≤c≤5 mM), close to those of natural aqueous environments. From these solutions an amorphous calcium phosphate, octacalciumphosphate or hydroxyapatite may form according to the conditions. The occurrence field of each phase is given as a function of pH and concentration. The genetic relationships among these phases are described and interpreted in terms of supersaturation and other physico-chemical parameters.

The effect of some common dopants, as magnesium and cadmium on nucleation, phase stability and crystal growth are also presented and discussed.

CALCULATING PRINCIPAL REFRACTIVE INDICES AND ORIENTATION OF THE OPTICAL INDICATRIX IN SELECTED TRICLINIC MINERALS: POINT-DIPOLE THEORY

Abbott, Richard N., Jr. (*Dept. of Geology, Appalachian State Univ.*)

Point-dipole theory was used to calculate the principal refractive indices and orientation of the optical indicatrix in selected triclinic minerals: kyanite, wollastonite, schizolite (Mn-rich pectolite), microcline, albite, walstromite ($BaCa_2Si_3O_9$), kaolinite, pyrophyllite-*1Tc*, Talc-*1Tc*, and triclinic forms of clinochlore and chloritoid.

A simple extension of point-dipole theory makes possible the calculation of not just the principal refractive indices, but also the orientation of the optical indicatrix in triclinic minerals. According to point-dipole theory, as extended by Abbott (1993), the relationship among structure, electronic polarizability, and optical properties can be summarized conveniently in four equations. The first equation (Cummins *et al.*, 1976; Pohl, 1978) gives the local electric field, **F**(k), at site k as a function of the local electric fields at all sites, k', in the unit cell,

$$\mathbf{F}(k) = \mathbf{E} + (1/V)\Sigma_{k'}\ L(kk')\,\alpha(k')\,\mathbf{F}(k'). \qquad (1)$$

The vector **E** is the macroscopic (externally applied) electric field, L(kk') is the Lorentz factor tensor for the pair k-k', α(k') is the electronic polarizability of species k', and V is the volume of the unit cell. The Lorentz factor tensors, L(kk'), depend only on the geometry of the structure, and were calculated using the method of Cummins *et al.* (1976). Equation 1 forms a system of linear equations solvable for the individual local electric fields, **F**(k).

The dielectric susceptibility tensor, χ, is then obtained from the local electric fields (Pohl, 1978):

$$\chi\mathbf{E} = (1/V)\,\Sigma_k\,\alpha(k)\,\mathbf{F}(k) \qquad (2)$$

Referred to a Cartesian base, **x** (column matrix of coordinate variables x, y, and z), the coefficients of the dielectric susceptibility tensor describe the surface of an ellipsoid,

$$\mathbf{x}^T\chi\,\mathbf{x} = 1. \qquad (3)$$

The principal axes of the ellipsoid are parallel to the principal axes of the optical indicatrix. The directions of the principal axes and their magnitudes (eigenvectors and eigenvalues, respectively) are found by diagonalizing the dielectric susceptibility tensor. The principal refractive indices are then simply related to the eigenvalues, χ_{ii}:

$$n_i = (\chi_{ii} + 1)^{1/2} \qquad (4)$$

The quantity, $\chi_{ii} + 1$, is the familiar dielectric constant. All calculations were referred to the D wavelength (λ_D = 5893 Å).

Electronic polarizabilities, α(k), for the constituent species (atoms and OH groups) were optimized for the best agreement between observed and calculated optical properties. As many as six electronic polarizabilities can be determined in this way for each mineral. Cations of the same element in symmetrically distinct sites were assigned the same polarizability. Four kinds of oxygen atoms were distinguished according to coordination: bridging oxygen (T-O-T, T = Si or ^{iv}Al), non-bridging oxygen (T-O-X_n, X = cation other than Si, ^{iv}Al, or H), oxygen not bonded to Si, ^{iv}Al, nor H (i.e., O-X_n), and hydroxyl oxygen (H-O-X_n).

The calculations show that the optical properties of a triclinic crystal (orientation of the indicatrix as well as refractive indices) can be modelled accurately from point-dipole theory. In addition, the calculations show that the electronic polarizability of an atom (or OH

ABSTRACTS

for the Plenary Lectures, Oral and Poster Sessions
of the **16th General Meeting**
of the
International Mineralogical Association
Pisa, 4–9 September 1994

Abstracts are listed alphabetically by the family name of the first author. Abstracts marked with • have been retyped; some were subjected to minor editorial revision.

FOREWORD

One thousand one hundred and sixty–two abstracts by authors from forty–seven different countries are collected in this volume devoted to the 16th General Meeting of the International Mineralogical Association, that is being held in Pisa, Italy, 4–9 September 1994.

This volume presents a complete overview of the research that is being carried on around the world in the field of mineralogy, illustrating the variety and the significance of the problems being studied in the various branches of the discipline.

What clearly emerges is the image of an extremely dynamic sector of the Earth Sciences, one at the same time linked in a fruitful connection with the disciplines of Chemistry and Physics.

The healthy balance between fundamental and applied research, thoroughly documented by the contributions gathered here, is another sign of the vitality of this discipline.

The scientific program of the 16th General Meeting has been prepared thanks to the intelligent and hardworking efforts of several persons and groups:

Commissions and Working Groups of IMA;

Program Committee – its action in preparing the main frame of the program and its interaction with the various Commissions and Working Groups of IMA were effectively directed and coordinated by Marcello Mellini;

Convenors of the various sessions – who were most generous with their time and expertise in soliciting contributions, in selecting papers for the poster and oral presentations, and in preparing the final schedule of the sessions;

Authors – who presented contributions of valuable scientific quality and who complied, with few exceptions, with the abstract guidelines.

The painstaking work of editing this volume was carried out by a single person, Marco Pasero, assisted by Letizia Ristori. He collected the abstracts, solicited the late authors, prepared the files on each contribution, compiled the author index, and carefully checked the work of the printer.

To all of the above, as well as to the institutions and organizations which sponsored the General Meeting or specific sessions, I would like to express the grateful acknowledgements of the Organizing Committee. Special thanks are due to the Italian National Research Council (C.N.R.) for its generous financial support.

Stefano Merlino
Chairman of the
16th General Meeting of IMA

group) depends on the local structural setting, i.e., polarizabilities are site-specific. Electronic polarizabilities are not strictly transferable and therefore only approximately additive.

Abbott, R.N., Jr. (1993). *Am. Mineral.*, **78**, 952-956.
Cummins, P.R., Dunmur, D.A., Munn, R.W. & Newham, R.J. (1976). *Acta Cryst.*, **A32**, 847-853.
Pohl, D. (1978). *Acta Cryst.*, **A34**, 574-578.

ANTIFERROMAGNETIC COUPLING OF FRUSTRATED SPINS AT T<1.4K IN BRAUNITE: A NEUTRON DIFFRACTION STUDY

Abs-Wurmbach I. and Ohmann S. (Inst. of Min. and Cryst., TU-Berlin) and Stüßer N. (BENSC, HMI-Berlin)

The present study is concerned with the magnetic structure of braunite, $Mn^{2+}Mn^{3+}{}_6O_8/SiO_4$. Its chemical structure can be derived from the α- Mn_2O_3 structure by a partial substitution of $2Mn^{3+}$ by Mn^{2+} + Si^{4+}. The structure may be described as a sheet structure with A-layers at z=0, 1/4, 1/2, 3/4 containing only Mn^{3+}(octahedral M2 and M3 sites) and, B-layers at z=1/8, 3/8, 5/8, 7/8 containing Mn^{2+} (antiprismatic M1 site), Mn^{3+} (octahedral M4 site) and tetrahedral Si [1]. The space group is $I4_1/acd$. This kind of structure is unique, allowing the Jahn-Teller ion Mn^{3+} ($3d^4$-configuration) to be incorporated in octahedra being more distorted than those of α-Mn_2O_3.

Braunite exhibits unusual magnetic behaviour. Magnetic susceptibilities measurements show an antiferromagnetic phase transition at about T_N=90 K [2]. But, it was found that braunite has a positive paramagnetic Curie-temperature at about θ_p=50K, a characteristic feature of strong ferromagnetic superexchange interactions. Furthermore, at low temperatures a new strong increase of susceptibilities is observed reaching a maximum at T=1K, thus indicating the interesting phenomenon of frustrated spins. Attempts to solve the magnetic structure from 4K neutron powder diffraction patterns have been problematic. The reason for this might be that not all spins have been entirely ordered down to 4K. Further neutron diffraction experiments at T<4K have been performed expecting total ordering of the spins. The temperature dependent powder diffraction diagrams are plotted in Fig.1. Indexing of reflections has been performed assuming the symmetry P4 for the unchanged nuclear cell. According to the results derived from magnetization and neutron diffraction experiments, the following model may be assumed: There exists a predominately ferromagnetic coupling in the A - sheets which are antiferromagnetically ordered to each other. The description of braunite as a layered structure [1] is in excellent agreement with its magnetic structure.

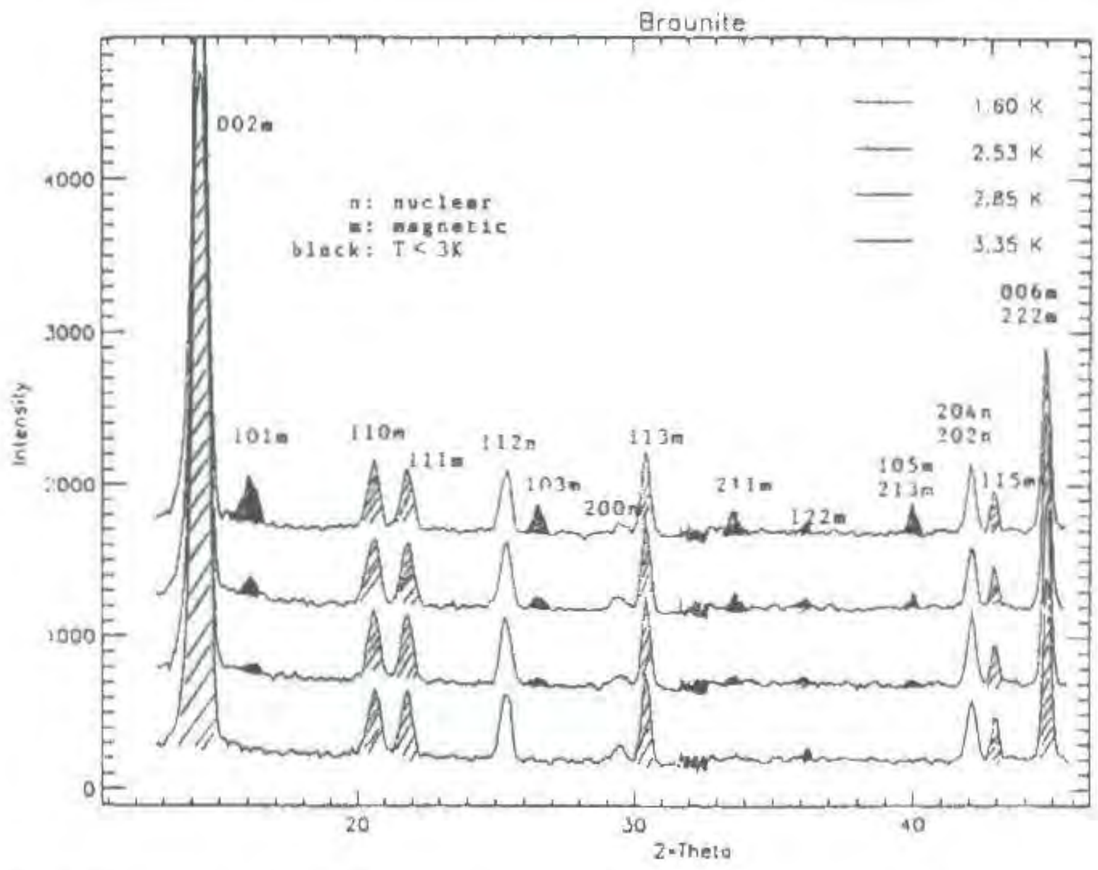

Fig.1: Neutron powder diffraction patterns of braunite at various temperatures

At T < 2.8K new reflections appear (101, 103, 211, 213) in accordance with our working hypothesis of frustrated spins present in the B-sheets above T=4K. Intensities of the magnetic reflections already observed at T≥4K remain unchanged down to 1.4K, thus indicating that new magnetic sublattices are arising from spins which have not been coupled at higher temperatures. The new reflections 101 and 103 might be explained by lattice planes built up from antiferromagnetically coupled Mn^{2+}- ions.

References:

[1]-Moore, P.B. & Araki, T. (1976): *Am. Min.*, **61**: 1226-1240.
[2]-Westerholt, K; Abs-Wurmbach,I. & Dahlbeck,R. (1986): *Phys. Rev.* **B34**, 6437-6447.

PETROLOGY AND GEOCHEMISTRY OF AL-P-MINERALS, IN DUMORTIERITE-, MUSCOVITE-, KYANITE-BEARING QUARTZITES OF THE FORMATION BARRAO DO GUACUI, DIAMANTINA, BRAZIL

Ackermand, D. (*Mineralogisches Institut, Univ. of Kiel, FRG*) and Morteani, G. (*Angew. Mineralog., Techn. Univ. of München, FRG*)

In the Upper Archean Barao do Guacui formation near Diamantina (Sierra do Espinhaco, Minas Geraes, Brazil) muscovite-kyanite quartzites rich in Al-phosphates, dumortierite, tourmaline and ilmenohematite are found. The whole rock chemical composition and the mineral assemblages define 5 main rock types:

A 1: Lazulite, kyanite, muscovite, quartz
A 2: Lazulite, augelite, kyanite, muscovite, quartz
A 3: Lazulite, amblygonite, tourmaline, muscovite, quartz
A 4: Lazulite, svanbergite, tourmaline, muscovite, quartz
B: Dumortierite, muscovite, quartz

In both the A1 aand A2 rock types, lazulites occur in lazulite/muscovite symplectite as patches in euhedral kyanite. In type A2 the lazulite grains are rimmed by augelite. The large blue lazulite grains typical for rocks of type A3 have no reaction rim and are in contact with euhedral amblygonite and tourmaline. In rocks of type A4, lazulite occurs as aggregates surrounded by a light brown margin consisting of a svanbergite/muscovite/quartz symplectite. Tourmaline as well as small titanohematite grains are rather homogeneously distributed within the matrix and the Al-P-phosphate-rich patches.The mostly euhedral dumortierite has never been found in contact with lazulite. The variation of X_{Mg} = Mg/(Mg + Fe) in lazulite (1.0 (A1) - 0.6 (A4)), and of X_{Sr} = Sr/(Sr+Ca) (0.5-1.0) and PO_4/SO_4 (2.0 - 1.2) in svanbergite functions of the bulk rock chemical composition and characterize the assemblage A4. In the lazulite porphyroblasts fluorine as well as XMg decrease from core to rim.

Lazulite, and possibly also the other phosphates, were formed in the early stages of the metamorphic history of the rocks, mostly in static conditions. According to regional literature on the tectono-metamorphic events in the Brazilian Shield (Viana, 1984), the metasediments and metavolcanic rocks of the Barao do Guacui formation should have experienced at least both the 2600 Ma Jequie-Aroense and the 570 Ma old Braziliano events. No information exists about the grade of the metamorphic events in the study area.

The chemical composition of the lazulite-bearing quartzites is characterized by high aluminium, phoshorus, fluorine, boron and low to very low sodium contents. The discussion of the protolith has to start from this peculiar composition.One possibility, discussed by Ackermand and Morteani (1994, in press) and by Schreyer (1987), is that the protolith was composed of volcanic rocks of acidic composition that had undergone a hydrothermal sericitic alteration. During the alteration processes Ca and Na were selectively depleted and Si, P, B and Al relatively enriched.

Considering upper Archean sedimentary processes responsible

for the formation of the quartzites, non-actualistic depositional environments have to be taken into account. Due to the lack of oxygen in Precambrian times, the deposition of phophorous-rich marine sediments is in fact hard to explain, nevertheless due to onset of photosynthesis, a local phosphate deposition cannot be excluded. The presence of magnetite-phyllites within the lazulite-bearing horizons may support the local availability of oxygen. The low Na content may then be explained for example by fresh water flash floods dissolving the highly soluble salts such as halite and/or soda. The second type of possible sedimentary environment is a closed lake system in a semi-arid to arid climate. Also in such an environment, elements like P and B may be accumulated and flash floods may supply clastic sediments and dissolve the highly soluble salts.

References:
Morteani, G. & Ackermand, D. (in press) Europ. J. Minerl.
Schreyer, W. (1987) in: Helgeson, H.C. (ed), Reidel publ., 265-296
Viana, H.S. (1984). Proleto Mapas Metalogenét., CPRM, Brasilia

CONTRASTING FEATURES OF FOLIATED AND MASSIVE HERCYNIAN CA GRANITOIDS FROM CALABRIA (ITALY)

Acquafredda P. , Di Battista P. (*Dept. Geomineralogico Univ. of Bari*) and Caggianelli A. (*DiTEc Univ. of Basilicata - Potenza*)

The integrated analysis of biotite and amphibole chemical data and of structural and compositional features of granitoid calc-alkaline (CA) complexes may increase the understanding of the conditions attending pluton emplacement as well as the definition of magmatic typology and tectonic setting. In this study we tried to define the spatial and temporal relationships for 10 Hercynian plutons of Calabria which belong to the CA suite and are metaluminous to weakly peraluminous. With this in mind we chiefly used data about the mineral chemistry of amphibole and biotite and re-examined available petrographic, structural and geochemical data in order to define in more detail the picture of the CA plutonism in Calabria. CA granitoids may be either foliated or massive (Rottura *et al.*, 1990). The foliation grades from very outstanding to weak and it is revealed by the preferred orientation of biotites, plagioclases and by the elongation of the mafic enclaves. Their composition changes from gabbroic to granodioritic, with a wide silica range (40-70 wt.%). Furthermore, they emplaced at different depths as it can be deduced from sparse contact metamorphic effects and from the mineral assemblage of the regionally metamorphosed country rocks.

Amphibole has a composition varying from Ts-Hbl to Act-Hbl, with Mg-Hbl being the more common type (Fig.1). Mg-Tschermak substitution ($Al^{IV} + Al^{VI} = Si + Mg$) mainly determined the variation in composition of amphiboles. The Al-in-hornblende geobarometer (Johnson & Rutherford, 1989) allowed an estimation of the depth of emplacement of the granitoids from levels of 5.5 to 0.7 kbar. Biotite, shows a wide range in the Al_t content from 2.5 to 3.4 (O=22) and its composition appears indicative of magma typology pointing to suites varying from Al-potassic to subalkaline. The distribution of the Mg/Fe ratio between coexisting biotite and amphibole turned out to be sensible to pressure of emplacement, the K_D value increasing with P (Fig. 2).

From the overall interpretation of the collected data the following information can be drawn:

a) a comparison of foliated versus massive granitoids allows to conclude that the former emplaced at deeper levels, probably along ductile shear zones whereas massive granitoids intruded at shallower depths in settings dominated by brittle deformation;

b) the early alignment and segregation of biotite flakes in foliated granitoid mushes prevented K_2O increase during differentiation and sometimes promoted the formation of low-K residual melts (Fig. 3);

c) foliated granitoids show a deeper contamination with crustal material in accordance with the presence of an Al-rich biotite;

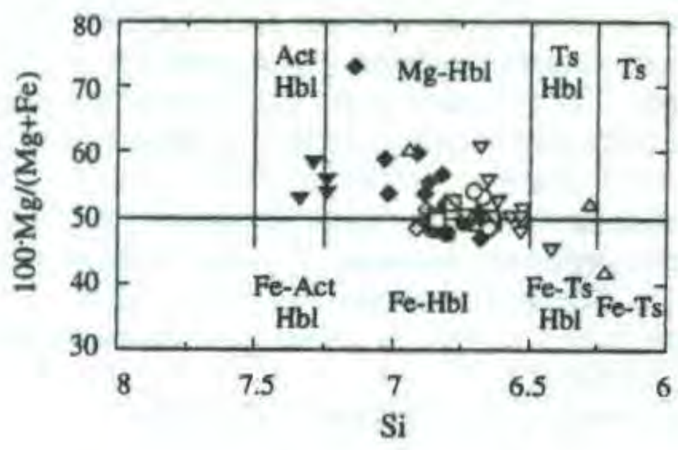

Fig. 1 - Amphiboles display a composition varying from Actinolitic hornblende (Act Hbl) to Fe Tschermakitic hornblende (Fe-Ts Hbl). Open symbols indicate foliated granitoids whereas closed symbols refer to massive granitoids.

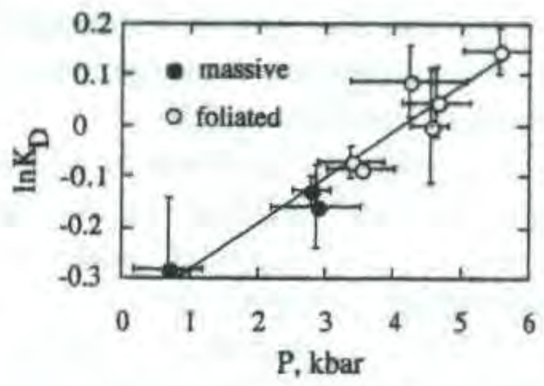

Fig. 2 - Diagram illustrating the sensitivity of the K_D value ($[Mg/Fe]_{Bt}/[Mg/Fe]_{Amph}$) to pressure of emplacement. Points are averages of some analyses for each plutonic mass.

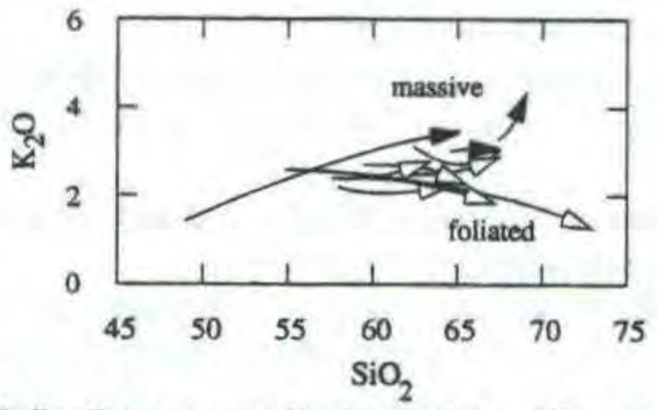

Fig. 3 - contrasting K_2O trends in foliated and massive granitoids. The early alignment and segregation of biotite flakes prevented the increase of K_2O during differentiation.

d) finally, younger Rb-Sr biotite cooling ages in foliated granitoids are coherent with a deeper emplacement and with a slow quasi-isobaric cooling.

References:
Johnson M.C. & Rutherford M.S. (1989). *Geology*, **17**, 837-841.
Rottura et al. (1990). *Lithos*, **24**, 97-119.

• BLUE AND GREEN TOURMALINES FROM GREGORIO PEGMATITE,BRAZIL

Adusumilli, Maria, S(*) ,Castro, Claudio de(**) ,& Bhaskara Rao, A.(*) *(*Inst. Geosciences, Univ. Brasilia. ** CECINE,Fed. Univ. Pernambuco, Recife)*

Green gem producing granitic pegmatites in Borborema region(RGN and PB States) are known since the World War II, but only recently the blue varieties have been recorded and are being coveted due to their precious nature, price and Cu2+ as colouring agent.The occurrences, one at São José da Batalha,PB(Fritsch et al 1989) and the other at Capoeira,RGN(Adusumilli et al,1993), have stimulated search to define controls of mineralization and regional exploration. A guide horizon of manganiferous laterite crusts in the colluvium, is proposed(Bhaskara Rao & Adusumilli, 1994, in press). for gem pegmatites.Gregório pegmatite is situated between the two occurrences and may constitute a link,in the exploration model.

Gregório pegmatite is located about 20 km SSW of Parelhas to Equador town,at an altitude of 270 m, at Serra dos Quintos and locally known as Quintos do Meio.The host rocks are biotite schists. The pegmatite has a nucleus Zone IV of rose and milky quartz; Zone III of perthitic feldspars with muscovite and quartz;Zone II feldspars and milky quartz with tourmalines and garnets; and Zone I feldpars and quartz; and masses of purple to rose lepidolite. Clevelandite occurs with lepidolite, indicating sporadic Na- and Li- phase activity. Neither the presence of complex phosphates nor the abundance of Li-silicates that characterise this pegmatite province, are noted.

Tourmalines are frequently black in aggregates; are green, blue and rose coloured sparsely. Prismatic crystals are upto 2 cm in size. They are transparent without solid inclusions; with vitreous luster; basal parting; associated with fragments and plates of lepidolite, milky and vein quartz, white clevelandite,and colourless micas. The fragments are compact and excellent for cutting. They are classified as gem elbaites, blue to green in colour.

These differ from tourmalines of other localities. These neither show the substitutions by lithium micas nor by quartz along the nucleus; also donot show colour zoning from the nucleus to the border. Thus, they are pegmatitic grown in the pneumatolytic phase when the B-rich fluids dominated. However, the colour of the green and the rose tourmalines is attruibuted to Fe 2+ and Fe 3+, Mn 2+,

Ti 4+ and possibly some Cr 3+; and the blue variety continues to owe its colouration to Cu 2+. The influence of charge transfer mechanism should also be considered in this explanation.

These tourmalines have a very good market.The presence of gem tourmalines in the Gregório pegmatite, and the blue variety, are significant in the exploration context. The following guides are proposed for exploration of gem pegmatites in this region.

l) Absence of typical Fe-Mn-Li phosphate minerals, characteristic of the granitic pegmatite region of Borborema Province (Adusumilli & Bhaskara Rao, 1994.in press)

2)Presence of Li-substitution through the minerals, specially lepidolites and spodumenes, besides occasional montebrasite-amblygonite.

3)Inicipient Na phase , evidenced through the well formed clevelandite aggregates in association with lepidolite.

4)Presence of oxides of Mn as masses; their transport in the colluvium, and resultant formation of manganiferous laterite crusts, due to lateritisation, covering the colluvial deposits containing gem tourmalines and overlying the gem pegmatites.

5)Frequent participation of Cu-Fe-S system in the evolution of the pegmatites, contributing Cu 2+ content of the tourmalines and hence their blue colouration.

6)Possible existance of other gem pegmatite deposits, as being evidenced through this occurrence,along the regional NNE-SSW trend of the biotite schists and gneisses, though these pegmatites cut across these structures and fill the fracture systems.

References:

Adusumilli, M.S., Castro, C., Milliotti, C.A., Bhaskara Rao, A., (1993)*XV SimpGeol.Nordeste, Natal. Extended Abstracts.* 142-144.
Adusumilli, M.S. Bhaskara Rao, A., (1994)*9 th. IAGOD Symp. Beijing. August(in press)*
Fritsch, E. et al., (1990). *Gems and Gemology,* 26, 189-205.
Bhaskara Rao,A. Adusumilli, M.S., (1994) *2 nd. SEGMITE International Conference. and Exhibition, Karachi. April (in press).*

Al/Si ORDERING TRENDS FOR THE TRICLINIC K-RICH FELDSPAR FROM X-RAY POWDER PATTERNS

Afonina G.G.(Inst. of Geochemistry, Siberian Branch of Russian Academy of Scienes, Russia)

Published resalts of crystall structure analysis of triclinic K-rich feldspars (Kfs) were used to obtaine the dependences of Σt_1, t_1O and Δt on t_1m and t_2O. In every case these dependences were approximated with two straigt differently inclined lines. Part of Kfs lie on the lines connecting tne last points on the charts. Regression analysis for the same reveal a similar dependence between $\Delta 2\theta(\bar{2}04-060)$ and Δt. This permitted establi-shing one-step and two-step Al/Si ordering trends in the triclinic Kfs.

In Kfs of one-step trends Al migrates into T_1O from T_1m twice faster than from T_2O or T_2m. In Kfs of two-step trends, at the first step Al migrates from T_1m to T_1O 1.5 times as slow as from T_2O or T_2m,and in the samples of the second step Al moves from T_1m into T_1O four times as fast as from T_2O or T_2m.

The regression equations connecting $\Delta t'$, $\Delta t''$ with $\Delta 2\theta(\bar{2}04-060)$ were obtained,where $\Delta t'$ corresponds to (t_1O-t_1m) for Kfs one step trends Al/Si ordering, $\Delta t'$ and $\Delta t''$ - for Kfs two-step trends of ordering. If Δt is calcu-lated from results of structure analysis or parameters of unit cells, $\Delta t'$ and $\Delta t''$ from $\Delta 2\theta(\bar{2}04-060)$, then equation $\Delta t=\Delta t'$ or $\Delta t=\Delta t''$ determine a trend of triclinic Kfs structure ordering.

The natural Kfs are investigated. In sam-ples with high Δt equations $\Delta t=\Delta t'$ is valid, while in samples with low Δt equalety $\Delta t=\Delta t''$ works.The values t_1O-t_1m for Kfs with the in-termediate ordering lie between $\Delta t'$ and $\Delta t''$.

GEOCHEMISTRY, MINERALOGY AND FLUID INCLUSIONS OF Sn-GREISEN MINERALIZATIONS IN THE SILJAN/GARBERG AND RÄTAN GRANITOIDS, CENTRAL SWEDEN

Ahl, M., *(Dept. of Geology and Geochemistry, Stockholm Univ., Sweden)*

A number of Sn-Pb-Zn-bearing greisen mineralizations are found in the northern part of the 1.65-1.8 Ga Transscandinavian Igneous Belt (TIB). Host rock for these are the most evolved parts of the ≈1.69 Ga Siljan/Garberg granites and the ≈1.70 Ga Rätan granitoids. These large post- to anorogenic batholiths were emplaced in environments exhibiting transitional features from compressional to extensional tectonics. The geochemistry of these late stage, high level emplaced granites show that they are highly evolved, as they are peraluminous, have an alkaline affinity, show A-type characteristics and have anomalously high F, Rb, Sn and Nb, as well as low Fe, Mg, Ti, Ba, Sr and Zr contents.

The greisen veins occur in zones bordering subvolcanic units and older units and are often structurally/fracture-controlled. Characte-ristic elements are Sn, Pb, Zn, Cu, W, Mo, As, Fe, F, Li, Be, Ag and Au. The mineralizations are spread over a wide area (≈10,000 km^2) and the mineral/metallic assemblages are somewhat different from place to place. They are small and economically insignificant.

In this investigation, two occurrences have been in focus, the Van and the Stora Flaten deposits. The main features for these greisen veins are cm to m wide dark alteration zones of quartz, mica minerals and chlorite in a red granite. These veins are characterized by a core of quartz, rimmed with Li-mica and ore minerals as cassiterite, galena, sphalerite, chalcopyrite, arsenopyrite and pyrite. Associated minerals are fluorite and topaz. In some of the greisen mineralizations, molybdenite, wolframite and scheelite also occur.

A preliminary study of fluid inclusions in quartz and fluorite, shows three major types of inclusions, containing aqueous, CO_2 (l)+(g) and solid phases.

A REVIEW: NONCLASSICAL PYRIBOLES-----WITH SPECIAL REFERENCE TO CALCIC ANALOGUE OF CLINOJIMTHOMPSONITE, AND QUADRUPLE AND RELATED CHAIN STRUCTURES IN METAMORPHISM

Akai J. , Konishi H. and Chiba A. (*Dept. of Geology and Mineralogy, Fac. Science, Niigata University*)

Since the first finding of ferromagnesian Triple Chain Silicates (TCS) from Chester Vermont USA (Veblen & Burnham ,1975, 1978), much interest has been focussed on biopyribole structure types. The same or similar minerals of Optical Microscopic (OM) size have been reported. (Widgiemooltha (Akai, 1981); Orijarvi (Shumacher &Czank, 1987)etc.). It has become urgnt problem to clarify whether calcic analogue of such pyriboles are present or not. Calcic analogue of clinojimthompsonite with width of 1000A which formed in metasomatic alteration was first found in Akatani.(Akai, 1982). Recently, Konishi (1991), and Konishi and Akai (1993) found calcic analogue of clinojimthompsonite of OM size from metamorphosed serpentinites in Japan. The most typical one is from Oeyama ophiolite, in Kyoto Prefecture, Japan. The calcic analogue of clinojimthompsonite is now in proposal as a new mineral. Its mineralogical data are as follows:

Chemical formmula : Ideal formula ; $Ca_2(MgFe)_8Si_{12}O_{32}(OH)_4$

Analytical result ; $(Ca_{1.924}\ Na_{0.039}K_{0.003})(Mg_{7.774}Fe_{0.197}Mn_{0.012}\ Cr_{0.017}Ti_{0.008}Al_{0.027})\ (Si_{11.984}Al_{0.016})O_{32}(OH)_4$

Space Group : C2/c

Lattice constants : a = 9.82 Å b= 27 .05Å c= 5.27 Å $\beta = 104.5^{\circ}$

Optical property: colorless or slightly pinkish in thin section and refractive index is lower than that of tremolite , birefringence is higher than that of tremolite in [001]section ; Cleavage angle 141

These triple chain silicates (or structures) can be classified and summarized based on compositional and genetic aspects (Table 1). It is suggested that such pyriboles or Chain Width Disorder in Pyriboles (CWDP) containing TCs may become characteristic indicators of characterisitc low grade metamorphism. For example, Ocean floor metamorphism is unique for formation of disordered pyriboles.

Calcic analogue of chesterite with width of 1500Å or more was also found in serpentinite from Yanahara and the other occurrences (Konishi , 1991; Chiba and Akai, 1994).

Quadruple chain structure which has length of 1000Å in **b** direction was found also with (42) structures (Chiba & Akai , 1994). These results further suggest that quadruple chain silicates larger than this

Table 1 Summary of occurrences of triple chain silicates (TCS) and related CWDP

A. Mg-Fe TCS : Jimthompsonite, chesterite, clinojimthompsonite (Optical Microscopic size)
   1. Reaction zone in serpentinite associated with metamorphism ; Chester, & other localities
   2. Thermally metamorphosed serpentinite ; Oeyama, Hayachine, Tari
   2'. Hydrothermally altered serpentinite (Grobety, 1992)
   3. Anthophyllite-cordierite rock ; Orijarvi , Yanahara

B. Ca(Mg,Fe) TCS : Calcic analogue of clinojimthompsonite (OM size)
   Metamorphosed serpentinite ; Oeyama, Tari, Hayachine

C. Ca(Mg,Fe)-TCS or Mg-Fe TCS , or CWDP (TEM size)
   1. Metasomatic alteration ; Akatani, Wagasennin, etc
   2. Ocean floor metamorphism (low grade metamorphism) ; Dredged specimen from Mariana Trench , Shimokawa
   3. Hydrothermal action (Geothermal area) ; Salton Sea (Yau, et al, 1986)
   4. Alteration of pyroxenes ;
   5. Ca-metasomatism ? ; rodingite (unpublished data)
   6. Ni ore mineralization process (this study) : Mariners mine

may be present in natural samples.

The next important point is their formation conditions. Some estimates based on natural samples are present : For jimthompsonite; (Orijarvi 550-630°C, 3-5 kb; Yanahara , 650 ±50°C and 4kb. etc) ; For calcic CWDP the following conditions for formation are suggested although they may not be thermodynamically strict ; (Akatani , < 300°C and low pressure, Salton Sea, 310-330°C). On the other hand, Calcic TCS with vacancy structure were derived at 500- 650°C, 600kg/cm2 by ion-exchange from Na-TCS (Akai & Saito, 1985). As is reviewed by Veblen(1992) or Maresch & Czank (1988) on CWDP in synthetic pyriboles, details are not clarified yet. However, frequent CWDP may depend largely on lower pressure < 5 kb or less. Presence of CWDP is suggesting a problem on thermodynamic stability of amphiboles.

Metamorphic nonclassical pyriboles of OM size are not so rare and show wide range of occurrences. So, it can be said that nonclassical pyriboles are one of important rock forming minerals.

References : Akai (1981) Abs. Sankoh Gakkai 72*;---- (1982) CMP, 80, 117-131; ----& Saito (1985) Bull. Min. 108. 21-28;---- (1988) Min. Geol. Sp. Is. 12, 105 -114; ---- (1993) Jour. Min. Soc. Jap. (KZ) 22, 95-111 *;---- et al. (1992) Abs. IGC 684.: Grobety (1992) Ph D. disset. ETH; Konishi (1991) Dr. Thesis Niigata Univ.; ---- & Akai (1993) Journ. Geol. Soc. Jap. 99, 679 -682; Chiba and Akai (1994) Abstr. Annu. Meet. Min. Soc. Japan *; Maresch & Czank (1988) Fortscr. Min. 66, 69-121; Shumacher & Czank (1987) Am. Min. 72, 345 -352; Yau et al. (1986) CMP, 94, 127-134; Veblen (1992) Rev in Min., 27, 181-229;----- & Burnham (1975) Abs. Trans Am. Geop. U. 56, 1076 ;---- (1978) Am. Min. 63, 1000-1009 (*: in Japanese)

THERMODYNAMIC PROPERTIES AND STABILITY RELATIONS OF HIGH-PRESSURE MANTLE MINERALS

Akaogi, M., Kojitani, H., Shiraishi, K. (Dept. of Chemistry, Gakushuin Univ.), Yusa, H. (Inst. Solid State Phys., Univ. of Tokyo) and Ito, E. (Inst. Study of Earth's Inter., Okayama Univ.)

Thermodynamic properties of silicates stable in the deep mantle are indispensable to calculate the phase relations at high pressures and high temperatures. Quartz-coesite-stishovite transitions in SiO_2 are widely accepted as pressure standards at high temperatures. We have measured the enthalpies of these transitions and heat capacities of the three polymorphs. The measured heat capacities decrease in the order of quartz, stishovite, and coesite above room temperature. This result is inconsistent with that by Watanabe (1982). Although the measured enthalpy for the quartz-coesite transition agrees with that by Akaogi and Navrotsky (1984), our new enthalpy data on the coesite-stishovite transition is about 10 kJ/mol smaller than the previous work. The coesite-stishovite boundary, calculated using the new enthalpy and heat capacity data, is more consistent with that by Zhang et al. (1993) than Yagi and Akimoto (1976).

The enthalpy for the $MgSiO_3$ orthopyroxene-perovskite transition was also measured, based on multiple measurements of perovskite. Using the data, the enthalpy for dissociation of Mg_2SiO_4 spinel to $MgSiO_3$ perovskite plus MgO was calculated as 86.1 ± 3.6 kJ/mol, which is about 11 kJ/mol smaller than that by Ito el al.(1990). The calculated slope of this boundary is -3 ± 1 MPa/K. Combining this slope with recent mantle convection studies, it is suggested that the upper mantle and the lower mantle convect separately, but intermittent mixing occurs between them. Our preliminary measurements suggest that the enthalpy for the orthopyroxene-perovskite transition in $(Mg_{0.92}Fe_{0.08})SiO_3$ is slightly smaller than that for $MgSiO_3$. The effect of iron substitution on the post-spinel transition boundary will be discussed.

MODEL FOR COMPUTING MINERAL FORMATION FROM BOILING FLUID: ACCOUNT OF DIELECTRIC CONSTANT.

Akinfiev N.N. (*Dept. of Chemistry, Moscow State Geological Prospecting Academy*)

Change in acidity and/or decreasing of ligands' concentrations are assumed to be the main physical-chemical reasons for mineral formation occurred while volatiles boiling away during fluid's exsolution process. In the present communication as a specific example of $PbS-H_2O-CO_2-NaCl-H_2S$ system it is shown that associated variation in dielectric permittivity of solvent mixture has also to be considered as a highly powerful factor of ore formation.

1. The water dissolution of nonpolar gases (CO_2, CH_4) gives rise to the reduction of dielectric constant ε_m of the medium. To compute ε_m it could be set that additive is the $\varepsilon^{1/3}$ value. So for H_2O-CO_2 mixture

$$\varepsilon_m^{1/3} = \Phi_{H2O} \cdot \varepsilon_{H2O}^{1/3} + \Phi_{CO2} \cdot \varepsilon_{CO2}^{1/3} ,$$

where Φ_{H2O} and Φ_{CO2} - volume fractions of H_2O and CO_2 with relative permittivities ε_{H2O} and ε_{CO2}. Decreasing in ε_m will accent the association reactions equilibrium to the products. For the detailed calculation of this effect it is convenient to use HKF state equation (Tanger & Helgeson, 1988): change in ε_m acts on the solvation part of Gibbs free energy of aqueous species $\Delta G_s = \omega \cdot (1/\varepsilon_m - 1)$, where $\omega = \eta \cdot Q^2/r$ refers to the absolute Born parameter of the species with charge Q and effective electrostatic radius r [Å], and $\eta = 1.66027 \cdot 10^5$ cal · Å/mole. So to compute equilibrium in the mixed fluid it is necessary to modify standard chemical potential of every species such as

$$\Delta G_m = \omega \cdot (1/\varepsilon_m - 1/\varepsilon_{H2O}) \qquad (1)$$

This approach enables oneself not to confine within examination of isolated reactions, but study equilibria of the whole system.

2. With the goal to estimate change in ε_m impact on the transport possibility of model $H_2O-CO_2-NaCl-H_2S$ fluid, calculations of PbS (galena) solubility were executed under typical natural ore formation conditions: T= 150-400°C and total pressure P=1 kbar. Concentration range of NaCl and H_2S 1.11 and 0,01 mole/kg_{H2O} were adopted. The initial concentration

of CO_2 was set to be 9.5 mole/kg that corresponds to the onset of boiling at 350°C. While the subsequent temperature lowering. CO_2 concentration decreases slipping along the saturation curve. The thermodynamic data from SUPCRT92 (Johnson *et al.*, 1991) were applied, and activity coefficients of ions were calculated using Debye-Hückel approach. The comparison of equilibrium composition of solution computed in two cases - before and after chemical potentials' modification according to (1) - gives one's evidence that variation of ε_m dramatically changes all the chemical properties of the soluti-

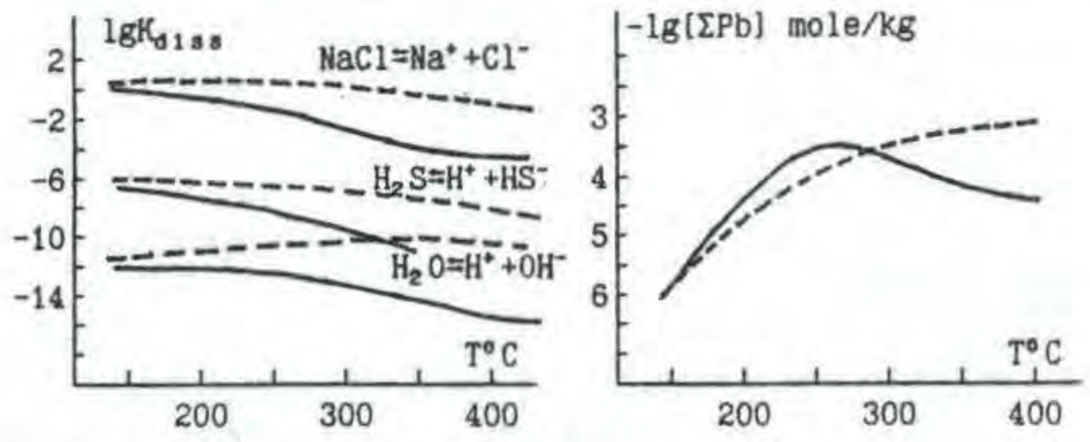

on. The main case is in a strong ions' association. Left fig. represents temperature dependence of some dissociation constants calculated without (dotted line) and with (solid line) account of ε_m change. Also the behaviour of Pb in the solution does change too. Thus at 400°C $PbCl_2^0$ is superior to all other chloride complexes, but not $PbCl_4^{2-}$ as it is expected. This effect causes the PbS solubility curve to have particularly pronounced maximum at 275°C (right fig.). Such a behaviour of Pb could favour its overdepositing and concentrating while moving fluid is cooling down.

The obtained results furnish distinct explanations for physical-chemical mechanisms of natural mineral formation.

References:
Tanger IV J.C., Helgeson H.C. (1988). *Amer. J. Sci.*, **288**, 19-98.
Johnson J.W., Oelkers E.H., Helgeson H.C. (1992). *Comp. Geosciencies*, **18**, 899-947.

DEHYDRATION AND REHYDRATION IN ZEOLITE YUGAWARALITE: A SINGLE-CRYSTAL X-RAY STUDY.

Alberti A. *(Inst. of Mineralogy, Univ. of Ferrara, Italy)*
Quartieri S. and Vezzalini G. *(Dept. of Earth Science, Univ. of Modena, Italy)*

Dehydration and rehydration processes and phase transformations of yugawaralite ($CaAl_2Si_6O_{16} \cdot 4.2H_2O$) were studied by single crystal X-ray diffraction. The crystal structure of samples dehydrated under vacuum for 24 hours at 20, 100, 150, 200 and 250°C were compared to that of a non-dehydrated sample. Rehydration behaviour was studied on the sample dehydrated at 150°C brought back to room conditions.

Yugawaralite is monoclinic, Pc, with ordered (Si,Al) distribution. The Ca atom is coordinated to four framework oxygens and four water molecules. Two of these molecules are disordered over two alternative oxygen positions. Another water site, with low occupancy, is present, and is not coordinated to Ca (Fig. 1a)

Yugawaralite held in vacuum at room temperature - even for relatively long times - does not show noticeable structural changes. Yugawaralite heated at 100°C loses the Ca non-coordinated water molecule, while the two disordered water molecules move in fully occupied sites intermediate between the two alternative positions present in the non-dehydrated sample. Ca remains 8-coordinated. When the mineral is heated at 150°C, two of the four water sites become empty. The Ca atoms are now 6-coordinated by four framework oxygens and the two residual water molecules. The reduction of the Ca coordination number causes an increase of T-O bond distances for the oxygens coordinated to Ca, compensated by an overall decrease of all the other T-O distances. Yugawaralite heated at 200°C shows a further 50% loss of the residual water and collapsing of the channel system: a sudden decrease of unit cell volume occurs (about 13%), the cell parameter *a* is doubled, the space group changes from Pc to Pn, and the structure is strongly squashed. Ca atoms are 6-coordinated, but now with five framework oxygens and one water molecule (Fig. 1b). Heating of the mineral at 250°C does not cause any noticeable modifications with respect to the structure at 200°C. When yugawaralite heated at 150°C is taken back to room conditions for two weeks, a complete rehydration occurs, with the water molecules in the same positions, and the same occupancies as in the non-dehydrated sample, whereas the framework maintains a slight deformation with respect to the untreated sample.

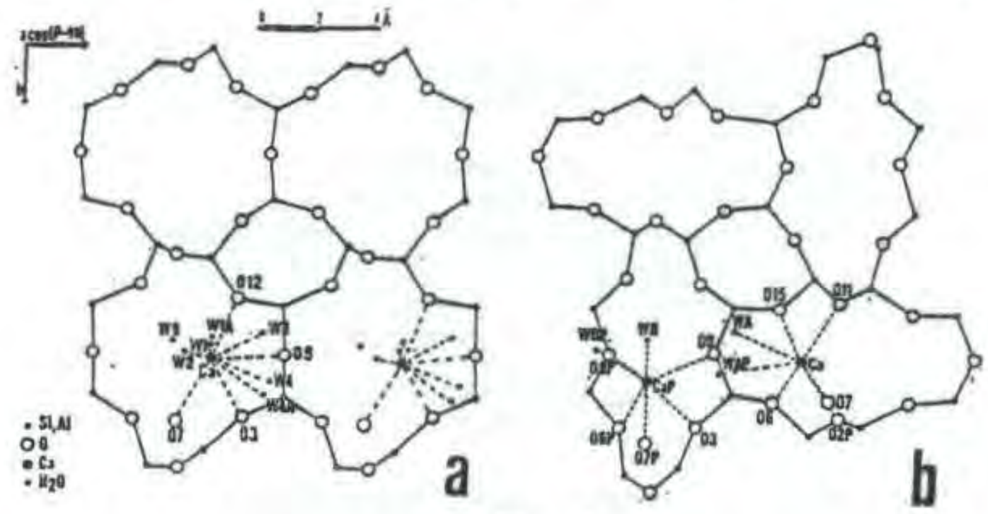

Fig. 1

Projection along [001] of non-dehydrated (a) and heated at 200°C (b) yugawaralite.

• MINERAL COMPOSITION AND REE GEOCHEMISTRY OF POSTMAGMATIC CALC-SKARNS FROM ITALY AND FAR EAST OF RUSSIA

Aleksandrov S.M. *(Vernadsky Inst. of Geochemistry and Analytical Chemistry of Russian Academy of Sciences, Moscow, Russia)*

Objects of study were calc-skarns of Elba (Calamita and Torre de Rio) and Capo di Bove in Tuscany, Italy, and Dal'negorsk deposit in Russia. All deposits are localized in exocontacts of granitic intrusions with limestones or, as exclusion, dolomites (Calamita).

In all deposits the following chronological sequence of skarn minerals was observed : wollastonite (Russia) – hedenbergite – ilvaite – garnet (Russia) – quartz, and constant presence of rhythmic-banded structures in metasomatic rocks. The stable composition of minerals in each deposit is related to the infiltration kind of skarn genesis.

The presence of rhythmic-banded structures is probably due to non-equilibrium thermodynamic conditions of the carbonate rocks replacement. This started from a development of wollastonite or hedenbergite on margines of equally grained marbles blocks near fluid-transported tectonic cracks and proceeded up to its full replacement. The crystal-growing trend in each early mineralic rhythms (wollastonitic in Dal'negorsk and hedenbergitic in all others) is directed toward the carbonatic rocks from the cracks. The front of replacement may have been curved or kept subparallelic to the cracks. Each rhythm reflects numerous repeatedly stops of chemical reactions at the time of replacement. Crossing rhythms in skarn structures are absent.

All the next secondary minerals (part of hedenbergites in Russia, ilvaite in Italy and garnet in Russia) are replaced pseudomorphically on early silicates in both sides between rhythms or as monomineralic front near the new tectonic cracks and have not changed the composition in each of investigated deposits.

The order of formation of skarn is reflected in the oxidation range of iron, that is maximal at the time of garnet formation. The Mg contents in hedenbergites are determined by the presence of carbonatic rocks and in Calamita reach up to 7.6%. All Mn is coming from hydrothermal solutions. Contents of REE in all deposits are monotonic and low, with little Ce-, Nd- and Gd-

maximums and, within one-order of variation, are similar to REE in marbles.

RARE-ELEMENT ALBITE PEGMATITES FROM THE CAP DE CREUS FIELD (EASTERN PYRENEES): P,T CONDITIONS OF FORMATION

Alfonso P., Melgarejo J.C. (*Dept. de Cristal·lografia, Mineralogia i Dipòsits Minerals, Univ. de Barcelona*)

In the Cap de Creus pegmatite field four types of granitic pegmatites have been stated according to their mineralogy and internal structure (Corbella y Melgarejo, 1993). Types I and II represent microcline-rich, barren or transitional pegmatites. Type III belongs to the beryl-columbite-phosphate subtype, and type IV to the albite subtype, according to the classification of Černý (1992). All these pegmatites crop out in separate areas related to the regional metamorphic grade.

Albite pegmatites represent the most evolved ones in the field and they are the richest in Nb-Ta-REE-Be-Li minerals. They occur within the cordierite-andalusite zone, in the outernmost part of the field. They are sparse, tabular-like and 1-2 m wide. Several units can be distinguished within these veins:

- border zone: fine-grained aggregates of quartz-muscovite;
- first intermediate zone: aplitic-sized aggregates of quartz, albite, columbite-tantalite, microlite and other REE-bearing minerals, muscovite and seldom beryl, apatite and montebrasite;
- second intermediate zone: similar mineralogy as above, but richer in primary phosphates as montebrasite, sarcopside, graftonite, lazulite and wyllieite;
- quartz core
- quartz-muscovite veins: they are richer in REE-Nb-Ta minerals and beryl; cassiterite, chrysoberyl, gahnite and nigerite can also be present;
- phosphate veins: formed by berlinite replaced by alluaudite, montebrasite, trolleite, lazulite, wyllieite, brazilianite and berillonite; Nb-Ta minerals can also occur;
- late clevelandite-chlorite veins: they are vugs rich in Ti-REE-Nb-Ta oxides and allanite.

The contacts with the host schists are sharp, but metasomatic phenomena are common at the exocontact: tourmalinization, graphitization, muscovitization and phosphatization (apatite).

Fluid inclusions have been measured in quartz, beryl and albite. They can be classificated in 5 types:

(A).- Multiphasic, with filling degree of 10-25%, salinity 36-39 wt eq % NaCl. Raman analysis of the bubble do not detect any component. Th are 290-370°C. They occur in the intermediate zone.

(B).- Multiphasic, with filling degree of 10-25%, salinity 31-32 wt eq % NaCl. Raman analysis of the bubble do not detect any component. Th are 270-318°C. They occur in the quartz core.

(C).- Monophasic, with CO_2 (76%), N_2 (20%), CH_4 (4%). Th_{CO2}(L) are 10-15°C. They also occur in the quartz core.

(D).- Multiphasic, with filling degree of 20%, salinity 34-36% wt eq % NaCl. Raman analysis of the bubble do not detect any component. Th are 260-290°C. They occur in the quartz-muscovite veins.

(E).- Triphasic or biphasic, with filling degree of 15-20%, salinity between 23-30%. They can contain or not halite as daughter crystal. Th are 280-330°C. They occur in cleavelandite veins.

According to the coexistance of both (B) and (C) types in the quartz core, we can state the conditions of formation of this unit: P= 2.2 Kb and T= 420-430°C. The second intermediate zone could tentatively occur between 440-540°C and P between 2.2-2.8 Kb. The quartz-muscovite veins could be formed at T<360°C.

References

Černý, P. (1991). *Geosc. Can.*,**18**:68-81

Corbella, M., Melgarejo, J.C. (1993). Proc. 8th. IAGOD Symposium. *Schweizerbart'sche Verlagsbuchhandlung*. Stuttgart, 295-302

THE CRYSTAL CHEMISTRY OF HIGH-ALUMINIUM PHLOGOPITE

Alietti, E., Brigatti, M.F. and Poppi, L (*Dept. of Earth Sciences, Univ. of Modena*)

Aimed at characterising the crystal chemical processes occurring in micas, this study affords insight into the structural changes that take place in phlogopite crystals with high Al^{3+} contents ($1.50 \leq {}^{[4]}Al^{3+} + {}^{[6]}Al^{3+} \leq 1.97$ atoms, calculated on the basis of $[O_{10}(OH)_2]$). The Al-rich phlogopite crystals studied are from skarns of the Predazzo and Monzoni Hills petrographic area (north-east Italy) and belong to $1M$ polytype.

Taking into account the ideal phlogopite composition $[{}^{[12]}K{}^{[4]}(Si_3Al){}^{[6]}Mg_3\ O_{10}(OH,F)_2]$, the Al^{3+} for Si^{4+} tetrahedral substitution in the crystals studied is mostly compensated for by the exchange vector $Si_{-x}\ Mg_{-y}\ Al_{x+y}$, where the subscripts x and y refer to the tetrahedral substitution of Al^{3+} for Si^{4+} and the octahedral substitution of Al^{3+} (and/or Fe^{3+}) for Mg^{2+} (and/or Fe^{2+}), respectively. The extent of tetrahedral substitution is lower than 40%.

The space group $C2/m$ (agreement factor: $0.025 \leq \mathcal{R} \leq 0.030$) and show:

— *tetrahedral sheet.* The tetrahedral mean bond lengths ($1.660 \leq$ <T-O>≤ 1.666 Å) are greater than those observed for the Mg^{2+} - true mica end members. The tetrahedra are quite regular: $1.0000 \leq TQE \leq 1.0002$; $0.03 \leq TAV \leq 0.91$; $110.6° \leq \tau \leq 110.3°$ (TQE and TAV as defined by Robinson *et al.*, 1971; τ is the flattening tetrahedral angle). Thus, with respect to ideal phlogopite, the increase in tetrahedral Al^{3+} produces more flattened tetrahedra which become more regular. The most significant difference in respect of the crystals of the phlogopite-annite join so far refined is that the tetrahedral ring rotation angle (α) is always higher than 10°. The α values come near both to those reported for trioctahedral brittle mica kinoshitalite $[{}^{[12]}Ba{}^{[4]}(Si_2Al_2){}^{[6]}(Mg_3)\ O_{10}(OH,F)_2]$ (Brigatti & Poppi, 1993) and to dioctahedral muscovite-$2M_1$ (Bailey, 1984). The lateral misfit between tetrahedral and octahedral sheets in Al-rich phlogopites is compensated for by a large tetrahedral ring rotation, whereas, in kinoshitalite, it is generally counterbalanced by single polyhedron and tetrahedral ring distortion;

— *octahedral sheet.* The octahedral sites follow the general trend of phlogopite, which is homoctahedral of type I (Weiss *et al.*, 1992), the M1 and M2 mean bond lengths being quite similar within the bounds of experimental error. The octahedral dimensions do not seem to have been markedly affected by tetrahedral features. This behaviour is even more evident if the M1 and M2 mean bond lengths are compared with the tetrahedral α angle.

References:

Bailey, S. W. (1984). *Reviews in Mineralogy*, **13**, 13-60.

Brigatti, M. F., & Poppi, L. (1993). *Eur. J. Mineral.*, **5**, 857-871.

Robinson, K., Gibbs, G. V., Ribbe, P. H. (1971). *Science*, **172**, 567-570.

Weiss, Z., Rieder, M., Chmielovà, M. (1992). *Eur. J. Mineral.*, **4**, 665-682.

DOSIMETRY WITH NATURAL KAOLINITES : APPLICATION TO THE STUDY OF PAST URANIUM TRANSFERS IN THE GEOSPHERE

Thierry Allard (*Lab. de Minéralogie Cristallographie, Univ. de Paris 6 et 7*), Jean-Pierre Muller (*ORSTOM, Dépt T.O.A. and Lab. de Minéralogie Cristallographie, Univ. de Paris 6 et 7*), Blandine Clozel (*DRGGP, BRGM*), Marie-Thérèse Ménager (*DCC/DESD/SCS/SGC, CEN-FAR*), Georges Calas (*Lab. de Minéralogie Cristallographie, Univ. de Paris 6 et 7*)

Several types of radiation-induced defects (RID) have been

detected in natural kaolinites by Electron Paramagnetic Resonance (EPR), and interpreted as hole-centers located on oxygen atoms of the kaolinite structure (Angel et al., 1974 ; Clozel et al., 1994). They are differenciated by their location within the kaolinite framework, the kinetics of their formation and their stability (Clozel et al., 1994). One radiation-induced defect, namely the A-center, is stable at the scale of geological periods and may provide a record of past radionuclide occurrence (Muller et al., 1992). Thus, our objective was to test the use of kaolinite as a natural *in situ* dosimeter for tracing past migrations of uranium in the geosphere. This could give useful informations on the processes governing the transport of radionuclides through various rock formations which are considered for the disposal of high-level nuclear waste. For that purpose, kaolinite is relevant because of its widespread occurrence, its high contact area with radioactive fluids and its high sensitivity to natural irradiation.

We first derived relations between the concentration of A-center and the radiation dose through artificial irradiations. We used natural kaolinites with varying degrees of crystalline order and chemical purity. Simulations of effects of naturally-occuring α-particles and γ-rays were carried out with He^+ ion-beams (Allard et al., 1994) and γ ^{60}Co source, respectively. The dose range was calculated to be consistent with radioactivity in uranium ore deposits (≤ 690 MGy). The concentration of A-center was measured using the least-square linear decomposition procedure of the EPR spectra according to Clozel et al., (1994). The production curves of A-center can be satisfactorily described by simple exponential functions in dose ranges which are sample- and radiation-dependent. This allows the determination of parameters relevant for a dosimetry with kaolinite, i.e. the radiation efficiency and the saturation level of A-center concentration. These parameters were correlated to the crystalline order of kaolinite in alpha-irradiation experiments.

Using these experimental results obtained on reference kaolinites, we tentatively calculated paleodoses of kaolinites from natural analogues of radwaste repositories. We present an example from an uranium-deposit hosted in a hydrothermally-altered tuff (Nopal, Mexico, Muller et al., 1990 ; Ildefonse et al., 1991). It is shown that these paleodoses can evidence ancient leaching or accumulation of uranium. They can also be used to quantify these past uranium transfers, provided that some constraints can be put : (i) on the age of the kaolinites and of the alteration events which were responsible for uranium migrations; (ii) on the contributions of ^{230}Th and ^{40}K to the dose absorbed by kaolinites; (iii) on the kinetics of leaching/accumulation of uranium (punctual or continuous event).

Allard, T., Muller, J-P, Dran, J-C, Ménager, M-T (1994). *Phys. Chem. Miner.* (in press)

Angel, B.R., Jones, J.P.E., Hall, P.L. (1974).*Clay Miner.* **10**, 247-255.

Clozel, B., Allard, T., Muller, J-P (1994).*Clays Clay Miner.* (submitted)

Ildefonse, P., Muller, J-P, Clozel, B, Calas, G. (1991). *Mat. Res. Soc. Symp. Proc.*, **212**, 749-756.

Muller, JP, Clozel B., Ildefonse P., Calas G. (1992). *Appl.Geochem.*, Special Issue **1**, 205-216.

Muller, J-P, Ildefonse, P., Calas, G. (1990). *Clays Clay Miner.*, **38**, 600-608.

MINERALOGY AND ELECTRON PARAMAGNETIC RESONANCE OF BERYL FROM THE KARATH AREA, SAUDI ARABIA.

Almohandis, A.A. (Dept. of Geology, King Saud University).

Pale green to yellowish green crystals of beryl occur in the Karath area, Saudi Arabia. The beryl-bearing pegmatite occurs at the contact of the Bani Thowr pluton with the young metamorphic rocks.
Small patches of beryl, thorium-monazite and columbite-tantalite were found near and inside the core of the pegmatite.

Mineralogical investigation and electron paramagnetic resonance were carried out on single crystals of the mineral at room temperature. X-band and Q-band spectra show essentially the same features. Thermally treated beryl gradually losses colour giving EPR lines of higher intensity and narrower line width. The EPR spectrum is attributed to ferric (Fe^{3+}) ions and manganese (Mn^{2+}) ions, at octahedral sites.

References:

Blak, R., Isotani, S., and Watnabe, S. (1982). Phys. Chem. Minerals, 8, 161-166.

Dvir, M. and Low, W. (1960). Phys. Rev., 119, 1587-1591.

Hawthorne, F.C. and Cerny, P. (1977). Can. Mineral., 15, 414-421.

VARIATIONS IN PYRITE CRYSTALS HABIT FROM CAMEROS BASIN (NE SPAIN)

Alonso-Azcárate, J.; López-Andrés, S.; Fernández-Díaz, L. and Rodas, M. *(Dept. Cristalografía y Mineralogía, Univ. Complutense Madrid).*

Pyrites from Cameros Basin, Soria-La Rioja NE Spain, represent one of the best natural examples of crystalline habit variation within a single mineral species. Some of these mineralizations are associated with a NW-SE schistosity band along the basin.

They are hosted across the basin by different formations of Upper Jurassic to Lower Cretaceous age. Pyrite crystals are found within different types of materials: lutites, sandstones, limestones and marls.

The pyrite deposits are located in the contact between permeable (sandstones) and impermeable materials (lutites and marls) that correspond to meandering and lacustrine depositional environments.

It has been traditionally accepted that these pyrites have got a diagenetic origin. However, recent sedimentologic and mineralogic studies on the Cameros Basin (Barrenechea, 1994) have pointed out that they could be related to the hydrothermal metamorphism that affected the basin. The presence of chloritoid, chlorite and illite inclusions within the pyrite crystals supports this interpretation.

The wide range of sulfur isotopic composition of these pyrites ($\delta^{34}S$ = -6.98 to 11.24‰) would indicate different sources for the S.

Pyrite crystals from Cameros Basin show a wide diversity of habits. Only three forms make up the majority of the morphologies: the cube *a* {100}, the octahedron *o* {111}, and the pyritohedron *e* {210}. The most common morphology is defined by cube faces {100} that can be perfectly smooth or show different degrees of striation. Acicular and thin platy habits, originated by an anisotropic development of equivalent *a* {100} faces, are not rare. Crystals corresponding to this last kind of morphologies always show perfectly smooth surfaces. Octahedral faces {111} appear combined with faces {100}. The relative morphological importance of both faces is variable. The pyritohedral faces *e* {210} can appear with or without cube faces. In the first case, cube faces show a heavy striation and, frequently, faces {hk0} can be also distinguished. Crystal aggregates and crystals showing split growth phenomena have also been found. A systematic pattern of changes in pyrite habit can be drawn within this basin.

The morphology of pyrite crystals grown from hydrothermal solutions is mainly controlled by two factors: temperature and supersaturation. The maximun temperature reached in the Cameros Basin ranges from 385°C to 410°C (Barrenechea, 1994); the pyrite crystals grew under these temperature conditions . The morphological diversity exhibited by pyrite crystals results from differences in the degree of supersaturation reached, during the growth proccess, in different regions of the basin. Changes in supersaturation level determine changes in crystal growth

mechanism. This affect the relative development of different faces. Murowchick and Barnes (1987) experimentally demonstrated that a general sequence of forms indicating increasing degree of supersaturation is cube to octahedron to pyritohedron. As these authors pointed out, mapping of pyrite habit could give interesting information to delineate zones of high supersaturation of hydrothermal fluids and zones of potential mineralization.

References:

Barrenechea, J.F. (1994) Ph D.
Murowchick, J.B. and Barnes, H.L. (1987): Am. Min. **72**, 1241-1250

DIAMANDS FROM AUTOLITHS IN UDACHNAYA PIPE

Altukhova Z.A.(Yakut.Inst.Geol.Sciences RAS)

Kimberlite breccias usually contain inclusions of kimberlite composition (autoliths). It is established in light of the Udachaya pipe that predominance of a particular type of autoliths affects both diamond grade and quality in the rock.

Comparison of diamonds from ultrabasic xenoliths,autoliths and the enclosing rock reveals important regularities in terms of diamond genesis. In serpentinized peridotite, diamond are predominantly rounded or of transitional type,fragments and octahedra are absent. Most diamonds have graphite inclusions. Snuff-colored diamonds are 3 times higher in quantity than steel-gray.

Diamond from fine grained (aphyric) autoliths also have distinctions. As compared to the enclosing rock, 50% of diamonds in autoliths are whole crystals. Half of them are octahedra, 25% - intergrowths, the other 25% - equal amounts of rhombododecahedra and transitional type stones.Like in peridotite, snuff-colored stones are 3 times higher than steel-gray. A distinctive feature of diamonds from autoliths is a high proportion of crystals with chromite inclusions (25%), as opposed to only 2% among those from the host rock. The host rock of porphyritic texture contains more fragment crystals and rounded diamonds (not found in autoliths) and less octahedra (3 times), rhombododecahedra and intergrowths.

For the eastern body of Udachnaya pipe, comparison of olivine-bearing and serpentinized porphyritic autoliths shows that the latter contain more diamond fragments,rounded crystals and rhombododecahedra but less stones of transitional type. The same tendency shows up on comparing morphologies of diamonds from olivine-bearing autoliths and the carbonatized ost rock. The latter contains 1,5 times less octahedra and trasitional crystals but 2 times more rounded crystals, rhombododecahedra and macles.

Carbonatized porphyritic autoliths have 1.5-2 times less diamonds of all morphologies except octahedra. However, there are more intergrowths, macles, colored diamonds and stones with graphite inclusions compared to serpentinized autoliths.

Morfological distinctions of diamonds from aphyric autoliths whose formation in thought to be related to special cooling conditions of a fluid phase of kimberlite magma indiindicate that these diamonds could have grown in situ considering a high proportion of stones with chromite inclusions and octahedra. In porphyritic autoliths,diamonds could be produced by disintegration of various diamondbearing rocks. This is evidenced by higher grade and better quality of diamonds in molten dunites and peridotites in comparison to kimberlite. Serpentinization and post-magmatic carbonatization adversely affect both the grade and uality of diamonds.

NITER AND GYPSUM AND THEIR DECAY EFFECTS IN A GRANITIC MONUMENT OF BRAGA (PORTUGAL)

Alves C.* and Sequeira Braga M.A., Depto. Ciências da Terra, Univ. Minho, Portugal (STEP/CT-90-0101). * JNICT Scholarship.

Soluble salts have been generally recognized as one of the most important decay agents in monuments. Nevertheless, few studies have been carried out concerning the effects of the different salt species. Previous studies have been done on several specific aims like field observations (Arnold & Zenhder, 1989); salt crystallization pressure (Winkler & Singer, 1972) and salt solubility and porosity structures of the building material (Hammecker, 1993).

In this paper are presented and discussed new results about soluble salts in granitic pillars and wall paintings in the Museu dos Biscainhos (Braga), where niter and gypsum are the main agents of decay.

XRD (fig. 1) and SEM analyses showed the presence of gypsum in granitic blocks and of niter in granitic blocks and wall paintings.

Gypsum occurs in the rupture surfaces of plates developed in granitic stones and has a strong decay effect. Nevertheless, gypsum was punctually found in efflorescences on granitic blocks. In this situation its decay effect is minimum. Niter crystallizes in the wall plasters and its responsible for the disruption of the paintings. The development of columnar crystals from crystallization nucleus in the pores of the plasters, or in the interface painting-plaster, seems to be the disruption mechanism. In the plaster it has not been observed this decay effect. Periodical observations have shown that the decay extends because of the proliferation of crystallization nucleus, related to the infiltration of solutions followed by evaporation, and not by the periodic dissolution and crystallization of efflorescence, mechanism pointed by Arnold and Zenhder, 1989. The high equilibrium relative humidity of niter does not allow the cycles of dissolution-crystallization. This observation has implications on the conservation works, since when salts like niter are present, the control of the environmental conditions in the monument could be of little use to stop the decay. Niter efflorescences observed in several granitic blocks seem to cause no significant stone decay. In the same blocks and laterally to the niter efflorescences, granular disintegration and plates have been observed. Aqueous extract chemical analyses, performed in niter efflorescences, plates and granular disintegration samples from three granitic pillars showed a decrease in nitrates and an increase in other anions, namely sulfates, in plates and granular disintegration relativelly to the niter efflorescences samples (fig. 2). These observations agree with the studies developed in sedimentary rocks, where niter crystallizes always at the block surface and not in the inner pores, because of the high solubility of this salt (Hammecker, 1993). This author concluded that niter does not originate important decay in the monuments stones.

As it was shown, gypsum and niter have very different decay behaviours. This alerts to the need of an accurate mineralogical determination of all the salts present in a monument.

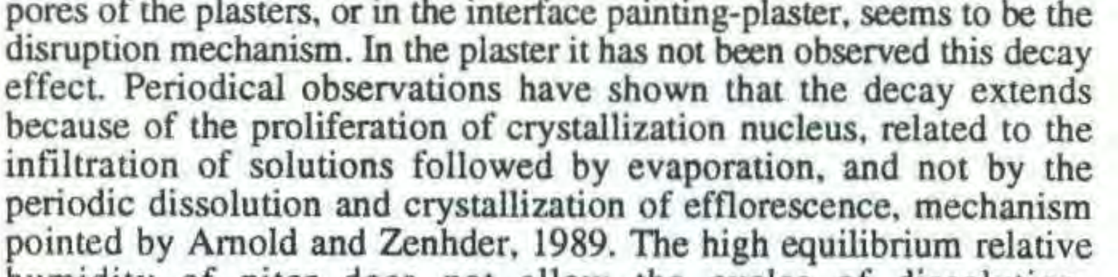

Fig. 1 - XRD spectra of niter efflorescences in granitic blocks.

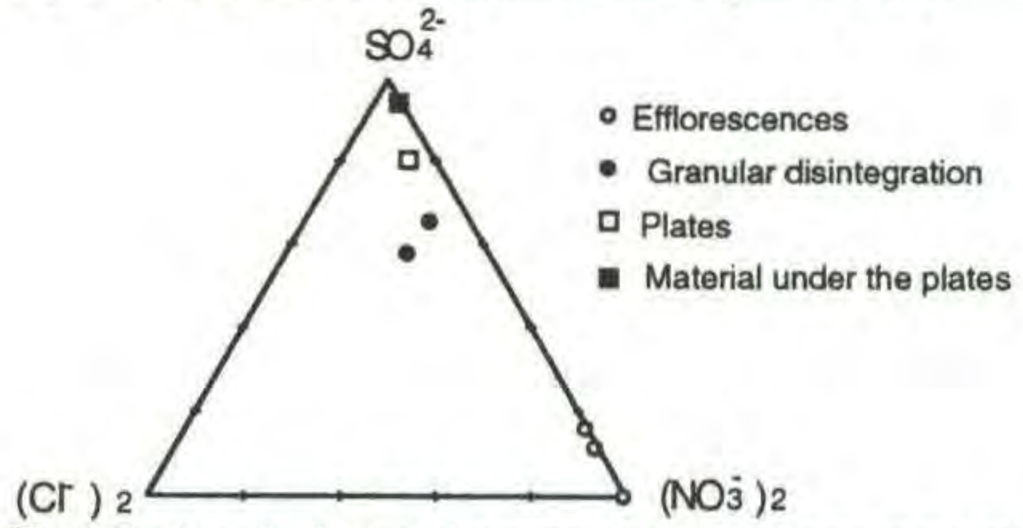

Fig. 2 Plotting of anionic molar composition of pathologies samples.

A. ARNOLD, K. ZEHNDER, *Atti 1° Simp. Int:, pp. 31-58*, Bari, 1989.
C. HAMMECKER, *Thèse Univ. Louis Pasteur, Strasbourg*, 1993.
E.M. WINKLER, P.C. SINGER, *Geol. Soc. America Bull., v. 81, p. 567-572*, 1972.

MICROCRYSTALLINE PROPERTIES OF MAGNETITE BY MEANS OF XRPD MEASURES

Alzetta G., Berti G., Tognoni E. (Dept. of Earth Sciences, Univ. of Pisa)

In order to gather information on crystallite size, grain size, magnetization and the associated relationships a natural magnetite sample from Punta Calamita (Elba Island) metamorphic formation has been studied.

Measures of magnetization induced by external fields were carried out on samples varying in granularity and magnetite content. Granulometric classes (5, 10, 15, 20 microns) were determined by a wet-sieving procedure which produced a satisfactory separation; the magnetite content was determined by quantitative analysis of powder X-ray diffraction patterns.

Microcrystalline properties of magnetite were investigated by determining the mean crystallite size and using the X-ray powder diffraction data obtained from a conventional Bragg-Brentano diffractometer.

Experimental data processing was carried out on XRPD patterns so as to evaluate the instrumental systematic effects and to render the results consistent. To this aim instrument calibration curves were calculated for several parameters (centroid, FWHM, lorentzianity of the peak shape, etc.) for standard and specimen data collections.

Thus, in order to observe true differences between the patterns, "Diffraction Instrumental Monitoring" was adopted to assess reproducibility, stability, as well as differences in instrumentation set up.

The variance method of peak analysis was used to determine the domains' mean size: the most common problems related to peak truncation were processed using Pseudo Voigt profile fitting.

Variance analysis was carried out on the peak profiles, while accounting for the peak regions where lattice microstrains produce negligible effects.

Results show that magnetization depends on both crystallite size and grain size.

CRYSTAL STRUCTURE OF PHENGITE-3T: THERMAL DEPENDENCE AND STABILITY AT HIGH P/T

Amisano-Canesi A., Ivaldi G., Chiari G. and Ferraris G.
Dip. Sci. Mineral. Petrol., Univ. Torino

Amisano-Canesi *et al.* (1994) have recently refined the crystal structure (space group $P3_112$) of two 3T phengitic muscovites: KZ from schists of North Kazakhstan [P ≈ 8 kbar, T ≈ 600°C; $(K_{0.93}Na_{0.03})(Al_{1.54}Fe_{0.25}Mg_{0.21}Ti_{0.04})(Si_{3.34}Al_{0.66})O_{10}(OH)_2$, a = 5.212(1), c = 29.804(6) Å] and DM from the pyrope-bearing whiteschists of Dora-Maira [P ≈ 30 kbar, T ≈ 700°C; $(K_{0.92}Na_{0.01})(Al_{1.41}Mg_{0.60}Ti_{0.02})(Si_{3.54}Al_{0.46})O_{10}(OH)_2$, a = 5.215(1), c = 29.755(5) Å]. Contrary to what was reported by Güven & Burnham (1967) for a muscovite-3T, KZ and DM do not show ordering in the two independent tetrahedral (*T*) and octahedral (*O*) sites, even if the latter two sites differ in size.

The same crystals used for the room temperature (RT) study were heated up to 600°C and single crystal diffraction data were collected and refined. For DM the crystal collapsed when the temperature was rised to 800° C; KZ, instead, was cooled from 600°C down to RT and a new set of diffraction data was collected and refined. After a second cycle of heating up to 800°C, KZ collapsed too.

The main characteristics of the structure at 600°C are (i) a regularization of the inter-layer K-polyhedron connected with a decrease in the ditrigonal distortion of the tetrahedral layer and (ii) a differential expansion of the two independent *O* sites which become of the same size.

In both crystals the termal expansion of the cell parameters is linear in the range 20 - 600°C ($\alpha \approx 0.8$ and 2.2×10^{-5} K^{-1} for *a* and *c*, respectively) and then increases sharply while approaching the structural collapse at 800°C. During cooling from 600°C the cell volume (V) of KZ shows a slight hysteresis ($\Delta V/\sigma \approx 5$ at RT), mainly due to an increase of the *c* value. Comparing the RT structural parameters of KZ before and after the heating cycle, the increase of *V* should be connected with an increase in the average value of the bond lengths in the smaller octahedron [from 1.943(2) to 1.953(2) Å] and in the K-polyhedron [outer bonds only: from 3.259(2) to 3.269(3) Å]. An overall increase of about 30% in the thermal parameters is also obtained after the heating cycle.

The differential expansion of the two independent *O* sites supports the hypothesis of Amisano-Canesi *et al.* (1994) that the presence of two independent *O* filled sites in 3T mica allows for larger flexibility with respect to monoclinic polytypes, where only one independent *O* site is present. An easier re-adjustement of the 3T structure under variation of *T* and *P* could justify an occurrence of phengite-3T greater than that of monoclinic polytypes in high-pressure metamorphic rocks (Sassi *et al.*, 1994). The hysteresis shown during the heating cycle by the volumes of the cell and of two coordination polyhedra might suggest caution in correlating structural parameters and chemical composition without taking into account the P/T paths of the samples.

References:
Amisano-Canesi A., Chiari G., Ferraris G., Ivaldi G., Soboleva S. V. (1994). *Eur. J. Mineral.* **6**, in press.
Güven N. & Burnham C.W. (1967). *Zeit. Krist.* **125**, 163-183.
Sassi F.P., Guidotti C.V., Rieder M., De Pieri R. (1994). *Eur. J. Mineral.* **6** , 151-160.

GEOCHEMICAL FEATURES OF CRUSTAL MELTS FROM CALABRIAN SERRE (ITALY)

Amore V., Paglionico A. (*Dept. Geomineralogico Univ. of Bari*)
Caggianelli A. (*DiTEc Univ. of Basilicata - Potenza*)
Del Moro A. (*Inst. Geocronologia e Geochimica Isotopica CNR PISA*)

Strongly peraluminous granitoids make up an integral part of the Hercynian magmatism in Calabria. Recent studies have shown that their origin is still controversial and that the contribution of crustal material is not exclusive. In particular, the Sr and Nd isotopic signature of the peraluminous granitoids doesn't match the isotopic composition of the restitic metapelites found in the lower crust section exposed in Southern Calabria (Caggianelli et al., 1991). Thus it was recently proposed that a purely pelitic source was unable to produce the overall features of the Calabrian peraluminous granitoids. This was in line with the conclusion of Miller (1985) which states: "very few Ps (strongly peraluminous) rocks derived entirely from pelitic sources". We have recently undertaken a petrological and geochemical study on a small outcrop (about 0.25 Km^2) of anatectic migmatites in order to define the features of the purely anatectic melts. They are exposed in the North-Eastern Serre in the neighbourhood of Squillace and are in contact with the Squillace-Petrizzi foliated calc-alkaline tonalites. A comparison with the more widespread peraluminous granitoids might shed light on the genesis of these rocks and help in evaluating the real contribution of crustal material to acidic magmatism.

The studied migmatites display a foliated raft or schlieren structure. The variable content in schlieren material determines the gradation from migmatites to granites l.s. The schlieren are made up of biotite, sillimanite, quartz ± plagioclase ± garnet. Schlieren are hosted in a medium grained granitic l.s. matrix with or without coarser K-feldspar.

In the migmatites quartz-biotite and quartz-plagioclase symplectites are widespread. They suggest, together with muscovite, the involvement of quartz, plagioclase and minor biotite in the melting process. Sillimanite occurs in fibrolitic aggregates and more commonly in the form of stubby prisms up to six centimeters in length. Stubby sillimanite often crosscuts or rims biotites, thus suggesting a growth at the expense of the dark mica. Garnet occurs in small quantities and displays trails in sigmoidal shapes formed during a dynamic metamorphic episode previous to partial melting. Sometimes pseudomorphs of biotite + quartz or biotite + plagioclase are present on garnet. They indicate rehydration reactions probably consequent on the crystallization of the leucosomes. Migmatite formation occurred by hydrous melting in the upper amphibolite facies and an important reaction was Ab + Ms + Qz + H_2O = melt + Al_2SiO_5. The absence of andalusite and the mineral assemblage of the neighbouring metapelites indicate pressures ranging from 4 to 5 kbar. An estimation of the PT conditions on the basis of the composition of residual garnet, biotite, muscovite and plagioclase indicated a pressure of 4-4.5 kbar and a temperature of 630-650 °C.

In binary scatter diagrams migmatites display generally linear trends. The value of the A/CNK molecular ratio increases as the SiO_2 content decreases, coherently with a restite-melt unmixing model and with an enrichment of peraluminous phases in the residue. Such a feature excludes a later magma stirring and an eventual control of major oxide variations by fractional crystallization. It can be observed a wide

variability in Ba (260 - 1609 ppm), K_2O (1.32 - 4.70 wt.%) and to a lesser extent in Rb (32 - 110 ppm) contents, in response to the varying proportions of K-feldspar. Thus the composition of melts varied from granodioritic to trondhjemitoid, depending on the stage of melting and/or source rock composition. The LREE content appears strongly controlled by monazite that typically occurs as inclusion in biotite. A subset of samples was selected for the determination of Sr and Nd isotopic composition. The $^{87}Sr/^{86}Sr$ initial ratio (Sr IR at 290 Ma) in two analysed migmatites turned out to be very high (0.7189 and 0.7180) whereas the εNd values were of -9.3 and -8.4. The examined granites display slightly lower values of Sr IR and slightly higher values of εNd (Sr IR = 0.7172 and 0.7161; εNd = -7.0 and -6.8). These biases in isotopic composition from migmatites to granites might appear suggestive of processes of contamination of leucosomes with the contiguous tonalitic magma.

The data collected in this study allow to extract some conclusions about the genesis of the Hercynian peraluminous granitoids in Calabria. With respect to the purely anatectic melts, here studied, they generally show important differences concerning higher K_2O/Na_2O ratio, Rb and P_2O_5 contents and decidedly lower Sr IR. The higher K_2O/Na_2O ratio possibly indicates that melting reactions involved more deeply the biotite breakdown. The lower values in Sr IR confirm that a purely anatectic origin is inadequate and that more complex models must be considered for their origin.

References:
Caggianelli et al. (1991). *Eur. J. Mineral.*, **3**, 159-180.
Miller, C.F. (1985).*J. Geol.*, **93**, 673-689.

NATURE, ORIGIN AND TRANSFORMATION OF A 7Å Fe PHASE IN SEDIMENTS : AN HRTEM AND AEM STUDY

Amouric M., Parron C., Casalini L. and Giresse L. (CRMC2 - CNRS, Univ. Aix-Marseille II, Luminy - Marseille)

Young marine green grains, from Fe-rich sediments, were studied by using HRTEM systematically combined with ponctual microchemical EDX analyse (Casalini et al, 1993). Results demonstrated these grains were made of a mixture of very small phases (mainly TO and TOT phyllosilicates) (figure 1) with a

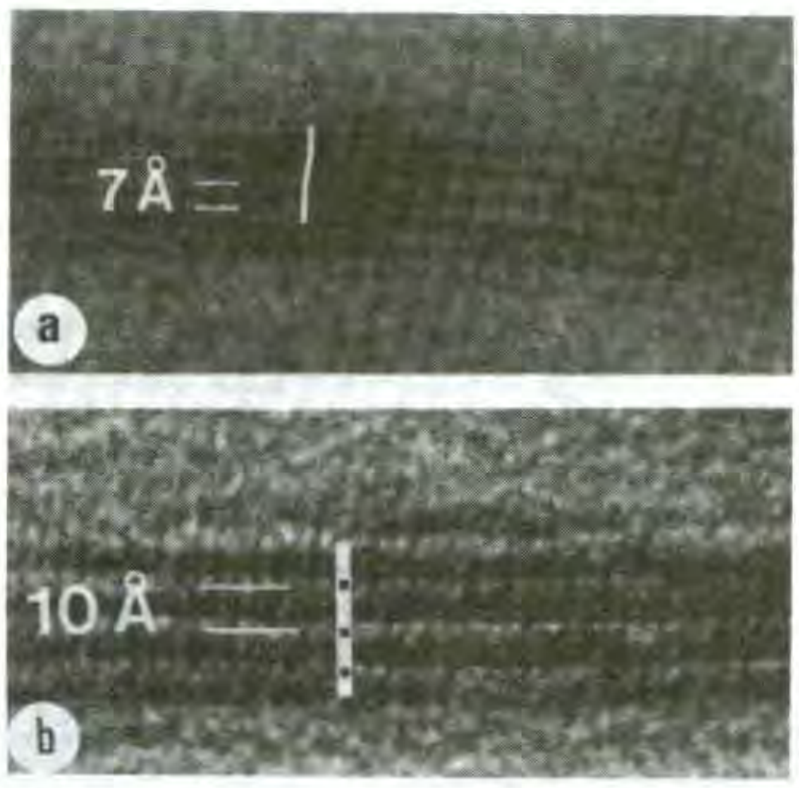

Figure 1 : a) Structure image of a predominant 7Å Fe (TO) phase (dool~7Å) exhibiting a faulted 1M polytipic sequence and b) Structure image of 10Å (TOT) phase (dool~10Å) with a pure 1M polytypic stacking sequence.

dominant 7Å Fe-specie. All the main phases, finely cristallochemically characterized, appeared intimately related in a same evolutionary process (Amouric et al, 1994). Each of them experienced different and well described transformation mechanisms. So first, a starting original Fe-rich Kaolinite transformed, via dissolution-recrystallization, into another particular 7Å Fe-rich phase, the composition of which may vary from a di-tri to a pure trioctahedral (Mg + Fe) pole. This Fe-rich TO mineral is effectively not a classical one. Then crystallization of a 10Å, rather dioctahedral K-rich phase occurs at the expense of it, through TO/TOT interstratified structures. Such an evolution takes place through a solid state mechanism in which one 10Å layer replaces one 7Å layer (figure 2). Another part of mica-like structures may

Figure 2 : Interstratified TO/TOT structure with a lateral transition in wich one 10Å layer replaces one 7Å layer.

also directly develop after dissolution of original Kaolinites. The development of 10Å K-rich phases could be significative of the beginning of the glauconitization process in these grains.

References :
Amouric M., Parron C. and Casalini L. (1994) clays and clay Miner. submitted.
Casalini L., Amouric M., Parron C. (1993) Bull-Miner. SFMC 5, 58-59

MINERALOGICAL EDUCATION AT THE BUCHAREST UNIVERSITY - ROMANIA

Anastasiu N. *(Dept.of Mineralogy, Bucharest University)*

The Department of Mineralogy - at the Bucharest University - has a distinguished tradition in education of academic level specialists in crystallography, mineralogy, petrography, volcanology, ore deposits geology and metallogeny, geochemistry, sedimentology and sedimentary petrology, instrumental analysis, experimental petrology and industrial deposits geology.

Ludovic Mrazec is the founder of the Romanian School of Mineralogy (100 years ago), and the first Romanian author of a general course of minerals & rocks. Other characters were Gh.Munteanu-Murgoci, Max Reinhard, David Roman, but since 1950, the main department personalities were Virgil Ianovici, Dan Giusca, Dan Radulescu.

At present, in MD there is a complex activity: it is organized academic year for currently courses, but more:courses for Ph.D. in four fields (Mineralogy, Petrography, Ore Deposits, Sedimentology), and training courses in the technique of microscopy, depositional systems and sequence analysis, structural petrology, too. MD staff organizes field trips for students and elaborates guide book for geological trips in igneous, metamorphic or sedimentary fields, and in classic mining regions.

In this department there is an academic staff and also research workers preparing the coming geologists and geologist engineers and study permanently in their field of activity.

There are two research group: * The "Group of Applied Mineralogy and Sedimentology", and * The "Group of Applied Petrology and Metallogeny" which have in attention monographic

studies, mineral assemblages studies, facies models, diagenesis, metallogenical models.

Many minerals and rocks collections are used by the students.

PROPERTIES AND STRUCTURES OF K-FELDSPARS FROM SOME GRANITE AND RELATED ROCKS: THE COMPARATIVE REMARKS ON THE ROMANIAN CARPATHIANS

Anastasiu N. and Fabian C. *(Dept.of Mineralogy, Bucharest University)*

In order to notice optical and structural variations of the potash feldspars of the quartz- feldspatic rocks (granitoids from Ogradena, gneiss and pegmatites from Cibin massif - South Carpathians) and some syenitoids (from Ditrau bodies - East Carpathians) has been carried out an investigation for the 2V and extinction angle, the refraction indices, triclinicity, twins and intergrowths.

The results of this examination (Ogradena massif) pointed out variations both of the 2V angle within large limits, between 60-94°, and the extinction angle (8-18°). At the boundary between the "massive" and the "gneissic" granitoids there is generally noticed a tendency of increase in the 2V values and, implicitly, of decrease in the %Or. This fact invalidates the gradual cooling as a singular phenomenon and confirms the dynamic control of the potash feldspar blastesis.

The form of primary crystallization of potash feldspars should have had a monoclinic symmetry, the present forms, with different triclinicity forms, being obtained by subsolidus transformations. The observations on potash feldspar also point out: the adaptation of the crystalline lattice of feldspar to dynamic conditions (stress, lamination) and their pointing out by the twins presence in the lattice and the variation of the optical properties; the possibility of existence, in the maximum deformation areas, of some potash feldspars with positive optical sign.

The kinematic control and the different intensity of the movements affecting the granitoids, respectively, explain the passing from the monoclinic to the triclinic symmetry (Δ values higher in the gneissic granitoids than in the massive one) and the omnipresence of cross twins. Also, the formation of the microcline as an initial triclinic phase would be hard to explain taking into account the presence of some optical parameters with variable limits.

- In the Cibin massif the potash feldspars are developed in some gneissic and/or pegmatitic rocks with migmatitic shapes. The optical and chemical characteristics point out a microclin with high triclinic symmetry and a not very high Or content. The mineralogy and the petro- structures in which is involved the K- feldspar (pertitic, or graphic structures, and different deformational stages)prove a late subsolidus dynamic genesis.

The kinematic control of the K- feldspar formation can explain, with thermodynamic arguments, the evolution of the diffusion coefficients and the chemical potentials of the minerals involved in the genetic reactions of the K- feldspar.

The structural shape of microclin is a good argument for the for its late blastesis in the evolution history of the Cibin's area gneissic rocks, and also for the fact that older amphibole, mica and/or plagioclase are involved in this blastesis which explain the K source.

The potash feldspars of the Ditrau massif appear in the anhedral crystal-grains, masses, pseudomorphs, veinlets-intimately intergrown with albite or oligoclase of replacement and exsolution perthites. The range of the optical properties of the potash feldspars (2V=70-80°, extinction angle (6-18°) leads to the spatial and asymmetric zonality as against the shape and petrographical composition of the massif . The investigation carried out by the X-ray diffraction and I.R. analysis confirmed the types of maximum and intermediary microcline (Δ = 0.9-0.5). These properties are due to the high instability of the potash feldspars and were acquired subsequently to their crystallization and selective remobilization processes in conditions of slow cooling.

X-RAY DIFFRACTION OF $SrTiO_3$ PEROVSKITE AT SIMULTANEOUSLY HIGH TEMPERATURES AND PRESSURES IN A DIAMOND ANVIL CELL

D. Andrault, G. Fiquet, P. Richet (Géomatériaux, Institut de Physique du Globe, Paris), Ph. Gillet (Sciences de la Terre, ENS Lyon) and J.P. Itié (Physique des Milieux Condensés, Université Paris VI)

Only synchrotron radiation can yield X-ray beams bright enough to perform X-ray diffraction experiments on samples brought to simultaneously high pressures and temperatures in a diamond anvil cell. We have thus set up a new system on the wiggler line of the DCI storage ring at LURE (Orsay, France) to make energy dispersive X-ray diffraction measurements on compounds whose pressure and temperature are measured from ruby fluorescence and blackbody spectroscopy, respectively. In our experiments, a CO_2 laser is used to heat the sample loaded in a membrane diamond anvil cell. Particular care was paid to design the optical system in order to maximize the ruby and blackbody signals, which are transmitted through optical fibers to a newly built DILOR multichannel spectrometer.

The first experiments have been performed on $SrTiO_3$ perovskite for which preliminary results will be presented. The temperazture dependence of the unit-cell parameters was determined as a function of temperature up to about 2000 K at 15 GPa. At this pressure, the room-temperature thermal expansion coefficient of this perovskite is lower than 10^{-5} K^{-1} at 15 GPa.

• PARTITIONING AND CRYSTAL FIELD STABILIZATION OF CHROMIUM 3+ IN COEXISTING PARAGENETIC MINERALS

Andrut M. and Langer K. *(Institut für Mineralogie und Kristallographie, TU Berlin)*

It has been qualitatively shown that the partitioning of $3d^N$-ions in systems as crystal/melt and crystal/crystal is dependent on the

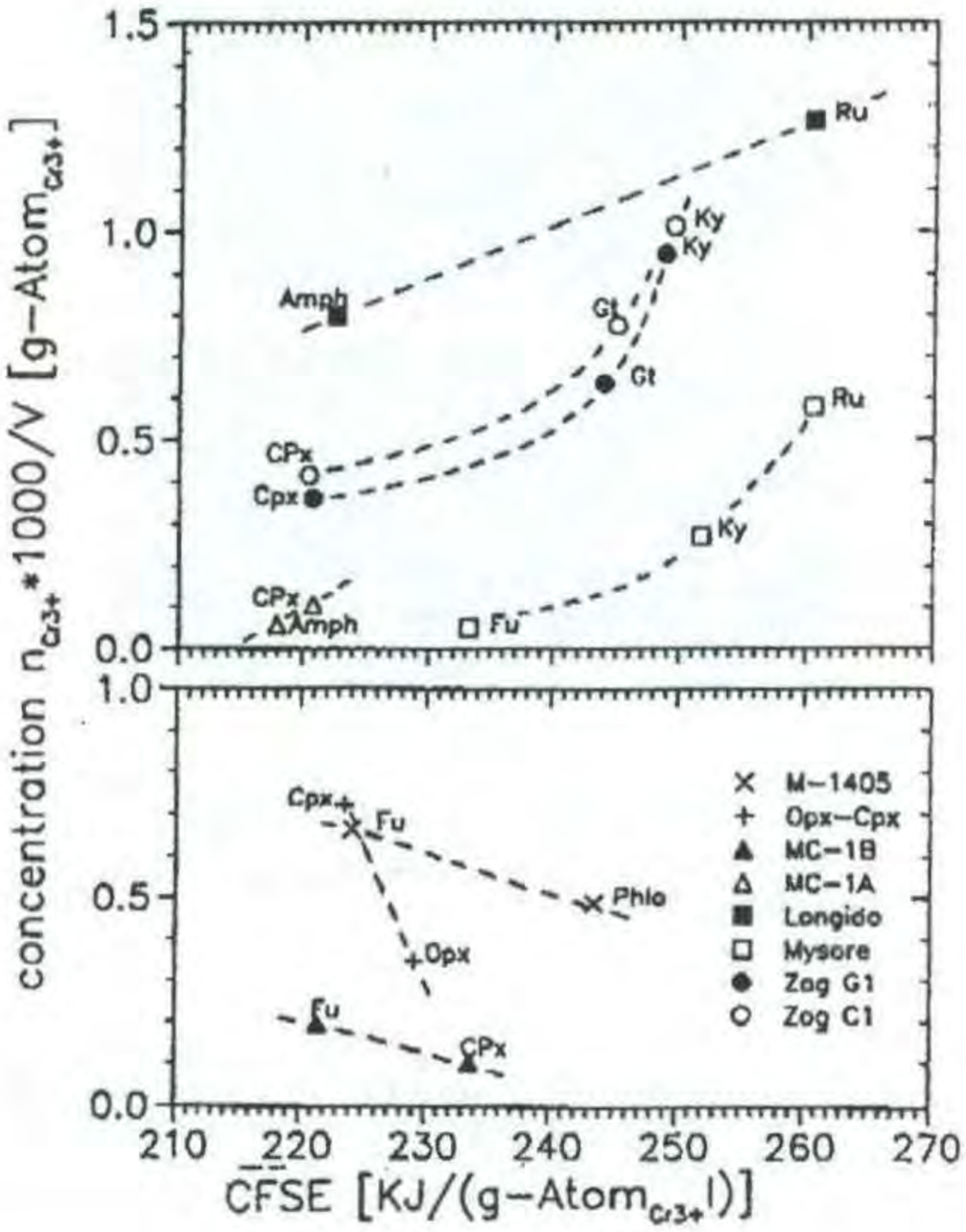

crystal field stabilization energy of the respective $3d^N$–ions in the structures of the phases involved (e.g. Burns, 1993). No quantitative proof of this concept is in the literature so far.

In contrast, the ionic radii concept states that the cation distribution is controlled, at least for trace concentration, by the size of the ion (Jensen, 1973).

A proof of the crystal field concept would be the existence of a quantitative relation between $CFSE_{3dN,Phase}$ and the concentration $C_{3dN,Phase}$ (Langer, 1988). Therefore we studied the polarized absorption spectra, from which 10Dq and, hence, CFSE, is to be extracted, and the concentration of Cr^{3+}, n_{Cr3+}*1000/V (V = molar volume) in [g–$atom_{Cr3+}$/l], in Cr^{3+}–bearing paragenetic minerals extracted from high pressure rocks. By a study of coexisting, paragenetic minerals, effects of different pT–conditions of their formation, which might obscure any quantitative relation between CFSE and concentration of Cr^{3+}, are avoided.

The results are represented in terms of $f(CFSE_{Cr3+}) = n_{cr3+}$*1000/V in [g–$atom_{Cr3+}$/l]. For most of the coexisting minerals there exists a clear dependence between CFSE and concentration. Deviation of distribution behaviour for some mineral pairs can be explained by influence of crystal chemical effects.

References:
Burns, R.G. (1993). Mineralogical Appl. of crystal field theory, 2nd ed., Cambridge
Jensen (1973) Thesis
Langer, K. (1988) in: Salje: Phys. properties and thermodynamic behaviour of minerals, Reidel

PHASE EQUILIBRIA OF $FeSiO_3$ PYROXENES

Angel R.J., Woodland AB, (*Bayerisches Geoinstitut, Bayreuth*) and Hugh-Jones D.A. (*Dept. Geological Sciences, University College London*).

Experimental studies of $FeSiO_3$ at P and T reveal two incompatible phase boundaries between Pbca and $P2_1/c$ as the recovered phases: Lindsley (1965) reversed a boundary with a shallow P-T slope at low pressures, while the results of Akimoto et al. (1965) indicate a much steeper boundary at higher pressures, as confirmed by experiments in Bayreuth.

We have therefore undertaken a single-crystal X-ray diffraction study of $P2_1/c$ clinoferrosilite in a diamond-anvil cell to attempt to resolve this discrepancy. We find that at room temperature the $P2_1/c$ phase inverts to a C2/c pyroxene phase at pressures in excess of 1.75 GPa. The transformation is first order, displays hysteresis, but has been reversed in the DAC between 1.48 and 1.75 GPa. The high-pressure phase is not quenchable to room pressure, so we conclude that Akimoto et al's reversals are of the Pbca ⇌ high-P C2/c phase boundary (the C2/c phase inverting to $P2_1/c$ on quenching), while those of Lindsley are those of the $P2_1/c$ ⇌ Pbca boundary. The phase diagram for $FeSiO_3$ therefore has the same topology as that recently demonstrated for $MgSiO_3$ pyroxene (Angel et al., 1992), with the interesting addition of a *separate* stability field for a *structurally distinct* high-temperature C2/c polymorph of $FeSiO_3$. The $P2_1/c$ - Pbca - High-P C2/c triple point is estimated to be located around 850°C and 4.5 GPa compared to 800-900°C and 7.6-7.9 GPa in $MgSiO_3$. Thermodynamic data for these phases will also be presented.

Lindsley (1965) *CIWY* 64:148. Akimoto et al. (1965) *JGR* 70:5269. Angel et al. (1992) *Nature* 358:322

MINERALOGY AND GEOCHEMISTRY OF GOLD-BEARING GOSSANS AND LATERITIC IRON CRUSTS IN THE AMAZON REGION, BRASIL

Angélica R.S., Costa M.L. and Pöllmann P. (*Geosciences Center, Univ. of Pará, Brazil and Inst. of Mineralogy, Univ. of Erlangen*)

Several supergenic gold deposits have been discovered in the Amazon region where gold is typically associated with the upper ferruginous horizons of the profiles. In the Igarapé Bahia mine and in the Águas Claras prospect (Carajás mining district) a typical gossan profile structuration can be observed with an oxidation zone at the top, an intermediate cementation or secondary sulfide zone and the primary sulfide zone at the base. In terms of mineral exploration in tropical rain-forest, one of the most important features of these occurrences is that superimposed lateritization processes obliterated originary gossans features, giving rise to a lateritic breccia-like iron crust and latosols with a new dispersion of gold and other elements. The consequent supergene profile can be described as follow, with its respective mineralogical composition:

Latosols	Al-goethite, kaolinite, gibbsite hematite, quartz
Latentic iron crust	hematite, goethite kaolinite, maghemite, gibbsite, quartz
Gossan	hematite, maghemite goethite
Saprolite	kaolinite, goethite, gibbsite, quartz
Supergene sulfide	cuprite, native copper, malachite
Primary sulfide	Chalcopyrite, pyrite, bornite, magnetite quartz
Wall-rocks	Meta-vulcanosedimentary rocks: coarse to fine sediments, basic volcanics and iron-formations.

In the Igarapé Bahia mine, mean gold contents in the gossans are 5 g/t, diminishing abruptly toward the latosols. Gold particles are extremely fine, and associated with sulfides in the primary environment and with iron oxi-hydroxides in the supergene zone, where they present high fineness. SEM-EDS analysis in isolated grains from quartz-veins (figure below) reveal a primary core with high fineness and a ferruginous rim or coating with elevated iron contents, in a good negative correlation between Au and Fe:

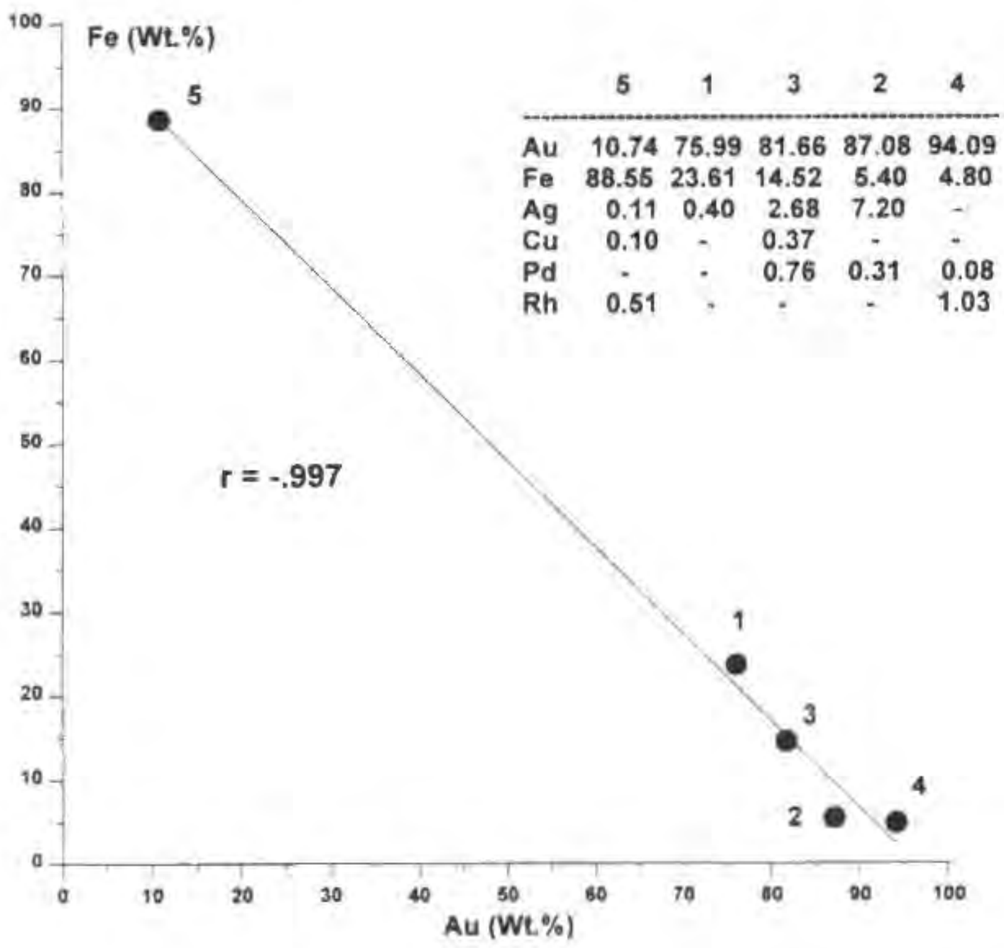

	5	1	3	2	4
Au	10.74	75.99	81.66	87.08	94.09
Fe	88.55	23.61	14.52	5.40	4.80
Ag	0.11	0.40	2.68	7.20	-
Cu	0.10	-	0.37	-	-
Pd	-	-	0.76	0.31	0.08
Rh	0.51	-	-	-	1.03

Presently, the gossans and lateritic crusts are the main target in gold geochemical exploration in tropical regions but in the case of the Amazon region they rarely outcrop. In the latosols, geochemical signals are weakened where these overburden act as a barrier in the discovering of new ore-bodies.

GEOCHEMICAL COMPOSITION OF SEDIMENTS FROM THE ORBETELLO LAGOON.

Angelone M., Anselmi B., Ghiara E., Gragnani R. and Monti A. (ENEA, AMB-ANV, CRE-Casaccia, Via Anguillarese 301, 00060 S. M. di Galeria, Roma)

Orbetello lagoon (Grosseto, Italy), is a shallow basin area of 27 km^2 and 1 m average depth, that is periodically affected by anoxic crisis that cause serious damage to the local economy.
Environmental multidiscliplinary research was carried out by ENEA with the aim of optimizing the restoration project (Bucci et al.,1990; Bonanni et al., 1992).

Since the objective of the present study was to investigate the geochemical composition of sediments. Cores and superficial sediments were analyzed for grain size composition and ^{137}Cs, ^{210}Pb, total organic (TOC) and inorganic carbon, total nitrogen (TN), organic and inorganic phosphorus, Fe, Mn and trace element (Hg, As, Cd, Se, Pb, Zn, Cu, Cr and Ni) contents.

According to Shepard (1954) sediments were classified as: silty clay, clayey silt and sand silt clay. In some cores ^{137}Cs profile showed probable reworking of sediments. Sedimentation rate ranges between 0.2-0.3 cm y^{-1}, in agreement with values found in other Italian lagoons (Orio and Donazzolo, 1987; Battiston et al., 1988; Anselmi et al., 1993).

The averages of TOC and TN contents are 5.26% (Std. D.=1.33) and 0.74% (Std. D.=1.78) respectively, that are similar to those found in different marine and lagoon environments (Suess 1973; Pelet and Debyser, 1977; Szefer and Skwarzec, 1988; Sfriso et al., 1988; Haugen and Lichtentaler, 1991). No significant variation with depth was observed suggesting that no important change of organic matter accumulation rate took place in the lagoon.
The mean TOC/TN ratios is 7.07 (Std. D.=1.68), suggesting a marine origin for organic matter.
Organic and inorganic phosphorus contents show a general decrease with depth, probably due to:
i) a selective enrichment of P at the interface water-sediment due to geochemical processes (Fe and Mn coprecipitation, clay adsorption, enrichment of P on organic substrate);
ii) precipitation of phosphate, from interstitial water, in the oxidized superficial sediments.

Trace element concentrations in core sediments decrease with depth according to pollution processes occurred in the XX century. High contamination level was found close by urban and industrialized areas.

References

Anselmi B., Ghiara E., Gragnani R., Narcisi B. and Paganin G.(1993). 9th Int. Conf. "*Heavy Metals in the Environment*", 2, 203-206. Toronto,12-17 September
Battiston G.A., Degetto S., Gerbasi R., Sbrignadello G. and Tositti L. (1988). *Sci. Total Environ.*, 77, 15-23.
Bonanni P, Caprioli R., Ghiara E., Mignuzzi C., Orlandi C., Paganin G. and Monti A.(1992) *Hydrobiologia*; 236/236, 553-568.
Bucci M., Ghiara E., Gragnani R., Izzo G., Morgana J.G, Naviglio L. and Uccelli R.(1990). Proceedings of an Int. Conf."*Marine Coastal Eutrophication*" Bologna, Italy, 21-24 March.
Haugen J. E. and Lichtentaler R. (1991). *Geochim. Cosmoch. Acta*, 55, 1649-1616.
Orio A.A., Donazzolo R. (1987). *Atti Ist. Ven. S.L.A.*, 11, 149-215.
Pelet R. and Debyser Y. (1977). *Geochim. Cosmoch. Acta*, 41, 1575-1586
Sfriso A., Donazzolo R., Calvo C. and Orio A.A. (1988). 3rd Int. Conf. "*Environmental Contamination*", 354-357. Venice, 26-29 September.
Shepard F. P. (1954). *J. Sed. Petr.*, 24, 151-158.
Suess E. (1973). Geochim. Cosmoch. Acta, 37, 2435-2447.
Szefer P. and Skwarzec B. (1988). *Marine Chemistry*, 23, 109-129.

CHEMICAL COMPOSITION PECULIARITIES OF FLUID INCLUSIONS IN QUARTZ OF THE PRAVOURMII TIN DEPOSIT, THE FAR EAST.

Antonov A.A., Panova E.G.. *(Dept. of Mineralogy, St.Petersburg Univ., Russia)*

The Pravourmii tin deposit is situated in (the Far East) and belongs to the category of cassiterite-quartz greisen formation. Ore formations are the veins and volumetric metasomatites in liparite. They are located in the closest exocontact of the Verchneurmii biotitic leucogranite massif. In accordance with the age interrelations of hydrothermal bodies, the following mineral assemblage, that correspond to certain stages of their formation, are distinguished in this deposit : early ore-free quartz veins in the granite (1a) and sericite-quartz greisen with a small content of wolframite and molybdenite (1b); ore quartz-topaz-siderophyllite greisen with cassiterite and wolframite (2); later quartz-tourmaline veins with tin sulphostanates and sulphides (3), the latest quartz-carbonate assemblages (4).

Statistical analysis of the chemical composition of fluid inclusions in quartz allows to distinguish the ore-bearing associations from the ore-free ones. The average contents of components in these inclusions vary in abroad range (%): (Ca^{2+} +Mg^{2+}) - from 22 to 85; (NH_4^+ +K^+) - from 7 to 44; (Cl^- +F^-) - from 8 to 61; HCO_3^- - from 17 to 64. It is established that the mentioned component contents are in a good correlation for the quartzes from the different assemblages. The maximum (NH_4^+ +K^+) and minimum (Ca^{2+} +Mg^{2+}) and HCO_3^- contents correspond to the early Mo-W-bearing greisens

• ORE VEIN FORMATION (TEST FOR ORE FORMATION THEORIES)

Apollonov V.N. *(Faculty of Geology, Moscow State University)*

Mineralogy and geochemistry of hundreds of ore deposits have been studied in detail at present. Based on this evidence, and on theoretical and experimental simulation, ore deposit genetic models are developed – where is the ore material from, how does it separate from the source, in which form is transported, how is it deposited to form an ore body. There is a lot of theories and models of ore genesis, and in the literature many discussions arise around mutually conflicting theories, that may go on for decades.

The attached figure shows a generalized sketch of the formation of ore veins located at a distance L from a source of radius R. Four situations are considered:

a – formation of a rhythmically zoned crystal,
b – a rhythmically banded vein,
c – a symmetrically banded vein,
d – a vein with distinct vertical zoning.

I have attempted to develop a theoretical model that describes the process of vein formation on the basis of R, L and of the following parameters:
– the time of separation of the ore material from the source (t_1);
– the time of transport to the vein site (t_2);
– the time of deposition in the vein (t_3);
– the rates of migration of the various components during separation from the source and transport to the vein.

By changing the starting conditions, I have obtained for different situations a generalized solution: R –> 0 , t_2 –> 0.

Scientists interested in the development of the model may contact the author either at the meeting or in writing, to discuss alternative solutions. Eventually, a volume collecting the contributions to this problem may be published.

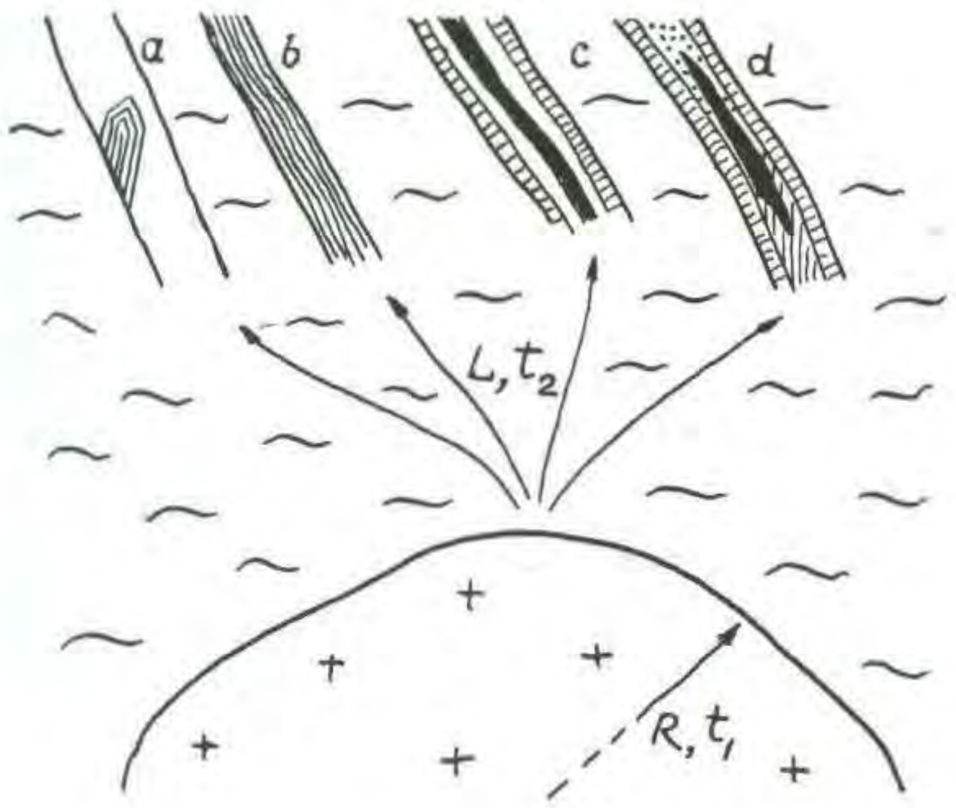

	Ti/(Ti+Cr+Al)	Cr/(Cr+Al)	Fe/(Fe+Mg)
Y793169(ulvö.)	0.70-0.92	0.24-0.81	0.96-0.99
Y793169(chro.)	0.06-0.15	0.61-0.70	0.82-0.95
A881757(ulvö.)	0.53-0.74	0.59-0.78	0.97-0.99
12064,9 (ulvö.)	0.64-1.00	0.00-0.72	0.98-1.00
12064,9 (chro.)	0.05-0.17	0.66-0.73	0.79-0.84
12031,21(chro.-ulvö.)	0.11-0.55	0.62-0.77	0.90-0.96

(ulvö: ulvöspinel, chro: chromite)

In Y793169 and A881757 ulvöspinel and chromite respectively crystallized at the last stage of crystallization in the mesostases, while in 12031,21 ulvöspinel continually grew on the chromite core. The Cr content in eucrites is depleted by the time when surface eucrite begin to crystallize after cumulate eucrite with spinel ended to crystallize. The difference of spinel crystallization and that of zoning trend of pyroxene reflect different bulk chemistry and crystal growth condition.

References:

Takeda, H. *et al.* (1993) Abstr. 18th Symp. Antarctic Meteorites, 25-27, NIPR.
Yanai, K *et al.* (1993) LPSC XXIV 1555-1556.
Takeda, H. *et al.* (1994a) LPSC XXV 1373-1374.
Takeda, H. *et al.* (1994b) Earth Planet. Sci. Lett. (in press).

CHEMICAL ZONINGS AND COOLING HISTORIES OF PYROXENE AND SPINEL IN LUNAR METEORITES, APOLLO 12 MARE BASALTS AND EUCRITES

Arai T. and Takeda H. (*Mineralogical Inst., Univ. of Tokyo*)

We studied pyroxene and oxide minerals in Y793169 and A881757 lunar meteorites, 12031 and 12064, low-Ti mare basalts of the Apollo 12 samples and the Y75011,84 eucrite to gain better understanding of the difference in crystal growth and cooling histories of basalts on planets of different sizes and chemistries.

Mineral chemistries and textures were examined by an electron probe microanalyzer (EPMA) and a scanning electron microscope (SEM), JEOL 840A with X-ray chemical map analysis (CMA) utilities.

Y793169 and A881757, Antarctic lunar meteorites, are new type of low-Ti mare basalts (Takeda *et al.*, 1993). Y793169 is a crystalline subophititc basalt with Fe-rich pyroxene, plagioclase and dark mesostasis. Pyroxene crystals reach up to 3 x 1mm. Mesostases contain ilmenite, ulvöspinel, chromite and troilite. Their ulvöspinel and chromite coexist as individual grains.

A881757 is equigranular and coarser-grained than Y793169, with crystal sizes between 2-4 mm and has been described as gabbro (Yanai *et al.*, 1993). This rock comprises Fe-rich pyroxene, plagioclase, a fair amount of chromian ulvöspinel, ilmenite and troilite. The chromian ulvöspinels are major opaque minerals and their Cr_2O_3 contents are homogeneous within the grains but are different between grains.

12031,21 is a pigeonite basalt and consisits of one large pigeonite crystal 5.2 x 1.8 mm in size attached matrices of plagioclase, ilmenite, troilite, silica and possible pyroxferoiite. The large pyroxene crystal shows several complicated chemical zoning trends nearly perpendicular to *c*-axis. In addition, Fe-metal and ulvöspinel-chromite are included in this crystal.The chromian ulvöspinel occurs as a rim of titanian chromite only on one side.

Y-75011,84 is a large crystalline clast in a polymict eucrite and shows a medium-grained subophititc textures and is composed of pyroxene, lath-shaped plagioclase and mesostases including ilmenite, troilite, Fe-rich olivine, Ca-phosphate and silica. Nd spinel was found in this polished thin section. The pyroxene crystal is up to 4.5 x 1.2 mm in size and shows extensive chemical zoning from pigeonite cores to subcalcic ferroaugite rims (Takeda *et al.*, 1994). Mesostases occur between pyroxene and plagioclase crystals. Besides relatively large crystals of ilmenite and troilite, a large part of mesostases is composed of dusty grains of ilmenite and troilite with a droplet-like shape.

Comparison of the chemical zonings of pyroxene in three rocks revealed that their trends are largely depend on the first phase to crystallize. In the lunar low-Ti basalts, pigeonite is the first phase but in the eucrite plagioclase grow together. Since the Ca content in Y75011,84 is depleted by the crystallization of plagioclase, pyroxene shows Ca poor trend. In 12031,21, rapid growth of pigeonite from super cooled melt induces Ca-rich zoning trend modified by later Fe-rich phase from a melt in the hollow crystal. Ti/(Ti+Cr) vs Fe/(Fe+Mg) trends in pyroxene of Y75011,84 are quite distinct from those of 12031, 12064 (Takeda *et al.*, 1994), Y793169 and A881757. The fact can be attributed to the fact that eucrite has less Ti content than mare basalt. Spinel data of Y793169, A881757, 12064 and 12031,21 are

THE STRUCTURES OF SHOCK-INDUCED ORTHOCLASE AND LABRADORITE GLASSES

Araki T., Okuno M., and Matsumoto T.
(*Dept. of Earth Sciences, Kanazawa Univ., Japan*)
Shono Y. (*Inst. for Materials Research, Tohoku Univ., Japan*)

The structures of shock-induced orthoclase and labradrite glasses have been investigated with X-ray diffraction method.

Two feldspars crystals were used for shock experiment; orthoclase($Or_{90}An_{10}$) and labradorite($Or_2Ab_{36}An_{62}$). Shock compression experiments were carried out under 38GPa(both crystals) and 43GPa(orthoclase). The obtained shock-induced glasses show higher refrective indices than those of the fused glasses.

The radial distribution functions D(r) for these glasses indicate that principle structures are TO_4(T=Si and Al) tetrahedra even in the shock-induced glasses. The details of D(r) curves for these shock-induced glasses differ from those for the fused glasses. The peaks of D(r) curves for shock-induced glasses are located at larger values of r than those for corresponding fused glasses. However, the D(r) curve for shock-induced orthoclase glass at 38GPa is similar to that for the fused labradorite glass, except 2.0<r<3.0 Å region. The peak positions of T-O and T-T atomic pairs of D(r) curve for shock-induced labradorite glass are similar to those for fused anorthite glass(Okuno *et al.*, 1985). Okuno *et al.* (1985) reported that the peak positions of the D(r) curve for shock-induced anorthite glass are similar to those for fused anorthite glass. Taylor & Brown(1979) reported that the structure of fused anorthite glass was different from those of alkaline feldspar glasses. They have explained that the structure of alkaline feldspar glass based on interconnected 6-membered rings of TO_4 tetrahedra found in trydimite, nepheline, however, that of calcic feldspar glass was consistent with 4-membered rings found in anorthite. Therefore, it may be indicated that the shock-induced orthoclase and labradorite glasses have the structure based on 4-membered rings found in more calcic feldspar glass. The densification of the shock-induced feldspar glass should be related to the linkages of TO_4 tetrahedra and this glass may be formed directly from cristalline phase without ordinary melting process.

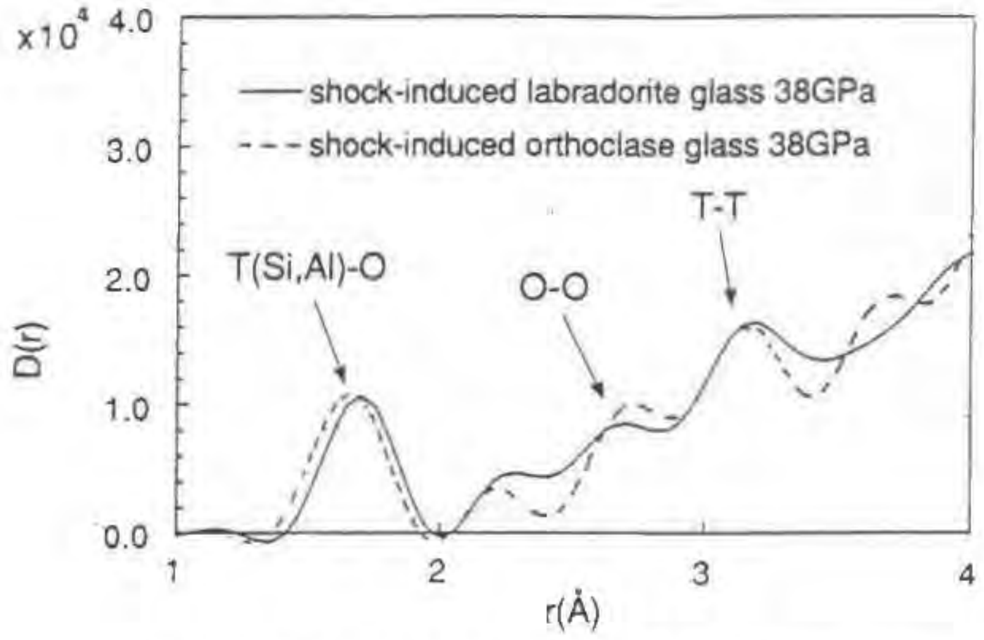

D(r) curves for the shock-induced orthoclase glass and labradorite glass at 38GPa.

References:

Okuno, M., Marumo, F., Syono, Y. (1985). *Mineral. J.*, **12**, 197-205.

Taylor, M. & Brown, Jr., G.E. (1979). *Geochim. Cosmochim. Acta*, **43**, 61-75.

CLASSICAL GEOTHERMOBAROMETRY VS. PETROGENETIC GRID APPROACHES: CONVERGENT RESULTS FOR HIGH-GRADE METAPELITES

Aranovich L.Ya. (*Inst. of Experimental Mineralogy, Chernogolovka*) and Berman R.G. (*Geol. Survey of Canada, Ottawa*)

An optimized set of both standard state and mixing thermodynamic properties has been obtained for the major Fe-Mg solid solution minerals of high-grade rocks: olivine, garnet, cordierite, orthopyroxene, biotite, and ilmenite. Tschermakitic substitution in orthopyroxene and biotite and F-(OH) substitution in biotite have also been accounted for. The new systematics are shown to be not only "internally", but also "externally" consistent, i.e. capable of reproducing experimental observations included and not included in the calibration.

Petrogenetic grids for high-grade metapelites have been calculated employing the derived data. The grid for the FMAS system predicts the transition from garnet-cordierite -to orthopyroxene-sillimanite assemblages in a narrow pressure range of 8.5 to 11 kbar between 800 to 1100°C, in good agreement with available experimental data. Compositions of the solid solution phases vary systematically along the transition curve, with only garnet exhibiting a maximum in its Mg/(Mg+Fe) ratio (*mg*). The grid is in very good agreement with observations on the minimum *mg* in orthopyroxene-sillimanite gneisses (~.6) and the maximum *mg* in cordierite-bearing rocks (~.50-.55).

For about 30 well-documented natural samples a comparison has been made between P-T estimates based on the grid and those calculated by direct application of Fe-Mg exchange and Fe-, Mg-, and Al orthopyroxene net-transfer geothermobarometers. For most of the samples the results show good agreement between the two approaches. This consistency indicates a high-temperature origin for these rocks as well as the ability of the exchange thermometers to monitor "near-peak" temperatures. For samples with the most aluminous orthopyroxene, systematic differences between Fe-Mg exchange and Al-in orthopyroxene temperatures can be explained by low-temperature Fe-Mg resetting, although there remain significant uncertainties in the calibration of thermodynamic properties of Al orthopyroxene end-members. Apparent discrepancy of petrogenetic grid vs. thermobarometry results for several samples can be attributed to the different response of rocks with strongly different bulk *mg* to varying P-T conditions.

MICROPOROSITY OF THE SOIL AS RELATED TO DIFFERENT PARTICLE SIZE DISTRIBUTIONS AND MINERALOGY

Aringhieri R. and Giachetti M. (*Ist. Chim. Terreno, C.N.R. Pisa*)

The most active part of the solid phase of the soil system is represented by both organic and inorganic colloid constituents. Among these, the inorganic colloid fraction is of importance because its role in determining foundamental physical properties of the soil such as soil structure and its stability, water storage capacity, and hydraulic conductivity. In addition the nature of its pore space system controls the transport of nutrient ions needed for plant growth (Aylmore & Quirk, 1967). Many of these properties are in fact closely linked to the microstructure and micropore system arising from a particular arrangement of the colloid particles and their nature. Despite of this only a few investigation on this subject have been carried out (Ristori et al.,1983 ; Murray et al., 1985).

In this paper the micropore size distribution (up to 100 Å) of fractions of different size grade from three soils differing in their mineralogy, and four natural clay minerals have been investigated by means low-temperature N_2 adsorption-desorption isotherms using a volumetric gas apparatus.

Specific surface area (SSA), specific pore volume (SPV), and the average pore radius (r) were calculated by applying the BET equation , whereas differential micropore size distributions were obtained from adsorption-desorption isotherms by using the Kelvin equation .

The results showed a maximum contribution of the finest fraction (0-2μm) to both specific surface area and microporosity of soils. Differential pore size distributions showed for all soils a maximum contribution to microporosity by pores having an effective radius of about 20 Å, thus indicating that this kind of pores contribute for the most part to the total microporosity of the soil.

Results obtained from natural clays also indicated for Montmorillonite and Illite systems the predominance of pores having effective radius of about 20 Å, whereas for the Kaolin system the major contribution to the microporosity was due to the predominance of pores of effective radius of about 10 Å. The relationship between these findings and the mineralogy of the soils needs however of further investigations, especially about the nature and origin of this kind of pores, and their function in a complex and extremely etherogeneous system such as the soil.

References:

Aylmore, L.A.G., & Quirk, J. P. (1967). *J. Soil Sci.*, **18**, 1-17.

Murray, R.S., Coughlan, K.J., Quirk, J.P. (1985). *Aust. J. Soil Res.*, **23**, 137-149

Ristori, G.G., Cecconi, S., Martelloni, C. (1983). *Agrochimica*, ***XXVII***, 20-27.

FORMATION OF BIOTITE IN A METAGREYWACKE COMPLEX, MECSEK MTS., HUNGARY: CONDITIONS OF LOW-T METAMORPHISM BASED ON ILLITE AND CHLORITE "CRYSTALLINITY", COAL RANK, WHITE MICA b_0-GEOBAROMETRIC AND MICROSTRUCTURAL DATA

Árkai P. *(Lab. for Geochemical Research, Hungarian Acad. Sci., Budapest)*, Lelkes-Felvári Gy. *(Hungarian Natural Science Museum, Budapest)*, Lantai Cs., Nagy G., Tóth M. *(Lab. for Geochemical Research, Hungarian Acad. Sci., Budapest)*

The investigated borehole Szalatnak-3 (with continuous core material) penetrated a Silurian metagrywacke complex, which is overlain by Triassic sediments. Basic dykes crosscut the sequence, moreover syenite body was found in the bottom of the borehole. Microstructural observations prove regional (dynamothermal) metamorphism overprinted by a contact (thermal) event.

The application of illite "crystallinity" (IC) method for the

metagreywacke samples, which contain di- and trioctahedral mica phases in strongly varying proportions, gave misleading results for determining metamorphic zones. In contrast, chlorite "crystallinity" (ChC) refers to transitional "anchi-/epizonal" (ca. 350°C) metamorphism. ChC data fit fairly well to conclusions obtained from chlorite geothermometric and coal rank data. On the basis of the b cell parameter of illite-muscovite, the complex was metamorphosed in a high thermal gradient regime.

Newly formed (metamorphic) biotite is widespread in the whole metagreywacke sequence. Microstructural observations and mineral chemical data refer to non-equilibrium transformations of detrital biotite --- chlorite --- newly formed biotite. Based on its post-tectonic (partly fissure filling) nature, the formation of biotite is attributed to the contact metamorphic heat effect and/or to an eventual infiltration metasomatism connected to the intrusion of syenite.

CHLORITE "CRYSTALLINITY" VS. ILLITE "CRYSTALLINITY" IN MONITORING METAMORPHIC GRADE: A CASE STUDY FROM THE SOUTH-ALPINE BASEMENT OF THE EASTERN ALPS, ITALY

Árkai P. *(Lab. for Geochemical Research, Hungarian Acad. Sci., Budapest)* Sassi F. P. and Sassi R. *(Dept. of Mineralogy and Petrology, Univ. of Padova)*

Illite and chlorite "crystallinity" indices (XRD peak widths abbreviated as IC and ChC) were determined in the Early Paleozoic, rather monotonous pelitic-silty complex of the South-Alpine basement of the Eastern Alps. The investigated 238 samples derived from eight localities between Sappada and Pontebba (Northern Italy), each represented by sample groups with n = 28 to 32.

Metamorphic grade in this area (related to the high-thermal-gradient Variscan metamorphism) ranges from diagenetic zone (to the east) through the anchizone up to the epizone (to the west), as pointed out by Sassi *et al.* (1974) and ascertained in detail by means of IC data (sensu Kübler, 1968, 1990) by Árkai *et al.* (1991) and recent unpublished data.

Fairly strong (r = 0.62-0.85) positive linear correlations were found between IC and ChC values, the latter having been measured on the 14 and 7 Å reflections of chlorite as ChC(001) and ChC(002). The ChC boundaries of the anchizone calculated by the linear regression equations between IC and ChC are very close to those obtained by Árkai (1991) on a smaller shale-slate-phyllite sequence (n = 82) in the Bükkium, innermost Western Carpathians, N-Hungary.

Although the ChC range of the anchizone is smaller than the corresponding IC range, the average value of the ChC turns out to be a reliable indicator of the metamorphic grade. Within the investigated eight populations, a perfect agreement was found between the IC- and ChC-based zone classification in 5 sample groups. Due to the statistical nature of the correlations, however, the zone classification in groups near to the high- or low-temperature boundaries of the anchizone became rather uncertain, presumably also due to a rearrangement of the chlorite polytypes. Anyway, this fact does not represent a drawback in monitoring the metamorphic grade basing on ChC data.

The applicability of chlorite "crystallinity" was also checked by significance tests of differences between the "crystallinity" averages of the sample groups. Out of the investigated 28 sample group-pairs the differences between the IC averages turn out to be significant in 25 cases at a significance level of P = 1 %, while the numbers of the cases with significant differences are 21 for the ChC(001) and 22 for the ChC(002). Consequently, the ChC method is less sensitive for identifying differences in metamorphic grade than the IC method. This fact can be explained by the smaller $\Delta^{o}2\Theta$ range of the ChC scale, comparing with the IC scale. Nevertheless, chlorite "crystallinity" can be regarded as a useful complementary tool, especially in certain (not uncommon) cases, where the interpretation of illite "crystallinity" is hindered by disturbing factors, such as the presence of discrete or mixed-layered paragonitic phases, margarite, etc.

References:
Árkai, P. (1991). *J. metamorphic Geol.*, **9**, 723-734.
Árkai, P., Sassi, R., Zirpoli, G. (1991). *Mem. Sci. Geol., Padova*, **43**, 293-304.
Kübler, B. (1968). *Bull. Centre Rech. Pau -SNPA*, **2**, 385-397.
Kübler, B. (1990). *Schweiz. miner. petrogr. Mitt.*, **70**, 89-93.
Sassi, F.P., Zanferrari, A., Zirpoli, G. (1974). *N. Jb. Geol. Paläont. Mh.*, **10**, 609-624.

CRYSTALLITE SIZE AND LATTICE STRAIN OF ILLITE-MUSCOVITE AND CHLORITE DETERMINED BY XRD: POSSIBILITIES AND LIMITATIONS OF THEIR METAMORPHIC PETROGENETIC APPLICATIONS

Árkai P., Tóth M. *(Laboratory for Geochemical Research, Hungarian Academy of Sciences, Budapest)*

Illite "crystallinity" (i.e., half height-width of the first basal reflection of illite-muscovite named also as Kübler-index or IC) has been applied world-wide for determining diagenetic and incipient metamorphic zones in pelitic and marly rocks for many years. Recently, structural and chemical changes of chlorite and its precursors expressed as chlorite "crystallinity" (ChC) and chlorite geothermometer proved to be useful empirical complementary indicators of metamorphic grade (≈temperature).

As to the general theorem, the line-broadening of an X-ray diffractometric reflection is the resultant of three main factors, namely: instrumental effects, crystallite size and lattice strain, each of which is rather composite. Several calculation methods elaborated originally for metals with rather simple structures are available for the determination of the crystallite size (i.e., the average size of those crystal domains in a given crystallographic direction, which scatter coherently the X-rays) and average lattice strain. The application of these methods for phyllosilicates needs precautions, for the real structure and chemistry of these minerals as well as their diagenetic - metamorphic evolution are much more complicated than the structural changes in metals.

In the present study crystallite size and lattice strain values obtained by various methods are compared. The test materials represent a metapelite series, which covers a range from deep or late diagenetic zone through the anchizone up to the epizone. Using natural "standards" for determining the instrumental line-broadening, the structural profiles were produced by Stokes' (1948) deconvolution method based on Fourier coefficients. The numerical results obtained by the variance method (Wilson, 1963), the Voigt deconvolution method (Langford, 1978) as single-line methods and by the Warren-Averbach analysis (Warren & Averbach, 1950) as multi-line method are compared using home-written programs and the PHILIPS APD-1700 software package.

Special attention is paid to the problems of natural "standards", the selection of which strongly influences the absolute results of the calculations. As the required preconditions are mostly not perfectly fulfilled in the cases of phyllosilicates, and as the adequate standards with infinite size and ideal structure are not available at present, the "absolute" values of mean crystallite size and lattice strain should be handled with great care and precaution, even if a fairly good agreement was found between the XRD-based crystallite size determinations and those obtained by other (TEM, SFM) methods in certain cases.

While the relationship between the mean crystallite size of illite-muscovite and chlorite and the metamorphic grade (≈temperature) is clear and can be explained by the Ostwald-ripening (Eberl *et al.*, 1990), the mean lattice distortion of these minerals is a complex parameter, which may relate to numerous types of lattice imperfections, the investigation of which falls far beyond the scope of the XRD technique.

Concerning the petrogenetic application of the results obtained by the methods listed above, not the absolute values, rather the relations (relative differences) in mean crystallite size and lattice strain calculated with a given method using a well defined, although arbitrary "standard" may provide new information about the

conditions of metamorphic (re)crystallisation, as compared to the conventional "crystallinity" studies.

References
Eberl, D.D., Srodon, J., Kralik, M., Taylor, B.E., Peterman, Z.E. (1990). *Science*, **248**, 474-477.
Langford, J.I. (1978). *J. Appl. Crystall.*, **11**, 10-14.
Stokes, A.R. (1948). *Proc. Phys. Soc. London*, **61**, 382-391.
Warren, B.E. & Averbach, B.L. (1950). *J. Appl. Physics*, **21**, 595-599.
Wilson, A.J.C. (1963). *Philips Technical Library*, Eindhoven.

• SPACE GROUP SYMMETRY OF MINERALS FROM ANALYSIS OF SELECTION RULES FOR INFRARED AND RAMAN SPECTRA

Arkhipenko D. and Moroz T. (*United Institute of Geology, Geophysics and Mineralogy, 630090, Novosibirsk 90, Russia*)

A primary crystal structure characteristic of minerals is associated with a distinct space group symmetry, which is not only the important value but also the way and method for setting the complex dependence "composition - structure - property" and defining the history of mineral formation in nature.

It has been known that X-ray diffraction method determines only 51 space groups from 230 uniquely; in other cases 2 to 5 space groups present the same rules of systematic absences of X-ray reflections. Previous investigations have shown the possibility to use non diffraction vibrational spectroscopy methods for defining a sp. gr. symmetry (Arkhipenko & Bokij, 1977). The suggested method includes the following steps:

1. Factor - group analyses for all models of sp. gr. with the same rules of systematic absences.

2. Experimental determination of IR and Raman symmetry modes for unit cell or its fragment.

3. The choice of space group on the basis of experimental and theoretical data.

Now we suggest the method for selecting one space group among the groups with the same rules of systematic absences, using the selection rules for Infrared and Raman spectra.

For example, diffraction group N4 has two space groups: C_{2h}^4 = P2/c and C_s^2 = Pc with the same conditions limiting possible X-ray reflections (Bokij & Poraj-Koshitz, 1964).

The character table of the point group C_{2h} signifies that only the A_g and B_g vibrations are Raman active and only A_u and B_u are infrared active for the component of the polarizability (α) or the dipole moment (T) belong to these species in this point group. A' and A" vibrations are both Infrared and Raman active in C_s point group (Nakamoto, 1986).

It immediately follows that IR and Raman frequencies present different values in C_{2h} point group and the same one in C_s.

Thus a simple comparison between IR and Raman experimental vibrational frequencies made possible to select one space group of symmetry among the groups with the same rules of systematic absences of X-ray reflections even for powder samples.

It is shown that almost all space groups may be theoretically differentiated; only 11 pairs of enantiomorphous groups cannot be distinguished.

The method has been applied to various minerals with CO_3^{2-}, SO_4^{2-}, PO_4^{3-} anions (dawsonite, hydrotalcite, carbonat- hydroxyapatite, alunite), lopezit - $K_2Cr_2O_7$, chrysotilasbest and to framework minerals (feldspathoids, zeolites).

References:

Arkhipenko, D.K. and Bokij, G.B. (1977). Crystallography, **22**, 1176.

Bokij, G.B. and Poraj-Koshitz, M.A. (1964). X-ray Analysis, V. 1, Moscow.

Nakamoto, K. (1986). Infrared and Raman Spectra of Inorganic and Coordination Compounds. John Wiley & Sons, Inc.

DYNAMIC X-SITE DISORDER IN SYNTHETIC SILICATE GARNET END-MEMBERS

Armbruster Th. (*Univ. Bern, Switzerland*) and Geiger C.A. (*Univ. Kiel, Germany*)

The silicate garnets of the general formula $X_3(Al,Fe)_2Si_3O_{12}$ represent one of the fundamental mineral groups found in the earth. Most natural garnets of the crust and uppermost mantle are solid solutions within the system $Mg_3Al_2Si_3O_{12}$ (pyrope) - $Fe_3Al_2Si_3O_{12}$ (almandine) - $Ca_3Al_2Si_3O_{12}$ (grossular) - $Mn_3Al_2Si_3O_{12}$ (spessartine) - $Ca_3Fe_2Si_3O_{12}$(andradite). We have synthesized single crystals of these five garnet end-members and investigated them by temperature dependent X-ray diffraction methods. The goal is to obtain a better understanding of the crystal chemistry of garnet as a function of composition and to investigate the nature of the disorder exhibited by the divalent cations.
Pyrope and almandine single crystals up to 1-2 mm in size were synthesized hydrothermally at elevated pressures and temperatures in a piston-cylinder device. Andradite was grown from a glass in the presence of PtO_2 also at high pressures and temperatures. Grossular and spessartine single crystals ranging up to approximately 200 microns in size were grown hydrothermally at lower pressures and temperatures, but with long run times, in cold-seal bombs. Data collection was undertaken on a CAD4 X-ray single crystal diffractometer at temperatures of 100 K, 293 K and 500 K. Reflection intensities were collected up to $\Theta = 50^o$ with MoKα X-radiation.
The divalent X-cation in garnet is eight-fold coordinated by oxygen anions forming a distorted dodecahedron. The X-site has 222 point symmetry with two crystallographically independent X-O bonds, such that four of the X-O2 bond lengths are slightly longer than the other set of four X-O4 bonds. The anisotropic thermal motion of the X-cation was studied by means of the difference mean-square displacement parameters, ΔU, evaluated along the two different X-O bonding vectors. ΔU values along the longer X-O4 vector are temperature dependent decreasing in the sequence Mg (pyrope) > Fe^{2+} (almandine) ≈ Mn^{2+} (spessartine) > Ca (grossular and andradite). Conversely, the ΔU's for the shorter X-O2 bonds show little or no dependence on temperature. The result is that the X-cations are dynamically disordered in a strongly anisotropic manner giving rise to a "rattling effect" within the dodecahedral site. If the X-site cations were statically ordered in subsites, as has been proposed in the literature, then the ΔU values should be largely temperature independent. The dynamic disorder of the X-cations can be graphically visualized using the program PEANUT (Hummel et al., 1991) by plotting the difference between the mean-square displacement parameters determined at 100 K and 500 K. These plots show clearly the anisotropic nature of the vibrational contributions and can, in addition, filter out any small contributions caused from residual static disorder. A similar analysis of the SiO_4 tetrahedra and AlO_6 and FeO_6 octahedra show that these polyhedral units can be described as rigid bodies.

Reference:
Hummel, W., Hauser, J., Bürgi, H.B. (1991). *J. Molecular Graphics*, **8**, 1307-1316.

ORDERING REVERSAL OF Mg/Fe INTRACRYSTALLINE PARTITIONING IN OLIVINE AT HIGH TEMPERATURE

Artioli, G. (*Dipt. Sci. Terra, Univ. Milano*), Gualtieri, A. (*Dipt. Sci. Terra,Univ. Modena*), Deriu, A. (*Dipt. Fisica, Univ. Parma*), Rinaldi,R. (*Dipt. Sci. Terra, Univ.. Perugia*), Wilson, C.C. (*Rutherf. Appleton Lab., U.K.*), Zanazzi, P F. (*Dipt. Sci. Terra, Univ. Perugia*).

In the crystal structure of olivine, $(Mg,Fe)_2SiO_4$, Mg and Fe can be distributed over two sites, M1 and M2, having slightly different octahedral configurations. Conflicting crystallochemical factors may influence the Mg-Fe ordering in the two sites, based on cation size, electrostatic potentials, and crystal field stabilisation; other factors influencing the Mg-Fe distribution are: composition, oxygen fugacity, pressure, and especially temperature.

The determination of the equilibrium:

$$Fe_{M2} + Mg_{M1} \Leftrightarrow Fe_{M1} + Mg_{M2}$$

expressed by the constant: K_D $[K_D = (Fe_{M1}/Mg_{M1})/(Fe_{M2}/Mg_{M2})]$ of the exchange reaction at different temperatures, provides the evaluation of cation partitioning. Several heating experiments on olivine, followed by quenching, and subsequent determination of K_D by X-ray structure refinements have been reported in the literature. Main results of these investigations are that K_D increases with temperature, *i.e.* iron tends to segregate into M1. However, olivines quenched from temperatures higher than 800°C have the same K_D as those of crystals quenched from 700°C, showing that the rate of cooling, also for very rapid quenching techniques, is lower than the speed of the exchange reaction at such temperatures as reported by a recent theoretical study placing the time constant of the Mg-Fe exchange reaction in the range of 10^{-2} - 10^{-4}s at 1000°C for compositions (Fe/Fe+Mg) in the range 0.1-0.5.

The only way to truly monitor this equilibrium above ~800°C is to carry out *in situ* experiments at high temperature in a controlled (non-oxidizing) environment. However, *in situ* single crystal X-ray data collections have proved unreliable due to experimental difficulties.

Single crystal neutron scattering experiments, allow the use of a sealed high temperature vacuum furnace which provides accurate control of the sample environment with negligible absorption or loss of accessibility to the neutrons; being only subject to the availability of large enough (≥1mm^3) single crystals.

Olivine single crystals with composition $Mg_{1.76}Fe_{0.24}SiO_4$ from a pallasitic meteorite were utilised in the present work. Full sets of Laue Neutron diffraction data were collected in two separate experiments on two different crystals at Room Temperature, 880°C, and 1060°C (first experiment); RT, 960°C, and 1030°C (second experiment; furnace stability ±5°C, in vacuum), on the SXD diffractometer line of the ISIS pulsed neutron source at the Rutherford Appleton Laboratory (UK). RT data reveal an essentially random distribution of Fe/Mg in the two sites with K_D ~1.0 in agreement with X-ray structure refinements on fragments of the same crystals. Oxidation of Fe^{2+} was ruled out by Mössbauer spectroscopy carried out before and after the high temperature neutron experiments on a few chips of the same single crystals.

The results indicate that at 880°C the Fe-Mg distribution is ordered with Fe tending to segregate into site M1, in agreement with literature data from quenching experiments (K_D =1.2-1.3). On the contrary, starting with the 960°C data, the structure refinements yield K_D values considerably smaller than one (0.6-0.5) and progressively diminishing to values near 0.3 at 1060°C, indicating preferential Fe segregation into site M2. This peculiar "***ordering reversal***" has never been observed before but it is confirmed beyond any reasonable doubt by the two separate experiments, on two different crystals and with slightly different experimental conditions. These results bear important implications as to the high temperature crystal chemistry of olivine, allowing the evaluation of thermodynamical properties of this phase at mantle conditions, with implications as to the physical properties of a mantle environment.

A large increase of the vibrational contribution to entropy with increasing temperature, which overrides the decrease of configurational entropy (ordering), might be the key to explaining how the ordering process is taking place with increasing temperature. Careful analysis of equivalent nuclear displacement parameters of the two sites at different temperatures should confirm this hypothesis.

EVOLUTION OF FOIDITE SERIES OF THE KOLA ALKALINE PROVINCE, RUSSIA: EVIDENCE FROM APATITE AND MELILITE CHEMICAL COMPOSITION.

A.Arzamastsev, L.Arzamastseva
(Geological Institute, Kola Sci.Centre, Apatity, 184200, Russia)

The distribution of Sr and REE in coexisting apatite, melilite and titanite in ultramafic alkaline intrusions and alkaline dykes has been studied. These data were compared with average concentrations of P_2O_5 and Sr in typical plutonic alkaline series: peridotite(PRD)-pyroxenite(PRX)-melilitolite (MLT)-melteigite(MLG)-ijolite(IJL)-urtite(URT)-nepheline syenite (NS).

The Sr distribution patterns differ in the Khibina foidite and ultramafic alkaline series of Kovdor, Vuoriyarvi, Sallanlatva, Ozernaya. The maximum Sr content in the Khibina foiditic series has been found in melanocratic foidolites. Besides, the apatite and titanite in these rocks are strongly enriched in Sr and REE. By contrast, in the Kovdor type series the maximal concentration of Sr and REE is typical for melilitolites, whereas the residual foidolites are depleted in these elements as well as the accessory apatite and perovskite.

The above differences between the Khibina and Kovdor type ultramafic alkaline series exhibit two particular evolutionary trends of fractional crystallization process, which was responsible for the entire ultrabasic-foiditic-phonolitic series. Parental olivine nephelinite melts are shown to be able to produce phonolite or melilitite derivatives, depending on fluid pressure.

Hydrous phases, appearing on the liquidus instead of clinopyroxene and olivine, result in melt compositions evolving toward the melilitite melt field, as is observed in the Kovdor, Vuoriyarvi, and Turiy Mys massifs. Crystallization of melilite, which has a relatively high Sr distribution coefficient causes depletion in Sr of the complementary members (foidolites and nepheline syenites).

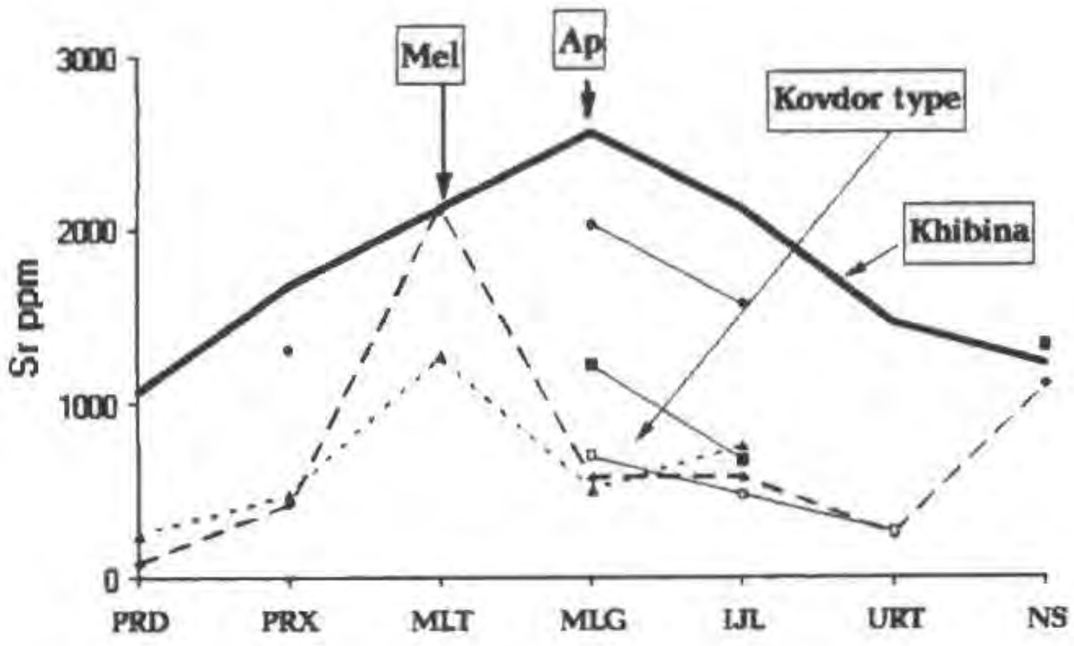

In the Khibina foidite series no important role of amphibole and phlogopite in the liquid evolution following the "phonolitic" trend should be expected. Melilitolite members of the series played no significant role and were reduced. This resulted in the enrichment of the Khibina melteigites and ijolites in Sr. As compared to apatite composition in the Kovdor foidites, the SrO content in those of the Khibina massif amounts to 3-6wt.%. Thus, the chemical composition of apatite and partly titanite in the Kola foidite series reflects the type of crystallization trends and depends on the presence or absence of melilitolite members.

STABILITY OF MINERALS AND DISTRIBUTION OF Zr AND Hf IN THE MELTING OF LAMPROITE AT UPPER MANTLE PRESSURE

A.M.ASAVIN, O.Yu. KHODYREV
(Vernadsky Institute of Geochemistry and Analytical Chemistry of Russian Acad. of Sci., Moscow, Russia)

The present study has been carried out in order to recognize the melting phase relationships of lamproitic rock and to obtain for the first time the distribution coefficients (K) of Zr and Hf in the solid phase/liquid equilibria in lamproite partial melting. To achieve the real equilibria experiments were made with artificial amorphous composition corresponding to mean composition of lamproites of Aldan (Siberia) at water unsaturated conditions under pressure 25 kbar and temperature range 1000-1300 C. Composition of clinopyroxene was characterized by low TiO2 0.6% and Na2O 1% versus high concentrations of these elements in the melt (TiO2 2.3%, Na2O 5%). The initial concentration of Zr and Hf were higher than the level of solubility. Baddeleite in the products of runs was established, with ZrO2/HfO2 ratio 0.85 and near 3% TiO2.

Zr and Hf were introduced in the melting equilibria in one series of runs as oxides in initial composition. The other series of runs introducing the elements as preliminary synthesized Zr,Hf-bearing garnet is being worked out. Due to above techniques stability of garnet has been clarified and reliable K of Zr and Hf in pyroxene/liquid and mica/liquid have been obtained.

In pyroxene/liquid K are 0.06 for Zr and 0.12 for Hf. It should be emphasized that K of Hf is higher than it for Zr. Moreover, these values are in order less than these in normal alkaline basalt systems. In phlogopite/liquid both K are less than 0.003. Melting phlogopite-bearing mantle is suggested to produce melts with high Zr and Hf concentration.

• ARE THE MANTLE XENOLITHS DERIVED GEOTHERMS CONVECTIVE OR CONDUCTIVE ? EVIDENCE FROM CENTRAL ASIA CENOZOIC ALKALINE BASALT NODULES

Ashchepkov I.V., Litasov Yu.D., Litasov K.D., Strizhov S.V., Ovchinnikov Yu.I. (*United Institute of Geology, Geophysics and Mineralogy, Russian Academy of Sciences, 630090, Novosibirsk, Russia*)

The positions of calculated geotherms for mantle xenoliths from Cenozoic volcanics of Central Asia (Vitim Plateau, Hentey Ridge, Tariat Depression, Dariganga Plateau, Minusa depression) were compared with those of other localities throughout the World (Eastern China, Eastern Australia, Patagonia).

Thermobarometer of Brey & Kohler (1990) or combination of methods of Bertrand & Mercier (1985) and Nickel & Green (1985) were applied to determine the temperature and pressure ranges. Xenoliths from the alkaline basalts produce PT plot close to the conductive oceanic geotherms but their relative position depends on many factors. Transbaikalian lherzolite alkaline basalt xenoliths (original data) are the most deep-seated among those described in literature. Estimated pressures up to 26-27 kbar were found for nodules from Burkal River (Hentey Ridge) and 28-30 kbar for Vitim Oligocene picrite-basalt tuffs. Vitim Quaternary xenoliths are more heated. All of the four locations of Quaternary garnet lherzolite xenoliths here produce individual PT ranges indicating temperatures higher than those for picrite basalt xenoliths. Burkal locations prolong the geotherm for Quaternary lherzolites from Vitim Plateau to deeper level. Mongolian garnet lherzolites from Tariat depression are close to Vitim Quaternary xenoliths but the majority of them corresponds to not so high pressure conditions. Upper part of mantle here is represented by pyroxenites with subsolidus lamellae.

The degree of heating seems to be correlated with the degree of metasomatism and abundance of amphibole and phlogopite veins in peridotites. Most cold Palei-Aike (Patagonia) slightly ferriferous lherzolites with amphibole probably are affected by subduction related melts. Vitim Oligocene mantle is more hot, and mainly phlogopite associations and amphibole veins without considerable enrichment in Fe are found here.

As regards Burkal garnet lherzolites, those containing submelted garnet show a lower degree of heating probably corresponding to the influence of volatiles (mainly CO_2) and tend to disequilibrium melting. Dry or carbon dioxide compositions of volatiles in mantle are typical for the hot Quaternary mantle in Central Asia. Phlogopites from Quaternary xenoliths reveal high concentration of fluorine. It probably creates an effect of extra high temperature solidus for peridotites.

Central Asia localities often contain hot (about 1300°C) cumulate pyroxenites or those ones that should have been at very high temperature originally. This means that intruded melts rapidly passed through the considerable vertical column, what may be typical for the dispersed continental hot spots. Three individual positions of the geotherm were found for different pyroxenites at the same location in Vitim for Oligocene xenoliths. Those for the high temperature pegmatoid pyroxenites reveal the trend close to adiabatic while anatectic green Cr-diopside websterites show the line close to conductive geotherm but shifted in the higher temperature field. Thus some of geotherms should be of conductive origin. Not only pyroxenites but also peridotites in some volcanoes create the PT trends crossing conductive curves. Together with the evident signs of the passage of the melts through the mantle column and regular distribution of the textures, this means that under the volcanoes the same passage of the different melts (basaltic, anatectic and hybrid) form local mantle diapirs. Their way of rising up seems to be individual. This conclusion is confirmed by the individual sets and compositions of the megacrysts supposed to be product of basalt melt crystallization in the supplying magmatic channels and chambers.

CRYSTAL GROWTH FROM SOLUTION: KINETICS AND SURFACE SUPERSATURATION

A.M.Askhabov
(Inst. of Geol., Komi Science Center, RAS, Syktyvkar, Russia)

Growth rates of different water-soluble crystals (potassium alum, ADP, KDP,epsomite e.a.) have been measured. For all these crystals growth kinetics in wide range of supersaturation are described by equation (Askhabov, 1993):

$$R = (K_d C_o/\rho)\times[\sigma - \tfrac{1}{2}\sigma^*(1+4\sigma/\sigma^*)^{1/2} + \tfrac{1}{2}\sigma^*], \quad (1)$$

Where $\sigma^* = K_d C_o/(\beta\rho)$, K_d- mass transfer coefficient, C_o- equilibrium concentration, ρ - density of crystals, β - kinetic coefficient of the face, σ - bulk supersaturation.

The empirical values of K_d and σ^* are the following:

$K_d = 6.4\times10^{-4}$ cm/s,
$\sigma^* = 0.055$ - for the (100) face of $NaClO_3$;
$K_d = 1.65\times10^{-3}$ cm/s,
$\sigma^* = 0.165$ - for the (110) face of $MgSO_4 7H_2O$;
$K_d = 2.42\times10^{-4}$ cm/s,
$\sigma^* = 0.04$ - for the (111) face of K-Al-alum.

Equation (1) may be used for determination of surface supersaturation σ_s (σ) for the crystal growing in the conditions of free and forced convection. For example, for the K-alum crystals growing in the free convection condition, the dependences σ_s (σ), based on experimental data R(σ) are following:

$\sigma_s = 0.02[(1 + 100\sigma)^{1/2} - 1]$ for {111}
$\sigma_s = 0.031[(1 + 64.5\sigma)^{1/2} - 1]$ for {001}

On the growth center σ_s is more, then one far from center. Because of it, gradients of supersaturation are appear on the face, and cause the formation of macrosteps. When the gradient achieve crytical values the morphological stability of growing crystal faces are lost. For the crystal growing in the dynamic conditions, σ_s achieves 0.80-0.90σ.

The processes of crystal growth from solution are controlled by combined mass transfer and surface kinetics. The ratio of their contribution are determined using the factor $\alpha = (1-\alpha\sigma/\sigma^*)^2$. The α values change in range from 0.2 (alum) to 0.9 (KBr). For the (101) face of KDP α = 0.45. Absolutly kinetic regime for the crystal growth from solution can not be achieved. Thats why only

experimental dependences $R(\sigma_S)$, got as result of calculations σ_S from σ, can be compared to theoretical models of crystal growth.

Analysis of $R(\sigma_S)$ data in the ranks of various growth models testifies about the cooperative character of crystal growth from solution. Furthermore, it is possible to evaluate quantitatively the contribution of different mechanisms. For example, the growth of octahedral faces of Al-K-alums is caused by mechanism of surface diffusion on 68% and direct jointing of particles on 32%. For prisma faces of ADP crystals and KDP dipiramidal ones the mechanism of surface diffusion is the main. Contribution of independant jointing of three-dimentional nucleous is not exceed 1-3% for the majority of studied crystals.

References:
Askhabov, A.M. (1993). *Doklady Academii Nauk*, 329, 737-740.

CELL PARAMETERS FOR Mg-, Al- AND Ni- SYNTHETIC END-MEMBERS OF THE COPIAPITE GROUP.

Atencio D. & Carvalho F.M.S. (*Inst. Geoctências, Univ. São Paulo*)

The general chemical formula of the copiapite group minerals is $(A^{(II)}_{1-3x}A'^{(III)}_{2x}\square_x)Fe^{(III)}_4(SO_4)_6(OH)_2.20H_2O$, where the A sites are completely filled by divalent cations (Ca, Cu, Fe, Mg, Zn) for $x = 0$, or two-thirds filled by trivalent cations (Al, Fe) for $x = 1/3$. The only phase synthesized in laboratory up to now is the equivalent of ferricopiapite. Synthetic equivalents of magnesiocopiapite and aluminocopiapite and the Ni-analogue (not known from natural occurrences) were obtained for the first time by the following procedure: mixtures of *p.a.* salts in stoichiometric ratios were soaked in water and maintained at room conditions until complete drying. Unit-cell parameters obtained from X-ray powder diffraction data using the program WIN-METRIC® (Registered Trademark of Sigma-C) are listed in Table 1. The agreement is good when compared to data for natural magnesiocopiapite and aluminocopiapite (Bayliss & Atencio, 1985) while the data for the Ni-analogue are similar to those for the copiapite-group compounds. XRD studies on Zn-, Fe^{3+}-, Mn- and Co- end-members synthesized by us are in progress.

Table 1. Cell parameters for synthetic copiapite-group end-members.

	Mg	Al	Ni
a(Å)	7.364(2)	7.358(1)	7.345(2)
b(Å)	18.875(6)	18.889(3)	18.83(1)
c(Å)	7.357(3)	7.356(1)	7.399(2)
α(°)	91.65(3)	91.69(1)	91.50(2)
β(°)	102.55(2)	102.452(9)	102.60(2)
γ(°)	99.03(3)	99.13(1)	99.30(3)

Reference:
Bayliss, P. & Atencio, D. (1985). *Can. Mineral.*, **23**, 53-56.

MINERALOGICAL AND PETROGRAPHICAL CHARACTERS OF THE BAHARIYA OASIS IRON ORES-BEARING MANGANESE MINERALS, WESTERN DESERT, EGYPT.

Attia, A.K.M. and Boulis, S.N. (Central Metallurgical Research Institute, P.O. Box 87, Helwan, Cairo, Egypt.)

ABSTRACT: The main purpose of this study is to shed some light on the iron-manganese mineral association in the Bahariya Oasis iron ore deposits in the Western desert of Egypt. About 50 samples collected from El-Gedida, Ghorabi and El-Harra areas were studied by means of a computer-controlled electron probe microanalyser and X-ray diffraction analysis. The main manganese minerals identified are pyrolusite, pyrosmalite, ramsdellite, and other amorphous minerals. They are finely dissiminated with hematite and goethite which are the most dominant iron-ore minerals of Bahariya Oasis. The grain size of the manganese minerals is usually less than 1 fm in diameter. In some cases they occur as cavity filling or individual crystals.

PETROCHEMICAL FEATURES OF IGNEOUS ROCKS IN THE RARE-ELEMENT PEGMATITE FIELD OF ELBA, ITALY

Aurisicchio C., Conte A.M. (C.S. for Experimental Equilibria in Minerals and Rocks - C.N.R., Rome, Italy) and Černý P. (Dept. of Geological Sciences, Univ. of Manitoba, Canada).

The famous rare-element granitic pegmatites in the island of Elba, in the Tyrrhenian Sea west of central mainland Italy, have been investigated since the 17th century. However, much of the abundant literature dealing with their mineralogy is outdated, and no meaningful information is available on their geochemistry and petrogenesis. Here we report the first petrochemical results of a comprehensive study of the Elban pegmatite field launched in 1990.

Two groups of igneous rocks are distinguished in the field. The plutonic GP (granodiorite-porphyry) suite constitutes the domal M. Capanne pluton of a relatively melanocratic (hb)-bi-granodiorite, locally with porphyry dikes. The leucocratic PEA suite consists of pegmatite, eurite and aplite dikes which crosscut the pluton, particularly on its eastern side where the pegmatites also penetrate its metamorphic envelope.

The A-*Q*-*P* (Le Maitre, 1989), A*b*-*Or*-*An* (Kosinowski, 1981) and *R1*-*R2* (De La Roche et al., 1980) diagrams classify the main plutonic rock as granodiorite, in part grading to monzogranite. The porphyries are monzogranitic, rarely quartz-monzodioritic. In contrast, all the PEA rocks show low Ca -monzogranitic to granitic compositions.

The $A=(Al-[K+Na+2Ca])$ vs. $B=(Fe+Mg+Ti)$ diagram of Debon & Le Fort (1983) and the *A/CNK* vs. *A/NK* diagram of Maniar & Piccoli (1989) sharply separate the GP suite of largely subaluminous granodiorites and sub- to metaluminous porphyries from the distinctly peraluminous PEA suite, in accordance with their respective mineralogies.

Chondrite-normalized REE abundances are virtually identical for both GP rock types: La_N averages at 80, La_N/Yb_N at ~13, with a moderate negative Eu anomaly and $Sm_N > Tb_N$ (except the LREE-enriched quartz-monzodioritic porphyry with La_N of 380). In contrast, the PEA suite has flatter patterns and lower LREE abundances: La_N of aplites, pegmatites and eurites averages at 16, 30 and 20, and La_N/Yb_N at 4, 6 and 7, respectively; Sm_N is slightly lower than Tb_N for all PEA rocks. The negative Eu anomaly is about the same as in the GP suite for pegmatites and aplites, but somewhat more pronounced in the eurites.

In terms of other trace elements, the PEA suite is poor in HFSE, LREE, Y, Ba and Sr, but enriched in Cs, Rb and in minor amount K, which however show considerable overlap.

Discrimination diagrams of Pearce et al. (1984) place both rock suites into the syncollisional fields. More significantly, the R1 vs. R2 plot of Batchelor & Bow*den* (198*5)* show the GP rocks trending from the pre-collisional (porphyries and some granodiorites) to the post-collisional (granodiorites) field, whereas the PEA suite fits late-orogenic parameters.

The post-collisional ranking of the granodiorites correlates with the post-tectonic (to anorogenic?) emplacement of the GP suite and related intrusions of the broader region. The melanocratic nature of most of the GP rocks, and their strong enrichment in Cs, and particularly Rb, correlate with their affiliation to the "alumino-Ca-Fe" domain of Debon & Le Fort (1983), both features suggesting a hybrid, heterogeneous protolith. The currently available data suggest that the PEA suite did not fractionate from the GP-generating magma but has a separate line of descent.

References:
LeMaitre,R.W. (1989). Blackwell,Oxford, 193 pp.
Kosinowski,M.H.F.(1982). Comp.& Geosci., 8, 1, 11-20.
De la Roche, H., Leterrier, J., Grand Claude, P., Marchal, M. (1980). Chem. Geol., 29, 183-210.
Debon, F., Le Fort, P. (1983). Trans. R. Soc. Edim. Earth Sci., 73, 135-149.
Maniar, P.D., Piccoli, P.M. (1989). Geol. Soc. Am. Bull., 101, 635-643.
Pearce, J.A., Harris, N.B.W.,Tindle, A.G. (1984). J. Petr., 25, 956-983.
Batchelor, R.A., Bowden, P. (1985). Chem. Geol., 48, 43-55.

THE DISTRIBUTION OF PGE IN HARDROCKS OF ALASKAN-TYPE INTRUSIONS .

Avdontsev S.N. (*Dept. of Petrology, VSEGEI*).

Plutons combined in this complex occur in the eastern Aldan Shield of the Siberian Platform . Intrusions have a similar concentrically zoned structure and are mainly composed of dunites surrounded by olivinites, wehrlites, clinopyroxenites and melanocratic gabbro (+/-hornblendites).

Three objectives were raised in the process of geochemical and topomineralogical surveying: **1**. More precise drawing of boundaries between rock varieties, which are difficult for identification (gradual contacts from dunites to olivinites, from Plag-clinopyroxenites to gabbro). **2**. Outlining and subsequent determination of geochemical anomalies after Pt for their later checking and definition as potential source zones for PGM placers. **3**. To obtain the new genetical information about the origin of rocks and massifs.

The various data obtained allowed general features of the genesis and history of formation of rocks and ores of intrusions to be determined. It was shown, that the main concentrations of PGM are not preferentially concentrated in the locations with maximum concentrations of chrome (i.e. maximum concentrations of CrSp), and the developing of CrSp segregations in dunites don't indicate the presence of significant PGM concentrations, contrast to stable correlation CrSp -> PGM observed in layered and some Alpine-type intrusions. The character of distribution of PGE (and REE) in the main rock varieties confirms the mechanism of intrusions consolidation during the process of ductile solid- state emplacement of mantle diapirs to the surface, with the complementary formation of dunite restite and mafic - ultramafic melts.

PHASE CHANGES IN MINERALIZED FILTRATION FLOWS

I.E.Azizov (Inst. Geol., Komi Sc. Cent., Ural. Div. of Rus. Ac. Sc., Syktyvkar, Russia)

The main criteria of the validity of the front approach for the description of processes, accompanied by phase changes are the condition of physical non-contradictivity (the appearance of effects of "superheating" and for "supercooling" in the vicinity of front being the physical contradiction).It is obvious that being physically contradictive the front unusable and a correct model is to be developed while taking account the appearance of finite zone of phase change.

In the present work physically non-contradictive description of vaporization processes in porous medium, saturated with fresh water and salt solutions in the framework of approach, based on the introduction of two-phase zone, has been developed for the first time.

The initial equations of heat and mass transfer we use: equation of continuity of vapor-water mixing (VWM); generalized Darcy's law for each phase; energy equation and equation of salt transfer. Inside one-phase zones this system of equations is closed by the reological and calorical equations, pressure P, temperature T and salt concentration c being the unknown functions. In a two-phase zone we use the condition of local phase equilibrium P=P(T) as additional closing equation. At the boundaries of two-phase zone we put the condition of mass balance, balance of moment, energy and mass of salt, solvated in liquid phase.

Here we describe only the most important results of our work.

The analysis of stable states of vapor-water system in inclined germetically closed porous column in the framework of front model leads us to the condition: if the temperature is strictly decreasing (increasing) functions of the depth,the states with vapor pillow (cap) are physically non-contradictive,otherwise the contradictions connected with the effects of "superheating" of water and/or "supercooling" of vapor are possible.

In the case of decomposition of smooth front of vapor generation in inclined germetically closed porous column well defined structure appears: water, VWM, vapor; VWM, vapor and so on. The generation of concrete structure depends on boundary temperature conditions at the ends of the column, on its length, and on the mass of water in the column. One of the must interesting phenomena which occur in two-phase zone is the phenomena of appearance of controversial flow of water and vapor.

While Pecle's number is increasing (Pe>10) the smooth front of vapour generation in one-dimensional filtrational flow is decomposed (if speaking about the drop-pressure mode), and the extended zone of phase change appears - two-phase zone with the criterion of existence.

In the case of large Pe the vapor generation in flow is closely connected with salt crystallization in pore space.

EXPERIMENTAL INVESTIGATION OF OL-OPX-ILM-RU ASSEMBLAGE OF Mg-Fe-Ti-Si-O SYSTEM AT HIGH PRESSURE

[1]Babich Yu.V., [2]Green D.H., [1]Sobolev N.V.
(1-*Inst. of Mineralogy and Petrography, Novosibirsk, Russia;*
2-*Geology Department, University of Tasmania, Hobart, Australia*)

The compositions and phase relations peculiarities of harzburgite assemblage (Ol+Opx+Ilm+Ru) of the titanium-enriched part of Mg-Fe-Ti-Si-O system were investigated at P=10-35 kbar, T=900-1350°C and within expanded oxygen fugacity range $Log_{10}(fO_2)$=FMQ±4 log.units (WC-WO_2-graphite(WCO), Ni-NiO(NNO), Fe_2O_3-Fe_3O_4(HM), C-saturated C-O-H fluid (CCO and GW_{max} buffers). Experiments were carried out on "piston-cylinder" type high pressure apparatus using conventional dabble capsule methods. Inspection of experimental products was performed optically and by electron microanalyser Camebax SX-55.

Using results of phase analysis and K_D between Ol(Opx) and Ilm in wide P-T-fO_2 range the testing of both Ol/Ilm and Opx/Ilm existing Fe/Mg exchange geothermometers (Bishop,1980; Andersen & Lindsley, 1981) was performed. It was established that temperature observed and calculated are in appropriate compliance only within narrow area with sufficiently low fO_2 value (no more than provided by NNO buffer) and differ considerably (>100°C) at more higher oxygen fugacity, where ilmenite solid solution contain more than 0.1mol.% of hematite. To exclude significant discrepancies of the geothermometers at oxidized conditions the modified semiempirical tentative versions of Ol/Ilm and Opx/Ilm

were derived. Corrected and simplified version of the orthopyroxene-ilmenite exchange thermometer is as following:

$$T(K)=(1715.7+1634*X_{Ilm}+2560.7*X_{Hem}+0.0124*P)/Ln(K_D),$$

where P - in bars, $K_D=(X_{En}/X_{Fs})^{OPX}/(X_{Gei}/X_{Ilm})^{ILM}$.
And improved version of olivine-ilmenite thermometer is given by:

$$T(K)=\{A_1+P*(A_2X_{Fa}+A_3X^{GI}+A_4)+A_5X_{Fa}+A_6X^{GI}+ +X_{Hem}(A_7+A_8X^{IG})\}/\{B_1-LnK_D+B_2X_{Fa}+ +B_3X^{GI}+X_{Hem}(B_4+B_5X^{IG})\} ,$$

where $X^{GI}=(X_{Gei}-X_{Ilm})$, $X^{IG}=(3X_{Ilm}+X_{Gei})/2$,
$K_D=(X_{Fo}/X_{Fa})^{OL}/(X_{Gei}/X_{Ilm})^{ILM}$, P -in bars, and coefficients are:

$A_1=-1575.28$	$A_5=1262.3$	$B_1=0.6819$
$A_2=3.61*10^{-3}$	$A_6=693.59$	$B_2=0.7842$
$A_3=1.328*10^{-3}$	$A_7=-1906.5$	$B_3=0.3721$
$A_4=-7.457*10^{-3}$	$A_8=-8624.1$	$B_4=1.9832$
		$B_5=-8.7764$

Estimation of the oxygen fugacity using fO_2-barometer (Eggler,1983) led to the appropriate results with mean error no more than 0.45 log.units through the all experimental range investigated.

References:
Andersen D.J.,Lindsley D.H.(1981).*Geoch.et Cosm.Acta*,**45**,847;
Bishop F.C. (1980). *Amer.Journ.Sci*,**280**,46-77;
Eggler D.H.(1983).*Geoph.Res.Lett.*,**10**,5,365-368.

THE ENERGETICS OF CATION ORDERING IN NATURAL BIOTITES.

Babushkina M.S., Nikitina L.P., Khiltova E.Yu. (*Institute of Precambrian Geology and Geochronology, St.Petersburg, Russia*).

The temperature dependence of degree of cation ordering and values of enthalpy and volume changes of isothermal Fe^{2+} redistribution reactions in biotites (X_{Fe}^{2+}=0.16-0.63) at 500,550,600 and 650°C with annealing times 240h was established. Milled in the agate vial in acetone by spacemill biotite powder (3-10 μm) was sealed in a quartz tube previously evacuated to a pressure less than 10^{-4} mm Hg. The fineness of temperature control was ∓10°C. Quenching was carried out in liquid nitrogen. The Fe^{2+} intersite distribution and unit-cell parameters were determined by Mössbauer and X-ray powder methods. The preference occupancy of M1 site by Fe^{2+} in the unheated biotites was established. The processes of ordering (Fe^{2+} redistribution from M2 to M1) or disordering (Fe^{2+} redistribution from M1 to M2) take place in different annealed biotites. At the same annealing temperature the degree of disordering increases with increasing of X_{vac}(M1) / X_R^{3+}(M2) ratio. The annealing during 240h allows us to achieve an equilibrium distribution practically for almost studied samples. The estimations of standard thermodynamic functions of redistribution reactions were obtained from intracrystalline ion exchange equilibrium Fe(M1) + Mg(M2) ⇔ Fe(M2) + Mg(M1) where Mg(Mi)=1-Fe(Mi), i=1,2. The ideal, regular and quasichemical solid solution models were used. The temperature dependencies of lnK (K-equilibrium constant of reaction) and ΔG (the change of free energy) are linear for each model. It permit us to calculate ΔH° and ΔS°. The values of ΔH° and ΔS° (table 1) indicate the substantial enthalpy and entropy effects of redistribution reaction of Fe^{2+} and Mg cations. The temperature dependencies of lnK and ΔG differ slightly for these models. The short-range order was determined in biotite structure in our earlier study. Consequently the interaction energy W_{Fe-Mg} is not equal to zero. So quazichemical model which best takes into account the real structure of solid solution was chosen. The volume effect (ΔV°) of redistribution reaction was estimated from the dependencies of molar volumes of annealed micas on Fe^{2+} content in M1 and M2 sites. The following expression of ΔV°as function of temperature was calculated for biotites:
ΔV°= -0.00102T + 0.789 /cal $bar^{-1}mol^{-1}$/ ∓0.02
Fist obtained values of enthalpy, entropy and volume effects of redistribution reaction of cations in biotites structures allow us to determine the equilibrium temperature of intracrystalline cation distribution.

Table 1

Solid solution model	Disordering		Ordering	
	ΔH°, Kcal/mol	ΔS°, cal/mol.K	ΔH°, Kcal/mol	ΔS°, cal/mol.K
Ideal	11.8∓2.5	12.7∓2.0	4.5∓1.0	3.2∓1.0
Regular (W_{Fe-Mg}=-1.92Kcal/mol)	18.3∓2.5	19.5∓2.0	11.2∓2.0	10.2∓2.0
Quazi-chemical	18.8∓2.5 (W_{Fe-Mg}=-1.92Kcal/mol)	20.2∓2.0	7.1∓2.0	5.1∓2.5

• CRYSTALLIZATION OF SPODUMENE FROM THE $R_2(Li,K,Na)O-MgO-Al_2O_3-SiO_2$ SYSTEM

Badau N. *(S.C. "CEROC" S.A., Cluj, Romania)*

The paper presents the study of the spodumenic vitroceramic from the complex $R_2(Li,K,Na)O-MgO-Al_2O_3-SiO_2$ system, using natural local raw materials (chemically treated steatite, rhyolite from Parva, bentonite) and TiO_2 as a nucleation agent in order to obtain some technical masses.

Products are obtained according to the glassware classical technological process followed by a directed crystallization. The spodumene crystallization diagrams were experimentally determined by the correlation of thermal analyses with the X ray diffraction method and electronic microscopy.

The glasses and the crystallized masses have been physico-chemically characterized (dilatometry, DTA, X-ray diffraction, electronic microscopy, density, hardness, chemical stability and chemical analyses).

The masses obtained are characterized by a microstructure specific for the spodumenic vitroceramic, the dimensions of prismatic and lamellar phase being of 1 to 4 μm.

References:
Berezhnoi A.I.: Glass Ceramics and Photositalls, Plenum Press, N.Y.–London, 1970, 444 p.
Bezborodov M.A.: Steklo cristaliceskie materialî, Izd.no nauki i techniki, Moskva, 1982.
Pavluskin N.M.: Osnovî tehnologhii sitalov, Stroizd. Moskva, 1979, 260 p.
Vogel W.: Structure and crystallization of glassed, Pergamon Press, Edition Leipzig, 1971, 246 p.

CHROME SPINEL AS A PROSPECTING AND PETROGENETIC INDICATOR

Bai Wenji

Chromite or chrome spinel occurring in the Earth is a mineral consisting mainly of 5 constituents: Cr_2O_3, Al_2O_3, Fe_2O_3, MgO and Feo. The authors have proposed a diagram with 4 constituents: Cr_2O_3, Al_2O_3, MgO and TFeO. This simple diagram can be suitable for the analyses by electron probe. The 4 constituents for chrome spinel have been shown by right–angled tetrahedron triaxially. So each analysis will be represented by two points which are the casting shadow on the two planes of right– angled tetrahedron (Fig.1A).

According to this simple diagram, three modeles of variation for chrome spinel chemical composition for chromite deposits in the Earth can be revealed. They are of ophiolite, continental centred intrusion and bedded intrusion. This diagram may show the trends of changes among the 4 contituents and differences of each rock body for each type (Fig. 1B).

By way of comparing the composition of spinels from meteorites, different chromite deposits, kinberlites, xenolithes in basalt and diamonds as a inclusion in kimberlite, representative chrome spinel chemical compositions have been plotted on the diagram, there appears will be a clear point area for each type of country rocks. The regular patterns in the diagram for the chrome spinels will be possible to point that they can distinguish the type of mafic– ultramafic complex and serve as a good indicator in prospecting work and can reflect an environment in which the country rock of the chrome spinel formed possibly.

For example, one of mafic–ultramafic complex in China consists of several rock facies, in which the dunite with high Al_2O_3 of chrome spinel contains chromite deposit only. So that dunite became a good taget ronge for the prospecting in that time. In another instance, we have known chemical composition of the chrome spinels from the chromite deposit in Tibet is more similar to that from diamonds as inclusion in kimberlites. In the

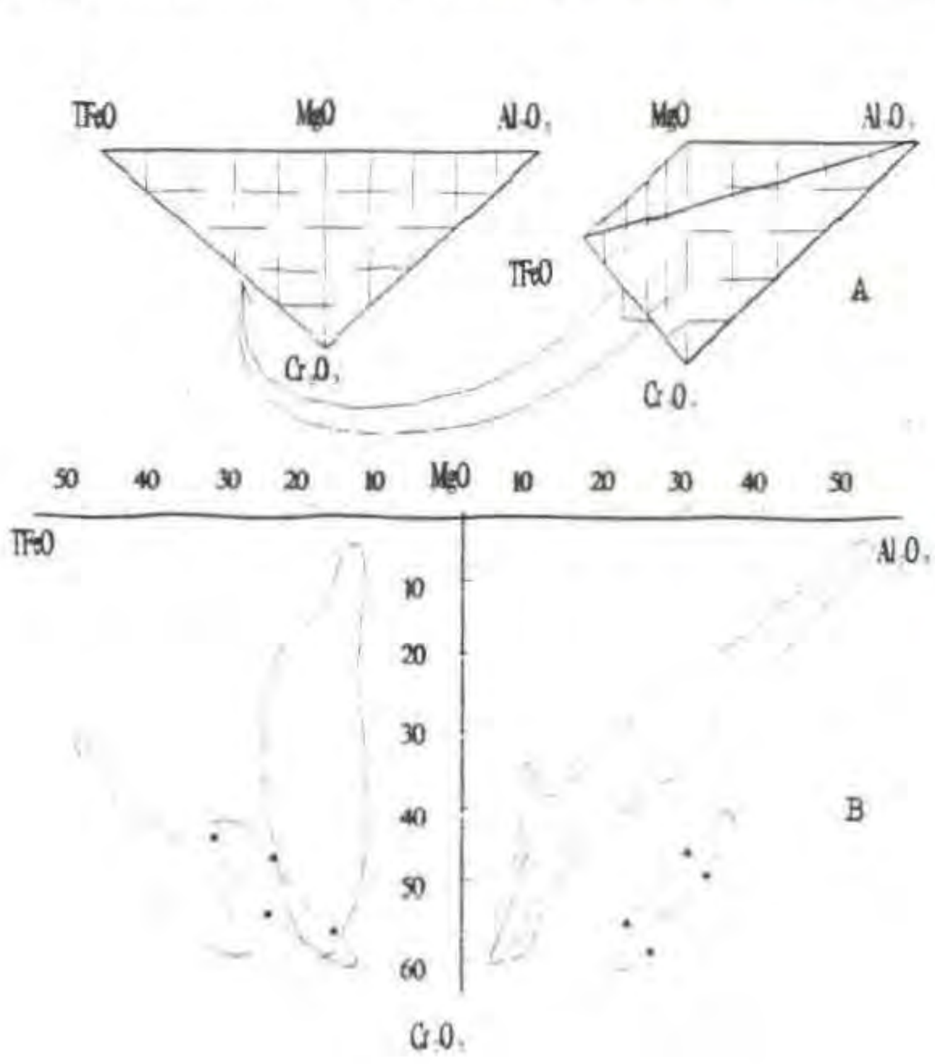

1– Ophiolites, 2– Bedded mafic–ultramafic intrusions, 3– Continental centred intrusions.

light of this comparing, in the later diamond– finding, the diamonds were found from the heavy mineral of the chromite ores in Tibet. The diamonds are part of unusal mineral assemblage including SiC, graphite, native chromium, native nickel and platinum group mineral. It is evidence in chrome spinel chemical composition to be useful in some prospecting.

References:
Bai, W. J., Robinson, P. T., Zhou, M. F. (1993). Mid–Continent Diamonds, GAC–MAC, 77–82.
Fang, Q. S. & Bai, W.J. (1981). Geological Review (Chnese) 27, 455–457.

CRYSTAL CHEMICAL SURPRISES OF SODIUM IN DEHYDRATED ANALCIME

Bakakin V.V.*, Alexeev V.I.*, Seryotkin Yu.V., Belitsky I.A., Fursenko B.A. and Balko V.P.* *(Inst. of Mineralogy & Petrography, *Inst. of Inorganic Chemistry, Russ.Acad.Sci., Novosibirsk, Russia)*

To clarify the peculiarities of dehydration and rehydration of analcime an X-ray crystal structure analysis was performed on one and the same single crystal of natural analcime in its original hydrated form (**I**) and dehydrated one (after heating at 550°C) (**II**). The original sample of analcime from Nidym river (East Siberia, Russia) (**I**) had a chemical composition close to $Na_{1.88}[Al_{1.88}Si_{4.12}O_{12}]\ 2H_2O$. Space group and unit cell parameters are as follows: **I** - Ibca, a=13.729, b=13.686, c=13.710 Å; V=2576 Å^3; Z=8; R=0.032; **II** - I2/a, a=13.730, b=13.489, c= 13.704 Å, β=90.05°; V=2538 Å^3; R=0.030.

Structure **I** follows relationships between Al fractions in tetrahedra and both lattice parameters and occupancies of the nearest Na sites, which were found by Mazzi & Galli (1978) for natural analcimes. Preserving position designations of these authors we can write for our sample **I**: T11 $Al_{0.46}$, T12 $Al_{0.16}$, T2 $Al_{0.31}$; M11 ($Na_{0.72}\square_{0.28}$), M12 ($Na_{0.45}\square_{0.55}$), M2 ($Na_{0.74}\square_{0.26}$).

The Al/Si-distribution in **I** and **II** is practically the same and all differences in the structures are due to a redistribution of Na-atoms as a result of changes in their surroundings. In **I** Na coordination is a very distorted octahedron - [6*o*]. Its quadrangular section (across two O-O-edges of two T-tetrahedra) is in the general case not plane [4*s*] but slightly tetrahedrized and may be designated as [4*t*']. The coordination polyhedron may be represented as [6*o*] = [4*t*'+2]. When water go away the Na-coordination changes from 6 to 4, Na-O distances shorten by ~0.06Å and the deformation of the T-framework occurs. Two M-sites (of three per formula unit) adopt plane trapezoidally distorted quadrangular configuration (extended notation [4*s*]), while third one in contrast adopt more pronounced [4*t*] configuration. The Na-O distances in the latter tend to increase (not to decrease). Na-atoms escape from this position and migrate to non fully occupied M1 and M2 sites. The (Na,□) - (Na,□) migration distances are near 4.2Å. The Na-distribution in **II** is as follows: M11 ($Na_{0.93}\square_{0.07}$), M12A and M12B ($Na_{0.00}\square_{1.00}$), M2 ($Na_{0.91}\square_{0.09}$). This Na-atoms redistribution leads to significant contraction along one of the axes (b).

The structure fragments of analcimes **I** and **II** in projection along [111] (Fig) show M-sites occupation and their coordination by H_2O and two O-O edges (shown in bold).

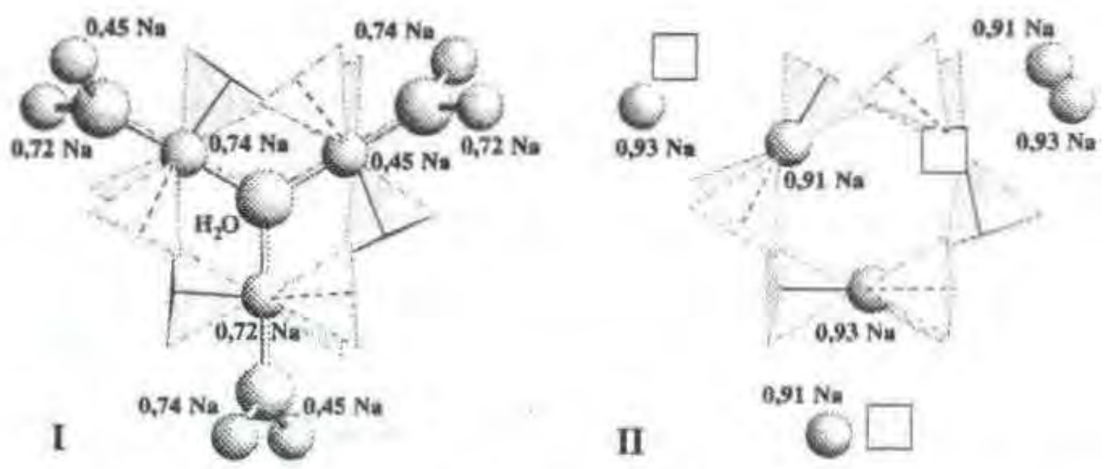

The following surprises of Na are found out in dehydrated analcime:

1. Fourfold plane trapezoidal Na-coordination; 4 Na-O within 2.39÷2.47Å, (mean 2.42Å); two O atoms from the next coordination sphere come closer to Na (3.2÷3.3Å in **II** instead of 3.6÷3.7Å in **I**).

2. The migrational redistribution of Na atoms resulting in one third of initial Na-positions become free and two thirds more occupied comparing to the original hydrated analcime. This process can be

expressed by following crystal chemical formulas (for idealized analcime composition $Na_2(H_2O)_2[Al_2Si_4O_6]$) :

I- $(Na_{1-x}\square_x)^{[6o]}\ (Na_{1-y}\square_y)^{[6o]}\ (Na_{1-z}\square_z)^{[6o]}\ (H_2O)_2\ [(Al,Si)_6O_{12}]$, where x+y+z = 1, [6*o*] = [4*t*'+2];

II - $Na^{[4s]}\square^{[4t]}Na^{[4s]}[(Al,Si)_6O_{12}]$.

Reference
Mazzi F. & Galli E. (1978) *Amer.Mineral.*, **63**, 448-460.

LOCAL STRUCTURE AROUND Eu^{3+} IN Na_2O-Al_2O_3-SiO_2 GLASSES DETERMINED BY LASER-EXCITED EMISSION SPECTRA

Baker, D.R. (*Dept. of Earth & Planetary Sci., McGill Univ.)*, Simkin, D. (*Dept. of Chemistry, McGill Univ.)*, and Marr, R. (*Dept. of Earth & Planetary Sci., McGill Univ.)*

Laser-excited emission spectra of Eu^{3+} in Na_2O-Al_2O_3-SiO_2 glasses have been measured at room temperature and at 10 K. Glasses studied include albite glass (dry and with 6.5 wt% H_2O), and peraluminous and peralkaline glasses with 75 mol % silica and Na/Al molar ratios of 1.68 and 0.6, respectively. Between 1.4 to 1.7 wt% Eu_2O_3 was added to the glasses and they were melted at 1 atm in air and at 3.0 GPa in a piston-cylinder apparatus. Glass samples were excited with an Ar^+ ion laser at both 457 and 476 nm with powers between 800 mw and 2.2 w.

The spectra of all glasses studied are similar and reflect $^5D_o \rightarrow {}^7F_{1,2}$ transitions. Peraluminous and albite glasses display very similar Eu^{3+} emission spectra with a maximum emission near 625 nm for an excitation of 457 nm and near 620 nm for an excitation of 476 nm. Neither composition, temperature, pressure, or for the albite glass, water, have a significant influence on the spectra of glasses with a molar Na/Al ratio equal to, or less than, one. These spectra for albite and peraluminous glasses resemble previously measured spectra in other silicate glasses. Spectra for the peralkaline glass span the same wavelength range as observed for albite and peraluminous glasses but demonstrate a shift in the maximum emission to near 614 nm for both excitation wavelengths and a narrowing of this major emission peak compared to the ones observed in the albite and peraluminous glasses. Pressure and temperature of glass synthesis have little effect on the spectra of the peralkaline glass.

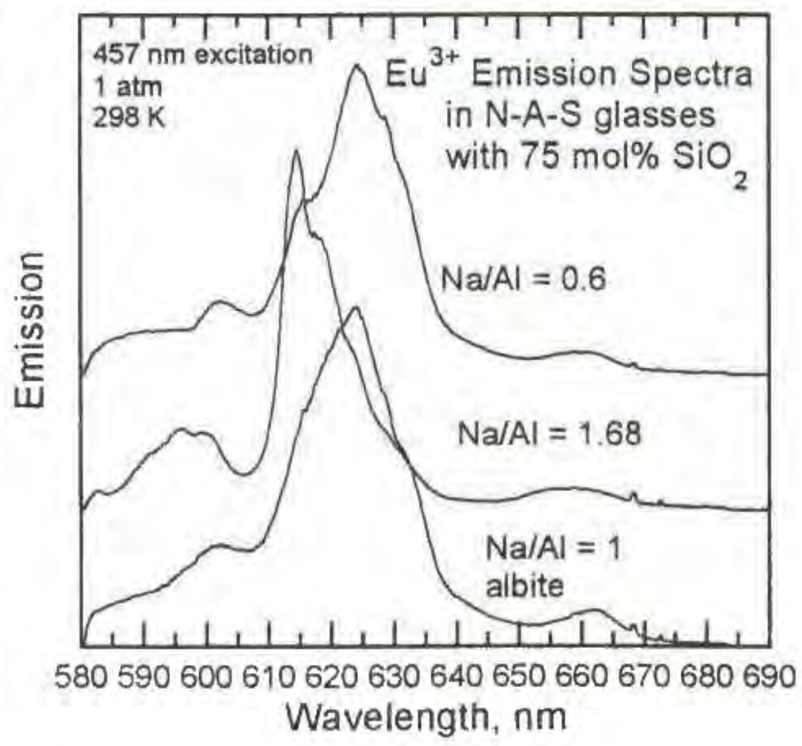

Spectra of all glasses are interpreted to reflect approximately 8-fold coordination of Eu^{3+} by oxygen with varying O-Eu-O bond lengths and angles. The insensitivity of the Eu^{3+} spectra to pressure is consistent with previous Raman and NMR studies of Na_2O-Al_2O_3-SiO_2 glasses which demonstrate little pressure effect on their structures at pressures up to 3.0 GPa. The similarity of dry and hydrous albite glass spectra, and of dry albite and peraluminous glass spectra indicate that the bulk polymerization of the glass does not exert a strong effect on the Eu^{3+} coordination in these glasses. However, spectral differences between the peralkaline and other glasses indicate that peralkalinity has a measurable effect on Eu^{3+} spectra and therefore Eu^{3+} coordination. The narrower peak in the peralkaline spectrum suggests the existence of more-regular oxygen coordination polyhedra around Eu^{3+} in this glass than those found in the peraluminous and albite glasses.

W-RUTILE FROM VEIN POST-SKARN MINERALIZATION OF THE BESTIUBE DEPOSIT, NORTH KAZAKHSTAN.

Baksheev I.A., Guseva E.V., Spiridonov E.M.
(Dept. of Geology, Moscow State Univ.)

Pyrrhotite-muscovite-quartz thin and short veins with Bi-Mo -W mineralization, as well as W-rutile, are widespread in the range of pyroxene hornfels halo. The hornfels occur around the smallest hypabissal quartz leucogabbro-norite, tonalite, plagiogranite intrusions. These veins cut skarnoid and calcerous skarn and in turn, they are crossed by molibdenite-quartz and gold-qartz veins.

Rare-metal veins are composed of quartz, hydroxylmuscovite, chlorite (ripidolite, corundophilite and others), dolomite, ferrodolomite, monoclinic pyrrhotite, chalcopyrite, rutile, F-apatite, scheelite, molibdenite, molibdoscheelite, sphalerite, arsenopyrite, Ni-Fe-cobaltite, Ni-linnaite, galena, bismutite, tetradymite, Pb-tetradymite, Sb-Pb-hedleyite, tetrahedrite, kobellite, cosalite, Ag-Pb-cosalite, cannizzarite. Pyrite, Ni-pyrite associate with the late sulfides Ag-tetrahedrite, chalcopyrite, Bi-Pb-sulfides. According to the homogenization of individual fluid inclusions with liquid CO2 in quartz the initial formation conditions of this mineralization are T=490-420°C, p=2.3-1.6 kbar, solution is KCl-NaCl-$MgCl_2$ with subordinate $CaCl_2$ amount, with salinity 25-22% NaCl equiv.

Molibdoscheelite, containing up to 2% MoO_3 and up to 3.5% SrO, composes nuclei of zonal scheelite crystals. Rutile forms the characteristic prismatic crystals and more rare tabular pseudomorphs on ilmenite. Rutile always contains 1-2% V_2O_3, 0.3-1.1% PbO, 0.2-0.4% Al_2O_3. W-rutile composes the nuclei of relatively large 3 mm long rutile crystals. W-rutile is oval, rounded in cross section. The boundary between W-rutile and rutile ring is clear. W-rutile contains 7.2-8.4 wt.% WO_3. Rutile of outer zones contains up to 1.4 wt.% WO_3. The chemical composition of the W-richest rutile (wt.%) is TiO_2 85.95, Al_2O_3 0.16, FeO 2.47, CaO 0.32, V_2O_3 1.65, PbO 0.67, WO_3 8.44, total 99.63 (microprobe "Camebax"). The positive correlation between W and Fe contents was established, with the W-richest rutile containing 2.6% FeO. An obvious isomorphism scheme is $2Ti^{4+} \rightleftharpoons Fe^{2+} + W^{6+}$. W-rutile is

slightly lighter in reflected light than W-poor rutile.

ASTHENOSPHERIC DEPTH METAMORPHISM OF CRUSTAL ROCKS VIEWED THROUGH THE ECLOGITE-GRANULITE SERIES OF THE ZŁOTE MOUNTAINS AND COMMON ECLOGITES OF THE BIALSKIE MOUNTAINS IN THE ORLICA-ŚNIEŻNIK DOME, NORTHEASTERN BOHEMIAN MASSIF

Bakun-Czubarow N. *(Inst. of Geol. Sciences, Pol. Acad. Sci.)*

HP metamorphic rocks, forming numerous but small bodies, are widely distributed throughout the Bohemian Massif. These rocks are represented by eclogites, granulites, garnet peridotites and exceptionally by calcsilicate marbles. Some of the HP rocks might have been previously equilibrated under ultrahigh pressures. UHP metamorphism involves mainly crustal rocks metamorphosed within the coesite stability field (Chopin 1987). Within the European Variscides an UHP metamorphism could be inferred from coesite pseudomorphs and quartz or potassium feldspar exsolutions in clinopyroxenes. In the eastern part of the Orlica-Śnieżnik Dome traces of UHP metamorphism were found in both the eclogite-granulite series of the Złote Mountains and in common eclogites of the Bialskie Mountains. The HP eclogite-granulite series of the Złote Mountains is built of prevailing acid granulites with intercalations of omphacite granulites and common eclogites. In the basic rocks the following HP mineral assemblages were recognized: 1. omp-grt-pl-Kfs-qtz-rt-ilm; 2. omp-grt-pl-Kfs-qtz-rt-ilm-ky; 3. omp-grt-pl-qtz-rt-ilm; 4. omp-grt-pl-qtz-rt-ilm-ky; 5. omp-grt-qtz-rt. The granulitic omphacites, with the highest jadeite content reaching 45% in grain cores, remain in equilibrium with unzoned oligoclases (An_{11-22}). Quartz pseudomorphs after coesite were recognized recently in omphacite granulites and eclogites. The pseudomorphs are usually composed of randomly oriented polycrystalline quartz aggregates, rarely with radial rims. They form either tiny inclusions (≥100 μm in diameter) in garnets of omphacite granulites and eclogites or minute rounded or bigger elongated inclusions (up to 300 μm in length) in eclogitic omphacites. In host minerals radial, and sometimes fragmentary concentric microfractures can be observed. Moreover in some domains of eclogitic omphacites needles and/or laths of exsolved quartz can be seen. The latter phenomenon may point to the pre-existance of nonstoichiometric omphacites with a vacancy end-member (CaEs) comprising up to 16 mol % of omphacite. Most likely the vacancies in omphacites were stabilized by pressures over 3 GPa, thus the rocks experienced pre-granulitic UHP metamorphism (~3 GPa at 700-800°C). After the UHP event the HP granulitic metamorphism followed. The beginning of cessation of the HP metamorphism has been dated for 352±4 Ma by means of Sm-Nd cpx-wr-ga isochrone (Brueckner et al. 1991). In the easternmost occurrence of common eclogites of the Bialskie Mountains the probable pseudomorphed coesites as well as quartz exsolutions in some domains of omphacite blasts have also been found. The starting of cessation of the HP metamorphism for the common eclogites in question was determined for 329±6 Ma (Brueckner et al. op cit.). Within the Saxothuringian Zone the eclogites of Central Erzgebirge (Schmädicke et al. 1992) and most likely those of the Münchberg Massif have experienced UHP metamorphism. In the southeastern part of the Moldanubian Zone in Lower Austria UHP metamorphism has been recorded in calcsilicate marbles previously containing potassium bearing clinopyroxenes (Becker, Altherr 1992). The rock complexes that recorded the UHP event outcrop in the outer parts of the Bohemian Massif. Most likely they were subducted to asthenospheric depths during an earlier Variscan or pre-Variscan collisional "Alpinotype" event (O'Brien, Carswell 1993).

References:
Becker H., Altherr R. (1992). *Nature*, 358, 745-748
Brueckner H.K., Medaris L.G., Bakun-Czubarow N., (1991). *Neues Jahrbuch Miner. Abh.*, 163, 169-196
Chopin C., (1987). *Phil. Trans. R. Soc. Lond.*, A 321, 183-197
O'Brien P. J., Carswell D. A., (1993). *Geol. Rundsch.*, 82, 531-555
Schmädicke E., Okrusch M., Schmidt W., (1992). *Contrib. Mineral. Petrol.*, 110, 226-241

THE EXPERIMENTAL STUDY OF THE As/Sb SOLID SOLUTION BEHAVIOUR IN Tl SULPHOSALTS

Balić Žunić T. (*Haldor Topsøe A/S, Copenhagen*), Makovicky E. (*Geological Institute, University of Copenhagen*) and Moëlo Y. (*Dept. of Material Sciences, University of Nantes*)

In the quaternary phase system Tl-Sb-As-S the compositions between $TlAsS_2$ (lorandite) and $TlSbS_2$ (weissbergite), as well as those between $Tl_5Sb_2As_{11}S_{22}$ and $Tl_5Sb_8As_5S_{22}$ (the presumed rebulite solid solution) were synthetized at 250°C and analysed by X-ray diffraction and microprobe.

In the lorandite-weissbergite system the miscibility gaps between 54 and 85 mol% $TlAsS_2$ and also (probably) between 24 and 34 mol% $TlAsS_2$ were recorded. The solid solution behaviour and miscibility gaps can be explained by the similarities and dissimilarities in the crystal structures of lorandite and weissbergite which were examined in detail. Both theoretical and experimental results suggest that lorandite and As-poor weissbergite are separated by a triclinic "weissbergite-like phase" $TlAs_{0.34-0.54}Sb_{0.66-0.46}S_2$ with a (probably) ordered As and Sb distribution.

The rebulite syntheses show that the Sb/As solid solution in this mineral extends from $Tl_5Sb_{3.6}As_{9.4}S_{22}$ to $Tl_5Sb_{5.3}As_{7.7}S_{22}$ at 250°C. At compositions exceeding 73 at% As, end-member rebulite appears in equilibrium with the phase close in composition to that of imhofite. At compositions below 59 at% As, the As-poorest rebulite coexists with the phase corresponding in composition to a new mineral from Allchar (Boronikhin *et al.*, 1992). Both rebulite and the new mineral have the same stoichiometric $Tl_2S:(As,Sb)_2S_3$ proportion (5:13) and probably are structurally closely related. Our syntheses indicate $Tl_5Sb_{7.5}As_{5.5}S_{22}$ composition for the new mineral in equilibrium with rebulite. The range of synthetic compositions did not allow to investigate the extent of the (probable) As/Sb solid solution of this mineral towards the As-poor end.

Boronikhin V., Cvetković Lj., Krajnović D., Gržetić I. and Pavićević M.(1992): International Symposium on Thallium, Belgrade 1992, 19.

THE DEFORMATIONAL HISTORY OF A QUARTZ-MYLONITE FROM MEDIUM GRADE REBRA SERIES (EAST CARPATHIAN, ROMANIA)

I. Balintoni, G. Bindea (*Inst. of Geology and Geophysics, Bucharest*)

In the East Carpathians, three different medium grade metamorphic sequences are known: Bretila, Negrisoara and Rebra. They were involved into Variscan and Alpine nappes. Rebra series is built up of micaschists paragneisses, amphibolites, marbles and black graphite bearing quartzites. A black quatzite from bucovinian nappe (uppermost basement Alpine nappe) was studied. On the mineralogical grounds, Balintoni, Gheuca (1977) recognised three pre- Alpine metamorphic events within Rebra series rocks: M_1 (St+Dis), M_2 (Cord+And) crystallised statically after forming of a penetrative foliation S_2, that sheared the older minerals, and M_3, retrogressive. The M_1 and M_2 events are pre- Variscan in age. S_2 foliation is the most conspicuous one in all rocks types, and the solely visible in the incompetent rocks. Generally it is parallel to

the lithon limits, but within competent lithons this foliation is plane-axial for a folded recumbent banding. In order to understand how the S_2 foliation has been generated we have chosen a folded quartz-mylonite to investigate it microstructurally. The thin sections were cut normally and parallel to the micro- fold axes (YZ and XZ- planes). No other lineation is visible macroscopically. (1) Mylonite type: it is a Boullier and Bouches (1978) type 4 mylonite, with a very clear differentiation banding, between graphite bearing and graphite lacking bands. The graphite bands have an average width around 500μm (maximum 1 mm) and the other 80μm (maximum 300μm). (2) Graine size and aspect ratio: in the graphite bands, the aspect ratio is generally 3:1; the grain width varies between 15 and 45μm, and the grain length between 45 and 150μm. Within the same band, the grain size is homogeneous. This is a mylonitic size. In the clear bands, aspect ratio decreases from 3:1 to 2:1 or 1.5:1, depending on the band width; the optimum grain size for quartz in these bands appears to be around 220/110μm, when they can grow freely. Variability of aspect ratio and the grain size were conditioned, by graphite screens lying between grains and at the band margins, inhibiting the growth. (3) Folding: after forming, the mylonite was primarly disharmonically folded (clear bands) and after that polyharmonically (clear and graphite bands together). The amplitude of folds is between 10 and 20 cm. Later on the folds were overturned and flattened, their limbs becoming parallel to the limits between lithons. Clear bands belong to class 1C and graphite bands to class 3 of folds (Ramsay, 1967). The width of graphite bands in fold hinges is twice that in limbs. The graphite bands behave much more incompetent than the clear bands. (4) Foliation: is represented by three component parts. First, the limbs of folds, parallel to the limits between lithons. Second, the mylonite banding with aspect of relic compositional foliation, within the lithons. Third, dimensional arrangement of plate quartz grains, parallel to the axial planes of folds. These aspects indicate the mylonite banding transposition. (5) LPO. Quartz c-axes LPO patterns, show maxim around Z axis, with a girdle through Y, and a secondary maximum in Y. The symmetry is like that in Tullis(1977) Fig. 4c, for coaxial plane strain, in combination with axial elongation. (6) Conclusions. The quartz mylonite has formed in transitional 2-3 deformational regime of Hirth and Tullis (1992). The strain can be so factorized : (a) simple shear parallel to layering (mylonitization and differentiation banding); (b) pure shear parallel to banding (the incipient disharmonic and polyharmonnic folding); (c) simple shear parallel to limits between lithons (overturning of the polyharmonic folds); (d) pure shear normal to layering (the flattening of folds and quartz c-axis LPO generated in plane strain regime); (e) static recrystallization without LPO randomising, because of the inhibiting grain growth action of graphite screens. In this way, S_2 foliation has formed during M_2 metamorphics event, at strain rate higher than normally.

A SUB-UNITS-BASED DESCRIPTION OF CANCRINITE-GROUP MINERALS .

Ballirano, P., Maras, A. (*Dept. of Earth Sciences, Univ. of Roma*)
Buseck, P.R. (*Dept. of Geology and Chemistry, Arizona State University*).
Wang, S. (*Arizona Materials Lab.*)

The family of cancrinite-minerals is composed by feldspathoids whose structure can be described in terms of stacking along z of layers built-up by six-membered rings of aluminosilicate tetrahedra. Complex stacking sequence minerals were observed leading to extremely high c parameters. The large number of atoms for unit cell, order-disorder phenomena, simplex substitution and stacking faults precluded the complete structure solution for some of these minerals. A different approach consists in identify sub-units inside the framework in order to understand the relationship existing between the chemical composition and the stacking sequence.

Up to now we have identify 7 different types of sub-units: large channels, cancrinite, sodalite, losod, liottite, 4X and 5X cages.

According to both analytical electron microscopy and IR spectroscopy it is possible to compare these idealized structures and the chemical data for the terms with known stacking sequence.

High resolution electron microscopy (HREM) allows to propose the stacking sequence for sacrofanite as ABCABCABACACABACBACBACABABAC, in accordance with the chemical data.

An unknown phase was also observed, characterized by rhombohedral symmetry and cell parameters a = 12.86 Å, c = 87.31 Å, derived by the stacking of 33 layers. Careful scrutiny of selected area electron diffraction (SAED) patterms outlines the presence of extra spots leading to a doubled c parameter. According to HREM photographs it seems possible to assign these spots to a superstructure. Due to symmetry constraints a rhomboedral stacking sequence must be composed by 3 blocks, each one shifted of 1 period with respect to the previous one: HREM shows the repetiton of 3 blocks of 11 layers leading to a proposed stacking sequence ABCABCABCABBCABCABCABCCABCABCABCA.

The role of sulphate groups is extremely important and its content for unit-cell is possibly the reason for the occurrence of different stacking sequences. SO_4 tends to occupy all the positions available inside the framework, allowing for minor substitutions, possibly according to the scheme proposed by Bonaccorsi *et al.* (1991) for davyne.

REFERENCES.

Bonaccorsi, E., Merlino, S., Pasero, M. (1990) *N. Jb. Miner. Mh.* **H3**, 97-112.

VOLCANIC ROCKS CRYSTALLINITY AND ENERGETIC EVOLUTION OF MAGMATIC SYSTEM OF VOLCANIC CENTRE

Baluev E.Yu. *(Inst. of Volcanic Geology and Geochemistry, Academy of Sciences, Russia)*

Karymsky volcanic centre (KVC) is one of the great ring structures in East Kamchatka. Its size is nearly 80x50 km. During KVC evolution a clear correlation existed between caldera sizes, which were put one into another, volume of pyroclastics related to caldera and degree of its welding. Volcanic effusive rocks from the early stages of KVC evolution are characterized by lower phenocrysts contents ,than those from the later stages.

The most high energetic and mostly depolymerized magmatic liquids were erupted in the initial stage of KVC evolution in the Early Pleistocene. This is confirmed by the presence of shield-like volcanoes, that were formed from aphyric and subaphyric volcanic rocks. The magmatic regime of this type could be rea-lized only in the open system by the fluid flow support. As a result, the relatively homogeneous state of magmatic liquids was well preserved even in the upper parts of magmatic columns at shallow depths. At the next stage, the increase of crystallinity and viscosity of magmatic liquids is observed. This processes is accompanied by the changing of volcanic cone morphology (stratovolcanoes are formed), the crystallization of magmas occurs at deeper levels, and the transition of magmatic system to closed conditions take place because of energy potential decrease. The important consequence of this transition is the formation acid magma chambers in the crust as a result of diffusion-infiltration metasomatism. Especially favorable conditions for this process

arise when upper part of basaltic fluid-conducting magmatic column is situated near the boundary of formation of rocks with different competence. This is supported by that the stage of acid pyroclastic eruptions, during the caldera-forming eruptions, had been preceded by the eruptions of basic lavas with maximum crystallinity. Besides, unlike basalts and basaltic andesites, correlation between structure belonging and quantity of phenocrysts is not characteristic of andesites and dacites. The further regressive development of KVC was caused by energy potential of generation zones of magmatic liquid, but already not only of basic but also of acid composition.

HIGH-POTASSIUM ANDESITES FROM THE FRONTAL PART OF ISLAND ARC AND THE ORIGIN OF CALC-ALKALINE MAGMAS (SW KAMCHATKA)

Baluev E.Yu. *(Inst. of Volcan. Geol. and Geochim., Academy of Science, Russia)*, Perepelov A.B. *(A.P. Vinogradov Inst. of Geochim., Academy of Sciences, Russia)*

The Pleistocene high-potassium andesites and some high-potassium basaltic andesites (HPA) were found on the south side of the Avacha Bay graben (SW Kamchatka), which structurally belongs to the Malko-Petropavlovsk transverse zone, which divides the East and South Kamchatka volcanic belts. HPA cover is not more than 14-15 km^2 in area on the land resulted from fissure eruption (its direction was NW).

HPA contain phenocrysts of plagioclase (34 vol.%), clinopyroxene (4%), orthopyroxene (2%) (frequently in the glomeroporhyric clus-ters), magnetite (1%), with magmatic embay-ment. The same minerals and also pigeonite, alkali feldspar and quartz are found among the microlites in the light brown glass of matrix. In the process of HPA liquid crystallization conform modification of mineral phase composition took place from phenocrysts to microlites. It was determined that HPA phenocrysts were born near the surface. Their further change was due to successive increase of liquid temperature from initial to final stage of crystallization. The reason was the decompression of magmatic liquid and accompanying oxidation of nonoxidation form of gases in the fluid phase.

The comparison of HPA with latites and trachyandesites from the rear zone and the frontal calc-alkaline andesites of the Kuri-le-Kamchatka island arc shows: 1. Plagioclase phenocrysts from HPA are somewhat more K than those from calc-alkaline andesites, however, both andesite types are characterized by the presence of orthopyroxene phenocrysts and pigeonite microlites; 2.Plagioclase phenocrysts from HPA are more Ca than, those from latites; 3.The Cu,Zn,B,Mg,U,Th concentrations in the HPA are higher, than in the above rocks, the Ti,K,Cr,V,Sr,Be concentrations are similar to those in trachyandesites and the Rb,Zr,Nb,Hf, REE concentrations are similar to those in latites; 4.The concentrations of other main and rare (Li,Ba,Ni,Co) elements correspond to the calc-alkaline andesites. Sr^{87}/Sr^{86} ratio in HPA is 0,7033. These peculiarities allow us to assume two alternative hypotheses of HPA origin: 1. The origin and the modification of calc-alkaline melts under the influence of degassing products of mantle substance; 2. HPA were generated at greater depths, than is characteristic of calc-alkalic andesites, by the participation of nonoxidation forms of the volatile mantle fluid components.

APPLICATION OF IR-SPECTROSCOPY FOR THE IDENTIFICATION OF IRRADIATED BERYLS

Banerjee, A. (Inst.f.Geowiss, Mainz University)

The changes of the vibrations of beryls between 4000 cm^{-1} and 3000 cm^{-1} caused by ionizing radiations were studied.

There are two types of water molecules in the channels of beryl: The characteristic absorption bands at 3590 cm^{-1} and 3655 cm^{-1} are due to water of Type-II and that at 3694 cm^{-1} is due to water of Type-I (WOOD & NASSAU, 1967) Moreover, another absorption band due to the fundamental vibration of water was also found,(WICKERSHEIM & ROBERT, 1959).

Several thin (0.3 to 0.5 mm) crystal plates of pale beryls without any inclusions were irradiated with X-ray (100 KV and 25 Amp). The ir-transmission spectra of the samples before and after the irradiation were obtained by an FTIR-spectrophotometer. The results were as follows:

The intensity of all of the absorption bands between 4000 cm^{-1} and 3000 cm^{-1} increased due to irradiation of the samples. However, the most significant increment of intensity was noted for the absorption band at 3663 cm^{-1}. This phenomenon might be used as a criterion for beryls irradiated with intense X-rays. Results of irradiation of beryls with other ionizing radiations will be published in due course.

References :
WOOD, D.L. & NASSAU, K.(1967). J.Chem.Phys.,47, 2220-2228.
WICKERSHEIM, K.A. & BUCHANAN, R.A.(1959). Amer.Min.,44, 440-445.

• ON THE COLOUR OF TOURMALINES FROM MOZAMBIQUE - THEIR CAUSES AND ALTERATIONS

Bank F.H., Bank H. and Henn U.(*Germ. Fund. for Gemstone Research, D-55743 Idar-Oberstein, Germany*)

Tourmalines from the famous pegmatite regions of the East-African state Mozambique possess a wide range of colours, including green-blue, green, olive-green, pink, red and brown. Multicoloured specimens like bicolour green/colourless or green/pink are also present as well as watermelons with a red core and a green border. A remarkable type of tourmaline crystals from Mozambique is partly corroded with the effect of detaching cores. Viewed in the direction of the c-axis the crystals look like a "bullock's-eye".

The tourmaline occurrences are located in the Alto Ligonha pegmatite fields (Muriane-Mine) which are mined since more than 40 years. The granitic pegmatites are distinctly zoned contain beryl of various colours, feldspar, quartz and mica (muscovite).

Chemical analyses of the tourmalines characterize a typical elbaite composition with varying contents of iron and/or manganese. These transition elements are responsible for the colour. The green tourmalines are coloured by iron and the red ones by manganese. The combination of both colouring elements causes certain mixed colours. The watermelon tourmalines show a distinct zoning of the iron/manganese ratio with higher manganese portions within the red core and higher iron contents at the border.

Some tourmalines from Mozambique show a remarkable alteration of colour effected by heat-treatment. Dark green stones turn into lighter green by using temperatures of about 600°C. Brown tourmalines have been found to get yellow at temperatures of 400°C and then pink at 550°C. At 600°C and higher temperatures the stones loose their colour. Over 750°C they start to get opaque and at 900°C they are totally opaque.

THE CHEMISTRY OF RUSSIAN TUNGSTATES

Barabanov V.F.(Dept.of Geochemistry,Univ.of St.Petersburg)

In the couse of many years studying wolframite deposits in the USSR (Barabanov,1961, 1975), the author collected experimental data on chemical compositions of wolframites from 27 deposits (162 chemical analyses) and scheelites (Barabanov,1980) from 27 deposits (60 chemical analyses).

From mineralogical, geochemical (Barabanov, 1971) and genetic investigations of these deposits, the author concludes that the composition of wolframites is largely determined by the composition of the rocks in which these wolframites are formed or which veins and ore bodies containing wolframites occur (Barabanov,1966). All other parameters (t,P,pH, Eh, etc.) are of minor importance for the mineralogenetic processes concerned (Barabanov, 1986).

References:
Barabanov,V.F.(1961).The mineralogy of wolframite deposits of East Transbaikalia,360 p.
Barabanov,V.F.(1966).Int.Geol.Rev.,8,770-782
Barabanov,V.F.(1971).Int.Geol.Rev.,13,332-334
Barabanov,V.F.(1975).The mineralogy of the wolframite deposits of Transbaikalia,v.2, 360 p.
Barabanov,V.F.(1980).Zapiski VMO,1-9,577-583
Barabanov,V.F.(1986).Abstracts of Eur.Meeting "Tungsten Deposits. Metallogeny,Exploration, Mineral processing,Mining", France,26-27

MODEL OF EVOLUTION OF GROWTH CONDITIONS OF NATURAL DIAMOND

Barashkov Yu.P. *(Lab. of Diamond Crystallogr. and Mineral., Yakut.Inst.Geol.Scienes)*, Beskrovanov V.V.

In natural flat-faceted octahedra, three volumetric, quasi-uniform areas (central, intermediate, peripheral) have been established that differ in morphological and physical characteristics and are continuous in time (Beskrovanov, 1992). All morphological varieties of natural diamonds can be explained as diffirent combinations of these three areas. The cental area shows seven species of diamond that have several features in common.The intermediate area is composed of two species characterized by alternation of zonally birefringent zones. The peripheral area is represented by a single species with the most perfect crystal structure.

Consider growth conditions of these quasi-uniform areas from the viewpoint of modern crystallography (Modern crystallography, 1980). Diamond species of the central area crystallized at high rate, under conditions of supersaturation and diffusion by a normal mechanism of growth. This is evidenced by structural imperfection, high density of dislocations, fibrous structure, primarily cubic shape and disposition at the genetic center of a crystal. In most cases, the size of central area is comparable to or somewhat larger than the critical size of a seed.

Zoning of the intermediate area is indicative of a layer-by-layer growth under diffusion-independent kinetic crystallization regime. Its crystallization conditions were characterized by some decreas in supersaturation and growth rate and periodical entrapment of impurities due to growth rate fluctuations. Because octahedral layers developed from the center of a face, im-purities accumulated between adjacent octahedral growth pyramids causing sectorial structure of a crystal. That supersaturation was high enough is indicated by a rtilinear-stepwise nature of zoning, i.e. an overlying layer started to grow before the previons layer covered the face completely.

The most perfect in structure peripheral area crystallized with a further decrease in supersaturation degree, growth rate and impurities content under kinetic regime, i.e. growth of a crystal was determined by kinetic of surficial processes rather than by volume diffusion, and supersaturation was uniform both near the crystal surface and infinitely far away from it.

Thus, changes in morphology and properties of the quasiuniform areas reflect evolution of growth conditions of natural diamond and evidence that a decrease of supersaturation and growth rate occurred during crystallization.

References:
Beskrovanov, V.V. (1992). Ontogenesis of diamond ,166, (in Russian).
Modern crystallography (1980), 3, 408 (in Russian).

CRYSTAL-CHEMICAL MODELS OF METAL ION CHEMISORPTION AT OXIDE-WATER INTERFACES

Bargar, J.R., Towle, S.N., Brown, G.E., Jr., and Parks, G.A. (Dept. of Geological & Environmental Sciences, Stanford University)

Adsorption reactions for aqueous metal ions onto (hydr)oxide mineral surfaces play a significant role in controlling their transport and dispersal in natural aqueous environments. Quantitative definition of the stoichiometry and structure of metal ion surface complexes is difficult but critically important for constructing accurate equilibrium models of metal ion transport in soils and groundwater aquifers. In principle, the adsorption behavior of metal ions at mineral-water interfaces should be governed by the same chemical factors that determine atomic arrangements in the bulk mineral: metal-ion charge, radius, coordination number, covalency, etc. Such factors are well described by existing crystal chemical principles, including Pauling's Rules (Pauling, 1929) and bond-valence-bond-length relationships (Brown and Altermatt, 1985). We hypothesize that these principles can be used to predict binding sites and constrain the coordination chemistry of metal-ion chemisorption at (hydr)oxide-water interfaces.

We demonstrate the relevance of these crystal-chemical principles to metal ion adsorption on mineral surfaces by comparing our predictions with two data sets: the local structure, composition, and mode of attachment of Pb(II) and Co(II) chemisorbed onto α-Al_2O_3 (sapphire) as determined using XAFS spectroscopy; and published pKa's for (hydr)oxide minerals. XAFS spectra from the system Pb(II)/α-Al_2O_3 indicate that chemisorbed Pb(II) is coordinated by four oxygen nearest-neighbors (three at 2.29Å, one at 2.53Å), with 0.5 Al second-neighbors at 3.79Å. In contrast, chemisorbed Co(II) is coordinated by six oxygen nearest-neighbors (at 2.08Å) with Co and Al present in the second shell, indicating that sorbed Co(II) occurs as inner-sphere, polymerized hydroxo- or oxo-bridged complexes. Application of Pauling's bond valence principle to these systems suggests that the most stable surface binding configuration for Pb(II) is one of two configurations: a monodentate (atop) geometry in which Pb is chemisorbed to surface oxygens that are *triply* coordinated by underlying Al to form [Al_3≡O—Pb] complexes, or a monodentate geometry in which Pb is bonded to a surface hydroxyl which is coordinated by *two* underlying Al atoms to form [Al_2=O H — Pb]. Both complexes are consistent with the experimentally-determined Pb-O and Pb-Al distances. The surface complex [Al-O—Pb] which has been used by several authors to model Pb uptake by α-Al_2O_3 is predicted to be *un*stable using the bond- valence-bond-length approach and is not consistent with our XAFS data. Additionally it should be noted that this simple theory requires a proton to be present in the [Al_2=OH—Pb] complex. The same principles will be applied to the system Co(II)/α-Al_2O_3 to constrain possible adsorption sites and stoichiometries.

As an additional test of the validity of the application of bond-valence-bond-length principles to surface modeling, we have used these principles to modify the MUSIC model (Hiemstra *et al.*, 1989a,b), *JCIS* **133**, 91, 105) of proton adsorption to (hydr)oxide surfaces in aqueous solution. We show that this approach accurately predicts surface acidity constants and therefore the charging behavior of (hydr)oxide surfaces.

References
Brown, I.D. and Altermatt, D. (1985), *Acta Cryst.*, **B41**, 244-247.
Hiemstra, T., van Riemsdijk, W.H., and Bolt, G.H. (1989a). *J. Colloid Interface Sci.*, **133**, 91-104.
Hiemstra, T., De Wit, J.C.M., and van Riemsdijk, W.H. (1989b). *J. Colloid Interface Sci.*, **133**, 105-117.
Pauling, L. (1929), *J. Amer. Chem. Soc.*, **51**, 1010-1026.

• IMPEDANCE SPECTROSCOPY OF FAYALITE UNDER DEFINED THERMODYNAMIC CONDITIONS

Barkmann Th. and Cemič L. (*Mineralogisch-Petrographisches Institut der Universität Kiel, Germany*)

Electrical conductivity of silicates is determined by the number of charge carriers, n_i, their effective charge, q_i and their mobility, μ_i;, so that, referring to all kinds of charge carriers

$$\sigma_{el} = \sum_i n_i \cdot q_i \cdot \mu_i$$

According to Nakamura & Schmalzried (1983) majority defects in fayalite are $Fe^{\cdot}_{Fe}$ and V''_{Fe}, which are described as the main charge carriers in fayalite (Sockel, 1973). At constant temperature and fixed a_{SiO2} the majority defect concentration and electrical conductivity should vary with the 6th root of oxygen fugacity, i.e.:

$$\sigma_{el} \sim fO_2^{1/6} \text{ (T=const., } a_{SiO2} = 1)$$

Impedance spectroscopy, in the frequency range 20Hz-1MHz, has been used to study the electrical conductivity of fayalite under variable oxygen fugacities and fixed a_{SiO2} at 1-atm pressure.

Impedance-fO_2-paths were found to be reversible using AgPd-electrodes. Therefore, Fe-loss to the electrodes is assumed to be negliglible and equilibria-conditions were established. The expected variation of electrical conductivity with fO_2 was confirmed at oxygen fugacities corresponding to the magnetite stability field.

Arrhenius plots of temperature dependent data lead to activation energies of 0.99 eV for the conduction process.

Barkmann, Th. & Cemič, L. (1993): Beih. z. Eur. J. Min., **5**,156.

Nakamura, A. & Schmalzried, H. (1983): Phys. Chem. Min., **10**, 27-45.

Sockel, H. G. (1973) in: Defects and Transport in Oxides, Seltzer, M.S. & Jaffe, R.J. (eds.), Plenum Press, 341-355.

RECENT ADVANCES IN THE STUDY OF THE PLATINUM-GROUP MINERALOGY OF THE LAYERED INTRUSIONS FROM KARELIA AND KOLA PENINSULA, RUSSIA

Barkov A.Yu., Pakhomovskii Ya.A. and Bakushkin Ye.M.
(*Geological Inst., Kola Sci. Centre of the Russian Acad. of Sci.*)

Early Proterozoic (2.4 Ga) mafic-ultramafic layered intrusions, widespread in the Karelia-Kola region, Russia, host various platinum-group element (PGE) deposits. The most diverse assemblages of platinum-group minerals (PGM), including more than 20 different PGM, were identified in the Lukkulaisvaara layered intrusion, Oulanka complex, Karelia (e.g. Barkov & Lednev, 1993; Barkov et al., 1993). Three new palladium minerals were found in Lukkulaisvaara (Barkov et al., in prep.).

Kivakka layered intrusion also forms part of the Oulanka complex. The PGM-bearing horizon is composed of olivine gabbronorite and gabbronorite and located at the border between two units, which comprise plagioclase-bearing pyroxenite and gabbronorite, respectively. PGM and rare electrum are closely associated with disseminated base-metal sulfides (BMS) (pyrrhotite, chalcopyrite and pentlandite). Merenskyite and moncheite are two principal PGM in the horizon, whereas both kotulskite and sperrylite are rare minerals (Barkov et al., in prep.). A continious range of composition for the merenskyite-moncheite solid solution was observed. The presence of intermediate phases of the merenskyite-moncheite series and kotulskite has been recorded in the Kovdozersky layered complex, Karelia (Barkov et al., unpubl. data). This is a first reported occurrence of PGM in this complex.

Previously, members of the merenskyite-moncheite series had been reported from the marginal part of the Burakovsky intrusion, Karelia (Trofimov et al., 1990), that is the largest layered intrusion known in Russia, as well as in Fennoscandia. Other PGM found there are Bi-rich kotulskite, sobolevskite, froodite and sopcheite. In addition, members of the laurite-erlichmanite series were reported from a chromitite horizon of the Burakovsky intrusion (Barkov et al., 1991).

A second occurrence of PGM associated with chromitite and scattered BMS was identified in the Imandrovsky layered complex, Kola Peninsula (Barkov et al., 1993). PGM are present as minute grains within hydrosilicates and at chromite-silicate grain boundaries. An amount of PGM inclusions in chromite is usually low (not more than 10-15 % total PGM). Only laurite-erlichmanite and very rare isoferroplatinum enclosed in chromites can be considered to represent a primary high-temperature association, while interstitial to chromite Pt- and Rh-based PGM (sperrylite, Rh-S-rich sperrylite, platarsite, Ir-free malanite (?), cooperite and hollingworthite) are late precipitated phases.

Mt.Generalskaya (Luostari) layered intrusion, Kola Peninsula, hosts a variety of PGM and rare tellurides (Barkov et al., in prep.). The most widespread PGM are members of the merenskyite-melonite solid-solution series and sperrylite. Kotulskite, Sb-rich kotulskite (up to 9.9 wt.% Sb), michenerite, hollingworthite, Ir-rich hollingworthite (19.1 wt.% Ir) are among the less abundant PGM. Telluropalladinite is very rare. These PGM were found accompanied by cobaltite-gersdorffite, hessite, altaite, Se-rich (10.5 wt.% Se) galena, tetradymite, rucklidgeite and argentopentlandite. A comparative study indicates that merenskyite-melonite series members located within altered silicates and quartz tend to be more Bi-rich and generally have lower Ni contents than those enclosed within BMS.

Fluid phase is thought to have played an important role in the formation of the investigated PGE deposits (e.g. Barkov & Lednev, 1993; Barkov et al., 1993).

References:

Barkov, A.Yu., Lednev, A.I.(1993). Eur. J. Mineral., **5**, 1227-1233

Barkov, A.Yu., Savchenko, E.E., Zhangurov, A.A. (1993). Mineral. Petrol. (in press).

Barkov, A.Yu., Lednev, A.I., Trofimov, N.N., Lavrov, M.M. (1991). Dokl. Acad. Nauk, **319**, 962-965 (in Russian).

Trofimov, N.N., Barkov, A.Yu., Lednev, A.I., Lavrov, M.M., Ganin, V.A. (1990). Dokl. Acad. Nauk, **315**, 703-706 (in Russian).

HRTEM STUDY OF CARLOSTURANITE: NEW POLYSOMES AND MICROSTRUCTURAL RELATIONSHIPS WITH ASSOCIATED PHASES

Baronnet A.[1], Belluso E.[2] and Ferraris G.[2]
[1]*C.R.M.C.*[2] , *Marseille* - [2]*Dip. Sci. Mineral. Petrol., Univ. Torino*

The inophite polysomatic series S_nX has been introduced by Mellini et al. (1985) in connection with the characterization of the serpentine-like mineral carlosturanite (S_5X) which widely occurs in serpentinites of western Alps. The building modules of the series are two (100) slices with compositions $X = Mg_6Si_2O_3(OH)_{14}\cdot H_2O$ and $S = Mg_3Si_2O_5(OH)_4$; for $n\rightarrow\infty$ serpentine composition is obtained. The cell parameters *b* (9.4 Å) and *c* (7.3 Å) are the same of lizardite; the value of *a* is $[(n+2)/2]\cdot 5.24$ Å for *n* even (lattice *P*) and $(n+2)\cdot 5.24$ Å for *n* odd (lattice *C*).

The examination by high resolution transmission microscopy (HRTEM) of several samples of carlosturanite from different localities of western Alps (Belluso & Ferraris, 1991) provided some new data.

Besides the three polysomes S_4X, S_6X and S_7X already reported by Mellini *et al.* (1985), the following new members have been found as chain-width defects in a matrix of carlosturanite (in parentheses the values of *a* in Å): SX (16.0), S_3X (28.8), S_8X (26.5), S_9X (57.4), $S_{13}X$ (80.0), $S_{14}X$ (42.0), $S_{15}X$ (91.6), $S_{17}X$ (101.1), $S_{20}X$ (58.0), $S_{22}X$ (65.0) and $S_{23}X$ (129.4). The most frequent polysomes are S_6X and S_7X, i.e. the members closer to carlosturanite composition in the direction of decreasing hydration. The member $S_\infty X$ (serpentine) is also well represented. It occurs under different morphologies ranging from lizardite to parachrysotile, through various kind of ondulation which could include antigorite as well. These phases and polysomes are in paragenesis with carlosturanite.

Two further generations of fibrous serpentine occur. One is represented by pre-carlosturanite chrysotile and is observed as rare relic within large single fibres of carlosturanite. No reactions between these two phases are evident. Instead, the abundant and mainly polygonal serpentine is clearly a later phase which derives from carlosturanite through solid state reactions. These reactions clearly begin at the (treble) joins between fibres of carlosturanite and proceede up to consumption of the original phase. Octahedral cations other than Mg (Ti, Mn, Fe) which occur in carlosturanite are no longer present in later phases.

All fibrous phases have in common the fibre directions and phenomena of epitaxy and/or topotaxy are clearly observed. In

particular, often the serpentine layers connect coherently different fibres.

Spatial relationships show that most fibres of carlosturanite nucleated independently; in some cases, however, nearly iso-oriented fibres originated *via* stepped {001} cleavage.

References:
Belluso, E. and Ferraris, G. (1991). *Eur. J. Mineral.*, **3**, 559-566.
Mellini, M., Ferraris, G. and Compagnoni, R. (1985). *Am. Mineral.*, **70**, 773-781.

MICROSTRUCTURES OF CHRYSOTILE AND POLYGONAL SERPENTINE FROM HRTEM AND SIMULATION DATA.

Baronnet A. and Devouard B. (*CRMC²-CNRS, Marseilles, France*)

Various serpentinite specimens from the Italian Alps have been carefully investigated by means of high resolution transmission electron microscopy (HRTEM) imaging and electron diffraction.

Normal chrysotile (x parallel to the tube axis) dominates as mostly spiral rolls in loose textures and as cylindrical rolls in compact textures. However, "theta" fibers appear also as elliptical rolls reinforced by lizardite bands stacked on the less curved parts of the inner tube wall. These bands are interpreted as overgrown material during and/or after the serpentine deformation. In compact chrysotile forming either colloidal 2-D crystals or glasses, the "theta" fibers typically locate where elastic stresses are at a maximum.

After the pioneering optical diffraction work on cylindrical lattice models by Whittaker (1953), the first experimental TEM evidence of fivefold symmetry in chrysotile (Devouard & Baronnet, Apr.1993) has been also confirmed from geometrical considerations made on curved lattices (Cressey & Whittaker, Dec.1993). We have performed a comprehensive set of 2-D Fourier transforms of cylindrical lattice models. Outer and inner tube diameters, the number of "curved" unit cells along the perimeter of each layer, and the radial stacking order/disorder were varied to cover most situations. It is shown that fivefold symmetry is ubiquitous and that fully ordered, semi-random and fully random radial stackings may be readily distinguished from the circumferential sharpness or diffuseness of 02*l*, 04*l* and 06*l* diffraction "wings".

Polygonal serpentines (PS), in the form of 15- and 30-sectored (rarely 29-sectored) cylindrical or spiral fibers are always found as veins or pockets in any chrysotile asbestos examined so far. PS's do not mix intimately in close- packed chrysotile but do so in entangled chrysotile material. For yet unknown reasons, carlosturanite evolves mainly as 15-PS (Baronnet *et al.*, 1994) whereas fibrous diopside produces almost exclusively 30-PS (Belluso *et al.*, 1993) in our samples. Successive sectors are linked in continuity by curved serpentine layers which maintain essentially the same radius of curvature along the sector boundary. In axial electron diffraction patterns of single fibers, this is marked by linear streaks connecting equivalent 00*l* reflections of successive sectors and such feature produces a typical "polygonization" of 0 2k l diffraction wings. The detailed analysis of the reciprocal and direct unit cells of successive lizardite-like sectors of PS's supports the martensite-like transformation (homogeneous shear) suffered by the layer stacking of one sector when going to the next one. This is consistent with the inferences of a recent dislocation model (Baronnet *et al.*, in press). Experimental axial EDP's of a number of single polygonal fibers and fast Fourier transform processing of their 2-D lattice simulations match correctly up to high spatial frequencies. Semi-random , one-layer and two-layer polytypes were included in the simulations. N-layered regular polytypes may be readily identified from the 10*N equispaced spots lying along the 020 diffraction ring.

Keeping fixed the radius of curvature of serpentine layers along sector boundaries has some bearing on the morphological classification of polygonal serpentine among serpentine varieties. While sectors may be compared to lizardite domains, intersectorial material may not be assimilated to narrow bands of chrysotile. Consequently, a circonferential description of PS as a polysomatic alternation of lizardite and chrysotile would not be correct. This intersectorial material differs from normal chrysotile which may or may not be present around the central hollow core.

References :
Baronnet, A., Belluso, E., Ferraris, G. (1994). *IMA 94 Abstr.*, this issue.
Baronnet, A., Mellini, M., Devouard, B. (1994). *Phys. Chem. Min.*, in press.
Belluso, E., Baronnet, A., Ferraris, G. (1993). *Plinius*, **10**, 44.
Cressey, B.A. & Whittaker, E.J.W. (1993). *Mineral. Mag.*, **57**, 729-732.
Devouard, B. & Baronnet, A. (1993). *Terra Abstr. Suppl. n° 1 to Terra Nova*, **5**, 351.
Whittaker, E.J.W. (1953). *Acta Crystallogr.*, **6**, 747-748.

LASER-HEATING IN A DIAMOND ANVIL CELL, RAPID COLLECTION OF DIFFRACTION DATA

Bassett, W.A. (*Geological Sciences, Cornell University, USA*)
Brister, K. (*CHESS, Cornell University, USA*)

A white x-ray beam from a synchrotron radiation source is directed through a portion of a sample under pressure in a diamond anvil cell. X-rays scattered in a fixed direction are collected by an intrinsic germanium detector and their energies analyzed. IR radiation from a CO_2 laser is focused onto the same portion of sample to heat it to temperatures of several thousand K. A PIN diode monitors the intensity of incandescent light from the hot sample so that diffraction patterns produced at different temperatures can be directed to up to 64 separate bins. Incandescent light analyzed by a grating spectrometer produces spectra that can be fit to greybody curves to determine temperatures. The diffraction patterns can then be displayed as a function of temperature. Preliminary experiments on KCl and $FeTiO_3$ show the disappearance of peaks due to melting and the shift of peaks due to heating.

VANADOMALAYAITE, $CaVOSiO_4$: A FURTHER NEW MINERAL FROM THE MANGANIFEROUS ORES OF EASTERN LIGURIA, ITALY

Basso R., Lucchetti G., Zefiro L. (*Dip. di Scienze della Terra, Univ. di Genova*) and Palenzona A. (*Ist. di Chimica Fisica, Univ. di Genova*)

Several studies of the manganiferous mineralizations in ophiolitic sequences of Eastern Liguria (Italy), carried out by different authors during the last fifteen years, have led to identify a significant number of uncommon minerals, included the new species: tiragalloite, saneroite, medaite, palenzonaite, strontiopiemontite, gravegliaite, reppiaite, mozartite and the present vanadomalayaite.

Vanadomalayaite, with ideal composition $CaVOSiO_4$, represents the vanadium analog of malayaite, $CaSnOSiO_4$, and titanite, $CaTiOSiO_4$. Vanadomalayaite fills with calcite, quartz and haradaite a small vein cutting metacherts at the Gambatesa mine, near the village of Reppia, Eastern Liguria. It has been found as very rare, subhedral, prismatic, isolated deep red crystals, with good {110} cleavage, not exceeding 0.4 mm in size. No twinning was observed. The mean chemical composition from microprobe analyses gives the empirical formula $Ca_{1.00}(V_{0.71}Ti_{0.26}Fe_{0.01}Al_{0.01})OSi_{1.01}O_4$, based on five oxygen atoms.

Single-crystal X-ray analysis ascertained the isotypy with malayaite and *A2/a* titanite. The crystal structure has been refined to $R = 0.026$ in the standard space group *C2/c*, confirmed by a long-exposure single-crystal rotation photograph, with $a = 6.526$, $b = 8.691$, $c = 7.032$ Å, $\beta = 113.88°$ and $Z = 4$.

The valency state of the vanadium, populating the octahedral site, is virtually 4+ in agreement with the mean bond distance and the formula neutrality. Both structural and chemical analyses suggest that the coupled substitution of primary importance in natural titanites $R^{3+} + OH^-$ for $R^{4+} + O^{2-}$, where *R* indicates cations in octahedral coordination, may be disregarded in vanadomalayaite.

Concerning vanadomalayaite, malayaite and the titanites submitted to structure refinement, the most relevant chemical variations are confined to the cations occupying the octahedral site. The radius of these cations strongly affects octahedron and cell sizes. On the basis

of the available data, the mean ionic radius of the cations in octahedral coordination is about linearly related to the mean octahedral bond length that in turn shows a nearly linear correlation with the cube root of the cell volume.

MECHANISMS OF FRAMEWORK CHANGE IN ZEOLITES

W. H. Baur (Inst. Kristallographie, Universität Frankfurt)

The tetrahedral frameworks of zeolites can adapt to physical (temperature and/or pressure) and chemical (sorption and/or cation exchange) influences by changing in various ways: the geometry of the angles T-O-T or O-T-O and the distances T-O can adjust, and in addition phase transformations, occasionally accompanied by changes in symmetry, can occur. It is surprising how flexibly the frameworks of the aluminosilicates (in the case of zeolites) and of other microporous compounds (such as the aluminophosphates) do respond to changing conditions. On the other hand, despite many adjustments in their detailed geometry some of the frameworks remain stable und even preserve approximately their overall dimensions.

The following instances are of particular interest because they illustrate the principles involved:

1. Microporous frameworks formed by TO_4 coordination tetrahedra are systems composed of rigid parts, the tetrahedra, and of bridging oxygen atoms serving as flexible hinges between the tetrahedra. Some of the most open tetrahedral frameworks display a pronounced resistance to collapse, even when undergoing radical changes in the chemistry of their embedded guests (ions or molecules). A study of empirically observed angular distortions in zeolite A (LTA) and a computer simulation show that this property is due to a self-regulating mechanism which allows changes in the dimensions of the framework only within limits set by chemically possible values of the T-O-T angles of the joint bridging oxygen atoms and which depends solely on the topological, symmetrical and geometrical properties of the three-dimensional nets underlying the frameworks. In **collapsible frameworks the hinges corotate and compression or tension at all hinges is exerted simultaneously in the same sense. In noncollapsible frameworks the hinges antirotate, and compression at one hinge necessitates tension at another hinge and vice versa** (Baur, 1992).
2. In-situ X-ray powder diffraction experiments show that zeolite NH_4 -rho exists in two forms when heated in vacuum. The **high temperature form has at 573 K a volume smaller by 6.7% than the low temperature form** at 295 K. At higher temperatures the framework contracts because the NH_4 -groups which at lower temperatures are located within the single eight rings of TO_4 tetrahedra and block their collapse assume at higher temperatures new positions located in the larger pores of the framework. The transformation between the two forms is reversible and is of the reconstructive type as far as the hydrogen bonds from the ammonium groups to the framework are concerned (Bieniok & Baur, 1992). An analogous behaviour is being displayed by Sr-rho. The framework of zeolite rho is collaspible in the sense discussed above.
3. Cation exchange of NH_4 for Na in natrolite, $Na_2Al_2Si_3O_{10}.2H_2O$, yields an anhydrous ammonium natrolite, $(NH_4)_2Al_2Si_3O_{10}$. The symmetry is reduced from space group Fdd2 in Na-natrolite to space group $P112_1$ in NH_4-natrolite. The volume of the unit cell of NH_4-natrolite is reduced compared with the original Na-natrolite by more than 4 %. The ammonium groups in the NH_4 -form occupy similar positions to the H_2O molecules in Na-natrolite. The Si-O and Al-O distances within the framework are strongly influenced by the hydrogen bonds from the NH_4 -groups. Hydrogen bonded oxygen atoms have, on average, larger T-O distances (0.01 Å) and smaller T-O-T angles (6.8°) than non-hydrogen bonded oxygen atoms of the framework. The effect of the hydrogen bonds on the T-O bond lengths is stronger than the influence exerted by changes in the T-O-T angles. This is the **first instance in which changes in the geometry of the framework of an aluminosilicate can be attributed solely to hydrogen bonding** effects. The contraction of the framework due to the exchange of NH_4 for Na is caused by tilting and twisting of the chains within themselves and not by a rotation of the chains as a whole around the hinges between the fibers (Stuckenschmidt et al., 1992). Similar observations apply to oxonium natrolite (Stuckenschmidt et al., in preparation). The NAT framework of natrolite is also collapsible.

References:
Baur, W. H. (1992). J. Sol. State Chem. **97**, 243-247.
Bieniok, A., Baur, W. H. (1992). Acta Crystallogr. B**49**, 817-822.
Stuckenschmidt, E., Kassner, D., Joswig, W., Baur, W. H. (1992). Eur. J. Mineral. **4**, 1229-1240.

MINERALOGY AND FABRICS OF MAFITES IN METABASITIC ROCKS OF THE SAXONIAN GRANULITE COMPLEX

Bautsch H.-J. (*Mus. Natur. Hist., Humboldt-Univ. Berlin*)
and Thieke H. U. (*Count. Off. of Geosc. Brandenburg*)

Within the matrix of felsic granulites of the inner part of the Saxonian Granulite Complex are local some larger boudin like bodies (up to 80 x 80 x 30 m) of metabasitic rocks. They have a characteristic foliation with different intensities constantly parallel one to another and to the felsic granulites.

The types of metabasitic rocks are: 1. pyroxenites (with 67 (42-90)% Px, 17 (0-45)% Gr, 3(0-25)% Ol, 6 (2-17)% Am); 2. pyroxene-granulites (with 40 (30-60)% Px, 14 (0-30)% Gr, 6 (0-18)% Am, 28 (12-49)% Pl); 3. serpentinites (with 55 (30-70)% Spt (Chrysotile), 21 (10-35)% Px, 8 (3-20)% Gr (symplectitic)).

In pyroxenites the proportion of ortho- to clinopyroxene is at 2 : 1. The composition of orthopyroxenes varies between enstatite (5% Fs) and hypersthene (43% Fs) with a preponderance of bronzite (16-22% Fs). The composition of clinopyroxenes varies between diopside (preponderant), augitic diopside and omphacite. The garnets has compositions near Alm_{44} $Pyr_{34}Gros_{20}$.

In pyroxene-granulites the proportion of ortho- to clinopyroxene is at 1 : 3. The compositions of clinopyroxenes varies in a broad range between diopside, diopsidic augite and omphacitic diopside corresponding with a variation of the orthopyroxenes (between 0-37% Fs). The garnets have average compositions near $Alm_{55}Pyr_{17}Gros_{27}$. The An - contents of the plagioclases are between 38-67%.

The fabrics in these metabasitic rocks were studied measuring more than 15.000 optical and morphological elements with the universal stage. In the pyroxenites the orthopyroxenes showes a distinct preferred orientation with a quasi - rhombic symmetry. [001] lies in (a b) with a peripheric maximum in b, while [010] and [100] forms girdles in (a c) vertical to (a b). A less distinct but on principle the same orientation patterns gives the clinopyroxenes in consideration the monoclinic optics. In pyroxene-granulites the clino- and orthopyroxenes gives on principle the same orientation patterns, sometimes distinct sometimes more diffuse.

From these results we conclude: The primary fabrics of the mafites in the pyroxenites and pyroxene-granulites are general homotropic with [001] -pyroxene and [100] -olivine parallel tectonic b and with girdles of the other crystallographic axes in (a c). The lattice orientation mechanism especially of the pyroxenes was a syntectonic recrystallisation with some intragranular rotation. The fabric formation was generated at granulite-facies metamorphism under deep crustal conditions in a triaxial stress field. There is no conformity of the fabric patterns with such of an origin from the upper mantle.

THE RESIDENCE OF RARE-EARTH ELEMENTS WITHIN GRANITE ROCKS. IMPLICATIONS FOR REE-BASED GEOCHEMICAL MODELING

F. Bea (*Dept. Mineralogía y Petrología,Univ. of Granada, Spain*)

The aim of geochemical modeling is to infer the behavior of

major mineral phases (and therefore P, T, Xvolatiles conditions) in a petrogenetic process by comparing actual trace-element distribution patterns to theoretical models, usually calculated from chemical equilibrium-based fractionation equations. Trace elements, to be usable in these equations, must be fractionated by major minerals and obey Raoult's or Henry´s law. In mantle-related igneous systems, REEs fulfill such requirements and are therefore successfully used to model basalt petrogenesis. In crust-related igneous systems, however, the situation is quite different. A systematic study with SEM, electron microprobe, and laser ablation ICP-MS on migmatites and granitoids from all over the world has revealed that most REEs (70-80% in subaluminous granites, 80-90% in peraluminous granites) dwell in accessory minerals, usually as major components. The only major minerals having significant REE contents are amphibole and garnet (HREE), and to a lesser degree (about 10x chondrite) clinopyroxene and feldspars (see Fig. 1). REEs in biotite, muscovite, and cordierite are near or below chondritic levels. The REE-bearing accessory mineral assemblage markedly depends on the rock peraluminosity and, in a lesser degree, on silica content. Strongly peraluminous granites (ASI >= 1.2) have monazite and minor xenotime, the relative importance of this latter increasing in high-silica granites. Meta-aluminous granites (ASI ≈ 1.0) have allanite, sphene, and occasionally REE-carbonates. Primary monazite and allanite may coexist when aluminosity is lower than ASI ≈ 1.1. Perakaline granites are usually very rich in REE-bearing accessories such as bastnaesite, allanite, monazite, xenotime and niobates. Apatite and zircon are ubiquitous in granite rock but their role as reservoirs of REEs is less important than previously thought. Fig. 1 shows LA-ICP-MS chondritic patterns of representative major and accessory minerals of granitoids.

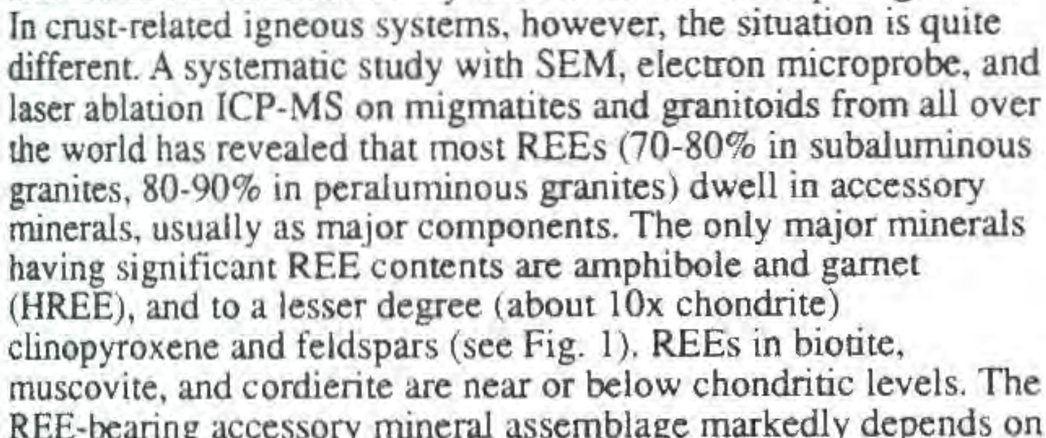

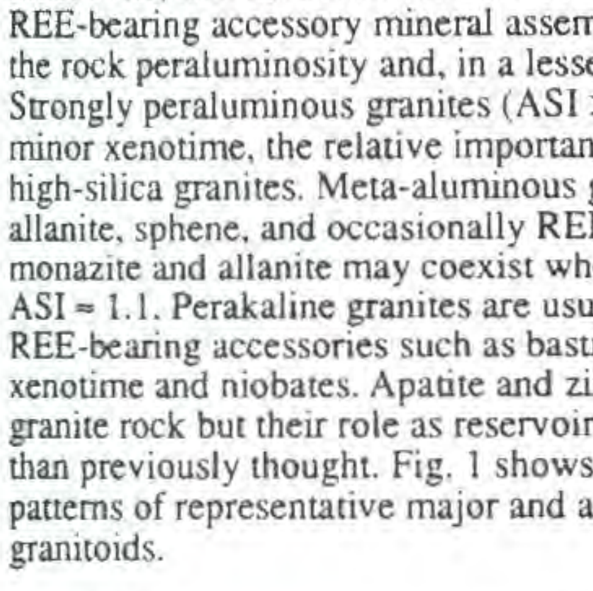

Fig. 1.- Chondrite-normalized patterns of REE in representative minerals of granite rocks. Data obtained by Laser Ablation ICP-MS. Amph, amphibole. Cpx, clinopyroxene. Grt, garnet. Opx, orthopyroxene.Crd, cordierite. Ms, muscovite. Bi, biotite. Pla, plagioclase. K-fsp, K-feldspar. Mo, monazite. All, allanite. Ap, apatite. Xe, xenotime. Sph, sphene. Zr, zircon.

These data mean that geochemical modeling of granite systems based on the REEs can neither be founded on equilibrium-based fractionation equations, nor provide any valuable information about the behavior of major minerals other than feldspars (due to their positive Eu anomaly) or garnet (which dramatically affects the LREE/HREE ratio, although very small amounts of xenotime produce the same effect). However, REE-based modeling is extremely useful to get information on accessory minerals and therefore about the bulk-chemistry of the system.

SILICON SELF-DIFFUSION IN QUARTZ.

F. Béjina and O. Jaoul. *(CNRS, Université Paris-Sud, 91405 Orsay)*

The silicon self-diffusion coefficient has been measured in β-quartz between 1400 and 1600°C, along the c-direction. We obtain :

$$D(\mathrm{cm^2/s}) = 1.5 \times 10^6 \exp(-7.2\mathrm{eV}/kT).$$

where k is the Boltzmann constant, and T is in kelvin.

We used very high-quality synthetic quartz, from SICN company, containing less than 1 ppm impurity and less than 10 ppm OH-related defects. Samples were polished and chemically etched in order to remove the cold worked layer. Then, the specimens were covered by RF sputtering with a 500–800 Å thick layer of 96% isotopically enriched $^{30}SiO_2$. This initially amorphous layer quickly recrystallizes epitaxially into β-quartz with a grain size between 1 and 50 μm, depending on the recrystallization temperature.

Annealings were performed under pressure (20 kbars) in a piston-cylinder apparatus designed to preserve the specimens from fracturing : in this way, the single crystals were maintained in the β-field. However, one series of experiments at 1400 and 1600°C was performed at room pressure without undergoing the phase transitions into cristobalite or tridymite : this probably results from a particular sluggishness of the transformation of high quality quartz in which nucleation seeds are missing.

Annealing durations t were chosen so that $2\sqrt{Dt}$ ranges between 500 and 1500 Å; at 1400°C, t is of the order of a few days, at 1600°C, a few hours. The diffusion profiles, analyzed with a combination of error functions, were measured by the mean of two different methods.

Rutherford Backscattering Spectroscopy (RBS) of 2 MeV α - particles gave a rapid view of the diffusion profiles, and a first rough estimate of D, by the use of the program RUMP (Doolittle, 1985, 1986). The specimens were then analyzed for their ^{30}Si concentration by the resonant nuclear reaction $^{30}Si(p,\gamma)^{31}P$ at 620.4 keV, by depth scanning with steps sometimes as small as 30 Å beneath the surface. Care was taken to have diffused specimens for which the total amount of ^{30}Si initially deposited has remained preserved. The activation energy of 7.2 eV is close to that of ^{30}Si diffusion in amorphous silica, in the temperature range 1110–1410°C (Brebec *et al*, 1980). We propose that diffusion occurs via Frenkel defects (one silicon interstitial associated with one silicon vacancy) involving interstitials moving inside an oxygen cage connecting two Si tetrahedral sites.

References :

Brebec, G., Seguin, R., Sella, C., Bevenot, J., Martin, J.C. (1980). *Acta Met.*, **28**, 327–333.

Doolittle, L.R. (1985). *Nucl. Instrum. Methods*, **B9**, 334–351.

Doolittle, L.R. (1986). *Nucl. Instrum. Methods*, **B15**, 227–231.

• DEVELOPING MINERALOGICAL DATABASE INFORMATION SYSTEM BASED ON THE COLLECTION OF THE FERSMAN MINERALOGICAL MUSEUM, RUSSIAN ACADEMY OF SCIENCE

Belakovskii D., Fiveyskiy D. *(Fersman Mineralogical Museum, RAS, Moscow)*

A project for developing a mineralogical database information system (MDIS) was supported by the Russian Fund of Fundamental Investigations. This MDIS is based on the oldest (since 1716) and largest (about 150,000 specimens) mineralogical collection in the former Soviet Union. The MDIS is designed to be accessible to both museum visitors and scientific community through networks.

According to the logical model of data the MDIS consists of two main parts. The first part includes the data related to mineral species. As a first step, the application for DOS was made (Clipper 5.1 and Microsoft C). It contains the mineral species names (complete up to December 1993) in English and Russian, group names, chemical formulas, crystal systems, references, presence in 4 most important Russian mineralogical museums. Fast context

search can be executed for any combination of data. Users may also:

- edit information in the database;
- input their own information into pre-existing empty fields and include it in the queries;
- work with a data file (*.dbf) in any compatible database system.

Using a special keyboard-screen driver the MDIS allows for on-screen editing by displaying chemical formulas using subscript symbols. This program will be distributed free during the 1994 IMA meeting.

The second part of the MDIS maintains data related to the Museum specimens. The database currently contains about 130,000 entries for the systematic, crystal, locality, gem collections. The data includes mineral names, localities, dates and sources of acquisitions. The processing of this data required compiling special glossaries for names of minerals and localities to allow for the numerous synonyms and different terms applied to identical mineral species or varieties. The conversion of mineral and locality names to approved names and modern geographic terms led to new ideas for organizing the collections and defining priorities for expanding them.

The next closest step for the MDIS is upgrading with synonyms and varieties of minerals, type localities, and new crystal-chemical formulas based on the structural-chemical classification of minerals being developed at the Fersman Museum by Prof. A. Godovikov.

CONTACT DIFFUSION IN PRECAMBRIAN BANDED PYROXENE GRANULITES

Belevtsev R. Ya. (Institute of Geochemistry, Mineralogy and Ore Formation, Kiev, Ukraine)

In Ukrainian shield there are banded pyroxene granulites which are represented contain hypersthene enderbite gneisses with little(1 to 300 cm thickness) agree steep dikes of two-pyroxene mafites and ultramafites. The mafites and ultramafites will come to 10-50 % and 1-5% of granulites correspondingly. The composition of enderbite gneisses correspond to trondhjemites, mafites - olivine tholeites , ultramafites - lherzolites and hypersthenites. The thickness of crystals of orthopyroxene (Opx), Ca-pyroxene (Cpx) and plagioclase (Pl) is 0,3 -0,6 mm in enderbite gneisses and mafites, 0,5-2,0 to 3-5 mm in ultramafites. The condition of two-pyroxene equilibrium had been calculated: T =800-900°C, P=200-500 MPa, P of water and oxigen very low. Hornblende, biotite, orthoclase and garnet are secondary minerals. There are a few generations of dikes. Latest cross dikes of iron mafites have large thickness (1-3 m). There are

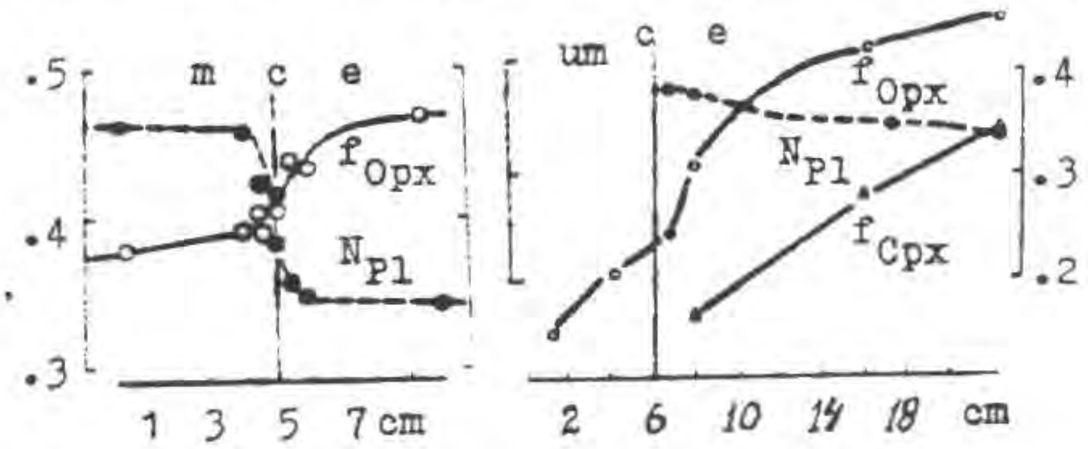

bimetamorphic zoning which has been traced to 1-2 cm and 5-10 cm from contact of mafitic and ultramafitic dikes correspondingly. Throuth these contacts diffusion transfer of components was under influence of gradient of concentration. From enderbite gneisses to mafites and ultramafites SiO2 and Na2O and to enderbite gneisses MgO, FeO, CaO migrated. The composition of pyroxenes and plagioclase normally has been changed in contact zoning (Fig.: m-mafite, umultramafite, e-enderbite gneisse, c-contact, f =Fe/Fe+Mg in pyroxenes, N= Ca/Ca+Na in plagioclase, with RSMA minerals). The change of concentration of component (C) in diffusion zones depend on distance x (cm), time t (c) and diffusion coefficient D (cm2/c): $C(x,t) = \mathrm{erfc}(x/2\sqrt{Dt})$. Hence characteristic Dt can be calculated: 1,5+0,5 cm^2 and 10+5 cm^2 for mafites and ultramafites correspondingly. Probably contact diffusion in granule complex had been realized at T=800-900°C throuth intergranular felsic melt. For dry dacitic melt (lgD=-11) contact zone of mafitic dike should be formed approximately during 5000 y. In contact zone of ultramafitic dike was more diffusion distance and also T 100 -200°C higher than in zone of mafites. Duration of diffusion transfer, that has been calculated by the data interdiffusion in Ca-pyroxene, have more value. The geological-petrological model of these processes is autometamorphism of dike set of mafites and ultramafites (2,9-2,0 GA) in the Early Archean trondhjemites (more 3,2-3,4 GA) of primary continental crust.

SOLID STATE PHASE TRANSFORMATIONS IN ANALCIME GROUP MINERALS IN A WIDE RANGE OF THERMODYNAMIC PARAMETERS.

Belitsky I.A., Fursenko B.A., Goryainov S.V., Bakakin V.V* and Seryotkin Yu.V. (*Inst. of Mineralogy & Petrography, *Inst. of Inorganic Chemistry, Russ.Acad.Sci., Novosibirsk*)

Zeolites and feldspatoids have a large varieties of microporou. frameworks and are very sensitive to the effect of pressure, temperature and changes of extra-framework cations. They are the best models to study the polyhedral tilt transitions in minerals, which were shown to be common in the Earth's crust (Hazen and Finger, 1984). Structural changes in elastic (flexible) and "collapsible"(in terms of Baur *et al.*, 1992) frameworks were studied by us earlier on the fibrous zeolites of the NAT structure type (Kholdeev *et al.*, 1987, Belitsky *et al.*, 1992).

The minerals of the ANA structure type: analcime, wairakite, leucite, pollucite and their cation-exchanged forms were chosen as an example of relatively rigid, "non-collapsible" framework. They were studied *in situ* at temperatures -170 ÷ 1000°C and pressures up to 100 kbar in DAC by X-ray diffractometry, IR and Raman microspectroscopy and thermochemistry (TG, TMA, DSC).

The high-temperature phase transitions with increasing in symmetry (analogous to 620-660°C inversion in leucite) were observed in cation-exchanged W-forms of analcime (cations in water W-positions) at lower temperatures: for example in K-analcime T_{tr} = 500-550°C.

In hydrated natural and cation-exchanged forms with extra-framework cations in S-positions (S-forms): analcime, wairakite, Li-, Ag-analcimes, Na-leucite a dehydration begins at 200-250°C accompanied by anisotropic contraction. At higher temperatures an expansion of dehydrated phases was observed giving rise to more isometric structures. Dehydrated S-forms can be preserved at ambient temperatures for a long time. Partial rehydration was observed when heating these forms in air up to 200-400°C. Structural changes during dehydration are smooth enough and allow the single crystals of dehydrated phases to be preserved and studied by the X-ray single-crystal diffractometry. The detailed results on crystal structures of dehydrated analcime are presented separately (Bakakin *et al*, 1994)

An isochemical phase transition was observed in hydrated wairakite at temperature 145-150°C (before dehydration) accompanied by anomalous changes in heat capacity, expansion, disappearence of polysynthetic twinning and increase in lattice symmetry.

The high pressure behavior of S and W forms of the ANA structure

type is different. A few phase transitions in analcime, wairakite and cation-exchanged analcimes were observed at pressures below 20 kbar accompanied by anomalous changes in Raman frequences and peak splitting in diffractograms reflecting lower symmetry and volume decrease of high-pressure phases.

The hydrated and dehydrated varieties of the same S-forms demonstrate different behavior under high-pressure. A number of phase transitions in dehydrated forms were distinctly seen visually under microscope in DAC. Most of them are reversible, but in wairakite at 3-4 kbar an irreversible phase transition was observed accompanied by drastic changes in optical properties, Raman spectrum and cell parameters. Two reversible transformations were detected in dehydrated analcime at 4 and 12 kbar, one in Ag-analcime at 3-4 kbar. All these high-pressure transitions were reproduced in various pressure-transmitting liquids (water, methanol-ethanol, glycerol). Water molecules did not enter in the ANA-type framework channels under high pressure at room temperature.

Experimental results show the relative rigidity and non-collapsible nature of the ANA-type structures. The observed phase transitions and structural changes are assosiated with relatively small distortions of the framework. At the same time significant changes have place in extra-framework cations and water molecules distribution among the possible S and W positions in the framework cavities.

References

Bakakin V.V., Alekseev V.I., Seryotkin Yu.V., Belitsky I.A., Fursenko B.A. and Balko V.P. (1994) This book, p.

Baur W.H. (1992) J.Solid State Chemistry, 97, 243-247.

Belitsky I.A., Fursenko B.A., Gabuda S.P., Kholdeev O.V., Seryotkin Yu.V. (1992) *Phys.Chem.Minerals*, 18, 497-505.

Hazen R.M. and Finger L.W. (1984) Comparative Crystal Chemistry. Jhon Wiley & Sons, New York, 1984, 231 p.

Kholdeev O.V., Belitsky I.A., Fursenko B.A., and Goryainov S.V. (1987) *Dokl. Akad. Nauk SSSR*, 297, 946-950.

• THERMOCHEMICAL STUDY OF FIBROUS ZEOLITES

Belitsky I.A. (*Inst. of Mineralogy and Petrology, Novosibirsk, Russia*) Kiseleva, I.A., Ogorodova L.P. (*Moscow State University, Moscow, Russia*)

Results of thermochemical studies of whole series of natural fibrous zeolites of three structural types, which have different ways of assembling the chains of alumino-silicate tetrahedra, are presented. We studied zeolites in the group of natrolite, including natrolite, tetranatrolite, mesolite, scolecite, gonnardite as well as thomsonite and edingtonite. All these minerals, apart from tetranatrolite and gonnardite, have overall ordered distribution. Zeolites were investigated by X-ray, chemical analysis, DTA, TG, high temperature heat flux microcalorimetry methods.

Thermochemical investigations included:

1. the measurements of the enthalpies of full dehydration of minerals using the two-step drop calorimetry technique;

2. the determination of the enthalpies of solution of these zeolites at 973K in lead borate solvent and their heat contents by "transposed temperature drop solution calorimetry" method;

3. the calculations of the standard enthalpies of formation of all zeolites studied. The enthalpy of transition of natrolite-tetranatrolite at 298.15K is 180kJ. Our results presented additional thermochemical properties of natrolite, mesolite and scolecite.

PETROGENESIS OF LEUCITE-BEARING NODULES FROM COLLI ALBANI VOLCANO EJECTA, LATIUM, ITALY

Belkin, H.E. (*U.S. Geological Survey*), Cavarretta, G. (*CNR, Univ. of Roma*) and Tecce, F. (*CNR, Univ. of Roma*)

Leucite-bearing nodules, ejected with pyroclastics during the pre- and syncalderic phases of the Tuscolano-Artemisio activity, were derived from the upper margins of the Colli Albani magma chamber. Textures and densities suggest that these nodules represent disaggregated marginal float cumulates or peripheral dikes of float cumulates. Cumulate clinopyroxene nodules with interstitial leucite are uncommon in the studied ejecta localities. Before eruption, the leucite-rich accumulations were affected by the passage of, reaction of, and subsequent precipitation of various phases from convectively percolating volatiles through the permeable crystal mush. This upward streaming of fluids has enriched the nodules in those elements most susceptible to volatile complexing (e.g., Li or Th as compared to Hf or Ta). Furthermore, the LREE enrichment noted in these rocks suggests the involvement of both CO_2 and H_2O as experimental evidence indicates LREE are not easily transported by pure CO_2 fluids.

Chemically and mineralogically these leucite-bearing nodules can be treated as a simple, two-component system: (1) primary magmatic leucite relatively depleted in REE (e.g. Nd = 18 ppm) with no Eu anomaly and (2) clinopyroxene (± mica and garnet) containing various included phases (typically apatite and titanite) that are enriched in REE (e.g. Nd = 118 ppm) with a small negative Eu anomaly. Major element chemistry reflects modal proportions of leucite and clinopyroxene (± mica); K_2O (4.5 to 20 wt.%) and CaO (0.5 to 18 wt.%) vary inversely. P_2O_5, indicative of modal apatite, varies from nil to 2.5 wt.%.

Petrographic, fluid inclusion, and electron microbeam studies document the passage of fluids during various stages of reaction and crystallization. Primary multiphase holocrystalline silicate-melt inclusions, typically in the iron-rich zones of the clinopyroxene, are relicts of a volatile-rich and REE-rich silicate melt infiltrating the leucite crystal mush. Later subcritical to supercritical solute-rich aqueous fluids reacted with and fractured host phases and were trapped as saline inclusions with common daughter crystals. The last major fluid event recorded by inclusions produced secondary two-phase (L+V), aqueous inclusions. These inclusions demonstrate formation at temperatures ranging from 150 to 375 °C, with salinities ranging from 0 to 5 wt.% NaCl equivalent. Evidence for boiling during some stages of their formation suggests that these fluids existed in cooler, shallower portions of the magma-chamber wall environment or were released after eruption during cooling of the pyroclastic deposits.

These leucite-bearing nodules record the complex and diverse environment and processes operating in the magma chamber margins of an alkalic magmatic system. These systems typically fractionate more quickly and, when vented by eruption, empty a greater proportion of their contents than do calc-alkaline systems. Furthermore, the Colli Albani magma chamber is situated in a thick sequence of Mesozoic carbonates linked by aquifers to Apennine sources of phreatic waters. These fluids interacted with the intruded magmas in zones of local contamination and hybridization and were responsible for phreatomagmatic eruptions in the late stages of Colli Albani volcanic activity.

• RARE-METAL APOBASIC METASOMATITES OF KOLA REGION (RUSSIA)

Belolipetsky A.P. and Petrov, S.I. (*Geological Inst. of Kola Science Centre, RAS*)

In the north-eastern part of the Baltic Shield (Kola region) unique geological formations are revealed – rare-metal apobasic metasomatites with anomalously high concentrations of Li (holmquistite), Zr (zircon) Y and REE (rare earth epidote – allanite), Nb (fergusonite) and Th (thorite). The indicated minerals in these metasomatites are rock-forming, their contents may reach 10-15% and more of the total rock volume.

The metasomatites are generated from gabbro-labradorites during metamorphic alteration. They form lense- or vein-shaped bodies commonly associated with fault system. The main rock-forming minerals are plagioclase, epidote, biotite and amphibole. The processes of autometasomatism are responsible for the formation of these rocks. At this stage the rare-metal mineralization in metasomatites is absent. Later processes of alkaline metasomatism and acid leaching result in albitization, silification and rare-metal mineralization. The indicated processes are conditioned by the action of alkaline solutions related to granite intrusions. In this case, the mineral composition is determined by geochemical character of parental granitoids. Being a geochemical barrier, host basites produce a peculiar kind of "traps" to accumulate rare-element minerals.

We distinguish two stages of rare-metal mineral formation. The first stage (Ar_2, 2800-3000 Ma) is connected with granodiorite-leucogranite intrusions and results in the formation of holmquistite metasomatites. They are characterized by high content of rare alkaline elements (Li, Cs). The main ore minerals are holmquistite and Cs-bearing biotite only. The next stage (Pt_1, 1700-2400 Ma) is associated with intrusions of peralkaline granites enriched by Zr, Y, REE, Nb, Th etc. The rare-element mineralization in metasomatites is more complex. We observe here high concentrations of zircon, rare-earth epidote-allanite, fergusonite and thorite. Chevkinite, monazite are common too.

Data from various mineral geothermometers and barometers indicate the range of formation temperature for rare-metal apobasic metasomatites from 550°C to 300°C. The range of pressure is 2-3 to 1-2 kbar.

References:

Akella, J., Vaidya, S. N., Kennedy, G. C. (1969) Phys. Rev., 185, 1135 - 1140.

Dziewonski, A. M. and Anderson, D. L. (1981) Phys. Earth. Planet. Inter., 25, 297 -356.

Belonoshko, A. B. and Dubrovinsky, L. S. (1994) American Mineralogist (submitted).

Kracek, F. C., and Clark, S. P. (1966) Handbook of physical constants, Geol. Soc.Am.Inc.,NY, 301-344.

Shen, G. (1994) Ph.D. Theses, Uppsala University

Zerr, A. and Boehler, R. (1993), Science, 262, 553- 555.

COMPUTER MODELING OF PROPERTIES AND PHASE TRANSITIONS OF GEOPHYSICALLY IMPORTANT MINERALS: MgO, SiO_2, AND $MgSiO_3$.

Belonoshko A. B. and Dubrovinsky L. S. (Theoretical Geochemistry Program, Institute of Earth Sciences, Uppsala University).

The Earth's lower mantle is believed to be mainly of Mg-Si-O composition. Therefore, investigation of phase diagram of this system is of specific interest for Earth scientists.

We have calculated new interatomic potentials for describing interaction in these minerals with GEMIN method (direct minimization of Gibbs energy) and applied these potentials for MD (molecular dynamics) simualtion of properties and phase transitions in Mg-Si-O system. The reliability of our procedure was checked for well studied NaCl.

We succeded to calculate properties in very good agreement with experimental data. We have applied two-phase MD simulation at constant pressure for simulation of melting to calculate PT (pressure-temperature) dependence of melting transition for NaCl (B1 and B2), MgO (periclase), SiO_2 (stishovite) and $MgSiO_3$ (perovskite). The calculated PT melting curves reproduce experimental data on melting transition (Akella et al, 1969; Kracek and Clark, 1966; Shen, 1994; Zerr and Boehler, 1993). Temperature of melting at core-mantle boundary (CMB) pressure (1.4 Mbar) is calculated to be from 6000 to 7000 K. Therefore, according to estimates of temperature at CMB, stishovite, periclase and Mg-perovskite are solid at CMB conditions.

We have fitted MD simulated data to equations of state, which are in agreement with existing experimental data and can be used for calculation of PVT properties under PT conditions of Earth interior (Belonoshko and Dubrovinsky, 1994). The calculated seismic parameter for Mg-perovskite is in better agreement with experimental data (Anderson and Dziewonski, 1982) than previously published.

PYROGROUPS IN THE NATURAL URANIUM PHOSPHATES AND ARSENATES.

Belova L.N., Gorshkov A.I., Dikov Yu.P., Doynikova O.A., Sivtsov A.V.
(Institute of Ore Deposits (IGEM RAS), Moscow)

The presence of pyrogroups was established in the natural autenite. This is the third occurence of natural phosphates with pyrogroups and the first occurence of natural uranium mica with pyrogroups.

Uranium micas with the unusual dark green or black colour attract our attention during more than 30 years. But if the cause of the unusual colour is usually connected with the presence of U^{4+} in the mineral's composition there is not a single opinion about the cause of its formation and position in the mica's structure.

The idea about interconnection of dark colour with the presence of fine-dispersed admixture of uraninite is not confirmed by several years investigations of authors.

The method of X-ray photoelectron spectroscopy was used for ascertaining the ratio of inequivalence uranium state in the mica's composition.

There was investigated the autenite with the next composition: UO_2 3.40; UO_3 59.8; CaO 6.04; P_2O_5 15.84; H_2O 14.12 %.

The next results were received. Uranium is present in two oxidation's states: U^{4+} and U^{6+}. The principal part (about 94%) is U^{6+}.

The character peculiarity of phosphorus is the presence of two independent structural groups: orthophosphate and pyrophosphate. Their ratio is PO_4 : P_2O_7 = 0.72 : 0.28.

The investigation of natural uranospinite with the 25% of U^{4+} by the same method estableshed the presence of about 4% pyroarsenates groups.

• A NEW MINERAL GROUP: COCONINOITE AND OTHER (Al,Fe)-URANYL-SULPHO-PHOSPHATES

Belova L.N., Gorshkov A.I., Doynikova O.A., Sivtsov A.V. *(Inst. of Geol. of Ore Deposits, Russ. Acad. Sci., Moscow)*

Three varieties of coconinoite from oxidation zone of U-V deposits in dark schists (Kyzylkumy) were studied.

The formula of their composition is: $A_4(UO_2)_2B_5(OH)_2 \cdot nH_2O$, where A = Fe, Al, Cr; B = PO_4, SO_4; n = 18.

Tiny plate-shaped crystals form spheroliths (< 0.2 mm) or fine crusts. Their colour is dependent from A cations in composition: olive-green (Fe, Al, Cr), sulphur (Al, Fe), cream-coloured (Al only). Glassy luster.

Our investigations were based on analytical transmission

electron microscopy (SAED, EDAX): The identity of SAED-patterns (with only slight differences in intensities) permitted us to consider these minerals as types of a common group of uranyl-phosphates with A-cation isomorphism: the end-member, only Al-type, and members of isomorphous series with ratio Al:Fe=4:1 and (Al+Cr):Fe=1:1. Composition of B anions is the same for all samples: PO_4:SO_4=4:1.

The data of SAED and X-ray powder diffraction were combined to define the previously unknown cell dimensions and space group. As result: a = 12.50, b = 12.97, c = 23.00 Å, β = 106.6°, $C2/c$ or Cc.

On the basis of our data the list of d/n, which was published by the discoverers (Young *et al.*, 1966), has been indexed. Parameters calculated therefrom: a = 12.47, b = 12.96, c = 23.08 Å, β = 106.76°.

Similarity in mineralogical and diffraction characters of xiangjiangite (Hunan, 1978), moreauite (Deliens & Piret, 1985*a*), and furongite (Hunan, 1976; Deliens & Piret, 1985*b*) with the studied minerals allowed us to assume their structural unity. Calculation of their published powder diffraction data on the basis of our data gives very similar values of cell dimensions. Xiangjiangite: a = 12.54, b = 12.98, c = 23.56 Å, β = 108.6°. Furongite: a = 12.50, b = 12.80, c = 22.86 Å, β = 104.9°.

Our investigation permitted us to consider coconinoite as a typical member of wide mineral group with a broad cation-anion isomorphism Fe-Al and P-S in its composition, and to regard moreauite, furongite and xiangjiangite as isomorphous members of coconinoite group (Belova *et al.*, 1993). Furongite and moreauite are especially phosphate- and at the same time especially Al-varieties. Xiangjiangite demonstrates both cation (Al>Fe) and anion (PO_4:SO_4=1:1) isomorphism in its composition.

Belova, L.N., Gorshkov, A.I., Doynikova, O.A., Mokkhov, A.V., Trubkiv, N.V., Sivtsov, A.V. (1993). *Doklady AN*, **329**, 772-775.

Deliens, M. & Piret, T. (1985*a*). *Ann. Soc. Geol. Belg.*, **108**, 365-368.

Deliens, M. & Piret, T. (1985*b*). *Bull. Mineral.*, **108**, 9-13.

Hunan Team (1976). *Acta Geol. Sinica*, **2**, 203-204.

Hunan Team (1978). *Sci. Geol. Sinica*, 183-188.

Young, E., Weeks, A., Meyrowitz, R. (1966). *Am. Mineral.*, **51**, 651-663.

MINERALOGY AND PROSPECTS OF TURQUOISE ON PAI-KHOY, RUSSIA

Belyaev A.A., Ievlev A.A. (*Inst. Geology, Komi* Sci. Centre, Ural Division, Russian Academy Sci.)

The first manifestation of turquoise in the European part of the USSR was discovered in 1979. It is situated on the Yugorsky peninsula in the middle streem region of Silova-yaha river (Pai-Khoy mountain range). Manifestation is located in the north limb of Middle-Silovskaya syncline structure and attracted to the zone of altered rocks of Late Devonian - Early Carboniferous age. Turquoise is located in three zones sub-concordant with stratification, with thickness of 1 to 3 meters, controlled by jointing and stratum separation. Fine impregnations of sulphide minerals and abnormally high content of phosphorus (P_2O_5 - 0.1-0.2%) are noted in unaltered rocks.

According to microprobe analyses the mineral contains (%): Al_2O_3 36.4-35.3; P_2O_5 38.9-37.2; FeO 2.6-2.0; MnO 0.07-0; CuO 3.7-3.1 in the green turquoise, 0.6-0.45 in the blue one; Na_2O 0.11-0.08; CaO 0.15-0.10; TiO_2 not discovered; Cr_2O_3 0.06-0. According to semiquantitative spectral analysis data it possesses (%): Y<0.004, V 0.003, Co and Nb 0.001, each, Be 0.0006, Ni and Yb 0.0004 each, Sc 0.0003, Sn 0.0002, Mo<0.0001, Ag 0.00001. Mossbauer spectroscopy gives the next correlation between the ferrous ions content: Fe^{+3}/Fe^{+2}=5.41. According to X-ray and IR-spectrum data the characteristics of studied material completely coincide with those of turquoise. Quartz and kaolinite are also detected.

The DTA-curve is characterized by intense endothermic effect at 352°C, weak endoeffect at 515°C and endothermic effect at 800°C. The unremitting loss of weight is fixed in the interval from 90 to 750°C. The total weight loss is equal to 17.85%, that is in good correlation with theoretic content of water in turquoise (17.72%).

The electron micrographs of some platy aggregates of turquoise reveal a dense collomorphous surface of this mineral. The aggregates are composed of plate particles of irregular form with jag borders, and splitting of peripheral parts into co-directional fragments is noted for many particles. The porous parts of platy turquoise are characterized by globular-plate aggregates. The main body of Pai-Khoy turquoise is present by spherical aggregates of radial structure.

In the authors opinion the obtained data on geological observations of the occurences of turquoise indicate a hydrothermal-metasomatic genesis of the mineral. The main criterions for prospects of turquoise on Pai-Khoy are: (1) availability of carbonaceous carbonate-siliceous turquoise-bearing formation of Khyzylkum type, (2) availability of horizon of ferrous jasper-like silicites of Famennian age, (3) progress of epigenetic processes resulting in leaching and re-distribution of ore elements, (4) availability of Cu, Zn sulfide or carbonate mineralization, (5) availability of turquoise locations and turquoise satellites (variscite, wavellite, amorphous phosphates, etc.). According to totality of these criterions or some of them the perspective and limited-perspective areas are determined on South-Easten Pai-Khoy.

It is necessary to mark the scientific importance of this turquoise location. It is situated in Arctic region where the physical type of weathering is predominant and the alluvial cover has the small thickness.

CHEMICAL AND STRUCTURAL FEATURES OF ALKALI FELDSPARES FROM RAPAKIVI GRANITES AND SOME RELATED ROCKS OF WIBORG, SALMI AND BERDIAUSH BATHOLITHES (RUSSIA)

Belyaev A., Shebanov A., Smetannikova O., Ermosh N. (Dept. of Geology, St. Petersburg University)

KFsp from rapakivi granites and related rocks have considerable variations of K, Na, Li, Rb content within massives, but in each of them there are regular variations of these elements concentration in the KFsps from various ovoid zones and groundmass.

1. The content of K in KFsp-ovoids from rapakivi granites increases from core to outer rim zones. That one of Na decreases and of Li remains approximately constant along this direction. Content of Rb decreases from central to middle zones and increases from middle to outer rim zones of ovoides.

2. The contents of K, Li, Rb in the KFsps from coarse-grained groundmass (between ovoides) are similar or higher than those in the outer rim zones of ovoids. The contents of these elements in the KFsps from fine-grained groundmass are considerably higher.

3. KFsps from monzonites (Salmi massif) and from metacrystals of metagabbroid xenolithes (Berdiaush massif) have higher content of K and Sr, lower of Na and similar of Li, Rb ones than KFsps of ovoids from rapakivi granites.

4. The ovoid-like KFsp-metacrystals (from 2 to 5 cm in diameter) were found in the country exocontact hornfels of the Salmi massif. The content of Na, Li, Rb in these KFsp-metacrystals is lower, and that of Sr is higher than in KFsp ovoids from rapakivi granites of Salmi massif.

Therefore, the regular variations of K, Na, Li, Rb, Sr contents in the KFsp ovoids accross the different ovoid zones are very similar to variations in metacrystals from xenolithes, monzonites and country hornfels.

X-ray structure studies of KFsp from ovoid-bearing rapakivi granites, monzonites and KFsp-xenocrysts from the diabase dyke crossing ovoid-bearing rapakivi granites of Salmi massif (Karelia, Russia) show following features:

5. KFsp from ovoides of rapakivi granites is represented by orthoclase-perthite (t_1=0.71-0.75). It contains 10-22%

of Ab-molecule in orthoclase structure(Ab^{Or}) in the ovoid cores and 5-6% of Ab^{Or} in the outer rim zones.

6. KFsp from monzonites is represented by orthoclase-perthite (t_1=0.71-0.75) with 14% of Ab^{Or}.

7. KFsp of metacrystals from metagabbroid xenolithes (Serdiaush massif)and KFsp-ovoides from rapakivi granites are very similar in Ab^{Or} contents(15%)in Or(t_1=0.61-0.66).

8.KFsp ovoid-xenocrystals included by the diabase dyke are represented by orthoclase-perthite(t_1=0.71-0.75) with 0-3% of Ab^{Or} in all zones of crystals.

We heated these KFsps at 900^0 C during 8 hours. The content of Ab^{Or} increased to 22-26% as a result of homogenization of KFsp.

The data given above allow to conclude, that ovoid-xenocrystals were included by the basaltic melt and were heated to the temperature about 900^0 C or higher. Later KFsp had exsoluted during following cooling and criptoperthites were formed. During experimental heating K-Na Fsps with criptoperthites have become homogeneous.

Therefore,the structure of KFsp-xenocrysts of hybridic rocks from mingling zones differs essentially from that one of KFsp-metacrystals of metasomatic hybridic rocks and monzonites.

GEOTHERMOMETRY AND GEOBAROMETRY IN THE S.ANNA TECTONIC WINDOW, SOUTHERN APUANE ALPS, TUSCANY, ITALY

M Benvenuti *(Dip. Sci. Terra, Univ. Firenze, Italy)*, P. Costagliola *(Museo Mineral. Litol., Univ. Firenze, Italy)*, P Lattanzi *(Dip. Sci. Terra, Univ. Firenze, Italy)*, G. Tanelli *(Dip. Sci. Terra, Univ. Federico II, Napoli, Italy)*

In the S. Anna tectonic window, greenschist-facies metamorphic rocks are the host of a number of barite-pyrite±iron oxides and/or polymetallic metamorphosed and/or metamorphogenic deposits (Lattanzi et al., in press). A number of geothermometers and geobarometers were applied to mineral assemblages in the deposits and their host rocks. When taken together they depict a consistent scenario for P-T conditions during metamorphism and mineralization at S. Anna, even if each of them suffers from inherent limitations and pitfalls.

Previous data. Carmignani et al. (1975) found that rocks at S. Anna show the same mineral assemblages occurring in other metamorphic rocks in the Apuane Alps, for which a P-T range of 350°-450° C and of 3-4 kbar is generally accepted. Based on the occurrence of biotite and on the composition of phengitic micas, Orberger (1985) suggested P-T conditions of ~400°-460° C and ~4 kbar. Cortecci et al. (1989) calculated S-isotopic temperatures of 380°-390° C for barite-pyrite and galena-sphalerite pairs from a barite-polymetallic vein.

Arsenopyrite geothermometry. Synkinematic arsenopyrite porphyroblasts occur in S.Anna rocks in apparent equilibrium with pyrite. The average (±1s) As content is slightly higher in the crystal rims (30.7±0.4 at. %) than in the crystal cores (30.0±0.2). The temperature ranges over which arsenopyrite with such compositions can stably coexist with pyrite are 350°-380°C for crystal rims and 300°-350° C for crystal cores (Scott ,1983), assuming that pressure influence is negligible (cf. Sharp et al., 1985).

Chlorite geothermometry. Although widely used, this geothermometer is not yet fully established (cf. de Caritat et al., 1993), and in particular it has been seldom applied in metamorphic environments. By extrapolation of the Cathelineau & Nieva's (1985) Al^{IV} vs. temperature regression, chlorites from metavolcanic and metapelitic rocks at S. Anna give temperatures of between 300° and 400° C, with a distinct frequency peak at about 340° C.

Phengite geobarometry. Phengitic micas in S. Anna rocks typically coexist with quartz and a Fe-Mg silicate (chlorite and/or, less commonly, tourmaline). Hence, their Si content provides minimum pressure estimates (Massonne & Schreyer, 1987) in the range 1.5-4.5 kbar (for T = 350° C), with a distinct frequency peak at 3.5 kbar.

Fluid inclusions. Pressure corrected (3.5 Kbar) microthermometric data for fluid inclusions in synmetamorphic mineralized veins provide trapping temperatures of about 350°-450° C, possibly indicating that mineralizing fluids were initially hotter than the host rocks. The (rare) occurrence of talc in S. Anna rocks has been reported by Orberger (1985); the intersection of the "talc in" isograd with fluid inclusion isochores occurs at P-T conditions of about 4 Kbar and 450° C.

In conclusion, all techniques consistently indicate that metamorphism and mineralization in the S. Anna tectonic window occurred in a temperature range of 350° to 450° C, at a pressure of ≥3.5 kbar

References:

Carmignani, L., Dessau, G., Duchi, G. (1975) *Boll. Soc. Geol. It.*, **94**, 725-758.

Cathelineau, M. & Nieva, D (1985). *Contr. Mineral. Petrol.*, **91**, 235-244.

Cortecci, G., Lattanzi, P., Tanelli, G (1989). *Chem. Geol.*, **76**, 249-257.

de Caritat, P., Hutcheon, I., Walshe, J.L. (1993). *Clays & Clay Min.*, **41**, 219-239.

Lattanzi, P., Benvenuti, M., Costagliola, P., Tanelli, G. (in press) *Mem. Soc. Geol. It.*

Massonne, H.J. & Schreyer, W. (1987). *Contr. Mineral. Petrol.*, **96**, 212-224

Orberger, B (1985) These Dr. INPL, Nancy, 263 p.

Scott, S.D. (1983). *Mineral. Mag.*, **47**, 427-435.

Sharp, Z.D., Essene, E.J., Kelly, W. (1985). *Can. Miner.*, **23**, 517-534

TEXTURAL AND S-ISOTOPIC (SHRIMP) FEATURES OF PYRITE FROM THE CAMPIANO DEPOSIT (SOUTHERN TUSCANY)

Benvenuti M. (*Dip.Sci.Terra, Univ. Firenze*), Eldridge C.S. (*Research School of Earth Sciences, The Australian National Univ., Canberra*) and Morelli F. (*Dip.Sci.Terra, Univ. Firenze*).

The massive sulfide deposit of Campiano occurs within the Southern Tuscany district. Other pyrite deposits in the district have been interpreted as pre-tectonic, possibly SEDEX-type deposits affected by Apenninic metamorphism and late-hydrothermal processes (Lattanzi & Tanelli, 1985). In comparison, pyritic bodies at Campiano show some distinctive features, mainly due to their close spatial association with the Boccheggiano fault, related to the post-Tortonian extensional stage of the Apenninic event.

Mineralogical and textural observations indicate a multi-stage process at Campiano. An early Fe-S-O mineral association was deformed, metamorphosed, and overprinted by a late-stage hydrothermal Cu-Pb-Zn(Fe) assemblage. Remnants of the earlier association are mostly constituted by a magnetite+pyrrhotite assemblage included within growth-zoned pyrite porphyroblasts. HNO_3 etching of the latter revealed the presence of three different pyrite generations (Py1, Py2 and Py3). Py1 occurs as rounded, subhedral crystals rarely exceeding a few tens of microns, very resistant to etching; it may show rosette structures possibly derived from colloform pyrite. Py1 is encased within growth-zoned Py2, which also hosts (and partially replace) the magnetite+pyrrhotite assemblage. Annealing textures, including 120° triple junctions, may be seen in Py2. The bulk of pyrite at Campiano is made up by Py3, which replaces Py2, but shows at least partial textural equilibrium with the polymetallic hydrothermal assemblage. Its strong reactivity to etching could point to fast crystal growth. Cataclastic deformation and pressure solution features commonly affect Py3.

Previous bulk S-isotope data on pyrites from Campiano (Cortecci et al., 1983; Benvenuti et al., 1993) consistently indicated an overall S-isotope homogeneity at the deposit scale (average $\delta^{34}S$=7.3±0.8), in agreement with the district average value of 9.3±1.4. S-isotope composition of associated massive pyrite and polymetallic sulfides (galena and sphalerite) generally reflects isotopic disequilibrium, although there is a slight tendency towards equilibrium between polymetallic sulfides and paragenetically late (i.e., Py3-dominated) pyrite. New S-isotope data of individual pyrite generations (*in situ* analyses) have been obtained by using a high resolution ion

microprobe (SHRIMP). Four polygenetic pyrites from different samples have been analyzed (Table 1).

Table 1

Sample No.	Mine Level	$\delta^{34}S$	description of analyzed point	Sample No.	Mine Level	$\delta^{34}S$	description of analyzed point
5	-125	9	core of Py1	10	-125	7	core of Py1
		8	surrounding Py2			8	surrounding Py2
		6	overgrown Py3			9	outermost rim of Py3
7	-125	9	core of Py1	22	-152	6	Py1 in rosette blades
		9	surrounding Py2			6	Py2 overgrowth
		8	fracture filling Py3			6	late stage Py3

Compositional variations are mostly within the analytical error (2σ=2‰), both within individual crystals and among pyrites from different samples. Such a homogeneous S-isotope signature at the deposit scale strongly suggests that a single source of sulfur was dominant during pyrite deposition at Campiano.

Although the time of formation and the depositional environment of this deposit are still partially obscure, the available mineralogical, textural and compositional features suggest the following evolution:

1) an oxidation state predominantly below the SO_2/H_2S fence;
2) precipitation of early Py1+Py2, at the expenses of a pristine magnetite+pyrrhotite assemblage;
3) leaching and partial remobilization of Py1+Py2 during a late hydrothermal stage, with deposition of Py3 without appreciable S-isotope fractionation.

Chemico-physical conditions estimated for deposition of the late Cu-Pb-Zn assemblage (T around 340°C; $fS_2=10^{-8}$-10^{-9}; $\delta^{34}S_{\Sigma S(fluid)}$ around 6.4‰: Benvenuti et al., 1993) can be reliable constraints to Py3 formation as well.

References

Lattanzi, P. & Tanelli, G. (1985). *Rend. Soc.It.Miner.Petrol.*, **40**, 385-408.

Cortecci, G., Klemm, D.D., Lattanzi, P., Tanelli, G., Wagner, J. (1983). *Mineral. Deposita*, **18**, 285-297.

Benvenuti, M., Morelli, F., Corsini, F., Masotti, S., Lattanzi, P., Tanelli, G. (1993) - *Mem. Soc. Geol. It.*, in press.

ENVIRONMENTAL IMPACT OF MINE WASTES IN THE BOCCHEGGIANO AREA (SOUTHERN TUSCANY): A PRELIMINARY REPORT

Benvenuti M. *(Dip. Sci. Terra, Univ. Firenze)*, Mascaro I *(Dip. Sci. Terra, Univ. Firenze)*, Corsini F. *(Dip. Sci. Terra, Univ. Firenze)* Lattanzi P. *(Dip. Sci. Terra, Univ. Firenze)*, Parrini P. *(Dip. Sci. Terra, Univ. Firenze)* and Tanelli G. (*Dip. Sci.Terra - Univ. Federico II in Napoli*)

Mining activity in the Boccheggiano area (southern Tuscany) dates back at least to Medieval age (XIII sec. A.C.). Up to the beginning of this century exploitation in the area mainly focussed onto polymetallic Cu(Pb-Zn-Ag) ores, particularly the so-called "Filone quarzoso-cuprifero di Boccheggiano" (FQC). This is a quartzose, copper-rich vein body emplaced along the Boccheggiano fault, a regional tectonic lineament related to the extensional stage of the Apenninic event (cfr. Benvenuti et al., 1993). The FQC yielded about 1.5 Mt ore at 4-8% Cu grade in the period 1889-1914.The low-grade ore was roasted and smelted in situ, leaving behind huge masses of slags and reddish roastings. Started in 1906, exploitation of pyrite bodies throughout the Boccheggiano area interested several massive bodies, including the Baciolo, Ballarino, Botroni, Molignoni, Rigagnolo, Valle Buia, and, since 1983, Campiano deposits, with a total production in the order of some tens of million tons (Tanelli & Lattanzi, 1983).

The most striking witnesses of such an intense and long protracted mining activity in the Boccheggiano area are represented by mine wastes. They are being the target of a detailed research program aimed to establish and quantify the environmental signatures that result from mining, mineral processing and smelting. One of the primary goals of this investigation is to provide information on the suite and concentration ranges of elements, and resulting mineralogical associations, in wastes, waters, soils, etc.. Another purpose is the study of elemental "geoavailability", i.e., the ease with which the elements can be liberated into the environment (cfr. Plumlee, 1994).

The data so far obtained can be thus summarized:

-1- Three basic types of wastes are present in the Boccheggiano area: (a) mine (N=11), (b) flotation tailings' (N=2), and (c) roasting and smelting wastes (N=1). Except for the latter type (c), related to polymetallic mineralization (FQC), all other wastes refer to pyrite exploitation.

-2- Main waste mineralogy is always characterized by ore/gangue phases of source mineral deposits: pyrite, gypsum, quartz, carbonates, chlorite, and micas. Type (c) waste materials mostly consist of quartz and hematite (roastings), and quartz, pyroxene, olivine, pyrrhotite and Cu-matte sulfides (slags).

-3- Secondary oxidation mineralogy commonly includes Fe-sulphates (jarosite, copiapite, fibroferrite, botryogen, siderotil), goethite, malachite, chrysocolla, anglesite, and native sulfur. Neogenic cassiterite, bismutite and/or bismite and (possibly) hydroxilbästnasite-Ce have been detected in type (a) wastes.

-4- Preliminary data concerning the bulk composition of waste samples consistently indicated high, albeit variable, metal contents (total ranges in ppm): Cu (90-2176), Pb (5-27800), Zn (77-15800), As (<0.1-1450). In particular, As and Pb are the most abundant metals in type (a) wastes, Zn and Pb in type (b), and Cu, Pb and Bi in type (c).

-5- Metal contents of waters draining the various types of wastes are generally high, though extremely variable (total ranges in ppm): Cu (<0.1-11); Zn (<0.1-14); Fe (0.2-2265). The observed depletion in metal contents of waters in the hot season with respect to winter time can be probably explained by reduced availability of leaching groundwaters.

References:

Benvenuti, M., Morelli, F., Corsini, F., Masotti, S., Lattanzi, P., Tanelli, G. (1993). *Mem. Soc. Geol. It.*, in press.

Plumlee, G. (1994). *SEG Newsletter*, **16**, 5-6.

Tanelli, G. & Lattanzi, P. (1983). *Spec. Publ. Geol. Soc. S. Afr.*, 7, 315-323.

A METALLURGICAL STUDY OF MEDIEVAL SLAGS FROM ROCCA SAN SILVESTRO (CAMPIGLIA M.MA, TUSCANY)

Benvenuti M. (*Dip. Sci. Terra, Univ. Firenze*), Mascaro I (*Dip. Sci. Terra, Univ. Firenze*) and Tanelli G. (*Dip. Sci.Terra - Univ. Federico II in Napoli*)

Metallurgical slags of medieval age have been found in two sites (A and B) within the Rocca San Silvestro seignorial castle (X-XIV sec. a.C.), located close to Campiglia Marittima (southern Tuscany). This region is long known for its mineral deposits, including Cu-Pb-Zn (±Fe,Ag,Sn) skarn and supergene ore bodies.

At site A small amounts of both furnace and tapped slags have been discovered, together with remains of three furnaces. Polymetallic slags are dominant, although a few lead slags also occur. Relics of johannsenitic pyroxenes in the slags strongly favour a provenance of mineral charge from adjoining Grotta Johannsenite skarn deposit. Slags from site A include matte sulfides (idaite, bornite, chalcocite, etc.) and metals (Ag-bearing lead, Cu and a Bi-rich alloy) dispersed in a Zn-rich fayalite+hedenbergite (±glass) matrix. Pb-Zn-bearing phases of the kirschsterite-glaucochroite series are characteristic of lead slags. The scarcity of litharge indicates that silver recovery by cupellation was probably limited to metallurgical assays for analytical purposes.

Sizable amounts of copper (tapped) slags are the only witnesses of metallurgical activity found at site B. A different source of ore (perhaps from the M.te Rombolo-M.te Spinosa-M.te Valerio area) and/or different smelting techniques with respect to site A are suggested by both mineralogical (absence of Pb-phases, covellite as the only metallurgical copper sulfide observed) and geochemical features (enrichment in FeO, Cu, Bi, and Sn, and depletion in Pb, MnO, P_2O_5, and K_2O with respect to slags from site A).

Tapped slags from both sites appear to have formed at temperatures between 1100° and 1150°C and $f(O_2)$ in the range of 10^{-10}-10^{-13} atm. Lower viscosities and metal contents of slags from site B consistently indicate a more optimised metal production than at site A.

A catalogue of Raman spectra of natural and synthetic minerals and their varieties : a useful tool for the application of Raman spectrometry in fields of earth sciences and industrial mineralogy.

Bény C., Gallas A.-M. (*Dept. Géochimie et Physico-Chimie, BRGM/DR, Orléans*), Lasnier B. (*M.L.R.O.-I.M.N., Univ. Nantes*) and Maestrati R..

Until now no extended Raman spectra catalogue exists in the fields of earth sciences and industrial mineralogy. This is probably due to the complexity of natural minerals and to the fact that the Raman spectra are dependent on the orientation of the sample and on the polarisation of the electric field of the laser beam.

However, such a catalogue is necessary for the characterization and identification of species, some of which can only be obtained only with the help of Raman spectrometry. The Raman spectra of over three hundred compounds have therefore been recorded and often, compounds have more than one spectrum corresponding to different crystallographic orientations, different laser beam polarizations or the use of different exciting radiations (to confirm some bands as Raman peaks to the case of the latter). Each spectrum is presented on a form that also contains the information relevant to the sample and the operating conditions.

The aim of this catalogue is to help the user of Raman spectrometry in the interpretation of the obtained data. In additonal to the spectra and the forms, it contains chapter on the theory of Raman and IR spectrometries, a chapter on the Raman spectrometric analysis of solid phases as inclusions or crystals, a chapter on some traps to avoid and on precautions to take, an index list minerals in alphabetical order and by family.

MINERALS, SOLIDS AND THEIR STRUCTURAL RELATIONSHIPS

Bergerhoff, G., Berndt, M., Brandenburg, K. and Radkowski, U.
(Institute for Inorganic Chemistry, Univ. Bonn)

The structure of the solid state is the key to the understanding of the chemical and physical properties. But to get a survey of the big amount of crystal structures known today by X-ray and neutron diffraction is only possible by using databases and appropriate programs. Minerals, mostly part of inorganic chemistry, are collected in the Inorganic Crystal Structure Database (ICSD), developed at our institute and now maintained and distributed by Fachinformationszentrum Karlsruhe, D - 76344 Eggenstein-Leopoldshafen, and Gmelin Institute, D - 60486 Frankfurt. The database is available on CD-ROM and On-line and contains full information on the crystal structure (cell dimension, space group, atomic coordinates, displacement parameters and conditions of measurement), bibliographic information and - for minerals - mineralogical name and origin.

A menue-driven and sophisticated retrieval program (for DOS and WINDOWS) allows to search for all interesting information: chemical composition, symmetry, minerals, author and year of publication, etc.To approach our goal the program has now been expanded to SIMILAR which compares structures and can search for structure types. First of all data for structure description have been standardized following Parthé & Gelato (1984). Afterwards correlation factors have been calculated for all isopointal structures. The user can now choose the degree of relationship in searching isotypes. To go beyond the boundaries of the space groups he can select certain formal structure types (e.g. AX_2, AB_2X_4, $ABC_2D_2X_7$), transform data to subgroups or supergroups and now compare data for similarity in a common space group..

All these comparisons are done on the algebraic level. But to confirm the relationships on the visible level the user can switch to the program DIAMOND. He can view any structure in full or any fragment, he can zoom and rotate the picture, he can measure distances and angles and he can superimpose two structures for immediate visual comparison.

With these programs we hope to give the crystallographic community appropriate tools for better understanding of crystal structures.

Reference:
Parthé, E. & Gelato, L. (1984). Acta Cryst. **A** 40, 169-183.

OPTIMIZED STANDARD STATE AND SOLUTION PROPERTIES OF MINERALS: OLIVINE, ORTHOPYROXENE, GARNET, CORDIERITE, ILMENITE, AND BIOTITE IN THE K_2O-FEO-MGO-CAO-AL_2O_3-TIO_2-SIO_2-H_2O SYSTEM

Berman, R.G. (*Geol Surv Canada*), Aranovich, L. Ya, (*Inst Exp Mineral, Chernogolovka*)

Major thermodynamic datasets have been derived to a large extent either without consideration of the mixing properties of minerals or using simplified ideal activity models. Because of the strong correlation between mixing and standard properties determined by phase equilibrium data, the growing body of high quality experimental data on solid solution bearing equilibria places important constraints not only on mixing properties, but also on standard thermodynamic properties. These constraints must be incorporated to obtain the greatest accuracy both in derived thermodynamic data and in geologically demanding applications such as thermobarometric and petrogenetic grid calculations.

In this study we have derived standard state and mixing properties of olivine (ol), orthopyroxene (opx), garnet (gt), cordierite (cd), ilmenite (il), and biotite (bi) in the system K_2O-FeO-MgO-CaO-Al_2O_3-TiO_2-SiO_2-H_2O from analysis of relevant phase equilibrium and thermophysical data. Solubility of Al_2O_3 in opx and bi was accounted for in addition to Fe-Mg mixing. Added confidence in the retrieved properties stems from consideration of data for ten linearly dependent Fe-Mg exchange equilibria among the above phases, as well as net transfer equilibria. The combined data set removes much of the ambiguities in mixing property magnitudes that arise in analyses of more restricted sets of data. Critical to successful analysis was the extension of the mathematical programming technique to include bulk composition constraints which force a fixed composition assemblage to be stable at experimentally studied conditions.

Results indicate that compatibility among the experimental data is improved markedly by incorporation of new Cp data on pyrope (Tequi *et al.*, 1991) and forsterite (Gillet *et al.*, 1991). Nonideal mixing parameters among these phases, although correlated, are well defined by the combination of experimental data, with $W_G^{Ol} > W_G^{Ilm} > W_H^{Bi} > W_H^{Gt} > W_H^{Opx} > W_H^{Cd}$, and 2.2 < W_G^{Ol}< 4.6 J/atom of isomorphous Fe-Mg. The few available brackets on the Al content of FMAS and FAS Opx (Lee and Ganguly, 1988) are in good agreement with the bracket in the FAS system (Kawasaki and Matsui, 1983), but indicate higher solubility than Harley's (1984) study. One implication is that Fe-Mg exchange temperatures for many granulites are not significantly reset in comparison with temperatures based on Al net transfer equilibria. Fe-Al interactions in both Opx and Bi are strongly negative, and have an important effect in geothermometry. Predicted phase diagrams for complex chemical systems are in reasonable agreement with available experimental data and with most observations based on natural assemblages.

References:
Gillet P., Fiquet G. (1991) *J. Geophys. Res.*, **96**, 11805-11816.
Harley, S.L, (1984) *J. Petrol.*, **25**, 665-696.
Kawasaki, T., Matsui, Y. (1983) *Geochim. Cosmochim. Acta*, **47**, 1661-1679.
Lee, H.Y., Ganguly, J. (1988) *J. Petrol.*, **29**, 93-113.

Tequi, C., Robie, R.A., Hemingway, B.S., Neuville, D.R., Richet, P. (1991) *Geochim Cosmochim Acta*, **55**, 1005-1010.

TUZLAITE, $NaCaB_5O_8(OH)_2{\cdot}3H_2O$, A NEW MINERAL WITH A PENTABORATE SHEET-STRUCTURE FROM THE TUZLA SALT MINE, BOSNIA AND HERZEGOVINA

VLADIMIR BERMANEC (UNIVERSITY OF ZAGREB), THOMAS ARMBRUSTER (UNIVERSITY OF BERN), DARKO TIBLJAŠ ((UNIVERSITY OF ZAGREB), DARKO ŠTURMAN (ROM, TORONTO), GORAN KNIEWALD (INSTITUTE RUDJER BOŠKOVIĆ, ZAGREB)

Abstract

Tuzlaite, $NaCaB_5O_8(OH)_2{\cdot}3H_2O$, is a monoclinic sheet-borate ($P2_1/c$, $\underline{a} = 6.506(1)$Å, $\underline{b} = 13.280(3)$Å, $\underline{c} = 11.462(3)$Å and $\beta = 92.97(2)°$, $\underline{V} = 989(1)$Å^3, $Z = 4$), occuring in nearly monomineral veinlets formed in the course of dolomitic marl diagenesis at the Tuzla salt mine located at the north-east part of Bosnia and Herzegovina. Intergrowths with halite have been observed where halite covers tuzlaite in later stages of diagenesis.

The crystal structure including hydrogen positions was solved and refined from X-ray single-crystal data to $\underline{R} = 2.8$, $\underline{R}w = 3.3\%$. Tuzlaite possesses a new type of pentaborate sheet-structure (Fig. 1) with four- and three coordinated boron (5:2Δ + 3T). Borate triangles and tetrahedra form ten-membered rings. The sheets are connected by Na and Ca which are coordinated to additional H_2O.

The new mineral is colorless to white. It is biaxial positive with following refractive indeces: $\underline{n}_X = 1.532(2)$, $\underline{n}_Y = 1.544(2)$ and $\underline{n}_Z = 1.561(2)$. The optical orientation is $Y = \underline{b}$, $Z:a = 14°$ (in acute angle β). Tuzlaite has one perfect parallel to {001}, hardness 2 to 3 and $\underline{D}_{meas} = 2.21$, $\underline{D}_{calc} = 2.23$. The chemical composition is : CaO 14.64%, Na_2O 10.25%, SrO 0.21%, B_2O_3 52.19%, Al_2O_3 0.26% and H_2O 21.66%. Tuzlaite is chemically related to the pentaborates probertite, $NaCaB_5O_7(OH)_4{\cdot}3H_2O$ and ulexite, $NaCaB_5O_6(OH)_6{\cdot}5H_2O$. The new mineral is named after the town Tuzla where it was found. The new mineral has been approved by the International Commission on New Minerals and Mineral Names.

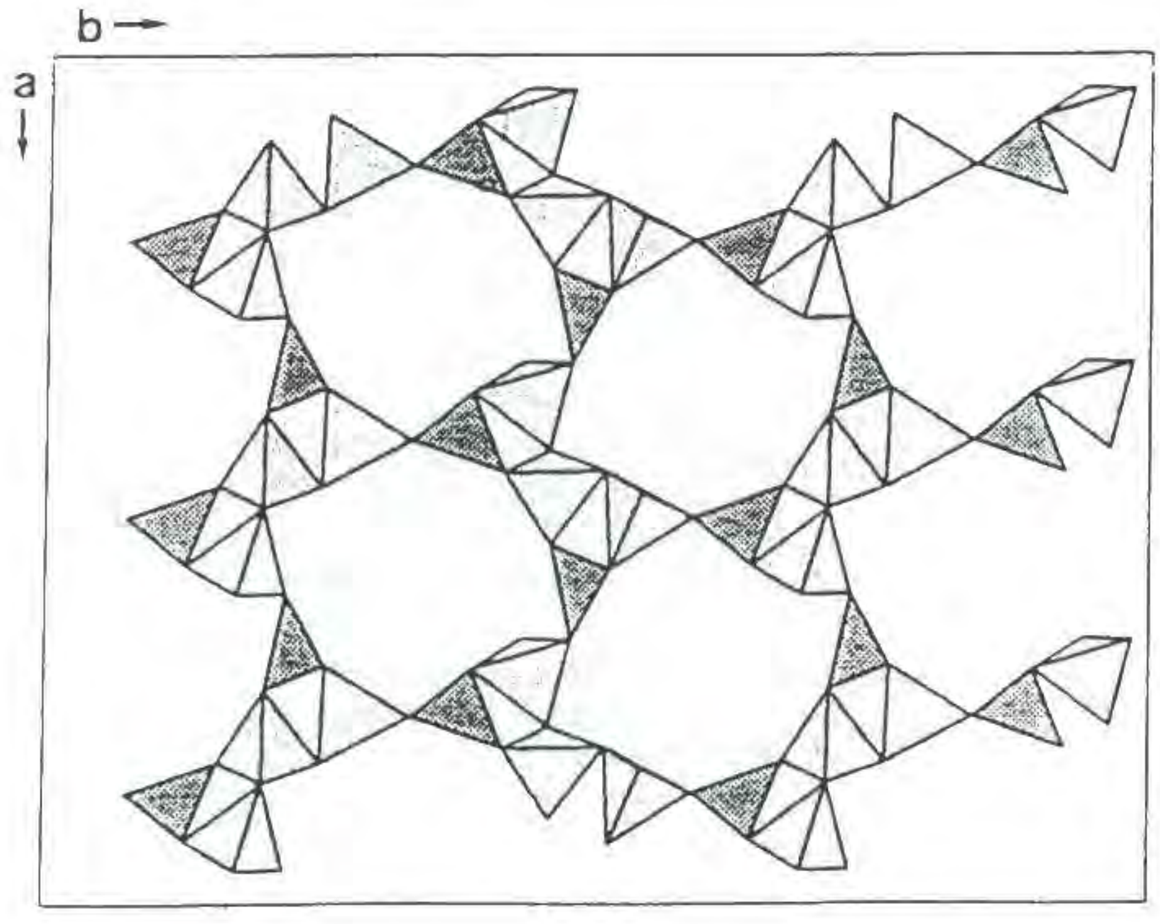

Fig. 1: Polyhedral model of a tuzlaite pentaborate sheet

References:

Ghose, S., Wan, Ch., Clark, J. (1978). American mineralogist, **63**, 160-171.

Menchetti, S., Sabelli, C., Trosti-Ferroni, R. (1982). Acta Crystallographica. **B38**, 3072-3075.

CERAMIC CLAYS FROM CEUTA (SPAIN) AND ITS POSSIBLE RELATION WITH SOME AMPHORIC ROMAN RELICTS

Bernal*, D., Cuevas**, J., Vigil de la Villa**, R. and García**, R. (*Dept. Prehistoria y Arqueología, Facultad de Filosofía y Letras; ** Dept. Química Agrícola, Geología y Geoquímica, Facultad de Ciencias. Universidad Autónoma de Madrid)

Some amphoric materials from Ceuta (Spain) being made for salt-preserving food have been dated as roman relicts. They are supposed to be manufactured using local clays, althoug there are not known excavations in ancient ceramic furnaces. Otherwise, it would be of interest to gain insight of their possible "in situ" manufacturing.

Several clay quarries exploited from the past for pottery or brick-making uses have been sampled in addition to some processed products in order to have a comparison with some amphoras collected in the "Museo Municipal de Ceuta". These materials are of Keay XIX tipe and some of them are from Ampurias. Three sites have been sampled. One of them "El Llano de las Damas", have a well documented origin established in the low middle age and some relicts of local vitrified pottery have been preserved. The others come from local potteries: "Alfar de Ingenieros" and "Fabrica de Ladrillos".

The 19 amphoric samples studied have been examined by means of XRD and chemical analyses of major and trace elements. Calcite, dolomite, quartz, feldspars are frecuent as non phyllosilicate components. Among the trace elements determined it can be outlined the significant contents of Pb(0-200ppm) and Zn(100-500ppm), specially in the clays from "El Llano de las Damas".

The unprocessed clays have been moulded and fired from 500 to 950°C to study similarities and firing temperatures. The main clay assemblages encountered in these materials are illite-kaolinite (80, 20%); kaolinite-illite-smectite (60, 25 and 15%); and illitic materials, corresponding to the three sites described in their respective order.

DETECTION AND MODELLING OF MICROCRYSTALLINE EFFECTS BY MEANS OF XRDP TECHNIQUE

Berti G. (Dept. of Earth Sciences - Univ. of Pisa)

With the aim of determining parameters of both instrument and sample systematic effects, the "Diffraction Instrumental Monitoring"

makes possible to evaluate the uncertainty and accuracy of the lattice d-spacing.

The instrumental parameters are calculated according to the mathematical theory of x-ray powder diffraction; the parameters' optimization is achieved by using the additive property of χ^2, thus constraining the involved models to converge simultaneously at the same minimum in a restrained Hilbert's space. To do this, the author uses DISVAR93 (centroid DISplacement and peak VARiance, 1993 update) (Berti et al., 1994), a package devised to process XRPD patterns. This package provides functions such as: data recording, visualization and zooming, peak/background separation, background fitting, profile fitting, etc. In particular, the package allows constrained optimization of the parameters affecting peak centroid and variance (Berti, 1993). This part covers the first two steps of the theory developed by Wilson (1963) which are necessary for complete reconstruction of the structural information from powder diffraction data.

On these bases, the image of the reciprocal lattice node, i.e. the diffraction peak fine structure, is analysed by means of both peak centroid stability and variation of variance from the peak maximum. This fine analysis allows precise isolations of the peak intervals where microstrains contribute negligibly to the intensity distribution, while the crystallite size (mosaicity) predominates (Berti, 1994).

Thus by defining the observed structure factor:

$$Fo = \{ Fm \bullet T(L(r^*)) \otimes T(\Phi(r)) \} \qquad (1)$$

in terms of unit cell structure factor, reciprocal lattice node, shape factor and aberrations, the microcrystalline arrangement along different crystallographic directions can be calculated as the mean distance between mistakes (Wilson, 1962) in the most general sense.

The model allowing calculations of microcrystallinity stems directly from (1) and fits experimental data.

The present approach, involves the convolutive synthesis of the last two steps (the third and fourth) of Wilson's theory. The third, developed by Alexander (1954), as well as the fourth require procedures with long computing times. Thus, here the third step has been carried out by means of a semplified procedure which uses pseudo-voigt functions for representing the full aberration contributions. In the meantime convolution of the crystalline structure and instrument components (the fourth step) was computed through Fast Fourier Transformation. Devices accounting for peak asymmetry and numerical artifacts, related to the FFT algorithm, were adopted, thus rendering reliable results.

The calibration curves deduced from diffraction instrumental monitoring (first and second steps) are currently used as warraties for the pseudo-voigt parameters representing the full instrumental contributions. Moreover, a normalizing scale factor is required for fitting experimental data

The results obtained are encouraging in that improvments to the presented approach are potentially capable to producing a numerical engine with high performance for detecting anisotropic microcrystalline effects.

References:
Alexander, E.L.,(1954).J.Appl. Physics, 25,155-161.
Berti, G., Giubbilini, S.,Tognoni, E.(1994). (submitted paper)
Berti, G. (1993). Powder Diffraction,8(2),89-97.
Berti, G. (1994). Adv. X-ray Analysis Vol. 37 (in press).
Wilson A.J.C. (1962). X-Ray Optics. Methuens Monog. London
Wilson A.J.C. (1963) Mathematical Theory of Powder X-ray Diffraction. Philips Tech. Library. Eindhoven The Netherlands.

CRYSTAL CHEMISTRY OF SALITES FROM MT. ETNA ALKALINE VOLCANICS

Bertolo S. and Nimis P. (*Dept. of Mineral. and Petrol., Univ. of Padova, Italy*)

Salitic mega- and phenocrysts from Mt. Etna (Sicily, Italy) were investigated by means of combined single-crystal X-ray diffractometry and WDS microprobe chemical analysis to obtain accurate site partitionings and to study in detail their chemical and structural features.

On the whole, the cation substitution mechanism is similar to that shown by other clinopyroxenes from sodic alkaline volcanic rocks (Dal Negro *et al.*, 1986), tri- and tetravalent cations in the M1 site ($^{[6]}Al^{3+}$, Fe^{3+}, Ti^{4+}) being balanced by both Si $\rightarrow$ $^{[4]}Al$ substitution in the tetrahedral site and (Ca^{2+}, Mg^{2+}, Fe^{2+}) $\rightarrow$ Na^{+} substitution in the M2 site. Minor differences between the studied samples are mainly related to their different Al contents (mainly $^{[4]}Al$). Decreasing $^{[4]}Al$ couples with decreasing Ca, as typically observed in clinopyroxenes from alkaline basic lavas (Dal Negro *et al.*, 1982). These variations are reflected by the negative correlation between T-Onon-bridging and M2-O3C2 distances.

The studied salites were compared with natural and synthetic clinopyroxenes crystallized from high- and low-pressure magmas. Chemical (*e.g.* low $^{[6]}Al/^{[4]}Al$ ratio) and structural parameters (*e.g.* high M1 site and cell volumes) suggest relatively low-pressure (< 5 kbar ?) conditions for both mega- and phenocryst crystallization.

References:
Dal Negro, A., Carbonin, S., Molin, G.M., Cundari, A., Piccirillo, E.M. (1982). *In:* Advances in Physical Geochemistry, S.K. Saxena (Ed.), vol. 2, Springer, Berlin Heidelberg New York, p. 117-150.
Dal Negro, A., Cundari, A., Piccirillo, E.M., Molin, G.M., Uliana, D. (1986). *Contrib. Mineral. Petrol.*, **92**, 35-43.

MINERALOGY OF TAILINGS FROM INGURTOSU MINE (SARDINIA)

Bertorino G., Caredda A.M., Ibba A., Fanfani L., Zuddas P. (*Dept. of Earth Sciences, Univ. of Cagliari*).

The mineralogy of sediments from abandoned ponds has been the subject of extensive studies (Blowes & Jambor, 1990; Blowes, *et al.*, 1991; Davis *et al.*, 1991). These have been aimed at clarifying the modalities and effects of mineralogical and geochemical processes occurring in the alteration of primary minerals responsible for environmental contamination in large areas where mining activity has been dismantled.

The Ingurtosu Pb-Zn mine (southwestern Sardinia) was in production from the beginning of the last century till 1968. The orebody consists mainly of galena/sphalerite veins in a quartz/siderite gangue. The minor constituents are pyrite, chalcopyrite, ankerite, dolomite, calcite, barite, cerussite, anglesite (Caboi *et al.*, 1993). The materials making up the tailings derive from different kinds of processing. Up to 1924 Pb and Zn concentrates were separated by gravimetric apparati and after that date by flotation.

The contamination process can be sketched as it follows: the sulphide minerals, still present in the tailing sediments due to incomplete separation of economic minerals from the gangue, oxidise readily in the vadose zone. Extensive sulphide weathering transfers high concentrations of SO_4^{2-}, Fe^{2+} and toxic metals to the streams, but no marked lowering of pH is observed in the water since the geochemical system is buffered by carbonates in the gangue (Caboi *et al.*, 1992).

The mineralogical investigation includes optical, XRD, SEM and EDS analyses of the sandy and clayey fractions of the tailings, as well as secondary precipitates from efflorescences deposited by waters filtering through the sediments.

Diffractometric analyses clearly showed that the main components of tailings of the larger grain sizes present a substantially uniform composition: i.e. slightly variable proportions of illite, quartz, siderite, ankerite, gypsum, anglesite and primary sulphides.

The finer grain sizes, which also contain quartz and gypsum, are prevalently made up of clay minerals, illite and at times kaolinite. Some samples are characterized by the presence of illite in association with another mixed-layer illite-montmorillonite mineral (Sródoń, 1984).

The encrustations, on the other hand, are made of Ca, Mg, Fe and Zn sulphates.

Microscopical observations and EDS microanalysis have pointed out that nearly all carbonate grains (siderite, ankerite), have alteration

rims made up iron oxides, where Zn, Cu and Pb are immobilized after sulphide oxidation. Alteration rims also indicate the presence of silicon (which is probably adsorbed) derived from aluminosilicate dissolution. SEM analysis and corresponding element X-Ray maps have shown non sulphide alteration rims also for sulphide grains.

A number of needle-shaped crystals made up prevalently of Fe and Zn sulphates were observed on the surfaces of unconsolidated grains.

In conclusion the mineralogical process that gives origin to the dissolution of toxic metals at Ingurtosu, is mainly due to the oxidation of sulphide minerals in soluble sulphates in a carbonate-buffered system.

References:

Blowes, D.W, Jambor, J.L. (1990). *Appl. Geochem.*, **5**, 327-346.

Blowes, D.W, Reardon E.J., Jambor, J.L., Cherry J.A. (1991). *Geochim. Cosmochim. Acta*, **55**, 965-978.

Cabot, R., Cidu, R., Cristini, A., Fanfani, L., Massoli-Novelli, R., Zuddas, P. (1992). *Water-Rock Interaction -WRI-7*, 367-370. Kharaka & Maest (eds).

Cabot, R., Cidu, R., Cristini, A., Fanfani, L., Massoli-Novelli, R., Zuddas, P. (1993). *Engineering Geology*, **34**, 211-218.

Davis, A., Olsen, R.L., Walker, D.R. (1991). *Appl. Geochem.*, **6**, 333-348.

Sródoń, J. (1984). *Clays and Clay Minerals*, **32** 337-349.

NEUTRON DIFFRACTION TO 25 GPa FOR STRUCTURAL STUDIES

J.M. BESSON

Physique des Milieux Condensés (CNRS URA 782), Université Pierre et Marie Curie. T. 13, E. 4, B. 77, 4 place Jussieu, F-75252 PARIS Cedex 05

Neutron diffraction experiments can now be performed up to 25 GPa, at least, with the Paris-Edinburgh cell, and yield fully refinable patterns on powder samples, by time-of-flight methods.

This is an increase by a factor of 10 over the range of pressure that was currently available four years ago. This range of pressure is necessary to provide significant information on the structural evolution of earth and planetary constituents, especially on the lighter elements which are difficult to probe by x-ray methods.

The principle and operation of the P.E. apparatus will be briefly described. Examples of results obtained under high pressure on minerals (e.g.: Brucite) and planetary constituents (e.g.: NH_3 - H_2O) will be given.

Extension of such structural studies by neutron diffraction to high temperatures ($T > 1000$ K) and higher pressures ($p > 2.5$ GPa) will be discussed, in view of its application to mineralogical studies.

THE EXPERIMENTAL STUDY OF U AND PB DISTRIBUTION BETWEEN ZIRCON AND THE SOLUTION OF VARIOUS COMPOSITION

Bezmen N. *(Inst.of Experimental Mineralogy RAS)*, Levchenkov O., Rizvanova N., Levsky L. *(Inst. of Precambrian Geology and Geochronology RAS)*.

The ability of zircon to accommodate U in substitution for Zr in its structure makes zircon a natural U-Pb geochronometer, potential source of U and Pb ore bodies and candidate for the ceramic immobilization of radioactive wastes.

The partition coefficients U(D_U) and Pb(D_{Pb}) depending on composition of solution (H_2O, 1M NaCl, 1M NaOH, 1M $NaHCO_3$, 1M Na_2CO_3, 2M Na_2CO_3 and 1M NaCl+0.5M HCl), temperature and the degree of zircon crystallinity have been determined.

The variations of D_{Pb} have been found from $1.5 \cdot 10^{-1}$ to $3.0 \cdot 10^{-2}$ under the interaction of metamict zircon with the solutions at T=400° C and P=1 kb while D_U were 150-200 times lesser. D_{Pb} increased from $4.0 \cdot 10^{-2}$ to $6.5 \cdot 10^{-1}$ in the temperature range from 200 to 600° C and decreased under the further raise of temperature. The changing of D_U was like to D_{Pb}: an increase in the 200-300° C range and a decrease at temperature over 400° C. The decrease of D_{Pb} and D_U can be explained by the formation of new solid phases (e.g.baddeleyite accommodating U from solution).

The distribution of Pb and U between crystalline zircon and 2M Na_2CO_3 solution at T=650-700° C and P=1 kb was characterized by the same partition coefficients.

The experimental results indicated that natural hydrothermal fluids were able to lead to the essential migration of Pb and U from zircon.

MINERALOGICAL MUSEUM CURATOR: SCIENTIST-CREATOR- RENOVATOR

Bhaskara Rao,A., Adusumilli, Maria S.*(Inst. of Geosciences, Univ. Brasilia)* and
Castro, C.*(CECINE, Fed. Univ.of Pernambuco, Recife)*

History of Man has much to do with our present state of development. Man's evolution through ages reveals his persistence and creativity. These are our sources of inspiration.Neverthless, though we should always recollect them,yet we should try to improve over them towards a better living. Libraries and museums are true repositories of our culture , heritage and evolution.

Mineralogical museums are no exception. They show the riches of the earth and enthuse in us the necessity to dig deeper into earth and discover the hidden resources and riches. This is only possible with a scientist- creator as a curator of a museum. He reveals the beauties, enlarges them, adds up his genius, and enthuses the youth by making minerals, metals and rocks indispensable for our living. A curator will induce and stimulate the needed consciousness towards nation's riches and development, fomenting progress within the reach of the community.

In developing countries the priorities are agriculture and industry. The raw materials for the industry are natural resources and minerals. The awareness towards this fact leads to the necessity of the countries to inspire the new generations towards earth sciences. The museums, which are the showrooms of our riches , thus demand a Curator who should not only be a scientist and creator but also a renovator. Only through renovation, museums can provoke interest in the people towards minerals, rocks, and earth sciences. This is the talent of the curator and his creative art, expected in furthering development through:

1) an operation within the realm of art of making old things look new.

2) an art of changing the disposition and distribution of the samples from time to time.

3) a mode of display , constantly differing from the earlier, by introducing new styles and materials.

4) an exhaustive preparation , exposition and renewal of presentation through posters.

5) an excellent concept, preparation and /or obtention of three dimensional models and their exposition.

6) obtention and exposition of geological and metallogenetic maps of different countries and at different scales.

7) exposition of some mineral/material forecast maps, landusage maps, geotechnical maps,environmental preservation maps etc. that depict the participation of geosciences in community affairs.

8) organisation and demonstration of the importance of raw materials and geosciences for the community, as for ex: gems, industrial minerals, metals, energy resources etc.

and

9) constant renewal of their disposition, display,lay out and similar features to call more attention for those that have been already exposed earlier.

Strategies to accomplish these attractive aspects depend on the authorities who should criteriously select a reputed scientist- thinker- and a communicator to be a curator, and give him some basic amenities and support, and leave him free to his creativity and growth. In this manner, it is certain that not only mineral museums start budding and flourishing, but also the search of the youth for knowing more of Geosciences to unearth and avail the known and unknown earth resources for better living. The present world situation doesnot differentiate much between the demand of the developed and developing world for the natural mineral resources. Thus this strategy is needed for both of them.

RADIATION DAMAGE IN ZIRCON AND MONAZITE

Biagini R. and Memmi. I. (Dept. of Earth Science, Univ. Siena)

Metamictization effects have been investigated in zircons and monazites characterized by different U and Th contents and by different ages. Even though no completely X-ray-amorphous zircon and monazite have been found, the samples show different degree of metamictization.

Six zircons from Sri Lanka (570±20 Ma), two monazites from Norway (1.64±0.9 Ga), one from Madagascar (1.65±0.5 Ga) and two from Alps (alpine age) were examined by X-ray (powder and single crystal) diffraction. U and Th contents were determined by Neutron Activation (zircons) and Electron Probe analysis (zircons and monazites). Density was determined on fragments using a pycnometer method.

Zircon crystals range from semi-transparent green to brownish-reddish in colour. U and Th contents are between 800 and 3000 ppm and between 150 and 500 ppm, respectively. As U and Th contents increase, X-ray powder diffraction patterns change: diffraction maxima decrease in intensity, shift to lower 2ϑ values, broaden and become asymmetric, due to increased contribution of diffuse-scattering component. Also density variation is related to U and Th increase, ranging from 4.80 (Th=150 ppm and U=800) to 4.10 g/cm^3 (Th=500 ppm and U=2890).

Monazites are semi-transparent and brownish-reddish in colour. ThO_2+UO_2 content range from 9.6 to 19 wt%. X-ray powder diffraction patterns do not show evident peak asymmetry or broadening; only a little shift towards lower 2ϑ values was observed in crystals with higher U, Th and Y content. These samples also show a density decrease from 5.28 to 5.01 g/cm^3.

Then in the studied samples different degrees of radiation damage have been found, mainly as function of different U and Th content, while the age seems to be ininfluent. Further, monazite, despite its very high U and Th content, displays only minor metamictization effects.

TRIOCTAHEDRAL MICAS FROM UNDERSATURATED POTASSIC VOLCANIC AREAS OF CAMPANIA, SOUTHERN ITALY.

Biasco A., Balassone G., Petti C. (*Dept. of Earth Sciences, Univ. of Naples)*

Biotites and phlogopites from volcanic, subvolcanic and metamorphic parageneses of Somma-Vesuvio, Ischia and Procida islands was studied by EPM-XRD, in order to asses to what extent different petrological conditions affect the crystallochemical features of these minerals. Chemistry of campanian trioctahedral micas is characterized by a rather wide compositional range. Volcanic samples, related to pyroclastics from Somma-Vesuvio and Ischia island, range from Fe-biotite to Mg-biotite, with Mg/Mg+Fe ratio ranging from 0.84 to 0.67. Al-Tschermak and $3(R^{+2})^{VI}=2Al^{VI}+(\square)^{VI}$, $3(R^{2+})^{VI}=Ti^{VI}+(\square)^{VI}$ substitutions are present in the octahedral layer. A Ba-rich biotite (BaO ~ 1.54 wt %) was also found in a volcanic assemblage, in association with leucite + clinopyroxene + garnet + olivine. Trioctahedral micas from subvolcanic and metamorphic ejecta found at Somma-Vesuvio and Procida island was chemically more random than the micas from volcanic products. They range from Fe-biotite , Fe-Mg-biotite (mainly in the subvolcanic samples) to high Mgv phlogopites (in some metamorphic samples). All subvolcanic samples are Si,Al-deficient and Fe'",Ti-rich, in some case with very high Fe'" content. Typical substitutions in the octahedral layer are similar to volcanic varieties. In the metamorphic phlogopites (Mg/Mg+Fe ratio around 0.93-0.98) Al-Tschermak substitutions in the octahedral layer are frequent. Any correlation between variations of fluorine amount and the different origin of the studied crystals can be observed. The most frequent polytypes, evidenced by XRD investigations, are 1M and 2M1. A good relationship is found between b-spacing and octahedral cationic radii. X-ray results pointed out distinctive features regarding volcanic and subvolcanic crystals. They are always characterized by higher b-spacing values, in contrast with metamorphic crystals showing lower b-spacing values. A good correlation is also found between the tetrahedral crystallographic parameters α (i.e. tetrahedral rotation angle) and $b_{octahedral}/b_{tetrahedral}$ ratios, but no indications related to different petrologic types can be drawn. The octahedral parameter ψ (i.e. octahedral flattening angle) is weakly correlated to α, in agreement with literature (Brigatti & Davoli,1990) and also in this case any clear relation with crystals from different petrologic environment can be emphasized.

References:

Brigatti, M.F. & Davoli, P. (1990). *Am.Min.*75,305-313.

POLYTYPIC SEQUENCES IN THE STRUCTURE OF A BETA-TYPE ZEOLITE FROM ANTARCTICA

Bigi S., Galli E., Quartieri S., Rossi A., and Vezzalini G. *(Dept. of Earth Science, Univ. of Modena, Italy)*
Alberti A. *(Inst. of Mineralogy, Univ. of Ferrara, Italy)*

A great number of zeolitic species was found in highly vesicular basaltic andesites from Mt. Adamson (Terra Victoria Land, Antarctica). Among the numerous zeolites found (heulandite, stilbite, mordenite, erionite, levyne, cowlesite, phillipsite, chabazite, thomsonite, scolecite, epistilbite) (Vezzalini *et al.*, 1993), the most interesting occurrence was that of a mineral related to the synthetic zeolite Beta (Newsam *et al.*, 1988; Marler *et al.*, 1993), and to the natural zeolite tschernichite (Boggs *et al.*, 1993). This mineral occurs as colourless, steep tetragonal dipyramids terminating in a basal pinacoid, usually isolated and, less frequently, twinned.

Beta structure has been described as an intergrowth of two polymorphs: tetragonal polymorph A (enantiomorphyc pair with a=b=12.5, c=26.6 Å, s.g. $P4_122$ or $P4_322$) and monoclinic polymorph B (s.g. C2/c, with a ≃ b =12.5$\sqrt{2}$, c=14.4 Å, $\beta = 114.5°$) (Newsam *et al.*, 1988), and tschernichite as a tetragonal mineral with a=12.88 Å, c=25.02 Å. Similarities in the X-ray diffraction patterns suggest that tschernichite, too, may consist of an intergrowth of polymorphs A and B (Boggs *et al.*, 1993).

Weissemberg and precession photographs of the mineral from Mt. Adamson showed overall features similar to those of Beta and

tschernichite: a) h0l and 0kl diffraction patterns always show two rods of diffuse reflections (extended along c*), followed by a rod of sharp reflections with h=3n and k=3n, thus indicating a disorder along c; the spacing between sharp reflections corresponds to $\simeq$ 13.3 Å; b) the hk0 layer shows an orthogonal symmetry with a$\simeq$b$\simeq$ 12.7 Å.

Selected area electron diffraction patterns did not show streaks, thus indicating essentially ordered domains of at least 10^7 Å^2; four-circle automatic diffractometer gave a=b=12.72 Å, c=26.64 Å, values which differ remarkably from those of both zeolite Beta and of tschernichite.

Starting from a (001) tetragonal layer-like building unit with a=b=12.72 Å (according to our unit cell parameters), only six frameworks with distinct stacking sequences are, in principle, possible: polytype A (c=26.64 Å, s.g. $P4_122$ or $P4_322$), polytype B (c=14.61 Å, β = 113.8°, s.g. C2/c), polytype C (c=27.96 Å, β = 107.6°, s.g. P2/c), polytype D (c=13.32 Å, s.g. $P4_2/mmc$), polytype E (c=26.64, s.g. $P2/m2/c2_1/m$), and polytype F (c=13.98 Å, β = 107.6°, s.g. P2/m). The structures D, E and F contain double-4 rings, and are thus believed to be less stable from an energetic point of view, although their presence in this natural sample cannot be excluded.

Preliminary investigations on a single crystal confirmed the presence of at least the two polytypes A and B. Work is in progress to check the presence of other polytypes, determine the frequency of each arrangement in the polytypic sequence, and perform the structural refinement of each polytype.

Thermal gravimetric curve and microprobe chemical analysis gave the formula $(Ca_{0.91}Na_{0.49}Mg_{0.05})\ (Si_{5.71}Al_{2.23})O_{16} \cdot 8.41H_2O$, which remarkably differs from that of tschernichite in both Si/Al ratio (2.56 for this sample, to be compared with the 3.0-3.7 range of tschernichite) and Na content (0.49 a.p.f., to be compared with 0.11 a.p.f. of tschernichite). X-ray powder diffraction also shows significant differences from those of Beta and tschernichite, especially in the low theta region.

References

Boggs R.C., Howard D.G., Smith J.V., Klein G.L. (1993). *Amer. Mineral.*, **78**, 822-826.

Marler B., Böhme R., Gies H. (1993). *Proc. Int. Zeolite Conf., Montreal, 1992*, pp. 425-432, Eds. R. von Ballmoos et al., Butterworth-Heinemann.

Newsam J.M., Treacy M.M., Koetsier W.T., de Gruyter C.B. (1988). *Proc. R. Soc. Lond.*, **A420**, 375-405.

Vezzalini G., Quartieri S., Rossi A., Alberti A. (1993): *Italian Antarctic Earth Sci. Newsletter*, **1**.

MINERALOGY IN AUSTRALIA - MUSEUMS AND SOCIETIES TO THE RESCUE?

W.D. Birch, *Department of Mineralogy, Museum of Victoria*

Mineralogy, the natural science, has an insecure future in Australia. It is no longer a mainstream study at tertiary level, and lacks a strong research base in the mining industry. The output of Australian mineralogical papers depends on a handful of individuals. Without a critical mass, the science has not been able to sustain a national specialist society or a journal.

Many of the rare or new species (and their associations) found in Australia over the past few decades have come to light through the activities of lone prospectors and hobby mineral collectors. In at least four states, mineralogical societies have sprung up to cater for the needs and interests of collectors. Links with museums having mineralogical collections and active curators have been important in the development of these societies. These links must be strengthened if the societies' contributions to Australian mineralogy are to continue.

ZIRCONIUM PHOSPHATE MINERALS IN PEGMATITE FROM WYCHEPROOF, VICTORIA, AUSTRALIA

Birch, W. D. (*Dept. of Mineralogy, Museum of Victoria*)

Three zirconium-bearing phosphate minerals, two of them new species, have been discovered in a late-stage pegmatite in a Devonian granite at Wycheproof, Victoria.

Wycheproofite, $NaAlZr(PO_4)_2(OH)_2.H_2O$, selwynite $NaK(Be,Al)Zr_2(PO_4)_4.2H_2O$, and kosnarite $KZr_2(PO_4)_3$ were early-formed minerals, which were followed by a suite of aluminium or iron-bearing phosphates, including wardite, eosphorite, cyrilovite, rockbridgeite, leucophosphite and a kidwellite-like mineral.

The zirconium phosphates, as well as wardite and eosphorite, crystallised under reducing conditions. Cyrilovite and later phosphates mark the onset of oxidising conditions, possibly accompanying interaction between the cooling granite and meteoric fluids.

The Zr-bearing phosphate suite appears to have crystallised from late-stage Zr-rich magmatic hydrothermal fluids, rather than as a result of alteration of zircon.

VERY LOW- AND LOW-GRADE ROCKS OF THE POZDIŠOVCE-IŇAČOVCE UNIT: FIRST EVIDENCE ON THE TERTIARY METAMORPHISM IN THE WESTERN CARPATHIANS

Biroň, A., Soták, J., Spišiak, J. (*Geol. Inst. Slovak Acad. Sci. Banská Bystrica, Slovakia*)

The Pozdišovce-Iňačovce unit forms the pre-Neogene basement of the east Slovakian part of the Transcarpathian Depression. Metasedimentary rocks of this unit (phyllitic schists, bituminous /graphitic/ phyllites, high-alumina phyllites, calcphyllites marbles, metapsammites, metatuffites) range from anchimetamorphic to epimetamorphic (lower greenschist facies) grade. On the basis of the fossil evidences, the age of these over-a-thousand-meter thick sequences was estimated Uppermost Palaeozoic, Mesozoic through Eocene. The complexes were influenced by post-Eocene thrusting, syntectonic low-grade metamorphism and later shearing processes.

Low-temperature metamorphism of the metasediments has been investigated on approximately 100 samples from borehole profiles by microscopic, electron microprobe and X-ray powder diffraction methods. In order of decreasing abundance the following minerals

were encountered: quartz, illite/muscovite, mixed-layer paragonite/muscovite (P/M), paragonite, chlorite, calcite, albite, dolomite, siderite, organic matter, pyrite, hematite, pyrophyllite, chloritoid, corrensite, tourmaline apatite and zircon. Secondary minerals are represented by kaolinite and rarely by mixed-layer illite/smectite.

The estimation of the physical conditions of metamorphism is based on the study of mineral assemblages. The most frequent there are the so-called non-diagnostic assemblages: illite/muscovite + paragonite + Qz ± chlorite ± albite ± organic matter. These are stable under the sub-greenschist as well as greenschist facies conditions. Generally, a characteristic feature of these rocks is ubiquity of the trace amounts of paragonite, and/or P/M (or metastable intermediate sodium potassium mica (Jiang & Peacor, 1993)). The P/M is usually considered a diagnostic mineral for middle anchizone metamorphic conditions. However, we have found this mineral phase in association with pyrophyllite and chloritoid. The explanation of this non-equilibrium will require a more detailed study.

Mineral assemblages useful for estimation of metamorphic temperatures were found in the rocks with high Al content. Lower temperature limit is determined by assemblages: illite + paragonite + P/M + corrensite + Qz or illite + paragonite + P/M + chlorite + corrensite + albite + Qz. The persistence of corrensite is indicative of the temperatures < 250 °C (lower anchizone, Shau et al., 1990). On the other hand, peak metamorphic conditions are documented by assemblages: illite/muscovite + pyrophyllite + paragonite + P/M + Qz, illite/muscovite + pyrophyllite + paragonite + P/M + chloritoid + Qz and illite/muscovite + chlorite + paragonite + P/M + chlorite + chloritoid + Qz. Chloritoid seems to have originated by the reaction: pyrophyllite + chlorite --> chloritoid + Qz + H_2O (Zen, 1960) under the lower greenschist facies conditions (approx. 350°C; Frey et al., 1988). It is very difficult to estimate pressure for the Pozdišovce-Iňačovce unit, because of the lack of geobarometers. However, taking into consideration some facts - e. g. chloritoid with low Mg content (X_{Mg} = 0.09-0.12) or white K-micas with rather low phengite component (max. Si = $6.6/O_{20}(OH)_4$) - for the present study, we tentatively estimate metamorphic pressure up to 5 kbars.

References:
Frey, M., Saunders, J.,Schwander, H. (1988).*J. geol. Soc. London*, **145**, 563-575.
Jiang, W.T. & Peacor, D.R. (1993).*Am. Mineral.*, **78**, 782-793.
Shau, Y.H., Peacor, D.R., Essene, E.J. (1990).*Contrib. Mineral. Petrol.*, **105**, 123-142.
Zen, E-An (1960).*Am. Mineral.*, **45**, 129-175.

• THE GEOCHEMICAL CHARACTERISTICS OF THE AUTHIGENIC SEDIMENTARY IRON SULPHIDES OF THE NORTH EAST BALTIC LOWER PALAEOZOIC

Bityukova L. (*Institute of Geology, Estonian Academy of Sciences, Tallinn*)

Diagenetic mineralization is widespread in the sequence of Vendian and Cambrian terrigenous sediments of the North East Baltic.

The natural sulphides studied are represented by various morphological forms: fine-grained framboidal pyrites formed in trace fossils (Tammeaid, 1991), crystalline aggregates, concretions and cementational type of pyrite. According to X-ray measurements (Kallaste, 1991) the dominating crystalline phase of natural sulphides is pyrite. Rarely sulphides consist of pyrite-marcasite mixture.

The distribution of 12 elements in sulphides was studied. Variation of the concentrations of microelements depends on the conditions of the formation and crystallochemical characters of sulphides (Vaughan & Craig, 1978). The main aim of the present work was the study of the effect of the facies condition of sedimentation on the compositional changes of the main morphological types of authigenic sulphides.

In the sulphides of the region under consideration the concentration of the Tl, As, Pb, Mo and Co has been estimated to exceed that of the host sediments.

The highest concentration of the microelements in the different morphological types of iron sulphides was found in the early diagenetic pyrites which fill the trace fossils in the argillaceous marine sediments of the Cambrian Lontova Formation. According to the X-ray studies this type of sulphide mineralization is represented only by pyrite with a cell parameter smaller than normal.

Diagenetic concretions have a cryptocrystalline structure and occur in several stratigraphic levels of the Vendian-Cambrian section. Also pyrites of these concretions have also a cell parameter smaller than normal. Pb, V, Ni, Co and Tl are concentrated in them. The highest concentrations were found in concretions of the Vendian Gdov Formation. Its sediments are formed in subcontinental conditions. In the Cambrian sediments the highest concentration of microelements was found in the concretions of Lontova and Lukati formations. Their sedimentation took place in the marine conditions.

The pyrites of the cementation type with normal cell parameters have stable concentration of microelements. This type of pyrite occurs mainly in the siltstones of the Cambrian Tiskre Formation. It formed in the conditions of the superposed diagenesis. The concentration of microelements in the cementation type of pyrite is far lower than in other morphological types.

Among the crystalline aggregates the lowest concentrations of microelements were found in pyrites from siltstones of the upper part of the Cambrian, which mostly have catagenetic genesis.

The above discussed distribution of elements determines the geochemical features of the formation processes of pyrite in the sediments of the Vendian and Cambrian of the North Baltic.

References:
Kallaste,T. (1991). Proc. Estonian Acad. Sci. Geol., 39, 50-60.
Tammeaid, I. (1991). Proc. Estonian Acad. Sci. Geol., 39, 95-97.
Vaughan, D.J.& Craig, J.R. (1978). Mineral Chemistry of Metal Sulphides. Cambridge University Press, 575 p.

MIXED-LAYER ILLITE/SMECTITE IN THE FOSSIL GEOTHERMAL FIELD HARGHITA BAI (EAST CARPATHIANS): CHEMICAL, MORPHOLOGICAL AND STRUCTURAL MINERALOGICAL EVIDENCES

BY
BOBOS I. (TECHN. UNIVERSITY of TIMISOARA), GHERGARI L. (UNIVERSITY of CLUJ NAPOCA) and SOBOLEVA S.V. (IGEM MOSCOW)

Mixed layer illite/smectite (I/S) of the pervasive argillic alteration from the Harghita Bai hydrothermal area has been studied by AAS, TEM and XRD. Thermodynamic fluctuations of hydrothermal convective systems has produced a multiple reaction series by which I/S are randomly (R=0) and ordered (R=1;R=2;R=3). A complete series of mixed layers I/S was evidenced. Chemical analysis shows a increases ofthe interlayer K content with decreases expandability. The fixing K per illite layers of hydrothermal solutions has a values between $0,08-0,64/O_{10}(OH)_2$. The morphology mixed layer I/S studied by TEM show changes from the flakey like habit to the lath like habit during the transition smectite to illite. Also, by TEM observed hexagonal plates habit for pure illite. Polytype were identified by electron diffraction (oblic texture method) and X-ray diffraction. 1M and $2M_1$ symmetry was found. XRD confirmed arrangements of mixed layer I/S changes from the random to ordered. Expandability varies between 90 - 5 % smectite layers.

This detailed observations on mixed layer I/S suggested the mechanism in which illite forms from smectite by dissolution, precipitation and growth.

• INFLUENCE OF LIVING ORGANISMS ON MINERAL EQUILIBRIA IN ENVIRONMENT

Bocharnikova E.A., Matichenkov V.V. (*Inst. Soil Science and Photos., Rus. Acad. of Sci., Pushchino*)

The various aspects of the mineral equilibria in environment (mineral stability, neoformation and transformation) under supergenic conditions are affected by dependence from content of soluble forms of mineral-forming elements in natural solutions (ocean, lakes, rivers, ground and soil waters). The forms and concentration of silicon substances are very important in this regard. They controls the various processes: dissolution, precipitation adsorption-desorption, complex formation and others. At the same time silicon is one of the most abundant nutrient for plants and microorganisms. The concentration of silicon is limited of plankton amount in ocean. An amount of $4{,}6.10^8$ t of Si is annually involved in biological cycle and $2{,}55.10^8$ t of Si are uptaken by plants every year. This amount is larger than the corresponding amounts for P, K or Ca. In different soil-plant systems silicon passes from lower soil horizons to upper ones, by the action of plants, in amounts from 100 kg Si/ha to more than 2000 Si/ha in year.

Soluble silicon substances (mono- and polysilicic acids) are uptaken by plant roots and transform in biolith forms. The plant debris, which contain a great amount of silicon bioliths are accumulated on soil surface. Plant silicon bioliths (opal type) return into the soil being dissolved in poly- and monosilicic acids. Consequently, as a result of the soil formation process, there is an increase of the amount of monosilicic, polysilicic acids and amorphous silica in mineral equilibria of the upper soil in terrestrial ecosystems.

The increase of silicon substances (mono- and polysilicic acids) has great effect on Al anion activity, Mg, Ca, Mn, Fe (Lindsey, 1979), pH, organic matter (Orlov, 1984). This process may change the direction of mineral neoformation in soil (increased amount of vermiculite, beidellite, soil chlorite), which is proved by observed data (Sokolova, 1985) and by our thermodynamic calculations.

The theoretical calculation shows that Pinus trees only during 300 years may destroy and transform 18% of clay minerals from lower horizons (from 7 to 30 cm of depth) into upper horizons. Other elements associated with clay (Al, Fe, Mg) move along soil profile with soil waters. By this way it is possible to account for the formation of podzol soil horizon in only 300 years, without considering other geochemical and biogeochemical processes which also reinforced it.

References:
Lindsey, W.L. (1979). *Chemical equilibria in soil*. John Wiley & Sons, N.Y.
Orlov, D.S. (1984). *Soil Chemistry*, Moscow, MGY.
Sokolova, T.A. (1985). *Clay minerals in humidity areas of USSR*.

SYNCHROTRON X-RAY FLUORESCENCE ANALYSIS OF FLUID INCLUSIONS: PROGRESS AND POTENTIAL

Bodnar R. J. and Mavrogenes J. A. (*Fluids Research Laboratory, Virginia Tech*)
Anderson A. J. (*Geology Dept., St Francis Xavier Univ.*)
Bajt S., Sutton S. R. and Rivers M.L. (*Dept. of Geophysical Sciences, Univ. of Chicago*)

One of the most promising directions in fluid inclusion research in recent years has been the application of synchrotron X-ray fluorescence (SXRF) techniques to analyze individual inclusions. SXRF is superior to many other techniques used for this purpose because SXRF (1) is non-destructive and (2) permits analysis of single inclusions. The analytical technique is straightforward and spectra are obtained on inclusions with minimal effort. However, a satisfactory protocol for interpretation of spectra to obtain quantitative information is still in the developmental stages, and large errors may result from incorrect assumptions.

We have initiated a project to identify those factors which most significantly affect the analytical results obtained with SXRF. Synthetic fluid inclusions containing known and variable concentrations of different elements were analyzed on beamline X26A at the National Synchrotron Light Source at the Brookhaven National Lab. Our results indicate that knowledge of the geometry of the inclusion and surrounding host phase, as well as the trace metal content of the host, are the most critical factors for accurate quantitative analysis. Furthermore, simple assumptions concerning the inclusion geometry, rather than actually determining the geometry of each inclusion analyzed, are likely to lead to errors in individual element concentrations that may be in excess of an order of magnitude.

One of the most important questions that must be answered relative to SXRF analysis of inclusions concerns the detection limits for various elements. These are being evaluated by analyzing solutions of known metal concentration contained in capillary tubes of various wall thicknesses and comparing the data with results from synthetic fluid inclusions containing the same solution composition. The results indicate that SXRF detection limits for various elements in homogeneous thick films cannot be applied to fluid inclusions. Rather, detection limits for individual elements in fluid inclusions are a function of inclusion thickness, element concentration and depth of the inclusion within the host mineral. For example, the detection limit for Sr in aqueous solutions in 11 μm inner diameter silica capillaries is approximately 250 ppm. However, for inclusions in quartz, the greater combined thickness of silica that the beam must pass through above and below the inclusion, and the abundant trace elements in the quartz, result in an increase in the background tenfold over that of silica glass capillaries. As a result, Sr could not be detected in any inclusions containing less than 1000 ppm Sr. Moreover, Sr was only detectable in inclusions containing 4,500 ppm if the inclusion thickness was greater than 5μm. Similarly, fluid inclusions containing 1,000 ppm Sr must be at least 100 μm thick for Sr to be detectable. Our synthetic fluid inclusions are rarely thicker than 20 μm, thereby establishing the detection limit for Sr at approximately 2500 ppm.

The much higher practical detection limits determined for metals of interest in most ore deposits studies (Cu, Pb, Zn, Au, Fe, Ag, Mn) preclude the use of SXRF to analyze metals in inclusions from many low temperature deposits, such as Mississippi Valley-type deposits. This occurs because the metal concentrations of the ore forming fluids are estimated to be only on the order of a few tens of ppm, which is significantly below the detection limits for metals in fluid inclusions using SXRF. Additionally, samples with high densities of fluid inclusions and/or with microscopic solid mineral inclusions are not well suited for SXRF analysis because it is rarely possible to obtain a beam path that passes only through a single inclusion of interest and does not intersect either another fluid or solid inclusion.

Our preliminary results document that the SXRF technique has great potential for determining the concentrations of various elements in individual fluid inclusions. Our results further show that use of detection limits determined from homogeneous thick films, as well as other simplifying assumptions in the interpretation of inclusion spectra, can result in significant errors in calculated concentrations. Finally, our results clearly prove that inclusion geometry and the path of the X-ray beam through the inclusion must be known precisely in order to obtain reliable and accurate quantitative information from the spectra.

CRYSTAL SIZE DISTRIBUTION OF SYNTHETIC AND SOIL GOETHITES.

Boero V.,*, Crosa M.*, Franchini- Angela M.**

*DIVAPRA- Chimica Agraria, Via P.Giuria 15, 10126 Torino.
**Dip. di Scienze Mineralogiche e Petrologiche, Via Valperga Caluso 37, 10125 Torino.

Surface area of goethites (α-FeOOH) may be very important in soil adsorption phenomena and can be estimated from the mean crystallite dimension (MCD), as determined by XRD line broadening (Schwertmann,1988).

Nevertheless the surface area determined via XRD is not always in agreement with that obtained by means other methods such as gas and dipoles adsorption.

The knowledge of the crystal size distribution may improve surface area determinations via XRD.

In this work some informations on such a distribution were obtained by studying changes in XRD line profile of synthetic

and soil goethite, caused by the dissolution with dithionite-citrate-bicarbonate (from 5 to 960 min at 25°C). The XRD spectra were analysed by the procedure described by Crosa *et al.*(1994).

The XRD spectra of the dithionite treated samples were compared with those of mixtures of synthetic goethite of different MCD, and discussed in terms of crystal size distribution.

References:
Schwertmann, U. (1988): Iron in Soils and Clay minerals, NATO ASI Series C217; Reidel, 203-250.
Crosa, M., Boero, V., Franchini-Angela, M. (1994). IMA 16th General Meeting (this issue).

THE TETRAHEDRITE-TENNANTITE MINERAL SERIES AND THEIR GENETICAL SIGNIFICANCE

Bogdanov K., Mladenova V. and Phillipov A. (*University of Sofia, Faculty of Geology and Geography, 1000 Sofia, Bulgaria*)

The minerals of the tetrahehdrite-tennantite (TD-TN) series with general formulae $(Cu, Ag)_6$ ^{TRG} $[Cu_{2/3}(Fe,Zn,Pb,Hg,Cd,Mn)_{1/3}]_6$ ^{TET} $(Sb, As. Bi, Te)_4$ ^{SM} $(S, Se)_{13}$ have been found in all volcanic hosted Pb-Zn ore fields (Spahievo, Zvezdel-Pcheloyad, Madjarovo, Lozen) in the Eastern Rhodopes, Bulgaria. The TD-TN minerals are most commonly observed in assemblage with sphalerite, chalcopyrite and galena (Lozen, Spahievo) as well as with Ag, Sb and Pb sulphosalts (Madjarovo, Zvezdel-Pcheloyad).

The TD-TN mineral series from the Eastern Rhodopes are characterized by widespread predominance of TD and constant presence of Fe, Zn and Ag. The Madjarovo and Zvezdel-Pcheloyad display higher Ag contents in both TD-TN minerals and ores as compared to Spahievo and Lozen ore fields where Mn was found in the TD-TN series.

According to $lgfS_2$-$lgfO_2$ diagram (fig. 1) and fluid inclusion studies the TD-TN bearing mineral assemblages in the main base metal deposits from the Eastern Rhodopes have been deposited at $lg\ fO_2$= -37-39, $lg\ fS_2$= -7-14 and pH 6-8 and temperatures 270-240°C.

The earlier gold-bearing mineral assemblages in the studied area where the fineness of gold is over 850 ‰ have been formed at values of $lgfS_2$ -6-8 and temperatures below 280°C. The Sb and Ag poor TN have been crystalized at $lg\ fS_2$ below -15. As a result of leaching from TD-TN the Ag has been fixed as electrum with fineness less than 700‰ in the late low temperature Au-Ag assemblages (240-180°C) in the studied deposits.

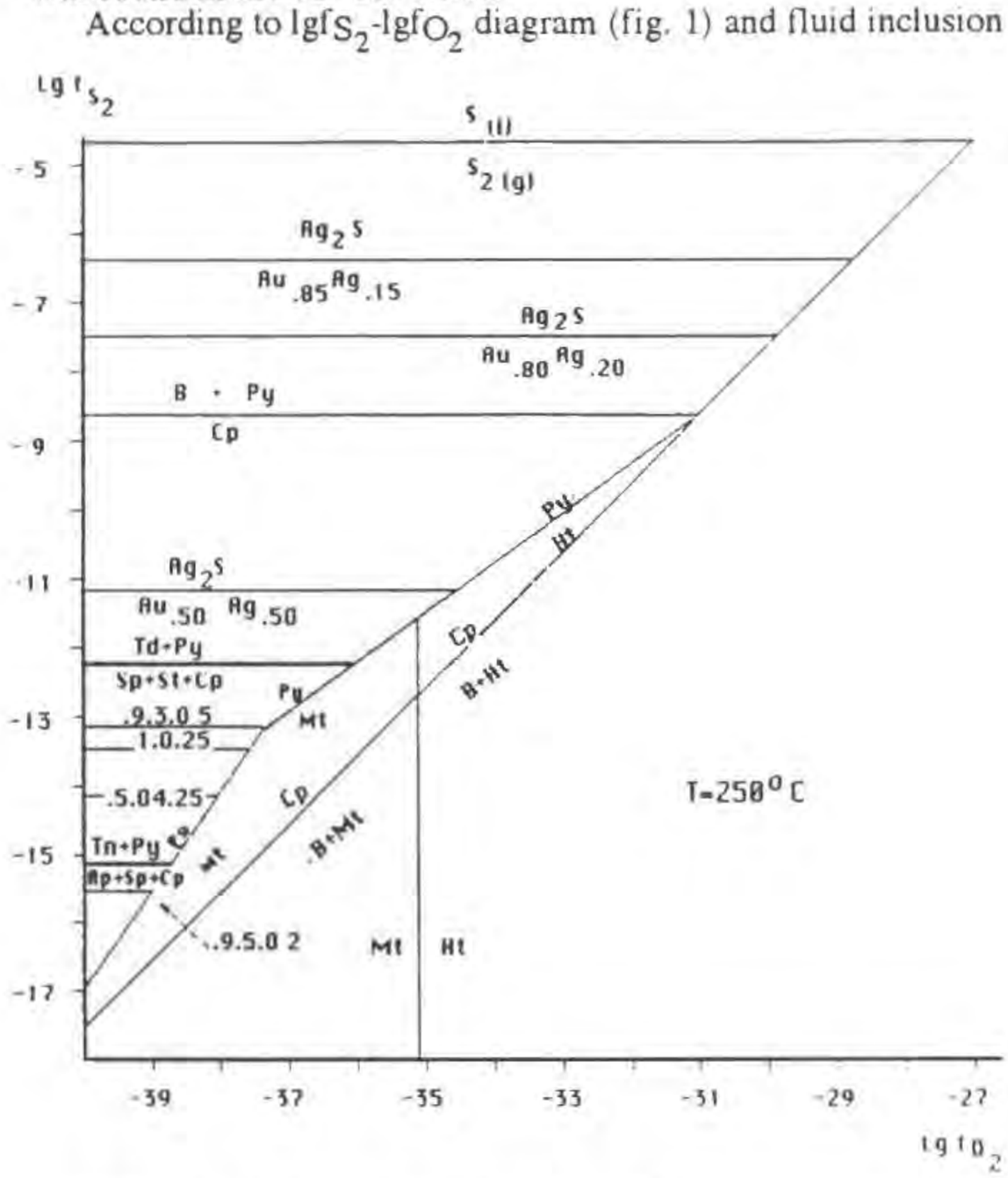

Fig. 1. $lgfS_2$-$lgfO_2$ diagram of tetrahedrite-tennantite assemblages from volcanic hosted ore fields in Eastern Rhodopes, Bulgaria

THE IMPORTANCE OF K IN THE OCCURRENCE AND STABILITIES OF MINERALS IN THE MILARITE (OSUMILITE) AND TUHUALITE GROUPS.

Boggs R.C. (Dept. of Geology, Eastern Washington Univ.)

The milarite and tuhualite groups are two structurally related groups of silicates (Boggs, 1986, 1987) with the general formulas $^{12}A^{9}B_2{}^{4}C_3{}^{6}D_2{}^{4}T_{12}O_{30}$ and $^{10}A_2{}^{9}B_2{}^{4}C_2{}^{6}D_2{}^{4}T_{12}O_{30}$ (with superscripts indicating the coordination of each site). K in the 12-fold A-site is important in stabilizing the milarite structure (hexagonal with double 6-membered rings) in preference to the tuhualite structure (orthorhombic pseudo-hexagonal with Na in the 10-fold A-site, and with double 6 repeat chains). The occurrence of similar minerals in the two groups that occur in both structural types (sogdianite and zektzerite, osumilite and tuhualite, and sugilite and emeleusite) appears to be controlled by the availability of K in the environment of occurrence.

All known milarite group members (except yagiite with about 35% K and 65% Na) have the A-site nearly fully occupied by either K or Ba. A recent observation of the substitution $^{D}Ca^{2+} + {}^{C}Al^{3+} \rightarrow {}^{D}(Y,REE)^{3+} + {}^{C}Be^{2+}$ in milarite by Černý *et al.* (1991) documents a range of substitution from milarite, $K•_2(Be_2Al)(Ca)_2Si_{12}O_{30}$ to $K•_2Be_3(CaY)Si_{12}O_{30}$. They suggest that the continued substitution of Y for Ca in the D-site with a corresponding substitution of • for K in the A-site would give a milarite group end member $••_2Be_3Y_2Si_{12}O_{30}$. I believe that this composition would be unstable in the milarite structure and instead an appropriate composition would be either $•_2Na_2Be_2Y_2Si_{12}O_{30}$ (tuhualite structure) or $K•_2Be_3Y_2(Si_{11}Al)O_{30}$ (milarite structure).

Many more members of the milarite group (13) are known than of the tuhualite group (3) as shown in the chart below which show the various members of the two groups with the equivalent members of the other group, many of which are synthetic (Sy) or hypothetical (**). The listed members of each group are given by the following symbols: Armenite (Ar), Brannockite (Br), Chayesite (Ch), Darapiosite (Da), Eifelite (Ef), Merrihueite (Me), Milarite (Mi), Osumilite (Os), Osumilite-(Mg) (Og), Poudretteite (Po), Roedderite (Ro), Sogdianite (So), Sugilite (Su), Yagiite (Ya), Zektzerite (Zk), Emeleusite (Em) and Tuhualite (Tu).

Milarite Group Members		Tuhualite Group Members	
Ar	$Ba(H_2O)_2Ca_2Al_3Si_9Al_3O_{30}$	**	$Na_2•_2Ca_2Al_2Si_{12}O_{30}$
Br	$K•_2Sn_2Li_3Si_{12}O_{30}$	Sy	$Na_2•_2Sn_2Li_2Si_{12}O_{30}$
Ch	$K•_2(Mg,Fe)_2(Mg,Fe,Fe^{3+})_3Si_{12}O_{30}$	**	$Na_2(•Na)Mg_2(MgFe^{3+})Si_{12}O_{30}$
Da	$K(•Na)(Mn,Zr)_2(Li,Zn,Na)_3Si_{12}O_{30}$	**	$Na_2Na_2(Mn,Zr)_2(Li,Zn)_2Si_{12}O_{30}$
Ef	$KNa_2(MgNa)Mg_3Si_{12}O_{30}$	Sy	$Na_2Na_2Mg_2Mg_2Si_{12}O_{30}$
Me	$K(•Na)(Fe,Mg)_2(Fe,Mg)_3Si_{12}O_{30}$	**	$Na_2Na_2Fe_2Fe_2Si_{12}O_{30}$
Mi	$K(H_2O)_{0.5}Ca_2(Be_2Al)Si_{12}O_{30}$	**	$Na_2Na_2Ca_2Be_2Si_{12}O_{30}$
Os	$K•_2Fe_2(Al,Fe)_3(Si,Al)_{12}O_{30}$	**	$Na_2•_2Fe_2Al_2Si_{12}O_{30}$
Og	$K•_2Mg_2(Al,Fe)_3(Si,Al)_{12}O_{30}$	**	$Na_2•_2Mg_2Al_2Si_{12}O_{30}$
Po	$K•_2Na_2B_3Si_{12}O_{30}$	**	$Na_2Na_2Na_2B_2Si_{12}O_{30}$
Ro	$K(•Na)(Mg,Fe)_2(Mg,Fe)_3Si_{12}O_{30}$	**	$Na_2Na_2Mg_2Mg_2Si_{12}O_{30}$
So	$K•_2Zr_2Li_3Si_{12}O_{30}$	Zk	$Na_2•_2Zr_2Li_2Si_{12}O_{30}$
Su	$KNa_2Fe_2Li_3Si_{12}O_{30}$	Em	$Na_2Na_2Fe_2Li_2Si_{12}O_{30}$
Ya	$(Na,K)(•,Na)Mg_2(Al)_3(Si,Al)_{12}O_{30}$	**	$Na_2•_2Mg_2Al_2Si_{12}O_{30}$
**	$K•_2Fe_2Fe_3(Si_{11}Al)O_{30}$	Tu	$Na_2•_2Fe_2Fe_2Si_{12}O_{30}$

Because of the range of possible substitutions many more members of both groups could exist. Possible occupancies based on reported occupancies and the similarities of the two structures are as follows:

	Milarite Structure	Tuhualite Structure
A-site	K, Ba, Na, Rb, Ca?	Na
B-site	H_20, Na, •, Ca?, K?	Na, •, Ca?, K?
C-site	Ca, Sn, Mn, Zr, Mg, Fe^{2+}, Na, Ti, Fe^{3+}, Al, Y, REE	Ca, Sn, Mn, Zr, Mg, Fe^{2+}, Na, Ti, Fe^{3+}, Al, Y, REE
D-site	Al, Li, Zn, Na, Mg, Fe^{2+}, Fe^{3+}, Be, B, Mn, Si	Al, Li, Zn, Na, Mg, Fe^{2+}, Fe^{3+}, Be, B, Mn, Si
T-site	Si, Al	Si, Al

New members of both groups can be expected in a wide range of low T - low P environments and new members of the tuhualite group should be particularly expected in low T - low P, Na rich environments.

References:
Boggs, R.C. (1987). Geol. Soc. Am., Abst. Prog., 19, 594.
Boggs, R.C. (1986). Abst. Prog., I.M.A. 14th Gen. Mtg, Stanford.
Černý, P, Hawthorne, F.C., Jambor, J.L. Grice, J.L. (1991). Can. Min., 29, 533-541.

ANALYSIS OF HEMATITE NANOCRYSTALLINE PARTICLES BY ANTIFERROMAGNETIC RESONANCE (AFMR) AND MÖSSBAUER SPECTROSCOPY.

Boizot B., Morin G., Ildefonse Ph., and Calas G. (Laboratoire de Minéralogie-Cristallographie, UA CNRS 09, Universités Paris 6 et 7 and IPGP), Bonnin D. (Laboratoire de Physique Quantique, ERA CNRS 676, ESPCI, Paris)

The temperature (T_b) of the magnetic transition from superparamagnetic to anti-ferromagnetic state is an important parameter which governs the properties of divided magnetic oxides. As T_b is largely dependent on the crystallite size, its determination provides a structural tool to assess the size and shape of these divided materials. We present data on hematite nanoparticles (size< 200 Å) studied with Mössbauer spectroscopy and AFMR in order to correlate the results obtained with these two methods. The temperature dependence of the Mössbauer and AFMR spectra have been studied between 90 and 450 K.

At room temperature, hematite particles smaller than 135 Å are characterized by a superparamagnetic doublet in Mössbauer spectroscopy and a Lorentzian shape in AFMR. Below the blocking temperature (T_b), Mössbauer spectra exhibit a magnetic sextuplet and AFMR resonances are weak and asymmetric. The AFMR line shape varies continuously with temperature. In addition, at one fixed temperature, the lineshape of AFMR and Mössbauer spectra shows important variations in the superparamagnetic state among the samples. Surface sites, in addition to the volume of the magnetic domains, may cause such variations.

T_b has been determined by AFMR and Mössbauer spectroscopy. The variation of AFMR signals with temperature allow an accurate determination of T_b which corresponds to a maximum anisotropy. T_b determined from AFMR increases from 160 to 220 K as the size of the magnetic domains of hematite particles increases. T_b is correlated with the assumed magnetic domain size of hematite nanocrystals.

Both AFMR and Mössbauer spectroscopy are then sensitive tools to investigate magnetic nanoparticles. However, AFMR can detect lower concentrations (100 ppm) of iron oxides particles than Mössbauer spectroscopy (1 %). The lower quantity of material required with AFMR allows its use for investigating highly diluted samples, such as the suspended materials transported in natural rivers. These nanocrystalline solids (i.e. size<100Å) are difficult to characterize by conventional structural tools. Preliminary spectra of these materials will be presented and discussed.

• THE STRUCTURAL-CHEMICAL DATA BASE OF SILICATE MINERALS

Bokij G.B., Vrublevskaja Z.V. *(Institute of Ore Mineralogy (IGEM) RAS, Moscow)*, Schedrin B.M., Burova E.M. *(Moscow State University, Moscow)*

An automatic data base of minerals has been realized on the basis of mineral classification. Up to day we have worked out an automatic base for silicates.

The investigation and using of minerals are very difficult without a rigorous classification. We suggest the system of classification where the lower taxon is a mineral species (Bokij, 1985). A mineral species corresponds to a simple substance or a crystalline chemical compound, obtained as result of geo- or cosmo-chemical processes. The suggested classification is combined with the chemical classification. On the first levels the classification is based on the anions. The system of the designation of minerals is decimal (Bokij, 1992) and connected with the Periodic Table.

Every mineral in this data base occupies a definite place in the mineral classification and it may receive a graphic picture of its structure.

References:
Bokij, G.B. (1985) *Notes of Union Mineral Society*, C **14**, 523 (in Russian).
Bokij, G.B. (1992) *Miner. Magazine* **14**, 47 (in Russian).

ORDER-DISORDER PHASE TRANSITION IN MICROSOMMITE: EXPERIMENTAL DATA AND MONTE CARLO SIMULATION

Bonaccorsi E., Merlino S. *(Dept. of Earth Sciences, Univ. of Pisa)* and Macedonio G. *(CNR CS Geol. Strutt. Dinam. App., Pisa)*

Minerals belonging to the davyne group are interesting not only for their crystal chemical features, but also for the ordering phenomena and the phase transitions that they exhibit when thermal and compositional conditions change. Taking in account the different $(SO_4)/Cl$ ratio, the minerals of the davyne group may be distinguished in:

microsommite	$[Na_4K_2(SO_4)]$	$[Ca_2Cl_2]$	$[Si_6Al_6O_{24}]$
davyne	$[Na_4K_2(SO_4)_{0.5}Cl]$	$[Ca_2Cl_2]$	$[Si_6Al_6O_{24}]$
quadridavyne	$[Na_4K_2Cl_2]$	$[Ca_2Cl_2]$	$[Si_6Al_6O_{24}]$

where microsommite and quadridavyne, respectively, display three- and four-fold unit cell with respect to the unit cell of davyne. The chemical formulae are written emphasizing the different structural units.

The following discussion refers only to the order-disorder transition which takes place in microsommite by changing the temperature. In microsommite each channel is ordered along *c*, with regular sequence of Na-populated layers, at the same level of $(SO_4)^{2-}$ group, and layers populated mainly by potassium. This ordered sequence may realize in two different but energetically equivalent ways; the ordered structure of microsommite is due to the regular distribution of such two possible configurations in the (**a**,**b**) plane. The ordering or disordering processes can be easily monitored by measuring the intensity I of the superstructure reflections, where $I = kQ^2$, with Q = order parameter. From equilibrium and kinetic experiences, the critical temperature and the activation enthalpy of the process could be evaluated (715°C; 30 kcal/mol).

For the above mentioned peculiarities (perfect order of the channels along *c*, order which may realize only in one of two ways, and long-range correlation in (**a**,**b**) plane of such ordered channels), this process can be properly described by a bidimensional Ising model for a "triangular" lattice. A Monte Carlo simulation with repulsive nearest-neighbor (NN) and actractive next-nearest-neighbor (NNN) couplings with null external field was performed for different lattice temperatures. Results reproduce: (1) the ground state configuration for low temperatures below a first phase transition to an intermediate ordered state which reproduces the

microsommite structure at room temperature, and (2) a second phase transition to a disordered state reproducing the microsommite behaviour at high temperatures. A parametric study was performed by varying the NNN/NN coupling ratio; it shows a decreasing of the first order-disorder transition temperature with decreasing NNN coupling. Calculations were performed on a 30x30 spin lattice with periodic boundary conditions. Between 100 and 500 Monte Carlo iterations were discarded until thermal equilibrium was reached, and about 1000 to 2000 iterations were retained for average computations. Results show the lattice configurations, the order parameter and the specific heat behaviour for different NNN/NN ratio coupling and temperatures.

STRUCTURAL MODEL OF Sb_2AsS_2: THE SYNTHETIC ANALOGUE OF PÄÄKKÖNENITE?

Bonazzi P., Borrini D. (*Dip. Sci. Terra, Univ. Firenze, Italia*) and Olmi F. (*C.N.R.- C.S.M.G.A, Firenze, Italia*)

During an experimental study on the pseudobinary system Sb_2S_3 - Sb_2As_3, a phase of composition equivalent to the formula $Sb_{2.12}As_{0.89}S_{1.99}$ was obtained, from presynthesized stibnite (Sb_2S_3) and a stibarsen - like intermetallic compound (Sb_2As_3), under dry conditions in sealed silica tubes at 480 °C.

The powder pattern of the synthetic phase is fairly similar to that of pääkkönenite, Sb_2AsS_2, a mineral discovered by Borodayev *et al.* (1982) in the antimony ore of the Kalliosalo deposit (Seinäjoki region, Finland). According to these authors, pääkkönenite is monoclinic with the following lattice parameters: a = 5.372(7), b = 3.975(5), c = 11.41(1) Å, β = 89.71(15)°, V = 243.6 Å^3.

Weissemberg photographs, performed on apparently single crystals of the synthetic phase, pointed towards an orthorhombic unit cell with parameters a = 10.7, b = 3.9, c = 22.6 Å, and Fmm2, F222 or Fmmm as possible space groups. Nonetheless attempts to solve the structure by direct methods in these space groups met with failure. In the C2/m space group (reflections re-indexed with the transformation matrix 1 0 0 / 0 -1 0 / -½ 0 -½), a more reliable solution was found by means of EEES (an automatic multisolution direct method of SHELX). The initial cycles of structure refinement were performed in the C2/m space group (R = 20 % with isotropic thermal parameters). Further LS cycles, carried out in the Cm space group, led to R = 9.6%. Cell parameters, determined using 25 high-theta reflections, are: a = 10.75(2), b = 3.959(3), c = 12.49(2) Å, β = 115.25(8)°, V = 480.8 Å^3.

The structure of synthetic Sb_2AsS_2 can be described as a sequence of sheets stacked along the **a** axis and mutually displaced by 1/2 b. Each sheet consists of $Sb_4S_4As_2$ ribbon - like units (parallel to the **b** axis) similar to the Sb_4S_6 chains of stibnite (Bayliss & Nowacki, 1972) but linked together by As - As bonds. Bond distances within the sheet range from 2.43 to 3.05 Å and interatomic distances between atoms belonging to different sheets are greater than 3.13 Å.

References:
Bayliss, P. & Nowacki, W. (1972). Zeit. Krist., **135**, 308 - 315.
Borodayev, Yu. S., Mozgova, N. N., Ozerova, N. A., Bortnikov, N. S., Oyvanen, P., Iletuynen, V., (1982). Internat. Geology Rev., **24** (10), 1234 - 1240.

CHALCOPYRITE AND SPHALERITE "DISEASES" - CRYSTAL GROWTH BY SOLID-STATE DIFFUSION

Bonev I.K and Radulova A. (*Geol. Inst., Bulg. Acad. Sci., Sofia*)

Some important aspects of the crystallography and origin of the chalcopyrite-sphalerite intergrowth-textures are still not well understood. An attempt has been made to obtain more information about their three-dimensional morphology, crystallographic relationships, spatial distribution, chemical features and geological setting, as a basis for discussion of their growth mechanisms, and for understanding the substantial diversity of the two types of inclusions - sphalerite and chalcopyrite.

1. Chalcopyrite inclusions in sphalerite - "chalcopyrite disease"

Only recently evidence was given for the metasomatic formation of this inclusions (Barton & Bethke; Bortnikov et. al., etc.), which was also proved experimentally (Eldridge et al.; Kojima & Sugaki; Bente & Doering, etc.). In addition to a microscopic study in doubly polished thin sections, we succeeded making a direct SEM study of chalcopyrite inclusions extracted from the sphalerite matrix. For these purposes a chemical procedure for selective dissolution of sphalerite was developed.

The following types of inclusions were found: 1. isometric crystals of pseudooctahedral or scalenohedral habit; 2. strongly branched dendrite-like fine skeletal crystals; 3. thin platy and needle-like crystals; 4. platy {112} twins. All inclusions are bounded by crystal faces, mainly {112} and {102}, and also by rough stepped surfaces. The two phases are in parallel crystallographic orientation. The well known "blebs", "dots", "lamellar", "quadrangle" and other forms are different sections of such chalcopyrite crystals.

It is assumed that the volume reduction during the topotaxic replacement of the sphalerite matrix (2-3 linear %) facilitates the diffusional flux and exchange of Cu^{1+} and Zn^{2+} on the interfaces (accompanied also by Fe^{2+} to Fe^{3+} transition) thus realizing layered growth of the included crystals. The common concentric or linear zoning is of epigenetic diffusional type, the larger and sparse blebs being located in more distant positions, under the control of rough defects (cleavage surfaces, twins).

The bulk microprobe analysis shows that the initial Fe content in the inclusion-free and inclusion-rich areas of sphalerite remains almost unchanged, the differences concern the Cu and Zn content.

2. Sphalerite stars in chalcopyrite - "sphalerite disease"

The sphalerite "stars" represent different sections of a skeletally developed "negative rhombododecahedron" (Vorontzov et al.; Shafranovskii; Bonev) in a parallel-axial orientation with respect to the matrix. The stress around the larger in volume sphalerite nuclei creating dislocation bundels (mainly in pseudododecahedral planes), thus controls the anisotropic diffusion and skeletal development of the inclusions. The stars are always accompanied by small characteristic {102} sector twins. In the twinned areas the a and c axes are exchanged ($2a/c$ = 0.970<1) , so that the local dilatational stress around the growing stars is relaxed. In some cases the bulk Zn content of sphalerite-bearing chalcopyrite is higher than the maximum acceptable for solid solutions Zn. The numerous sphalerite stars in such chalcopyrites are outposts of a bulk sphalerite replacement front, so being a manifestation of the metasomatic "sphalerite disease". The metasomatic and exsolution growth mechanisms are of the same type, the difference between them is mainly in the source of Zn ions. Other growth mechanisms proposed (Vorobyev; Marignac) have been also discussed.

Thus, it is assumed, that in the diffusional crystal growth in solid-state, especially during formation of chalcopyrite-sphalerite inclusions, the volume relationships are of great significance.

• KAOLIN AND ALUNITE ORE CHARACTERIZATION BY MULTISPECTRAL IMAGE ANALYSIS TECHNIQUES.

Bonifazi G.*, Gorga R.** (* *Dipart. Ing. Chimica, Materiali, Materie Prime, Metallurgia, Univ. "La Sapienza", Via Eudossiana 18, 00184 Roma; ** C.N.R. Ist. Trattamento Minerali, Via Bolognola, 7 00138 Roma)*

After a brief description of the geological characteristics of the median ridge of Roccastrada and Monticiano mountains (Grosseto, Italy) and an analysis of the main petrographical characteristics of the mineralization inside the Pliocene terrain in ignimbritic facies, chemical and mineralogical–petrographical detailed results are reported with particular reference to ore samples coming and directly sampled in the above mentioned area. Following detailed microscopic studies and extensive analyses carried out by microprobe, the possibility to utilize digital procedures able to define mineralogical maps related with the species of interest have been tested. Real colour images (RGB) have been thus acquired and processed to extract those textural and structural characteristics of interest for the further beneficiation steps. The procedures have been developed and tested with particular reference to:

– biotite relics partly kaolinized or surrounded by micro or sub micro granular kaolin;

– feldspar present as phenocrystals or partly substituted by kaolinitic and alunitic products;

– quartz elements immersed in a completely kaolinized matrix.

After the spectral identification (RGB components) of the different mineral species, their characteristics are defined following a "supervised" classification criteria, realizing this way: i) a classification of the different samples on the basis of the "kaolin quality content", ii) an analysis of the morphological characteristics of the different mineral species, iii) an evaluation of the degree of kaolinization and/or alunitization of the different original mineral species constituting the rocks. A discussion of the results is reported, with particular reference to the problems related with the processing of digital colour images resulting from petrographical thin sections.

THE WESTERN MEDITERRANEAN PERMO-TRIASSIC ALKALINE PROVINCE: A MINERALOGICAL OVERVIEW

Bonin B. (*Dept. des Sciences de la Terre, Univ. de Paris-Sud, Orsay*)

The amalgamation of discrete terrains of contrasting origins and compositions onto Pangæan mega-continent, was achieved in Upper Carboniferous and followed by subsequent breakup during the Permo-Triassic. Numerous alkaline magmatic complexes were emplaced during two discrete eruptive episodes: (i) Mid-Permian (280-265 Ma), (ii) Permo-Triassic (250-230 Ma). Isotopic data substantiate mantle origin and further crustal contamination overprints.

During the first episode, subvolcanic complexes were emplaced throughout the whole province, *i.e.* from Morocco to Corsica-Sardinia to the Alps to the Carpathians. They consist of an aluminous suite with major *biotite subsolvus* granite and minor gabbro, monzonite and syenite. Rock-forming minerals display an evolutionary trend toward Fe-enriched compositions but no extremely Mg-rich composition was detected. The suite is interpreted as a magma series defined by the gabbro -> monzonite -> granite liquid line of descent. The associated fractionating assemblage of olivine + clinopyroxene + orthopyroxene + plagioclase + amphibole + accessory minerals is exposed as gabbro-norite-anorthosite layered complexes. Silica-oversaturation and Al-rich composition of the residual melts were controlled by amphibole fractionation, while trace-element geochemistry was governed by accessory (apatite + zircon + allanite + chevkinite) assemblage.

The second episode, more restricted in area (Corsica-Sardinia, Alps), is characterized by the large range of highly evolved A-type granitoids, emplaced as subvolcanic ring-complexes and huge cauldrons. Granites and rhyolites of peraluminous (*biotite hypersolvus* and *subsolvus*), metaluminous (*fayalite hypersolvus*) and peralkaline (*arfvedsonite ± ægyrine hypersolvus* and *albitic*) compositions define two discrete associations: aluminous and peralkaline, both illustrating extremely Fe-enriched evolutionary trends. The chief rock-forming mafic silicate of the aluminous association is mica, with the biotite -> siderophyllite -> Li-mica ± celadonitic muscovite sequence. Rock-forming mafic silicates of the peralkaline association are olivine, clinopyroxene and amphibole, with the fayalite + hedenbergite -> Ca-amphibole -> Ca-Na amphibole ± silicic mica -> Na-amphibole + ægyrine sequence. Hydrothermal alteration effects have modified the original magmatic compositions, even at the volcanic level.

P-T PATHS FOR THE INTERNAL PENNINIC MASSIFS (WESTERN ALPS)

Borghi A., Compagnoni R. & Sandrone R.
(Dept. Mineralogical and Petrological Sciences - Univ.of Torino)

The Internal Penninic Massifs of the Western Alps (IPM) record a metamorphic evolution characterized by two main events: an eclogite facies "eo-Alpine" event (usually considered Cretaceous in age) and a greenschist facies "meso-Alpine" event (Upper Eocene in age). To better constrain the whole P-T path and, particularly, the transition between the two events, a petrographic and geo-thermobarometric study was performed on selected samples from the Monte Rosa, Gran Paradiso and Dora-Maira Massifs.

All the samples studied exhibit a similar Alpine evolution marked by two events.The older HP event occurred under LT eclogite-facies conditions (T = 500 - 550 °C; P = 12 - 15 kbar). The eclogitic climax is followed by a retrograde decompressional evolution, lower than the garnet stability field. The younger LP event is characterized by an initial prograde evolution under moderately decompressional conditions (T = 500 - 530 °C; P = 3-4 kbar). This event is marked by the development of oligoclase around albite, biotite after chlorite, Ca-amphibole and garnet. This post-eclogitic garnet generation displays a prograde and decompressional growth zoning.

P-T paths of the three IPM result to consists of two metamorphic peaks, which developed approximately at the same T, but at significantly different P. Consequently, the tectono-metamorphic history is characterized by a geothermal gradient progressively increasing from 12 to 40 °C/km.

The prograde part of the eo-Alpine trajectory is consistent with a process of subduction of oceanic lithosphere; its decompressional part is compatible with a moderately rapid uplift (0.6 mm/a), which occurred while subduction of cold oceanic lithosphere was still active. The meso-Alpine trajectory is consistent with the thermal re-equilibration, consequent to the continental collision.

• SPECIFIC FEATURES OF METAMORPHOSED ORES FROM RANGPO POLYMETALLIC DEPOSIT (SIKKIM, INDIA)

Borodaev Yu.S. (*Dept. of Geology, Moscow Univ., Russia*), Mozgova N.N. (*IGEM RAS, Moscow, Russia*) and Gandhi S.M (*Central Res. and Dev. Lab., HZL, Udaipur, India*)

Textures of the ore minerals due to deformation have been described in many types of deposits, but metamorphism of ore minerals has not been sufficiently studied yet. This investigation of metamorphosed ores is especially interesting because of current thinking (Mookherjee, 1967; Parilov, 1984; Starotsin et al. 1990) on possibility of appearance of sulphide melts or/and high concentrated brines–fluid melts due to metamorphism of ore.

Samples of metamorphosed ore from Rangpo polymetallic deposit have been studied by means of ore microscopy and EMPA. Sphalerite, pyrrhotite, calcopyrite, magnetite, arsenopyrite, and Co–sulpharsenides are the main ore minerals in the sample studied. Pyrite, galena and Ag–fahlores are less abundant. Rare minerals: molibdenite, sulphosalts, and native Bi and Ag. The ore minerals are intimately interlocked with silicate gangue (garnet, orthorhombic pyroxene, amphibole and others).

The interesting features of the ore are the following: 1. oblong shapes of sphalerite grains related to the schistosity of slates; 2. absence of chalcopyrite and/or pyrrhotite emulsion inclusions in sphalerite and vice versa star–shaped inclusions of sphalerite; 3. abundant post–metamorphic appearance of magnetite, capturing

curved pyrrhotite layers in schistose textures of ore; 4. droplets of chalcopyrite–pyrrhotite inclusions in magnetite porphiroblasts and numerous droplets of non–opaque inclusions in pyrrhotite grains; 5. myrmekitic ore microtextures formed by predominant galena intimately associated with minor Ag–tetrahedrite, native Bi and pyrrhotite between the big grains of sphalerite and magnetite; 6. filling the cracks in garnet idiomorphic grains by magnetite and sulphides without conducting veinlets and noticeable corrosion of the garnet grains; 7. zonal rhombic–shaped crystalls of Co–sulphoarsenides, formed by alternating zones of sulpharsenides and galena without conducting veinlets of galena; 8. finding of new unusual complex sulphide ("mineral G") $Cu_5Fe_6Pb_6$ $(Bi,Se,As)_2$ $(S,Se,Te)_{21}$ containing almost all (apart from Zn) ore forming elements; 9. absence of isomorfic Ag– and Bi–impurities in galena, notwithstanding these elements are available in Rangpo ores.

These features of the Rangpo ores resemble those found in the smelting products in furnaces. According to Edwards (1954), magnetite crystals are the common product of many matters, speisses and slags; magnetite in slags often contains droplets of different substances (f.e. Cu–sulphides); eutectic intergrowths, formed by Pb– and Cu–sulphides, occupy small intersticial areas in the smelting products; Cu–As–Sb–complex compound, which may be compared with "mineral G" from Rangpo, was observed in the matte, containing semimetals. Such resemblance permits to think that partial melting of natural ore minerals took place during metamorphism of the Rangpo ores. This point of view is supported by experimental works on sulphide systems (Brett & Kullerud, 1966; Lowrence, 1967 and others). They indicate that partial melting of sulphide association may occur at temperature around 700°C. According to Lowrence, the presence of fluxes (water vapour, fluorine and others) may significantly lower the melting point of Pb–Zn–Fe–sulphide ores.

SULFIDE THERMOMETRY: PROBLEMS AND OPPORTUNITY.

Bortnikov N.S. *(Institute for Geology of Ore Deposits, Petrography, Mineralogy and Geochemistry, Russian Academy of Sciences).*

Examples of application of mineral thermometry based on the component distribution are drawn. These data have also been employed to test for chemical equilibrium versus disequilibrium.

The distribution of iron and zinc between coexisting sphalerite and stannite from 12 tin deposits follows the Nernst Low and infer chemical equilibrium during mineral deposition. Experimental curves give temperatures of 150 to 330°C which are in good agreement with fluid inclusion data. However the contradiction in the thermometric expressions makes doubtful the application of this mineral pair in thermometry.

The distribution of cadmium and manganese between coexisting galena and sphalerite have been studied from more then 30 deposits. A large number of cadmium distribution points gave temperatures ranged from 150 to 420°C. These values tend to be about 40-200°C higher then the filling temperatures. The observed differences are considered to lie within pressure correction values. The assumption that coexisting sphalerite and galena were equilibrated with respect to cadmium distribution et majority deposits seems to be reasonable.

Several samples studied gave a good agreement between temperatures based on the manganese distribution and those estimated from filling and cadmium-galena-sphalerite geothermometer. However, most of the samples gave rather unreliable temperatures. From these results it is concluded that geothermometry based on manganese distribution between galena and sphalerite is not useful.

The arsenic contents in arsenopyrite from 12 deposits range from 28 to 33.3 at.% in assemblages with pyrite and from 30.5 to 33 at.% in assemblages with pyrite and pyrrhotite. The temperatures estimated on the arsenopyrite compositions tend to be more then 100°C higher then those obtained by different techniques. The differences may be explained as results of disequilibrium, and a pure experimental calibration.

The *FeS* contents in sphalerite coexisting with arsenopyrite + pyrite, arsenopyrite + pyrrhotite, arsenopyrite + pyrrhotite + pyrite range from 1.5 to 1.7 mole per cent, from 16.1 to 20.1 mole per cent and from 10.8 to 18.7 mole per cent. The temperatures estimated on the base of the arsenopyrite and sphalerite compositions are in the difference from those obtained by other techniques in the most deposits

• MINERAL FORMS OF PRECIOUS METALS IN OXIDIZED ORES OF SALAIR MINE AS IMPORTANT TECHNOLOGICAL FEATURES (WEST SIBERIA)

Bortnikova S.B., Lasareva E.V., Airijants A.A. *(United Institute of Geology, Geophysics and Mineralogy, Novosibirsk)*

1. Salair mine exploits a group of barite–nonferrous deposits with the accompanying gold and silver mineralization. Multi–stage history of ore–forming development was responsible for the complex composition of ores. Four major components (Pb, Zn, Cu, $BaSO_4$) together with the minor componentes Au, Ag, Cd, Se are liberated). Oxidized ores are quarried and enriched at the factory by gravitation and flotation. Recently hard types of ores have becom most typical. They are characterized by high contents of oxidized hard floated forms of metals in combination with fine intergrowth of the minerals. As a result the losses of precious metals increase during beneficiation.

2. Mineral forms of precious metals have been studied in through a comprehensive mineralogical investigation, including SEM method and microprobe analyses. It has been found that silver in unoxidized parts of ore bodies is mainly present as single minerals (hessite, argentite, pearceite) or as isomorphic substituent in sulphides (pyrite, galena) and sulfosalts of tetrahedrite group. Silver released during oxidation and destruction of primary inerals, which took place in hypergenesis zone, is partly redeposited as aggregates of achantite (sometimes with native silver and its amalgam) or single particles of chlorargyrite (AgCl) in goethite. Silver, after migration with underground water downwards weathering profile, precipitates in the secondary rims of acanthite with covellite and chalcocite in cementation zone. Generally acanthite makes up the inner part of complex reaction rims in galena, then covellite deposits, in which variable content of silver is present.

3. Gold is present in native form usually as lump– and wire–looking grains, typically 02–0.05 mm in size. Its fineness is 620 as average (max=800, min=520). 70% of grains are enveloped by iron hydroxide. Outer skins of grains may be divided in two types. The first, resulting from higher velocity of silver dissolution from the matrix, is very porous. As a rule these reaction rims were continuously developed around the gold grains. Lace–like interrupted outer skins of the second type probably appeared as a result of the secondary growth of colloidal gold on the surface of the grains. In addition, numerous small gold particles with high fineness are observed in the outer skins of iron oxide around primary gold. The authors believe that these gold particles were formed by hypergene processes during deposition of dissolved gold in iron hydroxide. Insignificant part of the gold (5–10%) is dispersed in the sulfides (pyrite, galena, sphalerite) probably

isomorphically. Sometimes goethite contains extremely thin scattering of gold.

4. The results we have obtained give a good mineralogical basis to decrease the losses of precious metals. It is now clear that only silver connected with sulfides, as well as that included in them, is extracted by flotation. At the same time, the silver minerals placed in oxides and carbonates of Fe, Pb, Cu are coming out in tailings. It has been found that gold present as relatively coarse sand (0.16–0.25 mm) is extracted by gravitational methods, but fine-grained gold associated with goethite and clay minerals is lost. Since the majority of gold in Salair mine has been mistakenly considered as scattered in sulfides, the main mineral processing method was flotation whereas gravitation was often expected from basic circuit. This explains why very high quantity of gold is regularly lost.

5. Our investigations allow to recommend a new technological line to upgrade the existing situation. This new circuit has, at its basis, essentially a new classifying principle of material separation. The finest fractions may be treated by modern Jigging technologies for enrichment of gold. Middle coarseness of substance needs reprocesssing by parallel shaking tables, which allow to extract native gold entirely. Electrochemical precipitation can be applied for silver enrichment. Gold and silver associated with sulfides may equally be treated by flotation with subsequent cyanidation of the resulting concentrates.

$^{13}C/^{12}C$- AND $^{18}O/^{16}O$-FRACTIONATION DURING SYNTHESIS OF $BaMg(CO_3)_2$ AND $PbMg(CO_3)_2$

Böttcher, M.E. (Geochem. Institute, Univ. of Göttingen, F.R.G.)

Equilibrium stable isotope fractionation during the low-temperature formation of ordered anhydrous carbonates as dolomite ($CaMg(CO_3)_2$) or kutnahorite ($CaMn(CO_3)_2$) is still an open question in carbonate geochemistry. No experimental determinations below 100°C have been carried out yet. Therefore, the $^{18}O/^{16}O$- and $^{13}C/^{12}C$-fractionation during the experimental formation of $BaMg(CO_3)_2$ (20°-90°C) and $PbMg(CO_3)_2$ (60°-100°C), two ordered rhombohedral double carbonates, have been investigated. The occurence of $BaMg(CO_3)_2$ (space group R3m; Effenberger & Zemann, 1985) as the mineral norsethite is known from sedimentary and hydrothermal environments (Mrose et al., 1961; Steyn & Watson, 1967).

Closed-system batch-experiments were performed using nesquihonite and witherite or cerussite as artificial precursors and diluted $NaHCO_3$ solutions. Run times at 20°C varied from several hours up to 289 d. The double carbonates were formed according to the overall reaction (Me= Ba, Pb): $MeCO_3 + Mg^{2+} + CO_3^{2-} \rightarrow MeMg(CO_3)_2$. Isotopic equilibration during norsethitization was demonstrated by the use of precursors and solutions with different isotopic compositions, and varying water-solid ratios and time. $^{18}O/^{16}O$ ratios of the acid-liberated CO_2-gas were evaluated assuming the fractionation factors due to the dissolution of $BaMg(CO_3)_2$ and $PbMg(CO_3)_2$ by phosphoric acid at 25°C to be 1.01164 and 1.01122, respectively.

^{18}O and ^{13}C are enriched in the final carbonates with respect to water and the sum of the dissolved carbonate species, respectively. The experimental results for the equilibrium $^{18}O/^{16}O$-partitioning between carbonates and liquid water are represented by (T in K):

$1000 \cdot \ln\alpha(BaMg(CO_3)_2 - H_2O) = 3.00 \cdot 10^6/T^2 - 4.67$, and

$1000 \cdot \ln\alpha(PbMg(CO_3)_2 - H_2O) = 3.47 \cdot 10^6/T^2 - 2.75$;

and for the $^{13}C/^{12}C$-partitioning between carbonates and gaseous CO_2 by:

$1000 \cdot \ln\alpha(BaMg(CO_3)_2 - CO_2) = 1.65 \cdot 10^6/T^2 - 8.59$, and

$1000 \cdot \ln\alpha(PbMg(CO_3)_2 - CO_2) = 1.96 \cdot 10^6/T^2 - 13.28$.

The results for $^{18}O/^{16}O$ as a function of temperature nearly halve those of the end-member carbonates (Friedman & O'Neil, 1977; Golyshev et al., 1981). Therefore, the experimental results may be used by analogy to estimate stable isotope fractionation in systems containing ordered double carbonates (Böttcher, 1993; Böttcher et al., 1993). For example, the equilibrium $^{18}O/^{16}O$-fractionation for dolomite and kutnahorite between 20° and 100°C is estimated from end-member relations to be:

$1000 \cdot \ln\alpha(CaMg(CO_3)_2 - H_2O) = 3.19 \cdot 10^6/T^2 - 4.42$, and

$1000 \cdot \ln\alpha(CaMn(CO_3)_2 - H_2O) = 2.96 \cdot 10^6/T^2 - 3.89$.

A close agreement with extrapolated experimental data of Matthews & Katz (1977) is observed for the dolomite containing system.

The spontaneous precipitation of a norsethite gel at 20°C according to Hood et al. (1974), followed by the alteration of the products at 20° or 60°C for 31 days, demonstrated isotope exchange reactions between solids and mother solutions, due to recrystallisation. However, isotope equilibrium was not reached within run time.

References:

Böttcher, M.E. (1993). *Doctoral thesis. Göttingen University.*

Böttcher, M.E., Hoefs, J. & Usdowski, E. (1993). *TERRA abs.* **5/1**, 336.

Effenberger, H. & Zemann, J. (1985). Z. Krist. **171**, 275-280.

Friedman, I. & O'Neil, J.R. (1977). *U.S.Geol. Surv. Prof.Pap.* **444-kk.**

Golyshev, S.I., Padalko, N.L. & Pechenkin, S.A. (1981). *Geochim. Int.* **18**, 85-99.

Hood, W.C., Steidl, P.F. & Tschopp, D.G. (1974). *Amer. Mineral.* **59**, 471-474.

Matthews, A. & Katz, A. (1977). Geochim. Cosmochim. Acta **41**, 1431-1438.

Mrose, M.E., Chao, E.C.T., Fahey, J.J. & Milton, C. (1961). *Amer. Mineral.* **46**, 420-429.

Steyn, J.G.D. & Watson, M.D. (1967). *Amer. Mineral.* **52**, 1770-1775.

POLYMERIZATION OF SILICATE MELTS

Bottinga, Y. (*Dept. of Geomaterials, I.P.G. and URA-734, CNRS, Paris*)

The internal structure of silicate melts is affected by changes in composition (X), pressure (P) and temperature (T), which provoke changes in bond lengths and angles causing contraction or expansion, but also changes in coordination and polymerization. The aim of this paper is to give an overall view of how polymerization affects thermodynamical, chemical, and transport properties of silicate liquids.

At low P most naturally occurring silicate melts behave unlike classical liquids, often their viscosity decreases and their compressibility increases with P. Only at high P have these melts the characteristics of classical liquids. This anomalous behaviour is the consequence of polymerization. X is the most important factor influencing the degree of polymerization; the great difference between the properties of liquid SiO_2 and Mg_2SiO_4 illustrate this perfectly. P is also an important parameter in determining the extent of polymerization. But in the T interval where magmatic processes are important, the influence of T on silicate melt polymerization is secondary.

The extent of polymerization as a function of X, P and T of most silicate melts has not yet been determined and we know only qualitatively how these three factors affect polymerization. This ignorance makes it impossible to extrapolate our knowledge of melts at P<10 kb to high pressures.

RAMAN MICROSPECTROMETRY OF KAOLINITES

Boudeulle M. and Panczer G. (*Laboratoire de Physico-chimie des Matériaux luminescents, Université Lyon I, France*)

Infrared absorption spectra of kaolinites devoted to the interpretation

of OH stretching vibrations in terms of known structures are numerous. On the contrary, the sarcity of Raman spectra is noticeable, due to the instrumental inadequacy and the weakness of spectra from clay powder samples, meaning that important structural informations are lacking. Such problems can be now overcome, using micro-spectrometers.

The particle size and crystallinity of known kaolinite samples from various origins have been previously characterized by X-ray diffraction, electron microscopy and diffraction.

Raman spectra, excited by the 488.0 and 514.5 nm lines of a Spectra Physics 2016 Argon ion laser at low power (< 50 mW), have been recorded from 10 to 4000 cm^{-1} using a 3-stages monochromator confocal XY Dilor spectrometer equipped with a CCD multichannel detector.

In the OH stretching region the presence of the band at 3685 cm^{-1}, first noted by Michaelian (1986), is confirmed. In the lattice vibration domain, together with bands common to all samples, some others appear "sample dependant" (117, 130, 143 and 516, 638 cm^{-1}), this dependance showing a priori some correlations with the genetics of the samples, hydrothermal, sedimentary or alteritic.

Although the assignation of the lattice bands could be only tentative, due to extensive mixing of vibrations, these differences would be discussed in the light of the structural and chemical characters of the materials, related to their presumed growth conditions.

References :
Michaelian, K.H. (1986). Can. J. Chem., 64, 285-289.

THE VARIATION IN AL CONTENT IN CHLORITE AS A RECORD OF GRAVITATIONAL COLLAPSE IN THE ARCHEAN CRUST : THE EXAMPLE OF THE HOLENARSIPUR GREENSTONE BELT (KARNATAKA, SOUTH INDIA)

Bouhallier H. (*Univ. Rennes, France*) & Guiraud M. (*Muséum Nat. Hist. Naturelle, Paris, France*)

Recent structural studies have documented diapiric instabilities within the Archaean Dharwar craton in the Holenarsipur area (South India). Diapiric strain fields are characterized by the occurence of linear troughs of supracrustals connected at foliation triple points. We have studied the P-T-X evolution recorded by metapelites in these two different settings. In the linear troughs the rock types consist in garnet-staurolite-epidote metapelites, staurolite-kyanite metapelites and garnet-staurolite-kyanite metapelites. Thermodynamic calculations based on THERMOCALC (POWELL & HOLLAND, 1988) indicate that all these rocks underwent the same peak conditions of metamorphism estimated at 7-8 kbar and 600°C and X_{H2O} around 1. The rock type in foliation triple points consists in garnet-chloritoid-chlorite bearing schists. However chlorite in inclusion in garnet or chloritoid occurs together with quartz and is Si-rich whereas chlorite in the matrix where quartz is absent is Al-rich. Calculations on phase diagram show that (i) in order for the PT conditions in the matrix minerals to be consistent with the rocks in linear troughs, values of X_{H2O} have to be lower, at about 0.5 and (ii) that the change in Al/Si composition in chlorite correspond to a prograde history from 470°C to 600°C and from 3 to 7-8 kbar. These results support the diapiric instabilities model.

Powell, R. & Holland T. J. B., (1988) Journal of Metamorphic Geology, **6**, 173-204.

HEAT CAPACITY, CONFIGURATIONAL HEAT CAPACITY AND VISCOSITY OF TITANOSILICATE MELTS

Bouhifd M.A and Richet P. (*Institut de Physique du Globe, Département de Physique des Géomatériaux*)

Titanium is an element whose abundance in silicate melts is significant, ranging up to 10 wt%, in alkali-rich, silica-poor compositions. This raises the possibility that titanium could affect significantly the physical properties of natural magmas.

Available data for titanosilicate liquids indicate a complex variations with composition and temperature. For example, the heat capacities of two titanosilicate melts ($Na_2TiSi_2O_7$-$K_2TiSi_2O_7$) display a unusual temperature dependence.

To complement these measurements, we have determined by drop-calorimetry the heat capacity and the configurational heat capacity of four alkali-titanosilicate liquids and glasses. We have also measured the high and low-temperature viscosity of these liquids with compressional and rotatory viscosimeters.

The variations of the heat capacity and viscosity as a function of temperature and composition will be discussed in the light of available structural data.

• CHARACTERIZATION OF TRIOCTAHEDRAL MICA SOLID SOLUTIONS OF THE SYSTEM K_2O-FeO-(Fe_2O_3)-Al_2O_3-SiO_2-H_2O-HF BY FTIR ABSORPTION AND MÖSSBAUER SPECTROMETRIES

Boukili B., Robert J.-L., Bény J.-M. (*CRSCM-CNRS, Orléans, France*)

The stability and phase relations of biotites have been investigated in the system K_2O-FeO-(Fe_2O_3)-Al_2O_3-SiO_2-H_2O-HF at 600°C and 720°C, 1 kbar PH_2O, under the fO_2 conditions set by the NNO, Co-CoO and MW buffers.

Starting compositions belong to the annite-siderophyllite join: $K(Fe_{3-x}Al_x)(Si_{3-x}Al_{1+x})O_{10}(OH,F)_2$, where x represents the extent of the Tschermak-type substitution. At 600°C, with the NNO buffer, annite (x=0) is associated with minor magnetite and sanidine. Along the join, the extent of the solid-solution range is restricted to $0 \leq x \leq 0.75$. The Co-CoO and magnetite-wustite buffering conditions produce essentially similar results. At high temperature (720°C), with the MW buffer, the solid solution extends up to x=0.8. Beyond this value, spinel, kalsilite and corundum are associated to mica.

The solubility of fluorine in the mica phase depends on the cationic composition: the maximum X_F value is 0.6 for annite at 720°C with the MW buffer. With NNO, X_F maximum is no more than 0.5 in annite and only 0.3 in more aluminous compositions. Beyond these solubility limits of fluorine, topaz and quartz are present.

FTIR spectrometry in the OH-stretching region shows that most of these micas exhibit a partial dioctahedral character which increases with fO_2. The general trends of variation of band wavenumbers in this region, as a function of the Al content (i.e. x), follow the general pattern previously established for magnesian micas: decrease of trioctahedral ν-OH and increase of dioctahedral ones. In the far infrared region the band assigned to the in-plane K-O vibrational motion (≈ 70 cm^{-1}), shifts as a function of composition (x and X_F). The shifts can be correlated to changes in the K-site configuration, and particularly to variations of the rotation angle of tetrahedra (α), which controls the extent of the solid solution ranges in the system studied.

Mössbauer measurements on these micas show that the Fe^{3+}/Fe^{2+} ratio decreases as the solubility of fluorine increases.

HIGH-TEMPERATURE X-RAY DIFFRACTION OF QUARTZ AND CRISTOBALITE

Bourova E. and Richet P. (*Dept. de Geomateriaux, IPGP*)

The cristobalite exists in two polymorphic modifications: the

low temperature phase α and the high temperature phase β. The structure and the elastic properties of the phase α are well-known, whereas the parameters of the phase β are discussible. The temperature of the α-β transition is about 270°C, but the coefficient of the thermal dilatation and the volume of melting of β-cristobalite are not so well known.

We observed the α-β transition of the cristobalite using the method of X-ray diffraction at high temperature. The main result is the very low thermal expansion of β-cristobalite from the α-β transition up to the melting point. Analogous experiments were made for quartz. We observed the low-high quartz transition at a temperature of about 573°C and quartz-cristobalite transition at a temperature of 1230°C.

These results will be presented and discussed in the light of the thermodynamics of melting of quartz and cristobalite.

THE DEVELOPMENT OF PLATINUM-GROUP MINERALS (PGM) IN LATERITES: MINERALOGICAL CHARACTERISTICS

Bowles J.F.W. (Mineral Science Ltd, UK)

This poster illustrates the mineralogical features of the Guma Water deposit, Sierra Leone with particular reference to textures suggestive of secondary growth. These features are characterised as:

Unconstrained growth in three dimensions.
Near-perfect development of mineral faces and interfacial edges.
Separation between source and deposit.
Corrosion features on some mineral faces.
"Overplating" of some mineral faces.
Zonation - colloform and cyclic textures.
Size - secondary PGM significantly larger than primary PGM.
"Sculpted" and step faced Pt-Fe nuggets.
Concomitant growth of PGM species.
Porous or "spongy" Pt-Fe nuggets.
Overgrowth of one phase by another.

The phenomena of unconstrained three dimensional growth, colloform and cyclic zonation, corrosion or resorption and continued growth are all familiar features of secondary growth in the supergene environment. The contrast in size between the PGM in the source rocks and those in eluvial and alluvial deposits indicates clearly that some secondary process has occurred whilst the geographical separation between source and deposit and the undamaged crystallographic form of the eluvial deposit indicates that the secondary process is neither *in situ* weathering nor mechanical transport. The mineral textures of concomitant growth and overgrowth are not exsolution textures indicative of cooling from an elevated temperature but show growth in the same environment possibly using one phase to provide a surface on which a second mineral can grow epitaxially. All of these features, taken together, are adequately described by solution, transport in solution and mineral growth in the secondary environment. This explanation also appears to have the potential to explain the "sculpted" or stepped surfaces and the porous or "spongy" nature of the Pt-Fe nuggets.

Reference:
Bowles, J.F.W. (1994). Chron. rech. miniére, in press.

INTERACTION BETWEEN MONTMORILLONITE AND POLLUTANTS FROM THE INDUSTRIAL WASTEWATERS: EXCHANGE OF Zn^{2+} AND Pb^{2+} FROM AQUEOUS SOLUTIONS.

Brigatti, M.F.(*), Corradini, F.(**), Franchini, G.C.(**), Mazzoni, S.(**), Medici, L.(*), Poppi, L.(*). ((*)*Dept. of Earth Sciences and* (**)*Dept. of Chemistry, Univ. of Modena*)

The dispersion of heavy metals in the environment as a result of industrial activities has received considerable attention in recent years. This research presents the results of experiments performed in order to describe the interactions between montmorillonite (sample SAz-1 from the Source Clay Repository of the Clay Minerals Society) and Zn^{2+} or Pb^{2+} solutions at different ionic strengths (from about 10^{-5} to 1 M) in order to observe changes in clay-solution system and in mineral crystal chemistry. In both types of solution the stationary state of exchange, attained within 20 minutes, depends on the solution's ionic-strength and can be interpreted by means of a Langmuir-type equation. Furthermore, the equation-adjusting coefficient (K) indicates that Zn^{2+} can be more easily exchanged by montmorillonite layers. In treated montmorillonite samples, the $d_{(001)}$ (60% relative humidity) decreases from 15.3 Å (value observed in untreated sample, mostly Ca^{2+}-saturated) to 12.85 (Zn^{2+}-exchanged montmorillonite) and 12.45 Å (Pb^{2+}-exchanged montmorillonite). Both values are closest to one-layer hydration. After the samples have been heated to 400° C, exchanged montmorillonite $d_{(001)}$ values decrease as the ionic radii of saturating cation ($d_{(001),\ Zn,\ 400°C}$ = 9.50 Å; $d_{(001),\ Pb,\ 400°C}$=10.0 Å). The closest packing is reached at T = 200°C for Pb^{2+} and at 380°C for Zn^{2+}-exchanged samples. These results, in conjunction with indications of thermal and infrared analyses, indicate the presence of:

— nearly one-layer water molecules in Pb^{2+}-exchanged montmorillonite;
— nearly two-layer water molecules highly cation-bonded and "brucitic-like" interlayers in Zn^{2+}-exchanged montmorillonite.

TRIOCTAHEDRAL MICAS-1M: CRYSTAL CHEMISTRY AND VARIATIONS IN LAYER GEOMETRY.

Brigatti, M.F., Poppi, L. *(Dept. of Earth Sciences, Univ. of Modena)*

In trioctahedral micas of the phlogopite-annite join, complex chemical variations can affect the geometry of the layer. These variations can be represented by a set of exchange operators which are extensively described in the literature. Unfortunately, the literature contains misleading information regarding the crystal chemical details and geometrical parameter variations when one or more exchange operators are active. This work deals with the structural variations of a series of trioctahedral true micas affected by the following exchange operators: $Mg_{-1}Fe^{2+}$, $Si_{-1}Mg_{-1}Al_2$, $Si_{-1}K_{-1}BaAl$, $Si_{-1}K_{-1}CaAl$, $Mg_{-1}Si_{-2}TiAl_2$, and attempts to point out the results obtained up to now. To this end, a large set (50 crystal data) of single crystal structure refinements, including a great number of unpublished data, was used.

Examination of the trends in the structure and in the geometrical parameters with compositional variation reveals that, starting from the ideal phlogopite structure:

— the exchange vector $Mg_{-1}Fe^{2+}$ produces a decrease in the average layer distortion and M1 and M2 octahedral sites become more distinct: M1 is more distorted and larger that M2;
— the exchange vector $Si_{-1}Mg_{-1}Al_2$ produces more regular tetrahedra and an increase in the tetrahedral edges, which is mostly compensated for by tetrahedral ring angle rotation α and does not particularly affect the octahedral sheet;
— the exchange vectors $Si_{-1}K_{-1}BaAl$ and $Si_{-1}K_{-1}CaAl$, produce larger and more distorted tetrahedra and enhanced flattening of the tetrahedral sheet. The interlayer cavity become more distorted and the presence of a divalent cation causes a reduction in interlayer separation;
— the exchange operator $Mg_{-1}Si_{-2}TiAl_2$ (Ti-Tschermak substitution) produces a decrease in the tetrahedral and octahedral thickness and an overall increase in the sheet's lateral dimension.

PRINCIPLES OF BUILDING OF STRUCTURE AND RADIATION CHARACTERISTICS OF THE MINERALS OF BIOLOGICAL ORIGIN

Brik A. and Gaver O. *(Inst. of Geochem., Mineralogy and Oreformation, Kiev)*

Under the minerals of biological origin as a rule they understand the minerals, which had grew in alive organism

(Lowenstam & Weiner, 1989). We have studied special features of structure of biominerals, phase transitions in these minerals and their radiation characteristics. The last one is connected with the fact that biominerals after Chernobyl accident are actively used in retrospective EPR dosimetry for reconstructing their dose loadings. The experiments in this paper we have carried out by EPR, NMR,X-ray difraction and gas chromatography methods.

We have discovered for the first time (Brik et al.,1992) the new reorientation effect in tooth enamel. It is well known that tooth enamel at (95-97)% consists of hydroxilapatite and it contains only (1-2)% organic substances and approximately the same amount of water. Tooth enamel consists of individual microcrystals - crystallites with size from dozens to thousand of nanometers. Crystallites are separated by thin water-organic interlayers they epitaxially had grown on. Since the size of crystallites is small the surface energy is essential in total energy of crystalite. Thus, organic matrix controls via surface energy of crystallite its properties, as well as the properties of biominerals as a whole. We have discovered that at T=180°C have intensive changes of properties of organic matrix and connecting with this changes effect spasmodic reorientation of crystallites takes place. We have studied this effect by methods mentioned above.

Nanocrystallinity of enamel results in the fact that its radiation sensitivity is about two orders more than hidroxilapatite formed in inanimate nature. So it appears that nature wisely provided human organism with rather highly sensitive dosimeter . We have studied (Brik et. al.,1993) by EPR method properties of radiation centers in tooth enamel and used these centers to determine the radiation doses taken by persons participating in elimination the accident consequences at Chernobyl Nuclear Power Plant. For dozens of persons the doses have already reconstrected within 0.25-1 Gy.

The second group of biominerals which we studied in this paper were mollusc shells.It is well known that mollusc shells are made up in the main of carbonats. We have studied the structure and EPR characteristics of radiation defects of mollusc shells from Chernobyl zone. By means of EPR method we have established that values of doses loading shells from Chernobyl reach the level of 10 Gy and from back-water near to the station about 20 Gy. The structure of shells as well as structure of tooth enamel consists of crystallites separated by water-organic interlayers. Mollusc shells even in a greater degree, than tooth enamel, are a convenient object for studies of organic and mineral substance interaction. It is connected with the fact, that carbonate in shells may be either in calcite or in aragonite form. At room temperature and normal pressure aragonite is unstable. But just it in the main is produced by a living organisms. We have studied phase transitions of aragonite-calcite in different types of shells. The studies have been performed with EPR, proton magnetic resonance, X-ray difraction and gas chromatographic methods. Because EPR signals of Mn^{2+} in calcite and aragonite are quit different EPR method may be used for obtaining detailed information about phase transition aragonite-calcite. Phase transition in shells for crystallites with different sizes take place at different temperatures (200-300)°C.

Thus the properties of biominerals are controlled by organic substance through surface energy of crystallites, or through spatially geometric parameters. We suppose that for pathologic mineral formations (calculi) in various organs the organic matrix sometimes can not control the properties of crystallites and that lead to uncontrolled growth of the crystallits and this mineral as a whole.

References:
Brik A.B.,Saduev N.B.(1992). *Mineral. Jornal*, 14, 91-94.
Brik A.B.,Saduev N.B.(1993). *Mineral. Jornal*, 15, 85-89.
Lowenstam H.A. & Weiner Sh.(1989) On the biomineralization. *N.-Y. Oxford Univ. Press.*

SYNCHROTRON X-RAY SPECTROSCOPY STUDIES OF MINERAL SURFACES

Brown, G.E., Jr., Liu, P. (Dept. of Geological & Environmental Sciences, Stanford University), and Kendelewicz, T. (Stanford Electronics Laboratory, Stanford University)

Within the past ten years, synchrotron x-ray spectroscopic methods have been used to probe metal ion sorption complexes on mineral surfaces and have provided the first direct structural and compositional information on such complexes at mineral-water interfaces *in situ*, i.e., with bulk water present and in contact with the surface. X-ray absorption fine structure (XAFS) spectroscopy, in particular, has become the method of choice for these studies, revealing, in favorable cases, the mode of metal ion attachment to mineral surfaces (inner *vs*. outer sphere and monodentate *vs.* bidentate) as well as the presence of monomers and/or hydroxo- or oxo-bridged oligomers involving the metal ion (e.g., Chisholm-Brause *et al.*, 1990). Using high-flux wiggler-magnet beam lines, solid-state multi-element array detectors, and fluorescence-yield XAFS measurements, sorbates containing metal ions with atomic number >23 (V) can be characterized when present at surface coverages ranging from a small fraction of a monolayer to many monolayers. However, while providing unique atomic-level information on metal ion sorbates, XAFS spectroscopy provides little direct information on the structure of the sorbent surface. In fact, it is common practice in such studies to assume that the hydrated surface has the same structure as the bulk mineral, which may not be true.

Because of their importance in controlling many of the geochemical processes at the Earth's surface, it is essential that we have a fundamental understanding of the bonding, reactivity and geometric structures of mineral surfaces, particularly when in contact with water. In order to gain such understanding, we have begun an experimental program that utilizes x-ray standing wave (XSW) measurements, surface EXAFS (SEXAFS), and photoemission spectroscopy to investigate the structure and reactivity of selected surfaces of single-crystal MgO, CaO, α-Al_2O_3, α-Fe_2O_3, TiO_2 (rutile), α-SiO_2, and ZnO under UHV conditions (≈ 10^{-11} torr), both before (clean) and after reaction with water and selected aqueous metal ion adsorbates. These oxides were chosen because of their relative simplicity and their geochemical and environmental relevance. To optimize surface sensitivity in our XSW and SEXAFS measurements, we have utilized Auger electron yield, which when referenced to total electron yield measurements, probes no deeper than 2 to 3 atomic layers. Our XSW studies of the clean, vacuum-cleaved CaO (100) and MgO (100) surfaces show that the surface atom positions are, within measurement error, the same as those in the bulk (vertical contraction of less than 0.5%). Ca SEXAFS data from the CaO (100) surface using Ca LMM Auger yield show that Ca-O distances are the same as those in the bulk. As expected for surface atoms, the coordination number of Ca is reduced relative to the bulk. Other XSW and photoemission results for other surfaces will also be presented.

References
Chisholm-Brause, C.J., O'Day, P.A., Brown, G.E., Jr., and Parks G.A. (1990)*Nature* **348**, 528-531.

Oxygen Isotopes in the Rapakivi Granites of South Greenland

P E Brown University of St. Andrews, Scotland

A E Fallick Scottish Universities Research and Reactor Centre, East Kilbride, Scotland

T J Dempster University of Glasgow, Scotland

The rapakivi suite of South Greenland intrudes early Proterzoic metasediments and formed synchronously with a period of extensional tectonics and low pressure granulite facies metamorphism. There are two main rapakivi facies, one black and the other white, the colour being given by the feldspars. The black rapakivi granites have an essentially anhydrous mineral assemblage, whereas the white rapakivis contain substantial amphiboles and micas. Intrusive relationships are present

between the two facies, though there are also gradational variations. Oxygen isotopes determined on a regionally representative set of samples are similar in both the black and white facies. $\delta^{18}O$ determinations on white feldspars (7) have a mean value of 10.1 (s 0.2) and on black feldspars (5) 10.0 (s 0.5). Quartz-feldspar fractionations are unexceptional. The mean of whole rock determinations (7) on both black and white is 9.5 (s 0.7). Overall these values are consistent with the rapakivi magmas having been derived by fusion of deep crustal material formed earlier in the Ketelidian erosional and tectonic cycle. Batches of magma which were to form the white facies contained more, but isotopically identical, fluids than the black facies. On cooling the magmas essentially behaved as closed systems and there has been no pervasive ingress of external hydrothermal fluids.

THE FE-MN DEPOSIT OF FIANEL - VAL FERRERA - SWISS ALPS : ITS MINERALOGICAL FEATURES.

J. Brugger (*Min. Petr. Inst. Uni. Basel, Switzerland*)

The deposit of Fianel (small scale iron production between the 17th and the 19th century) is embedded in Triassic carbonates belonging to the cover of the middle Penninic Suretta nappe. The deposit suffered an alpine metamorphism under green schist facies conditions. Three ores types occur in Fianel : (1) the iron-ore constituted by stratiform layers of hematite-quartzite (± apatite); (2) the iron-manganese ore mainly containing braunite, jacobsite and rhodonite; (3) a metric body of "pyroxenite" containing 90% pyroxene (> 60 % aegirine component), quartz and strontium-rich barite.

Mineralogical and structural data on two unusual parageneses from Fianel are presented :

1. A lenticular, stratiform metric body of rosa dolomite breccia with dolomite+hematite cement contains quartz vein with blue beryl, romeite crystals and a scheelite-powellite phase. Pure powellite and chernovite-(Y) are late phases found in cavities.
   In contrast to the type locality (Praborna, Piemonte, Italy), the romeite from Fianel is fluorine- and sodium-rich. The scheelite-powellite phase contains from 0.3 to 0.7 mol% of powellite. This "scheelite" is unique because of its high content of REE+Y (until 0.6 wt% Nb_2O_3 and 1.77 wt% Y_2O_3); the REE+Y anomaly is strongly correlated with arsenic (until 3 wt% As_2O_{10}).
2. Some decimetric layers of hematite quartzite contain up to 5 vol% of the red vanadate medaite grown within the alpine schistosity. Abundant palenzonaite and scarce pyrobelonite and saneroite associated with parsettensite are found in centimetric quartz-rhodonite-veins crosscutting these layers.

The significance of these parageneses in relation to the origin and metamorphic evolution of the deposit is briefly discussed.

THE CHEMICAL COMPOSITION OF MICA FROM THE GRANITES OF VERCHNEURMII COMPLEX INDICATION THEIR GEOCHEMICAL EVOLUTION.

Brusnizyn A.I. (*Dept. of Mineralogy, St.Petersburg Univ., Russia*)

The late Cretaceous Verchneurmii granitoid complex (VGC) and associated Sn, W and Bi deposits are located in the Priamuria area, the Far East. The VGC contains four granite phases. The micas from these rocks are characterized by the following changes of there chemical composition (from the early phases to the latest ones):

1. The Fe/Mg+Fe and Al/Si+Al+Mg+Fe ratios increase whereas the Ti content decreases. This regularity could be explained by the gradual decrease in crystallization temperature of the granites.
2. The Rb contents in micas increase while Ba become less in amount. Such behavior of these elements is determined in terms of the different distribution coefficients of Rb and Ba between the granite melts and micas. The Rb/Ba, Rb/K and K/Ba ratios in mica could be used as relative fractionation indices.
3. Mica from the youngest phase in the VGC is represented by Li-biotite that is considerably enriched in Cs, Nb, Sc, Ga, Sn and F. The accumulation of fluor-rich fluids in the latest portions of the melt has been an important stage in evolution of a rock forming process.

MECHANISM OF FORMATION OF Mg-Fe PHYLLOSILICATES IN A HYDROTHERMAL SYSTEM AT A SEDIMENTED RIDGE (MIDDLE VALLEY, JUAN DE FUCA)

M. Buatier (*Lab. de Sédimentologie, Université Lille)*:, G. Früh-Green (*Dept of Earth Sciences, ETH-Zürich*), A. M. Karpoff *CGS-CNRS, Strasbourg)* and J. McKenzie (*Dept of Earth Sciences, ETH-Zürich).*

The mineralogical and geochemical study of the hydrothermal minerals precipitated at the sedimented Juan de Fuca Ridge (Middle Valley) allows the characterization of newly formed silicates and the determination of their mechanisms of formation. The samples analysed for this study were collected during ODP Leg 139. This paper presents data on the newly formed phyllosilicates at Hole 858B located at the proximity of an active hydrothermal vent.

The background sedimentation in Middle Valley is represented by detrital minerals and biogenic components. Detrital phyllosilicates are illite, chlorite and smectite. These minerals represent the top of the sedimentary sequence but may be intercalated with pure hydrothermal sediments in Hole 858B. Neoformed and detrital phyllosilicates are clearly distinguished by their morphology seen by SEM and TEM and by their chemistry, whereby the hydrothermal phyllosilicates are Mg and Fe rich compared with detrital ones. The detrital or hydrothermal origin of the clay fractions is confirmed by stable isotope data, with $\delta^{18}O$ and δD ranging from 14‰ and -98‰ for the detrital phyllosilicates to less than 8‰ and approximately -40‰, respectively, in the hydrothermal phyllosilicates.

A mineralogical zonation with depth occurs in the sedimentary sequence at Hole 858B, Mg smectite is the major phyllosilicate in the hydrothermal unit at the top of the hole ; with increasing depth, corrensite becomes the dominant phyllosilicate, followed by swelling chlorite and chlorite at the bottom of the hole.

A fine characterization of these minerals has been investigated by HRTEM, AEM analyses and stable isotopes in order to constrain the mechanism of their formation, to approximate the temperature of formation and to discuss the sediment-fluid interaction processes in sedimented hydrothermal system. Corrensite, chlorite and swelling chorite are well distinguished by their chemistry and stacking sequence. Corrensite displays a 24Å stacking sequence ; its structural formulae is characterized by a very high Mg content and a Fe/Fe+Mg of about 0.08. Chlorite appears as crystallites with a 14Å stacking sequence and a Fe/Fe+Mg ratio of about 0.35. Chlorite is present at about 30 meters below sea floor. In the deeper sediments from Hole 858A (at 150 meters from the active vent) it is still the dominant phase but it is more Fe rich with a Fe/Fe+Mg between 0.5 and 0.6. Swelling chlorite occurs between 20 and 30 mbsf in Hole 858B, its chemistry and structure suggest that it is a corrensite/chlorite mixed layer. The stable isotope measured for each type of clay and for coexisting hydrothermal quartz permitted the temperature of formation of these phases to be calculated. Hydrogen isotope are relatively constant but oxygen isotopes show a decrease from values of 9.8‰ to values of 2.9‰ suggesting a high thermal gradient. The temperature calculated for a sample collected at 27.5 mbsf is approximately 240-250°C.

The variation of the chemistry of clay minerals with depth and the temperature gradient evidenced through the hole suggest a chemical evolution of the fluids from which the phases precipitated and local non equilibrium conditions of precipitation.

STUDY ON THE BEHAVIOUR OF VOLATILE ELEMENTS (F, Cl, S, C, B) IN MAGMATIC AND VOLCANIC PROCESSES

Buccianti A., Martini M. (Dept. of Earth Sciences, Univ. of Florence, Italy)

The main topic of this research is the study of the behaviour of volatile elements (in particular F, Cl, S, C and B) in magmatic and volcanic processes. The first aim is to use volatile elements so as to add a contribution in the understanding of the processes that controlled the genesis and the evolution of magmas in single volcanic systems. The second aim is to verify on a wider scale if these elements could characterize different tectonic settings.

A general account of the thermodynamics behaviour of H_2O and of other volatile species in melts has been given by Burnham (1979), who adapted these models to natural magmas and by Holloway (1981).

The use of multivariate statistical techniques of analysis of the data allowed the investigation of all the tectonic settings in this work, without losing information related to each single site.

The information obtained by the distribution of volatile elements is considered as being related to those processes that have influenced the evolution of the rocks. The study of primitive products, ruling out the loss of volatile elements due to fractionation or degassing processes, may provide information about the mineralogy of the mantle source. The study of the distribution of volatile elements in more differentiated products may provide information on the processes that have controlled their evolution. Thus the knowledge of the distribution of volatile elemets is important to understand how magma generated and how evolved after segregation from the source.

Rocks from different volcanic systems located in different tectonic settings as Mount Etna (Sicily), Sao Miguel (Azores Islands) and Lanzarote (Canary Islands) have been investigated. Taking into account only the most primitive rocks for each environment as well as the previous considerations, it has been possible to define the role played by apatite and phlogophite (Sao Miguel Island), phlogophite and perhaps amphibole (Lanzarote Island and Etna volcano) in the genesis of the analysed rocks. Thus the presence of these mineral could have controlled the distribution of the halogens in partial melts.

It has also been possible to see that the role played by fractionation of kaersutitic amphible may have characterized the evolution of alkaline rocks of Etna volcano. The results agree with the existence of a deep resevoir where the phenomenon could have developed. Moreover, the fractionation of amphibole and apatite seems to have played a role in the evolution of rocks of Sao Miguel island and the fractionation of apatite in the basaltic rocks of Lanzarote islands. The fractionation of these mineral phases, together with the degassing processes could have controlled the distribution of volatile elements during the evolution of the rocks (Buccianti, 1994).

References

Buccianti A. (1994). PhD Thesis, Dept. Earth Science, Univ. of Florence (Italy).

Burnham C.W. (1979). In: "*The evolution of igneous rocks*", Yoder (Ed), Princeton University Press.

Holloway J.R. (1981). In: "*Thermodynamics of minerals and melts*", Navrotsky & Wood (Eds), Springer, Berlin.

The genesis and tectonic settings of the Hungarian Variscan granitoids correlated with some other surrounding occurrences

Buda Gy. (*Dept. of Mineralogy, Eötvös L. Univ., Budapest*)

The conclusions are based on mineralogical, petrological and geochemical data of the Variscan granitoids of the Central Bohemian Pluton, West Carpathians, Hungary and South Alps. Detailed work has been carried out on the Hungarian granitoids and other data were collected from literature.

According to the mineralogical and geochemical data, the Variscan granitoids in Hungary, in Central Bohemian Pluton and in South Alps are S- or I-types; the majority of the West Carpathian granitoids are I-type.

The average leucocratic compositions of West Carpathian granitoids are considerable above the water-saturated cotectic surfaces, therefore they crystallized from water-undersaturated high temperature melt, at higher oxygen-fugacities, consequently magnetite and more oxidized biotite formed. The majority of granitoids belong to calc-alkaline trondhjemitic-suite and formed in the relatively thin continental crust (280-310 million years). Na-enrichment can be observed and the REE content is low (120-150 g/t).

The South-Hungarian so-called "in situ" migmatitic granitoids with very heterogeneous compositions crystallized from water-saturated melt. Low oxygen-fugacities prevailed, due to the low-temperature and sedimentary environment (graphite), consequently the biotite is slightly oxidized and ilmenite prevails. They contain medium-ordered K-feldspars in groundmass and highly ordered K-feldspar porphyroblasts. The former crystallized from water-saturated anatectic melt at slightly higher temperature with a relatively fast rate of crystallization and the second one formed from K-rich water solution at low temperature (K-metasomatism). The REE enrichments are considerable (240 g/t) caused by the high amount of accessories e.g. (allanite, zircon, apatite, thorite, RE-fluorcarbonate, etc.). These granitoids belong to the calc-alkaline monzonitic-suite. Their ages are between 340-360 million years.

In the case of the intrusions occurring along the Balaton-Velence tectonic-line and in the South Alps, the initial water-saturated melt became water-undersaturated due to the higher heat-flux. These melts intruded into the higher level of cooler continental crust (post-collision, hypabyssal plutons, 280 milion years) and produced a thermal contact aureole. Water-saturated eutectic melt formed at the later stage of differentiation and all constituents crystallized at once. These granitoids contain orthoclase formed at about 680°C. Slightly ordered K-feldspars crystallized at about 550°C, only in localized, water-enriched pegmatite "nests". The main temperature and pressure of crystallization were 2kbars and 680°C which was estimated from coexisting mineral assemblage of pelitic enclaves occurring in the upper part of the plutonic body, from the stability of biotites and from minimum melting of Ab-Or-Q system. These granitoids are slightly depleted in REE (70-160 g/t) due to intracontinental crustal differentiation. The enrichment in volatiles resulted in a higher amount of HREE at the final stage of crystal differentiation.

According to some major and trace elements, using Pearce's discrimination diagrams, the Hungarian Variscan granitoids formed in continent/continent collision belt and the West Carpathian granitoids originated either in a volcanic arc/continental collision zone or a subduction zone of oceanic and continental crusts.

The South Hungarian and Central Bohemian Variscan granitoids, belong to the same suite: S- or I-type, ilmenite-bearing, calc-alkaline monzonitic-suite. The granitoids of Velence-Balaton tectonic-line are: S-type, intrusive, hypabyssal, mostly magnetite-bearing, calc-alkaline granodioritic-suite and West Carpathians do not show any correlation with others: I-type, magnetite-rich, calc-alkaline trondhjemitic-suite.

It is supposed that the Central Bohemian and South Hungarian granitoids belonged to the Mezo-European platform. Later on, the South Hungarian crystalline plate was disconnected from Mezo-Europe by eastward movement of the South Alps along the tectonic line of Balaton-Velence.

THE GROWTH OF GEMS

Bukin G.V. (Joint Institute of Geology and Geophysics, Siberian Branch , RAS)

Research results of emerald, alexandrite, spinel and ruby growth are reported. It is only at the temperatures much lower than melting points of the above crystals and in the presence of mineralizers that the growth of the

above gems is possible. Melts of $Me^{I}_2O-V_2O_5$, MoO_3, Wo_3 (where M^{I} is Li, Na, K); $Me^{II}O-V_2O_5$, MoO_3, WO_3 (where Me^{II} is BaO, CaO, PbO) are used as crystallization media under flux conditions, while under hydrothermal conditions acidic solutions of complex composition are used, and complex fluorocompounds are suitable for gas transport technique.

P-T-X monomineral crystallization conditions of the grown gems are studied. Thus experiments show large phenakite, chrysoberyl and tridymite crystallization fields to be boundary to a small monophase crystallization field of $BeO-Al_2O_3-SiO_2$-flux $PbO-V_2O_5$ at the isotherm section of pseudoquaternary diagram. As for horizontal alexandrite crystallization and that by Ch.-ochralski technique, the growth is possible only from $BeO-Al_2O_3$ melts, supercooled below 1870°C.

The best gem crystal growth results were obtained in the closed 200-1000 cm^3 volumes by means of 1-3°C/mm temperature gradient at 900-1200°C for flux and gas transport systems, and 500-600°C for hydrothermal solutions.

Temperature ranges are mostly determined by crystalline media composition. Thus, the increase of incongruent emerald dissolution in $PbO-V_2O_5$ flux above 1200°C, with tridymite, phenakite and chrysoberyl growth, and viscosity increase up to 5-7 santipoise at the temperature below 1000°C, results in defective growth and capture of many inclusions. So, the temperature range of 1000°C-1200°C is the most suitable for the above flux.

The use of the oriented seeds or localization of single crystal growth centres yield the largest crystals of the best quality.

Crystal growth in closed volumes with temperature gradients under flux, hydrothermal and gas transport conditions is also preferable because it facilitates the introduction of iron group $3d_{1-8}$ ions: Cr, Ti, V, Fe, Mn, Ni, Co, which mostly effect color characteristics of gems, into some definite structural positions, in the required amounts and valencies.

Comparison of parameters and analysis of opportunities of various installations for crystal growth are given.

It is shown that in Russia techniques are developed to produce industrially gems that posses gemmological properties very similar to the natural stones.

STONE IN ARCHITECTURE OF ST.PETERSBURG, RUSSIA: FROM QUARRIES TO MONUMENTS AND BUILDINGS, FROM RAW STONE TO DETORIATED ONE.

Bulakh A.G. *(Mineralogy Dept., University of St.Petersburg)* and Abakumova N.B.

1. St.Petersburg was the first Russian town which was planned and designed in a really european style in the XVIII-XIX cc and decorated with natural stone that time.

2. Maintypes of stone are as follows (Abakumova & Boulah, 1977; Bulakh & Abakumova, 1987, 1993):
- microcline and plagioclase granites, almandine gneisses and talc-chlorite-carbonate shists from Finland and Sweden;
- quarzites and marbles from Karelia;
- marbles, calcite and dolomite limestones from Estland and from St.Petersburg's suburbs;
- marbles (real marbles and serpentinites) from Italy.

3. Colour of granites and gneisses depends on colour of feldspars and content of pyroxene, amphibole, biotite and garnet in rocks; colour of shists and serpentinites (italian "marbles" griotto, levant, siena etc.) is connected with the chemical composition of silicates and admixtures of hematite and goethite. The latter two minerals are main chromophores in sandstones, quarzites and also in marbles and limestones from Karelia. Glauconite in combination with goethite gives different colours to ordovician limestones from Estland and the St.Petersburg's suburbs.

4. Natural deterioration of stones involves their ferrugination, replacement of marbles' calcite with gypsum, chemical alteration and hydratation of biotite in granites and gneisses and, at last, the common frost weathering or rocks. Malachite, chrusocolla, atacamite, chalcantite and some others are compounds of bronze oxidation materials on stones.

5. Human-caused deterioration is a main reason of destroying processes. Barbarism and vandalism are stronger than strength and durability of any stone in St.Petersburg architecture. Unfortunately, restoration gives only a temporary success.

References:

Abacoumova, N., Boulah, A. (1977). *Revue de Gemmologie* A.F.G., **52**, 7-10.

Bulakh, A.G. & Abakumova, N.B. (1987). Natural Stone decoration of the centre of Leningrad. (In Russian). 197 pp.

Bulakh, A.G. & Abakumova, N.B. (1993). Natural stone decoration of main streets of Leningrad. (In Russian). 203 pp.

METALS IN SOLUBLE ORGANICS FROM ZONES OF ORE MINERALIZATION IN GOLD DEPOSIT SUKHOI LOG (RUSSIA).

Buslaeva E.Yu., Generalov M.E.(Ins. Geol. of Ore Deposits (IGEM), Moscow).

Large-scale gold deposit Sukhoi Log is situated near town Kropotkin in East Siberia. Ores of this deposit are represented by quartz-,quartz-carbonate, quartz-pyrite veins and bodies, enriched in disseminate sulphides (pyrite with minor pyrrhotite, chalcopyrite, galena, sphalerite and sulphosalts) in black shales. Black shales are carboniferous (about 0.8 wt. % C_{org}) quartz-chlorite-sericite rocks with abundant carbonate metacrysts. Carbonaceous matters in that shales are very fine-grained, some of their grains shows graphite-like anisotropy. They forms intergrows with quartz, micas and zone inclusions in carbonate metacrysts.

Previous data point on the importance of C-bearing compounds in the ore-forming process on this deposit. The gaseous phase of fluid inclusions in gold-bearing quartz contains 80-90% CO_2 and up to 0.5 % CH_4. Fluid inclusions in galena are enriched in hydrocarbons (63 %) and CO_2 (34 % of gaseous phase).

In this study we compare microelement compositions of black shales containing ore mineralization (mainly pyrite metacrysts up to several cm in size) and host black shale at the distance nearly 30 m from ore zone (Tab.1) with compositions of organic (chloroform, benzene-alcohol) extracts of these rocks.

Data of neutron activation analysis showed that compositions of studied black shales are very similar. Shale from ore zone is somethat enriched in Cu, Sb, Se, Hg, U. Data of NA analysis of organic extracts of these rocks are much more contrasting. In chloroform extract of black shale from ore zone the presence of Hg,Se,Re was estimated and Se,Re, Br were detected in benzene-alkohol extract. But none of them was detected in the same extracts from host black shale. It permits to

conclude the participation of metal-bearing organics (for example organoelement compounds) in the ore-forming process on black shale deposits.

Table.1 NAA data (in ppm) for black shale from ore zone (1) and host black shale (2).

	Mn	V	Cr	Co	Ni	Sr	Ba	Rb	Cs
1	380	133	200	13	100	240	450	140	5.4
2	851	124	160	22	130	310	420	115	3.9

	Sn	W	Zr	Hf	Ta	Br	Sc	U	Th
1	60	3.5	300	5.5	0.87	<1	24	1.8	11.0
2	80	4.8	250	5.5	0.68	<1	22	<0.5	9.2

	Cu	Zn	As	Sb	Mo	Te	Se	Ag	Au	Hg
1	320	75	31	17	8.8	2.0	1.6	0.7	0.11	1.50
2	190	115	55	11	10.0	4.4	1.1	0.8	0.29	0.45

	La	Ce	Nd	Sm	Eu	Gd	Tb	Tm	Yb	Lu
1	39	79	41	7.4	1.5	4.4	1.10	0.65	3.6	0.45
2	36	69	39	7.0	1.3	3.4	0.92	0.88	3.4	0.41

Acnowlegement: This work have been supported by the Russian Foundation of Fundamental Researches (project 93-05-9811).

GEOCHEMICAL STUDY OF TRAVERTINES OF THE HOT SPRINGS AT ALICUN DE LAS TORRES (GRANADA, S.E. SPAIN)

Caballero, E., Jiménez de Cisneros, C., Reyes, E., and Delgado, A. *(Dept. of Earth Sciences & Environm. Chem., Estación Exp. Zaidín, CSIC, Granada, Spain)*

A geochemical study is currently being carried out of the travertines related to hot spring water in the Alicún de las Torres area, where two natural aqueducts formed by travertines are to be found. The first aqueduct, which is still in the process of formation, is more than 1km long with a maximum height of 12m. The second and older of the two is 125m long and between 0,5m and 3m high. In this paper the geochemical nature of the formation is studied by determining the isotopic ($\delta^{13}C$ and $\delta^{18}C$), chemical (major and trace elements) and mineralogical composition of 18 samples taken from the travertines of the latter aqueduct.

The samples were taken in four vertical sequences along the length of the watercourse, and a minor increase in $\delta^{18}O$ can be seen from the bottom to approximately 2.5m. In the area nearest the surface this increase is more acute, probably due to a gradual isotopic re-equilibrium with the meteoric water present. In fact, the mean $\delta^{18}O$ value of the surface samples is the same as that of a carbonate precipate in equilibrium with the meteoric water of Alacún ($\delta^{18}O_w$ = -8.1‰), and at a temperature of 15.7°C, which is almost identical to the annual mean for the area. The deepest samples shared the same value of $\delta^{18}O$ = -9.5‰. If they are considered to have precipitated in equilibrium with the hot spring water ($\delta^{18}O_w$ = -9.2‰), the deposit temperature would be 17.3°C. From the values of $\delta^{13}C$ and the fractionation factors between CO_3Ca-CO_2 represented against the temperature, these values are very close to Bottinga's equilibrium line (1968), whilst the higher the sequence goes, the more the values diverge from this line.

The mineralogical study indicated that in the area nearest the surface (down to 0.5m) there is no gypsum, whilst this mineral accounts for up to 12% of the remaining samples. This confirms the isotopic exchange of the samples from nearest the surface with meteoric percolation water, responsible for the solubilization of the gypsum.

With regard to the remaining geochemical data which were determined, the travertines studied are mineralogically composed of high manganesian calcite (HMC). They also show a high Sr content, giving rise to a classification between "present-day" and "overlying", according to Cipriani et al. (1972), and an Fe and Mn content which is typical of this type of material.

Moreover, a vertical sequence has been ^{14}C dated, with results of 16300 years B.P. at the base, 14750 years in the intermediate area and 8780 years at the surface. This indicates that formation of these travertines began at the end of the last glacial period (16000 - 18000 y.B.P.) and that initial formation temperatures could therefore have been somewhat lower, since the surge water of that time must have had δ^{18}= values which were at least 1‰ lower.

References:

Botinga, Y. (1969). *J.Phys. Chem.* 72, 800-808.

Cipriani, N.; Ercoli, A.; Malesani, P. & Vannucci, S. (1972). *Men. Soc. Geol. Ital.* **11**, 31-46.

Ti-Zr-RICH OXIDES IN "CHROMITITE" LAYERS FROM THE BRACCO OPHIOLITE COMPLEX (EASTERN LIGURIA, ITALY)

Cabella, R[1]. and Gazzotti, M.[2] ([1] *Dept. of Earth Sciences, Univ. of Genova,* [2]*Dept. of Earth Sciences, Univ. of Modena*).

In the cumulitic gabbros from Bracco Ophiolitic Complex (BOC) "chromitite" layers, ranging in thickness from 1 mm to 10 cm, occur within melatroctolite lenses which consist of cumulus olivine with interstitial to poikilitic plagioclase and clinopyroxene. The "chromitites" occur both as monomineralic spinel layers and with interstitial plagioclase. The spinel compositions plot in the field of Cr-Spinel, as a consequence of their relatively high Al content. Moreover, TiO_2 content is always higher than 0.3 wt% suggesting an origin from cumulitic processes. In the Cr-spinel commonly are present polyphasic inclusions as silicates, sulphides and oxydes.

Very small grains (1 ÷ 50μm) of relatively rare Ti-Zr oxydes, loveringite, zirconolite and baddeleyite, have been observed under reflecting light microscopy and analyzed with a SEM and a ARL-SEMQ electron microprobe.

Loveringite was found principally in not altered inclusions along with Ti-pargasite and/or sulphides, or as grains dispersed in the serpentinitic matrix. Zirconolite and baddeleyite revealed an association together with altered inclusions of Ti-oxydes (Mn-ilmenite and/or rutile). Frequently, the same inclusions contain secondary titanite showing high ZrO_2 contents (1÷2 wt%).

The loveringite - zirconolite - baddeleyite (± Mn-ilmenite ± rutile) paragenesis was only observed into Moon rocks, alkalic complexes and also in layered basic complexes such as the Rhum complex (Williams, 1978), Laouni complex (Lorand *et al.*,1987) and Koitelainen complex (Tarkian & Mutanen, 1987).

However, while BOC occur in an oceanic (ophiolitic) environment, these layered basic complexes are from sub-continental origin.

This paragenesis may be related to the Cr-spinel crystallization step, after olivine fractionation, from a residual melt relatively enriched in incompatible elements like Zr and Ti. The apparent absence of zircon is possibly related to a weak or local undersaturation in SiO_2; the later orthopyroxene crystallization as

reaction rims surrounding skeletal olivine show a tendency to SiO_2 saturation of the interstitial melt. However, we cannot exclude the possibility that these mineral assemblages could be originated by a sub-solidus riequilibration and/or alteration of high temperature Ti- and Zr-rich phases like ilmenite or titanite.

References:
Lorand, J.-P., Cottin J.-Y., Parodi, G.C. (1987). *Can. Mineral.*, **25**, 683-693.
Tarkian, M. & Mutanen, T. (1987). *Min. & Petr.*, **37**, 37-50.
Williams, C.T. (1978). *Contrib. Mineral. Petrol.*, **66**, 29-39.

SR-RICH HOLLANDITE AND CRYPTOMELANE IN THE FE-MN OXIDE DEPOSIT OF THE CERCHIARA MINE (EASTERN LIGURIA, ITALY).

Cabella R., Lucchetti G. and Marescotti P. *(Dept. of Earth Sciences, Univ. of Genova)*

Cryptomelane group minerals (hollandite and cryptomelane) occur in massive braunite stratiform ores of the Cerchiara mine. Mn mineralizations were deposited interbedded to hematite-rich cherts at the bottom of the "Diaspri di Monte Alpe Formation" and re-equilibrated to prehnite-pumpellyite facies conditions (P=2-3 Kb, 250<T<300 °C) during Upper Cretaceous-Lower Cenozoic orogenic events. Hollandite and cryptomelane coexist with braunite + quartz ± hematite in massive ores or with braunite ± quartz ± carbonates ± Na-pyroxenes (namansilite, aegirine, Mn-bearing aegirine-augite) ± adularia ± albite in fracture filling assemblages.

The generalized formula $A_{1-2}Mn_8O_{16} \cdot nH_2O$ represents an isostructural series of manganese oxide minerals characterized by tunnels in their structures. The main end members are hollandite (Ba^{2+}), cryptomelane (K^+), manjiroite (Na^+) and coronadite (Pb^{2+}) according to the type of A-cation. From literature data SrO is lacking or very low; only few analyses of cryptomelane-hollandite from Falotta and Parsettens (Grison, Switzerland) have SrO in the range 0.55 - 2.62 wt% (Perseil, 1990). Cryptomelane and hollandite analysed from Cerchiara mine are solid solutions with very low or absent manjiroite substitution (up to 0,50 wt% Na_2O), also when they coexist with Na-rich phases; SrO content is always high, ranging from 1.93 to 3.72 wt%, both in K- and Ba-rich terms. The growth of K-rich and Ba-rich members in equilibrium conditions shows a limited extent of replacement between Ba^{2+} and K^+ ions suggesting a miscibility gap.

Hollandite and cryptomelane (SrO content up to 1.54 wt%) also coexist in Upper Jurassic quartzitic metaarenites (Maritime Alps) equilibrated under blueschists conditions (T=350° ± 50°C, P≤ 7kbars). Some analyses of these assemblages confirm a limited miscibility. The gap well agrees with literature data concerning both natural phases and synthetic products. The comparison of our data with hollandite-cryptomelane coexisting in different assemblages (varying from diagenetic conditions to sillimanite grade) shows no correlation between the miscibility gap extent and the different P-T conditions.

References:
Perseil E.A. (1990). *Schweiz. Mineral. Petrogr. Mitt.*, **70**, 315-320.

PROTON-MICROPROBE ANALYSIS PROVIDES NEW INSIGHTS INTO MINOR- AND TRACE-ELEMENT DISTRIBUTIONS IN DIFFERENT ORES

Cabri, L.J. *(CANMET, Ottawa, Canada)*

The proton-microprobe (μ-PIXE technique) is being used to study the minor- and trace-element distribution in many ore types. Among the advantages are fully quantitative, rapid, and relatively inexpensive analyses of specific mineral grains at concentrations ranging from about 3 to 50 ppm for a very wide range of elements. The MDL depends on the analytical conditions, elements sought, and the matrix. The disadvantages are that there are still relatively few proton-microprobes configured for mineralogical analysis and that the greater depth of penetration of protons, compared to electrons, requires greater care in selection of grains and in the interpretation of results. The advantages far outweigh the disadvantages.

New developments include pictorial displays of trace-element distributions by scanning proton-microprobe (e.g. Grime & Watt, 1993; Teesdale *et al.*, 1993), advances in on-line corrections of such displays for spectrum over-laps (Ryan & Jamieson, 1993), and evaluation of the accuracy and precision of the Guelph proton microprobe with the GUPIX program, using well-characterized silicate glasses and minerals (Czamanske *et al.*, 1993).

The proton-microprobe, when used in conjunction with other techniques has been used to study both the prospectiveness and the paragenesis of ores, and also to determine the mineralogical distribution of both economically useful elements as well as that of environmentally deleterious elements.

For PGE-bearing sulphide ores, the proton-microprobe has proven useful to quantify the distribution of elements such as As, Se, Ru, Rh, Pd, Ag, Sb, Te, and Tl. In base-metal and porphyry copper ores the elements are Ga, Ge, As, Se, Mo, Ag, Cd, In, Sn, Sb, Te, Pb, and Bi. In diamond exploration, using kimberlite indicator minerals, the trace elements for which the proton-microprobe is useful are Ni, Ga, Y, and Zr.

References:
Czamanske, G.K., Sisson, T.W., Campbell, J.L., Teesdale, W.J. (1993). *Amer. Mineral.* **78**, 893-093.
Grime, G.W. & Watt, F. (1993). *Nucl. Instr. Methods Phys. Res.*, **B75**, 495-503.
Ryan, C.G. & Jamieson, D.N. (1993). *Nucl. Instr. Methods Phys. Res.*, **B77**, 203-214.
Teesdale, W.J., Campbell, J.L., Halden, N.M. (1993). *Nucl. Instr. Methods Phys. Res.*, **B77**, 405-409.

ON THE OCCURRENCE OF REE-BEARING ACCESSORY PHASES IN THE CLAY-FRACTION OF PELITES: AN EXAMPLE FROM SOUTHERN APENNINES

Caggianelli A. *(DiTEc, Univ. of Basilicata, Potenza Italy)*
Fiore S. *(Istituto di Ricerca sulle Argille CNR Tito - Potenza Italy)*

The distribution of REE among minerals in shales is still argument of debate. It is generally accepted that clay minerals essentially concentrate REE (e.g. Condie, 1991) even though the possible role played by accessory phases (essentially zircon) was discussed by McLennan (1989) and Sholkowitz (1990). We recently demonstrated by SEM techniques the presence of accessory phases such as Ti-oxides, apatite and zircon and suggested that their influence on REE distribution could be dominant (Caggianelli et al., 1992). In this scenario the role of exchange reactions in the depositional environment in modifying REE content should be also considered (Cullers et al., 1975).

In this work we examined the whole rock and clay fraction from shales in the southern Apennines. We analysed selected samples by SEM techniques in order to have direct evidence on the eventual presence of accessory phases. Then we examined chemical and mineralogical data in order to infer the role of accessory phases in the distribution of REE.

SEM techniques allowed the identification of minerals such as a Ti oxide, zircon, apatite, xenotime, a Cr - Ni oxide and a Si - Al phosphate with high contents in LREE. In some instances BSE

techniques showed that some accessory phases may be found enclosed in single clay particles and that REE are present in amount large enough to be detected by EDS.

At a first glance the examined samples show a chondrite-normalized PAAS-like profile. However, normalizing REE contents to PAAS some important deviations can be enhanced. In detail, a pronounced enrichment in MREE and a depletion in HREE stand out.

A comparison of the chemical data between the whole rock and the <2μm fraction shows minor compositional differences. This is in agreement with the dominant weight of the clay fraction in the whole sediment. A correlation matrix between REE and mineral content in the <2μm fraction shows that none of the clay minerals is strongly correlated with REE. A moderate positive correlation can be deduced for illite and, to a lesser extent, for smectite. In examining correlation coefficients with major oxides and trace elements some important linkages do appear. In the <2μm fraction TiO2, Y, Zr are strongly correlated with REE while P2O5, Fe2O3 and Nb exhibit a moderate correlation.

In the whole rock counterpart a high statistical correlation exists between REE and TiO2, P2O5, Y, Zr and to a lesser extent with Rb. Worth noting is the strong correlation between P2O5 and Gd.

From the examination of these data it is confirmed the important role of accessory phases in affecting REE distribution in shales. It appears that phosphates are more important than zircon in controlling the distribution of some REE. The nature and mode of occurrence of the accessory phases found suggests that in part they may inherited from the source region and in part they formed in the depositional environment.

References:

Caggianelli, A., Fiore, S., Mongelli, G., Salvemini, A. (1992). Chem. Geol., **99**, 253-263.

Condie, K.C. (1991). Geochim. Cosmochim. Acta, **55**, 2527-2532.

Cullers, R.L., Chaudhuri, S., Arnold, B., Lee, M., Wolf Jr, C.N. (1975). Geochim. Cosmochim. Acta, **39**, 1691-1703.

McLennan, S.M. (1989). Am. Mineral. Soc., Rev. Mineral., **21**, 169-200.

Sholkovitz, E.R. (1990). Chem. Geol., **88**, 333-347.

PETROGENESIS OF A MIDDLE MIOCENE RAPAKIVI GRANITE, DEATH VALLEY, CALIFORNIA, USA

Calzia, J.P. *(U.S. Geological Survey, Menlo Park, California)*

The granite of Kingston Peak forms an elliptical batholith, 14.6 km long by 10.5 km wide, in the Kingston Range 45 km southeast of Death Valley, California. This hypabyssal granite is divided into (oldest first) a feldspar porphyry, quartz porphyry, and an aplite facies based on textural variations and intrusive relations. The feldspar porphyry and the quartz porphyry facies contain mafic xenoliths and are characterized by rapakivi textures and miarolitic cavities; aplite dikes and quartz veins are common in all three facies. The granite intrudes Early Proterozoic gneiss unconformably overlain by a thick sequence of sedimentary rocks consisting of the Middle and Late Proterozoic Pahrump Group and Late Proterozoic and Early Paleozoic miogeoclinal deposits; locally, the miogeoclinal deposits are disconformably overlain by sedimentary and volcanic rocks of the middle Miocene Resting Springs Formation. Biotite and hornblende from the feldspar porphyry facies yield concordant K-Ar ages of 12.1 and 12.4 Ma, respectively; hornblende also yields an $^{40}Ar/^{39}Ar$ age of 12.4 Ma. Andesite and basalt flows in the Resting Springs Formation yield conventional K-Ar ages of 12.5 to 11.1 Ma and are chemically and modally similar to the mafic xenoliths in the granite.

Chemical and isotopic data suggest that the calc-alkaline and metaluminuous feldspar porphyry and quartz porphyry facies were derived by partial melting of Mesozoic batholithic rocks at mid-crustal levels; the heat required for this melting event was probably transported into the crust by coeval volcanic rocks in the Resting Springs Formation and in adjacent mountain ranges. The aplite facies was derived by complex magmatic process(es) including fractionation of feldspars, hornblende, biotite, and Fe-Ti oxides and(or) assimilation of rocks similar in composition to the mafic xenoliths. Although steep linear patterns on lead isotopic plots suggest that the granite, the mafic xenoliths, and the coeval volcanic rocks are cogenetic, nonlinear major and trace element variation diagrams as well as strontium isotopic data preclude extensive magma mixing between these melts. Stratigraphic reconstruction of the Proterozoic, Paleozoic, and middle Miocene country rocks indicates that the granitic melt was emplaced at shallow (≈4 km) crustal levels in an actively extending orogen. Comparison of the observed crystallization sequence with experimental studies of granitic systems, combined with the abundance of titanite, magnetite, quartz, and amphibole, suggest that the feldspar porphyry facies crystallized at 675°C and at high oxygen fugacities ($fO2$ >NNO but <HM buffer curves). Late crystallization of hydrous minerals indicates that the volatile content (primarily H_2O) varied from less than 2 weight percent water near the liquidus to saturation near the solidus; the abundance of miarolitic cavities in the groundmass of all three facies indicates that the volatile phase was exsolved during late-stage crystallization of the granite.

INFLUENCE OF ACMITE CONTENT IN ORDER/DISORDER PROCESSES IN OMPHACITE.

Cámara, F.[1], Nieto, F. [1] y Oberti, R. [2] (1 *Departamento de Mineralogía y Petrología, Universidad de Granada-I.A.G.M. (C.S.I.C.),* [2] *C.N.R.-C.S. Cristallochimica Cristallografia. Pavia*)

Single-crystal X-ray structure refinement (SREF) was performed on 18 omphacite crystals with different acmite content. The samples are from eclogites belonging to the Nevado-Filabride Complex (Betic Cordilleras, SE Spain) and from eclogites and country-rock eclogites from Flemsøy, Western Norway. From the former locality three were found to be ordered with spatial group P2/n and the rest with C2/c. The two crystals from Flemsøy were P2/n. The omphacites have XNa 0.42-0.58 and show variable Fe^{3+} contents at M1 sites (0.0-0.32 a.f.u.). The ordered omphacitesshow Fe^{3+} not bigger than 0.12 a.f.u. and paired with Fe^{2+}, whereas the disordered crystals show variable Fe^{3+} and unpaired with Fe^{2+}. In spite of these Na contents (Jd-Di~1:1) most of the crystals are disordered, suggesting equilibrium temperatures higher than 850° C (Carpenter, 1981). As proposed by Rossi (1989), the acmite content in omphacites should have the same effect as a rise in temperature, and the order solvus should decrease steeply towards acmite. Omphacites equilibrated at temperatures below 850°C could show complete disorder. In fact, a lower temperature of 650° ± 50° C has been estimated from garnet-clinopyroxene pairs in these samples using the Ellis & Green calibration (1979) and considering Fe^{3+}=Na-Al in a 6 oxygen normalized formula. The P2/n pyroxenes of this group have low Fe^{3+} contents as deduced from SREF data and the Fe^{3+} is fully ordered at M11 while some Al still remains at M1. Several structural parameters also provide evidence of variable Fe^{3+} content at M1, such as an unusual enlargement of ***c*** and the volume of M2, and TAV changes with the charge at M2 following a clear trend to the acmite end-member value (fig. 1).

It is also worth considering the influence of kinetics, as ordering requires time for transformation and, unlike acmite content, rapid cooling or post-eclogite heating could prevent ordering in both

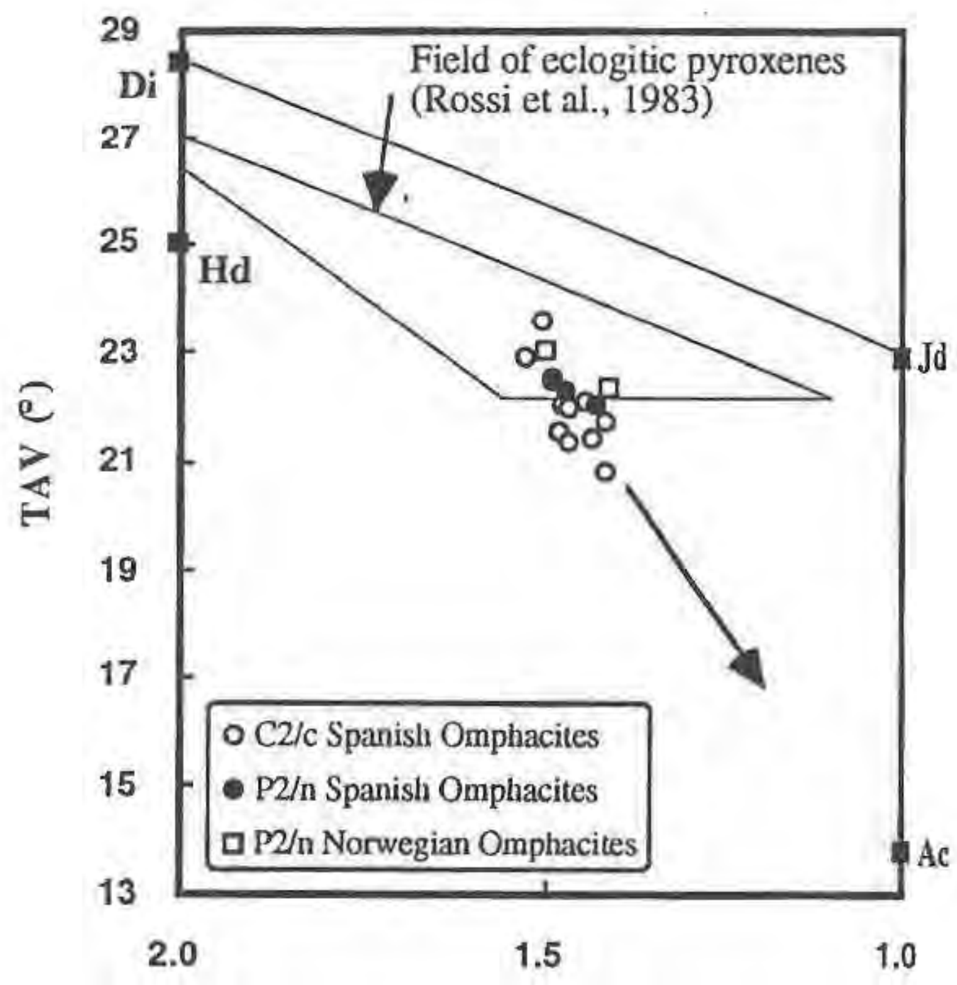

Figure 1

cases. A study on presence and development of microstuctures such as APD or exsolution lamella probably present in these pyroxenes is being carried out at present.

References:
Carpenter, M.A.(1981). *Contrib. Mineral. Petrol.*, **78**, 433-440.
Ellis, D.J. & Green, D.H. (1979). *Contrib. Mineral. Petrol.*, **71**, 13-22.
Rossi, G. (1989). *Eclogites and Eclogites Facies Rock*, Chp. 3, Elsevier, 237-270.
Rossi, G., Smith, D.C., Ungaretti, L. & Domeneghetti, M.C. (1983). *Contrib. Minrel. Petrol.*, **83**, 247-258.

APPLICATION OF POWDER ENERGY DISPERSIVE DIFFRACTOMETER TO CRYSTALLINE SAMPLE OF CANCRINITE.

Caminiti, R., Sadun, C. (*Dept. of Chemistry, Univ. of Roma*)
Maras, A., Ballirano, P. (*Dept. of Earth Sciences, Univ. of Roma*)

Only a few examples of the application of energy dispersive (ED) diffractometers are known. A prototype of an ED diffractometer in θ/θ geometry, equipped with a vacuum chamber fitted with a heating system (Caminiti, 1992) was used to study the effect of thermal processes on a cancrinite sample. The powdered specimen was located inside the sample holder forming an angle of 3° with the direct beam, corresponding to 15-35° 2θ for CuKα radiation.

Cancrinite is a rock-forming mineral and it shows a framework derived by the stacking along the z direction of layers buit-up by six-membered rings of silicoaluminate tetrahedra. This 3D arrangement leads to two cages and a large channel for unit cell, hosting extraframework cations and anions. Cancrinite is commonly non-stoichiometric and shows superstructures derived from the ordering of vacancies inside the large channel (Grundy & Hassan, 1982).

Our sample is non-stoichiometric with a 0.8 anion and cation deficiency: according to microprobe analysis the empirical formula is $Na_{6.3}Ca_{0.9}Si_6Al_6O_{24}(CO_3)_1F_{0.2}(H_2O)_2$.

The presence and the position of molecular water was studied using Fourier transform infrared (FT-IR) spectroscopy: the occurrence of two well developed absorption band located at 3607 and 3539 cm^{-1} points out to $O_{Framework}\cdots\cdots O_{H2O}$ distances of 3.1 and 3.0 Å, according to the Nakamoto plot (Nakamoto *et al.*, 1955)

The heating process was carried out increasing the temperature from room temperature up to 600°C, the acquisition time for every spectrum was 200 seconds. The diagrams show shifts, broadening and intensity changes for many peaks in the considered angular range. Other spectra were collected during the cooling process: according to the large FWHM typical of the instrumental set-up, it was not possible to immediately notice any cell parameters changes but intensity variations were evident.

Rietveld structure refinement of the treated powder show the sample is anhydrous with a nearly isotropical decrease of cell parameters, in fact the occupancy of the oxygen corresponding to the water was refined to 0.

FT-IR spectroscopy confirm the result showing no vibrational effect at all in the OH-stretching zone.

The changes in appearance of the spectra during the thermal cycles are probably due to framework distortions with a possible change in symmetry as the occurrence of a few extra peaks seems to indicate. The process starts at around 450°C and is perfectly reversible: according to the Rietveld refinement the intensities are changed due to the water loss and the anhydrous phase does not show any tendence to re-acquire molecular water: however the sample show a strong tendency to adsorb humidity.

REFERENCES.
Caminiti, R. (1992) XXI Congr. Naz. A.I.C., L'Aquila, Program and abstracts, 76, 139.
Grundy H.D. & Hassan, I. (1982) *Can. Mineral.*, **20**, 239-251.
Nakamoto, K., Margoshes, M., Rundle, R.E. (1955) *J. Amer. Chem. Soc.*, **77**, 6480-6488.

NEOLITHIC MINES IN THE GAVÀ AREA, CATALONIA, SPAIN: AIMS OF EXPLOITATION AND TECHNICAL ASPECTS

Camprubí A., Costa F., Salvany M.C., Sáez G., Arcas A., Melgarejo J.C. (*Dept. de Cristal·lografia, Mineralogia i Dipòsits Minerals, Univ. de Barcelona*)

The Mining Complex of Gavà (Baix Llobregat, Catalonia) was active during the Neolithic period (since 5700 b.p. until nearly 1000 years after), according to Alonso et al. (1978) and Villalba et al. (1990). Hence, these are probably the oldest gallery mines throughout Europe. According to the archaeologists, three potential materials could have been mined: phosphates for ornamentation, chert for tools or ochres for paintings. To solve the problem of the aim of such ancient mines, their geological mapping (surface and underground) has been performed.

The geology of the mining complex consists of Lower Silurian materials unconformably covered by 1-3 m of Miocene calcretes. The Silurian series consist of grey shales that enclose layers of chert, big chert nodules, and massive monomineralic oxide, jarosite and phosphate layers (Camprubí et al., 1993). Late hercynian and alpidic veins filled up by phosphates (mainly variscite, turquoise and strengite) crosscut the Paleozoic materials (Costa et al., 1993)

Three types of mining labors can be observed: trenches, pits and galleries. The trenches were opened close to the mountain ridges on mineralization. In them it is possible to observe the unconformity.

The mined galleries and some pits that communicate two levels of the mines run along phosphate veins. Other galleries that connect galleries in the same level run along thrust and fault surfaces. Neither galleries nor pits run along chert-rich or iron-rich layers. Hence, the aim of these works was mainly phosphates, and perhaps the other materials could have been mined as byproduct.

Other important aspect that can be deduced from the geological mapping is that most of the pits of access to the galleries were opened on calcretes. So, at the moment to open the pit, no mineral outcrops were in surface. This suggests an empyrical knowledge of the unconformity concept.

Though most of materials are soft, neolithic miners could have performed galleries along structural discontinuities because of their softer character.

References

Alonso, M., Edo, M., Gordo, L., Millán, M., Villalba, M.J. (1978). *Pyrenae*, **13-14**, 7-14.
Camprubí, A., Costa, F., Salvany, M.C., Sáez, G., Arcas, A. (1993). Las minas Neolíticas de fosfatos de Gavà (Catalunya). Unpub. Memory. Universitat de Barcelona. 63 pp.
Costa, F, Camprubí, A., Salvany, M.C., Sáez, G., Arcas, A., Melgarejo, J.C. (1993). In: Fenoll Hach-Alí, Torres-Ruiz & Gervilla (coord.): *Current Research in Geology Applied to Ore Deposits*, 715-718.
Villalba, M.J., Bañolas, L., Arenas, J. (1990). *Cahiers du Quaternaire*, **17**. Le silex de sa genèse à l'outil. Actes Vème Colloque International sur le silex, 275-285.

• MINERAL ASSEMBLAGE AND ORE GENESIS OF THE TELLURIDE - SULFIDE LODE DEPOSIT IN SICHUAN, CHINA

Cao, Z. (*Dept. of Mineral Resources, Chengdu College of Technology*)

The first ore deposit in the world with Te as the main ore-forming element has been discovered in Shimian county, Sichuan

province, Southwest China, and many experts are interested in the new type of ore deposit.

Geologists thought that it was impossible that tellurium could form a valuable mineral deposit, as it is among the scattered metals (the crust Clark Value is 0.002×10^{-6}, Litong 1976), even though it can be combined with Cu, Pb, Zn, Bi, Hg, Sb, Au, Ag, Pt group to form over 40 distinct minerals in natural world, which are often present as accessories in sulfide ores.

The Shimian tellurium deposit is located at podiform tectonic in Dadu river ductile shear structural zone. The thermometamorphic dome in Triassic system has controlled the occurrence of Te–ore veins. Wall rocks consist of coarse–grained marble, chlorite schist, biotite–amphibole schist. Mesozoic–Cenozoic granite belt crosses the region. Dolomite, pyrrhotite and tetradymite–tsumoite veins filled shear cracks. The ore vein is 0.3–0.6 meters in thickness and occurs in a group which consists of ore belt. The host rock alteration well developed in ferrodolomitization, muscovitization, albitization and silicization.

An ore grade so extraordinary is rare. Generally the ores present the following contents (wt%): Te 6.40–12.01, Bi 20.04, Cu 1.44–7.25, with a maximum Te 30.63, Bi 55.90 (massive Te–ore), Au average 10.96×10^{-6}, Ag 60–80 $\times 10^{-6}$ (analyzed by chemical method) and therefore they have a very high economic value. According to Lainik (1989), the ore deposit will come up to large scale in reserves.

The mineral assemblage in ores falls into three groups: tetradymite, tsumoite, tellurobismuthite, joseite–B, wehrlite and native tellurium; stuetzite, calaverite, vulcanite and native gold; pyrrhotite, pyrite and chalcopyrite; gangue minerals are dolomite, quartz, ferrodolomite, muscovite, etc.

Thermodynamic equilibrium computation and the phase diagram show that it is impossible to explain equilibrium relations of the mineral association with a simple telluride system. Some special paragenetic relationships and/or incompatible association may emerge in the ore fluid system.

The ores have two main tellurium minerals. Tetradymite (Bi_2Te_2S) often coarse–grained ({0001}, {10$\bar{1}$1}, {01$\bar{1}$2}), flaky ({0001}) euhedral cumulus crystal textures. Chemically, the mineral is pure (Te 33.60, Bi 60.88, S 4.65, average of 9 analyzed samples). Bi/Te/S atom percent is 41.52/37.7/20.76, in which S replace Te; a microenclave of tellurobismuthite has been observed with ore microscope. Minor elements in tetradymite are Se (0.353), Ag (0.133), Cu (0.054), Fe (0.04) etc. In tsumoite (BiTe), pyrrhotite shows a graphic exsolution texture. Chemical composition of tsumoite is Te 36.13, Bi 62.04, with accessory elements Sb (0.2), Fe (0.2), As (0.18), S (0.1), Zn (0.08), Cu (0.05), Ag (0.02).

Study of stable isotope geology and fluid inclusion suggest that the ore forming material derived from diapiric granite. From the study of the metallogenic process and of its physical–chemical parameters, we deduce that the telluride precipitated after the carbonate (dolomite) and the sulfide (pyrrhotite) stages. Finally, the ore–forming process ended with the silicate (quartz–muscovite) stage. Metallogenetic temperature of the ore deposit ranges from 185 to 253 °C (homogeneization). The depth of the mineralization is near to 1.5–2.5 Km. K–Ar isotopic dating in muscovite shows that the metallogenetic age is 144.2 Ma.

IDENTIFICATION OF MANUFACTURING TECHNIQUES AND USE OF ARCHAEOLOGICAL CERAMICS BY THIN SECTION.

Capel,J.(1), Delgado,R.(2) y Párraga,J.(2) *((1) Dpto. de Prehistoria y Arqueologia. Univ Granada, Spain.(2) Dpto. de Edafologia, Univ. Granada, Spain.)*

Some archaeological ceramics from different sites of the Bronze Age in Ciudad Real (Central Spain) have been studied. These sites are culturally related to "Motillas Culture" (Molina & Nájera,1978). The aim of this work is to identify, mineralogically and petrographically , the elements which can permit to obtain information about the manufacturation techniques of the pottery, and the mineralogical and/or chemical transformations produced by its use.

The samples were studied by means of XRD of both powder and oriented aggregates treated with ethylene glycol, and thin section petrographic microscopy.

From a mineralogical point of view, the results show that the ceramics were heated at temperatures between 700 and 800°C. Smectite has been detected in all samples, in varying proportions (6-16%), the greater amounts being present in those potteries of greater size. Taking into account that heating temperatures were above 700°C, the presence of smectite is anomalous (Güven,1991). Nevertheless, as phyllosilicates can be neoformed in different conditions, the presence of smectite can be attributed to the pottery use or to depositional effects. The neoformation of smectite by cooking use was deduced in previous papers (Capel et al.,1985). In order to corroborate the mineralogical conclusions, a thin section analysis was carried out.

Thin section examination completed the results obtained by XRD and allowed to come to some conclusions related to manufacturing techniques and pottery functionality. In relation with the ceramic making, phenocrystal and ore band orientation, both parallel to the potter walls, toghether with the existence of fissures also parallel to them, show a very accurate manufacturing process. Potters were made superposing clay rolls. This study shows that this technique was used in Middle Bronze Age as well as in End Bronze Age.

With respect to pottery use, it was possible to differentiate between alteration produced by functionality and deposition, by means of the study of the amounts of iron removed from minerals and its location in the ceramic matrix.

A group of great potteries (globular vessels and large bowls), presents large amounts of iron coated particles in the inner part of the walls and lower amounts in the outer ones. Another group of potteries, vessels of middle size, presents an homogeneous distribution of iron coating throughout the wall. These results, together with the previous mineralogical data, allow us to conclude that : the removal of iron was produced mainly in the innner walls due to the hydrolysis processes during the pottery use, while its homogeneous distribution is due to postdepositional processes during burial.

References:
Capel,J., Huertas,F., Linares,J. (1985). Miner.Petrogr. Acta, **29-A**, 563-575.
Güven, N. (1991). Reviews in Mineralogy, **19**, 497-552.
Molina, F.& Najera,T. (1978). Madrider Mitteilüngen, **19**, 52-74.

RATES OF INTERGRANULAR DIFFUSION DURING METAMORPHISM: CONSTRAINTS FROM COUPLED INTRACRYSTALLINE DIFFUSION IN GARNET

Carlson W. D. *(Dept. Geological Sciences, Univ. of Texas at Austin)*

In mid-Proterozoic rocks of the Llano Uplift of central Texas, garnets that grew in an early high-pressure metamorphic event were partially resorbed at their margins during later low-pressure metamorphism. Spectacular coronal reaction textures demonstrate that the rate of reaction was controlled by the kinetics of intergranular diffusion between reactants. As resorption progressed, partitioning of cations at the reactive interface between garnet and its breakdown products generated gradients in composition at garnet rims that were too large to be eliminated by intracrystalline diffusion. The steepness of these gradients measures the relative rates of the garnet resorption reaction and the intracrystalline diffusion of cations within garnet. It is therefore possible to obtain constraints on the rate of the resorption reaction (and thus on rates of material transport by intergranular diffusion) from experimentally determined values for rates of intracrystalline diffusion of cations in garnet.

The combined effects of simultaneous garnet resorption and intracrystalline diffusion were assessed by means of a discrete finite-element model. In the model, a garnet porphyroblast is regarded as a collection of thin, contiguous, concentric spherical shells of equal volume. Each shell is treated as a region of uniform composition. Resorption of the porphyroblast and diffusion within it are simulated by a series of incremental reaction steps in which resorption eliminates the outermost shell, and diffusional fluxes of cationic components into the next shell inward are computed from the composition of the resorbed shell and values for the partitioning of components between garnet and product phases. These values are uniquely defined by the requirement of material balance for the reaction, but they must be obtained by successive approximation in repeated simulations of each reaction zone. Diffusional fluxes at all interior boundaries between shells are computed from Fick's first law. Resorption rates and

intracrystalline diffusion rates are adjusted at each reaction increment to account for cooling, and the computation continues until both become negligible.

Well-constrained inputs to the model are the initial and final radii of the crystal; its initial compositional profile; the rock's cooling history; and experimentally determined rates of intracrystalline diffusion. Less well-constrained as an input parameter is the temperature dependence of the resorption rate (the activation energy for intergranular diffusion). Once values for these parameters are chosen, they fix the magnitude of the pre-exponential rate constant in an Arrhenius expression for the resorption rate. A single additional parameter, the initial temperature at which resorption begins, may be varied to obtain the best fit to the observed compositional profile. Alternatively, peak temperatures may be established from mineral exchange thermometry, permitting an estimate of the activation energy for intergranular diffusion to be extracted from the best-fit procedure.

Best-fit values for initial temperature are in reasonable agreement with mineralogic estimates of peak temperatures during the metamorphic event responsible for the resorption, which confirms that the model inputs (including the poorly constrained value for the activation energy for intergranular diffusion) are consistent with geologic reality. The simulations demonstrate that the kinetics of the resorption reaction require times on the order of 10 m.y. for the reaction to reach ~90% completion. This time scale in turn fixes within narrow limits the rates of intergranular diffusion responsible for the resorption reaction. However, because the reaction occurs over a narrow temperature range and because of the large uncertainty in the activation energy for intergranular diffusion, little confidence can be placed in extrapolation of those rates to higher or lower temperatures.

Constraints from this natural occurrence may allow refinement of experimental determinations of intracrystalline diffusion rates.The simulations are very highly sensitive to the *relative* rates of diffusion of Mn, Fe, Mg, and Ca in garnet. Published diffusion coefficients result in a calculated diffusion rate for Mg that is decidedly slower than that apparent in the Llano garnets. However, only a small adjustment in the literature value — changing the activation energy for Mg tracer diffusion by an amount that is about one-third of its stated uncertainty — brings all of the computed diffusion results into common agreement. Similarly, the rate of tracer diffusion of Ca in garnet, which is virtually unconstrained experimentally, is determined for the calcic almandines modeled in this study. The simulations are also sensitive to *absolute* rates of intracrystalline diffusion, although comparison to nature depends on accurate knowledge of the rocks' thermal history. For this natural occurrence, the experimentally determined rates may be slightly too slow, but again the required adjustment is small in comparison to the experimental uncertainty.

X-RAY PATTERN DECONVOLUTION IN IDENTIFICATION OF MIXTURES OF KAOLINITE WITH HALLOYSITE OR INTERSTRATIFIED KAOLINITE/2:1 MINERALS

Carnicelli S. (*Dept. of Soil Science - Univ. of Firenze*) and Mirabella A. (*I.S.S.D.S - Firenze*)

In the interpretation of x-ray patterns obtained from soil clay fraction, the contemporary presence of different mineral phases, only differentiated by subtle structural changes but of widely different genetic significance, create serious discrimination difficulties.

A classical problem in soil clay mineralogy is the distinction between Kaolinite and other minerals with very similar diffraction patterns, as Halloysite (0.7 nm) and Kaolinite interstratified with 2:1 minerals. Chemical intercalation techniques have been developed, exploiting different reactivity of Kaolinite and Halloysite, that induce shifts in peak position of one of the two minerals. Such methods, however, are time-consuming and technically difficult.

In theory, Kaolinite and Halloysite (0.7 nm) have different x-ray responses, the second showing a slightly higher d_{001} and tendentially broader peaks. Such differences are hard to exploit in mixtures, often leading to overlook one of the two minerals. The problem is furtherly compounded by the necessity to keep account of the possible presence of Kaolinite interstratified with 2:1 minerals, that in some diagnostic treatments may behave similarly to Halloysite (0.7 nm).

In recent years, computer analysis has been applied to help interpretation of x-ray data from soil clays (Moore and Reynolds, 1989). Use of such techniques could allow to resolve overlapping peaks and then differentiate phases with very similar behaviour.

To verify the potential of such techniques, the clay fraction from two soils, derived from different volcanic rocks and suspected to contain mixtures of different kaolinitic minerals, have been examined by a XRD deconvolution procedure, utilising the Marquardt algorithm and assuming that peaks are described by a pseudo-Voigt function. Intercalation with potassium acetate (Theng *et al.*, 1984) and heat treatments have been used to confirm mineral identification.

The samples from the different horizons of soil 9, developed on latitic lava, show a 0.72 nm peak characterised by a shoulder on the low-angle side; the deconvolution procedure allowed decomposition into two symmetric peaks, with maximum at about 0.72 nm for the more intense one and about 0.74 nm for the smaller.

The sample from the surface horizon of soil 83, developed on trachitic lava, showed similar features; in the deep horizon from this soil, a broad peak, centred around 0.74 nm, was dominant, but existence of a sharp 0.72 nm peak could not be discounted; in fact, deconvolution allowed discrimination of these two peaks.

These results could be interpreted as coexistence of Halloysite and Kaolinite in the same sample. The deconvolution procedure would then allow an estimate of the relative proportions of the two minerals.

The intercalation treatment, showed that only the sample from the deep horizon of soil 83 definitely contains Halloysite; the mixture with Kaolinite is confirmed by the persistence of a sharp 0.72 nm peak in the treated sample, while the 0.74 nm peak had shifted to 1.0 nm.

In the other samples, the 0.74 nm peak could not be attributed to Halloysite; it was insensitive to most diagnostic treatments, only shifting to higher angles, and becoming indistinguishable from the 0.72 nm peak, with heat treatments. This behaviour is common to Halloysite, and then not diagnostic for this mineral. The presence, in the same samples, of a 1.4 nm peak, showing various degree of collapse after K-saturation and heating, lends to attributing this peak to interstratification between Kaolinite and 2:1 minerals

These results show that definite identification of Halloysite requires the use of intercalation techniques. However, computer analysis of x-ray data allows acknowledgement of the presence of Halloysite-Kaolinite mixtures and the assessment of their relative proportions. This should be of significant help in evaluating genetic trends in soils where both minerals can exist.

References:

Moore, D.M. and Reynolds, R.C. Jr. (1989). Oxford University Press, Oxford. 332 pp.

Theng, B.K.G., Churchman, G.J., Whitton, J.S. and Claridge, G.G.C. (1984). Clays and Clay Miner., **32(4)**, 249-258.

METAMORPHIC VEINS WITH KYANITE AND ZOISITE MEGABLASTS IN THE ULTRAHIGH PRESSURE ZHU JIA CHONG ECLOGITE, DABIE SHAN, CHINA.

Castelli D., Compagnoni R. (*Dept. Mineralogical and Petrological Sciences, Univ. Torino, Italy*) and Xu S. (*Anhui Institute of Geology, Hefei, Anhui Prov., China*)

The Zhu Jia Chong eclogite occurs as a hectometric lens within oligoclase-epidote-two micas-garnet gneiss W of Taihu (Dabie Shan, Anhui Province) and consists of omphacite, garnet, clinozoisite, quartz, kyanite and porphyroblastic zoisite, amphibole and white mica. Coesite and diamond were also reported as inclusions in garnet (Xu et al., 1992). Accessory minerals are rutile, apatite, zircon and opaques. Eclogite-facies mineral assemblages show a polyphase retrograde evolution, which in later stages is characterized by the development of a variety of very fine-grained symplectites.

Within this eclogite, irregular veins and pods occur, which show a gradual transition to the country rock. They are up to ca. 50 cm thick and more than 10 m in length, with zoisite and kyanite megablasts up to 20 cm long and minor quartz and rutile. Idioblastic omphacite occurs only close to the contact with the country eclogite. During the

retrograde evolution, some kyanite is pseudomorphically replaced by aggregates of pale bluish-green paragonite. A second kyanite retrogression, also involving paragonite and zoisite, consists of a microscopic lamellar intergrowth of corundum and oligoclase.

The comparison between mineralogy and metamorphic evolution of country eclogite and veins suggests that the latter formed under eclogitic conditions, but during early stages of the decompressional history, most likely within the quartz stability field.

Reference:
Xu S., Okay A.I., Ji S., Sengör A.M.C., Su W., Liu Y., Jiang L. (1992). *Science, 256, 80-82.*

ON THE PHASE EQUILIBRIUM VERSUS PRESSURE PERICLASE + CORUNDUM ⇌ SPINEL: A QUANTUM-MECHANICAL CALCULATION

Catti M. and Valerio G.(*Dip.to Chimica Fisica Elettrochimica Univ. di Milano, Italy*)
Dovesi R. and Causà M.(*Dip.to Chimica Inorg., Fisica e Materiali Univ. di Torino, Italy*)

The ground-state crystal energies of cubic $MgAl_2O_4$ (spinel) and MgO (periclase) and of rombohedral α-Al_2O_3 (corundum) have been calculated at different volumes, relaxing the corresponding structures, by all-electron periodic Hartree-Fock methods. Basis sets of contracted Gaussian-type functions are employed for the 18 atomic (including *d*) orbitals representing each of the Mg, Al and O atoms. Mulliken net atomic charges z_{Mg}=1.86 (MgO), z_{Al}=2.30 (α-Al_2O_3), z_{Mg}=1.74 and z_{Al} = 2.24 e (spinel) are obtained. The elastic bulk modulus, the Murnaghan equation of state $p(V)$ at the athermal limit, the Mg-O and Al-O bond compressibilities and the binding energy have been derived for each phase (and the elastic constants C_{11} and C_{12} for spinel only). Comparison with existing experimental data is discussed. The enthalpy change for spinel decomposition into the simple oxides has been computed as a function of pressure, including a correction for the electron correlation energy based on local-density-functional the-ory. A decomposition pressure of 11 GPa at T=0 K is predicted, against values of 8 and 13 GPa derived from experimental thermodynamic data and from direct compression experiments (Irifune *et al.*, 1991), respectively.

References:
Irifune, T., Fujino, K., Ohtani, E. (1991). *Nature*, **349**, 409-412.

HYDROTHERMAL MINERAL OCCURRENCES IN THE SOUTHERN AND SOUTWESTERN PART OF KONYA, CENTRAL TÜRKİYE

Çelik*, M. and Temel, A.** (*SÜMMF, Dept. of Geo. Eng., 42040, Konya,Türkiye; **HÜ, Dept. of Geo. Eng., 06532, Beytepe, Ankara, Türkiye)

Various mineral associations formed as a result of hydrothermal alteration at 80-250℃ have been determined in the investigated area. These mineral associations are consist of silica polimorphs (quartz, tridymite, cristobalite), alunite group minerals (minamiite, jarosite, natroalunite, alunite, woodhousite, beaverite), layered silicate minerals (montmorillonite, halloysite, kaolinite, pyrophyllite, tosudite, rectorite etc.), framework silicates (ortoclase, sanidine, albite) and zeolites (heulandite, erionite, laumontite, stilbite).

Occurrence temperatures of above mentioned mineral groups are as follows; cristobalite and tridymite at 80-100 ℃; halloysite and montmorillonite below 100℃; kaolinite at 100-200℃; pyrophyllite at 200-350°C (Hayashi, 1989) and minamiite at 200-250℃ (Ossaka et. al., 1987).

Minamiite has been formed at acidic-neutral (pH=5.70-7.20) conditions. This mineral is generally pure; but in some places, it has been observed with paragonite, alunite and natrojarosite. Zeolite minerals have been formed at neutral-alcaline (pH=6.5-8.10) conditions. They are seen generally together silica polimorphs, natrosilite, jarosite and sometimes kaolinite and paragonite. Kaolinite and halloysite have been occurred at acidic (pH=4.15-6.30), while montmorillonite at alcaline (pH=7.20-9.30) conditions. In some places, clay mineral paragenesis are made from pure kaolinite, halloysite or montmorillonite.

According to wet chemical analysis results, minamiite contains 40-45 % Al2O3, 30-35 % SO3 and about 2-4 % CaO, Na2O and K2O, whereas kaolinite contains 35-37 % Al2O3, 45-46 % SiO2, 0.60-0.65 % Fe2O3, 0.1-2 % CaO. Mineralogical and chemical analysis result shows that clay minerals (kaolinite and montmorillonite) and minamiite can be used as an industrial raw material (ceramic, chemistry etc.).

References:
Hayashi, M. (1989). Geothermal Geoloyy.1, Alteration Mineralogy; Textbook for 20th International Group Training Course on Geothermal Energy, held at Kyushu University, Japan. 29p.
Ossaka, J., Otsuka, N., Hirabayashi, J., Okada, K. and Soga, H. (1987).Synthesis of minamiite, Ca 0.5 Al3(SO4)2 (OH)6; N.Jb.Miner.Mh., **2**.49-63.

Phase transitions in Steinbach tridymite

Cellai D., Carpenter M.A., Wruck B., Salje E.K.H. and Zhang M. *(Dept. of Earth Sciences, Univ. of Cambridge, Downing Street, Cambridge CB2 3EQ,, England)*

Tridymite is the parent structure of feldpathoids such as nepheline and kalsilite. The transformation behaviour of tridymite, from Steinbach tridymite, has been investigated over a range of temperature using X-ray single crystal diffraction, differential scanning calorimetry (DSC) and infrared spectroscopy (IR). The temperature dependence of diffracted intensity has been measured for reflections which violate the *c* glide absence to give a detailed characterisation of the sequence of phase transitions, which agree with the DSC and IR data.

Three phase transitions have been found in the temperature range 350 - 475 °C, and a model involving oxygen disorder will be discussed. In the temperature range 25 - 250 °C, the sequence and temperatures of phase transitions are strongly dependent on the thermal history. Crystals annealed in the stability field of the hexagonal phase develop the orthorhombic OP phase between ~ 100 °C and ~ 154 °C, which has not previously been reported for Steinbach tridymite.

MINERALOGY OF EXTREME FRACTIONATION IN RARE-ELEMENT GRANITIC PEGMATITES AT RED CROSS LAKE, MANITOBA, CANADA

Černý P., Teertstra D.K., Chapman R. (*Dept. of Geological Sciences, Univ. of Manitoba*), Fryer B.J. (*Dept. of Geology, Univ. of Windsor*), Longstaffe F.J. (*Dept. Geological Sciences, Univ. of Western Ontario*), Wang X.-J. (*Acad. Sinica, Guangzhou Inst. of Geochemistry*), Chackowsky L.E. (*Geol. Services, Manitoba Energy and Nat. Resources*), Meintzer R.E. (*Geol. Survey of Alabama*)

The Red Cross Lake pegmatite field is located in the Oxford Lake greenstone belt of the Sachigo Subprovince, in the northwestern part of the Archean Superior Province of the Canadian Shield. The field comprises highly evolved pegmatitic leucogranites with a progressively fractionated suite of tourmaline-bearing, spodumene and lepidolite pegmatites. All pegmatitic rocks are highly sheared to mylomitized, but the primary compositional features of virtually all minerals are well preserved.

The dikes of the lepidolite subtype are the most fractionated pegmatites ever encountered. They contain subordinate spodumene + quartz pseudomorphs after petalite and accessary schorl, elbaites, pollucite, beryl, amblygonite, apatite, cassiterite, manganotantalite, wodginite, microlite and zircon.

Bulk compositions of the lepidolite pegmatites show Li 1540-9755, Rb, 6219-14150, Cs 10-38-26976, Be 113-294, Ga 120-190, Sn 25-108, Nb 17-36, Ta 244-802 ppm, and K/Rb 2.6-1.6, K/Cs 16.0-0.7, Al/Ga ~750-500, Nb/Ta 0.074-0.024. Chondrite-normalized REE contents range from 2-0.3 for La to 0.1 - <0.01 for Yb and Lu, and $\delta^{18}O$ from +10.4 to +12.4‰.

Primary blocky K-feldspar attains Li 418, Rb 49835, Cs 4244, Tl 402, Ga 140 ppm, K/Rb 1.9, K/Cs 22.4, Rb/Tl 122, and Al/Ga 812. Late hydrothermal K-feldspar is virtually pure but is associated with discrete grains of a Rb-feldspar with K/Rb as low as 0.25.

Micas range from muscovite of moderate K/Rb 14.1 and K/Cs 40 to rubidian and cesian analogs of lepidolite with K/Rb 0.093 and K/Cs 0.019, respectively. The full range of Ms-to-Lpd fractionation is commonly exhibited by progressively zoned crystals as small as 100μm across.

The tourmaline group is represented by minor Mg-bearing schorl in the outer parts of the dikes, and predominant pale-pink rubellite which closely approaches the composition of ideal elbaite in the central parts.

Oxide minerals of Nb,Ta and Sn show Fe/Mn <0.086 and Nb/Ta < 0.057 in cassiterite, Fe/Mn <0.008 and Nb/Ta 0.087 in manganotantalite, Fe/Mn <0.007, Nb/Ta 0.037 and Ti/Sn < 0.004 in wodginite, and Nb/Ta 0.004 in microlite.

Beryl attains alkali contents as high as Li_2O 1.7, Na_2O 1.6 and Cs_2O 6.3 wt.%. Hafnium content of very rare zircon amounts to as much as 22.80 wt.% HfO_2.

The exocontact assemblage includes dravitic tourmaline, epidote, titanite, garnet close to Alm_{40} Gr_{30} Py_{30}, and strongly zoned trioctahedral micas with Mg/Fe (at.) <1.0, rarely > 1.0. Their outer zones display K/Rb and K/Cs ratios as low as 0.182 and 0.055, respectively.

Crystal-liquid and liquid-liquid fractionation coupled with selective complexing and mass-controlled diffusion rates could have cooperated to promote the extreme enrichment and fractionation of incompatible elements in the lepidolite pegmatites.

ANDALUSITE-BEARING VEINS AT VEDRETTE DI RIES (EASTERN ALPS): A GENETIC MODEL

Cesare B. (*Dept. of Mineralogy and Petrology, Univ. of Padova)*

Andalusite-biotite-quartz-bearing pegmatitic veins occur in the contact aureole of the Vedrette di Ries granodioritic-tonalitic pluton (Italian Eastern Alps). In two outcrops at different distances from the pluton, discordant veins formed during contact metamorphism, synchronously with the crystallization of andalusite and biotite within country-rocks. Andalusite veins are found only within andalusite-bearing hornfelses, and vein biotite occurs wherever host-rock garnet is partially replaced by biotite; no veins occur outside the area of contact metamorphic andalusite development.

The pegmatitic structure suggests that vein parageneses crystallized within fluid-filled cavities, and the orientation of fractures is consistent with a failure mechanism of hydraulic fracturing. Regimes of high fluid pressure in the host-rock are consistent with the estimated depth of emplacement of the tonalite, of about 10 km. Thermal, mechanical and chemical equilibrium among vein and host-rock is indicated by the strong control of host-rock composition on vein mineralogy, by the similar chemical composition of minerals in vein and host-rock, by lack of evidence for hydrothermal circulation, and by composition and density of fluid inclusions within veins.

A mechanism of *synmetamorphic veining* (Cesare, in print) is proposed to explain failure of rocks and subsequent mineral deposition within fractures. During hydrofracturing induced by dehydration reactions in response to heating in the aureole, fissures were immediately filled with locally-derived fluids. The lack of large-scale flux, together with high fluid pressures required by hydrofracturing, suggest fluid in the cavities was a virtually stagnant, passive medium, and that mass-transport toward fractures was driven by intergranular diffusion. Because temperature and fluid pressure values within veins were very close to those in the host-rock, vein assemblages are interpreted as the stable, high-T side of reactions taking place within pelitic schists during contact metamorphism, at the time when fractures opened. Veins from both outcrops formed within the stability field of andalusite, and only those from the highest grade zone of the aureole underwent further heating, with formation of sillimanite after andalusite. The whole process was controlled by heterogeneous dehydration reactions in the host pelite: once nucleation of product phases occurred, chemical components released by dissolution of reactant minerals were driven to precipitation sites by chemical potential gradients. Since nucleation was favoured at the strained grains of vein walls, andalusite and biotite simultaneously grew in vein and host-rock.

The proposed genetic model contrasts with generally adopted metasomatic mechanisms for the genesis of Al_2SiO_5-bearing veins, in not requiring large fluid/rock ratios or a highly "aggressive" fluid composition. The mechanism of synmetamorphic veining may be particularly useful in the interpretation of vein occurrences in medium- and deep-crustal rocks which have undergone extensive devolatilization.

References:
Cesare, B. Synmetamorphic veining: origin of andalusite-bearing veins in the Vedrette di Ries contact aureole, Eastern Alps, Italy. *J. Metamorphic Geol.* (in press).

ANDALUSITE-BEARING VEINS AT VEDRETTE DI RIES (EASTERN ALPS): PRESERVATION OF THE METAMORPHIC FLUID IN FLUID INCLUSIONS

Cesare B. (*Dept. of Mineralogy and Petrology, Univ. of Padova)* and Hollister L.S. (*Dept. of Geological and Geophysical Sciences, Univ. of Princeton, NJ)*

The andalusite-bearing veins that formed by hydrofracturing in the aureole of the Vedrette di Ries tonalite provide an excellent setting for preserving the metamorphic fluid in fluid inclusions. In the veins, quartz host grains, completely armoured by andalusite or in strain shadow areas, contain three types of fluid inclusions, recognized by means of petrographic and microthermometric study. Estimated fluid compositions are respectively: low-salinity H2O-CO2-CH4 mixtures with up to 35% CH4/(CO2+CH4) (type A); low salinity aqueous fluids (type B); H2O-free, CO2-CH4 fluids with the same carbonic speciation as A (type C). Carbonic types A and C often have a dark appearance, attributed to graphite coatings on inclusion walls. Textural evidence and calculated densities indicate the C-O-H-NaCl A type inclusions as the only generation likely to be trapped during vein formation. Along the cooling path of contact metamorphism, A type inclusions underwent strain-assisted re-equilibration, that caused a density increase at constant bulk composition. After rocks cooled below 350°C, unmixing occurred in the H2O-CO2-CH4 fluid mixtures, with formation of two immiscible fractions. Similarities of CO2/CH4 values, and textural occurrence suggest reworking or opening and re-trapping of unmixed

type A inclusions as mechanisms that led to the formation of metastable, pure carbonic type C inclusions. Aqueous type B, apparently trapped in a final, low temperature stage (225°C<T<350°C), could either be an independent fluid, or represent the H2O-rich fraction of unmixed A type C-O-H-NaCl fluids. If the uncertainties of quantitative approach to the C-O-H-NaCl system are taken into account, composition and density of the complex type A fluids, extrapolated from microthermometry, are in good agreement with the primary fluid values that can be independently predicted by geologic and petrologic data, and confirm the model of vein formation by hydrofracturing as a result of dehydration of graphitic metapelites.

CATION DIFFUSION RATES IN OLIVINES AND GARNETS -- NEW EXPERIMENTAL MEASUREMENTS AND IMPLICATIONS

Chakraborty, S. (*Bayerisches Geoinstitut, Universität Bayreuth, Germany*)

Data on diffusion rates of cations in minerals are useful for interpreting temperatures obtained from element exchange geothermometry as well as for constraining time scales of various geological processes. Two minerals that have been widely used for these purposes are olivines and garnets. However, in spite of the wide usage there remain major gaps in our knowledge of diffusion rates in these minerals. Here we report on the results of recent experimental studies aimed at removing some of these deficiencies.

Fe-Mg interdiffusion experiments performed on olivine diffusion couples at 1000-1100°C, $fO_2=10^{-12}$ bars show that single crystal/polycrystal diffusion couples used in experiments at low temperatures (<1100°C) may yield results that are difficult to interpret. Results from diffusion couples made out of two single crystals suggest that activation energies on the order of 240 kJ/mol are appropriate for extrapolation of volume diffusion data to lower temperatures. Composition dependence of Fe-Mg interdiffusion rates are much stronger near the Mg-rich end of the olivine solid solution series than that found in earlier studies.

Mg and Ca tracer diffusion experiments in garnets at 750-850°C, $fO_2=10^{-17}$ bars show that Ca tracer diffusion may be similar to or slower than Mg tracer diffusion rates, depending on the composition of the garnet. The newly determined Mg tracer diffusion coefficients are consistent with data from most previous studies. There is a significant pressure dependence of Mg tracer diffusion in garnet, in contrast to that in forsterite, another orthosilicate. Implications of these results for geothermometry and geospeedometry will be discussed.

DIFFUSIVE MIXING IN MULTICOMPONENT MELTS --- A PROBE FOR SPECIATION AND THERMODYNAMIC MIXING PROPERTIES

Chakraborty, S. (*Bayerisches Geoinstitut, Universität Bayreuth, Germany*)

When two miscible multicomponent melts mix by diffusion, the compositional evolution toward a homogeneous melt follows a path determined by the nature of diffusing species and the process is driven by chemical potential gradients. Therefore, analysis of experimentally observed diffusion paths in composition space provide information on speciation in melts on a long (thermodynamic or local equilibrium) time scale and constrain activity-composition relationships for various melt components.

Recent experiments in our laboratory provide data on interdiffusion of melts in the system K_2O-Al_2O_3-SiO_2 and $NaAlSi_3O_8$-$KAlSi_3O_8$-SiO_2 ± B_2O_3 ± P_2O_5 (haplogranitic system with added boron or phosphorus). The calculated species from observed diffusion paths allow some generalizations to be made. All oxide components of a melt are found to be coupled during diffusion. The nature of coupling determines transport rates of various diffusing species; weakly coupled components diffusing faster. It is found that P_2O_5 prefers to form a network of its own outside of the silicate network where it couples with all other components. The extent of coupling depends on the alkali:aluminum ratio of the melt. In contrast, B_2O_3 seems to simply couple with SiO_2 in these melts.

The thermodynamic mixing of oxide components in the investigated melts is found to be non-ideal even at the highest temperatures studied (1700°C). Calculated iso-activity contours in compositional space for various oxide components should help to constrain thermodynamic mixing models for these melts.

RAMAN SPECTROSCOPY IN MINERAL NANOPHASES

Champagnon B., Saviot L. (*Laboratoire de Physico-chimie des Matériaux luminescents, Université Lyon I, France)*

Materials composed of differents phases are analyzed by resonant Raman spectroscopy and Low Frequency Inelastic Scattering. It is shown that due to the selectivity of resonance phenomena, low concentration of a minor phase can be detected on samples analyzed under an optical microscope.

Furthermore, it is shown both experimentally and theoretically that the size of the nanocrystallits can be determined from the Raman spectrum. Confinement effects are observed when the crystellite diameters are of the order of few nanometers. Examples concerning greenockites, cordierite,etc... will be shown.

References :

Champagnon B., Andrianasolo B., Ramos A., Gandais M., Allais M.and Benoit J.P.(1993) J. Appl. Phys. **73**, 2775.

Duval E. PHYS. REV. B 46, 5795, (1992)

THERMODYNAMIC AND STOECHIOMETRIC CALCULATIONS IN PETROCALC : A PETROLOGICAL SOFTWARE TO MANAGE RELATIONAL DATABASES OF CHEMICAL ANALYSES.

Chat C. and Godard G. *(Laboratoire de Pétrologie Métamorphique, Université de Paris 7)*

PETROCALC is a Macintosh software package which allows management and processing of chemical analyses. Together with chemical analyses, definitions of mineral species, chemical components, end-members and user routines are stored in an interactive relational database. In order to customize the software functionnalities, these objects may be created, deleted, modified, sorted, selected, ..., recorded, exported to other software, etc.

A chemical analysis is a set of chemical components and their associated values (e.g., concentration of Al, molar fraction of Pyrope in a Garnet, ...). Each analysis belongs to a mineral species; analyses of the same species have the same chemical components. Definition of new chemical components or the use of preexisting ones is required when creating new species. Each species is related to a set of end-members. To create a new end-member, the specification of the related species and the definition of a set of formal equations describing its thermodynamic behaviour is required.

Different types of calculations are available in PetroCalc, for example :

• **Thermodynamic and stoechiometric calculations** : From a selection of analyses, PetroCalc deduces the related set of end-members involved and performs the calculation of all existing stoechiometric relations. For each relation, the equilibrium equation $\Delta G=0$ is build and simplified using **computer algebra** . Any pair of variables contained in this equation may be choosen to represent the equilibrium graphically. Figure 1 shows a P-T diagram of the reaction Paragonite = Jadeite + Kyanite + H20.

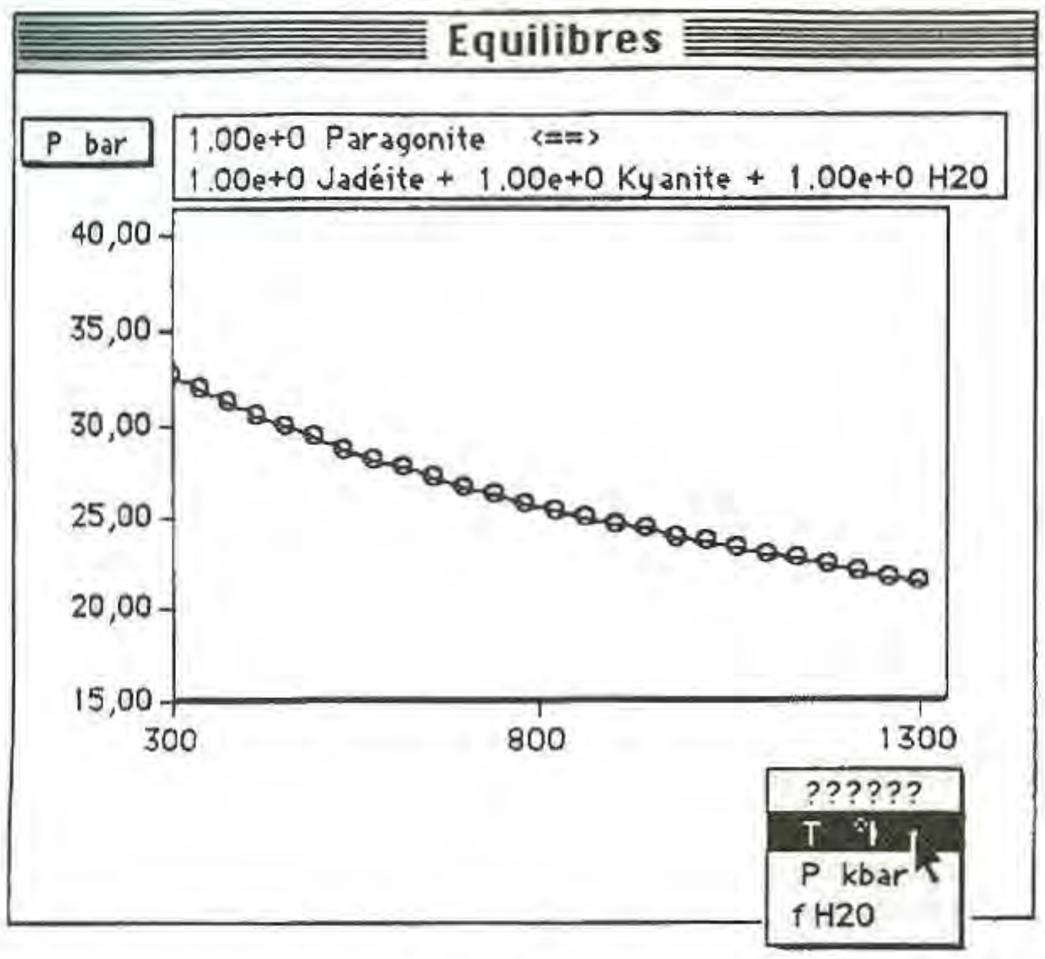

Figure 1

• **User calculations** : Using a Pascal-like programming language, the user creates or uses preexisting routines. These routines are, for example, structural formulae calculations, geothermobarometer, routines to plot analyses in a chemical diagram (ACF, AFM, etc.).

PETROGENETIC ASPECTS OF ORBICULAR GRANITE OF ROJARA, RAJASTHAN

Chattopadhyay,B. and Chattopadhyay,S.
(GSI,Jaipur, India)

Orbicular granite with orbs of various size and shapes (max. size 50cm X 30cm) has been observed in Rojara (25^{o} 13' : $73^{o}06'$) in an otherwise vast tract of coarse grained porphyritic Erinpura Granite Complex (ERG).

The enveloping rocks of the Erinpura granite include:(1) the ERG with average phenocryst 45.53% (11.20 SD). The phenocrsyts often show resorption and development of both pyterlitic and wiborgitic type of rapakivi intergrowth. This is intrusive into the metamorphic ensemble of Sirohi Group (Delhi Super Group) and shows development of thermal aureole along the contact. Compositionally it varies from granodiorite to alkali granite through quartz monzodiorite to quartz syenite (Fig.1). These granites have been subjected to strong ductile shearing along restricted zones leading to the formation of protomylonite to mylonite to phyllonite and development of S-C-C' fabric and (2) the Sumerpur granite (SG) which is nonporphyritic but sometimes show porphyry nature and is intrusive into the ERG. Minerallogically it varies from granodiorite to alkali granite through granite (Fig.1).

The nucleus of the orbicular granite has variable compositions :(i) crystal of quartz and K-feldspar,(ii) porphyritic granite showing rapakivi ovoids, (iii) schrol rock and (iv) biotite rich gneiss.

The shell of the orbicular granite is a medium grained alkali granite with k-feldspar far exceeding plagioclase. It is a granophyre with > 70% granophyric intergrowth. The matrix material of the orbicular granite is pegmatitic in nature with euhedral and resorbed crystals of feldspar. Tourmaline is present ubiquitously.

The orbicular granite is a product of interaction of ERG and SG. The R-mode factor analysis and paragenesis of Sumerpur granite suggests that mafics and plagioclases crystallised early followed by simultaneous crystallisation of K-feldspar and quartz (significant factor loading with opposite sign) producing granophyric intergrowth. The late phase of SG (generated due to partial melting of the crustal material under the influence strong ductile shearing, parallel to the regional Pali lineament, and supply of volatiles from the deeper part of the crust/mantle) utilised the enclaves of the enveloping rocks and the early phase of the same magma (which were often resorbed) as nucleus and wrapped around it as to form orbicules. Enrichment of the mother liquor with water vapour accounts for the coarseness of the matrix.

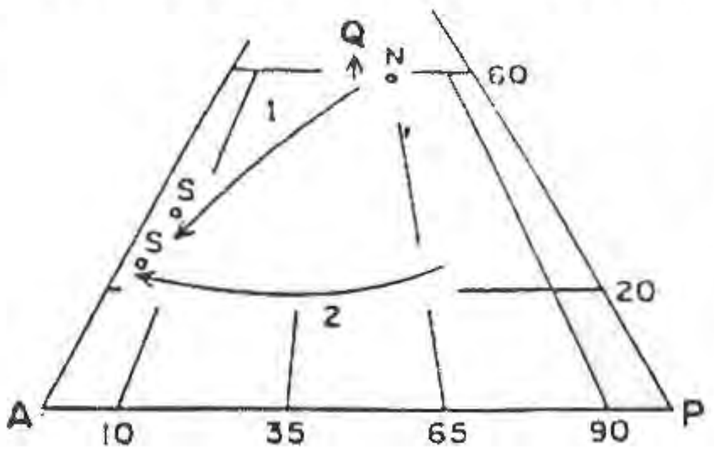

Fig. 1

1:SG trend
2:ERG trend
N:Nucleus
S:Shell

• GENESIS OF BLACK URANOPHANE

Chen Zhangru (*Mineralogical Dept., Beijing Research Institute of Uranium Geology*)

It is well known that uranophane is yellow, yet a kind of black uranophane was discovered in the oxidized zone of a granite-type uranium deposit in the south part of China (1).

Black uranophane surrounded by yellow uranophane is a compact aggregate, the mineral shows homogeneous black color under microscope. The results of wet chemical analysis show that composition of the mineral (5.8% CaO, 67.2% UO_3, 11.37% SiO_2 and 10.27% H_2O) is coincident with that of yellow uranophane, but 4.09% of tetravalent uranium exists in black uranophane.

Differential thermal and thermal gravimetric analyses, X-ray powder pattern and IR spectrum for the mineral have proved that it is uranophane, but few pattern lines of pitchblende can be found in the X-ray powder pattern of the mineral. No pitchblende has been discovered by microscope in the sample.

Formation conditions of the black uranophane are as follows:

1. Climate condition.

The uranium deposit is located in the humid subtropic zone. Annual rainfall and evaporation in the area where the deposit is located are 1600-2000 mm, 1300 mm respectively. The humid weather is helpful to oxidation of tetravalent uranium in uraninite and U-bearing accessory minerals from the granite.

2. Hydrochemical condition.

Hydrochemical condition of the uranium deposit is suitable to formation of the secondary uranium mineral assemblage.

Groundwater with pH value of 6.8–8.1 in the uranium deposit contains HCO_3^-, SiO_3^{2-}, Ca^{2+}, Na^+, which can provide Si and Ca, important components of uranophane. Groundwater with this sort of chemical property promotes uranium solution in water.

3. Host rock condition.

The Yenshan granite is the most important material resource for formation of uranophane. It provides U, Ca, Si forming uranophane. Based on analyses of $^{234}U/^{238}U$ isotope ratio in the granite, the results indicate that $^{234}U/^{238}U$ isotope ratio in the Yenshan granite varies from 0.873 to 0.978; but in the Indo-Chines granite it varies from 1.038 to 1.058. Calculation of ancient uranium content (2) shows that average migration rate of uranium in the Yenshan granite is 17.77%, maximum 47.7%. The revious $^{234}U/^{238}U$ isotope ratio and uranium migration rate in the Yenshan granite reveal that uranium in it is mobile and lost.

Ca, Si as important components forming uranophane come also from the Yenshan granite. Uranophane occurs in katagranite where contents of Ca, Si are lower than that of the granite (73.39% SiO_2, 0.90% CaO). Ca, Si lost in katagranite (70.43% SiO_2, 0.65% CaO) are used in formation of uranophane.

Some geologists consider that black uranophane possibly comes from full oxidation of pitchblende, although no pitchblende is found in the whole uranium deposit.

References

(1) Chen Zhangru et al., 1989. *Uranium geology*, Vol. **5**, N. 1, 8–14

(2) Zhang Baoju et al., 1979. *Annual Report of Beijing Research Institute of Uranium Geology*, Vol. **1**, 148–151

RE-EQUILIBRIA OF FLUID INCLUSIONS AT HYDROTERMAL CONDITION.

Chepkaja N.A., Kotelnikova Z.A. (*Inst. of Lithosphere of Rus. Acad. of Sci., Moscow*)

Re-equilibration of fluid inclusions during bringing the host crystal in P-T conditions different from trapping conditions has been confirmed by some experimental works. We have studied the modification of synthetic fluid inclusions during hydrothermal influence on host mineral. Fluid inclusions have been synthesized by growth of crystal of quarts on seed at 0.5 M solution of NaOH at 350 and 355 ^{o}C (crystal D and E respectively) and by the method of crack healing at the fluid H_2O-CO_2 with $X^{fl}_{CO_2}$=0.4 at 600^{o}C, 2 kbar (ex. 2099) and 800^{o}C, 3.65 kbar (ex. 2093).

Fluid inclusions have been studied by micro thermometric methods. Temperatures of homogenization of fluid inclusions was 294-300^{o}C (for 19 fluid inclusions in crystal) and 299-300^{o}C (for 20 fluid inclusions in crystal E). Temperature of ice melt varied from 0^{o}C to -1.25^{o}C for 53 fluid inclusions in crystal D and 30 fluid inclusions in crystal E. Temperatures of CO_2 homogenization of fluid inclusions was 21.5^{o}C at ex.2093 and 29^{o}C at ex.2099. Re-equilibration runs was made at 350-400^{o}C, P=300-1000 bars at solutions of NaCl with vary concentration with crystals D and E and at 500,1 kbar for ex.2099; 500^{o}C and 2.5 kbar for ex. 2093 (along isochore of 0.79 g/cc).

After runs at 500^{o}C temperatures of homogenization of all fluid inclusions in crystals D and E changed, at 400^{o}C and 350^{o}C they changed in a part of inclusions only. Composition of solutions in fluid inclusions did not change with exception of seven fluid inclusions, which had ice melt temperatures from -1.5^{o}C to -2.5^{o}C. The density of CO_2 reduce at both runs, the proportion of H_2O:CO_2 changed and varied for individual inclusions.

• ROLE OF f_{O_2} IN NATURAL DIAMOND FORMATION ACCORDING TO EXPERIMENTAL DATA

Chepurov A.I., Fedorov I.I., Sonin V.M. *(Inst. of Mineral. and Petrogr., Siberian Branch of Russ. Acad. Sci.)*

It is experimentally established that the diamond formation at "moderate" P–T parameters (50–60 kbar, 1300–1500 °C) takes place only in the presence of transition metals (Fe, Ni, Co, etc.). Carbon in sulfide and silicate melts crystallizes in the form of graphite even at P–T parameters of diamond stability. Under the action of a hydrogen–hydrocarbon fluid at these P and T parameters, transition metals are partially reduced from sulfides, silicates and oxides, and diamond is formed.

Stability of native transition metals accounts for the reducing fluid regime in processes of diamond formation. On the basis of experiments and thermodynamic calculations it is shown that under pressure of 40–60 kbar and temperatures of 1000–1500 °C the C-O-H and C–O–H–S fluids providing stability of diamond and native $Fe_{0.7}Ni_{0.3}$ or Fe and equilibrium of Fe/FeS consist chiefly of methane (40–90 mole %), water (5–30 mole %), hydrogen (up to 10–15 mole %). The total content of H_2S, CS_2, and COS is less than 1 mole %.

One can suppose that natural diamonds are crystallized under reducing conditions from silicate–metal or sulfide–metal melts. Properties and morphology of diamond crystals change by annealing under high pressure and dissolution, as redox environments change at higher levels in the Earth's crust.

• MINERALIZATION ASSOCIATED WITH DEEP-SEATED HYPERGENE ZONE IN THE MASSIVES OF ALKALINE-MAFIC AND ULTRAMAFIC ROCKS

Chernikov A.A. *(IGEM, RAS, Moscow)*

In deep parts from 500 to 2000 and more meters below the surface of Khibina and Lovozero (Kola peninsula) and other massives of alkaline–mafic rocks the supergene minerals widely spread in evaporite accumulations and permafrost rocks are present (Chernikov, 1992; Chernikov *et al.*, 1994). Natrite, thermonatrite, natron, halite, villiaumite, thenardite, melanterite, mirabilite, glauberite etc. belong to these minerals.

The studies carried on helped to find out that the main reason of convergent mineral origin in permafrost rocks, deep–seated hypergene zones and evaporites is connected with decisive and irreversible changes of physicochemical conditions during the processes of evaporation, freezing and underground water percolation into deep horizons of rocks; namely with alkalinity increase, mineralization and pressure growth in residual solution. But other factors differ essentially. That's why together with resemblances there is considerable distinction in mineral association, isotope characteristics and microadmixture of minerals.

There are speculations, confirmed by the actual material, that deep–seated hypergenesis is widely spread in all rocks and geological structures. But the main host minerals of high alkaline-mafic and ultramafic rocks are nepheline, lomonosovite, eudialite and others are less stable under the hypergene conditions. Various deep–seated hypergene minerals are widely spread just in these rocks. Since underground water has a high alkalinity (pH > 10) and almost 100% contents of (Na+K) among the cations in deep parts of massives of alkaline–mafic rocks, the more alkaline silicates substitute for less alkaline minerals. In water percolated zones,

zirsinalite and lovozerite substitute for eudialite. Ramsayite or adularia substitute for titanite etc. That's why the ultraagpaitic mineral association (Khomyakov, 1980; Semenov, 1980) is created, in which there are variable alkaline Ti–Zr–silicates, water–soluble Na–silicates and phosphates as well as ultra–alkaline minerals, villiaumite (50%), thermonatrite and cryolite (30% total alkalinity), etc.

References:
Chernikov, A.A. (1992). *Izv. RAS, Ser. Geol.*, 3, 118–126.
Chernikov, A.A., Dorfman, M.D., Dvourechenskaja, S.S. (1994). *Dokl. RAS*, 335, 84–87.
Khomyakov, A.P. (1980). *Scientific bases and utilization of the typomorphism of minerals*. M.: Nauka, 152–157.
Semenov, E.I. (1980). *Ibid*., 102–108.

KINETICS OF FSP CRYSTAL GROWTH FROM GRANITE MELT AT VARIABLE WATER CONTENT. EXPERIMENTAL STUDY.

Chevychelov V.Yu. and Simakin A.G.
(IEM, Chernogolovka, Russia)

Growth rates and delay times of heterogeneous nucleation of Fsp from granite melt are studied experimentally at total pressure 1 kbar and water content 4 and 2 wt.%. Special conditions are found to suppress volume crystallization and enhance growth on the Fsp seeds (Simakin & Chevychelov, 1990).

Based on the obtained experimental data melting diagram of used granite was ascertained.

It is found that morphology of Fsp varies from needle shape at ΔT=20-50°C, through dendrites aggregates at $\Delta T \geq$50-60°C to the normal spherolites at ΔT=160°C. At the unercoolings about 50°C stable fast crystals faces are splitided, glass inclusions are formed. This transition can be attributed to either diffusion driven instability or changing of growth mechanism (Sunagawa, 1984). Most crystals are elongated by **a**, only at small undercoolings few crystals with different orientation are noted.

It is found that delay time of heterogeneous nucleation of Fsp on the seeds of the same mineral attains from few hours at 4 wt.% up to few days at 2 and 0.7 wt.% of water content. On this parameter feldspar growth differs substantially from Pl growth from acid melt displaying practically no delay (Muncill & Lassaga, 1988).

Maximum growth velocities about $6 \cdot 10^{-8}$ cm/s for 4 wt.% and $3 \cdot 10^{-8}$ cm/s at 2 wt.% of H_2O content are observed at undercoolings about 40°C. Meanwhile predicted melts viscosities are the same near the liquidus.Difference in crystal growth rate and especially delay times can be attributed to change of melt structure at addition of water.

Experimental data on the dependence of crystal growth rate on the undercooling obtained are adequately interpreted with original model of diffusion transport and improved dependence of diffusivity from viscosity at a lower temperatures.

References:
Muncill ,G.E. & Lasaga, A.G.(1988). *Amer. Mineral.*, **73**, 982-992.
Simakin, A.G. & Chevychelov V.Yu.(1990). *Geokhimiya*, **5**, 682-690.
Sunagawa,I.(1984).*Mater.Sci. Earth Inter .*,63

TEACHING MINERALOGY AND CRYSTAL CHEMISTRY WITH COMPUTER GRAPHICS

Chiari G.
Dip. Scienze Mineralogiche e Petrologiche, Università di Torino

In mineralogy and crystal chemistry courses it is often useful to show crystal structures of minerals and inorganic compounds. This is traditionally done either by the use of drawings or three-dimensional models. Both techniques present some drawbacks. A drawing is static, in the sense that it cannot be modified according to need. To show a complex crystal structure it is essential to be able to change points of view, the number of atoms displayed and the conventions used to display bonds and atoms. Sometimes showing a single unit cell is not enough, since the structure can be better perceived by a larger portion of the crystal. Other times a unit cell is too much since the structure is too complex to be perceived at a glance.

The use of three-dimensional models can solve most of these problems, but has other drawbacks: they are costly and they cannot be seen from a distance in a large classroom.

An alternative to these methods is now available: a series of computer programs especially designed to display crystal structures. MOLDRAW, developed at Turin University, is one of these programs. It is very easy to use and can perform the following tasks: rotate the structure, change display modes (including Van der Waals radii selection which give a more real idea of the actual space occupied by the atoms), select crystallographic planes or directions for the projection, select co-ordination polyhedra around various atoms, cut a slice of given (modifiable) thickness along any crystallographic plane displaying the atomic content, and calculate on line important geometric features such as distances, angles, torsion angles, average planes, volume and lateral surface of polyhedra etc. A powder spectrum can be simulated: addition or removal of selected atoms is immediately reflected in the recalculated powder pattern. The changes of the powder pattern due to the substitution of a heavy atom in an isomorphous series can thus be very easily shown. Quality printouts allow the students to take copies of the structures home to study.

The problem of inserting the data in the program can be easily solved if one has access to a database such as ICSD (Inorganic Crystal Structure Database), now available in its new PC compatible form. The search for the structure is done using ICSD retrieval programs and the files obtained are automatically transformed into input files for MOLDRAW, each containing one structure with all the necessary information. Therefore there is no need for typing out co-ordinates etc. The students may be asked to study a given structure by retrieving it from ICSD (alternatively finding it in the literature and typing the information) and displaying it in detail with MOLDRAW. The display can be done either directly on the computer if the ratio student/machines is favourable and by means of colour transparencies obtained as printouts using an ink-jet printer, or by projecting slides taken directly from the screen.

It is useful, at least for one structure, to establish the connection between the computer models in their various forms and a physically built three-dimensional model. This can be constructed by the students using the tetrahedra, octahedra and cube-anti prisms plastic tools and bond of the MINIT system, for example. In order to understand how the atoms are bonded to each other MOLDRAW's slab feature can be effectively used. The framework of Zeolite structures (without oxygen atoms) are good examples for this task since they only require tetrahedra to build the model and they present high symmetry and produce beautiful final models.

Examples of these applications will be presented.

References:
ICSD - Inorganic Crystal Structure Database, FIZ, Karlsruhe.
Ugliengo P., Viterbo D., Chiari G. (1993). *Zeit. Krist.* **207**, 9-23.
MINIT - Cochranes of Oxford Ltd, Leafield, Oxford , England.

X-RAY DIFFRACTION ANALYSIS IN THE RESTORATION OF MICHELANGELO'S LAST JUDGEMENT

Chiari G.
Dip. Scienze Mineralogiche e Petrologiche, Università di Torino

During the restoration of the Last Judgement by Michelangelo in the Sistine Chapel two major problems arose with respect to the restoration of the vault: the presence of lighter lines, very roughly made, on the blue sky; and the need to decide whether to maintain or to eliminate the *modesty drapes*, or *"braghe"* (as they are popularly called) accumulated during the centuries.

The entire sky was painted using crushed Lapis Lazuli (the famous natural *ultramarine blue*) and was marked with lighter blue lines. Observations of thin sections showed that these lines were caused by the removal of the dark dirt layer rather than by being painted over with *tempera* or, worse, by a deterioration and discoloration of the lazurite. A trial to reproduce the effect using a paste obtained by mixing ash with water as a cleaning agent was successful, as the comparison of thin sections demonstrated.

Starting in 1563 (with Daniele Da Volterra) 40 *braghe* were painted to cover nudity. The board of experts decided that the oldest ones should be maintained and only the most recent (and aesthetically more displeasing) could be removed. Therefore the problem arose of determining the approximate age of the *braghe* in a scientific way, independent from art history considerations. This problem was tackled using different analytical methods by several people: 1) normal and ultraviolet light photography on the painting and in thin sections (Gabrielli N. and Morresi F.); 2) tristimulus colorimetry (Tabasso M. and Borrelli E.); 3) non-destructive X-Ray fluorescence using a portable device (Falcucci C. and Sciuti S.); 4) microprobe analysis on thin sections (Morresi F.); 5) X-ray powder diffractometry (Chiari G.). The entire research was co-ordinated and supervised by N. Gabrielli with the co-operation of G. Torraca.

The samples for the X-ray analysis (SIEMENS D5000 diffractometer equipped with Soller slits on the primary beam and graphite monochromator on the secondary beam; CuKα radiation) were obtained in part as remains of the previous sampling for the execution of thin sections, and in part purposely collected. This second series gave the best results since only the *tempera* layer was selected and analysed. Given the obvious necessity of reducing to an absolute minimum the amount of material taken for the analyses, it was decided not to recollect samples for the few cases in which only the mineralogical phases obviously contained in the mortar were present. In order to minimise the amount of each sample and to be sure not to lose any part of it during the subsequent manipulation, a special device was constructed that, working as a micro aspirator, allowed one to collect the grains detached by the scalpel point into a container to be opened directly in the laboratory. The few grains of material were deposited on a zero background quartz lamina (Smith D.K.-The Gem Dugout) using a drop of amyl acetate in order to increase the random distribution of the crystallites. Up to nine different phases were identified in many cases. It is worth noting the widespread presence of weddellite, the apparently ubiquitous calcium oxalate. The *braghe* were thus grouped into three well separated clusters: a) *bianco di S. Giovanni* as preparation and ochre based pigments, likely due to Daniele; b) preparation based on *lead white* (characterised by cerussite and hydrocerussite) and orpiment (AsS_3) as yellow pigment, which can be referred to Domenico Carnevali since his signature on Caron row was done with this technique; c) *lead white* preparation and a mixture of lead antimony oxides ($Pb_3Sb_2O_8$ and $PbSb_2O_6$) known as *Giallo di Napoli*. Since the latter pigment came into practice around 1750, its presence can be used as a *post quem* dating. Taking into account other considerations as well, a total of 17 *braghe* were removed, one of them on the basis of the X-Ray evidence alone. St. Peter and St. Bartholomew show a double drape, the first painted by Daniele and the second using Naples Yellow. It should be pointed out that there was a perfect consistency between all indications (when present) coming from the various methods applied. Art history considerations independently pointed to the same conclusions.

I am grateful to CNR - Committee 15 for funding the present research.

ORIGIN OF THE FUMAROLIC FLUIDS OF LA FOSSA CRATER (VULCANO ISLAND, ITALY), BASED ON δD AND $\delta^{18}O$ VALUES AND CHEMICAL DATA. IMPLICATIONS FOR VOLCANIC SURVEILLANCE.

Chiodini G.(Dept. of Earth Sciences, Univ. of Perugia), Cioni R.(IGGI-CNR, Pisa), Marini L.(ChemGeo, Pisa) & Panichi C.(IIRG-CNR, Pisa)

The δD value of the steam condensates is strongly, positively correlated with H_2O concentration and independent upon outlet T, whereas the $\delta^{18}O$ value is well, positively correlated with outlet T and independent on H_2O concentration. These observations suggest that, since 1979, the fumaroles of La Fossa crater have discharged mixtures essentially made up of magmatic water and marine-hydrothermal water. The contribution of meteoric water was very low in the period 1979-1982 and nil afterwards. The marine-hydrothermal component is characterized by δD close to +10 ‰, which is the value of local sea water. Its $\delta^{18}O$, with values in the +5 to +7.2 ‰ interval, is largely shifted with respect to local sea water, due to isotopic exchange with the ^{18}O-rich silicates of the rocks under high-temperature and low-permeability conditions (Panichi & Noto, 1992). The magmatic water, with δD values close to -20 ‰, is within the typical range of andesitic waters (Giggenbach, 1992), as expected for island arcs such as the Aeolian Arc to which Vulcano Island belongs. The $\delta^{18}O$ value of the magmatic water is generally of +3 to +4 ‰, although values as high as +5.5 to +6.5 ‰, which are within the typical range of magmatic water, were reached in the summer of 1988, when magma degassing extended into the kernel of the magma body.

All in all, both isotopic values and chemical data strongly support the dry model (Chiodini *et al.*, 1993 and references therein), which is therefore the landmark for the volcanic surveillance of the La Fossa apparatus. Considering that the maximum expected eruption (e.g. Frazzetta & La Volpe, 1991) is characterized by an early magma-water interaction, it is evident that this condition can be reached either by magma uprise into a wet environment or by water inflow into the magma body. Admitting that the occurrence of either one or the other phenomenon is preceded by substantial chemical and isotopic changes in the crater fumarolic system, the task of geochemical monitoring is to evaluate these variations, based upon the conceptual model of the system. Implicitly, if no relevant change is observed the risk of eruption should be minor.

Chiodini G., Cioni R., Marini L. (1993). *Appl. Geochem.*, 8, 357-371.

Frazzetta G. & La Volpe L. (1991). *Acta Vulcanol.*, 1, 107-113.

Giggenbach W.F. (1992). *Earth Planet. Sci. Lett.*, 113, 495-510.

Panichi C. & Noto P. (1992). *Acta Vulcanol., Marinelli Volume*, 2, 297-312.

GEOCHEMICAL MODELING OF HYDROTHERMAL SYSTEMS IN CARBONATE-EVAPORITE AQUIFERS

Chiodini G.(*Dept. of Earth Science, Univ. of Perugia, Italy*),
Frondini F.(*Dept. of Earth Science, Univ.of Perugia, Italy*)
and Marini L., (*CHEMGEO, Pisa, Italy*).

The theoretical composition of aqueous solutions in equilibrium with a mineral assemblage made up of calcite, dolomite, anhydrite, chalcedony (or quartz) and fluorite, has been calculated at different temperatures, PCO_2 and total molality of mobile species Na and Cl, considering the influence of ion complexing.

The mineral-solution equilibrium model is described elsewhere (Chiodini et al., 1991). The concentration of free ions and complex species of calcium, magnesium, sulphate, bicarbonate, fluoride, sodium and chloride has been computed:

1) every 25 °C, for temperatures from 0 to 100 °C, and every 50 °C, for temperatures from 100 to 200 °C;

2) every log-unit, for total Cl and Na molality from 0.001 to 0.1, setting $m_{Cl}=m_{Na}$;

3) every half log-unit, for PCO_2 from 0.1 to 100 bars.

Inspection of the ternary diagram HCO_3-SO_4-F (Fig.1), where theoretical total molalities, for $m_{Cl}=m_{Na}= 0.01$, have been used to construct a T-PCO_2 grid, shows that the HCO_3/SO_4 ratio is essentially a geobarometer, the SO_4/F ratio is practically a geothermometer, and the HCO_3/F ratio is a function of both T and PCO_2. In the considered range of m_{Cl} and m_{Na} the behaviour of these ratios does not change.

Fig. 1 reports also the measured values of several thermal springs fed by hydrothermal systems hosted in carbonate-evaporite reservoirs of Central Italy. These waters exhibit either Ca-SO_4 or Na-Cl chemical composition. The comparison of measured HCO_3, SO_4 and F molalities with theoretical values indicates that these waters have equilibrium temperatures in the interval 50-100 °C, independently on their chemical composition, while equilibrium PCO_2 is generally from 0.1 to 3 bar for Ca-SO_4 springs and more than 10 bar for Na-Cl waters. All in all, these characteristics suggest that Ca-SO_4 waters come from shallow aquifers communicating with outcrops of carbonate rocks while Na-Cl waters proceed from deeper aquifers covered by impervious rocks.

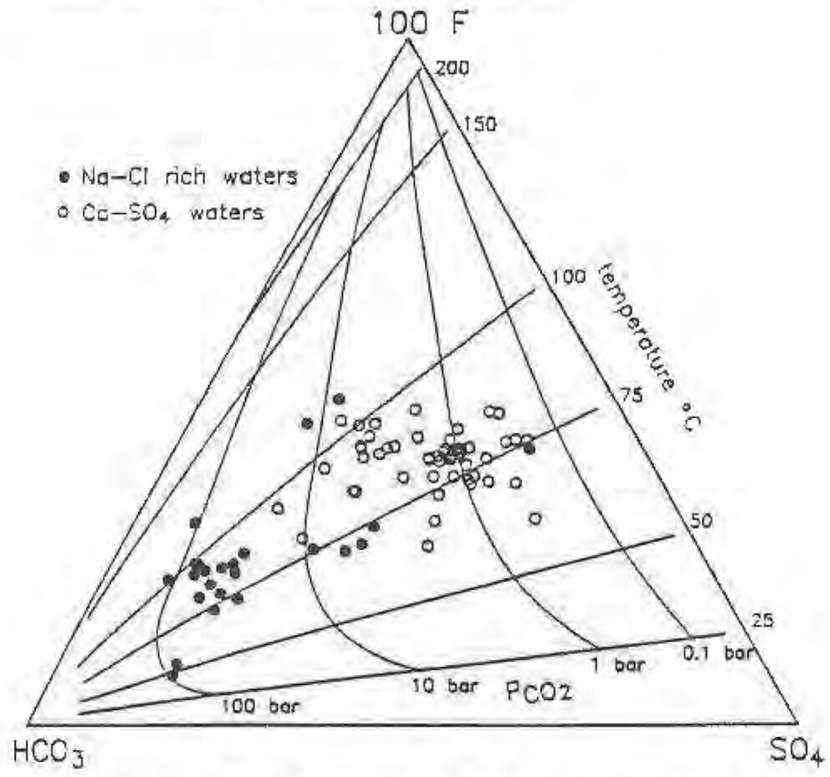

Fig. 1. Ternary diagram HCO_3-SO_4-F for $m_{Cl}=m_{Na}= 0.01$. Analitical data are from: Dept. of Earth Science, Univ. of Perugia (unpublished data), Bencini *et al.* (1977), Chiodini *et al.* (1991), Duchi *et al.* (1987), Duchi *et al.* (1985), Marini *et al.* (1986)

References:
Bencini, A., Duchi, V., Martini, M. (1977). *Chem.Geol*, **19**, 229-252.
Chiodini, G., Cioni, R., Guidi, M., Marini, L. (1991). *Geochim. Cosmochim. Acta*, 55, 2709-2727.
Chiodini, G., Giaquinto, S., Frondini, F., Santucci, A. (1991). *Geothermics*, **20**, 329-342.
Duchi, V., Minissale, A., Ortino, S., Romani, L. (1987). *Geothermics*, **16**, 147-157.
Duchi, V., Minissale, A., Romani, L. (1985). *Atti Soc. Tosc. Sci. Nat. Mem.*, **92**, 237-254.
Marini, L.,Chiodini, G., Cioni, R. (1986). *Geothermics*, **15**, 77-86.

TERRESTRIAL BUSERITE : ITS CHEMISTRY AND DEHYDRATION BEHAVIOR

Choi H. and Kim S.J. (*Dept. Geological Sciences, Seoul National University*)

Buserite is the name given by Giovanoli et al. (1971) to the 10-Å phase in the sea-floor manganese nodules. It has been reported from marine manganese nodules by Arrhenius and Tsai (1981), Chukhrov et al. (1984) and Ostwald and Dubrawski (1987). Terrestrial occurrences of the 10-Å manganate have not been reported (Ostwald and Dubrawski, 1987). Buserite is not listed in Fleischer's Glossary of Mineral Species (1991). However, terrestrial buserite has been identified from the Dongnam and Janggun mines, Korea.

Buserite is closely associated with 7-Å phase (usually rancieite) in manganese oxide ores of the supergene oxidation zones of manganese carbonate deposits. Both minerals are identified from one and the same flakes. The intensity ratios of 10-Å to 7-Å peaks are variable from sample to sample, and decrease with increasing dehydration. (Ca,Mg)-buserite and (Zn,Ca)-buserite have been identified from the Janggun and Dongnam mines, respectively. Dehydration and X-ray diffraction studies have been carried out for both minerals in order to know the nature of interlayer waters and their structural configuration.

Structural simulation for the X-ray powder diffraction patterns for both natural and synthetic samples shows that buserite has three interlayer waters between [MnO_6] octahedral sheets. Dehydration experiments by both the relative humidity control and gradual heating show that two types of water molecules are present in buserite, that is, the very weakly bonded water molecules and the weakly bonded water molecules. Dehydration taking place before 20% RH or about 50°C may be due to the removal of the very weakly bonded water which is assumed to be present bridging two interlayer waters bonded to [MnO_6] octahedral sheets. With gradual increasing dehydration, the 10Å peak gradually shifted to lower spacing (about 7.2Å) until no peak appears at about 60°C. It suggests that a considerable disordering takes place in the [MnO_6] octahedral sheets with removal of the very weakly bonded water. Dehydration taking place at above about 90°C may be due to the removal of two interlayer waters bonded directly to [MnO_6] octahedral sheets. The shift of 10-Å peak toward 7-Å between 50 and 90°C does not take place by a direct transformation, but by a gradual building of regular [MnO_6] octahedral layers from disordered phase. The disordered phase between 10Å and 7Å phases is also detected in the synthetic Ca- and Zn-buserite. (Ca,Mg)-buserite from the Janggun mine shows a slight rehydration by raising the relative humidity. Its basal spacing of (Ca,Mg)-buserite increased about 13% in intensity and sharpness. The present study supports that buserite is a valid mineral species.

References:
Arrhenius, G.O. and Tsai, A.G. (1981). *SIO Reference Series*, **81-28**, 1-19.
Chukhrov, F.V., Gorshkov, A.I., Drits, V.A., Sivtosov, A.V., Uspenskaya, T.Yu. and Sakharov, B.A. (1984). *Izvest. AN SSSR, ser. geol.*, **10**, 65-76.
Fleischer, M. (1991). *Glossary of mineral species*. Mineralogical Record, Arizona.

Giovanoli, R., Feitknecht, W. and Fischer, F. (1971) *Helv. Chim. Acta*, **54**, 1112-1124.
Ostwald, J. and Dubrawski, J.V. (1987) *N. Jb. Miner. Abh.*, **157**, 19-34.

UNCOMMON ROCK-FORMING MINERALS IN A VERY-HIGH-PRESSURE TERRANE, DORA-MAIRA MASSIF, WESTERN ALPS

Chopin C. (*Ecole normale supérieure, Géologie, Paris*), Amisano-Canesi A. (*Sci. mineralogiche, Univ. di Torino*), Brunet F. (*Bayerisches Geoinstitut, Univ. Bayreuth*) and Simon G. (*Mineral.-Petrogr. Institut, Univ. Kiel*)

In the southern part of the Dora-Maira massif, Italy, a quartz/coesite-rich phengite-pyrope-kyanite-talc-schist ("pyrope quartzite" or "whiteschist" *auct.*) occurs regionally as trails of boudins and lenses in the orthogneiss of the coesite-bearing terrane (Chopin *et al.*, 1991). Pyrope megablasts are 2 to 20 cm in size and include clinochlore, talc, kyanite and rutile, plus a variety of less abundant minerals, some of which represent new species or show uncommon features.

The most spectacular ones are members of a complete **silicate-to-phosphate solid solution** series. They range in composition from the ellenbergerite (neso)silicate end-member, $(Mg,Ti,\square)_2Mg_6Al_6Si_6Si_2O_{38}H_{10}$, space group $P6_3$ (Chopin *et al.*, 1986), to the quasi-isostructural phosphate, $(Mg,\square)_2Mg_{12}P_6P_2O_{38}H_9$, space group $P6_3mc$. The slight symmetry change from phosphate to silicate is due to cation ordering in the octahedral double chain (on the two-fold screw-axis) for the silicate. The purple colour of the silicate and the blue-green one of the phosphate are due, respectively, to Fe^{2+}-Ti^{4+} and Fe^{2+}-Fe^{3+} charge transfer // c, between face-sharing octahedra of the single chain (on the six-fold screw-axis). Structure refinements along the series, including the synthethic P-end-member, show that P and Si are equally partitioned among the two tetrahedral sites, although one (on the three-fold axis) has a free OH apex. Replacement of Si by P is charge-compensated primarily in the octahedral double chain (Mg for Al) and in the single chain (Mg for Ti, and non-monotonic, concomitant variations of the number of vacancies and protons along the series). With 20 to 50 % vacancy, the octahedral single chain appears as the flexible, regulating element of the structure. The silicate end-member is stable at very high pressures (> 27 kbar, Chopin *et al.*, 1992) whereas the phosphate end-member is stable down to 8 kbar or less (Beller, 1987; Brunet *et al.*, 1994); this offers interesting barometric prospects for the members of the series.

In **magnesiodumortierite**, a primary to early secondary phase, the two ellenbergerite-type chains of face-sharing octahedra, normally occupied by Al in dumortierite, contain Mg, which is dominant in the single chain (from $Mg_{0.65}\square_{0.35}$ to $Mg_{0.4}Ti_{0.3}\square_{0.3}$) and subordinate in the double chain (Al_2 to $Al_{1.2}Mg_{0.8}$, Chopin *et al.*, 1994).

Bearthite, $Ca_2Al(PO_4)_2OH$, occurs as an accessory mineral both in the pyrope-bearing rock and in metapelites of the same terrane (Chopin *et al.*, 1993). As a member of the brackebuschite group it has the smallest cation in each structural position, which may account for its stability at high pressures. However, an experimental study shows bearthite to be stable also down to very low pressures, up to 500°C at 1 kbar and up to 820°C at 10 kbar. That the first finding was in very-high-pressure rocks must therefore be fortuitous.

Magnesiostaurolite occurs exclusively as inclusions in pyrope megablasts. It has XMg = Mg/(Mg+Fe) in the range 0.80-0.95, virtually identical to that of the host garnet. Other uncommon features are the high lithium (*ca.* 1 wt.% Li_2O) and water contents, the absence of tetrahedral Al, and the structural position of Mg. The T2 tetrahedra normally occupied to 90-95 % by Fe show about 30 % vacancy (beside Mg, Li and Fe), whereas the neighbouring M4 octahedra, normally vacant to 95 %, show 25 % occupancy by Mg (Hawthorne *et al.*, 1993). This incipient change in coordination of the divalent cation may be the key to the Mg-staurolite paradox (a high-pressure phase with expectedly four-fold coordinated Mg) and to the complex thermodynamic behaviour of the staurolite series (*e.g.* reversals in Fe-Mg partitioning with garnet and chloritoid).

Magnesiochloritoid with XMg up to 0.95 was recently found in pyrope megablasts, together with talc and ellenbergerite. Its coexistence with talc implies for the prograde path an even steeper *P/T* gradient than previously thought, because *P* must have exceeded the stability limit of clinochlore + kyanite. Besides, Fe-Mg partitioning between magnesiochloritoid and garnet shows evidence of reversals from the normal situation (XMg)ctd > (XMg)gt. Whether temperature, composition, polytype or pressure is responsible for this anomaly is still presently explored.

References:
Beller, U. (1987): Diplomarbeit, Univ. Bochum
Brunet, F., et al. (1994): *Terra Abstracts*, **6**, EMPG V.
Chopin, C., et al. (1986): *Contrib. Mineral Petrol.*, **92**, 316-321.
Chopin, C., et al. (1991): *Eur. J. Mineral.*, **3**, 263-291.
Chopin, C., et al. (1992): *Terra Abstracts*, **4**, EMPG IV.
Chopin, C., et al. (1993): *Schweiz. mineral. petrogr. Mitt.*, 73, 1-9.
Chopin, C., et al. (1994): *Eur. J. Mineral.*, **6**, in press.
Hawthorne, F.C., et al. (1993): *Can. Mineral.*, **31**, 551-582.

LEAD TITANATE AS A PRESSURE CALIBRANT IN THE DIAMOND ANVIL CELL

Chou I-Ming and Haselton H.T., Jr. (U.S. Geological Survey)

The tetragonal-cubic phase transition in $PbTiO_3$ has been determined at pressures up to 7 kbar in a diamond anvil cell equipped with heating and cooling capabilities (Bassett et al., 1993). A chip of $PbTiO_3$ (about 350μm x 200μm x 40μm) was prepared from a crystal synthesized and characterized by Dr. Bing-Nan Sun (personal communication, 1994). The phase transitions, indicated by the movements of phase fronts, were observed optically at heating or cooling rates of about 1 °C/min and were recorded on videotape. The temperature intervals, in which the phase transitions occur, range from 0.8 to 2.8 °C depending on pressure. The temperature at which the movement of phase front starts (or ends) on heating (or cooling) was taken as the transition temperature [$T_{tr,h}$ (or $T_{tr,c}$); precise to ±0.4 °C and accurate to ±1.5 °C]. The transition temperatures were determined at 1 atm and along six isochores of H_2O. The density of each isochore was determined by the measured liquid/vapor homogenization temperature (T_h) using the equation of state of H_2O (EOSW) reported by Haar et al. (1984). Transition pressures ($P_{tr,h}$ and $P_{tr,c}$) along each isochore were calculated from the measured transition temperatures using the same EOSW. The results are listed in the following table.

$T_{tr,h}$ (°C)	$T_{tr,c}$ (°C)	T_h (°C)	Density (g/cm^3)	$P_{tr,h}$ (bar)	$P_{tr,c}$ (bar)
493.0	488.1	-	-	1 atm	1 atm
481.1	474.1	305.3	0.701	1906	1833
458.6	454.0	170.1	0.897	4887	4813
456.0	452.4	160.5	0.907	5094	5037
455.3	450.8	153.8	0.913	5255	5181
446.3	440.4	80.4	0.971	6861	6757
442.8	435.8	55.6	0.985	7280	7154

Least-squares regressions of the data give

$P_{tr,h}$ (bar) = 70217 - 142.35 $T_{tr,h}$ (°C), and

$P_{tr,c}$ (bar) = 68313 - 140.01 $T_{tr,c}$ (°C),

with the R-squared values of 0.9966 and 0.9987, respectively. Maximum differences between calculated and observed values of $P_{tr,h}$ and $P_{tr,c}$ are 210 and 143 bar, respectively. Some of the scatter is probably due to relaxation of the Re gasket between diamonds, which results in a slight deviation from isochoric behavior of the sample chamber. Regressions yield slopes for the phase boundary of -7.02 and -7.14 °C/kbar from the heating and cooling observations, respectively. They are less steep than the -8.4 (±0.3) °C/kbar reported by Samara (1971) for U-doped $PbTiO_3$; the variation may result from the compositional difference. The advantages of using $PbTiO_3$ as a pressure calibrant include the following: (1) the phase transition is rapid and the transition temperatures can be easily and precisely determined by observing the movement of phase fronts; (2) its phase boundary in P-T space intersects isochores of common geologic fluids at high angles and thus facilitates its applications; and (3) the phase transition covers the intermediate-temperature range of geologic

environments, with the α-β quartz transition applicable only at temperatures above 573 °C (Shen et al., 1993) and the tetragonal-cubic phase transition of $BaTiO_3$ applicable only at temperatures below 120 °C (Chou et al., 1993).

References:

Bassett, W.A., Shen, A.H., Bucknum, M., and Chou, I-Ming (1993). *Rev. Sci. Instrum.*, **64**, 2340-2345.

Chou, I-Ming, Haselton, H.T., Jr., Nord, G.L., Jr., Shen, A.H., and Bassett, W.A. (1993). *Eos*, **74**, 170.

Haar, L., Gallagher, J.S., and Kell, G.S. (1984). *NBS/NRC Steam Tables, Hemisphere Publ. Corp., Washington, D.C., 320pp.*

Samara, G.A. (1971). *Ferroeletrics*, **2**, 277-289.

Shen, A.H., Bassett, W.A., and Chou, I-Ming (1993). *Amer. Mineral.*, **78**, 694-698.

ORE TEXTURES AND ORIGIN OF Sb-Au MINERALIZATION IN THE NÍZKE TATRY MTS.

Chovan M. and Hurai V. (*Comenius University, Bratislava, Slovakia*)

Sb-Au mineralization in the Nízke Tatry Mts. is represented by vein-type hydrothermal deposits localized within regional mylonite zones and/or along faults hosted by Hercynian granitoides, migmatites and metamorphic rocks. During the last four decades, mining works have opened the Dúbrava deposit - the main antimony producer of Czechoslovakia. Country rocks of this deposit consist predominantly of biotitic granodiorites and tonalites. Elongated bodies of migmatites and gneisses represent relics of the crystalline cover.

Mineralization in the Dúbrava deposit has been formed during five stages separated in space and time. The earliest, high temperature stage is represented by lens-shaped, W-E trending quartz-pyrite veins up to several decimetres thick, containing also scheelite impregnations, wherever penetrating migmatites. Quartz veinlets with pyrite and molybdenite are located only in granitoides.

The second stage is represented by gold-bearing arsenopyrite and pyrite precipitated along with quartz either in form of impregnations in hydrothermally altered granitoides or along margins of the main quartz-sulphidic veins, following the N-S direction. Sectorial zoning is typical of these pyrites and arsenopyrites.

The third stage comprises earlier quartz + Fe-dolomite + sphalerite and later quartz + stibnite assemblages. Relatively frequent is symmetrically banded texture. The sphalerite is depleted in iron and associates with Pb-Sb sulphosalts. Majority of zinckenite in the earlier substage might have originated as a result of a temperature decrease, because the low temperature conditions are favourable for precipitation of the sulphosalts depleted in lead. Pb-rich sulphosalts occur very rarely in form of small inclusions in the zinckenite or robinsonite. Pyrite, as one of the earliest minerals of this stage, is obviously concentrically or sectorially zoned. Stibnite aggregates most commonly show mosaic structures and spindle-shaped, pressure-induced lamellae.

Primary senarmontite, native antimony, chalcopyrite and chalcostibite are rare.

The fourth stage is represented by quartz + dolomite + barite assemblage, accompanied by Ag-bearing tetrahedrite and Sb-Cu-Pb sulphides. Increased amount of Bi is manifested by the presence of chalcostibite, Pb-Sb-Bi sulphosalts and "horobetsuite". Intergrowths of these minerals create typical diffusional zoning and graphic structures.

The latest, barite stage forms independent veinlets with barite as the dominant mineral.

Fluid inclusion studies have demonstrated that the earliest, high temperature assemblages with scheelite, molybdenite and arsenopyrite have associated with immiscible $H_2O+CO_2(+CH_4)$, low salinity fluids at temperatures between 300-400°C and pressures about 2 kbars. Contrary to this, epithermal conditions are constrained for the latest stages. Decreasing homogenization temperatures with salinity indicate influx of diluted meteoric water into the mineral-forming solutions responsible for the formation of stibnite, tetrahedrite and barite. The majority of divalent cations in the aqueous fluid inclusions trapped in barite suggest a genetic link with Early Triassic evaporite formations.

Isotopic study on various sulphidic minerals has revealed predominantly mantle-derived source of sulphur with signs of crustal contamination indicated by a relatively narrow range of the $\delta^{34}S$ values from -1.7 to +6.3 ‰ in stibnite, sphalerite and pyrite. The $\delta^{18}O$ values between 3.3-8.5 ‰ indicate predominantly metamorphic and/or magmatic origin for water of the CO_2-rich aqueous fluids from the high temperature stages. The $\delta^{18}O$ values between -9.3 and +1.5 ‰ unequivocally imply participation of isotopically lighter meteoric water in later stages of the mineral-forming process.

References:

Sachan, H.K. & Kantor, J. (1990). *Geol. Zborn. Geologica Carpathica*, 41, 749-757.

THICK ANTI-PHASE BOUNDARIES IN SPHENE AND THE EFFECT OF THE 496 K PHASE TRANSITION: AN X-RAY DIFFRACTION STUDY

J. Chrosch, E.K.H. Salje (*Dept. of Earth Sciences, Univ. of Cambridge*), and U. Bismayer (*Min.-Pet. Inst., Univ. Hamburg*)

X-ray rocking curves at elevated temperatures were performed in synthetic Sphene, $CaTiSiO_5$, using a high resolution diffractometer in combination with a 120° (2θ) position sensitive detector. During the structural phase transition from the low temperature space group $P2_1/a$ to the high temperature space group A2/a (Taylor & Brown, 1976) the critical reflection (216) was investigated by tilting and rotating the crystal.

The line profiles and widths of the rocking curves and diffraction peaks were fitted with a combined Lorentzian and Gaussian function and compared with theoretical reflection profiles (Chrosch *et al.*, 1994). The temperature dependence of the rocking peak height could be calculated using the model of a macroscopic order parameter Q (Bismayer *et al.*, 1992; Salje *et al.*, 1993) yielding a critical exponent ß=0.16(2).

After the disappearance of the reflection (216) at approximately 500 K the remaining diffuse intensity yields a non-vanishing amount of anti-phase boundaries which are more than 200 times thicker (~25 Å) than those of the low temperature phase (~0.1 Å).

Boundaries of approximately the same order of magnitude were already obtained in electron diffraction studies (Van Heurck *et al.*, 1991).

References:

Bismayer, U., Schmahl, W., Schmidt, C., Groat, L.A. (1992). *Phys. Chem. Minerals*, **19**, 260-266.

Chrosch, J., Bismayer, U., Salje, E.K.H., Putnis, A., Schmidt, C., Kek, S. (1994) *in preparation.*

Salje, E.K.H., Schmidt, C., Bismayer, U. (1993). *Phys. Chem. Minerals*, **19**, 502-506.

Taylor, M. & Brown, G.E. (1976). *Am. Min.*, **61**, 435-447.

Van Heurck, C., Van Tendeloo, G., Ghose, S., Amelinckx, S. (1991). *Phys. Chem. Minerals*, **17**, 604-610.

MAGMATIC NATURE OF CRYOLITE IN GRANITES

Chtchekina T. I., Gramenitskiy Ye. N. (Moscow State University, Moscow)

Experimental investigations of the fluorine-bearing granite system (Gramenitskiy & Chtchekina, 1993) revealed a wide area of liquid immiscibility. Two coexisting melts were found: aluminosilicate and alkali-aluminofluorine ones. The latter is the independent component of the system and as the structure unit affecting on differentiation processes separates from aluminosilicate melt at final stage of

magmatic evolution. Thus phase relations in the system SiO2-Al2O3-Na2O-K2O-H2O-F may be treated as the direct model of cryolite-bearing granites formation.

Through-out the world near 15 localities of cryolite, associated with granites, are known. As a rule such granites represent the final phases of strongly evolved complexes (Bailey, 1980). These granites form post- or nonorogenic massifs, associated with regional faulting. Their age varies from Upper Proterozoic to Jurassic. Cryolite-bearing granites are usually peraluminous or peralkaline with sodium predominating relative to potassium and with high contents of F, Li, Rb, Zr, REE.

Three morphological types are characteristic of cryolite: a)uniform distribution in granites; b)nests or lenses; c)veins. The uniform distributed cryolite fits into the typical magmatic structure of granites. It crystallizes from F-saturated aluminosilicate melt. Experimentally, such saturation will proceed at the content near 3% fluorine in the melt. A similar concentrations of fluorine near 2.5-3% are noted in cryolite-bearing granites.

Nests and lenses of cryolite in the rocks are similar in morphology to the globular structure, observed in our experiments. The highest temperatures of such type cryolite formations is less than 590°. The solidus of aluminofluorine melt according to our experiments is about 530-550°.

The liquation of the alkaline-aluminofluorine melt leads to increasing of alumina to total alkalies ratio in the coexisting aluminosilicate melt and is attend by fractionation of alkalies: aluminosilicate melt is enriched by potassium, aluminofluorine one - by sodium with K_p = 7-8.

The concentration of Li and W in cryolite-bearing granites according to our experimental data is due to the extraction role of alkaline-aluminofluorine melt. The accumulation of F, Na, Li in liquating melt and the following evolution of fluid-magma systems at lowering temperature produce the processes of alkali-haloid metasomatism and the recrystallization of original, magmatic cryolite.

References:
Gramenitskiy, Ye.N., Chtcheкina, T.I. (1991). Geochemistry, 6, 821-840.
Bailey, J.C. (1980). Bulletin of the Geological Society of Denmark, 29, 1-45.

ORIGIN OF ARCHEAN GNEISS'S PROTOLITHS AND COMPOSITION OF ANCIENT MAGMAS (BY MELT INCLUSIONS IN ZIRCON)

Chupin S.V., Chupin V.P. (*Inst. of Mineral. and Petrogr., SB RAS, Novosibirsk, Russia*) and Bridgwater D. (*Geological Museum, Univ. of Copenhagen, Denmark*)

Melt inclusions in zircons from ancient tonalite-trondhjemite and charnockite gneisses were studied. The results provide unique information of the origin of different generations of zircon. And make possible to recognize the nature of protoliths (primary rocks) of gneisses, composition of magmas as well as characteristic features of primary-crustal magmatism in the early stages of the Earth's continental crust formation (Chupin *et al.*, 1993; Chupin *et al.*, 1994).

Primary melt inclusions (with glass) have been observed in zircon cores. The glass in these inclusions were determined by means of an optic method and by the analyzing chemical composition and Raman spectra of non-heated inclusions. The presence of glassy inclusions indicates fast cooling of melts. It is characteristic of volcanic and subvolcanic rocks.

The study revealed magmatic, perhaps, subvolcanogenic nature of protoliths of tonalite (3.33 Ga) and charnockite (about 3.3 Ga) gneisses of Aldan Shield and trondhjemite gneiss Uivak (3.73 Ga) of Canadian Shield. Protoliths of enderbite gneiss (>3.3 Ga) of Anabar Shield were likely to be of volcanogenic origin.

In some analyses of glass of inclusions from the cores of zircon from enderbite gneiss of Anabar Shield and from gneiss Uivak of Canadian Shield essentially sodium trachyandesite (about 57 mas.% SiO_2) and trachybasaltic compositions of melt were obtain. These melts from which the earlier cores of zircon were crystallized are supposed to characterize the primary basic substratum being a source of tonalite-trondhjemite magmas.

Essentially sodium trachyandesite (62.3 mas.% SiO_2) composition was obtained from glass of inclusions from zircon of tonalite gneiss and potassium-sodium rhyodacite composition - from zircon of charnockite gneiss of Aldan Shield. It is possible that these compositions are reflect the composition of initial magmas from which gneiss's protoliths were crystallized.

By results of melt inclusions investigations, geochronological and geological data it supposed that protoliths of tonalite and charnockite gneisses had common or close (in time) source of initial magmas. Probably these protoliths were united magmas series and potassium acid rocks were formed on the early stages of the Aldan Shield's continental crust formation.

References:
Chupin, V.P., Tomilenko, A. A., Chipin, S.V. (1993). *Geology and Geophysics (in Russian)*, **12**, 116-131.
Chupin, V.P., Chupin, S.V., Pospelova, L.N., et al. (1994). *Docladi Academii nauk*, in press.

THE ORIGIN AND CRYSTALLISATION CONDITIONS OF KYANITE GRANULITES (BY MELT INCLUSIONS IN KYANITE, GARNET AND OTHER MINERALS)

Chupin V.P. (*Inst. Mineral. and Petrogr., SB RAS, Novosibirsk, Russia*)

The deep-seated xenoliths of kyanite granulites, eclogites, and pyroxenites are found from Neogen (?) alkaline-basaltoid pipes in East Pamir. Among granulites occur separated massive and gneissose granulites (garnet + kyanite + quartz + sanidine) and kyanite granulites with fragments of eclogite rock assemblage.

All the rock - forming and accessory granulite minerals contain primary melt inclusions. This indicate magmatic origin of kyanite granulites. The melt inclusions were first established in kyanites.

Liquid CO_2 of high density was revealed in the fluid phase of melt inclusions. The data were obtained by cryometric and Raman spectroscopic methods. The calculations have shown high CO_2 content in melt (about 2 mas %). The melt composition are K-Na and K rhyodacites (according to the composition of melt inclusion glasses).

It was found, that kyanite granulites were crystallized at pressures above 15 kbar and temperatures not lower than 1050-1000°C.

Initial granulite melts were formed, perhaps, during anatexis of metapelite rocks and/or during fluid syntexis and partial melting of quartz eclogites at the depth of 60-65 km. Crystallization of such melts could have taken place at higher total pressures as a result of collision of lithosphere plates to form thick doubled crust in Pamir.

Thus, the acid magmas were generated in the deepest zones of the Earth s crust in collisional environment of Himalayan type with wide participation of CO_2. This permits one to use analogy with the fluid regime responsible for formation of ancient granulites but at lower PT-parameters of the latter.

Joseite A in bismuth mineralization of Bihor Mountains (Romania): its mineralogical characteristics and genetic significance

Cioflica G. & Lupulescu M. (*Dept. Mineralogy, Bucharest University*)

The most significant Laramian petrogenetic- metallogenetic event in the north-western part of Romania are connected with the emplacement of the granit pluton Baita-Dedes along a major NNE-SSW fracture and related dike suite. This intrusion produced an extended contact aureole , various thermal and metasomatic assemblages as hornfelses and calcic or magnesian skarns in the Permo-Mesosoic sedimentary rocks of the Bihor Realm, Baita Unit and Arieseni Unit, as well as in the Paleozoic metamorphites of the Paiuseni and Biharia Units.

The calcic skarns contain a Mo +/- W, Bi mineralization, in which the mineral joseit has been optically described by previous researchers. Our optical, electron microprobe, spectral reflectance, X-ray diffraction and microhardness data define this mineral as joseite A.

In reflected light joseite A appears as platy or long prismatic crystals, having a low polishing hardness, with perfect cleavage on (0001), white colour, no bireflectance and a very weak anisotropy in brownish, blue or grey tints.

The chemical composition, by mean of electron microprobe shows for the main elements the following values: Bi- 81.8970 %; S- 6.212 %; Te- 11.1006 % for an almost stoichiometric $Bi_{4.04}Te_{0.9}S_2$ formula. Small amounts of Sb, Pb, Cu, Se and As were also detected replacing the main cations as Sb and Pb for Bi and Se with As for Te.

The microhardness value is 45 kg/ mm^2 and the indentation shape is almost regular with straight borders.

The X-ray diffraction pattern is 3.08 (100); 2.24 (50); 4.40 (20); 2.57 (20); 1.96 (10) and 1.60 (5).

Field and laboratories observations point out the evolution of the metasomatic processes in the following sequence: after the magmatic stage the postmagmatic stage had a large extent with various mineral assemblages generated by infiltration metasomatism. In the first phase of this stage the calcic and magnesian skarns formed followed by Mo+/- W, Bi mineralization which open the metallization hydrothermal process. The relationships between minerals combined with experimental studies in the Bi-Te-S system emphasize joseite A deposition at the biginning of the Bi mineral sequence when f_{Te}/ f_S ratio is high but not at the values to permit the bismuth tellurides deposition.

COMPOSITIONAL LAYERING AND SYNERUPTIVE MIXING OF A PERIODICALLY REFILLED SHALLOW MAGMA CHAMBER: THE AD 79 PLINIAN ERUPTION OF VESUVIUS

R. CIONI, P. MARIANELLI, R. SANTACROCE, A. SBRANA (Dip. Scienze della Terra, Universita' di Pisa - Italy); L. CIVETTA (Dip. Geofisica e Vulcanologia - Universita' di Napoli - Italy); N. METRICH (Lab. P. Sue - CE/Saclay - Gif sur Yvette, France).

A detailed petrological study of the pyroclastic deposits of the AD 79 "Pompei" Plinian eruption of Vesuvius allowed: (i) the reconstruction of the thermal, compositional and isotopic ($^{87}Sr/^{86}Sr$) pre-eruptive layering of the shallow magma chamber; (ii) the quantitative definition of the syneruptive mixing between the different magmas occupying the different portions of the chamber, and its relationships with the eruption dynamics; (iii) the recognition of the variability of mafic batches having periodically supplied the chamber. During the eruption about 25-30% of magma was ejected as white K-phonolitic pumice, and 70-75% as grey K-tephri-phonolitic pumice. The white pumice Plinian fallout results from the drawing out of progressively deeper magma from a two-folded phonolitic body (T=850-900°C). The grey pumice results from syneruptive mixing involving three main end members, the phonolitic "white" magmas, mafic cumulates and a crystal-poor "grey" phono-tephritic magma, never erupted without being mixed. Mixing occurred within the chamber, triggered by a temporary destabilization of the Plinian column, and was characterized by a transition with time from physically "micro-mingled" to chemically hybridized pumice. After the re-establishment of the Plinian column, in the first stages of the grey pumice fallout, the amount of white magma mixed in the grey pumice was decreasing with increasing depth of tapping, but, after about 4-5 hours of grey pumice fallout, the mixing within the chamber was completed and the erupted grey pumice resulted from a constant mixing ratio (1.0-1.2). The grey magma had homogeneous composition with constant $^{87}Sr/^{86}Sr$ isotopic ratio (0.70749), as evidence of magmatic convection within it. No unambiguous liquidus phases were found testifying of its substantially overheated state (T=1000-1100°C); its very low viscosity was a main cause in the establishment of a physical discontinouity separating the white two-folded body from the grey one. The white/grey boundary layer possibly consisted of a multiply diffusive interface, periodically broken and recreated, supplying the phonolitic body through mixing of moderate amount of fractionated "grey" melts with the overlaying "white" magma. The presence of a large overheated mass testify of the young, growing stage of the AD 79 chamber, whose main engine was the periodic arrival of hot mafic magma batches. These were characterized by an overall moderately variable K-tephritic to K-basanitic composition, high temperature (about 1150°C), high volatile content (2.0-2.5% H2O+Cl+F+S), low viscosity (1-2x10^2 poises) and relatively low density (2500-2600 kg/m^3). The birth of the Pompei chamber should have followed the repeated arrival of these batches within a reservoir containing tephritic-phonolitic, crystal-enriched, magma, residual of the next preceding "Avellino" Plinian eruption (3,400 B.P.): about half of magma ejected during the AD 79 eruption could have been in fact inherited by the previous magma supply history of the chamber.

DE RE METALLICA AND DE LA PIROTECHNIA (AGRICOLA AND BIRINGUCCIO)

Cipriani C. (Mineralogical Museum, Univ. of Florence)

On the occasion of the fifth centenary of the birth of Georg Bauer, Agricola, rightly considered the father of Mineralogy, a contemporary of his should be remembered: Vannoccio Biringuccio, mine director and skilled metallurgist. Born in Siena in 1480, he died in Rome in 1537.

A comparison between his only work "De la Pirotechnia" and Agricola's famous "De re metallica" underlines the differences in style and approach. The former was written in Italian by an expert on the subject, the latter in Latin by a scholar. Yet there are many similarities between the two texts (in some cases translated literaly) and the illustrations.

Agricola's mention of Biringuccio's work does not do full justice to the influence the Italian man of action must have had on the German scholar.

On this subject several passages from the two works, written only twenty years apart, are commented upon.

The citations referred to concern: the amalgams of silver with their uses in metallurgy in the recovery of metal from minerals and from the residue of smelting; nitric acid for the recovery of silver used in the purification of hydrochloric acid; the ovens for copper metallurgy used in Saxony; brass metallurgy and the use of calamine; the minerals of manganese and their diversity from magnetite (lapis-magnes); the parting of gold from silver, in particular cupellation; and iron metallurgy, with regard to the various minerals, the processes of reduction in metal, and assays of qualitative analysis for copper.

• COMPOSITION AND EMPLACEMENT OF THE CAMPANIAN IGNIMBRITE, ITALY

Civetta L. *(Osservatorio Vesuviano, Ercolano)*, Orsi G., Pappalardo L. *(Dip. Geofis. e Vulcanologia, Napoli)*, Ort M. *(Dept. Geol. North Arizona University)*, Heiken G. *(Los Alamos Nat'l Lab. Los Alamos)*, Fisher R.V. *(Dept. Geol. Sciences, Univ. Calif., Santa Clara)*

The 34 ka Campanian Ignimbrite (CI) covered 30,000 km^2 with a volume of 250 km^3 DRE. The studied area is mostly in the Apennine Mountains with ridges of 1400 m a.s.l., including the Sorrento peninsula across the Bay of Naples. The CI sequence in distal areas is a basal fallout, dispersed eastward, beneath nonlayered massive poorly welded tuff.

SEM analysis shows the tuff to be from highly inflated magma. Anisotropy of magnetic susceptibility shows that the tuff spread radially from source but gravitationally drained down the Apennine slopes and valleys. Deposition occurred as gravity flows segregated from beneath the expanded transporting system and drained off slopes. Pumice and lithic fragments decrease in size with distance but lithic fragments are not vertically graded.

The CI ranges in composition from phonolite, to alkali trachyte, to trachyte. The basal fallout is phonolitic while the massive tuff was deposited in three homogeneous compositional units each successively less evolved. Each unit reached different distances from the vent, suggesting emplacement in three pulses. The chamber comprised two compositionally distinct magma layers with the most evolved at the top. The first pulse erupted the most evolved while the third the least evolved magma. The intermediate pulse erupted magma resulting from mixing of the two resident magmas. The flow generated by this pulse went farthest being most expanded and therefore able to cross rough morphology.

Developments in Electronic Cataloguing of the Mineral Collection at The Natural History Museum, London and Related Publications

A M Clark

Department of Mineralogy, The Natural History Museum, Cromwell Road, London SW7 5BD, U.K.

The collections in the Mineralogy Department of The Natural History Museum, London, consist of around 300,000 mineral specimens, 200,000 rocks and building stones, 30,000 ocean bottom deposit samples, and 5,000 meteorite specimens. Several of these collections have been placed on database systems in recent years; a description of these developments and the uses made of the data will be described. Currently a project is underway to place the catalogue of the largest of these collections, the systematic mineral collection, in electronic form. The network system being utilised in this project will be outlined, together with a description of the associated physical inventory of the collection, which is taking place in parallel with the database project.

Future developments will include: electronic access to elements of the database from outside the Museum; FRAX technology to store images of valuable (e.g. gemstone) material and type specimens; and publications derived from the electronic catalogue.

ASSESSMENT OF A SHALLOW MAGMATIC SYSTEM: THE CASE OF THE 1888-90 ERUPTION, VULCANO ISLAND

Clocchiatti R. *(G.S.T. Lab. Pierre Sue, CNRS-CEA, C.E./Saclay)*, **Del Moro A** *(Ist. di Geocronologia e Geochimica Isotopica, CNR Pisa)*, **Gioncada A.** *(Dip. di Scienze della Terra, Università di Pisa)*, **Joron J.L.** *(G.S.T. Lab. Pierre Sue, CNRS-CEA, C.E./Saclay)*, **Mosbah M.** *(G.S.T. Lab. Pierre Sue, CNRS-CEA, C.E./Saclay)*, **Pinarelli L.** *(Ist. di Geocronologia e Geochimica Isotopica, CNR Pisa)* **and Sbrana A.** *(Dip. di Scienze della Terra, Università di Pisa)*

This work deals with the study of the magmatic system feeding the last eruption of the volcano La Fossa, Vulcano island, Italy.

The petrogenetic mechanisms controlling the differentiation of erupted rocks have been investigated through petrography, mineral chemistry, major, trace and rare earth element and Sr, Nd and Pb isotopic geochemistry. In addition, melt inclusion and fluid inclusion data have been collected, both on juvenile material and xenolithic partially melted metamorphic clasts, in order to individuate the P-T conditions of the magma chamber feeding the eruption.

The erupted products, primarily compositionally zoned from latites to rhyolites, are heterogeneous due to syn-eruptive mingling. A very regular and continuous chemical zoning has been highlighted: rhyolites are the first erupted products, followed by thachytes and latites, while a reverse zoning reaching rhyolitic compositions was found in the upper part of the sequence .

The chemical and isotopic composition of the rhyolites indicates that they originated by fractional crystallization from latitic magmas plus assimilation of crustal material; trachytes represent hybrid magmas resulting from pre-eruptive mixing of latites and rhyolites.

The occurrence of magma-crust interaction processes, evidenced by the isotopic variations (87Sr/86Sr = 0.70474±3 to 0.70511±3; 143Nd/144Nd = 0.512550±6 to 0.512614±8; 206Pb/204Pb = 19.318-19.489; 207Pb/204Pb = 15.642-15.782; 208Pb/204Pb = 39.175-39.613), is confirmed by the presence of partially melted metamorphic xenoliths, having $^{87}Sr/^{86}Sr$=0.71633±6-0.72505±2 and 143Nd/144Nd=0.51229±7, in rhyolites and trachytes. AFC calculations indicate in a few percent the contribution of crustal material to the differentiating magmas.

Thermometric measurements on melt inclusions indicate that the crystallization temperatures of latites and trachytes were in the range of 1050-1100°C, while the temperature of the rhyolites appears to have been around 1000°C at the time of the eruption.

Compositional data on melt inclusions reveal that the magmas involved in the eruption contained about 1-1.5 wt% dissolved H2O in pre-eruptive conditions.

Some indirect data about the depth of the magma chamber derive from secondary fluid inclusions found in metamorphic xenoliths; these furnish low equilibration pressure data (30-60 MPa) allowing the location of the higher portions of the chamber at around 1500-2000 m of depth.

MINERALOGICAL CHARACTERISTICS OF CLAYS RESULTING FROM HYDROTHERMAL ALTERATION OF ANDESITE VOLCANIC ROCKS IN ESKİŞEHİR REGION WEST TURKEY

Çoban F. (İstanbul Tech.Univ.,Facult.of Min.)

Smectites from Mihalgazi hydrothermal deposit were studied. The studied area is situated in NE part of Eskişehir Province. In this region Eocene aged volcanic rocks are composed of andesite lavas and their pyroclastics. These volcanics show calc-alkaline character(Kibici, 1990).

Clay deposits were formed by reaction between K-bearing hydrothermal solutions and andesitic rocks (especially tuffs).Hydrothermal solutions ascended rising through the fracture systems and altered the volcanic rocks. Three different mineralogical associations were distingueshed in these clays
1- Smectite+Cristobalite
2- Smectite+Kaolinite+Feldspar+Quartz(Q)
3- Mixed-layer Illite/Smectite+Chlorite+Q

According to the X-ray diffraction and chemical data;dioctahedral smectite is the main mineral phase associated with kaolinite;K-Feldspar;mixed layer illite-smectite;kaolinite and silica phase; either quartz or cristobalite. Chlorite and allophane occur in small amounts in some samples. Dioctahedral smectites(Montmorillonite) are distinguished by their high iron and potassium content.

References:
Kibici;Y. (1990). Geol.Bull.Turkey;33;69-77.

Precious stone and Society.

New expositions in District Museum in Turnov.

Cogan M. (*District Museum in Turnov, Czech Republic*)

Precious stones have always played an extraordinary role in the human spiritual culture. We meet with them in the Epic about Gilgamesh, in Old and New Testament, in culture of the whole world. The Bohemian Kingdom and its stratums of precious metals and stones have been attracting Europeans since prehistorical ages. There still have been perceptible traces of Celtic output of Gold in the southern part of Bohemia. Bohemia used to be the biggest European silver producer in the middle Ages. Output and precious stones processing developed mostly during the rule of emperors Charles IV. and Rudolph II. for whom precious stones used to be means towards representation, connection with the Lord and with cosmic forces as well.

We meet with samples of symbolism and social events (even with a ideological signification of gems) much later. When geologist Andreas Eichler called Bohemia "the little Peru before the discovery of America" in 1820, when his colleague prof. Zippe raised Bohemian garnet to a mineralogical symbol of Bohemia in 1836, the Bohemian revival society comprehended pyrop as a patriotic expression. Turnov is one of the historical centres of the production of precious stones that has overlived till nowadays.

Turnov - a little town is placed in a geologically interesting region which is in the northern part of Bohemia (Czech Republic).

First mention of local stone cutters are from the 16th century and such sporadic production has been influencing the development of the town with its society till present days. A mineralogical variability of this region caused a mass collecting, but mostly the development of geology, mineralogy and gemology. The grinding union established a research station for precious stones analysis in 1935. When the II. World War was over there was founded the Institute of research of monocrystals being in use till nowadays here. The new expositions of mineralogy and gem grinding in the District Museum in Turnov (founded 1886) attempts on complex natural-historical and cultural-historical view of precious stones. The core of mineralogical part is geology and mineralogy of the region and the collection of precious stones from selected world finding places. The historical exposition shows the history of production and application of precious stones in Bohemia till nowadays, also new decorative minerals. The part of it is a cabinet with all sorts of precious stones used in goldsmithy and jewellery. Such comprehended exposition is a good base for future expert activities of the turnovian Museum - research educational programs for public, international symposiums, exhibitions and function of gemological centre.

The *silvery micaschists* of the Gran Paradiso Massif: a case of metasomatic transformation of granitoids within ductile shear zones.

F. Colombo, N. Ferrati, U. Pognante† (*Dip. Sc. Mineral. Petrol., Univ. Torino*)
J.R Kienast (*Lab. de Pétrologie, Univ. Paris VI*)

In the Gran Paradiso Massif (Italian Western Alps), *silvery micaschists*, whose origin is under debate, frequently occur within orthogneiss of the "Augengneiss Complex".

With the purpose to understand the *silvery micaschist* genetic processes, a geological and geochemical study was performed on a well exposed outcrop on the Valeille-Valnontey divide (Val d'Aosta). In this outcrop (100×500 m) gradual transitions from metagranitoid to orthogneiss and to *silvery micaschist* are evident.

Three main groups of *silvery micaschists* were distinguished: 1) garnet-bearing (±chloritoid) *silvery micaschist*, 2) chloritoid-garnet-kyanite bearing *silvery micaschist* and 3) quartz-poor chloritoid-bearing *silvery micaschist*.

The geochemical study of representative samples has shown that the transition from metagranite to *silvery micaschist* is accompanied by progressive and significant decrease in SiO_2, K_2O, CaO, NaO, Ba and increase in Al_2O_3, MgO, Ti, Zr, V and Sc. Mass balance calculations suggest a negligible volume increase in the transition from metagranite to orthogneiss, a small volume decrease (14%) in the transition from orthogneiss to garnet-bearing *silvery micaschist* and a significant volume decrease (35%) in the transition from garnet-bearing *silvery micaschist* to the quartz-poor, chloritoid-bearing *silvery micaschist*.

On both geological and geochemical ground, it is suggested that the *silvery micaschists* derive from a granitic protolith, which underwent a metasomatic process along ductile shear zones, developed either before or early in the Alpine high-pressure metamorphic history.

HIGH PRESSURE STRUCTURAL STUDY OF MUSCOVITE

Comodi P. and Zanazzi P.F. (*Dept. of Earth Sciences, Univ. of Perugia, Italy*)

The response of dioctahedral $2M_1$ mica to pressure has been studied by single crystal X-ray diffraction in a diamond anvil cell (DAC). Two samples with very different Na/Na+K ratios were refined: the composition is $(Na_{0.07}K_{0.9}Ba_{0.01}\square_{0.02})(Al_{1.84}Ti_{0.04}Fe_{0.07}Mg_{0.07})(Si_{3.02}Al_{0.98})O_{10}(OH)_2$, for a K-rich muscovite from W. Maine, USA (K-Ms) and $(Na_{0.37}K_{0.60}\square_{0.03})(Al_{1.84}Ti_{0.02}Fe_{0.10}Mg_{0.06})(Si_{3.03}Al_{0.97})O_{10}(OH)_2$ for a Na-rich muscovite from Nevada, USA (Na-Ms).

The samples were studied over a range of pressures with a Merrill Bassett DAC mounted on the Philips PW1100 diffractometer using monochromatized MoKα radiation. A steel foil 250 μm thick was used as gasket material and a 4:1 methanol:ethanol mixture as the hydrostatic pressure-transmitting medium. The pressure was monitored by measuring the wavelength shift of the Sm^{2+} fluorescence line (Sm^{2+}:BaFCl, Comodi & Zanazzi, 1993; precision 0.5 kbar).

Cell edges, measured at different pressures between 1 bar and 35 kbar, vary linearly, in the pressure range investigated, according to the following equations: $a_P = 5.195(2) - 1.54(3)\ 10^{-3}\ P$, $b_P = 9.020(3) - 3.06(5)\ 10^{-3}\ P$, $c_P = 20.068(6) - 23.5(3)\ 10^{-3}\ P$ for K-Ms, and $a_P = 5.165(2) - 1.51(4)\ 10^{-3}\ P$, $b_P = 8.964(3) - 3.12(7)\ 10^{-3}\ P$, $c_P = 19.798(6) - 19.9(4)\ 10^{-3}\ P$ for Na-Ms. Bulk moduli of K-Ms and Na-Ms are 490 and 540 (±30) kbar respectively (K'=4). This difference is due solely to the Na substitution for K in the interlayer region (Comodi *et al.*, 1994). Similar highly anisotropic compressibility patterns shown by both samples have

been found for other layer silicates (phlogopite, Hazen & Finger, 1978; lizardite, Mellini & Zanazzi, 1989).

The crystal structure of the K-Ms and Na-Ms were refined at 28 and 27 kbar, using 314 and 235 independent reflections for 40 parameters (R = 0.059 and 0.076 respectively). To avoid any bias introduced by using a reduced reflection data set measured at HP within the cell, the HP structures were compared with those determined with the same crystal mounting in the DAC at 0.5 kbar for K-Ms (R= 0.052, 319 independent reflections) and at 3.5 kbar for Na-Ms (R = 0.071, 212 independent reflections).

The main structural changes involve the interlayer region. The shorter inner K-O distances decrease more than the larger outer K-O distances: in K-Ms $<K\text{-}O>_{inner}$ changes from 2.847 at 0.5 kbar to 2.735 Å at 28 kbar, and $<K\text{-}O>_{outer}$ from 3.361 to 3.311 Å. The average value of the <K-O> bonds decreases from 3.104 to 3.023 Å, with a bulk modulus of 330 kbar. For the Na-Ms the $<K\text{-}O>_{inner}$ are 2.749 and the $<K\text{-}O>_{outer}$ are 3.354 Å respectively at 3.5 kbar and 2.642 and 3.304 Å at 27 kbar.

The intralayer region undergoes markedly smaller changes, at least in terms of volumes: no change in volume of Si,Al tetrahedra; only small volume decreases for the octahedral sites, larger for M1 than for M2. The differences of octahedral and tetrahedral compressibilities cause an increase in the ditrigonalization of tetrahedral layer in both samples studied. The rotation angle α changes from 11.3 to 12.7° in K-Ms and from 13.1 to 14.7° in Na-Ms.

The contribution by the compression of the 2:1 intralayer region to the thickness reduction along the [001] direction is about 6 times less than that due to the compression occurring in the interlayer region. Whereas the compressibility of intralayer thickness is 4.8 10^{-4} $kbar^{-1}$, that of interlayer is 27.7 10^{-4} $kbar^{-1}$. In terms of bulk modulus, K is 910 kbar for the intralayer and decreases to 290 kbar for K-O interlayer region. These values, compared with those measured for phlogopite by Hazen & Finger (1978), show that the larger compressibility of muscovite with respect to phlogopite is largely due to the greater compressibility of the dioctahedral layer compared to that of the trioctahedral layer.

References:
Comodi P, Zanazzi P.F., Guidotti C.V., Blencoe J.G., Sassi F.P. (1994). *Proceedings of the XVI IMA Meeting*, Pisa, Sept. 4-9.
Comodi P. & Zanazzi P.F. (1993) *J. Appl. Cryst.*,**26**,843-845.
Hazen R.M. & Finger L.W. (1978) *Am. Mineral.*, **63**, 293-296.
Mellini M. & Zanazzi P.F. (1989) *Eur. J. Mineral.*, **1**, 1, 13-20.

COMPRESSIBILITY OF $2M_1$ DIOCTAHEDRAL MICA: EFFECT OF NA⇔K SUBSTITUTION.

Comodi P., Zanazzi P.F.(*Dept. of Earth Sciences, Univ. of Perugia, Italy*), Guidotti, C.V. (*Dept. of Geological Sciences, Univ. of Maine, USA*), Blencoe J.G. (*Chemistry Div., Oak Ridge Nat. Lab., USA*), Sassi F.P. (*Dept. of Mineralogy and Petrology, Univ. of Padova, Italy*).

The influence of K⇔Na substitution on the baric behaviour of muscovite was determined by measuring the compressibility of two $2M_1$ samples having negligible phengitic component. The study was carried out by single crystal X-ray diffraction in a Merrill-Bassett diamond anvil cell.

The unit cell parameters of two crystals having composition $(Na_{0.07}K_{0.9}Ba_{0.01}\square_{0.02})(Al_{1.84}Ti_{0.04}Fe_{0.07}Mg_{0.07})(Si_{3.02}Al_{0.98})O_{10}(OH)_2$, K-Ms (7 mole % paragonite), from W. Maine, USA, and $(Na_{0.37}K_{0.60}\square_{0.03})(Al_{1.84}Ti_{0.02}Fe_{0.10}Mg_{0.06})(Si_{3.03}Al_{0.97})O_{10}(OH)_2$, Na-Ms (37 mole % paragonite), from Nevada, USA, were determined at pressures ranging from 1 bar to 35 kbar, by applying the least-squares method to the 2θ angles of 25-35 accurately centered reflections.

Isothermal bulk moduli, calculated from least-squares fit of pressure *vs* volume data to a Birch-Murnaghan equation of state, setting K' equal to 4, are 490 kbar and 540 kbar (both ± 30 kbar) for K-Ms and Na-Ms respectively. When the K' is not set at 4, K-Ms bulk modulus becomes 500 kbar with K' equal to 3.0 and Na-Ms bulk modulus becomes 550 kbar with K' equal to 2.9. Our data fit well with the compressibility data obtained through the elastic constants of muscovite measured with Brillouin scattering (Vaughan & Guggenheim, 1986), and the compressibility data obtained by Catti *et al.* (1994) for a $2M_1$ muscovite by powder neutron diffraction at kbar.

The lattice parameters decreased linearly from a=5.195(1) b=9.020(3), c=20.068(6) Å, β=95.76(2)° at 1 bar to a=5.147(1) b=8.921(6), c=19.34(2) Å, β=95.7(1)° at 34 kbar in K-Ms, a=5.165(2), b=8.964(3), c=19.798(6) Å, β=95.38(2)° at 1 bar a=5.122(4), b=8.870(6), c=19.09(2) Å, β=95.5(1)° at 35 kbar Na-Ms. Both samples show highly anisotropic compressibility patte as found for other layer silicates (phlogopite, Hazen & Finger, 19 lizardite, Mellini & Zanazzi, 1989). Linear compressibility coefficie parallel to the unit cell edges are β_a=29.6(6) 10^{-5}, =33.9(6) 10^{-5}, β_c = 11.7(2) 10^{-4} $kbar^{-1}$ (β_a:β_b:β_c = 1 : 1. 3.95) in K-Ms, and β_a = 29.2(8) 10^{-5}, β_b = 34.8(8) 10^{-5}, β_c 10.1(3) 10^{-4} $kbar^{-1}$ (β_a:β_b:β_c = 1 : 1.19 : 3.46) in Na-Ms.

The data indicate a small but nonetheless significantly great compressibility for K-Ms compared to Na-Ms. In particular the lat parameter compressibilities show that the difference in bulk modulus due entirely to the higher compressibility along the [001] direction K-Ms with respect to Na-Ms. Infact whereas the β_a and β_b coinci in K-Ms and Na-Ms, larger differences exist between the β_c valu The identical compressibility along a and b axes is due to very simil chemical compositions of the 2:1 tetrahedral and octahedral layers the two samples. In contrast, the substitution of 30 % more Na for in the interlayer region of the Na-Ms is the likely explanation for decrease of about 15 % in the compressibility along c axis of the Na Ms and the increase of 8% in its bulk modulus. The increase of t bulk modulus with the decrease of the interlayer cation size agrees wi the theoretical relationships proposed by Hazen and Prewitt (1977) in which the compressibility of a polyhedron is proportional to the cub of the mean bond distance and inversely proportional to cation form charge.

Analysis of high-pressure, high-temperature data of K-muscovi (Catti *et al.*, 1989) yields the following equation of state f dioctahedral K-mica V=Vo-1.6 P+0.04 T-0.66 X_{Na} where P and T a in kbar and °C, and X_{Na} is the mole fraction % of Na in the interlayer.

Because the two samples studied herein were constrain chemically such that the only significant variation was in terms of t Na-K ratio the observed variation of the compressibility impli that the 1 bar ΔV_{mix} curve shown in Guidotti *et al.* (1992) will chang its shape as a function of pressure. In the future, compressibil measurements on carefully chosen samples may provide insights as how increased pressure: 1) facilititates crystalline solution of phengi on natural muscovite, 2) affects the occurrence of different mi polytypes.

References:
Catti M., Ferraris G., Ivaldi G. (1989) *Eur. J. Mineral.*, **1**, 5, 625-632.
Catti M., Ferraris G., Hull S., Pavese A. (1994) *Eur. J. Mineral.*, (in press.)
Guidotti C.V., Mazzoli C., Sassi F.P., Blencoe J.G.(1992) *Eur. J. Mineral.*, **4**,283-297.
Hazen R.M. & Prewitt C.T. (1977) *Am. Mineral.*, **62**, 309-315.
Hazen R.M. & Finger L.W. (1978) *Am. Mineral.*, **63**, 293-296.
Mellini M. & Zanazzi P.F. (1989) *Eur. J. Mineral.*, **1**, 1, 13-20.
Vaughan M.T. & Guggenheim S. (1986) *J.Geophys. Res.*, **91**, 4657-4664.

METAVOLTINE FROM VESUVIUS: CRYSTAL STRUCTURE AND CRYSTAL CHEMISTRY

Comunale, G., Scordari, F., (Dip. Geomineralogico, Università di Bari, Italy), Bonazzi, P. and Menchetti, S., (Dip. Scienza della Terra, Università. di Firenze, Italy.)

Metavoltine from Madeni Zakh, Persia, was first described by Blaas in 1883. It is a hydrated alkaline iron sulphate which has long been confused with the synthetic compound known as Maus's salt. Previous papers concerning metavoltine and Maus's salt (Scordari et al., 1975; Giacovazzo et al., 1975; Scordari, 1977) have provided relevant contributions on this subject; however, the crystal structure of the natural phase was only roughly defined and

a number of crystal chemical problems concerning this mineral were still open to study.

This work was performed on a metavoltine sample from Vesuvius (the 1906 eruption). The structure was solved in $P\bar{3}$ instead of P3 as previously assumed (Giacovazzo et al., 1976). The lattice parameters are: a=9.545(2), c=18.09(1) Å. According to the structural study, the ideal unit cell content corresponds to $K_4Na_4ZnFe^{3+}{}_6O_6(SO4)_{12} \cdot 20H_2O$.

The structure can be described as a sequence of sandwich sheets of the ideal composition $[Na_2K_2Fe^{3+}{}_6O_2(SO_4)_{12}(H_2O)_6 Zn(H_2O)_6]^{4-}$ stacked along the c axis. Adjacent sheets are connected to each other by a layer of Na^+, K^+ and H_2O distributed on five independent structural sites. This layer, $[(Na^+{}_2K^+{}_2(H_2O)_3)(H_2O)_5]^{4+}$, shows substitutional and positional disorder, as made evident by the high values of the thermal parameters.

The precise structure determination has made it possible to establish the correct water content in metavoltine, and to clarify some crystal-chemical points, such as the constraints which control the $Na^+ \rightleftharpoons K^+$ substitution. From a mineralogical point of view, metavoltine from Vesuvius is noteworthy for its high content of octahedrally coordinated Zn, usually present as a minor substituent of Fe^{2+}.

References:
Giacovazzo,G., Scordari,F. and Menchetti,S. (1975). Acta Cryst. B31, 2171-2173.
Giacovazzo,G., Scordari,F., Todisco,A. and Menchetti S. (1976). Tschermaks Min. Petr. Mitt. 23, 155-166.
Scordari, F. (1977). Miner. Mag. 41, 371-374.
Scordari, F., Vurro, F. and Menchetti, S. (1975). Tschermaks. Min. Petr. Mitt..22, 88-97.

ALKALI-FELDSPAR SYENITES OF THE EASTERN BAHIAN ALKALINE PROVINCE (NORDESTE, BRASIL). THEIR RELEVANCE TO RAPAKIVI MAGMATISM

Conceição H. (*Inst. de Geociências, Univ. Federal de Bahia*) and Bonin B. (*Dept. des Sciences de la Terre, Univ. de Paris-Sud*)

Post-orogenic syenite plutons of the Eastern Bahian alkaline province postdate the Trans-Amazonian (2 Ga) orogenesis and constitute a linear belt of four discrete massifs, from north to south: Itiúba (1800 km^2), Santanápolis (180 km^2), São Félix (32 km^2), and Anuri (70 km^2). Emplaced along a north-south-trending 1000 km-long transtensional shear fault zone in mesozonal conditions, they display strikingly similar characteristics: (i) hypersolvus (*i.e.* one perthitic alkali feldspar) conditions of crystallization, (ii) extreme abundance of leucocratic alkali-feldspar syenite, occupying more than 95 % of the total area, (iii) occurrence of mafic syenites as discrete layers and autoliths, (iv) associated dyke swarms. Rock-forming mineral compositions indicate that anhydrous magmas crystallized at 900 to 850°C in a relatively oxidizing medium (NNO buffer).

Leucocratic alkali-feldspar syenites have intermediate (54-61 % SiO_2) and metaluminous compositions, with high K, Ba, Sr, P, Ti, and REE abundances. Its evolution was controlled by fractionation of clinopyroxene + apatite + monazite + zircon + Fe-Ti oxides. Mafic syenites are basic (45 % SiO_2) and yield extreme P, Ti, Y, Zr, and REE-enrichments. High REE contents (up to 2400 ppm) are correlated with highly fractionated patterns ($[La/Yb]_N \approx 100$). Thus, while syenites are cogenetic, they cannot represent melt compositions.

The Eastern Bahian syenites are interpreted as adcumulates yielding the [alkali feldspar + clinopyroxene + accessory minerals] fractionating assemblage. They precipitated at the roof of silicic magma chambers located at the ductile-brittle crust transition. Dyke swarm-filling alkali-feldspar granites represent the residual melts.

Further removal of the cumulative alkali-feldspar cap-rock by new magmas infilling the magma chamber would result in alkali-feldspar-bearing melts and ultimately in the development of the classical rapakivi texture through complex resorption-crystallization processes.

COMPUTER PROGRAMS FOR THE CALCULATION OF PETROLOGIC PHASE EQUILIBRIA

Connolly J.A.D. (IMP-ETHZ, Zuerich CH-8092)

There are a number of computer programs available for the calculation of petrologic phase equilibria from thermodynamic data. The intent of this talk will be to present a brief review of the capabilities and limitations of these programs. The phase equilibrium problem may be formulated in two ways: (i) the pressure, temperature and composition (i.e., the state) of a system is specified, and the stable minerals are to be determined; or (ii) the mineralogy of the system is specified, and the conditions for their equilibrium determined. Free energy minimization techniques are designed to solve the first formulation. In principle, free energy minimization techniques are capable of accurately treating systems with any degree of complexity. They are most well suited to problems where the bulk composition of the system is known, or variable in only one or two components. In general free energy minimization cannot be applied to crustal metamorphic rocks because heterogeneities, mineral zonation and disequilibrium make it difficult to define a thermodynamically relevant "bulk" composition. Several programs are available that employ FEM techniques to iteratively map phase relations as a function of two state variables (e.g., THERMOCALC I, Sundman et al. 1985; THERIAK, DeCapitani & Brown, 1987), but these techniques are impractical in the context of the multivariable problems common in petrology where the exact composition of the system cannot be specified. For this situation, a solution to the second formulation of the phase equilibrium problem is more efficient because there are only a finite number of possible phase assemblages within the parametric space of any system. The most popular program of this type is PTX or PTAX (Berman et al., 1986) which can be used to determine stable univariant equilibria as a function of pressure, temperature, fluid composition or the activity of a component or phase for systems in which the remaining phases have fixed compositions. THERMOCALC II (Powell & Holland, 1990) and PERPLEX (Connolly, 1990) have this capability, but are also able to treat mineral solutions and to make calculations as a function of the bulk composition of a system. For solution phase calculations, THERMOCALC II computes the numerically exact equilibrium compositions of any specified assemblage, but it does not determine the stability of the equilibrium. In contrast, PERPLEX does determine the stability of solution phase equilibria, but it uses an approximation that becomes infeasible for mineral solutions with more than six compositional degrees of freedom. Both THERMOCALC II and PERPLEX are also capable of computing mineral modes for a specified bulk composition.

Most of the above computer programs have specific advantages that make them uniquely useful in certain situations. The source codes for THERIAK and PERPLEX are generally available, and thus these programs can be run on any computer with a FORTRAN compiler. The PTAX and THERMOCALC II programs are available only in compiled versions for IBM and MacIntosh, respectively, personal computers. All the programs with the exception of THERMOCALC II have associated computer programs for generating graphical output.

References:
Berman, R.G., Brown, T.H., Perkins E. (1987). *Am. Mineral.*, 72, 861-862.
Connolly, J.A.D. (1990). *Am. J. Sci.*, 290, 666-718.
DeCapitani, C., Brown, T.H. (1987). *Geochim. Cosmochim. Acta*, 51, 2639-2652.

Powell, R., Holland T.J.B. (1990). *Am. Mineral.*, 75, 376-386.
Sundman B., Jannson B., Andersson J-O. (1985). *CALPHAD*, 9, 153-156.

RELATIONSHIPS AMONG LAMPROITIC, KAMAFUGITIC AND ROMAN TYPE MAGMAS: MINERALOGICAL, PETROLOGICAL AND EXPERIMENTAL DATA

CONTICELLI S. *(Dip. Scienze della Terra, Università di Firenze)*

Fractional crystallisation, crustal contamination, mixing and combination of them, working on parental magmas having kamafugitic and lamproitic affinities besides the more common Roman Type (further portioned in HKS and KS) are though to be responsible for the genesis of the wide compositional spectrum of potassic-alkaline volcanites in Central Italy. The close spatial and time associations of these mafic potassic magmas, having different mineralogical and geochemical characteristics from each other, usually found in different areas in the world, represent an unique opportunity for studying the processes that brought to their genesis.

Rocks with *lamproitic* affinity in Italy are plagioclase free, with clinopyroxene characterised by Ca, Si and Al not sufficient to fill the respective sites. Geochemically they are characterised by high K/Na, Ni/Sc and LILE/HFSE values and have the highest contents in incompatible as well as compatible elements among all basic potassic volcanites. Rocks with *kamafugitic* affinity are still plagioclase-free, with clinopyroxene characterised by low Al, only rarely not sufficient to fill the T site. Geochemically they are characterised by K/Na and LILE/HFSE values as high as those of lamproitic ones, but with lower Ni/Sc values, and have consistently high incompatible and compatible elements abundance. It is worth to note the extremely high and variable Sr abundance. *Roman Type* have highly variable mineralogical and geochemical characteristics, covering the entire compositional gap between the previous two groups and volcanites with calc-alkaline affinity. Leucite is the most representative mineral, plagioclase is present and increase in quantity from HKS to KS rocks. Clinopyroxene range from diopside to salite in composition with Al amount higher than those found in kamafugites and lamproites. K/Na values are also highly variable, whereas consistently low Ni/Sc and high LILE/HFSE values are peculiar of both HKS and KS rocks. Initial Sr and Nd isotopic ratios in the most mafic rocks are highly variable, even though HKS and kamafugites from Central Italy cluster the value for Sr isotopes of 0.710, whereas lamproites and associated rocks range from 0.712÷0.716.

Melting experiments on the most primitive compositions of each group of alkaline potassic magmas from Central Italy revealed that none of them were in equilibrium with a "regular" mantle source paragenesis. Beside different X_{CO2} is required during partial melting in order to account the differences in terms of chemical and mineralogical composition observed. Experiments on kamafugites and HKS mafic compositions reveals that Ca-rich silicates are predominant in their source, along with mica, olivine and either spinel or garnet. Experimental data integrated with geochemical data suggest that a residual source prior to metasomatism may be claimed for the genesis of lamproites, kamafugites and HKS north of Rome. Metasomatism with K- and LILE- rich fluids prior to partial melting should have occurred. Geochemical evidence suggest that the metasomatizing agent was characterised by a bimodal compositions. A Ca-poor metasomatic agent, probably related to melting of upper crustal rocks, may be responsible for the evolution of the source of lamproitic and related magmas (South Tuscany), whereas a $CaCO_3$-rich metasomatic agent may be responsible for the evolution of the source of kamafugites and HKS magmas. This possibility agree well with experimental data. Beside these data coupled to isotopic data corroborate the hypothesis that even the $CaCo_3$-rich agent may have been released by a crustal reservoir enriched in a carbonaceous component.

NOMENCLATURE OF ZEOLITES: WORK OF TH CNMMN SUBCOMMITTEE

Coombs D.S. *(Geology Dept., University of Otago, Dunedin, N. Zealand)* (Subcommittee Chairman)

Questions being considered include:

(1) The definition of a mineral zeolite. What are th truly essential features of a zeolite? To what extent ma elements other that Si and Al occupy tetrahedral sites (as lovdarite, viséite, pahasapaite)? Should the definitio allow for possible end-member cases which contain no H (consider pollucite, hsianghualite) or in which Si is th only tetrahedral cation? Are T—(OH,F)—T bond acceptable in the framework? Should the definition allow "interrupted" framework structures (e.g. parthéite roggianite) in which one corner of some tetrahedra i occupied by an (OH) group which is not shared with other tetrahedra? The definition must be acceptable t mineralogists. Can it also be compatible with requirement of workers in other fields?

(2) A suitable hierarchy of terms from *species* and series (where there is a compositional range) to *structural type* and *sub-groups* or *groups* to *family* or *group* for zeolites a a whole.

(3) Where a topologically identical structure forms a compositional series, should separate species status be given according to the dominant extra-framework cation? This would accord with general CNMMN practice that a separate name is given where a major structural site is occupied by a chemical component different from that in the equivalent site of an existing mineral. With very few exceptions (harmotome and phillipsite, perhaps chabazite and herschelite, analcime and wairakite), this has not been done for zeolites.

(4) If the answer to (3) is Yes, about a dozen series such as chabazite, phillipsite, and ferrierite would, on presently available data, require about 30 species names. Should authors be allowed to propose completely new names? Should a system of prefix modifiers be recommended? Or should a Levinson-like system be adopted with names such as chabazite-Ca, chabazite-Na, chabazite-K; ferrierite-Mg, ferrierite-K, ferrierite-Na, with chabazite and ferrierite (e.g.) retained as series names and for undifferentiated members? Should exceptions be allowed, e.g. by retaining both phillipsite and harmotome?

(5) Framework Si:Al ratios vary widely in some zeolites, e.g. analcime, heulandite, chabazite. Should this be an allowable basis for recognizing separate zeolite species? Consider the case of clinoptilolite and heulandite.

(6) How should order-disorder relationships and symmetry differences in topologically identical structures be handled? In some zeolites, e.g. analcime, topologically identical structures are known with a wide variety of different space-group symmetries, but essentially identical compositions. No-one (?) argues for separate names in some of these cases, but perhaps the space group symbol (in brackets?) could be placed after the name where this is important. What about natrolite-tetranatrolite, and orthorhombic and tetragonal edingtonite?

(7) In other cases, topologically equivalent structures, e.g. scolecite-mesolite-natrolite, barrerite-stellerite-stilbite have different symmetries that appear to be related to differences in composition. Can species status be based satisfactorily on this combination of factors?

(8) Should changes associated with partial dehydration or over hydration be grounds for awarding species status?

Some thinking and provisional conclusions of the Subcommittee will be discussed.

Br/Cl RATIO INCREASE IN FUMAROLIC SALAMMONIAC FROM VULCANO (AEOLIAN ISLANDS - ITALY).

Coradossi N. *(Dept. of Earth Sc., Univ. of Florence)*, Garavelli A., Vurro F. *(Geomineralogical Dept., Univ. of Bari)*, Salamida M. *(ENEL Laboratory, Bari)*.

Since the last eruption in 1888-1890, "La Fossa" crater of Vulcano changed into a typical state of fumarolic activity of various intensity. An increase of volcanic activity was recorded in the years 1921-1926, 1978-1982 and since 1985 to onward. In particular, from 1987 to 1993 the maximum temperature of the crater fumaroles increased from 330 to about 700 °C. Around the fumarolic vents, whose emission temperature values are less than 300°C, salammoniac, NH_4Cl, is the most abundant sublimate. In this phase, the Br/Cl ratio determination result especially interesting because it is closely related to the Br/Cl content of fumarolic gases.

A previous work (Coradossi *et al.*, 1985) reported that both temperature and Br/Cl ratio in NH_4Cl samples from Vulcano crater increased from 1970 to 1978. In particular, from 1977 to 1978 a high bromine content was registered. This study show a similar Br/Cl ratio increase in salammoniac samples deposited in the fumarolized area of Vulcano from 1992 to onward. The high bromine content in the investigated sublimates is related to a change in the composition of fumarolic gases with time, caused either by local fractionation processes, or to an increase of bromine in volcanic fluids. The first hypothesis could be the result of a mobilisation of salammoniac deposited under the ground surface during periods of reduced fumarolic activity, while the latter could be due to an increase of magmatic component of the volcanic fluids.

References:
Coradossi, N., Pinarelli, L., Bertolini, G.L. (1985). *SIMP Rend.*, **40**, 299-309.

MEDIUM RANGE ORDER IN BORATE AND SILICATE GLASSES.

Cormier L., Galoisy L. and Calas G. (*Laboratoire de Minéralogie-Cristallographie, Université Paris VI et VII, IPGP and URA CNRS 09- FRANCE*)

Static structural disorder usually prevails in multicomponent glasses. As a consequence, the medium range order in glasses, i.e. the structure beyond the first coordination shell, is not well understood. We present X-ray absorption spectroscopy (XAS) data at the Ni-K edge (8333 eV) on Ni-bearing polymerized borate and silicate glasses. The spectra were recorded using synchrotron radiation light source DCI at LURE (Orsay, France). The spectra were recorded in transmission mode at about 4.5K to limit thermal disorder effects.

EXAFS spectra of alkali-poor borate glasses (up to 20 wt.%) show the presence of three distinct shells of neighbors around Ni (O_1, B, O_2, respectively). Such a complex structure is usually not observed in glasses because of static disorder. With higher proportions of alkali, only two shells remain (O_1 and B).

These results indicate the modification of the borate network when alkalis are added to B_2O_3 glass. The structure of B_2O_3 glass consists of neutral boroxol rings and BO_3 triangles with bridging oxygens. When alkalis are added, the B_2O_3 network starts to depolymerize and EXAFS data are consistent with the presence of truncated boroxol rings, at low alkali content. 6-coordinated Ni^{2+} is grafted on these boroxol rings with $d(Ni\text{-}O_1)=2.05$Å, $d(Ni\text{-}B)=3.2$Å and $d(Ni\text{-}O_2)=4.2$Å (Cormier *et al*, in prep.). The permanence of these ordered domains in alkali borate glasses is then a property of the first stages of their depolymerization process. At higher alkali content, disorder increases by a disappearance of the boroxol rings domains despite the presence of majority ^{III}B.

In all silicate glasses investigated, some contribution of Si second neighbors is apparent, the intensity of which is proportional to the concentration of 4-coordinated Ni^{2+}. This indicates an ordered connection between $^{IV}Ni^{2+}$ and the glassy network. In K-bearing glasses, Ni prevails in 4-coordination and is surrounded by 4 Si second neighbors, indicating that NiO_4 tetrahedra are connected to the silicate framework (Galoisy and Calas, 1993). In presence of other cations, these ordered Ni-bearing domains are less important, but the variations of the Ni-O-Si angle as a function of the radius/charge ratio indicate how the nature of the cations influence the structure of the ordered 3-dimensional silicate framework.

In both borate and silicate glasses, this possibility to associate a coordination state to a medium range order structure opens the possibility to investigate the nature of glass-to-melt transformation processes.

References:
Galoisy and Calas, Geochim.Cosmochim. Acta (1993), **57**, 3627-3633.

SULFUR ISOTOPIC COMPOSITION OF FUMAROLIC GASES FROM VULCANO ISLAND DURING 1979-1993

Cortecci G. and Ferrara G. (*Dept. of Earth Sciences, Univ. of Pisa*)

After the explosive eruption during 1888-1890, the volcanic activity at Vulcano (Aeolian arc archipelago, north of Sicily) was restricted to a fumarolic stage, the discharged fluids at the Fossa Grande crater being constituded mainly by H_2O and CO_2 along with acid gases including both H_2S and SO_2. Maximum outlet temperature began to change from 300°C in 1978 in concomitance with a strong seismic event and achieved 660°C in 1993. This heating phase was accompanied by increasing flow-rate and remarkable fluctuations in the chemical composition of fluids, as well as by the appearance of new vents. In order to more groundedly contribute to the refinement of the geochemical model of the crater fumarolic system in view of implications for volcanic surveillance, data on chemical and total sulfur isotopic compositions of fluids from Cortecci *et al.* (1992) were implemented with additional data, all these dealing with samples collected between 1979 and 1993; seventy out of ninety samples, however, refer to 1988-1993 years.

Before late 1984, nearly constant $\delta^{34}S(\Sigma S) = +3 \pm 0.3‰$ is displayed by fumaroles, thus suggesting a single major source of sulfur likely related to degassing of an andesitic magma at depth. Afterwards, the $\delta^{34}S$ decreases and varies between –2.7 and +1.6‰, due to the influence of shallow hydrothermal fluids carrying isotopically light volatile sulfur from leaching in the underground of previously accumulated elemental sulfur ($\delta^{34}S$ = –5.4 to –1.2‰, average –4.2 ± 1.3‰) and hydrothermal pyrite ($\delta^{34}S$ = –11.5 to –5.9‰, average –9.0 ± 2.3‰). These geochemical events were concomitant with enhanced seismic activity in the area possibly accompanied by intrusion of seawater into the volcanic system. In particular, the peak in the local seismicity in August 1988 was preceded in July by a notable rise of $\delta^{34}S$ in fumaroles from $-1.8 \pm 0.6‰$ to $-0.2 \pm 0.1‰$, as expected from an increased contribution of the magmatic component in the fluids. The $\delta^{34}S(\Sigma S)$ kept between –0.5 and +1.2‰ until early 1989, then fell down to –2‰ after a few months. The pre-1984 isotopic signature in the gases has been no longer restored.

In binary plots, available $\delta^{34}S$–H_2O and $\delta^{34}S$–CO_2 data points from 1984 to 1993 samplings arrange, without any clear-cut distinction in space and time, along fairly well defined negative and positive trends, respectively (see fig.1). Mixing would seem to be confirmed between a deep magmatic fluid ($\delta^{34}S \approx +3‰$) with approximately 76 mole%H_2O and 22 mole%CO_2, and a shallow hydrothermal fluid of variable isotopic ($\delta^{34}S \approx -11.5$ to $-1.2‰$) and chemical composition (94 to 98 mole%H_2O and 1.4 to 2.4 mole%CO_2), the chemistry inferred for the end members being taken from Chiodini *et al.* (1993). The model works well enough also when $\delta^{34}S$–ΣS, $\delta^{34}S$–H_2S/SO_2 and $\delta^{34}S$–HCl/SO_2 data points are considered. The gaseous sulfur species

in the shallow fluid may be, however, appreciably enriched in ^{34}S with respect to parental S-bearing minerals (Grinenko and Grinenko, 1967). In this case, the model appears to be even more fitting.

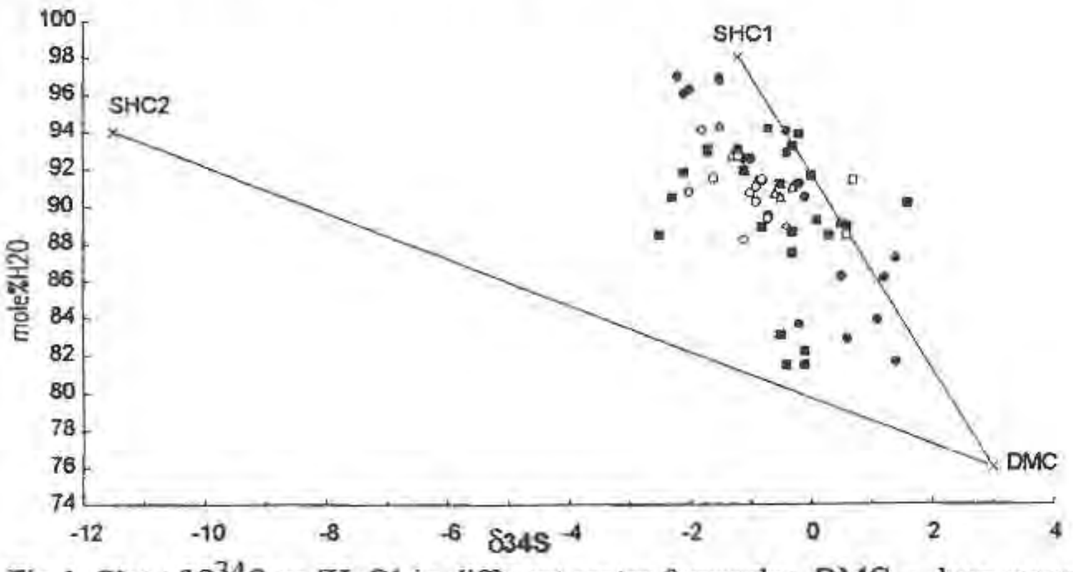

Fig.1. Plot of $\delta^{34}S$ vs $[H_2O]$ in different crater fumaroles. DMC = deep magmatic fluid; SHC1 and SHC2 = limiting data points of the shallow hydrothermal fluid.

References:
Grinenko, V.A. & Grinenko, L.N. (1967). *Geokhimiya*, **9**, 1049-1055.
Cortecci, G., Ferrara, G., Maiorani, A., Turi,B. (1992). *Proceedings of Water–Rock Interaction Symposium (WRI-7) / Park City/Utah.* Kharaka & Maest (eds), pp. 911-914. Balkema, Rotterdam.
Chiodini, G., Cioni,R., Marini, L. (1993). *Appl. Geochem.*, **8**, 357-371.

Al-Fe PHOSPHATES IN THE GAVÀ-BRUGUERS AREA, CATALONIA, SPAIN

Costa F., Camprubí A., Salvany M.C., Sáez G., Arcas A., Melgarejo J.C. (*Dept. de Cristal·lografia, Mineralogia i Dipòsits Minerals, Univ. de Barcelona*), Fontan F. (*Lab. de Mineralogie et Cristallographie, Univ. P. Sabatier, Toulouse*)

In the Catalonian Coastal Ranges the Silurian series contains many phosphate showings: some examples can be observed at the Miramar Mountains (Camprubí et al., 1993) in Southern Catalonia, and in Gavà-Bruguers area. In the Gavà-Bruguers area (20 Km. SW Barcelona) is where more different types of phosphate mineralization occur, as representative of P mobilization due to different geological processes:

Stratiform mineralization: It occurs at the basal units of the Silurian series, interbedded with gray shales and chert nodules, chert, nontronite, magnetite layers and massive jarosite layers. The mineralization consists of centimetric levels of apatite, variscite and strengite. The strengite unit can achieve 2 m thick. These mineralizations have been interpreted as sedimentary-exhalative in origin (Costa et al., 1993). During the Hercynian orogeny all these sediments were affected by regional metamorphism (very low grade), three folding and thrusting phases, and faulting during the Alpidic cycle.

Vein mineralizations: They are closely related to the sediments described above. Two types of veins occur:

a) prekinematic veins: they appear to form later than the first folding stage and the cleavage, and previous to the other stages. They are mainly composed by variscite and/or strengite. These veins have been interpreted as remobilizations during metamorphism.

b) postkinematic veins: they crosscut all the above sediments and foliations. The primary minerals are crandallite, turquoise, variscite and strengite. Veins can be monomineralic or formed by two phosphates or few more. Jarosite can also be found in some veins. In certain cases these minerals occur as latter phases in quartz veins. These veins represent late Hercynian hydrothermal events, but some of them could be related to the Alpidic faulting.

Limestone replacement: Late Silurian-Early Devonian limestones were replaced by ankerite or siderite, probably due to hydrothermal fluids related to Hercynian thrusting. Tinticite nodules or veins formed during late meteoric phenomena (oxydizing environment) on the above minerals (Melgarejo et al., 1988).

All these minerals were affected by meteoric replacement. Tinticite nodules were replaced by a new generation of late phosphates, including dufrenite and calcioferrite. Montgomeryite and collinsite are widespread in veins or pseudomorphs of the early formed phosphates.

References:

Camprubí, A., Costa, F., Salvany, M.C., Sáez, G., Arcas, A., Melgarejo, J.C. (1993). *Bol. Soc. Esp. Min.*, **16,1**, 55-56.
Costa, F., Camprubí, A., Salvany, M.C., Sáez, G., Arcas, A., Melgarejo, J.C. (1993). In: Fenoll Hach-Alí et al. (eds.) *Current Research in Geology Applied to Ore Deposits*, 715-718.
Melgarejo, J.C., Galí, S., Ayora, C. (1988). *N. Jb. Miner. Mh.*, **10**, 446-453

PRELIMINARY FLUID INCLUSION DATA ON QUARTZ FROM CARRARA MARBLE, TUSCANY, ITALY

Costagliola P., Cipriani C. (*Museo. Mineral.Litol., Univ. Firenze*) & **Lattanzi P.** (*Dip.Sci. Terra, Univ. Firenze*)

The famous Carrara marble is a metamorphosed Jurassic limestone belonging to the Apuane Alps (AA) complex. The complex, consisting of a Palaeozoic basement and of a Mesozoic-Cenozoic cover, underwent metamorphism (P≈3-4 Kbar; T=350-450 °C) and two main deformational stages D_1 (27 m.y.) and D_2 (8-12 m.y.).

A number of mineral deposits, mainly hosted by the basement, have provided fluid inclusions (FI) belonging to the H_2O (CO_2)-NaCl system having a salinity around 5-10 wt.% NaCl eq. and temperature of homogenization (Th) 200-250 °C. However, fluid inclusions with higher salinity (up to 33 wt% NaCl eq.) have been documented and appear to be restricted to late- or post-metamorphic structures (Lattanzi *et al.*, 1992; Hodgkins & Stewart, 1994). A fluid inclusion study in quartz from veins and cavities hosted in the Carrara marbles was undertaken; the aim is to collect information about metamorphic hydrology in the higher levels of the complex, in lithotypes that did not locally contribute to fluid production (H_2O) through devolatilization reaction. Veins are localized in the so called "Macchia Bianca" that is interpreted as a sedimentary structure isoclinally folded together with enclosing marble (Franzini *et al.*, 1987). According to these Authors, cavities and veins were emplaced, during D_2 stage, along boudins produced preferentially in correspondence of Macchia Bianca levels, due to the rheological discontinuity with the surrounding marbles.

Preliminary data were obtained on two specimens from the Mineralogic Museum of Università di Firenze. Salinities of the fluid inclusions are in the range 5-15 wt.%, whereas Th fall between 180 and 230 °C. Microthermometry and Raman analysis indicate that only very few inclusions contain CO_2, with no systematic relation to sample location, Th and salinity. On a broad scale, NaCl eq. content and Th do not differ significantly from the values observed in the basement. Salinity shows an appreciable positive correlation with respect to Th (Fig. 1); this may indicate a mixing between two end members fluids, one (A) characterized by low temperature and salinity and the other (B) by higher temperature and salinity. (A) may indicate contributions of meteoric fluids, whereas (B) could reflect the presence of a "salinity reservoir" that became progressively involved by metamorphic circulation during the late stages of metamorphism. This reservoir could be represented either by evaporitic beds occurring in the nearby formations, or by basinal brines expelled during deformation (cf. Lattanzi *et al.*, 1992; Hodgkins & Stewart, 1994).

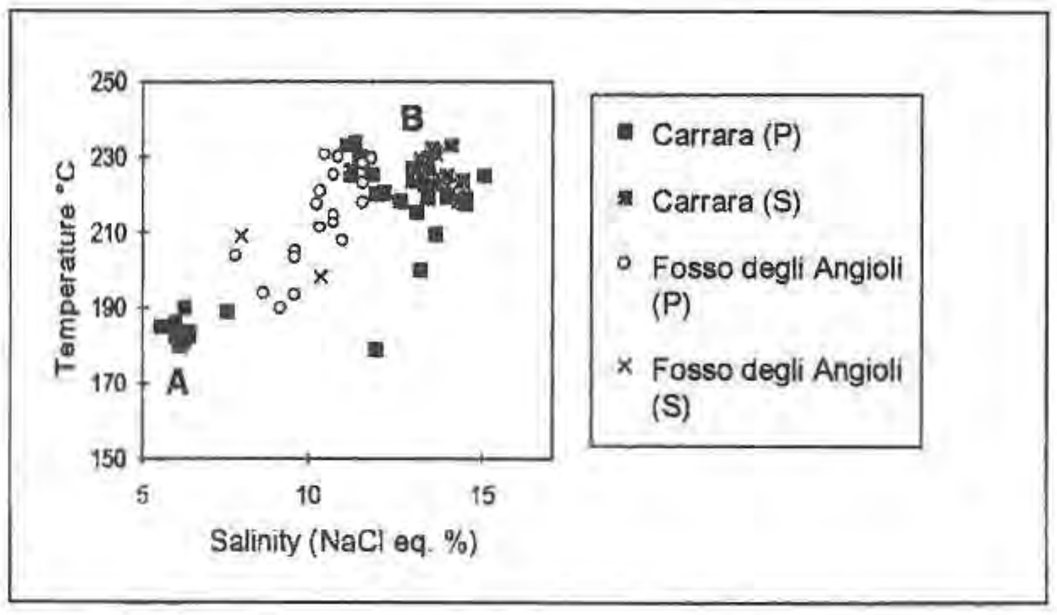

Fig. 1 - Th-NaCl diagram of fluid inclusions in quartz from Carrara marbles (P=primary; S=secondary)

Hodgkins M.A. & Stewart K.G. (1994). *J. Struct. Geol.*, **16**, 85-96
Lattanzi P., Benvenuti M., Costagliola P., Ruggieri G. & Tanelli G. (1992). *Plinius*, **8**, 94
Franzini M., Orlandi P., Bracci G. & Dalena D. (1987). *Min. Rec.*, 18, 263-296

DENSITY, EXPANSIVITY AND COMPRESSIBILITY OF CaO-Al_2O_3-SiO_2 LIQUIDS

Courtial P., Dingwell D.B. and Webb S. (*Bayerisches Geoinstitut, Universität Bayreuth, 95440 Bayreuth, Germany*)

The volumetric properties of aluminosilicate liquids are important in understanding the thermodynamics of magmatic systems. An equation of state, or the temperature and pressure dependence of volume is essential for calculation of magmatic phase relations at pressure and determining the direction and rate of magma transport in the Earth.

In order to obtain a model as a function of temperature, pressure and composition, we are determining densities, expansivities and compressibilities of melts in simple ternary aluminosilicate systems. The strategy is to investigate joins radiating from SiO_2 to various stoichiometries on the alkali or earth-alkaline aluminate. We present here volumetric measurements made in the CaO-Al_2O_3-SiO_2 system (see figure).

Density measurements have been made using both Pt and Ir-based double bob Archimedean systems. Densities have been determined in the temperature range of the liquidus up to 1800 °C. The results of the two set-ups are in good agreement for determinations on the same compositions. Compressibilities have been determined on melts using the ultrasonic method at 3, 5 and 7 MHz from the melting point up to 1600 °C. The measurements of the longitudinal waves propagating in the melts were performed in the reflection mode with the transducer acting as both sender and receiver.

Density measurements show that the liquid density increases with the decreasing of SiO_2 content. With the same (Al_2O_3/CaO) ratio, our data suggest a density change about 8 % for low SiO_2 content up to 60 mol %. Concerning the compressibilities measurements, the addition of Al_2O_3 and CaO to SiO_2 allows an increase of the bulk modulus up two twice that of the SiO_2 value.

Along the joins investigated, density determinations indicate an ideal behaviour of this property above 40 mole % of SiO_2. A deviation from this trend of over 5 % is however observed for the lowest SiO_2 contents. A more restricted number of compressibility measurements also suggest a deviation from ideal behaviour for SiO_2-poor melts.

The structural specificity of aluminum appears to have measurable consequences for melt properties. The non-ideality of volume with composition along the silicate-aluminate joins will be discussed in terms of the possible structural sources.

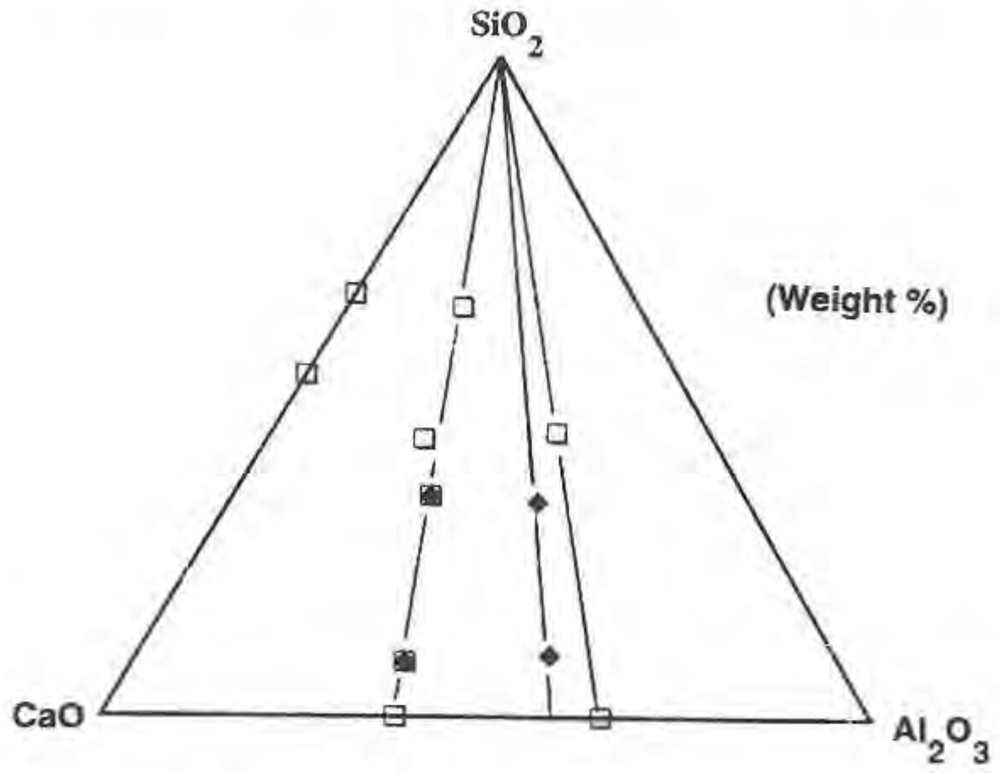

Open symbols: density measurements
Solid symbols: compressibility measurements

ATMOSPHERIC GASES IN AMBER

Craig H. (UCSD, La Jolla CA) and Horibe Y. (Tokai Univ., Japan)

The fundamental problems in amber-gas research are the diffusivities of air gases (N_2, O_2, and Ar) in the amber matrix, and the interpretation of the measured compositions. Horibe & Craig (1988) found D = 0.85 (N_2 and Ar) and 3.0 (O_2) × 10^{-10} cm²/sec, and Hopfenberg *et al.* (1988) found D = 5-8 × 10^{-13} cm²/sec for propane. D values for N_2, O_2, Ar are 3-5 orders of magnitude > propane in polymer glasses: thus the Horibe-Craig and Hopfenberg data are consistent. Landis & Snee (1991) reported a null-measurement (no release of neutron-generated ^{39}Ar) of D ≤ 1.5 x 10^{-17} cm²/sec. Landis & Snee and Berner & Landis (1988b) claim that the propane data do not follow Fickian kinetics, but Hopfenberg *et al.* showed clearly that they do. Until independent studies by careful protocols confirm one set of values, *nothing* can be said about the age of gases in ambers.

The most curious observation in the Berner & Landis gas data is that "reconstructed" O_2 lies between narrow limits of ~ 21% to 35%. These values are precisely those in modern air and in air dissolved in solvents such as water and organic fluids similar to plant resins, so that one must wonder how Nature arranged the composition of the Cretaceous atmosphere so that O_2 never strayed outside them. Berner and Landis (1988a) measured N_2, O_2, Ar, and CO_2 in three Canadian ambers by successive crushing. The sum of (O_2 + CO_2) was assumed to be the *original* O_2 concentration because of respiration. They claim (1988b) that in samples in which Ar was measured "the O_2-rich end member ("primary gas") is found to exhibit airlike N_2/Ar ratios". However all but two of their data cluster close to the composition of gases *in a solution phase* in water or organic solvents such as benzene and cyclohexane (O_2~34%) which are reasonable surrogates for an amber matrix. Thus their "O_2-rich end members" have solution-like N_2/Ar ratios, *not* air-like ratios. They also list N_2, O_2, and CO_2 data for Baltic amber and resins, but no Ar data are given, so that these data are useless for interpreting the origin of the gases.

The N_2/Ar ratio is 83.6 in air, and 38- 42 in air dissolved in water, benzene, and cyclohexane. Horibe and Craig (1987) measured N_2/Ar ratios of 37-41 in 20 ambers, interpreted as atmospheric gases dissolved in tree sap, with consumption of O_2 by respiration in the original groundwater source to the roots and in the tree. We now report data on 35 ambers, recent resins and gums in which the mean N_2/Ar ratios are 40.10 in ambers and 37.1 in the resins. Three Baltic "bone" ambers with very high bubble contents have ratios of 47, 53,

and 61, indicating an excess of bubbles relative to the initial bulk phase. In Baltic, Dominican, and Canadian Tertiary ambers, [O_2 + CO_2] ranges from 11.2 - 37.3% of total gas, with lowest values in the three bone ambers with high N_2/Ar ratios. The range in Canadian Cretaceous ambers is 14.5 to 26.0% (and N_2/Ar = 40.9-43.6), indicating no evidence for any excess O_2 relative to modern air.

In both the Berner & Landis data and our data the N_2/Ar ratios indicate that amber and resin gases are derived from solutions that initially had the composition of modern air, in which O_2 has been consumed by respiration and oxidation reactions and CO_2 from these sources has been added. Our model assumes that gases derived from groundwater and via transpiration-exchange in leaves migrate from sap to the oleoresin precursors of amber within the tree, and are extruded with them when the bark is ruptured. This model accounts for the observed gas chemistry, and for the micro-bubble swarms in bone amber which we interpret as the result of high-P gas extrusion. No matter what diffusivities are assumed for air gases in amber, there are no compositional inconsistencies in the existing data that require a higher O_2 content in the Cretaceous atmosphere.

Berner, R.A. & Landis, G.P. (1988a,b). *Science* **239**, 1406, and **241**, 721.

Hopfenberg, H.B., Witchey, L.C., Poinar, G.O. (1988). *Science* **241**, 717.

Horibe, Y. & Craig,H. (1987). *EOS* **68**, 1513. (1988).

Horibe, Y. & Craig, H. (1988). *Science* **241**, 720.

Landis, G.P. & Snee, L.W. (1991). *Paleo. Paleo. Paleo.* **97**, 63.

HELIUM - Nd - Sr & Pb ISOTOPIC COMPONENTS OF THE ETHIOPIAN MANTLE PLUME(S?)

Craig H., Scarsi, P., (SIO/UCSD, La Jolla CA, USA) & Ferrara, G. (Istituto Geocronologia e Geochimica Isotopica, Pisa).

$^3He/^4He$ ratios provide a unique "primordial signature" for the study of MORBs *vis-à-vis* OIB hotspots. Relative to the uniform MORB $^3He/^4He$ ratio: $R = 8 \times R_A$ ($R_A = 1.4 \times 10^{-6}$ in air He), the 16 globally-active "High-^{3}He" hotspots range from R/R_A = 11.3 to 30, reflecting ^{3}He derived from a Primitive Mantle (PM) undegassed component in which Nd-Sr isotopic ratios are ≈ "Bulk Earth" values. The Ethiopian plume $^3He/^4He$ signature was established in 1976 by sampling volcanic gases in the Rift Valley from 6° to 12°N (Tendaho Graben). $^3He/^4He$ ratios in these gases range up to 15.1 R_A at 7.3°N in the Corbetti Caldera area, showing that a mantle plume of the "High-^{3}He" type is a component of the Ethiopian Flood Basalts. (Passive upwelling of asthenosphere cannot produce basalts with "High-^{3}He" R/R_A values). We have now extended this work with He-Sr-Nd-Pb data on basalts over the same Rift section, and in the Northern Afar Depression up to 15°N, 40°E. (Pb data: TBA, Pisa).

$^3He/^4He$ ratios in olivine phenocrysts range from 5.2 to 17.0 R_A, with maxima at 8°N in the Rift Valley (17 R_A), where the maximum value was also found in volcanic gases, and at 13.5°N in the central Afar Depression (13-14.2 R_A). The Sr-Nd data are generally similar to those of previous studies (Betton & Civetta, 1984; W. Hart *et al.*, 1989; Schilling *et al.* 1992) and show two mixing trends, toward DM and HIMU endmembers, from a PM component sited at 7.5°N on the Rift axis, in the region of the highest $^3He/^4He$ ratios.

Basalts with HIMU-type Sr-Nd ratios were found at Arafali (Eritrea) in an outlier of Afar Axial range basalts similar to those at Manda Inakir and Lake Asal in Djibouti, discovered by Vidal *et al.* (1991). These HIMU basalts are similar to, but more extreme than, those in the "46°E anomaly" in the Gulf of Aden (Schilling *et al.*, 1992): in our section HIMU-trend basalts also occur at 6.6°N in the S. Rift, on the northern edge of Lake Abaya. Our data map into PM ("High-^{3}He"), DM, and HIMU plume components on the "depleted" side of the PM - Bulk Earth ratios. The HIMU sites (Djibouti, Arafil, S. Ethiopian Rift, and Gulf of Aden) are of special interest: they show no preference for common radial distances from the Schilling "torus-headed plume", as they are 70, 450, 550, and 650 km from its presumed center in the central Afar. The Arafil and Djibouti sites lie on a locus ~ parallel to, and close by, the edge of the Red Sea, near the N and S ends of the Danakil Horst, while the other two are along strike in the Rift Valley and the Gulf of Aden, indicating a possible tectonic control of HIMU emplacement. The association of HIMU and PM trends in close proximity raises the question of whether there are two Ethiopian plumes, or two manifestations of a single plume.

Similar geographical couplings of plume components, observed in the "Low-^{3}He" - HIMU, Cook Islands (R/R_A = 5.5-6.8) and "High-^{3}He", PM-containing, Austral Islands (R/R_A = 9.3-13.0), where the change in plume-persuasion occurs precisely at the intersection with the Austral Fracture Zone, and in the eruptions of the Easter hotspot plume along the East Rift of the Easter Microplate (Poreda *et al.*, 1993), may also be influenced by regional tectonic structures. In Ethiopia the He-Sr-Nd coupling is not as clearcut as in the Austral-Cook chain lavas: in the HIMU samples R/R_A = 6.3-8.6 at Arafil, 12.3 in a W. Afar exposure, 7.0 in a central Rift site, and 5.2-6.3 in the southern Rift. Nevertheless, HIMU-PM associations are becoming interesting: do they originate in a *single* plume at the core-mantle boundary, segregated by percolation in the boundary layer?

Betton, P.J. & Civetta, L. (1984). *Earth. Planet. Sci. Lett.* 71, 59-70.

Hart, W.K., WoldeGabriel, G., Walter, R.C., Mertzman, S.A., (1989). *J. Geophys. Res.* **94**, 7731-7748.

Poreda, R.J., Schilling, J-G., Craig, H., *Earth. Planet. Sci. Lett.* **119**, 319-329.

Schilling, J-G., Kingsley, J-G., Hanan, B.B., McCully, B.L. (1992). *J. Geophys. Res.* **97**, 10927-10966.

Vidal, Ph., Deniel, C., Vellutini, P.J., Piguet, P., Coulon, C., Vincent, J., Audin, J. (1991). *Geophys. Res. Lett.* **18**, 1913-1916.

SURTSEYAN VS STROMBOLIAN AND EFFUSIVE ACTIVITY IN THE M.TE PORRI SUCCESSION (SALINA, AEOLIAN ARCHIPELAGO, ITALY): EVIDENCES OF A THREE COMPONENT MAGMA MINGLING

CRISCI GM*, DE ROSA R**, MAZZUOLI R*** & VENTURA G*

*Dip.Sci.Terra,UNICAL,Cosenza,**Dip.Geomin.,Univ.Campus,Bari, ***Dip.Sci.Terra,Univ.Pisa

On the western flank of M.te dei Porri (Salina Island), the renmants of a small volcanic centre was recognized, testifying of the initial phases of activity of the M.te dei Porri stratovolcano. It consists of a tuff-ring resulting by the emplacement of hydrovolcanic pyroclastic surges and fall deposits (HP), covered, without unconformities, by strombolian lapilli (SD) and a lava flow (LF). The HP juvenile clasts range in composition from early erupted basaltic andesistes to late erupted andesites, frequently containing mafic cumulates. SD lapilli exhibit an overall andesite basaltic composition and contain abundant quartzite xenolithes and xenocrysts. Quartzites are commonly rimmed by rhyolitic glass and plagioclase-clinoyroxene aggregates. LF shows macroscopic textural evidences of mingling between HP-type and SD magmas. The HP component is characterized by a very high phenocrysts content (50-55 vol%) and can be interpreted as a sort of crystal-mush of HP. Ratios between incompatible elemements indicate that fractional crystallizzation was the main operative process in the evolution of HP rocks. SD basic rocks show a different geochemical signature being enriched in K2O, Sr and incompatible elements (i.e. Rb, Ba, Zr, U, Th) in respect to the HP magma.

Whole of the data suggests the following model: a) the basic magma (SD) rises through the metamorphic basement and suffers a significant contamination by including and partially melting crustal material; b) SD magma enters a shallow magma chamber where resident magma (HP) was undergoing a FC process; the lower portions of the reservoir were occupied by an high-viscous, nearly

rigid crystal-mush; c) SD magma pushes up the crystal-mush triggering the eruption; d) the eruption starts with the emission of the lower mafic magma and then of andesites because of the small volume (and therefore low thickness) of differentiated liquids; e) SD magma ascent breaks the crystal-mush and is erupted;the last eruptive phase is characterized by the contemporaneous slow effusion of both SD and HP lowest magmas (LF).

XRD LINE PROFILE ANALYSIS OF SYNTHETIC AND SOIL GOETHITES.

Crosa M.*, Boero V.* Franchini- Angela M.**
*DI.VA.P.R.A.- Chimica Agraria, Via P.Giuria 15, 10126 Torino.
**Dip. di Scienze Mineralogiche e Petrologiche, Via Valperga Caluso 37, 10125 Torino.

Intrinsic line broadening (WHH) can be used to calculate, by the well known Scherrer Formula, the mean crystallite dimension (MCD) if the contribution from strain can be neglected. WHH of soil iron oxides is usually taken from differential X-ray diffraction (DXRD) profile obtained subtracting the XRD profile of a sample free of all or part of the Fe oxide minerals from that obtained from the untreated sample (Schulze, 1981).

In the present work the precision and reliability of this technique is evaluated by means of a fitting program (Enzo *et al.*, 1985) , in order to compare the results obtained from a conventional XRD pattern with a DXRD one.

Significative improvements have been reached when the XRD-DXRD method was modified by a procedure which takes into account, as imput parameters for analysis, beside the WHH, the following ones, obtained from the sample free of iron oxides: baseline, peak positions, Lorentz/ Gauss proportions and asimmetry. In this way the goethite parameters of soil untreated sample resulted more accurate and precise, expecially as concerns WHH.

The fitting procedure, used also to optimize step and counting time in XRD scanning, is analysed and discussed.

References:
Schulze, D.G. (1981). Soil Sci. Soc. Am. J., **45**,437-440.
Enzo, S., Polizzi, S., Benedetti, A. (1985). Z. Kristallogr., **170**, 275-287.

CRYSTALLOGRAPHIC EVIDENCE FOR Ti-OXY SUBSTITUTION IN BIOTITES FROM METAPELITES

Cruciani G. (*Inst. of Mineralogy, Univ. of Ferrara, Italy*), Guidotti C.V. (*Dept. of Geological Sciences, Univ. of Maine, USA*) and Zanazzi P.F. (*Dept. of Earth Sciences, Univ. of Perugia, Italy*)

The substitution mechanism $^{[6]}(R^{2+}) + 2(OH)^{-} = {}^{[6]}(Ti^{4+}) + 2O^{2-}$ (i.e. Ti-oxy substitution) in biotites has been proposed by several authors (Bohlen *et al.*, 1980; Dymek, 1983; Bol *et al.*, 1989). Nevertheless the Ti-oxy substitution is commonly neglected owing to the difficulty of its recognition on the basis of the incomplete chemical data typically obtained by electron microprobe analyses.

However, the recent single-crystal structural results of Cruciani & Zanazzi, (1994) support the occurrence of Ti-oxy substitution. Specifically, variation of the *c* lattice dimension of biotite is largely a function of the distance between the hydroxyl group position on the octahedral sheet and the interlayer K^+ cation. Hence the loss of the proton as in the proposed Ti-oxy substitution should lead to a decreased repulsion between the then absent proton and the interlayer K^+ and be reflected by an inverse relationship between increasing Ti content and shortening of the *c* cell parameter, as observed by Cruciani & Zanazzi. However, to test this model more rigorously, it was necessary to study a suite of biotites for which the TiO_2 content was the only significant compositional variable.

Hence, we measured the cell parameters variation on single crystals of biotites from metapelites of W. Maine (USA). Samples were chosen from a metamorphic suite showing increasing TiO_2 contents in the biotites as a function of increased metamorphic grade. TiO_2 varies from 1.48 wt% to 3.32 wt%, but the other compositional variables (Al, Si, Mg/Fe Ratio, and Fe^{2+}/Fe^{3+} Ratio) are narrowly constrained (Guidotti *et al.*, 1988; Guidotti & Dyar, 1991). The H^+ content, of the biotites of Western Maine, measured by uranium extraction, has been shown to vary inversely with metamorphic grade (Dyar *et al.*, 1991). Moreover, a clear, inverse correlation has been found between the H^+ content and the sum of highly charged cations (Dyar *et al.*, 1993).

For this new suite of biotites we have studied, the inverse correlation between TiO_2 content and the mica-layer thickness along $\mathbf{c}^*$ is quite clear, as shown on the Figure on which the preliminary new data are plotted ($y = 10.175(15) - 0.057(9)\ x$; $R^2 = 0.91$).

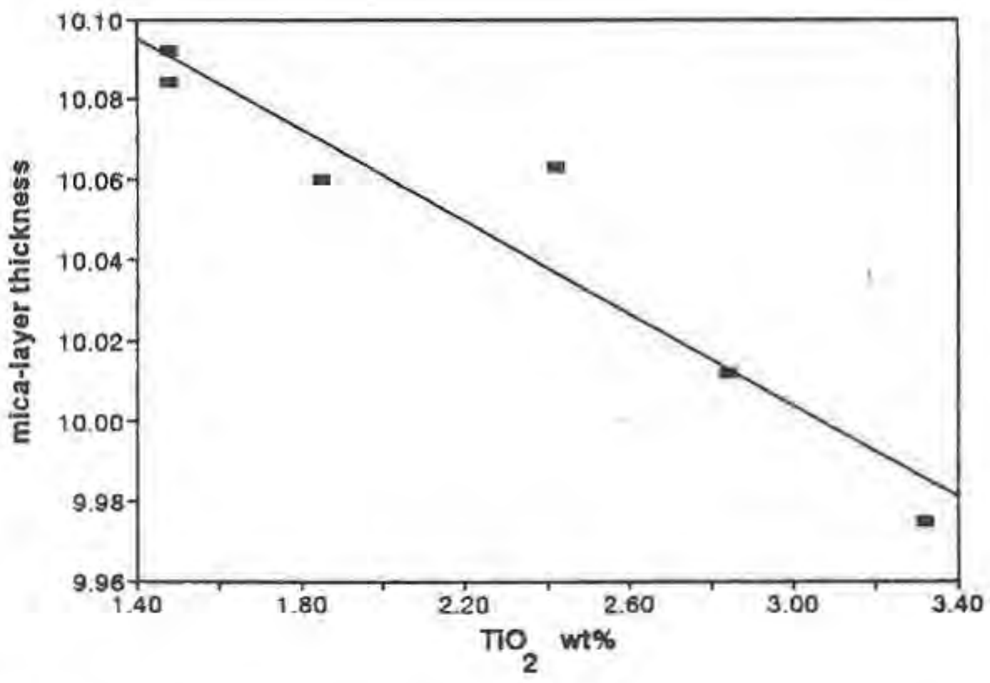

References:
Bohlen, S.R., Peacor, D.R., Essene, E.J. (1980). *Am. Mineral.*, **65**, 55-62.
Bol, L.C.G.M., Bos, A., Sauter, P.C.C., Jansen, J.B.H. (1989). *Am. Mineral.*, **74**, 439-447.
Cruciani, G. & Zanazzi, P.F. (1994). *Am. Mineral.*, **79**, 289-301.
Dyar, M.D., Colucci, M.T., Guidotti, C.V. (1991). *Geology*, **19**, 1029-1032.
Dyar, M.D., Guidotti, C.V., Holdaway, M.J., Colucci, M. (1993). *Geochim. Cosmochim. Acta*, **57**, 2913-2918.
Dymek, R.F. (1983). *Am. Mineral.*, **68**, 880-899.
Guidotti, C.V., Cheney, J.T., Henry, D.J. (1988). *Am. Jour. Sci.*, **288**, 270-292.
Guidotti, C.V. & Dyar, M.D. (1991). *Am. Mineral.*, **76**, 161-175.

SELF-DIFFUSION OF CATIONS IN GARNET AND PYROXENE MINERALS

Cygan R.T., Schwandt, C.S., and Westrich, H.R. (*Geochemistry Department, Sandia National Laboratories*)

Accurate diffusion coefficients for cations in silicate minerals are often required for evaluating petrologic processes. The experimental determination of diffusion coefficients also provides a basis for evaluating diffusion mechanisms and the limit of their use in thermal history models; changes in diffusion mechanisms often complicate the extrapolation of high temperature diffusion data to the lower

temperatures. A matrix of experimental runs for examining diffusion in garnet and pyroxene is used to determine the dependence of diffusion on oxygen fugacity at lower crustal temperatures (800°C to 1000°C). A diffusion couple is comprised of a thin film with an enriched isotope that is produced by the thermal evaporation of a metal oxide onto a polished surface of the mineral. The oxygen fugacity of the anneals is controlled and maintained by electronically-regulated mixtures of CO and CO_2. The annealed diffusion couples are subsequently analyzed by depth profiling with an ion microprobe. Typical penetration depths of diffusion are less than 0.15 μm. Use of the thin film approach allows for the determination of diffusion coefficients with values as small as 10^{-24} m^2/sec with a relative uncertainty of 15 percent.

Self-diffusion of ^{25}Mg in pyrope and ^{44}Ca in grossular garnet have been determined at Q-F-M conditions and 800°C, 900°C, and 1000°C using this approach. The self-diffusion activation energies of 147 ± 21 kJ/mole for Mg in pyrope and 155 ± 10 kJ/mole for Ca in grossular are obtained from the best fit of the diffusion coefficients to an Arrhenius relation. The corresponding frequency factors (D_o) are 2.57 x 10^{-15} m^2/sec for pyrope and 7.2 x 10^{-16} m^2/sec for grossular. Diffusion measurements of ^{25}Mg in oriented crystals of orthoenstatite were performed at 800°C, 850°C, and 900°C at I-W conditions. The activation energies for Mg diffusion in enstatite are considerably higher than those observed for pyrope. They vary from 254 ± 19 kJ/mole for the (001) orientation to 344 ± 36 kJ/mole for the (100) orientation. However, only minor diffusion anisotropy is observed within the temperature range of the experiments. The enstatite data are also in excellent agreement with the Ganguly & Tazzoli (1994) model based on cation exchange kinetics.

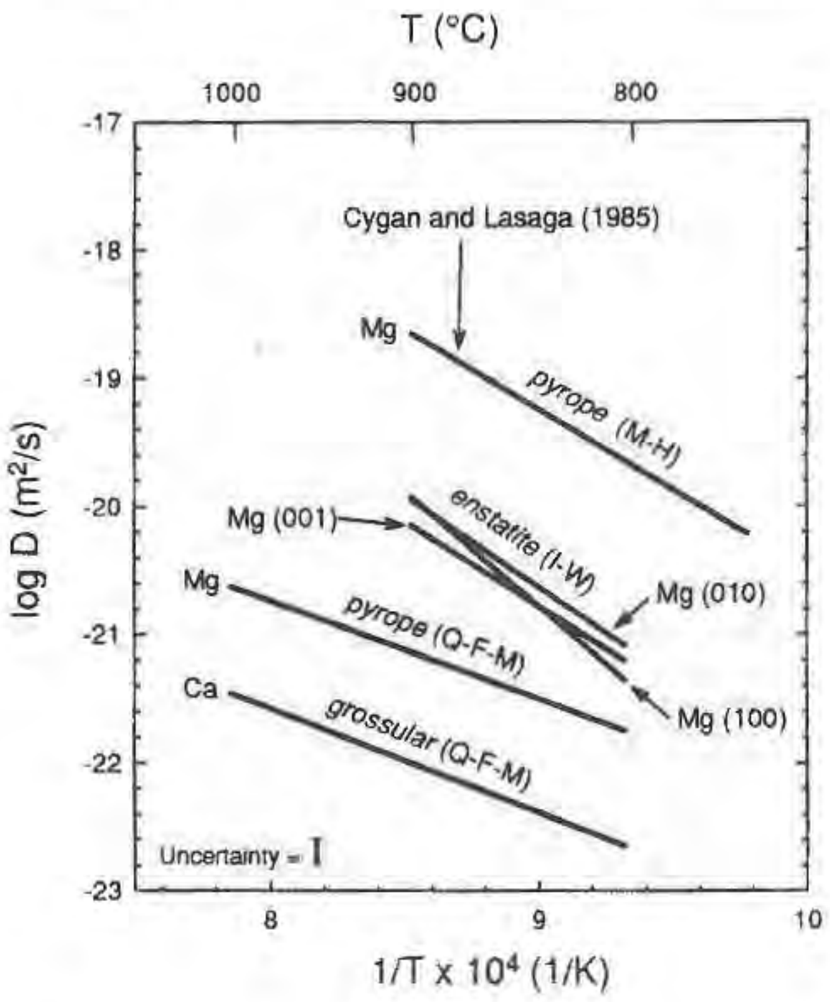

References:
Cygan, R.T. and Lasaga, A.C. (1985). *Am. J. Sci.*, **285**, 328-350.
Ganguly, J. and Tazzoli, V (1994). *Am. Mineral.*, **79**, in press.

Research sponsored by the Geosciences Program of the U.S. Department of Energy Office of Basic Energy Sciences under contract DE-AC04-94AL85000.

"AMPHIBOLOIDS" - A POSSIBLE STRUCTURAL SERIES

Czank, M. (Mineral. Inst. Univ. Kiel, Germany)

Most of the chain silicate structures can be described as a modular structures. In the polysomatic series of the pyriboles, either pyroxene-like and mica-like slabs (Thompson, 1970) or I-beams (Veblen *et al.*, 1978), both extending parallel to the chains, can be chosen as structural modules. Each member of the series has chains of the same periodicity (P=2), but of different mulitplicity (M=1,2,3,...). In the homologous series of the pyroxenoids the moduls can be pyroxene-like and wollastonite-like layers which are parallel to (001) of pyroxene (Takéuchi and Koto, 1976). Each member of the series has single chains (M=1) but of different periodicity (P=3,5,7..... ...—> ∞ (≡2)) which run parallel to **c**.

It has been shown that carlosturanite can be regarded as a member of a polysomatic series with vierer chains (P=4; M varies) (Mellini *et al.*, 1985). A similar series including the structures with vierer loop-branched (*IB*) chains (e.g. howieite) can be derived by choosing slabs of half the width of the haradaite chain as the modules.

Analogous to the pyroxenoids, a new structural series can be derived by choosing (001) layers of amphibole and of howieite (Fig.1), which could be called "amphiboloids" (M=1,*IB*; P varies). The end-member amphibole has a crystal chemically effective chain period of P=2 and chain multiplicity of M=2.

Chain mulitplicity faults and chain periodicity faults are common in these structural series and they lend credence to the possible existence of such structures as stable phases (Czank and Liebau, 1980). In the "amphiboloids" discrete faults within the end-members, but no other stable structures have as yet been found.

Using the above modular structural principles, an almost infinite number of new possible chain silicate structures, such as vierer-, sechser-, achter-, etc. double, triple, quadruple, etc. chains (P and M varies) can be derived.

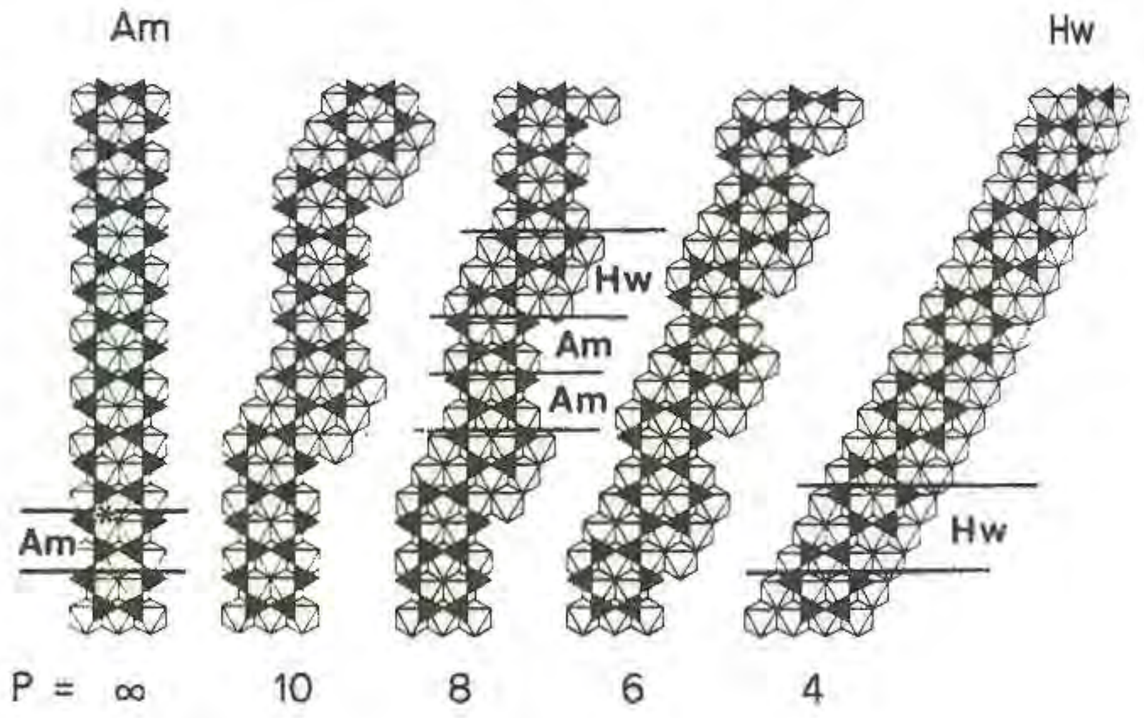

Figure 1. Structural series of "amphiboloids": $M^{2+}_{(7/2)P-8}M^{3+}_{6}[Si_{4P-4}O_{11P-10}](OH)_{P+6}$, (P=4,6,.....—>∞). Am=amphibole, Hw=howieite, P=chain periodicity. M4 position in Am is not shown. The modul layers of Hw and Am are indicated and the building principle of the series is given examplary for P=8.

References:
Czank, M., Liebau, F. (1980). Phys. Chem. Miner., **6**, 85-93.
Mellini, M., Ferraris, G., Compagnoni R. (1985). Am. Miner., **70**, 773-781.
Takéuchi, Y., Koto, K. (1977). Min. J., **8**, 272-285.
Thompson, B.J., Jr. (1978). Am. Miner., **63**, 292-293.
Veblen, D.R., Buseck, P.R., Burnham, C.W. (1977). Science, **198**, 359-365.

NATIVE GOLD IN THE BAIA MARE MINING DISTRICT

Damian Gh. and Damian Fl.(*Dept. of Geology, Univ. Baia Mare*)

The hydrothermal ore deposits of the Baia Mare district are related to Neogene volcanic rocks (Badenian - Upper Pannonian). Three areas can here be distinguished as resulting from: (1) the association of the ores with volcanic rocks of different ages,and (2) the prevalence of metals in the ores.

I. The western area (Ilba - Băița) with Sarmatian pyroxenic andesites and ore veins containing mainly base metal sulphides and subordinately gold and silver. Gold occurs both in the base metal ores, forming microinclusions in chalcopyrite, galena, sphalerite, pyrite, and quartz and in the Au - Ag ores, where it is included in quartz. At Ilba about 60 percent of observed gold grains occur in quartz, having the fineness of 720. The fineness increases at Băița, i.e. of 760. Small amounts of gold appear included in goethite, i.e. 8 and 4 percent, respectively.

II. The central area (Săsar) with quartz andesites of Pannonian age and Au - Ag ore veins or stock works. Gold is associated either with quartz (about 30 percent), iron oxides (5 percent), sulphides (38 percent) and carbonates. The gold in the quartz veins has nearly the same fineness (610-763) as compared to the gold associated with pyrite in the stock works (640-730).

III. The eastern area (Dealu Crucii - Cavnic) with pyroxenic andesites of Pannonian age and ore veins bearing both base metal sulphides and gold. At Baia Sprie the gold is mostly associated with sulphides (mainly pyrite, about 68 percent) and has a fineness of 715-740 as compared with the gold in quartz (about 31 percent) of significant lower fineness (650). At Suior most of the gold is included in quartz (80 percent) in the upper part of the vein and associated with sulphides (82 percent) in the lower part. The gold fineness is of 730-785. The gold in the Băiuț area (Breiner) is included either in pyrite or sphalerite (about 60 percent) or in quartz (40 percent) and shows a higher fineness (875-980). Most of the gold in the Văratec ores is related to chalcopyrite (32 percent) and quartz (40 percent) and shows also a relatively high fineness (800-860).

The average size of gold grains (inclusions) varies from 0,05 mm, when associated with sulphides, to 0,02 mm, when associated with quartz.

PIXE (PIGE), SEM AND RAMAN OBSERVATIONS ON FLUID INCLUSIONS FROM A PORPHYRY COPPER DEPOSIT FROM THE APUSENI MOUNTAINS, RUMANIA.

Damman, A.H. (1), Kramer, J.L.A.M (2), Rieffe, R.C. (1) & Vis, R.D. (2). *((1) Inst. of Earth Sciences, (2) Physics Dept., Vrije Univ., Amsterdam).*

Quartz crystals from a porphyry copper deposit in the Apuseni Mountains, Rumania (Pintea, 1993), contain three types of primary and pseudo-secondary fluid inclusions. Type-1 inclusions are highly saline, consisting of various daughter minerals that may form up to 90% of the volume of the inclusion and a small vapour bubble. Type-2 inclusions contain a large vapour bubble and a small, often practicly invisible, rim of liquid. Type-3 inclusions contain a vapour bubble of variable width and a rim of liquid, containing one or more daughter minerals. Types-1 and -2 inclusions are very common; type-3 inclusions are much more rare.

PIXE (proton induced X-ray emission), PIGE (proton induced γ-ray emission), SEM and Raman analyses on these inclusions show the following results:

1) PIXE- and SEM-spectra of type-1 inclusions contain strong K, Ca, Al and Fe-lines and weaker, but still clearly distinguishable S, Cl, Cr and Ti-lines. Strong Na-lines are frequently found in the PIGE spectrum of these inclusions. Microscopic observations, Raman- and SEM analyses of type-1 inclusions show the presence of Cr-bearing hematite, anhydrite, halite, sylvite and Al-silicates, presumably clay minerals. Ti also occurs in PIXE spectra of quartz next to the fluid inclusions, suggesting the presence of small rutile needles in the quartz.
2) PIXE analyses of type-2 inclusions show two distinct types of spectra:
2a) Spectra containing strong Fe- and Cu-lines and
2b) Spectra containing strong Mn-, Fe-, Zn-, Pb-, and Br-lines and distinctly weaker Cu-lines.
3) Type-3 inclusions contain all elements present in the types-1 and -2 inclusions.

According to Pintea (1993 and personal communication) types-1 and -2 inclusions represent a contemporaneous, immiscible hydrosaline melt (type-1) and a vapour (types-2a and -2b). Optical observations combined with analytical data suggest that:

a) The type-3 inclusions were most probably formed by heterogeneous trapping of immiscible types-1 and -2 inclusions.
b) Al, K, Ca, Na, Cr, Cl, S are strongly enriched in the hydrosaline melt during melt/vapour separation.
c) Mn, Cu, Zn, Pb and Br are strongly enriched in the vapour during melt/vapour separation.
d) The contemporaneous occurrence of types-2a and -2b inclusions suggests that chemical differentiation has taken place in the vapour, presumably shortly after the melt/vapour separation.

References:
Pintea, I. (1993). Abstract ECROFI XII, Archiwum Mineralogiczne XLIX, 165-167.

SOME ACCESSORY MINERALS IN GRANITOIDS FROM HUNGARY

Dani Z. and Buda Gy. (*Dept. of Min. Eötvös L. Univ. Budapest*)

Two type of granitoids can be distinguished in Hungary. The first one is syncollision, "in situ" migmatite (360 m. years) with heterogen composition, it outcrops in Mecsek Mts. and is covered by thick sediments in other part of South Hungary. The other type is a postcollision granitoid (280 m. years) with composition from quartzdiorite to granite. This occurs in the Velence-Mts. and can be discovered in drill holes along the Balaton-Velence faults-zone. This granite is intrusive type with thermal contact aurole. The main crystallization temperature of this granite was about 680 °C and the cooling was rapid.

The main accessory minerals in syncollision granitoid are fluor-apatite, titanite and zircon. The fluor-apatite euhedral, often zoned. Sometimes the core is black or dark grey, perhaps from carbon-content indicating sedimentary origin. Titanite is either euhedral or subhedral. The first one is bigger in size with primary origin. The second one forms small grains originated from alteration of biotite. The primary one is sometimes rich in Nb, and zoned caused by variable Nb-content. Zircon is euhedral, zoned, often has more than one cores. The cores usually are hydrozircons, with U- and Th-content. Zonation is caused by change of Fe-, Ca- and Al-content. Hf-content is varying. Result from zircon-morphology shows overlapping between mixed crustal and mantle origin calc-alkaline granitoid and subalkaline granitoid at 800°C crystallization temperature. Other frequent accessory minarals are allanite, secondary RE-fluorcarbonate minerals, pyrite, epidote, rutile, monazite and thorite-uranothorite. Allanite is euhadral, zoned, commonly has epidote-rim, often altered. Secondary allanite can be observed too. Secondary RE-fluorcarbonate minerals are subhedral, inhomogen, formed from allanite by F^-, CO_3^{2-} bearing hydrotermal solutions. Monazit also has primary and secondary origin. Other rare accessory minerals are sulphides (galena,

tetrahedrite, chalcopyrite, arsenopyrite), ilmenite, cassiterite, huttonite.

Apatite, zircon, titanite and allanite are the main accessory minerals in the postcollision granitoid. Apatite usually occurs as an inclusion in biotite. Zircon generally is weakly zoned, sometimes with Ca-free core and Ca-rich rim, which indicates the zircon formed from early to late crystallization. The results from zircon-morfology show subalkalkaline character (with mixed crustal and mantle origin) according to classification of J. P. Pupin and 800-850 °C forming temperature. Titanite has two origin: primary and secondary formed from the alteration of biotite. Allanite and secondary RE-fluorcarbonate minerals are main REE-bearing accessory minerals. Allanite is euhedral, zoned. Alteration often can be observing with thorite veins. Secondary RE-fluorcarbonate minerals is subhedral with inhomogen composition formed by alteration of allanite. Other accessory minerals are epidote, thorite-uranothorite, rutil, zoizite and galena.

The syncollision granitoid (South Hungary) is rich in REE due to the REE-bearing accessory minerals. The more differentiated postcollision granitoid (Velence Mts.) has lower REE-content, richer in heavy REE originated from intracontinental differentiation.

APPLIED MINERALOGY AND METAL RECOVERY FROM THE OLYMPIC DAM CU-U-AU-AG DEPOSIT, SOUTH AUSTRALIA

Danti, K.J. and Grguric, B.A.
(*Western Mining Corporation Ltd., Olympic Dam Operations*)

Olympic Dam Operations is an expanding producer of uranium oxide and refined copper, gold, and silver. The operations consist of a mechanised underground mine, a flotation circuit to separate copper sulphides from uranium and gangue minerals, a hydrometallurgical plant to extract uranium from flotation concentrates and tailings, a copper smelter to produce blister (anode) copper, and a copper refinery to produce electrorefined and electrowon copper cathode, and refined gold and silver. All mineral processing and metal refining takes place at the mine site.

The Olympic Dam deposit is hosted by a hematite-rich hydrothermal breccia complex which occurs entirely within a Mid-Proterozoic A-type granite. The ores are lithologically and mineralogically diverse, with more than 25 ore and gangue minerals each exhibiting specific grinding, flotation, leaching, and smelting properties. Most of the economically recoverable metals occur in chalcocite, bornite, chalcopyrite, electrum, uraninite-pitchblende, coffinite, brannerite, and minor occurrences of digenite, djurleite, roxbyite, covellite, idaite, acanthite, native copper, gold, and silver. Minerals containing currently subeconomic metal concentrations include cobaltian pyrite, carrollite, molybdenite, galena, florencite, bastnäsite, monazite, and xenotime. Deleterious elements occur as Pb-, Hg-, As-, Ag-, and Bi-tellurides and selenides which are intergrown with the copper sulphides. The gangue mineralogy consists of hematite, magnetite, sericite, chlorite, quartz, siderite, dolomite, barite, anhydrite, gypsum, fluorite, tourmaline, zircon, and apatite. The size, shape, abundances, and intergrowth characteristics of these minerals vary spatially throughout the deposit.

Ore delivered to the metallurgical plant is the product of blending ores from several sources throughout the orebody to meet optimal copper:sulphur ratios and grades. Key factors identified to date which directly influence overall metal recoveries during ore processing include copper and uranium grades, copper:sulphur and iron:silica ratios, and the relative proportions of both of acid soluble to insoluble copper- and uranium-bearing minerals. Mineralogy, morphological characteristics, and textural relationships exert the basic, primary control on these parameters. Applied mineralogy is utilised on-site to address both immediate and long term problems caused by processing and refining highly variable ores. An important objective of Olympic Dam's mineralogical research effort is to provide, in a timely manner, high quality mineralogical data when necessary to all stages of mineral processing and metal recovery.

Computerised optical microscope-based image analysis systems have been extensively used to provide quantitative mineralogical analyses of materials including plant feed, plant and laboratory concentrates, tailings and concentrate leach residues, furnace slags, flash furnace oxidation products, blister copper, electrowon and electrorefined copper cathode, and precious metal-bearing refinery slimes. Image analysis in conjunction with scanning electron microscopy and electron microprobe analysis has also been used to: 1) study the effects of refractory corrosion in the flash furnace, 2) characterise the distribution of uranium-bearing minerals in plant feed, concentrates, and tailings, 3) study the geochemical behaviour of copper, uranium, and gangue minerals during leaching in the hydrometallurgical circuit, and 4) identify and quantify the mineralogy of deleterious elements.

Experience and financial benefits gained by Western Mining Corporation at Olympic Dam and at its nickel operations in Western Australia through the utilisation of applied mineralogy has shown clearly that on-site mineralogical laboratories are not only justifiable but necessary in today's highly competitive metal markets.

LOW GRADE METAMORPHISM IN CLAY MINERALS: SETTING UP A METHOD FOR CRYSTALLITE SIZE AND MICROSTRAINS DETERMINATION

Dapiaggi M. and Setti M. *(Dip. Scienze della Terra-Univ. di Pavia)*

A detailed study of the microstructural[1] and physico-chemical characteristics of the clay minerals involved in diagenetic-metamorphic reactions is certainly a basic step in the knowledge of their behaviour as indicators of low grade metamorfism.

A number of indicators has been proposed to study the transition between diagenesis and low grade metamorphism. The most widely used is the Kübler "crystallinity" index (IK) for illites, related to the organic matter maturation, was originally developed for the discover of the so-called oil-window, that is of the commercial accumulation of oil in a range of depth and geothermal gradient between 65.5 and 150° C (Pusey III, 1973). Due to the problems related to the presence of complicated tectonic frameworks, complex parageneses and variable K contents among the samples, the Kübler Index should be used paying particular attention to its limitations.

A new method was set up for the study of the mineralogical associations commonly found in the sedimentary environment during burial diagenesis and incipient metamorphism. A lot of physico-chemical variables may influence either the presence of certain mineral species or their microstructural characteristic. In particular, the chemical composition of the whole rock, its porosity and the presence of interstitial fluids play an important role in the definition of the actual characteristic of the rock. The first stage of the method was therefore a detailed study of all these variables while, in a second time, oriented preparations of the clay fraction ($<2\mu m$) were analyzed via X-ray Powder Diffraction. The presence and the type of order of expandable material (interstratified minerals) was detected using the Srodon method (Srodon, 1980, 1984) on ethylen-glycol preparations. The complex paragenes found suggest the use of a

[1] the term "microstructural" will be referred, from now on, to all the defects which affect lattice periodicity, leaving its structure undisturbed (small crustallite size, microstrains, grain boundaries, stacking faults, dislocations, etc.)

program of pattern decomposition, in order to distinguish among the various mineral species present in the samples; moreover, the program allows a direct calculation of the crystallite size and of the microstrains of the powdered material, through the Warren-Averbach method (Warren and Averbach, 1952). The program used was the one proposed by Enzo *et al.* (1988)

The method was tested on a set of kaolinites synthesized under different conditions, such as starting composition, crystallization time and temperature (Huertas *et al.*). As a result, the crystallite size determination (Dapiaggi and Setti, 1993) were in good agreement with the synthesis conditions of the kaolinites, giving thus a physical meaning to these calculations. The method was applied to samples from the Western Ligurian Flysch Units (Maritime Alps, Northwestern Italy) and it could be used, through a precise determination of the microstructural characteristics of the minerals, for the determination of the metamorphic grade in any similar environment; even it has not been tested yet for this purpose, it may be applied for the discover of the oil-window.

References:

Dapiaggi, M. and Setti, M. (1993). *Proceeding of the 3rd European Powder Diffraction Conference (EPDIC3)*, Vienna, 25-28 September, 1993. In press.

Enzo, S., Benedetti, A. and Polizzi, S. (1988). *J. Appl. Cryst.*, **21**, 536-542

Huertas, F. J., Huertas, F. and Linares, J. (1993). *Applied Clay Science*, 7, 345-356

Pusey III, W. C. (1973). *World Oil*, **176/5**, 71-75

Srodon, J. (1980). *Clays and Clay Minerals*, **28**, 401-411

Srodon, J. (1984). *Clays and Clay Minerals*, **32**, 337-349

Warren, B. E. and Averbach, B. L. (1952). *J. Appl. Phys.*, **23**, 497

AN ^{57}Fe MÖSSBAUER EFFECT STUDY OF FRANKLINITE

De Grave E., Vandenberghe R.E. (*Dept. of Subatomic and Radiation Physics, Univ. of Gent)*, Vochten R. (*Dept. of Chemistry, Univ. of Antwerp)* and Kruk R.P. (*Dept. of Radiospectroscopy, Jagellonian University, Kraków*).

Franklinite crystals were collected from the Sterling Hill deposit, Sussex Co., New Jersey. The cubic lattice parameter of the spinel compound, determined using a Guinier-Hägg camera and silicon powder as internal standard, was found to be 0.8451 nm. No impurity phases were detected. The chemical formula derived from AAS is close to $Zn_{0.7}Mn_{0.3}Fe_2O_4$.

Mössbauer spectra were collected at variable temperatures in the range 4.2 - 500 K. A longitudinal external field of 55 or 60 kOe was applied at selected temperatures. The Curie temperature T_C was found to be 240±5 K. Above T_C the spectra consist of slightly broadened ferric doublets with a small but consistent asymmetry in peak depths. Following the suggestion of Vogel *et al.* (1976), these doublet spectra were adequately described by a superposition of two components. However, some fine structure in the residual function remained and the goodness-of-fit lowered significantly if three doublets, all with equal line widths Γ, were fitted. The obtained Mössbauer parameters (Γ=0.27 mm/s) at room temperature are listed in Table 1. The temperature variations of these parameters show a normal behaviour. Based on the δ^{Fe} values, D1 and D2 can be assigned to octahedral (B sites) Fe^{3+} ions and D3 to tetrahedral (A) ones. The appearence of two distinct B sites has been attributed to clustering of Mn and Zn (Vogel *et al.* , 1976).

At temperatures between ≈30 K and T_C the spectra reflect a complicated relaxational behaviour with apparently two distinct spectral components with a different temperature variation.

Table 1. Quadrupole splitting ΔE_Q, center shift δ^{Fe} (both in mm/s) and fractional area RA of the three doublets D1, D2, and D3 fitted to the spectrum of franklinite at ≈300 K.

doublet	ΔE_Q	δ^{Fe}	*RA*
D1	0.38(1)	0.36(1)	0.64(3)
D2	0.53(2)	0.37(2)	0.30(3)
D3	0.47(5)	0.24(3)	0.06(3)

The spectrum at 4.2 K shows an asymmetric six-lines pattern. When fitted with two symmetrical components, hyperfine fields of approximately 497 and 510 kOe were obtained, with relative areas of 0.24 and 0.76. The center shifts are equal (0.47 mm/s against Fe), but the quadrupole shifts $2\varepsilon_Q$ differ, i.e. -0.16 and 0.06 mm/s respectively. The spectrum at 4.2 K in an applied field of 55 kOe is shown in Fig.1. Qualitatively, it can be explained by local spin canting and spin reversal as observed earlier by Morrish and Clark (1975) for synthetic Zn-rich (Mn, Zn) ferrites.

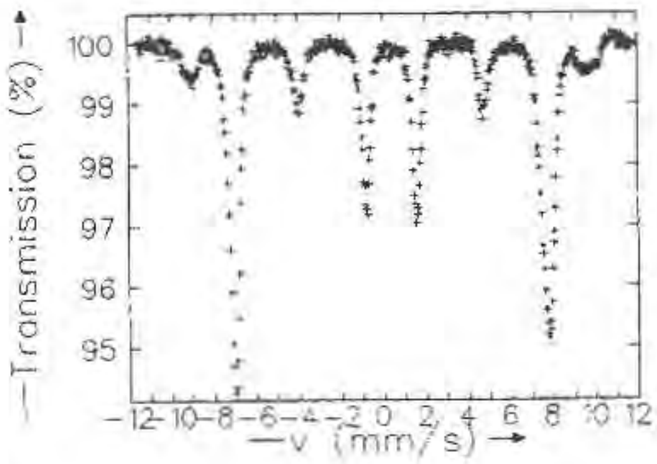

Fig.1. Mössbauer spectrum of franklinite at 4.2 K in an applied field of 55 kOe.

References:

Vogel, R.H., Evans, B.J., Swartzendruber, L.J. (1976). *AIP Conf. Proc.*, **34**, 125-127.

Morrish, A.H., Clark, P.E. (1975). *Phys. Rev.* **11**, 278-286.

ISOTOPIC STUDY OF BENTONITES FROM LOS TRANCOS DEPOSIT (CABO DE GATA, S.E. SPAIN)

Delgado, A., Reyes, E. and Caballero, E. *Dept. of Earth Sciences & Environm. Chem.,*
Estación Exp. Zaidín, CSIC, Granada, Spain

In order to study the genesis of the bentonite in ore found at Los Trancos, the isotopic composition of 23 bentonite samples was determined, taken both from surface outcrops and from core probes. The determination of $\delta^{18}O$ values was carried out on the lesser fraction of 2μm of these samples. Analysis of δ^2H was carried out on the total sample (bentonite), since it has a high percentage of smectite (over 90%) and the other minerals detected contain no hydrogen in their structure.

The $\delta^{18}O$ values show a mean value of 21.26‰ (σ = 1‰). The δ^2H values show great dispersion (σ = 22‰); their mean value is of -90‰. Since natural processes, such as water mixtures, evaporation processes, isotopic exchanges with the rock, etc. could not account for such dispersion, there must have been postformational exchanges of the smectite with the different types of water to which the area has been exposed.

If this explanation is confirmed it would be one of the most significant natural examples to support the hypothesis that hydrogen exchanges are possible in minerals of clay at low temperatures (Linares, 1987; Bird & Chivas, 1988; Longstaffe & Ayalon, 1990; Kyser & Kerrich, 1991).

Therefore, only the $\delta^{18}O$ smectite values can be used to determine the types of water and temperatures involved in the processes of bentonization . If the typical composition of meteoric water in the area (-6‰ > $\delta^{18}O$ < -4‰) and that of sea

water ($\delta^{18}O$ = 0‰) is considered together with the most frequent values in the smectites (+20‰ to + 23‰), one must conclude that if meteoric water has intervened in the process of bentonization, it would have temperatures of between 10°C and 30°C, whilst if sea water had intervened, the temperatures of the process would have been between 35°C and 55°C.

Of the two types of water proposed, the following evidence appears to point towards the intervention of meteoric water: a) Field evidence indicates that some samples have originated in a meteoric environment, whilst other, edaphic, samples belong to a paleosoil sandwiched in the top-lying carbonates. Both groups show isotopic values which are very similar to those of the rest of the samples of the ore. b) The other secondary phases present in the ore which appear to be syngenetic with the bentonites, calcite filling fractures and disseminated in the bentonite itself in the form of nodules and silica (opal-A) produced by alterations in the tobaceous materials, were originated in equilibrium with the meteoric water, at environmental temperatures of between 15°C and 25°C.

The morphology of the Los Trancos ore, with a band of tufa intensely altered to bentonite around a late andesite dome, indicates that mechanical and thermic effects must have favoured a rapid hydration of the tufa and quite possibly the formation of a protobentonite. Later, an intense circulation of meteoric water must have completed the process of bentonization, making its distinctive isotopic mark on the bentonites.

References:

Bird, M.I. & Chivas, A.R. (1988). *Chem. Geol.* **72**, 249-265.

Kyser, T.K. & Kerrich, R. (1991). In: *Stable Isotope Geochemistry (Ceochem. Soc.)* **3**, 409-422.

Linares, J. (1987). *II Congr. Geoquim. España.* 55-62.

Longstaffe, F.J. & Ayalon, A. (1990). *Applied Geochem.* **5**, 657-668.

THERMAL PROPERTIES of TiO_2.

de Ligny D., Westrum, Jr., E. F. and Richet, P.
(*Département des géomatériaux, Institut de Physique du Globe de Paris*)

The rutile form of TiO_2 is a common accessory mineral in metamorphic and igneous rocks. In addition, the heat capacity of several rutile-type compounds like stishovite was estimated using Kieffer vibrational modeling. The thermodynamic properties of rutile have a geochemical and theoretical interest. Unfortunatly, available calorimetric data show an unusual scatter of more than 5% for the heat capacity of rutile at high temperature. In view to make and test correctly a model for TiO_2, a new investigation of its thermal properties was needed.

We have thus redetermined the heat capacity of rutile from 5 to 1800K from adiabatic calorimetry and drop-calorimetry measurements. The thermal expansion was determined up to 1600K from high temperature volumes measured by X-ray diffraction experiments performed in an energy dispersive configuration in the wiggler line of the DCI storage ring of LURE (Orsay).

A Kieffer-type vibrational modeling constructed with available Raman, I.R and inelastic neutron scattering data will be presented. This new model will be faced to the experimental measurements and previous modeling.

REE IN GARNETS FROM POLYMETAMORPHIC SCHISTS IN THE CENTRAL STRUCTURAL DOMAIN, NE BRAZIL.

De Lima, E.S. (*Dept. of Geology, Federal Univ. of Pernambuco*), Vannucci, R., Bottazzi, P., Ottolini, L. (*CNR, Univ. of Pavia*)

Major-element mineral chemistry from the Serido Formation, Central Structural Domain, NE Brazil, has been used to investigate the P/T variations during the Brasiliano metamorphism (600-450 m.y.). It was shown that: 1) The Serido rocks underwent a polyphasic metamorphic evolution; 2) Minerals crystallized during the first metaphorphic phase re-equilibrated (biotite and garnet) during the second metamorphism, particularly in areas where it reached high amphibolite facies conditions. In these areas garnet show a fairly flat major-element profile, suggesting that re-equilibration and diffuion processes might have acted during the Brasiliano metamorphism (De Lima 1986, 1987a, b, 1992).

The samples investigated in the present study come from the staurolite (SV-2), sillimanite (SS-21) and sillimanite/cordierite (SS-40) zones. Pressures and temperatures using garnet-plagioclase and garnet-biotite exchange reactions vary from 1.5 kbar/540°C (staurolite zone), 5.5 kbar/660°C (sillimanite zone), 4.7 kbar/680°C (sillimanite/cordierite zone), which reflect P/T conditions during the second metamorphic event in the area.

The analysed samples correspond to metapelites, whose mineral assemblage reflect two metamorphic crystallization. The main foliation is defined by the alignment of biotite, plagioclase and quartz. Garnets inthese samples show three morphological signatures. Sample SS-40.1 has euhedral to subhedral garnet prophyroblasts, which show overgrowth type morphology. The second type garnet (SV-2) represents euhedral to subhedral inclusion-free porphyroblast, and the third type of garnet (SS-21) represents porphyroblasts with trail oriented inclusions.

Rare earth elements were measured with an ion-probe. The REE distribution in these garnets reflect the same behavior as Y. They are HREE-enriched, and show negative Eu anomaly (values from rim to core, Yb/Ce; Eu/Eu*: SV-2: 54,400-120,609; 0.16-0.28; SS-40: 84,250-54,818; 0.11-0.20; SS-21: 750-41,360; 0.26-0.56). The Eu_N/Eu^*, Yb_N/Gd_N, Yb_N/Dy_N values in these garnets presents two distinct patterns: a) a step-like profile with core values higher then rim values (samples SV-2 and SS-40); b) an increasing profile from rim to core (sample SS-21).

The REE chemical compostion in garnets from the Serido Formation corroborates De Lima's *et al.* (1992) suggestion of two different growth stages for garnets in the Serido Formation, were garnet in sample SS-21 crystallized during a single continuous growth stage, whereas samples SV-2 and SS-40 were formed by a two-step growth.

References

De Lima, E.S. (1986). PhD Thesis, UCLA, 218p.

De Lima, E.S. (1987a). Rev.Bras.Geociencias vol.17:315-323

De Lima, E.S. (1987b). Acad.Bras.Ciencias,vol.59:233-241

De Lima, E.S., Vannucci, R., Bottazzi, P., Ottolini, L. (1992). 37º Cong.Bras.Geologia,vol.1:436-437.

GENETIC RELATIONSHIPS BETWEEN MIGMATITES AND ANATECTIC GRANITES IN SOUTH GALLURA (SARDINIA): PETROLOGICAL, GEOCHEMICAL AND ISOTOPIC (Sr, Nd) EVIDENCE

Del Moro A. *(IGGI, CNR, Pisa)*, Di Pisa A. *(Inst. of Geol. Min. Sci., Univ. of Sassari)* , Macera P. *(Dept. of Earth Sciences, Univ. of Pisa)* & Oggiano G. *(Inst. of Geol. Min. Sci., Univ. of Sassari)*

A High Grade Metamorphic Complex (HGMC) crops out in Northern Sardinia, essentially consisting of migmatites. It is separated from a medium-grade terrane by an oceanic suture zone (Cappelli *et al.*, 1991). This picture is ascribed to the Hercynian orogeny (Carmignani *et al.*, 1992). The aim of this paper is to depict the anatectic process occurred in Southern Gallura and to infer the genetic relationships between migmatites and the associated parauthochtonous anatectic granites (Oggiano & Di Pisa, 1988; Macera *et al.*, 1989).

Two main lithologies, metatexites and diatexites, are recognizable among the Southern Gallura migmatites corresponding to two different field appearences and geographical distributions. The former, ML migmatites (to the East), consist of high-grade Sil-bearing gneissic rocks texturally preserving in-solidus metamorphic fabrics, the latter, TP migmatites (to the West), show strong evidence of anatectic homogenization and/or compositional differentiation by melt segregation processes. Available geochronological data on granites indicate that the anatexis occurred in a time span ranging from 310 to 300 Ma (Macera *et al.*, 1989). Thermo-barometric extimations of partial melting conditions in TP migmatites, based on Gt-Bt geothermometer and Gt-Pl-Sil-Qtz geobarometer, yield T and P values ranging from 650 to 750°C and from 5 to 7 Kbars, respectively.

The geochemical data are normalized to a representative sample of our collection (ML/1) having chemical composition very similar to the European Shales (ES) and representing, in our opinion, a reliable protholith. Granites and leucosomes show depleted incompatible and RE element patterns in respect to ML/1. Melanosomes show more or less specular patterns. No meaningful variation for silica, alumina and soda contents, but depletion in calcium is observed in some granites. Both the high incompatible, but Rb and K, and transitional element depletions in granites, along with the specular enrichment of these elements, except the ferromagnesian ones, in restitic melanosomes, suggest for granites a low-grade partial melting of a ML/1-type source likely involving the breakdown of biotite.

Sr and Nd isotopic compositions, calculated at 300 Ma, allow us to distinguish two main populations each of them being constituted by both migmatites and granites. The first one (ML metatexites and A group granites) has higher Sr isotopic ratios (0.715/0.716) and more negative ε Nd (-7.6/-7.9) than the second population (TP diatexites and B group granites) (0.710/0.711; -5.1/-6.4).

Geochemical patterns show a strong internal coherence within each population, suggesting a possible direct linkage between migmatites and granites having similar Sr and Nd isotopic ratios. A and B group granites, in turn, likely represent the melt fractions extracted and there is no field evidence to suspect their provenance from strongly different protholiths, as they both are parauthochtonous granites.

The noticed variability of the Sr and Nd isotopic compositions might be ascribed to the isotopic heterogeneity of the source. The group A granites possibly derive from more pelitic portions, the group B granites from more arenaceous ones. On the other hands, assuming a chemical and isotopic equilibrium partial melting process, A and B melts would leave restites with higher (ca. 0.715) and lower (ca. 0.711) Sr isotopic ratio, respectively. Partial melting processes in the HGMC of Southern Gallura appear to be mainly controlled by the breakdown of micas producing highly peraluminous melts (A/CNK molecular ratio ranging from 1.1 to 1.3). In particular B group melts often show Al_2SiO_5 as liquidus phase, suggesting for them a mica-rich rather than a Qtz-feldspatic protholith. This means that the contribution of an arenaceous material to the Sr isotopic composition of B group granites might represent only a minor component, whatever the age of sediments is. Furthermore, the absence of melanosomes/restites with Sr isotopic composition similar to the ML/1 and A group granites ones, leads us to infer a more complex evolution of the Sr isotopic systematics in the whole area.

In terms of initial Nd isotopic composition, the difference between the two populations is governed by the monazite and/or allanite behaviour during the partial melting process.

References:
Cappelli, B., Carmignani, L., Castorina, F., Di Pisa, A., Oggiano, G., Petrini, R. (1991). *Geodinamica Acta*, **5**, 101-118.
Carmignani, L., Barca, S., Cappelli, B., Di Pisa, A., Gattiglio, M., Oggiano, G., Pertusati, P.C. (1992). *IGCP 276, Newsletter*, **5**, 61-82.
Macera, P., Conticelli, S., Del Moro, A., Di Pisa, A., Oggiano G., Squadrone, A. (1989). *Per. Min.*, **58**, 25-43.
Oggiano, G. & Di Pisa, A. (1988). *Boll. Soc. Geol. It.*, **107**, 471-480.

HIGH-PRESSURE ANATECTIC MIGMATITES IN THE AUSTROALPINE ULTEN UNIT: GEOCHEMICAL, Sr AND Nd ISOTOPIC INVESTIGATION

Del Moro A. (*Ist. Geocronologia e Geochimica Isotopica, C.N.R., Pisa)*, Martin S. (*Dip. Geologia, Paleontologia e Geofisica, Univ. di Padova)* and Prosser G. *(Fac. di Scienze, Univ. della Basilicata, Potenza)*

The Ulten unit is a high-grade basement complex located in the Upper Austroalpine system of the Eastern Alps (Western Trentino, Italy). It mainly consists of Ky-bearing migmatites and gneisses, which derive from partial melting and deformation of previous metapelites. Minor aluminous granulites, Grt-Ky restites and pegmatitic rocks are associated to leucosome bodies within migmatites. The high-grade basement includes lenses of Grt- or Spl- peridotites and Grt-metabasites, which rarely contain eclogite-facies relics (Benciolini & Poli, 1993).

Estimated P-T peak metamorphic conditions range from 1.2-1.7 Gpa and 800-850°C (Benciolini & Poli, 1993; Benciolini, 1993) or ≥1.4 Gpa and 700-750°C (Hoinkes & Thöni, 1992; Hauzenberger *et al.*, 1993) when dehydration or fluid-present melting are considered, respectively. Using the dataset of Holland & Powell (1990), P-T peak conditions of 833±33°C and 1.55±0.16 Gpa have been obtained on migmatites, restites and gneisses (Martin *et al.*, in prep.). These high P-T conditions have been probably achieved within the deep portions of a colliding wedge during the Variscan Orogeny (Lower Carboniferous).

Migmatites, gneisses and restites define unmixing lines in binary variation plots of major (with the exception of K_2O) and ferromagnesian trace elements versus SiO_2 content. Leucosoma-rich migmatites attain 77% in SiO_2 whereas the alumina content increases until 35% in the more refractory specimens. The A/CNK molecular ratio varies between 1 and 8.5 from a stromatic migmatites to restitic granulites.

Leucosoma-rich migmatites are enriched in SiO_2, CaO, Na_2O and depleted in Al_2O_3, TiO_2, FeO tot., MgO, Zr, Cr, Ni, Sc, Co,V and REE tot. relative to restitic granulites. Both LREE and HREE patterns are similar although REE are more abundant in restites with respect to migmatites. Thus partial melting produced a plagioclase-rich "granitic" leucosome leaving as residues femic and REE-rich accessory phases within restites.

The Sr isotopic ratios of migmatites, restitic granulites and enclosed metabasite pods, calculated at the minimum metamorphism age of 330 Ma (Lower Carboniferous), are 0.7056-0.7185 independently of the lithology while eps. Nd(330) values range between -2.9 and -10.9.

No smooth correlation exists between the isotopic parameters mentioned above either for migmatites or for restitic granulites. However, the $^{87}Sr/^{86}Sr$ isotopic composition does generally decrease as the Sr concentration increases (from 120 to 1330 ppm) in migmatites. The decoupling of the Sr and Nd isotopic systematics supports the metasomatic addition of low Nd/Sr ratio aqueous fluids to the original material.

The observed Sr chemical-isotopic values do not correspond to those typical of pelitic to graywacke metasedimentary rocks but can reflect the effects of a syn-metamorphic process.

A $^{87}Sr/^{86}Sr$ isotopic ratio as low as 0.7055 is suggested for the hydrous solution(s) that metasomatized the granulite-migmatite complex.

These isotopic features suggest the following hypothesis: the Ulten unit may be interpreted as a deep mèlange-type zone which behaved as an isotopically undefined material between different end-members. The mixture of different tectonically emplaced rock types may have represented the source of an atypical $^{87}Sr/^{86}Sr$ isotopic ratio within the aqueous fluids. The presence of mafic and ultramafic rocks within the tectonic mèlange could explain the relatively low initial $^{87}Sr/^{86}Sr$ values calculated for the migmatite-granulitic complex.

Benciolini N. & Poli S. (1993) Terra Abs., EUG VII, 398.
Benciolini N. (1993) Simp. CROP-Alpi Centr., Sondrio.

Hoinkes G. & Thöni M. (1992) in "Pre-Mesozoic Geology in the Alps" Springer-Verlag, 485-494.
Holland T.B.J. & Powell R. (1990) J. Metam. Geol., 8, 89-194.
Hauzenberger Ch.,Höller W., Hoinkes G., Klözli U. & Thöni M. (1993) Terra Nova Abs. 4, 13.
Martin S., Prosser G., Godard G., Kienast J.R. & Morten L., in preparation.

SUPPORTING MINERAL COLLECTIONS: A ROLE FOR THE SOCIETY OF MINERAL MUSEUM PROFESSIONALS

DeMouthe J.F. (California Acad. of Sci., San Francisco, CA, USA <jdemouthe@calacademy.org>), Harlow G.E., (American Museum of Nat. Hist., New York, NY, USA <gharlow@amnh.org>), and Francis C.A. (Harvard Univ. Mineral. Museum, Cambridge, MA, USA)

Mineral collections and the mineralogists who curate them play a primary role in mineralogy, through exhibitions, education of the public, scientific research and the support of research by providing specimens, data and information. Museums are under increasing pressure to justify their function and mission which requires museum professionals to communicate more effectively among themselves and with the public, supporters and those who utilize their collections. Likewise, museum mineralogists need to coordinate their activities to be more effective.

The Society of Mineral Museum Professionals (SMMP), formerly Mineral Museums Advisory Council (MMAC), aims to meet these challenges in a variety of ways. The mission of the society is to "foster recognition of mineral science collections as essential scientific, educational and cultural resources; to promote support for growth, maintenance and use of collections and exhibits; to advance museum practice through cooperation in the development, review and dissemination of information."

Current activities and projects of the Society include:
⇒ An annual meeting at the Tucson Gem and Mineral Show which includes a program on an important issue or topic in museum and collection work;
⇒ regional meetings where members can get together for a program or discussion;
⇒ publication of a newsletter 2-4 times annually;
⇒ maintenance of a Museum Hot-Line for stolen specimens (which will soon be accessible through the Internet);
⇒ sponsorship of exhibitions at mineral shows or professional meetings to foster the Society and its goals;
⇒ establishment of liaisons with other professional societies to exchange information and work toward mutual goals (a liaison presently exists with the Mineralogical Society of America and will soon exist with the Mineralogical Association of Canada);
⇒ maintenance of a list of collections, collection management policies, and other resources at member's institutions;
⇒ selection of the recipient of the annual Carnegie Mineralogical Award sponsored by the Carnegie Museum of Natural History;
⇒ development of a workshop on standards and goals for mineral collection data bases and a mineral collections networking group on the Internet to provide contacts and resource lists for curators and scientists.

Presently the Society is predominantly a North American organization, but it looks forward to a broader membership and seeks cooperation with other organizations around the world. Further information and membership forms are available through the authors.

PGE MINERALS FROM BROKEN HILL, NEW SOUTH WALES

Dennis, G.R., Elvy, S., Gray, N., Williams, P.A.
(*Department of Chemistry, University of Western Sydney Nepean, Australia*)
and French, D.A. (*CSIRO, North Ryde, Australia*)

PGE mineralization of exceptionally high grade has long been recognised from deposits to the east of Broken Hill, NSW, Australia (Mingaye, 1892). It is largely confined to gossan pods and stringers after sulfides in shear zones adjacent to or in contact with ultramafic members of the Broken Hill Block (Barnes, 1988). The nature of the PGE minerals present has been speculated upon, but hitherto never proven .

Platinum mineralogy is simple; remnant sperrylite, $PtAs_2$, is present in gossan fragments. It is observed to be oxidized to native platinum, Pt. This observation is in accord with previous predictions concerning the fate of sperrylite in the supergene zone (Plimer and Williams, 1988). Some of the native Pt has associated Pd and Fe in solid solution. Braggite, PtS, isoferroplatinum, Pt_3Fe, and tetraferroplatinum, PtFe, are also present.

Palladium mineralogy is much more complex. The Pd minerals paolovite, Pd_2Sn, stibiopalladinite, $Pd_{5+x}Sb_{2-x}$, native palladium, Pd, and palladium-platinum, palladium-copper and palladium-bismuth alloys have been identified as isolated grains together with two new phases of composition $Pd_8Te_{3-x}Hg_x$ ($x \leq 0.7$) and $Pd_8Te_{3-x}Bi_x$ ($x \approx 1$). The latter phase may be related to Pd_8Te_3 or to $Pd_{20}Te_7$ and has been synthesised on the basis of the latter overall stoichiometry. These tellurides are associated with native bismuth grains, tellurian bismuth alloys and blebs of native gold.

Fragments of primary pyrite, pentlandite, pyrrhotine and chalcopyrite are preserved *in situ*. Alteration of pentlandite to violarite has been noted in drill core which has intersected primary mineralization (Giles, 1974).

Associated secondary mineralogy is curious; anglerite, $PbSO_4$, and iodargyrite, AgI, are common in the gossan. New secondary Cu-Pd oxides corresponding to the formulae Cu_2PdO_3 and $Cu_5Pd_2O_7$ occur in veinlets of chrysocolla.

Mobilization of Pd from the original sulfide ores is evident. The element has been transported some distance from the sulfide lenses into the surrounding rocks and redeposited, associated with malachite. No evidence for the transport of Pt to the same extent is observed.

No discrete Rh, Ru, Os or Ir minerals have been found separately. However, significant amounts of these elements are present, presumably in solid-solution, in some of the abovementioned species and submicroscopically, as found using PIXE methods.

Barnes, R.G. (1988). *Bull. Geol. Surv. New South Wales*, **32**, 101-103.
Giles, C.W. (1974). "The Ultramafics of the Broken Hill District and their Associated Mineralisation," B.Sc. (Hons) Thesis, University of Adelaide, 68 pp.
Mingaye, J.C.H. (1892). *J. Roy. Soc. New South Wales*, **26**, 371-3.
Plimer, I.R. and Williams, P.A. (1988). In "Geoplatinum 87", Ed. Prichard, H.M., *et al.*, Elsevier, 83-92.

GEOTHERMAL STRUCTURE OF SENGAN AREA, JAPAN, BY FLUID INCLUSIONS THERMOMETRY

De Vivo B., Fedele L., Raia F. and Tarzia M. (*Dip. di Geofisica e Vulcanologia, Università di Napoli, Italy*)
Sasada M., Sasaki M. and Sawaki T. (*Geol. Survey of Japan, Tsukuba, Japan*)

The Sengan geothermal area, north-east Honshu, is located in the Hachimantai volcanic region at the border between Akita and Iwate Prefectures. It is one of the largest-scale active geothermal fields in Japan, with three operating geothermal power stations (Ohnuma, Matsukawa and Kakkonda). We report here the new results obtained by fluid inclusion studies from three wells (SN3, SN5 and SN6K) and we discuss them together with the results already published obtained from SN7D (De Vivo & Sasada, 1992) and SN1 (De Vivo *et al*, 1992) wells. The boreholes SN5 and SN7D are located immediately north of Akita-Yakeyama volcano in the Sumikawa geothermal system area; SN3 and SN6K are located south of Akite-Yakeyama, and SN1 is west of Kakkonda geothermal power plant. The boreholes cross volcanics (lavas and pyroclastics) and Pleistocene lacustrine silt deposits, with SN7D and SN5 reaching Tertiary intrusive "granitic" rocks. Palaeozoic sediments and Cretaceous granitic rocks crop out at the peripheral zone of the Sengan area. The maximum depth is 2474 m in SN7D. The maximum in-hole temperature is 310°C at 1740 and 1921 m in the same borehole. Fluid inclusions occur mainly along fracture trails in the igneous quartz of the tonalite and volcanic rocks, as well as in late hydrothermal veins of calcite, quartz, anhydrite and wairakite. They are of secondary origin. An average of six core samples at different depths have been studied by fluid inclusions for each borehole. Three thermal events occurred in the geothermal system: contact metamorphism, ore mineralization and geothermal alteration. These events

are characterised mineralogically by biotite-actinolite, sphalerite, galena; Ca-Al silicates and zeolite clay minerals respectively (Takeno & Noda, 1987). The widespread coexistence of L-rich and V-rich inclusions indicates extensive boiling in the hot-water dominated system. The overall scenario shows the presence of three types of inclusions: a) L-rich, with low salinity (≈ 0.1 wt % NaCl equiv.) and low Th (≈ 150°C); isotopic data indicate that these fluids are of meteoric origin (Ueda et al., 1991); b) L-rich and V-rich with very low salinity and Th from moderate (≈ 200°C) to high (≈ 380°C); c) L-rich and V-rich with daughter minerals, with salinities ranging from ≈ 4 to 40 wt % NaCl equiv. These fluids show to contain, in addition to Na^+, as well other components (Mg^{2+}, Ca^{2+}, Li^{+}). The deep fluids in Sengan area are, at least partially, of magmatic source, originating from Tertiary intrusive bodies, as confirmed by $\delta^{18}O$ and $\delta^{34}S$ isotopic data (Ueda *et al*, 1991).

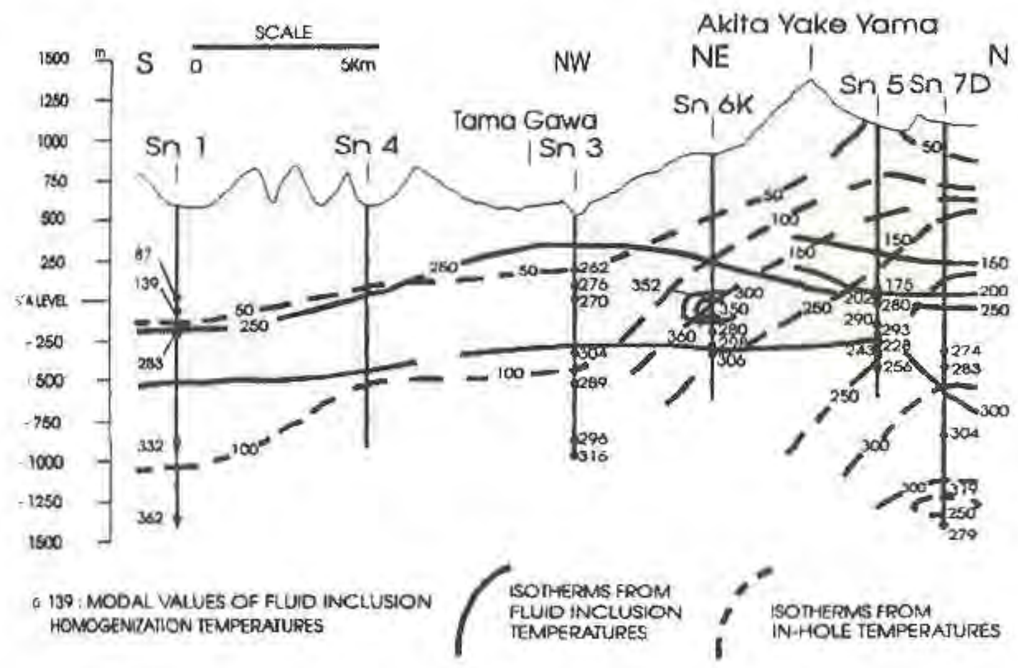

The comparison of the Th values with in-hole temperatures indicates that a cooling of about 200-300 °C occurred in the South part of the Sengan area. In the northern part, in correspondence of the Sumikawa geothermal system, in-hole temperatures agree with Th, indicating that this system has cooled not as much. The cooling of the southern sector is probably the result of a shift of the heat source and/or of a falling water table.

References:

De Vivo B. & Sasada M. (1992). *J. Geoth.. Res. Soc. Japan*, **14**, 101-113.
De Vivo B., Raia F., Sasada M., Sawaki T. (1992). *7th Int. Symp. Water-Rock Interaction, Balkema*, 1445-1450.
Takeno N. & Noda T.(1987). *Rept. Geol. Survey Japan*, **266**, 233-249.
Ueda A., Kubota Y., Katoh H., Hatakeyama K., Matsubaya O., (1991). *Geochem. Jour.*, **25**, 223-244.

SYNTHETIC CHRYSOTILE FIBERS : FROM CYLINDRICALLY TO CONICALLY WRAPPED STRUCTURES. IMPLICATIONS FOR THE GROWTH MECHANISMS OF CHRYSOTILE.

Devouard B. and Baronnet A. (*CRMC²-CNRS, Marseilles, France*)

Since the theoretical work of Whittaker (1953) and the HRTEM observations of Yada (1967), mainly, chrysotile is well known to consist in cylindrically wrapped 1:1 silicate layers.

Natural samples can display various tubular structures, varying in the crystallographical axis of the tube (ortho- and para-chrysotiles), the stacking of successive layers, and possibilities of spiral and/or helicoidal wrapping.

Synthetic chrysotile often shows conically wrapped structures (Yada, 1977). We observed these rather peculiar fibers, which are probably related to local excess of supersaturation, along with the usual cylindrical structures mentioned above. In such structures, the conicity angle is related to a constant rotation of the serpentine layer from one turn to the next. As a consequence, conical fibers are neither ortho- nor para-chrysotile, the crystallographic directions varying continuously with respect to the fiber axis. We will discuss the control of the conicity by the layer stacking structure, on the basis of both HRTEM and EDPs.

Another interesting point is that conical fibers display continuous variations of curvature both radially and along the tube axis. Step bunching of packets of serpentine layers tends to remain visible on the outer surfaces of conical fibers, while the minimal radius of curvature do not vary within the core of a same fiber. These experimental facts advocate for a growth model of chrysotile in which the elastic energy stored in curved layers should play a prominent role.

In addition, synthetic samples allow one to observe easily the whole fibers -either cylindrical or conical. A few puzzling microstructures encountered in natural fiber sections (such as incomplete fibers sections or overgrowths) can be explained on the basis of the 3D morphology development of those synthetic fibers. Early stages of growth are also found, consisting in curved packets of serpentine layers, not yet closed as tubes.

Beyond the theoretical interest of curved lattices -chrysotile is one of the few examples of such structures, along with graphite nano-tubes (e.g. Zhang *et al.*, 1993) and a few sulfosalts of the cylindrite group (Williams & Hyde, 1988)- the observation of synthetic chrysotile gives clues to a better understanding of the growth mechanisms of serpentines in their natural environments.

References :
Whittaker, E.J.W. (1953). *Acta Crystallogr.*, **6**, 747-748.
Williams, T.B. & Hyde, B.G. (1988). *Phys. Chem. Min.*, **15**, 521-544.
Yada, K. & Iishi, K. (1977). *Am. Mineral.*, **62**, 958-965.
Yada, K. (1967). *Acta Crystallogr.*, **23**, 704-707.
Zhang, X.F., Zhang, X.B., Van Tendeloo, G., Amelinckx, S., Op de Beck, M., Van Landuyt, J. (1993). *J. Crystal Growth*, **130**, 368-382.

MICRO-RAMAN STUDIES ON AMPHIBOLES

Sybrand A de Waal (*Department of Geology, University of Pretoria* and Danita de Waal (*Department of Chemistry, University of Pretoria*)

Micro-Raman spectra of members (arfvedsonite, katophorite, ferro-winchite, ferro-richterite and richterite) of a single chemically zoned amphibole crystal and co-existing ferro-actinolite show four distinct groups of lines. The normalized line intensities (NLI's) of the first group (ca. at 1088, 978, 895, 576, 542, 367 and 222cm^{-1}) show strong positive correlations with the total cationic iron in these amphiboles, as calculated from electron microprobe analyses. In the second group (ca. at 1066, 1028, 929, 679 and 381 cm^{-1}) the NLI's display strong dependency on the Ca in the relevant mineral formulae. The NLI's of the third group (a single line at ca. 743cm^{-1}) correlate with total titanium in the octahedral sites, but show the richterite to deviate from the general trend. The NLI's of the fourth group (a single weak line at ca. 437cm^{-1}) could not be confidently correlated with any of the cation proportions in the calculated amphibole formulae. Raman lines at wavenumbers above 600cm^{-1} are generally taken to result from vibrational modes involving tetrahedra and those below this value are ascribed to M-O (octahedral) and A-O (alkali site) vibrations and distortion of tetrahedral chains (Della Ventura et.al. 1991, 1993). These assignments are discussed in the light of the present findings.

References:
Della Ventura, G., Robert, J.-L., and Benny, J.-M.(1991) *American Mineralogist*, **76**, 1134-1140.
Della Ventura, G., Robert, J.-L., Benny J.-M., Rautsepp, M., and Hawthorne, F.C. (1993) *American Mineralogist*, **78**, 980-987.

CH_4-H_2O-NaCl FLUID INCLUSIONS AT WELLENBERG, SWITZERLAND; IMPLICATIONS FOR THE SAFETY OF A PLANNED RADIOACTIVE WASTE REPOSITORY

Diamond L.W. *(Mineralogy-Petrography Institute, University of Berne, Switzerland)* and Marshall D.D. *(Mineralogy-Petrography Institute, University of Lausanne, Switzerland)*

Switzerland's final underground repository for low- and intermediate-level radioactive waste is planned to be built in carbonaceous marls of the Palfris Formation at Wellenberg. As part of a broad geological assessment of the long-term safety of the site, fluid inclusions have been analysed in quartz-calcite veins and vugs recovered from boreholes within the marls.

From the fluid inclusions, two contemporaneous but immiscible vein fluids have been identified in all examined boreholes and at all examined depths (170-1400m): (1) a weakly saline, CH_4-saturated aqueous "liquid" (mol: 97.9% H_2O, 0.6% NaCl, 1.5% CH_4, <0.1% CO_2; $\bar{V}$ = 19cm^3/mol), and (2) a conjugate, H_2O-saturated methane "vapour" (mol: 3.2% H_2O, 95.3% CH_4, 1.5% CO_2; $\bar{V}$ = 46cm^3/mol). The vein minerals precipitated from this two-phase system between 190-280°C, over a wide span of fluid pressures, from 400-2500 bars.

The range of formation temperatures is interpreted to reflect prolonged fluid migration into the veins, coinciding with, and outlasting, the local peak of Alpine metamorphism at ~20 Ma. Whereas fluid temperatures remained rock-buffered, the spread in fluid pressures reflects a fluctuating hydrodynamic regime during cavity opening and mineral deposition, largely independent of the lithostatic load. The fluctuations are ascribed to variable relative rates of porosity generation and fluid migration, dictated in turn by changing rates of regional deformation. Model calculations suggest the lowest deduced fluid pressures were in fact sub-hydrostatic.

A variety of fluid inclusion and mineralogic evidence indicates that the two vein fluids were generated in the immediately adjacent wall rocks, that is, within a geochemically and hydrodynamically closed system. CH_4 presumably evolved from progressive thermal decomposition of wall rock carbonaceous matter during Alpine metamorphic heating, whereas the NaCl-H_2O component was derived from sea water originally trapped in rock pores during sedimentation and later diluted by H_2O evolved by metamorphic dehydration of matrix clay minerals. The observed state of immiscibility in the veins is thus a direct consequence of in-situ fluid production below the CH_4-H_2O-NaCl solvus.

The major-component chemistry of the fluid inclusions matches some of the free gases and ground-waters found upon drilling impermeable sections of the Palfris Formation. Dilute, aqueous NaCl solutions are present which match the ancient "liquid" phase trapped in inclusions, while free CH_4 gas has its analogue in the conjugate "vapour" phase of the inclusions. Even sub-hydrostatic pressures are locally measured in the boreholes today, in parallel with the inclusion evidence for under-pressured fluids during metamorphism. The down-hole fluids thus appear to be emanating from vugs in nearby wall rocks, which today still contain Alpine metamorphic fluids.

The simplicity of the metamorphic fluid history, the absence of fluids of external origin, and the remarkable geochemical correlations between metamorphic fluid inclusions and present-day down-hole fluids, imply that zones of the Palfris Formation have remained hydrodynamically tight for many millions of years. There is therefore good reason to expect that such zones will remain impermeable well into the future, and hence they may provide a hydrodynamically safe environment for disposal of radioactive waste.

OPTICAL SPECTROSCOPY AS A TOOL TO DISCERN NATURAL AND SYNTHETIC EMERALDS

J. Díaz, A. Lorenzo, J. García Solé and F. Jaque (Dpto. de Materiales, Univ. Autónoma de Madrid)
M. A. Hoyos and I. Vara (Dpto. de Geología, Univ. Autónoma de Madrid).

The optical spectroscopy (absorption, luminescence and life-time) of natural (Colombia) and synthetic (Chatham and Lechleitner) emeralds has been studied in the temperature range 10-300 K. Many differences have been found in the spectroscopy, characteristics that can be used to discern natural from synthetic gems. In fact it has been observed that the R lines associated with the $^4A_2$ ---> ^2E transition are narrower and well defined in synthetic crystals than in natural gems. Fig. 1 shows the emission spectra at 10K with excitation at 450 nm for natural (——) and synthetic (---) gems.

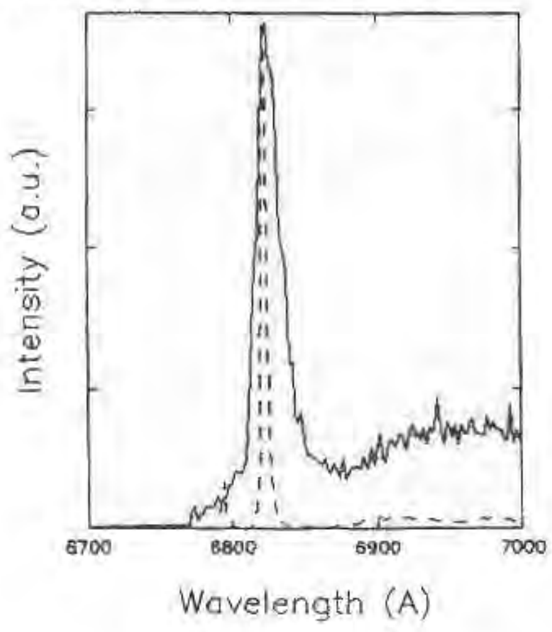

The life-time of the natural samples (12 μs at 10 K) is faster than in synthetic crystal (1.2 ms at 10 K), indicating that a strong variation in the energy distance between the $^4T_2$ and ^2E levels could take place in natural samples. The temperature dependence of the decay-time in the range 10K-300K has been studied in both kind of crystals. No variation with temperature was observed in natural gems.

In relation with the vibronic broad bands due to the $^4A_2$ ---> $^4T_2$ transition they are also narrower in synthetic samples than in natural gems.

Finally, the optical absorption, in the infrared region has also been analyzed showing differences between synthetic and natural samples. In particular, the optical spectroscopy associated with Fe^{3+} and OH impurities, in the IR region, is discussed.

WATER IN GRANITIC MELTS: EXPERIMENTAL STUDIES OF STRUCTURE-PROPERTY RELATIONSHIPS.

Dingwell D.B., C. Romano, K-U. Hess and N. Bagdassarov *(Bayerisches Geoinstitut, Universität Bayreuth 95440 Bayreuth, Germany)*

The role of dissolved water in influencing the behavior of granitic magmas is one of the central themes of igneous petrology. A number of recent experimental studies on the composition dependence of the solubility of water in melts, the speciation of dissolved water, and the

properties of hydrous melts provide valuable new input for models of the physical and chemical thermodynamics of hydrous melts.

The solubility of water in granitic melts is significantly compositionally dependent. Recent solubility data for the effects of Cs, Rb, K, Na, Li, F, B and P on the pressure- and temperature-dependence of the solubility of water in granitic melts indicate that the complexity of existing solubility models is not sufficient.

Infrared spectroscopic investigations of the kinetics and speciation of water in granitic glasses indicate that the temperature dependence of a equilibrium between chemically (OH) dissolved and physically (H_2O) dissolved is large and that kinetic corrections for the effect of quenching on the speciation of water can be used to delineate the chemical thermodynamics of water solution in melts.

Recently obtained, high precision, viscosity data for the effect of depolymerizing agents such as excess alkalies on the viscosity of granitic melts allows for the parameterization of the effect of depolymerization on viscosity, and indirectly aids the interpretation of structure-property relations in hydrous melts.

Consideration of the physics of water mobility in hydrous granitic melts indicates that the concentration dependence of water diffusion in melts is a simple consequence of the permeability of the melt structure to water molecules and that the detached mobility of water in silicic magmas provides for the special case of magma fragmentation due to the lag time between diffusive bubble growth and shear stress relaxation in the bubble walls.

^{27}Al MAS NMR STUDY OF AL IN STRAIGHT AL-O-SI CONFIGURATIONS USING ZUNYITE AND HARKERITE

Dirken, P.J. (Dept. of Geochemistry, Univ. of Utrecht, The Netherlands).

The well-known correlation between the ^{27}Al isotropic chemical shift and the Al-O-Si intertetrahedral angles in framework aluminosilicates (Lippmaa et al., 1986) is useful in a number of fields. It is used in NMR studies of amorphous solids, to give an estimate of ring sizes and angle distributions. Secondly, it is useful in studying Al/Si ordering in framework aluminosilicate minerals like zeolites and leucite. A third application of this correlation is in assigning NMR resonances to specific sites in a crystal structure.

Zunyite ($Al_{13}Si_5O_{20}(OH,F)_{18}Cl$) contains two unique crystallographic groups. The first is an Al_{13} group, the second a Si_5O_{16} group (pentamer), which has 180° intertetrahedral angles. It is formed by a central Q^4 site and 4 surrounding Q^1 sites. The zunyite structure has been studied carefully by ^{27}Al NMR by Kunwar et al. (1986), but only at low spinning speeds (<5 kHz). Kunwar et al. (1986) found two Al resonances both for the Al_{13} complex (∂_{iso} 72 and 9 ppm).

In the present study, high (11-13 kHz) spinning speeds are used and two additional signals appear in the spectrum (Figure 1). The first signal at -3.4 ppm (peak position at 11.7 T field) is from an impurity, the other signal has an ^{27}Al isotropic chemical shift of 46.8 ppm and is believed to be from excess Al occupying the central Q^4 site of the pentamer. This is made plausible by comparing the NMR results of zunyite with those of harkerite ($Ca_{24}Mg_8[AlSi_4(O,OH)_{16}]_2(CO_3)_8(BO_3)_8(H_2O,Cl)$). Harkerite contains an $AlSi_4(O,OH)_{16}$ pentamer with Al in the central $q^4(1Si)$ site, surrounded by 4 Si atoms in tetrahedral coordination. The Al-O-Si angle in this structure is 176°. The spectrum shows a signal with an isotropic chemical shift of 44 ppm, which is close to the 46.8 ppm signal of zunyite. Therefore, it is believed that the coordinations of Al in both minerals are similar and that as a result, the Si_5O_{16} pentamer contains Al in a $q^4(1Si)$ configuration. Quadrupole effects, electrostatic interactions and ^{29}Si MAS NMR strengthen this assumption.

Because the 46.8 ppm and 44 ppm signals are from Al in a framework configuration, it can be correlated with Al-O-Si intertetrahedral angles (Lippmaa et al., 1986). The 44 ppm fits the correlation very well; the 46.8 ppm signal of the zunyite pentamer, however, does not. A possible reason could be, that the zunyite adapts to the incorporation of Al in the pentamer by narrowing the intertetrahedral angles to 171°. In any case it is clear, that the range of Al-O-Si angles in the correlation of Lippmaa et al. (1986) can be extended to 176°.

References:
Kunwar, A.C., Thompson, A.R., Gutowsky, H.S., and Oldfield, E. (1986) *J. Magn. Res.*, **60**, 467-472.
Lippmaa, E., Samoson, A., and Mägi, M. (1986) *J. Amer. Chem. Soc.*, **108**, 1730-1735.

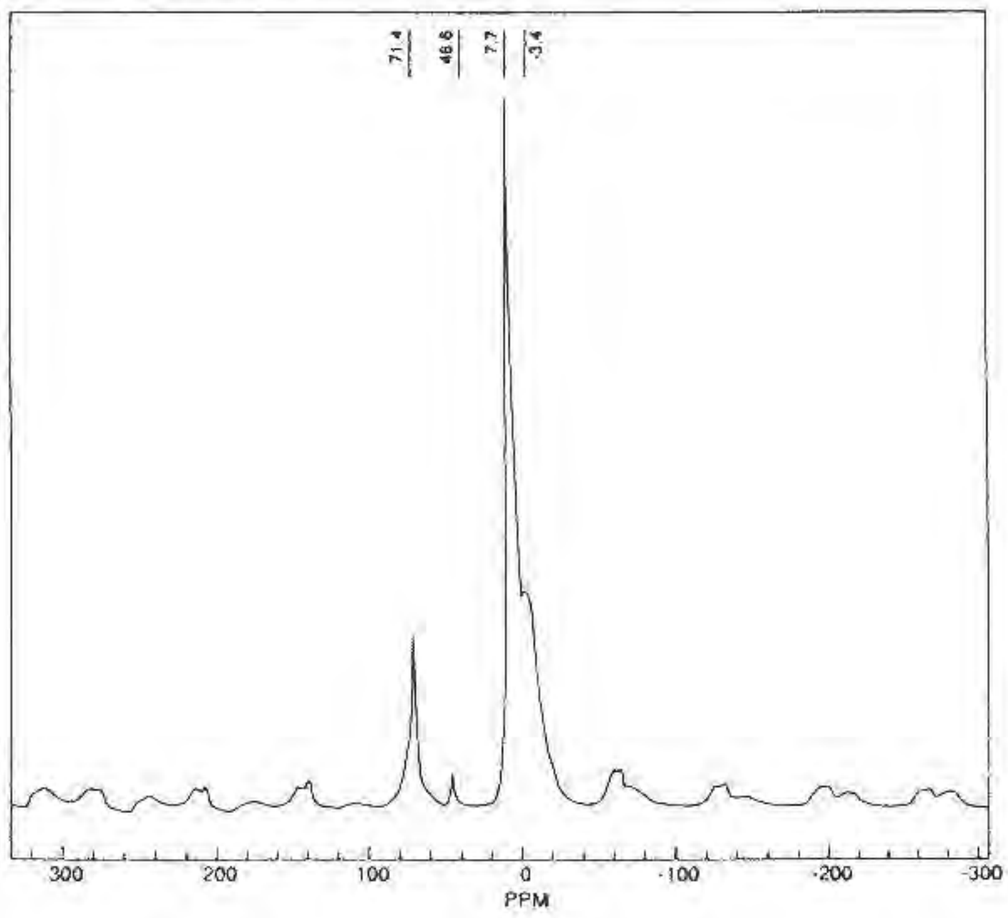

Figure 1. ^{27}Al MAS NMR spectrum of zunyite at a magnetic field of 11.7 T.

`MINERALOGICAL AND PETROLOGICAL FEATURES OF UPPER-CRETACEOUS-TERTIARY VOLCANIC SERIES OF ARMENIA, LESSER CAUCASUS

Djerbashian R., Mnatsakanian A.(*Institute of Geological Sciences, Armenian Acad. of Sci., Yerevan, Republic of Armenia*)

The territory of Armenia is a part of fault-fold building of Lesser Caucasus. Its tectonic structure due to Latest Cretaceous collision includes the southern margin of Eurasian plate (the Somcheto-Karabakhian megablock) and northern faulted projection of Iran-Arabian platform (the Central Armenian megablock). The Upper Cretaceous-Tertiary volcanic series are formed in mentioned megablocks and evolve further in different geodynamic environments. According to the age, minerology, petrochemical parameters and degree of differentation the following series may be distinguished.

Upper Cretaceous (K_2) bimodal calc-alkaline series consist from Ol+Cpx+Pl basaltes, Ol dolerites, Opx+Cpx+Pl andesibasalts - Amph + Pl + Opx rhyodacites, Bi+Pl+Q+Ksp rhyolites. It is related to rifting and destruction of Somcheto-Karabakhian paleoisland volcanic arc.

Middle Eocene(P_2^2) calc-alkaline series is related with early stage of collision and localized in the suture zone and within the limits of Central Armenian megablock. In the northrn, Bazum-Sevanian zone of deep compression this series is continuosly differentiated and represented by Opx + Cpx + Ol + Pl basaltes, Opx + Cpx + Pl + Amph andesibasaltes and andesites, Amph + Q + Bi+Cpx rhyodacites and rhyolites. In the southern Vaik-Zangezurian zone of deep tension this series is represented by shortened weekly differentiated row Opx+Cpx+Pl+Ol basaltes - Opx+Cpx+Pl andesites. This series is developed further in Upper Eocene.

Upper Eocen (P_2^3) K-Na subalkaline series is formed on the middle stage of collision and localized in the same structural zones. In the Bazum-Sevanian zone it also is represented by continuously differentiated row Cpx+Amph+Pl trachybasaltes, trachyandesites - Pl+Ksp+Bi+Amph trachy-rhyolites. In the Vaik-Zangezurian zone series consists from shortened row Cpx+Amph+Pl trachybasaltes - trachyandesites.

Upper Eocene-Oligocene (P_2^2 - P_3) K-alkaline series is localized within cratonized Tezhsar block of the Bazum-Sevanian zone. It constitutes volcano-tectonic ring structure and is represented by Bi+Ksp+Amph trachytes and Ksp+Lc+Bi+Amph phonolites.

The chemistry of phenocrysts and their assemblages was studied. The results show that their crystallisation occurs at the shallow depth and high temperature conditions of the intermediate magmatic chambers in which the values of alkality, $P(H_2O)$ and $P(O_2)$ vary in wide range. The distribution of major and trace elements between coexisting mafic phases correlates with the high temperature side of corresponding exchange reactions. The values of T_{sol} for basaltic members studied series estimated by Ol-liquid and Opx-Cpx geothermometer constitute: for K_2 950-1050°C, for P_2^2 1000-1150°C, for P_2^3 1100-1200°C; by Cpx-Amph geotermometer for trachytes P_2^3 - P_3 series 1000-1100°C.

Values oxygen fugasity estimated by Mgt-Jl geotermometer are in the range: for K_2 series $LogfO_2$ = -9-12, for P_2^2 calc-alkaline series of compression zone $LogfO_2$ = -8.5-12.5, of tension zone $LogfO_2$ = -16-18; for P_2^3 subalkaline and P_3 K-alkaline series $LogfO_2$ = -14-16.5. Degree of SiO_2 differentation for studied series show a positive correlation with degrre of oxidation of fluid phase. Compositional evolution of mafic phenocrysts from K_2 series to P_2^2 and P_2^3 - P_3 one shows that the increase of Mg/Mg+Fe ratio in anhydrous phase is accompanied by its decrease in water-bearing phase. This points to the succesfull elevation of the intratelluric crystallization temperature in the intermediate chambers due to heat flood increase from magmatic source in time.

The variety of petrochemical types of volcanic series for territory under study according to Sr isotopic rations reflects both the magma source heterogeneity as well as different independent evolutionary processes which is characteristic for the regions of collisional tectogenesis.

PETROLOGICAL, MINERALOGICAL, AND GEOCHEMICAL PECULIARITIES OF CONTINENTAL PLUME-BASALTS FROM DIFFERENT GEODYNAMIC ENVIRONMENTS

Dmitriev Yu.I.(*Inst. of Geol. of Ore Dep., Petr., Mineral., Geoch., Russian Acad. Sci.*)

Basaltic mantle-plume related magmatism is responsible for eruptions of flood-basalts on continental platforms. In terms of geodynamic regimes the manifestations of flood-basalt magmatism occur in following environments: (a) zones of unimpeded localized spreading such as continental rifts transformed into mature oceans (Mesozoic flood-basalts of Brazilian Platform preceding opening of the South Atlantic Ocean, (b) areas of unobstructed diffuse spreading such as intracontinental extensional basins (Late Paleozoic-Early Mesozoic flood-basalts of Tungusska Basins on Siberian Platform), and (c) regions of restricted spreading such as continental rifts failed to open into full-size oceans (Late Paleozoic-Early Mesozoic flood basalts of Pan-Xi Rift on South China Platform, which stopped to open on the stage of initial oceanic basin due to compressive stress from collided South and North China plates). Comprehensive studies of flood basalts mentioned have revealed their specific features.

Brazilian flood -basalts related to the rift opened into the ocean are accompanied by distinctly subordinate basic tuffs and intrusive bodies and occur in association with considerable amount of intermediate and acid lava. Basalts are mainly olivine-free and enriched in Si, Fe, K, Ba, but depleted in Mg and Cr. The time of lava-pile formation was rather short (several Ma).

In flood-basalt association of Siberian intracontinental basin the role of intermediate and acid lavas is insignificant. Extrusive, intrusive, and volcanogenic rocks occur in about equal proportion. Basalts as a rule contain olivine and are enriched in Mg. The formation of the lava pile took time of the order of tenth Ma.

Basaltic rock association of the failed rift zone on the South China Platfo resembles Brazilian flood-basalts b predominance of extrusive rocks and basal enrichment in Fe and K. At the same ti insignificant role of andesites an rhyolites among Pan-Xi Rift lavas and commo presence of olivine in basalts make the similar to Siberian flood-basalts. Geochemica pattern of the South China Platform basalts i intermediate between Brazilian and Siberia basic lavas. Flood-basalts of southern Chin show indications of low grade melting of th magma source material such as limite distribution of lavas and presence of highe alkalinity rocks.

The peculiarities of plume-basalts erupte under different conditions can be used a geodynamic regime indicators for ancient floo basalts and as hints for prediction o tectonic evolution trends of present day are of the flood-basalt magmatism.

METALLIC CLUSTERS IN SULFIDE MINERALS

Dmitrieva M.T.(*Inst.of Geol. of Ore Dep.,Pet Min., Geoch. Russ., Acad. of Sci. Moscow)*

The cluster formation in the structures natural minerals has not been discussed widely as the same problem concerning th chemical compounds.

The Fe-Ni cube clusters in pentlandi $^{VI}[Fe_uNi_v]^{IV}(Fe_xNi_{y\ z})S_8$ has been considere (Rajamani & Prewitt, 1973) as the "specif aspect" which appears to stabilize th structure.

The second example of cube clusters build Cu-Fe cations was revealed (Dmitrieva , 197 in K-bearing sulfide - djerfisherite $K_6Na(Fe,Cu,Ni)_{24}S_{26}Cl$. The Me-Me distance (2,76A) the structure is close to correspondi distance(2.531A) in pentlandite structur indicating metallic bonding. The simil clusters is expected to exist in thalfesini $Tl_6(Fe,Ni,Cu)_{25}S_{26}Cl$ structure although th structure of this mineral has not been solved. The (Fe_8S_{14}) cluster discovered in bartoni structure (Evans & Clark, 1981) are close related to the clusters reported f pentlandite $(Fe,Ni)_8S_{14}$ and djerfisheri $(Cu,Fe)_8S_{14}$.

The other type of clusters can be observed in minerals of chalcopyrite series- talnakhit $Cu_9Fe_8S_{16}$, mooihoekite $Cu_9Fe_9S_{16}$ and haycockit $Cu_4Fe_4S_8$. The length of bond Fe-Fe (2.48A) an Cu-Cu (2,56) in metal octahedra (Hall,1975) allow us to consider them as octahedra clusters.

It has been shown that the isomorphism limit in minerals with cube clusters are controlle by cluster presence. The crystallochemica peculiarities of minerals with clusters ar discussed on the basis of total number o d-electrons in clusters.

References:
Rajamani, V., Prewitt C.T. (1973). Can. Miner. 12, 178-187.
Dmitrieva M.T., Ilyuchin (1975). Doklady Acad. Nauk SSSR, Earth Sci. Section ,223, 343-346.

Evans, H.T.Jr, & Clarc, J.R. (1981). Am. Mineral., 66, 298-308.
Hall, S.R. (1975). Can. Mineral., 13, 168-172.

MAGMATIC EPIDOTE-BEARING TTG SUITE IN THE RETEZAT MASSIF (SOUTH CARPATHIANS)

Dobrescu A., Stoian T., Robu L. (*Dept. of Mineralogy and Petrology, Institute of Geology and Geophysics, Bucharest*)

The Retezat Granitoid Massif is a large pluton outcropping on an area of about 180 sqkm, in the Precambrian Crystalline terrains of South Carpathians. It consists mainly of tonalitic, trondhjemitic and granodioritic rocks, approximating a TTG suite.

The main mineralogical character of this suite is the presence of magmatic epidote and muscovite within plagioclase-quartz-alkali feldspar-biotite assemblage; accessory minerals as apatite, sphene, zircon, rutile, garnet, tourmaline, magnetite and ilmenite are found. No amphibole has been identified.

In terms of major elements, the rocks are calc-alkaline, high-Al, showing a low-K, trondhjemitic differentiated trend. The presence of magmatic muscovite and high corundum-normative values suggest a peraluminous nature of the parental magma. Rare earth elements geochemistry shows low REE contents (7REE < 100ppm), depleted HREE (La/Lu_{cn}~10-140) and small negative or no Eu anomalies (Eu/Eu*> 0.4).

Based on the TTG rocks mineralogy and (REE) geochemistry, we tried to suggest a petrogenetic process and the possibility of magmatic epidote crystallizing from such a magma, even its using as a PT indicator of crystallization.

The sulfides of alkali metals and their phase relations in K-Fe-Cu-S system

Dobrovolskaya M.G., Nekrasov I.Ya.
35 Staromonetny per. Moscow 109017, Russia

New investigations of minerals related to the group of alkali metals sulphides contribute to better understanding of their parageneses formation. In 1963 P.Ramdohr mentioned the "mineral C" in stone meteorite. In 1966 this sulphide was described as a new mineral by L.Fuchs, who named it "djerfisherite". Later on this mineral has been found in different geological environments: Cu-Ni ores of Norilsk deposit, alkalic rocks and pegmatites of the Khibina, Lovozero, Murun massifs (Russia), Coyote Peak (California, USA), kimberlites of South Africa and Yakutia.

The new mineral rasvumite ($K.Fe_2S_3$) has been determined in alkalic rocks and pegmatites of Khibina massif in association with djerfisherite ($K_6(Cu,Fe,Ni)_{24}S_{26}Cl$) and other K-bearing sulphides [Sokolova et al. 1970]. Then rasvumite, bartonite ($K_3Fe_{10}S_{14}$) and erdite ($NaFeS_2 \cdot 2H_2O$) have been found in alkalic diatreme of Coyote Peak [Czamanske et al. 1977]. Erdite was discovered also in pegmatite of nepheline-syenite rocks of Lovozero massif [Khomyakov et al. 1982]. Other Na-bearing mineral chvilevite $Na(Cu,Fe,Zn)_2S_2$ was found in Pb-Zn ores of Akatuy deposit, Russia [Kachalovskaya et al. 1988). New sulphides - murunskite ($K_2Cu_3FeS_4$), Tl-bearing murunskite and thalcusite were found in charoitic rocks of Murun massif [Dobrovolskaya et al. 1987].

Thus a group of K,Na,Tl-bearing sulphides was introduced into the mineralogy. Accumulation of data on their occurence and study of phase relations in (K,Na)-(Fe,Ni)-Cu-S systems permited to reveal their mineral parageneses. They depend from K, Na, S_2 ($\mu_K, \mu_{Na}, \mu_{S_2}$) activity rather than whole rock composition. Diagrams of phase relations in K-Fe-Cu-S system showed that chemical composition of alkali metals sulphides and a sequence of their parageneses depend from μ_K and μ_{Na} values. This is caused by replacement of K by Na, S by Cl, Fe by Ni or Cu. There are three modifications of djerfisherite differing by chemical composition and corresponding to various genetic types of sulphide mineralization.

Studies of phase relations in (K,Na)-(Fe,Ni)-Cu-S-H_2O system lead to the conclusion, that sulphides of alkali metals group were crystallized in non-equilibrium conditions. Only djerfisherite is stable whereas other K,Na-bearing sulphides are non-stable. This is confirmed by destruction of murunskite grains, transformation of rasvumite, formation of K-Cu-Fe-bearing sulphides which differ by chemical composition, but occur in association with djerfisherite and other sulphides.

XRD AND TEM STUDY OF SZAIBELYITE FROM ITS TYPE-LOCALITY (RÉZBÁNYA)

Dódony I. and Lovas Gy.A. (Dept. of Mineralogy, Eötös Loránd University, Budapest)

In the course of a systematic reinvestigation of several Hungary-related minerals the study of szaibelyite $Mg_2(OH)[B_2O_4(OH)]$ from its type-locality was undertaken. The type specimen of this mineral was first described by Peters (Peters, 1861) and has remained poorly characterised ever since due to its relative complex paragenesis. It occurs in massive contact marble in the form of radial aggregates of fine bundles of asbestiform crystallites in intimate coexistence with other boron bearing Mg-minerals like kotoite and fluoborite. The lack of up-to-date descriptive data of szaibelyite has raised recently some confusion between this mineral and an other one called ascharite (Feit, 1891) which give a special actuality to the present work.

A tedious preparatory process consisting of dilute acid treatment, repeated sedimentation and hardness selective separation resulted in a visually monomineralic szaibelyite sample, that was suitable for X-ray powder diffraction study. The data collection was performed on a Siemens D5000 theta-theta diffractometer using copper radiation. The processing of the raw intensity data was carried out on its integrated computer system and software. The subsequent unit cell calculations were made using a local version of the UNITCELL program (Appleman & Evans, 1973). The refinement converged to the unit cell parameters of a=12.571(1), b=10.4025(9), c=3.1333(4) Å and ß=95°54.2(9)' in the monoclinic $P2_1/a$ (14) spacegroup. Figures of Merit F_{20}=38(.017,32) and M_{20}=26 show the reliability of the indexing of the 60 suitably resolved reflections in the 5-79°2Θ angular range.

A Rietveld analysis of the powder pattern of szaibelyite was also undertaken using the DBWS-9006PC program (Young, 1993). Starting with the monoclinic structural model of Takéuchi and Kudoh (Takéuchi & Kudoh, 1975) the refinement converged to the R factors of R_P=14.1, R_{WP}=18.4, R_B=10.0 and R_F=5.8 in spite of the difficult-to-handle fibrous preferred orientation. The final atomic parameters showed no significant deviation from the Takéuchi model. The refinement results prove that the crystal structure of the szaibelyite from Rézbánya is monoclinic and has the same atomic arrangement as determined for a szaibelyite sample from Königshall-Hindenburg, Germany (Takéuchi & Kudoh, 1975). Despite of the strong two-fold pseudosymmetry of the corner-sharing chains of double Mg octahedra, no indications of the presence of polymorphic variations was found in the powder pattern.

The TEM observations were performed under a JEOL 100CX microscope. The intensive radiation damage of szaibelyite limited the usable illumination time and/or brightness making the high resolution imaging especially difficult.

The [001] elongated crystallites occur in bundles in which the individual fibres are randomly oriented around their c axis. The mean size of the crystals is in the 100 nm range in cross section and the most common faces observed are (100) and (010).

The most characteristic real structural feature of this type specimen is the (100) twinning producing weak diffuse scattering parallel to the a* axis in the selected area electron diffraction patterns. This phenomenon may explain the line broadening observed in the high angle region of the powder pattern. The thickness of the twin lamellae is a few nm. No polytype modifications or periodic twinning of the basic crystal structure were observed.

The results of the above structural measurements made on the material of the type locality confirm the priority of the of the original description of szaibelyite (Peters, 1861). In spite of the low accuracy of the early chemical analysis, the original description of szaibelyite (Peters, 1861) proved to be valid and in good accordance with the recent results.

Acknowledgement: This study was supported by the Hungarian National Research Found (OTKA) under the contract no. of T 007545.

References:

Appleman, D.E., Evans, H.T.Jr. (1973): Job 9214: Indexing and least-squares refinement of powder diffraction data. Report PB2-16188, U.S. Dept. of Commerce, National Technical Information Service
Feit, W. (1891). Chem.-Ztg. **15**, 327

Peters, K.F. (1861) 2. Teil. S.-B. Akad. Wiss. Wien,**44**,81-155
Takéuchi, Y., Kudoh, Y. (1975). Am.Min.,**60**,273-279
Young, R.A. (1993). The Rietveld Method, IUCr Monographs on Crystallography 5.,Oxford University Press,p30.

STRUCTURAL RELATIONSHIP BETWEEN PYRITE AND MARCASITE

Dódony I. (*Dept. of Mineralogy, Eötvös L. Univ., Budapest*), Pósfai M. and Buseck P.R. (*Dept. of Geology, Arizona State Univ., Tempe, AZ*)

Pyrite is the most common sulfide mineral; it is widespread in ore deposits and common in many sedimentary, metamorphic, and igneous rocks. It exhibits a range of interesting structural characteristics, such as penetration twins (Donnay *et al.*, 1977), epitaxial inter- and overgrowths with its polymorph, marcasite (Brock & Slater, 1978; Gait & Dumka, 1986), and the occurrence of a variety of morphological types. Of particular interest are samples that contain crystals with non-cubic morphology (such as radial and colloform assemblages), since these may reflect special conditions of formation. As part of a larger effort to establish the relationships among microstructure, composition, and macroscopic appearance we studied pyrite spherules from Recsk, Hungary, using high-resolution transmission electron-microscopy (HRTEM) imaging and selected-area electron-diffraction (SAED).

Many pyrite crystals contain planar faults perpendicular to one of the [001] axes. A comparison between HRTEM micrographs and images simulated for defect model structures shows that the faults can be interpreted as single (101) layers of marcasite that disrupt the regular sequence of (002) layers in pyrite. In [100] projection, S-S pairs are oriented on both sides of the fault plane parallel to each of the two body diagonals in either the (0-11) or the (011) plane of pyrite, instead of lying alternately in the (0-11) and (011) planes. The S-S pairs' centers of gravity (the Fe atoms) are shifted by ±0.23[020], depending on whether the fault plane lies between two layers of S-S pairs oriented parallel to (0-11) or (011), respectively. Such an arrangement can be obtained if one part of the ordered pyrite crystal is rotated by a 2_1 screw axis parallel to [100]. The faults result in a recognizable contrast change in the sequence of (002) layers in HRTEM images obtained from [100]- or [110]-type directions. In Figure 1 both types of faults (i.e., "left" and "right" oriented marcasite lamellae, marked by L and R) occur in the pyrite matrix.

Preliminary analyses by energy-dispersive x-ray spectrometry indicate that some pyrite crystals contain significant concentrations of As. We are continuing to investigate whether the As-content of pyrite is related to the occurrence of marcasite lamellae in pyrite. We are also examining the abundance and genetic significance of these faults.

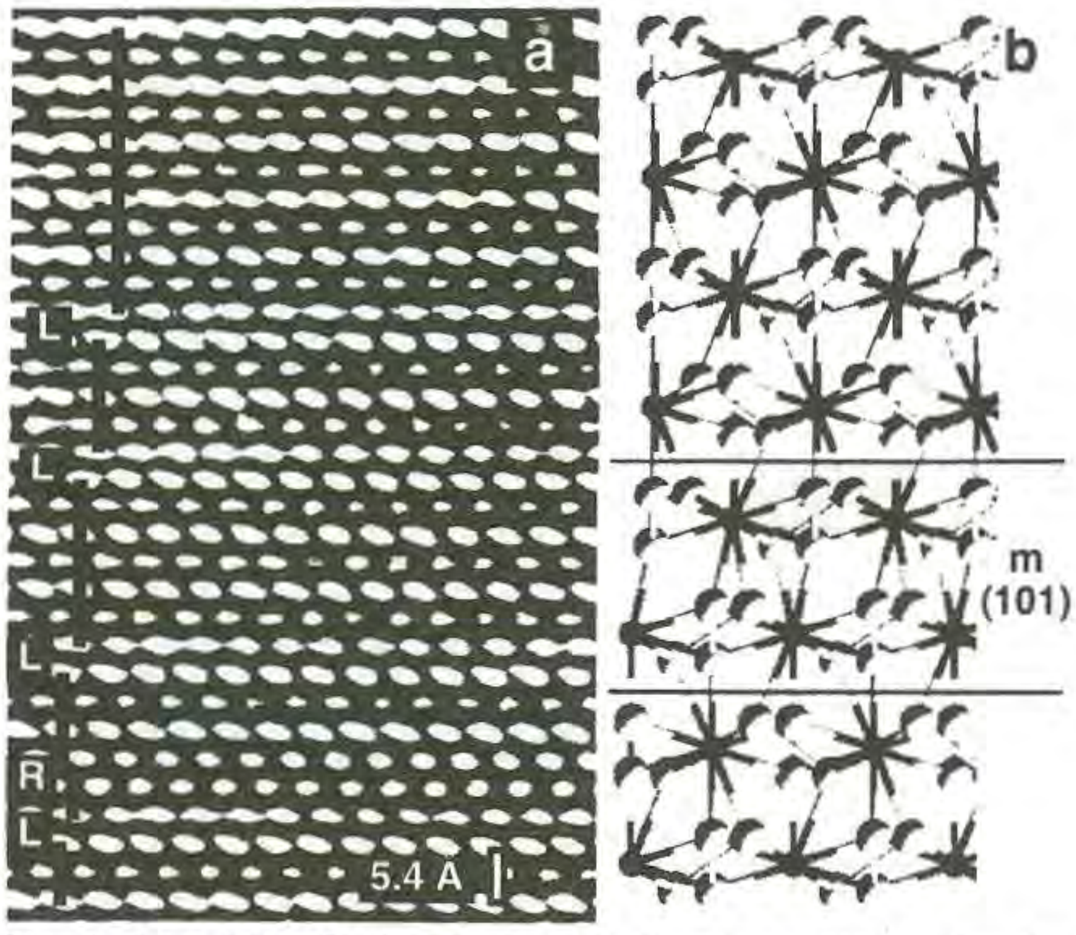

Fig. 1. (a) [-110] HRTEM image of disordered pyrite. The fault planes are marked L and R, indicating the orientation of the marcasite (101) layer. The broken lines mark pyrite (110) planes. (b) Structure model for an "R" fault in the same projection as in (a).

References:
Brock, K.J. & Slater, L.D. (1978). *Am. Mineral.*, **63**, 210-212.
Donnay, G., Donnay, J.D.H., Iijima, S. (1977). *Acta Cryst.*, A33, 622-626.
Gait, R.I. & Dumka, D. (1986). *Can. Mineral.*, **24**, 685-688.

COOLING HISTORY FROM PYROXENE CRYSTAL CHEMISTRY AND TEM-TEXTURES IN ANTARCTIC FRO90011 ACAPULCOITE

Domeneghetti M.C. (*CNR, C.S.C.C. Pavia*), Molin G., Salviulo G. , Stimpfl M. (*Dept. of Mineralogy and Petrology, Univ. of Padova*) and Tribaudino M. (*Dept. of Mineralogical and Petrological Sciences, Univ. of Torino*)

The Antarctic FRO90011 meteorite was found during the 199 Italian expedition. The sample, which weighs 1.8 g, was classified b Maras et al. of the EUROMET team as an acapulcoite achondri (Folco L., 1992). FRO90011 shows an achondritic coarse granoblasti texture with approximate chondritic composition. Clino- an orthopyroxene composition is $En_{51}Fs_5Wo_{44}$ and $En_{85}Fs_{12.4}Wo_2$ respectively. The crystal chemistry of Pbca and C2/c pyroxene sing crystals and the TEM texture of Pbca pyroxene were investigated t reconstruct the evolutionary history of the meteorite parent bod (Ganguly & Ghose, 1994; Molin *et al.*, 1991a; Molin *et al.*, 199 Watanabe *et al.*, 1985). Orthopyroxene Fe^{2+}-Mg ordering at the M and M2 sites yields a closure temperature of 575±20 °C accordin to Molin *et al.*, (1991a) and a cooling rate of the order of the degree pe hour using kinetic constants of Saxena *et al.*, (1989). Clinopyroxe Fe^{2+}-Mg ordering at the M1-M2 sites yields a closure temperature o 513±50 °C according to Molin *et al.*, (1991b) and, as i orthopyroxene, a qualitative cooling rate of a few degrees per da TEM investigations on orthopyroxene show a few thin clinopyroxe lamellae, not larger than 20Å, parallel to (100) and rare one unit cel Guinier Preston zones. EDAX analysis did not reveal significan chemical differences between global and lamella-free zones.

The above data are interpreted as consistent with fast cooling due t rapid radiative heat loss.

References
Folco, L. (1992). *Meteoritics*, **27/3**, 221-222.
Ganguly, J. & Ghose, S. (1994). *Geoch. Cosm. Acta*, (in press).
Molin, G.,Tribaudino, Brizi, E. (1994). *Mineral. Mag.*, **58**, 143-150.
Molin, G.M., Saxena, S.K., Brizi, E. (1991a). *Earth and Pl. Sc. Lett.* **105**, 260-265.
Molin, G. & Zanazzi, P.F. (1991b). *Eur. J. Mineral.*, **3**, 863-875..
Saxena, S.K., Domeneghetti, M.C., Molin, G.M., Tazzoli, V. (1989) *Phys. Chem. Min.*, **16**, 421-427.
Watanabe, S., Kitamura, M., Morimoto, N. (1985). *Earth Planet. Sc. Lett.*, **72**, 87-98.

A STRUCTURE MODEL FOR *Pbca* ORTHOPYROXENES

Domeneghetti M.C. (*CNR, CSCC, Pavia*), Molin G.M. (*Dept. of Mineralogy and Petrology, Univ. of Padova*) and Tazzoli V. (*Dept. of Earth Sciences, Univ. of Pavia*)

A file containing the results of X-ray single-crystal structure refinements and chemical analyses of about 200 *Pbca* orthopyroxenes with different composition and degree of order has been created. Multiple linear correlations between structural and compositional parameters were searched using the SPSS program. The coefficients and constant terms of linear equations which allow to predict cell parameters and interatomic distances for any orthopyroxene, starting from its crystal-chemical formula, were calculated. The coefficients referring to the cation-oxygen mean bond distances of the regular polyhedra M1 and SiB appear to be nearly correlated to the ionic radii of the cations at these sites, thus justifying the introduction of <M1-O> and <SiB-O> bond

distances in the linear equations used for determining or checking M1 and SiB site populations. From the predicted distances, the geometric refinement program DLS-76 yields the relevant atomic positions, which agree satisfactorily with those measured experimentally. The same results were obtained faster using coefficients which directly express the correlation between the atomic fractions at the structural sites and the atomic positions. The calculation of the atomic positions makes it possible to study the effects induced on the structure by any variation of chemical composition and cation distribution; in particular it has allowed to simulate the structural properties of fictive end-members. The structure simulation may also allow a spectroscopist, who has determined the chemical composition and the Fe distribution of an orthopyroxene, to obtain its structural parameters with a good approximation.

The coefficients and constant terms of linear equations which express the atomic fractions as a function of cell parameters, atomic positions and mean atomic numbers at M1 and M2 sites were also calculated in order to test the possibility of predict, for any orthopyroxene, its cation distribution. These coefficients allows a crystallographer who has collected the X-ray single crystal diffraction data of a sample, to obtain a rough evaluation of its site population before the results of the chemical analysis are available.

The goodness of these predictions will be continously improved by adding to the "orthopyroxene file", as they become available, data referring to compositions still poorly represented.

The simulation of the atomic positions will be used in the next modelling step ("energy simulation") in order to develop a structure-energy model for the orthopyroxene (work in progress). The Gibbs free energy minimization principle will be applied to the results of lattice-energy and entropy calculations to predict the degree of order at equilibrium for any orthopyroxene at various T and P conditions.

EVALUATION OF POLLUTANT EMISSIONS DURING FIRING OF ITALIAN BRICK CLAYS

Dondi M., Ercolani G., Fabbri B. and Marsigli M.
(CNR-IRTEC, Faenza, Italy)

Fluorine, sulfur and chlorine contained in the raw materials used by the ceramic industry are the source of pollutant emissions during the firing process. Environmental protection paid an increasing attention to the reduction of these stack emissions. In Italy, clean air norms have been applying since two decades in the tile industry and they have recently been extended to the heavy-clay production too.

In this situation, a study concerned in the pollution hazards connected with firing of different heavy-clay products was undertaken. Fluorine, sulfur and chlorine contents of 250 clays currently used by the Italian brick industry were evaluated (Dondi *et al.*, 1993). In addition, a parallel was drawn between 104 brick clays and the corresponding fired products in order to get an indirect evaluation of pollutant release during firing.

Fluorine, sulfur and chlorine, and main components as well, were analyzed by means of X-ray fluorescence spectrometry. The decrease in F, S and Cl concentrations between clay and fired product, on anhydrous base, was assumed to be the loss during firing.

Concentrations vary in the 500-1300 ppm range for fluorine (870 ppm on average), 100-6200 ppm for sulfur (660 ppm on average) and 10-1000 ppm for chlorine (100 ppm on average). Fluorine distribution is quite similar in the various geological units, while S and Cl contents are fairly distinct among the different formations.

The data obtained account for moderate fluorine release, mainly 0 to 40% of the original content. This trend can be mainly referred to the widespread use of carbonate-rich raw materials. In fact, the higher emissions (40 to 80%) occur in clays with low carbonate content.

The situation of sulfur is more complex due to the widespread use of S-rich oil and coal as combustibles. In fact, both sulfur losses and gains are recorded. Most products show a sulfur release (0 to 60%) or a limited gain (0 to 20%). Significant increases of sulfur content in the fired products occur mainly when coal is used.

Owing to the poor thermal stability of alkaline chlorides, Cl loss during firing is generally high (50-100%).

Dondi M., Ercolani G., Fabbri B. (1993). *Proc. 10th Int. Clay Conference, Adelaide, South Australia*, in press.

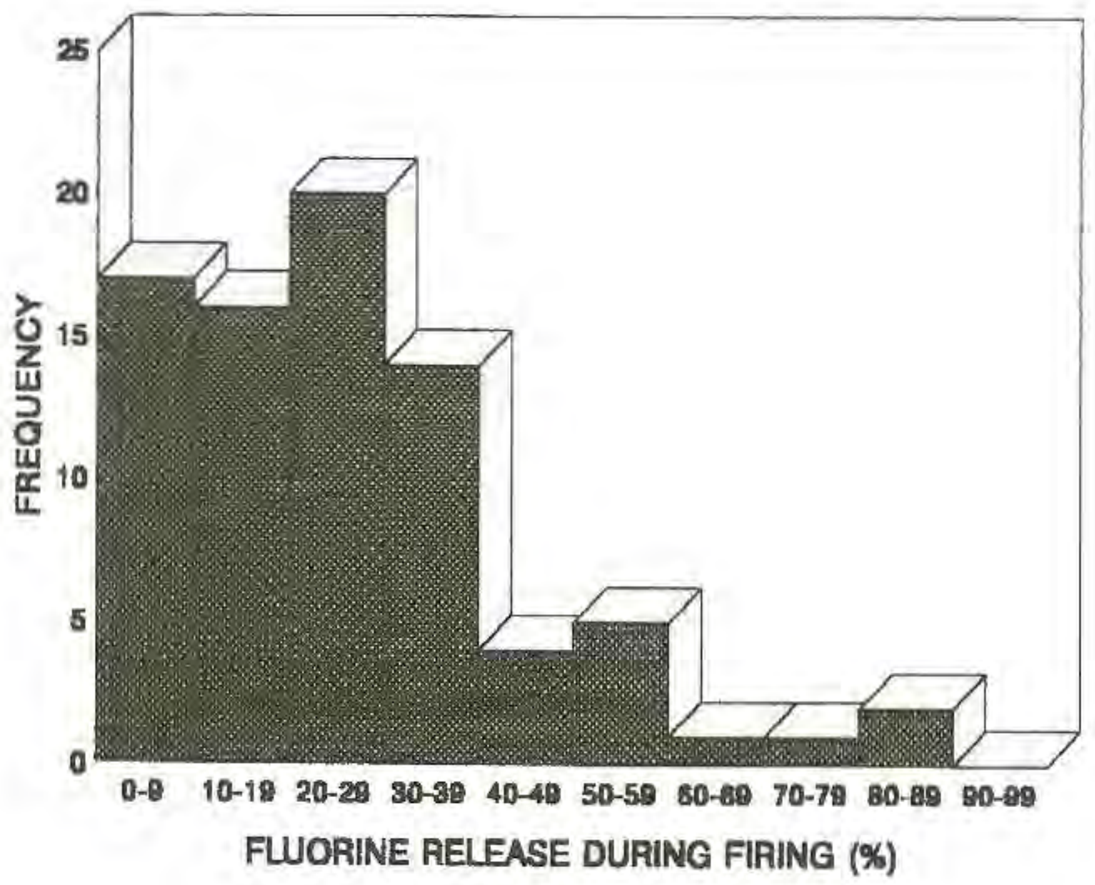

MAGMATIC EVOLUTION OF MT. ETNA (SICILY): Sr-Nd ISOTOPES AND TRACE ELEMENT DATA

D'Orazio M., Armienti P., Innocenti F., Petrini R., Pompilio M., Tonarini S. *(DST-Univ. of Pisa, IMP-Univ. of Trieste, IIV-CNR - Catania, IGGI-CNR - Pisa)*

Eastern Sicily was affected since Upper Trias by a widespread intra-plate basaltic magmatism with a dominant Na-alkaline affinity. Mt. Etna volcanic system represents the youngest and northernmost episode of this magmatic sequence. The early activity in the Etnean area started with the outpouring of tholeiitic, transitional and mildly alkaline lavas from subaerial and submarine fissural activity. Subsequently, a series of large central volcanoes ("Trifoglietto", "Cuvigghiuni", "Serra Giannicola Grande", "Ellittico", "Mongibello recente") were built up whose distribution indicates a westward and then northward migration of the eruptive focus. All these volcanic centres produced Na-alkaline rocks ranging in composition from alkali basalts to trachytes. The occurrence of evolved products testifies that the evolution in distinct shallow magma chambers operated during the building of the volcanic system. By contrast, a set of volcanological and geochemical evidences suggest that present day activity (dominantly hawaiitic) is probably fed by a complex system of dikes.

Sr-Nd isotopes and ratios of incompatible trace elements, allow to divide Mt. Etna volcanics in two major groups (see figure). Group I ($^{87}Sr/^{86}Sr = 0.70304 \div 0.70333$, $^{143}Nd/^{144}Nd = 0.51290 \div 0.51297$, $Ba/Nb = 9 \div 14$, $Th/Ta = 1.5 \div 3$, $Rb/Ta = 5 \div 12$) is characterised by a negative correlation between $^{87}Sr/^{86}Sr$ and $^{143}Nd/^{144}Nd$ and by relatively low LILE/HFSE ratios. The tholeiitic products of the initial activity and the alkaline lavas pre-dating the building of the Trifoglietto volcanic centre, all belong to this group. Group II rocks ($^{87}Sr/^{86}Sr = 0.70331 \div 0.70370$, $Ba/Nb = 10 \div 21$, $Th/Ta = 2.5 \div 3.8$, $Rb/Ta = 10 \div 23$) show an increase of Sr-isotopic and LILE/HFSE ratios accompanied by almost constant $^{143}Nd/^{144}Nd$ values (0.51287 ± 2).

This group includes the volcanic rocks erupted since the building of the Trifoglietto volcano until Present.

It cannot be excluded *a priori* that crustal contamination is involved in the genesis of Etnean lavas, however this hypothesis is weakened by the following considerations: 1) the high Sr contents of Etnean lavas requires that the increase of $^{87}Sr/^{86}Sr$ ratio, due to crustal contamination, cannot realise without a concurrent significant change in major element chemistry; 2) no one of the available crustal materials has the geochemical and isotopic features required to explain the trends observed within Etnean volcanics.

To better constrain the mantle sources of Mt. Etna lavas, we compared their geochemical and isotopic data with those obtained on a set of selected sample belonging to Hyblean rocks and mantle xenoliths.

Group I lavas show Sr-Nd isotopic and LILE/HFSE ratios overlapping with the alkaline Hyblean volcanics (alkali basalts up to melanephelinites) and are interpreted as a product of the interaction between a MORB-like source and a relatively enriched lithospheric component. The former is indicated by the Hyblean tholeiites ($^{87}Sr/^{86}Sr \approx 0.70275$, $^{143}Nd/^{144}Nd \approx 0.51315$), whereas the latter is suggested by the occurrence of metasomatised mantle xenoliths with Sm/Nd < CHUR and $^{143}Nd/^{144}Nd$ ranging from 0.51289 to 0.51299.

Group II lavas exhibit geochemical and isotopic features involving at least a third component, revealed during the most recent activity (< ~ 80 ka B.P.). It must be enriched in LILE, U, Th and ^{87}Sr and relatively depleted in Ta and Nb. Moreover it guarantees the almost constant $^{143}Nd/^{144}Nd$ ratio of Group II lavas. These geochemical features are compatible with mantle enrichments induced by dominantly aqueous and alkali-rich fluids.

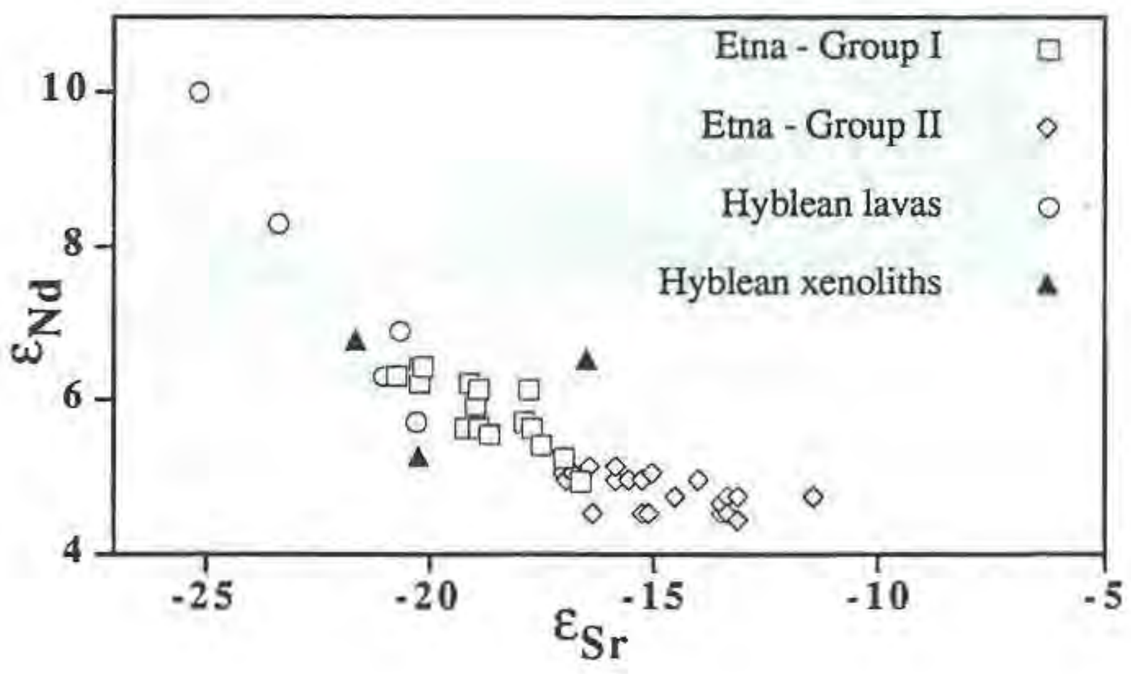

THERMINEOS AND GEM-LTEP: DATABASES AND COMPUTER SOFTWARE FOR THERMODYNAMIC CALCULATION IN MINERALOGY

Dorogokupets P.I., Lashkevich V.V., Zorkaltsev A.V., Vasiltsov V.A. (*Institute of the Earth Crust, Irkutsk, 664033, Russia*)

THERMINEOS and GEM-LTEP are a collection of C++ programs and databases with easy to work with interface for calculation of thermodynamic properties of minerals and related substances, as well as for computer modelling of thermodynamic processes in mineralogy and geochemistry.

THERMINEOS are a thermochemical and thermophysical databases for elements, minerals, gases and aqueous phases (Dorogokupets et al., 1989; 1993). The THERMINEOS maintains the database of elements' standard thermodynamic properties, special databases for thermochemical and thermophysical properties of minerals, the databases of aqueous and gaseous phases, published databases for minerals, and some other equations of state for solids and gaseous phases. Service utilities maintain output data in the format of the reference-book, as well as in user-defined formats.

GEM-LTEP is a modification of SELECTOR software (Karpov, 1981) based on minimization of Gibbs energy of a multisystem and uses a new version of the interior point method (Dikin, Zorkaltsev, 1980) for calculation chemical equilibria. It can be used for calculation T-P, T-X, P-X diagrams, stability fields of minerals, chemical mass transfer and computer simulation physico-chemical phenomena in mineralogy and geochemistry.

Nowadays this software works under the DOS but in future releases there'll be a Windows version too. It can be demonstrated and we need to know other people's opinions on these programs to improve them in the future.

HIGH TEMPERATURE DEFORMATION AND EARLY PARTIAL MELTING IN DIOPSIDE

Doukhan J.C. (*Univ. Lille, France*) and Jaoul O. (*Univ. Paris-Sud*)

The rheology of pyroxenes may affect the rheology of a number of rock forming assemblages, especially in the deep continental crust and the upper mantle. Diopside is the Mg end member of the clinopyroxene solid solution $(Mg,Fe)CaSi_2O_6$ (most natural samples contain also minor amounts of Al, Cr, and Na). High temperature creep of gem quality diopside single crystals was investigated with applied stress σ ranging from 50 to 170 MPa, and in ranges of temperature (T ≈ 1000-1320°C) and oxygen fugacity ($f_{O2} \approx 10^{-18}$-10^{-9} Mpa) representative of the upper mantle. Compression orientations were chosen to test either the (100)[001] glide system which is known to be active at the lower temperatures or other potential systems like {110}1/2<110>, {110}[001], (100)[010] and (010)[100].

Above 1000°C, the equivalent {110}1/2<110> glide systems appear to be the easiest ones. Two contrasted deformation regimes are also observed depending on T and f_{O2} conditions. Below a critical set of these parameters (typically T < 1130°C and $f_{O2} < 10^{-14}$ MPa, while solidus $T_S \approx 1350$°C) well reproducible experiments lead to the creep law $\dot{\varepsilon} = A\, f_{O2}^{m} \exp(-Q/RT)$ with m ≈ -1/5 and Q ≈ 540 kJ/mol. In contrast above these critical T and f_{O2}, creep becomes more or less insensitive to temperature and oxygen fugacity (see figure).

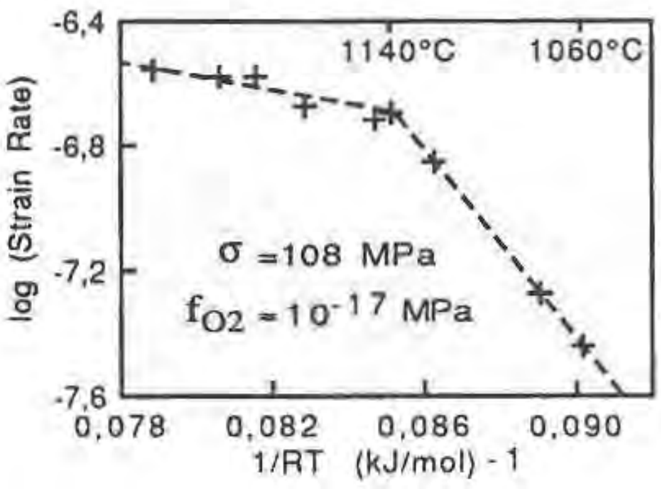

Representative steady state creep experiment at constant stress. Crosses represent experimental points. Oxygen fugacity slightly increased with T.

Transmission electron microscopy (TEM) investigations on the deformed samples show that for both deformation regimes, the expected {110}1/2<110> systems were activated. In both cases mobile dislocations are confined in their glide planes and exhibit orientations parallel to simple crystallographic directions. Hence, the contrasted behaviours below or above critical T and f_{O2} do not stem from a change from glide controlled to climb controlled dislocation motion. However, in the samples deformed in the "high temperature" regime, tiny rounded precipitates are systematically observed. For short test duration and/or just above critical T and f_{O2}, these precipitates are quite small (10 to 100 nm). For long test duration (15 days) and/or at higher T and f_{O2} their size becomes appreciably larger (up to 1 μm) and their volume proportion may reach 5 to 8 %. Such precipitates pin the mobile dislocations and decrease their mobility. This explains, at least qualitatively, the observed change of the creep laws.

We annealed our diopside material under confining pressure and observed that precipitation persists (for instance up to 1500 MPa at T≈1200 °C). We also investigated by TEM some diopside grains from mantellic nodules rapidly brought to the surface by volcanic explosions. A number of them yield the same precipitates.

Crystallographic and chemical characterizations performed by TEM show that the small rounded precipitates nucleated at the beginning of the annealing (with or without applied stress) are amorphous and

constituted of almost pure silica. Their shape strongly suggests that they were a molten phase which reverted to glass during cooling. As they grow their chemical composition also evolves. They become enriched in Al, Na, Fe, Ca while the surrounding matrix is correspondingly depleted in these elements.

Diopside thus begins to melt incongruently from temperatures well below (up to 250°C below) its conventional solidus T_S. These observations question the stability of diopside and the published phase diagrams as well. We called this phenomenon Early Partial Melting (EPM), and we believe that EPM was not detected earlier because of the small size of the glass precipitates.

We propose the following model for the first stage of EPM: in diopside the major point defects are cationic vacancies, their charges being electrically compensated by the change Fe^{2+} -> Fe^{3+}. Vacancy concentration increases with T and f_{O2} as well as Fe^{3+} concentration. However there is a limit to this process above which SiO_2 precipitates. Then tiny silica precipitates absorb the surrounding cations (Al, Na,...), that decreases their melting temperature. Such a process might be very important for the first stages of partial melting in rock assemblages representative of mantle composition.

A QUANTUM MECHANICAL STUDY OF MAGNESIUM SILICATES.

Dovesi R. (*Dept. Inorganic, Physical and Materials Chemistry, Univ. of Torino*) and D'Arco, Ph. (*Lab. de Géologie, E.N.S., Paris*)

Results of quantum-mechanical calculations performed with CRYSTAL92 (Dovesi *et al.*, 1992) on magnesium-silicates are presented. CRYSTAL92 is a standard *ab initio* program for the study of the electronic structure of crystalline compounds; it can be run on medium size workstations and obtained on request from the authors.

The first application refers to the relative stability of cubic, tetragonal and orthorhombic phases of $MgSiO_3$ -perovskite as a function of pressure (D'Arco *et al.*, 1994 a). The calculated orthorhombic unit cell is the most stable, in agreement with experiment. The relative stability and the effect of pressure is interpreted in terms of bond population analysis, and is mainly determined by the oxygen-oxygen repulsion.

The relative stability of $MgSiO_3$-ilmenite, $MgSiO_3$-perovskite and (MgO+stishovite) assemblage phases as a function of pressure is then discussed (D'Arco *et al.*, 1994 b); the geometry of the four compounds has been fully optimized at nine volumes, and the equation of states has been derived therefrom. The critical points of the method (electronic correlation terms; basis set size and cost effects; zero point energy contributions), which can haevily alter the relative stability of the three phases, are discussed. It turns out that in the explored range of pressure (0<P<60GPa) the mineralogical assemblage periclase-stishovite has higher enthalpy than $MgSiO_3$-ilmenite and perovskite and that ilmenite trasforms to orthorhombic perovskite around 29.4 GPa, in good agreement with the extrapolation to 0K of experimental measurements.

Dovesi, R., Saunders, V.R., Roetti, C. (1992). CRYSTAL92 User's Manual, *Università di Torino, Torino.*
D'Arco, Ph., Sandrone, G., Dovesi, R., Orlando, R., Saunders, V.R. (1994 a). *Phys. Chem. Minerals*, in press.
D'Arco, Ph., Sandrone, G., Dovesi, R., Aprà, E., Saunders, V.R. (1994 b). submitted for publication.

THE STRUCTURE OF LOW ALBITE AT HIGH PRESSURES AND TEMPERATURES: COMPARISON WITH ALKALI-SUBSTITUTED FELDSPARS

Downs R T and Ribbe P H (*Carnegie Inst of Washington, Geophys Lab* , and *Dept Geol Sci, Virginia Tech, Blacksburg*)

Using X-ray diffraction, the crystal structure of ordered low albite from Crete has been refined by Downs, Hazen, and Finger (1994; *Amer Geophys Union abstract*) at 0.44, 1.22, 2.68, and 3.78 GPa to reasonable precision (exception: atomic parameters ~|| **c***, which was the axial direction in the Merrill-Bassett diamond anvil pressure cell).

Volume measurements at 14 pressures up to 4.05 GPa yielded a bulk modulus of K_o = 54(1) GPa with a pressure derivative of K_o' = 6(1).

Comparison of the steric details of these low albite (LA) structures with those refined at 13 K (Smith et al., 1986; *Am Mineral* 71 *727*), 273 K (five modern determinations), and at 773, 1023, and 1243 K (Winter et al., 1977; *Am Mineral* 62 *921*) provides a detailed analysis of the primary structural changes occuring with pressure (P) and temperature (T).

As expected, compression and expansion are largely limited to tilting and rotating of the framework AlO_4 and SiO_4 tetrahedra which accompany decreases in 5 of 7 Na-O bond lengths with P and increases in 5 of 7 Na-O bonds with T. The volume of the MO_7 polyhedron is inversely correlated with the "distortion" of the inter-tetrahedral *T*-O-*T* angles and the "distortion" of the *M*-O distances from their respective means (using a parameter defined by Baur, 1974; *Acta Cryst* B30 *1195*). The volume changes in the NaO_7 polyhedra by no means account for all of the unit cell volume changes: inter-tetrahedral tilting and rotating are dominant. At most oxygen atoms, the *T*-O-*T* angles follow analogous trends from high T to high P. Interestingly, the trends of most structural parameters extrapolate well with unit cell volume from low microcline to LA at high T to LA at 13 K, but under compression the structure behaves differently. A distance least-squares (DLS) Rietveld refinement of an alkali-exchanged Li-feldspar (Deubener et al., 1991; *Am Mineral 76 1620*) provides insight into changes under compression.

• THE QUESTIONS OF SYSTEMATICS AND ISOMORPHISM IN RHABDOPHANE GROUP

Doynikova O.A., Belova L.N., Gorshkov A.I., Sivtsov A.V. (*Inst. of Geology of Ore Deposits, RAS, Moscow*)

It was shown that rhabdophane group consists of the following minerals: rhabdophane (and its TR–varieties), ningyoite (its analogue is the later "discovered" tristramite), brockite (its analogues are smirnovskite and greyite).

Two samples from Mineralogical Museum RAS, brockite and smirnovskite, and numerous ningyoite samples from different deposits were studied. A new Ca–variety of rhabdophane–like phosphate has been established. All the minerals present hexagonal syngony.

The questions related to the cation variability were considered on the basis of crystallochemical data of the analytical TEM (SAED, EDAX) and literature data. We have established a wide range of variability of the amount of Ca, U, TR, Th in natural phosphates of this group. Similarity of structural motifs allowed us to consider cation isomorphism of the whole group according to the example of ningyoite. The substitution $[SiO_4]$–$[SO_4]$ is not excluded. Diagram of cation composition has been proposed. Possible structural positions of isomorphous cations have been discussed.

The most probable isomorphous scheme is: $2\ TR^{3+} = U^{4+}\ (Th^{4+}) + Ca^{2+}$. The predominance of Ca over U in ningyoites can be explained by the substitution: $TR^{3+}[PO_4] = Ca^{2+}[PO_3OH]$.

Substitution of structural H_2O by the OH–group can take place in compensation. The existence of defects (vacant TR–positions) also makes heterovalent replacement easier.

Such isomorphism has genetic validity because in nature the rabdophane–like minerals are closely associated with organics, which promotes active involvement of atomic hydrogen in processes of mineral formation.

Reference:
Doynikova, O.A., Gorshkov, A.I., Belova, L.N., Sivtsov, A.V. (1993). *Zap. VMO*, **3**, 79–88.

TRIOCTAHEDRAL FERRUGINOUS MICA COEXISTING WITH MUSCOVITE: EVIDENCE FROM HYDROTHERMAL EXPERIMENTS

Drabek M (Czech Geol Survey, Prague), Rieder M (Inst Geol Sci., Charles University, Prague) and Memmil (Dept of Earth Sciences, Univ. of Siena)

Pairs of coexisting dioctahedral and trioctahedral micas are common in metamorphic and igneous rocks, and their chemical variations could be valuable in understanding petrologic histories of those rocks Although the biotite field is defined by the inverted ternary system, phlogopite - eastonite - annite - siderophyllite, in the present experiments, we started with annite as the first approximation and allowed it to react with muscovite

The experiments were conducted at 1 kbar and with f(O2) imposed by the nickel-bunsenite buffer Most runs started with end members (or micas of a similar composition) that were allowed to approach the solvus from outside, but we succeeded also in bracketing the trioctahedral limb of the solvus from the inside The micas' shifts in composition were monitored by the position of the 060 and 331 diffraction peaks and selected run products were analyzed by a transmission electron microscope (TEM) equipped with an EDS microanalysis

By devising a regression algorithm, we succeeded in relating the shift in degrees two-theta with run temperature (1/T K) and duration of the run and thus were able to estimate run times necessary to achieve chemical shifts of a needed magnitude This made the experimenting more thoughtful and time-economical

Unfortunately, the data show that treating the join as binary or pseudobinary cannot be justified, because the composition of the trioctahedral micas deviates from the binary approximation prohibitively, something that has not been recognized or adequately stressed by other researchers who experimented in related synthetic systems Instead, the composition of muscovite and the trioctahedral micas coexisting with it must be interpreted in terms of six components Si, Al, K, Fe, H, O A trivariant assemblage in such a system (fixed by three intensive parameters temperature, pressure, fugacity of oxygen) contain five phases vapor plus four solids The latter are muscovite, trioctahedral mica (on the annite - siderophyllite join), hercynite-type spinel and K-feldspar

MODULATING IN QUARTZ HAS BEEN DETECTED.

Drebushchak V.A., Dementiev S.N. (Inst. Mineralogy & Petrography, Novosibirsk).

The incommensurate phase in quartz as a new stable one was predicted and than was found to exist within 1.4 K temperature range between the α and β phases. The phase is characterized by a modulated structure with a period incommensurate to that of the quartz lattice and can be observed only at cooling. Advances in these investigations were summarized in (Dolino, 1988).

We have carried out thermoanalytical investigation of the α - β phase transition on quartz samples, both natural and synthetic. The high-quality specimens were selected. The modulated phase existing in a wide temperature range (up to 10 K) was found out for the first time. The phase can be observed both at heating and cooling (Drebushchak & Dementiev, 1993).

Since the temperature range of the existence exceeds that of thermal hysteresis, we discovered the explanation (Dolino, 1988) of the phase to be wrong. The discrepancies are as follows: i) the stable phase exists within the temperature range of hysteresis; and ii) the second order phase transition is announced to exist, which shows vague (and irreproducible) features and has never been detected before.

We have detected the stable modulated phase, and furthermore the stages of generation of the structure were detected as well (Drebushchak & Dementiev, 1994). The Figure shows the dilatometric (a) and calorimetric results for the same sample. Both peaks are split. Each individual stage is caused by modulating the structure with 1, 2, and 3 wave excitations. The total width of the peaks are different due to different conditions of the heat supply.

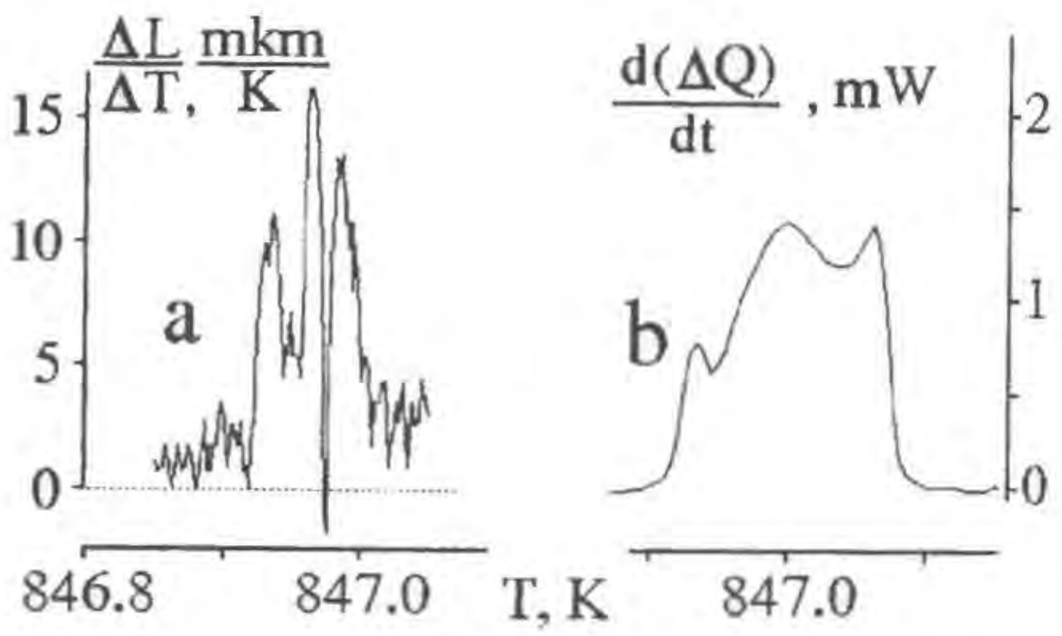

The splitting of the dilatometric (a) and calorimetric (b) peaks due to modulating the structure with sequential 1, 2 and 3 wave excitations.

The wide temperature range of the phase existence allows us to analyze the relationship between length and temperature. The modulating wave vector fits equation $q \sim (T - T_o)^{1/2}$ well, but with $T_o \cong T_c$, not $T_o \cong T_c$ - 10 K (Axe & Shirane, 1970). The high-temperature limit of the range of modular structure existence does not show the phase transition.

References:

Axe, J.D. & Shirane, G. (1970). Phys. Rev. **B1**, 342-349.

Dolino, G., in S. Ghose, J.M.D. Coey, E. Salje (Eds.), (1988) *Structural and Magnetic Phase Transitions in Minerals*, Springer-Verlag, New York, Berlin, Heidelberg, London, Paris, Tokyo, 17-38.

Drebushchak, V.A. & Dementiev, S.N. (1993). *Geokhimiya*, No.9, 1341-1353.

Drebushchak, V.A. & Dementiev, S.N. (1994). *Thermochimica Acta*, (submitted).

• MODULAR FEATURES OF Mn, Fe, Co, Ni–CONTAINING OXIDES AND HYDROXIDES

Drits, V.A. and Gorshkov, A.I. (*Geological Inst. and Inst. of Ore Mineralogy, RAS, Moscow*)

Oxides and hydroxides whose cation compositions are represented by Mn, Fe, Co, and Ni are characterized by a variety of structural features. These features can be classified in terms of modular crystallography if layers, islands, rods, walls, and channels are used as the basic building units. Buserites and birnessites have layer structures and differ in the structure and composition of interlayers, the layer stacking, and for the presence or absence of superperiodicity.

Asbolanes are structures that consist of two–dimensionally continuous MnO_2 layers which alternate with island–like layers of either a different cation composition or a different valency or coordination for Mn. Thus asbolanes are mixed–layer minerals whose layers are incommensurate in the (001) plane. Two or three sublattices are needed to describe the periodicity of these minerals.

A number of asbolane varieties were found whose island–like layers contain either Ni, or Ni and Co, or Co^{3+} and Mn^{2+}, or Mn^{3+} etc.

The basic building unit of Mn and Fe oxihydroxides with channel structures is a rod or chain consisting of edge–sharing MnO_6 or FeO_6 octahedra. The systematics of these minerals is based on the following:

- channel structures are formed by combinations of ribbons that consist of octahedral chains linked through shared edges;
- the ribbons are linked through common octahedral apices and form the walls of the channels;
- variation in the width and height of the walls gives rise to the different structural varieties;
- unit cell parameters depend on both wall dimensions and odd/even number of octahedral chains in the ribbons that alternate in the given direction parallel to the wall.

Mn oxides are classified into four groups: pyrolusite, hollandite, todorokite, and ramsdellite, which include the known and recently discovered structures, as well as hypothetical channel structures.

The forms of the structural heterogeneity of Mn and Fe oxyhydroxides are determined by disordered mixed–layering and mixed–channeling, intergrowth of layer and channel components and by other types of structural defects.

MINERAL CHEMISTRY OF METAPELITES AND METABASITES IN RELATION TO P–T–t PATHS OF SIKKIM, EASTERN HIMALAYAS.

Dubey, C. S. (Dept. of Geology, Univ. of Delhi)

The Sikkim area forming a part of the Lesser Himalaya is a domal structure constituted by low to high grade metamorphic rocks characterised by inverted metamorphism. Geologically, the oldest rocks of Eastern Sikkim are represented by the Darjeeling Formation associated with amphibolite bands along with kyanite–sillimanite, staurolite and garnet zones, while the Daling Formation is characterised by low grade chloritoid and chlorite zones. The chemical analysis of various metamorphic minerals showed that Fe/Fe+Mg ratio in general decreased from low to high grade metapelites with slight variations in staurolite zone. The Na/Na+K ratio exhibited increase in low to medium grade zone whereas it decreased in the high grade kayanite–sillimanite zone.

The metapelites of Eastern Sikkim area underwent two phases of prograde metamorphism, each culminating into a retrograde metamorphic episode (Fig. 1). The first event was prograde regional metamorphism, M_1, during which S_1 and S_2 schistosity were formed. During this episode of metamorphism chlorite, chloritoid, biotite, garnet, staurolite and kyanite were formed. Most of the prograde minerals (chlorite to staurolite) in this phase of metamorphism were formed by continuous reactions except for kyanite (without almandine) which was formed probably by discontinuous reaction. The chemical zoning of garnets in garnet zone show a normal growth zoning. The chemical zoning of garnets in staurolite zone show a normal growth zoning followed by an inverse chemical zoning in the outer part of core. Different geothermometers revealed temperatures upto 465 to 527°C in garnet zone and 555 to 576°C (Core parts) in staurolite zone. The maximum pressure in core parts of garnets in staurolite zone was inferred upto 6.6Kbr.

The M_1 metamorphism was followed by a retrogressive phase M_{1a} due to which the prograde minerals from chlorite to kyanite showed alteration effects. The evidences of this retrogressive phase is inverse chemical zoning in the outerpart of cores alongwith presence of retrograded chlorite in the garnets from staurolite zone, decrease of Zn in outer core parts of staurolites. The temperatures and pressure of this retrogressive

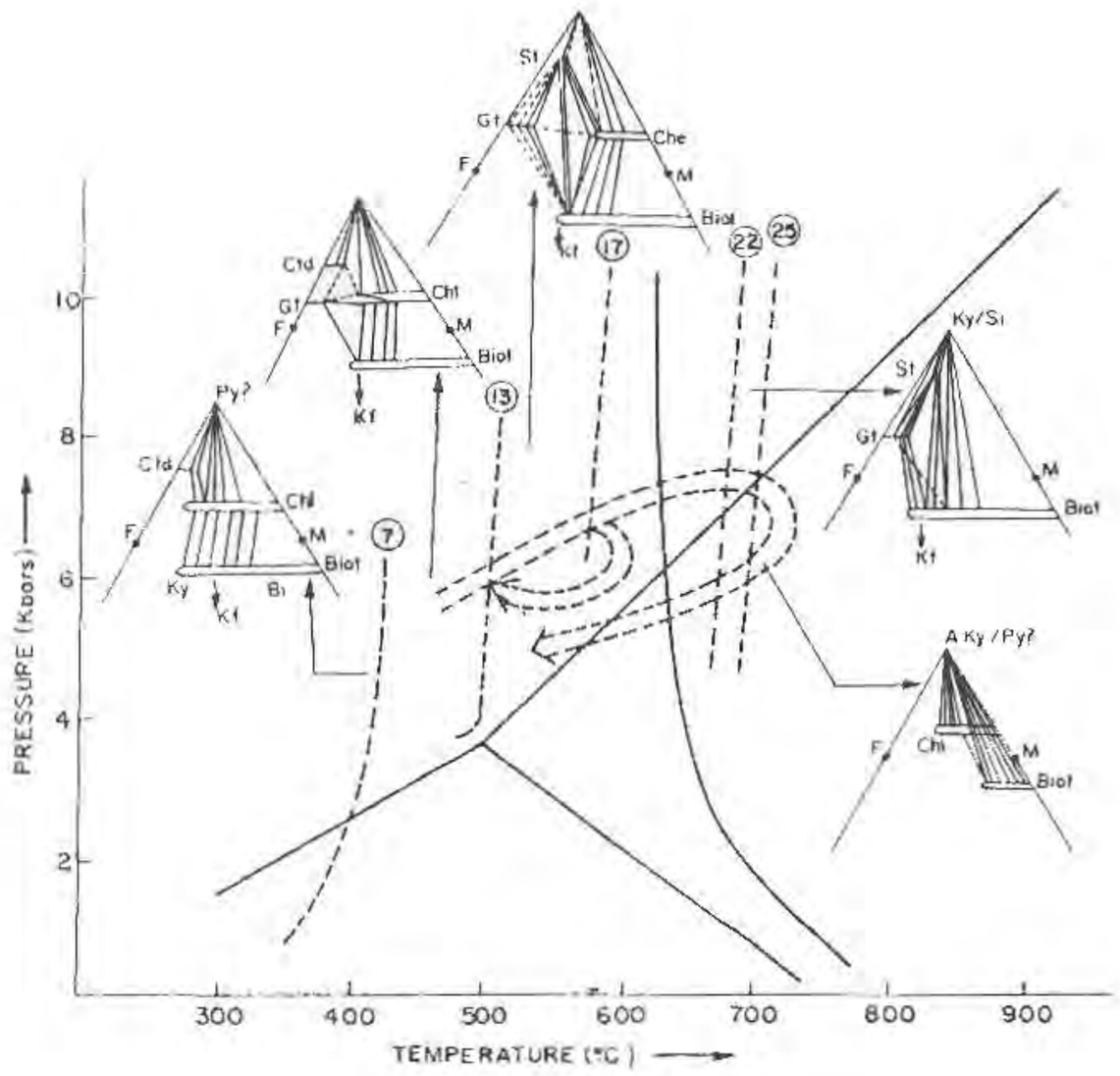

FIG.1

event is inferred from outer core parts of garnets in staurolite zone from 492 to 522°C at 5.7Kbr pressure.

M_2, metamorphism was again a prograde type during which garnet, staurolite, kyanite and sillimanite (with almandine) were formed. The garnets in staurolite zone show another prograde normal zoning from outer part of cores to inner parts of rim. The other evidences in favour of such type of prograde metamorphism are inclusion free rims of earlier multistage garnets, idioblastic inclusion free later formed garnets and staurolite, presence of staurolite inclusion in staurolite, increase of Zn content in Fe–rich staurolite, presence of k–richer muscovite, Ca–rich plagioclase and zoned k–feldspar. The presence of garnet in kyanite–sillimanite zone formed during this metamorphic phase is attributed to an increase in content of Zn in staurolite which possibly acted as an internal buffer. The temperature and pressure during M_2 metamorphic phase reached in the range of 630 to 695°C at 6.9–7.3Kbr respectively in kyanite–sillimanite zone. This metamorphic episode M_2 again culminated into retrograde metamorphism M_{2a}, during which the rims of the multistage garnet were chloritised. The other evidences are replacement of k–rich feldspar by muscovite, reverse zoning of garnet at rim, pseudomorph of chlorite after idioblastic garnet, decrease in Zn content of staurolite. Prograde as well as retrograde biotite were the main constituents of amphibolites. The studies in the Eastern Sikkim area therefore reveals polymetamorphic conditions of rocks as revealed by Staubli(1989) in NW Himalayas.

Reference :
Staubli, A. 1989. Jour. Met. Geol., v. 7, no. 1, pp. 73–94.

The possibility of "post-stishovite" phases of silica at pressure up to 100 GPa.

L. S. Dubrovinsky, S.K.Saxena, A. B. Belonoshko (*Theoretical Geochemistry, Institute of Earth Science, Uppsala University*)

During experiments with iron and amorphous silica placed in DAC at 800 kbar and room temperature the reflections were observed which can be explained by crystallization of silica. The

observed reflections can not be explained by formation of stishovite, because very intensive stishovite reflections (211), (220), and (002) (corresponding distances are 1.44, 1.40 and 1.26 A at 800 kbar) are not observed but, in the same time, reflections at 1.50, 1.49 and 1.42 A appears.

The possibility of existence of SiO_2 in structural modifications of $CaCl_2$, CaF_2, $PbCl_2$, disordered NiAs. Fe_2N and α-PbO_2.was discussed previously (Tsuchida and Yagi, 1989; Dubrovinsky at al, 1989a, 1989b; Bukowinski and Wolf, 1986; Liu at al., 1978; Sekine at al., 1987). It was shown (Dubrovinsky at al, 1989a) that disordered NiAs, Fe_2N and α-PbO_2 are the same structural modifications and further we will consider only α-PbO_2 modification. We have succeeded to interpret the diffraction pattern by appearance of SiO_2 with α-PbO_2 structure.

According to Dubrovinsky et al (1989a) SiO_2 in α-PbO_2 modification can stably exist from 300 to 2000 kbar. In contrast, according to Sherman (1993) SiO_2 (α-PbO_2) is not stable compare to stishovite up to at least 1600 kbar. We calculated structure and properties of this phase by MD (molecular dynamics) and GEMIN (minimization of Gibbs energy) methods using new transferable interaction potential for silica phases. According to GEMIN method SiO_2 (α-PbO_2) is more stable than stishovite by 6 kJ/mole and, according to MD calculations, stishovite is more stable. However, the difference of energies is small according to both methods. Hence, this phase can exist metastably and its appearance at crystallization of amorphous silica at pressure 800 kbar is in agreement with Oswald rule.

References:

Tsuchida, Y., Yagi, T. (1989): Nature, v. 340, N 6230, 217-220.

Dubrovinsky, L.S., Piloyan, G.O., Ryabchikov, I.D. (1989a): In: Mineralogy. Nauka, 1989, 33-40.

Dubrovinsky, L.S., Piloyan, G.O., Ryabchikov, I.D. (1989b): Trans. of Academy of Sciences of USSR, 1989, v.304, N 2, 424-426.

Bukowinski, M.S.T., Wolf, G.H. (1986): J. Geophys. Res., v. 91, N 135, 704-710.

Liu, L., Basset, W.A., Sharry, J. (1978): J. Geophys. Res., 1978, v. 83, 2301-2305.

Sekine, T., Akaishi, M., Setaka N. (1987): Geochim. Cosm. Acta, 1987, v.51, 379-381.

Sherman, D.M. (1993): J. Geophys. Res., 1993, v. 98, 11865-11873.

• PYROXENIC CERAMIC MASSES OBTAINED FROM PERLITE

Duca M. *(Res. Instit. Glass Ceram., Cluj, Romania)*

We intended to obtain some microstructures which could confer physical–mechanical properties and chemical resistance to the pyroxenic masses obtained from the $CaO–MgO–SiO_2+yAl_2O_3$ system.

By melting a mixture of perlite, dolomite, marble and sand some glasses have been crystallized; 1,5% Cr_2O_3 as crystallizing agent was added to the mixture.

The pyroxenic masses were prepared according to the same technology used for vitroceramics. The mixture was melted at 1450°C and the glass crystallized subsequently.

The microstructure of the obtained masses consists of acicular diopside crystals 2 to 3 μm in size, representing 90 to 95 percent, the remaining 5 to 10 percent representing the glass phase; the crystallized masses have been physico–chemically characterized (thermal analyses, X–ray diffraction, density, resistance to abrasion, hardness and chemical stability).

By their higher qualities pyroxenic masses can be employed in manufacturing devices with a high resistance to wearing, grinding devices, inner parts of some mills, plate for various industries, substitutes for metals, insulators, thread conductors for textile industry.

References:

Junina L.A., Kuzmenko M.I., Iaglov B.N. (1974): Piroxenoviesitalli, Izd. BGU, Minsk, 222 p.

Lipovski I.E., Dorofeev V.A. (1972): Osnovi petrurghii, Izd. Metalurghia, Moskva, 320 p.

Pavluskin N.M. (1979): Osnovi tehnologhii sitalov, Stroizdat., Moskva, 260 p.

• MICROSTRUCTURE AND SOME PROPERTIES OF EXPERIMENTAL MATERIALS FROM THE $Li_2O–MgO–Al_2O_3–SiO_2$ SYSTEM

Duca V. *(Dept. of Mineralogy, Univ. of Cluj, Romania)*

This paper illustrates a series of experiments carried out to obtain the synthesis of pyroxenic masses with pre–established properties.

Raw materials used are spodumene from Contu, talc from Cerisor, sand from Surduc and boric acid. Small TiO_2 quantities (rutile–anatase concentrate) and $ZrSiO_4$ were added, both of them obtained from the Surduc sand.

By melting the mixture we obtain a glass, to which a crystallization thermic treatment is applied. Melting occurs at 1450°C with a 1.5 hours interval of maximum temperature.

The crystallization method was elaborated according to the data supplied by DTA. Resulting materials contain about 90 percent of crystalline phases and about 10 percent of glass phase. The main mineral component is β spodumene accompanied by minor "O silica" quantities, characteristic of the compositional domain under discussion.

Data concerning the chemical analyses, as well as analyses carried out through DTA, RX, dilatometry, IR absorption spectrometry, optic and electronic microscopy, are presented. Moreover, Vickers hardness and specific weight have been determined.

Samples have been tested in aggressive environments.

References

Pavluskin N.M. (1979): Osnovi tehnologi sitalov, Stroizdat., Moskva, 260 p.

Rapp J.E. (1973): Thermal Expansion Coefficient – Crystallinity Relations in $Li_2O–Al_2O_3–SiO_2$" Glass Ceramics, Amer. Ceram. Soc. Bull., 52, 6, 499–504.

• MINERAL ASSEMBLAGES OF ALKALINE MASSIFS AND THE PROBLEM OF TECHNOGENIC DEPOSITS

Dudkin O.B. *(Geol. Inst., Kola Centre of Rus. Acad. of Sci.)*

The mining waste and beneficiation tailing dumps are often termed technogenic deposits. However, according to V.I. Vernadsky, technogenic deposits is an ecologically neutral mass of mineral substance which undergoes a controllable alteration (V.I. Vernadsky, *Meditation on naturalist*, Moscow 1977). An optimal object to illustrate this problem are the currently mined deposits in alkaline massifs. They are the large apatite mines in the Khibiny massif, the rare–metal deposit in Lovozero massif, the iron ore and

phlogopite mine of Kovdor massif. There are massive accumulations of mine waste and beneficiation sands ranging from tens to hundreds million tons. The mineralogy of ores and mining waste were studied in detail. The ores contain very diverse minerals. Nepheline, apatite, aegirine, forsterite, diopside, phlogopite, calcite, baddeleyite, magnetite are accumulated in the beneficiation sands and mine waste. Calcite, nepheline, apatite are slowly soluble. The micas pass into hydrate forms. Compound alkaline titanium– and zirconium–silicates easily decompose. Villiaumite, natural NaF, and sodium carbonates are rapidly soluble.

Two types of alteration processes can be selected: explosive hypergenesis of mine waste and conservation diagenesis of beneficiation sands. Vast surface of rock fragments in mine waste is exposed to combined effect of atmospheric O_2, H_2O, CO_2 and alteration of minerals is very quick. The changes of minerals are somewhat different from the surfacial natural processes slowly going on in the surface rocks. For example, natural NaF in mine and mine waste is quickly dissolved by water and aqueous solution dries in the rock cracks to form $Na_2CO_3 \cdot 10H_2O$ which breaks the rock into fragments. Films of gaylussite and opal develop on the surface of nepheline grains. Sulfide–bearing sövite crumbles to sand within 2–5 years. The sewage of mines contains up to 120 mg/l F^-, 24–26 mg/l SiO_2 and Na^+, 140 mg/l CO^{2-}. The grain size of beneficiation sands is 0.01–0.30 mm. Flooded sands quickly become compact. Filtration of water slows down. The access of oxygen stops. As a result, minerals are essentially preserved. The grains of calcite, sulfides, magnetite, nepheline maintain their properties for 15–50 years.

The study of minerals alterations in the mining waste and beneficiation tailings shows: ecologically neutral technogenic deposits may be created with slowly going useful changes of their substance. The necessary conditions of environment are complete control of sewage and minimum erosion and deflation. If these conditions are observed, useful slow dissolution, self–cementation and decomposition of rock blocks may be attained by means of natural agents and catalysts.

NATURAL CONTROL OF THE THERMAL STABILITY OF FISSION TRACKS IN ZIRCON

Dunkl I. (Laboratory for Geochemical Research, Hungarian Academy of Sci., Budapest)

At the interpretation of the fission track (FT) results yielded on slowly cooled or reheated formations the most important factor is the thermal stability of the tracks in the dated minerals. There are two ways to determine the time-temperature (tT) dependence of the thermal stability of the latent fission tracks in the lattice of a uranium bearing mineral.

(1) Laboratory annealing experiments of different duration and temperature should indicate the tT fields of the total and the partial track stability as well as the zone of track instability in a given mineral. The extrapolation of several months long experiments to geological time periods is acceptable in the case of apatite and natural glasses. However, the extrapolation of results yielded by annealing of zircon is hardly sufferable, as the structure of zircon is always contains a dense and sensitive alpha-recoil track background. Thus, early papers of FT dating presented totally inconsistent tT fields on the stability of tracks in zircon (see arrows in Fig.).

(2) Fission track dating of zircons from formations of known thermal history should give information about the position of fields of different track annealing in the Arrhenius diagram.

The metamorphic history of Paleozoic and Mesozoic formations the Bükk Mts. (Inner Western Carpathians, Hungary) is well umented (Árkai, 1983), thus the FT data can be used as the lt of a long-term natural annealing. The duration of the tamorphic overprint was 20-30 Ma, its limitation is given by the ination of marine sedimentation prior the deformation and the appearance of metamorphic formations as detritus. The temperature conditions are registered by the organic transformation, illite 'crystallinity' and carbonate composition.

The boxes in Fig. represent the different units with different metamorphic grades. The borders of 'zero' and 'total' disappearance of tracks run probably between the boxes.

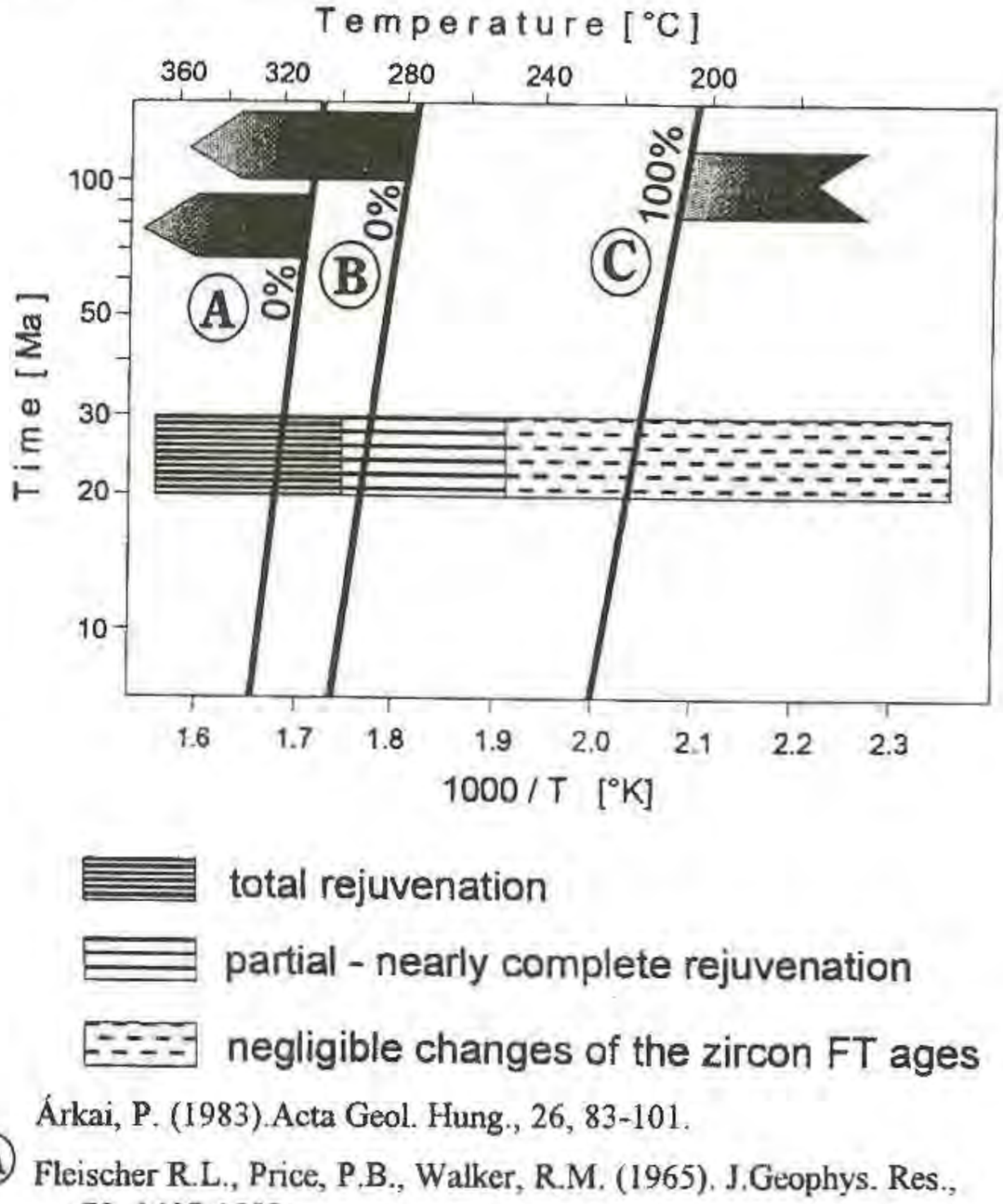

Árkai, P. (1983).Acta Geol. Hung., 26, 83-101.

Ⓐ Fleischer R.L., Price, P.B., Walker, R.M. (1965). J.Geophys. Res., 70, 1497-1502.

Ⓒ Koul, S.L., Wilde, A.R., Tickoo, A.K. (1988). Tectonophysics, 145, 101-111.

Ⓑ Krishnaswami, S. et al. (1974). Earth Planet. Sci. Lett., 22, 51-59.

THE REDISTRIBUTION OF COPPER IN ALUMOSILICATE PHASES UNDER REDOX POTENTIAL CHANGE.

Durasova N.A., Kochnova L.N., Ignatenko K.I. (*Vernadsky Inst.of Geochemistry and Analytical Chemistry,Moscow)*

Experimental studies included synthesis of copper-containing glasses and glass ceramics forming main types of rocks using buffer mixture Ni-NiO (whose fO_2 is close to that of natural conditions) at T 1300-900°C for 6-12 hours. Partially recrystallized ceramics were synthesized at temperatures below liquidus. In some glasses Fe was substituted for Co to prevent its disturbing influence on the Cu^{2+} determination by EPR method. A part of the material obtained as grains was heated at T 500°C for 10 days at fO_2 of air. Then initial and heated samples were treated with hydrochloric solutions. It had been calculated % of the copper loss from the initial and heated glasses and ceramics.

A considerable mobilization of copper with hydrochloric from thermally treated phases of both glasses and ceramics is mentioned. A large removal is mentioned for andesite and basalt phases. It was established certain forms of existence, oxidation degree of copper in the initial glasses sythesized at fO_2 N-NiOamd differences heated at fO_2 of air obtained by EPR method and method of luminescence in glasses of granitic eutectie composition.

The results obtained attest for the presence of copper in low oxidation degrees Cu^{+1} in the initial glasses (Cu^{+1} is detected by the luminescence method) and for the appearance of the Cu^{+2}signal in samples heated in the air. The formation of layers enriched in copper

in heated grains is detected by the electron spectroscopy method for chemical analysis performed for the glass compositions listed above in the "MEKHANOBR" Institute. Sizes of layers enriched in copper (110-120 nm) in heated samples were determined by the ion microprobe measurements.

The results obtained allow one to present a mechanism of the Cu^{+1} element of variable valence from the area of redox potential existed in the inner parts of the phase to the area of another redox potential of the phase surface connected with gas atmosphere, water solution,etc.

We can suppose the copper migration in volcanogenic formation when oxidation regime is changed on the basis of the experimental modelling performed, wich allowed us to elucidate the copper distribution in glasses and ceramics at solidus T, when fO_2 is chenged.

CRYSTAL CHEMISTRY OF TOURMALINE: A GUIDE TO METAMORPHIC EVOLUTION OF METAPELITES

Dutrow, B.L. and Henry, D.J. *(Dept. of Geology & Geophysics, Louisiana St. Univ.)*

Tourmaline (*tur*), a ubiquitous metamorphic mineral, develops in a plethora of bulk compositions and is stable from conditions of diagenesis through partial melting. It effectively monitors the history and evolution of metamorphic rocks due to a combination of its refractory nature, chemical complexity and responsiveness to the environment of formation.

Metapelites often contain detrital *tur*. These constituents commonly retain their morphological and chemical integrity as cores with metamorphic *tur* overgrowths (*ovg*). Application of $Al-Fe-Mg$ and $Ca-Fe-Mg$ discrimination diagrams together with allied compositional data on the detrital cores (Henry & Guidotti, 1985; Henry & Dutrow, 1992), illustrate that ≥ 10 source rocks commonly contribute detritus to individual samples of metasediment.

During low grade metamorphism, *tur* exhibits pronounced polarity that is most notable where nucleation occurs on detrital *tur*. Morphologically, this is manifest as asymmetric *ovg* of *tur* dominantly at the (+)c-axis. Chemically, the contemporaneous *tur ovg* at respective c-poles display significant differences in major and minor element concentration *i.e.* compositional polarity. With increase in metamorphic grade, morphological and compositional polarity diminish and disappear in the staurolite (*st*) zone. Compositional polarity complicates traditional interpretation of intercrystalline element partitioning involving *tur* and coexisting phases. Two possible partition coefficients can be calculated from the same mineral pair *e.g.* the polar differences in Mg-Fe produce partition coefficients that are significantly dissimilar. This apparently derives from the decoupling of Mg and Fe in *tur*, probably related to Mg-specific exchange components *e.g.* $\square AlNa_{-1}Mg_{-1}$. Crystal structure refinements of aluminous dravite have confirmed this coupled substitution and indicated that Mg may be found in both Y and Z octahedral sites (Hawthorne et al., 1993). However, **internal** partition coefficients calculated between the poles of individual *tur* grains or contemporaneous internal zones, behave systematically. These coefficients approach one for samples at increasing grade or for contemporaneous zones within a single zoned *tur*.

As metamorphic grade increases, *tur* retains compositional zoning from the earliest stages of *ovg*. Discontinuous zoning is common and is generally marked by a distinct color change. These zones appear to reflect punctuated *tur* growth probably associated with discontinuous reactions. For instance, *tur* growth observed in a *st* zone schist coincides with the discontinuous *st*-forming reaction that involves significant amounts of muscovite (*mus*) consumption. *Mus* containing B, at levels of several 100 ppm, is released to the fluid which permits *tur* nucleation on preexisting *tur* grains. Discontinuous zoning implies that B was sporadically available during the rock's growth history. *Tur* may serve a sensitive monitor of discontinuous reactions which release B to the system. The distinct chemical discontinuities that separate core-*ovg* and chemical zones are retained even into the sillimanite zone. This implies very limited volume diffusion within *tur*, most likely a consequence of the complicated heterovalent substitutions involving numerous sites.

Tur chemistry, textures and modes can also signal open vs. closed behavior of metamorphic fluids. Irreversible thermodynamic modeling of the development of anomalously high concentrations of chemically homogeneous *tur* in prograde *mus*-rich pseudomorphs after *st* indicate that B must have been added to the metapelite from external sources, while other constituents must have been removed (Dutrow & Foster, 1992). Thus, even at high grades of metamorphism, *tur* is an effective chemical monitor of evolution.

References:
Dutrow, B. & Foster, C.T., (1992) GSA Abstracts, 24, A218.
Henry, D. J. & Guidotti, C. V. (1985) Am. Min. 70, 1-15.
Henry, D. J. & Dutrow, B. L. (1992) CMP, 112, 203-218.
Hawthorne, F. *et.al* . (1993) Am. Min. 78, 265-270.

FERRIC IRON, H, AND LIGHT ELEMENTS IN SILICATES FROM METAPELITES IN WESTERN MAINE, USA

Dyar M.D. *(Dept. of Geology & Astronomy, West Chester Univ.)* and Guidotti C.V. *(Dept. of Geological Sciences, Univ. of Maine)*

Since the advent of the electron microprobe there has been a precipitous decline in wet chemical measurements, and thus the practices of neglecting or estimating Fe^{3+} contents and assuming ideal H^+ stoichiometry have become commonplace. Minor and light elements that are difficult or impossible to analyze by electron probe, e.g., Li, F, B, and Be, have received similar treatment. However, recent work based on ion microprobe data has called attention to problems arising from ignoring these latter constituents. In the absence of complete analyses measured on coexisting minerals from petrologically well characterized rocks, it was inevitable that such difficult to analyze components would be ignored, thereby promoting an unfortunate practice of merely assuming certain stoichiometries. We contend that site substitution models, activity models, geothermometers, geobarometers, and thermodynamic models of mineral reactions are incomplete without measurement of H^+, Fe^{3+}, and other constituents needed for a complete chemical analysis.

To support our contention, we present here H^+, Fe^{3+}, and light element data obtained in conjunction with electron microprobe analyses of over 500 petrologically well-constrained, Fe-bearing hydroxyl silicates. Light elements, measured using PIGE (proton-induced gamma-ray emission spectroscopy), ion probe, and electron probe, vary widely according to mineral assemblages and modes, e.g., ranging from 0.01-0.35 for wt% Li_2O and for 0.12-1.54 wt% F in micas. H^+ and Fe^{3+}, analyzed using uranium-extraction methods and Mössbauer/wet chemical analysis, respectively, also show extensive variation in the minerals studied. In Al-, Ti-, and Si-saturated metapelites, we observe the following:

Oxide assemblage	Mineral	$Fe^{3+}/\Sigma Fe$	wt%H_2O
graphite-ilmenite	biotite	8-12%	4.52-3.21
graphite-ilmenite	muscovite	16-63%	2.54-4.96
graphite-ilmenite	chlorite	6-13%	8.80-10.41
graphite-ilmenite	staurolite	3-10%	1.43-1.78
graphite-ilmenite	tourmaline	15-25%	2.44-2.80
graphite-ilmenite	garnet	5%	<0.1
magnetite	biotite	19-27%	3.31
magnetite	muscovite	65-75%	3.75
hematite	biotite	46%	3.99
hematite	muscovite	82%	3.71

For most of these minerals, H^+ varies systematically as a function of metamorphic grade. Biotite, muscovite, and chlorite are deficient in H^+ relative to their generally-assumed stoichiometries except in garnet-grade rocks. Moreover, oxysubstitution (or deprotonation) involving only H^+ and Fe^{3+} exchange is rare. Instead, the related substitution of $H^+_{mineral} + (Fe,Mg)^{2+}_{mineral} \rightarrow (Fe^{3+},Al^{3+},\frac{1}{2}Ti^{4+},etc.)_{mineral} + \frac{1}{2}[H_2]_{gas}$ is extremely common. This mechanism accounts for the great majority of R^{3+} and R^{4+} substitution (apart from the Tschermak and $Fe^{3+} \leftrightarrow Al_{vi}$ substitutions), reducing or eliminating the need to invoke vacancies for charge balance.

For hydrous phases, our data show that errors will be inherent for calculations assuming negligible light elements, stoichiometric H, and all Fe as Fe^{2+}. For example, in muscovite from graphite-bearing metapelites, the $Mg/Mg+Fe^{2+}$ ratio will be systematically in the range of about 0.1 too high when incomplete analyses are used. For magnetite-bearing rocks, the error in the ratio is at least twice that. Furthermore, the common assumption that the presence of Fe^{3+} in hydrous phases is completely balanced by H^+ deficiencies (e.g., that normalization to 22 O for micas allows one to ignore both H^+ and Fe^{3+}) is misleading and incorrect.

Cooling rate histories from garnet - biotite equilibrium

Ehlers K. (*Dept. of Earth Sciences, Monash Univ.*) and Powell R. (*School of Earth Sciences, Univ. of Melbourne*)

Dodson's (1986) solution of the temperature-dependent diffusion equation may be used to determine cooling histories from geothermometrically-inferred closure temperatures. If a mineral pair such as garnet-biotite equilibrated at the start of cooling, continued to equilibrate during cooling, then such closure temperatures, T_c, are a strong function of grain size and cooling rate (s). Thus garnet grains of different size which equilibrated with biotite, within *one* rock or thin section, will close at different temperatures, and thus should record different stages of the thermal history. The application of Dodson's equation in the deduction of thermal histories is straightforward if a garnet grain is known to be cut, for example, through its center, but the section position is normally unknown. However, using a single garnet grain cut at an unknown section position, an apparent closure temperature can be determined using an exchange geothermometer, and, with an observed radius, an apparent cooling rate can be calculated. From this apparent closure temperature and apparent cooling rate a family of solutions of possible actual closure temperatures and cooling rates can be calculated for a family of assumed actual grain radii. This family of solutions forms a locus on a $\ln s - T_c$ diagram. With many analyses of garnet grain centers in a thin section, garnets of a particular size which give *higher* closure temperatures will normally be cut closer to their centers. Using this, the cooling history of a rock may be determined. This approach is tested with a Monte Carlo simulation. The calculated cooling histories provide potentially important constraints on the tectonic evolution of metamorphic terrains.

References:
Dodson M. H. (1986) *Material Science Forum* 7, 145-154.

GRANITIC DYKES IN THE BENI BOUSERA PERIDOTITIC MASSIF (INNER RIF, MOROCCO)

Elbaghdadi.M., Tabit, A., Duthou, J.L. (*Dept. of Earth Sciences, Faculte of Science–Semlaia, Marrakech*)

The acidic dykes in Beni Bousera body are separated in two types of injection different by their structural position. The first type is represented by garnet leptynite which is in equilibrium with metamorphic formation surrounding the peridotite body. The age of emplacement was pre–Silurian. The second type of injection is related to the latest stage of emplacement of peridotite–kinzigite association. Datings suggest an alpine age. Injection of cordierite granite dykes occurred as well.

Structural study shows that the orientation of the leptynite injections follows the massif border, but the cordierite granite dykes cross–cutting layering and foliation in the peridotite does not show any preferring direction.

The Beni Bousera's acidic pods have a peraluminous and leucocratic character that indicate a crustal S–type origin. The anatectic magma is formed by partial melting of the surrounding rocks during the hot emplacement of peridotite. The sedimentary source is isotopically and chemically heterogeneous.

Isotopic dating of the emplacement of these acidic injections yeld an age of 20.2±0.4 Ma which is contemporaneous to the alpine metamorphism culmination.

THE FIRST OCCURRENCE OF PGM IN A CHROMITE DEPOSIT IN THE EASTERN DESERT, EGYPT

Elhaddad M.A. (Geol.Dept., Assiut University, Egypt)

Laurite, osmiridium, iridosmine and palladium-tellurium- antimony- arsenic alloys were first recorded in the basement rocks of Egypt.

The Pt-minerals were found in a massive chromite lenses hosted in a serpentinized peridotite in Gebel Lawi (Southeastern Desert). The PGM are represented as grains of random distribution ranging in size from < 10 to 40 microns. Their occurrence do not seem to be correlated with stratigraphic position.

Osmium, iridium.and ruthenium predominate in the chromite grains over platinum, palladium and rhodium which is a typical common feature for phiolitic comple xes. Mineral phases containing palladium and tellurium were associated with intercumulus nickel sulphides and arsenides.

The PGM were correlated with those of other localities worldwide on one hand and those from non-ophiolitic complexes on the other.

We believe that the latter phases have developed in response to weathering and/ or low temperature hydro-thermal alterationprocesses, while the PGM -bearing sulphides and alloys have formed by a change in both the oxygen and sulphur fugacities as well as mineral equilibria of the magma caused by an increase of volatiles.

SOME ASPECTS OF IGNIMBRITIC RHYOLITES OF DOKHAN VOLCANICS, SOUTH WEST SAFAGA, EASTERN DESERT, EGYPT

By

M.M. EL-RAHMANY

Faculty of science, Al-Azhar University, Cairo, Egypt.

The present study have revealed that the south west safaga ignimbritic rhyolites are formed mainly of acid volcanic glass, interatulluric crystals and lenticular glass shards (fiamme), and are chiefly fine grained, ill sorted welded rhyolitic tuffs. Granulometric analyses, textural patterns, welding, compaction and devitrivication are discussed. The studied ignimbrites are in close association with an

assemblage of rhyolite, rhyodacite and andesites. The ignimbrites were erupted with explose violence as a turbulent mixture of hot expanding gases and gas-emitting lava fragments, at relatively low pressure. Also, chemical classification proved their calc-alkaline character, while their petrochemistry suggests that the studied ignimbrites and associated volcanics are related by a common fractionation scheme.

PETROGENESIS OF ANORTHOSITE-RAPAKIVI GRANITOIDS OF THE NAIN PLUTONIC SUITE, LABRADOR: NEW DATA AND PERSPECTIVES

Emslie R.F., Hamilton M.A., Thériault R.J. *(Geological Survey of Canada, Ottawa, Canada)*, and Prevec S.A. *(GÉOTOP, Université du Québec à Montréal, Canada)*.

The Nain Plutonic Suite (NPS), about 1.3 Ga, underlies some 19,000 km^2, intruding the boundary zone between the Nain Province (middle to late Archean basement) and the Churchill Province (late Archean and early Proterozoic basement) to the west. Small intrusions of mantle-derived troctolite with highest ε_{Nd} @ 1.3 Ga (near -3.0) are present in both eastern and western sectors of the NPS. Nd isotopic signatures of all other igneous units of the NPS reflect their geographic positions relative to the inferred boundary between the Nain and the Churchill Provinces (ε_{Nd} <-10, and ε_{Nd} > -10, respectively). Anorthositic rocks have variable and significant contributions of crustal Nd but notably lower I_{Sr} than the granitoid rocks. Ferrodiorites are similar isotopically to the anorthositic group and have chemical and mineral compositions more akin to the anorthositic group than the granitoids.

Major granitoid batholiths associated with the Nain Plutonic Suite are dominantly metaluminous, extending locally to weakly peraluminous compositions. They crystallized at pressures averaging about 3.5 kbars, but up to 1 kbar lower in the south. Redox conditions were typically 1 to 3 log fO_2 units below the FMQ buffer. The subvolcanic-volcanic Flowers River Igneous Suite (FRIS) intrudes Notakwanon batholith at the southern end of the NPS, overlapping the younger end of the age range for the NPS within errors, but comprising largely peralkaline compositions. Individual samples of FRIS rocks span the range from weakly peraluminous to metaluminous to peralkaline, inviting the inference that liquid lines of descent related to those of NPS granitoids have been involved in FRIS evolution. Trace element chemistry of the FRIS is remarkably similar to the more fractionated NPS granitoids, particularly Notakwanon batholith. Comparative geochemistry of the granitoid batholiths of the NPS suggests that the FRIS was derived from similar source materials, but is distinctly more evolved. Initial Nd isotope compositions in all but one FRIS granite sample are in the range (ε_{Nd} = -9.7 to -7.8, n=10), in accord with derivation from crustal sources similar to those found for the three principal NPS granitoid batholiths that intruded Churchill Province crust (ε_{Nd} = -9.7 to -7.7, n=9).

Aluminous orthopyroxene megacrysts in NPS anorthositic rocks have indicated crystallization pressures (6.2 to 11.0 kbar) consistent with deep crust to upper mantle depths. NPS rapakivi and rapakivi-like granitoid rocks are products of crystallization from magmas derived in large part by partial melting of the lower crust. These granitoid rocks show the influence of sources similar to the basement gneisses, but were augmented by materials with much shorter crustal residence time, offering support for contemporaneous basaltic underplating of the lower crust. Isotope and elemental geochemistry and mineral compositions in major rock units of the NPS, coupled with knowledge of the timing of intrusive events, allows the essential features of petrogenesis to be assessed and points to a model that may have wider application. Separation of granitoid partial melts at the lower crust left depleted, hot, plagioclase-pyroxene granulite crustal residues which were assimilated concurrently or subsequently by mantle-derived basaltic magmas. This process permitted development of large volumes of anorthositic magma in upper levels of deep crustal to uppermost mantle magma chambers by plagioclase flotation; concurrently, fractionation moved residual liquids toward ferrodiorite compositions. Upward movement of buoyant anorthositic magmas followed crustal paths preheated by earlier passage of granitoid magmas. Relatively small volumes of high density, Fe-rich, ferrodiorite melts were expelled to higher crustal levels.

COMPOSITION OF LIGNITE FLY ASH: VARIATION WITH PARTICLE SIZE AND MICROANALYSIS

Enders, M. & Bambauer, H.U. *(Inst. of Mineralogy, Münster)*

About 30 % of the German electricity supply is produced from the combustion of brown coal. German power plants produce annually approx. 10.Mio t of brown coal fly ash. This material reacts hydraulically with water. Most of the fly ash is used with the products of flue gas desulphurization for sanitary landfilling. Economic and compositional reasons restrict the usage as an admixture to concrete. The detailed knowledge of quantitative minera-logical and chemical composition is important to predict the behavior of fly ash in the landfill and concrete.

High Ca/S fly ashes from the mining area S Leipzig were classified by dry sieving (< 100μm, 63-100 μm, 45-63 μm, 32-45 μm, 20-32 μm, < 20 μm). The sieving process was supervised with laseroptic particle size determination. The obtained material was analyzed with optical and electron microscopy, XRF, XRD. The composition of submicron particles was determined with AEM-Methods.

Optical examination leads to the determina-tion of five basic particle types, which show almost no intergrowth. Mineralogical each of them consists of a certain paragenesis of minerals and amorphous components. Quartz is a common thermally fragmented relic from the coal. Glassy spheres are the thermal conversion products of clay minerals. Devitri-fication of the glasses produces anorthite and gehlenite. Opaque spheres are composed of hematite and magnetite and some marcasite, which survived the combustion process. Anhydride occurs as small idiomorphic crystals and as a thin surfacelayer on other particles. Agglomerates consist of thermally altered clay minerals which welded together during the coal combustion.

The combination of dry sieving, laser-granulometric particle size determination and XRD/XRF data revealed a strong correlation between particle size and composition of the fly ashes. SiO_2, Al_2O_3, K_2O and Rb increase linearly with particle size. In contrast CaO, MgO, Ba, Mn and Sr decrease. S, Na, As, Pb and Zn are due to vaporisation/condensation processes highly enriched in the submicron range. The Oxides of Fe, P and Ti and the elemental content of Cr, Cu, Th and V display almost no variation with particle size. X-Ray intensities of mineralogical components vary with their major chemical constituents (quartz, anhydride, lime, hematite). The combination of chemical and mineralogical data offers a calibration method for quantitative XRD-analysis. The calibration line includes the matrix change with particle size. Therefore it can be used independently from matrix effects.

The glassy spheres are important for the hydraulic reaction of fly ashes in concrete and sanitary landfilling. Their main constituents are CaO, SiO_2 and Al_2O_3. Their Al/Si ratio indicates kaolinite as precursor mineral. Glassy spheres with CaO > 25 wt-% are soluble in acetic acid. The remainder with CaO < 25 wt-%. are soluble in strong acids (HNO_3, HCl). This indicates the existence of different types of glassy spheres. Low Ca-spheres are homogeneous. They show only a slight hydraulic activity. They are enriched in the coarse fractions of the fly ash. High Ca-spheres consist of glass, gehlenite and inclusions of lime. They are easily soluble and react hydraulically.

In mixtures of fly ash and deionized water ettringite and gypsum crystallize within a few days. During ettringite formation the glass

composition did not change. This is evidence for a second reservoir for easy soluble Al, Ca, S besides the glassy spheres.

Most of the anhydride crystals contain aluminium and other elements. Al/Si ratios exclude kaolinitic glass as heterogeneous seed in the anhydride cores. Anhydrides are probably intergrown with aluminium-sulfates. These anhydride crystals could be the easy accessible reservoir of Al, Ca and S for the fast ettringite formation.

From chemical analysis (XRF, colormetric) it is possible to determine the CaO-content in sulfates, lime and glass. The maximum soluble CaO-content in glass is 25 wt-%. The distribution of CaO between lime, glass and anhydride is controlled by the pSO_2, the temperature and the viscosity of the glassphase.

Our results show a clear relation between particle size and composition of coal conversion residues. They can be used for the prediction of hydraulic activity of high Ca/S fly ashes.

CONTRIBUTIONS TO THE PROBLEM OF "INVISIBLE" GOLD

England, K.E.R., Vaughan, D.J. (*Dept. of Geology, Univ. of Manchester, England*), Zeng, R. (*Inst. of Geology, Academia Sinica, Beijing*), Borrini, D. (*Dip. Scienze della Terra, Firenze, Italy*) and Parish, R.V. (*Dept. of Chemistry, UMIST, England*).

Gold-bearing arsenopyrite and arsenian pyrite (<0.4 at%) have been synthesised using hydrothermal methods (500°C at pressures of 1-2 kbar) and naturally occurring auriferous arsenopyrite and pyrite samples examined optically and by electron probe microanalysis. The latter were obtained from a wide range of localities including some previously studied (in France, South Africa, Ghana and Canada) and others studied for the first time (China and Zimbabwe).

A wide range of analytical and spectroscopic techniques were applied to try and gain further understanding of the nature of "invisible" (by optical microscopy) gold in arsenopyrite and arsenian pyrite. In addition to routine optical, electron microprobe and scanning electron microscope studies, these have included transmission electron microscopy, X-ray absorption spectroscopy (EXAFS), X-ray photoelectron spectroscopy (XPS) and ^{197}Au Mössbauer spectroscopy. There was no evidence from electron microscopy for optically "invisible" particulate gold. Unfortunately, attempts to use EXAFS to study the locus of gold in both arsenopyrite and auriferous pyrite were frustrated by the problem of overlap between the As K-edge and the Au L-edge, although future synchrotron systems incorporating more intense sources and more sensitive detectors may overcome this difficulty.

A Mössbauer spectrum of auriferous arsenopyrite from the Howard Mine, British Columbia, Canada showed a very broad absorption peak at +3.6 mm/s clearly demonstrating that the gold is not metallic gold but chemically bound, probably within the arsenopyrite lattice. The linewidth (~6 mm/s) could arise from an unresolved doublet or a range of sites. The data are consistent with gold in the form of Au(I) (or possibly Au(III)). X-ray photoelectron spectra for an auriferous arsenopyrite sample from Ghana (Ashanti Mine) yielded a peak attributable to the $Au4f_{7/2}$ transition. The position of this peak (at a binding energy of 84.61 eV) strongly suggests gold in the form of Au(I) rather than metallic gold ($Au4f_{7/2}$ at 84.0 eV) or Au(III) ($Au4f_{7/2}$ at ~ 87 eV). The crystal chemistry of auriferous arsenopyrite (and arsenian pyrite) will be discussed in the light of these data.

PETROGENESIS OF THE SOVGAVAN THOLEIITE-ALKALINE BASALT FLOOD-PLATEAU, SIKHOTE-ALINE: MODEL OF ISOTOPIC-GEOCHEMICALLY ZONED MANTLE DIAPIR.

Esin S.V (*United Institute of Geology, Geophysics and Mineralogy, Universitetsky pr 3, Novosibirsk, 630090, Russia*)

The Sovgavan tholeiite-alkaline basalt plateau was formed at the inner part of the Asian active continental margin between 14.7-5.4 m.a. The plateau is composed by low-Ti and high-Ti quartz and olivine tholeiite basalts, olivine and alkaline olivine basalts, basanites and hawaiites.

All basaltic magmas were generated from one mantle source, that is a garnet-peridotite mantle diapir. On the basis of Sr-isotopic and geochemical data concluded that the magmas were produced by a heterogeneous diapir source that includes N-MORB, EMI (DUPAL-type) and EMI (non-DUPAL-type) components.

The mantle diapir has probably a zoned structure, according to isotopic, geochemical (REE, HFSE, LILE) characteristics and modal composition. Zonation is probably formed by infiltration of melts that are produced by low degrees of melting from deep-seated to upper part of the diapir. Tholeiite magmas and alkaline magmas were generated in upper and middle parts of the diapir and in its deep-seated parts, respectively.

In the upper part diapir material reacts with litospheric part of the mantle. Its base is of HIMU-type isotopic geochemical composition, as it was an ancient subducted slab. As a result, high-Ti tholeiite magmas are formed here.

It is proposed that primary magmas form magmatic chambers in the litospheric mantle where processes of crystal fractionation take place. The "secondary" magmatic chambers were found at the Moho-boundary, where tholeiitic melts reacted with granulites of the base of the crust.

• MINERALOGY OF THE KOROSTEN RAPAKIVI GRANITES (UKRAINIAN SHIELD)

Esipchuk K.Ye., Skobelev V.M., Verkhoglyad V.M. Inst. Geochem., Mineral. & Ore Form., Acad. Sci. Ukraine, 252142 Kiev, Ukraine

The Korosten rapakivi granite complex (1770-1737 Ma) is composed of several intrusive phases. The older granites (1770 ± 2 Ma) are made up of pyroxene-amphibole ± fayalite ovoidal granite, followed by amphibole-biotite and biotite granites. These porphyritic granites contain coarse, medium and small ovoids or are ovoid-free. The younger phase (1747-1737 Ma) is a fluorite-topaz zinnwaldite albite granite. Stocks and dykes of biotite and biotite-amphibole granite- and syenite-porphyries were emplaced at the same time. The two felsic phases bracket the emplacement (1760 ± 2 Ma) of basic rocks (anorthosite and gabbro-norite).

Fo_{5-8} olivine was observed in granite and quartz-monzonite in contact with gabbro and anorthosite. Augite predominates on orthopyroxene, amphibole is ferrohastingsite, sometimes grünerite. Biotite of the annite-siderophyllite series is Fe-rich and Mg-poor. The abyssal counterparts of ovoidal rapakivi granites contain Mg-richer and alkali (especially Na)-depleted mafic minerals, while biotite is Ti-rich. The younger albite granite contain Li-bearing zinnwaldite.

Alkali feldspar is more sodic in the older rapakivi granite and more potassic in the younger granite. From older to younger granites, Be, Sr, Pb, Li contents decrease, while Rb, Cs abundances increase. In typical rapakivi granite, plagioclase is zoned with a An_{32-40} core and An_{15-27} rims. Ovoidal alkali feldspar megacrysts mantled by oligoclase rims is a very common texture.

Accessory minerals are typically prismatic dipyramidal zircon, fluorite, apatite, anatase, allanite and ilmenite. Topaz, cassiterite and columbite occur in the younger granite. Trace-element contents of zircon within typical ovoidal rapakivi granites are lower than within ovoid-free granites: 290 - 1700 ppm U, 200 - 1200 ppm Th, 1750 - 6000 ppm Y, 370 - 930 ppm Yb, respectively.

THE PETROLOGY AND GEOCHEMISTRY OF LAVAS FROM THE IBLEAN PLATEAU: IMPLICATIONS FOR THE SOURCES OF ALKALINE AND THOLEIITIC MAGMAS IN THE PLIO-PLEISTOCENE.

Esperanca S. (Dep. Earth Sci., Monash Univ., Australia), Ferrara G. (Ist. Geoch. Geocr. Isotopica, C.N.R. Pisa, Italia), Mazzuoli R. (Dip. Sci. Terra, Univ. Pisa, Italia), Trua T. (Dip. Sci. Terra, Univ. Pisa, Italia).

The volcanic products of Plio-Pleistocene age of the Iblean

plateau are characterized by magmas with alkaline and tholeiitic affinities. The alkaline trend is defined by foidites, basanites, and occasional evolved trachybasalts, whereas the tholeiite trend shows mainly basaltic and basaltic andesite compositions.

The most primitive (Mg# 67-69) alkaline magmas that do not show cumulate textures are characterized by a wide compositional range in K_2O (0.5-1.5wt%), TiO_2 (1.7-2.5wt%), and incompatible elements such as Rb (5-10 ppm) and Zr (150-250 ppm). The alkaline basalts and basanites with higher K_2O content have an incompatible trace element pattern that resemble that of OIB magmas. The tholeiites display relatively homogeneous compositions with low K_2O contents and incompatible trace element abundance patterns similar to MORB-type magmas.

Field evidence indicates a close spatial and temporal relationship between the eruption of the alkaline and tholeiitic magmas suggesting that the tectonic regime in eastern Sicily in the Plio-Pleistocene was permissive of a variety of magma types.

Preliminary Pb isotopic compositions were obtained for samples from two volcanic successions, the V.ne dell'Oddiero (a series of subaqueous pillow lavas and hyaloclastites interbedded with shallow marine limestones) and the thick subaereal lavas of the Risicone river. These data indicate the influence of multiple mantle sources in the generation of the Iblean magmas in the Plio-Pleistocene. They also suggest that both successions analysed sampled these sources.

The alkaline magmas reflect the interaction or mixing of two magma sources, one characterized by radiogenic $^{206}Pb/^{204}Pb$ isotopic compositions (19.4-20.0) that could represent the older continental lithosphere or a plume-type OIB component, and a second MORB-like component with less radiogenic Pb. In contrast, the tholeiitic magmas have sampled a third Pb source with a less radiogenic $^{206}Pb/^{204}Pb$ (<19.2) for a higher $^{207}Pb/^{204}Pb$ and $^{208}Pb/^{204}Pb$ that could represent recently reworked mafic crust/mantle.

The variability in Pb isotopic compositions of individual samples can be correlated with major and trace element chemistry. In general, alkaline rocks with more radiogenic Pb isotopic compositions have higher TiO_2, K_2O/TiO_2, Sr/Zr and lower Zr/Nb. Evolution in the alkaline trend is accompanied by small shifts towards less radiogenic $^{206}Pb/^{204}Pb$. These data further suggest that the tholeiites of the Risicone river succession may have interacted with alkalic magmas at depth, but have evolved by melting larger proportions of a source that appears to have an older component, possibly in a shallower magma chamber.

These trends in Pb isotopic composition show the susceptibility of this isotopic system to heterogeneity in the source of alkaline magmas. The variations observed indicate that, most likely, the alkalic magmas have had primarily independent ascent paths and have not resided for long periods of time in deep magma chambers.

CUMMINGTONITE: Mg-Fe ORDERING AND THERMODYNAMIC PROPERTIES

Evans B.W., Ghiorso M.S., Yang H. (*Dept. of Geological Sciences AJ-20, University of Washington, Seattle WA 98195*) and Hirschmann M. (*Division of Geological & Planetary Sciences, California Institute of Technology, Pasadena, CA 91125*)

The crystal structures of 24 heat-treated and 6 unheated natural ferromagnesian clinoamphiboles have been refined from single crystal X-ray intensity data. Site-preference for Fe^{2+} is in the order: M4>>M1=M3>M2. Fractionation is more pronounced in unheated samples than in samples equilibrated at high temperatures (600°-750°C). A weak preference of Fe^{2+} for M1 over M3 is found in the heat-treated material. Assuming that Ca is restricted to M4, and that Mn orders on M4 to a degree comparable to Fe^{2+}, our X-ray results are broadly consistent with the results of Mössbauer spectroscopy.

Variation in cell-volume with Fe/(Fe+Mg) is linear, and no dependence of volume on ordering state was detected. When corrected for impurities, extrapolated endmember molar volumes are 26.33 J/bar for magnesiocummingtonite and 27.84 J/bar for grunerite.

These results indicate that at minimum a 3-site model (M13, M2, M4) must be utilized to successfully reproduce the configurational entropy of cummingtonite solid solutions at metamorphic temperatures. We have derived a general 4-site formulation for the molar (vibrational) Gibbs free energy of ferromagnesian amphibole which is expressed in terms of site mole fractions and comprises macroscopic endmember properties and temperature independent cation-ordering exchange-energies, intra-site regular solution parameters, and "reciprocal" energy parameters accounting for the non-coplanarity of the vertices of composition-ordering space. When reduced to the 3-site model, we require, in addition to endmember properties, values for only 8 parameters, 7 of which can be derived by non-linear regression analysis of the ordering data. The last parameter requires phase equilibrium constraints involving cummingtonite and at least one other ferromagnesian mineral, and from the wealth of experimental data provided by Fonarev and coworkers (Fonarev, 1988) we choose the reversal brackets of the two-phase loop for orthopyroxene and cummingtonite (+quartz and H_2O) at 2940 and 4900 bars determined by Fonarev and Korolkov (1980). Endmember data for magnesiocummingtonite are obtained by minor adjustment of the enthalpy of anthophyllite as required by intercrystalline Fe-Mg partitioning data, and for grunerite from the experimental work of Lattard & Evans (1992). We retain consistency with the database of Berman (1988) throughout.

Predicted phase equilibrium curves based on our calibration of cummingtonite solution parameters are in excellent agreement with four additional independent sets of experiments by Fonarev and coworkers (Fonarev, 1988) on cummingtonite in equilibrium with magnetite, orthopyroxene, olivine, quartz, and H_2O. Where necessary, these calculations incorporate the solution properties of olivine and orthopyroxene derived by Sack & Ghiorso (1989). Excellent agreement is also obtained in a comparison of predicted macroscopic K_D for Fe^{2+}-Mg exchange between cummingtonite and olivine or orthopyroxene with compositions of natural parageneses extracted from the literature.

When plotted as functions of macroscopic X_{Fe} and temperature, G^{ex} and H^{mix} become progressively more asymmetric towards lower temperatures, with pronounced minima at X_{Fe}=2/7, which is the composition of the ordered compound with M4 filled by Fe and M1, M2, and M3 filled by Mg. Their temperature dependence arises from S^{config} which reflects the variation in degree of cation ordering as a function of temperature. At 600°-800°C both endmember components exhibit small positive departures from ideality, but at lower temperature there are positive and negative departures depending on composition.

The thermodynamic data can be used to constrain the P, T, fH_2O and fO_2 conditions accompanying the crystallization of cummingtonite from dacitic and rhyolitic magmas and the equilibration of cummingtonite in a variety of metamorphic rock-types.

References:
Berman, R.G. (1988). *J. Petrol.*, **29**, 445-522.
Fonarev, V.I. (1988). Mineral equilibria in Precambrian iron formations (in Russian). Moscow, 294p.
Fonarev, V.I. & Korolkov, G.J. (1980). *Contrib. Mineral. Petrol.*, **73**, 413-420.
Lattard, D. & Evans, B.W. (1992). *Eur. J. Mineral.*, **4**, 219-238.
Sack, R.O. & Ghiorso, M.S. (1989). *Contrib. Mineral. Petrol.*, 102, 41-68.

MATERIALS AND FEATURES OF FLAT TERRACOTTA ROOFING TILES FROM CARNIA (NE ITALY)

Fabbri B. and Dondi M.
(*CNR-IRTEC, Faenza, Italy*)

The flat terracotta roofing tile from Carnia (NE Italy) represents a very typical roofing article in the Italian scene (Puntin, 1981). Really its use is connected with the traditions of some areas in central Europe, Austria and south Germany in particular.

This product was largely diffused in western Carnia up to the middle of the 20th century, and the existence of different production units in the area up to that moment is well documented.

The tiles often show a partial coloured coating, mainly green, but also red and white elements are frequent, while blue ones are

very rare. In most cases, the coloured tiles do not constitute the entire roofing, but they serve to compose ornamental motifs or inscriptions or symbols.

Coloured and not coloured tiles were studied from a technological point of view, in order to recover this cultural heritage and possibly stimulate the renewal of an artisan production activity. To this purpose, the chemical and mineralogical compositions of both bodies and coatings were determined by XRF and XRD respectively.

The white coating resulted to be constituted by a layer of lead-containing transparent glass (50 to 100 μm thick) applied on an engobe layer the thickness of which varies from 150 to 300 μm. The green coating was different due to the presence of copper in the transparent glass and to the reduced thickness (50 to 100 μm) of the engobe layer. Red tiles did not show any engobe and the transparent glass contained iron.

Body composition resulted quite variable, but it always dealt with calcium-containing materials (about from 2 to 10 % CaO). The variations in composition were not referable to the type of roofing tile (coloured or not, white or red or green) but to the provenance of the artifacts. It was clear, indeed, that local raw materials had been used, which had been extracted from very small deposits. Really, no large clay formations exist in the territory.

All the tiles were characterized by a homogeneous firing degree and a maximum firing temperature from 900°C to 1000°C could be deduced. Their optimum state of conservation certainly is a consequence of the good firing level and the suitable microstructure of the product.

Puntin, E. (1981). In: *DARTE*, L.Ciceri ed., Società Filologica Friulana, Udine, 253-270.

THERMODYNAMIC MODELING OF THE PHASE RELATIONS IN THE $MgO-FeO-Al_2O_3-SiO_2$ SYSTEM AT PRESSURE AND TEMPERATURE OF MANTLE.

Fabrichnaya O.B. (*Inst. of Earth Sciences, Uppsala University; Vernadsky Inst. of Geochem. & Analyt. Chem., Moscow*)

The phase relations in the system $MgO-FeO-SiO_2$ are important for understanding the mineral composition of Earth's mantle. Based on the available experimental data in the $MgO-FeO-SiO_2$ system, I have evaluated the mixing properties of the solid solutions and enthalpies of fictive phases in the $FeO-SiO_2$ system. I have used the thermodynamic properties of the pure phases from (Saxena *et al.*, 1993) and the assessment was performed using the THERMOCALC program (Sundman *et al.*, 1985). The solid solutions were described using asymmetric regular model in a Redlich-Kister form: $G^{ex} = x_1x_2[A_0+A_1(x_1-x_2)]$, where x_1 is Fe/(Fe+Mg), x_2 - Mg/(Fe+Mg) in phases. The entropies, temperature dependence of C_p and equation of state parameters for fictive end-members were estimated using data on structural analogues.The phase diagrams of the compositions $Mg_2SiO_4-Fe_2SiO_4$ and $MgSiO_3-FeSiO_3$ calculated at temperatures 1273-2073 K and pressures up to 30 GPa using our data base are in a good agreement with available experimental determinations. The assessed data were used to calculate phase diagrams of the $Mg_4Si_4O_{12}-Mg_3Al_2Si_3O_{12}$ (En-Py) and $Fe_4Si_4O_{12}-Fe_3Al_2Si_3O_{12}$ (Fs-Alm) systems at 1273 K and pressures up to 20 GPa. The model of complete disorder on two octahedral positions was used to describe the solid solutions of garnet majorite $a_{Py}=X_{Py}^2$. The calculated phase diagrams are in a good agreement with experiments (Akaogi & Akimoto, 1977). The value of maximal solubility of $Mg_4Si_4O_{12}$ in garnet was obtained 43 mol.% being in a better agreement with (Akaogi & Akimoto, 1977) than with (Kanzaki, 1987). However, the calculated phase diagrams of En-Py and Fs-Alm joins are within experimental uncertainty, that confirms the reliability of our database.

References:
Akaogi, M. & Akimoto, S., (1977). *Phys. Earth Planet. Inter.*, 15, 90-106.
Kanzaki, M. (1987). Phys. Earth Planet. Inter., 49, 168-175.
Saxena, S. K., Chatterjee, N., Fei, Y., Shen, G., (1993). Thermodynamic data on oxides and silicates. Springer Verlag, New-York.
Sundman, B., Jansson, B., Anderson, J.-O. (1985). *Calphad*, 9, 153-190.

THE GOLD CONCENTRATION IN IRON SULFIDES (THE EXPERIMENTAL INVESTIGATION)

Fadeev V.V., Koserenko S.V., Kalinichenko A.M. *(Vernadsky Inst. of Geochem. and Analyt. Chem.)*

Natural objects of very different genesis are characterized by abnormally high concentrations of gold in the iron sulfides. The role of sulfides as the natural concentrators of gold is well–known. However, the mechanism of its accumulation is incomprehensible. The general task of our investigations is to clarify the mechanisms of gold concentrating.

Two general ways of gold–bearing sulfides formation in the hydrothermal processes may be proposed. The first one is primary formation of a mineral–concentrator on which gold concentrates later. Another one is the simultaneous coprecipitation of macro– and micro–components. The influence of surface sorption plays a very important role in both the processes for concentrating mixtures.

The starting point of our investigations was the study of the solid phase by methods of X–ray phase analysis, chemical phase analysis, Mössbauer spectroscopy, PMR, NAA, EPR. By means of laboratory modelling, the formation conditions of the iron sulfides were clarified. The transition ways from one sulfide type into another were detected. The pyrite is the main concentrator of gold in nature. That is why the model of the pyrite formation from hydrotroilite in "aging" processes was studied in more detail. We had revealed three stages of the pyrite formation: the forming of the hydrated hydrotroilite, its dehydration and transition to pyrite. Three types of precipitates have been isolated and their ability to sorb gold was considered in two–phase systems. To detect quantitatively gold the method of sorption radioactive indicator (^{195}Au) has been applied. The gold was sorbed in all the phases. Temperature ranges and microcomponent concentrations in experiments which corresponded to the natural hydrothermal processes were T = 25–200 °C, C_{Au} = 10^{-12}–10^{-3} g/ml, pH = 3–12.5. The temperature range 100–200 °C was used only for pyrite because the other phases are not stable under heating. The following kinetic of sorption and sorption quantitative data were obtained:

– The obtained isotherms of gold adsorption are described by the Langmuir equation. The equilibrium gold concentrations of solutions decrease for the field of the saturation in the hydrotroilite–pyrite series. This shows the decrease of the sorption ability of the precipitates relatively to precipitate mass under aging.

– The sorption ability of the pyrite does not change essentially in the temperature range 25–200 °C. The value of the saturation increases a little with temperature increase.

– The sorption of gold decreases 5–10 times with transition in the alkaline pH range in all precipitates.

A number of gold–bearing sulfides were studied by PMR technique. The presence of hydrogen–containing groups (OH^-, HS^- or HS_2^-) was established and the correlation between contents of gold and hydrogen–containing groups was discovered. The experimental data we have obtained permit us to suggest the sorption mechanism of gold–sulfide coprecipitation as a result of the formation of unstable chemical compounds of gold–sulfide type on the surface and in the volume of the sulfides. The aging of these compounds leads to formation of the stable sulfides and disseminated form of gold.

ANOMALOUS Nb-Ta DISTRIBUTION IN THE ANIMIKIE RED ACE PEGMATITE, FLORENCE COUNTY, WISCONSIN, USA

Falster, A. U., Wm. B. Simmons, and K. L. Webber *(Department of Geology and Geophysics, University of New Orleans)*

The Animikie Red Ace pegmatite in Florence County,

Wisconsin, is a highly fractionated late Penokean pegmatite with a pronounced Li-Rb-Cs-Be-Mn-Ta-enrichment trend. It is a pegmatite of the rare-element subgroup of the orogenic class and belongs to the complex spodumene-lepidolite type of Cerny. The steeply dipping dike has a maximum exposed dimension of 600 x 3.5 meters and displays complex zonation. From the margin inward, the following zones can be distinguished: a) a rubellite-bearing wall zone with comb structure (WZ), b) a nearly tourmaline-free outer intermediate zone (OIZ), c) a tourmaline- and phosphate-bearing middle intermediate zone (MIZ), d) a microcline-rich inner intermediate zone (IIZ), e) a core margin with altered spodumene (CM), and f) a spodumene-quartz core (C). Besides these concentric zones, the following irregular zones and replacement bodies can be distinguished: g) a saccharoidal albite aplite which crosscuts other zones, h) albite replacement units, i) lepidolite replacement units, and j) keelward lepidolite pods.

Nb-Ta oxides exhibit two distinctly anomalous trends: 1). Columbite-tantalite occurs in all zones from the wall zone to the late - stage replacement bodies; and 2). Ta concentration of columbite-tantalite rims is bimodally distributed within the pegmatite with the highest concentration occurring in the wall zone and in the middle intermediate zone. Normally, the Ta/Ta+Nb ratio of columbite-tantalite is considered an indicator of fractionation within a pegmatite and increases in the most highly evolved interior replacement zones. Highest Ta/Ta+Nb ratios in the wall zone is the opposite of what is expected and indicates that the Animikie Red Ace pegmatite crystallized from a melt that was the product of a high degree of fractionation prior to its emplacement. This conclusion is substantiated by the following observations:

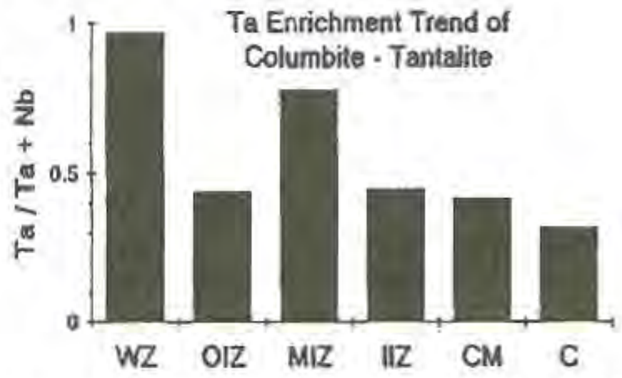

1). Existence of other rare, highly fractionated minerals such as tantite, wodginite, and rhodizite in the wall zone.
2). The occurrence of rubellite in the wall zone instead of the interior zones, which is unknown in other pegmatites.
3). Whole-rock Cs contents of pegmatite zones mimic Ta contents with maxima in the wall zone and the middle intermediate zone.

LANTHANIDE ORTHOPHOSPHATE SYNTHESIS

Falster, A. U., Wm. B. Simmons, and K. L. Webber (*Department of Geology and Geophysics, University of New Orleans*)

Rare-earth-element (REE) and yttrium (Y) orthophosphates have been synthesized in high purity and sufficient size to be suitable as standards for electron microprobe analyses. Crystals up to 5 mm were readily grown using a new technique which utilizes trisodium phosphate and sodium tungstate as a flux with the appropriate REE or Y oxide. Lanthanide oxides are mixed with the flux and fused at 1200 °C for four hours and then cooled at a rate of 20 °C per hour to 1000 °C, followed by slower cooling of about 5 °C per hour to a temperature of 600 °C and then a rapid cooling to room temperature within 12 hours. The resulting solid is dissolved in distilled water to recover the orthophosphate crystals. The light REE (La, Ce, Pr, Nd, Sm, Eu, and Gd) orthophosphates crystallize in the monazite structure, the heavy REE (Tb, Dy, Ho, Er, Tm, Yb, Lu, and Y) in the xenotime structure. Intermediate REE orthophosphates crystallize in both monazite- and xenotime-structure types in the same batch. This technique eliminates the problem of lead contamination associated with synthesis using lead pyrophosphate flux and has the added advantage of greater ease of crystal recovery since the flux is water soluble.

IN-SITU HIGH TEMPERATURE XAS STUDY OF Ti GLASSES AND MELTS.

Farges F. (*Lab. de Physique et Mécanique des Géomatériaux, Université Marne-la-Vallée, Noisy le Grand, France*), G.E. Brown Jr. (*Dept. of Geological and Environmental Sciences, Stanford University, Stanford and SSRL, USA*), Gan H., Navrotsky A. (*Princeton Univ., Princeton, USA*), P. Richet (*Dept. des Géomatériaux, Institut de Physique du Globe and CNRS, Paris*).

Lange and Navrotsky (1993) recently suggested that change in the Ti-coordination in some Ti-bearing super-cooled liquids may be a possible structural explanation for some unusual variations in the heat capacities (Cp) between T_g and T_l. In order to ascertain this hypothesis, we have undertaken an in-situ high temperature (300-1600 K) X-ray Absorption Fine Structure (XAFS) spectroscopy study of Ti-glasses and melts. Data was collected on wriggler beam line IV-1 (SPEAR storage ring working at 3 GeV and 100-40 mA; located at SSRL, California), using a Si-111 double-crystals monochromator and a fluorescence mode, running under a He_2 atmosphere. Glasses compositions where the heat capacities variations have been measured includes: (1) concentrated glasses like NTS2 (or $Na_2O.TiO_2.2SiO_2$; in mole%) and KTS2 ($K_2O.TiO_2.2SiO_2$), and (2) more Ti-diluted glasses: potassium trisilicate, potassium disilicate and potassium metasilicate with 8, 6 and 4 moles% TiO_2, resp. TiO_2. The other examined compositions were: ($0.05TiO_2$·$0.06K_2O$·$0.06CaO$ ·$0.08Al_2O_3$·$0.76SiO_2$) and ($0.05TiO_2$·$0.11CaO$·$0.08Al_2O_3$·$0.76SiO_2$).

XAFS spectra were recorded with 0.2 eV points in the Ti-K edge region in order to extract the normalized pre-peaks intensities and positions.The XAFS oscillations were fitted considering an temperature-induced anharmonicity in the Ti-O potential shape (see Farges, Fiquet, Andrault and Itié, this issue). Rutile ($^{[6]}TiO_2$) and the defective spinel $Ni_{2.7}{}^{[4]}Ti_{0.7}O_4$ were used as model compounds to extract anharmonic parameters with temperature. $^{[4]}$Ti-O anharmonicity was confirmed to be negligible, because of the most rigid character of this bond (1 valence unit; in contrast to $^{[5]}$Ti-O and $^{[6]}$Ti-O bonds). In fact, Ti-O anharmonicity behaves exactly as Ge-O (see Farges, Fiquet, Andrault and Itié, this issue) because of their identical bond strengths.

With increasing temperatures, all glasses-to-liquid transitions undergo nearly identical structural changes (ca., independant of the Ti-content). A slight increase in the Ti-K pre-edge intensity is observed for temperatures greater than T_g. Detailled interpretations of the normalized pre-edge intensities and anharmonic data reduction show no drastic changes around the Ti-coordination environment with increasing temperatures. They will be discussed in details. No evidences for Ti-nucleation were observed probably because of the low Me-O (Me=Na, K and Ca) bond strengths of the 2nd neighbors cations around Ti.

Lange, R.A., Navrotsky, A. (1993) *Geochim. and Cosmochim. Acta*, **57**, 3001-3011.

HIGH TEMPERATURE NMR STUDIES OF MOLTEN OXIDES.

Farnan, I., Trumeau, D., Florian, P., Massiot, D. and Coutures, J-P. (Centre de Recherches sur la Physique des Hautes Températures. CNRS 45071 Orléans, France)

The ability to carry out NMR experiments at temperatures where most refractory oxides are molten is providing new insights into the behaviour of these materials in the liquid state. Structural information is obtained by the interpretation of the NMR chemical shift. Empirical relationships between cation coordination and chemical shift have mainly been established at room temperature and these have been used to interpret data obtained at temperatures more than 2000°C higher. It is important in this work to verify that the high temperature shifts obtained in the NMR spectrum are the result of structural changes occurring in the liquid due to changes in temperature or composition.

Investigation of the influence of other effects that can result in shifts in the NMR resonance is of great importance. The first step in investigating this is to observe more than one nucleus in the liquid by NMR. The observation of different shifts for different nuclei indicates that changes in the bulk magnetic susceptibility of the sample with temperature are not dominating the shifts obtained. Also important are the possible influences of unpaired electrons, we have documented important changes in the shift behaviour of aluminate liquids at very high temperature that demonstrate the reduction of aluminium and the presence of a highly temperature dependent paramagnetic shift. The aerodynamic levitation device used in our laboratory allows the temperature range of these liquids to be extended significantly (~200°C

of supercooling for Al_2O_3) due to the low rates of heteronuclear nucleation in containerless conditions. This is important because we need to understand changes in chemical shift over as large a range as possible since effects are often fairly small for aluminate liquids when compared with aluminium in silicate liquids, say. Our sparse knowledge of the 'intrinsic' effect of temperature on chemical shifts tells us that small paramagnetic shifts need to be interpreted with care. In order to investigate this more fully and constrain the microscopic behaviour of the liquid more thoroughly by its NMR response we are extending our range of experiments to low frequency nuclei such as ^{89}Y and ^{25}Mg.

IRON-BEARING MINERALS IN THE LOWER MANTLE AND CORE

Fei Y. (*Geophysical Laboratory and Center for High Pressure Research, Carnegie Institution of Washington*)

With recent development of high-pressure and high-temperature techniques (the multi-anvil apparatus and high-temperature diamond-anvil cell), the physical conditions (pressure and temperature) of the Earth's lower mantle and core can be simulated in laboratory. We have studied a variety of iron-bearing materials related to the lower mantle and the core including $(Mg,Fe)SiO_3$-perovskite, $(Mg,Fe)O$-magnesiowüstite, and phases in the systems Fe-O and Fe-S at high pressure and high temperature. The oxidation state and location of iron in $(Mg,Fe)SiO_3$-perovskite have been studied with ^{57}Fe Mössbauer spectroscopic techniques over the temperature range 30 - 450 K. The maximum solubility of iron in $(Mg,Fe)SiO_3$-perovskite as a function of temperature at lower mantle pressure was determined by Mössbauer spectroscopy, x-ray diffraction, and electron microprobe analyses. The role of ferric iron (Fe^{3+}) in the lower mantle will be discussed in conjunction with the new simultaneous high *P-T* experimental result on $FeFeO_3$ which confirms previous suggestion that the high *P-T* structure of $FeFeO_3$ is isostructural with $MgSiO_3$-perovskite.

FeO and FeS, important constituents of the Earth's core, have been studied under simultaneous high *P-T* conditions by using an externally double-heated diamond-anvil cell and synchrotron x-ray diffraction techniques. The structure of the high *P-T* metallic FeO has been determined by *in situ* x-ray diffraction measurements for the first time. The x-ray diffraction data of FeO at 96 GPa and 900 K are consistent with NiAs-type structure. The structure of FeS at simultaneous high *P-T* was also determined to be hexagonal with a (2a,c) cell. The phase diagrams of FeO and FeS were determined up to *P-T* of 100 GPa - 1100 K and 30 GPa - 900 K, respectively.

P-V-T EQUATIONS OF STATE OF MANTLE-RELATED MINERALS

Fei Y. (*Geophysical Laboratory and Center for High Pressure Research, Carnegie Institution of Washington*)

$(Mg,Fe)_2SiO_4$-wadsleyite, $(Mg,Fe)_2SiO_4$-spinel, $(Mg,Fe)SiO_3$-perovskite, and $(Mg,Fe)O$-magnesiowüstite are important constituents of the Earth's mantle. Experimental measurements of *P-V-T* properties of these phases are crucial for developing accurate mineralogical and compositional models of the Earth's interior. We have systematically measured *P-V-T* equations of state for $(Mg,Fe)_2SiO_4$-wadsleyite, $(Mg,Fe)_2SiO_4$-spinel, $(Mg,Fe)SiO_3$-perovskite, and $(Mg,Fe)O$-magnesiowüstite up to a pressure of 30 GPa and a temperature of 1100 K by using an externally heated high-temperature diamond-anvil cell and synchrotron x-ray diffraction techniques. The experiments were conducted under hydrostatic or quasi-hydrostatic conditions, using neon as a pressure transmitting medium. Pressures were determined by measuring the lattice parameter of internal standards such as Au and NaCl. The *P-V-T* equations of state of Au and NaCl have been critically examined based on directly measured compression isotherms at high temperatures (up to 1100 K). The experimental *P-V-T* data for the mantle-related phases were fitted to the Mie-Grüneisen thermal equation of state. A set of thermophysical parameters, including isothermal bulk modulus K_{T0}, temperature and pressure dependence of the bulk modulus, Debye temperature θ_D, Grüneisen parameter γ_0, and the volume dependence q, was determined for each individual phase. The consistency between the derived thermophysical data and the available thermodynamic data has been critically evaluated through thermodynamic relations.

MINERALOGICAL AND CHEMICAL COMPOSITION OF THE ORDOVICIAN IRONSTONES IN THE IBERIAN PENINSULA: PROVINCE OF ZAMORA.

Fernández A. and Moro M. C. (*Dpto.Geología, F. Ciencias, Univ. Salamanca. 37008 Salamanca*).

The Ordovician ironstones in the Iberian Peninsula are well represented, in the NW region, where the most important deposits are located such as Coto Wagner, Vivaldi and S. Bernardo in the province of León; those of Guadramil, Marao and Moncorvo in the NE of Portugal and those of the Alcañices Synform in the province of Zamora, studied from different points of view by Fernández (1994). All these mineralizations are located at the top of the Armorican Quartzite (Arenig) in layers of different thicknesses, interstratified within the sandy and pellitic metasediments of the top of this formation. All of them seem to be related to the first of the three great transgressive phases that occurred during the Ordovician that gave rise to an important development of the ironstones on the margins of Gondwana (Young, 1989).

The mineralizations studied in the province of Zamora are arranged in several levels ranging between 0.2 and 2 m in thickness at the top of the upper member of the Pielgo Quartzite formation (Arenig). Mineralogically, they are formed of magnetite, hematites, chamosite, biotite, quartz and apatite, as essential minerals, and zircon, tourmaline, graphite, rutile, ilmenite, muscovite and/or illite as accessory minerals. Occasionally, antophilite and garnets appear as essential minerals.

The chemical composition of these minerals has been determined with a Camebax SX50 electronic microprobe (M.E). They are anomalous contents in Cr, V, Ba and Ni. Additionally, in the magnetite, which is the predominant oxide, trace elements, rare earths and oxygen isotopes have been analyzed chemically in a number of representative samples.

Regarding the analytical results obtained, the Co/Ni < 1 ratio of this oxide suggest the sedimentary origin of the magnetite. The content and distribution of the elements of the rare earths group (REE) are similar and all of them show a clear negative anomaly in Eu and also a slight positive anomaly in Ce, in this case indicating the diagenetic or metamorphic formation of this mineral (Fryer, 1977). The $\delta^{18}O$ values obtained for the magnetites (+2.6‰ to +8.7‰) suggest that a zoning probably exists in these mineralizations with respect to the temperature of the low-grade metamorphism affecting them or with respect to differences in the depth of the sedimentation basin. In any case, these values lie within the established range for metamorphic waters.

The chemical-structural characterization of the chamosite ($Si_{2.94}$ $Al_{1.062}$) ($Al_{1.554}$ $Fe_{3.302}$ $Mg_{0.855}$ $Mn_{0.043}$ $\#_{0.246}$) has permitted the calculation of fO_2, fS_2 and the T of formation of these mineralizations, obtaining values ranging between -38.8 and -30.7 for log fO2 and between -13.3 and -9.5 for log fS_2 and T of 200ºC and 330ºC, respectively (Walshe, 1986). These T more or less correspond to those of the metamorphism, although they are slightly lower. In the stability diagram of Gole (1980) these conditions of fO_2 and fS_2 suggest that the magnetite is stable close to the hematite-magnetite limit, which in the Log fO_2 -T diagram is defined by the MH buffer (6 Fe_2O_3 = 4 Fe_3O_4+O_2).

Acknowledgments

This work has been carried out within the D.G.I.C.Y.T.(M.E.C. España) and Castilla-León Autonomy Community (Projects: PB-91-0563 y SA-15/09/92).

References:
Fernández, A. (1994). *Tesis Doctoral* Univ.Salamanca, (in prep.).
Fryer, B. J. (1977). *Geochim. Cosmochim. Acta*, 41, 361-367.
Gole, M. J. (1980). *Amer. Miner.*, 65, 8-25.
Walshe, J. L. (1986). Econ. Geol., 81-6, 681- 703.
Young, T. P. (1989). In: Young, T.P. y Taylor, W. E. G.(Eds.), Phanerozoic ironstones, *Geol. Soc. Lond. Spec. Publ.*, 46, iv-xxv.

The salinity differences largely reflect differences in the NaCl content of the fluid.

The suggested model is one of calcite-quartz reaction in a open system, in the presence of an aqueous fluid with contrasting salinities. This prevented from a rise in the CO_2 content of the fluid. The compositional gradient of the fluid across the aureole probably resulted from the mixing of an aqueous high-salinity fluid, for which, in the absence of stable isotope evidence a magmatic derivation can not be excluded, and a "metamorphic" low-salinity one.

COMPLEX MULTIPHASE FLUID INCLUSIONS IN WOLLASTONITE FROM THE MERIDA (SPAIN) CONTACT METAMORPHIC DEPOSIT. EVIDENCE FOR FLUID MIXING.

Fernández-Caliani, J.C. *(Univ. of Huelva)*, Casquet, C. *(Univ. Complutense of Madrid)* and Galán, E. *(Univ. of Sevilla)*

The Mérida wollastonite deposit was formed within Lower Cambrian marbles as massive replacements of quartz-rich psammitic intercalations by calcite-quartz-fluid reaction triggered by the nearby emplacement of an Hercynian granitic pluton. The marble outcrop actually is a "screen" separating an earlier, roughly concordant, dioritic intrusion from the granitic pluton, which is discordant to the regional and local structures.

Fluid inclusions are very abundant in wollastonite as polyhedral prismatic primary inclusions, arranged parallel to the long axis of the host crystal. The size is very variable with the long dimension ranging from 5 μm to 100 μm. However most of the inclusions fall between 25 and 50 μm.

According to the phase contents at room temperature, two general types of primary inclusions are recognized: *type I*), liquid or gas-liquid low-salinity aqueous inclusions; and *type II*), multiphase gas-liquid-solids inclusions. The latter are the most abundant, and because of the peculiar filling and the significant variations shown by their microthermometric properties are of particular interest to understand the nature of the fluids involved in the formation of wollastonite.

Multiphase inclusions consist of a gas bubble, a liquid and several solid phases. The following have been identified by SEM-EDS analysis of open inclusions: wollastonite, calcite, apatite, quartz, halite and precipitates of Ca-Mg-Na-K chlorides. Up to six solid phases can be found in a single inclusion. In most cases however, wollastonite and calcite are the only solids present. Also, more than one crystal of the same phase can occasionally be found in a single inclusion. Most of the solids are considered to be daugther minerals precipited out from the fluid at different temperatures during cooling of the aureole. Halite has only been found in the proximity to the granite contact. The solids, except the chlorides, do not show appreciable changes on heating to ca. 500º C. On the average the solid assemblage accounts for about 15% of the total volume of the inclusion. The gas/liquid volume ratio is 5-20% as a general rule.

On fast cooling, complete freezing of the liquid takes place between -60º and -105º C to a pale brown speckled solid assemblage. No evidence of CO_2 or other unmiscible gases could be detected.

On heating, first melting (T_E) is detected at temperatures between -50º and -40º C. However close to the granite contact values of T_E as low as -70º C have also been found, coinciding with the presence of halite in the solid assemblage. In respect to the final melting temperature (T_M) of the frozen liquid, a clear distinction exists between close and far-to-the contact inclusions. In the latter case, final melting takes place by disappearance of the ice at temperatures in the range -3º to -20º C, with most of the values falling between -3º and -11º C. In the first case instead, values of T_M range from -11º C to -40º C. Halite disappearance in proximal inclusions takes place in the range 250º to 310º C in the presence of the gas bubble. Disappearance of the latter is observed between 220º and 300º C. Above 300º C many inclusions decrepitate.

All the data above suggest that the fluids involved in the formation of the Mérida wollastonite can be modelled in the system NaCl-$CaCl_2$-H_2O. Values of T_E under -52º C can be explained as metastable eutectic melting of Ca-hydrates in highly saline inclusions. The amount of CO_2 in the fluid had to be very small, and largely represented by its content in calcite. After recalculation the X_{CO_2} of the initial fluid had to be lower than 0,05. The fluid was probably saturated with wollastonite, calcite (and quartz) and begun to precipitate these phases in the inclusions inmediately after being trapped at temperatures well above 500º C. Salinities of the residual fluid are very variable, ranging from high salinity fluids (about 40 wt % NaCl equiv.), close to the granite contact, to low-salinity ones, far from it (about 5 wt % NaCl equiv.).

GEOCHEMISTRY OF PLAGIOCLASES FROM PAIMAN RANGE (NW ARGENTINA): PRELIMINARY RESULTS BY LAM-ICP-MS

Fernández-Turiel J.L., López-Soler A., Querol X., Saavedra J. *(CSIC Spain)* and Toselli A. *(Univ. Nac. Tucumán, Argentina)*

Laser ablation microprobe - inductively coupled plasma mass spectrometry (LAM-ICP-MS) has been used to determine the trace and major elements of plagioclases, directly on solid sample and without any previous sample preparation. The preliminary results obtained allow us to confirm the possibilities of LAM-ICP-MS on single point geochemical analysis of minerals. The study was focused in the geochemistry of plagioclases from the milonitic zones of Paimán Range (Famatina System, La Rioja Province, Argentina) in order to determine the chemical modifications introduced in these milonitic granites as consequence of the tectonic events.

The analytical method employed to study the centimetric plagioclase crystals is correct in terms of spatial resolution (the diameter of laser crater can be modified from 30 to 300 μm) and sensitivity, with detection limits at sub-ppm level (the REEs are determined easily).

The analyses were performed with a FISONS PlasmaQuad PQ 2+ spectrometer, equipped with a laser ablation microprobe FISONS LaserLab in the ICP-MS Laboratory of the Institute of Earth Sciences "J. Almera" of the CSIC (Spain). The operative conditions for the ICP-MS were: RF power, 1350 kW; plasma argon flow rate, 14.0 L min^{-1}; auxiliar flow rate, 1.0 L min^{-1}; carrier gas flow rate, 1.20 L min^{-1}. The ablation was performed on Q-switch mode with a Nd:YAG laser, working at 1064 nm and 850 V.

The tuning was stablished using the ^{139}La isotope (silicate glass SRM 612). The major elements (Si, Al, Na, K and Ca) were determined in *peak jump* mode, and the trace elements (Rb, Sr, Ba, REE, etc., until forty different elements) in *scanning* (DUAL) mode. The calibration strategy was based in the use of the isotope ^{48}Ca as internal standard and in the stechiometry of major elements. This method allow us to reduce drastically the bias introduced by the volume differences of the ablations.

We have observed a similar distribution, as consequence of their petrogenetic behaviour, among: a) Rb, Ge, Y and REEs; b) Sr, Ba and W; c) Pb, Zn, Ga and B; d) Li, Cs and Tl; and e) In y Cd. The REE present variations in total contents from point to point analyzed, nevertheless, in a single megacrystal show a similar trend respect the chondritic composition, reflecting clearly the Eu possitive anomaly.

In conclusion, the preliminary results demonstrate the effectiveness of the LAM-ICP-MS for the rapid analyses of trace and major elements in feldspars, opening new and original perspectives in the study of these minerals (e.g., Jenner et al, 1994).

References:

Jenner, G.A., Foley, S.F., Jackson, S.E., Green, T.H., Fryer, B.J., and

Longerich H.P. (1994). *Geochem. Cosmochem. Acta*, 58: 5099-5103.
López, J.P. and Toselli, A.J. (1993). *XII Congreso Geológico Argentino*, Actas, III: 39-42. Mendoza.

THE LEAD ISOTOPE COMPOSITION OF THE SUBLIMATES FROM THE FUMAROLES OF VULCANO (AEOLIAN ISLANDS, ITALY): INFERENCES ON THE DEEP FLUID CIRCULATION

Ferrara G. *(IGGI, C.N.R., Pisa)*, Garavelli A. *(Dept. Geomin., Univ. of Bari)*, Pinarelli L.*(IGGI, C.N.R., Pisa)* & Vurro F. *(Dept. Geomin., Univ. of Bari)*

The fumarolic fluids of Vulcano (Aeolian Islands, Italy) consist of a mixture of both deep and shallow components. The final products, the fumarolic gasses and the sublimates associated with them, provide information on the complex interactions that occur at depth. Since radiogenic isotopes do not undergo fractionation after they are incorporated in a fumarolic gas, they can be used directly to characterize the components that mixed. Lead isotopes are particularly suitable, because sea water, which plays an important role in the formation of the fumarolic fluids of Vulcano, contains only negligible amounts of Pb (about 10^{-12} g/g). Therefore, the lead present in the fumarolic gasses (and sublimates) is derived from the magmatic component and the water that interacted with the host-rocks.

The lead isotope compositions of the lead sulfosalt sublimates collected from the Fossa Crater of Vulcano in 1924, and between 1989 and 1993, are given here. The lead isotope ratios of most of the samples are the same within the range of analytical error, regardless of their collection date. The only samples that display slight variations are those collected in 1993.

On the whole, the compositional range of the lead isotopes of the sublimates overlaps that of the latitic-rhyolitic activity of Fossa, and differs substantially from that of the pre-Fossa trachybasaltic activity. Also, the Pb isotope composition of the sublimates is quite different from that of the Calabrian basement rocks.

The data presented here show that the magma presently degassing at Vulcano has the same lead isotopic composition as the products of the recent activity of Fossa, while the fumarolic fluid circulation of Vulcano has not involved the basement rocks that host the magma chamber.

THE NEW TITANOSILICATE NAFERTISITE AS MEMBER OF A POLYSOMATIC SERIES WHICH INCLUDES MICA

Ferraris G.[1], Khomyakov A.P.[2], Soboleva S.V.[3], Belluso E.[1], Ivaldi G.[1] and Pavese A.[4]
[1]*Dip. Sci. Miner. Petrol., Univ. Torino* - [2]*IMGRE, Moscow* - [3]*IGEM, Moscow* - [4]*Dip. Sci. Terra, Univ. Milano*

Nafertisite is a new mineral from Khibina massif (Russia) with chemical composition $Na_3Fe^{3+}{}_5Fe^{2+}[Ti_2Si_{12}O_{34}]O(OH)_6 \cdot 2H_2O$; it is monoclinic P2/c or $P2_1/c$ with a = 5.353(4), b = 16.176(12), c = 21.95(2)Å, β = 94.6(2), Z = 2.

Only crystals showing some disorder have been found. By comparison with bafertisite and astrophyllite, a model of the structure has been deduced which is able to account for chemistry, morphology, cleavage and X-ray diffraction intensities. Mica-like TOT layers are present where the *O* sheet is only partially occupied by Fe octahedra. Actually, the *T* sheets are hybrids where, through the insertion of Ti-octahedra, the silicate net is split into strips consisting of a new type of branched amphibole double chains. The corresponding strips consist of disilicate groups in bafertisite and branched pyroxene chains in astrophyllite. Alkali atoms are located in the inter-layer space, as in mica . Two-layer P2/c and $P2_1/c$ structural models were tested. They differ only for the relative position of *T* and *O* sheets and produce close sets of calculated diffraction intensities; the overall agreement is slightly in favour of the P2/c model.

In a polysomatic series BM_n, with $M = Na(M^{2+})_3[Si_4O_{10}]O(OH)$ (mica module) and $B = Na_2(M^{2+})_4[Ti_2Si_4O_{14}]O(OH)_4$ (bafertisite module), bafertisite, astrophyllite and nafertisite ideally are the members with n = 0, 1 and 2, in the order. Taking into account real compositions (i.e. minerals belonging to bafertisite and astrophyllite groups), the following general formula is obtained for the polysomatic series: $[A,\square]_{2+n}[M,\square]_{4+3n}[X_2T_{4+4n}O_{14+10n}](OH,O)_{5+2n}$, with A = Na, K, Ba, ... ; M = Fe^{2+}, Fe^{3+}, Mg, Mn, Ca, ...; □ = vacancy; X = Ti, Sr, Nb, Al, ...; T = Si, Fe^{3+}, Al, ... The total number of oxygens is 19 + 12n; some of them correspond to OH (p) or H_2O (q) groups, the values of *p* and *q* depending on the number of cationic charges.

The described polysomatic series is built up by a mechanism similar to that known for biopyriboles and the two series share the *M* module. According to Egorov-Tismenko & Sokolova (1990), bafertisite is also a member of the polysomatic series seidoserite-nafakite which includes a large number of titanosilicates, all containing the bafertisite TOT layer. Ideally, members of the BM_n series are based on *P* lattice when *n* is odd and on *C* lattice when *n* is even (*b* axis doubled). Whereas the dimensions of the building modules are similar in directions [100] (5.4 Å) and [001] (11.0 Å), they differ along [010]: 6.8 and 5.0 Å for *B* and *M*, in the order. If *m* is the number of layers along [001], ideally BM_n polysomes have $a_n \approx$ 5.4 Å, $b_n \approx$ (6.8 + n5.0)Å (x2 when *n* odd) and $c_n \approx$ m11.0 Å.

As in phyllosilicates, polytypes differing for stacking and/or number of layers along [001] are possible. Besides, within the ideal TOT layer the two *T* sheets can be connected by 2 or 2_1 axis. Presumably, both types of layers are disorderly present in nafertisite crystals; they occur as individual phases in astrophyllite.

References:
Egorov-Tismenko, Yu. K., Sokolova, E. V. (1990). *Mineral. Zh.* **12**, 40-49.

TUNGUSITE: NEW DATA, RELATIONSHIP WITH GYROLITE AND STRUCTURAL MODEL

Ferraris G.[1], Pavese A.[2] and Soboleva S.V.[3]
[1]*Dip. Sci. Miner. Petrol., Univ. Torino* - [2]*Dip. Sci. Terra, Univ. Milano* - [3]*IGEM, Moscow*

Tungusite is a fibrous hydrous silicate of Ca and Fe from cavities of spherulitic lava (Lower Tunguska river, East Siberia). It was firstly described by Kudriashova (1966).

New chemical analyses, electron and X-ray powder diffraction data, and comparison with gyrolite and reyerite show that the ideal formula of tungusite is:

$$[Ca_{14}(OH)_8](Si_8O_{20})(Si_8O_{20})_2[Fe_9(OH)_{14}].$$

Two formula units are within a triclinic cell with a = 9.715(9), b = 9.719(8), c = 22.08(4) Å, α = 90.1(1), β = 98.4(2), γ = 120.0(1)°.

A structural model for tungusite is derived by splitting the double tetrahedral layer of reyerite (Merlino, 1988) and inserting a trioctahedral sheet *X*, wich at maximum contains 9 cations.

A substitutional solid solution represented by the formula

$$[Ca_{14}(OH)_8](Si_{24-y}Al_yO_{60})[Na_xM_{9-(x+z)}\square_z(OH)_{14-(x+y+2z)} \cdot (x+y+2z)H_2O]$$

exists between tungusite (M = Fe^{2+}, x = y = z = 0; green color) and gyrolite (M = Ca, x = 1, y = 1, z = 6; white color).

Polytypes due to different relative positions between the tetrahedral and the octahedral *X* sheets are possible and shall be discussed.

References:
Kudriashova, V.I. (1966). *Dokl. Akad. Nauk SSSR*, **171**, 1167-1170.
Merlino, S. (1988). *Min. Mag.*, **52**, 247-256.

REACTION MECHANISMS AND TEXTURES OBSERVED BY TEM DURING THE HYDRATION OF BIOTITE TO CHLORITE: A CASE STUDY FROM THE KLODZKO-ZLOTY STOK AREA, S.W. POLAND.

Ferrow E.A. (*Dept. of Min. & Petrology, Lund University*)

The alteration of biotite to chlorite is a common reaction during the retrograde metamorphism of amphibolite rocks to greenschist rocks. The reaction textures produced, the compositions and fugacities of the fluids present, and the amount of mass transferred depend on the reaction mechanisms adopted.

Veblen and Ferry (Veblen & Ferry, 1983) proposed two independent reaction mechanisms. In the 1:1 reaction mechanism, one biotite is altered to one chlorite by replacing the interlayer K cations by a brucite-like layer. For the rocks studied here, the 1:1 mechanism gives:

$$1Bio + 1.78Mg^{2+} + 2.53Fe^{2+} + 1.38Al^{3+} + 0.56H_4SiO_4 + 4.88H_2O + 2.44O_2 \Rightarrow 1Chl + 1.53K^{+} + 0.20Na^{+} + 0.38Ti^{4+}$$

The hydration reaction results in an increase in volume and requires the addition of substantial octahedral cations. The presence of a brucite-like layer in biotite, first reported by Baños et al. (1983), was considered as an example of the 1:1 mechanism. Later, Ferrow and Ripa (1991) published a micrograph showing the insertion of brucite-like layer in biotite by such reaction mechanism.

In the 2:1 reaction mechanism two biotites are altered to one chlorite by a brucite-like layer replacing the talc-like layer in biotite. For the case study, the 2:1 mechanism gives:

$$2.00Bio + 8.46H_2O + 0.21Fe^{2+} \Rightarrow 1.00Chl + 1.00Mg^{2+} + 0.76Ti^{4+} + 1.44Al^{3+} + 4.92H_4SiO_4 + 5.77O_2 + 3.09K^{+}$$

The reaction results in a decrease in volume and releases considerable Al^{3+} and Si^{4+} to the fluid. Veblen and Ferry (1983) reported the termination of a mica layer into a chlorite layer and correctly suggested that the brucite-like layer was inserted by the 2:1 reaction mechanism. However, it is only recently that Baginski and Ferrow (1994) showed a very nice example of this reaction mechanism and the corresponding volume decrease.

Yau et al. (1984) observed the transformation of 14 phlogopite layers to 10 chlorite layers with no volume decrease. Based on this observation, they suggested a third reaction mechanism, 3:2, where the 1:1 and 2:1 reaction mechanisms alternate. For a constant volume change, the 3:2 mechanism gives:

$$1.50Bio + 0.57Ca^{2+} + 0.39Mg^{2+} + 1.37Fe^{2+} + 5.50H_2O + 1.61O_2 \Rightarrow 1.00Chl + 2.31K^{+} + 0.38Ti^{4+} + 0.30Na^{+} + 1.80H_4SiO_4$$

While the first two mechanisms require or release Al during hydration, the third mechanism conserves Al. Moreover, the Ti released to the fluid crystallizes as sphene in the immediate grain boundaries and along the basal planes of the biotite-chlorite intergrowths. The observation that both the 1:1 and the 2:1 reaction mechanisms prevail agrees very well we the finding of Ferrow and Ripa (1991). However, the 3:2 reaction mechanism has not been imaged by TEM yet. Nevertheless, I report evidence for a new 3:2 type reaction mechanism where brucite-like layers are inserted in pairs by simultaneous addition of the 1:1 and 2:1 reaction mechanisms (Fig. 1).

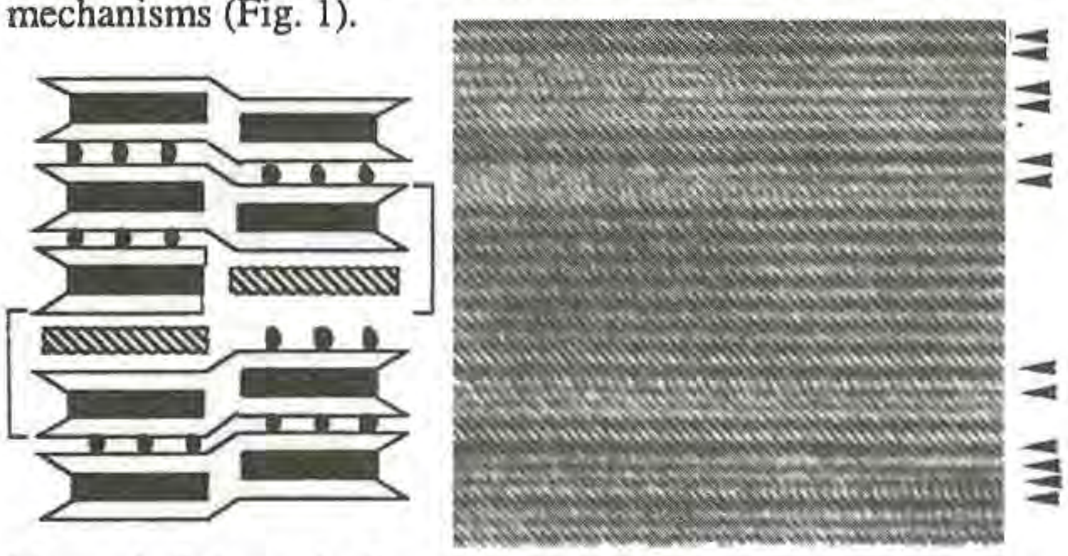

Figure 1. Schematic diagram of a 3:2 type reaction mechanism and the experimental HRTEM image showing pairs of brucite-like layers (arrows) within biotite. Two chlorite-like structures are indicated.

References:
Baginski, B. & Ferrow, E.A. (1994). *Terra abstract*, **5**, 398.
Ferrow, E.A. & Ripa, M. (1991). *Lithos*, **26**, 271-285.
Olives Banos, J., Amouric, M., De Fouquet, C., Baronnet, A. (1983). *Am. Mineral.*, **68**, 754-758.
Veblen, D.R. & Ferry, J.M. (1983). *Am. Mineral.*, **68**, 1160-1168.
Yau, Y.C., Lawrence, A.M., Essene, E.J., Peacor, D.R. (1984). *Contrib. Mineral. Petrol.*, **88**, 299-306.

CORRECTING CRYSTAL TILT IN HRTEM IMAGES: THE CASE OF ORTHOPYROXENE

Ferrow E.A. (Dept. of Min. & Petrology, Lund University); Zou X.D. and Hovmöller S. (Dept. of Structural Chemistry, Stockholm University)

Experimental HRTEM images of minerals are sensitive to specimen thickness, crystal tilt, defocus, and beam tilt. The conventional approach in interpreting experimental TEM images is based on visual comparison with images simulated over a range of specimen thickness and defocus values. If the crystal is tilted, which is very common for minerals, then tilt axis and tilt angle need to be included. Simulating HRTEM images with so many unknown parameters demands a very heavy computer calculation. Furthermore, the solution obtained is not unique. If the crystal tilt can be determined and removed from the experimental images using other independent techniques, much less calculations are needed to find the suitable thickness and defocus for simulating images to fit the experimental image.

Recently, Hovmöller et al. (1994) reported that, using the crystallographic image processing (CIP) program system CRISP (Hovmöller, 1992), crystal tilt can be determined and corrected directly from experimental HRTEM images. This is done in three steps. Firstly, a Fourier transform of the HRTEM image is calculated and the crystal symmetry is determined from the phases and the amplitudes of the diffraction spots. Secondly, the position of the tilt axis and the magnitude of the tilt are determined from the deviation of the amplitudes and phases. Finally, symmetry constraints are imposed on the phases and amplitudes and a tilt-free image is retrieved by calculating the inverse Fourier transform.

In order to investigate the potential of CRISP for correcting crystal tilt in HRTEM images of minerals, orthopyroxene was taken as an example. Livi & Veblen (1989) have shown that experimental HRTEM images of orthopyroxene exhibit an asymmetry in the sizes and intensities of the light features corresponding to the alternating tetrahedral chains. Moreover, they found that the asymmetry was due to crystal tilt and beam misalignment. In order to interpret these experimental images they simulated a series of images for different tilt angles wiht fixed specimen thickness and defocus. The image which gave the best fit to the experimental image was used to estimate the amount of the tilt.

In this study images were calculated for a series of crystal tilts and thicknesses, under the Scherzer defocus condition. The tilt axis was estimated and the undistorted image was reconstructed using CRISP. Figure 1a is an example of an image tilted by 0.70 degrees; and Figure 1b is the same image after the tilt has been corrected. An untilted image and its kinematic projection are also included (Figs. 1c & 1d). The tilt correction gives a remarkable improvement in presenting the structure features of orthopyroxene. It is worth

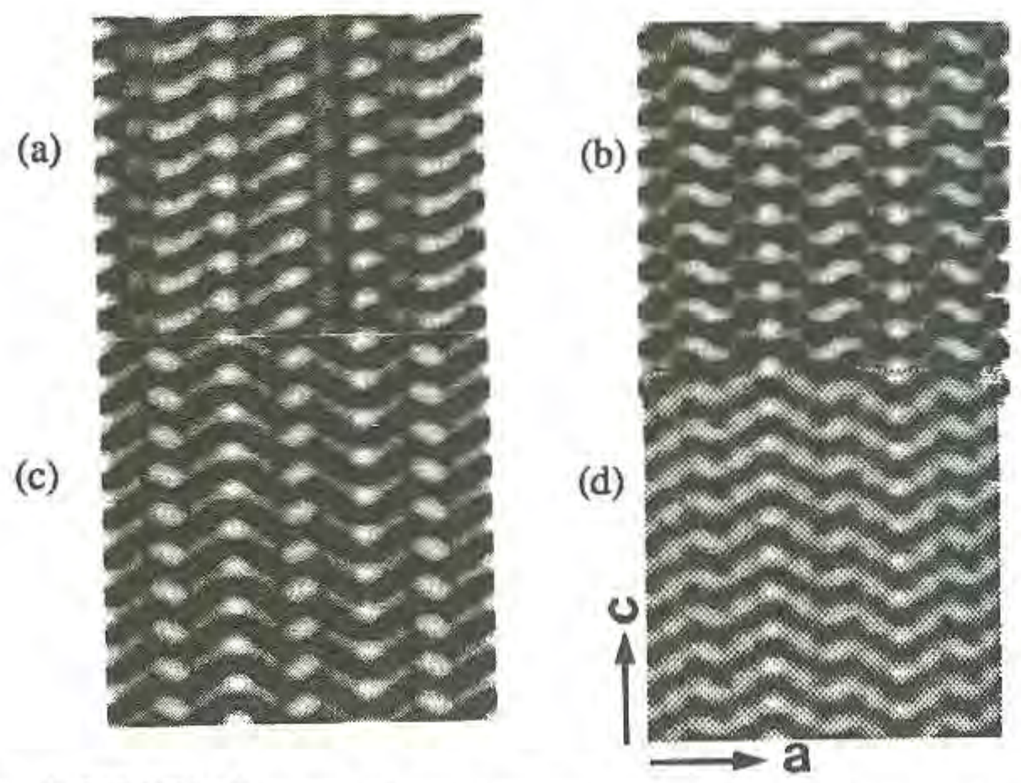

Fig. 1. HRTEM images of orthopyroxene projected along the b-axis.

mentioning that although the crystal is 159 Å thick, it is still possible to retrieve structure projections by CIP. However, we also found that, depending on the crystal thickness, there is a limit to the amount of tilt that can be corrected using CIP. Nevertheless, the result shows that it is possible to determine and correct for crystal tilt directly from experimental images by CIP. Once the effect of crystal tilt is removed from the micrograph, it is then easy to estimate the specimen thickness and defocus by image simulation.

References:
Hovmöller, S. (1992). *Ultramicrosc.*, **41** (123), 121-136.
Hovmöller, S., Larine, M., Zou, X. (1994). In ICEM13. Paris.
Livi, K.J.T. & Veblen, D.R. (1989). *Am. Mineral.* 74, 1070-1083.

• CRYSTAL CHEMISTRY AND MINERALOGY OF THE VOLCANIC EXHALATION PRODUCTS OF THE LARGE TOLBACHIK FISSURE ERUPTION (KAMCHATKA, RUSSIA)

Filatov S.K and Semenova T.F. (*Dept. of Crystallography, St. Petersburg Univ.*), Vergasova L.P. (*Inst. of Volcanology, Rus. Ac. Sci.*)

In this paper the most complete list of minerals from the volcanic exhalations of the Tolbachik eruption is presented. Among the 100 minerals identified 44 are signaled for the first time in the volcanoes of Kurilo-Kamchatsky region and 13 are new minerals. The list has been prepared on the basis of the data collected during a 17-years survey of the exhalation products of the Large Tolbachik Fissure Eruption, which are unique as regards the variety of gas composition. The products of exhalation were investigated by a set of modern crystal chemical methods which include X-ray poly- and single crystal studies, crystal structure determinations, X-ray microprobe analysis, high temperature powder diffraction. Minerals of Tolbachik exhalations correspond to 13 classes of chemical compounds and are represented mainly by chlorides, oxychlorides, sulphates and oxysulphates of copper, sodium and potassium.

Crystal chemical methods were used to investigate the forms of metal transport by volcanic gases. Based on the determination of crystal structures of new minerals, as well as on data published in the scientific literature, the authors identified the $[OCu_4]^{6+}$ tetrahedra as the most "strong" groups in the structure of some minerals (oxysalts, oxides). In these phases oxygen is not forming the acid residuals SO_4, SeO_3Cl, etc..., or the OH-groups and the H_2O molecules, but rather it contributes to the formation of these polyhedra. $[OCu_4]$ tetrahedra are polymerized through common vertices and edges. Up to day ten different types of polyions composed of $[OCu_4]$ tetrahedra were identified, characterized by finite groups, endless chains, layers, networks. The analysis of bond lengths and angles in the tetrahedra was carried out; the obtained data were used as a basis for the development of a new branch in crystal chemistry, which describes in details the crystal structures of the compounds with $[OT_4]$ tetrahedra, the forms and size of the tetrahedra, the types of polymerization, the conditions of their origin.

This field of crystal chemistry represents a theoretical basis for the determination and the prediction of the exhalation minerals and the ore forming processes. It is suggested that the formation of tetrahedra around the strongest anions is typical not only of a crystalline material but also of a gaseous phase, where they represent the most strong fragments of a future structure. The presence of structural fragments in a gaseous phase simplifies the process of crystallization; in particular it can explain the nearly instantaneous crystallization of chemical compounds having complex composition and complex structure, which are rather common among exhalation minerals. Thus the determination of the crystal structures of exhalation minerals can bring information on probable forms of mass transport in volcanic gases.

ON A NEW GENETIC TYPE OF PLACER GOLD-EOLIAN

Filippov V.Ye, Nikiforova Z.S. *(Yakut Inst. of Geol. Sciences, Russian Acad. Sciences, Russia).*

Among various mineralogical aspects of gold under a keen discussion is the problem of toroidal and hollow spheroidal gold genesis. Nowadays, there are some hypotheses as to the origin of these unique shapes of gold: chemogenic (Petrovskaya, 1973; Machaires, 1970; Lowenstein, 1982; Dilabio et.al., 1988; Fressinet et.al., 1988); mechanogenic in a hydrodynamic medium (Izbekov, 1985, 1980; Giusti, 1986; Dunn, 1929; Klominsky et.al., 1988), biogenic (Yablokova, 1972; Watterson, 1985). The hypotheses are contradictory and fail to explain all the diversity of intermediate shapes, as well as a mechanism and conditions of their formation.

While studying typomorphic features of gold particles and comparing with geologic-geomorphologic setting this gold has been found in, we have hypothesized that the unusual shapes of gold originate under eolian conditions. For the purpose of confirming this hypothesis, we carried out an experiment to investigate the transformation of gold flakes under eolian conditions. During the experiment, we have observed the sequence of transformation of gold flakes into toroidal and later, hollon spheraidal shapes. There were obtained experimentally various configurations of gold particles analogous to those discovered in nature and characterized by marks of eolian action. These are ubiquitous in various regions of the world and are typical of all platforms within North and South America, southern Africa, Australia, West Europe and South Africa. The age of this gold ranges widely from Riphean up to Cenozoic.

Gold which has undergone the eolian action is characterized by definite typomorphic features and is classified into groups. Gold particles toroidal and hollow spheroidal in region, gold particles are from 0.1 to 0.25 mm in size, the surface is finely shagreen or polished. Spheroidal gold has an internal partition which divides the spheroid into two hollow chambers. Fineness of gold is high (960-990%.). The second group is epresented by massive flat gold particles with ridges along the edges of these particles, as well as by lumpshaped ones with smooth polished projections. Gold particles are 0.25 mm and more in size. Average fineness of gold varies and depends on the composition of primary sources.

Thus, the genesis of toroidal and hollow spheroidal gold is related with a mechanical transformation of flaky gold under eolian conditions. We identify gold particles with marks of eolian action as a new genetic type of placer gold called "eolian gold". Since eolian gold has a widespread occurrence and forms high concentrations of metal, we recommend to pros pect eolian gold placers.

References.
Dilabio R.N. et. al. (1988). *Econ. Geol.* 83. 153-162.
Dunn E.J. (1929). *Geology of gold.* London. 303.
Freyssinet P.H. et. al. (1988).*jour of Geoch.* 32. 17-31.
Giusti L. (1986). *Gandion jour Earth Sci.* 23. 1662-1672.
Isbekov E.D.(1985). *The formation and evolution of placev deposits*, Russia. 190.
Klominsky et. al. (1983). *Sbornik Gel.* 25. 111-186.
Lowenstein P.L. (1982). *New Guinea Geol. Survey.* 9. 1. 245.
Machairas G. (1970). *Bur Recherches Geol. Min Bull.* 11. 3. 72.
Petrovskaya N.V. (1973). *Natur Gold*, Russia. 347.
Watterson J.R. (1985). *Precambrian Researsh.* 30. 321-335.
Yablokova S.V. (1972). *DAN.* 205. 4. 933-936.

CLINOPTILOLITE TUFF FOR THE CLEAN FOOD-CHAIN OF MAN

Filizova, L. (Inst.Appl. Mineralogy, Bulg. Acad.Sci.)

The Bulgarian experience in providing for the clean food-chain of man dates from 1985 (Hinkovski et al,1988).Clinoptilolite tuff with rhyolitic composition and oligocene age from the Eastern Rhodopes has been used.

The clinoptilolite (CLI) contents is 70%. The non-zeolite minerals are quartz, K-feldspar, montmorilonite, celadonite. According to the composition the CLI is calcium-rich and potassium-rich type (Tsitsishvili et al, 1992).

Drinking and waste water can be cleaned by NH_4,Sr,Pb,Zn, Cu, Mn-ions with ion-exchange capacity alkCLI < 1,3 < calCLI. Overdoses of herbicides in soil are immobilized and soil fertility is insured (Filizova et al,1985).

After the radioactive contamination of Bulgarian territories caused by the Chernobyl accident some measured for cleaning of water, food and wine have been carried into effect The decontamination of food products by means of contact with the appropriate CLI grain-size fraction insures: 98% of drinking waterfrom Cs-137; 83% of pork meat and sausages; 50% of poultry meat; 72% of cheese; 98% of milk, as well as 55% cleaning from Sr-90. CLI as a 10% addition to the daily portion of animals redused with 50% the contents of Cs-137 and with 44% of Sr-90 in cow and sheep milk;45% of Cs-137 in sheep meat; 54% of Cs-137 and 37% of Sr-90 in pork meat; 70% of Cs-137 and 41% of Sr-90 in poultry meat.The total activity of a coctail of isotopes in green fodder of milky cows is reduced with 74% in their milk. A speeded extraction of isotopes and increasing of the total activity to 300% in the excrements of those cows has been observed(Hinkovski et al, 1988; Nat. Conf., 1992).

References:

Hinkovski, T., Marinov, V., Djoreva, M.(1988). The experience of Bulg. Acad. Sci. Agric., 279 p.

Tsitsishvili, G.V., Andronikashvili, T.G., Kirov, G.N., Filizova, L. (1992). Natural Zeolites. Ellis Horwood Ser. Inorg. Chem.

Filizova, L., Stojanova, K., Kirov, G.N. Bulg.Pat. 40009, 1985.

Nationale Conference "Population Defence from Desasters and Accidents" (1992), Sofia. Abstr.

CRYSTAL CHEMISTRY OF RARE EARTH ELEMENTS IN APATITE AND CALC-SILICATES

Fleet M.E. and Pan Y. (*Dept. of Earth Sciences, Univ. of Western Ontario*)

The crystal chemistry of rare earth elements (REE) in apatite has been investigated by hydrothermal synthesis of individual REE-substituted crystals of general formula $Ca_{10-x-2y}Na_yREE_{x+y}(P_{1-x}Si_xO_4)_6(F,OH)_2$. For 11 REE, and similar equivalent bulk compositions and run conditions, the pattern of REE uptake by fluorapatite is LREE enriched and peaks at Nd, as in many igneous and metamorphic apatites. A weak 4*f* crystal field effect is also discernible. Refined X-ray structures of La-, Nd- and Gd-bearing apatites yielded the following occupancies for REE in the Ca(1) and Ca(2) sites: La [0.023; 0.093], Nd [0.049; 0.104], Gd [0.039; 0.076], reported as [Ca(1); Ca(2)]. The structure of Dy-apatite is in progress. The REE and Na occupancies are consistent with site preferences deduced from bond valence calculations (Brown, 1981). In particular, the bonding requirements of the A anion (OH, F, Cl, O) exert a considerable influence on the site preference of cations in apatite. Cuspidine $[Ca_4Si_2O_7(F,OH)_2]$, a minor phase in some of the experimental products, is HREE enriched and substitution of REE appears to be limited to $Ca_2NaREESi_2O_7(F,OH)_2$. The X-ray structure for a twinned crystal of $Ca_2NaLuSi_2O_7(F,OH)_2$ shows that Lu is restricted to Ca(3) and Ca(4), and Na to Ca(1) and Ca(2); the coupled occupancies being $Lu_{1-x}Ca_x$ for Ca(3) and $Na_{1-x}Ca_x$ for Ca(1), with $x = 0.15$. Again, Lu and Na occupancies are consistent with site preferences deduced from bond valence calculations. The correlation with bond valence is being extended to predict REE site preference in other calc-silicate phases with multiple Ca positions.

Reference:

Brown, I.D. (1981), *in Structure and Bonding in Crystals*, II, 1-30

IN SITU MONITORING OF THE QUENCH PROCESS AND THE LIQUID SOLID TRANSITION OF HIGH TEMPERATURE LIQUIDS BY ^{27}AL NMR.

FLORIAN P., MASSIOT D., POE B.(*), FARNAN I. and COUTURES J.P. (*CNRS - CRPHT, Orleans FRANCE, * also at Dept. of Chemistry, Arizona St. Univ., USA*)

Improvements to our very high temperature, aerodynamically levitated, laser heated NMR set-up (Coutures *et al.*, 1990 and Boe *et al.*, 1993) mean that it is now possible to obtain a resolved ^{27}Al spectrum in aluminum bearing refractory liquids in one scan and to repeat the measurement every 50 ms. It is thus possible to monitor in situ, the cooling of a sample from 2500°C down to crystal or glass, including the undercooled liquid and the liquid coexisting with the solid during crystallisation, by ^{27}Al NMR (chemical shift and line width). The temperature is measured simultaneously, optically by IR emission and from the Curie law behaviour of the observed magnetisation. We report results on the cooling of liquid Alumina (Al_2O_3 T_{liq}= 2054°C, $CaAl_2O_4$ T_{liq}= 1605°C, $Y_3Al_5O_{12}$ T_{liq} = 1940°C among others).

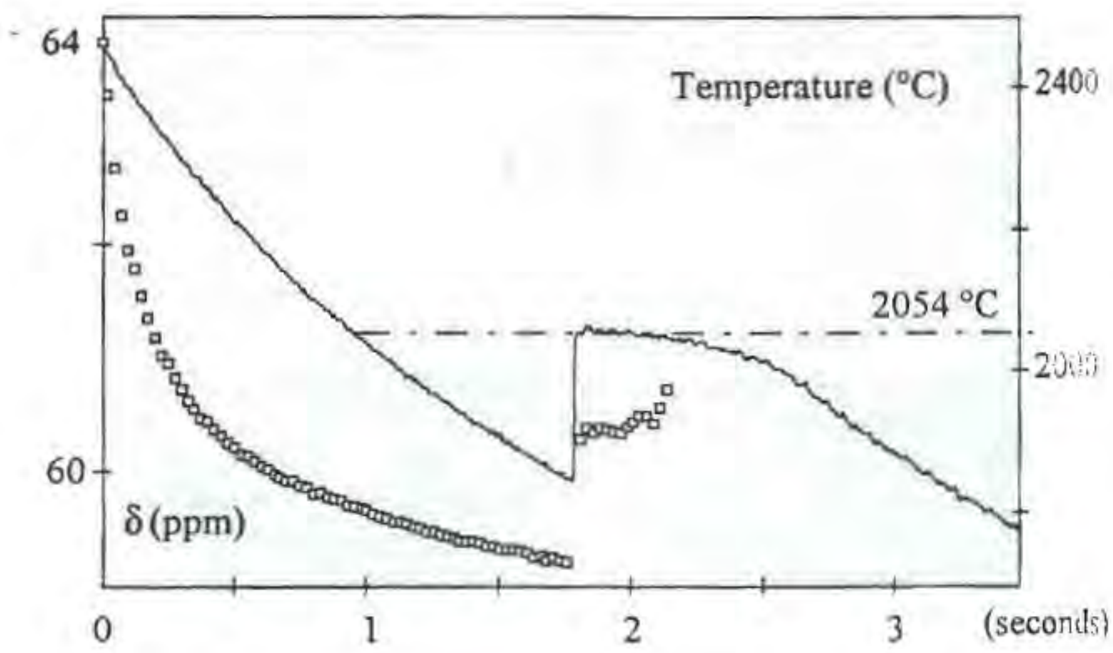

Figure reports the observed variation of chemical shift for a 3 mm diameter air levitated droplet of liquid Al_2O_3 at 2450°C down to crystalline α-Al_2O_3 at 2054°C through undercooled liquid phase in less than 2.5 seconds. We observe a discontinuous change of the chemical shift (several ppm) at the crystalllisation where the linewidth is a minimum (~100Hz) and increases continuously up to more than 250 Hz at the disapperance of the liquid signal. The two observed behaviors give structural (chemical shift) and dynamical (T_2 relaxation times from linewidth) description of the cooling liquid which can be interpreted in terms of aluminium average coordination and shear relaxation times.

In aerodynamic levitation conditions heterogeneous nucleation is minimized and for $CaAl_2O_4$ and $Y_3Al_5O_{12}$ both crystal and glasses can be obtained from the levitated liquid samples depending on the experimental conditions. These two different cooling path leading to a quenched melt or a crystal can be traced through aluminum time resolved NMR.

references :
Coutures J.P., Massiot D., Bessada C., Echegut P., Rifflet J.C. and Taulelle F., *Cr. Acad. Science*, **310**, 1041-5, (1990).
Poe B.T., Mc Millan P.F., Coté B., Massiot D., Coutures J.P., *Science*, **259**, 786-788, (1993)

EXPERIMENTAL STUDIES RELEVANT TO ULTRAHIGH-PRESSURE METAMORPHISM

Rockenberg T., Schreyer W., Skrok V., and Wunder B. (Research Group on High-Pressure Metamorphism, Institut für Mineralogie, Ruhr-Univ. Bochum)

The results of Experimental Mineralogy and Petrology over the past 30 years or so have laid the foundations for recognizing the scientific fact of ultrahigh-pressure metamorphism. Thus it is now established that rocks initially formed within the continental or oceanic crust have been subducted - at least over the past 500 million years - to mantle depths of up to some 140 km, where quartz and graphite were converted to coesite and diamond. Experiments have defined the stability fields of other high-pressure minerals such as pyrope, Mg-staurolite, Mg-chloritoid and Ti-ellenbergerite that occur in the ultrahigh-pressure rocks as well. It is of crystal chemical interest that hydrous phases of the $MgO-Al_2O_3-SiO_2-H_2O$ system including chlorite with Mg in sixfold coordination become unstable between about 50 and 60 kbar in favor of others (MgMgAl-pumpellyite = $Mg_4^{[7]}Mg^{[6]}Al_5Si_6O_{21}(OH)_2$, pyrope) that contain Mg in higher coordination. A very surprizing aspect of the system at pressures above some 60 kbar is that completely new and unexpected phase compatibilities were found such as forsterite + diaspore and forsterite + corundum.

In the $CaO-Al_2O_3-SiO_2-H_2O$ system zoisite becomes unstable at P>60 kbar through breakdown into grossular + kyanite + coesite + H_2O. Conversely, lawsonite remains stable up to at least 100 kbar. At this pressure and >1000°C it breaks down to grossular + "topaz-OH" ($Al_2SiO_4(OH)_2$) + stishovite + H_2O.

Considerable progress has been made in the system $MgO-SiO_2-H_2O$ which is of interest for the metamorphism of hydrated mantle rocks. The synthesis of pure antigorite could be achieved using talc and brucite as starting materials at 50 kbar, 500°C. Antigorite remains stable up to some 45 kbar, at 550°C, where it breaks down to clinoenstatite + forsterite + H_2O. Talc is more pressure- and temperature-resistant as it breaks down to enstatite + coesite + H_2O at some 60 kbar, 750°C. The very silica-poor hydrous phases D (= "Chondrodite-OH", $Mg_5Si_2O_{10}H_2$) and A ($Mg_7Si_2O_{14}H_6$) could be synthesized at 50 kbar, 900°C and 80 kbar, 700°C, respectively. Their stability fields can probably be reported at the meeting. However, it remains doubtful as to whether or not these phases can appear within the much more siliceous mantle rocks: The assemblage forsterite + H_2O forming an efficient chemical barrier was found to be stable at 70 kbar as low as 700°C relative to assemblages of $MgSiO_3$ with silica-deficient hydrous phases.

The extension of experimentation to higher pressures and simultaneously lower temperatures allows predictions on the mineralogy in the cold portions of old subduction zones. There, the synthetic phase MgMgAl-pumpellyite may be stable in hydrated mantle rocks, while phase Pi ($Al_3Si_2O_7(OH)_3$) and "topaz-OH" may appear in more aluminous rocks of sedimentary origin. "Topaz-OH" was found to break down at 150 kbar, 1000°C, to the less hydrous assemblage diaspore + $Al_5Si_5O_{17}(OH)$, another high-pressure phase first synthesized by Eggleton et al. (1978). The very existence of these hydrous phases allows the retention of water to great, hitherto unexpected depths. Although metamorphic rocks containing these phases may never reach the Earth's surface because of phase breakdown during subsequent heating, the knowledge of their probable presence in subduction zones is of paramount geophysical interest. Thus Experimental Petrology may also be instrumental for deriving knowledge of the physical and chemical behavior of very deeply subducted Earth materials under in-situ conditions.

References:
Eggleton, R.A., Boland, J.N., Ringwood, A.E. (1978). Geochem. Journ., **12**, 191-194.

Thermal events in low-Ca pyroxenes and augites from a suite of equilibrated L-class chondrites

Folco L. and Mellini M. *(Dip. Scienze della Terra, Siena)*

Pyroxenes are expected to bear detectable temperature records of three mineralogical processes, which, for decreasing temperature, are: (re-)crystallization, exsolution, and intracrystalline cation ordering. As exsolutions and site partitioning are time-dependent phenomena, cooling rates can be obtained. Relationships between equilibrium temperatures, cooling rates and petrographic types on equilibrated ordinary chondrites can constrain the still controversial thermal model of parent bodies.

We are reporting on an ongoing pyroxene geothermometry study of a complete suite of equilibrated L-chondrites (Tab.1). Care was taken to select unshocked specimens to avoid possible thermal overprints. Brandon, a highly shocked chondrite, was however included as undeformed L7 samples are so far unavailable. Minimal crystallization temperatures, obtained by applying the geothermometer of Lindsley (1983), mainly show that values for low-Ca pyroxenes are significantly lower than those of coexisting augites. This thermal gap continues to be a systematic feature in the thermal history of chondrites, as first stressed by McSween and Patchen (1989). Two orthopyroxene grains from each type 5 and 6 samples were analysed by single crystal diffraction method for cation partitioning determinations. According to Molin and Ganguly (1992), data was then converted into equilibrium temperatures of the intracrystalline Fe-Mg M1-M2 exchange. Search for L4 and L6/7 low-Ca pyroxenes is hampered by crystal imperfections (as evidenced by x-ray diffraction patterns).

Data indicates complex and diversified thermal records at high and low temperatures; the crystallization temperature discrepancy showed by low-Ca pyroxenes and coexisting augites, likely inherited from primary chondrule crystallization processes, calls for an accurate reading of data even within a suite of chondrites conventionally defined as "equilibrated".

Tab.1. Minimal crystallization and ordering temperatures.

sample	class		mcT °C			ordT °C
			Low-Ca Pxs	augites	difference	
FRO 90052	L4	S1	800 (710÷970)	1145 (1100÷1210)	345	
New Almelo	L5	S1	835 (770÷870)	960 (880÷1010)	125	460±35
Park	L6	S1	795 (745÷850)	1000 (960÷1050)	205	360±35
Brandon	L6/7	S5	780 (715÷870)	1015 (980÷1040)	235	

FLUID INCLUSIONS EVIDENCE OF POLYMETAMORPHISM IN LAPLAND GRANULITE BELT

Fonarev V.I. (*Inst. of Experimental Mineralogy, Russian Acad. of Sci.*) and Kreulen R. (*Inst. of Earthsciences, Univ. of Utrecht*)

Fluid inclusions in minerals of the Lapland granulites belt are investigated. As was established, using a consistent system of mineralogical thermometers and barometers, metamorphism of the region occurred in 4

major temperature stages: (M1) 860-925↑C, (M2) 780-810↑C, (M3) 675-720↑C, (M4) 565-605↑C. The underlying Lapland granulites rocks of the Tanaelv belt complex were metamorphosed into on prograde stage at T=590è20↑C. In Lapland granulites several groups of fluid inclusions differing in temperatures of melting (composition) and temperatures of homogenization (density) are discovered. These groups correspond to M1-M4 metamorphic stages. The first two stages were differed by a specific character of fluid with $N_2>CH_4$ (M1) and $CO_2>CH_4(N_2)+H_2O$ (M2). The next stages were characterized by aqueous-bicarbonate fluid with a marked predominance of CO_2. In garnet-biotite plagiogneisses of the Tanaelv belt complex only one group of bicarbonate (with lost water) inclusions is fixed. The values X_{H2O} at metamorphism Lapland granulites at the stage M3 (0.25-0.41) and M4 (0.30-0.46) are defined. For less metamorphosed rocks of the Tanaelv belt X_{H2O}=0.46-0.55.

This work was supported in part by Russian Fund of Fundamental Investigations (Grant No. 93-05-8848).

THE GEOCHRONOLOGICAL EVOLUTION OF THE CABO FRIO TECTONIC FRAGMENT, RIO DE JANEIRO, BRAZIL, AND ITS BEARING IN THE BRAZIL-AFRICA CORRELATION

Fonseca A.C. (Dept. of Geology, Univ. of Rio de Janeiro), Cordani U.G. (Inst. of Geosc., Univ. of São Paulo*), Bigazzi G. (C.N.R. - Pisa) and Kawashita K. (*)

The coastal area of Brazil, east of Rio de Janeiro, and including the localities of Cabo Frio, Arraial do Cabo and Búzios, is referred in this work as "Cabo Frio tectonic fragment". It becomes a key region for a Brazil-Africa correlation, within because of its possible direct link with the western portion of the Congo-Angola Craton, exposed along the Angolean coast (Fonseca et. al, 1979).

Two main lithological units which occur in: ortho and paragneisses (Heilbron et al., 1982) The orthogneisses have granitic-granodioritic-tonalitic compositions, with amphibolitic enclaves and intercalations. The paragneisses are metapelites, with intercalations of amphibolite, quartzites and calc-silicate rocks, metamorphosed in upper amphibolite facies, in intermediate pressure conditions. Basalt dykes and diabase and intrusive alkaline rocks related to Mesozoic tectonism also occur in the area.

Most Sm-Nd and Rb-Sr whole-rock isochrons obtained on single-outcrop samples of the orthogneisses yielded age values around 2000 Ma, suggesting an Early Proterozoic age for the emplacement of the sequence (Fonseca, 1994). The low Sr initial ratios of the isochrons could be related to a mantelic derivation, but the ε°_{Nd} negative values (-7) indicate the contribution of crustal materials.

Sm-Nd and Rb-Sr isochron work carried out in the paragneisses (Fonseca, 1994) yielded consistent results around 540 Ma, indicating a Lower Paleozoic age for their regional metamorphism, and thus relating them to one of the last episodes of the agglutination of West Gondwana (Brito Neves and Cordani, 1991). Their T_{DM} Sm-Nd model ages are of the order of 1600-1300 Ma, and correspond to weighted mean values in relation to the ages of the different sources of the sediments. They represent always maximium values for the depositional events, and preclude the idea of the orthogneisses been their only source.

The younger tectonomagmatic episodes are also represented in the geochronological pattern of the orthogneisses, especially in their ^{40}Ar-^{39}Ar mineral ages of about 600-500 Ma, as well as in some Rb-Sr and Sm-Nd apparent results of intermediate age, which are probably caused by partial rejuvenation.

For the Meso-Cenozoic thermal history of the region, two thermal pulses are detected by the fission-track method applied to apatite and titanite (Fonseca., 1994). The signification of the first one, around 190 Ma, is difficult to access, and the second pulse, between 84 and 34 Ma, is deal to the alkalic magmatism which affected large areas in Southern Brazil, and specially a major tectonic zone in Rio de Janeiro State, to which belongs the Cabo Frio and many other alkalic intrusions (Fonseca et al., 1979).

The geochronological evidence allows to correlate the terrain including the orthogneisses with the western part of the Congo-Angola Craton, where the Lower Proterozoic Eburnean orogeny predominates as the main tectonomagmatic episode. However, the already mentioned rejuvenation at about 600-500 Ma indicates that the Cabo Frio tectonic fragment was part of the reactivated border of the Congo-Angola Craton, overprinted by the Brasiliano/Pan African orogeny.

REFERENCES

BRITO NEVES, B.B. and CORDANI, U.G.; 1991. Prec. Res., 53, 23-40.

FONSECA, A.C.; 1994. Dr. Sc. Thesis, IG/USP, 186p.

FONSECA, M.G. et al., 1979. Folha RJ, Vitoria e Iguape, DNPM.

HEILBRON, M. et al.: 1982. An. Acad. Bras. Ci., **54(3)**, 553-562.

THE PHOSPHATE MINERAL ASSOCIATION OF FREGENEDA PEGMATITES (SALAMANCA, SPAIN)

Fontan, F.*(Univ. Paul Sabatier, Toulouse, France)*; Roda, E.; Pesquera, A.; Velasco, F.*; (Dept. de Mineralogía y Petrología, Univ. del País Vasco/EHU, Spain)*

In the Fregeneda area different pegmatitic types can be distinguished. The most common type correspond to simple pegmatites with homogeneous internal structure, but Li and Sn-bearing pegmatites are also relatively widespread. The pegmatites are located north of the Lumbrales granite, most of them intruding into rocks of the Schist-Metagraywacke Complex. A limited number of pegmatites, which are located in an intermediate zone, between the barren pegmatites and the most evolved Li and Sn-bearing bodies, carry a complex association of Fe-Mn phosphate minerals. The study of these phosphates has allowed the identification of primary phases as wyllieite, graftonite, sarcopside, ferrisicklerite and triplite; and secondary phosphates as heterosite, rosemaryite, alluaudite and vayrynenite. Besides other phosphate minerals as Mn-rich apatite. In this study, their main characteristics including their chemical composition, analyzed by microprobe and their unit-cell parameters, are reported.

One of the most common transformation mechanisms in similar associations is the oxidation of the transition metal cations simultaneous with the Na-leaching in wyllieite to generate rosemaryite and the Li-leaching in triphylite (not detected here) to generate ferrisicklerite and later heterosite, so that rosemaryite, ferrisicklerite and heterosite are topotactic alteration products. The occurrence of sarcopside exsolution lamellae in ferrisicklerite and heterosite is an evidence of the replacement processes of the former by the latter. On the other hand, the Na-metasomatic reemplacement of the early phosphates as ferrisicklerite and graftonite, producing alluaudite is also well developed in this association. Nevertheless, the replacement of wyllieite by alluaudite can not be rejected as it has been observed in other similar associations. With regard to the vayrynenite, this is the fourth occurrence of this rare mineral, appearing closely associated to alluaudite, although its genetic relationships have not yet been established.

The occurrence of this phosphate association in these pegmatites is in agreement with the pegmatite fields zonation, so that the phosphate-bearing pegmatites are those with an intermediate degree of fractional crystallization, and besides they appear between the barren and the more evolved pegmatites with Li and Sn.

ACCESSORY MINERAL BEHAVIOUR DURING DIFFERENTIATION OF COMPOSITE GRANITE PLUTONS IN THE ERZGEBIRGE (GERMANY)

FÖRSTER, H.-J. (*GeoForschungsZentrum Potsdam*)

The Hercynian granites in the Erzgebirge metallogenic province have been traditionally classified into two major plutonic series, the Older (OIC) and Younger (YIC) Intrusive Complexes of probably pre- and post-Westphalian ages, respectively. The granitoid rocks often form composite bodies built up by a succession of up to four texturally and geochemically distinct sub-intrusions, of which impressive examples are the Kirchberg (Ki, OIC) and Eibenstock (Ei, YIC) granite suites located in the western Erzgebirge. These plutons, which underwent extended differentiation resulting in deviating geochemical patterns (Table1), have been selected for examination of their REE-Y-Th-U-bearing accessory mineral paragenesis.

The occurrence of **allanite** and **thorite**, both strongly altered and hydrated, is evidently restricted to the Ki granites. Allanite has been exclusively detected in the least evolved, first sub-intrusion at conditions of CaO exceeding 1.6 wt.%. Electron microprobe analyses revealed discrete and highly variable compositions with respect to U (< 0.1 - 20 wt.%), Y (< 0.1 - 6.5 wt.%), LREE (0.2 - 5.2 wt.%), and HREE (0.1 - 2.9 wt.%) in thorite. These suggest a multiple growth of thorite during magma differentiation.

Monazite is a common constituent of all Ki and Ei granite intrusions, except of the allanite-bearing Ki1 granite. Noteworthy is that striking differences exist between both suites with respect to the concentration of U and the substitution mechanism for accomodation of Th and U into the monazite lattice. In general, the amount of Th (Ki: 2 - 33 wt.%, Ei: 2 - 34 wt.%) substituted for the LREE's as well as the sum (Gd+Dy) increase, and the La/Nd ratio decreases with progressive differentation.

Xenotime is present during the entire evolution of the Ei suite, but is lacking in the early (1, 2) and latest differentiates (4) of the Ki magma.

Table1: Behaviour of whole-rock trace elements and accessory mineral assemblages in the Kirchberg and Eibenstock granite suites

	Kirchberg (OIC) Ki1 ---> Ki4	Eibenstock (YIC) Ei1 ---> Ei4
sum REE (ppm)	313 ---> 61.8	71.6 ---> 5.8
sum LREE	292 ---> 39.4	61.4 ---> 4.1
sum HREE	14.6 ---> 30.6	10.0 ---> 1.7
Y	20 ---> 47	19 ---> 3
Th	27 ---> 37	17.3 ---> 1.5
principal accessories	allanite thorite, uranothorite U-poor monazite xenotime (Yb) Th-Y-REE-rich uraninite apatite (mostly early) zircon	U-rich monazite xenotime (Dy) Y-REE-poor uraninite apatite (mostly late) zircon

Uraninites found in the Ki granites contain substantial amounts of Th (4.8 - 7.2 wt.%), Y (1.3 - 3 wt.%), and REE's (1.6 - 3.5 wt.%). In contrast, uraninites from individual Ei sub-intrusions display markedly lower contents of the elements mentioned.

The nature and compositional characteristics of the accessory minerals controlled much of the deviations in the trace-element geochemistry observed between both granite suites, and reflect the melt compositional changes during progressive differentiation. However, most of the accessories are characterized by strong compositional variabilities at a variety of scales both within single grains and among samples from the same sub-intrusion. Complex and non-uniform chemical patterns are best displayed by monazite and thorite. These variations among accessory minerals must be carefully considered when predicting the magmatic evolution of granite suites.

SIMULATION OF GARNET GROWTH PATTERNS USING FORWARD MODELS OF METAMORPHIC TEXTURES

Foster, C. T. (*Dept. of Geology, University of Iowa*)

Forward modeling techniques based on differential and irreversible thermodynamics have been used to simulate growth of garnet porphyroblasts in metapelites as they progress along a P-T path. The method involves a two step procedure: 1) the Gibbs'90 program (Spear et al., 1991) is used to calculate the overall whole-rock reaction at the hand-specimen scale along a specified P-T path; 2) this information is used as input to Seg93 (Foster, 1993), a program that uses local equilibrium and irreversible thermodynamic principles to determine the material transport paths and reaction mechanisms by which the whole rock reaction progresses. The development of the rock texture is modeled by using the local reactions to calculate how the distribution and mode of minerals in the rock change along each segment of the P-T path.

The example shown in Figure 1 was calculated for a polymetamorphic rock from northwest Maine, USA that experienced an isobaric thermal pulse which grew garnet and staurolite (stages I+II), a cooling period during which the pressure increased 500 bars (stage III), and a second isobaric thermal pulse which grew more staurolite and sillimanite (stages IV+V). Calculated local reactions involving garnet porphyroblasts are strongly influenced by the proximity of other porphyroblasts in the rock. This causes garnets in different locations to have distinct growth/dissolution histories that produce a variety of garnet growth zoning patterns (Figure 2). The calculated patterns are similar to Ca zoning maps obtained from garnets in pelites near Rangeley, Maine, USA.

References:
Spear, F.S., et al. (1991). *Am. Mineral.*, **76**, 2009-2012.
Foster, C. T. (1993). *Geol. Soc. Amer. Abstracts*, **25**, 264.

FIGURE 1: CALCULATED THIN-SECTION TEXTURE WITH SIX DIFFERENT GARNET CONFIGURATIONS

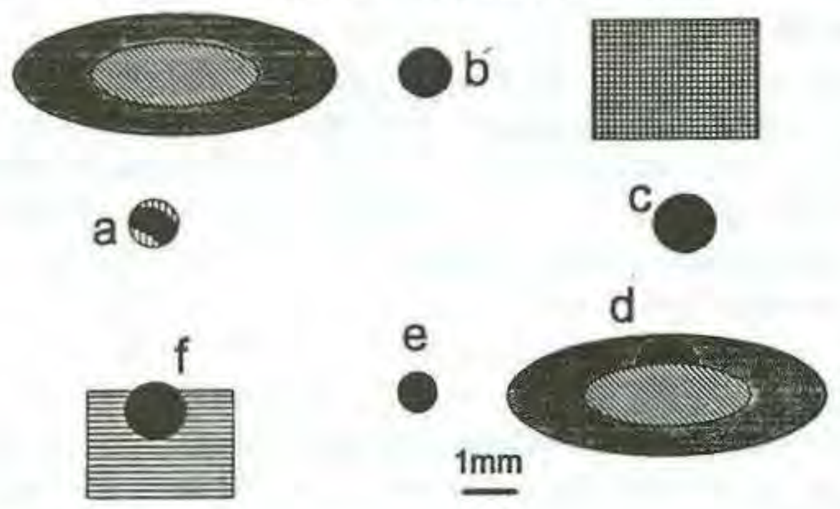

FIGURE 2: CALCULATED GARNET ZONING PATTERNS

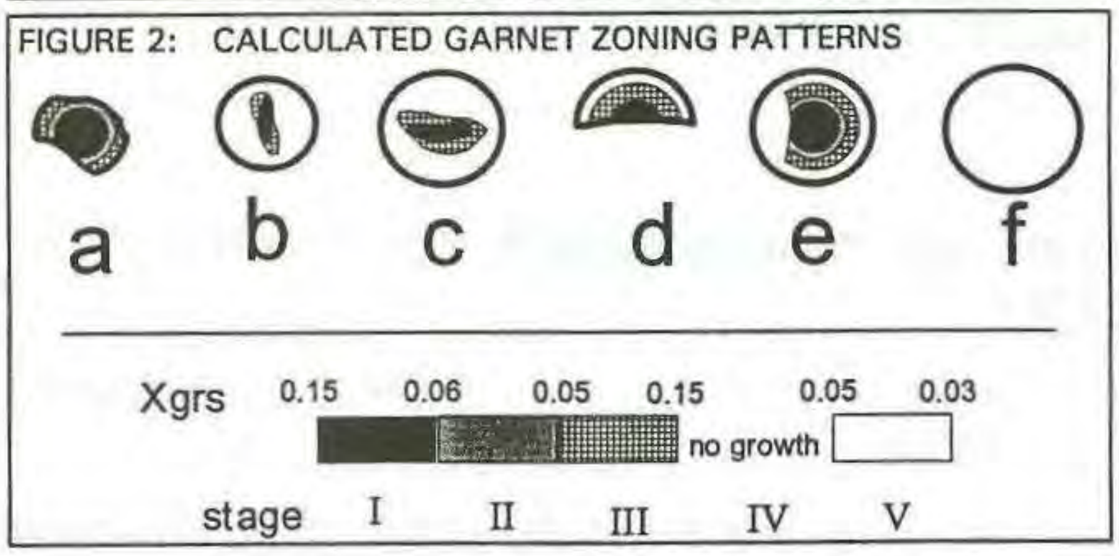

THE ROLE OF PLAGIOCLASE CRYSTALLIZATION, RETENTION AND RECYCLING IN THE EVOLUTION OF CALC-ALKALINE MAGMAS: DATA FROM VOLCANOES OF AEGEAN AND AEOLIAN ARCS

FRANCALANCI L. (*Dipartimento di Scienze della Terra, Università degli Studi di Firenze, Italy*)

It is remarkable that plagioclase, which often represents the most abundant mineral phase of calc-alkaline rocks, has usually an important function in generating the variable petrologic features of arc magmas. Different magmatic processes all implying the key role of plagioclase, are invoked for explaining most of the geochemical and petrographic variations of calc-alkaline volcanics.

The abundance of low-MgO high-alumina basalts in arcs and their paucity elsewhere has recently suggested that a special feature of arc magmatism is responsible for their peculiarities. Several authors consider the low-MgO high-alumina magmas as fractionated hydrous liquids that have partially degassed and crystallized prior to eruption. At relatively high pressure, a high magmatic H_2O content reduces the total proportion of plagioclase in the crystallizing assemblage, thus originating low-MgO high-alumina magmas.These magmas are also present in the Aeolian arc (e.g. Filicudi, Salina), but they are not found in all the volcanoes of the archipelago (e.g. Alicudi; Peccerillo & Wu, 1993). In the light of previous considerations, some major and trace element variations observed among the calc-alkaline less evolved rocks of Aeolian arc (Francalanci et al., 1993) seem to be explained suggesting different pressure of magma crystallization during their ascent to the surface. Polybaric evolution, implying different processes but also a different role of plagioclase, have been also suggested for explaining the variations from calc-alkaline (evolution at lower pressure) to more potassic magmas at Stromboli (Francalanci et al., 1989).

An extensive crystallization of plagioclase occurs at lower depth, especially when a prior fractionation of mafic phases at higher pressure led to the origin of high-alumina liquids. During their ascent, magmas can reside and evolve in crystallizing and convecting reservoirs sited at lower levels in the crust. Here, significant processes of crystal sorting, retention, accumulation and recycling take place. Due to its lower density, plagioclase plays again the main role in such kind of mechanisms. Evidence for the occurring of these processes are also present at the Aeolian (e.g. Filicudi; Francalanci & Santo, 1993) and Aegean (e.g. Nisyros) arcs. In particular, a very complex evolution has been found for the Nisyros magmas: AFC and mixing processes are hypothesised to occur in a convecting magma chamber, where they are associated to the delicate balance of crystallization, crystal settling, sorting and retention (Francalanci et al., 1994). Vigorous convection leads both to plagioclase retention, generating high-porphyritic and Sr-rich rocks, and to recycling of previously accumulated plagioclase, causing the decrease of Sr isotope ratios found in the most evolved rocks.

Francalanci, L., Manetti, P. & Peccerillo, A. (1989). *Bull Volcanol.*, **51**, 355÷378.
Francalanci, L. & Santo, A.P. (1993). *Acta Vulcanol.*, **3**, 203÷227.
Francalanci, L., Taylor, S.R., McCulloch, M.T. & Woodhead, J. (1993). *Contrib. Mineral. Petrol.*, **113**, 300÷313.
Francalanci, L., Varekamp, J.C., Vougioukalakis, G., Defant, M.J., Innocenti, F & Manetti P.(1994). *Boll. Volcanol.*, submitted.
Peccerillo A. & Wu T.W. (1992). *J. Petrol.*, **30**, 1295÷1315.

COOKEITE IN METABAUXITE FROM ALPI APUANE, ITALY

Franceschelli, M., Memmi, I., Pannuti, F. (Dept. of Earth Sciences, Univ. of Siena)

Cookeite, that is Al-Li rich di-trioctahedral chlorite (Bailey and Lister, 1989), was found in a metamorphic bauxite belonging to the Triassic "Breccia di Seravezza Formation" (Authochton Unit, Alpi Apuane).

The cookeite-bearing metabauxite has a strong residual chemical character and its chemical composition is: SiO_2=30-35%, Al_2O_3=34-37%, Fe_2O_3=10-14% and K_2O and CaO < 2%. The Li content ranges from 1100 to 1400 ppm

During Alpine Orogeny, the Authochton Unit rocks underwent polydeformation (D_1-D_2 folding phase, Carmignani et al., 1978) and low-temperature metamorphism, (pyrophyllite+quartz zone, Franceschelli et al., 1986).

The cookeite-bearing metabauxite, 1 m thick, is schistose with evident porphyroblastic texture, due to chloritoid porphyroblasts (up to 3 mm in lenght). The matrix consists of fine-grained cookeite, pyrophyllite, muscovite, margarite, diaspore, hematite and rutile, moderately oriented according to the S_1 schistosity.

Cookeite occurs in two microstructural sites:
- as fine to medium-grained crystals growing on an original pisolite,
- as medium-grained grains interleaved with pyrophyllite, muscovite and margarite.

It was identified mainly by X-ray powder methods, based on the values of d(060) and of the intensity ratio 003/(003+004). The identification was confirmed by chemical analyses that were performed by electron microprobe, apart from Li and B that were determined by ion microprobe. Cookeite has quite a homogeneous chemical composition that, on average, is :

$$(Al_{4.1}\ Fe^{2+}_{0.04}\ Mg_{0.02}\ Li_{0.72})\ (Si_{3.185}\ Al_{0.8}\ B_{0.015})\ O_{10}\ (OH)_8$$

Its composition is comparable with the ones reported by Jullien and Goffé (1993) for metamorphic cookeite, that are characterized by Li contents in the range 0.7-1 a.f.u.

The association cookeite-pyrophyllite-margarite-chloritoid-diaspore of the cookeite-bearing metabauxite can supply further constraints to T and P of Alpine metamorphism of Alpi Apuane. This association, according to Jullien and Goffé (1993), indicate T conditions of 350-370 °C and pressure lower than 5 kb.

The occurrence of cookeite in a metabauxite of the Breccia di Seravezza Formation (that is the first occurrence in low-grade metamorphics of Alpi Apuane), not only enriches the mineralogical knowledge of the Alpi Apuane metamorphic rocks, but also supplies further details, mainly about metamorphic temperature conditions, and confirms that cookeite is a quite common mineral in low-grade Al-rich metapelites, where it can be used as index mineral.

References:
Bailey, S.W. & Lister, J.S. (1993). *Clays and Clay Minerals*, **37**, 193-202.
Carmignani, L., Giglia G., Kligfield R. (1978). *J.Geol.*, **86**, 487-504.
Franceschelli, M., Leoni L., Memmi I., Puxeddu M.. (1986). *J.metamorphic Geol.*, **4**, 309-321.
Jullien, M. & Goffé B. (1993). *Schweiz.Mineral.Petrogr.Mitt.*, **73**, 349-355.

MINERAL STANDARDS FOR GEOCHEMISTRY

Francis C.A. (*Mineralogical Museum, Harvard Univ.*), Dyar M.D. (*Dept. of Geology and Astronomy, West Chester Univ.*), McGuire A.V. (*Dept. of Geosciences, Univ. of Houston*), and Robertson J.D. (*Dept. of Chemistry, Univ. of Kentucky*)

Mineralogical museums serve science by routinely loaning specimens from their collections to researchers for a wide variety of specific investigations. Museum curators can broaden the impact of their collections on scientific research by participating in the selection, preparation, characterization, and distribution of

minerals for use as reference standards. The mineral standards described below were mostly drawn from the Harvard University mineral collection.

Recently, McGuire *et al.* (1992) developed a set of 13 common rock-forming minerals to be used as standards for the quantitative analysis of oxygen using electron microprobes equipped with multielement W-Si (also known as LDE1 and PC1) crystals. Usually oxygen is calculated assuming fixed stoichiometry. The new standard set permits more complete chemical characterization of minerals and enables investigators to more readily address such questions as Fe^{2+}/Fe^{3+} ratios and cation nonstoichiometry. The set is comprised of albite, almandine, biotite, corundum, dolomite, enstatite, forsterite, gahnite, hematite, kaersutite, muscovite, quartz, and sillimanite. Approximately 40 sets of these minerals have already been distributed to laboratories worldwide by the senior author.

Currently, a set of 9 mineral standards for microprobe analysis of light elements (Li, Be, B, and F) is being developed. Gem quality single crystals of danburite, ferrian dravite, elbaite, hambergite, kornerupine, lithiophilite, lithian muscovite, phenacite, and spodumene have been selected for complete chemical characterization by a combination of techniques: major and minor elements by electron microprobe analysis, Fe^{2+} and Fe^{3+} by Mössbauer spectroscopy, H by uranium extraction, and Li, Be, B, and F by proton-induced gamma-ray emission analysis (PIGE), prompt-gamma neutron activation analysis (PGNAA), and wet chemical methods. The chemical data are supplemented by physical data (unit cell dimensions, specific gravity, and optical data) and their geologic modes of formation have been researched.

The authors invite a dialogue with investigators aimed at identifying mineral standards not currently available to meet the needs of the research community.

References:
McGuire, A.V., Francis, C.A., Dyar, M.D. (1992). *Amer. Mineral.*, 77, 1087-1091.

NEW DATA ON CRYSTALLOCHEMISTRY AND PROPERTIES OF THE POLLUCITE - ANALCIME SERIES MINERALS

Frank-Kamenetskaya O.V., Rozhdestvenskaya I.V., Kaminskaya T.N., Zorina M.L., Gordienko V.V. and Kostitsyna A.V. *(St.Petersburg University, RUSSIA)*

The structural causes of an excess of Si, of a change of water type and quantity and of a weak birefringence of minerals in pollucite - analcime series (Cs,Na)(1-x)Al(1-y)Si(2+y)O6·nH2O are dicussed. New structure data on Na-pollucites from various pegmatite localities have been obtained by X-ray analysis and treated invoking IR-spectroscopy and DTA data.

X-ray single crystal analysis showed the following. The occurence of a weak birefringence and of forbidden X-ray reflections are attributable to the decrease of pollucite's symmetry up to tetragonal (sp.gr. $I4_1/acd$) or orthorhombic (sp.gr.Ibca) owing to different occupancies of Na position. The proposal that symmetry decrease is a consequence of the Al ordering in tetrahedric positions have not been supported. The Al/Si ratios in tetrahedra deduced from average T-O distances are in good agreement with the chemical compositions and in all cases more than 1/2. Excess charge due to Al(+3)↔Si(+4) substitution is compencated not only by a deficite of alkaline cations.

X-ray thermal powder diffraction, IR spectroscopy and differential thermal analysis revealed that no less than two types of water occured in the structure of intermediate pollucite - analcime solid solutions. The water molecules occupy only one crystallographic position but are connected with the structure variously. As Na content decreases in pollucite - analcime series the number of water molecules, which interact with Al/Si framework most strongly (H2O-II) increases against the background of the decrease of the total (H2O-I + H2O-II) water molecules' amount. These data allow to refine the scheme of isovalent substitution:

Na + n1(H2O-I) ↔ Cs + n2(H2O-II),

where n1 > n2.

The conception of cluster structure of sodium pollucites (Beger, 1969) is advanced. It permits to explain the chemical composition variations of pollucite-analcime series minerals mentioned above.

Reference:
Beger R.M. (1969). *Z.Krist.*, 129, 280-302.

NEW RELEVANT DATA ON THE CRYSTAL CHEMISTRY, AND ON THE GENETICAL PROBLEM OF ALLUAUDITES AND WYLLIEITES.

Fransolet, A.-M. *(Lab. Minéralogie, Univ. Liège)*, Antenucci, D. *(ISSeP, Liège)*, Fontan, F. *(Lab. Minéralogie, Univ. Toulouse)* and Keller, P. *(Inst. Mineralogie, Univ. Stuttgart).*

In the last decade, we have collected numerous field observations and chemical data, which allow us to assert, according to Moore & Ito (1979), that the occurrence of rosemaryite, $NaMnFe^{3+}Al(PO_4)_3$, involves the formation of a "primary" wyllieite, $Na_2MnFe^{2+}Al(PO_4)_3$, unoxidized and without lattice vacancy. The problem of the replacement of Fe^{3+} by Al is also discussed.

New wet chemical data for hagendorfite from the type locality, and for various alluaudites *s.s.* from Rwanda pegmatites show that Mn also shares the X(1) position with Na, frequently and significantly. Since Moore (1971) suggested the existence of an ideal term, $NaCaMnFe^{2+}{}_2(PO_4)_3$, another possibility, $NaMn_2Fe^{2+}{}_2(PO_4)_3$, is also proposed.

The crystallochemical role for H_2O was tentatively explained by the existence of H_4O_4 replacing the PO_4 tetrahedra (Huvelin *et al.*, 1972). A plot of all the wet chemical analyses available in the literature, and of new chemical data shows that the amounts of H_2O tend to increase inversely with the Na_2O contents. Owing to the recent description of an alluaudite-like compound, $NaCdIn_2(PO_4)_3$ (Antenucci *et al.*, 1993), H_2O could occur in the channels, which appear along [001] when all the X(2) sites are vacant.

Relevant electron microprobe data for alluaudite closely associated with ferrisicklerite - heterosite from the Mont Kibingo pegmatite, Rwanda, tend to demonstrate that, in contrast with the opinion of Moore & Ito (1979), the occurrence of $NaMnFe^{3+}_2(PO_4)_3$ also involves the existence of a former $Na_2MnFe^{2+}Fe^{3+}(PO_4)_3$ without lattice vacancy. This new hypothesis forces us to consider that alluaudite *s.l.* could occur as a primary phase in particular phosphate associations. This is the case for hagendorfite closely associated with arrojadite in Hagendorf-Süd, as well as for alluaudite associated with both fillowite and graftonite in the Buranga and Rusororo pegmatites.

References

Antenucci, D., Miehe, G., Tarte, P., Schmahl, W.W. & Fransolet, A.-M. (1993): *Eur. J. Mineral.*, 5, 207-213.

Huvelin, P., Orliac, M. & Permingeat, F. (1972): *Notes serv. géol. Maroc*, 32, n° 241, 35-49.

Moore, P.B. (1971): *Amer. Mineralogist*, 56, 1955-1975.

Moore, P.B. & Ito, J.(1979): *Mineral. Magazine*, 43, 227-235.

THE DARFUR DOME IN W-SUDAN - THE PRODUCT OF A SUBCONTINENTAL MANTLE PLUME?

Franz, G., Pudlo, D., Urlacher, G., and Volker, F.*
(Fachgebiet Petrologie, TU Berlin; * Geologisches Institut, Universität Karlsruhe)

The Darfur Dome is one of several major Cenozoic (35 Ma to Recent) volcanic provinces in N-Africa, and its origin is possibly linked to a subcontinental mantle plume. It is situated in the central part of the N-African plate, in a pre-Neoproterozoic basement, which was reworked during the Late Proterozoic and which is covered by a thin layer of Cretaceous sandstone. The area of regional uplift extends over ~ 800 ×1400 km (referring to the 600 m a.s.l. contour line), maximal uplift is ≤ 500 m, and uplift rates are estimated to be in the order of 15 - 25 m/Ma. The central part of the area is characterized by a negative Bouguer anomaly (-90 to -104 mgal over an area of ~ 400 × 500 km).

Three major volcanic fields (Marra Mountains, Tagabo Hills, Meidob Hills) and many isolated volcanic occurrences cover an area of ~ 45.000 km^2 . Magma generation in each of the three fields is similar. Nearly primitive basanitic rocks show HIMU-like Sr-, Nd-, and Pb isotopic signatures with $^{206}Pb/^{204}Pb$ ratios around 20. Especially in the young Meidob volcanic field (< 7 Ma) they form a suite of chemically well coherent rocks. Assimilation of crustal material produced small amounts of trachytic (which occur as pumice and ignimbrites) and, more rarely, hawaiitic to benmoreitic compositions, well in accord with trace element and isotopic characteristics.

Many features of the Darfur Dome are consistent with model calculations for large scale mantle plumes. The major differences are, however, that no high-Mg rocks (komatiites, picrites) have yet been found, and that magma output rates are one order of magnitude less than in OIB (e.g. Hawaii) and two orders of magnitude less than in CFB.

STONES IN MONUMENTS: NATURAL AND HUMAN-CAUSED DETERIORATION.

Franzini M. *(Dept. of Earth Sciences, Univ. of Pisa).*

The term deterioration, referred to stones in monuments, has a very wide meaning: it covers all the alterations that the bulk or the surface of a stone undergoes as from its installation.

A full understanding of the deterioration in a monument needs a lot of additional information besides the ones that can be gathered through the check-up of the monument and laboratory analyses, namely:

- stone variety and, if possible, quarry of provenance;
- chemical, mineralogical, physical data on the fresh stone;
- workings undergone by the stone;
- knowledge of the surroundings of the monument, climatic and microclimatic data;
- period of accomplishment;
- history of protective treatments;
- modifications undergone by the monument during its existence, with special attention to restoration events.

All these data have to be valued to identify the various deterioration processes and to distinguish between the ones that have been at work in the past from those which are presently working, taking into account that often two or more deterioration processes may act at the same time.

We must try to distinguish deteriorations due to natural causes (thermal disaggregation, dissolution, wind abrasion, etc.), from those generated by human activities (air pollution, badly carried out restorations, visitors' impact, etc.), and from deteriorations produced by natural processes induced by human activities (soluble salts crystallization, Ca-oxalate coatings, calcium carbonate and gypsum deposits, etc.).

A complete understanding of the deterioration processes and of their causes is indispensable to plan restoration, to arrange suitable protection measures, and to foresee routine maintenance.

THE "LEANING" TOWER OF PISA. STONES, MORTARS AND DECAY PRODUCTS.*

Franzini M., Leoni L., Lezzerini M., Sartori F. (*Dept. of Earth Sciences, Univ. of Pisa*) and Veniale F. (*Dept. of Earth Sciences, Univ. of Pavia; "International Committee for the Safeguard of the "Leaning" Tower of Pisa"*).

The "Leaning" Tower of Pisa is a eight-story, cylinder-shaped structure made of the so-called infill-masonry, that is of two stone walls separated by an infill, about 2.30 m thick, composed of rock fragments and stones cemented with mortar. An helicoidal staircase within the masonry climbs from the ground floor to the belfry. In this structure up to 13 different lithotypes have been identified; for most of them the geological source formation (sometimes the quarry, too) was also recognized. By far the most abundant lithotype is San Giuliano marble, a dominantly white, fine-grained marble, which forms most of the external facing. In the internal facing this is again the dominant lithotype up the fourth story, being substituted from there upward by the Agnano breccia, a highly variable calcareous breccia, often porous and poorly cemented. The Filettole dark-grey limestone ranks third in frequency, having been mostly employed in the external facing dark bands. Much less frequent are other rocks such as "Panchina" (a highly porous calcarenite), granodiorite from Elba Island, "Macigno" (a feldspathic sandstone), and Verrucano quartzite. Carrara marbles (both white and dark-grey varieties) are frequently present, but only as replacement materials.

The infill is composed of fragments of the same lithotypes

which make up the walls, cemented by a strong mortar exhibiting frequent voids of different size. The ratio of rubble to mortar is practically constant at 2.0 all over the masonry. On the contrary the sand component of the mortar shows significant variations of grain size and abundance with the stage of construction.

All these materials are affected by more or less advanced decay processes. The physical degradation is mostly related to natural causes. Temperature excursions, particularly marked on the monument southern side, deeply damages the San Giuliano marble, ultimately producing a mass of calcitic crystals lacking intercrystalline connections ("marmo cotto" = "baked marble"). Wind abrasion and pitting affect all the stones, particularly those of the south-western quadrants, exposed to the dominant Libeccio wind, but only up to the third story. Marine spray from nearby (5 miles) Tyrrhenian Sea brings about crystallisation of sodium chloride and other soluble salts (mostly Ca-sulphate) on the surface and within the stone first layers, producing disaggregation of calcite crystals similar to "marmo cotto".

The observed chemical weathering seems to be related to both natural causes and pollution. Acid rains (due to the presence of SO_4^{--}, HCO_3^- and NO_3^- anions) cause corrosion, dissolution and washing away of carbonatic material on the exposed surfaces and precipitation of black-crust-forming salts in the more sheltered areas. Gypsum appears as the most abundant product of chemical weathering; this phase is the main component of the black crusts, but it is also diffused on all the monument surfaces not washed by frequent water runoff. Gypsum is present in significant amounts even in internal spaces such as the internal cylinder and the staircase; in these locations it seems to be connected with acid dew ensuing from condensation of atmospheric components in confined rooms. Even more worrying is the presence of gypsum as a decay product of the infilling mortar; analyses of core samples show in fact that a process of acid sulphatic attack on this material is going on. This implies a significant water circulation just within the tower masonry, which is also proved by the conspicuous, secondary deposits of calcite (travertine-like) encrusting the walls and the ceiling of the staircase.

* By permission of the "International Committee for the Safeguard of the "Leaning" Tower of Pisa".

THE MINERALOGICAL COLLECTIONS OF THE NATURAL HISTORY MUSEUM OF PISA UNIVERSITY

Franzini M., Perchiazzi N. (*Dept. of Earth Sciences, Univ. of Pisa*).

The Natural History Museum, formerly named "Galleria", was founded in 1591 by the Grand Duke Ferdinando I dei Medici. The oldest mineralogical collection presently preserved was established in 1842, when L. Pilla came from Naples to Pisa with his collection of Vesuvian rocks and minerals. The most part of the collections is due to the intense work of A. d'Achiardi, director of the Mineralogical Museum from 1880 to 1903. In 1985 the zoological, palaeontological and mineralogical collections were transferred in the Certosa di Calci, the present seat of the Natural History Museum. The mineralogical collections are computerized and available for study purposes and grow about 500 samples/year, thanks to the collaboration with the Earth Sciences Department of Pisa University and with amateurs. A list of the samples and of the species is available on floppy disks on request. Some informative data on the collections are briefly reported in the following tables; in addition, 237 admixtures of minerals and 56 uncertainly classified samples are catalogued.

The Types collection		
APUANITE	Burpalite	Calcioancylite-(Nd)
Canavesite	Cascandite	COQUANDITE
DACHIARDITE	DINITE	FIEDLERITE-1*A*
FIEDLERITE-2*M*	FRANZINITE	Hiortdahlite-I
Hiortdahlite-II	Jervisite	Liottite
PERETAITE	PITIGLIANOITE	PORTITE
Rittmannite	Sapphirine-1*A*	STIBIVANITE-2*O*
TUSCANITE	URANOPOLYCRASE	VERSILIAITE

Among the preserved types, hiortdahlite-I, fiedlerite-2*M* and dinite are neotypes while portite is a nekrotype. The types discovered in Tuscany are reported in small caps.

A large number (near 500) of mineralogical localities and 279 species are presently represented in the rich Tuscan regional collection, whose historical value is increased by the presence of 21 discredited Tuscan species. Among the recently discovered Tuscan minerals, the alteration minerals (43 species) of the Etruscan iron slags of Baratti beach, firstly studied in the Museum, are well represented by 170 samples.

The mineralogical exhibition is located in a 500 m² room, mostly dedicated to the systematic and to the regional Tuscan shows. In addition, some showcases with informative panels are devoted to the *color in minerals*, *fluorescent minerals*, *meteorites* and *diamond*. Fine samples from classical Tuscan mineralogical zones are present in the regional exhibition (about 300 m² and 300 samples): Elban hematite and pyrite, Apuan Alps geocronites, cubic pyrites from Niccioleta and Gavorrano mines, Monte Amiata antimonites and cinnabars. Elba island, the most famous Tuscan mineralogical zone, is represented by very fine nineteenth-century samples of hematite, pyrite and ilvaite from Rio Marina and by the fine pegmatitic druses with centimetric crystals of elbaite, beryl, pollucite, orthoclase from S. Piero in Campo.

References:

Cipriani, C., Franzini, M. (1993). *Atti e Memorie dell'Accademia Toscana di Scienze e Lettere La Colombaria*, **58**, 377-416.

Collection	*Samples*
Systematic	7868
Regional Tuscan	6819
Petrographic	777
Fossil coals	47
Hydrocarbons	34
Meteorites	28

Systematics of the collections		
Class	*Species*	*Samples*
Elements	21	548
Sulphides	110	2368
Halides	44	439
Oxides	103	1426
Carbonates	56	1455
Borates	23	108
Sulphates	84	1010
Phosphates	151	745
Silicates	276	6286
Organic	4	9

CO_2+H_2O FLUIDS IN LEUCOSOMES IN MIGMATITES FROM THE DEEP FREEZE RANGE (TERRANOVA BAY, ANTARCTICA).

Frezzotti M.L., Giorgetti G., Palmeri R. (Dept. of Earth Science, Univ. of Siena)
Burke E.A.J. (Inst. of Earth Science, Vrije Universiteit, Amsterdam)

Deep Freeze Range is a portion of the southern Wilson Terrane situated between the Campbell and Reeves Glaciers. It is characterized by two tectono-metamorphic sequences: a metasedimentary monometamorphic sequence (including the Priestley Formation Auct.) and a polymetamorphic sequence mainly consisting of granulitic and migmatitic rocks.

During the Cambro-Ordovician Ross orogeny both the metasedimentary and the polymetamorphic sequences were intruded by granitoid plutons (Granite Harbour Intrusive Complex) and they

experienced a prograde regional high T-low P metamorphism ranging from lower greenschist to upper amphibolite facies and to anatexis.

A fluid-inclusion study was performed on four samples (one gneiss, one migmatitic gneiss and two stromatic migmatites) from the high grade monometamorphic sequence.

High-grade gneisses and mesosomes of monometamorphic migmatites consist of biotite + quartz + plagioclase + K-feldspar ± garnet ± cordierite + graphite plus accessory minerals which grow along the main foliation. Fibrolitic sillimanite may be present as inclusions in both garnet and cordierite.

Graphite-free leucosomes have a granitic/granodioritic composition with garnet ± cordierite as restitic phases.

The coexistence of garnet + cordierite + K-feldspar and the relics of sillimanite within cordierite and garnet suggest the A'KFM model reaction (1) Bt + Sil + Qtz = Grt + Crd + Kfs + V as responsible for the formation of the pelitic gneisses. Under reduced P_{H2O} this previous reaction is considered to be the main reaction forming the monometamorphic migmatites. The P-T estimates inferred from geothermobarometric methods indicate that reaction (1) was overstepped at T about 700-750 °C and P=4-5 kbar (X_{H2O}=0.5), with relatively constant retrograde pressures suggesting an isobaric cooling.

Relatively abundant CO_2±H_2O fluid inclusions occur in clusters and intracrystalline trails only in leucosomes: microthermometry and Raman analyses reveal a fluid composition of 48 mol% CO_2, 51 mol% H_2O and 1 mol% NaCl, with a water activity of about 0.5. CO_2 liquid homogenization temperature (ThL) ranges from -25.8 to +29.3 °C.

CO_2 with traces of CH_4 fluid inclusions are abundant both in leucosomes, and in graphite-bearing mesosomes and gneiss. Their melting temperature (Tm) ranges between -56.9 and -62.7 °C; ThL ranges from -34.7 to +28.1 °C.

Widespread decrepitation phenomena affect CO_2 inclusions in migmatites: this can be inferred from their variable size, their irregular shape and the occurrence in clusters of two-phase CO_2 inclusions, without visible water, but associated with three-phase CO_2 inclusions.

CO_2-dominated fluid inclusions with variable amounts of N_2 and CH_4 typically occur in the gneiss and in mesosomes. Tm ranges from -57.2 and -61.9 °C, while homogenization occurs to the vapour in mesosomes (ThV from -11.4 to +25.4 °C) and to the liquid in the gneiss (ThL from -9.2 to +18.7 °C).

Late two-phase aqueous inclusions are always present in all the samples studied.

The occurrence of CO_2+H_2O fluids is controlled by migmatitic structure and their density is consistent with the P-T conditions of the migmatitic event: these features indicate that their formation is related to migmatization by partial melting with a low H_2O activity (X_{H2O}=0.5). CO_2+H_2O fluids without CH_4 in graphite-free leucosomes, cannot be explained by vapour-absent partial melting of graphite-bearing mesosomes: this would have produced mixed CO_2-CH_4 fluids in the leucosomes by a reaction such as Bt + Sil + Qtz + C = Grt + Crd + Kfs + L + CO_2 - CH_4. We conclude that free oxidizing pure CO_2 fluids ± H_2O were present during high-grade metamorphism and triggered partial melting reactions.

High-density CO_2+CH_4 fluids characterize the retrograde evolution of these rocks at lower temperatures: isochore distribution, indicating successively higher densities, supports a substantially isobaric cooling history (P-T counterclockwise path).

GEOCHEMISTRY OF THE MARMORE TRAVERTINES (VALNERINA, CENTRAL ITALY)

Frondini F. and Zanzari A.R. (*Dept. of Earth Sciences , Univ. of Perugia*)

The Marmore area (Valnerina, Central Italy) is characterised by a travertine deposit of almost 1 km^2 and up to 110 m thick, standing unconformably on the Mesozoic limestones of the Umbria-Marche sequence. The travertine is deposited by the waterfall, 160 m high, that the Velino river forms falling on Nera river from the south-eastern rim of the valley.

A geochemical study has been carried out to define the relationships between travertine, depositing water and compositional changes occurring during diagenesis in meteoric environment.

Thirty-eight samples were collected from six drillings at depth ranging from 0 to 110 m. All the samples were analysed for the content of the following elements: Ca, Mg, K, Na, Li, Si, Ti, Al, Fe, Mn, Zn, Sr, Ba, Cl, S. Were also sampled and analysed the waters of the Velino river before and after the fall and the water from a well drilled in the travertine.

Analytical data of the waters show the effect of calcite precipitation due to the rapid degassing during the fall and leading to a variation in pH and to a sharp decrease in HCO_3, Ca, Mg, SO_4 and some trace elements as Ba, Sr, Mn, Zn and Fe.

The calculated distribution coefficients for Mg and Sr show values, respectively D_{Mg}=0.04 and D_{Sr}=0.132, within the range of values given by literature (Veizer, 1983).

Because the depth of sampling is related to the age of the sediments, elemental changes during increasing diagenetic equilibration of $CaCO_3$ with meteoric water are shown plotting trace elements content against depth.

Na, Sr and S show a depletion with depth while Mg shows an enrichment.

The behaviour of Na and Sr can be explained as the result of multiple dissolution-reprecipitation events that lead to a decrease in concentration for those elements with D < 1.

Analogously the decrease of S can be related to the depletion of sulphate ions, replacing carbonate ions in calcite, occurring during the solution-precipitation cycle.

Finally there are two possible causes for the increase in the Mg/Ca ratio with depth:

1) The equilibrium constant of calcite changes with $MgCO_3$ molefraction; very low Mg-calcite is less soluble than pure, or nearly pure, calcite (Thorstenson and Plummer, 1977), and for this reason in multiple dissolution-reprecipitaton events the solid phase tends to be enriched in Mg.

2) Pure, or nearly pure, calcites require solutions with extremely low Mg/Ca ratios in the aqueous phase to maintain thermodynamic equilibrium while the ground waters of the regional aquifer, interacting with the deeper levels of the travertine deposit, are characterised by higher Mg/Ca ratios.

The Mn content, that has a strong positive correlation with Fe content, does not show any significant correlation with the depth of sampling and the diagenesis and, reflecting the redox conditions of the depositing water, gives interesting paleoenvironmental information.

References:
Thorstenson, D. C. & Plummer, L. N. (1977). *Am. Jour. of Science*, 277, 1203-1223.
Veizer, J. (1983). *Reviews in Mineralogy*, 11, 265-299.

EXTREMELY PHOSPHORUS-RICH ALKALI FELDSPARS FROM RARE-METAL GRANITES IN THE BOHEMIAN MASSIF (CZECH REPUBLIC)

FRÝDA J. AND BREITER K. (CZECH GEOLOGICAL SURVEY, PRAGUE)

During a systematic investigation of Variscan granites along the Bohemian-Bavarian border, it was found that the Křížový kámen granite is a new P-rich granite type. Both feldspars (albite and K-feldsdpar) are the main phosphorus reservoirs in this granite. This finding initiated a research of feldspars in other highly differentiated, P-enriched granites within the Bohemian Massif (Breiter, 1993), in the Southbohemian pluton (Homolka - granite) and in the Karlovy Vary pluton (Podlesí - granite).

The average contents of P_2O_5 in K-feldspars (Křížový kámen 0.57 wt.%, Homolka 0.77 wt.%, and Podlesí 0.83 wt.%) were always greater than the average contents of P_2O_5 in plagioclases (Křížový kámen 0.23 wt.%, Homolka 0.23 wt.%, and Podlesí 0.39 wt.%). Also, there was a considerably heterogenous

distribution of P_2O_5 within single grains of both plagioclase and K-feldspar from all granitic rocks studied. The analyses of feldspars yielded partitioning coefficient of phosphorus between K-feldspar and plagioclase ranging from 1.5 to 2.5.

Our data generally agree with a theoretical mechanism of phosphorus substitution: $Al^{3+} + P^{5+} = 2\ Si^{4+}$ (Simpson 1977). Only for K-feldspars from the Podlesí granite the measured data suggest a statisticaly significant difference from the above substitution mechanism. The P-contents in K-feldspar from this locality (up to 2.5 wt.% of P_2O_5) represent the highest P-contents in natural feldspars known to date. These high contents suggest that the behavior of phosphorus is not strictly stoichiometric, similar to observations made on experimentally grown P-rich alkali feldspars (London et al., 1990).

The incorporation of phosphorus into feldspars is possible because the crystallization of apatite is metastably suppressed throughout the main stage of peraluminous granitic magma crystallization. The apatite crystallized during the late stages and the phosphorus contents of both the granitic melt and feldspars sharply dropped (the average P_2O_5 content of feldspars from the Homolka granite is roughly five times greater than in a late-stage aplite). The granites studied conserved nearly all phosphorus of the granitic melts and the alkali feldspars are main phosphorus reservoirs. This fact has important implications for trace-element modeling of peraluminous granitic melts.

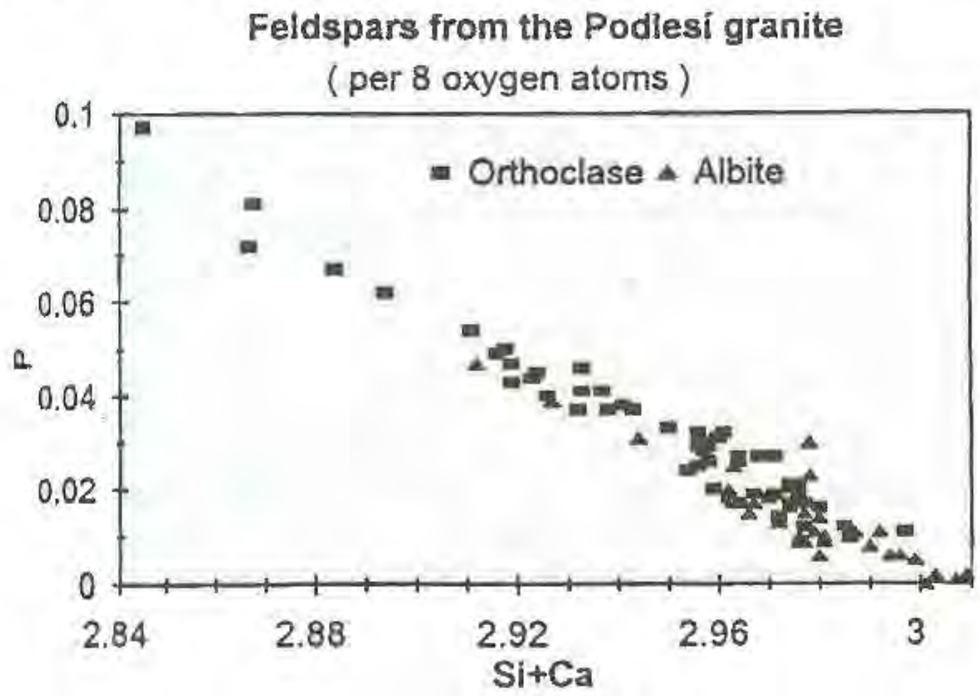

References:
Breiter, K. (1993). *Metallogeny of collisional orogens of the Hercynian Type*, Ed. Seltmann, R., Potsdam, 18-19.
London, D. (1992). *Am. Miner.*, **77**, 126-145.
London, D., Černý, P., Loomis, J.L. (1990). *Can. Miner.*, **28**, 771-786.
Simpson, D. R. (1977). *Am. Miner.*, **62**, 351-355.

CHANGES IN IRON OXIDATION STATE AND DEPROTONATION INDUCED BY ANNEALING OF NATURAL TOURMALINES

Y. Fuchs (*Lab. Mineral. Exp. Appl., Université UPMC, Paris)*, M. Lagache *(Lab. Geol.. ENS, URA 1316 du CNRS, Paris)* and G. Linares *(D.R.P., UPMC, Paris, URA 71 du CNRS)*.

Mössbauer effect spectrometry of natural tourmalines from various origins shows different distributions of Fe^{2+} and Fe^{3+} in the Y and Z octahedral sites (Hermon *et al.*1973; Mattson & Rossman, 1984, 1987a; Saegusa *et al.*1979). The occurence of intervalent iron was also described by Mattson & Rossman (1987b) and attributed to the delocalization of an electron between Y and Z sites (Ferrow *et al.*1988).

Two samples of tourmaline from the Humboldt Range hydrothermal field (Paulet *et al.*1991) were analyzed using a Mössbauer effect spectrometer. The first sample has only divalent iron in both sites. The second sample shows divalent iron in the Z site, divalent and trivalent iron in the Y site and a delocalized electron hopping between Y and Z site. These two samples were annealed under hydrothermal conditions (500°C and 50 MPa) for 20 days in limited oxidizing conditions. Mössbauer spectra of the annealed tourmalines show no change in the oxidation state of Fe in the Z site but important changes in the Fe^{2+}/Fe^{3+} ratio in the Y sites: Fe^{3+} scarcely appears in the Y site of the first sample and in the second sample there is an increase of the Fe^{3+} in Y site and a decrease of the amount of intervalent iron. This result is interpretated as a localization in the Y site, of the electron which was hopping between Y and Z sites. IR spectrum of the sample before and after annealing confirms that the stretching absorbtion band of the OH is moving toward lower frequencies. This result is consistent with OH surrounded by more trivalent cations. IR spectrum also shows a strong deprotonation of the tourmaline after annealing so that it is possible to assume that the development of trivalent cation in Y site is charge compensated by deprotonation.

We discuss the importance of this phenomenom in natural tourmalines and its significance to the interpretation of fluids involved at different stages of hydrothermal processes.

References:
Ferrow, E.A., Annersten, H., Gunardawana, R.P. (1988). *Min. Mag.* ,**52**, 221-228.
Hermon, E., Simkin, D.J., Donnay, G., Muir, W.,B. (1973). *Tschermaks Min. Petr. Mitt.*, **19**, 124-132.
Mattson, S.M. & Rossman, G.R. (1984). *Phys. Chem. Minerals*, **11**, 225-234.
Mattson, S.M. & Rossman, G.R. (1987a). *Phys.Chem. Minerals*, **14**, 163-171.
Mattson, S.M. & Rossman, G.R. (1987b). *Phys.Chem. Minerals*, **14**, 94-99.
Paulet, P.H., Fuchs, Y., Maury, R., Foit, F.F. Jr., Rosenberg, P.E. (1991). *C.R. Acad. Sci. Paris*, **313, II**, 1155-1162.
Saegusa, N., Price, D.C., Smith G. (1979). *Journ. Phys.* coll. C2, **40**, 456-459.

GEOCHEMICAL AND ISOTOPIC (^3H, D, ^{18}O) STUDY OF THE NATURAL SPARKLING MINERAL WATER FOUND ON THE W' SLOPE OF THE MONTE VULTURE VOLCANO AND BOTTLED BY THE MONTICCHIO-GAUDIANELLO Co. (PROVINCE OF POTENZA, SOUTH ITALY).

Fuganti A. (Univ. Trento/Italy), Morteani G., Preinfalk C., Blamart D. (TU München/Germany), Bulgarelli G., Festa A. (Monticchio Gaudianello Co./Italy)

On the Southern and Western flanks of the Quaternary Monte Vulture volcano (1322 m) springs produce natural sparkling mineral water. The mineral waters used by the Monticchio Gaudianello Co. are captured from springs and drilled wells in an area about 2 km NW of where the two Monticchio lakes formed in a caldera structure. The drillings showed that the aquifer is contained in a series of interstratified, porous, fractured, strongly altered nephelinites and phonolites.

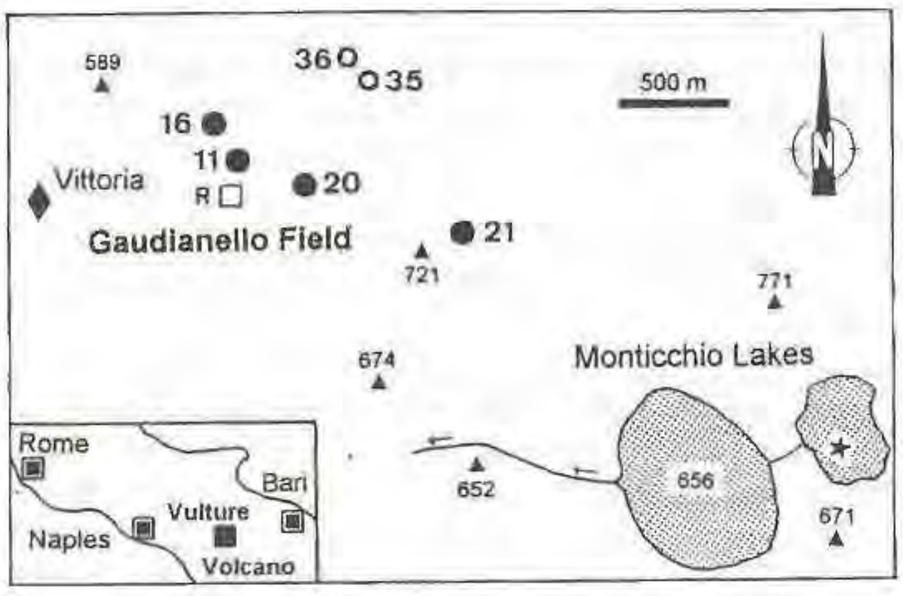

Fig. 1: Topographic sketch of the Monticchio Gaudianello area with no. of the sampled wells, springs, the pluviometer and of the Monticchio lakes

In Tab. 1 the technical, chemical and isotopic (^3H, D, ^{18}O) data of the water produced from the springs and wells and of that from the Monticchio lakes and of the local rainfall are given. The water flow in the aquifer is directed from the watershed to the NW. The T.D.S. of the water increases from the watershed to the most distant wells and springs in the NW.

Tab. 1: Technical, chemical and isotopic data of the water of the springs, the wells, the Monticchio lakes and of the local rainfall

Source	Elevation [m]	Vert. length [m]	Static level [m]	Horiz. length [m]	^3H	δD ‰	$\delta^{18}O$ ‰	T.D.S. mg/l	CO_2 mg/l
Spring (♦)									
Vittoria	555					-58			
Horizontal Wells (○)									
35	557			183	< 0.6	-58	-9.0	800	950
36	545			230	< 0.7	-56	-9.1	1200	900
Vertical Wells (●)									
16	634	69	51		< 0.8	-60	-9.3	1600	800
11	642	80	44		< 1.0	-58	-9.0	1300	900
20	646	96	54		< 0.8	-58	-9.1	850	1400
21	724	201	137		< 1.0	-57	-9.1	424	440
Lake Water (★)									
Small L.	658	5				-44	-5.3		
Small L.	658	32				-59	-8.6		
Rain Water (R □)						-61	-8.9		

^3H values in tritium unit (T.U.) with 1 T.U. = 0.119 Bq/l
δD (±2 ‰) and $\delta^{18}O$ are given against V-SMOW.

The increase of the T.D.S. of the water is the result of a leaching of the volcanic country rocks. The δD and $\delta^{18}O$ of the rain water are -61 and -8.9 ‰ (V-SMOW) and very similar to the water of the springs and wells and to the deep water of the small Monticchio lake and have to be considered of meteoric origin (see e.g. Mongelli et al. 1975). The water of the small Monticchio lake at -5 m is enriched in δD and $\delta^{18}O$ by around 20 and 3 ‰ as compared to the meteoric water. This can be interpreted in terms of evaporation stratification.

The low tritium contents (< 0.8 T.U.) of the waters from the wells indicate that these waters are older than 40 years. From the distance of about 3 km between the watershed and the wells and an age older than 40 years a flow velocity of less than 75 m/year in the highly fractured and porous aquifers can be calculated.

An important question still under investigation is the role of the Monticchio lakes in the recharging of the aquifers. The many settlements along the shores of the lakes are a potential source of contamination. But the low flow velocity is a guarantee that a potential organic contamination from domestic sewage will not influence the quality of the water produced by the Gaudianello Co.

References:
Mongelli, F., Panichi, C. & Tongiorgi, E.(1975). *Arch. Oceanogr. Limnol.*, **18**, 167-188.

DISLOCATION DISSOCIATION IN MANTLE OLIVINES

Fujino K. (*Dept. of Earth Sciences, Hokkaido Univ.*), Kohlsted D.L., Karato S. (*Dept. of Geology and Geophysics, Univ. of Minnesota*), and Bai Q. *(GeoForschungZentrum Potsdam)*

Dissociated dislocations in natural olivines derived from the upper mantle and in experimentally deformed olivines, have been observed with high-resolution electron microscopy to examine the correlation between the dislocation dissociation and the hydration in olivine. We have found dissociated [010], [011] and [001] dislocations in naturally deformed olivines from the Uenzaru peridotite, northern Japan, while the dissociations of only [010] dislocations are observed in olivines from San Carlos and in olivines experimentally deformed at dry and subsequently annealed at wet conditions.

The most common type of dissociation of [010] dislocations is the same among the natural and the experimental olivines, and the dissociation is $[010]=1/4[01\bar{1}]+1/4[01\bar{1}]+1/4[011]+1/4[011]$, with the stacking faults parallel to $(02\bar{1})$, (010) and (021) planes, while the dissociation of [001] dislocations is $[001]=1/2[00\bar{1}]+1/2[001]$, with the stacking fault of (001) plane. The separation between the partial dislocations ranges from 5 to 20 nm. All the observed dissociated dislocations have the same character; namely, the Burgers vectors of the partial dislocations are of the type 1/4<011> or a combination of two such Burgers vectors, and the stacking faults are parallel to {021}, (010) or (001). This observation indicates that all these dissociations are formed by the same scheme. Calculations using anisotropic elastic constants of olivine show that the energy of the dissociated dislocations is lowered from that of the parfect dislocation in all the cases by up to 66%.

The fact that all the [010] dislocations are dissociated into partial dislocations in examined olivines including those from San Carlos which are considered to have been at the dry condition, indicates that the [010] dislocations are always dissociated into partials by their high instability of perfect dislocations, while the dissociation of [001] dislocations may be induced by the presence of hydrogen or water.

IN SITU X-RAY OBSERVATION OF SILICATE PEROVSKITE UNDER LOWER MANTLE CONDITION

Funamori N., Yagi T., Kondo T., Uchida M. and *Utsumi W. (*Inst. for Solid State Physics, Univ. of Tokyo,* *now at *Dept of Earth and Space Science, State Univ. of New York at Stony Brook*)

In spite of its importance, little studies have been so far carried out to clarify the thermoelastic property of silicate perovskite under lower mantle condition. Using Drickamer-type high pressure apparatus employing sintered diamond as an anvil material, we have succeed for the first time to carry out an in situ x-ray observation under lower mantle condition (Funamori & Yagi, 1993). The results indicates that the orthorhombid perovskite structure is stable at the condition of the top of the lower mantle and that the pressure dependence of α is relatively small ($\delta_T=(\partial \ln\alpha/\partial \ln V)_T=3$) compared to earlier estimates. However, the temperature in this experiment was measured by indirect method and has some ambiguity. Furthermore, a large uniaxial stress component in Drickamer type apparatus (Funamori et al., 1994) might give systematic errors in the unit cell determaination.

In order to overcome these problems and to determine the thermoelastic properties under lower mantle conditions accurately, we have re-measured the thermal expansion under pressure using the MA8-type double stage mult-anvil apparatus which can generate higher pressure than the cubic anvil type apparatus and has smaller uniaxial stress component compared to that in the Drickamer-type apparatus. By improving the x-ray diffraction geometry and the sample assembly, we have succeeded to obtain a high quality x-ray diffraction pattern up to 2000K at above 20 GPa. Up to the present, transformation of $MgSiO_3$ from a pyroxene structure to a perovskite structure could be observed in situ and the uint-cell volume of the perovskite was determined with the accuracy of 0.15%. The detailed description of the latest experiments and the results of the analysis well be presented at the meeting.

References:
Funamori N. and Yagi T. (1993). *Geophys. Res. Lett.*, 20, 387-390.
Funamori N., Yagi T., and Uchida M. (1994) *J. Appl. Phys.*, in press.

SYNCHROTRON X-RAY DIFFRACTION STUDIES ON STRUCTURAL PHASE TRANSITIONS IN OXIDES AND SILICATES AT HIGH PRESSURES IN DAC.

Fursenko B.A., Belitsky I.A., Politov A.A* and Seryotkin Yu.V. (*Inst. of Mineralogy & Petrography*, **Inst. of Solid State Chemistry, Russ.Acad.Sci., Novosibirsk*)

Synchrotron radiation (SR) facility of the Inst. of Nuclear Physics of the Russ.Acad.Sci. in Novosibirsk was used. Experiments were made on the "Diffraction cinema" station of the VEPP-3 storage ring.

SR beam from wiggler (E=2GeV, I=100-200 mA) was monochromatized using curved Ge-monochromator ((220) plane, λ=0.93Å), collimated to 0.2x0.2 mm or smaller and directed to the small powder sample compressed in DAC (Fursenko *et al.*, 1985) between two diamond anvils and surrounded by metal gasket with pressure transmitting liquid. Diffracted rays were detected by the position sensitive detector (PSD) with linear resolution 0.1 mm

situated on the vertical goniometer (sample to PSD distance was 250 mm).

Typical exposure time for the framework aluminosilicates at high pressures was 5-10 min for satisfactory statistics and even lower for special kinetic experiments. It is to be compared to 30-60 s exposures for simple oxide minerals such as zincite. Further decrease of exposure time could be reached using energy dispersive (ED) method, but as was shown by our preliminary comparative study on the same objects the resolution of the ED diffraction patterns is too poor to work with complex framework silicates structures of low symmetry.

Pressure was measured by ruby fluorescence, known mineral compressibility or derived from graduation of the Belleville springs.

A number of reversible phase transformations in oxides and silicates were studied. High-pressure reconstructive phase transition in zincite ZnO (from wurtzite to NaCl structure) at 80 kbar, though reversible, was shown to have a large hysteresis (down to 50 kbar), which was enlarged drastically in Zn-doped oxide (down to near atmospheric pressure) (Fig. 1).

Fully reversible phase transitions were detected in fibrous zeolites: natrolite, scolecite and mesolite below 20 kbar. Strongly anisotropic compression of edingtonite was observed at pressures up to 40kbar. Preliminary results were obtained for laumontite and hydrosodalite.

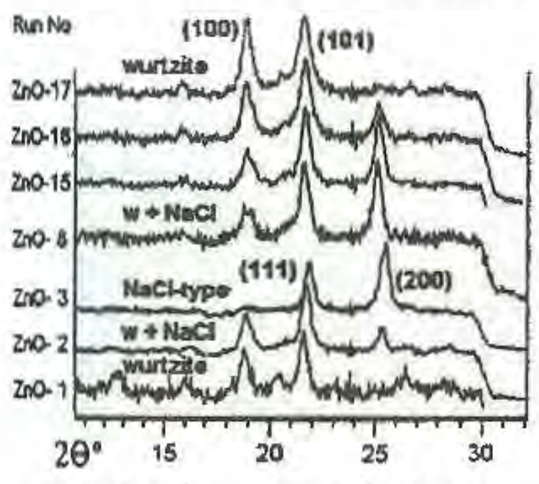

Fig.1. ZnO ↑

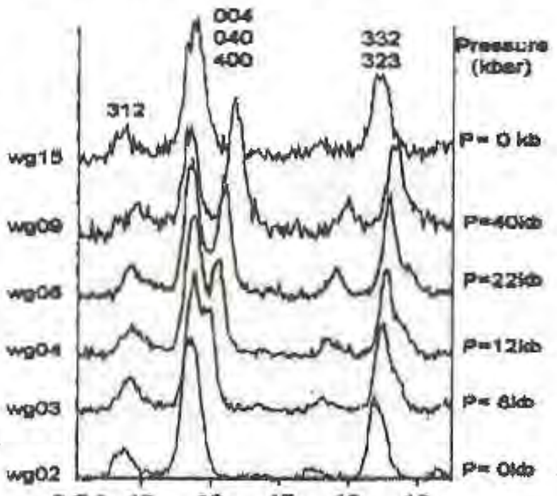

Fig.2. Wairakite→

Wairakite - a Ca-member of analcime group with chemical composition $Ca_{0.97}Na_{0.06}K_{0.03}Al_{1.95}Si_{4.04}O_{12}$ 2.06 H_2O was studied in more details. The results were practically the same, when wairakite was compressed in water, methanol:ethanol mixture, and glycerol, showing no penetration of pressure transmitting liquid into the framework channels of the ANA-type framework.

Strong splitting of 004, 040, 400 diffraction maxima with increasing pressure (Fig.2) and distinct slope changes on pressure dependence of individual peaks' positions are interpreted as a phase transition near 17.5 kbar. This suggestion is supported by Raman spectroscopy data, showing a distinct discontinuity in band frequencies pressure dependence (Goryainov *et al.*, 1993). Although the resolution of our diffractograms is not sufficient to make a final conclusion, lowering in symmetry from monoclinic to triclinic is supposed. All changes observed at high pressure up to 50-60 kbar are fully reversible, but amorphization beginning above 80 kbar.

References

Fursenko, B.A., Litvin, Yu.A., Kropachev, V.D., and Kholdeev, O.V. (1985), *Pribory i technika experimenta*, N5, 174-178.

Goryainov, S.V., Belitsky, I.A., and Fursenko, B.A. (1993) *J.Raman Spectroscopy*, in press.

REFRACTORY CERAMICS IN SEVERE ENVIRONMENTS

Gabis V.M. (*Ecole Sup. Energie et Matériaux, Univ. of Orléans*)

Behaviour of refractory ceramics in severe environments depends for a large part on microstructure and minor phases. Two case stories are presented to illustrate this point.

The first example concerns interaction between several oxides and aluminium alloys. Excepted corundum, all materials react with molten aluminium, within less than one hour. At the refractory/aluminium interface a gas layer is always observed as well as a thin alumina layer on the metal side of the gas layer. Oxygen which is necessary to yield the alumina layer is transported from the outer atmosphere to the refractory through the molten alloy. Corrosion mechanism is always reduction. Ellingham diagrams are not always able to predict refractory corrosion. More complete thermodynamic calculations are necessary.

The second example concerns clogging deposits of alumina inside submerged nozzles used for steel continuous casting. At high temperature, alumina-graphite refractory generates gaseous products by a reduction mechanism of secondary oxides by carbon. Liberation of CO(g) at the refractory-alumina killed steel interface yields oxidation of the dissolved aluminium and enhances the precipitation of alumina. Several solutions are proposed to prevent this clogging phenomenon.

DIAMONDS PHOTOLUMINESCENCE AT ROOM TEMPERATURE

Gaft M. (Geology Group, Open Univ. of Israel)

The photoluminescence (PL) of diamonds has been studied mainly at 77 K where luminescence centers (LC) are characterized by zero-fonon lines. At 300 K they are nearly absent and the broad vibronic bands are difficult to identify. The aim of this paper is to measure and ascribe the diamonds PL at 300 K. Interpretation was done on the basis of a comparison between PL at 77 and at 300 K. The experiments were carried out on "pure type" diamonds, each with specific type of LC (Table).

Several types of N3 at 300 K with different proportions between zero-fonon line at 415 nm and its vibronic replicas at 429, 440, and 452 nm were detected. Sometimes this line is nearly

LUMINESCENCE PARAMETERS OF DIAMONDS AT 300 K

LC	SPECTRAL-KINETIC PARAMETERS				PS
	λ,LM nm	HW nm	λ,EX nm	DT us	
N3	440	50	370	0.02-0.04	LINE AT 415 AND BANDS AT 429, 440, 452 and 465 nm
nN3?	440	50	370, 340	0.02-0.04	LINE AT 416 nm IS ABSENT
A	450-470	100	230	0.025 100, 3000	MAIN BAND FOR THE SORTING
H3	535	67	340	0.02, 7.5, 7700	WEAK SHOULDERS AT 505 AND 520 nm.
H4	520	67	340	0.020	WITHOUT STRUCTURE
S3	535	65	340	2-3, 24	LINE AT 497 nm
S2	540	85	340	2-3, 240	WITHOUT STRUCTURE
S1	575	100	340	0.02, 5-6 200, 2100	WITHOUT STRUCTURE
575	575	33	340	0.025	LASER EXCITATION
578	675	58	340	0.01, 200	LINE AT 657 nm
640	685	70	380	?	SHOULDER AT 638 nm
788	788	5	340	?	TOGETHER WITH S1

λ,LM - LUMINESCENCE MAXIMUM; HW - HALF-WIDTH;
λ,EX- EXCITATION MAXIMUM; DT - DECAY TIME

absent and its disappearance is accompanied by excitation band broadening.

The cause may be the N3 clusters formation with the following concentration quenching resulting from energy migration. The transfer is evidently of the emission-reabsorption type, namely, emission by one LC and its reabsorption and emission by the other LC. This is explained by the similarity of the energies of emission and reabsorption. In the luminescence of the sensitizer, only the intensity of the absorbed part diminishes, the rest remaining unchanged.

This allows to explain our data as follows. A feature distinguishing the N3 center is that its absorption is similar to its excitation and presents a mirror reflection of its PL. The line at 415 nm is present in the emission and in the absorption spectra being subjected to the concentration quenching. This is confirmed by the fact that this process is particularly prominent in the yellowish diamonds which are characterized by elevated N3 contents.

THE S. R. PERREN GEM AND GOLD ROOM, ROYAL ONTARIO MUSEUM, TORONTO, CANADA

Robert I. Gait *(Dept. of Mineralogy)* & Fang-Pin Lee *(Exhibit Design, Royal Ontario Museum, Toronto, Canada)*

The S. R. Perren Room, the first stage of the much larger Earth Sciences Gallery, opened in 1993. It is a 100 square metre, innovative, permanent exhibit of over 1000 items from the Royal Ontario Museum's gem and gold collections. In addition to the traditional gems, unusual, rare, and soft gem materials, faceted for the connoisseur collector and museums are displayed. Laboratory-grown crystals, gem substitutes, and imitations are also brought to the attention of the public.

The entire exhibit is illuminated by a glass fibre optic system connected to only 13 light sources. Each source contains a 150 watt metal halide bulb that produces light with a colour temperature of 4000°K (an approximation to daylight). The bulbs have a life expectancy of 6000 hours, equivalent to an estimated one and a half years of museum use. The flexible nature of the glass optic fibres allow the light to be taken to virtually anywhere in the display. In most instances the optic fibres are fed into lenses of various sizes depending on the area of the pool of light required. Thus the objects can be lit from underneath, behind, or from above without any elaborate electrical wiring. The fibre optic system was chosen because lighting is of critical importance to gem displays. Some of the text panels are backlit by a woven fabric made from plastic optic fibres that distributes the light evenly along its length and breadth. This is the first museum gallery in north America to be lit exclusively by fibre optics.

The colourful gems are presented on a neutral background of finely-sandblasted, colourless, acrylic stands and platforms. The gems are elevated or held in position by very thin, stainless steel dental wire posts, drilled into the acrylic. These mounts allow the gems to easily adjusted for optimum viewing and lighting.

The ambient light in the room comes entirely from the display cases, enhanced by reflections off the polished granite floor. The warm wood panelling and low ceilings provide an intimate and opulent setting for the dazzling gems and the richness of the gold specimens. Special care was taken to ensure that the groups and positions of individual gems were complimentary to one another. Thus even with over 100 items in a single case, they appear to be composed and well spaced.

The text is in English and French and inside the cases it is kept to a minimum. Additional information is provided outside the cases in large format booklets. In these, information about each of the 960 gems, jewellery, lapidary objects, and crystals is available to the visitor.

Two touch screen audiovisual stations outside the room are "user-friendly" and in almost continual use. The visitor can choose from three main topics: How faceting enhances a gemstone; how stars and cat's eyes are formed; or where the colours come from in precious opal.

There are 70 gold specimens on display including some spectacular pieces from Canada; six nuggets from California (weighing from 70 to 180 troy ounces) and a few small, but beautiful, examples of crystalline and wire gold.

METHODOLOGY FOR LOCATION OF ORIGINAL QUARRIES OF BUILDING STONES. APPLICATION TO MALAGA CATHEDRAL (SPAIN)

Galán E., Carretero, M.I. and Mayoral E. (*Dept. of Crystallography and Mineralogy, Univ. of Sevilla, Spain*)

Many times it is necessary to localize the original quarries from which stones of a particular building were extracted. These stones could be use for future restoration labours and for testing in the lab (artificial ageing tests, physical properties determination, control of the efficacy of conservation treatments, etc.). Generally the review of historical documentation give us information about the geographical setting of quarries and the situation of the stones in the monument, but, this information have to be proved. The comparative study of stones from quarries and monuments should basically include the following determinations:

1) Mineralogical and petrographical studies.
2) Chemical analysis of major, minor and trace elements.
3) Stable isotopes determinations.
4) Physical properties of quarry materials and unweathered building stone (water absorption, ultrasonic velocity, porosity and porous system, density, bulk density, compression strength, etc.).
5) Statistical analysis of the results.

This methodology was applied to Málaga Cathedral stone represented in the main façade and towers, which, according to the historical literature, came from Almayate (Miocene-Pliocene limestones) and Cerro Coronado (Permotriassic sandstone) in Malaga. The conclusion of the comparative study carried out on quarries and building stones was consistent with the information available from the historical documentation.

ROCKS OF THE NORTH-WESTERN REGION OF THE UKRAINIAN SHIELD

Galiy S.A., Skobelev V.M., Esypchuk K.Ye., Kogut K.V. (*Inst. of Geochem., Mineral. and Ore Form., Kiev, 252142, Ukraine*)

Series of nickel-bearing maphic-ultramaphic intrusive massifs of different sizes (from one to hundred square km) was found in the North-Western Region of the Ukrainian Shield during the last years. All they are located in zones of deep faults limiting the Shield or dividing one into different tectonic megablocks. All they are proterozoic (2050-1990 Ma), unmetamorphozed, discordant with more ancient metamorphic rocks and ultrametamorphic granitoids of basement. The rocks of these massifs are characteristic by low isotopic ratio of $^{87}Sr/^{86}Sr$ (0.7026)

and positive value of Nd (+2.8), and ones belong toperidotite-pyroxenite-gabbronorite formation.

The nickel-bearing massifs are layered intrusions. Majority of them are monophasic. Both evident and cryptic layerings are observed in the massifs. That is why very wide diapason mineral paragenes and variable chemical composition of the same minerals are characteristic for rocks of the massifs.

Main rockforming minerals are olivine, clyno- and orthopyroxenes, plagioclase, hornblende. Biotite,chlorite, serpentine, K-feldspar, quartz, carbonates, graphite are secondary minerals. Typical accessory minerals are apatite, zircon. Ore minerals are represented by ilmenite, magnetite, spinel (seldom), sulphides, nuggets gold and platinum (very seldom), bismuthids (seldom).

Different schemes of crystallization and succession of crystallization of cumulate minerals are observed in different massifs. Diversity of temperature conditions of crystallization of magmas is characteristic also, e.g. subsolidus temperature of crystallization of different rockforming minerals in the same intrusion could vary crystallization of the same mineral into different layers of the same intrusion could reach about 200-300°C. In such cases composition of the same minerals varies also strongly, e.g., ratio Fe/Fe+Mg varies from 0.21 to 0.64 for olivines of the Prutovskaya intrusion, from 0.18 to 0.57 for orthopyroxenes, from 0.32 to 0.58 for biotites, from 0.38 to 0.74 for chlorites; composition of clynopyroxenes varies from $Fs_{42}Vol_{52}$ to $Fs_{36}Vol_{24}$; composition of plagioclase varies from An_{77} (in garrizites) to An_7 in granophires). It is an obvious case of cryptic layering.

Lithostatic pressure into cameras of crystallization of different intrusions of the nickel-bearing formation was almost constant (300-500 Mpa), therefore all ones are mezoabissal. In the same time pressure of water and oxygen could vary in wide diapason even into different parts of the same intrusion or during process of crystallization.

Main sulfide mineral paragenes are: chalcopyrite-pentlandite-pyrrhotite, pentlan dite-cubanite-chalcopyrite-pyrrhotite and pyrite-violaryte-makinavite. It is observed zone distribution of the mineral paragenes both lateral, and vertical, it is fixed in increase of role of Fe-Cu associations (troiylite+putoranite+cubanite) directly as deep incriases. Ore sulfide paragenes were formed under temperature from 730 to 150 °C.

ENVIRONMENT OF NICKEL AT TRACE LEVEL IN SAN CARLOS OLIVINE.

Galoisy L., Calas G. (*Laboratoire de Minéralogie-Cristallographie, Université Paris VI et VII, IPGP and URA CNRS 09- FRANCE*) and Brown G.E., Jr (*School of Earth Sciences and SSRL, Stanford University, Stanford, CA 94305 USA*)

X-ray absorption spectroscopy (XAS) provides a direct access to the determination of the sites occupied by trace elements in minerals. We present results on the location of minor amounts of nickel (5000 ppm) in San Carlos olivine using Ni-K edge EXAFS. Spectra have been recorded at the Stanford Synchrotron Radiation Laboratory (SSRL) on wiggler beam line 4-3. A 13 element diode-array detector and a (220)Si monochromator were used. Ni_2SiO_4 olivine and spinel were used as references.

The comparison of San Carlos and Ni_2SiO_4 EXAFS spectra indicates different environments of Ni^{2+} in both structures. The Ni-O distance d(Ni-O)=2.07Å in San Carlos indicates a preferential location of Ni atoms in the M1 sites. This direct determination confirms the predictions from crystal field theory and previous data on more concentrated Mg-Ni olivines. Inded crystal field stabilization energy are expected to drive Ni^{2+} cations in the smaller M1 sites of the olivine structure (Burns, 1993). Relaxation effects may be directly derived from the discrepancy between the experimental Ni-O distances and the cation-oxygen distances expected from structure refinement data (Brown, 1982). Ni-O distance is significantly smaller than the Mg-O distance in the M1 site of forsterite (2.101 Å) and even smaller when considering the average M1 cation-oxygen distance in natural olivines. Relaxation effects are thus important during Mg to Ni substitution.

The intracrystalline distribution of Ni in the olivine structure may be constrained by modeling EXAFS spectra, considering the various possible structures around Ni located at M1 sites. Heterogeneous distribution of Ni may be excluded and the Ni-Mg ordering in the M1 chains will be discussed. A comparison with Fe-K edge EXAFS data obtained on the same sample will be presented to show the different behavior of these two transition elements.

Reference:
Brown, G.E.,Jr. (1982). *Rev. Miner.*, **5**, 275-381.
Burns, R.G. (1993). Mineralogical Applications of Crystal Field Theory. *Cambridge University Press.*

EPITAXY OF ACHTARANDITE ON GROSSULAR

Galuskina I.O.*, Galuskin Ye.V.* (*Inst. of Ore Deposits, Petrog., Miner. and Geoch.(IGEM), Moscow, Russian Acad. of Science*) and Winiarska A. (*Inst. of Physics, Silesian Univ., Poland*)

The problem of the achtarandite (a pseudomorph after an unknown mineral from the Vilui river , Yakutia) - is a mystery for more then 200 years (Lyakhovich, 1952, Kleber & Pascal, 1960, Kuznetsova & Schafranovsky, 1966). Metacrystals of the achtarandite, vesuvianite (viluite), grossular and diopside are found in skarned limestones and dolomites (Pz_1) in the field of spread of diabasic dikes (T). Groundmass of the rock was altered and consists of chrysotile, garnet (series grossular- hydrogrossular, with a-cell parameter from 11.85Å to 12.12Å), calcite and saponite. As a subordinate minerals kaolinite, penninite, clinochlore, hematite, goethite and other are noted.

The achtarandite crystals (less then 15 cm) occurred in form of {112} or a combination of {112} and {11$\bar{2}$}. From the set of 308 achtarandite crystals noted as growing on the 100 grossular crystals (1-2 cm in size) 292 were found as growing epitaxially (Fig.1). The achtarandite crystallized simultaneously with outer zone of grossular and viluite. On grossular crystals the induction surfaces with achtarandite were noted. Their morphology indicate the relatively high growth rate of achtarandite. Character of the pseudomorphs show that achtarandite was forming case-like crystals (thickness of wall: 2-4 mm), central part of which was filled by substrat minerals. The achtarandite "case" was substituted oriently by the polycrystalline aggregate of hydrogrossular (a-cell parameter from 11.95Å to 12.06Å). Inclusions of achtarandite in viluite were substituted by host-mineral (viluite) with preservation of primary zonality of the "case" and inheritance of the host-crystal orientation.

Fig.1. Epitaxy of achtarandite (A) on grossular (G), (112)A ‖(112)G or (112)A‖(11$\bar{2}$)G.

Achtarandite crystallized in a cubic system. Its "a" cell-parameter was very similar to grossular, but both minerals differ in the symmetry classes ($\bar{4}$3m in achtarandite). Achtarandite composition was close to the compositions of grossular and vesuvianite. Greatest crystals of achtarandite were mentioned in portions of the rock poor in viluite and diopside. Absence of quartz in the rock, under consideration sequence of minerals crystallization and the

*- *till 10.1994 at the Department of Earth Science, Silesian Univ., Poland.*

characteristic compositional features of grossular indicate that achtarandite contained Ca and Al as main chemical components and was easily hydrated. As a result we suppose that achtarandite was in fact the mineral similar to mayenite ($12CaO \cdot 7Al_2O_3$, $\bar{4}3m$, a=11.97Å). Extraordinary large sizes of achtarandite crystals can be explained by an influence of kinetic factors, a mechanism of growth and a stabilizing influence of impurities.

References:
Lyakhovich, V.V. (1952). *Dokl. Akad.Nauk.SSSR*, **82**, N4, 625-628.
Kleber, W. & Pascal, I. (1960). *Neues Jahrb. Mineral., Abhandl.*, **94**, H.2, 1266-1276.
Kuznetsova, V.G. & Schafranovsky, I.I. (1966). *In* "Genesis of mineral individuals and aggregates". Moscow, 97-103.

REGENERATED AND NEOGENIC MINERALS FROM POLYGENETIC DEPOSITS

Gamyanin G.N. *(Yakut Inst. of Geol. Sciences, Russian Acad. of Sciences)* .

The seguence of magmatism and metallization occurrences is controlled by geodynamic evolution of the Verkhoyano-Kolyma folded area. As a result, in zones of long-lived deep faults distinguished is a juxtaposition of various types of metallization, different in time and composition. Juxtaposition of antimony (Sb) and silver polymetallic (SP) metallization on te gold quartz (GQ) one, as well as of gold silver (GS) metallization on the gold rare-metal (GRM) and cassiterite sulfide (CS) result in a formation of polygenetic deposits characterized by a peculiar mineral composition.

Besides the well-known geological features of polygenetic deposits distinguished are mineralogical ones. They are related with a regeneration of major minerals of early metallization when juxtaposed by later one, as well as with a generation of unusual neogenic minerals which have not met in juxtaposing metallization types. Morphological habit and composition of regenerated minerals considerably differ from minerals analogous for juxtaposing metallization types. Unlike the early turbid coarse-grained aggregates, regenerated quartz, for example, is represented by an aggregate of transparent rice-shaped grains or small crystal-like druses. Pyrite and arsenopyrite form skeletal and mantle-like crystals, and sphalerite forms globular grains. The composition of regenerated minerals is characterized by a decreasing set of trace elements and we observe an increase in maior elements in juxtaposing metallization types.

For example, when juxtaposing Sb metallization on GQ, impurities of antimony increase in arsenopyrite (to 1%) and pyrite (to 17%), as well as the cobalt and nickel impurities in arsenopyrite (to 2%) by a factor of 100, whereas Ag concentrations in all minerals decrease by a factor of 10-100. Conversely, when juxtaposing GS metallization on GRM and CS, Ag impurities increase in all minerals by a factor of 10-20, and tetrahedrite becomes high-argentian (Ag>30%). In any case, regenerated sphalerite becomes low-ferruginous (Fe<2%). Regenerated minerals compositionally differ from their counterparts in juxtaposing metallization types.

As a result of mutual reaction interaction, neogenic minerals comprise usually major components of juxtaposing types: Au+Sb- aurostibite, aupoantimonite; As+Pb+Sb- arsenic-bearing lead sulphoantimonites; Sn+Pb+Sb- tin-bearing lead sulphoantimonites, etc. A combination of neogenic and usual minerals give rise to a generation of peculiar intergrowth structures, i.e. subgraphic, zonal kindey-shaped, diamond-shaped lenticular, etc.

The revealed features of regenerated and neogenic minerals are diagnostic for polygenetic deposits.

THERMODYNAMICS OF (Ca,Mg,Fe,Mn)-GARNET SOLID SOLUTION: NEW EXPERIMENTS, OPTIMIZED DATA SET, AND APPLICATIONS TO THERMO-BAROMETRY

Ganguly, J. and Cheng, W. (*Dept. of Geosciences, Univ. of Arizona*)

Most geothermo-barometers involve garnet as one of the reacting phases. Thus, an accurate knowledge of the thermodynamic mixing properties of multicomponent garnet solution is of central importance in the field of geothermo-barometry. Optimized data sets for the mixing properties in the binary joins of (Fe,Mg,Ca,Mn)-garnet have been provided by Ganguly and Saxena (1984) and Berman (1990), which have found extensive applications in phase equilibrium calculations of natural assemblages involving garnet.

In this work, we report a large number of new experimental data of garnet composition in equilibrium with kyanite, anorthite and quartz (Gross + 2 Ky + Qz ⇌ 3 An: GASP) in the Ca-Mg-Mn, Ca-Mg-Fe-Mn and Ca-Mg-Fe systems. These data have been modelled, according to a modified form of multicomponent subregular formulation (Cheng and Ganguly, 1994), by constraining the Fe-Mg binary values to Hackler and Wood (1989), Ca-Fe values to Berman (1990), and Fe-Mn values to O'Neill et al. (1989), along with the available experimental and observational data on the compositional dependence of K_D(Fe-Mn) and K_D(Fe-Mg) between garnet and coexisting phases to develop a self consistent model of the binary and ternary interaction parameters of (Ca-Mg-Fe-Mn) garnet, which are summarized below. Application of these data to several metamorphic terrains yield consistent P-T estimates, which are compatible with the nature of the aluminosilicate polymorph, whenever it is present in the assemblage of interest, and other petrological constraints, and which also show limited scatter when the garnet compositions in an isothermal-isobaric suite change widely.

Parameter	W(H)	W(S)	W(V)
Ca-Mg	19768	3.5	0.012
Mg-Ca	8620	3.5	0.058
Ca-Fe	873	1.69	0.0
Fe-Ca	6773	1.69	0.03
Ca-Mn	475	0	0
Mn-Ca	475	0	0
Mg-Fe	2117	0	0.020
Fe-Mg	695	0	0.003
Mg-Mn	10115	5.2	0
Mn-Mg	10115	5.2	0
Fe-Mn	620	0	0
Mn-Fe	620	0	0

W(H), W(S) and W(V) are respectively the enthalpic (J/mol), entropic (J/mole-K) and volumetric (J/mol) contributions to the subregular free energy parameter on one-cation basis (W(G) = W(H) - TW(S) + (P-1)W(V)). The ternary interaction parameters can be calculated from the binary terms according to the Cheng and Ganguly (1994) formulation.

References:
Berman, R.G.(1990) American Mineral. 75, 328-344.
Ganguly, J. & Saxena, S.K. (1984) American Mineral. 69, 88-97.
Hackler, R.T. & Wood, B.J. (1989) American Mineral. 74, 994-999.
O'Neill, H. St.C., Pownceby, M.I. & Wall, V.J. (1989) Contrib. Min. Pet., 103, 216-222.
Cheng, W. & Ganguly, J. (1994) Geochim Cosmochim Acta (in press)

CATION ORDERING GEOSPEEDOMETRY OF ORTHOPYROXENE: APPLICATIONS TO METEORITES AND SKAERGAARD INTRUSION

Ganguly, J., (*Dept. of Geosciences, Univ. of Arizona*), Domeneghetti, M.C. (*Dept. of Earth Sciences, Univ. of Pavia*) and Molin, G. (*Dept. of Mineralogy and Petrology, Univ. of Padova*)

In orthopyroxene (OPx), Fe^{2+} and Mg fractionate as a function of temperature between two non-equivalent octahedral sites, M1 and M2. Mueller (1967) developed a kinetic theory of isothermal order-disorder process of Fe and Mg in ferromagnesian silicates as function of time (t), which can be applied to numerically simulate the change of ordering state in a continuously cooling system (Ganguly, 1982). This permits determination of the cooling rate of a natural crystal around the closure temperature (T_C) of its Fe-Mg ordering process by obtaining a satisfactory match between the observed and simulated quenched ordering states.

We have refined the calibration of Molin et al. (1991) of the equilibrium intracrystalline fractionation of an OPx crystal (X_{Fe}= 0.23) from Johnstown meteorite using bulk compositional constraint according to very accurate microprobe data (collected against synthetic standards with very high counting statistics, and averaged over a large number of spot analyses), and assuming that Fe^{2+} and Mn fractionate similarly (Hawthorne and Ito, 1978). No Fe^{3+} ion was needed to maintain charge balance. The refined calibration is as follows: $\ln K_D = -3062/T(K) + 0.888$, where $K_D = (Fe^*/Mg)^{M1}/(Fe^*/Mg)^{M2}$, and $Fe^* = Fe^{2+}$+ Mn. For X_{Fe} = 0.10 - 0.50, the disordering rate constant, K^+, can be expressed as (Ganguly et al., 1994) $\ln K^+ (min^{-1}) = 26.2 + 6.0X_{Fe} - (31,589)/T(K)$.

The above data yield $T_C \approx 375$ °C for the Johnstown OPx sample and a cooling rate around T_C of ~ 7 °C/10^3 yr, with an uncertainty of a factor of ~10. The cooling rate represents slope at ~ 375 °C of an 'asymptotic cooling model', $1/T(K) = 1/T_o + \eta t$, with η = 1.8(E-8) $K^{-1}y^{-1}$ or of an 'exponential cooling model', $T(K) = T_o\exp(-\alpha t)$, with α = 11(E-6) y^{-1}. These results are in accord with the qualitative conclusions of Mori and Takeda (1981) and Molin et al. (1991) about the very rapid cooling rate of Johnstown meteorite, which seems to be counter-intuitive in view of the homogeneous chemical compositions of the very large crystals found therein. Work is currently in progress to constrain the size of the parent body using the quantitative cooling rate as a constraint.

We have also determined the site occupancies of several OPx crystals (X_{Fe}= 0.35 - 0.40) separated from the marginal border group, base of lower zone 6, and Uttental plateau of the Skaergaard intrusion. The above calibrations of K_D and K^+ yield T_C of these samples in the range of ~ 380 to 425 °C, and cooling rates around T_C from ~7 to 155 °C/10^3 yr, with an uncertainty of a factor of two. Comparison of these results with the thermal models of Norton and Taylor (1979) of the Skaergaard intrusion suggests cooling via convective fluid circulation around 400 °C through rocks with permeabilities of at least 10^{-12} cm^2.

We have calculated the relationship between cooling rate, quenched ordering state and bulk composition of binary Fe-Mg orthopyroxene. The results show that for Fe-poor OPx compositions, such as commonly encountered in meteorites, the retrieved cooling rate is extremely sensitive to errors in the site occupancy determination, and the geospeedometer is impractical for OPx with $X_{Fe} < 0.15$.

References:
Ganguly, J. (1982) Adv. Phys. Geochem. 2, 58-99.
Ganguly, J., Yang, H. and Ghose, S. (1994) Geochim. Cosmochim. Acta, in press.
Hawthorne, F.C. and Ito, J. (1978) Acta Cryst. B34, 891-893.
Molin, G.M., Saxena, S.K. and Brizi, E. (1991) Earth Planet. Sci. Let. 105, 260-265.
Mueller, R.F. (1967) J. Phys. Chem. Solids, 28, 2239-2243.
Norton, D. and Taylor, H.P.,Jr. (1979) J. Petrology, 20, 421-486.

EFFECT OF INTERFACE IRREGULARITIES ON DIFFUSION PROCESS AND THE FRACTAL BEHAVIOR OF DIFFUSION FRONTS

Ganguly, J., Norton, D. (*Dept. of Geosciences, Univ. of Arizona*) and Chakraborty, S. (*Bayerisches Geoinstitut, Bayreuth*)

The nature of diffusion fronts in a semi-macroscopic scale is a problem of considerable interest in solid state sciences. Sapoval et al. (1985; 1986) have carried out theoretical analysis of diffusion process from the point of view of 'percolation theory', and have shown that completely 'random walk' diffusion in a square lattice is charactertized by an irregular front with a fractal behavior.

During the course of our on-going experimental investigation of multicomponent cation diffusion in aluminosilicate garnets using diffusion couples, we have examined a number of diffusion zones at different resolutions under electron microprobe. Two dimensional x-ray maps of the diffusion zones at a resolution of 1cm ≈ 5 μm revealed the diffusion fronts to be always irregular. Further, the diffusion zones were found to develop very complex element distribution patterns as a consequence of very small initial irregularities (~ 0.2 μm) on the interface, which amplified during the diffusion process. These findings need to be carefully considered in the interpretation of complex diffusion patterns in natural minerals in terms of tectonic and petrological processes.

Irrespective of the complexities of the interdiffusion zones, the diffusion fronts that we have examined so far showed fractal behavior, but with a characteristic dimension of 1.17 ± 0.03 as opposed to 1.76 ± 0.02 calculated by Sapoval et al. (1985). It seems very likely that multicomponent diffusional exchange (which is not a completely random walk process) is characterized by fronts with fractal dimension of 1.76 ± 0.02. Thus, fractal analysis may provide a means for distinguishing if a homogeneous core composition of a natural crystal represents original composition (i.e. unaffected by diffusion), or is a result of too much diffusional exchange of elements with an adjacent phase leading to homogeneity at the core at a concentration level different from the original composition. This is of considerable importance in the interpretation of temperature determined from 'plateau' core compositions of coexisting minerals, and in the calculation of cooling rate from

concentration profiles between adjacent mineral grains with concentration plateaus near the cores (e.g. Lasaga, 1983)

References:
Lasaga, A. (1983) Adv. Phys. Geochem. 3, 81-114.
Sapoval, B.R., Rosso, M. and Gouyet, J.F. (1985) J. Physique Lett., 46, L-149 - L-156.
Sapoval, B.R., Rosso, M. and Gouyet, J.F. (1986) Solid State Ionics, 18 & 19, 21 - 30.

THE EXOTIC HIGH TITANIFERROUS OXIDES FROM XENOLITHS IN KIMBERLITES

Garanin V.K.*), Kostrovitskiy S.I.**), Kudrjavtseva G.P.*), Varlamov D.A.***) *(*) Dept.of Geology, Moscow Univ., **) Inst.of Geochemistry, Irkutsk, ***) Inst.of Experimental Mineralogy, Chernogolovka)*

Oxides of unusual composition have been established in garnet grains from the kimberlite concentrate of Yakutian pipes (Sytykanskaya, International, Yagodka) and Aldanskaya dyke. The oxides are characterized by high titanium, chromium, zirconium contents and are closest to the minerals of armalkolite-kennedeite-redledgite group with the $(Mg,Fe)Ti_2O_5$ theoretical formula and of the crichtonite-loveringite-lindsleite-mathiasite with the $AM_{21}O_{38}$ (A=Sr,Pb,Ca,Na,U,TR; M=Fe,Cr,Ti,Zr,Mg) theoretical formula. A rare mineral shrilankite and a Zr-Fe-Ti-phase are also found. The latter has never been described for the Earth rocks. Inclusions of these minerals in garnet have needle-like shape, sometimes drop-like shape and often form intergrowths with rutile, ilmenite rarer with chromespinel. The host garnet regardes to lerhzolite paragenesis (for Cr-Ti-phases) and eclogitic or granulitic (for Zr-Ti-phases).

Cr-armalkolites are characterized by wide variations of chromium (1,7-23,0 wt.% Cr_2O_3), which displays a negative correlation with titanium contents. Admixtures of ZnO (up to 0,94 wt.%) and Nd_2O_3 (up to 0,45 wt.%) are constantly present in Zr-armalkolite with contents of ZrO_2 ranging from 2,5 to 7,9 wt.%. Shrilankite distinguishes by small admixtures of iron (1,1 wt.% FeO), strontium (0,48 wt.% SrO) and calcium (0,22 wt.% CaO) and is close by the composition of $Zr_{0,33}Ti_{0,66}O_2$ to this mineral from Ceilon placers (Willgallis et al.,1983). The Zr-Fe-Ti-phase replies by its composition to the formula $ZrFeTiO_5$ and has been described in nature for the first time. Its synthetical analogue is known (Lattard, 1987).

The thermodynamic parameters of garnet crystallization are: P=10-20 kbar, T=950-1050 C, fO_2=-10-11. They indicate the upper mantle origin of garnets. Morphology of the oxide minerals in the garnet grains directs to the subsolidus formation of inclusions. The obtained data testify to the primary magmatic nature of the Ti-Zr-Cr-phases and do not go into the scheme of their origin within the processes of mantle metasomatism (Erlank et al., 1987).

References:
Erlank,A.J., Waters,F.G., Hawkesworth,C.J. et al. (1987), *Mantle Metasomatism*. London, Acad.Press, 221-311.
Lattard,D. (1987). *Contr.Miner.Petrol.*, v.97, 264-278.
Willgallis,A., Siergmann,E., Hettiaratchi,S. (1983). *Neus.Jahrb.Min.Monatsh*, 151-157.

EVOLUTION OF SUBLIMATE DEPOSITION SINCE 1988 THROUGH 1993 AT LA FOSSA CRATER OF VULCANO (AEOLIAN ISLANDS - ITALY)

Garavelli A. *(Geomineralogical Dept., Univ. of Bari)*, Garbarino C., *(Inst. of Giac. Miner., Geol. and Geoph., Univ. of Cagliari)* Laviano R., and Vurro F. *(Geomineralogical Dept., Univ. of Bari).*

Geochemical surveillance of active volcanoes is traditionally carried out by the analysis of volcanic fluids evolving in fumarolic field. An anusual method of geochemical volcanic surveillance, based on sublimate collection and analyses, has been tryed since summer 1988 at "La Fossa" crater of Vulcano. Since then, a remarkable increase both in emission temperatures and in fluid output has been registered in the crateric fumarolized area of the island, accompanied by significant variations in the chemical and isotopic composition of the volcanic fluids (Barberi *et al.*, 1991).

Volcanic sublimates were collected in the years 1988-1993 directly on the ground of the area; in the sampling sites temperatures were measured.

Chemical and mineralogical analyses showed interesting variations occurred on the phases collected since the beginning of the present volcanic crisis to onward. In particular, while in 1988 sulfur, salammoniac, and sassolite, were the only sublimates occurring in the area, since 1990 also Bi-sulfides (bismuthinite), Pb-Bi sulfosalts (galenobismutite, cannizzarite, lillianite and cosalite), sphalerite and pyrite were collected on the ground around fumarolic vents with emission temperatures higher than 450 °C. Since october 1992, the new mineral barberiite, whose occurrence is due to the high fluorine content in volcanic gases emitted, was also collected (Garavelli & Vurro, 1994).

Microprobe analyses on Bi-sulfides and Pb-Bi sulfosalts showed both a PbS/Bi_2S_3 ratio decrease and a selenium content increase in 1993 sublimates if compared with same phases collected in previous years. Greenland & Aruscavage (1986), on the basis of geochemical and volcanological studies at Merapi volcano (Indonesia), stated that selenium content increases in correspondence with pre- sin- and post-eruptive periods. For this reason the particular abundance of this element in 1993 Vulcano sublimates might be a very useful information for volcanic surveillance. The PbS/Bi_2S_3 ratio decrease in 1993 products with respect to the 1990 ones, could be ascribed to a Pb and Bi different source in Vulcano fumarolic fluids.

The sulfide and sulfosalt assemblage recognised among fumarolic products from Vulcano crater was also used to obtain fO_2 and fS_2 values of volcanic fluids indirectly. In fact, at a fixed temperature, the fugacity of oxygen and sulfur in ore forming fluids at the time of deposition of sublimates largely controls the mineralogy of these particular volcanic deposits. For this research, the stability fields in a fO_2 and fS_2 diagram of collected phases (ZnS, Bi_2S_3 and FeS_2) at a temperature of 600 °C have been compared. The contemporaneous presence of the collected phases is allowed only for $fO_2 < 10^{-18}$ and fS_2 ranged between 10^{-1} and 10^{-4} (Garavelli, 1994); the results obtained are quite similar to those estimated for Vulcano directly by measurements on the ground (Carapezza M.L. *et al.*, 1993).

References:
Barberi, F., Neri, G., Valenza, M., Villari, L. (1991). *Acta Vulc*, 1, 95-106.
Carapezza, M.L., Gurrieri, S., Nuccio, P.M. & Valenza, M. (1993). *"Riassunti Conv. Ann. G.N.V.", Roma 8-10 Giugno 1993*, 80-81.

Garavelli, A. (1994). *Ph. Thesis*, 1-168.
Garavelli, A. & Vurro, F. (1994). *Am Mineral.*, **79**, 381-384 (in-press).
Greenland, L.P. & Aruscavage, P. (1986). *J. Volc. Geoth. Res.*, **27**, 195-201.

TRANSPORT, VOLATILIZATION AND CONDENSATION MECHANISMS AS DEDUCTED FROM THE STUDY OF VOLCANIC SUBLIMATES PRESENTLY OCCURRING AT THE FOSSA CRATER (VULCANO ISLAND - ITALY).

Garavelli A., Laviano R., and Vurro F. *(Geomineralogical Dept., Univ. of Bari)*

Volcanic sublimates are solid phases directly condensed from a gaseous volcanic steam. The results obtained from a mineralogical and geochemical study of these phases may be successfully used to improve knowledge of volcanic exhalations (metal content, condensation mechanisms, fO_2 and fS_2, etc.). In particular, the sampling method initially described by Le Guern & Bernard (1982), which consists in silica tubes (L = 1 m, Ø = 33 mm) introduced as deep as possible into fumarolic vents, has proved very useful. Phases collected at different temperature values on the inner walls of the sampling tubes, represent the deposition product from a gaseous phase that has suffered scarcely any atmospheric contamination, and are thus especially useful.

This research was carried out in the Fossa Crater fumarolized area of Vulcano (Aeolian Islands, Italy) during the years 1988-1993; in the same period a sudden increase in maximum and average emission temperatures was registered in the area, as well as an increase of fumarolic fluid output.

Contemporaneous sublimate collection and temperature measurement on the ground, allowed us to verify that in the crateric fumarolized area of Vulcano in the years 1988-1993, at temperatures lower than 300°C the only solid condensed phases were salammoniac, NH_4Cl, sassolite, H_3BO_3, sulfur and the new mineral barberiite, NH_4BF_4; when temperature increased above 450°C Bi-sulfides and Pb-Bi sulfosalts (bismuthinite, Bi_2S_3, galenobismutite, $PbBi_2S_4$, cannizzarite, $Pb_4Bi_{5+x}S_{11.5+1.5x}$) were the most abundant condensed phases; over 650°C no sublimates were collected (Garavelli, 1994). The deposition rule of sublimates on the ground which emerged is quite different from that deduced on the basis of the products collected on the inner walls of the silica tube. This is due to atmospheric contamination and to the dilution processes of the fumarolic fluids from which the mineralogical phases condensed on the ground. In fact, in the higher temperature parts of sampling tubes, Me-S-Cl compounds were the most abundant collected phases; DRX powder analyses indicated the presence of $Bi_{19}Cl_3S_{27}$ and Pb_4SCl_6. Associated compounds are Bi-sulfides and Pb-Bi sulfosalts, whose morphology and mutual relationships with sulfochlorides suggest that sulfosalt occurrence was due to sulfochlorides previously grown. This hypothesis may also explain the particular abundance at Vulcano of the non-stechiometric sulfosalt cannizzarite, whose occurrence in nature is a very rare event, and which it has been possible to synthesise in Pb-Bi-S systems only in the presence of small amounts of chlorine (Graham *et al.*, 1953).

However, the fact that sulfochlorides were collected suggests that Me-S-Cl complexes play a very important role in the metal transport processes and the condensation mechanisms of volcanic fumarolic fluids with high HCl content.

The occurrence in sampling tubes of S-Cl and As-S-Cl solid compounds suggest that, in addition to the metals, arsenic and even a part of sulfur may be transported in volcanic steams as volatile chlorides.

References:
Garavelli, A. (1994). *Ph. Thesis*, 1-168.
Graham, A.R., Thompson, R.M., Berry, L.G. (1953). *Am. Miner.*, *38*, 536-544.
Le Guern, F. & Bernard, A. (1982). *J. Volc. Geoth. Res.*, **12**, 133-146.

DEFORMATION AND METAMORPHISM AT THE NORTH AMERICA - INTERMONTANE BELT BOUNDARY; NEW CONSTRAINTS FROM THE BIG SALMON COMPLEX, YUKON TERRITORY, CANADA

Gareau, S. A. *(Min.-pet. Institut, Univ. Bern, and Geological Survey of Canada)* and Mortensen, J.K. *(Dept. of Geological Sciences, Univ. of British Columbia, Canada)*

Lithologic assemblages which comprise the southern Big Salmon complex, including biotite-hornblende metaplutonic rock of mid-Mississipian age, biotite quartzite to semi-schist, hornblende gneiss and minor marble, resemble those of Yukon-Tanana terrane, a pericratonic assemblage occupying a critical position in the Cordillera, between North American strata and far-travelled terranes.

The wide range in orientation of fabrics in these units differentiates the study area from the Teslin suture zone as documented along trend to the north. The suture appears to have been cut out along late, high-angle faults which juxtapose the southern Big Salmon complex against unmetamorphosed Cache Creek Group rocks to the west. The southern Big Salmon complex would be part of the transitional region between the steeply-dipping suture zone originally located to the west, and more gently-dipping rocks to the east.

Regional ductile deformation affected a moderately foliated/strongly lineated Mississipian (344Ma) orthogneiss, but probably predates emplacement of an undeformed hornblendite of Early Jurassic (or older?; 198Ma U-Pb sp) age. Moderate foliation and strong lineation in a biotite-hornblende tonalite of earliest Jurassic (206Ma) age suggest that deformation continued at least until that time.

Mylonitic fabrics in the marginal part of the Lone Tree biotite±hornblende±garnet granodiorite and in surrounding metamorphic rocks formed during an Early Cretaceous deformational event coeval with, and related to Lone Tree pluton emplacement at about 122 Ma. Absence of fabrics in a biotite granodiorite to granite intruding metamorphic rocks in the northeastern part of the area imply that all deformation had ceased by Early Paleocene (64Ma) time. This unexpectedly young plutonic body cooled very rapidly and had an important thermal impact on at least the northern part of the study area. All hornblende and biotite K-Ar dates from samples of the northern region are latest Cretaceous or younger. Mineral assemblages and textures in samples from six calc-silicate bands attest to strong contact metamorphism and possible influx of a water-rich fluid phase.

SITE POPULATIONS IN NI-MG-OLIVINES FROM OPTICAL ABSORPTION SPECTRA: EQUILIBRIUM AND KINETICS OF CATION DISTRIBUTION

Garsche, M. and Langer, K. (*Institut für Mineralogie und Kristallographie, TU Berlin*, Germany)

The intracrystalline cation distribution in olivines has attracted considerable attention in recent years. In synthetic Ni-Mg olivines a strong partitioning of Ni^{2+} into the smaller M1 site has been observed in a series of structure refinements (Boström, 1987; Ottonello et al., 1989). In this study we establish a method by which quantitative site distribution information can be obtained from optical absorption spectra. We studied the kinetics of the order-disorder reaction $Ni(M2)+Mg(M1) \rightleftharpoons Ni(M1)+Mg(M2)$ and the equilibrium cation distribution between 450 °C and 800 °C using optical spectroscopy.

Olivine crystals, $(Mg_{1-X}Ni_X)_2SiO_4$, were grown by a flux method, using Li_2MoO_4 as the solvent. The crystal structures of olivines with variable X_{Ni} have been refined from single crystal

X-ray diffraction data. Subsequent to data collection these crystals were prepared for the microscope spectrometric technique according to Hu et al. (1990). Polarized electronic absorption spectra were taken in the range from 35000 cm^{-1} - 4000 cm^{-1}. The absorption values of the transitions $^3A_2 \rightarrow {}^3T_1(F)$ and $^3A_2 \rightarrow {}^3T_1(P)$ (Ni^{2+} in M2) in E//X and E//Z remain linear with concentration over the entire compositional range (see Figure).

The kinetics of the Ni,Mg exchange in olivines with $X_{Ni}=0.30$ and $X_{Ni}=0.50$ have been investigated by means of isothermal annealing experiments between 450 °C and 550 °C. The change of Ni^{2+} in M2 is determined from the linear absorption coefficient of the electronic transition $^3A_2 \rightarrow {}^3T_1$ (P).
Evaluation of the data with the Mueller formalism yields activation energies of 170 (181) kJ/mole for the ordering process

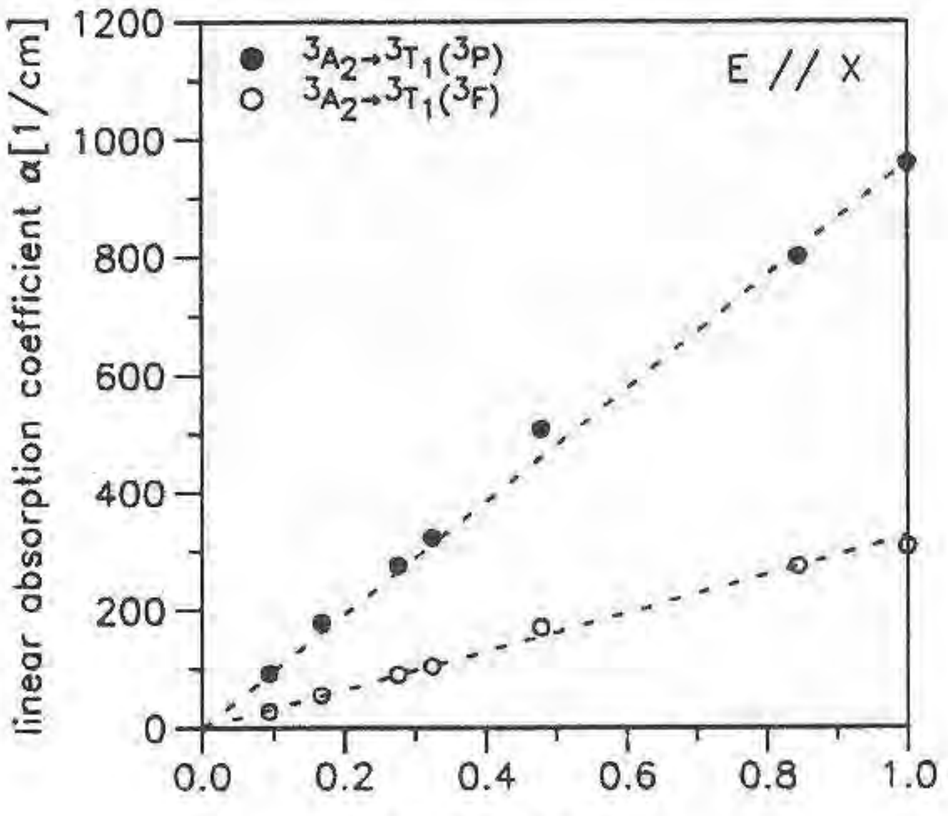

Correlation of the intensities of two spin-allowed bands (Ni^{2+} in M2) with the fraction of Ni^{2+} in the M2 site

and 251 (199) kJ/mole for the disordering process for crystals with $X_{Ni}=0.30$ ($X_{Ni}=0.50$).

Additional annealing experiments were performed in the temperature range between 550 °C and 800 °C. A plot of the site fractions $x_{Ni(M2)}$ in equilibrium versus temperature reveals a linear trend up to about 800 °C. $RT\ln K_D$-values show a slight increase from 18 kJ/mole at 450 °C to 20 kJ/mole at 800 °C.

References:
Boström, D.(1987). Amer.Mineral. 72, 965-972.
Hu, X., Langer, K., Boström, D.(1990). Eur.J.Mineral.2, 29-41.
Ottonello, G., Della Giusta, A., Molin, G.M.(1989). Amer. Mineral. 74, 411-421.

MINERALOGICAL AND THERMODYNAMIC MODELING OF HEAVY METAL MOBILITY AT SALAIR MINE DUMPS

Gas'kova O.L., Kolonin G.R., Bortnikova S.B. (United Institute of Geology, Geophysics and Mineralogy, Novosibirsk)

The Salair mine one of the oldest in Russia exploits both the primary barite-containing sulphide ores and oxidizing zone (with Au, Ag and barite recovering) during 200 years. Three mine tailings of different age formed during last 60 years, were the main testing objects. The obtained results reflect mineralogical ore composition, their geochemical characteristics, component distribution according to grain-size fraction and their change degree in the near surface conditions. The thermodynamic modeling of geochemical mobility of a large group of toxic metals (Fe, Cu, Pb, Zn, Cd and others) was carried out with the use of the free energy minimizing program "GIBBS". The interaction of the near-surface waters with sulphides was examined both depending on the red-ox conditions (degree of aeration) and the reaction progress (ξ - reactor approach by H.Helgeson). This simultaneous examination was the most important point to consider (Kolonin and Gaskova,1992).

The significant mineral-geochemical reasons of our elaborated model are: a) the presence of carbonate minerals, restricting the acidity of solutions by pH>5, except the primary mine waters in the career and near the buried pit mining with pH~4; b) a considerable quantity of FeS_2 with respect to other sulphides that are promoted to the oxidizing process; c) complete predominance of goethite and other ferrous hydroxides among the secondary ferrous minerals; d) formation of covellite, bornite and acantite as shells on other sulphides (sphalerite, galenite); e) Cd presence in sphalerite (up to 0.3%) and its very high contents in acid mine waters (up to 84.3 mg/l).

In the investigation process one evaluated a possible formation of specific barrier impenetrable for oxygen and other chemical agents

In the investigation process one evaluated a possible formation of specific barrier impenetrable for oxygen and other chemical agents which is named "hardpan" (Blowes,1991). This "hardpan" can sufficiently protect sulphide minerals situated beneath against intensive oxidizing dissolution with the following pollution of subsurface waters.

The following generalized results may be presented as the most interesting from theoretical and practical point of view:
1) the quantitative characteristics of three types of possible mobility conditions of toxic metals in reduced, intermediate and oxidizing conditions and comparison of the received results with other authors data (Spycher and Reed, 1992; Brimhall and Crerar,1992);
2) the influence of ratio of pyrite and chalcopyrite contents in oxidized products on the toxic metals mobility in carbonate conditions;
3) evaluation of possible formation of protective shells of Cu and Ag sulphides as well as anglesite and other secondary minerals to lower mobility of nonferrous metals;
4) prediction of most effective natural precipitants of toxic metals in the surraundings of sulphide mine tailings.

References:
Kolonin,G.R. & Gas'kova,O.L. (1992). In: Y.K. Kharaka and A.S.Maest (eds.) Proceedings of the Sympos. on Water-Rock Interact.1071-1074.
Spycher,N.F. & Reed,M.H. (1992). Ibid., 1087-1090.
Brimhall,G.N. & Crerar,D.A. (1992). In:I.S.E. Carmichael and H.P. Eugster (eds.) Thermodynamic Modeling of Geological Materials, Ch.8, 247-353.
Blowes, D.W. et al.(1991). Geochim.et Cosm. Acta. 55. 965-978.

DEFINITION OF MINERAL TEXTURAL TYPES AIMING AT THE BENEFICIATION OF ALJUSTREL AND NEVES-CORVO VOLCANOGENIC MASSIVE SULPHIDE ORES

Gaspar, O. C. (*Instituto Geológico e Mineiro, Portugal*)

The textures of the ores, the fine mineral intergrowths, the complex distribution of the deleterious minor elements, and the low base metal contents in some ore types, pose many technological problems to the beneficiation of the volcanogenic massive sulphides occurring in the Iberian Pyrite Belt. In particular the colloform

textures and fine intergrowths of the base metal sulphides with pyrite impose extremely fine liberation sizes (K_{80}=15 to 25 μm).

The mineralogical, textural and metallogenic studies have provided an understanding of the distribution of vertical and lateral metal zoning in the ore bodies (Gaspar & Pinto, 1991; Gaspar, 1991; Leitão, 1993). Mapping of the ore types, carried out by mine geologists, and the metal zoning patterns computed from data base have shown that ore types are distributed as ore lenses, and that vertical base metal zone exists in several orebodies. Excluding the case of some Neves-Corvo orebodies where zoning is more complex due the resurgence of hydrothermal recurrences of ore deposition, all the orebodies show higher copper grades at the footwall and increasing zinc and lead grades toward the hangingwall. A lateral zoning sometimes also occurs, showing higher grades near the discharging sites of the late Cu-rich hydrothermal solutions.

Since ore processing efficiency is affected by ore textures, and because the same mineral often shows different textural features, a relationship between the textures of the feed ores and those of the middlings must be established for all ore types defined at the deposit scale.

To design efficient ore dressing plants that can treat the different ore types of Aljustrel and Neves-Corvo deposits, methods of determining the mineralogical and textural characteristics of the several Aljustrel and Neves-Corvo ore types, and of their behaviour during grinding and concentration processes has been developed jointly with the mining companies Pirites Alentejanas, SA, E.D.M, SA, and SOMINCOR, SA.

For supplying, on time, the information needed for the optimization of the concentration processes, an empirical method, based both on the definition of the different ore types, and on semiquantitative microscopical data, was also developed

References:
Gaspar, O.C. & Pinto, A. (1991). Mineral Mag.,**55**, 417-422.
Gaspar, O.C. (1991). Comun. Serv. Geol. Portugal, **77**, 27-52.
Leitão, J.C. (1993). Symposium on Polymetallic Sulphides of the Iberian Pyrite Belt, Évora, October. Ed. APIMINERAL, Lisboa, 1.12, 21p.

A P-T-t PATH FOR SOME HIGH-PRESSURE ULTRAMAFIC/MAFIC ROCK-ASSOCIATIONS AND THEIR FELSIC COUNTRY-ROCKS BASED ON U-PB SHRIMP-DATING OF MAGMATIC AND METAMORPHIC ZIRCON DOMAINS. EXAMPLE: SWISS CENTRAL ALPS

Gebauer D. *(Department of Earth Sciences, ETH Zürich, CH-8092 Zürich, Switzerland)*

Numerous boudinaged garnet-peridotite and eclogite bodies occur in high-grade gneisses of the Alpine Adula-Cima Lunga nappe system. Geo-thermobarometric data (e.g. Evans and Trommsdorff, 1978 and Heinrich, 1986) demonstrate a significant P-T increase to the S suggesting low, i.e. subduction related geothermal gradients. SHRIMP-ages are reported for various rock types from the two classical areas of Cima di Gagnone (CdG, ≥ 20 kbar, 750 °C) and Alpe Arami (AA, ≥ 25 kbar, 850 °C). All U-Pb data collected so far were obtained within distinct zircon domains that, based on their cathodoluminescence patterns, indicate either magmatic or various types of metamorphic origins.

At AA zircons from two gar-peridotite samples record pre-Alpine ages (1.72 Ga, ~ 650 Ma and 456 Ma) that probably reflect intergranular melting and formation of trapped mantle liquids. Although the peridotites have suffered extreme Alpine P-T conditions, zircon domains that registered this episode, could only be found in one sample, which contains metamorphic zircon domains that average 36.3±1.4 Ma (unless otherwise stated, all errors are given as 95% c. l.).

Zircons extracted from two types of gar-pyroxenites that occur as layers and boudins within the gar-peridotites at AA have formed magmatically under still HP-conditions at 35 Ma (errors < 1 Ma). The same was found for magmatic zircons of an eclogite that also formed under HP-conditions 35 Ma ago. The few spots placed so far into the magmatically resorbed, metamorphic cores of these eclogite zircons yield ages from 41 Ma to 45 Ma.

The zircons of the two pyroxenites and two peridotites contain variably small amounts of inherited cores or, in the cases of the peridotites, of whole grains of Phanerozoic, Proterozoic and Archean ages. Obviously, the HP pyroxenite and eclogite melts inherited differently old zircons of various ages from the peridotitic sources and resorbed them to various degrees. Between these old magmatic cores of the gar-pyroxenites and the 35 Ma old zircon domains, domains in the range of ~ 40 Ma to 45 Ma can occur, indistinguishable in age from the metamorphic Alpine cores of the eclogite zircons. These oldest Alpine zircon domains may have formed over an extended period of time during prograde metamorphism in the course of deep subduction of the peridotite. Therefore, they may record the closest age estimate on the maximum burial of the peridotites that was reached before final melting of the heterogeneous peridotite sources at 35 Ma. The latter probably occurred during decompression (uplift) and produced the high-pressure eclogite and gar-pyroxenite melts that incorporated both 40 Ma to 45 Ma old metamorphic zircons as well as the much older, Pre-Alpine zircon cores from the polymetamorphic and polyanatectic peridotite sources.

The country-rock gneiss at AA was found to be a Hercynian granite (297 ± 3 Ma) proving tectonic intermingling of the mafic/ultramafic rocks with the granitic host-rock. At CdG tectonic introduction of the mafic/ultramafic rock association can not be proven geochronologically. This is based on a 528 ± 6 Ma age of the gabbroic, MORB-type eclogite protolith and a Panafrican formation age (592± 8 Ma, 1 std. dev.) of the youngest detrital zircon grain in the semipelitic country-rock gneisses. This implies post-Panafrican deposition. On the other hand, as no Caledonian or Hercynian detrital zircons were found so far in this rock, a pre-Caledonian deposition (Cambro-Ordovician) is likely and possibly coeval with the formation of the Cambrian MORB-type protolith of the dated eclogite at CdG. There is no geological evidence that this Cambrian, gabbroic protolith and its presently surrounding sedimentary precursor escaped metamorphism during the Caledonian and/or Hercynian orogenesis until the Alpine subduction. Thus, it is very likely that these rocks have been probably transformed under amphibolite facies conditions already during the Hercynian and/or Caledonian orogenic cycles. However, due to the absence of partial melting in the immediate metasediments of the eclogite at CdG, that formed above 20 kbar and 750 °C, tectonic juxtaposition under still HP-conditions during the Alpine cycle is nevertheless probable for petrological reasons (HP-relics in the metasediments; Heinrich, 1986).

The Cambrian age of the low-pressure protoliths of the CdG eclogite is in good agreement with a 521± 8 Ma protolith age of an amphibolite at the Simano - Leventina nappe boundary near Biasca (Gebauer, 1993 and unpubl. data). This rock is also associated with ultramafic rocks (Loderio) and has a very similar geochemical signature to the corresponding CdG eclogites (Schaltegger, pers. comm.). Thus, apart from the different mantle origins and depths of partial melting of the ultramafic rocks at AA and CdG, their protolith ages are also grossly different. In contrast, the Alpine metamorphic sequence of events along the P-T path coincides for the HP-section with that found at AA, 42.4±2.9Ma and 34.7±0.9 Ma, respectively. However, opposite to the zircons in the 35 Ma old HP melts at Alpe Arami, the coeval zircon domains in the gar-peridotite at CdG do not show any undisturbed and concentric, oscillatory growth zoning. This indicates that they did not precipitate freely within a melt. The same holds true for the magmatic, Cambrian zircons of the eclogite at CdG that not only contain metamorphic domains at 35 Ma but also even younger ones at 30 Ma±1.5 Ma. The latter might have formed as a result of destabilization of pyroxene during amphibolite facies retrogression.

The probable peak of Alpine metamorphism in the granitic and metasedimentary country rocks at AA and CdG occurred at 33.0±0.6 Ma, as determined from metamorphic domains within detrital zircons at CdG and magmatic zircons within a deformed leucosome inside the Hercynian metagranite at AA. This 33 Ma event is also registered in U-poor, metamorphic domains rimming only about 2 Ma older domains of zircon from the garnet-pyroxenites, one eclogite and one peridotite at AA and may be related to P-T conditions around the eclogite - granulite facies boundary. The youngest event, only found at AA and post-dating the last of the four deformation phases (e.g. Möckel, 1969), was the emplacement of numerous pegmatite dikes at 25.5±0.8 Ma. This event still or again occurred under amphibolite facies conditions. It was probably coeval with both reheating during intrusion of intracrustal granites similar to the Novate granite and introduction of large amounts of fluids. A number of zircon domains within mainly the felsic country-rocks record this youngest of the four Alpine (Eo-/Oligocene) metamorphic (and structural?) stages. Interestingly, this latest event recorded by the zircons could not be found in any of the zircons extracted from the samples of CdG. This can readily be explained with the fact that the pegmatites and the 26 Ma old Novate

granite occur in the southern steep belt and not in areas of overall flat lying structures further N in the nappe system, like at CdG.

The data obtained so far indicate that deep subduction of continental lithosphere ≥ 80 km, post-dating subduction of Mesozoic oceanic crust, continued between ~ 45 Ma to 40 Ma. The second time marker on the P-T-t-curve is related to partial melting of the peridotitic sources above 1000 °C ~ 35 Ma ago. At this stage, the garnet-pyroxenites and eclogite formed magmatically, possibly during ± isothermal uplift of the heterogeneous and polymetamorphic mantle material. Tectonic intermingling of the cooling peridotites and eclogites with the felsic country-rocks must have occurred during rapid uplift after 35.2± 0.9 Ma and probably was completed by 33.0±0.6 Ma as the Hercynian and pre-Hercynian zircons from the country-rocks do not show metamorphic domains older than 33 Ma. Both the age signatures in the 33 Ma old metamorphic zircon domains of the felsic and ultramafic/mafic rocks as well as the structural data on these rocks (e.g. Möckel, 1969) are in line with this conclusion. The country-rocks were thus subducted to less extreme depths as the mafic/ultramafic rocks. Therefore, they were not or only partially melted during this third geological episode that can be marked geochronologically on the P-T-t curve. The fourth Alpine metamorphic age is so far only detected at CdG by 30±1.5 Ma old metamorphic zircon domains that probably formed during amphibolite facies retrogression of the host eclogite. There are at present no constraints on the further cooling path at CdG. At AA, 25.5±0.8 Ma ago considerable magmatic and fluid activity must have existed under still or again amphibolite-facies conditions. This Upper Oligocene episode is probably responsible for complete or at least partial rejuvenation of numerous mineral ages obtained within the southern steep belt (Rb-Sr, K-Ar, U-Pb monazite and Sm-Nd).

The 3 youngest ages in the southern steep belt define the last part of the 8 stages on the P-T-t path. They are biotite ages that range from 18 Ma to 20 Ma and fission track ages that are around 15-18 Ma for zircon and around 10 Ma for apatite (Naeser and Gebauer, unpubl., Hurford, 1986 and Seward, pers. comm.).

Geodynamically, the corner flow or orogenic wedge model - in combination with uplift caused by buoyancy, extensional faulting and erosion - seems to fit the observed age pattern best as it accommodates both subduction and uplift processes within a single P-T-t loop at plate tectonic speeds.

HALAGURITE - THE MISSING MEMBER OF THE Mn-Mg-Fe PYROXENE QUADRILATERAL

Gehör S., Laajoki K. (Dept. of Geol.,Univ. of Oulu, Finland) and Devaraju T. (Dept. of Studies in Geol., Univ. of Karnatak, India)

Results of recent investigations into natural manganese-bearing pyroxenes have suggested a possible Mn-Mg-Fe-pyroxene quadrilateral. The granulite-facies manganese-bearing iron-formations of Southern Karnatak, India, contain Ca-poor Mn-Fe-Mg orthopyroxenes as lamellae with Ca-rich clinopyroxene. The widths of the orhopyroxene lamellae vary from 3 to 10 um (Fig.1). According to microprobe studies this orthopyroxene in

Fig. 1

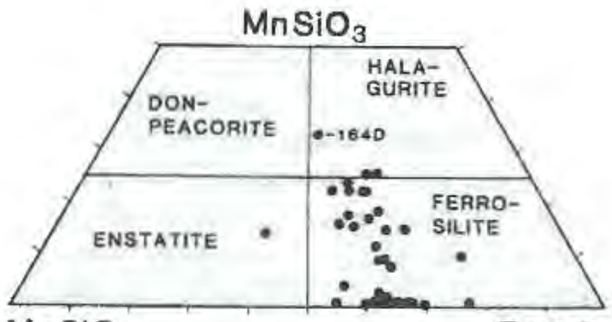

sample 164D contains from 17.27 to 18.50 % MnO and falls into the $FeMnSi_2O_6$ field of the predicted quadrilateral. Due to its high magnesium content, from 9.4 to 10.7 %, it nevertheless occupies the corner opposite the $FeMnSi_2O_6$ end-member point. The averaged chemical formula of the grains studied is $Ca_{0.110}Mn_{0.624}Fe_{0.664}Mg_{0.611}Si_2O_6$.(Table). This new orthopyroxene is tentatively named halagurite.

Transmission electron microscope measurements made by Dr. I. Dodony at Eötvös Loránd University, Hungary, revealed a kanoite-type $P2_1/c$ space group for halagurite. Optical and mineral chemical data on 43 orthopyroxenes from the Halaguru iron-formations prove that there is a continuous solid solution from Mn-free ferrosilite to halagurite (Fig. 2) and, consequently that the main Mn-Mg-Fe-pyroxene quadrilateral really exists.

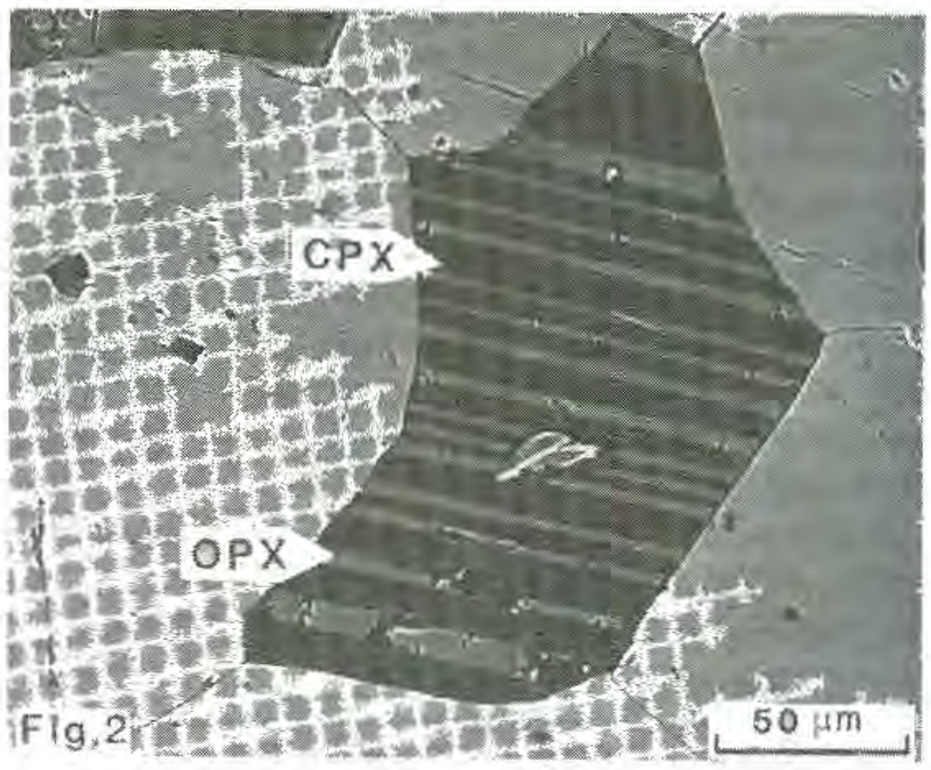

Fig.2

Microprobe analyses of OPX; Sample 164D. Column 7=average of Nos. 1-6

	1	2	3	4	5	6	7
Na_2O	0.00	0.04	0.06	0.03	0.05	0.04	0.04
MgO	10.79	9.60	9.66	9.46	9.41	9.37	9.72
Al_2O_3	0.05	0.05	0.05	0.05	0.05	0.05	0.05
SiO_2	50.46	49.44	50.26	49.80	49.57	49.63	49.86
CaO	1.75	2.40	2.70	2.33	2.34	2.78	2.38
TiO_2	0.00	0.01	0.02	0.03	0.03	0.05	0.02
V_2O_3	0.01	0.02	0.01	0.02	0.01	0.00	0.01
MnO	17.53	18.40	17.27	17.67	17.42	17.51	17.63
FeO	20.10	19.66	18.42	18.65	18.78	18.42	19.00
ZnO	0.02	0.08	0.03	0.02	0.05	0.02	0.04
Total	100.76	99.69	98.50	97.99	97.73	97.88	98.76
Cations	(on the basis of 6 oxygen)						
Si	2.0090	2.0043	2.0366	2.0331	2.0319	2.0302	2.0242
Ti	0.0000	0.0002	0.0006	0.0010	0.0009	0.0016	0.0007
Al	0.0026	0.0022	0.0022	0.0023	0.0022	0.0023	0.0023
Fe	0.6693	0.6667	0.6241	0.6368	0.6439	0.6301	0.6452
Mn	0.5911	0.6318	0.5927	0.6110	0.6049	0.6067	0.6064
Mg	0.6406	0.5801	0.5833	0.5754	0.5752	0.5716	0.5877
Ca	0.0746	0.1042	0.1174	0.1018	0.1028	0.1217	0.1038
Na	0.0000	0.0033	0.0046	0.0027	0.0036	0.0031	0.0029
MNSIO3	29.92	31.86	30.91	31.74	31.39	31.43	31.21
FESIO3	33.88	33.62	32.55	33.08	33.42	32.65	33.20
MGSIO3	32.43	29.26	30.42	29.89	29.85	29.62	30.25
CASIO3	3.780	5.260	6.120	5.290	5.340	6.310	5.340

NEAR INFRARED AND ^{57}FE MÖSSBAUER SPECTROSCOPIC INVESTIGATIONS ON ALMANDINE GARNET SOLID SOLUTIONS

Geiger, C.A. (*Mineralogisch-Petrographisches Institut der Univ. Kiel*)

Single crystal near infrared and powder ^{57}Fe Mössbauer spectroscopic measurements have been undertaken on $Fe_3Al_2Si_3O_{12}$-$Mg_3Al_2Si_3O_{12}$ and $Fe_3Al_2Si_3O_{12}$-$Mn_3Al_2Si_3O_{12}$ garnet solid solutions. The Mössbauer hyperfine parameters are shown in Figure 1a and 1b.

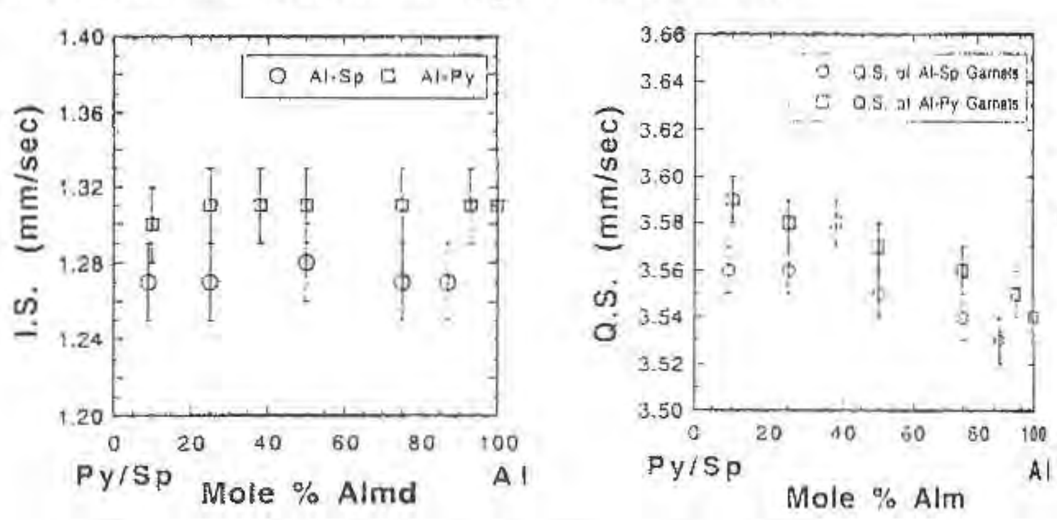

Fig.1) Isomer shifts and quadrupole splittings.

The presence of Mg or Mn^{2+} in neighboring edge-sharing dodecahedra, where the X(1)-X(2) distance is about 3.5 Å, does not significantly influence the magnitude of the electric field gradient at the Fe^{2+} dodecahedral sites. The quadrupole splitting in garnet, which is a qualitative measure of site distortion, is neither affected by garnet chemistry nor by increasing pressure (Huggins, 1977).

Conversely, the NIR spectra show measurable shifts in the three t_{2g} electronic d-level bands (Fig. 2). The spectra can be interpreted as indicating that the Fe^{2+}-dodecahedral site distortion decreases with increasing pyrope component and increases with increasing spessartine component. The d-orbitals of Fe^{2+} are sensitive to localized site distortions caused by neighboring dodecahera of different composition and different geometry.

In the crystal field model, $\Delta = 1/R^5$, where Δ is the crystal field splitting and R is the cation-oxygen distance. This relationship is in agreement with the diffraction averaged X-O bond lengths along the Al-Py binary, but not for Al-Sp solid solutions, where Δ increases with increasing spessartine component (Fig. 2).

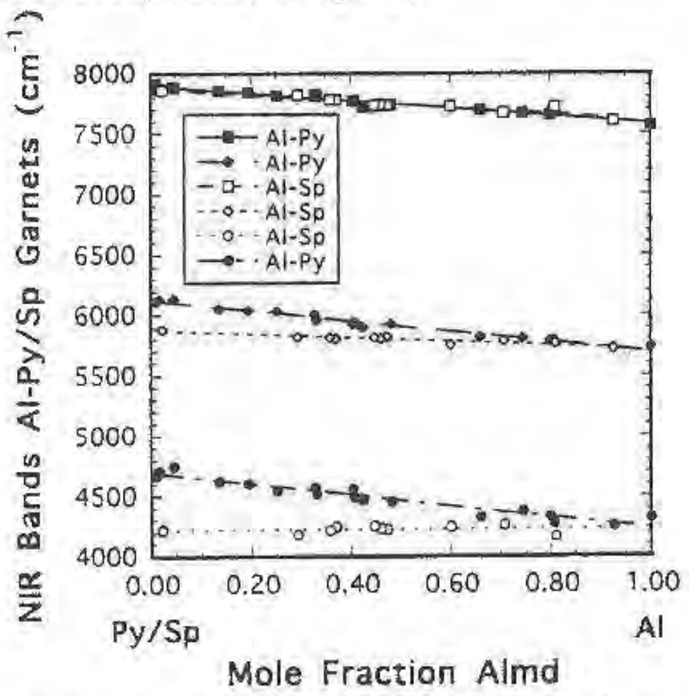

Fig. 2. Band positions of the three t_{2g} electronic transitions in Al-Py and Al-Sp garnet solid solutions.

References:
Armbruster, T., Geiger, C. A., and Lager, G.A. (1992). *Am Min.*, 77, 512-521.
Huggins, F.E. (1976). In Strens, R.G.J. ed., J. Wiley, New York, 613-640.

BINARY MOLAR VOLUMES OF MIXING OF GARNETS IN THE SYSTEM $Fe_3Al_2Si_3O_{12}$-$Mn_3Al_2Si_3O_{12}$-$Mg_3Al_2Si_3O_{12}$

Geiger, C.A., von Saldern, Ch., and Feenstra, A.
(*Mineralogisch-Petrographisches Inst. der Univ. Kiel and Univ. Bern*)

Molar volumes of garnet solid solutions are required for quantitative applications of many of the existing geobarometers. We present volume of mixing data for the three garnet binaries $Fe_3Al_2Si_3O_{12}$ (almandine)-$Mg_3Al_2Si_3O_{12}$ (pyrope), $Mn_3Al_2Si_3O_{12}$ (spessartine)-$Fe_3Al_2Si_3O_{12}$, and $Mg_3Al_2Si_3O_{12}$-$Mn_3Al_2Si_3O_{12}$, which can be used in thermodynamic calculations involving Ca-poor garnet solid solutions.

The change in the molar volumes along the three binaries result from an exchange of the divalent cations Mg^{2+}, Fe^{2+}, and Mn^{2+} in the dodecahedral site. Deviations from ideal mixing are expected to be minimal because the ionic radii of all three cations are similar (0.89 Å, 0.92 Å and 0.96 Å, respectively). This has been verified experimentally by X-ray powder diffraction refinements made on synthetic solid solutions. The deviations from ideality in all three binaries are very small. These excess volumes of mixing can be fitted with an asymmetric mixing model, where $V^{xs} = X_1X_2(X_1W_{12} + X_2W_{21})$. Preliminary best fit interaction parameters for the three binaries are $W_{Al\text{-}Py}$= 0.0(1), $W_{Py\text{-}Al}$= 0.7(2); $W_{Al\text{-}Sp}$= 0.4(1), $W_{Sp\text{-}Al}$= 0.1(1); and $W_{Py\text{-}Sp}$ = 0.4(1), $W_{Sp\text{-}Py}$= 0.3(1) in cm^3/mole.

The assumption of ideal volumes of mixing for all three binaries will not lead to significant errors in geobarometric calculations for crustal conditions.

A crystal chemical model has been formulated, following Born and Zemann (1964), in an attempt to understand the observed binary volumes of mixing. The model has been tested with X-ray data along the pyrope-grossular ($Ca_3Al_2Si_3O_{12}$) binary (Ganguly *et al.*, 1993). It can be shown that the degree of tetrahedral rotation, assuming a garnet framework of rigid tetrahedra and octahedra, is correlated with the excess volume of mixing. This model predicts that the smaller of the two X-site cations in a binary solid solution should have increased amplitudes of vibration within a more distorted X-site with increasing solid solution of the larger X-site cation or the larger volume component. Due to the increased vibrational freedom of the smaller cation, any excess vibrational heat capacities should mimic the observed positive excess volumes of mixing in binary garnet solid solutions.

References:
Born, L. and Zemann, J. (1964). *Cont. to Min. Pet.*, **10**, 2-23.
Ganguly, J., Cheng, W. and O'Neill, H. St. C. (1993). *Am. Mineral.*, **78**, 583-593.

COHENITE FROM MINERAL ASSOCIATIONS CONNECTED WITH HIGH-TEMPERATURE VOLCANOGENIC GASEOUS JETS (KAMCHATKA, RUSSIA).

Generalov M.E.*, Glavatskikh S.F.* (*Ins.Geol. Ore Deposits (IGEM), Moscow;*Ins.Volcanology, Petropavlovsk-Kamchatsky)

The association of native metals and alloys (Fe, Cu, Al, Zn, Pb, Sn, Ti, Cu-Zn, Sn-Sb-Ag) was early (Glavatskikh, 1990) discovered on the 2-nd volcanic cone formed during the Big Tolbachik's Fissure Eruption (1974-1976), Kamchatka. This association is presented by fine-grained material connected with wall alterations of the volcanic slag around high-temperature gaseous jets.

We have studied heavy magnetic fraction of this material which have been derived without crushing. Besides predominant jagged, curved plate-like grains of native iron in some samples rounded, yellowish-grey grains 0.05-1 mm in size with metallic luster were discovered. After studies in polished sections these grains were identified as aggregates of native iron and iron carbide. Carbide phase forms here plate-like inclusions in Fe-matrix

and carbide-iron eutectics. Content of carbide in these aggregate is 50-90 vol. %.

Composition of carbide (by microprobe data (mass.%): 92.5 - 92.8 Fe; 0.2 - 0.4 Mn; < 0.1 Cr; 0.4 - 1.3 Si is very close to the composition of stoichiometric Fe_3C phase. Composition of matrix is: 95.1 Fe; 0.1 Mn, < 0.1 Cr; 1.0 Si. Weight deficite of weight may be explained by the presence of fine-grained carbide inclusions in the matrix.

Optical properties of carbide are correspondent to properties of cohenite. Microhardness of the carbide is 1100 - 1300 kG/mm². Diffraction data (d , (I)): 2.40 (5); 2.27 (4); 2.23 (3); 2.12 (5); 2.07 (4); 2.03 (10); 1.992 (6); 1.867 (3); 1.771 (4); 1.693 (2); 1.591 (2); 1.526 (3); 1.360 (1); 1.332 (2) proves that the carbide is cohenite (orthorombic, Pbmn, a = 4.54±0.02, b = 5.09±0.01, c = 6.73±0.01 Å). Additional lines point on the presence of α - Fe (Im3m, a = 2.86 Å) and unidentified cubic (Fd3m (?)) phase with a = 5.44 Å.

Observed correlations between native iron and cohenite in studied aggregates shows that in this case the main portion of cohenite have been crystallized from Fe - C melts. In the system Fe-C it is possible at temperatures from above 1200°C (start of Fe_3C crystallization) to 1147°C (formation of Fe-Fe_3C eutectic). Minor part of cohenite may be produced as a result of the solid-phase exolution α - (Fe,C) --> γ - Fe + Fe_3C.

Presence of cohenite in the association connected with the action of high-temperature volcanogenic fluids shows not only their reduced character but also the enrichment of these fluids in carbon-bearing compounds which may controls metal transportation by endogenic fluids.

Acnowlegement: This work have been supported by the Russian Foundation of Fundamental Researches (project 93-05-9811).

A NEW THERMODYNAMIC DATABASE FOR THERMOBAROMETRY

Gerya T.V. and Perchuk L.L. *(Dept. of Petrology, Moscow Univ.)*

The database provides the GEOPATH program (Gerya and Perchuk, 1990) with thermodynamic data used for calculations of temperature (T), pressure (P) and CO_2-H_2O fugacity. The database contains an internally consistent data (Perchuk, 1990; Perchuk et al., 1989) on thermodynamic properties of mineral solid solutions and standard thermodynamic values for geothermometric, geobarometric and "fluid-bearing" equations. In contrast to other datasets (Holland & Powell, 1985; Berman, 1988) the system discussed has been created on the basis of experimental data with the solid solutions involved. A thermodynamic treatment of available experimental data for 27 reactions includes the following excess Geebs free energy models for biotite, garnet, orthopyroxene, spinel (Gerya & Perchuk, 1990) and CO_2-H_2O cordierite

Bt: $G^e = -4405\,X_{Phl}X_{East} - 24577\,X_{Ann}X_{East}$, **East** $=KAl_3AlAl_3O_{10}(OH)_2$

Opx: $G^e=(-1409+1.052T)X_{En}X_{Fs}+(-2527-0.0309P)X_{Ok}X_{Fs}$; **Ok**$=AlAlO_3$

Crd: $G^e=3392X_{Crd\text{-}CO2}X_{Crd\text{-}H2O}-5537X_{Crd\text{-}Dry}X_{Crd\text{-}H2O}-196X_{Crd\text{-}CO2}X_{Crd\text{-}Dry}$

where **Crd-CO_2** $= CO_2$ in Crd chanels, **Crd-Dry** $= (Mg,Fe)_2Al_4Si_5O_{18}$

fluid: $G^e = 2020\,X_{CO2}X_{H2O}$. **Ol**: $G^e = 1441\,X_{Fo}X_{Fa}$

The level of consistency, L_C, (Perchuk, 1990) and an accuracy of thermodynamic data for each given reactions are estimated statistically.

References:

Berman R.G., (1988). *J. Petrol.* **29.** 445-522.

Gerya T.V. & Perchuk L.L. (1990). *Geokchimia.* **10**, 1412-1418.

Holland T.J.B., & Powell, R., (1990). *J.Metam.Geol.* **8**, 89-124.

Perchuk L.L., (1990). In: *Progress in Metamorphic and Magmatic Petrology.* Ed. Perchuk L.L. Cambridge University Press. 93-111.

Perchuk L.L., Gerya T.V. & Nozhkin A.D.(1989). *Metam.Geol. 7*, 599-617.

Perchuk L.L. and Gerya T.V. (1990). In: *The Baltic Shield.* Ed. Gorbachev R.M. Abstracts. Lund, Sweden. 72-73.

Standard thermodynamic data for some thermobarometric reactions

No	Reaction at 1000, K	ΔH°	ΔS°	ΔV°
	Exchange			
1	1/3Prp + 1/3Ann = 1/3Alm + 1/3Phl	-7000	-4.589	-0.0238
2	1/3Prp + 1/2Crd_{Fe} = 1/3Alm + Crd_{Mg}	-6587	-2.889	-0.0158
3	1/3Ann + 1/2Crd_{Mg} = 1/3Phl + 1/2Crd_{Fe}	-413	-1.700	-0.0080
4	1/3Prp + Fs = 1/3Alm + En	-3566	-1.717	-0.0231
5	1/3Ann + En = 1/3Phl + Fs	-3434	-2.872	-0.0007
6	1/2Crd_{Fe} + En = 1/2Crd_{Mg} + Fs	-3021	-1.172	0.0073
7	1/3Phl + OK = 1/3East + En	140	-1.282	0.0322
8	1/3Ann + OK = 1/3East + 1/2Fs	-3294	-4.154	0.0315
9	1/3Prp + 1/2Fa = 1/3Alm + 1/2Fo	-2337	-1.422	-0.0152
10	1/3Fo + Fs = 1/3Fa + En	-1229	-0.295	-0.0078
11	Crd-CO_2+H2O =Crd-H_2O +CO_2	1708#	3.342	-1.1058
	Net-transfer reactions			
12	En + 1/3Ok = 1/3Prp	-1234	-0.030	-0.0679
13	Fs + 1/3Ok = 1/3Alm	-4800	-1.747	-0.0910
14	En + Ok + 3/2Qtz = 1/2Crd_{Mg}	-5695	3.133	0.4571
15	Fs + Ok + 3/2Qtz = 1/2Crd_{Fe}	-2674	4.305	0.4498
16	1/3Prp+2/3Sil+5/6Qtz = 1/2Crd_{Mg}	1095	2.924	0.5436
17	1/3Alm+3/2Sil+5/6Qtz=1/2Crd_{Fe}	5492	5.813	0.5594
18	1/3Phl+ Qtz=En +1/3Kfs+1/3H_2O	4094	8.203	-0.1354
19	1/3Ann + Qtz = Fs +1/3Kfs+1/3H2O	660	5.331	-0.1361
20	1/3East+Qtz=Ok+1/3Kfs+1/3H2O	954	9.485	-0.1676
21	1/2Fa + 1/2Qtz = Fs	-267	-0.699	-0.0445
22	1/2Fo + 1/2Qtz = En	-1496	-0.994	-0.0524
23	1/3En + 1/3Spl = 1/3Fo + 1/3Ok	2915*	0.566	0.0017
24	4/2En + 1/3Spl = 1/3Fo + 1/3Prp	1681**	0.536	-0.0662
25	2En + 3/2Spl = 3/2Prp + 3/2Qtz	898	-0.299	0.0445
26	1/2Crd + H2O = 1/2Crd·H2O	-1228	-10.256	-0.1899
27	1/2Crd + CO2 = 1/2Crd·CO2	-20824$	-11.927	0.3630

#$\Delta G = G^o + PT\,4.271\times10^{-4}$; * $\Delta Cp = -2.339$; ** $\Delta C_p = -2.339$; $ $\Delta G = G^o + 4.271\times10^{-4}PT$

PETROLOGY AND GEODYNAMIC SETTING OF CEFALIKDAG GRANITOID (KAMAN REGION - CENTRAL ANATOLIA)

Geven A. (Dept. of Geological Eng., Middle East Technical University)

The Cefalıkdag granitoid, a Santonian-Campanian pluton composed of Küçükçürtepe megacrystic granite, Savcılıebeyit hornblende granite and Kaletepe microgranite, intrudes the Pre-Mesozoic metamorphic rocks of Central Anatolian Crystalline Complex. Cefalıkdag granitoid is metaluminous to peraluminous and calk-alkaline in character. Major and trace element behaviours indicate to a fractional crystallization process for the evolution of the Cefalıkdag granitoid. According to

chemical and mineralogical characteristics, the source material is suggested to be of magmatic origin (I-type) although S-type characteristics are present. Cefalıkdag granitoid is of continental crust origin and discriminant diagrams indicate a post collisional tectonic environment.

Regional data suggests that the continental crust was thickened due to the ophiolitic obduction from İzmir-Ankara suture zone and partially melted after the collision of Tauride-Anatolide platform with Kırşehir massif. As a result of this, during the rise of the newly formed granitic magmas in the continental crust, co-genetic but compositionaly different rocks of Cefalıkdag granitoid were formed due to contamination.

Ghiorso, M.S. (1987). *Reviews in Mineralogy*, **17**, 443-465.
Ghiorso, M.S. (1990). *Contrib. Min. Petrol.*, **104**, 645-667.
Ghiorso, M.S. (1994). *Geochim. Cosmochim. Acta*, submitted.
Ghiorso, M.S., Evans, B.W., Hirschmann, M.M., Yang, H. (1994). *Contrib. Min. Petrol.*, submitted.
Ghiorso, M.S. & Kelemen, P.B. (1987). *Geochem. Soc. Sp. Publ.*, **1**, 319-336.
Ghiorso, M.S. & Sack, R.O. (1991). *Contrib. Min. Petrol.*, **108**, 485-510.
Ghiorso, M.S. & Sack, R.O. (1994). *Contrib. Min. Petrol.*, submitted.
Hirschmann, M. (1991). *Amer. Min.*, **76**, 1232-1248.
Hirschmann, M. & Ghiorso, M.S. (1994). *Geochim. Cosmochim. Acta*, submitted.
Sack, R.O. & Ghiorso, M.S. (1989). *Contrib. Min. Petrol.*, **102**, 41-68.
Sack, R.O. & Ghiorso, M.S. (1991a). *Contrib. Min. Petrol.*, **106**, 474-505.
Sack, R.O. & Ghiorso, M.S. (1991b). *Amer. Min.*, **76**, 827-847.
Sack, R.O. & Ghiorso, M.S. (1994a). *Contrib. Min. Petrol.*, in press.
Sack, R.O. & Ghiorso, M.S. (1994b). *Contrib. Min. Petrol.*, in press.
Sack, R.O. & Ghiorso, M.S. (1994c). *Contrib. Min. Petrol.*, submitted.

AN INTERNALLY CONSISTENT SET OF THERMODYNAMIC SOLUTION MODELS AND AN ASSOCIATED STANDARD STATE THERMODYNAMIC DATABASE FOR THE COMPUTATION OF PHASE EQUILIBRIA IN MAGMATIC SYSTEMS

Ghiorso M.S. (*Dept. Geolog. Sci., Univ. of Washington, USA*), Sack R.O. (*Dept. Earth and Atmosph. Sci., Purdue Univ., USA*), and Hirschmann M.M. (*Div. Geolog. Planet. Sci., CalTech, USA*)

We have developed an internally consistent set of thermodynamic solution models and a standard state (endmember) properties database for the analysis and computation of phase equilibria in magmatic systems. Our standard state database extends the work of Berman (1988) to include additional endmember solids *and properties of several molten silicates*; while associated internally consistent solution models include formulations for activity-composition relations of liquids of magmatic composition within the system SiO_2-TiO_2-Al_2O_3-Fe_2O_3-FeO-MnO-MgO-NiO-CoO-Na_2O-K_2O-P_2O_5-H_2O (Ghiorso & Sack, 1994; Hirschmann & Ghiorso, 1994), and for solid solutions of the majority of the igneous rock forming minerals. The latter include models for (Mg,Fe^{2+},Ca,Ni,Co)-olivines (Hirschmann, 1991; Hirschmann & Ghiorso, 1994), (Mg,Fe^{2+},Ca)-pyralspite garnets (Berman, 1990; Berman & Koziol, 1991), (Na,Mg,Fe^{2+},Ca)^{M2}(Mg,Fe^{2+},Ti,Fe^{3+},Al)^{M1}(Fe^{3+},Al,Si)$_2^{Tet}O_6$-pyroxenes (Sack & Ghiorso, 1994a,b,c), (Mg,Al)-melilites (Charlu *et al.*, 1981), (Mg,Fe^{2+})-cummingtonites (Ghiorso *et al.*, 1994), (Mg,Fe^{2+})-biotites (Sack & Ghiorso, 1989), (Na,Ca, K)-feldspars (Elkins & Grove, 1990), (Na,K,Ca,[])-nephelines, (Mg, Fe^{2+})(Fe^{3+},Al,Cr)$_2O_4$-(Mg,Fe^{2+})$_2TiO_4$ spinels (Sack & Ghiorso, 1991a,b), and (Fe^{2+},Mg,Mn^{2+})TiO_3-Fe_2O_3 rhombohedral oxides (Ghiorso, 1990; Ghiorso & Sack, 1991). These models and the associated standard state database form the basis of a software package (MELTS, Ghiorso & Sack, 1994) which may be used to model igneous processes such as (1) equilibrium or fractional crystallization, (2) isothermal, isenthalpic or isochoric assimilation, and (3) degassing of volatiles. Calculations are performed using energy minimization methods (Ghiorso 1985, 1987, 1994; Ghiorso & Kelemen, 1987) and are applicable to magmatic liquids ranging in composition from highly alkalic basalts to tholeiites to rhyolites, over the temperature (T) range 900°-1700°C and at pressures (P) up to 4 gPa. Utilizing MELTS, phase equilibria are predicted by specifying bulk composition of the system and either (1) T and P, (2) enthalpy (H) and P, (3) T and volume (V), or (4) H and V. Phase relations in systems open to oxygen are calculated by directly specifying the f_{O2} or the T-P-f_{O2} evolution path.

The MELTS software package is written in ANSI C and is accessed via an X11/Motif graphical user interface. It is designed to run on "UNIX" level workstations.

References:
Berman, R.B. (1988). *J. Petrol.*, **29**, 445-522.
Berman, R.B. (1990). *Amer. Min.*, **75**, 328-344.
Berman, R.B. & Koziol, A.M. (1991). *Amer. Min.*, **76**, 1223-1231.
Charlu, T.V., Newton, R.C., Kleppa, O.J. (1981). *Geochim. Cosmochim. Acta*, **45**, 1609-1617.
Elkins, L.T. & Grove, T.L. (1990). *Amer. Min.*, **75**, 544-559.
Ghiorso, M.S. (1985). *Contrib. Min. Petrol.*, **90**, 107-120.

Island arc regime of the Central Eastern Desert of Egypt : Mineralogical and geochemical evidences.

By
Ghoneim.Mohamed Fouad
Geology Department .Facuty of Science .Tanta University Egypt

Central Eastern Desert of Egypt includes widespread occurrences of non-alkaline metavolcanic rocks (770 +12 Ma) and calc-alkaline granites (between 850 to 614 Ma).These rocks exhibit geological and geochemical characteristics similar to rocks developed in island arc tectonic regime. Nevertheless, they are treated separately and uncorrelated by the authors. In the present paper a compiled 250 chemical analyses are presented for major, trace and EMP data (amphiboles,pyroxene,mica,felspar and opaque minerals). Geochemical and mineralogical treatment of the data favour the argument of production of I-type granite from the M-type extrusive metabasalts and meta-andesites. Morever,there are evidences of partial melting during arc-arc collision and/or suturing. The same data point to generation of pre-cratonisation first cycle during the evolution of the Nubian Shield It has been later activated during the Pan-African cratonisation second cycle. The second cycle has been achieved similar with some modification to the first cycle but not unique and independent.

HEAVY METAL OXIDES FROM COMBUSTION PROCESSES: A CHEMICAL AND PHYSICAL INVESTIGATION

Gianfagna A.*, Diociaiuti M.°, Burragato F.*, Baldo G.°, Paoletti L.°
(* *Dipartimento di Scienze della Terra, Università di Roma "La*

Sapienza"; ° Laboratorio di Ultrastrutture, Istituto Superiore di Sanità, Roma.)

Fly ashes, mainly constitude by cenospheres, are product during fuel oil combustion (Smith, 1962). Cenospheres are spheroidal, black particles with a spongy structure and sizes from about 10 to 200 μm. They are constituded by an amorphous component rich in C, S, Si. Their structure is characterised by both hollows, in the volume, and holes at the surface.

Many microcrystalline phases can be observed inside the cenospheres; such phases are very small in sizes, generally less than one micron, and are prevalently composed by sulphates (of Ca, Fe, Ba, Mg, ...) and by metal oxides. Pratically all metal oxide phases contain V, Fe and Ni, sometimes together with Al, Ti, Cr, Zn and Mn (Burragato et al., 1993; Paoletti et al., 1993).

In this work we studied the crystal-chemistry of suth metal oxide phases because their importance from the environmental, toxicological and health point of view, due to the presence of an high concentration of heavy metals. Because of the very small sizes of the phases of interest, analytical scanning and trasmission electron microscopy techniques were used. In particular the selected area electron diffraction (SAED), the energy dispersion X-ray spectrometry (EDXS) and the electron energy loss spectroscopy (EELS) were performed.

The distribution of the detected metal oxide phases shows three distinct clusters: **a)** V-Fe, **b)** Fe-Ni and **c)** Ni-V.

The **a)** cluster represent about 30% of the detected metallic oxide phases; V and Fe ranging from about 15 to 85% and from about 60 to 40%, respectively.

The **b)** cluster represent about 38% of the detected metallic oxide phases; Fe and Ni ranging from about 70 to 30% and from about 40 to 60%, respectively.

The **c)** cluster represent about 32% of the detected metallic oxide phases; Ni and V are present into 1:1 ratio.

The crystal-chemistry of these phases would indicate two different structures: *spinel type* (V-Fe and Fe-Ni) and *ilmenite type* (V-Ni). TEM and EELS investigations allowed to individuate specific features corresponding to the assumed structures. Morphological and crystallographic features for phase **a)** and **b)** agree with a cubic symmetry (octahedral habit), whereas phase **c)** presents lamellar habit and hexagonal symmetry.

Through EELS it was possible to discriminate V^{4+} in the V-Ni phase (*ilmenite type*) and V^{5+} in the V-Fe phases (*spinel type*).

The high vanadium oxidation state is correlated to the high temperatures (above 1000°C) and P_{O_2} present during the combustion processes. Moreover, the spinel-ilmenite transition may be attributable to the relative cooling of the cenospheres during flue arise.

References:

Burragato F., Diociaiuti M., Gianfagna A., Paoletti L. (1993) *Proceeding of Multinational Congress on Electron Microscopy*, Parma, Italy, September 13-17, pp. 265-266.

Paoletti L., Diociaiuti M., Gianfagna A., Viviano G. (1993) *Mikrochim. Acta*, **110**, in press.

Smith W. S. (1962) *Atmospheric Emission from Fuel Oil Combustion. An Inventory guide*. U.S. Departement of Health, Education and Welfare, PHS Publication n. 999-Ap-2.

VANADIUM-BEARING CLINOHUMITE IN METASOMATIC VEINS FROM ADAMELLO (ITALY)

Gieré R. *(Geophysical Laboratory, Carnegie Institution of Washington)*, Graeser S. *(Mineralogisch-Petrographisches Institut, Universität Basel)*, Reusser E. *(Institut für Mineralogie und Petrographie, ETH Zürich), and* Guggenheim R. *(REM-Labor, Universität Basel)*

Vanadium-bearing clinohumite has been discovered in metasomatic veins from the contact aureole of the Adamello Batholith (Provincia di Trento, Northern Italy). The clinohumite crystals are characterized by a deeply blue color, a color not yet reported for the humite group minerals. The vein paragenesis consists of clinohumite+forsterite+calcite, and occasionally also contains titanian clinohumite. The large modal abundance of blue clinohumite results in a striking color contrast between the veins and the white dolomite marble host-rock.

In thin section, the clinohumite crystals are easily recognised by a pronounced pleochroism ranging from light blue to colorless. Titanian clinohumite, on the other hand, exhibits a pleochroism ranging from golden yellow to colorless.

Electron microprobe analyses revealed the presence of considerable amounts of vanadium (up to 0.22 wt.% V_2O_3). The studied clinohumites are devoid of titanium ($TiO_2 < 0.025$ wt.%), and thus the V-K_α line could be used for analysis yielding higher count rates than V-K_β. Analyses were made for two samples from different veins, because they contain crystals with slightly different color shades: in one vein clinohumite is relatively light blue and has an average content of 0.06±*0.01* wt.% V_2O_3 and 0.37±*0.02* wt.% FeO, whereas in the other vein it exhibits a darker blue color and contains an average of 0.20±*0.01* wt.% V_2O_3 and 0.75±*0.10* wt.% FeO. The concentrations of all other analyzed components are similar and relatively constant in the two samples, i.e. [in wt.%] ZnO = 0.02, MnO = 0.05 , and SiO_2 = 38.1. In both specimens, however, the fluorine and MgO contents show a considerable variation, resulting from substitutions involving these two components as well as V, Fe, and OH. The obtained correlation matrix documents that fluorine does not correlate with any of the analyzed components, and thus the variation in F must be due to the OHF_{-1} exchange. This is in contrast to the incorporation of F into titanian clinohumite, which takes place at a constant OH content (along $TiO_2Mg_{-1}F_{-2}$). A good correlation is found between Fe and V (r = 0.914), suggesting that the incorporation of V is coupled to that of Fe. Evaluation of the linear regression data indicates that the exchange VFe_2Mg_{-3} best describes accommodation of V into clinohumite. This exchange would imply that V is present in a bivalent oxidation state, a conclusion that remains to be verified spectroscopically.

The two clinohumite specimens exhibit almost identical unit cell parameters. The sample richer in V_2O_3, though, appears to have a slightly larger unit cell with the following dimensions: a = 13.74±*0.01* Å, b = 4.734±*0.002* Å, c = 10.28±*0.01* Å, β = 100.14±*0.05* °, and V = 658.0±*1.0* $Å^3$.

Two populations of calcite, both coexisting with dolomite, occur in the clinohumite-bearing veins: one variety contains 5 - 5.6 mole% $MgCO_3$, indicating a minimum formation temperature of approximately 525 - 550 °C for the dolomite-hosted veins (estimated P_{total} = 2kb). This temperature is consistent with conclusions drawn from stable isotopic data and thermodynamic calculations for mineral assemblages in other veins. The second population contains an average of 3.5 mole% $MgCO_3$, suggesting that calcite partially re-equilibrated during cooling (~ 465 °C).

Vanadium is not detectable in the dolomite marble host-rock (V < 12 ppm), and therefore, had to be deposited from the metasomatic fluid which also carried Si, Fe, and F. The fluid was most likely of magmatic origin, derived from a nearby tonalite intrusion. Field observations suggest that the veins were formed simultaneously with the tonalite emplacement. As documented by the occurrence of V-bearing spinel (~ 0.25 wt.% V_2O_3) in other veins from the same outcrop, vanadium has been transported during several stages of metasomatism.

CRYSTAL STRUCTURE AND THERMAL DECOMPOSITION OF THE COQUIMBITE-TYPE COMPOUND $Fe_2(SeO_4)_3 \cdot 9H_2O$

Giester G. and Miletich R.
(Institut für Mineralogie und Kristallographie, Universität Wien, Austria)

Crystals of $Fe_2(SeO_4)_3 \cdot 9H_2O$ were slowly grown at T=295K from concentrated aqueous solutions of $Fe_2(SeO_4)_3$ with excess H_2SeO_4. Preliminary X-ray work revealed the presence of streaks and diffuse reflections and considerable effort was necessary to yield a single crystal suitable for X-ray structure investigations.

The belonging to the coquimbite structure-type (Fang & Robinson, 1970; Giacovazzo et al., 1970) assumed by chemistry and cell metrics, was established by the structure refinement: space group $P\bar{3}1c$, a=11.190(5)Å, c=17.518(5)Å, V=1899.7Å^3, Z=4, R=0.042 for 803 unique data up to $\sin\Theta/\lambda = 0.6$Å^{-1}. The crystal structure features a $[Fe_2(H_2O)_6(SeO_4)_3]$ framework consisting of isolated $[Fe3(Ow1)_6]^{3+}$ octahedra and $[Fe1Fe2_2(Ow3)_6(SeO_4)_6]^{3-}$ clusters which are connected to each other only by hydrogen-bonds. Channels running parallel to [100] within the framework contain non-framework H_2O molecules (Ow2). Based on the sites of the hydrogen atoms obtained from difference-Fourier summations a complete hydrogen-bonding scheme can be given.

The thermal behaviour obtained from TGA experiments (303-873K, flowing N_2, heating rate: 0.5K/min) revealed an almost identical decomposition of the title compound compared to that one of coquimbite (Cesbron, 1964). The mass loss (dm=-23.6wt.%) between 353K and 523K can be attributed to the complete dehydration ($9H_2O$ p.f.u.=23.07 wt.%); a further step at 693-753K (dm=-50.1wt.%) reveals the final decomposition by the release of $3SeO_3$. The corresponding DTG curve in the range 353-523K shows one peak (373K) with a shoulder (355K) and two further peaks (411K, 513K) indicating that the dehydration actually proceeds in at least four distinct steps at partially coinciding temperature intervals.

References:
Fang, J.H. & Robinson, P.D. (1970) *Am. Mineral.*, **55**, 1534-1540
Giacovazzo, C., Menchetti, S., Scodari F. (1970) *Lincei, Rend. Sc. Fis. mat. e nat.*, **49**, 129-140
Cesbron, F. (1964) *Bull. Soc. franç. Min. Crist.*, **87**, 125-143

NATURE OF BLUE AND GREEN COLOURING CENTERS IN APATITES STUDIED BY *EPR* AND OPTICAL SPECTROSCOPY.

L.G.Gilinskaya, R.I.Mashkovtsev (United Inst. of Geology, Geophysics and Mineralogy, Universitetsky pr.3, 630090 Novosibirsk, Russia

A number of important crystallostructural peculiarities of widely spread polygenic mineral apatite $Ca_5(PO_4)_3(F,Cl,OH)$ have been found by EPR studies to date. Our previous investigations have shown that paramagnetic centers in apatite can be used as original probe of structural and chemical peculiarities formed as a result of *a)* isomorphous substitution, *b)* deviation of composition from stoichiometry, or *c)* post-crystallization influence, in particular by temperature and/or pressure.

In the present work blue and green natural apatites with S and Si impurities are investigated by EPR method and optical spectroscopy in order to establish the model of colour centers.

We found that paramagnetic centers $SO_3^-(S=^1/_2)$ and $SiO_3^-(S=^1/_2)$ are accompanied with isomorphous substitution of phosphorus by sulphur and silicon and with the above mentioned colouring. However these centers are formed only under certain conditions. The principal condition for the formation is isomorphous entering of actinoide ions in the form of U^{4+} and Th^{4+} to Ca^{2+}II positions. When forming the nearest environment, the actinoide ions shift oxygen atoms of the neighboring PO_4^{3-} anions, as well as substitutional SO_4^{2-} and SiO_4^{4-} anions. The anions are thus broken (PO_4^{3-}->PO_3^-, SO_4^{2-}->SO_3, SiO_4^{4-}->SiO_3^{2-}), resulting in formation of paramagnetic radicals by means of electrons capture (PO_3^{2-}, SO_3^-) or loss (SiO_3^-) by the broken structural fragments. In samples containing S or Si as impurity yet not having isomorphous U or Th ions (or with concentration less than a few units of 10^{-4}%) the paramagnetic centers are not formed; the samples are colourless in this case.

We have determined g-factor values and structural location of SO_3^- and SiO_3^- centers, and studied their temperature-dependent and X-ray irradiation behavior and correlation with samples colour and its intensity. The models of colour centers are proposed on the basis of experimental results.

We found that the appearance of blue colour of natural apatites is caused by SO_3^- centers having characteristic optical transition between $3e$ and $6a_1$ orbitals at $\lambda \approx 600$nm. Green colour is correlated with more complicated defect - SiO_3^- radical in complex with rare-earth ion, $SiO_3^- + TR^{3+}$ (Ce^{3+}). Wide bands at 590, 660 and 680 nm correspond to this complicated defect in the optical spectrum.

IS MAGNESITE STABLE TROUGHOUT THE EARTH'S MANTLE.

Gillet Ph., Guyot F. and Martinez (ENS Lyon, France)

Carbonates are minor constituents of the Earth's mantle, nevertheless they are essential actors of the internal CO_2 cycle: they carry CO_2 from the surface to the mantle and may act as C host at depth. We present a series of experimental evidences and calculations which show that magnesite is stable to at least 2000 km in the mantle.

In-situ Raman spectroscopy shows that magnesite is stable up to 30 GPa and 2500 K. Experiments in the presence of silicates representative of mantle mineralogy show that magnesite is stable with $MgSiO_3$ perovskite and MgO up to 50 GPa and 2500 K.

In order to discuss the stability of magnesite at greater depth, its thermodynamic properties have been calculated using vibrational modelling and available room temperature equation of state.

The specific heat and entropy of magnesite have been calculated from IR and Raman data recorded at high pressures and temperatures. Comparison with available (T<1000 K) calorimetric data is excellent and leads to confident extrapolation at higher temperatures.

Molar volumes V(P,T) of magnesite have been computed up to 4000 K and 100 GPa using a modified Mie-Grüneisen equation of state. The static part is calculated from a third order Birch-Murnaghan equation of state whereas the thermal part is calculated using the vibrational density of states model used for calculating the specific heat. The proposed equation of state reproduces well the measured thermal expansion at room pressure.

These data are then used to calculate the decarbonatation curves ($MgCO_3=MgO+CO_2$) as well as other reactions involving silicates at pressure and temperature conditions relevant to deep Earth processes. The geotherm crosses the calculated decarbonation curve between 2500 and 2900 km depth. All the results suggest that magnesite may be the carbon host in most of the mantle. The possible rôle of magnesite in the control of upper and lower mantle oxygen fugacity is also discussed.

TEXTURAL EVIDENCE OF SUPERCOOLING IN INTRUSIVE PILLOWS OF THE GUARDIA MARINA BEACH (SARDINIA ISLAND, WESTERN MEDITERRANEAN, ITALY)

Gimeno,D. & Pujolriu,Ll. (*Dept. Geoquímica, Petrologia i Prospecció Geològica, Universitat de Barcelona, 08071 - Barcelona, Spain*).

The Guardia Marina beach contains outcrops of

subalkaline basaltic pillow lava within a Miocene sedimentary sequence of shallow marine facies. Recent work (Assorgia & Gimeno, 1994) has showed the coeval growth of pillows at the magma–water and magma–sediment interfaces, as well as a recurrent process of pillow-growth from feeder dikes. The intrusive pillows are characterized by the presence of peperitic drops of basalt within the sediment (wall rock) in a halo a few centimeters thick around the pillow border.

The comparative study of the pillows (intrusive and extrusive) and dikes shows several stages in the crystallization history of the magma. Fresh samples of pillow rims are characterized by a prevalence of brown glass. The presence of phenocrysts is restricted to olivine, radially aggregated glomerules of plagioclase phenocrysts, and large twinned augitic clinopyroxene phenocrysts. A second generation of acicular and skeletal microlites of plagioclase and dendritic and skeletal clinopyroxene is also present. The entire paragenesis shows a distinctive idiomorphic character.

Glass of the rim of the intrusive pillows shows microperlitic jointing around foci of thermal anisotropies (altered olivine phenocrysts), as well as transition from ductile to brittle behaviour (peperitic drops and lobulate digitation inside of the sediment, microfaulting, etc.)

The tops of feeder dikes and the cores of massive or poorly vesiculated fresh pillows are texturally similar to the rims of the pillows. Large numbers of plagioclase skeletal microlites are present, so the texture can be denoted as porphyric-intersertal. Locally, the phenocrysts are smaller in size than those in the pillow rim, but no traces of important corrosion have been detected.

The dikes are characterized by a substantially smaller proportion of glass, hence very few intersertal spaces exist. Olivine phenocrysts are small and subidiomorphic or rounded. The clinopyroxene has undergone intense corrosion and embayment. Some plagioclase glomerules are rounded due to resorption. The texture is porphyritic and mesocrystalline.

References:
Assorgia,A. & Gimeno,D. (1994). Geologie in Mijnbown, **72**, 1-11 (in press).

Acknowledgements: Field work was partially funded by the University of Barcelona and Cirit Grants of the Autonomous Government of Catalonia (D.G.).

SEM AND HRTEM STUDY OF CHLORITE-PARAGONITE-MUSCOVITE INTERGROWTHS IN PORPHYROCLASTS OF A LOW GRADE METAMORPHIC QUARTZITE FROM VERRUCANO FORMATION (NORTHERN APENNINES, ITALY)

Giorgetti G., Memmi I. (Dep. of Earth Science, Univ. of Siena), Nieto F.(Ist. of Mineralogy and Petrology, Univ. Granada)

Low grade metamorphosed clastic rocks from Triassic Verrucano Formation (Northern Apennines, Italy) contained detrital and metamorphic minerals along with porphyroclasts of intergrown phyllosilicates: differences in chemical and mineralogical compositions between the clasts and the matrix can be sometimes observed (Franceschelli et al., 1991).

A scanning and transmission electron microscopy study has been performed on a quartzite (qtz+chl+ms+pg+ab as matrix constituent) containing subrectangular or barrel-shaped phyllosilicate intergrowths, up to 200 μm in diameter (made up by chl+pg+ms), in order to investigate their origin. These porphyroclasts are quite abundant and randomly oriented in relation to the main metamorphic foliation.

SEM-EDS analyses reveal that they are predominantly constituted by chlorite-$(Mg_{4.17}Fe_{4.33}Al_{3.22})(Si_{5.38}Al_{2.62})O_{20}(OH)_{16}$-with minor paragonite-$(Na_{1.87}K_{0.05})(Fe_{0.11}Al_{3.97})(Si_{5.97}Al_{2.03})O_{20}(OH)_4$-and muscovite-$(K_{1.69}Na_{0.11})(Mg_{0.13}Fe_{0.19}Ti_{0.06}Al_{3.72})(Si_{6.15}Al_{1.85})O_{20}(OH)_4$-lamellae, both parallel and transversal to the chlorite cleavage planes.

One representative clast has been chosen for TEM analyses. Both SAED patterns and lattice fringe images show several hundred angstrom sized lamellae of defect-free chlorite occurring as a perfectly ordered IIb polytype.

Na and K micas occur either as lamellae up to 200-300 Å thick or as one or few layers intergrown in chlorite packets. Electron diffraction pattern both from pg and ms lamellae (according to the AEM composition) exhibites splitting of the (00l) reflections indicating the presence of both micas in all the areas. Both micas are 2M polytype and occur in partially desoriented packets. Thier lattice fringe images show the typical "mottled" contrast and high defective zones.

Often the three phases are not parallel intergrown: electron diffraction patterns sometimes show two sets of rows of (00l) reflections with different periodicity (10 and 14 Å) making small angles (5-10°).

HR images of intergrown lamellae of micas and chlorite show high defective structures: single 10 Å layers can be recognized in packets with 14 Å periodicity causing characteristical deformation contrast close to the 10Å layer. A solid state transformation mechanism of one chlorite layer laterally changing into one mica layer has been observed. This process implies the substitution of a brucite-like layer by the mica interlayer cations with a decrease in volume (Olives et al., 1983).

The chemical analyses of these high-defective zones deviate from defect-free chlorite composition towards muscovitic and paragonitic ones; this deviation can be interpreted as a contamination of chlorite by both micas.

Considering structural and chemical features, we interpret these phyllosilicate intergrowths (according to Franceschelli et al.,1991) as the product of partial transformation of detrital chlorites into muscovite and paragonite during the metamorphic process: this process implies reactions involving a K- and Na-rich metamorphic fluid in equilibrium with the matrix mineral association.

References
Franceschelli, M., Memmi, I., Gianelli, G. (1991). Contrib. Mineral. Petrol., **109**: 151-158.
Olives, J., Amouric, M., De Fouquet, C., Baronnet, A. (1983). Am. Mineral., **69**: 754-758.

METASOMATIC REPLACEMENT OF SINGLE CRYSTALS: MODEL EXPERIMENT, CRYSTALLOGENETIC THEORY

Glikin A.E. and Sinai M.Yu. (*Crystal Genesis Lab, Crystallography Dept., St. Petersburg Univ.*).

The generalized concept of metasomatic replacement after single crystals was obtained by numerous in situ experiments with 130 low-temperature systems and by theoretic analyzing of their results on the basis of crystallogeny (Glikin & Sinai, 1991).

The classification of products unites all known and first discovered types of structure and morphology. Structural types are: 1) monocrystals, 2) polycrystal aggregates, 3) holes, surrounded by crystal aggregates. They correspond to the types of phase equilibria in systems: 1) isomorphic, 2) non-isomorphic with mutual solubility decreasing of components, 3) non-isomorphic with mutual solubility increasing of components. Morphological types are: vicinal, face and habit pseudomorphs (corresponding primary crystal features are remained), then localized, dissipated and translocated "automorphs" (correspond to the information of primary crystal place). They

depend on kinetic properties: diffusion, crystal nucleation, growth and dissolution.

Some integral parts of metasomatism, limiting process courses and product features, are analysed through phase diagrams: reaction volume deficit or excess determines process mechanism and kinetics; instability leads to box-like pseudomorphs and holes. Other parts are limited by kinetics and cannot be predicted definitely: effect of inclusions on product structure and morphology; crystal disorientation in epitaxial replacement products. Effect of primary inclusions is very strong; products of their interaction with a solution are classified as pointed above for crystal replacement. These and other characteristics are closely interconnected.

Monocrystalline replacement proceeds in isomorphic substance rows being realized through two mechanisms. 1) Volume deficit leads to a rapid replacement being characterized by intensive inclusion implantation into a crystal and limited by a diffusion in a solution; the final pseudomorphs are peculiar spongy crystals and display a poikilitic or a graphic structure at sections. 2) Volume excess leads to an extremely slow replacement being characterized by a continuous border with autoepitaxial accretions around crystals and limited by a diffusion in crystals.

Polycrystalline replacement is realized through a dissolution of an initial crystal and a simultaneous intergrowth of products into a primary crystal (pseudomorphs) or their growth distantly (automorph). Replacement rate and mechanism depend on volume deficit or excess too. Box-like pseudomorph formation depends on a curvature of solubility isotherms and on a quantitative relationship between crystal and solution volumes.

Hole-forming replacement (negative pseudomorph formation) is realized through dissolution of an initial crystal and a simultaneous precipitation of a dissolved substance owing to a temperature decreasing.

A hypothesis of rapakivi-type structure formation, basing on synopsized results, was suggested. In short, such a rock appears to be a secondary one after anortosite. Apparently, it consists of innumerable combined polymineral pseudomorphs and automorphs after primary feldspar crystals with a wide range of composition. Porphiroblasts are monocrystalline pseudomorphs, thus, rounded and faced ones are related to the first and second types consequently; their zonality is connected with inclusion implantations and with an evolution of a solution composition. Orbiculars are localized automorphs. These and other morphological phenomena substantiating the hypothesis were observed as in rapakivi from Vyborg so in experiments.

Reference:
Glikin, A.E. & Sinai, M.Yu. (1991). *Proceed. of Russian Miner. Soc.*, **120**, 1, 3-17.

PETROCALC : A PETROLOGICAL SOFTWARE TO MANAGE RELATIONAL DATABASES OF CHEMICAL ANALYSES.

Godard G. and Chat C. *(Laboratoire de Pétrologie Métamorphique, Université de Paris 7)*

PETROCALC is a Macintosh software package which allows management and processing of chemical analyses. Together with chemical analyses, definitions of mineral species, chemical components, end-members and user routines are stored in an interactive relational database. In order to customize the software functionnalities, these objects may be created, deleted, modified, sorted, selected, ..., recorded, exported to any other software, ..., using a Macintosh-like interface with pull-down menus and multiwindowing.

A chemical analysis is a set of chemical components and their associated values (e.g., SiO2, Aliv, Xpyrope, ...). Each analysis belongs to a mineral species (e.g., garnet, ...); analyses of the same species have the same chemical components. Definition of new chemical components or the use of pre-existing ones is required when creating new species. Each species is related to a set of end-members (e.g., pyrope, ...). To create a new end-member, the specification of the related species and the definition of a set of formal equations describing its thermodynamic behaviour is required.

The main types of calculations available in PetroCalc are :

- **User procedures** : The user can use preexisting procedures or customize the software by writing his own procedures to perform structural formulae calculations, geothermobarometry, ... These procedures are created using a Pascal-like programming language.

- **Thermodynamical calculations** : Using computer algebra, the software can solve thermodynamical formulae to determine equilibrium conditions from a set of chemical analyses.

- **Stoichiometric calculation** : Calculation of stoichiometric relations among a set of analyses can be performed in order to determine stoechiometric coefficients.

PetroCalc is "Free Ware" but needs a runtime version of the commercial relational database system 4th Dimension. The package includes : the application v2.0; a database with all usual species, related components and user procedures; a user manual with its accompanying demonstration database; a runtime version of 4th Dimension. Minimum hardware requirements are an Apple Macintosh running at least system 6, with 2 Mb RAM available and a hard disk.

• NATURAL STRUCTURAL–CHEMICAL CLASSIFICATION OF MINERALS

Godovikov A. A. (*Fersman Mineralogical Museum, RAS. Moscow, Russia*)

1. The natural character of a classification is its major requirement. Relevance should be given to chemical features, paragenetical relationships, sequence in nature, more than to formal features such as isostructurality, similarity in M:X ratio, etc... For example it appears unnatural to separate vanadates characterized by V with coordination number (CN) 4 (placing them in the same class with phosphates and arsenates) from vanadates which present a different CN for V (5 or 6) but are closely connected with the previous ones. A lot of similar examples exist.

2. The proposed classification is based on the following aspects and considerations.

a) Type of constituting elements, distinguished on the basis of their belonging to s– f– d– or p–types, ceno– or noncenosymmetric ones.

b) Type of chemical bonding, taking into account not only the intermediate ionic–covalent, but also metallic–covalent, metallic–covalent–ionic and more complex character.

c) Fundamental properties of atoms: electronegativity, force characteristics (FC), nuclear numbers,...

d) Crystallochemical treatment of the amphotery, explaining the increase of the basic properties with the increase of the CN of the cation and, on the contrary, the increase of the acidic properties with the decrease of the coordination number of the cation.

e) Detailed mineralogical–crystallo– chemical systematic of cations, derived taking into account the fundamental properties of the elements, their belonging to sidero–, chalco– or lithophilic types.

f) Numerous information on the crystal structures of minerals, as well as the different variants of their structural classifications.

g) Diverse chemical properties of minerals: acid–basic characteristics, solubilities, stabilities at various physical–chemical conditions,....

3. We succeeded in developing a classification of minerals presenting taxons which include up to some dozens of minerals (in one case even more than 180 mineral species) related each other not only on the basis of structural features, but also on the basis of conditions of formation, paragenesis, clearly indicating the physical–chemical aspects for the transition from one taxon to the other and stressing the "natural" scientific basis of mineralogy.

SALIOTITE, A NEW HIGH-PRESSURE, LOW TEMPERATURE METAMORPHIC PHYLLOSILICATE MINERAL: ORDERED 1:1 COOKEITE/PARAGONITE MIXED LAYER.

Goffé B. (CNRS, ENS, Paris), Baronnet A.(CNRS, CRMC2, Marseille), Jullien M. (ENS, Paris), Morin G. (Univ. Paris)

Abstract.

Saliotite has been found in Permo-Trias metapelites in two occurrences: the first is in the Alpujarrides nappes of the Sierra Alhamilla (Betic chain, Andalucia S.E. Spain) and the second is in western Crete. In Andalucia, saliotite occurs in schist foliation as deformed lamellae, intergrown with pyrophyllite, paragonite, cookeite and calcite including relics of aragonite. In Crete, saliotite has only been found under electron transmission microscopy as 300Å slabs interlayered in cookeite. Saliotite is optically biaxal negative, $1.58<n_\alpha<1.59$ and $1.58<n_\beta<1.59$, $1.59<n_\gamma<1.6$, biref= 0.007, 2V = 0-50°(obs.). Based on electron and ion microprobe analysis the empirical formula is $Si_{3.1}\ Al_{3.8}\ Mg_{0.01}\ Fe_{0.03}\ Ca_{0.02}\ K_{0.04}\ Na_{0.41}\ Li_{0.5}\ O_{9.86}\ (OH)_5$, corresponding to the ideal formulae : $[Si_3Al]\ Al_3Li_{0.5}Na_{0.5}\ O_{10}\ (OH)_5$. The crystal unit-cell is monoclinic with a=5.158(1), b=8.914(3), c=23.83(2)Å, ß=94.23(4)°, V=1093(1)$Å^3$, Z=4. The calculated density is 2.75 g/cm^3. The strongest diffraction lines in the X-ray oriented powder pattern are : (dÅ/I/hkl) 23.76/60/001; 11.89/40/002; 7.93/30/003; 4.75/80/005; 3.396/100/007; 2.966/50/008. Transmission electron microscopy confirms the nature of a perfectly regular 1:1 ordered interstratification (R=1) of cookeite (di-trioctaedral chlorite, 14Å) and paragonite (di-octaedral mica 9.5Å). At the hundred-Å scale the saliotite is mainly intergrown with lamellae of cookeite and less frequently with paragonite.

The deformation of saliotite in the main metamorphic foliation, its inclusion in calcite veins containing relics of aragonite, and the widespread crystallisation of cookeite and paragonite in the late metamorphic structures demonstrate the early crystallisation of saliotite during the high-pressure (HP) metamorphic stage. This HP stage is attested by the regional cristallisation of aragonite and ferrocarpholite. Thermodynamic calculations result in a minimum pressure of about 8 kbar at 280-320°C for aragonite-ferrocarpholite-pyrophyllite assemblage formation. In Western Creta, temperature is estimated around 380-400°C for a minimum pressure of 10 kbar (Theye et al 1992). This temperature condition could be a maximum for the stability of saliotite that could be considered as relic in Western Creta.

Saliotite is a new HP-LT mineral. It is stable along very cold geotherms (8-10°C/km) in the stability field of pyrophyllite (300-400°C). Its breakdown gives peculiar paragonite-cookeite intergrowths that occurs through exsolution type mechanism. Its partial preservation together with aragonite and ferrocarpholite is due to a cooling path during decompression.

Theye, T., Seidel, E., Vidal, O.(1992) *Eur. J. Min.*, **4**, 487-507.

3-D PETROGRAPHIC IMAGING USING SCANNING ACOUSTIC MICROSCOPE

Golan G., Shoval S.*(Dept. of Physics and Geology, The Open University of Israel)*, and Pitt C.W. *(Dept. of Electrical Engineering University College London, UK)*

The potential performance of a novel Scanning Acoustic Microscopy (SAM) technique for achieving high resolution 3-D acoustic images, by employing thermal effects and image subtraction methods, has been studied and demonstrated on sedimentary and magmatic rock samples from Israel.

The experiments with the SAM were carried out in the Wolfson Unit laboratories at University College London, UK. Focal length, in the reflection mode, was taken as a parameter. Effective scanned surface of the rock planes was in the order of 800^2 µm. It was found that using the image subtraction technique, short periods of sample heating had lead to a better pattern selectivity, due to the strong temperature dependency of the rock samples' elastic parameters.

The obtained results indicate that this technique provides improved petrographic imaging. This capability stems from the SAM potential to distinguish between various minerals and rock components. SAM technique emphasizes the fabric of different crystals and their boundaries. Furthermore, it identifies composition variations in single crystals, presence of zoning and inclusions. SAM is sensitive to the distribution of accessory materials and oxides. It allows for the detection of fine features of fossil or micro-structures e.g. ooliths. By defocusing the acoustic beam in various planes below the rock surface, a three-dimensional reconstruction is possible.

SAM capability to penetrate into opaque minerals is suitable for the investigation of ore deposits. As a non-destructive testing method, it is useful for the examination of ancient pottery.

SAM does not provide direct mineralogical analysis, however, the minerals content in such measurements can be estimated according to their specific acoustic mineral signatures.

The Rio Jacare mafic-ultramafic complex (Brazil): a metamorphosed piece of a great layered complex yielding tholeiitic affinities.

E. GOMES*, B. PLATEVOET*, J.J. BATISTA** and B. BONIN*

The Rio Jacare mafic-ultramafic complex belongs to the São Franscisco craton (Bahia state, Brazil). It consists of a 30 km-long, 1 km-thick elongate body, which is 2.2 Ga old (Sm/Nd and U/Pb methods), but has been metamorphosed during the Transamazonian orogenesis. The rock suite is subdivided into two series (Brito, 1984) of metamorphosed rocks: the lower series is made up of 400 m-thick metagabbro with some layers of ferro-amphibolite; the 600 m-thick upper series is composed of metagabbro with a particular zone, the Magnetitite Zone (M.Z) which is made up of amphibolite, magnetitite, ferro-amphibolite and some layers of anorthosite. The complete rock sequence is representative of cumulates metamorphosed in the amphibolite facies conditions. The magmatic origin is supported by numerous preserved primary structures typical of cumulates, such as pyroxenite, leucogabbro, ferrogabbro, magnetitite and anorthosite. Reaction of pyroxenes, oxides and plagioclase with a H_2O-rich fluid is responsible of the crystallization of Ca-rich and Ca-poor amphiboles, garnet and sometimes mica:

Cpx + Opx + Pl1 + Ox1 + Fluid (H_2O) -> Grt + Ca amp. + Cum + Pl2 + Ox2 + SiO_2

The reaction is very similar to that proposed by Barink (1984) to explain the metagabbro formation of the Smith-Wakeham belt (Quebec). The amphibole-garnet-plagioclase association yields a temperature of 590 ± 40 °C for a presure of 0,55 GPa.

The M.Z. includes an important volume of magnetitite which is now the greatest lode of V-bearing Ti-magnetite in Brazil. The M.S. is discontinuous, the principal lode of V-bearing magnetite is located in the district of Novo Amparo. Several drillings have crosscut the M.Z. Subzones limits and correlations between drilling cores were established with reference to the prograde succession of cumulates. Laterally, massive magnetitite disappears to the North, where only plagioclase-bearing magnetitite occurs. The total thickness of magnetitite (30m in the drilled area) is also decreasing from South to North and increases again at the extreme North.

Large variations of magnetite compositions are observed due to subsolidus reequilibration effects. Cr contents are always low, indicating an evolved parental magma. V contents are stable or increase with degree of reequilibration of magnetite, indicating that V probably remains within magnetite structure during reequilibration processes. The maximum value of about 4% of V_2O_3 was observed in magnetite within pyroxenite, and only 2% within magnetitite, which could be due to weak incorporation of V into pyroxene and also because major crystallization of oxides implies a drastic partition of V available from the parent melt between crystallizing minerals. However, increasing oxygen fugacity, which probably instigates massive crystallization of magnetitite (Spencer & Lindsley, 1981; Reynolds, 1985), also induces decreasing incorporation of V within magnetite structure.

The Rio Jacare complex can be considered as a piece of a fossil magmatic chamber. It is a new example of a large tholeiitic reservoir like Bushveld or Stillwater layered complexes, with important development of magnetitite layers. The observed sequence of cumulates also indicates that the parental magma was already evolved, Cr-poor and contains maximum amounts of Fe, Ti and V, typical of compositions of tholeiitic ferrobasalt.

NEW MODEL OF THE EARTH'S DEGASSING

Goncharov G.N. (*Dept. of Geochem., univ. of St.-Petersburg*)

Application of the methods of calculation of parameters of electronic structure of iron atoms, geometric and energy characteristics of their positions in minerals (Goncharov, 1991 a,b) for interpretation of experimental spectroscopic, in situ, high-pressure studies of minerals (Champion *et al.*, 1967; Huggins, 1976; *et al.*) allowed us to propose a new model of differentiation of Earth's depth zones (Goncharov, 1992). As pressure rises, it takes place transition of the electronic charge from ligand orbitals to *3d-*, *4s-* and *4p-* orbitals of iron; this leads to an increase in covalence of bond and then to a reduction of Fe^{3+} -ions in case of many of ligand environments under high pressures, corresponding to upper mantle and transition zone of the Earth. Analogous process of Fe^{2+}- reduction can be under more high pressure in the lower mantle and core. Decrease probably twice of values of the radii of ligand atoms because of oxidation of ligands to state of neutral atoms due to iron reduction under high pressure and temperature should lead to division thereof between the Earth's primordial material and crust through the mechanism of diffussion. Between the proofs of formation of ascending diffussion flows of neutral atoms of ligands in the Earth's solid mantle are: 1) clearly defined inverse correlations between the K value (the abundance ratio of element atoms in external Earth's shells and carbonaceous I type (C I) chondrites) and the radii of atoms of anion-forming elements of subgroups VI-A and VII-A; 2) the presence of Fe^{3+} in deep-seated xenoliths of mantle origin in contrast to parental chondrites in which Fe^{3+} is practically absent and other proofs.

The most low energy transition with charge transfer for $Fe^{3+}L_6$ - complexes ($t_{1g} \rightarrow t^*_{2g}$) leads to the following sequence of ligand oxidation as related to pressure rise:

$$I^- = S^{2-};\ Br^- = CN^-;\ Cl^-;\ SO^{2-}_4 = O^-_2;\ H_2O;\ F^-.$$

The $Fe^{2+} \rightarrow Fe^{1+}$ conversion requirs a much higher pressure as compared to $Fe^{3+} \rightarrow Fe^{2+}$, but sequence of ligand oxidation with increase of pressure is the same.

Elevation of flows of the oxidated ligand atoms to upper zones of the Earth leads to Fe^{2+} oxidation. Subduction of material saturated with Fe^{3+} and ligand atoms into mantle as the pressure rises leads to a progressive reduction of Fe^{3+} and separation of oxidated ligands from them; ligands form fluid flows in increasing order of value of energy transition with charge transfer $Fe^{3+} \leftarrow L$, as moving to the back subduction zones. In accordance with the chemical affinity of ligands with metals, extracted from country mantle and crust rocks in the ascent of fluid flows, the usual (for instance, the Pacific metallogenic belt) regional metallogenic zoning appears. Capacity of ascending mantle of fluid flows to extract metals from enclosing rocks is primarily determined by the geodynamic environment.

The formation of fluid flows can be determined by fluid accumulation in local mantle volums which project onto surface as "hot spots". Ascent of separate columns of fluids leads to formation of enormous ore bunches and deposits, localized in isometric structures of different type. In this case, the ascending fluids of different ligands fall in line, resulting in formation of complex deposits (Bushveld megapluton).

The report concerns also a new approach to explanation of the evolution mechanism of ore-forming and environmental processes in the Earth's history.

References:
Champion, A.R., Vaughan, R.W., Drickamer, H.G. (1967). *J. Chem. Phys.*, 8, 2583-2590.
Goncharov, G.N. (1991, a). *Geokhimiya*, 3, 388-397.
Goncharov, G.N. (1991, b). *ZVMO*, 5, 81-94.
Goncharov, G.N. (1992). *ZVMO*, 4, 1-14.
Huggins, F.E. (1976). *Ph. and ch. miner. and rocks*, 613-640.

Gorelikova N.V. and Patyk-Kara N.G.
(Inst. of Geol. of Ore Dep., Petrog., Mineral. and Geochem., Russian Acad. of Sci.)

Metacolloidal zircon in the fine-impregnated ores from volcanites of Kazakhstan

The new type of zirconium mineralization has been revealed in the Devonian volcanic rocks from orogenic depressions at the Central Kazakhstan. The most essential feature of this deposit is the fine-grained type of zirconium mineralization, unusial texture of zirconium ores and paragenesys Zr with P. Predominant minerals of ores are quartz, kaolinite and hydromicas on the data of IR spectroscopy, X-ray diffraction and differential thermic analysis. Some part of Zr (up to 26 percents of total ZrO_2 content) is solved in acids. The intergrow of fine zircon grains with 10Å micas, kaolinite, quartz, hematite, hetite and calcite was revealed by the use of TEM with "Kevex", microdiffraction and local energy-dispersion analysis. The zircon grains have formed globular or monometric aggregates with the features of hexagonal crystal cut. The size of zircon grains is o,n — o,onμ. Ranges from poor crystal aggregates to high level microcrystals in ores were recognized with the help of microdiffraction. Besides zircon crystals, there is metacolloidal zircon, similar with gelzircon. The latter mineral is characterized by lower value of density, refractive index, double-refraction and not crystal structure which mainfests itself as broad reflections, corresponding to zircon. This mineral form fine dispersive, heterogenous rounded aggregates or fine corrosium rims (1-10μ), overgrowed biotite crystals. Textural and morphological features of zirconium ores suggest that deposition of ore elements took place at low temperature and colloidal solutions took part in ore formation. In our opinion, as a result of this process coagulative mixtures were formed. Later they were crystallized in colloidal aggregates with fine, not perfect zircon crystals in the ageing process. That is why we observe the different degree of zircon crystal perfection.

The data, giving in this paper, allow consider this deposit as a new genetic type of zirconium mineralization, connected with low temperature hydrothermal processes.

FLUORESCENT MINERAL ANOMALIES IN THE LITHOSPHERE (THEORY AND APPLICATIONS)

Gorobetz B. (*Inst. of Mineral Resources VIMS; College of Geodesy and Cartography of Moscow*), Portnov A. (*Moscow Inst. of Prospecting Geology MGRI*)

Spectra of photoluminescence (PL) of 2500 samples of some 100 minerals, excited by UV lamps or lasers, were deciphered. It allowed to reveal that overwhelming majority of mineral substances fluoresce due to PL centres formed by transition elements with incomplete f- and d-shells: U, TR, W, Mo, Ag, Mn, Cr, V, Ti, entering minerals as impurities or much more rarely as intrinsic elements. In addition to the "classical" fluorescent minerals - calcite, fluorite, scheelite, zircon, ruby, uranium salts - it occured that PL is peculiar to apatite (almost always), feldspars (from some sort of veins), datolite, danburite, meyonite, barite, dozens of ironless "ore" minerals contaning titanium, manganese, tin, lithium, berillium, boron. Still, fluorescent minerals occupy a very small part of volume of the Earth crust. Their macroscopic outcroppings are distributed extremely inhomogeneously forming fluorescent anomalies. Two main factors are responsible for that phenomenon.

1) The clarks of many luminogenous metals are so low (10^{-6} - 10^{-3} %) that rock-forming minerals turn out to have no PL to be visible (e.g. feldspars in granites and granitoides). 2) The mechanism of concentration self-quenching or quenching by iron suppresses PL of centres formed by some elements from iron group having the clarks of the order of 0.1 -1%. Thus the bulk of the Earth crust is represented by quasinon-fluorescent background of rock-forming minerals. And only in some specific localities of the crust peculiar processes of geochemical differentiation, accompanied sometimes by ore-forming, result in accumulation of the luminogenous transition elements as PL centres in some vein, alteration and ore minerals. It took place in some post-magmatic hydrothermal and alteration processes as well as in some placers and zones of oxidation of ores. So PL centres in peculiar assemblages of minerals can trace such geological bodies. For example, carbonatites are traced by Mn^{2+} in calcite, by Ce^{3+} and Eu^{2+} in apatite, sometimes by Ti^{4+} in buddeleyite: mica pegmatites are traced by Eu^{2+} in plagioclases and sometimes in microcline; different skarns may be traced by Mn^{2+} in calcite, scapolite, by Ce^{3+} and Eu^{2+} in datolite; hydrothermal veins may be traced by Mn^{2+} in calcite, by Eu^{2+} and Yb^{2+} in fluorite, by Eu^{2+}, Ti^{3+} in barite etc.

• DISTINCTIVE FEATURES OF CHEMISTITES - A NEW VARIETY OF SERPENTINITES WITH THE HYDROTALCITE-LIZARDITE BASE PARAGENESES FROM SOUTH-EAST PART OF BALTIC SHIELD

Goroshko A.F. (*Karelian Geolog. Expedition, Geol. Committee of Karelia*)

Chemistites were discovered as a new rock and prospective Ni-Mg ore for hydrometallurgical refining and are studied since 1989. Chemistites have been known in the three mafic-ultramafic intrusions in south-east part of Baltic shield, Republic Karelia, Russia. These are: Hursula two-phase intrusion of olivinite-peridotite formation (AR) occurring into Archean green-stone belt; Kutshenogorsky olivinite intrusion (AR) into Archean granitoid rocks; Burakov layered pluton (PR). In the latter one the large lenticular blinde chemistite body (8x2.5 km, thickness 0,3-0,9 km) has been studied during geological exploration of Aganosorsky Ni-Mg deposit. Chemical composition of chemistites is similar to that of the enclosing serpentinite, wt%: SiO_2 - 37.83, Al_2O_3 - 0.43, Fe_2O_3 - 7.21, FeO - 2.09, MgO - 37.83, CaO - 0.47, NiO - 0.32, l.o.i. 15.0-17.75, surplus CO_2 - 1.80 (Steinberg & Tchashuchin, 1977). Mineral composition: group of hydrotalcite (brugnatellite, coalingite, pyroaurite) 12-22%, lizardite - 73-81%, magnetite - 1-10%. Other minerals: chamosite, chrisotile, calcite, dolomite, chromite; clay and sulphide minerals less than 0.05%. Chemistites have peculiar features: 1) A high acid solubility (in 5-10% H_2SO_4 or 2-3N HCl, at 15-25 °C, air pressure) - 80-95% Ni, 35-60% Mg, 15-30% Fe can be extracted in solution during 4 hours. This largely distinguishes them from other varieties of serpentinites, as well as from Ni-ore of weathering crust, in which acid solubility for Ni is less than 10-35%. 2) Acid soluble phases include: hydroxide, hydrocarbonate; the acid insoluble phases are: oxide, sulphide; the silicate phase (serpentinite) is slightly soluble. 3) Physical metastability due to decomposition of massive "in situ" rocks to aleurite powder by shaving the lithostatic load during some days. 4) High porosity (3-12%). 5) Low electrical resistance (35-65 ohm/m). 6) High polarization (10-30%).

Chemistites originate through an autometamorphic serpentinization taking place in the middle of the magmatic camera where the residual melt presents the highest concentration of CO_2. Dissociation of CO_2-H_2O fluid at the temperature of formation of lizardite prevented to reach pH = 10.49 (brucite precipitation) (Varlakov, 1986) and kept pH = 8.0-8.4 (chamosite precipitation); pH comes down to 6.0-6.5 near the borders of the reacting serpentinite grains. Ni, Mg, Fe were redistributed from all volume to the outlying area of serpentinite grains into hydrotalcite. This was corroborated by the results of the microanalyses and by dynamic of leaching. Physical change to fine powder is due to the effect of hydraulic microwedging in Quaternary permafrost zone.

References:

Varlakov A.S. (1986). *Petrology of serpentinization process of folding areas*. Moscow, 224 pp.

Steinberg, D.S., Tchashuchin, I.S. (1977). *Serpentinization of ultramafites*. Moscow, 312 pp.

NATURAL HETEROEPITAXIAL DIAMONDS (CARBONADO) IN AVACHITES OF KAMCHATKA

Gorshkov A.I., Seliverstov V.A., Sivtsov A.V. (*In-t of Geology of Ore Deposits, RAS, Moscow*), Baikov A.I., Anikin L.P. (*In-t of Volcanology, FEB RAS, Petropavlovsk-Kamchatskii*), Dunin-Barkovskii R.L. (*In-t of volcanic Geology and Geochemistry, FEB RAS, Petropavlovsk-Kamchatskii*).

Avachite is melanocratic basaltic rocks (SiO_2 about 50 mas. %, MgO 14-16 mas.%), which consist of phenocrysts of olivine, clinopyroxene, etc. (60%); stock or dyke of avachite intrude Pleistocene-Holocene volcanites of volcano Avachinskii's Somma. These rocks contain small angular grains of carbonado with rough, irregular surface. The paper is dedicated to results of investigation of these polycrystal polymineral aggregates with Electron Microscope JEM-100c, equipped with EDS "Kevex-5100" and ASID.

Scanning electron and X-ray images permit to identify isolated diamond's crystals of size 6-7 mkm, accociating with quartz, feldspars and rutile (?). Application of selected area electron diffraction together with EDS analysis of isolated particles of suspensional specimens gave the possibility to identify next minerals: diamond's microcrystals of size 1-7 mkm (a=3.55 *nm*), and associated with them fine dispersed polycrystalline aggregates of cubic carbon of silicide α-SiC (a=4.36 *nm*), isolated particles of native silica (a=5.42 *nm*) and graphite. The main additive phases are quartz, K- and Na-feldspars, and chlorite scarcely.

Experimental results obtained and analysis of published data, including data on diamond's artificial synthesis, show that carbonado from avachites of Kamchatka were formed under reducing conditions, comparatively low temperatures and geostatic pressures. Mineral-substrate is presented by α-SiC. Diamond polycrystalline tex-

ture was dictated by polycrystallic composition of α-SiC. It is believed that cubicm carbon silicide was formed in a melt as a result of carbonic fluid - native silicium or, possible, carbonic fluid - SiO_2 reactions. Thus, uniqueness of avachite carbonado-bearing melt is determined by (1) the high pressure of hydrocarbon gases, (2) the presence of hydrogen among vagmatic fluids, needed to depress the grow of graphite crystallites, and (3) presence of the mineral-basement α-SiC.

WATER TRACER DIFFUSION IN SINGLE CRYSTAL ZEOLITES. RAMAN MICRO-SPECTROSCOPY STUDY.

Goryainov S.V. and Belitsky I.A.
(Inst.of Mineralogy & Petrography, Russ.Acad. Sci.,Novosibirsk)

Many of the physico-chemical properties of zeolites depend on the water mobility in the channels of aluminosilicate framework. Usually, the water diffusion in zeolites is investigated by powder macrotechniques. Tiselius (Barrer,1971, p.4) used the method of optical microscopy to study the water diffusion in heulandite single crystals at sorption.Different diffusion models were calculated by Derouane et al.(1988). Chabazite dehydration and sorption of water were studied by Valueva & Goryainov (1992) by thermochemical and Raman spectroscopy methods. Raman study of single crystals using microscope allows to observe directly the spatial-temporal dependences of concentrations of diffusing molecules. The purpose of this presentation is to describe deuteron-proton exchange reaction in zeolites and to find the water diffusion parameters from Raman data.

Raman spectra were recorded by OMARS 89 (DILOR) 512-channel spectrometer fitted with OLYMPUS microscope. The kinetics of isotopic substitution H→D in the single crystals placed into vaporous or liquid heavy water has been investigated at 19-180 or 19-104°C, respectively. Following natural zeolites were studied: natrolite (Khibiny),chabazite (Khilok r.),scolecite (Podkam.Tunguska r.) from Russia, and mesolite from India (Poona).

A model of water tracer diffusion is proposed. The $H_2O(n_1)$,$HDO(n_2)$,and $D_2O(n_3)$ molecular concentrations are calculated for the crystal of the orthorhombic symmetry at the deuteration of initial H_2O-sample. A way is shown to find the diffusion coefficients D* (D_1*, D_2*, and D_3*), equilibrium constant K and deuteron-proton exchange rate a from experimental data.

The water diffusion coefficients for natrolite placed in liquid D_2O appeared to be 1.5-2 times higher than those for sample in vaporous D_2O. 1.5-1.6 times higher water diffusion occurs along [001] than along [110] at 20 °C in vapor, Table 1.

Table 1. Tracer diffusion coefficients for water in zeolites.

Zeolite	Direction	T,°C	D*, m^2/s	E,kJ/mol	D_2O medium
Natrolite	[001]	20	$0.74\ 10^{-15}$	52 ±0.5	Liquid
	[110]	20	$0.47\ 10^{-15}$	55 ±0.5	
	[001]	20	$0.45\ 10^{-15}$	56.5±1	Vapor at
	[110]	20	$0.3\ 10^{-15}$	59.5±1	17.5 torr
Scolecite	[110]	19	$0.9\ 10^{-15}$	-	
Mesolite	[110]	19	$0.36\ 10^{-15}$	-	
Chabazite		19	$0.4\ 10^{-11}$	-	

. Method of K determination is following. n_1 or n_3 are found at the distance where n_2 reachs maximum in the sample, and $n_1=n_3=n$ according to the model. Then K is calculated as $K=[(1-2n)/n]^2$. Rate a is found at the first stage (small time) of reaction. In initial H_2O-sample placed in D_2O medium, the HDO yield is proportional to the rate a and the constant K.

In the case $D_1^*=D_2^*=D_3^*=D^*$ and overlapping bands of H_2O, HDO, and D_2O in the region of O-D or O-H vibrations, the diffusion coefficient is determined at time t from the relation $D^*=x_2^2/t$ at the distance x where the relative intensity of O-D or O-H band is equal to 0.48, non-depending of K. In the case of distinct O-D bands of HDO and D_2O, D* can be found from the spatial dependence of n on leading edge.D* is found as $D^*=x_2^2/4t$ at the distance x_2 where the ratio I_2/I_{2max} of O-D band intensities for HDO is equal to calculated Y(K): for example, Y(3)=0.55, Y(4)=0.53.

Thus, calculations of single crystal zeolite deuteration are given and a method is shown to obtain water diffusion parameters and constants of $H_2O+D_2O=2HDO$ reaction from the spatial dependences of H_2O, HDO, and D_2O contents measured by Raman microprobe.

References:
Barrer R.M. (1971) In: Molecular sieve zeolites-II. (Gould R.F.,ed.) American Chem.Soc., Washington, p.1-36.
Derouane E.G.,Andre J.-M., Lucas A.A.(1988) *J. Catalysis*,110,58-73
Valueva G.P., Goryainov S.V. (1992) *Geol.& Geophys.*, N12, 81-85.

PERIODIC PRECIPITATION IN GEL: THE RULE OF THE CRITICAL SUPERSATURATION.

Goshka L.L., Kolosov S.I., Ruzov V. P.
(Dept.Experim. Phys, Univ. of Syktyvkar)

The comparison of the results of experimental investigations and numerical simulations will be presented in the paper.

The periodic precipitation was observed as the result of diffusion of $CuSO_4$ solution through the silica-gel acidified by HCl.The concentration range of the $CuSO_4$ was (0.1 - 1.0) mol/l.

Following regularities were obtained:

- the space law: $Y_{i+1}/Y_i - a_1$
  Y_i is the ring coordinate in gel,
  in our case a_1- 1.08 ± 0.02;

- the width law: dY_i/Y_i-a_2
  dY_i is the ring width and
  a_2- 0.06 ± 0.01

- Wagner's law: $Y_i^2/t - W$

  t is ring formation time, the constant W depends on the reagents concentrations, in our case W- (-0.10) p[Ca] + 0.16

The theoretical approach. Two reagents U and V are separated by gel and diffuse towards one another. The diffusion destroy steady state. It can lead to the precipitation due to the chemical reaction:

$$U + V \rightleftarrows Z$$

The precipitation occurs in some location in gel if one of two conditions is satisfied:

a) the precipitate already exists in this location;

b) the concentration product exceeds the steady one, such as $u*v > s*L$ $(s>1)$

where u and v are the concentrarions of U and V, constant "s" is the critical supersaturation, and L is steady concentration product.

We suppose also that the chemical reaction velocity is infinite. Such simplification leads to zero width of the rings. The analisys of the model shows that such simplification is volid only for s-value and diffusion time period long enough.

As the result of chamical reaction the system transmits to steady state $v*u=L$.

The results of numeric calculations.

We obtained the space law and Wagner's law for time interval large enough.

If value s-constant increases the spacing constant a_1 decreases.

If s -> 1 the distance between the neighbour rings becomes infinitly large to infinite. One can suppose that in this case it means that the ring width tends to infinite.

Göske, J., Pöllmann, H. & Dickschas, D. (Erlangen, Forchheim)

Investigations on xenolites in the tertiary basalt from Maroldsweisach / Lower-Frankonia

In the north of Bavaria, on the border between Frankonia and Thuringia tertiary basaltic extrusions are forming a vein-system, described as Heldburger Gangschar. One of these volcanoes is the Zeilberg near Maroldsweisach in Lower-Frankonia.

The tertiary basalt from Maroldsweisach is fractionated from exterior nephelinbasanite to nephelintephrite (Huckenholz, H.G. & Werner, C.D.). In the center, the quarry from Maroldsweisach is well-known because of its secondary zeolite-paragenesis and mesozoic xenolites. Contact metamorphism and hydrothermal-metasomatism reactions of mesozoic carbonatious rocks with the surrounding basaltic-extrusion causes the formation of various secondary and tertiary mineral paragenesis. Spinel - peridotites occur as well. At the Zeilberg, xenolites from räth- and dogger-sandstones as well as high metamorphic lias-clays with belemnit-rostres are well-known (Jakob, 1976). From surrounding rocks, nucleus of xenolitic contact areas and new metamorphic facies are observable (Jakob & Matouschek, 1979).

The xenolites show on intensive pyrometamorphism in the brim-area. In the border-area these can be distinguished between metasomatic contact areas of the basaltic rock and xenolites. Bigger xenolites remain unchanged in the center and are metamorphosed to the rim-area (Göske, J. & Pöllmann, H.). The presence of zeolites and CSH-phases can be due to a hydrothermal mineralisation of a primary thermal transmutated xenolitic rock. This hydrothermal mineralisation causes likewise a new entity of minerals and contact-areas. Besides the zeolite-facies, due to contact metasomatism, hornblende-hornfels, pyroxen-hornfels and sanidinite-facies are developed.

Particularly in strong decomposed limy xenolitic rocks hydrolysis and metasomatosis to secondary minerals assembled with participation of volatile phases as CO_3^{2-}, Cl^-, SO_4^{2-} takes place. This secondary minerals are partly changed due to weathering-solution to tertiary-paragenesis.

Three formation-areas for the mineralisation can be distinguished :

1. basalt with accompanying tuffs
2. xenolites and reaction zones
3. primary not influenced mesozoic sediments

The main-paragenesis can be distinguished :

1. zeolitic mineral facies
2. CSH-phase facies
3. pyrometamorphism facies (incl. sanidinite facies)
4. contactmetamorphism - metasomatism facies
5. tertiary-paragenesis

The rare mineral-paragenesis and their formations conditions are described and the variation of the chemistry and of the mineral stock in xenolites are discussed.

Göske, J. & Pöllmann, H. : Untersuchungen an Xenolithen und Mineralneubildungen in tertiären Vulkaniten N-Bayerns - Geol.Bl.NO-Bayern, In Vorb.

Huckenholz, H.G. & Werner, C.D. : Die tertiären Vulkanite der Heldburger Gangschar (Bayr.-thür. Grabfeld) - Ber.Dt.Min.Ges. Bh.Eur.J.Min. 2, 1-42 (1990).

Pöllmann, H. & Dickschas, D. : SiO_2-Minerale aus Maroldsweisach / Ufr., In Vorb.

Pöllmann, H. : Die Afwillit-Portlandit Paragenese im Basalt des Zeilbergs bei Maroldsweisach/Ufr. - Aufschluß 42, 257-266, Göttingen (1991).

Scheinpflug, R. : Der Zeilberg bei Maroldsweisach. - Privatverlag, Lohr am Main, Ostpreußenstr. 7 (1983).

TRIOCTAHEDRAL MICAS AS INDICATORS OF THE COMPOSITIONAL EVOLUTION OF Sn-Li-Rb-Cs-F GRANITES, AN EXAMPLE: THE EIBENSTOCK PLUTON (WESTERN ERZGEBIRGE/GERMANY)

Gottesmann B., Tischendorf G., and Förster H.-J. (*GeoForschungsZentrum Potsdam, Germany*)

The majority of the Hercynian granitoids of the Erzgebirge region are interpreted as belonging to two main plutonic series, the Older (OIC) and the Younger Intrusive Complex (YIC). The granites of both complexes underwent extended, but distinct differentiation which is best displayed by the Kirchberg (Ki; OIC) and the Eibenstock (Ei; YIC) plutons in the western Erzgebirge. Both massifs are composite bodies built up by a succession of four texturally and geochemically distinct sub-intrusions.

Specific features of compositional variations characterizing the Kirchberg and Eibenstock granites are reflected, among other things, by the chemical, optical and X-ray (d_{060}) characteristics of their trioctahedral micas.

Complete analyses of mica concentrates showed that the Kirchberg granites contain common Mg-Fe biotite. In contrast, the Eibenstock granites show a succession of siderophyllite - protolithionite - zinnwaldite reflecting differentiation from Ei1 to Ei4 granite. Furthermore, electron microprobe studies on single grains revealed that some of the micas in distinct sub-intrusions (Ei1, Ei2) are intensely zoned, with decreasing Fe content from the core to the rim.

In the Erzgebirge, nearly unzoned Mg-Fe biotites are characteristic for granites spatially associated with W-Mo mineralization (Kirchberg). In contrast, strongly zoned F-rich Li-Fe micas are a diagnostic feature of those granites producing topaz-bearing tin mineralization (Eibenstock).

ACTIVITY MODELS AND FUNCTIONS OF STATE FOR FLUIDS AND FLUID MIXTURES: TESTING PROCEDURES FOR CONSISTENCY USING EXPERIMENTAL RESULTS FOR MINERAL EQUILIBRIA

Gottschalk M. (Mineralogisches Institut, Universität Tübingen)

Equations of state for fluids and fluid mixtures are essential for the evaluation of metamorphic equilibria. For a wide range of metamorphic conditions fluid mixtures and their properties are of great interest. In conjunction with internally consistent thermodynamic databases, these equations are used to evaluate metamorphic equilibria. For example in the fluid system H_2O-CO_2-CH_4 the function by *Kerrick & Jacobs* (1981) is widely used. Beside this a large number of equations are available now for various conditions. For pure fluids like H_2O and CO_2 most functions of state deliver similar results. But for fluid mixtures large differences in the calculated fugacities can be observed.

With the help of experimental results for mineral equilibria the functions of state can be tested for consistency. This has already be done for example by *Ferry & Baumgartner* (1987), but the tools available now are improved and extended.

One general testing procedure is using linear programming. With this tool general information can be obtained about whether some existing experimental phase equilibrium is consistent with the used function of state or not. Besides other data, enthalpies and entropies for each phase involved are required. But these values also have their errors and influence the test. Another testing procedure is to use an 1/T

- ln K_{red} diagram. With the help of heat capacities and molar volumes the equilibrium constant, involving the fugacities and activities of fluid species, is reduced to 298 K and 0.1 MPa. This reduced equilibrium constant is then plotted against 1/T. In such a diagram a straight line must separate stable parageneses. Slope and intercept of this line are directly related to the change of enthapy and entropy of the reaction. But enthalpies and entropies are not needed for the calculation of the plot. If the stable parageneses can not be separated by a line, this is an indication that the equation of state employed is invalid for the required conditions.

References:
Ferry, J.M., Baumgartner, L. (1987). Mineralogical Society of America. Review in Mineralogy **17**, 323-366.
Kerrick, D.M., Jacobs, G.K. (1981). Am.J.Sci. **281**, 735-767.

HOW TO SYNTHESISE LARGE AMPHIBOLES: METHOD AND FIRST RESULTS

Gottschalk M. (Mineralogisches Institut, Universität Tübingen)

Experimental research with amphiboles and especially with calcic amphiboles has been hampered for a long time by small the grain size of the reaction products. The diameter of synthetic amphiboles usually lies in the range of 3 µm or smaller. As a result in most cases it is very hard to analyse synthesised amphiboles with the electron microprobe. The precise composition of the run products must be known, however, for the determination of phase equilibria and the development of mixing models.

Another problem which hinders experimental work with amphiboles is the common abundance of chain disorder in synthetic material. For the successful thermodynamic interpretation of experimental results, well ordered amphiboles are required.

A new experimental technique has been developed using principally oxides in addition to $CaBr_2$ and $MgBr_2$ as starting materials, which allows the synthesis of large amphiboles. No seeds are used. The use of Ca-halogenides is not new in experimental petrology. CaI_2 has been used by several authors, but without large success. Amphiboles containing F are much easier to synthesis than their OH counterparts. It seems that the speciation and the transport properties in the fluid phase containing halogenides (except Iodine) are more advantageous for amphibole growth than in halogene free fluids.

In the system Al_2O_3-CaO-MgO-SiO_2-H_2O-CO_2 crystals of tremolite-tschermakite solid solutions grow at 500 MPa and 700 °C as large as 50x50x500 µm and therefore analyses with the microprobe are easy. The composition of the amphiboles produced under these conditions is remarkable. In the parageneses anorthite-talc-clinochlore-amphibole-H_2O, amphiboles have a uniform composition of $Tr_{46}Ts_{46}Cum_8$, which comes very close to pure hornblende. At this conditions this is much more than previously reported by *Cao et al.* (1986), *Jenkins* (1988) and *Cho & Ernst* (1991), but is close to the maximum tschermakite contents observed by *Jasmund & Schäfer* (1972). In other parageneses the tschermakite contents are lower. The synthesis of amphiboles with additional Na_2O is also very successful with similar results.

HRTEM examinations of amphiboles synthesised with the new procedure show, that they are well ordered and chain disorders are rare (< 1%). It can also be demonstrated that chain disorder can be induced or prevented by the choice of starting materials.

References:
Cao, R.-L., Ross, C., Ernst, W.G. (1986). Contrib.Mineral.Petrol. **93**, 160-167.
Cho, M., Ernst, W.G. (1991). Am.Min. **76**, 985-1001.
Jasmund, K., Schäfer, R. (1972). Contrib.Mineral.Petrol. **34**, 101-115.
Jenkins, D.M. (1988). Contrib.Mineral.Petrol. **99**, 392-400.

EVIDENCE OF LIQUID IMMISCIBILITY IN IGNIMBRITES: ULTRAPOTASSIC, LATITE AND RHYODACITE MELTS AS MEMBERS OF PETROGENETIC SERIES IN THE NORTHERN ARMENIA

Gouchtchine A. V. (Institute of Mineralogy, Geochemistry & Crystal Chemistry of Rare Elements, RAS, Moscow)

High- and ultrapotassic rocks represent the collisional stage of Paleogene magmatism in the Northern Armenia. The volcanic glasses of contrasted compositions were identified by us in Late Eocenian vitriphiric ignimbrites from Alaverdy district. In fiammes of globular-fluidal structure low potassic acid matrix (1.2-1.5 % K2O) contains two kinds of microglobules which correspond to latite (4.5 % K2O) and to ultrapotassic dacite (12.0-13.7% K2O; 0.2-0.3% Na2O).

These two kinds of glasses are very close by their chemistry to the puissant ignimbritic layers and to lava flows widely distributed in the region. The ultrapotassic melts, whose density was less than 2.33-2.35, were accumulated in the upper parts of magma chambers above the latite magma zone (density 2.41-2.43). This model is consistent with natural relations in differentiated ignimbritic flows.

Appearance of ultrapotassic melts offers the most plausible explanation to the extraordinary trends with high degree of potassium accumulation, for example: from latite to ultrapotassic rhyodacite, strongly depleted by sodium. Ultrapotassic dacite, latite and lowpotassic rhyodacite glasses correspond to the end members of petrogenetic series of low-, high- and ultrapotassic kinds. The magma mixing processes with absarokite, basalt or latite source melts were obviously responsible for appearance of wide compositional spectrum of Late Eocenian volcanic rocks.

A RAPAKIVI-CHARNOCKITE ASSOCIATION IN THE NATAL METAMORPHIC PROVINCE, SOUTH AFRICA

Grantham, G.H. (Dept. of Geol., Univ. of Pretoria) and Thomas, R.J. (Geol. Survey of South Africa).

Texturally, the granitoids exposed in the Umzumbe and Margate Terranes of the Natal Metamorphic Province may be subdivided into a megacrystic porphyritic suite (the Oribi Gorge Suite) and a medium-grained equigranular suite (the Margate Granite Suite). The ~1050Ma (U/Pb) old Oribi Gorge Suite (Thomas *et al.*, 1993) locally displays rapakivi textures and was emplaced syntectonically (Jacobs *et al.*, 1993).

Mineralogically, the Oribi Gorge Suite is characterised by biotite + hornblende + garnet ± orthopyroxene ± clinopyroxene. One pluton (Oribi Gorge Pluton) also contains fayalite which is locally partially replaced by orthopyroxene. Orthopyroxene - clinopyroxene thermometry suggests crystallisation temperatures of ~1050°C. Barometry using fayalite - orthopyroxene suggest pressures ~6.5kb. These P-T constraints suggest a primary origin for the charnockite.

The ~1000Ma old (Rb/Sr) (Eglington *et al.*, 1986) Margate Granite Suite is characterised by biotite + garnet ± orthopyroxene. The Margate Granite Suite does not show rapakivi textures and may therefore be similar to the even-grained granites of the Wiborg Massif decribed by Vorma (1976). The orthopyroxene in the Margate Granite Suite is developed in aureoles where the Margate Granite Suite is intruded by the Oribi Gorge Suite and also where the Margate Granite Suite intrudes other mafic lithologies and consequently some of the orthopyroxene in the Margate Granite Suite is secondary and metamorphic. The idiomorphic shape and chemistry of garnets in the Nicholson's Point Granite of the Margate Granite Suite suggest that they may be primary in origin.

The granitoids have major and trace element chemistries typical of rapakivi granites in that they exhibit high high FeO/(FeO+MgO) ratios, high alkalis in relation to CaO, K_2O>Na_2O and high Ba, and Zr (and F in the Oribi Gorge Suite) (Vorma, 1976). In addition the Oribi Gorge Suite is characterised by high TiO_2 and high P_2O_5 contents and SiO_2 contents which vary between ~54% and 70%. The Oribi Gorge Suite is tholeiitic in

character, displays A-type and within-plate type chemistry. The chemistry of the Nicholson's Point Granite of the Margate Granite Suite is virtually identical to that of the Wiborg Massif (Vorma, 1976).

The chemistry and petrography of the Oribi Gorge Suite support the genetic relationship between rapakivi granites and charnockites suggested by numerous authors and additionally, may merely reflect a shallower depth of emplacement for the rapakivi granite with charnockites occuring at greater depths.

References:

Eglington, B.M., Harmer, R.J. and Kerr, A. (1986). *Transactions of the Geological Society of South Africa*, 89, 199-214.

Jacobs, J., Thomas, R.J. and Weber, K. (1993). *Geology*, 21, 203-206.

Thomas, R.J., Egington,B.M., Bowring, S.A., Retief,E.A., and Walraven. (1993) *Precambrian Research*, 62, 83-101.

Vorma, A. (1976). *Geological Survey of Finland*, Bulletin 285, pp. 98.

RUBY / SAPPHIRE - Cr-SILICATE ROCKS: METASOMATIC PRODUCTS OF GREYWACKE SCHIST AND SERPENTINITE, SOUTHERN ALPS, NEW ZEALAND

Grapes, R. H. (Research School of Earth Sciences, Victoria Univ. of Wellington, New Zealand).

Boulders of ruby/sapphire corundum - fuchsite - margarite - tourmaline (locally known as "Goodletite") occur in moraine derived from the northern part of the Southern Alps, New Zealand. Such rocks have never been found insitu but some larger boulders retain a partial selvage of serpentinite indicating that they are associated with lenses of ultramafic rock (the Pounamu Ultramafic Belt) that occur within garnet zone quartzofeldspathic (greywacke) schist of the Alps.

Corundum typically occurs as single and interpenetrating barrel-shaped crystals (up to 5mm x 2mm) that are spectacularly colour zoned from pale pink to dark ruby-red and from pale blue to deep violet. Cr_2O_3 ranges up to a maximum of 12.9wt% (in 5 μm thick lamellae) and variation of SiO_2, TiO_2, FeO, Fe_2O_3, and V_2O_3 with respect to Cr-content is shown in Fig.1. Highest concentrations of Si, Ti, Fe^{2+} and V occur in blue corundum and Cr and Fe^{3+} in red corundum. Concentration maxima of the former elements lie close to 2% Cr_2O_3 suggesting a narrow "substitution window" that may coincide with optimal lattice distortion caused by incorporation of larger Cr and Fe^{3+} atoms into the corundum structure. Zoning profiles show an inverse relationship between Cr, Fe^{3+} and Ti, Fe^{2+} and V implying substitutions of $(Fe, V)^{3+} = Cr^{3+}$ and $(Si,Ti)^{4+} + Fe^{2+} = 2(Cr, Fe)^{3+}$.

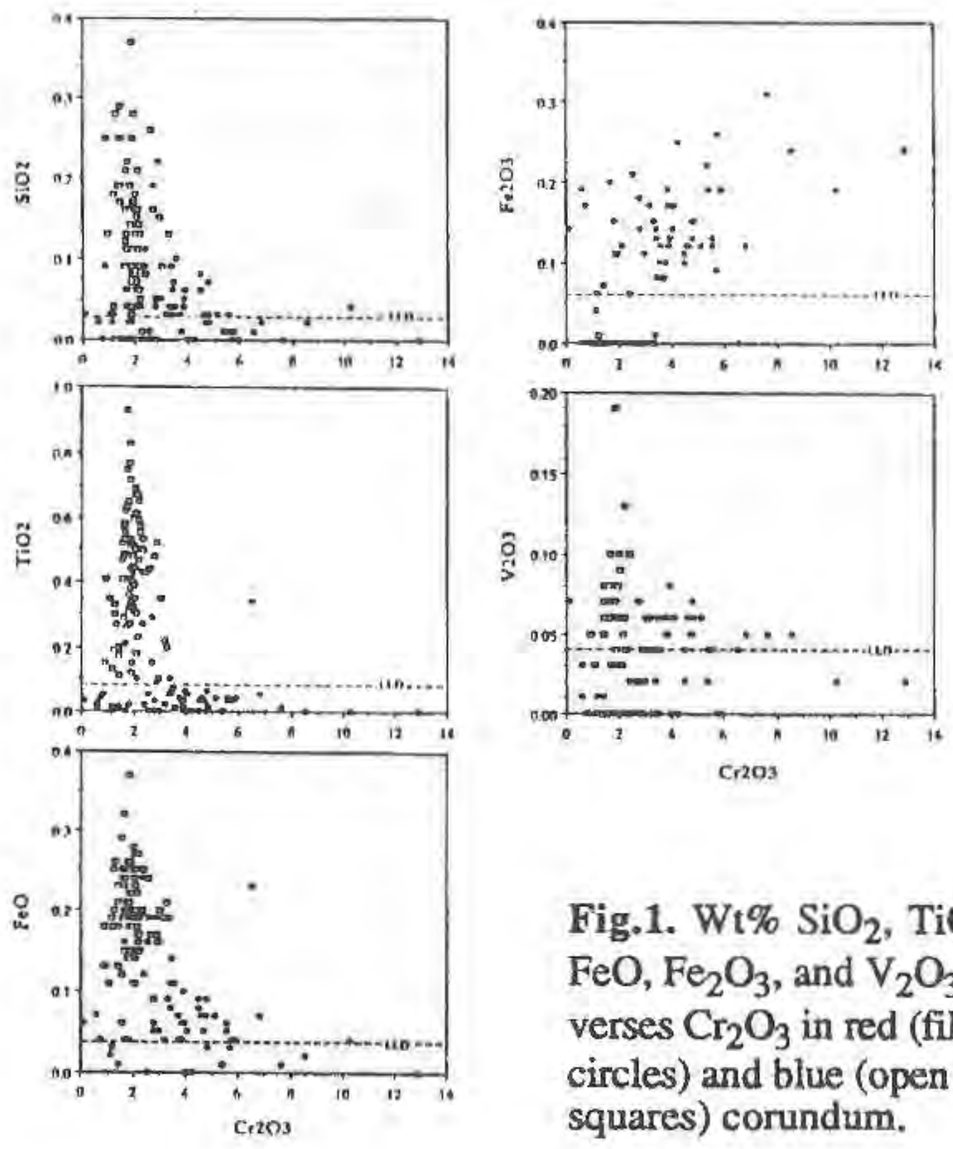

Fig.1. Wt% SiO_2, TiO_2, FeO, Fe_2O_3, and V_2O_3 verses Cr_2O_3 in red (filled circles) and blue (open squares) corundum.

The corundum is set within a matrix of fuchsite (0.6 - 1.9% Cr_2O_3; up to 2.0% BaO) and margarite (0.3 - 0.9% Cr_2O_3; 0.8 - 2.6% Na_2O). Rare boulders have cores of corundum/margarite surrounded by a zone of nearly pure fuchsite that is in turn rimmed by chlorite (X_{Mg} = 0.8; 1.2 - 1.4% Cr_2O_3) and then serpentinte. Tourmaline (1.9 - 3.3% Cr_2O_3) occurs as veins and/or late stage crystals throughout the micaceous matrix.

Textures indicate that corundum has grown at the expense of fuchsite and margarite and is also partly retrograded to these minerals. In the absence of K-feldspar and anorthite-rich plagioclase or epidote, corundum-producing reactions appear to have been

$fuchsite_1/margarite_1 = corundum + fuchsite_2/margarite_2 + H_2O$.

Schist/serpentinite reaction experiments and natural occurrences indicate that these unusual rocks are the result of extreme metasomatism of greywacke schist during amphibolite grade metamorphism. Experiments at 2kb/450°C produced chlorite and then mica-rich zones in schist starting material away from the serpentinite contact. At higher temperatures corundum formed from K and Ca-micas. Comparison of bulk compositions of quartzofeldspathic schist and the micaceous matrix of the "goodletite" together with isocon analysis, indicates that conversion of the former to the latter requires a 50-60% mass weight loss with conservation of Al, K, Ca, volatiles, depletion in Si and all other major/trace elements with enrichment in Cr.

The origin of the corundum/Cr-silicate rocks in the Southern Alps of New Zealand may have relevance to that of the corundum/fuchsite bodies within Archean ultramafics, southern Africa.

LABORATORY MODELLING OF CHARNOCKITE MELTING AND TEMPERATURE ESTIMATES IN CHARNOCKITE COMPLEXES

Graphchikov A.A.,Konilov A.N. *(Institute of Experimental Mineralogy Russian Academy of Sciences)*

The melting of assemblages biotite + orthopyroxene + quartz and biotite + sanidine + quartz and stability field of the mineral assemblage biotite+ orthopyroxene +sanidine+ quartz, modeling charnockites, were studied in the system KAlO2-MgO-FeO-SiO2. The experiments were performed in the temperature range 650 - 900 C, at 100 - 800 MPa and the mole fraction of water in the fluid X(H2O) = H2O/(H2O + CO2) = 1.0, 0.5, 0.3 and 0.1-0.15. Synthetic minerals have been used in the starting mixtures.

It has been established that the increase of Fe-content of biotite results in a considerable decrease of temperature of the solidus of biotite + quartz as well as of the existing temperature of charnockite assemblage. The P-T position of the assemblage biotite (phlogopite-annite)+ orthopyroxene + sanidine + quartz has been calculated using thermodynamic and experimental data. With decreasing of water mole fraction in the fluid melting reactions and stability field of charnockite assemblage remove to higher pressures. At a CO2 molar fraction of 0.9-0.8, that is typical for fluid inclusions from migmatite complexes, melting should occur at P >1500 MPa and T >850 C. That is in contradiction to conditions for migmatization estimated from the mineral geobarometer/geothermometer.

The analysis of the glasses in the products of the experiments showed that they contains an insignificant amount of FeO and MgO. Fe - content of the melt is

greater than that of biotite and orthopyroxene coexisted with it. As an example glass composition recalculated to 100 wt.% is (run 412, 800 C, 500 MPa, XH2O)= 1): SiO2- 79.30; Al2O3- 10.10; FeO- 1.34; MgO- 0.09; K2O-9.17. Aqueous fluid in the system studied contains quenched-vapor precipitates with SiO2 content from 80 to 90 wt.%.

OCCURRENCE OF FERRIKAOLINITE PARTICLES IN SYNTHETIC FE-KAOLINITES

*Grauby O., **Petit S., *Amouric M. and **Decarreau A.
(* *CRMC2, Univ. of Marseille, ** Lab. Petrology of Surface, Univ. of Poitiers*)

In kaolinites, 1 : 1 aluminous phyllosilicates, Fe^{3+} for Al octahedral substitutions may occur. The presence of iron in these minerals is even used as an indicator of its lateritic origin. However, as natural minerals, kaolinites generally contain only small amounts of ferric iron (up to almost 2% Fe_2O_3). Recently, an experimental study based on mineral synthesis (Petit & Decarreau, 1990), has showed that higher ratios of Fe for Al substitution (up to almost 7% Fe_2O_3) may exist, which probably does not represent a structural limit.

The ferric end-member, unknown as natural species, is called ferrikaolinite. This ferric mineral, similar to the kaolinite, with an ideal $Si_2Fe^{3+}{}_2O_5(OH)_2$ structural formula, is at the present time considered as a fictitious end-member in the thermodynamic simulations of the clay solid-solutions (Fritz, 1981 ; Trolard & Tardy,1989). It was interesting then to know if it was possible to completely substitute Fe^{3+} for Al in the network of kaolinite.

In this study, syntheses of ferrikaolinite were conducted using ageing at 200°C of (1) a silicoferric coprecipitate and (2) a silico-ferric-aluminous coprecipitate, with water in excess in both cases. In the first experiments, 2:1 clays and hematite were generally obtained, whereas in the second experiments kaolinite was produced.

XRD and IR spectroscopy of the products obtained through the way (2) revealed that kaolinites were synthesized, and Mössbauer spectroscopy indicated that iron was strictly ferric.

The TEM study and the coupled EDX chemical microanalysis revealed the existence of two groups of clay particles :

- very numerous hexagonal particles, with low iron content ($\leq$ 6% of Fe_2O_3)
- few small almond-shaped particles, completely substituted in iron. The chemical composition of such particles was this of a pure ferrikaolinite.

These direct prooves, obtained thanks to the TEM, are still supported by the occurence of specific infrared signals related to concentred iron in the network of the kaolinite. In the OH stretching vibrations zone, the absorption band situated at 3535 cm^{-1} corresponds to the Fe_2OH groups and in the OH bending vibrations region, a more discreete signal due to Fe_2OH groups, appears at 800-818 cm^{-1}.

All these analytical data tend to demonstrate the existence of ferrikaolinite with $Si_2Fe^{3+}{}_2O_5(OH)_2$ as structural formula. So, this mineral was evidenced and characterized for the first time.

References :

Fritz, B. (1981). *Sci. Géol. Mem.*, **65**, 197p.

Petit, S. & Decarreau, A. (1990). *Clay Miner.*, **25**, 181-196.

Trolard, F.& Tardy, Y. (1989). *Clay Miner.*, **24**, 1-21.

THERMODYNAMIC DATA FOR MG-STAUROLITE CONSISTENT WITH PHASE-RELATIONS IN THE SYSTEM $MGO-AL_2O_3-SIO_2-H_2O$

Grevel K.-D. and Fockenberg T.
(Research Group on High-Pressure Metamorphism, Institut für Mineralogie, Ruhr-Universität Bochum, Germany)

The high-pressure phase Mg-staurolite $Mg_4Al_{18}Si_8O_{46}(OH)_2$ (MgSt) was investigated experimentally by Fockenberg & Schreyer (1993). In this study thermodynamic data for Mg-staurolite are obtained using mathematical programming analysis on the basis of the Berman-dataset (Berman, 1988), a simple activity model for clinochlore (Holland & Powell, 1990) and an equation of state for water which can be extrapolated to high pressures (Grevel & Chatterjee, 1992). The linear constraints of the mathematical programming problem were taken from the results of the bracketing experiments by Fockenberg & Schreyer (1993). Considering the following equilibria including the phases clinochlore (Chl), corundum (Co), orthoenstatite (En), kyanite (Ky), pyrope (Py), talc (Tc), and water (H_2O)

3 MgSt = 4 Py + 11 Co + 12 Ky + 3 H_2O

5 MgSt + 11 H_2O = 4 Chl + 13 Co + 28 Ky

3 MgSt + 1 H_2O = 4 Tc + 19 Co + 8 Ky

1 MgSt = 4 En + 5 Co + 4 Ky + 1 H_2O

the subsequent thermodynamic data for Mg-staurolite were derived. The c_p-coefficients were choosen according to Berman & Brown (1985):

$H^0_{f,298}$ = -25215046.3 J mol^{-1}

S^0_{298} = 957.83 J K^{-1} mol^{-1}

$V = 44.29 \cdot (1 - 0.07385 \cdot 10^{-5}(P - 1) + 0.000155 \cdot 10^{-8}(P - 1)^2 + 1.1194 \cdot 10^{-5}(T - 298.15) + 0.000766 \cdot 10^{-5}(T - 298.15)^2)$ J bar^{-1} mol^{-1}

Starting with these data, other high-pressure phases of the system $MgO-Al_2O_3-SiO_2-H_2O$, e.g. MgMgAl-Pumpellyite, can be included.

References:
Berman, R.G. (1988). J. Petrol., **29**, 445-522.
Berman, R.G. & Brown, T.H. (1985). Contrib. Mineral. Petrol., **89**, 168-183.
Fockenberg, T. & Schreyer, W. (1993). Terra Abstr. supplement No. 4 to Terra Nova **5**, 9.
Holland, T.J.B. & Powell, R. (1990). J. metam. Geol., **8**, 89-124.
Grevel, K.-D. & Chatterjee, N.D. (1992). Eur. J. Mineral., **4**, 1303-1310.

CRYSTAL STRUCTURE RELATIONSHIPS OF REE CARBONATES

Grice, J.D. (Mineral Sciences Division, Canadian Museum of Nature, Box 3443, Station D, Ottawa, Ontario, Canada. K1P 6P4)

As (CO_3) groups do not polymerize due to simple bond-valence considerations, the crystal structures of carbonate minerals tend to be layered, with (CO_3) slabs being interleaved with layers of large cations predominantly alkaline, alkaline-earth and rare-earth cations. This rather simple arrangement gives rise to very few structure types but a large number of mineral species. The great diversity of species results from: 1) the numerous possible substitutions of cations; 2) variability of cation:(CO_3); 3) the

variation in thickness of the carbonate layer; 4) addition of an (H_2O) layer; and 5) the addition of other anionic groups such as $(SiO_4)^{4-}$, $(PO_4)^{2-}$, $(BO_4)^{5-}$ and $(SO_4)^{2-}$. The thickness of the carbonate layer is determined by the orientation of the triangular polyhedron, which in its two extremes may be either "flat-lying" or "standing-on-edge". Combinations of these two extremes give rise to a large diversity in slab thickness which may in some minerals accommodate a variety of other anions and cations.

REE minerals with discrete, flat-lying $[CO_3]$ layers include moydite-(Y) (Fig.1, Grice & Ercit, 1986), baiyuneboite-(Ce), cebaite-(Ce), cordylite-(Ce), and huanghoite-(Ce); discrete, inclined to standing-on-edge $[CO_3]$ layers include ancylite-(Ce), bastnäsite-(Ce), parisite-(Ce), röntgenite-(Ce), sahamalite-(Ce), synchysite-(Ce), and zhonghaucerite-(Ce). Fewer REE minerals have combinations of discrete and mixed $[CO_3]$ layers. Included in this group is donnayite-(Y) (Fig. 2, Grice & Perrault, 1975), lanthanite-(La), mckelveyite-(Y) and tengerite-(Y). A few complex REE carbonate minerals have no discrete $[CO_3]$ layers but still consist of slabs; petersenite-(Ce) (Fig. 3, Grice *et al.*, 1994), mineevite-(Y) and new $Na_{15}Y_2(CO_3)_9(SO_3F)Cl$.

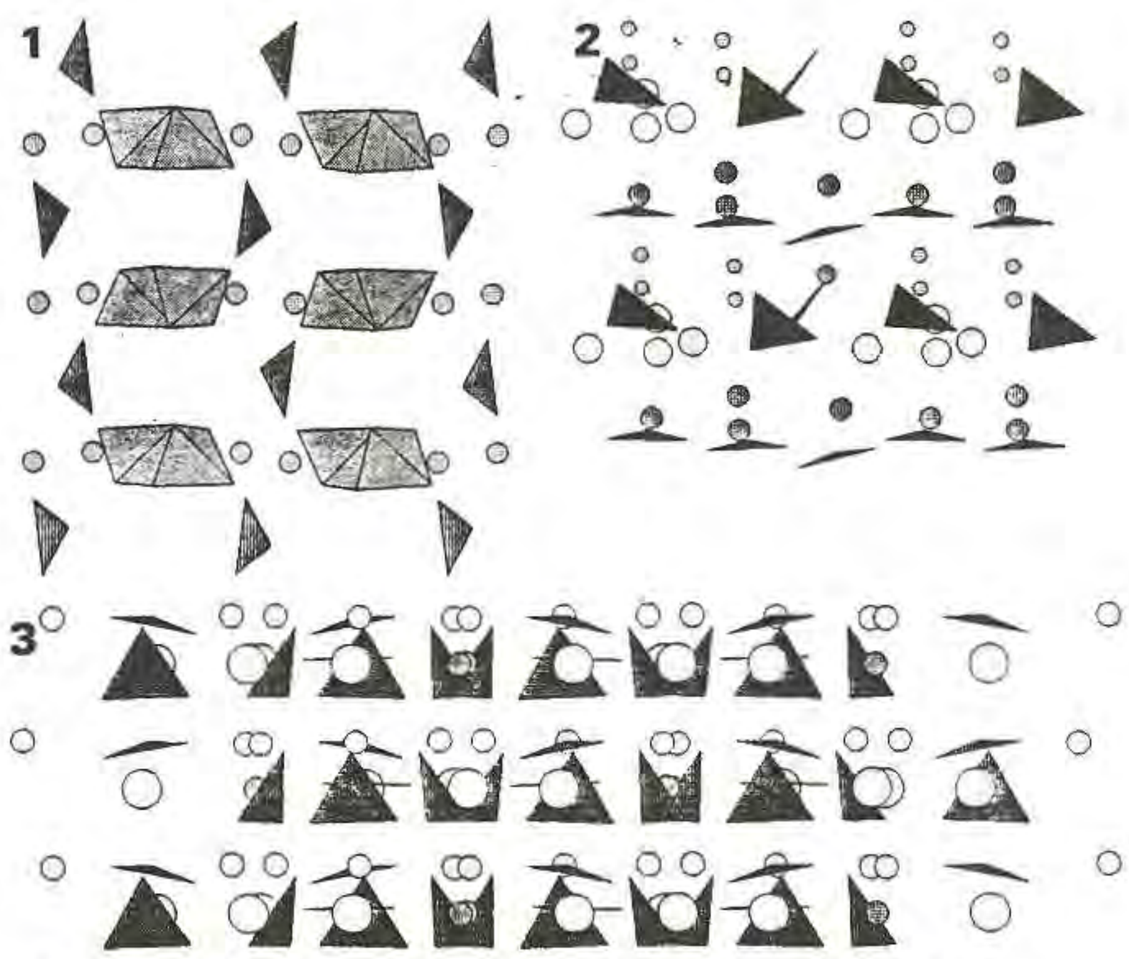

Fig.1. Moydite-(Y) with $[CO_3]$ and $Y[B(OH)_4]$ layers.
Fig.2. Donnayite-(Y) with flat $[CO_3]$, $[SrO_{10}]$ and a thick slab containing H_2O, $[YO_9]$, $[NaO_6]$ and $[CO_3]$.
Fig.3. Petersenite-(Ce) with flat-lying $[Na_3(CO_3)]$ layers and thick $[REE_2Na(CO_3)_4]$ slabs.

References:
Grice, J.D. & Ercit, T.S. (1986). *Can. Mineral.*, 24, 675-678.
Grice, J.D. & Perrault G. (1975). *Can. Mineral.*, 13, 209-216.
Grice, J.D., Van Velthuizen, J. & Gault, R.A. (1994). *Can. Mineral.*, 32, in press.

ESTIMATION OF EXOGENIC COMPONENT OF ORE -FORMING FLUIDS OF MAGNESIAN-MAGNETITE DEPOSIT (EAST SIBERIA)

S.Grishina , M.Masurov, G.Fon-der-Flaas, S.Masurova

Formation of magnesium-magnetite type deposits on Siberian platform was resulted from interaction between basalt melts and evaporites, maximum recrystallisation being find in the layered series of carbonates and salts.

The mixing of gases, released during crystallisation of melts with products of melting, dissociation and dissolving of country rocks produce ore-forming fluid. Additionally, interaction with basinal brines occures at the contact with intrusion after cooling of magma.

Inclusions in various minerals were studied to estimate contribution of exogenic compounds in ore-forming fluid of Korshunovskoye Fe-ore deposit. Inclusions in halite were found the most informative for fluid evolution study. The Cambrian evaporite formation here, intruded by dolerite sills and pipes, contain numerous generations of halite, which record distinct fluid events, correspondent to various stages of magmatic and hydrothermal activity:

- moderate salinity brine in chevron inclusions from unaltered rock salts far from central part of diatreme;
- N_2-bearing fluid in altered rock salts at a distance of 9 km from central part of diatreme;
- CO_2-bearing fluid + C-like material in halite at the contact with apophysis of granulated basalts;
- CO_2-H_2S-S_8-bearing fluid in the vicinity with breccia pipe;
- high salinity $CaCl_2$-bearing fluid in halite from halite-magnetite rocks from the central part of diatrem.

Inclusions containing supersaline brine (70 % of $CaCl_2$) and daughter pyrrhotite crystals, dissolving at heating in the range from 500 till 560°C were supposed to be relicts of ore-forming fluid.

HRTEM Study of (100)-Stacking Faults in Kyanite

Grobéty B.H. and Veblen D.R. (*Dept. of Earth and Planetary Sciences, Johns Hopkins University*)

(100)-stacking faults are common planar defects in kyanite (Boland *et al.*, 1977). Two formation mechanisms for these faults are known: (1) The dissociation of the perfect (100){001} dislocation (Lefebvre & Menard, 1981) leads to the formation of (100)-stacking faults connecting the two partials. The observed displacement vecors are 1/2[001] and 1/2[011]. (2) The same (100)-stacking faults with 1/2[011] displacements can be relicts of the transformation of staurolite into kyanite. Wenk (1980) observed such faults along the boundary between both minerals in topotactic intergrowths from Alpe Sponda, Switzerland. The positions of these stacking faults within the unit cell and the atomic arrangement along the fault planes are not known. Two different models were proposed: Lefebvre & Menard (1981) locate the stacking fault along the aluminum octahedral layer in the kyanite structure. This position, along which only aluminum-oxygen bonds and no silicon-oxygen bonds have to be broken, is energetically the most favorable and does not alter the nearest neighbor relationship across the fault plane. Wenk, however, put the stacking fault along the layer of empty octahedra. As a consequence, the arrangement of the SiO_4- tetrahedras across the fault is drastically changed. They are not isolated, but are instead connected in pairs across the fault. Considering the mechanism of the transformation of staurolite to kyanite proposed by Wenk (1980), this choice is not obvious. According to this mechanism kyanite is formed through the elimination of the staurolite oxy-hydroxy-layer by nonconservative (010)-stacking faults. Changes in the fault vector create stacking faults in the newly formed kyanite, which are also situated within the octahedral aluminim layer and not along the layer of empty octahedra.

High resolution transmission electron microscopy (HRTEM) of stacking faults in kyanites from the Campolungo area, Lepontine Alps, Switzerland, and the Rieserferner area, Northern Italy, together with contrast simulations using the EMS-program package (Stadelmann, 1987) allowed experimental determination of the fault position within the unit cell. The simulations were done using the multislice approach and the method of periodic continuation (Fields & Cowley, 1978).

The contrast of the stacking faults in HRTEM images shows mirror symmetry relative to the contrast of the surrounding matrix. This mirror symmetry is expected for stacking faults lying within the aluminum octahedral qlayer and shows up in the contrast simulations.

which fit the experimental images very well (Fig. 1). The (100) stacking faults are, therefore, positioned in the aluminum octahedral layer, independent of their formation mechanisms.

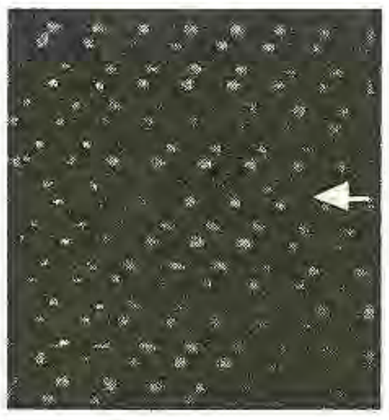

Fig 1. Digitally recorded and Fourier filtered HRTEM image of a (100)-stacking fault. The position of the stacking fault is indicated with a white arrow. The inset shows a contrast simulation for a defocus value of -100 nm and a sample thickness of 15 nm.

The Campolungo kyanite contains, in addition to the (100)-stacking faults, previously undescribed nonconservative (110)-stacking faults. They connect the terminations of relict staurolite layers and have a projected displacement component along **a***. A new 4-layer polytype was observed in the Rieserferner kyanite, containing two unit cell layers in normal positions, followed by two layers in twin position along **a***.

References

Boland, J.N., Hobbs, B.E. & McLaren, A.C. (1977). *Phys. Status Solidi*, **39**, 631-641.

Fields, P.M.& Cowley, J.M. (1978). *Acta Crystallographica*, **A34**, 103-109.

Lefebvre, A. (1982).*Phys. Chem. Min.*, **8**, 251-256.

Lefebvre, A. & Menard, D. (1981). Acta Cryst., **A37**, 80-84.

Stadelmann, P.A. (1987). *Ultramicroscopy*, **21**, 131-146.

Wenk, H.-R. (1980). *Am. Mineral.*, **65**, 766-769.

PGE MINERAL TYPES AND THEIR CONCENTRATING LEVELS IN THE LUKKULAISVAARA MASSIV (NORTHERN KARELIA)

T.L.Grokhovskaya, I.P.Laputina *(Inst.of Ore Deposits Geology RAS, Moscow)*

Sequence of the layered mafic-ultramafic Lukkulaisvaara massif (2,4 Ga) comprises five principal stratigraphic units which are lower marginal gabbro-norite, ultrabasic,norite, gabbro-norite and gabbro series of 5 km general thickness. Most complicated structure features the noritic series;its middle part is critical zone composed by combination of cumulates, typical for noritic series with exceedingly diverse in composition and texture rocks ranging from micrograined to pegmatoid ones. Micrograined rocks of critical zone are close to microgabbronorites composing the dyke-like bodies of different thickness and length.

Most sufficient concentrating of platinum metalls occures within critical zone and subconformable microgabbronorite body developed in the top of norite series. The latter contains three horizons with anomalous PGE concentrations: in upper endocontact (0.5-2m of thickness with PGE content up to 2 ppm); in lower endo- and exocontacts where the low-sulfide platinum mineralization is featured by the highest PGE concentrating with respect to sulfides (0.5-5m of thickness with PGE content up to 20 ppm); within the body itself whose ore zone is presented by schlieren and veins of pegmatoid plagiopyroxenites in which PGE concentrations are commensurate to sulfide component and mount up to 20 ppm. Low-sulfide platinum mineralization in critical zone is characterized by spotted distribution of PGE enriched olivine-bearing norites, taxitic and fine-layered rocks. Unusial trait of ore horizons within the critical zone is high variety of Pt/Pd ratio with Pd predominance in western part of massif and strictly Pt prevalence (with factor 10 and more) in its eastern part. Besides, the abnormally increased PGE content levels were discovered within ultrabasic series in peridotites with intergrained chromite and sulfide dissemination (1-3ppm of PGE content).The different platinum-metals paragenesises are peculiar to each level of low-sulfide mineralization. Mostly numerous PGM association is developed within the microgabbro-norite body and presented by sulfides, sulphoarsenides, bismuth-tellurides and antimonides (Grokhovskaya *et al.*,1992). Sperrylite and Bi-tellurides of Pt and Pd are established in rocks of the critical zone (both among intergrained Po-Pn-Cp, Cp-Po, Cp dissemination and in main as well H_2O- and Cl-bearing silicates), so kotulskite and merenskyite predominant in western part of the massif, whilst sperrylite and moncheite do in eastern one.

PGM from ultrabasic series associate with low-sulphur paragenesis of sulfides (mostly troilite and Fe-pentlandite with Fe/Ni ratio up to 2 prevail here) in difference to basic series. An other important trait of this mineralization is wide development of native Cu in silicates and sulfides. By special way of Camebax-microbeam microprobe analyses it has been shown that spots of different shape and of irregular distribution enriched by Pt (0.1-35.3 wt%), Pd (0.1-79.9), Rh (0.07-1.0), Ir (0.02-0.3),Os (0.05 -0.48), Ru (upto 0.12) are presented within native pure copper. The alloys Cu_5Pt and Cu_5Pd are mostly frequent. Besides, it has been established into sulfides, silicates and native Cu and Te, the tiny inclusions (1-15mk) of sperrylite with admixture Rh (1.9wt%), $(Pt,Ir,Rh)_2(As,S)_3$, $CuTe_2$, Cu_3Te_2 (up to 1,0 wt% of Pt,Pd), and also unknown ealier phases as (Pd,Cu)(Bi,Te),(Cu,Pd)$(Te,Bi)_2$, $(Pt,Cu)Te_2$ contained admixture of Rh,Ru,Ir,Os.

• CONCEPTION OF MINERALS EFFECTIVE STEADINESS

Grudev A.P. *(All-Russian Sci. Res. Inst. of Mineral Res., Moscow)*

More realistic estimates of probability of detecting particular minerals in the Nature requires expansion of firmness concept outside classical thermochemical method of approach. In connection with that it was introduced the concept of "Minerals Effective Steadiness" (MES), recommended in the form of any functional of three particular functions of stability (see the matrix below).

PARTICULAR FUNCTIONS OF STABILITY (PFS)	SUMMARIZED INTERCHANGE FLOWS (SIF) (1) Energy SIFe	(2) Mass SIFm	(3) Information SIFi
(1) Thermochemical PFStc orthostability	(1.1) Standard thermodynamic potentials, atomization energy, etc.	1.2 Chemical potentials (too activities, concentrations etc.)	(1.3) Mixing functions, considering with ordering of structures estimates
(2) Kinetic PFSkn pseudostability	(2.1) Activation energy; intereselection of partners by HARD/SOFT pr.	(2.2) Equilibrium constants; kinetic coefficients etc.	(2.3) Impactness of minerals transformations; catalysis and biocatalysis
(3) Topological PFSt quasistability	(3.1) Spatial arrangement of matter of mineral individual and aggr.	3.2 Morphogranulometry of blocks, clusters and domains	(3.3) Fractal measureness of aggregates; interm. and protocompounds in sol.

Each of PFS is to consider in the aspects of each of three individual but closely conjugated flows of interchange by energy, mass and information between evolving mineral matter and geological surroundings. The author obtained results exacting PFS for surrounded elements of the matrix-MES given above.

References (all in Russian):

Grudev, A.P. (1988). *Doklady Akad. Nauk SSSR*, **303**, 1460-1463.

Yakhontova, L.K. & Grudev, A.P. (1978). *Supergenesis zone of ore deposits*. Moscow State University Press.

HIGH TEMPERATURE PHASE TRANSITIONS IN NATURAL KAOLINITES

Gualtieri A. (Earth Sciences Dept., Univ. of Modena, Italy)
Artioli G. (Earth Sciences Dept., Univ. of Milan, Italy)
Bellotto M. (CISE, Tecnologie Innovative, Segrate Milan, Italy)
Clark S.M. (SERC Daresbury Laboratory, Daresbury, UK)

In spite of the wealth of studies dealing with the solid-state reactions in kaolinite at high temperature, there is no general agreement on the reaction path followed during kaolinite decomposition, mullite formation, as well as on the structural characteristics of the intermediate phases (Bellotto, 1993). The large discrepancies among the reported experimental results are partly due to the different degrees of disorder of the starting kaolinite and this aspect must be considered in the modelling of the reaction path in the kaolinite-mullite sequence. Non-isothermal and isothermal time-resolved energy dispersive powder diffraction data using synchrotron radiation were collected at beamline 9.7 at Daresbury Lab. on two kaolinites showing a different degree of stacking disorder. The quantitative assessment of the faults density has been performed on the basis of a novel structure model describing the statistical occurrence of disordered layers in kaolinite (Artioli et al., 1994). The non-isothermal runs performed at different heating rates from $10°C/min$ to $100°C/min$ in the temperature range 25-1400$°C$ allowed a preliminary interpretation of the reaction mechanisms (Bellotto, 1993). The isothermal runs were performed in the ranges 500-700$°C$ (dehydroxylation reaction in kaolinite) and 1200-1400$°C$ (mullite formation). A fast pre-isothermal heating rate of $100°C/min$ was used. Profile fitting techniques were employed for the quantitative estimate of the conversion rates of kaolinite and mullite. The analysis of the conversion vs. time curves for the kaolinite dehydroxylation is consistent with a diffusion controlled process for both kaolinite samples described with a Ginstling-Brounshtein or with a first order kinetic reaction. The apparent activation energies obtained using a Ginstling-Brounshtein equation (KGA1: 40.1(6) KCal/mol; KGA2: 26.0(2) Kcal/mol) confirm our earlier estimates based on non-isothermal data (Bellotto, 1993) and show that the dehydroxylation is greatly influenced by the starting material structural state. The process is possibly connected with the proton diffusion through the transforming material, which is related to both the hydroxyl diffusion out of kaolinite, and the change in coordination of the aluminum cations from six to four. At the highest reaction rates the mechanism is limited by heat transfer in the boundary layer surrounding each decomposing kaolinite particle. This has great effect on the initial stages of the reaction and is well apparent from the time-resolved data at the highest isothermal temperatures. The results are consistent with an apparent Avrami kinetic behavior and they are in agreement with the data reported by Criado et al.(1984), and previously unexplained. A structural model for metakaolinite based on simulations of powder spectra and DLS modelling is derived. It consists of a collapsed three dimensional structure in which both Al and Si are in tetrahedral coordination. A minor percentage of residuals hydroxyls are retained up to the total collapse of this pseudo-structure into amorphous phase which behaves as a single phase gel during the mullite nucleation and growth processes. This would imply homogeneity in such amorphous phase. However an induction period is present, probably associated with the necessary diffusion of Si out of the forming domains of mullite. The apparent activation energy of mullite formation are slightly different in the two samples (KGA1: 121(6) Kcal/mol; KGA2: 95(4) Kcal/mol), which might indicate either small chemical modulations in the amorphous precursor, or a defect-controlled growth of mullite.

References

Artioli G., Bellotto M., Gualtieri A., Pavese A. (1993). Clays and Clay Min., submitted.

Bellotto M. (1993). European Powder Diffraction Conference, EPDIC-3, Abstracts, 4.

Criado J.M., Ortega A., Real C., Torres De Torres E. (1984). Clay Min. **19**,653-661.

• PECULIARITIES OF GENESIS AND STRUCTURE OF RUTILES OF YEGORJEVSKOE ORE FIELD (SALAIR RIDGE)

Gubareva D.B., Arkhipenko D.K., Nesterenko G.V. (*United Institute of Geology, Geophysics and Mineralogy, SD RAS, Novosibirsk, Russia*)

Mineral structure is a good informative source about T, P, t - influences. Thus, investigation of minerals with mobile structure elements, different polymorphic modifications, is of great importance to solve problems of their genesis.

Titanium dioxide is one of such minerals. In nature it exists as anatase, brookite, rutile. The last is the widespread mineral in different kinds of rocks.

Its unique specimens from the gold–bearing weathering crust of Yegorjevskoe ore field with features of the phase transition anatase–rutile and rutiles synthesized in lab from X–ray amorphous anatase under different T, t – heating conditions were studied and compared by means of X–ray powder diffraction (XPD).

Natural rutiles were represented by brown, red and honey-yellow crystals with morphology typical for anatase (tetragonal bipyramids). But X–ray data showed the presence of only rutile modifications. XPD allows to uniquely distinguish these modifications (ASTM, cards 21–1272, anatase; 21–1276, rutile).

The obtained XPD data showed that the experimental values of intensities of natural rutiles reflections (Iexp) do not correspond to their calculated values (Icalc), i.e. they are anomalous. Calculated values of intensities and spacings (d, A) for anatase and rutile were obtained using computer programs. The degree of abnormality was estimated by the ratio Icalc/Iexp. In result it was found that the degree of abnormality for the same name X–ray reflections of natural rutiles is different. As regards the spacings they correspond to their calculated values. X–ray characteristics of synthesized rutiles (d, A, I) correspond to their calculated values independently of heating conditions of synthesis.

The observed anomalous intensities of the reflections of natural rutiles show that their structures (a) differ from the ideal pattern, (b) are characterized by different degree of defectivity. All the studied rutiles were formed as a result of phase transition anatase–rutile and are authigenic relict minerals; the mentioned weak differences among their structures reflect different conditions of their genesis with complex T, P, t – influences. Thus, we conclude that the origin of these rutiles is absolutely different, and they could appear in the products of the weathering crust from different mother rocks.

THE PERCOLATIVE PHASE TRANSITION UNDER THE METAMORPHISM OF COALS.

Gufan Y.M., Losev N.F. and Mochtchenko I.N.
(North Caucuses Scientific Center, Rostov-on-Don, Russia)

The thermodynamic model of coal microstructure has been developed for the various metamorphic stage. The coals of medium and high ranks is described as a stratiform polymer produced by the aromatic rings and other functional groups(OH, O, CO, S, SO etc). These groups are connected in quasi-plane fragments which formed the coaxial, spiral, stratiform, packed and other space structures. The main goal of our paper has been the modeling of quasi-plane fragment of coal microstructure, there space dispositions were not analyzed.

We proposed that these fragments are formed by the C, H, O, S atoms and vacancies which chaotic occupy The knot of plane hexagonal net. The last is not real atomic lattice, it is only topological coordinate system which let any continuous

deformations conservating the topological equivalence. The dependence of quasi-plane fragment structure from the concentration of aromatic rings was calculated in the framework of the percolation theory.

It has been shown the percolative phase transition was existed in coal system under the aromatic concentration been equal to 0.5. When the concentration is less than 0.5, the coal system contains graphite-like clusters of only finite sizes. When the concentration is more than 0.5, the infinite clusters are existed in system.

Proceeding from electronic properties of graphite-like cluster, we proposed that they were responsible for the coal electronic conductivity and calculated he last for the different stage of metamorphism . The obtained results satisfactorily coincide with the experimental dates. Particularly, the obtained percolative transition corresponded the beginning of the sharp rising of electronic conductivity which had been observed in real coals under the carbon concentration near 92 %.

The carbon concentration was used as an order parameter characterizing of metamorphic stage. The connection between the aromatic ring concentration and the carbon one was determinated using the approach of the stochastic occupating and the cluster approach. The last gave a more exact agreement with experimental dates.

Using the elaborated model we also estimated the connection energy between different functional groups in coals, their concentrations and aromatic stage for coals of different ranks. The obtained results show some sides of structure transformations taken place under the metamorphism.

^{29}SI AND ^{27}AL MAS NMR SPECTRA OF NATURAL MONTMORILLONITE IN CHINA

Guo, J., Li, L., Yuan, H., Yang, N., Wang, D., and Chen, F.
(*Magn. Reson. & Atomic and Mol. Phys. Lab., Acad. Sinica*)

The presence of aluminium in tetrahedral coordination in montmorillonite has a direct influence on the surface acidity and cracking activity of bentonites (Rupert, et al., 1987). Since Thompson (1984) has detected the presence of partial aluminium in four—fold coordination in Wyoming bentonite using MAS NMR, the problem on the presence of natural mont— morillonites containing tetrahedral coordination aluminium has been discussed (Woessner, 1989; Morris, et al., 1990).

In this paper the seven samples of bentonites from China have been investigated. M124 and M125 are from Heishan, Liaoning. M1 Yangyuan, Hebei. M13, M14 and M15 Gaozhou, Guangdong and M11 Wuping, Fujian. Apart from that M15 is a acid—treated commercial bentonite, the others are natural samples. Based on the data of XRD, chemical analysis and IR, the principal mineral is Ca—montmorillonite (ca. 80%), the main impurity mineral is quartz and only a small amount of feldspar occur in these samples. The ^{29}Si and ^{27}Al MAS NMR spectra of bentonites were recorded on Burker MSL—400 spectrometer using single pluse sequence.

The ^{29}Si NMR spectra of the samples all show two sharp and symmetrical peaks. The ^{29}Si chemical shift of main peak is at about —93 ppm which is due to montmorillonite in the samples and the other at about —107 ppm attributed to α—quartz or at about —109 ppm similar to that of crustobalite. These results are consistent with XRD. However, the ^{27}Al spectra of these samples are quite different. The intensity of the peaks at 53. 9 to 56. 7 ppm, which belong to Al(IV), varies from sample to sample.

According to the data of XRD and ^{29}Si and ^{27}Al spectra of the studied bentonites, it can be speculated that this Al(IV) should belong to montmorillonite in bentonites rather than to other aluminosilicate minerals. Montmorillonite is a 2:1 layer silicate. Structurally, there are two possibilities, one is that aluminium atoms substitute silicon atoms in Si—O4 tetrahedral sheets and other is due to dehydroxylation of Al—$O_4(OH)_2$ octahedral sheets by heat— or acid—treated bentonites. Beidellite is a typical example of former. The ^{29}Si and ^{27}Al spectra of beidellite reported by Nadeau, et al., (1985) is quite different from the spectra of our samples in both the ^{27}Al (IV) chemical shifts and the shape of ^{29}Si peak.

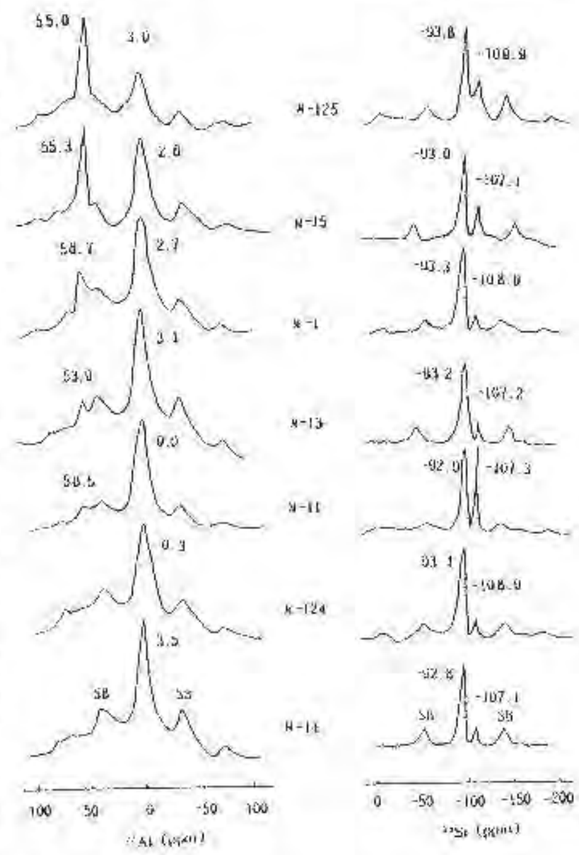

MAS NMR spectra of bentonites

The bentonites from Gaozhou were treated by heat or acid. ^{27}Al spectra of these products exhibit a peak of Al (IV) at 53 to 55 ppm, showing that the local environment of of aluminium ions in four—fold coordination obtained by the two methods is same. Nevertheless, their ^{29}Si spectra is distinct. The ^{29}Si spectra of natural bentonites is similar with that of acid—treated commercial bentonites. From these, it may be considered that the Al(IV) in the studied bentonites result from the interreaction of the montmorillonite with natural acid—bearing water.

TiO_2 NANOPARTICLE COATINGS INVESTIGATED WITH SCANNING FORCE MICROSCOPY

Gutmannsbauer, W., Haefke, H.
(Institute of Physics, University of Basel, Switzerland)
Bange, K.
(Schott Glaswerke, Mainz, Germany)

TiO_2 is one of the most extensively studied transition metal oxides. The increasing interest does not only stem from its remarkable optical and electronic properties but also from commercially available products, e.g. antireflection coatings, interference filters, laser mirrors, solar cells etc. Depending on the coating conditions (deposition parameters) TiO_2 can perform different modifications: amorphous (ρ=3.81 g/cm^3), anatase (tetragonal, ρ=3.84), brookit (orthorhombic, ρ=4.17) and rutile (tetragonal, ρ=4.26). With increasing density the refractive index is also getting higher.

Various preparation methods, such as sol-gel, dip coating and reactive deposition can be used for the fabrication of coatings with desirable optical, mechanical and chemical properties. Studies have been performed to relate optical as well as structural properties to the deposition technique and parameters, respectively (Meyer *et al.*, 1993).

It is generally accepted today that many technical material problems of glasses and oxidic coatings are surface problems. For example, the optical properties of such coatings are strongly affected by the surface roughness. Up to now, the surface topography and roughness of oxidic nanoparticle coatings have been studied with several techniques, such as stylus technique, light microscopy and scattering, various interferometric techniques and electron microscopy. Unfortunately, scanning electron microscopy (SEM) is limited by spatial resolution and transmission electron microscopy (TEM) has the disadvantage that it is an indirect method, i.e. only a reproduction of the surface is analyzed. Moreover, these techniques are not well suited to provide accurate values for the roughness of a sample surface. The recently

introduced method of scanning force microscopy (SFM), also termed atomic force microscopy (AFM), allows to study the sample surface from the micrometer down to the nanometer scale. The roughness of the sample surface is acquired simultaneously while measuring the topography.

In this study, we have investigated the surface morphology of TiO_2 nanoparticle coatings produced by various reactive deposition methods: ion beam sputtering (IBS), ion plating (IP) and electron beam evaporation (RE). Depending on the deposition techniques used the films show different growth behaviour: Films prepared by RE exhibit a polycrystalline structure in the well-known anatas modification, whereas the films grown by IP and IBS show an amorphous structure. Additionally, we have observed the formation of rutile crystallites in the amorphous TiO_2 films obtained by IBS. The rutile nucleation occurs above a critical film thickness of TiO_2. A possible explanation for the formation of the rutile phase might be compressive stress, arising from the bombardment of the growing film by atoms and ions (Davis, 1993). In order to reduce this stress, the IBS and IP films change to a denser state and form finally the rutile phase at the surface region.

References:
Meyer, E., Haefke, H., Güntherodt, H.-J., Anderson, O., Bange, K. (1993). *Glastech. Ber.*, **66**, 30-37.
Davis, C. A. (1993). *Thin Solid Films.*, **226**, 30-34.

NEW INSIGHTS INTO BIOMINERALIZATION PROCESSES BY SCANNING FORCE MICROSCOPY

Gutmannsbauer, W., Lüthi, R., Reimann, P., Haefke, H., and Güntherodt, H.-J.
(Institute of Physics, University of Basel, Switzerland)
Hänni, H.A.
(Institute of Mineralogy and Petrography, University of Basel, Switzerland)

Biomineralization refers to the processes by which organisms form minerals. The shell growth of nacre forming molluscs (e.g., bivalvia (mussels)) is a biomineralization process which is related to similar processes in the human body. Compared to human bones, the shell of a mussel is a suitable model, for studying biomineralization processes.

Minerals forming the shells have been studied by scanning and transmission electron microscopy (SEM and TEM), and by x-ray diffraction (XRD) (Erben, 1970, Mutvei, 1970) so far. Concerning the surface structure, SEM is limited by spatial resolution and TEM needs special sample preparations (e.g., replica techniques) which can alter the surface. The recently introduced method of scanning force microscopy (SFM) allows to study the crystal surface from the micrometer down to the nanometer scale. In this study, shells of salt- and freshwater mussels were used.

Operating the force microscope in the contact mode, the crystalline as well as organic components of the shell were imaged. The crystalline minerals are tabular aragonite crystals ($CaCO_3$, orthorhombic) in the so-called nacreous layer (mother of pearl) and calcite ($CaCO_3$, trigonal) in the prismatic layer. The aragonite crystals can form different shapes in the mussels. We observed different growth structures of aragonite, e.g. spiral and concentric patterns, varying from saltwater to freshwater mussels. On the top surfaces of these crystals, a structure was revealed that we believe to be the so-called organic matrix. It is assumed that the organic matrix influences strongly the growth of the covered crystals (Lowenstam & Weiner, 1989).

References:
Erben, H. K. (1970). *Biomineralization*, **2**, 15-46.
Mutvei, H. (1970). *Biomineralization*, **2**, 48-72.
Lowenstam, H. A. & Weiner, S. (1989). *Oxford Univ. Press.*

CORE-MANTLE INTERACTION: RESULTS FROM DIAMOND-ANVIL CELL EXPERIMENTS

Guyot F. (*CHiPr, University of Stony Brook*) and Poirier J.P. (*Géomatériaux, IPG-Paris*)

Laser-heated diamond-anvil cell (DAC) allow to approach CMB conditions in the laboratory. Here, we will briefly discuss the results brought by this technique as well as possible future ways of getting more significant data.

The first experimental results were obtained by the Berkeley group [1], [2] who studied chemical reactions between silicates and liquid iron at about 70 GPa and high temperatures by electron probe and x-ray diffraction on samples recovered at ambient pressure and temperature. In a more detailed study, using analytical transmission electron microscopy (ATEM), involving samples synthesized at pressures ranging between 70 GPa and 130 GPa and high temperatures, Goarant et al (1992) [3] studied the reactions between metal and silicates at the scale of individual grains. In some of the samples, reasonable local equilibrium could be checked by ATEM. It was observed that metal-silicate interfacial tension does not seem to counteract the penetration of molten metal within the silicates. Besides its obvious meaning for metal-silicate segregation in early planetary bodies, this statement also implies that metal from the core could migrate within the lower mantle, especially if the two media are in chemical disequilibrium. Poirier and Le Mouel [4] have calculated the depth of penetration using reasonable physical parameters and have found that a thin layer of a few tenth of meters might be invaded by molten metal at the bottom of the lower mantle. Such a limited contact zone between core and mantle might still be large enough to modify the compositions of lower mantle and crust over geological times.

All these experiments suggest that dissolution of oxygen in liquid iron is enhanced by high pressures. Actually, even without pressure, a complete miscibility of Fe-FeO liquids has been suggested at temperatures relevant to the CMB [5], and this enhanced miscibility does not require to be related to a possible metallic character of FeO at high pressures. This leads to a shift of the oxygen fugacity stability fields of silicates in silicate-metal assemblages; in DAC experiments where samples are prevented to equilibrate with any outside medium, silicates evolve according to reductive destabilization reactions such as:

$FeSiO_3$ --> Fe + SiO_2 (stishovite) + O (in the metal) (1), or
FeO --> Fe + O (in the metal) (2).

Any parameter that might affect the redox state of the starting material, such as adsorbed water or organics, will change the results, since the intrinsic oxygen fugacity of the sample will then be changed. In future experiments, much attention has to be paid to a careful characterization of the redox state of the starting material (ie by annealing it under controlled oxygen fugacity). It is also clear that the experimental results might be very different in multi-anvil presses, if they were to operate at such high pressures, since the redox conditions are then controlled, at least partially, by the nature of the cell assembly.

To illustrate the role of the redox state of the starting material in DAC experiments, we showed that San Carlos olivine mixed with graphite tranforms at high pressures (40 GPa) and temperatures into an assemblage of iron free $MgSiO_3$ perovskite and MgO periclase coexisting with pure Fe [6], indicating that reductive destabilisation reactions similar to (1) and (2) have taken place. Similarly, synthetic nickel-bearing olivine annealed at its minimum stability point in fO_2 transforms into a nickel-free perovskite-magnesiowustite assemblage coexisting with (Fe,Ni) alloy [7]. DAC experiments without a pressure medium thus preserve some redox characteristics of the starting materials. Such redox effects might also strongly influence the siderophilic or lithophilic character of a given element. The experiments of Goarant et al (1992) [3] suggest a siderophilic behaviour of chromium and manganese at high pressures, in agreement with previous experiments performed at lower pressures [8]. This behaviour might however be very dependent on the oxygen fugacity of the starting material. Also, there have been some discrepancies between multi-anvil press and DAC studies about the siderophilic behaviour of nickel at high pressures and temperatures [6], [9]. Such differences might be resolved if the intrinsic redox conditions prevailing during the experiments are carefully examined. This should increase much the significance of CMB and core formation data from laser-heated DAC experiments.

References:
[1] Knittle E. and Jeanloz R. (1989) *Geophys. Res. Lett.*, 16, 609. [2] Knittle E. and Jeanloz R. (1991) *Science*, 251, 1438. [3] Goarant F. et al. (1992) *J. Geophys. Res.*, 97, 4477.[4] Poirier J.P. and le Mouel J.L. (1992) *Phys. Earth Planet. Int.*, 73, 29. [5] Ringwood A.E. and Hibberson W. (1991) *Earth Planet. Sci. Lett.*, 102, 235. [6] Guyot F. et al. (1992) *EOS* ., 73, # 43, 64. [7] Malavergne V.et al. (1994) *EGS abstracts Grenoble April 1994*. [8] Ringwood A.E. et al. [1990] *Nature*, 347, 174. [9] Urakawa (1991) *Earth Planet. Sci. Lett.*, 105

TOPAZ-BEARING GRANITES, COMMON LATE-STAGE PHASES OF RAPAKIVI GRANITE COMPLEXES

Haapala I. (*Dept. of Geology, Univ. of Helsinki)*

The rapakivi granites are felsic members of bimodal gabbroic-granitic complexes found in many Precambrian shield areas. The plutonic-volcanic complexes are usually 1.75 to 1.0 Ga in age and they were emplaced in cratonic extensional tectonic environments, but rare Archean and Phanerozoic rapakivi complexes are known as well. The early granitic phases of the complexes are hornblende-biotite±fayalite granites, followed by biotite granites; in many complexes the last intrusive phases are represented by topaz- and siderophyllite-bearing microcline-albite granites and corresponding topaz-bearing porphyry (ongonite) dykes. The topaz of these late-stage granites is in part magmatic, in part metasomatic in origin. The granites are geochemically specialized showing the characteristics of the tin granites, and Sn-Be-W-Zn-Pb mineralization is associated with them in several areas (Rondonia and Amazonas in Brazil, SE Missouri in the U.S.A., southern Finland, Russian Karelia, the Ukraine, China).

The Tertiary topaz rhyolites of the western United States show many similarities with the Precambrian topaz-bearing rapakivi granites: bimodal magmatic association (basalt-rhyolite), A-type geochemical characteristics, very high Fe/(Fe+Mg) in biotite and in less common hornblende and fayalite, extensional tectonic setting, Precambrian crustal source and associated Be-Sn-W-Mo-F mineralization. Despite the age difference, these similarities probably reflect similarities in petrogenesis and geotectonic environment of these magmatic suites.

MODULATION IN SYNTHETIC ÅKERMANITE

Hagiya K., Ohmasa M., Kusaka K., Haga, N. (Dept. of Life Sci., Himeji Inst. of Tech.) and Iishi K. (Dept. of Miner. Sci. and Geol., Yamaguchi Univ.)

Incommensurate phases of synthetic åkermanite were found by Hemingway *et al.* (1986) and Seifert *et al.* (1987) independently. Recently Iishi *et al.* (1989) grew single crystals of åkermanite solid-solution $Ca_2Mg_{1-x}Co_xSi_2O_7$ and also found satellite reflections in electron diffraction patterns throughout the series. The modulated structure of Co end-member was determined by Hagiya *et al.* (1993) based on the five-dimensional description. The arrangement of the constituent tetrahedra is indicated in Fig.1. Thus some features of spectroscopic studies (Seifert *et al.*, 1987, Merwin et al., 1989) could be attributed to the effect of the modulation in the structure.

The effect of substitution of metal atoms to the modulation was newly investigated with a sample in the $Ca_2MgSi_2O_7$-$Ca_2FeSi_2O_7$ system. The features of diffraction patterns of the sample is quite similar to those of the Co-åkermanite but faint diffuse streaks were observed between satellites around main reflections. The cell parameters, the components of the modulation wave and the intensities of the satellite reflections were determined on an Enraf-Nonius CAD-4 diffractometer with Mo$K\alpha$ radiation monochromatized by graphite. The basic structure is tetragonal $P\bar{4}2_1m$, unit-cell dimensions a=7.8577(8), c=5.0127(6)Å, V=309.50Å^3, Mg/Fe=0.58(1), Z=2, M=288.42, D_x=3.095g·cm^{-3}. The positional and thermal parameters were refined to R=0.091 for 758 unique reflections. The ratio Mg/Fe was determined by the refinement of the occupancy at metal site. The modulated structure is also tetragonal $P^{P\bar{4}2_1m}_{p4mg}$, $\mathbf{k}_1$=0.298×(**a***+**b***), $\mathbf{k}_2$=0.298×(-**a*** +**b***) where $\mathbf{k}_1$, $\mathbf{k}_2$ wave vectors and **a***, **b*** reciprocal lattice vectors of the basic structure. The wave length of the modulation is 18.6(1)Å and slightly shorter than that of the Co-åkermanite (19.04Å). *REMOS*, a least-squares program developed by Yamamoto (1984) was employed to refine the modulated structure on F according to the multi-dimensional treatment (higher than three dimensions). The configuration of the network formed with metal and silicon tetrahedra is similar to that found in the Co-analogue (Fig.1). The amplitude of Mg occupancy at the metal site is very small and suggests that Mg and Fe atoms are in a disordered state.

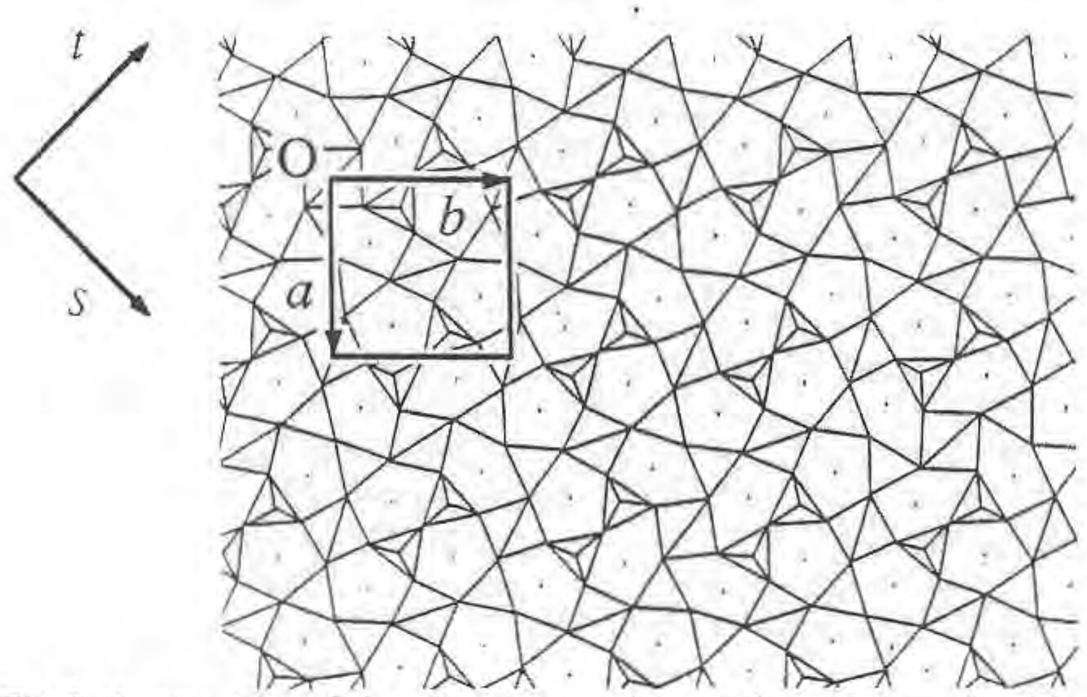

Fig.1 A part of modulated structure viewed along the c axis. The origin of the modulation is indicated by O, together with the outline of the basic structure. S and t indicate the directions of the internal coordinates.

References:
Hagiya, K., Ohmasa, M. & Iishi, K. (1993) *Acta Cryst.*, B**49**, 172-179.
Hemingway, B.S., Evans, H.T.Jr, Nord, G.L.Jr, Haselton, H.T.Jr, Robie, R.A. & McGee, J.J. (1986) *Can. Mineral.*, **24**, 425-434.
Iishi, K., Fujimoto, K. & Fujino, K. (1989) *Neues Jahrb. Mineral. Monatsh.*, 219-226.
Merwin, L.H., Sebald, A. & Seifert, F. (1989) *Phys. Chem. Minerals*, **14**, 752-756.
Seifert, F., Czank, M.& Schmahl, W. (1987) *Phys. Chem. Minerals*, **14**, 26-35.
Yamamoto, A. (1984) *REMOS* 82.1. Natl. Inst. Res. Inorg Mater., Tsukuba, Ibaraki 305, Japan.

APPLICATIONS OF ORE MICROSCOPY AND CATHODOLUMINESCENCE MICROSCOPY TO PYROMETALLURGICAL PRODUCTS

Hagni R.D. (Dept. of Geology and Geophysics, Univ. of Missouri-Rolla)

Reflected light microscopy (RLM) and cathodoluminescence microscopy (CLM) have been applied to a wide variety of pyrometallurgical research and industrial products. These products have resulted largely from pyrometallurgical research projects supported by the Department of the Interior's Mineral Institutes program administered by the Bureau of Mines through the Generic Mineral Technology Center for Pyrometallurgy. The University of Missouri-Rolla serves as the headquarters for the Pyrometallurgy Center but the research projects have been carried out at about 15 universities in the United States. The writer and his students have served for the past 13 years as the Process Mineralogy Group within the Center for providing mineralogical expertise on many of those pyrometallurgical research projects. In addition, he has been very involved in the mineralogical study of many industrial pyrometallurgical problems.

In most of those studies of pyrometallurgical products reflected light microscopy has been found to provide the most useful information. Scanning electron microscopy-energy dispersive spectroscopic analysis (SEM-EDS) and electron probe microanalysis (EPMA) have been used as ancillary techniques to obtain semi-quantitative and quantitative chemical analyses of phases selected under the

reflected light microscope. Cathodoluminescence microscopy has been found to be uniquely suited to the recognition and study of the non-opaque phases present in pyrometallurgical products. Such phases typically exhibit strong cathodoluminescence due the incorporation of activator trace elements at the high temperatures at which those phases have crystallized.

RLM has been found to be especially effective in the study of the mineralogy of flash furnace products. Mineralogical reactions that take place in the flash furnace can be observed directly in suspended particles, and the extent of their fragmentation and agglomeration can be evaluated. RLM study of bath smelting products from complex Co-Ni-Cu-Pb-Zn ores has provided information on partitioning of those metals between phases in the matte. RLM examination of problem lead drosses has shown significant differences in mineralogy from typical lead dross from the Viburnum Trend. RLM study of the mineralogy of a slag from a secondary copper smelter showed why it was difficult to pull off. RLM of roasted refractory gold ores provide data on their mineralogy and permeability to cyanide solutions. Microscopic analyses of dusts from lead and copper smelters provide mineralogical information regarding pyrometallurgical and environmental concerns. Electric arc furnace (EAF) dusts have been studied by RLM to determine their mineralogy as an aid to selection of pyrometallurgical treatment processes to render these dusts non-hazardous. Current RLM studies involve the mineralogy of products from the direct reduction smelting of iron ores and the treatment of pyrometallurgical wastes to render them non-toxic.

CLM has been found to be especially useful in the study of phosphorus-bearing minerals in ores, beneficiation products, and pyrometallurgical products. Apatite and collophane contain trace amounts of Mn and REE that activate blue to gray CL. Their presence, abundance, and distribution are readily determined by CLM. The mineralogy of ceramic build-ups in electric induction furnaces are uniquely studied by CLM. Spinel exhibits bright green CL, forsterite shows red CL, calcium hexaluminate is dark green, corundum is red, and rare earth silicates show pink CL.

The application of RLM and CLM to pyrometallurgical products to determine their mineralogy, phase abundances, phase compositions, and textural intergrowths are important in monitoring a variety of pyrometallurgical research results and in resolving many industrial pyrometallurgical problems.

COMPARISON OF THE ORE MINERALOGY, ORE TEXTURES, PARAGENETIC SEQUENCE, AND MODE OF OCCURRENCE OF PERMIAN SHALE- AND SANDSTONE-HOSTED COPPER-SILVER DEPOSITS AT PAOLI AND CRETA, OKLAHOMA, U.S.A.

Hagni R.D. (Dept. of Geology and Geophysics, Univ. of Missouri-Rolla)

The shale-hosted (Flowerpot Shale, Guadalupean Series) copper-silver ore deposit at Creta in southwest Oklahoma and the sandstone-hosted (Wellington Formation, Leonardian Series) silver-copper ore deposit are similar in many respects. They are stratabound deposits, contained in Permian sedimentary rocks, and comprised of economic to near economic amounts of copper and silver. Ore microscopic study of the ores shows, however, that they differ significantly in their mineralogy, ore textures, paragenetic sequence, and mode of occurrence.

Copper occurs mainly as anilite and digenite in the Creta deposit, with smaller amounts of djurleite, chalcocite, geerite, and yarrowite (Hagni, 1988). Silver is present at Creta mainly as stromeyerite, associated with smaller amounts of argentiferous djurleite and argentiferous chalcocite. In contrast, copper in the Paoli deposit occurs mainly as chalcopyrite, chalcocite, digenite, and covellite; silver is present only as native silver (Thomas, Hagni, and Berendsen, 1991).

Recent ore microscopic study (Hagni, 1993) of the ore textures at Paoli shows that whereas small amounts of the copper sulfide mineralization occur as replacements of disseminated, diagenetic, pyritohedral pyrite crystals and as partial replacements of carbonate cement between clastic quartz sand grains, the most important forms of copper sulfide grains are those that have been deposited by the replacement of hematite. The replaced hematite grains have irregular shape, range greatly in size, and have formed as replacements of carbonate cement in the host sandstones. This mode of copper sulfide occurrence at Paoli is totally unlike that at Creta where the copper sulfide grains occur as replacements of 120 µm megaspores, 40 µm colloform pyrite grains, and 10 µm or smaller pyrrhotite crystals.

The replacement of hematite grains at Paoli was initiated by the formation of covellite and followed successively by chalcocite, digenite, bornite, and chalcopyrite. Sulfide minerals stable under more oxidizing conditions were deposited first, and they were followed by sulfides stable under progressively more reduced conditions. This replacement process resulted in a paragenetic sequence of ore mineral deposition that consists of: pyrite (oldest)-goethite-hematite-covellite-chalcocite-digenite-bornite-chalcopyrite (youngest). The sequence of copper minerals at Paoli is the reverse order of those deposited at Creta and it is unusual for most copper ore deposits elsewhere. The paragenetic sequence at Paoli is interpreted to indicate that the host red-bed sandstones experienced an early introduction of reducing fluids that formed disseminated and cementing pyrite. Subsequent oxidation of that early pyrite to form hematite and minor goethite probably occurred at the leading edges of roll fronts of oxidizing groundwaters. The shapes of the ore deposits at Paoli indicate that the copper ore fluids were ones that moved in the form of roll fronts along Permian stream channels. The paragenetic sequence shows that the ore fluids became progressively more reducing during the deposition of the copper sulfides.

The Paoli and Creta copper deposits are interpreted to have formed by replacement from epigenetic fluids. The differences in ore textures are the resulted of selective replacement of different pre-existing materials.

References:
Hagni, R.D. (1988) Proc. 7th IAGOD Symp., Lulea, Sweden, 163-166.
Thomas, C.A., Hagni, R.D. and Berendsen, P. (1991) Ore Geology Reviews, **6**, 229-244.
Hagni, R.D. (1993) N-C Sec., Geol. Soc. Am. abs., 25, 23-24.

FIVE-COORDINATED TRIVALENT MANGANESE IN VESUVIANITE: A SPECTROSCOPIC STUDY

Hålenius U. (*Dept. of Mineralogy, Swedish Museum of Natural History*)
Annersten H. (*Dept. of Earth Sciences, Univ. of Uppsala*)

The cation distribution in vesuvianite, ideally $X_{19}Y_{13}Z_{18}O_{68}W_{10}$ with essentially X=Ca, Y=Al, Fe, Mg, Z=Si and W=OH,F (Groat and Hawthorne, 1992), has been the subject of a number of recent publications, e.g., Dyrek et al. (1992), Fitzgerald et al. (1992) and Groat and Hawthorne (1992). However, the site distribution of manganese, which may occur at relatively high concentrations in vesuvianite, has so far not been studied in detail. In the present work vesuvianites from highly oxidised piemontite-kentrolite-rich skarn assemblages at Jacobsberg, Filipstad, Sweden have been studied by means of EMP, Mössbauer spectroscopy and polarised optical absorption techniques at atmospheric conditions as well as at elevated pressures (~50 kb) using DAC-techniques.

The optical absorption spectra of the present samples reveal, in addition to some very weak and sharp bands, one intense and strongly polarised absorption band (O >> E) at ~18,000 cm^{-1} (FWHM~2,500 cm^{-1}) and a weak, relatively broad (FWHM~4100 cm^{-1}) and essentially unpolarised band at ~11,500 cm^{-1}. The intensities of these two bands display excellent positive correlations to sample Mn-content. DAC-experiments at ~50 kb show an energy shift of the band at 18,000 cm^{-1} of ~10 cm^{-1}/kb. The polarisation, energy position, width and pressure effect of this band indicate that it is caused by a spin-allowed electronic d-d transition in Mn^{3+} at the square pyramidal Y(1)-site, which is of C_{4v}-symmetry.

The molar extinction coefficient of the band at 18,000 cm^{-1} can not be determined directly from the sample chemistry and only a lower limit for this parameter may be obtained. The reasons for this is as follows. The Mn-content of the most Mn-rich vesuvianite crystals exceeds 1 a.p.f.u., which is the upper limit for the number of five-coordinated positions (Y(1)). This indicates that manganese may be present in different valence states and/or at different sites in the investigated samples. As no additional intense absorption bands are observed in the spectra of the high-Mn samples, it is suggested that any surplus manganese occurs in the divalent state. In addition to this, Mössbauer ^{57}Fe experiments on some of the present samples indicate that fair amounts of ferric iron (up to 0.15 a.p.f.u.) are located at the pentacoordinated Y(1) -site. Furthermore, Cu^{2+}-contents of up to 0.5 a.p.f.u. are encountered in these samples. Optical absorption spectra of the high Cu-samples reveal an absorption band at ~15,600 cm^{-1}, which in accordance to Dyrek et al. (1992), is assigned to an electronic d-d transition in divalent copper at the Y(1)-site. Taking these indications of Fe^{3+} and Cu^{2+} incorporation at the Y(1) site into consideration, a minimum ε-value of ~300 $l \cdot mole^{-1} \cdot cm^{-1}$ for the Mn^{3+}-band at 18,000 cm^{-1} is obtained. This extinction coefficient value is comparable to what is observed for absorption bands caused by spin-allowed d-d transitions in trivalent manganese at distorted octahedral sites in a number of silicates, as e.g., andalusite and piemontite.

Symmetry considerations restrict the number of symmetry-allowed transitions in a $3d^4$-cation at a C_{4v}-site to one. The weak Mn-correlated absorption band at 11,500 cm^{-1} is accordingly assigned to a symmetry-forbidden d-d transition in trivalent manganese at the Y(1)-site.

Additional very weak and sharp absorption bands at ~20,000 and ~21,000 cm^{-1} are tentatively assigned to spin-forbidden d-d transitions in Mn^{3+} at the Y(1)-site.

References:

Dyrek, K., Platonov, N., Sojka, Z. and Zabinski, W. (1992). *Eur. J. Mineral., 4, 1285-1289.*

Fitzgerald, S., Leavens, P.B. and Nelen, J.A. (1992): *Mineral.Petrol.,46, 163-178.*

Groat, L.A. and Hawthorne, F.C.(1992). *Can. Mineral., 30, 19-48.*

FERROUS IRON AND THE COLOUR OF MAGNUSSONITE

Hålenius U. and Lindqvist B. (*Dept. of Mineralogy, Swedish Museum of Natural History)*

Magnussonite is a rare manganese arsenite, originally described from Långban, Sweden (Gabrielsson, 1956) and later identified at Sterling Hill, New Jersey, USA (Frondel, 1961). The magnussonite formula ($Mn_{18}[MnAs_6O_{18}]_2Cl_2$) defined by Moore and Araki (1979) on the basis of a structural refinement was later redefined by Dunn and Ramik (1984). Based on new EMP- and water-analyses they proposed $Mn_{10}As_6O_{18}(OH,Cl)_2$ as the ideal magnussonite formula.

Magnussonites from Långban invariably display greenish colour hues, while at Sterling Hill greenish as well as brownish magnussonites occur. Chromophoric elements (3d-elements) in reported magnussonite analyses are confined to Cu, Fe and Mn. The cause for the frequently noted greenish colour of magnussonite has never been established, but Moore (1970) considered the possibility of divalent copper as a chromophore.

The present study has been carried out on a dozen magnussonite crystals from four different Långban samples and single crystals obtained from hydrothermal syntheses of Fe-doped magnussonite. The material has been studied by means of EMP, polarised optical absorption and high-pressure DAC techniques.

In contrast to previous studies on magnussonite, which report an isotropic mineral character, all the studied natural crystals are characterised by a weak optical anisotropy (measured birefringence equals 0.001) and a distinct pleochroism. The optical character of these anisotropic crystals is uniaxally negative and E > O.

The polarised optical absorption spectra of the natural material are characterised by a narrow (FWHM≈900 cm^{-1}) and non-pleochroic absorption band at 23,750 cm^{-1}, which marks the field-independent $^6A_1(S) \rightarrow {}^4A_1{}^4E(G)$ transition in Mn^{2+} and a broader (FWHM≈2,700 cm^{-1}) distinctly pleochroic (E > O) absorption band at 15,300 cm^{-1}. The intensity of the latter band displays a strong positive correlation with sample FeO-content (R^2=0.94), which varies for the present samples from 0.25-2.42 wt-%. The energy of the band shifts towards higher values at increasing sample pressure (9.5 cm^{-1}/kb). The band widths, the excellent linear correlation of band intensity with FeO-content as well as the response to high pressure (44 kb DAC-experiment) suggest that this absorption band is caused by a spin-allowed electronic transition in ferrous iron. The fact that the absorption spectra of Fe-doped synthetic magnussonite crystals grown hydrothermally under reduced conditions display an absorption band of corresponding character (band energy, band width and extinction value) is an additional evidence for the proposed band assignment to a Fe^{2+} d-d transition. In addition to the two already mentioned bands there appears a band at 14,200 cm^{-1} in spectra of most iron poor natural magnussonite crystals. This absorption band, which is assigned to a spin-allowed d-d transition in Cu^{2+}, displays a FWHM of 2,200 cm^{-1} and its intensity is well correlated with the sample CuO-content (R^2=0.88), which for the present crystals varies from 0.53-3.88 wt-%.

From the present study it is concluded that greenish colours in magnussonite may be caused by the presence of ferrous iron as well as divalent copper. Due to an intensified UV-absorption with increasing copper content and a comparably low extinction coefficient of the 14,250 cm^{-1} Cu-band, copper containing magnussonites are weakly greenish coloured. Fe-bearing magnussonites are more strongly coloured in blueish green hues as a consequence of a less intense UV absorption edge and a higher extinction coefficient for the Fe^{2+}-band at 15,300 cm^{-1}.

References:

Dunn, P.J. and Ramik, R.A. (1984). *Amer. Mineral.*, 69, 800-882.

Frondel, C. (1961). *Arkiv för Mineralogi och Geologi*, 2, 571.

Gabrielson, O. (1956). *Arkiv för Mineralogi och Geologi*, 2, 133-135.

Moore, P.B. (1970). *Arkiv för Mineralogi och Geologi*, 5, 55-62.

Moore, P.B. and Araki, T. (1979): *Amer. Mineral.*, 64, 390-401.

COMPUTER AIDED DATABASE OF THE INFRARED SPECTRA OF MINERALS.

F.Hanousek, CaterSoft Prague, Czech Republic

E.Večerníková, Instit.of Inorg. Chemistry ASCR, Prague, CR

T.Řídkošil, Region. Museum of the Czech Paradise,Turnov, CR

Automation in spectrochemical analysis has produced a tidal wave of data requiring processing. Automated spectral comparison with

library data in a similarity for identity search give adequate results where the analysis is of a relatively simple nature of virtually pure compounds.

The IR spectroscopy is in most cases for identifying of the structure of minerals a very informative single technique together with XRD or EMS methods. Indeed, infrared spectroscopy was used as one of the principal methods of identifying new compounds, establishing the structure of complex anions, classifying materials as regards crystal structure, studying isomorphous rerationships and polymeric transformations and qualitatively analysing of several crystal phases.

We are concerned in our work to identify different mineral species by IR spectroscopy as one of tools for deriving information of the structure and composition of theirs. Our collection of IR spectra have in this time up to 1200 well defined pure mineral species (XRD or EMS defined).

All our collection of the IR spectra of the minerals keep the recommended guide-lines of the Optical Spectroscopy Subcommittee as follows:

1. Spectra in our collection are stored in full raw form, without previous data manipulation (e.g. smoothing, baseline correction etc.) apart from conversion to absorbance units.
2. The spectra collection are submitted in the ASCII library format and (on request) also in the JCAMP -DX format on the commercially available low cost magnetic medias (floppy disc).
3. The sample purity should be stated with at least one other measurement as secondary verification (XRD, EMS).

All IR spectra are measured in our institute, on grating spectrometer Pye - Unicam PU 9512 connected with computer in the interval between 4000 -200 cm^{-1} , in the form of KBr (TlBr)pellets, under strictly controlled constant conditions. The data obtained on this instrument are at last the same quality as obtained from FTIR spectrometer, and in many cases are of better quality.

Software pack include library routines and searching procedures and routines for spectra file manipulation (spectra subtraction, smoothing, baseline correction, spectra deconvolution, 1st and 2nd derivatives, peak search etc.).

The goal of this spectra collection is to identify the different mineral species by IR spectroscopy and deriving information concerning the structure and composition of minerals with employing full automated computer aided methods. This collection is intended not only for mineralogical or inorganic spectroscopical use, but in the field of teaching of those disciplines also. Most of the IR data are previously unpublished and were obtained specifically for this collection.

Distribution of Cr(III) in trioctahedral layers of stichtite studied by ion-exchange chromatography

Hansen H. C. B., (*Chemistry Dept., Royal Vet. & Agricult. Univer., Copenhagen*) and Koch C.B. (*Phys. Dept., Tech. Univer. Denmark)*

Stichtite is a layered Mg-Cr(III) hydroxide carbonate belonging to the pyroaurite-sjögrenite group. Positively charged trioctahedral metal hydroxide layers alternate with interlayers of charge compensating anions and water molecules. It has a general composition of $Mg_{8-x}Cr^{III}_x(OH)_{16}(CO_3)_{x/2}$, with x = 2 - 2.65. The cation distribution in trioctahedral hydroxide layers of pyroaurite-type compounds may affect the stacking polytype, the free energy of formation and the charge distribution in the interlayer, which in turn may influence the mechanisms of interlayer reactions. Regular cation ordering may be detected by diffraction techniques. In most cases local ordering is more likely to occur and this may be determined by spectroscopic methods (Koch & Hansen, 1994). However, here we have taken advance of the substitution inertness of Cr(III). Multinuclear Cr(III) hydroxy fragments present in the stichtite is assumed not to cleave during acid digestion (Spiccia & Marty, 1986) and hence may be separated by ion-exchange methods.

The cation distribution of one natural and two synthetic stichtites have been analysed. Chromatographic separation of monomeric and polymeric (almost only dimeric) hydroxo Cr(III) complexes showed that for both the natural and the synthetic stichtites the content of Cr(III) found in polymers amounts only to 10 - 20 % of the content which would be present if Cr(III) was randomly distributed in the hydroxide layers. This implies that Cr-Cr nearest neighbours is a thermodynamic unstable configuration, giving rise to a more or less ordered cation distribution in the trioctahedral hydroxide layers of stichtite. For the synthetic stichtites ($Mg_{5.70}Cr^{III}_{2.26}(OH)_{16}(CO_3)_{1.07}$) the following frequencies for the three-cation groupings coordinating one OH could be calculated: 3Mg: 32 %, 2MgCr: 51 %, Mg2Cr: 16 % and 3Cr: < 1 %. In infrared spectra two different absorptions in the OH stretching region were observed, which could be assigned to OH coordinated to 3Mg and OH coordinated to 2MgCr or Mg2Cr, respectively.

References

Spiccia, L. & Marty, W. (1986) Inorg. Chem., **25**, 266 - 271.
Koch, C.B. & Hansen, H.C.B. (1994) Proc. 10th Int. Clay Conf. Adelaide (in press).

EXPERIMENTAL MINERALOGY OF TOURMALINE GROUP: THE BINARY SYSTEM TSILAISITE - DRAVITE, $Na[Mn_xMg_{1-x}]_3Al_6(BO_3)_3Si_6O_{18}(OH)_4$, AT T = 375-700°C AND P = 2000 AND 3000 BARS.

Haralampiev, A.G. and Grover, J.E. (*Department of Geology, University of Cincinnati*)

As part of a larger project to investigate the stability of tourmaline in the system $Na[M]_3Al_6(BO_3)_3Si_6O_{18}(OH)_4$, where M = Mg, Fe^{+2} and Mn^{+2}, synthesis and reversal experiments have been made on the dravite (Mg) - tsilaisite (Mn) join at 2000 and 3000 bars pressure and temperatures in the range 375°-700°C using mixtures of constituent oxides, oxalates or carbonates with H_2O and B_2O_3 in excess (Haralampiev & Grover, 1993).

FIGURE 1 is a hypothetical binary phase diagram showing regions in T - X_{Mn} space at 2000 bars where we believe tourmaline, garnet and a two-phase mixture of tourmaline and garnet might occur. As X_{Mn} [= Mn/(Mg+Mn)] increases, the amount of tourmaline in the run products decreases, relative to Mn-rich garnet or to an equivalent low-temperature garnet break-down product. Rhodochrosite (Rds) or Mn-chlorite may replace garnet at 600°C for some intermediate compositions, and appear generally at lower temperatures when the composition is Mn-rich. Replacement of garnet by chlorite at temperatures lower than about 550° is consistent with Hsu's [1968] results on the stability of spessartine in a H_20-bearing system. The lower boundary of the two-phase field slopes upward with increasing Mg content, consistent with a decrease in garnet stability (and a concomitant increase in tourmaline stability) as the pyrope component increases at this relatively low pressure. Specific phase assemblages that appear in our synthesis runs at intermediate compositions and temperatures vary somewhat with time: with longer runs the two-phase field for Tur+Grt expands and therefore extent of this field is not clear, yet. At high-manganese compositions (X_{Mn}=1.0) tourmaline appears only in a narrow temperature range: assemblage at 425° is Tur+Rds±Ab and at 500°C - Tur+Grt±Ab. The upper boundary for the two-phase region is

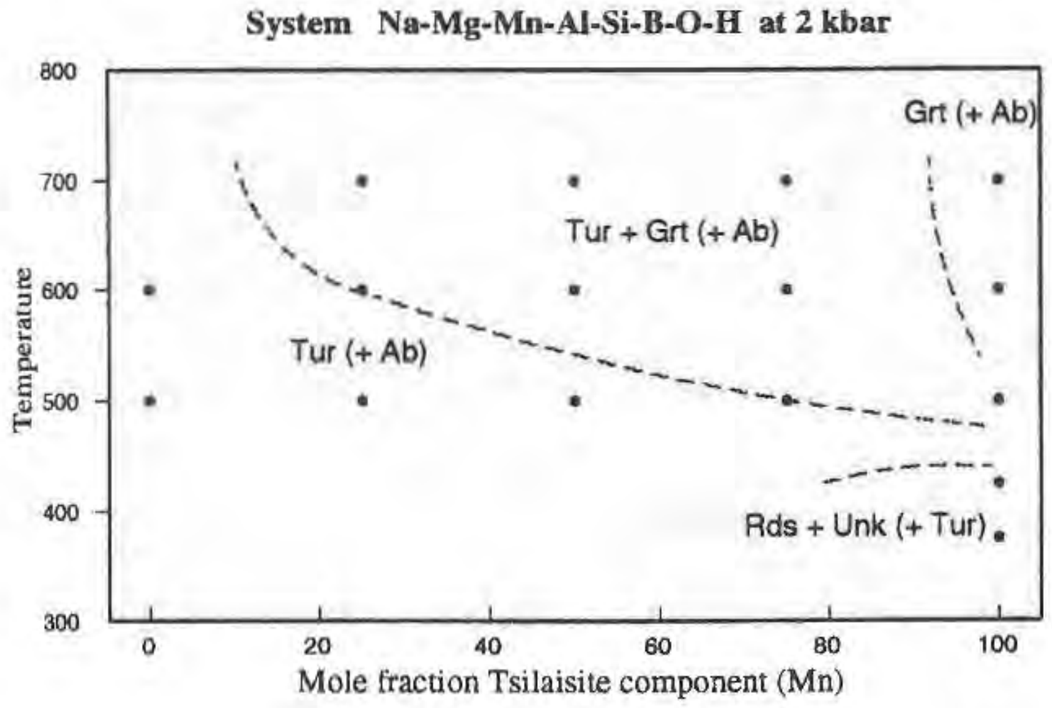

Figure 1.

fixed with reversed results, between 500° and 600°C and delimit a single-phase Grt field (± high-Ab ± Corundum).

Another effect related to the association Grt+Tur is separation of *c* and *a* cell parameters of our synthetic tourmalines in two distinct clusters. First is with *c*-cell lengths of the order of 7.14 to 7.16 Å and represent tourmalines that coexist with garnet in the two-phase field of FIGURE 1, while the second cluster (forming linear trend with *c*-values between 7.21 and 7.18 Å) represent tourmalines that occur without garnet (±Ab). The simplest explanation for these trends is that tourmalines coexisting with spessartine are depleted in Mn, relative to those that have formed as single-phases with compositions close to bulk values. By this model, increasing Mn in Tur (relative to Mg) would increase the *c*-cell parameter.

These results are consistent with the apparent absence of tsilaisite in nature, and compatible with Haralampiev's (1992a,b) observation that Fe^{+2}-Mn tourmalines coexisting with Fe-bearing spessartines from the Latinka pegmatite, Rhodope Mountains, Bulgaria, are never more Mn-rich than about $X_{Mn} = 0.3$. Thus, the partitioning of Mg and Mn between synthetic garnets and tourmalines is probably analogous to that for Fe^{+2} and Mn in natural systems.

REFERENCES:
Haralampiev, A.G. (1992a). GSA Abstr. & Progr., **24**, 7, A259
" , Dinolova E., (1992b). Compt.Rend de l'Acad. Bulg. Sci., **45**, 1, 25-27.
" , Grover, J.E. (1993). GSA Abstr. & Progr., **25**, 6.
Hsu (1968). J.Petrology.

GEOCHEMISTRY AND PETROGENESIS OF LATE MESOZOIC AND TERTIARY EXTENSION-RELATED ALKALINE VOLCANIC ROCKS OF THE PANNONIAN BASIN (CENTRAL-EASTERN EUROPE).

Harangi S.[1], Tonarini S.[2], Vaselli O.[3] and Manetti P.[3] (*[1] Eötvös University of Budapest, [2] C.N.R. - Institute of Geochronology and Isotope Geochemistry Pisa, [3] University of Florence*)

The Pannonian Basin (PB) is a back-arc-type area, where extensive extension occurred during the Late Tertiary due to the subduction of the European plate beneath the PB microplate. Late Tertiary extension-related alkaline volcanic rocks (nephelinite to transitional basalt, ultrapotassic basalt, trachyte) reflect the nature of the mantle beneath the PB, whereas Early Cretaceous alkaline mafic rocks of the Mecsek Mts. (Southern PB) provide information on the mantle before the subduction-related metasomatism occurred.

The Early Cretaceous Mecsek mafic rocks and the Late Tertiary basanites from the peripheral areas of the PB (Nógrád-Gömör /NG/, Graz Basin /GB/) show the most depleted Sr and Nd isotopic ratios (ϵNd=4.5-6, ϵSr=-30 to -14; Fig. 1) and could represent magmas extracted directly from a St Helena-type OIB asthenospheric mantle. Alkaline basalts from the central PB have lower Nd (ϵNd=0.3-3.3) and higher Sr (ϵSr=-10 to -3) isotopic ratios (Fig. 1) and resemble Gough-type OIB. Miocene trachytes of the Little Hungarian Plain (LHP, Western PB) can be considered as a precursor of the extension-related basaltic volcanism in the PB. They have more depleted isotopic ratios (ϵNd=3.9, ϵSr=-15.1; Fig. 1) than the basalts of the central PB. The ultrapotassic leucite-bearing basalt of Bár (Southern PB) is unique in the PB and show transitional character between plagioleucitites (Group III) and lamproites. This rock may be related to the lamproites of the Vardar Zone.

Trace element variation of PB alkaline mafic rocks is consistent with 2% to 15% degrees of partial melting of garnet-peridotitic mantle. Trace element ratios and Sr-Nd isotopic signatures of PB alkaline volcanics indicate an involvement of crustal material in their genesis. Crustal contamination during the ascent of magmas can be excluded based on some characteristic trace element ratios (Rb/Nb, Th/Nb, K/Nb etc.) and ϵSr vs. Sr relationship. Contamination by crustal material may occur, however, via hydrous fluids or melts released from subducted slab. The Early Cretaceous alkaline volcanics of the Mecsek Mts. could have originated from an uncontaminated asthenospheric mantle, whereas the Late Tertiary alkaline basalts could have been formed from a slightly metasomatized mantle. Metasomatism of the mantle was resulted from both H_2O-rich fluid and silicate melt migration. Positive correlations between ϵSr and LILE/La ratios suggest that the enrichment process could not be related to the Tertiary subduction event, but an ancient one.

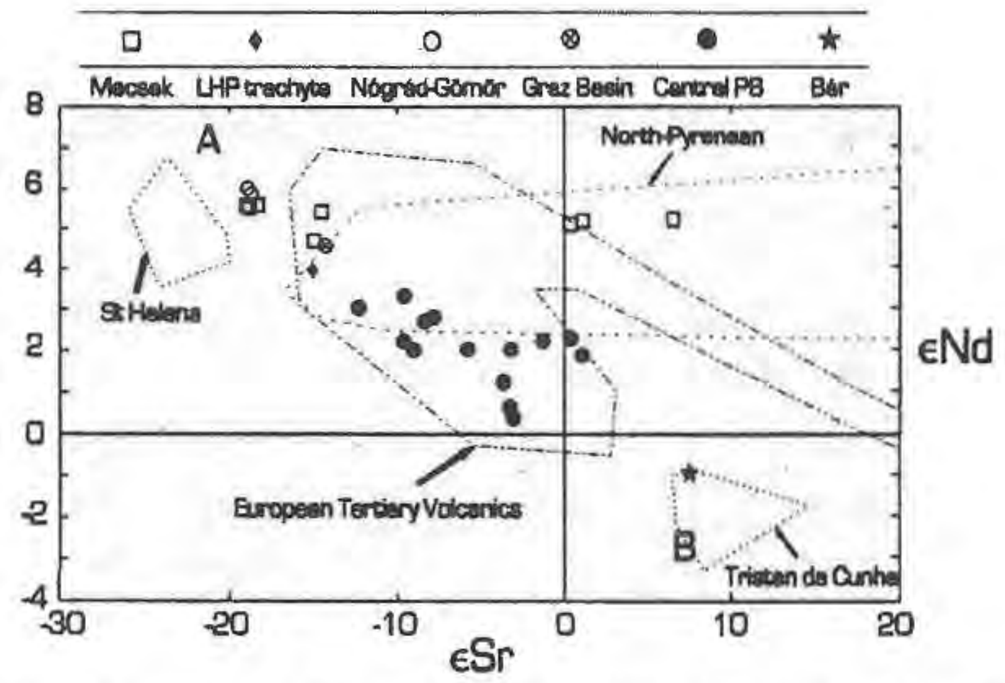

Figure 1. - ϵSr vs. ϵNd distribution of the Mesozoic and Tertiary alkaline volcanics of PB.

CRYSTAL CHEMISTRY OF HIGH P/T, METASOMATIC, BARIAN MICAS FROM INCLUSIONS IN SERPENTINITE, MOTAGUA FAULT ZONE, GUATEMALA.

Harlow G.E. (American Museum of Natural History, New York, NY, 10024-5192 USA <gharlow@amnh.org>)

One to three coexisting micas with relatively high barium content, particularly in grain rims adjacent to late-stage Ba-rich phases, have been found in jadeitites, albitites, and micaceous rocks from a serpentinite-matrix melange along the Motagua Valley of Guatemala, recently described by Harlow (1994). Barian phengite ($\leq$ 4.7 wt. % BaO) and phlogopite ($\leq$ 1.3 wt. %) ± paragonite, preiswerkite or banalsite ($BaNa_2Al_4Si_4O_{16}$) are found in the jadeitites (blueschist-to-greenschist-like conditions -- $100^o < T < 400^o$ C; $5 < P < 11$ kb). Barian phengite, from ~1.2 to $\leq$ 8.9 wt. % BaO (0.5 cats/22 oxygen), dominates in mica-rich rocks (greenschist grade -- $T_{max} < 400^o$ C; P = 3 to 8 kb) coexisting with minor celsian, cymrite ($BaAl_2Si_2O_8 \cdot H_2O$), hyalophane and/or barite. Barium is elevated in the late-stage metasomites in the serpentinite-melange environment

with potassium micas forming the main reservoir of barium in these rocks. Barium content in phlogopite is always lower than in coexisting phengite, with an exchange coefficient D(Ph/Phl) = 1.2 to 9.5. Coexisting paragonite and late stage preiswerkite have low but not always negligible barium content, as high as 0.3 wt. % BaO.

Zoning, primarily of phengite, has been studied extensively to evaluate the exchange relationships and compositional evolution. Zoning is commonly step-wise and infrequently continuous or oscillatory. The principal exchanges (a positive sense of exchange will increase the left-hand side of an equation) observed are:

[a] $^{vi}(Mg, Fe^{2+}) + {}^{iv}Si \Leftrightarrow {}^{vi}Al + {}^{iv}Al$

[b] $K^+ \Leftrightarrow Na^+$

[c] $3\cdot{}^{vi}(Mg, Fe^{2+}) \Leftrightarrow 2\cdot{}^{vi}Al + {}^{vi}\square$

where $\square$ = vacancy. Barium enrichment in K-micas requires a charge-coupling mechanism:

[d] $Ba^{2+} + {}^{j}A^{x} \Leftrightarrow (K^+,Na^+) + {}^{j}B^{x+1}$

Phlogopites are relatively rare in these rocks and are often corroded or intergrown with chlorite. Generally, Ba contents vary less than Na; otherwise no consistent relationships are found.

Data for phengite in jadeitites is limited but the following is observed: i) Ba enrichment is described by

[e] $Ba + {}^{iv}Al \Leftrightarrow K + {}^{iv}Si$ (a feldspar-like exchange)

in most cases. However, phengite enrichment (positive [a]) in certain rocks leads to [a] + [e]:

[f] $Ba + {}^{vi}(Mg, Fe^{2+}) \Leftrightarrow K + {}^{vi}Al$.

ii) In all samples Ba content is positively correlated with the degree of trioctahedral character (positive [c] exchange) and possibly with XII-fold site occupancy. iii) K/Na vs. Ba varies among samples.

Data for phengite in mica-albite rocks and albitites show i) Ba enrichment by exchange [e] in all but one sample for which exchange [f] is applicable. This single sample contains cymrite and comes from the same location as the jadeitites which manifest exchange [f]; ii) the same relationship of Ba content with XII-fold site occupancy as above; and iii) variable correlation of Ba content with trioctahedral character, K/Na variation.

An interesting interpretation of these data is the possible minor, unforeseen, vacancy replacement exchange, perhaps of the form:

[g] $Ba + 2\cdot{}^{vi}(Mg, Fe^{2+}) \Leftrightarrow {}^{xii}\square + 2\cdot{}^{vi}Al$.

Moreover, Ba substitution into phengitic muscovite may depress the phengite content due to the commonly observed [e] exchange. Extrapolation to zero Ba content increases Si content, and presumably predicted P. However, manifestation of the [f] exchange may record a paragenesis with rising P/T, implied by the phengite component of the exchange and the probable pressure-volume penalty for tetrahedral aluminum substitution with Ba incorporation in the mica structure. This higher P/T interpretation is consistent with the coexistence of cymrite, a high P indicator, with Ba-rich mica in the relevant rock.

Micas manifest considerable chemical variance in these rocks and record much about the fluid and paragenetic evolution. The complex and sometimes heterogeneous chemical variation in mica (e.g., K/Na vs Ba) must reflect those abundances and changes in the metasomatic fluid. Increased trioctahedral character with barium content suggests an increase in ferromagnesian content of the fluid and/or an increase in stability of a Ba-phlogopite component in phengite. Barium may fluctuate in some of the local environments but, in general, abruptly rises to saturation of celsian or cymrite. Barium is probably made available by destabilization of barite (decrease in fO_2) within a sedimentary component in the serpentinite melange.

References:
Harlow, G. E. (1994) *Journal of Metamorphic Geology* **12**, 49-68.

GEOTHERMAL AND FLUID EVOLUTION OF THE VARISCAN CRUST DEDUCED FROM THE KTB DRILLING

Harms U., Huenges E. *(KTB Project-Group, NLfB, Hannover)* and Kohl Th. *(Geophysics, ETH Zürich)*

The KTB Hauptbohrung in SE Germany has up to now penetrated more than 8700 metres of Variscan Basement, consisting of amphibolite facies metagraywackes, amphibolites and metagabbros.

The detailed investigation of post-Variscan tectonics, retrograde and low-grade mineralizations, fluid inclusions, petrophysical parameters and related age determinations allow an exemplary study of the 300 Ma lasting thermal evolution.

The deduced P-T-t conditions and fluid pulses constrain the thermal evolution in at least five late- and post-Variscan phases. The middle Carboniferous crustal uplift and granite intrusions disturbed the mid-crustal isotherms. At the same stage the upper crust was elevated up to 7 km. Aqueous Na-Cl-rich granite-derived fluids governed the system and mobilized N_2 and CO_2 during intrusions at a geothermal gradient of about 50 - 60°C km^{-1}. Formation of vein-tourmaline was caused at local high water/rock ratios in a hydrothermal system rich in boron at upper greenschist facies conditions.

A second phase during upper Carboniferous compression is characterized by graphite (and pyrite) mineralizations from C-O-H-rich fluids at about 400°C and 1.5 to 2 kbar. The Permian to Cretaceous evolution is poorly preserved, but K-Ar isotope data of clay-fraction micas point to thermal events. The third phase during upper Cretaceous compression generated a large crustal scale thrust at a gradient of about 40 °C km^{-1}.

The following Paleogene/Neogene and subrecent extensional phases during the formation of the nearby Cheb rift are associated with the formation of Ca-Cl-rich inclusions at a geothermal gradient of 23 - 26°C km^{-1}.

The recent temperature profile shows an unexpected high geothermal gradient of 28 ± 1°C km^{-1} between 2 and 8 km depth; the vertical heat flow density in 8 km depth is 78 ± 13 mW m^{-2}. The radiogenic heat produces cumulative 8 ± 1 mW m^{-2} from 8 km depth to the surface .

The recent fluid regime is characterized by groundwaters down to 2 km depth and saline Ca-Na-Cl-rich waters from about 3 km depth further on. Up to 0.6 m^3 nitrogen and methan gas mixtures are dissolved in 1 m^3 of this fluid. Fluid bearing fracture zones with partly immense reservoirs were found especially between 3 and 5 km depth and additionally at about 7 and 8.7 km depth. Below 6 km depth formation pressure gradients are increasing from 10 to 13 ± 0.5 MPa km^{-1}.

Geothermal modelling is applied - on the basis of the data given above, the known conductive heat conductivity and crustal structure - to estimate:

- the effect of the deformation of the temperature field due to tectonic elevations,
- the geothermal relevance of fluid transport and the duration of fluid migration with respect to possible deformations of isotherms,
- the possible effect of hydration heat derived from exothermal hydration of minerals and
- the impact of Oligocene/Miocene basaltic volcanism and heat transport from the Moho.

GOLD AND PLATINUM-GROUP MINERALS FROM ALLUVIAL DEPOSITS OF CENTRAL ALBERTA, CANADA.

Harris D.C and Ballantyne, S.B. *(Geological Survey of Canada, Ottawa)*

Native gold and platinum-group-minerals (PGMs) are present in the sand bars of the North Saskatchewan River and in Pleistocene fluvial gravel horizons of the land-based gravel operations near the City of Edmonton, Alberta. The most abundant PGMs are Pt-Fe alloys with minor Os-Ir-Ru alloys and rare native platinum, hongshiite and sperrylite. The Pt-Fe alloys occur as platelets <400um, as rods up to 600um and as spheres <100um. In composition, the alloys range in (Fe,Cu,Ni) contents from 10 to 31 at. % with as much as (in wt.%) 4.3 Os, 6.4 Ir, 7.1 Rh and 4.4 Ru. X-ray powder diffraction shows that the alloys are ferroan platinum and SEM studies reveals numerous inclusions of copper iron sulfides, native osmium, cooperite, irarsite, laurite, hollingworthite and several unidentified phases.

The Os-Ir-Ru alloys vary widely in composition, but belong to the compositional fields of osmium, iridium and ruthenium.

Pristine gold grains range in fineness from 550 to 950 with some grains containing as much as 8.0 wt.% Pt and 4.0 wt.% Pd.

The exact origin of the PGMs and gold is unknown. Mafic-ultramafic intrusions (Alaskan-type) or Alpine basic to ultrabasic (ophiolite complex-type) have not been documented in Alberta. One possible source is the reworking of paleoplacers channels. A second possible source is the kimberlites and lamproites that are being discovered in the province.

ROCK DEFORMATION AND SWINGING OF ISOGRADE SURFACES IN METAMORFIC ROCKS OF THE SEBEŞ MTS. (SOUTH CARPATHIANS) ROMANIA

Hârtopanu I., Hârtopanu P.(*Inst. of Geology and Geophysics, Bucharest, Romania*)

Two major synformal folds, connected to the M_2 metamorphic event, occur in the south-west and in the south-east part of the Sebeş Mts.

The outcrop area of these folds largely overlaps the sillimanite grade metamorphism in the area. An antiformal fold occurs between the synforms showing staurolite-kyanite zone metamorphism like the other areas of the Sebeş Mts. We suggest that the coincidence between synforms and the higher degree of metamorphism (and vice versa) could possibly mean that a rapid folding event, responsible for the folding of the isotherms was followed by a relaxation meaning temperature rise within synforms and its drop within antiforms. This means that a faster deformation (folding) is interposed between two episodes of possible mineral blastesis. The relaxation and further persistence of the same conditions enabled the presence of two generations of kyanite (± staurolite) in the staurolite-kyanite zone. At the same time in manganese rich rocks a new spessartite is formed, occurring as schlieren on the account of an older one; in metapelitic rocks, apart from a pervasive neoformation of phyllosilicates, a new spessartite results on behalf of almandine. In the western synform along the western border between sillimanite/staurolite+kyanite zones, the kyanite progressively changes to sillimanite, being altered to muscovite, biotite and plagioclase, while sillimanite grows or nucleates on biotite. The eastern border of the sillimanite zone in the western synform is represented by an older tectonic plane marked by chloritoid and sillimanite bearing mylonites. This plane extends further off the sillimanite zone, showing in places small patchy areas with sillimanite zone metamorphism within the kyanite-staurolite zone.

It is concluded that swinging of isograde surfaces must coincide with a D_2 folding controlled swinging of the isotherms.

PYROPHANITE FROM DELINEŞTI , ROMANIA.

Hârtopanu P., Cristea C., Stelea G. *(Inst. of Geology and Geophysics, Bucharest, Romania)*

Delineşti Mn-Fe ore is situated in northern part of Semenic Mts, in the Sebeş-Lotru Series. It is metamorphosed in almandine amphibolites facies. Pyrophanite was found in hybrid ore which is a result of thermal, metasomatic and hydrothermal change of gondite or carbonate ore by acid granite intrusions and pegmatites. Pyrophanite appears as veins in hybrid gondite ore where it is associated with spessartite-calderite, acmite, monazite, hematite, dannemorite and quartz. In carbonate hybrid ore, pyrophanite is dispersed and it is associated with rhodonite, pyroxmangite, rhodochrosite, spessartite-calderite and yellow alkali amphiboles. Another pyrophanite-bearing association is: albite, microcline, acmite, phlogopite, spessartite-calderite, hematite, yellow alkali amphiboles and monazite.

Lattice constants of pyrophanite calculated on the base of X-ray data are: a=5.133 Å, c=14.26 Å, V=325.381 Å^3. IR analyses of pyrophanite display absorption spectra resembling the ilmenite's ones. Chemical composition inferred from wet classical method display the following contents (in weight percentages): MnO=40.5, TiO_2=52.3, Fe_2O_3=6.1; microprobe analyses show: MnO=39.40, TiO_2=57.40, Al_2O_3=0.04, SiO_2=0.3 and total Fe=2.0.

Pyrophanite is related to hydrothermal veins, being consequently considered as post-metamorphic; it is younger than the Fe^{+3}, Na, K, B, F metasomatosis, and older than Ba-feldspars, barite, bementite, neotocite. Pyrophanite and monazite are intimately associated and most probably, point to the fact that they have resulted from the thermal and metasomatic change of an initial metamorphic Ce- and Y-rich titanite. Pyrophanite from hybrid carbonate ore was formed in this way.

THE CRYSTAL CHEMISTRY OF FELDSPATHOIDS AND THEIR RELATIONSHIP TO THE ZEOLITES

Hassan I. *(Department of Geology, University of Kuwait)*

Feldspathoid is a comprehensive term that may have different meaning for different authors. As a result, different minerals are considered as feldspathoids. The feldspathoids are best defined as anhydrous framework aluminosilicates that contain alkali and alkali earth elements, but contain no volatile anions and are similar in composition to the feldspars (*i.e.*, they contain the same or similar atoms), but contain less silica than the alkali feldspar. Thus the feldspathoids have Si/(Si+Al) ratio less than 0.75. Nepheline and leucite best fit this definition.

The mineral groups that will be considered in detail include sodalite, cancrinite, and scapolite; minerals commonly considered as feldspathoids. However, these are the only framework aluminosilicates that contain large volatile anions such as Cl^-, SO_4^{2-}, CO_3^{2-}, OH^-, and H_2O. These minerals have chemistries and structures that are quite different from that of the feldspars or the feldspathoids, proper. However, their structures are closely related to the zeolites, but they are not zeolites, proper.

The structures of the cancrinite-group minerals are characterized by parallel six-membered rings consisting of alternating AlO_4 and SiO_4 tetrahedra. The hexagonal symmetry is the result of the stacking of such six-membered rings in an AB... sequence. This stacking gives rise to large continuous-channels that are formed by twelve-membered rings of alternating AlO_4 and SiO_4 tetrahedra. These are among the largest channels known, even for zeolites. The cancrinite structure also consists of small cages, known as ε-cages in zeolite chemistry. The sodalite-group minerals have strong structural similarities to the cancrinite-group minerals, but the former have an ABC... stacking sequence that leads to cubic instead of hexagonal symmetry. This sequence leads to an offset of the C-type layer and gives rise to a network of large β-cages in the sodalite-group minerals. Some cancrinite-type minerals have structures that are based on more complicated stacking of six-membered rings. Some examples of these minerals and their stacking sequences are liottite (ABABAC...), afghanite (ABABACAC), and franzinite (ABCABCBACA...). Some zeolites also have structures that are based on similar stacking of six-membered rings, *e.g.*, offretite (AAB...), erionite (AABAAC...), levynite (AABCCABBC...), and chabazite (AABBCC). The ε- and β-cages are also used as building blocks in many zeolite structures such as zeolite A, offretite, and faujasite.

As a family, sodalite, cancrinite, and scapolite, has a unique chemistry in that they are the only aluminosilicate minerals that contain large volatile anions and they have a close structural relationship to the zeolites, but not to the feldspars or the feldspathoids, proper. Therefore, a new group name, *i.e., zeoloids*, may be appropriate for these minerals.

Sodalite- and cancrinite-group minerals commonly contain superstructures that may be commensurate or incommensurate. In the case of the cancrinite-group minerals, the superstructures can be rationalized as the effect of cation and anion ordering on the sites that are located in the channels. HRTEM image of cancrinite shows ordering of vacancies in the channels.

Several sodalite-group minerals contain incommensurate-modulated structures that arise from modulations of the framework oxygen-atom positions. The different sizes of clusters, e.g., $[Na_4.SO_4]^{2+}$ and $[Na_4.H_2O]^{4+}$, which occur in nosean are ordered. The degree of order influences the positional modulations of the framework oxygen atoms. The cluster ordering, which is enhanced by the net charge differences between the clusters, accounts for the two well-defined framework oxygen-atom positions in some sodalite-group minerals. This type of cluster ordering also gives rise to APBs, which also occur in scapolite.

GEOLOGY AND PETROCHEMISTRY OF WADI ISBAIYA AREA, SOUTH SINAI EGYPT

Hassen, I. and Buda, Gy. (*Dept. of Min., Eotvos. L. Univ., Budapest*)

Late Precambrian granitoid rocks occurring within a large area of South Sinai are divided on the basis of geology and petrology into Older and Younger assemblages.

Geological, petrological and geochemical studies of Wadi Isbaiya area indicate that there are different types of granitoid rocks: Older granitoids (phase I), Younger granitoids (Phase II and III).

The Older granitoids consist of quartz-diorite, granodiorite and quartz monzonite. The phase II includes Hb. Bt. granite and monzogranite, while phase III consists of alkali feldspar granite, syenogranite, quartz-syenite and granophyre.

The Older granitoids are enriched in xenolith. The second phase hosts some xenoliths and is transected by numerous dyke swarms. The third phase is more or less free of xenoliths, whereas dykes are extremely rare.

The phase I shows calc-alkaline trend and is enriched in Sr, Ba, Rb, Ti, Zr,Y, Nb and P. They contain moderate Ni and Cr indicating relatively low-P fractionation

Younger granites are distinguished by their enrichment in Si, Na, Y and impoverished in Ba, Sr Zr, V and Zn compared to the Older phase. High contents of Y may be in relation to genesis of these rocks (magmatic origin).

The phase III contains 75-77% SiO2 and also is characterized by meta-aluminous and peraluminous affinity. The high K2O/Na2O and Fe*/(FeO*+MgO) are also characteristic features of post-tectonic, "A-type" granite.

Late Precambrian crustal evolution in South Sinai occured in a strongly compressional tectonic environment except of the alkali granite (phase III) which tends to be extenstional type.

The suite exhibits typical features characteristic of I-type granites (phase I and II), while phase III is closed to A-Type granites.

Magmas of the early granitoids were probably derived from magmas produced by partial melting of a modified oceanic crust at an active continental margin during the late stage of Pan-African orogeny with addition material from continents [contaminated or assimilated of Early Pan-African (gabbroid or dioritic country rocks)], while the later post tectonic intrusion may have been formed by progressive fractionation of that magma.

THE IMPORTANCE OF LIGHT LITHOPHILE ELEMENTS IN ROCK-FORMING METAMORPHIC MINERALS

Hawthorne F.C. (*Dept. of Geol. Sci., Univ. of Manitoba*)

The light lithophile elements (H,Li,Be) are not detectable by electron-microprobe analysis, and it is only recently that B can be determined accurately by this method. This situation led to the neglect of these constituents in analytical work and crystal-chemical considerations of most important metamorphic rock-forming minerals. However, things have changed in the last 10 years. Crystal-structure refinement combined with electron- and ion-microprobe analysis and bulk chemical techniques have shown that the light lithophile elements play important roles in several rock-forming metamorphic minerals.

Staurolite may be written as $A_4B_4C_{18}D_4T_8O_{40}X_8$ where A = Fe^{2+},Mg,□(vacancy); B ≈ Fe^{2+},Mg,Li,□; C ≈ Al,Fe^{3+},Mg,Ti; D = Al,Mg,□; T = Si,Al; X = OH,F,O^{2-}. Careful AA, H-extraction line and ion-microprobe work showed that both Li and H are key variable constituents of staurolite. Taking the additive component of staurolite as $\square_4Fe_4^{2+}Al_{16}(Al_2\square_2)Si_8O_{40}[(OH)_2O_6]$, the principal heterovalent exchanges in staurolite are $^{A}Fe^{2+\,B}\square_2H_2$ $(^{A}\square\,^{B}Fe^{2+}\square_2)_{-1}$ and $^{B}LiH(^{B}Fe\square)_{-1}$. The long-denoted enigmatic character of staurolite now begins to come clear: two of the principal chemical variables, H and Li, are invisible to the electron microprobe, and were *assumed* to be absent and constant, respectively. As a consequence of this, the chemical formula was wrong, activity models were inappropriate, and conflicting results from experimental and field studies were common. This unsatisfactory situation has now been resolved with our understanding of the role of H and Li in the staurolite structure.

Vesuvianite may be written as $X_{19}Y_{13}Z_{18}T_5O_{68}X_{10}$ where X ~ Ca; Y ~ Al,Mg,Fe^{2+},Fe^{3+}; Z = Si; T = B,□; W = OH,F,O^{2-}. Crystal-structure refinement showed the presence of unassigned electron-density in the structure; polarized infrared spectroscopy suggested the presence of BO_n groups, and the presence of B was confirmed by electron-microprobe analysis. Stereochemical arguments indicate that B must be replacing H in the structure, and the great variability of H in vesuvianite was confirmed by bulk determination of H_2O. Vesuvianite can contain up to ~4 B apfu (~4 wt% B_2O_3) and is a potentially significant sink for B in metamorphic rocks.

The general formula for alkali amphiboles may be written as $AB_2C_5T_8O_{22}X_2$ where A = Na,K,□; B = Na,Ca,Mn^{2+},Fe^{2+}; C = Mg,Fe^{2+},Al,Fe^{3+},Li; T = Si,Al; X = OH,F,O^{2-}. Until recently, Li was thought to be restricted to the unusual orthorhombic amphibole holmquisite, in which it is a B-group cation occupying the M4 site. However, crystal-structure refinement of (red) amphiboles from a metamorphic manganese deposit at Kajlidongri, India, indicated extremely low X-ray scattering at the M3 site, compatible with occupancy of this site by (Mg,Mn) and either Li or □. Bulk AA analysis showed high Li values (Li_2O ~ 1 wt%) and this was confirmed by ion-microprobe analysis. The new amphibole leakeite, ideally $NaNa_2(Mg_2Fe_2^{3+}Li)Si_8O_{22}(OH)_2$, was described from this region, and the manganese equivalent was discovered at the Grenfell Manganese Mine in Australia. The effect of Li on amphibole stability has not yet been examined experimentally, but the high Fe^{3+} (and Mn^{3+}) contents suggest that these compositions are characteristic of high $f(O_2)$ conditions (and not poor-quality chemical analyses, as has been sometimes assumed previously).

It is notable that in geochemically suitable environments, many common rock-forming minerals can incorporate major amounts of light lithophile elements into their structures. Such substitutions frequently involve two light-lithophile elements (e.g., H and Li, H and B) or one light-lithophile element and a change in valence state (e.g., Li and $Fe^{3+} \rightarrow Fe^{2+}$). All of these substitutions are invisible to the electron microprobe, and highlight the importance of using

crystal-structure refinement and new microprobe methods (ion microprobe, micro-L-edge XANES, micro-XPS) for adequate characterization of metamorphic minerals.

THE ROLE OF HYDROGEN IN CONTROLLING THE STRUCTURAL UNIT IN OXIDE AND OXYSALT MINERALS

Hawthorne F.C. (*Dept. of Geol. Sci., Univ. of Manitoba*)

Hydrogen plays a very important role in the structure and chemistry of the oxide and oxysalt minerals. The characteristics of this role can be examined in a simple and intuitive fashion within the framework of bond-valence theory. For any crystal structure, the structural unit can be defined as the strongly bonded part of the structure; the structural units are linked together by interstitial species, usually alkali and alkaline-earth cations and H_2O groups that are involved in much weaker bonding. These structural units thus constitute structure modules from which one or more structures or structure types may be built.

In oxide and oxysalt minerals, H most commonly has a coordination number of [2]. Usually, this arrangement undergoes a spontaneous distortion with the H cation moving off-centre towards one of the two coordinating anions. The tightly bonded OH^- or H_2O° groups that result can be thought of as oxyanions or ligands, and are extremely polar. The bonding associated with these two groups is extremely directional in nature. On the oxygen side of each (OH or H_2O) group, it functions as an anion, whereas on the hydrogen side of each group, it functions as a cation. Furthermore, the strength of this chemical bonding is very different: on the anion side of each group, the bonding is usually relatively strong ($\sim$1.2 v.u. for OH, $\sim$0.4 vu for H_2O), whereas on the cation side of each group, the bonding is usually relatively weak ($\sim$0.20 vu for OH and H_2O). It is because of these unusual characteristics of its normal 'oxyanions' that H has such a unique structural role in oxide and oxysalt minerals.

The structural unit of a mineral is the strongly bonded part of the structural, and usually involves bonds of $> \sim 0.3$ vu. This means that the anionic side of the OH and H_2O groups can be part of the structural unit, whereas the cationic side cannot. Thus in both groups, H tends to truncate the strongly bonded network of the structural unit. As an example, consider the structural unit of artinite, $[Mg_2(CO_3)(OH)_2(H_2O)_3]$, shown below:

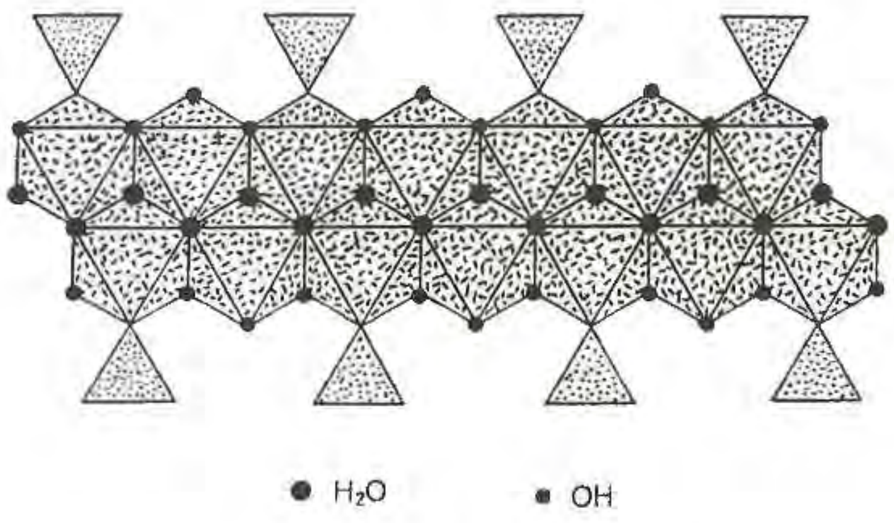

The structural unit is a ribbon of edge-sharing $Mg\phi_6$ octahedra (dashed) flanked by CO_3 triangles (dotted). The anions in the centre of the strip are H_2O groups; they allow the octahedra to link in two directions within the plane of the ribbon, but prevent linkage orthogonal to the ribbon. The OH anions at the edge of the strip allow the octahedra to link only in one direction, along the length of the ribbon, and prevents linkage in two directions orthogonal to the length of the ribbon.

The role of OH and HO groups is to 'tie off' the polymerization of the structural unit in specific directions. Hence H plays a crucial role in controlling the dimension of polymerization of the structural unit, and through this, many of the physical and chemical properties of a mineral. We will explore the importance of this role in controlling the diversity and complexity of mineral structures as a function of pressure and temperature.

AN APPLICATION FOR GEOCHEMICAL ANALYSES: THE STUDY OF DECAY MECHANISMS OF A SANDSTONE BUILDING IN THE SOUTH WEST OF SCOTLAND.

Hayles, C. S. and Bluck, B. J. (*Dept. of Geology and Applied Geology, Univ. of Glasgow*)

Culzean Castle, property of the National Trust for Scotland, lies on a cliff top above the Firth of Clyde. The Castle has been built over three main periods, the most important of which was designed by Robert Adam and completed between 1777 and 1792. The permeable volcanigenic lithic arenite used to construct the Castle and its outbuildings are of different origin and as such weathering to varying extents according to position, architectural design, degree of exposure, and mineralogical properties. Comparing the quarry stone with that on the building provides an opportunity to determine the prominent forms and rates of weathering in lithic arenites buildings.

Samples from the building have been examined using XRF, XRD, and SEM. These have been compared with material from the quarries to identify major chemical redistributions involving carbonates, silicates, sulphates and chlorides in the stone of the building.

Ingress of moisture throught the stone exceeds egress, prohibiting the stone from drying out. This provides a mechanism for internal decay. The hygroscopic nature of the stone activates salt crystallisation (halite, gamma calcium sulphate) thus inducing the phenomena of contour scaling. As these acidic solutions are retained within the stone the carbonate cement can be either cracked, and filled in with a silicate cementing agent, or dissolved and reprecipitated towards the exterior surface of the stone by capillary action. The growth, volume change, and thermal expansion of swelling clays such as chlorite also have a destructive effect on the stone.

THERMAL STABILITY AND POZZOLANIC ACTIVITY OF CALCINED CLAYS

He C. (Geological Inst., Univ. of Copenhagen)

Four commonest clay minerals, kaolinite, illite (American Clay Minerals Society, IMT1), Ca-montmorillonite (STx1) and Na-

montmorillonite (SWy1) were investigated in detail. Samples were calcined at three to four temperatures according to their thermal reactions revealed by DTA. Chemical and physical properties of the calcined clay minerals were investigated. All samples, untreated and calcined, were mixed with $Ca(OH)_2$ in the presence of simulated cement pore solution, and with ordinary Portland cement, respectively. The reaction rate of these mixtures was monitored by chemical shrinkage tests. Reaction products were again studied by XRD, DTA, SEM, EMPA, as well as alkali and acid solubility tests. Technological properties of the clay-cement mortars were studied by flow, and by compressive strength tests after reaction for 2, 7, 28 and 91 days. A fly-ash was also studied as a reference sample.

Our study confirmed that calcination is very effective in activating the pozzolanic properties of clays. The latter can be quantified using the following three indicators:

(1) XRD amorphous phase increases markedly by calcination. During dehydroxylation of kaolin at 550°C, intensity of the diffuse band increases by 78%, at 800°C by 95% but it drops abruptly to 43% at 950°C when the formation of mullite takes place. For illite the background area increases by 3% at 650°C, 14% at 790°C and 53% at 930°C, whereas the (001) reflection decreases accordingly.

(2) In the alkaline solubility tests, with 0.5N NaOH, soluble Al in kaolinite increases dramatically with increasing calcination temperature. At 800°C, it increases up to 665% of the value for uncalcined kaolinite but at 950°C it drops to 175%. In illite, the alkali-soluble Al in illite increases with the calcination temperature to 480% at 650°C and to 534% at 930°C. For Ca-and Na-montmorillonite at 830°C, it increases to 2000% and 3500%, respectively.

(3) In the compressive strength test after 28 days curing, the cement-pozzolan mortar containing 30% kaolin calcined at 550°C and beyond, has more than 2 times compressive strength of the mortar with uncalcined kaolin and ~115% of pure ordinary Portland cement (OPC) mortar. Pozzolanic activity of illite is rather poor. Although calcination at 930°C enhanced the mortar compressive strength by 40%, it still is about 80% of that for pure OPC mortar and about 90% of that of fly ash-cement mortar. Montmorillonite has fairly good pozzolanic activity. The optimum calcination temperature for Ca-montmorillonite is 830°C by which the mortar compressive strength is 160% of that for uncalcined clay and 125% of that for pure OPC mortar. Na-montmorillonite, for the optimum temperature of 830°C, has 260% compressive strength of uncalcined and 113% of pure OPC mortar.

The reaction products of clay-$Ca(OH)_2$ mixtures differ according to the composition of starting clays. For the same clay they are the same but their amounts vary with calcination temperature, suggesting variability in pozzolanic activity.

Combining the complete laboratory results with practical (cost and technical) considerations, the following calcination temperatures are recommended: kaolinite, 550°C; illite (poor pozzolan) 930°C; Ca-montmorillonite, 730°C and Na-montmorillonite, 830°C.

Gibbsite Formation in Subtropical Soils of China

He J.Z., Li X.Y., Xu F.L. (Dept. of Soil Science, Huazhong Agricultural Univ.)

The occurence of gibbsite in subtropical soils of China is mainly attributed to the action of weathering processes of high intensity and of great duration. For example, the gibbsite in red soils (ultisols) and latosols (oxisols) of the region is generally recognized as the last product of progressive weathering of clay minerals, and its coexisting minerals are mainly kaolinite and iron oxides. In the last decade, gibbsite has been identified in many mountain soils of the region, especially those derived from granite and located at higher altitudes, and its amount may be larger than that in the corresponding horizontal soil. This gibbsite was explained as a relict of hot and humid palaeoclimatic conditions. However, evidence confirming its formation under other environments and during initial stages of weathering has become increasingly recognized. We have investigated more than 160 mountain soil samples in subtropical China. The comprehensive analyses of the soil parent materials, texture, coexisting clay minerals, climates and topography show that the gibbsite in the mountain soils located at higher altitudes is mainly formed under the conditions of intensive eluviation and rapid desilicification and in the initial weathering stages of aluminosilicates, such as plagioclases, rather than inherited from that of palaeoclimatic conditions (Xu et al.,1990; He et al., 1992). Furthermore, our latest results show that some of the gibbsite in the mountain soils may be formed from hydroxy interlayered smectite (He et al., 1993). It is found that the 1.4-nm intergrade mineral in yellow soil of the Mang Mountains (25°N, 113°E) is derived from montmorillonite, and the hydroxy-Al in the interlayer of 1.4-nm intergrade mineral may free from the interlayer and crystallize into gibbsite.

On this basis, it may be concluded that there are three machanisms for gibbsite formation in the subtropical soils of China. First, gibbsite is the last product of progressive weathering of clay minerals. Second, gibbsite is formed under the conditions of intensive eluviation and rapid desilicification and in the initial weathering stages of alumilosilicates. Third, gibbsiite is formed from the interlayered hydroxy-Al of smectite. The forming mechanism may depend on various soils. One mechanism may be predominant in one kind of soil, and two or three mechanisms may also control the formation of gibbsite altogether in another kind of soil.

References:
He, J.Z., Li, X.Y., Xu, F.L. (1992). Pedosphere, 2, 63-69.
He, J.Z., Li, X.Y., Xu, F.L. (1993). Chinese Sci. Bulletin, 38, 2096-2098. (in Chinese)
Xu, F.L., Li, X.Y., Huang, Q.Y. (1990). Acta Pedologica Sinica, 27, 293-300. (in Chinese)

IRON, BRAZIL TWINS, AND THE FORMATION OF THE SILICA POLYMORPH MOGANITE

Heaney, P.J. *(Dept. of Geol. & Geophys. Sci., Princeton Univ.)*

Following the discovery of moganite by Flörke *et al.* (1984), powder X-ray diffraction has revealed that this silica polymorph is present in virtually all unaltered microcrystalline "quartz" varieties (Heaney and Post, 1992). Subsequent studies have indicated that the concentration of moganite is dependent on depositional environment. Whereas most microcrystalline silica contains between 5 and 20 wt % moganite, chert from evaporitic environments typically includes 20 to 50 wt % moganite (Heaney *et al.*, 1992). The purest natural moganite (up to 85 wt %) occurs within the welded tuff of the Mogan Formation in Gran Canaria, Spain. An electron probe investigation of this material indicates

that moganite grows in intimate association with hematite, aegerine, and Fe-rich feldspar (Heaney and Vicenzi, 1994).

Transmission electron microscopy of moganite from Gran Canaria suggests that the formation of this metastable polymorph is promoted by the substitution of $[Fe^{3+} + Na^{+}]$ for Si^{4+}. Trace quantities of Fe and Na in moganite laths were clearly discerned by energy dispersive X-ray spectroscopy. No other iron-rich phases were detected by imaging or electron diffraction in the areas selected for analysis. Moreover, moganite nodules from Gran Canaria frequently exhibit coloration like that observed in citrine and amethyst, which also are enriched in tetrahedrally coordinated Fe^{3+} (Cohen, 1985).

The inclusion of Fe^{3+} and Na^{+} within the quartz structure would appear to induce oscillations in chirality: Amethyst exhibits unusually high concentrations of Brazil twin domains (Schlössin and Lang, 1965), and moganite is effectively twinned at the unit-cell scale according to the Brazil law (Miehe and Graetsch, 1992). The induction of Brazil twinning may be a steric effect associated with interstitial Na^{+} and the greater ionic radius of Fe^{3+} compared with Si^{4+}. The coupled substitution of these species may force framework displacements with $\mathbf{b} = 1/2$ [110], thereby creating Brazil twin boundaries (McLaren and Phakey, 1966).

References:
Cohen, A.J. (1985) *Am Mineral*, **70**, 1180-1185.
Flörke, O.W., Flörke, U., and Giese, U. (1984) *Neues Jahr Mineral Abh*, **163**, 325-336.
Heaney, P.J. and Post, J.E. (1992) *Science*, **255**, 441-443.
Heaney, P.J., Sheppard, R.A., and Post, J.E. (1992) *GSA Abstr.*, **24**, A231.
Heaney, P.J. and Vicenzi, E.P. (1994) *Eos*, submitted.
McLaren, A.C. and Phakey, P.P. (1966) *Phys Stat Sol*, **13**, 413-422.
Miehe, G. and Graetsch, H. (1992) *Eur J Mineral*, **4**, 693-706.
Schlössin, H.H. and Lang, L.R. (1965) *Phil Mag*, **12**, 283-296.

BIOTITES AS PETROGENETIC INDICATORS IN HERCYNIAN GRANITES OF THE FICHTELGEBIRGE (NE BAVARIA, GERMANY)

Hecht L. (Dept. of Applied Mineralogy, Techn. Univ. of Munich)

The Hercynian granites of the Fichtelgebirge are peraluminous monzo- and syenogranites which can be subdivided into two main groups, the "older granites" (326 ± 2 Ma) and the "younger granites" (306 to 286 Ma; Richter & Stettner, 1979; Carl & Wendt, 1993). Among other factors these two main groups differ in chemical composition and in the types of their enclaves. It is still under discussion which genetic processes were involved to what extent in the formation and differentiation of the granites.

The biotites of these granites have been investigated by petrography and geochemistry in detail (Hecht, 1993). At least six biotite generations can be indentified. The formation and/or transformation of the different biotite generations can be associated to genetic processes like partial melting (restites), magma mixing, magma fractionation and postmagmatic metasomatism. Most important for the reconstruction of these differentiation processes was a biotite generation which form small single grains included in larger quartz grains. This primary biotite is preserved from secondary alteration processes and reflects the magma fractionation. The results of biotite investigation together with the whole rock data lead to the following conclusions:

(a) Mafic magmas were involved in the formation of the older granites, probably by magma mixing. (b) Locally abundant restite minerals (biotite and others) in the younger granites suggest that restite unmixing is involved in the formation of these granites. (c) Magma fractionation (crystal fractionation) played an important rule in the formation of both granite groups. (d) The younger granites were strongly affected by early postmagmatic alteration which most probably also changed the whole rock composition.

References:
Carl, C. & Wendt, I. (1993). *Z. geol. Wiss.*, **21**, 49-72.
Hecht, L. (1993). *Münchner Geol. Hefte*, **10**, 221 p.
Richter, P. & Stettner, G. (1979). *Geologica Bavarica*, **78**, 144 p.

SYNCHROTRON INFRARED SPECTROSCOPY OF EARTH AND PLANETARY MATERIALS

Hemley, R. J., Mao, H. K., Hanfland, M., Li, M., Goncharov, A., and Meade, C. (*Geophysical Lab and Center for High Pressure Research, Carnegie Institution of Washington*).

Synchrotron radiation can be used for infrared spectroscopy to study a wide range of problems in mineralogy and planetary science, and forms a natural complement to synchrotron x-ray techniques. We describe recently developed synchrotron IR techniques and applications utilizing beam line U2B at the VUV ring at the NSLS, Brookhaven National Laboratory. The radiation source has 100-1000 higher brilliance than conventional sources; it is also more stable and its pulsed character can be utilized for time resolved studies. The experiments were performed in the near to mid-IR, from 1-15 μm or 650-10,000 cm^{-1}, using conventional Fourier transform spectrometers. Both vibrational and electronic excitations are probed, which in turn can be used to study crystallographic transitions, electronic transitions, metallization phenomena, and thermodynamic properties of materials. With the high brightness and low divergence of the source, measurements can be made with high spatial resolution, including the studies on microscopic samples (at length scales near the diffraction limit of the light) and measurements of the spatial distribution of phases and composition in bulk samples. Both conventional and custom built IR microscopes have been employed. One of the most important applications of the synchrotron infrared technique has been in the study of materials at ultrahigh pressures with diamond-anvil cells. Most of the experiments to date have been carried out on hydrogen, the most abundant element in the solar system and the primary constituent of the giant planets. For these experiments new micro-optical systems have been constructed for interfacing with diamond-anvil cells, usually contained in optical cryostats. A number of new phenomena in dense hydrogen have been documented, including the observation of extraordinary enhancement of the intramolecular stretching modes in the solid above 150 GPa (>1.5 Mbar) at low temperature. Other applications include the study of ices, hydrogen-water mixtures, and hydrogen component in dense silicates quenched from high pressure. New developments include the implementation of custom built microscope designs with large working distance reflecting objectives for high-pressure cells in optical cryostats and furnaces.

ATOMIC RESOLUTION IMAGING OF MINERAL SURFACES

Henderson G.S. (*Dept. of Geology, Univ. of Toronto*) and Wicks F.J. (*Dept. of Mineralogy, Royal Ontario Museum*)

Atomic resolution imaging of insulator mineral surfaces is now possible using Atomic Force Microscopy (AFM). However, there is controversy over whether the images produced by the AFM are true representations of the atomic structure, or whether the images are merely an ensemble of averaged atomic positions. Much of the controversy results from a lack of understanding of the interaction between the AFM tip and the mineral surface and will only be solved with detailed theoretical calculations. However, a number of features observed in "atomic-resolution" images of layered silicates and other minerals would indicate that

true atomic-resolution is being achieved with AFM. These features include excellent correspondence between calculated and observed structures, images of defects and single atoms, as well as, surface adsorbed cations, and observation of more than one type of mineral structure in a single image. In studies involving Cs^+ adsorption onto silicate sheets the AFM is able to image the Cs^+ ions bonded into siloxane rings. Images of 1:1 layer silicates have been obtained in which both the octahedral and tetrahedral sheets are observed simultaneously. Neither of these results would be possible if the AFM images were composites of averaged atomic positions. Further, in recent work involving materials whose structures are unknown, excellent agreement is obtained between the AFM images and proposed structures simulated by molecular modelling. Any averaging of atomic positions would have to be on a very small scale but even this appears unlikely given that the Mg atom sites have been resolved in both 1:1 and 2:1 layer silicates.

A DEVELOPING SCIENTIFIC ROLE FOR MINERALOGY MUSEUMS

Henderson Paul. *(Dept. of Mineralogy, The Natural History Museum, London, UK.)*

Information technology (IT) is providing a new opportunity for natural history museums to develop significantly the relevance and use of their mineralogical collections and expertise. The worldwide investment in mineralogy in museums is large yet currently the impact from that investment is relatively low. A fuller role for museum mineralogists can be achieved through a coordinated multi-national approach in which IT plays a major part. The aims would be: (i) to improve both the efficiency and the effectiveness of the relevant museum function and (ii) for the museums' output to be contributing more to current regional and world issues.

The environmental and resource issues on the world stage are clearly ones that can and do involve mineralogists. Museum research groups will need to ensure that their studies of mineral behaviour encompass relevant properties, including those that relate to mineral-water interaction and secondary mineral formation, if they are to help solve some of these issues. The resources available to any individual museum are likely to be insufficient for it to study the full range of mineral properties and/or geographical regions. A planned international collaboration is now necessary. Geographical distance is no longer an impediment to the feasibility of such an initiative. The components of an initiative are outlined.

vesuvianite. Cell dimensions range from usual values to unusually large values as shown in Fig. 1.

Vesuvianite is fine grained and is usually closely associated with fine grained hydrogrossular. There is a close relation in cell dimensions between vesuvianite and associated

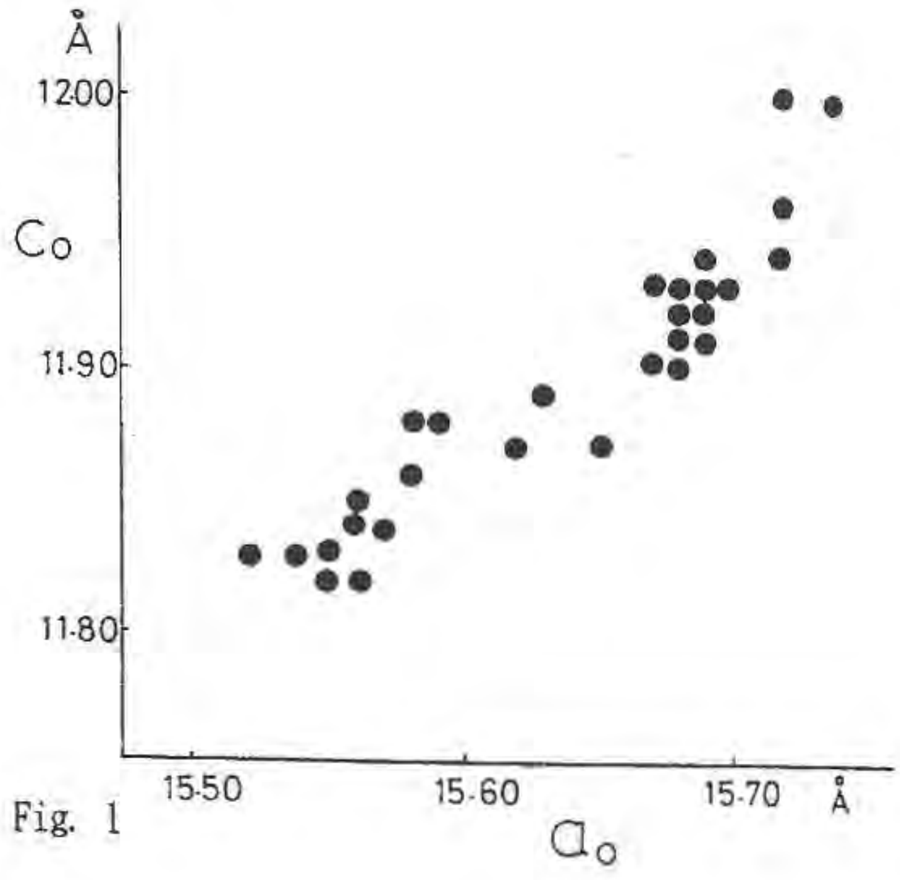

Fig. 1

hydrogrossular as shown in Fig. 2. Wide variation in cell dimension of hydrogrossular has been well known and is the result of substitution of silica by hydroxyl ions. The relationship shown in Fig. 2 may show that vesuvianite with

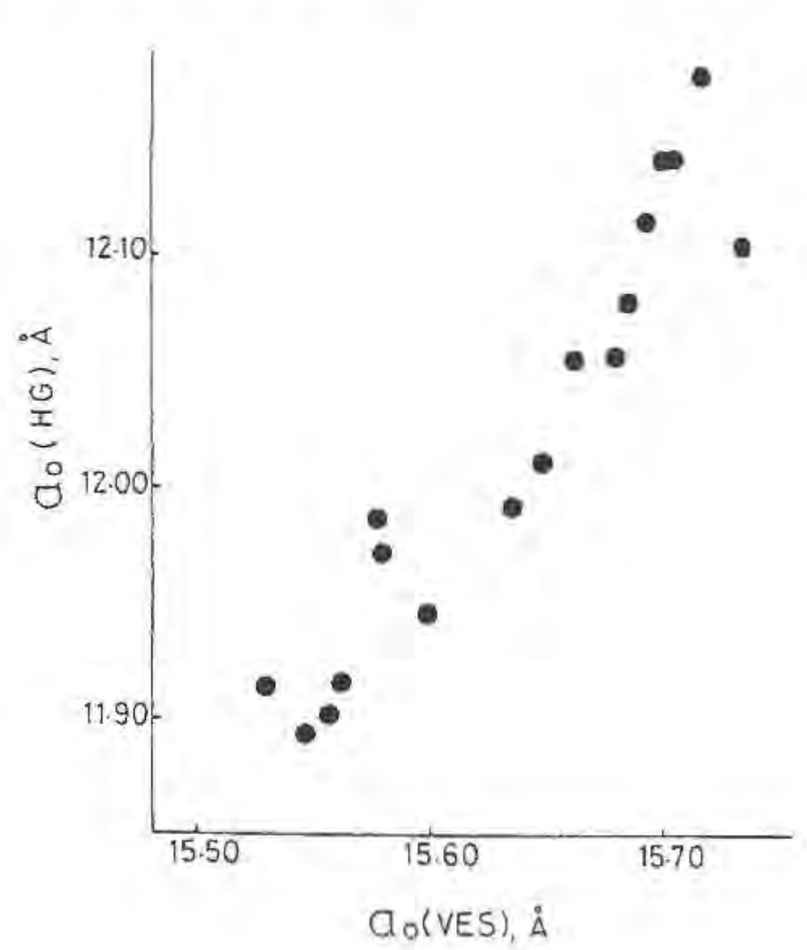

Fig. 2

large cell dimensions contains hydroxyl ions substituting silca.

Chemical composition of gehlenite and bulk compositions of alteration products which are consisting of vesuvianite and/or hydrogrossular show that there are small change in silica, alumina and water contents. Alteration of gehlenite with addition of water resulted in vesuvainite with large cell dimensions and those with addition of silica and subtruction of alumina resulted in vesuvianite with small cell dimension.

VESUVIANITE FROM KUSHIRO, HIROSHIMA PREFECTURE, JAPAN

Henmi, C., Kusachi, I. and Henmi, K. (Dept. of Earth Sciences, Okayama Univ.)

Mineralogically zoned skarns comprised of gehlenite zone and wollastonite zone occur at Kushiro, Hiroshima Prefecture, Japan. Vesuvianite occurs as an alteration product of gehlenite. There is wide variation in cell dimension of

GRANODIORITIC AND DIORITIC INTRUSIONS IN LATE KAROO TIMES: GENESIS AND ECONOMIC IMPLICATIONS

A. Henning, W.A. van der Westhuizen, H. de Bruiyn and G.J. Beukes *(Dept. of Geology, Univ. of the Orange Free State)*

A 6 m thick transgressive granodioritic sheet intruded a dolerite sill in the Speelmanskop area 20 km north of Cradock in the Eastern Cape Province, South Africa. The sheet changes upwards into a 15 m thick concordant sill.

Geologically the area is underlain by dolerite, intrusive into sandstone and intercalated shale lenses of the Katberg Formation of the upper Beaufort Group, Karoo Sequence. In places, the granodiorite sheet is intrusive into sandstone of the Katberg Formation and seems to have evolved by fractional crystallization from a mantle source with minor contamination by sedimentary material. Small plumes, a few cm in diameter and up to a meter in height, consisting of feldspar, graphite, prehnite and quartz occur in the upper parts of the sheet. The carbon contained in the rising plumes, concentrated as a layer of graphite nodules and associated felsic material in the upper part of the granodiorite body.

Mineralization in the form of chalcopyrite, gersdorffite, cobaltite and nikkelite occurs in the graphite nodules. Gold and silver concentrations of up to 0.32 and 3,9 ppm respectively were reported for this horizon of variable thickness (1 meter in places).

A dioritic intrusion, containing pyrite, occurs to the north of the granodioritic intrusive. The diorite appears to have originated from a lower crustal source and evidence of *in situ* fractionation is apparent in the dioritic body. No relationship could, however, be ascertained between the diorite and either the dolerite or the granodiorite. Evidence is presented to show that the granodiorite and the dolerite have originated from the same source, with the granodiorite being the more evolved product.

A CUSPIDINE AND BULTFONTEINITE-BEARING SKARN FROM CHESNEY VALE, VICTORIA, AUSTRALIA

Henry, D. A. (*Dept. of Mineralogy, Museum of Victoria*)

At Chesney Vale in northern Victoria, a Devonian granite has intruded and contact metamorphosed a sequence of Ordovician shales and mudstones. Fine-grained, banded calc-silicate rocks occur approximately 20 m from the granite contact and represent a small calcareous unit interbedded with the shales.

A metamorphic assemblage consisting largely of grossular and diopside with minor wollastonite has been overprinted by a fluorine-rich metasomatic event. Primary skarn minerals are garnet (andradite-grossular) and vesuvianite (fluorine-bearing). The major fluorine-bearing phases are cuspidine $Ca_4Si_2O_7(F,OH)_2$ which occurs as patches and veins and fluorite which occurs as small grains throughout the rock. Minor patches of bultfonteinite $Ca_2SiO_2(OH,F)_4$ occur with vesuvianite. A hydrated retrograde assemblage includes epidote-clinozoizite and prehnite with minor phases including afwillite, foshagite, rosenhahnite, talc and tobermorite.

The granite at Chesney Vale is a high-level intrusion (pressure of <1 Kb). The observed assemblage in the skarn indicates magmatic temperatures (<600°C), and low $X_{(CO2)}$. The presence of the fluorine-bearing minerals cuspidine, bultfonteinite and vesuvianite, and the occurrence of fluorite veins in nearby granites, suggest a magmatic source for the skarn-forming fluids.

This is the first occurrence of cuspidine in Victoria and the first record of bultfonteinite in Australia.

METAMORPHIC FLUIDS IN HIGH GRADE MARBLES AND CALC-SILICATE ROCKS OF THE CENTRAL MOJAVE DESERT, CALIFORNIA: EVIDENCE FROM CALCULATED PETROGENETIC GRIDS

Henry, D.J., Neuffer, P. and Sella, G. F. (Dept. of Geology and Geophysics, Louisiana St. Univ.)

A series of polymetamorphic granulite and upper amphibolite facies marbles and calc-silicate rocks are exposed in the central Mojave Desert and preserve mineral assemblages and compositions diagnostic of the evolving fluid conditions during the metamorphic history. These metasediments were exhumed in Miocene time by detachment faulting and locally produced a greenschist facies overprint on the high grade rocks. Two proximal areas, the Harper Lake domain (HL) and West Hinkley Hills domain (WHH), contain similar packages of sedimentary rocks but have distinctive mineral assemblages that are primarily a function of differences in fluid composition. The range of metamorphic fluids was evaluated using petrogenetic grids calculated from compositions of coexisting minerals in diagnostic samples.

The HL domain underwent an initial granulite facies metamorphism at 800-850°C and 7.5-9 kbar involving predominantly CO_2-rich fluids. Calculated petrogenetic grids involving characteristic mineral assemblages such as scp-qtz-di±cal±an±kfs for calc-silicates and cal-dol-di-fo±spl±phl establish that the composition of the metamorphic fluid is variable but $X(CO_2)>0.7$. There is an upper amphibolite facies overprint (750-800°C and 10-12 kbar) that involves the stabilization of czo, grs and prg in calc-silicates at $X(CO_2)=0.4$-0.6 and of chl and chu in marbles at $X(CO_2)=0.05$-0.1.

In contrast, the WHH domain underwent a peak upper amphibolite facies metamorphism at 650-750°C and 6-7 kbar involving H_2O-rich fluids ($X(H_2O)\approx0.8$) with later H_2O-richer fluids ($X(H_2O)> 0.9$) introduced at slightly lower temperatures. The WHH calc-silicates were modeled with characteristic assemblages such as wo+vsv+grs+cal+di±qtz±an±kfs and scp+vsv+grs+cal+di+an+kfs+spn+bt and the marbles with the assemblage cal+dol+di+fo+spl+hbl+chl.

A POLYMETAMORPHIC ORIGIN OF REACTION TEXTURES IN A GRANULITE TERRANE CONFIRMED BY SM-ND DATING OF GARNET

Hensen, B. J., Zhou, B and Thost, D.E. (*Department of Applied Geology, University of NSW, Kensington, 2033, Australia*)

Reaction textures have been widely used to derive pressure-temperature-time (P-T-t) paths for metamorphic rocks. On this

basis both near isobaric cooling and near isothermal decompression paths have been proposed for granulite facies terranes. Time constraints are often lacking and it is tacitly assumed that the textures, and the derived sequence of events, can be attributed to a single metamorphic episode. This assumption is unlikely to be universally applicable because rocks habitually cool back to ambient conditions without textural evidence for re-equilibration. Dry rocks in particular react only under special conditions involving deformation and/or fluid influx. It is possible therefore that mineral assemblages and reaction textures in a single rock record segments of P-T paths that are unrelated.

Such a case is documented, by garnet Sm-Nd chronology, for some mafic granulites with spectacular two stage garnet breakdown textures. The geochronological evidence shows that the garnet formed at c. 1000 Ma, at 850-900°C and 10 kbar, whereas the garnet breakdown reactions producing symplectites of orthopyroxene and plagioclase, and orthopyroxene, plagioclase and spinel respectively, took place at c. 500 Ma and c. 750°C and 6-4 kbar, in response to reheating and decompression, during a second granulite facies metamorphic episode.

The results show that the garnet cores still record the earlier high P-T event and also retain a memory of the timing of this event. The subsequent reheating to 700 -750 °C at c. 500 Ma did not reset the Sm-Nd isotope system within garnet cores. Therefore it is concluded that the closure temperature of Sm-Nd system for garnet in these rocks is in excess of 700 °C.

Our data demonstrate that, in the absence of reliable criteria for heating or cooling and without age constraints, reaction textures cannot be assumed to record pressure or temperature changes in a single tectono-thermal event.

Kainite forming reactions in the system Na-K-Ca-Mg-Cl-SO_4-H_2O and safety aspects of repositories for hazardous wastes in salt formations

Herbert H.-J. (GSF-Institut für Tieflagerung, Braunschweig)

The underground disposal of hazardous wastes in salt formations requires to investigate the effects of an accidental inflow of water or brine into the repository, as the fluid phase is considered to be the major pathway for the release of noxious compounds into the biosphere. The kainite forming reactions of water with potash formations are of special interst for the safety assessment because of the corrosive chemistry of the resulting solutions and the huge volume changes to be expected. These reactions are:

water+halite+carnallite + kieserite+ anhydrite (1)

water+halite+sylvite + kieserite+ anhydrite (2)

They have been investigasted in large scale in situ experiments. A comparison of the experimental data and the results of thermodynamic model calculations on the basis of the Pitzer equations (Pitzer, 1973) with the geochemical computer code EQ3/6 (Wolery, 1992) will be presented.

The reactions can be described accurately by using the six component system Na-K-Ca-Mg-Cl-SO_4-H_2O. There is a good agreement between experimental data and the model calculations. In both reactions the resulting solutions are six component solutions with high Mg-concentrations. Reaction (1) yields at 25°C a solution at the invariant point IP19 of the six component system with 93.5 moles Mg/1000 molesH_2O. From reaction (2) results a constant solution at point IP21 with 73.0 moles Mg/1000molesH_2O. IP 19 is in equilibrium with the minerals dissolved in reaction (1). Therefore the reaction stops when this composition is reached. In reaction (2) the resulting solution IP21 is constant but not invariant. This solution is not in equilibrium with kieserite. It continues to dissolve kieserite while forming huge amounts of kainite, without changing its composition. The composition will change only when either kieserite or sylvite or water are no longer available in the system. If kieserite is exhausted first, the composition of the solution will stay at point IP21. No further dissolution is possible. If sylvite is exhausted and kieserite exists in excess the composition will move to point IP19 and stay there; an invariant composition has been reached. No further dissolution is possible. If both sylvite and kieserite are available in unexhaustible quantities the reaction will continue until the entire water of the system is used up by the formation of kainite ($(KMgClSO_4)_4$*$11H_2O$).

The mass balance calculations show, that reaction (1) can lead to a doubling of the volume of the initialy intruding solution. 1m^3 intruding NaCl solution forms 1.92 m^3 IP19 solution. During the reaction 1.36 m^3 carnallite and 0.2 m^3 kieserite can be dissolved and 0.34 m^3 kainite will precipitate. In reaction (2) 1 m^3 NaCl solution can form 2.2 m^3 kainite by dissolving 0.96 m^3 sylvite and 1.22 m^3 kieserite. In this reaction theoretically all the water of the intruding solution can be used up as hydration water of the precipitated kainite.

These results show that for the safety assessment of a repository in salt formations it is necessary to understand the reaction types which can take place in detail. In one case 1 m^3 of intruding water leads to the formation of almost 2 m^3 of brine which can become contaminated and may leave the repository. In another case the water is completely used up and therefore a water intrusion doesn't present a major danger for the repository.

The combination of experimental in situ data and geochemical calculations based on Pitzer's ion interaction model and the HMW-database (Harvie *et al.*,1984) turned out to be a powerful tool for the understanding of the complex reactions in high saline brines.

References:
Harvie, C.E., Moller, N. Weare, J. H. (1984). Geochim. Cosmochim. Acta, **48**, 723-751.
Pitzer, K. S. (1973). J. Physical Chemistry, 77, 268-277.
Wolery, T.J. (1992): UCRL-MA-110662-PT-I, LLNL.

• QUANTUM MECHANICAL STUDIES OF MINERAL INTERFACES

Hess A.C. (*Solid State Theory Group, Molecular Sciences Research Center, Pacific Northwest Laboratory, Richland, U.S.A.*)

Although geological processes are often viewed on the macroscopic scale, the underlying chemistry is controlled by molecular scale phenomena. The study of atomic scale processes has traditionally been the realm of the chemical physics community which has employed computational quantum mechanics and molecular dynamics in conjunction with experimental spectroscopic and diffraction experiments to study microscopic phenomena Recent advances in quantum mechanical methods are allowing researchers to accurately describe chemical speciation, adsorption and chemical reactions occurring at the interfaces of geophysically important systems. Therefore, a brief description of the current state-of-the-art in atomic scale ab initio quantum mechanical methods will be presented.

In particular, the application of ab initio periodic Hartree-Fock theory and periodic gaussian basis density functional theory to the surface chemistry of several faces of MgO, CaO, Al_2O_3, ZnO and TiO_2 will be discussed. Attention will be focused upon the determination of the clean surface electronic and atomic geometric structure and morphology as well as the structure and energetics of several molecular species adsorbed on the external surfaces of these minerals. Comparisons to available experimental data will be made and conclusions drawn when warranted.

Viscosities of haplogranitic melts: Comparison of the effects of excess alkalies and alkaline earths.

Hess, K.-U., D.B. Dingwell and S.L. Webb (*Bayerisches Geoinstitut, Universität Bayreuth, 95440 Bayreuth, Germany)*

The addition of oxide components, such as the alkali and alkaline

earth oxides, in excess of the (alkali + alkaline earth)/aluminum ratio equal to 1 have a marked fluxing effect on the rheology of granitic liquids. These components are examples of a general observation that has lead to the description of excess alkalies/alkaline earths as network-modifying or depolymerizing agents in silicic melts.

The viscosities of granitic melts containing up to 20 wt.% addition of the alkali oxides (Cs_2O, Rb_2O, K_2O, Na_2O, Li_2O) and the alkaline earth oxides (BaO, SrO, CaO, MgO) have been determined in order to investigate in detail the relationship between depolymerization of these melts and their resultant viscosities. The high temperature viscosities have been determined using the concentric cylinder method whereas low temperature viscosities were determined using the micropenetration method. The combined datasets (high and low temperature viscosities) reveal the following trends. The excess alkali melts illustrate a strongly nonlinear decrease in viscosity at all temperatures. A molar comparison of their effects indicates that the alkalies behave very similarly. A slight variation is observed such that viscosity at a constant stoichiometry increases with alkali size. In contrast, the effects of the alkaline earths on the viscosity are complicated by an additional feature. The effect of the alkaline earths on viscosity is less than that of the alkalies. This is increasingly the case with reducing temperature. The effect becomes so extreme that at the lowest investigated temperatures, the viscosities of the alkaline earth bearing melts increase with decreasing cation size; the opposite of the trend observed for the alkalies. This contrast between the low temperature viscosities of the alkali- and alkaline earth-bearing granitic melts may result from the lower entropy associated with nonbridging oxygens in the alkaline earth-bearing melts.

TRANSITION MECHANISMS OF GRAPHITE TO DIAMOND UNDER SHOCK COMPRESSION

Hirai H., Kondo K., Kukino S., and Ohwada, T. (*Res. Lab. Engr. Matls. Tokyo Inst. of Technology*)

Transition mechanisms of graphite to diamond under shock compression is quite important for understanding carbon behavior under high-pressure, as well as diamond genesis in space. Diamond has been synthesized by both static and dynamic high-pressure techniques, however transition mechanism of graphite to diamond have not been resolved. Especially under shock compression, it has been a hot issue what mechanism controls the transition. Shock-induced phase transition occurs in nanosecond order, thus a martensitic (diffusionless) mechanism has been proposed to explain such rapid conversion (Decarli & Jamieson, 1961). While, reconstructive (diffusive) mechanism was also reported by high-temperature experiments using glassy carbon (e.g. Setaka & Sekikawa, 1981). Transition mechanism under inequilibrium condition such as shock compression strongly depends both on material parameters, namely crystallinity, crystallite size and microtexture of starting material, and on experimental parameters, namely loading duration and cooling rate. In this work, several kinds of graphitic materials, natural graphite, carbon black, glassy carbon and so on were selected and characterize in detail prior to shock compression. Developing a sample assembly, shock compressions were carried out. Cooling rate was estimated by one dimensional thermal diffusion equation. And, dependence of microtexture of the graphites and of cooling rate on the transition mechanism under shock compression was discussed.

References
Decarli, P.S. & Jamieson, J.C. (1961) Science, 133,1821.
Setaka, N. & Sekikawa Y. (1981) J. Mater. Sci. Lett. 16,1728.

Trace elements and isotopes in basalts as tracers of mantle evolution

A.W. Hofmann (Max-Planck-Inst. f. Chemie, 55020 Mainz, Germany)

Much of our knowledge about the deep interior of the Earth is derived from basalts. Mid ocean ridge basalts demonstrate that the upper mantle (above 660 km) has been depleted in incompatible elements, and that this depletion is complementary to the enrichment of the continental crust. However, the volume of depleted mantle exceeds that of the upper layer and the depleted elements in the upper mantle must be partially replenished from the lower mantle. A mechanism for this is the rise of plumes from the core-mantle boundary. The plume flux into the upper mantle must be limited to a few large plumes, so as to avoid complete mixing of the 2 layers. Smaller plumes presumably rise from the base of the upper mantle. All plumes contain recycled lithospheric material, traced by chemically fractionated components produced by near surface processes, i.e. melting, hydrothermal and sedimentary processes. No plume comes from a truly primordial reservoir. For example, the Hawaiian plume, which shows a trend toward an apparently primordial $\varepsilon(Nd) = 0$, as well as high, apparently primordial $^3He/^4He$ ratios, also contains constant Th/U = 3.0 and Nb/U = 50, with no correlation with either Nd or He isotopes and no trend toward primitive values of Th/U - 3.8 and 4.2 and Nb/U -30. In addition, $\delta^{18}O$ values of Hawaiian tholeiites are lower than primitive-mantle values of 5.5 to 6.0. Thus, if the Hawaiian plume is derived from the core-mantle boundary, its source was most likely created by the sinking of former lithosphere to the core-mantle boundary. When plumes rise from the lower mantle, their heads transfer lower-mantle material to the upper mantle and create continental flood basalts or large oceanic plateaus, which may be accreted onto existing continents and form juvenile continental crust. The conversion generates ultramafic differentiates, which are returned to the upper mantle and replenish its isotopic and incompatible element budget with lower-mantle material.

• IN SITU VIBRATIONAL SPECTROSCOPY OF MINERALS AND ITS RELEVANCE TO THE GEOSCIENCES

Hofmeister A.M. *(Dept. of Earth and Planetary Sciences, Washington University)*

Vibrational spectroscopy is a powerful tool for investigating the composition and thermal state of the Earth's interior, as well as to study the basic properties of materials. Determinations of the mantle's expansivity, compressibility, various T and P derivatives, and a reasonable approximation for the equation of state V(P,T). Establishing the geotherm requires additional information on the pressure and temperature dependence of thermodynamic properties such as heat capacity and entropy. *In situ* measurements of vibrational spectra can provide all of these variables using semi-empirical models developed by Brout (1959), Kieffer (1979) and Hofmeister (1991) and ambient condition measurements of V. Currently, infrared and Raman data can be collected at mantle pressures (100 GPa) from microsamples in a diamond anvil cell, and temperature measurements can be made of miscoscopic samples through absorption studies of macroscopic samples through reflectivity measurements. Correct interpretation of *in situ* spectra requires complete characterization at ambient conditions.

Recent research in our laboratory involves measurement of IR spectra of gases, phases in the $MgO–FeO–SiO_2$ system, and analogues as a function of pressure. Tridymite, perovskites and iron oxides have been measured at elevated temperatures. Current endeavors concern modification of the experiments to attain high temperatures during compression. Our work is coordinated with calorimetric experiments at high temperatures by P. Richet (IPG) and with Raman spectroscopic studies by A. Chopelas (Max Planck Inst., Mainz). These collaborations allow refinement of the thermodynamic models for sufficient accuracy (± 1%) to be useful under mantle conditions. This report focusses on examples of recent studies, applications of the results, and prospects for the future.

The SiO_2 polymorph tridymite undergoes multiple displacive transition with temperature. Symmetry analysis (Hofmeister *et al.*, 1992) can be used to predict allowed pathways. As the number of IR bands vary among the possible structures, IR spectroscopy as a

function of T can be used to ascertain space group. At room temperature, tridymite has roughly 16 IR bands, fat too few to be consistent with monoclinic or orthorhombic symmetries. At 220°C a transition to a structure with eight IR bands occurs. Above 450°C, the high tridymite structure $P3/mc2$ possesses seven IR modes. We propose that a hexagonal phase of tridymite ($P6_322$ with 8 IR bands) is stable from ~450 to 220°C, and that another phase exist from ~220 to 100°C ($R32$ with 19 IR bands). Assignment of different space groups through spectroscopy and crystallography can be attributed to differences in scale, in that diffraction may be affected by twinning, strain, and stacking disorder.

High pressure IR absorption measurements of β–$(Mg,Fe)_2SiO_4$ at ambient temperature show that OH is stable to 15 GPa (Cynn and Hofmeister, in review). The pressure dependencies of the near–IR water bands confirm that one hydroxyl is located on the bridging oxygen and is strongly hydrogen bonded and the other is located on the oxygen unattached to an Si and is not hydrogen bonded. The structural incorporation of hydrogen in wadsleyite suggests that this phase may be stable over a wider range of mantle conditions than previously supposed, and thus may be of greater proportions volumetrically than just the transition zone. The pressure dependence of the lattice models are close to those used by Chopelas (1991), and thus the thermodynamic quantities she derived are essentially correct.

Large (~20%) drops in vibrational frequencies of alkali halides at the transition of the B1 phase to B2 imply that the bulk modulus K_T *decreases* during transformation, due to the decrease in bond strength as ionic separation increases. Calculation of the $K_T(P)$ from the initial volume and the vibrational frequencies are in excellent agreement with previous determinations of the equation of state for NaCl–B1 and NaF–B1. For NaCl–B2, these calculations, with one measurement of volume, constrain V(P) and $K_T(P)$. After transformation at 32 GPa, K_T of NaCl–B2 is 117±3 GPa, 17.5±2.5% less than that of B1. Results derived for KCl, KBr and KI are similar such that parameters of their B2 phases are better constrained than those of B1, due to their large stability fields for B2. The compositional dependence of the changes in $K_T(P)$ and V derived from our data and from previous IR measurements of RbBr and RbI are compatible with a simple ball–and–spring model. The B1–B2 phase transition should not be unique: a decrease in K_T is expected for the rutile–fluorite transition.

Current and future work involves interfacing a CO_2 laser with our FTIR for the simultaneous generation of IR data at elevated P and T. This capability will allow inferences of space group and measurement of the P and T derivatives of C_P, S and K_T at mantle conditions.

THE PHYSICAL AND CHEMICAL PROPERTIES OF MINERALS WITH MODULAR CRYSTAL STRUCTURES

Hofmeister, W. (Institute for Gemstone Research, Idar-Oberstein, at the Johannes Gutenberg-University Mainz, Germany)

To describe certain crystal structures with means of modular constructions is not to have a more sophisticated way of structural characterization. Modular crystal structures are built as reactions on physico-chemical conditions during crystal growth using energetically alternative ways of structural freedom.

Prehnite, $Ca_2Al(Si_3AlO_{10})(OH)_2$, is a sheet silicate which crystallizes in two polymorphic forms with space groups P2cm and P2/n depening on the ordering scheme of Si and Al in tetrahedral voids (Baur et al., 1991). There is never a total order of Si and Al on the two tetrahedrally coordinated positions, maximum order amouts to a ratio of 80:20 for the two different sites. Different stacking of unit cell modules results in this distinct crystal chemistry and physical properties like piezoelectricity are induced in the same way, depending on the verification of maximal non isomorphic subgroups of the Pncm space group symmetry.

Topaz, $Al_2SiO_4(F,OH)_2$, is another mineral which is known to show anomalous optical and physical effects (piezo-/ pyroelectricity e.g.). It is usually known to crystallize in space group Pnma, which does not allow any of the sometimes observable electric charcteristics. The replacement of F by OH in the topaz structure reduces local symmetries and it can be shown, that a replacement ratio of 28.6 mol.% F by OH is an upper limit of normal, natural stability. Maximum observed replacement amounts to ca. 29 mol-% F by OH (Deer et al., 1982). The distinct chemistry, accompanied by distinct physical parameters is due to symmetry reduction by different stacking of principle structural modules.

Pumpellyite, $CaAlAl_2(SiO_4)(Si_2O_6OH)(O/(OH)_2)$ and the Fe^{3+} analogon julgoldite $CaFe^{3+}Fe^{3+}_2(SiO_4)(Si_2O_6OH)(O/(OH)_2)$ are isomorphic and chemically closely related. But they do not form a solid solution though their specific element contents are known to result in complete solid solution in other crystal structures. Chemical twinning of the same principle structural module results either in pumpellyite or julgoldite but in between the crystal structures of epidote $CaFe^{3+}Al_2(SiO_4)(Si_2O_7)(O/OH)$ or (clino)zoisite $CaAlAl_2(SiO_4)(Si_2O_7)(O/OH)$ are stabilized depending on the chemical supply (Hofmeister, 1990). Thus the typical pumpellyite-epidote paragenesis is copied by the julgoldite-(clino)zoisite paragenesis.

These few examples give more evidence of the powerfull concept of modular crystal structures. Certain topics of solid solution problems, chemical and physical characteristics, paragenesis and phase transitions are better understood and easily predicted.

References:

Baur, W. H., Joswig, W., Kassner, D. & Hofmeister, W. (1990). Prehnite: Structural Similarity of the Monoclinic and Orthorhombic Polymorphs and their Si/Al Ordering. J. Solid State Chem., **86**, 330-333.

Deer, W. A., Howie, R.A. & Zussman, J. (1982) Topaz. Rock-Forming Minerals / Orthosilicates, **1A**, 801-815.

Hofmeister, W. (1990). Kristallchemie und Pseudosymmetrie bei kohärent-polysynthetischer Verzwillingung von Archätypen zu mimetischen Kristallstrukturen. Habilitationsschrift Univ. Mainz.

RAPAKIVI FELDSPARS IN THE MOUNT SCOTT GRANITE, OKLAHOMA, U.S.A.

Hogan, J.P., Price, J.D. and **Gilbert, M.C.** (*School of Geology and Geophysics, Univ. of Oklahoma, Norman, OK 73019 U.S.A.*)

Recent work on the fine-grained Mount Scott sheet-granite indicates: 1) Rapakivi textures are widespread, and 2) these textures have significance in evolution of the granite not previously recognized.

In hand-sample, the A-type Cambrian Mount Scott Granite, of the Southern Oklahoma Aulacogen is readily recognized by the presence of dark-grey, and to a lessor extent buff-red, ovoid alkali feldspar phenocrysts ($\approx$4-8 mm) set in a finer-grained ($1 \leq$ mm) buff-red microgranite to granophyric matrix of predominantly alkali-feldspar and quartz. In thin-section, the dark-grey alkali-feldspar phenocrysts are exsolved antiperthites, whereas the buff-red alkali-feldspar phenocrysts are exsolved perthites. Both phenocrysts exhibit variable amounts of resorption. Angular subhedral crystals change to anhedral ovoid shapes apparently as the extent of resorption increases. The rim (0.05-0.8 mm in width) of optically-zoned plagioclase may be albite twinned. Rapakivi feldspars are overgrown by perthitic orthoclase with numerous quartz inclusions. Commonly, granophyric orthoclase and quartz nucleated on ovoid phenocrysts and grew outward to define the matrix.

Reconstructed feldspar compositions from microprobe analysis confirm the presence of three distinct alkali-feldspars. Ovoid antiperthites were anorthoclase ($\approx Or_{17}Ab_{74}An_9$), ovoid perthites were sanidine ($\approx Or_{45\text{-}64}Ab_{35\text{-}52}An_{0.5\text{-}3}$), and matrix perthites were also sanidine ($\approx Or_{56\text{-}72}Ab_{28\text{-}43}An_{0.1\text{-}1}$) but are consistently more potassic. Plagioclase rims of these rapakivi feldspars are sodic-oligoclase ($\approx Or_{0.5\text{-}4}Ab_{78\text{-}88}An_{8\text{-}17}$). The center of rims are An_{17} and contacts with core and with matrix alkali-feldspar are $An_{8\text{-}10}$. Magmatic plagioclase also occurs as distinct crystals. Texturally, some plagioclase crystals appear to have crystallized early, whereas others are distinctly late. Compositions of isolated plagioclase are similar to rapakivi rims

($\approx Or_{0.8-9}Ab_{79-94}An_{8-15}$). Two-feldspar geothermometry yields temperature estimates of ≈640°C. Our preliminary interpretation is that 640°C records the temperature at which grain-scale chemical reequilbration ceased. This suggests rapid cooling of this granite body, consistent with emplacement in a near-surface subvolcanic environment.

Textural evidence and geochemical data point to a complex crystallization history. Projection of normative compositions on to Q-Ab-Or ternary are consistent with magma generation at pressure of approximately 4 kb "dry" (a depth of ≈15 km) and a period of crystallization at 2 kb at a reduced H_2O activity of 0.5 (a depth of ≈8 km). Amphibole geobarometry also yields pressure estimates of ≈2 kb. Stratigraphic constraints indicate that late crystallization pressures were at near-surface conditions in the 500 bar range. Geophysical modelling of the crustal structure beneath the Southern Oklahoma Aulacogen suggests the top of an inferred mafic intrusion at a depth of 15 km. The Cambrian brittle-ductile transition as well as the basement-cover contact is modeled at 8 km. We suggest Mount Scott magma originated at ≈15 km. The inferred mafic intrusion at 15 km acted either as a source for the magma or as a heat source for partial melting of the crust. The magma then rose along crustal-scale fractures associated with rifting. Ascent of the magma was temporally arrested a depth of 8 km along the brittle-ductile transition and/or the basement-cover contact. During ponding, Mount Scott magma partially crystallized before it ascended *en masse* to its final emplacement level beneath a temporally equivalent extensive rhyolite volcanic pile.

We interpret the formation of rapakivi feldspars in the Mount Scott granite to be the result of decompression during magma ascent (e.g. Nevekasil, 1991) whereas microgranite to granophyric matrix records rapid crystallization at the emplacement level. Subsolidus reequilibration has to a limited extent modified the original magmatic chemistry and texture of feldspar crystals. However, through careful analysis of these crystals we are beginning to construct a more accurate representation of the crystallization history of this A-type granite.

GEOCHRONOLOGY AND GEOTHERMOBAROMETRY OF THE PREALPINE CRYSTALLINE BASEMENT IN THE ÖTZTAL ALPS (AUSTRIA)

Hoinkes G., Thöni M., Bernhard F., Kaindl R., Lichem Ch., Tropper P. (*Inst. of Mineralogy and Petrology, Univ. of Graz*)

A five-year research programme (S47) dealing with the prealpine evolution of crustal rocks in Austria was carried out from 1988 to 1993 with the financial aid of the Austrian Science Foundation to decipher the magmatic and metamorphic evolution of the Austro-alpine Ötztal crystalline basement (S4705). Based on geochemical data of the metaigneous rocks, Rb-Sr- and Sm-Nd-ages of the metaigneous and metasedimentary rocks and geothermobarometry of metapelites the following picture of the geological evolution of the Ötztal basement may be derived:

(1) The protolith of the most wide-spread rock types, the metapelitic-and-psamitic gneisses and schists, is of proterozoic age. Sm-Nd-analyses of garnet-staurolite-Al_2SiO_5-rich micaschists yield nearly concordant T_{DM}^{Nd}-ages of 1.57 to 1.70 Ga.

(2) The oldest magmatic ages of 520 to 580 Ma are measured on basic to intermediate metaigneous rocks (gabbros, diorites, tonalites).

(3) Metagranitoids predominately show geochemical crustal signature with a few exceptions of small metagranite bodies associated with metabasites.
Based on Sm-Nd-whole rock ages and zircon-evaporation data the time-span of acid magma crystallization is thought to be between 480 and 515 Ma.

(4) The numerous Rb-Sr-whole rock ages from the literature and our work around 430 and 450 Ma are thought to indicate a caledonian metamorphic event. This interpretation is supported by Rb-Sr-muscovite ages of up to 460 Ma from migmatites.

(5) Gabbros from the central Ötztal eclogite zone - yielding the older magmatic ages of 520 - 530 Ma - were almost completely metamorphosed to eclogites and subsequently to amphibolites. Garnet-clinopyroxene whole rock Sm-Nd-isochrones from the eclogites yield variscan ages of 373 - 343 Ma probably dating an early variscan high pressure event.

(6) Sm-Nd-ages of garnets from metapelites range between 343 and 331 Ma and probably date the temperature climax of the variscan metamorphic cycle.

(7) A clockwise variscan PT-loop is reconstructed by geothermobarometric methods including relative geothermobarometry of zoned garnets (Gibbs' method) and thermobarometry with equilibrium implications (TWEEQU) of the KFMASH-assemblages in equilibrium with garnet rims. TWEEQU implies a chemical equilibration of 620° C and 6 - 7 kbar whereas the proceeding of high pressure metamorphism during which garnet cores were formed in the range of 10 - 12 kbar.
From the eclogites, however, a much higher pressure of about 20 kbar was derived by Miller (pers. com). The retrograde variscan P-T-path is well constrained by spectacular garnet breakdown textures of spherical fibrolite and biotite intergrowth and by a textural crystallisation sequence of the Al_2SiO_5-polymorphs from early kyanite to subsequent sillimanite and late andalusite formation.

A RE-EXAMINATION OF THE MUSCOVITE-ALMANDINE-BIOTITE-SILLIMANITE GEOBAROMOMETER

Holdaway M.J., Mukhopadhyay B., (Dept. Geol. Sci., SMU), Dyar M.D. (Dept. Geol. & Astron.,West-Chester Univ.), Guidotti C.V. (Dept. Geol. Sci., Univ. Maine), Dutrow B.L. (Dept. Geol. & Geophys., LSU).

The muscovite-almandine-biotite-sillimanite (MABS) geobarometer, most recently calibrated by McMullin et al. (1991), has potential as a geobarometer for medium-grade pelitic metamorphic rocks. However, calibrations to date have not been entirely satisfactory.

The calibration of McMullin et al. (1991) uses an annite activity model that produces unrealistically low ideal activities and compensates for these low activities with estimated Margules parameters involving Mg and Fe with Al and Ti in biotite. We have examined activity models for annite. Whereas a number of activity models are theoretically possible, most of them produce similar activity values. We believe that the best model is:

$$X_K \, X_{Fe}{}^3 \, X_{OH}{}^{\alpha}$$

In this model, all Fe^{3+} resides in octahedral sites. X_K = K/(K + Na + ❑), X_{Fe} = Fe^{2+}/(Fe^{2+} + Mg + Mn + Ti + Fe^{3+} + Al^{vi} + ❑) equivalent to Fe^{2+}/3, X_{OH} = OH/(OH + F), and α = OH + F. Vacancies in the twelve-fold site may well be H_3O^+. Substitution of O for OH and tetrahedral solid solution are considered to be coupled to octahedral 3+ and 4+ site occupancy. Other activity models for annite are also being tested.

The preferred activity model for muscovite is:

$$X_K \, X_{Al}{}^2 \, X_{❑} \, X_{OH}{}^{\alpha}$$

In this model X_K = K/(K + Na + ❑), X_{Al} = Al^{vi}/2, $X_{❑}$ = ❑.

When these activity models are used in conjunction with the end-member thermodynamic properties of Berman (1988) and McMullin et al. (1991) and the garnet model of Berman (1990) the calibration yields unrealistically high pressure (2-3 kbar high) for a suite of 49 muscovite-garnet-biotite-Al silicate- (sillimanite or andalusite) bearing pelitic metamorphic rocks from west-central Maine, USA. For these

rocks, we have either determined or estimated by grade Fe^{3+}, H_2O, and E in biotite and muscovite.

McMullin et al. (1991) used three different suites of assemblages to calibrate this geobarometer. Each suite comprised a limited number of samples, and one of the suites was from the Maine rocks discussed above. These authors obtained empirical fit parameters which they used as Margules parameters for quaternary Fe^{2+}-Mg-Al-Ti biotite solid solution. When we use the activity model described above, in conjunction with an improved set of a-X parameters for quaternary Ca-Mg-Fe^{2+}-Mn garnets (Mukhopadhyay et al.,this volume) the need for Margules parameters is reduced. We used W_{FeAl} = 64 kJ, W_{MgAl} = 73 kJ, consistent with our garnet-biotite geothermometer. It was necessary to make small adjustments in ΔH_f° for annite (-5139 kJ/mole), and almandine (-5170 kJ/mole). These values are in good agreement with those obtained by Robie et al. (1978) and Harlow and Newton (1992). These enthalpy values do not violate the Ferry-Spear experimental data, which yields ΔH of the Fe-Mg exchange reaction as $+48.0 \pm 6$ kJ when corrected flor non-ideality in Fe-Mg garnet.

References:
Berman, R.G. (1988) J. Petrol., **29**, 445-522.
Berman, R.G. (1990) Am. Mineral., **75**, 328-344.
McMullin, D.W.A., Berman, R.G., & Greenwood, H.J. (1991) Can. Mineral., **29**, 889-908.
Harlow, D.E., & Newton, R.C. (1992) Am. Mineral., **77**, 558-564.
Robie, R.A., Hemingway, B.S., & Fisher, J.R. (1978) USGS Bull. **1452**.

A PETROGENETIC GRID APPROACH TO GEOTHERMOMETRY AND GEOBAROMETRY

Holland, TJB (Dept Earth Sciences, University of Cambridge) and
Powell, R (Dept Geology, University of Melbourne)

Geothermometry/geobarometry, in which the mineral compositions for some presumed preserved equilibrium mineral assemblage in a rock are substituted into many mineral equilibria in order to calculate pressure and temperature, rarely provides all the pressure-temperature information available in a rock. In particular, the path to and from the metamorphic peak is critical from the point of understanding orogeny. Information relating to the path commonly occurs in mineral assemblage changes, mineral and mineral mode changes, which can be deduced from the petrography and mineral chemistry. These chemical and textural changes in the rock can be compared with the equivalent changes as predicted from the thermodynamic modelling. Whereas conventional geothermometry/barometry just gives a point on the pressure- temperature path, using calculated petrogenetic grids is capable of providing path information. With the software, THERMOCALC, the calculation of such petrogenetic grids for systems which approximate those of rocks is a rapid and relatively simple task. The use of this approach is illustrated with examples of rocks from well-studied terrains.

ORDER-DISORDER MODELS FOR COMPLEX MINERALS

Holland, TJB (Dept Earth Sciences, University of Cambridge) and
Powell, R (Dept Geology, University of Melbourne)

The lack of effective models for order-disorder in complex silicates is an important limiting factor in performing reliable calculations of mineral equilibria for application to rocks. Models need to be sufficently flexible so that a wide range of behaviour is possible, but should not involve too many adjustable parameters as there are insufficient data for most minerals to determine them. New results will be presented comparing the applicability of Landau theory with nearest neighbour approximations to various rock-forming minerals. Particular emphasis is placed on being able to handle non-ideal multicomponent solid-solutions efficiently. We show that a fictive end-member approach is a powerful way of approaching the modelling, allowing the easy incorporation of the end-members of minerals involving order-disorder into internally-consistent thermodynamic datasets, as well as into the calculation framework of software such as THERMOCALC.

OPTICAL ABSORPTION STUDY OF TERRESTRIAL HIBONITE

Holtstam D. (*Swedish Museum of Natural History*)

Hibonite, $CaAl_{12}O_{19}$, belonging to the hexagonal magnetoplumbite (M) structure type, is a rare mineral found in both cosmic and terrestrial rocks. Whereas meteoritic hibonites often are dichroic in orange or blue, the variety from the type locality at Esiva, Madagascar has *O* pale brown and *E* grey. Electron microprobe analyses and polarized optical absorption spectroscopy data in the range from 300 to 2200 nm have been obtained on Madagascan hibonite.

The major impurities are Ti (0.62 apfu), Mg (0.56 apfu), Fe (0.34 apfu) and REE (0.10 apfu). The E⊥c spectrum can be resolved into three broad (FWHM~6000 cm^{-1}) bands at 21 900, 18 000 and 12 900 cm^{-1}. The former two are assigned to $Fe^{2+} \rightarrow Ti^{4+}$ intervalence charge transfer (IVCT), whereas the low-energy band is likely to result from $Fe^{2+} \rightarrow Fe^{3+}$ transitions. In the E$\|$c spectrum the presence of several broad, unresolved bands is indicated.

The crystal structure (*e.g.*, Utsunomiya *et al.*, 1988) contains five unique Al sites: three with octahedral, one with tetrahedral and one with trigonal bipyramidal (5-fold) coordination. IVCT can *a priori* be assumed to occur between face-sharing Al(4)-Al(4) or edge-sharing Al(5)-Al(5) and Al(1)-Al(5) octahedra, respectively. The polarization of the bands clearly indicates that at least two of the types are involved.

Optical measurement under high pressure (47 kbar) in the diamond-anvil cell show enhancement of the intensities of the bands by 30 to 60%, but no significant shift in energy.

A narrow (FWHM=2000 cm^{-1}) band centered at 5400 cm^{-1}, present in both principal vibration directions, is attributed to spin-allowed *d-d* transitions of Fe^{2+} at the tetrahedral site. Concentration of divalent ionic species into this site is in accordance with predictions based on electrostatic calculations for the structure type.

Reference:
Utsunomiya, A., Tanaka, K., Morikawa, H., Marumo, F., Kojima, H. (1988). *J. Solid. State Chem.* 75, 197-200.

IDENTIFYING INORGANIC PHASES WITH QUANTITATIVE ANALYSIS DATA AND A CHEMICAL CLASSIFICATION SYSTEM FOR INORGANIC COMPOUNDS

Hölzel, A.R. *(Systematik in der Mineralogie)*

A new and safe search strategy uses the sum of oxides or elements for related groups. A crystal-chemical search-algorithm solves the problem of solid solution series. The idea behind this grouping method is that a search is not conducted for individual elements, but for groups of elements. Elements are grouped according to the size of cations or related anions, in the same manner in which they are grouped in the chemical formula. A mineral database provides for the quantitative analysis with singular fields and fields for groups.

Singular fields: SiO_2, H_2O, CO_2, B_2O_3, RE_2O_3(sum of RE-oxides), Halogenides, and Pt-group elements (PLT).

Additional fields for the groups:

SL / SF	sum of S, Se, Te oxides / elements
AT / AE	sum of P, As, Sb, V oxides / elements
LS / LE	sum of large-sized cation oxides / elements
MS / ME	sum of medium-sized cation oxides /elements
ES	sum of SL, AT, LS, MS, I_2O_5, GeO_2, SiO_2
EE	sum of PLT, SF, AE, LE, ME, Cl, Br, I, Ge, Si

The light elements and their oxides, etc. (of Li, Be, N and F) are not included in this scheme.

This grouping strategy is realized not only in a database, but also in a standalone program. This program makes possible an automatic search with a batch file, for example with the results of an ICP analysis. It is also possible to combine the results of chemical analysis with X-ray data.

Data for Mullite: SiO_2 29.0, Al_2O_3 69.6, TiO_2 0.8, Na_2O 0.2, K_2O 0.1, and the strongest X-ray lines: 3.39, 3.428 and 2.206

Run	Element	%	Range	Range	Hits
1.	Si	(29.0)	± 5	'qualitative search'	1058
2.	Al	(69.6)	± 5	'qualitative search'	451
3.	SiO_2	29.0	± 5	from 24 to 34 %	104
4.	MS	70.6	± 5	from 65 to 75 %	6
5.	ES	99.7	± 5	from 94 to 99 %	4
6.	X-ray	3.39	± 2	from 3.32 to 3.45	3
7.	X-ray	3.43	± 2	from 3.36 to 3.49	2
8.	X-ray	2.21	± 2	from 2.17 to 2.25	1

Result: 4 hits by chemical and 1 hit together with X-ray data!

This search scheme with the automatic working program is primary build for minerals. The database is expandable for all inorganic compounds by using an adapted classification system, or the chemical composition.

This classification system will perform the searches to defined compounds, to substance classes and for the identification by using quantitative chemical analysis data. This system follows the periodic classification of the elements. It is subgrouped according to their ionic-radii and chemical behavior.

It is possible to take any chemical compound into the presented classes. NaCl is consequently classified into 1Ac and 7A. A further refinement uses the atom-% to expand these classes. The complete classification for NaCl with the atom-% is " 1Ac 50.0, 7A 50.0".

The search with these classes will collect all alkalihalogenides with alkali/halogene ratios equal 1:1. A further selection with Na and Cl narrows the result down to NaCl and related halogenides.

1Aa:	H D T	1Ab:	Li	1Ac:	Na K Rb Cs
2Aa:	Be	2Ab:	Mg	2Ac:	Ca Sr Ba Ra
3Aa:	B	3Ab:	Al Ga In	3Ac:	Tl
4Aa:	C	4Ab:	Si Ge	4Ac:	Sn Pb
5Aa:	N	5Ab:	P As Sb Bi	6Aa:	O
6Ab:	S Se Te Po	7A:	F Cl Br I	8A :	Ar Kr Xe
1B:	Cu Ag Au	2B :	Zn Cd Hg	3Ba:	Sc Y La - Lu
3Bb:	Ac - Cf	4B:	Ti Zr Hf	5B :	V Nb Ta
6B:	Cr Mo W	7B :	Mn Tc Re	8Ba:	Fe Co Ni
8Bb:	Ru Rh Pd Os Ir Pt				
GLE:	1Ac 2Ac Tl Pb Ag Au Cd Hg Y, La-Lu, 3Bb				
GME:	2Ab 3Ab Sn Cu Zn Sc 4B Nb Ta 6B 7B 8Ba 8Bb				
GEE:	GLE GME 4Ab 5Ab 6Ab Cl Br I V				

Not included in GEE: H (D T) Li Be B C N O F and noble gases.

A further subclassification is using "GLE and GME" to differ the cations into two classes. This by their cation-radii, GLE for the large, GME for the medium to small radii. A selection to compounds with similar cationradii is possible in this way, also a search to solid solution series. GEE contains all elements detectable using a microprobe.

$Me[XO_4]\cdot 6H_2O$ (Me=Mg, Cu, Zn, Mn, Fe, Co, Ni; X=S, Se, Te) is classified on the base of 24 atoms to:
1Aa 50.0, 6Aa 41.7, 6Ab 4.2, (2Aa 1B 2B 7B 8Ba) 4.2 and GME 4.2, GEE 8.3. It is possible to collect the whole class directly with "GME 4.2" instead of 2Aa etc.

USE OF Sr-ISOTOPIC SIGNATURES FOR HABITAT DETERMINATION ON A FOSSILS STAG'S MANDIBLE FROM THE SITE OF HOMO ERECTUS HEIDELBERGENSIS

Hölzl S.*, Horn P.* and Storzer D.** (* *Min.-Petr. Inst., Univ. Munich, Germany,* ** *Mus. Nation. d'Hist. Nat., Paris, France*)

We report a pilot study to an investigation aimed at identifying the habitat of *Homo erectus heidelbergensis* (*H.e.h.*) by using the Sr isotopic ratio as tracer.

The idea was to compare Sr isotopic signatures in bone dentine and tooth enamel (in this case from a stag found in the very same stratum at Grafenrain/Mauer, Germany as the mandible of *H.e.h.*) with those of the bedrock units (hence soils and, inherently, plants grown thereupon) from potential habitats, in order to identify the predominant grazing area of the animal.

The applicability of the method requires that the potential habitats of then living animals show differing Sr isotope signatures.

In the case of *H.e.h.* respective the fossil stag's mandible we were faced with the splendid situation that the excavation site is situated at the junction of regions with rather different lithologies and $^{87}Sr/^{86}Sr$ isotopic ratios: Muschelkalk: 0.708, Keuper: 0.71-0.72, Buntsandstein: 0.72-0.74 and Basement: 0.75-0.90.

A further condition is that Sr isotope exchange processes (sediment/tissue) did not completely erase the original isotope signature. To prove that and in order to find a remainder of the original Sr isotope signatures we applied (beside bulk analyses) a crafty and laborious sample treatment of stepwise mechanical and chemical cleaning and etching.

As can be seen from the $^{87}Sr/^{86}Sr$ release pattern it was possible to isolate sites (phases?) from the enamel of the stag's tooth which did exchange Sr with the sediment (0.7094-0.7118) and those which clearly did not. This material has a $^{87}Sr/^{86}Sr$ ratio of 0.7208, that must be attributed to Buntsandstein (New Red Sandstone of Lower German Triassic) excluding other potential habitats from the wider area.

Independent proof for almost no cation exchange in enamel we get from uranium radiography.

CARPATHIAN ARC MESOZOIC OPHIOLITES: PETROLOGY AND GEOCHEMISTRY

Hovorka D. (*Faculty of Natural Sciences, Comenius University, Bratislava, Slovak republic*)

During late Cretaceous and Tertiary principal reconstruction of Cenozoic as well as Palaeozoic in Carpathians took place. One of the most topical geological problems is the reconstruction of the type and geodynamic setting of the ophiolites. Based on the field and laboratory studies, an attempt to sum up the whole set of available/original data is presented.

Within the Mesozoic terranes in the area under consideration 3 main magmatic rock-sequences originated: a) calc-alkaline volcanics, b) alkaline volcanics, c) ophiolites. Petrological and geochemical problems of the ophiolites will be discussed in the following.

Basal members of a completely developed ophiolite complex, e. g. spinel peridotites and their serpentinized derivatives are known to be present in the form of serpentinite mélanges: the Meliata-Rudabanya Unit in the Western Carpathians (Upper Triassic in age), Transylvanian nappes in the Eastern Carpathians, the Severin nappe in the Southern Carpathians. The Jurassic age of both is the most probable. Gabro and plagioclase peridotite bodies known from the Szarvaskö complex (the Bükk Mts., Hungary) as well as similar bodies from the southern Apuseni Mts. (the "Mures ophiolites", Romania) have pronouncedly tholeiitic character and should be attributed to the level of ophiolite cumulates. Among the relics of the ophiolite complexes, volcanic members of tholeiitic affinity are the most widespread. They are known to occur in the Meliata-Rudabanya unit, The Szarvaskö complex, the Darnó Hills occurences (both N. Hungary). Numerous fragments of tholeiitic volcanics (together with gabbroids and radiolarites) are known to occur in several tectonic units in the Eastern Carpathians (territories of the Ukraine and Romania). Based on tholeiitic volcanics pebbles occurences in Lower Cretaceous conglomerates, it can be supposed that they are most probably Triassic-Jurassic in age.

As one of the evidences of the oceanic crust consumption, the known occurrences (the Meliata-Rudabanya unit, the "black flysch" of the Transylvanian nappes) of the blueschists should be used.

No complete ophiolite complex (in the Coleman's 1977 definition) is present in the Carpathians. Known tectoniccaly dismembered ophiolite developed in Triassic-Jurassic time-span. Close spatial association of calc-alkaline volcanics with ophiolites in the southern Apuseni Mts. (Romania) are in favour rank them among "island arc ophiolites".

ISOFERROPLATINUM IN A PLATINUM-GOLD PLACER FROM NORTHWESTERN CHINA

Huang Dianhao, Chen Keqiao, Wu Chengyu and Yu Shimei (*Institute of Mineral Deposits, Chines Academy of Geological Sciences, Beijing 100037*)

Isoferroplatinum was identified among several platinum group elements (PGE) minerals from an alluvial-diluvial platinum-gold

placer related to chrome-bearing ultrabasic rocks in the Qilian Mountains, Northwestern China. The mineral is shaped as rounded grains or platy grains (0.6–1.8 mm), with bright yellowish white reflection color and isotropic optical feature under reflected light microscope. Microprobe analysis yields 90.48–91.56% Pt and 8.56–9.10% Fe, with the molecular formula of $Pt_{2.85-3.00}Fe$. X-ray powder diffraction analysis of two samples measured by Gandolfi camera gives the following lines: sample N. 2, 2.230(8), 1.931(10), 1.366(7), 1.165(10), 1.115(5), and sample N. 6, 2.233(10), 1.934(4), 1.367(7), 1.166(9), 1.117(5). The a_0 values were determined as 3.863±0.001Å (N. 2) and 3.868±0.003Å (N. 6), with unit-cell volume of 57.63±0.04Å^3 and 57.90±0.10Å^3, respectively. These data are consistent with those of the natural and synthetic isoferroplatinum documented by Cabri et al. (1975). The studied isoferroplatinum is associated with native gold, osmium, iridosmium and chromite. This assemblage provides a valuable indicator for prospecting primary PGE ores in the area.

THE MINERAL ASSEMBLAGES AND THE P-T-t PATH OF GRANULITIC IRON-FORMATION IN LAIHE, CHINA

Huang W.K., Wang M.Z. and Gong G.H. (*Guangzhou Institute of Geochemistry, Academia Sinica*)

Two mineral assemblages in Laihe iron-formation, Laioning province are as follows: (1) eulite(Fs_{87}) + hedenbergite + quarts+ magnetite + laihunite. (2) grunerite + ferro-edenite hornblende+ quartz+ magnetite+ carbonite+ Fe-jimthompsonite. Both "100" and "001" lamellae of eulite in hedenbergite appearred and the "001" lamellae were turned from the pigeonites. Therefore, there were continuous stages during the forming of pyroxenes: (a) Opx_I-Cpx_I(homogeneous facies), (b) Opx-Cpx-Pig(lamella), (c) Opx_{II}-Cpx_{II}(both with lamellae). Accoridng to H. W. Jaffe's diagram(1978) and the geothomometer, the Opx_{II}-Cpx_{II} is formed at 740°C and 7-7.8 x10^{8}pa, the Opx-Cpx-Pig at 820°C and 8x10^{8}pa, and the Opx_I-Cpx_I at 800.5-815.9°C whill assuming the lamella content for a percentage of 4-8. Compared with the pressure of 13x10^{8}pa of Archaean terrenes having laihunite in Qianan and the subsolidus phase related to pyroxenes, it is plausible to presume that the pressure for Opx_I-Cpx_I is 11-13x10^8 pa. Therefore, an *ITD* type of P-T-t path for granulite iron-formation in Laihe would be constructed. It might represent the tectonic environment of old basement, which was unconformably covered by the granite-greestone terrene in Laioning province.

The homogeneous laihunite(without the relict minerals) did not contected with quartz immediately, between them a rim of eulite and hendenbergite existed. It is suggested that the laihunite might be formed at the same condition of granulite facies with T>742°C and P>7-7.8x10^{8}pa.

References:
Jaffe,H.W.(1978). *Am.Mineral.*, 63 ,1116-1136.

STUDY OF CATION EXCHANGE IN THE EARLY STAGES OF A MONTMORILLONITE LONGEVITY EXPERIMENT: MODELLIZATION AND TEMPERATURE EFFECT

Huertas F.J., Cuadros J. and Linares J. (*Estación Experimental del Zaidín, CSIC, Granada, Spain*)

Introduction. Bentonites are being investigated to be used as a barrier in Nuclear Waste Disposals. One of the main problems of these materials is their conversion into illite. The first step of this transformation is the K adsorption in the smectite interlayer, which severely influences the transformation rate. Our data correspond to the shorter runs of experiments on montmorillonite illitization at different temperature and K concentration conditions. So, they only deal with ion exchange. Data on temperature effect on cation exchange in smectites existing in literature cover the range up to 40-50°C, and conclude that it is hardly appreciable.

Experimental. The fraction <20 μm of a bentonitic material (97% smectite) from Cabo de Gata (Almería, SE Spain) was treated under all combinations of the following conditions: 60, 120, 175, 200°C; 0.025, 0.05, 0.1, 0.3, 0.5, 1 M in KCl concentration; 1, 5, 15 days. The solid and solution run products were analysed for K, Na, Mg and Ca, and the CEC was independently determined.

Results and discussion. The only process observed was K exchange for the original cations (Ca, Mg, Na). As it was expected, equilibrium was attained in the exchange raeaction even at the shortest run time.

No temperature effect could be detected on the exchange isotherms. The calculations made to describe and modellize the exchange reaction also showed that temperature was not relevant, though the temperature range of the experiments was so wide.

The study of the exchange isotherms revealed the presence of two consecutive steps in the overall exchange as K concentration increased. First, Na was extensively removed (~63% of Na equivalent fraction) without appreciable remotion of Ca and Mg. During the second step Ca and Mg were also exchanged. Since Ca and Mg showed the same behaviour, Ca+Mg data were used in all calculations (Garrels & Tardy, 1982). As the experiments were closed systems, the ion exchange was not complete. The steps were described by means of a simple Langmuir equation. It was found that the second step began at a K concentration in the solution of 0.018 M.

The overall exchange process was modellized using a combination of Langmuir-type terms (Sposito, 1982):

$$X_{ad} = X_{in} + \sum_n \frac{A_n C_n}{1 + A_n C_n}$$

X_{ad} is the equivalent fraction of the adsorbed K, X_{in} is the equivalent fraction of K initially present in the smectite, A_n is an experimental parameter different for each ion, and C_n is the concentration of each ion in solution (eq/l). This model accurately fitted the experimental data. A_n presented the following values for each cation: K 11, Ca+Mg 0.18, Na 10^{-16}. This expression has a direct physic meaning. It can be used to describe heterovalent, poliionic exchange reactions, whose rigurous thermodynamic study is complex for theoretical and experimental reasons (Goulding, 1983).

This study show that Na is readily displaced by K even at very low K concentrations. Nevertheless, Ca and Mg are more energetically adsorbed in the smectie interlayer and are only displaced at high K concentrations. Bentonites containing Ca and Mg should be used as barrier in Nuclear Waste Disposals in order to prevent K entrance in the interlayer, which is the first stage of its transformation into illite.

References:
Garrels, R.M. & Tardy, Y. (1982). *Developments in Sedimentology*, vol. **35**, 423-450.
Sposito, G. (1982). *Soil Sci. Soc. Am. J.*, **46**, 1147-1152.
Goulding, K.W.T. (1983). *Advances in Agronomy*, **36**, 215-264.

COMPRESSION OF (Mg,Fe)SiO_3 ORTHOPYROXENES

Hugh-Jones D.A. (*Dept. Geological Sciences, University College London*) and Angel R.J. (*Bayerisches Geoinstitut, Bayreuth*)

Orthopyroxenes across the enstatite-ferrosilite join were compressed to 8.5 GPa in a diamond anvil cell and unit cell parameters and structures were determined using single crystal

X-ray diffraction techniques. Equations of state (EOS's) were calculated from the data for all pyroxene compositions studied.

The volume variation with pressure (to 8.5 GPa) of pure $MgSiO_3$ orthoenstatite shows a discontinuous break at ~4 GPa, with both parts of the EOS exhibiting very different values of K_T and K'. Structural data shows that this discontinuity corresponds to a change in compression mechanism of the orthoenstatite: below ~4 GPa the silicate tetrahedra are essentially incompressible, whereas above this pressure the Si-O bonds shorten with no associated distortion of the tetrahedra. This abrupt change in compressibility is accompanied by a discontinuous change in the rate of kinking of the chains, and the degree of tilt of the tetrahedra from the (100) plane.

A compressibility study on a $(Mg_{0.6}Fe_{0.4}SiO_3)$ orthopyroxene reveals that its EOS also displays a discontinuous break corresponding to a change in compression mechanism. In this case, the break in the EOS occurs at ~3 GPa, and the nature of the change in the rate of tilting of the tetrahedra and kinking of the chains is different to that observed in pure $MgSiO_3$.

High pressure experiments on orthoferrosilite ($FeSiO_3$) are still in progress and it appears highly likely that a similar change in compression mechanism will occur at an even lower pressure. Compression of natural orthopyroxene crystals show that the effect of the presence of calcium is to smear out the break in the EOS causing it to appear continuous to ~6 GPa.

THE MICROMOUNT MINERAL COLLECTIONS AT THE DENVER MUSEUM OF NATURAL HISTORY

Hurlbut J.F. (Dept. Earth Sciences Denver Museum of Natural History)

This historical collection is made up of the gifts of two major collections. The largest and more famous being the gift of Paul and Hilde Seel. This collection of over 10,000 items gathered from all over the world contains many specimens that were collected in the 1920's and 1930's. Many specimens were collected at type localities. Some of these famous localities are no longer available for collecting, making this collection of great value for further study. The fact that most minerals in the collection have several specimens from the same location increases the possible study value.

Lists of the minerals, by country, and type locations are available to researchers. Requests to study specimens will be considered.

METAMORPHIC EVOLUTION OF THE ECLOGITIC ROCKS IN A PRE-ALPINE COLLISIONAL BELT IN THE SOUTH CARPATHIANS, ROMANIA

Iancu V.[1], Johan V.[2], Maruntiu M.[1], Ledru P.[2] ([1] *Inst. of Geol. and Geophys., Bucharest, Romania;* [2] *BRGM, Orléans, France*)

Eclogitic rocks are present in the pre-Alpine nappe stack situated in the basment of the South Carpathians; they are encountred in some litho-tectonic entities or are directly related to deep-seated shear zones.

Taking into account petrographical and structural data, lithologic or structural control, type of metamorphic evolution and nature of associated protoliths, four types of eclogitic rocks have been distinguished.

a. Eclogites as infracrustal tectonic lenses with retrograde type evolution in the Sebes Group are associated with HP granulites and garnet lherzolites. The paragenetic association of the eclogitic stage is Cpx + Grt + Ky + Amp + Zo + Ru. Cpx inclusions in Grt show a core with Jd_{24-25} and a corona with Jd_{18-22}; Cpx in the matrix is Jd_{26}. Garnet composition is variable from core (Py_{44}) to rim (Py_{51}). A decompression stage is indicated by destabilisation of jadeitic Cpx to Di + Pl symplectites and Sp + An , Cor + Pl in kyanite coronas in the associated banded rocks. Amphibolitic facies re-equilibration yielded zoned Amp + Pl (An_{49-60}) and muscovite. Structural and mineral proofs point out to M_1 and M_2 retrogression in MP and locally LP conditions together with the crustal-supracrustal, continental type rock assemblages.

b. Eclogite nuclei dispersed in the Cumpana Group are associated with granulitic facies rocks and augen gneisses in a polymetamorphic migmatitic complex. Their eclogitic parageneses are represented by Omp(Jd_{38-42}) + Grt (Py_{42-46}) + Ky +Winchite + Ru + Zo + Qt. An decompressive event is marked by Cpx (Jd_{15}) + Pl(An_{21}) symplectites, coronitic textures (Sp+Pl) around Ky, followed by an amphibolitic facies retrogression with Amp + Pl + Bi. There are prograde, unequilibrated high-grade rocks (mafic - ultramafic, felsic) intimately associated, suggesting an initially prograde evolution, before retrogression.

c. In ocean-like crustal rocks of the Lotru Group, the retrogressed eclogites are associated with garnet-bearing metagabbros and peridotitic rocks with well-preserved magmatic textures. The garnet with inclusions of Amp and Pl(An_{19-25}) shows a zonal distribution of pyrope content from core (Py_{19}) to rim (Py_{27}). In the matrix, Di + Pl(An_{30}) are intimately associated in equillibrated aggregates while around the garnet the coronas of pargasitic Hb + Pl(An_{61-42}) develop. Phase relations reflect a retrograde reequilibration under amphibolite facies conditions during orogenic uplift.

d. Eclogitic rocks with well-developed tectonitic facies (high-grade mylonites) in the Leaota Mts. exhibit a direct structural control to deep-seated shear zones. They are related to white micaschists, metagabbros and metagranites containing prograde granulitic parageneses. Some differences in mineral chemistry are related to whole rock composition. Eclogitic paragenesis in Mg-protoliths is Grt + Omp(Jd_{41-46}) + Amp(Win) + Ky + Ru + Phen + Zo. Pyrope contents of the garnet vary from 25 in the core to 36 in the rim. In ferrous protoliths, pyrope contents of zoned garnet are 12 (core)-16 (rim), Cpx I is Jd_{39} and Cpx II (Jd_{14-24}) forms symplectites with Pl (An_{3-10}). Amphibole inclusions in garnet consist of feroan pargasite, zoned amphibole in the matrix is Mg-taramite (core) and EdHb (rim). Superimposed amphibolite to greenschist facies parageneses may also occur.

MINERALOGICAL, TEXTURAL AND STABLE ISOTOPE STUDIES OF THE CARMINA ZINC-LEAD STRATIFORM DEPOSIT (THE DEMANDA MOUNTAIN RANGE, SPAIN)

Ibáñez J. A., Velasco F. and Pesquera A. (Dep. of Miner. and Petrol., Univ. País Vasco)

The Carmina deposit is a deformed sediment hosted zinc-lead deposit that occurs in the Upper Cambrian of Demanda Mountain Range This massif is located between Burgos and La Rioja provinces at the north of Spain, and it is regarded as the connection of the Cantabric chain of mountains and the Iberian one. The paleozoic stratigraphic sequence on the Demanda Mountain Range includes Cambrian, Ordovician and Carboniferous metasedimentary rocks, mainly sandstones and shales with occasional dolostone beds in the lower part. These paleozoic rocks have been affected by three hercynian deformation phases accompanied by a low to very low grade regional metamorphism whose intensity increases towards the northwest (Colchen, 1974).

The mineralization has got a tabular morphology and approximately 2 m. thickness with a perfect parallelism of the primary layering with the regional foliation. Contacts with the host rock are quite sharp. The textural and structural features reveal a strong deformation (Ibañez *et*

al., 1993). The ore body shows a vertical zoning made up of two different layers predominantly composed, from the footwall to the top, of sulfides (galena and sphalerite) and quartz respectively. A third kind of association composed of dolomite has been observed from fragments gathered from the old mine dumps. The mineralization shows banded and/or brecciated structures composed dominantly of sulfides together with host-rock fragments, quartz and dolomite. Occasionally fine layers of chloritized metasediments appear inter-laminated with the sulfides.

The primary paragenesis in the deposit, which is characterized by a very simple sulfide mineralogy, consists mainly of sphalerite, quartz, dolomite and galena with lesser amounts of pyrite, marcasite, calcite and chalcopyrite.

Owing to the regional deformation and metamorphism we can see the paragenesis affected by foliation, folds, boudinage, stretching, brecciation, flaser structures and pressure shadows. This effects are also displayed microscopically by means of foliation processes and recrystallization microtextures with triple junction angles and annealing phenomena. Brecciated textures, with or without remobilization, are important and affect the primary mineralization. In these breccias, the disoriented fragments of sulfides, quartz, carbonates and schists are inside a matrix composed of galena, quartz and sphalerite.

The carried out preliminary sulfur isotope data (galena and sphalerite) show homogeneous $\partial^{34}S$ values around +30 ‰, very close to the value of the Cambrian sea-water sulfate. Moreover the very negative $\partial^{13}C_{PDB}$ (-13 to -15‰) values from carbonates suggest the incorporation of organic carbon from black shales to the hydrothermal solutions; while the variation of $\partial^{18}O_{SMOW}$ (+26‰ to +19) values are very similar to the oxygen isotope data of the Cambrian dolostones.

The described facts suggest that the Carmina mineralization could be considered a normal product of sedimentary basin evolution and classified as a SEDEX lead-zinc deposit (Sangster, 1990). Sulfide precipitation took place during the Upper Cambrian clastic sedimentation in an intracontinental rift system by uprising hydrothermal fluids, conducted along active growth faults. Grain size was upgraded by overprinting low grade regional metamorphism. In conclusion, according to the geological setting, morphology, mineralogical associations, isotopic data and the effects of deformation and metamorphism, we could favour for the Carmina ores a synsedimentary sea-floor exhalative origin.

References:
Colchen, M. (1974). Mem. I.T.G.E. **85**, 162-171
Ibañez, J.A. Velasco, F. Pesquera, A. (1993). Bol. Soc. Esp. Miner, **16-1**, 59-60
Sangster (1990). Appl. Earth. Sci. **99**, 21-42

PHOSPHATE PHASE TRANSITION IN WEATHERING ZONE OF ZAOSTROVSKOE DEPOSIT, MIDDLE TIMAN, RUSSIA

Ievlev A.A.(Dept. of Mineralogy, Inst. of Geology, Syktyvkar, Russia)

Zaostrovskoe phosphate-bauxite deposit of Middle Timan belongs to linear-contact type. It was formed as a result of weathering of shale-carbonate rocks in contact zone of shales and carbonate rocks of the Upper Riphean. There are two horizonts in productive layer: phosphorites in the lower part and phosphate-bearing bauxites and allites in the upper part. Phosphorite horizont comprises the breccia-like rocks which are gradually changed by phosphate-bearing argillites in the upper part of horizont.

The source of phosphorus for Zaostrovskoe deposit was the underlying Riphean shale-carbonate rocks locally riched in phosphorus. Processes of weathering of phosphorus-bearing rocks led to the concentration and re-distribution of phosphorus in weathering profile. Epigenetic processes during the period of buring of the deposit under conditions of swamped lagoon had the greatest effect. Swamp water penetrated inside the rocks and caused the dissolution of phosphate minerals and phosphorus transportation to the lower parts of weathering profile, where phosphorus precipitated on carbonate geochemical barrier in the form of apatite. In the upper part of weathering profile the sta⁄ying part of phosphorus concentrated mainly in alumophosphates. Phosphate component in breccia-like rock is present by nearly-ideal fluorapatite with minor content of isomorphic carbonate ions. Ideal X-ray diagram and good preservation of fluorapatite crystals testify to high structural perfection of fluorapatite. Crystals are fine, stick-like and distributed evenly inside the clay substrate of breccia (muscovite).

In argillite breccia phosphate is Sr-bearing fluorapatite. Crystals are fine, stick-like, but in contrast to phosphate breccia they collect and compose some little parts of material entirely. Clay material is present by muscovite and kaolinite.

In allite phosphate is present by one or two minerals of Al-Sr-Ca-phosphates like crandallite and goyazite. Muscovite and kaolinite are also the components of allite.

Therefore the evolution of phosphate minerals in weathering profile is discovered: fluorapatite → Sr-fluorapatite → Sr-alumocalcium phosphate. There are two general tendences. First one is the transition of Ca-phosphate into Al-Ca phosphate. It is universally recognized way of weathering of phosphate minerals which here does not achieve the last stage of Al-phosphate. Hence, it is middle stage of weathering. Second tendency is the process of introduction of strontium in phosphate: primarily as isomorphic admixture in fluorapatite structure and then the formation of Sr-phosphates.

HELIUM ISOTOPES IN ROCKS AND MINERALS OF KOLA SUPER DEEP HOLE SD-3

Ikorsky S.V., Kamensky I.L. *(Geol. Institute, Kola Sci. Cent. of Russian Academy of Sci.)* and Smirnov Yu.P. *(Sci. Prod. Center „Kola Super Deep Hole")*

About 100 core samples from the Kola Deep Hole were studied for contents and isotope composition of helium. The work lasted for about 10 years. Two methods were used to release helium from samples: 1) full melting to release all helium and 2) crushing to release inclusion helium.

The work was made by means of a Ukrainian mass-spectrometer MI-1201 modified by us to perform the analyses in static regime. Now we can measure the $^3He/^4He$ ratio = $1 \cdot 10^{-8}$ for $1 \cdot 10^{-6}$ cm^3 STP.

As it is known the rocks stripped by SD-3 are Precambrian. From surface down to 6842 m depth these are Lower Proterozoic volcanogenic-sedimentary rocks of the Pechenga series (2.4 - 1.9 Ga), then down to 12212 meters these are Archean strongly metamorphised (2.8 - 2.9 Ga) rocks (gneisses, schists, amphibolites). The age of the last metamorphism is 1.9 - 1.7 Ga. At this time the formation of numerous quartz veins took place.

The main types of rock (gneisses, amphibolites, schists, diabases, gabbro, sandstones, limestones, aplites and others) and two kinds of minerals (rock-forming amphiboles from Archean part of the hole and quartz from veins throughout its section) were investigated.

The main results are: contents of helium vary in a

wide range (10^{-6} cm^3/g) from 1 up to 2806, $^3He/^4He$ ratio (10^{-8}) ranges from 1.8 up to 13.5.

The principal consequences are:

1) The $^3He/^4He$ ratios do not depend on completeness of releasing of helium from samples. Both melting and crushing gave the same results for the same samples. Step-wise heating showed an absolute monotony of $^3He/^4He$ for all steps of temperature (3 - 10) steps for 3 samples.

2) There are two zones with higher 3He/4He ratios than the radiogenic value ($^3He/^4He$ $2 \cdot 10^{-8}$). The first is from 3.3 km down to 6 km and 3He/4He is about $(10 - 13) \cdot 10^{-8}$. The second is from 6.8 km down to 8-8.5 km where 3He/4He is $(7-10) \cdot 10^{-8}$. For other parts of the section we have radiogenic or approximately radiogenic $^3He/^4He$ ratios. Inside these zones the $^3He/^4He$ ratio does not depend on either rock type and mineral or helium content in neighbour samples.

3) The $^3He/^4He$ ratio and both ^4He and ^3He contents are independent in relation to uranium, thorium and lithium. There have been made about 500 analyses for uranium and thorium throughout the section of SD-3 and 35 analyses of lithium for samples with different $^3He/^4He$ ratios.

4) There are two possible ways to explaine the increase of $^3He/^4He$ ratio in the named zones. The first was announced earlier by Tolstikhin, it is the consequence of bringing of mantle helium by ultrabasic magma, forming the diabasic strata of the Pechenga series. The second is that two these zones are controlled by important structural elements: Luchlompolsky fault and Proterozoic - Archean boundary. We believe that mantle helium went through thesame structures during the last metamorphism 1.9 - 1.7 Ga ago.

Therefore, there is no increase of $^3He/^4He$ ratio at the SD-3 bottom,and for the middle part of the section the increase is explained, in our opinion, by tectonic reasons.

PARAGENETIC STUDY OF BISMUTH SULFOSALT ASSEMBLAGES FROM ROMANIAN SKARN DEPOSITS

Ilinca Gh. (*Instit. of Geology and Geophysics, Bucharest, Romania*)

In several areas from South-western Banat (Sasca Montană, Oraviţa-Ciclova, Ocna de Fier) and Apuseni Mts.(Valea Seacă, Băiţa Bihor), Romania, copper-rich sulfide deposits are among the major results of interaction between Upper Cretaceous-Palaeocene calk-alkaline magmatic bodies (generally called *banatites*) and sedimentary deposits of Permian and Upper Jurassic-Lower Cretaceous age. They contain various bismuth sulfosalts as ubiquitous, minute grains or individual crystals associated with hematite, magnetite, pyrite, arsenopyrite, chalcopyrite, tetrahedrite-tennantite, luzonite, enargite *etc.* Only the most common of the identified bismuth carriers for which chemical data are available, will be cited here: galenobismutite $Pb_{0.98-1.09}Bi_{1.78-2.08}S_4$, cosalite $Cu_{0.20}Pb_{2.24}Bi_{2.28}S_5$, lillianite $Cu_{0.07}Pb_{2.99}Bi_{2.19}S_6$, pavonite $Ag_{1.16}Bi_{3.33}S_5$, hammarite $Cu_{1.83-2.00}Pb_{1.19-0.25}Bi_{4.07-4.52}S_9$, krupkaite $Cu_{2.04}Pb_{2.40}Bi_{6.49}S_{12}$, wittichenite $Cu_{3.06-3.21}Bi_{0.95-0.99}S_3$, emplectite $Cu_{1.02-1.14}Bi_{0.87-0.98}S_3$, bismuthinite and native bismuth. A doubtful phase with a $PbS:Sb_2S_3$ ratio of about 54:36 mole percent, matching the composition of kobellite but with no Fe or Sb, was also frequently found.

The ore deposits in the mentioned skarn environments are extremely complex and distinguishing between the deposition stages may therefore seem difficult. A detailed paragenetic study reveals a general trend of evolution, especially as concerns the Cu-Pb-Bi-components which have proved to represent sensitive tracers in discriminating the different periods of deposition. The sequence of evolution given further on is essentially schematic and it ignores many local variations in mineralogical composition, but it suggests that the most significant factors in the diversification of the mineral assemblages are the thermal decomposition and the metasomatism of a quite simple starting material.

Three stages of deposition have been inferred:

- Stage 1 (Fe ± Co, As). The sequence started with Fe-oxides (hematite, magnetite) which were gradually replaced by pyrrhotite, marcasite and pyrite, pointing to a continuous increase of sulfur fugacity. Sometimes (*e.g.* at Oraviţa-Ciclova), significant amounts of arsenopyrite and minor cobaltite accompanied the Fe-sulfides.

- Stage 2 (Bi ± Pb, Zn, Cu, Ag, Te). Mainly Pb-Bi sulfosalts were formed (*e.g.* Oraviţa-Ciclova, Ocna de Fier). Their sequence display a general tendency towards increased $PbS:Sb_2S_3$ ratios. The highest temperature phase - galenobismutite - commonly breaks-down to form cosalite and lillianite, both associated with secondary bismuthinite and bismuth. Cosalite has been observed to pseudomorph fully or partially galenobismutite, or to contain tiny bladed inclusions of pavonite, bismuthinite and bismuth. Locally, the typical members of this stage are bismuthinite, native bismuth, tetradymite and tellurobismuthite. Seemingly, isolated galena grains and sphalerite containing chalcopyrite+mackinawite exsolution blebs are contemporary to this stage.

- Stage 3 (Cu ± Bi, W, Mo, Au). The main ore deposition event; it correlates with a strong copper metasomatic front that significantly affects the previously formed ore minerals. Chalcopyrite commonly pseudomorphs pyrite and may locally contain cubanite lamellae of obvious metasomatic origin. Specific dissolution-deposition structures formed by tetrahedrite-tennantite, enargite or luzonite point to the fact that at least in part they were formed during the reaction between arsenopyrite and copper-rich solutions. The effect on Pb-Bi sulfosalts is yet more striking. Mutual boundaries between chalcopyrite and galenobismutite or cosalite show reaction rims with hammarite, krupkaite, wittichenite and emplectite. Sometimes, hammarite forms pseudomorphs after galenobismutite or cosalite being constantly associated with secondary bismuthinite and bismuth. Other replacements result in specific textures such as chalcopyrite-bismuthinite symplectites. Primary bismuth minerals formed during this stage are scarce; usually, they are restricted to minor wittichenite or emplectite occurring as exsolution blebs in chalcopyrite. Gold, scheelite and molybdenite are also contemporary with stage 3, but their relationships with other minerals suggest simultaneous crystallisation.

DIFFUSION OF HYDROGEN IN DIOPSIDE AND PYROPE.

J. Ingrin, S. Hercule, (*CNRS, Université Paris 11, Orsay*),

Pyroxenes and garnets are basic constituants of the upper mantle and the lower mafic crust. Natural pyroxenes generally incorporate a large quantity of water as hydrogen point defects (Skogby and Rossman, 1989; Ingrin et al, 1989; Skogby et al., 1990), while pyrope garnets incorporate a relatively low proportion of water (Bell and Rossman, 1992). No data yet exists on the kinetics of hydrogen exchange with such mineral phases.

The kinetics of hydrogen diffusion in diopside single crystals has been investigated through dehydration experiments performed in air between 700 and 1000°C. Samples oriented along [001], [100]* and [010] crystallographic directions were cut in thin slices of less than 1 mm thickness and about 4 x 4 mm across. The decrease, with time of heating, of the OH^- concentration was measured from the integral of the OH^- absorption bands of infrared spectra taken on a few mm^2 area at the center of the sample slices. The fit of diffusion data to an Arrhenius law gives an activation energy of 109 ± 25 kJ/mol and 146 ± 17 kJ/mol, and a preexponential term of 3.2×10^{-8} and 1.7×10^{-6} m^2s^{-1} for orientations [001] and [100]*, respectively. The behavior along the three orientations can be considered as isotropic, within the uncertainty of the data. We propose that the kinetics of dehydration (or hydration) of diopside crystals recovered from nodules can be analyzed

through the isotropic diffusion law: $2.4 \times 10^{-7} \exp[-128\ kJmol^{-1}/RT]\ m^2s^{-1}$.

The kinetics of dehydration of diopside is effectively slower than the kinetics of dehydration of olivine. However, if olivine may undergo extensive dehydration during ascent with magma, dehydration of diopside may be also significant if we take into account the lower grain size of this latter mineral as observed in nodules. The low concentration of OH^- defects in olivine cannot be fully explained by its rapid dehydration. We agree with Bell and Rossman (1992) that the OH^- content of diopside in the mantle conditions is probably higher than the OH^- content of olivine.

Preliminary results from hydrogen extraction experiments performed on garnet give an upper value of 2×10^{-14} m^2/s for the rate of hydrogen escape at 800°C, around one order of magnitude below the rate observed for diopside. Thus, a higher dehydration during ascent cannot be argued to explain the lower concentration of OH defects measured in natural garnet compared to pyroxenes.

References :
Bell, D. R., Rossman G. R. (1992). *Science*, **255**, 1391-1397.
Skogby, H., Rossman, G. R. (1989). *Amer. Miner.*, **74**, 1059-1069.
Skogby, H., Bell, D. R., Rossman, G. R. (1990). *Amer. Miner.*, **75**, 764-774.

REACTIONS BETWEEN MOLTEN IRON AND SILICATES AT HIGH PRESSURE

Ito, E., Sato, K., Morooka, K., Katsura, T. *(Institute for Study of the Earth's Interior, Okayama Univ.)* and Ujike O. *(Dept. of Earth, Toyama Univ.)*

Reactions between molten iron and silicate melt at high pressure were investigated by employing a uniaxial split-sphere apparatus and mixtures of pure iron and ferromagnesian silicates as the starting materials. The experimental pressure was varied from 10 to 26 GPa at temperatures of 2500-2600°C. It was confirmed that certain amount of Si(up to about 3 %) dissolved in molten iron from silicate melt at pressures higher than 20 GPa and the dissolution is enhanced with increasing pressure. Many small spherical blobs composed of SiO_2 and FeO present in coalesced iron grains were interpreted as the quenched immiscible liquid formed during cooling. Therefore, O also dissolved in molten iron under the experimental conditions. Nevertheless any evidence for dissolution of Mg was not obtained. Consequently, the present study indicates that Si and O are important light elements of the Earth's core if the core segregation were proceeded in the deep magma ocean. Dissolution of K and small amounts of REE in molten iron were also observed. Chemical evolution of the core and the mantle will be discussed based on the recent core formation model and the present experimental results.

MÖSSBAUER STUDY OF THE KINETIC OF THE RADIATION - CHEMICAL OXIDATION OF IRON IN THE AMPHI BOLE STRUCTURE.

Ivanitskiy V.P., Voznyuk P.O. *(Ukrainian Acad. of Sci., Institute of Geochemistry, Mineralogy and Ore Formation, Kiev)*

The kinetic of the radiation-chemical oxidation of iron in the structure of Ca- amphibole has been studied using the Mössbauer spectroscopy. Gamma-irradiation has been performed using g-ray photons of ^{60}Co isotope. The absorbed dose had values varying in range of 120 to 640 MGy, the power of the absorbed dose had the value of 23 Gy/s.

It has been determined that the irradiation leads to stimulation of the reaction of the radiation-chemical oxidation of iron ions in the non-equivalent octahedral sites M1, M2 and M3. The kinetic of the processes of the accumulation of iron Fe^{3+} can be described by the equation:

$$\alpha = 1 - \exp(-kt^n),$$

where α is the ratio of oxidized ions Fe^{3+} to total number of iron ions, **k** and **n** are certain constants which depend upon the constant of oxidation rate of iron ions, upon the nature of the mineral and number of intermediate stages of the oxidation processes, respectively. Here k = 0,00047, n = 0,36108.

The obtained value of $n < 1$ indicates that the phenomenon of diffusion is the dominating factor in the processes of radiation-chemical oxidation of iron in Ca-amphiboles.

The values of the radiation yield $G(Fe^{3+})$ and values of the irradiation energy (E) required for the oxidation of one ion Fe^{2+} were calculated from Mössbauer data of α. It was found that values of $G(Fe^{3+})$ and E depend upon the absorbed dose and vary in the ranges of 0,0271 to 0,0089 ion/g and of 3,626 to 11,196 Kev, correspondingly.

CATION ORDERING, LATTICE STRUCTURE AND THERMODYNAMICS OF NI-MG OLIVINES

IVANOV M. V. *(Institute of Precambrian Geology and Geochronology, Russian Academy of Sciences, Nab. Makarova 2, St. Petersburg 199034, Russia).*

The statistical theory of binary two-sublattice solid solutions recently developed in terms of the cluster variation method allows us to compare and join information on long- and short-range ordering and thermodynamics of silicates in one picture. The properties of the solid solution are described in the theory by sets of cation coordination numbers and energetic parameters. The theory is applied to Ni-Mg olivines. The set of cation pairs with energies which can affect the thermodynamic properties of the crystal is determined through the analysis of the inter-cation distances. This determines the number of energetic parameters (4), needed to describe ordering and thermodynamics of Ni-Mg olivines. The available experimental X-ray data on cation ordering in Ni-Mg olivines allow us to determine only three of these parameters. The whole set of parameters is determined by a fitting procedure on the base of X-ray data combined with available experimental data on olivine-oxide equilibrium. These experimental data are discussed from the point of view of the sign of the solid solution asymmetry.

ORIENTATION OF NEMATIC LIQUID CRYSTALS (NLC) ON SURFACES OF MAGNETIC MINERALS

G.Yu.Ivanyuk and M.G.Tomilin (*Geological Institute of Kola Science Centre of the Russian Academy of Sciences and S.I.Vavilov State Optical Institute*)

Thin layers of homogeneously oriented NLC applied to an optical quality surface as a free layer may image the microheterogeneity of electrical (Hairyatdinov & Chuvyrov, 1980), magnetic (Tomilin & Ivanyuk, 1993) and van der Waals characteristics of surfaces of minerals (Billard, 1980). Local deformations of the NLC layer over the underlying surface can be observed with a simple optical microscope in polarized light. Optical orientation of NLC is determined by methods of optical compensation. An analysis shows that NLC can be used for nondestructive testing of twinned, zoned, tessellated crystals of magnetite, ilmenite and pyrrhotite as well as the magnetite relics in a kenomagnetite matrix. Domain pattern typical for polycrystals of pyrrhotite and tesselated domain patterns in magnetite were also

obtained. With the NLC technique it has been possible to determine an orientation of magnetite magnetization vectors.

The NLC technique is very easy to use and does not require sophisticated equipment. It provides unique and valuable information about magnetic properties and microstructure of minerals and opens wide areas for application in mineralogy, geology and engineering as well as in solid state physics, for example: nondestructive testing of physical heterogeneities in the ferromagnetic crystals and alloys; imaging patterns of magnetic fields; paleomagnetic investigations; scientific photography.

References.
Billard, J. (1980). Bull. de Miner., 1980, **3-4**, 444-451
Hairyatdinov, J.A. & Chuvyrov, A.N.(1980). Doklady Akademii nauk SSSR, 1980, **2**, 437-439
Tomilin, M.G. & Ivanyuk, G.Yu. (1993). Liquid Crystals, **5**, 1599-1606

• MINERAL POLYMORPHISM AND ITS TECHNOLOGICAL MEANING

Izoitko, V. (*Mechanobr, St. Petersburg*)

It is widely assumed that the main role in beneficiation is played by structural and textural peculiarities of ores.

However, the investigations of the last years have shown that mineral capacity to form polymorphic modifications with similar composition and different structure is not less important. These modifications differ in many properties: surface energy, fragility, magnetic ability, solubility in acids, ability to oxidize and flotate. Thus, the monoclinic pyrrothite oxidizes quicker than the hexagonal one, maximum flotation velocity being with a sulphur to iron atomic ratio, ≈ 1.1. In the course of flotation hexagonal molybdenite is accumulated in the concentrate, with loss of the rhombohedral 3R forms.

In the digenite–djurleite–chalcosite group the ability to flotate increases simultaneously with the ratio of copper to sulphur.

Changes of composition and properties are also characteristics of the isomorphous series: ferberite–hübnerite, calcite–dolomite and others.

NEW DATA ON LOW METAMORPHISM IN BRIANCONNAIS DOMAIN OF PREALPES, SWITZERLAND

Jaboyedoff M., Thélin, P. and Girod, F. (X-ray Laboratory, Inst. Mineralogy, Univ. of Lausanne)

The Swiss "Préalpes médianes" are a stack of several nappes of Penninic origin (Briançonnais domain), located on the NW border of the Helvetic nappes. This unit is classically divided into the frontal "Préalpes médianes plastiques (PMP)" and the interior "Préalpes médianes rigides (PMR)".

New data on very low grade metamorphism has been produced by XRD using the Scherrer width ("illite crystallinity") and the evolution of the clay mineral parageneses, focussing in particular on mixed-layered clay minerals.

Numerous measurements of the Scherrer width (SW) at the half maximum (001 reflection of illite) show evidence for an increase in the degree of metamorphism from diagenesis in PMP to deep anchizone conditions in the trailing part of PMR, along an horizontal NW-SE cross section; this gradient may implie transported metamorphism during alpine mouvments.

Detailed work on mixed-layer clays shows that all parameters as degree of ordering-disordering ("Reichweite" descriptor), interstratification rate and composition of each component (illite, smectite, chlorite) may be used to caracterize finely thermal conditions during diagenesis. XRD signals (air-dried and glycolated patterns) were fit with computerized simulations in order to constrain the properties (especially ordering-disordering and interstratification rate) of the mixed-layered clays and the proportions of all involved clays.

As in the famous Gulf Coast profiles, it is possible to find evidence of progressive zonation recorded namely by increasing illite/smectite ratios in mixed-layered clays within the diagenesis. So on, in the "Préalpes", this indicator may be used in a combined way with the SW decreasing within the anchizone.

Particuliar lithologies, bauxites by example confirm the SE-NW gradient by the passage of kaolinite-boehmite-diaspore assemblage to diaspore-pyrophyllite paragenesis.

HIGH - PRESSURE AMPHIBOLITES AND THE ORIGIN OF TONALITIC - TRONDHJEMITIC MELTS IN THE SHEAR ZONE, VARISCAN BASEMENT OF THE WESTERN CARPATHIANS

Janák M.,[1] Pitoňák P.[2] , Spišiak J.[2] *([1] Dept. Mineral. Petrol. Comenius University, Bratislava, Slovakia, [2] Geological Inst. Slovak Acad. Sci., Banská Bystrica, Slovakia)*

The origin of tonalitic to trondhjemitic melts by partial melting of amphibolites is evidenced by textures, composition, P-T conditions and REE contents in the Variscan basement of the Western Carpathians

Tonalitic to trondhjemitic veins and segregations originate in amphibolites of inhomogeneous, banded structure, with alternating mafic and felsic layers in the thickness of several mm to dm. They enclose massive, garnet and clinopyroxene-bearing lenses, with relics of high-pressure conditions, highly retrogressed. Banded amphibolites (leptyno-amphibolites) are involved in the thrust sheets and slices within the high-grade, pre-Alpine basement of the Western Carpathians, e.g. in the Tatry Mts. they form the base of the upper unit, thrust over the lower (micaschist) unit as a consequence of Variscan, SE-vergent thick-skinned thrusting.

Banded amphibolites show inhomogeneous, migmatitic texture, the mafic and felsic parts differ in composition. Tonalitic to trondhjemitic leucosomes are composed mainly of quartz and plagioclase (albite to oligoclase), minor garnet (almandine-rich) and amphibole (pargasite to hornblende) are also present. The mafic part exhibits amphibolite composition, dominated by amphiboles above plagioclase and quartz. Individual bands are different in geochemistry. REE content in the felsic bands is low, with flat distribution pattern, or slightly positive Eu anomaly, indicating an origin of tonalitic to trondhjemitic melt from basaltic (metabasite) source. The mafic, amphibolite part is slightly enriched in REE, exhibiting also nearly flat distribution pattern. It is inferred, that both-felsic and mafic parts may represent segregations of more homogeneous parental rock, obliterated by partial melting, deformation and retrogression. Garnet and clinopyroxene-bearing lenses can represent such a rock, recording peak P-T conditions of about 750° C and 10 kbars, near the transition of high-pressure amphibolite, granulite and eclogite facies. At such conditions, partial melting of amphibolite (hornblende + plagioclase) leading to the origin of tonalitic / trondhjemitic (plagioclase + quartz) melt is suggested, based on experimental phase equilibria. Owing to the lower-crustal pressure conditions exceeding 10 kbars, fluid-absent dehydration-melting of amphibole was probably effective, garnet and clinopyroxene (diopside) being the residual phases. Locally, at the presence of H_2O-rich fluid, however, the melt can be produced at lower P-T conditions, crystallizing amphibole from the water-saturated melt, as indicated by large amphiboles in the leucosome.

The presence of the melt is capable of substantial weakening of the rheology in the partially melted rock, enhancing its deformation. As inffered from the textures, the melt has been mostly focused into the domains of the lowest stress, forming veins and segregations in the shear bands. The pathways for the migration of liquid were probably microfractures, facilitating the interconnectivity of interstitial melt, flowing down the pressure gradient during decompression.
High-pressure garnet and clinopyroxene-rich lenses represent most probably residual left-overs after partial melting and ductile deformation.

Fe-Mg INTERDIFFUSION IN OLIVINE UP TO 9 GPa AT T=600-900°C. EXPERIMENTAL DATA AND NUMERICAL SIMULATION. IMPLICATIONS FOR THE ACTIVATION VOLUME OF CREEP IN THE EARTH's UPPER MANTLE.

O. Jaoul, Y. Bertran-Alvarez, (*CNRS, Université Paris 11, Orsay*), R. C. Liebermann, , (*CHIPR , USB, Stony Brook, N.Y.*) and G. D. Price, (*UCL, London*)

We have measured the interdiffusion coefficient of Fe/Mg in San Carlos olivine (average composition Fo_{90}) at temperatures T = 600 to 900°C and pressures from P = 0,5 to 9 GPa. These data are essential for estimating the closure temperatures of geothermometers based on Fe-Mg exchange in olivine in contact with other phases (e.g. spinels) and for establishing a firm basis to understand how high T plastic deformation of olivine depends on pressure.

These measurements were performed by preparing olivine samples covered by a thin layer of fayalite at Orsay. The specimens were annealed at high P-T in a uniaxial split-sphere apparatus (USSA-2000) at Stony Brook (Bertran-Alvarez *et al.*, 1992).

The Fe-Mg interdiffusion profiles were analyzed by Rutherford Back Scattering (RBS) in France. The results yield a pre-exponential factor $D_o = 7.7 \times 10^{-8}$ cm^{2}s^{-1}, and an activation energy $E^* = 147 \pm 58$ kJ.mole^{-1}, in the expression $D = D_o \exp(-E^*/RT) \exp(\varepsilon X_{Fe}) \exp(-PV^*/RT)$. Our data are best fitted with $\varepsilon = 3$, X_{Fe} = Fe/(Fe + Mg) around 0.1, and $V^* = -0.5 \pm 0.6$ cm^{3}mole^{-1}. Effectively, the activation volume V^* is equal to zero in the range of P and T investigated.

Comparisons of the present results obtained at relatively low temperature under extrinsic conditions for diffusion with other Fe-Mg interdiffusion data at higher temperature (≥ 1125°C) under intrinsic conditions allow us to conclude that the activation volume for migration V_M^* is close to zero whereas that for formation is $V_F^* \sim 5.5$ cm^{3}mole^{-1}. This conclusion has important implications for the creep sensitivity to pressure which is the sum of V_F^* for Fe-Mg diffusion and $(V_F^* + V_M^*)_{Si}$ for silicon self diffusion (Jaoul, 1990) ; the experimental determination of this latter activation volume is currently underway in our laboratories.

Numerical simulations involving energy minimizations performed with the CASCADE and PARAPOCS codes in London offer excellent confirmation of these experimental observations: one finds $V_M^* \sim 0$ and $V_F^* \sim 4.8$ cm^{3}mol^{-1}.

The activation energy E^* for Fe/Mg interdiffusion deduced from the present experiments as well as the preexponential factor D_o enable precise estimates of the closure temperatures of geothermometers based on the Fe-Mg exchange between olivine and spinel.

References :
Bertran-Alvarez, Y., Jaoul, O., Liebermann, R.C. (1992). *Phys. Earth Planet. Int.*, **70**, 102-118.
Jaoul, O., (1990). *J. Geophys.Res.*, **95**, 17631-17642.

UNIQUE GEM VARIETY OF CHLORITE FROM KORSHUNOVSK IRON-ORE DEPOSIT (EAST SIBERIA)

Jitova L.M.,Mazurov M.P.,Saharov V.K.(Korshunovsk GOK and Novosibirsk Inst. of geol.)

The composition, gem prpoperties and crystallization conditions of chlorite, found only in Korshunovsk deposit in East Siberia, have been researched by methods of translucent microscopy, IR-spectroscopy and x-ray-structural analysis.

Gem variety of chlorite is the compact monomineral reniform aggregate of deep green colour of different shades.It is typical for chlorite a thin concentric banding and radially-fibrous picture, formed by flabellate orientation of chlorite flakes with silvery-pearly reflux.The silvery-pearly radiality in combination with different shades of green create the mysterious pictures, reminding fantastic plant landscapes.

Inside the iron-ore diatreme of Korshunovsk deposit, formed under basalts and evaporites interaction, are found cavities from 30 to 3 metres,localized among magnetite ore and pyroxene skarns. Incrustations of reniform chlorite aggregates increase on the walls of these cavities.

It was distinguish some morphological varieties of reniform chlorite, depending on it location inside the cavities: elongate pseudo-stalactites, hanging down from the top of cavity, and radially-fibrous reniform incrustations of lateral walls and bottom of cavity. Incrustations are growing sequently one after another, forming large lace bands with thickness up to 2,0 m.

Reniform aggregates of chlorite consist of spherulites, growing under geometrical selection conditions. Spherulites are formed by cone-like radiated tufts of split flakes,tightly adjoining to each other. Repeated split and helicoidal convolution of flakes, during the growth of spherulites, create a flaser-radiated microstructure of spherulite aggregates.

The most perfect (001) cleavage is the reason of silvery-pearly reflux of chlorite flakes.The more intensive pearly flakes are oriented by their plane cleavage parallel to the cut. So, brightness of decorative picture and intensivity of silvery-pearly reflux depend on orientation cut section relatively the centre of spherulite. Cross sections have a dark convergence-zonal pictures similar to malachite one. Inclined axial sections display all transitions from star-like to fireworks-like pictures, when silvery-pearly rays die out radiate off the spherulite centre, or dark rays flare up by pearly brilliance flying away.

Two varieties of gem chlorite were distinguish, after their decorative and other properties: transparent chlorite and untransparent pearly chlorite.

It was determined that anisotropy of microhardness of chlorite aggregates expressed in increase of microhardness on cross sections of spherulites. Transparent chlorite has higher microhardness compare to pearly chlorite (79,6-119,8 kg/mm2-for pearly chlorite, 148,9-183,5 kg/mm2 - for transparent chlorite).

Coincidence of the everage value of specific weight with volume weight (or, in other words, real and everage density) is also typical for transparent chlorite, indicative of porosity absense and compact packing of flakes in spherulite.

Variations of iron content in chlorite composition create different fine shades of green. The more iron chlorite is deeper is colour.

It was determined, that chlorite aggregates are represent by chlinochlore. Transparent chlorite is a mixture of clinochlore with amesite. Interchange of packets with different interplanar spaces in chlorite structure is the reason of high density and there by of valuable gem properties of transparent chlorite. So, transparent chlorite is able to be conserved in thin slabs (up to 2-3 mm), to be well polished and to be used in jewellerie.

The origin of gem variety of chlorite is conditioned by recrystallization of skarns and ores over the distinctive hydrothermal high-temperature karst, which takes place in Korshunovsk deposit.

ALUMINO-WINCHITE-BEARING ECLOGITES FROM THE SOUTH CARPATHIANS, ROMANIA: MINERAL ASSOCIATIONS AND METAMORPHIC EVOLUTION

Johan V.[1], Maruntiu M.[2], Iancu V.[2], Ledru P.[1]
([1] *BRGM, Orléans, France;* [2] *Inst. of Geol. and Geophys., Bucharest, Romania*)

Alumino-winchite-bearing eclogites occur within a pre-Alpine deep-seated shear zone in Leaota Mts., in the south-eastern part of the South Carpathians (Romania). They are intimately associated with garnet-bearing gabbros and amphibolitized eclogitic rocks (Sabau et al., 1986; Iancu&Maruntiu, 1993).

Mineral assemblages and solid inclusions in the well-zoned garnets and in kyanite indicate the following stages in the metamorphic evolution of the eclogites.

(I) **Pre-eclogite stage:** paragonite + zoisite + quartz + winchite + rutile + apatite + zircon inclusions in the almandine-rich garnet cores.

(II) **Early-eclogite stage:** disappearance of paragonite, and appearance of phengite, kyanite needles and scarce omphacite crystals as inclusions in the pyrope-rich garnet rims. Kyanite blasts, containing small inclusions of winchite + zoisite + omphacite + rutile, develop in the matrix.

(III) **Peak-eclogite stage**: crystallization of large oriented omphacite and kyanite crystals in equilibrium with well-developed winchite and inclusion-free garnet.

(IV) **Late- to post-eclogite stage:** abundant phengite, locally replacing kyanite. Rare secondary paragonite and albite, as well as the post-deformation clinozoisite, indicate incipient retrogressive evolution.

The estimated peak metamorphic conditions are T ≈ 780-860 °C at a minimum pressure of 20-22 kb. A P-T-t path, based on numerous reactions and geothermo-barometers is proposed.

Winchite included in garnet is Al-rich. Its formula indicates extensive Tschermak's substitution. The compositions of winchite are given in table 1.

Table 1. Selected microprobe analyses of winchite

	A	B	C
SiO_2	46.95	52.96	52.76
TiO_2	0.33	0.34	0.15
Al_2O_3	15.54	11.53	10.23
Cr_2O_3	0.02	0.05	0.08
FeO_t	10.02	7.07	8.01
MnO	0.10	0.00	0.00
MgO	12.38	14.44	15.20
CaO	7.74	6.72	6.76
Na_2O	4.29	4.25	4.30
K_2O	0.35	0.22	0.18
Total	97.72	97.58	97.67
Si*	6.602	7.303	7.270
Al^{IV}	1.398	0.697	0.730
Al^{VI}	1.178	1.176	0.931
Ti	0.035	0.035	0.016
Cr	0.002	0.005	0.009
Fe^{3+}	0.583	0.285	0.583
Fe^{2+}	0.595	0.531	0.340
Mn	0.012	0.000	0.000
Mg	2.595	2.968	3.122
Ca	1.166	0.993	0.998
Na_B	0.834	1.007	1.002
Na_A	0.336	0.129	0.147
K	0.063	0.039	0.032

A=winchite included in garnet, B=winchite included in kyanite, C=winchite (core) in the matrix;
* number of atoms calculated on the basis of 23 (O).

References:
Sabau, G., Tatu, M., Gabudeanu, D. (1986). D.S. Inst. Geol. Geofiz., Bucuresti, **1**, 70-71.
Iancu, V. & Maruntiu, M. (1993). Roman. J. Min., **76**, Suppl. 1, 16-18.

PGE MINERALIZATION IN ALASKAN TYPE COMPLEXES: NEW GENETICAL ASPECTS

Johan Z. (*BRGM, Orléans, France*)

Two types of PGE mineralization can be distinguished within Alaskan-type complexes: (1) Ir-rich isoferroplatinum accumulation associated with chromite "schlieren" in dunite; (2) PGE sulphide- and arsenide-bearing mineralization appearing as a late phase in clinopyroxenite. In both cases, base-metal sulphides are missing or rare, and are later than the PGE mineral phases. Consequently, the mechanism of PGE concentration by high-temperature MSS cannot be applied. The mineralization associated with clinopyroxenites results from a high-temperature fluid which is related to the evolution of the intercumulus liquid and the high activity of volatiles (As,Sb).

The origin of platinum accumulations in dunite is still controversial. Isoferroplatinum is everywhere interstitial to chromite. Euhedral chromite and clinopyroxene are included in Pt_3Fe, which also fills fractures in chromite and clinopyroxene grains. Solid inclusions filling negative crystals in isoferroplatinum from Milverton, Australia, (Johan et al., 1991) and Nizhni Tagilsk, Russia, have been studied. The following associations were observed: (1) cpx+mu+ttn+ap+anh+glass; (2) cpx+ampf+ttn+ap+glass; (3) cpx+amph+mu+alb+ap+glass; (4) amph+bi; (5) cpx+amph+mu+glass.

Clinopyroxene is strongly zoned. The cores are enriched in iron (7-10 mol.% Fs) and contain 4-5 mol.% Jd; the rims are jadeite-rich (28-56 mol.%) and impoverished in Fe (2-6 mol.% Fs). The amphibole composition is close to the tremolite end-member and contains up to 0.6 wt.% F. Rare inclusions of edenitic hornblende associated with phlogopite were observed. The latter shows extensive solid solution with annite (XFe = 0.43) and siderophyllite (Al[IV] = 2.24), and contains 1.4 wt.% TiO_2 and 0.1 wt. % Cl. Fluorine concentration is systematically below the microprobe detection limit. Muscovite exhibits significant phengitic (19 mol.% celadonite) and paragonitic (14 mol.%) substitutions; XMg = 0.90-0.94, TiO_2 concentration varies from 0.3 to 0.7 wt.%. Fluorine was not detected in muscovite from N. Tagilsk, but can reach 0.4 wt.% at Milverton. Apatite is a pure F-apatite end-member.

Titanite shows high Al_2O_3 concentrations (2.5 wt.% at N. Tagilsk, 4.0 wt.% at Milverton) and an F-content of 0.1-0.14 wt.%. The residual glass is silica- and alumina-rich (SiO_2 62-65; Al_2O_3 16.5-18.0 wt.%). Its MgO and FeO contents are respectively less than 0.5 and 0.3 wt.%. Na/(Na+K) varies strongly between inclusions from 0.34 to 0.56. Analytical totals suggest a water content of 11-15 wt.%. Isoferroplatinum penetrates along the albite grain boundaries and Pt_3Fe inclusions were observed in phlogopite.

The mineral associations in silicate inclusions indicate an extremely high water activity in magmatic liquid and a high total pressure. The absence of olivine and orthopyroxene can be explained by their reaction with liquid at high $a\ H_2O$, giving rise to phlogopite and amphibole. The composition of H_2O-rich initial liquids, calculated from modal analyses and mineral chemistry, is strongly variable from one inclusion to the other. This suggests a liquid-liquid immiscibility process. The origin of isoferroplatinum is related to the evolution of a fluid-rich magmatic liquid.

References:
Johan Z., Slansky E., Ohnenstetter M. (1991). *C.R.Acad.Sci. Paris*, **312**, sér.II, 55-60.

PETROLOGICAL EVOLUTION OF THE CINOVEC GRANITE CUPOLA, CZECH REPUBLIC: MINERAL CHEMISTRY CONSTRAINTS

Johan Z. and Johan V. *(BRGM, Orléans, France)*

Samples from a 1596 m deep borehole in the Cínovec (Zinnwald) granite cupola known for its W-Sn mineralization, have been studied. The drilling traversed greisens in the apical part of the cupola, then zinnwaldite granite (ZG) to the depth 730 m, and finally protolithionite granite (PG) (Stemprok & Sulcek, 1969; Cocherie *et al.*, 1991). Besides the accessory minerals commonly occurring in granitic complexes (zircon, xenotime, monazite, thorite), the minerals pyrochlore, columbite, ilmenorutile, rutile, REE-carbonates (bastnaesite, synchysite) and REE-oxyfluorides have been identified. Accessory minerals are excellent indicators of geochemical and petrological evolution of the cupola. The Cínovec cupola originated from a strongly evolved, Na-,K-, incompatible elements- and volatile (F, CO_2, H_2O)-rich magmatic liquid. The apical part of the intrusion was enriched in volatiles, causing a lowering of the liquidus temperature. The crystallization of albite (Ab) first started in the deeper part of the intrusion (PG), being delayed in the ZG. K-feldspar (Kf) precipitated after Ab. The precipitation of a large amount of feldspars (about 50 vol.% of the intrusion) led to a strong increase in concentration of F, CO_2, H_2O and incompatible elements, in the residual magmatic liquid. This

liquid gave rise to F-rich micas (Mi) containing inclusions of zircon, thorite, monazite and xenotime.

The Rb distribution shows a strong enrichment in Rb for Kf and Mi from the apical part of the intrusion (0.8 and 2.0 wt.% Rb_2O respectively), unlike for Ab which shows rather constant (0.15-0.2 wt.%) Rb_2O concentration along the drillhole. The K_{Rb} between Kf and Ab strongly increases in the apical part, whilst that for the pair Mi-Kf is remarkably constant. This indicates a drastic change in crystallization conditions after the precipitation of albite, presumably the appearance of a fluid phase.

The magmatic stage ends with the crystallization of quartz, the onset of which is immediately preceded by that of niobo-tantalates (they represent the main stock of W within the cupola) and cassiterite. It is followed by a mineral association which precipitated from an interstitial F- and CO_2-rich fluid phase characterized by high Ca-activity and transporting REE and LIL elements. This assemblage comprises fluorite and bastnaesite formed at early stages, and synchysite and pyrochlore which precipitated at the late-stage evolution of the fluid when its F/CO_2 ratio was lowered due to the crystallization of a substantial amount of fluorite. This residual fluid phase is again characterized by high Ca-activity, and high concentrations in Pb, Ba, Sr, Bi, As, U, W, as shown by the composition of a silica- and uranium-rich, defect (2+,5+) pyrochlore.

The fluid phase is not in equilibrium with accessory mineral phases included in micas. Zircon, thorite and xenotime are strongly hydrated and fluorinated, and are enriched in REE due to the interaction with fluids. Furthermore, pyrochlore metasomatically replaces columbite crystals; the replacement is particularly intense in the lower part of the ZG where columbite is virtually absent, in contrast with the uppermost part of the cupola where columbite is widespread but pyrochlore is absent.

The vertical distribution of xenotime, monazite and thorite indicates that PG is enriched in P and Th with respect to the ZG. The occurrence of W-rich columbite in the transition zone between PG and ZG, and the substitution mechanism of W in the columbite crystal structure (Johan & Johan, in press) indicates an important variation in fO_2 at this petrological boundary. The early stages of evolution are characterized by fO_2 lower than that of the HM buffer, whilst the mineral association resulting from the fluid phase has been formed at fO_2 higher than indicated by HM equilibrium.

References:
Cocherie, A., Johan, V., Rossi, Ph., Stemprok, M. (1991). In Pagel and Leroy (eds): *Source, Transport and Deposition of Metals*., Balkema, Rotterdam, 745-749.
Johan, V. & Johan, Z. (in press). *Mineral. and Petrol.*
Stemprok, M. & Sulcek, Z. (1969). *Econ. Geol.*, **64**, 392-404.

A HRTEM STUDY OF POLYSOMATISM IN TITANIAN CLINOHUMITE FROM MAGMATIC VEINS IN THE TERTIARY GARDINER COMPLEX, EAST GREENLAND.

Johnsen, O. (*Geological Museum, University of Copenhagen*)

Nielsen & Johnsen (1978) described titanian clinohumite (Ti-CL) as a major constituent in up to 20 cm wide veins splitting off from a pyroxenitic ring dyke and intruding dunite in the Tertiary Gardiner Complex , East Greenland. The centres of the veins are dominated by magnetite octahedra or aggregates of Ti-CL.The bulk of the veins is composed of apatite felt, antigorite, phlogopite, magnetite, eckermannite and minor forsteritic olivine.

The present study of this unusual occurrence of Ti-CL has been initiated in order 1) to detect and characterize polysomatic defects as previously found in Ti-CL and other Mg members of the humite group (e.g. White & Hyde, 1982), 2) to map the distribution of these defects and other microstructures petrologically, and 3) to record the defect "history" of the associated minerals in the vein.

As pointed out by Thompson (1978) olivine (O) and the humite group minerals norbergite (N), chondrodite (NO), humite (NOO) and clinohumite (NOOO) comprise a polysomatic series. Members with uneven numbers of O slabs are monoclinic, the others are orthorhombic. To emphasize the membership of the series the monoclinic minerals are set with the a axis as the diad axis, space group $P2_1/b$.

The results so far, based on crushed powder samples on holey carbon coated Cu-grids studied using a TEM Philips 430 microscope at 300 kV, show that Ti-CL from Gardiner ranges from entirely defect free to highly defective. The enclosed HRTEM image shows an area with a high density of polysomatic faults looked down the b axis. The inserted image is a magnified part of an area showing Ti-CL units with units of titanian chondrodite (Ti-CH) and one NO_7 unit. The arrays of bold white spots correspond to the M(3) octahedra that accommodate all Ti (Fujino & Takéuchi, 1978) and thus represent N slabs while the arrays of light white spots represent O slabs. This interpretation of the images is confirmed by a through-focus series in combination with a corresponding computed series and supplemented by substitutional simulations.

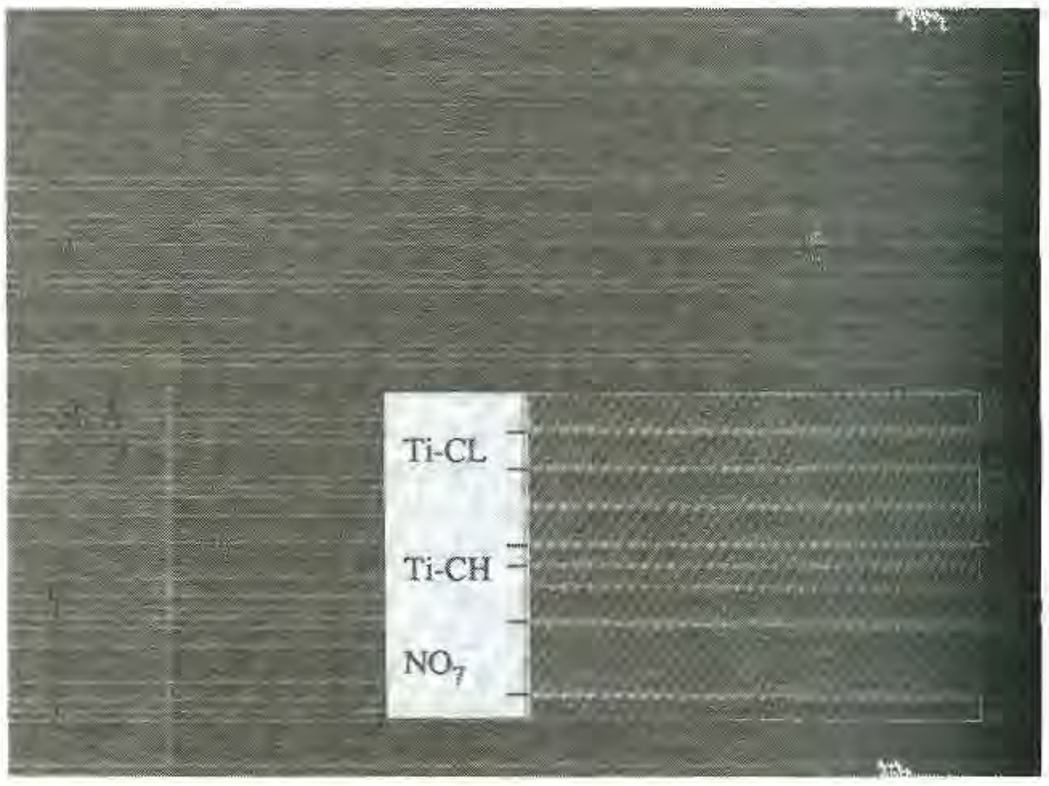

Only polysomatic units with uneven numbers of O slabs have been detected, in order of decreasing frequency: 3 (=Ti-CL), 1 (=Ti-CH), 7, 9, 5 and 15. Counts over sequences of >100 polysomatic units embedded in normal Ti-CL show that the Ti-CL stoichiometry is maintained and consequently the dimensions in the c* direction counterbalanced. Adjustments usually take place within a maximum of 5 units. The most frequent successions of the "pathological" units are 1-1-7 and 1-1-1-3-9 occurring with distinct polarity. Oscillations in the Ti activity during crystallisation may be responsible for the formation of polysomatic units with high activity favouring Ti-CH and low activity creating $NO_{>3}$ units. Ion milled samples from petrographic thin sections may give indications of the growth direction.

References:
Fujino, K. & Takéuchi, Y. (1978). Am. Mineral. **63**, 535-543
Nielsen, T.D.F. & Johnsen, O. (1978). Min. Mag. **42**, 99-101.
Thompson, J.B., Jr. (1978). Am. Mineral. **63**, 239-249.
White, T.J. & Hyde, B.G. (1982). Phys. Chem. Minerals **8**, 55-63.

• THE CAVITY MINERALS OF THE SILICA GROUP OCCURRING IN THE BASALTS OF THE DECCAN VOLCANIC PROVINCE OF INDIA WITH SPECIAL REFERENCE TO THEIR GEMMOLOGICAL PROPERTIES AND USES

Joshee S.P. and Phadke, A.V. (*Dept. of Geology, Univ. of Poona*)

The Deccan volcanics covering over half-a-million square kilometres of western India are largely bereft of any economically important mineral deposits other than the basalts used in construction, and small deposits of bauxite and laterite.

The basaltic rocks, however, are a veritable storehouse of many beautiful cavity (and vein) minerals like zeolites, phyllosilicates and a wide range of silica minerals. The silica minerals occur more commonly in the *aa* type lavas wherein they fill, either partly or wholly, cavities of various sizes and shapes ranging from small more or less round vescicles and lenticular bodies, to broader or

narrower veins sometimes extending up to ten metres. As the host rocks weathers at a relatively faster pace, the silica minerals get released and could be collected from the fields, streams and rivers.

The widest range of silica minerals anywhere in the world occurs in the area, and includes rock crystal, crystobalite and amethyst as well as innumerable microcrystalline varieties like chalcedony, carnelian, sard, plasma, crysoprase, prase, onyx, banded agates, zebra agates, jaspers of various colours, as well as beautiful moss-agates, tree-agates and bloodstone for which the areas have long been famous. The occurrence of these varieties is discussed with regard to their geographical distribution in the province.

The lapidary industry which utilizes these materials is located at Cambay and other centres where age-old traditional methods are employed even today to produce beads and cabochons of various shapes and sizes for use in inexpensive jewellery.

The physical properties, XRD characters, and thermal behaviour are discussed supplementary to gemmological properties of this plentifully occurring mineral group.

INFLUENCE OF PRESSURE ON STACKING DISORDER AND MIXED-LAYERING: HRTEM STUDY OF CHLORITE COOKEITE.

Jullien M., Goffé B. (*Lab. de Geologie, Ecole Normale Supérieure de Paris*) and Baronnet A. (*Centre de Recherche sur les Mécanismes de la Croissance Cristalline de Marseille*).

Cookeite $LiAl_4Si_3AlO_{10}(OH)_8$ is a di,trioctahedral Al-Li-rich chlorite. It occurs not only in its classical pegmatitic environment but also in a wide variety of metamorphic rocks (metapelites, metabauxites...) over a narrow temperature range, i.e. between 250 and 450 °C, and between pressures from 1 to 15 kbar (Vidal & Goffé, 1991). An HRTEM study of natural cookeites from these environments reveals a progressive ordering of the stacking sequence as a function of increasing pressure, thus affecting polytypism and mixed-layering (Baronnet, 1992).

Polytypism: At low pressure, below 4-5 kbar, all cookeites exhibit great stacking disorder with the 1-layer disordered polytype. Between 4 and 8 kbar the stacking sequence becomes more and more ordered with the appearance of the 2-layer polytype. At high pressure, above 8-9 kbar and up to 14-15 kbar, we observe the perfectly ordered 2-layer polytype associated with complex polytypes of 3, 4, 5, 6, 8 and 10 layers. The basic structures of these long-period polytypes are essentially constituted by the 1-layer, 2-layer and 2-layer twinned structures.

Mixed-layering: pressure favours spectacularly and probably constrains the mixed-layering of the association cookeite/paragonite. At low pressure, below 8 kbar, we observe complete segregation of these two phases. For pressure above 8-9 kbar, regular periodic or quasi-periodic cookeite/paragonite mixed-layer structure appears. The regular mixed-layer mineral saliotite consisting of 1cookeite/1paragonite (Goffé *et al.*,1994), coexists with a mixed-layer structure which have very long quasi-period made of *n*cookeite/1 paragonite with $22 < n < 26$.

This study demonstrates the influence of pressure on crystalline microstructures, stacking disorder and mixed-layering. It allows one to define the thermodynamic stability fields of these polytypic structures, as is the case for polymorphs.

References:

Baronnet, A. (1992).In: Minerals and Reactions at the Atomic Scale: Transmission Electron Microscopy. P. R. Buseck, ed. *Rev. Mineral.* **27**, 231-288.

Goffé, B., Baronnet, A., Morin, G. (1994). *Eur. J. Mineral.*, submitted.

Vidal, O. & Goffé, B. (1991). *Contrib. Mineral. Petrol.*, **108**, 72-81.

EVOLUTION OF CARBON AND REDOX STATE DURING UPWELLING OF GRAPHITE-BEARING ASTENOSPHERE

A.A. Kadik, *(V.I.Vernadsky Inst. Geochemistry. and Analytical Chemistry,Russia,Moscow)*

Electrochemical measurements of the oxygen fugacities (fO_2) of coexisting minerals (Ol,OPx,CPx,Spl,Gar) of mantle peridotite xenoliths from Mongolia and the Baikal region (central Asian) indicate that the evolution of the upper mantle beneath continental rift systems is characterized by a wide range of redox conditions mainly in the range between the wustite-magnetite (WM) and the iron-wustite buffer (IW). Main part of slightly depleted lherzolite are moderately reduced (around WM and WM-2). At 800-1200 °C,10-20 kbar the range of oxygen fugacities correspond to the complete spectrum of *C-O-H* fluid saturated by carbon. This conclusion confirms by the presence of rare and extremely fine-graned (2-3 *mk*) crystals in minerals and carbon dissolved in olivines and pyroxenes (5-100 *ppm*).

The observed evolution of oxygen fugacities is closely linked to the distribution of volatile species. H_2O and CO_2 would be dominant volatiles for more depleted and oxidized peridotites and CH_4 - for more reduced and less modified part of peridotites. We interpret highly reduced peridotites as a relict from erlier lower-fO_2 regime in the outer layers of primitive Earth . By comparing the measured fO_2 with carbon-CO-CO_2-carbonate equilibria we find the data not to be consistent with hypothesis that oxidation state of the upper mantle is buffering by *C-O* fluid in equilibrium with elemental carbon. Our data support that oxygen fugacity of the fertile upper mantle is weakly buffered by ferric/ferrous redox equilibria.Correlation between fO_2 of minerals and the composition of the spinel lherzolites (Mongolia) in terms of degree of extraction of the basaltic component indicates decreasing of *fO2* during partial melting. It is expected, that redox state of primary melt has been controlled by reactions: $C(graphite) + 2Fe_2O_3(melt) + O^{2-}(melt) = CO_3^{2-}(melt) + 4FeO(melt)$.

It is suggested, that the carbon-melt-crystal reactions during *(1)* fluid - absent melting in presence some amount of free carbon or *2)* fluid- absent melting of carbon-bearing minerals may be reason of the carbon-species formation in basaltic magmas. The reaction between graphite and basaltic melt $C(graphite) + O^{2-}(melt) + O_2 = CO_3^{2-}(melt)$ *(1)* may lead to formation in magma 0.1 - 0.5 % *wt.* CO_2 , observed generally in basaltic glasses. It was shown that carbon is incompatible element in the melt + carbon-bearing olivines,pyroxenes equilibria (*D= C* in melt/*C* in crystal = 10 - 100) (Kadik & Shilibreeva,1994) and during the fluid-absent

partial melting magma will be enriched in carbon in comparison with crystalline rest. CO_2 content in melt during partial melting in the absent of the free carbon may be enough high (several hundreds *ppm*).

Melts that finally segregate from that source and erupt on the earth's surface may than be more oxidized than the mantle source at depth prior to partial melting. The extent of melt oxidation relative to the mantle source may be directly proportional to the depth of graphite exhaustion.

References:
Kadik, A.A.,Shilobreeva S.N. (1994). *Lunar Planet. Sci. Conf. 25th.*

THE EFFECT OF ADSORPTION ON THE TRANSFORMATION OF ALUMOSILICATES DURING SOLUTION.

Kadoshnikov V.M., Manichev V.J. *(Department of Radiochemistry of Environment Inst. of Mineralogy, Geochemistry and Ore Formation, Ukr. Ac. of Sci., Kiev)*

The description of the transformation of silicates and alumosilicates that takes into account only changes of physico-chemical parameters of the dispersive medium is found to be incomplete since it does not take into account the considerable changes of the surface energy on the solid phase which appear due to the adsorption.

The investigation on the kaoline dissolving by the carbon dioxide solution in the presence of the soil acids has shown that during the adsorption of the humine acid on the kaoline surface the value of the free solution energy is changed. During this process the adsorption does not hange the incongruent character of the kaoline dissolving but increases the solubility of the mineral mainly for the augmentation of the silica extraction from the mineral into the dispersive medium. This effect is supposed to be caused by the reducing of the bonds (linkage) between the atoms of the surface phase with one another and with the matrix.

This phenomenal is simultaneously connected with the reduction of the chemical bonds of the silica and the aluminium and with the increased reaction capacity of such surfaces.

„MAURITZITE" AN IRON-RICH SMECTITE FROM ERDŐBÉNYE (HUNGARY), THE PHASES OF ITS MODIFICATION

Kákay Szabó O. *(Hungarian Geological Survey)*

A mineral of cylindrical shape, composed by balls of size from 2 to 5 mms and of a black velvet colour, filling the vesicles of the pyroxene andesite in neighbourhood of Erdőbénye was called *mauritzite* by L. Tokody (1) in honour of the late Professor B. Mauritz. However the statements of Tokody seemed to questionable to M. Fleischer (2) and it is by now a mineral under discussion (C. Hintze (3), H. Strunz (4)). According to new investigations (O. Kákay (5), by optical, chemical, X-ray, thermal, infrared, Mössbauer, SEM and transmission methods, the mauritzite is a *layer silicate between the di- and trioctahedral smectites.*

There are considerable subtitutions *in the tetrahedral layer where Si* is substituted by *Al* and Fe^{3+}. *In the octahedral layer cation sites occupied* by Fe^{3+}, Fe^{2+} and *Mg*. The interlaminar space contains large amount of water. The quantity of exchangeable cations is small.

$$(Ca_{0.14}\,Na_{0.03})(Fe^{3+}_{0.88}\,Fe^{2+}_{0.45}\,Mg_{1.43})^{VI}(Si_{3.32}\,Al_{0.42}\,Fe^{3+}_{0.26})^{IV}O_{10}(OH)_2$$

In the octahedral layer the value of $Fe^{3+}+Fe^{2+}$ substitution is 1.33, the high value of Fe^{3+} substitution results in a deficit of cations (-0.24). The sum of octahedral positions occupied by Fe^{3+}, Fe^{2+} and vacant octahedral positions is higher then the number of Mg positions: ($Fe^{3+}+Fe^{2+}$+def.ofcat.=0.88+0.45+0.24=1.57>1.43=Mg)

Genesis and alteration:

The original pyroxenes were transformed from inosilicates to phyllosilicates by the cation mobilizing effect of water derived from steam phase during crystallization of pyroxene andesite. Poorly crystallized smectite phases of variable Fe and Mg content replace very often primary magmatic minerals. Their chemical composition is nearly identical but they are not of identical crystal phase. This results in an uncertainty in the literature on iron saponites. The mauritzite, however, is a specific crystal phase: it crystallized from fluids derived from the magma under high pressure and high temperature in the vesicles of andesite. Mauritzite remained without further change only in the deep zones of the subvolcanic body. This is why it is so rare. Passing from the deep zones of the laccolith toward the surface mauritzite undergoes alteration under decreasing pressure and temperature. In the successive rearrangements of the structure of mauritzite first, the Mg, Fe cations leave the octahedral layer resulting in collapsed lattice structure. The remaining material enriched in SiO_2 is rearranged to new silicates (illite, chalcedone, quartzine, hyalite, trydimite and quartz).

References:
Tokody, L. (1957). *Ann. Hist. Nat. Mus. Nat.* Hungary., **8**, 17—21.
Fleischer, M. (1957). *Discussion. Am. Min.*, **42**, 407.
Hintze, C. (1967). *Handbuch der Mineralogie.*, **III**. 451.
Strunz, H. (1970). *Mineralogische Tabellen.* Leipzig, 551.
Kákay Szabó, O. (1983). *Földtani Közlöny.*, **113**, 333—356.

STUDY OF MINERALS BY NMR

Kalinichenko A.M. (Inst. of Geochemistry, Mineralogy and Ore Formation of Ukr.Ac. Sc.,Kiev)

The NMR method can be used for solving various problems of crystallochemistry, geochemistry and mineral genesis.

1.The determination of crystalline distribution of cations.

It should be noted that NMR of ^{1}H, ^{27}Al, ^{29}Si gives the great posibilites for the investigation of crystallochemical peculiarities of micas, amphiboles, hydrogrossular and zircon. NMR of H (PMR) is of the greatest importance, since protons are present in considerable quantities in both containing water and nominally waterless minerals.

The clustered distribution of octahedral cations in micas and amphiboles has been established, moreover, the size of Fe-Mg clusters in phlogopite and the phlogopite clusters in muscovite were found by complex using data obtained by PMR and ESR.

New scheme of isomorphism $Si^{4+} \rightarrow Al^{3+} + H^{+}$ has been proposed as a result of the study of the isomorphism character in hydrogrossular by NMR. By the same way for zircon it was proved that both crystalline and amorphous phase of malacon contain OH-groups. The validity of the zircon crystallinity degree determined by NMR has been confirmed by the X-ray evidence.

2.The investigation of fluid inclusions.

The method of the quantitative determination of the water and sodium content in the fluid inclusions of some minerals is offered. It has been shown that in the quartz-felspars veins the sodium content in the quartz is considerably larger than in the felspars while the water content is considerably smaller. This phenomenon is considered to be connected with the different content of the sodium and the water during the crystallization of felspars and quartz. Thus NMR data can be useful for the investigation of the ore-formation processes.

3.The description of the mineral genesis.

The study of PMR spectrums of nominally waterless minerals (pyroxenes, andalusite, sillimanite, sulfides and others) shows that both the admixed phases and the inclusions of protons in structure of minerals (so-called "the proton corrosion") can be revealed from these spectrums. It is assumed that the content of such protons indicates the degree of minerals hydrolysis and, therefore, the intensity of hydrothermal processes.

The analysis of the results obtained by PMR permits to recommend this method for the express determination of the ideality degree of various mineral structures.

SILVER IN COPPER AND LEAD MINERALS

Kalinin A.A. *(Geol. Inst., Apatity, Russia)*

Available data on Ag deposits (Sidorov et al.,1989) show that Ag mineralization was formed due to late hydrothermal alteration of high-temperature sulfide ores; metasomatic processes favour mobilization of Ag dispersed as an isomorphic admixture in early sulfides. With a view to evaluate isomorphic capacity of minerals in respect of Ag we analysed data on Ag-content in sulfides and their analogues from massive sulfide, copper-nickel sulfide, copper-molybdenum porphyric and polysulfide hydrothermal ore formations with a focus of attention on Cu and Pb minerals.

As a result of study of Cu sulfides we obtained the following raw of minerals in succession of increase of Ag-content:cubanite - chalcopyrite - bornite - digenite and anilite - chalcocite - klockmanite - covellite - tetrahedrite group (tennantite - tetrahedrite - freibergite). The minerals at the beginning of the raw contain 0.03% Ag (cubanite) and at the end of it 34% Ag (freibergite). The least favourable minerals for isomorphic silver are double sulfides of Cu and Fe. In the structures of these minerals Cu occupies tetrahedral emptinesses between 4 S atoms (Kostov & Kincheva-Stefanova, 1984); Ag-content increases accordingly the increase of Cu content from cubanite to bornite. Other minerals of the raw contain structural groups with triangular coordination of copper atoms. As soon as the same triangulars AgS_3 are characteristic of Ag sulfide (acanthite) it explains a sharp rise of Ag admixture in Cu sulfides (digenite - covellite) up to 0.6%. And the most favourable for Cu-Ag isomorphism are friable and frame-type structures of tetrahedrite-group minerals where complete isomorphic substitution of Cu in triangular position is possible (4 formula units,i.e.23 mass.%), and 2 additional atoms of Ag (up to 34%) may be mobile in conducting cells (Mozgova & Tsepin, 1983).

The raw of Ag-isomorphic capacity of lead minerals is the following: altaite - clausthalite - galena - boulangerite - kobellite, i.e. from telluride to selenide and sulfide and then to Pb sulfosalts. During the late evolution there are formed Pb-Ag, the Ag sulfosalts and native silver. The sulubility of Ag_2S in PbS is known not to exceed 0.6 mol.% even at 600°C (Amcoff,1984). A sharp rise of isomorphic substitution appears if Bi or Sb enters the structures of Pb minerals together with Ag: $2Pb^{2+} \rightarrow Ag^{+} + Bi(Sb)^{3+}$, it explains high content of Ag admixture in Pb sulfosalts.

In case of intergrowths of Fe-Ni-Co, Fe-Cu, Cu and Pb sulfides Ag distributes among Cu and Pb minerals only, the coefficient of Ag-distribution to Cu sulfides, tellurides, selenides and sulfosalts varies from 2 to 4.

References:

Sidorov A.A.,Konstantinov M.M.,Eremin N.A., Savva N.E.,Kopytin V.I.,Safronov D.N.,Naiborodin V.I.& Goncharov V.I. (1989). *Silver (geology, mineralogy, genesis, ore deposits).* "Nauka", Moscow (in Russ.)

Kostov I.& Kincheva-Stefanova J. (1984) *Sulfide minerals. Chrystal chemistry, paragenesis, systematization.* "Mir",Moscow (in Russ.)

Mozgova N.N.& Tsepin A.I. (1983). *Tetrahedrites.* "Nauka",Moscow,(in Russ.)

Amcoff O. (1984) *Mineral. Deposita*, 19,63-69

MĂGURENI HILL, PRELUCA VECHE: A NEW OCCURRENCE OF HYDROTHERMAL SEPIOLITE

János Kalmár, Péter Kovács-Pálffy, Mária Földvári
Hungarian Geological Survey, Budapest

In the western slope of Măgureni Hill (Preluca Veche, Romania) an interesting sepiolite occurrence is developed. Sepiolite and accompanying minerals (steatite, saponite, kaolinite, vermiculite) fill veins, 1-5 cm thick, in neighbourhood of some pegmatite lodes which traverse crystalline limestones and dolomites of early Paleozoic? age (Măgureni Carbonate Formation).

The amount of sepiolite in this veins is 85-90%. Sepiolite forms white or light greenish, nacreous, fibrous agregats or felty sheets in thinner, millimeter-size joints of the marbles. The 0.5-2 nm thick sepiolite needlets, of rhombic or polygonate cross-section are displayed in parallel, catenular or star-like agregats, having small quantities of the other clay minerals, secondary carbonates and amorphous silica-drops set into holes of this network.

In this paper, utilising DTA, XRD, IR and SEM-investigations, a detailed mineralogical study of the sepiolite is presented. The microchemical analyse of some sepiolite samples shows a little concentration of Fe, Ni, Co and Zn, which substitute Mg giving small deformation of the lattice.

Genetically, the sepiolite from Măgureni Hill resulted by interaction between Mg-bearing carbonatic host rocks and silica-rich residual solutions during the final stage of the pegmatitic event. - Financial support for this study was provided by the National Scientific Fund (OTKA T 7636).

INSIGHT INTO MT. ETNA PRIMARY MELTS FROM STUDY OF MINERALOGY AND MAGMATIC INCLUSIONS

Kamenetsky V.S.[1,2], Clocchiatti R.[1], Armienti P.[3], Innocenti F.[3]
([1] LPS, CNRS, Saclay, [2] Vernadsky Inst. of Geochemistry, Moscow, [3] DST - Univ. of Pisa).

During the eruptive history of Mt. Etna the initial subalkaline (so called tholeiitic and transitional basalts with $K_2O<0.6$ wt.%) character of volcanics changed to alkaline one ($K_2O>1.2$ wt.%), which is maintained up to present. In order to explain this transition, the mineralogy and magmatic inclusions in olivine have been studied in the most Mg-rich tholeiites (Aci Castello, Aci Trezza, Adrano),

transitional (Paterno) and alkaline (Maletto, Spagnolo, Timpa di Acireale) basalts, using electron microprobe and heating/freezing stages techniques.

Mineral assemblage consists of olivine, spinel, clinopyroxene, ±orthopyroxene. Olivine is the dominant phase with maximum Fo content gradually increasing from 86 mol.% in tholeiites, to 88 mol.% in transitional and up to 89-90.5 mol.% in alkaline basalts. Cr-Al spinel occur as inclusions in olivine phenocrysts and display the wide range of compositions in terms of Cr# and TiO_2 (Fig.1.). The spinel from subalkaline, alkaline basalts and the majority of Mt. Maletto spinel form distinct compositional groups. The relationship between Fo values of the most primitive olivine from alkaline samples and the Cr# of coexisting spinel indicates a near-primary nature of their parental melts, whereas tholeiites lie fairly far from the mantle array, defined by Arai, 1987. Clinopyroxene Mg# (maximum and range) corresponds closely to that of olivine, suggesting its very early crystallisation. Orthopyroxene (Mg# up to 86 mol.%) has been found as inclusions in the most magnesian olivine from tholeiitic lavas only.

The crystallisation temperatures evaluated from the study of melt inclusions in olivine reveal no contrast between samples of different affinity, correlate positively with $Fo_{90.5-78}$ and range from 1250° to 1100°C. The pressure of crystallisation is apparently higher than 300 MPa as indicated by the density of CO_2 primary inclusions in olivine.

Relatively high SiO_2 contents (50-54 wt.%) characterise most of melt inclusions in olivine from tholeiites, anyway Ne-normative melts, enriched in K_2O and P_2O_5 (~1.5 wt. %) melts are also recorded. The primary melt of alkaline rock from Maletto has relatively low MgO (10 wt.%), FeO (7 wt.%) contents and unusually high CaO/Al_2O_3- 1.4. We consider that fractionation of such a melt can produce the spectrum of magmas parental for the historical and present-day volcanics.

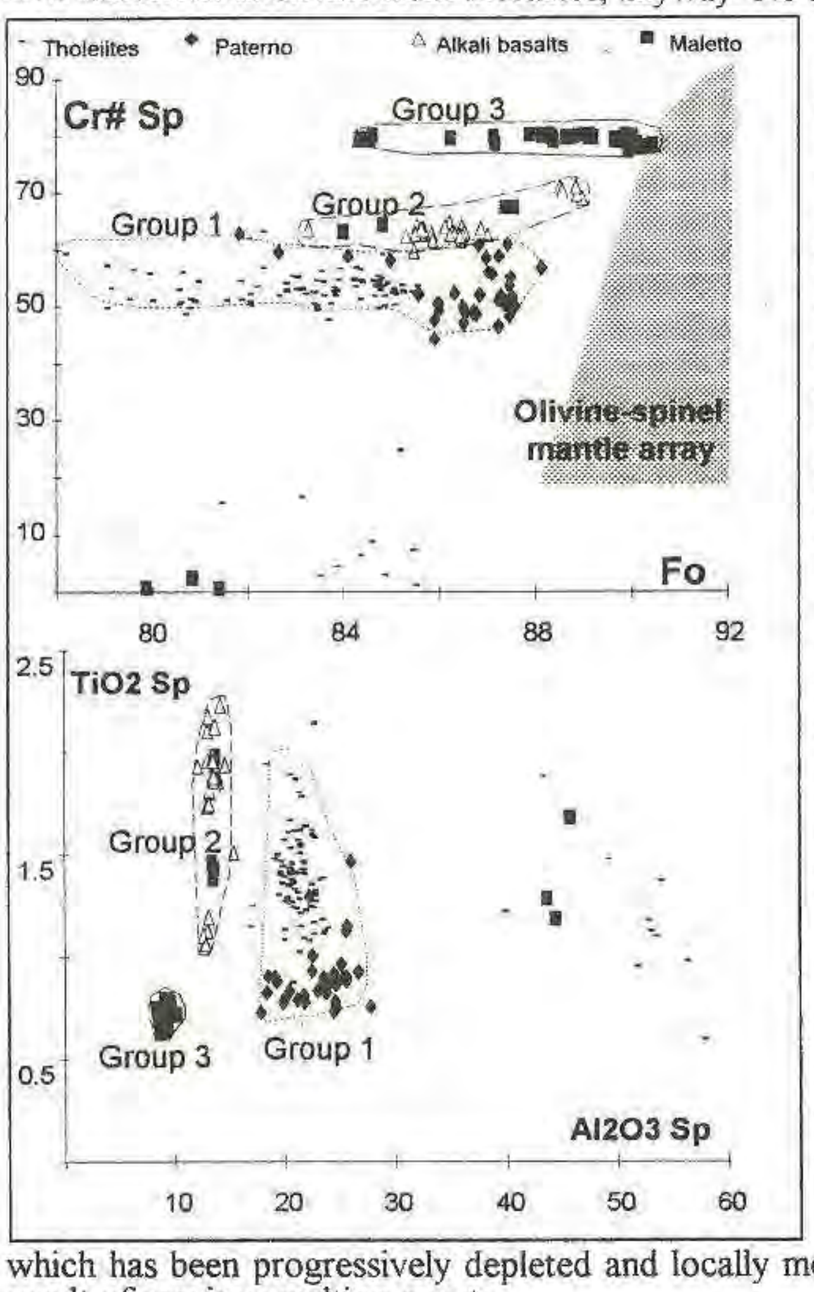

The large compositional range of etnean primitive melts is attributed to various extents of melting of a MORB-like mantle source, which has been progressively depleted and locally metasomatised as a result of previous melting events.

References: Arai, S. (1987). *N. Jb. Miner. Mh.*, **8**, 347-354.

CATHODOLUMINESCENCE AND INFRARED STUDIES OF ARKHANGELSK DIAMONDS

Kaminsky F.V., Zakharchenko O.D. *(TsNIGRI, Moscow, Russia)*, and Milledge H.J., Taylor W.R., Woods P.A *(Dept Geological Sciences, University College London, U.K.)*.

Macrodiamonds (~5-6 mm size) and microdiamonds (<1 mm size) from three kimberlite pipes (Lomonosova, Pomorskaya and Karpinski) of the Zolotitsa field, Arkhangelsk province, northwest Russia, have been characterized by cathodoluminescence (CL) and infrared spectroscopic (IR) methods. CL provides information on diamond growth zonation while IR methods can be used to characterize the state of nitrogen impurity aggregation and hence the thermal history of a diamond (Taylor *et al.*, 1990).

The Arkhangelsk pipes intrude a thick sequence of late-Proterozoic terrigenous sedimentary rock which overlies Archean basement of the Kuloi extension of the eastern Kola Craton. Unlike many kimberlite pipes elsewhere, the upper, crater-facies parts of the pipes are well preserved. Dating of perovskite from one of the pipes (Sinitsyn *et al.*, 1991) gives an Ordovician age (~462 Ma). Xenoliths of garnet dunite, garnet harzburgite, and eclogite have been recorded in drill-core from the Arkhangelsk pipes (H. Downes, S. Sablukov & L. Budkina, pers. comm.), and studies of the concentrate minerals (Sobolev et al., 1992) show that garnet±spinel lherzolite was also sampled by the pipes. Peridotitic garnet thermometry (W.L. Griffin, pers. comm.) indicates that a thick lithosphere and cool cratonic geotherm of ~36-37 mWm^{-2} prevailed at the time of kimberlite emplacement. Within the diamond stability field under these conditions, lithospheric temperatures would have been ~900°C at 140 km depth and ~1100°C at 190 km depth.

The morphologies of Arkhangelsk macrodiamonds include a high proportion of cube, skeletal cube, and resorbed (i.e. dodecahedral and tetrahexahedral) external forms relative to octahedral forms. This indicates the presence of several distinct macrodiamond populations. The internal morphology of 10 representative Arkhangelsk macrodiamonds has been revealed by CL and optical birefringence (BR) studies of polished sections. The CL images show that the macrodiamonds have experienced multiple growth histories and BR patterns show remarkably sharp boundaries between different growth horizons. In one case, a sharped-edged octahedron has been overgrown by a cube form, in another stone a colourless "central-cross" form has been overgrown by an orange cube form, and in other cases complex rhythmic growth zones and sector growth are revealed.

IR spectroscopy shows that the orange cube is a pure type Ib diamond overgrowth on a type IaA core. At ~900°C, type Ib diamond containing ~100-200 ppm nitrogen can only survive for ~1 million years (and less at higher temperatures) without aggregation to the IaA form. Thus the orange diamond overgrowth must represent an Ordovician diamond growth event that occurred immediately prior to kimberlite eruption. In the same kimberlite pipe, a fully aggregated type IaB octahedral diamond is present. If this diamond resided in the mantle at moderate temperatures, say ~1100°C, then its nitrogen aggegration characteristics indicate that it must be several billion years old. Therefore in the one pipe there is evidence for both Palaeozoic and Precambrian diamond growth events.

Unlike the macrodiamonds, the Arkhangelsk microdiamonds are commonly of sharp-edged octahedral external form without cubic overgrowths. The microdiamonds have presumably grown in a region of the mantle isolated from late-stage diamond growth events.

References:

Sinitsyn, A.V., Ermolaeva, L.A., Grib, V.P. (1991). *Extended Abstracts, 5th International Kimberlite Conference, CPRM-Special Publication*, **2/91**, 367-369.

Sobolev, N.V., Pokhilenko, N.P., Grib, V.P., Skripnichenko, V.A., Titova, V.E. (1992). *Soviet Geology and Geophysics*, **33**, 71-78.

Taylor, W.R., Jaques, A.L., Ridd, M. (1990). *Am. Mineral.*, 75, 1290-1310.

GROUNDMASS MINERALS IN THE KUNDELUNGU KIMBERLITES, SHABA, ZAIRE.

Kampata D.M. *(Géol. et Miner. Univ.Cath.Louvain, Belguim)*

Moreau J .*(Géologie Mineralogie, Univ.Cath.Louvain, Belguim)*

Nixon P.H *(Dept of Earth Sciences, The University of Leeds, U.K.)*

Two kimberlitic provinces are currently recognised in Zaire: the diamond-rich kimberlites from Mbuji Mayi in the East Kasai region (Mbuji Mayi), and the the diamond-poor kimberlites from the Kundelungu plateau in the Shaba region.

In the Kundelungu area, about 24 kimberlite pipes croup out along two alignments which trend north-south corresponding to the eastern and western borders of the plateau. The kimberlite pipes were probably intruded into the western border of the Bangweulu block, which was cratonized at about 1800 Ma.

The minerals of the kimberlite groundmass are olivine, monticellite, spinel, perovskite, ilmenite, calcite and serpentines. The enclosed megacrysts are Cr-rich and Cr-poor pyrope, Cr-

diopside, enstatite, olivine and ilmenite. Almost all pipes contain crustal inclusions and mantle nodules (lherzolites and eclogites).

Olivine in the groundmass occurs as small (<0.3mm) euhedral-to-subhedral single crystals or as serpentinized euhedral crystals surrounded by a monticellite corona. The forsterite content in the solid solution ranges between 85.6 and 91.3 mole % for both types of olivine.

Monticellite presents two distinct morphological varieties : small, isolated idiomorphic crystals (5 to 10 mm) and epitaxial coronas which surround olivine crystals. Both have similar compositions, containing 11 to 19 mole % kirschteinite and 2.5 to 7 mole% forsterite.

Spinel occurs as small (0.2mm) euhedral to subhedral crystals randomly distributed throughout the groundmass or as reaction fringes around ilmenite. Their chemical composition exhibits a characteristic trend, traversing Haggerty's (1976) prism at similar Fe/Fe+Mg ratios and showing a distinct hiatus in the sequence of crystallization.

Ilmenite is found as isolated anhedral crystals or intergrown with spinel, rutile and perovskite. It defines a trend close to Haggerty's magmatic Mg-enrichment trend (Haggerty *et al.*, 1979).

Perovskite occurs as euhedral to subhedral crystals or a complex pseudomorphs after ilmenite or spinels. It is the major carrier of the rare earth elements and other trace elements (Nb, Th, Ta, etc.).

Serpentine (essentially chrisotile and lizardite) and carbonates are the dominant secondary phases in the groundmass. Pyrite, phlogopite, barite and apatite are also present.

The mineralogical similarity between the different kimberlite pipes in the Kundelungu area suggests their consanguinity.

References:
Haggerty, S.E.(1976). *Mineral. Soc. Amer.* **3**, 101-300.
Haggerty, S.E., Hardie, R.B.II, McMachon, B.M. (1979). *Amer. Geophys.*1,*Union,* 245-259.

A UNIQUE ASSEMBLAGE OF LEAD FLUORIDE MINERALS FROM THE GRAND REEF MINE, GRAHAM COUNTY, ARIZONA

A.R. Kampf (*Natural History Museum of Los Angeles County*)

Six new lead fluoride minerals have been found in the oxidized zone of the Grand Reef mine, an epithermal Cu-Pb-Ag deposit in Graham County, Arizona. Grandreefite, $Pb_2SO_4F_2$, pseudograndreefite, $Pb_6SO_4F_{10}$, laurelite, $Pb(F,Cl,OH)_2$, and aravaipaite, $Pb_3AlF_9{\cdot}H_2O$ were described by Kampf et al. (1989). Artroeite, $PbAlF_3(OH)_2$, has been approved by the CNMMN. Another mineral, of composition $PbCa_2AlF_6(OH)_3$, is still under study. These minerals are found in quartz-lined vugs that are enveloped by layers of galena and fluorite. Secondary copper sulfates such as linarite and caledonite dominate the mineralization outside of the vugs containing the Pb-F minerals, but are absent within the vugs. Acidic supergene sulfate-rich solutions are thought to have freed Pb and F from the layers of earlier-formed galena and fluorite. The layers of galena and fluorite apparently also served as a barrier preventing Cu^{2+} from entering the vug and limiting the amount of SO_4^{2-} available relative to F^-.

The structures of grandreefite (Kampf, 1991) and artroeite have been solved completely and the structure of pseudograndreefite has been partially solved. The grandreefite and pseudograndreefite structures consist of layers based upon the β-PbF_2 (fluorite) structure with SO_4 groups between layers. The artroeite structure contains edge-sharing dimers of $AlF_3(OH)_3$ octahedra linked together via bonds to Pb atoms to form approximately close-packed layers. In grandreefite Pb is in eightfold coordination with a relatively balanced distribution of bond distances. In artroeite Pb is in ninefold coordination with a very lopsided distribution of bond distances that can be attributed to the lone pair effect.

Twinning and poor crystal quality have thus far hampered the determination of the structures of the other new minerals. The laurelite structure is probably related to that of penfieldite (Merlino, Pasero, and Perchiazzi, personal communication). Evidence suggests that the structures of aravaipaite and the mineral of composition $PbCa_2AlF_6(OH)_3$ are closely related.

Because of limited resources, scientific research in a mineralogical museum often requires significant interaction with outside individuals and institutions. In this study, the specimen containing the first four new minerals was brought to the author's attention by W.W. Besse, then a graduate student at California State University at Los Angeles. This and other specimens, as well as information concerning the deposit, were provided by several mineral dealers and collectors, R.A. Bideaux, L. Presmyk, D. Shannon, and W. Thompson. Microprobe analyses were conducted by P.J. Dunn of the Smithsonian Institution and E.E. Foord of the U.S. Geological Survey (Denver, Colorado), L.L. Jackson also of the USGS (Denver) made water determinations, G.R. Rossman of the California Institute of Technology assisted with IR spectroscopy, and C. Strouse and S. Khan of the Department of Chemistry and Biochemistry, University of California, Los Angeles provided the facilities for the structure determinations.

Kampf. A.R. (1991). *American Mineralogist*, **76**, 278-282.
Kampf, A.R., Dunn, P.J., Foord, E.E. (1989). *American Mineralogist*, 74, 927-933.

Neo-granite pluton at the Kakkonda Geothermal Field, Northeast Japan: Petrological characteristics of the Quaternary pluton as the heat source

Kanisawa,S., Ishikawa,K. (Tohoku Univ.,Sendai,Japan), Doi,N. and Kato,O. (Geothermal Engineering Co.Ltd., Iwate, Japan)

The Kakkonda geothermal field is one of the most prominent liquid-dominated geothermal systems belong to the Sengan geothermal area, Northeast Japan. A neo-granite pluton is confirmed at the bore holes of 1,950 - 2,770m depth, which is considered to be one of the heat source of the area. Chemical composition of the pluton ranges from quartz diorite of SiO_2 65% to adamellite of SiO_2 75%. Observed well temperature is up to 350 °C, which is higher than the closure temperature of K-feldspar. K-Ar ages of minerals of the pluton have the range from 0.068 to 0.34 Ma, which may indicate the subsequent ages passing the closure temperature of each mineral. The intrusive age of the pluton might have been older than the obtained data, and slightly younger than 0.7 - 1.0 Ma, from the relation between the ages of the adjacent Tamagawa Welded Tuffs (TWT). The TWT are thought to be related genetically to the pluton because of their closely association with the pluton in space and time. Trends of chemical composition of the pluton, however, have a slight difference from those of the TWT; i. e., the former are lower in Al_2O_3, P_2O_5 and higher in MgO contents than those of the latter. The difference is due to the crystal segregation and elutriation of

particles during flowage of pyroclastic rocks, or to lateral zoning of composition in magma chamber. Major and trace element chemistry of the pluton, however, shows similar characteristics of those of the Pleistocene acidic pyroclastic rocks from southern part of northeast Honshu, Japan.

The genetic relation between the pluton and the Tamagawa Welded Tuff should be further studied in detail.

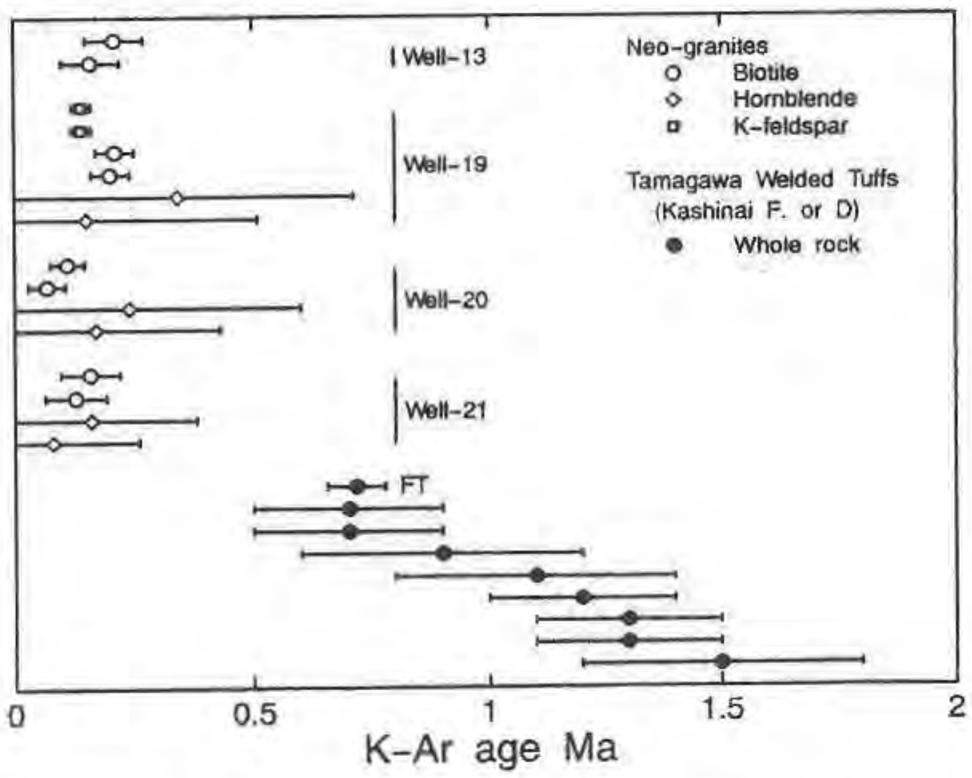

Fig.1. Results of K-Ar age determination of plutonic rocks and Tamagawa Welded Tuffs (TWT).

STAUROLITE SCHIST AND AMPHIBOLITE TERRAINS OF THE SERBO-MACEDONIAN MASSIF UNDER GEOTHERMO-BAROMETRY CONSIDERATION

Karamata S.[1], Fed'kin V.[2], and Cvetkovic V.[1]

(1 - Faculty of Mining and Geology, Belgrade University, Belgrade, Yugoslavia; 2 -Inst. of Experim. Miner., Russian Acad. of Sciences, Chernogolovka, Moscow distr., Russia)

Different rock types - staurolite metapelites, amphibolites, dyke complex rocks etc., have been studied with a special emphasis on mineralogical geothermobarometry. Detailed microprobe investigation of compositions of co-existing minerals, their zoning, inclusions and contacting mineral portions permitted the reconstruction of physico-chemical conditions of metamorphism at the different stages of the region geological development. The PT path of the metamorphic evolution was computed on the basis of the internally consistent and experimentally supported system of mineralogical geothermometers, geobarometers and water fugacity indicators. At least three stages of mineral formation were reconstructed for Serbo-Macedonian metamorphic complexes.

The most ancient granulite stage is fixed in the contact aureole of the Bistrice ultrabasic massif, located in the southern part of the Serbo-Macedonian block. Maximum metamorphism parameters (T = 600-870 ^{o}C, P = 7.8-9.3 kbar) have been estimated for Cpx-bearing garnet amphibolites which seem either to preserve (or to inherit) tracks of the most ancient and most high-level metamorphism of the ophiolite plate remnants, overthrusted (or intruded ?) on (into) the Paleozoic base. The first stage of thermal history of the region must have been interrupted by tectonic movements from time to time and reflects conditions of subisobaric cooling.

The physico-chemical conditions for the amphibolite facies were fixed in alumina and basic rocks at some distance from the Bistrice ultrabasic massif boundary and in the north part of the Serbo-Macedonian block. The compositions of co-existing minerals from micaceous schists of the Lebane-Medvedya area and from amphibolites and Sta-bearing rocks of the Batochina region show a retrograde P-T trend from T = 560-600 ^{o}C, P = 6.7-7.1 kbar to T = 470-520 ^{o}C, P = 1.5-2 kbar. The beginning of this (second) stage reflects conditions of a rapid uplift of the Earth's crust portion, which gradually reaches conditions of a normal geothermal gradient.

The third, final stage of the thermal history of the Serbo-Macedonian massif is likely to have occurred later than the other two and is related to the development of a later dyke complex of basic composition. Garnet-amphibole and garnet-biotite parageneses of this complex show some features inherent in prograde metamorphism and are characterized by conditions from the green schist facies (and lower), T = 370-420 ^{o}C, P = 0.3 - 0.7 kbar to epidote-amphibolite facies, T = 500-520 ^{o}C, P = 3-4 kbar. The P-T trend of this stage coincides in slope with that of the second (amphibolite) stage and seems to fix the latest position of the geothermal gradient.

DIAMOND FROM MINAS GERAIS, BRAZIL: AN UPDATE ON SOURCES, PRODUCTION AND CHARACTERISTICS

Karfunkel, J., Chaves, M.L.S.C. *(Dept. of Geology,Federal University of Minas Gerais,Brazil)*,and Svisero, D.P. *(Inst. of Geoc. Univ. of São Paulo, Brazil)*

The State of Minas Gerais (MG) was the main diamond producer worldwide for almost 150 years. In 1870, 2/3 of the world production still came from Brazil, mostly from MG, declining a decade later to about 3% of the 3.140.000ct mined in 1880. In 1991 Brazil contributed about 1.5% to the world diamond production of 100.000.000ct, with 220.000ct comming from MG.

About 98% of the diamond produced in MG come from alluvial deposits and less than 2% from Middle Proterozoic metaconglomerates in the Diamantina district.

The two main source areas are located in the Diamantina region of the Espinhaço Range, and in western MG. The Jequitinhonha River and its tributaries, Espinhaço Range, constitute the most important area. Mining is conducted there by companies as well as by thousands of diggers *(garimpeiros)*. Grades of 0.008 to 0.2 ct/m3 are reported from alluvial deposits, while the Proterozoic metaconglomerates contain up to 1.75ct/m3, with a minerable average between 0.3 to 0.7ct/m3. Most of Espinhaço diamonds are of gem quality with an average colour from G to J and an average size around 0.5ct. Dodecahedra and octahedra are the most common crystallographic forms. Carbonados and ballas rarely occur.

In the western part of MG, mainly in the Alto Paranaíba and São Francisco basins, some localities such as Coromandel and Rio Bagagem became famous as a result of periodic findings of large diamonds, some weighing over 100ct, including the *Presidente Vargas* with 726.6ct. Average estimated grades are 0.04 to

0.1ct/m3. Simple dodecahedral (63%) and octahedral habits (35%), are the most commons.

Although many theories try to explain the origin of the diamonds in MG, all are mined from sedimentary deposits: Precambrian metaconglomerates, Cretaceous conglomerates, and recent alluvial and colluvial gravels. Two fundamental problems remain una nswered: i) the nature of the primary source rock, and ii) their geographic situation.Mineral inclusions indicate ultramafic origins - the most accepted theory today.

The 1.7-1.6 Ga age for the metaconglomerates of the Espinhaço Range with the source area in the cratonic region towards the west is regarded as plausible. These diamonds and those mined in western MG may have similar age and source areas even though a source from Cretaceous kimberlitic intrusions are postulated by some authors (the latter without economic diamond content up to day). Another theory for the origin of the MG diamonds is their transport and deposition during the late Proterozoic glaciation (about 1 G.a.), followed by Cretaceous and later concentration by alluvial processes.

Although much ongoing research attempts to resolve the origin of the diamonds in MG, it may be hampered by the possible erosion of craters and diatremes, such that the remaining root zones are sterile and/or buried under hundreds of meters of sediments. The future will show if the source rock and area can be identified, located, and economically explored. The study of diamond production from secondary deposits in MG over the past 250 years suggests, that there will be no significant increase in production during this century.

POLYANION STRUCTURES IN SILICATE MELTS

Karlsson K.H. and Fröberg K. *(Department of Chemical Eng., Åbo Akademi Univ., Finland)*

The existence of some kind of medium range order in silicate melts and glasses has been a generally accepted fact at least since Bockris and coworkers published their papers in the mid 1950ies. When adding more than some 15...20 mol-% alkali oxide to silica, already stoichiometry requires discrete polyanions. But the extraordinary stability of the melts excludes structures reminding of any elementary cell. High temperature NMR show that in the acidic range glasses and melts have common structural features, while low temperature NMR gives a Q^n distribution that at least is not in contradiction with stoichiometry nor with Raman, when suggesting the concentration of 4-rings decreasing and of 3-rings increasing towards disilicate composition. Based on high temperature voltammetry a polyanion model has been suggested that below some 27 mol-% alkali oxide include 6-rings as well. A feature of the model is that it predicts Si-O-Si angles that fall within the quoted error margins calculated from X-ray diffraction on sodium silicate glasses.

The model takes into account two different types of reactions. Breaking of oxide bridges, but with preserved number of anions, is considered as neutralisation, while a breaking resulting in a splitting of the anion is considered as depolymerisation. The former leads to oxide dents with an ability to form chelate type complexes with a metal oxyanion, while the latter can on the most form a singular complex bond with the anion. When a chelate is formed with, say, an aluminate or ferrite ion, the metal looses much of its identity, while many properties due to the silicate anion remain almost unchanged. Thus it is the soda/silica ratio that determines the properties of the melt, while the alumina changes Q^3 configurations to Q^4 but hardly affects the size of the anion. This explains for instance why small alumina additions hardly affect the viscosity all.

NEW VARIETIES OF HINGGANITE-GADOLINITE GROUP MINERALS FROM ALKALINE-GRANIT PEGMATITES OF WESTERN MONGOLIA

Kartashov P.M. and Lapina M.I. (Institute of Geology of Ore Deposits of RAS, IGEM RAN, Moscow)

In Tatyana alkaline-granit pegmatite (Mongolian Altai), hingganite-gadolinite group minerals were found in two situations. Brown zonal crystals from the microclin-quartz complex of axial part of vein were described in (Kartashov et al.,1993). Here they associate with genthelvite, bavenite, allanite, cyrtolite, thorite, britholite, chevkinite, fergusonite and xenotim. The grains of hingganite coloured light-gray up to colorless and looking homogenious, were found within pseudomorphoses after REE-eudialyte from block zone of the pegmatite together with zircon,allanit and calcit.

Earlier, we have determined three zones (generations) in gadolinite-(Y) crystals from microclin-quartz complex Gd-I,Gd-II and Gd-III (from centre to periphery), that differ greatly in ratio LREE/HREE+Y - 0.68, 1.11, 0.11. The mineral was referred to low-ferroan gadolinite, but taking into account isomorphism according scheme $REE^{3+}Fe^{2+}=Ca^{2+}Fe^{3+}$, on the triangular diagram $REE_2Fe^{2+}Be_2Si_2O_{10}$-$REE_2Be_2Si_2O_8(OH)_2$-$CaREEFe^{3+}Be_2Si_2O_{10}$ compositions Gd-I and partially Gd-II fall in hingganite field, while Gd-III ones appear on the hingganitecalciogadolinite boundary line. A more detailed investigation of Gd-II enriched with LREE made it possible to discover microzones (up to 10 mkm) and spots corresponding in their composition to gadolinite-(Nd)(Nd>Ce>Y), hingganite-(Nd)(Nd>Ce>>Y) and hingganite-(Ce)(Ce>Nd>Y).

Three phases:two selectively yttrian (up to 84 wt% from REE+Y) low and high calcian ones, and a REE-rich phase, were determined within colorless grains from pseudomorphoses. In these, LREE/HREE+Y ratio reaches 0.02, 0.002 and 0.79, respectively. The first phase forms independent zones and in fact is hingganite-(Y). Two others were found closely accreted. Since the isomorphic scheme $REE^{3+}Fe^{2+}=Ca^{2+}Fe^{3+}$ can't be obviously applied to them, due to Fe valency, and their compositions can not be described with traditional calcian minals calciogadolinite $CaREEFe^{3+}Be_2Si_2O_{10}$ and $REE_2CaBe_2Si_2O_{10}$ minasgeraisite, we introduced a new minal of composition $CaREEFe^{2+}Be_2Si_2O_9(OH)$ connected with gadolinite by isomorphous substitution $REE^{3+}O^{2-}=Ca^{2+}OH^-$. The compositions are fall within the hingganite field along the same line (52 at% Hng), forming two dots groups which differ in Ca contents (40 and 17 at% of the new minal), on the triangular diagram gadolinite-hingganite-new minal. Extremely Ca-rich (12-13 wt% CaO) compositions fall into two groups dependig on REE contents: REE-rich ones contain up to 35 at% of minasgeraisite minal, while those REE unsaturated ones - up to 47 at% of the suggested minal.

The combined diagram of gadolinite group minerals from Tatyana pegmatite in coordinates Y-REE-Ca show well temporal evolution of the compounds: Ca content falling and REE-growth from Gd-I to Gd-II, and growth of Y and Ca contents from Gd-II to Gd-III. Hingganites from pseudomorphoses continues this succession to the highly-yttrian and highly-calcian compositions.

Earlier, we have determined Gd-III enrichment with Eu,Ca and Fe, as the result of penetration metasomatic solutions into pegmatite. Hingganites from pseudomorphoses are sharply nonhomogeneous in Eu distribution. Low Ca phases enriched with REE (up to 34 wt% REE_2O_3) and respectively Eu (up to 1.5 wt% Eu_2O_3) are intergrow with Ca-high selectively yttrian REE-poor (<0.06 wt%) Eu-free phases. This nonhomogeneity may be explained only by decay of solid solution. Formation of stable Y-Ca-HREE and Y-REE-LREE isostructural phases reflects optimal combinations of radii and charges of cations.

The two kinds of heterogeneity are typical for the investigated minerals - the **syngenetic** type reflecting changes in environment composition and appearing as concentric zonation, and the **epygenetic** one, connected with solid solution decay, and expressed in spot-like distribution. The former type is the most evident in zonal crystals from axial zone of pegmatite, while the latter one - in hingganite from apoeudialyte pseudomorphoses.

References: Kartashov P.M., Voloshin A.V., Pakhomovsky Y.A. (1993) **Proc. Rus. Mineral. Soc.,3,65-79.**

THERMODYNAMIC MODELLING OF MINERAL-FLUID EQUILIBRIA WIHT PLATINUM GROUP ELEMENTS

Karzhavin V.K., Torokhov M.P., Zhangurov A.A. (Geol.Inst.Kola Sci.Centre Russian Acad.Sci., Apatity)

The Imandra lopolith is assigned to the formation of platinum bearing, differentiated gabbro and norite intrusions of ancient platforms. Its origin is related with the magma of tholeitic composition, with the Fenner trend of crystallisation according to the study of previous investigators. Correlation with other plutons of this formation showes, that it differs in geochemical and metallogenic specialization. Accoding to all features it is similar to the Bushveld intrusive complex. Under the present data geological section of the intrusion is represented in general by:

1. A lower chromite bearing layered zone composed of alternating melanocratic norites and plagiopyroxenites with mesocratic norites and gabbronorites, underlain by a schlir horisont with nodules of chromite, where the evidence of the precrystallization differention can be observed.
2. The main zone of relatively homogeneous mesocratic gabbronorites.
3. An upper layered zone, composed of meso-, leucocratic gabbro and plagioclasites.
4. A near-roof zone of gabbro- and gabbrodiorites with the Ti-Mgt, highly vanadium ore.

The rocks composing the intrusive, form a single syngenetic row from plagiopyroxenites of near-bottom part to gabbrodiorites of the near-roof zone. By chemical composition, the rocks of the intrusion can be referred to the alkaliearths. The distribution of PGE in the section of the intrusive complex is irregular.

The aim of this work is to purity the most common and typical features of PGE distribution in the complex multicomponent native system, the model of which could be correct enough for the qualitative and quantitative estimation of mineral and fluid phases composition, as well as the conditions of massif formation. Using the method of physic-chemical modelling (Newton minimization of the Gibbs free energy) the investigation of the multisystem based on the chemical compounds of the near-bottom part of the massif was undertaken. The fluid phase is represented by the most real and informative components of the system C - H - S - O, in equilibrium with the solid phase, bearing 43 different minerals. The PGE are represented in element and sulphide forms. The given multisystem was studied as open for input or output of some components in a wide range of temperatures and pressures. The following results were obtained from the study:

1. Melt crystallization as of dry character.
2. Associations and compounds of minerals (rocks) of the lower chromite bearing zone, determined in the pluton, are perfectly reconstructed by the method of mathematical modelling, using the weighted mean composition of this zone. The use of the weighted mean composition of the whole pluton gives a negative result, that allows us to conclude about the partition of the preliminary melt of the intrusion to the secondary melts in the pre-crystallization period. One of this secondary melts responds evidently to the chemical composition of the lower zone.
3. PGE mineralization concentrated in chromitites, represented by dissiminated spinelides in leucocratic gabbro. In the ore-bearing rocks the PGE content is one order of magnitude lower. This result is in good agreement with the character of RGE distribution in the native object.
4. The obtained results make it possible to predict the RGE mineralization occurences with the similar approach also in other parts of the intrusion section.

CONDITION INSTABILITY AS A CHARACTERISTIC FACTOR OF CRYSTAL FORMATION

I.A.Kasatkin, O.S.Grunsky, A.E.Glikin (*Crystallography Dept., Crystal Genesis Lab, St. Petersburg Univ.*).

Some features of natural minerals are not reproduced in model experiments. Rich-faced crystals with low-dense forms and multiended crystals are the striking examples. Thus, it is obviously that experimental conditions are setted with a contempt of some important factors. We have suggested instability to be one of them. This factor operates in all cases of a mineral formation but it is still investigated too poorly, because experimenters try mainly to ensure stable conditions.

Effect of supersaturation instability on crystal morphology has been investigated for ammonium dichromate and Al-K-alum as aqueous-soluble mineralogical models. Mainly three laws of varying of supersaturation were realized: 1) a monotonous increasing, 2) a monotonous decreasing, 3) a non-monotonous changing with increasing followed by decreasing. Crystals with specific features (including predicted ones) were really obtained.

While supersaturation increases, a crystal morphology evolves according to the scheme: arising of a fine striation and its subsequent coarsening turning into a "multiended" and "multiedged" crystal formation. Macroscopic ridges of a final relief can form some non-ordinary crystallographic orientations. Besides, every ridge bounds a column-like or plate-like specific body in a crystal. A degree of a morphological evolution according to the described scheme is directly proportional to a crystal habit sensitivity to supersaturation variations and inversely proportional to an intensity of a solution stirring during a crystal growth process.

Convex quasi-cylindrical and quasi-spherical surfaces as well as some faces with a low reticular density occur only in cases of a non-monotonous changing (increasing followed by decreasing) of supersaturation during a growth. Other morphological features can arise in a wide range of growth conditions.

Autooscillations of growth rates owing to fluctuations of a supersaturation near crystal surfaces are an example. Thiourea crystal growth from aqueous solutions at constant supersaturations is characterized with such oscillations what were registered by an automatic laser interferometer. Their amplitude reaches 150 % of average values and slightly falls with a supersaturation decreasing. Analysis of frequency spectra of oscillations has displayed their periodicities. An oscillation period is inversely proportional to a supersaturation and varies from tens of minutes to tens of seconds; oscillations are irregular if a supersaturation is higher than some critical value. The oscillations of (001) rates are connected with the periodic capture of inclusions but such a correlation has not been obtained for (110).

Another example of instability effect is a formation of a solid solution crystals with zones of different average compositions and with inhomogenous distribution of components within zones. Such an instability is corresponded with a solution composition evolution taking place due to a crystallization and with growth rate fluctuations. These phenomena have been discovered for synthetic arcanite-tarapacaite mixed crystals grown in aqueous solutions.

At last, metasomatic and recrystallization processes are characterized by specific instabilities connected with their own nature as well as with external influences. Apparently, a replacement is accompanied certainly by a directed variation of a solution

composition whereas a recrystallization proceeds only due to temperature/pressure oscillations or gradients.

Thus, a condition instability is an extremely significant factor of crystal formation and must be investigated especially in detail.

SERPENTINE DISSOLUTION IN SULPHURIC ACID

Kasikov A.G., Neradovsky Yu.N., Kosyakov A.I.
(Russian Ac Sci, Kola Science Centre)

Serpentine solubility has been studied from copper-nickel ores of the Kola Peninsula in 2-50% sulphuric acid at T = 20-80°C and im sulphuric acid containing oxidizing additives (1-5% NHO_3, Cr(1V)). The starting copper-nickel ore, monomineral serpentine fractions and their polished preparations were subjected to treatment with acid for 8 hours. The folloving structural varieties were investigated: antigorite, chrysotile and lizardite represented by well crystallized and amorphous aggregates.

It has been established that the crystallized chrysotyl-asbestos and antigorite do not react with acid as long as 8 hours, cryptocrystalline serpentine only up to 4 hours. Serpentine stability in time decreases 2-fold with oxidizer addition to sulphuric acid solution.

Under conditions of serpentinite polymineral medium, the serpentine solubility increases in comparison with monomineral sample. In mineralized ores, easily soluble serpentine phases are present which react already during specimen treatment with 2% sulphuric acid at room temperature.

High solubility was found to be characteristic of serpentine gererations of cryptocrystalline structure which seems to be caused by the presence in serpetine structure of oxidized iron and mixed-laminated aggregates in whose structure nimite was found by x-ray dosimetry.

Serpentine interaction with acid occurs, apparently, by diffusion. In this case, magnesium iron and aluminium are leached from its structure and it is transformed into a high-siliceous compound with an increased content of water nickel and chromium featuring the properties of silicate gel.

GROWTH OF BIOGENETIC CALCITE IN THE GEL

Katkova V.I. and Rakin V.I. *(Inst.geology, Komi Sci.Cent., Ural Div., Rus.Acad.Sci.)*

Calcite is one of the most abundant biominerals. It can be product of metabolic processes of macroorganism itself or a result of bacterial vital activity.

The aim of our work was to obtain crystal deposit as a product of bacteria.

Silicagel was chosen as the medium of crystallization for the reason that it is neutral for crystal growth and suitable to direct ion diffusion for crystallization.

For modeling of biomineralization process the following bacterial cultures were used: E.Coli, St.Aureus, Proteus, Klebsiella. We employed the cultures of bacteria maintained in the carbohydrate and albuminous media.

To establish whether the gel was bacteria-penetrable, several experiments were carried out. E.Coli culture and carbohydrate solution were placed on different sides of the gel column. In 24 hours, flakes observed on the other side of the gel, indicated the presence of the bacteria. Thus, the size of pores in the gel proved to be larger than the size of the bacteria.

The mixture of nutritious medium and the bacteria culture was placed over the silicagel in a cylindrical tube. On the opposite side of the column, $CaCl_2$ solution of 0.1 M concentration was put. Crystal nucleation and growth were most active at temperature over 30°C.

According to X-ray diffraction obtaining deposit in the all experiments was identified as calcite. The maximum size of crystal did not exceed 0.5 mm. SEM photographs showed that the crystals were completely covered by an organic film. It was confirmed by IR-spectra. The mechanism calcite formation is following : bacteria ferment carbohydrate and albumen with accompanying production of, in particular, carbonic acid and carbonic dioxide. Calcite nuclei form in the course of interaction between carbonic acid and calcium ions. In some system with time crystalline aggregates were gradually acquiring a yellow shade because bacteria can produce pigments.

Crystal deposit was appearing in the form of Liesegang rings in the gel column in most experiments. In some cases (Klebsiella) crystals were nucleated only at a surface of glass tubes. The gel's acidity varied in the range 4-9 (pH) and however the crystals grow only in the bound 5-7. In the course of crystallization and bacteria life the acidity of gel changes.

Crystals as spherical aggregates without evident faces were formed only in the presence E.Coli with carbohydrate. Rounded crystals with little faces formed in the presence of Klebsiella, Proteus and albumen. At this crystals the faces of one rhombohedron are either $\{10\bar{1}4\}$, or $\{10\bar{1}3\}$, while in the presence of Klebsiella the form $\{10\bar{1}4\}$ was observed.

The mixture of E.Coli and St.Aureus with carbohydrate lead to formation facetted crystals characterized by 2 simple forms: rhombohedrons $\{10\bar{1}4\}$ and $\{3\bar{3}04\}$ when the gel's initial pH value equaled 5 and rhombohedrons $\{10\bar{1}4\}$ and $\{1\bar{1}01\}$ formed at pH=7.

Thus it was established that crystals of calcite are growing independently from nutrient solution and kind of bacteria in vitro. However in vivo another minerals (calcium oxalates, calcium phosphates, urates, magnesium ammonium phosphates) can form in the result of bacteria activity too.

In the most cases cleavage rhombohedron $\{10\bar{1}4\}$ was present on the crystal shape, but the sharp rhombohedrons $\{3\bar{3}04\}$, $\{1\bar{1}01\}$ were appearing occasionally. We suppose the formation of certain rhombohedron is related to solution acidity and kind of bacteria.

RETENTION OF Cd AND OTHER HEAVY METALS BY BENTONITE CLAY MINERALS (EXPERIMENTAL STUDY)

Ke J.J. (Institute of Chemical Metallurgy, Academia Sinica, CHINA)

The disposal without attendant pollution of waste containing heavy metals, whether soil, sewage sludge or industrial effluents, is becoming a matter of increaing concern, because many heavy metals form stable complexes with biomolecules and their presence in even small amounts can be detrimental to plants and animals. Cadmium is one of the most hazardous heavy metals. Some heavy metals are retained in soils due to the content of humic acid and

inorganic ion exchangers, among these some clay mineral are prominent. The retention of Cd and other heavy metals by bentonite clay mineral has been studied in this work.

The laboratory experiments for the adsorption of heavy metals on bentonite,a clay with a high content of montmorillonite, and then treatment of this slurry under hydrothermal conditions to retain heavy metals have been carried out. Montmorillonite is made up of negatively charged silicate layers and has a composition $(Al,Mg)_{2-3}(Si,Al)_4O_{10}(OH)_2 \cdot nH_2O$ with interlayer cations compensating the positive charge deficiency of silicate layers. The chemical composition of this clay is variable due to considerable atomic substitution possible in this clay, but the major constituents are always Si, Al, Mg and water along with considerable amounts of exchangeable cations. These exchangeable cations are present along with water molecules inside the interlayer spacings of the clay framework. The interlayer space in montmorillonite clay is substantial, permitting it to as a host compound and, therefore, it is possible to adsorb some exchangeable cations present in the interlayer spacings of the clay mineral.

The experimental results show that the order of retention was Ni > Cu > Zn > Cd, which reflects the adaptation of metals ion to the silicate lattice of bentonite clay mineral. Cadmium as one of the most hazardous pollutants is not satisfactorily fixed by the silicate lattices of clay mineral. In such a case, a more promising approach is transforming cadmium into sulphide, which can be done by adding a small amount of sulphur under hydrothermal conditions as shown in the following reactions. According to the disproportionation of elemental sulphur under hydrothermal conditions, it follows:

$$4S^{\circ} + 4H_2O \rightarrow 3H_2S + SO_4^{2-} + 2H^{+} \qquad (1)$$

Meanwhile, the reaction of Cd^{2+} with S^{2-} produces a precipitate of CdS,

$$Cd^{2+} + S^{2-} \rightarrow CdS \qquad (2)$$

CdS formed resists acid attack at pH>1.

It has been shown from the experiments that the hydrothermal sulphidizing in neutral or slight acid suspension seems more suitable for insolubilizing Cd. The retention of Cd increased with hydrothermal temperature from 150° to 240°C and the amount of sulphur added. Only traces of cadmium are leached out after hydrothermal treatment. It appears that this method may be adapted for fixation of Cd in contaminated waste water, soil and sludge.

References:
Ke, J.J., Sorence, E. (1992). Mineral Process and Extractive Metallurgy Review. 9,107-124.
Ziper, C. et al. (1988). Soil Sci. Soc. Am. J. 52,49-53.
Hereas, H. (1988). German Patent DE 3205717c2.

THE MINERALOGICAL AND GEOCHEMICAL ROLE OF Fe-Mn-PHOSPHATE MINERALS IN THE EVOLUTIONARY PROCESS OF GRANITIC PEGMATITES - NEW RESULTS FROM NAMIBIA

Keller, P. (Institut für Mineralogie und Kristallchemie, Universität Stuttgart)

Minerals of the triphylite-lithiophilite and triplite-zwieselite solid solution series are primary components of many granitic pegmatites. Keller *et al.* (1994a) demonstrate recently that the phosphates of both series are sometimes cogenetic but more frequently triplite-zwieselite is the earlier mineral of more or less complex crystallization sequences. The intergrowth of triphylite-lithiophilite and triplite-zwieselite were used to test for compositional zoning and to determine the intercrystalline main element partitioning. The triplite structure has preference for Mn, Mg, and Ca. In the cases where diffusion can possibly be excluded, the following equation was determined for the Fe/(Fe+Mn) ratio: [Fe/(Fe+Mn)tripl.] = [Fe/(Fe+Mn)triph.] / {2.737-1.737[Fe/(Fe+Mn)triph.]} with R = 0.988 (Keller *et al.*, 1994b).

The Fe/(Fe+Mn) ratio of both phosphate series were applied in the interpretation of granitic pegmatites of Namibia. They belong to the Namaqua province, partly exposed along the southern border of Namibia, and the more important Damara province, developed in the western part of central Namibia, where different pegmatite belts can be distinguished. As evident from field observations, the pegmatites of the two provinces and of some belts differ with respect to many features. Nevertheless, it was possible to quantify the relation between K/Rb of K-feldspar and Fe/(Fe+Mn) on the basis of triphylite-lithiophilite for many pegmatites of the Damara province, predominantly of the Karibib belt. A preliminary correlation equation with R=0.90 is: K/Rb = 5.5exp{3.0[Fe/(Fe+Mn)]}. Although there are some misfitting exceptions, e.g. pegmatites strongly altered by metasomatic processes, which need further investigations, it is evident that abundant schörl or biotite does not significantly alter the Fe/(Fe+Mn) ratio. The Fe silicates may only affect the content of phosphate minerals in a pegmatite.

As already known, the K/Rb ratio varies very sensitively, not only within one pegmatite but also within a feldspar crystal. Thus mean values of a large number of analyses are necessary for scientific and exploration purposes. The opposite is observed for the Fe/(Fe+Mn) ratio of phosphate minerals. Especially triphylite-lithiophilite is chemically homogeneous when it occurs free of other primary minerals forming Fe-Mn-Mg solid solutions and in addition all crystals within a usually narrow zone display the same Fe/(Fe+Mn) ratio. On the other hand, successively changing Fe/(Fe+Mn) ratios were detected, following the fractionation trend according to the pegmatite zonation and to the mean K/Rb ratios. Such effects and the compositional zonation are more distinct for minerals of the triplite-zwieselite series. Taking these observations into account, evident relationships between some economically interesting mineralization and the Fe/(Fe+Mn) ratio of a pegmatite is not a surprising result.

References:

Keller, P., Fransolet, A.-M., Fontan, F. (1994a). *N. Jb. Mineral.*(in press).
Keller, P., Fontan, F., Fransolet, A.-M. (1994b). *J. Mineral. Petrogr.* (submitted for publication)

CHEMICAL AND MORPHOLOGICAL FEATURES OF ARSENOPYRYTE CONCERNING IT S USE AS A GEOTHERMOMETER

Kerestedjian T. N., (*Geol. Inst., Bulgarian Acad. Sci., Sofia*)

Since 1960 arsenopyrite is extensively investigated in respect to it's possible use for geothermometry. Distinct compositional sector zoning, very typical for the bulk of hydrothermal and hydrothermal-metasomathic arsenopyrites appeared to be one of the greatest problems restricting arsenopyrite geothermometer. A detailed analysis of mineral's composition in precisely determined crystal areas revealed a number of dependencies, very useful for understanding the sophisticated way of inscribing the genetic information in the mineral. The main results of the study can be shortly defined as follows:

1. Arsenopyrite's composition can completely be characterised by just one numeric value - the As/S ratio. This permits us to compare the composition of different crystal areas by their intensity in BSE images only (excluding rare cases with significant external impurities).

2. Being one of the few minerals with contrastly different in composition crystal sectors, arsenopyrite demonstrates constant relations between these compositions, defined with the following unequations:

$$C_{101} < C_{210} < C_{010} < C_{120},$$

where C_{hkl} is the composition of the four respective sectors, found definitive for nearly all known arsenopyrite crystals.

3. Last relations were extended further on quantitative level, to reveal strongly correlated linear dependencies between C_{101} (participating with no exceptions in all arsenopyrite crystals) and the respective C_{hk0}, permitting so far the use of only one composition value (C_{101}) for characterisation of the whole crystal.

4. A pronounced dependence between C_{hkl} and the morphology (bounding+elongation) was established as an addition to already known dependence composition-growth rate, specific for every crystal face.

Restrictions coming up by zoning, as well as formulae for estimating geothrmometrically representative compositions are discussed.

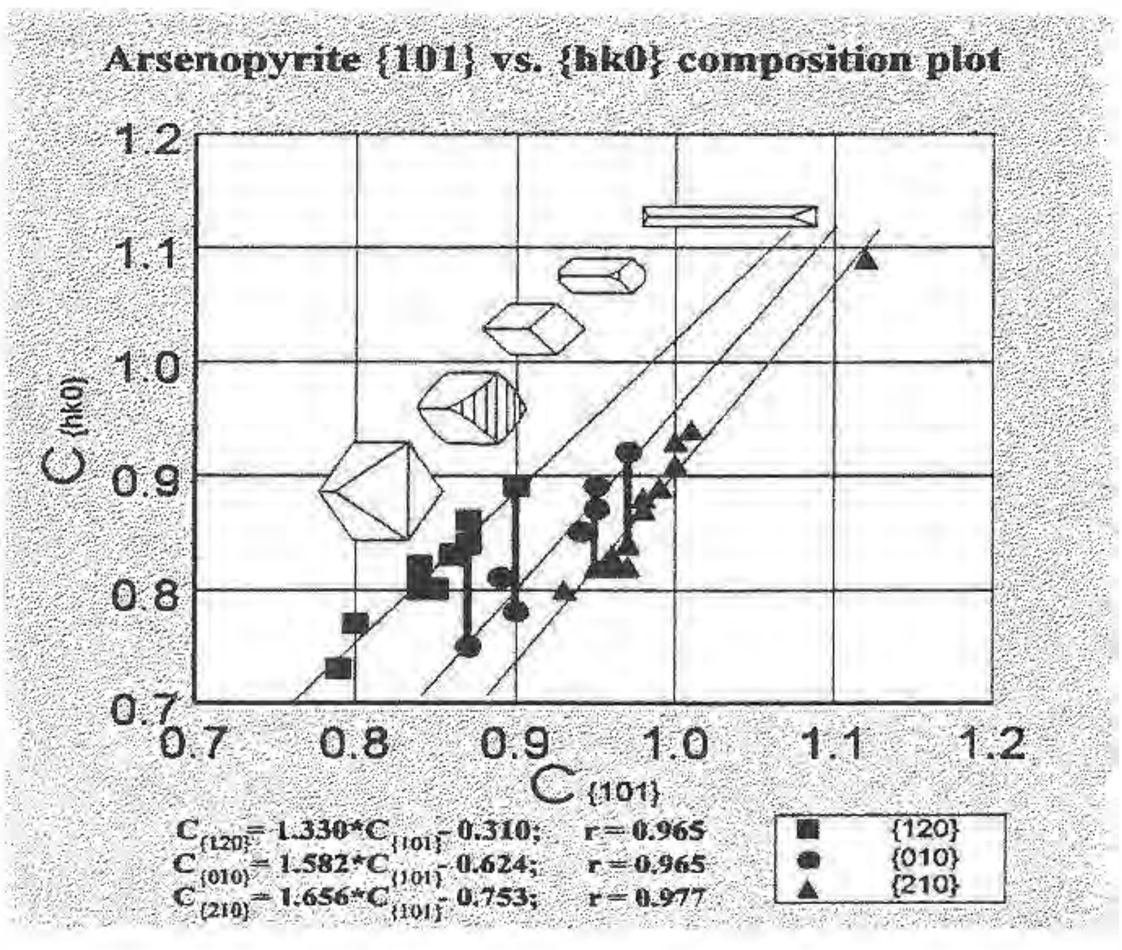

THERMAL DEFORMATION AND DEHYDROXYLATION IN NATURAL TRIOCTAHEDRAL AND DIOCTAHEDRAL MICAS

KHILTOVA E.YU., BABUSHKINA M.S.
(Institute of Precambrian Geology and Geochronology of Russian Academy of Sciences, St-Petersburg, Russia)

The absence of reliable information on physico-chemical characteristics of rock-forming minerals at high T and P (especially on iron-bearing silicates) restrains the thermodynamical approach in phase modelling for deep zones of the Earth. The joint x-ray, infrared and Mossbauer experiments were carried out to study the structural changes in micas under the temperature in vacuum.

X-ray high-temperature powder-diffraction data reveal the anisotropy of thermal expancion in trioctahedral Fe-Mg series and negative expancion in some directions of the structure in ferrous ones. The equation for composition dependencies of MTEC are obtained: $\alpha_V = 54.5 - 0.07 X Fe^{2+} + (0.06 * 10^{-3}) X^2 Fe^{2+}$; $\alpha_{33} = 17.8 - 26.7 X Fe^{2+}$; $\alpha_\beta = 0.7 - 16.3 X Fe^{2+}$; the degree of anisotropy $\Delta = 1.5 X Fe^{2+}$. The axis of the least expansion α_{33} in Fe-Mg micas changes its orientation with chemical composition and decreases to negotive values with Fe^{2+} content increasing. Al_{IV} occupation of octahedra reduces the degree of anisotropy. After 400C the character of thermal expansion in phlogopites changes. In biotites besides thermal expansion the oxidation of iron due to decomposition of OH^- groups takes place. The complete oxidation in ferrous biotites terminates at 600C. In micas with the less Fe^{2+} content the temperature is higher. Phlogopites conserve OH^- ions up to 900C.

Mean thermal expansion coefficients, orientation of MTEC tensor and ellipsoids of MTEC for muscovites are calculated. The changes in muscovite structure up to 600C are caused by thermal expansion. Decomposition of OH^- groups and dehydroxylated phase formation start after 600C. Two phases of muscovite exist simultaneously from 600C to 800C .The stretching vibrations of OH^- ions can be determined up to 900C. The stuctural changes are reflected in frequency and intensity of stretching and other vibrations in infrared spectrum. The most essential changes are observed in the range of Si-O-AL vibrations.

MECHANISM AND KINETICS OF LOW-TEMPERATURE OXIDATION OF Mg,Fe-OLIVINE

Khisina N.R., Khramov D.A., Kleschev A.A. (*Inst. of Geochemistry and Analytical Chemistry of Russian Acad. of Sci., Moscow*), Taylor, L.A.(Planetary Geosciences Institute, *Univ. of Tennessee, Knoxville, TN, USA*)

Olivine samples ($Mg_{1.78}Fe_{0.22}SiO_4$) were annealed at 700 °C at fO_2 = 0.2 bars for periods ranging from 5 to 146 h and guenched in air. Initial and oxidized samples were studied with X-ray powder diffraction, transmission electron microscopy, thermomagnetic analysis and Mossbauer spectroscopy. Oxidation of olivine resulted in formation of ferri-olivine, magnesioferrite (as major oxide phase) and magnetite (minor oxide phase). Ferri-olivine- formula = $Mg_{0.5-0.5}(Fe^{3+})_{1.0}SiO_4$, forms planar (001) precipitates 6 A thick within the olivine host. Magnesioferrite exsolves as fine-grained precipitates (50-60 A) filling interstices between the ferri-olivine planar precipitates. The orientation of the olivine host and

magnesioferrite precipitates were determined from electron diffraction data. The Curie (Neel) point of magnesioferrite produced in olivine at 700 °C was determined to be 330 °C, corresponding to a stoichiometric magnesioferrite with a cation inversion parameter of x=0.811 and a cation distribution formula of $(Mg_{0.189}Fe_{0.811})^{IY}(Mg_{0.811}Fe_{1.189})^{YI}$, as per O'Neil et al. (1992).

Oxidation rates were expressed through the time dependence of the $(Fe^{3+})_{tot}$ / Fe_{tot}, $(Fe^{3+})_{f\text{-}ol}$ / Fe_{tot}, and $(Fe^{3+})_{oxi}$ / Fe_{tot}, where $(Fe^{3+})_{oxi}$ is the Fe^{3+} ions in oxide phases, $(Fe^{3+})_{f\text{-}ol}$ is the Fe^{3+} ions in ferri-olivine, $(Fe^{3+})_{tot} = (Fe^{3+})_{oxi} + (Fe^{3+})_{f\text{-}ol}$, $Fe_{tot} = (Fe^{3+})_{tot} - (Fe^{2+})_{tot}$. Oxidation kinetic data obtained for samples with average grain size of 70mkm, annealed at 700 °C (*Khisina et al.*, in press) show two stages of oxidation corresponding to the formation of ferri-olivine in the first stage

olivine $- O_2 =$ ferri-olivine + forsterite

and magnesioferrite in the second stage

olivine + O_2 = magnesioferrite + forsterite + SiO_2

During the first stage, an increase in $(Fe^{3+})_{tot}/Fe_{tot}$ was found to be limited by the rate of increasing $(Fe^{3+})_{f\text{-}ol}/Fe_{tot}$. The linear rate law with a rate constant, $k_{f\text{-}ol} = 1.23 \times 10^{-3}\ s^{-1}$ was calculated for this first stage. At the end of the first stage, the $(Fe^{3+})_{f\text{-}ol}/Fe_{tot}$ was found to reach a steady state value. During the second stage, $(Fe^{3+})_{tot}/Fe_{tot}$ was found to increase due to increasing $(Fe^{3+})_{oxi}/Fe_{tot}$, and a parabolic rate-low constant, $k = 3.28 \times 10^{-3} s^{-1}$ was determined.

Kinetic data, complimented by electron microscopy results, lead to the conclusion that ferri-olivine is not an intermediate, metastable phase in the oxidation process, concluding in formation of magnesioferrite and magnetite. Magnesioferrite is exolved directly from the olivine matrix due to oxidation and is not an isochemical product of the decomposition of ferri-olivine.

References:
O'Neil, H.St.C., Annersten, H., Virgo, D. (1992) *Amer. Mineral.* 77, 725-740.
Khisina, N.R., Khramov, D.A., Kolosov, M.V., Kleschev, A.A., Taylor, L.A. *Amer. Mineral.*, in press

MÖSSBAUER SPECTROSCOPY STUDY OF OLIVINE+FERRIOLIVINE+SPINEL ASSEMBLAGE PRODUCED BY OXIDATION OF OLIVINE

Khisina N.R., Khramov D.A. (*Inst. of Geochemistry and Analytical Chemistry, Russian Academy of Sciences, Moscow*)
N.O.Ovchinnikov (*Inst. of Geology and Geochronology of Precembrian, Russian Academy of Sciences, S.-Peterburg*),
A.A.Kleschev (*Moscow State Univ.*)

$Mg_{1.78}Fe_{0.22}SiO_4$ olivine samples oxidized in air at 350-700 °C were investigated with X-ray powder diffraction, transmission electron microscopy, thermomagnetic analyses and Mössbauer spectroscopy. Microtexture of oxidized olivines was found to have either (001) ferriolivine planar precipitates of 6A in thickness or (001) ferriolivine planar precipitates + isometric precipitates of spinel (magnesioferrite) of 5-6nm in size (Khisina et al., 1992). Mössbauer spectra of both initial and oxidized olivines were recorded at 298 K and 573 K and the following results were obtained.

(1) δ and ε parameters for the $(Fe^{3+})_{Fol}$ doublet (Table 1) were found to be consistent with room temperature parameters of Fe^{3+} in ferrifayalite (Kan & Coey, 1985).

(2) δ and ε parameters for Fe^{2+} in the M1 and M2 sites of the olivine structure did not change with increasing amount of ferriolivine (olivine + ferriolivine assemblage, Table 1). However these parameters were found to be noticeably changed with the spinel (magnesioferrite) appearence (olivine + ferriolivine + spinel assemblage, Table 1). These changes were found to correlate to the data indicated that b and c unit cell parameters of olivine matrix anomalously decreased and the olivine lattice become distorted (compressed) within the oxygen close-packed (001) plane as spinel appeared (Khisina et al., in press). The distortion of the M1 and M2 olivine polyhedra caused by spinel precipitation is appeared to change the δ and ε parameters of Fe^{2+} in Mössbauer spectra of oxidized olivines.

(3) The $Fe^{2+}(M1) / Fe^{2+}(M2)$ ratio value does not increase with increasing ferriolivine mole fraction, therefore the composition of ferriolivine was assumed to be $Mg_{0.5}v_{0.5}(Fe^{3+})_{1.0}SiO_4$ (v - vacancies).

Table 1

Fe^{2+}(M1)		Fe^{2+}(M2)		Fe^{3+}(Fol)	
δ	ε	δ	ε	δ	ε
initial olivine					
1.146(4)	1.458(2)	1.167(4)	1.541(2)		
ol + Fol					
1.143(1)	1.459(3)	1.170(2)	1.536(2)	0.402(1)	0.409(2)
ol + Fol + Sp					
1.109(4)	1.492(1)	1.197(3)	1.509(1)	0.403(2)	0.419(3)

References:
Kan, X. & Coey,J.M.D. (1985). *Amer. Mineral.*, **70**, 576-580.
Khisina, N.R., Khramov, D.A., Kolosov, M.V., Meshalkin S.S. (1992). *Doklady of Russian Acad. of Sci.*,**324**, No4, 866-870.
Khisina, N.R., Khramov, D.A., Kolosov, M.V., Kleschev, A.A., Taylor, L.A. *Amer. Mineral.* (in press)

V.G. Khitrov, A.A. Chernikov, and S.S Dvourechenskaja (IGEM RAS, Moscow)

DIFFUSION PROCESSES IN MINERALS AND ROCKS OF THE WEATHERING CRUST

Diffusion processes in the natural environment is closely associated with the sorption and the transformation reorganization in minerals (Chernikov, 1992). The sorption is the initial case of supergene alteration of the rocks and minerals. Sorbate diffuses in the crystal structure of minerals transforming it.

The traces of sorbate diffusion are observed, sometimes along the cracks, the fractures, the planes of cleavage, the interlayer or interglanular space and vacant spaces of the crystal lattice.

This reveals the peculiarity of the modification in the weathering crust in dependence of physical-chemical environment condition of different rocks and crystal lattice of the primary rocks forming minerals, which define the means of sorbate diffusion.

Ultrabasic, basic, and partially mediosilicic rocks contain mainly mafic minerals, including trioctahedric layering silicates. In these rocks divers means of diffusion and further transformative processes proceed. As result a serpentine of type A structure, saponite and chlorite (♂ and ♂'), further also vermiculite and varieties of montmorillonite (Mg-Fe^{3+}, Fe^{3+} and Al-Fe^{3+}), and vermiculite-montmorillonite mixing-layered formation, illite 1M (if the rock contains phlogopite) and other phases are formed (Khitrov, Kotelnikov, Zinchuk, 1988; Kotelnikov, Zinchuk, Khitrov, 1988).

On the top of that profile a formation of ochre and an accumulation of aluminium oxide take place.

Accordingly, lesser divers paths diffusion proceed at the alteration of acid rocks, which are enriched of quartz, K-feldspar and dioctahedric layering silicates. In the bot-

tom of profiles illite 2M or 1M (if the rock contain a muscovite or biotite), then montmorillonite-illite mixing-layered formation, and infrequently - montmorillonite (in case of the weathering of tuffas) are presented.

The peculiarity of transformation of these rocks from bottom to top of the profiles causes longer conservation of dioctahedric layering minerals including the kaolinite consequently forming later.

References

1. Chernikov A.A. (1992). Izvestiya RAS, ser. geol., No 3, 118-126. 2. Khitrov V.G., Kotelnikov D.D., Zinchuk N.N. (1988). In Book: "Hypergenez i Rudoobrazovanie". M.: Nauka. 15-28. 3. Kotelnikov D.D., Zinchuk N.N., Khitrov V.G. (1988). Ibid. 29-38.

CHERNOBYL-DERIVED HOT PARTICLES AS TECHNOGENIC MINERALS: COMPOSITION TYPES AND STABILITY

Khodorivski M.S.[1], Proskura N.I.[2] Sinitsyn V.A.[1] and Kulik D.A.[1]
([1] Ukrainian Acad. Sci., Institute of Geochemistry, Mineralogy and Ore Formation, Kiev; [2] Minchernobyl, Chernobyl Research Centre, Ukraine)

Studies of the Chernobyl-derived hot particles matrix composition have shown that they are mainly uraniferous. About half of such particles >10 μm in size contain significant amounts of both U and Zr. The U-bearing hot particles were classified into two types by means of the electron microprobe and XRD structural analysis: fuel (1) and fuel-construction (2).

The fuel hot particles (1) are small pieces of the nuclear fuel elements, disintegrated by explosion but not fused. They are essentially uraninite UO_2. The hot particles of type (2) were formed by an increase of temperature and partial melting of nuclear fuel. They can be considered as a solid solution of $(U,Zr)O_2$ composition (Tepikin et al., 1992) or as mechanical inclusions of UO_2 into Fe- or Si-matrix. The type (2) particles with $(Zr,U)SiO_4$ composition (Kiselev et al., 1992) - the so-called *chernobylite* - commonly occur under the shelter of 4-th (broken) Chernobyl NPP unit. These are in fact the uraniferous zircon. The conditions of formation of hot particles in question permit to regard them as technogenic minerals.

Limiting equilibrium solubilities of various types of hot particles were estimated using a method of multisystem isobaric-isothermic potential minimization implemented into the proprietary SELEKTOR++ code (Karpov et al., 1993). The calculations of solubility were performed for the hydrochemically different typical natural waters of the 30-km reservation zone of Chernobyl NPP.

It was found that the limit equilibrium dissolved U concentrations in the aerated natural waters are in the range $n\cdot10^{-3}$ - $n\cdot10^{-2}$ mg·(kg $H_2O)^{-1}$ (in the case when the dissolution of uraninite is accompanied by the solid-phase oxidation reactions), and may reach $n\cdot10^{-2}$ mg·(kg $H_2O)^{-1}$ in the case of metastable dissolution of UO_2.

The solubility of U-bearing hot particles sharply decreases when the oxidating conditions change to reducing (suboxic) ones. It was calculated to be $n\cdot10^{-6}$ mg·(kg $H_2O)^{-1}$ in the low-acidic reducing bog water and $n\cdot10^{-4}$ mg·(kg $H_2O)^{-1}$ in the low-alkaline, reducing river water. The Fe-U-bearing hot particles are the most stable and the U-bearing hot particles are the most soluble (in the range: U-, Si-U-, Fe-U-hot particles in the aerated natural waters). The precipitation of UO_2 may occur at the cost of U leached from the Si-U- and Fe-U-hot particles (due to low U solubility and significant Fe and Si-bearing matrix solubility at reducing conditions).

Insufficient thermodynamic data on the aqueous Zr species does not permit to obtain quantitative estimates of Zr-bearing hot particles solubility. At qualitative level, the solubility of the $(U,Zr)O_2$ and $(Zr,U)SiO_4$ hot particles is found to be much lower than that of the "pure" U- bearing particles.

References:

Tepikin, V.E., Rybalko, S.I., Rybakova, E.A., Zimin, Yu.I. and Petelin, G.I. (1992). *Chernobyl, NPO "PRIPYAT" Publication*, 18 p. (in Russian).

Kiselev, A.N., Nenagliadov, A.Yu., Surin, A.I. and Checherov, K.P. (1992). *Moscow Institute of Atomic Energy Publication*, 120 p. (in Russian).

Karpov, I.K., Chudnenko, K.V. and Kulik, D.A. (1993) *Amer. J.Sci.*, submitted, 50 pp.

THE ALTERATION OF CARBONATE MINERAL FORMATION AND SOIL SOLUTION COMPOSITION IN CHERNOZEMS OF CENTRAL PRECAUCASUS (RUSSIA) DUE TO IRRIGATION.

Khokhlova O.S., Arlashina E.A., Kovalevskaya I.S., Morgun E.G. *(Inst. of Soil Sci.& Photosynthesis Russian Academy of Sci., Pushchino, Moscow region, Russia).*

The purpose of our investigation was to study the changes of calcareous material and soil solutions composition in chernozems due to irrigation. We examined non-irrigated chernozems and irrigated ones since 1956. The soils studied are derived from loess deluvial clay loams on the north-western slope of Stavropol' upland, Central Precaucasus (Russia). For researching of carbonate minerals the complex of morphological and instrumental methods was used. Soil solutions were displaced by immiscible liquid (alcohol) and their composition was analysed by routine methods. The calcareous accumulations were classified according to Ovechkin (1984).

From the morphological observations segregating forms of carbonates (white soft spots) and migrational ones (veins) predominate in non-irrigated and irrigated soils respectively.

The white soft spots contain 48-54% of calcite, veins - 7-15% as follows from the thermal analysis data. Besides, calcareous material in veins of irrigated soils are dissociated at lower temperatures than that in non-irrigated chernozems probably due to less size and more loose packing of calcite crystals in calcareous accumulations. This alteration happens in calcite of irrigated soils because processes of its dissolution- recristallization are often repeated. Carbonate minerals have no time to be crystallized well.

X-ray diffraction patterns show that calcite in migrational forms of carbonates (veins) from both soils is characterized by the presence of some magnesite component. Segregating forms (white soft spots) are composed of pure calcite with stable lattice that follows from IR spectra. Variety of calcite mineralogical features in migrational and segregating forms is consistent with different mechanisms of their formation. As migrational forms are more abundant in irrigated soil, the magnesian calcite formation is intensified due to irrigation.

From the data on soil solution composition Ca and Mg content in irrigated chernozems is higher, than that in non-irrigated ones. Elevated content of Ca in soil solutions indicates on the growing carbonate mobility. This assumption is supported by the stable segregating carbonate forms are transformed into the mobile migrational ones due to irrigation. The increase of Mg content in soil solutions is reflected in larger part of magnesite component in calcite of calcareous accumulations of irrigated chernozems. The magnesite component in calcite may be also increased owing to

the Mg partitioning effect (Arnaud&Herbilon,1973), as the intensification of water regime results to the enhancing of the number of carbonate dissolution-reprecipitation cycles.

Thus the prolonged irrigation causes alteration of water regime of chernozems and leads to some changes in soil solutions composition and carbonate mineral formation. Segregating forms of carbonate accumulations in irrigated chernozems are replaced by migrational ones with another calcite mineralogical characteristics. Finally, irrigation results to the changes of the mechanism of accumulation and chemical peculiarities of calcareous material.

References:

Arnaud, St.R.& Herbilon, A.J., 1973. *Geoderma*, **9**, 279-298.
Ovechkin, S.V.1984. In: *Soils and soil cover of forest and steppe zones of the USSR and their rational use*. Moscow, USSR, 184-189. (in Russian).

OPTICAL ABSORPTION SPECTRA OF ROCK-FORMING BIOTITES AND PHLOGOPITES

Khomenko V.M. *(Dept. of Spectroscopic Methods, Inst. of Geochemistry and Physics of Minerals, Kiev)*

Biotite samples from granitic rocks (Ukrainian Shield), as well as phlogopites from carbonatite intrusion (Karelia), ultrabasic rocks (Ural) and from kimberlites (East Siberia) were studied by optical spectroscopic method, in region 27000 - 5000 cm^{-1}. It was established that electronic absorption features of biotite and phlogopite are controlled by the intensities ratio of the absorption bands of three main optical absorption centres (OAC): $Fe^{2+}Ti^{4+}CT$ (strong broad band at 24000cm^{-1}, *E*⊥*c*), $Fe^{2+}Fe^{3+}$ CT (strong band at 14000 cm^{-1}, *E*⊥*c*) and Fe^{3+} in tetrahedral sites (strong UV-absorption and sharp *dd*-transition peaks at 25000, 22470, 20200, 19050 and 15380 cm^{-1}, *E*∥*c*). Tetrahedrally coordinated Fe^{3+} ions were found in biotites from some syenites and in phlogopites from kimberlites besides typical tetraferriphlogopites from carbonatite rocks. Cr^{3+} ions contribute to the optical spectra of phlogopites from some ultrabasic rocks.

Certain qualitative and quantitative combinations of the above OAC are typical for biotite of every granitoid complex studied, as well as for every phlogopite generation in carbonatite intrusions.

It was shown, that the oxygen fugacity was a main factor which caused the OAC combination in phlogopite-biotite micas.
Normally there is an inverse dependence between Ti^{4+} and Fe^{3+} concentration in these minerals. Phlogopites show an inverse pleochroic scheme when Fe^{3+}/Ti^{4+} ratio exeeds 5,2.

RECENT CONTRIBUTION TO THE MINERALOGY OF ALKALINE ROCKS

Khomyakov A.P. (Inst. Miner. Rare Elem., Moscow, Russia)

The author has been involved in the discovery of 65 IMA-approved minerals in alkaline massifs of the Kola Peninsula and other regions, 30 of them - since 1983. These discoveries have significantly furthered our knowledge of the chemical and structural diversity in the mineral world. In particular, they made it possible to considerably expand the list of minerals of phosphorus and rare elements (Li, Sr, REE, Zr, Nb), to establish new types and groups of compounds, to reveal ion-exchange and other useful properties in many minerals, and to find a large number of previously unknown structural types and building units, such as the 18-membered cyclosilicate radical in megacyclite.

The bulk of the new minerals have been found in the deep sectors of the Khibina and Lovozero massifs (Kola Peninsula) in the hyperagpaitic rocks, very specific pegmatitic and hydrothermal nepheline syenite derivatives (Khomyakov, 1990, 1993), containing as characteristic minerals a great variety of water-soluble sodium salts, in particular, the most alkaline carbonates (natrite), silicates (natrosilite), and phosphates (olympite) known in nature. The finding of their large concentrations in derivatives of the alkaline magmas signifies the discovery of an earlier unknown phenomenon - a natural substance being in the peralkaline condition - and readily explains the gigantic size of the rare-metal and phosphate deposits associated with the agpaitic magmatism and their extraordinary mineral diversity.

The process of formation of nepheline syenite derivatives, including hyperagpaitic ones, clearly defines three successive stages - increasing (I), maximum (II), and decreasing (III) alkalinity - which is represented by the alkalinity vs. time Λ-shaped curve, designated as the "alkalinity wave" (Khomyakov, 1983, 1990). The latter accounts satisfactorily for many features of the derivatives, in particular, the development of agpaitic mineral associations in the axial zones of miaskitic pegmatites and of miaskitic associations in the axial zones of agpaitic pegmatites. The principal characteristic of the alkalinity wave is its amplitude whose magnitude and, respectively, the mineral diversity of the corresponding derivatives decrease in going from the hyperagpaitic types through the intermediate ones (Langesundfjord etc.) to the miaskitic types. The same amplitude is matched by the same types of mineral assemblages irrespective of the scale of the processes and size of the forming bodies. This may explain the seemingly paradoxical similarity in the mineral composition of the gigantic pegmatitic fields in the Khibina-Lovozero and Ilimaussaq (S. Greenland) alkaline complexes, on the one hand, and the mineral microsegregations in the small pegmatitic and other formations in the Mont St.-Hilaire alkaline complex (Canada), on the other.

References:

Khomyakov, A.P. (1983). In: The Evolution of Mineralogy and Geochemistry and Their Relation to the Study of Mineral Resources (ed. F.V.Chukhrov), pp. 66-82. Nauka, Moscow.
Khomyakov, A.P. (1990). Mineralogy of Hyperagpaitic Alkaline Rocks. Nauka, Moscow.
Khomyakov, A.P. (1993). Geokhimiya, 8, 1183.

MINERALOGICAL AND FLUID INCLUSION EVIDENCE OF HETEROGENEOUS ORE-FORMING FLUIDS AT THE GREISEN-RELATED ORE DEPOSITS

Kigai I.N. (Instit. of Geology of Ore Deposits, Petrogr., Mineralogy and Geochemistry, IGEM, Russia Acad. of Sci., Moscow)

Detailed studies of wall-rock alterations at various tin and tungsten vein-type deposits have shown the development of typical metasomatic zoning with primary formation of monomineral mica, topaz or tourmaline rear zones, practically devoid of quartz, at the expence of quarz-bearing granitic or sedimentary country rocks. Those alterations were followed by quartz ± cassiterite ± wolframite ore precipitation with scarce sulfides and simultaneous silicification of mica, topaz or tourmaline. Analysis of such mineralization style led the present author to suggestion of wall-rock alteration under influence of a liquid which have been produced by the condensation of a silica-deficient gas phase of a heterogeneous fluid (Kigai, 1979).

D.White et al. (1971) proposed a model of vapor-dominated heterogeneous systems referring to modern hydrothermal systems of the Larderello, Italy, the Geisers, California, some recent mercury and (less obvious, - I.K.) to older porphyry copper deposits. But the behaviour of silica during wall-rock alteration and successive ore precipitation can be used as a reliable criterion of much older mineralization related to such heterogeneous fluids (this should be the case of all types of ore assemblages conjugated with the wall-rock alterations of hydrogen metasomatism style).

Another possible criterion could be derived from comparative fluid inclusion studies of wall-rock alteration minerals and ores. Being formed from solute-deficient gas phase, the condansates of this gas had to contain essentially lesser quantities of sodium and potassium chlorides, silica and some other non-volatile solutes (and enriched in volatile acids which allow them to perform a hydrogen metasomatism, i.e. greisenization). Using eutectic temperatures and daughter minerals' melting and transformation temperatures we could estimate the composition and percentage of major solutes in captured fluids. But the finding of remnants of inclusion sets evidencing heterogeneity of fluids during the wall-rock alteration is a very complicated task. First difficulty is related to extremely small size of primary inclusions in alteration minerals and scarsity of large (> 15 μ) inclusions allowing good freezing stage studies. Second one was found to be a consequence of very often complete transformation of primary composition of gresening fluids by later more concentrated ore precipitating solution. This is suggested by the wide superimposition of ore assemblages upon greisens and tourmalinites with the frequent conversion of latters to economic or low grade ore[a].

Having studied several tin/tungsten deposits in Siberia and Middle Asia of the former USSR we have met only one deposit-the Trudovoye tin-tungsten mine in Kirgizia, about 100 km south of Issyk Kul lake - where we managed to find earlier low concentrated (<5 wt % NaCl + KCl) water solutions, with filling temperatures over 400°C, showing all transitional types to carbon dioxide-dominated and nearly pure carbon dioxide inclusions, i.e. with clear indications to "boiling". Greisenization have started at fluid pressures over 2 kbar. Main greisen minerals are quartz and lepidolite. Later ore minerals of the same stage of mineralization (quartz, fluorite, wolframite and cassiterite) have been precipitated mostly in the gradually opening veins from much more concentrated liquid NaCl-KCl solutions starting from higher than 14 wt% NaCl eq. and finishing with 6.5 wt% at the very end of the stage.

References:

Kigai, I.N., Samovarov, Yu.V. (1989). Zapisky VMO, **108**, #2, 8-24 (Proceed. All-Russ. Miner. Soc., in Russian).

Kigai,I.N. (1979). Osnovnye parametry prirodnykh processov endogennogo rudoobrazovaniya. **2**, 7-34. Novosibirsk: Nauka Publishers (in Russian).

White, D. E. et al.(1971). Econ.Geol., **66**, 75-97.

GEOMETRICAL AND LATTICE DYNAMICAL STUDIES OF $P6_3/mmc$, $C222_1$ and $P2_12_12_1$ TRIDYMITES

Kihara K. (*Dept. of Earth Sciences, Kanazawa University*)

Disorder of oxygen atoms in $P6_3/mmc$, $C222_1$ and $P2_12_12_1$ tridymites were analyzed in geometrical and lattice dynamical points of view. In all steps of calculations, silicon atoms were fixed on the X-ray positions in the X-ray cells at 155°C for $P2_12_12_1$, at both 170°C and 380°C for $C222_1$ and at 460°C for $P6_3/mmc$, and only the positions of oxygen atoms were varied in comparison with prescribed values of Si-O=1.61 Å and O-O=2.64 Å, both independent of temperature.

According to the present calculations, six-membered rings of SiO_4 units are all collapsed in these forms, and SiO_4 units can take different orientations in forming tridymite frameworks: six in $P6_3/mmc$ and $C222_1$, and three in $P2_12_12_1$. Atomic distances and angles in the *ideal* frameworks are about equal for the three forms: <Si-O> (mean Si-O) = 1.611 Å, <O-O> = 2.629 Å, and <Si-O-Si> = 147°.

The tridymite framework structures undergo thermal vibrations in two kinds of pair-wise rotational modes, at the Γ-point, of SiO_4 units joined by the apical oxygen atoms. One of the rotational modes is about <100> (or <210> for the hexagonal case) with the lowest frequencies among optic modes, and the other <010> with the second lowest frequencies. The rotational mode about <100> is remarkably soften as temperature approaches to the hexagonal-orthorhombic transition from below. The behavior of atoms at the hexagonal-orthorhombic transition is explained in terms of coupled softening of the two rotational modes of neighboring local domains in different orientations. The $C222_1$ structure is readily soft for displacements in lattice modes of an optic branch from about $a^*/6$ to the Brillouin zone center.

ORTHORHOMBIC DISTORTION OF PYROLUSITES

Kikuchi T., Miura H. and Yoshino T. (*Division of Earh and Planetary Sciences, Hokkaido Univ., Japan*)

There are some pyrolusites of which lattice is slightly distorted to orhtorhombic form from the tetragonal one (Potter & Rossman, 1979). The sharpness of (310) reflection varies from one locality to others. Among them, the structural refinement of pyrolusite from Imini mine, Marrakech, Morroco by Rietvelt method revealed that the cell is orthorhombic with a=4.3821(3), b=4.4347(3) and c=2.8744(2) Å. Even in such a case, no distinctive chemical composition has been recognized. Pyrolusite contains 1-2 wt% H_2O in most cases. We have estimated that the orthorhombic distortion is caused by the chemisorped water which diffused in the structure. The chemical formula of such a hydroxidized specimen can be expressed by $Mn^{4+}_{1-x}Mn^{3+}_xH_xO_2$. We have examined the possible contributions of Mn^{3+} ions and hydrogen ions to the lattice distortion.

Contribution of tri-valent manganese ions

The MnO_2-$V^{5+}Mn^{3+}O_4$ system has been studied experimentally to introduce Mn^{3+} ions in the pyrolusite structure. The oxide mixture was sealed in a Pt-capsule and held at 900 °C under 25

kbar to prevent reduction. The solid solubility of $V^{5+}Mn^{3+}O_4$ component in MnO_2 was less than 50 mol%. The lattice parameter *a* increased and *c* decreased slightly with increase of $V^{5+}Mn^{3+}O_4$-component. However, the (310) reflection was sharp and the tetragonal system was maintained. The change of lattice parameters can be explained by Jahn-Teller effect of Mn^{3+} ions. One dimensional elongation of octahedra will be caused exclusively in the planes vertical to the *c*-axis, keeping the 4-fold screw axis of the rutile structure. This means the orthorhombic distortion can not be caused by Mn^{3+} ions.

Contribution of hydrogen ions

We calculated the lattice energy of hydroxidized pyrolusites, $Mn^{4+}_{1-x}Mn^{3+}_xH_xO_2$, by using Born-Mayer form based on the model that the hydrogen ions occupy the ocatahedral interstitial positions making a hydrogen bonding in the structure as shown in Fig. 1. This structure is similar to manganite one. The lattice parameters for a given x were obtained to minimize the lattice energy. The results are listed in Table 1. The values shown in the table is not absolute one because of the uncertainty of coeficients used in the calculation. From the results, it is however deduced that the introduction of hydrogen makes the cell orthorhombic. It is also seen from Fig. 1 that the electrostatic repulsive force along *b*-axis will be larger than that along *a*-axis, since the hydrogen ions and the Mn ions make a row along *b*-axis at the same z-parameter.

The present paper supports well a work of de Wolff (1959). He indicated that the pyrolusite which could be a pseudomorph after manganite shows some broad reflection lines.

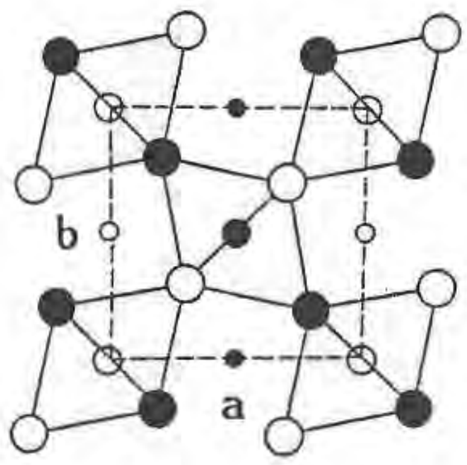

Fig. 1. Hypothetical model of hydroxidized pyrolusite

○, ● : O^{-2} at z=0 , z=0.5
○, ● : Mn^{+4-x} at z=0 , z=0.5
○, ● : H^{+x} at z=0 , z=0.5

Table 1. Calculated lattice parameters of hydroxidized pyrolusite

x	*a* (Å)	*b* (Å)	*c* (Å)	*b/a*
0.00	4.4424	-	2.8359	-
0.10	4.4609	4.6113	2.7461	1.034

References:
de Wolff, P.M.(1959). Acta Cryst. , **12**, 341-345.
Potter, R.M. & Rossman, G.R.(1979). Am. Miner. **64**, 1199-1218.

YAFSOANITE, CHEREMNYKHITE, KUKSITE AND OTHER NEW OCCURENCE IN KURANAKH GOLD DEPOSIT (ALDAN, YAKUTIA)

Kim A.A. *(Yakut Inst. of Geol. Sciences, Russian Acad. of Sciences, Russia).*

Kuranakh gold deposit is one of the famous in Aldan mining region. It is located in the central part of the Kuranakh graben at the contact between Cambrian carbonate and Jurassic terrigenous deposits. The gold deposit represents an elongated sheets. It is located in the N.-W and submeridional fault system. Primary ore bodies are pyrite-quartz and adular-quartz metasomatite that remain as relicts among desintegrated clay-limonite product of oxidation.

In the gold deposit the unknown so far telluride-sellenide and tellurate associations have been studied in detail. In primary pyritic-adular metasomatite a telluride association (gold, koloradoite, sylvanite, altaite) has been found. Of most interest are rare lowtemperature calcite hydrotermal veins. Minerals of Te-Se association (gold, koloradoite, sylvanite, altaite, naumannite, claustalite, tiemannite, cinnabar, orpiment) are preserved as the smallest inclusions in calcite. Various complex of secondary minerals is observel as a colloform and drusoid aggregate, and as single crystals, and also as pseudomorphic neogenesis in the interstices between the lathes of calcite. All abovementioned minerals, have corroded contact with calcite very often.

In the telluratic association yafsoanite $(Zn,Ca,Pb)_3TeO_6$, kuksite $Pb_3Zn_3TeO_6(PO_4)_2$, cheremnykhite $Pb_3Zn_3TeO_6(VO_4)_2$ are new minerals (they have been comfirmed by CNM IMA). V, Si variety of dugganite and dekluasite are the first finds in Yakutia. Formulae of cheremnyhite, kuksite and dugganite (Williams,1978) reflect the composition of extreme members of the isomorphous series. In fact we deal with termidiate composition with wide isomorphism in V, Si-As series, and limited in V,Si-P series. In close association with tellurate highdispersion extraordinary silicate phases have been found. Phase 1 is trioctahedral mineral of the montmorillonite group, with the composition between saponite and sokonite; phase 2 is trioctahedral phyllosilicate with Pb and Te in and Te in and in thetrahedron; phase 3 is silicate with Zn, Mn, Te. General formula of minerals is $[n*H_2OM^{+2}](Mg,Zn)_3(Si_{4-x-y}R^{+3}_xR^{+4}_y)O_{10}(OH)_2$; key M^{+2}-Ca,Mg,Pb; R^{+3}_x-Al,Fe; R^{+4}_y-Te, Mn; x-0,3-0,5; y-0,0-0,9. Under favourable conditions phases 2 and 3 may be presented as a new mineral.

References.
Williams S.A.// *Amer. Miner.* 1978. Vol. 63. N 9-10. P. 1016-1019.

EVOLUTION OF AMPHIBOLITES AND RESTITES IN MIGMATITES FROM SE TRANSDANUBIA (HUNGARY)

Király E. (Dept. of Petrology and Geochemistry, Eötvös L. University, Budapest, Hungary)

The South-East Transdanubia is a part of the microcontinent of Tisia. Metamorphites of these areas have complex, polymetamorphic history. Stages of the polymetamorphism: a Barrow-type, almandine-amphibolite facies metamorphosis (Szederkényi, 1974) (1), a metamorphosis under high temperature and low pressure (2), a post-orogenic potassium metasomatosis (Buda, 1985) (3) and a retrograde greenschist facies metamorphosis (T<450°C) (Árkai, 1985) (4).

Samples of amphibolites and restites gathered from Görcsöny Area (from core), Mórágy Hills (from surface) and western Mecsek Mountains (from core) show different metamorphic stages. These three areas are separated from each other by faults and their relationships to each other are uncertain.

Microscopic observation and textural analysis were used to determine the sequence of minerals and mineral parageneses, and exact composition of clinopyroxenes, garnets, amphiboles and plagioclases were measured by electron microprobe for geothermometry & geobarometry.

(1) The first metamorphic event is characterised by garnet (alm_{59-62}, pyr_{21-24}, gro_{12-14}, sp_{2-3}), amphibole (tschermakite, magnesio-hornblende), biotite, quartz and plagioclase (Ab_{59-66}) assemblage observed only in Görcsöny Area. Its pT conditions are: 570-580°C and 5-7 kbar by Plyusnina's thermobarometry, but 480°C and 7,5 kbar from sample of another core. Gr-hbl thermometry shows 593-648°C (Graham & Powell,1984) and 400-510°C was given between 6 and 7,5 kbar by Blundy & Holland's thermometry.

(2) Most of the clinopyroxenes (ferro-diopside) and amphiboles often with zoning (from actinolite to magnesio-hornblende and from silicic edenite to edenitic hornblende) developed under the second event. (Some of exsolved clinopyroxenes in amphiboles containing a little chromium were texturally different from these.) The temperature from amphiboles and plagioclases developing by second stage is between 540°C and 560°C below 2 kbar (Plyusnina's method) and between 416°C and 529°C (Blundy & Holland's method). Clinopyroxenes altered partly or totally to amphibole aggregates on cooling. Clinopyroxenes may indicate the highest temperature of this stage but the temperature obtained from amphiboles should be lower. The temperature of melting (685°C) may be very close to that where clinopyroxenes appear. This stage might be correlated with granitization.

(3) The alterations of amphibole to biotite and the plagioclase to microcline are the indicators of the potassium metasomatosis (Buda, 1985). It might have occurred between the second and the third stage.

(4) The second event was followed by the third one almost continuously with decreasing temperature. Amphibole aggregates were replaced by aggregates of plagioclase, calcite, chlorite and quartz. It can be also investigated on samples from Ibafa. Temperature of this is 346-435°C by Blundy & Holland's thermometry. But some inclusion in amphiboles produced on higher temperature (410-476°C) and amphibole inclusions in plagioclases developed on higher pressure condition (7-8,5 kbar) maybe under the first stage (?).

References:

Árkai, P. et al.(1985). Acta Geol. Hungarica 28(3-4) 165-190.
Blundy J.D.& Holland T.J.B. (1990). Contrib Mineral Petrol 104 208-224.
Buda, Gy. (1985). unpubl. Ph.D. Theses 148.
Graham C.M.& Powell R. (1984). J. met. Geol. 2 13-31.
Plyusnina, L.P. (1982). Contrib Mineral Petrol 80 140-146.
Szederkényi, T. (1974). unpubl. Ph.D. Theses 184.

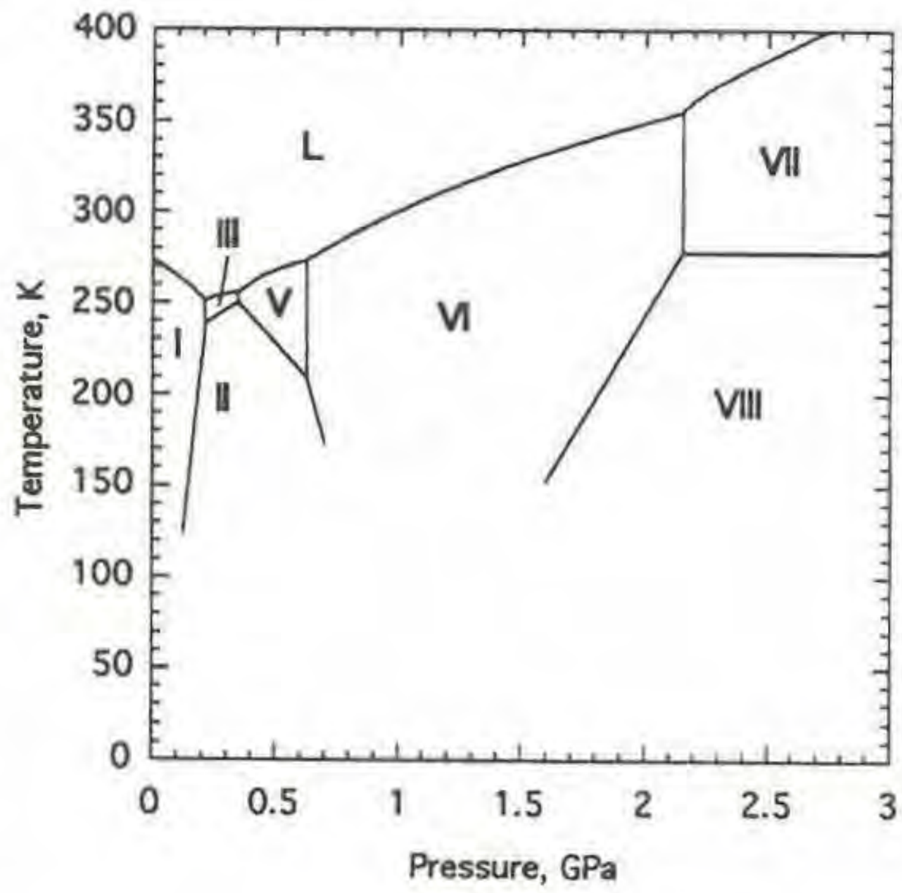

size within the pressure cell using the sliding piston normally used for deformation experiments. We have made rate measurements between 158 and 223 K, over which range the rate of I –> II increases by many orders of magnitude for a fixed value of $P - P_e$ where P is the applied hydrostatic pressure and P_e the equilibrium pressure of the transformation. The morphology of ice II inclusions also is a function of temperature, grading from plate-like structures at warmer temperatures to more equant shapes at low temperatures. The extremely high aspect ratio of the ice II inclusions at warm temperatures suggests a stress enhancement, perhaps assisted by localization of latent heat, at the edges of the growing inclusions.

The reverse transformation II –> I runs less rapidly than I –> II under comparable conditions, which we attribute to the change of sign of the latent heat and volume change of transformation, and possibly a difference in the relative rheologies of the two phases.

The ice I –> II transformation can also be induced nonhydrostatically. The parameter controlling rate of transformation at fixed temperature under nonhydrostatic conditions is $\sigma_1 - P_e$, where σ_1 is the maximum principal stress. The presence of nonhydrostatic stress also causes the orientation of the flat ice II inclusions to align normal to the direction of σ_1.

We have not been able to induce the I –> II transformation in bulk below 158 K, but we have evidence that limited transformation of I to II at high stresses and low temperatures leads to a shear instability in ice I. This instability is distinct from brittle failure of most rocks in that it occurs at a differential load that is very insensitive to P. Close analogies between ice I –> II and olivine –> spinel (large volume change, distinct kinetic retardation at low temperature, and positive latent heat) suggest that the shear instability in ice I may be closely related to the mechanism of deep earthquakes.

KINETICS OF PHASE TRANSFORMATIONS IN ICE

Kirby, S.H. (*U.S. Geological Survey, Menlo Park, CA*), Durham, W.B. (*Univ. of California, Lawrence Livermore National Laboratory, Livermore, CA*), and Stern, L.A. (*U.S. Geological Survey, Menlo Park, CA*)

Water ice is an unusual mineral in that it has at least eight different stable crystalline polymorphs below 2.5 GPa (see phase diagram below). Most transformations between polymorphs display temperature-dependent kinetic retardation. For example, virtually all the known high-pressure phases of ice can be returned metastably to 0.1 MPa if depressurization occurs at temperatures below 100–150 K.

We have encountered and documented phase transformations among ices I, II, III, V, and VI as part of a study of the mechanical properties of those phases, and we have formally studied the kinetics of the ice I – ice II transformation in the forward and reverse directions. Those transformations involve a sufficiently large volume change that we are able to monitor their progress by sensing sample

U-Th AND Au-Bi-Te-Zn MINERALIZATION OF THE UNIQUE RARE METAL-TIN DEPOSIT SYRYMBET (REPUBLIC OF KAZAKHSTAN).

Kiseleva G.D., Laputina I.P., Chukhrova O.F. (Institute of geology of ore deposits, Russian Acad. Sci., Moscow), Tyuleneva V.M. (All-Russian Institute of Mineral Raws, Moscow, Russia).

The deposit is localized at the contact between highly-differentiated granites and vendian metasediments. The economic ore bodies are hosted mostly in vendian sediments. The whole area of the deposit is covered by weathering crust, which represents a new own economic type of the rare metal-tin mineralization. The deposit was formed as a result of long-duration multistage process. At least six stages of the mineral formation were distinguished. The host rocks were altered into hornfels, skarns and greizens. More than 70

newly formed minerals have been established. The ores contain a great number of the trace-elements. The main economic mineral is cassiterite. Rather rare for tin deposits gold, tellurium, zinc and uranium-thorium mineralization was established. It was proved that the tin mineralization was followed by Au-Bi-Zn-Te one. U-Th mineralization is manifested within the main productive greizen stage and is represented by the evolution row of minerals in which composition from the beginning to the end of the greizen process increases the Th content and decreases the content of U (Th-uraninite - U-monazite - U-fluocerite - Th-monazite - thorite).

The deposit is characterized by the great number of the mineral forms for one and the same element. Five minerals of Sn have been found (cassiterite, varlamoffite, hydrostannate, stannite, stannoidite), three - of Au (native gold, electrum, maldonite), two - of Te (joseite, tetradymite), six - of Bi (native bismuth, wittichenite, bismuthinite and minerals mentioned above); besides, Bi is a constant trace-element in the cassiterite. The native zinc - very rare natural mineral - has been detected in the association with the bismuth minerals. The extremaly rare mineral of In - roquesite - has been also determined in the association with bornite.

The main accompanying elements are Bi, Mo, Be, W, Y, Nb, Cu, F, Pb and Zn, the most of them being of economic interest. The geochemical halo of tin is accompanied by the haloes of Cu and As. The upper boundary of the vast Bi halo is confined to the central part of the ore body, the lower one coinciding with the granite roof. The haloes of W and Mo are situated at the underore part of the body.

The unique reserves of this deposit, the diversity of ore and accompanying elements, the variety of the mineral forms of their manifestation are considered to be the result of the long-duration multistage mineral-forming process. The occurrence of Au and U in the ores reflects the Au-U metallogenous specialization of the North-Kazakhstan ore province.

• THE COMPOSITION OF FLUID-CONTENT MINERALS AND THE CHLORINE ROLE AT FORMATION OF THE PGE-BEARING HORIZONS; IOKO-DOVYREN LAYERED MASSIF, NORTHERN TRANSBAICALIA, RUSSIA

Kislov, E.V., Konnikov E.G., Orsoev D.A. (*Buryatian Geol. Inst, Ulan-Ude, Russia*) and Pushkarev E.V. (*Inst. of Geol. and Geochem., Ekaterinburg, Russia*)

The Ioko-Dovyren massif stretches on 26 Km length with thickness of 3.5 Km and was emplaced 740 Ma in the Proterozoic Olokit pericontinental sedimentary basin. The massif sequence comprises plagioclase lherzolites, dunites, troctolites, olivine gabbros and olivine gabbronorites. The PGE-bearing horizons were revealed at the gabbroic part of the massif and traced for 19 Km.

The lowest and richest horizon I is confined to the transition area from rhythmic layered troctolite-olivine gabbro sequence to massif olivine gabbro. The horizon II is confined to transition area from olivine gabbro to olivine gabbronorites.

The PGE bearing rocks are characterized by presence of the disseminated sulphides (up to 7 vol. %) and OH-bearing minerals (phlogopite, biotite, zoisite, prehnite, actinolite, chlorite), sometimes K-feldspar and quartz.

The phlogopites from olivine gabbronorite and leucogabbro of horizon I have higher Cl (0.08-0.34 %) than F (0.0-0.15 %). The altered phlogopite contains less halogens (both F and Cl - 0.06 %). The low-temperature metamorphic zoisites and prehnites are halogens-free.

The phlogopites and biotites of PGE-bearing rocks of horizon II also contain more Cl (0.08-0.58%) than F (0.04-0.25%) except for the one from the plagioclase-bearing peridotite (0.18-0.44 % f and 0.10-0.16 % Cl). The postmagmatic amphiboles, chlorites and altered biotites contain no more than 0.15 % of Cl+F with varying proportions. The zoisites at these rocks are halogens-free too.

Most of phlogopites and biotites from younger sulphide-bearing gabbronorites contain more Cl (0.11-0.51%) than F (0.02-2.00%), being in association with fluorapatite (1.94-3.24% F and 0.22-1.07% Cl).

The halogen contents of apatites, phlogopites and biotites point to a relatively chlorine-rich, fluorine-poor environment during the crystallization of these minerals with halogen enriched at the chamber top. As the altered biotites and phlogopites, amphiboles, chlorites are Cl- and F- poor, the low temperature metamorphic clinozoisites and prehnites are halogen-free, the Cl is unlikely to have been introduced by circulation of low- to moderate-temperature meteoric waters.

These features suggest that the PGE mineralization formed in process of upward migration of residual melt or juvenile fluids evolved during solidification of ultrabasites and layered sequence of Yoko-Dovyren massif.

CHEMICALLY SECTOR ZONED GARNET IN THE SANBAGAWA METAMORPHIC ROCK

Kitamura M., Wallis, S.R. and Hirajima, T.
(*Dept. of Geology and Mineralogy, Kyoto Univ., Japan*)

The Sanbagawa belt is a regionally high P/T metamorphic belt. Chemically sector zoned garnet is first found in a rock sample from one of the metamorphic zones (oligoclase-biotite zone) in the Besshi area, Japan, while texturally sector zoned garnets have been reported in metamorphic rocks (*e.g.*, Jamtveit & Andersen, 1992)

The host rock is mainly composed of a compositional banding of biotite + garnet-rich and hornblende-rich bands several cm thick each other. The garnet in the bands is coarse-grained (up to 1 cm) and shows normal concentric growth zoning patterns.

Within the compositional banding of the host rock, there are a number of thin layers (< 1 cm) with a striking pink color that consist dominantly of quartz and garnet. The layer consists dominantly of fine-grained (up to 100μm) quartz and garnet with subordinate amounts of large (< 5 mm) dolomite porphyroclasts. The garnet crystal in the layers can be divided into three regions; core, mantle and rim. The core is Fe-rich (around $Mg_{0.5}Fe_{1.9}Ca_{0.4}Mn_{0.2}$). The mantle (around $Mg_{0.4}Fe_{1.7}Ca_{0.7}Mn_{0.2}$) shows the chemical sector zoning characterized by the symmetrical element distribution, where the high Fe/Mg regions appear mainly around the corner of the {110} faces. The sector zoning was interpreted to be formed during the growth. The rim (around $Mg_{0.4}Fe_{1.8}Ca_{0.6}Mn_{0.2}$) shows no such a sector zoning.

Chemical sector zoning is generally formed by element distribution among more than two crystallographically non-equivalent growth sectors. On the other hand, all the sector zoned garnet in question shows no change of crystal habit bounded by {110} faces throughout the crystal growth, and the compositional heterogeneity was observed on the isochronal surface of the {110} sectors. The present sector zoning is therefore a new type of chemical sector zoning.

This new type of sector zoning was interpreted to be formed by the difference in step densities between the center and edges of the growth surfaces in the stability field of polyhedral shapes of a crystal, since the difference caused the different lateral growth rates of the steps and resulted in the heterogeneous element distribution.

References:
Jamtveit,B. & Andersen,T.B. (1992) *Phys.Chem.Min.*, **19**, 176-184.

• METASTABLE DIAMOND SYNTHESIS - PRINCIPLES AND APPLICATIONS

Klages K.P. (*Fraunhofer-Institut für Schicht- und Oberflächentechnik (FhG-IST), Braunschweig, FRG*)

The first synthesis of diamond under conditions of its metastability

was achieved reproducibly by Eversole at Union Carbide Corporation in the early 50's, even before the high-pressure-high-temperature experiments at General Electric were successful. Nevertheless it took almost 30 years until the scientific-technical community was generally convinced of the feasibility of continuous low-pressure diamond growth from activated gas phases. Since then, however, diamond CVD technology has progressed considerably: A multitude of deposition processes is now available to grow diamond films, textured and heteroepitaxial (on Si) deposition has been achieved, and new technological applications of diamond films, utilizing their outstanding physical properties, are continuing to emerge. Simultaneously, the understanding of which molecular species and physico-chemical processes are relevant for the CVD growth of the metastable diamond phase has developed exceptionally rapidly, thanks to data-bases for chemical gas phase reactions in C-H-O systems being available from the research on flames and combustion.

The lecture is intended to give an overview of growth processes and applications of diamond films. Emphasis will be laid on examples from the work at FhG-IST.

TURQUOISE GEM MATERIAL: NATURAL AND VARIOUS MODIFICATIONS AND SUBSTITUTES

Klein, C. (*Dept. of Earth and Planetary Sciences, Univ. of New Mexico*) and Werner, G. (*Albuquerque, New Mexico*)

High quality, good color, durable turquoise gem material of natural (mineral) origin is rapidly becoming scarce. Because of the craftsmanship needed to drill and shape the hard natural material for use in jewelry and because of the high price of the bulk material, a large industry has arisen in the alteration (improvement) of originally poor quality material (of turquoise composition) and in the production of various turquoise substitutes. The public that buys turquoise jewelry or turquoise set in sterling silver (as is typical from the southwestern part of the USA) is generally unable to distinguish the various types and hence is vulnerable to fraud.

"Unnatural" turquoise includes the following types: A. Stabilized turquoise which is originally poor quality turquoise (referred to as "chalk" in the trade) that has been chemically impregnated and hardened. This stabilization is the result of impregnation with organic resins, which under controlled conditions causes polymerization of the turquoise into a permanently hardened and stable state. This impregnation generally enhances the blue color of the original "chalk", and makes the final product durable and attractive. The color produced is similar to that of a hydrous natural gem grade turquoise. B. Oil treated turquoise in which the color of the natural material has been enhanced by impregnation with organics such as mineral oil, paraffin, or oil-based polishes. All such additives are by nature unstable. Therefore, these treatments generally result only in a temporary improvement of color, with subsequent fading. Oil treated turquoise can be subsequently sealed to lengthen the color retention. C. Treated turquoise which means natural or stabilized turquoise that has been altered to produce a change in the coloration of the natural mineral; this involves dying of the material to enhance its color. D. Reconstituted turquoise which means turquoise dust and/or particles, or nuggets bonded together with plastic resins and generally packed with other mineral fillers so as to imitate natural turquoise with mineral matrix. E. Imitation turquoise which includes any natural or synthetic compound or mineral that is manufactured or treated so as to closely approximate turquoise's appearance. This includes turquoise colored plastics (with or without fine mineral matrix), glass, enamel and dyed chalcedony.

Material in category C(dyed) can generally be distinguished by a well-trained eye; those in categories D and E (reconstituted and imitation) can generally be identified by some physical tests. However, those in categories A and B, can in most cases only be identified and distinguished by elemental microanalysis for H, C, and N. Since 1985 G.W. and Robert North at the New Mexico Bureau of Mines, have tested many types of turquoise (natural gem quality and the various alterations) by this method. Furthermore, major element chemical analysis and X-ray powder diffraction techniques have also been used. For categories A and B, as compared with natural gem turquoise, the amounts and ranges of C and H values are distinctive:

	Weight % C	Weight % H
Natural gem turquoise	< 0.15	1.46 - 2.05
Stabilized (cat. A)	2.5 - 20	2.4 - 3.6
Oil-treated (cat. B)	0.2 - 0.3	2.0 - 2.1

In addition to the above types of alterations or imitations, there is synthetic aluminum hydroxide, $Al(OH)_3$, that is dyed a turquoise color. This can be identified only by X-ray diffraction techniques. Furthermore, there is a tough, very good turquoise-colored synthetic material that consists mainly of CaO(38.0), TiO_2(4.0), Al_2O_3(2.2), P_2O_5(2.4), all in weight percentage, and C = 16.22, H = 1.12, N = 10.37 weight %. This material is a true Persian blue with excellent hardness and durability.

CHRYSOBERYL GROWTH FROM THE HYDROTERMAL SOLUTIONS

Kljakhin V.A. (Institute mineralogy and petrography Siberian Branch, RAS)

The data reported on solibility of alexandrite in 1 mole sodium salts of basic inorganic acids and recrystallization of chrysoberyl into seed crystals in hydrotermal conditions at 873 K. Solubility of alexandrite was determined by the weight loss of the block. The highest solubility was obtained for Na_2CO_3 solution. Na_2CO_3-0,118 mole/litre, (NaF-0,063 mole/litre, Na_2CO_3-0,042 mole/litre).

Experiments were performed on recrystallization scheme. Na_2CO_3 was taen as the basic solvent. We estimated the influence of the solvent concentration on the growth rate, mass transfer stability over time and the influence character of the additional components introduced into the solvent. In all experiments a stable growth of the seed crystals is observed (up to 0,15 mm/ /24 hours), but multi-head growth with numerous "punctures" occurs. The growth rate of seed crystall increases with increasing concentration of the solvent Na_2CO_3. Addition of NaF, $NaNO_3$ and Na_2SO_4 does not essentially effect the growth rate. The colour of chrysoberyl obtained from carbonate and carbonate-fluoride solution is light yellow-green. In the presence of nitrates and sulphates it becomes dark-brown. In some sample disontinuity - effect of the cat'seyes - is observed.

THE REAL STRUCTURE AND PROPERTIES OF APATITES

Knubovets R. (Dept. of Geology, The Open Univ. of Israel, Ramat-Aviv)

The real structure of apatite significantly differs from its idealized model. There is no atom which has less than two nonequivalent crystallochemical positions in the real structure of apatite. The following features were found: presence of hydroxyl groups forming and non forming hydrogen bonds, non-equivalence of the different positions of fluorine atoms, partial condensation of the ortophosphate groups to pyrophosphates, localization of the carbonate ions, replacing the ortophosphate group, or on the hexagonal axis.

The structural characteristics of natural phosphates are typomorphous and suitable for geological research and genetic studies. An explanation of the paradox of oxyapatite formation in geological systems genetically similar to the mantle in extremely reducing environments is proposed. Structural typomorphism of apatite was successfully used to reveal kimberlite pipes. It turned out that apatites with Eu^{2+} luminescence, condensation of ortophosphate groups, formation of OH...O hydrogen bounds may serve as a marker for the detection of kimberlite pipes while analyzing magnetic anomalies.

The crystal lattice of phosphate is dynamic. High pressure or heat treatment of apatites result in the relocalization of anions from one structural position into another. Distribution of various ions between their non-equivalent structural positions is of great importance to mineral properties.

For example, dynamics of hydroxyl groups determine to a large degree the acidic thermal treatment process which is used to remove fluorine from natural phosphates in the production of mineral fertilizers. The fluorine content of Kovdor apatite is two or three times less than that of the Khibin apatite. However, it is much more difficult to remove fluorine from the structure of Kovdor apatite compared to Khibin apatite. It was shown, that one of the reasons for this is an increased content of hydrogen bonds in Kovdor apatite which inhibits diffusion along the hexagonal axis.

Another example is the influence of carbonate ion mobility in the apatite structure on the properties of Karatau raw materials. Classification of Karatau phosphate rocks into two categories: high quality and regular ones, was based on the quantity of P_2O_5 in an ore. However, the so called high quality ores, in spite of their high P_2O_5 content, turned to be unsuitable for production of elementary phosphorous because of the relocation of the carbonate ions from one crystallographic position to another in the apatite structure.

Crystallochemical analysis facilitates the prediction of mineral properties, the prevention of technological failures and the optimization of phosphorite processing.

POLARIZED FTIR-SINGLE-CRYSTAL SPECTRA OF NATURAL STAUROLITE

Koch-Müller M., Langer K.(*TU Berlin*) and Beran A.(*Universität Wien*)

Staurolite, an important rockforming mineral with variable chemistry and OH^- content, has the ideal formula $Fe_4Al_{18}Si_8O_{46}(OH)_2$. However, this formula is not consistent with the observed OH^- content of natural and synthetic staurolites (Holdaway et al 1986: 2.8 - 4.2 H pfu; Lonker 1983: 1.8 - 3.6 H pfu; Fockenberg 1992: 2.88 - 4.44 H pfu). This deviation from the ideal formula with respect to the OH^- content is maintained by the formation of vacancies in the T2, M3 and M4 sites (Ståhl et al 1988; Hawthorne et al 1993). There are two main substitution mechanisms:

(1) $Al^{3+} + 3\,O^{2-} = \square + 3\,OH^-$ (M3, H1)

(2) $Fe^{2+} + 2\,O^{2-} = \square + 2\,OH^-$ (T2, H2)

The protons involved have been localized by Takeuchi et al 1972 (H1), Tagai & Joswig 1985 (H1) and Ståhl et al 1988 (H1 and H2), but until now no single-crystal spectra exist, which could confirm the proton positions. Therefore, polarized FTIR absorption spectra of staurolite from Pizzo Forno have been measured in different orientations in the range 4000 - 3000 cm^{-1}. The spectra in Fig. 1 show two relativly sharp bands at 3675 and 3576 cm^{-1} (E ∥ a) and a broad band at 3451 cm^{-1} with a shoulder at the low energy side (E ∥ a) and a broad band at 3340 cm^{-1} (E ∥ c). The pleochroism and the energy of the broad band at 3451 cm^{-1} is in accordance with OH^- valence vibrations of the protons H1. The observed halfwidth of this band is caused by the variation of the chemical environment due to different occupancy of the coordinating T2 sites. The sharpness and the pleochroic scheme of the band at 3675 cm^{-1} can only be explained by OH^- valence vibrations of H2 protons in a non-varying chemical environment. Then, the band at 3576 cm^{-1} is expected to be due to an additional type of hydrogen atom (H3). From the pleochroic behaviour, the observed halfwidth and bond valence considerations we conclude, that these protons are also bonded to O1 in a bifurcated hydrogen brigde to O5 of a vacant T2 site. The band at 3340 cm^{-1} is probably due to a fourth proton position.

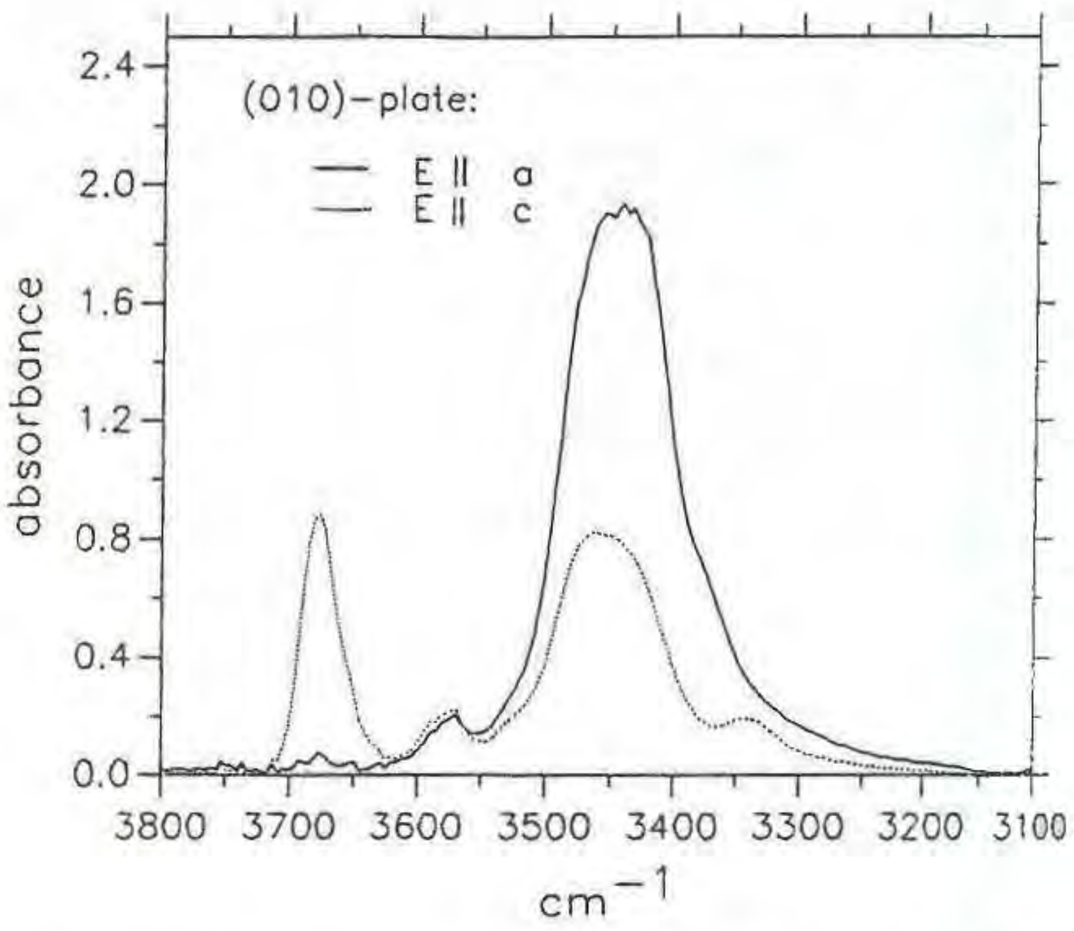

Fig. 1: Polarized staurolite spectra in the OH vibrational range. Crystal thickness: ca 11 µm.

References:

Fockenberg, T. (1992). Ber. Deutsche Min. Ges., 4 , 1, 82.

Hawthorne, F.C., Ungaretti, L., Oberti, R., Caucia, F., Callegari, A. (1993). Can. Min., 31 ,551-582.

Holdaway, M.J., Dutrow, B.L., Borthwick, J., Shore, P., Harmon, R.S., Hinton, R.W.(1986). Am. Mineral., 71 ,1135-1141.

Lonker, S.W. (1983). Contrib. Mineral.Petrol., 84 ,36-42

Ståhl, K., Kvick, Å., Smith, J.V. (1988). J. Sol. State Chem., 73, 362-380.

Tagai, T.& Joswig, W. (1985). N. Jb. Miner. Abh., 153, 177-215

Takéuchi, Y. Aikawa, N. Yamamoto, T. (1972). Z. Kristallogr., 136 , 1-22.

MECHANISM OF CARBONATIZED PERIDOTITE PARTIAL MELTING.

L.N.Kogarko, A.H.Pacheco

(Vernadsky Inst. of Geochemistry RAS. Moscow Madrid University)

During the investigation of the unique harzburgite nodule from the Montana Clara Volcano (Canary island archipelago) for the first time the evidence of the primary carbonate melt was discovered. This carbonate is enriched in calcium and it occurs together with glass containing sulphide globules. In addition to primary olivine and orthopyroxene there are pockets of fine grained minerals belonging to the second generation (more magnesium olivine, sodium bearing clinopyroxene, less aluminous spinels) due to the metasomatic interaction of primary carbonatite melt and harzburgite. The possibility of the metasomatic interaction of carbonatite melts with mantle material with the formation of similar mineral assemblages was demonstrated exeprimentally (1) and it was suggested during the investigations of nodules of continental and oceanic mantle (2,3). The interaction takes place according the reaction:

$$\underset{enstatite}{4\,MgSiO_3} + \underset{dolomite}{CaMg(CO_3)_2} = \underset{forsterite}{2\,Mg_2SiO_4} + \underset{diopside}{CaMgSi_2O_6} + 2CO_2$$

However primary carbonatites in this mantle nodules were not discovered. In our work we for the first time observed the evidence of carbonatite melts themselves and mineral assemblages arising during metasomatic interaction of primary carbonatite melt with mantle material. Very often carbonate forms in the investigated nodules rounded oval segregations immersed into glass where

numerous very small sulfide globules having the composition of monosulfide of Ni, Fe and Cu are also present. In our opinion the character of interrelationships between carbonate, glass and sulfides testifies to the processes of immiscibility which occurred during the adiabatic decompression of mantle which may result in the appearance of carbonate liquids close in composition to natural calcite carbonatites. Therefore the investigated unique mineral assemblage including carbonate and glass can be considered as a micro model of the generation of the carbonatitic magmas during the processes of the partial melting of carbonatized metasomatized oceanic mantle. The development of carbonatite magmatism on Canary Islands (Lanzerote), Cape Verde Islands is likely to be related to the partial melting of carbonatized mantle in the South Atlantic, which took place over a vast territory.

References:
1. Green,D.H. and Wallace,M.E. 1988 *Nature*, 336, 459-462
2. Yaxley,G.M.,Crawford, A.J and Green,D.H. 1991 *Earth Planet.Lett.*,107,305-317
3. Eric H.Hauri, Nobumichi Shimizu, Julie J.Dieu and Stanley R.Hart 1993 *Nature* vol. 365

AGE AND ORIGIN OF GRANITOIDS ALONG THE PACIFIC COAST OF MEXICO

Köhler, H., *Schaaf, P., *Morán-Zenteno, D. & Solís-Pichardo, G.
Mineralogisch-Petrographisches Institut der LMU München, Germany; (* now: Instituto de Geofisica, UNAM Mexico City, Mexico).

The objective of this project has been to determine the ages and petrogenetic setting of the undeformed and deformed granitoids of the Guerrero and Xolapa Terranes along the Pacific coast of Mexico, bounded by Puerto Vallarta to the north and Salina Cruz to the south. 13 intrusive bodies of different dimensions have been studied. In total 150 whole rock and 50 mineral concentrate samples have been analyzed using the Rb-Sr and Sm-Nd method.
We used Rb-Sr whole-rock systematics to investigate the intrusion ages of the magmas, well aware of the problems of interpretation inherent to this isotopic system. These whole-rock dates were, where possible, compared with biotite Rb-Sr ages for verification. In some cases, only biotite ages are available in which case we have interpreted these as minimum ages of emplacement.
The results of the Rb-Sr dating indicate a considerable spread of emplacement and cooling ages. The emplacement ages for undeformed granitoids range between latest Lower Cretaceous (~100 Ma) and Oligocene (~25Ma). The orthogneisses of the Xolapa Complex rendered latest Jurassic/earliest Cretaceous (130-140 Ma) ages.
A plot of intrusion age versus geographic position along the coast indicates a younging of plutonic activity from NW to SE. Arc magmatism migrated along the pacific continental margin of Mexico over a distance of 1000 km during a period of ca. 75 Ma. Notably discordant to this trend are the intrusion ages of the orthogneisses at the Jurassic/Cretaceous boundary.
This trend is mirrored by the biotite cooling ages which also display a systematic younging toward the SE including the biotite cooling ages of the orthogneisses. This suggests that along this 1000 km long portion of the continental margin between 85 and 15 Ma before present, Rb-Sr closing temperature in biotite was reached at progressively later times toward the SE, independently of the emplacement ages of the plutons.
Geochemical data characterize the granitoids as M-, I-, to S-type granites. To further characterize the petrogenetic relationships among the granites, Sr and Nd isotope systematics of these rocks have been examined. Like the intrusion and cooling ages, the ε-Sr-, the ε-Nd-values, and the Nd model ages exhibit considerable scatter: ε-Sr values vary between -12 and +275, while those of ε-Nd lie between -8 and +7. The Nd model ages, which are without exception older than the corresponding emplacement age, range between 1200 and 200 Ma.
On a ε-Sr versus ε-Nd diagram, the data plot initially along the Sr-Nd Mantle Array, subsequently curving in the direction of the Phanerozoic Crust trend. The values of most of the individual intrusives along this trend, which include present day MORB through OIB to continental crustal isotopic signatures, occupy only a small portion of the entire trend. Exceptions to this are two complexes in the NE, whose values span the entire range of the whole population.
Plotting the model ages of the granitoids as a function of distance along the coast yields a systematic relationship which, with two exceptions, is very similar but opposite in sense to those of the emplacement and cooling ages. Beginning with the complexes in the NW and continuing to the SE for a distance of 800 km, the data describe a trend of increasing model ages from 200 to 800 Ma. This spatial and temporal pattern of model ages documents either an increasing proportion of older continental crust contamination of the melt fractions, or an increase in the age of the crust contaminating the melt, from the NW to the SE. In the case of the two exceptions to the model age trend mentioned above ages vary between 400 and 1200 Ma. These ages attest to a distinct and complex petrogenetic setting for these plutons, in which emplacement of strongly contaminated melts and lightly contaminated melts alternated with time.
The heterogeneous isotopic data along the batholithic belt of the Mexican Pacific coast underline its complex tectonic setting, due to the emplacements of the paleotrench, changes in the geometric plate tectonics interaction, truncation of the continental margin and different stages of continental thickening and uplift.
The data presented in this summary synthesize research carried out by Schaaf (1990), Moran-Z. (1992) and Solis-P. (1994, in prep.).

References
Schaaf, P. (1990). Diss.Univ.München
Moran-Zenteno, D. (1992). Ph.D.Thesis. UNAM Mexico

THREE NEW TELLURIDE MINERALS FROM ARCHEAN GOLD DEPOSITS IN THE HATTU SCHIST BELT, ILOMANTSI, EASTERN FINLAND

Kojonen K., Johanson B. and Pakkanen L. (*Geological Survey of Finland*)

Several gold deposits have recently been discovered in the Archean Hattu schist belt, Ilomantsi, eastern Finland, 80 km east of the town of Joensuu (Nurmi & Sorjonen-Ward, 1993). The gold mineralizations occur with sulphide disseminations in quartz-carbonate veins and shear zones in hydrothermally altered tonalites, quartz-feldspar porphyry dykes, quartz-tourmaline veins and mica schists. In the northern part of the belt, gold is found in altered felsic porphyries in contact with komatiitic ultramafic rocks.

Most of the gold is in native form intergrown with pyrite, arsenopyrite, rutile, native bismuth and tellurides of Au, Ag, Tl, Bi, Pb and Fe (Kojonen *et al.*, 1993). The tellurides include altaite, tsumoite, hedleyite, tellurobismuthite, unnamed Bi_3Te_2, rucklidgeite, volynskite, hessite, frohbergite and melonite. Minor amounts of gold are incorporated in electrum, calaverite, montbrayite and petzite.

The three new telluride minerals found in Hattu schist belt have chemical compositions corresponding approximately the chemical formulae: Ag_8TlTe_5, NiSbTe and AuSbTe (Table 1). The first new telluride mineral A (Ag_8TlTe_5) (Johanson *et al.*, 1991, Kojonen & Kristen, 1993) appears greyish in reflected ligth in air and dark grey in oil immersion. The gray tinge is slightly paler than that of hessite. Bireflectance was not observed in the grains studied and anisotropy is weak. The polishing hardness is about the same as that of hessite. The second new telluride mineral B (AuSbTe) is greyish white in colour, darker than altaite and weakly anisotropic. Bireflectance was not observed in the grains studied. The polishing hardness is lower than that of frohbergite but about the same as that of altaite. The third new telluride mineral C (NiSbTe) is light brownish in colour resembling pyrrhotite in colour. It has weak bireflectence both in air and oil immersion and the anisotropism is clear. The polishing hardness is higher than that of altaite.

Table 1. Chemical composition of new telluride minerals from Hattu schist belt, Ilomantsi Finland.

	A.	B.	C.
Au	0.75	43.1	0.00
Ag	47.5	0.00	0.00
Bi	0.00	0.15	0.14
Tl	15.6	n.d.	n.d.
Te	36.0	28.7	50.6
Sb	0.14	26.4	23.7
Hg	0.00	0.15	0.42
Ni	0.02	n.d.	23.7
Fe	0.02	0.03	0.02
As	n.d.	n.d.	1.30
Tot	100.03	99.43	99.87

A) $Ag_{7.85}Au_{0.05}Tl_{1.38}Te_5$, B) $Au_{1.01}Sb_{1.04}Te$,
C) $Ni_{2.04}Sb_{0.98}Hg_{0.01}As_{0.09}Te_{2.0}$, n.d. = not determined

Although these three telluride minerals cannot sufficiently defined because of their very fine grain size and rare occurence (only in one sample each) their homogenous chemical composition suggests that they represent new mineral species.

References:

Johanson, B., Törnroos, R. and Kojonen K. (1991). *Current Research 1990, Geological Survey of Finland, Special Paper* **12**, 91-96.

Kojonen, Kari, Johanson Bo, O'Brien Hugh and Pakkanen Lassi (1993). *Geological Survey of Finland, Special paper* **17**, 233-271.

Kojonen, K. and Kristen. D. (1993) *Scientific and Technical Information* Vol. **X, 6**, 191-196.

Nurmi, P. A. and Sorjonen-Ward, P. (1993): *Geological Survey of Finland, Special paper* **17**, 386 p.

PYROPE AND ORTHOPYROXENE INCLUSIONS IN DIAMOND: CHEMICAL VARIATIONS AND GEOTHERMOBAROMETRY.

Kolesnik Yu.N. (Inst. of Mineralogy, Geochemistry and Ore Formation, Ukr. Acad. of Sci., Kiev), Sobolev N.V., Yefimova E.S.(Inst. of Mineralogy and Petrography, Siberian Branch, Russian Acad. of Sci., Novosibirsk), Vishnevsky A.A. (Inst. of Mineralogy, Geochemistry and Ore Formation, Ukr. Acad. of Sci., Kiev)

44 inclusions in diamonds consisting both of pyrope (Py) and orthopyroxene (Opx) are considered. Most of them (25) have been obtained from kimberlite on the East Siberian Platform. The rest belong to kimberlite of S.Africa (published data).

The compositions of Opx and Py touching in inclusions form relatively narrow cluster in respect to scatter of the nontouching inclusions compositions. For example the aluminum contents of Opx touching in inclusions confine into interval 0,23-0,44 wt.% but those compositions nontouching in inclusions cover the Al contents interval 0,1-1,9 wt.)%. That can be explained, as we believe, by achievement of the diffusive equilibrium in touching inclusions. If the Opx or Py grains are armoured by diamond separately, each of them can evolve separately only at outer P,T conditions variations.

Therefore the geothermobarometry of touching inclusions can define in principle pressure and temperature of the last equilibrium of minerals. The nontouching inclusions can reveal the history of evolution of minerals confined in diamonds. The equilibrium pressure of Opx+Py association is estimated using the recently proposed geobarometer.

It is recalibrated incorporating the determination of the high temperature equilibrium fractionation of cations among nonequivalent sites in Opx. The exerimental equilibrium conditions of Opx and Py in MAS, CMAS, FMAS, CFMAS systems have been described without introduction of additional empirical constants. The published variants of geothermometers are used.

As a result we have obtained P and T of the last Opx+Py equilibrium in touching inclusions. They are located in the diamond stability field and approximate the shield geotherms calculated (Pollack & Chapman, 1977) for the surface heat flow 35-40 mW/m2. A scatter of the P,T estimation in nontouching inclusions reveals, as we believe, the reduction of mantle temperature beginning from Precambrian.

References:
Pollack H-N., Chapman D.S. (1977). Tectonophysics 38, 279-296.

DIFFUSION-CONTROLLED GROWTH OF GARNET CORONAS IN ARCHEAN GABBRO-NORITE (YENISEI RIDGE, RUSSIA)

Kolobov V.Yu. and Kouznetsova R.P. (United *Institute of Geology, Geophysics and Mineralogy, Novosibirsk, Russia*)

Coronal zones between plagioclase and olivine or pyroxene are prominent examples of reaction structures in metabasite. Mineral composition and structure of coronas depend on metamorphism conditions (P, T), chemical composition of reactant minerals and mass transfer parameters. Garnet coronas in gabbro-norite from Kansk series of Yenisei ridge (Eastern Siberia) are placed between crystals of plagioclase and orthopyroxene. According to mineral thermobarometry the metamorphism of Kansk series underwent in conditions of granulitic facies at temperature of 700-900°C and pressure of 6-8 kbars (Reverdatto, 1988).

There are two zones distinguished in the coronas. External zone at the plagioclase contact represented by garnet. This zone reaches about 1-2 mm width. It is red coloured and well differentiated in the rock. Internal zone consists of quartz and clinopyroxene, sometimes with single grains of garnet. The thin monomineral layer of quartz with width of 0.1 mm appears in some regions close to external garnet zone. Microprobe analysis data witnesses on chemical non-uniform of minerals in the coronas. In particular the average content of FeO, MgO and CaO in garnet near to the external bound with plagioclase are respectively 27.75, 4.07 and 8.12 wt %. In opposite near to the orthopyroxene contact these components reach the concentration of 29.15, 3.79 and 7.17 wt %. Remarkable, that the chemical composition of plagioclase near to garnet rims and away from them is also different. Away from garnet coronas plagioclase composition is An_{47}, but in close contact - An_{45}. These facts point to the limited mobility of species in process of metamorphic reactions.

Theory of the irreversal thermodymanics has been used to form the basis of algorith and numerical simulation computer program applied to model the growth of diffusion-controlled reaction coronas (Sheplev et al., 1991). Stability fields of growing coronas were constructed in coordinates of relative phenomenological diffusion coefficients for SiO_2-Al_2O_3-FeO-MgO-CaO system. The quality estimation of mass transfer parameters was obtained for metamorphism of metabasites under conditions of granulitic facies.

References:

Reverdatto V.V. (1988), Dokl. AN SSSR, v. 302, N 5, p. 1196-1200 (in Russian).

Sheplev V.S. et al. (1991), Soviet Geology and Geophysics, v. 32, N 12, p. 1-12.

MINERAL EQUILIBRIA AS THEORETICAL BASE FOR DECISION OF PROBLEMS OF ENVIRONMENTAL PROTECTION

G.R.Kolonin *(United Institute of Geology, Geophysics and Mineralogy, Novosibirsk)*

1. Mining activity is very important process when huge quantities of minerals, ores and rocks are removed on the earth surface and placed under conditions unusual for their stability. In this connection many problems of environmental protection depend on our understanding of chemical properties of both potentially hazard minerals and useful ones capable for absorbing or neutralizing any toxic, acid or other undesirable components. It is the reason why the mineralogical approach to mineral equilibria including study of dissolving, volatility, absorbtion, ion exchange and other types of reactions should be the real theoretical base for technological thinking.

2. From this point of view the first mineralogical task is the investigation of toxic properties of minerals as reflection of their specific physical-chemical properties. Ratios of total contents of toxic components at observed conditions to their extremelly permissible concentrations can be used as convenient indicators of toxic abilities of minerals named by us "coefficients of toxicity". The example with sulphide minerals presented usually in tailing dumps of many Siberian mines will be discussed. It is possible to design similar rows for any other mineral types, including ones, containing volatile toxic components.

3. There are many other types of minerals (first of all asbestos, then quartz, fluorides, chlorides and so on), which have high toxicity in their dust forms. Of course, it depends on chemical composition, crystal-chemical peculiarities, solubility and other characteristics of their activity. Recently it was illustrated in the book "Health effects of mineral dusts" (Rev.in Miner.,v.28,1993). In general we advance this second task to attract special attention of mineralogists.

4. Complex mineralogical-geochemical approach could be very fruitful when different sorts of deviations of salt or cation-anion exchange with a participation of human or animal bones and teeth take place, as well as cases of allogenic inner mineral ("stone") formation. The best example of this third task is the unfinished story with the mystery of endemic Kashin's-Beck's (or "urovskaya") bone disease located in the East Transbaikal region. It was Prof. A.P. Vinogradov, who has explained it on the base of the similar point of view as the result of the Ca deficit and its Sr compensation in 1949. The opposite hypothesis about phosphorus excess in water, rocks and other environmental components has been discussed for the last ten years. Many similar problems of use of mineral fertilizers are open yet.

5. The fourth mineralogical task in this context is the study of protective properties of many types of minerals and rocks. The next sorts of water-rock (mineral) interaction take place in both natural and technological conditions: chemical sorption of heavy metals and other cations, physical absorption, ion- exchange. General ion-exchange capacities and influence of physical-chemical conditions as well as of kinetic peculiarities must be studied by experimental methods as the real scientific basis for the arranging of rather cheap and reliable mineralogical barriers for toxic components. Its positive feature is the excellent possibility to utilize similar products after usage by means of high temperature treatments.

6.The next important task in the problem under discussion is the search for the best modes of nuclear waste disposal. To be extremely brief we mention only the Ringwood's SYNROC based in highest extent on the mineral equilibria approach and completely corresponding to Shuiling's term "geochemical technologies".

• GEMSTONE TREATMENT

Komov I.L. *(Inst. of Geoch., Mineralogy and Ore Formation, Kiev)*

Considerable amount of the off-grade material with faded colours and pale patterns occurs together with high-standard semi-precious stones. This decreases the gem and decorative quality of stones and sometimes precludes their use for such purposes. The colour, contrast range of pattern, and brightness of different minerals and aggregates can be changed by γ-irradiation combined with physical and chemical treatment of the original samples. A number of methods to change or intensify the colour have been developed (different types of physico-chemical treatment, including treatment by heat and pressure, impregnation with chemical reagents which facilitate colour reactions, ionising radiation etc.). These processes are called ennobling. Man-made heat treatment and ionizing radiation, in fact, reproduce the effect of the same factors produced on minerals under natural conditions. Each mineral has its own most precious colour and colour density. The deviation from these parameters considerably decreases the prices of semi-precious stones. When ennobling low-standard natural corundum, it is possible to intensify the dark-blue colour of leucosapphire and to weaken the colour of black corundum. The colour of natural orange, yellow, and orange-brown sapphire is due to the presence of centres of ions such as Fe^{3+}, Ti^{3+}, and Cr^{3+}. Similar colours can be obtained in synthetic corundum from Ni^{3+} and Cr^{3+}, as well as by additional heating. Natural colourless or light-yellow corundum may be ennobled through irradiation or annealing. Depending on the kind and conditions of irradiation, topaz can be coloured brown or blue. But after γ-irradiation, the colour is unstable and weakens as it becomes affected by sunlight. The reactor-induced irradiation, when the mineral becomes blue or dark blue, is the most efficient method of ennobling topaz. One of the important tasks of the gemmologist is to identify the treatment which may have been used to modify the colour or appearance of the gemstones being examined.

THE REE-Nb MINERALIZATION OF BIRAYA CARBONATE DEPOSIT, EASTERN SIBERIA, RUSSIA

Konev A.A., Chernikov V.V., Dneprovskaya L.V. *(Inst. of the Earth' Crust, Irkutsk, Russia)*, Vorobiev E.I. *(Inst. of Geochemistry, Irkutsk, Russia)*

A REE-Nb deposit in carbonate rocks bearing similarities to carbonatites of alkaline formations was studied in the Biraya river basin area, Vitim-Patom Highland. This occurrence resembles the Bayan Obo deposit of China. Carbonate rocks contain up to 4-5, sometimes 15 wt % of REE oxides occurring in monazite.

Carbonate rocks form layers 300 m thick and 7-10 km long. The complex enclosing them is represented by gneisses, schists, amphibolites, granitoids (Pt_1 and R). Carbonate rocks are crossed by granite-pegmatites, syenite-pegmatites and alkaline syenites (C-P). The isotope dates of the carbonate rocks vary from 1600-1700 to 350-375 M.yr.

The wall rocks are fenitized and carbonatized. Aegirine, richterite and magnesioarfvedsonite develop in them. Carbonate rocks are composed by ankerite, sometimes by calcite and magnesite. The $FeCO_3$ content in ankerite and magnesite varies from 21 to 55 mol.%. Calcite contains up to 7%, ankerite - to 3.5% of SrO. Of the carbonates strontianite, norsethite, benstonite were established. The content of apatite, sulfides and magnetite is increased. The deposits of magnetite in carbonate rocks are of commercial significance.

The monazite prevails among rare minerals. There

occur also aeschynite, blomstrandine, fersmite, tantalite-columbite, ilmenorutile, fergusonite, allanite, chevkinite, perrierite, bastnasite.

The following isotope data were obtained for ankerite: Sr^{87}/Sr^{86}=0.70434; $\delta^{18}O_{smow}$ = 5-7.9‰ ; $\delta^{13}C_{PDB}$ = 5.8-10.3‰ . The last values are not characteristic of carbonatites.

Comparison between Biraya and Bayan Obo shows that these deposits have features in common: 1) linear-layer shape, 2) increased Fe-content in carbonate, 3) the occurrence of nepheline-free alkaline metasomatites, 4) the similarity of mineralization. However, there are essential distinctions: 1) higher metamorphic grade of the Biraya sequence, 2) more important role of bastnasite in Bayan Obo because of fluorine abundance there and its deficiency in Biraya, 3) larger scale and higher concentrations of useful components in Bayan Obo.

Authors concluded that the Biraya deposit is of metamorphic-metasomatic origin and resulted from the action of alkaline mantle fluids saturated with rare elements.

Ti-Cr-V OXIDES IN METAMORPHOSED SCHISTS, LAKE BAIKAL AREA

Koneva A.A., Piskunova L.F. (*Inst. of Geochemistry, Irkutsk, Russia*)

A series of Ti-Cr-V oxides has been found in kyanite-sillimanite-cordierite-graphite schists in precambrian metamorphic rocks of the Olkhon suite, west shore of the Lake Baikal. These oxides occur mainly as thin lamellae in rutile and rather seldom as homogeneous mineral grains, their sizes varying from 5-10 to 100-150 mcm in length. Sometimes they are in intergrowth with eskolaite-karelianite, $(Cr,V)_2O_3$. The latter exhibits wide isomorphism of Cr and V: from 40 to 90 mol.% of Cr_2O_3.

It was established through electron-microprobe analyses that Ti-Cr-V phases under study belong to two homologous rows:

1 - $Ti_{n-2}(Cr,V)_2O_{2n-1}$ (n=3,4,5,6,8,9,12,14,18);

2 - $Ti_{n-4}(Cr,V)_4O_{2n-2}$ (n=5,7,9,11).

The first row corresponds to synthetic Ti-Cr homologous series (Andersson-Magneli phases).

The most frequent phase is $(V,Cr)_2Ti_3O_9$, which corresponds to schreyerite (V/Cr>1) or olkhonskite (V/Cr<1). The minerals form a continuous isomorphic row with $Cr_2Ti_3O_9$ content varying from 11 to 75 mol.%. Sometimes they associate with a mineral with the formula $(V,Cr)_2TiO_5$, which seems to be chromian berdesinskiite. Other Ti-Cr-V phases are rare in occurrence.

The variation of V/Cr ratio in the same phases is due to its difference in thin layers inherited from sedimentation.

HRTEM OBSERVATION OF OXIDIZED OLIVINES FROM THE OZE-HIUCHIGATAKE VOLCANIC ROCKS IN CENTRAL JAPAN

Konishi H. (*Dept. of Geological Science, Grad. School of Science & Technology, Niigata University*) and Akai J. (*Dept. of Mineralogy and Geology, Faculty of Science, Niigata University*)

Oxidized olivines occur in dacitic andesites in the Oze-Hiuchigatake volcano, central Japan, which provide geochemical and petrographical evidence of magma mixing of dacitic andesite magma and olivine augite basalt magma (Yokose, 1989; Konishi & Akai, 1994). The oxidized olivines have been described as iddingsite by Yokose (1989). The oxidized olivine crystals have been studied by HRTEM. The crystals contain magnetite, enstatite, laihunite and other unidentified materials, which must be formed by olivine oxidation.

The intergrowths of magnetite and enstatite have a lamellae-like appearance. The platelets are laying on (100), (010) or (001) plane of olivine and their size are about several hundred Å in width and about one micron in length. The platelets have enstatite cores although Moseley (1984) reported that the platelets have magnetite cores and magnetite can be the first phase to precipitate (Figure 1). The structural relations between host olivine and these minerals are as follows:

(1) [100]Ol // [111]Mt, [001]Ol // [110]Mt
(2) [100]Ol // [100]En, [010]Ol // [001]En, [001]Ol // [010]En
(3) [100]Ol // [010]En, [010]Ol // [001]En, [001]Ol // [100]En
(4) [100]Ol // [001]En, [010]Ol // [100]En, [001]Ol // [010]En
(5) [100]Ol // [041]En, [010]Ol // [100]En, [001]Ol // [01$\bar{4}$]En
(6) [100]Ol // [01$\bar{1}$]En, [010]Ol // [100]En, [001]Ol // [001]En

The relations (3), (5) and (6) were confirmed for the first time. Enstatite has many stacking disorder along the a-axis. A new stacking sequence (+--) was found for the first time, which repeats 20 times or 270Å along the a-axis (Figure 2). The stacking sequence with small disorder is up to about one micron along the a-axis.

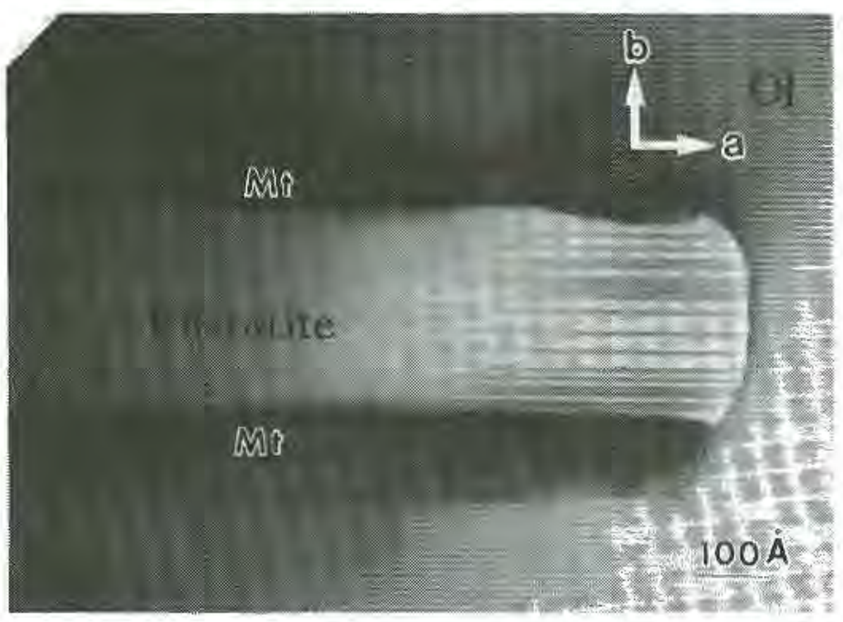

Fig. 1

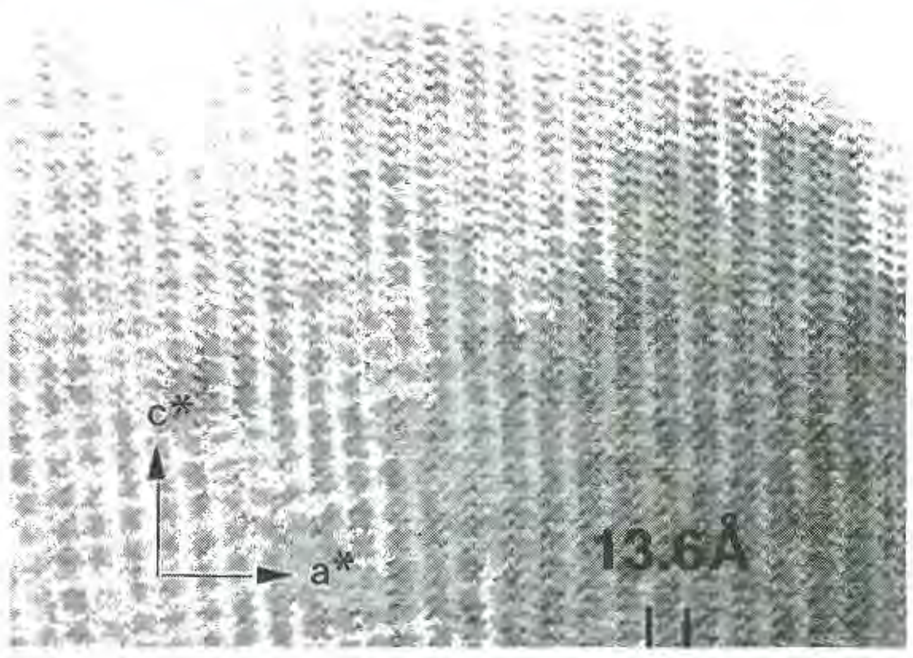

Fig. 2

Disordered intergrowths on (001) of olivine and laihunite, and GP zones were observed. This assemblage was found in olivines in andesites from the Abert Rim, Oregon by Banfield et al. (1990) and were estimated to be formed by olivine oxidation.

The olivine crystals may be oxidized in mixing of higher fO_2 dacitic andesite magma and lower fO_2 olivine augite basalt magma. The formation of intergrowths of laihunite and olivine may correspond to another episode of olivine oxidation.

REFERENCES:
Banfield J. F., Veblen D. R. & Jones B. F.(1990). *Contrib. Mineral. Petrol.*, **106**, 110-123.
Konishi H. & Akai J. (1994). *Mineralogy & Petrology* (in press).
Moseley D. (1984). *Am. Mineral.*, **69**, 139-153.
Yokose H. (1989) *J. Mineral. Petrol. Economic. Geol.*, **84**, 301-320. (in Japanese with English abstract)

PSEUDO-SYMMETRY ELEMENTS AS TOOLS FOR THE RECOGNITION AND DEFINITE CHARACTERIZATION OF MODULAR CRYSTAL STRUCTURES

Konrad, J. and Hofmeister, W. (Inst. f. Geosci., Univ. of Mainz)

In modular crystal structures special atoms or groups of atoms are related by pseudo-symmetry elements (PSE). Therefore the presence of PSEs in a crystal structure gives evidence of its modular structural character.

Since many crystal structures are centrosymmetrical, it is expedient to check a possible modular crystal structure for "centres of symmetry", which do not belong to the crystal´s real space group symmetry. The pseudo-centres of symmetry describe an approximately centrosymmetrical relation between atoms or groups of atoms in special limited spheres of the real crystal structure. Their average position can be calculated by means of the relative atomic coordinates of atom pairs related by the pseudo-centre. Average positions of other PSEs can be calculated in a similar way.

If PSEs have been determined in a crystal structure they are added to the crystal symmetry and considered equivalent to the "real" symmetry elements. It is expedient to look for pseudo-centres, because centres of symmetry are generally placed in the origin of centrosymmetrical unit cells and comparing possibly related crystal structures is made easy. Considering all centres of symmetry a modular structure can now be separated into (centrosymmetrical) subcells (modules). These modules may differ in chemical composition or orientation or chemical composition, orientation, metrics, and global structure and even in the topology of the modular building blocks.

The relation of a module to its corresponding crystal structure is not always obvious as the actual module may only be present as a subcell. Since metrics and positions of the subcells are known with respect to the metrics of the modular structure, atomic coordinates can be transformed, and the structures, built up by each module, can be calculated.

The relation of the real crystal structures and the crystal structures of the modules reveals the crystal chemical reasons for the building of modular crystal structures. New findings on the genetical interdependence of chain-silicates will be presented

CHEMICAL EVOLUTION OF THE LOVOZERO ALKALINE INTRUSION (KOLA PENINSULA): EVIDENCE OF ROCK FORMING MINERALS.

Korobeinikov A.N. and Laajoki K. (*Geol. Inst., Kola Sci. Centre, Russ. Acad. Sci.; Dept. of Geology, Univ. of Oulu*).

The Lovozero massif is the biggest distinctly layered intrusion of peralkaline feldspathoid syenites in the world. The present study concerns petrological aspects of rock forming mafic silicates and feldspathoids chemistry. Data obtained on clinopyroxenes chemistry with a use of electron microprobe (Korobeinikov & Laajoki, 1993) evidence that crystallization of pluton started from its upper parts. This lead to nosean syenites formation (upper border group). After that, the central rhythmically layered group of urtite-foyaite-lujavrite was formed. Chemistry of clinopyroxenes from eudialyte lujavrites shows their comagmatic and most evolved nature as to other plutonic rocks, although there are structural evidences of later emplacement of eudialyte lujavrites into pluton.

Clinopyroxenes are strongly zoned and show common for all plutonic rocks compositional trend from augite and diopside in nosean syenites (cores of grains) to aegirine-augite and aegirine in layered series of urtite-foyaite- lujavrite and eudialyte lujavrites. The gap in clinopyroxene compositional trend established in Mg-Na-(Fe^{2+}Mn) and other plots is attributed to amphibole crystallization due to critical vapour pressure at certain stage of magmatic evolution. Amphiboles evolve from richterite (cores of pyroxene-amphibole intergrowths) in nosean syenites to eckermannite and later to magnesio-arfvedsonite in other rocks.

The comparison between clinopyroxene crystallization trends for Lovozero and East Greenland intrusions (Larsen, 1976) have been made. It is asumed that the main reason for geochemical differences between these two layered intrusions was the different initial magmas alkalinity and the rate of its subsequent increase. More agpaitic nature of the Lovozero magma caused it's more oxidized character due to water dissociation by alkalies. The result of it was intensive growth of Mg/Fe^{2+} in mafic silicates during magmatic evolution. At late stages of the Lovozero crystallization the deficiency of ferrous ion had caused strong Ti-enrichment of pyroxenes due to breakdown of pyroxene - Fe-Ti-oxide titanium buffer. The same reason is responsible for the big amount of johannsenite end-member in Lovozero middle stage's pyroxenes.

The rock forming nosean of the earliest rocks - nosean syenites contains a number of sodalite and pyrrhotite inclusions. Sodalite inclusions are mostly anhedral and located in various parts of host nosean. But largest sodalite inclusions located in the cores of nosean grains are close to euhedral. Sodalite usually contains bigger amounts of iron than coexisting nosean (averages - 0,88 and 0,41 respectively). It is suggested that sodalite crystallized as a first phase of nosean syenites being accompanied by sulphide melt unmixing and formation of nearby pyrrhotite blebs. The subsequent increase of oxygen activity along with agpaicity index caused the crystallization of nosean instead of sodalite-sulphide assemblage.

We believe that many of the above mentioned chemical peculiarities were caused by oxidizing behaviour of water in highly alkaline magma of the Lovozero pluton.

References:
Korobeinikov A.N., Laajoki K. (1993). *Geokhimia*, 8, 1143-1150 (in Russian).
Larsen L.M. (1976). *J.Petrol.*, 17, 258-290.

• STUDIES OF PYRITE FORMATION MECHANISM IN AQUEOUS SOLUTIONS AT LOW TEMPERATURE AND PRESSURE

Koserenko S.V., Khramov, D.A., Fadeev, V.V., Kalinichenko A.M., Marov, I.N., Evtikova G.A., Rusakov, V.S. *(Vernadsky Inst. of Geochem. and Analyt. Chem.)*

The experimental studies of pyrite formation in aqueous solutions at low and elevated temperatures by use of X-ray phase analysis, chemical phase analysis, Mössbauer spectroscopy, proton magnetic resonance PMR), neutron activation analysis (NAA), electron paramagnetic resonance (EPR) were carried out. It was shown that in the conditions of our experiments the initial sediment consisted of X-ray amorphous sulfide (Fe:S ≈ 1:1) and elemental sulfur. The conditions of experimental runs included the following parameters: 25–250 °C; pressure in the range of 1–50 atm; ≈ 0.1M H_2S solution; $Fe(OH)_3$ was used as the initial reagent; pH 5.0–8.5. The sulfide fraction of the sediment along with the adsorbed H_2O was found to contain the structure protons presumably localized within the OH– and HS– groups (Bokyi & Bondar, 1979). Thus the primary sulfide phase was considered as a compounds of FeOHHS

composition. In the process of sediments aging the equilibrium pyrite formation was ascribed inn terms of the following reaction: $FeOHHS + S^\circ \dashrightarrow FeS_2 + H_2O$.

The synthesized sediments, both the initial and aged ones, were studied by Mössbauer spectroscopy on ^{57}Fe nuclei and by EPR. Iron was found to exist predominantly in a form of Fe^{2+}. Fe^{2+}–ions in FeOHHS and FeS_2 crystalline structures occurred in low spin state [ISS: $3d^6t2g$ ($\uparrow\downarrow\uparrow\downarrow\uparrow\downarrow$)].

Close vicinity of Fe^{2+}–ions at the initial and final stages of iron sulfide sediment formation was not markedly disturbed, i.e. all structural changes on aging processes gives rise to structural changes in anion sublattice of solid phase.

The experimental results are interpreted as an evidence of two step pyrite formation mechanism within broad conditional range corresponding to the natural sedimentary, hydrothermal–sedimentary and low temperature hydrothermal processes. The first step involves the formation of metastable phase–precursors (FeOHHS). The sediment aging results in the removal of hydrogen–bearing structurally localized groups as well as formation of pyrite sulfur and dehydration of the sediment. The direct formation of pyrite crystallization nuclei in the initial solution is supposedly favored by acid environment (pH 3.5–4.5).

Presented pyrite formation mechanism is valid in redox conditions corresponding to FeS_2–S° buffer. The formation of pyrite in substantially more reduced conditions (FeS–FeS_2 buffer) could be expressed by the following scheme (Schoonen & Barnes, 1991):

FeS	-->	FeS	-->	Fe_3S_4	-->	FeS_2
amorphous		mackinavite		greigite		pyrite

References:
Bokyi, G.B. & Bondar, A.M. (1979). *Doklady Akad. Nauk SSSR*, **248**, 956–959.
Schoonen, M.A. & Barnes, H.L. (1991). *Geochim. Cosmochim. Acta*, **55**, 1495–1504, 1505–1514, 3491–3504.

HYDROTHERMAL EXCHANGE OF ALUMINUM IN QUARTZ AT VARIOUS ACIDITIES

Koshchug D.G. (*Dept. of Geology, Moscow State Univ.*),
Fediushchenko S.V. (*Dept. of Geology, Moscow State Univ.*),
Hafner S.S. (*Inst. of Mineralogy, Marburg Univ.*),
Chernucha F.P. (*Dept. of Geology, Moscow State Univ.*)

Aluminum concentration in hydrothermally recrystallized polycrystalline quartz was measured by electron paramagnetic resonance (EPR) in order to study the change of aluminum concentration under experimental conditions which may be related to natural geochemical processes (metasomatic, hydrothermal, pegmatitic, etc.). Correlation between point defects in quartz and physicochemical parameters of mineral forming media has been studied extensively, in particular using EPR. Nevertheless, published results are ambiguous and partly contradictory.

Recrystallization experiments were carried out at 400°C and 0.1 GPa in H_2O or 0.001, 0.01, 0.1 molar HCl, or 0.002, 0.02, 0.2 molar NaOH. Some of recrystallizations have been done in the presence of feldspar as a source for aluminum in the fluid. Titanium autoclaves and platinum or gold ampoules have been used for the recrystallization. Aluminum concentration was measured at 77 K using a special reference sample. Before EPR measurements initial and recrystallized samples were gamma irradiated with a dose of 100 Mrad.

It was found that aluminum concentration in quartz decreased by a factor of 6 after recrystallization in acid solutions and H_2O. In more basic solutions aluminum concentration increased, reaching maximum in 0.02 molar NaOH, and subsequently decreased. Aluminum concentration in quartz recrystallized in 0.02 molar NaOH without feldspar reached its initial value and exceeded it for 30 % in the presence of feldspar.

In general aluminum concentration in quartz for the system under consideration depends mainly on the chemical composition and pH of the fluid, and on the interaction of aqueous aluminum species with the quartz surface. Chemical composition and pH of the fluid were determined on the basis of equilibrium thermodynamics (Borisov, 1992). Concentration of aqueous aluminum species decreases in the order $Al(OH)_4^- > Al(OH)_3 > Al(OH)_2^+ > Al(OH)^{2+} > Al^{3+}$. Calculated pH and pOH ranged between 4 and 9, and 6.5 and 1.5, respectively.

Quartz dissolution studies (Gratz, 1993, and references cited therein) showed that negative charging of quartz surface depends on the OH^- activity. Above the point of zero charge negative surface charge increases from acid to basic solutions reaching saturation at pOH less than 2. Increasing of aluminum concentration in hydrothermally recrystallized quartz is determined most probably by the increasing of negative surface charge. Decreasing of aluminum concentration in quartz recrystallized in high basic solution may be explained by the saturation of surface charge and by the decreasing of concentration of positively charged aluminum hydroxides in the fluid.

Obtained results show that aluminum concentration in quartz measured by EPR may be used as an indicator of pH or pOH of the hydrothermal system under consideration. Of course, detailed studies of surface reconstruction and specific site-binding are necessary to elucidate the machanisms of surface reactions.

Borisov M.V., Shvarov Yu.V. (1992) Thermodynamics of geochemical processes. Moscow Univ., Moscow.
Gratz A.J., Bird P. Geochim. et Cosmochim. Acta (1993) 57, 965-991.

WATER, COUNTRY ROCKS AND MAGMA INTERACTION DURING CRYSTALLIZATION OF ELDJURTA GRANITE (CAUCASUS)

Kostitsyn Yu.A. (Institute of mineralogy, geochemistry, and crystallic chemistry of rare elements, Moscow)

Eldjurta biotitic granite was intruded into Palaeozoic migmatites and gneisses of the Great Caucasus. It was dated by isochrone Rb-Sr method on minerals as 1982±8 Ty [Zhuravlev & Negrey, 1993], so it is one of the youngest granitic plutons on the Earth surface.

Rb and Sr concentrations and Sr and O isotopic compositions were determined in 30 samples from 4.7 km vertical section of the granite and some country rocks: marble, gneiss, skarn, as well as in ore metasomatite from Tyrnyauz W-Mo deposit, localized above the pluton.

Upper part of the granite exhibits constant initial Sr isotopic composition near 0.70685, and smooth decreasing of $\delta^{18}O$ from +9.1‰ at depth 2.5 km to +6.6‰ at top endocontact. Pronounced postmagmatic alterations in the vertical section are absent. Published oxygen isotopic composition of quartz and biotite in the section [Liakhovich & Gurbanov, 1992] allow us to calculate equilibrium temperatures (660-770°C), that suggest penetration of meteoric waters from above immediate into Eldjurta magma. Meteoric water/magma ratio is evaluated from 0.1-0.8 at the top endocontact to 0.007-0.03 on 2.5 km below it. So, we must suppose a circulation meteoric waters from the magma. Those granitic samples, with hard subsolidus alterations of minerals as well as aplites, have $\delta^{18}O$ from +9.5 to +10.1‰, i.e., after crystallization of the main magma portions, receiving of meteoric water into the magma chamber was terminated.

The granite located just below have concurrently decreasing $^{87}Sr/^{86}Sr$ (from 0.70741 to 0.70673) and $\delta^{18}O$ (from +9.1‰ to +7.0‰) as depth increase. These data, as well as distribution of Sr concentrations, are consistent with a model including assimilation of about 6% crust rocks by granitic melt during crystallization (AFC) [DePaolo, 1981] with ratio assimilation to crystallization rates about 1:10. Probably, this part of the granite represents another (earlier than the above one) injection from deep source immediately into country rocks.

Mezocratic enclaves have higher concentrations of less radiogenic Sr as compared with the granitic samples and possibly represent bubbles of more mafic (basaltic?) melt, which was cause of crust melting beneath Caucasus. It is not improbable also that these enclaves are mafic residues from melting area.

Sr and O isotopic compositions in ore metasomatite (0.70810 and +5.4‰), skarn (0.70897 and +6.0‰) and marble (0.70823 and +17.7‰) suggest that main transport medium in ore formation was meteoric water, likely the same that washes the upper part of the granitic body.

Zhuravlev, A.Z., Negrey, E.V. (1993) Reports of Russian Academy of Sciences. **332**, 482-485.

Liakhovich V.V., Gurbanov A.G. (1992) Geochemistry. **6**, 800-812.

DePaolo D.J. (1981) Earth and Planetary Sci. Letters. **53**, 189-202.

ELECTRON PARAMAGNETIC RESONANCE DEFECTS IN AMETHYSTS FROM BULGARIA

Kostov R.I. (*Geol. Institute, Bulg. Acad. of Sciences, Sofia*)

Ten amethyst samples of different genesis (from vein Pb-Zn polymetallic deposits and from granitoid and volcanic host rocks) from Southern Bulgaria have been chosen for an electron paramagnetic resonance (EPR) study.

They have been studied also by infrared spectroscopy, thermoluminescence and for trace element content (Kostov, 1983; 1992). EPR previous data have been obtained mainly for E_1, Al and Fe centers in vein amethyst from the Madjarovo Pb-Zn deposit in the Eastern Rhodopes Mountains (Kostov & Bershov, 1984; Kostov & Hafner, 1992).

Polycrystalline samples up to 200 mg have been studied at room temperature on a Varian Associates spectrometer in the X band. The following signals have been observed in the EPR spectra: Fe^{3+} at g=4.3, Fe^{3+} or Fe-bearing phases at g=2 (very strong and broad signal), the E_1, Ge and Mn centers. In the g=2 region of the EPR spectra a narrow signal has been observed, which has been interpreted as the superposition of hole centers (their similar g_1 and g_2 values) and the g_3 values have been used for their identification (g= 2.060-59, 2.054-52, 2.049-48, 2.044-42, 2.038, 2.034, 2.029, 2.023-22 and 2.019-17).

The two main types of EPR spectra are with a strong broad signal at g=2 and with the same signal, but of a lower intensity with a superimposed sharp g=2 signal. The first type EPR spectra are common for samples from the Pb-Zn deposits and a correlation to the intensity of the amethyst colour is suggested. The Fe^{3+} signal at g=4.3 has been observed in almost all of the EPR spectra and Ge centers have been found characteristic to the samples from volcanic rocks. Hole centers in the g=2 region probably point to local geological and geochemical peculiarities.

Acknowledgement. The author thanks the Deutsche Forschugsgemeinschaft for financial support of this study at the University of Marburg in Germany.

References:

Kostov, R. (1983). *Rev. Bulg. Geol. Soc.*, **44**, 3, 294-303.

Kostov, R.I. (1992). Amethyst. A Geological-Mineralogical and Gemmological Essai. Private Edition, Sofia, 249 pp.

Kostov, R.I. & Bershov, L.V. (1984). *Izv. Acad. Nauk SSSR, Ser. Geol.*, 11, 93-105.

Kostov, R.I. & Hafner, S.S. (1992). *Compt. Rend. Acad. Bulg. Sci.*, **45**, 1, 29-31.

THERMODYNAMIC PROPERTIES OF Sr, Ba - BEARING FELDSPAR SOLID SOLUTIONS

A.Kotelnikov and I.Chernysheva (*Inst. for Exp. Mineral., Russian Acad. of Science, Chernogolovka, Moscow distr.,142432, RUSSIA*)

The feldspar solid solution in the systems: Na-Sr, Na-Ba, K-Sr, K-Ba and Ca-Sr, Sr-Ba, Ca-Ba have been studied under hydrothermal conditions at 700 - 900°C and P=2kbar. Thermodynamic functions of synthetic binary feldspar solid solutions have been obtained by the method of X-ray and cation-exchange reactions. We studied following reactions:

$$2Na(K)AlSi_3O_8 + Sr(Ba)Cl_2 = Sr(Ba)Al_2Si_2O_8 + 2Na(K)Cl + 4SiO_2 \quad (1)$$

$$Ca(Sr)(Ba)Al_2Si_2O_8 + Sr(Ba)(Ca)Cl_2 = Sr(Ba)(Ca)Al_2Si_2O_8 + Ca(Sr)(Ba)Cl_2 \quad (2)$$

The Sr, Ba partition between feldspars and aqua - chloride fluid is not ideal. The values of excess mixing functions (excess cell volume, excess free energy of mixing) have been calculated. Margules model of solid solution has been used to describe these excess mixing functions. Margules parameters for the different feldspars are listed in Table 1. The excess volumes and free energies of mixing are in a good accordance to the difference of the ionic radius of isomorphic elements.

Table 1. Margules parameters for binary feldspar solid solutions.

System	Excess volume W1	Excess volume W2	t°C	Excess free energy W1	Excess free energy W2
	cc/mol			kJ/mol	
Na-Sr	5.24	3.35	800	11.79	0.89
Na-Ba	10.84	6.44	800	12.55	16.51
K-Sr	-0.88	-3.47	700	11.10	4.50
K-Ba	0.68	0.68	800	4.42	5.82
Ca-Sr	4.47	0.40	800	15.97	15.97
Sr-Ba	0.74	-0.02	800	9.23	9.23
Ca-Ba	-	-	800	31.00	41.02

THE SYSTEM H_2O-CO_2-NaCl AT 400-800°C, P=1-5kbar

Kotelnikova Z. *(Inst.of Lithosphere, RAS,Moscow)* and Kotelnikov A. *(Inst.for Experim.Mineralogy, RAS, Chernogolovka, Moscow distr)*

The system H_2O-CO_2-NaCl has been studied at 400 - 800°C, P = 1 - 5 kbar by the synthetic inclusions method. The homogenic fluid field increase with pressure increasing (T=const) and decrease with temperature increasing (P=const). We have not detect phase surface extreme at P=3kbar. The NaCl solubility dependence (T=const) is not linear: pressure increasing from 1 to 2 kbar produces 10mol% solubility increasing; pressure increasing from 3 to 5 kbar produces 4 mol% solubility increasing only. If the H_2O-CO_2-NaCl system diagram type is similar to one of H_2O-CO_2, the critical curve extreme of the ternary system may locates at pressure a little bit more then 5kbar.

It is difficult to determine the coexisting phase compositions using microthermometry technic owing to uncertainties of measurements of phase volumes and homogenization temperature to gaseous phase. The ternary system tie lines positions (at 700°C and 5 kbar) approximately correspond to lines connect following points: 9 mol% NaCl; 76 mol% H_2O; 15 mol% CO_2 and 2 mol% NaCl; 13 mol% H_2O; 85 mol% CO_2.

MINERALOGICAL CRITERIA OF SULPHIDE AND SILICATE FORMATION IN THERMOGRADIENT CONDITIONS AT ELEVATED P-T-PARAMETERS

Kotov N.V., Maslenikov A.V., Poritskaya L.G. (St.Univ.,Inst.Precambrian Geol.& Geochronol. Rus.Ac.Sci. St-Petersburg, Russia)

Minerals formation processes modeling in thermogradient conditions is great important at mineralogenetic problems investigation of fault zones.It was realized using cold seal Tuttle reactor with the work zone temperature 600°C decreasing in cold part to 200°C, 1kbar. The temperature ranges were measured along the central stick of reactor by means of independent thermocouple before experiments.The starting material situated in the working part of the central stick during runs at the constant P-T-parameters.Dissolution of this material leads to its transport in wapour phase and precipitation of newly formed minerals in low grade zone.The mineral synthesis processes are realized in the systems buffered by Ni-NiO and Fe-Fe_3O_4 reactors walls.After runs finishing, quenching and degermetization of reactor the central stick was studied in the scanning electron microscope chamber by means of local microanalysis (CamScan-4,Link).

The behaviour of some widespreades silicates and sulphides on the base of mineralogical criteria of phase formation was investigated.It was established that pyrite at 600°C,1kbar breaks in the reactors work zone with sulphur loss that leads to formation of well crystallized pyrrhotite crystals at the reaction between S and dissolved Fe in thermogradient zone at 450-350°C.The plate formed marcasite crystals are formed on the central stick near its low temperature part.Like this the chalcopyrite breakedown in high temperature work zone is the reason of pyrrhotite and bornite crystallization.The feldspar and argentite mixture dissolution leads to thermogradient fayalite and pyrrhotite crystallization in 500-600°C-zone Than the pyrrhotite cover zone are seen up to 350°C temperature marke.Finally plate formed marcasite is observed on the central stick cold part.At the same time native Ag-whiskers formed after argentite appear in the work zone.On the whole the sulphide formation process is realized more quickly than the incongruent feldspar dissolution.Thus,according to the electron microscope investigation the substitution of pyrrhotite by mica disperces crystals is revealed.

The abovementioned method shows the important features both minerals crystallization and minerals substitution and precipitation. This is analogous to minerals formation processes in the thermogradient fault zones.The method is important at the investigation of mineral sequences formation in ore deposits. The results of experimental mineralogical observations are the potential base of paragenetic mineral analysis on the way of some concrete ore-metasomatic systems investigation.

NATIVE GOLD CRYSTALS GENESE IN PRODUCTIVE QUARTZ VEINS OF MURUNTAU DEPOSIT (WESTERN UZBEKISTAN)

Kotov N.V., Maslenikov A.V., Poritskaya L.G.

The native gold disperced crystals are the main form of its existence in productive veined quartz of unique world gold deposit Muruntau (Central Kysyl-Kum,Western Uzbekistan). This deposit of variscan age is localized in low grade metamorphosed black shales (O-S). According to N.Kotov & L.Poritskaya (1992) the consequence of vein metasomatic rocks is following: 1.Productive quartz-veins-I and assotiated with these biotite-twofeldspar metasomatites. 2.Productive column-like quartz--veins-II accompanied with chlorite-sericite-albite metasomatites. 3.Quartz-veins-III singenetic to sericitolites with organic matter and poor Au-Ag-mineralization.Gold separation (with grain size 0.05-0.3mm) from productive quartz veins by means of different methods without particules deformation shows predominants of octahedra and cubooctahedral forms. Investigation of fine sections quartz-gold intergrows by means of scanning electron microscope method (CamScan-4,Link) shows the quartz-inclusions in gold crystals, that are confirm to crystal habitus.This indicates the time breake of gold grows with the gold forming process recurence.On the whole the quartz crystallisation don't disturb the regular gold crystals grows.Distribution of gold fineness on the crystal is stable with variation 950-985.Special investigations of singenetic gas-liquid-inclusions in quartz shows that their cross size (0.001-0.005mm) is less than abovementioned ones for gold crystals.The absence of gold particules in gas-liquid-inclusions is the main feature of productive vein quartz.Some of these inclusions are rather microchannel provided the fluide moving from gold crystals area formation.All these data are the evidence of both gold and quartz material simultanious grows.The gold particula-

rus regular form could be explaned by the concordance of gold and quartz dissolution curves.In comparison with this the quartz-sulphides dissolution curves are different, so the gold-sulphides intergrows in productive quartz are not typical.Muruntau gold deposit is the unique object to study the gold crystal forming processes in industrial gold ores.

References:
Kotov N.V., Poritskaya L.G. (1992). Int.Geol. Rev.,34,No.1,77-87.

PHOTOSORBING PROCESSES IN THE SUBSURFACE AREA OF MINERALS

Kotova O.B.(*Inst.of Geology, Ural Division of Russian Academy of Sciences*)

Researching the mineral surface, we consider it as the border of two areas, where there are interconnected processes; therefore in the future it would be named the subserface area of minerals. Among great number research methods of the subsurface area there is method, basing on the study of stimulated processes by light during connecting gas area moleculas with crystal surface, basing on the great number borders between molecularic and electronic processes in the adsorbing layer and in the subsurface crystal area.

The investigation of photostimulating reactions, in which surface centres take part, allows to obtain the information about subsurface crystal area.At that time the participation of centres in photoprocesses opens the possibility to carry out selective reactions and other practical supplements. By this method the subsurface area of some minerals was researched. In the paper it would be showed the power engineering of electronic transition, which bring to formation of adsorbing centres on the mineral surface. The investigation of the mechanisms of the formation of adsorbing centres allows to retrace the dynamic of development of processes from elementary act of the induction dissociation adsorbtion to the mechanism of complex border formation. It is showed, the elementary act of the dissociative adsorbtion in the case of formation photoinductive centres is accompanied by luminescence, it allows to investigate energy processes by sight. Particular attention in the paper are gived adsorbing processes, as a result, hydratating groups and carbon groups are formed, because they are marks of electronic processes and they take place in the technological application during separating processes of mineral partical by electrostatic methods.

THE MODELLING OF ZONED LAYER GROWTH AT THE CONTACT OF DOLOMITE AND QUARTZ

Kouznetsova R.P., Sheplev V.S. and Kolobov V.Yu.
(*Institute of Mineralogy and Petrography, Novosibirsk, Russia*)

Zoned reaction bands at the contact of incompatible minerals and rocks are source of important information about P-T conditions, duration of processes, mass transfer, composition of intergranular fluid, etc. For solving direct and inverse problems of diffusion zoning the theory and computer program were developed, which permit to estimate main characteristics of growing layer sequences: diffusion coefficients of species, concentration profiles in intergranular fluid, layer growth rates, etc. The stability criterion was obtained to choose the only mineral layer sequence from several ones permitted by the equations of steady-state diffusion.

Zoned reaction bands at the contact of carbonaceous and silicate rocks are well known. The theory and computer program were applied for investigation of zoned layer growth at the contact of dolomite and quartz in the SiO_2-MgO-CaO-H_2O-CO_2 system. The stability fields of all possible sequences in the space of mobility coefficients of diffusion species were determined at several fixed P-T-X_{CO_2} conditions. For an example, by the reaction:

$$3CaMg(CO_3)_2+4SiO_2+H_2O=Mg_3Si_4O_{10}(OH)_2+3CaCO_3+3CO_2$$
dolomite quartz talc calcite

the quartz|talc|talc+calcite|dolomite zoning forms at any diffusion coefficients. The another case, by the reaction:

$$5CaMg(CO_3)_2+8SiO_2+H_2O=Ca_2Mg_5Si_8O_{22}(OH)_2+3CaCO_3+7CO_2$$
dolomite quartz tremolite calcite

the quartz|tremolite|tremolite+calcite|dolomite zoning can forms only. At T=600°C, P=2kbars and X_{CO_2}=0.5 zoned bands form, which consist of talc, tremolite, diopside and forsterite. There are four independent reactions between quartz, dolomite and these minerals. This case is more complicated. More than 25 mineral sequences can form at the contact of dolomite and quartz in the space of diffusion coefficients.

The results of investigations can be used for the determination of the forming conditions of natural and experimental zoning.

"CODIM" - A NEW COMPUTER SYSTEM FOR OPTICAL DIAGNOSTICS OF OPAQUE MINERALS

Kovachev V. V., Straschimirov S. B. and Giurov Ch. P. *(Dept. of Economic Geology and Dept. of Applied Geophysics, Univ. of Mining & Geology of Sofia)*

CODIM is a new diagnostic info-system and computer programs for preliminary determination of opaque minerals. It is based on the processing of data obtained through the quantitative measurements of their reflectivity and microhardness. These two parameters of the minerals could be measured precisely through the nowadays conventional devices such as photometers and microhardness testers which alloy measurements over relatively small (> 20 mkm) mineral grains. The diagnostic is realized on three steps - comparison of the reflectivity spectrum, comparison of the microhardness and checking other available data for the mineral.

The practical experience suggest that the usual direct diagnostic of the minerals based on their reflectivity sometimes is not very definitely. It is due to the absence of standardizing the grade of polishing for the measured mineral and standard mineral and the difficulties to determine the cut orientation for anisotropy minerals. These problems could be successfully avoided if we use a computer supported evaluation of the shape of the reflectivity spectrum (RS) (Kovachev et al., 1985). It is based on the method of the less squares which evaluate the difference between the forms of standard RS and measured RS for unknown mineral and as a result a correct comparison is guaranteed. Selection of minerals is made on the basis of a general integration coefficient which includes parameters of shape and absolute different value of RS.

Microhardness is used as a supported parameter which is compared directly and it's involving increases the reliability of diagnostic. The liaison between the measured parameters (reflectivity and microhardness) and other optical properties of the minerals could be established through the specially designed info-system for standard minerals including data for their color, isotropism, bireflectance, color dispersion, structure (space group, parameters of unit cell), chemical composition (formulae, trace elements), paragenesis, locality and references.

Data for the standard minerals were included in case when the determinations of the main parameters were done over one and the same mineral grain (Criddle and Stanley, 1986; Chvileva et al., 1988, personal data). The database contains all the basic characteristics for more then 900 standard minerals and the system is open. The system is very selectively which gives a possibility for a diagnostic of minerals with very close optical properties, such as minerals from tennantite-

tetrahedrite group, Pb-Sb sulphosalts, colusite group, platinum group and others.

The software is realized on IBM compatible personal computer including DOS version. The system's work speed is increased if mathematical processor is used. The database is open and it can be updated if it is necessary.

The system CODIM could be successfully used in laboratory studies of ores, rocks, coals, metals, alloys, waste products of raw materials, and in the educational process as well. The effect of the system could be multiplied if it is designed as a new complete apparatus including a proper computer arrangement.

References:
Kovachev, V. V., Straschimirov, S. B., Rangelov, B. I., Pavlov, I. (1985). In: *"Physics of Minerals and Ore Microscopy", Proceedings of the 13th General Meeting of the IMA, Varna,* publ.: HBAS, Sofia, 233-242.
Chvileva, I., Bessmertnaia, M., Spiridonov, E. 1988. *Spravochnik-opredelitel rudnih mineralov v otrasenom svete (Guide for ore mineral identification in reflected light)* - in Russian.- M., Nedra, 168 p.
Criddle, A. J. and C. J. Stanley. 1986. *The quantitative Data file for Ore Minerals.* British Museum (Natural History). 420 p.

FLUORAPATITE FROM ŢIBLEŞ NEOGENE SUBVOLCANIC MASSIF (EAST CARPATHIANS, ROMANIA)

Kovacs M. (CUARŢ Company Baia Mare, Romania), Molnár F. (Dept. of Mineral., Univ of Budapest), Kovács P.P. (Hung. Geol. Survey, Budapest), Lupulescu M. (Dept. of Mineral. Univ of Bucharest)

The Tibleş Mts. belong to the Subvolcanic segment of the Neogene volcanic chain of the East Carpathians and consist of calc-alkaline intrusive rocks - mainly monzodiorites, diorites and microgranodiorites (Udubaşa et al, 1983). A postmagmatic association, very rich in mineral species was here described (Kovacs et al, 1985) in the contact area of a Paleogene sedimentary xenolith (150 m in length) with a monzodiorites body. Many minerals and especially apatite, phlogopite and rutile are very well represented.

Well developed columnar crystals of fluorapatite, up to 3 cm in length, occur especially on the joints of the brecciated igneous rocks from the endocontact zone. The apatite are intimately associated with pseudohexagonal crystals of fluorphlogopite (of max. 1 cm in size). Besides CaO (54.46), P_2O_5 (39.27) and F (2.62) the chemical analysis of fluorapatite show the presence of Cl (0.36) and OH (0.06).

The complex assemblages which include, besides fluorapatite and fluorphlogopite, more than 30 minerals (silicates, sulphides, oxides and hydroxides) were formed in a large temperature range. Taking into account the relations among minerals, the fluorapatite appears as the first crystallised phase, a fact confirmed also by microthermometric studies (T_h = 410-460 C).

Fluorapatite from Tibleş Mts. represents a novelty for the Neogene volcanic chain of East Carpathians (Romania) due both to its mode of presentation, composition and especially to its morphological features.

References:
Kovacs, M., Radu, P., Talpos, S., (1985) - *D.S.Inst. Geol. Geophys.* **LXIX/1**, 13-30
Udubaşa, G., Edelstein, O., Răduţ, M., Pop, N., Istvan, D., Kovacs, M., Pop, V., Stan, D., Bernad, A., Gőtz, A., (1983) - *Ann. Inst. Geol. Geophys.*, **LXI**, 285-295, Bucureşti

VOLCANOLOGY AND MAGMATOLOGY OF THE SÁGHEGY VOLCANO (LITTLE HUNGARIAN PLAIN, PANNONIAN BASIN, HUNGARY).

Kovács R.[1], Harangi S.[1], Vaselli O.[2] and Coradossi N.[2]
([1] *Eötvös University of Budapest,* [2] *University of Florence*)

Sághegy is one of the best exposed volcanoes in central-eastern Europe. It was active 5 Ma ago and there is an excellent view into its inner structure due to the intensive quarrying. The volcanic activity of Sághegy belongs to the Late Miocene-Quaternary extension-related alkaline basaltic volcanism of the Pannonian Basin.

The basaltic magma probably rised along a northwest-south-east tectonic line which cuts several other volcanoes (Somló, Kabhegy, Tihany) of the Pannonian Basin. Owing to the interaction between the silicate melt and external water the volcanic activity started with phreatomagmatic explosive eruptions resulted in fine grained tuffaceous layers with bombs derived from the sedimentary basement. It was followed by Strombolian-type eruptions in the inner part of the tuff ring. Massive lava flows feeded from the central fissure are considered to be the last products of the first volcanic phase. Then, several smaller scoriaceous tuff cones were formed at the marginal parts of the volcano, whereas, lava fountain activities occurred around the central fissure. Sheeted lava flows closed the second pyroclastic explosive phase. The central and parasitic vents were filled by columnar basalts.

No significant petrological and chemical variation can be recognized in the volcanic products of Sághegy. Most of basalts have slight hypersthene-normative composition and are classified as alkali olivine basalts and trachybasalts. Compared with the basaltic products of the volcanoes of the Little Hungarian Plain, the Sághegy basalts show the most silica-saturated character. Mantle xenoliths occur subordinately in them. The relatively high mg# ($mg\# = Mg^{2+}/(Mg^{2+}+Fe^{2+}) = 0.64\text{-}0.70$) and the FTSE abundance (Ni=200-220ppm, Cr=300-400ppm) indicate that they could be close to the primitive liquid composition. Their trace element distribution is similar to that of Gough-type OIB having positive Rb, Ba and K anomalies compared to the average OIB (Figure 1). Petrogenetical model calculations suggest that the small geochemical variation in the Sághegy basalts can be explained in terms of 7% to 8% degrees of partial melting process.

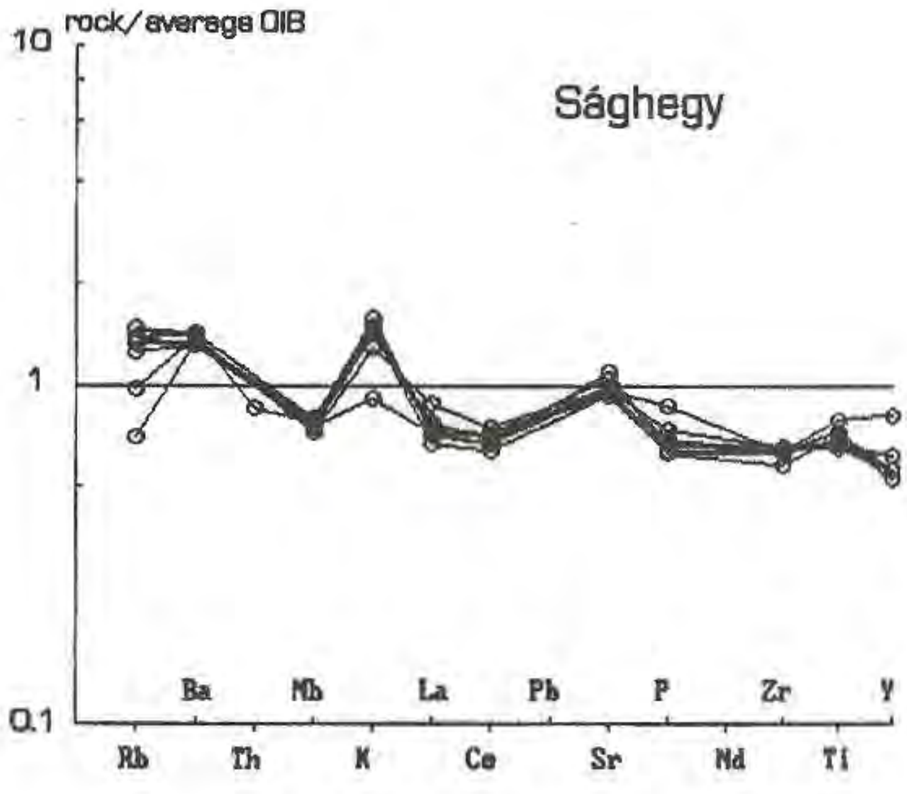

Figure 1 - OIB normalized trace element pattern of the Sághegy basalts.

QUATERNARY (Ca–Fe–Mg–Mn) GARNET: DISPLACED EQUILIBRIUM EXPERIMENTS AND COMPARISON TO CURRENT GARNET MODELS

Koziol A.M. *(Dept. of Geology, University of Dayton)*

Garnet (grt) in metamorphic rocks is primarily a Fe–Mg aluminosilicate solid solution [i.e. almandine (alm) – pyrope (prp)] with lesser but significant amounts of Ca and Mn [grossular (grs) and spessartine (sps)]. Details of the mixing properties of grt must be known for accurate application of mineral geothermometers and geobarometers for understanding metamorphic terrains. This study addresses some of the complexities of grt solid solution by experimentally determining the activity of 10–18 mole % grs with the Fe–Mg–Mn composition of Alm 64.5 Prp 10.5 Sps 25.

The activity of grs was measured by the displaced equilibrium technique, where the equilibrium position of the reaction 3 anorthite = grs + kyanite + quartz is displaced to lower pressure by solid solution in the grs garnet. Starting materials were homogeneous synthetic garnet mixed with anorthite, kyanite and quartz, with Li_2MoO_4 added as a flux. 3/4 inch diameter NaCl medium piston–cylinder apparatus was used. Experiments were conducted at 1012 °C, 13.4 kbar; 1000 °C, 12.7 kbar; 912 °C, 8.5 kbar; and 870 °C, 8.2 kbar. Corresponding reversed final mole fractions of grs in garnet and activity coefficients of grs (in parentheses) are: 0.171 (1.25); 0.157 (1.27); 0.125 (1.28); 0.91 (1.23); and 0.98 (1.20).

Results from this study may be directly compared to previous studies of ternary garnets (Koziol and Newton, 1989) because of similar compositions, including a similar Mg/Mg + Fe value. Addition of 21 – 23 mole % sps component does not significantly change the activity coefficient of grs at a fixed Mg/Mg + Fe value, implying ideal or nearly ideal mixing of sps with grs–alm–prp garnet.

These results generally agree with the model of Berman, proposed in 1990, for quaternary garnets. Values for the activity coefficient of grs predicted by Berman's model are smaller but within uncertainty limits for the compositions studied here.

Ten years ago garnet solid solution properties were poorly known. With concerted effort in the areas of displaced equilibrium experiments, calorimetry, and molar volume determinations (see Ganguly *et al.*, 1993, for the most recent work), garnet is becoming one of the better–defined mineral solid solutions.

References

Berman, R.G. (1990). *Amer. Mineral.*, **75**, 328–344.

Ganguly, J., Cheng, W., and O'Neill, H.St.C. (1993). *Amer. Mineral.*, **78**, 583–593.

Koziol, A.M. and Newton, R.C. (1989). *Contrib. Mineral. Petrol.*, **103**, 423–433.

CERVELLEITE AND SOME NEW UNNAMED SILVER MINERALS FROM THE CHADAK DEPOSIT, UZBEKISTAN, CENTRAL ASIA.

Kozlov V.V., Fadeeva N.G. (Inst. of Geol. and Geophys., Uzbekistan) and Levin V.L. (Inst. of Geol. Sciences, Kazakhstan)

Chadak gold–silver mine is situated in the north–eastern part of the Kurama ridge, West Thian Shan, Uzbekistan. Gold and silver–bearing veins (259±10 Ma) located in late Paleozoic andesitic tuffs and flows near monzonite–granodiorite multiple intrusion. These veins were formed during four stages of mineral deposition: (1)quartz+calcite+ adularia stage with electrum and acanthite (main ore–forming stage); (2)Ca–silicates stage with early wollastonite ± garnet substage and late Fe– oxyde and Pb,Zn,Fe, Cu, Bi, Ag–sulfide substage; (3) quartz + ankerite±chlorite stage with pyrite, Ag–Cu sulfides, Ag–Au and Ag–Sb minerals; (4) quartz+ hematite stage with minor Cu, Bi–sulfides.

More then 150 minerals have been identified in gold–bearing hydrothermal veins. Among them some rare and new unnamed minerals have been studied using electron microprobe (Cameca MS–46 and JEOL–733 instruments).

Cervelleite occurs as isotropic greenish grey inclusions up to 50μm in second–stage galena with acanthite, hessite, wittichenite, electrum and unnamed minerals. For a load of 20g the range of microhardness obtained from 10 indentations was 73–98 (mean 85). Chemical composition (average of 17 analyses), wt.%: Ag 66.81–69.92 (68.2); Cu 1.26–3.79(2.92); Bi n.d.–0.96(0.13);Te 20.81 –23.44 (22.16); Se n.d.–1.72 (0.72); S 4.94–5.95 (5.36). The average gave a formula identical to cervelleite one (A.Criddle et al.,1989) with substitutions of some elements: $(Ag_{3.88}Cu_{0.27})_{3.98}Te_{1.01}(S_{0.97}Se_{0.05})_{1.02}$.

Unnamed mineral F (ideal formula Ag_8BiTeS_5) occurs as moderate anisotropic brownish grey tabular grains up to 30 μm, which intergrown with cervelleite in galena. Chemical composition (average of 3 analyses, wt.%): Ag–59.12; Cu 4.75; Bi 14.39; Te 8.45; S 11.08; Se 0.86; Total 98.65. The formula calculated to 16 atoms: $(Ag_{7.87}Cu_{1.07})_{8.94}Bi_{0.88}Te_{0.85}(S_{4.88}Se_{0.18})_{5.12}$.

Unnamed mineral X6 (ideal formula $AgCuBiS_3$) occurs as anisotropic light brownish grey inclusions up to 150 μm in galena with Ag–rich wittichenite. Chemical composition (average of 2 analyses, wt. %): Ag 24.55; Cu 12.74; Bi 43.37; S 19.83; Total 100.49. The formula calculated to 7 atoms: $Ag_{1.08}Cu_{0.88}Bi_{0.88}S_{2.88}$.

Ag–rich wittichenite occurs in a matrix of galena and sphalerite as grayish brown anisotropic pleochroic (blue–red) grains up to 100 μm in size. Chemical composition (wt.%):

Ag	Cu	Bi	S	Total	Formulae
13.06	29.55	39.39	18.01	100.01	$(Cu_{2.4}Ag_{0.8})_{3.0}Bi_{1.0}S_{2.8}$
13.07	29.01	39.36	17.96	99.40	$(Cu_{2.4}Ag_{0.8})_{3.0}Bi_{1.0}S_{3.0}$
18.96	23.95	38.66	17.88	99.45	$(Cu_{2.0}Ag_{1.0})_{3.0}Bi_{1.0}S_{3.0}$

Ag–low (up to 4.7 wt.% Ag) and Ag–free wittichenite also occurs.

Unnamed mineral B1 (ideal formula $AgCu_3S_2$) occurs as a weakly anisotropic grayish blue fine inclusions (up to 50 μm) and microveinlets in sphalerite, quartz and andradite. Chemical composition (average of 2 analyses, wt. %): Ag 54.54; Cu 25.50; S 19.13; Total 99.17. The formula calculated to 6 atoms: $Cu_{3.04}Ag_{0.84}S_{2.12}$.

Unnamed mineral X5 (ideal formula $Pb_2Bi_4Te_3(S,Se)_5$) occurs as yellowish white anisotropic grains up to 50 μm in calcite with pyrite, galena and unnamed Se– rich sulfotellurides and sulfosalts. Chemical composition (wt.%) Pb 22.02; Bi 45.33; Ag 0.52; Te 20.05; S 6.29; Se 4.26; Total 98.46. The formula calculated to 11 atoms: $Pb_{2.04}Bi_{4.18}Te_{3.01}(S_{3.78}Se_{1.03})_{4.78}$.

These minerals were introduced during second stage mineralization by relatively high fO_2 (Mt–Hem buffer), low f_{Te2}/f_{S2} (acanthite–hessite equilibria), low CO_2 (<3mol. %) and high salinity (20–35wt.% NaCl eq.) fluids at temperatures 350 – 220°C. The fluids precipitated a complex assemblage of hematite 1, magnetite, pyrite, sphalerite, chalcopyrite, galena, and hematite 2 in gangue of andradite, epidote, quartz, sericite and calcite.

Reference:

Criddle, A.J., Chisholm, J.E., Stanley, C.J. (1989). *Eur. J. Miner.*, 1, 371–380.

PEGMATITIC ALLANITES–EPIDOTES FROM KARKONOSZE GRANITOIDS, SW POLAND: CHEMICAL COMPOSITION AND FLUID INCLUSIONS

Kozlowski A. *(Inst. Geochem., Fac. Geol., Warsaw University)*

Four varieties of allanites were found in pegmatites of the Variscan granitoids of Karkonosze Mts.: a) zoned allanites brown in the centre and yellow at the margins, b) allanites similar to (a) with pale yellow–greenish or colourless epidote–clinozoisite rim, c) zoned allanite like (a) or (b) but with corroded epidote (REE–epidote)–clinozoisite inner core (Fig.), d) crushed epidote–clinozoisite core cemented with brown to orange–yellow allanite.

By electron microprobe all major and minor elements were determined in allanites–epidotes, including La, Ce, Pr, Nd, Sm,

Dy plus Y, Th and Pb. The analyses, recalculated to 12.5 (O), were considered using the formula: A1 A2 M3 M2 M1 O(OH) [$T3O_4$][T2 $T1O_7$]. Basis of the crystallochemical interpretation was discussed in Smulikowski & Kozlowski (1994). Main composition variations occurred in the sites A2 and M3 (Fig.). The site A2 may contain up to 0.6 Ce, 0.25 La and 1 REE+Y p.f.u.

Fluid inclusions in the epidote cores have homogenization temperatures (Th) up to 320°C and when overheated and decrepitated - to 350°C. The latter Th is also typical of the earliest allanite zone. Outwards the grain Th decreases, occassionally with boiling phenomena (inclusions D and E in Fig.). Outermost zone yielded Th 180-200°C.

Early epidotes were crushed, then corroded and replaced by allanite formed from hot REE-bearing solutions inflowing through newly opened fractures. Late epidote-clinozoisite rims appeared after exhaustion of REE (and possibly iron) in the parent solution.

Reference:

Smulikowski, W., Kozlowski A. (1994). *N.Jb.Min.,Abh.* in press.

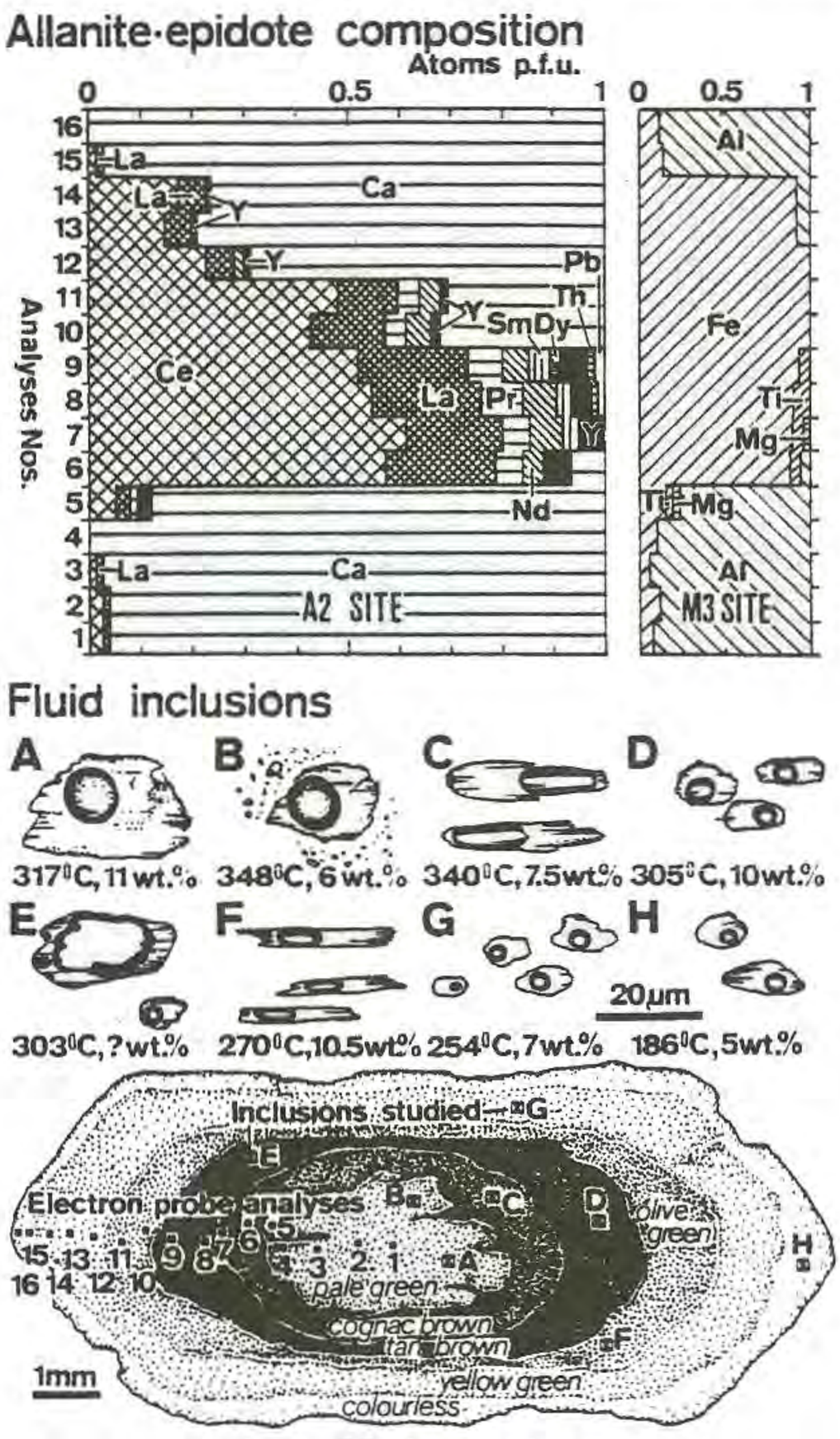

• FLUORITE OF ORE FORMATIONS

Krasilshchikova O.A. and Tarashchan A.N. (*I.G.M. & Ore formation, Ac. Sci. Ukraine, Kiev*)

Composition of optically active centers in fluorite (Krasilshchikova et al., 1991) have been compared and their results have been summarized for a set of ore formations presenting different by their genetic features. These formations are: 1. Rare-earth carbonatite (Kazakhstan, Buryatia), 2. Rare-metal metasomatite (Ukrainian shield, eastern Siberia), 3. Rare-metal greisen (Kazakhstan, Primorie, Urals), 4. Lead-zinc hydrothermal (Scandinavia, British Isles), 5. Mercury-fluorite (Karpathia, Donbass, Caucasus), 6. Bitumen-carbonate fluorite (Scandinavia, Donbass), 7. Quartz-fluorite (Baikal region, Polar Urals).

For fluorites of these formations typomorphic COAC have been identified which are peculiar only for the earliest stages of fluorite-forming process. Special features of COAC of the mentioned ore formations (number in accordance) are: 1. High concentrations of OAC: Mn^{2+}, Ce^{3+}, Sm^{3+} (X-ray luminescence spectra), Eu^{2+} (Photoluminescence spectra). 2. High concentrations of OAC: Mn^{2+}, Gd^{3+}, Ce^{3+}, Sm^{3+}, Dy^{3+} (XRL-spectra), Yb^{2+} (PL-spectra). Absorption spectra typomorphic for fluorites of both mentioned formations are similar and show high concentrations of TR-stabilized color centers. Thermoluminescent curves also reveal high concentrations of thermally excited OAC. 3. Extremely high concentrations of OAC: Mn^{2+}, Gd^{3+} (XRL-spectra), Yb^{2+} (PL-spectra). High concentrations of $(YO2)^{\circ}$ centers (absorption spectra). Extremely high concentrations of thermally excited OAC. 4. High concentrations of Ce^{3+}, Eu^{3+}, Nd^{3+} (XRL-spectra), Eu^{2+} (PL-spectra) together with O^-, O_2^- and O_3^- color centers. 5. High concentrations of optically active centers: Ce^{3+}, Sm^{3+}, Sm^{2+}. Medium concentrations of color centers and thermally excited OAC. 6. Low concentrations of TR^{3+} and TR^{2+} centers. Presence of bitumen in the form of photoluminescence centers. Fluorites of two last formations are also characterized by low concentrations of thermally stimulated centers.

This sequence of COAC is formed in fluorite structure as a result of geochemical and physical-chemical changes of ore-forming media: alcalinity-acidity conditions and irreversible decrease of temperature, pressure and concentrations of mineral-forming components.

Therefore the questions related to the formational and genetic attribution of fluorite can be solved together with many problems of global, regional, local and microzoning of fluorite-bearing mineralization on the basis of COAC studies.

References:

Krasilshchikova , O.A., Tarashchan A.N, Nechaev, S.V. (1991). *Mineral. Zhurn.* 13, 25-42.

PRINCIPLES OF METASOMATISM

Krasnova N.I.(*Inst.of Earth Crust,S.Petersburg University,Russia*)

The main features of metasomatic mineral formation are discussed. Mostly only their certain combinations appear to be acceptable indicators of the metasomatic origin of minerals and mineral assemblages. This features are as follows: 1-pseudomorphs-the most convincing and adequate sign of the metasomatic processes;2-undisplaced relicts of a primary mineral and structural pattern relicts of a substratum; 3- inherited features of chemistry,isotopic composition,and x-ray structural features of precursor minerals; 4-marked change in the composition of veins crosscutting the rocks of different composition; 5-the arrangement of individual zones in the metasomatic columns according to the mobility of components; 6-chain arrangement of crystals in combination with signs of protolith corrosion; 7-direction of growth vectors of crystals from the contacts of a fissure into a wallrock; 8-the absence of gravitational effects.

There are also some typical structural-textural features of metasomatic rocks: 1-rhythmic aggregates; 2-the fine- to medium-grained nature of the primary textures; 3-high density of dislocations and block or "poikilitic" nature of the crystals.An explanation of the chemical replacement reactions must be strictly based on quantitative-mineral calculations of the thin-sections examined with allowance for

volume effects and changes in the porosity during metasomatism.

The better the investigator selects the facts that indicate the metasomatic nature of a geological material, the more reliable will be all the subsequent physicochemical calculations of the conditions of mineral formation.

NEW DATA ON THE PROBLEM OF ULVOSPINEL OCCURENCE IN TI-MAGNETITE EXSOLUTION STRUCTURES

Krasnova N.I.[1] @ Krezer Ju.L.[2] (1-*Inst.of Earth Crust, S.Petersburg Univ.*, 2-*MECHANOBR, Russia*)

Microstructural peculiarities and chemical composition of ingrowths in Ti-magnetite from various rocks of some of Kola Peninsula massifs were investigated using the electron probe microanalysers SEM-501 and CAMEBAX. The samples were preliminary etched by concentrated HCl that allowed to analyze even the ultrathin (about 1 mkm) latticed ingrowths. All the ingrowths fall into the following groups: 1-ilmenite-geikielite; 2-spinel-magnetite and magnomagnetite; 3 -spinel-pleonaste; 4 -spinel-herzinite. For the most of them composition data are adduced for the first time. Diagnostics for two specimens are confirmed by the x-ray studies of laminated phases (in one case-ultrathin latticed ingrowths) isolated from Ti-magnetite after its periodic treatment in HCl and magnetic separation. This laminated phases proved to be of the ilmenite-geikielite group that is in disagreement with the conventional opinion on their belonging to the ulvospinel phase. Up to now no ulvospinel has been found among the various ingrowth types in the studied titano-magnetites.

Some spinel and ilmenite inclusions have been developed as skeleton or isometric crystals simultaneously with growth of magnetite grains; the others have appeared as a result of titanomagnetite exsolution at decreasing temperature. Correct diagnostics of the laminated and other phases in magnetite necessary for both the mineralogists and geophysics is possible only when a complex of up-to-date research methods is used.

EXPERIMENTAL MODELLING OF ORE ELEMENTS PARTITIONING BETWEEN PHASES IN FLUID-MAGMATIC SYSTEMS.

I.F.KRAVCHUK
Vernadsky Institute of Geochemistry, Moscow

Experimental modelling of ore elements behavior in fluid-melt equilibria is the main approach to determine partitioning coefficient of metal magmatucally evaluated, to elucidate the factors, controlling element fraction, to estimate ore-bearing ability of magmatic melt. Sealed platinum and gold capsules were used in some types high pressure bombs with optimal quenching systems. The phases after runs were separated and analysed by some methods. Usually we approached to equilibria from the both sides, adding ore elements to melt or to fluid.

The main results are:

1. Measurements of partitioning coefficients of Zn and Mo between granodiorite melts with various Al contents and aqueous salt fluid at 1000°C, 2, 4 kbar demonstrate the significance of compositions of melt and pressure as fators of ore elements fractionation in magmatic processes. Experimental data give evidence for opposite effect of pressure for Zn and Mo: K_{Zn} is reduced by a factor 4-5 as the pressure increases from 2 to 4 kbar, K_{Mo} increases in 3 times at the same conditions. Experimental results also show the various speciation of Mo and Zn in fluid.
2. The study of Cu and W partitioning between two fluid phases of the heterogenic fluid at 800°C and 1 kbar demonstrates the high extractive ability of high density fluid phase. The value of coefficient partitioning for W is close to 10-14 , the value for Cu is 8-10.

Experimental and literature data are used for discription of ore elements partitioning in dependence on chlorine concentration in fluid, Al content in melt and pressure.

FELDSPAR SOLID SOLUTIONS AND RANGES OF THE MINERAL CHANGES DURING MAGMATIC DIFFERENTIATION WITH REGARD TO (ANTI)RAPAKIVI TEXTURES AND PLZONATION.

Kravtsova E.I.(Inst.Precambr.Geol.Geochronol., Russian Academy Sci.,St.Petersburg)

Trends of different magma crystallization in the ternary Fsp-system were being revised in parallel with analysis of natural feldspar compositions to improve the physicochemical model. The extension and low-temperature terminations of the allowable trends of feldspar change during magma differentiation are discussed at various P_{H2O}, presence of fluids and additions of Qtz.

Same correlations for position and length of the low-temperature section of solidus curve, where alkali feldspars coexist in peritectical relations, are of special interest as the development of anti- and rapakivi textures is possible there for the melts, initially or in consequence of fractionation plotting rather close to the area itself.

At crystallization of magmas from immiscibility fields the section above represents the gap between two rows of feldspar changeability. The compositions of the end phases of the trends and width of the gap depend very much on conditions and change even at Pconst with accumulation of SiO2 in the melts. These data are useful as the indicators of rock origin environment. But analyis is complicated sometimes by the fact, that before the emergence of the mentioned gap disruptions appear in the series of (pseudo) binary Pl-loops as magma crystallization trends approach the cotectic (Kravtsova, 1991, 1992). Nevertheless, the phenomenon corresponds largely to the frequency of occurrence of natural Pl compositions, that is illustrated by the examples of numerous contrast normal zonations of Pl from volcanic series. The compositions of the zones approximate to the ranges of Huttenlosher or Boggild solvi and may result from resorption of more basic Pl by acid one, content of An in those phases depending on conditions and composition of parental magma. Sometimes they fit the intermediate interval, that is possible when the Pl-gaps above merge together with further fall in T. There are no such sharply defined zonations in Pl of intrusive rocks, where compositions of the mineral has had time to change up to the boundary of a gap by the moment of its emergence and is able to keep pace with shifting of that boundary while the gap is widening at T decrease. Less equilibrium expansion of the latter will stimulate the formation of reversed zonations in basic Pl of the corresponding rocks and normal one in acid Fsp.

The gap conforming to peristerite solvus would influence on the course of the latest stages of Pl crystallization, stimulating mag-

matic albitization, provided P_{H2O} exceeds 5 kb and NaKFsp can't appear already. At lower P_{H2O} (except dry conditions in presence of cotectical Qtz) fractional crystallization of even calc-alkaline magmas may end with the mentioned above peritectical reactions of alkali feldspars. The assay shows that antirapakivi textures could be predominantly formed at low P_{H2O} or in the dry system pure of Qtz and rapakivi textures develop probably just before or simultaneously with Qtz solidification, when dry conditions give way to P_{H2O} environment, peritectical reactions both KFsp to NaKFsp and An, dissolved in Or, to Olig-Ab taking place.

References:
Kravtsova, E.I.(1991). Granites and Geodynamics, SovGeoInfo, Moscow, 49-50.
Kravtsova,E.I.(1992). 29th IGC, Kyoto, Japan,Abstract vol.2 of 3, 538.

CRYSTALLIZATION OF ALKALINE LARNITE-NORMATIVE MAGMA AT VARIOUS REDOX CONDITIONS.

Krigman L.D. and Kogarko L.N.*(Vernadsky Inst. of Geochemistry RAS. Moscow)*

Strongly silica-undersaturated high calcium alkaline magmas are important for understanding the genesis and evolution of melilite-bearing rocks. Here we present the results of 1 atm. melting experiments with synthetic turjaitic melt at various redox conditions (QFM buffer and air). Loop technique was used to avoid iron losses. Oxygen fugacity in the furnace was regulated and checked by solid electrolytic cells. The composition of phases were determined by EMPA.

The results of our study show that redox conditions change the phase assemblages and the trends of residual melts evolution. The order of crystallization at QFM is: liquid(L) +olivine (Ol) + melilite (Mel); L + Ol + Mel + clinopyroxene (Cpx); L + Ol + Mel + Cpx + nepheline (Ne). Melilite is a predominant phase at all temperatures. In air the crystallization proceeds in order: L + spinel (Sp), L + Sp + Cpx; L + Sp + Cpx + Mel; L + Sp + Cpx + Mel + Ne. Ol is absent. Cpx predominates among the crystalline phases. It contains high Fe and anomaly low silica (42 wt.% only).

The trend of melt changes during the crystallization. Initial crystallization of Ol and Mel results in rapid growth of Fe/Mg values, while Na-Fe ratio changes insignificantly. As Temperature falls and oxygen fugasity grows the feild of Cpx-cryctallisation increases and Na/Fe values rise steeply, while Fe/Mg values are nearly constant. Another effect of high oxygen potential is the increasing silica content in the melt due to greater quantity of Sp among solid phases. Similar trends of melt evolution are observed in natural volcanic and plutonic suites (Nyiragongo, Oahu, Kugda).

INTERPRETATION OF PHASE RELATIONS IN THE RARE-ALKALI-METAL METASOMATIC ROCKS OF PEGMATITE FIELDS, KOLA PENINSULA

Krivovichev V.G. *(Dept. of Mineralogy, St.Petersburg Univ., Russia)*

The rare-metal pegmatite fields (Voronia, and Kolmozero) in the Kola peninsula are accompanied by linear zones of hydrothermally altered rocks formed before the pegmatites were emplaced. These metasomatites are always associated with pegmatites and share their geochemical characteristics and trends of mineral formation.

Thermodynamic analysis is carried out for some components of the mineral system Li-Na-K-Ca-Mg-Al-Si-H_2O in which the mineral equilibria using hornblende, holmquistite, biotite, chlorite, plagioclase and quartz are considered. The calculations are realized on the basis of quantitative estimation of activities of the components in solid (minerals) and liquid (mineral forming media) solutions. The method of calculations of thermodynamical constants of minerals is proposed based on the analysis of mineral equilibria and study of the composition and properties of relicts of mineral forming media. Seven types of metasomatic columns are established. Each of them origin is depend on K^+/Li^+ ratio in solutions and on mineralogical and petrographical features of the initial substratum. It is shown that all of the zonatations revealed in rare-alkaline-metal metasomatites are the result of variations in acidity-alkalinity of solutions caused by their interaction with the rocks of more basic composition. This led to a single and unidirectional sequence of segregation of paragenetic mineral associations.

STRUCTURAL SETTING OF GEMS AT THE EASTERN PAMIR.

Kruglov V.A. and Terekhov E.N. Unemployed, Inst. of the Lithosphere, Russian Ac. of Science, Moscow, Russia.

The special structural - geochemical mapping of areas of wide occurences of gems, have made in the Eastern Pamir (Tadjik Republic , former USSR).

Many occurences of ruby, beril, tourmaline, garnet, scapolite, sphen, cordierite are known in the region which is named "Kukurt gems field". Our structural study was mainly based on the materials on the special phototheodolite survey. In the course of field work all structural information, sampling points and gems findings were put on the phototheodolitic images. In Moscow, these images were transformed into topographic maps by means of special apparatus and then geologic maps (scale 1 : 10 000) were compiled using additional geologic information.

The most part of gems are confined to the peripheral zone of a granite-gneisses dome, which is separated from unmetamorphic rock in the south by a wide strike-slip zone (The Muskol fault). The structural study showed that the granite-gneisses dome moved along this strike-slip zone with a slight rotation. These deformations took place at the brittle-plastic conditions that resulted in formation of pegmatites, veins, recumbent folds and small nappes origineted at the peripheral zone of the dome, which concentrates such gems as: tourmaline, beril, sphen, scapolite, garnet, ruby.

The Muskol fault is a favourable place for finding ruby. In this zone, there are many disseminated ruby in the marble and gneisses and lenses of corundum-fuchsite rocks, thickness up to first meters. The latter contain high-quality ruby.

For the first time, the blue corundum occurence in unmetamorphic rocks was revealed in the Eastern Pamir south of the Muskol fault. Corundum- bearing rocks with grafites, tourmalines, rutiles, magnetites, kyanites and muskovites form bodies of complicated form. They are confined to boundaries of marbles and schists. Corundum-bearing rocks are metasomatites and are characterized by high

K_2O (up to 10%), TiO_2 (up to 6%), Al_2O_3 (up to 50%), F (up to 4000 ppm), Ba (up to 2500 ppm), Zr (up to 700 ppm), Cr (up to 1000 ppm), La (up to 250 ppm) and Ce (up to 450 ppm), with La_n / Yb_n ratio = 150-200. All these characterics evidence that the corundum-bearing rocks are close to alkalic magmatic rock middle composition by some typical elements. This magmatic rocks form dykes and mark the Muskol fault in eastern part.

According to our and experimental data (Andersen, 1987), high temperature alkalic solutions can transport Al_2O_3 and deposit it in the favourable conditions (boundaries of rocks of various composition). Such a situation was at the Eastern Pamir, at Neogene time, when deep metamorphic rocks with high concentration of Al_2O_3 upthrust over the structures of the upper level of the Earths crust. The thrusting was accompanied by alkalic volcanism and accordingly by alkalic solutions. The latter are responsible for origination of corundum-fuchsite rocks at the strike-slip zone and corundum-bearing metasomatic rocks among unmetamorphic units.

PRISM- AND BASIS-PARALLEL SUBGRAIN BOUNDARIES IN QUARTZ: A MICROSTRUCTURAL GEOTHERMOBAROMETER

Kruhl, J.H. (Geol.-Pal.Inst., JW Goethe-Univ. Frankfurt/M.)

Subgrain patterns in quartz from rocks, affected by prograde and retrograde low- and high-pressure amphibolite and granulite facies metamorphism as well as by contact metamorphism, have been studied. At pressures ranging from less than 1 Kbar to 10 Kbar, in the stability field of the (trigonal) low-quartz, prism-parallel subgrain boundaries are dominant whereas basis-parallel subgrain boundaries are not developed. However, in the stability field of the (hexagonal) high-quartz both, prism- and basis-parallel subgrain boundaries, occur and form typical rectangular ("chessboard") patterns. The low-high-quartz boundary exactly represents the boundary between these two types of subgrain patterns. If during the tectonometamorphic history the low-high-quartz boundary is crossed the two subgrain patterns are subsequently formed, independently of the P-T conditions changing from the low- to the high-quartz field or the other way. The likely reason behind the change from one to the other subgrain pattern is that in high-quartz prism-[c] glide becomes at least as easy as <a>-glide. This is supported by theoretical considerations on the 'ease of glide' in low and high quartz (Baëta & Ashbee 1969).

The results of experimental quartz deformation suggest that "water" has some influence upon the change from <a> to [c] glide. However, such a view is not supported by the empirical data. On the contrary, the change from one to the other subgrain pattern, or from one to the other glide system, appears to be unaffected by XH_2O.

The transition from low- to high- quartz occurs at 573°C and 0 Kbar and changes to higher temperatures at higher pressures (c. 810°C at 10 Kbar) (Yoder 1950). Therefore, the occurrence of the different subgrain structures can serve as a thermobarometer. The advantage of such a thermobarometer is: (1) The two types of subgrain patterns can be clearly and simply distinguished by optical microscopy. (2) Because subgrains are formed at low dislocation densities they register even weak deformations. (3) In contrast to (high-angle) grain boundaries, subgrain boundaries are stable during post-deformational annealing. Therefore, they may preserve indications of earlier deformation events.

Consequently, the occurrence of chessboard subgrain patterns in quartz represents a practicable geothermobarometer with far-reaching possibilities of application.

References:

Baëta,R.D. & Ashbee,K.H.D. (1969). Am.Miner.54, 1574-1582.
Yoder,H.S. (1950). Trans.Amer.geophys.Union 31, 827-835.

REE-BEARING ARSENITES AND ARSENATES FROM THE M.LEONE NAPPE (BINNTAL-REGION, CH / ITALY)

Krzemnicki M. (*Min.Petrogr.Inst., Univ. Basel, Switzerland*).

The Monte Leone nappe (ML-nappe), a lower penninic unit in the Western Alps, is famous for its outstanding mineral deposits, i.e. the sulfosalt-deposit in the Lengenbach dolomite and the hydrothermal As-mineral-deposits within the cristalline rocks of the ML-nappe.

This study focusses on the mineral chemistry of the complex Rare Earth Element (REE)-As-oxides, which occur in Alpine-type fissures in the ML-gneisses of the Binntal-region. Due to the rapid uplift of the penninic units during the Alpine orogenesis, a very intense hydrothermal activity occurred, remobilizing the pre-Alpine As, Cu, Bi, REE sulfidic deposits (Graeser & Roggiani, 1976). The enriched hydrotherms preferentially migrated along discrete fractures within the ML-nappe.

Detailed qualitative and quanitative spectroscopic analyses with the Electron Microprobe (EMP) on a number of **arsenites** (cafarsite, asbecasite) and **arsenates** (agardite-(Y), cervandonite-(Ce), chernovite-(Y) and gasparite-(Ce)) from different sample localities within the ML-gneiss were carried out.

Different to the primary description (Graeser,1968), the EMP-analyses of cafarsite and asbecasite revealed the presence of REE (La,Ce,Nd,Y) in all the mineral samples (REE_2O_3 up to 2.0 wt%). The REE seem to substitute for calcium. The composition of the cafarsite is significantly different in each locality. This indicates a mineralisation process in a very disequilibrated, rapidly cooling environment (Edenharter *et.al.*, 1977).

Heinrich and Eadington (1986) calculated a thermodynamic model with As-hydroxyde-complexes for metamorphic conditions. This is the basic model for understanding the hydrothermal transport of As in the ML-nappe. The REE have been characterized formerly as relatively immobile elements. But recent studies have shown, that these elements are migrating in hydrothermal fluids under various conditions, forming complexes with F^-, Cl^-, CO_2 and possibly reduced sulfur species, i.e. H_2S, HS^- and S_2^- (Cullers & Graf, 1984; Gieré, 1993).

The presence of fluorite, fluorapatite and mimetite suggests that F^- and Cl^--complexes were mainly responsible for the hydrothermal migration of the REE within the ML-nappe. But also H_2S, as the main dissolving agent of the primary As-sulfides (tennantite and ±arsenopyrite), could have played a important role for the REE-mobilization. It's also possible that the migrating REE were complexed by As-species, e.g. $(AsO_3)^{-3}$.

The REE-bearing As-minerals in the ML-gneisses are oxidation products of a remobilized As, Cu, REE-sulfide deposit. The increasing oxygen fugacity of the whole rock during Alpine metamorphism gave rise to the formation of REE-bearing arsenites, followed by the cristallisation of the REE-bearing arsenates. Mineral samples from different localities in the Binntal-region indicate a mobilization of As and REE on a regional scale, affecting the whole Penninic ML-nappe.

References:

Cullers, R.L. & Graf, J.L. (1984). *Elsevier, Developments in Geochemisty* , Nr. 2, 300-316.
Edenharter, A., Nowacki, W., Weibel, M. (1977). *Schweiz. Min. Petrogr.Mitt.*, **57**, 1-16.
Gieré, R. (1993). *Chem. Geol.*, **110**, 251-268.
Graeser, S. (1968). *Schweiz. Min.Petrogr.Mitt.*, **48**, 367-375.
Graeser, S. & Roggiani, A.G. (1976). *Rend.Soc.Ital.Min.Petrogr.*, **32**, 279-288.
Heinrich, C.A. & Eadington, P.J. (1986). *Econ. Geol.*, **81**, 511-530.

SAPPHIRES FROM AN ALKALI BASALT IN THE KAMAFENTE-DISTRICT IN SW-RWANDA (AFRICA)

Krzemnicki M. (*Min.Petrogr.Inst., Univ. Basel, Switzerland*).
Hänni H.A. (*Min.Petrogr.Inst., Univ. Basel, Switzerland*).

East-Central Africa is well known for rich gemstone deposits, e.g. in Kenya, Tanzania and Uganda. A new sapphire-deposit from

the Kamafente-district (Rwanda) has been investigated recently by the authors.

The western border of Rwanda follows the western branch of the Great African Rift, an intracontinental extension-suture,which has been tectonically active from early Tertiary up to nowadays. An intense extensional faulting has occured along this rifting structure; the precambrian basement was rotated and uplifted besides the main fault, accompanied by granitoid intrusions and continental basalt-volcanism.

The sapphires from SW-Rwanda are associated with a specific alkali-basalt flow. They are mainly of deep blue color, often showing a so called silk (submicroscopic inclusions, i.e. hematite-ilmenite or rutile).

The color in these sapphires is caused by the Fe^{2+}/Fe^{3+} intervalence charge transfer (IVCT). An UV-visible-near IR-spectra reveals a broad absoption peak, centered at 890 nm, which correspondences with the IVCT-absorption maxima at 870 nm (Fritsch & Mercer, 1993).

Sapphires from basalts are supposed to cristallize under physical -chemical conditions of the lower crust. The formation of a Al_2O_3-complex is only possible in a Si-poor and Al-rich, high pressure / temperature environment. The sapphires have been transported by a basic magma (basalt) up to the earth-surface. The heat, chemical-("aggressive fluid-milieu) and physical-(impact-) stresses during the transport cause the so called "primary corrosion" of the sapphires (Coenraads, 1992). The surfaces of the sapphires from SW-Rwanda have been studied by Scanning Electron Microscopy (SEM). They all show heavy corrosion features, due to the transport in the basalt.

The inclusions have been analyzed by qualitative spectroscopy (EDS). The final identification of mineral inclusions is still in progress, however on the basis of SEM-EDS spectra following minerals are expected: zircone, hematite, ilmenite, uranpyrochlore and phyllosilicate-minerals.

Due to the rapid decomposition in a tropical humide climate, the main sapphire-deposits are of aluvial-type. They are exploited with traditional methods by the local population.

References:
Coenraads, R.R. (1992). *Journ. of Gem.*, **Vol. 23**, 151-160..
Fritsch, E. & Mercer, M. (1993). *Gems & Gemology* , **29**, 151.

A HYDROUS MAGNESIUM SILICATE PHASE F SYNTHESIZED AT 17 GPA and 1000 °C: CRYSTAL STRUCTURE AND STRUCTURE-COMPOSITION RELATIONS

Kudoh Y., Nagase T. (*Both at: Institute of Mineralogy, Petrology, and Economic Geology, Faculty of Science, Tohoku University*)
Sasaki S. (*Research Laboratory of Engineering Materials, Tokyo Institute of Technology*)
Tanaka M. (*Photon Factory, National Laboratory for High Energy Physics*)
Kanzaki M. (*Department of Inorganic Materials, Tokyo Institute of Technology*)

The cation-disordered crystal structure of phase F, a non-stoichiometric, hydrous silicate synthesized in a uniaxial, split-sphere, multi-anvil apparatus at conditions of 17 GPa and 1000 °C (Kanzaki, 1991), have been solved and refined in space group $P6_3cm$, using X-ray data of a small single crystal of a size 18x24x30 μm measured with synchrotron radiation (λ=0.7075 Å) at Photon Factory. The composition and unit cell for phase F, assuming 18 oxygens per cell, are $Mg_{3.35}Si_{5.51}H_{7.28}O_{18}$, a=5.073(3) Å, c=14.013(9) Å, V=312.3(5) $Å^3$. The structure contains layers with many features of superhydrous phase B (Pacalo & Parise, 1992; Kudoh et al., 1994) like units, with the layers of oxygen atoms stacked in the ABCBAC type doubled cubic closest packing arrangement. Two types of layer units with the composition $Mg_3(SiH_2)_3O_{12}$ and $Mg_2Si_3O_{12}$ stacked in disorder along the c axis. Sharing of faces between tetrahedra and octahedra is avoided through the presence of vacancies. There is, however, no long-range order in the occupation of these sites, as indicated by the lack of superstructure. These features are similar to those of phase E, $Mg_{2.13}Si_{1.09}H_{3.41}O_6$ (Kudoh et al., 1993).

References:
Kanzaki, M. (1991). *J Phys. Earth Planet. Inter.*, **66**, 307-312.
Kudoh, Y., Finger, L.W., Hazen, R.M., Prewitt, C.T. & Veblen, D.R. (1993). *Phys. Chem. Minerals*, **19**, 357-360.
Kudoh, Y., Nagase, T., Ohta, S., Sasaki, S., Kanzaki, M. & Tanaka, M. (1994). *Proceedings of the 14th AIRAPT Conf.*, in press.
Pacalo, R.E.G. & Parise, J.B. (1991). *Am. Mineral.*, 77, 681-684.

NEW DATA ABOUT THE DIAMOND INTERNAL STRUCTURE AND ITS GENESIS

Kudrjavtseva G.P., Garanin V.K. (*Dept. of Geology, Moscow University*)

A study of microadmixtures, mineral and fluid inclusions, the defecteness, the isotopic composition and optical properties of natural diamond different zones synonymously testifies the discreteness of the natural diamond formation.

There are four stages in the diamond genesis: the origin of the diamond crystals nucleus (1) with participating the crust carbon during the subduction processes (Haggerty, 1986), additional growing of diamond in mantle conditions in eclogite.(2) and peridotite (3) zones of Earth; excess growing of diamond in the protokimberlitic magma (Garanin, Kudrjavtseva, 1990; Navon et al., 1989). Each of zones are characterized by different diamond morphology, the definite set of mineral inclusions and the specific optical properties.

New data about zonal structure of Arkhangel's diamond crystals are discussed. System of absorption N3 type is established in central part of diamonds. This system is not found in peripherical parts of diamonds.

It was determinated, at last, two generations of diamond in Mg-Al-eclogites. The most younger among these generations with the small concentration of nitrogen mostly of cubic habit should be considered as the source of type II diamond, which has unique semiconductive properties.

The bringing to light the differences in chemical composition of the same named minerals from inclusions in diamond and diamond-bearing rocks (eclogites and peridotites) indicates that typomorphism of the minerals from inclusions in diamond it is not possible to use as an undirect criteria of diamond grade estimation of kimberlites. Besides this, the small size of mineral inclusions in diamond do not let us to find them in mass quantity in heavy fraction of kimberlite rocks and alluvial deposits. The

most effective in undirect diamond grade estimation is the typomorphism of minerals which made up of the diamond bearing xenoliths. The long evolution of diamond material, the discretness of its genesis and interactions berween diamond and kimberlite fluid predeterminate the borders of the using the known criterion of diamond grade and let us to suggest the new ones.

The modern technology of searching and estimation the diamond potential of kimberlites should be based on the two groups of factors defining the opportunity of diamond formation (the diamond potential) and the conditions of its safety (the real diamond grade). It was discussed the complex diamond grade kimberlite estimation methodology which was worked out in the Moscow State University and let us on the database to carry out the operative estimation of diamond grade kimberlites.

References:

Haggerty,S.E. (1986). Nature, v.320, no.6, 34-38.

Garanin,V.K.,Kudrjavtseva,G.P. (1990). *Lithos*, v.25, no.1-3, 211-217.

Navon,O.,Spettel,B.,Hutcheon,I.H. et al. (1989). *Ext.Abstr.Proceed.* of 28th IGC, Washington,69-72.

SAPPHIRINE IN METAMORPHIC ROCKS OF RUSSIA AND UKRAINE

Kulish E.A., Institute of Geochemistry, Mineralogy and ore formation;Ac.Sci.Ukraine,Kiev.

Within the Aldanian, Anabarian and Ukrainian shields sapphirine has been established in Archean, more rarely Lower Proterozoic, high-alumina, quartzless, high-magnesia rocks of two types. 1.Primary sedimentary and volcanogenic-sedimentary rocks, subjected to regional metamorphism ander the conditions of low subfacies of granulite facies and high subfacies of amphibolite facies. Sapphirine occurs in paragenetic equilibrium associations (intergrowths) with hypersthene, cordierite, phlogopite (biotite), spinel, garnet, plagioclase, orthoclase (microcline),sillimanite, corundum, magnetite et al. 2.Products of metasomatise (granitization) of metamorphosed basite-ultrabasite ortho- and pararocks, gneisses and shists, containing unaltered alumina enstatite-hypersthene, plagioclase, diopside, biotite (phlogopite), spinel, hornblend, garnet, olivine, magnetite, graphite et al. Metasomatose has polystage, directed, zonal regressive character. Si, K, Al, H_2O, F, Cl, B are supplied, Fe, Mg, Ca, Mn, et al. are evacuated. Fe is evacuated more actively than Mg, that causes the creation of low- iron minerals, at the same time their magnesiality as a whole is higher during lost stages of metasomatose. Regime of Eh is of relatively wide range. Metasomatose takes place with successive gecrease of PT within amphibolite facies. Interrelations of minerals are multistage ones, reactional, minerals are more or less of zonal structure. Sapphirine is represented by polygrain aggregates, simplectites, by grains of lens - like, columnar, limbate, veinlet, tabular, porphyroblastic and another form. Rarely more or less distinet flattened hexagonal prisms with rigid vertical striation. Pleochroism varies widely from colourless, grey, yellowish, blueish tint to dark-blue, sometimes with greenish tint. Sapphirine is developed on enstatite-hypersthene, spinel, plagioclase, more rarely on garnet, sillimanite, hornblende, diopside, olivine, corundum et al. Sapphirine is substituted by cordierite, garnet, phlogopite, microcline, corundum, sillimanite, kornerupine et al. Sapphirine is stable under metasomatic conditions within wide rauge of PT, unstable when fluids saturated with Si, K, Fe, B are present. Chemical composition of sapphirines is relatively variable. (FeO ·100):(FeO+MgO) =0-18. Noticeable isomorphism Mg-Fe-Al is mentioned, sometimes Cr, Ni, Co contents are noticeable. Ferruginity increases the line sapphirine cordierite biotite (phlogopite) kornerupine hypersthene garnet spinel.

PETROGENESIS OF EARLY CAMBRIAN GRANITOIDS OF LESSER HIMALAYA, INDIA.

KUMAR, Santosh. (Dept. of Geology, Banaras Hindu Univ.)

The granitoid magmatisms are known to occur during the Early Cambrian (560±20 Ma) period in the Chaur, Champawat, Mandi and Jaspa regions of Lesser Himalaya. Rapakivi-textures (sensu lato) have commonly been reported in the Chaur and Champawat granitoids (Chadha, 1980; Powar & Pande, 1966). A perusal of existing data including the new data set of Chaur and Champawat granitoids indicate their diverse tectono-magmatic environments.

The Chaur granitoids have variable foliated to non-foliated structures with a common bt(±hb) - gt - kf (+ perthite) - plag - qz - sph - zir - Fe-Ti oxides - tourm mineral assemblage. The Champawat granitoids show medium- to ocarse-grained textures and belong to granodiorite - adamellite series having a common bt(±hb±cpx) - plag - kf - qz - zir - rut - sph - Fe-Ti oxides - tourm mineral assoication. Surmicaceous enclaves are commonly hosted in Chaur granitoids whereas surmicaceous as well as rounded to ellipsoidal dark-coloured fine-grained magmatic enclaves are hosted within Champawat granitoids.

Geochemical evidences suggest typical peraluminous (S-type) syncollisional nature of Chaur granitoids characterized by high Rb, depleted Ba and Sr relative to potential metasedimentary sources and strong depletion of HFS elements (Zr, Nb and REE). However, Champawat granitoids show slightly metaluminous to peraluminous anorogenic (A-type) affinity (shown by magmatic enclaves) characterized by enrichment of Nb, Y, Zr, Th, U and LREE suggesting the derivation of Champawat granitoids by the partial fusion of anorogenic (Proterozoic ?) crust. The required heat-flow was perhaps contributed by the mantle-derived magma. These granitoids differ markedly to those of typical Fennoscandian rapakivi granites described by Haapala and Rämö (1990).

References :

Chadha, D.K. (1980). Rec. Res. Geol., **6**, 325-329.
Haapala, I. & Rämö, O.T. (1990). Geol. Soc. Am., Spl. paper 246, 275-286.
Powar, K.B. & Pande, I.C. (1966). Curr. Sci., **15**, 519-520.

STRUCTURE AL IMPURITY IN ROCK-FORMING QUARTZ AS AN INDEX OF GEOCHEMICAL FEATURES OF GRANITOIDS.

Kurasova S.P. (*Dept. of Geology, Moscow State Univ.*),
Boev A.G. (*Dept. of Geology, Moscow State Univ.*),
Chernukha F.P. (*Dept. of Geology, Moscow State Univ.*),
Gurbanov A.G. (*IGEM, Russian Acad. Science*),
Koshchug D.G. (*Dept. of Geology, Moscow State Univ.*),

Quartz from different acidic magmatic rocks has been studied extensively by different analytical methods including electron paramagnetic resonance (EPR) in order to find out the correlation between the content of impurities and physicochemical conditions of rock-forming media. However, complex investigation and comparison of EPR data to the results of conventional analyses have not been carried out yet, though such approach seems to be mostly essential for geological interpretation of EPR data. The aim of this work is to reveal the correlation between the geochemical features of rock forming quartz and content of structural aluminum substituted for Si measured by EPR.

Quartz from magmatic and metamorphic formations of Great Caucasus (Proterozoic and Paleozoic) has been chosen for the investigations. More than 60 quartz samples of gneissic, granodiorite-plagiogranite, granite-migmatite, gabbro-diorite-plagiogranite, early orogenic diorite-granite and late orogenic diorite-granite origin have been studied by conventional methods (X-ray fluorescence, ICP, neutron activation, atomic absorbtion) and by EPR.

EPR measurements of aluminum content (Al_{EPR}) in quartz were carried out at 77 K using a special reference sample. Before the measurements all samples have been gamma irradiated with a dose of 100 Mrad.

It was found that concentration of Al_{EPR} in the rock-forming quartz from magmatic granitoids and in situ granites is several times higher than in quartz from migmatites and orthogneisses. Al_{EPR} for differentiated early-orogenic granitoid formation increases from early intrusion phases (diorite and granodiorite) to late phases (biotite granite and, especially, two-mica granite). Al_{EPR} is extremely low for granitoids subjected to intensive secondary hydrothermal alteration.

Al_{EPR} increases with increasing of aluminum content in rock and Li content (Figure) in rock-forming quartz.

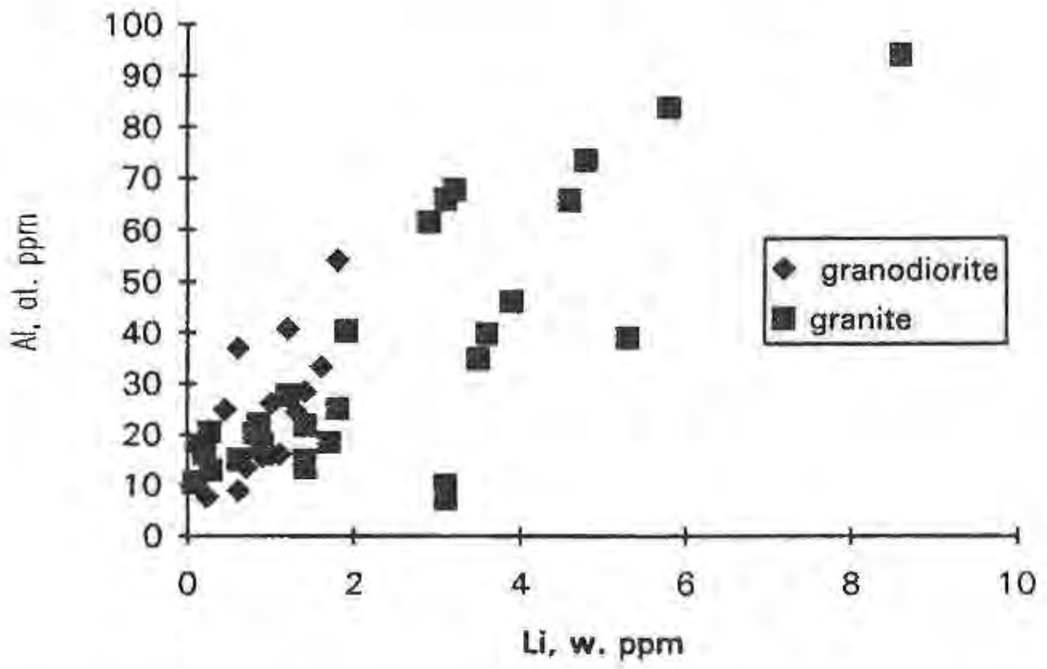

Al_{EPR} correlates mainly to Li content in quartz and, to a minor extent, to aluminum content in rock for granites. There is no correlation of Al_{EPR} and content of Na or K in quartz. It means that Li is a main charge compensating ion in the substitution of Al^{3+} for Si^{4+} in quartz from rocks under consideration.

MICROMETEORITES

Kurat G., Brandstätter F. (*Naturhistor. Museum, Vienna*), Koeberl C. (*Inst. of Geochem., University of Vienna*), and Maurette M. (*CSNSM, Orsay-Campus*)

The Earth collects about 40.000 t/a of extraterrestrial matter, most of it as dust in the mass range 10^{-8} to 10^{-2}g (Hughes, 1978). This most common extraterrestrial matter on Earth was not available for study until fairly recently, when samples were recovered from blue ice near Cap Prudhomme, Antarctica (Maurette at al., 1991). We have studied a collection of dust particles in the mass range 1-47µg by INAA, ASEM, EMPA, and optical microscopy. A surprisingly large proportion of the black and irregularly shaped particles turned out to be unmelted micrometeorites. They consist of either phyllosilicates, or olivine and/or pyroxene, or mixtures thereof.

Mineral abundances and compositions indicate a relationship to the rare chondrite classes CM and CR. Bulk major and trace element compositions best fit that of CM chondrites with the exception of some elements which are either depleted (Ca, Ni, S, less commonly Na, Mg, and Mn) or enriched (K, Fe, As, Br, Rb, Sb, and Au) in micrometeorites as compared to CM chondrites. Most of these differences have terrestrial causes (leaching and condensation of certain phases) but some (olivine-pyroxene abundances, olivine compositions, bulk C contents) appear to be primary features. Thus, the most common extraterrestrial matter accreting on Earth today is probably a matter of its own but related to some rare chondrite classes.

References:
Hughes, D.W. (1978). In: *Cosmic Dust* (ed. J.A.M. McDonnell), Wiley, Chichester, 123-185.
Maurette M., Olinger C., Christophe Michel-Levy M., Kurat G., Pourchet M., Brandstätter F., and Bourot-Denise M. (1991). *Nature* **351**, 44-47.

A CORRELATION BETWEEN ENERGY AND SPATIAL PARAMETERS OF MINERALS AS A MEANS FOR ENLARGEMENT OF THERMODYNAMIC DATABASE

Kurepin V.A. *(Institute of Geochemistry,Mineralogy and Ore Formation, Ukr.Acad.Sci.,Kiev)*

There is a correlation between energy and spatial effects of complete replacements of A by B in the AX series of compounds ($X = X_1,X_2,X_3,...$) having the same coordination of atoms A and similar bond between them and surrounding atoms (Kurepin,1992,1993). These correlations may be expressed by

$$_{\Delta}e = (a + b\ (_{\Delta}s)^{m})n$$

where $_{\Delta}e$ is the difference between BX and AX in an energy parameter (bond energy, enthalpy, Gibbs energy , entropy or heat capacity), $_{\Delta}s$ is the difference in a spatial parameter (interatomic distance in a binary compound or molar volume), a and b are coefficients, m and n are equal to 1 or -1.

The relations between energy and spatial effects of BA replacement in compounds of main subgroup elements

differ from analogous relations for compounds of transition elements and elements of the 1b and 2b subgroups.

These correlations can be used for estimating thermodynamic constants of mineral BX if its molar volume and constants of its structural analog AX are known. For instance, $_{\Delta}Hf$ of ferrous mineral FeX may be calculated using data for its magnesian analog MgX

$$_{\Delta}H_f(FeX) = {}_{\Delta}H_f(MgX) + {}_{\Delta}H_{FeMg}$$

or using data for Mn, Co, Ni and other analogs.
The $_{\Delta}e$-$_{\Delta}s$ correlations of many BA replacements have been determined and used for estimating thermodynamic functions of minerals.

References:
Kurepin, V.A.(1992). *II Int. Symp."Thermodyn. Natur. Proc."Abstracts,Novosibirsk*,33.
Kurepin, V.A. (1993). *Geochem. Int.*,30, 18-30.

• OPTICAL HIGH-PRESSURE INVESTIGATION OF BASALT GLASS AS A MODEL OF DEEP-SEATED MELTS

Kuryaeva R.G., Kirkinsky V.A. *(Institute of Mineralogy and Petrography, Novosibirsk, Russia)*

A study of silicate glasses provides a valuable information on a structures and some properties of native melts. It is especially important for petrologic and geophysical aims to know the compressibility of glasses, modelling deep seated melts.

A method of refractive index measurement for isotropic substances at pressures up to 5 GPa using a diamond anvil cell and a polarizing-interference microscope has been developed by the authors. The error of this measurements is not more than 0,005 at maximum pressure.

According to Mueller's theory of photoelasticity a change in refractive index of isotropic substances under pressure takes place owing to a change in the number of oscillators per unit volume (density) and a polarizability variation of the ions at the cost of the structure deformation. The dependence of the refractive index (n) from these factors is expressed by $\delta n/\delta\rho=(n^2-1)(n^2+2)(1-\lambda_0)/6n\rho$, with ρ substance density, $\lambda_0=\Delta RV/R\Delta V$ strain-polarizability constant, R molar polarizability. λ_0 values are known to be very similar for isostructural substances. As most rock-forming magmatic melts contain more than 50 mol % SiO_2, it is interesting to study the "normal" glasses - their structure models with continuous structural network. Vitreous SiO_2 and silica-rich glasses are known to exhibit similar anomalous elastic behaviour at high pressure. The baric coefficients of the compressibility increase with increasing pressure up to 2-3 GPa, go through a maximum and thereafter decrease with a pressure growth. Such behaviour suggests that compressibility character and therefore the strain-polarizability constants are similar for glasses of this type. Measuring the refractive index under high pressure and taking into account the strain-polarizability constant one can know the density of glasses under high pressure.

We have studied the behaviour of refractive index of fused silica and natural glass of tholeiite basalt at high pressure up to 5,0 GPa. For both glasses the pressure dependence of the refractive index in the range up to 1,0 GPa is close to linear. The baric coefficients of the refractive index of vitreous SiO_2 and basaltic glass (dn/dP) are 12,5 MPa and 12,0 MPa respectively. At pressures higher than 1,0 GPa the baric coefficient for both glasses increases, reaches a maximum near 2,2-2,4 GPa and thereafter it decreases with pressure growth up to 5,0 GPa. So the refractive index exhibits an anomalous behavior under pressure, identical with that of the silicate glasses compressibility. Using the measured refractive index of fused silica at high pressure up to 5,0 GPa and its known compressibility in this pressure range, the strain-polarizability constant $\lambda_0=0,20$ was obtained. This constant was applied to a calculation of the equation of state of basaltic glass at pressures up to 5,0 GPa, using the density-refractive index relationship. The increase of the density of the basaltic glass at maximum pressure is 12%. The compressibility of the same basaltic glass, which was measured by photomethod, is in good agreement with that obtained by the refractive index measurement.

Determined compressibility of basalt glass is significantly greater than of plagioclases. It means that at high pressure some alcalic plagioclases are lighter than melt and can ascend at crystallization, forming anorthosite and similar rocks. This work was performed with the financial support of the Russian Foundation for Fundamental Investigations, project 93-05-9456.

Isotopic and Temporal Evolution of Oceanic Island Volcanism

Kurz, M.D. *(Dept. of Marine Chemistry & Geochemistry, Woods Hole Oceanographic Institution, Woods Hole MA 02543)*

Isotopic studies of oceanic volcanic rocks provide crucial information regarding long lived heterogeneities within the earth, and the processes by which melts are extracted from the mantle. An understanding of the causes of the temporal evolution from single oceanic island volcanoes is important to understanding both the microscopic scale of melting, and the global heterogeneities. Geochronology of oceanic island lava flows on the important 1 Ka to 100 Ka time scales is now possible using a combination of ^{14}C dating and surface exposure dating with cosmic ray produced nuclides (such as ^{3}He). Hawaiian volcanoes are a key example of systematic geochemical variability over such short time scales. At Mauna Loa volcano, there is a correlated change in the He, Sr, Nd, and Pb isotopic compositions of the erupted lavas at approximately 10 Ka, suggesting a major change in the mantle source; the decrease in $^{3}He/^{4}He$ ratios at that time suggest that the hotspot source was removed from Mauna Loa. This major change is followed by shorter time scale (roughly 1 Ka) variations in Sr, Nd, and Pb isotopes which require either an axially heterogeneous Hawaiian plume, or that the isotopes are affected by melting and melt migration processes. Kilauea volcano, which is just adjacent to Mauna Loa on the island of Hawaii, displays complex isotopic variability on much shorter time scales (100 to 1000 years). Seismic and geological evidence that the magma chamber beneath Kilauea is much smaller than Mauna Loa suggests that the difference between these time scales is partly due more effective homogenization during magma storage at Mauna Loa. Due to the shorter residence time in a magma chamber, the Kilauea lavas are more sensitive to differences in size and geochemistry of individual magma batches, thus providing key constraints on fractional melting at depth in the upwelling region. Such variations have not been observed in other oceanic island volcanism, suggesting that Hawaiian volcanism is unique due to the combination of large upwelling velocity, large temperature anomally (i.e., great depth of melting), and thick lithosphere. However, there are still too few isotopic studies with the necessary geochronology, and preliminary studies of Galapagos volcanoes suggest some temporal evolution on such time scales. The existing data demonstrate that isotopic and trace element geochemistry, in combination with stratigraphy and newly available geochronology, are important probes of melting and melt migration processes within mantle plumes.

• DEFORMATION OF STIBNITES IN THE MADSAN ANTIMONY VEINS (NIGDE MASSIF, TURKEY): AN IMPLICATION ON P-T CONDITIONS OF LOCAL DEFORMATION

Kuscu I. and Erler A. (*Dept. of Geol. Eng., Middle East Tech. Univ.*)

The Madsan antimony deposit is located at the southeastern part of the Nigde province (south-central Turkey). It lies at the southeastern part of the Nigde Massif, close to its boundary with Ecemis strike slip fault. The deposit consists of a series of epithermal veins hosted by marbles and gneisses of the Gümüsler Formation of the Massif. The veins have a simple mineralogy as

quartz, calcite, stibnite and pyrite as major constituents, and cinnabar in trace amounts.

Stibnite is characterized by its extreme sensitivity to any kind of deformation because of its ductility and low strength. Thus, it may serve as a guide to tectonic conditions, that is pressure and temperature of deformation evidenced by a set of textures. These are pressure lamellae and annealing as the main textures, and curvature, offset of pressure lamellae and fracture filling textures as the textures of minor importance. These were developed in three successive deformation phases. Pressure lamellae represent the first order deformation in the region, while the second order deformation is represented by curved pressure lamellae and local annealing texture, and the third order deformation is characterized by truncation and offset of pressure lamellae.

This deformations are likely to occur at temperature reaching up to 180°C and pressure at about 2 bars. Geological evidences support the idea that first order deformation is explained by the southward thrusting of the Nigde Massif with the deposit over the Ulukisla Basin. The second order deformation is due to an increase in internal compressive forces and increasing dislocations and lattice diffusion within the stibnite structure after deformation has ended. The third order deformation is the direct result of younger normal faulting close to the deposit.

COMPOSITION, MANTLE DISCONTINUITIES AND SEISMIC PROPERTIES OF THE MOON

Kuskov O.L., Fabrichnaya O.B. *(Vernadsky Institute of Geochemistry and Analytical Chemistry, Moscow)* **and Saxena S.K.** *(Uppsala University, Uppsala)*

To constrain composition of the Moon we have calculated the stable phase assemblages and their seismic properties by the method of minimization of Gibbs free energy whether various compositional models are consistent with the seismic observations (Nakamura, 1983) for the lunar mantle at the depths of 100 and 1000 km. Internally consistent thermodynamic computation of phase equilibria is carried out for the FMAS and CFMAS system. The standard free energies of end members required to describe the compositions of the phases in the CFMAS system (Opx, Cpx, Pl, Ol, Gr, Sp) and mixing properties of the solid solutions have been derived. The calculations give the mineralogical changes in dependence on temperature and pressure throughout the lunar mantle. P-wave and S-wave velocities were calculated for a series of proposed bulk composition models. Compositional models for the Moon (impactor composition, Orgueil composition, etc.) and earthlike compositions (pyrolite, lherzolite) were considered. It has been found that impactor and Orgueil models are very unlikely for the lunar mantle. Within reasonable temperature adjustment in the temperature profile, all of the terrestrial compositional models come close to the seismic data below the 500-km discontinuity. It has been found that a composition being enriched by Al_2O_3 (up to about 6 wt.%) and having the pyrolite contents of the other major oxides ("lunar pyrolite") is adequate to describe the seismic properties of the lunar lower mantle. Within the uncertainty of calculations and resolution of seismic data an Al-rich model with a terrestrial Ol/Px ratio and unusually enriched in garnet has the best fit to the lunar lower mantle physical properties. In spite of uncertainty of the seismic data it is shown that none of the analyzed compositional models satisfies the seismic constraints simultaneously in the upper, middle and lower mantle. Phase changes in any model considered are not able to explain the nature of the 500-km discontinuity. The transition from spinel to garnet field causes the jumps of 0.2 km/sec in Vp and 0.05 km/sec in Vs in comparison with the seismic jumps of 0.8 km/sec in Vp and 0.40 km/sec in Vs. A conclusion is made that the lunar mantle is chemically stratified.

FROM MINERALS TOWARDS SUPERCONDUCTORS

Kuz'micheva G.M. *(Academy of Fine Chemical Technology of the Name M.V.Lomonosov, Moscow, Russia)*
Gorchakova O.E. *(All-Russian Institute of Scientific and Technical Information, Moscow, Russia)*

The data based on the crystallochemical analysis of superconducting phases showed that their structures derive from the structures of the minerals. However, the composition of the minerals corresponds to the maximal stability of the structure, while the composition of the superconductors is on the limit of stability.

According to the structure and mean number of valent electrons per cation (e/K) the superconducting non-metallic phases are divided into three groups:

$$\sim 0.2 \le e/K < 2.1, \quad 2.1 \le e/K \le 3.0, \quad 3.0 < e/K \le 6.0.$$

The basic structural feature of the superconducting non-metallic phases of the first group is the clusters isolated or binded in the rectilinear chains (borides, carbides, Chevrel phases, imperfect oxides). The base of the structure of the second group phases is the one-, two-, three-dimensional framework from polyhedra, in the centre of which are the cations with variable formal charge (structural types of spinel, perovskite or derivative from the last). The peculiarity of the structure of the third group phases is imperfection (intercalation compounds, bronzes).

Taking into account the properties of organic superconductors - fullerides and graphite intercalation compounds - they can be attributed to the group one and three respectively.

A comparison of crystal structures A_xC_n (fullerides) and LnB_{12} (rare-earth dodecaborides) shows that they are similar. The C_n ($n \ge 60$) molecules form a crystals whose structures are regarded as a face-centred cubic (fcc), hexagonal close packing (hcp), body-centred tetragonal (bct) and body-centred cubic (bcc) configuration of the molecules. Cations (A) occupy octahedral and tetrahedral interstitial sites. Borides with UB_{12} - type structure (the first group of non-metallic superconducting phases) have fcc packing of the B_{12} - polyhedral clusters where the cations (Ln) fill all the octahedral positions. A possible correlation of critical temperature of fullerides A_xC_n with their composition and symmetry of molecules C_n known for the first group of superconductors was discussed.

The calculated weighted-mean cation radius (r_A,A) for A_3C_{60}-superconducting compounds and for A_3C_{70}-compounds is in the range 1.12÷1.54 and 1.20÷1.60 respectively. Phases with r_{Amax} being on the limit of the structure stability have the highest transition temperature (T_{cmax}). Cations in structure A_4C_{60} (bct) and A_6C_{60} (bcc) were located in the tetrahedral sites with r_{Amax}=1.48A. The phases with a structure that can be described by a coherent growth of different molecules packing might also be formed. These phases may have the superconducting properties with a higher or a lower T_c value as compared to the individual phase.

For graphite intercalation compounds A_xC_n ($n \ge 2$) the relationship between the atom radius (or the weighted-mean atom radius), pressure, composition, polymorphic modifications of the graphite matrix and critical temperature was found. These properties unite intercalates (the third group of superconducting phases) with compounds of graphite.

The subdivision of superconducting non-metallic phases into three groups based on the electron concentration of the cations and depending on the relative character of the interaction is useful in searching for new phases with possible superconducting properties. All the theses are corroborated by experiments.

THREE WAYS OF IMPURITY INFLUENCE ON THE DEFECT STRUCTURE OF QUARTZ CRYSTALS

Kuz'mina M.A., Moshkin S.V., Punin Yu.O.
(Dept. of Geology, Univ. of St. Petersburg, Russia)

The study of the structural impurity influence on defect structure of quartz crystals from hydrothermal veins of the Urals was carried out. Some large crystals were exposed to the

gamma-radiation to reveal their radiation coloration, since it was known that this coloration connected directly with the structural impurities of Al, Na, K, Li and H, which were presented in quartz crystals (Mineralogy . . . , 1979). After that they were sawn along third axis into plates, in which concentration and distribution of various kinds of defects within of zones and sectors of grown faces were studied.For investigation the following methods were used: spectral analysis, optical and infrared spectroscopies, X-ray diffraction, optical polarizing microscopy and chemical etching.

As the result for "light-smoky - dark-smoky - olive - citrine quartz" row (that corresponded to general consequence of quartz crystallization in hydrothermal veins of the Urals (Eshkin et al., 1983)) it was established that: a) the concentration of such structural impurities as Al, Li, and H increased in this row, and the concentration of Na and K was practically constant; b) the a and c parameters of the unit cell increased in this row, (c parameter increased rapidly from light-smoky to dark-smoky quartz, while a parameter - from dark-smoky to citrine quartz); c) the number of various kinds of blocks decreased in this row (microblocks - in 1.2 times, mesoblocks - in 2.0 times, and macroblocks were observed for smoky quartz only); d) the dauphin twins were observed in smoky quartz mainly (their number decreased with increasing of colour intensity), and the brazil twins were typical for the olive and citrine quartz (their number increased with a rising of concentration of citrine color centres); e) the number of syngenetic cracks increased in this row.

The formation of the defect structure of a single crystal in process of its growth is determined by following processes: the generation of defects, the disappearance of them, the regrouping and inheritance of various defects on growing crystal face. The reconstruction of the defect structure of quartz crystals in grown sectors <R> and <r> has revealed three ways of structural impurity influence on it in the process of growth:

1) Some kinds of plastic defects and cracks in quartz crystals were formed by effect of the internal strains, which appeared on the boundaries of grown zones and sectors with different concentrations of structural impurities. These strains were calculated with use of parameters of unit cell in neighboring zones (sectors). A direct proportional dependence between number of cracks in unit volume and values of maximum normal strains, which achieved 0.1 of quartz breaking point, was observed. Also the similar dependence between values of "intensity of strains", which characterized maximum tangent strains, and relative change of the density of mesoblocks and brazil twins in the direction of growth was determined.

2) Kinds of formed defects depended on nature and concentration of structural impurities. In the row from light-smoky to citrine quartz the density of all kinds of blocks decreased and the number of brazil twins and cracks increased. In this row a critical intensity of the strains increased (it was determined as a value, above which a generation of mesoblocks on grown face prevailed over their disappearance and regrouping); this fact gave evidence that plastic properties of quartz decreased in this raw.

3) Kinds and concentration of the structural impurities have influenced on development of defect structure in crystal growth mainly by means of breaking of motion and regrouping of dislocations. In light-smoky quartz chaotic dislocations were reorganized in microblocks easily, and then microblocks developed into meso- and macroblocks; on the contrary, in olive and citrine quartz number of micro- and mesoblocks was small, and macroblocks were absented.

References:

Mineralogy and crystallophisics of jewelry varieties of silica. (1979). Moscow. (russ).

Eshkin V. Yu., Karyakina T. A., Bogdanova G. N. (1983). In "New ideas in genetic mineralogy", Leningrad, 82-86. (russ).

SPECIAL FEATURES OF LUMINESCENCE OF FELDSPARS FROM METASOMATIC ROCKS.

Kuznetsov G.V. and Tarashchan A.N.
(Inst. Geochem., Mineral. and Ore Format., Kiev)

In X-Ray luminescence (XL) spectra of feldspars of any composition (K, Na, Ca) the wide band of irradiation with maximum varying from 445 to 480nm is always observed. Generally accepted model of the center i-s charge defect on alumino-oxigen tetrahedral complexes $[AlO_4^{4-}]$ (simplified - A-center). Detailed analysis of the shape of the band in spectra of various feldspar samples has shown that it has complex structure and is the superposition of two different bands with maxima ~ 440-450 nm and ~ 500-510 nm.

In majority of feldspars from granitoides of magmatic and metamorphic origin the ratio of intensities of these bands is practically constant. We suppose that these are two structurally different modifications of A-centers (A_1 ~ 445 nm and A_2 ~ 510 nm). Centers A_1 are prevailing over A_2 centers.

During XL-studies of metasomatic rocks from varions regions (Ukraine, Siberia, Kazakhstan) it has been established that XL spectra of corresponding feldspars have their specific features. With general low concentration of A - centers the ratio of intensities of A_1 and A_2 bands changes substantially (the part of A - centers increases). The same features are proper for feldspars from pegmatites subjected to metasomatic changes. We connected these changes with greater stability of A_2-centers in metasomatic process. New luminescent characteristic (metasomatic factor f_m) is proposed in order to defect metasomatic process and its degree. The value of f_m reflects the ratio of concentrations of A_1 and A_2 centers and is determined by configuration of XL-spectrum within the range of irradiation of these centers.

A set of limitations are mentioned for the use of f_m for studies of rocks of definite geochemical types.

HYDROTHERMAL QUARTZ EVOLUTION: STRUCTURAL IMPURITY CONCENTRATION CHANGE

Kuznetsov S.K., Lutoev V.P. (*Inst. Geol., Komi Sci. Cent., Ural Div., Rus. Ac. Sci.*)

The concentration of Al- and Ge- paramagnetic centres in hydrothermal quartz from quartz veins of Subpolar Ural were measured by ESR. Six basis generations of quartz were investigated. The most early quartz veins were formed in Upper Proterozoic, and late ones were formed in Permian period. The late quartz is well-formed crystals of smoky, citrine or amethyst colour.

It was ascertained that Al-centres concentrations in different quartzes change from 5 p.p.m. to 160 p.p.m. The fluctuation of Ge-centres concentrations is higher and belongs to range from invisible values to 1.6 p.p.m. The concentrations of these centres positively correlate and essentially rise in generation sequence of quartzes. The average concentration of Al-centres is increased from 9 p.p.m. to 25 p.p.m., and it of Ge-centres - from 0.01 p.p.m. to 1.3 p.p.m. The most higher concentrations are registered in citrine quartz's crystals. Note, that the most late quartz generation, presented by the amethysts, differs by relatively low the centres' concentrations from other quartz.

It is possible, that the founding tendencies are geochemistry law for hydrothermal mineralization, which can occur at the change of physical-chemical parameters of crystallisation, for example, the temperature decreasing and alkalinity of the solution. The metamorphic process of quartz veins, causing the

recrystallization and crushing of quartz, has essential role in impurities concentrations change. In this process the centres concentrations are decreased.

• THE FEATURES OF MORPHOLOGY OF DIAMOND CRYSTALS FROM METAMORPHIC ROCKS.

Kvasnitsa V.N. (*Dept. of Diamond problems, Inst. of Geochem., Mineral., and Ore formation, Acad. Sci. of Ukraine, Kiev*)

The characteristic features of diamond from metamorphic rocks of Kazakhstan and deposits of Ukraine give the possibility to judge about the specific conditions of their crystallization, that is a short time stay of the mineral forming substance at the conditions of diamond stability. Such microcrystals grew by diffusion way. Unlike mantle diamonds, the diamonds from metamorphic rocks present the following typical features: spheroidal and skeletal forms, aggregates, not uniform intrinsic structure, enrichment in impurities, abundance of the crystals with cubic habitus, normal (partially microblock) mechanism of growth most crystals. All these features evidently show that the crystals grew with a high rate in mineral forming substance oversaturated by carbon. A great number of centers of crystallization and high defectness of the crystals are main causes of a small dimensions of the diamonds. An additional factor of crystallization is probably a high specific surface energy of the microcrystals. An investigation of the morphology of diamonds from metamorphic rocks show that, as for microcrystals from mantle, an octahedron is not the only smooth boundary surface. There are also cube, rhombic dodecahedron and other forms. Wide morphological variety of diamond microcrystals included into a single crystal of garnet as well as autoepitaxy are particularly significant phenomena. By all above features the diamonds from metamorphic rocks are close to synthetic diamonds, especially to those grown in gaseous substance under the condition of metastability.

NEW OPPORTUNITIES FOR THE GEOSCIENCES AT THE ESRF

Å. Kvick

European Synchrotron Radiation Facility
B.P. 220, F-38043 Grenoble Cedex, France

ESRF, the European Synchrotron Radiation Facility, is a third generation dedicated synchrotron facility being constructed as a joint venture between 12 European countries in Grenoble, France. The facility is presently in an advanced commissioning stage and the general user program will start during 1994. The ESRF is located in a section of Grenoble with a rich scientific infrastructure. In addition to French research institutes such as CNRS, CEA and IBS there are international institutes including EMBL, Max-Planck laboratories as well as the next door high-flux neutron reactor of the Institute Laue Langevin.

The ESRF will during the next few years develop 30 facility beamlines mainly on insertion devices. Many of the remaining bending magnet ports will be developed by independent consortia of scientists in so called Collaborating Research Groups (CRG:s).

Naturally many of the proposed beamlines are suited to experiments in the geoscience areas. Table 1 gives a list of beamlines that are particularly relevant to studies in the geosciences. The ESRF beamlines are listed under their beamline number and the CRG:s under their acronyms. a summary of all beamline characteristics can be found in the ESRF beamline handbook[1].

[1] ESRF Beamline Handbook.

Table 1

Beamlines suitable for Geoscience research listed according to disciplines. The radiation source is given in parenthesis; U=undulator, W=wiggler and BM=bending magnet.

Diffraction, Crystallography	BL2 (W), BL5 (W), Swiss/Norv (BM)
Elastic diffuse scattering	BL17 (W), D2AM (BM)
EXAFS, SEXAFS	BL8 (U), BL18 (U), IF (BM), Gilda (BM), Swiss/Nov (BM)
High Pressure	BL2 (W), BL3 (W), BL5 (W), BL8 (U)
Magnetic scattering	BL12 (W)
Microcrystal diffraction	BL1 (U)
Nuclear diffraction	BL11 (U)
Powder diffraction	BL15 (BM--W), Swiss/Norv (BM)
Small angle scattering	BL1 (U), BL4 (U)
Surface scattering	BL7 (U), IF (BM)
Topography	BL16 (W), Swiss/Norv (BM)

The first beamlines have operated since November 1992 and many experiments of geophysical significance have already been performed. The talk will outline the technical capabilities of the beamlines and will provide examples from high pressure experiments such as on single crystal H_2, powder diffraction, Mössbauer and topography.

GEOCHEMISTRY OF TRACE ELEMENTS IN SOME SALT-AFFECTED SOILS

Labib F.B. (Prof.) and Rahim I.S. (Ing.)
Soils & Water Use Dept., National Research Centre, DOkki, Cairo, Egypt.

The main object of this research work is to recognize the mineral source of five trace elements (Fe, Mn, Zn, Cu and B) in some salt-affected soils in Egypt.

Three profiles from the northern part of the Delta and another one from El-Fayoum were selected, sampled and analysed.

The obtained results from heavy minerals identification and trace elements determination lead to the following conclusions:

- The main source of iron in these soils is opaque minerals as heamatite , magnetite , pyrite and calcopyrite . Also epidote , augite , hornblende and biotite contribute to the total content of iron in soils.
- The Mn - bearing minerals are: pyrolusite, manganite and rhodonite as opaque grains. It is evidently that fertilizers are one of the sources of Mn in these soils.
- The clay minerals are positively correlated with Zn content and the Zn as sphalerite and gahnite could not be detected in the heavy minerals counts.
- The opaque calcopyrite can be one of the sources of Cu in such soils. however, chemical and organic fertilizers besides the pesticides and atmospheric fall-out contribute considerably to Cu content in soils.
- The extractable boron in these soils is highly correlated with high salt content , evidently in the form of borax and karnite salts. the mineral source of boron in the sand fraction is tourmaline.

Referances:

Abdou, F.M. et al.(1980). Egypt. J. Soil Sci. 30,1.29-43.
Berrow,M.L. and Reaves, G.A.(1984). Proc. Int. Conf. Envir. Contam. (London, July 1984) 331-370.
Black,C.A.et al.(1982). Amer. Soc. Agron. Inc. Madison, Wisconsin.
Cottenie,A. et al.(1982). Lab. of Analytical & Agrochemistry, State Univ. Ghent, Belgium.
Jackson, A. L. (1960). Constable Co., Ltd., London.
Kassem,Y.S. & Elwan, A.N.(1980). Egypt.J. Soil Sci.,20,1,57-63.
Kerr,P.F.(1962). Mc Graw Hill, New York-Toronto -London.
Keys to Soil Taxonomy (1992). SMSS Tech. Monog. No.19 Fifth Edition, Pocahontus press, Inc. Blacksburg, Virginia.
Krauskopf,K.B.(1982). Soil Sci.Soc. Amer. Madison Wisconsin.
Labib,F.B. et al.(1987). Agrochimica,33,1-8.
Milner,H.B.(1962).Allen and Unwin Ltd., London.
Norvell,N.A.(1982). Soil Sci.Soc.Amer.Inc. Madison, Wisconsin.
Sposito,G. & Page,N.L. (1985). Marcel Dekker Inc., New York.
Wahab, M. (1977). Ph.D. Thesis, Fac. Agric., Ain-Shams Univ., Egypt.

OWENSITE, $(Ba,Pb)_6(Cu,Fe,Ni)_{25}S_{27}$, A NEW MINERAL FROM THE WELLGREEN Cu-Ni-Pt-Pd DEPOSIT, YUKON, CANADA

Laflamme, J.H.G., Cabri, L.J. and Szymański, J.T. (*CANMET, Ottawa, Canada)*, Roberts, A.C. (*GSC, Ottawa, Canada)* and Criddle, A.J. *(The Natural History Museum, London, England)*.

Owensite [ideally $(Ba,Pb)_6(Cu,Fe,Ni)_{25}S_{27}$], is a new mineral found in samples from the Wellgreen Cu-Ni-Pt-Pd deposit, Kluane District, Yukon Territory, Canada (Cabri *et al.*, 1993). The mineral, which is very rare, occurs as small anhedral grains ranging from 6 x 12 to 43 x 110 μm, and is closely associated with pyrrhotite, magnetite, chalcopyrite and pentlandite. Owensite is opaque with a metallic lustre and a black streak. The mineral is pale brownish grey in plane-polarized reflected light, isotropic. Reflectance spectra and colour values were determined. Owensite displays cubic symmetry and has a unit-cell parameter of a = 10.349(1) Å and V = 1108.4(3) Å^3, with strongest lines of 3.460(40,300), 3.281(40,310), 2.996(90,222), 2.378(90,331), 1.835(100,440) and 1.779(40,433). Its crystal structure has been determined as cubic, a = 10.349(1) Å, space group *Pm3m* (Szymański, 1994); D (calc) = 4.78 g/cm^3 for Z = 1, based on the empirical formula derived from the electron-microprobe analyses. Structurally, owensite is closely related to djerfisherite $K_6Na(Fe,Ni,Cu)_{24}S_{26}Cl$ but is unusual in that it is totally devoid of the chlorine and monovalent metals found in the latter mineral. In owensite, the djerfisherite Cl site is occupied by a S atom, and the Na site is occupied by one of the (Fe,Cu) atoms. There is some positional disorder with the Pb atom attributed to the $6s^2$ electrons. The structure has been refined to 5.2% for absorption-corrected X-ray diffraction data collected with MoKα to 2θ = 100°. Owensite honours DeAlton R. Owens (1934-) of the Canada Centre for Mineral and Energy Technology, Ottawa, for his contributions to mineralogy, particularly in the field of electron microbeam analyses.

References:
Cabri, L.J., Hulbert, L.J., Laflamme, J.H.G., Lastra, R., Sie, S.H., Ryan, C.G., and Campbell, J.L. (1993). *Explor. Mining Geol.* 2, 105-119.
Szymański, J.T. (1994). *Can. Mineral.* (submitted).

MÖSSBAUER EFFECT STUDIES OF SYNTHETIC TOURMALINE

M. Lagache *(URA 1316 du CNRS, ENS, Paris)* , Y. Fuchs *(Lab. Minéralogie Exp. Appl., UPMC, Paris) and* G. Linares *(D. R. P., UPMC, Paris, URA 71 du CNRS)*.

Tourmaline was synthesized at temperatures of 400, 500, 550, 600, 650°C , and pressures from 40 to 100 MPa using the reaction observed in natural assemblages (Fuchs & Lagache, 1994): chlorite + albite + boron --> tourmaline + mica + iron oxyde + oxygen. Experiments lasted from 15 to 142 days. The chlorite used as reagent is a natural iron-rich chlorite from the Monte Fondoli hydrothermal system (Trento, Italy). A Mössbauer effect spectrum of this chlorite shows that more than 93% of the Fe is divalent. The experiments were run at the different temperatures in three ways: material in sealed gold vessels, material in sealed platinum vessels, and with or without Ni-NiO buffer. All reactions were complete but the two at 400°C, even after 142 days. The products were analyzed by XRD and Mössbauer spectrometry. In all experiments above 550°C the iron oxide crystallized as magnetite.

The synthetic tourmalines were studied by Mössbauer effect spectrometry. The Fe^{3+} (25 to 60 % of the total iron) is located in the Z site and Fe^{2+} in the Y site following the Goldschmidt's first rule. SEM microprobe analyses were also performed on these synthetic tourmalines. The structural formulae calculated on the basis of the SEM microprobe analyses show no discrepancy with the iron site attribution based on MES. The Fe^{2+}/Fe^{3+} ratio varies in relation to the temperature and oxygen fugacity conditions. On the basis of these results some interpretations of the Mössbauer spectra of natural tourmalines are discussed.

Y. Fuchs & M. Lagache (1994) *C.R. Acad. Sci. Paris*, **in press.**

MINERALOGY OF A RARE-ELEMENT PEGMATITE ASSOCIATED WITH RAPAKIVI GRANITE AT LUUMÄKI, FINLAND

Lahti, S. I., (Geological Survey of Finland,Betonimiehenkuja 4, 02150 Espoo, Finland)

Granitic pegmatites especially those containing rare-elements are scarce within the 1.54--1.65 Ga old rapakivi granite intrusions in Finland. Locally small pegmatite bodies with miarolitic cavities are common. Characteristic accessories in the pegmatites are topaz and fluorite; in addition, beryl, columbite, tourmaline, cassiterite, bertrandite, certain sulphides and REE minerals are locally observed.

The Luumäki pegmatite dyke, which situates in the northern corner of the Viborg rapakivi intrusion in SW Finland, is exceptionally large and rich in rare minerals (Lahti & Kinnunen 1993). The dyke is about twenty metres wide and well zoned. A massive quartz core about 10 m wide makes up the core of the dyke. The core is surrounded by three separate zones referred here as intermediate, wall and border zone.

Large pockets, which are lined with crystals of quartz, feldspars and locally yellow, yellow green or blue green transparent gem beryl, are characteristic in the central parts of the pegmatite. The pockets, which may be at the maximum two metres long, are partly filled with brownish red clay or in cases with hard microcrystalline quartz, jasper.

The grain size of the pegmatite increases gradually from the narrow fine-grained border zone nearest to the host rapakivi granite towards the quartz core. The main minerals in the border, wall and intermediate zone are reddish brown albitic plagioclase, microcline, quartz, biotite and muscovite. The border and wall zone, which are mineralogically simple, are characterized by graphic feldspar.

The intermediate zone is enriched in rare minerals. Large crystals of common beryl, topaz and thorium-rich monazite-Ce are common. Topaz crystals, which may weigh several kilograms, are locally replaced by fine-scaled muscovite and fibrous margarite. Hematite-goethite accumulations, crystal aggregates of ferro-columbite and wolframian ixiolite replaced by thorium-rich pyrochlore-microlite, euxenite and cassiterite are locally encountered. Since 1986 the pegmatite has been mined for gem beryl and other gem minerals.

Two generations of beryl can be distinguished in the pegmatite. The older beryl generation or common beryl occurs as large altered prismatic crystals up to 30 cm in diameter in the intermediate zone. Corroded crystals or crystal fragments of the younger beryl generation, i.e. transparent gem beryl, occur with bertrandite and clay minerals in the pockets associated with altered crystals of common beryl. The fluid inclusion studies indicate a crystallization temperature between 400° and 460° C for the gem beryl in the pocket mineralizations.

Lahti, S.I. & Kinnunen, K.A. (1993) *Gems & Gemology* 29, 30-37.

APPLICATION OF CATHODOLUMINESCENCE TO SYUDY MICROSTRUCTURAL MARKERS AND FLUID INCLUSIONS IN QUARTZ

Lai Yong (*Dept. of Geology, Peking University*)

Linhai gold deposit is located approximately 40 km south-east of Jinzhou City, Liaoni Province. The gold－bearing quartz veins are surrounded by the migmatizated plagiogneiss of late Archean age in which the extended fracture are the perfect space for quartz growthing.

The cathodoluminescence is used to study the quartz growth feature and its generations. Usually, the trace elements (e.g. Mn, Ag, Mo, Cr, Sm, Eu, Er) in crystal are the activator that influnce the formation of luminescence center. When the streams of electrons from cathode are directed onto the crystal surface, the luminescence center cause crystal luminescence. The composition of ore－bearing fluid has been changing during the growthing of minerals. So the same minerals which have different generations or the growth zones of a mineral crystal have different luminescence under the cathodoluminescence microscope. It is helpful to distinguish the different generation minerals and a crystal microstrctural marakers in which the fluid inclusions can be finded. More detail data can be gotten by means of studying fluid inclusions indifferent growth zone.

The luminescence of quartz and other minerals show that the alteration has been subjected to at least three episodes, and the gold mineralization strongly correlate with the second. Detail P－T－V－X properties of ore－bearing fluid were determined from the fluid inclusions trapped in the growth zone of quartz. The mechanism of both ore bodies location and metallognic dynamics are determined from the physicochemical phase diagrams of ore－bearing fluid system.

BORON-BEARING CHIAVENNITE AND OTHER LATE-STAGE MINERALS OF THE PROTEROZOIC LITHIUM-PEGMATITES OF UTÖ, STOCKHOLM, SWEDEN

Langhof J. and Holtstam D. *(Swedish Museum of Natural History)*

The famous Utö granitic pegmatites, which transect the old iron mines (probably mined already in the 12th century), were the first recognized lithium pegmatites in the world. The pegmatite dikes are the type locality of spodumene, petalite, manganotantalite and holmquistite (Smeds & Cerny, 1989). Although their scientific value was appreciated early, they were regarded as "wallrock" of no economical importance. The mining operations ceased in 1878 and today the dikes are inaccessible to *in situ* observations, but the waste heaps of the iron mines contain plenty of material reflecting the complex mineralogy of the pegmatites. The investigated associations originate from dump material collected in recent years.

The two main pegmatite bodies show different zoning. The northern dike partly displays a vertical layering across its tabular form, whereas the southern pegmatite shows a more symmetrical zoning pattern. Furthermore, aplitic dikes containing lithium minerals transect the banded iron formation (Pilava-Podgurski, 1956) and could be considered as offshots of the main dikes.

Three different late-stage mineral associations have been observed: (1) chiavennite, milarite and bavenite in small cavities close to the contact between narrow (0.1-0.3 m) "aplitic" dikes and magnetite-skarn wallrock, (2) helvite-genthelvite, chiavennite and milarite in druses or as fissure infillings of albite-rich zones of the main dikes and (3) wickmanite replacing stokesite in fissures transecting cassiterite-bearing albite-rich zones of the main pegmatites. Other late formed accessory minerals noted include *i.a.* apatite, manganite, epidote, friedelite, sphalerite, holmquistite and calcite.

The average composition of the Utö chiavennite (ideally $CaMnBe_2Si_5O_{13}(OH)_2 \cdot H_2O$) based on 12 point analyses (WDS) of 4 different grains, except for B and Be that were measured on a single grain using an ion microprobe, is: Na_2O 0.39, Al_2O_3 3.17, MgO 0.07, SiO_2 53.99, CaO 10.81, K_2O 0.02, Fe_2O_3 2.38, MnO 10.44, BeO 8.95, B_2O_3 1.03 and H_2O 10.20 (calc.). Cell parameters obtained from powder XRD are: *a* 8.905(3) *b* 31.229(9) and *c* 4.775(2) Å. Boron could be incorporated by the charge-coupled substitution $B^{3+}+Al^{3+} \leftrightarrow Be^{2+}+Si^{4+}$.

Members of the helvite group occur as single crystals and crystal groups exhibiting an oscillatory zonation, ranging from Mn-dominant cores to Zn-rich margins. The chemical composition, expressed as molar proportions of the end members, ranges from 2.9% danalite, 53.6% helvite and 43.5% genthelvite to almost pure end member genthelvite. The helvite group minerals show no fluorescence effect under SW or LW ultraviolet light. Presence of late-stage Mn- and Zn-rich solutions and local break-down of early formed beryl, are necessary conditions for the formation of chiavennite and helvite-genthelvite. Utö is the third known world occurrence of chiavennite, earlier been described from Chiavenna, Italy and the Oslo Region, Norway.

References:
Pilava-Podgurski, N. (1956). *Sveriges Geologiska Undersökning*, **C 541**, 1-54.
Smeds, S.-A. & Cerny, P. (1989). *Geologiska Föreningens i Stockholm Förhandlingar*, **111**, 361-372.

COMPLEX INVESTIGATION OF ELPIDITES CHEMICAL COMPOSITION

M.I.Lapina, A.V.Mokhov, and P.M.Kartashov
(Institute of Ore Deposits (IGEM RAS), Moscow)

Elpidite is a conventional name of aqueous so-

dium zirconium silicate $Na_2Zr(Si_6O_{15}) \times 3H_2O$. However, beside the sodium elpidite, its isostructural K- and Ca- varieties have been found. Therefore, as a matter of fact, the existence of elpidite group of minerals with the isomorphous substitution between Na, K and Ca should be admitted. Investigations have been performed with the TEM and does not allow estimate any real percentage of those elements and its limits. This restriction was the result of conventional analysis style on TEM based on EDS spectrum normalization to 100 percent.

The aim of present work was to estimate the concentrations of Na, K and Ca and recalculate former TEM results in order to define the limits for isomorphous capacity of elpidites. Using the TEM of "JEM 100C" type combined with the EDS spectrometr have analysed more than 10 elpidite samples from Mongolia, Canada and Kola Peninsula, Russia. All those minerals have been checked by electron microdiffraction for the elpidite-style internal structure. Two samples from all studied-Na-elpidite from Lovozero massif and Na-K-Ca-elpidite sample X6Y-9002/1 from Mongolia - were found to be the most homogeneous on microscopic level. The samples were analysed with the "Camebax-Microbeam" microprobe. In order to avoid sodium loss, the analyses were performed under following conditions: 20 kV; 1.5 nA , 1 sec.

More than 130 microprobe analyses of different elpidite particles which had been obtained earliez with the use of VOSTOK software on the TEM, have been recalculated using the microprobe data. The results plotted on a three-dimentional diagram show a style and limits of isomorphous elements substitutions in the elpidite structure.

• THE ACCUMULATION KINETICS OF $[AlO_4]^\circ$ CENTERS IN QUARTZ.

Larikov A.L. (*Institute of Geochemistry, Mineralogy and Ore Formation, Kiev, Ukraine*)

The interest to accumulation process of paramagnetic centers $[AlO_4]^\circ$, detected by ESR and optical spectroscopy, is justified by the substantial role of quartz in rock minerals. Aluminum is the most pervasive impurity in natural quartz. The radiation effects in natural quartz is an important source of information about geological history of the rocks (Larikov et al., 1991).

The recent investigation on the behavior of aluminum impurities centers permits to derive kinetics equations for this process. The equations described the process of holes trapping at oxygen ions, the escape of alkali ions and two recombination variants of the $[AlO_4]^\circ$ centers. In first case the alkali ions are trapped again, in the second proton is trapped forming centers $[AlO_4/H]^\circ$ (Halliburton et al., 1981).

The kinetics equations agree very well with the experimental results. The sum of $[AlO_4]^\circ$ + $[AlO_4/H]^\circ$ centers trend to maximum. The maximum is defined by the probability of escape of the alkali ions and its trapping by aluminum center, as well as by aluminum content.

The second curve with typical maximum decreases to a value which is determined also by the probabilities of hole trapping and proton trapping at aluminum center.

The equations permitto obtain, on the basis of the experimental data, the probability of the processes, related to peculiarities of quartz structure and its impurities.

The accumulation kinetics of $[AlO_4]^\circ$ centers permit to ameliorate the laboratory procedure of irradiation for the evaluation of the age of the rock contained quartz.

References:

Halliburton, L.E., Koumvakalis, N., Markes, M.E., Martin, J.J. (1981). *J Appl. Phys.*, **52**, 3565–3574.

Larikov, A.L., Shumski, A.A., Brik, A.B., Matyash, I.V. (1991). *Geochemya*, **10**, 1510–1513.

IGNEOUS ROCKS OF THE 1.87-1.82 GA OLD AKITKAN ANOROGENIC VOLCANO-PLUTONIC BELT: A SOURCE OF ORE MATERIAL OF THE HERCYNIAN RARE METAL AND POLYMETALLIC DEPOSITS OF THE NORTH BAIKAL REGION

Larin A.M., and Neymark L.A., *(Inst.of Precambrian Geology and Geochronology RAS)*

North Baikal Region (NBR) is situated in southern surrounding of the Siberian platform and belong to a typical polycyclic Early-Late Proterozoic orogenic domain which was partly reworked during the Hercynian orogeny. Within the NBR the Akitkan anorogenic volcano-plutonic belt (AAVPB) can be distinguished, which traced more than 1000 km along the margine of the NBR and Siberian platform. U-Pb zircon age for the most part of the AAVPB igneous rocks yields 1866+/-6 Ma. Igneous rocks of this belt exhibit within-plate features and silicic rocks are represented by A-type granites. The granites and acid volcanics are characterized by high contents of K, F, Rb, Zr, Y, Nb, Ba, U, Th, Pb, Be, Sn and REE.

The number of deposits (rare metal pegmatites and quartz-amazonite veins, tin-polymetallic skarns, polymetallic veins and stratabound carbonate-hosted Pb-Zn deposits) are spatialy associated with AAVPB. There are different opinions about the age and genesis of these deposits and ages of them estimated by various authors differ from Early Proterozoic to Late Paleozoic.

Pb-Pb and U-Pb isotopic systematics were studied in different magmatic rock types of the AAVPB and in different ore deposit types. The following results were obtained.

1. Zircon from rare metal quartz-amazonite vein demonstraites a concordant U-Pb age of 321+/-11 Ma.

2. Galenas from deposites are characterized by homogenous Pb isotope compositions within each deposit and the data are radiogenic.

3. Pb-isotopic data for the acid-leached feldspar residues from igneous rocks of the AAVPB, pegmatites and quartz-amazonite veins as well as ore galenas form linear trend in the $^{207}Pb/^{204}Pb$ - $^{206}Pb/^{204}Pb$ plot. This trend represents "T_1-T_2 isochron". For T_1 = 1866 Ma (U-Pb age of the AAVPB magmatic rocks) the estimation T_2 = 320 Ma has been obtained. This age estimation is of a good agreement with U-Pb age of a quartz-amazonite veins.

The new geochronological and Pb-isotopic data suggest that studied rare metal, tin-polymetallic, polymetallic deposits including stratabound carbonate-hosted Pb-Zn deposits of the NBR were formed during Hercynian tectonic event at the cost of crustal material of the AAVPB.

CATION DISORDER EFFECT ON MAGNETIC PROPERTIES IN $ZnFe_2O_4$ SPINEL

Larsson L., Annersten A. *(Inst. of Earth Sciences, Uppsala Univ.)* and Nordblad P. *(Inst. of Technology, Uppsala Univ.)*

The temperature dependent, intracrystalline cation distribution in $ZnFe_2O_4$ spinel is of importance for the magnetic properties, as observed in the vicinity of the magnetic ordering temperature ($T_N \approx$

10 K) by Mössbauer spectroscopy and magnetization measurements. The strength of the magnetic couplings and the distributions of the hyperfine fields are found to be dependent on the number of ferric ions, available in the tetrahedral site. In this spinel, at such low temperatures, there is a co-existence of magnetic phases.

$ZnFe_2O_4$ is usually considered as a totally ordered spinel, i.e. all Fe^{3+} ions in the octahedral B-site, represented by the inversion parameter, x = 0. The disorder, and consequently x, increase with the number of Fe^{3+} ions in the tetrahedral A-site.

A previous X-ray diffraction refinement study on the very same samples of this synthetic $ZnFe_2O_4$ spinel presented increasing disorder with increasing annealing temperature (O'Neill, 1992): x(650°C) = 0.087(22) to x(950°C) = 0.198(19). Also our low temperature Mössbauer spectroscopy study shows evidences of divergence from total order and further, supports the obtained x-values.

In order to characterize the magnetic features, magnetization measurements were performed in a SQUID magnetometer in zero field cooling and in field cooling. The results with a splitting of the susceptibility curves, strongly indicate spin glass like properties for $ZnFe_2O_4$. With increasing disorder there is a trend of increasing magnitude of the susceptibility (from the order of 10^{-3} to 10^{-2} emu/g), and spin glass transition temperature. T_N, however, is found to be nearly unaffected by the degree of order. For the most ordered sample, T_N is higher than the spin glass transition temperature, indicating an antiferromagnetic region occurring between the high temperature paramagnetic and low temperature spin glass like regions.

The Mössbauer spectra were recorded at 4.2 K, slightly below T_N, both in zero field and in applied external magnetic fields. With increasing disorder there is a simultaneous increase of the magnetic hyperfine fields from 46.5 T to 49.4 T (weighted mean values). Several sub-sets of six-line patterns with different hyperfine fields, derived from different local surroundings of the ferric ions, contribute to the resulting spectra. The 2:nd and 5:th lines are present, also in the in-field spectra, pointing at a non-collinear alignment of the magnetic moments. The distribution of the resulting hyperfine fields, in direction as well as in magnitude, is dependent on the cation distribution, observed as an increasing strength of magnetic couplings between the two sites, and an increasing collinearity of magnetic moments with increasing disorder.

References:
O'Neill, H.St.C. (1992). *Eur. J. Mineral.*, **4**, 571-580.

NEW ADVANCES IN GEOSPEEDOMETRY: APPLICATIONS TO TECTONIC RATES IN THE CASCADES CORE COMPLEX, WASHINGTON, USA

Antonio C. Lasaga, David A. Evans, Mark T. Brandon, Jay J. Ague (Department of Geology & Geophysics, Yale University, P.O. Box 6666, New Haven, CT 06511)

At equilibrium, the chemical composition of any given mineral is a function of pressure, temperature, and the composition of any minerals and/or fluid composition with which it is in reversible contact. If kinetics are also important, then the composition will be a function of the growth rate and mechanism of the mineral as well as of the surface kinetics in the mineral and of the transport processes along grain boundaries either dry or through the presence of a fluid medium. Chemical zonation in minerals is a result of the combined effects of 1) the initial growth zonation in the crystal, 2) the variation in the composition at the boundary of the grain as a result of changes in external conditions and 3) diffusion (usually bulk) within the mineral grain. If the variation of diffusion coefficients with chemical composition, P and T are known, then the chemical zonation can be used to infer powerful deductions about the variations in external conditions that the particular grain experienced.
Note that nowhere is time included in P-T paths except with additional geochronology. Interestingly, the expected modifications by 2) and 3), however, lead to a potentially much more powerful inversion that can extract detailed P-T-t paths, not just a cooling or heating rate. The power of such an inversion has only very recently been appreciated and applications of zoning profiles to constraining possible tectonic processes are just now being carried out.
We have applied the new geospeedometry approach to metamorphic rocks in the Cascades Core Complex. The Chiwaukum Schist on the NE side of the late Cretaceous Mount Stuart batholith shows evidence of a low-P contact metamorphism, followed by a higher-P amphibolite-facies regional metamorphism. The new geospeedometric methods have been applied to garnet crystals from the Chiwaukum Schist collected along an east-west 3.5 km-long profile oriented perpendicular to the contact with the batholith. The results support the conclusion of some workers that emplacement of the batholith was followed by burial and regional metamorphism. Burial from about 11 km to at least 22 km and then subsequent uplift to about 8 km, all occurred between 95 Ma, the age of the batholith intrusion, and about 87 Ma, the estimated age for cooling of the schist below 500 C. The geospeedometry for different garnets predicts a thermal history with variable cooling rates. The obtained geospeedometric T(t) functions, however, can be quite nicely fitted by a a very fast uplift and erosion model with uplift rates around 0.8 to 1 cm/yr (8 to 10 km/Myr). Rapid unroofing appears to follow shortly after the climax of crustal thickening within the Cascade metamorphic core and may be related to erosional and/or tectonic denudation within a mountainous collisional orogen.

SPATIAL SCALES ASSOCIATED WITH MINERAL KINETICS AND METAMORPHIC IMPLICATIONS

Antonio C. Lasaga, and Danny M. Rye (Department of Geology & Geophysics, Yale University, P.O. Box 6666, New Haven, CT 06511)

A critical concept that is needed to appraise properly the dynamics of systems that couple both fluid flow and the kinetics of chemical reactions is that of steady state. The establishment of steady state producs a region that is never close to equilibrium. Such non-equilibrium spatial regions are commonly accepted as playing a key role in low-temperature geochemistry. However, the extent of this region for metamorphic systems is shown to reach lengths ranging from fractions of meters to at least hundreds of meters. Of great note is that these conclusions were reached using kinetic data measurable in laboratory time scales at high temperatures. The interplay of these steady state spatial scales with the different length scales of lithologic units can lead to complex non-equilibrium behavior. At steady state, any locality not at equilibrium will remain so, until one of the reactant phases is completely consumed. As reactant phases are consumed, the region of non-equilibrium will shift in a manner governed by the details of fluid flow, the thermal evolution, and the chemical kinetics within the reaction zone. Such steady

state non-equilibrium regions can have a siginificant effect on our models of isograd development. For example, equilibrium $T - X_{CO_2}$ reaction curves may be significantly overstepped during metamorphic events. Furthermore, the overstepping of metamorphic reactions results in the possibility that several reactions can occur concurrently, including metastable reactions. In fact, this possibility requires us to keep track of all possible metastable reactions when considering observed phase assemblages. Extensive reaction far from invariant points in open systems and the concurrent operation of several metastable reactions will produce a sequence of mineral assemblages that, in some instances, would be consistent with the sequence of reactions predicted by an equilibrium model. This drastic deviation from the scenario based on no-flow and infinite-kinetics leads to the conclusion that isobaric invariant points and singular points may not necessarily be the loci of identifiable isograds in the field. To properly interpret the field data, additional factors such as mineral abundances, rock texture, heating rate and reaction kinetics must be introduced. These concepts can be illustrated with data on the contact aureole around the Marysville Stock, Montana, USA.

"DECOUPLED" ELEMENT PARTITIONING AND ZONATION IN GARNET AND BIOTITE FROM AMPHIBOLITE-FACIES METAPELITES OF WEST SUDAN

Lattard D. and Brunsmann A. *(FG Petrologie, Technical University, Berlin, Germany)*

Metamorphic rocks often show disequilibrium by mineral zoning and reaction textures, reflecting successive stages of their P-T evolution. P-T estimates for each stage are usually gained from several geothermobarometrical calculations based on different mineral equilibria. The pre-requisite for these calculations is that the distribution of *all* elements between the mineral phases at the considered locations reflects *one single* equilibrium stage. However, since the kinetics of intracrystalline diffusion is not only mineral- but also element-specific, single elemental concentrations at one point of a crystal may correspond to different equilibrium stages during the metamorphic evolution. The zonation patterns for different elements or - in case of unzoned crystals - the elemental concentrations throughout the crystal may thus be "decoupled".

We report here examples of decoupling of the concentrations of Ca vs. Fe, Mg and Mn in garnet and of Ti, Al, Na and K vs. Fe and Mg in biotite from metapelites of the basement of the Meidob Hills (W-Sudan). The (presumably pan-African) metamorphic evolution of this basement is characterized by a clockwise P-T path with peak conditions in the upper amphibolite-facies (T: 700-750°C, P: 7-9 kbar) followed by decompression and cooling (Lattard et al., 1993). The metapelites contain Grt-Bt-Sil-Qtz-Pl ±Ky±Ms±Kfs±Gr±Ilm.

Only the largest garnet porphyroblasts (r>2.5 mm) have kept prograde zoning with concentric bell-shaped Mn patterns in the core. All porphyroblasts show a strong increase of the Mn content at their rims, reflecting retrograde garnet resorption. Both prograde and retrograde zoning involve Mn, Mg and Fe, which reflects equilibria with other Fe-Mg-Mn phases. Ca shows more complicate, occasionally acentric, prograde zoning patterns governed by the GASP equilibrium. The Ca contents at the rims vary strongly, with generally low values, but also high (prograde) ones locally preserved, e.g. in pressure shadows. This implies that the re-equilibration of the GASP assemblage on the retrograde path occurred only very locally, in relation to deformation patterns.

Biotite crystals are occasionally zoned, e.g. with increasing Al contents towards neighbouring kyanite. The composition of the biotite crystals is highly dependent on their textural position. Mg/Fe is higher in crystals in direct contact with or enclosed in garnet as in matrix biotite, as already reported in other metapelites (e.g. Tracy et al., 1976; Robinson, 1991). However, primary biotite inclusions differ from crystals grown in embayements in garnet porphyroblasts through lower K/Na and, in some samples, higher Ti and Al contents. This indicates that the last retrograde biotite re-equilibration involved only Fe-Mg exchange with garnet on a local scale.

In both garnet and biotite, the Fe-Mg exchange appears to outlast other processes of re-equilibration during the retrograde path. Garnet-biotite thermometers can thus record closing temperatures for this exchange. On the contrary, geobarometric equilibria involving redistribution of Ca in garnet (GASP) or of Al in biotite (Patino Douce et al., 1993) probably record earlier stages of the metamorphic evolution. Because of the decoupling of the Fe-Mg partitioning from that of Ca (garnet) or Ti, Al, Na and K (biotite) during the retrograde evolution of such metapelites, multi-equilibrium geothermobarometry (e.g. TWEEQU of Berman, 1991) must be used with great caution.

References:
Berman, R.G. (1991). *Can. Mineralogist*, **29**, 833-855.
Lattard, D., v. Goerne, G., Franz, G. (1993). *In*: "Geoscientific Research in Northeast Africa", U. Thorweihe & H. Schandelmeier, eds. Balkema, Rotterdam, 161-163.
Patino Douce A.E., Johnston, A.D., Rice, J.M. (1993). *Am. Mineralogist*, **78**, 113-131.
Robinson, P. (1991). *Am. Mineralogist*, **76**, 1781-1810.
Tracy, R.J., Robinson, P., Thompson, A.B. (1976). *Am. Mineralogist*, **61**, 762-775.

PGE-BEARING ANORTHOSITES OF PANSKY TUNDRA LAYERED INTRUSION: ORIGIN FROM PLAGIOCLASE CRYSTAL MUSH

Latypov[1] R.M., Halkoaho[2] T.A.A., Alapieti[3] T.T.([1]Geological Institute, Kola Science Centre, Apatity, Russia,[2] Department of Geology, University of Turky, Finland. [3] Department of Geology, University of Oulu, Finland)

Anorthosites are confined to the lower layered unit of Pansky Tundra intrusion composed mainly of gabbronorites with minor amounts of norites. Anorthosites are found to differ strongly from mafic rocks in that they (1) form dykes and sills intruding gabbronorites and containing them in the form of xenoliths, (2) show intensive deuteric alterations with simultaneously fresh surrounding gabbronorites, (3) have abruptly higher whole-rock Fe/Fe+Mg and Fe^{3+}/Fe^{2+} ratios, alkali and volatile contents, (4) are characterized by decoupling of whole-rock Fe/Fe+Mg ratios and An contents of plagioclase, (5) host about 80% of sulfide mineralization enriched in PGE, with the rest being contained in gabbronotites directly surrounding ore-bearing anorthosites.

Origin of anorthosites is attributed to injection into partly consolidated gabbronorites the plagioclase crystal mush originated by accumulation of plagioclase in the residual melt of the inrusion magma chamber. The mush is supposed to be emplaced throuth the series of feeders and spread out predominantly concordant with gabbronorites layering forming simple sills and systems of subparallel sills.

Crystallization of mush containing trapped highly differentiated and fluid-saturated residual melt can explain evolved composition of anorthosites and their intensive deuteric alterations. Primary inhomogeneity in degree of differentiation of trapped melt in different parts of mush intensified by its equilibration with varying amounts of unterstitional mafic minerals can produce broad range of whole-rock Fe/Fe+Mg ratios compared with the limited variability of average An contens of plagioclase. Concentration of Fe,Cu,Ni, PGE and related elements in the residual melt could lead to liquation of immiscible sulfide liquid in the mush that provided formation of PGE-rich sulfide mineralization in anorthosites bodies. The similar one in gabbronorites can be connected with expulsion of some of the transporting melt into host rocks during emplacement of crystal mush.

A BENTONITE DEPOSIT FROM SOUTHERN ITALY (S. CROCE DI MAGLIANO, CB): TRACE ELEMENTS DISTRIBUTION AND CRYSTALLOCHEMISTRY OF THE EXPANDABLE PHASE.

Laviano R. (Dept. Geomineralogico, Univ. of Bari) and Mongelli G. (DiSGG, Univ. Basilicata)

A set of 11 Bentonite samples were collected from S. Croce di Magliano (Cb province, southern Italy).

Concentrations for major elements and Ba, Ni, Cr, V, Rb, Sr, Zr, Nb, Sc, Th, U and REE for the whole rock and the <2μm size fraction, were obtained by XRF and INAA. The mineralogical assemblage was determined by XRD and SEM-EDX investigations.

In the whole rock are recognised clay minerals, quartz, cristobalite, feldspars, carbonates, micas, apatite, Fe- and Mn-oxi-hydroxides and zeolites. Among the clay minerals a Ca-Na beidellite with Fe and Mg in the octahedral sheet is the more abundant phase. Its crystallinity degree is high (v/p = 0.90 Å) and the crystallites size ranges from 80 Å to 100 Å. A related typical crystallochemical formula is:

$$(K_{0.08}Ca_{0.71}Na_{0.30})(Ti_{0.03}Fe_{0.43}Al_{2.60}Mg_{0.75})(OH)_4(Si_{7.47}Al_{0.53})O_{20}$$

Concerning the trace elements distribution, REE show a large variability both for the whole rock (La 63-128× chondritic, Yb 2.8-14.0× chondritic) and the <2μm size fraction (La 51-134× chondritic, Yb 2.7-13.3× chondritic). Furthermore, as for the whole rocks, data normalised to the upper continental crust (Condie, 1993) reveal a subset of samples significantly depleted in Sc, V, Cr and Ni, probably suggesting that material with different original composition contributed to the formation of the studied bentonite deposit.

Reference:
Condie, K.C. (1993). *Chem. Geol.*, **104**, 1-37.

• THE CHARACTERIZATION AND PROVENANCING OF WHITE AND COLOURED MARBLES USED IN ANTIQUITY

Lazzarini L. (*L.A.M.A.,Dip. Storia dell'Architettura, I.U.A. Venezia*).

The word marble comes from the Greek verb "marmairo", which means "to shine", and is correctly applied either ethymologically or petrographically to metamorphic carbonatic rocks. The great fortune of crystalline marbles throughout the centuries as statuary and architectural stones, derives from their generally homogeneous and isotropic fabric, very good workability and easy polish, as well as from their abundance, especially in the Mediterranean area. It was in fact there, more precisely in the Cyclades that white marbles started to be used from the third millennium BC for small idols, also diffused outside the Cycladic islands. However the apexes of marble use were reached later in the Greek and Roman era, and more recently in the neoclassic and contemporary periods.

The identification of white and coloured marbles used in the past through a scientific characterization provides very valuable information for historical and archaeological studies, as well as for authentication of doubtful artifacts and the determination of marble sources for restorations. Up to now there does not exist a single analytical technique which may solve the problem of white marble provenance, in spite of the fact that traditional minero-petrographic studies, trace-elements and ESR analyses, stable C and O isotopic measurements have been fully applied for the solution of the problem, the advantages and disadvantages of all these techniques being fully discussed in the paper. At present the most successful approach is the combination of detailed petrographic studies in thin section and isotopic analysis, both taking advantage of a well developed international data bank on reference marble standards from ancient quarries. A few case-studies of identification of the marble of statues and monuments. as well as an example of how archaeometric studies of the "Rosso Antico" and "Cipollino Verde" marbles may help Earth sciences, are presented.

EXSOLUTION, DISLOCATIONS, DISSOLUTION AND REPRECIPITATION IN ALKALI FELDSPARS

Lee, M.R., Parsons, I. (*Dept. of Geology and Geophysics, Univ. of Edinburgh*), Waldron, K (*Dept. of Geology, Colgate Univ.*)

The morphology and periodicity of exsolution microtextures in strain-controlled coherent crypto- and micro-perthitic alkali feldspars are functions of bulk composition and cooling rate. Median bulk compositions adopt zig-zag or lozenge morphologies, devoid of dislocations, to minimise elastic strain. The process involved is Na-K interdiffusion down chemical potential gradients dominated by elastic strain energy. The total energy is ~2.5-4 kJmol^{-1} and it provides the driving force for subsequent intra-crystal solution-reprecipitation which leads to the pervasive development of turbidity and sub-grain formation.

There are no detailed studies of the microtextures in Or-rich alkali feldspars typical of many subsolvus granites. We have used an HF etching and SEM technique, and TEM, to characterise K-feldspars from several granites. All contain straight lamellar micro- and crypto-perthites in which strain is partly relieved by sets of edge dislocations forming extended elliptical loops with long axes parallel to b and in the Murchison plane (~$\bar{6}$01). These dislocations provide pathways for water ingress into crystals, accounting for the common observation that exsolution lamellae are often the site of turbidity. In and around lamellae, albite and adjacent orthoclase are replaced by microporous subgrain textures. Elsewhere in most crystals solution-reprecipitation along fractures leads to pervasive recrystallisation. Dislocations are exploited during weathering to form etch pits and are often sites of clay mineral growth. The microtextural evidence shows that the main mechanism of ^{18}O exchange in feldspars at low T is likely to be solution-reprecipitation. The cryptoperthites form at T<400°C and the dislocations at even lower T, and it is clear that the reactivity of common alkali feldspars will increase and their Ar retentivity will decrease markedly at this T.

VOLCANIC FLUIDS FROM VULCANO (AEOLIAN ISLANDS, ITALY): CONSTRAINT FROM BORON ISOTOPIC COMPOSITION AND CONTENT

Leeman W.P. *(Keith-Wiess Rice Univ., Houston, USA)*; Pennisi M., Tonarini S., Ferrara G. *(IGGI, CNR, Pisa, Italy)*; and Pennisi A. *(DST, Univ. of Catania, Italy)*

$^{11}B/^{10}B$ ratio has been determined on condensates of fumarolic fluids of Fossa Grande (F5 fumarole), covering a span of time of about 20 years. $^{11}B/^{10}B$ ratios, reported in permil to NBS

standard SRM 951, vary from -4 to +3, with a general increase with time observed from 1978 to 1992. This trend is interrupted (significant $\partial^{11}B$ decrease) in 1985, 1989 and, in particular, in 1993 when significant changes in B concentration were recorded, together with other geochemical parameters.

The isotopic evolution of B cannot simply be related to a sea water input into the volcanic system because of the positive correlation observed between $\partial^{11}B$ and boron concentration. In fact, SW is enriched in ^{11}B and has a B concentration of about 5 ppm, while the boron content of condensates is about 30 times higher.

$\partial^{11}B$ from condensates of medium to high temperature fumaroles have been determined since 1992. The isotopic characterization of the fumarolic field is under study.

$\partial^{11}B$ and $^{87}Sr/^{86}Sr$ on hydrothermal waters of Vulcano were determined with the aim to better understand the volcanic system. Sr isotopic compositions provide a clear picture of the relation between geothermal fluids and associated rocks, and so a combinated B and Sr isotopic study can be useful to understand the sources of thermal water. The analyzed thermal waters of Vulcano have B and Sr contents ranging from 2 to 9 ppm and 0.5 to 2 ppm respectively and $\partial^{11}B$ ranging from -7 to 0.92 permil. The Sr isotopic composition varies from 0.7047 to 0.7067 (rocks isotopic composition is in the range 0.7044-0.7053; Del Moro personal communication). The combined isotopic data are correlated by an exponential curve (r^2= 0.91), with ^{11}B and ^{87}Sr enriched end-member toward SW values and the depleted ^{11}B and ^{87}Sr ones related to the volcanic rocks. The fit according to an exponential curve is strongly linked to the higher value of $\partial^{11}B$; in order to verify the validity of this relationship Vulcano thermal waters were compared for $\partial^{11}B$ and $^{87}Sr/^{86}Sr$ with the first data belonging to Mount Etna thermal waters. These latter vary from -5 to +20 permil and 0.7035 to 0.7088 for $\partial^{11}B$ and $^{87}Sr/^{86}Sr$ respectively, suggesting an interaction between at least two reservoirs. The depleted $\partial^{11}B$ and $^{87}Sr/^{86}Sr$ reservoir seems to be associated to the volcanic rocks, while the enriched one could be: 1) SW, in the thermal waters sampled near the coast; 2) water equilibrated with marine sediments in those sampled at the edge of the volcanic edifice.

INDIUM IN BASE-METAL SULFIDES FROM VARIOUS OCCURRENCES : NEW DATA

O. Legendre (*BRGM, Orléans, France*)

Economic concentrations of indium in sulfide ores, although present in various types of deposit, seem to be commonly related to polymetallic volcanogenic massive sulfide deposits (VMS) or xenothermal-type deposits (XT) on condition that tin is also present.

The economic carriers of indium in such deposits are sphalerite, chalcopyrite and, to a lesser extent, minerals of the stannite-kesterite series (*i.e.*, $Cu_2(Zn,Fe)SnS_4$).

A survey of indium content in sphalerite, chalcopyrite and stannite-kesterite from VMS and XT deposits of England, France, Portugal, Bolivia, Tasmania and Japan was carried out using an electron-probe micro-analyser. The results are presented in Table 1.

Particular attention has been paid to the mode of In incorporation in the analysed phases. In sphalerite, the known coupled substitution of InCu for Zn has been recognised for all samples.

In stannite and kesterite, which present the highest In concentration among the three phases analysed, the mechanism of incorporation corresponds to that described by Shimizu *et al* (1986) for sakuraiite, but with (Fe,Zn)In substitution instead of CuSn.

In chalcopyrite, presence of In is correlated to an excess of Cu relative to stoechiometry, with the correlation being close to one In for one Cu. Incorporation of In in the chalcopyrite structure therefore seems to be a coupled substitution of CuIn for Fe.

Analyses of coexisting stannite-sphalerite pairs and derived temperatures based on the geothermometer of Nakamura *et al.* (1982) show that partition of In between the two minerals is directly related to the temperature of formation of stannite and sphalerite, In being preferentially enriched in stannite at high temperatures.

Thus, it appears that In is preferentially concentrated in minerals having a sphalerite-type structure, i.e. a tetraherdron-based structure with a metal/sulfur ratio of 1, provided that charge balance is maintained and that the replaced cation has an ionic radius similar to that of In^{3+}. This observation does not preclude the presence of In in other minerals such as sulfosalts, or cassiterite. Incorporation of In in sphalerite-type minerals in an ore-forming process also seems to be related to crystallization order rather than being strictly controlled by crystal structure.

Table 1: Range of In content (wt%) for the analysed phases

Localisation	**Stannite**	**Sphalerite**	**Chalcopyrite**
Ste Agnes, Eng.	0.31-0.38	—	0.12-0.18
St George, Eng.	0.01-0.12	0.01-0.03	0.00
Les Chaillats, Fr.	0.00-0.03	0.00-0.07	0.00-0.05
Corvo, Port.	0.00-2.04	0.00-5.45	0.00-0.14
Chilena, Bol.	0.02-0.04	0.00-0.07	—
San Luis, Bol.	0.00-0.42	0.00-0.38	0.00-0.05
Oonah mine, Tas.	0.01-0.1	—	0.02-0.05
Ikuno, Jap.	0.30-4.42	0.02-0.41	0.06-0.15

References:

Nakamura Y. and Shima H. (1982). *Geol. Soc. of Japan Joint Meet.* A-8

Shimizu M., Kato A. and Shiozawa T. (1986). *Canadian Mineralogist*, **24**, 405-409

NEW MINERALS OF ALUNITE: THEORETICAL FORECAST

Legkova G.V. (*Inst.of Geochemistry,Mineralogy and Ore Formation, Ukrainian Academy of Sciences*)

Alunite is a stratified sulphate having the formula of classic composition $X_1Y_3[ZO_4]_2(OH)_6$, where X - K^+, Na^+..., Y - Al^{3+}, Fe^{3+}..., Z - S^{6+}, W^{6+}... The chemical structure of alunite may be represented schematically as follows:

```
           / O – Y(OH)2 – O \
X – O – Z – O – Y(OH)2 – O – Z – O –
           \ O – Y(OH)2 – O /
```

Usually in mineral forming medium, where the alunite is crystallized, not only complex ions $Y(OH)^{+}{}_{2}$ but ions $Y(OH)^{2+}$ and Y^{3+} are present (Kashkay, 1970). It is supposed that the formation of new minerals of alunite group depends on the entering the $Y(OH)^{2+}$ or Y^{3+} ions in the crystal structure. The crystallization of minerals takes place when maximum concentration of ions mentioned in a solution.

At higher acidity and lower temperature of a solution (compared to those of 'classic' alunite) it is assumed the formation of new mineral, with the participation of complex ions $Y(OH)^{2+}$, having the formula $X_1Y_3[ZO_4][YO_4](OH)_3$ and chemical structure similar to alunite one:

```
           / O – Y(OH) – O \
X – O – Z – O – Y(OH) – O – Y – O –
           \ O – Y(OH) – O /
```

The alunite crystallization with Y^{3+} ions in structure is possible at even smaller values of P_h and temperature. Then a new mineral has the formula $X_1Y_3[ZO_4]_2[YO_3]_2$, and its schematical structure is more complicated but remains similar to alunite:

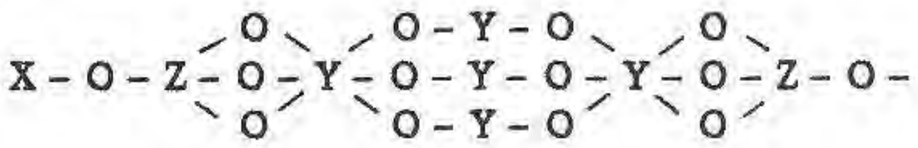

It has been suggested the chemical reaction of new mineral formation as the transformation of feldspar by acidic solutions. It was estimated the fields of stability for new minerals.

To confirm by experiment the existence of these theoretically predicted minerals, it is necessary to use not only generally accepted X-ray diffraction and thermal methods but electron probe microanalysis as well.

References:
Kashkay, M.A. (1970). *Alunites, their genesis and use.* Moscow, Nedra, v.1, 400 p.

PAULINGITE, A NEW OCCURRENCE FROM VINARICKÁ HORA, CSFR

Lengauer C.L., Giester G. and Tillmanns E.
(*Institut für Mineralogie und Kristallographie der Universität Wien*)

Paulingite, first described by Kamb & Oak (1960), had only been reported from localities in U.S.A. and Canada, until Hlousek *et al.* (1988) described paulingite together with phillipsite in cavities of basaltic rocks of Vinarická Hora in the north of Kladna (CSFR). Because the samples exhibit perfectly developed, colourless dodecahedral crystals with a diameter up to 2 mm, a detailed investigation of this occurrence was done by EMX, TGA and single crystal X-ray analyses.

Based on an EMX analysis of four different crystals and a TGA with 3.1 mg sample the structural formula (Z=16) is $(Ca_{2.58}K_{2.30}Ba_{1.39}Na_{0.76})\ (Al_{11.52}Si_{30.59}O_{84}) \cdot 33H_2O$ with minor amounts of Mg (0.05), Sr (0.12) and Fe (0.04) at the Me sites. With respect to literature data (Tschernich & Wise, 1982), the investigated paulingite is characterized by a significantly lower Si/Al ratio of 2.66 and a high Ba-content. A thermal treatment of some crystals at 570 K yielded only diffuse reflexions indicating the decomposition of paulingite. This is in aggreement with the thermogravimetric measurement, which showed a two step weight-loss at 350 K (-11 wt. %) and 600 K (-3 wt. %), respectively. The refractive index is 1.476(2).

Weissenberg and precession photographs display no forbidden reflexions, thus confirming space group *Im3m*. The obtained lattice parameter have a value of a_o = 35.100(5) Å, which is higher than the reported data according to the low Si/Al ratio. The single crystal refinement confirms the framework structure given by Gordon *et al.* (1966). By difference fourier synthesis three fully and some partially occupied Me sites and two groups of water sites were detected in the channels.

References:
Gordon,K.E. Samson,S. & Kamb,W.B. (1966). *Science*, **154**, 1004-1007.
Hlousek,J. Veselovský,F. & Rychlý,R. (1988). *Cas.Mineral.Geol.*, **33**, 109.
Kamb,W.B. & Oak,W.C. (1960). *Amer.Mineral.*, **45**, 79-91.
Tschernich,R.W. & Wise,W.S. (1982). *Amer.Mineral.*, **67**, 799-803.

THE GRADE OF METAMORPHISM IN THE META-PELITES OF THE INTERNAL LIGURID UNITS (NORTHERN APENNINES, ITALY)

Leoni L., Marroni M., Sartori F., Tamponi M. (Dept. of Earth Sciences, Univ. of Pisa)

The metamorphic grade of the Internal Ligurid Units (Northern Apennines, Italy) has been investigated in metapelites through mineral assemblages, illite "crystallinity", polytypism and b_o and chlorite "crystallinity".

All these Units, known as Cravasco-Voltaggio (CV), Mt.Figogna (MF), Mt.Gottero (MG), Colli-Tavarone (CT) and Bracco-Val Graveglia (BVG), consist of well preserved ophiolite sequences and the associated sedimentary covers which are interpreted as remnants of the Western Tethys oceanic lithosphere. During the pre-Oligocene orogenesis this oceanic lithosphere, involved in subduction processes, has been deformed and tectonically dismembered into several units displaced from west to east. From the Sestri-Voltaggio line these Units succeed each other eastward in the following order: Cravasco-Voltaggio, Mt. Figogna, Mt. Gottero, Colli-Tavarone, and Bracco-Val Graveglia.

Every metamorphic indicator points to very-low grade metamorphic conditions for all the Internal Ligurid Units. Within these overall conditions a well defined trend is however evident. An increase of metamorphic grade is well recognizable from east to west.

On the basis of the illite "crystallinity" index the following temperatures of metamorphism have been estimated: 300-350°C (Cravasco-Voltaggio U.), 270-320°C (Mt. Figogna U.), 250-300°C (Mt. Gottero U.), 200-250°C (Colli-Tavarone U.) and 180-230°C (Bracco-Val Graveglia U.). These values are in a good agreement with those estimated from the metamorphic parageneses of the associated metabasites (Cravasco-Voltaggio, Mt. Figogna and Bracco-Val Graveglia Units) or are consistent with the tectonic setting proposed by the most recent geological models (Mt. Gottero and Colli-Tavarone Units) (Marroni, 1994).

The illite b_o shows a decrease from the western Units to the eastern ones; the pressures of metamorphism estimated through this parameter are 7 Kb for Cravasco-Voltaggio U., 6 Kb for Mt. Figogna U. and near to 4 Kb for Mt. Gottero, Colli-Tavarone and Bracco-Val Graveglia Units. These baric conditions are similar (Cravasco-Voltaggio U.) to or definitely higher (Mt. Figogna U.) than those estimated through the metabasites parageneses (6 Kb and 3-4 respectively), but strictly coherent with the recognized deformation features (Marroni, 1994). For Mt. Gottero U. no data from metabasites are available, but again the pressure value estimated in the present study (4 Kb) appears consistent with the tectonic setting. On the contrary the metamorphic pressures of Colli-Tavarone U. and Bracco-Val Graveglia U. appear overestimated with respect to those inferred from the geological data; for Bracco-Val Graveglia U. the mineral assemblages of metabasites point to a 2-3 Kb pressures. Such a discrepancy probably suggests a failure of mica b_o parameter to work as a reliable geobarometer at the onset of anchizone (temperatures below 250°C).

The opposite seems to be true for mica polytype content and chlorite "crystallinity"; these indicators of low grade metamorphism don't show any significant variations in the more metamorphic units (Cravasco-Voltaggio and Mt. Figogna Units), while significant variations related to the metamorphic grade are observed in low anchizone-late diagenesis zone (Mt. Gottero, Colli-Tavarone and Bracco-Val Graveglia Units).

References:
Marroni, M. (1994). Mem. Soc. Geol. It. (in press).

HEAVY METALS IN RECENT SEDIMENT OF TUSCANY CONTINENTAL SHELF.

Leoni L. (Dept. of Earth Sciences, Univ. of Pisa), Sartori F. (Dept. of Earth Sciences, Univ. of Pisa), Nicolai I. (Dept. for the Environment, E.N.E.A.).

As a contribution to a research program on the environmental quality of Tuscany continental shelf the distribution of heavy metals (+ Ba and As) in the bottom sediments of the area off the Tuscany coast (west-central Italy) has been investigated. The data collected on numerous surface sediments and core samples show that Ba, Cr, V, Ni, Co, Cu, Zn, Pb and As distributions result from the influx of materials both from natural and anthropogenic sources.

In the northernmost part of the surveyed area (Magra River mouth - Meloria Shoals basin) most of the positive concentration anomalies are to be ascribed to the man's influence. Pb, Zn, Cr and As show the highest and most widespread enrichments, while Cu and V have lower and more limited positive anomalies. Ni and Co distributions exhibit only few and small areas of moderate enrichment.

In the central zone (Meloria Shoals - Elba Islan basin) too the positive anomalies most conspicuous as to outcrop area those related to anthropogenic contributions; they chiefly involve Pb, Zn, Cu, As and, in part, also V. Local concentrations of Cr, Ni, Co and, to some extent, also of Zn and V, appear essentially related to natural sources; occasionally high, but commonly restricted to limited areas of coarse sedimentation, they mirror influx of natural materials derived from small mineralizations or from basic and ultrabasic magmatic rocks (ophiolites).

In the southernmost area of Tuscany continental shelf (Elba Island - Argentario Promontory basin) only a diffuse As positive anomaly covers a wide area: core data suggest an origin mostly related to anthropogenic activities, but for some parts the presence of As-rich natural materials from nearby mineralizations may also be inferred. In this basin the positive anomalies of Pb and Zn are restricted to a small area between Elba Island and Follonica Gulf; most likely they are chiefly due to inputs of modern contaminants, though a contribution of natural materials from Eastern Elba mineralizations can not be ruled out. Again, the conspicuous enrichments of Co, V, Pb and As observed in the sediments of a small area close to Montecristo Island are to be ascribed to a contribution of contaminated materials from man's activities. On the opposite, the low and restricted anomalies of Cr and Ba within the gulf of Follonica are related to natural causes such as the influence of mineralizations in the Cornia River basin.

MELTING RELATIONS IN THE Fe - Ni - S SYSTEM AT HIGH PRESSURES AS APPLIED TO THE FORMATION OF MAGMATIC SULPHIDE DEPOSITS

Leontievsky K.V., Kirkinsky V.A. (Institute of Mineralogy and Petrography, Novosibirsk 90, Russia)

During studies of inclusions in diamonds from kimberlites deposits of various world regions many sulphides have been found, the overall content of which is comparable with that of silicates. Sulphides include the following minerals: pyrrhotite, monosulphide solid solution $(Fe,Ni)_{1-X}S$, pentlandite, chalcopyrite, cubanite, pyrite, troilite, violarite-like phase, millerite, djerfisherite. Rounded forms of many inclusions suggest that sulphides have been trapped by host mantle minerals in the liquid state. As inclusions in diamonds provide the most reliable data on the mantle geochemistry, these facts are decisive evidence that sulphide play a significant role in deep-seated rocks. To clarify phase equilibria of native sulphides in the mantle, an investigation of Fe-Ni-S system, which represents the principal composition of sulphide phases at the depth, has been carried out at 6 GPa in a high-pressure "anvil-pit-toroid" apparatus using graphite ampoules.

Melting diagram of the FeS - NiS system at 6 GPa relates to III Roseboom type: the complete series of solid solutions with the minimum point at 1050°C and FeS content of about 35 mol. %. Equilibrium compositions of solidus and liquidus phases in the Fe-rich part system have been determined.

In the ternary Fe-Ni-S system at 6 GPa and 900°C the monosulphide solid solution $(Fe,Ni)_{1-X}S$ with pyrrhotite structure (Mss), that contains up to 1,8 at. % Ni, is in equilibrium with (Fe,Ni) alloy, Mss (1,8 to 38 at. % Ni) coexists with the melt and Mss, containing 38 to 50 at. % Ni, is in equilibrium with Ni-rich phase $(Ni,Fe)_9S_8$ decomposing under quenching. Pentlandite is not stable at the experiment parameters, hence in diamond inclusions it has been probably formed in the process of subsolidus reactions at lower temperature. A wide melt region exists in the system under experiment conditions, which is displaced towards Fe and Ni enrichment as compared with the region existing at atmospheric pressure. Therefore iron and nickel might concentrate in a liquid sulphide phase at temperature below silicate solidus, that may cause high migrational ability of these elements in the mantle.

A preservation of the wide region of sulphide phase at such high pressure is partly connected with the presence of additional components: carbon and oxygen. Carbon from the ampoule is soluble in sulphur-poor phases: (Fe,Ni) alloy and sulphide melt. Oxygen, which release at thermal decomposition of the container material, is fixed as admixture phase- wustite, detected in the products of the runs. Redox conditions of high pressu- re experiments are similar to C-CO buffer.

Rather low melting temperatures in the Fe-Ni-S system at high pressures, especially in the presence of some oxygen phases, suggest that sulphide melts can move at stresses and crack formation in mafic and ultramafic rocks at 'subsolidus temperatures as ore magmas. Deep-seated essentially sulphide melts in some cases appear to be a medium of native diamond crystallization.

HIGH-PRESSURE AND ULTRAHIGH-PRESSURE METAMORPHIC ROCKS IN NORTHERN KAZAKHSTAN

Lepetyukha V.V., Reverdatto V.V. and Ten A.A.
(Inst.Geol., Geophys.and Mineral., Siberian branch of Russ.Acad.Sci., Novosibirsk, Russia)

The Kokchetav anticlinorium situated in northern Kazakhstan is a Precambrian median massif surrounded by Caledonides. The Proterozoic core of the anticlinorium consists of metapelites and metabasites intensely deformed, foliated, crumpled into folds of various shape and amplitude, undergone two stage of metamorphism. By character of metamorphism, two blocks, eastern (EB) and western (WB), separated by a probable meridional fault can be distinguished. Micaceous and feldspathic disthene- and garnetiferous schists of the WB contain diamond inclusions; metabasites are eclogite boudins formed under P > 40 kbar and T = 800-1000°C. Mica schists, porphyroids and quartzites of the EB contain disthene, sillimanite, garnet, plagioclase, etc.; cordierite, gedrite and staurolite are found sporadically. Metabasites bed within schists as boudins or teared sheets; they are eclogites, amphibolites and amphibolized dolerites. Eclogites are found as boudins only, but the rest of metabasites occur mainly in the form of plate-like deformed bodies. Besides, there are lenticles of serpentinites, spinel- and garnetiferous pyroxenites and garnet-talc schists. Eclogites of the EB were formed under P = 12-14 kbar and T = 600-700°C, spinel pyroxenites - about 20 kbar and T = 900°C; the stability of gabbro allow us to determine P < 10-12 kbar. These estimations based on mineral thermobarometers testify to very heterogeneous pressure distribution during the first metamorphism stage. Pressure gradient made up no less than 1 kbar/km.

The first stage of metamorphism was 530 m.y. ago (U-Pb isotopic data for zircons; Claoue-Long et al., 1991). The second stage of metamorphism connected with amphibolite origin was 517

m.y. ago (Ar-Ar isotopic data for micas; Shatsky et al., 1993) at P about 7 kbar and T = 600-650°C.

The distribution of PT-parameters over the Earth' s surface during the second metamorphism stage was nearly even within the accuracy of determination. The formation of metapelite mineral associations occured and depended on both stages of metamorphism, however influence of the later one was felt to be more intense within the EB. It is possible to attract two mechanisms for explanation of the nature of metamorphism: considerable subsidence of the part of the crust and shearing deformations in the rocks; they both took part in pressure generation.

The first mechanism was apparently predominant with respect to the WB, and the second played a leading role in the EB where subsidence was less substantial. The grounds for that are much higher total pressure in the WB than in the EB, and extreme heterogeneity in pressure distribution in the EB. The model of direct subduction as a sole reason of high-pressure metamorphism seems to be unbelievable concerning the EB especially. Additive increase in pressure in the crust during the first metamorphism stage which could exceed 40 kbar according to numerical experiments was conditioned by slow sheared flowing within superviscous inhomogeneous medium. A proper theory on the basis of Stokes equation was developed by Ten (1993).

References:
Claoue-Long J.C. et al. (1991). *Geology*, 19, 710 - 713.
Shatsky V.S. et al. (1993). *Terra abstr.* No 4 to *Terra nova*, 5, 23.
Ten A.A. (1993). *Dokl.Akad.Nauk (Proceed.Acad.Sci.)*, **323**, 322 - 324 (in Russian).

DEGASSING KINETICS OF NATURAL CORDIERITES

Lepezin, G.G., Osorgin, N.Yu., Sokol, E.V. and Shvedenkov G.Yu. (*United Institute of Geology, Geophysics and Mineralogy, Novosibirsk, Russia*)

Degassing kinetics of cordierites has been studied using chromatography. Four specimens were investigated. Their chemical compositions are:

(1) $Na_{0.08}(Mg_{1.98}Fe_{0.03}Mn_{0.01})[Si_{5.03}Al_{3.95}O_{18}]$
(2) $Na_{0.06}(Mg_{1.57}Fe_{0.41}Mn_{0.07})[Si_{4.98}Al_{3.96}O_{18}]$
(3) $Na_{0.02}(Mg_{1.47}Fe_{0.58})[Si_{4.99}Al_{3.98}O_{18}]$
(4) $Na_{0.23}(Mg_{0.09}Fe_{1.72}Mn_{0.10})[Si_{4.99}Al_{3.98}O_{18}]$

The experiments were carried out under isothermal conditions at temperatures 600, 700, 750, 800, 900, 1000°C. (tabl.1). The results were treated by an equation, describing diffusion from sphere

$$\frac{M_t}{M_\infty} = 1 - \frac{6}{\pi^2}\sum_{n=1}^{\infty}\exp\left(\frac{Dn^2\pi^2 t}{r_o^2}\right)$$

Where M_∞ is the initial H_2O and CO_2 contents; M_t is H_2O and CO_2 content left after annealing; t is time, r_o is average size of cordierite parties. Activation energy is determined from Arrhenius equation and is equal to 31.4-43.7 Kcal/mole for H_2O and 48.4-78.7 Kcal/mole for CO_2 (tabl.1). The durations of cordierites degassing at different temperatures are summarized in tabl. 2.

Table 1
Kinetic parameters of H_2O and CO_2 diffusion in cordierites in the range from 873 to 1073 K

	N	Fe/(Fe+Mg)	Δ	$D_o, cm^2/s$	E, Kcal/mole
H_2O	1	0.015	0.223	$1.9*10^{-2}$	31.4
	2	0.230	0.234	$3.3*10^{0}$	42.7
	3	0.283	0.260	$5.0*10^{-1}$	37.4
	4	0.953	0.139	$4.7*10^{0}$	43.7
CO_2	1	0.015	0.223	$1.8*10^{0}$	48.4
	3	0.283	0.260	$2.8*10^{6}$	78.7

Table 2

	N	r_o, cm	700 °C	500 °C	300 °C
H_2O	1	0.05	5 d.	306 d.	$1.10*10^{3}$ y.
		0.2	73 d.	1.3 y.	$1.70*10^{4}$ y.
	4	0.05	1 d.	9.6 y.	$1.98*10^{5}$ y.
		0.2	162 d.	154 y.	$3.10*10^{6}$ y.
CO_2	1	0.05	310 d.	560 y.	$3.30*10^{7}$ y.
		0.2	14 y.	$8.90*10^{3}$ y.	$5.30*10^{8}$ y.
	3	0.05	3.5 y.	$1.30*10^{5}$ y.	$7.60*10^{12}$ y.
		0.2	56 y.	$2.10*10^{6}$ y.	$1.20*10^{14}$ y.

y. - years, d. - days

For example, at 700 °C and r =0,05 cm it takes 5-10 days and 310 days -35 years to liberate 95% of H_2O and CO_2 respectively. At T=300°C and r=0,05 cm the experimental duration for degassing of H_2O must be equal to $1.1*10^{3}$-$1.98*10^{5}$ years and to $3,3*10^{7}$-$7,6*10^{12}$ years for CO_2 respectively. By this means evidences indicate also that at T<700°C, r_o>0,1cm it is impossible to degass cordierites completely under the experimental conditions. The obtained data is important for practice and theory of experimental petrology. In the first place, they are permitted to estimate the experiment caring out. Secondly, it is possible to correct while in evolving of the fluid composition with the help of H_2O and CO_2 contents in cordierites.

CALCULATION OF THE DURATION OF THE MINERAL-FORMING PROCESSES (THE EXAMPLE OF CORDIERITE)

Lepezin G.G. and Sokol E.V. (*Institute of Mineralogy & Petrography, Novosibirsk, Russia*)

According to theoretical views formation of disorder phases in prograde metamorphic reactions is practically universal phenomenon. Ordering is often slow process, and it can be used as a time-scale. The hexagonal--> orthorhombic ordering transformation in cordierite is the convenient model for the investigation of structural evolution during the prolonged temperature subjection.

We found that indialites (Δ=0.0) and intermediate phases (Δ=0.10-0.16) were common in the fused sediments (ex-argillytes) from Chelyabinsk coal field (S.Ural).Their rock forming conditions may be described as a dry annealing. The typical assemblage is Cordierite+Mullite+Tridymite+Quartz±Cristobalite±Pseudo-Brookite. Glass was not detected.

There is the number of experimental studies of the changes in the structural states of Mg-cordierites in dry sistems (Langer & Schreyer,1969; Putnis,1980; Putnis & Bish, 1983; Schreyer & Schairer,1961). We attempted to evaluate these kinetic data with Avraamy-Erofeev equation. The curve lnk=f(T) is complex-shaped, depending on the type of TTT-diagram (Putnis & Bish,1983). The low-temperature interval of this curve (T<1280°C) is the most interest for the real geological sistems. Activation energy (E) and preexponential multiplier (ko) were calculated with Arrhenius equation for this case $k = 8.1 \cdot 10^{15}\exp(-\frac{150000}{RT})$, the error of equvation for Δ ($\alpha = \Delta/0.31$) is 10%.

The temperatures of formation the cordierite-bearing associations from fused sediments varied from 800 to 1100°C, the real Δ.-

values were 0.10-0.16. Based on the gained kinetic parameters the durations of structural transformations in high-cordierites were calculated by the Avraamy-Erofeev equation. These values fall into the interval 0.5 to 22 years.The results are consistent with the real time of burning (0.5-3 years) and active smouldering (10-20 years) of the coal waste heaps. Wide spreading of high- and intermediate structural states in cordierites in crystalline fused sediments strongly suggests that the crystallization of a disordered phases within the stability fields of the ordered polymorphs may be realized not only in the experiments with the highly metastable starting materials (glass) but in the some dry natural assembleges as well.

The same method of calculation was used for the estimation the time interval of hexagonal-->orthorhombic transformation in cordierites (Δ=0.24-0.29) from high-temperature hornfels (upland Sangilen, Sibiria, Russia). The results were follows : if Δ=0.25 and T=800°C, then τ=13 mln.years; if Δ=0.25 and T=750°C, then τ=400mln.years. These results may be considered as essentially overstate. This means that the catalitist effect of fluid phase on the reaction rate should be considered. At the same time Δ-values of natural cordierites are statistically dependent on the metamorphic conditions: $\bar{\Delta}$=0.24,S=0.03,n=111 (epidote-amphibolite facies); $\bar{\Delta}$=0.26, S=0.03,n=84 (amphibolite facies); $\bar{\Delta}$=0.27, S=0.02, n=77 (granulite facies).

Thus the experimental and natural materials suggest that order --> disorder transformation in cordierite may be principally used for the solution the kinetic problem of petrology.

References:

Langer,K.,Schreyer, W. (1969). Amer. Mineral.,54,1442-1459.

Putnis,A. (1980). Contrib. Mineral. Petrol.,74, 135-141.

Putnis,A. & Bish,D.L. (1983). Amer. Mineral., 68, 60-65.

Screyer,W. & Schairer,J.F. (1961). J.Petrol., 2, 324-406.

EFFECTS OF SPECIMEN THICKNESS ON ILLITE "CRYSTALLINITY" MEASUREMENTS

Lezzerini M. and Tamponi M. (*Dept. of Earth Sciences, Univ. of Pisa*)

Specimen thickness is the main experimental factor controlling the results of illite "crystallinity" (I.C.) determinations. Several authors (Krumm and Buggish, 1991 and literature cited therein) have pointed out the effects of this factor and warned against non standardized samples preparation. Some of them also proposed procedures to eliminate the problem: Krumm and Buggish (1991) suggested determination of I.C. on very thin sedimentation slides with a thickness (expressed as density of material on the slide) of 0,25 mg/cm^2 or less, while Frey (1988) merely recommended to avoid thin slides. The problem has been re-examined in this study on three sets of pelitic samples from Palombini Shale Formation (Northern Apennines, Italy) covering a wide range of I.C., which encompasses metamorphic grades from late diagenesis to early epizone. The collected data show that I.C. values are strongly dependent on specimen thickness when thin slides are used (density of material below 0.5 mg/cm^2); then the procedure proposed by Krumm and Buggish (1991) would require a very careful control of the suspension density in order to obtain a nearly constant density of the sedimentation slide of about 0.25 mg/cm^2; even in this case, however, application of this procedure seems to be difficult because of the low intensities of the mica (001) peak which are commonly obtained.

For densities of the sedimentation slides above 0.5 mg/cm^2 the variation of I.C. with thickness is much less marked, but not negligible as assumed by Frey (1988).

In a plot of "crystallinity" index (Kübler index) versus density of the slide the points result aligned along straight lines with a moderate slope; samples with different crystallinities are ranged on subparallel lines.

On the basis of these results the following procedure is suggested:

a) preparation of thick sedimentation slides (density of the material greater than 0.5 mg/cm^2);

b) measurement of the specimen density and I.C. index;

c) plotting of the experimental data in the graph presented herein and normalisation of the I.C. values to a selected reference thickness.

As a reference, whatever thickness could be chosen. However a value in the range 1-4 mg/cm^2 is suggested, since, in our experience, this is the most common thickness of sedimentation slides prepared from pelitic samples. The average value of this range (2.5 mg/cm^2) would most likely allow a reliable confrontation also with old literature data.

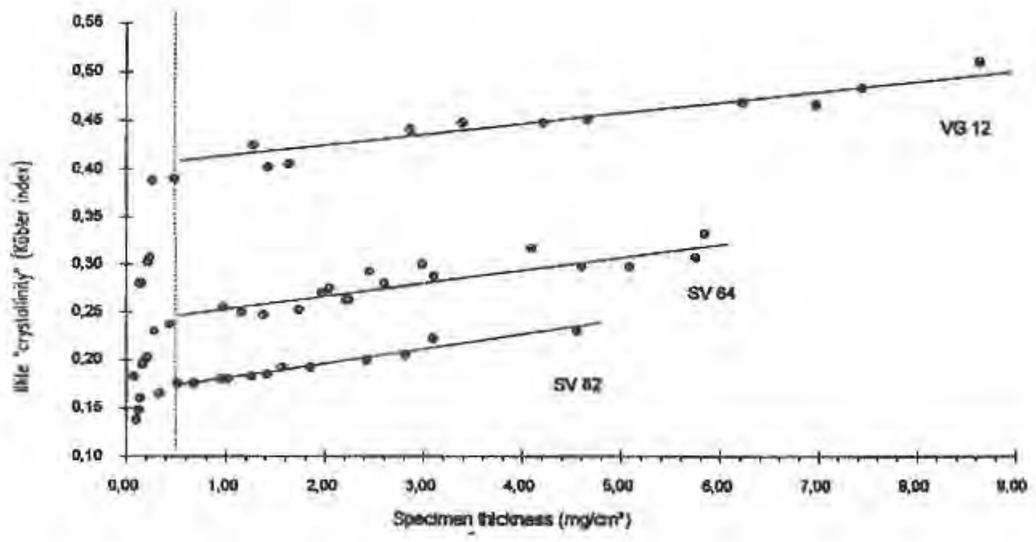

References:

Frey, M. (1988). Discontinuous inverse metamorphic zonation, Glarus Alps, Switzerland: evidence from illite "crystallinity" data. Schweiz. Miner. Petrogr. Mitt., **68**, 171 - 183

Krumm, S., Buggish, W. (1991). Sample preparation effects on illite crystallinity measurement: grain-size gradation and particle orientation. J. metamorphic Geol., **9**, 671 - 677

The Existence of the Negative Valence State of Gold in Sulfide Minerals and its Formation Mechanism

Li Jiuling[1], Feng Daming[2], Qi Jeng[1] and Zhang Guilan[1]

([1]Institute of Mineral Deposits, Chinses Academy of Geological Sciences, Beijing 100037, China; [2]Beijing University of Science and Engineering, Beijing 100081 China)

In recent year"invisible gold" occurring in sulfide minerals of Carlin disseminated type gold deposits has attracted wide attention. At present, the most important progress on "invisible gold"comes from the study of Mossbauer spectra. F. E. Wagner et al (1986–1992) confirmed that in gold–bearing pyrite and arsenopyrite there exist "Chemical bound gold" that is different from not only native gold (Au $^{\circ}$) but also other known gold compounds. The chemical valence state of such "Chemical bound gold " in arsenopyrite and pyrite, however remains unclear.

The "invisible gold" – bearing arsenopyrite and pyrite occurring in Carlin–type gold deposits of Guang Xi; China, and hydrothermally synthesized gold–bearing pyrite and marcasite are investigated in detail, particularly by X–ray photoelectron spectrum (XPS) analyse. The binding energy was adjusted to give the values of 82.5eV–83.5eV for the Au $4f_{7/2}$peak of these minerals. They were obviously lower than Au $4f_{7/2}$84.0eV of metal gold (Au $^{\circ}$). The data of the binding energies of gold–bearing sulfides measured are notably lower than those of Au $^{\circ}$, $Au^{1+}$and Au^{3+}in other gold compounds, indicating that the gold in these sulfides is neither zerovalent nor positive valence (nor loses its valence electron), but gains or shares such a valence electron or elections in

combining with anather element. Therefore we suggest that there is gold occurring in a negative valence state in the lattice of these sulfides, as it replaces some sulfur and is combined with sulfur by the covalent bond. This paper also preliminarily discusses the possibility and the formation mechanism from the chemistry and geochemistry of gold, the crystal chemistry of arsenopyrite, pyrite and marcasite, the geochemical environment and in combination with the synthetic experimental conditions.

STUDY ON PHYSICOCHEMICAL CONDITIONS OF THE FORMATION OF SOME BERYL- AND AQUAMARINE-BEARING GRANITE-PEGMATITES IN CHINA*

Li Zhaolin, Mao Yanhua and Lei Lihong (Department of Geology, Zhongshan University)

Rare element granite-pegmatites are widely distributed in the northwestern and southeastern parts of China, and especially famous are those occurring in Keketuohai, Xinjiang and in Mufushan, Hunan. The origin of pegmatite has been a subject of much controversy. This paper studies mainly the physicochemical conditions under which pegmatites of the above-mentioned two areas were formed, with a view to probing into the origin of these pegmatites. In 1985-1991, the authors discovered for the first time melt inclusions and melt-fluid inclusions in beryl, aquamarine and rock crystal from pegmatites of the above-mentioned two areas, thus providing the basis for solving the origin problem. The Keketuohai granite-pegmatites ore field is Hercynian in age, and is located in Paleozoic metamorphic system. The Mufushan pegmatites are Yanshanian in age and are distributed in Late Yanshanian granite or in the contact zone between the granite and the metamorphic rock in Mid-proterozoic strata. In both areas all of pegmatite contain beryl. Aquamarine occurs largely in association with rock crystal in geode within pegmatite veins of the later stage.

In beryl and aquamarine crystals from pegmatites of the two said areas occur inclusions of various types. The melt inclusions and melt-fluid inclusions are characterized by $C_{Si}+A_{Si}$, $nC_{Si}+nA_{Si}+G$ and $L+G+C_{H.D}$, $nC_{E.D}+nC_{H.D}+A_{Si}+L+G$ phases respectively. Homogenization temperatures of melt inclusions are: Beryl 700-1140°C; aquamarine 890-905°C, while homogenization temperature of melt-fluid inclusions are: beryl 700-960°C; aquamarine 640-905°C. In addition, gas-liquid inclusions sometimes in association with melt inclusions are also found in beryl and aquamarine of the two said arias, and the following phase characteristics are found: G+L, L+G, L+$G_{CO_2}+L_{CO_2}$. Homogenization temperature of gas-liquid inclusions: beryl 180-410°C; aquamarine 180-350°C. Temperature measurement on inclusions shows slightly different results for the two said areas: temperature of formation is 1140-180°C for pegmatite from Keketuohai, but 990-180°C for pegmatite from Mufushan. Ore fluid analysis and micro-gas analysis have been conducted on beryl and aquamarine. The result shows that the ore fluid from Mufushan pegmatite is intermediate to slightly alkalic in nature, Eh=76.64-89.98 mV, cations $Na^{+1}>K^{+1}>Ca^{+2}>Mg^{+2}$, anions $HCO_3^{-1}>Cl^{-1}>SO_4^{-2}>F^{-1}$. The K + Na content is higher and the Ca^{+2} content is lower in beryl than in aquamarine. The ore fluid has a salinity of 21-25.3 Wt% NaCl, a density of 0.95-1.04g/cm^3, gas composition: $H_2O>CO_2>CO>H_2S>CH_4$. In comparison, the ore fluid from Keketuohai pegmatite has a similar cation property with anions $SO_4^{-2}>HCO_3^{-1}>Cl^{-1}>F^{-1}$, showing an intermediate to slightly acidic property, Eh=68.69-108.91 mV, and was formed in a relatively reducing environment.

The study shows that pegmatite is of milt-solution character and magmatic origin in two said areas, formation temperatures are: beryl 1140-180°C, aquamarine 905-180°C, nature of ore fluid is Na-K-Ca-CO_3-Cl-SO_4-F or Ca-Na-K-SO_4-HCO_3-Cl-F.

* The project supported by National Science Foundation of China and Laboratory of Ore Deposit geochemistry Institute of Geochemistry Academia Sinica.

L-liquid phase; G-gas phase; $C_{H.D}$-infusible crystalline phase; $C_{E.D}$-fusible crystalline phase; A_{Si}-amorphous silicate; L_{CO_2}-liquid CO_2; C_{NaCl}-crystalline NaCl.

MULTISTAGE METAMORPHIC EVOLUTION OF OVERPRINTED SAPPHIRINE-BEARING KYANITE-ECLOGITES IN CENTRAL RHODOPE, N. GREECE: EVIDENCE OF GRANULITE-FACIES METAMORPHISM

Liati A. (*Dept. of Mineral Resources Engineering, Technical University of Crete*) and Seidel E. (*Mineralogisch-Petrographisches Institut, Universität zu Köln*)

In central Rhodope of northern Greece, kyanite-eclogites were discovered in the area of Thermes. They are strongly overprinted and contain abundant symplectites of clinopyroxene+plagioclase and amphibole+plagioclase. Less abundant are symplectites of spinel+plagioclase, corundum+plagioclase and, rarely, sapphirine+plagioclase, all forming at the expense of kyanite. Biotite+plagioclase symplectites occur in some cases; they probably formed at the expense of preexisting phengite. The initial high-pressure paragenesis was: garnet+omphacite+kyanite+zoisite(+phengite).

Sapphirine, Fe-Mg-spinel, corundum, högbomite and, rarely, orthopyroxene occur as products of the overprinting metamorphism. Sapphirine, Fe-Mg-spinel, corundum and, partly, högbomite are associated with rutile(+ilmenite)+plagioclase. Part of högbomite coexists with Fe-Mg-spinel+rutile. Formation of sapphirine, Fe-Mg-spinel and, in part, högbomite is ascribed to reaction between omphacite+kyanite+ilmenite, while part of högbomite resulted by reaction between Fe-Mg-spinel+rutile.

For the high-pressure stage of metamorphism, minimum PT conditions were 19 kbar, 700°C, while for part of the overprinting metamorphism ca. 11 kbar, 780°C. The kyanite-eclogites of Thermes, after the high-pressure stage entered the granulite-facies field thus recording the highest overprint temperatures identified in the Rhodope.

The rock unit bearing the granulite-facies overprinted kyanite-eclogites belongs to the highest P and T thrust nappe and represents probably the deepest levels of the Rhodope crystalline rocks.

JANKOVIĆITE, A NEW SULFOSALT MINERAL FROM ALLCHAR, MACEDONIA: CRYSTAL STRUCTURE AND CRYSTAL CHEMISTRY

Libowitzky E., Giester G. and Tillmanns E. (*Institut für Mineralogie und Kristallographie, Universität Wien, Austria*)

Jankovićite, $Tl_5Sb_9(As,Sb)_4S_{22}$, a new sulfosalt mineral from the Allchar region, Macedonia, has recently been described by Cvetković et al. (1994). The crystal structure was determined by direct methods from 6450 reflections, measured on a four-circle X-ray diffractometer, and refined to a final R-value of R/R_w = 0.062/0.038. The cell parameters are a_o = 7.393(4) Å, b_o = 8.711(5) Å, c_o = 17.58(1) Å, α = 103.81(3)°, β = 91.81(3)°, γ = 109.51(3)°; space group P1, Z = 1.

The three crystallographically different Tl atoms are coordinated irregularly by eight sulfur atoms each with Tl-S distances between 2.890 and 3.778Å, AsS_3 pyramids are almost regular with As-S from 2.250 to 2.351Å. Sulfur coordination polyhedra around antimony atoms Sb(1), Sb(2), Sb(3) and Sb(4) are basically distorted trigonal pyramids with average Sb-S distances of about 2.5Å, next nearest S atoms are about 3Å apart. Sb(5) has a 2+2 coordination with two S atoms at a distance of about 2.4Å and two at about 2.8Å.

The structure consists of kinked chains of SbS_n polyhedra //c which are connected by AsS_3 pyramids to form buckled layers // (100) (cf. fig. 1). These Sb-As-S layers are interconnected via Tl atoms in eight coordination. Tl(3) and Sb(1) occupy statistically a split-atom position, 0.68Å apart, with a site occupation factor of one half each. The As sites are partially substituted by antimony. The structure shows close similarities with that of rebulite, $Tl_5Sb_5As_8S_{22}$ (Balić-Žunić et al., 1982).

References:

Cvetk... Lj., Boronikhin, V.A., Pavićević, M.K., Krajnović, D., Gržet... Labowitzky, E., Giester, G. & Tillmanns, E. (1994). *Mineral... rol.* (submitted)

... T., Šćavnićar, S. & Engel, P. (1982). *Z. Kristallogr.*, ... 5.

Fig.1. The structure of jančovicite viewed along the b-axis. Atoms in decreasing size represent Tl, Sb, As, S. Tl3/Sb1 occupy a split-atom site with 1/2 occupation each.

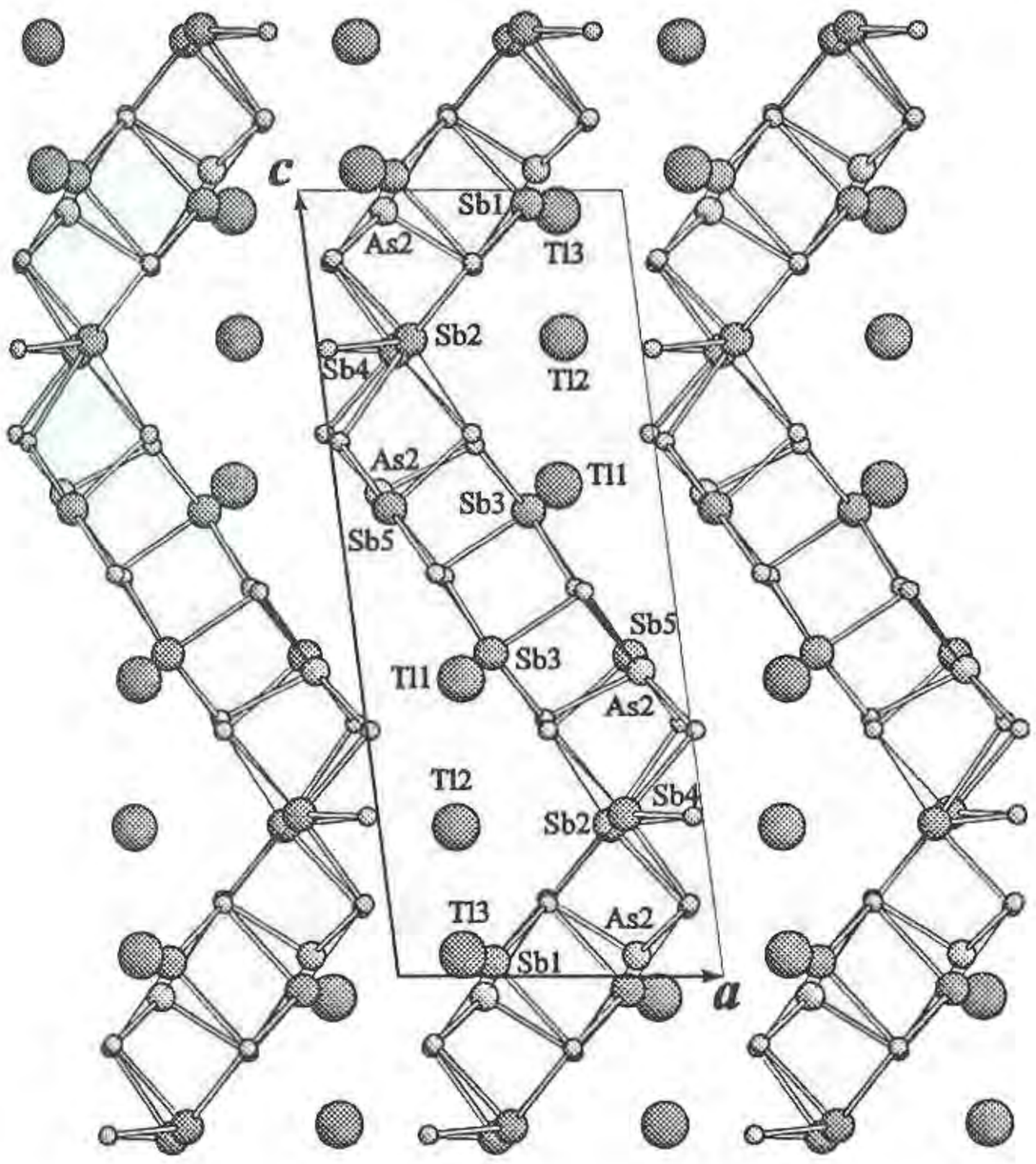

ELASTICITY DATA BASE FOR THE HIGH PRESSURE PHASES OF MANTLE MINERALS

Liebermann, R. C., Sinelnikov, Y. D., Li, B., Meng, Y. *(all at Center for High Pressure Research and Dept of Earth and Space Sciences, University at Stony Brook)*, Gwanmesia, G. D., Cooke, J. A. *(Dept of Physics, Delaware State University)*, and Rigden, S. M. *(Research School of Earth Sciences, Australian National University)*

Laboratory investigations of the elastic and thermal properties of minerals provide the experimental data base used to define the equations of state for these solids. These equations of state may be applied to calculations of phase diagrams and to interpretation of seismic models in terms of the mineralogy and chemical composition of the Earth's interior. This endeavor requires accurate measurements of the elasticity of upper mantle minerals and their high-pressure polymorphs as a function of pressure and temperature. This paper summarizes the current state-of-the-art in these investigations using various experimental techniques, including Brillouin spectroscopy for single crystals, ultrasonics for polycrystals, and static compression of powders and single crystals using *in situ* X-ray diffraction. We will focus on the properties of the high-pressure phases of mantle minerals, with special emphasis on recent studies of beta and spinel phases of Mg_2SiO_4, majorite-pyrope garnets and stishovite, and on the extent to which these different techniques provide complimentary data on the elastic behavior of these important mantle phases.

MECHANISMS OF PHASE TRANSFORMATIONS IN SAN CARLOS OLIVINE AT HIGH PRESSURES

Liebermann, R. C., Wang, Y., Martinez, I., Guyot, F., Reeder, R. J. *(all at Center for High Pressure Research and Mineral Physics Institute, University at Stony Brook)*, Galoisy, L. *(Laboratoire de Minéralogie-Cristallographie, Universités de Paris 6 et 7)* and Cuny, D. *(Géomatériaux, Institut de Physique du Globe-Paris)*

Natural San Carlos olivine $(Mg_{0.91}Fe_{0.09})_2SiO_4$ crystals have been compressed and heated in a uniaxial split-sphere apparatus (USSA-2000) under conditions of known deviatoric stress and temperature gradient, and examined by powder X-ray diffraction and analytical transmission electron microscopy (ATEM).

Specimens of the ß-phase have been synthesized at P=14 GPa and T=1500K in times of 5 to 90 min. In experiments of short run duration, the fine-grained olivine transformed completely to the ß-phase, whereas the coarse single crystals of olivine were only partially transformed to the ß-phase. These partially-transformed crystals consist of olivine cores surrounded by rims of ß-phase crystals which have grown inward from the boundary of the original olivine crystals. The Fe content of both the olivine cores and ß-phase rims is identical with that of the starting material on both the electron microprobe and the ATEM scale. The ß-phase rims consist of a series of finger-shaped crystals which nucleate on and grow normal to the boundary of the olivine crystals. There is no evidence that their growth rates are related to either the direction of maximum principal stress or the crystallographic orientation of the olivine crystals. Thus, the growth process is isotropic and systematically related to the run duration.

Assemblages of $(Mg,Fe)SiO_3$ perovskite and magnesiowüstite were synthesized at P=26 GPa and temperatures and run durations from 1000-1900K and 2 min to 14 h, respectively. Within the analytical precision, the iron-magnesium partitioning coefficient between the magnesiowüstite and perovskite $K^{Fe\text{-}Mg}_{mw\text{-}pv}$ appears to be independent of both T and run duration, and in

reasonable agreement with the results of previous studies. It is important to note that the disproportionation reaction of olivine to perovskite plus magnesiowüstite is complete at 1600K within 2 min. However, the grain size is affected by run duration, being about 20 nm at 1600K for 2 min and 1000 nm at 1900K for 1.5 h. TEM studies are underway to characterize the microstructural features in these specimens and to compare with those observed in specimens produced in diamond-anvil cell experiments.

PODIFORM CHROMITITES FROM PRECAMBRIAN OUTOKUMPU OPHIOLITE COMPLEX, EASTERN FINLAND

Liipo, J.[1], Vuollo, J.[1], Nykänen, V.[1], Piirainen, T.[1], Tuokko, I.[2] and Pekkarinen, L.[3] (1=University of Oulu, Department of Geology, Oulu, Finland; 2=Finnminerals Oy, Kajaani, Finland; 3=Outokumpu Finnmines Oy, Outokumpu, Finland)

The Outokumpu ophiolite complex (1.97 Ga), known for its Cu-Co-Zn-Au ores, occurs as a dismembered sequence of upper mantle peridotites and an incomplete crustal sequence comprising dunites, pyroxenites, gabbros and mafic volcanics. The upper mantle peridotites are harzburgites, dunites and lhertzolites in terms of relict minerals. A well-preserved podiform Cr deposit is assosiated with the harzburgite-dunite transition.

The podiform chromitite was found in a disused talc quarry, and its size is still unknown. The chromitite samples show typical structures of ophiolitic chromites, such as massive and nodular textures. The nodular chromite consists of subrounded coarse grains, while the massive type is commonly dissected by sets of fractures. The chromite grains vary in shape from euhedral to rounded grains ranging from few millimeters to 40 millimeters in size, though the largest grains are frequently cataclastic. Primary silicates are not preserved in the chromitite. The fracture network and the intergranular silicates are composed of kämmererite and magnesite. Gersdorffite and nickeline occurs either in the ferritchromite as sub- or anhedral grains or in the secondary silicates as euhedral grains from 2 to 100 µm in diameter. The platinum-group minerals, such as laurite, irarsite and osarsite, occurs in gersdorffite as minute exsolution lenses, which is the main diffrence between studied and Mesozoic podiform chromitites.

On the basis of the mineralogy, mineral chemistry, and platinum-group element distribution, chromitites from Outokumpu ophiolite complex are analogous to Al-rich podiform chromitites of Mesozoic age, indicating that ore forming and mantle processes were similar to those that took place in the Phanerozoic to procude podiform Cr ores.

Podiform chromitites of approx. 2.0 Ga age are known at present only from Outokumpu ophiolite complex, though ophiolite complexes of same age have been regocnized from Canadian (Purtuniq ophiolite) and Fennoscandian (Jormua and Outokumpu ophiolites) Shields.

AN ATTEMPT OF DETERMINATION OF ISOTOPE COMPOSITION OF FE, NI AND CU IN MINERALS OF PGE-CU-NI DEPOSITS IN NORIL'SK AND SUDBURY

Likhachev A.P.(TsNIGRI, Moscow), Kiricov A.D. and LiFatu A.V. (MEKHANOBR, Saint Peterburg)

The problem of ore components sourse of PGE-Cu-Ni deposits is not solved. Modern genetic concepts admit participation of cosmic material (Sudbury), or mantle substance and the Earth's core (Noril'sk) in ore formation. The data characterizing isotope composition of ore-bearing elements can fasilitate the solving of these problems. In this connection, we undertook an attempt of analysing isotope composition of Fe, Ni and Cu from Noril'sk region, the samples of Oktyabrsky deposit were studied which represent massive ore and dessiminated mineralization in picrite gabbro-dolerite. In Sudbury, massive pyrrhotite and chalcopyrite ores from the Creighton deposit were studied. Pyrrhotite, chalcopyrite, pentlandite, magnetite and olivine were analysed. Isotope measurements were made by the SIMS method 1MS4F mass-spectrometer Cameca firm with the 0,3 relative percent error, while the determination of element content was done on the CAMSKAN microprobe with the 1,0 relative percent error. The developed methodology of determination of isotope element composition took into consideration the following factors: isotope heterogeneity; isobar superpositions of complex (multiatomic) ions; isobar superpositions of atom ions; mass discrimination. The $^{57}Fe/^{54}Fe$, $^{56}Fe/^{57}Fe$, $^{58}Fe/^{54}Fe$, $^{56}Fe/^{54}Fe$, $^{58}Ni/^{60}Ni$, $^{64}Ni/^{60}Ni$, $^{61}Ni/^{60}Ni$, $^{62}Ni/^{60}Ni$, and $^{63}Cu/^{65}Cu$ ratios were determined. An example of obtained date is shown in Fig. The obtained data point to considerable differences in isotope relations between examined elements both within the limits of each deposits and between the deposits. The most distinct is the deposit and all the Noril'sk ore types and the coincidence of isotope characteristics of essentially chalcopyrite Sudbury ores with Noril'sk ores. In orders ascertain the nature of observed isotope variations the analysis of systematic sample collections is required.

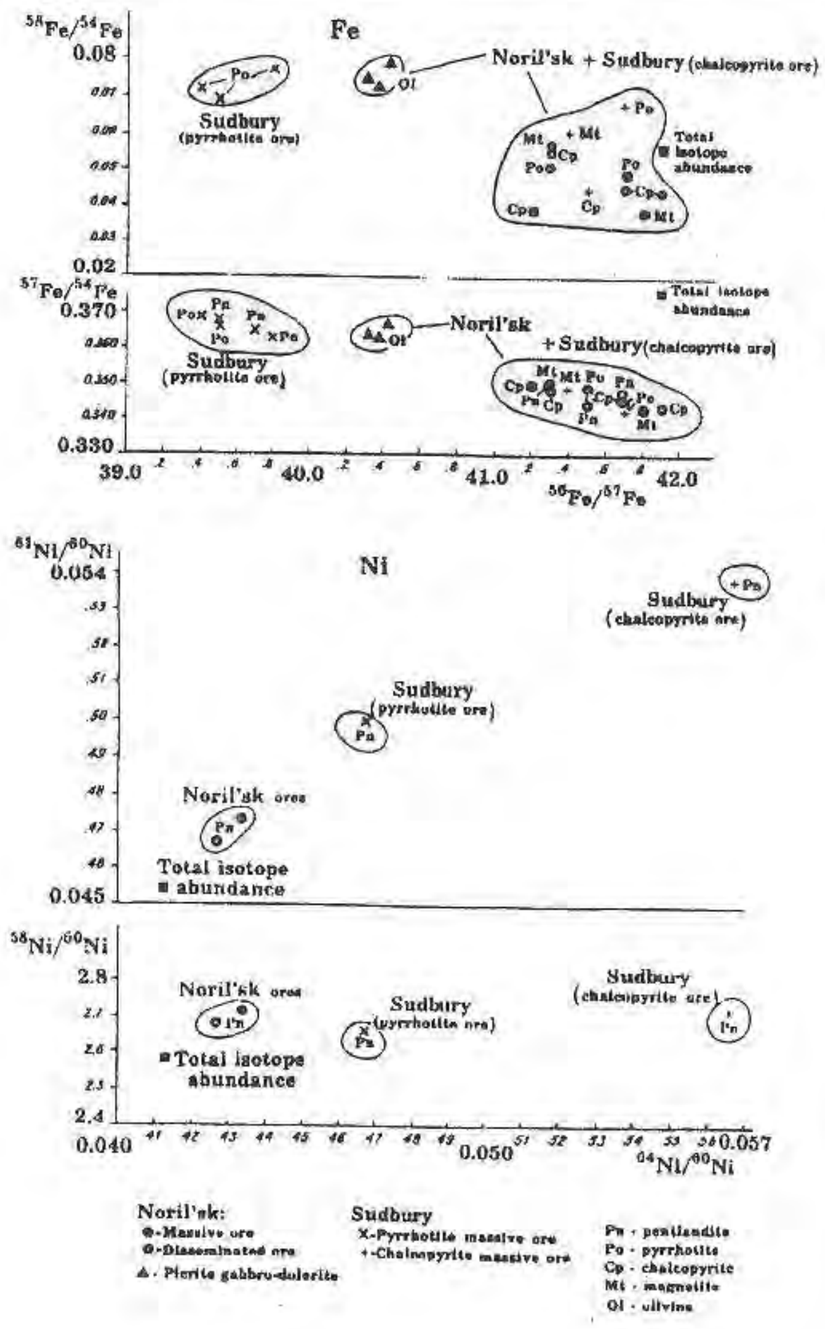

CONTACT METAMORPHIC REACTIONS BEHAVIOUR DURING AMPHIBOLES FORMATION IN AMYGDALOIDAL METABASITES

Likhanov I.I.[1], Reverdatto V.V.[1], Memmi I.[2]
(*1-Inst. of Mineralogy and Petrography, Novosibirsk, Russia, 2-Univ. of Siena, Italy*)

Rare assemblages from metabasites of contact aureole of the Kharlovo gabbro massif (Altay, Russia) have been studied in detail to determine the relationship between reaction history and compositional zoning of minerals. Arfvedsonite and hornblende were formed at T=525-550°C and P=1.5 kbar in middle part of contact aureole according to the following reactions:

$$0.8\ Chl + 0.27\ Bt + 0.83\ Cal + 1.38\ Mag + 1.68\ Sph + 1.4\ Ab = 1.5\ Hbl + 1.58\ Ilm + 4.65\ H_2O + 0.83\ CO_2;$$

$$0.02\ Chl + 1.18\ Ab + 0.21\ Cal + 0.14\ Mag = 0.1\ Arf + Olg + 0.02\ H_20 + 0.21\ CO_2.$$

The reliability of reactions are confirmed by experimental investigations on ordering of acid plagioclases and calcite solubility decreasing in fluid with increasing temperature, and by comparison of the calculated volume ratios of minerals with the observed volume ratios of phase contents.

Based on detailed mineral chemistry and phase relation investigations a reaction model describing the reaction mechanisms of the rock microtextures is proposed. The relationship between real mineral reaction mechanisms and scales of mass transfer is established.

The arfvedsonite formation took place under conditions of local saturation of H_2O-CO_2 pore solution by Si, Na and Fe, and short duration of thermal metamorphism as a result of local metasomatic diffusion controlled reaction connected mainly with Na and Si leaching during incongruent dissolution of acid plagioclase.

Mass balance analysis and compositional and content of coexisting mineral variations show that the mass transfer of main petrogenic components was limited by smallest volumes (microsites) on the order of 0.06-0.1 mm^3.

THE STRUCTURAL CLASSIFICATION OF MINERALS

Lima-de-Faria, J. (Centro de Cristalografia e Mineralogia, Instituto de Investigação Científica Tropical, Lisbon, Portugal)

The classification of animals and plants has not changed much since Linnaeus's proposal (1735), because, at the time, its detailed study was already possible, particularly with the help of the microscope, and consequently, a natural classification based on their internal structures could be established. On the contrary, the criterion for the classification of minerals has changed throughout the ages (from practical purposes, to physical properties, and to chemical composition) following the development of the mineralogical science. These changes were always a step further in the direction of the internal structure of minerals. Only after the first determination of a crystal structure was carried out (Bragg, 1913) was it possible to reach the internal structure of minerals. Since then most of the mineral structures have been studied, and the time is now ripe to develop a real natural classification, replacing the classical chemical classification by a structural classification of minerals. In 1983 the author proposed a structural classification of minerals which may be considered as an extention of the structural classification of the silicates to the whole domain of minerals.

The strong opposition to the chemical classification proposed by Cronstedt (1756) lasted for more than one hundred years. A clear parallelism may be established between the replacement of the physical by the chemical classification and the proposed replacement of the chemical by the structural classification. Dana said in his "System of Mineralogy" (1850), " ... chemistry has opened to us a better knowledge of the nature and relation of compounds; and philosophy has thrown new light on the principles of classification. To change is always seeming fickleness. But not to change with the advance of science is worse; it is persistence in error ... ". A similar statement could now be applied to the structural classification. However, with the present knowledge of the structural characteristics of minerals and of the history of mineralogy, it may well be that the acceptance of the structural classification of minerals instead of taking one hundred will take only a few years.

References:

Dana, J.D. (1850). The system of mineralogy. John Wiley, New York, third edition.

Lima-de-Faria, J. (1983). A proposal for a structural classification of minerals. Garcia de Orta, Série Geologia, 6, 1-14.

Linnaeus, C. von (1735). Systema naturae, sive regna tria natura systematice proposita per classes, ordinis, genera et species. Theodorum Haak, Leiden.

Sintering properties of Kyanite and Its Application in Refractories

Binyin Lin Shaowei Zhang
(Wuhan Iron and Steel University, Wuhan 430081, P. R. China)

Abstract

The effects of chemical composition, grain size and calcining temperature on the mullitization behavior, expansibility, bulk density and apparent porosity of kyanite concentrate from different orefields of China have been analysed by x-ray diffraction, SEM and OM. Based on the above analysis, the application of kyanite in refractories has been studied. The results as follows:

1. The decomposition and the mullitization behavior of kyanite (1) the temperature of initial decomposition of kyanite is 1100℃; (2) the temperature of marked decomposition of kyanite is 1300℃ (or 1350℃). At the temperature, the formation amount of mullite gets 3/4 of theory formation amount (the mullite content is over 60%), the range of marked decomposition temperature is 1300-1450℃ or 1350-1450℃; (3) the temperature of complete decomposition is over 1450℃. (4) the proper calcining heat must be over 1500℃ owing to the existence of kyanite-pseadomorph. (5) the temperature at which kyanite transforms into mullite is influenced by grain size and impurities; high-impurity and large grain of kyanice lay behind about 50℃.

2. The relationship between the sintering properties of kyanite and the mullitzation behavior

The expansibility, bulk density and apparent porosity in calcining process are related to the mullitization behavior, the characteristics of which are listed in table 1.

Table 1. The relationship between the sinterability of kyanite and the mullitization behavior

Temp. (℃)	degree of mullitization	characteristic of decomposition	expansibility	bulk density	apparent porosity
1100-1300 (1350)	low	some decomposition	some increase	some decreas	some increase
1300-1450 (1350)	very high	marked decomposition	marked increase	marked decrease	marked increase
>1450	complete	complete decomposition	decrease	increase	decrease

3. Application

Kyanite has been applied in refractories successfully as,

1)Production of high-quality high-alumina bricks

Owing to large expansion of kyanite, it can't be used to produce refractory brick directly. This is given in many data books but the author has successfully used them in Al_2O_3-SiO_2 system refeactories. The refractoriness under load of the refractories is high while the creep and reheating linear change are low. 2)Synthesis of mullite grog. 3)Production of mullite refractory slurry. 4)Swelling agent of unshaped refractories.

DISLOCATION OF THE OLIVINE IN SIXIANGKOU CHONDRITIC METEORITE FROM JIANGSU, CHINA

Lin C—Y., Zhang F—S., Wang H—N., Guo Y. and Xu H—Z.
(Center for Materials Analysis, Nanjing University)

Sixiangkou meteorite is a olivine — bronzite chondritic meteorite falled in the territory of Sixiangkou town, Taizhou city, Jiangsu province of China in June 15 of 1989. It is composed mainly of olivine, diopside and bronzite with typical chondule texture. The inhomogeneity in the chemical composition and the dense dislocation have been found in the olivine. The mole percent of fayalite ranges from 21.7% to 46.0%. Therefore the Sixiangkou meteorite would be refered to as L—group chondrite (Van Schmus, 1967).

The bright field images show two main types of dislocation in the olivine. One is relatively straight and parallel to [001]. The other is slightly bended and parallel to [100]. The Buurgers vector for both of them are parallel to [001]. Consequently, the straight one is the screw dislocations and and the bended is the edge dislocations. Based on the statistics of 25 photomicrographes, the dislocation density ρ is $4.13\times10^{10}/cm^2$. Sometimes the jogs and small dislocation loops can be found as well. However, the dipole, network and helical dislocation have never been found.

The authors come to the conclusion that the Sixiangkou chondritic meteorite was formed under a rapid condensation and was not thermally metamorphosed strongly. The dislocation of the olivine was formed as a consequence of the shock of high strain rate at the temperature of 800—1000℃.

References:
Van Schmus, W. R. et al. (1967) Geochim. Cosmochi. Acta, 31, 747—765.

THE PHASE TRANSFORMATION AND THE PREFERRED ORIENTATION OF THE SUPERPLASTIC DEFORMED TZP CERAMICS

Lin C—Y. and Zhang Z—D.
(Center for Materials Analysis, Nanjing University)

The Y_2O_3 stabilized tetragonal zirconia polycrystals (3Y—TZP) has been superplastically compressed and elongated between 1500 and 1600℃ up to strains near 248%. The preferred orientation of the tetragonal zirconia crystals has take place during the process of deformation. The c axes trend to parallel to the elongating direction and the a axes trend to parallel to the compressing direction. It shows that the superplastic deformation gradually turns to plastic one in the late stage of deformation and this transition is related to the obvious growth of zirconia grains. The particle size of undeformed 3Y—TZP is 0.35～0.42μm on an average. The size of the compressed and elongated 3Y—TZP is 1.98μm and 1.80μm respectively.

The portion of monoclinic zirconia in the 3Y—TZP ceramics has increased as a result of the superplastic deformation. The volume percent of the monoclinic zirconia Vm of undeformed 3Y—TZP ceramics calculated with the help of the calibration curve(Taraya et al., 1984) is only 4～5%. The Vm of the compressed 3Y—TZP is 14.5% and the Vm of the elongated 3Y—TZP is up to 65.1%. This phase transformation can occur only at the temperature below 1000℃ and with the particle size above the critical size for the $t\rightarrow mZrO_2$ transformation. Consequently, it happened after the growth of zirconia grains during the cooling process.

In addition to the growth of zirconia grains, the remained stress after deformation and the lattice and/or boundary defect formed during the process of deformation also influence the phase transformation in the deformed TZP ceramics, especially in the elongated one.

References:
Taraya, H., et al. (1984) J. Am. Ceram. Soc., 67, 119—121.

• MORPHOGENETIC TYPES OF THE LEUCOXENE FROM DEVONIAN ORES OF YAREGA DEPOSIT (RUSSIA).

Lisitsina M.A. (*VSEGEI, St. Petersburg, Russia*)

Unique Yarega deposit of leucoxene ores is situated in the north-east of the East European platform. The Middle-Upper Devonian sandy-claycy titanium-bearing formation is 120 m thick and lies on the Riphean slates. Ore bodies occurring at the base and top of formation are formed of quartz leucoxene conglomerates and sandstones. Rutile, anatase, brucite, zircon, tourmaline, pyrite, sphalerite, monazite, gold, etc., are found in ores besides leucoxene.

The typomorphism of leucoxene from the lower, middle and upper part of formation was studied. The following morphotypes of leucoxene were observed: 1. crystals, which are cut without traces of corrosion; 2. round-oval lenticular grains; 3. xenomorphic grains. Juxtaposition and penetration twins along 0001 are often found. The goniometric study allows to consider, that the examined leucoxene have a cutting identical to ilmenite. The color of leucoxene varies from black to grey, the grey color is more usual. The specific gravity of leucoxene is 3,3-3,6 g/cm^3. The leucoxene from the lower placer has a bimodal distribution of the granulometric fractions, the rest of leucoxene has an unimodal distribution. Microprobe analyses of uncut segregation of leucoxene indicated a complex, multiphase structure; sometimes the structure is zonal: Si-nucleus is surrounded by Ti-phases, which is replaced by complex Fe-Ti-Si phase, and the outer zone is Si-Ti phase. Silicon can be found in the form of silica, aluminosilicates and amorphic or crystalline phases of titaniumsilicate. Leucoxene from Riphean slates is composed of ilmenite-rutile-anatase; leucoxene from conglomerate of the lower placer is composed of anatase-rutile and leucoxene from the upper layer is composed of rutile. The chemical and geochemical composition of leucoxene from different layers of the section proves that some of them have the inherited set of elements from the Riphean leucoxene. In the lower place besides the above mentioned leucoxene there is leucoxene of quite a different type. It contains lower quantities of Ni, Co, Cu and larger quantities of Ti, Ag, Pb. The leucoxene from the upper placer contains minimum quantities of Ti and much more of Mg, Ca, Cu, Cr, TR.

The investigations indicate the presence of two genetic types of leucoxene in Yarega deposit: pseudomorphic after ilmenite and authigenic xenomorphic leucoxene. The last one is located mainly at the base of titanium-bearing formation near the contact with the Riphean slates, where the influence of infiltration processes is greatest. The obtained data indicate the polygenic nature of leucoxene ores in this deposit.

STUDY OF THE KINETICS OF THE DEHYDROXYLATION MECHANISM IN LAYER SILICATES AND ALUMOSILICATES

Litovchenko A.S., Kalinichenko E.A., Dekhtyaruk N.T. (*Inst. of Geochemistry, Mineralogy and Ore Formation, Ukraine Science Academy, Kiev*)

Structural transformations of hydroxyl-containing minerals are

usually accompanied by destruction of the OH-groups (the dehydroxylation effect). This effect can be evoked by temperature, electric field, radiation, etc. This effect is followed by partial or complete rebuilding of a substance structure. There is a number of compounds, in which the dehydroxylation effect does not change the structure but results in a local redistribution of charge. It is need to note that the dehydroxylation mechanism depends on a nature of an external influence source. Temperature is the most wide-spread source of such influence. The temperature of destruction of the OH-groups depends on composition and structural peculiarities of a mineral. But, according to literary data the clear connection between the dehydroxylation effect and the structural peculiarities of a mineral has not be established. Many characteristic features of this effect remain unclear (the behaviour of the OH-groups before their destruction, the shape and the height of the barrier, the mechanism of getting over the barrier by a proton, etc.).

The subject of this work is the study of the physical nature of the dehydroxylation mechanism. This is of a great importance for the understanding of mineral transform kinetics. The results of study of layer silicates and alumosilicates (kaolinite, muscovite and phlogopite) have been summarized in this work. In these compounds as a result of influence of temperature no changes of cations valency occur, therefore the dehydroxylation effect results in the formation of H_2O molecules and not H_2 molecules.

For the investigation of the dehydroxylation mechanism the data of NMR of ^{1}H, ^{27}Al, and ^{29}Si, IR-spectroscopy, electroconductivity have been used. Checking of the mineral cell parameters was carried out by X-ray analysis. Some specimens were investigated in the wide ranges temperature (300 K - 1200 K) and pressure (10^5 - $8*10^8$ Pa).

Earlier (Litovchenko A.S. *et al.*, 1991) we have established that there is the intensive reorientation movement of OH-dipols in kaolinite before destruction of the OH-groups. Pressure also has been found to influence the dehydroxylation effect in muscovite.

The analysis of literature and our experimental data permitted to suppose that the dehydroxylation effect may be described by the following scheme. OH-groups are known to be arranged by pairs in the structure of layer minerals. The calculations show that during the destruction of the OH-group it is energetically profitable for the proton to diffund to the neighboring OH-group in the same cisoctahedral limits. In order to explain the physical nature of the dehydroxylation we use the model of sp^3-hybridization of OH-groups orbitals. In the case of dioctahedral structures two orbitals form the bonds with the octahedral cations, the proton becomes localized on the third orbital and the fourth one is vacant. Such situation is described by the double minimum potential (D.M. potential) with the height of the barrier about 5 eV (about 2 eV by experimental data). The curve of the potential energy of the proton in muscovite is asymmetric since the proton passed from oxygen to the ion OH^- - not to the ion O^{2-}. The calculations show that the Si - Al distribution and the position of K^+ interlayer cation influence the value of asymmetry. The barrier height of D.M.potential is modulated by the thermal movement of the OH-dipol so that the proton can cross the barrier to the vacant orbital of the neighboring OH-group. This results in the formation of a H_2O molecule which diffunds into the interlayer space. In trioctahedral micas there are no vacant orbitals of the OH-groups where the proton would come. Such orbital is formed when the bonds with the octahedral cations break. This process proceeds under the higher temperature in comparison to the similar process in dioctahedral micas. This fact explains the differences between the thermostability of muscovite and phlogopite.

Reference:
Litovchenko A.S., Ishutina O.D., Kalinichenko A.M. (1991). *Phys.Stat.Sol.(a)*, 123, k 57

HIGH-PRESSURE MELTING EQUILIBRIA OF UPPER MANTLE SUBSTANCE IN TERM OF MULTICOMPONENT SYSTEM: EXPERIMENTAL DATA ON THE SPINEL/GARNET -OLIVINE - ORTHOPYROXENE - CLINOPYROXENE JOINS

Litvin Yu.A. (Inst. of Experim. Mineralogy, Russian Ac. Sci.)

Magmatic evolution of the Earth's mantle is strongly affected by the liquid-solid phase equilibria inherent to the real mantle substance, but our understanding of the equilibria remains incomplete. The varieties of the equilibrium assemblages as well as their physico-chemical systematics may be identified no sooner that with high - pressure experiment.

The Earth's upper mantle is composed of multicomponent silicate substance well idicated by ultramafic and mafic xenoliths from depths to 300 - 400 km (Haggerty & Sautter, 1990). Contribution of the Na_2O - CaO - MgO - FeO - Al_2O_3 - SiO_2 system into the composition of mantle substance is about 99 wt%. In term of the 6-component oxide system, the join spinel (Sp) - olivine (Ol) - orthopyroxene (Opx) - clinopyroxene (Cpx) and garnet (Ga) -Ol - Opx - Cpx are perfectly representative for spinel - peridotite and garnet - peridotite facies, respectively.

The liquid-solid phase relations for the join Sp - Ol - Opx - Cpx were determined in experiments at 2.0 GPa. The boundary phases correspond by their compositions to rock - forming minerals of fertile mantle peridotite KLB - 1 representing undepleted mantle composition (Takahashi, 1986). In the melting diagram of the polythermal section $Ol_{12}Opx_{48}Sp_{40}$ - $Ol_{12}Cpx_{48}Sp_{40}$ of the Sp - Ol - Opx - Cpx join, direct evidence has been found that the initial melting of the system is peritectic. The main liquid-solid equilibria of the spinel - peridotite mantle system are presented by the 5-phase pseudo - invariant peritectic point Ol + Opx + Cpx + Sp + L (at 1450 C) as well as the 4-phase univariant curves Ol + Opx + Cpx + L; Ol + Opx + Sp + L; Opx + Cpx + Sp + L; and Ol + Cpx + Sp + L. The systematics of the liquid-solid and solid-solid equilibria is depicted in frames of a composition tetrahedron and presented by three - dimentional diagram which is crucial to analyse the processes of magma generation and rock - forming differentiation for conditions of the spinel-peridotite facies.

The new data on the Sp-Ol-Opx-Cpx join combined with the earlier on the Ga-Ol-Opx-Cpx join at 4.0 GPa (Litvin, 1991) gave a chance to clear up the transition of liquid-solid equilibria of spinel-peridotite facies into these of garnet - peridotite facies for the interfacial boundary, and to discuss the pressure dependence of the upper mantle melting equilibria in the 2.0 - 10.0 GPa pressure range.

References:
Haggerty,S.E.&Sautter,V.(1990).Science,248,49.
Takahashi,I.(1986).J.Geophys.Res.,91,9367.
Litvin,Yu.A.(1991).Physico-Chemical Studies of Melting Relations of the Deep Earth's Substance(in Russian),Nauka,Moscow(Monograph).

AN EXPERIMENTAL STUDY OF THE AMPHIBOLITE - ECLOGITE TRANSITION

Liu, J.[1], Ernst, W. G.[1], Bohlen, S. R.[2], and Liou, J. G.[1] (*1. Department of Geological and Environmental Sciences, Stanford University, Stanford, CA 94305, USA. 2. US Geological Survey, 345 Middlefield Road, Menlo Park, CA 94025, USA*)

We have conducted experiments on the amphibolite-eclogite transition at 650-950°C, 8-26 kbar, with f_{O_2} defined by QFM, H_2O/rock ratio of 1:25, using quartz tholeiite glass as starting

material. Experiments lasted 4-34 days. Results shown in Fig. 1 delineated four P-T regions based on the garnet-in, plagioclase-out, and amphibole-out boundaries as pressure increases. Mineral assemblages (accompanied by Ti-phases) of these regions are plagioclase + hornblende + clinopyroxene, garnet + clinopyroxene + hornblende + plagioclase, garnet + clinopyroxene + hornblende, and garnet + clinopyroxene, corresponding to amphibolite, garnet-amphibolite, amphibole-eclogite, and eclogite facies, respectively.

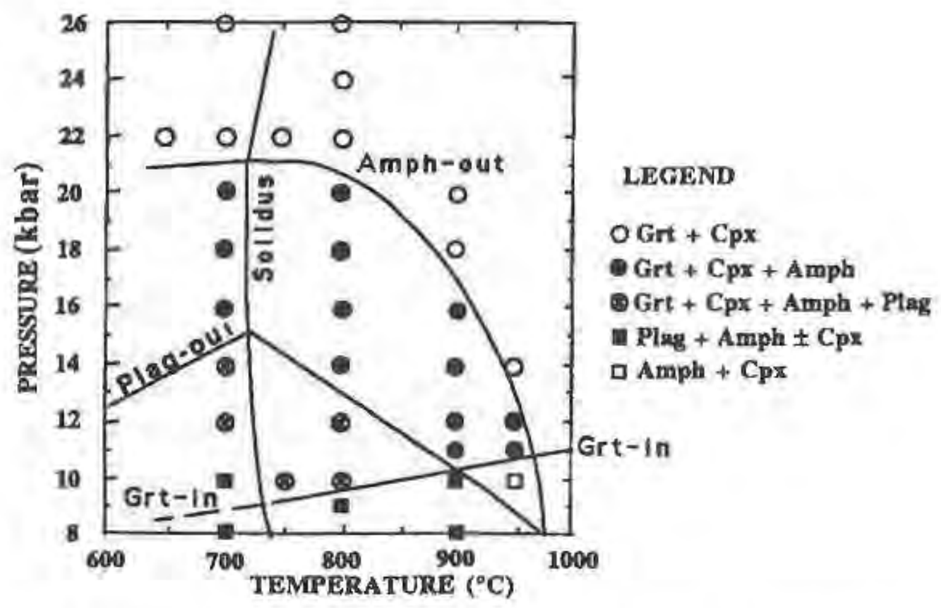

Fig. 1 Amphibolite-eclogite transition in a basaltic system

Rutile, ilmenite and titanite are the associated Ti-phases: ilmenite is stable at P ≤14 kbar at T ≥ 800°C; rutile is stable at P ≥ 16 kbar at T ≥ 800°C, and P ≥ 14 kbar at T ≥ 700°C; titanite is stable at P ≤ 16 kbar at 700°C. The solidus of this system is located between 700-750°C at P > 10 kbar. Quartz occurs in all run products at T ≤ 700°C, whereas 10-15% interstitial melt is ubiquitous in experiments at T ≥ 750°C.

P-T boundaries for the synthesis fields indicate that garnet grows between 10 and 11 kbar at 900 and 950°C, demonstrated by reversal experiments, and between 9 and 10 kbar at 750 and 800°C, with a slope of 5 bar/°C. Plagioclase breaks down between 14 and 16 kbar at 700°C and disappears through melting between 12 and 14 kbar at 800°C, and between 10 and 12 kbar at 900°C, with a negative slope in the supersolidus region. Clinopyroxene occurs as a minor phase at low pressure at T ≥ 800°C, and occurs at P ≥ 16 kbar at 700°C. Amphibole breaks down between 20 and 22 kbar at 650 to 800°C, between 16 and 18 kbar at 900°C, and between 12 and 14 kbar at 950°C.

Compositional data have been obtained inasmuch as all synthetic phases, even at temperature as low as 650°C, are coarse enough to be identified and analyzed by electron microprobe. Phases are homogeneous and change compositions and proportions systematically, compatible with equilibrium crystallization. The compositional ranges of garnet are $Alm_{50-52}Gro_{30-32}Pyr_{10-12}Spe_{3-5}$, $Alm_{44-48}Gro_{30-33}Pyr_{13-20}Spe_{3-4}$, and $Alm_{47-50}Gro_{23-28}Pyr_{24-28}Spe_{0-1}$ at 700, 800 and 900°C, respectively. Jadeite content of clinopyroxene increases as pressure increases: it increases, for example, from Jd_{21} at 16 kbar to Jd_{36} at 26 kbar at 700°C, and from Jd_6 at 10 kbar to Jd_{22} at 24 kbar at 800°C. Amphiboles synthesized at 700-950°C are calcic: they are magnesio-hornblende, pargasitic hornblende, and ferroan pargasite at 700, 800, and 900°C, respectively.

Those data have allowed construction of a petrogenetic grid in order to document details of mineral reactions involved in the transition from amphibolite, through garnet-amphibolite, granulite, and amphibole-eclogite to eclogite facies in a pressure range of 6-12 kbar at 700-950°C. This is critical for a better understanding of crustal-scale processes such as formation of eclogite from hydrated oceanic basalt and amphibolite and its effect on slab buoyancy. Eclogite assemblages, coexisting with vapor, appear after amphibole breaks down; hydrous minerals are unstable at P ≥ 22 kbar and T ≥ 650°C. This has important implications for sources of H_2O in the mantle, especially with regard to the processes of warm oceanic crust subduction and continental collision.

REACTIONS DURING LOW-TEMPERATURE METAMORPHISM OF ALUMINOUS SHALES

Livi K.J.T., Ferry J.M. and Veblen D.R. (*Dept. of Earth and Planetary Sciences, Johns Hopkins University*)

Very low-temperature metamorphism of shales and slates has been traditionally studied by X-ray powder diffraction. Using this technique, phase identification and determination of grade (illite "crystallinity") has been possible on very fine-grained material. With improved electron microbeam techniques, the texture and compositions of individual grains can be determined. Lack of geothermometers and diagnostic reactions in shales with average aluminum contents still prevent the estimation of metamorphic variables. However, aluminous shales contain several index minerals that have the potential for defining temperature and fluid compositions.

To this end, T-X phase relations among kaolinite (ka), chlorite (chl), pyrophyllite (py), margarite (ma), sudoite (di-trioctahedral chlorite)(su), chloritoid (ctd), calcite (cc), dolomite (do), and quartz (q) in the system Ca-Fe-Mg-Al-Si-H-O-C were calculated using the program PERPLEX (Connolly, 1987), the database of Holland and Powell (1990; 1993, personal communication), and natural data from Theye et al. (1992) for Fe-Mg distribution between su and chl. Chl, su, ctd, and do were considered to be ideal Fe-Mg solid solutions. The fluid was assumed to be saturated with graphite and obey the equation of state of Connolly and Cesare (1993).

Conclusions are: (1) Su (with cc + do + q) has a broad X_{CO_2} stability range but a narrow temperature range in Mg-rich shales (0.05-0.6 X_{CO_2}, 300-340°C at 2 kb). This assemblage is a useful geothermometer. Careful examination of powder X-ray patterns may reveal the presence of su masked by coexisting trioctahedral chl. (2) There are few stable reactions that form su and ctd without the reactant do. (3) Equilibria involving carbonate minerals, especially those involving ma, are incompatible with CH_4-rich fluids. In addition, the majority of stable reactions tend to enrich the fluid in CO_2, and there are no mechanisms to enrich a fluid in CH_4. This supports the suggestion of Mullis (1987) that CH_4-rich fluids in fluid inclusions in quartz veins are probably derived from decomposition of hydrocarbons and kerogen. (4) Univariant or divariant reactions between coexisting aluminosilicates (ka, py, or ma) and do are potential indicators of temperature or fluid composition. The assemblage su + py + do + cc + q + graphite has a very limited temperature and fluid composition range (T = 325-330°C and X_{CO_2} = 0.21-0.25 at 2 kb) for the mineral compositions found at Guggenegg in the Glarus Alps, Switzerland. (5) Univariant or divariant decarbonation reactions may be used to calculate or limit time-integrated fluxes involved in the formation of ma, su, and ctd. The T-X_{CO_2} slopes of many of these reactions indicate that little fluid flux is necessary to drive reactions, especially at intermediate X_{CO_2}. This is consistent with field observations that find ka + py, ma + py, and ctd + py assemblages relatively rare. Reactions in epizone-grade slates from the Urseren Zone, Switzerland, yield fluxes on the order of 10^4 cm for the formation of ctd (assuming a temperature-distance gradient of 3.3×10^{-5} °/cm). Formation of su in the anchizone at Guggenegg records a flux of 10^3 cm.

The T-X calculations of metamorphic conditions derived for the aluminous Liassic black shales can be correlated with illite "crystallinity" grade boundaries (Frey, 1978). The ka = py reaction occurs at somewhat higher T than the onset of the anchizone in the Liassic shales. This reaction then places an upper limit to the diagenetic zone at about 300-325°C for low to intermediate X_{CO_2} values and 2 kb. Minimum formation temperatures for the epizone index minerals, ctd and ma, are around 350°C at 3 kb. Kisch (1987) estimated the lower boundary of the anchizone to be around 200-250°C and the upper limit to be 300°C. Despite the discrepancies, calculations show that it is now possible to estimate many of the desired metamorphic parameters from low-temperature shales and slates.

References

Connolly, J. & Cesare, B. (1993). *J. Metamorphic Geol.*, **11**, 379-388.
Connolly, J & Kerrick, D. (1987). *CALPHAD*, **11**, 1-55.
Frey, M. (1978). *J. Petrol.*, **19**, 95-135.
Holland, T.J.B. & Powell, R. (1990). *J. Metamorphic Geol.*, **8**, 89-124.
Kisch, H. (1987) in Low Temperature Metamorphism, Frey ed., 227-300.

Mullis, J. (1987) in Low Temperature Metamorphism, Frey ed., 162-199.
Theye, T., Seidel, E. & Vidal, O. (1992). *Eur. J. Mineral.*, **4**, 487-507.

EARLY MINERALOGY IN SCOTLAND AND ITS CONTRIBUTION TO SCIENCE

Livingstone A. (*Dept. of Geology, Royal Museum of Scotland*)

The paper chronologically outlines the development of mineralogy in Scotland from the 1780s to 1900 by highlighting the main characters involved. Eminent figures in the Scottish University Museum world include John Walker (1731-1803) who was utilising a hardness scale some 40 years before Mohs, and his protégé Professor Jameson (1774-1854) who held the Chair of Natural History for 50 years. Walker was a man of great vision and the Father of Scottish Natural History and Mineralogy. Robert Jameson (of jamesonite) was a prolific collector and writer producing numerous mineralogical textbooks. Walker's University Museum collection was removed by his Trustees upon his death. Jameson commenced amassing a large natural history collection for teaching purposes which eventually totalled over 74,000 specimens including 7000 mineral specimens.

As the University Museum collections rapidly expanded under Jameson's Keepership pressure became so great that a new Museum was sought by Jameson. The current Royal Museum of Scotland resulted largely from Jameson's efforts and was founded in 1854, the year of his death. Surrounding and interacting with Jameson were a number of mineral dealers and collectors. Alex Rose (1781-1860) a mineral dealer founded the Edinburgh Geological Society in 1834. Thomas Allan (1777-1833; of allanite) and Robert Allan (1806-1863) both merchant bankers by profession amassed large collections. Later followed Patrick Dudgeon (1817-1895) and Professor Matthew Forster Heddle (1828-1897) Professor of Chemistry at St. Andrews University, both of whom donated/sold large mineral collections to the Royal Museum of Scotland. Heddle wrote 'The Mineralogy of Scotland' (1901) which is still the only major work on Scottish Mineralogy.

CAUSES OF COLOR IN SERPENTINE MINERALS

M. Logar (Dep. of Mineralogy, University of Belgrade)
V. Poharc-Logar (Dep. of Mineralogy, Univ. of Belgrade)
B. Kasalica (Dep. of Physics, Univ. of Belgrade)

Diffuse reflectance spectra of six vein serpentine minerals were measured in the 50000-5000 cm^{-1} region, using λ9 Perkin Elmer instrument. Specimens of variable thickness (0.1 to 0.5 mm) polished on the both sides were prepared for transmittance (T) and diffuse reflectance measurements using $R_{45,0}$ device to avoid specular reflectivity. Typical spectra are shown in the fig., where $K_t=-lnT*d^{-1}(mm)$ and $f(R_\infty)=K/S$. The color specification (CIE, illuminant C) of the transmitted and reflected light is: $d_c(T)=577$ nm, $p_c(T)=46.1$ %; $d_c(R)=520$ nm, $p_c(R)=4.9$ %.

The shape of the absorption curve and, therefore, the actual color of the serpentine minerals, depends on K/S relation.

Spectral distribution of absorption coefficient K depends on the energies of the electronic transitions in Fe^{3+}(0.68 %) and Fe^{2+}(0.58 %). Those are in octahedral sheet replacing Mg. The main contribution to K offers Fe^{3+}->O charge transfer band (peak at ~37000 cm^{-1}), which is spread over the visible region, overlapping weak d - d transitions bands. Two peaks at ~13500 and ~11000 cm^{-1} are caused by Fe^{2+}->Fe^{3+} and T_{2g}->E_g (Fe^{2+}) respectively, rather then $^4T_{1g}$ and $^4T_{2g}$ (Fe^{3+}).

Spectral distribution of the scattering coefficient S arises from the textural inhomogeneities. Calculated from Kubelka formulas, S was found to have $\nu(cm^{-1})$ dependence: $S=const*\nu^{3.2}$. Compared to the empirical data (Kortum & Oelkrug, 1964), that correspond to particle size smaller then wavelength in the blue region.

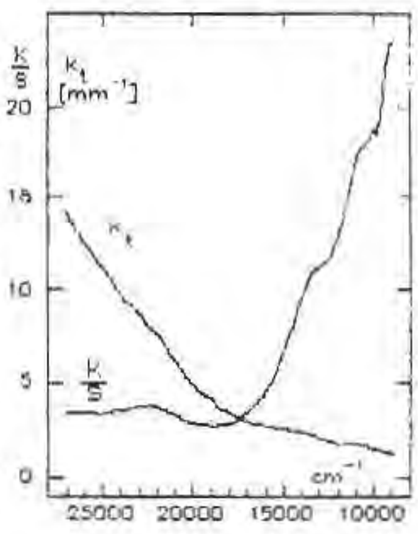

Reference:
Kortum, G. & Oelkrug, D. (1964). *Z. Naturforsch*, **19a**, 28.

NEW SUBGROUP OF CR–AL SERIES IN MICA

Lu Anhuai, Chen Guangyuan, Sun Daisheng
(*Dept. of Geology, China Univ. of Geosci.*)

Due mainly to their complex compositions and wide distributions as well as important roles in rock and ore formations, minerals in mica groups, the most abundant phyllosilicate, are still paid great attention to by geologists. Generally the micas can be classified at group level as true micas with compensation primarily by monovalent interlayer cations and brittle micas with compensation primarily by divalent interlayer cations in the formula unit. Furthermore, the two groups are divided into subgroups on the basis of their octahedral occupancy as dioctahedral subgroup corresponding to Mg–Fe series and trioctahedral subgroup corresponding to Al series considered before.

In fact, many of the major rock–forming silicate minerals appear to be capable of accomodating substantial substitution of Cr into their crystal structures and even more the isomorphous replacement between Cr and Al in octahedral sites in some minerals is quite complete, e.g. in spinel group like $MgCr_2O_4$—$MgAl_2O_4$, in garnet group $Ca_3Cr_2Si_3O_{12}$— $Ca_3Al_2Si_3O_{12}$ and in pyroxene group $NaCrSi_2O_6$— $NaAlSi_2O_6$ etc.. Recently the substitution of Cr for Al in octahedral positions in natural micas is widely reported and the maximum levels of Cr substitution may be far greater, especially at low pressure, than hitherto suspected. The natural chromian muscovite shows the value of Cr_2O_3 up to 24.7% corresponding to 1.45 Cr atom per formula unit (11 oxygens) with a maximum 81.9% substitution of Cr for Al on octahedral sites (Treloar, 1987). Data of 118 chromian muscovites from different corners of the world including 41 from Chinese samples completed by auther are brought together for setting up the relationship between Cr and Al on octahedral sites shown in Fig.1. This plot shows evidence for extensive solid solution between octahedral Cr and Al which is rarely demonstrated before. Unfortunately the end member of Cr in the solid solution has not been discovered in nature, while the another end member of Al is known as muscovite.

As with complete solid solution of Mg–Fe series corresponding to trioctahedral subgroup, phlogopite $KMg_3(Si_3Al)O_{10}(OH)_2$—biotite $K(Mg,Fe)_3(Si_3Al)O_{10}(OH)$—annite $KFe_3(Si_3Al)O_{10}(OH)_2$in mica group, Cr–Al series corresponding to dioctahedral subgroup is also indicated here at first time, chrome mica $KCr_2(Si_3Al)O_{10}(OH)_2$— chrome aluminium mica $K(Cr,Al)_2(Si_3Al)O_{10}(OH)_2$— aluminium mica i.e. muscovite $KAl_2(Si_3Al)O_{10}(OH)_2$. Because of Cr–bearing muscovites reported in old literatures through never yet with Cr_2O_3 values in excess of 4.81%, usage of the term fuchsite to cover a range in Cr_2O_3 content more than 4.81% is discouraged in mineralogy. It may not be debatable that classification and nomenclature of minerals in mica group should be reviewed in detail. Tentative classification at subgroup level being advanced here is chromo–alumino–mica and magnesio–ferro–mica according to types of completely isomorphous replacements among cations in

octahedral sites in natural true micas which are rather systematic so far known.

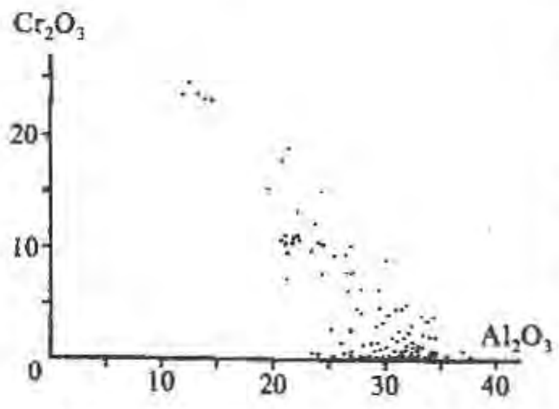

Fig.1 Substitution of Cr for Al

Since the element of Cr riches in mantle-derived rocks, especially chrome mica is usually generated from crystalline basements of basic to ultrabasic metavolcanics in the earlier geological era or related to remobilization from the crystalline basements in the later geological era and sometimes occurs in hydrothermal altered ultrabasic rocks in ophiolite suites, characteristics of systematic evolution emphasis on phylogeny of the new subgroup of Cr-Al series will be helpful to recognize the geological history from the early origin of crust to the late crust evolution and from rock formation to ore formation.

Multimedia Technique in Mineral Database

Lu Jun (Institute of Mineral Deposits, Chinese Academy of Geol. Sci.)

During 15th IMA General Meeting, the present author reported a multi-language mineral database. It involves mineral name (in English, Chinese, Russian respectively), chemical formula, JCPDS number and mineral data analyzed by electron probe, infrared spectroscopy and XRD. It is obvious that the data types involved in the above database are only digital and character types. In fact, we are often able to obtain various graphs or images in the course of mineralogical studies. For instance, correlation diagram between chemical compositions of minerals, gray or color images from both optical and electron microscopes (SEM or TEM). If all of these information are stored in a database, it will be very convenient to mineralogists. Before multimedia technology emerged, it was very difficult to do this.

The emergence of large-capacity compact discs, high-speed CPU and high-speed digital signal processing technique makes it possible to establish multimedia DBMS, image-text DBMS, that involves graphs, text, images, and sound. In order to store image fields in a DBMS, we have to take into account two problems: 1. image access format; 2. image compress code standard. Now there have been more than two kinds of access format, e.g. TIF and TGA etc.. For still image, JPEG compress standard has often been used. Image-text DBMS may run under both DOS and WINDOWS environments so that mineralogists will be able to choose one from these two environments.

On the basis of multi-language mineral database, the present author selected DOS mode to establish multimedia mineral database which involves hand-specimen image of minerals and some of TEM topography image and electron diffraction patterns.

References:
Lu Jun (1990) Microcomputer system for identification of minerals. 15th IMA General Meeting ABSTRACTS Vol.2 p.709.
Lu Jun (1990) Some applications of microcomputer to mineralogy. 15th IMA General Meeting ABSTRACTS Vol.2 p.1014.
Smith, D.G.W. and Leibovitz, D.P. (1986) MinIdent: A data base for minerals and a computer programme for their identification. Can. Min. v.24, p.695-708.

STUDY ON THE FEATURE OF ZIRCONIUM AND ZIRCON FROM BAUXITE IN HENAN PROVINCE

Lü, X. (*Inst. of Non-ferrous Mineral Resources and Geology of Henan, China*)

The bauxite in Henan is diaspore type ore, the same with the major types of our country in Guizhou and Shanxi province. The deposits hosted in ore-bearing Benxi group middle Carboniferous above the weathering erosion surface of Cambrican or Ordvican carbonatite. From bottom to top, the lithological characters of ore-bearing system are ferruginous clay, bauxite and kaolinitic clay. The ore is composed of diaspore, kaolinite, illite, chlorite, montmorillonite, limonite etc. The ore structure and texture is campact ; massive, oolitic and saccharodial texture. The contents of main chemical composition are: Al_2O_3 65-70%, SiO_2 5-15%, Fe_2O_3 2-4%, TiO_2 2.5-3.5% and loss 13-14%.

Based on statistics, the minimum content of Zircomium is 425×10^{-6}, the maximum content is 991×10^{-6}. The contents of Zircomium are different in different zones. In the same zone, the Zr content is positive corrolated with the content of Al Ti, negative corrolated with the content of SiO_2. In vertical section, from bottom to top, the content of Zircomium changes from low to high, then again to low, the lithological characters change from ferruginous illite clay to bauxite, then to kaolin clay. As the ore grade changes from poor to rich, the content of zirconium changes from low to high. So, Zirconium is one of indicative elements of bauxite.

The author enriched the zircons from bauxite, clay and related rocks by artificial panning and study its mineralogical features in detail by microscope, electron microscope spectrum methods etc, and get many clear photoes of zircons. The elements of zircons are SiO_2 31.42-31.71%, ZrO_2 65.40-65.51%, HfO_2 2.98-3.19%, The stronger lines of the zircons in the power diffraction pattern average 0.333nm, 0.251nm, 0.1710nm, 0.1631nm. The study indicates that the zircons in bauxite with different colour: colourless, pink, purple, light purple, brown, light brown etc. The crystal shapes are variey. They have bipyramid ditetragonal prism and pyramid tetragomal prism from short to long in length, bipyramid and allotriomorphic particles etc. The zircons with different colour and shapes proved that the bauxite came from different sources. Most of the zircons have polished scratch in their surfaces, it show that the zircons had been carried over some distance. The study indicates that Zirconium of bauxite mainly contents in zircons. The analysis shows the more zircons, the more diaspores in buaxites in the same deposit . So there are the more zircons the richer Al_2O_3 in bauxite.

The author also studied the mineralogical characteristics of the zircons from carbonitite of ore-bearing basement and in nearby weathering metamorphic rocks, that their age is older than bauxite's, for example, granite-gneiss, striped-migmatite etc. Throgh comparison, the same crystal forms and colour of the zircones have been founded from them and from the bauxite. It proved that the sources of bauxite are

from basement rocks and related metamorphic rocks around sedimentary area.

The study on Zirconium distribution and the features of Zirconium minerals in the bauxite and related rocks will benefit the prospecting of high quality bauxite and the research for the material sources and formed environment of bauxite.

CRYSTAL CHEMISTRY OF TOURMALINES FROM THE CRUZEIRO PEGMATITE, MINAS GERAIS, BRAZIL

Lucchesi S., Federico M., Graziani G. and Andreozzi G.B. *(Dip. Scienze della Terra, Univ. of Roma "La Sapienza", Italy)*

A crystal chemical study was carried out on tourmalines from the Cruzeiro pegmatite (Governador Valadares, Minas Gerais State, Brazil). This Li-, B-, Be-, Nb-, Ta- and Zn-enriched, miarolitic pegmatite consists of three internally zoned dykes which intrude into the quartzites of the Serra da Safira complex.

Tourmalines were collected in the outer, wall and internal zones and in the pockets of n° 1 and n° 3 dykes. Crystals were investigated by means of an electron microprobe (Cameca-Camebax WD system), an ion microprobe (Cameca IMS 3f) for H, Li, Be and B and an X-ray single-crystal diffractometer (Siemens P4).

Structural data were collected with $Mo_{K\alpha}$ radiation and unit cell parameters were determined from 26 independent reflections and their Friedel pairs, from 85° to 95° 2ϑ. X-ray intensity data were collected in the range $3° < 2\vartheta < 95°$ with the ω-scan method. Structure refinements were carried out by means of the SHELX-TL PC program.

An extensive chemical study already presented (Lucchesi *et al.*, 1993) clarified the coupled substitution mechanisms operating in the tourmalines of Cruzeiro. The composition of the border and the wall zone tourmalines is referable to aluminous, alkali-deficient schorl (Foit & Rosenberg, 1977) with Mg ranging from 0.02 to 0.95 a.f.u.. The chemical composition of tourmalines from the inner zone and pocket is referable, on the contrary, to OH-rich (OH+F up to 4.57 a.f.u.), alkali-deficient elbaite with a relatively wide range of Y-site substitutions (Fe^{2+} from 0.00 to 1.04 a.f.u. and, sporadically, minor contents of Mn, up to 0.51 a.f.u., and Zn, up to 0.22 a.f.u.).

All the crystals, particularly those occurring in the pockets, are also characterized by an ubiquitous deficient B content (from 2.48 to 2.94 a.f.u.), never sufficient to achieve the full site occupancy required by stoichiometry.

Unit cell parameters of the elbaite-dominant tourmalines range between $\underline{a}$ = 15.8318(6) to 15.9246(6) Å and $\underline{c}$ = 7.0998(3) to 7.1302(3) Å, while the schorl-rich samples are characterized by larger unit cell dimensions (up to $\underline{a}$ = 15.9842(6) Å and $\underline{c}$ = 7.1581(3) Å).

Unit cell variations are in line with those reported in literature for the elbaite-schorl series (Epprecht, 1953; Foit, 1989) and the higher $\underline{c}$ values characteristic of the tourmalines from the wall zone may be ascribed to minor dravite content.

Structural variations are related to chemical composition and in particular:
T-O from 1.617 to 1.624 Å,
B-O from 1.375 to 1.378 Å,
Z-O from 1.906 to 1.917 Å,
Y-O from 2.000 to 2.047 Å,
X-O from 2.672 to 2.700 Å.

References:

Epprecht, W.(1953). *SMPM*, **33**, 481-505.
Foit, F. F., Jr. (1989). *Am. Min.*, **74**, 422-431.
Foit, F. F., Jr. & Rosenberg, P. E. (1977). *Contr. Min. Petr.*, **62**, 109-127.
Lucchesi, S., Federico, M., Graziani, G., Andreozzi, G., Mendes, J. C. (1993). *Plinius*, **10**, 171-173.

EFFECT OF VOLATILE EXSOLUTION ON THE OXIDATION STATE OF BASALTIC MAGMAS DURING PRESSURE DECREASE AND CRYSTALLIZATION

Lukanin O.A. (*Vernadsky Inst.Geohem. & Analyt. Chem., Moscow*),
Lukanin A.O. (*Geological Inst., Russian Academy of Sciences, Moscow*)

Computer simulation results of basaltic magmas redox state changes caused by gases exsolution (H_20-H_2 or CO_2-CO) during magmas uprising to the surface and their crystallization are presented. Variations in fluid composition, volatile content in the melt, oxygen fugacity and ferric-ferrous ratio in the melt were calculated for the closed system with all volatiles retained in the melt and for the open system with the successive separation and removal of the gas phase (Lukanin & Lukanin, 1993). The model of water-bearing magmas used accounts the solubility of H_2 in silicate melts according to experimental data (Zharikov *et al.*, 1988; Bezmen *et al.*, 1991) that differs from previous calculations, in which H_2 solubility was neglected (Candella, 1986).

Calculations performed in the framework of the simplified model has shown that decompression degassing can be an effective mechanism for fO_2 increase in magmas near surface (by more than 1 or 2 orders of magnitude), provided reduced magmas ($fO_2 < WM$) are relatively high in volatiles ($H_2O > 2$ and $CO_2(+CO) > 0.5$ wt.%), that is, when the degassing of water-bearing magmas begins at pressure >1-2 kbar and the degassing of dry carbon-bearing magmas at >5 kbar. Therefore the exsolution of CO_2-CO rich gas phase from the low-volatile ocean tholeiitic melts ($H_2O < 0.1$-0.5; $CO_2 < 0.1$-0.3 wt.%) at pressures below 1-3 kbar, evidently, can not essentially influence on their oxidation state. The degassing of initially reduced low-volatile basaltic magmas during their crystallization (crystallization degassing) plays more important role in fO_2 increase in forming residual melts. Relative fO_2 increase during crystallization is the greater, the lower is initial fO_2 value in magmas before saturation of volatiles and the more fractional is the degassing, as in case of decompression degassing.

The oxidation effect of decompression and crystallization degassing decreases with increasing of fO_2 in magmatic system. When basaltic magma fO_2 reaches the level of the FMQ-NNO buffers equilibria, the degassing practically does not effect on the fO_2. Moreover, as crystallization is proceeding, there arise new factors that retard the fO_2 increase. These factors are the crystallization and fractionating Fe-Ti-oxides and oxygen consumption by sulphide sulphur oxidation in magma (Carmichael & Giorso, 1986). As a result, the future cooling and crystallization of magma may proceed under the self-buffering conditions of the system, when fO_2 maintains at FMQ-NNO level, as one can observe in differentiated basaltic series.

References:

Bezmen, N.I., Zharikov, V.A., Epelbaum, M.B. *et al.* (1991). *Contrib. Mineral. and Petrol.*, **109**, 89-97
Candela, P.A. (1986). *Geochim. et Cosmochim. Acta*, **50**, 1205-1211.

Carmichael, I.S.E. & Giorso, M.S. (1986). *Earth Planet. Sci. Lett.*, **78**, 200-210.
Lukanin, O.A. & Lukanin, A.O. (1993). *Petrology*, **1**, 250- 256.
Zharikov, V.A., Persikov, E.S., Bukhtiyarov, P.G. *et al.* (1988). *Dokl. Acad. Nauk SSSR*, **300**, 953-957.

Bi- minerals from Baita Bihor skarn deposit (Romania) - mineralogical characteristics and substitutions: implications for ore fluids chemistry

Lupulescu M.V. (*Mineralogy Dept., Bucharest Univ.*)
Lupulescu A. (*Insitute of Geol. & Geophys., Bucharest*)

The ore deposit of Baita Bihor (Bihor Mountains, Romania) contains a large number of bismuth minerals which open the mineralizing hydrothermal process in the grossular- andradite and wollastonite skarns.

Our electron microprobe, structural, spectral reflectance and micro-hardness study points out the following mineral record: joseite A , tetradymite, ingodite, bismuthinite, aikinite, gladite, friedrichite, Pb- rich cuprobismutite, pavonite and cosalite.

The relationships between minerals show that at the beginning of the mineralizing process the structural layered minerals as ingodite, joseite A and tetradymite formed, followed by cosalite, pavonite, Pb-rich cuprobismutite and by the members of the bismuthite - aikinite homologues series deposition.

The minerals of the Bi-Te-S system (ingodite, joseiteA and tetradymite) are indistinguishable by optical means and their chemical compositions by electron microprobe indicate very poor substitutions. The most common , but not so extended are the replacement of S by Se and Te by Sb. Only in one sample a small part of the Bi atoms are replaced by Pb in the layered structure of joseite A.

In the cosalite composition, $Pb_{1.86}Bi_2S_5$, cation substitutions are limited. Minor replacement as interstitial Cu atoms by silver occurs. The value of this mineral is as an indicator of the limiting thermal conditions at the time of mineralization.

In the bismuthinite - aikinite homologues series the substitution of Pb for a part of bismuth atoms in the BiS_5 square pyramide varies from 0.95 % lead atoms in bismuthinite ($Bi_{1.86}Pb_{0.04}S_3$) to 5 % lead atoms in gladite ($Pb_{0.77\text{-}0.95}Cu_{1.02\text{-}1.07}Bi_{4.58\text{-}4.65}S_9$) to 13 % atoms in the friedrichite composition ($Pb_{4.59}Cu_{4.79}Bi_{6.96}S_{18}$). To balance the charge, 1.3 % copper atoms in bismuthinite, 6.6 % atoms in gladite and 13.7 % atoms in friedrichite are added in the tetrahedral interstices. No silver atoms were detected because they do not have any favorable position in these mineral structures. Sulfur is common replaced by Se and then by Te.

The possible extended Bi by Pb replacement in the Pb- rich cuprobismutite ($Cu_{7.4}Bi_{10.9}Pb_{1.05}S_{23}$) is in the octahedral positions occupied mostly by Bi in the cuprobismutite unit cell.

The composition of pavonite shows the substitution of silver by copper and of bismuth by lead to give the following formula:

$(Ag_{0.48}Cu_{0.62})_{1.1}(Bi_{2.86}Pb_{0.09})_{2.95}(S,Te)_{5.09}$ or
$(Ag_{0.36}Cu_{1.03})_{1.39}(Bi_{2.78}Pb_{0.19})_{2.97}(S_{5.02}Te_{0.09}Se_{0.09})_{5.2}$.

The substitution degree in the bismuth minerals record at Baita Bihor ore deposit is more extended in the pavonite and aikinite-bismuthinite homologues series comparing with the minerals which belong to the Bi-Te-S system. The trace element composition points out a more complex chemistry (Hg, As, Se, Ni, etc.) for the hydrothermal fluids able to generate the mineral associations of low and medium temperature against the high temperature mineral assemblages. These data can be correlated with the changes in the f_{S2}/ f_{Te2} ratio which lead the mineral deposition. The depositional sequence begins with sulfotellurides of bismuth formed under increasing f_{S2}/ f_{Te2} were these minerals are stabilized with respect to pure bismuth tellurides (unidentified here) and continues with bismuth sulfosalts and then sulfides deposition under high f_{S2}.

Bismuth minerals occur in many other places in the western part of Romania, being a characteristic feature of the mineralizations related to Upper Cretaceous - Paleocene magmatism. This data are in good agreement with the observation that bismuth minerals are generated in continental arc tectonic setting which involves the continental crust contribution.

VOLCANIC-HOSTED GRAPHITE MINERALIZATION IN THE EXTERNAL ZONES OF THE BETIC CORDILLERAS (SOUTHERN SPAIN)

Luque, F.J., Barrenechea, J.F. and Rodas, M. (*Dpto. Mineralogía. Univ. Complutense, Madrid*)

Graphite mineralization related to volcanic rocks is a very uncommon type. It has been only recognized, up to now, at Borrowdale (Cumberland, England; Strens, 1965). The present paper deals with the mineralogic study of a similar deposit associated to Jurassic volcanic rocks in Southern Spain.

The volcanic rocks occur in discontinuous outcrops along a WSW-ENE band of about 250 Km long and 5-10 Km wide in the Subbetic Zone of the external parts of the Betic Cordilleras. These rocks mainly correspond to pillow-lava and pillow-breccia flows, being interbedded within Jurassic carbonate pelagic sequences (mainly marls and limestones). The volcanic rocks, together with their subvolcanic counterparts (sills and dikes), originated in the mantle and were extruded through a thinned continental crust as a fissure volcanism in a distensive to transtensive regime (Comas *et al.*, 1986; Puga *et al.*, 1989).

The studied mineralization is located in one of these volcanic outcrops, near Huelma (Jaén province). The host rock corresponds to an alkaline basalt; graphite has not been found in the surrounding carbonate sediments. The most abundant primary minerals in the basalts are olivine, augite and plagioclase, often zoned. Rutile is the main accesory phase. The petrographic study shows that these rocks have undergone different degrees of alteration. Their textures range from intergranular to ophitic and intersertal.

Graphite mineralization in the volcanic rocks occurs in a highly altered level as rounded to irregular pockets, small nodules and fracture fillings. X-ray diffraction (XRD) studies reveal the presence of quartz and, less commonly, calcite in the mineralized bodies.

The specific study of graphite was performed by means of reflected light microscopy, XRD, thermal analysis (DTA-TG) and transmission electron microscopy (TEM). When neccesary, graphite was isolated by acid (HF + HCl) treatment.

Graphite appears as randomly distributed flaky xenomorphous crystals with high reflectance values. The results indicate a perfect three-dimensional order, as deduced from the mean (002) spacing ($d_{(002)}$ = 3.355 Å), and the presence in the XRD patterns of other basal and non-basal reflections of the hexagonal graphite structure. In addition, a remarkable feature is the recording of two peaks at 2.08 Å and 1.97 Å, which correspond to the (101) and (012) reflections of the rhombohedral modification of graphite. The calculated degree of graphitization ranges from u=0.8 to u=1.

On the basis of the c_o parameter of graphite, and according to the geothermometrical estimation of Shengelia *et al.* (1979), a temperature of formation about 700-750 °C has been determined. From the field and mineralogical evidence, graphite is thought to be formed from the assimilation and reduction of carbon contained in the surrounding carbonate rocks.

Nevertheless, such a high temperature of formation and the presence of the rhombohedral phase of graphite appear to be in disagreement (Kwiecinska, 1980). This fact is also observed in the Borrowdale deposit and could suggest that the process of graphitization in fluid-deposited mineralizations is developed in a different way from that taking place during the evolution of organic matter due to prograde metamorphism.

References

Comas, M.C., Puga, E., Bargossi, G.M., Morten, L. & Rossi, P.L. (1986). *N. Jb. Geol. Paläont. Mh.*, 25, 386-404.
Kwiecinska, B. (1980). *Polska Akad. Nauk, Prace Mineralogiczne*, 67, 5-79.
Puga, E., Portugal, M., Díaz de Federico, A.; Bargossi, G.M. & Morten, L. (1989). *Geodinamica Acta*, 3, 253-266.

Shengelia, D.M., Akhvlediani, R.A. & Ketskhoveli, D.N. (1979). *Dokl. Akad. Nauk SSSR*, 235, 132-134.
Strens, R.G.J. (1965). *Geol. Mag.*, 102, 393-406.

OPTICAL ABSORPTION OF IRRADIATED CHALCEDONY

Lutoev V.P. *(Inst. Geol., Komi Sci. Cent., Ural Div., RASci.)*

Colours of chalcedonies are usually connected with chromatic inclusions and peculiarities of light diffraction on microstructures of the chalcedony aggregate. The colour of α-quartz microcrystals, which compose chalcedony, does not practically influence on resulting colour. One of the effective factors of modification of α-quartz colours is ionized radiation, which stimulates the appearance of the colour centres. The radiation effects in macrocrystalline quartz are studied in detail, as a rule ones are disregarded when the microcrystalline quartz is investigated.

The purpose of this work is investigation of γ-radiation influence on absorption spectra of chalcedonies in visible and ultraviolet regions (1.6 ÷ 6.2 eV). The electron spin resonance (ESR) of chalcedony powders and blocks was studied too.

The objects were spherulitic zone agates from Timan (Northern Russia). The specimens were cut out from zone of transparent colourless gomogeneous longfiber chalcedony. They are consist of 97 ÷ 99% of silica and 0.5 ÷ 1.5% of water and some quantity of impurities of Al, Na, K, Fe, Mg, Ca. X-ray index of crystallinity is 4.5 ÷ 6.5. The smoky colour appears in chalcedonies after γ-irradiation (dose is about 10^4 Gy).

No bands in visible region are registered in origin chalcedonies. The inexpressive bands 2.1 eV and 2.6 eV were detected in γ-irradiation chalcedonies. $[AlO_4e^+]^0$ - smoky colour centres of α-quartz may cause these bands. Centres like those in the chalcedonies were observed by ESR. Their concentration in the origin samples is 2 ÷ 10 p.p.m. and after irradiation increases to 10 ÷ 30 p.p.m.

The absorption spectra of chalcedonies in the ultraviolet region resemble the absorption spectra of citrine Fe-doped quartz. They consist of the intensive broad (linewidth is about 1.5 eV) band at 5.6 eV and less intensive poorly resolved band at 4.9 eV. By analogy with Fe-doped quartz crystals we consider that the above-mentioned bands are caused by ligand-cation transitions of electronic charge, i.e. $O^{2-} \rightarrow Fe^{3+}$. It is confirmed by the registration of anisotropy ESR spectrum at g≈4.3 in nearly directed chalcedony specimen. This spectrum is evidently caused by Fe^{3+}-impurities of the quartz microcrystals of the chalcedony.

γ-irradiation does not change intensities of bands at 5.6 eV and 4.9 eV, but it significantly broadens longwave shoulder of absorption spectra. By subtraction of spectra a new component at 4.4 eV with halfwidth 1 eV was found in absorption spectra of irradiated chalcedony. The longwave bound extends on visible region.

The lowtemperature annealing destroys the band at 4.4 eV and it restores by repeating of irradiation. The irreversible destruction of the band probably occurs at annealing temperatures higher then α-β transition point. The paramagnetic species with the same radiate and temperature reaction exist in chalcedonies, as ESR method showed . They include oxigen hole centres (g_{zz}= 2.068, 2.052, 2.030) and electron E'-centres typical for quartz macrocrystal. The hole paramagnetic centres and organic radicals probably special for chalcedonies were also found. However a simple interdependency between radiate band and any paramagnetic species was not found yet.

MINERAL REACTION KINETICS IN VIEW OF EXPERIMENTAL RESULTS: PAST, PRESENT AND FUTURE

Lüttge, A. *(Inst. f. Mineralogie, Petrologie u. Geochemie), Univ. Tübingen*

Past: For decades the interest of many (experimental) petrologists working on metamorphic petrology focussed on equilibrium, phase relationships, and the stability of minerals and parageneses. The petrogenetic grids which resulted allow us to quantify the stability conditions of many metamorphic assemblages.

Therefore, the step beyond equilibrium, the study of reaction kinetics, was also made possible on the basis of such data. Thus, we learned to study the dynamic mode, the processes which produce metamorphism. The goals were to quantify these processes and the parameters which are relevant. During the 70's and 80's several authors have studied the mechanisms and kinetics of a small number compared with the large number of reactions which are relevant to metamorphism of mineral reactions using mostly mineral powders as starting materials. One main result of this work was the observation that the overall mechanism of heterogeneous mineral reactions occurs via a dissolution-transport-crystallization mechanism over a wide range of P-T-x conditions, and that there is a catalytic effect of water, even if it is present only in very small amounts. Most of the reactions are interface controlled and the determination of the rate limiting steps showed that the dissolution of reactants is often critical. Thompson & Rubie (1985) and Kerrick et al. (1991) have given excellent reviews of this experimental work.

However, up to now there is only a very limited number of data available, especially for activation energies, which are quite difficult to determine. In addition there has been criticism of experimental methods using mineral powders, because of the problems of surface defects and large porosities which may not apply to nature, but in any case such powder experiments provide important information on mechanisms, rates, and activation energies of mineral reactions.

Present: A recent study by Lüttge & Metz (1993) using a rock cylinder of a siliceous dolomite shows that the results are essentially the same as those from earlier studies using mineral powders. The comparison can be done using a concept of splitting the rock into microsystems which can be compared directly with the situations observed in a powder mixture. On the basis of these results, it seems reasonable that experiments using mineral powders are useful as a first step to study the influence of kinetic variables. Experiments with rock samples can become a "bridge" to connect these results with observations made in nature.

Some other interesting aspects of present kinetic studies are:
- the behavior of single crystals used as reactants,
- the formation of metastable phases, and side reactions,
- approach to equilibrium.

An important approach is the study of the initial phase of the reactions. To do this it is necessary to use more sophisticated experimental equipment to achieve very short run-up times. The results of such experiments give us much better insight into the beginning of dissolution of reactants and the nucleation of run products. With this method it is possible to study the kinetics as a function of only small variations in the set of starting parameters, because the heating rate, for example, determines the dissolution of the reactants.

Future: Thompson & Rubie (1985) and Kerrick et al. (1991) present useful suggestions for future research to quantify the processes involved in metamorphic reactions. Over and above that, it seems necessary to study the processes occuring in the fluid phase in more detail. SEM/TEM methods, EDX, WDX and X-ray diffraction techniques provide information about the solids at the beginning and at the end of each run. Measurements of conversion can determine the rate of a reaction, but the fluid phase during the reaction is still nearly a black box. A better understanding of the mechanisms of overall heterogeneous reactions requires a much better knowledge of speciation, and concentrations of species in the fluid phase. Therefore extraction and spectroscopic techniques are valuable and should be used and developed. Each approach which helps to split

the overall mechanism into smaller parts which can be quantified will be a substantial step forward.

References:
Kerrick, D.M., Lasaga, A.C., Raeburn, S.P. *in* Kerrick, D.M. (ed.) (1991). *Rev. in Miner.*, **26**, 583-671.
Lüttge, A., Metz, P. (1993). Contrib. Mineral. Petrol. **115**, 155-164.
Thompson, A.B., Rubie, D.C. (eds.) (1985). Advances in Phys. Geochem., **4**, Springer.

PHASE TRANSITIONS AND STRUCTURAL EVOLUTION OF OCEANIC FERRO-MANGANESE NODULES

Lysiuk G.N. (*Institute of Geology, Ural Division, Russian Academy of Sciences*)

Phase transformations study of minerals from pelagic ferromanganese nodules was conducted in three directions:

a) characterizing of matter from different growth zones of nodules. It allowed us to follow the nodule matter evolution from a nucleation moment till a modern state;

b) high temperature heating in dry air;

c) experimental modelling metamorphic processes at high temperatures and pressures in different media (neutral, acid, alkaline). On this basis ane can predict ways of nodule matter transformation.

The investigaton of variation in physical properties of predominant crystalline phase (10 Å phase) showed that reflecting coefficient and hardness values are increased along with coming from a periphery zones of nodules to a centre. That is a consequence of the degree of mineral crystallinity is increased in this direction and the growth from a centre to a periphery goes through several stages for a long period of time.

High temperature heating of nodule samples up to 1000°C results in amorphous phase to be transformed to jacobsite. On the basis of experimental modelling metamorphic processes, PT-diagrams for fields of crystalline phases stability were revealed. Hydrothermal processing samples in neutral medium results in crystalline phases of two structural types: olivine structural type (tephroite, fayalite) and spinel structural type (magnetite, hausmannite, $NiMn_2O_4$, $NiFe_2O_4$, $CoFe_2O_4$). In acid medium, fields of stability of crystalline phases are distinguished with the following mineral associations: hematite, tephroite - jacobsite - braunite; tephroite - jacobsite - hausmannite. In alkaline medium braunite, tephroite, jacobsite, hausmannite are formed.

The formation of hematite and braunite under treatment in acid media is in accordance with the results of studies of mineral phases in metamorphic ferromanganese nodules. It is important in view of ferromanganese ores genesis, as we can now describe the processes of recrystallization of manganese and iron hydroxides and the formation of the elements' oxides.

Ferrites and manganites $MnFe_2O_4$, $FeFe_2O_4$, $MnMn_2O_4$, $NiMn_2O_4$, $NiFe_2O_4$, $CoFe_2O_4$) are formed as at high temperatures in dry air as under hydrothermal conditions in neutral media. Synthesis of cobalt and nickel and manganites is of practical interest. Until now it is not known what phases nickel and cobalt belong to. We can say of them only on general. As seen from our experiments the formation of these phases leads to an enrichment of nodule ore and favours a following extraction of the elements. Note that these compounds are not formed under treatment in acid and alkaline media as a consequence of leaching.

The data obtained provides an opportunity to reveal main evolution tendencies in ferromanganese nodule phase constitution as well as to synthesize new crystalline phases from the initial matter of nodules.

GRAIN BOUNDARY DIFFUSION IN MANTLE SILICATES

Mackwell S. and Fisler D. *(Dept. of Geosciences, Penn State Univ.)*

Grain boundary diffusion rates have been determined for oxygen in fayalite and silicon in enstatite using a reactive growth technique. Thin polished slices of quartz were imbedded in finely ground powders of iron oxide or natural olivine, and treated at high temperatures in a controlled oxygen environment under a light uniaxial load. Under the conditions of the experiments, a thin layer of polycrystalline fayalite or enstatite formed at the interface of the powders and the quartz. We measured the thickness of the reaction phase as a function of oxygen fugacity and temperature for times ranging from 4 to 200 h. The thickness of both the fayalite and enstatite increased parabolically with time, indicating that the rate of growth of the reaction phases was controlled by diffusion of chemical species through the reaction phase.

We utilized platinum inert marker experiments, measured dependencies of growth rate on oxygen fugacity, and previously published diffusion data to determine the species rate-limiting the growth of the reaction phase. On the basis of these observations, we determined that the species controlling the growth of the fayalite rim was oxygen, diffusing along a grain boundary path. Using the measured grain size of the reaction rim, $d \simeq 1\ \mu m$, we obtained a mean grain boundary diffusivity for oxygen in fayalite of

$$\bar{D}_O^{gb}\,\delta = 1.28\times10^{-3}\ f_{O_2}^{-0.17}\ e^{-540/RT}\ m^3s^{-1},$$

where δ is the grain boundary width (in m), and the activation energy is in kJ/mol. This result is reported as a mean diffusivity as the reaction phase was grown in an oxide activity gradient.

Similarly, we determined that the species rate-limiting the growth of the enstatite rim was silicon, diffusing along a grain boundary path. From the measured grain size of $d \simeq 1\ \mu m$, we calculated a mean grain boundary diffusivity for silicon in enstatite of

$$\bar{D}_{Si}^{gb}\,\delta = 3.3\times10^{-9}\ f_{O_2}^{0.00}\ e^{-411/RT}\ m^3s^{-1}.$$

CARBONATIZATION OF SERPENTINITE IN THE MURCHISON GREENSTONE BELT, KAAPVAAL CRATON : IMPLICATIONS FOR GOLD MINERALIZATION

Madisha M. E. (*Dept. of Geology, Rand Afrikaans Univ.*)

The Murchison Greenstone Belt deposits represent Archean lode gold deposits hosted by a semi-brittle-ductile shear zone (the Antimony line) characterized by intensely deformed and carbonated mafic and ultramafic units of the greenstone sequence. Mineralization is hosted by ultramafic lithologies that display distinct hydrothermal alteration zonation characterized by massive introduction of CO_2 and alkalis (K and Na). The alteration zonation is defined by serpentinite → talc-carbonate → quartz-carbonate±fuchsite. Mineralization occurs in quartz-carbonate veins which are almost entirely hosted by quartz-carbonate rocks. The presence of fibrous quartz and carbonate grains in mineralized veins and the presence of undeformed veins that are parallel to and crosscut the deformed quartz-carbonate assemblages, suggest a syn- to post-tectonic emplacement of the veins.

The quartz-carbonate zone is characterized by the presence of quartz and carbonates which influence the mechanical properties of the rocks relative to other alteration zones. Subsequent deformation will, therefore, result in brittle deformation of quartz-carbonate rocks, which accounts for the preferential occurrence of mineralized quartz-carbonate veins in these rocks. Alteration is, therefore, of fundamental importance in the localization of the mineralization as it creates a sequence consisting of a variety of mineral assemblages

(lithologies) characterized by contrasting physical properties (i.e. **competency**). This will, therefore, make certain lithologies (quartz-carbonate rocks) preferable hosts.

The fact that this well-known alteration sequence of serpentine → talc-carbonate → quartz-carbonate±fuchsite can be constrained by a T-X_{CO_2} phase diagram allows the distinction between carbonate phases from the alteration sequence and those contained by crosscutting mineralized veins. The presence of dolomite and magnesite in these veins suggest that the alteration and subsequent mineralization could be a result of;

1) two distinct fluid events or
2) a single fluid with a complex evolution

ANCIENT CERAMICS : THE MINERALOGICAL AND CHEMICAL APPROACH

Maggetti M. *(Institute of Mineralogy and Petrography, Univ. of Fribourg)*

Chemical methods were used for solving some cultural-historical problems on ceramics, 100 years before the first application (1933) of mineralogical methods.The lecture will show some examples of a successful application of both approaches in archaeometric studies of ancient ceramics.

First, the theoretical bases of the application of chemical (X-ray fluorescence, neutron-activation) and mineralogical (microscopy, X-ray diffraction, Hg-porosimetry) procedures in the study of ancient ceramics are presented. Selected case studies are then discussed to study questions about the provenance (local or non-local production, i.e. import), the techniques (selection and preparation of raw material, addition of degreasing-components, firing temperatures, kiln-atmosphere) and the burial processes (chemical alterations/changes/reactions, clay-mineral generation, secondary pore-obstructions, destabilization of firing-phases). The study of ancient ceramics (provenance, techniques, burial changes) should include the chemical, as well as the mineralogical method, as they both show advantages and disadvantages.

MINERALOGY OF PLACER GOLD OF THE PREPOLAR URALS

Maiorova T.P. (Inst. Geol., Komi Sci. Centre, Ural Div. Russian Acad. Sci.)

Gold placer province of the Prepolar Urals stretches as a wide belt along its western slope and includes Central Ural longitudinal structural zone comprised by Proterozoic metamorphic rocks and the considerable part of Western Urals zone composed the Paleozoic clastic and carbonate deposits. Alluvial valley and terrace gold placers of Quaternary age prevail in the region.

Fine gold particles 0.1-1 mm predominate in the region. Only in the alluvium of small rivers the gold particles have larger size - 2 mm and above. Typically the moderate roundness of gold varies from good to weak in different placer regions. Lamellar and scaly gold particles prevail, but almost always some grains of other morphological types are present lump-like, crystallomorphic, rod-like and other ones.

Placer gold of the region is various by chemical composition. Its fineness ranges from 507 to 998 fine, but high-purety gold prevails in the majority of regional placers. Hg and Cu as well as Ag are the main admixtures. Hg content ranges from 0.1 to 8.17 wt.%, Cu content - from 0.02 to 6.5 wt.%. But 0.1-0.73 wt.% values for Hg (72%) and 0.02-0.15 wt.% ones Cu (84%) have the largest frequency of occurrence. Examination of data on chemical composition of placer gold using triangular diagrams, correlative and factor analyses reveals 4 types of gold : Ag, Ag-Hg, Ag-Cu and Ag-Cu-Hg ones. Each of these gold types is characterized by certain interval of fineness variation, content and ratio of the main admixture elements, specifics in distribution within geological structures of the Prepolar Urals. Investigation of internal structure of gold particles and character of distribution of the main elements (Au, Ag) in them allows to estimate the degree of gold alteration under the influence of weathering processes which are very intensive in many regions. In addition 17 microadmixture elements - Cu, Hg, Pd, Pb, Fe, Ti, Zn, Ni, Sb, Zr, Al, Ca, Mn, Si, Mg, As, Nb, have been recognized in placer gold of the region. Their contents are at about 10^{-2}-10^{-4}%. Cluster analysis of the relative quantities of these elements in gold reveals 2 groups of microadmixtures. The first group includes mainly lithophile elements. The second one - mainly chalcophile elements. Siderophile elements are distributed among them. In each group smaller element associations reflecting the specifics of ore mineralization in placer regions are distinguished.

Obtained data on mineralogy and typomorphic features of placer gold suggest the genetic types of sourcer lode corresponding to placers of the Prepolar Urals and their commercial use.

ISOMORPHIC AND MINERAL FORMS OF Ta AND Nb ADMIXTURES IN CASSITERITES FROM RARE-METAL PEGMATITES AND TIN-BEARING PEGMATITES

Makagon V.M. and Shmakin B.M. (*Institute of Geochemistry, Irkutsk, Russia*) **and** Wedepohl A.I. (*MINTEK, Randburg, Republic of South Africa*).

Cassiterites from rare-metal pegmatites of the Sayan Mountains (Eastern Siberia), which are of Li-Sn and Li-Cs-Ta types, granitic pegmatites of the Bastar deposit (India) of the Li-Sn type and Sn-bearing pegmatites from the Uis deposit, Namibia, and Tokwane deposit, Swaziland, were studied by means of electron microprobe and scanning electron microscope by Yu.D. Bobrov (Irkutsk) and A.I. Wedepohl (Randburg) respectively. Bulk chemical analyses of cassiterite crystals were also done, by means of quantitative emission spectroscopy, by I.E. Vasilyeva (Irkutsk) and by ICP-MS at MINTEK (Randburg).

In the cassiterites from granitic pegmatites of the Sayan region both isomorphic and mineral forms of Ta and Nb admixtures take place. For the isomorphic case mean Ta contents ranging from 0.45 to 1.49 mass % are found, for samples from different parts of the Sayan Mountains. Isomorphic Nb admixture takes place to a lesser extent than for Ta. Substitution for Ta with Fe compensation is possible in two different ways: 1) $2Sn^{4+} \leftrightarrow Ta^{5+} + Fe^{3+}$ and 2) $3Sn^{4+} \leftrightarrow 2\,Ta^{5+} + Fe^{2+}$. Some points in the cassiterite are characterized by high Ta and Nb contents without Fe compensation. The mechanism in this case might be $5\,Sn^{4+} \leftrightarrow 4Ta^{5+} + \square$.

Mineral inclusions in Sayan cassiterite are tantalite-columbite with Sn^{2+} replacing some of the Fe or Mn, and possibly $Sn_4(Nb,Ta)_6O_{23}$. In these phases there are Ta and Nb concentrations of up to 68 and 28% by mass, respectively.

Cassiterite from the pegmatites of the Bastar deposit contains isomorphic admixtures Ta(0.86 mass %) and Nb(0.03%) without marked Fe compensation. Mineral inclusions have the composition of microlite. Some of these

inclusions contain up to 22% Pb and can be described as plumbomicrolite.

Small mass percentages of isomorphous Ta and Nb (0.15 and 0.21 respectively) are found in cassiterite of the Uis pegmatites, Namibia. There are also fairly frequent inclusions of columbite-tantalite with Nb values ranging from 38 to 49% and Ta values ranging from 8 to 23%, by mass.

Where the tin-bearing cassiterite from Tokwane, in NW Swaziland was concerned, the average isomorphic content of Ta is 0.58% by mass but no Nb was detected. Infrequent inclusions consist of two phases, probably tanteuxenite and tantite both containing Ta, Nb, Ti and Ca, U, Sn. There are smaller amounts of the Ca, U in the tantite. There is a considerable amount of Sn in both phases i.e. 7 to 38 mass per cent. Y may be present in both phases but could not be confirmed due to overlapping peaks. Ta and niobium in these inclusions range from 32 to 59 mass % and 2 to 8% mass per cent respectively.

It is concluded that isomorphic Ta tends to occur to a larger extent in cassiterite from pegmatites than does Nb. A variety of Ta - Nb mineral inclusions can also be found in these cassiterites, the most common ones being tantalite-columbite or pyrochlore-microlite. Some additional components such as Pb, Bi, U and Sn can occur in these phases.

EVOLUTION OF MINERAL SEQUENCES OF ALPINOTYPE ULTRABASITS

Makeyev A.B., Bryanchaninova N.I. (Russ. Acad. of Sci., Institute of Geology, Syktyvkar)

For fifteen years we have studed the alpinotype ultrabasits of the Polar Ural. Mineralogical data on typochemism and typomorphism of rock-forming silicates (olivine, ortho-, clinopyroxenes), accessory minerals (chrome spinellide and sulfide) obtained in course of topomineralogical investigations allow to distinquish different ultrabasite complexes according to dunite-harzburgite ratio and to indicate various genesis of these complexes. Ontogenetic explorations of the minerals, paragenetic and typomorphic analyses gave a necessory materials for building of scheme of evolution of the mineral sequences. They are drawn maps for Voykaro-Synynsky, Riyzsky, Syumkewsky massifs, which show spatial change of various characteristics of complexes, rocks and minerals.

Evolution of mineral sequences of alpinotype ultrabasits is conditioned by changing the intensive parameters of the mineral-forming environment: fall the temperature and pressure in process of the formation of rocks. There are six stages in the history of the formation of ultrabasits massifs: mantle, regional metamosomatic, pegmatitic, regresive and progressive metamorphic stages and hypergenesis.

Each of the stages are charactarized by definite group of minerals. Those minerals which are presented in the mineral sequences of different stages are distinquished by composition and some of physical properties.

Evolution of composition of main rock-forming silicates from mantle to regional metasomatic stages consists in purifying of isomorphic admixtures in olivine and orthopyroxene and accumulation of Ca, Cr in clinopyroxene.

The main indicators of mineral sequences are chrome spinellide. Evolution of the composition of chrome spinellide pass from chrompicotite to chromite and then to magnetite by carring out Mg,Al,Zn,Ni and accumulating Fe^{2+}, Fe^{3+},Mn,Ti,V. By Mussbauer spectroscopy has been determined a gap of solid solution in natural series of chrome spinellide bitween chromite and magnetite.

We found more than fifty sulfide in ultrabasits of the Polar Ural. They may be divided into three groups, according their compositions. The first generation is connected with the pegmatite process. The main minerals are Cu-Fe-Ni sulfide: troilite, Fe,Cu-pentlandite and chalcopyrite. The second sulfide generation was formed in the autometamorphism (α-lisarditisation). The main minerals are Ni-pentlandite, heazlewoodite and millerite. The third generation includes Cu-Ni and rare metals sulfide, arsenide, sulfoarsenide and sulfosalt, which were formed in the progressive metamorphism process. All of the sulfide contain platinum group elements about 0,1%.

All these materials gave a posibility to constract a petrologic model of alpinotype ultrabasit massifs of the Polar Urals. It allows for deep quantitive forecast of chromite content which has proved successful of several objects. A set of prospecting signs and evaluation criterias permit to give reliable answers to the questions: where, how much and what quality chrome ore should be expected on each given ultrabasite massif.

MODULAR CLASSIFICATION OF COMPLEX SULFIDES

Makovicky, E. (*Geological Institute, Univ. of Copenhagen*)

Crystal structures of many complex sulfides (especially sulfosalts) can be described as composed of rods, blocks or layers of simple, archetypal structures that are recombined by the action of structure-building operators into a complex structure.

The apparent contradiction between the polyhedral and modular approaches to structural classification is resolved by the principle of hierarchical description (we deal with structures with indistinctly expressed 'backbones' of strongly bonded units). Primary (or first-order) configurations are polyhedra common to the entire 'phyllum' of compounds (BS_3 and BS_5, seldom BS_4 and BS_6 groups for sulfosalts). Secondary (second-order) configurations are the groupings (clusters, chains, layers, etc.) built from these polyhedra via the strongest B-S bonds. Tertiary (third-order) configurations are dimensionally higher units obtained by composition/interplaiting of secondary configurations via secondary B-S bonds, around lone electron pair micelles, etc. Quaternary configurations (groups, formations) are obtained by enveloping of these groups by, or their combination with, coordination polyhedra of other elements. Quinary configuration is the packing of quaternary (or ternary) configurations into a large-scale structural pattern. Example: jamesonite $FePb_4Sb_6S_{14}$; SC1:SbS_5 pyramids; SC2: triple chains Sb_3S_7 SC3: lone electron pair micelles Sb_6S_{14}; SC4: diamond-shapec rods $FePb_4Sb_6S_{14}$; SC5: herringbone packing of above rods connected into rod-based layers. Hierarchical classification systematizes and interrelates various approaches used for sulfides, sulfosalts, high-T superconductors, etc.

The modular (or: fragment-recombination) structures often build homologous series, either based on an accretional or on a variable-fit principle. Cases combining both principles are fairly common (Makovicky 1989, 1992a). Homologous series of accretional type are the original concept (Magnéli, 1953) for series that became later known as polysomatic series (Thompson, 1978). They can either be extensive (variable N), or only pairs of homologues (N_1 and N_2), or combinatorial (combining N_1 and N_2 in different proportions in one structure).

Crystal chemistry of complex sulfides or other recombination structures requires categories more general than homology. Merotypic structures (merotypes, meros = part) are composed of two (or more) types of alternating layers (blocks). One set of these are common to all merotypes (they are isotypic, homeotypic or related via homologous expansion/contraction); the layers (blocks) of the other set(s) differ for different merotypes.

Homologous series may form subsets of merotypic families; members with one layer set missing exist as well. Examples: hutchinsonite homologues, high-T superconductor families.

Plesiotypic structures (plesiotypes, plesios = near, close) are built on the same overall principles: (a) they contain fundamental structural elements (blocks, layers) of the same general type and (b) mutual disposition/interconnection of these elements follows the same general rules but (1) they contain additional structural elements that differ from one member of the family to another, (2) details of the fundamental elements may also differ (homologous or non-homologous expansion, truncation, slip planes) and (3) details of the relationships sub (b) may differ as well. Diagrams expressing the degree of kinship can be constructed for the plesiotype family. Merotypes and homologous series can enter a plesiotype family as subsets.

Examples: rod-based Pb-Sb-Bi sulfosalt structures (Makovicky, 1993); families of modified phyllosilicate structures, REE sulfide families (Makovicky, 1992b).

Magnéli, A. (1953). *Acta Cryst.*, **6**, 495-500.

Makovicky, E. (1989). *N. Jahrb. Miner. Abh.*, **160**, 269-297.

Makovicky, E. (1992a). *Modern Persp. in Inorg. Crystal. Chem.*, Parthé, E. (ed.), Kluwer Acad. Publ., 131-161.

Makovicky, E. (1992b). *Austral. J. Chem.*, **45**, 1451-1472.

Makovicky, E. (1993). *Eur. J. Mineral.*, **5**, 545-591.

Thompson, J.B. (1978). *Amer. Mineral.*, **63**, 239-249.

PGE CONTAINING PHASE SYSTEMS AND PGE DISTRIBUTION COEFFICIENTS FOR MAGMATIC SULFIDE DEPOSITS

Makovicky, E., Barnes, S.J. and Karup-Møller, S. (*Univ. of Copenhagen; Univ. de Quebec; Technical Univ. of Denmark*)

Experimental research on PGE behaviour in magmatic sulfide deposits attempts (1) to establish phase relations that explain the mineral assemblages observed in them and (2) to obtain distribution coefficients for PGE between solid phases and melts for further use in fractionation models. Our research in the phase systems Pd-Fe-S, Pd-Ni-S, Pd-Cu-S, Pd-Fe-Ni-S, etc., enabled us to establish distribution coefficients mss/sulfide melt and alloy/sulfide melt for Pd at 900° and 725°C.

Between 900°C and 550°C the Pd-Fe-Ni-S system contains a field of sulfide melt, with the boundaries between 20 and 50 at % S. The broad melt field contracts progressively towards the Ni-Pd-S side of the system with decreasing temperature.The melt coexists with mss for the entire range of Fe-Ni substitution at 900°C (Fig. 1) but - according to our revision of the Fe-Ni-S system - it is prevented from doing so in the low-Pd portions of the Pd-Ni-Fe-S system at 725°C. This is caused by the large $(Ni,Fe)_{3\pm x}$ S_2 solid solution field (an important collector of Pd at low S fugacities).

For the association melt-alloy, the alloy undergoes significant enrichment in Fe and especially in Pd - its degree varies with overall Ni and Pd contents in the charge. In the geologically most important association melt - mss, logarithm of the Pd and Ni distribution coefficients shows a linear dependence on molar contents of S in mss . At 900°C, the distribution coefficient mss/liquid for atomic proportions of Pd changes by 4 orders of magnitude between 50 and 54.5 at % S on the ln scale; that for Ni changes by about 2.5 orders of magnitude. Principal trends for 725°C are the same as, or parallel to, those for 900°C (Fig. 2). The distribution coefficients obtained for Pd by Fleet et al. (1993) straddle the regression line defined by our data (Fig. 3). For Ni, they lie on the regression line. Therefore, use of our results for fractionation models at different sulfur fugacities and for derivation of S fugacities that existed during deposit formation, based on the observed fractionation of PGE, appears justified.

Fleet, M.E., Chryssoulis, S.L., Stone, W.E. and Weisener. C.G. (1993). *Contrib. Mineral. Petrol.*, **115,** 36-44.

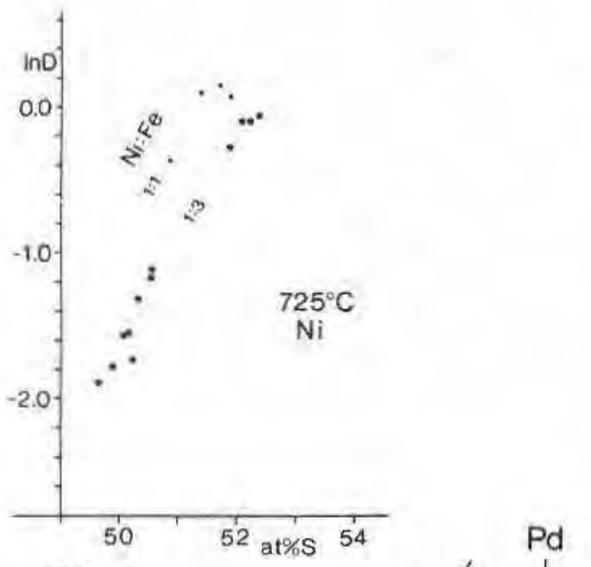

Fig.2

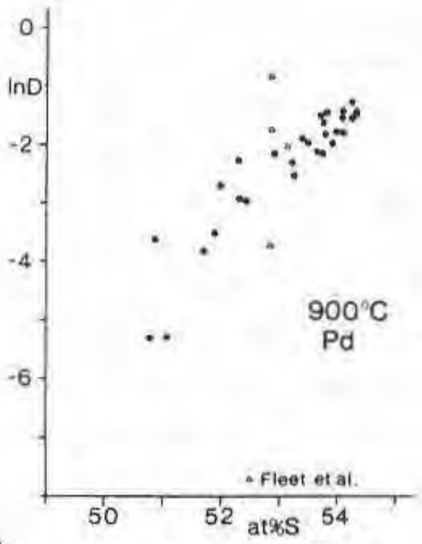

Fig.3

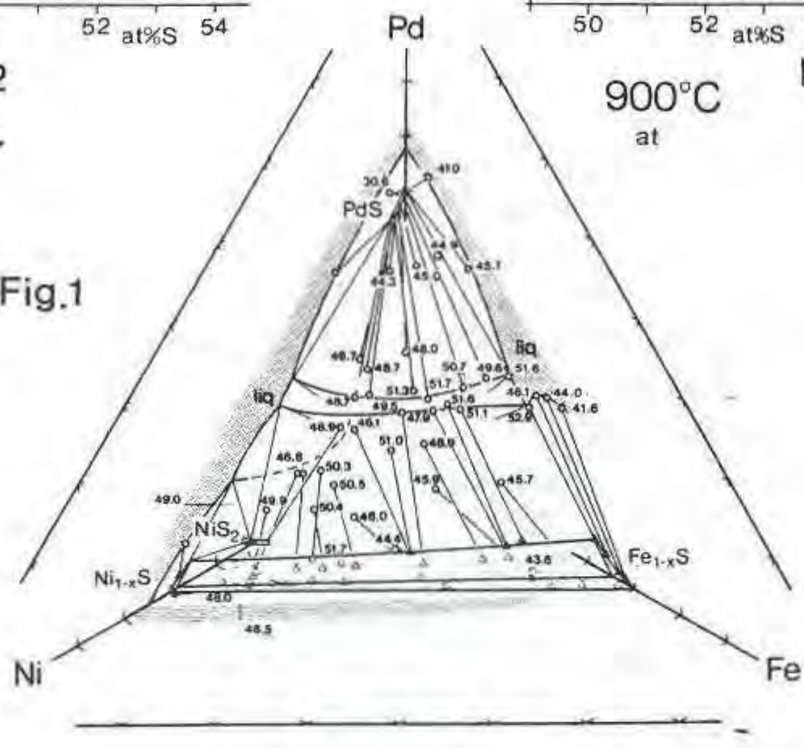

Fig.1

ON THE PHASE SYSTEMS Cu-Fe-Au-S AND Cu-Rh-S

Makovicky, M., Makovicky, E., Karup-Møller, S. and Rose-Hansen, J. (*Univ. of Copenhagen and Danish Technical Univ., Lyngby*).

The low-Au portions of the Cu-Fe-Au-S system were studied by means of dry syntheses from pure elements in evacuated silica glass tubes at 1000°, 900° and 700°C. At 1000°C the sulfide melt stretches as a broad belt between $Cu_{2-x}S$ and $Fe_{1-x}S$. At the lowest S contents, in association with various Fe-Au-Cu alloys, it dissolves traces (0.05-0.03 at %) of Au. At moderate S contents, in association with increasingly Au-rich alloys it dissolves about 3 at % Au. For high S contents, up to 8-10 at % Au was observed in this melt, still without associated alloys or metal melts. Bornite is virtually Au-free on S-poor side and contains up to 1.8 at % Au on the S-rich side; pyrrhotite is nearly Au-free (0.01-0.10 at % Au) even for Cu-richest concentrations (~ 3 at % Cu) associated with Au-bearing sulfide melt. Au contents exsolve from bornite and iss on quenching.

At 900°C, low-S bornite dissolves traces (< 0.06 at %) of Au in association with Cu-rich (Cu, Au) alloys. S-rich bornite has 0.5-1.5 at % Au in association with melt that contains 4-7 at % Au; in eutectic residuals the Au contents reach 11.4 at % Au.

Similarly, iss dissolving 0.5-1.0 at % Au coexists with sulfide melt that for elevated S contents has >4 at % Au and in the residual, quench eutectic even 12.4 at % Au. Pyrrhotite with up to 4 at % Cu again dissolves only 0.02-0.14 at % Au (even if

associated with iss that has 0.7 at % Au). Analysis of the phase system is complicated by the loss of S from the melt on quenching so that its microprobe data are displaced towards the line $Fe_{1-x}S$-$CuFeS_2$-$Cu_{2-x}S$. 700°C served as a reference temperature. Microprobe data confirm that at this temperature iss still dissolves 0.4-0.5 at % Au, pyrrhotite only traces, and bornite from 0.0 to ~1.5 at % Au, according to the fugacity of sulfur. The studied phase system describes distribution of Au in Cu-rich sulfide magmatic deposits, such as the Skærgaard intrusion in Greenland.

At 900°C the phase system Cu-Rh-S contains five binary solid phases: ~RhS_3,Rh_2S_3,Rh_3S_4,$Rh_{17}S_{15}$ and high digenite, two sulphide melts, Cu-Rh alloys as well as three ternary phases: cubic $(Rh,Cu)S_{3-x}$, lath-like ~$Cu_{1.5}Rh_3S_8$ and cubic $CuRh_2S_4$. Solubility of Cu in Rh_2S_3 and Rh_3S_4 is very low; $Rh_{17}S_{15}$ dissolves 3.7 at% Cu. The Cu-rich melt appears to extend only to ≤ 2 at% Rh; it is involved in ternary associations S-melt-~$(Rh,Cu)S_{3-x}$ and melt-digenite-$(Rh,Cu)S_{3-x}$. Associations with cuprorhodsite $CuRh_2S_4$ can be used to separate S-rich and S-moderate regions of the phase system; those with Cu-Rh-alloys represent S-poor associations. This allows preliminary classifi cation of PGE deposits into groups according to S fugacity.

At 725°C all the above mentioned Rh sulphides persist; solubility of Cu in Rh_3S_4, Rh_2S_3 and $Rh_{17}S_{15}$ increases (to ~5 at% Cu in the latter). Ternary thiospinel ~$CuRh_2S_4$ is associated with digenite. Principal associations are Cu-Rh-digenite, digenite-$Rh_{17}S_{15}$-alloy, digenite-$Rh_{17}S_{15}$-Rh_3S_4 and $CuRh_2S_4$-Rh_2S_3. At 500°C Cu_2S and CuS dissolve at most traces of Pd (0.02-0.04 at%) whereas Cu still dissolves 10 at% Rh; Rh dissolves only minor amounts of Cu. The association digenite-$Rh_{17}S_{15}$ divides the phase system into S-rich and S-poor regions. High-S regions contain associations CuS-~$(Rh,Cu)S_3$, ~$(Rh,Cu)S_3$-Rh_2S_3, digenite-Rh_2S_3-$Rh_{17}S_{15}$. Rh_3S_4 appears unstable at 500°C. Again we observe the lath-like phase, ~$CuRhS_3$. $Rh_{17}S_{15}$ dissolves ~1.3 at% Cu in association with sulphides whereas up to ~3.5 at% Cu in association with alloys.

The phase system Cu-Rh-S is being investigated because of the importance of Cu-rich assemblages for the mineralogy of Rh in PGE deposits.

This research was financially supported by EEC and Danish State Research Council.

HIGH-PRESSURE RAMAN AND X-RAYS STUDIES OF ZEOLITES UP TO AMORPHIZATION

Malezieux J-M. (*Institut de Géodynamique, Université de Bordeaux 3)* and Gillet Ph. (*Ecole Normale Supérieure, Lyon*)

Raman spectra of natural zeolites (mesolite, scolecite) have been obtained up to 115 kbar and to 60 kbar, respectively for mesolite and scolecite, using a diamond anvill cell with Kbr as pressure-transmitting medium to avoid fluid penetration, and a DILOR XY microraman spectrometer equipped with a CCD detector. Spectra were collected on grains closest to the ruby chip used for pressure determination.

The following features are observed :

1°) With increasing pressure, the O-T-O bending modes, in the 430-540 cm^{-1} region, exhibit a frequency shift versus pressure of the order of 0,25 cm^{-1} $kbar^{-1}$ in the case of mesolite and 0,33 cm^{-1} $kbar^{-1}$ in the case of scolecite.

2°) The E specy mode of mesolite at 532 cm^{-1} splits at pressure close to 45 kbar. The splitting is of the order of 20 cm^{-1} at 90 kbar. No splitting of the corresponding mode is observed in scoletcite spectra.

3°) At pressure in excess of 100 kbar in the case of mesolite and 60 kbar in the case of scolecite, amorphization is observed, marked by the appearance of very broad bands in the 200-600 and 800-1100 cm^{-1} regions, analogous to those observed in the pressure-induced amorphous aluminosilicates e.g. feldspars.

4°) The streching modes of the H_20 molecules represented by a set of 5-6 well-defined bands between 3200 and 3600 cm^{-1} are reduced to a single broad band in the amorphous phase.

5°) Recrystallization phenomenon appears on the edges of scolecite sample during the decompression, and well-defined bands replace the broad ones in the low-frequencies range.

Preliminary X-rays data are also presented using the same high-pressure device than the one used for Raman experiments. They confirm the crystal to amorphous transition in zeolites.

• SOME REGULARITIES IN CHLORINE DISTRIBUTION BETWEEN MAGMATIC MELTS AND WATER FLUIDS

Malinin S.D., Kravchuk I.F. (*Vernadsky Institute of Geochemistry and Analytical Chemistry, RAS, Moscow, Russia*)

Chlorine is an important component of magmatic–fluid melt systems in view of its complexing ability with petrogenic, ore and rare earth elements in magmatic processes.

On the basis of the available experimental data on chlorine distribution between NaClsolutions and magmatic natural and synthetic melts of various compositions at 800–1200°C and 0.6–3 kbar (F. Delbove, J. Webster, S. Malinin, I. Kravchuk et al.) it was found that the values of the ratio of the partition coefficients (D) to those related to diluted NaCl solutions (D°), at the same P and T values, combine in common curves independently of the melt compositions.

The established regularity affords an opportunity to quantitatively reproduce chlorine solubility values in any magmatic melts for wide ranges of chlorine concentrations in fluid, on the basis of a minimum number of experimental data.

Moreover, since $D/D° = \gamma_{NaCl}$, we have an independent way to determine the values of the activity coefficients of NaCl in fluid solutions.

• MAGMATIC FLUIDS AS MINERAL TRANSPORT MEDIA. SOLUBILITY DATA ON SCHEELITE AND FLUORITE IN SUPERCRITICAL SALT SOLUTIONS

Malinin S.D., Kurovskaya N.A. (*Vernadsky Institute of Geochemistry and Analytical Chemistry, RAS, Moscow, Russia*)

The occurrence of tungsten ore deposits linked to magmatic intrusions raises the problem of the fluid transport ability for tungsten. Scheelite solubilities in water solutions of NaCl (0.2 – 34 m), $CaCl_2$ (0.2 – 2.5 m) and NaCl–$CaCl_2$, at 600–800°C and 2 kbar total pressure, has been studied starting from the concept that ore mineral solubility data determine the upper limit of transport ability of fluids. For comparison the solubilities of fluorite at the same conditions have been studied.

All the experiments were performed in sealed Pt capsules by quench method. Synthetic monocrystals of scheelite and fluorite were used.

Solubilities increase rapidly with increasing NaCl and $CaCl_2$ concentrations attaining 75 g/l and 54 g/l in the 34m NaCl solution for scheelite and fluorite respectively. Solubilities are higher in $CaCl_2$ solutions than in NaCl solutions, notwithstanding the presence of the common ion Ca in both phases. For both minerals the solubility at 800°C is 0.5–1 order of magnitude higher than at 600°C. Solubility data as a function of $NaCl/CaCl_2$ ratio present a minimum in composed solutions. The obatained data explain the anomalously high tungsten contents in gas–fluid inclusions in quartz from a series of deposits (Transbaikal area tungsten deposits).

Both diagrams with scheelite and fluorite are very similar, indicating the common nature of solution reactions in both systems.

Species identification of W and F in fluids through the method of slope quantification on solubility diagrams was carried out. Neutral complex species Na_2WO_4NaCl, $CaWO_4xCaCl_2$, NaFNaCl and CaF_2CaCl_2 were proposed.

These results indicate that minerals considered as sparingly soluble at room temperature can be transported by salt solutions at high temperatures.

High solubility of both minerals makes reliable effective W and F transport by supercritical fluids; this, combined with positive

solubility dependence on temperature, provides the opportunity for their deposition from saturated solutions by cooling.

Dilution of magmatic fluid may be another reason of the deposition.

• MEMBRANE FORMS OF MINERALS AS RESULT OF CRYSTALLIZATION FROM POROUS MEDIUM

Malishevsky D.I. *(IGEM, RAS, Moscow, Russia)*

The mineralization of large karst caverns of Middle Asia (Kugitangtau Mountains, Turkmenistan) was investigated. The karst caverns have been formed in Jurassic limestones since late Cretaceous age to the present time. Their development was controlled by fault zones. The main part of mineralization is made of calcite–gypsum–aragonite flowstone aggregates with various morphologies. Depending on the velocity and the way of flowing of water solutions, the following morphological aggregates can be recognized: stalagmites, stalactites, "tubes", "curved tubes", tubes with thickenings, coralloids, helictites, cave pearls, etc. Precipitation of colloidal carbonates form "moon milk".

Gypsum aggregates form various crusts and stalactites, fibrous crystals (length to 1.5 m), gypsum "flowers" (antolite), gypsum "hedgehogs", gypsum "spiders" etc.

Long (few meters) calcite tubes, growing in few months, present zonal texture: the inner part of calcite tube with radial–fibrous texture is composed by magnesian calcite but the outer part consists of pure calcite. The direction of growth is from center to rim. It was shown that mineral forming solution penetrates through supply channel in the central part of the tube with further diffusion to the outlines of growing mineral. The gypsum aggregates which formed on porous substrate of limestones or clays are large bend and splitted columnar intergrowths.

Membrane forms of mineral are the result of the capillary way of mineral growth with interphase difference of electrical potentials and formation of double electrical layers. Thus, there is an asymmetrical distribution of charged particles near boundaries. Filtrations of mineralized solution through limestones with positive electric–kinetic Z–potential equal +34.78 mV increases concentration of solution above dripstones, which is the reason of mineral crystallization. A porous medium of mineral crystallization is characteristical not only for the karst caverns but also for disintegrated powder rocks in weathering crustes and many other geological objects.

GEOCHEMISTRY AND MINERALOGY OF PLATINUM GROUP ELEMENTS IN ULTRABASITES OF THE ALASKAN-TYPE INTRUSIVES.

Malitch K.N.(All-Russian geological institute (VSEGEI)), St Petersburg.

We have conducted a detailed mineralogico-geochemical study of concentrically-zonal platinum-bearing ultrabasic massifs situated in several regions of Russia: Urals (Nizhnij Tagil), marginal parts of the Siberian platform (Konder, Chad, Sybach, Guli), Far East (Feklistov). The intrusives have concentrically-zonal structure and are mainly composed by dunites which surrounded to periphery by metadunites, werhlites, clinopyroxenites and melanocratic gabbroids.

1. It was established that there is a similar pattern of distribution of platinum group elements (PGE) in clinopyroxenites and melanocratic gabbroids. They are characterized by a predominance of non-refractory PGE (Pt, Pd, Rh), in contrast to the dunites and chromitites in which the more refractory PGE (Ir, Os) predominate. According to the level of concentrating of rare-earth elements (REE) dunites and metadunites give in abruptly clinopyroxenites and melanocratic gabbroids. In addition to this metadunites, according to the character of distribution of REE, demonstrate all features of postdunite rocks.

2. With the help of electroimpulsive desintegration from the samples of chromitites,having weight 2-6 kg there where established more than 300 grains of platinum-group minerals (PGM) which have the size of 30-300 micrometers. There was studied morphology of PGM grains, their inner structure, mineral associations, chemical composition of minerals (Camscan, Link-10000). There are predominant crystals of isoferropalatinum of cubic, cubooctahedral, octahedral form having the size less than 0.1 mm. Large grains of PGM have, as a rule, irregular form. In chromitites there were determined the following PGM: mainly isoferroplatinum; secondary - chollingvortite, irarsite, sperrylite, erlichmonite, iridosmine, tulaminite; rare - laurite, platarsite, osmium native, chongshite, heversite etc. In grains-aggregates of PGM there were established several mineral associations of various age. The conclusion was done about polygenic nature of formation of platinum mineralization of chromitites. Identity in mineral composition and geochemical peculiarities of PGM from placers and chromitites determine the latter as the main source of platinum - bearing placers associated with such type intrusives.

3. The data obtained allow us to establish the factors which control the distribution of native platinum mineralization inside large dunite bodies which form the central parts of the massifs. The maximum concentrations of platinoids are confined to areas of dechromespinelization of definite chemical composition, geometric size and texture. In particular the Cr_2O_3content in chromspinellids serves as an additional mineralogical criterion for determination of the prospectivity for platinoids. Vein-forming and "streaky disseminated" chromspinellids are most prospective for PGM according to this parameter.

4. The character of distribution of platinum group metals at the rock and mineral levels can be well explained from the point of view of differentiation of PGE during fractional fusion of the mantle substratum with formation of an ultramafite-mafite melt and a complementary ultrabasic restite and their subsequent continuous evolution. The heavy refractory platinoids are accumulated in the dunite restite while the melt of clinopyroxenite-gabbro composition is enriched in REE and non-refractory platinoids. Some difference of geochemical platinoid and REE specialization in ultramafites of zoned structure is caused by relative accumulation or transformation of PGE and REE in mantle substratum during the process of its transference to the surface.

XPS INVESTIGATION ON TI-BEARING GARNETS FROM M.VULTURE (ITALY)

Malitesta, C., Losito I, Sabbatini L.(*Dept.of Chemistry,Univ.of Bari*)
Scordari, F. , Schingaro, E. (*Geomineralogical Dept.,Univ. of Bari*)

A study on the coordination environment and the oxidation state of Ti in some melanitic garnets has been performed by X-ray Photoelectron Spectroscopy. The investigation has been extended to the Fe2p signal in order to compare the Fe^{3+}/Fe^{2+} ratios provided by this technique with those yielded from Mössbauer investigations (Pedrazzi et al.,1994). To the purpose XPS measurements have been performed on the same powdered samples already used for the Mössbauer study. For all the examined samples XPS analyses consisted mainly of two steps:

a) the quantitative determination of the atomic species present in the samples;

b) the fitting of the Ti *2p* and Fe $2p_{3/2}$ spectra.

The step a) allowed, through the analysis of the narrow scans of

Si, Al, Fe, Ca, Ti, O: 1) to check whether differential charging affected the measurements; 2) the atomic percentages of the mentioned elements to be determined with an average accuracy of ± 10% and comparisons with chemical results via EPMA to be made. The step b) allowed the determination of the oxidation states of Ti and Fe. The results can be summed up as follows:

i) **Ti *2p* signal**. The best fit was obtained with three doublets of gaussian-lorentzian peaks, one assigned to Ti^{3+} and two to Ti^{4+}. The latter can be interpreted as due to the presence of Ti^{4+} into two sites of the garnets structure: octahedral and tetrahedral.

ii) **Fe $2p_{3/2}$ signal**. The best fit was obtained with three components: two Fe^{3+} peaks and one Fe^{2+} peak according to the model suggested by McIntire and Zetaruk (1977) for the compound Fe_3O_4. The estimated Fe^{3+}/Fe^{2+} ratios consistent with the Mössbauer results were obtained.

References

McIntyre, N.S. and Zetaruk, D.G. (1977) - *Analytical Chemistry*, **49**, 1519-1529.

Pedrazzi, G, Ortalli, I., Schingaro, E., Scordari, F. (1994) - 16th General Meeting of the International Mineralogical Association, 4- 9 September, 1994 - Pisa, Italy.

• THE RELATIONSHIPS BETWEEN NITROGEN AGGREGATION AND ISOTOPIC COMPOSITION OF NITROGEN AND CARBON IN DIAMONDS.

Maltsev K. *(Vernadsky Institute of Geochemistry and Analytical Chemistry, Moscow, Russia)*

Data are presented on the study of isotopic composition of carbon in diamonds from several kimberlite pipes and deposits of Jakutia and Ural and of forms of aggregation of nitrogen, with the aim to clarify the mechanism of diamond formation.

Main results are:

1. A correlation was found between $\delta^{13}C$ and the amount of nitrogen within various aggrgation centres, which reflects the growth temperature and geological history of diamonds.

2. The diamonds with $\delta^{13}C = -4.5‰$ grew at high temperature, while the diamonds with $\delta^{13}C$ in the range between $-2‰$ and $-8‰$ grew at different temperatures.

Our data confirm the idea that enrichment of primitive carbon ($\delta^{13}C = -4.5‰$) of the diamonds in light isotope is related to the fractionaction of carbon isotopes in fluid in the process of its movement through the mantle at various temperatures. The realization of this mechanism implies that carbon is present in the fluid in two forms: light CH_4 (reduced form) and enriched carbonate (oxide form). The growth of diamonds is connected with these two forms of carbon.

THE CAUSES AND CONSEQUENCES OF KOMATIITIC MAGMAS POLYGENESIS

MALYUK B.I. *(Institute of Geology & Geochemistry, Ukrainian AS, 290053 Lviv, Ukraine)*

SLIVKO E.M. *(Department of Geology, Lviv State University, 290005, Lviv, Ukraine)*

From the view of present knowledge preeruptive batches of komatiite magmas cannot be regarded as the result of any simple petrogenetic process. Even primary komatiite melts have had complex composition due to mantle source heterogeneity and laterally gradiented shape of melting zones. Further contributions might be expected from small-scale adiabatic melting of suspended source remnants during initial primary melt ascent. Another ones of different values were polybaric fractionation, crustal contamination and mixing with evolved tholeiitic melts within the common subsurface stratified magma chambers and volcanic conduits. Finally, most komatiite melts reached surface has been affected by flowage differentiation as well as thermal erosion of less refractory flow base rocks.

When komatiite magmogenesis is considered as the succession of generation, transport and crystallization processes, the magma composition reached the surface can be expressed as:

$M = L + S$

where L - melt composition, S - solid phases composition. Melt composition or L also can be written as:

$L = X_1 + X_2 + X_3 + X_4 + R$

where $X_1 ... X_i$ - contribution of:

X_1 - partial melting,
X_2 - fractional crystallization,
X_3 - contamination,
X_4 - hybridism,
R - "enigmatic" processes.

While L = 1, all X and R can reach any value from 0 to 1, but the matrix of these values would be different for another magma batch even. Solid phase composition also can be showed as:

$S = Y_1 + Y_2$,

where Y_1 - intratelluric crystals,
and Y_2 - xenogenic matter.

All of these parameters are highly variable and should be studied in each particular case.

Polygenic nature of most komatiite magmas is responsible for some major geochemical, mineralogical and metallogenic consequences. First, trace element addition and extraction should be highly variable at the different stages of komatiite magma evolution and the single element contribution from the one process could be enhanced or reduced by another one in compatible or selective incompatible mode. Second, some distinct accesory minerals such as chromespinels should be expected to represent chemical reequilibration resulted from refractory and contaminated phases contribution. Finally, metallogenesis in relation to komatiites also cannot be described by a simple magmatic process (in the case of Ni ores) or metamorphic one (in the case of Au epigenetic ores). The actual history of metal concentrations within komatiites appear to be the long-termed complicated process with different sources involved.

SPECIATION OF HEAVY METALS AT THE HYDROUS METAL OXIDE/WATER INTERFACE: THE LEAD CASE

Manceau A., Boisset M.C., and Charlet L. *(Environmental Geochemistry Group, Univ. of Grenoble)*

Chemical reactions at the mineral/water interface, important in an array of disciplines, are of environmental significance as such reactions greatly affect the mobility and speciation (toxicity) of metal ions. The structural environment of metals at this interface determines their potential for remobilization to the aqueous environment and can change the physical/chemical state of the sorbent. Hydrous oxides are among the most important sorbents found in natural systems, including soils, because of their abundance and high structural disorder.

The specific affinity of hydrous oxides for lead is very strong and can result in high geochemical partitionings such as that found in oceanic nodules where lead concentrations associated with (Fe,Mn) oxides can amount to ≈0.5%. The high affinity of lead for the Earth's surface materials is also at the origin of its higher concentrations in the uppermost horizons of contaminated soils. A detailed knowledge of lead speciation and interactions with minerals and organics at a

molecular scale is therefore vital to assessing the hazard that these contaminations represent and a prerequisite for remediation.

The sorption mechanism of lead on various Fe and Mn oxides including hydrous ferric and manganese oxides, goethite, and birnessite was investigated by extended X-ray absorption fine structure (EXAFS) spectroscopy and useful results were obtained for samples with less than 2000 ppm Pb. For each of these sorbents the nature of reactive surface sites and the structure of lead surface complexes was determined. These examples demonstrate the existence of a direct structural relationship between the nature of the sorbent and the kind of lead complex formed at its surface. These laboratory experiments were complemented by studies of soil materials originating from sites contaminated by various process industries including synthesis of lead organometallics for gasoline antiknocks, Pb-Zn smelting, and recycling of Pb-batteries. Preliminary results show that the speciation of lead in these soils varies with the source of contamination.

STATIC AND DYNAMIC STUDIES OF THE REACTIONS OF INORGANICS AT THE HYDROUS OXIDE/WATER INTERFACE BY SYNCHROTRON-BASED AWAXS AND FLUORESCENCE-YIELD AND DISPERSIVE EXAFS TECHNIQUES.

Manceau A., Charlet L., Silvester E., Spadini L.(*Environmental Geochemistry Group, Univ. of Grenoble)* and Bouchet-Fabre B. (*LURE, Orsay, France)*

Minerals that are formed at the Earth's surface are typically finely divided, some of them being amorphous to X-ray diffraction. The resulting high surface area and density of defects impart them with a high chemical reactivity and explains their key role in controlling the mobility and speciation of trace metals in the environment.

It will be shown how recent achievements in synchrotron-based techniques allow a mechanistic description of the different surface assisted phenomena to be elucidated. Specifically, the potential of the anomalous wide angle X-ray scattering (AWAXS) technique used in combination with fluorescence-yield extended X-ray absorption fine structure (EXAFS) for determining the structure of surface complexes and the nature of active surface sites will be illustrated, taking as an example the adsorption of cadmium on Fe oxides. The first application of energy-dispersive EXAFS to time resolved studies of redox reactions catalyzed by mineral surfaces will also be presented. At present with this technology it is feasible to follow chemical reactions with half lives in the ms to s time range. Finally, new opportunities offered to the environmental geochemistry community by third generation storage rings will be discussed.

• PETROGRAPHY OF THE SÄÄKSJÄRVI ULTRAMAFIC BODY IN SOUTHWESTERN FINLAND WITH SPECIAL EMPHASIS ON THE CHEMISTRY OF CALCIC AMPHIBOLE

Mancini F., Marshall B. and Sutinen M. (*Dept. of Geology, University of Turku, Finland*)

The Sääksjärvi ultramafic body is located in a proterozoic orogenic belt in SW Finland, the Kylmäkoski belt. The country rocks are represented by high grade allumina-rich gneisses and amphibolites. The ultramafic body contains metaperidotites and subordinate metapyroxenitic and metagabroic amphibolites. Prograde mineral assemblages in metaperidotite include: i) olivine + Ca-amphibole; ii) olivine + Ca-amphibole + orthopyroxene; iii) olivine + Ca-amphibole + Cr-spinel. Instead, lizardite and chlorite (phlogopite) occur as retrograde and replacing minerals. Textural relationships indicate an amphibole + olivine, (Fo_{76-82}), reaction relation to orthopyroxene, (En_{77-81}), whereas beads of chrome spinel, Cr_2O_3=29÷43wt%, were inherited from the magmatic stage. In the genetically related amphibolites, calcic amphibole shows (100) and ($\bar{1}01$) lamellae of cummingtonite, and coexists with minor plagioclase, quartz and Fe-Mg cummingtonite.

The ratio Fe^{+3}/Fe^{+2} in the Ca-amphibole formulae has been evaluated using the 15eNK method of recalculation. The $Mg/Mg+Fe^{+2}$ ratio is positively correlated with the $MgO/MgO+FeO_t$ ratio of host rock. Also octahedral Al vs. Al_2O_3 (rock) show positive correlation. The analyzed calcic amphiboles exhibit solid solution toward hornblenditic compositions, with the substitutions *Ed* ($NaAl_{-1}Si_{-1}$) = 0.19 ÷ 0.41 and *Ts* ($Al_2Mg_{-1}Si_{-1}$) = 0.46 ÷ 0.6. Minimum P-T conditions of crystallization, P=5±1 Kbar; T=650°C, have been inferred with respect to the compositional gap between tremolite and hornblende, (Mish and Rice, 1975; Smelik et al., 1991). The substitution $(Fe^{+2}Ca_{-1})^{[M4]}$ is also relevant and indicates 10.5÷11.7 moles% of cummingtonite component in solid solution, which agrees with the observed cummingtonite lamellae, and further supports the reaction: *Fe-Mg cummingtonite + olivine = orthopyroxene + H_2O.*

In the H_2O-Na_2O-CaO-MgO-Al_2O_3-SiO_2 petrogenetic grid, (Jenkins, 1981 and 1983), the maximum P-T metamorphic estimates for the Sääksjärvi ultramafic body, cross the "chlorite-out" isograd, corresponding to the sillimanite-garnet-biotite zone in the country rocks. This is further supported by the composition of relic chrome-spinel, which was enriched in allumina, Al_2O_3=21÷30wt%, as a consequence of the breakdown of chlorite.

References:
Jenkins, D.M. (1981). Contrib. Mineral. Petrol., 77, 166-176
Jenkins, D.M. (1983). Contrib. Mineral. Petrol., 83, 375-384
Mish, P. & Rice, J.M. (1975). J.Petrol., 16,1-21
Papunen, H. & Vorma, A. (1985). Geol. Surv. Finland Bull., 333, 123-144
Smelik, E.A., Nyman, M.W., Veblen, D.R. (1991). Am. Mineral.,76, 1184-1204

A GLADSTONE-DALE SURVEY OF THE CARBONATE MINERALS

Mandarino, J.A. (*Dept. of Mineralogy, Royal Ontario Museum*)

A Gladstone-Dale survey of the carbonate minerals was undertaken to determine the compatibility of the optical, density and chemical data for each mineral. The compatibility index (C.I.) is based on the two Gladstone-Dale equations, $K_p = (\bar{n}-1)/D$ (i.e., the physical constant) and $K_C = \Sigma(k_n p_n/100)$ (i.e., the chemical constant). In these equations, $\bar{n}$ is the mean index of refraction, D is the density, k's are the Gladstone-Dale constants for each constituent and p's are the weight percentages of the constituents. The author (Mandarino, 1979) defined the compatibility index as $C.I. = 1-(K_p/K_C)$. He also proposed the following scale to express the compatibility of the pertinent data for a compound: ±0.000 to ±0.019 (superior), ±0.020 to ±0.039 (excellent), ±0.040 to ±0.059 (good), ±0.060 to ±0.079 and > ±0.079 (poor).

Data were taken from the literature for the 203 known carbonate minerals. Insufficient data were available to carry out the calculations for nine species: bastnäsite-(La), dypingite, gregoryite, hydroscarbroite, natrofairchildite, plumbonacrite, susannite, tundrite-(Nd) and zincrosasite.

The first round of calculations for the remaining 194 species resulted in the following distribution among the compatibility categories: superior 74 (38.1 %), excellent 52 (26.8 %), good 31 (16.0 %), fair 6 (3.1 %) and poor 31 (16.0 %). The minerals which fall into the poor category are: lokkaite-(Y), thorbastnäsite, motukoreaite, sharpite, barringtonite, cordylite-(Ce), comblainite, joliotite, tuliokite, bastnäsite-(Y), ewaldite, indigirite, bismutite, brianyoungite, barstowite, wyartite, phosgenite, synchysite-(Y), widenmannite, otavite, defernite, carbonate-cyanotrichite, tengerite-(Y), kettnerite, rabbittite, rutherfordine, brugnatellite, georgeite, nullaginite, voglite and azurite. These are listed in decreasing order of the compatibility index, i.e. lokkaite-(Y) with C.I. = -0.455 has the worst compatibility and azurite with C.I. = -0.080 has the best compatibility within the poor category.

Working with this list, better data were sought for the species to see if any could be raised to better compatibility categories. It is apparent that the very nature of some of the minerals in this list prevents the measurement of good data, but in some cases it was found that the data used for the calculations were in error. For example, the data used for otavite were taken from the *Mineral*

Powder Diffraction File Data Book, where the index of refraction given as 1.842 results in a poor compatibility index of -0.113. Using the more complete optical data (Fleischer *et al.*, 1984) for otavite (ω = 1.830 and ϵ = 1.605), the new mean index of refraction, 1.755, gives a compatibility index of 0.002 which places the mineral in the superior category.

Barringtonite presents another example. The calculated density given in the original description is 2.825 g/cm^3, but this is based on an incorrect unit cell volume. The density calculated from the correct unit cell volume is 2.46 g/cm^3. The indices of refraction given for this mineral are α 1.458, β 1.473 and γ 1.501 ($\bar{n}$ 1.477) which are very close to the data for lansfordite, α 1.456, β 1.469 and γ 1.508 ($\bar{n}$ 1.478). Barringtonite and lansfordite are, respectively, $MgCO_3 \cdot 2H_2O$ and $MgCO_3 \cdot 5H_2O$. It is quite possible that the optical data given for barringtonite were measured on material which really was lansfordite. Based on a comparison of the optical data for magnesite, barringtonite and landsfordite, a more reasonable value for the mean index of refraction for barringtonite is 1.573; this changes the compatibility index from 0.211 to 0.038, i.e. from poor to good.

References:
Mandarino, J.A. (1979). *Can. Mineral.* **17**, 71-76.
Fleischer, M., Wilcox, R.E. & Matzko, J.J. (1984). *Microscopic Determination of the Nonopaque Minerals.* U.S. Geological Survey Bull. 1627.

THE PERFECT MINERAL PROPOSAL OR DESCRIPTION

Mandarino, J. A. (*Dept. of Mineralogy, Royal Ontario Museum*)

In terms of new mineral proposals submitted to the Commission on New Minerals and Mineral Names (CNMMN) of the IMA, the perfect mineral description is often rarer than the mineral. Over the years, the CNMMN has striven to obtain better data from proposers of new minerals and, although there has been marked success with many proposals, there is still room for improvement.

This abstract does not allow space for a detailed analysis of the problems with new mineral proposals and published descriptions, but the following paragraphs outline some areas where more attention should be given.

Chemical data. Chemical analyses by electron microprobe have become the norm. About 94 % of the proposals sent for voting in 1993 contained chemical data obtained by electron microprobes. More proposals contain multiple analytical data as well and the CNMMN encourages this practice. The average number of analyses carried out per proposal in 1993 was 9; the range was 1 to 40 and the most frequent numbers of analyses per proposal were 3, 10, 5 and 9 in that order. Some improvement in the choice of standards could be made in a few cases, for example, some members question the use of metal standards for the determination of cationic constituents in nonmetallic minerals.

Crystallographic data. More attention should be given to the presentation of X-ray powder diffraction data. Calculated spacings often are calculated for a unit cell slightly different from that presented as the defining cell. More precise unit cell parameters usually are obtained from least-square refinements of the powder data. The precision attached to measured spacings should be consistent with the diameter of the camera used. The a:b:c ratio frequently is given as the ratio of the three dimensions of a crystal rather than the ratio of the unit cell parameters! Although we do not require crystal structure determinations (the number of proposals with structures reached 37 % in 1993), such information is extremely valuable in assessing the validity of a proposed new species.

Optical data. For nonopaque minerals, the indices of refraction should be measured for the standard wavelength 589 nm. It is surprising that many contradictions, such as optic signs and values of calculated 2V which do not match the indices of refraction, exist in optical data. Complete orientations and dispersion statements frequently are omitted from proposals. The situation with data for opaque minerals is getting better but could be improved to avoid contradictory statements. Notable among these are inconsistencies between the reflectance values and the statements describing anisotropy, bireflectance and pleochroism. Abstracts of proposals sent for voting now contain the complete reflectance data supplied by the proposers.

Physical data and appearance. The physical properties most frequently omitted from proposals are: streak, cleavage, fracture and tenacity. Many people seem to have forgotten that streak is the colour of the powdered mineral and can be observed when a sample is prepared for an X-ray powder diffraction pattern. A common mistake is the assignment of a vitreous lustre to a mineral which has indices of refraction greater than ~ 1.8; weakly absorbing minerals with high indices of refraction have adamantine lustre. It is very important to give a short description of the mineral including the kinds of aggregates and their dimensions as well as the dimensions of the individual crystals.

Miscellaneous data. Full information on the choice of names should be given including the connection of the mineral to the person for whom it is being named. Information on where the type material is preserved is a requirement. Details on the locality, including associated minerals, are also very important.

Careful use of the current version (930329) of the check-list for new mineral proposals, available from the Chairman or any member of the CNMMN, could lead to the preparation of a perfect proposal and, subsequently, to a perfect mineral description.

X-RAY DIFFRACTION MICROPROBE FOR HIGH-PRESSURE STUDIES

Mao H., Hu J., Shu J., Finger L. W., Fei Y., Meade C., Kingma, K. J., and Hemley R. J. (*Geophysical Laboratory, Carnegie Institution of Washington*)

An x-ray diffraction microprobe has been developed for studying structural properties of minerals under various pressure and temperature conditions. Polychromatic x-ray beam from the X17C superconducting wiggler beamline at National Synchrotron Light Source is collimated to a size less than 10μm X 10μm for probing microscopic samples in diamond cells.

X-ray diffraction of single crystals at high pressure requires the development of techniques for maintaining hydrostatic hydrostatic environment and probing diminishing sample sizes as the results of the tradeoff for higher pressures. We showed that solid helium is a suitable medium up to 55 GPa. Wüstite and stishovite crystals of 5 - 10μm have been studied.

The effect of nonhydrostatic stress is determined by polycrystalline x-ray diffraction in the direction deviated from the compressional axis by an angle varying from 0 to 90°. The relation of uniaxial strain to the phase transition of wüstite is demonstrated.

Constraining models of the Earth deep interiors requires equation-of-state data on minerals at simultaneous high *P-T* conditions. Polycrystalline x-ray diffractions to 100 GPa and 1100 K have been routinely performed with externally heated diamond cells. Diffractions of iron and $MgSiO_3$-perovskite at 70 GPa and 3000 K have been achieved with internal resistance heating and CO_2 or YAG laser heating. Microprobing with intense x-ray source is essential for resolving volume variations in a steep temperature gradient inherently associated with these experiments.

TETRADYMITE FROM THE DASHUIGOU TELLURIUM DEPOSIT, SICHUAN, SOUTHWEST CHINA

Mao J., Chen Y., Lei Y., Zhou J. and Yen J. (Institute of Mineral Deposits, CAGS), Yang B. (Sichuan Company of Nonferrous, Rare and Noble Metals, China)

The Dashuigou tellurium deposit, Sichuan, southwest China, is the first deposit dominanted by tellurium in the world. Tetradymite is the most important ore-forming mineral in the deposit. It occurs as aggregates of big euhedral crystals with diameters of 0.3 to 6 mm, which form either almost pure tetradymite massive ore or breccia ore which is composed of calcite breccias, pyrrhtite breccias, and interstitials of tetradymite together with tellurbismuth, wehrlite, native tellurium, native silver, native gold, chalcopyrite, calcite and quartz. All the tetradymite shows perfect cleavages along (0001) plane.

Optical properties In reflected light the tetradymite is creamy white, shows weak reflected pleochroism, and clear optical anistropy. The reflectance given for tetradymite in literature varies over a wide range. The values obtained here are: O 59.9% and E 45.5%. The measurements were made photometrically under oil with Leiz green filter (obsorption peak at 526 μ), using a carborundum standard. The mineral may take a good polish and its polished surface is often planar. The hardness of the tetradymite was measured by Π MT-3 type micrometer of hardness as 20-80 kg/mm^2, which is equal to 1 to 2 Moss hardness. Its specific gravities of 7.15 to 7.28 g/cm^3 were obtained by the method of hydrostastic weighing in carbon tetrachloride.

Chemical composition Ten chemical analyses of tetradymite from the Dashuigou tellurium deposit gave: Bi 57.65-58.68%, Te 35.20-36.40%, and S 4.59-5.36%, and trace elemnts Ag 230-340 ppm, Se 160-280 ppm, Fe 310-2800 ppm, Sb 100-280 ppm, and Au 1.4-10.7 g/t. It may be noted that the noble elments Au and Ag are quite enriched in the tetradymite. In fact, the tetradymites are so rich in Au, Ag, and Se elements that they can be recovered as by-product in the mine.

X-ray diffraction Five X-ray diffraction patterns for the tetradymite were obtained with a copper target, 45 kv, and a current 45 mA. The diffraction patterns are similar to those of the tetradymite taken by Pauling (1975). Their unit cell dimentions are a: 4.2048-4.5225 and c: 29.5008-29.6170.

Sulfur isotopes Ten samples of the tetradymite were chosen to be analysed for sulfur isotopes. The result shows that their $\delta^{34}S$ ranges from -0.5‰ to 2.1‰ with an average of 0.5‰.

Dicussion and conclusion Tetradymite is one of rare minerals. Since its discovery in 1851 (Jackson, 1851), it has been reported and/or studied in the United States, Japan, the former Soviet Union, Korea, China, India, and so on. Because tellurium is one of rare-scattered elements, tetradymite recognized in the past usually occur as rare mineral in some sulfide metal deposits, gold deposits, and tungsten deposits. It is in the Dashuigou tellurium deposit where tetradymite so greatly accumulates and occurs as massive aggregates of big crystals.

The tetradymite in the Dashuigou tellurium deposit is an odinary mineral, but contains a lot of trace elements, such as Fe, Pb, Sb, Se, Ag, and Au. It should be emphasized that grades of Se, Ag, and Au in the ore composed predominantely of tetradymite reach economic value.

Furthermore, the sulfur isotopes of the tetradymite experienced high homogenization and all the values are distributed near $\delta^{34}S$=0‰. This perhaps indicates that the sulfur was derived from some magmas.

Reference: Jackson, C.T. (1851) Am. As, Pr 4, 324-325.
Pauling, L. (1975) Am. Mineral., 60, 994-997.

CRYSTAL CHEMISTRY AND IR SPECTROSCOPY OF CANCRINITE-GROUP MINERALS .

Maras, A. & Ballirano, P. (*Dept. of Earth Sciences, Univ. of Roma*)

About 30 samples, pertaining to the cancrinite-group minerals, from different italian localities were investigated using both analytical electron microscopy and IR spectroscopy.

The chemical data were obtained by means of an electron microprobe Cameca SX50, the experimental set-up was: 10 s of counting time, beam diameter 10μm, 15 kV and 15 nA.

IR spectra were collected on a Perkin Elmer FT 1760 with a nominal resolution of 4 cm^{-1}.

The davyne-group (Bonaccorsi, 1993) is characterized by Cl as prevailing anion with one SO_4 group at maximum for every sub-cell.

IR spectroscopy outlines the presence of significant amounts of CO_3 groups that, according to structure refinements of minerals pertaining to the cancrinite-vishnevite serie, could be housed by the large channels: minor amounts of F were also detected whereas no evidencies of the presence of molecular water were observed.

Quadridavyne samples investigated are non-stoichiometric with a 0.5 anion and cation deficiency for every sub-cell, raising a different possible explaination for superstructures in davyne-group as due to the ordering of vacancies, according to schemes similar to those described by Grundy & Hassan (1984) for cancrinite.

A correlation between the a parameter and the position of the absorption band located at around 680 cm^{-1} was observed along with a relationship involving the K content and the a parameter.

Liottite and afghanite show a SO_4/Cl ratio close to 1 with a small prevalence of SO_4 for liottite. Only one sample of afghanite contains minor amounts of molecular water, all the others are anhydrous; these sample, as well as all the cancrinite-group minerals analyzed, are characterized by a strong tendency to absorb humidity that is loss at 50°C. The same correlations obtained for davyne-group were observed for liottite and afghanite.

Franzinite is characterized by SO_4 as prevailing anionic group with minor amounts of Cl and F; IR spectroscopy failed to detect molecular water and CO_3 groups.

Giuseppettite and sacrofanite are also characterized by prevailing SO_4 groups but significant amounts of molecular water were observed on IR spectra.

REFERENCES.

Bonaccorsi, E. (1993) *Plinius*, **9**, 16-22.
Grundy & Hassan (1982) *Can. Mineral.*, **20**, 239-251.

MINERALOGICAL CHARACTERIZATION AND GEMOLOGICAL POSSIBILITIES OF ALEXANDRITE, EMERALD AND PHENAKITE FROM FRANQUEIRA (NW. OF SPAIN), THE FIRST SPANISH OCCURRENCE OF THIS MINERAL ASSEMBLAGE.

Marcos-Pascual, C., Moreiras D. B., Paniagua, A., (*Dept. of Geology, Univ. of Oviedo*) Fernández-Díaz, M.R., Garcia-Granda, S. *(Dept. of Physical and Analytical Chemistry, Univ. of Oviedo)*

The chrysoberyl, emerald and phenakite gemstone deposit of Franqueira is the only one known in Spain with this mineral association. It is located in the NW part of the Iberian Peninsula, in the granitic domain of the Galicia - Tras os Montes zone . In Franqueira, a pegmatite body crosscuts an ultramafic rock of dunitic character and associated gabbroic lithologies. In the contact between

the pegmatite and the dunite a metasomatic zone has been developed. Alexandrite, emerald and phenakite have grown in this zone.

Alexandrite appears as euhedral or subhedral twinned porphyroblasts - in size up to 1 cm - in the phlogopite or as skeletal intergrowths within emerald.

Emerald appears as euhedral prismatic crystals with sizes of up to 10 cm. Sometimes it can replace the alexandrite and phenakite.

Phenakite appears as short subhedral and colourless prismatic crystals up to 3 cm in size.

These minerals have been characterized by their chemical and physical properties, including: The internal characteristics; the specific gravity; the optical properties (colour, pleochroism and the principal refractive indices).

Their crystalline structures have been refined using single-crystal X-ray methods. Termogravimetric and infrared spectroscopic studies in order to determine the H_2O content in emerald have been made. Chemical analysis of minor elements in these minerals are considered in the structural refinement.

Finally, the gemological possibilities of these minerals will be drawn.

DO DISORDERED BIOPYRIBOLES BEHAVE AS A PHASE OR A PHASE MIXTURE? AN EMPIRICAL OBSERVATION

Maresch W.V. (*Inst. Mineralogie, Univ. Münster, Germany*) and Czank M. (*Mineralogisch-Petrographisches Inst., Univ. Kiel, Germany*)

Several lines of reasoning have led to logical if not yet completely definitive conclusions on the relative stabilities of the ordered biopyriboles. These include textural evidence of reaction sequences involving biopyriboles in natural occurrences (e.g. Veblen & Buseck, 1981), energy calculations on the basis of structure determinations (e.g. Abbott & Burnham, 1991), and theoretical models of polysomatic series, such as the axial next-nearest-neighbour Ising or ANNNI model (e.g. Price & Yeomans, 1986). By contrast, the thermodynamic properties and the reaction behaviour of disordered biopyriboles are still a matter of considerable speculation (e.g. Veblen & Buseck, 1981; Maresch & Czank, 1988). How are "microscopic" observations to be related to "macroscopic" properties?

1) Equal numbers of double-chain and triple-chain slabs parallel to (010) can be thought of as being combined in a crystal and shuffled in card-deck fashion through an infinite variety of possible disordered states until the rigorously ordered ...232323... sequence of chesterite is attained. The bulk composition of the crystal remains constant. At what stage will the macroscopic, physico-chemical properties of the crystal be essentially those of chesterite and not those of a mechanical mixture of amphibole and jimthompsonite? Will a chesterite crystal continue to react as a modified, homogeneous entity as disorder increases, or at what stage will it disproportionate again into a heterogeneous mechanical mixture?

2) The polysomatic model predicts that continued polymerization of single chains will eventually lead to a sheet silicate through an infinite possible series of intermediate, both ordered and disordered polysomatic states. The bulk composition must change. Consider the following reactions:

$$\text{TREMOLITE} + 3\text{calcite} + 2\text{qtz} \Leftrightarrow 5\text{diopside} + 3CO_2 + H_2O \quad (A)$$

$$\text{TALC} + 3\text{calcite} + 2\text{qtz} \Leftrightarrow 3\text{diopside} + 3CO_2 + H_2O \quad (B)$$

How far will the location of reaction (A) continuously shift towards or even coincide with (B) for tremolite of increasing degree of polymerization and disorder? Or at what point will homogeneously reacting, disordered, hybrid tremolite crystals disproportionate to a mechanical mixture of biopyriboles?

These important questions still remain to be tackled in a rigorous way, but we have obtained HRTEM images of synthetic lamellar pyroxene/amphibole intergrowths in the system CaO-MgO-SiO_2-H_2O. The experiments were run at P/T-conditions where pyroxene reacted to amphibole via a solution/precipitation mechanism. This process can be clearly observed at crystal terminations, where the double chains were stable and grew, whereas the single chains were not, and reacted out to form deep embayments into the crystal. The disordered biopyriboles obviously behaved as mechanical mixtures down to the unit-cell scale, where some discrete lamellae were less than two double-chains wide. Similar observations on other types of biopyriboles have not been possible, because reactions are usually topotactic. Nevertheless, intracystalline terminations of wide-chain biopyriboles in both natural and synthetic amphiboles are usually remarkably strain-free.

Until a more rigorous approach can be developed, we suggest that to a first approximation disordered biopyriboles can be regarded as mechanical mixtures, at least during reactions under hydrothermal conditions. The results of careful eperiments with synthetic biopyriboles should yield information directly applicable to natural ordered analogues, even if the synthetic material involved is structurally disordered.

Abbott, R.N., Jr., Burnham, C.W. (1991). *Am. Mineral.*, **76**, 728-732.

Maresch, W.V., Czank, M. (1988) *Fortschr. Mineral.*, **66**, 69-121.

Price, G.D., Yeomans, J. (1986). *Mineral. Mag.*, **50**, 149-156.

Veblen, D.R., Buseck, P.R. (1981). *Am. Mineral.*, **66**, 1107-1134.

TYPES OF THE STATES OF MATTER IN THE UNIVERSE;PLACE OF MINERAL FORMATION

Marfunin A.S.(Dept.of Mineralogy,Moscow University)

A system covering all the types of matter can be presented by three diagrams:
-Big Square of the Universe (density-temperature,absolute maxima 10^{32} K and 10^{94} g.cm^{-3}) including states of the entire Universe,
-The Universe with temporal structure,
-Galactic Universe.

The closed space of the diagrams includes all the states (including minerals and stuff of Life),for all galaxies,from the beginning up to the end of the Universe,and could be valid for all Universes with antropic values of fundamental physical constants.

There are two kind of consequences from the system:general and mineralogical.

The system can be considered as a Model of the Universe. Types of the states of matter are stages of the evolution of the Universe ("a drawing of the Divine Plan").

Formula of the Space:$H_{90}He_{10}he_{0.001}$ ("he" =heavier than Hydrogen and Helium elements).

Genetic classification of stars,genetic system of elements,"Arrow of Time" for the Universe with temporal structure and "Network of Time" repeated trillions times for galactic Universe,terminal states of the evolution (superdense White Dwarfs,Neutron Stars,Black Holes,and Mineral states and Stuff of Life) are considered.

Temporal algoritm of the gavitational transformations determines stellar and planetary scenarios of the evolution ("Wohltemperiertes Universum").Consequences from the evolutionary system are compared with some general concepts:Philosophical Systems,Time,Substance,Infinity,Genesis.

Largest area of mineral formation is H-He-he interstellar medium.

Hydrogen of this "superhyperhigh vacuum"

state (10^{-24} g.cm^{-3}, i.e. one hydrogen atom in cubic centimeter) is the only material for star formation and for synthesis of all elements in stars.

Extremely dispersed all other ("he") elements in H-He-he medium in form of interstellar micromineral dust and molecules are the only source of matter for planets and Life. Bulk volume of mineral dust in our Galaxy can be estimated as about 60 trillions of Earth masses.

Characteristics of micromineral formation in H-He-he Space include:

ultra-low pressure mineral condensation and ice-rock accretion;
generations of minerals, presolar minerals;
secondary alterations;
Light extinction, scattering, polarization;
size and habitus, intergrowths;
variation of composition;
cosmothermometry.

Relations of interstellar mineral dust to formation of planets, asteroids, meteorites, and comets; role of minerals as substratum for Life, and antropicity of geological evolution are considered.

MAFIC MAGMA BATCHES AT VESUVIUS. A GLASS INCLUSION APPROACH TO THE MODALITIES OF FEEDING STRATOVOLCANOES

Marianelli P.[1], Métrich N.[2], Santacroce R.[1] and Sbrana A.[1]
([1]Univ.di Pisa, Scienze della Terra, Pisa, Italy; [2] Lab. Pierre Süe, GST, CE-Saclay.France)

Glass inclusions in olivine and diopside phenocrysts from pyroclasts of various eruptions of Vesuvius are representative of the magmas having supplied the volcano in the last 4-5,000 years. During this interval the volcano alternated open conduit activity (e.g.1944 and 1906 eruptions) with long rests interrupted by Plinian and Subplinian eruptions (e.g. 3,360 BP "Avellino", AD79 "Pompei", AD472 "Pollena"). The eruptive behaviour was conditioned in all cases by the presence of shallow reservoirs: two cases are distinguished: (i) small and very shallow, 1906-type, and, (ii) large and deeper Plinian-Subplinian. Lapilli of 1906 lava fountains contain olivine (Fo_{90-91}) including Cr-spinel (Cr#>76) and volatile-K-rich tephritic glass (MgO ~ 9 wt%, H_2O = 2.2 wt%; Cl = 0.4-0.5 wt%; S = 0.15-0.2 wt%; F = 0.18-0.2 wt%), which represents the first recognized Vesuvius primary magmas. Mg-poorer olivine (Fo_{83-89}) also occurs in 1906 and 1944 products; it formed within the shallow reservoir, together with pyroxene and leucite, between 1200°C and 1130°C, from slightly evolved K-tephritic melts (MgO = 6-8 wt%); these summarize the compositional evolution of the resident magma, as resulted of the complex, repeated processes (new magma injections, magma mixing, crystal settling, magma extractions) acting through out the life time of the chamber. The Plinian and Subplinian pumice contain diopside, phlogopite and minor olivine (Fo_{85-87}) representing adcumulates wrenched from the chamber walls.

These crystals result from rapid crystallization of the fresh magma batches periodically supplying the chamber before reaching thermal equilibrium and mixing with resident magmas. Glass inclusions in these minerals have therefore been regarded as representative of the magmas supplying the Plinian-Subplinian chamber(s). They range from K-basalt to K-tephrite (MgO = 6-8 wt%), with homogenization temperature of 1130-1170°C. The "Avellino" glass inclusions have K-basaltic compositions, contrasting the mostly K-tephritic Pompei and "Pollena" inclusions (which are quite similar each other and comparable to magmas having fed the volcano in the recent period of activity). The "Avellino" glasses also display lower Cl and P contents in respect to the younger tephritic melts, and these variations should reflect primary features of the mantle-derived magmas. These facts indicate that: (i) important changes occurred at depth between 3,360 and ca. 2,600 BP (possible birth of the "Pompei" chamber); (ii) the rising magma batches in the last 2,600 years have been essentially homogeneous, a feature consistent with the steady magma supply rate to Vesuvius. Both primary and near-primary Vesuvius magmas, as illustrated by melt inclusions, emphasize high K, P, Cl and volatile contents, with high K_2O/H_2O (2-2.5), K_2O/TiO_2 (1.5-2.8) and Cl/P (0.8-1.2) ratios consistent with a metasomatized mantle source.

CORRELATIONS BETWEEN CHEMICAL COMPOSITIONS AND PHYSICAL PARAMETERS OF LUDWIGITES. EXAMPLES FROM ROMANIAN OCCURRENCES.

Marincea Şt. (*Institute of Geology and Geophysics, Bucharest*)

Samples of ludwigite from several Romanian localities were analysed in order to refine and enlarge the correlations between physical parameters and chemical composition. Some such data were previously found by Aleksandrov (1982). All the samples originate in magnesian skarns from the Banatitic Province, related to the Late-Cretaceous-Paleogene magmatism i.e. Ocna de Fier (the type locality for ludwigite), Băiţa Bihor, Pietroasa, Maşca-Băişoara and Cacova Ierii.

Wet-chemical and microprobe analyses showed that the major compositional variation is given by the substitutions of Mg^{2+} by Fe^{2+} in the M(1) - M(3) structural positions. The content of vonsenite in solid solution ranges between 1.72 and 14.35 mole percent. The substitutions in the M(4) structural positions are minor, pointing to low contents of azoproite (up to 0.70 mole percent), alumoludwigite (up to 12.54 mole percent) and chestermanite (up to 0.02 mole percent). Consequently, the variations of some physical parameters esentially correlate with the vonsenite content in a direct but nonlinear manner: a) the mean reflectance value (between 9.235 and 11.52 %); b) the "a" cell parameter (between 9.194 and 9.280 Å); c) the cell volume (between 340.37 Å^3 and 348.55 Å^3); d) the frequency related to the ν_5 antisymmetric stretching vibration of the $[BO_3]^{3-}$ group in the infrared absorption spectra (between 1240 and 1272 cm^{-1}); e) the calculated specific gravity (between 3.79 and 3.88). Other parameters (i.e. the "b" and "c" cell parameters; the frequencies on the infrared absorption spectra related to the ν_2 symmetric bending and to the ν_1 symmetric stretching of the $[BO_3]^{3-}$ group e.a.) are only slightly dependent on the variations of the vonsenite content.

References:

Aleksandrov, S.M. (1982) Geochemistry of boron and tin in magnesian skarn deposits. *Nauka Ed.*, Moskow, 272 p. (in Russian).

SPECTROSCOPIC INVESTIGATION OF CALCIUM TARTRATE CRYSTALS.

Markov V.P., Popov K.G., Tikhonov N.A.
(Syktyvkar University, Syktyvkar, Komi, Russia)

Element-organic combinations play a significant role in mineralogy of human. Usually, they are small soluble salts of wine, milk or anther

kind of acids. They imagine itself a crystals of complex structure.

This work is devoted to spectroscopic investigation of structure and properties of calcium tartrate tetrahydrate (CTT) $CaC_4H_4O_6 * 4H_2O$ crystals. CTT crystals was grown in silica-gel during opposite direction diffusion of wine acid ($H_2C_4H_4O_6$) and calcium chloride ($CaCl_2$). As a result of diffusion regime of growth, filter and localizing ability of gel the CTT crystals are of a best quality with dimension till 1 sm, transparent, colorless or small yellow [1].

There were as following methods used in our investigations: X-Ray diffractometry, Differential thermal analysis, Optical dencitometry and Raman spectroscopy.

The crystals of CTT had high perfection. This result exceeded by X-Ray double-crystal investigations. The half width of the rocking curves for different reflections was 13÷20". This fact give a possibility to observe microblocks in CTT crystals by X-Ray double-crystal topography and to measure their small angle grains values.

Differential thermal analysis of the CTT was carry out. At the range 60°÷270°C the crystal structure destroyed (endothermic twin peaks at 170°C) and removed four molecules of structural water. By heating at 500°÷900°C two new crystal structures were appeared. Any differences in thermal effects among white, yellow and yellow-white crystals were not found.

Optical spectrum of transmission of CTT crystals was registered in visible part of light (350÷700 nm). There are three regions of wave length with local maximums of optical density D: 420÷480 nm (blue region) - D=0.46; 540÷560 nm (green region) - D=0.38; 660÷690 nm (red region) - D=0.28.

The Raman spectrum of CTT crystals was excited with Ar-laser light with 100 mW and wave length 514.5 nm. The 90° scatted nonpolarized light was registered by double monochromator at resolution of 6 sm^{-1} (see figure).

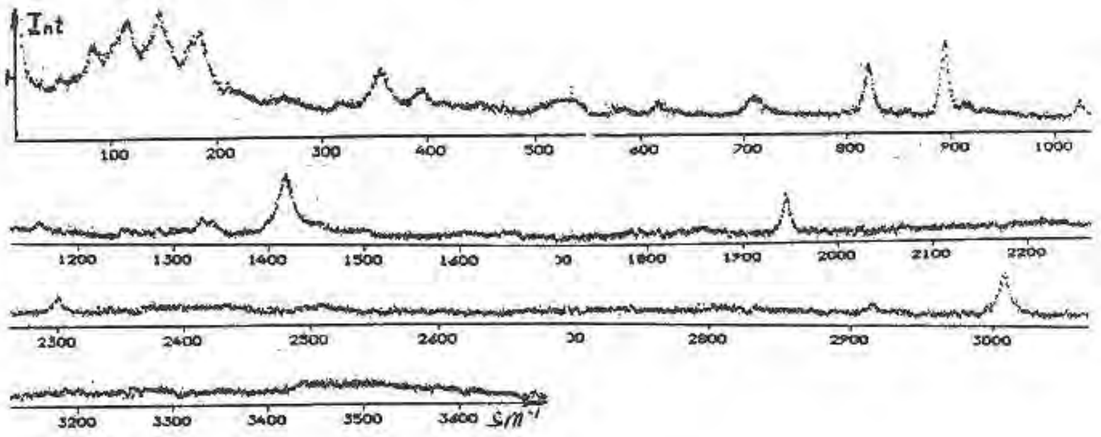

References:

1. Ruzov V.P. et.al., Crystal Growth In Gel: Investigation of Nucleation Processes. Cryst. Res. Techn., v.25,(1990), p.737-746.

THE SIGNIFICANCE OF P ENRICHMENT IN ALKALI FELDSPAR, SOUTH MOUNTAIN BATHOLITH, NOVA SCOTIA

Martin, R.F. (*Dept. of Earth & Planetary Sciences, McGill Univ.*), Kontak, D.J. (*Nova Scotia Dept. of Mines & Energy*) and Richard, L.R. (*Dept. of Geology, Dalhousie Univ.*)

The 370 Ma peraluminous South Mountain Batholith (SMB) of Nova Scotia (eastern Canada) consists of granodiorite, monzogranite, leucomonzogranite and leucogranite. Granitic pegmatites, deuteric alteration and mineralization are locally abundant in the latter two phases. Bulk analyses of the perthitic K-feldspar (Kfs) indicate a strong correlation between concentration of phosphorus and degree of fractionation, as indicated by concentrations of Rb, Ba, Sr and Eu. The Kfs in pegmatites may even contain in excess of 1.0 wt% P_2O_5; that in the monzogranite also shows a notable enrichment in P (0.1-0.4% P_2O_5). Electron-microprobe analyses indicate that 1) P is structurally bound in both K-rich and Na-rich phases (berlinite substitution: Al + P = 2Si), 2) its concentration is erratic, even on a local scale (<100 μm), and 3) it generally favors the K-rich phase over albite in a perthitic intergrowth. X-ray-diffraction scans and unit-cell refinements confirm orthoclase (Or) as the dominant polymorph in this batholith. Highly ordered microcline (Mc) does occur, but only in areas of intense deformation or hydrothermal alteration, as near the East Kemptville Sn deposit. The scarcity of Mc in such a composite batholith is consistent with relative depletion of the granitic magma in dissolved H_2O and rapid cooling. Subsidiary factors that also could have impeded the inversion of Or to Mc are the peraluminous bulk-compositions and the presence of structurally bound P. Elevated whole-rock P_2O_5 reflect the presence of P-rich Kfs rather than of other P-bearing phases like apatite. The appearance of secondary phosphates in mineralized centers (*e.g.*, East Kemptville) may indicate local fluid-mediated release of structurally bound P from orthoclase upon its conversion to microcline).

SUCCESSIVE PARAGENESES IN METAULTRAMAFIC ROCKS OF THE SOUTH CARPATHIANS

Măruntiu M. (*Inst. of Geology and Geophysics, Bucharest, Romania*)

Three groups of ultramafic rocks occur within the medium-grade polymetamorphic terrains of the South Carpathians. Prior to the generalised medium-grade (kyanite-staurolite zone) M_1-M_2 events of the country rocks, these groups are characterised by distinct PT-t evolutions of parageneses as follows:

a. the subcontinental lherzolitic rocks hosted by continental supracrustal rocks of the Sebeş Group show a continuous retrograde path from HP-HT garnet-bearing parageneses (*ol+opx+cpx+grt*) to two successive spinel-bearing parageneses (*opx+cpx+spl* like coronas around the garnet, representing a decompression stage in granulitic facies, and *ol+opx+amp+spl* in S_1 foliated assemblages of high-amphibolite facies) and then to chlorite parageneses (*ol+amp+chl±anthop±tlc*) in S_2 foliated assemblages; bodies of harzburgitic compositions in the same litho-tectonic assemblage show relics of partial melting generated ol+spl aggregates with typical textures and effects of silicic metasomatoses in granulitic facies (opx neoblasts and veins) in turn followed by amp+spl and amp+chl bearing assemblages in amphibolitic facies M1-M2 events;

b. in the dunitic, harzburgitic and pyroxenitic rocks of the dismembered ocean-like crust of Lotru Group there are evidences for nearly isobaric cooling of HT Cr-spinel protoliths to the secondary spinel assemblages (megacrysts of Al-opx exhibit microblastic *spl+opx+cpx* along highly shear planes) followed by continuous retrograde evolution in the amphibolite (*ol+amp+chl+tlc*) and greenschists (*serp+brc*) facies;

c. the plagioclase wehrlitic rocks in continental bimodal (amphibolites+metagranites) association of Cumpăna Group are characterised by: 1. prograde evolution of the magmatic *ol+cpx±opx +spl+pl* paragenesis to generalised *ol+cpx+opx+spl* one, and *ol+cpx+opx+grt+cor* paragenesis only along the margins of the bodies, and 2. retrograde path to high (*ol+amp+spl*) and medium (*ol+amp+chl*) amphibolite facies.

Extensive recrystalisation in medium to low amphibolitic facies has been accompanied by Si, Al, Ca and CO2 metasomatic processes which are responsable for widely distribution of hydrated parageneses with talc, chlorite, tremolite-actinolite, antigorite, magnesite, dolomite and quartz.

Consequently, the different origins for ultramafic rocks in various metamorphic crustal sequences have been emphasised as well as their different significances in terms of tectono-

metamorphic evolution of the litho-tectonic entities in the prealpine nappe stack of the basement of the South Carpathians.

STRUCTURAL DATA AND CHEMICAL COMPOSITIONS OF MG-CHLORITES FROM SOME ULTRAMAFIC BODIES OF THE SOUTH CARPATHIANS (ROMANIA).

Măruntiu M., Robu L. and Stelea G. (Institute of Geology and Geophysics of Bucureşti)

Mg-chlorites contained by the ultramafic bodies had been observed at the contact between ultramafic bodies and the country crystalline rocks, like veins or irregular zones, being generated by the metasomatic phenomena, developed in the metamorphic processes.

Ultramafic bodies are associated with medium-grade metamorphic rocks, sometimes retrograded.

The mineral assamblages associated with Mg-chlorites are: chlorite+amphibole (actinolite), chlorite+biotite or chlorite +amphibole+talc.

Chemical compositions emphasized a high Mg content for majority of chlorites and significant aluminium content.

Variations of octahedral cations contents (5 to 6) and the vacancies (from 0 to 1) point out a tri-trioctahedral structure for all chlorites, but all chemical features emphasize a clinochlore member of chlorites series, with an obvious aluminous characters for some of them.

Substitutions in the octahedral positions between $Al \leftrightharpoons Mg$, $Mg \leftrightharpoons Fe^{3+}$, Fe^{2+} or $Mg \leftrightharpoons Cr$, Ni determine small variations of b parameter, which increase with increasing of Mg, Fe^{2+}, Fe^{3+}, Cr, Ni content.

The higher Al content of some chlorite is emphasized by IR absorbtion spectra, registering characteristic absorbtion bands for **Si-O-Al** or **Si-O-Mg** vibrations in the domains 750 - 850 cm^{-1} and 450 - 700 cm^{-1}.

• METASOMATIC TOURMALINIZATION PROCESSES IN THE PEGMATITIC ROCKS OF APUSENI MOUNTAINS (ROMANIA)

Marza I. *(University of Cluj-Napoca)*

A pegmatitic vein with metasomatic tourmaline occurs in the pegmatitic sub-province of Apuseni Mountains, which belongs to the meso-metamorphic unit of Somes (sillimanite, kyanite, staurolite, almandine, etc...). The vein with tourmaline crosses retromorphic biotitic gneisses. The size of the vein is: 10 meter width and 50 meter in length. The pegmatitic vein contains metasomatic tourmaline (T2) and crystals of tourmaline (T1) which formed at the same time of the pegmatitic crystallization processes.

The neosome was formed from solutions enriched in boron, which concentrated in the tourmaline T2 in the final stage of the crystallization of the pegmatitic solutions on the proto-pegmatitic paleosome. The neosome produced substitutions and corrosion on primary minerals (feldspars and quartz). Contents of 80-90% of tourmaline in the pegmatitic vein suggested the presence of preexisting rocks rich in tourmaline.

THE NEW TYPE OF WATER IN BERYL

Mashkovtsev R.I. (*Inst. of Mineralogy and Petrography, Novosibirsk, Russia*)

The present communication describes results of a spectroscopic study of synthesized beryls in the IR and near IR regions and author demonstrate the existence of one more form of water associated with the heavy alkali ions. The beryls were grown in autoclaves from solutions containing Li,Na,K,Rb, and Cs separately and also as mixtures.

Besides the well-known bands related to type I and II water vibrations were also observed additional bands in samples doped with K, Rb, and Cs ions. The additional bands at 7102, 5192, 3704, and 1604 cm^{-1} relate to the new type III water.

Since the third type of H_2O are observed in beryls, containing heavy alkali ions, it would be reasonable to consider that there is an interrelationship between these cations and the water molecules. The wave numbers of the type III water molecules varies only slightly from the type I water wavenumbers, whereas their axes of symmetry are identically directed.Thus one might suggest that the small perturbence experienced by the water molecules is determined by the alkali ions situated at distances significantly greater than in the case of type II H_2O. Recent structure refinements of beryl assigns H_2O molecules, as well as the larger alkali ions to the 2a sites (Artioli et al., 1993). Hence the type III water molecules and heavy alkali ions are arranged in the neighboring 2a positions.

Reference:
Artioli,G.,Rinaldi,R.,Stahl,K.,Zanazzi,P.F. (1993). *Am.Mineral.*, **78**, 762-768.

THE CHANGE OF MINERAL EQUILIBRIUM IN SOIL BY HUMAN AGRICULTURAL ACTIVITY

MATICHENKOV V.V. (*Russia, Pushchino, Inst. Soil Sci. and Photos. RAS*)

The mineral equilibrium in soil depends on soil formation factors (parent material,climatic, relief,time and live organisms). The agricultura leads to change of some factors (climatic - melioration and change of live organisms-plants). We studied the follow problems of this aspect of mineral equilibrium: 1) the influence of plants on balance of silicon in soil in virgin and cropped soils, 2) the ways of restoration,protection and optimization of this balance. The complex of various soils (Soddy Podzolic, Grey Forest, Chernozem and Chestnut soils were investigated.

Using of reference sources and elaborating by us algorithm we have calculated the follow data: Silicon is involved in biological cycle of $4,6 \cdot 10^8$ t annually. Soil-paint systems are a major object of terrestical biogeochemical silicon cycle when the common average content of soluble silicon compounds is $3,5 \cdot 10^8$ t of Si and the annual increase of soluble silicon substance is $3,1 \cdot 10^8$ t of Si. In upper soil horizons it is maximum of soluble and potential soluble silicon compounds, because in this place it is more intensive weathering and biogeochemical processes in which silicon takes part. It was calculated that on an average $2,75 \cdot 10^7$t of Si was out irretrievable from field with crop every year. $9,0 \cdot 10^6$t of Si is out from natural cycle every year when forests are cut down.

The human agricultural activity had broken breaks balance of mobile, light soluble and mineral forms of silicon; in so doing natural processes hadn't been restorating restorated this balance during near 100 years. We have observed, that agriculture made more active the processes of transformation and migration of mineral compounds (Si,Al,Fe).The decrease of mobility of silicon substances in higher soil horizon has negative influence on plant and soil fertility. Moreover in higher horizon we have observed the destruction af alkaline and sour solution forms of Si and their migration in down horizons The sour solution forms of Si were carried out from upper horizon also. And we ha-

ve observed the increase of differentiation along this soil profils. The content of Si in alkaline extract was changed in the same fashion that in the sour solution.

Summing up we can conclude that intensive agriculture destroys the silicon state and balance in ecosystem by means of plants (out irretriable with crop). The transformation of silicon compounds in upper soil horizon results in degradation as living part of ecosystem as mineral part and general destruction of land. Because of this it is necessary to restore silicon state and balance in agro-ecosystems.

We have conducted some experiments with amorphous SiO_2 and two kinds of silicon-rich industry wastes in greenhouse and field experiments. The silicon status, change of additional silicates and mineral neoformation were controlled by of element analyzing, x-ray, IR-spectroscopies and electronic microscopy.

The application of high active amorphous silicates had great influence on soil mineral phosphates (Ca-, Al-, Fe-). Our investigations showed possibility of the reaction of replacement Si on P in soil.

Conclusions:

1. The great amount of Si was involved by live organisms, essentially by plants.
2. The intensive agriculture pressure caused to negative changes of mineral equilibrium in soil.
3. The silica metal industry wastes can be used for restore and preserve of mineral equilibrium in cooper soils.

BARIUM-FREE BURBANKITE FROM POÇOS DE CALDAS, MINAS GERAIS, BRAZIL.

Matioli P.A., Atencio D., Coutinho J.M.V. (*Inst. Geociências, Univ. São Paulo*)

Barium-free burbankite - $(Na,Ca)_3(Sr,Ce)_3(CO_3)_5$, hexagonal - occurs as a latest interstitial filling mineral in the nepheline sienite from Pedreira da Prefeitura ("City Hall Quarry"), Poços de Caldas, Minas Gerais, Brazil. Associated minerals in the fracture are calcite, fluorite, natrolite, analcite, pyrite, manganoan ilmenite, strontianite, ankerite, kutnahorite, gaidonnayite and an unidentified chlorite-like mineral (cf. also Ulbrich & Ulbrich, 1992). Barium-free burbankite forms colorless to yellowish euhedral, individual or radial aggregates of prismatic to acicular crystals up to 10 mm. The mineral is opticaly uniaxial negative with ω = 1.620 and ε = 1.600. X-ray powder-diffraction data for the Brazilian sample are virtually identical to those cited in the literature. EDS analysis showed the presence of Sr, Na, Ca and Ce. Poços de Caldas burbankite differs from the samples from other occurrences (chemical analyses of burbankite from several localities quoted by Fitzpatrik & Pabst, 1977) by the absence of Ba. Barium-free burbankite was synthesized by Chen & Chao (1974).

References:

Chen, T.T. & Chao, G.Y. (1974). *Can. Mineral.*, **12**, 342-345.
Fitzpatrik, J. & Pabst, A. (1977). *Am. Mineral.* **62**, 158-163.
Ulbrich, H.H.G.J. & Ulbrich, M.N.C. (1992). Roteiro de Excursão, v.5, 37o. Congr. Bras. Geol.

MD SIMULATION OF CRYSTALS AND MELTS IN THE SYSTEM $CaO–MgO–Al_2O_3–SiO_2$

Matsui M. (*Dept. of Earth and Planet. Sciences, Kyushu Univ.*)

Transferable interatomic potentials have been developed for use in computer simulations of both crystals and melts in the $CaO–MgO–Al_2O_3–SiO_2$ system. The potentials are composed of pairwise additive Coulomb, van der Waals and repulsive interactions. The net charges, q's, on the Ca, Mg, Al, Si, and O ions are constrained as $q(Ca) = q(Mg) = \frac{2}{3}q(Al) = \frac{1}{2}q(Si) = -q(O)$, in order to preserve the requirement of transferability between materials with different composition. Necessary energy parameters were obtained and tested using both the static WMIN and dynamic MD calculations for crystals in the system $CaO–MgO–Al_2O_3–SiO_2$.

The crystals studied here have a wide variety of structural topologies; including oxides(periclase, lime, corundum, and spinel), nesosilicates(olivines, garnets, and sillimanite), inosilicates (pyroxenes), and tectosilicates(cristobalite and quartz). Some high pressure phases, such as coesite, stishovite, wadsleyite, ringwoodite, $MgSiO_3$ ilmenite and perovskite, $CaSiO_3$ perovskite, are also included.

In spite of the simplicity of the potentials and the diversity of the structural types, our MD simulations are quite satisfactory in reproducing accurately the observed structures of these crystals, including the symmetries of the crystal lattices, the unit-cell parameters, the coordination numbers of the cations, and the Ca–O, Mg–O, Al–O and Si–O bond distances. The MD simulated bulk moduli of these minerals are also found to agree well with the measured values.

The MD calculations are further successfully used to reproduce reasonably well the measured (or estimated) densities of various melts in the system $CaO–MgO–Al_2O_3–SiO_2$, and their temperature and pressure dependence.

CLOSE PACKING OF IDENTICAL ELLIPSES

Matsumoto T. (*Dept. of Earth Sciences, Kanazawa Univ., Japan*) and Tanemura M. (*Inst. of Statistical Mathematics, Tokyo, Japan*)

In contrast with the closest packing of circles, with plane group p6mm, periodic close packings of ellipses with 6 contacting neighbours do not always have the maximum density $\rho = \pi/2\sqrt{3}$. Nowacki(1948) indicated five different densest packings of ellipses in four plane groups : p2, c2mm, p2gg and p31m, in 54 types of periodic patterns of ellipses. In all of these five packings, every ellipse is in contact with 6 neighbour ellipses. These packings could be considered to be the densest among the possible forms of ellipse packing.

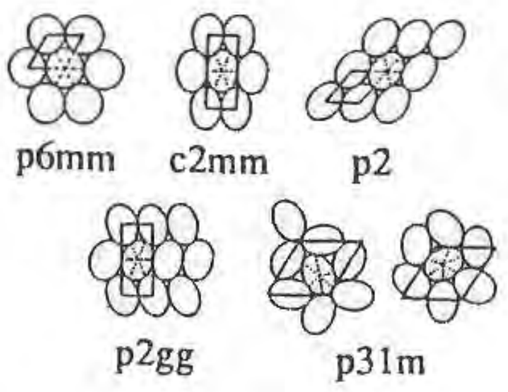

Close packings of circles and ellipses. Nowacki(1948)

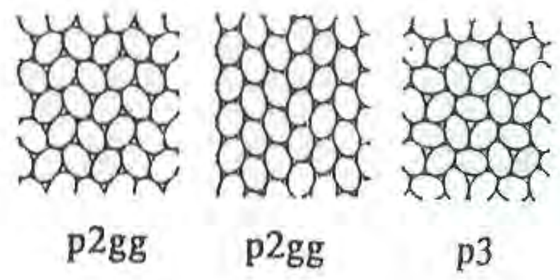

Close packing of ellipses. Grünbaum & Shephard(1987)

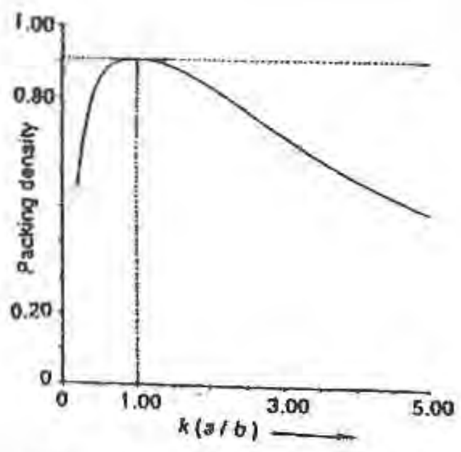

Density for p3 packing of ellipses.

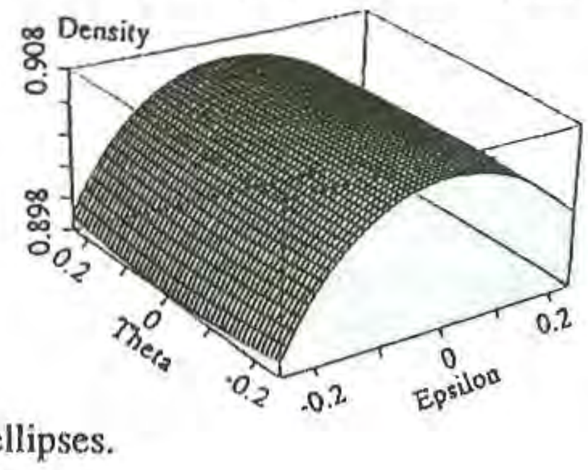

Density for p31m packing of ellipses. Tanemura & Matsumoto(1992)

Matsumoto(1968) and Matsumoto and Nowacki(1966) have shown that the first two of the above densest packings of ellipses, p2 and c2mm, always attain the above maximum density. That of the third, p2gg, cannot exceed this maximum density. The former two packings, p2 and c2mm, are derived from the densest packing of circles, p6mm, by affine transformation, while the p2gg packing of ellipses can never attain the maximum density of ρ.

Tanemura and Matsumoto(1992) have shown that the density of p31m packing of ellipses, the fourth one of the above list, never exceeds the above maximum density ρ. Grünbaum and Shephad (1987) showed four new types of periodic patterns of ellipses, three of them, p3, and two p2gg, with 6 contacting neighbours. We are calculating the density of these three packings, by neumerical calculation and by expanding form in term of ε = k-1(near k=axial ratio of ellipse = 1) and θ (tilting angle of ellipse).

For p3 packing, we obtain the following equation as expanding form in term of ε and θ :

$$\rho(k,\theta) = \pi/2\sqrt{3}\cdot\{1-3/32\cdot\varepsilon^2+1/128\cdot(17-90\sin^2\theta+240\sin^4\theta -160\sin^6\theta)\varepsilon^3-3/4096\cdot(411-1440\sin^2\theta +3840\sin^4\theta-2560\sin^6\theta)\varepsilon^4\}+O(\varepsilon^5).$$

This means the density attains the maximum only when k=1($\varepsilon = 0$) namely, circle packing.

References:

Grünbaum, B. & Shephard, G.C. (1987). Tilings and Patterns, Freeman, New York.

Matsumoto, T. (1968). *Z. Krist.*, **126**, 170-174.

Matsumoto, T. & Nowacki, W. (1966). *Z. Krist.*, **123**, 401-421.

Nowacki, W. (1948). *Schweiz. Mineral. Petrogr. Mitt.*, **28**, 502-508.

Tanemura, M. & Matsumoto, T. (1992). *Z. Krist.*, **198**, 89-99.

MINERAL CHEMISTRY OF THE YEMENI VOLCANIC ROCKS

Mattash*+** M.A. and Buda* Gy. (*Dept. of Mineralogy, Eotvos L. Univ., Budapest*, Board of Mineral Exploration, Yemen**)

Yemen area was situated on the Afar triple-junction in the late Oligocene. During the late Oligocene-early Miocene (synrift phase) and late Miocene-Recent (postrift phase) due to continental extension resulted in the extrusion of large volumes of igneous effusive rocks (2000 m) as a result of numerous endogenic processes which have been generated domal up-lift (3666 m) and continental splitting. According to the radiometric age data the extrusion of the synrift and postrift-related igneous activity can be regarded contemporaneous with the formation of the mid-oceanic ridges in the Gulf of Aden and Red Sea (30-15Ma, and 10-0Ma respectively).

The Yemeni Cenozoic volcanic rocks have an almost continuous graduation from one type to another over a range of silica concentrations from less than 50% to greater than 70% SiO_2. The majority either have SiO_2 concentrations of less than 50% or greater than 67% indicating a marked bimodal character. In other words, the acidic/basic ratio of the Yemeni volcanics is over 0.5, whereas the intermediate rock types compose no more than 5% of the whole volume.

Olivine phenocrysts have high forsterite content (Fo_{91-75}, in their cores), whereas these values decrease at the rims and within the groundmass olivines (Fo_{75-40}), consequently the early-formed olivine crystals contain some Ni and are significantly richer in Mg, than the late-formed crystals. This can be elucidated as the function of falling in temperature (rims and groundmass). The MgO content of the olivines from some Quaternary (Marib) alkali olivine basalts is the highest (MgO=49.13 wt.%), whereas the lowest value is obtained from some differentiated late Miocene basaltic rocks from Aden (MgO=22 wt.%). The former indicates a deeper (mantle zone) origin, and the latter has developed (differentiated) in a relatively shallow magma chamber. The MnO content of the olivines attains up to 2 wt.% in some differentiated basaltic rocks of the southern part of the Yemeni Tertiary volcanics, and decreases in the olivines of the northern part (0.12-0.63 wt%).

Pyroxene from basalts shows a composition variation from Mg-rich augite to ferroan diopside (salite), and less commonly to aegirine-augite. The early-formed augite phenocrysts contain $En_{48}Wo_{45}Fs_7$, but the late-formed augites contain $En_{32}Wo_{43}Fs_{25}$, with an average composition represented by the molecular formula $En_{42}Wo_{44}Fs_{14}$ for the cores, and $En_{34}Wo_{43}Fs_{23}$ for the rims and groundmass pyroxenes. It seems clear that the $CaSiO_3$ content of both phenocrysts and groundmass pyroxenes approximately remains constant, and that they appear over the Skaergaard trend. In addition, the early-formed magnesian rich augites contain some Cr (Cr_2O_3 up to 1.09 wt.%), but the Cr content rapidly decreased, indicating fractional crystallization. The clinopyroxenes mostly show normal zoning, but concentric and hour-glass structure are also found with an increased Fe:Mg ratio toward the rims. Optically these rims are characterized by yellow and green colour, indicating an enrichment in the content of ferric and Ti ions. The majority of the clinopyroxene composition plots within the alkali basaltic clinopyroxene field. Moreover, the pyroxenes plotted in the ferroan diopside (salite) field are considered as a characteristic feature of the alkaline suite. Titanaugite is also identified either as phenocrysts or at the rims of some augite phenocrysts. It is distinguished from common augite by its high TiO_2 content (2.9-5.34 wt%), and also by the high contents of Al and Fe^t. In some samples titanaugite appears to be rimmed with an outer zone of greenish aegirine-augite indicating the degree of alkali enrichment in the latest stages of crystallization. The relatively lower value of the Al^{vi} (octahedral position), and the lower Al^{vi}/Al^{iv} proportion values of the analysed pyroxenes indicate that these pyroxenes are of low pressure origin.

Plagioclase in basalts has the composition range from $An_{87}Ab_{12}Or_1$ in the cores of the early-formed plagioclase phenocrysts, to $An_{60}Ab_{38}Or_2$ at the rims and within the groundmass plagioclase. Optical properties of plagioclase that measured by Universal Stage indicate that most of the plagioclase are fundamentally of high temperature origin. The occurrence of nepheline in the basalt of the younger volcanics (late Miocene-Quaternary) indicates that the younger basalts are more alkaline compared with the Oligo-Miocene basalts.

HALLOYSITE AND OTHER HYDROTHERMAL-RELATED MINERALS OF CAPALBIO GROSSETO (TUSCANY-CENTRAL ITALY).

Mattias P. (*), Crocetti G. (*), Barrese E. (**), Falco F. (**)
(*) = Dept. of Earth Sciences, Univ. of Camerino.
(**)= Dept. of Earth Sciences, Univ. of Calabria,Cosenza.

Near Capalbio (Grosseto), in the northern area of Monteti hill, in Pozzo Picciolente locality, outcrops metalliferous deposits of pyrite and Mn minerals, originated by hydrothermal actions affecting low grade metamorphites (phyllites and argillaceous schists), belonging to the Verrucano formation of Carboniferous-Permian age.

The hydrothermalism produced very large alteration processes with formation of argillaceous phases also, outlined, in the past, during the researches of extractive and mining activities.

By field researches, laboratory analysis (XRD, DTA, TG, IR, SEM and TEM) and optical observations on mineralogical microscope, a continuos range of variation from unaltered to completly altered rocks has been identified. All the aspects of the process can be pointed out following the muscovite alteration phases:

-muscovite and/or sericite->illite->halloysite-10Å and/or

-muscovite and/or sericite->illite->mixed layers->smectite.

The hydrothermalism, favored by some important faults, on a almost limited area with a very strong intensity, with the formation of high purity phases.

A particular emphasis has been given to the study of halloysite-10 Å. The chemical analysis is the following:

SiO_2	Al_2O_3	Fe_2O_3	CaO	MgO	Na_2O	K_2O	H_2O^-	P.al F.	TOT.
43.21	36.33	0.41	0.30	0.09	0.01	0.01	5.32	14.47	100.14

with traces of :

V=14, Cr=46, Ni=17, Sr=10, Zr=8, Ba=13, La=1, Ce=15 (in ppm).

The halloysite-10Å showed all the passage to the halloysite-7Å

and some characteristic morphologies as tubular, bath etc, produced in different environmental and genetic microconditions. In the tubular crystals the size is also 5-7 μm, where the dimensional ratio is 20:1.

The Atterberg limits, determined on pure materials, give the following values: WP=38, WL=49 with IP=11.

A)SEM micrographs

B)TEM micrographs

Among the other clayish newformed minerals, the most important are illite and smectite with irregular mixed-layers.

The smectite is dioctahedral with 20.19% of Al_2O_3 e 2.61% of MgO. The illite, with all the passage to muscovite-sericite mica, is related to sequence of alteration of the parent rocks. Clearly terms of "open illite" have been, often also, observed. In the past some terms of this "open illite" were described with specific names as: "illidromica", "idromica" e "andreattite" (Andreatta, 1947-48; Andreatta, 1949; Andreatta, 1949a; Pellizzer & Guidetti, 1959; Pellizzer & Guidetti, 1959a).

Besides pyrite, limonite-goethite and Mn-minerals that have been object of mining programs, the other newformed phases are mainly the following: cristobalite α, quarzo (variety jalino, ametista, citrino e latteo) and jarosite.

According to the previous phases, other "residual" minerals have been observed: mica muscovite-sericite, quarzt, feldspar, kaolinite e chlorite, forming the basament rocks.

References:
Andreatta,C.(1947-48)-*Mem.Accad.Sc.Ist.di Bologna*,S.X.,**5**,1-17.
Andreatta,C.(1949)-*Per.Min.*,**18**,11-31.
Andreatta,C.(1949a)-*Clay Min.Bull.*,**3**,96-99.
Pellizzer,R. & Guidetti,G.(1959)-*Rend.Soc.Min.It.*,**15**,181-190.
Pellizzer,R. & Guidetti,G.(1959a)-*Rend.Soc.Min.It.*,**15**,215-231.

MINERALOGICAL CHARACTERIZATION OF TEXACO PETROLEUM COKE GASIFICATION SLAGS

Mavrogenes, J.A., Craig, J.R. (*Dept. of Geological Sciences, Virginia Tech*) and DeCanio, S. J. (*Texaco Beacon Labs*)

Gasification of coal and petroleum coke is a promising method that can not only burn waste without air pollution, but very efficiently generate gases which may be used in chemical synthesis, electrical generation or heat production. Texaco has conducted an extensive pilot plant test program at the Montebello Research Laboratory to optimize the Texaco Gasification Process using petroleum coke, the residuum solid remaining after refining, as a feed stock. When used for electrical production, this system is so efficient that it produces more electricity than conventional burners, yet the only by-products are pharmaceutical grade sulfur and V-rich slag. To insure proper flow through of material, oxygen fugacity is carefully regulated throughout the system to control the Vanadium valence state. This study was undertaken to examine vanadium-rich slags in order to identify phases, characterize their behavior, and attempt to predict methods to modify them. Vanadium phase equilibria is presently poorly understood, in large part because of the multiple oxidation states of vanadium (-1, 0, +2, +3, +4, and +5) and the difficulty of unequivocally identifying the valence state(s) in many compounds. The operation of these gasifiers at approximately 1400°C is well above the melting point of V_2O_5 (658°C) but considerably below the melting temperature of VO_2 and V_2O_3 (1637°C and 1937°C respectively). If $f O_2$ can be regulated to keep the gasifier conditions within the V_2O_5 field, slag material would more likely remain molten and more easily flow out of the bottom of the burner. The purpose of this ongoing research program is to accurately determine the valence state of V within phases in slags collected from specific regions within the gasifier. Our ultimate goal is to help define the $f O_2$ present within the gasifier during operation by analyzing the products of gasification.

The oxidation state of pure V phases is readily determined by microprobe analysis alone, where V_2O_5 (V^{5+}) is 56% V, VO_2 (V^{4+}) is 61.4% V, and V_2O_3 (V^{3+}) is 68% V. However, V valence in multi-element phases (especially those containing other elements of variable variance such as Fe) cannot be resolved by microprobe analysis alone. Depending upon air release into the cooling gasifier, samples were categorized as oxidized or reduced. Oxidized samples contain: fine grained (Ca, Mg, Fe, V) oxide matrix of variable composition, (Fe, V, Ni) spinel, (Mg, Al, Fe, V, Ni) spinel, V_2O_5 laths, Al-Si glass blebs and Ni sulfides. Reduced samples contain: crystalline Ca-silicate matrix, subhedral to euhedral (Mg, Al, Fe, V) spinel, a subhedral V oxide, Fe and Fe-Ni Sulfides, Fe-Ni alloys, and complex Ca-oxide matrix. The small grain size of phases within these slags (2-50 μm) precludes the use of X-ray photoelectron spectroscopy (XPS) and X-ray absorption near-edge spectroscopy (XANES) on individual phases to determine Fe and V valence states. Furthermore, X-ray diffraction (XRD) analyses are inconclusive due to the small grain size and low abundance of individual phases within the slag. Raman spectra collected in air do not help determine the V valence within a phase because laser heating oxidizes the sample, however Raman spectra collected from standards in vacuum at low temperatures (-180°C) yield peaks characteristic to each valence state. Raman spectra in conjunction with microprobe analyses, help resolve the valence state of V within complex V-bearing phases.

CONTRASTING BEHAVIOUR OF AMPHIBOLITES AND METAPELITES DURING SHEAR ZONE METAMORPHISM, DUE TO STRAIN PARTITIONING AND CHANNELIZED FLUID FLOW: A CASE STUDY FROM THE EASTERN ALPS.

Mazzoli C., Peruzzo L. and Sassi R. *(Dept. Mineralogy and Petrology, University of Padova, C.so Garibaldi 37, 35137 Padova, Italy)*

Several sectors of the northernmost part of the Austroalpine Nappe which are in direct, tectonic contact with the Tauern Window (Pennides), are affected by shear zone metamorphism. Its effects are particularly evident to the north of Brunico (Bruneck), where the so-called "Cima Dura-Durrek Complex" outcrops. This complex consists of pre-Alpine metamorphic rocks, in which metapelites and metasemipelites of different types prevail, making up a thick sequence in which amphibolites, horneblende gneisses and acidic sheet-like gneisses are interlayered, as well as minor quartzites and marbles. The whole sequence is tightly folded. The limbs are very steep, and become subvertical (*i.e.* coincident with the axial plane) in the northernmost parts.

Important effects of Alpine mylonitic deformations and related metamorphic crystallization are widespread within the whole Cima Dura Complex, and define the most typical and common feature which may be recognized in it both in field and in thin section. Alpine mineral assemblages clearly belong to the greenschist facies and are chronologically related to the mylonitic deformation.

However, the distribution of the Alpine deformational and metamorphic overprints is not homogeneous, because discrete rock portions do not display any of them whereas others are completely reworked.

Specifically, amphibolites which repetitively occur as layers, lenses and large boudins at various distances from the tectonic boundary between the Austroalpine and Pennidic units, display everywhere the same, foliation-related, mineral assemblage Pl + Hbl ± Grt, identical to that occurring in the amphibolites of the pre-Alpine basement outside the shear zone, and irrespective of the distance from the above mentioned major tectonic boundary.

Therefore, foliation and mineralogy occurring in the amphibolites within this Alpine shear zone are both pre-Alpine: due to strain partitioning, the amphibolite bodies escaped Alpine deformational and metamorphic reworking.

On the contrary, the metapelitic sequence in which the amphibolites are interlayered, display everywhere an important greenschist facies metamorphic reworking, texturally related to the pervasive Alpine mylonitic foliation.

Furthermore, basing on microstructural analyses of the metapelites, the Alpine overprints in them may be classified into two deformational and metamorphic stages:
(i) the older stage produced the main mylonitic foliation and the texturally related mineral assemblages, which are to be related to the biotite-almandine zone;
(ii) the younger stage produced: 1) a further, local mylonitization, which also affected the mineral grains crystallized during the older Alpine stage; 2) the crystallization of randomly oriented muscovite and chlorite flakes; 3) the local, retrograde alteration into chlorite of several biotite and garnet crystals formed during the older Alpine stage.

Such water-controlled alteration processes developed statically in some sites, so that chlorite pseudomorphs were produced preserving the undisturbed shape of the original biotite and garnet crystals; in other sites they were also controlled by simultaneous shear, so that, *e.g.*, the original garnet crystals were dismembered and chloritized, and their various fragments were distributed in trails along the reactivated mylonitic foliation surfaces.

In conclusion, the rock sequence involved in this Alpine shear zone acquired variously differentiated metamorphic and microtextural features: *a)* strain partitioning during the main Alpine shearing stage produced from one side, in the deformation shadows, the survival of pre-Alpine foliation and mineral assemblages within the amphibolite bodies, and from the other side, in the surrounding metapelites, a widespread, deformational and metamorphic reworking; *b)* a combination of strain partitioning and channelized fluid flow during the late Alpine shearing stage produced a further textural and mineral differentiation within the metapelites, with the appearance of juxtaposed microdomains in which either records of water-mineral interactions do not occur, or they are widespread and display various textural features according to whether they are located or not along reactivated mylonitic surfaces.

VOLCANISM AND TECTONIC PROCESSES IN THE MAIN ETHIOPIAN RIFT: AN EXAMPLE OF MAGMATICALLY ACTIVE CONTINENTAL RIFT

Mazzuoli R.(*Dip. Sci. Terra, Univ. Pisa, Italy*), Boccaletti M.(*Dip. Sci. Terra, Univ. Firenze, Italy*), Tortorici L.(*Ist. Geof. e Geol., Univ. Catania, Italy*), Trua T.(*Dip. Sci. Terra, Univ. Pisa, Italy*), Ventura G.(*Dip. Sci. Terra, Univ. Cosenza, Italy*)

The Main Ethiopian Rift (MER) is the northern branch of the East African Rift system; it extends northeast towards the Red Sea-Afar-Gulf of Aden system thus separating the Somali block from the Nubian block. The magmatism played a major role in development of the MER. Geochemical constraints indicate that the composition and type of volcanism vary significatively along the Rift system from Afar depression up to the MER. In the sector connecting the Afar to the MER, the Plio-Quaternary basaltic lavas show a plume-magma signature. In this area, following the working model of Schilling, the flattened mantle plume intersects the rifting zone. The geology of a key area located south of Addis Abeba, indicates that from 2 Ma up to 0.4 Ma the MER volcanism was characterized by huge volumes of rhyolitic ignimbrites and domes whereas in most recent times these products are interbedded with basaltic lavas which mainly occur along the rift axis. The basalts have geochemical characters suggesting an important contribution of the lithosphere in the mantle magma source. Petrological data and geochemical modelling indicate the fractional crystallization plus crustal assimilation as the main process for producing the rhyolite liquids from the parent basaltic magma. Such a process has profound implications for crustal evolution beneath the MER because it implies the presence of large magmatic reservoirs and large volumes of ultramafic cumulates.

The type and the age of volcanic events and the complex fault patterns, suggest that an important tectonic phase occurred at around 2 Ma produced an oblique extension along the NE-SW trending strike slip faults which could be responsible for the large basaltic magma intrusions into continental crust and their differentiation and interaction with crustal material.

MÖSSBAUER SPECTROSCOPY OF HIGH-PRESSURE PHASES AND OXYGEN FUGACITY OF THE MANTLE

McCammon C.A. (Bayerisches Geoinstitut, Universität Bayreuth, D-95440 Bayreuth, Germany)

The dominant high-pressure phases inferred to be present in the Earth´s mantle can be synthesised in the laboratory and examined using a wide variety of techniques to characterise the properties of these phases and correlate results with bulk geophysical and geochemical data to produce a unified description of the Earth´s interior. Mössbauer spectroscopy is a powerful tool for studying properties such as oxidation state because it is sensitive to the environments of Fe^{2+} and Fe^{3+} in the high-pressure structures.

Mössbauer studies of upper mantle-derived minerals have been crucial for estimating the upper mantle oxidation state (e.g. Wood et al. 1990 and references therein). The relatively high upper mantle oxygen fugacity (near QFM) is a consequence of Fe^{3+} concentration in the modally minor phases clinopyroxene and spinel (O´Neill et al. 1993), so changes in mantle mineralogy could likely cause changes in mantle oxidation state. Below 400 km in the Earth´s mantle, the low-pressure assemblage of olivine + pyroxenes ± spinel ± garnet transforms to β-$(Mg,Fe)_2SiO_4$ + $(Mg,Fe)SiO_3$-rich garnet, and at approximately 550 km to γ-$(Mg,Fe)_2SiO_4$ + $(Mg,Fe)SiO_3$-rich garnet. To investigate the minimum Fe^{3+} content of these transition zone phases, they were synthesised at their low f_{O_2} stability limits (in equilibrium with Fe metal and SiO_2) at high pressure and high temperature in a multianvil press. All run products were analysed using X-ray diffraction, the electron microprobe and Mössbauer spectroscopy. Although no Fe^{3+} was detected in the starting materials, measurable amounts of Fe^{3+} were found in all run products. While concentration of Fe^{3+} in the modally minor phases clinopyroxene and spinel results in an upper mantle oxygen fugacity near QFM, the ability of all major transition zone phases to accommodate Fe^{3+} implies that in an isochemical mantle, the oxygen fugacity of the transition zone must be lower than that of the upper mantle.

The inevitable presence of Fe^{3+} in transition zone minerals is likely to have significant effects on physical properties such as electrical conductivity, and the magnitude of these effects partly depends on the partitioning of Fe^{3+} between crystallographic sites, both within a single phase and between different phases in the transition zone. As an initial step in characterising the crystal chemistry of Fe^{3+} in transition zone phases, several samples of $(Mg,Fe)SiO_3$-rich garnet were synthesised in a multianvil press at varying f_{O_2} conditions. Mössbauer spectra of the quenched samples were recorded at a series of temperatures between 80 and 300 K. Although the amount of Fe^{3+} is relatively small (maximum $Fe^{3+}/\sum Fe \sim 0.15$), well-defined parameters for Fe^{3+} could be determined through systematic fitting of all spectra. The temperature variation of the centre shift and area ratio data provide an estimate of the Mössbauer Debye temperature and intrinsic isomer shift, while the temperature variation of the quadrupole splitting indicates the change in site distortion. The only fitting model that produced realistic values for these parameters indicates that Fe^{3+} occupies both the tetrahedral and octahedral sites in the garnet structure, where the partitioning appears to be related to both Fe^{2+} and Fe^{3+} content. The data can be used to speculate on the partitioning of Fe^{3+} between transition mantle phases, and the likely implications for physical and chemical properties.

References:

O´Neill, H. St. C., Rubie, D.C., Canil, D., Geiger, C.A., Ross II, C.R., Seifert, F., and Woodland, A.B. (1993) in *Evolution of the Earth and Planets*, E. Takahashi, R. Jeanloz, and D. C. Rubie, Eds., American Geophysical Union, Washington D.C., 73-88.

Wood, B.J., Bryndzia, L.T., and Johnson, K.E. (1990) *Science*, **248**, 337-345.

THE CRYSTAL CHEMISTRY OF FERRIC IRON IN THE LOWER MANTLE

McCammon C.A. (Bayerisches Geoinstitut, Universität Bayreuth, D-95440 Bayreuth, Germany)

Ferric iron is likely has a significant effect on lower mantle properties such as electrical conductivity despite its low abundance relative to cations such as ferrous iron, magnesium and silicon. Both

major lower mantle phases likely contain ferric iron at lower mantle conditions: McCammon et al. (1992) demonstrated that $(Fe,Mg)SiO_3$ perovskite contains measurable amounts of ferric iron at its minimum fO_2 stability limit, and McCammon (1993) concluded that (Fe,Mg)O likely contains ferric iron on the basis of experiments on the endmember Fe_xO. Determination of the amount and location of ferric iron in these phases has been problematical because of the small amounts involved, but is important to characterising properties such as electrical conductivity because of the likely role of ferric iron in the conduction mechanism. To address this problem, a systematic study of these phases has been undertaken using Mössbauer spectroscopy, where variables such as oxygen fugacity, pressure, temperature and composition have been varied to generate series of spectra that can be analysed with realistic fitting models.

To characterise the nature of the iron sites in $(Fe,Mg)SiO_3$ perovskite, $^{57}Fe_{0.05}Mg_{0.95}SiO_3$ was synthesised using a multianvil press, and Mössbauer spectra of the quenched sample were recorded at a series of temperatures between 80 and 300 K. Although the sample contains a relatively small amount of ferric iron ($Fe^{3+}/\Sigma Fe$ ~ 0.05), well-defined parameters for ferric iron could be determined through systematic fitting of all spectra. The temperature variation of the centre shift and area ratio data provide an estimate of the Mössbauer Debye temperature and intrinsic isomer shift, while the temperature variation of the quadrupole splitting indicates the change in site distortion. A similar series of measurements were made on bernalite, $Fe(OH)_3$, a recently described mineral with a perovskite-like structure (Birch et al. 1993). Since ferric iron occupies only the octahedral sites, bernalite provides an excellent opportunity to characterise the nature of octahedral ferric iron in a perovskite-like structure. Comparison of results for $(Fe,Mg)SiO_3$ perovskite and bernalite strongly suggests that the ferric iron in $(Fe,Mg)SiO_3$ perovskite occupies the octahedral site almost exclusively.

To study the nature of ferric iron in (Fe,Mg)O, a suite of samples were synthesised at atmospheric pressure and varying temperatures and oxygen fugacities in a gas-flow furnace. Cubic cell parameters were determined using X-ray diffraction while Mössbauer data were used to calculate ferric iron contents. The cubic cell parameter decreases linearly with increasing ferric iron content, and the ferrous iron Mössbauer data show consistent trends which can be used to infer possible defect structures. The ferric iron content of (Fe,Mg)O increases with increasing oxygen fugacity, in agreement with previous work (e.g. Valet et al. 1975). All previous work, however, was based on chemical and thermogravimetric analysis, which gave minimum ferric iron contents close to zero. In contrast, the Mössbauer data show that the minimum ferric iron content is much larger: $Fe^{3+}/\Sigma Fe$ ~ 0.03 for the composition Fe/(Fe+Mg) = 0.2. These results indicate that (Fe,Mg)O contains significant ferric iron in equilibrium with Fe metal at lower mantle temperatures. Analysis is underway to extract information about the probable location of ferric iron as a function of iron content. Results can be used to speculate on the partitioning of ferric iron between lower mantle phases, and the likely implications for physical and chemical properties.

References:
Birch, W.D., Pring, A., Reller, A. and Schmalle, H. (1992). *Naturwissen.*, 79, 509-511.
McCammon, C. (1993). Science, 259, 66-68.
McCammon, C.A., Rubie, D.C., Ross II, C.R., Seifert, F., O'Neill, H. St. C. (1992). *Amer. Mineral.*, 77, 894-897.
Valet, P., Pluschkell, W. and Engell, H. (1975). *Arch. Eisenhüttenwes.*, 46, 383-388.

THE ORIGIN OF $(OH)_4$ DEFECTS IN QUARTZ AND THEIR BEHAVIOUR ON HEATING

McConnell J.D.C. *(Dept. of Earth Sciences, Univ. of Oxford)*

It is generally accepted that water plays an extremely important role in the behaviour of minerals in metamorphism not only in terms of facilitating diffusion and diffusion mechanisms but also in the context of the deformation of minerals such as quartz where it is has long since been accepted that the presence of water leads to the phenomenon of hydrolytic weakening. The mechanism of this process is, however, not well understood since until recently it has not been clear how water is incorporated in the quartz structure.

Recent *ab initio* calculations on the mechanism of the incorporation of water in quartz have now been completed. These calculations indicate that the preferred mode of incorporation involves the replacement of Si by H_4 leading to the development of $(OH)_4$ groups comparable to those found in the hydrogarnet structure.The *ab initio* calculations also indicate that the energy asssociated with the incorporation of interstitial water molecules in quartz is prohibitive. The energy data from these *ab initio* calculations have been used to derive a phase diagram for the system quartz-water at low water contents. In the modelled phase diagram the solubility of water in quartz at a pressure of 1.0 GPa passes through a maximum at 0°C and thereafter decreases with increasing temperature implying that dehydration must occur on heating. The mechanism of dehydration within the quartz crystal is described. This involves the aggregation of $(OH)_4$ defects and the development of free water at very high pore pressures.

Careful heating experiments on wet quartz in the electron microscope endorse the *ab initio* calculations and indicate that the $(OH)_4$ defects aggregate on supersaturation to form rafts as a transitional stage in the overall dehydration process. Electron diffraction contrast theory is used to establish that the Burgers vector associated with these rafts is approximately 1Å. This expansion is shown to be compatible with the characteristics of the $(OH)_4$ group in hydrogarnets, and with the results of the *ab initio* stress calculations. The role of these $(OH)_4$ rafts in dehydration and in hydrolytic weakening is discussed.

FERRIC IRON IN UPPER MANTLE MINERALS

McGuire A.V. (*Dept. of Geosciences, Univ. of Houston*) and
Dyar M.D. (*Dept. of Geology & Astronomy, West Chester Univ.*)

Studies which attempt to determine increases (oxidation) or decreases (reduction) in mantle rock $Fe^{3+}/\Sigma Fe$ ratios due to metasomatic processes require an understanding of ferric iron contents in minerals of unmetasomatized mantle peridotite. Mössbauer spectroscopy offers a method of measuring $Fe^{3+}/\Sigma Fe$ ratios on mineral separates from mantle rock samples. Studies comparing measured Mössbauer results with $Fe^{3+}/\Sigma Fe$ calculated from electron microprobe data show agreement only for spinel. *Calculated* $Fe^{3+}/\Sigma Fe$ values for silicate minerals (garnet, pyroxene, amphibole) are completely random and inaccurate, and $Fe^{3+}/\Sigma Fe$ for these minerals must be measured spectroscopically.

Early studies considered spinel to be the only mantle phase of significance in evaluating mantle oxygen fugacity and redox reactions, and these studies only presented data on spinel. More recent works recognize the value of examining all coexisting phases in a mantle assemblage, as follows.

Olivine is not generally considered to be a Fe^{3+}-bearing phase, and, indeed, Mössbauer spectra of olivine separates from unmetasomatized peridotite show no Fe^{3+}. Spectra of olivine from a modally metasomatized spinel-amphibole peridotite from Dish Hill, CA show 1-6% $Fe^{3+}/\Sigma Fe$, suggesting that under oxidizing metasomatic conditions, olivine may incorporate Fe^{3+}. TEM studies of these olivines indicate that Fe^{3+} is accommodated as lamellae of laihunite intergrown with olivine.

Orthopyroxene (opx) Mössbauer spectra show 1-14% $Fe^{3+}/\Sigma Fe$ with no variations related to metasomatism. Crystal chemical constraints may limit the ability of Al-rich and Cr-rich mantle opx to accommodate Fe^{3+} and to react during metasomatism.

Clinopyroxene (cpx) separates from unmetasomatized spinel peridotite contain 12-24% $Fe^{3+}/\Sigma Fe$. Cpx in modally metasomatized spinel peridotite is more oxidized with 32-34% $Fe^{3+}/\Sigma Fe$; whereas $Fe^{3+}/\Sigma Fe$ values are not notably oxidized (16-18%) in cpx from a xenolith that experienced Fe-Ti metasomatism. Al-augites from spinel pyroxenite xenoliths appear to have higher $Fe^{3+}/\Sigma Fe$ (23-31%) than cpx in spinel peridotites. Cpx separates from 3 garnet peridotite xenoliths exhibit $Fe^{3+}/\Sigma Fe$ of 14-27%, similar to the range of values observed for spinel peridotites.

Spinel data show a range of $Fe^{3+}/\Sigma Fe$ values, with variation

correlated both to tectonic setting and metasomatic history. Suboceanic abyssal spinel peridotites exhibit the lowest known spinel $Fe^{3+}/\Sigma Fe$ values of 5-25%. Spinel separates from unmetasomatized peridotite xenoliths contain 14-33% $Fe^{3+}/\Sigma Fe$. $Fe^{3+}/\Sigma Fe$ in spinel from metasomatized spinel peridotite xenoliths ranges from 30-40%. While both spinel and cpx exhibit metasomatic oxidation, their $Fe^{3+}/\Sigma Fe$ values are not clearly correlated, suggesting that oxygen fugacity is not the sole parameter controlling Fe^{3+}/Fe^{2+} ratio. Crystal chemistry, metasomatic fluid compositions, etc. are also important.

Ferric iron contents of mantle garnets are low (1-15% $Fe^{3+}/\Sigma Fe$), and correlate strongly with garnet peridotite texture and composition. "Hot-sheared" garnet peridotites contain garnet with the highest Fe^{3+} contents, and garnet "cold-coarse" samples exhibit the lowest Fe^{3+}.

Ferric iron contents of mantle-derived amphiboles are extremely variable with $Fe^{3+}/\Sigma Fe$ ratios from 27-100%. Fe^{3+} is strongly correlated with H^+ content, and reflects both sample transport history (in less oxidized kaersutite) and variations in the oxidation state of mantle metasomatic fluids. Few Mössbauer studies have been performed on mantle-derived phlogopites; values of 23-64% $Fe^{3+}/\Sigma Fe$ are reported.

Ongoing work is in progress to continue characterization of the interrelationships among Fe^{3+}, H^+, and bulk composition of coexisting mantle minerals from within carefully constrained tectonic, geologic and petrologic contexts.

STRUCTURE AND DYNAMICS IN ALUMINOSILICATE LIQUIDS

McMillan P.F. *(Dept. of Chemistry, Arizona State University)*

We have used vibrational and NMR spectroscopic techniques coupled with MD simulations to explore the structure and dynamic behaviour of aluminosilicate glasses and liquids. In-situ high temperature Raman spectra of SiO_2 show an anomalous frequency increase in the principal low frequency band, indicating anharmonic narrowing of the SiOSi angle. This is joined by configurational effects above T_g, resulting in the anomalous volume behaviour of SiO_2 glass and supercooled liquid.

Structural relaxation in liquid SiO_2 is accompanied by Si-O-Si bond breaking, consistent with the magnitude of the activation energy for viscous flow. This observation is combined with recent results on the mechanism of structural relaxation in silicate liquids to propose an energetic model for viscous relaxation in SiO_2, involving O^{2-} transfer via formation of a ^{V}Si intermediate.

^{27}Al NMR experiments combined with MD simulation give insight into the coordination behaviour of Al in high temperature liquids in the CaO-Al_2O_3-SiO_2 system, and the effects of substituting Mg for Ca are investigated. High T vibrational data for these liquids indicate that the aluminosilicate structural units persist on a vibrational timescale (10^{-13} s), although O^{2-} exchange reactions between them, via ^{V}Si and ^{V}Al intermediates, occur on at least a 10^{-11} s timescale.

Simulations of silicate liquids at high pressure indicate that O^{2-} and Si^{4+} diffusivities increase, and viscosities decrease, until 10-12 GPa, in agreement with experiment.

These observations are discussed in terms of local energetics, and the barriers to formation of highly coordinated network forming (Si, Al and O) species. The model is generalized to ternary aluminosilicate systems, to provide a rationalization for the observed viscosity maximum at constant silica content, in high silica rock-forming melt compositions.

A NEW OCCURENCE OF LAITAKARITE AND WITTITE IN A URANIUM DEPOSIT IN THE SWISS ALPS

Meisser N. *(Musée géologique, Univ. of Lausanne, Switzerland)*

A remarkable uranium-bismuth-lead-selenium paragenesis was discovered in the uranium deposit of "La Creusaz" near the village of "Les Marécottes" in the "Aiguilles Rouge Massif", Valais, Switzerland. Laitakarite, $Bi_4(Se, S)_3$, and wittite, $Pb_8Bi_{10}(S, Se)_{23}$, occur in quartz-pitchblende-pyrite-chalcopyrite breccia veins which cut the prevariscian gneissic basement hosting the carboniferous Vallorcine granite. These Bi-Pb-Se-minerals crystallised during a late deposition-stage without carbonates; native bismuth, selenian galena, bismuthinite and weibullite-like mineral also occur.

Laitakarite is the most abundant bismuth mineral of the paragenesis, macroscopically, it forms millimetre sized metallic gray masses. Microscopically, laitakarite appears as acicular crystals with a strong cleavage, xenomorphic masses replace pitchblende or form laths in wittite. Cell parameters for La Creusaz laitakarite are: a=4.21(1) Å; c=39.91(7) Å; C=9.47, for the hexagonal lattice. Electron microprobe analysis shows high lead content, from 4.4 to 12.5 wt. % and tellurium substitues partially selenium up to 2.1 wt. %.

Wittite forms sporadic centimetre sized masses or xenomorphic grains associated with laitakarite. X-ray diffraction powder patterns for La Creusaz wittite are very close to that of "Falun" (Sweden) and "Nevskoe" (Russia) wittite. Wittite from La Creusaz always contains silver, from 0.7 to 0.9 wt.% and antimony, but never copper.

	LAITAKARITE				WITTITE	
	Creusaz			Falun	Creusaz	Falun
Ag	-	-	-	-	0.88	0.34
Cu	-	0.01	-	-	-	0.05
Pb	12.53	4.65	4.44	3.78	32.13	34.85
Bi	66.97	74.72	75.78	78.29	44.44	44.96
Sb	0.13	0.14	0.12	-	0.09	-
Se	11.53	15.37	15.70	13.83	11.75	7.63
Te	2.12	0.90	0.85	0.10	0.05	-
S	4.72	3.38	3.21	4.07	10.56	12.51
Total	98.00	99.17	100.10	100.07	99.90	100.34

GROWTH HISTORY AND CRYSTAL CHEMISTRY OF MEMBERS OF THE ELBAITE-TSILAISITE SERIES

Melchiorre G.[(1)], Scandale E.[(1)] and Lucchesi S.[(2)] *([(1)]Dip. Geomineralogico, Univ. of Bari, Italy, [(2)]Dip. Scienze della Terra, Univ. of Roma, Italy)*

Yellow-colourless tourmaline crystals from pegmatite pockets in aplite veins (Elba Island, Italy) have been studied by XRD topography, electron microprobe analysis and single crystal structure refinement.

The studied tourmalines exhibit colour zoning perpendicular to and parallel to the c axis: the transition from the inner yellow regions to the colourless ones suddenly occurs.

The yellow regions (y.r.) are dislocation-free and are characterized by growth bands and growth-sector boundaries whereas in the colourless - prismatic, pedion and pyramidal - growth sectors bundles of dislocations can be observed perpendicular to the growing faces .

The colourless regions (c.r.) show also diffraction contrasts typical of macromosaic textures. The corresponding grains are characterized by screw dislocations parallel to c and are joined by tilt-boundaries in which edge dislocations ($\underline{b} = 1/2\langle 11\bar{2}0\rangle$) parallel to c have been observed.

Therefore the growth history can be reconstructed as follows: 1) the y.r. developed by 2D-nucleation or direct incorporation of growth units; 2) the c.r. resulted from simultaneous multinucleation, by screw-dislocation mechanism, of different

crystalline individuals that, as growth went on, were joined by tilt-boundaries.

The electron microprobe analyses show variations of the minor element concentrations corresponding to chemical sector zoning, in the y.r., and to chemical zoning crossing the regions of different colour. Of particular interest, the amount of manganese reaches values up to 9.5 wt. % MnO in the y.r. and drops below detection limit in the c.r..

The structural refinements from colourless fragments are consistent with data reported in literature for ideal elbaite, whereas those from several yellow fragments are consistent with different intermediate members of the solid solution series between the elbaite - tsilaisite end members.

In conclusion the transition between differently coloured regions abruptly occurred by sudden drastic changes of the P-T-x growth conditions after which the growth mechanisms, the chemical composition and the structural parameters of the tourmalines were modified. Growth marks recorded the P-T-x changes. In fact by comparison with beryl varieties from pegmatite pockets of the same locality (Scandale *et al.*, 1990; Graziani *et al.*, 1990), it can be concluded that both the y.r. and pegmatite beryls are characterized by the same distinctive structural defects (general growth marks, typical of the environment). It can be also concluded that chemical sector zoning and chemical zoning can be considered specific growth marks - typical of the local growth medium.

This paper confirms the importance that growth-history reconstruction and growth marks can play for systematic investigations of compositional variations of minerals. In fact they can pilot the selection of mineral fragments for structural refinements and they can also be helpful in relating the chemical variations to the driving mechanisms.

References:

Graziani, G., Lucchesi, S., Scandale, E. (1990). *Phys. Chem. Minerals*, **17**, 379-384.
Scandale, E., Lucchesi, S., Graziani, G. (1990). *Eur. J. Mineral.*, **2**, 305-311.

THE OCCURRENCE OF PLATINUM GROUP AND Ag-Au-V-Cr-REE MINERALS IN LOWER SILURIAN SEDIMENTARY-EXHALATIVE (SEDEX) SULPHIDE MINERALIZATION, POBLET, CATALONIA, SPAIN.

Melgarejo J.C. (*Dept. de Cristal·lografia, Mineralogia i Dipòsits Minerals, Univ. de Barcelona*), Jorge S. (*Depto. de C. Experimentales y Geodinámica, Burgos*), Taylor R.P., Jones P. (*Dept. of Earth Sciences, Carleton Univ. Ottawa*)

The Llandoverian series of the Prades Mountains (Southern Catalonian Coastal Ranges) contain several sedimentary-exhalative (SEDEX) deposits, whose thickness can reach up to 30 m. Typically, the deposits consist of decimetre-thick layers of quartzite and exhalative sediments, interbedded with black shales. The SEDEX deposits and their host rocks were deformed and metamorphosed during the Hercynian Orogeny. In addition to the regional metamorphism (under anchimetamorphic conditions), the deposits also have been affected by contact metamorphism related to the emplacement of late Hercynian granitoids.

Some important, and perhaps unique, feature of the Silurian SEDEX deposits in this area are: (a) the exhalative sediments consist of thin, alternating, monomineralic layers of apatite, chalcedonic quartz, anorthite (An_{100}), amphibole, biotite, titanite, calc-silicate minerals (mostly pyroxene), and sulphides; (b) the high abundance of Ti-bearing minerals, particularly titanite and Ti-bearing oxides; (c) their high V-Cr contents (up to 2100 ppm and 550 ppm, respectively), as is indicated by the abundance of V-rich minerals such as vuorelainenite $\{(Mn^{+2},Fe^{+2})(V^{+3},Cr^{+3})_2O_4\}$, goldmanite $\{Ca_3(V,Cr,Al,Fe^{+3})_2(SiO_4)_3\}$, and a V-Ti-Cr-Fe-Y oxide mineral), and by enrichments of these elements in biotite (up to 0.4 wt% V_2O_3), amphiboles (up to 5.8 wt% V_2O_3, 0.6 % Cr_2O_3), pyroxene, andalusite, chlorite, and titanite.

The most abundant sulphide is pyrrhotite, with lesser chalcopyrite, löllingite, arsenopyrite, galena, and sphalerite. Other ore minerals include Ti-Cr-V-bearing oxides (vuorelainenite, niobian rutile). Arsenopyrite replaces löllingite or Pd-bearing löllingite and has grown as idiomorphic poikiloblasts. Pyrite or marcasite also are common as "birds eye-like" replacements after pyrrhotite. Other accessory minerals include allanite and monazite, which occur as small disseminated crystals. All of the minerals display evidence of having been affected by Hercynian metamorphism (annealing of pyrrhotite-galena-chalcopyrite-sphalerite aggregates), sulphidization processes (pyrite replacing pyrrhotite, and arsenopyrite replacing löllingite) and the development of poikiloblasts (arsenopyrite, pyrite, titanite).

Löllingite, which is the most common Pd-bearing mineral, occurs as small grains (up to 100 microns) inside arsenopyrite. The palladium contents (0-3 wt%) is quite variable both within, and between, individual löllingite grains. Other palladium-bearing minerals (AsPd, native palladium, stibiopalladinite), only occur at the contact between löllingite and arsenopyrite. Electrum, native bismuth, Ag-Au-Pb-Bi tellurides and selenides (e.g., hessite, petzite, clausthalite, altaite) also can occur in other positions inside the arsenopyrite poikiloblasts. The relationship between the Pd-bearing löllingite and Pd-bearing minerals indicates that the latter were generated by palladium that was liberated from the löllingite structure during the sulphidation processes. This suggests that the Pd was easily accomodated within the structure of the arsenopyrite. Other elements (such as Ag, Au, Se, Te, Sb), also appear to have been introduced during the sulphidation process, which occurred during metamorphism and deformation.

AMPHIBOLE COMPOSITION IN ROCKS OF PREDAZZO VOLCANO-PLUTONIC COMPLEX (SOUTHERN ALPS, ITALY)

Menegazzo Vitturi L. (*Dept. of Environmental Sciences, Univ. of Venice, Italy*) Visonà D. and Zantedeschi C. (*Dept. of Mineralogy and Petrology, Univ. of Padova, Italy*)

Various small igneous bodies arranged in a ring of 2 km diameter constitute a multipulse subvolcanic pluton outcropping near Predazzo in the Southern Alps. This intrusive complex cuts a Ladino-Carnic volcanic sequence; its emplacement occurred between 237 and 230 Ma ago (Laurenzi *et al.*, 1994).

The igneous complex is composed mainly of monzodiorites and monzonites in the outer part and leucogranites and granites in the inner part, small bodies of monzosyenites and syenites are also located in the eastern side (Lucchini, 1967).

Amphibole occours in almost all lithotypes and also in the metavolcanites as thermal-metamorphic minerals or in veins with quartz and rare plagioclase.

Metamorphic and subsolvus reactions produced amphiboles of actinolitic horneblende and actinolite composition. Hornblende with actinolitic rims is characteristic in the monzodiorites and monzonites; Mg-hastingsite with pargasitic rims is typical in leucomonzonites; pargasitic hornblende is sometimes found in granites. The amphibole of the last three occurrences was produced by reaction between clinopyroxene and magma.

The differences in amphibole composition suggest two different magmatic sources: a calc-alkaline magma which may have generated monzodiorites and monzonites; and a more alkaline magma with lower a_{H2O} and higher fo_2 which may have generated leucomonzonites, granites and probably also syenites.

A peculiar crystal chemistry feature of the examined amphibole is the well-defined correlation between Cl and Ti. It suggests that Ti as well as ^{IV}Al, K and Fe^{2+} is correlated with Cl incorporation in Cl- bearing Ca-amphiboles.

References

Laurenzi, M., Visonà, D., Zantedeschi, C. (1994). *ICOG 8*, 5-11 July 1994.

Lucchini, F. (1967). *Mineral. Petrogr. Acta*, **13**, 195-215.

MODELLING THE GARNET STRUCTURE VIA CRYSTAL-CHEMICAL DATA

Merli M., Callegari A., Caucia F., Leona M., Oberti R. and Ungaretti L. *(Dip. Scienze della Terra, Univ. di Pavia; CNR-CS Cristallochimica e Cristallografia, Pavia)*

Present knowledge on garnet solid-solutions is characterized by an apparent dichotomy: deviations from ideality for thermodynamic parameters of mixing are reported anytime Ca substitutes for Mg,Fe,Mn at the X site, whereas estimates of the unit-cell edge can be obtained within the experimental errors from linear combinations of the ionic radii of the chemical constituents. Non-ideal behaviour of garnet solid-solutions involving Ca at the X site is discussed on the basis of single-crystal X-ray structure-refinement (SREF) results by Ungaretti (1994). We report here some details of a comparative crystal-chemical study carried out on 250 garnets characterized by using combined SREF+EMP analyses. This sampling is representative of garnet compositions reported in the literature. The final R_{sig} for the reflections up to $\sin\theta/\lambda = 0.90$ Å^{-1} (i.e. 40° θ for the MoKα radiation) are in the range 1.0-1.5%; the difference between the mean atomic numbers obtained from SREF and those calculated from EMP analyses is always lower than 2% (i.e. lower than the sum of the estimated errors). Site populations were derived by integrating all the crystal-chemical information from SREF with EMP results, converted into end-member percentages and used as independent variables. Unit-cell edge and oxygen coordinates were the dependent variables. Multiple regression analysis and statistic evaluation both of the sampling and of the results were performed by means of program SPSS/PC 4.0.

First attempts towards structure modelling were made in the Mg-Fe-Mn-Ca-Al-Si-O system, by selecting the samples with $a \leq 11.85$ Å. Good results were obtained in the hypothesis of an ideal solid-solution behaviour, which implies linear combinations of crystal-chemical parameters. As an example, the linear equation obtained to predict the unit-cell edge on the basis of site-population has R = 0.9987, standard error = 0.005 and F and t-test probability = 0. However, analysis of the residuals showed that their distribution is not random, and that systematic although slight overestimates near the end-members and corresponding underestimates in the middle of the joins are present.

A non-linear approach was thus undertaken, and a model for non-ideal mixing was chosen on the basis of the available thermodynamic data. Subregular mixing for Py-Gr, Py-Al and Al-Gr, ideal mixing for Sp-Py, Sp-Al and Sp-Gr joins, and empirical correction for the low An and Uv contents were adopted in the hypothesis of a binary interaction model. R = 0.9995, standard error = 0.003 and a random distribution of the residuals were obtained for the unit-cell volume. The calculated ΔV of mixing is positive, with a maximum value of 6 Å^3 at $Py_{40}Gr_{60}$, in full agreement with the results obtained by Ganguly *et al.* (1993) in the (synthetic) Py-Gr join. Similar results were obtained for the Al-Gr (+ 4.5 Å^3 at $Al_{30}Gr_{70}$) and Py-Al (+ 3 Å^3 at $Py_{70}Al_{30}$) joins.

Complete structure modelling was then performed within this non-ideal model and predictive equations for the oxygen coordinates have been obtained with very high reliability level (Merli, 1994). The results will be presented in terms of unit-cell edge, mean bond lengths and polyhedral internal angles; their statistical evaluation and their crystal-chemical implications will be discussed.

Ganguly, J., Cheng, W., O'Neil, H.St. (1993). *Am. Mineral.*, **78**, 583-593.

Merli, M. (1994). Ph.D. Thesis. Università di Pavia.

Ungaretti, L. (1994) 16th IMA Meeting, Pisa (Italy).

OD STRUCTURES IN MINERALS

Merlino S. and Pasero M. *(Dept. of Earth Sciences, Univ. of Pisa)*

The concepts of polytypism and polysomatism play a central role in the study and discussion of the modular features of minerals.

OD theory presents a neat definition of polytypism, a definition relying on precise symmetry concepts, and allows a rigorous discussion of the structural relations in polytypic families and more generally of a wide class of disorder phenomena. After shortly recalling the terminology and the basic concepts of OD theory (OD layers, OD groupoid families, MDO structures) it will be shown how the OD approach may: a) easily describe and discuss the relationships within complex structural families; b) be helpful in guessing reliable structures for new natural and synthetic compounds.

a) Structural relationships. As significant examples the sursassite–pumpellyite–ardennite family and the spinel–spinelloids group will be discussed. In both cases the constituting layers, the symmetry properties of each family, and the MDO structures will be presented.

b) Heuristic power of OD approach. It will be shown how the OD approach may be helpful to unravel structures of new natural and synthetic compounds. The case of penkvilksite will be discussed: penkvilksite presents two distinct forms, with monoclinic and orthorhombic symmetry, respectively, which represent two MDO structures within one family of OD structures built up by two different kinds of layers. The OD approach to the polytypic relationships between the two forms was fundamental to the development of a reliable model for the orthorhombic form.

In contrast to the rigid, symmetry–based definition of polytypism afforded by the OD approach, polysomatism may be defined as arising from different ways of stacking two or more structurally compatible units, which substitutes the quite rigid constraints of symmetry with less definite metrical requirements.

It seems interesting to present and discuss a wide structural series where the distinctive features of the two concepts are conspicuously displayed. This series, which comprises both natural (minerals of the aenigmatite–rhönite group) and synthetic phases ($CaFe_3AlO_7$, SFCA, etc.), is a polysomatic series with spinel–type (S) and pyroxene–type (P) structures as end–members.

The OD character of the various polysomes in the series (PSPS....; PSSPSS....; PSSSPSSS....) will be discussed, and it will be shown that: a) each family has two MDO polytypes, the former triclinic (MDO1; 1*A*), the latter monoclinic (MDO2; 2*M*); b) there are only two types of OD groupoid families in that series:

$$P\ 1\ (2/m)\ 1 \quad \{\ 1\ (2_1/c_{1/2})\ 1\ \}$$

$$P\ 1\ (2/a)\ 1 \quad \{\ 1\ (2_1/c_{1/2})\ 1\ \}$$

the first symbol corresponding to $P(S)_{2n+1}P(S)_{2n+1}$.... polysomes, the second second to $P(S)_{2n}P(S)_{2n}$.... polysomes.

X-RAY QUANTITATIVE PHASE ANALYSIS OF CLINOPTILOLITE TUFFS, CRYSTAL-CHEMISTRY-BASED APPROACH

Meshalkin S.S., (*V.I.Vernadsky Inst. of Geochem. & Analyt. Chem., Russian Acad. of Sci.*)

Clinoptilolite is a very important zeolite of industrial application. It plays an important role in human health and environment protection in Russia. Rocks of new deposits discovered and products of industrial processing have to be certified. The most effective method to certify it is X-ray powder qualitative and quantitative analysis. We discuss here the main difficulties in the analysis of the hard-to-study rock - clinoptilolite tuff and report our achievements in this field.

Clinoptilolite tuffs are complex systems consisting of few (5 -6 or more) minerals. The degree of crystallinity of these minerals is often low as a result the diffraction maxima are wide. Natural tuffs often contain an amorphous component appears on the diffractogram as a very wide hump. The intensities of diffraction maxima of clinoptilolite changes for different samples because chemical composition of the mineral varies within a wide range.

We have analyzed the literature data concerning the X-ray qualitative and quantitative analysis of clinoptilolite tuffs and proposed a new approach based on the modern methods of X-ray data collection and processing as well as crystal-chemistry of clinoptilolite. The location and superposition of analytical maxima of the main impurities in the tuffs have been analyzed and the most informative part of diffractogram has been selected. Crystal-chemical data have been used to calculate intensities and location of all peaks in the interval of interest. Deconvolution code has been applied to precisely estimate the true intensities of analytical peaks of each phase. We proposed an algorithm of quick and accurate qualitative and quantitative phase analysis of clinoptilolite tuffs.

Samples of some clinoptilolite deposits have been studied by the method proposed and recommendations have been given to perform the optimum rock processing.

DIAMONDS AND INCLUSIONS FROM S.E. AUSTRALIA - UNUSUAL PHYSICAL AND CHEMICAL PROPERTIES

Meyer, H.O.A. (*Dept. Earth and Atmos. Sci., Purdue University*), Milledge, H.J. (*Dept. Geol. Sci., University College London*), and Sutherland, L. (*Div. Earth Sci., Australian Museum*)

Diamond occurs in Tertiary alluvial gravels, overlain by basaltic lavas, in the Copeton region of New South Wales, Australia. The primary source of the diamonds is uncertain. The diamonds are relatively good in quality but have a reputation of being difficult to cleave and polish. Recent studies have shown the diamonds to have unusual carbon isotopic signatures with $\delta^{13}C$ values between -3.3 and +2.4 °/oo compared to the worldwide range of -2 to -30 °/oo. Furthermore, although olivine inclusions of the ultramafic inclusion suite have been identified (Sobolev et al. 1984), clinopyroxene and garnet inclusions are calcium-rich and a chemically distinct to both ultramafic and eclogitic suite inclusions. Also unusual is that coesite is a relatively common inclusion. Thus in terms of occurrence, properties and inclusions, diamonds from the Copeton region differ markedly from diamonds from other worldwide localities.

A suite of diamonds from the Copeton-Bingara area has been assembled with the aim of characterizing the morphology, cathodoluminescence properties, micro-infrared spectroscopy, nitrogen aggregation, carbon isotopes and inclusion chemistry. Seventy-one diamonds, ranging in size from 0.06 to 0.65 ct, have a generally similar appearance in that most have become relatively rounded by resorption (assuming that the original morphology was octahedral). A large number of specimens display several hemispherical-like cavities with rough surfaces, and many show micron sized circular features. Both these features appear to be typical of Copeton area diamonds and are generally not encountered elsewhere.

Initial examination using micro infrared (IR) and cathodoluminescence (CL) indicates the diamonds belong to two distinct groups. Diamonds in one group are generally yellow in color, show rather featureless blue CL, and have very high nitrogen contents. Because of the thickness of the diamonds conclusions based on IR measurement are at this point tentative, but relative estimate of nitrogen aggregation states suggest most are type IaB, with possible nitrogen contents approaching 3000 ppm. The large amount of resorption displayed by the diamonds would suggest the CL show evidence of internal zonation if it existed; none is apparent in diamonds of this first group. Diamonds in the second group are generally white, with less regularly morphology, show variable CL, sometimes indicating complex zonation, and a variable but lower nitrogen content as low as 10 ppm. Some are definitely inhomogeneous. A few paler diamonds (i.e. yellow/white) have intermediate nitrogen content. Also the position of the platelet peak (i.e. platelet size) in the IR spectra varies widely both within and between specimens. It appears that platelet development in the diamonds belongs to two distinct temperature regimes.

The relationship of inclusion type to diamond group is unknown at this time. Detailed examination of inclusion chemistry and CL of internal surfaces revealed on polished surfaces of the diamonds is underway. However, the known occurrence of two distinct inclusion suites (ultramafic and calc-silicate), and the presence of two groups of diamonds based on color, nitrogen content, and CL response, suggests at least two, and possibly more, geochemical environments in which the diamonds formed. The calc silicate suite (Ca-rich cpx and garnet plus coesite) is generally unique to S.E. Australia and may be considered to reflect diamond growth in a subducted lithospheric environment. Evidence to support this suggestion requires further work, currently underway, but also has to be consistent with the geological evolution of South Eastern Australia.

References:

Sobolev, N.V. et al. (1984) Dokl. Akad. Nauk. SSSR, **174**, 172-178.

STRUCTRUAL REFINEMENT OF MONAZITE-(Ce)

Mi Jinxiao & Shen Jinchuan(*Test Centre, China Univ. of Geosci.*)

Monazite($CePO_4$) was one of commonly occurred and most important rare earth minerals. The crystal structure of monazite was early determined by Kokkoros in 1942 and later Ueda (1967) and Ghouse (1968) reinvestigated and refined the crystal structure. But the structural refinement by four-circle diffractometer has not been reported by now. The authors refined the cell parameters and crystal structure of monazite-(Ce) by using Rigaku RASA-5RP high power Automatic Four-circle Single Crystal Diffractometer. A fine crystal grain of monazite from Tongcheng, Hubei, China, was used for the crystal structure refinement. Least-squares refinement gave the monoclinic cell parameters $a = 6.7843(17)$, $b = 6.9891(12)$, $c = 6.4592(10)$ ($\times 10^{-10}$m), $\beta = 103.626(16)^\circ$, $Z = 4$, $P2_1/n$. Intensities were collected with graphite monochromated Mokα_1 radiation ($\lambda = 0.70926$) in 2θ from 2° to 69°; a total of 1106 ($F > \sigma(F)$) independent reflections were collected with h from 0 to 10; k from 0 to 11; l from -10 to 10.

There were four $CePO_4$ molecules in unit cell of monazite. All atoms occupied the sites of 4e in Wyckoff letter. The heavy

atom(RE) was obtained from E−map by direct method strategy using SHELX−76 and SHELX−86. The atomic coordinates of light atoms (P,O) were obtained from Difference Fourier map. Multi−circle full matrix least−squares led to the R factor of 0.06. The final coordinates and isotropic temperature factors were presented in Table 1; and interatomic distances in table 2.

Table 1. Atomic Coordinates and Isotropic Temperature Factors

ATOM	X(A)	Y(B)	Z(C)	U11
CE	.2186(2)	.3409(2)	.8995(2)	.0068(2)
P	.1951(6)	.3366(6)	.3879(6)	.0044(6)
O(1)	.1164(18)	.1668(19)	.4990(19)	.0117(19)
O(2)	.3733(17)	.2863(17)	.2907(18)	.0078(18)
O(3)	.2499(17)	.4909(17)	.5538(18)	.0086(19)
O(4)	.0283(19)	.3974(19)	.1946(20)	.0128(21)

Table 2. Monazite: interatomic distances($x10^{-10}$m)

atoms	distances	atoms	distances	atoms	distances
Ce—O(2)	2.449	Ce—O(1)	2.554	P—O(3)	1.504
O(4)	2.457	O(4)	2.572	O(2)	1.529
O(3)	2.468	O(1)	2.624	O(4)	1.535
O(3)	2.520	O(1)	2.795	O(1)	1.545
O(2)	2.527	Mean:	2.552	Mean:	1.528

The crystal structure of monazite−(Ce) is isostructural with that of cheralite, (Th,Ca,Ce)PO_4 . The atom P is lying in the centre of slightly distorted PO_4 tetrahedron. The cerium atom forms nine coordinated polyhedron which connect isolated PO_4tetrahedra. Ghouse(1968) reported the coordination number of cerium atom was eight. Ueda (1967) discribed the polyhedron 9−coordinated, but the distances of Ce−O given by him were unreasonable: the shortest distances were only 2.29($x10^{-10}$m) and 2.30; the largest ones were 2.96 and 3.31. The average distance of Ce−O given in this paper is 2.552, and the shortest distance is 2.449; the largest is 2.795. The average distance of PO_4 tetrahedron is 1.528; the O−P−O angles vary from 103.4 ° to 113.1 ° . Apparently, the structure of monazite refined in this work is more precise and reasonable than the data reported before.

References:
Finney, J.J. & Rao, N.N. (1967) *Am. Mineral.* **52**, 13−19.
Ghouse, K.M. (1968) *Indian J. Pure Appl. Phys.*, **6**, 265−268.
Miyawaki, R & Nakai, I (1987) *Rare Earth*, **11**, 39−42.
Ueda, T.(1967) *J. Jpn. Assoc. Mineral. Petro. Econ. Geol.*, **58**, 170−179.

CRYSTALLOGRAPHIC STUDY OF KIRSCHSTEINITE EXSOLUTION LAMELLAE IN METEORITIC OLIVINES

Mikouchi T., Takeda H., Miyamoto M. (*Mineralogical Inst., Univ. of Tokyo*), Ohsumi K. (*Photon Factory, KEK*), and McKay G.A. (*SN4 NASA/JSC*)

Ca, Fe-rich olivine, kirschsteinite ($CaFeSiO_4$) is a rare terrestrial mineral, but is a common phase in the oldest basalt in the solar system (angrite). Olivine crystals (~500 μm in diameter) from the angrite LEW86010 meteorite show spectacular exsolution lamellae of kirschsteinite. The lamellae orientation reported by previous investigators (Prinz *et al.*, 1988, McKay *et al.*, 1989) is not in line with results by us (Mikouchi *et al.*, 1993). In order to obtain further constraint on the crystallography of kirschsteinite lamella, we have examined orientation of the lamellae for another two olivine single crystals and got the same results. Moreover, the olivine in the LEW86010 thin section originally used by the above authors was analyzed by synchrotron radiation (SR) with the Laue method at beamline 4B (BL-4B) of the Photon Factory (PF), KEK (Ohsumi *et al.*, 1991, Ohsumi *et al.*, 1993) and the lamellae directions were compared.

The crystal system of olivine (forsterite-fayalite solid solution series) is orthorhombic, and its space group is *Pbnm*. Kirschsteinte belongs to the same crystal system and the space group. The precession photographs of the $(hk0)^*$ and $(h0l)^*$ planes give the cell dimensions of the host olivine as: a 4.79±0.03Å, b 10.39±0.05Å and c 6.06±0.03Å. The faint reflections just inside the host olivine were recognized on the $(hk0)^*$ and $(h0l)^*$ nets. The cell dimensions of the exsolved phases are: a 4.87±0.05Å, b 11.14±0.10Å and c 6.36±0.05Å, which well accord with the reported cell dimensions for kirschsteinite (Sahama & Hytönen, 1958). The host olivine and exsolved kirschsteinite are found to share crystallographic orientations.

Examination by an optical microscope and SEM of the oriented olivine single crystal revealed that all polished olivine crystals parallel to (100) include exsolution lamellae up to 10 μm in width. The distance between them is typically 50-100 μm. The lamellae were parallel to the a axis. The two sets of the lamellae are symmetrically related with respect to the crystallographic b and c axes and found to be parallel to (031) and (0$\bar{3}$1). The result using SR is consistent that the lamellae are parallel to (031) and (0$\bar{3}$1), but is different from the orientations parallel to (011) and (0$\bar{1}$1), (001) and (011), or (001) and (031) reported previously (Prinz *et al.*, 1988, McKay *et al.*, 1989).

One possibility which can explain the difference of the lamellae directions and the width is that the previous data were based on the measurements on non-oriented thin sections, consequently, the lamellae tend to give larger values and they might have mistaken their crystallographic axes. Another possibility is that the lamellae of several directions may truly exist. However, the planes parallel to (031) and (0$\bar{3}$1) are dense plane of atomic distribution considered from atomic structure of olivine. Taking notice of (031) and (0$\bar{3}$1) planes, quadruple cell can be derived for the twin lattice of pseudomerohedry, because the ratio of the cell dimension of the b axis and c axis is almost $\sqrt{3}$: 1 (Fig.1). Such twinning in monticellite ($CaMgSiO_4$) is uncommon, but {031} are known to be twin planes (Larsen *et al.*, 1941) and olivine also has twinning on (031). The lamellae in this case might be a kind of twin of a different but similar phase, because the only difference between olivine and kirschsteinite is the cell dimensions and chemical composition.

References:
Larsen, E.S., Hurlbut, C.S., Buie, B.F., Burgess, C.H. (1941). *Bull. Geo. Soc. Am.*, **52**, 1841-1868.
McKay, G., Miyamoto, M., Takeda, H. (1989). *Meteoritics*, **24**, 302.
Mikouchi, T., Takeda, H., Mori, H., Miyamoto, M., McKay, G. (1993). *Lunar Planet. Sci.*, **XXVI**, 987-988
Ohsumi, K., Hagiya, K., Ohmasa, M. (1991). *J. Appl. Cryst.*, **24**, 340-348.
Ohsumi, K., Miyamoto, M., Takase, T. (1993). *18th Symp. Antarctic Meteorites*, 192-194.
Prinz, M., Weisberg, M.K., Nehru, C.E. (1988). *Lunar Planet. Sci.*, **XIX**, 949-950.
Sahama, T.G. & Hytönen, K. (1958). *Am. Miner.* **43**, 862-871.

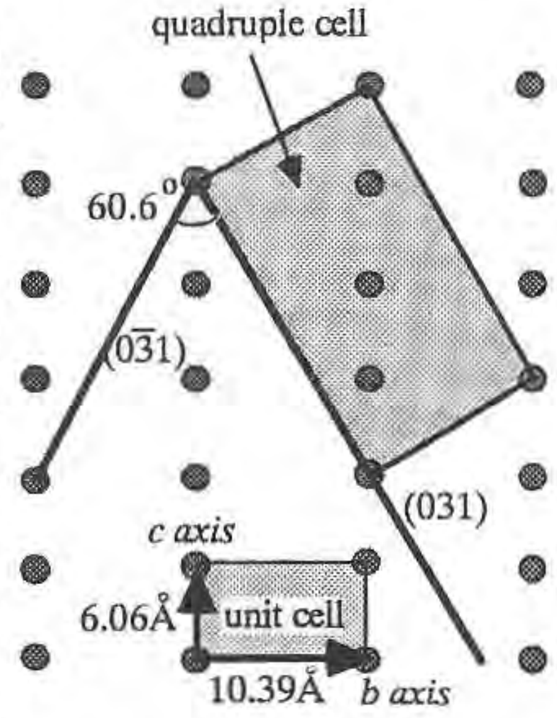

Fig.1 : Schematic illustration of (100) plane of olivine

SPECTROSCOPIC AND X-RAY DIFFRACTION INVESTIGATIONS OF YAKUTITE FROM THE POPIGAI CRATER

Milledge H.J., Ross N.L., Woods P.A. *(Dept Geological Sciences, University College London, U.K.);* Verchovsky A.B. *(Earth and Planetary Sciences, Open University, Milton Keynes, U.K.).*

It has been found that in some meteorite impact craters, such as the Oligocene Popigai crater in Siberia, pre-existing graphite has been converted to a polycrystalline form which contains both cubic (diamond) and hexagonal (lonsdaleite) tetrahedral structural components (Frondel & Marvin, 1967).

This material is highly variable in appearance, ranging from transparent white flakeswhich resemble diamond cleavage fragments, through yellow translucent flakes, to black specimens whose morphology retains the platy appearance of its graphite precursor. X-ray diffraction (XRD), birefringence (BR), infrared microspectroscopy (IR), FT Raman (FTR), cathodoluminescence (CL), scanning

electron microscopy (SEM), and stable isotope mass spectrometric (MS) investigations have been made of selected specimens of polycrystalline diamond-lonsdaleite ("yakutite") from the Popigai crater.

XRD photography shows that the specimens exhibit a range of particle sizes, with the cubic structure predominating, and very strong preferred orientation which does not support the mechanism of formation suggested by Valter et al. (1990), which requires the hexagonal axis of lonsdaleite to be normal to the c-axis of the original graphite precursor. BR, which should increase as the non-cubic component increases, has not proved a reliable indicator of hexagonal diamond content in these specimens. FTR spectra show a broadening of the normal 1332 cm^{-1} diamond Raman line such as might be expected for small particle sizes, but without the associated spectral shift. IR, however, in addition to confirming the dominance of cubic diamond, indicates the presence of CO_2 in some form analogous to that encountered in rare mine diamonds (Schrauder and Navon, 1993); SEM photographs confirm the presence of decrepitation phenomena also seen in some specimens. Furthermore, unusual CL colours seen in the CO_2-bearing diamond are also seen in the yakutite material. MS data for the various morphological types has also been obtained. The range of phenomena observed will be illustrated.

References:
Frondel C., Marvin U.B. (1967) *Nature*, **214**, 587-589.
Schrauder M., Navon, O. (1993) *Nature*, **365**, 42-44.
Valter A.A. et al. (1990) *Mineral. Mag. USSR*, **12(3)**, 3-15.

STUDIES OF REDDISH MICROCRYSTALLINE QUARTZ FROM GRANITE-TYPE URANIUM DEPOSITS, SOUTH CHINA, USING TRANSMISSION ELECTRON MICROSCOPE(TEM)

Min M. and Zhang F. (*Dept. of Earth Sciences, Univ. of Nanjing*)

The granite-type uranium deposits are one of the most important commercial uranium deposit types in China. It contains at least 35 percent of China's uranium reserve. Reddish microcrystalline quartz is an important uranium-bearing gangue mineral in the deposits. Two kinds of occurrence forms for U element have been distinguished in the mineral: visible uranium, which occurs as visible U-minerals under optical microscope and invisible uranium, which can not be found in the form of visible uranium minerals under optical microscope. Few previous studies have been reported on invisible uranium. Present paper introduces the study results on invisible uranium in the mineral using TEM. It is investigation for the first time in China.

Ultramicro-pitchblende and ultramicro-coffinite were firstly found in the aggregate of reddish microcrystalline quartz from the granite-type U-deposits by means of TEM. The ultramicro-pitchblende grains commonly range between 0.1μm and 1μm in size. EDS spectra and wavelength-dispersive (WD) electron microprobe analyses indicate major UO_2(81.32-85.17wt%), with minor Al, Si, Fe and K. It may replace micro-pyrite along cracks. Ultramicro-coffinite grains vary from 0.2μm to 0.5μm in size. It contains UO_2(50.86-65.43wt%), SiO_2(25.70-29.41wt%) and traces of Al, K, Fe and S. These U-minerals occur intertitially to quartzes and along cracks, and are often surrounded by clay minerals or ferric minerals. The latter may be attributed to irradiation transformation from silicates and ferrous minerals. It is negated that invisible uranium element in the U-bearing microcrystalline quartz was adsorpted by microquartz and contained ferric minerals, which was commonly reported in previous literatures. Reddish tone of the microcrystalline quartz aggregate results from contained micro-ferric mineral grains, i.e. goethite, water-goethite and hematite. The ferric minerals and clay minerals, rimming the ultramicro-uranium minerals, may perhaps be radiation-damaged products of original ferrou minerals and silicate minerals (Simmons & Caruso, 1985).

Close association of ultramicro-pitchblende and ultramicro- coffinite in reddish microcrystalline quartz may be due to: (1) their similar forming physico-chemical conditions (temperature, pressure, pH and Eh etc.) (Min, 1992); (2) chemical transformation each other; (3) phasic transformation from U_3O_8 to UO_2 (Dymkov, 1973).

References:
Simmons, G., Caruso, L. (1985). DOE/ER/04972-T2, 214-220.
Min, M. (1992). On genesis of uranium minerals. Beijing: Atomic Energy Press House. 136-159.
Dymkov, U. M. (1973). Characteristics of pitchblende. Moscow, 89-103.

MINERALOGY AND APPLICATION OF ZEOLITE RESOURCES IN JAPAN COMPARED TO THAT IN OTHER COUNTRIES IN THE WORLD

Minato H. (*Professor Emeritus, The University of Tokyo*)

A fiew kinds of natural zeolites are used as nonmetallic resources in recent from about 1960 in Japan. About 150,000 t of zeolite resources are supplied per year such as for soil conditioning material to paddy soil and farm soil and golf links, pet or cat sand, admixture for feeding stuff of domestic animals, admixture for domestic animal excrement, paper industry clay, gas adsorbent and ion exchanger, catalysis and its supporter and etc.. Utilizations as showen in this report are effective for problems of environmental protection, for instance, gas adsorbents for SO2, CO2, NH3 and etc., deodorizer and ion exchangers for NH4 in town waste water, waters in river, lake, pond and etc., holding materials of fertilizer in soils, heavy metallic ions in waste waters such as town waste water, industrial one, that from metallic mine and etc.. From about 15 zeolite quarries and mines worke and supply the zeolite products, in granular shape, powder and fine powder as sutable forms to each different utilizations. The zeolite minerals are limited to clinoptilolite and mordenite, and they are formed mainly by burial diagenetic reactions and associated with hydrothermal reactions. and they are main component minerals in zeolitic tuffaceous rocks associated with caly minerals of montomorillonite, ceradonite, chlorite and etc., and low cristobalite, quartz, feldspars and etc..

Each zeolite minerals, clinoptilolite and mordenite, are divided to three groups, Na, K and Ca type by their exchangeable cations. The differences bring about their special physicochemical properties, differences in thermal stability between Ca type clinoptilolite and alkaline type one and high adsorption capacity for CO2 and N2 gases in Na type mordenite and etc.. These characters on the zeolites are principal properties for their utilization. An example,

Na type mordenite, from Itado, Akita Pref., is used for adsorbents of oxygen generator and nitrogen genrator.

To day, natural zeolite is one of new kinds of nonmetallic resources.

In other countries.

Asia.

Korea: Clinoptilolite with mordenite occur from east area and used for agriculture, stockbreeding.

China: Clinoptilolite and mordenite ore worked from about 80 zeolite localities and mainly used for cement industry and mixing material for concrete.

Indonesia: Clinoptilolite with mordenite is occurred from about 60 localities, 2 or 3 of the localities are worked and the zeolite is used for agriculture, mainly.

Mongoria: Zeolite, mainly clinoptilolite, occurs from about 10 localities and its utilizations are tested.

East Russia: Clinoptilolite locality is found from the Kamchatka Peninsula and chabazite licality is from near Nikolaevsk on Amur.

Oceania.

Australia: Ca type clinoptilolite occur from New England Orogen, northwestern area of Newcastle, and is used for agriculture, stockbreeding, water treatment and etc..

New Zealand: Mordenite localities are found.

Europe. In Bulgaria, Hungary and Yugoslavia, zeolite is worked and used mainly for mixing material of cement. Slovakia, Rumania, Greece and Turkey have zeolite, also.

America. U.S.A. with Alaska and Cuba have many zeolite mines and utilize them in various applications. Argentina, Chile and Mexico have zeolite resuorces, also.

References:
Minato, H. (1991). Sekko& Sekkai, No.235, 531-546.
Natural Zeolite and its Utilization,-Proc. Int. Symp. Miner. Prop. & Utili. Natural Zeolites, 1992, (1994), Ed. Minato et al.,- Tokyo Univ. Press, Tokyo, Japan.

EXPERIMENTAL STUDY OF THE RELATIVE WATER SOLUBILITY IN ALUMINOSILICATE MELTS UNDER T=900-1100°C, P=2 KBAR ON THE TRITIUM AUTORADIOGRAPHICAL DATA

Mironov A.G., Epelbaum M.B., Chekhmir A.S. (Buryat Geol. Ins., Ulan-Ude; Ins. of Exp. Min. Russ. Acad. of Sci.)

The aim of the experiments is the study of the themperature dependence water solubility in basalt and granite melts. It is debatable for the basalt melt up to now. The experiments have been carried out with the use of radioactive tracer method. The tritium was used as a tracer in the water (^3HHO+ $+H_2O$) with quantitative 10-15 MBc/g. The experiment conditions: T=900-1000°C, P=2 kbar, duration - 3-5 hours. The glass samples radio activity was measured by the autoradiographical method on the nuclear emulsion plate (MR) with the resolution about 10-20 micron and exposition - 5-20 days. The beforehand melting glasses with known water concentration were used: granite glass - 2,8-4,5 mas%, basalt glass - 3,9 mas%.

The autoradiographic data obtaned have shown that water solubility at the pressure 2 kbar in basalt melt is higher than in obsidian and the temperature dependence has different trend: in basalt melt solubility increases with temperature whereas in obsidian - decreases. It was found that the water solubility is more higher in mixing zone of granite and basalt melts and water-bearing melt-rock interaction zone. The edgings of basalt glass (10-20 micr.) around the parcial melting plagioclase crystals are very enriched with water while the contact of the pyroxen crystals and water-bearing basalt glass did not reveal such kind of edging.

This regularities have been found due to measuring of the basalt glass water concentration in the intercrystalline space using of the local tritium autoradiography with the high resolution. The essential water loss from basalte and granite glass surface was being established also under observation during two years. It depends on the presence of two forms water existence in aluminosilicate melt: molecular water and hydroxil group. The molecular water evaporats more quicly from basalt glass surface than from granite glass.

The high water solubility in basalt melt allows to suppose the presence of water-bearing basite magma influensing on the island arc magmatism formation and on the origin of gabbro-granite series.

ELECTRICAL CONDUCTIVITY OF RING SILICATES

Mirwald P.W. *(Inst. Mineralogy a. Petrographiy Univ. Innsbruck)* and Schmidbauer E. *(Inst. Applied Geophysics Univ. München)*

Most silicates are electrical insulators at room temperature and they exhibit a semiconducting bahavior only at high temperatures. Electrical measurements on Mg-cordierite and beryl samples revealed anisotropic AC-resisitivity at temperatures above 300 °C (Schmidbauer & Mirwald, 1993, Mirwald & Schmidbauer, 1993). This finding may be related to the channel structure of these ring silicates. To explore further this apparently structurally controlled phenomenon and to delineate possible systematic tendencies in electrical behavior by comparison, the AC-resisitivity of tourmaline (schörl) was studied in addition.

Measurements of the AC-resisivity (20 Hz - 1 Mhz) were carried out on oriented single crystal cubes (≈ 4 mm) in the temperature range of 300 - 800 °C in a N_2 atmosphere (99.999%). The measurements were conducted with a Hewlett-Packard LCR-meter (type 4284 A) using a four terminal pair configuration.

The samples of the three minerals studied were of good quality as ensured by microscopy, by IR-spectroscopy and by electron microprobe and/or X-ray fluorescence methods.

The impedance data, plotted in the complex impedance plane (real part Z´ vs. imaginary part Z´´), revealed in general several semicircular arcs which may be associated with different conduction processes. From an extrapolation of a semicircle towards the Z´-axis

Table 1: Survey of resisivity data

Mineral	Orientation	Activation energy (eV)	R_{DC}^{AC} range (Ohm)	Temperature (°C)
Cordierite	// c	I*: 0.75	$10^3 - 10^7$	250 - 725
	// c	II: 0.83	$10^6 - 10^7$	560 - 790
	// a	I: 0.85	$10^6 - 10^7$	600 - 840
Beryl	// c	I: 1.2	$10^4 - 10^7$	400 - 800
	// c	II: 1.8	$10^5 - 10^7$	600 - 800
	// a	I: 1.6	$10^6 - 10^7$	680 - 800
Tourmaline	// c	I: 0.85	$10^5 - 10^7$	400 - 700
	// a	I: 0.89	$10^5 - 10^7$	400 - 700

*: conduction mechanism I and II respectively

in the low frequency region, the DC resistivity R_{DC}^{AC} was determined. From log R_{DC}^{AC} vs. 1/T plots, activation energies of charge transport processes were derived.

Table 1 gives a survey of the results. Except for tourmaline, two conduction mechanisms are found in the [001] direction. No resisivity anisotropy was detected for tourmaline which may be related to its specific cation configurations in the channels. Due to the considerable chemical variability of each mineral, no distinct conduction process could be assigned to an experimental semicircle yet. It is probable that activation energies < 1 eV are related to electronic processes while above 1 eV ionic conduction may be involved.

References:
Schmidbauer, E. & Mirwald, P.W. (1993). *Mineralogy and Petrology, 48, 201-214.*
Mirwald, P.W. & Schmidbauer, E. (1993). *Ber. Dtsche Mineralog. Ges. 1, 1993, 192.*

SHOCK METAMORPHIC EVOLUTION BY IMPACT EXPERIMENTS

Miura Y. (Fac. of Sci., Yamaguchi Univ., Yamaguchi 753, Japan)

It has been considered that quartz minerals, anorthite (An)-poor plagioclase, and Fe-rich feldspars (or pyroxenes) are formed by magmatic crystallization of the Earth or Earth-type planets under high temperature condition of the magma. However, Miura et al. (1992a, b) reported that when similar high-temperature can be obtained at impact processes, shocked phases can be formed under impact condition.

The purposes of the present study are to obtain direct evidence for solid-liquid-vapour reaction process of impact from mineralogical data of shocked materials, and to apply the impact experimental data to formations of silica and plagioclase phases on primordial lunar and Earth-type planetary bodies and asteroids followed crystallization at major shock metamorphism (i.e. shock metamorphic evolution).

Target rocks of impact experiments are gabbroic anorthosite, granite, basalt and sandstone with impact velocity from 2 to 7 km/sec. Experimental procedure of impacts are the same method by Miura (1991).

The various shocked quartz minerals with low-, high-, and normal-X-ray calculated density can be obtained in the artificial impact crater experiments of various type target rocks. Fine-grained shocked quartz aggregates crystallized from vaporization of feldspar (F) or quartz (Q) are shown by the increased abundance of shocked quartz (SQ) and feldspar (SF) at the 'fine ejecta': that is, SQ/SF=3.0 and 5.6 in granite and gabbroic anorthosite, respectively. This type of shock metamorphism is the largest shock wave under solid-vapour reaction.

There are two types of shocked (diaplectic) plagioclase

1) 'Small compositional change type': Chemical compositions of 'large coarse-grained fragments' broken by impact reveal partly anomalous diaplectic feldspar grains with irregularly wavy (undulate) extinction and nonstoichiometric composition' which can be found at the wall rocks of artificial and natural impact craters.
2) 'Large compositional change type': Fine-grained plagioclase (-like) composition found in fine ejecta of artificial impact craters reveals decrease of An-content and mixture of projectile to form Fe-rich feldspars or pyroxenes. In fact, plagioclase from Kohyama gabbroic anorthosite (bytownite-labradorite) changes to albite (i.e. decrease of An_{40} mol.%). The type of diaplectic plagioclase shows intermediate to maximum degree of shock wave.

The shocked materials formed by large impact with solid-liquid-vapour reactions can be found in shocked quartz aggregates and projectile mixture, as follows:

1) 'Very fine-grained shocked quartz' (SQ): Analytical data of SEM with EDX indicate that shocked quartz formed by the largest shock wave shows 'fine-grained aggregate' of silica composition (about 1 μm) with 'dendritic texture' (i.e. queched texture from vapour-melt condition) and large parts of amorphous state .
2) 'Mixture of Fe-projectile and feldspar': Projectile of Fe or Cu was melted to produce mixtures of Cu/Fe and plagioclase, various types of droplets and mantle-core concentric structure. The shocked concentric texture of impact experiment is well similar to the planetesimal structure, which impact materials consists of Fe-rich in the core, and Cu (and Al, Mg, Ca, K, Na, Si)-rich in the mantle of the concentric texture.

The overall process which is called as shock metamorphic evolution can be applied to lunar impact and recrystallized rocks (cf. the lunar rocks of KREEPy and lunar rocks with major feldspar and tiny quartz aggregates).

The impact experimental results and major scientific significances in this study can be summarized as follows:

1) Shocked phases of quartz, An-poor plagioclase, Fe-rich feldspar and Fe-rich pyroxene can be formed by shock metamorphic evolution.
2) Shocked quartz aggregates with 'dendritic texture' is formed by rapid cooling process under 'solid-melt-vapor' reaction.
3) Shocked quartz aggregates can be formed in all types of target rocks (such as anorthosite, granite, sandstone, and basalt).
4) Major two types of shocked (diaplectic) plagioclases are obtained: a) large coarse-grained feldspars with partial anomalous chemistry, b) fine-grained plagioclase (-like) grains with low An-content.
5) Primordial and evolved surfaces of Earth-type planetary bodies and the Moon reveal shock metamorphic evolution which is suggested by artificial impacts in this study.
6) The initial stage of impact process can be obtained in artificial impact craters, though almost all major shock metamorphic phases can be found in well-developed terrestrial impact craters.

References:
Miura, Y. (1991) Shock Waves (Springer-Verlag), 1, 35-41.
Miura, Y., Kato, T. and Imai, M. (1992a) Meteoritics, 27, 261-262.
Miura, Y., Takayama, K., Kato, T., Kawashima, N. and Yamori, A. (1992b). Shock Waves (Springer), Proc. Intern. Sympo. Shock Wave, 18, 403-408.

FORMATION PROCESS OF KAOLINITE IN THE HYDROTHERMAL SYNTHESIS

Miyawaki R., Tomura S., Inukai K., Shibasaki Y., Okazaki M. (*Nat. Indust. Res. Inst. Nagoya*), Samejima S., Satokawa S., and Kamori M. (*Engin. Res. Assoc. for Art. Clay*)

Two formation processes of kaolinite in hydrothermal reactions, one from an amorphous mixture of silica and alumina (Miyawaki *et al.*, 1992), and the other from a mixture of amorphous calcium silicate and aluminum chloride (Miyawaki *et al.*, 1993), were studied by XRD, IR, DTA-TG, TEM, and high-resolution solid state ^{29}Si- and ^{27}Al-MAS/NMR.

The amorphous mixture of silica and alumina was prepared with commercially available silica-sol and alumina-sol, while the amorphous calcium silicate was prepared with diatomite and calcium hydroxide.

The amorphous mixture of silica and alumina with distilled water, or the amorphous calcium silicate with aluminum chloride solution, was hydrothermally treated in a Teflon pressure vessel at 220°C for reaction times varying from 1 to 144 hours.

The amorphous mixture of silica and alumina consisting of Q^4 state silica changed into an intermediate amorphous with Q^3 state. The intermediate amorphous phase converted into crystalline kaolinite with spherical shape (Q^3 state). The yield and crystallinity of kaolinite increased with an increase in the reaction time. On the other hand, the coordination number of aluminum changed from a mixture of six- and four- coordinations to six-coordination. The TEM observation clarified that spherical kaolinite is more abundant than platy kaolinite in the earlier stages of crystallization of kaolinite with the spherical kaolinite changing to a platy morphology with increasing hydrothermal reaction time.

On the other hand, during the hydrothermal treatment of the amorphous calcium silicate with Q^1 and Q^2 state, an intermediate amorphous phase with the Q^3 state silica structure was formed prior to the crystallization of kaolinite. The ^{29}Si-MAS/NMR spectra suggest that the intermediate phase has a similar structure to that of the intermediate phase in the reaction system with the amorphous mixture of silica and alumina. However, no spherical particles were detected in the present reaction process, presumably due to the coexistence of calcium and chloride ions. Conversion of the starting material to the intermediate amorphous phase as well as to kaolinite occurred in a shorter reaction period in comparison to those from the amorphous mixture of silica and alumina. This characteristic is attributed to a lower degree of polycondensation of silica in the amorphous calcium silicate.

If an SiO_4 tetrahedron is the basic reaction unit in the hydrothermal reaction system, a direct reaction path from a starting material to kaolinite is possible. However, the two reaction steps with the intermediate phases observed in the present syntheses suggest that a cluster of polycondensed SiO_4 tetrahedra is the basic reaction unit in the present syntheses. This prediction can be confirmed by the fact that the difference in the structure of the starting material greatly affects the formation of kaolinite. It is also noteworthy that both the starting materials with different structures

changed into kaolinite through the intermediate states having similar structures.

References:
Miyawaki, R., Tomura, S., Inukai, K., Shibasaki, Y., Okazaki, M., Samejima, S., Satokawa, S. (1992) Clay Sci., **8**, 237–284.
Miyawaki, R., Tomura, S., Inukai, K., Okazaki, M., Toriyama, K., Shibasaki, Y., Kamori, M. (1993) Clay Sci., **9**, 21–32.

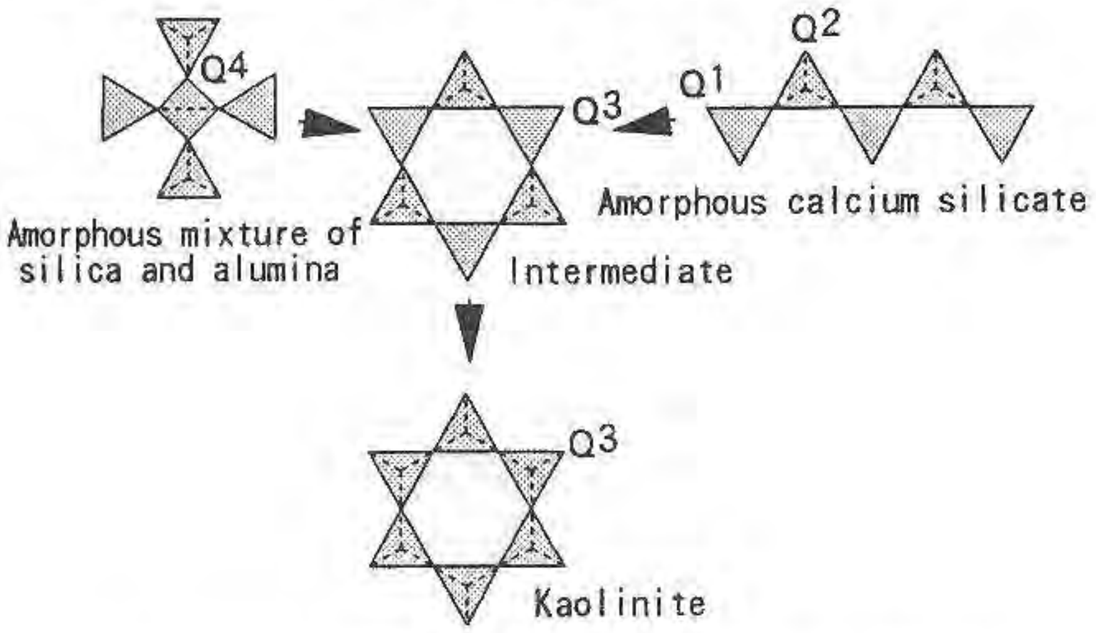

Fig. Schematic illustration of formation processes of kaolinite.

COMPLEX MINERALOGY OF Sn-, Sb- AND Mn-ENRICHED SULFIDE ORE IN GORDA RIDGE SEDIMENTS

Moëlo Y. (*IMN, Univ. of Nantes, France*), Oudin, E. (*Grenoble, France*) and Koski, R. (*USGS, Menlo Park, USA*)

The first study of mineralized sediments from Escanaba Trough (Gorda Ridge, northeast Pacific Ocean) revealed various complex sulfides : tetrahedrite, boulangerite, franckeite and a stannite-like mineral (Koski et al., 1990 ; Oudin, 1991). The reexamination of two Sn-, Sb- and Mn-enriched samples from this area brings new data concerning the mineralogical expression of these elements.

In the first sample, enriched in Sn together with Sb and Mn, tin precipitates first in wurtzite as numerous stannite-like inclusions having the original composition $Cu_2(Fe_{1.6}Zn_{0.4})SnS_5$. Then franckeite is formed as epitaxial lamellae on partially dissolved pyrrhotite crystals ; its structural formula is close to $(Pb_{5.24}Sn_{0.90}Mn_{0.08})_{\Sigma 6.22}Sn^{4+}{}_{2.00}Fe_{0.96}Sb_{2.00}S_{13.94}$. Finally, very fine lamellae of a herzenbergite-type mineral appear with Sb-rich alabandite in the outer, colder part of the sulfide crust. The lamella composition varies significantly, between $(Pb_{0.5}Sn_{0.5})S$ (= teallite) and the Mn-dominant new pole $(Mn_{0.65}Sn_{0.20}Pb_{0.15})S$.

In the second, Sb-enriched sample, curved lamellae, similar to franckeite, have been observed also in the outer, colder wall, in close association with galena and Fe-poor sphalerite. These lamellae have an original composition close to $Pb_{15}Sb_4Fe_7Cu_5S_{32}$, analogous to that of "mineral B", $Pb_6Bi_2Fe_5Cu_4S_{18.5}$ (Karup-Møller, 1970). These two minerals have probably homologous composite structures (SnS-type layers alternating with (Fe,Cu)S layers of the valeriite-type).

References:
Karup-Møller, S. (1971). *Can. Mineral.*, **10**, 871-876.
Koski R.A., Shanks, W.C., Bohrson, W.A. and Oscarson, R.I. (1988). *Can. Mineral.*, **26**, 655-673.
Oudin, E. (1991). Doct. Thesis, Toulouse Univ., 482 p.

A TECHNIQUE OF STANDARD SAMPLES PREPARATION FOR LOCAL X-RAY ANALYSES.

A.V.Mokhov, M.I.Lapina, A.I.Tsepin
(Institute of Ore Deposits (IGEM RAS), Moscow)

High demand to the resolution of analitical methods is typical of modern mineralogical studies. But quality of standard samples becomes critical for meeting such demand. One of the most important prerequisites for getting exact and correct results using microprobe or TEM is the complience of standard samples with such requirements as: (1) known chemical composition which was determined by independent methods; (2) uniform elements distribution; (3) a stable temporal behaviour of the sample; (4) stability of the sample in vacuum or under the influence of electron beam; and some other. One of the most important difficulties is the inhomogeneity of standard samples. During homogeneity control of choosed standard samples with the use of micro robe alone, erroneous results could be obtained because of various reasons. In order to avoid such mistakes we propose to perform a combined investigation of provisional standard samples. The study pattern is as follows.

1. The most clean and optically homogeneous grains of a mineral of known chemical composition are being selected from a crushed sample.
2. A suspension of the mineral is prepared with the routine technique, and its qualitative TEM analysis is made, which allows to reveal any possible phase or chemical inhomogeneity. At the same time a control of particles structure could ormed using the electrone microdiffraction.
3. A quantitative analysis of fine graines under electron microscope is made using VOSTOK software [1] which makes possible estimates of composition variations from a particle to particle.
4. Separated homogeneous graines are analysed with the microprobe, a special attention being paid to the abscence of porosity, to grain stability under electron beam and to stability of registered intensities in time.

With the use of that technique we have prepared and analysed standard samples of thorite, thorianite, aegirine, dyopside, Y-garnet, tectite, sanidine, olivine, and some other minerals.

****

[1]. A.V.Mokhov.//Izvestiya RAN, seriya geologicheskaya, 1986, 4, 99-104 (In Russian).

MAFIC GRANULITES FROM NORTHEN APENNINES CRETACEOUS MELANGES

Montanini A., Vernia L., Meli S. (*Istituto di Petrografia, Univ. of Parma, Italy*)

Mafic granulites from Northern Apennines occur as blocks in sedimentary melanges of Cretaceous age, together with huge olistoliths of ophiolitic rocks and rare amphibolites and gneisses. They are the unique occurrence of deep continental basement rocks in the Northern Apennines. The associated ultramafic rocks (i.e. the External Ligurides peridotites) have been recently interpreted as subcontinental mantle emplaced at shallow depth during the incipient ocean formation (Piccardo et al., 1992).

Deformed rocks with mylonitic, blastomylonitic and "mortar" textures are frequently observed. The undeformed samples range from xenoblastic to granoblastic poligonal. Granulitic assemblages consist of plagioclase (labradorite), clinopyroxene and variable amounts of orthopyroxene, red-brown amphibole (Ti-rich pargasite), garnet, green spinel, magnetite, ilmenite, biotite, apatite, zircon, sphene. Some olivine-bearing samples show orthopyroxene-spinel symplectites at the contact between olivine and plagioclase. Rare garnet occurs in olivine-free samples as rims of spinel or as reaction product between clinopyroxene and spinel.

Geothermometric estimates (780-850°C) based on the clinopyroxene-orthopyroxene equilibria are in agreement with granulite-facies conditions. A rough pressure estimate (7-10 kbar) can be obtained considering the olivine-out and the garnet-in curves for natural and synthetic basaltic systems.

Major and trace element composition of the mafic granulites reflects cumulus processes involving plagioclase and pyroxenes. The igneous protoliths could have been derived from the underplating of subalkaline (tholeiitic) magmas at the base of the crust. Subsequent cooling and partial hydration have yielded the observed corona reactions and the red-brown pargasite.

However, most samples have undergone more or less extensive retrogression strictly related to mylonitization. Green, blue-green and pale-green amphiboles with compositions ranging from Ti-poor horneblende to actinolite partially replace clinopyroxene and pargasite. Clinopyroxene may be also replaced by epidote + chlorite+ sphene (together with green hornblende). Orthopyroxene is often converted to chlorite (± talc), whereas plagioclase may be sericitized.

The extent of this retrogression is extremely variable: some samples show only negligible amounts of acicular green amphibole locally rimming clinopyroxene, whereas other rocks are almost completely converted into a low-temperature assemblage consisting of sericite + actinolite + chlorite ± epidote + Fe-Ti oxides. The retrometamorphic processes affecting the granulitic assemblages have not been isochemical, causing mobilization of several major and trace elements (Na, K, Ca, Rb, Sr).

It is proposed that these mafic granulites could belong to the deep crust uplifted and sheared during the rifting which led to the opening of the Ligurian Tethys, according to the mechanism of simple shear proposed by Lemoine et al. (1987).

References

Lemoine, M., Tricart, P., Boillot, G. (1987). *Geology*, **15**, 622-625.
Piccardo, G.B., Rampone, E., Vannucci, R. (1992). *Acta Vulcanol.*, **2**, 313-325.

• NON-DESTRUCTIVE TESTS IN STONE CONSERVATION

Montoto M. (*Dept. of Geology, Group of Petrophysics, University of Oviedo*)

General principles of non-destructive tests, NDT, used for the characterization of the state of internal deterioration of monumental stones are described.

A petrophysical approach to these studies is considered; besides, rocks are non homogeneous and polyphasic materials, full of internal discontinuities with anisotropies at different scales; those circumstances can not be ignored for a realistic petrophysical interpretation of data obtained under NDT.

A case history is presented: the study of the internal state of deterioration (internal fractures and zones of different degree of weathering) of a granitic Megalith under ultrasonic tomography.

This tomography is based in the analysis of the velocity variations of longitudinal waves traveling between known emitter/receiver position located around granite slabs of the Megalith. The exact path-ways followed by the waves are initially unknown and depend on the distribution of the elastic characteristics within the medium. As mentioned, rocks are non homogeneous materials and any wave traveling through them will suffer continuous refractions, that is a deviation in its path-way. This is the first problem that algorithms of tomography have to solve to deduce the real path-way between pairs of transducers.

Therefore, tomography provides a mapping of the variations in the velocity of propagation of ultrasonics through the interior of the material; later, those values have to be petrophysically interpreted in terms of internal cracking and weathering.

The practical difficulties implied in these studies are summarized:

a) accurate location of the emitter/receiver coordinates
b) injection and reception of signals ("ultrasonic pulse technique")
c) location of the first arrival of the wave: field equipment for displaying and storing the signals;
d) algorithms for image reconstruction (SIRT);
e) integration of the previous geological and petrophysical information with the information of the tomograms, petrophysical interpretation;
f) interpretation of the internal state of deterioration.

ARGENTOPENTLANDITE ASSOCIATED WITH HYDROTHERMAL ORES RELATED TO ACID VOLCANISM OF SE SPAIN (EL CHARCON, AGUILAS ZONE)

Morales-Ruano, S. & Fenoll Hach-Alí, P. *(Department of Mineralogy and Petrology, University of Granada)*

The Fe-Cu-Pb-Zn mineralizations at El Charcón (Aguilas, Spain) constitute a system of veins related to volcanic rocks and hosted within metamorphic materials of Triassic age. They include several sulphides such as chalcopyrite, sphalerite, cubanite and argentopentlandite. For more details on the geology, mineralogy, geochemistry and ore forming processes in this area, the reader is referred to Morales *et al.* (1994).

Argentopentlandite is a scarce mineral. It has only been described in no more than ten world deposits and always related to Co-Ni mineralizations associated to skarns (Shishkin *et al.*, 1971), Ni-Cu deposits associated with ultramafic rocks, (Vuorelainen *et al.*, 1972; Scott & Gasparrini, 1973), metamorphosed Fe-Ni sulphide deposits (Groves & Hall, 1978), or orebodies closely associated with tourmalinites (Benvenuti, 1991). Argentopentlandite from El Charcón is the first report for Spain and it is also the first occurrence in which argentopentlandite is associated with hydrothermal systems related to acid volcanism.

The El Charcón argentopentlandite has a reddish- to pinkish-brown colour in reflected light and tarnishes slowly in air to a slightly darker colour. It is isotropic, without visible cleavage and alteration products, and it has not internal reflection. This sulphide is typically associated with chalcopyrite grains. It always occurs within these grains as small individualized anhedral to subhedral patches up to 100 μm (some of them including small sphalerite stars), as poorly-developed dendrites, or as intergrowths with cubanite, but never around the margins of chalcopyrite grains. There are not lamellar or symplectite-like intergrowths (Groves & Hall, 1978) between chalcopyrite and argentopentlandite.

The El Charcon argentopentlandite was analyzed by electro microprobe (CAMECA SX-50) using as standards $CuFeS_2$ (Fe,Cu), synthetic Ag_2S (Ag), NiAs ((Ni), CoS (Co) and ZnS (S), accelerating potencial was 20kV with a sample current of 30nA. The average formula obtained from 11 analyses ($Fe_{5.21}$ $Ni_{2.76}$ $Ag_{1.00}$ S_8) suggests that Ag occupies specific crystallographic sites within the pentlandite lattice (Scott & Gasparini, 1973).

The spectral reflectance of argentopentlandite from El Charcón was measured using a SF Zeiss microphotometer. The values for four wavelengths measured in air relative to SiC standard are: 470nm (27.9%); 546nm (32.8%); 589nm (35.6%) and 650nm (37.0%). All the other values of the spectral curve agree with those given in the literature.

The El Charcón chalcopyrite including argentopentlandite has always lamellar twins and also includes the same type of sphalerite inclusions as argentopentladite, which indicates that chalcopyrite was formed above 400°C. The fluid inclusions of quartz crystals paragenetic with argentopentlandite indicate a homogenization temperature between 405 and 508°C. The maximum thermal stability limit of argentopentlandite is 455°C at low pressures (Mandziuk y Scott (1977). Consequently, the El Charcón argentopentlandite could have been formed at temperature around 400-450°C and within this temperature interval, the log fS_2 would be around -9 and -16 atm., according to the Mandziuk & Scott (1977) diagram. All this suggests that our argentopentlandite has the same hydrothermal origin as their paragenetic ores which are related to the acid volcanism which has affected the Aguilas zone.

References:

Benvenuti, M. (1991). *Eur. J. Mineral.*, **3**, 79-84.
Groves, D. & Hall, S.R. (1978). *Can. Miner.*, **16**, 1-7.
Mandziuk, Z.L. & Scott, S.D. (1977). *Can. Mineral.*, **15**, 349-364.
Morales, S.; Fenoll, P. & Both, R. *This volume*.

Scott, S.D. & Gasparrini, E. (1973). *Can. Miner.* , **12**, 165–168.
Shishkin,N. &Mintekov,G.(1971).*Zap.Vses.Min.Obs.*,**100**, 184–191.
Vuorelainen, Y, & Hakli, T.A. (1972). *Am. Minerl.*, **57**, 137–145.

MINERALOGY, GEOCHEMISTRY AND METALLOGENY OF THE HYDROTHERMAL ORES OF SOUTHEASTERN SPAIN (AGUILAS–SIERRA ALMAGRERA)

Morales–Ruano, S.[1]; Fenoll Hach–Alí, P.[1] & Both, R.[2] ([1]*Department of Mineralogy and Petrology, University of Granada;* [2] *Department of Geology and Geophysics, University of Adelaide*)

The base metal ore deposits of the Aguilas (El Charcón, Ermita de la Cuesta de Gos and Reina del Cielo) and Sierra Almagrera (El Arteal and El Jaroso) zone are related to the potassic calcalkaline and shoshonitic volcanism of southeastern Spain (Lopez Ruiz & Rodriguez Badiola, 1980). This volcanism was, in turn, influenced by a N–S compression during the Upper Miocene that produced various regional fractures. The mineral deposits always take the form of veins located in the fault zone (with direction E–W at Aguilas and N–S in the Sierra Almagrera) that has brought into contact metamorphic basement rocks of the Lomo de Bas unit with those of El Cantal and Las Palomas (Alvarez, 1987).

The mineralogy consists of Cu–Fe–Zn–Pb sulphides, Fe–Ni sulpharsenides, Bi–Ag–Pb sulphosalts and fahlores, with variations in abundance between deposits (Morales Ruano, 1994).

A study of fluid inclusions in quartz in the Aguilas area indicates polysaline fluids ($CaCl_2$, KCl, $MgCl_2$, NaCl, H_2O) in the majority of the deposits, with the exception of the lowest temperature fluid inclusions of stage II of El Charcón. The values of homogenization temperatures, salinity and density differ for each deposit (Table 1).

The paragenetic sequence determined from microscopic textural study, together with the chemistry of phases analysed by electron microprobe and microthermometric data of fluid inclusions, have enabled interpretation of the characteristics of the ore–forming fluids (pH < 5.8; log fO_2 = –36.1 to –43.2; log fS_2 = –13.0 to –15.2; log fH_2S = 10^{-2} to 10^{-3}). Under these conditions the dominant sulphur species in the fluid would be H_2S.

Table 1: Fluid inclusion microthermometric data

	CHARC.I	CHARC.II	ERMITA	REINA
Homog. T	405–508°	160–310°	203–402°	180–320°
Salinity	16–21%	2–8%	2–22%	14–22%
Density	0.62–0.80	0.74–0.94	0.69–1.03	0.87–1.02

Sulphur isotope analyses give $\delta^{34}S$ values between 1.5 and 5.0 ‰, with galena having the lowest value. The value of $\delta^{34}S_{fluid}$ is estimated to have been between 2.0 and 6.3 ‰. $\delta^{34}S$ values follow the sequence $\delta^{34}S_{ZnS} > \delta^{34}S_{fluid} > \delta^{34}S_{PbS}$. Finally, the value of Δ ($\delta^{34}S_{H2S} - \delta^{34}S_{fluid}$) calculated for the above pH and fO_2 conditions is between 0 and 0.5 ‰. These data indicate a magmatic or hydrothermal origin for the sulphur and equilibrium isotopic crystallization.

Transport of the metals must have been in the form of chloride complexes, given the polysaline nature of, and the lack of evidence for either organic or sulphur–bearing components in, the fluid inclusions.

The wide range of homogenization temperatures observed in each deposit indicates that cooling of the fluids was the major controlling factor determining the precipitation of the metals. Variations in salinity are a further factor to be considered, although fluctuations within each deposit are of minor importance. The influence of H_2S in the fluid can be discounted, since it remained constant within each deposit. Variation in pH can also be discounted, in view of the lack of evidence for boiling of the fluid or of reaction of the fluid with the host rock.

References:
Alvarez, F. (1987). *Ph. Thesis. Salamanca University*. 371p.
Lopez Ruiz,J. & Rodriguez Badiola,E.(1980). *Est. Geol.*, **36**, 5–63.
Morales–Ruano, S. (1994). *Ph. Thesis. Granada University*. 346p.

SILVER-GOLD ALLOYS AND SILVER-ANTIMONY INTERMETALIC COMPOUNDS OF SHKOL'NOE DEPOSIT (KURAMA RIDGE, TADJIKISTAN): INTERGROWTHS, COMPOSITION AND THERMODYNAMIC CONSTRAINS.

Moraley G.V. *(Institute of Geology of Ore Deposits, Petrography, Mineralogy and Geochemistry, Russian Acad. of Sciences)*

The silver-gold Shkol'noe deposit is located within the Kandjol ore field in the south-west part of the Kurama Ridge. The number of Permian quartz - calcite veins with Ag-Au mineralization occur in the Middle Carboniferous altered granodiorites.

Five stages of mineralization are recognized in the veins: I - quartz and calcite; II - quartz, calcite, adularia, sericite, sulfides, freibergite, Ag-Sb and Ag-Pb-Bi sulfosalts, acantite, naumannite, allargentum, dyscrasite, Ag-Au alloys and native bismuth; III - grey quartz and blue-grey calcite; IV - carbonates - quartz - chlorite, with abundant sulfides, rare fahlore, Pb-Sb, Ag-Pb-Sb sulfosalts, nickeline; V - barite - galena with minor quartz, calcite, pyrite, chalcopyrite, Ag-fahlore.

Silver-gold mineralization was formed during the II stage. At the beginning of the stage rhythmically - banded quartz-adularia-calcite assemblage "A" with electrum-I was precipitated. Then barren tabular quartz-calcite assemblage "B" was formed. At the end of the II stage massive quartz-calcite assemblage "C" with electrum-II, kustelite and native silver was precipitated. The Ag-Au alloys are the latest minerals both in assemblages "A" and "C". The dyscrasite and allargentum were recognized in assemblage "C" only. They are resorpted by electrum-II.

The extremely high fineness variability in the range from 70 to 25 wt.% of Au in the electrum and kustelite is a peculiar feature of the Ag-Au alloys. The gold content in electrum-I, coexisting with sulfides and gangue minerals, range from 50 to 70 wt.%. Native silver, kustelite (~25 wt.% of Au) and low Au electrum-II (35-50 wt.% Au) occur in intergrowths with high Ag fahlore and Ag-Sb sulfosalts. Electrum-II associated with sulfides, quartz and calcite is relatively enriched in gold (50-70 wt.% Au). Electrum-II intergrown with dyscrasite and allargentum has narrow variations of the fineness (45-55 wt.% Au). Cu, Sb, As, Bi, Se, and Te are the most common trace elements in Ag-Au alloys.

Unusually high contents of Au (up to ~12 wt.%) was found in Ag-Sb minerals. Two alternative explanations of this phenomena can be proposed. The first one is admixture of gold resulted from intimate intergrowths with gold bearing minerals. The second one is the isomorphous substitution of silver by gold in allargentum and dyscrasite. The second explanation seems to be preferable because in the grains of allargentum and dyscrasite without

visible electrum inclusions the determined Au content are high enough (up to 9.75wt.%).

Au-Ag mineralization was formed at 300-160°C and 83-6 bar. The electrum-I was formed at temperature ~300-250°C, $lgfS_2$ from -9.0 to -12.6 and $lgfO_2$ from -31.2 to -39.9. The electrum-II, kustelite and native silver were precipitated at temperature 300-160°C, $lgfS_2$ from -10.1 to -17.8 and $lgfO_2$ from -32.0 to approximately -48.0. The dyscrasite and allargentum were formed at 260-160°C, $lgfS_2$ from -12.3 to -15.6 and $lgfO_2$<-37.0. There is evidence that precipitation of Au-Ag minerals resulted from boiling and mixing of at least two solutions different in salinity.

MINERALOGY AND GEOCHEMISTRY OF BAUXITE-PHOSPHORITE DEPOSIT IN THE MIDDLE TIMAN (RUSSIA)

Mordberg L.E. (VSEGEI, Sankt-Petersburg, Russia)

Devonian bauxite-phosphorite deposit in the Middle Timan is underlain by Rifean dolomites and is overlain by Eifelian-Givetian quartz sandstones. Total profile attains 27m. Underlying dolomites contain 0.1-1.5% of P_2O_5 in form of francolite.

Mineralogy of the deposit is very interesting (Kolokoltsev et al., 1987). Rock-forming elements are francolite, crandallite, svanbergite, diaspore, sericite and chamosite. Goethite, kaolinite and celestine are sometimes present, as well as pyrite and marcasite. Francolite is more widespread in the lower part of the deposit. It is replaced with crandallite upwards in the section. Svanbergite is distributed irregularly. Diaspore is a mineral of the upper part of the deposit. The top of bauxite layer is kaolinized and contains pyrite and marcasite as a rule. Sericite and chamosite are transitional minerals, but the highest content of mica is near the footwall. Geochronological study (Kolokoltsev et al., 1990) determines 4 generations of mica, two of which are older than the deposit (540 and 420Ma), and the third and the forth are younger (370-350 Ma and 320-300Ma correspondingly). Sulphides are typical for the upper kaolinized zone.

The content of P_2O_5 varies from 0.3 to 25%, and its highest content occurs in the lower part of the deposit. There is no distinct bound between bauxite and phosphate zones, because crandallite and svanbergite are often occurred together with diaspore, and phosphorus content in bauxite zone is sometimes high too. However, in general, bauxite layer occurs higher than phosphate one. Sr content varies from hundreds of ppm to 5.2%, and its high amounts (more than 1%) are characteristic for rocks rich in phosphorus.

Phosphate zone is also richer in U (29ppm) and Y (147ppm), than bauxite zone (correspondingly 16ppm and 120ppm). Contents of Zr and Pb are decreased from bauxite zone towards the top and the bottom, whereas contents of Ni, Co and Rb are increased in these directions. Th content is increased from the bottom to the top of the deposit. Th/U ratio is close to 1, that is very low. It originates from relatively high U content (from 18 to 63ppm) and ordinary Th contents (9-40ppm). For comparison, Th/U in bauxites of the world is estimated close to 4 ; and for the nearest Schugor bauxite deposit Th/U varies from 6 to 25 in different zones because of very high Th contents (up to 700ppm) and ordinary U contents (2-21ppm). Rb content is very high for weathering profiles (up to 200ppm), and strongly depends on mica amount. High positive correlation of Rb and K is observed.

The stages of minerals formation can be described as follows: (1) Francolite and older generations of mica were inherited from the source rocks during weathering; (2) The supplying of alumosiliceous material and its weathering led to diaspore, crandallite and svanbergite formation. The problem of Sr source is not quite clear now; but the presence of phosphorus created geochemical barrier, which has prevented removal of this very mobile element; (3) On the diagenetic stages, supplying of Si and S led to formation of kaolinite and pyrite in the upper part of profile, as well as to formation of chamosite and celestine; (4) On epigenetic stages, twice mica was formed as a result of hydrothermal activity. The deposit described is unique both geochemically and mineralogically, because of very rare combination of rock-forming elements, their amounts and mineral forms.

References:

Kolokoltsev, V.G., Lisitsyna, M.A. & Mordberg, L.E. (1987). *Proc. KOMI ASSR X Geol. Conf.*, Syktyvkar, 146-150 .

Kolokoltsev, V.G., Lisitsyna,M.A., Mordberg, L.E., Nesterova, E.N. and Rublev, A.G. (1990). *Chem. Geol.*, **84**, 86-87.

BIOOXIDATION PROCESSES IN A COMPLEX GOLD ORE FROM NW SPAIN USING *Thiobacillus ferrooxidans*

Moreno T., Lunar R., Sierra J., Oyarzun R. (Dept. de Cristalografía y Mineralogía, Univ. Complutense, Spain) and Maturana H. (Dept. de Minas, Univ. de La Serena, Chile).

Bacterial leaching is an attractive alternative process for the dissolution of gold-bearing refractory ores e.g. arsenopyrite. Since arsenic and sulphur gases e.g. SO_2 produce many environmental problems, biooxidation is now being considered as serious alternative to the conventional techniques to allow gold liberation (Attia et al., 1985; Errington et al., 1987, Rossi, 1990, Maturana et al., 1993). The conventional techniques involve either roasting or flotation of the Au-Fe-S-As refractory ore before cynide leaching for gold recovery.

Au-arsenopyrite ores account for most of the Northwestern Spain gold resources. Conventional treatment of these ores by flotation or roasting before cyanide leaching would result in either economic or environmental problems. A composite sample from one of the deposits (Albores) was selected to test whether it could be subjected to biooxidation induced by *Thiobacillus ferrooxidans*. The tests were designed to observe adaptative mechanisms of *T. ferrooxidans* and alteration processes in the primary minerals.

The chemical composition of the ore is: 12.8 % Fe, 9.8 % S, 9.1 % As, 0.15 % Pb, 46 g/t Ag and 17 g/t Au, with arsenopyrite as the main mineral phase and minor amounts of pyrite, sphalerite, galena, chalcopyrite, tennantite-tetrahedrite, acanthite, ruby silvers and electrum.

Adaptation of *T. ferrooxidans* was achieved increasing pulp density from 2 % to 10 % in 44 days. Changes in pulp density were made when a value of 10^8 bacteria/ml was reached. This process was performed in two erlenmeyers and a batch reactor at pH 1.8. The adapted bacteria were used in the biooxidative tests and the best results were achieved at pH 2.0.

Previous adaptation of bacteria allowed rapid population growth during the leaching tests and absence of the *lag* phase. Corrosion holes in arsenopyrite of both inorganic and biologic origin were detected by SEM microscopy. Precipitation of goethite and jarosite was of minor importance.

References:

Attia, Y., Litchfield, J., Vaaler, L. (1985). *Proc. of AIME Annual Meeting, New York, 1985.*

Errington, M., Gibbs, H., Pooley, F.(1987). *Proc. Hydrometallugy 87, Manchester, U.K.*
Maturana, H., Lagos, U., Flores, V., Gaete, M., Cornejo, L., Wiertz, J.V. *FEMS Microbiology Reviews, 11, 215-220.*
Rossi, G. (1990) *Biohydrometallurgy. McGraw-Hill, 609 pp.*

LOCATION OF Fe^{3+} IMPURITIES IN Fe-DOPED $\alpha Al(OH)_3$: EXPERIMENTAL AND CALCULATED EPR POWDER SPECTRA

Morin G., Ildefonse Ph., Calas G., and Dubertret B. (Laboratoire de Minéralogie-Cristallographie, UA CNRS 09, Universités Paris 6 et 7 and IPGP), Bonnin D. (Laboratoire de Physique Quantique, ERA CNRS 676, ESPCI, Paris), Bouzat, G. (Aluminium Pechiney)

Aluminium hydroxides, as well as their dehydrated derivatives, usually contain iron impurities which may be used to understand their formation conditions. They are also considered as model compounds to understand the mechanisms of the homovalent Al-Fe substitution in minerals. However iron occurs under various species in these materials: isolated Fe^{3+} cations incorporated in the lattice, adsorbed cations or trapped Fe-oxyhydroxides. Spectroscopic tools are the choice methods to analyze these different forms, but the low concentrations encountered (10-100 ppm) put severe limitations. We present new data on Fe-bearing gibbsites electron paramagnetic resonance (EPR) at both X- and Q-band, and diffuse reflectance spectroscopy (DRS) of natural and syntheticgibbsites, $\alpha Al(OH)_3$ with an iron content between 30 and 250 ppm. EPR spectra of polycrystalline gibbsite have been modelled in order to determine the sites occupied by Fe^{3+} in the gibbsite lattice as well as to quantitatively estimate sites occupancies.

EPR powder spectra of the samples studied yield two kinds of signals : (i) a broad resonance centered around geff =2.0 related to associated superparamagnetic iron oxyhydroxides, and (ii) sharp lines related to diluted Fe^{3+} substituted to Al in the gibbsite structure. EPR powder spectra simulations evidenced that Fe^{3+} occurs in the two non-equivalent six-coordinated Al-sites: Al1- (B^0_2 = 0.0.1485 cm^{-1} ; B^2_2 = 0.0692 cm^{-1}) and Al2 (B^0_2 = 0.0858 cm^{-1} ; B^2_2 = 0.0501 cm^{-1}). Site occupancy of Al2-octahedron, whose principal distorsion axis is close to the stacking direction, is three times larger than that of Al1-octahedron whose principal distorsion axis lies almost inside the sheets. Zero Field Splitting intrinsic parameter derived from superposition model analysis, and bond length are higher for the Fe-OH bond ($|\overline{b_2}|$ = 0.38 cm^{-1}, R_0=2.08 Å) than for the Fe-O bond ($|\overline{b_2}|$ = 0.26 cm^{-1}, R_0=2.02 Å). That could explain the low affinity of Fe^{3+} for pure hydroxyl coordination and may be a chemical limitation explaining the lack of solid solution in $\alpha Al_{1-x}Fe_x(OH)_3$ and more generally the incomplete Fe to Al substitution in hydroxyl-bearing phases.

In some samples, a third Fe^{3+} site with maximum rhombic symmetry is observed. Relative absorbance of this spectrum with respect to those of both structural Al1 and Al2 sites indicates that it contributes for a small part of the total iron content in the samples. This site is interpreted as Fe^{3+} at strained sites within the surface sheets of gibbsite crystallites.

For all samples, the main feature on raw and second derivative DRS spectra is a band at 37000 cm^{-1} related to O→Fe charge transfers due to substituted Fe^{3+} in $\alpha Al(OH)_3$. Both EPR and DRS measurements of structural Fe^{3+} are well correlated to the total iron content and no saturation of structural sites is observed up to 250ppm total Fe. Besides, structural Fe^{3+} is at lower level in samples which exhibit two DRS bands at 18700 cm^{-1} and 20200 cm^{-1} related to hematite and goethite respectively.

In $\alpha Al(OH)_3$, the relative partition of iron between lattice substitution and segregated oxides can be accurately determined with appropriate spectroscopic tools. Applications of this method to natural environments will be presented to trace the different populations of gibbsite occuring in weathering profiles.

MINERALOGICAL AND CHEMICAL COMPOSITION OF SILURIAN Al (Fe-Ca) PHOSPHATES IN THE IBERIAN PENINSULA; PROVINCES OF ZAMORA AND HUELVA.

Moro, M.C.(*); Cembranos, M.L.(*); Fernández, A.(*) and Pérez del Villar,L.(**)
(*)Dept. Geology. Univ. Salamanca. (**)CIEMAT. Madrid.

Abstract:

The mineralizations of Silurian Al (Fe-Ca) phosphates in the Iberian Peninsula are associated with levels of cherts and/or lidites normally from the upper Wenlock of the different series established by Robardet and Gutiérrez Marco (1990). The best known, mainly in the form of variscite, are located in the provinces of Barcelona, Huelva and Zamora, those of the latter province being the most important owing to the number and quality of the occurrences. According to some authors, these mineralizations were already known to the Arabs (Arribas *et al.*, 1971); and may be that also to the Romans or even before (Campano *et al.*, 1986)

The levels of cherts and/or lidites hosting these mineralizations, interstratified within vulcano-sedimentary Silurian series, are composed mainly of microcrystalline quartz , with chlorite, illite, muscovite and biotite as accessories and traces of orthoclase, millisite and crandallite. Geochemically, they are enriched in P_2O_5, V, Ba, Cr, Cu, Ni and Zn. The content and distribution of the elements of the rare earth's group (R.E.E) are similar to those of cherts from ocean floors (Moro *et al.*, 1994)

Two type of Al (Fe-Ca) phosphates mineralization are associated with these siliceous rocks. One consist of stratiform Al (Fe-Ca) phosphates, with a laminated or concretionary textures (oncolites). In the second type, Al (Fe-Ca) phosphates fills the fissure network crosscutting the siliceous host-rocks or is associated with quartz lodes, both having a massive texto-structure (Moro *et al.*, 1992).

The mineralogical composition of the types and subtypes of these phosphate mineralizations, essentially variscite, has been determined by polarization microscopy, X-ray diffraction (XRD), differential thermal analysis (DTA), thermogravimetric analysis (GT), scanning electron microscopy with a coupled dispersive energy analyzer (SEM and DEX) and with a Camebax SX 50 electronic microprobe (EM). Variscite is seen to be the main phosphate mineral while strengite, the intermediate members of the variscite-strengite series, crandallite, millisite and turquoise are always present as accessory minerals.

From the chemical point of view, both morphological types differentiated display anomalous contents in V, Cr, Cu and Zn and, occasionally, in Ni and Co. The distribution spectra of the REE of the stratiform phosphates are similar to those of the siliceous host rocks and also to those of marine phosphorites not associated to upwelling marine currents.

Acknowledgments

This work has been carried out within the D.G.I.C.Y.T.(M.E.C. España) and Castilla-León Autonomy Community (Projects: PB-91-0563 y SA-15/09/92).

References:

Arribas,A; García,E; Martín Pozas,J.M.; Nicolau,J.; Salvador,P. (1971). *Stvdia Geologica Salmanticiensia*, **II**, 115-132.

Campano,A; Rodriguez,J.A.; Sanz,C.(1986). *Instituto de Estudios Zamoranos "Florian de Ocampo"*. Anuario.

Moro,M.C.; Gil,M.; Cembranos,M.L.; Pérez del Villar,L.(1992). *III Congr. Geol. Esp. y VIII Congr. Latinoamericano Geol. Salamanca.* **3**, 212-217.

Moro,M.C.; Cembranos,M.L.; Gil,M.; Fernández,A.;Pérez del Villar. (1994). *Bol. Soc. Esp. Min.*, **17-1**, (in press).

Robardet,M.; Gutierrez Marco,J.C.(1990). In: *Pre-Mesozoic Geology of Iberia*. R.D. Dallmeyer & E. Martínez García (ed.). Springer-Verlag. Berlin, Heidelberg, 383-395.

LIQUID AND FLUID IMMISCIBILITY DURING MAGMATIC EVOLUTION OF THE LÅNGARSHOLMEN CARBONATITE RING-TYPE INTRUSION FROM NORTHERN ALNÖ, SWEDEN.

Morogan V. and Lindblom S. (Dept. of Geology and Geochemistry, Univ. Stockholm)

The Alnö alkaline-carbonatite complex is made up in its northernmost part, at Långarsholmen, of a ring-type intrusion. The plutonic rocks of the ring complex exhibit the order of emplacement pyroxenite -> (silico)-sövite -> ijolite, and are surrounded by a breccia zone. Preliminary mineral chemistry and fluid/solid inclusions studies suggest that the northernmost ring complex and the main intrusion at Alnö have had a somehow different magmatic evolution, implying different evolution of fluid phases also.

At Långarsholmen, the mafic silicate magma started to crystallize Al-diopside of 0.11 CaTs content during a mid-crustal stage of evolution (ca. 5-6 kb and 1175°C). At this stage, the mafic magma was immiscibily coexisting with a Mg-bearing calcitic melt, recorded in the abundant carbonate inclusions of composition $Ca_{0.82}Mg_{0.12}Fe_{0.03}Mn_{0.01}CO_3$, trapped by the crystallizing Al-diopside. The two immiscible melts seem to have separated at ca. 5kb and 1150°C, in good agreement with late experimental studies.

After separation, the carbonatite magma fractionated cc+ap+dol (cf. dolomite inclusions in primary apatite). Around 4kb, a CO_2-bearing fluid (d=0.85) was present and became trapped as fluid inclusions (type A1) in the primary apatite, formed during the mid-crustal stage. The residual calcitic melt was emplaced into the upper crust and gave rise to sovite. Fluid inclusions (type A2), trapped during recrystallization of primary apatite indicate an evolution of the fluid phase towards a late (Na+K) hydro-carbonic fluid during cooling at shallow depths of final emplacement.

The pyroxenite magma crystallized Al-di/di+ap+mt during its ascent, and was initially in contact with a saline hydro-carbonic fluid trapped as inclusions (type B2 reluctant to dissolution up to 550°C) in diopside and apatite. The pH_2O started to increase and Fe-pargasite began to replace the pyroxene. It appears that the fluid present at this stage was aqueous and contained ca. 40% NaCl.

With decreasing PT, the fluid splited into two immiscible phases of high- and low-salinity (inclusions of type B1 and C1, respectively). At shallow depths of final emplacement, the composition of the fluid phase was most probably controlled by the supply of volatiles from external sources as indicated by the dilution trend of some B1-type fluid inclusions.

The ijolite does not show signs of liquid immisciblity with the sövite at Långarsholmen, and exhibits mostly postmagmatic activity of fluid phases. Its relations with the pyroxenite and sövite in the area are unclear. Most likely, the ijolite is related to the intrusion of the Alnö main complex.

PETROGENESIS OF THE DITRAU COMPLEX, EAST TRANSYLVANIA, ROMANIA

Morogan V. (Dept. of Geol. and Geochem., Univ. Stockholm), Upton B.G.J. (Dept. of Geol. and Geophys., Univ. Edinburgh), and Bindea G. (Inst. of Geol. and Geophys., Bucharest).

The Ditrau complex, eastern Transylvania, is included in the prealpine Pietrosu-Bistrita thrust nappe of the eastern Carpathians. The complex is divided by a WE fault into a northern (i.e. Jolotca area) and a southern (i.e. Ditrau s.s. area) part, with the southern part down-faulted. The intrusion comprises four igneous rock series: alkali gabbro/syeno - diorite, syenite/quartz syenite, nepheline syenite, and alkali granite and is cut by a large variety of dykes, including alkali basalt, basanite/tephrite and tinguaite.

In the northern part, the alkali gabbros are prevailing and they are intimately associated with syenite/quartz syenite. Ovoid to lenticular bodies of mafic rocks (from a few cm thick up to a metre or more) with lobated and crenulated margins are enclosed and veined by syenite in a way recalling the net-veined intrusions. The mafic rock also forms pillow-shaped bodies with chilled margins against the syenite, displaying a quenched fabric under the microscope. The syenites grade into quartz syenites, and are associated with alkali granites. A discrete ultramafic body (kaersutitic peridotite) occurs in the Jolotca area.

In the southern part, the syeno - diorites predominate and are associated with syenite/monzonite in a way similar to the net-veined intrusions. These rocks are intruded and locally transformed (scapolitized) by a younger suite of nepheline syenites.

Mineralogically the rocks are relatively simple: the gabbroic and dioritic facies involve plagioclase (from An60 to An15) + diopsidic pyroxene + abundant amphibole (kaersutite/pargasite ->pargasitic hornblende ->rarely actinolite) + titanite (up to 20%) ± apatite. The ultramafic rock consists of olivine (Fo80) + diopside + abundant kaersutite oikocrysts ± phlogopite ± apatite ± oligoclase. Very characteristic of the mafic rocks intimately associated with the syenite is the coexistence of several populations of plagioclase +albite ± interstitial and/or rims of microcline + abundant biotite, which may reflect a mixing episode.

Al and Ti contents of amphibole indicate a range of crystallization temperatures from ≥1000°C to ≤850°C for gabbros and diorites, respectively.

Major and trace element variations of plutonic rocks suggest that the Ditrau magmas have been derived from a volatile rich alkali basalt parental magma. It appears that the most primitive magmas reaching high levels were already relatively highly fractionated. Incompatible-element patterns show that the alkali gabbro/syeno-diorite series may have resulted from further fractionation and mixing with an already crustal contaminated syenitic magma. Nepheline syenite (phonolite) magmas may have had a parent similar to the basanite/tephrite dykes, abundant in the area. Incompatible elements of syeno-diorites from the southern part indicate contamination by the nepheline syenite magma, possibly during a metasomatic event. Incompatible-element patterns of alkali granites suggest a crustal origin of the granitic magma.

SULFATION MECHANISM IN LIMESTONES: EFFECT OF SO_2 AND NO_2 IN HUMID AIR AND KINETICS OF REACTION

Moroni B. and Poli G. (*Dept. of Earth Sciences, Univ. of Perugia, Italy*)

In the modern polluted atmosphere the reactivity of carbonate rocks with sulfur oxides can be considered a primary cause of stone decay. The aim of this work was to study the conceptual and quantitative aspects of the processes of sulfation through the evaluation of the effects of different amounts of SO_2, alone or combined with NO_2, on the atmospheric corrosion of a limestone.

Experiments were carried out in an apparatus deliberately designed for the purpose, and performed at constant temperature (25°C), relative humidity (100% or less) and dynamic flow conditions (300cc/min). The specimens consisted in little slabs cut from the same block of material, a limestone belonging to the "Scaglia" Cretaceous-Tertiary lithostratigraphic formation.

The progress of reaction was monitored through different analytical techniques: liquid chromatography (HPLC) and X-ray fluorescence (XRF) were used to quantify the change in the bulk chemical composition with respect to total sulfate ion and total sulfur respectively; X-ray diffraction (XRD) was used to follow the reaction mechanism and, through the application of the Rietveld method, to determine the relative quantities of the parent minerals and the reaction products. The occurrence and the textural features of the reaction products were observed by Scanning Electron Microscopy (SEM), whereas the relationships with the substratum were analyzed by means of EPMS elemental maps.

The analytical data obtained by the different methods are in good general accordance. As regards HPLC and XRF, in particular, the experimental points were fitted by means of the same kind of exponential curve accounting for the progressive change in the rate of sulfation. This curve is characterized, in the first part, by a linear trend, whose slope is directly correlated to the SO_2 concentration in

the atmosphere, and reaches a steady state after a few days from the beginning of the reaction.

On the other hand, XRD analysis revealed that calcium sulfite hemihydrate, $CaSO_3*1/2H_2O$, and gypsum, $CaSO_4*2H_2O$, are the main products of reaction; gypsum, in particular, is the only product in the presence of NO_2, evidencing the role of this gas in the oxidation of SO_2 to SO_3. Therefore the following mechanisms of reaction may be proposed in the two cases:

$$CaCO_3 + SO_2 + \tfrac{1}{2}H_2O \rightarrow CaSO_3 * \tfrac{1}{2}H_2O + CO_2 \xrightarrow{\frac{1}{2}O_2 + \frac{3}{2}H_2O} CaSO_4 * 2H_2O$$

$$CaCO_3 + SO_3 + 2H_2O \rightarrow CaSO_4 * 2H_2O + CO_2$$

SEM observation evidenced that the reaction products form on the surface of the samples, and that they begin growing on from preferential sites of lower energy.

Some efforts were also made in order to determine the rate laws and the rate constants of the reactions. This aim was pursued either for the overall sulfation mechanism (HPLC and XRF data) or for the single steps of the process (XRD data), and led to the conclusion that whatever the order at the beginning of the reactions, it keeps constant only in the first, linear part of the curves. This particular feature may be interpreted as an evidence of the change in the diffusion processes promoting the reactions. Our data are in general agreement with those reported in previous works and point out the role of atmospheric SO_2 concentration in the extent of adsorption, of NO_2 in the oxidation of SO_2 to SO_3, and of solid state diffusion in the mechanisms of reaction. Work is still in progress in order to examine thoroughly the kinetic aspects of the reactions and the relationships with the chemico-physical properties of the material.

The validity of the experimental findings has been successfully verified through the analysis of homologous samples taken from monuments. In particular, the presence, at the top of the substratum, of a Ca-depleted layer as observed by EPMS elemental maps may be regarded as another evidence of the role of diffusion in the deterioration processes.

COMPOSITION AND PHASE RELATION OF THE AL-P-PHASES IN CELESTITE-, MUSCOVITE-, KYANITE-BEARING QUARTZITES FROM THE PASSO DI VIZZE / PFITSCHER JOCH (SOUTH TYROL, ITALY).

Morteani, G. (*Angew. Mineralog., Techn. Univ. of München, FRG*) and Ackermand, D. (*Mineralogisches. Institut, Univ. of Kiel, FRG*)

In the Penninic Lower Schieferhülle units of the Tauern Window at Passo di Vizze/Pfitscher Joch (South Tyrol, Italy), a metaquartzite band several tens of meters wide and one km long contains layers of a quartz-muscovite-kyanite-tourmaline-staurolite-celestite-assemblage with additional lazulite, svanbergite, goedkenite and apatite as phosphates. The layers contain up to 15 vol.% phosphate minerals. Previous work has established the P-T-conditions of peak metamorphism at about 550°C and 7 kbar (Selverstone et al., 1984). The age of the protolith is thought to be Permo-Triassic (Lammerer & Morteani, 1992). The bright blue lazulite results is, from microprobe analysis, a lazulite-scorzalite$_{ss}$ $(Mg,Fe^{2+})\ Al_2\ (OH)\ (PO_4)_2$ with Mg/Fe substitution only. Colorless svanbergite has a marked woodhouseite component (Sr,Ca) $Al_3\ (OH)_6\ (PO_4)\ (SO_4)$ showing Sr/Ca and P/S substitutions, and goedkenite has an approximately constant composition corresponding to $Sr_{0.9}\ Ca_{1.9}\ Al\ (OH)\ (PO_4)_2$. In tourmaline X_{Mg} varies from the core to the rim from 0.15 to 0.70 and X_{Mg} in staurolite is 0.25. Euhedral apatites are Sr-rich, whereas the small and anhedral apatites in contact with aluminum phosphates are Sr-poor.

Three parageneses are observed: A) lazulite, svanbergite, apatite, and tourmaline, B) lazulite, svanbergite, goedkenite, apatite, and celestite, and C) staurolite and tourmaline. All three parageneses also contain quartz, kyanite, muscovite, and ilmenohematite. Staurolite is never in contact with the phosphate phases. The parageneses reflect the whole rock composition.

Microscopy, careful microprobe X-ray area scans and chemical analysis by microprobe show that anhedral apatite is a corrosion relict in lazulite, and svanbergite rims lazulite grains. Goedkenite usually forms isolated patches in the phosphate-, and coelestite-rich parts of the rocks. From such observations the following sequence of reactions can be suggested:

1.) Apatite + kyanite + Mg^{2+} → lazulite + quartz + Ca^{2+}
2.) Apatite + celestite + kyanite → goedkenite + quartz + S^{6-}
3.) Lazulite + celestite + Ca^{2+} → svanbergite + Mg^{2+}

It can be supposed that Fe-Al-phosphates are, due to their extensive compositional variability and their refractive nature, very valuable geothermometers that can record a consistent part of the P-T-path of metamorphic events up to conditions of upper amphibolite facies.Unfortunately only very few experimental data about the stability relations of Fe-Al-phospates for the P-T-range of greenschist to amphibolite metamorphism exist.

References:

Selverstone, J., Spear, F., Franz, G, & Morteani, G. (1984). Journ. of Petrol., 25, 501-531.
Lammerer, B & Morteani, G (1986). Mitt. Österr. Miner. Ges., 135, 185-197.

THE PECULIARITIES OF CRYSTAL GROWTH MECHANISM OF SLIGHTLY SOLUBLE COMPOUNDS UNDER HIGH SUPERSATURATION

Moshkin S.V. (Dept. of Geology, Univ. of St.Petersburg, Russia)

The majority of data about crystallization kinetics of slightly soluble compounds gives evidence that the crystal growth mechanism of these compounds differs from classic dislocation one. For gypsum, barite, celestite, silver chromate and some other compounds the dependencies of growth rate (V) on relative supersaturation (S) have an exponential nature. On the other hand the relative high crystal growth rates of these compounds under small supersaturations (S<0.25) do not conform to the theory of growth by means of two-dimension (2-D) nucleation. This character of kinetic dependencies may be explained if the mixed growth mechanism, under which 2-D clusters are formed between steps of the dislocation spiral, should be assumed.

The model of this mechanism with following supposition base was considered: 1) the 2-D clusters are formed between the steps, and when a moving step captured these clusters the effective length and density of breaks of this step increase; 2) an average size of clusters is proportional to critical one; 3) the influence of steps train on 2-D nucleation reduces to decreasing of surface supersaturation beetwen the steps. Basing on these suppositions following equations may be received:

$$V = W + K * \exp(-A / \ln(S+1)) / \ln(S+1)^3, \qquad (1)$$

where: W is the rate of growth by means of steps train motion (A. Chernov, 1961), K - coefficient independent of supersaturation and includes the clusters form factor, A - ordinary exponential coefficient of 2-D nucleation.

To control the applicability of the model the experimental dependencies of growth rate of {-111} and {120} faces of gipsum crystals on value of relative supersaturation at three temperatures was established using the method described in detail in (S. Moshkin et al., 1980). The obtained dependences are in good agreement with equation (1).

References:

A.A.Chernov.(1961).Uspehi Fis. Nauk. 73, 277-331. (russ.)
S.V.Moshkin, A.V.Nardov, T.G.Petrov. (1980). Kristallografiya, 25, 1307-1310. (russ.)

NEW GROWTH OF SULPHIDES ON THE SURFACE OF POLISHED SECTIONS

Mozgova N.N., Efimov A.V., Kuzmina O.V. (IGEM RAS, Moscow, Russia), Borodaev Yu.S. (Dept. of Geology, Moscow Univ., Russia)

1. Solid state diffusion play an important role in transformation of ore minerals, but has not be sufficiently studied yet (Moh, 1973). New formed sulphides on the polished sections or on the surfaces of ore samples after long storage may help in understanding of mechanism of ion diffusion in minerals. Some instances of such new formed silver and copper sulphides have been described (Chen et al., 1980; Walenta, 1984). As known Ag and Cu are the most mobile atoms.

2. New growth of Ag- and Cu-sulphides were found on the surfaces of polished sections after storage for 10-30 years in the laboratory at room temperature. Polished sections represent different kinds of ores from various types of deposits. All of them contain some Ag- or/and Cu-bearing minerals (native Ag, chalcocite, covellite, chalcostibite, bornite, enargite, tennantite, tetrahedrite and some other Ag- and/ or Cu-sulphosalts). New formed were examined optically, by scanning electron microscopy, energy-dispersion method and X-ray diffraction.

3. The results obtained demonstrate that acantite and Cu-sulphides are the main minerals among new formed compounds. Morphological types of individuals were recognized: dendrites, thin needle-like crystals (so-called whiskers), columnar crystals, filaments, noduls of spheric, botryoidal or irregular forms, flakes, thin films. Size of dendrites varies from 0.1 to 0.8 mm (length) and from 0.005 to 0.1 mm (width) with variations of l/w ratio from 7 to 40. Other anisotropic individuals have the lesser dimentions. Isometric noduls usually reach 0.05-0.06 mm in diameter. Colours of new formed sulphides are also varied: silver-white, blue-grey, indigo-blue, bronze, beige, black. The anisometric individuals ussually form bush-like aggregates. The Ag- and Cu-sulphides occur sometimes directly on the primery ore grains in the polished section, covering all surface of grains or growing only on their boundaries. But they often spread and migrate onto surface of adjacent phases, including non-opaque minerals and the epoxy mounting medium. New formed and initial ore minerals ussually differ in chemical composition. For example acantite (Ag_2S) grows on native Ag; chalcocite (Cu_2S) or djurleite ($Cu_{1.93}S$) on bornite; acantite and chalcocite (or djurleite) on Ag-bearing tetrahedrite-$(Ag,Cu)_{10}(Fe,Zn)_2Sb_4S_{13}$.

4. The filament growth of Ag or Cu sulphides on silver or copper after reaction with gaseous H_2S at room temperature has been studied in chemistry and metallurgy (Drott, 1960; L. Baclund, P. Baclund, 1964 and others). Crystal morphology of sulphides is due to the density gradient of the reacting gas in atmosphere (Hashimoto & Tanaka, 1955). The transport of material to the tips of the crystal occurs by diffusion of metals. Formation of new growth of sulphide in our samples was evidently the same. Cu and Ag sulphosalts and sulphides being non-stoichiometric compounds have composition fields and part of Cu or Ag atoms are mobil in their structures. These mobil atoms can migrate onto the surface of the grains and react with H_2S as native metals. These minerals can lose some metals changing their composition in the limit of their field of homogeneity (without decomposition).

New data about briartite.

Mozgova N.N.(IGEM RAS, Russia), Nenasheva S.N.(Fersman Mineralogical museum), Borodaiev Yu.C.(Dept of geology, Moscow Univ, Russia), Tsepin A.I.(IGEM RAS, Russia).

In sample from Tsumeb type locality (collection Fersman mineralogical museum), **Cu**-rich briartite (rare complex sylphide **Ge**) in xenomorphic grains (up to 1-2 mm) in renierite was found. The chemical composition of mineral (14 microprobe analyses) varies (in wt %): **Cu** 34.10-35.83; **Ag** 0.00-0.13; **Zn** 10.86-13.89; **Fe** 2.54-4.10; **Ge** 14.30-15.91; **Ga** 1.96-3.42; **As** 0.15-0.32; **S** 31.79-32.65; total 98.69-101.64. From impurities was found **V** and **Sb**, rarely **W** and **Sn**. Comparing experimental data with literature shows general interval of Cu variation in briartite 31.6-35.8 wt %, respectively ~0.25 **Cu** atom per briartite formula $Cu_2(Zn, Fe)GeS_4$ (or 0.5 atoms per unit cell). During the recounting the analyses on more exploring complex **Ge** sylphide — renierite (on 33 atoms) this interval is ~1 **Cu** atom, that is comparing with that of renierite, where it, according to L. Bernstein, explained through the substitution pair **Zn(II)+Ge(IV)≠Cu(I)+As(V)**.

Statistical work of results of analyses shows two most important, independent from each other back bonds **Cu-S** and **Zn-Fe**; -- coefficients of correlation -0.973 and -0.983 respectively with the level of importance of 0.532 for 95% trusting probability. The same dependence in smaller scale was found in synthetic briartite (8 microprobe analyses), consisting only basic elements (**Cu**, **Fe**, **Zn**, **Ge** and **S**), in which the quantity of Cu varies from 31.51up to 34.96 wt %. (on 0.11 atoms in briartite formula).

This data shows that compensational isomorphism, which was found in renierite, in briartite was not shown, although it has the same quantity of Cu variation with renierite. The purposes of back dependent Cu-S in briartite may be:1) presenting Cu (I) and Cu(II) and decreasing Cu(II) with the increasing of consistence of Cu in mineral; 2) forming in cuprum-rich briartite bonds of Cu-Cu, the same as in pairs of Hg-Hg in HgCl; 3) particular Cu transforming with the increasing of its quantity in atomic state with disposing in emptinesses of briartite structure. (clathrates structure).

It's not excluded that **Cu**-rich briartite, which gives during the recounting on 33 atoms correlations, which are near to ideal mineral formula $[Cu_9(Zn_3Fe)_4(Ge_{3.5}Ga_{0.5})_4]_{17}S_{16}$, may be independent mineral specie, if it'll be crystallochemistry individual enough.

Good chemistry and structural similarity of known complex sylphides **Ge** (renierite, germanite and briartite) attests that it is convenient to prefer to join them at one group in mineralogical classifications.

PECULIARITIES OF COMPOSITION OF Ag-BEARING FAHLORS

Mozgova N.N., Nenasheva S.N., Tsepin A.I. (IGEM RAS, Moscow, Russia), Borodaev Yu.S. (Dept. of Geology, Moscow Univ., Russia), Hariya Yu. (Hokkaido Institute of Technology, Sapporo, Japan)

Fahlores (tetrahedrite-tennantite series)

are the most wide-spread sulphosalt minerals. The ideal general formula $Me_{12}SMe_4S_{13}$, where Me (metals)= Cu (main element), Ag, Zn, Fe, Cd and others substituting metal elements, SMe (semi-metals)= As, Sb, Bi, Te is widly used and chemical composition data of fahlores are often calculated on the base of 13 anoms.

The negative correlation between Ag and S in fahlores has been reported by some authors. Poor microprobe analyses hase been discussed as possible reason of this (Hall, 1972; Shimada & Hirovatari, 1972). The decrease of S atoms in S2 site with increasing Ag content has been recently established by X-ray single crystal method (Rozhdestvenskay et al., 1989). According to Samusikov et al. (1988), disappearance of the 13-th S-atom is the cause of well known change of a curve in the plot a_0 -Ag content (at approximalely 4 Ag atoms).

The data base of 17 sets of 556 microprobe analyses of Ag-bearing fahlores from various kinds of ore deposits (authour's and published data) were processed using the statistics method. All microprobe data were normalized to 16 cations. The Ag content widely vary from 0,n to 9,6 atoms per formula unit (the most often to 6.5 atoms). Comparison of our microprobe analyses of the same three fahlore samples conducted in three laboratories (in Russia and in Japan) showed no significant influence of different analytical conditions on determination of composition of the minerals.

The results obtained show as follows:

1. The S contents in Ag-bearing fahlores widely vary and often are noticeably less then 13 atoms per formula unit.
2. The negative correlation between S and Ag contents exists in such minerals of different types of ore deposits and fit a linear equation to the results.
3. The inclination of these linear Ag - S relations appreciably varies in different kinds of ore deposits as well as in different pairs of co-existing fahlores and various generations of fahlores on the same deposits.
4. The younger (newformed after metamorphism) fahlores contain less S concentration than the early stage samples in metamorphosed stratiform polymetallic deposit (Rajpura-Dariba, India).

These results allow as to conclude:

1. The main reason of variation of Ag - S relations is evidently geochemical environment during formation of fahlores (especially S fugacity).
2. The widely used formula calculation on the base of 13 S atoms is not correct for Ag-bearing fahlores.
3. The decrease of S content from ideal 13 S atoms may hardly be responsible for the known change of the a_0 - Ag relation because of monotonucs character of Ag - S correlations. This point needs further studies.

THE EFFECT OF Na-BEARING THERMAL SOLUTIONS ON Ca-Mg-BENTONITE SORPTION OF Sr AND Cs.

Mukhamet-Galeyev A.P, Kudrin A.V, Nikonov B.S.
(Inst. of Ore Deposit Geolology & Geochemistry, Moscow)

A great part of radioactive wastes have been solidified into Al-P-Na glass matrix in Russia. Sodium is the most soluble and mobile component of the matrix. Ca-Mg-bentonite is very suitable material for a sorption barrier and rather typical mineral for a weathering crust of basic rocks on a possible repository area. Thus the goal of this paper was to investigate the effect of heated Na-bearing solutions on Ca-Mg-bentonite sorption of Sr and Cs, which are ones of the most principal mobile fission products.

Bentonite samples were treated by 0.1, 0.3 and 1.0 m NaCl solutions at 170, 210 and 250°C during 0.5-6 months.

As XRD and solution analysis show the bentonite alterations were mainly limited exchanging Ca and Mg by Na, which proceeded at high temperatures slower than at 20°C. The Si concentrations were caused by quartz solubility, which do not depend on NaCl contents, but increase with temperature growing. Al values were two orders of magnitude more than those of kaolinite solubility with quartz existence.

Sorption isotherms of Sr and Cs on the untreated bentonite have been fitted by Freundlich equation (fig):

$\log[Sr]_s = 1.13\pm0.13 + 0.561\pm0.035 * \log[Sr]_l$

$\log[Cs]_s = 1.66\pm0.13 + 0.740\pm0.050 * \log[Cs]_l$

where $[]_s$, $[]_l$ are respectively Sr and Cs sorbent (meq/g) and solution (meq/mL) concentrations. The sorption of Sr has been three times better than that of Cs at 10^{-6} meq/mL solution content, but the Sr isotherm slope was less than that of Cs, so the sorption of the elements have been equal at 10^{-3} meq/mL.

The action of NaCl solutions at 170-250°C resulted significant increasing of the sorption of both Sr and Cs (fig). Particularly, the isotherm slopes grew with Na content in solution, and the isotherm intersections increased with temperature. The distribution ratios of both Sr and Cs have been enlarged more than 5 times.

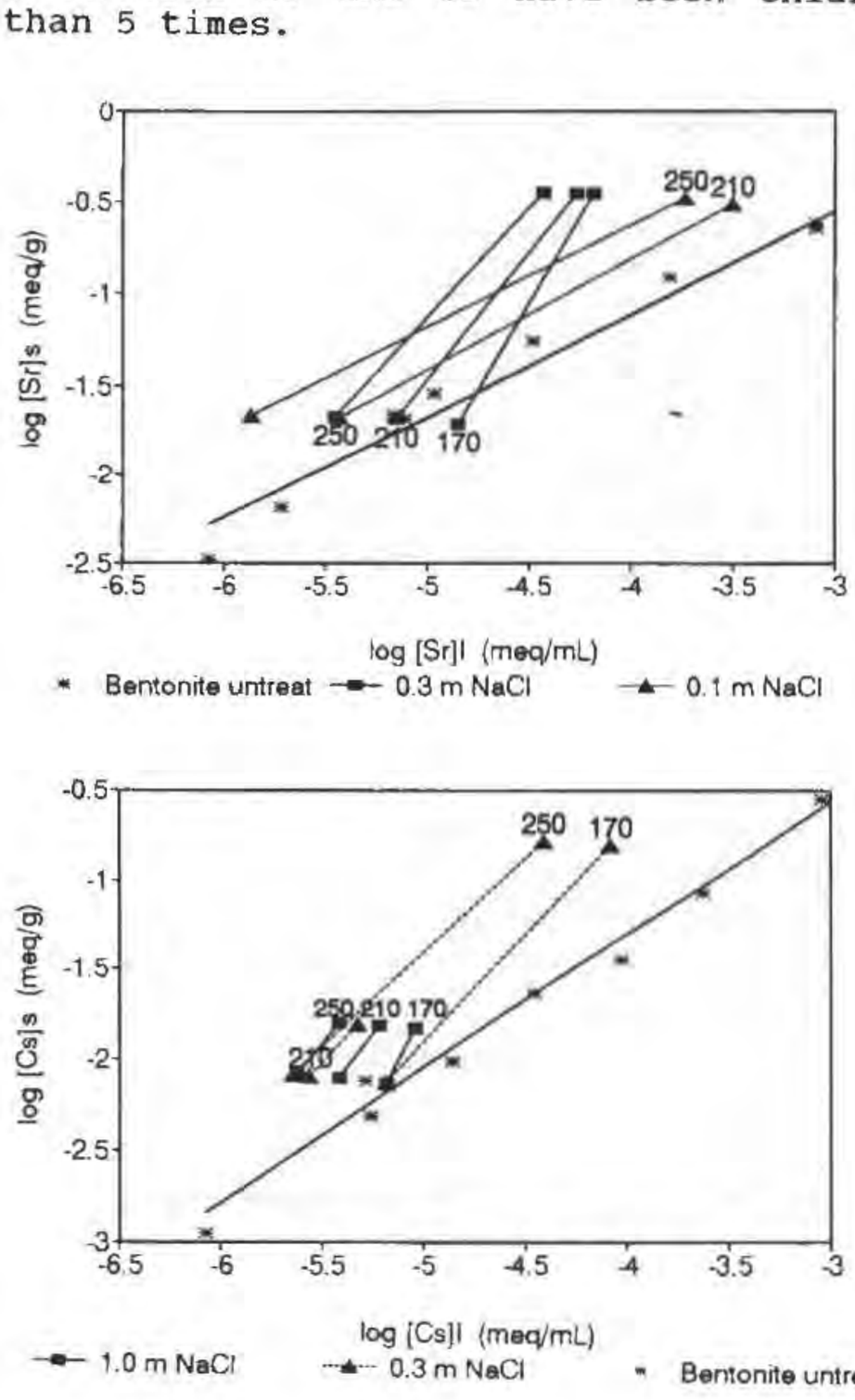

Figure. The sorption isotherms of Sr and Cs on Ca-Mg-bentonite untreated and treated in 0.1-1.0 m NaCl solutions at 170-250°C.

GARNET-BIOTITE GEOTHERMOMETER: A RE - CALIBRATION

Mukhopadhyay B., Holdaway M. J. (Dept. Geol. Sci., SMU), Guidotti C. V. (Dept. Geol. Sci., Univ. Maine), Dyar M. D. (Dept. Geol. & Astron., West Chester Univ.), Dutrow B. L. (Dept. Geol. & Geophys., LSU)

The garnet-biotite geothermometer is the only mineralogic thermometer that can be applied to the medium grade pelitic metamorphic rocks. Several authors have calibrated this thermometer based on the original Fe-Mg partitioning experiments of Ferry and Spear (1978). Problems exist with each of these calibrations.

We have used Ferry-Spear's (1978) experimental data to obtain a garnet-biotite geothermometer by taking into account: (1) correct $\ln K_D$, (2) a minor correction for Fe^{3+} in garnet and biotite (in light of recent Fe^{3+} determinations), and (3) a correction for nonideality of Fe-Mg garnet according to the model of Hackler and Wood (1989). This calibration yields the equation (T in K, P in bar):

$$T = \frac{48476.78 + 0.311 * P + 3RT\ln(\gamma_{Mg}^{Gt} / \gamma_{Fe}^{Gt}) + 3RT\ln(\gamma_{Fe}^{Bt} / \gamma_{Mg}^{Bt})}{18.91 - 3R\ln K_D}$$

which is solved by the method of iteration because of the temperature dependent γ terms on the right hand side of the equation.

We have re-evaluated all available experimental phase equilibria, calorimetric, X-ray diffraction, and natural Mn-Mg partitioning data for quaternary Ca-Mg-Fe^{2+}-Mn garnets. This results in a much improved set of a-X relationships with the following Margules parameters (in J, K, bar) that are used in conjunction with the formulations presented by Mukhopadhyay et al. (1993) to obtain the $RT\ln(\gamma_i/\gamma_j)$ terms:

$W_{FeMg}^{G} = -11600 + 10.4T - 0.030P$; $W_{MgFe}^{G} = 32000 - 20.0T + 0.020P$;
$W_{FeCa}^{G} = 7770 + 0.099P$; $W_{CaFe}^{G} = 2620 + 0.064P$;
$W_{MgCa}^{G} = 27000 - 28.4T + 0.177P$; $W_{CaMg}^{G} = 72000 - 8.0T + 0.050P$;
and $W_{MgMn}^{G} = W_{MnMG}^{G} = 19000$ (all pfu).

We have applied this calibration to 72 coexisting garnet-biotite pairs from graphite-ilmenite- bearing aluminous rocks of staurolite-, staurolite + andalusite-, staurolite + sillimanite-, and sillimanite-bearing assemblages of M3 in west-central Maine, USA which crystallized at about 3.1 kbar (Holdaway et al., 1988). For these rocks, $Fe^{3+}/(Fe^{2+} + Fe^{3+})$, H_2O, and F of biotite have either been analyzed or estimated by grade. Garnet compositions are peak-T compositions with a 2% correction for Fe^{3+}. Application of the garnet-biotite geothermometer to this data base tightly constrains (2.54 % average standard deviation per zone) T to values about 50°C higher than realistic values if Fe^{2+}-Mg-Al-Ti mixing in the octahedral site of biotite is assumed to be ideal. A value of -9000 J pfu for ΔW_{Al} in biotite corrects for this discrepancy. This correction yields T-values that are consistent with the aluminum silicate phase diagram of Holdaway and Mukhopadhyay (1993). For the low Ti content of these biotites, a similar ΔW_{Ti} correction is not necessary. The -9.0 kJ value of ΔW_{Al} is reasonable in light of natural paragenetic data. Further experimental data are needed to constrain ΔW_{Ti} and ΔW_{Al}. The assumption of ideal Fe-Mg mixing in biotite is consistent with natural observations.

References:

Ferry, J. M., & Spear, F. S. (1978): Contrib. Mineral. Petrol., **66**, 113-117.

Hackler, R. T. & Wood, B. J. (1989): Am. Mineral. **74**, 994-999.

Holdaway, M. J. & Mukhopadhyay, B (1993) Am. Mineral. **78**, 298-315.

Holdaway, M. J., Dutrow, B. L., & Hinton, R. W. (1988) Am. Mineral. 73, 20-47.

Mukhopadhyay, B., Basu, S., & Holdaway, M. J. (1993) Geochim. et Cosmochim. Acta, **57**, 277-283.

CRYSTAL-CHEMISTRY OF IRON AND TITANIUM FROM NATURAL CLAY MATERIALS

Muller J-P. (*ORSTOM, Dépt. TOA and Lab. de Minéralogie-Cristallographie, Univ. de Paris 6 et 7*), Allard T., Malengreau N., Lauquet G. and Calas G. (*Lab. de Minéralogie-Cristallographie, Univ. de Paris 6 et 7*), Delineau T. (*Lab. Environnement et Minéralurgie, ENSG Nancy*).

Iron and titanium are ubiquitous elements in clay materials. They can be substituted in the clay lattices or expressed as separated phases like oxides, oxyhydroxides or gels. Moreover, the latter can form coatings or inclusions. It is of a special importance to determine the different forms under which Fe and Ti occur because they (i) can be used as witnesses of physico-chemical conditions of formation and evolution of clay materials, (ii) play an important role in the reactivity of these materials and during the transfer and exchange of matter in the environment and, (iii) affect the quality of commercial clays. However, the location of Fe and Ti with respect to clay(s) structure is often uncertain, on account of the low level of Fe and Ti concentrations encountered in most natural samples as well as of the finely divided nature of Fe- and Ti-phases, which preclude the use of conventional methods. The objective of this paper is to demonstrate that (i) diagnostic absorption bands in Electron Paramagnetic Resonance (EPR), in second-derivative Diffuse Reflectance Spectroscopy (DRS; in the visible and UV regions) and in FTIR diffuse reflectance (in the near and mid-infrared regions; NIR and MIR) allow analysis of the status of trivalent iron and of titanium in natural clay materials and, (ii) these spectroscopies allow the detection of Fe and Ti down to 1-100 ppm, on account of their high sensitivity. Spectra of raw and chemically treated kaolins from different environments, including reference samples, will be used as examples.

Diagnostic spectral features for the various Fe- and Ti-species in kaolins were defined using experimental spectra of natural and synthetic, reference samples and calculated spectra: (1) EPR signals show the presence of ferric ions in two distinct sites in the structure of kaolinite, referred to as $Fe_{(I)}$ and $Fe_{(II)}$; although both correspond to substituted iron, they are distinguished by the intensity of site distortion, $Fe_{(II)}$ being substituted for Al^{3+} and related to domain of high "crystallinity" (Muller & Calas, 1993; Gaite *et al.*, 1993); (2) absorption bands in the NIR (at 7025 cm^{-1} and 4465 cm^{-1}) and in the MIR (at 875 and 3598 cm^{-1}) are also due to iron in $Fe_{(II)}$ sites (Delineau *et al.*, 1994); (3) DRS in the visible region and EPR spectrometry enable definition of the size, the nature and the distribution of Fe-phases (Malengreau *et al.*, 1994a); (4) DRS in the UV region enables distinction of features due to rutile, anatase and Ti-gel, at 24810, 27860 and 29400 cm^{-1}, respectively (Malengreau *et al.*, 1994b). One striking result is that, while oxides and/or oxyhydroxide-like phases coat kaolinite particles, Fe- and Ti-gel-like phases are often occluded between kaolinite lamellae.

References:

Delineau, T., Allard, T., Muller, J-P., Barres, O., Yvon, J., Cases, J-M. (1994). *Clays Clay Minerals* (in press)

Gaite, J. M., Ermakoff, P., Muller, J-P. (1993). *Phys. Chem. Minerals*, **20**, 242-247.

Malengreau, M., Muller, J-P, Calas, G. (1994a). *Clays Clay Minerals* (in press)

Malengreau, M., Muller, J-P, Calas, G. (1994b). *Clays Clay Minerals* (submitted)

Muller, J.P. & Calas, G. (1993). In *Kaolin Genesis and Utilization*, H. H. Murray, W. M. Bundy and C. C. Harvey, eds. The Clay Minerals Society of America, Boulder, Colorado, 261-289.

GEOCHEMISTRY OF SULPHID INCLUSIONS AND TREVORITE FROM VOLCANIC ROCKS OF BAIKAL RIFT ZONE.

Murav'yeva, N.S., Senin, V.G., Vernadsky Inst. Geochemistry &Anal. Chemistry Russian Academy of Sciences, 19 Kosygin st., Moscow 117975, Russia

Sulphides from Neogene-Quaternary volcanic rocks of Baikal Rift Zone (BRZ) occur as inclusions in mega- and phenocrysts, in pyroxenite xenoliths and as individual grains. Sulphides involve pyrrhotite, monosulphide solid solution (MSS), pentlandite, pyrriteand chalcopyrite. The sulphides host rocks are represented by differentiated effusive series. The rock compositions vary from alkaline basalts to intermediate and acid rocks

Microprobe measurement showed Ni contents in sulphides from BRZ range from 0.03 wt.% to 21.26 wt.% and are inversely correlated with ferrous (Fe) contents. Sulphides formed during different stages of basaltic magma's evolution are revealed to have different Ni contents: in high pressure products - megacrysts and pyroxenite nodules Ni content is > 1 wt.% Ni, while in sulphides from basaltic differentiates Ni content is < 1 wt.%. Ni.

The sulphides from the pyroxenite nodules are nonuniform in mineral and chemical composition. Ni contents in sulphides from.a pyroxenite nodule are often within a range of Ni contents for megacrysts from the rocks of one volcanic field..Ni-magnetites and trevorite ($NiFe_2O_4$) in pyroxenite nodules from Tokinsky Stanovik Mountains were discovered. Trevorite, the rare terrestrial mineral, probably is singenetic with sulphides.

The structure - morhpological features coupled with composition features suggested that the origin of sulphides from the rocks of Baikal rift zone is geterogenic. Some of them represent the products of liquid immiscibility, while for other ones the fluid phase must .played an important role. The fluid related with mantle metasomatism could be responsible for sulphides on the early stages of evolution of alkaline basaltic magmas, wheras the sulphides from basaltic differentiates could be related with fluids generated on late (pre-eruptive) stages of the magma degassing

NEW DATA ON MINERALOGY OF Au-Sb DEPOSITS OF TIEN-SHAN

Mustafin S.K.(Institute of geology of National Academy of sciences of Kirghiz Republic).

Au-Sb deposits of Tien-Shan are represented by jasperoid and vein types. The mineral composition of these deposites is diverse. Their hypogeneous mineralization was studied.

1. The Hg-bearing gold and stistaite were discovered in carlyne-type ores.

Hg-bearing gold is associated with quartz. It is represented by irregular grains 0.1-1mm in size. Their composition is quite uniform: (mas.%) Au - 97.3; Hg - 2.5; Ag <0.1.

Grains of stistaite 0.1-4mm in size forms intimate eutectoidal intergrows with native Pb. Most homogenous stistaite grains shows composition: Sb - 45.96-48.07; Sn - 36.60--40.48; Pb - 11.01-11.73; As - 1.14-1.37; Te - 1.48. Composition of native Pb is: Pb - 82.30--91.16; Sb - 2.06-6.85; Sn - 2.70-6.46; Te - 0.13-0.26. Aggregates of stistaite and native Pb contains also up to 0.0n % Cu, Zn, Hg, S, up to 120 ppm Bi and 20 ppm Ag.

2. At the vein-type deposits for the first time the folloving minerals and varieties were discovered: native Sb, hubnerite, Sb-bearing gold, Se-bearing Au-Ag sulphide.

Native Sb forms aggregates up to 100mm in size and partly is replaced by stibnite. Impurites in native Sb are:(ppm) Au -0.9; Ag - 5; Bi - 120 and As (0.1-0.7 mas.%). The composition of the gaseous phase of fluid inclusions in native Sb is (vol.%): N_2 - 82.2; O_2 - 13.4; CH_4 - 0.2; C_2H_4 - 0.1; CO_2 - 0.2; CO -0.3; H_2O - 1.6.

Hubnerite forms crystals 0.05-2mm in size within massive stibnite ores. These crystals have compositional zoning. Composition of the core zones is: MnO - 23.20-24.11; FeO - 1.54--1.73; WO_3 - 74.25-75.10 and MnO - 17.90-21.18; FeO - 4.07-5.17; WO_3 - 74.76-76.93 - at the rim zones.

Sb-bearing gold is a phase formed in result of aurostibnite decomposition. It have structures of "mustard gold" and forms aggregates 0.01-4mm in size. Sb content in this gold can reach 2.60 mas.%.

Se-bearing Au-Ag sulphide shows composition (mas.%): Au - 32.47-41.52; Ag - 46.32-58.59; S - 7.24-9.68; Se - 0.55-2.14. Unsimilar to compositions of known Au-Ag sulphides uytenbogaarditite and petrovskaite, which have been discovered earlier. Inclusions of such phase have crystal-like form (50 μm in size) were founded in electrum (mas.%): Au - 60,64-61,68; Ag - 35,62-38.14; Se - 0.44-0,75.

These minerals may be considered as indicators of ore-forming processes.

MAGMA CHAMBER REPLENISHMENT BY PICRITIC MATERIAL IN THE LESOTHO BASALT FORMATION, SOUTHERN AFRICA

C.A. Myburgh, H. de Bruiyn, W.A. van der Westhuizen and G.J. Beukes (*Dept. of Geology, Univ. of the OFS)*

The well known Karoo Sequence of Southern Africa covers large tracts of the subcontinent and is characterised by extensive volcanic activity at the final stages of its development. The Maluti Mountains of Lesotho are predominantly composed of a series of chemically homogeneous, highly amygdaloidal basaltic lava flows of varying thickness. Picrites have previously been described along with the basalts, olivine basalts and andesites. Subordinate intercalated pyroclastics and sandstones occur intermittently in the volcanic pile.

A 50 m thick basaltic lava flow in the Katse Dam area consists of ophitically and subophitically intergrown plagioclase and clinopyroxene at its highly altered base and top. No olivine is present at the top and only a few crystals were noted at the base. The centre of the flow is, however, dominated by cumulus olivine crystals and clinopyroxene phenocrysts and is chemically manifested by an enrichment in MgO, FeO, Ni and Cr and depletion in Al_2O_3 and CaO.

The presence of cumulate olivine crystals in the centre of the flow is ascribed to flow differentiation which indicates a greater flow velocity near the centre than at the margins. The development of olivine cumulates indicates a residence time in a magma chamber prior to eruption.

Changes in the chemical composition of this flow, relative to others in the area, indicates that it is the product of a magma chamber that has been replenished by a primative picritic magma.

EXPERIMENTAL, IN-SITU, HIGH-TEMPERATURE, HIGH-PRESSURE STUDIES OF RELATIONS BETWEEN PROPERTIES AND STRUCTURE OF SILICATE MELTS RELEVANT TO MAGMATIC PROCESSES.

Mysen, B. O. (*Geophysical Lab., Carnegie Institution of Washington, Washington DC, USA*)

The degree of polymerization (NBO/*T*) of natural magmatic liquids at 1 bar and moderate pressure range between 1 (e.g., basalt) and near 0 (e.g., rhyolite). Spectroscopic data (NMR, Raman) of silicate glasses and melts (at magmatic temperatures) in this NBO/*T*-range are consistent with coexistence of a small number of structural units in the materials (Q-species with 2, 1, 0 nonbridging oxygen per silicon, Q^2, Q^3 and Q^4). Alkali metals and alkaline earths connect across the nonbridging oxygens with oxygen coordination numbers derived from x-ray data suggested to range from 5 to 10 with an apparent positive correlation between the oxygen coordination number and the ionization potential of the metal cation.

The equilibrium among these units, $2Q^3 \Leftrightarrow Q^2+Q^4$, is a systematic function of bulk chemical composition [metal cations, Al/(Al+Si), $Fe^{3+}/(Fe^{3+}+Si)$, and Ti/(Ti+Si)], temperature (above the glass transition range), and pressure. In binary alkali silicate melt systems, the ΔH of the equilibrium ranges from -30 kJ/mol to 30 kJ/mol where ΔH correlates negatively with ionization potential of the metal. In alkaline earth silicate systems, the temperature effects are small. Increasing pressure drives the equilibrium to the right.

For typical alkali silicate melts the oxygen exchange frequency among the units derived by modeling ^{29}Si and ^{17}O NMR data increases from several kHz at 25°C to several hundred kHz at 1000°C. Viscosity and diffusivity derived from these data accord with results from direct experimentation.

The configurational changes above the glass transition temperature range resulting from the temperature-dependent species distribution contributes only 10-20 % of the total configurational heat capacity of the melts. The main contribution to the configurational properties appears to be in the metal-oxygen polyhedral changes. The logarithm of the activity coefficients for the Q-species at magmatic temperatures, $\ln \gamma^{Q_i}$, are linear functions of the $\ln X^{Q_i}$, where X^{Q_i} is the mol fraction of the species. At magmatic temperatures (>800°C) these relations among mol fraction and activity coefficient depend only on the mol fraction of the species (which, however, is a function of temperature and bulk composition).

$Al^{3+} \Leftrightarrow Si^{4+}$ substitution is yield positive correlation between Al/(Al+Si) and ΔH of the speciation expression for highly polymerized melts (NBO/$T \leq 0.5$). For more depolymerized systems (e.g., NBO/T=1, haplobasalt,), an additional expressions, $3Q^2 \Leftrightarrow 2Q^2+Q^3$, is required. The ΔH for the latter expression is positive for melts with large electropositive metal cations (e.g., Na^+ and K^+), but with smaller charge-balancing cations (e.g., Li^+) the ΔH is negative. The preferred substitution of Al^{3+} in highly polymerized structural units and the concomitant changes in unit distribution can be correlated with viscosity changes as a function of Al/(Al+Si) of the melts.

Components such as Ti^{4+} and Ti^{4+} affect rheological and thermodynamic properties greatly. Unusual variations in behavior with temperature, pressure, and bulk compositions are also observed. These variations are consistent with structural data which indicate multiple coordination states of these cations. Low concentrations tend to favor network-modifying roles (e.g., octahedral) with gradual transformation to tetrahedral concentration with increasing concentration. Increasing pressure may cause coordination transformations from tetrahedral to octahedral. Increased temperature has the opposite effect.

MODELING HAPLOBASALTIC LIQUID STRUCTURE AT HIGH TEMPERATURE: EFFECT OF ALKALI METAL AND ALUMINA CONTENT

Mysen, B. O. (*Geophysical Lab., Carnegie Instn. Washington, Washington DC, USA*)

The anionic structure of aluminosilicate melts between 25° and 1460°C has been determined along the joins $Li_2Si_2O_5$-$Li_2(LiAl)_2O_5$ (LS2-LA2) and $Na_2Si_2O_5$-$Na_2(NaAl)_2O_5$ (NS2-NA2) with micro-Raman spectroscopy. In these systems, Li^+ and Na^+ serve both to charge-balance Al^{3+} in tetrahedral coordination and as network-modifiers. Raman spectra of all samples indicate that Al^{3+} is in tetrahedral coordination so that the NBO/*T* equals unity for all compositions studied. This NBO/*T* value mimics that of basaltic liquids. The Al/(Al+Si) ranges between 0 and 0.3. The Al/(Al+Si) covers the range of most natural magmatic system. The range in ionization potential of the metal cations covers that of most network-modifying cations in magmatic liquids with the exception of Mg^{2+}. The influence on the melt structure of principal chemical components in natural basaltic magmatic systems can be addressed, therefore, from structural studies in the LS2-LA2 and NS2-NA2 systems.

In the Al-free endmember systems, the three species, Q^4, Q^3, and Q^2 coexist and the expression, (1) $2Q^3 \Leftrightarrow Q^2+Q^4$, describes the equilibrium. The ΔH for reaction (1) (ΔH_1) is 17.1±0.7 kJ/mol for NS2 melts, whereas its value is only 6.8±1.3 kJ/mol for LS2 melts. Substitution of Na- or Li-charge-balanced Al^{3+} for Si^{4+} results in stabilization of an additional, more depolymerized structural unit, Q^1, and an additional equilibrium, (2) $3Q^2 \Leftrightarrow 2Q^2+Q4$, is needed for a complete description of the equilibria. The LS2-LA2 system, the ΔH_2 for this reaction ranges between ~0 and -87 kJ/mol, whereas in the NS2-NA2 system, the ΔH_2 is positive with values between 16 and 37 kJ/mol. Equilibrium (1) is also affected by equilibrium (2) in the Al-bearing melts, so that in the NS2-NA2 melt system, the reaction is now driven to the left with temperature (ΔH_1 = -10 - -15 kJ/mol), whereas in the LS2-LA2 system, equilibrium (1) shifts more strongly to the right with temperature than in the absence of Al (ΔH_1 is positively correlated with Al/(Al+Si) in the range 6 - 48 kJ/mol).

The temperature-dependence of the Raman frequencies of (Si,Al)-O^- stretch bands (O^- denotes bridging oxygen) is linear in the NS2-NA2 system with the temperature-dependent frequencies, $1/\nu(\partial\nu/\partial T)$, in the range of -1.4•10-5 K^{-1} to -4.1•10-5 K^{-1} (R-values from regression between 0.98 an 1.00). The absolute value of $1/\nu(\partial\nu/\partial T)$ is greater for bands assigned to (Si,Al)-O^- stretching in structural units with the largest number of nonbridging oxygens (i.e., Q^1). The Al^{3+} in NS2-NA2 melts and glasses resides principally in the most polymerized of the coexisting structural units because the Raman frequencies of (Si,Al)-O^- stretch bands in more depolymerized units is relatively insensitive to Al/(Al+Si). Qualitatively similar behavior was observed for the $1/\nu(\partial\nu/\partial T)$ of the analogous bands in spectra of LS2-LA2 glasses and melts in the Al/(Al+Si) range 0-0.2. All the (Si,Al)-O^- stretch bands, however, are considerable more sensitive to Al/(Al+Si) in the LS2-LA2 system than in the NS2-NA2 melt and glass system. This difference indicates that as the ionization potential of the charge-balancing cation increases, aluminum becomes more evenly distributed among the coexisting structural units. With Al/(Al+Si)>0.2, the $1/\nu(\partial\nu/\partial T)$-values for the 950 cm^{-1} [assigned to (Si,Al)-O^- in Q^2 units] and 1100 cm^{-1} [assigned to (Si,Al)-O^- in Q^3 units] bands in the spectra of LS2-LA2 melts change at temperatures between 1200° and 1300°C. This change might reflect a redistribution of Al^{3+} among the structural units at these temperatures.

Properties of magmatic liquids that depend on bond strength and distribution of structural units (e.g., thermochemical and rheological properties) depend, therefore, on the ionization potential of the metal cation(s) and on the Al/(Al+Si) of the melts. Activties of structural units, and, therefore, liquidus phase relations will be similarly affected.

PHASE RELATION OF CALCIC AMPHIBOLES IN HIGH PRESSURE AND TEMPERATURE

Na K.C. and Cho M. (*Dept. of Geological Sciences, Chungbuk National Univ. Cheongju, 360-763, Korea; Dept. of Geological Sciences, Seoul National Univ. Seoul, 151-742, Korea*)

Amphiboles approaching edenite, richterite, tschermakite, pargasite, sadanagite and tremolite solid solutions were synthesized at temperatures of 750-1,070℃ and fluid pressures of 0.5-20Kb in NCMASH system. Conventional hydrothermal technique and piston-cylinder apparatus were employed at low and high pressures, respectively. Gel mixtures of the edenite and sadanagite compositions, along with exess H_2O, were used as starting material.

Edenitic amphiboles(Amp) occur with clinopyroxene(Cpx) + forsterite(Fo) at high pressure(> 6Kb) and Cpx + Fo + 15Å sodic phase(Sph) at lower pressures. Both assemblages convert at high temperatures to an amphibole-free assemblage, Cpx + Fo + Sph. 15Å sodic phase persists to very high temperatures. In sadanagite composition, more edenitic amphiboles(Amp) coexist with Cpx + Sph, Cpx or spinel, Sph + corundum, zoisite + corundum, and Cpx + spinel + liquid. 10Å Sph is characteristic in this system. The boundaries between the observed assemblages are determined by more than ten reversal experiments using the mixture of low and high temperature products.

Compositions of synthetic amphiboles are variable depending on P, T, and mineral assemblages, and their ranges on the basis of 23 O atoms(anhydrous formula) are: Na^{A} = 0.68-0.96; Na^{M4} = 0.22-0.57; Al^{VI} = 0-0.57; and Al^{IV} = 0.47-1.00 in edenite composition. In particular, Al and Na contents vary significantly with mineral assemblages. For example, Al changes from 0.47-0.52 at 1Kb to 0.80-1.00 in the Amp + Cpx + Fo assemblages at 6-20 Kb. Edenitic substitution increases in intermediate pressure, on the other hand, tschermakitic substitution in high pressure. Edenitic and cummingtonitic substitutions increase with temperature. In sadanagite composition, their ranges are: Na^{A} = 0.86-0.99; Na^{M4} = 0.11-0.46; Al^{VI} = 0.34-0.49; and Al^{IV} = 0.73-1.36. Compositions of synthetic amphiboles in more aluminous environment are variable depending mainly on their mineral assemblages, and the most edenitic and pargasitic amphiboles occur in Amp + Cpx field at more than 10 Kb.

DIAMOND PARAGENESIS DIAGNOSTICS BASED ON OPTICAL CHARACTERISTICS OF STRUCTURAL NICKEL

V.A.Nadolinny[1], V.P.Afanasyev[2], N.P.Pokhilenko[2], V.M.Zuev[3], O.P.Yuryeva[1], S.M.Bezborodov[3], S.I.Mityukhin[3] ([1]*Institute of Inorganic Chemistry, Russian Academy of Science,* [2]*Institute of Mineralogy and Petrography, Russian Academy of Science,* [3]*"Almazy Rossii-Sakha" Co.*)

The investigations carried out recently permitted one to conclude that luminescent centers S2, S3 and 523.8 nm well known in diamonds were associated with the Ni impurity <1>. Since Ni is characteristic element of ultramafic parageneses practically to be absent in eclogite parageneses, the structural Ni impurity would be expected to find in the ultramafic paragenesis diamonds missing in eclogite paragenesis ones. The hypothesis was tested by investigation of more than 400 diamond crystals with preknow paragenetic belongment. It was found that the centers S2, S3 and 523.8 nm were absent in eclogite diamonds. In diamonds of ultramafic parageneses they are either present or absent but in this case instead of them (very seldom together with them) there are luminescent centers H3, H4 and 490.7 nm associated with plastic deformations. Antogonistic relations between Ni and deformation luminescent centers lead to conclusion that in the process of the plastic deformation there is as a rearrangement in electron state of Ni centers at the expense of electrons transfer to the brocken bonds in the dislocation cores as transformation of extended Ni defects. The coexistence of nickel and deformation centers is possible evidence of nonuniform deformation of crystals. The line of investigations seems very reasonable to evaluate the paragenetic belongment of diamonds, still requiring further studies to discovery all the types of Ni-centers and forms of their manifistication in the physical properties of diamond.

References:
V.A.Nadolinny, A.P.Yelisseyev (1993) *Diamond and Related Materials*, 3, 17-21.

Structural changes of $CaGeO_3$, $MgGeO_3$ and Mg_2GeO_4 under high pressure at room temperature

Nagai T. and Yamanaka T. (*Dept. of Earth and Space Science, Osaka Univ.*)

It has been reported that many materials become amorphous solids under high pressure at kinetically low temperature as exhibit a phase transition to a high pressure stable phase. Recently our group (Yamanaka et al., 1992) discussed pressure-induced amorphization of GeO_2(low-quartz form) and proposed that the amorphization is a precursor phenomenon of the transformation to high pressure stable phase. However, it is necessary to conduct more researches of the relationship between the mechanism and crystal structures systematically. In this study we focused on pyroxene and olivine structure which have basically closed packed oxygen atoms. The arrangements of the oxygen atoms of $CaGeO_3$(wollastonite form), $MgGeO_3$(clino-pyroxene form) and Mg_2GeO_4(olivine form) at ambient pressure and temperature approximates a cubic closed packing of first two and a hexagonal closed packing of the last.

$CaGeO_3$: In situ X-ray diffraction measurements by using a DAC up to 27 GPa at room temperature show that the diffraction profile of $CaGeO_3$ changes at about 6GPa and 15GPa. The change at 6GPa is characterized by the appearance of two new peaks and the disappearance of all wollastonite peaks except 101 diffraction peak. Two new peaks can be indexed as neither garnet nor perovskite which have been reported as high pressure stable phases of wollastonite type $CaGeO_3$. The 101 diffraction peak represents the stacking of close-packed oxygen layers. The profile is subsequently changed from about 15GPa. Two new different peaks, which have not been identified, appear and other diffraction peaks include the 101 diffraction peak of wollastonite type $CaGeO_3$, are vanished above 20GPa. Andrault et al. (1992) reported the change of the Ge-O bond length based on XAFS data of $CaGeO_3$ under high pressure. According to their data, the Ge-O distance of $CaGeO_3$ is quasi-constant up to 7GPa and increases from 7 to 12GPa and decreases again above 12GPa. They suggested that the coordination change of germanium from fourfold to sixfold occured. We concluded that there is some modification of wollastonite structure above 6GPa. The modification may be resulted from the coordination change of germanium, but the periodicity of the direction of oxygen stacking is retained. And above 15GPa, wollastonite type $CaGeO_3$ may transform to an unidentified phase.

$MgGeO_3$: In situ X-ray diffraction measurements by using a

DAC up to 35 GPa at room temperature show that the diffraction patterns of $MgGeO_3$ start to change at about 10GPa and only two peaks are visible at 35GPa. One peak may be indexed as a clino-pyroxene form but another may not be. And the peak is not assigned as illmenite and corundum forms of $MgGeO_3$. XAFS data by Andrault et al.(1992) indicated that the Ge-O bond length of $MgGeO_3$ decreases up to 8.5GPa and then increases at least up to 31GPa. It seems that some modification occurs around 10GPa as a result of the coordination change of germanium. And the modification may be led to an unidentified phase which has sixfold germanium atoms.

Mg_2GeO_4 : In situ X-ray diffraction measurements by using a DAC up to 35 GPa at room temperature show that all diffraction peaks of Mg_2GeO_4 vanish at between 25 and 30GPa. And after decompression no diffraction peak are observed. In the case of Mg_2GeO_4, pressure-induced crystalline to amorphous transition occurs and this transition may be irreversible.

Our X-ray diffraction data indicate that some modification of $CaGeO_3$, $MgGeO_3$ and Mg_2GeO_4 structures take place under high pressure at room temperature. It is suggested that such modification may be a precursor phenomenon of the transformation to a high pressure phase. However, the observed high pressure phases may not be identified to any high pressure phases reported before. And it seems to be depend on the degree of the modification that only Mg_2GeO_4 of three samples shows a pressure-induced amorphization. The modification in Mg_2GeO_4 may be smaller than that of $CaGeO_3$ and $MgGeO_3$ from the view point of germanium coordination.

References:

Yamanaka T., Shibata T., Kawasaki S. and Kume S. (1992). in *High Pressure Research* edited by Y. Syono and M. H. Manghnani, 493-501, AGU, Washington, D. C.

Andrault D., Madon M., Itie J. P. and Fontaine A. (1992). *Phys. Chem. Minerals*, **18**, 506-513.

Chemical state analysis of light-elements in earth and planetary minerals by SR-XANES microprobe

Nakai I. (*Science Univ. of Tokyo*), Terada Y. (*Univ. of Tsukuba*) and Tsuchiyama A. (*Univ. of Osaka*)

Introduction

Chemical state analysis of elements in a mineral provides useful information for the study of the origin and history of mineral formation and subsequent alterations of the mineral. However, it has been difficult to obtain two-dimensional information of the chemical state of light elements by conventional analytical techniques such as Mössbauer spectroscopy and ESR. In this study, we have applied the XANES (X-ray Absorption Near Edge Structure) technique to solve the above problem. This technique provides information on the electronic structure of an element in a sample. Especially, a combination of the XANES technique with X-ray fluorescence detection using a Si(Li) detector and Synchrotron Radiation (SR) X-ray micro beam makes it possible to obtain XANES spectrum of trace elements in a small sample area nondestructively. Here we report chemical state analyses of the light elements in some important meteorites and geological samples.

Experimental

We have measured the XANES spectra of Ti, Cr, Fe in some meteorites (chondrites: YAMATO691, Allende, Murchison, Krymka and Semarkona) and that of S in a sediment rock from Takanosu, Akita, Japan. XANES measurements were made using monochromatized radiation with Si(111) double crystals for Ti, Cr and Fe, and InSb(111) double crystals for S at the Photon Factory, KEK. Samples were placed on a XY stage in a vacuum chamber. Fine parallel beam of desirable size was obtained by a focusing mirror (BL-4A) or a set of vertical and horizontal slits (BL-8B).

Results and Discussion

Figure 1 shows the Cr-K XANES spectra of chondrules in the meteorites with reference to the spectrum of metallic chromium. It shows that chromium in the chondrule of Allende meteorite exists in the trivalent state. On the other hand, the spectrum of YAMATO 691 shows a doublet peak at the absorption edge indicating that both divalent and trivalent chromium exist in the chondrule as a component of a silicate. Clear existence of divalent chromium in a silicate phase has never been identified experimentally until this study. Our XANES spectra of the Ti and Fe-K edge also indicated the existence of trivalent titanium and metallic iron in the YAMATO 691 meteorite. Consequently, it is found that this meteorite was formed in a highly reducing condition.

Figure 2(a) shows a sketch of the sediment rock sample. The sample consists of two parts, the gray part and cream one. From the XANES spectra given in Fig. 2(b), it was observed that the gray part contains sulfur of both sulfide and sulfate, while the cream part contains sulfate sulfur. It is considered that this difference in the chemical state of sulfur was caused by weathering. In this way, we have established the chemical state analysis of the light elements in earth and planetary minerals.

We acknowledge the cooperation of Drs. S. Nakashima, K. Ogata and S. Hayakawa.

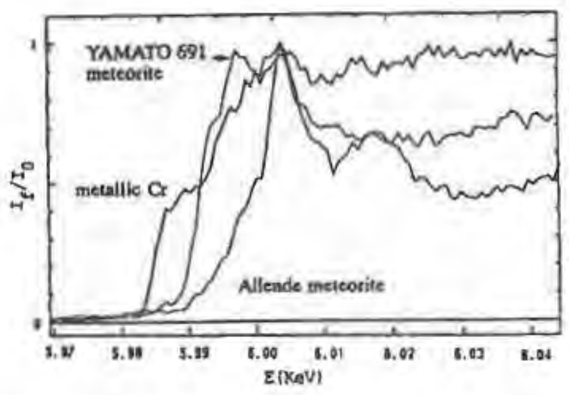

Fig. 1. Cr K-XANES spectra of metallic Cr, YAMATO 691 and Allende meteorites.

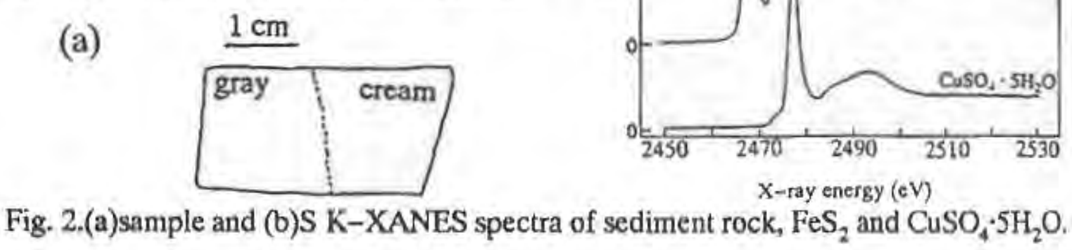

Fig. 2.(a)sample and (b)S K-XANES spectra of sediment rock, FeS_2 and $CuSO_4 \cdot 5H_2O$.

PRECISE DETERMINATION OF LATTICE PARAMETERS USING A GANDOLFI CAMERA FOR A VERY SMALL-SIZED CRYSTAL: AN APPLICATION TO POLYTYPES OF MOLYBDENITE

Nakamuta Y. (*Department of Earth & Planetary Sci., Kyushu University*)

A Gandolfi camera is a kind of Debye-Scherrer cameras and has a special attachment devised to obtain a powder pattern directly from a single crystal of down to 30 μm in size (Gandolfi, 1967).

In this study, the authors intended to determine precise lattice parameters of a mineral from a diffraction data obtained by a Gandolfi camera (57.3 cm in diameter). The powder diffraction data recorded on a film was read with a microdensitometer. A profile-fitting technique using a split-type pseudo-Voigt function was applied to determine diffraction-peak positions precisely. When the specimen was less than 100μm in size, the absorption error was found to be negligible. Therefore, lattice parameters were determined by the $\cos^2\theta$ extrapolation method after the correction for radius and shrinkage errors. Fig. 1 shows the $\cos^2\theta$

extrapolation for silicon. The plots of *a*'s calculated from individual diffraction lines are linear in the range from 2θ = 27° to 180°. The lattice parameter obtained is 5.4306(1) Å, which is in good agreement with that reported for silicon (5.43054(17) Å, Parrish(1960)).

Molybdenite has the two modifications, $2H_1$- and 3R-polytypes. $2H_1$-molybdenite occurs more abundantly in nature than 3R-one, and the latter is often associated with $2H_1$-molybdenite. The precise determination of their lattice parameters by a conventional method using a diffractometer is usually very difficult because of their eminent basal cleavage and the coexistence of both polytypes in most samples containing 3R-molybdenite. By using a Gandolfi camera, each fine-grained molybdenite crystal picked up from a mixture of $2H_1$- and 3R-polytypes was found to have an individual polytype, then the precise lattice parameters of it could be determined on the basis of the powder data obtained by a Gandolfi camera. The lattice parameters obtained for $2H_1$- and 3R-molybdenites are a= 3.1601-3.1609 Å, c= 12.290-12.301 Å and a= 3.1624-3.1635 Å, c= 18.369-18.387 Å, respectively.

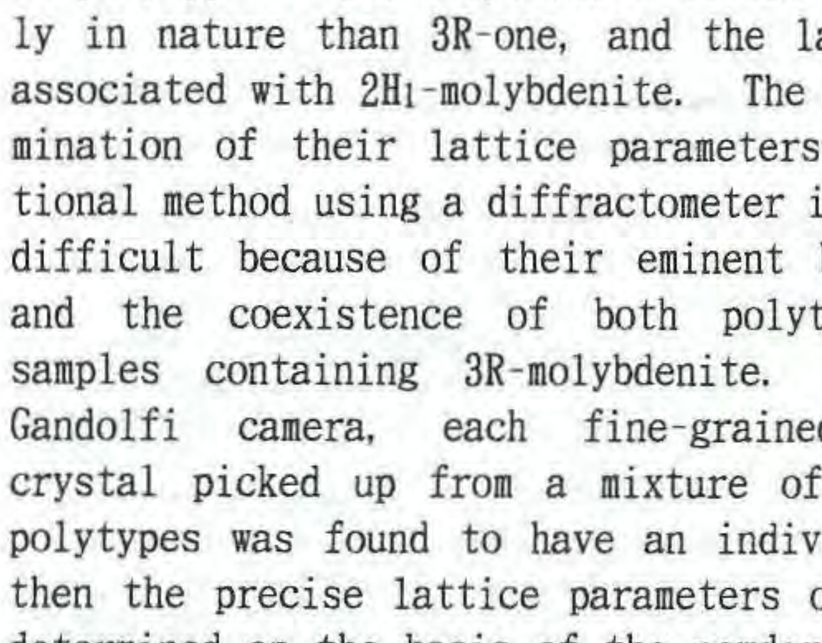

Fig. 1 Plots of *a* against $\cos^2\theta$.

References:
Gandolfi, G. (1967). Miner. Petrogr. Acta, **13**, 67-74.
Parrish, W. (1960). Acta Cryst., **13**, 838-850.

Anti-rapakivi mantled feldspar textures in alkaline volcanic rocks from Oki-Dogo, Japan

Nakano S. (*Dept. of Earth Sci., Shiga Univ.*)

Anti-rapakivi mantled feldspars consisting of plagioclase (or anorthoclase) cores and sanidine rims are commonly found in alkaline volcanic rocks (lava and dyke) from Oki-Dogo island, Japan. The feldspar textures are much variable in a crystal and in each crystal. The three characteristic cases were already studied: hypersthene-augite trachyte lava (Nakano,1992), alkali rhyolite lava (Nakano & Suwa, in press) and olivine-hedenbergite trachyte sheet (Nakano & Akai, 1992).

The feldspar textures consist of two contrasting types: one is microscopically complicated two-feldspar textures varying from mantled feldspars to perthitic feldspars, and another is fine cryptoperthitic textures. The former is considered to record magmatic resorption processes (Rahman and Mackenzie, 1969: Nekvasil, 1992). The latter show subsolidus exsolution process after the magmatic process. The cryptoperthitic textuers are nearly common in all the rocks. The common features of the microscopic two-feldspar textures have been also recognized, which is independent of rock type and occurrence but with a systematic variation through the rocks. This fact shows that the same magmatic process forming mantled feldspars and related two-feldspar textures occurred inevitably in each rock independently of subsolidus cooling, and supports the interpretation that they formed during ineviatble crystallization course with magmatic resorption reactions.

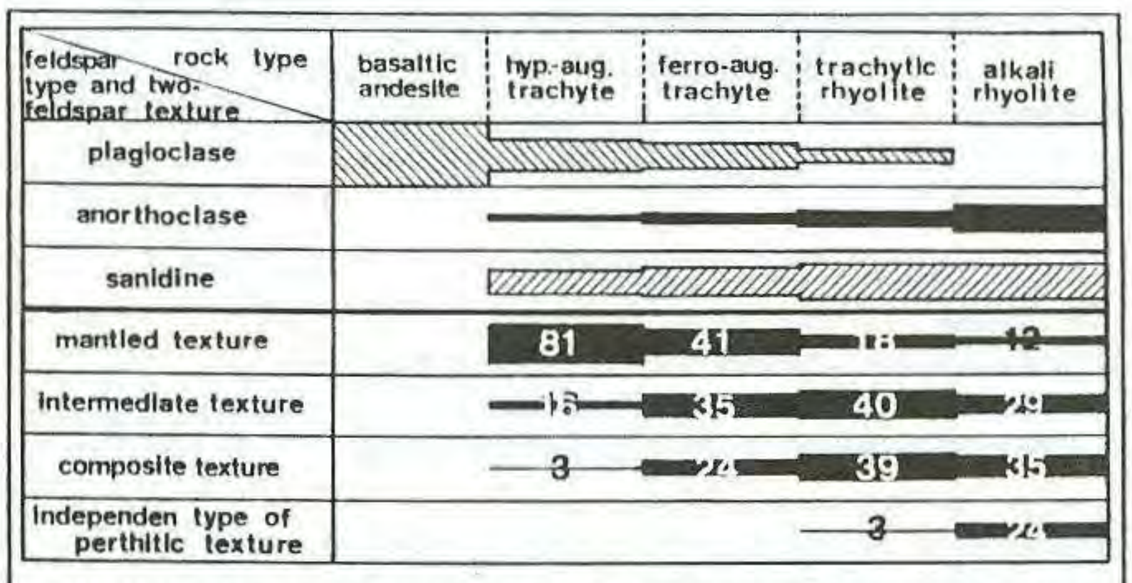

Variation diagram of mantled feldspar textures through the lava rocks with an increasing order of differentiation index towards the right, showing frequency of phenocrystic-feldspar types and textures. "Intermediate" means modifications of mantled texture, and "composite" means those apparently with perthitic texture.

● APPLIED MINERALOGY FOR TESTING AND DETERMINING QUALITY OF THE ENGINEERING MATERIALS

Nakhla F.M. *(Dept. of Mining Eng., Univ. of Cairo)*

Over the past two decades, applied mineralogy has made considerable progress to characterize many engineering materials indispensable for the rapidly developed modern technology that is controlling the different stages of industrial production. The most important engineering materials include metallic and non-metallic industrial minerals, coal, iron, steel, alloys, electronic substances, building and crushed stones, gravels, sand, glass, refractories, ceramics, bricks, cement, the insulating materials, plastics, wood, rubber, paints and paper.

Methods of applied mineralogy provide accurate and highly reliable information for revealing the physical, chemical, mineralogical, textural, structural and mechanical properties of the solid materials. These characteristics determine the quality of the engineering substances and their appropriate utilization in the industrial and technical fields. Mineralogical study may also help to solve certain problems for locating the most favourable sites of important engineering projects, foe example dams, tunnels, bridges, the railway tracks, thermal and nuclear power plants, building new installations of the mining,

metallurgical, chemical and petroleum industries for the socioeconomic development.

The role of applied mineralogy for testing and determining quality of the engineering materials is displayed in the following examples.

1. Identification of various properties of soils, nature and composition of different rock types, by the relevant methods of applied mineralogy, would decide most suitable locations for laying down the foundations of important engineering constructions. The specifications and quality of engineering materials and composition of various ingredients forming the concrete aggregate are confirmed by highly reliable methods such as microscopic examination, electron probe scanning and X-ray diffraction analysis.

2. Since the advent of the industrial age onwards, various methods of applied mineralogy have been in service of mineral industry starting from the prospection, detailed exploration, sampling, the economic evaluation, through exploitation by the suitable mining methods, mineral processing, to the extraction of valuable metals and marketing.

3. In metallurgy, nature, composition, textures and structures of metals, alloys and their slags inclusions, particularly in steel, may influence their mechanical properties, resistance to corrosion and uses in engineering purposes. The slag inclusions in steel are commonly in the form of synthetically formed opaque or transparent minerals. The opaque inclusions consist of graphite, sulphides as alabandite or pyrrhotite, and some oxides, for example magnetite, ilmenite, chromite and rutile. The transparent inclusions occur in the form of silicates such as fayalite, enstatite, wollastonite, spessartite, various forms of silica and some oxides. Microscopic study by the polarized transmitted and reflected light is the principal method for determining mineralogy of the slag inclusions in iron and steel.

4. Different types of clay minerals of high quality and standard specifications are extensively used in the chemical, metallurgical and petroleum industries. Quality and uses of clays in various engineering and industrial purposes could only be revealed and ascertained by adopting relevant techniques commonly used in applied mineralogy.

THE COMPOSITION OF THE Ni-Cu ORES OF THE NORIL'SK REGION

A.J. Naldrett and **M. Asif**, Department of Geology, University of Toronto; **V.A. Fedorenko**, TsNIGRI, Moscow; **V.Ye. Kunilov** and **A.I Stekhin**, "Noril'sk Nickel", Noril'sk; **P.C. Lightfoot**, Ontario Geological Survey, Sudbury; **N.S. Gorbachev**, Institute of Experimental Mineralogy, Moscow

Three principal intrusions host Ni-Cu-PGE sulfide mineralization in the Noril'sk mining camp, the Noril'sk I, Main Talnakh and Northwest Talnakh (also known as Kharayelakhsky) intrusions. This paper is concerned with the composition of the ores associated with these bodies. Three principal ore types are present; disseminated sulfide in picritic- and taxitic-gabbro dolerite; massive ore forming sheets at the base of the intrusions (or within the underlying country rocks as at the Northwest Talnakh intrusion) and "Copper ore" which forms a halo around massive ore and also occupies zones of brecciated country rock (both argillite and dolerite) at the tops of intrusions. Analytical data obtained by us on samples selected systematically from drill core, and collected underground and from surface stockpiles of ore from specific underground locations, have been combined with mine data that was made available to us.

It is found that in the case of all three intrusions, Pt, Pd, and Au increase and Rh, Ir, Ru and Os decrease with increasing Cu; Ni shows little change with variation in Cu until Cu exceeds about 15 wt% when recalculated to 100% sulfide, where-upon it starts to decrease. When data are recalculated to metal content in 100% sulfide, it is found that the metal content of the sulfides of the disseminated ore is characteristic of a given intrusion but varies greatly between the three intrusions. That from the Noril'sk I intrusion is highest with average Ni and Cu (in wt%) and Pt, Pd, Rh and Ir (in ppm) being 6.62, 15.97, 60, 106, 3.00 and 0.42 respectively; disseminated ore from the Main Talnakh intrusion averages 6.78, 15.05, 25, 65, 1.75 and 0.23 respectively; while that from the Northwest Talnakh intrusion averages 3.96, 9.48, 5.40, 193, 0.30 and 0.036 respectively. In each case the disseminated and copper ore describe a trend with copper that is significantly enriched in Pt and Au with respect to Cu in comparison with the trend described by the massive ore. Pd in massive, disseminated and copper ore all lie on the same trend, although the massive ore is poorer in both Cu and noble metals than the other two ore types. Although they decrease with increasing Cu, Rh, Ir, Ru, and Os are higher at a given Cu content in the disseminated and copper ore than in the massive ore.

All of the above characteristics are attributed to fractional crystallization of mss (monosulfide solid solution) from a single sulfide liquid. The massive ore is highly enriched in cumulus mss; the copper ore, which forms as a halo around the massive ore, represents fractionated liquid that has seeped away into the enclosing sediments as fractionation has proceeded. The disseminated ore has crystallized with less efficient separation of cumulates and fractionating liquid. The compositional trends can be modelled assuming the following partition coefficients between mss and sulfide liquid ($D^{mss/sul.\ liq.}$); Cu = 0.1; Pd = 0.1; Pt = 0.05; Au = 0.001; Rh = 4; Ir = 4.

The differences between ore associated with each of the three intrusions can be modeled as a consequence of the sulfides having derived metals from different volumes of magma which have passed through the channels now occupied by the ore bearing intrusions.

GRANITIC CHAMBER-TYPE PEGMATITES OF UKRAINE: NEW DATA ON MINERALOGY, GEOCHEMISTRY AND FLUID INCLUSIONS

NAOUMKO I.M. *(Institute of Geology and Geochemistry, Ukrainian AS, 290053, Lviv, Ukraine)*

Chamber-type pegmatites are genetically and spatially related to rapakivi-like biotite-hornblende granitoides of Korosten pluton in northwestern part of the Ukrainian Shield. New mineralogical, geochemical and fluid inclusions data obtained from the gemstone-

bearing paragenetic associations of leaching zones (albitized and topazized rocks) and chambers allow to provide further appropriate detalization of mineral-forming conditions during postinversion stage (below 573°C) of pegmatitic process.

Mineralogy. Recent mineralogical findings can be listed as follows:

- ilmenorutile with the composition of

$$Fe_{0.128}(Nb_{0.175}Ta_{0.057})_{0.232}*$$
$$*(Ti_{0.642}Sn_{0.004})_{0.646}O_{2.000}$$

in association with topaz and siderite in the leaching zones;

- carbonaceous matter with the simplest formula as $C_{491}H_{386}O_{87}S(N)$ [Ginzburg et al, 1987] that corresponds to oxidised higher kerite and is associated with felspars, smoky quartz, morion and topaz in chambers.

Geochemistry. Carbon isotopic composition from siderite ($\delta^{13}C$ = -15,7 ÷ -9,8 °/oo) and calcite ($\delta^{13}C$ = -15,5 ÷ -14,3 °/oo), as well as kerite ($\delta^{13}C$ = -35,5 °/oo) are defined (here and below PDB Standard used).

Fluid Inclusions. At the first time primary inclusions are found and investigated that are formed near solid particles media during repulsion, joint growth and their trapping by growing topaz crystals in leaching zones. Both solid (albite ?) and fluid (complex CO_2 with L CO_2 = 20-35%, essentially gaseous with G = 90-95%) inclusions are defined. They were formed during extensive boiling of mineral-forming fluids that suggests for heterogenous medium of gemstones crystallization.

Within the zones of amethyst colouring from growth pyramids of major positive rhombohedron in quartz crystals from chambers the primary essentially gaseous inclusions (G = 95-97%) with carbonaceous matter on their wells are found. The high methane content of volatiles from inclusions studied (27-43 vol.%) as well as inclusions from albite (55-57 vol.%) and accesory beryl (71-75 vol.%) suggest for carbonaceous matter were possibly derived from sublimation and polymerization of fluids hydrocarbon components.

New results also obtained concerning $\delta^{13}C$ of CO_2 from fluid inclusions in quartz zoned crystals from chambers:

"honeycomb" quartz: -10,8 ÷ -12,1 °/oo,
morion: -11,2 ÷ -13,9 °/oo,
"dusting" zone: -15,1 °/oo,
ice-coloured: -16,6 °/oo,
uncoloured: -10,9 °/oo.

Such carbon isotopic distribution is explaned by two-step injection of fluids with deep-seated-compounds predomination into pegmatite bodies: 1) around α-β quartz transition point resulted in "honeycomb" cracking, 2) under-crystallisation of uncoloured quartz.

STRUCTURAL AND PHASE TRANSFORMATION OF GLAUCONITE IN Mg-, Ca-, Na- CARBONATE MEDIA UNDER ELEVATED P_{H_2O} - T -CONDITIONS.

Nauruzbaev K. A., Kotov N. V., Goilo E. A. and Frank-Kamenetskii V. A. *(Department of Crystallography, State University, St. Petersburg, Russia)*

Some runs with glauconites with addition of Mg-, Ca-, Na-carbonates under P_{H_2O} = 1 kbar, T = 300 - 500°C were carried out. The yield runs were studied by means of X-ray diffraction methods (DRON - 2.0, CuK_α). Addition of $MgCO_3$ to glauconite at 400°C lead to formation of (Mg,Al)-serpentine-like phase, and biotite + serpentine at 500°C. In the presence of $CaCO_3$ glauconite transforms into biotite (400°C), and biotite + hedenbergite + quarz (synthetical) (500°C). It was found the formation of aegirine + analcite at alteration of glauconite in $2MNa_2CO_3$ solutions (300°C). The increase of temperature up to 400°C leads to formation of such assotiation as aegirine + biotite + cordierite. The formation of biotite + acgirine take place at T = 500°C. The processes of layer silicate transformation with structural inheritance is common feature of topotactical reactions in hydrotermal conditions at short run durations (for example 1hr - 3 days; Frank-Kamenetskii V. A., Kotov N. V., Goilo E. A. Layer silicate transformations under elevated p-T - parameters. Leningrad, Nedra, 1983, 151 p.).

The new unique phenomen at this work is synthes of pyroxens after such starting layer mineral as glauconite at the same hydrothermal run conditions. The direction of transformation is caused by nature of glauconite, containing Fe^{3+} in dioctahedral structural positions.

COPPER-NICKEL MINERALIZATION IN ALPINE-TYPE ULTRABASITES OF KARAGINSKY ISLAND (THE WESTERN BERING SEA)

Nazimova Ju.V. *(All Russian Mineralogical Society, St.Petersburg, Russia).*

Sulfur copper-nickel mineralization of the Karaginsky Island is located in ultrabasites within the Karaginsky Ophiolite Complex.

Vein-disseminated mineralization formed on the early stage of ore deposition and accompanied by local antigoritization of the wall ultramafic rocks. Chalcopyrite is the main mineral of this stage. It is characterized by the stoichiometry of the composition and the low content of the minor elements. Chalcopyrite is accompanied by cubanite, pyrite, sphalerite, magnetite, bravoite, violarite.

The formation of the massive ores, enriched by Ni and Co, took place on the later stage of mineralization. The deposition of these ores is accompanied by the intensive processes of antigoritization and rodingitization. New generations of chalcopyrite, pyrite, cubanite, sphalerite, magnetite become the main minerals of this stage. The main features of them are the nonstoichiometry of the chalcopyrite, presence of structural impurities of Ni and Co in pyrite, magnetite and Mn in chalcopyrite, and also the increasing of Fe in sphalerite. Bravoite and violarite contents are considerable increases. It should be emphasizes that comparing with first stage the concentration of Co in these minerals is 2 times higher.

Sulfide mineralization is formed during the active hydrothermal alteration of ultrabasic rocks by ore- and S-bearing fluids. The ores under consideration may be attributed to the new type of copper-nickel mineralization in ultramafic rocks.

CONCLUSIONS ABOUT THE PETROGRAPHIC STUDY OF THE ANCHIMETAMORPHIC COMPLEX WITH META-ANTHRACITE FROM "ARMENIS-RÂUL LUNG" (BANAT AREA-ROMANIA)

NEDELCU C.(SC."PROSPECTIUNI"SA. MINERALOGICAL LABORATORY)

The anchimetamorphic complex from Armenis-Râul Lung-Râul Alb is a lower Liassic age. This complex belongs to the alpine cover of the Danubian Domain on wich the Getic Nappe has been superposed in Austrich and Laramic phase.

For the realisation of the study I have used the microscopic methodes of analysis (in the transmited and reflected light)thermodifferentiale,thermogravimetric,X-ray diffraction,chemicals,etc.

In the Armenis-Râul Lung-Râul Alb area,this anchimetamorphic complex is made of metasandstones,meta-argillites with Czekanowskia track and meta-anthracites. Only in the metasandstones have been developed "false little veins" of quartz recristallised from the detrital granules. Those "false veins"have chalcopyrite and cubanite inclusions. In the metasandstones matrix, in the meta-argillites and in the meta-anthracites pores there are illite with a high degree of cristallinity (3-4 mm index Kübler), new born pyrrhotite and pyrophyllite next to kaolinite and quartz relicts. The meta-anthracites are made, predomonantly, of collinite, telinite, semifusinite, singenetic (kaolinite, quartz, illite, chlorite) and epigenetic (pyrophyllite and hematite) minerals.

The vitrinites are optical strongly pleochroical, anisotropic, reflectanded (R=6,60%) and bireflectanded and partly converted into coke, pyrocarbone and semigraphite. Sometime, the same, the vitrinites are replaced by the calcite, quartz and illite.

The generation of the coke, pyrocarbone and semigraphite took place in the time of riching the plastic phase of the vitrinitic organic matter with a strong dagasation (a hydrogen loss in the shape of CH_4 and oxygen in the shape of CO_2). $CO_2$with calcium in the geological environment made the calcite.

In the same time from the kaolinite and quartz in the meta-anthracite pores the pyrophyllite was formated. The pyrocarbone is considerated a carbonic product."of temperature" made in the coals beeing in the thermally contact with intrusion rocks, but this is not the case in the anchimetamorphic complex from the Armenis. The existance of the equilibrum quartz + kaolinite → pyrphyllite + water is stable at about 300°C and 1 Kbarr is an indication upon the thermo - barric conditions of the carbonic mezophase, while the coke, pyrocarbone and semi-graphite have been formated.

GEOCHEMISTRY OF CASSITERITES AND THEIR INCLUSIONS FROM TIN AND TUNGSTEN DEPOSITS IN PORTUGAL

Neiva A.M.R. (Dept. of Earth Sciences, Univ. of Coimbra)

Euhedral crystals of cassiterite from granitic pegmatites and quartz veins and their inclusions and anhedral crystals of cassiterite of a massive sulphide deposit from a volcano-sedimentary complex were analysed by electron microprobe. The dark zones in cassiterites containing inclusions of Nb- and Ta-bearing oxide minerals are generally enriched in Nb, Ta and Fe, while the light-coloured zones are relatively pure. No change in chemical composition of dark zones was found with increasing distance from these inclusions. These elements are incorporated in the cassiterite lattice. The cassiterites with mainly inclusions of rutile are among the poorest in Nb, Ta and Fe and generally no chemical distinction was found between their dark and light-coloured zones, but locally the former has more Ti than the latter. The analysed cassiterites from a volcano-sedimentary complex do not show any significant inclusion. Their brownish-coloured zones have more Fe than the light-coloured zones. Most of the analysed cassiterites show Fe > Mn and Nb > Ta preference. The cation distribution in these cassiterites suggests that $2\,(Nb, Ta)^{5+} + (Fe, Mn)^{2+} \rightleftarrows 3\,Sn^{4+}$ might be an important mechanism for Ta, Nb, Fe and Mn incorporation in cassiterite.

Columbite-tantalite is the predominant Nb- and Ta-bearing oxide mineral included in cassiterite, but Sn-ixiolites and W-bearing columbites were also found as inclusions in cassiterite. In these ixiolites and columbites there is a tendency for Ta and Ta/(Ta+Nb) to decrease and Nb to increase from core to rim and the core of this columbite is enriched in W. Some columbite-tantalites present a similar behaviour, in others Ta and Ta/(Ta+Nb) increase and Nb decreases from core to rim, but complexely oscillatory zonation was also revealed.

The rare inclusions of ilmenite have more Nb than Ta. Nb is positively correlated with Mn and Fe+Mn and Ti is negatively correlated with Mn, Mn+Fe, Nb and Nb+Ta. There is also the positive correlation between Fe+Mn and Nb+Ta.

Rutile contains Nb > Ta and Fe > Mn. Their analysis reveal substitutions of the type $2\,(Nb, Ta)^{5+} + (Fe, Mn)^{2+} \rightleftarrows 3\,Ti^{4+}$.

NON-STOICHIOMETRY OF CHROMITE FROM THE BUSHVELD COMPLEX, SOUTH AFRICA.

J. Nell (Min. & Proc. Chem. Div., Mintek) and H. Pollak (Dept. Physics, Univ. Witwatersrand)

A study was undertaken to document variations in the Fe^{3+}/Fe^{2+} ratio and cation-to-oxygen stoichiometry in a suite of chromite samples from the Bushveld Complex, South Africa, using ^{57}Fe Mössbauer spectroscopy. Data were collected at 298 K and at 77 K. Two distinctly different types of chromite (labelled I and II) were identified. Both types are paramagnetic at 298 K, but at 77 K type II chromite becomes magnetic, while type I chromite remains paramagnetic. Typical paramagnetic spectra of the two types are given in Figures 1 and 2.

The paramagnetic spectra were fitted by attributing the area under the high velocity envelope to 50 % of the ferrous iron present in the sample. We achieved the best fit to the data by using a quadrupole field distribution for Fe^{2+}, together with one Fe^{3+} doublet in the case of type I chromite, and two Fe^{3+} doublets for type II chromite. Due to the extensive overlap of the paramagnetic sub-spectra no attempt was made to allocate $Fe^{2+}$and Fe^{3+} to octahedral and tetrahedral sites. The Fe^{3+}/Fe^{2+} ratios of type I chromite varied between 0.2 and 0.4 while for type II chromite it varied between 0.7 and 1.3. Within the experimental uncertainty the calculated cation-to-oxygen stoichiometry ratios of type I chromites were close to ideal (3 : 4), while type II chromites were found to be significantly non-stoichiometric with values as low as 2.92 : 4 (i.e. deviation from stoichiometry, δ, = 0.08).

The cation-to-oxygen stoichiometry ratios of type II chromite are similar to values found for magnetite equilibrated at high

temperatures (1400 °C), and under oxygen partial pressure (PO_2) conditions close to the hematite stability field (Dieckmann, 1982). The relationship between δ, PO_2 and temperature for the natural chromites will obviously be different from magnetite, but the fact that such large values for δ can only be attained at high temperatures argues against a low-temperature, post-magmatic, oxidation mechanism for the formation of type II chromites.

At present it is not possible to determine whether type II chromite is a primary liquidus phase or whether it is a high-temperature oxidized equivalent of type I chromite. The occurrence of non-stoichiometric type II chromite may, however, be consistent with the formation PGE-rich chromitite layers from a reaction between non-stoichiometric chromite and FeS as suggested by Naldrett and Lehmann (1988).

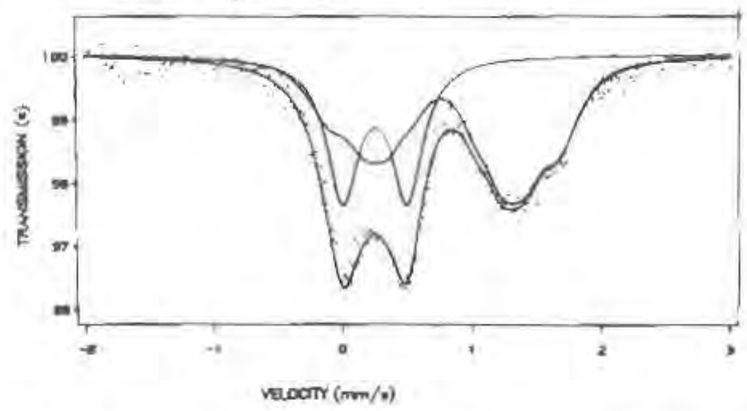

Fig. 1. Mössbauer spectrum of a typical type I chromite at 298K.

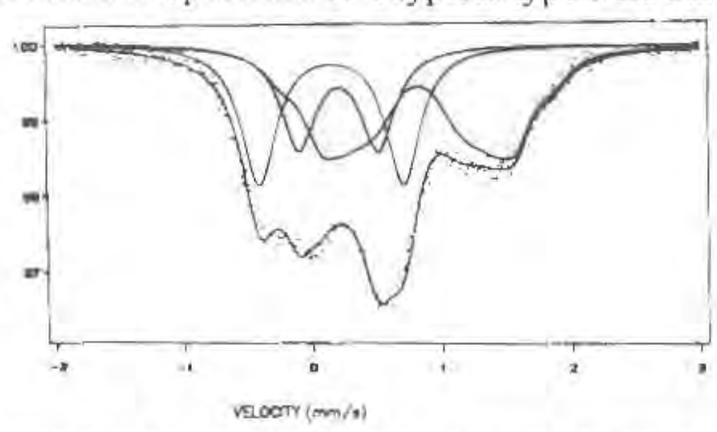

Fig. 2. Mössbauer spectrum of a typical type II chromite at 298K

References:
Naldrett, A.J. & Lehmann, J. (1988) *Geoplatinum '87*, 93-109
Dieckmann, R. (1982). *Ber. Bun. Phys. Chem.*, **86**, 112-118

• ON THE FLOCCULATION OF PYRRHOTITE AND MAGNETITE IN FINE POWDERS

Neradovsky Yu.N., Maksimov, V.I. *(Kola Sci. Centre, Russ. Ac. Sci.)*

Flocculation of the mineral particles can play both positive and negative role in the technological processes (Pirogov *et al.*, 1985; Yoon *et al.*, 1987; Edwards *et al.*, 1980).

There is the problem of the considerable flotation losses of sulphide minerals in the dressing of Cu–Ni ores, consisting of serpentinites. Investigation of the minerals interaction in various stages of the beneficiation process has shown that one of the reasons for a decrease of the flotation properties of sulphide is the flocculation of magnetite on the surface of the magnetic pyrrhotite grains.

It has been established that in the course of the ore grinding down to 100 micron, pyrrhotite and magnetite, dispersed in the silicate, transform into the free state and begin to interact one with another like ferromagnetic minerals. In this case, the large grains of the monoclinic pyrrhotite (100–50 micron) attract the fine (< 10 micron) ones and also grains of magnetite. As a result a sulphide–oxide mantle of the minerals fine grains is formed on the surface of the magnetic sulphide. The presence of magnetite in the mantle decreases abruptly the flotation capacity of the coarse grains of sulphide. We have obtained data about the magnetite content in the mantle which leads to the loss of the flotation capacity of pyrrhotite.

Small parts of magnetite and pyrrhotite also form a independent floccules which consist of particles with similar size. Their flotation properties depend on the correlation of minerals. Magnetite entraps in its floccules also the grains of nonmagnetic minerals, which results in flotation losses.

The specific feature of the pyrrhotite and magnetite flocculation in fine powders is that the formation of the sulphide–oxide fine-grained mantles is observed only on the coarse grains of sulphide but not on those of oxide. In this connection we suppose the presence of any cement on the sulphide surface.

References:
Pirogov, B.I., Tarasenko, V.N., Kravtsov, N.K. (1985). The problems of a directed alteration in technological and technical properties of minerals. –L., Mekhanobr, 34–43.
Yoon, R.N., Xu, Z., Chen, W. (1987). "Floccul. biotechnol. and separ. sust. proc.". Intern. Symp., San Francisco, Calif., July 28 – Aug. 1, (1986), Amsterdam, 707–716.
Edwards, C.R., Kirkic, W.B., Agar, G.E. (1980). Int. I. Miner. Process, 7, 332–342.

ALUMOGOETHITES FROM BAUXITE PROFILES OF THE NORTH ONEGA BASIN (RUSSIA)

Nesterova E.N. (VSEGEI, Sankt-Petersburg, Russia)

Lower Carboniferous laterite and bauxite profiles of the North Onega basin (North of the Russian Plate) are developed on different rocks: (1) Proterozoic Serpentinites; (2) Proterozoic metamorphosed diabases; and (3) Devonian clays and sandstones. Alumogoethites from these profiles were studied. The results of investigation are as follows:

(1) Goethite from the lower montmorillonitekaolinite-goethite zone of laterite profile after serpentinites does not contain Al admixture, while AlOOH amount in goethite from the upper gibbsite-goethite zone varies from 11 to 25mol.%. This profile was formed during 2 stages; and gibbsite zone with alumogoethites was generated at the latest stage.

(2) The degree of Al-Fe isomorphism in goethites from laterites after diabases increases gradually from the lower montmorillonite-goethite-kaolinite zone (9%) to the upper goethite-gibbsite zone (24mol.%). Such a distribution is typical for laterite bauxite profiles.

(3) The bauxite-bearing profile over Devonian sediments is characterized by increasing of AlOOH amount in goethite from the lower zones (0 - 9mol.%) to the upper bauxite zone. The highest degree of isomorphism is in gibbsite bauxites (up to 21.5mol.%), while in boehmite bauxites it is no more than 14mol.%. These patterns allow to consider these bauxites as lateritic ones; their sedimentary genesis, suggested by some researchers, is not confirmed by our data.

Additional investigation of alumogoethites from different weathered rocks, which are related with bauxites and laterites genetically, shows the following:

(1) Carboniferous kaolinite weathering profile, which replaces bauxites and laterites laterally and is developed over Devonian sandy clays, contains goethites with up to 8.2mol.% of AlOOH. The highest degree of isomorphism occurs near laterites over crystalline rocks; and the farther from them, the lower Al-Fe isomorphism. It is almost absent farther than 2km. The contents of some trace elements, which are accumulated in laterites, are decreased in the same direction (Mordberg and Nesterova, 1993). It allows to consider alumogoethites from kaolinite profiles as an indication of nearest laterite occurrence.

(2) Goethite from pisolitic iron ores, which overly bauxites, contains 7.8 - 13.3mol.% of AlOOH, and these ores can be considered as the upper part of bauxite profile.

(3) The shingle of weathered rocks were found in the basal part of Devonian sedimentary stratum. Goethite from

these shingle is characterized by the presence of 8mol.% of AlOOH in its structure. It indicates, that Pre-Devonian weathering epochs took place within the North Onega basin; and the conditions of weathering were close to lateritic one. Probably, most of Pre-Devonian weathering profiles were eroded, but some of them could be buried.

Typomorphic features of natural goethites can be used not only for the purpose of modelling of bauxite genesis, but also for predictive estimation.

Reference:
Mordberg, L.E. and Nesterova, E.N. (1993). *Resource Geol. Special Issue*, No.16, 157-168.

• CAPABILITIES OF MINERALOGICAL DATABASES: AN ILLUSTRATION USING THE *MINERAL* DATABASE

Nichols, M.C. *(Materials Synthesis Department, Sandia National Laboratories, California)*

Mineralogical databases have become very useful for identification as well as for research on both new and well established minerals and mineral groups. New implementations of the mineralogical database MINERAL for Windows and for Macintosh will be used to illustrate how such databases can help solve mineralogical problems. Simple searches of the MINERAL database using single fields, as well as complex searches utilizing combinations of different fields (e.g. elements, appearance, crystal system, powder diffraction data, etc.) along with search parameters such as .AND., .OR. and .NOT. will be demonstrated. MINERAL also allows a range of values to be specified as input for a search.

Comparison of questionable species with the entire database can be used to show similarities with other species. Comparison or even sorting of crystallographic parameters present in MINERAL can be used to demonstrate similarities between minerals or to show one or more relationships within a mineral group.

MINERAL has been used as a research and teaching tool by universities, libraries and museums, as an identification tool by mineral exploration companies, and by mineral collectors to keep track of their collections. Frequent updates from the literature have made it valuable for those who wish to have access to the most current mineralogical data.

Having the identical database for both the Windows and Macintosh platforms allows greater accessibility by users in the mineralogical community and will mean that improvements or changes made for one platform will be identically available to all users. Making chemical formulas available with the appropriate symbols, subscripts and superscripts, and ensuring that the mineral names contain all the appropriate diacritical marks enhances the usefulness of the database.

Input regarding future capabilities and features for MINERAL will be solicited.

THE 'MINERAL' DATABASE

Nickel, E.H. *(Division of Exploration & Mining, CSIRO))*

The MINERAL database is a computerized compilation of mineral data consisting of over 4000 records, including all valid mineral species and about 600 unnamed minerals.

The data include name, chemical formula, appearance, crystallographic parameters, hardness, measured and calculated densities, up to four literature references including the latest structural reference, type locality, author(s) of the name, the 8 strongest X-ray powder diffraction reflections and their intensities, group classification name and symbol, and a symbol that indicates the validity status of the mineral. There is also a "notes" field that contains additional information.

Most of the data fields are rapidly searchable using the software supplied with the database. Versions currently available include those for IBM PC (both WINDOWS and non-WINDOWS versions) and Macintosh computers.

The information in the database is continually updated, and updates are available to subscribers at 6-monthly intervals

rift": the magmatic arc is associated with backwards development of a marginal basin. The tholeiite products resulted by partial melting of upper mantle material above the Benioff plane and the calk-alkaline products by partial melting of the subducted plate.

After completion of the ophiolite suite, the assemblage underwent a clockwise rotation (according to palaeo-magnetic informations).

The Mesocretaceous and Neocretaceous deformations led to the above mentioned tectonic units of the South Apuseni Mts. and to their petrographic variation in terms of ophiolitic distribution/ composition.

ALPINE OPHIOLITES OF THE SOUTH APUSENI MOUNTAINS (ROMANIA): A REVIEW OF GEOCHEMICAL CHARACTERISTICS AND TECTONIC SETTING

Nicolae I., (*Inst. of Geology and Geophysics, Bucharest, Romania*)

The most significant ophiolitic occurrences of the Romanian Carpathians are located in South Apuseni Mts. The author of the present poster treats the ophiolite meaning in "*largo senso*", that is ophiolites are to be formed/found in various geotectonic settings.

Ophiolite rocks of the South Apuseni Mts. are related to seven tectonic units; vertical columnar sections intend to expose petrographic peculiarities of these ophiolitic assemblages. A survey of the actual stage of chemical knowledge (major as well as minor elements, REE, Sr^{87} / Sr^{86} ratios, isotopic K-Ar ages, *etc.*) is taken into account.

Numerous diagrams are listed in order to comment the South Apuseni Mts. ophiolitic tectonic setting. Accordingly, it is confirmed that five of above mentioned seven tectonic units (Căpîlnaş-Techereu Nappe, Bedeleu Nappe, Hospea Nappe and Rimetea Nappe) are of magmatic arc type, whereas two of them (Feneş Nappe and Criş Nappe) are of marginal basin setting.

The magmatic arc ophiolites consist of a basal tholeiitic series and a superposed calc-alkaline series. The marginal basin ophiolites are composed of basic rocks, mainly volcanics.

A schematical ophiolitic evolution suggests that rock formation is related to subduction of oceanic crust to the "Transylvanian

• THE ORIGIN OF PROTEROZOIC GOLD-COPPER DEPOSITS IN THE BIDJOVAGGE DISTRICT, FINNMARK, NORTHERN NORWAY, AS DEDUCTED FROM REE AND Nd-Sr ISOTOPIC DATA ON CALCITE

Nie F.J. *(Institute of Mineral Deposits, Beijing)*, Bjørlykke A. and Nilsen K.S. *(Dept. of Geology, Univ. of Oslo)*

Gold- and copper-bearing calcite veins, quartz-calcite veins and calcite-containing massive copper ores are widely distributed within A, B, C and D deposits in the Bidjovagge district, Finnmark, Northern Norway (Bjørlykke *et al.*, 1987). Rare earth element (REE) and Nd-Sr isotopic characters of calcites from all the four deposits have been determined. According to petrographic evidences, REE patterns (twelve samples) and Nd-Sr isotope data (twenty-eight samples), calcites have been classified into four types: (1) Three early vein calcites from A and C copper deposits show almost flat REE curves and slightly positive Eu anomalies. (2) Two late vein calcites from C and D deposits have flat light REE curves, positive heavy REE curves and negative Eu anomalies. Two secondary calcites from the late veins correspond to this type. A Sm-Nd isotope age of 1858 ± 72 Ma for primary calcite crystallization has been given based on fifteen calcites. The Sm-Nd calcite age is in well agreement with previously published U-Pb age on davidite of these ore deposits (Bjørlykke *et al.*, 1990). (3) REE patterns of the earliest vein calcite from B gold-copper deposit has overall negative slope and negative Eu anomaly whereas one early vein calcite and one secondary calcite from the early vein show "U"-shaped REE patterns. All these three early vein calcites are characterized by high gold and scandium content and (4) Two late vein calcites from the B deposit have almost flat slope and negative Eu anomalies. Sm-Nd data on seven vein calcites are relative scattered, and gave an isochron of 1809 ± 150 Ma, identical to the age of vein calcites from A, C and D ore deposits. In contrast, Nd-Sr-isotope data on secondary calcites from early and late veins are strongly scattered and do not show colinearity with 1858 Ma or 1809 Ma isochron lines.

REE patterns, εNd(T) and εSr(T) values indicate that ore-bearing solutions for these vein calcites from the A, C and D ore deposits derived their metals from mafic volcanic-related fluids. A possible source for the ore-forming fluids seems to be the diabase sills. In contrast, isotopically more evolved source such as albite felsite and syn- or post-tectonic high level granitoid intrusive (albite diorite) are probably metal source for these veins calcites in the B ore deposit. For these secondary calcites from the C ore deposit, relative high initial εNd(t) values at 1858 Ma imply that much recycled high radiogenic Nd-component was incorporated by re-crystallization and re-mobilization of primary calcite. Three samples of secondary calcite from the B ore deposit, which obviously deviated from 1809 Ma isochron are easily explained as product of syn- or post-ore metamorphic or metasomatic event.

All Rb-Sr isotope data for twenty-eight calcite samples do not display any isochron relationship. The excess data scatter is probably due to low Rb-content in calcite and incomplete Sr-isotope equilibration during hydrothermal fluid evolution and/or subsequent geologic event.

ON THE DIAMOND HYDROGENESIS THROUGH AQUASOL ENVIRONMENT

Niedbalska A. (DiaTech Ltd. Co., Łomianki)
Sałaciński R. (Dep. of Geology, Warsaw Univ.)
Szymański A. (Fac.of Chem. Warsaw Politechn.)

Forty years history of diamond synthesis as before to leave many unanswered questions in the sphere of large natural diamonds genesis. Geochemistry, free radicals as low temperature catalysts and magnetic field influence on the crystal nucleation and growth are not analysed.

Uncomon development in the last ten years in chemical engineering of advanced materials synthesis suggest for researchers necessity to happen again a deep petrological analysis of the diamond nucleation and overgrowth.

Presented before data, our own experiences and petrological knowledge suggests the pneumatolitic aquasol environment as potential source of a diamond ungrowing in the Earth crust.

Natural diamond were nucleated probably in the silicate melt at magmatic step of the magma differentiation, but overgrowth up to large crystals rather was connected with pneumatolitic step. At the pneumatolitic processes the postmagmatic solutions are enriched with volatile components which shows chromite former, ferrite former and carbide former tendencies.

With that step occur mineralization based on the decomposition of the organic compounds included into migrated gaseous fluids.

Pneumatolitic processes of magma differentiation may be a second step of diamond nucleation and long time on seed diamond crystal overgrowth. That process may be creative up to end of the hydrothermal processes running out magma differentiation.

Presented suggestions are verified by the large anhedral diamond crystals occured into pegmatitic quartz veins of Brasilian itacolumite.

METAMORPHISM VERSUS DEFORMATION IN THE ECLOGITIZED GRANITOIDS OF THE MONTE MUCRONE AREA, SESIA-LANZO ZONE, ITALIAN WESTERN ALPS

Nieto J. M. (*Dpto. Mineralogía y Petrología, Univ. Granada, Spain*) and Compagnoni R. (*Dipt. Scienze Mineralogiche e Petrologiche, Univ. Torino, Italy*)

The "Eclogitized Micaschist Complex" (EMC) of the Sesia-Lanzo Zone is a portion of the Variscan continental basement of the western Alps, recrystallized under eclogitic conditions during the Alpine orogeny. In the central part of the EMC, a large body of garnet-omphacite-phengite orthogneiss, which derived from Alpine recrystallization of late-Variscan granitoids, locally preserves small portions of the undeformed igneous protholith. In some of these metagranitoid portions, cm- to dm-thick shear zones may be found, which commonly have a central millimetric part mainly consisting of pink zoisite.

In the massive portions of the eclogitized metagranitoid domainal equilibria prevail. During a first metamorphic stage, the igneous plagioclase is pseudomorphically replaced by jadeite + zoisite + vermicular quartz, and the igneous biotite is pseudomorphically replaced by a Ti-rich phengite and surrounded by a double reaction rim consisting of an inner garnet corona and an outer Ti-poor phengite + vermicular quartz corona. At this stage, textural relicts of the igneous biotite are still preserved, but biotite is re-equilibrated to metamorphic composition. In a second metamorphic stage, jadeite + zoisite progressively disappear and are replaced by white mica and quartz intergrowths. In the biotite site, the biotite is replaced by omphacite + phengite + titanite, and coronitic garnet is progressively re-equilibrated to grossular-richer compositions. Geothermobarometric estimates indicate for both stages similar metamorphic conditions (T= 570 ± 30 °C and P= 16 kbar), and structural evidence suggests that the second stage assemblage was produced by the enlargement of the equilibration volumes in the rock, made possible by the infiltration of an aqueous fluid.

In the shear zones, the igneous mineral sites become progressively flattened and toward the central part, more strained portion the rock exhibits a mylonitic texture and consists of thin alternating layers of granoblastic quartz and jadeite + vermicular quartz, respectively. The central portion of the shear zone is usually composed of interlocking prismatic crystal of randomly oriented zoisite. The isotropic orientation of both zoisite and jadeite indicates that the eclogitic minerals developed statically at the expense of an already sheared granitoid. The presence of jadeite, still including vermicular quartz, supports the interpretation that the alkali pyroxene is not the result of HP deformation and recrystallization of former jadeite, but the direct breakdown product of pre-existing albite. Therefore, the shear zones, crosscutting the Monte Mucrone metagranitoids, are pre-Alpine or prograde Alpine mylonites, statically recrystallized under eclogitic conditions. The lack in the shear zones of the second stage metamorphic assemblage is interpreted as a consequence of the metasomatic processes connected to mylonitic deformation, which leached out Ca, Fe and Mg from the shear zone, i.e. the elements essential to the omphacite growth.

MANTLE ECLOGITES: T, P and f_{O_2} EQUILIBRIUM CONDITIONS and DEPTHS of FORMATION.

Nikitina L.P., *Simakov S.K and Ivanov M.V. (*Institute of Precambrian Geology and Geochronology Russian Academy of Sciences; *All Russian Geological Research Institute, Russia*)

Equilibrium conditions of mantle eclogite formation are determined on the basis of investigation of eclogite xenoliths from kimberlite and lamproite pipes (Jakutia, South Africa, Australia, and North America) by using garnet-clinopyroxene thermobarometer (Nikitina & Ivanov,1993) and garnet-clinopyroxene oxygen barometer (Simakov, 1993). Thermobarometer permits us to estimate the temperature and pressure conditions for garnet-clinopyroxene assemblages with sodium-rich pyroxenes in the range of 650-700≤T≤1650-1700°C and 20-25≤P≤65-70kb. Oxygen barometer is suitable for assemblages in which garnets contain Cr_2O_3 less than 1.0 wt.%. Accuracy of garnet-clinopyroxene thermobarometer was tested by comparison of P-T estimates for diamond-bearing and graphite-bearing eclogite xenoliths with the diamond-graphite univariant curve by (Bundy et. al 1961).

Eclogites occur in the mantle at depths from 50-60 to 200-220km and crystallize at temperature from 800 to 1550-1600°C and pressure from 20-25 to 60-65 kb. Diamond-bearing eclogites are formed at pressure over 35-45kb and temperature below 1250-1300°C. Their parageneses correspond to EMOD and WM buffers mainly. Water is the main component of fluids. On the C-O-H diagram the compositions of fluids are close to ones extracted from natural diamonds and to the point of crossing

of H_2O and CO_2 lines. Diamond-free eclogites correspond to another type of fluids: their compositions are shifted into reduction area of C-O-H diagram close to intersection of CO and CH_4 lines. The main component of this fluids is CH_4.

This investigation was supported by Russian Basic Research Foundation (N 17778A).

References:
Bundy,F.R. et. al. (1961).J. Chem. Phys,35. 383-391.
Nikitina L.P. & Ivanov M.V. (1993).Docl. Russ. Acad. Sci., 331, N2, 214-216.
Simakov S.K.(1993). Docl. Russ. Acad. Sci., 332, N1, 83-84.

THE LIQUIDUS MINERAL ASSEMBLAGES OF ARMENIAN POST-COLLISIONAL NEOVOLCANICS.

Nikogosian I.K.(*Inst. of Geological Sci., Yerevan, Armenia*), Magakyan. R. (*Vernadsky Inst. of geochemistry, RAS, Moscow*), Melkonian R.L (*Inst. of Geological Sciences, Yerevan, Armenia*).

The post-collisional magmatism is broadly manifested in the contact zone of Arabian and Eurasian continental plates. The volcanism of this type is presented by high-alkaline Neogen-Quaternary volcanic suites of Kaphan, S-E Armenia, Lesser Caucusus. Based on the major and trace element contents two types of series are distinguished in this volcanics: basanitic and subalkaline.

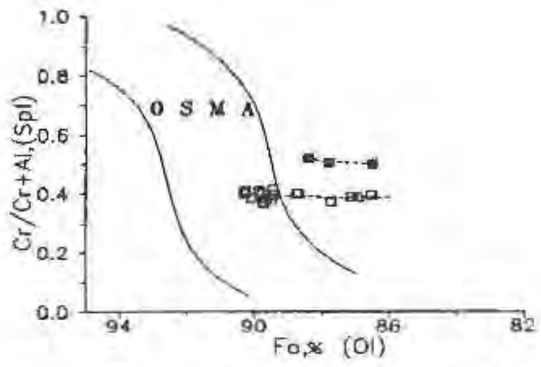

Fig. Compositions of spinel inclusions in olivine phenocrysts from the studied rocks. OSMA - composition of Ol-Sp mantle assemblages (Arai, 1992).

The detailed microprobe investigations of olivine crystals and spinel inclusions there in has been carried out, for the rocks of both series, and show the following results:

The spinel-olivine assemblages of studied rocks cannot be interpreted as disintegration products of mantle nodules for more high CaO contents in olivine and TiO_2 and Fe_2O_3 contents in the spinel, and presence of melt inclusions in olivine.

The earliest primary liquidus olivine-spinel assemblages of both series was determined (Fig): $Fo_{90.3\text{-}86}$, Cr/Cr+Al(Spl)= 0.40 mol% for basanitic series and $Fo_{88.5\text{-}86}$, Cr/Cr+Al(Spl)= 0.50 mol% for subalkaline series.

Systematic difference of spinel compositions for host-olivine of the same compositional interval confirm the conclusion, that studied series belong to the different types of magmas.

The most magnesian compositions of studied olivines corresponded to the range of olivine assemblages of the primary mantle associations ($Fo_{87\text{-}92}$,Arai, 1992), that can be the base for more detailed estimations of composition and early crystallization conditions of primary melts of the series, on experimental or calculation grounds.

Reference: Arai S. (1992). Mineral. Mag., 56, 173-184

CLINOPYROXENE GEOBAROMETER FOR BASALTIC SYSTEMS

Nimis P. (*Dept. of Mineral. and Petrol., Univ. of Padova, Italy*)

An updated and improved version of the crystal-structure simulation program of Ottonello *et al.* (1992), a procedure that enables calculation of the structural parameters of a *C2/c* clinopyroxene (Cpx) of known chemistry without requiring direct X-ray diffraction analysis, has been used to investigate the structural variations of experimental Cpx synthetized under controlled physico-chemical conditions.

The sensitivity of Cpx to the crystallization pressure has been calibrated by means of the crystal-structure simulation of published chemical analyses of experimental near-liquidus Cpx synthetized from dry basaltic starting materials at increasing pressure (0-24 kbar). The good internal consistency of simulated cell and site volumes variations with changing pressure has allowed construction of an empirical geobarometer based on the well-known cell volume *vs.* M1 site volume relationship. In spite of the quite wide range of silica, alumina and alkali contents in the starting materials, simulation data have enabled reproduction of the experimental pressures within ± 2 kbar (= 1σ; maximum error < 6 kbar; N = 29).

The proposed *structural* geobarometer is strictly applicable to *C2/c* Cpx crystallizing from melts of *basaltic* composition ($Mg/(Mg + Fe^{2+})_{Cpx}$ = 0.7-0.9), except for high-alumina basalts, in the absence of garnet. It is therefore suitable for many natural Cpx occurring as mega- or phenocrysts or forming cumulate pyroxenites. For basalts with *normal* contents of Al_2O_3 (< 18 %), variations of major elements in the melt do not reduce the accuracy of the geobarometer.

Application of the new geobarometer to natural Cpx megacrysts from the Hyblean Plateau (SE Sicily, Italy) yields pressure values (12-16 kbar) indicating that they have formed at mantle depths within the stability field of spinel, consistently with their equilibrium mineral assemblages.

References:
Ottonello, G., Della Giusta, A., Dal Negro, A., Baccarin, F. (1992). *In*: Advances in Physical Geochemistry, Thermodynamic Data, S.K. Saxena (Ed.), Springer, New York Berlin, p. 194-238.

CRYSTAL CHEMISTRY OF DANALITE FROM DABA SHABELI COMPLEX (SOMALIA)

Nimis P., Molin G., Visonà D. (*Dept. of Mineral. and Petrol., Univ. of Padova, Italy*)

An E-W gabbro-syenite belt occurs in the crystalline basement of N Somalia, consisting of multipulse bodies with an age of ca. 690 Ma. Among these bodies, the Daba Shabeli Complex (about 70 km SSE of Berbera) is notable for the occurrence of danalite-bearing granites, representing differentiates of mantle-derived magmas produced in deep chambers. These granites occur as coarse-grained, often porphyric, alkali-feldspar dykes with rapakivi texture. Mafic minerals are biotite (*mg* = 0.24-0.39 and Cl up to 1%), amphibole (Fe-edenite with Fe-actinolitic horneblende rims and Cl up to 1.7%), magnetite, ilmenite and large (up to 30 mm) reddish-brown rounded danalite crystals (Visonà, 1994).

Danalite $[(Fe,Mn,Zn)_8(BeSiO_4)_6S_2]$ is a cubic ($P\bar{4}3n$) beryllo-silicate (sodalite group, helvite subgroup). Its structure shows alternating Si (TA) and Be (TB) tetrahedra, which are linked to form a 3D framework. Several works have addressed its chemical and physical properties (*e.g.* Kwak & Jackson, 1986) but, to our knowledge, only two structural refinements have so far been carried out (Hassan & Grundy, 1986).

A sphericized crystal from Daba Shabeli (at. Fe:Mn:Zn = 0.65:0.23:0.12) was investigated by means of single-crystal X-ray diffractometry (XRD), and subsequently analysed with a WDS electron microprobe (EMP) and an ion microprobe (for Be). XRD data were collected up to $2\theta \leq 70°$. Structural refinement was carried out using the STRUCSY program, starting from helvite atom coordinates (Holloway *et al.*, 1972). Scale factor, atom displacement parameters, Fe and O coordinates, and Fe occupancy were allowed to vary in four isotropic and three anisotropic minimization cycles to R = 2.13%. A slightly better fit was then obtained by also varying Be occupancy, yielding a final R = 2.11%. Calculated (EMP) and observed (XRD) electron densities on each site agree within 0.2 e^-.

As previously observed (Hassan & Grundy, 1986), Be is completely ordered. Be occupancy < 1 (see Table) suggests that small fractions of Si (< 0.02 apfu) may substitute for Be, as found in helvite (Mn end-member) by Holloway *et al.* (1972). However, Si and Be polyhedron geometries are similar to those of the completely ordered danalites studied by Hassan & Grundy (1986). We conclude that Si and Be ordering may be considered as complete within analytical uncertainty.

References:
Hassan, I., Grundy, H.D. (1986). *Am. Mineral.*, **70**, 186-192.

Holloway, W.M., Giordano, J.R., Giordano, T.J., Peacor, D.R. (1972). *Acta Cryst.*, **B28**, 114-117.
Kwak, T.A.P., Jackson, P.G. (1986). *N. Jb. Miner. Mh.*, **10**, 452-462.
Visonà, D. (1994). *Bull. Ist. Agronom. Oltremare*, special issue (in print).

Table - Selected structural refinement data.

a(Å)		8.2127(8)			
obs. non-eq. refl.		339			
R %		2.11			
	occ.	*x/a*	*y/b*	*z/c*	Beq
S	1.000	0	0	0	0.984
Si(TA)	1.000	0	1/2	1/4	0.530
Be(TB)	0.983(9)	1/2	0	1/4	0.780
Si(TB)	0.017(9)	"	"	"	"
Fe	1.003(7)	0.1689(0)	0.1689(0)	0.1689(0)	0.742
O	1.000	0.1408(2)	0.1394(2)	0.4121(3)	0.755
TA-O(Å)	1.623(2)				
TB-O	1.638(2)				
Fe-O	2.026(2)				

RARE ZEOLITES FROM SIKHOTE-ALIN, RUSSIA

Nistratova I.E. and Nistratov Y.A. (*Institute of Ore Deposits, Petrography, Mineralogy & Geochemistry of RAS, Moscow*)

Recently some rare zeolites were found in Paleogene volcanic rocks from Sikhote-Alin Range.

Ferrierite is discovred in andesitebasalt near Kraskinskoye in the south of the region. Amygdales and vugs, 0.5 to 2 cm in diameter, are filled by only ferrierite or also heulandite and calcite. Ferrierite forms fibrous aggregates on the walls of the vugs. It appeared after heulandite but before calcite. Heulandite and ferrierite are enriched by Sr and Ba, perhaps due to hydrothermal alteration of volcanites. This is the first discovery of ferrierite in Russia.

Dachiardite was detected in hidrated trachiriodacite glasses near the Belogorscoye gold mine in the north of the Sikhote-Aline Range. Dachiardite occurs (in microscopic leaching crusts) in the following cristallization sequence: smectite (or illite-smectite), clinoptilolite, mordenite, dachiardite, cristobalite (or adular). Dachiardite forms radial aggregates of sabel-like cristals. Cristal individs (to 1.2 mm long) are simpl fibers along b. Chemical analisis obtained by a CamScan electron microscope with X-ray AN-87/S unit results in the formula:

$K_{1.4}Ca_{1.0}Na_{0.3}[(Al_{3.5}Si_{20.4})O_{48}] \cdot 14H_2O$

with Si/Al=5.78. In the associated clinoptilolites Si/Al ratio ranges from 5.7 to 7.7, possibly due to activity of silicon. This is the first discovery of dachiardite in acid glass; it's richest in Ca and resembles the "svetlozarite" proposed by Maleev(1976).

Referenses:
Maleev, M.N. (1976). Zapisky Vses. Mineral. Obsh., 105, 4, 449-453.

ORIGIN OF THE ALMANDINE PHENOCRYSTS IN INTRUSIVE ANDESITES FROM THE RODNA MOUNTAINS (SUBVOLCANIC ZONE, EAST CARPATHIANS, ROMANIA)

Niţoi E., Marincea Şt., Ureche I. (*Institute of Geology and Geophysics, Bucharest*)

Not previously described, garnet-bearing andesites represent an intrusive manifestation of the second cycle of the Neogene volcanism in this area. They occur as dykes intruded in some metamorphites belonging to the Bretila Series (Precambrian in age) or in sedimentary deposits of Paleogene age. Petrographically, they are quartziferous andesites with hornblende and biotite, always containing normative (CIPW) corundum.

Garnets occur as subhedral to euhedral phenocrysts (0.5 to 2 mm in size) free of inclusions and without reaction rims. They are very uniform in composition: dominantly almandine (between 49.96 and 55.08 mole percent), subordinately pyrope (between 21.87 and 28.15 mole percent), minor grosular (up to 5.78 mole percent) and spessartine (up to 10.57 mole percent). No significant compositional differences occur between various phenocrysts and between core and rim within the same phenocryst. The physical parameters (i. e. the refraction index of 1.794 and the cell edge of 11.552 (±0.007) Å) also indicate an almandine. Garnet is allways surrounded by clusters of plagioclase crystals or enclosed in idiomorphic plagioclase phenocysts. This plagioclase (2-3mm in size) is identical in form and composition (An=42-52%) with the one found elsewhere in the host rock.

The chemical composition, the preference of garnet to some rocks of calc-alkaline series (quartziferous andesites and dacites) and its constant association with plagioclase, indicate genetic relationships between garnets and their host rocks. This paper points out that the garnets represent products of crystallisation from intermediate calc-alkaline magma in an early stage of its evolution rather than accidentally included xenocrysts.

X-RAY AND ^{57}Fe MÖSSBAUER STUDIES OF OLIVINE-RELATED THIOGERMANATES

Nord, A G[x] and Ericsson, T (Dept. of Mineralogy, Inst. of Geology, University of Uppsala)

Thiogermanates $(Fe,M)_2GeS_4$, with M = Mg, Mn, or Zn, have been prepared from pure ground elements mixed in stoichiometric proportions. Each mixture was kept in a gold capsule, inserted in a silica tube, evacuated, and slowly heated to 800°C where the temperature was maintained for a week; then quenched in cool water.

X-ray powder diffraction data were obtained with a Guinier focusing camera ($CuK\alpha_1$ radiation, R = 40.00 mm, internal standard Si). The Guinier photographs were evaluated with a computer-controlled film scanner and associated programs, giving accurate unit cell dimensions. The solid solutions crystallize with the olivine structure (space group Pbnm), with two distinct octahedral metal sites.

The ^{57}Fe Mössbauer spectra resemble those of iron-containing olivines. At room temperature there are two strongly overlapping doublets with a centroid shift (relative metallic iron) around 0.9 mm/s and a quadrupole splitting around 3 mm/s. At liquid nitrogen temperature the two crystallographic sites show a strong difference in hyperfine fields, ~25 and ~6 Tesla in Fe_2GeS_4. At even lower temperatures there is a clear change in the shape of the Mössbauer spectra, indicating a second magnetic transition.

The metal cation partitioning is almost random in the (Fe,Mg) thiogermanate, with a somewhat stronger ordering for the (Fe,Mn) and (Fe,Zn) solid solutions. The data obtained are compared with results for olivines and olivine-related $(Fe,M)_3\square(PO_4)_2$ sarcopsides.

[x]Present address: RAÄ/RIK/Analys, Södra Malmgården, P. O. Box 5405, S-114 84 Stockholm, Sweden

EXSOLUTION KINETICS IN PYROXENES

Nord G.L. (*United States Geological Survey*)

The geologic application of exsolution kinetics in pyroxenes is

still confined to comparing relative sizes of lamellae of similar composition. To advance beyond this stage experimentally determined rate laws are required that measure kinetic parameters as a function of time, composition, temperature and oxygen fugacity. The greatest experimental difficulty is isolating a single mechanism. The simplest mechanisms to isolate are those that do not involve nucleation such as cation order-disorder and spinodal decomposition and coarsening.

Cation order-disorder involves diffusion of Mg and Fe over the distance between M1 and M2 sites. Activation energies for this process, appear to fall into two groups, approximately 250 kJ/mole for Mg-rich samples and 170 kJ/mole for Fe-rich samples (Sykes-Nord & Molin, 1993). These two groups were calculated from disordering experiments fitted to the chemical rate law of Mueller and imply a change in the order-disorder mechanism with composition, although this change has not yet been defined.

Spinodal decomposition and coarsening involve diffusion of Ca as well as Mg and Fe over one-half the wavelength (λ) of the exsolution lamellae. Activation energies for coarsening as determined by isothermal heating experiments on synthetic clinopyroxenes range from approximately 270 to 525 kJ/mole. Coarsening rates are constrained by the slower bulk diffusivity of Ca. The characteristic diffusion distances and activation energies of spinodal decomposition and coarsening compared to those of cation order-disorder are so dissimilar that exsolution should be considered a relatively high temperature process and order-disorder a relatively low temperature process.

The activation energy for spinodal decomposition can be determined by experimentally defining C-shaped "extent-of-transformation" curves on a time-temperature-transformation diagram. Because spinodal decomposition is instantaneous there is no starting curve as in a nucleated process. The curves therefore must define points in time during the development of spinodal decomposition and coarsening that can be keyed to specific changes. In real space this change is the development of periodic exsolution lamellae from the nonperiodic fluctuations present in the quenched material and is observed by transmission electron microscopy. This change is more precisely defined in reciprocal space as the development of satellites from diffuse streaks as observed in electron diffraction patterns. Cahn (1968) pointed out that the depression of the nose of the curve (maximum transformation rate) from the temperature of the spinodal (T_s) is a function of the activation energy, Q, $(T_s-T_{nose})/T_s = 2RT_s/Q$. Also, the slope of the bottom of the C-curve defines the activation energy. This curve defined by Nord and McCallister (1983 and unpublished) for $Wo_{25}En_{31}Fs_{44}$ only constrains the activation energy to between 240 and 400 kJ/mole.

In general, the rate law $\lambda \propto t^{1/n}$ has been used to describe coarsening in lamellar systems where $n = 3$ or 2. A linear fit to a ln λ, ln t plot of the coarsening data for $Wo_{25}En_{75}Fs_0$ (McCallister, 1978) results in $n \approx 3.2$ at 1300°C, $n \approx 4.0$ at 1200°C and $n \approx 5.8$ at 1100°C. Similarly a fit of the coarsening data for $Wo_{25}En_{31}Fs_{44}$ (Nord and McCallister, 1983) results in $n \approx 3.3$ at 1000°C, $n \approx 3.1$ at 900°C and $n \approx 6.6$ at 800°C. Even with the large uncertainties associated with the measurements, the fits suggest that n increases with decreasing temperature. This indicates that there is an additional factor(s) to consider. One possibility that may reduce the coarsening rate of the lower temperature experiments is a rapid increase in spontaneous strain in the pigeonite lamellae that arises from the $C2/c \rightarrow P2_1/c$ transition. Without the loss of coherency at the lamellar interface, coarsening will be suppressed. If the pigeonite lamellae in the higher temperature experiments are coarsened at temperatures above the transition temperature they would be free to coarsen without the additional spontaneous strain of the displacive transition.

It is apparent that there may be more than one mechanism affecting the kinetics of even the simplest transformations in pyroxenes. It will be the task of future experiments to better define these mechanisms.

References:

Cahn, J.W. (1968) *Trans. Met. Soc. AIME*, **242**, 166-180.

McCallister, R.H. (1978) *Contrib. Mineral. Petrol.*, **65**, 327-331.

Nord, G.L., Jr. & McCallister, R.H. (1983) *Proc. Electron. Micro. Soc. Amer.* 182-185.

Sykes-Nord, J.A. & Molin, G.M. (1993) *Amer. Mineral.*, **78**, 921-931.

TRANSFORMATION OF NATIVE GOLD IN EXOGENIC ENVIRONMENT.

Novgorodova M.I., Generalov M.E., Trubkin N.V.
(IGEM RAN, Moscow).

Exogenic history of native gold starts from oxidation zones of the upper part of ore deposits. The predominant part of gold from oxidated ores is residium kept the main peculiarities of gold from primary ores. Only the small part of gold is newly formed after the decomposition of gold-bearing minerals. Nevertheless soluble gold complexes to be formed at atmosphere pressure and temperature are responsible for enrichment of weathering crusts during long geological time.

The leading process of chemical transformation of gold is diffusion of silver impurities from volume to boundaries and dislocations in gold grains with further leaching of Ag by surficial water. High grade rims and stringers take rise ultimately through some intermediate stages of zonal distribution of silver impurities. At the high sulphur activity the gold-silver sulphides form as thin rims on primary gold, rarely as small individual grains

Decomposition of various gold-bearing minerals leads to formation of extremely fine-grained mixture of gold with oxides, tellurates and other secondary minerals which aggregates named mustard gold for their brownish colour. Both gold sulphides and mustard gold are formed in situ by decomposition of primary gold minerals so they occur in oxidation zones but not in weathering crust and placers.

In weathering crust (the South Urals) formed on paleozoic shales and gneises with gold-sulphide-quartz veins and dissemination the secondary gold mineral phases (named by author rusty gold) were found. They consist from fine-dispersional mixture of various Fe hydroxides, gold particles and new gold mineral phase - Au-hydroxide. Results of detail electron-microscopy study, microprobe analysis and X-ray powder data have shown that the gold hydroxide AuO(OH,Cl) has crystal structure of NaCl-type (a = 4.9 A, Fm3m). Gold hydroxide contains minor impurities of Fe, Si, Al and changeable Ag. Under optical microscope rusty gold has a violet colour with numerous small inclusions and rims of yellow metallic gold.

Minor gold impurities were determined in lepidocrocite, hematite, magnetite with unit cell parameter of these minerals being without changes.

Experimental studies of Fe- and Au-hydroxides were carried out. Au- and Fe-hydroxides synthezied from alcalic solutions of $HAuCl_4$ and $FeCl_3$ under normal temperature and pressure have been investigated by electron microscopy and IR-spectroscopy. It was found that real structure of synthezied Au-hydroxides differs from natural ones and belongs to type of gigantic cluster compounds $Au_q(O, OH, Cl)_n$, where $q > n$. Metal skeletons of gold clusters have sizes from 20 to 300 A, cuboctahedron form, cubic crystal structure (a = 3.92-3.96 A, Fm3m, inner distance Au-Au in cluster is 1.77-1.80 A). There is not miscibility between synthetic AuOOH and FeOOH. Coexisting phase with metallic gold is feroxigite (δ -FeOOH) but not akaganeite (β - FeOOH).

Difference between crystal structures of natural and synthetic gold hydroxides in dependance of kinetic factors of mineralogenesis is discussed. Chemical and mechanical transformation of gold in placers are considered.

HFI IN GERMANATES AND IN RELATED SILICATES

G. V. Novikov and L. V. Sipavina

Hyperfine interactions (HFI) in germanates Fe_2GeO_4, $FeGeO_3$, and $CaFeGe_2O_6$ were studied by ^{57}Fe gamma-resonance. The data on relative silicates were revised.

Spinel Fe_2GeO_4, the structural analog of the high-P cubic (s.g. *Fd3m*) phase of Fe_2SiO_4, was synthesized at normal pressure. Fe^{2+} ions in the spinel are accommodated in octahedral positions. The local magnetic field on ^{57}Fe nuclei appears at about 16 K, at 4.2 K its value is close to saturation, nevertheless relaxation of magnetic moments takes place up to 4 K. Some specific features of ^{57}Fe spectra of Fe_2GeO_4 are discussed.

$FeGeO_3$, the structural equivalent of the high - T, unquenchable monoclinic phase of $FeSiO_3$ (s.g. *C2/c*), orders magnetically at T_N = 53 K. The electric field gradient (EFG) main axes q_{zz} on ^{57}Fe nuclei in M1 and q_{xx} in M2 positions are parallel to the internal magnetic field at 15 - 53 K and are assumed to be about parallel to the crystallographic b axis. Below 14K spins of Fe^{2+} in both M1 and M2 positions change the orientation with respect to EFG tensor main axes, the spin-canting transition is assumed. Some contradictory data on magnetic properties of chain silicates (S. Ghose et al., (1987), J.Linares et al., (1983), A. Wiedenmann and J.-R. Regnard, (1986), A. Wiedenmann et al., (1986)) are discussed.

In monoclinic Ca-Fe chain germanate (s.g. *C2/c*), which is the hedenbergite structural analog, Fe^{2+} ions favor M1 octahedra, from 5 to 25 % of them were determined in M2 distorted polyhedra in samples studied.

Using textured samples and temperate applied magnetic field, the sign of EFG tensor main component q_{zz} on ^{57}Fe nuclei in germanates and in some silicates was determined at room temperature. The original two-step algorithm of hyperfine ^{57}Fe pattern quantitative interpretation was used. The principal ideas of the algorithm (G.V. Novikov, (1987)) are to be presented. Some results are given in Table 1. The data accumulated give the background for comparative analysis of properties of germanates and silicates.

Table 1. Local fields in germanates and related silicates

Site	T (K)	I.s. (mm/s)	Q.s. (mm/s)	H (kOe)	η	q_{zz} sign	
			Fe_2GeO_4 (T_N=16K)				
Oct.	300	1.113	2.914	0		-	a
Oct.	4.2	1.24	2.86	145	0.2	-	
			$FeGeO_3$ (T_N=53K)				
M1	300	1.162	3.007	0		+	
M2	300	1.154	2.233	0		+	b
M1	16.7	1.27	3.30	105.0	0.1	+	a
M2	16.7	1.28	2.40	332.1	0.1	+	
M1	4.2	1.28	3.26	183.0	0.1	+	
M2	4.2	1.28	2.28	312.6	0.1	+	
			$CaFeGe_2O_6$				
M1	300	1.152	2.003	0		+	
M2	300	1.165	2.678	0			
			$FeSiO_3$ (T_N=45K)				
M1	300	1.184	2.506	0		+	
M2	300	1.134	1.932	0		+	
M1	4.2	1.000	3.000	199.0	0.1	+	a
M2	4.2	1.26	2.000	321.4	0.4	+	
			$CaFeSi_2O_6$ (T_N=41K)				
M1	300	1.193	2.245	0		+	
M1	4.2	1.31	2.61	186.2	0.1	+	a
M1	4.2	1.32	2.56	184.5	0.4	+	

[a] H is assumed to be parallel to q_{xx}
[b] H is assumed to be parallel to q_{zz}

References

S. Ghose et al., Phys. Chem. Minerals 14, 36 (1987).
J.Linares et al., J.Magn.Magn.Mater. 31-34, 715 (1983)
A. Wiedenmann & J.-R. Regnard, Solid State Comm. 57, 499 (1986).
A. Wiedenmann et al., J. Phys. C19, 3683 (1986).
G.V. Novikov, VINITI Reports No 4112-B87, No 7404-B87, No 7533-B87 (1987) (in Russian).

XAFS Studies of Iron in the teeth of Chitons

Numako C. (*Univ. of Tokyo*), Nakai I. (*Sci.Univ. of Tokyo*), Okoshi K. (*Senshu Univ. of Ishinomaki*) and Ishii T. (*Nat. Inst. Rad. Sci.*)

Introduction It has been known that several kinds of animals have iron oxides such as magnetite (Fe_3O_4) or iron hydroxide oxide (FeOOH) in their bodies. Many biologists reported that pigeon, honey bee and some kinds of fishes which migrate between fresh water and the sea keep small magnetite crystals in their brain. It is said that these animals use magnetite as a compass in order to know the direction on the earth. On the other hand, it is famous that chitons, which belong to Polyplacophora, accumulate iron in their teeth as magnetite at high concentration. Fig. 1 shows a structure of a radula of chiton which has many teeth. The teeth become maturated gradually from the top of the radula (part A) to the end (part D) in the mouse. It has not been ascertained yet, however, what kind of biological functions iron in the teeth has. The purpose of this study is to investigate the chemical forms of iron in the teeth of chitons, and to examine crystal formation mechanism in them.

Experimental A radula of chiton was separated from the body and was kept in alcohol. The Fe K-absorption spectra of the radula of chiton were measured using synchrotron radiation at Photon Factory, National Laboratory for High Energy Physics, Tsukuba, Japan. Samples were placed in polyethylene bags during the measurements. For a comparison, Fe K-absorption spectra of some Fe compounds were measured as standards of known chemical formula and structures: i.e., Fe, Fe_2O_3, Fe_3O_4, α-FeOOH, β-FeOOH, and γ-FeOOH.

Results and Discussion The Fe K-XANES spectra of the radula of chiton are presented in Fig. 2, and are compared with some of the standard materials. The overall spectral shapes from part A to D of the radula gradually change, but any chemical shift of the pre-edge peaks could not be observed among the spectra. Moreover, the spectra of the teeth were identical to none of the standard materials. A result of X-ray powder diffraction analysis of the maturated teeth showed that the diffraction pattern was magnetite. From XANES

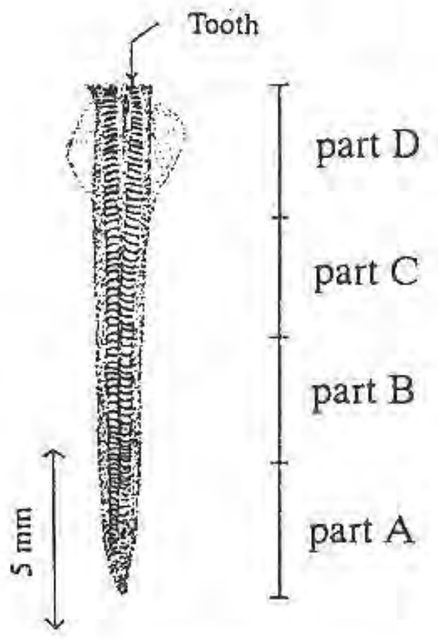

Fig. 1 The structure of the radula of chiton.

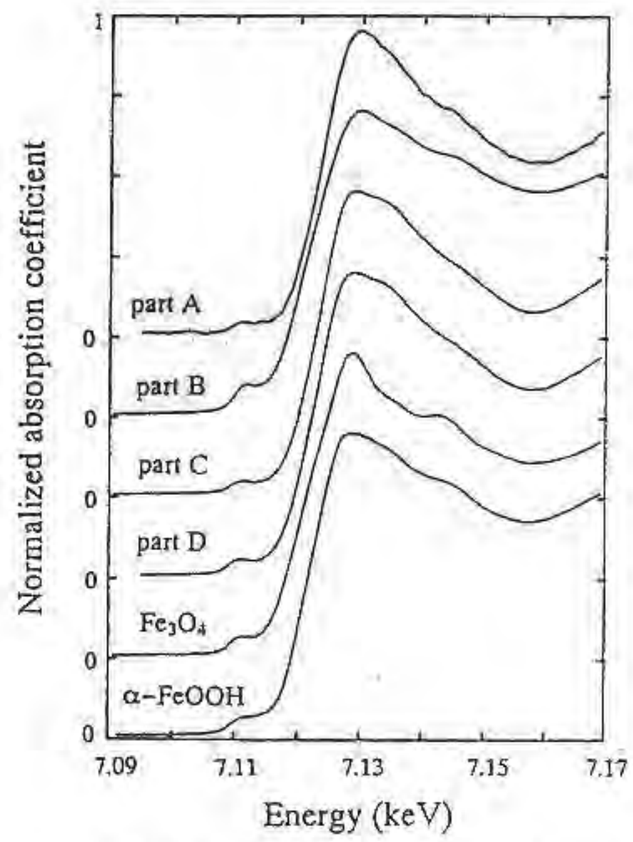

Fig. 2 Fe K-XANES spectra of teeth of chiton and standard materials.

spectra of the teeth, however, even most maturated part D was not very close to that of magnetite. It is interesting that the results of XANES spectra don't agree with that of X-ray diffraction. It is considered that the teeth of chiton contain both magnetite and other amorphous components different from magnetite. Some biologists reported that this amorphous component could be a starting material of magnetite formation in the teeth. This may be a key material in the accumulation of iron from organic tissues into the teeth and will be a subject of our future research.

$Mn^{2+}_2SiO_3(OH)_2 \cdot H_2O$, A NEW PYROXENE RELATED CHAIN SILICATE FROM THE NCHWANING MINE, KALAHARI MANGANESE FIELD, SOUTH AFRICA

Nyfeler D., Armbruster Th. (*Univ. Bern, Switzerland*), Dixon R. (*Geolog. Survey, South Africa*) and Bermanec V. (*Univ. Zagreb, Croatia*)

$Mn^{2+}_2SiO_3(OH)_2 \cdot H_2O$ is an orthorhombic chain silicate (space group $Pca2_1$, $Z = 4$, $a = 12.672(9)$, $b = 7.217(3)$, $c = 5.341(2)$ Å occurring as pin-cushion-like aggregates together with calcite, bultfonteinite and chlorite at Nchwaning mine, located in the Kalahari Manganese Field, Northern Cape Province, South Africa. The aggregates are formed by light brown, transparent needles which average 1 x 0.1 x 0.05 mm in size. The crystal structure including H positions was solved and refined from X-ray single-crystal data to $R = 2.5$, $R_w = 2.8$ %. The structure consists of layers containing laterally linked so-called pyroxene-building units: an edge-sharing double chain of octahedra topped with a 'Zweier-single chain' of SiO_4 tetrahedra. Symmetry equivalent building units are turned upside down and laterally linked to the former unit. This arrangement yields a double layer structure with hydrogen bridges linking the double layers. A striking feature of the structure is the fact that one MnO_6 corner is formed by a H_2O molecule. The new mineral is biaxial negative with the refractive indices $\alpha = 1.681(1)$, $\beta = 1.688(2)$, $\gamma = 1.690(2)$ and $2V_x = 54.4(4)^o$. The optical orientation is $X=b$, $Y=a$, $Z=c$. The mineral has two perfect cleavages parallel to (010) and (100). The calculated density is 3.202 g/cm^3. The tetrahedral chain and octahedral distortion of the new mineral is compared with pyroxenes having Mn^{2+} on M1 (synthetic $MnSiO_3$ ($P2_1/c$ clinopyroxene), and johannsenite $CaMn[SiO_3]_2$). In addition, distance least square refinements were applied to test whether cations with smaller (Mg) and larger ionic radii (Ca) could substitute for Mn^{2+} in $Mn^{2+}_2SiO_3(OH)_2 \cdot H_2O$. It was found that Mg and Ca analogs would also yield reasonable structure models.

FURTHER INSIGHTS INTO AMPHIBOLE COMPLEXITY

Oberti R. *(CNR-CS Cristallochimica e Cristallografia, Pavia)*

The discovery and crystal-chemical characterization of three new amphibole end-members derived by unforeseen polyvalent substitutions [leakeite, $NaNa_2(Mg_2Fe^{3+}_2Li)Si_8O_{22}(OH)_2$ with Li^+ ordered at M3 (Hawthorne *et al.*, 1992); $CaCa_2(Mg_4Al^{3+})Si_5Al_3O_{22}F_2$, with Ca^{2+} at A; $NaNa_2(Mn^{2+}_2Mn^{3+}_3)Si_8O_{22}O_2$, with Mn^{3+} ordered at (M1 + M3) and O^{2-} at O3] has recently given further complexity to the amphibole compositional space. In order to understand whether or not these end-members represent an oddity due to very peculiar conditions of crystallization, a systematic examination of rock-samples for which anomalous amphibole unit-formulae had been published was performed; it showed that octahedral Li is frequent in alkali amphiboles from manganiferous metasediments and from peralkaline granits (Hawthorne *et al.*, 1993). ^{M3}Na-bearing amphiboles have also been recognized; ^{A}Ca has been found both in other localities and in synthetic F-pargasite.

These findings show that cation distribution in amphibole is much more subtle than previously recognized, at least at peculiar (but not rare) P,T,X conditions of crystallization. This implies the need for detection and modelling of cation distribution between independent structural sites with the same coordination. A systematic comparative crystal-chemical study has been therefore carried out with the aid of the data base available at the CSCC, which presently contains more than 700 single-crystal structure refinements (SREF). This work shows the presence of: a) $^{[6]}Al^{3+}$ disorder between M2 and M3 in pargasite with composition near to the end-member, but $^{[6]}Al^{3+}$ order at M2 in F-pargasite (Oberti *et al.*, 1995); b) $^{[4]}Al^{3+}$ disorder between T1 and T2 well before the stoichiometric limit of 2 apfu in pargasite and kaersutite crystallized at very high T (low- to high- P) conditions; c) $^{[6]}Fe^{3+}$ disorder between M1 and M3 in the presence of almost complete dehydrogenation. As it is the case of the new end-members, crystal-chemical arguments show that the observed cation distributions are determined mainly by local charge-balance constraints.

It can be concluded that the amphibole structure is even more flexible than we thought, and can therefore adapt itself to the most various P,T,X conditions of crystallization. This is of course the reason why amphiboles are nearly ubiquitous in the Earth's crust (and not so rare in the upper mantle) and are therefore important indicators of petrogenetic conditions. However, these results indicate that the amphibole structure cannot be modelled on a straightforward site-assignment basis. Although the situation is simpler in the case of more canonical compositions, in general a reliable starting set must be built up with very accurate and complete site-populations as those obtained by integrating SREF+EMP+SIMS (for Li and H) analyses performed on the same crystal. Moreover, first attempts towards structure modelling have shown that site dimensions are affected at variable extent by the composition of adjacent structural sites.

These results also indicate that a complete chemical characterization should be performed in the case of amphiboles, especially in Li-bearing and magmatic environments. The lack of Li and/or H determination is in fact the reason of incorrect recalculation of many amphibole unit-formulae, with obvious implications on the estimates of petrogenetic (e.g. fO^{2-}) conditions.

Hawthorne, F.C., Oberti, R., Ungaretti, L., Grice, J.D. (1992). *Am. Mineral.*, **77**, 1112-1115.

Hawthorne, F.C., Ungaretti, L., Oberti, R., Bottazzi, P., Czamanske, G. (1993). *Am. Mineral.*, **78**, 733-745.

Oberti, R., Hawthorne, F.C., Ungaretti, L., Cannillo, E. (1995). *Can. Mineral.*, submitted.

PETROGENETIC GRID FOR ULTRAHIGH-PRESSURE METAMORPHISM IN THE MODEL SYSTEM $CaO-MgO-SiO_2-CO_2-H_2O$

Ogasawara Y. Liou J.G. and Zhang R. (*Dept. of Geological & Environmental Sciences, Stanford University*)

Recent findings of talc-bearing and magnesite-bearing assemblages from UHP eclogite and garnet peridotite (e.g., Zhang & Liou, 1994) and dolomite-coesite assemblage (Okay, 1993) in central China required a petrogenetic grid for the model system $CaO-MgO-SiO_2-CO_2-H_2O$. The *P-T* grids shown below were calculated for eight minerals at varied X_{CO2} using non-ideal mixing of CO_2-H_2O and the data set by Holland & Powell (1990). The results indicate that the *P-T* grid strongly depends on X_{CO2}; the invariant points A, B, C and D are stable at both X_{CO2} conditions. At $X_{CO2}=0.001$ (Fig. **a**), Di-Tc-Co assemblage is stable at P=26 ~ 31 kb, Di-En-Ms assemblage is stable from 20 to 38 kb, and dolomite can not coexist with coesite. At $X_{CO2}=0.4$ (Fig. **b**), all stable invariant points and univariant reactions shift toward lower-*P* and higher-*T*, and the Do-Ms-Qz (Co) stability field expands. The narrow stability field of Do-En assemblage appears between 690 and 850 °C. For ultramafic composition indicated by Di-En-Fo triangle, the talc-bearing assemblages are restricted to

retrograde stage whereas the mafic rocks may contain Di-Tc-Co as peak and Di-Tr-Qz as retrograde assemblages (*P-T* path shown as an arrow in Fig. **a**). The calculated *P-T* grids will be significantly modified with additional components and phases or using different thermochemical database. Nevertheless, they illustrate the observed paragenesis in Dabie UHP terrane and the inhomogeneity of fluid phase during the UHPM at mantle depth.

References:
Holland, T.J.B., Powell, R. (1990). *J. Metamorphic Geol.*, **8**, 89-124.
Okay, A.I. (1993). *Eur. J. Mineral.*, **5**, 659-675.
Zhang, R., Liou, J.G. (1994). *Amer. Mineral.* (in press).

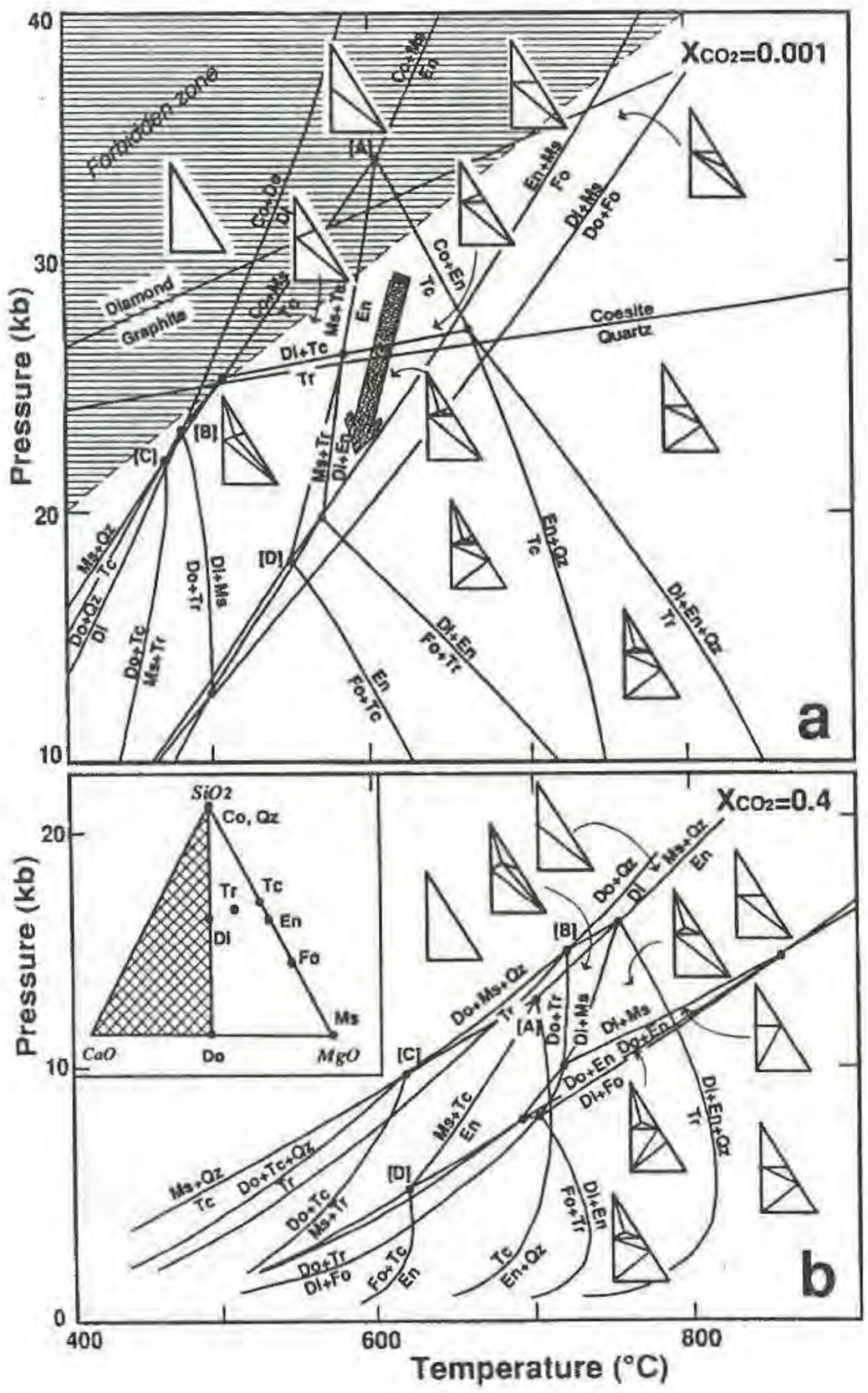

MICROCRYSTALLOGRAPHY IN MINERALOGY BY SYNCHROTRON RADIATION

Ohsumi,K.(*Photon Factory,Natl Lab. for High Energy Physics*), Hagiya,K.(*Dept. of Life Sci., Himeji Inst. of Tech.*), Miyamoto, M. (*Miner. Inst.,Univ. Tokyo*) and Ohmasa,M.(*Dept. of Life Sci.,Himeji Inst. of Tech.*)

In order to analyze micro-textures in complicated crystal aggregates, and to refine structures of submicrometer-sized crystal particles or twinned domains, an equipment and software system was developed using the Laue method combined with polychromatic synchrotron radiation. This development was carried out at beamline 4B of the Photon Factory(PF), KEK and was successfully applied to some inorganic specimens. In the second stage of the development, micrometer size areas of larger specimens were analyzed. In particular, this method is important for studying micro areas of minerals which have been sectioned for analysis by optical microscopy. In this way, crystallographic information may be obtained from the exact same area of samples as is probed by optical microscopy, EPMA or Raman spectroscopy. The development of the micro area diffraction system at beamline 4B and its recent results are described below.

Due to the limited space around beamline 4B of PF, a micro- beam is produced by using a micro-pinhole. The newly developed equipment for structural studies of micro area was designed to combine a micro-pinhole and with an imaging plate (IP; Fuji Co. LTD.) read out system. The experiment is carried out in vacuum to minimize air scattering, but it is not necessary to open the chamber to obtain diffraction data from a different micro area or with different crystal orientation. The micro-pinhole is set at a distance of 7mm from the sample position. The diameter of the micro beam was measured to be 8μm full width at the half maximum by scanning an ion chamber with a slit. The IP detector covers -60 to 165 degrees in two-theta with a cylindrical camera radius of 100 mm.

This apparatus has been applied to olivine in a thin section of L6 chondrite, and the structure refinement including the site occupancies of Mg and Fe over M1 and M2 sites was successfully carried out based on the intensities of Laue spots. The orientation of pyroxene in a micro lamella structure in a thin section of a meteorite was also determined by this technique.

A NEW COBALT ARSENATE HYDRATE MINERAL FROM ASHIO MINE, TOCHIGI PREFECTURE, JAPAN

Okada, A. (*Inst. Phys. Chem. Res.*), Ii, H. (*Chiba Univ.*) and Takeuchi, H. (*Showa Corp.*)

Ashio Mine is a copper mine found in 1610, locating at Ashio, Tochigi Prefecture, Japan. The geology in the vicinity of Ashio Mine is mainly composed of Paleozoic slate, sand stone and chert, and rhyolite injecting the host sedimentary rocks. Ore deposits consist of metalliferrous veins and replacement deposits which occur in the Paleozoic strata and rhyolitic inject bodies (Kusanagi, 1954, 1957). The metalliferrous veins are typical xenothermal ore deposits and more than 200 veins, 16 cm wide on average, distribute in the minerallized area. The replacement deposits named Kajika ore deposits, range up to several ten meters in diameter. Two types of ores, massive ores and disseminated ones, are found in the mineralized deposits. Primary minerals in the metalliferous veins are mainly pyrite and chalcopyrite with accessory amounts of pyrrhotrite, sphalerite, galena, native gold, native bismuth, bismuthinite, arsenopyrite, wittichenite, stannite, cassiterite, wolframite and marcasite. Secondary minerals are native copper, native silver, chalcocite, bornite, cuprite, malachite, azurite, vivianite, ludllamite, melanterite and so on. In the replacement deposits, the main mineral assemblage is either chalcopyrite-pyrrhotite or sphalerite-pyrrhotite with minor pyrite, arsenopyrite, stannite, cassiterite, native bismuth, bismuthinite and sphalerite. During the mineralogical investigation of the ore minerals from Kajika ore deposit in Ashio Mine, reddish purple crystalline aggregates, about 0.1 mm in size, were found on the surface of the black-colored, mineralized area composed mainly of bismuth-pyrite-wolframite assemblage. X-ray powder diffraction analysis by using Debye method and electron microprobe analysis under the electron microscopic observation indicated that the reddish purple material is composed of $CoHAsO_4 \cdot H_2O$. The $CoHAsO_4 \cdot H_2O$ mineral is isostructural to koritnigite, $ZnHAsO_4 \cdot H_2O$, which was found at Tsumeb in Southwest Africa (Keller *et al.*, 1979), and cobaltkoritnigite, $(Co,Zn)HAsO_4 \cdot H_2O$, from Saxonian Erzgebilge and Bauhaus mining area in Richelsdorf Mountains (Schmetzer *et al.*, 1981), and has a triclinic lattice (space group: P1) with a_0=7.87, b_0=15.7, c_0=6.72 Å, α=94.3°, β=96.9° and γ=90.3°. The X-ray powder pattern is in good agreement with that of synthetic $CoHAsO_4 \cdot H_2O$ (Zettler *et al.*, 1979). Ashio mine's cobalt arsenate hydrate mineral does not contain significant amount of zinc, and consists of the cobalt end-

membered component. This new phase is presumably a weathering product from Co-beaing species like cobaltite, CoAsS.

References

Keller, P., Hess, H., Süsse, P., Schnorrer, G. and Dunn, P. J. (1979). *Tschermaks Min. Petr. Mitt.*, **26**, 51-58.

Kusanagi, T. (1954). *Japanese J. Petrol. Mineral. Econ. Geol.*, **38**, 8-18.

Kusanagi, T. (1957). *Japanese J. Petrol. Mineral. Econ. Geol.*, **41**, 263-312.

Schmetzer, K., Horn, W. and Medenbach, O. (1981). *Neues Jahrb. Miner. Mh.*, **6**, 257-266.

Zettler, F., Riffel, H., Hess, H. and Keller, P. (1979). *Z. anorg. allgem. Chem.*, **454**, 134-144.

GRANULITE FACIES PRECURSORS OF ULTRA-HIGH-PRESSURE METAMORPHISM IN DABIE SHAN, CHINA

Okay, A.I. (Dept. of Geology, Istanbul Technical Univ.)

Ultra-high-pressure eclogite and calc-silicate with coesite and diamond inclusions in garnet, pyroxene and dolomite occur in a felsic gneiss dominated large area in Dabie Shan in central China and suggest that a large piece of continental crust has been metamorphosed at pressures of over 30 kbar and at temperatures of 800° ±50° C during the Triassic. The protoliths of these ultra-high-pressure rocks could either be sedimentary and magmatic rocks of the upper continental crust or Precambrian metamorphic basement rocks. Petrology of some garnet-pyroxenites in Dabie Shan sheds light on this problem and indicates that, at least some of the protoliths of the ultra-high-pressure rocks, were granulite facies basement rocks of Precambrian age.

The garnet-orthopyroxenite intercalated on metre scale with eclogite and garnet-clinopyroxenite forms a 50 m thick and several hundred meter long lens in felsic gneiss in Dabie Shan. The garnet-orthopyroxenite consists mainly of enstatite and poikilitic pyrope-rich garnet with minor clinochlore, Ti-clinohumite, olivine, magnesite and rutile. The equilibrium P-T conditions in the garnet-orthopyroxenite, as determined from the Fe-Mg exchange equilibria between garnet and enstatite, and Al solubility in enstatite were 740° ±50° C and over 40 kbar pressure. Pressures of over 28 kbar are also indicated by inclusions of quartz pseudomorphs after coesite in garnet from the adjcining eclogites.

The garnets in the orthopyroxenite contain large number of inclusions of sapphirine, clinochlore, enstatite, talc, corundum, gedrite, hornblende and phlogopite, typical minerals of the granulite facies metamorphism. Phase relations among the inclusion minerals indicate that they have formed at similar temperatures of 730° ±30° C as the ultra-high-pressure metamorphism but at much lower pressures of 4±2 kbar. This early granulite facies metamorphism was most likely part of a Precambrian event genetically unrelated to the Triassic ultra-high-pressure metamorphism. This is supported by recent Sm-Nd data on eclogites indicating reworking of a Precambrian continental crust.

If most of the protoliths of the ultra-high-pressure rocks were Precambrian granulite facies metamorphic rocks, as it seems likely, there must have been no externally derived fluid phase present during the ultra-high-pressure metamorphism and the dry felsic gneisses that form the bulk of the ultra-high-pressure metamorphic terrain, did probably never developed full ultra-high-pressure assemblages.

PYRITE FROM RECENT AND FOSSIL GEOTHERMAL SYSTEMS OF KAMCHATKA

Okrugin V.M., Chubarov V.M. and Okrugina A.M. (Inst. Volcanology, Petropavlovsk-Kamchatsky)

Pyrite (Py) is the most abundant mineral in geothermal systems of Kamchatka. Py was studied by the methods of scanning electron microscopy, microprobe analysis and atomic-fluorescent spectroscopy. Py is characterized by variety of forms: from oolites and framboides, dendrites to idiomorphic crystals reaching the most diversity in recent thermal springs. We have found thin Py incrustations (2-8 mk) around plant remnants in springs, "microtubes" with a diameter of 2-5 mm, composed of apatite, opal and Py, as well as microincrustations on the surface of rock fragments and minerals. Py from the fossil Au-Ag epithermal systems (low- and high-sulphide types) is characterized by more crystalline forms. Py was found to contain As (up to 10.2%), Hg (up to 20.5%, occasionally with As up to 5.6%), Te (up to 0.6%), Mn (up to 0.8%) Cu (up to 0.7%), Ag (up to 0.2%), Au (up to 0.4%). The above elements are distributed unevenly. Two types of their zonal distribution are recognized: classic concentric and more complicated, mosaic, spotted. Some regularities have been revealed between the mineral composition of epithermal Au-Ag ores, their spatial position and composition of elements-admixtures in Py. In South Kamchatka, Py has almost everywhere As, in Central Kamchatka, Cu, sometimes Te. Au forms in contemporary Py local clusters.

FIELD AND THEORETICAL STUDY OF CHLORITOID AND STAUROLITE DECOMPOSITION IN THE ANDALUSITE STABILITY FIELD, TONO CONTACT METAMORPHIC AUREOLE, NE JAPAN; IMPLICATIONS FOR PELITIC PHASE RELATIONS UNDER LOW PRESSURES.

Y. Okuyama-Kusunose (*Geol. Museum, G.S.Japan*)

Low-pressure metamorphism is characteristic in regional high heat flow terranes, and in thermal aureoles around igneous plutons. Low-*P* pelitic phase relations are commonly described by reactions involving andalusite(And), sillimanite(Sil) and cordierite(Crd) in the model pelitic system(KFMASH). Their mutual relations to medium-*P* phase relations involving staurolite(St) and garnet(Grt) are not, however, well understood due to the relative instability of these minerals in normal pelitic compositions under low pressures: the low-*P* phase relations in the KFMASH system have been considered to be a simple extrapolation of medium-*P* phase relations (e.g., Spear & Cheney, 1989), or to include a Crd-Cld join instead of the And-biotite(Bt) and St-Bt joins (e.g., Powell & Holland, 1990).

A different topology on the low-*P* phase relations is recently proposed by Okuyama-Kusunose (1994), based on the reaction relations observed in Fe-rich metapelites of the contact aureole around the I-type Tono granodiorite mass, northeast Japan, and other localities. The phase relations newly proposed

involve a model univariant reaction, chlorite (Chl)+Cld+muscovite(Ms) = And+Bt+quartz(Qtz)+ H_2O (II), located in the middle-grade temperatures (520-530 °C) of the stability field of andalusite. Two invariant points, with coexisting And-Bt-Chl-Cld-Crd (ABCCC) and And-Bt-Chl-Cld-St(ABCCS), exist in the low-*P* and high-*P* ends, respectively, of this reaction. The latter invariant point has a high-*P* equivalent located in the kyanite field in the previous studies. However, the observation of reaction (II) in the stability field of andalusite leads to a conclusion that this high-*P* equivalent must be metastable.

This paper reports a further occurrence of extremely Fe-rich assemblages, including Cld, Grt and St, from the Tono contact aureole. The aureole is divided into the paragonite, andalusite, and sillimanite zones on the basis of the formation and phase transition of Al_2SiO_5 minerals. The andalusite zone is further subdivided into lower and upper subzones by the formation of Crd through the reaction, Chl+Ms+Qtz = And+Bt+Crd+ H_2O(III). The assemblages newly found are shown in Fig. 1, with ranges in X_{Fe} of phases. A thermodynamic analysis of these assemblages confirms the topology proposed by Okuyama-Kusunose(1994). The topology predicts that, in metapelites of the normal compositions, the And-St assemblage is limited between the invariant point ABCCS (3.2 kbar, 532 °C) and the triple point of Al_2SiO_5. The analysis also suggests a stable extension of St-breakdownreaction, St+Ms+ Qtz = Al_2SiO_5+ Bt+Grt+H_2O, in the andalusite field.

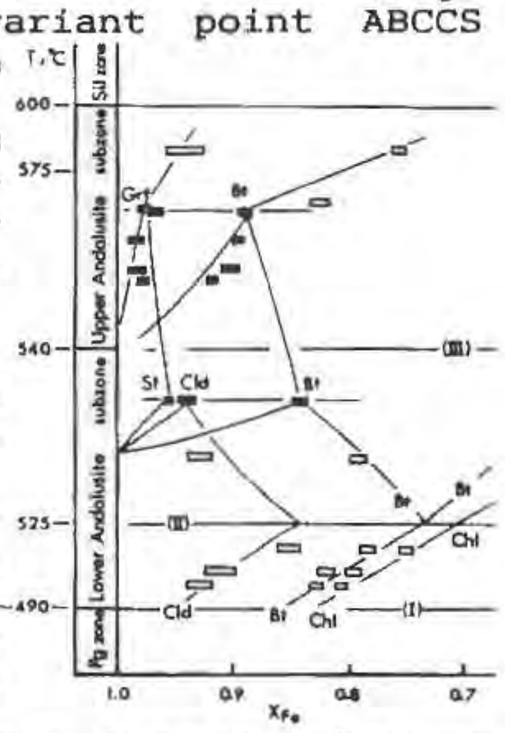

Fig. 1; An empirical T-X_{Fe} diagram showing Fe-rich assemblages in the Tono contact metamorphic aureole.

References:
Okuyama-Kusunose, Y.(1994) *J. Metamorph. Petrol.*, 12, 153-168.
Powell, R. & Holland, T. (1990) *Amer. Mineral.*, 75, 367-380.
Spear, F.S. & Cheney, J.T. (1989) *Contrib. Mineral. Petrol.*, **101**, 149-164.

DISPLAY AND SAMPLE MANAGEMENT SYSTEM IN THE GEOLOGICAL MUSEUM, GEOLOGICAL SURVEY OF JAPAN

Y.Okuyama-Kusunose, Y. Banno, C. Matsue, and M. Bunno (*Geological Museum, Geological Survey of Japan*)

Geological Museum of the Geological Survey of Japan (GSJ) was founded in 1980 at the time of removal of the GSJ to the Tsukuba Science City, Ibaraki Prefecture, in the suburb of Tokyo Metropolis. The Geological Museum is a 2-story building in annex to the main building of GSJ. The Museum building furnishes a central hall and four exhibition room one of which is for systematic display of minerals, rocks and fossils, and storage rooms and laboratories. The Museum Section has much older history, being founded in 1952, for systematic management of geologic samples used for research at GSJ. In the IMA session, we will introduce our Museum mainly focused on the display of mineral specimens and the sample management system.

Most of the geologic samples on display and in storage are collected in the Japanese Islands, and classified into five categories, namely, the R, M, F, B and D collections. The total numbers of registered samples are 60,251 in rocks (R collection), 13,934 in fossils (F collection), and 30,656 in minerals (M collection, numbers at March 28, 1994). A large number of rock samples are collected during the survey for quadrangle series. B and D collections are boring cores (B collection) and a group of samples from ore deposits (D collection), respectively. These two collections consist of a large number of individual samples of various rock (mineral) types in a single registration. The numbers of registered samples are constantly increasing, with the largest increment during the 1993 fiscal year being recorded in M collection (20 % increase). As for the M collection consists of individual samples of relatively high quality, the D collection is used as a principal source of mineral samples for exchange and scientific use. The present number of D collection is as small as 66, but they include as many as 6000 individual samples from 66 ore deposits and other mineral localities most of which are characteristic to geological setting of Japanese Islands as an active volcanic arc.

Registration numbers are given on a first-come-first-served basis in each of the five categories. At the time of registration, the sample names, localities, names of collector, and the other information concerning to geological features of the samples must be reported by filling a form that must also be presented together with samples. The registration procedure was first designed 15 years ago when GSJ decided to construct a computer-aided sample management system. The samples are managed according to information reported in a form on a database named GEMS-II-T (GEological Museum sample management System, ver. II-T) which is constructed on a NEC PC-9801 series computer. Because this computer is dominant only in Japan, and because our system is not connected to network, presently it is not accessible outside the Museum. Lists of samples whatever stored on the database can be obtained on this system according to sample numbers, type of samples, localities, and other geological features. However, the numbers of samples stored on the database is limited, especially on minerals, due to a chronic lack of hands for the computer work. Efforts are continued to breakthrough this bottleneck, together with updating of the system and simplification of the registration procedure.

ILLITE-SMECTITE INTERSTRATIFIED MINERALS IN THE SMECTITE-TO-ILLITE TRANSITION

Olives J. and Amouric M. *(CRMC2 - CNRS. Marseille)*

In a hydrothermal smectite-to-illite conversion series, high-resolution transmission electron microscopy revealed, in most of the samples, the coexistence of pure smectite, pure illite and interstratified illite-smectite. The observations suggest the existence of two transformation mechanisms : (i) dissolution of smectite and crystallization of illite (Fig. 1) ; (ii) solid-state transformation of one smectite layer into one illite layer (Fig. 2) (Amouric & Olives, 1991). It is likely that the interstratified minerals are formed by the solid-state mechanism, whereas pure illite crystals are produced by dissolution-crystallization.

The illite-smectite interstratification sequences are disordered, in most cases, but locally ordered sequences are also observed

(Fig. 3). Analytical electron microscopy results show that the general evolution is from montmorillonite to illite, which implies a chemical modification of all the structural levels (interlayer, tetrahedral and octahedral).

First electrostatic lattice energy calculations have been made with our "overlap method" (Olives, 1986), of more rapid convergence than the classical Ewald's or Bertaut's methods. We obtain the following energies : (i) -80.16 MJ/mole for an illite of composition $K_{0.75}(Si_{3.25}Al_{0.75})Al_2O_{10}(OH)_2$; (ii) - 82.00 MJ/mole for a smectite of composition $(Na, K)_{0.35}Si_4(Al_{1.65}Mg_{0.35}O_{10}(OH)_2$ (dehydrated montmorillonite) ; (iii) -162.14 MJ/mole(corresponding to $O_{20}(OH)_4$) for the ordered interstratified is, with the structure .... $O_m(TIT)_iO_m(TIT)_s$ ... (I, T and O are respectively the interlayer, tetrahedral and octahedral levels ; i refers to the above illite composition, s to the smectite one and m denotes the middle composition between i and s), this structure being that which corresponds to the minimum of the energy . Then, the energy of the interstratified mineral is approximately equal to the sum of the energy of pure illite and that of pure smectite. This is in agreement with the observed coexistence of these three phases in our samples.

Amouric, M. & Olives, J. (1991). *Eur. J. Mineral*, **3**, 831-835.
Olives, J. (1986). *Acta Cryst. A*, **42**, 340-344.

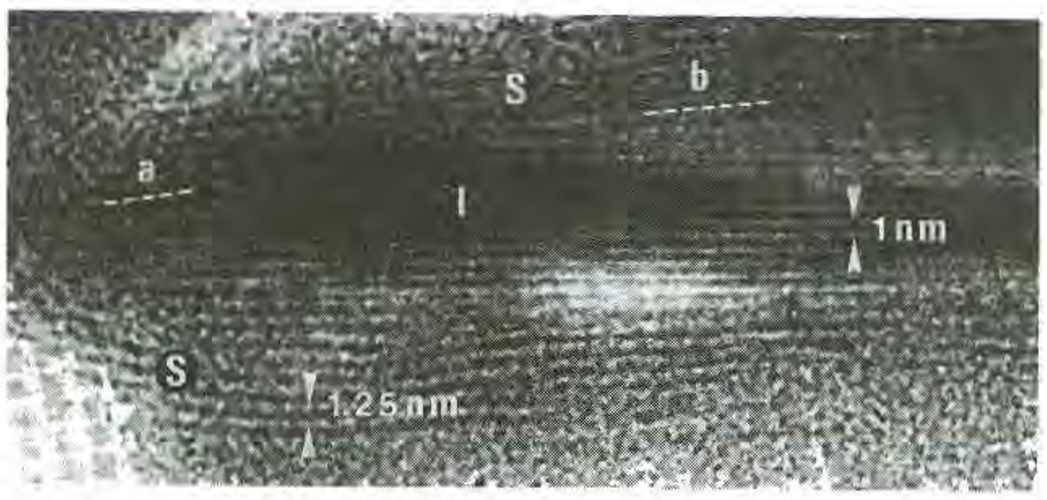

Fig. 1 : The darkly contrasted illite crystal I grows at the expense of surrounding smectite S, cutting the smectite layers (with a small angle) in the upper part of the image (a, b zones).

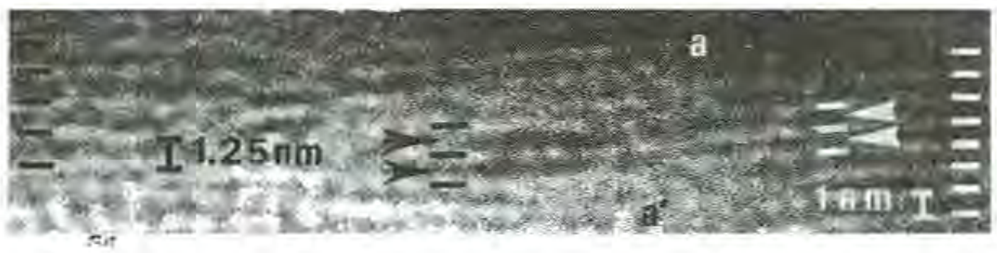

Fig. 2 : Lateral transition between smectite layers (left part) and illite layers (right part). A continuous lateral transformation : 1 smectite layer→1 illite layer is observed (indicated by arrows).

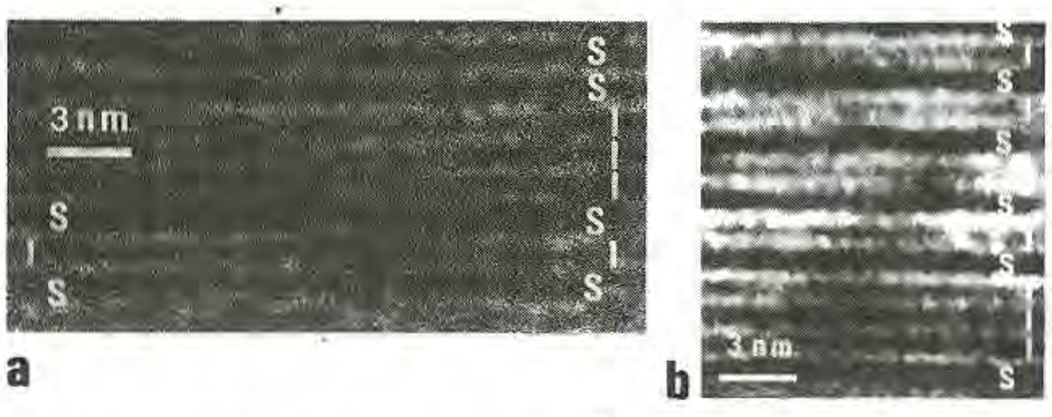

Fig. 3 : Interstratification sequences (I = illite layer, S = smectite layer): (a) disordered type ; (b) IS ordered type

FLUID-INCLUSION DATA OF COLOMBIAN EMERALDS : TOTAL HOMOGENIZATION BY SALT DISSOLUTION.

Ordoñez,F.H.R.,Schultz-Güttler,R.A.,Svisero,D.
(University of São Paulo , Brasil)

Partial results of an ongoing research on the origin of the Emeralds of Colombia are presented. The deposits are confined along two belts on the eastern and western flanks of the "Cordilheira Oriental"near Bogota, Colombia.

Most studies in the past concentrated on one or the other deposit only.Here,fluid inclusion studies on a total of five deposits (Muzo,Pacho,Yacopi,Coscuez,Chivor)with altogether 450 fluid inclusions (FI)studied complement the existing data.

The most important finding of the microthermometric measurements is that all FI from all deposits showed **PARTIAL homogenization by vapor disappearance before TOTAL homogeni - zation by salt dissolution** (**Halite** at Muzo, Pacho,Chivor and Coscuez,but **Sylvite** at Yacopi).The temperatures of partial homogenization are 210±30°C and those of total homogenization 330±30°C.Emeralds from Chivor showed slightly higher temperatures of 370± 30°C. These results reconfirm data given by Ottaway et al.,1986,from Muzo and by Giuliani et al.,1992,from Coscuez, but not those given by Kozlowski et al.,1986,from Somondoco.

As a first approximation of the complex chemistry of these fluids,the data are displayed in the model systems $CaCl_2$-NaCl-H_2O and $CaCl_2$-KCl-H_2O **respectively.One notes very high salt concentrations** of about 40 to 50% by weight for all deposits.

Minimum pressures of sealing of these FI are estimated by the method of Solovava et al.,1992, in the model system NaCl-H_2O using the difference of temperature between the **vapor disappearance** and **salt dissolution.** Pressures determined this way are **independent** from any estimated thickness of former overburden based on the geological history. Since the system NaCl-H_2O shows a quite high vapor pressure along the Liquid(L)-Solid(S)-Vapor(V)coexistence curve and the slope of the halite dissolution (L+S/L)curves should not be strongly dependent on the presence of other dissolved ions,the pressures so estimated may very well be maximum pressures of closing and formation of those FI. The values found define a mean of about 1400 bars. It is therefore likely that the mean conditions of the formation of the FI's and consequently of the emeralds are about 330 to 370°C and about 1400 bars pressure.

This pressure translates to about 5 km of former overlying rockstrata at the time of formation of these emerald deposits and , if one considers the lithostratigraphy of the "Cordilheira Oriental" as shown by Dengo & Covey,1993, appears reasonable.

Dengo,C.A.,Covey,M.C.(1993)Bull AAPG,77, 1315-1337
Giuliani,G.,Sheppard,M.F.,Cheilletz,A.,Rodriguez,C. (1992)Compte Rend.l'Acad.Sc.(Paris),314, 269-274
Kozlowski,A.,Metz,P.,Estrada,H.A.J.(1988) N. Jb. Min. Abh., 159, 23-49
Ottaway,T.L.,Wicks,F.J.,Spooner,E.T.C.(1986) Fluid Inclusion Research , 19 , 322
Solovava,I.,Girnis,A.,Gruzkova,A.,Naumov,B.(1992) Geochem. Intern. , 29, 64-74

• STUDY OF ANORTHOCLASE MICROSTRUCTURE FROM KILIMANJARO

Organova N.I., Marcille I.M., Borutsky B.E. *(IGEM RAN)*, Zacharov N.D. *(IKRAN)*, Salyn' A.L. *(GIN RAN, Moscow, Russia)*

X-ray (powder diffractometer, Guinier camera, Smith method), chemical (microprobe) and electron microscopy (TEM and HRTEM) study of anorthoclase sample with formula $Or_{24.2}Ab_{65.2}An_{9.5}Cn_{0.5}SrFsp_{0.6}$ has been carried out. Unit cell dimensions are: a = 8.25(2), b = 12.93(4), c = 7.13(2) Å, α =

92.62(2), β = 116.24(11), γ = 89.57(2)°. Powder diffraction displayed only one triclinic phase, X-ray pattern by Smith method has shown albite and pericline twins.

Electron microscope patterns contain dark stripes (K-rich phase) with lengthening along $(\bar{2}01)$ plane instead usual $(\bar{6}01)$ one. There are lamellae of two kinds – with mean thicknesses 65 or 400 Å .

Careful investigation of diffractometer profiles has shown that some of them are wider than others. It is because Na- and K-phases have different but close contents.

The exsolution of this sample has taken place after monoclinic-triclinic transition. Such sequence of events is connected with the history of Kilimanjaro sample (Organova *et al.*, 1992).

An analogous case has been described in Transbaikal feldspar sample (Chisina & Bochkaev, 1981). Possibly similar conditions existed in Antarctic Ca-rich anorthoclase (Tagai *et al.*, 1988).

References:
Organova, N.I., Marcille, I.M., Zacharov, N.D., Borutsky, B.E., Salyn, A.L., Ivanov, V.P. (1992). *Izv. Ac. Sc. Ser. Geol.*, **12**, 47–58 (in Russian).
Chisina, N.R. & Bochkaev, F.I. (1981). *Miner. Jour.*, **3**, 36–49 (in Russian).
Tagai, T., Takeda, H., Tachikawa, Schropfer, L.H., Fuess, H. Kaminura, U., Kyll, P.R. (1988). *N. Jb. Miner. Mh.*, **1**, 9–20.

TWO NEW MINERAL PHASES FROM PIEDMONT AND TUSCANY, ITALY

Orlandi P. (*Dept. of Earth Sciences, Univ. of Pisa*)

Phase-1, $PbFe_6^{3+}(PO_4)_4(OH)_2$,belonging to the alunite group, is the phosphate analogue of plumbojarosite.

It occurs as millimetric vitreous red trigonal pyramidal crystals associated with vanadinite, opal, pyrite, cubanite,sphalerite, galena, grossular, diopside, and others within the cavities of an ultramafic rock outcropping near Balangero, Piedmont, Italy.

Preliminary data indicate that phase-1 shows symmetry and crystallografic features very similar to those of plumbojarosite (symmetry of diffraction effects $\bar{3}2/m$; $a = 6.78(1)$, $c = 16.98(4)$ Å). The X-ray powder pattern and Weissenberg photographs of phase-1 and plumbojarosite are almost identical.

Preliminary microprobe chemical data indicate that Pb, P and Fe are the main costituent chemical elements; S and As are also present as minor elements.

Phase-2, ideally $Fe^{3+}V_3^{3+}Ti_3^{4+}Sb^{3+}O_{13}OH$ is the vanadium analogue of derbylite, or the antimony analogue of tomichite.

It was found at Buca della Vena mine, where derbylite and V-bearing derbylite crystals were already found in the past (Mellini et al., 1986).

Phase-2 occurs as 0.1 mm prysmatic black crystals within small cavities in calcite and dolomite veins associated with acicular tufts of stibivanite-2*M*. At Buca della Vena mine further vanadium minerals occur: stibivanite-2*O*, karelianite, and V-rich varieties of apuanite and versiliaite.

Phase-2 was identified by an X-ray powder pattern obtained with a Gandolfi camera which turned out almost identical to that of derbylite, and on the basis of a semiquantitative SEM-EDS chemical analisis: V, Ti, Fe and Sb (in order of decrescent abundance) were the only elements revealed.

Phase-1 and phase-2 are still not completely characterized and yet not again submitted to the I.M.A. Commission on New Minerals and Mineral Names.

References:

Mellini, M., Orlandi, P., Vezzalini, G. (1986). *Mineralogical Magazine*, **50**, 328-330.

MINERALOGICAL FEATURES OF THE PGE-BEARING HORIZONS, IOKO-DOVYREN LAYERED MASSIF, NORTHERN TRANSBAIKALIA, RUSSIA.

Orsoev D.A., Kislov E.V., and Konnikov E.G. (*Buryatian Geol. Inst., Ulan-Ude, Russia*).

The Ioko-Dovyren massif stretches on 26 km length with thickness of 3.5 km and was emplaced 740 Ma in the Proterozoic Olokit peri-continental sedimentary basin. The massif sequence comprises plagioclase lherzolites, dunites, troctolites, olivine gabbros and olivine gabbronorites. The PGE-bearing horizons were revealed at the gabbroic part of the massif and traced for 19 km.

The lowest and richest horizon I is confined to the transition area from rhytmic layered troctolite - olivine gabbro sequence to massiv olivine gabbro (500-600 m above of cumulus plagioclase first appearence). It is composed of concordant veins, lenses of coarse-grained, taxitic troctolites, olivine gabbros, pegmatites and anorthosites with thickness up to 5m.

The horizon II is confined to transition area from olivine gabbro to olivine gabbronorites. It consists of concordant veins, lenses of taxitic leucogabbros, pegmatites, microgabbros, gabbronorites, norites, plagioclase-bearing peridotites with thickness up to 3 m.

The PGE-bearing rocks are characterized by presence of the disseminated sulphides (up to 7 vol.%) and OH-bearing minerals (phlogopite, biotite, zoisite, prehnite, actinolite, chlorite), sometimes K-feldspar and quartz. In troctolites and olivine gabbros the sulphide mineralization presents troilite, hexagonal pyrrhotite, ferrous pentlandite, rarely cubanite and chalcopyrite. More PGE-rich anorthosites are characterized by two sulphide association: i) cubanite, pentlandite, chalcopyrite and hexagonal pyrrhotite; ii) high nickel-bearing pentlandite, talnakhite, bornite, chalcopyrite and godlevskite. The mackinawite is common, sphalerite, galena, copper and pyrite are rare minerals.

The tulameenite, zvyagintsevite, moncheite and tetraferro-platinum were found in association with cubanite and chalcopyrite at anorthosites and form aggregates or separate grains.

CONTRASTING MECHANISMS FOR STIBNITE PRECIPITATION AT MARI ROSA AND EL JUNCALON ANTIMONY DEPOSITS: IMPLICATIONS IN TEXTURAL FEATURES AND TEMPERATURE OF MINERALIZATION.

Ortega L. and Vindel E. (*Dept. Cristalografía y Mineralogía, Univ. Complutense de Madrid*)

Mari Rosa and El Juncalón are late Hercynian vein-type antimony deposits hosted by Upper Precambrian metapelitic rocks in Central/Western Spain and are spatially related to Upper Carboniferous-Lower Permian granitoids. Main mineralized veins at Mari Rosa correspond to small bodies of massive stibnite hosted within dilation zones occurring along low-angle compressional faults. At El Juncalón the mineralization occurs along subvertical strike-slip faults.

The mineral paragenesis developed along three hydrothermal

episodes. Of these only the second episode was of some importance and led to the deposition of a stibnite ore containing up to 30 ppm Au at Mari Rosa and up to 0.4 ppm at El Juncalón. Striking differences between both deposits are observed regarding textural features: massive stibnite occupy most of vein cavities in Mari Rosa while mostly quartz with discrete stibnite occurs at El Juncalón.

Fluids associated to ore deposition belong to the H_2O-NaCl-CO_2-CH_4-N_2 system, with the exception of CO_2, absent in El Juncalón mineralized areas. They evolved with a progresive cooling from initial circulation temperatures close to 400°C in the early stages to around 150°C in the late episodes. At Mari Rosa, massive stibnite deposition resulted from a boiling process developed at 300°C and 0.9-1 Kb. Unmixing of the fluid was induced by sudden pressure drops in dilational jogs during the low-angle faults movements. Simple cooling of the fluid, with no salinity changes, was the driving mechanism for stibnite deposition around 250°C at El Juncalón.

These contrasted precipitation mechanisms account for most of the textural features of the deposits, with massive mineralization at Mari Rosa and low stibnite/quartz ratios at El Juncalón. According to Drummond and Ohmoto (1985), boiling at $T \leq 300$°C will result in the precipitation of similar amounts of quartz and metals and is clearly different from cooling, which would deposited about ten times more silica with the same amount of metals.

Differences in temperature of stibnite precipitation between Mari Rosa and El Juncalón can also be explained in terms of the mechanism of precipitation involved in each deposit. Ore solutions are likely to be saturated in antimony only below 270°C (Munoz *et al.*, 1992). According to experimental data (Wood *et al.*, 1987; Krupp, 1988) decrease of fluid temperature from 350°C to 200° would dramatically reduce antimony solubility (up to ten times), leading to precipitation of stibnite even from initially undersaturated solutions. Therefore, simple cooling seems to be an adequate mechanism for stibnite precipitation. However, phase separation during boiling in Mari Rosa must have led to a strong partitioning of antimony towards the liquid phase according to Spycher and Reed (1989), which would have resulted in saturation and sudden precipitation of stibnite at 300°C.

References:

Drummond S.E. & Ohmoto H. (1985): *Econ. Geol.* **80**, 126-147.

Krupp, R.E. (1988): *Geoch. et Cosmoch. Acta*, **52**, 3005-3015.

Munoz M., Courjault-Rade P. & Tollon F. (1992): *Terra Nova* **4**, 171-177.

Spycher, N.F. & Reed, M.H. (1989): *Econ. Geol.*, **84**, 328-359.

Wood S.A., Crerar D.A. & Borsick M. (1987): *Econ. Geol.* **82**, 1864-1887.

$^{87}Sr/^{86}Sr$ DATA OF CELESTITE ORE DEPOSITS IN SPAIN

Ortega M.[1], Barbieri M. [2], Rodríguez M. [1], Arana R. [3] and Trudu C.[2]

1. *Dpto. Mineralogía y Petrología. Univ. de Granada, Spain.* 2. *Dipto. Scienze della Terra. Univ. di Rome, Italy.* 3. *Dpto. Química Agrícola, Geología y Edafología. Univ. de Murcia, Spain.*

Introduction

Strontium and especially celestite outcrops and ore deposits are found at many locations in Spain. This study presents the first isotopic data from the most important celestite deposits with the aim of achieving a better understanding of their genesis. The Sr isotopic values were measured using a Finnigan MAT-262 spectrometer at the Geochemical Laboratory of the University of Rome (Italy).

Characteristics of the ore deposits

The deposits studied are located in SE Spain, in the provinces of Granada, Murcia and Jaén. According to their geological context they can be grouped as follows: Betic Cordilleras ("Montevives", MO; "Fortuna", FT; "El Saltador", ES; "Lorca", LO and "Las Gacias", GA), and the "Jaén" (J) deposit in the Guadalquivir basin (Table).

Table 1. Characteristics of primary mineralizations.

Ore deposit	Host rocks/Age	Morphology	Mineralogy
MO(1,2)	marnes with gypsum/UM	well stratified	celestite
FT(3)	dolomies/J-C	stratified	celestite
ES(4)	calc-schists/PT	lenticular	celestite
LO(4)	dolomitic limestones/T	stratified	celestite*
GA(5,6)	limestones/calc-schists/T	massive	celestite
J(7)	marnes with gypsum/T	nodules	celestite

UM: Upper Miocene; C: Cretaceous; J: Jurassic; T: Triassic; PT: Permian-Triassic. * Galene, fluorite. 1: Ortega et al. (1973); 2: Martín et al. (1984); 3: Alías et al., (1979); 4: Arana & López (1983); 5: Arana & López (1982); 6: López (1988); 7: Sanz et al. (1984).

Isotopic data

Table 2 summarises the most significant isotopic data obtained in this study. Each datum represents a mean value of five measurements. All the analyses present an error of $\pm$ 0.00002 (2 σ).

Discussion and Conclusions

Table 2. Isotopic data

Geological context	Ore deposits	$^{87}Sr/^{86}Sr$
Betic Cordilleras	MO	0.70855
	FT	0.70772
	ES	0.70889
	LO	0.70901
	GA	0.70954
Guad. Basin	J	0.70857

There is a marked diversity of isotopic values in the different deposits studied, regardless of their geological context. Projection of the isotopic data of celestite from "MO" deposit on the curve of De Paolo & Ingram (1985) indicates that the Sr has a marine origin and the data agree with the isotopic values of the Miocene sea. The carbonate fraction, which should represent the stromatolitic component, presents a higher isotopic value (0.70887) than the celestite, which demonstrates that the stromatolitic carbonate was replaced by celestite within the mixing zone with participation of freshwater and sea water, as proposed by Martín et al. (1984).

The deposits in the province of Murcia present highly variable isotopic values. The data obtained at "FT" agree with a diagenetic genesis of the deposit. The isotopic values are characteristic of the beginning of the Tertiary, according to the curve of De Paolo & Ingram (1985). Activity of sulphate water may have been involved in this genesis (López, 1988). The "ES", "GA" and "LO" deposits all present isotopic values indicative of formation under epithermal temperatures, without the action of sea water and with an important supply of radiogenic ^{87}Sr from silicate rocks. In fact, the parent rock of the "ES" deposit has a value of 0.70884, which is very similar to that of the deposit itself.

In the "J" deposit the isotopic values found in the massive celestite of the nodules (Table 2) reflect the contribution of the Triassic parent marls, whose silicate fraction would have provided the ^{87}Sr with the highest isotopic value. The isotopic variations detected inside a single celestite nodule are exclusively due to the growth process of the nodule and the continuous supply of Sr from the parent rock (0.70855) down to the last generations of beautiful celestite crystals (0.70862 and 0.70869).

References

Alías, L.J., Fernández, M.T., Ortíz, R. (1979). *Est. Geol.*, **35**, 433-436.

Arana, R. & López, V. (1982). *Bol. Soc. Esp. Min.*, **5**, 123-133.

Arana, R. & López, V. (1983). In: L. hom. C. Felgueroso, 21-33.

De Paolo, D. & Ingram, B.L. (1985). *Science*, 227, 938-941.

López, V. (1988). Ph. Thesis, Univ. Murcia, 352, (unpublished).

Martín, J., Ortega, M., Torres, J. (1984). *Sed. Geology.*, **39**, 281-298.

Ortega,M., Arana,R., Rodríguez,M.(1973). *Cuad. Geo. Univ. Granada*, 5, 5-19.

Sanz, C., Ortega, M., Rodríguez, J., Velilla, N.(1984). *Bol. Geol. Min.* XCV-III,268-276.

• ON GENERAL FEATURES OF PORPHYROBLAST FORMATION

Ostapenko G.T. *(Inst. of Geochemistry, Mineralogy and Ore Formation, Academy of Sciences, Kiev, Ukraine)*

General mechanism of porphyroblast formation proceeding from the existence of thin intergranular fluid film was analysed. It has been shown that the formation of porphyroblast as a solid body, replacing the same volume of a matrix (mineral, rock) is possible due to the rise of an extra pressure (EP), exerted by the growing

porphyroblast on the matrix. The rise of considerable crystal pressure at metamorphic PT–conditions was experimentally proved by the author using the periclase hydration reaction as an example.

It was found that EP values vary weakly along grain contacts. For the stationary process of porphyroblast growth a quantitative dependence of EP upon rate constants for porphyroblast crystallization and matrix dissolution (which, in their turn, depend on film thickness, surface reaction rate and other factors), their molar volumes, solubility and theoretical value for crystallization pressure was found. Moreover equations for rates of stationary crystallization and dissolution as functions of the above mentioned factors were obtained.

General thermodynamical conditions for idiomorphism of a porphyroblast which is in contact with other crystals were formulated. Crystal "striving" for idiomorphic shape in quasi–isotropic matrix was estimated both for static (absence of growth) and dynamical (when porphyroblast grows) conditions.

Explanations for formation of mineral porphyroblasts with different grade of idiomorphism in metamorphic rocks were given.

References:
Nikitina L.P.(1986)The thermodynamic of silicate solid solutions.,Leningrad,Nauka,152p.(in Russian).

LONG AND SHORT RANGE ORDER AND THERMODYNAMIC PROPERTIES OF OLIVINE SOLID SOLUTIONS OF DIFFERENT COMPOSITIONS.

Ovchinnikov N.O.and Nikitina L.P.(Inst.Precambrian Geol.& Geochronology Rus.Ac.Sci., St.-Petersburg,Russia)

The distribution of isomorphic cations between non–equivalent positions (long range order) of natural $(Fe_x Mg_{1-x})_2 SiO_4$ (0<X(Fe)<0.30) and synthetic $(Fe_x Mg_{1-x})_2 GeO_4$ (0<X(Fe)<0.35) and $(Fe_x Ni_{1-x})_2 SiO_4$ (0<X(Fe)<1.0) olivines was studied by Messbauer method.

The Fe–Mg long range order degree in silicate and germanate olivines was found to be very small.The replacing Si with Ge in the anion group of Fe–Mg olivine structure has no influence on cation distribution.

The replacing Mg with Ni essentially changes the character of cation distribution.In Fe–Ni olivines we establish the high degree of long–range order(Fe in M2)and differences of long–range order and unit cell units compositional dependences with X(Fe) equal to 0.0–0.3(1 group),0.3–0.5(2 group) and 0.5–1.0(3 group). The calculations according to quasichemical treatment for multisite low symmetrical solid solutions(Nikitina,1986)show the existance of short range order(the dominating formation of asymmetrical atom couples),which is confirmed by Messbauer data.The deviation from ideal state is negative(for the 3 group W(Fe–Ni)= -4.3 ± 1.3 kcal/mol).

In Mg–Ni olivines the high degree of long range order(Mg in M2),without differences in long range order compositional dependences was established by many scientists.According to quasichemical treatment calculations the existance of dominating formation of symmetrical atom couples (clastering) was found.The deviation from ideal state is positive(W(Mg–Ni)= 1.7 ± 0.8 kcal/mol)despite the high degree of long range order.

We suppose that the existance of compositional differences of solid solution structural characteristics and the sign of deviation from ideal state in olivine solid solutions are the result of long and short range order degree changes.

The compositional and temperature dependences of thermodynamic functions of mixing (activities of components;Gibbs free energy and exess free energy;enthalpy of mixing) for the Fe–Ni and Mg–Ni olivine solid solutions are obtained.

MINOR AND TRACE ELEMENTS IN MINERALS OF EQUILIBRATED METEORITES AND UPPER MANTLE ROCKS AS INDICATORS OF THERMAL HISTORY

Palme H.[1] and Zipfel J.[2] *([1]Mineralogisch-Petrographisches Institut, Universität zu Köln, 50674 Köln; [2]Max-Planck-Institut für Chemie, Mainz, 55020 Mainz, Germany)*

The application of microchemical methods for the analysis of trace elements in minerals of meteorites and upper mantle rocks has produced a wealth of new data. Not only concentrations but also zoning patterns of trace elements within single mineral grains are now routinely determined. Since the distribution of trace elements among minerals of equilibrated rocks is, in general, temperature dependent information on equilibration temperatures and/or cooling rates can be deduced. The application of these data is, unfortunately, limited by the rudimentary knowledge of relevant diffusion coefficients, in particular, at low temperatures.

Olivine and pyroxene are the most abundant minerals in upper mantle rocks and undifferentiated meteorites which also may contain large metal fractions. As diffusion in olivine and metal is much faster than in pyroxene, equilibria involving olivine and metal record lower temperatures (500°C to 700°C) than equilibria with pyroxenes (800°C to 1200°C), given sufficiently slow cooling rates.

Examples: The REE-distribution between orthopyroxene (opx) and clinopyroxene (cpx) was found to be strongly dependent on temperatures determined by the enstatite-diopside solvus. Upper mantle rocks and equilibrated meteorites (silicate inclusions in IAB-iron meteorites and Acapulcoites) plot on the same correlation line. This implies that the Al_2O_3 content of opx has little influence on the incorporation of REE into opx since opx in meteorites has low Al_2O_3 contents. Deviation from the correlation was used to infer late addition of REE to the Acapulco meteorite (Zipfel et al., in prep.).

The Ca contents of olivine (ol) in cpx and opx containing rocks are strongly temperature dependent (Köhler and Brey, 1990). Rapidly cooled xenoliths in alkali-basalts have ol with high Ca (500 to 700 ppm) preserving upper mantle p,T-conditions. A steep CaO-increase at the outermost rim reflects short duration heating by the host magma (Zipfel and Wörner, 1992). Large peridotite bodies may have low CaO in ol indicative of slow cooling. Rocks of the Zabargad peridotite have ol zoned in CaO with Ca as low as 50 ppm. From these data cooling rates can be calculateded which then may be transformed into uplift rates (Zipfel et al. 1991). Olivine of silicate inclusions in IAB-iron meteorites and Acapulcoites, well equilibrated chondritic meteorites, is zoned in CaO with Ca-contents as low as 30 ppm. Apparently, these meteorites cooled slowly with CaO-diffusion frozen in at temperatures below 500°C. Quantification of cooling rates is, however, uncertain primarily because of the uncertainty involved in extrapolating high temperature diffusion coefficients to low temperatures.

Similarly low equilibrium temperatures as recorded by CaO in olivine are derived from Ni distribution between olivine and metal. IAB-silicates and Acapulcoites have Ni-contents in olivine from 3 to 11 ppm, depending on the prevailing fO_2 and corresponding to temperatures of around 600°C.

Conclusions: From these data and from the knowledge of diffusion coefficients cooling rates at different temperatures can be calculated. Hopefully, this will finally lead to a better understanding of the thermal history of terrestrial and

extraterrestrial rocks and allow, for example, to calculate the size of meteorite parent bodies or estimate reliable uplift rates of large ultramafic massifs on Earth.

References: Köhler T. and Brey G. (1990) Geochim. Cosmochim. Acta **54**, 2375-2388; Köhler T. et al. (1991) N. Jb. Miner. Mh. **9**, 423-431; Zipfel J. and Wörner G.(1992) Contrib. Mineral. Petrol., **111**, 24-36; Zipfel J. et al. (1991) Beih. z. Eur. J. Mineral. Vol. 2, No. 1,1190 (abstract).

ON SELECTIVE CAPTURING OF INCLUSIONS IN DIAMOND IN CONNECTION WITH THE UPPER MANTLE COMPOSITION PROBLEM

Pal'yanov Yu.N., Khokhriakov A.F., Borzdov Yu.M., Doroshev A.M., Tomilenko A.A. and Sobolev N.V. **(United Inst. of Geology, Geophysics and Mineralogy, Novosibirsk, Russia)**

The mantle substance is best preserved in diamond which, by virtue of its physical properties, is the ideal container for minerals captured during crystallization. Thus syngenetic inclusions in natural diamond are the main source of information on chemical and phase composition of the upper mantle rocks. When studying inclusions in diamonds from different deposits, it has been ascertained that the most frequently occurring minerals captured in diamond growth are sulphides, chromite, olivine, garnet, pyroxenes, rutile. However, the following question is still open: to what extent does the averaged composition of inclusions correspond to the diamond formation medium composition? This problem may be solved by modelling the process of capturing inclusions by diamond single crystals grown in different artificial systems.

Diamond single crystals were grown in the Fe-Ni-C system using the high pressure setup of the "split sphere" type at 5.5-6.5 GPa, 1300-1600^{o}C. The size of single crystals was from 0.1 up to 2 carats. Phase composition of inclusions was determined by X-ray, chemical analysis was performed using the Camebax microanalyzer. Fluid inclusions were studied by volumetric, Raman-spectroscopy and gas chromatographic techniques.

The following phases were identified as inclusions: tenite, wustite, spinel, garnet, orthopyroxene, diamond and fluid. Tenite (γ-Fe0,3 Ni0,7) occurs primarily as negative diamond crystals. Wustite (Fe0,95Ni0,050) forms triangular and hexagonal crystals in epitaxial growing with diamond. Spinel is a complex solid solution with the following basic components: magnetite - 74.8, chromite - 18.5, - fayalite - 6.1 and picrochromite - 0.6 (mol.%). Spinel appears as needle crystals. Garnet falls in pyrope-grossular-almandine group (by composition). Orthopyroxene is chemically close to ferrosilite with small calcium and sodium impurity. Garnet and orthopyroxene form disperse inclusions in the shape of a rain drops or their aggregates. Diamond occurs as octahedral and cubooctahedral crystals. Fluid is a compound solution of liquefied gases in liquid alcans appearing as tubular, disk-shaped and faceted inclusions. The source of the substance forming inclusions that differ radically from crystallization medium in composition is microimpurities in the starting materials, adsorbed gas phase on high pressure cell substance and elements of the container diffusing into melted metal. It has been established that with a certain ratio of crystallization parameters, growing diamond crystals capture phases which are not typical for the system on the whole, and, vice versa, sometimes they do not capture the main phase of crystallization medium - melted metal. Thus in diamond crystallization, inclusions are captured selectively, and their phase and bulk chemical composition does not adequately represent the crystallization medium composition. This should be taken into account in developing the upper mantle substance models.

VILLAMANINITE AND OTHER CU-RICH PYRITE TYPE DISULFIDES: A REVIEW.

This work is devoted to the memory of Prof. Dr Günter H. Moh (1929-1993)

Paniagua, A., Marcos-Pascual, C., Moreiras, *(Dept. of Geology, Univ. of Oviedo)* D. B., Fenoll, P., *(Dpt. of Mineralogy-Petrology, Univ. of Granada)* Friedl, J., Wagner, F. E. *(Dpt. of Physics, Tech. Univ. München)*

Villamaninite, (Cu, Ni, Co, Fe)$(S,Se)_2$, represents the Cu-rich portion of pyrite type disulfides, including the end-member CuS_2 (Paniagua, 1989, Oudin *et al.*, 1990). This paper synthesize the results of a multimethod approach to the knowledge of the mineralogical characteristics and genesis in its type-locality: Providencia mine, Leon, Spain.

The electron microprobe analyses on samples of this deposit show a wide range of solid solution in the FeS_2-CoS_2-NiS_2-CuS_2 series (Ypma *et al.*, 1968, Paniagua, 1989, 1991), being the villamaninite composition formally established between the CuS_2-$Cu_{0.5}Ni_{0.5}S_2$-$Cu_{0.33}Ni_{0.33}(Co+Fe)_{0.33}S_2$-$Cu_{0.5}(Co+Fe)_{0.5}S_2$ according to the IMA CNMNMN. Sulfur is substituted by selenium up to 9.12 wt. % Se. Microprobe analyses made under enhanced analytical conditions (Paniagua, 1991) show important amounts of trace elements, being Zn (<0.9 wt. %), Ag (<0.7 wt. %), As (<0.5 wt. %), Hg (<0.5 wt. %), Au (<0.4 wt. %) and Sb (<0.2 wt. %) the most significant ones.

After ^{197}Au Mössbauer experiments on gold-bearing villamaninite (Friedl *et al.*, 1991) can be concluded that gold is present in a chemically bound state, different from those of any gold mineral studied to date except for gold ditellurides. This implies at least two different cation sites in the villamaninite structure, in disagreement with a pyrite type structure *sensu stricto*. This fact, together with a slight degree of anisotropy previously observed, moves to carry out a single-crystal X-ray diffractometric study (Moreiras *et al.*, 1991).

After this study becomes clear that villamaninite is not cubic, but pseudocubic, being the best fits obtained for the monoclinic $P2_1$ space group. The villamaninite cell parameters increase with the Cu content, as expected for a pyrite-type disulfide. The slight distortion of the cubic symmetry for villamaninite is in agreement with the expected Jahn-Teller distortion of Cu^{+2} in octahedral sites.

Reflectance and Vickers hardness measurements show a linear decrease with the increase in cell parameters (Paniagua *et al.*, 1987).

The relations between chemical composition, cell parameters and physical properties can be explained in terms of successive occupation of antibonding levels along the FeS_2-CoS_2-NiS_2-CuS_2 series.

Fluid inclusion and sulfur isotopic data (Paniagua, 1993, Paniagua *et al.*, 1993) suggest that the studied disulfides were precipitated from saline brines under shallow conditions at mean temperatures of 120° C and nearly hydrostatic pressure at pH 8-9 in an epithermal

environment. The most significant fluid parameters were calculated from disulfide composition, fluid inclusion and isotopic data, resulting $fO_2 \leq -54.0$ and fS_2 ranging between -16.6 and -17.8.

Friedl, J., Paniagua, A., Wagner, F. E. (1991). *N. Jahrb. Miner. Abh.*, **163 (2/3)**, 247-254.

Moreiras, D., Marcos, C., Paniagua, A., Díaz-Fernández, M., García-Granda, S. (1991). *N. Jahrb. Miner. Abh.*, **163 (2/3)**, 254-256.

Oudin, E., Marchig, V., Rösch, H., Lalou, C., Brichet, E. (1990). *C. R. Acad. Sci. Paris*, **310-II**, 221-226.

Paniagua, A. (1989). *N. Jahrb. Miner. Abh.*, **160 (1)**, 8-11.

Paniagua, A. (1991). *N. Jahrb. Miner. Abh.*, **163 (2/3)**, 241-247.

Paniagua, A. (1993). Unpubl. Th. Doc. Univ. Oviedo, 337 p.

Paniagua, A., Marcos, C., Moreiras, D., González-Prado, J. (1987). Bol. Soc. Esp. Mineral., **10-2**, 177-183.

Paniagua, A., Fontboté, L., Fenoll, P., Fallick, A. E., Moreiras, D. B., Corretgé, L. G. (1993). Proc. 2nd. Biennial SGA Meeting, Granada, 531-534.

Ypma, P. J. M., Evers, H. J., Woensdregt, C. F. (1968). *N. Jahrb. Miner. Mh.*, **1968**, 174-191.

FEATURES OF LAMPROITIC ROCKS OF MOLBO RIVER (WESTERN ALDAN, RUSSIA)

Panina L.I. (*United Institute of Geology, Geophysics and Mineralogy, Novosibirsk, Russia*)

Melt inclusions in rock-forming minerals of the Molbo rocks have been studied. Additional mineralogical investigations of Mesozoic olivine-leucite rocks of the river Molbo related by some researchers to leucitites (*Arsenyev&Nechaeva*, 1955), and by others to lamproites (*Konev et al.*, 1988) were performed. The rocks form about 1,5 m thick dike situated among Late Cambrian metamorphic rocks. Replaced olivine and leucite, apatite, rare pyroxene and phlogopite represent phenocrysts of these rocks. The groundmass is usually devitrified glass. The rocks contain (wt.%): 46-47 SiO_2, 1.2-1.4 TiO_2, 8.3-9.1 Al_2O_3, 9.8-12.1 FeO, 5.3-9.8 MgO, 4.2-6.8 CaO, 0.8-1.7 Na_2O, 6.6-9.6 K_2O, 0.9-1.4 BaO.

It was established that pyroxene pertains to low-alumina (0.2-0.5 wt.%), low-iron (FeO/FeO + MgO - 16-21 mol.%), low-titanian (0.2-0.3 wt.%) diopsides. Pyroxene phenocrysts commonly contain crystallites of fresh leucite with 3.5 wt.% of FeO and olivine crystallites (Fo_{82-84}). Pseudoleucite phenocrysts are made up of K-feldspar with 1.5-2.5 wt.% FeO. In zoned phlogopites from centre to periphery the contents of TiO_2 increase from 6.4 to 8.3 wt.% and the contents of Al_2O_3 decrease from 11 to 5.2 wt.%.

The investigations of melt inclusions showed that pyroxene was crystallized at 1180-1240 C, apatite at 1150-1030 C. The initial melt was low-alumina (6-8 wt.%) high-magnesian (4-8 wt.%) and rich in Ba and Sr. This melt preserved agpaitic character of alkalinity at all crystallization stages. High abundances of SO_3 and Cl are common to this melt (up to 0.37 and 0.47 wt.%, respectively) which promoted crystallization of baritocelestine at magmatic stage. The data obtained favor the relation of considered rocks to lamproites, to its low-titanian varieties.

References:
Arsenyev, A.A., Nechaeva, E.A. (1955). *Dokl.AN SSSR*, **104**, p.910-911.
Kohev, A.A., et al. (1988). *Dokl.AN SSSR*, **299**, p.707-710.

ON THE MINERALOGY OF KIMBERLITES OF UKRAINIAN SHIELD

Panov B.S., Melyakhovetsky A.A., Krivonos V.P, Morozova G.V. (Donetsk Technical University)

In the Priazovian part of the Ukrainian Shield in 1990 there have been revealed pipes of kimberlites broke the granites with the age of 1700 Ma. On their chemical composition kimberlites of the Priazovje are similar to kimberlites of Siberian and Chinese Platforms distinguishing from them by higher contents of K_2O(1,46%), TiO_2 (3,56%) and lower contents of MgO (18,27%). Taking account of component concentration of Mg(69,8-70,7%), Ca(14,9-16,7%), Cr(17,5-20,3%), in garnets from Priazovian kimberlites, it appears that these garnets are very closed to another ones from diamond-bearing provinces of Yakutia and other world. Chrome-spinellids are characterized by high contents Cr_2O_3(52,15-54,35%), valuable variations of TiO_2(0,22-3,68%) and unconstant concentrations of FeO(14,57-21,11%). In graines of ilmenite from Priazovian kimberlites the quantatity of TiO_2 is up to 46%, Mg-7%, Cr_2O_3-0,3%. The content of FeO in ilmenite is nearly 47%. On peculiarities of their composition studied minerals are proximit to analogous accessory minerals of diamond-bearing kimberlites from other world's regions. It is suggested that the existance of kimberlitic pipes in South-Eastern part of the Ukrainian Shield can be used as an evidence of their occurrence in other geoblocks of this part of the Russian platform.

References:
Knyazkov, A.P., Krivonos, V.P., Panov, B.S. et al (1992) of Ukr. Sc. Ac. 6, 84-88. (in Russian).
Sobolev, N.V., Kharkiv, A.D., Pohilenko, I.P. (1986) Geologia i Geophisika 7, 18-27 (in Russian).

FLUORITE AS AN INDICATOR OF RARE-METAL ORE FORMATION

Panova E.G. *(Dept. of Mineralogy, St. Petersburg University, Russia)*

Fluorite is one of the most abundant vein mineral of Akchatay W-deposit, Kazachstan. It presents in quartz-muscovite, quartz-topaz, quartz-wolframite greisens, in quartz veins, and in the most late quartz-tourmaline and quartz-carbonate veins.

Fluorites from quartz-wolframite greisens are accumulated the maximum quantities of rare-earth elements (REE) characterized by the minimum ratios of Ce group REE sum to Y group REE sum (0.27-0.37). These ratios correspond to the lowest pH of the mineralforming media. For the fluorite from post- and pre-ore paragenesis these ratios are more higher (0.48-0.66).

Concentrations Mn^{2+} in fluorites were determined by EPR and thermoluminescence methods. The data obtained show that the maximum concentration of this element correspond to fluorite from quartz-wolframite greisens.

The relative Eh values were obtained using the Er^{3+}/Er^{2+} ratio determined by photoluminescence method. For fluorites from quartz-wolframite greisens this ratio is near 1, for fluorites from pre-ore mineralization is near 2, and for fluorites from late veins is near 5.

Thus, the data obtained show that the most favorable conditions for wolframite deposition are the lowest pH and Eh values as compared with ore-free and ore-poor mineralization.

MINERALOGICAL OBSERVATIONS ON NON-ASBESTIFORM SERPENTINE VEINS

Papp G. (*Dept. of Mineralogy & Petrology, Hungarian Natural History Museum, Budapest*)

Mineralogical composition and microtextural features of samples of non-asbestiform serpentine veins of different macroscopic properties mainly from localities of the Carpathian Basin were studied by petrographic microscopy, X-ray powder diffraction,

infrared spectroscopy, thermal analysis and transmission electron microscopy. Special attention was paid to samples that proved to contain polygonal serpentine (PS).

Macroscopic properties and composition: The splintery and massive brittle veins were found to consist of PS+chrysotile (except for fine splintery antigorite-"picrolite"). Massive "soft" and fibrous but non-asbestiform veins were found to consist of chrysotile+lizardite. A massive banded vein contained chrysotile+PS and chrysotile+antigorite assemblage.

Detectability of polygonal serpentine: Apart from the direct TEM observation of the polygons in ion-thinned samples, it is the presence of rod-shape serpentine particles with a diameter of ≥ 0.1 μm in powdered samples, that seems to be an unambiguous proof of the presence of PS. Experiences with samples abundant in PS suggest that IRS is unsuitable for the detection of PS. This is the case for thermal methods, too, however the "splitting" of the major endothermic peak around 650-700°C (Morandi & Felice, 1979) were observed frequently in such materials. X-ray powder patterns of PS-rich samples can be characterized by chrysotile-2M and lizardite-1T (occasionally multi-layer lizardite) type reflections with a higher quantity and quality of observable peaks than those of the PS-free samples with chrysotile and/or lizardite composition.

Microtextural features observed by TEM in ion-thinned and replica samples: In splintery chrysotile+PS veins parallel growth of long PS rods and chrysotile fibres is dominant. Voids between the larger individual grains or clusters of PS are filled with (frequently deformed) chrysotile, incomplete PS or fragments of PS.

In a massive chrysotile+PS vein separate PS individuals were found in unoriented chrysotile "fabric".

The most peculiar microtextural phenomenon observed in non-asbestiform lizardite+chrysotile and antigorite+chrysotile veins was the alternation of thin lizardite (antigorite) lamellae with thin layers composed of chrysotile tubes. Chrysotile may form oriented intergrowths with these lizardite (antigorite) lamellae.

Observations on polygonal serpentine: Incomplete growth of the polygonal serpentine is abundant in splintery veins. "Open" sector boundaries of the incomplete polygons tend to close by chrysotile-like curvature or by small "half-polygons" of PS. The irregularity of PS may also be pronounced in axial direction resulting in a telescope or cam-wheel like shape.

XRD patterns of "bulk" samples and SAED patterns taken perpendicularly to the axial direction (a^*) of single PS grains suggest that both chrysotile-2M and lizardite-1T like layer stacking of PS is possible. SAED patterns taken from axial direction proved the existence of other stacking types, too (Dódony, 1993).

The contrasts observed in the sectors of polygonal serpentine of some veins indicate high density of faults in the layer stacking. SAED patterns of some individual PS grains revealed the presence of ordered multi-layer varieties. Multi-layer PS may dominate in several veins as indicated indirectly by the example of non platy multi-layer "lizardites" (in fact PS-s; Papp, 1990) known for long time from Unst and other localities.

References:
Dódony, I. (1993): *Microscopia Elettronica*, **14** (2) Suppl., 249-252.
Morandi, N. & Felice, G. (1979): *Mineral Mag.*, **43**, 135-140.
Papp, G. (1990): *Annls. hist.-nat. Mus. natn. hung.*, **82**, 9-17.

FORMATION OF THE SULFATE MINERALS IN THE OXIDATION ZONE OF THE PYRITE DEPOSIT AT WIEŚCISZOWICE (SW POLAND) - A STABLE ISOTOPE APPROACH

Parafiniuk J. (*Inst. of Geochem., Mineral. and Petrogr., Univ. of Warsaw*)

Results of the stable isotope analyses of copiapite, fibroferrite, gypsum, pickeringite and epsomite from the oxidation zone of the pyrite-bearing sericite-chlorite schists at Wieściszowice, SW Poland, have been presented. Isotope ratios of sulfur and oxygen in the sulfate ion as well as isotopic composition of oxygen and hydrogen of the crystallization water were employed to examine the formation and stability conditions of these minerals in the oxidation zone.

The $\delta^{18}O$ (SMOW) values of the sulfate ion in minerals vary in narrow intervals: -4.9 to -2.6‰ for gypsum, -4.2 to -1.6‰ for fibroferrite, -5.7 to -1.6‰ for copiapite, -6.2 to -3.6‰ for pickeringite, and -5.5 to -4.5 for epsomite. These data show that the pyrite oxidizing agent was mainly Fe^{3+}, in spite of the availability of molecular oxygen, since oxygen incorporated in the sulfate ion is derived mostly from the meteoric water. This pathway of the formation of sulfate under acid condition involves a vigorous oxidation of ferrous to ferric iron by bacteria e.g. Thiobacillus ferrooxidans. It is also supported by the almost completely absence of the ferrous sulfates in the studied paragenesis.

Sulfur isotope composition of the sulfate minerals is similar to that of pyrite for which $\delta^{34}S$ (CDT) value is 1.6‰. Gypsum and fibroferrite are slightly enriched in ^{34}S and their av. $\delta^{34}S$ value is 2.7 and 2.3‰, respectively, whereas copiapite, pickeringite and epsomite show small depletion with av. $\delta^{34}S$ values of 1.4, 1.4 and 0.7‰, respectively. This fractionation is interpreted rather as resulting from mineral crystallization than from the pyrite oxidation. The earlier formed, less soluble minerals have bound isotopically heavier sulfur than those more soluble, for crystallization of which a higher concentration of solution is necessary.

Gypsum, fibroferrite, copiapite and pickeringite were examined monthly during a year for their crystallization waterisotope composition. Gypsum reveals nearly constant isotopic composition during a whole year ($\delta D \approx -57$‰, $\delta^{18}O \approx -0.9$‰, SMOW). For fibroferrite only minor variation were detected: from -76‰ in winter to -62‰ in summer in the δD values, and from 1.0‰ in winter to 5.8‰ in summer in $\delta^{18}O$ values. The copiapite and pickeringite crystallization water close reflects the annual changes of the isotope composition of the atmospheric precipitation. Their δD values range from -97‰ in both in winter to -55 and -64‰ in summer, respectively. The respective $\delta^{18}O$ values reveal minor variation: from 3.1 and 1.1‰ in winter to 7.6 and 6.1‰ in summer.

The results above pointed out that the isotopic composition of the sulfates, appearing due to weathering, is potentially a good indicator of their formation and behaviour in the sulfide oxidation zones.

TITANIUM ENVIRONMENT AND COORDINATION: XANES ANALYSIS AND MULTIPLE SCATTERING CALCULATIONS

Paris E. (Dip. di Scienze della Terra, Univ. di Camerino, Italy)
Romano C. (Bayerisches Geoinstitut, Univ. Bayreuth, Germany)

Titanium can be found in mineral structures in both tetrahedral and octahedral coordination and,in silicate glasses, it assumes a variety of polyhedral geometries, with the average coordination number varying from 4 to 6. This structural role can be investigated by X-ray absorption spectroscopy (XANES-EXAFS) which gives information on bond distances and coordination numbers. In particular, regarding the XANES

region, changes in the position and intensity of the resonances in the experimental spectra of both Ti-bearing minerals and glasses suggested to investigate in detail the structural role and local geometry of Ti by using multiple scattering calculations (MS).

XANES spectra have been calculated using clusters of oxygens in different types of 4,5,6-fold polyhedra and in a series of geometrical environments, symmetries and degrees of distortion around the Ti atoms. The calculations allowed to evaluate the influence of each of these parameters on the Ti K-edge XANES spectra. In particular, it has been investigated the correlation between type of coordination and intensity of the pre-edge peak and its relations with the polyhedral simmetry and how various types of polyhedral distortion affect the shape of the absorption spectra.

Comparison with the experimental Ti XANES spectra of silicate glasses and minerals is satisfactorily and give insights into a systematics of titanium structural behavior by X-ray absorption spectroscopy.

EXPERIMENTAL STUDY OF SR, BA PARTITION BETWEEN PLAGIOCLASE AND AQUA-CHLORIDE FLUID AT 550-800 ^{0}C AND P=1-2KBAR.

M.Parmousina and A.Kotelnikov, (*Inst. for Exp. Mineral., Russian Acad. of Science, Chernogolovka*), I. Chernysheva (*Vernadsky Inst. Geochem. and Anal Chem, Russian Acad. of Science, Moscow)*

The goal of this work is to study a Sr, Ba partition between feldspar and fluid in the wide temperature range to study a minor elements behavior during geochemical processes in the Earth crust. We used $NaAlSi_3O_8$ - $CaAl_2Si_2O_8$ synthetic glasses and cleaned natural plagioclases as starting materials. Cold seal hydrothermal equipment with external heating and autoclaves were used. Temperatures regulated to $\pm5^0$C, pressures $\pm$50 bars. Run duration ranged from 60 to 220 days. Atomic absorption and microprobe analyses were used to determine solution and feldspar compositions.

Sr partition between plagioclase and fluid was studied at 550 and 600 ^{0}C (P=1kbar). Partition coefficient (Kp) Sr(Ba) between Pl and fluid described as: $Kp=X^{Pl}_{Sr(Ba)}/X^{fl}_{Sr(Ba)}$ Sr partition coefficient dependence on the plagioclase composition are linear:

$$\ln Kp=2.916-3.969*X^{Pl}_{Ca} \quad (550^0C) \quad (1)$$

$$\ln Kp=2.206-3.549*X^{Pl}_{Ca} \quad (600^0C) \quad (2)$$

Ba partition between plagioclase and fluid was studied at 550 600 ^{0}C (P=1kbar) and 800 ^{0}C (P=2kbar). Ba partition coefficient dependence on the plagioclase composition are linear:

$$\ln Kp=2.599-5.736*X^{Pl}_{Ca} \quad (550^0C) \quad (3)$$

$$\ln Kp=2.671-8.454*X^{Pl}_{Ca} \quad (600^0C) \quad (4)$$

$$\ln Kp=2.731-5.494*X^{Pl}_{Ca} \quad (800^0C) \quad (5)$$

Barium enrich plagioclase relative to fluid with temperature increasing.

FLUID STUDIES IN MINERALS BY GAS CHROMATOGRAFY,NMR AND ESR.

Pasalskaya L.F., Kalinichenko A.M.,Matyash I.V., Bagmut N.N..
(Inst.of Geochemistry,Mineralogy and Ore Formation, Ukraine Science Academy,Kiev).

Gas chromatography, nuclear magnetic (NMR) and electron spin (ESR) resonances have been used for quantitative determinations of fluid components, captured by minerals during crystallization.

Among them: gas chromatography with the thermal extraction of fluids in inert atmosphere for CO_2 ,CH_4 ,H_2 ,CO determinations; NMR as nondestructive method for determination of liquid water in inclusions; ESR- for diagnostic of organic substance and microquantities of carbonates in minerals.

This complex of methods allows to establish the origin of fluids, evolved from minerals by heating them in inert atmosphere too. For example, we discovered the solid organic substance in the fine fractions of synthesis quartz, extracted it, treating these fractions by concentrated HF solution. The carbonized remnant of this organic substance formed after heating it in inert atmosphere at 823 K produces in vacuum the ESR signal (g=2,003).

Modern performance about mechanico-chemical processes and our investigations allow to conclude that the discovered solid organic substance is formed on the large new surface area by the mechanico-chemical reactions during mineral grinding.

It quantity and composition are determined by properties of grinding samples and conditions of grinding.

This solid organic substance is destroyed with formation of a number of volatile components, including carbohydrogens at heating in inert atmosphere or vacuum of fine fractions of minerals. But, we consider, that the thermal decrepitation is more correct then grinding, because in the first case we can decrease the influence of surface processes by the selection of the fraction size. We applied ESR not only to check the size of fractions, but for diagnostic of organic substance, captured by minerals during crystallisation, too (Pasalskaya *et al.*,1988).So, ESR signal with g=2,003, observed in the big fraction of the samples, heated at 823 K showes, that they contain organic substance. The study of fluid components in such samples by destructive methods is difficult.

NMR as nondestructive method may be used for quantitative determinations of liquid water , Na^+, Li^+ and other ions in the solutions of fluid inclusions (Pasalskaya *et al.*,1989)

It is known, that NMR line parameters are bound with the mobility and quantity of nucleuses. This allows to receive the information about various fluid forms, for example: liquid water in fluid inclusions, constitutional and absorptional water, individual H_2O molecules, semultaneously.

So, we discovered the interlayer molecules of H_2O and CO_2 in zonal flogopit crystal and other micas, using NMR, ESR and gas chromatography (Kalinichenko *et al*,1989).

Therefore, the application of the complex of methods, including gas chromatography, NMR and ESR may provide more reliable, sometimes unique information about chemical composition and origin of fluids.

References:

Pasalskaya,L.F.,Kalinichenko,A.M.,Matyash,I.V. (1988).*Dopov.Acad.Nauk UkrRSR, Ser.B*,**9**,25-28.

Pasalskaya,L.F.,Proshko,V.Y.,Kalinichenko,A.M. (1989).*Dopov.Acad.Nauk UkrRSR,Ser.B*,**12**,11-13.
Kalinichenko,A.M.,Pasalskaya,L.F.,Pavlishin,V.I (1989).*Mineral.Journal*,**11**,67-71.

OD CHARACTER IN PbFeCl, A NEW LEAD AND IRON (III) HYDROXYCHLORIDE WITH A NOVEL STRUCTURE-TYPE

Pasero M., Perchiazzi N., Bigi S.*, Franzini M., Merlino S. (*Dept. of Earth Sciences, Univ. of Pisa; * Dept. of Earth Sciences, Univ. of Modena)*

A new phase – a hydrated hydroxychloride of lead and iron – has been recently sampled within the Etruscan iron slags of Baratti beach, near Piombino, Southern Tuscany, Italy. Associated minerals are goethite, fiedlerite–1*A*, fiedlerite–2*M*. In what follows we shall refer to this new phase with the acronym PbFeCl, with reference to its ideal chemical composition, $Pb_2Fe^{3+}Cl_3(OH)_4{\cdot}H_2O$, derived on the basis of both electron microprobe analyses and structural data. PbFeCl represents the product of the interaction between sea–water and metallurgical iron slags containing sporadic lead spherules. Therefore, just because of the role played by humans in producing the slags, it cannot be considered as a new mineral according to the guidelines recently assumed by the I.M.A. Commission of New Minerals and Mineral Names.

PbFeCl occurs as small yellow crystals tabular {001}, elongated [100] with rectangular outline, and dimensions up to 0.3 mm long and 0.05 mm across. Twinning is ubiquitous, with (001) as twin plane.

PbFeCl is monoclinic, space group $P2_1$, with a = 6.253(3) Å, b = 8.033(5), c = 9.221(6), α = 102.98(8)° (a non standard setting was chosen for the sake of consistency with the OD–groupoid family symbol, as given by Dornberger–Schiff & Fichtner, 1972). It displays a previously unreported structural type. The crystal structure of PbFeCl (R = 0.082 for 1119 reflections, single–crystal data collected with Mo$K\alpha$ radiation) is characterized by layers, parallel to (001), formed by 9–coordinated Pb atoms. The lead coordination polyhedra comprise 5 chlorines, 3 hydroxyls and a water molecule in a tri–capped triangular prism. Such layers alternate with layers characterized by column of edge–sharing $[Fe^{3+}(OH)_6]$ octahedra running along [100], and structural voids which host a complex hydrogen bonding system between hydroxyls and water molecules towards chlorine anions.

PbFeCl belongs to a family of Order–Disorder (OD) structures formed by equivalent layers. It is worth to note that OD character is a very common peculiarity among lead hydroxychlorides, as it has been described in other structural families (laurionite – paralaurionite, Merlino *et al.*, 1993; fiedlerite–1*A* – fiedlerite–2*M*, Merlino *et al.*, 1994).

The basic OD layer in PbFeCl is periodic in the two directions a = 8.03 Å, and b = 6.25 Å (γ = 90°), the width of the layer being c_0 (= c sin α) = 8.99 Å. The OD–groupoid family symbol reads:

$$\begin{matrix} P & 2_1 & m & (a) \\ & \{n_{½,2} & 2_{½} & (2_2)\} \end{matrix}$$

There are two possibilities of stacking of the layers, differing only in the direction of the translational component associated with the n glide normal to a. The glide can be either $n_{½,2}$ (translation $+b/4 + c_0$; in the following "+") or $n\bar{}_{½,2}$ (translation $-b/4 + c_0$; in the following "–"). Therefore two Maximum Degree of Order (MDO) structures may exist within this family:

1. When the stacking sequence is ++++ (or ––––) two monoclinic structures in twinning relationships are obtained, both with space group $P2_111$, corresponding to the above–described structure (MDO1 and MDO1').

2. When the stacking sequence is +–+– a structure with orthorhombic symmetry and space group $P2_1ca$ is obtained (MDO2).

According to the polytype notation, the two MDO structures should be called PbFeCl–1*M* and PbFeCl–2*O*, respectively.

References:
Dornberger–Schiff, K. & Fichtner, K. (1972). *Krist. Techn.*, **7**, 1035–1056.
Merlino, S., Pasero, M., Perchiazzi, N. (1993). *Mineral. Mag.*, 57, 323–328.
Merlino, S., Pasero, M., Perchiazzi, N. (1994). *Mineral. Mag.*, 58, 67–75.

THE ENRICHMENT OF SOLUBLE ORGANICS FROM BLACK SHALES OF SREDINNY RIDGE (KAMCHATKA) IN ORE ELEMENTS.

Pashkova O.Yu., Buslaeva E.Yu.,Generalov M.E. (Institute Geology of Ore Deposits (IGEM))

Black shales of Sredinny Ridge (Kamchatka, Russia) are host rocks of a number of Au-, Cu-, W-ore occurences. The region where the studied probes of black shales were collected is rich in industrial deposits of placer gold. The supposed source of placer gold here is quartz veins connected with these black shales.

The main goal of our study was determination of metals accumulation in soluble organics in black shales in order to clear up the role of these black shales in the formation of ore occurences.

The hot extraction of these carbonaceous rocks (C_{org} 0.3 - 0.9 mass.%) was carried out using chloroform and ethanol-benzene (1:2) as extractives. The contents of elements in extracts were determined by the INAA method. The results were equaled with the same of average contents in the Earth crust (after A.P. Vinogradov, 1962). The last ones were normalized on Mn which was presented in each extract. The data of analyses were also normalized on that element. The comparison of obtained results leads to important conclusions.

1. There are lot of elements in extracts (mainly metals) which contents are higher than the average contents in the Earth crust. More elements were determined in chloroform extracts (10 - 13) than in ethanol-benzene ones (4 - 8).

2. The highest contents of Se, Re, Hg, Au, W, Sb were determined both in chloroform and ethanol-benzene extracts.

3. The accumulation of elements in soluble organics may be connected with the presence of organoelement compounds or some other compounds with organic ligands.

•GEOLOGICAL STRUCTURE AND MINERALOGY OF CHAMBER PEGMATITES OF VOLYN

Pavlishin V. I. (*Inst. of Geol., Miner. & Ore Formation, Acad. Sciences of Ukraine, Kiev*)

The chamber pegmatites of Volyn are genetically and spatially related to the rapakivi–like granites of Korosten pluton. The pluton consists of platform–type intrusions and is surrounded by highly metamorphosed formations. About a quarter of the Korosten pluton area is occupied by gabbro–anorthosite massives, the rest consists of granitoid rocks. The most probable age of Korosten pluton is equal to 1770 million years.

In accordance with textural evidences granites are divided into five varieties: γ_1, γ_2, γ_3, γ_4, γ_5. The utterly differentiated chamber pegmatites are mainly localized in the γ_2 granites gravitating towards the contact with hybrid γ_1 granites (Lazarenko et al., 1973).

Within the limits of Korosten pegmatite field the chamber pegmatites are found in only one region. The latter is a part of endocontact zone of a granite massif with the length about 22 km and as broad as 0.3–1.5 km. The zone adjoins the western contact of the gabbro–labradorite massif. The relation of the chamber pegmatites to the endocontact zones adjoining the basic rocks is an important peculiarity of the disposition of the Volyn chamber pegmatites.

Mineral composition of the Volyn chamber pegmatites is variable and contain alltogether about 100 minerals.

The chamber pegmatites are genetically and spatially related to enclosing rapakivi-like granites. Graphic aggregation from outer zones of pegmatites have been formed during the magmatic stage of pegmatite formation; the next mineral-forming stage is connected with recrystallization phenomena. During this stage the graphic aggregations have been influenced by fluids which favoured the growing of larger pegmatoid blocks and differentiation of monomineral zones.

The main mass of quartz crystals and other minerals have been formed after the quartz transition (≈600°C). The crystallization of minerals proceeded from gaseous, boiling and liquid solutions.

Metasomatic mineral formation is common for the whole postmagmatic process of pegmatite development but it occurs mostly in an underchamber region (the leaching zone), where the intensive processes of quartz dissolving and microcline albitization took place, due to the influence of alkali solutions. Dissolved silica proceeded to the chamber and was a nourishment source for the crystal growth (Kaliuzny et al., 1971; Lazarenko et al. 1973).

References:

Kaliuzny, V.A., Vozniak, D.K. et al. (1971). Mineral forming fluids and parageneses of minerals of pegmatites of zanorysh type from Ukraine. Kiev, Naykova dumka (216 p.; Ukrainian).

Lazarenko, Eu.K., Pavlishin, V.I. et al. (1973). Mineralogy and genesis of Volyn chamber pegmatites. Lvov Vyshcha shkola (360 p.; Russian).

HUMAN BODY MINERALIZATION AND TRENDS IN BIOACTIVE CERAMIC IMPLANTS

Pawlikowski M., (Lab. Biomineralogy, AGH, Krakow)

Constant Eh, pH and t ^{o}conditions of human body as well as biological processes conduct to crystalization of various solid phases in human tissues. They represent necessary minerals and the group of dangerous one. Necessary minerals are present in teeth and bones. Dangerous are observed in muscules, blood vessels, lungs, thyroid, kidneys, gallblader, tumors of cancer etc. Mineralization of heart, blood vessels, cartilage, lungs, tumor of cancer is present in two forms i.e. as secret and visible. Secret mineralization is detected only by sensitive chemical methods. Visible mineralization present as grains and crystals which is possible examin using classic mineralogical methods. Secret mineralization may pass into visible one.

The mineralization developes because of many reasons as: restruction of tissues, genetic defects of biological structures, ilnesses, pollution of environment etc.

The knowledge concerning mineral phases present in human tissues constitutes the base for preparation of implants.

There are various trends in preperation and grafting of implants. Following types of bone implants are used: autogenous bone, allogenic bone, xenogenic bone, tricalcium phosphate (TCP), hydroxyapatite, composites (natural and synthetic polimers, calcium sulfate), calcium aluminiate ceramics, glasses and glass ceramics.

Our investigation are focused on hydroxyapatite produced at 40^{o}. Obtained phosphates as well as hydroxyapatite are grafted into bone of rabbits. Implants are grafted with autogenic marrow and stromal cels separated from bone marrow.

Autogenic bone marrow is used now for acceleration of healing of fractured bones. Up to now 56 patients was treated this method with the good results and full, fast healing of the fractures.

Now the investigations are performed on rabbits with grafted, powdered hydroxyapatite. The results show stimulating character of apatite on acceleretion of healing of fractured bones.

INTEGRATED ISOTOPIC AND TRACE ELEMENT STUDIES OF MAGMA GENESIS AND EVOLUTION: THE CASE OF SOME ITALIAN VOLCANOES

PECCERILLO A. (Istituto di Scienze della Terra, University of Messina, Italy)

Isotopic investigations of igneous rocks have provided an inpressive advancement in our understanding of magma genesis and of the nature and evolution of their sources. Variation of stable and radiogenic isotopic signatures in igneous rocks, however, depend on both heterogeneous sources and on the interaction between magmas and crustal rocks. Detailed petrological and geochemical studies in conjunction with isotopic investigations are the best approach to discriminate between the two processes. In the present paper the case of some Italian volcanoes is discussed and the implications of integrated petrological, trace element and isotopic studies for the solution of the source heterogeneity vs. magmas contamination dilemma are explored.

The Roman Comagmatic Province is characterized by variable $^{87}Sr/^{86}Sr$, $^{143}Nd/^{144}Nd$, Pb and oxygen isotopic compositions. Overal variation of these parameters clearly indicate an interaction between mantle and upper crustal end-members. Detailed studies of single volcanic suites indicate that these trends largely depend on source heterogeneities but have also been affected by magma contamination processes. The northern sector of the Roman province is a key zone in which both processes operated extensively and they can be discriminated by careful scrutiny of petrological, trace element and isotopic data.

The Aeolian arc consist of calcalkaline to potassic volcanics which show a range of trace element and isotopic compositions. Again, variations of geochemical parameters appears to be the effect of both source heterogeneity and magma contamination. AFC processes have been important during the generation of acidic magmas. However, the discrimination of the effect of low pressure and mantle processes is more difficult to constrain for mafic magmas, even though several geochemical and isotopic data suggest that crustal assimilation had an important role for several mafic Aeolian volcanics.

GEOLOGICAL, GEOCHEMICAL AND ISOTOPIC STUDY OF THE MATTONI NATURAL SPARKLING MINERAL WATER FOUND NEAR KYSELKA, NW BOHEMIA (CZECH REPUBLIC)

Pecek J. (*Aquatest Co., Karlovy Vary, Czech Republic*), Fuganti A. (*Università Trento, Italy*), Morteani G., Blamart D., (*T. U. München, Germany*)

In the surroundings of the village of Kyselka, 10 km NE of the renown spa of Karlovy Vary in NW Bohemia (Czech Republic) the Mattoni Co. produces natural sparkling mineral water from springs and wells. The locations of the springs, wells and the sampling points of the river water investigated are given in Fig. 1.

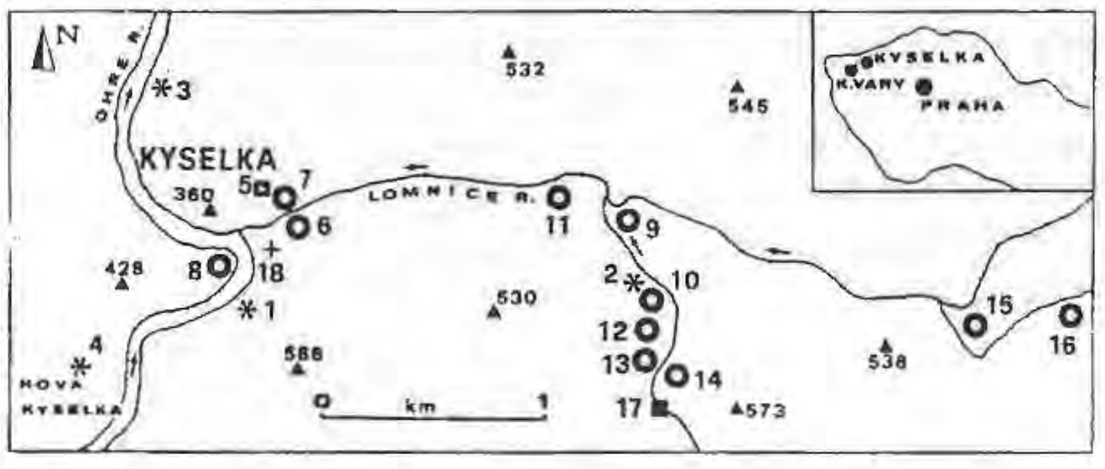

Fig.1: Location of the investigated springs, wells and of sampling points of the rain water in the surroundings of Kyselka.

The country rocks from where the mineral water is produced are Hercynian granites and the alkaline basalts belonging to the Tertiary volcanism of the Doupovsky Hory. The tectonic contacts between the granites and the volcanic rocks are NE-SW, NW-SE, N-S and E-W striking faults. Tritium values low as 0.3 TU, point to an age of the water older than 40 years. Values of 9.2 indicate a mixture of old and recent water. The old water comes predominantly from the wells within the granite. The water from wells in the Tertiary volcanic rocks related to the volcanism of the Doupovsky Hory connected to the Ohre rift system is at the contrary young. The waters from the wells in the granites show also a much higher mineralization than those from the volcanic rocks. All produced waters are from δ D and $\delta^{18}O$ values meteoric in origin and in agreement with the modern water equation given by Craig (1961) and similar to that of the springs of Karlovy Vary. The differences in mineralization between the waters coming from the granite and those coming from the volcanic rocks as well as the higher age of the water from the granites indicates that the water from the granites comes from a much deeper and/or slower water circuit than those from the volcanic rocks. No isotope data exists on the CO_2 found in the mineral waters. From what supposed by Weinlich et al. (1993) from the study of other mineral springs in the Ohre rift the CO_2 found in the mineral waters of Mattoni can be supposed to be of volcanic origin and therefore be connected to the Tertiary magmatism that produced the volcano of the Doupovsky Hory.

References:
Craig, H. (1961). *Science*, **133**, 1833-1834
Weinlich,F., Brauer, K. Kämpf, H., Strauch, G. and Weise, S. (1993). *Z. geol. Wiss.*, **21**, 135-142.

MÖSSBAUER INVESTIGATION ON TI-BEARING GARNETS FROM M. VULTURE (ITALY).

Pedrazzi,G., Ortalli I. (*Inst. of Physical Sciences, Univ. of Parma*)
Schingaro E., Scordari F. (*Geomineralogical Dept., Univ. of Bari*)

The results of a Mössbauer investigation on titaniferous garnets from M. Vulture, a volcanic massif located in the eastern side of Southern Appennines (Italy) are presented. The study was undertaken to investigate the structural role and the oxidation state of iron in some natural melanites and to derive the iron site populations.

The garnets structure presents three non-equivalent crystallographic sites: dodecahedral (X), octahedral (Y), tetrahedral (Z). Ti-bearing garnets are, perhaps, the most complex within the garnets group from a compositional viewpoint and in these compounds iron may be located in all the available sites. Hence their Mössbauer spectra consist of several contributions, characterized by a certain degree of overlapping of the different components, especially in the low velocity region.

The results of the measurements performed on 10 samples from different pyroclastic deposits of M.Vulture may be summed up as follows: a) the spectra of most samples have been fitted with four doublets, corresponding to Fe^{2+}(X), Fe^{2+}(Y), Fe^{3+}(Y), Fe^{3+}(Z); b) three out of ten samples show an additional contribution whose interpretation is not straightforward. Preliminary results have not yet allowed it to be unambiguosly assigned to Fe^{2+}(Z), as suggested by Kühberger et al. (1989); c) from the comparison with the large amount of literature data on similar compounds it has been found out that the Mössbauer spectra of the examined samples (as well as of all melanitic and schorlomitic garnets) can be fitted according to two different models, here named Model 1 (Amthauer et al., 1976) and Model 2 (Schwartz et al., 1980). They differ mainly for the position of the low velocity component of the Fe^{2+}(X) doublet, respectively at ~ -0.6 mm/s for the former and ~ 0 mm/s for the latter as shown in Fig.1 for the sample LC2. The two models are indistinguishable from a statistical standpoint and yield slight but systematic differences for the estimated occupancies of Fe^{3+}(Y) and significant differences for Fe^{3+}(Z) occupancies. Comparison with the results obtained through independent techniques (EPMA, XRD) and low temperature (T=77 K) Mössbauer measurements allowed to ascertain that Model 1 is to be considered the correct one; d) The influence of the thickness effect have been evaluated according to the method proposed by Rancourt et al. (1993) and through the calculation of the transmission integral.

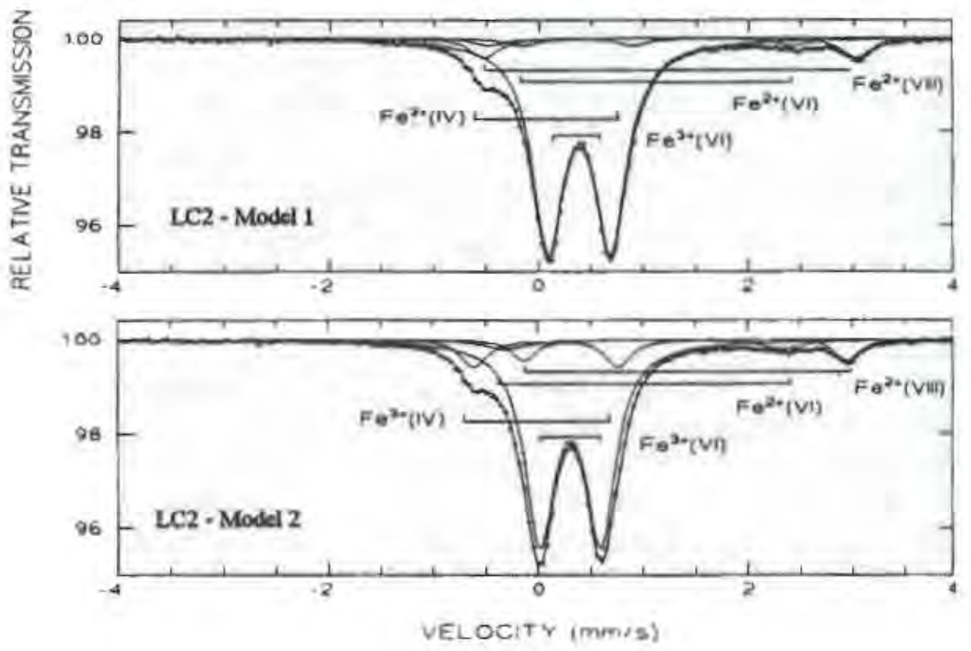

Fig. 1

References:
Amthauer, G., Annersten, H., Hafner, S.S. (1976). *Zeit. Kristall.*, **143**, 14-55
Kühberger, A., Fehr, T., Huckenholz, H.G., Amthauer, G. (1989). *Am. Mineral.* **16**, 734-740.
Rancourt, D.G., McDonald, A.M., Lalonde, A.M., Ping, J-Y. (1993) . *Am. Mineral.*, **78**, 1-7.
Schwartz, K.B., Nolet, A.D., Burns, R.G. (1980). *Am. Mineral.*, **65**, 142-153

BELOVITE-(Ce): SPECIFICATION OF THE FORMULA AND DISTINCTION FROM STRONTIUM-APATITE.

Pekov I.V.*, Chukanov N.V.**, Yeletskaya O.V.*, Khomyakov A.P.*** (**Dept. of Geology, Moscow University; **Inst. Chemical Physics Chernogolovka, Moscow distr.; ***IMGRE, Moscow).

To specify the formula of belovite-(Ce) authors studied the representative collection of specimens from Lovozero and Khibiny massifs (Kola peninsula). The collection contains museum material and new finds: 14 specimens from 10 pegmatite bodies including the holotype from Mt.Maly Punkaruaiv (Lovozero) (Borodin & Kazakova, 1954). Fluorapatite, the natural and synthetic strontium-apatite were studied for comprasion. We use the electron probe, H_2O-determination, X-ray powder measurement, IR-spectroscopy.

Mean chemical composition of belovite-(Ce):

$$(Sr_{2.90}Ca_{0.09}Ba_{0.08})_{3.07}Na_{0.94}(Ce_{0.50}La_{0.32}Nd_{0.11}Pr_{0.03}Sm_{0.01}Th_{0.01})_{0.98}$$
$$(P_{3.01}Si_{0.03}O_{11.99})(F_{0.79}OH_{0.4})_{1.2}.$$

The ideal formula: $Sr_3Na(Ce,La)(PO_4)_3(F,OH)$. In all specimens F > OH. X-ray powder diffractograms of belovite-(Ce) contain reflections 0001 (7.16-7.19Å, I=10-40%) and 0003 (2.385-2.395Å, I=3-7%). This fact corroborates the trigonal symmetry (space group $P\bar{3}$) for belovite-(Ce) with cation-ordered structure (Nadezhina *et al.*, 1987; Miyawaki & Nakai, 1993) in contrast to hexagonal apatite ($P6_3/m$) and strontium-apatite ($P6_3$) (Pushcharovsky *et al.*, 1987). X-ray diagrams of these minerals do not contain reflections 0001 and 0003 owing to special extinction. In general view IR-spectra of belovite-(Ce) and strontium-apatite are similar. However, belovite-(Ce) spectrum has the supplemental splitting of bands in region of banding vibration of $(PO_4)^{3-}$. Apatite and strontium-apatite spectra contain two lines in this

region, but belovite-(Ce) spectrum has clearly separated triplet (548,570,595 cm^{-1}). Probably, this effect is a consequence of ordered cation disposition in belovite-(Ce) structure in comprasion with apatite.

So, belovite-(Ce) $Sr_3Na(Ce,La)(PO_4)_3(F,OH)$ (but not $Sr_3NaCe(PO_4)_3OH$ (Nadezhina *et al.*, 1987; Miyawaki & Nakai, 1993) and not $(Sr,Ce,Na,Ca)_5(PO_4)_3(OH,O)$ (Borodin & Kazakova, 1954)) is a rare earth mineral proper (name according to Levinson rule). It distinct by the stable stoichiometry, well-ordered structure and trigonal symmetry. Its X-ray diagram and IR-spectrum are individual characteristics that allows to clearly identify this mineral and to differ from strontium-apatite $(Sr,Ca)_5(PO_4)_3(F,OH)$ (Efimov *et al.*, 1962) in particular.

References:
Borodin L.S. & Kazakova M.E. (1954) *Dokl.AN USSR*, **96**, 3 (in Russian).
Nadezhina T.N. *et al.* (1987) *Min.Zhurn.*, **9**,2 (in Russian).
Miyawaki R. & Nakai I. (1993) *Handbook Phys.Chem.R.E.*, **V.16**.
Pushcharovsky *et al.* (1987) *Crystallography*, **32**,4 (in Russian).
Efimov A.F. *et al.* (1962) *Dokl.AN USSR*, **142**,2 (in Russian).

SILVER MINERAL ASSEMBLAGE OF SARBAJ MINE (NORTH KAZAKHSTAN).

Pekov I.V.*, Karpenko V.Yu.** (*Dept. of Geology, Moscow University; **Ilmenski reservation, Ural, Russia).

Small but rich silver manifestation was occurred newly on Sarbaj skarn iron deposit (North Kazakhstan). Silver minerals form crusts, druses, beautiful crystals and massive aggregates in cavities of carbonate veins in chloritizied pyroxene skarn. Early white calcite is the main vein mineral. It contains sulfide impregnation. Age succession of ore minerals: pyrite → chalcopyrite → sphalerite → grey ore → arsenopyrite (or löllingite). The late assemblage was occurred in cavities only. Vein minerals: late calcite, chlorite, quartz, Mn-siderite, zeolites. Silver minerals prevail in ore assemblage: native silver, acanthite (main), proustite, pearceite (widely-distributed), stephanite, pyrargyrite, polybasite, allargentum, argentopyrite, stromeyerite, xanthoconite, mckinstryite, also native arsenic, Ag-rich grey ore (8-13% Ag), löllingite, goethite, hematite and insignificant quantity of stibnite, cleyophane, late pyrite, chalcopyrite, marcasite. Native silver forms twisted wire-sheep crystals which make assemblages to 200 kg. Pearceite and polybasite was discovered in all isomorphous series limits from $(Ag,Cu)_{16}As_2S_{11}$ to $(Ag,Cu)_{16}Sb_2S_{11}$ including As/Sb=1 composition. Often pearceite crystals (to 12 mm) form twins ("butterfly") by (201) and (102). Transparent cherry-coloured polybasite crystals (to 2 mm) is of interest. This polybasite is a copper-free (<0.01% Cu), but its crystals contain fine chalcopyrite impregnation. Kidneys of native arsenic (to 10 cm) were occured in several veins. Allargentum forms fine ingrowths (to 30 mkm) in arsenic. Some veins contain spherical cavities after leaching of arsenic kidneys with incrustation of proustite, Sb-proustite (to 35-40% mol.Ag_3SbS_3) and beautiful transparent xanthoconite crystals (to 5 mm). Authors measured goniometrically unusual pseudomorph after prismatic dyscrasite crystals (to 4 cm). It consist of mckinstryite and stromeyerite aggregate with thin chalcopyrite crust.

Silver mineral assemblage forms at the late stage of hydrothermal process by low temperature and high oxydative potential. One can illustrate it with the help of mineral thermometers (argentopyrite - below 150-170°C; stromeyerite + mckinstryite - below 95°C; needle-shaped crystals of low-temperature orthorhombic acanthite) and consecutive crystallization mineral series. Changing in time of iron minerals clearly fixes the oxydative potential rise and S^{2-}-activity lowering: pyrite → siderite → hematite → goethite. The majority of silver minerals were crystalized with goethite and hematite jointly at the lowest S^{2-}-activity conditions. Silver-rich veins are a lead-poor. Galena is practically absent in this system that favour the development of various silver mineral assemblages.

Research on Relation of Tunnel Structure to Electric Properties of Tourmaline

Peng M.S., Wang H.Y.
(Zhongshan University, 510275, the P.R.China)

Tourmaline's general formula can be written as $WX_3Y_6(BO_3)_3[Si_6O_{18}](OH, F, Cl)$, where W stands for Na or Ca, X is Mg, Fe, Mn, Al etc, and Y may be Al, Fe, Cr and V. Its crystal structure is dominated by complex trigonal ring composed of silicon and oxygen tetrahedral,with space group R_{3m}-C_{3v} and without symmetry center . As a result of this kind of structure, tourmaline has piezoelectricity and pyroelectricity , Especially , the discovery of pyroelectricity in 1824 promoted the rapid development of dielectric physics.

Natural tourmalines coming from Xinjiang Autonomous Region (sample T1 and T2), Hunan Province (sample T3) and Yunnan Province (sample T4 and T5) of China belong to isomorphic series of schorl and dravite according to electron microprobe analysis. The contents of Fe and Mg in tourmalines increase gradually from sample T1 to T5, on the contrary , Na decreases step by step. As to genese, samples T1 and T2 belong to pegmatitic type, T3 is due to hydrothermal type, T4 and T5 are metamorphic type.

Because of limitation of geometric shape,we only get such a set of piezoelectric parameters data , for instance , elastic constant (S^E_{11} and S^E_{33}) , dielectric constant ε^T_{33} , piezoelectric constant (d_{33} and d_{31}) by means of transimission circuit method. Pyroelectric constant is measured by dynamic method. As compared with the data of wide-applied piezoelectric ceramics and rock crystal, these samples have not industrial values as their parameters incline towards too low values. However,when the mathematical model of parameter and component is established, we discover there is an apparent correlativity between parameters and contents of Na,Fe,Mg and so on. For example,the multivariate regression equation of d_{33} and Na, Fe and Mg is following:

$$d_{33}=13.026-0.784\,\alpha_{Fe}-0.282\,\alpha_{Mg}-2.258\,\alpha_{Na},$$

with a correlation coefficient is 0.984. To be more exact, sodium has a positive correlativity with these parameters, but iron and magnesium have negative one and sodium make a greater contribution to these parameters than iron and magnesium do. Combining with analyses of polarized Raman spectra, infrared spectra and nuclear magnetic resonance, we find hydroxyl occupies the tunnel structure and is parallel to C axis in all samples, over which sodium ion stands. So in the tunnel there are two type ions with different charge symbols. When tourmaline vibrator resonates or is heated, these ions of two sorts can take place ion displacement, as a result, the piezoelectric and pyroelectric effects can be got enhancement. With respect to Fe and Mg, their contributions to parameters can be fulfiled only by way of symmetry of crystal structure and are less than that of Na. But we also find that water which exists in the tunnel structure can run low the piezoelectric and pyroelectric effects.

References:

Tatli & Ozkan,(1987),*Phys.Chem. Minerals*,14,172-176.
Peng et al,(1989),*Annual Report of the Director Geophys. Lab.*,U.S.A.

TOURMALINITES AND TOURMALINE-BEARING ROCKS IN THE PALEO-PROTEROZOIC METAMORPHOSED EVAPORITIC SEQUENCE, NORTHEASTERN CHINA

Peng Q.M. and Xu H. (Dept. of Geol., Changchun Uni. of Earth Sciences, Changchun, 130061, P.R.C.)

Stratiform tourmalinites and tourmaline-bearing rocks are common in many geological settings, especially the Proterozoic- Paleozoic SEDEX type deposits (Slack et al., 1984). The origin and significance of these rocks have been studied extensively in the last decades. It was suggested that these rocks can serve as indicators for origin of the associated ores (Plimer, 1986, Slack et al., 1984 and Slack et al., 1993). The boron was infered to be derived from the underlying sediments, most probably evaporites (Slack et al., 1993).

The Stratiform tourmalinites and tourmaline-bearing rocks in eastern Liaoning and southern Jilin province, northeast China crop out extensively in the lower portion of the Paleoproterozoic volcanic-sedimentary sequence (Liaohe Group), as hanging walls of the stratabound borates. The tourmalines exist as: (1) stratiform turmalinites that consist mainly of tourmaline and quartz (<1mm); (2) bands or lamina in the quartzo-feldsparthic rocks; (3) bands or veinlets in the borate hosting magnesian marbles and (4) coarse grained tourmaline in the quartz veins and pegmatitic veins associated with the granites. Poikiloblastic texture s common in the (1) and (2) types. The abundance of tourmaline is remarkably high adjacent and overlying the borate ore bodies (suanite ludwigite and szaibelyite). This suggests a genetic link between the tourmalinites and the underlying borates. Microscope study revealed that both the tourmaline and quartz resulted from boron and silica metasomatism in the tuffs or clastic sediments. Geochemistry of those rocks indicates that the tourmaline-rich and tourmaline-poor quartzo feldspar rocks are analogous in major and trace element patterns.

Tourmalines of different occurrences in the sequence belong to schorl-dravite series. Within Al-Fe-Mg and Ca-Fe-Mg diagram, the (1) and (2) type tourmaline fall in the Fe3+-rich and Ca-poor metapellite and metapsammites defined by Henry and Guidotti (1985). Mg/Fe ratio of the tourmaline varies from 2.64 in the magnisian marbles to 0.74 in the quartzo-feldspar rocks. This suggests that chemistry of the host rocks may be the major control over the Mg/Fe of the tourmalines.

Boron for formation of the tourmaline-rich rocks in the sequence came from leaching of the under lying evaporitic borates. The pre-metamorphism hydrothermal activities resulted in leaching, transport and precipitation of boron. This case study provides a good example showing the genetic relationship between tourmaline-rich rocks and their boron sources in a evaporite-related sequence that may host large or superlarge SEDEX type mineral deposits.

References:

Henry, D.J and Guidotti, C.V.(1985), American Mineralogist, 70, 1-15.
Plimer, I.R. (1986), Mineral. Deposita, 21, 263-270.
Slack, J.F., Herriman, N., Barnes, R.G. and Plimer, I.R. (1984), Geology, 12, 713-716.
Slack, J.F., Palmer, M.R., Stevens, B.P.J. and Barnes, R.G. (1993), Economic Geology, 88, 505-541.

NORMAL COORDINATE ANALYSIS OF INTERNAL VIBRATION OF LUDWIGITE

Peng Wenshi, Zha Fubiao and Xie Xiande (*Guangzhou Institute of geochemistry, Academia Sinica*)

The formula of ludwigite is $(Mg,Fe^{2+})_2Fe^{3+}BO_3O_2$ and its space group belongs to D_{2h}^{16}-Pbam, Z= 4. The site symmetry of BO_3^{3-} ion is Cs. Among three B-O bond lengths, two of them are comparable.Therefore, the site occupancy of BO_3^{3-}ion can be considered to be C_{2v} for the convenience of calculation.

Table 1 gives the band frequencies and assignments of ludwigite.

Table 1. Band frequencies and assignments of ludwigite

band assignments	υ_3	υ_2	υ_4	M-O		
frequencies(cm^{-1})	1250	706	622	476	396	334

According to the GF matrix method presented by Wilson, the normal coordinate analysis is focused on the establishment and solution of the secular equation: $|GF-E\lambda|=0$, where E is the unit matrix, $\lambda=4\pi^2C^2\upsilon^2$, $G=UgU^{\sim}$ and $F=UfU^{\sim}$, g is the kinetic energy matrix related to the mass of atoms and their space geometry arrangement, f is the force constant matrix concerning with the potential energy and U is a transformation matrix.

Based on group theory analysis the internal vibrations of ludwigite can be represented as $\Gamma_v=3A_1+B_1+2B_2$, in which the contributions of the bond length internal coordinates to normal vibrations are $\Gamma(\Delta r)=2A_1+B_2$, and the contributions of bond angles are $\Gamma(\Delta\beta)=2A_1+B_2$. Apparently, one redundancy is A_1. Therefore, it is necessary to select the change of angle between the B-O bonds and the molecular plane,ie $\Gamma(\Delta\alpha)=B_1$.

The g matrix can be obtained through the unit vector method presented by Wilson and the U matrix can be deduced from the projection operator. Under the operation of the U matrix, the g matrix and f matrix (the general valency force field) can be reduced to the quasi-diagonalized matrix of the same form.

Because the number of the required force constants is greater than the number of measured frequencies, it is necessary to use the simplified force field. With the mode of class B_2,the elements of the G matrix and F matrix(U- B simplified force field) are given as follows:$G_{11}=0.20$, $G_{12}=G_{21}=0.16$, $G_{22}=0.24$, $F_{11}=K+F$, $F_{12}=F_{12}=-0.85F$, $F_{22}=1.96H+0.63F$,where K,H and F are the stretching force constant, the bend force constant and the repulsion force constant between non-bonded atoms, respectively. After repeated fitting calculation, the following results are got:

Force constants(N/m): K=345, H=78, F=120.
Calculated frequencies(cm^{-1}): υ_3=1252, υ_4=623.

Obviously, the calculated frequencies are in good coincidence with the measured values. Potential energy distribution can provide an objective criterion for the band assignments. The normalized potential energy distribution can be calculated from $Via=F_{ii}Lia/\lambda a$. The potential energy distribution of BO_3^{3-}ion in ludwigite is presented as follows:

BO_3^{3-}	υ_3	υ_4
S_3	0.71	0.20
S_4	0.30	0.79

Because S_3 comes from the operation of the projection operator on bond length and S_4 results from the operation on bond angle, the assignment of υ_3 and υ_4 to the stretching vibration and bend vibration are apparently reasonable.

Reference

Wilson, E.B.Jr.et al.,(1955). *Molecular vibrations*, McGraw-Hill Book Company, New York, pp. 54-240.

HIGH-PRESSURE METAMORPHISM IN THE ROCKS FROM THE RED CLIFF AREA, GREAT CAUCASUS, RUSSIA

Perchuk A.L. *(Institute for Ore Deposits Geology, Petrology, Mineralogy & Geochemistry, RAS, Moscow)*

The Red Cliff area in the Great Caucasus provides a good example of group B eclogites (Coleman et al, 1983) interlayered with garnet micaschists. Prograde metamorphic changes in the eclogites are expressed petrographically as inclusions of glaucophane, epidote, paragonite, omphacite and quartz in garnet with homogeneous core and zoned margins with Mg number increase to the rim. PT-estimates show temperature increase from 520 to 700°C while pressure (minimum values) changed from 13 to 16 kbar. Similar temperature peak has been calculated for garnet micaschists. Pressure of 18 kbar and water activity of 0.6 have been obtained by joint solution of the paragonite-omphacite-kyanite (Holland, 1979) and phengite (Massone & Schreyer, 1987) barometric equations for eclogite and garnet micaschists, respectively, at the temperature peak, 700°C.

Retrograde stage of metamorphism is documented in wide spectrum of symplectite-forming reactions in eclogites, and replacement of phengite by biotite with subsequent growth of chlorite after garnet and biotite in garnet micaschists. Mineral equilibria show decompression till the amphibolite facies conditions, 8 kbar and 600°C.

Studies of fluid inclusions from eclogites reveal their aqueous composition of low salinity (0-9 wt% NaCl equiv.). Calculated isochores clearly demonstrate that the inclusions relate to the amphibolite facies event.

References:

Coleman, R. G., Beatty, L. B. & Brannock, W. W. (1965). *Geological Society of America Bulletin*, 76, 483-508.

Holland, T. J. B., (1979). *Contributions to Mineralogy and Petrology*, 68, 293-301.

Massonne, H. J. & Schreyer, W. (1987) *Contributions to Mineralogy and Petrology*, 96, 212-224.

GIBBS CHEMICAL POTENTIALS OF WATER AND ALKALIES DURING GRANITIZATION

Perchuk L.L and Gerya T.V. *(Depr. of Petrology Moscow State Univ)*

A few reactions in the Precambrian complexes may indicate granitization and charnockitization processes. Two major hydration reactions among them are Opx+Kfs+H_2O=Bt+Qtz and Kfs+Opx+Cpx+H_2O = Hbl+Qtz+ (K_2O). They are acompanied by simultaneously operating continues reactions, such as Mg-Ts(Opx)+Qtz+(K_2O)=Kfs+En, Pl1 + (K_2O)=Pl2+Kfs+(Na_2O) and Bt(Sid)+Qtz+(K_2O)= Bt(Phl)+Kfs+ (H_2O) recorded in unique textures and mineral compositions showing perfect mobility of H_2O and alkalies (Perchuk & Gerya, 1993). All the above reactions are governed be major thermodynamic parameters, i.e. temperature (*T*), pressure (*P*), $\mu_{CO2,fl}$, $\mu_{H2O,fl}$, $\mu_{K2O,fl}$ and $\mu_{Na2O,fl}$.

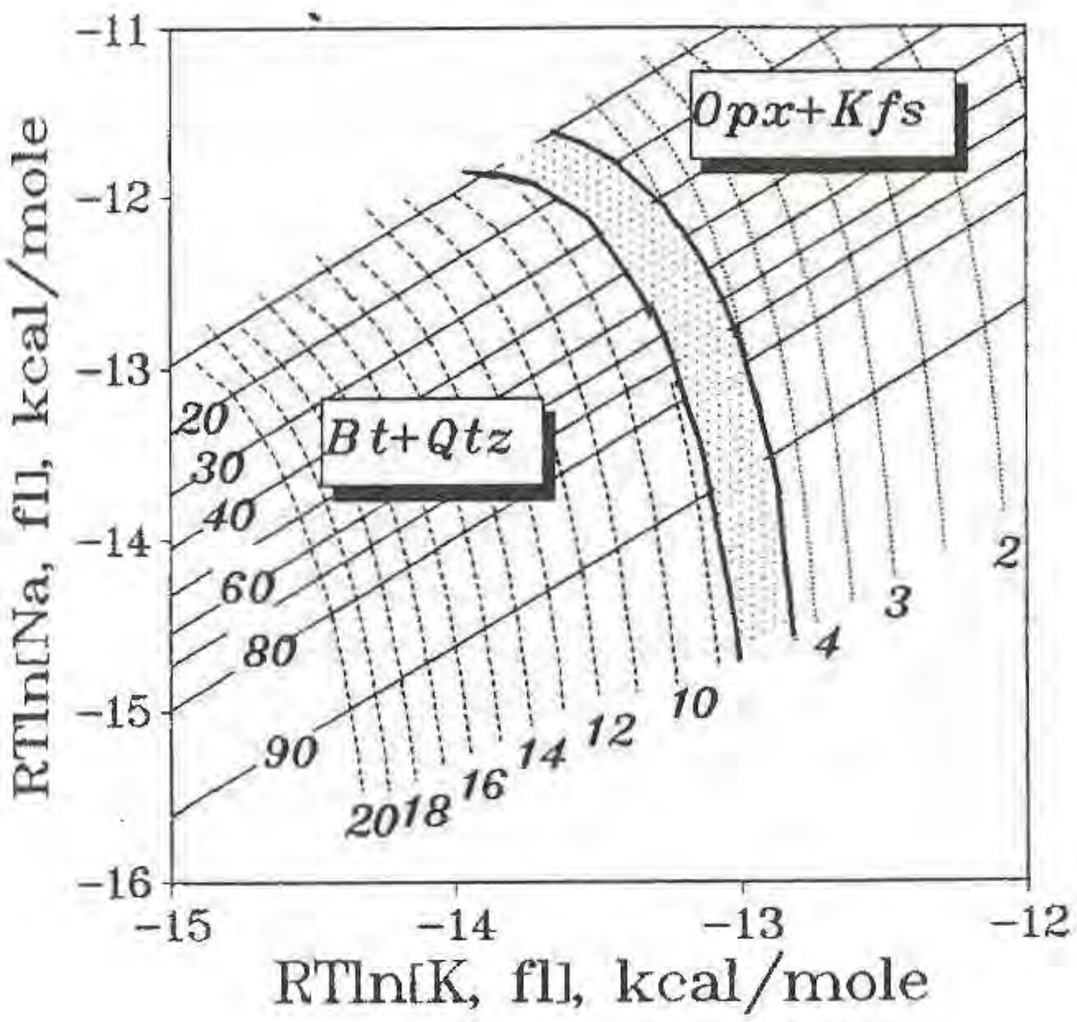

The quantitative diagrams calculated in coordinates of relative chemical potrntials, $\mu_{K2O,fl}$ - μ_{H2O} and $\mu_{K2O,fl}$ - $\mu_{Na2O,fl}$ at given *P* and *T* measured using data on mineral thrmometry and barometry. An example of such diagram calculated at *P*=5 kbar, *T*=700°C and water activity 0.35 is shown below. The diagrams suggest that increase in alkali potentials leads to charnockitization of gneissic complexes, whereas their decrease, or an increase in $\mu_{H2O,fl}$ promotes granitization. Mineral facies of granites and charnockites are indicated in the diagrams and allow to predict changes in mineral compositions of the rocks.

References:

Perchuk, L.L., Gerya, T.V. (1993). Fluid control of charnockitization. Chemical geology. 108, No 1-4, p.175-186

SPECIFIC BISMUTH MINERALIZATION OF MIAROLITIC PEGMATITES WITHIN THE MALKHAN FIELD, CHITA OBLAST, RUSSIA

Peretyazhko I.S. and Zagorsky V.Ye. (Vinogradov Institute of Geochemistry, Siberian Branch of Russian Academy of Science), Irkutsk, 664033, P.O. Box 4019

A newly discovered Malkhan field of miarolitic pegmatites in Central Transbaikalia is the main source of collection specimens and gem tourmaline within Russia. The Malkhan pegmatites are remarkable for their enrichment in Bi, which results in the diverse Bi mineralization in the pegmatites and wide primary dispersion haloes in the country rocks (Zagorsky & Peretyazhko,1992). In primary quartz-feldspar complexes increased Bi contents are observed in quartz, micas, feldspars (up to 15 ppm) and in accessory columbite-tantalite, struverite, U-polycrase-euxenite, hematite (up to 0.5%). Bismuthinite is found sometimes in association with bismutite. Most of Bi mineralization is observed in the near-pocket lepidolite-albite complexes and in the pocket filling material, containing up to 300 ppm of Bi. Native bismuth, bismutite, bismutotantalite, bismutomicrolite, bismutomicrolite-bismutobetafite, bismutopyrochlore, Bi-rich tourmaline, and a new mineral - bismutocolumbite have been discovered.

Bismutocolumbite $Bi(Nb_{0.8},Ta_{0.2})O_4$ is found in the pocket material of the Danburitovaya vein as crystals and fragments of black crystals with well-developed faces {h0l} and {hk0}. The size of its prismatic crystals is up to 2 mm long and 1 mm across. H=5.5 by Moos. Cleavage: {001} perfect. Density: (meas.)=7.56 g/cm^3, (calc.)=7.67 g/cm^3. Biaxial (+), α=2.38(2), β=2.42(2), γ=2.47(2) (579 nm). Unit cell data: Orthorhombic, Pcnn, (Å): a=4.992(3), c=5.677(3), b=11.731(5), V=332.45(6) Å^3, Z=4 (Peretyazhko et al., 1992). Microprobe investigations indicate the presence, in some veins, of grains of minerals, corresponding by composition to members of an isomorphous series intermediate between bismutotantalite, stibiotantalite, stibiocolumbite, and bismutocolumbite. It may also indicate complete miscibility of solid solutions in the minerals of ABO_4 structural type, where A - Bi,Sb; B - Ta, Nb.

Bi minerals of pyrochlore group. Varieties, forming the continuous series from microlite to bismutomicrolite (0.5-30 % of Bi_2O_3) are the case in the lepidolite-albite near-pocket complexes. The linear increase of cell parameters, decrease of reflection intensity with odd indices as opposed to reflections with even indeces, increase in refraction indeces (1.96-2.14) and density (5.46-6.92 g/cm^3) are observed with the Bi increase. Some grains have Ti contents higher than 20 atomic%, and there are even grains, possessing 30-33 atomic% of Ti, that corresponds by composition to bismutobetafite. It is established, that Bi^{3+} in microlites replaces Ca^{2+} in A position under relatively constant Na^+ quantity. F is removed from the structure ($O^{2-}\rightarrow 2F^-$) and Ta^{5+},Nb^{5+} are replaced by Ti^{4+},Sn^{4+} in B position, that is described by the ideal structural formula $Na_1(Ca,Bi_X)_1(Ta,Nb)_{2-Y}(Ti,Sn)_Y(O,F_{1-Z})_7$, where X=Y+Z is within a range of 0-1. Bismutomicrolite grains with the zones size up to 300-400 micron, corresponding to stibiomicrolite and stibiobetafite, have been found under microprobe study. The fine-grained brown-

yellow aggregate, corresponding to bismutopirochlore (unknown in the nature) by microprobe and X-ray diagnosis, develops after columbite-tantalite grains from the pocket material in one of the vein.

Elbaite-liddicoatite tourmalines from some veins contain up to 0.5% of Bi_2O_3. This is the first finding of Bi-rich tourmaline in the world (Peretyazhko et al., 1989). Such tourmalines are marked also by increased Pb contents (up to 0.54% of PbO). Microprobe study doesn't provide any independent Bi- and Pb-bearing phases. It is presumed, that Bi^{3+} and Pb^{2+} are isomorphously replace Na^+ and Ca^{2+} in X position. When Na^+ and Ca^{2+} are replaced by Bi^{3+} and Pb^{2+} the charge compensation is due to triads [2Li,Al] formation in the Y octahedron on one hand and via deprotonization, which follows the scheme $(Pb,Bi)_{[X]} + 2Li_{[Y]} \rightarrow Al_{[Y]} + (Na,Ca)_{[X]} + H^+$ on the other hand. Bi mineralization in pegmatites appears due to accumulation of this element in the process of granite-pegmatites system evolution. It should be noted, that the leucogranites and genetically associated pegmatites are enriched in Bi 100-400 times higher than the Clark of acid intrusive rocks.

References :
Zagorsky V.Ye. & Peretyazhko I.S. (1992). Pegmatites with precious stones, Central Transbaikalia. Novosibirsk, Nauka Press, 224, (in Russian).
Peretyazhko I.S. et al. (1992). Zapiski Vsesoyuznogo Mineralogicheskogo Obshestva, 121, No.3, 130-134.
Peretyazhko I.S. et al. (1989). Doklady Akademii Nauk SSSR, 307, No.6, 1461-1465.

SPECTROSCOPIC STUDIES OF REACTIONS AT THE AQUEOUS-SULFIDE MINERAL INTERFACE

Persson P. (*Dept. of Inorganic Chemistry, Umeå Univ., Sweden*)

Although not as naturally abundant as oxide minerals, sulfides and reactions at their surfaces play an important role in both geochemical and industrial processes. In reducing aquatic environments adsorption onto sulfide mineral particles may be the mechanism which controls the aqueous availability of many metal ions. Furthermore, a coupled adsorption/reduction reaction at sulfide surfaces has recently been proposed as a possible way of forming ore deposits of noble metals (Bancroft & Hyland, 1990). Sulfides in oxidizing systems are also of great interest, primarily because of the connection to the problem of acid mine drainage. The main technological use of sulfides is as an ore source of base metals such as Cu, Zn and Pb. In the separation process of the individual metal sulfides from the crude ore, the surface chemistry of the sulfides are of outmost importance. In this paper, surface reactions of sulfides relevant to the ore extraction, and metal ion adsorption reactions will be discussed.

The metal sulfides are extracted by specifically hydrophobating their surfaces with organic anions, usually alkylxanthate ions ($ROCSS^-$), in an ore/water mixture. To optimize the conditions in this so called flotation process, it is vital to know the mode of attatchment of the alkylxanthate ions. By use of diffuse reflectance Fourier transform infrared spectroscopy three different adsorption modes, previously suggested (Leja, 1982), have been established. Depending on the structure of the sulfide, the extent of surface oxidation and the solubility of the metal alkylxanthate, the alkylxanthate ions can be adsorbed as a surface complex, surface precipitate, or as the neutral oxidized form dialkyl dixanthogen (ROCSS-SSCOR). Examples of the three mechanisms will be given and related to the surface properties of the metal sulfides.

Adsorption of metal ions on hydrated sulfide mineral surfaces is usually explained by either a cation-exchange mechanism or by surface complex formation similar to that on oxides. The relative solubility of the sulfides determines which of the two reactions that will occur. Co(II) on ZnS will be used to exemplify surface complex formation and Cu(II) on ZnS as an example of cation-exchange. To obtain structural data, the systems have been studied by means of *in-situ* X-ray absorption spectroscopy (XAS). The XAS data shows that most likely both surface -OH and -SH groups are active in the surface complexation of Co(II). The ZnS surfaces also induce four-coordination of a fraction of the oxygen-ligated Co(II) surface complexes. The structural differences of Co(II) and Cu(II) on ZnS will be discussed, and comparison will be made with surface complexation of Co(II) on ZnO.

References:
Bancroft, G.M., Hyland, M.M. (1990), *Mineral-Water Interface Geochemistry*, eds. Hochella, M.F, Jr., White, A.F., Reviews in Mineralogy, 23, 511-558.
Leja, J. (1982), *Surface Chemistry of Froth Flotation*, Plenum Press, New York.

THE SYSTEM Ag-As-S: CRYSTAL GROWTH EXPERIMENTS WITH APPLICATION TO MINERALOGY.

Pertlik, F. and Rosenstingl, J. (Institut für Mineralogie und Kristallographie der Universität Wien).

Investigations of phase relationships in the system Ag-As-S including the growth of single crystals from molten metall solutions were described e.g. by JAEGER and VAN KLOSTER (1912), ROLAND (1970 a, b), BLACHNIK and WICKEL (1980), investigations under hydrothermal conditions e.g. by BÉLAND (1946) and PEACOCK (1947).

To enlarge the knowledge (or hypotheses) about the transport of metal elements, especially silver, and the formation of sulfide ore deposits in nature, experiments in the system Ag-As-S under the following hydrothermal conditions were performed: Ammonia water or aqueous solutions of alkaline hydroxides, range of temperature from 100° C to 250° C, saturation vapour pressure. Single crystal of the compounds Ag_3AsS_3 (trigonal and monoclinic), $AgAsS_2$ (rhombohedral), Ag_3AsS_4 and $Ag_7S_2(AsS_4)$ as well as $NH_4Ag_2(AsS_2)_3$, $NH_4Ag_2AsS_4$ and $(NH_4)_5Ag_{16}(AsS_4)_7$ were revealed (ROSENSTINGL, 1993, AUERNHAMMER et al. 1993).

The oxidation state of arsenic and therefore the formation of arsenic(III) or arsenic(V) sulfides is controlled by the concentration of the alkaline solvent (pH value) and the excess of sulfur. This might be the reason for the numerous arsenic(III) sulfide minerals in comparison to only two arsenic(V) sulfides (sulfarsenates): Fangite, $[Tl_3(AsS_4)]$, and Billingsleyite, $[Ag_7S_2(AsS_4)]$ (STRUNZ, 1993).

References:

Auernhammer, M., Effenberger, H., Irran, E.,

Pertlik, F., Rosenstingl, J. (1993). J. Solid State Chem. 106, 421-426.
Béland, R. (1946). Ph. D. Thesis, University of Toronto.
Blachnik, R., Wickel, U. (1980). Z. Natf. 35 b, 1268-1271.
Jaeger, F.M., van Kloster, H.S. (1912): Z. anorg. Chem. 78, 245-269.
Peacock, M.A. (1947): Univ. Toronto Stud., Geol. Ser. 51, 85-87.
Roland, G.W. (1970,a). Met. Trans. 1, 1811-1814.
Roland, G. W. (1970, b). Eccon. Geol. 65, 241-252.
Rosenstingl, J. (1993). Nat. Dipl. Univ. Wien.
Strunz, H. (1993). Lapis (Extra Edition) 12/93.

• NUCLEAR WASTE DISPOSAL: MINERALOGICAL AND GEOCHEMICAL ISSUES REVISITED IN A SOCIOTECHNICAL CONTEXT

Petit J.C. (*Commissariat a l'Energie Atomique, 92265, Fontenay aux Roses Cedex, France*)

For more than twenty years a large consensus amongst the scientific and technical community has been slowly constructed for the management of nuclear wastes. The basic idea in most countries is that their long-term confinement should be best guaranteed through their final disposal in a deep geological formation. The classical concept is based on a multi-barriers system where the host rock acts as the "ultimate shield" against the dispersion of radionuclides in order to minimize the impact, if any, on the biosphere. Because of this key role ascribed to the geological barrier, and also because the behaviour of the technological barriers themselves must be assessed in geological conditions and over very long periods of time, geosciences have been increasingly influencial in this field of research. It is noticeable that mineralogy and geochemistry have been particularly mobilized by scientists in this context. In fact, the research in this field has essentially followed two symmetrical approaches, based on either the science and technology, on the one hand, or Nature itself, on the other hand, as the primary resource of justification and demonstration. We will-show that natural analogues (e.g. of technological materials, geochemical processes, etc.) play the key epistemological role of strongly linking together the science and technology fields with the realm of Nature.

In this context, we will illustrate how major mineralogical and geochemical issues have been dealt with and how their better undertanding has contributed to increasingly reliable long-term extrapolations. Important examples, concerning processes involving the different barriers of current disposal concepts (waste matrices, metallic canisters, engineered and geological barriers), will be discussed: i. mineral dissolution for both crystalline and amorphous solids; ii. trace elements speciation; iii. colloidal transport and retention on mineral surfaces; iv. trace elements "trapping" on/in minerals (sorption, ion exchange, co-precipitation); v. fracture flow, water/rock interactions and rock permeability, etc. In particular, we will underline the specific contribution on these key issues of energetic ion beam analytical techniques (Rutherford Backscattering Spectrometry, Resonant Nuclear Reaction Analysis, Elastic Recoil Detection Analysis, etc.) which we have applied for more than a decade in this field. Finally, we will underline new directions of research which may reveal important for the future.

THE RELATIONSHIP BETWEEN MINERAL TEXTURES AND EXTRACTIVE METALLURGY

Petruk W. (*CANMET, Dept. of Natural Resources, Canada)*

The primary requisite for a successful extractive metallurgy operation is to grind an ore to liberate the minerals so that they can be concentrated or to expose mineral surfaces so that the minerals can be leached. The ease or difficulty of liberating or exposing the mineral grains is dependent upon the mineral textures. In particular, mineral grains with straight grain boundaries and a weak bonding to other minerals are easily liberated and readily concentrated into high grade concentrates. In contrast mineral grains that have re-entrant boundaries and are strongly bonded to their neighbours are not easily liberated and will not produce high grade concentrates, even with regrinding. Similarly, inclusions that occur along fractures and grain boundaries can be readily exposed and leached. Whereas minute random inclusions in large grains will not be liberated or exposed unless they occur along planes of weakness.

The amenability of an ore to texture destruction, and hence to mineral liberation, is dependent upon its depositional history. Consequently selecting a liberation model for predicting grind sizes requires a sound knowledge of the ore textures and the depositional history of the deposit.

U-Pb-ZIRCON AND Rb-Sr DATING OF GNEISSES FROM SOUTH-EASTERN RHODORPES, BULGARIA

Peytcheva I. *(National Museum "Earth and Man", Sofia)*

There are two opposite concepts about the way and the time of formation of plagoclase- and two-feldspars-gneisses from the Belorechka group in SE Rhodopes. According to the majority of the authors they are Early Archaean sediments and volcanites, metamorphosed twice in amphibolite facies (probably at the end of the Archaic and Proterozoic) and with imposed late greenshist metamorphism. According to the second concept they are Alpine granites, plastic deforfed almost simultaneously with their formation.

The accessory zircon has been separated from a 25 kg sample (I-4a). It is sharp-dipyramid and it is desposed in the field of the crustal authochtone and subauthochton granites on the Pupin's morphological classification diagram. Altough the cristals are bright and transparent, slightly rounded cores, oveprinted with optically equial zircon rims are fixed in them in transmitted light. The zircons have been separated according to their size and colour. The points, corresponding to the different fractions, demonstate a complex discordant picture. The presence of inherited zircon is obvious. It is older than 575 Ma - the $^{207}Pb/^{206}Pb$ age of the biggest zircon fraction, which has been studied. Above the relict phase in the following process of granite formation is to be found a new-grown phase, making up the basic mass of the small zircon fractions. The corresponding points are disposed almost concordantly and determine the age of this process according to the low intercept with the concordia at $T = 331 \pm 8$ Ma. About the same value (330-339 Ma) vary the $^{206}Pb/^{238}U$ apparent ages of all zircon frations.

Rb-Sr isotope system was studied in whole-rock (20 kg and 1 kg) and monomineral samples. The age of the last metamorphism in the area is $T = 34 \pm 1$ Ma. It exseeds greenshist facies in intensity. The isotope measurements of the whole-rock samples allow an errorchrone to be drawn with an age $T = 377 \pm 27$ Ma and initial ratio $^{87}Sr/^{86}Sr = 0.7065 \pm 0.0005$ (MSWD = 122). A separate errorchrone for the plagioclase-porphyroblastic gneisses from the southern part

of the explored area (belonging to the Lower Archaean Strajetzka group, according to D.Koshucharov, 1987) determine an age an age T=367 ± 71 Ma. Within the error's limit it coincides with the age, determined by U-Pb method. The most probable explanation of the crustal, but not high initial strontium ratio (~ 0.707), having in mind the piculiarities of zircons, is the metamorphism or partial melting of comperatively young vulcanogenic-sedimentary material with low ratio Rb/Sr.

References:
Кожухаров Д. (1987). *Geol.Balc.* **17**, 2, 15-38

CHAMBER PEGMATITES FROM CENTRAL RHODOPES, BULGARIA - MINERAL PARAGENESES, CHEMISTRY, AGE DETERMINATION

Peytcheva I, Sekyranov A., R Arnaudova, V.Arnaudov
(Nat. Museum "Earth and Man" and Geol. Inst., Sofia)

Two types of pegmatites are known in the Central Rhodopes of Bulgaria - deformed and non deformed. The deformed are supposed to be "old" (Precambrian ?) or to be Alpine metamorphic pegmatites. The non deformed chamber pegmatites are presumably in connection with non exposed Tertiary granites.

A 100 m long and to 6 m bright pegmatite body from the second group was followed and a lot of samples are collected. There are in the caverns potassium feldspars, quartz (colourless, smoky quartz, citrine, amethyst), albite (cleavelandite), micas (biotite in the merge parts to muscovite in the central one), garnet (almandine-spessartines), beryl (aquamarine, goshenite, morganite), tourmaline (sherl to elbaite), Ta-Nb minerals, zircon and other minerals.

Structural and chemical investigations of potassium feldspars and garnets allow the following conclusions to be made:

1. All potassium feldspars of the pegmatite are "orthoclase", but the Al/Si degree of order decreases from the out to the central (adularian) zones.

2. The Na content decreases in the same direction.

3. The Rb increases, and Ba and Sr decrease from the out to the block zone of the pegmatite. The hydrothermal stage of crystallisation marks a new moment of the rare elements chemical behaviour: in the adularia zones falls the Rb content pronounced, Ba increases in a narrow 0.5 cm zone to 1.39 w.% . Mn, Sr, P, Zr increase too, but they are presumable in own minerals - spessartine, apatite, zircon, included in the adularia.

4. Garnet changes from $Pyr_{1.47}Alm_{31.80}Spes_{66.73}$ to $Alm_{4.80}Spes_{95.70}$ in the central parts of some caverns. In the spessartine caverns crystallises the Mn-rich beryl morganite.

The Rb-Sr isotope cooling age of the pegmatite body is determined on two adularias from a zoned crystal, albite and potassium feldspar from the block zone at T= 35.4+/-1.8 M a $(^{87}Sr/^{86}Sr)_i$ = 0.7091 +/- 0.0036).

ZIRCONS IN BIOTITES OF MOLDANUBICAN GRANITES

Pfaffl, F. A. (State Soil Res. Inst. Dept. of Geology, Zwiesel, Germany)

In the porphyritic edge layer of the Hohenauer-Granite (Leuko-granite-gneiss), Passau-Forest, in the south-east of Germany, there are microdines which are up to 5 cm big and the latter have biotites which very often contain zircons with radiation zones. The internal construction of the microclines shows clear zones by putting the biotites which has a mantle out of quartz and plagioclase near to the stages of growth. The biotite shows whirls in the form of circles, a phenomen on which has not been observed in the Moldanubicum. The biotites are added on the lines of growth; the broad side is very often directly or with an edge added on the lines of growth. They have got an olive-brown to a glazing or a shining brown (n_x) pleochroism or a red-brow to a chestnut-brown pleochroism and that shows that they contain of lot of titan oxide. Besides, you can see a mantle made of quartz and a combination with plagioclases. The biotites contain accessory zircons with clear zones of colours and radioactivity. By means of a chemical diadochy in the structure of the zircons it is possible to put in the structure certain substances of Y, Th and even U, where as Th and U cause a certain amount of radioactivity. The clear and precise thin-section of the zircons which is made vertically to the c-axis shows when they cut a very strong refexion of the light: n_o = 1,906. When we tried to find out their age according to the U-Pb-methode, we came to the result that they were 316-325 million years old (do Velbert-dm).

References:
Frasl, G. (1963). Jb. Geol. BA, Wien, 106, 405-428.
Hoppe, G. (1963). Abh. dtsch. Akad. Wiss. 1-130.
Pfaffl, F. (1964). Geol. Bl. NO-Bayern (printing).
Pupin, J. P. (1980). Contrib. Min. Petrol. 73, 220.
Ramdohr, P. (1958). Akad. Wiss. Berlin, 4, 1-9.

THERMAL BEHAVIOUR OF FIBROUS ZEOLITES OF THE NATROLITE GROUP

Phadke A.V.and Apte Aditi
(Dept. of Geology, Univ. of Poona)

The basaltic lava flows belonging to the Deccan Volcanic Province of India (DVP) bear numerous cavities, varying in size and shape. The occurrence of zeolites is especially profound in 'pahoehoe' type rather than the 'aa' type lava flows in the western region of the DVP. The fibrous zeolites are especially gorgeous and their thermal characters are equally interesting and informative in respect of their crystal structure and the manner in which the H_2O molecules are bonded with other ions.

Thermal curves of scolecite and mesolite, the two members of the natrolite group, from different localities in Maharashtra, India and natrolite from Germany, for comparison, were recorded at a heating rate of 10 °C/ minute in air, up to 1000 °C. The data on present investigations significantly differs from previous literature (Gottardi and Galli, 1985).

Natrolite from Germany shows a clear and sharp water loss in a single step around 380 °C, about 50 °C higher than the results of Reeuwijk (1972).

Scolecite, $Ca_8(Al_{16}Si_{24}O_{80}).\ 24H_2O$, instead of two major steps of loss of water, shows three distinct steps, (i) in the narrow range around 250 °C nearly equaling the next two, (ii) a double reaction with peaks at 425 °C and 480 °C, and (iii) around 550 °C.

The remaining water escapes gradually beyond this temperature. These steps are clearly reflected in the TG and the DTG curves. The first step corresponds to the expulsion of water from the site farthest away from Ca, one of the Na sites of Natrolite. The two sites nearer and somewhat asymmetrical with Ca are emptied after this in succession.

Thermal curves of Mesolite, $Na_{16}Ca_{16}(Al_{48}Si_{72}O_{240}) \cdot 64\ H_2O$ are much more complex with a major loss around 238 °C to 270 °C in a double reaction. Three or even four steps of further water loss, in some cases, take place in a manner similar to scolecite. By analogy, the double reaction peak in the range 238 °C - 270 °C is here attributed to the expulsion of water from the scolecite type channels, and the water from the natrolite type channels is driven off in the next step. There are marked steps of water loss even beyond 400 °C. The different steps of water expulsion are clearly reflected in the TG and the DTG. The peak temperatures of the thermal curves (DTA & DTG both) show higher values with larger sample amount.

Succesive phase transitions above 700 °C are also well reflected in the DTA curves.

References :

Gottardi, G., & Galli, E. (1985). *Natural Zeolites*, 409 p.

Reeuwijk, L.P. Van (1972). *Amer. Mineral.*, **57**, 499 - 510.

MAGMA FLOW-DIRECTION INDICATORS IN A LARGE DIABASE DIKE IN SOUTHERN NEW ENGLAND, U.S.A.

Philpotts A.R. (Dept. Geology & Geophysics, Univ. of Connecticut)

Many recent magma flow-direction studies based on measurements of anisotropy of magnetic susceptibility have concluded that flow in giant diabase dikes is commonly unidirectional and predominantly horizontal. However, in a large diabase dike that crosses southern New England, seven independent flow-direction indicators show that the flow was complex, with both forward and backward movement, and on average was in an upward direction.

The 50-m-wide Higganum dike can be traced as a series of en echelon segments for 450 km from Long Island Sound to the coast of Maine. In Connecticut, a segment of this dike is down faulted into the Mesozoic Hartford basin where it is seen to connect with the first flood basalt in that basin. Granophyre melts derived from partial melting of wallrocks along this dike were intruded into the dike while it was still flowing. Because of the high viscosity and low diffusion rates of these liquids, felsic streaks are still preserved within the first few centimetres of the dike's margins. The deformation of these streaks preserves a record of part of the flow history of the dike.

Granophyre that intruded the dike early exchanged alkalis (but not Si and Al) with the enclosing basaltic magma so as to establish a distribution similar to that between immiscible iron-rich and silica-rich liquids. This granophyre, therefore, is relatively K-poor. By contrast, granophyre that entered the dike after most of the ferromagnesian minerals had crystallized, is relatively K-rich. The granophyre's composition can thus be used to indicate the relative time at which the felsic melt entered the dike.

The most useful flow direction indicator was formed when the granophyre liquids were streaked off in the flow direction of the basaltic magma. These straight streaks are commonly recumbently folded by periods of backflow. Other flow indicators include: imbrication of phenocrysts near contacts; breaking and shearing of phenocrysts; granophyre segregations attached asymmetrically to phenocrysts; reidel shears; and ramp structures.

Flow-direction measurements within one en echelon segment of the Higganum dike show that as the magma rose, it spread laterally toward the ends of the segment. Thus the primary flow pattern was upward but fan like. However, at every site where measurements were made, the last recorded movement was backflow, which was almost always in the reverse direction of the forward flow, that is, down toward the center of the fan. This indicates that the center of the en echelon segment acted as a conduit that focused both forward and backward flow. Also, the fact that the final flow direction was downward rather than upward indicates that the magma was not forced up by the local wallrocks closing in behind the magma as it buoyantly rose.

The Higganum dike is interpreted to have formed from a linear array of intrusive fingers, with each finger spreading laterally to form an en echelon dike segment as it rose through the lithosphere. This argues for a laterally extensive magma source at depth instead of a local one from which the magma spread laterally.

• CHEMICAL APPROACH TO STONE CONSERVATION

Piacenti F. *(Centro di Studio sulle Cause di Deperimento e Metodi di Conservazione delle Opere d'Arte, C.N.R. – Univ. of Florence, Italy)*

The materials to be used for the protection and consolidation of stone in monuments exposed to the atmospheric agents must have unique properties. They must, in fact, not only perform their specific role but also be extremely stable in order to provide long lasting, colourless, reversible treatments, permeable to water vapour.

These materials may be hardly be found among those created for other industrial applications.

Those actually in use do not generally meet these requirements: they are reactive species leading to irreversible treatments, to severe reduction of the permeability of the surface to water vapour, and even to changes in colour.

Reconsideration of the effect expected from "consolidation" treatments has lead to define its aim not in the restoration of the original properties of the stone, but in the aggregation of the loose material present on its surface, in order to prevent its loss. Elastic materials with good aggregating properties may therefore be used to achieve this result.

Fluorinated elastomers have been tested for this role. An hexafluoropropene–vinylidenfluoride copolymer having 360000 a.m.w. was tested with success: on a calcarenite having 36% porosity, 35 g/s.m. of this product provided 70% increase aggregation of the surface (measured by abrasion), 85% reduction in the capillary absorption of liquid water, only 25% reduction in the permeability to water vapour. This product is stable to U.V. irradiation, oxidation, and provides reversible treatments even after prolonged aging.

The protection of stone exposed to the open air is mainly protection from rain which collects pollutants from the atmosphere and brings them in contact with the surfaces exposed. Rain and the pollutants are then absorbed in the porous stone structure and are the cause of its decay.

Protection of stone is best achieved not by occlusion of the pores, which must be avoided at all costs, but by changing the wettability of the walls of its pores by water. Fluids immiscible with liquid water, capable of coating the pores without occlusion, appear to be the appropriate answer to this problem.

Some perfluoropolyethers were tested for this use since they seemed to possess all the properties required for this application. The development of some new functionalized perfluoropolyethers, mono–, di– and tetra–amides, which have shown a very good behaviour as protective agents for stone, will be presented and discussed.

VIBRATIONAL SPECTRA, THERMAL PARAMETERS AND THERMODYNAMIC FUNCTIONS FOR MINERALS OF THE OLIVINE GROUP

Pilati, T. (*Dept. of Physical Chemistry and C.N.R. Centre, Univ. of Milan*), Demartin, F. (*Inst.of Structural Inorganic Chemistry, Univ. of Milan*) and Gramaccioli, C.M. (*Dept. of Earth Sciences, University of Milan*)

For minerals of the olivine group, such as forsterite Mg_2SiO_4, fayalite Fe_2SiO_4, tephroite Mn_2SiO_4, monticellite $CaMgSiO_4$ and glaucochroite $CaMnSiO_4$ vibrational spectra in the whole Brillouin zone have been calculated, using a rigid-ion Born von Karman model, with empirical atomic charges and force fields derived from best fit to the available Raman-IR spectra of these minerals and to the experimental phonon dispersion curves of forsterite and quartz (for the procedure here used, and applied to forsterite, chrysoberyl, bromellite, corundum, and quartz see: Pilati *et al.*, 1990, 1993,1994).

The agreement with the experimental data is good; however, some reinterpretation of the available data in the literature has been necessary, especially for the low frequencies.

From these calculations, also atomic displacement parameters (anisotropic) have been evaluated for all the atoms in these crystal structures: with the only exception of a single O atom in monticellite, the agreement with the corresponding crystallographic data is remarkably good, even at different temperatures. This agreement has been essential for checking the validity of the empirical force fields used here, and also indicates essential reliability of the estimated thermal- motion tensors involving different atoms. On these grounds, an average corrected value of 1.633 Å for the Si-O bond distances in these compounds can be deduced.

Even the calculated values of thermodynamic functions, such as entropy, are in good to very good agreement with the observed values; for the minerals containing Fe and Mn, these values are consistent with complete magnetic disorder above 100K. For fayalite, if the values suggested by Burns (1985) and Hofmeister (1987) for the electron contribution to entropy are accepted, the calculated values at high temperature are almost coinciding with the experimental data. Like for all the minerals so far studied by us, even at room temperature there is a substantial zero-point contribution to vibrational energy and thermal parameters.

The results obtained confirm the possibility of developing empirical force fields which are transferable, at least within wide groups, and the essential need of good experimental data for fitting the field (particularly as low frequencies in IR and Raman spectra, and as phonon dispersion curves).

References:

Burns, R.G. (1985) in: Reviews in Mineralogy, **14**, 277-316, edited by Kieffer, S.W. & Navrotsky, A. Washington D.C.: The Mineralogical Society of America.

Hofmeister, A.M. (1987) *Phys.Chem.Minerals*, **14**, 499-513.

Pilati, T., Bianchi, R., Gramaccioli, C.M. (1990) *Acta Cryst.* **B46**, 301-311.

Pilati, T., Demartin, F., Gramaccioli, C.M. (1993) *Acta Cryst.* **A49**, 473-480.

Pilati, T., Demartin, F., Cariati, F., Bruni, S., Gramaccioli, C.M. (1993) *Acta Cryst.* **B49**, 216-222.

Pilati, T., Demartin, F., Gramaccioli, C.M. (1994) *Acta Cryst.* B50, in the press.

TOPOTAXY RELATIONS IN THE TRANSFORMATION PHOSGENITE-CERUSSITE.

Pina C.M.(1); Fernández-Díaz L.(1) and Prieto M.(2)
(1) *Dpt. Cristalografia y Mineralogia. Univ. Complutense of Madrid*
(2) *Dpt. Geologia. Univ. of Oviedo.*

Phosgenite ($Pb_2Cl_2CO_3$) and cerussite ($PbCO_3$) are two secondary lead minerals that form in supergenic deposits as an alteration product of galena and anglesite. The crystallization of both phases is strongly controlled by the ph of the medium. Phosgenite grows at pH values around 5, while cerussite nucleation requires a basic pH. Crystal growth experiments in a porous silica gel transport medium allows to study both processes. Phosgenite is the first phase in nucleating. Afterwards, the physicochemical evolution of the system determines that phosgenite crystals become unstable and transform into cerussite. This transformation is controlled by a solvent mediated dissolution-recrystallization mechanism, similar to that proposed by Cardew & Davey (1985) for some polimorphic transformations. The transparency of the gel allows to follow the process by means of optical microscopy. The transformation starts in one point of the phosgenite crystal and, soon, an advancing front is defined. The transformation proceedes throughout the bulk of the initial phase preserving the external shape of the crystal. The final pseudomorph of phosgenite is built by aggregates of parallel fibrous crystals of cerussite elongated along [001]. The long axis of the fibres form a 45° angle with the direction [100] of the initial phosgenite crystal.

Cerussite shows orthorhombic aragonite-type structure. The space group is Pmcn, with a = 5.1800(7)Å, b = 8.492(3)Å, and c = 6.134(3)Å. In this structure, the Pb atoms are pseudohexagonally arranged in layers parallel to (001). These layers are separated by "corrugated" layers of CO_3 groups that also show a pseudohexagonal arrangment. Each CO_3 group is surrounded by six Pb atoms, and each Pb atom has nine immediate oxygen neighbors.

Phosgenite structure shows P4/mbm symmetry, with a = 8.160(4)Å, and c = 8.883(6)Å. In this structure, the Pb and Cl atoms define layers parallel to (001). These sheets are connected by CO_3 groups. The carbonate groups have the usual shape and lie in {110} mirror planes. In phosgenite, lead is coordinated by five Cl and four O atoms (Giuseppetti & Tadini, 1974).

The transformation of phosgenite into cerussite provides an interesting example of topotaxy. The main orientation relations that have been found are as follows:

(001) phosgenite || (010) cerussite
<110> phosgenite || <001> cerussite

These relations coincide with those described as epitaxy by von Vulteé (1950). They can be discussed according to the main strructural features of both phases: the distribution of CO_3 groups defining layers in both structures, and the coordination number of Pb atoms.

References:

Cardew, T.T. & Davey, R.J. (1985). Proc. R. Soc. Lond. A **398**, 415-428.

Giuseppetti, G. & Tadini, C. (1974). Tschermaks Min. Petr. Mitt., **21**, 101-109.

Vultée, J. von (1950): Fortschrift Mineral. **29/30**, 297-378.

IMMISCIBLE, HYPERSALINE CO_2-H_2O FLUIDS ASSOCIATED WITH REE AND MoS_2 MINERALISATION IN THE DITRAU ALKALINE MASSIF, TRANSYLVANIA, ROMANIA.

Pintea I. (*Institute of Geology and Geophysics, Bucharest, Romania*) and **Diamond L.W.** (*Mineralogy-Petrography Institute, University of Bern, Switzerland*)

Dioritic-hornblenditic rocks in the NW part of the Ditrau alkaline massif

host hydrothermal veins with a complex REE mineralogy, including silicates and phosphates, Mo-Bi-Cu-Fe sulphides, Ti-Fe-Mn-Th oxides, and carbonates. Quartz from these veins contains fluid inclusions of three main compositional types: (1) hypersaline aqueous inclusions saturated in CO_2 vapour, halite and other salts; (2) dense CO_2-rich inclusions with a weakly saline aqueous liquid; and (3) inclusions with intermediate compositions between 1 and 2, consisting of liquid CO_2, vapour CO_2, aqueous liquid, halite, and other salts.

Petrographic, microthermometric and phase equilibrium analysis suggests that the three inclusion types represent hydrothermal fluids which were in an immiscible state during mineral deposition. Thus, type 1 inclusions correspond to a hypersaline liquid phase, type 2 inclusions correspond to the conjugate vapour, and type 3 inclusions are heterogeneously trapped mixtures of the two end-members.

The nepheline phenocrysts which mainly occur in the inner part of the massif (Ditrau Valley) contain fluid inclusions representing a heterogeneous low-temperature high salinity fluids. These are aqueous brines with NaCl, KCl, etc, and the homogenization temperature ranged below 300 ^oC suggest hydrothermal genetic conditions.

• THE MINERAL CHEMISTRY AND TEXTURES OF WITTICHENITE, MIHARAITE, CARROLLITE, MAWSONITE, AND In–Bi–Hg TENNANTITE FROM NEVES–CORVO (PORTUGAL)

Pinto A. *(SOMINCOR, Portugal)*, Bowles J.F.W. *(Open University, UK)* and Gaspar O.C. *(I.G.M., Portugal)*

The Neves–Corvo mine is located in the Iberian Pyrite Belt in the South of Portugal. The deposit consists of five volcanogenic sulphide ore bodies known as Neves, Corvo, Graça, Lombador and Zambujal. Since it was opened in 1988 the mine has become the major European producer of copper and tin. The Neves ore body has two important subdivisions known as Neves Norte and Neves Sul. The Neves Norte ore body is mainly composed of polymetallic pyrite ores with some highly cupriferous ores at the base and its is these copper ores which are considered in this contribution.

The ore at the base of Neves Norte is particularly copper–rich and consists largely of chalcopyrite and bornite. Tin sulphide minerals, especially stannite and mawsonite, are present. In addition there are several mineral associations which are described here for the first time from within the Pyrite Belt. These associations include:

1. Carrollite ($CuCo_2S_4$) containing small inclusions of cobalt–rich pyrite.

2. Tennantite containing significant quantities of In (up to 2.7%), Hg (up to 1%) and Bi (up to 8%).

3. Selenium–bearing galena containing up to 30% of clausthalite (PbSe) end–member. The galena often contains inclusions of naumannite (Ag_2Se).

4. Wittichenite (Cu_3BiS_3), miharaite ($Cu_4FePbBiS_6$), stromeyerite (AgCuS) and nekrasovite ($Cu_{26}V_2Sn_6S_{32}$).

The purpose of this work is to communicate the mineral chemistry and textures of these unusual phases with a view to contributing to the studies of this ore.

Wittichenite and miharaite are usually to be found, as here, associated with bornite–rich ore. Indeed the first description of miharaite (Sugaki *et al.*, 1980) shows the association of miharaite with wittichenite, galena and chalcopyrite in bornite–rich skarn ores (Mihara Mine, Japan) and in a quartz vein deposit (Okutsu–cho, Japan). Roquesite and bismuth–rich tennantite with wittichenite are associated with copper ores in the Sn–W deposit of Cinovec, Czechoslovakia (Novak *et al.*, 1991). Carrollite often occurs as euhedral grains replaced by chalcopyrite, bornite or other copper minerals (Uytenbogaardt and Burke, 1971) and this is exactly the association to be found at Neves–Norte.

All these associations have in common a higher temperature paragenesis compared with that normally found in the Iberian Pyrite Belt. The ore appears to bear comparison in some respects with the stringer ore described by Marcoux and Moelo (1993). There is a clear comparison with the bornite–rich ores of the North Lyell section of the Mt. Lyell massive sulphides (Markham, 1968) where tennantite, galena, copper sulphides, mawsonite, stromeyerite and wittichenite (?) are present in the calchopyrite–bornite ores. In the Mt. Lyell deposit these ores are probably near to the stockwork of the massive sulphides deposit and it is likely that the highly cupriferous ore at the base of the Neves–Norte represents a similar situation.

References:

Markham, N.L. (1968). *Mineral. Deposita*, **3**, 199–221.

Marcoux, E. and Moelo, Y. (1993) In: Current Research in Geology Applied to Ore Deposits, Eds. P. Fenoll Hach–Ali, J. Torres–Ruiz, F. Gervilla, Granada.

Novak, F., Jansa, J. and David, J. (1991). *Véstnik Ustrednihoústavu geol.*, **66**, 173–181.

Sugaki, A., Shima, H. and Kitikaze, A. (1980). *Amer. Mineral.*, **65**, 784–788.

UTILIZATION OF ICP-EMISSION SPECTROSCOPY IN THE ANALYSIS OF FLUID INCLUSION DECREPITATES

Piperov N.B., Bonev I.K. and Atanasov S. *(Bulg.Acad.Sci., Sofia, Bulgaria)*

In this communication we share our experience in applying the D-ICP method the basic principles of which were developed some 10 years ago (Thompson *et al.*, 1980; Alderton *et al.*, 1982). An aerosol, obtained by the decrepitation of fluid inclusions in the material studied, is transported by carrier gas to the plasma of a multichannel ICP-spectrometer.

The analytical train, including the heated reactor (decrepitator) on line between the nebulizer system and plasma torch, offers a new possibility for calibration, even in the case of hot reactor.

The material studied is a late, low temperature (Th = 132-150^oC) hydrothermal quartz. The evolution curves of the alkaline (Na, K), alkaline earth (Ca, Mg), and ore (Cu, Zn, Fe, Pb) elements feature a single, well shaped maximum at ca. 230^oC, that could be related to the decrepitation of fluid inclusions. The chalcophylic elements (S, As) are released from the sample at temperatures higher than 400^oC, probably due to sulphide microimpurities.

The dependence of the analytical signal on the mass of the sample was checked for Na, K and Ca, and sample weights of 0.00 (empty reactor), 0.30, 0.50, 1.00, 1.50, 2.00 and 3.00 g (1.25-1.60 grain fraction). The relationship is linear, but presence of an intercept suggests that fluid inclusions are not the only source of Na.

We believe also that grain size analysis may be helpful in the bulk analysis of fluid inclusions (Piperov & Penchev, 1973; Piperov *et al.*, 1979). It may be expected that analytical signal from fluid inclusions *versus* grain size of the samples in logarithmic mode is a straight line with slope +1. For Na, K, Ca, Al, Fe, Cu and Zn, and 8 grain fractions in the range 0.062-1.60 mm, straight lines were obtained, but the slope was always higher than 1 (1.4-3.3). Some corrections are possible.

References:

Alderton, D.H.M, Thompson, M., Rankin, A.H. Chryssoulis, S. (1982). *Chem. Geol.*, **37**, 203-213.

Piperov, N.B., Penchev, N.P. (1973). *Geochim. Cosmochim. Acta*, **37**, 2075-2097.
Piperov, N.B. Penchev, N.P., Zidarova, B.P. (1979). *Chem. Geol.*, **27**, 215-231.
Thompson, M., Rankin, A.H., Walton, S.J., Halls, C., Foo, B.N. (1980). *Chem. Geol.*, **30**, 121-133.

CHARACTERISATION OF HEMATITE - ILMENITE EXSOLUTIONS USING TEXTURAL IMAGE ANALYSIS.

Pirard E. *(Applied Geology, Univ. of Liège, Belgium)*
and Duchesne J.C. *(Petrology, Univ. of Liège, Belgium)*

A large number of hematite-ilmenite samples collected in Norwegian anorthositic complexes (Egersund-Ogna, Bjerkrem-Sogndal, Ana-Sira...) have been characterised by chemical and petrographical methods. In order to improve our knowledge about geothermometry, possible recrystallisation processes and local heterogeneity, video image analysis has been tried.

Efficient image analysis firstly requires that an optimal procedure for image segmentation (separation of individual phase images) be designed. In the present study, tophat transformations and directional tophat transformations appear to give particularly good results on hemo-ilmenite grains in polished sections. Such segmentations allow for a simple two dimensional estimate of the global hematite to ilmenite (H/I) ratio to be derived. The stereological problem of estimating phase proportions from two dimensional sections of an anisotropic material is further discussed. Ratios estimated by image analysis are thereafter critically compared to the chemical data from the same samples.

More powerful capabilities of image analysis are illustrated : H/I from successive generations of exsolutions, spatial variability (zonation) of the H/I ratio in contact with magnetite, interlamellar distances and lamellae thicknesses. H/I ratios on a grain by grain basis are also computed using directional mathematical morphology transforms.

Careful use of image analysis appears to correlate very nicely with chemical data and leads to a detailed investigation of the intrinsic mechanisms of hematite-ilmenite exsolutions.

THE INVESTIGATION OF SUBMICROSCOPIC STRUCTURE IN MODIFIED KAOLINITES

Plastinina M.A., Fedorenko Yu.G., Zlobenko B.P., Kadoshnicov V.M. *(The Inst. of Geochemistry, Mineralogy and Ore-formation Ac.Sci. Ukraine, Kiev)*

The solution of general problem - to establish an interconnection between kaolinites structure defects and their formation conditions as well as consequent history, includes as one of components an investigation of defects nature by XRD and IR-spectroscopy.

Coherent scattering regions (CSR) sizes along "c" axis are an objective characteristic of kaolinite crystals which values, according to an experiment, have a high degree of linear correlation with Hinckly Index (HI) for samples with specific surface (S) value not exceeding 30 m^2/g. The complex experimental investigation of defects nature which are changing the CSR size allows, on the one hand, to determine the certain factors contributing into a total HI value and, on the other-to carry out a certain testing of kaolinites structural disorder theoretical models.Modified kaolinites are of certain interest in above purpose because of they allow to carry out a more selective differentiation of reasons responsible for the change of submicrocopic parameters.

With the use of XRPD, IR-spectroscopy and S-measuring the kaolinites were studied being modified by the next kinds of treatment:

1) deintercalation from formamide molecules by normalized water washing (H_2O and D_2O);

2) normalized mechanical treament (grinding within an agate mortar);

3) an isothermical warming up at T=734 K of different duration.

As a initial material for an investigation the kaolinite from Prosyanov deposit (Ukraine) was used having the next characteristics: CSR size along "c" axis - 46 nm, HI - 1.42 rel.units, content of low-defect phase %ldp - 56, microstrains value - 0.008.

It was established that CSR sizes along "c" axis:

were decreased in case (1) while HI value decreasing and S value remained unchanged;

remained unchanged in case (2) while HI value decreasing and S value remained unchanged;

were increased by 1.5-2 times in case (3) while conversion degree α >0.65 and retained their origin values while α <0.65.

It was shown that above three methods of treatment are differently influencing upon kaolinites IR-spectroscopic characteristics within a range of their OH-groups stretching vibrations. With the use of IR-spectroscopic data the nature of defects in deintercalated kaolinites was determined, and the features of kaolinite structural hydroxyles behaviour while its destruction after mechanical and thermic influence were established.

The explanation of the observed changes in XRPD-pattern of deintercalated kaolinites has been proposed. It does not contradict data of helicoidal structure of kaolinite crystals and modern model of its structural disorder,which excludes defects of $\pm$b/3-random layer shifts-type (Plançon et al., 1989).The conclusion was made that the decrease of %ldp could not always described by the known parameters of the expert system of Plançon and Zacharie (1990).

References

Plançon A.,Giese R.F., Snyder R.,Drits V.A., Bookin A.S. (1989). Clays & Clay Miner., **37**, 203-210.
Plançon A. & Zacharie C. (1990). Clay Miner., **25**, 249-260.

• SOME NEW ASPECTS OF ELECTRONIC ABSORPTION SPECTROSCOPY OF OXYGEN BASED MINERALS

Platonov A.N. *(Inst. Geoch., Miner. and Ore Formation, Ukrainian Acad. Sci., Kiev)*, Langer K. *(Inst. Mineral. Kristall., Techn. Univ., Berlin)*

Transitions between ground and excited electronic states, $\psi - \psi^*$, as LM– and MM–charge transfer as well as dd–transitions of 3d–ions give rise to absorption bands in the UV/VIS/NIR spectral ranges of transmission spectra of oxygen based minerals. The bands are characterized by their energy position ν in cm^{-1}, half band width $D\nu_{1/2}$ in cm^{-1}, linear or integral absorption coefficient $\alpha = \log(I_0/I)/t$ or $\alpha_i = (1/t) \cdot \int \log(I_0/I) d\nu$, respectively, and – except for cubic crystals – their polarization dependence, as well as by typical p– and T–dependancies of these properties.

In chemically complex natural minerals, such spectra mostly consist of complex superpositions of all types of the aforementioned transitions which, despite of the progress in curve fitting procedures, are still difficult to be resolved in many cases.

Provided the bands are correctly assigned to the respective excitation, then the spectra allow for the extraction of information that is related to local properties, i.e. to the "micro–system" subject

to excitation, within the matrix of the whole real crystal. Thus, electronic absorption spectroscopy is subsidiary to the crystal-averaging diffraction methods of crystal structure research.

Recent progress in this field, achieved in our laboratories covers method, theory and applications:

Polarized single crystal spectra can now be recorded with a local resolution down to about 3mm in a spectral range down to approx. ν = 10,000 cm^{-1} (λ = 1,000 nm). This enables e.g. to obtain polarized single crystal spectra of small synthetic crystals, grown under controlled (p, T, x, f_i)-conditions to contain only one type of "micro-system", with minimum size of about 10 μm. Such spectra greatly contribute to solve band assignment problems of the chemically more complex natural minerals. The spectral range, accessible to such locally resolved measurements extends now to about ν = 40,000 cm^{-1} (λ = 250 nm) in the UV and, thus, allows for studying the structure and polarization of the LM-CT related UV-absorption edges.

As far as dd-transitions are concerned, those of $3d^3$-configurated tetravalent manganese structurally isolated octahedra $(Mn^{IV}O_4)^{8-}$ could be characterized (Wildner & Langer, 1994). Ligand field theory has been extended to trigonal fields, using calculations similar to those of König & Kremer, 1977), for the case of octahedral Co^{2+} with point symmetries $\bar{3}$m, 3m, and 3 (Wildner & Langer, 1994b). Temperature dependencies, within the range 77 - 597 K, of dd-transitions of Cr^{3+} in octahedral sites of various point symmetries, with or without inversion centre, have been obtained (Taran et al., 1994). Models of Cr^{3+}-distribution in the complex structure of sapphirine could be derived from polarized spectra of Cr^{3+}-bearing sapphirines (Langer et al., 1994). Crystal field theory shows the cubic crystal field parameter 10Dq to be proportional to $(R_{M-O})^{-5}$ (cf. e.g. Burns, 1993). Thus, it is possible to derive local M-O distances in 3d-ion centered sites of 3d-ion bearing solid solutions. Comparing such distances $R_{M-O,sp}$ with those obtained from X-ray structure refinements $R_{M-O,x}$, an experiment that averages distances of all sites of the same crystallographic position, show often typical discrepancies that indicate that $R_{M-O,x}$ are rather fractional sums $\Sigma_i x_i R_{Mi-O}$ for the respective ions i than real distances . This should independently be verified by X-ray absorption spectroscopy.

Progress was also achieved with respect to the theoretical interpretation of the intercrystalline distribution behaviour of $3d^N$-ions, in that for a series of Cr^{3+}-bearing mineral parageneses from the mantle, the distribution coefficients $(K_{D,Cr3+})^{ph1/ph2}$ were found to quantitatively correlate with the respective difference in the crystal field stabilization energy $(\Delta CFSE_{Cr3+})^{ph1-ph2}$ (Andrut & Langer, this conf.). Locally resolved electronic spectroscopy was also used to elucidate the kinetics of the intracrystalline order/disorder reaction

$$Ni(M1) + Mg(M2) \quad \underset{K_o}{\overset{K_d}{\rightleftharpoons}} \quad Ni(M2) + Mg(M1)$$

in $(Mg_{1-x}Ni_x)_2SiO_4$ olivine solid solutions with x = 0.3 and x = 0.5 (Garsche & Langer, this conf.). Activation energies for the order, o, or disorder, d, reaction are

o:	170(5) KJ/Mole	d:	251(39) KJ/Mole (x=0.3)
	180(1) KJ/Mole		199(30) KJ/Mole (x=0.5)

Electronic spectra of mantle minerals from kimberlitic xenoliths and kimberlites themselves, and the values of colourimetric quantities calculated from such spectra, have successfully been used in tracing the genetic relations of such rocks as well as in diamond prospection of such mantle material from more than 200 kimberlite pipes in Yakutia, the Eastern European Platform, South Africa and China (Matsuk et al., 1994).

• THE APPLICATION OF COLOURIMETRIC PARAMETERS OF MINERALS IN GENETIC MINERALOGY

Platonov A.N. and Matsuk S.S *(Inst. of Geochem., Mineral. and Ore Formation, Kiev)*

For the solution of some genetic questions, particularly the genetic correlation of mantle plutonic rocks, the authors have used the objective colourimetric parameters of minerals (ICI-system), which are calculated from their optical absorption spectra. Such parameters may be essentially regarded as a general spectral characteristics of coloured minerals, as they provide numerical data for the features of optical absorption spectra (relative intensity of the absorption bands of different colour centers, bands dependence on concentration, character of spectral band shift under the influence of second-sphere cations, etc...). The colourimetric parameters may be used in comparative studies of the minerals taken from mineral associations that differ in composition and P,T-conditions of formation.

This method proved to be fruitful for the study of rock forming minerals (garnets, ortho- and clinopyroxenes, olivines, spinels, kyanites) from various mantle parageneses, which are represented by the plutonic xenoliths in the kimberlite pipes of Siberia and South Africa. On the colourimetric diagrams which are plotted for each mineral, the colour points of the studied samples from different parageneses form strictly determined areas ("colour fields") according to specific (typomorphic) combinations of chromophore centers (Cr^{3+}, Fe^{2+}, Fe^{3+}, Fe^{2+}-Fe^{3+}, Fe^{2+}-Ti^{4+}) for minerals of every paragenesis.

The comparative colourimetric analysis of the mantle minerals in kimberlites is capable to solve the following problems:

1) the genesis of diamond and accessory minerals in kinberlite;

2) the recognition of composition and facies attribution for the plutonic mantle rocks;

3) the evolutionary studies with regard of the plutonic magmatic chambers, the upper mantle substance differentiation etc.

KINETICS OF THE MAIN SULFIDE MINERALS OXIDATION IN EXOGENETIC PROCESS (THE COMPUTATION MODEL)

Pluysnin A.M., Gunin V.I., Mironov A.G. (Buryat Geological Institute, 6, Sahyanovoj str., Ulan-Ude, 670042, Russia)

The experimental study of the pyrite, pyrrhotite, chalcopyrite and galena oxidation was carried out at 25°C and 1 bar pressure. It was established that the oxidation process proceeds according to some parallel and consective reactions, the metastable sulfur forms (polytionate and tiosulfate) being formed (Pluysnin et al., 1990). The stechiometric equations were proposed. The order and velocity of main reactions were found.

On the basis of the kinetics data obtaned the computation model of the sulfides oxidation has been worked out. The model allows to evaluate the changes of the initial and new formation solid phase, to control the solution composition at any time and any distance of dispersion streams.

The computation simulation made it possible to modify the sulfide minerals ratio, oxigen concentration in the solution, water exchange intensity and jointing. The results of computation simulation allou to prognosticate the character of mineral distribution and deposition, the length and contrast of the geochemical dispersion streams, solid phase ratio in solution under different geochemical conditions.

References:

Plyusnin A.M., Mironov A.G., Belomestnova N.V., Chernigova S.E. (1990). Geokhimiya,1,51-60.

This work was supported by the Russian Fundamental Research Foundation, contract 93-04-14019.

PHASE RELATIONSHIPS INVOLVING SAPPHIRINE APPLIED FOR THERMOBAROMETRY OF ALUMINOUS GRANULITES

Podlesskii K.K. (*Institute of Experimental Mineralogy, Russian Academy of Sciences*)

Based on experimentally studied reactions in the MgO-Al2O3-SiO2 (MAS) system and volume properties of minerals, an internally consistent thermodynamic description of phase relationships involving orthopyroxene, spinel, pyrope, cordierite, alumina silicates, quartz, sapphirine and corundum has been obtained for temperatures from 700°C to 1500°C and pressures from 2 to 30 kbar. The derived phase relationships take into account a variable

solubility of alumina in solid solutions of orthopyroxene and sapphirine, as well as a variable water content in cordierite. Distribution of iron and magnesium between sapphirine and coexisting minerals has been calibrated based on empirical data using thermometers and barometers developed by Aranovich & Podlesskii (1989) for the FeO-MgO-Al2O3-SiO2 (FMAS) system. Application of the results to natural assemblages observed in aluminous granulites of the Eastern Siberia demonstrates consistency of the estimates based on sapphirine-bearing reactions with the P-T paths previously reported for related complexes. In some cases, sapphirine-bearing assemblages provide estimates of temperature below 700°C and that of pressure below 5 kbar, which implies that occurrence of this mineral in a rock cannot be considered a firm evidence of a very high-grade origin.

Reference:
Aranovich, L.Ya. & Podlesskii, K.K. (1989) *Geol. Soc. London, Spec. Publ.*, 43, 45-61.

THE HIGH PRESSURE STABILITY OF HYDROUS PHASES IN BASALTIC AND ANDESITIC SYSTEMS : AN EXPERIMENTAL STUDY TO 7.7 GPa.

Poli S. (*Dip. Scienze della Terra, Univ. of Milano*) and Schmidt M.W. (*Département Terre, CNRS - URA10, Clermont Ferrand*)

Phase relationships in synthetic basaltic and andesitic systems were experimentally investigated at water saturated conditions from 2.2 GPa up to 7.7 GPa, from 550 °C to 950 °C, in order to monitor the stability of hydrous phases in the subducted crust and to constrain the reactions causing the release of water to the mantle wedge.

Water reservoirs in the subducted oceanic crust at depth higher than amphibole stability field, i.e. P > 2.2-2.5 GPa, are represented by lawsonite (11 wt.% H_2O), Mg-chloritoid (8 wt.%), talc (5 wt.%), epidote (2 wt.%), in mafic rocks, and lawsonite, epidote, phengite (4 wt.%) and staurolite (2 wt.%), in intermediate compositions.

The stability field of lawsonite extends to ca. 800 °C and to 880 °C at 77 kbar in mafic and intermediate compositions, respectively. The breakdown of lawsonite above epidote-out, namely for pressure higher than 3.0-3.2 GPa, is governed by a continous reaction with a steep positive slope involving garnet and clinopyroxene. Phengite is the hydrous phase with the largest stability field found here, being stable to 7.7 GPa 920 °C. Talc, staurolite and, in one single experiment, brucite contribute in minor amounts to the water balance in mafic and intermediate rock compositions.

A model for water release from the subducted slab is developed profiting by thermal models for subduction zone environments. Up to 1 wt.% and 2 wt.% H_2O in mafic and intermediate rocks, respectively, can be stored at depth higher than 200 km by these hydrous phases. Dehydration rate is high down to amphibole-out (70-80 km) but it strongly decreases below. The large stability field of phengite may greatly enhance the role of sediments at increasing depth. Water release at depth higher than 200 km through progressive lawsonite and phengite breakdown will greatly simplify the generation of amphibole peridotite in the mantle wedge.

ABOUT THE GENETIC AND CRYSTALLOCHEMICAL INFORMATIVITY OF FE $^{3+}$/FE - RELATION IN BIOTITES.

Polshin E.V.,Belevtsev R.Ya. and Dudko V.N.(*Ukrainian Acad. Sci., Institute of Geochemistry, Mineralogy and Ore Formation, Kiev*)

On basis of study of chemical data for 390 biotite samples from garnet-containing metapelites has been shown that the histogram of $f = Fe^{3+}/Fe$ relation had a two peaks. The same histogram constructed on the Mossbauer data has a one peaks at f = 0.08 only (Fig.1). It is supposed that the second peaks on the chemical histogram is due to mistakes of chemical analysis.

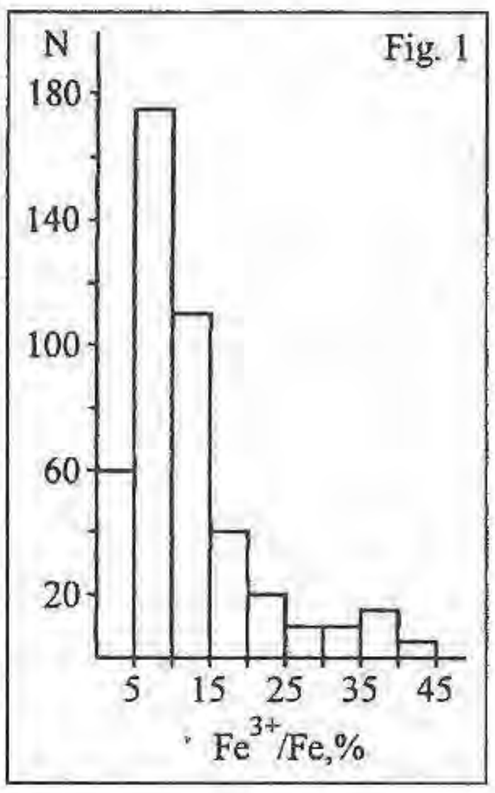

The position of first peaks does not depend on the facial conditions and composition of enclosing rocks. It does not depend on nearly oxidize-reduce potential also.

It is supposed that the nature of such constancy is analogous to one of constant relations between a basic chemical elements in biotite and this peak may be considered as a sign of the biotite chemical composition.

We assume that the position of this peak is determined possibly with the features of conjunction of tetra- and octahedral layers of biotite structure. The f-deviation for the biotite sample from the ideal value 0.08 is determined with interaction of internal and external factors as temperature, oxidize-reduce potential and etc. The degree of influence of each factor may be cleared up on series of special collected samples.

In [1] the diagram with parameters Ti/Fe^{3+} - Fe^{2+} has been proposed for the facial dividing of biotites. In the studied group of biotites the concentration of optical active centers of Ti was increased and of Fe^{3+} - Fe^{2+} decreased with increasing of temperature. In our group of biotites the correlation factor between these parameters equal only + 0.018.

But the use of value f = 0.08 for the diagram with $y = Ti/0.08Fe$ (instead of Ti/Fe^{3+} chem.) and $x = 0.92Fe$ (or $y = Ti/Fe$ and $x = Fe$) allowed to set up the correlation (r = -0.81) between these parameters and to divide biotites from the rocks with the different degree of metamorphism (see Fig.2).

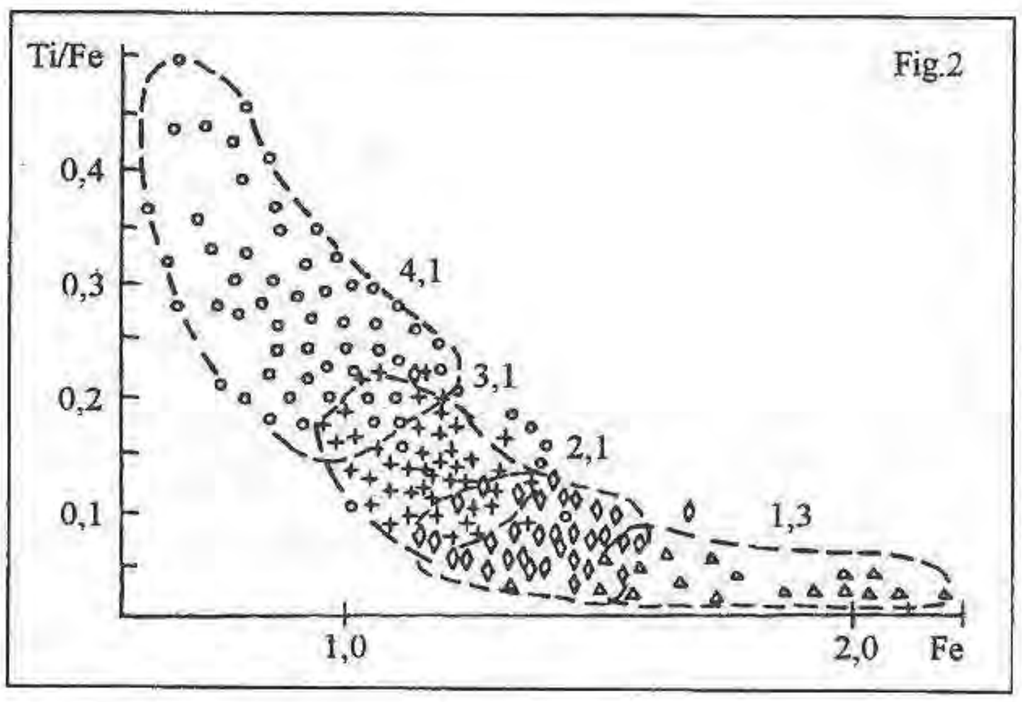

References:
Homenko V.M.,Platonov A.N.,Tcherbakov I.N. et al.(1989). *Mineral. jurnal*,11,N4.36-44 (in Russian).

EQUATIONS OF STATE AND THERMODYNAMIC PROPERTIES OF MINERALS: A SELF-CONSISTENT MODEL APPROACH.

Polyakov V.B. and Kuskov O.L. *(Vernadsky Institute of Geochemistry and Analytical Chemistry, Moscow)*

A self-consistent mathematical model for calculating the

equation of state (EOS) and thermodynamic properties of minerals is suggested. The model combines the Kieffer model vibration spectrum with the Born-Mayer potential, describing volume dependence of static lattice potential energy.

A distinctive feature of the model is its self-consistency that means a mutual agreement of the vibration spectrum and the static lattice potential energy. A way of the agreement consists in calculating the Born-Mayer potential parameters, given the model vibration spectrum, by the least-squares method using the equation of state along the zeroth isobaric curve. In addition to customary used thermodynamic quantities the reduce isotopic partition function ratios (β-factors) are taken as model input data. This provides a means for more reliable evaluating parameters of the model vibration spectrum, especially of its high-frequency part. The self-consistent model for construction of the EOS has been applied for periclase, lime, corundum, forsterite and grossular garnet. The model validation for adequacy has shown a good accuracy of the model predictions and has suggested broad potentials for application of this model to extrapolating experimental data as well as to calculating EOS and thermodynamic properties of minerals. The model seems to be available for calculating reference equations of state of minerals characterized by the lack of phase transformations in a wide range of P-T values for the purpose of using them as calibrated standards. Appropriate package of the calculation programs for the IBM personal computer has been made.

THERMAL DIFFUSION FROM HORNBLENDE AND BIOTITE AND THEIR POTASSIUM-ARGON DATES

Ponomarenko A.N., Spivak D.Y., Kalinichenko A.M. (*Ukrainian Academy of Sciences Institute of Geochemistry*)

Up to now, we have had no definite answer to the question about radiogenic argon migration mechanism. Some authors [1] note that the fluid regimen of the rock formation has influenced the mechanism of loss and capture of isotopical Ar. We have found free CO_2 molecules in hornblendes and micas. We conjectured that character of CO_2 emission from the minerals points to possible diffusional argon loss under the low temperature [2].

To gain a better insight into the link between CO_2 and values of isotopical ag8e, we explored the biotites and hornblendes from the rocks of the Ukrainian Shield. The character of the CO_2 emission from the explored minerals is assumed to be analogous to argon emission.

Some minerals were dated by application of the U-Pb method. The received values of isotopical age for metamorphic and magmatic rocks fall into a certain order: $age_{zircon} > age_{hornbl.} > age_{biot.}$

We examined the curves of CO_2 emission from the hornblendes and biotites as well as the 2contents of the high-temperature CO_2 emitted at 800 K or higher temperature.

We were led to the following conclusion:

- the smaller is the value of isotopical date by biotite and hornblende, the greater is the shift of the CO_2 emission

- there is also a corellation between the high-temperature CO_2 and the isotopical age by biotite and hornblende (table 1).

Table 1

N	N of sample	CO2 vol%	K-Ar age Ma	Remarks
1	T-31-86	41/31	1540/2185	Bi/Am
2	1008-a	45/70	1600/2580	-//-
3	51-72	50/80	1640/2370	-//-
4	K-1-4/81	60/50	1780/2130	-//-
5	992	70/67	1780/2080	-//-
6	ÅM-8-2-80	60/60	1890/2100	-//-

Potassium-argon dates for biotites are in the time interval of 1500-1900 Ma. and for hornblendes - in the interval 1900-2600 Ma.

Observational data suggest that despite the possible post-crystallization loses of radiogenic argon, the received values of K-Ar age by biotites and hornblendes has reflect the succession of geological events.

Magmatic rocks, aged 2600 Ma., had been changed by regional metamorphism 2000 Ma. The local metamorphism manifested itself again in several regions of the Ukrainian Crystalline Shield about 1600-1800 mln y. ago.

References

Lohov *et.al., (1987). Abstracts of Re ports delivered at the geologicak seminar at Zvenigorod.*,**2**,134-141.

Kalinichenko *et.al., (1988). Mineralogical Journal.*,**10**,44-50.

• MINERAL ASSOCIATIONS AND CONDITION OF FORMATION OF GOLD BEARING VEINS AND HYDROTHERMALLY ALTERED ROCKS OF DEPOSIT MAY (NORTHERN KARELIA)

Poritskiy M.S., Buiko A.K. *(Inst. Precambrian Geol. and Geochronology, R.A.S., St. Petersburg)*

1. The gold deposit is situated in Pana–Kuolayarvi riftogenic zone. Ore bodies are located in subvertical deep fault zone, traced by dikes of basic composition.

2. Metasomatic mineral assemblages are superimposed on metamorphic ones of svevofennian age (1800–1700 Ma).

3. Hydrothermal processes proceeded in four stages: a) carbonate–chlorite stage; b) quartz–actinolite veins; c) ore veins with epidote–quartz–albite–biotite metasomatites near the vein; 4) carbonatization.

4. Ore minerals in Au–bearing veins were formed in two stages: a) native gold, chalcopyrite, pyrite, tsumoite (BiTe) and clausthalite (PbSe); b) galena, pyrrhotite, sphalerite, cobaltite, altaite (PbTe), hessite (Ag_2Te) greenockite (CdS).

5. The ore in the deposit is represented by native gold of 988–787 fine. Fineness decreased in the second stage of ore–forming process. It can be explained by the penetration of silver in gold structure under rise of temperature.

6. According to geochemical investigations, during the processes of hydrothermal alteration of wall rocks near the vein gold concentrated with quartz.

7. The temperature of formation of quartz–actinolite veins was 400 °C, that of Au–bearing quartz veins was 500 °C; pressure under metasomatic processes was estimated as 50 MPa.

PRIMITIVE MELTS OF THE TROODOS OPHIOLITE (CYPRUS) TRAPPED AS INCLUSIONS BY CHROMIUM SPINELS.

Portnyagin M.V., Sobolev A.V., Dmitriev L.V. (*Vernadsky Institute of Geochemistry, Moscow*), Danyushevsky L.V. (*University of Tasmania, Geological Department*)

Olivine-phyric ultramafic dykes, the latest in the Troodos dyke complex (Desmons et al., 1980), are comagmatic to the type II Upper Pillow Lavas (UPL), transitional to the most depleted high-Ca boninite-like ultramafic lavas of the Troodos Ophiolite (Sobolev et al., 1993). The dykes are strongly altered having small relicts of fresh olivine phenocrysts but well-preserved spinel grains. Thus, melt inclusions trapped by spinels during crystallization may preserve original compositions unaffected by post-magmatic alteration. Olivines and spinels in the dykes are usually very magnesian (up to Fo93.5) and chromium-rich (Cr# up to 80) respectively, indicating that the melt inclusions may represent primitive unfractionated melts.

To eliminate possible effects of crystallization inside inclusions after trapping, spinel grains have been heated up to 1300 °C during 30 sec, kept at this temperature for 3 min and then quenched. Heating experiments have been performed using a high-temperature heating stage (Sobolev et al., 1980), characterized by a high quenching velocity (ac. 300 °C at temperatures above 1000 °C). A total of 50 spinel grains 0.5-1 mm in diameter have been studied. After quenching each grain has been mounted into epoxy and gradually ground until melt inclusions have been opened onto the surface. Approximately 10% of the grains studied contained primary melt inclusions 10-120 μm in size. Usually groups of 2-4 inclusions of different sizes have been found close to the center of the grains. Most of the inclusions have spherical or elliptical shapes. Quenched inclusions can be divided into two types according to their phase composition: glassy inclusions and inclusions containing quenched glass and small evenly-destributed olivine crystals up to 10 μm in size, which comprise up to 40 vol.% of inclusions. Fluid bubbles are present in both types. Each spinel grain contains inclusions of one type only.

Compositions of inclusions larger than 30 μm have been analyzed by electron microprobe Cameca MS-50 (GEOMAR Forschung Zentrum, FRG), using scaning mode (5-10 μm for glassy inclusions, 20 μm for inclusions with olivine crystals). From three to five different areas have been analyzed within each inclusion and averages have been accepted as inclusion compositions. Variations of MgO between different analyses within each inclusion are less than 1.5 wt.%. Host spinel grains are unzoned and vary in composition (Cr#) from 77.4 to 81.3 mol.%.

The presence of olivine within some inclusions indicates their trapping at temperatures higher than 1300 oC, that evidences undependently for the high temperature nature of Troodos boninite-like magmas (Sobolev et al., 1993). Furthermore a good correlation between compositions of host-spinels and melt inclusions (Figure) shows that the olivine crystals observed have crystallized inside of inclusions rather than trapped together with melt at temperatures lower than 1300°C.

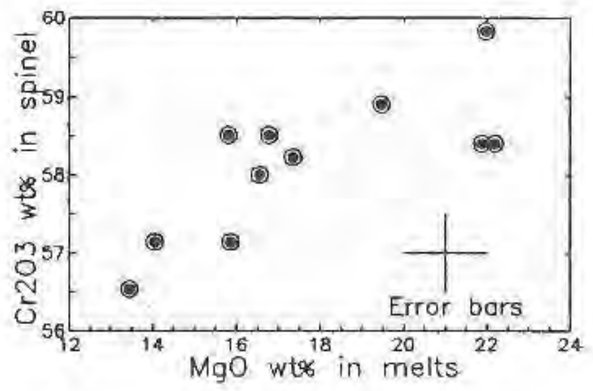

The inclusions vary widely in composition from 13 to 22 wt% of MgO. All major element contents, except FeO* and Na_2O, fall within the field of dyke and lava rock composition and form the trends close to the lines of olivine control. Higher Na content of melt inclusions most likely reflects Na depletion of rocks during post-magmatic alteration. Very low Fe* contents of melt inclusions may be accounted for by crystallization of magnetite or Fe-rich spinel onto walls of inclusions during the experiment or in nature due to oxidation of melt as a result of breakdown of water (Sobolev et al., 1983). Such process is not to affect significantly the concentrations of other elements.

Thus, we conclude that chromium spinel may preserve as a melt inclusions essentially unaffected primitive melts trapped during their growth. Based on the data obtained we believe that crystallization of Troodos ultramafic dykes took place from the very magnesium (at least 20 wt%) magmas at the temperature higher than 1300°C.

Desmons, J. et al. (1980) Ofioliti, 5, 22-26;
Sobolev, A.V. et al. (1993) Petrology, 1993, 1, 4, 379-412;
Sobolev, A.V. et al. (1980) Proc. 11th Lunar Conf., New York: Pergamon Press, 105-116;
Sobolev, A.V. et al.//C.R. Acad. Sci. Paris., 1983, 296, 275-280

X-RAY AND NEUTRON DIFFRACTION STUDY OF CORONADITE AND CESAROLITE

Post J.E. (*Smithsonian Institution*)

Coronadite ($Pb_{1.0-1.4}Mn_8O_{16}$), the Pb-bearing member of the hollandite mineral group, typically occurs as fine-grained masses, that are not suitable for single-crystal diffraction studies. TOF powder neutron diffraction data were collected for coronadite samples from Morocco and Australia, and their crystal structures were refined in space group I2/m using the Rietveld method. The Pb positions are disordered in the tunnels of the hollandite-like framework about a site displaced approximately 0.5 Å from (0,0,0).

Cesarolite is a poorly characterized Pb manganese oxide described from Tunisia (Buttgenbach & Gillet, 1920). Examination of samples from the original locality reveal two intimately mixed Pb manganese oxide phases: 1) a dense, dull-gray phase that is revealed by powder X-ray diffraction to be poorly crystalline coronadite and 2) a shiny, metallic phase, $Pb_{.54}Mn_2O_4$, that yields sharp powder diffraction lines that are indexed by an R-centered hexagonal unit cell with a=2.8106(1), c=20.386(1); although electron diffraction patterns show superstructure reflections. Partial structure information from the second phase indicates a layer-type structure, analogous to that of chalcophanite.

Reference:
Buttgenbach, H. & Gillet, C. (1920)
Amer. Min. 5, 211.

ON THE POLYGENETIC NATYRE OF SOME ORE TANTAL- BEARING MINERALS IN THE AMAZONITE-ALBITIC RARE METAL GRANITES OF RUSSIA

Povarennykh M.Yur. (Inst. of Geology of Ore Deposits, Russian Academy of Sciences, Moscow)

Data concerning typomorphism (typical feature complex containing chemical composition, crystal morphology, peculiarities of inner structure and paragenetic association) of Ta-bearing minerals (especially of the columbite-tantalite mineral group although with the pyrochlore-microlite one, kassiterite and wolframite) from the Aetykinskiy, Orlovskiy and Maikul'skiy massifes of amazonite-albitic rare metal granites is given. Combined with the information on the geology, mineralogy and petrography of the massifes, it is used as an argument in the determination of the genesis of rare metal minerals and the formation of the massifes itself.

The earlier injections and deep sited facies of the later granite injections contain crystals of columbite-tantalite mineral group without revealed zonal-sectoring pattern with even anatomical inner structure, orthorhombically ordered, relatively more hard and less tender. They are predominantly anisometric of tabular, fibrous, foliated habit, elongated by [001] and platenned by [010], with relatively narrow set of crystal forms. They are characterized by the Fe-Mn-columbitic composition with the Mn/Mn+Fe ratio varying from 0.28 to 0.49 and Ta/Ta+Nb - from 0.04 to 0.29 and reduced trace element content. Their nearest paragenetic association consists of inner parts of

coarse-grained amazonite and dark gray "pea-like" quartz with the oriented albitic inclusions, dark silver gray zinnvaldite, albite N 0-5 with the polysynthetic twinning, elongated zirtolite crystals with the domination of (101) form over (211).

The later injections and nearest endocontact facies of the earlier granite injections contain crystals with coarse or complicated zonal-sectoring anatomical pattern (polyzonal, oscillating), disordered within the orthorhombical system up to completely disordered ixiolites and ordered monoclinic wodginites, relatively more tender and less hard. They are predominantly isometric of columnar habit shortenned by [001], slightly elongated by [100], and thick tabular , slightly platenned by [001], ordinary with very wide set of crystal forms. As a rule, they are characterized by the Mn-Ta-columbitic composition with the Mn/Mn+Fe ratio varying from 0.45 to 0.97 and Ta/Ta+Nb - from 0.2 to 0.94 and enlarged trace element content (>0.15 % Sc_2O_3, >0.4 % WO_3, >0.2 % SnO_2, >0.35 % TiO_2). Their nearest paragenetic association consists of outer zones of coarse-grained amazonite and dark gray quartz, fine-grained light gray quartz and intensive blue green amazonite, albite with the so called "chess"-like extinction, light silver gray lepidolite, topaz poikiloblasts with fine-grained albitic inclusions, pod-like kassiterite crystals shortenned by [001] with the reduced tetragonal prysm facets, mutual pseudomorphs with pyrochlore-microlite.

It is shown that the established facts may be interpreted using the suggestion of polygenetic nature of rare metal minerals (magmatic and hydrothermal metasomatic), connected with intraplutonic evolution of the ore-magmatic systems of the massifes from the single portions of melt, saturated by volatile components, without a significant external matter introduction in it. Among the investigated massifes, in the row of post magmatic alteration degree Maikul`skiy and Orlovskiy plutons depend the extreme positions: the first as the representative of minor and the latter - of greater alteration degree; Aetykinskiy massif depends the intermediate position.

MULTIPLE OUTLIER DETECTION IN THE AVERAGE PRESSURE- TEMPERATURE METHOD

Powell, R (Dept Geology, University of Melbourne) and
Holland, TJB (Dept Earth Sciences, University of Cambridge)

The average pressure-temperature method of calculating the conditions of formation of mineral assembalges involves combining, in a least squares sense, the equilibria for a set of independent reactions between the end-members of the phases in the mineral assemblage which are also in the thermodynamic dataset. As well as being efficient and statistically sound, the method allows the calculation of the uncertainties on the resulting conditions of formation. If the statistics of the calculation suggest that one or more items in the input data are outliers (χ^2 test fails), it is important to be able to appraise the input data to identify the causes of the problem. This is straightforward if only one item of data is at fault, but if several may be, it becomes a nasty combinatorial problem. An alternative approach to multiple outlier detection is outlined which is based on the least- median-of-squares method. Once identified, outliers can be removed, and the usual least squares method applied: this can be described as a reweighted least squares approach.

THE LEAST SQUARES METHOD IN GENERATING INTERNALLY CONSISTENT THERMODYNAMIC DATASETS

Powell, R (Dept Geology, University of Melbourne) and
Holland, TJB (Dept Earth Sciences, University of Cambridge)

Internally-consistent thermodynamic datasets based on the large body of experimentally-bracketted mineral equilibria as well as calorimetry and other measured properties provide the means for calculating mineral equilibria with software such as THERMOCALC. The Powell and Holland methodology for fitting the experimental data to generate a thermodynamic dataset is based on least squares. Recent advances in this approach are reviewed. It is reiterated that experimental brackets may be modelled with a Gaussian distribution, and that as a consequence a least squares approach is desirable as well as efficient. Apart from the statistical justification for using least squares, a significant advantage of the method is that uncertainties in the thermodynamic data are calculated as part of the regression. It is shown how these uncertainties may then be used to calculate uncertainties on the positions of mineral equilibria involving solid solutions.

DIFFUSIVE EQUILIBRATION OF MINERALS DURING COOLING

Powell, R, White, LR, and Ehlers, K (University of Melbourne)

In an important paper, Dodson (1973) presented an analytical solution for diffusion of an element at low concentration in a slower diffusing phase in a faster diffusing reservoir during cooling, with particular reference to isotopic systems. Recently Ehlers and Powell, via extensive numerical experimentation, have shown the range of applicability of Dodson's equation for element exchange between minerals during cooling, and proposed an empirical extension of the equation to extend that range. New analytical extensions of Dodson's equation will be presented, and the implications of the results for peak temperature and cooling rate estimation will be illustrated.

Reference:
Dodson (1973) *Contribs. Mineral. Petrol.* **40**, 259-274

MINERALOGY AND GEOCHEMISTRY OF LACUSTRINE FACIES WITH MAGNESIUM CLAYS (KEROLITE-STEVENSITE / SEPIOLITE) IN THE MADRID BASIN MIOCENE (SPAIN).

POZO M., MORENO A. *(Dpt. Q.A. Geología y Geoquimica, U.A. de Madrid)*. CASAS J. *(C. Ciencias Medioambientales. C.S.I.C. Madrid.)* & MARTIN RUBI J.A. *(I.T.G.E. Madrid)*.

The Miocene Intermediate Unit (Aragonian-Vallesian age) of the Madrid Basin has as a characteristic the existence of important deposits of sedimentary magnesium clays, which have been interpreted as marginal lacustrine facies, forming a belt to the south and east of Madrid city, and marking a lateral transition from open lacustrine deposits to arkosic alluvial fan materials prograding NW-SE wards with source from the Spanish Central Range.

The kerolite-stevensite deposits studied in this work are located at the lower part of the intermediate unit whose strata are well exposed in quarries and outcrops near Esquivias village, 40 km south of Madrid. These clays are characterized by their pinkish to pale brown color and previous mineralogical research showed that they are composed of stevensite or mixed layers (kerolite-stevensite) with a structural formula:

$(Si_{8})(Al_{0.13}\ Mg_{5.60}\ Fe_{0.05})\ O_{20}(OH)_4.\ X_{0.18}.$

The lithostratigraphic logs show an alternation between pinkish clays-sands and green to yellowish grey mudstones-siliciclastic sands bounded at bottom and top by laminated fine sand with dark mudstone in deltaic cycles.

The presence of nodules (calcite, authigenic quartz, sepiolite) in pinkish clays and of clinoptilolite in sands and greenish mudstones indicates early diagenesis processes. Other postsedimentary features like desiccation cracks, prismatic structure, bioturbation (roots, burrows) and pedogenic

micromorphologies (oriented birrefringent clays, cutans, glebules, pedotubules) seem to be related with paleoedaphic conditions especially abundant at top of the better developed pinkish beds.

From a mineralogical point of view two different associations have been observed:

a) Pinkish clays-(sands): kerolite-stevensite / stevensite-(sepiolite-illite-quartz-calcite).

The geochemistry of pinkish clays indicates (as does mineralogy) the predominance of Si and Mg in all the samples studied being remarkable the negative correlation between magnesium and those elements related to detritals (Al,Fe,K,Ti).

The texture of Mg-silicates in pinkish clays showing "honey-comb" microfabric and common colloform morphologies suggest neoformation in a saline medium under severe evaporation conditions. Sepiolite content in these clays and in nodules associated point to a later drop in the water salinity (calcite cements). The formation of sepiolite by dissolution-precipitation during trioctahedral phyllosilicates instability is inferred.

b) Green-grey mudstones: Mg-Al smectite-illite / mica-feldspars (Ca-Na,K)-quartz-(kaolinite).

The Mg-smectites (saponite) associated with inherited minerals (quartz, feldspar, Al-smectite, illite, kaolinite) in green mudstones are interpreted as a result of transformation of Al-smectites and neoformation during early diagenetic stages.

The results let us establish a very shallow lacustrine environment (mud flat) in which kerolite-stevensite facies are related to palustrine ponds development where authigenic Mg-clays are formed. The alternation of green mudstones and sands with pinkish clays indicates cyclic shift of the lake shoreline during expansive and retractive episodes in arid to semiarid climatic conditions. Correlation between detrital input with green facies and pinkish clays with shallowing upward features in confined environment have been observed.

CRYSTAL STRUCTURE OF Cr-RICH PYROPE: TEMPERATURE AND CRYSTALLINE FIELD DEPENDENCE

Prencipe M., Ferraris G. and Ivaldi G.
(*Dip. Sci. Mineral. Petrol., Univ. Torino*)

Occurrence of Cr-rich pyrope from kimberlites has been reported by several authors (e.g. Sobolev *et al.*, 1973). Due to the larger radius of Cr^{3+} (0.61 Å) with respect to that of Al^{3+} (0.53 Å), which normally occupies the octahedral site, an apparent contradiction arises regarding the ease of Cr^{3+} to get into this site, whereas e.g. Fe^{3+} (0.64 Å) is not usually found. The contradiction seems even more acute, considering the shrinking effect of pressure over the coordination polyhedra.

In order to address the problem, the crystal structure of a Cr-rich pyrope $[(Mg_{2.3}Fe_{0.3}Ca_{0.4})(Al_{1.7}Cr_{0.3})Si_3O_{12}]$ coming from a garnet peridotite xenolith (Carswell & Dawson, 1970) has been refined, at 290K and 970K, through single crystal X-ray diffractometry (Mo K_α radiation).

The values of cell edge are 11.557 Å and 11.630 Å at 290 K and 970 K, respectively (linear thermal expansion coefficient: $1.0\ 10^{-5}\ K^{-1}$). Anisotropic refinements over 300 independent reflections ($2° < \theta < 40°$; R=0.016 and R=0.018 for room and high temperature data respectively) yielded oxygen coordinates (0.0334 0.0479 0.65232) at 290 K and (0.03412 0.04865 0.65383) at 970 K. Equivalent thermal parameters for the cubic (X), octahedral (Y) and tetrahedral (Z) sites and oxygen (in $Å^2$) are 0.0094, 0.0045, 0.0049 and 0.0089 at 293 K, and 0.0255, 0.0114, 0.0110 and 0.0191 at 970 K. Refined occupancies are in close agreement with the chemical analysis.

The ratio between the volumes of X-site and Y-site, at room temperature, is 2.26, which is similar to that of a Cr-free garnet (2.28), with very similar X-site and Z-site composition $[(Mg_{2.2}Fe_{0.4}Ca_{0.4})Al_2Si_3O_{12}]$, measured by the Authors. The thermal expansion coefficients for the X and Y-sites are 4.0 K^{-1} and 2.7 K^{-1}, respectively, and are similar to those of the Cr-free garnet (4.2 K^{-1} and 2.8 K^{-1}, respectively). This suggests a similarity in the values of compressibility of the same sites, so that even at high pressure the ratio between the X-site and Y-site volumes should be nearly identical for the two garnets. It results that, with respect to purely aluminum member, in the Cr-rich garnet there is not an expansion of the Y-site at the expense of the X one, as could rather be expected on the ground of geometrical consideration: factors other than geometrical features must therefore be invoked in order to explain the stability of cromium in the octahedral site of the structure.

Among transition metal ions, Cr^{3+} has one of the highest crystal field stabilization energy (CFSE) in a octahedral enviroment, due to its $3d^3$ external electronic configuration. Consequently, some shortening in the cromium-oxygen distance increases the stabilization; this may well explain the presence of conspicuos amount of cromium, substituting aluminum, in very high pressure pyrope. On the other hand, Fe^{3+} ($3d^5$ configuration) has not CFSE so that it cannot enter into the structure without considerable destabilization, because of steric hindrance.

The influence of Cr-O distance over the CFSE was noted during the experiment: provided the temperature dependent crystal field splitting of d orbital in T_{2g} and E_g subsets, as the temperature increase, the energies of the spin allowed $^4A_{2g} \rightarrow {}^4T_{2g}$ and $^4A_{2g} \rightarrow {}^4T_{1g}$ transitions decrease due to increasing Cr-O distance; as a result, our garnet changed colour from ruby-red to dark green when the temperature was raised up to 600 K.

In conclusion, with the consideration of crystal field stabilization effects, the stability of cromium in pyropes is no longer neither a contradiction nor a mistery; moreover it underlines the fact that, expecially in the case of transition metals, not always ions can be simply regarded as hard spheres.

References:

- Carswell D. A. & Dawson, J.B. (1970). *Contr. Mineral. and Petrol.*, 25, 163-184
- Sobolev N.V., Lavrent'ev, Pokhilenko N., Usova L. (1973). *Contrib. Mineral. Petrol.*, 40, 39

FES: PHASE RELATIONS AND CRYSTAL STRUCTURES

Prewitt C. T. and Fei Y. (*Geophysical Laboratory, Carnegie Institution of Washington*)

Although FeS appears to be a simple compound, investigators have tried for many years without much success to determine the stability relations and crystal structures of phases having this composition at varying temperatures and pressures. Progress has been limited because of the difficulty of maintaining stoichiometry and in characterizing phases that cannot be quenched to ambient conditions. Recent high-pressure (HP), high-temperature (HT) diffraction experiments on FeS using synchrotron radiation provide new information about crystal structures and phase relations in this system. The experiments were performed at room temperature with monochromatic x-radiation and also using an externally-heated diamond-anvil cell with polychromatic radiation on beamline X17C at the National Synchrotron Light Source. Previously, most work on characterizing FeS has been as a function of temperature at room pressure or of pressure at room temperature. By extending our measurements at simultaneous temperatures and pressure, we confirmed the presence of at least five different phases and numbered them from I to V.

Troilite (FeS I) is the stable phase at low temperatures and pressures. As the temperature is raised at room pressure, troilite undergoes a transformation to an intermediate HT phase (FeS IV) at 420 K, which then transforms to FeS V at about 600 K. FeS V has the NiAs structure with cell edges $A=B=3.44$ Å and $C=5.88$ Å, and space group $P6_3/mmc$. Troilite has a hexagonal cell related to that of FeS V by the matrix transformation (2,1,0/-1,1,0/0,0,2). At room temperature with increasing pressure, troilite transforms to a phase with the MnP structure (FeS II) at 3.4 GPa $(1,1,0/0,0,\frac{1}{2},\frac{1}{3},-\frac{1}{3},0)$ and then to a previously unknown structure (FeS III) at 6.7 GPa. Because the diffraction patterns of FeS II and FeS IV are similar and because no data intermediate diffraction data were available, King and Prewitt

(1982) proposed that these phases could have the same structure, that of orthorhombic MnP. However, Keller-Besrest & Collin (1990) concluded that FeS IV is hexagonal with a 2*A*, *C* cell. In the present study, we confirm that the phases are distinct and different. Cell refinement using diamond-cell, synchrotron x-ray data shows that the MnP orthorhombic cell provides a better fit to the HP data, and *in-situ* high-*P*, high-*T* XRED measurements indicate that FeS IV is a separate phase that does have the 2*A*, *C* cell as reported by Keller-Besrest and Collin.

Even with high-quality synchrotron x-ray data, it has been difficult to determine the symmetry of FeS III because diffraction patterns from different experiments are not consistent with each other, probably because of preferred orientation effects and because more than one phase is often present. However, it has been possible to index peaks that occur consistently in x-ray patterns at several different pressures on a monoclinic cell with a=5.121(2) Å, b=5.577(2) Å, c=3.328(2) Å, and β=95.95(4)° at 15 GPa. Preliminary indications are that the structure is still related to that of NiAs, but with significant distortions of the simple NiAs structure.

With new diffraction data obtained at simultaneous temperatures and pressures up to 900 K and 20 GPa, it has been possible to determine phase boundaries and crystal structures that clear up many questions that have existed regarding the FeS phase diagram and crystal chemical relationships. For example, the slope of the phase boundary between Fes I and FeS IV is negative and that between FeS IV and FeS V is positive. The results also provide new insight to the complete range of previous physical measurements on FeS, including the shock wave studies by Ahrens (1979) and Brown *et al.* (1984).

References:
Ahrens, T. J. (1979) *J. Geophys. Res.* 84, 985-998.
Brown, J. M., Ahrens, T. J., Shampine, D. L. (1984) *J. Geophys. Res.* 89, 6041-6048.
Keller-Besrest F., Collin G. (1990) *J. Solid State Chem.* 84, 194-210.
King H. E., Prewitt C. T. (1982) *Acta Crystallogr.* B38, 1877-1887.

MODELLING OF DEFECTS AND DIFFUSION IN MINERALS

G D Price and L N Vočadlo (Research School of Geological and Geophysical Sciences, University College London and Birkbeck College, London).

Defects in solids can be modelled using either quantum mechanical or atomistic approaches. Recent advances using both Hartree-Fock and Local Density Approximation methods to model defects in LiF, MgO and quartz will be reviewed. Atomistic simulations of defect formation based on the Mott-Littleton methodology are now well established and provide good estimates for formation enthalpies and migration enthalpies. The progress being made towards the calculation of absolute diffusion rates, involving the evaluation of defect formation and migration entropies will be outlined. Specifically, we will discuss our calculations of the absolution rate of ionic diffusion in MgO. We have used the super-cell approach to calculate *absolute* ionic diffusion coefficients for both cation and anion diffusion in MgO. We have found that the migration route is not straightforward and that there is in fact a bifurcation of the saddle surface. Using Vineyard theory and by applying an anharmonic correction to the predicted quasi-harmonic phonon frequencies we have calculated the attempt frequencies for both the migrating species. In conjunction with our results for calculated activation enthalpies, this has enabled a quantitative analysis of both the extrinsic and intrinsic régimes of the diffusion equation. As a result of our calculations, we believe that current experimental techniques are only able to sample the extrinsic régime.

AB INITIO CONSTANT PRESSURE MOLECULAR DYNAMIC STUDIES OF MANTLE MINERALS

G D Price and R M Wentzcovitch (Research School of Geological and Geophysical Sciences, University College London and Birkbeck College, London)

We will discuss the development of an ab initio constant pressure extended molecular dynamics method with variable cell shape. This is a symmetry conserving method which allows for efficient structural searches and optimizations in spaces with preselected symmetry groups. We have used this technique to study the zero temperature behaviour of $MgSiO_3$ and $CaSiO_3$ perovskites up to pressures which exceed those within the Earth's mantle. The predicted structural and elastic properties are in outstanding agreement with those inferred from experiment. We estimate the enthalpy difference between orthorhombic and cubic polymorphs of $MgSiO_3$-perovskite is so great as to preclude the cubic phase to be entropically stabilized under expected mantle conditions. We find the bulk modulus of $CaSiO_3$ to be very similar to that of $MgSiO_3$, and infer that Ca enrichment of the lower mantle is unlikely to affect the average bulk modulus of the region. We will also present data on the high pressure behaviour of Mg_2SiO_4-olivine and the clino-enstatite polymorph of $MgSiO_3$.

BIMODAL BEHAVIOUR IN PRECIPITATING (Sr,Ba)CO_3 AND (Sr,Ba)SO_4 SOLID SOLUTIONS

Prieto, M.; Fernández, A. *(Dpto. de Geologia, Univ. de Oviedo)*, Fernández-Díaz, L. *(Dpto. de Cristalografía, Univ. de Madrid)* and Putnis, A. *(Dept of Earth Sciences, Univ. of Cambridge)*

Complete series of solid solutions strontianite-witherite and barite-celestite can be synthesized by precipitation from aqueous solutions. However, there is a contrast between the possible chemical variations and the natural occurrences. Although there are not miscibility gaps, there is a lack of complete, natural solid solution of these minerals. In this work, nucleation experiments were carried out to study the factors that promote this bimodal behaviour. Crystals were obtained by counter-diffusion of $SrCl_2$+$BaCl_2$ and Na_2CO_3 or Na_2SO_4 through a silica gel column. The composition of the solids was analyzed by electron microprobe.

In the case of solid-solution aqueous-solution systems (SSAS), the formation criteria of sólid phases can be found from the "solidus" and "solutus" relationships of Lippmann (Glynn & Reardon, 1990). From these relationships one may compute the solid and aqueous phase compositions for a series of possible thermodynamic equilibrium states. These values can be displayed by means of χ_{Sr} - $\chi_{Sr,aq}$ plots, where χ_{Sr} and $\chi_{Sr,aq}$ are the mole fraction of the Sr-endmember in the solid and the activity fraction of Sr^{2+} in the fluid.

In the case of (Sr,Ba)CO_3 there is no thermodynamic reason to justify a bimodal behaviour. Values of $\chi_{Sr,aq}$ between 0.15 and 0.30 correspond to equilibrium values of χ_{Sr} between 0.48 and 0.69. However, in the case of (Sr,Ba)SO_4 , the equilibrium χ_{Ba} - $\chi_{Ba,aq}$ curve shows that only a very narrow range of aqueous phase compositions can coexist in equilibrium with solid solutions in the range $0.1<\chi_{Sr}<0.9$. This explains the scarcity of natural (Sr,Ba)SO_4 of intermediate composition from equilibrium considerations.

However, precipitation in SSAS systems occurs when a certain supersaturation level has been reached. In the case of the solid solution $C_xB_{(1-x)}A$, the supersaturation is done by (Prieto *et al. 1993*):

$$\beta = \left[C^+\right]^x \left[B^+\right]^{(1-x)} \left[A^+\right] \Big/ (K_{CA}\ a_{CA}\ )^x\ (K_{BA}\ a_{BA}\ )^{(1-x)}$$

where $[C^+]$,$[B^+]$ and $[A^-]$ are the activities of the ions in the aqueous solution. K_{CA} , K_{BA} , a_{CA} and a_{BA} are, respectively, the solubility products and the activities of the two endmembers of the SS. Therefore, for a given AS composition one must compute the $\beta(x)$ function for the entire compositional range from $x=0$ to $x=1$.

The $\beta(x)$ function is not enough to explain the effective precipitation behaviour. The present nucleation experiments demonstrate that the effective composition of the nuclei is not the one for which the system is more supersaturated, but that one for which a specific supersaturation threshold is before overpassed. For this reason, the experimental χ_{Sr} - $\chi_{Sr,aq}$ pairs do not agree with the equilibrium values. Anyway, in the case of $(Sr,Ba)CO_3$, the effective χ_{Sr} - $\chi_{Sr,aq}$ curve does not show a bimodal kinetic behaviour. On the contrary, the experimental χ_{Sr} - $\chi_{Sr,aq}$ pairs for $(Sr,Ba)SO_4$ show a clear bimodal tendency. Therefore, following to Baldasari & Speer (1979), the lack of a complete, natural solid solution strontianite-witherite can be explained because these carbonates are usually formed from the precursor sulphates celestite and barite.

Finally, a relationship between bimodal tendency and compositional zoning of high gradient has been observed. This phenomenon is very sharp in the case of barite-celestite (Putnis *et al.*, 1993), but $(Sr,Ba)CO_3$ crystals are basically homogeneous.

References

Baldasari, A. & Speer, J.A. (1979). *Am. Min.*, 64, 742-747.

Glynn, P.D. & Reardon, E.J. (1990). *Am. J. Sci.*, 290, 164-201.

Prieto,M. Putnis,A. & Fernández,L.(1993). *Geol. Mag.*,130, 289-299.

Putnis,A., Fernández, L. & Prieto, M. (1992). *Nature*, 358, 743-745.

CLAY MINERALS OF DRYLANDS AND IRRIGATED STEPPE SOILS IN THE RUSSIAN PLAIN

Prikhod'ko V.Ye. (Inst. of Soil Science and Photosynthesis RAS)

Clay minerals of south and odinary chernozems, dark and light chestnut, solonetz complex and brown desert steppe soils were investigated. They have light, medium and heave loam texture. Irrigation terms make up from 10 to 100 years. The irrigation rates came to 2000-5000 m^3/ha. It was carried out sweet waters containing a negligible amount of suspended particles.

Upper horizons of nonirrigated soils contain less clay content than parent roaks. Under the effect of irrigation clay accumulation in upper-horizons of soil profile takes place in the case if coarse fractions contain layered silicates in a state of individual particles or of aggregates which are able to a physical disintegration up to the size of clay particles. In these conditions the forming of clay fraction occurs with a bigger intensity than the loss of clay particles as a result of destruction and migration. If reserve of layered silicates too little in coarse fractions irrigation can lead to the loss of clay fraction from upper horizons.

In composition of clay fraction montmorillonite (36-58%) preveils, illite makes up 23-37%, kaolinite and chlorite are 17-35% (mable). Upper part of drylands characterizes decrease of chlorite and increase of illite compared with parent materials. That testifies about chlorite destruction. The illite content increases due to illitization process and as a result of a physical disintegration of mica and illite particles, contained in coarse fractions. These processes are confirmed by increase of the potassium content and decrease of the magnium content in clay fraction of the upper soil part compared with the C horizon. From north to south of steppe zone the potassium content in clay fraction increases. In this direction illitization process intensifies in upper horizons. Medow chestnut soil characterizes by maximum its increase. Under irrigation illitization process and destruction of chlorite in 0-50 cm layer intensify.

The labile structure superdispersion cheifly peculiar to the lower horizons of nonirrigable soils extende to the entire soil profile of irrigated soils. Na ion from irrigation subsoil waters is responsible for it.

The main changes of the clay material under pedological processes in natural conditions and under irrigation take place in the upper 0-50 cm layer, in the lower horizons they realize in the intercrack mass and some cutans on which soil solutions have the greatest influence.

TABLE. Clay mineral content (%) in nonirrigated soils

Minerals	Horizon	Chernozem odinary	Chernozem south	Chestnut* d.	Chestnut* c.	Chestnut* l.	Chestnut* m.	Solonetz	Brown soil
Kaolinite +chlorite	A	25	30	27	30	25	22	25	20
	C	27	33	31	26	31	30	30	31
Illite	A	27	28	26	30	35	37	34	32
	C	26	28	25	29	32	32	31	30
Swelling minerals	A	48	42	47	40	40	41	41	48
	C	47	39	44	45	37	38	39	39
Clay content	A	15	29	32	51	19	22	19	11
	C	18	34	33	50	33	31	30	15

*- d - dark; c - common, l - light, m- medow.

LATTICE ENERGY: AN OVERVIEW ON THE CPX MODELING

Princivalle F., Tirone M. (*Istituto di Mineralogia e Petrografia, Univ. di Trieste*)

Lattice energy calculation is a useful instrument to explain the microscopic and macroscopic properties of minerals. This abstract want to provide some informations on lattice energy and multicomponent generalizations with special regards to Cpx. The internal energy is given by $U=U_{coh}+U_{vib}$ where the cohesive energy is the lattice energy at 0 kelvin. In this model the vibrational contribution is neglected. Lattice energy calculations in the ionic approach are performed as follows:

-Coulomb energy: by means of the Ewald method (Tosi, 1964) assuming charge and atomic position fixed.

-Repulsive energy: by the application of the Born-Haber cycle as proposed by Ottonello (1987).

-Dispersive energy. This component is the effect of the polarizability and polarization attitudes of atoms and in some terms correct the effects of partial covalent bonds. The contribution is divided in dipole-dipole and dipole-quadrupole energies.

The calculations may concern Cpx in the system Ca-Na-Mg-Fe^{2+}-Fe^{3+}-Al-Si. The Cpx's structures were obtained by means of the DLS program (Baerlocher et al., 1977) utilizing the necessary bond distances from the data base reported in Ottonello et al. (1991). The data of enthalpy reported in Ottonello et al. (1991) and in part from reaction analysis computed here were used to obtain lattice energy through the Born-Haber cycle. The repulsive coefficient calculations are performed through the Minuit program (James and Ross, 1977),

adopting the repulsive formulation proposed by Gilbert (1968): $U^{R}_{i,j} = (\rho_i+\rho_j) \exp [(r_i+r_j)/(\rho_i+\rho_j)]$ where r are the ionic radii (Shannon, 1976) and ρ are the hardness parameter. In this way we obtain a repulsive coefficient for each atom and this must be considered presently the optimum for the lattice energy calculations in Cpx.

The method of the virtual crystal, assuming an average potential by a weighted sum of the atomic potential in each site, gives results of some interest for sistems of two or three components but the method fails for more complex sistems. This is an evident limit of the method as reported in de Fontaine (1979). An inprovement could be the formulation of the pair probabilities. Unfortunately it is of difficult application because it needs the distance betwen single species in the solid solutions and not the average distance obtained by the usual X-ray diffraction metods.

The repulsive parameters can be used to compute the distribution of atoms in multicomponent system and therefore short range order and Fe-Mg distribution. This could be done considering a superlattice structure formed by a reasonable number of lattices with a composition rapresentative of the sample. The calculation of the lattice energy for different atoms distribution allows to compute the free energy and in consequently to choose the configuration with the lower free energy as the most probable.

REFERENCES

Baerlocher C., Hepp A., and Meier W.M. (1977) DLS-76.
de Fontaine D. (1979) Solid state phys., 34, 74-274.
Gilbert T.L. (1968) J. Chem. Phys., 49, 2640-2642.
Ottonello G. (1987) Geochim. Cosmochim. Acta, 51, 3119-3135.
Ottonello G., Della Giusta A., Dal Negro A., and Baccarin F. (1991) In: Advances in Physical Geochemistry, Vol. 9, Saxena S.K. (ed.).
Shannon R. D. (1976) Acta Cryst.,.A32, 751-767.
Tosi M. (1964) Solid state phys., 16, 1-120.

ARE NEW MINERALS USEFUL?

Pring A. (*Dept. of Mineralogy, South Australian Museum*)

Approximately 50 new mineral species are described in the scientific literature each year. Many of these new species occur only as tiny grains or in very small quantities and are generally not of great importance in rock forming processes. The description of a new mineral requires the synthesis of data from a wide range of experimental methods, both modern and classical, yet despite the fact that this work unquestionably requires considerable scientific skill and intellectual input, it is considered by many in the geosciences as little more than mineralogical stamp collecting. One obvious reason for its apparent low esteem in the geosciences is that it is very difficult to construct a coherent long term research program in which new mineral description is a central theme; after all, the discovery of a new species is generally associated with a large element of serendipity and it is unimaginable (in Australia at least) that a national scientific research council would fund new mineral work. At the same time we, mineralogical taxonomists, are also partially to blame for the low esteem in which our discipline is held. In general we tend to think of new minerals merely in mineralogical terms rather than considering them in the broader context of inorganic materials. After all, minerals are naturally occurring inorganic compounds and some new minerals are also new inorganic compounds. Some new inorganic compounds, because of their chemistries and structures, have interesting properties, be they physical, electronic, optical or magnetic, which have applications in technology. Similarly some of the new minerals described each year will have novel properties which may make these minerals of technological interest. New minerals can be considered in four broad, somewhat overlapping, categories (i) new end members, (ii) new polymorphs, (iii) known synthetic compounds found as minerals, and (iv) minerals which have new structure types and chemistries. From a technological point of view minerals with new and novel structures and chemistries are most likely to be of potential interest. In this paper a number of recently described new minerals will be considered in terms of novel new inorganic compounds; particular attention will be paid to new minerals which may be of technological interest. By taking a broader view of our subject we can more fully exploit our discoveries and at the same time raise the scientific profile of descriptive mineralogy.

• THE QUANTITATIVE ANALYSIS OF PETROGRAPHIC STRUCTURES OF THE FERRUGINOUS QUARTZITES OF THE KOLA PENINSULA

Pripachkin P.V., Voitekhovsky Yu.L. (*Geol. Institute, Kola Sc. Centre, Russian Academy of Sciences*)

Rhythm banded structure characterized by alternation of fine layers of almost monomineral quartz and ore magnetite is the main dustinguishing feature of ferruginous quartzites (FQ). Moreover, a relationship between the degree of ore-potential and textural features was observed. FQ with low ore mineral content are characterized by fine banding. On the contrary, FQ with low ore mineral content are characterized by coarse-banded textures.

The origin of banding and its relationship with ore-potential is problematic. From the synergetics point of view, the authors consider that high ore concentrations and pronounced non-uniform textures are concurrent evidences of the evolution of the FQ complex as a thermodinamically open system (Pripachkin, 1991). Correspondingly the traces of the process should be displayed through all levels of its structural hyerarchy.

This premise allows to establish the evolutionary sequence of the FQ textures on the basis of their petrographic structures. The method of quantitative characterization of those structures was given (Voitekhovsky, 1992).

We studied the unclearly banded (1) and plicated (2) textural types of the Petchegubsk FQ deposit. The statistical distribution of the quartz-quartz, quartz-magnetite, magnetite-magnetite contacts, as well as of the different coordinations for quartz and magnetite grains, were found for both types. These distributions determine the peculiar features of the petrographic structures. The level of their ordering is characterized by the entropies of the distributions we mentioned above. For the types (1) and (2) the entropy (given as % of the maximum possible value) is: 76 and 62, respectively, as regards the distribution of intergrain contacts; 89 and 89, respectively, as regards the coordination between magnetite grains; 91 and 85, respectively, as regards the coordination between quartz grains. Therefore the study confirms the hypothesis of the concurrent ordering of quartzites in the range from the unclearly banded to the plicated ones, through texture and structure levels of organization.

References:

Pripachkin, P.V. (1991) Geol. synergetics, Alma-Ata, 65-68
Voitekhovsky, Yu.L. (1992) Proc. Rus. Miner. Soc., 2, 34-40

• THE INFLUENCE OF SURFACE SUBSIDENCE AND REACTIVATION OF FAULTS DURING THE EXPLOITATION OF COAL RESERVES ON MODERN MINEROGENESIS IN WASTE HEAPS

Privalov V.A. , Panova E.A., Privalova N.A. (*Donetsk Technical University*)

Nowadays 1257 waste heaps, with total volume of extracted rocks near 1.7 km^3, are known in the Donets coal basin. The studies carried out in recent years have revelead a distinct difference in chemical composition between rocks from coal-bearing strata in situ and rock mass of waste heaps, especially situated in the immediate vicinity of geological faults reactivated during under ground mining. For instance, precise measurements for such waste heaps, compared with other ones and also with original composition of Carboniferous series, have indicated: i) increase of concentrations of some elemennts (e.g. Fe, Ti, Al, Pt); ii) higher contents of ferriferous minerals; iii) neocrystallization of the following minerals: native sulphur, ammonium chloride, mascagnite, halotrichite, pickeringite, alunogen, realgar. Field observations and detailed geochemical and mineralogical surveys have shown that location of all major anomalies are controlled by fracturing pattern and distribution of fault traces. In some cases, anomalous radiation was found. Behaviour of faults during the exploitation of coal reserves is a phenomenon by which the relative

stability of rocks falls down along a surface and the parts separate, displacing apart one from the other. They more commonly occur as a zone of discrete fractures with level of ground strain e up to 0.05. This allows to calculate pressure of 0.5–1 kbar (P=eE, where E=10–20 kbar). Such P/T conditions correspond to the formation of low pressure granulitic metamorphic facies and, as a result, mineralogical alteration and redistribution of elements may be due to this process. An additional peculiarity, connected with surface subsidence and reactivation of faults, is that immediately after failure the rocks become highly permeable channelways for fluid flows.

HYDROTHERMAL ALTERATION AND FLUID INCLUSIONS AT CABEZA LIJAR TUNGSTEN DEPOSIT (SPAIN)

Protano G. and Riccobono F.
(Inst. of Mineralogy and Petrography, Univ. of Siena, Italy)

Ore geology and petrography. The tungsten deposit of Cabeza Lijar is one of most significant intrabatholitic orebodies of the Sierra de Guadarrama (Spanish Central System). It consists of a swarm of closely spaced wolframite-bearing quartz veins hosted by a porphyritic, medium to fine-grained, late-hercynian leucogranite. The mineralized veins are subvertical with N100-120°E strike, ranging in thickness from less than 1 cm to 50 cm. A system of garnet-bearing aplite dykes also runs practically parallel to the ore veins. The ore veins show a metalliferous paragenesis mainly consisting of wolframite, subordinate chalcopyrite and minor quantities of molybdenite, scheelite, pyrite, cassiterite, sphalerite, bismuthinite and stannite. The main gangue minerals are quartz and muscovite. The wolframite is by far the main ore mineral and, together with molybdenite, the first metalliferous phase to crystallize. Among the gangue minerals muscovite precedes quartz in the order of deposition and in many instances seems coupled with Cu-Zn-Sn sulphides. Ore deposition postdates hydrothermal alteration of selvages and the main vein-filling sequence is wolframite-muscovite-quartz.

Hydrothermal alteration of host rock. The host-rock is always heavily and symmetrically altered very close to the mineralized veins. Hydrothermal alteration of selvages is sharply zoned and consists of two different bands: an inner purely feldspatic rim and a thicker outer envelope consisting of an intergrowth of quartz and feldspars. A narrow feldspatic rim usually borders the mineralized veins. It is constitued by albite and microcline with traces of quartz and biotite. The thicker outer band consists of a quartzose aggregate with scattered small feldspatic eyes (microcline+albite) and muscovite nests. At a relatively short distance from the veins (1-40 cm) the transition to fresh rock occur quite abruptly through a thin silicized zone. A greisen-type alteration assemblage is present along the mineralized fractures and within the leucogranite as irregular areas.

Fluid inclusion study. A fluid inclusion study was carried out on ore (wolframite) and gangue (quartz) minerals from the mineralized veins and on quartz from the quartz-feldspatic selvages and from the greisen. As the wolframite was absolutely opaque to the visible light, petrographic study and microthermometric measurements of the trapped fluids were performed with near IR (0.8-1.2 μm) radiations.

Two main types of fluid inclusions were distinguished.

a) Type I are primary two-phase (L+V) inclusions with F=0.70-0.90, trapped in both wolframite and quartz from ore veins, in quartz from quartz-feldspatic selvages and from greisen. They are aqueous fluids with low concentration of one or more volatile phases which frequently nucleate as chlatrate during freezing. Th values range from 200 to 400°C and salinities from 3-11 wt % NaCl eq. In this family of inclusions, those trapped in quartz of the quartz-feldspatic selvages have the highest Th and salinities: 350-400°C and 8-11 wt % NaCl eq. respectively. Type I inclusions found in the wolframite have Th values of 305-350°C and salinities of 5.1-8.8 wt % NaCl eq.. The fluids in quartz from mineralized veins have a range of homogenization temperatures and salinities of 230-340°C and 3.5-7.5 wt % NaCl eq. respectively. Slightly different values (Th=200-310°C and salinities=3.5-9.5 wt % NaCl eq.) are shown by inclusions trapped in quartz from the greisen.

b) Type II are secondary aqueous two-phase (L+V) liquid-rich (F=0.95) inclusions, with low Th (150-260) and salinities (1-2 wt % NaCl eq.). They are present in all the types of quartz studied.

Conclusions. The microthermometric data indicates that type I fluids are responsible for the main alteration-mineralization phenomena at Cabeza Lijar. Type II inclusions represent the product of a late barren hydrothermal event. Hydrothermal circulation along the mineralized vein-system seems to have undergone progressive dilution as the temperature dropped. The quartz-feldspatic alteration of the selvages probably represents the first episode, whereas wolframite growth in fractures predates quartz deposition. Many similarities exist between the alteration-mineralization style at the Cabeza Lijar tungsten deposit and that of several W-Mo-Sn deposits of the european hercynian orogen, now interpreted as porphyry-like ores.

PATHOLOGY OF MINERAL INDIVIDUALS AS A RESULT OF DISTURBTION OF THEIR ADAPTATION TO UNFAVOURABLE ENVIRONMENT

Yu.O. Punin and G.E. Demidova *(Cristal Genesis Lab., Crystallography Dept., St.Petersburg Univ.)*

Crystal as a self-organising system imitates many features of development of alive organism during it's formation. Phenomena violating well-known laws of geometrical and phisical crystallography were defined as a "pathology of mineral individuals".This term states the existance of specific ways of crystals development, which are quite different from "normal" growth (dendrites, spherulites, twins, twisted and curved crystals, etc.)

Pathological processes of crystal growth are the result of adaptation of growing crystals to unfavourable conditions of crystallisation and are caused by some pathological factor or a group of such factors. They are, for example, inhomogeneity of medium, deformations and so on.

Large variety of pathological processes of growth, specific features of forms and structures of pathological crystals and their wide spreading provide rich posibilities for interpreting and reconstruction of the conditions of mineral genesis.

Macrodefects, which disturb a regularity of inner structure and outer form of crystals have a growth nature. A growth of crystals is a three-stage process which includes a transfer of a substance in a mother medium to a growth front, it's adsorbtion on a crystal surface and incorporation into a crystal lattice. At each stage special types of defects arise (diffusional, adsorbtional and absorbtional ones).

The list of pathology phenomena includes also the defects, caused by morphology reconstruction processes during dissolving, regeneration and sudden change of crystallisation conditions. Polycrystalline imitations of single crystals, such as epitaxy textures and pseudomorphes are the exterme cases of pathology.

The classification of the pathological growth phenomena is proposed on the basis of natural crystal defects study and experimental investigation of the model high-soluble compounds. The thermodynamics and kinetics of crystals pathology development are considered in details. The standard collection "Pathology of Crystals" is being created. It illustrates the morphological types and main peculiarities of pathology development. This collection is based on pairs of samples (natural and artifical crystals) with similar type of defects.

• A NEW HYPOTHESIS ON THE GENESIS OF THE Fe–Mn OCEAN NODULES

Punin Yu.O., Smetannikova O.G., Demidova G.E., Smolskaya L.S.
(St. Petersburg State University, Russia)

A Complex investigation of ferro–manganese ocean nodules (FMN) from three region of Pacific Ocean was performed; it included the study of their morphology, inner structure and zonal variations of chemical and mineral composition. All the investigated FMN display some common features, irrespectively of their size and morphology. These are:

1. Regular rhythmical zoning with two types of layer texture, the dendritic and massive ones (D and M respectively). Each zone of a given texture has fine zoning of second order.

2. The close correlation between relative layer thickness and their texture, the D–layers being two–three times thicker than M–layers. This suggests a higher growth velocity of D–layers.

3. The asymmetry in the inner structure of FMN corresponding to their morphological asymmetry.

4. The regular rhythmical variations of chemical composition of FMN, the D–layers being enriched in Mn, Ni, Cu and M–layers being enriched in Fe and Co. It was also observed a fine chemical zoning of second order.

5. The zonal variations of mineral composition of FMN.

These data are not consistent with the existing theories on the origin of FMN. A new hypothesis is proposed, based on the auto–oscillation mechanism of ore substance precipitation. Two types of layers with different texture and composition are built by two different heterogeneous processes, which occur simultaneously but with periodical predominance of one or the other.

The D–layers are formed by contact coagulation of colloidal particles of Fe,Mn–hydroxides. The M–layers grow by absorption of Mn^{2+} ions with autocatalytical oxidation. The combination of these two non–linear heterogeneous reactions, with diffusive transport of colloidal particles and Mn^{2+} ions to the growing surface of nodules, leads to oscillatory kinetics of precipitation. The alternating action of these two mechanisms is caused by the alternating exhaustion and enrichment of diffusive layer by two forms of ore substance, namely colloidal particles and ions.

The proposed hypothesis explains qualitatively all main peculiarities in FMN structure and composition, as well as other known data on their behaviour.

• NEW STRUCTURES OF SILICATES AND RELATED COMPOUNDS

Pushcharovsky D.Yu. (*Dept. of Geology, Moscow State University*)

The new ideas on crystal chemistry of silicates, based on author's structures studies, are reviewed.

1. The structure investigation of jaffeite $Ca_6[Si_2O_7](OH)_6$ (a 10.035, c 7.499 Å, sp. gr. P3, Z=2, 871 reflections, R_{aniso} 0.030) allowed to complete the isotypic serie fluoborite $B_3[Mg_9(F,OH)_9O_9]$ – jeremejevite $B_2[B_3Al_6(OH)_3O_{15}]$ – painite $CaZrB[Al_9O_{18}]$. All these structures contain the octahedral frameworks, formed by double bands, in which octahedra share the edges. On the contacts of these bands there are trigonal and hexagonal channels. The trigonal channels are filled by pyrogroups $[Si_2O_7]$ (jaffeite), by trigonal Zr–prisms and B–triangles (painite) or by $[BO_3]$–triangles (fluoborite, jeremejevite).

2. The study of K–nenadkevichite $(K,Na)2\{(Nb,Ti)_2[Si_4O_{12}](O,OH)_2\}1.6H_2O$ (a 14.69, b 14.164, c 7.859 Å, β 117.87°, sp. gr. Cm, Z=4, 1443 reflections, R_{aniso} 0.055) explained its microtwinning mechanism. The refined mass coefficents of twinned components are 0.47 and 0.48. In spite of monoclinic symmetry and the excess of K and Ti the similarity of K–nenadkevichite with orthorhombic nenadkevichite but not with monoclinic labuntsovite was shown.

3. The new family of band silicates includes revdite $Na_{16}[Si_4O_6(OH)_5]_2[Si_8O_{15}(OH)_6](OH)_{10}\ 28H_2O$ (a 53.83, b 9.972, c 6.907 Å, β 96.78°, sp. gr. C2, Z=2, 1785 reflections, R_{aniso} 0.084), synthetic $Cs_4(NbO)_2[Si_8O_{21}]$ (Crosnier *et al.*, 1990) and $K_4(NbO)_2[Si_8O_{21}]$ (a 33.920, b 10.950, c 7.737 Å, α 74.42, β 72.10, γ 89.81°, P1, Z=5, 8820 reflections, R_{aniso} 0.045). Their double bands are considered as the superposition of two vlasovite–like bands $[Si_4O_{11}]$. The mechanism of one dimensional commensurate modulation in $K_4(NbO)_2[Si_8O_{21}]$ with the volume of the unit cell ≈ 5 times bigger in respect to $Cs_4(NbO)_2[Si_8O_{21}]$ and modulation vector q=0.4a* is primarily connected with the change of tilt angles between Si–tetrahedra, which realize the contacts between two parts of silicate bands.

4. Tsaregorodtsevite $N(CH_3)_4[Si_2(Si_{0.5}Al_{0.5})O_6]_2$ is the first mineral with $N(CH_3)_4$–cations (TMA), which occupy the positions in the channels of sodalite–like tetrahedral framework. Its orthorhombic (sp. gr. I222) to cubic (sp. gr. I432) HT–transformation at 970°C was studied. The decrease of the unit cell volume, fixed in the annealed samples, is connected with the destruction of the channel fillers. The mutual disposition of Si, O–anions and cations in structures of TMA–silicates allows to emphasize the dominating role of silicate complexes (Shapelev, 1990). Thus, besides the zeolites (Kawahara & Kohara, 1992) this group of silicates does not obey the main concept of silicate crystal chemistry, which assumes that cations determine the constitution of silicate structures.

References:

Crosnier, M.P., Guyomard, D., Verbaere, A., Piffard, Y. (1990). *Europ. J. Solid State Inorg. Chem.*, 27, 435–442.

Shepelev, Yu.F. (1990) Thesis of D. Sci. Dissertation. Inst. of silicate Chemistry. St. Peterburg.

Kawahara, A., & Kohara, S. (1992). Abstr. of 29–th IGC, Kyoto, v.3/3, 696.

Alteration of REE-bearing accessories in granitoids from the Mecsek Mts.

Puskás Z., Gál-Sólymos K. (*Dept. of Petrology and Geochemistry, Eötvös L. Univ.) and Buda Gy. (Dept. of Mineralogy, Eötvös L. Univ.*)

Electron microprobe analyses were carried out on heavy mineral separates from the syncollision Variscan granitoid occurring in Mórágy (Mecsek Mts., South Hungary).

The main REE-bearing minerals are allanite and RE-fluorcarbonates, beside these sphene, zircon, apatite, epidote and thorite were found too.

The rock is slightly altered porphyroblastic microcline-bearing amphibole- biotite-monzogranite.

Fresh primary allanite is very rare, generally altered by F^- and CO_3^{2-}-rich hydrothermal solutions.

The alteration products, as thorite and one part of the RE-fluorcarbonates remained inside the altered allanite. The other parts were transported by solutions, and crystallized as RE-fluorcarbonates in the fractures of the rock.

Secondary allanite formation can be observed too, either as an overgrowth on former epidote, or replacing epidote and calcite. This type of allanite is depleted in U and Th. The breakdown and leaching of primary allanite resulted in the formation of Ce-epidote too.

Primary thorite is rare and occasionally altered to thorogummite. It occurs more commonly in a fine-grained form, which has been originated from allanite during the hydrothermal alteration.

The REE-content of the primary sphene is rather low (0.3 w%). Nb occurs irregularly or forms a vein-like enrichment zone inside crystal and commonly altered to Nb-bearing rutile and calcite.

MICROSTRUCTURES ASSOCIATED WITH PHASE TRANSITIONS

Putnis, A. (*Department of Earth Sciences, University of Cambridge, CB2 3EQ England)*

This paper reviews the microstructures which form as a result of phase transitions in minerals, with particular emphasis

on the origin of the so-called tweed microstructures in minerals undergoing cation ordering and disordering. The nature of the tweed microstructure can to some extent be inferred from diffraction contrast experiments in transmission electron microscopy (TEM) and structural models based on such observations will be discussed, specifically regarding the length scale of ordering and strain in the structure. Such structural models of the tweed are then compared with the conclusions drawn from spectroscopic measurements (NMR and IR) in a number of systems. It is concluded that in tweed microstructures which result from symmetry changes driven by cation-ordering, the local degree of order is not itself modulated. A model based on twin-related domains of the low symmetry form is consistent with experimental observations. Mechanisms of coarsening of the tweed microstructure to form the lamellar twinning observed in the fully ordered structure are briefly reviewed.

MINERALOGICAL STRATIGRAPHY OF METAMORPHIC COMPLEXES IN THE URALS

Pystina Yu.I., Pystin A.M. (Institute of geology Komi Science Center, Syktyvkar, Russia)

Accesory minerals of several metamorphic complexes of the Urals have been studied with the purpose of stratigraphic division and age correlation of these objects. It has been reveded that zircon, apatite, sphene, tourmaline, rutile were the most informative minerals for stratigraphic investigations. Zircon is of particular interest in these minerals series as comparatively stable in metamorphic processes and usually represented by a number of morphological types.

Mineralogical criteria for making the division of metamorphic series and to carring out the correlation of contemporary metamorphic objects spatially separated have been developed. It is shown that the next features may be used as criteria: specific composition of accesory minerals and their relativus; typomorphic mineral associations and major minerals; morphological features of some minerals and, first of all, of zircon (colour, habitus, degree of roundness and surface character, coefficient of elongation and dimensions, internal structure of crystals, etc.); spectroscopic features of minerals and thire isotopic age. On the base of mineralogical criteria with the use of other data (lithology, degree of metamorphism, character of folding, etc.) the geological structure of definite regions in the Urals here metamorphic complexes are found, has been clarified.

GEOLOGICAL STUDY AND PROSPECTING MINERALOGICAL MAPPING IN JIEHE GOLD DEPOSIT

Qi, J. and Li, L. *(Gold Geological Institute of MMI, LangFang, P.R.C.)*

Situated in the northeastern part of Zhaoyuan county, Shandong province, Jiehe gold deposit is a typical mesothermal deposit hosted in Guojialing granodiorite (135—100Ma.). The granodiorite is bounded on the northeast by the Archean Jiaodong group (2670Ma.) and on southwest by Linglong granite (118—170 Ma.). The Archean Jiaodong group and Guojialing granodiorite with abyssal assimilation of the Archean Jiaodong group form in turn the primary and secondary source of gold supply while the NE trending faults cutting Guojialing granodiorite give rise to the formation of the deposit. The ore in the deposit occur near the fault as quartz—pyrite veins, cross—cutting pyrite veinlet and pyritized greisenized granodiorite. Through research in the physical properties of minerals in the deposit, it is found that the thermoelectrical coefficient of pyrite and the integral intensity of quartz and microcline increase with the increase of gold tenor. Using these physical properties of minerals as parameter, three mineralogical maps are made showing the following regularities. (1) The known orebodies of the deposit occur in anormalous areas where the thermoelectric coefficient is larger than 140μv/℃ while the integral intensity of quartz and microcline are larger than 4R (Roentgen) and 15R (Roentgen) respectively. (2) The extreme—value points of gold tenor and extreme—value points of the physical parameters occur approximately in the same location. (3) The orebodies and the anormalous zones of the mineralogical parameters are quite similar in outline. (4) Except for the known orebodies, four more other anormalous zones which indicate four hidden unknown orebodies are displayed in the mineralogical maps of the physical parameters. According to the indication of the maps, the unknown hidden orebodies have been found.

The Volta Grande Pegmatites (Minas Gerais. Brasil): granitic pegmatites rich in Rb and rare elements.

Quéméneur J.*(Dept. Geol. IGC. UFMG, Belo Horizonte, Brasil)* and Lagache M *(Lab. Geol.Ecole Normale Supérieure Paris).*

The Volta Grande pegmatites occur near the city of São João del Rei in the south of the Minas Gerais state.They are associated with Early Proterozoic (Transamazonic) granites dated (Rb/Sr) 1932±32Ma (Quéméneur &Vidal 1989). These granites and pegmatites are hosted by gneisses and amphibolites of the archean greenstone belt of the Rio das Mortes Valley. The studied pegmatites can be classified as the albite-spodumene type of Cerny (1990) and they are very similar to theWeinebene pegmatites in the Koralpe, Austria (Göd 1989).

These pegmatites form large bodies, up to 1200 x150 x10m. elongated paralelly to the foliation of the amphibolites. The pegmatitic bodies show unusual mineralogical zoning (Quéméneur 1987) with a large central granitoid zone containing spodumene, quartz, microcline, albite and muscovite and a irregular border zone composed of fine aplitic albitite or columnar association of spodumene and quartz. Pockets of lepidolite and lenses of giant spodumene crystals occur in the granitoide zone. The pegmatites develop a large metamorphic aureole in the amphibolites with zinnwaldite and holmquistite.

The Volta Grande pegmatites are geochemically characterized by a high content in Rb and Li.The feldspars and micas were analysed using electron microprobe (Petrographie Paris6), ICP (Ecole des Mines St Etienne) and wet chemistry (Ecole Normale Supérieure Paris). These minerals show exceptionaly high content in Rb similary to those of Red Cross Lake pegmatite in Manitoba (Cerny et al. 1985).

	Rb2O%*	Rb2O%m	Cs2O%*	Cs2O%m	K/Rb	Rb/Cs
micro	3.70-4.31	4.25	0.04-0.15	0.10	3.0	44
musc	3.22-4.24	3.90	0.07-0.24	0.13	2.1	28
lepid	5.52-7.85	6.92	0.34-0.46	0.38	1.1	18
Zw 1	4.28-6.42	5.39	0.43-0.63	0.52	1.1	9.0
Zw 2	2.55-3.82	2.99	0.36-1.04	0.77	2.47	2.67

Table n°1:Content in Rb , Cs and K/Rb and Rb/Cs ratio of the micas and K-feldspars of Volta Grande.*Minima and maxima values. m: mean values.Zw1: zinnwaldite near of the contact with pegmatite, Zw2: zinnwaldite far from the contact.

The partition coefficient of K-Rb par can be calculated for the K-feldspars and micas of the Volta Grande pegmatites. The K/Rb atomic relation in microclines and muscovites are respectively:

K/Rbmicro= 7

K/Rbmusc = 4.7

Cmusc/micro= (K/Rbmusc)/(K/Rbmicro)=4.7/7=0.67

The sanidine-solution partition coefficients Csanidine/solution and Cmusc/solution were experimentally determined (Lagache 1968) and Volfinger1970) these are respectively 2.22 and 1.82;it corresponds to: Cmusc/Csan = 0.82. This value ar similar to those calculated for Volta Grand.The calculated coefficent of lepidolite using the Volta Grande datas is the following: Clep/solution=2.45/3=0.82. This value is similar to those experimentally obtained by Volfinger&Robert 1980

with other trioctaedral micas(phlogopite:0.90-aestonite:0.65).The zinnwaldite of the contact aureole also show exceptionally high content in Rb. Its partition coefficient with muscovite is: (K/Rb)zw/(K/Rb)musc= 2.36/4.7= 0.50.

We suggest that the Rb-content of pegmatite increased probably during the cristallization of the pegmatite, due to the high partitioning coefficients of microcline and muscovite. This explains the high Rb-content in the lepidolite.cristallized in late stages On the other hand, in the contact aureole the low zinnwaldite coefficient causes a decrease of the Rb-content. Most of the Cs remains in the solution and is incorpored into minerals formed by late stage;although high Cs-content can be found in the extern border of the contact zone (Zw2 Tab. 1).

References:
Cerny, P.(1990). *Geol. Rundschau,79/2*, 183-226.
Cerny, P., Pentighaus, H. , Macek, J.J. (1985). *Bult. Soc. Geol. Finland*, **57**, 217-230.
Göd, R. (1989). *Mineralium Deposita*, **24**, 270-278.
Lagache, M. (1968). *C.R. Acad. Sci. Paris*, **267**, 141-144.
Quéméneur, J. (1987). *Revi Bras. de Geociências*,**17(4)**, 595-600.
Quéméneur, J.& Vidal, P. (1989). *4 Simposio Geol. Minas Gerais An.* 7, 135-148.
Quéméneur, J., Lagache, M., Correia Neves, J.M. (1993). *C.R. Acad. Sc. Paris*, **317**, 1425-1431.
Volfinger, M. (1970).*These 3ème cycle Univ. Paris.*
Volfinger, M., Robert, J.L. (1980).*Geochimica Cosmochiimica Acta* , **44**, 1455-1461.

CA-MAGNESITE PRESENCE IN SALINE LAKE SEDIMENTS FROM SPAIN.

Queralt I., Julià R., Plana F. and Giralt, S. (*Inst. "Jaume Almera", CSIC, Barcelona*)

The eastern part of the Iberian Peninsula is one of the most extensive areas of saline lakes in Europe.

Several samples of lake sediments obtained from cores in Lake Salines (SE, Spain) and in Gallocanta Lake (central part of Spain) contain calcium magnesite. This mineral phase is well characterized by their X-ray diffraction (XRD) plot features. The main peaks exhibit systematic shift (towards higher basal d-spacing) respect to those reported for pure magnesite, suggesting a magnesite expanded cell dimensions.

The results of chemical analyses exhibit a fixed calcium content (8% mol $CaCO_3$) in the magnesite structure. No other cations were detected. Comparison of our X-ray data for this Ca-magnesite with those of other magnesium-rich carbonates suggests structural analogies with the R-3 symmetry group.

Supplementary data provided from scanning electron microscopy, microprobe chemical analysis, infrared spectra, and atomic absorption analysis allow us to consider the presence of Ca-bearing magnesite with the chemical formula $(Mg_{0.92},Ca_{0.08})CO_3 \cdot 3H_2O$ as a frequent metastable phase in lake deposits. We interpret this phase as a result of the changing Mg/Ca ratio in the host water during the precipitation process. The bedrock composition of the catchement area and the hydrological balance are the main factors controlling carbonate precipitation.

CANAPHITE: AN UNCOMMON CONDENSED PHOSPHATE IN LAKE SEDIMENTS

Queralt I., Julià R., Plana F. (*Inst. "Jaume Almera", CSIC, Barcelona*) and Seret G. (*Univ. of Louvain la Neuve, Belgium*)

Canaphite, the first example of condensed phosphate occurring as a mineral phase ($CaNa_2P_2O_7 \cdot 4H_2O$), was defined as a new mineral by Peacor *et al.* (1985) studying samples from the Paterson area, New Jersey. The redefined crystal structure (monoclinic, Pc group) was described by Rouse *et al.* (1988). No other occurrences have been reported at the moment.

After extraction of the small size fraction and treatment of several samples of La Cruz Lake recent sediments (Cuenca, Spain),little aggregates of canaphite have been obtained and identified by routinary X-ray diffraction procedures. The main diffraction peaks are in excellent agreement with those reported in literature and the refined cell parameters (a=5.676, b=8.575, c=10.509, β=106.29°) are not far from those previously reported.

Scanning electron microscopy observations allow us to recognize that canaphite occur in different samples, appearing in three different morphologies: a) radiating clusters of euhedral long prismatic crystals (up to 100 μm in size), b) spherical nodules and c) tabular crystal aggregates. Microprobe analyses exhibit little differences in chemical composition between the different morphologies. Raman analysis show a single spectrum with main vibrational modes at 358.1, 472.9, 741.8 and 1030.7 cm^{-1}.

References:
Peacor, D.R., Dunn, P.J., Simmons, W.B., Wicks, F.J. (1985). *Mineralogical Record*,**16**,467-468.
Rouse, R.C., Peacor, D.R., Freed, R.L. (1988). *American Mineralogist*,**73**,168-171.

CHARACTERIZATION OF HYDROTHERMAL PROCESS IN TUNGSTEN ORE DEPOSITS OF THE SPANISH CENTRAL SYSTEM.

E. Quílez(1); E. Vindel(1); J. Sierra(1); J.A. López-García(1); M.C. Boiron(2) and M.Cathelineau(2).
(1)Dept. Crist. y Mineralogía. Univ. Complutense, Madrid. Spain.
(2)CREGU, BP23, 54501 Vandoeuvre-les Nancy Cedex, France.

The W(±Sn,Mo) deposits from central part of the Spanish Central System are closely related to peraluminous leucogranites and monzogranites emplaced at shallow depths. The low K/Rb ratio and high content in Rb, Sn, W and Nb allow to clasify these granites as fertile. This hydrothermal process has been dated by K/Ar method. The results show that it can be described as an early hydrothermal event (300-290 M.y.) related partly to the end of the magmatic activity in this area.

Two clearly defined metallogenic stages can be distinguished: a first one consisting of W(±Sn,Mo) deposits and a later of Fe-Cu-Zn sulphides. In all the veins, quartz is the main gangue mineral. The most important types of associated hydrothermal alteration are greisenization (390°-300°C) and chloritization (305°-285°C). The alteration shows a zoned spatial distribution of secondary mineral assemblage with greisenization confined to the areas closer to the veins, and chlorite in the external zone. The chemical variations related to these alterations are important, but are restricted to the wallrocks adjacent to the veins. The W-bearing quartz veins and greisens are structurally controled. They are associated to faults related to a transtensional strike-slip tectonic regime, with SE-NW compression. This tectonic regime displays similar features to the Permian and Upper Carboniferous deformational stages described by other authors in the same area.

Four hydrothermal stages have been defined on the basis of fluid composition and the thermobarometric conditions: *(1)* An early high-temperature (470°-350°C) brine (53-43%wt.eq.NaCl) of magmatic origin has probably circulated during a first phase of faulting causing subsequent greisenization and LREE enrichments of the altered zones. *(2)* The second hydrothermal stage results in the circulation of a H_2O-NaCl-CO_2-CH_4-N_2 fluids of moderate salinity (9-2%wt.eq.NaCl). The temperature range was wide (150°-450°C) and the pressures lithostatic above 1 Kb. The process was characterized by the dilution of CO_2 until exhaustion in the system. It was favoured by a pressure drop and

by the dilution and cooling resulting from the solutions mixing, during this stage. Isotopic data evidence the participation of meteoric waters in the process. In terms of immiscibility, no evidences of a genetic relationship between stage (1) and stage (2) have been found. *(3)* Low to moderate salinity solutions (1-8%wt.eq.NaCl) circulated at minimum temperatures in the range of 150° to 250°C and pressures above 200 bars. *(4)* The latest fluids are represented by cooler (120°-90°C) aqueous solutions of higher salinities (over 15%wt. eq.NaCl) that contain significant amounts of $CaCl_2$ and $MgCl_2$.

The complex carbonic-aqueous fluid plays an important role in the transport of tungsten at acid pH and low fO_2. The precipitation of the tungsten is directly related to the loss of CO_2 in the system. This CO_2 loss produced a probably slight pH increase and, as Dubessy et al. (1987) pointed out caused the increase in the dielectric constant of the fluid and correlatively the desestabilization of neutral species. In addition, it can be observed a decrease of temperature and salinity during the hydrothermal evolution in all studied mineralizations, which promoted a decrease of the ionic strength in the solutions. All these factors favoured the precipitation of wolframite.

References

Dubessy, J; Ramboz, C; Nguyen-Trung, C; Cathelineau, M; Charoy, B; Cuney, M; Leroy, J; Poty, B. and Weisbrod, A. (1987). Bull. Minéral. 110. 261-281.

FELDSPAR GEOTHERMOMETRY ON GRANULITE-FACIES METAPELITES FROM SRI LANKA

Raase P. (*Mineralog.- Petrograph. Inst., Univ. Kiel*)

Two-feldspar geothermometry revised by Kroll et al. (1993) is shown to be a valuable tool for deciphering the retrograde temperature development in high-grade metamorphic rocks. In the metapelites from the Highland Complex of Sri Lanka for which very high peak metamorphic temperatures have been reported (Schenk et al., 1988), several feldspar generations have been analyzed:

1. Large antiperthite grains (up to 2cm) have bulk compositions with high Or contents (Or19-21 at An25-32, Or33 at An9). No primary alkali feldspar is found.
2. High-temperature recrystallizates in strongly flattened granulites with platy quartz contain coarse string perthite (Or62-74, An3.8-2.5) and plagioclase with low Or content. Seldom mesoperthite and antiperthite are found together.
3. Low-temperature recrystallizates in metapelites without platy quartz contain string perthite (Or78-87, An2.6-1.1).
4. Fine-grained late recrystallizates and rims of very fine string or film perthite.

Plagioclase in generations 2-4 is low in Or (<2.5) except some inclusions in garnet (Or6), and devoid of antiperthitic domains.

Assuming that the Al/Si exchange between plagioclase and alkali feldspar is frozen in at high temperatures while alkali exchange continues, a minimum temperature of feldspar recrystallization can be calculated by the two-feldspar geothermometer revised by Kroll et al. (1993). Two-feldpar temperatures for recrystallizates (generation 2) in strongly flattened metapelites from the central and southeastern part of the Highland Complex are in the range 780-900°C, for recrystallized feldspars (generation 3) in metapelites from the western and central part in the range 640-710°C, and for late fine-grained recrystallizates (generation 4) about 560-570°C (calculated using Margules parameters from Fuhrman and Lindsley, 1988). These temperatures compare well with results from garnet-pyroxene thermometry in metabasites (Schumacher et al., 1990): about 820°C for core compositions of coarse garnet and orthopyroxene, 700°C for garnet-clinopyroxene rims, and 640°C for orthopyroxene-plagioclase symplectites.

Bulk compositions of relict antiperthites (generation 1) from 6 metapelite samples suggest peak temperatures of metamorphism of 960-1020°C (or even higher if Margules parameters of Elkins and Grove, 1990, or Lindsley and Nekvasil, 1989, are used). These high temperatures far above the minimum temperature of fluid-absent melting of metapelites might be unrealistic and probably result from the Margules parameters which are not well constrained at high temperatures. Maximum metamorphic temperatures of about 900°C are suggested from relics of inverted pigeonites (Schenk et al., 1988).

References:

Elkins, L.T., Grove, T.L. (1990). *Am. Mineral.*, **75**,544-559.
Fuhrman, M.L., Lindsley, D.H. (1988). *Am. Mineral.*, **73**, 201-215.
Kroll, H., Evangelakakis, C., Voll, G. (1993). *Contrib. Mineral. Petrol.*, **114**, 510-518.
Lindsley, D.H., Nekvasil, H. (1989). *EOS Trans. Am. Geophys. Union*, **70**, 506.
Schenk, V., Raase, P., Schumacher, R. (1988). *Terra Cognita*, **8**, 265.
Schumacher, R., Schenk, V., Raase, P., Vitanage, P.W. (1990). *In:* Ashworth, J.R., Brown, M. (eds.) *Allen & Unwin*, London, 235-271.

MINERALOGY AND MAGNETIC PROPERTIES OF BAKED CLAYS IN PLIOCENE COAL DEPOSITS OF THE DACIC BASIN, ROMANIA

Rădan S., Rădan S.C., Rădan M. and Vanghelie I. (*Inst.of Geology and Geophysics, Bucharest, Romania*)

The Upper Pliocene coal deposits of the Dacic Basin contain numerous occurrences of baked and/or fused sedimentary rocks generated by natural spontaneous burning of lignite seams. Usually, these rocks consist of hardened red clays and sands with brick-like appearance (porcelanite), but sometimes they show a slaggy or vitreous texture with marked vesicularity and dark color (clinker). A few magnetic anomalies have been detected in some heat affected areas, suggesting important changes in mineralogy and magnetic properties of these rocks during the post-depositional thermal perturbation.

The main non-clay minerals determined in thin sections and by X-ray techniques within the original rocks (not affected by heating) are represented by angular quartz and quartzite grains, plagioclase, microcline and orthoclase, with scarce white mica, subordinate calcite, dolomite and minor siderite, and few amounts of anatase.

Clay mineral assemblages are dominated by illite (average content, 41%) with important percentages of smectite (29%) and kaolinite (26%) and sporadically chlorite (4%). The argillaceous material included within the coal seams as clay interbeds or finely disseminated clay fraction is composed mainly of kaolinite (average content, 70%), with subordinate illite (16%) and smectite (14%). The floor of the lignite beds consists of clays rich in smectite (average content, 51%), associated with illite (24%) and kaolinite (21%) and accidentally chlorite (4%).

The heat-affected rocks show modified mineral assemblages, which can be correlated with the increasing temperature, in the successive stages from slight baking to more or less total fusion, towards the burnt coal seam.

X-ray diffractograms of some samples of clay-porcelanite sequence point out the gradual lowering and disappearance of clay mineral reflections, starting with smectite and going on with kaolinite, chlorite and finally illite. Among the non-clay minerals, first to break-down are the carbonates, followed by quartz, and later, by feldspars. Consequent to the increasing temperatures, cristobalite and various amounts of hematite appear, the latter at the expense of goethite, hidrogoethite and iron sulfides.

The clinker-containing sequences show even more interesting and rich newly-formed mineral assemblages, consisting of hematite, cristobalite, tridymite, β-quartz (?), mullite, spinel, cordierite and

magnetite (?). The low temperature quartz and the feldspars are no more found within the scoriaceous mass of the clinker.

The mineral transformations induced in these clays by heating during the natural burning of coal beds, prove that the porcelanite and clinker forming temperature reached at least 1100 - 1200° C, easily exceeding the Curie point of ferromagnetic minerals. The baked clays show very important values of magnetic susceptibility (2580 x 10^{-6} - 161000 x 10^{-6} u. SI) and remanent magnetization (150 - 5900 mA/m) as compared with natural non-affected clays (65 x 10^{-6} - 755 x 10^{-6} u. SI and 0.01 - 30 mA/m respectively). As a consequence, the occurrences of the thermally affected deposits are recorded as important anomalies by the magnetic mapping.

The paleomagnetic studies provided, also, interesting data concerning mineralogical evolution of clays during heating processes. In this respect, laboratory techniques used for thermal demagnetization require repeated magnetic susceptibility and remanent magnetization determinations, on samples heated in steps, up to 700° C. X-ray analyses carried-out on such samples revealed similar mineral transformation processes as described in natural clays and porcelanites.

PBC ANALYSIS OF THE CHALCOPYRITE STRUCTURE

Radulova, A. S. (*Departement of Mineralogy, University of Geneva*)

The analysis of the chalcopyrite structure is based on the periodic bond chain (PBC) method. The procedure includes the determination of: 1. the order of decreasing d_{hkl}: 101, 112, $1\bar{1}2$, 103, 200, 004, 202, etc. 2. the order <uvw> - the most probable PBC bearing directions - <111>, <100>, <131>, <110>, <021>, <351>, <331>, etc. 3. the PBC on the projections of the structure along <uvw>. The PBC. are <110> and <021> - zigzag chains with composition respectively: Cu-S-Fe-S and Cu-S-Cu-S-Fe-S-Fe-S. (interatom distance no more than 2.302 Å). The only slices with two or more PBC (F-forms) are 112 and $1\bar{1}2$. The pinacoid contains one <110> chain because in the order d_{hkl} the first (001) elementary slice is 004 - too thin for two <110> chains. S - forms are {001}, {100}, {102}, {124}, {136}. K - forms are {103}, {101}, etc.

The theoretical habit of the chalcopyrite crystals is a combination of {112} and $\{1\bar{1}2\}$. Their faces are energetically equivalent. The only difference is the composition of the surface - cations for {112} and anions for $\{1\bar{1}2\}$. It may be the reason for the different developement of these forms in the natural chalcopyrite crystals as in the case of the sphalerite.

References:

Hall, S.R. & Steward, J.M. (1973). *Acta Cryst.*, **29**, 579-585.
Hartman, P. (1963). *Z. Krist.* **119**, 65.
Hartman, P. (1987). In: Sunagawa, I. (ed) *Morphology of crystals, Terra Pub., Tokyo*, 269-319.
Hartman, P. & Perdoc, W. (1955). *Acta cryst.*, **8**, 49-52.
Jevsikova, N. (1965). *Zap. Vses. Miner. Obshtestva*, **94**, 129.
Kostov, I. (1961). *Géoch. et Gîtes Métal.*, **2**, 121.
Radulova, A. (1991). *Compt. rend. Acad. bulg. Sci.*, **44**, 63-66.

SHAPE OF GROWING CRYSTAL. COMPUTER SIMULATION.

Rakin V.I. *(Inst.Geol., Komi Sci.Cent., Ural Div., Rus.Acad.Sci.)*

A computing model of a system "crystal polyhedron - solution" was created. The kinetic regime of crystal growth was analyzed. The model object was K-alum sulfate crystal, that belongs to cubic syngony. Main simple forms are octahedron, cube, rhombododecahedron. Crystal shape computing was conducted on the basis of data on crystal form kinetics for a certain range of supersaturation (Rakin, 1990). Growing process was realized by calculation of the mass balance in the system during growth of crystal faces. Dissolving of the crystal was not proposed. Crystal shape development for different physical and chemical conditions of growth has been studied. The situation modelled are closely related to same ones in real experiment. It was examinated the following experimental conditions:

1. Isothermal system. System closed for heat and mass transfer.
2. Isothermal system. Influence of specifical chemical admixtures on the growth rates of the crystal forms.
3. Heat exchange with environment. Constant and managed regimes of the process.
4. Solvent exchange (evaporation) with environment. Constant and managed regimes.
5. Mixed heat and solvent exchange with environment. Managed regimes of the process.

For numerical presentation of the crystal shape the shape factor was introduced:

$Sf = V^{1/3} \times S^{-1/2} \times (4\pi/3)^{-1/3} \times (4\pi)^{1/2}$,

where V - volume, S - surface area of the crystal (Rakin & Bogdanov, 1991)

It was found that correlation between shape factor and supersaturation through out alone crystal growth was not observed. And therefore the concept of "steady shape" of the crystal was defined. The crystal shape aspires to "steady shape" at continious and stationary growth conditions, independently from initial shape of crystal-seed. It was found that steady shape dependanted on growth conditions, and change of chemical composition of the solution influenced on steady shape strongly than changes of physical parameters. Although average statistical shape calculated for some crystals is not the "steady shape", but it is possible at the prolonged process of growth. According to this statistical view the crystal shape of mineral depends on growth conditions.

To solve the problem of crystal homogeneity it is necessary to keep condition, when the crystal shape has a less quantity of simple forms (f.e. - octahedron for K-alum sulfate crystals).

The number of dynamic equilibrium of system "crystal - solution" was suggested:

$G = V_s \times (dC/dt)_{ext} \times (dM/dt)^{-1}$,

where V_s - volume of the solution, (dM/dt) - mass growth rate of the crystal, $(dC/dt)_{ext}$ - change of the solution concentration due to external factors.

System "crystal - solution" become balanced after the some time at the constant conditions (f.e uniform evaporation of the solvent). It was shown that the number G would be equal to one during the process for getting of the crystal-octahedron as big as possible. Thus the such managed regime of crystal growth is more perfect.

References:

Rakin, V.I. (1990). *Abstracts, 15 General Meeting of the IMA, Beijing, China*, 397-398
Rakin, V.I. & Bogdanov, G.Ye.(1991). *Abstracts, Intern. conf. "Centenary of space groups", Leningrad, Russia*, 115-116

IN SITU REFINEMENT OF GOLD FROM QUARTZ VEINS, NARKAGWE, SUKUMALAND GREENSTONE BELT, TANZANIA

Rammlmair, D.[1], Lyatuu, D.[2] and Makyao, F.[2] ([1] BGR, Hannover, FRG; [2] Madini, Dodoma, Tanzania)

Gold mineralization at Nyarkagwe, in the center of the Sukumaland Greenstone Belt, is restricted to quartz veins and shear zones crosscutting Nyanzian pillow lavas and basic subvolcanics which are overlain by carbon- and pyrite-rich sediments and felsic tuffs.

Metamorphism of the area is of low grade. Shear zones and quartz veins act as hot fluid conduits. Amphibole, chlorite and epidote be-

sides pyrite, pyrrhotite and chalcopyrite are common at such shear zone alteration halos.

The Nyarkagwe area lies in the center of a major dome structure which is elongated in EW direction. The main compressional stress was active in NS direction and generated a set of shears and dilatational quartz veinlets, giving way to EW- and vertical dilatation.

These tectonic features are arranged in a sinistral Riedel shear system with a reverse Riedel shear system component. The main trends of shear zones and of quartz veins are E-W (D, sinistral), SE-NW (P, sinistral), NE-SW (R, sinistral) and N-S (R', dextral). Mineralization occurs in all directions, but not in all of the shear zones and quartz veins. The dip directions of the EW striking quartz veins are variable, but only N-dipping veins in the northern part and S-dipping ones in the southern part of the area are mineralized.

Some quartz veins (D) may show a continuous strike of up to two km, others (P, R) occur as "en echelon" veinlets pinching out vertically and horizontally, others show some sort of flecturing, both in vertical and horizontal direction. So-called flats (almost horizontal dilatational veinlets) are reported to show the highest grades of mineralization.

The gold contents of the investigated quartz veins and shear zones do not correlate with the colour of quartz veins (white to black), neither with any of the trace or major elements or with the mineral assemblages, nor with the amount of post emplacement shearing. Mineralization is controlled by the following factors: intrusion of granitoid bodies (engines) in a tectonically fertile environment (promoter) into basic and felsic host rocks (probable sources of the gold), emplacement of quartz veins and shear zones (fluid conduits and areas of deposition).

The quartz vein and shear zone internal refinement of primary gold (with some 20% Ag) to a secondary gold (with 2 to 17 % Ag, in situ refined) is completely controlled by the availability of fluids, provided by quartz internal microshears, and changing fluid chemistry and oxigen fugacity, buffered by the retrograde mineral assemblages of the contact metamorphic aureole (scapolite, amphiboles, epidotes, chlorites, prehnite, sulfates, carbonates, chlorides, sulfides, hydroxides).

Individual gold grains of individual quartz veins show a high variety in shape, porosity and chemistry. Primary undeformed gold has a shiny and smouth surface, the typical golden colour, anhedral (quartz interstities) to subhedral, rarely euhedral shape and have no or little porosity, and normal silver-contents (15 to 20%). Tectonically and hydrothermally overprinted gold grains on the other hand are flat to well rounded grains, have a dull and rough surface, yellowgreyish colour and an extremely high degree of porosity, and low silver-contents (2 to 15 %).

Individual gold grain analyses (ICPMS) showed that Ag, PGE and other elements are depleted in altered grains.

RADIOGENIC ISOTOPES OF THE LUUMÄKI RARE-ELEMENT PEGMATITE, WIBORG RAPAKIVI BATHOLITH, FINLAND

Rämö O.T. (*Dept. of Geology, Univ. of Helsinki*), Lahti S.I., and Vaasjoki M. (*Geol. Surv. of Finland*)

A gem beryl-bearing granite pegmatite dike has recently been described from the north-central part of the Wiborg rapakivi granite batholith (Lahti & Kinnunen, 1993). The dike is 20-m wide, cuts sharply its rapakivi granite (wiborgite) wallrock, and consists of a massive quartz core surrounded by three zones of feldspar-mica-quartz pegmatite (wall, intermediate, and border). The main minerals of the pegmatite are quartz, microcline, albite, biotite, and, locally, muscovite. The border and wall zones are mineralogically simple whereas the intermediate zone contains about 20 rare minerals, in particular, large crystals of beryl, topaz, and monazite-(Ce). In order to date the pegmatite and to shed light on its petrogenesis, we have carried out a radiogenic isotope study of monazite and microcline of the intermediate zone and microcline of the border zone.

Two monazite fractions, containing 0.8565% Pb and 0.1385% U, yield almost concordant U-Pb ages with a mean $^{207}Pb/^{206}Pb$ age of 1628±2 Ma. Microcline fractions from the intermediate and border zones have relatively high contents of Pb (102.7 ppm and 109.3 ppm, respectively) and show Pb isotope ratios of 6/4 = 16.41, 7/4 = 15.46, and 8/4 = 35.74 (intermediate zone), and 6/4 = 16.54, 7/4 = 15.49, and 8/4 = 35.82 (border zone). Stacey & Kramers (1975) μ_2 values are 9.91 (intermediate zone) and 9.98 (border zone).

The monazite is strongly enriched in LREE with 1.344% Sm, 7.498% Nd, and $^{147}Sm/^{144}Nd$ of 0.1084. The initial ε_{Nd} value of the monazite is –0.9±0.5 and the T_{DM} model age (DePaolo, 1981) 2014 Ma.

In terms of Rb-Sr systematics, the monazite is low in Rb and relatively unradiogenic (Rb 0.96 ppm, Sr 69.97 ppm, $^{87}Sr/^{86}Sr$ = 0.71848) whereas the microclines are low in Sr and strongly radiogenic (intermediate zone: Rb 747.0 ppm, Sr 13.30 ppm, $^{87}Sr/^{86}Sr$ = 6.3068; border zone: Rb 935.1 ppm, Sr 27.11 ppm, $^{87}Sr/^{86}Sr$ = 3.7099). The three mineral fractions define a Rb-Sr errorchron with an age of 1581±420 Ma (2σ, M.S.W.D. = 141) and $^{87}Sr/^{86}Sr_i$ of 0.7176±0.0054 (2σ). With its remarkably low Rb/Sr of 0.014, the monazite yields a well-constrained $^{87}Sr/^{86}Sr_i$ of 0.71755±0.00007 (2σ), compatible with the initial ratio of the three-point errorchron.

We interpret the 1628±2 Ma U-Pb age of the monazite as the crystallization age of the Luumäki pegmatite. The pegmatite is thus somewhat younger than the youngest granite types on the northern flank of the Wiborg batholith, dated at 1631–1634 Ma (Vaasjoki *et al.*, 1991).

The initial Nd isotopic composition (ε_{Nd} –0.9±0.5) and the alkali feldspar μ_2 values (9.91, 9.98) of the Luumäki pegmatite are similar to those of the eastern Finnish rapakivi granites (ε_{Nd} (1640 Ma) –2.9 to –0.2, μ_2 9.57 to 9.98; Rämö, 1991) and indicate that the magmatic evolution of, and subsolidus processes in, the pegmatite did not substantially affect the Nd and Pb isotopic systematics inherited from deep crust. The initial $^{87}Sr/^{86}Sr$ of 0.71755±0.00007 of the pegmatite is, however, distinctly higher than the initial $^{87}Sr/^{86}Sr$ of 0.7075±0.0021 calculated for the eastern Finnish rapakivi granites (unpublished data by the authors) and suggests that some upper crustal relatively high $^{87}Sr/^{86}Sr$ strontium was incorporated into the pegmatite magma in the course of its evolution.

References:

DePaolo, D.J. (1981). *Nature*, **291**, 193–196.

Lahti, S.I. & Kinnunen, K.A. (1993). *Gems and Gemology*, **29**, 30–37.

Rämö, O.T. (1991). *Geol. Surv. Finland Bull.*, **355**, 161 p.

Stacey, J.S. & Kramers, J.D. (1975). *Earth. Planet. Sci. Lett.*, **26**, 207–221.

Vaasjoki, M., Rämö, O.T., Sakko, M. (1991). *Precambrian Res.*, **51**, 227–243.

TRANSFORMATION OF GRAPHITE TO DIAMOND UNDER SUPERCRITICAL CONDITIONS OF SHEAR FLOW .

Kasskazov A.V., Novgorodova M.I. (Ins. Geol. of Ore Deposits (IGEM), Moscow).

Recent finds of non-kimberlitic diamonds cannot be accounted for by the xenogenous or impact nature of the diamonds that advance new genetic problems. One of this finds is microne-size diamonds of cubic or octahedral habit encountered in mantle-derived xenoliths of spinel peridotites with extensive secondary plogopitization and graphitization (the Tuvish diatreme, Southern Gissar Range). Microne-size diamond inclusions in graphite were detected in the course of complex examination of graphite crystal surface by SEM and microdifraction.Plastically-deformed state of the graphite whose structure answered generally to the 2H polymorf has been determined. The distortion of graphite structure and its local amorfization were detected in the centre of intersections of slip bands of different directions ("deformation stars").

We consider the process of graphite amorphization and origin of microne-size diamonds as the rezult of a local "thermal explozion" cauzed by shear flow of graphite. The concept of thermal explosions of gas (Semenov,1928) was previously called upon to explain the nature of diamonds collectors and direct diamond nucleation in hydrocarbon masses. Experiments on graphite shear flow (under a hydrostatic pressure up to 10 kbar and normal temperature) have shown the formation of areas with sp^3- hybridization.

The "thermal explosion" in shear flow of a viscous body is accounted for by the fact that the material can not release dissipating heat by thermal conductivity. This phenomenon results in turn in overheating instability, that leads to microexplosion effects with local increase of temperature up to the melting temperature and consecuent local generation of extremely high pressure. This pressure alone or together with the effect of chemical catalitical reactions can result in nucleation and crystallization of high-pressure solid phases.

The mathematical calculations of shear flow (Turcotte,Schubert, 1982) under supercritical conditions in a graphite grain (considering the special frictional and thermal conductivity properties of graphite) have demonstrated that overheating instability may lead to local rise of temperature up to T=4000 K in the tension region of the grain (taking the dimension of this region of about 10^{-6} m and assuming the total evaporation of graphite, we estimated the pressure as about 60 kbar). Considering the high rate of the diamond nucleation under this temperature and pressure, we have shown (Novgorodova,Kasskazov 1992) the possibility for the diamonds to be formed in the graphite under the effect of thermal explosions caused by shear flow in rocks to be beyond the thermodynamic stability field of diamonds.

References:

Semenov,N.N.(1928)Journ. of Russia Phys.-Chem. Soc.,v.60,n.3,247-250.

Turcotte,D.L.,Schubert,G.(1982)Geodynamics, part2,730p.

Novgorodova,M.I.,Kasskazov,A.V.(1992)Docl.RAN v.322,n.2.,379-381.

TEM INVESTIGATION OF SPINEL LHERZOLITE EXPERIMENTALLY DEFORMED AT HYPERSOLIDUS CONDITIONS

Raterron P. and Doukhan N. (*Univ. of Lille, FRANCE*), Bussod G.Y. (*Bayerisches Geoinstitut, Bareuth, GERMANY*)

In order to assess the effect of small melt fraction (1-7 vol.%) on the rheology of the Earth's mantle, natural and hot-pressed spinel lherzolites, consisting of 60% olivine, 25% enstatite, 13% Cr-diopside, and 2% Cr-spinel, were tested in compression in a Griggs-Blasic apparatus at 1.0 GPa confining pressure, with 1.5 wt.% water added, and at hypersolidus temperatures (900°-1100°C).

Steady state hypersolidus deformation at strain rates of 10^{-7} to 10^{-6} s^{-1}, results in deviatoric flow stresses of 100 to 400 MPa for strains exceeding 15%. The textural development and melt topology of the deformed samples, investigated by Bussod & Christie (1991), indicate that the rheology is controlled by dislocation creep (n≈3) in the dominant phase olivine, which forms a solid skeletal framework. Flow is accommodated by dynamic recrystallisation, whereby the grain size is inversely proportional to the flow stress, and results in the redistribution of melt at triple grain edges and in a network of channels anisotropically wetting recrystallized grain boundaries.

One reports here an detailed investigation by transmission electron microscopy (TEM) of the defect micro-structures present in the deformed crystalline phases, with a particular emphasis on the relation between melting and micro-mechanisms responsible for deformation.

Reference:

Bussod, G.Y. & Christie, J.M. (1991). *Jour. Petrol.*, Special Lherzolites Issue, 17-39.

SYNTHESIS OF H_2S - BEARING FLUID INCLUSIONS

Razina M. (*Dept. of Geology, Moscow State University, Moscow*), **Kotelnikova Z.**, (*Inst. of Lithosphere RAS, Moscow*), **Kotelnikov A. and Migdisov A.**(*Inst. for Experim.Mineralogy RAS, Chernogolovka*)

Phase relations of the system H_2S-H_2O in wide range of P-T parameters (300 - 600°C, P=200 - 1000 bar) have been investigated experimentally using method of synthetic fluid inclusions. Traditional method of H_2S freezing into the capsule by liquid nitrogen has many uncertainties: 1) H_2S and O_2 are always freezing both into the capsule, causing reaction of H_2S oxidation to S^o. 2) It is impossible to get the sufficient mole fraction of H_2S in mixture H_2S - H_2O.

Method of generation of H_2S using hydration reaction of Al_2S_3 during the run has been used. Calculations of the system H_2S - H_2O - Al_2O_3 at the experimental parameters show us that the process of H_2S oxidation to S^o is suppressed. Solubility of Al- phases in fluid is negligible. Our method permits one to get fluid containing 50 mol% of H_2S. Fluid composition had been controlled using gas chromatography method and weight method.

Healing of the cracks in the quartz with fluid inclusions formation is rather long time process and requires the sufficient duration of experiments (more one month).

The solid H_2S melting temperature in H_2S - H_2O -bearing inclusions is -82 -85°C. Liquid H_2S phase had been observed in inclusions containing high dense fluid. Gas - hydrate H_2S*6H_2O had been identified at -20°C. Melting temperature of H_2S*6H_2O reaches +27°C.

ROLE OF SILICATE BUFFERS IN THE FRACTIONATION OF Cs AND Sr BETWEEN FLUID AND SOME OF Al-Si MINERALS (ILLITE-SMECTITE PHASES AND ANALCIMES) at 250-300°C, $P_{sat.}$-1 KBAR

Redkin A.F. and Hemley J.J.
(IGEM Russian Ac. of Sci, Moscow and U.S.Geological Survey, Reston VA)

Zeolites, smectites, and mixed-layer phases, which have a notable ability to sorb a variety of ions and organic pollutants, have now found wide utility in sewage and runoff water treatment, as a potential barrier in underground radioactive waste burial, and even in detoxification inside living animal bodies. The capability of keeping heavy ions within the structure of zeolites, smectites, and mixed-layer phases is a function of the aqueous solubility of these minerals in a given overall physicochemical system. We investigated such relations both experimentally and through thermodynamic simulations using available data bases.

Our investigation of sorption (ion-exchange equilibria) for Cs and Sr on Na-analcime and Na-montmorillonite (which changed to illite-smectite during experiments) in water and chloride solutions showed that the tendency of these phases to fix Cs and Sr depends upon both the nature of the assemblage and its role as a pH buffer in the system. Leachability of Cs and Sr from illite-smectite phases under the above PT conditions is a minimum in albite-containing assemblages (albite-microcline-muscovite and quartz-albite-muscovite) at pH's lower than 6 (at 250-300°C), whereas from polucite and Sr-analcime in albite-analcime bearing assemblages it is a minimum near pH 8. Leachability or solubility for the single minerals, however, (analcite or illite-smectite) is relatively constant over the pH range of 3 to 9, and one to several orders of magnitude higher than when the buffer assemblages are used. This illustrates the importance of the buffers in maximizing radionuclid containment in underground waste burial.

TRACE ELEMENTS AS PROBES OF MINERAL SURFACE SITES DURING CRYSTAL GROWTH

Reeder R.J. (Dept. of Earth and Space Sciences, State University of New York, Stony Brook, NY 11794 USA)

Many kinds of evidence demonstrate that a site in the bulk crystal structure may have several different configurations on the surface during crystal growth. Such incorporation sites commonly occur as kinks within growth steps, and differences in sites may exist not only between nonequivalent faces but also within an individual face. Incorporation sites may differ in their attachment kinetics, as well as their affinities for trace element uptake during growth. Where certain growth mechanisms segregate sites of different types on the crystal surface, site selective trace element incorporation occurs, resulting in intrasectoral or sectoral zoning.

Trace elements that differ in their size, charge, and electronic configuration may act as sensitive "probes" of the structural character of surface sites, according to their relative affinities for incorporation. Sites of distinct types are found to be spatially segregated at nonequivalent vicinal faces of spiral growth hillocks, and trace element distributions provide a direct measure of surface site differences. This approach requires that trace element concentrations have not been altered after incorporation, and therefore may be limited in some high-temperature systems.

Low-temperature solution growth experiments involving coprecipitation of a wide variety of both divalent metal cations and complex anions into calcite single crystals have shown the usefulness of this approach. Calcite $\{10\bar{1}4\}$ surfaces growing by the spiral mechanism with step orientations parallel to $<\bar{4}41>$ contain at least four distinct cation incorporation sites and as many anion sites. First-order models based on an unrelaxed surface reveal differences in kink site coordination and size, which are consistent with observed trace element distributions determined by synchrotron X-ray fluorescence microanalysis. The structural distinction among surface sites explains the differences in growth step velocities observed by atomic force microscopy. It is further found that surface CO_3 sites incorporate complex anions, including SO_4^{2-} and SeO_4^{2-}, which are sensitive to site size and coordination geometry. Similar investigations of other minerals will help in understanding the detailed behavior of surfaces during crystallization.

MAGMA CHAMBER PROCESSES PRE-DATING THE CULMINATING ERUPTION AT THE LATERA CALDERA, AS EVIDENCED BY PLUTONIC CLASTS.

Renzulli A., Nappi G. *(Ist.Vulc..e Geoch., Univ. of Urbino, Italy)*
Upton B.G.J. *(Dept.Geol. and Geoph., Univ. of Edinburgh, U.K)*

The Pitigliano Formation, consisting of pumice flows, welded tuffs and subordinate lavas, represents the products of the culminating, paroxysmal phase of the eruptions giving rise to the Latera caldera. It is compositionally zoned from phonolite at the base to tephritic phonolite at the top. The Formation contains abundant cognate and xenolithic plutonic clasts. These are mainly syenitic, ranging from leucocratic foiditic syenites (with hauyne, and SiO_2 up to 61.4%) to mesocratic foiditic syenites (SiO_2 down to 46.6%). However, quartz syenites with up to 70.6% SiO_2 form a minor proportion of the plutonic clasts.

The silica-undersaturated and silica-oversaturated clasts show contrasting textures: the foiditic syenites are relatively porous, with drusy cavities whereas the quartz syenites have little or no void spaces. It is inferred that the quartz syenites have experienced a longer and more complex cooling history than the foiditic syenites and that the latter may therefore be younger. We interpret the more-abundant leucocratic-mesocratic foiditic clasts as cognate fragments sampled from the innermost (and youngest) zones of side-wall and/or roof nodules from the magma chamber boundary layer, whereas the

quartz syenites may represent outer (and crustally contaminated) zones (xenoliths from previous stages of crystallisation).

Mineral chemistry and whole-rock major and trace element compositions of the leucocratic foiditic syenites closely match those of the phonolitic tephra in the lower part of the Pitigliano Formation. The leucocratic foiditic syenites are therefore regarded as crystallisation products from residual magma in the upper zone of the chamber, whose bulk composition approximated to the phonolitic minimum in the residual system. At this stage compositional convection along the boundary layer had effectively ceased. Interstitial liquids became progressively enriched in "incompatible elements" which were ultimately mainly accomodated in sphene and apatite, both of which are ubiquitous accessory minerals. Conversely, the quartz syenite xenoliths are depleted in incompatible elements and this dilution was probably promoted by assimilation of upper crustal rocks which commonly have lower incompatible element contents than any parental K-rich magma of the Roman Province.

It is believed that the Pitigliano Formation magma chamber had a low aspect ratio, that heat loss was predominantly through the side-walls and that crystallisation was rapid in relation to convection. In addition, the presence of both leucocratic and mesocratic foiditic syenite clasts (and occasionally composite leucocratic-mesocratic lithic fragments) suggests that some modal layering was present in the side-wall (and/or roof) cumulates reflecting a cyclical crystallisation process. The liquid line of descent of the magmas seemed to be controlled by alternating "true" cumulate fractionation (mesocratic foiditic syenites) and slowly cooled equivalents of the bulk liquid composition (leucocratic foiditic syenites).

The phenocryst assemblage in the volcanic sequence is regarded as mixtures of free-growing crystals in the central magma reservoir, derivatives from the youngest partly liquid mush along the chamber walls (crystal mush layer) and crystals stripped from the inner side-wall margins (cognate accidental xenocrysts).

THE CRYSTAL CHEMISTRY OF FELDSPAR MINERALS

Ribbe, P.H. *(Dept. of Geol. Sci., Virginia Tech, Blacksburg)*

Most natural feldspars, MT_4O_8, fall within the composition range $(Na,K)_x(Ca,Ba)_{1-x}Al_{2-x}Si_{2+x}O_8$ [buddingtonite, $NH_4AlSi_3O_8$, is a fifth rare end member]. Only a few minor *M*- and *T*-site substituents have any significance to the properties of these minerals.

Historically, advances in understanding the crystal chemistry of these feldspars have proceeded mainly from crystal structure determinations, including some at elevated temperatures (low and high albite, monalbite, sanidine, anorthite) and, more recently, some at high pressures (anorthite, microcline, low albite). This substantial array of structure refinements, combined with those from related, synthetic structures (M^{1+} = Li, Ag, Rb, H; M^{2+} = Eu, Sr, Pb), and with thermodynamic measurements, infra-red and Raman spectroscopy, and with lattice parameter measurements collected as functions of temperature (T), pressure (P), and composition (X), form the data base. Apart from Al,Si order-disorder, structural changes are primarily related to inter-tetrahedral (*T*-O-*T*) angle variations and the accompanying *M*-O bond length adjustments. Limited O-*T*-O angle variations are observed, especially where *T* = Al. $(Al,Si)O_4$ tetrahedra expand slightly with T, but they are essentially incompressible.

Landau theory has been applied to various phase transitions observed in alkali and alkaline-earth feldspars involving spontaneous strain with PTX and with Al,Si and even Na,K order-disorder.

The figure summarizes some of the phase transitions discussed in this review. [A chemical symbol defines the feldspar; the subscripts *o* and *d* = order and disorder; ⇔ indicates chemical substitution, ⇑ indicates increases in P or T.]

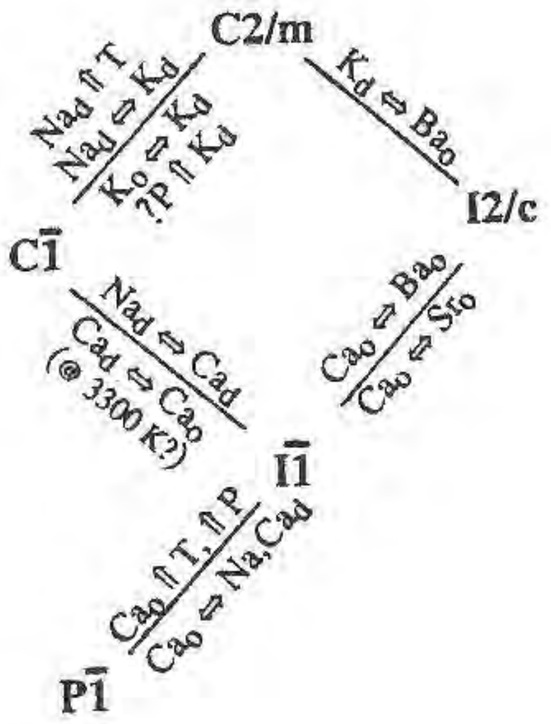

AMPHIBOLES FROM OPHIOLITIC GABBROS OF NORTHERN APENNINE (ITALY): EVIDENCE FOR INTERACTION WITH SEAWATER-DERIVED HYDROTHERMAL FLUIDS

Riccardi M. P., Tribuzio R. and Messiga B. *(Dip. Scienze della Terra, Univ. di Pavia; CNR - CS Cristallochimica e Cristallografia, Pavia)*

Ophiolitic rocks from Northern Apennine were subjected to low pressure metamorphism, characterized by a complex retrograde evolution. Petrologic investigations on the ophiolitic intrusives highlight two distinct metamorphic events. The first, responsible for the exposure of the gabbro-peridotitic complex on the sea-floor, was characterized by high dT/dP gradients (granulite facies conditions) and was accompanied by ductile deformation. The second metamorphic event, presumably related to infiltration of seawater-derived hydrothermal fluids, was accompanied by brittle deformation. Both deformed and undeformed intrusives are actually crosscut by sets of parallel fractures filled with amphibole (± plagioclase). In order to unravel the metamorphism related to the brittle deformation, we collected electron and ion microprobe data on amphiboles from Mg-Al- and Fe-Ti-gabbros, and from the included veins.

Both Mg-Al- and Fe-Ti-gabbros are characterized by minor Ti-pargasite, either of igneous origin or related to the high dT/dP ductile event. Ti-pargasites are commonly overgrown by zoned amphiboles (hornblendes to actinolites) showing gradual outward decreasing of edenitic substitution ($Na_{(A)}$ from 0.7 to 0.3 apfu), coupled with Ti lowering; glaucophanitic substitution is invariably subordinate ($Na_{(M4)} < 0.2$ apfu). In Fe-Ti-gabbros, the rims of zoned amphiboles have extremely high Fe contents, which are probably related to the release of iron due to the replacement of igneous Fe-Ti-oxides by titanite.

Based on textural relations, we distinguished different amphibole generations within the veins. The compositional evolution of vein amphiboles (hornblendes to actinolites) bears close similarities to that observed for the amphiboles which statically developed within the gabbros. The older vein amphiboles have high values of edenitic substitution ($Na_{(A)}$ = 0.7 apfu) and Ti contents close to 0.1 apfu.

The trace element composition of hornblendes and actinolites is strongly controlled by the microstructural domain, i.e. by the composition of the precursor minerals. Hornblendes and actinolites, from either gabbros or included veins, invariably show lower REE, Y, Zr, and F than Ti-pargasites; they also show a wide compositional range for Cl and B, generally with higher contents with respect to Ti-pargasites.

The major element evolution of amphiboles from the ophiolitic gabbros and the included veins indicates low pressure conditions and progressively decreasing temperature (from amphibolite to greenschist and low grade facies). As a whole, the

halogen and trace element composition of hornblendes and actinolites is consistent with crystallization in the presence of seawater-derived hydrothermal fluids. We concluded that the amphibole-bearing veins cutting the gabbros operated as preferred channelways for introduction of the fluids. The high value of edenitic substitution and of Ti in the early amphiboles from the veins suggests that the interaction with seawater-derived hydrothermal fluids occurred under high thermal conditions.

CONFIGURATIONAL PROPERTIES OF SILICATE MELTS: COMPRESSIBILITY AND HEAT CAPACITY

Richet P. (*Laboratoire des Géomatériaux, Institut de Physique du Globe, Paris*)

Outside phase transition regions, solids keep a constant configuration. Their properties being determined by essentially fixed interatomic potentials, they can be termed *vibrational*. The properties of liquids also include vibrational contributions. However, liquids undergo continuous structural changes in response to temperature or pressure variations. These changes results in the existence of so-called *configurational* contributions to the physical properties of melts. Their importance lies in that they are at the roots of the differences between the properties of liquids and solids.

In this paper, we will discuss the relevance of configurational contributions to the entropy and volume of silicate melts. From extensive calorimetric measurements performed since the late 70's, the relative importance of vibrational and configurational contributions to the heat capacity and entropy is relatively well known. The implications for the temperature and composition dependence of the viscosity will be briefly mentionned.

Analogous data for the compressibility and volume of silicate melts are generally lacking. It has long been known that equilibrium compressibilities at high temperatures can be obtained from ultrasonic measurements. Recently, it has been shown that vibrational compressibilities could be determined from Brillouin scattering measurements. We will present some results obtained by combining these two different techniques.

Finally, available data suggest that sound velocities in glasses are a sensitive function of thermal history. The possibility of using Brillouin scattering measurements for investigating the thermal history of natural glasses will thus be discussed.

THERMODYNAMIC PROPERTIES OF MINERALS AT HIGH TEMPERATURES

Richet P. (*Laboratoire des Géomatériaux, Institut de Physique du Globe, Paris*)

Thermodynamic properties of minerals have been extensively investigated during the last decades. Surprisingly, however, most of this experimental effort has been devoted to low or moderate temperature conditions. Most of the available data for temperature ranges close to the melting point have been gathered a long while ago, at a time when generally samples could not been well enough characterized.

In view of rapidly increasing temperatures along the geothermal gradient, the need for new high-temperature thermodynamic measurements was thus obvious. In this paper, we will review calorimetric results recently obtained in our laboratory on a series of important minerals. Particular attention will be paid to the heat capacity of minerals in phase transition regions and in the premelting range.

We will also discuss some new determinations of thermal expansion coefficients made with a very simple high-temperature heating stage used to make X-ray diffraction measurements with synchrotron radiation.

GRAIN SIZE EVOLUTION DURING FIRST-ORDER PHASE TRANSITION IN SUBDUCTED SLABS

Riedel M. R. (*Project Group Thermodynamics, Univ. of Potsdam*) and Karato S. (*Dept. of Geology and Geophysics, Univ. of Minnesota*)

The grain size reduction due to first-order phase transformations can dramatically reduce the strength of subducting slabs that in turn will affect the fate of subducted slabs. We have studied the grain size evolution during a first order phase transition with time-varying supersaturation numerically on the basis of a nucleation and growth model. A three dimensional simulation algorithm is used in which not only the nucleation and growth of individual new grains, but also the effects of grain impingement is taken into account. The microstructures are characterized by two different morphological functions, the grain size distribution and the cluster size distribution. Both functions are scaleable in terms of the Avrami length and Avrami time, which are related to the peak nucleation and growth rates. The presence of preferred nucleation sites (heterogeneous nucleation) such as grain boundaries significantly modifies the microstructures when the spacing of nucleation sites is much larger than the Avrami length, the main effects being a reduced percolation threshold and an elongated grain shape.

Using the experimental data on the kinetics of olivine-spinel transformation, we have simulated the microstructural evolution during this phase transformation for a realistic p,T-profile in a subducting slab. The results indicate that the amount of grain size reduction is sensitive to the slab temperature (i.e., slab velocity): grain size reduction is significant for a cold slab but not significant for a warm slab.

MINERALOGY OF BIOTITES FROM THE WIBORG RAPAKIVI BATHOLITH

Rieder M. (*Dept. of Geology, Charles University, Prague*), Haapala I. (*Dept. of Geology, Univ. of Helsinki*) and Povondra P. (*Dept. of Geology, Charles University, Prague*)

Mineralogical studies have been made of biotite separated from nine chemically analyzed rock specimens representing the main granite types of the classic Wiborg batholith in southeastern Finland: wiborgite, pyterlite, various biotite granites and topaz-bearing granites. The micas were chemically analyzed, their unit-cell dimensions, polytypes and some other physical properties were determined.

All the analyzed micas plot near the annite-siderophyllite corner of the Fe-Mg-Li triangle of triochtahedral micas. Their Fe/(Fe+Mg) ratio varies from 0.8 to 1.0, being lowest (0.80 to 0.88) in the biotites of various biotite-hornblende±fayalite granites (dark wiborgite, wiborgite, tirilite) and highest (0.92 to 1.00) in the siderophyllite (containing 1.2 to 1.6% Li_2O) from the topaz-bearing granites. The TiO_2 content of the micas varies inversely with Fe/(Fe+Mg), being highest in dark wiborgite (3.98%) and lowest in topaz-bearing granites (0.18%). The content of fluorine is high in lithian siderophyllite (4.2 to 4.9%). In the annite-phlogopite-$KFe_3^{3+}AlSiO_{12}(H_{-1})$ diagram the biotites plot below the magnetite-hematite oxygen fugacity buffer line. Lowest oxygen fugacity (below the fayalite-quartz-magnetite buffer line) is indicated for the annite of the dark wiborgite, and highest

oxygen fugacities for the siderophyllites of the topaz-bearing granites which plot between Ni-NiO and magnetite-hematite buffer lines. Inasmuch as the topaz-bearing granites have undergone various subsolidus reactions, it is possible that the composition of the micas was readjusted during late magmatic or post-magmatic stages.

Four crystals from each mica sample were examined for polytypism. Although 1M was expected and found to be most frequent, a surprising wealth of polytype stackings were observed. So, for example, siderophyllite from pyterlite contains polytypes 5M, 3Tc and 1M, whereas lithian siderophyllite ("protolithionite") from the topaz-bearing granite at Kymi yielded polytypes 2M1, 3T and unresolved complex structures. A large variety of polytypic structures is usually reported from pegmatites or hydrothermal veins, where conditions of relatively quick nucleation prevail, and a relative monotony is reported from abyssal or metamorphic rocks. The different pattern observed here may be associated with the rather unique chemistry of these micas and its structural consequences.

MINERAL PHYSICS CONSTRAINTS ON UPPER MANTLE AND TRANSITION ZONE MINERALOGY

Rigden S.M. (*Research School of Earth Sciences, Australian National University*), Liebermann R.C. (*Center for High Pressure Research and Dept of Earth and Space Sciences, Univ. at Stony Brook*) and Gwanmesia G.D. (*Dept of Physics, Delaware State University*)

The experimental data base that can be used to interpret seismological velocity-depth and density-depth profiles in the Earth's deep interior is provided by measurements of elasticity and density as a function of pressure and temperature in the laboratory. In spite of regional variations in seismic models as a function of tectonic setting persistent features remain. In the upper mantle, a region of lower than expected velocities occurs around 200km in depth, followed by normal gradients of velocity which can be reconciled with expected upper mantle mineralogy. Although there are some tradeoffs between the magnitude of velocity discontinuities at ~400 and 660 km depth and velocity gradients in the transition zone, the gradients appear higher by almost a factor of two for shear waves than for those calculated for adiabatic compression of most candidate mineral phases.

Matching of the detailed seismological structure with an appropriate mineral assemblage requires accurate laboratory measurements of elasticity as well as an appropriate method for extrapolation beyond the range of experiments and into the high-pressure, high-temperature regime of the mantle. Not all of the required laboratory elasticity data are available. Ultrasonic data have been obtained in our laboratories for the beta and spinel phases of Mg_2SiO_4 and majorite garnet to 3 GPa. There are indications that pressure derivatives of the shear modulus of majorite-rich garnets may be high enough to go some way towards explaining high velocity gradients in the transition zone. However, an important part of the required data set that is missing is that of the temperature dependence of elasticity for these phases. We will review the available data for the important upper mantle and transition zone phases with emphasis on the elasticity measurements and report on progress to determine the temperature dependence of elasticity.

Geosciences Facilities at the Advanced Photon Source

Rivers, M.L. (Center for Advanced Radiation Sources and Dept. of Geophysical Sciences, Univ. of Chicago)

The Advanced Photon Source (APS) is a 7 GeV, third generation synchrotron facility presently under construction at the Argonne National Laboratory, USA. The APS is optimized for the use of radiation produced by wigglers and undulators. The APS undulators will have a brilliance (photons/mrad^2/mm^2/sec/0.1% bandwidth) which is 10^4 times larger than bending magnet radiation from existing synchrotron sources. The APS wigglers will provide high brilliance to energies beyond 100 keV.

Geo/SoilEnviroCARS, a group of earth, soil and environmental scientists in the Consortium for Advanced Radiation Sources, plan to construct and operate a sector at the APS for geoscience research. This sector will contain five experimental stations, three on a bending magnet beamline and two on an insertion device beamline. The insertion device straight section will be equipped with both a wiggler (critical energy up to 32 keV) and an undulator (fundamental energy tunable from 4.5 to 13 keV).

There will be facilities on both the bending magnet and insertion device stations for the following types of studies: high pressure diffraction in the diamond-anvil cell using both energy dispersive and angle dispersive techniques; high pressure diffraction in a large multi-anvil press; x-ray absorption spectroscopy, including microspectrocopy with beam sizes of 1-2 μm, and surface spectroscopy; powder diffraction; microcrystal diffraction; x-ray fluorescence microprobe analysis with 1-2 μm beam size and sub-ppm sensitivity.

The Geo/SoilEnviroCARS facility at the APS will be operated as a user facility with nearly all of the beam time allocated on the basis of peer-reviewed proposals. The sector will be equipped with sample preparation laboratories and a laser laboratory for high pressure work. Argonne is constructing a residence facility with convenient access to the synchrotron where users can live they are working at the APS.

We hope that construction of the Geo/SoilEnviroCARS facility will begin in 1994, with first beam on the bending magnet beamline in late 1995 and first beam on the insertion device beamline in 1996. The entire sector should be complete and fully operational in 1998.

THE BEHAVIOUR OF METAMICT AND CRYSTALLINE ZIRCON UNDER HYDROTHERMAL TREATMENT

Rizvanova N.G., Levchenkov O.A., Levsky L.K., Belous A.E. (*Inst.of Precambrian Geology and Geochronology RAS*), Bezmen N.I. (*Inst. of Experimental Mineralogy RAS*)

The data of Cathodoluminescence, X-ray Diffraction and Microprobe Analysis provide some evidences that the rate and scale of zircon transformations under hydrotermal treatment depend on both the treatment conditions and the degree of structural damage of mineral.

At the same time interpretation of variations in metamorphically induced U-Pb isotopic discordance requires thorough understanding of zircon-fluid interactions.

The analyses on the interaction of a metamict zircon with solution such as H_2O, 1M NaCl, 1M NaOH, 1M $NaHCO_3$, 1M and 0.1M Na_2CO_3 at temperature 400°C, P=1 kb and t up to 7 days have been performed. The behaviour of the zircon at its treatment by 2M Na_2CO_3 solution at T=400-800°C, P=1-5 kb and for 3-14 days has been studied in more detail.

The reconstruction of defective and enriched by impurities zones of zircon (concentration exqualization of impure elements and raising of crystallinity) begun at 400°C and P=1 kb. The metamict zircon zones are dissolved with the formation of baddeleyite accommoding U from solution and silicate phase enriched in Zr and impure elements. This process is intensified with pressure rise. Considerable lead loss (up to 90%) under above conditions has been established. The appreciable quantity of U migrates from the zircon only in the solution of 2M Na_2CO_3.

Crystalline zircon has been treated by the solution of 2M Na_2CO_3 at T=400-800°C, P=1 and 5 kbar and t=7 days. Data obtained evident that the migration of U and Pb from crystalline zircon is observed only during its dissolution at T above 650°C.

Experimental study shows appreciable U and Pb losses for metamict zircon. It could take place at lower P-T than greenschist grade facies metamorphism. The uranium and lead loss from crystalline zircon took place under conditions corresponding with granulite facies of metamorfism.

FRESH- AND SEAWATER-BASALT INTERACTIONS UNDER LOW TEMPERATURE GRADIENT (140-200°C). AN EXPERIMENTAL STUDY

Robert C. and Vidal O. (Département de Géologie, Ecole Normale Supérieure, Paris, France.)

Robert and Goffé (1993), showed that clays and zeolites, occurring as secondary phases in continental basalts, crystallized in water rich environments, *during* the cooling of the flow. They suggested that the distribution and the composition of clays and zeolites depended on the variations of temperature with distance and time. In this case, significant mass transport, driven by the temperature variations, must have developed through the flow.
The present experiments were designed to determine if significant amounts of mass transport can be induced in response to variations of temperature with distance. Basalts were reacted with freshwater and seawater (fluid/rock ratio of 10) under a low temperature gradient (140-200°C) for 150 days at 200 bars. Basalt powder was sealed in perforated gold capsule (3.5 cm) to enable exchanges of solution. The gold capsules were set at one extremity of a gold tube (15 cm long) along with pure water. Temperature varied as a function of distance representing a thermal gradient between the two ends of a single hydrothermal system. After quenching, the walls of the tube were observed with a SEM, in order to identify which phases precipitated outside the capsule from the solution. Results are as follow :
1) *Freshwater-basalt interaction* converted all the reactant to iron-saponite (Fe > Mg in octahedral sites) inside the capsule placed at the cold extremity. Different zeolite species (chabazite-phillipsite-analcime-wairakite) crystallized outside the capsule, all along the tube, as a function of tempearture. Mg saponite (Mg > Fe) occurred exclusively at the hottest extremity, coexisting with wairakite.
2) *Seawater-basalt interaction* led to the crystallization of anhydrite and Mg rich-saponite inside the capsule placed at the hot extremity. Outside the capsule, Mg content of saponites decreases with decreasing temperature. Zeolites did not crystallized.
Experimental results suggest the following conclusions :

- The thermal gradient controls i) the distribution of mineral species (smectites *versus* zeolites and zeolite species distribution) and ii) the continuous chemical change within the same mineralogical species (from Mg rich-smectites to Mg poor-smectites).

- The initial composition of the fluid used as starting material appears to be of major importance on the crystallization of zeolites.

The experiments demonstrate the effectiveness of dissolution, precipitation and mass transport under a thermal gradient. The spatial distribution of phases is consistent with local equilibrium between solution and solid phases. Interpretation of results is therefore possible using activity diagrams. The phase relations in the seawater-basalt system involving only phyllosilicates as Mg-bearing saponite and iron-bearing saponite can be depicted by using a $Log(aMg^{++})/(aH^{+})^2)$ vs $Log(aFe^{2+}/(aH^{+})^2)$ diagram. Calculations show that with increasing temperature up to 200 °C, Mg decreases in solution in order to maintain equilibrium between solution and saponites. As a result, Mg saponite precipitates. The crystallization of Mg rich-phase under conditions of highest temperature whereas Fe bearing species occurs under conditions of lowest temperature is in good agreement with field observations.

Robert & Goffé (1993). Geochim. Cosmochim. Acta., **57**, 3597-3612.

TETRAHEDRALLY COORDINATED M^{2+} CATIONS IN MICAS: THE RULE AND NOT THE EXCEPTION

Robert J.-L., Lahlafi M., Sergent J. and Penthier M. *(CRSCM-CNRS, Orléans, France)*

Tetrahedrally coordinated divalent cations are more and more frequently observed in natural micas as well as in their synthetic analogues. The characterization of this coordination could be realized by various methods: XRD on single crystals when available, FTIR absorption spectrometry (both in the OH-stretching wavenumber region and in the 1200-400 cm^{-1} range) and UV-visible absorption spectrometry for transition elements.

The most evident case of tetrahedral coordination of a divalent cation is that of Be^{2+} which is present as a major component in bityite: $Ca(Al_2Li)(Si_2AlBe)O_{10}(OH)_2$, and may enter the tetrahedral layer of lepidolite solid solutions, up to several thousand ppm.

Magnesium is also frequent in tetrahedral coordination. Since the pioneer work of Seifert & Schreyer (1971), several cases of tetrahedrally coordinated Mg have been observed. Particularly in high-Ti phlogopites from lamproites (beyond 0.35 Ti a.p.f.u. calculated on the basis of 11 oxygens), and their synthetic equivalents. The incorporation of $^{[4]}Mg$ in these titanium-rich micas is required to allow the dimensional fit between the tetrahedral and the octahedral layers. It is also observed in synthetic high-Cr phlogopite-like micas in which the high stabilization energy of Cr^{3+} in six-fold coordination provokes the migration of Mg from the octahedral to the tetrahedral layer.

As to $^{[4]}Co^{2+}$ and $^{[4]}Ni^{2+}$, they are commonly observed in low-Al micas obtained in experimental systems, but at present, there is no evidence for $^{[4]}Fe^{2+}$ in micas.

Generally, the tetrahedrally coordinated divalent cations favor the trioctahedral micas, and the vicinity of local trioctahedral configurations in mixed triocta-dioctahedral mica solid solutions.

Reference:
Seifert F. & Schreyer W. (1971) Contrib. Mineral. Petrol., 30, 196-215.

FRANKHAWTHORNEITE, $Cu_2^{2+}Te^{6+}O_4(OH)_2$, A NEW Cu^{2+} OXYSALT MINERAL WITH AN INFINITE FRAMEWORK STRUCTURE, FROM THE CENTENNIAL EUREKA MINE, JUAB COUNTY, UTAH, U.S.A.

Roberts, A.C., Harris, D.C. & Stirling, J.A.R. (*Geol. Surv. Canada, Ottawa*), Grice, J.D. (*Can. Mus. Nature, Ottawa*), Criddle, A.J. (*Nat. Hist. Museum, London*), Jensen, M.C. (*Mackay School of Mines, Reno*), Moffatt, E.A. (*Can. Concerv. Inst., Ottawa*).

Frankhawthorneite, ideally $Cu_2^{2+}Te^{6+}O_4(OH)_2$, is a very rare constituent on the dumps of the Centennial Eureka mine, Main Tintic subdistrict, Juab County, Utah, U.S.A. (lat. 39°56'38"N, long. 112°07'18"W). It occurs as 0.1 mm-sized medium leaf green crystals, or as crystal groupings, on drusy white quartz and is associated with mcalpineite ($Cu_3TeO_6 \cdot H_2O$), pyrite, hematite, acanthite, chryscolla, connellite, enargite, hinsdalite, svanbergite and an unidentified Cu-Zn-Te-bearing pale green botryoidal crust. Individual vitreous transparent crystals are prismatic to stubby bladed, are subhedral to euhedral, have slightly curved faces with forms {010} major and {100} and {011} minor, and are elongate [001] with a length-to-width ratio of approximately 3:1. The mineral is monoclinic, space group $P2_1/n(14)$ with unit-cell parameters refined from powder data: $a = 9.095(3)$, $b = 5.206(2)$, $c = 4.604(1)$Å, $ß = 98.69(2)°$, $V = 215.5(1)$Å^3, $a:b:c = 1.747:1:0.884$, $Z = 2$. Averaged electron-microprobe analyses gave CuO 45.20, TeO_3 48.77, H_2O (calc.) [5.05], total [99.02] wt.%; this yields the empirical formula $Cu^{2+}_{2.03}Te^{6+}_{0.99}O_{4.00}(OH)_{2.00}$, based on O = 6 and with H_2O calculated to give 2(OH). D (calc.) for the empirical formula is 5.44 g/cm^3. All pertinent physical, chemical, optical and

crystallographic properties are tabulated, as is a fully indexed X-ray powder-diffraction pattern. The mineral name honours Dr. Frank C. Hawthorne, Professor of Mineralogy, University of Manitoba, Winnipeg, Manitoba, Canada, for his many outstanding contributions to the fields of mineralogy and crystallography, and, more specifically, for his on going studies of the crystalchemistry of Cu^{2+} oxysalt minerals.

The crystal structure has been refined to $R = 5.5\%$, $R_w = 4.7\%$ for 631 unique reflections of which 485 were observed, based on the criteria [$F>5\sigma(F)$]. Cu^{2+} is in octahedral coordination with a distinct Jahn-Teller effect of one axis of the elongated polyhedron and Te^{6+} is in regular octahedral coordination. Bond valence sums (eu) are: Cu(1.98), Te(5.66), O1(1.59), O2(1.26) and O3(1.96); the bond valence sums indicate 4 oxygen atoms and 2 hydroxyl groups in the structure. The mineral has an infinite framework structure of edge-sharing [CuO_6] and [TeO_6] octahedra. Eby & Hawthorne (1993) denote this as a M=M framework. Each pair of edge-sharing [CuO_6] octahedra is cross-linked to the next pair of [CuO_6] octahedra. The square-shaped open channels which parallel [010] most likely contain H atoms associated with O2. These and other important aspects of the structure will be diagrammatically illustrated.

Reference:

Eby, R.K. & Hawthorne, F.C. (1993). *Acta Cryst.*, **B49**, 28-56.

MORPHOLOGICAL ASPECTS OF ZIRCONS FROM GRANITOID ROCKS OF THE PETREANU MASIFF (SOUTH CARPATHIANS - ROMANIA).

Robu I.N. and Robu L. (Institute of Geology and Geophysics of Bucureşti)

The Petreanu Masiff is composed by two distinct granitoid bodies: (1) Furcătura granitoid observed in the northern part of the masiff and (2) Petreanu granitoid, which had been met in the western and southern part of this.

All geological data (mineralogical,petrological, structural and geochemical) point out for these masiffs a different geological evolution: Furcătura granitoids, formed as a result of a magmatic activity (an intrusion accompanied by metasomatic processes - sodic metasomatosis) and Petreanu granitoids, formed due to an intense alkaline metasomatosis (mostly potassic), which affected Nisipoasa and Bodu crystalline formations.

The different origin of these masiffs is emphasized by the zircons morphology: Furcătura granitoid contains zircons specified for (1) Al-calc-alkaline environment and (2) subalkaline-alkaline one and Petreanu granitoid body includes zircons characterizing (1) calc-alkaline medium and (2) subalkaline - alkaline one.

Morphological variations of zircons from both granitoid bodies had been determinated by the different crystallization conditions and the geological processes which affected the country rocks: (1) - the initial different growth conditions, pointted out by the different zircons groups, characterizing for each body and (2) - the later metasomatosis processes determining the grows of zircons with the similar morphological features for both bodies.

CORRELATIONS BETWEEN CHEMICAL COMPOSITION AND STRUCTURAL CHARACTERISTICS OF WHITE MICAS FROM PEGMATITES BODIES (LOTRU MOUNTAINS - ROMANIA)

Robu L., Stelea G. and Vanghelie I. (Institute of Geology and Geophysics of Bucureşti)

White micas are one of the most important minerals of pegmatites bodies, which, together with feldspars, black micas and quartz compose pegmatites rocks.

Pegmatites bodies are associated with the polymetamorphic medium-grade crystalline formations (biotite+garnet±sillimanite±kyanite gneisses, micaschists and amphibolites) of Lotru (LG) and Sebeş (SG) Groups.

Two generations of pegmatitic bodies had been identified: (1) in concordance with M_1 metamorphic moment, like lenses and budines in the crystalline formations and (2) according to M_2 moment of metamorphism, like discordance veins.

Chemical composition of white micas points out an important celadonite component for micas of pegmatites from both groups, with an obvious higher value for micas of SG.

Other components (paragonite, Ca-paragonite, Fe^{2+}-celadonite, Fe^{3+}-celadonite) do not present a systematic variations.

Variation of cation composition from white micas, determined by the chemical substitutions ($K \rightleftharpoons Na,Ca$) or ($Al \rightleftharpoons Mg,Fe^{2+},Fe^{3+}$) induced some exchanges of values of b and d_{oo2} parameters.

Structural features, identified by X-ray powder diffraction emphasized a $2M_1$ polytype.

The high Al content and obvious Mg amount from white micas are showed by IR absorbtion spectra, registering characteristic absorbtion bands for Si-O-Al vibrations in the domain 700-800 cm^{-1} and for Mg-O-Si vibrations at the values of intensity between 550 and 675 cm^{-1}.

Crystallochemical features of White micas point out the low temperature and low pressure for the crystallization environment.

COMPOSITION AND STRUCTURAL STATE OF ALKALI FELDSPARS FROM THE FREGENEDA PEGMATITES (SALAMANCA, SPAIN)

Roda, E.; Pesquera, A.; Velasco, F. *(Dept. de Mineralogía y Petrología, Univ. del País Vasco/EHU, Spain)*

Different pegmatitic types, ranging from barren to Li- and Sn-bearing pegmatites have been recognized in the Fregeneda area. The pegmatites are located North of the Lumbrales granite, which is a parautochtonous, two-mica granite that was deformed during the third phase of Hercynian deformation. Most of the pegmatites intrude into rocks of the Schist-Metagraywacke Complex, that in this area consists of an alternation of quartzites, graywackes, schists and pelites.

The alkali feldspars associated to these pegmatites were analyzed by means of FRX, ICP and NA. Therefore, their structural state was characterized by X-ray powder diffraction.

Textural differences between the K-feldspar from the different pegmatite types have been observed. In this way, the most common is a perthitic coarse grained feldspar. The intergrowth varies from vein to patch perthite, whereas film and bleb perthites have been less commonly observed. Veins and patchs are very irregular, and usually show the albite twin. Perthites are more important in the less evolved pegmatites relative to the Li and Sn-bearing ones. The second petrographic type is only associated to the more evolved pegmatites, and it correspons to a coarse cuneiform K-feldspar, that grows perpendicularly to the contacts with the host-rock. Finally, the third type corresponds to a xenomorf albitized K-feldspar, with a clouded aspect. On the other hand, the presence of graphic quartz-feldspar interqrowths is frequent in the less evolved pegmatites, as well as deformation evidences as kinkig, undulatory extinction, etc.

The structural state of feldspars is a measure of the average Al/Si

distribution over the non-equivalent tetrahedral sites. It is usually determined from the unit-cell parameters, that let us know the (t1o+t1m) and (t1o-t1m) values for triclinic feldspars, and 2t1 for monoclinic phases, using the Kroll & Ribbe (1987) method. Results indicate variation in the structural state, from low microcline to orthoclase, with intermediate order degrees. A relation between the pegmatite type and the order degree of the feldspars has not been detected, since in all the types K-feldspars with different structural state coexist. This suggests that the evolution after their formation was different for the different pegmatitic bodies. Thus, the presence of a disordered feldspar indicates a rapid decompression or a low activity of processes that could favour the inversion. On the contrary, ordered K-feldspar suggests a slow crystallization rate, or the influence of hydrotermal fluids or shear phenomena (Eggleton & Buseck, 1980). Besides, the presence of granophyric intergrowths and albitization are signals of a fluid phase activity could be a catalyst for the exsolution processes.

On other hand, the plot of a versus $b \times c$ parameters reveals a certain deformation in the intermediate microclines as well as in some maximum microclines. In this last case, deformation can be explained taking into account that these low microclines show characteristics that correspond to the irregular microclines described by Bambauer et al., (1989). As the structural state, a relation between the deformation of the K-feldspar and the pegmatite type has not been found.

With regard to their Or content, the Hovis (1986) method, based on the unit-cell volume, seems to be the most reliable, since the obtained results are in agreement with the FRX and ICP data. Thus, the Or content vary from 86,8 % to 100% according to the Hovis method, whereas the analytical results show very low contents in Na_2O (< 0.1%) and in CaO (< 0,4%). Variations in the major elements contents have not been detected. On the contrary, there are significant differences in the trace elements contents depending on the pegmatitic type. The feldspars associated to the less evolved pegmatites are the poorest in Cs (7-28 ppm), Li (1-6 ppm), Rb (500-600 ppm) and Zn (1 ppm), and show higher K/Rb ratio than those from the Li-rich pegmatites, whereas these exhibit the richest feldspars in Li (29-218 ppm), Rb (2900-4700 ppm) and Cs (106-713 ppm), the poorest in Ba (5-44 ppm) and the lowest K/Rb ratios (Roda et al., 1993). With regard to the Sn-bearing pegmatites, their K/Rb ratio shows intermediate values, whereas their contents in Ba (971 ppm) and Sr (536 ppm) are the highest. These pegmatites show characteristics of the most evolved terms in a given pegmatitic sequence, so, this group of pegmatites can not be related by simple fractional crystallization with the rest of the types. In contrast, the other pegmatites show congruent trends, thus, in a first aproximation, they are genetically, as well as spatially, related to each other.

References:
Bambauer,H.U.,Krause.C.,Kroll,H.(1989).*Eur.J.Mineral.*,**1**,47-58.
Eggleton, R. A. & Buseck, P. R. (1980). *Contrib. Mineral. Petrol.*, **74**, 123-133.
Hovis, G. L. (1986). *Amer. Mineral.*, **71**, 869-890.
Kroll, H. & Ribbe, P. H. (1987). *Amer. Mineral.*, **71**, 1-16.
Roda, E., Pesquera, A., Velasco, F. *Current research in Geology applied to ore deposits, La Guioconda, Granada.*, 653-656.

COMPARATIVE STUDY OF THE TRANSITION BETWEEN DIAGENESIS AND LOW GRADE METAMORPHISM IN SILICICLASTIC AND CARBONATE CRETACEOUS MATERIALS. CAMEROS BASIN (NE SPAIN).

Rodas, M.; Alonso-Azcárate, J.; Barrenechea, J.F. *(Dept. Cristalografía y Mineralogía, Univ. Comp. Madrid)* and Mas, J.R. *(Dept. Estratigrafía, Univ. Comp. Madrid).*

The Cameros basin is located in the northwesternmost part of the Iberian Ranges. It represents a singular case in the geological background of the Mesozoic basins of this area, as anomalously high subsidence and sedimentation rates took place within the basin during the Late Jurassic-Early Cretaceous.

This is the only basin of the Iberian Ranges where the Mesozoic sediments were affected by a low-grade metamorphic event.

A total of 390 samples were collected along six stratigraphic sections through the Urbion and Enciso Groups.

Sediments of the Urbion Group (DS2, DS3, DS4 and lower part of the DS5 depositional sequences, Figure 1) consist of lutites and sandstones, which essentially correspond to meandering fluvial systems.

The Enciso Group (upper part of the DS5 depositional sequence, Figure 1) is formed by alternating limestones and marls, with ocasional sandy and muddy interbeddings, mainly corresponding to shallow lacustrine deposits.

The mineralogical characterization of these materials shows significant differences as a function of their lithology (siliciclastic or carbonate rocks).

The mineral assemblages recognized in the siliciclastic materials of the Urbion Group have been used to detect changes in the degree of metamorphism:

- Low-grade metamorphism: quartz, chloritoid, illite, chlorite, paragonite and mixed-layer muscovite/paragonite.
- Very low-grade metamorphism: quartz, illite, chlorite, pyrophyllite and rectorite.

The mineral assemblage in the carbonate rocks of the Enciso Group shows less variations than in the Urbion Group, being mainly composed by illite and chlorite. In order to estimate the metamorphic conditions, variations in the illite and chlorite "crystallinity" indices have been measured.

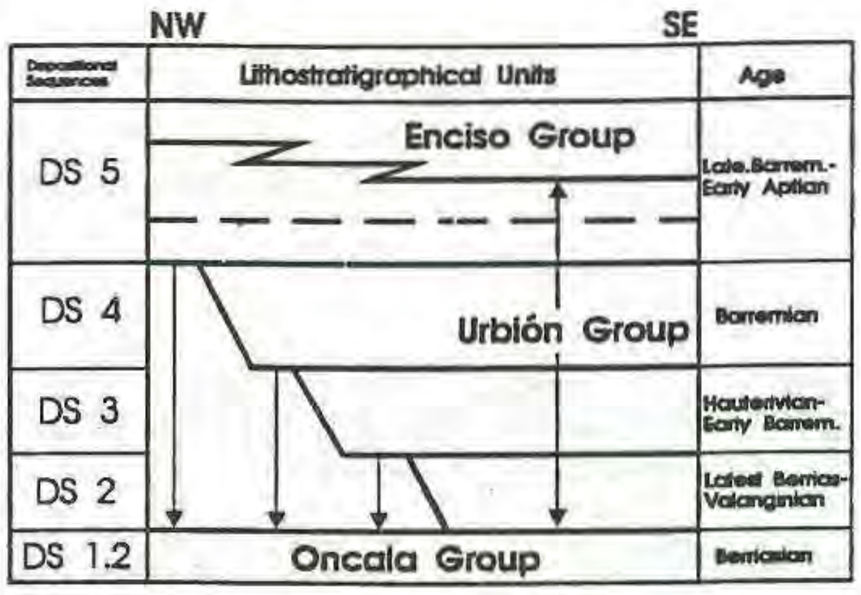

Figure 1: Depositional sequences defined by Mas *et al.* (in press) for the Cameros basin (NE Spain).

Illite "crystallinity" cannot be regarded as a reliable indicator of the degree of metamorphism in the siliciclastic materials of the Urbion Group, due to the consistent presence of paragonite and mixed-layer muscovite/paragonite associated to the illite 10 Å peak.

In summary, the mineralogical and sedimentological data obtained in this part of the basin, indicate a progressive decrease in the metamorphic grade as we move from the depocentral areas to the eastern sector, marked by the transition from epizonal to anchizonal conditions.

References:
Mas J.R.; Alonso, A.; Guimerá, J. (in press): *Rev. Soc. Geol. Esp.*

FLUID INCLUSION CRUSHING AND HOMOGENIZATION STUDIES OF CALCITE VEINS FROM YUCCA MOUNTAIN, NEVADA, TUFFS: ENVIRONMENT OF FORMATION

ROEDDER, E., Earth & Plan.Sci., Harvard Univ., Cambridge MA, 02138; WHELAN, J. USGS, Denver CO, 80225; and VANIMAN, D.T., Los Alamos National Laboratory, Los Alamos, NM 87545.

Calcite vein and vug fillings at four depths (130-314m), all above the present water table in USW G1 bore at Yucca Mountain, Nevada, show two principal types of primary fluid inclusions: either full of liquid or full of vapor. With rare exceptions, the liquid-filled inclusions have no vapor bubbles. The vapor-filled inclusions provide evidence that a sepa-

rate vapor phase was present in the fluid during crystallization of these calcites.

Crushing stage studies of the vapor-filled inclusions were reported in our earlier paper (G.S.A. Abst. with Prog. V.25, no.6, p. A-184, 1993) as indicating trapping of an air-water-CO_2 vapor phase at <100°C. Those studies, made using microscope immersion oil as the mounting medium, showed the oil sucking into the inclusions, and hence implied <1 atm pressure at room temperature. The amount of oil entering was assumed to be a measure of the partial pressure of H_2O in the vapor at the time of trapping (now condensed to an invisble film of liquid water), and hence a measure of the temperature of trapping.

Our new studies reveal that the vapor inclusions now contain gas at essentially 1 atm at room temperature; the entry of oil noted earlier came from the dissolution of methane in the immersion liquid used. When crushing was in glycerol, in which methane is relatively insoluble, no fluid was sucked in, nor was there any vapor expansion, i.e., the pressure in the inclusions is now about 1 atm. These inclusion data impose some useful constraints on the depositional environment for these calcites, but leave several ambiguities. The lack of bubbles in even relatively large liquid inclusions suggests low trapping temperatures, probably well under 100°C. The two types of inclusions require trapping from a heterogeneous system of liquid + vapor and suggest two possible environments: the liquid phase could have been merely a film on the walls of an otherwise vapor- or air-filled vein or vug opening, in a system above the water table (i.e., unsaturated), or the vapor phase could represent exsolution (effervescense) of a gas such as CO_2 in an essentially liquid-saturated system (below water table). However, the presence of gases at essentially 1 atm. pressure in the vapor inclusions requires that the veins were open to the surface at the time of trapping, and precludes any significant hydrostatic head at trapping. Hence the calcite must have crystallized from a down-flowing fluid film on the walls of a vein that was open to the surface. The crushing studies using glycerol do not discriminate between air, methane, and CO_2, but do preclude any significant partial pressure of H_2O in the vapor at the time of trapping, and hence suggest trapping at low, perhaps even ambient temperatures. Gas analyses of the vapor phase inclusions are planned.

The inclusion data also do not place constraints on the time of crystallization nor on the origin of the gases in the vapor inclusions. The air, CO_2, and methane all could have been of surface origin, dissolved in the down-flowing water, or could have been evolved from deep groundwaters in the underlying Paleozoic limestones and then redissolved in the down-flowing cold surface water films. In either case, exsolution of these gases from the liquid film would be expected on warming during the fluid descent.

LUMINESCENCE OF GEM AND ASSOCIATED MINERALS FROM FORSTERITE SKARNS OF PAMIR

Rogozhin A. (Inst. of Mineral Resources VIMS, Moscow)

The luminescence properties of samples collected from unique association of gem minerals in the S.-W. Pamir (Kukhilal) were investigated. These are rose spinel, clinohumite, forsterite, the mineralisation being confined to magnesian marbles over wich forsterite-magnesite, enstatite and forsterite-spinelite skarns are developed. Geochemical features of this mineralisation apart from enrichment in magnesium are high contents of chromium (spinel) and titanium (dravite in pegmatites, clinohumite), and low iron contents. The X-ray and UV lamp/laser-induced luminescence spectra of spinel, clinohumite, forsterite, enstatite, talc, phlogopite, apatite, calcite, magnesite, dolomite, fluorite, feldspars and some other minerals were measured. Relatively low contents of iron (a well known luminescence quencher) explaine the rich variety of bright luminescence wich visual appearance in the samples studied ranged from violet (apatite) to deep red (spinel). Some minerals manifested not documented previously or at least not well known luminescence spectra and corresponding centres (e.g. Mn^{2+} in spinel, Ti^{4+} in clinohumite, talc et al). The majority of minerals demonstrate luminescence due to Mn^{2+}-ions: forsterite (630 nm), enstatite (655 nm), clinohumite (625 nm), phlogopite (570 nm), apatite (580nm), dolomite (580 nm, 630 nm), calcite (630 nm), magnesite (580 nm) and even spinel (512 nm) (the luminescence bands maximum wavelengths are put in the brackets).

Gem clinohumite is the second most important mineral of the mineralisation investigated. Transparent samples of clinohumite varied from practically colourless to heavy orange. The average TiO_2 concentrations in the yellow-orange clinohumite are about 2.5% while Fe_2O_3 concentration ranges from 0.02 to 0.4 % wich is not enough for effective luminescence quenching. Clinohumite colour is due to charge transfer transitions in Ti^{3+} - Ti^{4+} pairs (Platonov, A.N., 1976). In the luminescence spectra of clinohumite we found two bands with maximum wavelengths at 550 and 625 nm. The relative intensities of the bands varied in favor of the shortwave one as the intensity of yellow-orange colour grew. We assign the longwave band to Mn^{2+}-centres and the shortwave one - to Ti^{4+}-centres. Characteristic properties of luminescence spectra of many magnesian silicates studied are broad bands with maximum in the range from 420 to 600 nm depending on the excitation mode wich we assign to titanium-oxigen complexes. Such bands were registered in fluorescence spectra of (apart from clinohumite) forsterite, enstatite, phlogopite, talc , chrisotile, brucite.

We believe that the luminescence spectra data form a basis for obtaining mineral genesis information. Besides, the distinctive luminescence features of Kukhilal minerals proved to be useful for mineral identification, prospecting and for automatic sorting technique development.

References: Platonov, A.N. (1976). Origin of Colour of Minerals. Naukova dumka:Kiev, 264 p.

TEXTURES OF URANIUM ORES IN THE WESTERN CARPATHIANS , SLOVAKIA

Rojkovič I. (Geological Inst. SAV, Bratislava)

Uranium mineralization results from various ore - forming processes that are reflected also by ore textures. U-Mo stratiform mineralization is related to the Permian volcanic and volcanoclastic rocks and U-Cu-(Pb-Zn) mineralization to sandstones with abundant organic matter. Tabular and lens-shaped ore bodies are arranged conformable to surrounding rocks. The disseminated and banded mineralization retains sometimes original cross-bedding of the rock. Uranium associated with organic matter occurs in more porous vitrinite (telinite). The uraninite distribution pattern follows original plant tissue even in the folded coal fragments. Deposition of uranium on pyrite, Ti-oxides

(replacing Fe-Ti oxides), Fe-hydroxides is documented by EMA, FT reprints and α-autoradiography. Uranium minerals are related to Ti oxides (leucoxene) originated by alteration of Fe-Ti oxides and they are also associated with framboidal pyrite.

The Upper Permian diagenesis originated stratiform accumulations of U, Mo, Cu and other elements close to source of ore elements (granits, acid tuffs) and permeable horizon by the reduction and adsorption processes at temperatures ranging from 100 to 150°C from fluids of 27.1-33 equiv. wt. % NaCl according to fluid inclusions study. The Pb-U dating has yielded the ages from 270 to 240 Ma (Kolektiv 1984). Larger variability of the isotopic composition of $\delta^{34}S$ and $\delta^{13}C$ in the stratiform ores suggests mixing of meteoric solutions with fluids of volcanic origin and their complex history (Rojkovič et al. 1993).

The stratiform mineralization is overlapped by later, remobilization-related, stratabound U, Mo and Cu mineralization confined mostly to ore-bearing horizons. The coal matter has been crushed and folded during early Alpine orogeny. The secondary cracks were filled with younger quartz - carbonate - sulphide mineralization intersecting original plant tissue. This mineralization evidently postdates uranium sorption by organic matter (Rojkovič et al. 1992).

Higher grade uranium mineralization has been identified in the structures concordant to Alpine cleavage and inside tectonic faults, forming veins and stockworks crosscutting the horizons with the U - Mo mineralization. The vein mineralization in the Permian sequences encloses fragments of pre-existing ore layers.

Uranium-rich mineralization is represented by the uraninite, creating colloform, concentric and botryoidal aggregates and veinlets. Major ore minerals are: uraninite, molybdenite, U-Ti oxides and pyrite. They are accompanied by chalcopyrite, tennantite, galena, sphalerite, arsenopyrite, coffinite, brannerite, quartz, Fe-dolomite, siderite and apatite (Rojkovič et al. 1993). Relics of exsolution structures from a solid solution of Fe-Ti oxides has been found even in hydrothermaly altered rocks. They are replaced by Ti and U-Ti oxides preserving euhedral shape in volcanic rocks and they are rounded in the sedimentary rocks. The stratiform ores were remobilized 100-130 Ma ago (Kolektiv 1984) at temperatures up to 250-270°C.

References:

Kolektiv (1984). Czechoslovak uranium deposits. (SNTL, Prague), 365 p. (in Czech)

Rojkovič, I., Franců, J., Čáslavský, J. (1992). Geol.Carpath., Bratislava, 43, 27-34.

Rojkovič, I., Novotný, L., Háber, M. (1993). Mineral. Deposita, 28, 58-65.

• POSITION OF PRECIOUS METAL MINERALIZATION IN METALLOGENY OF THE BANSKA STIAVNICA - HODRUSA ORE DISTRICT.

Rojkovičova L., Onačila, D., Lexa, J., Štohl, J. (*Dionyz Stur Institute of Geology, Bratislava, Slovakia*)

Middle Slovakia Neovolcanic Region covers approximately 5000 km². It consists of several isolated andesite stratovolcanoes of different size. The interval of activity is from 17 to 7 Ma. The Banskà Stiavnica is the largest and from the point of view of metallogeny the most conspicuous volcanic structure within the Region. The central zone of the stratovolcano is the site where multistage metallogeny of Au, Ag, Pb, Zn, Cu, Fe mineralization of different genetic types took place. The central volcanic zone had been developing from simple crater to caldera type structure and finally ending by resurgent dome, presently known as the Banská Stiavnica horst.

In general there were recognized two main metallogenetic stages (Štohl & Lexa, 1990) associated to the volcanotectonic evolution of the central zone of the Banská Stiavnica stratovolcano.

1. Precaldera stage – as a whole it is represented by "intrusion related" type of metallogeny: iron skarn type (a), copper porphyry (b), and stockwork and disseminated base metal ± quartz-gold mineralization (c). In more detail they are described as follows:

(a) magnetite skarn mineralization formed at contacts between granodiorite and limestone – dolomite of Mesozoic basement complex. Mineralization is of contact replacement type and is associated with Mg Ca skarn minerals. There is no gold present in this type.

(b) disseminated stockwork – like base metal mineralization is bound to apical portions of the subvolcanic granodioritic body at its contact with overlaying volcanic complex. It is characterized by simple mineral association with sphalerite and galena predominating over chalcopyrite and pyrite. Accessory precious metal mineralization is represented by native gold, electrum polybasite and hessite. Recently discovered Au mineralization associated with base metal minerals is located in similar structural environment next to base metal stockwork on subhorizontal extension fractures. Precious metal mineralization is developed in quartz, sulphide and carbonate minerals, in the association with acanthite, hessite, Ag–sulphotellurides (Jelen et al., 1992). Mutual relation of the two former mineralization types is not clear to date.

Cu, Mo, Au skarn porphyry type mineralization is bound to endo and exo – contacts between the granodiorite porphyries and dolomites, dolomitic limestones (Mg skarns). Gold occurs in close association with pyrrhotite, pyrite and chalcopyrite, in association with marcasite, valleriite, molybdenite, sphalerite, galena, millerite, altaite, magnetite and hematite.

2. Postcaldera stage is of vein type. It is associated with horst forming processes within framework of extension tectonic regime. Epithermal vein mineralization is represented by three different types: (a) polymetallic vein ± Au with transition to Cu ± Bi mineralization at depth, (b) Ag – Au veins with minor base metal mineralization and (c) Au – Ag veins located at marginal faults of the horst.

Base metals ± Au veins (a) are developed mainly in the propylitized pyroxenic andesite, quartz – diorite porphyry and granodiorite host rock of the Stiavnica Ore District. Vertical zoning of the vein development has been well defined: Au, Ag, As, Sb association located mostly in the upper portions of the veins and Au, Ag, Cu, Bi, W association, located 500 – 600 m below the surface (Jelen et al., 1992).

Ag, Au veins with base metals (b) are developed predominantly in the Hodrusa Intrusive Complex (granodiorite, diorite, quartz - dioritic porphyry) host rocks. Characteristic features of these veins are quartz – carbonate gangue minerals and precious metal mineralization (pyrargyrite, stefanite, miargyrite, polybasite, acanthite, gold, electrum), accompanied by galena, sphalerite, chalcopyrite, pyrite and marcasite.

Au – Ag stage (c), situated at the marginal part of the horst, occurs in the amphibole – biotite andesitic host rocks and is related in time and space with rhyolite volcanism. Gold is present in pyrite as well as finely dispersed in a zone of silica metasomatites, in association with acanthite, galena, sphalerite, chalcopyrite and marcasite.

References

Štohl, J., Lexa, J. (1993). *IUGS/UNESCO deposit modelling Workshop*.

Jelen, S., Háber, M., Kalinaj M., Bebej, J. (1992). *Conference Proceedings*, 81–89.

• ISOTOPIC SYSTEMATICS ACROSS A BLEACHING FRONT IN A CHARNOCKITE (KHONDALITE BELT, SOUTH INDIA)

Roller G. (*Max-Planck-Institut für Chemie, Mainz; Min.-Petr. Inst., Univ. München*) and Köhler H. (*Min.-Petr. Inst., Univ. München*)

Investigations of the high-grade terranes in southern India have

yielded important information on the genesis of granulites worldwide. Of special interest to the scientific comunity was the in situ charnockitisation and the transition from amphibolite to granulite facies. Another phenomenon often described is the bleaching of dark charnockites. Contrary to prograde charnockitisation, the process responsible for bleaching remains poorly understood. Therefore, this study focuses on the effects a bleaching process has on the Rb-Sr- and Sm-Nd systematics in order to evaluate element-mobility and the significance of geochronological data in such rocks.

Across the bleaching front in a charnockite of the Ponmudi unit (Khondalite Belt, South India) a rock column of about 16 cm was cut from a hand specimen and further devided into 16 cubes of approximately identical size. The cubes were analysed by isotope dilution for Sr, Rb, Nd and Sm. The results demonstrate that during the bleaching process Sm, Nd and Rb were added, while Sr was removed from the system. Nd and Sr isotopes define a binary mixing line of two elements having different isotope ratios. The data is consistent with granulitic lower crust beeing contaminated with a component showing an isotopic signature typical of continental upper crust. Due to this severe modification of element concentrations and isotope ratios, none of the samples from the bleached part are suited for age calculations. The addition of an upper crustal component leads to higher $^{143}Nd/^{144}Nd$ isotope ratios within the bleached charnockite and hence lower $\varepsilon(Nd)$ values and Nd model ages. The cubes of the unaltered charnockite define a Rb-Sr-isochron of uncertain significance. In contrast, biotite-whole rock and garnet-whole rock ages (460 Ma and 480 Ma, respectively) are geologically significant, and support the early Paleozoic age of metamorphism and consequently the distinct tectonic setting of the Ponmudi unit within the high-grade terrane of South India. Moreover, these metamorphic ages support a genetic relationship between the South Indian Khondalite Belt and the Highland complex of Sri Lanka.

STRUCTURAL PROPERTIES OF MANTLE MINERALS

Ross N.L. (*Dept. Geological Sciences, University College London*).

Understanding the structural behaviour of mantle phases as a function of pressure and temperature is fundamental for interpreting seismological and thermal models of the Earth's interior. In particular, equations of state (EOS) of mantle phases are vital input into whole-Earth models. The EOS most currently used in the treatment of experimental compression data of minerals is the third-order Birch-Murnaghan EOS. This EOS is valid as long as higher order powers in the Taylor expansion of F in finite strain, f, are small, the crystal undergoes homogeneous strain, and there are no phase transitions. Recent high-pressure single-crystal X-ray diffraction studies of important mantle phases, however, have shown the following:

- They do not obey EOS systematics;
- They compress inhomogeneously;
- They show changes in compression mechanism with increasing pressure;
- They undergo displacive phase transitions.

Therefore the EOS of mantle minerals cannot be extrapolated from room pressure, but must be measured *in situ* at high pressure. In this talk, the structural behaviour of mantle phases at high pressure will be reviewed and the implications of the above factors on the phase stabilities and equations of state of mantle phases will be discussed.

SPECIMEN CARE: IRON SULFIDES ALTERATION IN MUSEUM ENVIRONMENT

Rossi P. (*Dip.Sci.Terra, Univ. Firenze*), Cipriani C. & Costagliola P. (*Museo Mineral. Litol., Univ. Firenze*)

Iron sulfides alteration is one of the most common problems faced by museum curators dealing with specimens care (cf. Howie, 1977). Oxidation reactions take place on the surface and in the fractures of the samples leading to severe specimens damage. Specific research on this subject, a study of alteration processes in 44 samples of pyrite from ore deposits from Southern Tuscany and Isola d'Elba, is now in progress at the Museo di Mineralogia e Litologia dell'Università di Firenze.

The examination of altered pyrite through X-ray diffraction clearly revealed the presence of sulphates. In particular szmolnokite ($FeSO_4.H_2O$), as a major constituent, rozenite ($FeSO_4.4H_2O$) and melanterite ($FeSO_4.7H_2O$) are the main products of pyrite oxidation.

The specimen alteration index was obtained, for each sample, by comparing the intensity of selected X-ray diffraction peaks of sulphates with those of pyrite. That index was then compared with other parameters held to be responsible of alteration such as trace elements content (As, Co, Ni and Mn), crystal habit, textures and structures as observed in reflected light. The time span from sample collection to the present (the "age" of the specimen) is not exactly known, thus it was roughly approximated by the date on which the specimen was acquired by the Museum. As alteration is probably the result of many factors (e.g. textures, chemical composition, storage conditions, etc.), among which the time elapsed since the samples have been exposed to the atmosphere is conceivably the most important, it is difficult to evaluate the contribution of each single factor, other than time, without knowing the "age" of the specimens. Nevertheless fracture density appears to be the parameter that is best positively correlated with the degree of alteration.

Selected specimens were etched by oxidizing H_2O_2 solutions and/or subjected to controlled atmosphere in a climatic test chamber, for comparable times. Pyrite alteration was monitored by measuring Fe released in solution and by changes in colorimetric parameters of crystals surface. These experimental runs provide further evidence that specimen fracture, more than the other feature, is responsible for the alteration. In accordance with Howie (1992), it was confirmed that relative humidity, in particular beyond 60% threshold, considerably increases alteration processes.

Isolation of the specimens from the atmosphere was retained to be the best method to protect them from oxidation. The surface of the specimens was then treated with synthetic resins which are also used in the preservation of monuments. All the resins used (Paraloid B52, Akeogart CO, Akeogart CO+Kynar and Dry-film) did not significantly alter the original appearance of the specimens. Experimental runs showed that Akeogard CO +Kynar was the most suitable resin for our purposes.

References:
Howie, F.M. (1977). *Newsletter of the Geological Curators Group*, **10**, 497-513
Howie, F.M. (1992). *The care and conservation of geological material*, F.M.Howie, Butterworth-Heinemann, 138 pp

KINETICS OF HIGH PRESSURE PHASE TRANSITIONS IN SUBDUCTING LITHOSPHERE

Rubie D.C., Hogrefe A.R., Sharp T.G., Seifert F. (*Bayerisches Geoinstitut*)
Stein S. *(Northwestern University)*
Kirby S.H. *(U.S. Geological Survey)*
Ross II C.R. *(University of Nebraska)*

The constituent low-pressure minerals of oceanic lithosphere (e.g. olivine and orthopyroxene) become thermodynamically unstable at a depth of about 400 km in the mantle and transform to higher-density phases such as β-$(Mg,Fe)_2SiO_4$ (modified spinel structure), γ-$(Mg,Fe)_2SiO_4$ (spinel structure), $(Mg,Fe)SiO_3$ (ilmenite structure) and garnet rich in the $(Mg,Fe)SiO_3$ component.

Such phase transformations may fail to occur at the equilibrium pressure in subducting slabs because of low temperatures, in which case the low-pressure minerals persist metastably to a depth determined by the reaction kinetics. It has been suggested that a wedge of metastable peridotite extends to a depth >650 km in some subduction zones. This metastable wedge affects the driving force for subduction through the transformation-induced density change and the state of stress in the slab through the volume change. It has previously been proposed that deep-focus earthquakes originate by a shear instability, known as transformational faulting, which develops in the metastable wedge when phase transformations occur under stress.

Transmission electron microscope (TEM) studies of experimentally-reacted samples show that the mechanism of the $(Mg,Fe)_2SiO_4$ olivine (α) to spinel (β or γ) transformation involves incoherent nucleation of spinel on olivine grain boundaries and either diffusion- or interface-controlled growth. The transformation kinetics in the stability field of either β or γ can be described by a rate equation which incorporates rates of nucleation and interface-controlled growth. A modification of this equation can also be used to model transformation rates under conditions of continuously changing pressure and temperature in subduction zones, provided the rates of nucleation and growth can be estimated as a function of temperature and pressure from experimental data. Experimental growth rate data for the α–β and α–γ transformations in Mg_2GeO_4, Ni_2SiO_4, Mg_2SiO_4 and $(Mg,Fe)_2SiO_4$ together with limited nucleation rate data for γ-Ni_2SiO_4 enable a semi-quantitative estimate of olivine-spinel transformation kinetics in subduction zones to be made. The transformation rate equation is evaluated along temperature-depth-time paths, calculated in two-dimensional thermal models of subducting slabs, to determine the depth of transformation.

Results of the kinetic calculations show that in slowly subducting slabs of young lithosphere (e.g., Aleutian) temperatures are high enough for olivine to transform to β–$(Mg,Fe)_2SiO_4$ close to the depth of the equilibrium phase boundary. In rapidly subducting slabs of old lithosphere (e.g., Tonga), temperatures in the slab interior are relatively low and consequently olivine persists to depths of 600 km or more. Transformation of metastable olivine to γ-$(Mg,Fe)_2SiO_4$ takes place over a narrow depth interval because the evolved latent heat results in a temperature increase of up to 150 °C which produces a runaway reaction rate. The boundary of the resulting metastable wedge coincides with an isotherm which in the present model is at approximately 600 °C. The maximum depth to which metastable olivine can survive in a subduction zone depends primarily on the thermal parameter ϕ, which is the product of the age of the lithosphere and the rate of subduction. The maximum depths of deep-focus earthquakes also correlated strongly with the thermal parameter, and our results are therefore consistent with their origin by the transformational faulting mechanism.

TEM studies of phase transformations in a model peridotite (hot-pressed forsterite + $MgSiO_3$ clinoenstatite aggregates), reacted in the stability fields of β- and γ-Mg_2SiO_4 + stishovite (16-21 GPa and 1000-1600 °C) for times up to 30 hours, show that the kinetics of pyroxene breakdown reactions at high pressure are much more sluggish than those of olivine. Whereas forsterite reacts rapidly (<2 h) to β-Mg_2SiO_4 at 16 GPa and 1200 °C, metastable clinoenstatite persists at 20 GPa and 1500 °C for times up to 30 h. At higher pressures (21 GPa and 1250 °C), clinoenstatite transforms polymorphically to metastable ilmenite which subsequently reacts on a slower time scale to the stable γ-Mg_2SiO_4 + stishovite assemblage. These results suggest that metastable $(Mg,Fe)SiO_3$ clinopyroxene is likely to survive to considerably greater depths than olivine in subduction zones and may transform directly to metastable ilmenite. The clinoenstatite to ilmenite phase transformation, like that of olivine to γ-spinel, results in a large negative volume change and high latent heat production and may also result in transformational faulting, particularly in pyroxene-rich lithologies.

PHYSICO-CHEMICAL STUDY OF THE SEDIMENTS IN THE RIVER ARA, HUESCA, SPAIN.

Rubio, V. (Dpto. Geografía, U. Autónoma of Madrid), Vigil de la Villa, R., Cala, V. and García, R. (Dpto. Geología, U. Autónoma of Madrid).

The study of the sediments of the river Ara in the province of Huesca, Spain, using several physicochemical analysis, allows the recognition of the origins of some of the materials found in their composition.

The minerals of the sand fraction, those connected with the clay fraction and the minor elements, show certain processes and associations that, along with the identification of river terraces, cones, glacis and even morrainal deposits, help in the explanation ot the geological origins of the Huesca Pyrenees.

The application of a multivariate factorial analysis to the data using the BMDP-4M computer program, helped in the interpretation of the results.

In the sediments that were studied, carbonate is found in the thickest textural fraction, while quartz concentrates itself in the finest textural fraction. The microelements seem to show differences as far as their dynamic is concerned, thus, chrome, lead and nickel, are associated with manganese metallic oxides regardless of their degree of crystallinity while copper and zinc are associated with phyllosilicates.

A manifestation of the alteration will be related with the formation of iron and manganese metallic oxides.

As far as the set of clay minerals is concerned there can be observed several differences related with their origins, illite that seems to have an inherited granitic origin, would be auchthonous, while sepiolite and smectite might may have been produced by the alteration of feldspar, amphiboles and phylosilicates present in the original material.

STABILITY OF DICKITE IN PERMO-TRIASSIC SEDIMENTS (BETIC CORDILLERAS, SPAIN)

Ruiz Cruz, M.D. (*Departamento de Química Inorgánica, Cristalografía y Mineralogía, Univ. de Málaga, Spain*)

In the Maláguide Complex (Betic Cordilleras, Spain) dickite is widely developed in detritic Permo-Triassic sequences (Ruiz Cruz & Puga, 1992). Lateral extension is large (in the order of several hundred of km) whilst vertical extent is limited to the lowest 20-50 m of these sequences. The interpretation of this restrictive formation of dickite in sequences in which the maximum stratigraphic charge was not greater than 400 m is the aim of this work.

This Complex contains rocks from Paleozoic to Early Miocene age classically considered as non-metamorphic. Mäkel (1985) differentiates three lithostratigraphic Units: a) The Paleozoic Unit; b) The Triassic rock Unit and c) The Mesozoic and Tertiary rock Unit. Our study is concerned with Upper Paleozoic (Carboniferous) and Triassic rock Units.

Clay mineral patterns

In Carboniferous and Permo-Triassic rocks, three zones have been identified, based on clay mineralogy:

Zone	Lithostratigraphy
1.- *Illite -(chlorite)*	Sandstone member (Upper Permo-Triassic)
2.- *Dickite-mica*	Conglomerate member (Lower Permo-Triassic)
3.- *mica-chlorite*	Greywacke member (Carboniferous)

1.- In the upper Permo-Triassic illite is the dominant clay mineral (60-100%). IC values are variables from 0.4 to 1.2.
2.- In the lower Permo-Triassic, dickite is the dominant phyllosilicate. IC values in this zone vary from 0.25 to 0.46.
3.- Carboniferous rocks are characterized by the mica-chlorite assemblage. $2M_1$ is the only politype determined and IC is <0.35.

Chemical data

The analyzed chlorites show an intermediate composition, with a Fe-content decreasing in the order Carboniferous>Permo-Triassic (1.70-3.20). Al content is in the range 2.62-3.00, being the Lower Permo-Triassic chlorites the richest in this element. Si content ranges between 2.71 and 3.11, showing the Permo-Triassic chlorites the highest Si contents. The octahedral occupancy is also variable. In the Permo-Triassic members octahedral totals are

<5.75. The range of octahedral occupancy in the Carboniferous member is 5.77-5.94. The tetrahedral Al, according the Si variations is notably greater in Carboniferous chlorites. Temperatures in the order of 150-200ºC, for lower Permo-Triassic and 300-350ºC, for Carboniferous can be deduced from the regression lines by Cathelineau (1988) and Hillier & Velde (1991).

Microprobe analysis of illite-mica shows K+Na contents ranging from 0.74 to 0.95, being 0.80 the medium value in the illite zone, 0.85 in the dickite zone an 0.88 in the mica-chlorite zone. Si content is also variable between 3.08 and 3.53. Only a few of the samples within each group can be considered as phengites and so, used as geobarometer from the diagram by Massone & Schreyer (1987). Assuming temperatures in the order of 200ºC for the Permo-Triassic members and 300ºC for the Carboniferous one, we can deduce pressures in the order of 2-4 Kb and 3-5 Kb for these members, respectively.

Conclusions

1.- The existence of a clear discontinuity in the chemical composition of chlorites between Carboniferous and Permo-Triassic materials clearly indicates that a variscan metamorphism affected the Paleozoic sequences in the Málaga area. Chemical data indicate temperatures probably higher than 300ºC and pressures of 3-5 kb.

2.- Diagenesis is characterized in the lower Permo-Triassic by intensive disolution processes and development of kaolinite and quartz. In the upper Permo-Triassic early burial diagenesis is indicated by development of K-feldspar, carbonates and scarce illite.

3.- In the lower Permo-Triassic, diagenetic assemblages were strongly affected by the alpine metamorphic event. Two types of transformation coexist in the conglomeratic member, related to this event, which have been developed in a relatively short interval of time: kaolinite → dickite and dickite → mica/chlorite. The reached temperatures were in the order of 150-200ºC and pressures in the range of 2-4 kb.

References

Cathelinau, M. (1988) *Clay Miner.*, 23, 471-485.
Hillier, S. & Velde, B. (1991) *Clay Miner.*, 26, 149-168.
Mäkel, G.G. (1985) Gua Papers of Geology, 22, 263 pp.
Massone, H.J. & Schreyer, W. (1987) *Contr. Mineral. Petrol.*, 96, 212-224.
Ruiz Cruz, M.D. & Puga, E. (1992) *Actas III Congreso Geol. de España*, 329-334.

MAIN SEQUENCE OF MINERAL PARAGENESIS DEVELOPMENT AND ITS SIGNIFICANCE FOR THE EVOLUTION CLASSIFICATION OF ROCKS, ORES AND DEPOSITS.

Rundqvist D.V. (Vernadsky State Geological Museum, Moscow).

The sequence of mineral paragenesis development in the process of deposits formation bears the important information about the phylogenetic origin of deposits and their relationships. This assertion is based on the early derived general geogenetic law of development - parallelism of ontogeny and phylogeny in geological history. As consequence there is a suggestion analogous to the general Berr law in biology -- in succession of the general sequence of paragenesis development the primary members reflect the belonging to the general type whereas the later members belong to the more fraction taxons of the evolution classification (see scheme):

Using these general principles we meet however a lot of yet unsolved problems. In particular, the choice of the time scale of formation, since many deposits are telescoped and formed during several epochs. It is not clear also how to determine correctly the more early members

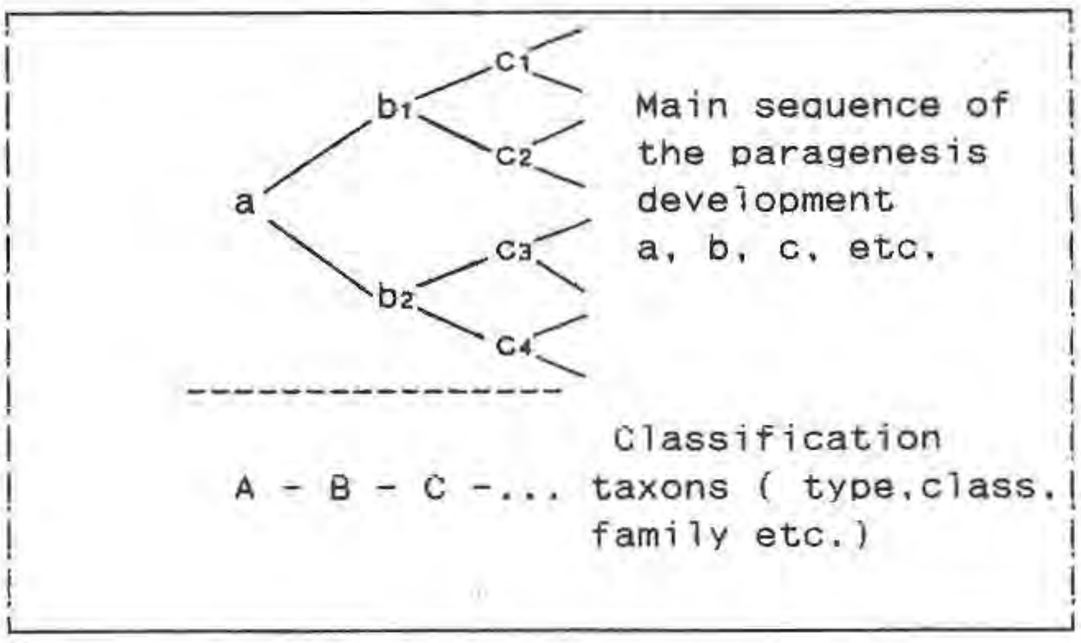

of the main sequence: in which cases the preore metamorphic and magmatic paragenesis should be taken in mind. The convergence of the late mineral paragenesis (similar in different evolution rows) also makes difficult to use principles above discussed.

The strong and weak features of this classification are considered in detail on the examples of paragenesis development for tin and gold deposits in Russia.

The precise definition of the principles of main sequence formation makes it possible to propose the international joint program "The creation of natural evolution classification of mineral paragenesis and economic ore deposits".

The principal significance has the estimation of progressive and regressive branches of evolution. For the first the increasing of features divergency is typical whereas for the later the increasing of of features convergency is typical. The evolution classification unites together the paragenesis rows and branches of the magmatic rocks as well as their hydrothermal varieties (veins, metasomatites and ores). In this relation the classification proposed represents the natural classification of the mineral species.

GEOTHERMOBAROMETRY OF MANTLE PERIDOTITES FROM CAPE VERDE ISLANDS

I.D.Ryabchikov, L.N.Kogarko, T.Ntaflos, G.Kurat
Institute for Geology of Ore Deposits, Moscow; Vernadsky Institute of Geochemistry, Moscow; University of Vienna; Museum of Natural History, Vienna.

Mantle nodules from Sal Island are mainly represented by harzburgites and low-calcium lherzolites belonging to spinel peridotite facies. They contain interstitial glass with the included microphenocrysts of Cpx, Ol, Cr-rich spinel and sulphide globules with the associated Ni-Fe metallic alloys. There are two varieties of glass: silica-rich with low concentrations of Mg, Fe, Ca and high contents of K and Na and Mg-rich variety with low alkali contents. Two pyroxene geothermometers and Ca-in-olivine geobarometer (Brey, Kohler, 1990) yield high temperatures and relatively high pressures - up to 1300 C at 30 kbar, while harzburgites are characterized by lower temperatures (800-1100 C). Oxygen fugacities estimated from the compositions of primary spinels lie near Ni-NiO buffer, whereas secondary spinels (microphenocrysts in glass and recrystallized rims of primary crystals reacted with melt) show very reduced conditions appreciably lower than QFM which is consistent with the presence of metallic phases included in glass. Geothermobarometry of Cape Verde peridotites reveals zoning in lithosphere composition (more depleted harzburgites above less

depleted low-Ca lherzolites) consistent with the model of residual mantle column (Plank, Langmuir, 1992) produced by partial melting of ascending diapir. Low redox potential exhibited by minerals included in interstitial glass is possibly due to the desulphurization reactions triggered by sharp decrease in pressure during the eruption of magma with entrained peridotitic xenoliths.

References:

1. Brey G.P., Kohler T. 1990. *Geochim. Cosmochim. Acta*, vol. 31, p. 1353

2. Plank T., Langmuir C.H., 1992. *Journ. geophys. Res.*, , vol. 97, p.19749.

THERMODYNAMIC MODEL OF SOLID DISSOLUTION IN AQUEOUS FLUIDS.

RYZHENKO B.N. (Vernadsky Institute of geochemistry and analytical chemisty, Moscow, Russia).

According to thermodynamics the rate of solid dissolution depends on chemical component activity difference (in solid and surface solution layer), not on the current total concentration of solute. A strict definition of "chemical component" activity should be related to certain species of chemical element in the solution. All other species transform to choosen one due to complexing reactions which are usually fast running in aqueous solutions.

As a resalt we have an expression for any element concentration of solid-aqueous solution system.

$$1.\quad m_t = \alpha \beta_t (1-\varphi_t) + m_{ini}\varphi_t$$

$$2.\quad \varphi_t = \exp\left(-\frac{k\mathcal{D}t}{\beta_t\mathcal{D}-k}\right) \quad . \quad k = \frac{k^\circ S}{V} \quad . \quad \mathcal{D} = \frac{\mathcal{D}^\circ S}{Vd}$$

where m_t - total concentration of the element at moment t;

m_{ini} - initial concentration of the element;

α - saturation activity of the species choosen as a chemical component of the element;

β - complexing coefficient of the element which is equal to the ratio of total concentration of the element/activity of its species choosen as a chemical component in the surface aqueous solution at time t;

k° - rate constant of solid/aqueous solution reaction (average value for all elements of the solid);

$\mathcal{D}^\circ$ - diffusion coefficient of the aqueous species of the element (average value for all aqueous species of the element);

S - contact square of solid/aqueous solution;

V - volume of the aqueous solution of the system (if molality, so it is the volume of 1 kg of water);

d - linear diffusion distance of the surface aqueous layer.

The model explanes
(1) The pH - dependence of dissolution rate
(2) The temperature -dependence of dissolution rate
(3) The effect of aqueous solution mineralization on the dissolution rate
(4) The relation of solubility and dissolution rate.

It was shown that several weeks are enough to get saturation of congruently solids at ordinary experimental mixing or natural rock porosity. For incongruently soluble solid it demands several times more.

APPLICATION OF POSITRON ANNIHILATION SPECTROSCOPY TO MINERALS

Sachanbiński M. (*Inst. of Geological Sciences, Univ. of Wrocław*) and Chojcan J. (*Inst. of Experimental Physics, Univ. of Wrocław*)

Positron annihilation spectroscopy (PAS) uses positrons and positronium atoms (Ps - the positron-electron bound state) as probes for the research of matter in different states. The characteristic feature of the probes is their strong tendency to become localized in low-electron-density sites of condensed matter. This makes PAS a suitable tool to the exploration of the electron density "holes" which are related to structural elements and/or defects in crystals or atomic-scale pores in amorphous materials for example. The holes "seen" by the Ps atoms have a size ranging from 0.1 to 3 nm and they can be studied even in complex materials as information on the holes are usually easily extracted from the proper positron annihilation data.

Till now we have applied PAS to cryptocrystalline variety of quartz as well as to opal, tektite (Chojcan & Sachanbiński, 1993a), mica, gadolinite-(Y), feldspar, calcite, flogopite, obsidian and amber (Chojcan & Sachanbiński, 1993b). We used measuring apparatus of standard design made in Institute of Experimental Physics of Wrocław University i.e. spectrometers for measurements of positron annihilation lifetime spectra as well as one-dimensional angular correlations of positron annihilation radiation. The collected data show that some minerals from the cryptocrystalline variety of quartz as well as tektites, opals, obsidians and ambers contain different empty pores with sizes of the order of 1 nm which trap the Ps atoms before their decay. The largest pores are observed for the examined samples of ordinary opal and agate (about 3 nm in diameter) whereas the smallest pores are detected in the investigated specimens of tektite (less than 1 nm in diameter). Simultaneously the estimated concentration of the pores in tektites (0.12 nm^{-3}) is more than ten times greater than in ordinary opals and agates. In the case of other minerals studied i.e. calcite, feldspar, mica, gadolinite-(Y) and flogopite the positron annihilation spectroscopy does not reveal any nanopores.

From the results obtained it follows that positron annihilation spectroscopy can successfully contribute to a knowledge on microstructure of minerals especially those where positronium atoms are formed. The utilization of PAS in mineralogy seems to be promising and in the nearest future this technique should join the set of traditional spectroscopies using by mineralogists.

References:

Chojcan, J. & Sachanbiński, M. (1993a). *Acta Phys. Polon. A*, **83**, 267-271.

Chojcan, J. & Sachanbiński, M. (1993b). *in* "Proc. of XXVIII Zakopane School of Physics on Condensed Matter Studies by Nuclear Methods", E.A. Görlich and K. Tomala eds., Jagiellonian Univ. & Inst. of Nucl. Phys., Cracow, 296-298.

ACTIVITY-COMPOSITION AND PHASE RELATIONS IN QUADRILATERAL AND NATURAL PYROXENES

Sack R.O. (*Dept. Earth-Atmosph. Sci., Purdue Univ., USA*), and Ghiorso M.S. (*Dept. Geolog. Sci., Univ. Washington, USA*)

We have developed a model for the thermodynamic properties of clino– and orthopyroxenes in the composition space defined by $CaMgSi_2O_6$ and the exchange vectors $Fe(Mg)_{-1}$, $TiAl_2(MgSi_2)_{-1}$, $Fe^{3+}(Al)_{-1}$, $Fe^{3+}Al(MgSi)_{-1}$, $Mg(Ca)_{-1}$, and $NaAl(CaMg)_{-1}$. The model is formulated assuming (1) molecular type mixing for the coupled exchange substitutions $TiAl_2 \Leftrightarrow MgSi_2$, $Fe^{3+}Al \Leftrightarrow MgSi$, $Al_2 \Leftrightarrow MgSi$, and $NaAl \Leftrightarrow CaMg$ (and their ferroan equivalents) and that (2) Fe^{2+} and Mg^{2+}, and Al^{3+} and Fe^{3+} display long–range non–convergent ordering between M2 and octahedral M1 sites, and octahedral M1 and tetrahedral sites, respectively. The molar vibrational Gibbs energy is described by a Taylor expansion of second degree in seven linearly independent composition and ordering variables, which is extended to third degree to account for asymmetry in the mixing of Ca and Mg, and Ca and Fe on the M2 site, and is further modified for the assumption that the standard state properties of Ca end–member components of clinopyroxenes are linearly dependent on the coordination number of Ca^{2+} on the M2 site.

The model for the quadrilateral ($Mg_2Si_2O_6$–$CaMgSi_2O_6$–$CaFeSi_2O_6$–$Fe_2Si_2O_6$) subsystem successfully accounts for (1) Fe–Mg partitioning relations between orthopyroxenes, pigeonites, and augites, (2) calorimetric data for $CaMgSi_2O_6$–$Mg_2Si_2O_6$ pyroxenes, and (3) the T–P–X systematics of both the reaction pigeonite = orthopyroxene + augite, and miscibility gap features, over the temperature and pressure ranges 800–1500°C and 0–30 kbar. The calibration is achieved with the simplifying assumption that all regular–solution–type parameters are *constants* independent of temperature. It is predicated on the assumptions that (1) the Ca-Mg substitution is more nonideal in Pbca pyroxenes than in C2/c pyroxenes, and that (2) entropies of about 3 and 6.5 J/K–mol are associated with the change of Ca from 6– to 8–fold coordination in the M2 site in magnesian and iron clinopyroxenes, respectively. The model predicts that Fe^{2+}–Mg^{2+}, M1–M2 site preferences in C2/c pyroxenes are highly dependent on Ca and Mg contents, and that the pigeonite stability field extends to pressures as high as 40.3 kbars. The proposed model is internally consistent with our previous analyses of the solution properties of spinels, rhombohedral oxides, and Fe–Mg olivines and orthopyroxenes (Sack & Ghiorso, 1989, 1991a, b; Ghiorso, 1990a; Ghiorso & Sack, 1991).

Our calibration of the extension of the model to Ti–, Al–, Fe^{3+}–, and Na–substituted pyroxenes has been accomplished utilizing (1) constraints on miscibility gaps in $CaMgSi_2O_6$–$CaMg_{1/2}Ti_{1/2}AlSiO_6$–$CaAl_2SiO_6$ pyroxenes, (2) constraints on long–range Fe^{3+}–Al^{3+} ordering in $CaFeAlSiO_6$–rich pyroxenes, (3) constraints on the Al–contents of orthopyroxenes coexisting with forsterite and spinel in the MAS subsystem, (4) energetic inequalities imposed by pyroxene absences within accessible composition space, (5) composition data on coexisting pyroxenes and liquids derived from published experimental studies ($IW \leq f_{O_2} \leq NNO$) and those reported here (f_{O_2} = 0.21 bar), and (6) chemical potentials of endmembers and exchange components in liquids defined by the thermodynamic melt model of Ghiorso & Sack (1994). Model parameters have been extracted by regression, imposing bounds on parameters dictated by size mismatch considerations, considerations of homogeneous equilibria, and by analogy with oxide structures. The resulting calibration, incorporated in the MELTS software package (Ghiorso & Sack, 1994), successfully predicts experimentally determined liquidus compositions, temperatures, and symmetry states for pyroxenes crystallizing from a variety of silicate melts, ranging from basalts through rhyolites to potash ankaratrites.

References:

Ghiorso, M.S. (1990) *Contrib. Min. Petrol.*, **104**, 644-667.
Ghiorso, M.S. & Sack, R.O. (1991) *Contrib. Min. Petrol.*, **108**, 485-510.
Ghiorso, M.S. & Sack, R.O. (1994) *Contrib. Min. Petrol.*, submitted.
Sack, R.O.& Ghiorso, M.S. (1989) *Contrib. Min. Petrol.*, **104**, 42-68.
Sack, R.O.& Ghiorso, M.S. (1991a) *Contrib. Min. Petrol.*, **106**, 474-505; **107**, 415.
Sack, R.O.& Ghiorso, M.S. (1991b) *Am. Min.*, **76**, 827-847.

AN ATTEMPT TO DETERMINE THE METAMORPHIC GRADE OF LOW-T METAMAGMATIC SUITES USING CHLORITE "CRYSTALLINITY"

Sadek Ghabrial D. and Árkai P. *(Laboratory for Geochemical Research, Hungarian Academy of Sciences, Budapest)*

Chlorite "crystallinity", i.e., the half-height width of the first and second XRD basal reflections of chlorite abbreviated as ChC(001) and ChC(002), proved to be a useful metamorphic grade indicator in metapelitic and -silty rocks.

In the present study ChC and other properties of chlorite and its precursor phases from metapelitic rocks are compared to those of associated magmatic suites of the Bükkium, innermost Western Carpathians, Hungary.The magmatic suites are represented by Jurassic ophiolitic basic-ultrabasic sequence that contains differentiated plagiogranite bodies and Triassic basaltic and andesitic lava and pyroclastic rocks. As it was determined earlier by complex (mineral paragenetic, illite "crystallinity" and coal rank) studies, the grade of the Alpine (Cretaceous) regional transformation in the investigated Mesozoic formations varies from the deep or late diagenetic zone (Darnó Hill, southwestern Bükk Mts.), through the diagenetic/anchizone boundary (Szarvaskő area, western Bükk Mts.) up to the high-T anchizone and epizone (Lillafüred area, eastern Bükk Mts.).

The changes of ChC(001) and ChC(002) averages determined on whole rock samples and <2 μm grain size fractions of metamagmatic rocks using air-dried and ethylene glycol-solvated preparations correlate fairly well with the differences in metamorphic grade determined on the basis of indicative Ca-Al-silicate mineral assemblages of the metamagmatic rocks and of the illite "crystallinity" data of the surrounding metasediments. Systematic, significant ChC differences were obtained between the intrusive (gabbroic, subordinately granitic), the hypabissal (diabase) and the volcanic (pillow basalt) members in the ophiolitic suite of the Szarvaskő area. Considering also the inferred steep geothermal gradient, these differences refer to an ocean-floor (hydrothermal) metamorphic event which preceded the Cretaceous regional (dynamothermal) overprint.

COMPLEMENTARITY BETWEEN MONOELECTRONIC AND MULTIELECTRONIC APPROACHES IN XAFS CALCULATIONS

Sainctavit Ph and Arrio M.A. (*Laboratoire de Minéralogie - Cristallographie, CNRS URA9, Universités Paris VI et VII, IPGP - FRANCE*)

Various recent techniques of XAFS simulations have been developped that allow to extract valuable information from X-ray Absorption Fine Structures. The information can be either related to the knowledge of the local organisation around the absorbing atom or related to the precise determination of the electronic ground state properties of the absorbing atom. Two approaches are available : monoelectronic or multielectronic calculations. The combination of the two methods allows to calculate K, L and M edges of almost any atom in the periodic table.

Multiple scattering calculations are monoelectronic calculations that suit well to K edges of almost any atom (Z>4) and $L_{2,3}$ edges of heavy atoms (Z>50). These edges correspond to transitions towards states that are far from being pure atomic states since they are much hybridized with the neighbouring atoms. In multiple scattering calculations both initial and final

states are monoelectronic wave functions and the final state is constructed from the superposition of an atomic state with the contributions from all the neighbouring atoms. In the method, covalency is treated explicitly although electronic correlations are not : much information can be gained about middle range organisation and covalency.

A multielectronic technique as the ligand field multiplet approach developped by B.T.Thole is well suited to the simulation of edges where the photoelectron orbital in the final state undergoes strong correlations. This is the case of $L_{2,3}$ edges of transition metals and $M_{4,5}$ edges of lanthanides and actinides. For these edges, the photoelectron orbital in the final state is mainly atomic with slight perturbations from the neighbours. It is then essential to treat exactly the correlations between the electrons in the open shells and between the opens shells (the photoelectron orbital and the core orbital in the final state). The influence of the neighbouring atoms is mainly treated by crystal field parameters that are determined by other spectroscopies (UV-visible spectroscopy). When covalency has to be introduced it is developped in the framework of Configuration Interaction where parameters injected in the calculation have to be extracted from UPS or XPS.

We shall present the application of the two theoretical techniques for compounds where it is hard to distinguish between crystallographic and electronic information. The first case is related to the spin transition compound $Fe^{II}(Phen)_2(NCS)_2$. Fe^{II} ion is bounded in octahedral symmetry to six nitrogen atoms. When the temperature is below 90K Fe^{II} (S=0) is in the low-spin state and when the temperature is above 90K Fe^{II} is in the high spin state (S=2). By comparing experiments and calculations for the two spin states at K edges (multiple scattering caluclation) and $L_{2,3}$ edges (multiplet calculations) it is possible to separate electronic changes from crystallographic changes that occur during the transition. We shall also present additional results concerning X-ray Magnetic Circular Dichroism on oxyspinels and sulphospinels at $L_{2,3}$ edges of transition metals. We show that covalency can be large and that a model where hybridization and correlations are treated is to be introduced in order to understand the spectra.

HIGH-TEMPERATURE CRYSTAL STRUCTURE OF FELDSPAR: I. SANIDINE.

Saito, S.*, Shimizu, M.** and Kimata, M.**, (*Inst. of Mat. Sci.* & Geosci.**, Univ. of Tsukuba*)

The design of a newly revised radiative air-cooled crystal heater (Kimata et al., 1991) is described below, based on an electric resistance principle. The method presently used involves the air-cooled prop for a resistance heater and an external shield of heat-resistant plastic film (Kapton) air-cooled. The requirement of stability for the duration of experiment could be fullfiled in the PID action for temperature variation accompanied by the change of diffractometer angle chi; elimination of 'chimney effect'. This resistance heater can be mounted on a Rigaku AFC diffractometer.

Sanidine, $KAlSi_3O_8$, is one of typical silicate minerals crystallizing at high temperatures. The sanidine from the Eifel (Volkesfeld), Germany, is of $Or_{82}Ab_{18}$ composition. Crystal data for the present sample at 900 ^{o}C are space group C2/m, a = 8.627(3), b = 12.966(4), c = 7.155(2) A, β = 115.70(2) ^{o}, V_{cell} = 721.4(2) A^3, whereas those at 23 ^{o}C are C2/m, a = 8.537(2), b = 13.014(2), c = 7.181(2) A, β = 115.99(1) ^{o}, V_{cell} = 717.0(3) A^3. The former and the latter structures were refined to R = 0.056 and 0.047 for the 729 and 807 observations with $F>3\sigma F$, respectively. Thermal expansion of the present sanidine up to 900 ^{o}C is caused by expanded <M-O> bond length and larger T(2)-OA2-T(2) angle. The view (Smith & Brown, 1988) that the T-A2-T angle in alkali feldspars is controlled mainly by crumpling around the M atom is strongly confirmed by observation of the present thermal behavior of sanidine geometry. Of great interest is an apparent shrinkage of the T-O distances at 900 ^{o}C, which may be merely the result of the swinging-arm effect from increased thermal vibrations (Ohashi & Finger, 1974 & 1975).

Table 1. Bond distances and T-O-T angles in sanidine.

	23 ^{o}C	900 ^{o}C
<M-O> A	2.935(4)	3.013(6)
<T1-O>A	1.655(3)	1.640(4)
<T2-O>A	1.646(3)	1.626(4)
T-OA2-T^{o}	135.4(3)	141.7(3)

References

Kimata, M., Shimizu, M., Saito, S. (1991). Trans. Amer. Cryst. Assoc., 27, 301-308.

Smith, J. V. & Brown, W. L. (1988). Springer-Verlag, 67p.

Ohashi, Y. & Finger, L. W. (1974). Carnegie Inst. Washington Yearbook, 72, 539-544.

Ohashi, Y. & Finger, L. W. (1975). Carnegie Inst. Washington Yearbook, 73, 569-572.

CRYSTALLIZATION FEATURES OF GOLD THIN PHASES IN QUARTZ

Sakharova M.S., Ryakhovskaya S.K. and Turchkova A.G.
(Dept. of Geology, Univ. of Moscow)

Thin and ultrathin phases of gold are wide spread in natural gold-quartz associations but the nature of these formations is not enough studied. The process of gold precipitation on natural and synthetic quartz in hydrothermal systems (100-200^{o}C) is experimentally investigated and the features of morphology and crystallites distribution are considered in this paper. It is established that thin and ultrathin gold particles (from 0.1 to 30 microns) are the faceted crystals during the first stage of the process. Germ centres are located on dislocations outputs as energetically favorable places or they form epitaxial accretions with quartz. The differences of gold accumulations on the different quartz facets are revealed: maximal one is on pinacoid and minimal one is on the prism facets.

The influence of quartz metamorphism features on the gold crystallization is studied. The proportionality is obtained between gold precipitation and the deformation degree of quartz during gold precipitation on synthetic quartz which was undergone of mechanical deformations (loading from 0.9 to 4.8 thousand bars/cm^2) analytically and by the calculation method of dislocation density and density of germ centres. The gold crystallites distribution on the surface has the local point character under small loadings and coinsides with the dislocations outputs. Gold crystal-

lites are located along boundaries of blocks and quartz grains when the pressure increases. First they form interrupted chains and then do continuous aggregates and linear zones.

The influence of hydrothermal quartz metamorphism is revealed (etching by Na_2CO_3 with concentration from 1.0% to 2.5%). The intensification of gold precipitation process occurs when the degree of quartz etching increases. Crystallization centres are edges of sharp faceted negative etching figures of quartz. Morphology complication of precipitated gold in the course of time is connected with the twin appearence and next germ crystallites increasing.

The data obtained allow to reveal the reasons of thin gold particles rise in quartz associations and quartz metamorphism significance in the gold accumulation.

ATOMIC ORDERING IN MINERALS: KINETIC PROCESSES

SALJE E.K.H. (*Dept. of Earth Sciences, Univ. of Cambridge*)

Ordering processes in minerals, such as Al,Si ordering in feldspars, requires changes of site-occupancies but not long-distance diffusion. The driving force of cation ordering is identified as the excess Gibbs free energy of the equivalent thermodynamically stable states. The resulting rate laws are discussed and compared with experimental observations. Different rate equations based on Landau-Ginzburg, Glauber and Kawasaki theories are compared, it is shown that Al,Si ordering in anorthite follows the predictions of a Landau-Ginzburg approach but not a simple Ising type behaviour.

Local correlations between kinetic events in cation/vacancy ordering in framework structures lead to "partial conservation" of the order parameter (Salje, 1993). Mixing non-conserved and conserved kinetic processes leads to a bifurcation behaviour with uniform states for mainly non-conserved order parameter and periodic pattern formation if more than 1 out of 12 steps is conserved. Possible correlations with experimental observations are discussed.

References:
Salje, E.K.H. (1993). *J. Physics: Condensed Matter.*, **5**, 4775-4784.

ENERGETICS OF DEFECT STRUCTURES: SOME CONCEPTS AND RESULTS

Salje E.K.H. (*Dept. of Earth Sciences, Cambridge University, Downing Street, Cambridge CB2 3EQ, UK*)

The influence of defects on the thermodynamic stability of minerals is best observed under conditions close to the transition point to another mineral phase. The experimental results show that defects can (de)stabilise a mineral phase under equilibrium conditions and greatly reduce the kinetics of the transition between two phases with localized point defects being less important than extended defects (such extended defects include the deformation clouds around point defects, line defects and planar defects).

The upper temperature bound for the stability of a mineral is changed in a non-linear fashion when the defect density is increased (the plateau effect). In case of small defects concentrations, isolated defects have a weak influence on the stability, whereas high defect densities generate continuous defect fields. These fields couple quadratically with the relevant configuration coordinates which leads to a strong renormalization of the transition temperature.

A novel approach for the description of planar defects and surfaces structures is reported.

OCELLAR, MICROGRAPHIC, AND RAPAKIVI TEXTURES IN RAPAKIVI GRANITES OF SOUTHEASTERN FINLAND

Salonsaari P.T. and Lintala J.M. *(Dept. of Geology, Univ. of Helsinki, Finland)*

Three common textures occur in hybrid rocks and magmatic mafic enclaves (MME) of the bimodal Jaala-Iitti complex, SE Finland: 1) quartz with amphibole ±augite rim (ocellar texture), 2) alkali feldspar megacrysts with plagioclase-quartz intergrowth (micrographic texture), and 3) alkali feldspar megacrysts rimmed by plagioclase ±quartz ±amphibole (rapakivi texture). Two sources for quartz and alkali feldspar megacrysts are proposed. First, they are transferred during hybridization from the partially crystallized rapakivi granite magma (felsic end-member) to the hybrid magma and especially to the MME magma. Second, megacrysts are derived from the disaggregated (rapakivi) granite xenoliths.

Occurrence of mantled textures in hybrid rocks indicates thermal disequilibrium between the xenocrysts and the host magma. After disaggregation of the xenoliths and partial melting of the megacrysts, plagioclase with quartz and/or amphibole are crystallized forming mantled xenocrysts. Alkali feldspar megacrysts also show exsolved albite and formation of concave quartz at the margin of the alkali feldspar.

Coeval occurrence of rapakivi granite batholiths and diabase dykes indicates bimodal magmatic association. However, in the rapakivi granites of the Wiborg batholith, SE Finland, indications of large scale hybridization or xenolith assimilation are rare; the Jaala-Iitti complex is a local exception. Mafic magma may form layers below larger rapakivi granite batholiths. These layers may act as a heat source for partially crystallized rapakivi granite magma producing partially melted alkali feldspar megacrysts and common micrographic alkali feldspar-quartz intergrowth. Cooling of the reheated magma causes growth of plagioclase mantles around the corroded alkali feldspar crystals in changed physicochemical conditions.

NOMENCLATURE OF MINERAL SPECIES OF Cu-Ag ISOMORPHOUS TETRAHEDRITE

Samusikov V.P., . Gamyanin G.N. (Yakut Inst. of Geol.Sciences, Russian Acad. of Sciences, Russia)

Broad variations in the Ag content in tetraedrite resulted in the appearance of disordered names of mineral species in this isomorphous series. Any name mentioned in scientific literature has no definite Ag content boundaries. It also concerns to the most used term "freibergite" Ag concentrations in which are interpreted variously. Certain difficulties in practical activities are accounted for absence in common nomenclature of mineral species of , Cu-Ag tetrahedrite series.

Riley (1974) showed that the cell parameter (a_o) of tetrahedrite varies with Ag concentrations; up to 22% Ag — a_o increases (10.386-10.59 Å) and over 22% Ag-a_o decreases (10.59-10.47 Å). He suggested to name the specimens with a reverse a_o — Ag dependence as "freibergites" (see Figure). On the other hand, the data on synthetic specimens of high-argentian tetrahedrite (Pattrick & Hall, 1983) as well as on individual analyses of their natural counterparts (Hilin & Guanxin, 1990) suggest a direct a_o—Ag dependence in this isomorphous series, when Ag concentrations are observed to be over 22%. The problem of designation of these specimens has not solved yet.

We have analyzed and compared specimens from three groups: 1) up to 22% Ag; 2) over 22% Ag, with a direct a_o—Ag dependence; 3) over 22% Ag, with a reverse a_o -Ag dependence. As to the third group specimens, a decrease in sulphur contents is established to be the reason for dimishing a_o. When Ag accounts for 36-38%, the sulphur deficiency is about one atom on a formula basis (a_o — 10.49-10.47 Å).

In specimens from the first and second groups the sulphur content is theoretical, i.e. 13 atoms, at any Ag content. This is a common isomorphous series of Cu-Ag substitution in tetrahedrite. In one of the

Ag pollymetallic Yakutian deposits we have discovered and studied the end argentic member of the series (Ag-52%, Cu-0.7%; a_o-10.90 A). It differs from freibergite (Riley, 1974) by ao parameter and sulphur contents, being the argentic counterpart of tetrahedrite. In accordance with the requirements of New Mineral International Commission, we suggest to consider this mineral species as independent and to name it "tarynite" (for the locality). Based on the above, we suggest a nomenclature of mineral species of Cu-Ag tetrahedrite series (see Figure).

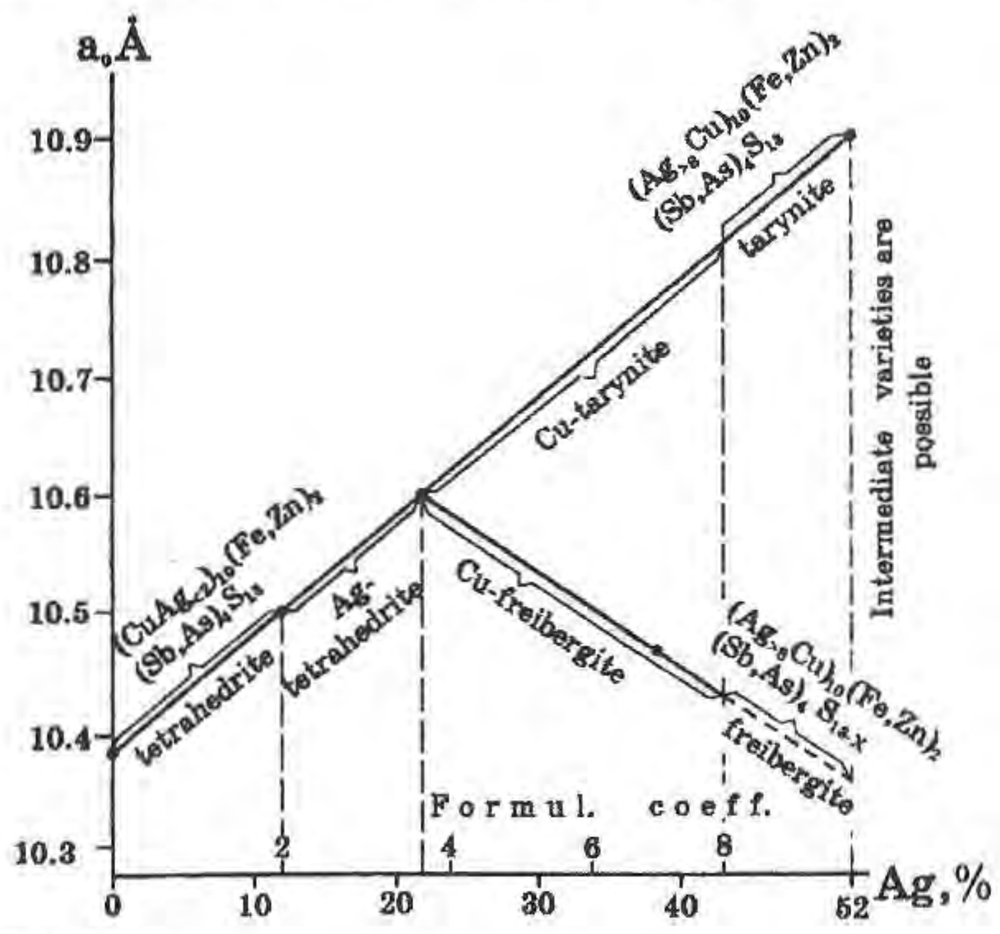

References.
Hilin,L. & Guanxin,W.(1990). Acta Miner . Sin., 2,119-126.
Pattrick,R.A. & Hall, A.J. (1983). Miner.Mag., 47,441-451.
Riley,J.F. (1974). Mineral Deposita,.9-2, 117-124.

"TURBIDITY" IN ALKALI FELDSPARS FROM GRANITIC PEGMATITES

Sanchez L. (*MNCN-CSIC Madrid, present adress: CRSCM-CNRS Orleans*), Sobrados I. (*Inst. Cien. Materiales CSIC Madrid*), Menendez E. (*Inst. Cien. Const. Eduardo Torroja CSIC Madrid*), Rouer O. (*CRSCM-CNRS Orleans*), Sanz J. (*Inst. Cien. Materiales CSIC Madrid*), and Garcia-Guinea J. (*MNCN-CSIC Madrid*).

Alkali feldspars from pegmatites of Brasil and Spain have microscopic to submicroscopic inclusions giving a "turbid" and "clouded" appearence. Inclusions are isotropic, irregular and spatially associated with patch/vein lamellae in network and/or isolated masses. Inclusions have no detectable lines in XRD and microprobe analyses show strong varibility: SiO_2 40-46 wt%, Al_2O_3 30-40 wt%, K_2O up to 5 wt%, Na_2O up to 0.5 wt%, FeO up to 2.5 wt%, MgO up to 1.3 wt%, CaO up to 0.4 wt%, P_2O_5 up to 0.35 wt%, F up to 2000 ppm, Cl up to 5500 ppm. Dark coronas around them are richer in Cl, Fe, Mg. Thermal analysis up to 600 °C shows a TG curve with multiple steps of water loss up to 11 wt%. An homogeneous matrix with a clot appearance is observed in transmission electron microscopy containing crystals inside. Electron diffraction patterns show an amorphous nature. ^{29}Si-MAS-NMR spectra show one or two broad lines at approximately -87 and -91.6 ppm from Si in the Q^3 environment. ^{27}Al-MAS-NMR spectra show one or two broad lines at approximately -70 and -3 ppm due to Al in IV and VI coordination.

Inclusions with a "turbid" appearance are kaolin-like amorphous materials. They may be interpretated as a product of the interation of early rock with Cl-rich aqueous fluids from the late tranformation stage in the pegmatitic process. This interation is associated with Na-feldpar patch/vein-lemellae formation of perthites.

Plagioclase zoning in lavas from Filicudi island, Aeolian arc, Southern Tyrrhenian Sea, Italy: a Nomarski Differential Interference Contrast study.

Santo A.P. (*Dip. di Scienze della Terra, Firenze, Italy*), Clark A.H. (*Dept. of Geological Sciences, Queen's University, Kingston, Canada*) and Manetti P. (*Dip. di Scienze della Terra, Firenze, Italy*)

Reflected-light Nomarski Differential Interference Contrast (NDIC) microscopy provides exceptional resolution of the zoning and, thereby, growth history of individuals grains of plagioclase through the imaging of microtopographic relief produced by the dissolution of more calcic zones by concentrated fluoboric acid. This technique has been applied to representative lavas of the Filicudi island volcanic centre of the Aeolian arc.

Five main eruptive centres with complicated geometrical relationships are exposed on Filicudi. The rocks constitute a calc-alkaline suite, ranging from basalt through basaltic andesite, to high-K andesite. Plagioclase, the major phenocrystic phase, forms euhedral-to-subhedral grains with normal, oscillatory and reverse zoning, and a wide overall compositional range (An_{50-90}). Petrogenetic modelling implies the involvement of fractional crystallization, the mixing of basic with more evolved magmas, and crustal contamination. NDIC microscopy clarifies the mode of interaction of these processes through the definition of complex internal features in plagioclase not observable in transmitted light.

The plagioclase is characterized by alternations of euhedral zones with oscillatory zoning, and patchy or sieve-textured domains. Internally, the patchy zones are either very finely-textured or coarser and chaotic. Dissolution surfaces are very commonly developed. Whereas all plagioclase phenocrysts display complex growth histories, those in basaltic and basaltic-andesite members are more complicated than those in high-K andesites.

THE PARAGONITE-MUSCOVITE SOLVUS: NEW RESULTS

Sassi F.P. (*Dept. Min. Petr., Univ. of Padova, Italy*), Guidotti C.V. (*Dept. Geol. Sci., Univ. of Maine, Orono, USA*), Blencoe J.G. (*Chem. Div. Oak Ridge Nat. Lab., Oak Ridge, USA*) Sassi R. (*Dept. Min. Petr., Univ. of Padova, Italy*) and Selverstone J. (*Dept. Geol. Sci., Univ. of Colorado, Boulder, USA*)

The nature of the Pg-Ms solvus and its geothermometric potential have been discussed in numerous previous papers, but field, experimental and thermodynamic investigations of Pg-Ms solvus pairs have yielded conflicting results. For example, graphical and calculated Pg-Ms solvi based on experimental data for synthetic, binary Pg-Ms micas are inconsistent with solvus data for natural, quasibinary Pg-Ms micas. To resolve these and other discrepancies among the various types of solvus data for Pg-Ms micas, we have conducted a series of investigations to determine how Pg-Ms solvus relations are affected by P, T and the phengite content of muscovite.

Na-K and geothermometric data for 28 natural, quasibinary Pg-Ms pairs were analyzed in detail in an effort to determine precisely the P-T-X limits of the binary solvus. The data are rather scattered, making it impossible to ascertain the effects of P on solvus relations, but the

T-X morphology of the solvus is clearly discernible. Thus, the data were used to develop parametric (non-thermodynamic) equations for an "average" binary solvus. Consistent with previous results, the new solvus is strongly asymmetric toward paragonite, and the Pg limb is steeper than the Ms limb. However, calculated solvus critical constants (critical T = 796°C, critical X = 34 mole % Ms) deviate significantly from corresponding values obtained from thermodynamic models developed by previous investigators.

Our parametric equations for an "average" binary solvus yield three geothermometric formulations that can be used to calculate equilibration temperatures for natural, quasibinary Pg-Ms pairs. The first two expressions are "paragonite-based" and "muscovite-based", respectively. The third one is "closure-based", because it yields equilibration temperatures that vary with the degree of solvus closure:

$$T = 796.5 + 415.47 ln\left[1 - \left(X_{ms}^{Ms(Pg)} - X_{ms}^{Pg(Ms)}\right)^2\right].$$

Comparison of the temperatures calculated from the three geothermometers yields information on the mutual consistencies of the Na-K compositions of coexisting Pg and Ms with respect to their utility in Pg-Ms thermometry.

Appropriately selected chemical data for 139 natural Pg-Ms pairs indicate the effects of Fe and Mg on the P-T-X topology of the Pg-Ms solvus. With increasing P, the Ms limb shifts markedly toward end-member Ms, whereas the Pg limb shifts only slightly toward end-member Pg. P-induced broadening of the solvus reflects increasingly nonideal Na-K mixing as the phengite content of muscovite increases.

Due to (1) the effects of P and T on the stability relations of Pg-Ms pairs, and (2) the wide scatter of the data for Pg-phengitic Ms pairs, practical applications of Pg-Ms solvus geothermometry are restricted to quasibinary Pg-Ms pairs that equilibrated at pressures between approximately 2 and 8 Kbar. Within this pressure range, the utility of Pg-Ms solvus thermometry is limited thermally to approximately 300-700°C by the decomposition of K-saturated paragonite at temperatures between approximately 580 and 700°C, and by steepening of the solvus limbs at temperatures below 300°C.

References

Blencoe J.G., Guidotti C.V. & Sassi F.P. (1994). *Geoch. Cosmoch. Acta* (in press).

Guidotti C.V., Sassi F.P., Blencoe J.G. & Selverstone J. (1994). *Geoch. Cosmoch. Acta* (in press).

Guidotti C.V., Sassi F.P., Sassi R. & Blencoe J.G. (1994). *J. Metam. Geol.* (in press).

ASCENT RATE OF ULTRADEEP (> 300 KM) ULTRAMAFIC SAMPLE : CONSEQUENCE FOR DEPTH OF KIMBERLITE MAGMA GENERATION

Sautter V. *(C.N.R.S., Université Paris 11, Orsay)* and Doukhan N. *(Université des sciences et techniques de Lille)*.

Ultramafic xenoliths of ultradeep origin (> 300 km) have been recognized in Jagersfontein kimberlite pipe (Haggerty & Sautter 1990, Sautter *et al.* 1991). These specimen (less than 3 cm in diameter) are characterized by garnet crystals showing pyroxene exsolution lamellae along {111} planes of the host. Reconstitution of pyroxene in garnet give high Si garnets stable at pressure in exces of 130kb placing xenoliths origin at or close to the 400 km seismic discontinuity. Thermodynamical constrains allow to define the following evolution of such deep samples: (1) transport from the transition zone (130 kb - 1400°C) to the base of the lithosphere (45 kb - 950°C) inducing pyroxene exsolution in garnet (2) capture by cretaceous kimberlite of Jagersfontein and transport to the surface.

The question of depth of kimberlite magma generation have been reassessed from these samples and syngenetic majorite inclusions in diamonds. According to Ringwood *et al* 1992, kimberlites result from partial melt in the transition zone thus transport directly ultradeep xenoliths and xenocrystal of diamonds with their high pressure inclusion to the surface. Pyroxene exsolutions from garnet provide a basis for evaluation of transport mechanism from 400 to 150 km. Exsolution rate constants are unknown. However, in ultradeep sample JAG 92P2 pyroxene exsolutions are chemically zoned over 1000 nm (Doukhan et *al* 1994).: Si, Na, Ca decrease towards garnet host whereas Al, Fe, Mg increase. Such cross diffusion is consistent with pyroxene growth from "majorite". The chemical homogeneity of garnet host indicates that interdiffusion of Al and Si which occured exclusively in octahedral site is faster compared to pyroxene where redistribution of Al-Si involves both octahedral and tetrahedral sites. Exsolution reaction is thus controlled by interdiffusion of Al-Si in the growing pyroxene. Sluggishness of Al-Si diffusion in pyroxene (Sautter *et al.* 1988) and transformation kinetics deriving from parabolic law require at least one million year for reaction to go to completion. This precludes fast uprising in a kimberlite magma rooted in the transition zone. On another hand survival of diffusion gradients in samples that finally reequilibrate at 950°C 45 kb indicates that lithospheric residence, before ultimate transport to the surface, was short less than 28500 years.

We conclude that ultradeep samples first crystallized at depth in the convective asthenosphere, then were carried to the base of the lithosphere at slow ascent rate. This would be consistent with the ten to twenty millions years required for samples to be transported from 400 to 150 km in uprising part of a convective cell. Explosive kimberlite would be the ultimate transport agent through the lithosphere.

References :

Haggerty S.E. and Sautter V. (1990) *Science* , **248**, 993-996.
Sautter V, Haggerty S.E. and Field S (1991) *Science*, **252**, 827-830.
Ringwood A.E, Kesson S.E. Hibberson W. and Ware N. (1992) *E.P.S.L.* ,**113**, 521-538.
Doukhan J.C., Sautter V. and Doukhan N (1994) *P.E.P.I* ,in press.
Sautter V , Jaoul O. and Abel F. (1988) *E.P.S.L.*,**89**, 109-114

NEW RESULTS OF THE STUDY OF AMBER-LIKE FOSSIL RESINS (AFR)

Savkevich, S.S. *(Russian Mineralogical Soc., St. Petersburg)*

The study of the AFR in the last-time was caused by the necessity to develop the long time neglected scientific part of mineralogy - organic mineralogy.
Especially the interest of research was the revision of the minerals of the AFR, which were first described in the nineteenth century. The diagnostic characteristics were determined, which could be used for the systematic scientific registration of the samples of the old and new localities.

Because the structure of the AFR (highly polymerized organic structures) cannot be determined by conventional chemical or x-ray methods, some modern physical methods were used to determine some properties of the structure of the AFR. The IR-spectrometry turned out to be very useful, especially in combination with some other, mainly thermal methods.

By the revision of several AFR-localities in the former USSR we found out that in one locality at least two minerals of AFR occured. This was confirmed by the analysis of the minerals of other localities, e.g. Canada, Dominican Republic, Germany (Halle). On the other hand the same minerals, e.g. Succinite (the "real" amber), appear in other places like Netherlands, Great Britain, Ukrainia, Siberia or in the USA. For this reason names like "Dominican Amber", "Baltic Amber", "Romanian Amber" etc. are misleading. They do not define the mineral of AFR. Archaeometry should consider this fact if the origins of the minerals in the jewellery of an archaeologic discovery have to be determined.

Our investigations in the geological and geochemical history of the sediments (rocks), which contain these resins, and in different physical features of the AFR have demonstrated that the structure of AFR is unstable and can change with pressure, heat and/or oxidizing conditions, especially in early stages.This was confirmed by the transformation of the Succinite to Roumanite. Also sulfur can intrude in the high-polymerized lattices because of the permeability of the AFR for gases and liquids.

By different combinations of above mentioned physical and chemical conditions result in different minerals of the AFR and their continuous series (similar Ab-An, Garnets etc.).

GEOCHEMISTRY OF FLUID INCLUSIONS IN GRANITIC ROCKS IN JAPAN - A PRELIMINARY STUDY -

Sawaki T., Sasada M. and Sasaki M. (Geological Survey of Japan)

Several types of fluids are trapped in the granitic rocks of Cretaceous to Tertiary ages exposed in Japan. Fluid inclusions in the granitic rocks consists of (1) aqueous two-phase liquid-rich, (2) aqueous two-phase vapor-rich, (3) monophase liquid, (4) CO_2-bearing aqueous and (5) halite and/or other daughter mineral-bearing multiphase.

Monophase liquid inclusions may be formed by trapping low-temperature meteoric water, and the other 4 types of inclusions probably trapped fluids under cooling processes of the crystallized granitic magma, unless different hydrothermal episodes were super-imposed.

Halite-bearing fluid inclusions and vapor-rich inclusions are more frequently in Tertiary granitic rocks than in Cretaceous ones. They are also common in granitic rocks intruding contemporaneous volcanic rocks. That is, the shallower plutons have the more saline fluids in inclusions. Experimental data on NaCl-H_2O system and solidus of granitic rocks also shows that highly saline fluid in which halite is stable at room temperature are trapped in inclusions at shallower depths.

Preliminary gas analyses by a quadrupole mass spectrometer show relatively low gas contents of the inclusions in granitic rocks at the shallower depths. This suggests that the inclusions were probably formed by trapping degassed fluids separated from magmatic fluids.

THERMAL AND CHEMICAL STATE OF THE EARTH'S CORE

Saxena S. K. (*Inst of Earth Sciences, Uppsala University*)

Recent experimental data on the melting and phase transformations of iron and nickel to pressures as high as 200 GPa provide important information to understand the nature of the Earth's solid inner core and liquid outer core. Recently Boehler (1993) determined the melting temperature of iron in a diamond-anvil cell to a pressure of 200 GPa; these temperatures are lower than those found in shock-wave experiments. The existence of a new phase β with an unknown structure at high pressure was established in recent studies (Boehler, 1993; Saxena et al.1993).

Based on new experiments on the stability of the β phase and melting of iron to a pressure of 150 GPa (Saxena et al.,1994) an internally consistent thermodynamic data base is now available with which to model the iron phase diagram and the core energetics. This thermochemical and experimental data show that iron melts at the central core pressure of 363.85 GPa at 6350 $\pm$ 350 K and the central core temperature corresponding to the upper temperature of iron melting is 6150 K. The pressure dependence of iron melting temperature is such that we can explain the inner solid core and the outer liquid core with a simple model. The inner core is nearly isothermal (6150 at the center to 6130 K at the inner-core/outer-core boundary) and made of hexagonal closest packed (hcp) iron and ~1 per cent solid ($MgSiO_3$ + MgO). By including less than 2 per cent of solid impurities with iron, the outer-core densities along a thermal gradient (6130 K at the base of the outer core and 4000 K at the top) can be matched with the average seismic densities of the core.

References

Boehler R. (1993). *Nature*, 363, 534-536.
Saxena S. K., Shen G., Lazor P (1993). *Science* 260, 1312.
Saxena S. K., Shen G., Lazor P (1994). *Science* In Press.

COORDINATION CHEMISTRY OF THE MINERAL WATER INTERFACE

Schindler, P. W. (*Dept. of Inorg. Chemistry, Univ. of Bern*)

Metal atoms at mineral surfaces are coordinatively undersaturated. Exposition to an aquatic environment leads to formation of surface functional groups such as -OH or -SH that are coordinated to the surface atoms. The presence of a dissociable proton and one or two lone pairs explains that such groups exhibit both Bronsted acidity and basicity. In addition the lone pairs suggest Lewis basicity.

The surface functional groups can thus react with dissolved metal aqua ions to form inner sphere binary surface complexes. The reaction can proceed with or without proton displacement. In addition, the surface functional groups can coordinate with metal-ligand complexes which leads to formation of ternary surface complexes. Another type of surface complex is formed by replacing the functional groups coordinated to surface atoms by dissolved ligands.

The stoichiometry and the thermodynamic stability of surface complexes can be deduced from experimental and computational procedures adapted from solution chemistry. The evaluation is, however, not straightforward since the calculations require knowledge of the acting surface potential, a quantity that can only be obtained on the basis of an assumed model for the electrified interface. Different models may result in differences in both stoichiometry and stability of the postulated species. Additional information from spectroscopy is of great help in discriminating between the outcome of the different model calculations.

Stable surface complexes are important in interpreting and predicting adsorption phenomena in technology as well as in the environment. Transient surface complexes have been assumed as precursors for the activated complexes in dissolution and nucleation processes as well as in heterogeneous electron transfer reactions.

MELANITIC GARNETS FROM M.VULTURE (ITALY): A CHEMICAL AND STATISTICAL STUDY

Schingaro, E., Scordari, F.(*Geomineralogical Dept., Univ.of Bari*)

The crystal chemistry of 153 melanitic garnets from different stratigraphic sequences of M.Vulture volcanic deposits has been investigated by electron microprobe analyses, crystallographic (Scordari and Schingaro, 1994) and spectroscopic methods (Pedrazzi et al., 1994; Malitesta et al., 1994).

The aim of the present work was to investigate the chemical variability of the garnet samples within and among the studied stratigraphic sequences and to have an insight into the substitutional mechanisms affecting their crystal structures. To this purpose statistical analyses by univariate and multivariate techniques have been performed on electron microprobe data, namely on seven *variables* (major and minor oxide percentages, such as CaO, MgO, MnO, FeO, Al_2O_3, TiO_2, SiO_2) and 153 *individuals*.

Univariate techniques (*box-and-whiskers plots, stem and leaf displays, non-parametric tests*) allowed the real variable distributions to be compared, both qualitatively and quantitatively. Multivatiate techniques (*Principal Component Analisys, PCA*) allowed to examine the structure of the data array and seek to display relationships among sets of individuals graphically in as few dimensions as possible.

The following results have been obtained:

a) the majority of the total variability of the garnets compositions is related to changes in Si, Ti, Fe and Al contents, hence it is accounted for by four out of the seven original variables;

b) on the basis of the Fe/Al and Si/Ti ratios the the occurrence of four groupings has been revealed, to which most of the individuals (with the exception of few outliers) belong. These groupings are consistent with the statigraphic classification of the examined volcanic units.

c) relationships between variables have been revealed which may be interpreted as the result of the combinations of multiple substitutional mechanisms. The latter may lead couple of chemical species to vary sometimes in the same direction (direct relationship), sometimes in opposite directions (inverse relationship). This has to be accounted for to explain both the 'observed' relationships and the failure to reveal 'expected' correlations.

Both the geometrical and the chemical results provided by the crystallographic investigations are consistent with those obtained on chemical grounds.

References

Malitesta, C., Losito, I., Sabbatini L., Scordari, F., Schingaro, E. (1994) - 16th General Meeting of IMA, 4-9 September 1994- Pisa, Italy

Pedrazzi, G., Ortalli, I., Schingaro, E., Scordari, F. (1994) - 16th General Meeting of IMA, 4-9 September 1994 - Pisa, Italy

Scordari, F. and Schingaro, E. (1994) - 16th General Meeting of IMA, 4-9 September 1994, Pisa, Italy.

THE TEMPERATURE DEPENDENCE OF THE Fe^{2+}/Mg^{2+} DISTRIBUTION IN SYNTHETIC ORTHOPYROXENES

Schlenz H. and Kroll H. (Dept. of Mineralogy, Univ. of Münster)

The intra-crystalline order/disorder-distribution of Fe^{2+} and Mg^{2+} on the M1 and M2 sites of the orthopyroxene structure can be used to estimate the cooling rates of orthopyroxene-bearing rocks. This requires that the temperature dependencies of the rate constant k and the distribution constant K_d are precisely known. k can be taken from the work of Anovitz et al., 1988 . There are a number of models (e.g. Ganguly,1982; Shi et al., 1992; Yang & Ghose, 1993) to calculate K_d which all give different results. Unfortunately small differences of K_d produce large deviations in the calculated cooling rates. We present a model which is entirely based on site occupancies determined by X-ray structure refinement. The excess Gibbs free energy due to non-convergent ordering is described by an expansion that is derived from the reciprocal solution model. The contributions of the configurational and the non-configurational entropy are separated in this expansion:

$$\Delta G^{ord} = -1/2[\Delta G^{0}_{exch} + (L_{M2} - L_{M1})X]Q + 1/4[\Delta G^{0}_{rec} - (L_{M2} + L_{M1})]Q^2 - TS_{conf} \qquad (1)$$

Two compositions of synthetic orthopyroxenes were ordered at 850°C, 800°C, 675°C, 650°C and 550°C with kinetic experiments at 650°C and 550°C. In addition experiments at a constant cooling rate from 850°C down to 250°C were performed to confirm the temperature dependence of k as suggested by Anovitz et al.. Together with the available X-ray data we fitted our data to equation (1) at equlibrium condition. Cooling rate calculations based on our model for the T,X -dependence of Kd adequately reproduce the Fe^{2+}, Mg^{2+} site occupancies of a variety of slowly cooled natural samples.

References:

Anovitz et al., Am Mineral 73: 1060-1073 (1988)

Ganguly, J., In: S.K. Saxena, Ed., Advances in physical geochemistry, Vol.2, 58-99 (1982), Springer Verlag, New York.

Kroll et al., Phys Chem Minerals, in press (1994).

Schlenz et al., Phys Chem Minerals, in press (1994).

Shi et al., Phys Chem Minerals 18: 393-405 (1992).

Yang, H., Ghose, S., Abstract, Geol. Society of America, 1993 Annual Meeting.

VARISCAN Sm-Nd AND Ar-Ar AGES FOR ECLOGITE-FACIES ROCKS FROM THE ERZGEBIRGE, BOHEMIAN MASSIF

Schmädicke, E. (Dept. of Earth Sciences, Univ. of Washington, Seattle), Mezger, K. (Max-Planck-Institut für Chemie, Mainz), Cosca, M.A. (Inst. de Minéralogie et Pétrographie, Univ. Lausanne) and Okrusch, M. (Mineralogisches Inst., Univ. Würzburg)

The Erzgebirge Crystalline Complex (ECC) is one of the rare examples of the occurrence of both, 'crustal' eclogites and mantle-derived garnet-bearing ultramafics (GBU) in the same tectonic unit. Thus, the ECC represents a key complex for studying tectonic processes such as crustal thickening and incorporation of mantle-derived material into the continental crust. Nevertheless, no age determinations have been carried out on HP rocks from the ECC hitherto, and - in contrast to the other eclogite- or GBU-bearing units in the Bohemian Massif - the HP event has been assumed to be related not to the Variscan but to an older orogenic cycle.

This study is the first attempt to date HP metamorphism in the Erzgebirge for which a Variscan age can be derived from Sm-Nd and Ar-Ar data. 'Crustal' eclogites and a mantle-derived pyroxenite both indicate a Carboniferous metamorphic age. Sm-Nd garnet-whole rock tie lines define ages of 337 ± 5, 349 ± 7, 361 ± 4 (eclogites) and 353 ± 7 Ma (pyroxenite). ^{40}Ar-^{39}Ar spectra of phengite from two eclogite samples give plateau ages of 348 ± 1 and 355 ± 1 Ma which coincide with the Sm-Nd age data. This overlap of ages obtained with different isotopic systems - for which an apparent difference in blocking temperatures of about 300 K is generally assumed - indicates extremely fast uplift rates. Cooling rates may well be in the order of 100 K/Ma, or even higher. Therefore, the closing temperature of the specific isotopic system is of minor importance, and the data indicate the age of HP-metamorphism and not a point of the cooling path as in slowly cooled rocks. Such rapid tectonic processes with an uplift in a time-span of only a few million years (and probably with a burial in a similar order) might be the reason for isotopic disequilibrium. Inspite of textural equilibration and metamorphic temperatures in excess of 800°C, in three of the four investigated samples, clinopyroxene, garnet and the whole rock do not define a line in the Nd-isotope diagram. The metamorphic clinopyroxenes seem to have inherited their isotopic signature from magmatic precursors and failed to equilibrate with the whole rock during the short episode of metamorphism.

EXPERIMENTAL DETERMINATION OF THE PVTX PROPERTIES IN THE SYSTEM (H_2O+40 WT% NaCl) - CO_2 AT ELEVATED TEMPERATURE AND PRESSURE

Schmidt C. and Bodnar R. J. (*Fluids Research Lab.,Virginia Tech*)

Fluid inclusions containing H_2O, CO_2 and NaCl as the major components are common in metamorphic and igneous rocks and in many hydrothermal deposits. However, little is known about the PVTX properties of H_2O-CO_2-NaCl mixtures at elevated pressures and temperatures, particularly at high salinities. The synthetic fluid inclusion technique combined with a hydrothermal diamond anvil cell provides a means to obtain information about these properties.

The solvus and the P-T slopes of iso-Th lines were determined for bulk fluid densities above the critical density for a constant composition of 40±0.1 wt.% NaCl and 5±0.1 mole% CO_2 (both relative to H_2O). Synthetic fluid inclusions were formed in cold-seal pressure vessels at constant pressures of 2 and 4 kbar and temperatures between 350° and 700°C. The inclusions were analyzed

on a gas-flow heating/cooling stage to determine the temperatures of halite dissolution [Tm (NaCl)] and total homogenization [Th (L-V)].

The formation temperatures were regressed as a function of Th (L-V) for each isobar. The iso-Th lines were located by solving the two regression equations for the same Th value to obtain formation temperatures corresponding to the homogenization temperature. A linear fit to the P-T datapoints was used to determine the iso-Th line. The pressure of the one-phase/two-phase boundary was obtaineded by extrapolating the iso-Th lines to the total homogenization temperature corresponding to that line. Molar volumes were calculated from the known bulk composition of the inclusions, the density of the aqueous phase + halite at room temperature, and the density of the CO_2-rich phase, which was obtained from Raman spectroscopic CO_2-peak separation at 32°C or from microthermometric measurements of the CO_2 homogenization temperature.

Addition of 40 wt.% NaCl to an aqueous solution containing 5 mole% CO_2 causes a significant shift of the solvus towards higher pressures. The addition of 5 mole% CO_2 to an H_2O-40 wt.% NaCl fluid has only a small effect on Tm(NaCl), which increases from 323° to about 335°C. The slopes of the iso-Th lines decrease from 28 bars/°C for Th(L-V) of 400°C, to 6 bars/°C for Th(L-V)=600°C.

ORIGINS OF MINERALOGY: THE AGE OF AGRICOLA

Schneer C.J. (*Dept.Earth Sci. Emeritus, U. of New Hampshire*)

The Age of Agricola was also the century of Copernicus and the beginning of the scientific revolution. The printing of 30,000 works between Gutenberg's Bible and Rülein von Calw's *Bergbüchlein* in 1500 fueled the cultural explosion of the Cinquecento. It was the age of the Italian algebraists—the *cossistas* del Ferro, Tartaglia, Ferrari and Cardan— the age of Reformation and the Inquisition and the wars of religion, but also an age that created a science of harmony through the mathematical reduction of music (Zarlino and V.Galileo) and symmetry in art (Dürer), architecture (Palladio) and nature. Minerals were then a class of *fossilium*, or *oryctos*(Gr.) described in the 16th century by metallurgists and mining men (Birunguccio), physician-scholars who studied medical properties of minerals (Cardan, J.C.Scaliger, Agricola, Rösslin, Kentmann, Gesner, Paracelsus, Boetius de Boodt), and artists like the potter Palissy. Their learning was rooted in the medieval sciences of harmony, geometry, astronomy and arithmetic, as interpreted by humanist scholars such as Erasmus and the printer Frobenius of Basel, and the pervasive Hermeticism. Their mineralogy was philological—starting from Theophrastus, Pliny and the medieval encyclopedists—following Aristotle and Averroës, but modified by their practical experience.

Modern ideas of symmetry groups, reticular structure and corpuscular chemistry grew out of the identification of the elements with the five Platonic solids in works of Piero della Francesca, Pacioli and Leonardo in the 15th century; Dürer, Nifo, Clavius, Scaliger, Candalla in the Age of Agricola; applied to minerals by Kepler, Descartes, Hooke, and Steno in the 17th and leading to the six *formes primitives* of Haüy in 1784.

Rejecting alchemy, the Age of Agricola undertook the natural classification of minerals and provided an empirical and mathematical basis for the later development of morphological and structural crystallography and corpuscular chemistry.

SELF-SEALING OF THE WASTE SULFURIC ACID LAKE OF THE TiO_2 PLANT AT ARMYANSK, CRIMEA, UKRAINE.

Schuiling, R.D. (*Dept.of Geochemistry, Utrecht University*) and Gaans, P.F.M.van (*Dept.of Physical Geography, Utrecht University*)

The TiO_2-plant at Armyansk discharges its waste sulfuric acid and other effluents into an "acid collector" of 42 km² surface area. Under the semi-arid climatic conditions, such a surface represents the equilibrium between effluent production and evaporation. In the course of its operation since 1969, the pH of the lake has decreased to a value of 0.9. This decrease was slowed down, due to buffering by the surrounding sediments, as corroborated by mass balance and equilibrium modelling. At the bottom of the lake a 10 to 50 cm thick layer of natrojarosite has developed, which is underlain by a hardground of iron oxides cemented by gypsum, that separates the jarosite at pH of 0.9 from the underlying calcareous clay with pore water pH of 6.2. After perforation of the iron crust the pore-water shows strong degassing, showing that the reaction crust acts as an effective seal. The crust is also a barrier for heavy metals from the effluent. Notably arsenic, vanadium and chromium are largely immobilized by isomorphic substitution in the reaction zone.

It is suggested that similar seals can replace conventional isolations in disposal sites, the more so since they will show a strong tendency to repair themselves after damage. Such seals can be obtained by the interaction between two chemically contrasting wastes, or between a waste and a suitable geological formation. Current experiments demonstrate the feasibility of this combined isolation/ immobilization environmental technology.

MUTUAL EXSOLUTION TEMPERATURES IN HORNBLENDE AND CUMMINGTONITE AND THEIR POSSIBLE SIGNIFICANCE AS EVIDENCE FOR VARYING REGIONAL METAMORPHIC COOLING RATES.

Schumacher, J. C.[1], Klein U.[2] and Czank M.[2] ([1]*Mineralogisch-Petrographisches Institut, Univ. of Freiburg, FRG;* [2]*Mineralogisch-Petrographisches Institut, Univ. of Kiel, FRG*)

Within the amphibolite facies, hornblende (HBL) and cummingtonite (CUM) typically coexist in low-Ca amphibolites. Upon cooling, HBL and CUM may mutually exsolve lamellas in two orientations, which are nearly parallel to either (100) or (10$\bar{1}$). Optimal phase boundary theory (OPB) predicts lamella orientations, which are functions of variations in a, c and β (Robinson *et al.*, 1977 and refs. therein). These parameters are both T and composition dependent.

The extent of the effects of the T and composition have been investigated on natural HBL-CUM pairs from the middle-amphibolite facies in southwestern New Hampshire, USA (SWNH) and the upper amphibolite-facies in central Massachusetts, USA (CM). Transmission electron microscopy (TEM) imaging of exsolved HBL and CUM pairs shows that multiple generations of lamellas can be distinguished based on average lamella width and orientation. Subparallel orientations differ up to 4°.

The T dependence of the lattice parameters was measured using a Guinier film camera with heating attachment installed. The data that was used to calculate the lattice parameters was collected at elevated T (25-600°). Over this T range, the β angle decreases 0.4°, the a increases about 0.5Å and c increases about 0.02Å for both HBL and CUM. Based on these data, OPB calculations indicate that T dependence of the (10$\bar{1}$) and (100) lamella orientations are the is most strongly influenced by Δa and Δc , respectively. Although theoretically either of these lamella orientations should yield T data, in practice only the (10$\bar{1}$) lamellas are useful. The relatively minor changes in c with T combined with the higher sensitivity of lamella orientation to extremely small variation in Δc limit the usefulness of the (100) lamella at present.

Estimated exsolution T's in both HBL and CUM range

from about 580 to 300 °C in both CM and SWNH samples. Lamella with maximum width yield the highest *T's*, but at equivalent *T's*, HBL lamellas in CUM are a factor 3-5 narrower than the CUM lamellas in HBL suggesting diffusion of one or more of the HBL components (Ca?) is a rate limiting step. The CM samples show at least four generations of exsolution, while the SWNH samples show at least three generations suggesting that CM locality cooled more slowly. This interpretation is in accord with reconstructions of the *P-T* history indicating that, relative to the SWNH locality, the CM locality cooled at deeper levels of the crust. Additionally, temperatures of exsolution are essentially the same for several generations of lamellas at both localities. At constant *T*, the key differences are both spacing and width of lamellas. At SWNH the lamellas are more closely spaced and narrower than those at the CM locality which further suggests lower cooling rates for the CM locality at given T's along the retrograde leg of the *P-T* path.

References:
Robinson, P., Ross, M., Nord Jr., G. L., Smyth, J. S., and Jaffe, H. W., 1977, Am. Miner., **62**, 857-873.

CONTINUOUS, DISCONTINUOUS AND OSCILLATORY ZONING IN GARNETS FROM REGIONAL METAMORPHIC MICA SCHISTS AND PHYLLITES, WESTERZGEBIRGE, GERMANY

Schumacher, R.[1,3], Rötzler, K.[2] & Maresch, W.V.[3] *([1]Mineralogisch-Petrographisches Institut Kiel, [2]GeoForschungsZentrum Potsdam, [3]Institut für Mineralogie, Münster)*

Zoning patterns of garnets in **mica schists** with ilmenite, rutile, biotite, plagioclase, quartz, ± staurolite and ± chloritoid and in **phyllites** with white mica, biotite, chlorite, plagioclase, quartz, ilmenite, rutile, ± clinozoisite are studied in detail by microprobe using elemental X-ray intensity mapping images (MAPS) and quantitative analysis. The garnet zoning patterns can be correlated with their metamorphic history.

Most garnets in both rock types show continuous zoning with increasing almandine and pyrope and decreasing spessartine and grossular components from core to rim. However, in some samples the MAPS images show sharp discontinuities and even oscillatory changes in spessartine or grossular components on a µm scale, which are not seen in pyrope and almandine components. Together, these changes indicate a more complex growth and resorption history of the garnets.

Oscillatory zoning patterns may be more common than originally thought, but can easily be missed during quantitative analysis, because they occur within short distances. The investigated zoning patterns did not show up in the backscatter images, but were found by the MAPS analysis that were carried out with wave length dispersive spectrometers, across areas of garnet up to 2 mm across. The measurements required measurement durations of up to two days. This technique is a more sensitive method to determine zoning patterns and to understand the reactions that formed them.

P-T estimates of various metamorphic stages are obtained by application of conventional thermobarometry and of the TWEEQU program (internally consistent thermodynamic dataset of Berman, 1991) to assemblages formed at the different P-T stages.

In the **mica schists** several generations of white mica (Si = 3.4 to 3.1 p.f.u.) and plagioclase can be distinguished. Early albite is found as rare inclusions in garnet; relict oligoclase occurs in the matrix; texturally later albite porphyroblasts have late oligoclase rims. The zoned garnets in the mica schists are interpreted to have began growth at maximum P-T conditions (10-12 kbar, 500-520°C) and to have continued to grow during uplift at still increasing T along a clockwise P-T path. Retrograde zoning at the rims is characterized by increasing spessartine contents and reverse zoning of the grossular, almandine and pyrope components. In a few samples oscillatory zoning in respect to the grossular component (sample E 514: 25.7 mole % in the core, decreasing to 8.2 mole %, then increasing to 14.4 mole % and decreasing again at the extreme rim) is weakly correlated with opposite zoning patterns of the spessartine component. The discontinuous changes in composition may be related to reactions involving white mica, chlorite and changes in plagioclase composition. The more diffuse zoning patterns of Fe^{2+} and Mg are likely to be caused by later internal homogenization.
The zoned garnets in the **phyllites** are interpreted to have grown during heating at high pressures up to maximum P-T conditions of about 9 kbar and 480°C (based on: garnet transitional core/rim area, a second generation of white mica with Si = 3.3 p.f.u., biotite, chlorite, rutile and ilmenite) and during uplift at still increasing temperatures. Rim compositions are affected by garnet consuming reactions involving white mica, biotite, chlorite and clinozoisite. Garnet in a clinozoisite-bearing phyllite (sample E 24B) shows a continuous decrease in spessartine component from core (28 mole %) towards the rim (16 mole %) and, over about 50 µm at the rim, a discontinuous, oscillatory increase, decrease and further increase (30 mole %). These changes are correlated with a contrasting, but weaker zoning in almandine component (48 mole % in the core, 58 mole % towards the rim, 48 mole % at the extreme rim), which may have been partially homogenized due to later diffusion that may have more strongly affected Fe^{2+}. So far, no evidence in support of open-system behavior of the fluid phase could be found in the mica schists and phyllites. Consequently, we attribute the oscillatory changes in garnet composition to regional metamorphic reactions .

Reference:
Berman (1991) Can. Min. **29**

MINERALOGY AND CRYSTALLOCHEMISTRY OF BIOTITES FROM THE GEORGIAN METAMORPHIC ROCKS

Schwelidze I. (Geological Institute of Georgian Academy of Sciences, Tbilisy, Georgia

Chemical, X-ray and electron diffraction (oblique texture patterns) study of biotite samples from different metamorphic rocks of Abkhasia and Upper Svanetia has revealed the strong dependence both composition and structure from the genesis. Biotites from metapelites as a rule are of eastonite-siderophyllite compositions whereas biotites from metabasites are of phlogopite-annite series. With increasing of the metamorphic alteration degree (from biotite to migmatite zones) Fe content rapidly falls with the parallel increasing of Mg content.

With increasing of the metamorphic alteration degree from metapelites to metabasites there occurs the sequence of polytypes $Md \rightarrow 1M \rightarrow 2M_1$. The initial stages of metapelites metamorphic alteration are characterized by polytype Md formation under conditions of low temperature and low pressure; by the pressure increasing this semi-random polytype transforms to the ordered 1M polytype. In metabasites under high pressure conditions the polytype $2M_1$ is formed as a result of dickite alteration.

CRYSTAL CHEMISTRY OF TITANIAN GARNETS FROM M. VULTURE (ITALY)

Scordari, F., Schingaro, E.(*Geomineralogical Dept., Univ. of Bari*)

Ti-rich garnets have usually intricate crystal chemistry because of both the compositional complexity and the uncertainty about iron and titanium oxidation states. Consequently, calculation of the stoichiometry and cations site assignements are not trivial problems. The combination of complementary techniques may help to shed light on these controversial questions.

In this study melanitic garnets occurring in alkaline undersaturated igneous rocks from M. Vulture, Basilicata (Italy) are analyzed.

The chemical composition was investigated by means of electron probe micro-analysis (EPMA). Informations provided by chemical

and single crystal diffraction (XRD) data allowed the atoms to be initially lodged in the available sites of the garnet structure. The distribution model completion was obtained after Mössbauer (MS), X-ray Photoelectron Spectroscopy (XPS) and Infra-Red spectroscopy (IR) investigations. Finally the results of 153 EPMA and of 31 XRD analyses were subjected to statistical investigation (Principal Component Analysis, PCA) to delineate the chemical exchanges that affect M. Vulture garnets.

The salient crystal chemical results from independent techniques can be synthetized as follows:

1) cation replacements involve chiefly Y (Al-Fe-Ti) and Z (Si-Ti-Fe) sites and subordinately X (Ca-Fe-Mn) site;

2) ferrous iron is present in X, Y and perhaps Z sites, while ferric iron is located in Y (prevalent) and Z sites;

3) titanium seems to be present in the oxidation states 3+ (Y) and 4+ (Y and Z);

4) OH^- groups (~1% atoms per formula unit) seem to enter the structure both through the usual hydrogarnet and the $Fe^{3+}(Y)+O^{2-} \leftrightarrow Fe^{2+}(Y)+OH^-$ mechanism.

"About classification of minerals"

Semenov E (Institute of Mineralogy,Geochemistry and Crystalchemistry of Rare Elements,Moscow)

Author (Semenov 1991,Semenov et all 1981) published on russian two types of systematic of all known minerals. One is based on position of main chemical elements (atoms) in Periodical Table,another on position of their ion (counting valency).

So order for separate minerals and their isomorphic groups of silicates: Na 1+; Be-Fe-Pb 2+; Al,Fe,TR 3+; Ti,Zr 4+; Nb 5+; U 6+. Complicated minerals like eudialyte (silicate of Na,Ca,Fe,TR,Zr) are grouped according to main ion -Zr- with maximum valency (v-4) minimum radius (R) and potential (R/V) in the class of Zr silicates. Such ions (Zr,Ti,Nb) are amphoteric and have low migration ability during processes of hypergenous and postmagmatic alteration.These elements usually determine type of paragenesis,of reaction series (for instance, alteration rims of Zr - hydrosilicates - lovozerite, terskite etc- around endialyte).

Similiarity of volume and unit cell dimensions,x-ray powder diagramme are main features of one group minerals.Highest (pseudo) symmetry and minimal cell volume are very important and characteristic for each mineral group.

Some tens of mineral names are mentioned in my tables as unsatisfactory. For instance hydromagnesite or my new mineral monohydrocalcite:they have no real(structural etc) connection with magnesite and calcite.I think CNMMN of IMA could discuss this problem and propose new names.

References

Semenov E et all "Mineralogical Tables" p.1-398 Moscow,Nedra 1981

Semenov E "System of minerals" p.1-333 Moscow,Nedra 1991

SILVER HALIDES FROM THE OXIDATION ZONE OF THE GAI DEPOSIT, THE SOUTHERN URALS, RUSSIA.

Sergeev N.B., Kuznetsova O.Yu., Laputina I.P. (Inst. of Geology of Ore Deposits, Petr., Miner. and Geochem., Moscow, Russia).

Silver halides occur in the oxidation zone of the Gai base-metal deposit in the Southern Urals (Sergeev et al., 1994). A great deal of the minerals concentrates in the leaching zone in the lower part of the weathering profile. Bedded friable native sulfur-quartz ores contain an average of 52 g/t Au and 389 [illegible] with local concentrations up to 1.6 kg/t [illegible].

The halides are the principal [illegible] minerals; native silver, electrum, aca[illegible] and uytenbogaardtite are less abundan[illegible] silver halides occur as grey, green, blac[illegible] or horn-like aggregates, and rarely [illegible] octahedral crystals. Most are less than [illegible] across. They are intimately associated [illegible] amorphous silica and secondary quartz. El[illegible] microprobe analysis revealed that the [illegible] consist of chlorargyrite, iodargyrite, em[illegible] and iodembolite. Native gold and s[illegible] electrum and uytenbogaardtite found [illegible] inclusions in silver halides.

The composition (Ag > $\sum$ Cl+Br+[illegible] textural relations of halides suggest [illegible] replacement origin after silver-b[illegible] minerals. Partly their formation may be [illegible] supergene migration of silver as [illegible] complexes under arid climatic conditions.

References:

Sergeev N.B., Zaikov V.V., Laputina [illegible] Trofimov O.V. (1994). *Geology of Ore Depo* 36, 2 (in press).

PECULIARITIES OF SERPENTINE CHEMISTRY AS AN INDICATOR OF CRYSTALLIZATION CONDITIONS OF KIMBERLITE MAGMA

Shamshina E.A.,Altukhova Z.A.(Yakut.Inst.Geol.Sciences RAS)

Serpentine, a major rock-forming mineral of kimberlite, replaces large and small olivine grains as pseudomorphs, makes up the matrix, and fills interstices between autoliths (makes up a cement). Microprobe analysis of the above three varieties of serpentine in kimberlites from Leningradskaya, Vostok, Yakutskaya, Mir pipes in Yakutia clearly revealed compositional differences between the varieties both within a pipe and from pipe to pipe.

Serpentine of the larger (more than 2 mm) pseudomorphs has low Al and variable but usually low Fe contents. It exhibits,in general, small amounts of isomorphic replacements. Its oversaturation in Mg determines insignificant replacement (up to 0.06 f.u. per 3 f.u. Mg); its ferric Fe replaces Si (up to 0.20 f.u. per 2 f.u. Si) rather than Al. Higher Fe contents are observed only in the larger pseudomorphs from the Vostok pipe wherein Mg replacement by ferrous Fe reaches 0.48 per 3 f.u. Mg. Pseudomorphs of 1-2 mm size have a similar composition. Smaller (less than 1 mm) pseudomorphous serpentines have low Si and moderate Fe and Al contents. Si isomorphic replacement reaches 0.09 f.u. ferric Fe and 0.16 f.u. Al per 2 f.u. Si. In the Vostok pipe a clear increase of Al content of serpentine with decreasing size of pseudomorphs is seen.

Matrix serpentine has lower Mg and Si, hence a higher degree of isomorphic replacements. Mg is usually replaced by ferrous Fe (up to 0.30 f.u. per 3 f.u. Mg) and Si by Al (up to 0.12 f.u. per 2 f.u. Si). In lower horizons of Yakutskaya pipe, matrix serpentine is so much rich in Al that the latter replaces not only Si but also Mg (up to 0.27 f.u. per 3 f.u. Mg).

Serpentine cement is characterized by consistently high Al contents and widely varying isomorphic replacements of both Mg and Si. Mg is replaced by Al up to 0.30 f.u. and ferrous Fe up to 0.48 f.u. per 2 f.u. Si.

Thus, larger serpentine pseudomorphs formed during pre-kimberlite stage, smaller pseudomorphs during kimberlite magma emplacement, matrix serpentine resulted from residual melt, and serpentine cement from the effect of a post-magmatic fluid.

CLINOENSTATITE AS A CATALYST FOR THE PHASE TRANSFORMATION OF OLIVINE TO SPINEL

Sharp T.G. and Rubie D.C.(*Bayerisches Geoinstitut*)

The polymorphic phase transformations between olivine (α), modified spinel (β) and spinel (γ) forms of $(MgFe)_2SiO_4$ are important to dynamic processes within the Earth's mantle. Of particular importance are the transformations that occur within subducting lithosphere where relatively low temperatures result in

slow reaction kinetics and the metastable persistence of olivine. It has been proposed that metastable olivine can persist to depths of up to 650 km before transforming to the spinel structure (Sung and Burns, 1978). It has also been proposed that the metastable reaction of olivine to spinel under stress can result in transformational faulting (Kirby et al., 1989) or anti-crack faulting (Green and Burnley, 1989) which may account for deep focus earthquakes that occur in rapidly subducting lithosphere. The kinetics and mechanisms of α to γ- to β-phase transformations have been well documented for the pure Mg_2SiO_4 system using transmission electron microscopy (TEM) (Brearley et al., 1992), but the Fe-bearing system is only now being examined. In addition to olivine, enstatite comprises approximately 25% of oceanic lithosphere yet the role of enstatite in high pressure phase transformations has not been previously considered. We are combining multi-anvil experiments with TEM to investigate the mechanisms and kinetics of the olivine to spinel and β-phase transformations in the presence of the high-pressure form of enstatite, high clinoenstatite.

Transformations in the $(MgFe)_2SiO_4$ -$(MgFe)SiO_3$ system are being investigated by hot pressing and reacting mixtures of San Carlos Olivine and enstatite. The hot pressing step is critical for kinetic and mechanistic studies because it produces a starting sample with relatively large grains (up to 20 μm), low defect densities, and stable grain boundaries. The samples are then reacted at $\approx$ 14 GPa and 900 to 1000 °C for up to 12 hours. At these conditions high-clinoenstatite does not transform to higher pressure phases, but it does influence the phase-transformations of olivine by catalyzing the nucleation of metastable spinel within the stability field of β-phase. We find that in all of the reacted samples spinel occurs in contact with high-clinoenstatite with a specific crystallographic relation where $(111)_\gamma$ // $(100)_{en}$ and $[-110]_\gamma$ // $[010]_{en}$. The spinel structure is kinetically favored over that of b-phase because it nucleates coherently at olivine-enstatite boundaries forms a low-energy interface with the pyroxene. This orientation relation is only seen in Fe-bearing system, implying that the presence of Fe may effect reaction mechanisms. After longer run durations the spinel transforms to β-phase, indicating that the spinel formed metastbly in the stability of β-phase.

At the conditions used in our experiments nucleation kinetics are dominated by the catalytic effect of the high-clinoenstatite. This enhanced nucleation of spinel relative to β-phase is relevant to the transformations that occur at relatively high temperatures where nucleation kinetics are rate limiting (Rubie and Ross, 1994). At higher temperatures olivine is expected to transform to β-phase near the equilibrium boundary rather than being transformed metastably to spinel. The enhanced nucleation of the spinel structure in the presence of high-clinoenstatite may expand the temperature range over which olivine reacts directly to spinel in subducting slabs.

Brearley, A.J., Rubie, D.C., and Ito, E. (1992) Phys. Chem. Minerals **18**, 343-358.

Green, H.W.II, and Burnley, P.C. (1989) Nature 341, 733-737.

Kirby, S.H., Durham, W.B., and Stern, L.A. (1991) Science **252**, 216-225.

Rubie, D.C. and Ross, C.R. II (in press) Phys. Earth and Plan. Interiors.

Sung, C-M and Burns, R.G. (1978) Phys. Chem. Minerals **2**, 177-197.

MELT EVOLUTION DURING CRYSTALLIZATION OF ROCKS OF UDOKAN LAVA PLATEAU (SIBERIA)

Sharygin V.V. and Kalugin V.M. (*United Institute of Geology, Geophysics and Mineralogy, Novosibirsk, Russia*)
Stupak F.M. (*Institute of Natural Resoures, Chita, Russia*)

Volcanism of the Udokan lava plateau (ULP) took place in three stages from miocene to holocene. Hawaiite, mugearite, trachyandesite and trachyte represent first stage. More basic and alkalic rocks (olivine melanephelinite, basanite) have started and trachytes have completed each following stage (Stupak, 1987).

Thermobarogeochemical studies of the ULP rocks have shown that there are not essential deviations in evolution of melt parent of each ULP stage. Parent basic melt of each stage were initially rich in Al_2O_3 and alkalis (on heated glasses in minerals of earlier rocks). Residual glasses of inclusions hosted by minerals of earlier rocks (melanephelinite and others) compositionally correspond to later rocks of stages (Litasov, 1992). Residual glasses in minerals of later rocks are close to more acidic rocks (Sharygin *et al.*, 1992).

Microprobe analysis of crystalline phases in melt inclusions has also revealed presence of rhonite trapped by minerals of basanite and melanephelinites, as well as amphibole and mica in minerals of hawaiites and later rocks. Possibly, the existence of these minerals is an evidence that initial melt were Al-saturated and poor in H_2O, and its further enrichment in H_2O led to formation of amphibole and mica.

Compositional study of melt inclusions and the ULP rocks has indicated some differences in evolution of initial melt under various conditions. Namely, at the final stages of evolution the initial melt under close microsystem conditions (e.g., melt inclusions in minerals) can overcome "trachytic barrier" and evolve toward more siliceous compositions, while volcanic activity of ULP (e.g., open macrosystem) are limited by trachyte formation.

References:

Litasov, Yu.D. (1992).
Thermobarogeochemistry of mineral-forming processes, Novosibirsk, issue 2, p.16-29.

Sharygin, V.V., Kalugin, V.M., Stupak, F.M. (1992).
Ibid., p.7-15.

Stupak, F.M. (1987):
Cenozoic volcanism of the Udokan ridge, Nauka, Novosibirsk, 168p.

Union College' s mineral collection : its scientific significance

Shaw G. and Lupulescu M. (*Geology Dept, Union College*)

The Union College mineral collection consists of several collections acquired by the college over a long period. The core of the collection consists of two major acquisitions: the Wheatley Collection and the Pfordte Collection. In addition to these there are many specimens gifts from various donors and other specimens collected over the years by college faculty. A part of it is the Italian Collection which contains 128 specimens with various mineral associations from Vesuvius lavas. The Union College collection has more than 7000 mineral specimens.

Prof. Silliman, in one of his " Reports on the Minerals" exhibited at the World' s Fair in New York , remarked " that the sulphates and molybdochromates of lead in Mr. Wheatley' s Collection are the most magnificent metallic salts ever obtained in lead mining, and unequalled by anything we have seen in the cabinets of Europe".

The collection contains 473 mineral species, covering almost the entire mineral systematics. Some goups of minerals such as native elements (19 mineral species), borates (19 mineral species), carbonates (31 mineral species) are especially well represented.
The number of mineral species, specimens with basic crystallographic forms or unusual morphology, the variety of twins and mineral associations, mineral pseudomorphs and some very rare mineral species are of real interest for the mineralogists and students of mineralogy.

The mineral specimens are arranged according to Dana' s system and within each mineral class, according to Hey' s chemical index

system. For easier access to the specimens and to provide additional security for the collection, all specimens have been entered in a computer file system. Digital images are stored in the same files.

The following varieties are particularly well represented and deserve special notice: native silver; native copper from the Keweenaw Peninsula, some associated with native silver and pyrargyrite; twinned, well developed (3 cm) crystals of native bismuth from Cobalt, Ont.; tellurium and nagyagite from the type locality, Nagyag; lamellar twinned sylvanite from Nagyag; every variety of fluoride from the USA and foreign localities; very large crystals of spinel from Monroe, NY; superb tetragonal dipyramids of anatase; metagenetic and geniculate twinned or acicular crystals of rutile in quartz; brilliant crystals of ruby sphalerite; and superb specimens of chalcocite from the Bristol Mine, CT.

Molybdates, phosphates, vanadates, arsenates and sulphates are an important part of the collection. Wulfenite (41 specimens), pyromorphite (68 specimens), mimetite (22 specimens), vanadinite (12 specimens) and anglesite (43 specimens) from the Wheatley Mine and from many around the world are especially well represented, some with very well developed crystallographic forms. Some the specimens are very characteristic for these species and were used for figures or were otherwise mentioned in " Dana' s Textbook of Mineralogy".

The collection preserves specimens from some very well-known mineral localities, old mines, and from many type localities long since exhausted. Many specimens, by their crystallographic forms and their specific association, very nicely characterize the mineralogical features of some mineral districts, not only in the USA but elsewhere in the world. As such, the collection would be especially important to those interested in the history and characteristics of some important, old ore deposits.

- GENESIS OF QUARTZ IN RAPAKIVI GRANITES: MORPHOLOGICAL AND PHYSICO-CHEMICAL EVIDENCE

Shebanov, A.D. and Belyaev, A.M. (Dept. Geology, Univ. St. Petersburg, Russia).

Genesis of quartz in rapakivi granite remains an important mineralogical problem. The sequential crystalllization of three discrete quartz generations is discussed.

* Type (i), composed of the fine-grained anhedral crystals of the groundmass, is also observed as inclusions in K-feldspar ovoids and as chains of grains along outer rims of K-feldspar lamellae of the trachitoid rapakivi facies. It crystallized directly from the melt.
* Type (ii) within the groundmass is made up of euhedral crystals and sporadic intergrowths with rims of the ovoids. The rounded or pseudo-hexagonal crystals have an average diameter of 0.5 to 2.2 cm. Any major rapakivi minerals can be included within this type.
* Type (iii) comprises vermicular thin lamellae of quartz localized within feldspar ovoids. This type is comparable in size with and often subparallel to the string perthites and probably exsolved as a result of subsolidus alteration of alkali feldspar.

The three types of crystals were separated from different zones of ovoids, K-feldspar lamellae and groundmass of the different phases of rapakivi granites from Wiborg and Berdyaush batholiths and were studied by thermally-induced luminescence and IR spectrometry. Parameters of unit cells were determined. From the data obtained so far, the maximum amount of structural Al and alkalies is contained within type (i) and the minimum within type (iii).

While type (ii) is intermediate, thermoluminescence data yield high intensities of the Li-Al(O^-) centres, corresponding to high (about 6 to 11 ppm) Li and B contents. IR patterns are similar to quartz within metasomatic apogranitic veins. Water-salt gas-liquid primary fluid inclusions yield maximum homogenization temperatures of 490-500°C. After taking correction for pressure into account, temperature of cristallization is estimated as about 500-630°C. It is suggested that crystallization of type (ii) took place during late-magmatic to autometasomatic stages in a volatile-saturated environment.

ELEMENT PARTITIONING OF DIOPSIDE AT HIGH P-T

Shen G. (*Inst. of Earth Sciences, Uppsala University*)

A natural diopside sample with 1.5 wt% of iron was laser-heated in diamond anvil cell at pressures between 300 and 700 kbar. The heated area was subsequently analyzed by electron microprobe. It is shown that the diopside breaks down into a Mg-rich phase and Ca-rich phase; Si/O ratio for both phases is very close to 1:3; Fe is preferentially partitioned into the Mg-rich phase. For molten area, similar results were obtained; however, Fe is found to be strongly localized to less than 1 μm in diameter, comparing to the heated spot of about 25 μm in diameter. Since the iron partitioning between liquid and minerals will strongly affect the density relationship between them, those data should be considered when modelling the density profile for melts and minerals in Earth's lower mantle.

Because of the small size (<1 μm) of Fe-rich spot, quantitative analysis is still in progress. Preliminary result shows that the iron-rich spot contains as high as 68wt% of Fe, some amounts of Si (18wt%), but low Mg and Ca (3wt% and 1.5wt% respectively). Implications for the lower mantle's differentiation with those partitioning data together with some recent results on high pressure melting of silicates will be discussed.

A REEVALUATION OF THE CRYSTAL CHEMISTRY AND STRUCTURE OF THE SCAPOLITE GROUP MINERALS

Sherriff, B.L. and Teertstra, D.K. (Department of Geological Sciences, University of Manitoba)

Scapolite is a tetragonal framework aluminosilicate with general formula $M_4T_{12}O_{24}\cdot A$ with M = Na(+K) + Ca+(+Fe^{2+}), T = Si + Al(+Fe^{3+}), and A = Cl + CO_3(+ S species). H plays a significant but as yet poorly understood role in the anion site (OH, H_2O, HCl, HS, HCO_3, HSO_4). Once details of the stoichiometry are understood, scapolite may be an important indicator of Eh, pH, volatile activities and perhaps of P,T conditions over a wide range of planetary geologic environments.

We have reviewed 498 bulk chemical and electron microprobe analyses of scapolite presented in the literature, along with 103 determinations of cell parameters, 14 structure refinements and our additional work. Solid solutions are continuous and there is no break in the series.

The T-sites seem to be well-ordered across the series. Previous X-ray studies have suggested a high degree of Si-Al disorder even towards the end-member in which Si/Al = 1.0. However, the actual ordering pattern probably

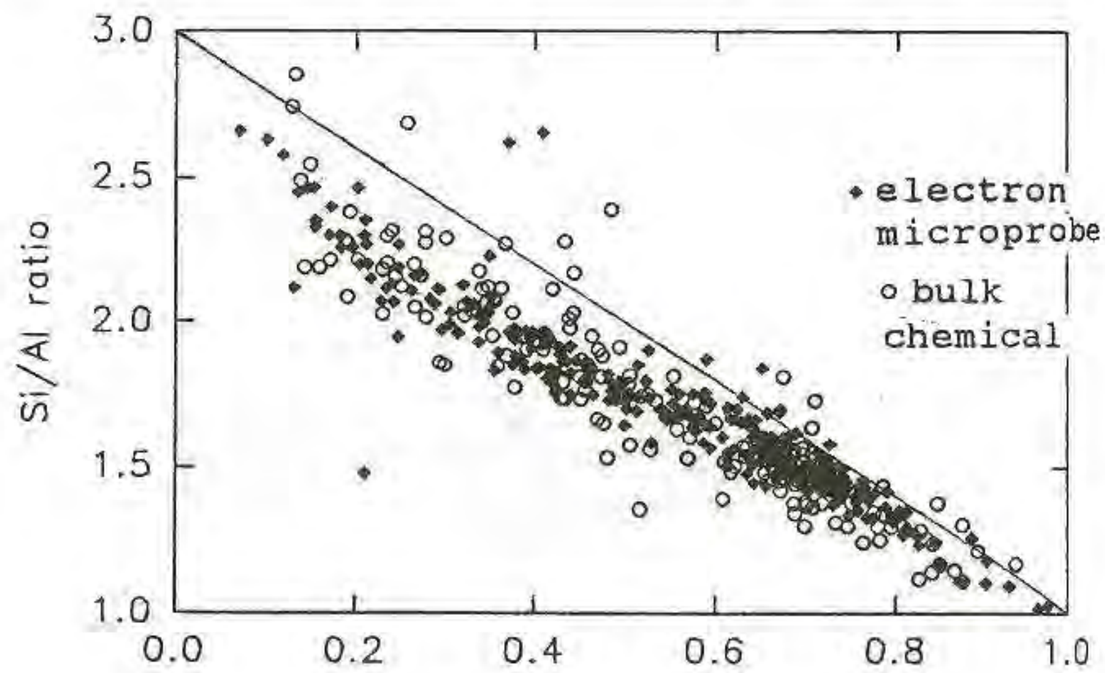

Fig. 1. A plot of Si/Al vs. $M^{2+}/\Sigma M$ (= mol.% Me) shows that the series extends from natural end-member meionite (Me) $Ca_4Al_6Si_6O_{24}\cdot CO_3$ but not to the often-quoted end-member marialite (Ma) $Na_4Al_3Si_9O_{24}\cdot Cl$. Si/Al ratios range from 3.0 to 1.0 (mean 1.7). The $Ca^{2+}+Al^{3+}$ = $Na^{+}+Si^{4+}$ plagioclase substitution (indicated by the diagonal line) is not followed, we have shown that scapolites are relatively Na-rich.

minimizes the number of energetically unfavourable Al-O-Al bonds and reduces the configurational entropy. DOR and MAS NMR data document a constancy in short-range T-site order across the series. ^{27}Al spectra resolve two Al environments; Al prefers one environment and enters a second one as Si/Al ratios decrease. ^{23}Na spectra show only one environment for Na across the series. The X-ray data show apparent disorder because alternating stacking sequences are averaged in this type of long-range measurement.

The substitutions $M^{+} = M^{2+}$, $T^{4+} = T^{3+}$ and $A^{-} = A^{2-}$ are independent and constrained only by availability of sites and requirements of net electroneutrality. The M site has vacancies (Σ less than 4). The A site seems to be filled, and contains the maximum possible amounts of Cl. There is no special Cl-free variety "mizzonite"; however, samples with S>C should be named as a new species.

THERMODYNAMIC SIMULATIONS OF GEOCHEMICAL HETEROGENEOUS EQUILIBRIA

Shi PF., and Saxena S.K. *(Inst. of Earth Sciences, Uppsala University)*
Eriksson G. *(LTH, RWTH-Aachen)*

A geochemical version of the computer package ChemSage (Eriksson & Hack, 1992) has been developed to simulate heterogeneous equilibria in hydrothermal, metamorphic and magmatic systems (Shi *et al.*, 1993). The Gibbs free energy minimization technique is used in this approach. The multicomponent C-H-O-S-N-Ar fluid model coded in SUPERFLUID (Belonoshko *et al.*, 1992), the modified HKF model (Shock & Helgeson, 1988) coded in SUPCRT92 (Johnson *et al.*, 1992) for calculating the standard properties of aqueous species, and in AQSMIX (Shi *et al.*, 1993) for calculating the non-ideal properties of aqueous solutions, and the comprehensive EOS for solid and solid solutions (Saxena *et al.*, 1993), are employed in ChemSage. Thermodynamic properties for silicates, carbonates, oxides, sulfides, halides, and their solid solutions, have been assessed, resulting in the internally consistent GEOCHEM.TDB (Saxena *et al.*, 1993; Shi *et al.*, 1993); the dataset for aqueous solution species within SUPCRT92 has been combined with the modified and evaluated data from NEA-TDB and other sources, yielding the unified AQUEOUS.TDB (Shi *et al.*, 1993).

Some applications for complex geochemical systems are reported here. The calculations of solubilities of CH_4, CO_2, NaCl, KCl, FeS, PbS, ZnS, $CuFeS_2$, $BaSO_4$ and $CaCO_3$ in fresh and saline waters, and speciations in aqueous/gaseous phases have been compared with available experimental data. The stabilities of various graphite-bearing assemblages under hydrothermal conditions have been calculated. Furthermore, thermodynamic simulations of geochemical processes relevant to formation and evolution of unconformity-type U deposits and Proterozoic Au deposits have been preformed.

References:

Belonoshko, A.B., Shi, PF., & Saxena, S.K. (1992). *Computers Geosci.*, **18**, 1267-1269.
Eriksson, G., & Hack, K. (1992). *ChemSage Handbook*. RWTH-Aachen.
Johnson, J.M., Olekers, E.H., & Helgeson, H.C. (1992). *Computers Geosci.* **18**, 899-947.
Saxena, S.K., Chatterjee, N., Fei, YW., & Shen, GY. (1993). *An Assessment of Thermodynamics of Oxides and Silicates*. Springer, New York.
Shi, PF., Saxena, S.K., & Eriksson, G. (1993). *SKB-Report*, UU93-1.
Shock, E.L., & Helgeson, H.C. (1988). *Geochim. Cosmochim. Acta*, 52, 2009-2036.

THE MODE OF SUBSTITUTION IN THE SOLID SOLUTION OF Ag SULFOSALTS MINERALS

Shima, H. (Dept. of Mineral and Mining Eng., Yamaguchi Univ.)

A large number of minerals containing Ag exist and occur in ores usually as minute minerals, which makes it difficult to identify them. However, recently EPMA analyses have greatly improved it. Most of them occur in the form of sulfosalts minerals, which consist of Ag, another metallic element, and semimetal elements such as As, Sb, and Bi. These minerals form widely ranging solid solutions in nature, making their chemical compositions complex. They are roughly classified into following three groups;

1) sulfosalts containing Cu and Ag
2) sulfosalts containing Pb and Ag
3) sulfosalts containing Ag and two kinds of semimetals

These three groups are sub-classified into nine 4-component systems shown below. These 4-conponent systems have been studied by many researchers. The present author has determined the phase relations of the nine systems by synthetic experiments. These results are summarized here. Characteristics of the mode of substitution in the solid solution of sulfosalts minerals in the systems are discussed. Here are three instances of the phase relations on the systems of the groups mentioned above.

It is made clear that most of Ag sulfosalts minerals form solid solutions in large extent, being caused by each specific mode of substitution; 1) substitution between Cu^{+} and Ag^{+} in the Cu-Ag sulfosalts, 2) substitution between $2Pb^{2+}$ and couple of $Ag^{+}+Bi^{3+}$ (or Sb^{3+}, As^{3+}) in the Pb-Ag sulfosalts, 3) substitution between two semimetals in the two semimetals sulfosalts. In these cases the limit of solid solutions varies according to conbination of the elements and their atomic radii.

Ag-sulphosalts minerals

Cu-Ag-Bi-S system
Cu-Ag-Sb-S system
Cu-Ag-As-S system
Pb-Ag-Bi-S system
Pb-Ag-Sb-S system
Pb-Ag-As-S system
Ag-Bi-Sb-S system
Ag-Bi-As-S system
Ag-Sb-As-S system

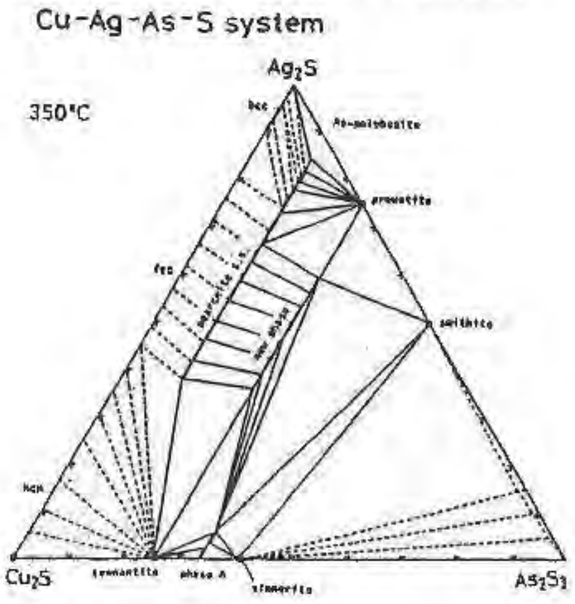

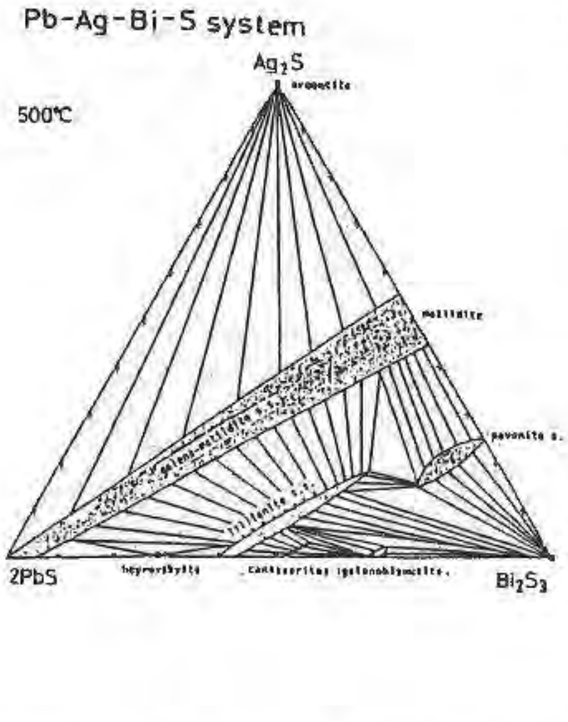

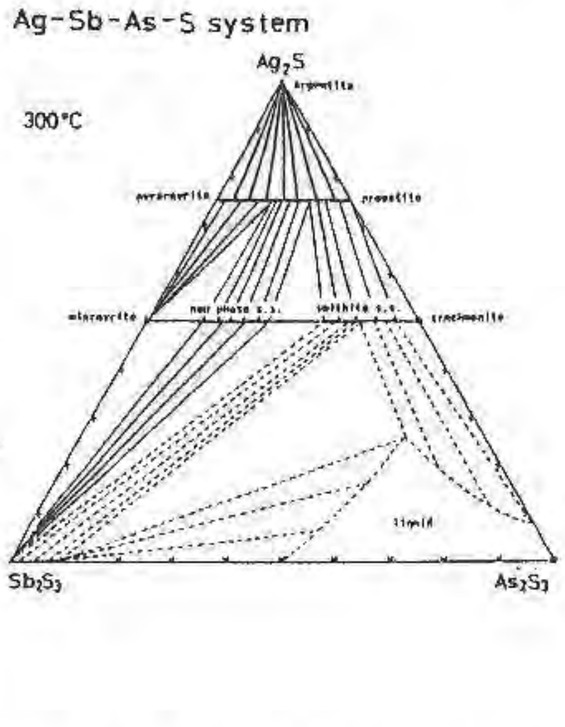

EFFECT OF H_2O ON THE Mg_2GeO_4 OLIVINE-SPINEL PHASE TRANSITION

Shimobayashi,N., Shimizu,Y. and Kitamura, M.
(*Dept. of Geol. & Mineral., Kyoto Univ.*)

Magnesium orthogermanate, Mg_2GeO_4, is known as an analogue of Mg_2SiO_4, one of the most important consistuents of the Earth's upper mantle. It transforms from the olivine structure (α) to the

spinel structure (γ) at much lower pressures than the others exhibiting the olivine-spinel phase transition. In the present study, isothermal experiments were carried out to make a Time-Temperature-Transformation (TTT) diagram for the olivine-spinel transformation in Mg_2GeO_4 under the conditions with or without H_2O.

Mg_2GeO_4 olivine was prepared from reagent grade MgO and GeO_2. The mixture was heated at about 1140K and at atmospheric pressure for 2 days. Powder X-ray diffractometry confirmed a single-phase Mg_2GeO_4 olivine. Mg_2GeO_4 spinel was synthesized hydrothermally from the olivine using Au-capsules held at 0.07GPa and 733 to 1058K. The powder X-ray diffraction pattern showed that most of the products consisted of both olivine and spinel. Estimates of the volume fraction transformed (ξ) was determined on the basis of the relative intensities of two olivine peaks ((210), (311)) and two spinel peaks ((220), (422)). Using the completely-transformed Mg_2GeO_4 spinel, additional experiments on the reverse transition to olivine were also carried out by heating in air at higher temperatures than transformation temperature (Tc=1083K at atmospheric pressure).

By fitting the experimental data at each temperature to the Avrami equation, specific times were derived at which the olivine-spinel phase transition is first detectable (10% transformed) and virtually complete (90% transformed). By plotting the logarithm of the time against the temperature (or its reciprocal), we obtained a TTT diagram for the Mg_2GeO_4 olivine-spinel phase transition (Figure 1).

The slopes of the curves at temperatures far from Tc in both parts of Figure 1 (above Tc and below Tc) reflect the activation energy for diffusion (see Putnis, 1992). The results for the activation energies of the transition were obtained as below;

35± 4 kJ/mol [olivine ⇒ spinel: H_2O-saturated],

645±325 kJ/mol [spinel ⇒ olivine: dry condition].

The latter value does not seriously contradict to a value of 438kJ/mol proposed by Rubie et al. (1990) as the activation energy for growth in the olivine-spinel phase transition of Ni_2SiO_4, while the former value is too small. The remarkable differency between the present activation energies suggests that the existence of H_2O promotes the olivine-spinel phase transition.

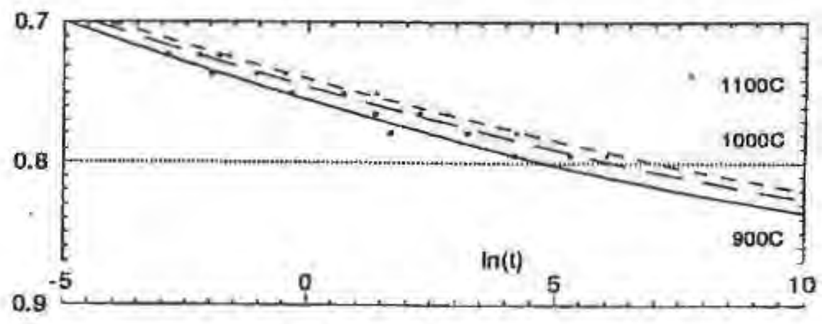

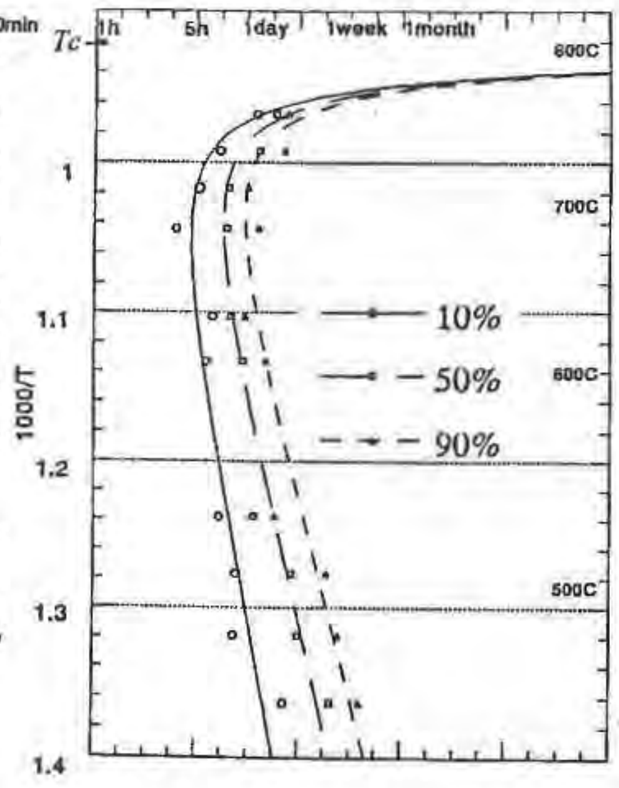

Figure 1 Time-Temperature-Transformation diagram for the phase transition in Mg_2GeO_4; olivine⇒spinel under a H_2O-saturated condition (lower part) and spinel⇒olivine under a dry condition (upper part). In each part, three curves represent the time & temperature at which the transformation is 10%, 50% and 90% complete, respectively.

References:

Putnis,A. (1992) Introduction to Mineral Sciences, Cambridge.

Rubie,D.C., Tsuchida,Y., Yagi,T., Utsumi,W., Kikegawa,T., Shimomura,O. and Brearley,A.J. (1990) *J. Geophy. Res.*, **95**, 15829-15844.

STUDY OF LIQUID UNDER PRESSURE AT PHOTON FACTORY

Shimomura . O (Photon Factory, KEK, Japan)

Structural investigation of liquid under pressure is one of the research fields that have been largely developed by use of synchrotron radiation. Liquid and amorphous materials have no structural coherency, so that the diffraction profile is very broad and weak. The characteristic of wide energy range and high brightness of synchrotron radiation make it possible to give a reliable profile.

A cubic anvil type high pressure apparatus, named MAX80 at the Photon Factory (PF), has a relatively large sample volume to embed an internal heater. MAX80 sits at the bending magnet beam line at the Accumulation Ring where x-ray energy up to 150 keV is available. Therefore, MAX80 is quite suitable to study liquid materials under pressure.

There are mainly three groups at PF who are studying liquid under pressure; Tsuji group of Keio Univ. is the first group (Tsuji et al., 1989) and treats mainly metals, Kawamura group of Tokyo Inst. Tech. mainly silicates and Ohno group of Japan Atom. Ener. Res. Inst. treats ionic crystals.

So far an energy dispersive method has been adopted because of following reasons;

(1)very sharp receiving slit system is required to eliminate the scattering and diffraction of pressure transmitting medium,

(2)very wide energy range is suitable, and

(3)reduction of measuring time is required due to the instability of liquid sample.

Pressure dependencies of nearest neighbor distance and the first coordination number for liquid Se, Te, Bi and Cs are obtained. The coordination numbers increase gradually with increasing pressure, which suggests that the phase transition takes place continuously in liquid.

For liquid ionic crystal such as KCl, comparison with molecular dynamics calculation is now proceeding. An inverse Monte Carlo calculation is trying to explain the behavior of molten silicates.

More recently, a radial soller slit system has developed to measure the diffraction profile with an angle dispersive method in a short measuring time.

Reference:

Tsuji, K et al., (1989) *Rev. Sci. Instrum.*, **60**, 2425-2428

Polarized IR Spectra of Optically Anomalous Topaz under FTIR Spectroscopy

K.SHINODA & N.AIKAWA

Department of Geosciences, Faculty of Science, Osaka City University

3-3-138, Sugimoto, Sumiyoshi, Osaka 558, JAPAN

Optical anomaly widely observed in minerals generally means that minerals have optical properties different from their accepted crystal symmetry. The optical anomaly in topaz which has been well-known as showing a sectoral texture has been suggested to be caused by the ordering of hydroxyl/fluorine. However, direct evidence of the ordering of hydroxyl/fluorine has not been observed. Polarized micro-FTIR study revealed reversed deviations of polarized absorbance distribution due to OH^- dipoles at neighboring two sectors in an optically anomalous topaz. The reversed deviations of absorbance distribution indicates reversely ordering states of hydroxyls at the two sectors. The anomalous optical properties in topaz can be considered due to the reduction of symmetry governed by the ordering of hydroxyl/fluorine.

Polarized infrared absorbance spectrum of an optically anisotropic crystal was formulated for the crystallographic analysis of hydrous component in the crystal under FTIR spectroscopy (1). The adequacy of the formulation was

1. Shinoda, K. & Aikawa, N. *Phys. Chem. Minerals* **20**, 308-314 (1993)

confirmed by comparison of calculated interference fringes with those identical to the observed one in polarized absorbance spectra of an optically anisotropic crystal. The formulation of the spectrum proposed an experimental constraint for correct measurements of polarized absorbance spectra, which request us to set the optically anisotropic crystal at its extinction position. Under this experimental constraint, polarized absorbance distribution due to OH^- dipole in topaz was measured. From observed symmetrical distribution of absorbance, the orientation of OH^- dipoles in topaz was determined to lie in the (010) and inclined 27° from <001> based on the formulation of polarized absorbance under FTIR (2). However, polarized absorbance distributions of optically anomalous topaz from Brazil measured at neighboring two sectors were asymmetrical and reversely deviated. The asymmetry of absorbance distribution shows inclined absorption axes in the crystal, which indicates the reduction of symmetry from orthorhombic. The inclined absorption axes must be brought about by unbalanced distribution of OH^- dipoles because the OH^- dipole is an oriented and intense absorber of IR light. The reverse deviation of absorbance can be regarded to result from reversely deviated distribution of OH^- dipoles, consequently, two different ordering states of hydroxyls between the two sectors. Since the degree of deviation of absorption axis from a principal orientation is consistent with the deviation of extinction positions from the perfect cleavage, the degree of deviation of absorption axis must mean the degree of ordering of hydroxyl/fluorine. After annealing the same specimen at 950°C for 5 hours, the sectoral texture disappeared but the absorptions due to hydroxyls remained, where a symmetrical distribution of absorbance was observed. Disappearance of sectors and symmetrical distribution after annealing can be regarded to result from the disordering of hydroxyls. Therefore, optical anomaly in topaz can be governed by the ordering of hydroxyls.

2. Shinoda, K. & Aikawa, N. *Phys. Chem. Minerals* in press (1994)

NEW DATA ON SULFATE-PHOSPHATE MINERALS

Shiryaeva L.L. (Dept.of Mineralogy, Inst.of Geology, Syktyvkar, Russia)

We studied the minerals of sulfate-phosphate group which occupied the intermediate position between sulfates and phosphates. 12 minerals of this group is known: svanbergite, woodhouseite, destinezite, hinsdalite, corkite, hotsonite, wilkeite, kribergite, orpheite, ardealite, peisleyite, delvauxite.

These minerals are weakly studied and their identification is difficult due to similar chemical compositions and structures and wide isomorphism both in cation and anion parts of chemical composition of these minerals.

We studied the samples of svanbergite from Timan, Polar and Subpolar Urals and Brazilia, destinezite from Pai-Khoy, Czechoslovakia and Germany, wilkeite from the USA, hinsdalite from Bulgaria, hotsonite from the South Urals.

Grystal forms of sulfate-phosphate minerals are distinguished from the electron micrographs.

Chemical compositions of sulfate-phosphate minerals were studied and their comparison with the literature data was carried out. Optical and mossbayer spectra were obtained for destinezites and diadochites. On the base of these data the similarity of structural position of Fe was shown. It was found that destinezite had only three-valent Fe placed in non-distorsed tetrahedral positions in the structure. Diadochite has three-valent Fe placed in three different distorsed tetrahedral positions.

Termal and weight loss curves were obtained for all studied samples. On the base of thermal and chemical data we stated that de-sulfatization of destinezites and diadochites took place in wide temperature interval.

Unhomogeneous composition of Timan and Polar Urals svanbergites was shown by microprobe investigations. Florensite and gorceixite inclusions were found in pseudo-cubic crystals of svanbergite. La and Ce were in all studied samples.

Due to wide isomorphism the X-ray identification of svanbergite, woodhousaite, gorceixite, florensite is difficult because their atomic cells have the similar structure. We didn't find the correlation between lattice constants and chemical compositions of these samples. Lattice constants for the samples, which are close to svanbergite by chemical composition, lie in limits a_o = 6.94 - 6.98 Å, c_o = 16.35 - 16.90 Å. The exact identification of svanbergite, woodhausaite and similar crystallographic minerals needs the co-mplex of several physical and chemical methods.

The diagram of sulfate and phosphate ions content in studied sulfate-phosphates is created on the base of chemical and microprobe data. Wide variability in sulfate and phospate ions content is exist. Destinezite is more stable in this item. The homogeneity in distribution of sulfate and phosphate complexes in the limits of an individe is stated.

IR-spectra obtained during experiments may be the standart ones.

ALKALI FELDSPARS AND MICAS FROM PEGMATITES IN THE SOUTHWESTERN USA

Shmakin, B.M., Zagorsky, V.Ye., and Afonina, G.G. (*Institute of Geochemistry, Russian Academy of Sciences, Box 4019, Irkutsk 33, 664033 Russia*)
Foord, E.E. and Brownfield, M.E. (*U.S. Geological Survey, Box 25046 Denver Federal Center, Denver, CO 80225 USA*)

Results of chemical and structural studies are presented for a suite of 73 potassium feldspars and 45 micas from granitic pegmatites in the Southwestern USA. Localities sampled included the Myers pegmatite, Canon City, CO; the Harding pegmatite, Dixon, NM; the Petaca district, Petaca, NM; the White Picacho district, Wickenburg, AZ; all of Precambrian age, and Cretaceous pegmatites from the Peninsular Ranges Batholith (PRB) in San Diego County, CA. Major, minor and trace elements were determined for the feldspar and mica samples, and structural states were determined for the feldspars.

All feldspars were analyzed for K,Na,Li,Rb,Cs by flame photometry and for Ba,Sr,Pb and Tl by emission spectrography. The levels of element concentrations are close to those of other world-wide rare-metal and miarolitic pegmatites. Maximum contents of 7700 ppm Rb, 2600 ppm Cs and 760 ppm Tl were found in potash feldspars from the "spotted zone" near the core of the Harding mine. Regional geochemical pecularities exist for the White Picacho rare-metal and for the Little Three and Himalaya miarolitic pegmatites. In all cases examined, the later generations of K-feldspar contain more Rb,Cs and

Tl than earlier ones in the same pegmatite body. Overgrowths on some crystals from miarolitic cavities show a more primitive element signature (i.e. increased Ba and Sr, decreased Rb, Cs and Tl).

Structural states were determined for 44 of the feldspars by a powder-diffraction X-ray method. All of them belong to the series: high microcline (ordered orthoclase) - intermediate microcline - maximum microcline. The majority of samples have Δt values >0.9 and none have $\Sigma t_1 < 0.84$. Ten samples have Δt values < 0.5 and three samples have Δt between 0.6 and 0.64. All samples (N=7) from miarolitic cavities of the Little Three mine pegmatite, the White Queen mine pegmatite and the Elizabeth R mine pegmatite, including two overgrowths (rims) have Δt values between 0.0 and 0.3 and Δt" values between 0.16 and 0.34. These values are less than those of the surrounding pegmatite because of temperature and rates of crystallization plus the hindering effect of ordering by large cations (Rb and Ba).

Complete chemical analyses were done by V. A. Grigoryeva for 2 biotites, 32 muscovites and 11 lepidolites. Ba,Sr,Pb,Zn,Sn and Tl were determined by emission spectrography. Lepidolites from the Stewart and Himalaya mines have the highest F and Si contents. Muscovites from the Himalaya mine have the highest Sn contents, as much as 1400 ppm. Muscovites frequently contain more Sn than lepidolites, reflecting prior extraction of Sn by cassiterite and muscovite. Tin contents in the Himalaya, Little Three and some of the White Picacho muscovites are higher than any of the others. Samples of muscovite from the Harding mine have the lowest Sn content of all. More than 1000 ppm Zn is present in biotite from the Myers quarry, CO as well as in the muscovite from Petaca (Globe mine). Zn contents in micas from the White Picacho district are also elevated.

The expected elemental fractionation trends are present in both the feldspars and micas. The greater the degree of pegmatite evolution, the higher the content of rare alkalies (Li,Rb,Cs,Tl) in both feldspars and micas along with F in micas. Feldspars and micas from the Harding mine, White Picacho district and the Himalaya mine are the most chemically evolved of all of the examined samples. Depth of emplacement, greater than 12 Km, of the Harding pegmatite and the pegmatites in the White Picacho district precluded the development of miarolitic cavities such as found in the pegmatites of San Diego County, CA. The concentrations and ratios of admixture elements in rock-forming minerals depend upon different evolution sequences (series), degree of differentiation (paragenetic type) of the pegmatites and the time of mineral formation.

INFRARED STUDY OF THE HYDROXYL GROUP IN APATITES FROM THE SENONIAN PHOSPHORITES, MISHASH FORMATION, ISRAEL

Shoval S., Knubovets R., Gaft M. (Geology and physics groups, The Open Univ. of Israel, Tel-Aviv), Nathan Y. (Geological Survey of Israel, Jerusalem) and Pregerzon B. (Rotem-Amfert-Negev, Yeruham, Israel)

The characteristics of hydroxyl groups in, both, bulk phosphorites samples and shark teeth from the Senonian Mishash Formation of Israel were examined by FT-IR. Samples from other phosphorite deposits as well as magmatic and synthetic apatites were run for comparison.

Concentrated IR disks were prepared using 5-10 mg of sample in 150 mg of KBr to observe the relatively weak OH bands in the spectrum. The disks were dried for 24 hours at 110, 290 and 350°C to remove stable water bands which mask the OH stretching band. Immediately after heating, the dried disks were re-pressed (without re-grinding) to improve the resolution.

Sedimentary marine apatites are known to be francolite (fluor-carbonate-apatite). In spite of this, after heating at 290 and 350°C most of the samples show a clear, albeit weak band at 3540 cm^{-1}. This indicates the presence of structural hydroxyl in OH...F position (1). Nahal Zin samples contained in general more hydroxyl groups than those from Zefa-Arad (Fig. 1). Samples from Russeifa and El Hassa (Jordan) showed similar spectra. Stronger bands in the same frequency were observed in synthetic as well as magmatic fluor-apatite (e.g. Kola). The fossil shark teeth also show a stronger band which is accompanied by a shoulder at 3570 cm^{-1} (Fig. 1). The stronger band at 3540 cm^{-1} indicates a larger amount of hydroxyls in the OH...F position, while the shoulder at 3570 cm^{-1} indicates an additional type of structural hydroxyls, probably in OH...O position (2). These results are confirmed by the presence of two types of libration weak bands of hydroxyl groups at 670 and 630 cm^{-1}. The 3540 cm^{-1} band is also observed as a shoulder in some of the unheated samples.

The difference between the samples may be connected to their origin or diagenesis. In the shark teeth the hydroxyls may well be residual. In conclusion, it appears that OH is a small common constituent of francolites.

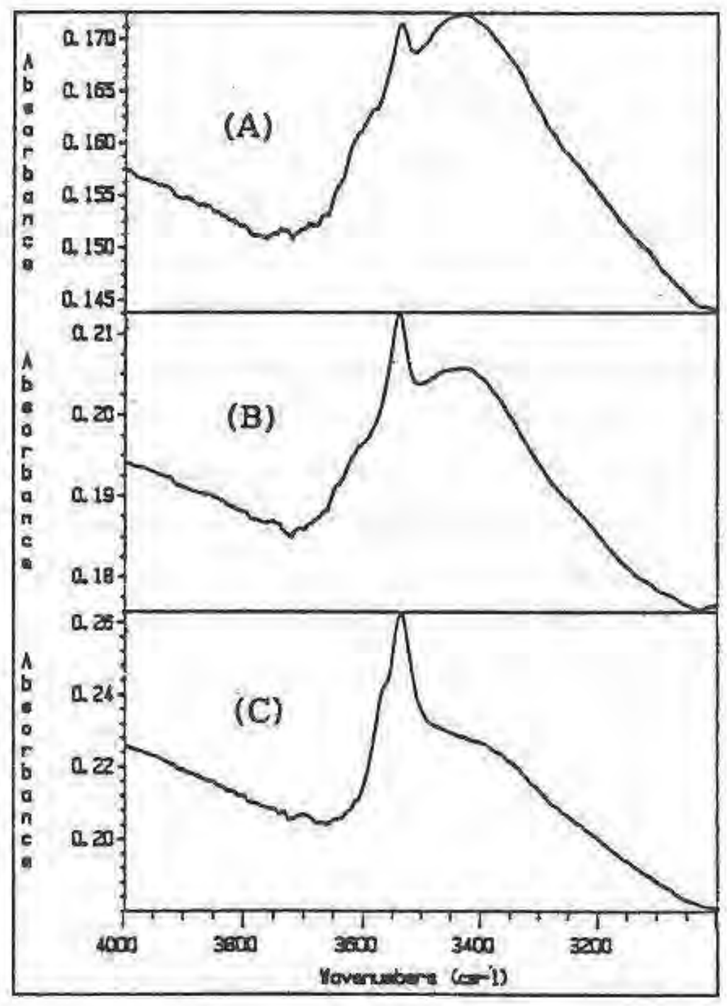

Fig. 1 - Infrared spectra (after heating the disks at 350°C) of samples from Zefa-Arad (A), Nahal Zin (B) and Senonian shark tooth (C) in the OH stretching region.

References:
1. Young, R., van Der Lugt, W., Elliott, J. (1969) *Nature*, 223, 729-730.
2. Knubovets, R. (1994) *Reviews in Chemical Engineering* (in press).

• STUDY OF QUADRUPOLE SPLIT IN MÖSSBAUER STUDY OF PYRITES FROM TWO SULPHIDE DEPOSITS OF INDIA

Shrivastava K.L. (*Dept. of Geology, Fac. of Engineering, J.N.V. University, Jodhpur, India*)

The Mössbauer study of pyrite samples, collected from a wide and gradual range of geological conditions covering early diagenesis to high grades of metamorphisms and associated with rich to poor basemetal mineralization at Amjhore pyrite deposit and Rajpura–Dariba polymetallic sulphide deposits of India, have been performed.

The study was carried out with a Mössbauer spectrometer, consisting of an electromechanical drive in the constant acceleration mode. A proportional counter with accessory electronics was backed by 8K channel analyzer and a micro computer. The radiation source was 25 mci ^{57}Co. All Mössbauer spectra were recorded at room temperature (300°K), in transmission geometry and were analyzed with the help of computer system VAX 11/730.

In sedimentary Amjhore pyrite deposit, not associated with any basemetal mineralization, the globular and framboidal pyrite from

carbonaceous shale showed Quadrupole Split value of 0.650 mms^{-1}. In sedimentary metamorphosed polymetallic sulphide deposit of Rajpura–Dariba the pyrite samples collected from unmetamorphosed black chert, mildly metamorphosed calc – silicate rock, followed by gradual higher grades of garnet – graphite – mica schist, tremolite vein, coarse diopside vein and finally kyanite – graphite – mica schist demonstrate Quadrupole Split values of 0.644, 0.629, 0.622, 0.624, 0.620 and 0.616 mms^{-1} respectively. The black chert shows a little, calc silicate and garnet–graphite – mica schist shows rich, tremolite vein and diopside vein show poor and kyanite – graphite – mica schist shows very poor basemetal mineralization associated with the pyrites.

It is concluded that the Quadruple Split values show a gradual increase along with the increasing order of diagenesis and metamorphism of pyrites.

THE PROBLEM OF KINETIC PHASE TRANSITIONS IN MINERALS

Shtukenberg A.G., Punin Y.O., Kotelnikova E.N. and Soukharjevsky S.M. (Geological Faculty, Univ. of St. Petersburg)

Order-disorder phase transitions are well known in minerals. The arrangement of different atoms in one equivalent position system may be regular or chaotic. Transition between these two cases is a thermodynamic phase transition of first or second order and each phase have a definite field of its thermodynamic stability. So the degree of structural order in minerals is widely used for determination of mineral forming conditions. But there are also kinetic phase transitions (KPT) where stability of phases defined by kinetic factors. Kinetic factors may shift strongly the point of phase transition. In some cases KPT may be observed even when equilibrium phase transition is unknown. Analysis of available data showed that KPT may often occure in minerals.

For order-disorder KPT determination several groups of methods are applied. They are : X-ray diffraction methods: spectroscopic methods and optical methods.

Two types of KPT was suggested: ordering and disordering.

1. Disordering (phases are formed with less degree of order then thermodynamically stable ones). Theoretical mechanism of this process was investigated but experimental exploration of this mechanism is obviously insufficient. Such process take place in many minerals for example in feldspares.

2. Ordering (phases are formed with greater degree of order then thermodynamically stable ones). Subpositions of one lattice position may be equivalent in volume of crystal and non-equivalent on growth surface. This leads to ordered component distribution through one position. Growth face structure causes normal selection which was investigated in quartz crystals and some other minerals. Growth step structure causes tangential selection which was studied worse then normal selection on example of $(Zn.Cu)SeO_4 * 6H_2O$ crystals.

We have investigated KPT on the model systems – three perfect isomorphic rows of alums. Alums crystals have been grown from low-temperature aqueous solutions. Unlike the end members of isomorphic rows mixed crystals display lower symmetry of optical properties than original alum one (space group Pa3). In one crystal different growth sectors have different optical indicatrix orientation and birefringence. Such optical properties suggest lower crystal symmetry. The value of birefringence is the increasing function of solid solution concentration. There are no data about the equilibrium phase transitions in such alum crystals. Calculations show that lattice misfit strains have no significant contribution to optical anomalies appeared. Unit cell dimensions (X-ray monocrystal diffraction data) in growth sectors <100> and <111> respectively are similar up to 0.001 Å. Thus these data lead to idea that KPT of ordering type take place in alums.

EPR spectroscopy has shown that kinetic ordering may work in alums but scheme of its display should differ strongly from scheme described for quartz and some other crystals. To this day the mechanism of KPT in alums is unknown. Here we can deal with interlacing of both type of KPT ordering and disordering.

Generally the problem of KPT appearence contains many obscure items and alums crystals show it distinctly.

SORBENTS, CERAMICS AND GLASSES AS RELIABLE DISPOSAL FORMS OF NUCLEAR WASTE

G.Shvedenkov, V.Kovalev (*United Institute of Geology, Geophysics and Mineralogy, Novosibirsk*)

The accumulation and long-term storage of high-level nuclear liquid waste posess a major problem for production of nuclears. The prerequisites for using acid alumosilicate glasses as a matrix are: higher chemical stability owing to formation of silica gel coating on its surface; the radionucleids are close to the soda rock in respect to the geochemical specialization; acid melts give glasses easily. The radionucleids are established to hold tightly in old natural volcanic glasses ,undergoing hydration and devitrification. The aluminosilicate glasses and ceramics with incorporated radionucleids provide the most equilibrium compositions with geochemical environment and the close fitting with geological formation (granitic massifs) for the underground disposal of wastes. For this reason the leaching with ground water for the sufficient time for its stabilization becomes minimal and uncontrolled distribution of radionucleids into environment is prevented in the surroundings.

But liquid waste must be immobilized by incorporation into a solid matrix. The bentonite may be used as an initial material for waste glass. The modelling water mixture of nitrate stable Cs,Sr and Ce was used for extraction and contained (g/l) 25.8 Ce,3.8 Sr ,8.7 Cs and 0.4$(C_4H_9)_3PO_4$. The bentonite fraction of Kamalin deposit (East Siberia) was collected for ion exchange experiment. Specific surface area was determined as 400-520 m2/g using the BET nitrogen adsorption technique. The cation exchange capacity averages between 60-110 mg-equivalent to 100g of dry matter. Bentonite samples are composed primarily of the mixlayered beidellite with nontronite component (80 %). They contain addition minor amounts of glauconite, plagio-clase, α-crystobalite and calcite.

The solid materials and standard solution, containing the elements simulating radionucleids were shaken in glass bottles for 10,15 and 30 hours and at constant temperature 30,60 and 80 +1 C. The solution (ml) to clay (mg) ratios were approximately as follows 1:10. The distribution of Cs, Sr, Ce,Ca, Na and K was determined by atomic absorption and colorimetry. The rate of ion exchange was rapid during the first hour and changed slowly thereafter. The tendencies of content increase Ce (up to 4.5 mass %), Sr (up to 2.66%), Cs (up to 4.5%) are cleary recognized in bentonite after ion exchange. By contrast, concentrations of Ca, Na and K are reduced from 1.82 to 0.56%,from 0.12 to 0.41% and from 1.27 to 1.08% respectively. Differential thermic analyses realized to establish mineral transformation during heating of bentonites saturated with components of modelling active solution. One exothermal and five endothermal peaks appeared in all DTA diagrams: 480 C-oxidation Fe^{2+};130-140 C - loss of molecular water; 660 C - loss of hydroxyl water; 870-890 C - generation of β-crystobalite,plagioclase, μ-cordierite and britolite mixture; 1115 C - initial stage of melting;1290 C - liquidus. The synthesis of britolite $Ca_3TR_7(PO_4)(SiO_4)O_2$ detected by X-ray analysis unambiguosly suggest the 3-butyl phosphate absorption by initial montmorillonite. The clay was brought up to the melting

tempeture in fifteen minutes, maintained there for one hour and then cooled in air.The shock heating of bentonite is the production of determining factor for monolithic high silica glass. The powders of glasses and clay sinters (average specific surface area 0.3 m2/g) were treated with distilled water, 5% (NH4)2CO3 and 1N HCl during 1,5 hours at 80 C.

Tab. Concentrations of leached Ce,Sr and Cs(1.0 E-3 mass %) from glass/sinter.

	H_2O	$(NH_4)_2CO_3$	HCl
Sr	n.d./n.d.	n.d./n.d.	2.3/n.d.
Ce	80/30	3.9/3.6	620/600
Cs	2.7/2.7	5.3/6.1	9.3/7.0

It is significant that the sinters of bentonite hold the changing cations as well as glasses. An experimental value for the leaching rate of the final product varies about 3 E-7 gram of glass/cm2/day.

QUANTITATIVE PHASE ANALYSIS OF ROCKS AND ORES

Sidorenko G.A.(*Com.of Geology of Russia, Institute of Mineral Resources, VIMS*)

The quantative phase analysis (QPA) is necessity of rock's type determination and evaluation of ores' quality. QPA is the complex of physical and chemical methods for determination:

(a) form of elements' place in the sample (independent mineral phase, isomorphic or sorbed admixture),

(b) diagnostics of minerals and quantitave determination of mineral's phases concentration.

In QPA "mineralogical analysis" and "phase analysis" are the synonyms. Base for diagnostics of minerals is determined by individual property. Base for QPA is determined by intensity of this property for every mineral phase in rocks, ores.

QPA use different methods: optical microscopy, X-ray diffraction, thermal analysis, IR-, NGR-, NMR-spectroscopy, magnitometry, qunantum optics, luminescence, chemical phase and thermochemical analysis. Many methods of QPA provide control of result's correctness. Using of standard samples of phase composition allows to conduct metrological evaluation of each method. System of such evaluation for QPA methods was worked out. In concrete case the choice of QPA meethod is determined by the object and requirements on accuracy and express of analysis.

Complex of 2-3 methods of QPA gives the optimum results.

References:

Sidorenko G.A. Metrology in Mineralogical investigations. In book *Problem of genetic and applied mineralogy*. M."Nauka", 1991, p.209-215.

Ostroumov G.V., Sidorenko G.A., Lyubimova L.N. *Journal of Analytical Chemistry*, 1988,v.**94**. N 2,p.360-367.

Dyakonov J., Sidorenko G.A. *et al. Powder Diffraction*, v.7, N 3,1992, p.137-141.

Ostroumov G.V., Masalovich H.S.,Sidorenko G.A. *Journal of Analytical Chemistry*, v.**91**, N 12, 1986, p. 2175-2180.

A SIMPLE MODEL FOR TREATMENT OF EXPERIMENTAL DATA ON CRYSTAL GROWTH FROM THE MELT.

Simakin A.G.
(IEM, Chernogolovka, Russia)

There are several models based on experimental data available for evaluation of crystal growth rates from silicate melts . Some of them are totally empirical (e.g. Dearnley,R. ,1993), others are proposed in attempt to separate effects of different factors (Kirkpatrick, R.J.,1975; Muncill & Lasaga,1988). Basically model should include several components: influence of chemical diffusion, influence of viscosity on the growth particle mobility, influence of melt structure in regard ability of suitable for growth unites, mechanism of growth.

1. Elimination of contribution of long range chemical diffusion from experimental data obtained in the multicomponent melts. In many cases crystals grown from viscous silicate melts have elongate habitus. Mass - transport conditions on the tip of such crystal is quite different from conditions near the plain face. We include in our model series representation of Ivantzov function.

2. Evaluation of diffusivity at relatively large undercoolings. There is no experimental data on the diffusive mobility of network forming components in the temperature range of crystallization. We can estimate such dependence with compensation rules (Winchell,1969) for diffusion and viscosity and assuming that diffusion activation energy for network-forming components is near the same as activation energy for viscosity (Simakin, 1993). It follows from this treatment that only for strong liquids like Q melt diffusion is inversely proportional to viscosity in other cases diffusion decreases more slowly as compared with viscosity. Rate of crystallization velocity decrease is similar to that of diffusivity at large undercoolings.

3. Reduced growth rate(V_r) (Kirkpatrick, 1975) obtained with new approach reflects growth mechanism more correctly. It is found that nonlinear part of dependence $V_r(\Delta T)$ at small undercoolings corresponds to spiral growth mechanism in the case of $NaPO_3$ (Avramov,1988) and resumably An growth.

4.Treatment of experimental data on the Fsp growth. General model accounting long-range diffusion as well as $D(\eta)$ dependence at large undercoolings was used to interpret experimental data on Fsp growth (Chevychelov & Simakin in this issue). The only non-adjustable parameters remained is crystal width which is taken from experimental data directly. More slow growth of Fsp from granite melt with about 2 wt.% of water as compared with the same melt with 4 wt.% of water can be connected not with diffusion effects but rather with influence of water on the melt structure.

References:

Avramov,I. et al (1988). *J.Crystal Growth*,**87**, 305-310.

Dearnley,R. (1993). *Mineral.Mag.*,**57**,337-348.

Kirkpatrick, R.J.(1975). *Amer.Mineral.*,**60**, 798-814.

Muncill,G.E. & Lasaga, A.G.(1988). *Amer. Mineral.*, **73**, 982-992.

Simakin, A.G. (1993). *Petrology*, **1**, 550-556.

Winchell,P.(1969). *High Temp. Sci.*,N1,200-215.

EVIDENCE ON A POSSIBLE NAGYAGITE - "ARSENIAN-NAGYAGITE" SERIES IN THE ORES OF SACARAMB GOLD- SILVER TELLURIDE DEPOSIT, ROMANIA.

Simon G. *(Dept. of Mineralogy, Univ. of Bucharest)* and
Alderton D.H.M. *(Dept. of Geology, R.H. College, Univ. of London)*

Nagyagite is the most complex sulfo-telluride of lead, gold and antimony, first described at Sacaramb (formerly Nagyag), Romania. In spite of its abundance and importance in the ores of Sacaramb, the mineral still remains poorly-characterized. Its structure, exact chemical composition and formula are still uncertain. An important variation in the chemical composition of nagyagite from the type locality has been recently confirmed using electron microprobe analyses (Simon, Alderton and Bleser, unpublished data). Also, a possible new mineral species, a sulfo-telluride of lead, gold and arsenic has been recently mentioned in the same deposit (Simon *et al.*, 1993).

In the Sacaramb gold-telluride deposit the "arsenian- nagyagite" occurs as rims around the early formed altaite, petzite, stutzite, sylvanite I (primary), tellurantimony, hessite+sylvanite II (as a decomposition product of γ and\or χ phase), krennerite and coloradoite. This mineral often shows clear zoning with nagyagite sensu-stricto, which is reminiscent of the most common zonation structures of tetrahedrite group. Three and sometimes four layers totally different in As and Sb content may be easily seen. The shape of the "arsenian - nagyagite" grains in these zoned crystals seems to be a hexagonal one.

In plane polarized light the "arsenian-nagyagite" is moderately reflecting and very slightly bireflectant and pleochroic. Near the nagyagite it is darker and shows a grey slightly greenish tint.

The electron microprobe analysis of this zoned crystals show significant variations not only of As and Sb but also of Au, Te and Pb, for both nagyagite and "arsenian- nagyagite". Nearly 200 electron microprobe analysis of nagyagite and "arsenian nagyagite" plotted in various diagrams, suggest that there is no correlation between Sb and Te in nagyagite, nor between As and Te in "arsenian-nagyagite". The As vs. Sb diagram displays a negative correlation, suggesting a substitution between these two elements (fig.1). On the other hand, there is a significant variation of Sb and As due to the large variation of the other chemical elements that constitute the nagyagite and "arsenian-nagyagite", respectively. The Sb/As atomic ratio in the calculated chemical formula (based on 5 atoms of Pb) varies in the zoned crystals from 1.27- 1.60/0 to 0.04/1.30- 1.50 (in at%) with an apparently continuous trend between these two end values. The complete substitution between Sb and As suggests the presence of a possible series between these two end members, nagyagite and "arsenian - nagyagite" respectively.

The optical properties and the drawn out reflectance curves, also support the above mentioned idea.The reflectance curves and the quantitative color of different chemical members of nagyagite-"arsenian- nagyagite" possible series are plotted between these two end members reflectance curves (fig. 2), and quantitative color determinations.

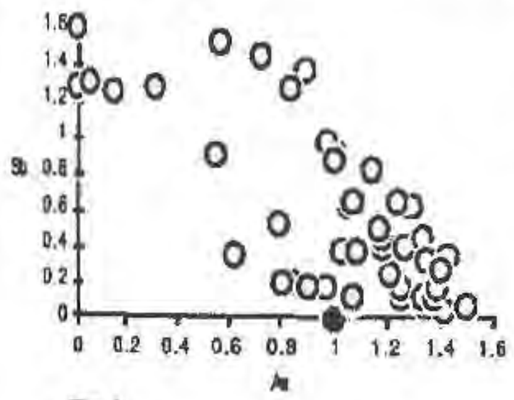

Fig 1.

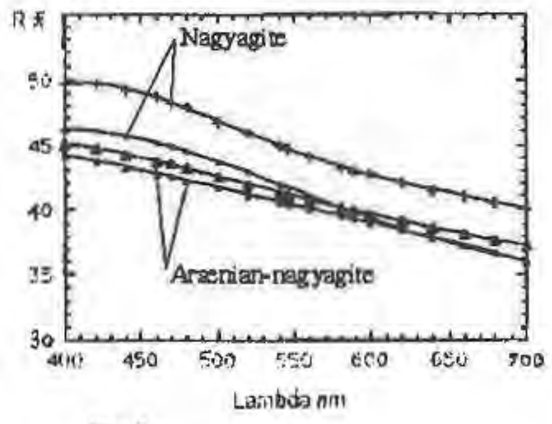

Fig. 2.

If the nagyagite chemical formula of $Pb_5Au(Te,Sb)_4S_{5-8}$ is correct, then As should be added too, substituting for Sb. In such a way the "arsenian-nagyagite", with a chemical formula of $Pb_5Au(Te,As)_4S_{5-8}$ might be a new mineral species. Unfortunately the structural data are still laking for defining a new mineral species.

Some new Mossbauer spectroscopy data carried out on nagyagite from type locality have indicated that the valency of Au is 3+ and the Sb is 3+ (Udubasa *et al.*, 1993). Taking into account of all this data it seems to be more probable a 2- valency of Te and a substitution between Sb and As, then a substitution between Te and Sb and/or As in the chemical formula of nagyagite and "arsenian-nagyagite". Of course only further structure data will confirm or not these suppositions.

References:

Simon, G., Alderton, D.H.M., Bleser, T. (1993). submitted to *Mineral. Mag.*

Udubasa, G., Wagner, F., Friedl, J. (1993). *Rom. J. Mineralogy*, 76, supl. 1, 50.

FORMATION OF HOLLOW PRODUCTS OF METASOMATIC REPLACEMENT

Sinai M.Yu. and Glikin A.E. *(Crystal Genesis Lab., Crystallography Dept., St.Petersburg Univ.)*

Different variants of hollow products of replacement after monocrystals were studied experimentally. So-called box-like and negative forms were received during a low-temperature modelling at low-temperature systems of aqua-soluble salts. Their formation conditions and mechanisms were defined.

1. Formation of box-like pseudomorphes under isothermal conditions. A deficit of a new phase volume comparing with a replacing phase one is the reason of these phenomena what realize in two ways (A, B).

A) Product precipitation occurs in systems with the specific curved isoterms of a joint solubility. Correspondently, different quantities of product are crystallized during the different stages of the process. A polycrystal product rim replaces outer zones of a primary crystal at a gently sloping segment of the Schreinemackers's diagram isotherm at the first stage characterized by a small volume deficit. Then, product crystals grow slightly while a relict of a primary crystal dissolves rapidly at the second stage what characterized by a great volume deficit and by an abrupt segment of the isotherm.

B) Precipitated products have a non-soluble composition while the amount of dissolved reagent is limited. They form a polycrystal rim replacing outer zones of a primary crystal. If these products require all original amount of dissolved reagent, the relict of primary crystal dissolves afterwards without any precipitation of new phases.

2. Formation of negative pseudomorphes under temperature decreasing. These products are presented by holes appeared instead of the original crystals. These phenomena are characteristic ones for the systems with the joint increasing of solubility of both salt components. Primary dissolved component precipitates owing to temperature decreasing while the primary crystal dissolves. That dissolving substance grows up locally the solubility of the precipitating substance and prevents the new phase formation at the place occupated by the primary crystal.

Experimental examples.

1A. Box-like pseudomorphs of Tutton's salt $K_2Cu(SO_4)*_6H_2O$ after $CuSO_4*5H_2O$ and of KCl (or KBr) after $K_2Cr_2O_7$. One can see in situ under microscope a formation of numerous small crystals of the new phase on the original crystal dissolving surfaces contacting with the solution. During the first short moment of the reaction (5-10 min) the new crystals grow together forming a box-like aggregate copying an original crystal habit. Then relict of the primary crystal dissolves completely and box- like form remains.

1B. Box-like pseudomorphs of nickel chromates after the crystals $NiSO_4*7H_2O$ during their reaction with aqueous solution of K_2CrO_4. Forming box-like aggregate copies many peculiarities of primary surface morphology and consists of radially-fibrous and bud-like fragments of the product substance.

2. The replacement of the crystals $NaNO_3$ at the cooling supersaturated solution $K_2Cr_2O_7$. The crystal $NaNO_3$ dissolves intensive just as numerous fine crystals of $K_2Cr_2O_7$ precipitates outlining the original crystal. A habit of the primary crystal can be identified.

Reference:

Sinai M.Yu. & Glikin A.E. (1989). Izvestiya VUZov. *Geologiya i Razvedka*, 4, 31-35.

GOLD DISTRIBUTION IN KARSTIC NICKEL IRON ORES AND OLD LATERITIC WEATHERING CRUSTS, LOKRIS AREA, GREECE

Skarpelis N. (Dept.of Min. Res. Eng., Techn. Univ. of Crete)

Laterites attracted last years increased interest of exploration geologists for gold concentrations. Lateritic supergene gold deposits are associated with variably developed lateritic profiles or with reworked weathering products. The nickel-iron ores of Central Greece are exploited and processed for the production of ferronickel alloy.

They were formed after the destruction of Lower Cretaceous weathering crusts, by transportation and redeposition of the lateritic material under marine conditions, either on ultramafics or on karstified carbonate rocks during the Cenomanian transgression. Deposition of the ore was muntistage. Mineralogical and geochemical differences between successive ore beds are identified. Relics of the old weathering crust, containing Ni-nontronite, are found at the footwall of a few nickel iron ore deposits lying on serpentinites. Ophiolitic lithologies and more acidic rock types were the parent rocks of the lateritic material.

Mineralogical and multi-element, including gold, chemical analyses of samples of nickeliferous iron ore, the underlying serpentinite and the nontronite, revealed a significant enrichment of several major and trace elements from top to bottom of the ore bodies. Gold concentrations range between 2 to 55 ppb. The pattern of gold distribution along vertical profiles is erratic. The structure of gold dispersion is not indicative of a mechanical or chemical transportation and deposition of the element. The lack of significant gold values into the ore and the old weathering crust is discussed.

REACTIONS OF ASBESTOS AND OTHER FIBROUS MATERIALS

Skinner, H.C.W. (Dept. of Geology & Geophysics, Yale Univ., New Haven, CT 06520)

Scanning Electron Microscopy and High Resolution Electron Microscopy have made it possible to identify and to 'quantify' the proportion of fibrous materials in our environment. Of particular import are the results on particles suspended in air and in lung tissues. The concentration of fibers have been documented for several workplace environments and related to disease such as cancers and the pneumoconioses, e.g. asbestosis. Mandated reduction in occupational exposure, commencing in the 1970's, appears to have lowered the incidence of asbestosis but the mechanism(s) of disease induction by fibrous, or other mineral particles, remains under study.

The reactions of mineral materials in the biological regime that could contribute to the induction and promulgation of disease, such as surface properties, composition and crystal structural differences of the many fibrous species that have been studied over the past 30 years will be reviewed. The hypothesis of "foreign body" response will be considered in light of studies on water-rock interactions.

Reference

Skinner, H.C.W., Ross, M. Frondel, C. (1988) *Asbestos and Other Fibrous Materials: Mineralogy, Crystal Chemistry and Health Effects*. Oxford Univ. Press, New York.

OH INCORPORATION IN FLUXGROWN CLINOPYROXENES

Skogby, H. (*Dept. of mineralogy, Swedish Museum of Natural History*)

The pyroxenes are among the nominally anhydrous silicates which have been shown to contain small amounts of structurally bound OH. Reported concentrations of hydroxyl in pyroxene, as determined by infrared spectroscopy, range from 10 to 2400 ppm OH. The IR spectra of natural pyroxene are complex with several different absorption bands of different polarization in the OH region, indicating that the OH ions reside in different local environments. These environments as well as the mechanisms controlling hydroxyl incorporation in pyroxene are poorly known.

This presentation describes hydrogen incorporation in synthetic clinopyroxenes, during and after crystallization. Samples of diopsidic composition have been synthesized by fluxgrowth methods using a $Na_2B_4O_7$ flux to obtain single crystals suitable for infrared spectroscopy. The samples, which were grown both in air and under controlled f_{O_2}/f_{H_2} using a CO_2-H_2 gasmixing furnace, contain low concentrations of unwanted Na and B.

An effective way to incorporate hydrogen is heat treatment of samples containing reducible elements (e.g. Fe^{3+} and Mn^{3+}) under hydrogen atmosphere at temperatures above 700°C, which cause hydrogenation up to OH concentration levels as reported for natural samples. The OH bands in IR spectra of most of the hydrous synthetic pyroxenes are similar to those of natural diopsidic pyroxenes in terms of band positions and polarization. The spectrum of endmember diopside (neglecting the Na and B contamination) display a single band centered at 3425 cm^{-1}, whereas spectra of Fe-containing samples have four bands centered at 3625, 3525, 3440 and 3330 cm^{-1}.

There are more than one mechanism for pyroxene hydrogenation. Hydrogen is accomodated according to the reduction-hydrogenation reaction $Me^{3+} + O^{2-} + 1/2H_2 = Me^{2+} + OH^-$, where Me is either Fe or Mn. The changes in oxidation state of Fe and Mn can be traced by Mössbauer spectroscopy and optical spectroscopy. However, also other incorporation mechanisms are active since also samples devoid of reducible elements accomodate hydrogen during similar treatment, although to a lesser extent.

LOCAL LEVEL OF UNIQUE VOLCANIC ROCKS IN THE PECHENGA VOLCANIC SUCCESSION AND ITS SIGNIFICANCE IN ORE FORMATION (KOLA PENINSULA, RUSSIA)

Skuf'in P.K.(*Geol. Inst., Kola Sci. Centre, Russia*)

The rock succession of the lower Proterozoic ore-bearing Pechenga structure, formed during the time period 2.35-1.85 Ga, is characterised mainly by basaltic volcanites. They form about 90% of this entire 10 km-thick succession, from andesite - basalts and trachybasalts through tholeiitic basalts to picritebasalts and picrites,under the conditions of dilation movements. The final stage of picrite-basaltic volcanism was of the most importance, because recently many authors have suggested, that the Ni-bearing gabbro-wehrlite intrusions and ferropicrites of the upper Matert formation make up a genetically related volcano-plutonic association (Marakushev et al., 1986). Picrites form the lower, middle and upper parts of the Matert rock sequence (Skuf'in & Fedotov, 1989) and the most important of them - the middle level. It is the level of volcanic rocks which differs much from uniform basaltic masses of the common Pechenga rock succession. And just here appeared such unusual volcanic high-iron rocks, as eucrites, alkali ferrobasalts, ferro-rhyolites, high-silica ferrorhyolites (kahusites), etc.This level is represented by four beds of rhyolitic coarse-grained welded tuffs, interbedded with globular subalkali picrites and variolitic alkali basalts. Numerous clasts in the welded tuffs (paleoignimbrites) are

represented by porphyric volcanic rocks of the above mentioned differentiated association. The rounded microclinic and high-temperature quartz phenocrysts are morphologically similar; the electron microprobe compositions of microclinic phenocrysts from eucrites, ferrorhyolites, kahusites and others are identifical too.
The petrochemical features of these high-differentiated rocks and the trends of their magmatic evolution are rather similar, as well as their REE spectra. A common genetic process explains the origin of this exotic volcanic group - it is the process of magmatic liquid immiscibility. Partly this process was modelled in the globular and variolitic picrites of this level. The variolitic globules in the differentiated picrites are enriched in alkali metals, especially in potassium, and also in TiO2 and SiO2, and considerably depleted in MgO, FeO as well as in Ni,Co and other ore metals. It is suggested, that the entire many-kilometer thick basaltic succession of mature stage of the Pechenga volcanic evolution is a manifestation of permanent delation movements; in such conditions large uniform masses of Fe-tholeiites developed. But the local collision movements, distinguished due to insignificant folding phase, were responsible for the stagnation of the magmatic chamber, the enrichment of parental magma in mantle alkali fluids, the intense processes of magma liquid immiscibility in subalkali iron melt, the appearance of the local strata of unique volcanic high-differentiated rocks in monotonous basaltic Matert formation and finally to the occurrence of the ore- bearing gabbro-wehrlite intrusive formation.

References:
Marakushev A. A., Bezmen N. I., Skuf'in P. K., Smolkin V. F. (1986). *Metallogeny of Basic and Ultrabasic Rocks, Theophrastus Publ., Athens,* 359-389.
Skuf'in P. K. & Fedotov Zh. A.(1989). *Dokl. Acad. Nauk SSSR,* 305, No 4, p. 956-962 (in Russian).

THERMODYNAMIC MODELING OF WATER-MINERAL-ROCK INTERACTION :THE "FLUID" SOFTWARE PACKAGE

Skvirsky,A.L., *Institute of Precam.Geology, Russian Acad.Sci St.Petersburg,199034,RUSSIA*

A new thermodynamic approach to model geochemical system's behavior has been proposed. It utilizes a principle of minimization of the Gibbs free energy of a system to find its equilibrium state. A system with chemical interactions is treated as solid (mineral and mineral solid solutions) and aqueous phases (charged and neutral aqueous species) set under mass and charge conservation laws constraints. The highly efficient numerical procedures make automatic selections of chemical components to be in the final equilibrium state from the specified list, depending on input constrains and perform quantitative estimation of equilibrium composition at pressure and temperature given.

The use of derived approach finally evolved in effective implementation of the method for an ordinary PC computer - the "FLUID" Software Package. The "FLUID" Package combines virtually all the popular databases of standard thermodynamic properties :Holland and Powell,1990 and Berman,1988 for minerals and gases;SUPCRT92 for minerals, gases and aqueous species;plus equivalent EQ3/6 database for low temperature/pressure data. It can also deal with mineral solid solutions using non-ideal mixing model of Helffrich and Wood,1990. An aqueous phase nonideality is treated via B-dot equation of Helgeson,1969. The input specifies the bulk composition of the system and the phases and components to be considered in calculations. The output consists of the quantities of phases in the system at equilibrium and the composition of the fluid phase.

INFLUENCE OF THE COMPOSITION OF SOLUTION ON THE STRUCTURE ORDERING IN POST-OLIGOCLASE ADULARIA

Słaby E. (*Inst. of Geoch., Min. and Petr., University of Warsaw*)

Structure of feldspar, one of the most important rock-forming mineral, has been a subject of continuous research efforts for many years. Many creditable contributions refer to recognizing reasons for the development of disordered structures in hydrothermal feldspars. Studies on feldspar structure concern almost exclusively a feldspar crystallizing from the solution freely in voids. Literature devoted to the structure of alkali feldspars, which are post-plagioclase pseudomorphs, practically does not exist. Adularia of this nature occur in Permian ryodacite from Zalas and Miękinia, at the north as well as the south edges of the Krzeszowice ditch. The adularia were formed through break-up of the oligoclase framework and migration of Ca.

The kinetics of crystal growth depends on the composition of the solution. Therefore in order to determine the growth kinetics of post-plagioclase adularia, a correlation between the composition of the solution causing adularization of the plagioclase, and the structure state of the newly formed feldspar was ascertained. Both in Miękinia and Zalas a distinct zonality in distribution of hydrothermal parageneses is present, indicating a consequent variation of the concentration ratio mK^+/mH^+ (Słaby, 1987, 1990). Products of the plagioclase - solution interaction are: Ist zone - albite and adularia, IInd zone - smectite-illite (or kaolinite) with little amount of albite and adularia, IIIrd - zone - calcite with little amount of albite and adularia. Finding the mK^+/mH^+ ratio corresponding to any given paragenesis requires a knowledge about the temperature, at which the paragenesis was formed. The necessary thermal data has been obtained from water composition of the Zalas intrusion using the Fournier thermometer (Fournier, 1981). Information derived from papers dealing with similar processes indicate, that those values are very probable.

By means of investigating structural state of adularia from each zone the relevant data on the composition of the solution have been assigned. The structure of the post-oligoclase adularia from Zalas and Miękinia shows a similar tendency concerning order-disorder as the freely crystallizing adularia. In the latter the order-disorder depends on growth speed (Akizuki & Sunagawa, 1978). It has been found in current series of examinations that the more is the ratio mK^+/mH^+ the more disordered structure of adularia develops. Lower concentration of both K^+ and H^+ favours the structure state of adularia being more ordered. Structural state of post-oligoclase adularia has been derived by the Su *et al.* method (Su *et al.*, 1986). Adularia from the first zone have got distinct sector structure and $\Sigma t_1 = 0.58\text{-}0.64$, from the second one $\Sigma t_1 = 0.6\text{-}0.75$, from the third one $\Sigma t_1 = 0.7\text{-}0.75$. Adularia from the third zone do not show sector structure. Investigation of the structural state of hydrothermal feldspar and accompanying paragenesis proves to be an effective petrographic tool useful for the determination of kinetics of hydrothermal processes.

References:

Akizuki M., Sunagawa J. (1978): Min.Mag., **42,** No 324.
Fournier R. O. (1981):Chapter 4 in "Geothermal systems: principles

and case histories", Ryback L. & Muffler L. J. P. (eds), Wiley - New York, p. 109-143.
Slaby E. (1987): Arch.Min. **XLIII**, z.2
Slaby E. (1990): Arch.Min. **XLVI**, z.1-2.
Su S. C., Ribbe P. H., Bloss F. D (1986): Amer. Miner. **71**, 1285-96.

SUBMICROSCOPIC EXSOLUTION REACTIONS IN METAMORPHIC MINERALS: THE CASE OF AMPHIBOLE

Smelik, E. A., *Dept. of Geological & Geophysical Sciences, Princeton University, USA*

In recent years an increased number of transmission-analytical electron microscope (TEM-AEM) studies of common metamorphic minerals have revealed that they may contain a wide array of complex exsolution microstructures that had gone previously undetected. This is especially true for the amphiboles. TEM-AEM examination of optically homogeneous amphibole shows that they commonly contain numerous submicroscopic exsolution lamellae of one, two, or even three other amphiboles. The abundance of exsolution microstructures in amphibole minerals attest to the large miscibility gaps that exist between members of the four major groups (calcic, ferromagnesian, sodic, and sodic-calcic). The cation size variation allowable in the M4 crystallographic site largely controls these inter-group miscibility gaps. Miscibility gaps also exist within amphiboles series, notably between actinolite and hornblende in the calcic series and between anthophyllite and gedrite in the ferromagnesian series. Exsolution in these series involves cation exchange among the M2, T1, and A sites in the amphibole structure. Crystallographic analysis of the exsolution microstructures suggests that lattice misfit largely controls the orientation of the lamellae. Exsolution mechanisms can also be inferred from the microstructures. Evidence for heterogeneous and homogeneous nucleation and growth, and spinodal decomposition have been observed. New observations suggest that exsolution microstructures play an important role during the initial stages of hydration or retrograde alteration in amphibole. In exsolved orthoamphibole, there is evidence for submicroscopic fluid channelization, controlled by the exsolution microstructure. In these samples, the gedrite lamellae are altering to a mixture of chlorite plus quartz while anthophyllite lamellae remain unaffected, thereby forming walls between narrow channels of high fluid flux.

A CALORIMETRIC STUDY OF EPIDOTE GROUP MINERALS

Smelik, E. A., *Dept. of Geological & Geophysical Sciences, Princeton University, USA*; Franz, G., *Fachgebiet Petrologie, Technische Universität, Berlin, FRG;* and Navrotsky, A., *Dept. of Geological & Geophysical Sciences, Princeton University, USA*.

Enthalpies of drop-solution in molten $2PbO{\cdot}B_2O_3$ at 975 K have been measured for a series of natural Al-Fe epidote group minerals. Three compositions of orthozoisite and seven compositions of monoclinic epidote and clinozoisite have been studied in order to examine the energetics of the $Al \leftrightarrow Fe^{3+}$ exchange. For the orthorhombic series, the enthalpy of drop-solution decreases with increasing Fe content, from 495 ± 5 kJ/mol for the Al endmember to 480 ± 4 for orthozoisite with about 15 mol% Al_2Fe component (~2.5 wt% Fe_2O_3), which approaches the solubility limit of Fe in the orthorhombic structure. For the monoclinic series, the composition $Ca_2Al_2Fe^{3+}Si_3O_{12}(OH)$ is considered an endmember. The enthalpy of drop-solution decreases with increasing Al content from 518 ± 6 kJ/mol at 96 mol% Al_2Fe (~16 wt% Fe_2O_3) to a minimum of 478 ± 3 kJ/mol at about 65 mol% Al_2Fe (~11.4 wt% Fe_2O_3), and increases with further Al substitution to a value of 501 ± 3 kJ/mol at 46 mol% Al_2Fe (~7 wt% Fe_2O_3). This trend suggests a positive enthalpy of mixing for the monoclinic series, and indicates a possible miscibility gap. The calorimetric data further suggest that the monoclinic and orthorhombic series should be considered as separate solid-solution series. Enthalpies of formation from the elements at 1 bar, 298.15 K have been calculated for Fe-free orthozoisite and the Fe-rich monoclinic endmember. The results are -6,883 ± 9 kJ/mol and -6,470 ± 9 kJ/mol, respectively. These results are consistent with those from phase equilibrium studies and the previous calorimetric results of Kiseleva and Ogorodova (1987).

References:
Kiseleva & Ogorodova (1987) *Geochem. Internatl.*, **24**, 91-98.

METALS AND OTHER ORE-FORMING COMPONENTS IN LATE MAGMATIC FLUIDS OF GRANITE PEGMATITES (ON INCLUSIONS IN HONEYCOMB QUARTZ).

Smirnov S.Z. (*United Inst. of Geol., Geophys. and Mineral. Novosibirsk, Russia*),
Bakumenko I.T. (*Univ. of Lvov, Ukraine*),
Ishkov Yu.M. (*Geol. Inst., Ulhan-Ude, Russia*)

Honeycomb quartz from different types of granite pegmatites has been studied to define contents of different metals and other mineral-forming components, involving in formation of ore deposits, connected with residual granite pegmatites. Honeycomb quartz are typical of relatively high-temperature pegmatites. It forms a core of zoned crystals (morion or pinky quartz), which grew on the walls of pegmatitic chamber.

Recent thermobarogeochemical studies (Kosukhin et al., 1984) has shown that honeycomb quartz crystallized from later portions of pegmatitic melt with coexisting fluid. These quartz crystals contain fluid and melt inclusions which confined to honeycomb fissures. Only fluid inclusions were used for investigating late magmatic fluid. In general, inclusions of aqueous and aqueous - CO_2 solutions with low density (0.3 - 0.5 g/cm^3) are common, while inclusions with high-density are rare and may be later or necked down in origin.

Honeycomb quartz was collected from three localities of granite pegmatites, differing in degree of ascent from parent magmatic body (e.g. transferring degree) and partly in mineralogy. Pegmatites of the Kent massif (Kazakhstan) are autochthonous (nontransferred) and contain berg crystal and fluorite as principal minerals of pegmatitic chamber (berg-crystal-bearing type). Pegmatites of Volyn are characterized by low transferring degree and mainly contain topaz and beryl. Pegmatites of the Zolotaya Gora (Transbaikalian) are similar to the Volynian ones (topaz-beryl type) but were ascended far from parent magma source.

Compositions of inclusions was examined by cryometry and laser-spectral-mycroanalyse procedure, developed in Ulhan-Ude (Ishkov & Reif, 1990). The main component of fluid is Na in chloride and hydrocarbonate forms. All analyzed solutions contain Fe, Cu, B in small amounts and also Mn and Be in trace amounts. The fluids of the Kent pegmatites are rich in Fe, Cu and B (1.0, 5.5 and 1.3 grams per kilograms of solution, respectively). Fluids of topaz-beryl pegmatites from Volyn are poorer in these elements (0.043 - 0.073 g/kg Fe and 0.011 - 0.059 g/kg Cu). In addition, fluids of the Volyn pegmatites contain 0.03 - 0.1 g/kg Mn. Contents of Fe and Mn in the fluids of the Zolotaya Gora topaz-beryl pegmatites don't exceed limits of sensitivity, and Cu content is slightly less than in the Volynian pegmatites (0.017 - 0.003 g/kg). Unlike the berg-crystal-bearing pegmatites from Kent, the fluids of topaz-beryl pegmatites from Zolotaya Gora and Volyn contain Be

in very small amounts (0.002 g/kg and 0.001 g/kg, respectively). Boron content of the fluids of the Transbaikalian pegmatites (0.043 g/kg) is higher than in the Volynian ones 0.01 g/kg), but don't exceed those in the Kent pegmatites.

Mineralogical features of postmagmatic assemblages show that minerals of the main ore components (Fe, Cu) are scarce with exception of the latest low-temperature associations and authometasomatic changes. In contrast to minerals of Fe and Cu, minerals of Be are omnipresent in both early and late hydrothermal assemblages of topaz-beryl pegmatites in spite of very low Be content. Boron mineralization is absent in all investigated pegmatites.

References:

Kosukhin O.N., Bakumenko I.T., Chupin V.P. (1984):
Magmatic stage of forming of granite pegmatites.
Nauka, Novosibirsk, 136p.

Ishkov Yu.M., Reif F.G. (1990):
Laser-spectral analyses of the inclusions of ore-bearing fluids in minerals. Nauka, Novosibirsk , 93p.

CRYSTALLIZATION FEATURES OF W-RICH TANTAL-NIOBATE FROM RARE-METAL GRANITE MELT (ON EXAMPLE OF ARY-BULAK ONGONITE MASSIF, SIBERIA)

Smirnov S.Z. and Kuzmin D.V. (*United Institute. of Geology, Geophysics and Mineralogy, Novosibirsk, Russia*)

Tantal-niobium mineral in topaz phenocrysts from the Ary-Bulak ongonite massif was initially described as columbite (Naumov *et al.*, 1990). This mineral occurs as crystallites or trapped phases of melt inclusions hosted by topaz. In quartz phenocrysts its crystallites are scarce. Crystallites of tantal-niobate usually form stellar aggregates with 0.5-1 mm in size. Distribution of crystals and aggregates in the host topaz are chaotic. They occur in both central and outer zones of topaz phenocrysts.

Compositional study of tantalo-niobates due to the EMA and SEM has shown that Nb, W, Fe, Mn and Ta are major components. Contents of W in this mineral (up to 18-24 wt.% WO_3) are found to be unusually high for tantal-niobate group.

Two groups of compositions of tantalo-niobate are distinguished. The first group is richer in Nb, Ta, Mn and poorer in Fe, W than second ones. All microprobe analysis are calculated well on formulae AB_2O_6 (columbite). However the content of W varies in single crystal from 7-9.5 wt.% WO_3 (most common of columbite) to 24 wt.% WO_3 (unusually high for columbite). BSE-images has revealed composition heterogeneity of crystallite with 24 wt.% WO_3. Heavier elements (Ta, W) are mainly concentrated in thin (about 1 mk) outer zone.

Tantal-niobate was formed at the latest stage of ongonite melt crystallization simultaneously with topaz phenocrysts. Composition of the earlier crystals corresponded to Ta-Nb-W solid solution with columbite structure. Later this solid solution turned into Ta-Nb-phase (columbite) and W-phase (wolframite). Formation of W-rich rim of crystallites witnessed to increasing of W-activity toward the final stages of tantal-niobate crystallization.

Reference:

Naumov V.B., Solovova I.P.,Kovalenko A.I. *et al* (1990):
Gechem. Intl., **8**, pp. 1200-1205.

MODELING OF TUNGSTEN DISPERSION HALOES FORMATION UNDER DIFFUSION INTERACTION BETWEEN ACID SOLUTIONS AND HOST ROCKS

Smirnova O.K. and Khodanovich P.Yu.
(Buryat.Geol.Inst., Russian Acad. of Sciences)

Hydrothermal ore formation always originates under interaction between water solutions and wall rocks. Most active interaction forestalles economic ores formation. Large volumes of altered wall rocks that were related with ore bodies formation and are an integral part of deposits are the result of such interaction. Primary dispersion haloes of ore bodies which are fixed around their by geochemical mapping and wide used for searching of deep located and non outcroping ores are certain atributes of ore bodies.

Authors suggest the solution of tungsten primary dispersion haloes formation problem under its redistribution from fluids transit zone to wall rocks in the process of their diffusion interaction. Under this conditions diffusion of components into wall rocks is complicated by mineral reactions on the forming metasomatic column zones borders.

In the basic of numerical calculations macrokinetic model of local-equilibrial metasomatic replacement (by D.S.Korzhinsky) with using schemes of reversible chemical reactions was taken. Principles of such model were maked by V.N.Balaschov. In this model systems of differencial transport equations of material balance and those of equations of mineral production are used. In limit cause of local chemical equilibration kinetic equations of mineral production are reconstructing to equations of masses action law, writing equalibria correlation. Numerical solutions of equation systems were realized by V.I.Gunin's program on PC.

Characteristic replacement processes were modeling: plagioclase by calcite on the frontal zone border; calcite by scheelite and rodochrozite at the intermediate zone border. Composition of primary model fluid was maximal correlated with sulfide-tungsten deposits fluids. The model fluids contented (mol/kg H_2O): H_2CO_3 (0,5-0,05); $WO4^{-2}$ (0,1-0,2); Mn^{+2} (1,0-0,1); HCl and HF were introduced in different concentrations (from 0 to 0,1 mol/kg H_2O). Calculations were done for temperature 250-300° C and pressure 1 kbar. Regular variation of persipitated scheelite contents along metasomatic column with maximum in intermediate zones was established. Tungsten contents in fluid decreases to frontal column zones and is maximal near fluids transit zone.

The computation results conform very well to data of scheelite distribution in the natural metasomatic berezite columns on sulfide-tungsten deposits. For such columns synmetasomatic scheelite dissemination and increased tungsten trioxide contents (to 0,02-0,03 %) in the intermediate column zones are characterized by chemical analysis. The main factor of tungsten and other metals concentration in medium zone of metasomatic column is leaching (decreasing of acidity) of acid solutions under their reactions with wall rocks owing to their buffer properties.

Described correlations allow to conclude that significant volume of primary geochemical dispersion haloes on sulfide-tungsten deposits are forming in premineralization beresitization process. They forestall economic ores formation and may be partially separated from them spatially and structurally.

MINERALS OF UZBEKISTAN

Smirnova S.K., (Inst. of Geol. and Geophys., Uzbekistan)

Since the first evidence on minerals in Uzbekistan by Abu-Raikhan-al-Beruni (973-1048), the famous uzbek encyclopaedist of the early Middle Ages there were many advances especially during the later part of our century.

Uzbekistan is a very interesting province for mineralogists. The list of minerals numbers at present more than 700 minerals and about 140 mineral varieties, they constitute about one third of all minerals of the Earth.

There are 24 minerals in native state. Among them native gold, silver, graphite and sulfur often form deposits, the others (tellurium, selenium, mercury, iron, copper, bismuth, lead, zink, platinum metals etc.) occur in very small amounts. Recently native chromium has been discovered by M. Novgorodova, R. Jusupov, L. Morgunova, S. Badalov et al., 1983) in gabbro-diabasic dykes and in terrigenic rocks.

Among the carbides khamrabaevite (Ti,V,Fe)C has been found by R. Jusupov and M. Novgorodova (1984) in basalt of Chatkal ridge and in gabbro-diabasic dykes (Kurama ridge) as inclusions in suessite. The mineral was named for Ibrahim Khamrabaev, academician, an expert of geology and ore deposits in Central Asia.

Among the silicides suessite (Fe_3Si) was discovered. It is the first earthly analogue of mineral from the meteorite North Haig.

More than 40 tellurides of gold, silver and bismuth occur in many mineralized veins. Some new, but unnamed sulfotellurides of Ag, Sb, Bi, Pb and Sn were discovered.

Sulfides are widely spread in mineral deposits. As a rule they are studied in detail. Four new minerals were discovered by V.Kovalenker et al. (1979. 1981, 1982, 1984) in gold deposits in Kurama and Chatkal mountains. There are kuramite (Cu_3SnS_4), chatkalite ($CuFeSn_2Se$) - both were named for occurrence, nekrasovite ($Cu_{26}V_2Sn_6S_{32}$) was named for russian mineralogist and geochemist Prof. I. Ja. Nekrasov, mochite (Cu_2SnS_3) was named for Prof. G. Moh.

The amount of sulfates consist of those of Ca, Sr, Ba, Na, K etc. They are present in the form of huge beds of gypsum, anhydrite or in the form of nodules of barite and celestite. Among the sulfates there is uklonskovite ($NaMg[SO_4](OH)*2H_2O$) was discovered by M. Slusareva and named for Alexander S. Uklonsky, academician, the founder of mineralogical school in Uzbekistan.

The list of minerals also contains many carbonates, phosphates, oxydes, halides, tungstates, molibdates, vanadates of various genesis.

Silicates number more than 190 minerals. They mainly occur in form of feldspars, feldspatoids, micas, amphiboles and pyroxenes in igneous and sedimentary rocks and also in metasomatites and veins.

The first finds of some mineral varieties are of interest, they are: vanadiferous cassiterite and stibial colusite were discovered by E. Spiridonov and A. Badalov (1984), antimonial and arsenious mawsonites (E. Nikolaeva et al., 1984), seleniferous emplectite (V.Kovalenker et al., 1984), high thorian kasolite (E. Dunin-Barkovskaja, 1989) etc.

The information about minerals of Uzbekistan was compiled in the Mineralogy Laboratory of the Institute of Geology and Geophysics Uzbekistan Academy of Sciences by Maria I. Moiseeva and Svetlana K. Smirnova and edited in form of two monographs (1975-1977, 1989).

Noteworthy advances in mineralogy had been made by mineralogists of Uzbekistan. At present they continue their researches and soon we'll learn much new minerals.

References:

Minerals of Uzbekistan (1975-1977), volumes 1,2,3,4. p.p.1616.
New Information on Minerals of Uzbekistan (1989), p.p.316.

NEW TRENDS IN COMPUTER-BASED TEACHING OF MINERALOGY AND CRYSTALLOGRAPHY.

Dorian G.W. Smith, Dept. of Geology, and **Michael Abley**, Dept. of Soil Science, Earth Sciences Bldg., University of Alberta, Edmonton, Alberta, Canada, T6G 2E3

The IMA Catalogue of Software for Mineralogists (Smith, 1992) included about 900 items in 21 different fields. Although much of this software is aimed at research, "Teaching of Mineralogy and Crystallography" includes 75 items related to a wide range of topics from crystal structure simulation to mineral identification. However, day-to-day use of some of the available software in the classroom, has left a very clear impression that students regard much of it as either trivial, amateurish or outdated. We must realise that many of today's students are thoroughly familiar and comfortable with computers. They are accustomed to the devices, standards, conventions and conveniences offered by major, multi-national software houses for word processing, databases, imaging and, of course, video games. If we are to realise the potential of computers in teaching, it is essential that programs developed for this purpose do not lag far behind state-of-the-art software in the wider public domain. The Windows™ program for PC/compatible computers, offers not only a convenient *shell* for running existing software, but also provides a vehicle and a standard for future program development.

Instrumentation costs for modern mineralogy are high. Currently, a powerful desk-top computer may cost less than, for example, a student petrographic microscope. We believe we are at the beginning of a trend towards reducing these instrumental costs by simulating their performance and output via computers. Recently, Tindle (1994) reported an on-going project at the Open University (U.K.) aimed at using imaging capabilities of computers to create a "virtual microscope" which would offer not only a simulation of optical microscope images but also provide features not available on a real instrument - *e.g.*, simultaneous viewing of a thin section under plane polarised light and crossed Nicols. Kohut *et al.* (1993) described an interactive program ("MAX") written as an aid for teaching clay mineralogy by simulating X-ray powder diffractometer patterns.

At this meeting, we shall introduce **Mineral Master©**. This software consists of three components which run under Windows™: an image/textual/numerical database; a search-match component; and a tutorial/quiz section to test users' progress. The initial version includes 110 relatively common minerals typically covererd in an undergraduate course. The database contains one or more 640x480-pixel/256-colour, scanned images for each mineral. Photographs of hand specimens, many supplementary stereomicroscopic, petrographic thin section and electron beam images, crystal structure and crystal morphology representations and spectral or graphical displays, are all included. Textual and numerical data draw heavily on the **MinIdent-PC** database, including fields for formula, symmetry, space group, cell dimensions, composition, Mohs' hardness, Vickers' hardness, density, reflectance, indices of refraction, colour(s) in thin section and the 5 strongest X-ray powder diffraction lines. If appropriate, both ranges and means for these data are made available. Additional fields contain commonly-used hand specimen characteristics, generalised descriptions, notes on geological occurrence, literature references and comments on stored images.

Mineral Master has been developed in Visual Basic™ for PC/compatible platforms equipped with a CD ROM drive and an SVGA monitor. Activities are accessed through menus and buttons, either via mouse or keyboard. Images can be expanded to full screen at any time; additionally, zooming and panning features are included to facilitate detailed examination at higher magnifications.

We believe that such software, coupled with modern networking trends, could not only mitigate the escalating costs of equipping mineralogical teaching laboratories, but should also widen the availability of teaching facilities, particularly in under-developed countries. The approach provides a visually stimulating and more inspiring learning environment than conventional, text-based systems. Furthermore, to some extent, students can tailor their learning programs to their particular needs, strengths and weaknesses, and apportion their time individually. They may also test their progress confidentially with assessment by an objective, non-threatening machine.

References:

Kohut, C.K., M.W. Abley, and Dudas, M.J., (1993). J. Nat. Resources & Life Sci. Educ., **22**, 169-172.

Smith, D.G.W., Ed., (1992). Working Group on Databases Computer Applications, International Mineralogical Association, 197 pp.
Tindle, A.G., (1994). Min. Soc. Bull. 102, 9-13.

A SYSTEMATIC APPROACH TO REPRESENTING MINERAL CRYSTAL-CHEMICAL STRUCTURE FORMULAS

Smith, D. K.[1], Roberts, A. C.[2] and Bayliss, P.[3] [1]*The Pennsylvania State University, Univeristy Park, PA 16802, USA.* [2]*Geological Survey of Canada, 762-601 Booth Street, Ottawa, Ontario, Canada K1A 0E8.*, [3]*Mineralogy, Australian Museum, P. O. Box A285, Sydney, N. S. W., Australia.*

Throughout the mineralogical and crystal-chemical literature, there are many different methods that have been used to represent the general crystal structure formula. This lack of consistency leads to considerable confusion. Also there is confusion caused by the simultaneous use of the same letter code to represent a structure site and the element in that site. This presentation will introduce an approach to a standard use of the English alphabetic characters in a manner that does not lead to ambiguity between site symbols and element symbols.

Many of the English characters are used individually to designate elements in chemical formulas, so it is necessary to avoid the use of these characters in any standard structural formula representation. The characters A, D, E, G, L, M, Q, R, T, X, and Z, however, are available. In order to deviate as little as possible from common usage, the early letters are assigned to the larger cation sites and the later letters are used for the smaller sites and the anions. Thus, T retains its use for representing tetrahedral coordination sites. X and Z are used for anions. There are sufficient other letters to cover all the structural configurations in mineral and alloy structures.

This scheme for representing the structural groups found in the mineral world has been used for the Mineral Group subsection of the Powder Diffraction File. Its success in this application suggests that it should be adapted for all uses of mineral structural formula in texts and scientific literature.

GEOCHEMICAL EVOLUTION AND GENESIS OF VOLCANITES WITHIN EARLY PROTEROZOIC PECHENGA-IMANDRA-VARSUGA BELT (KOLA PENINSULA).

Smolkin V. F. & Skuf'in P. K. (Geol. Ins., Kola Sci. Centre, Russ. Acad. Sci., SU-184200 Apatity, Russia).

The Pechenga-Imandra-Varsuga belt is a unique paleorift system, which has undergone a full cycle of evolution (arch-structure - rifting - orogeny and metamorphism). This NW-SE trending belt extends discontinuously over c. 700 km in the Kola Peninsula from the Caledonides of N. Norway to the western coast of the White Sea. The following stages of its evolution have been recognised: pre-riftogenic (2.56-2.30), early riftogenic (2.30-2.20), later riftogenic (2.20-1.95) and orogenic (1.95-1.85 Ga) [Smolkin, 1992]. Volcanic processes operated in the course of 11 periods of variable duration, which were interrupted by the sedimentary cycles. The composition of volcanic associations changed upwards: basaltic, andesitebasaltic, picritebasaltic, trachybasaltic, basalt-ferropicritic, picrite-basalt-andesitic, and andesite-dacite-rhyolitic. Some volcanic associations altered laterally. As the riftogenic processes evolved, the initial 87Sr/86Sr ratio in volcanites first decreased from 0.7041 (2.32 Ga, andesitebasalts) to 0.7021 (1.98 Ga, tholeiitic basalts) and then increased again to 0.7043 (1.86 Ga, andesites and dacites). It is suggested that in the early pre-riftogenic stage, eruption of the mantle basaltic melt occurred, with melting of the granite-gneiss basement and mixing of heteroabyssal melts of variable compositions. It is based on the study of isotopic system and also the changes in K/Ti, Ti/Rb, V/Cr, La/Ce ratios and the REE-distribution patterns. Mantle and mantle-crustal high-alkalic melts were erupted in the early riftogenic stage. In the mature stage of the riftogenic system, the generation and eruption of two types of melts occurred. They are represented by subabyssal tholeiite basaltic and abyssal ferropicritic types. There were two independent mantle sources for them: depleted and metasomatically enriched. For the picrites and genetically related to them intrusive gabbro-wehrlites, the increased 87Sr/86Sr ratio (0.7032 and 0.7030) and the decreased ε Nd=+1.5 ratio (1.99-1.97 Ga) have been established. Ferropicrites and gabbro-wehrlites have the same primary-magmatic mineral paragenesis (olivine, Ti-augite, plagioclase, kaersutite, Ti-chromite, ulvospinel and ilmenite). But as distinct from the volcanites, the intrusions are characterised by extensive processes of contamination, which had a profound impact in the formation of sulphide Cu-Ni ores. The interrelations between the ferropicrites and basalts show that during the tectonic inversion, specific conditions for mixing of their parental melts existed. And finally, in the orogenic stage, the thermal influence on the upper crust resulted in the formation of crustal-mantle and crustal melts. Outside southern margins of the PIV belt, granite and granodiorite domes arose (1.94 Ga). Volcanic rocks were metamorphosed in greenstone and amphibolite facies (1.79-1.72 Ga), which caused the recrystallisation of Cu-Ni ores and some disturbance in isotopic systems. Simultaneous emplacement of postorogenic monzodiorites took place during this stage.

References:
Smolkin V.F.(1992). Komatiitic and picritic magmatism of the Early Precambrian of Baltic Shield. Nauka, St. Petersburg. 278p.

HARD X-RAY MICROPROBE AND MICROIMAGING TECHNIQUES BASED ON BR AGG-FRESNEL CRYSTAL OPTICS AT THE EUROPEAN SYNCHROTRON RADIATION FACILITY.

A.Snigirev
European Synchrotron Radiation Facility, B.P.220, 38043 Grenoble, France

It has been shown recently that combination of microfocusing optics with the high brilliance x-ray beams provided by the third generation synchrotron radiation sources like ESRF opens up new capabilities to develop hard x-ray microprobe and microimaging technique. Bragg-Fresnel optics demonstrated unprecedented and very promising performance in terms of efficiency, resolution, energy tunability and stability.

There are many uses for hard x-ray micro- and submicrobeam including diffraction, imaging and fluorescence experiments. Linear microprobe with 1μm beam width was realized at the ESRF Microfocus beamline to measure diffraction from a small samples of 10-100μm sizes: fibers, wires, starch particles etc. Small angle scattering camera with spot size of 2μm and angular resolution 10^{-4}rad was designed and used to study turkey tendon collagen.

Microfluorescence technique is of particular interest for elemental analysis of very small samples in biology and earth science. Scanning fluorescence microprobe based on linear, circular and elliptical Bragg-Fresnel lenses was tested on Microfocus and Troika Beamlines. Resolution of about 0.7μm and flux 10^8-10^9ph/s have been achieved. Mapping of different metallic masks and micrometeorite inclusions has been made with the microbeam.

A microprobe beamline dedicated to microfluorescence, micro-

diffraction, microtomography and microimaging is designed to be installed at the ESRF. The performance of this beamline will be presented as well.

ULTRAHIGH PRESSURE MINERAL ASSEMBLAGES OF DIAMONDIFEROUS METAMORPHIC ROCKS FROM KOKCHETAV MASSIF (NORTHERN KAZAKHSTAN)

N.V. Sobolev, V.S. Shatsky, M.A. Vavilov *(Institute of Mineralogy and Petrography, Russian Academy of Sciences, Siberian Branch, Novosibirsk 630090, RUSSIA)*

Diamondiferous metamorphic rocks occupy the territory no less than 100 km² within Kokchetav massif. They are represented mainly by mylonite gneisses (up to 80%), garnet-pyroxene and garnet-pyroxene-carbonate rocks which occur as lenticular, banded or vein-like bodies within these gneisses of Zerendin rock series. Microdiamonds are observed in hundreds of doubly polished plates and thin sections mostly as inclusions in garnets and zircons. Sometimes they are present as inclusions in clinopyroxene and kyanite. Diamond presence in rounded pseudomorphs after garnets and their preservation within different secondary assemblages is also typical. No diamonds were observed in intergranular space between of garnets and pyroxenes. The majority of diamonds are cubo-octahedra, with varying development of cube and octahedral faces (80% of all observed diamonds have a size less than 20 micrometers). The diamond presence always correlates with a presence of graphite. High temperature (about 900°C) eclogites found within the diamondiferous mylonite gneisses are the only rocks which do not contain either diamond or graphite.

A number of pyroxene grains included in garnets and zircons from all types of diamondiferous rocks show variable K_2O concentrations up to 1.55% in the cores. The phengite inclusions contain up to 5% TiO_2 and the titanites up to 13.5% Al_2O_3. Fe-Mg garnets contain mainly from 9 to 19% CaO. Coesite as monocrystalline grains is included in zircons. Only traces of quartz are detected by Raman spectroscopy in a number of such inclusions. Coesite-diamond and coesite-pyroxene polymineralic inclusions with K-bearing clinopyroxene are also found in zircon grains.

Zircon is considered the high-strength mineral container uniquely protecting coesite from transformation into quartz. A series of independent indicators of ultrahigh pressures are present in all types of diamondiferous rocks besides of diamond itself. They include abundant coesite preserved as inclusions in zircon only, K-bearing clinopyroxene, Al-rich titanite, Ti-rich phengite found both as inclusions in garnets and zircons.

CHANGING OF THE CHEMICAL COMPOSITION AND INNER STRUCTURE OF THE ALKALI FELSPARS IN THE VERTICAL SECTION OF GRANITE MASSIVE ELDJURTI

Sobolev R.N.(Dept. of Geology, Moscow State Univ.)

It is known that chemical composition (K,Na), symmetry Si-Al ordering), character of decay (K-Na ordering - pertites) and 2V of alkali felspars (A.F.) depend on conditions of it formation and existing. Conseqvently, if we know these characteristics, it's possible to reconstruct conditions of A.F. formation, as well as rocks which they form. We've studied these characteristics of A.F. taken from hole drilles in Eldjurti granite massive from it upper contact till depth about 5 km. This massive is on the North Caucasus, 40km to the north from volcano Elbrus. K-Ar age is 2 million years. In this vertical section were studied aiso biotite, glass and fluid inclusions. A.F. are as phenocrysts and in ground mass. Chemical composition was studied on microprobing Camscan-4; X-ray investigation by diffractometr DR=H-YH-1; results were calculated on computer by special programs.

Si-Al ordering. All A.F. are of monoclinic symmetry: 1. from the upper contact to the depth 1000m sanidines (0-150m intermediate; 150-600 intermediate and low; 600-1000m low) and 2. deeper orthoclases (1000-4500 high, deeper intermediate).

2V. Increase with depth: 0-150m less than 40° (minimum in the interval 0-30m); mostly fluctuate from 40 to 60° (sometimes less then 40) from 150 to 600; in the interval 600-1000m - 40-60° and deeper than 1000m - 50-60°.

Character of decay (pertites). Till the depth 150m all A.F. are homogeneous; in the interval 150-600m homogeneous and crypthopertitic (mostly in the border zones of grains); from 600 till 1000m crypthopertitic and rare homogeneous (in ground mass); 1000-15000 cryptho- and micropertitic; 1500-4500 micropertitic; deeper - micropertitic (ground mass) and pertitic (phenocrysts).

Chemical composition. K_2O concentration varies from 9 to12 (phenocrysts) and from 11 to 12 mas % (ground mass). In a wholle concentration increase with depth. K_2O content in border zones of grains is about 1% higher than in cores. Na_2O concentration varies in the limit 1 - 2 (phenocrysts) and 0.5-1 mas % (ground mass). In a wholle concentration decrease with depth. Na_2O content in border zones of grains is about 1 mas% less than in cores.

Changing of all characteristics is interconnected.

It was established that process of ordering began in phenocrysts befor groud mass crystallization. Phenocrysts began to grow during magma intrusion then grew simultaneously with A.F. from ground mass. Magma crystallization occured in some stages (zones) from the upper contact (apical zone) to the centre of the massive. Magma has high temperature and was "dry".

MINERAL ASSEMBLAGES AND CHEMICAL COMPOSITION OF PB-BI SULPHOSALTS AS INDICATOR OF STABILITY OF THE SYSTEM PB-Bi_2S_3 IN NATURE

Soboleva L.N. (Dept. of Geology, Moscow Univ)

The sulphosalts were studied from Cara-Oba (Kazakhstan), Ustarasay and Chokodam (Uzbekistan), Bukuka (Russia, Zabaykalye) and other ore deposits by the following methods: ore microscopy, electron-microprobe analyses and X-ray powder microanalyses. For these minerals are typical:

1. Separation in space from Bi sulphosalts of another chemical composition, which can be found in them only as the mineral-microinclusion. This is a result of Pb-Bi sulphosaits, bismuthinite and galena inner structure autholisium from extra concentrations of Cu, Ag, Sb at low temperatures.

2. In these deposits only 4 minerals, of the PbS-Bi_2S_3 system, were founded in a significant amount: bismuthinite, galenobismutite, cosalite and galena. All these minerals are stable at the temperatures less than 270°C. Other Pb-Bi sulphosalts: cannizzarite, bursaite, lillianite, heyrovskite - are stable only at relatively high temperatures and are rare in the nature.

3. All these minerals form closely intergrown mixtures. There are two typical mineral assemblages: bismuthinite - galenobismutite and cosalite - galena. The intergrowths of bismuthinite - cosalite are rare, but intimate intergrowths of galenobismutite - cosalite and galenobismutite - galena are not established.

4.Chemical compositions of bismuthinite, galenobismutite, cosalite and galena were studied by electron microprobe analyses and results are in good general agreement with their theoretical compositions. Concentrations of trace elements not exceed the isomorphous capacity at low temperatures. Relationships between Cu:Ag:Sb are determined by the composition of the mineralizing fluids.

MELT INCLUSIONS IN MINERALS AS INDICATORS OF ROCKS AND ORES FORMATION BY LIQUID IMMISCIBILITY

Sokolov S.V., (*All-Russian Inst. of Mineral Resources*)

Hypotheses for origin of rocks and ores by liquid immiscibility in magmatic systems are usually based on indirect evidence: (1) coexistence of contrasting rock compositions, which could not be explained by crystal fractionation; (2) some features of bulk compositions of such coexisting rocks and data on trace element's distribution between them; (3) presence of emulsion structures; (4) experimental modeling of liquid immiscibility at PTX- parameters applicable to magmatic processes. Perhaps, only liquation-type melt inclusions seem to be direct indicators for manifestation of magmatic liquid immiscibility.

It has been found experimentally (Romanchev et al.,1972) that crystallization of layered magmatic systems is attended with simultaneous trapping of droplets of immiscible liquids by minerals in accidental proportions. This type of melt inclusions is known to exist in a number of rock-forming minerals of volcanic and plutonic rocks ranging in composition from basic to acid and alkaline, their pegmatite and ore derivatives, in carbonatites and also in mantle nodules and lunar basalts.

Many publications (see, for example, summary by E.Roedder, 1984) and our results of inclusions study (Romanchev & Sokolov, 1979; Sokolov, 1989) testify to various types of liquid immiscibility:

1. Silicate - silicate, typical for ultrabasic-basic and alkaline magmas.
2. Silicate - saline; it is manifested by in the splitting out of carbonate and alkaline-halide liquids from respectively alkaline and granite melts.
3. Ore - silicate, characterized by separation of sulfide, oxide and metal liquid fractions.

The compositional resemblance of liquation inclusions to corresponding rocks (basalts, pyroxenites, rhyolites, carbonatites) confirmed by above-mentioned geological and geochemical criteria allows to conclude that liquid immiscibility is a real process of magmatic differentiation that gives rise to a broad spectrum of rocks. In addition, it plays an effective ore-generating role, because layering of magmas leads in many cases to separation and accumulation of oxide, sulfide, phosphate, rare-metallic and complex ores.

References:

Roedder, E, (1984). *Fluid inclusions. Reviews in Mineralogy*, vol. 12.

Romanchev, B.P., Kogarko L.N., Krigman L.D. (1972) *Geokhimia*, No. 10, 1307-1311.

Romanchev B.P., Sokolov S.V. (1979). *Geokhimia*, No. 2, 229-240.

Sokolov S.V. (1989). *Geokhimia*, No. 12, 1683-1693.

• TSAREGORODTSEVITE: A NEW NATURAL FELDSPATHOID WITH ORGANIC CATION

Sokolova E.V. *(Dept. of Crystallography, Moscow State Univ.)*

Tsaregorodtsevite was found in metamorphic rocks in the Northern Urals (Pautov *et al.*, 1993). Crystal structure and structural transformations of tsaregorodtsevite were investigated using X-ray single-crystal technique (Sokolova *et al.*, 1991, 1993). The crystal chemical formula of tsaregorodtsevite is $[N(CH_3)_4][Si_2(Si_{0.5}Al_{0.5})O_6]_2$, it is orthorhombic, *I*222, a = 8.984(3), b = 8.937(2), c = 8.927(2) Å, D_x = 2.01 Mg m^{-3}, Z = 2, R = 0.047 for 516 unique observed reflections. Si and (Si,Al) tetrahedra form the 1:5 aluminosilicate framework that is topologically similar to that of sodalite, $Na_8(Al_6Si_6O_{24})Cl_2$.

The isolated polyatomic organic groups $[N(CH_3)_4]^+$ (TMA) are discovered for the first time in natural minerals. They represent intraframework cations at the corners and center of the cell. (TMA)-groups are connected with O atoms of the framework by hydrogen bonds.

A systematic thermoanalytic study using X-ray single-crystal technique has shown two transformations of tsaregorodtsevite framework on heating. Weight loss was fixed at 660-950°C and was due to the destruction of (TMA)-cations. The two phases are characterized as follows: I (870°C): tetragonal, *I*422, a = 8.908(1), c = 8.925(1) Å, R = 0.044, 408 reflections; II (970°C): cubic, *I*432, a = 8.817(3) Å, R = 0.047, 39 reflections. Both modifications exhibit the same structure type and retain the tsaregorodtsevite framework. However, increasing disorder of Si and Al atoms culminate in a change of interatomic distances and symmetry. Similar tendency was predicted on an example of sodalite (Hassan & Grundy, 1984).

Hassan, I. & Grundy, M. (1984). *Acta Crystallogr.*, **B40**, 6-13.

Pautov, L.A., Karpenko, V.Yu, Sokolova, E.V., Ignatenko, K.I. (1993). *Zap. Vses. Miner. O.*, **122**, 128-135.

Sokolova, E.V., Rybakov, V.B., Pautov, L.A. (1991). *Doklady Akad. Nauk SSSR*, **317**, 884-887.

Sokolova, E.V., Rybakov, V.B., Pautov, L.A., Pushcharovskii, D.Yu (1993). *Doklady Rus. Akad. Nauk*, **332**, 309-311.

PETROLOGY AND EVOLUTION OF TRANSITIONAL ALKALINE - SUBALKALINE GRANITOIDS FROM SERRE - DRAMA (NE GREECE): EVIDENCE FOR FRACTIONAL CRYSTALLIZATION, MAGMA MIXING AND ASSIMILATION

Soldatos T. (Dept. of Miner., Petrol. & Econ. Geol., Univ. of Thessaloniki), Poli G. (Dept. Earth Sciences, Univ. of Perugia), Cristofides G., Eleftheriadis G. (Dept. of Miner., Petrol. & Econ. Geol., Univ. of Thessaloniki) and Tommasini S. (Faculty of Earth Sciences, Univ. of Amsterdam)

The Serre-Drama or Vrondou intrusive complex is an Oligocene composite pluton which intrudes marbles and shists of the Lower Tectonic Unit of the Western Rhodope Massif, adjacent to its western boundary with the Serbomacedonian Massif. New and literature gechemical data of the pluton are discussed to clarify basic/acid magma interactions and to revise petrogenetic schemes in a monzonitic intrusive suite.

The pluton consists mainly of hornblende-biotite quartz-monzonites that occupy two thirds of the exposed area, and has gradational contacts with biotite-hornblende monzogranites (granite) and granodiorites, and obscured contacts with the more basic rock-types: clinopyroxene-hornblende monzonite and porphyritic monzonite with subordinate cumulate gabbro and lamprophyric dykes. Microgranular enclaves (ME) of diorite to quartz-monzonite composition are abundant in all rock-types except the gabbro and the lamprophyre. The main salic mineral constituents are quartz, K-feldspar (perthitic orthoclase and microcline) that in the monzonite forms megacrysts, and oligoclase to acid labradorite plagioclase with characteristic patchy zoning. The main ferromagnesian minerals in order of abundance are common hornblende, biotite, and clinopyroxene (mostly in monzonite and gabbro). Among the accessories are titanite, very abundant, apatite, epidote, allanite, zircon, and opaques.

Samples from the strongly deformed quartz-monzonite at the southern contacts and the detached Elaion small body, exhibiting a

gneissic texture, overlap geochemically with the rest of the Serre-Drama samples that do not show any metamorphic signature at all. This feature coupled with field constraints, such as the gradational contacts between the deformed and the non-deformed rocks, having gneissic and intrusive textures respectively, suggest a syn-intrusional deformation.

From geochemical point of view all the samples show roughly regular lines of descent for major elements, but very scattered patterns for most of the trace elements. Interesting feature is that ME samples can be subdivided into two groups at different K_2O, Rb, Ba, Sr, La contents. The same holds for samples showing an actual monzonitic character. Linear programming models using published data on minerals like K-feldspars, biotite, and accessories seem to exclude that such a geochemical feature could have derived from unamixing processes between a magma with less monzonitic affinity and those minerals. On the other hand the two sample groups cannot have derived from each other through processes at shallow level. These conclusions support the hypothesis that two parental magmas with different affinity coexisted.

Their evolutionary trends led to the formation of monzonites and of quartz-monzonites, granodiorites and monzogranite respectively. However, patterns cannot be easily recognized due to strong geochemical overlapping, and this can suggest, on the other hand, that both the two magmatic reservoirs influenced shallow level environment. Trace element constraints together with variable isotopic ratios, support the hypothesis that assimilation plus fractional crystallization processes may be responsible for the evolutionary trends, even if simple crystal fractionation can be suggested for the genesis of very acidic products.

A model is presented whereby magmas at different affinities underwent assimilation plus fractional crystallization in an intracrustal magma chamber(s) to yield more evolved liquids. Influx of hot primitive magmas into the base of the chamber(s) could have facilitate assimilation, but eventually lead also to mixing processes that complicated the geochemical patterns.

• DICKITE OF JURASSIC SEDIMENTARY ROCKS OF TALINSKAYA ZONE OF GAS AND OIL ACCUMULATION (WESTERN SIBERIA)

Solotchina E.P., Kazansky Y.P. and Kazarbin V.V. *(Geology Institute of Sib. Div. RAS, Novosibirsk, Russia)*

Dickite is the widespread mineral of Jurassic terrigenous rocks of Talinskaya Zone of gas and oil accumulation (Western Siberian Platform). The problem of its genesis is controversial. There are two different points of view: on the one hand, it is the typical hydrothermal mineral and on the other hand it may be authigenic catagenetic mineral of sedimentary rocks.

A lot of the dickite samples from gravelstones and sandstones cement of the Sherkalinskaya suite (Lower Jurassic) were investigated (1). Besides that, dickite samples from the siderite geodes of the kaolin weathering crust which is underlying the Lower Jurassic deposits (2), from the material of space cavity filling in the Pre-Jurassic base (3) and from Ak-Tashkoye hydrothermal deposit (Altai) (4) were studied for comparison.

By means of scanning electron microscopy two morphological varieties of the studied dickite were determined. The dickite samples (1), (2) are attributed to the first type. Their aggregates are represented mainly by laminar elongated pseudohexagonal crystals with rough "attacked" surface and look like ordered kaolinite. The (3), (4) samples are referred to the second type. Their aggregates are represented by tabular (rarely laminar) pseudohexagonal crystals with distinct contours with flat smooth, sometimes stepped surface. The crystals are very closely packed.

All the investigated dickites present the same X-ray powder diffraction patterns with narrow distinct lines and infrared spectra. However we managed to find structural differences between the determined morphological varieties with the help of the Fourier analysis of profiles of X-ray diffraction lines. By means of this method the parameters of dickite's fine crystal structure (size of coherent scattering regions, CSR, and crystal lattice microstrains, E) were determined in the direction normal to basal planes. For the first type of dickite it was found that CSR size is D= 400 A, relative RMS-microstrains E = 3.10^{-3}. The second type of dickite has D twice as much and E one half as much as that found for the first type.

Thus, we explain the morphological and structural differences of the studied dickites in terms of their different genesis. We think that the first type is the product of catagenic processes in porous space of terrigenous rocks and weathering crusts and the result of replacement of kaolinite. The second type is typically hydrothermal. The formation of the authigenic dickite in the Lower Jurassic clastic oil-bearing rocks improves their reservoir properties.

STRUCTURE AND REACTIVITY OF MINERAL SURFACE COMPLEXES: A STUDY OF THE SORPTION OF Cd(II) ON FeOOH

Spadini L., Manceau A., and Charlet L. *(Environmental Geochemistry Group, University of Grenoble)*

Reactions at the solid-water interface between aqueous solutes and oxides play a major role in geochemical and environmental systems Significant improvement in the accuracy of presently used predictive tools can be expected from increased knowledge on the structure and the reactivity of the surface complexes. EXAFS spectroscopy is one of the few methods which provides molecular level information about the structure of the products of interfacial reactions. To this end, samples were prepared of Cd adsorbed on αFeOOH (goethite) and HFO (amorphous FeOOH) at surface coverages ranging from 11 to 100% and 1 to 90% respectively. The cation Cd(II) was choosen due to (i) its relevance to environmental systems, and (ii) its low tendency to polymerize and precipitate, thereby reducing the possibility of solution nucleation.

EXAFS spectra analysis yields two distinct Cd-Fe distances at 3.2_9 and 3.4_9 Å, corresponding respectively to edge (E) and double corner (DC) linkages between the Cd and Fe (H_2O,OH,O) octahedra. For αFeOOH, at low surface coverage, Cd-Fe surface complexes involving edge sharing are mainly formed whereas at high coverage DC linked complexes predominate. Structural considerations requires that 4 oxygens are shared between the Cd-Fe atoms in an edge linkage vs. two to three in a DC linkage. These results imply that the affinity of Cd is higher toward surface complexes involving edge sharing and/or a high number of shared oxygens. The same relative affinity exists for Fe(III) ions sorbing on αFeOOH during the crystal growth process. This indicates that Cd(II) and Fe(III) ions have the same relative affinity for goethite functional groups and form similar surface complexes. This finding is supported by EXAFS analysis of a $\alpha(Cd_{.005}Fe_{.995})OOH$ coprecipitation sample in which it is shown that Cd substitutes for Fe in the goethite structure. For Cd-HFO samples, the relative amount of E and DC linkages is constant regardless of the surface coverage and equals that found for Cd-αFeOOH at low surface coverages. This is thought to be caused by the high amount of high affinity sites on the amorphous sorbent.This result can be understood in the light of most recent models of the structure of hydrous ferric oxides which indicate that the amount of high affinity surface sites, i. e. free edges, is much higher for HFO than for αFeOOH.

In the range of surface coverage considered, no polymerization or surface precipitation processes were observed. This indicates that Cd is a very suitable agent to probe the nature of surface reactive sites.

CARBON AND OXYGEN ISOTOPE RECORDS OF FLUID MIXING AND FLUID-ROCK INTERACTION IN CARBONATES FROM THE ZINC-LEAD DEPOSIT OF SAN VICENTE (CENTRAL PERU)

Spangenberg J.[1], Fontboté L.[1], Sharp Z.D.[2], and Hunziker J.[2]
([1]Département de Minéralogie, Uni. Genève, [2]Institut de Minéralogie, Uni. Lausanne)

Carbon and oxygen isotopic characterization of host and gangue carbonates were used to constrain the mechanism of ore precipitation in the Mississippi Valley-type Zn-Pb deposit of San Vicente. The $\delta^{13}C$ and $\delta^{18}O$ values were measured for different carbonate phases (see table) from samples taken at the San Vicente mine following a hierarchical sampling sheme.

Carbonate phase (n)	$\delta^{13}C$ ranges (‰ PDB)	$\delta^{18}O$ ranges (‰ PDB)
Dark replacement dol., I (29)	0.5 to 2.5	-9.6 to -6.3
White sparry dolomite, II (115)	-0.1 to 1.7	-11.8 to -7.3
Late filling dolomite, IIId (10)	-0.3 to 1.1	-12.5 to -9.8
Late filling calcite, IIIc (25)	-11.5 to 0.7	-15.1 to -9.1
Dol. replacing evaporite, EPd (7)	-0.4 to 1.0	-12.1 to -9.8
Cal. replacing evaporite, EPc (11)	-4.5 to 0.8	-16.1 to -9.5

For a given carbonate generation no significant differences were observed between: 1) the three mineralized dolomite units, 2) different mantos in the same dolomite unit, and 3) samples from crosswise profiles performed at the same manto.

However significant isotopic variations were detected at the textural scale. The figure shows the distribution of the median isotopic composition of the carbonate phases in the $\delta^{13}C$ vs. $\delta^{18}O$ space.

In the dark replacement dolomite (DRD) increasing hydrothermal alteration is recognized through increasing grain size between very fine-grained (Ivf), fine (If), and fully recrystallized medium-grained (Im) DRD. The hydrothermal alteration is recorded by an isotopic shift towards lower $\delta^{13}C$ and $\delta^{18}O$ values (trend A in the figure).

In the subgenerations of the white sparry dolomite (WSD) the isotopic trend is inverse, towards heavier isotopic composition from t1 towards t6 (trend B in the figure), where: t1 = spots of WSD, t2 = fine veinlets of WSD, t3 = ordered bands of WSD, t4 = zebra texture, t5 = crosscutting veins of WSD, and t6 = WSD in breccia. Trend B corresponds to the isotopic shift towards heavier $\delta^{13}C$ and $\delta^{18}O$ values reflecting the evolution of the mineralizing fluid (e.g. parent fluid of IIt1) by interaction with the host dolomite.

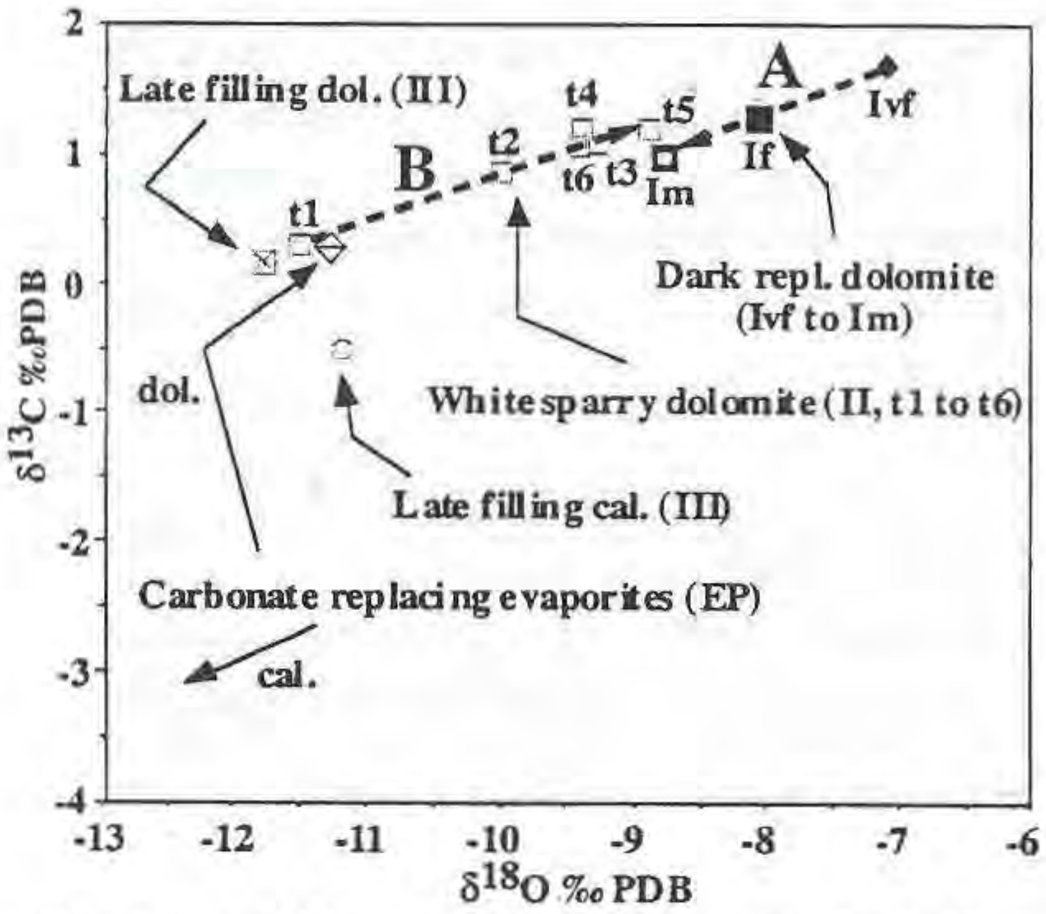

Quantitative models of the $\delta^{13}C$ vs. $\delta^{18}O$ covariations in the different carbonate generations are in line with geological and petrographic observations. The precipitation of the syn- and post-ore carbonate generations (EP, II, III) involve mixing of the native formational fluid (e.g. parent fluid of Ivf) with a hot acidic extraformational fluid. The isotopic evolution of the host dolomite and of the subgenerations of the white sparry dolomite are explained by interaction of the mineralizing fluid with the host carbonate and previously precipitated gangue carbonates.

ELASTICITY OF SOLID SOLUTION SERIES FROM GHZ ULTRASONIC INTERFEROMETRY

Spetzler H., Chen G., Getting I.C. (Dep. of Geological Sciences, CIRES, Univ. of Colorado, USA)

The development of a GHz ultrasonic interferometer opens opportunities to study the elasticity systematics of mineral solid solution series. Such studies in the past have usually been inconclusive because of the unavailability of large samples required by other methods and the lack of precision in the data when small samples are used. With the GHz ultrasonic interferometer, acoustic wave travel times through samples of a few hundred microns can be measured to an absolute accuracy of several parts in 100,000. Combining the travel time data with the sample size measured by laser interferometry, we obtain acoustic velocities through samples of sub-millimeter sizes to high precision.

We choose to study the solid solution series of olivine and garnet, possibly two of the most abundant phases in the mantle. Both form solid solution series by different cations occupying the same structural site in the crystals. We have measured olivine with different Mg/(Mg+Fe) ratios over a small temperature range and observed that the P-velocities vary linearly with the Mg/(Mg+Fe) ratios. From the forsterite end (Mg/(Mg+Fe)=100%) to Fo72 (Mg/(Mg+Fe)=72%), the P-velocity of olivine along the b-axis drops from 7.872 (km/s) to 7.223 (km/s) (about 9% reduction). The normalized temperature derivative changes monotonically from -5.48×10^{-5} /K to -6.73×10^{-5} /K (about 20% increase in absolute values). We are now in the process of mapping the elasticity vs. the Mg/(Mg+Fe) ratio in garnet.

If these relationships between composition, temperature and velocity hold at high pressure and temperature appropriate to Earth's interior, then an increase of 1% in Fe/(Mg+Fe) ratio in olivine reduces the velocity an amount equivalent to that resulting from a temperature increase of 70 K.

EPISODIC METAMORPHIC REACTIONS: MICROSTRUCTURAL CONTROLS ON THE DEVELOPMENT OF COMPOSITIONAL HIATUSES IN GARNET PORPHYROBLASTS IN THE MERAN-MAULS BASEMENT OF THE EASTERN ALPS

Spiess R. *(Dept. of Mineralogy and Petrology, Univ. of Padova, Italy)* and Bell T.H. *(Dept. of Geology, James Cook Univ., Townsville, Australia)*

Within the Variscan portion of the Meran-Mauls Basement of the Austro- Alpine of South Tyrol eight near orthogonal foliations have successively developed and been preserved as inclusion trails in some garnet porphyroblasts. These foliations are commonly truncational with respect to one another and do not have a spiral character indicating 630° of porphyroblast rotation. The earliest garnet cores formed during the second of these deformation events with subsequent growth occurring during the sixth, seventh and eighth deformations.

Compositional zonation in garnet porphyroblasts from two samples from the one outcrop show significantly different patterns for the most recent stage of garnet growth. They vary from smooth to abrupt reductions in grossular and spessartine content (and a rise in XMg) in different microstructural sites. Where the deformation event, in which the bulk of the garnet porphyroblast grew, was partitioned such that it was only weakly developed against the porphyroblast, the transitions were smooth. Where the deformation was more intensely developed against the earlier bulk of the garnet, the transition was more abrupt.

This can be explained in terms of a significant hiatus in porphyroblast growth, with dissolution of the earlier-formed garnet where the partitioning of deformation against the porphyroblast rim was strong, and a much weaker, to insignificant, hiatus in growth where little or no shear occurred against the rim. It indicates a strong microstructural controlon the sites of porphyroblast growth and associated chemical reaction within syntectonically metamorphosed rocks, resulting from the effects of intensity of foliation development on the access of material to the growth site.

Dissolution of garnet and cessation of porphyroblast growth took place during the development of a subhorizontal foliation. Growth recommenced during subsequent development of a near-vertical foliation, recording the peak of metamorphism around 600°C and 6kbars. An increase in spessartine and a drop in XMg contents in portions of the outermost rims of these garnet porphyroblasts, indicates retrogression commenced soon afterwards, generating partial resetting rather than further growth. The only younger deformation present in these samples, which developed a horizontal foliation, was associated with alteration of garnet and biotite to chlorite and may have caused this resetting of the rims. However, this is uncertain and even unlikely if this latter event was Alpine in age.

SITE OCCUPANCY IN GARNET BY CHANNELLING ENHANCED MICROANALYSIS

Spigarelli S., Rinaldi R. (*Dip. Scienze della Terra, Univ. di Perugia*), Balboni R. (*CNR-LAMEL di Bologna*) e Frabboni S. (*Dip. di Fisica, Univ. di Modena*)

The X-ray emission modulation upon electron beam orientation at channelling conditions in a TEM/EDS can be profitably exploited to provide detailed structural information through a quantitative approch generally referred to as ALCHEMI (Atom Location by Channelling Enhanced MIcroanalysis). We used this technique for the determination of cation partitioning in pyrope and titanium-rich garnets (general formula $X_3Y_2Z_3O_{12}$).

Two main modes of operation exist: planar and axial ALCHEMI. They require the alignment of the crystal with respect to the incident beam direction, so that different atomic species lie on alternate planes (planar geometry) or along atom columns (axial geometry) with significantly different projected potentials. The channelling experiments give the distribution of the cations between the octahedral (Y) site and the dodecahedral (X) + tetrahedral (Z) sites.

The procedure we employed for selecting the appropriate orientations consists of the following: 1) simulation and inspection of the crystal structure for selecting the diffracting conditions; 2) use of an appropriate computer code (Stadelmann, 1987) to obtain, from n-beam dynamical calculations in the Bloch wave scheme, the electron flux in the crystal for different orientations. We thus selected three zone axes, [111], [211], and [311], and five planar configurations, (444), (420), (400), (211), and (220), for channelling experiments. They were performed using a Philips CM30 analytical transmission electron microscope (AEM) fitted with a LaB_6 electron gun operating at 100kV and an EDAX 9900 X-ray analyzer. The specimen was oriented in all experiments using the Kikuchi line method and spectra were collected using a Gatan low-background Be double tilt heating/cooling holder operating at 77K for total counting times of 100s and counting rates of 3000 counts s^{-1}. The specimen thickness in the probed area was estimated to be 100-150 nm.

The entity of the channelling effects measured from the variations of the integrated elemental intensities over the incident beam orientations was statistically significant for all the different diffracting conditions. Axial orientations provided better result than the planar geometry for all the crystals analyzed, as the channelled versus non channelled count ratios in the former proved to be one order of magnitude greather than in the latter.

For the pyrope garnet the population distribution of the elements calculated from spectra collected in [111] zone axes is in good agreement with that obtained through X-ray structure refinements of the same material and with indipendently obtained crystal chemical parameters.

For the titanium rich garnet, in which determination of the location and oxidation states of the cations distributed among the tetrahedral (Z) and octahedral (Y) sites, have been extensively discussed in the literature, the axial spectra provided information concerning the distribution of Al, Fe and Ti between these sites. The relative site preference for those tetrahedral sites not occupied by silicon obtained from channelling effects is in the order: Al >> Ti ≈ Fe from which one can infer an octahedral site preference for Ti and Fe.

Moreover our results show that for the axial channelling geometry the delocalization of X-ray generation appears to be negligible for first order partitioning calculations.

References

Stadelmann, P.A. (1987). *Ultamicroscopy*, **21**, 131-145.

NEW MINERALS OF Bi-Pb-Te-S AND ALEXITE, KOCHKARITE, RUCKLIDGEITE IN CONTACT METAMORPHOSED KOCHKAR GOLD DEPOSIT AT SOUTHERN URALS

Spiridonov E.M., Apollonov V.N. (Dept. of Geology, Moscow State University) , Pokusaev V.I. (YuzhUralzoloto)

Altaite with tellurobismuthite lamelli, tellurobismuthite with altaite lamelli, galena with tetradymite lamelli ...(Chvileva et al., I988) caused by solid exolution of protominerals like rucklidgeite and alexite occur in plutonogenic hydrothermal gold - telluride deposits. Similar minerals usually occur in metamorphosed ores.

Kochkar deposit in Southern Urals Hercinides where gold-telluride ores, enclosing beresites and listvenites, wall-rock granitoids and lamprophiric dykes were metamorphosed to hornfels of hornblende fascies is a classic example. Age of mineralization is C_{I-2} , age of metamorphism P_2 .

Ore aggregates are granulated. They contain newly formed biotite, actinolite, pirrhotite, turmaline, diopside, andradite ... Metaberesites contain porphiroblastes of oligoclas-bytownite, clinozoisite...

Ore are abundant in galena, tetradymite Bi_2Te_2S, tsumoite Bi_2Te_2, sulfotsumoite Bi_3Te_2S and other bismuth sulfotellurides. Newly formed minerals are alexite $PbBi_2Te_2S_2$ and $Pb_2Bi_2Te_2S_3$, $PbBi_4Te_4S_3$, $PbBi_6Te_6S_4$ - formed from tetradymite; $PbBi_2Te_2S$ formed from tsumoite; $Pb_2Bi_3Te_2S_3$ formed from sulfotsumoite.

In abundance of galena and bismuthinite newly formed minerals are cannizzarite (abundant) and cosalite. When bismuthinite is abundant bonchevite $PbBi_4S_7$ and galenobismuthinite $PbBi_2S_4$ occur.

Tellurobismuthite Bi_2Te_3 and altaite PbTe presence is usually accompanied by newly formed kochkarite $PbBi_4Te_7$ (Spiridonov et al., I989). When altaite is sometimes abundant this leads to formation of rucklidgeite $PbBi_2Te_4$ (Zavjalov et al., I977). Kochkarite also occurs in galena, but rucklidgeite only in very low sulfide quartz veins.

Double tellurides and sulfotellurides of Bi - Pb were formed at contact metamorphism of ores at altaite - tellurobismuthite and galena - tetradymite ... interaction followed by annealing of newly formed mineral phases. Size of metamorphogene telluride and sulfotelluride grains can reach I5xI5x5 mm. Both macro- and microscopically the Bi-Pb-Te-S new minerals are close to tetradymite. Their reflectance values are substantially lower than these of tetradymite and closer to galena. VHNumber is very low. The minerals are distinctly anisotropic having individual reflectance spectra.

The work was financed by the Russian Fundamental Research Fund, Grant 93-05-I4594.

References:

Chvileva T.N., Bezsmertnaya M.S., Spiridonov E.M. et al. (I988). Reference Book for Determination of Ore Minerals in Reflected Ligth. M. Nedra, 504 p. (in Russian).

Spiridonov E.M., Ershova N.A., Tananaeva O.I. (1989).Geology of Ore Deposits, 31, N 4, 98-102 (in Russ.).
Zavjalov E.N., Begizov V.I., Stepanov V.I. (1977). Zap. VMO, 106, N 1, 62-68.

WESTERN CARPATHIANS MESOZOIC PRIMITIVE ALKALINE VOLCANICS

Spišiak J.[1] and Hovorka D.[2] *([1]Geological Inst. Slovak Acad. Sci., Banská Bystrica, Slovakia,[2] Faculty of Sciences Comenius' University, Bratislava, Slovakia)*

In several Mesozoic tectonic units (Silesian, Tatric and Fatric ones) of the Western Carpathians, different alkaline effusive and rarely also intrusive rocks of the Cretaceous age (approx. 100 Ma) are known. Olivines, pyroxenes and less frequently also amphiboles form megacrysts; locally their glomerophyric accumulations are present. Fine-grained devitrified matrix (up to 40 vol. %) is another constant rock component. Clinopyroxenes are quantitatively the most abundant and genetically the most significant minerals in all rock types. Clinopyroxenes are characteristic for sector and oscillatory zoning. Sector zoning (hourglass structure) is expressed through two very different types of sectors: pyramidal and prismatic. Pyramidal sectors are enriched in Mg, Si and depleted in Fe, Al, Ti , as opposed to prismatic ones. Oscillatory zoning is common. Abundant are rims enriched in Ti, Al^{IV} and Fe and depleted in Mg, Al^{VI}. Rimward Ti-Al^{IV} enrichments are a result of polybaric crystallization during the ascent of the magma. The composition of Cpx microlites corresponds to that of phenocrysts rims.

Cpx composition and zoning document:

- phenocryst cores especially those of Cpx (partly also Hbl) originated under high-pressure conditions as a product of fractional crystallization (23 kbar, 1260° C),
- phenocryst rims of Cpx and Hbl (partly also mafic micas) crystallized under a considerable pressure decrease during the melt ascent.

These were also the conditions for the crystallization of microlites in the matrix and Cpx and Hbl in the resorbed xenolith parts.

Following Cpx classification (IMA) these Cpx correspond to diopside. The nature of Cpx phenocrysts documents a rapid ascent of the melt which was contamined by a resorption (mostly of carbonates) of xenoliths. Variable composition of the rocks under discussion is a result particularly of fractional crystallization and xenolith assimilation. Based on their chemical composition the rocks under consideration correspond with alkaline basalts/basanites, locally even picrites. In general, the rocks have low SiO_2 (cca 41%) and high TiO_2 and P_2O_5 contents (3.2 and 0,8% respectively). Characteristic features of these rocks are: elevated Cr (280 ppm) and Ni (190 ppm) contents; elevated contents of incompatible elements such as Ba (650 ppm), Sr (700 ppm) and LREE; also high Nb (78 ppm), V (245 ppm) and Zr (305 ppm) is detected. On the other hand, the contents of compatible elements are relatively low: Y (24 ppm) and HREE . In different discrimination diagrams (*Pearce* and *Cann* 1973, *Mullen* 1983, *Meschede* 1986 etc.) the rocks under consideration are projected mostly in the field of alkali basalts (WPA, OIA; *Hovorka* and *Spišiak* 1993). The normalized REE pattern is considerably enriched in LREE, shows slight positive Eu anomaly and low HREE contents. . The rocks are similar to Mesozoic alkaline rocks in the Northern Calcareous Alps *(Trommsdorff et al.* 1990) and Hungary (Dobosi 1986, 1987) in composition and occurrence.

The presence of primitive alkaline volcanics is a consequence of embryonal rifting in their respective units.

References:
Dobosi, G. (1986) *Ofioliti, 11, 19-34.*
Dobosi, G. (1987) *Neu. Jb. Mineral. Abh., 156, 281-301.*
Dobosi, G. & Horváth, I. (1988) *Neu. Jb. Mineral. Abh., 158, 241-356.*
Hovorka, D. & Spišiak, J. (1993) *Jb. Geol., B-A., 136, 769-782.*
Meschede, M. (1986) *Chem. Geol., 56, 207-218.*
Mullen, E.D. (1983) *Earth Planet. Sci. Lett., 62, 53-62.*
Pearce, J.S. & Cann, J.R.(1973) *Earth Planet. Sci. Lett., 19, 290-300.*
Trommsdorff, V., Dietrich, V., Flisch, M., Stille, P., Ulmer, P. (1990) *Geol. Rdsch. 79, 85-97.*

MINERAL SPECIES FIRST DESCRIBED FROM ITALY

Stalder, H.A. *(Naturhistorisches Museum, Bern)*, Cipriani C. *(Museo di Storia Naturale, Univ. of Firenze)* and Hölzel, A.R. *(Systematics of Minerals, Ober-Olm near Mainz)*

Since more than 10 years the IMA-Commission on Museums (CM) is working at a Catalogue of Type Mineral Specimens (CTMS). In 1990 the "IMA Reference Sample Catalogue" (H.J. Rösler et al., Freiberg, 1990, a computer database) appeared as a result of the first data collection. - But because this catalogue was far to be complete and had too many mistakes, only an interne distribution of outprints for CM-members wás organized. - The activity of the CM however initiated in the last years in much museums a more careful and more systematical search for type mineral specimens, this most valuble mineral heritage. It was also possible to get informations directly from the literature. Now there exists a card file index with approximately 3 times more data than in the first catalogue. - The data from the minerals first described from Italy are now the first ones given into a computer database.

The exemple of the italian minerals is very significant. Only from three countries (USA - 620, Russia - 365, Germany - 250) have been described more species than from Italy with 175 ones (approx. the same as from Sweden). - In the CTMS are listed the original publications of all today valid mineral species (all authors, with the year and the journal), the type localities (as precise as possible, including informations about changements of names with country borders) and the depositories of type specimens (with some details of the latter).

The whole italian list and (on the basis of specific mineral species) the most important problems concerning the CTMS will be discussed.

Table: Number of mineral species described from a specified locality (resp. area), the percentage of the species which are documented by type specimens and the place of depositories for the respective type specimens.

	Vesuvio		Larderello		Baveno	
	n	%	n	%	n	%
18th century	2	0	-	-	-	-
19th century	41	34	1	100	-	-
20th century	14	86	5	80	5	80
total	57	45	6	83	5	80
depositories	Firenze 6 Napoli 4 Paris 15 London 4 Washington 2		Firenze 3 Washington 3 Paris 1		Milano 4 Paris 2 London 1	

NEW DATA ON THE CRYSTAL PHASES OF THE $BaO - Ba_2SiO_4 - Al_2O_3 - Mg_2SiO_4 - MgO$.

D.A. Stavrakeva
Higher Institute of Chemical Technology
1756 - Sofia, Bulgaria.

The crystal phases Ba_2SiO_4, $Ba_3MgSi_2O_8$, $BaMgSiO_4$, $Ba_2MgSi_2O_7$, $BaMg_2Si_2O_7$ and Mg_2SiO_4 of the section $2BaO.SiO_2 - 2MgO.SiO_2$ represent an interest for obtaining of the Ba-Mg special cement and refractory materials.

The region $BaO-Ba_2SiO_4-Al_2O_3-Mg_2SiO_4-MgO$ is important for the synthesis of new materials.

By the X-ray microanalyser of the compositions of this part, which were termal treated at 1550°C - 1 hour, the following phases were determinated: Magnesium Aluminum Oxide, Barium Aluminum Oxide, Barium Magnesium Aluminum Oxide, Magnesium Silicate, Barium Magnesium Silicate, Barium Aluminium Silicate, Periclase and Corundum.

The Magnesium Aluminum Oxide (Spinel) ordinarily is without admixure and it is presented as $Mg_{1,09-1,13}Al_{1,91-1,94}O_4$.

The Barium Aluminum Oxide appears as a $3BaO\ Al_2O_3$ with isomorphic admixture of MgO-1,19 ÷ 3,27%, Na_2O-0,40÷0,93% and SiO_2- 1,02-4,00%.

The Barium Magnesium Aluminum Oxide is $2BaO\ MgO.4Al_2O_3$ with BaO-41,25÷44,84%, MgO- 5,35÷6,14% and Al_2O_3 - 49,70÷52,61% or $4BaO.2MgO.11Al_2O_3$ with BaO-34,48%, MgO - 4,42% and Al_2O_3 - 61,11%.

The Magnesium Silicate is a phase with variable composition from $13MgO.5SiO_2$ to $23MgO.8SiO_2$, which has different composition from that of Forsterite ($2MgO.SiO_2$). It is orthorombic.

The composition of the Barium Magnesium Silicate is $2BaO.2MgO.SiO_2$, which contains as an isomorphic admixture Al_2O_3 to up 4,12 wt.%.

The Barium Aluminum Silicate is $Ba_2Al_2SiO_7$, which contains or not Magnesium. Its composition varies: BaO - 68,58÷75,32%, Al_2O_3- 9,73÷17,56%, SiO_2 - 10,01÷13,93%, MgO - to up 5,99% and Na_2O to up 1,20%.

All the new crystal phases are presented from very well formed idiomorphic individuals.

INTERMEDIATE RANGE STRUCTURE IN SILICATE LIQUIDS AND GLASSES: NMR RESULTS

Stebbins, J.F. and Sen, S. (*Dept. of Geological and Environmental Sciences, Stanford University, Stanford CA 94305 USA*)

A number of spectroscopic and scattering techniques have provided considerable information about short-range order in silicate glasses and liquids, including first and second neighbor coordinations and distances. Short range structure probably controls the major features of melt energetics. Medium range order (MRO) implies non-random correlations at length scales beginning beyond a few Angstroms and may include clustering of cations and/or of anionic units. The presence of MRO may have major effects on nucleation kinetics, conductivity, viscosity, and component activities, but its detection and quantification remains one of the major and most discussed challenges in the science of amorphous materials.

We have recently used several new NMR techniques to address this question. For ^{29}Si in a variety of glasses, we have found that spin-lattice relaxation rates are controlled by direct coupling to the electronic spins of paramagnetic impurities, such rare earth or transition metal cations. Because this coupling is strong, quantifying its effects can give information about structure to at least several nm. In a study of $Li_2Si_4O_9$ glasses (Sen and Stebbins 1994) we found that even in rapidly quenched, optically homogeneous samples, nanoscale heterogeneities are developed, resulting in Li-rich and Li-poor regions with a fractal structure at a scale of at least 1-3 nm. Similar work has found that clustering of rare earths in SiO_2 glass can be detected even when only 2 to 4 atoms are present in each cluster. In contrast, studies of the dynamics of exchange of silicate species just above the glass transition in $K_2Si_4O_9$ (Farnan and Stebbins 1992, and in prep.) show that all species exchange at a rate consistent with bulk viscosity, suggesting that larger-range structure does not play a role. This fits well with the less clustered nature of K vs. Li liquids.

References:
Farnan, I. Stebbins, J.F. (1992) *Trans. Am. Geophys. Union*, **73**, 43.
Sen, S., Stebbins, J.F. (1994) *Physical Review*, in press.

• ICP AND XRF: TWO COMPLEMENTARY METHODS FOR ELEMENTAL DETERMINATION OF GEOLOGICAL SAMPLES

Steiner J.D., Bonvin D. and Kohler A.
(*ARL/Fisons Instruments, En Vallaire Ouest C, CH-1024 Ecublens*)

ICP (Inductively Coupled Plasma) is well known as a technique providing high performance for trace elements. Determination well below ppm levels for most elements can be achieved, even in some cases to ppb levels.

XRF (X-ray Fluorescence) is generally used for major elements using preparation of samples as fused beads. Trace detemination can be done for concentrations above ppm levels.

Using the same basic sample preparation, international geochemical standards have been measured using both ICP and XRF techniques. Results will be discussed and the complementary aspect of both techniques will be shown.

AQUA-COMPLEX $2SiO_3$-H_2O-$Me^{n+}2Me^{m+}O_4$ AS AN UNIVERSAL FORM OF MINERAL SUBSTANCE EVOLUTION

Stenina N.G., Distanova A.N. (*Inst. of Geology*)
Berezin Yu.A. (*Inst. of Pure&Applied Mechanics*)
SB RAS, Novosibirsk, Russia

Aqua-complexes in the form of their segregations of submicron-micron size were discovered as impurity inhomogeneities in natural quartz by transmission electron microscopy (TEM) (Fig. 1) (Stenina et al., 1984). TEM combined with other methods data on the interpretation of these defects allowed the aqua-complex to be presented as follows (Fig. 2). Chemical identification of Me^{n+}, Me^{m+}, O′ positions may be proposed basing on joint analysis of our and literature data. This is Me^{n+} - one- two valent cations such as Li, Na...Fe^{2+}, etc.; Me^{m+}-polyvalent cations Al, Fe^{3+}... U, REE, etc. and such volatiles as B, P, As, Te; O′-volatiles: O, F, Cl, S. The weak donor-acceptor Si—O bonds and hydrogen H^+...O

bonds provide crystalline continuum of quartz matrix saturated with individual aqua-complexes and their segregations. TEM study showed the growth nature of these defects.

The fact that these impurity inhomogeneities represent the

Fig. 1. Aqua-complexes segregations as impurity inhomogeneities ("voids") in hydrothermal quartz

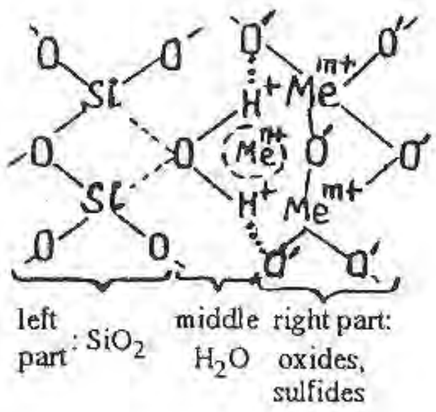

Fig. 2. Aqua-complex

portions of mineral-forming medium allowed to reconsider traditional view of minerals as the static units of mineral substance in favour of their dynamic consideration according to which mineral forms record only the specific moments in the development of mineral substance. This new concept of mineral is proved by the data of minerals behaviour in real fluid-silicate systems. Basing on the predominant role of silica-water-metaloxide species in the formation of silicate phases it was predicted and experimentally established the criterium of ore-bearing capacity of hydrothermal quartz (Stenina et al., 1988). Investigation of structural-chemical transformations of silicate minerals within the rocks seria from country gabbro to granites showed that redeposition of silicate substance occur via aqua-complexes

$$2SiO_3\text{-}H_2O\text{-}Me^{n+}2Me^{m+}O_4'.$$

The data indicating the principal role of aqua-complexes in the mineral substance transformation, redeposition and transference make to propose the existence of unified energetical structure managing the chemical composition of specific complexes. Quantum-chemical approach to the understanding of aqua-complex nature allowed to predict Au-Fe association within aqua-complex that was experimentally confirmed by X-ray images in Fe and Au characteristic radiation. Basing on this it may be concluded that aqua-complexes are responsible for geochemical associations.

Aqua-complex presented in Fig. 2 describes all variety of minerals: 1) Quartz - left part of the complex; 2) Nonwater silicates - left and right parts; 3) Water silicates - all three parts; 4) Complex oxides, sulfides - right part. These mineral forms arise as a result of aqua-complexes disruption in response to the evolution of fluid-silicate system under changing thermodynamical and chemical parameters.

References:
Stenina, N.G., Scherbacova, M.Ya., Bazarov L.Sh., Mashkovtsev, R.I. (1984). *Phys. & Chem. Min.* **10**, 180-186.
Stenina, N.G., Sotnikov, V.I., Koroluk, V.N., Kovaleva, L.T. (1988). *Geochimiya*. No. 5, 641-653.

• THE ROLE OF MICROLITES DURING THE COOLING AND CRYSTALLIZATION OF RHYOLITIC MELTS

Stevenson R.J., Sharp T.G., Dingwell D.B. (*Bayerisches Geoinstitut, Universität Bayreuth, Germany*)

Microlites occur as small flow-aligned crystals in the groundmass of volcanic glasses. They have an important role in the physical properties of erupting volcanic materials as they can crystallize during magmatic ascent or during surface flow, and can influence the rheological properties of cooling lava flows.

From parallel plate viscometry measurements with strain rates appropriate to the interior of lava domes, a difference in log viscosity of 0.6 Pa s was found for the more viscous microlite-rich (>10%) and microlite-poor (<1%) natural calc-alkaline rhyolitic obsidians from samples of identical bulk chemistry from the same lava flow. This difference may result from either compositional changes in the melt during crystallisation, or the physical effect of suspended microlites on the rheological properties of the suspension, or both. Separating these effects is especially difficult for microlite-rich samples where the microlites are closer together than the spatial resolution of electron microprobe analyses. The microlites themselves are also too small for characterization by electron microprobe techniques thereby requiring a microanalytical technique with high spatial resolution.

As part of our investigation of the effects of suspended crystals on the rheological properties of magmatic suspensions, we have used transmission electron microscopy (TEM) to chemically and analytically characterize the microlites and determine the composition of the interstitial glass in microlite-rich samples.

TEM imaging of microlite-rich samples shows a large population of previously unrecognized crystals, "nanolites", that are approximately 0.1 by 3, μm in size and invisible to backscattered-electron imaging and optical microscopy. The nanolites and the larger microlites have been identified as orthopyroxene, clinopyroxene, calcic-amphibole, and plagioclase. In addition, a complex pyroxene intergrowth has been observed that consists of a Ca-poor orthopyroxene core mantled by a Ca-rich clinopyroxene rim. Glass compositions associated with these crystals show depletions of Ca and enrichments of K with respect to crystal-poor flow bands from the same sample. This indicates that small compositional heterogeneities can lead to rheological variations associated with the formation of flow banding in lavas.

THE SURFACE ATOMIC STRUCTURE OF CALCITE AND ITS EFFECT ON REACTIVITY

Stipp, S.L.S. *(Anal. Chemistry, Univ. of Geneva)*,
Gutmannsbauer, W. and Lüthi, R. *(Physics Inst., Univ. of Basel)*.

The surface of calcite after cleavage is highly reactive. Near-surface analytical techniques (x-ray photoelectron spectroscopy, XPS, and low-energy electron diffraction, LEED) show that the $\{10\bar{1}4\}$ face does not behave as a simple termination of the bulk structure. Cleavage of this ionic solid leaves "dangling bonds" that cause a restructuring of the atomic lattice at the surface that changes, whether the sample is in contact with ultra-high vacuum after fracture, or with the humidity of ambient air (Stipp and Hochella, 1991). Atomic Force Microscopy (AFM) images taken at high resolution in air also show a unit cell that is not as expected for a termination of the calcite lattice but that can be explained by a surface covered with hydration species: CaOH and CO_3H (Stipp *et al.*, 1994). New LEED and high resolution AFM images, obtained from samples cleaned and cleaved in ultra-high vacuum will demonstrate the effect of adsorbed and hydrolysed water on the surface atomic structure. Topographic scale images collected in vacuum, in air and under solutions containing foreign anions or divalent trace metals will be compared to demonstrate the effects that both a hydrolyzed and an adsorbed water layer can have on such interface processes as adsorption, surface diffusion and formation of a solid-solution by solid-state diffusion. These studies also present a good example of the use of surface and near-surface techniques for solving problems in mineralogy and in interface geochemistry.

References:
Stipp S.L. & Hochella M.F., Jr. (1991) *Geochim. Cosmochim. Acta* **55**, 1723–1736.
Stipp S.L.S., Eggleston C.M. & Nielsen B.S. (1994) *Geochim. Cosmochim. Acta*, in press (July).

DENSITY FUNCTIONAL THEORY: NEW WINDOWS INTO PLANETARY INTERIORS

Lars Stixrude (Earth & Atmospheric Sciences, Georgia Tech) and R. E. Cohen (Geophysical Laboratory, Carnegie Institution of Washington)

With recent advances in solid state theory and computation, first

principles-based theory is becoming an increasingly important geophysical probe. It is now possible to investigate materials with large unit cells (up to Z=20), and a variety of physical properties including atomic and electronic structure, elasticity, phase stability, lattice vibrations, and the effects of temperature. Because of their accuracy and their ability to make predictions independent of experiment, these methods hold the promise of rapid advances in our understanding of the composition and state of planetary interiors.

A variety of methods will be illustrated using silicate perovskite, hydrogen and iron as examples. All the techniques rely on various approximations to density functional theory (DFT) to obtain the total energy of a crystal structure and are completely independent of experimental data. First principles methods, such as the Linearized Augmented Plane Wave (LAPW) method, readily achieve fully converged solutions of the Schrödinger-like Khon-Sham equations even for complex crystal structures (e.g. *Pbnm* perovskite). They require only an approximation to the many-body exchange-correlation terms. We will show results using the Local Density Approximation (LDA), which replaces these terms at every point in space by the exact result for an electron gas of the same local density, and functionals which go beyond LDA by including gradient information (GGA), important in 3d transition metals.

To investigate high temperature properties, liquids and melting, we extract the essential physics of these elaborate electronic structure calculations in the form of simple models, amenable to statistical mechanical simulations. We describe a new Slater-Koster tight-binding model which eliminates the need for pair-interaction terms by assigning the arbitrary zero in the band structure so that the total energy is given by a sum over the bands. We find good agreement with energies of distorted structures not included in the inversion, elastic constants and phonon energies of Fe, Si and Xe. The quasiharmonic phonon spectrum and the cell model partition function calculated with the SK model are used to determine high temperature elastic properties, phase stability and seismic velocities and to compare directly with geophysical observables.

PHYSICS OF DEEP EARTH MATERIALS FROM FIRST PRINCIPLES

Lars Stixrude (School of Earth & Atmospheric Sciences, Georgia Tech) and R. E. Cohen (Geophysical Laboratory, Carnegie Institution of Washington)

First principles calculations, though they first appeared in the earth science literature nearly 20 years ago, are just now emerging as a major probe of planetary interiors. They are completely independent of, and thus complementary to experimental methods. They represent a major advance in accuracy and applicability over earlier, *ab initio*, approaches, such as electron gas type models, because they make no approximations to the nature of bonding - ionic, covalent and metallic materials are equally amenable to first principles theory. We show results based on state-of-the-art Linearized Augmented Plane Wave (LAPW) calculations of $MgSiO_3$ perovskite and iron. The method achieves essentially fully converged solutions of the Schrödinger-like Khon-Sham equations. The only approximation is to the many-body exchange-correlation terms, for which we use the Local Density Approximation (LDA) and the Generalized Gradient Approximation (GGA).

Our understanding of the composition and state of the lower mantle rely primarily on our knowledge of the properties of silicate perovskite, its most abundant constituent. An important issue for many years has been the possible existence of a phase transition in $MgSiO_3$ perovskite under lower mantle pressure-temperature conditions. Based on analogy with other perovskite materials and electron gas computations, a phase transition was predicted from the observed orthorhombic phase to higher symmetry tetragonal and cubic phases. Our LAPW results, however, show that the orthorhombic phase is enormously favorable energetically relative to the high symmetry structures and that phase transitions are highly unlikely below melting. This means that the large and growing body of data on the only $MgSiO_3$ perovskite structure ever observed is geophysically relevant and that other explanations must be sought for recently observed lower mantle seismic reflectors near 710, 900 and 1200 km depth.

First observed nearly a decade ago, the origin of elastic anisotropy in the earth's inner core remains unknown. Though models have been proposed, our ignorance of the elastic properties of the phase of iron, or even which phase is stable under core conditions prevents progress. Our LAPW calculations in the GGA approximation represent the largest compression range (nearly two-fold) over which theory and experiment (including equations of state, phase transitions and magnetic moment) have been compared for a transition metal. The results show that the bcc phase of iron is mechanically unstable at high pressure, and is thus unlikely to exist in the inner core, as has frequently been proposed. We address the elastic properties of the inner core and evaluate current models of its anisotropy by predicting the elastic constants of the hcp and fcc phases with a new, Slater-Koster (SK) tight-binding Hamiltonian. The parameters of the Hamiltonian are determined by inverting LAPW band structures and total energies, thus extracting the essential physics from the elaborate electronic structure calculations. High temperature elasticity, phase stability and seismic velocities are determined by calculating the quasiharmonic phonon spectrum and the cell model partition function.

CRYSTAL STRUCTURE OF ROCK-FORMING AND GEM CHLORITE FROM ANGARO-ILIMSK TYPE OF IRON DEPOSITS, RUSSIA.

Stolpovskaja V.N., Mazurov M.P., Palchik N.A., Zhitova L.M.,(*UIGGM, Novosibirsk, Russia*).

In the iron skarn deposits of the Angaro-Ilimsk type chlorite is typically associated with destructive alteration of magnetite ores, skarns, dolerites and other host rocks. Where retrograde alteration is intense, large amounts of fine-grained chlorites occur interstitial to pyroxene, magnetite, calcite, apatite, titanite, forsterite, garnet; where alteration in a lesser degree, medium- and coarse-grained chlorites in close association with calcite and halite fill in veins and cavities. The rosette, scale aggregates of splitting platy grains of chlorite on recrystallized magnetite druses are very typical for brecciated ores.

Only inside the iron-ore diatreme of Korshunovsk deposit, formed as result of basalt-evaporite interaction, are found unusual cavities filled in reniform monomineral aggregates of unique gem variety of chlorite.

The rock-forming and gem varieties of chlorite are very similar each other in composition and band configurations in the infrared absorption spectra. They are trioctahedral Mg-chlorites-clinochlores with very low Fe content in the range from Fe = 0.15 to Fe = 0.47, and with the higher Al content, ranging from Al = 1.75 to Al = 2.62.

As with the published spectra of clinochlores the strongest Si-O band is splitted into 2-3 components, one of these has the highest wavenumber for chlorites at about 1100 cm^{-1}. The band near 660 cm^{-1} is as a rule solitary. With increasing Al content the band 760 cm^{-1} appears and increases in intensity, whereas the highest frequency band of the interlayer hydroxyl ions shifts to lower wavenumbers from 3650 to 3575 cm^{-1} (Farmer, 1974).

Among studied materials it can be singled out the group of the more siliceous, silvery-pearly gem chlorites. Two peculiarities of their spectra are not typical of chlorites with similar composition. In the first, the wavenumber of the highest frequency OH-band is too large. And of the second, it is presence of the absorption band around 620 cm^{-1} as a well-defined shoulder. Among the natural chlorites a such band is given only by those of high iron content (Shirozu & Isida, 1982), but it is not our case. However, the absorption spectra of the reported in the literature aluminous serpentines with the same Al content are entirely compatible with those of studied gem chlorites (Serna & White, 1979; Shirozu & Isida, 1982).

As known, Mg-chlorites can be considered as a stabilized Al-serpentine polymorphs, and both modifications have no clear diffraction distinctions at the boundary Al contents. Preliminary X-ray results indicate that in the diffractograms of high-siliceous samples there is the reflection near 14 Å, however all the odd 00l-lines are extremely wide. Apparently, the such mineral as the trioctahedral 14 Å chlorite is being formed only.

Thus, along with the typical Mg-chlorites of the considered deposits there are intermediate serpentine-like minerals. According to the TEM results, no particular serpentine particles are found. Obviously, high density, viscosity, transparency and other gem chlorite properties, useful for treatment, are due to the own structural peculiarity of the studied minerals.

References:
Farmer, V.C. (1974). In: *The infrared spectra of minerals*, 331-363.Mineralogical Soc. Lond.
Serna, C.J. & White, J.L. (1979). Mineral. Mag.,**43**, 141-148.
Shirozu H. & Isida K. (1982). Mineral. J. **11**, 161-171.

Gedanite and Gedano-Succinite

Stout, E.C., Beck, C.W. (*Amber Research Lab., Dept. of Chemistry, Vassar College, Poughkeepsie, New York)*
Kosmowska-Ceranowicz, B.*(Museum of the Earth, Warsaw)*

Gedanite, found along with succinite (in environs of Gdansk), was described and named by Helm in 1878. He also described a fossil resin that had long been known among the amber workers as "friable amber". He declared friable amber to be a variety of succinite, undeserving of a new mineralogical name (Helm, 1896). He found no succinic acid in gedanite, and only 1.13 and 1.70 % in friable amber, i.e. much less than in succinite, but warned that the two resins are difficult to distinguish and that they are often confused with one another by mineralogists and collectors. More recently, Savkevich (1970,1983) has designated friable amber as gedano-succinite and declared it as well as gedanite to be resins of the same botanical origin as succinite but diagenetically changed as a result of different depositional processes.

By means of infrared spectroscopy (IRS) and gas chromatography / mass spectrometry (GC/MS), we have studied eight specimens that are labeled ' gedanite' in mineralogical collections of Europe and the U.S.A. The 60 components identified by their mass spectra are, with the exception of very small amounts of fatty acids and alkanes, almost all the same that Mills *et al.* (1984/5) have found in succinite, including all 14 diterpene resin acid derivatives. A specimen in the Musée National d'Histoire Naturelle in Paris contains 5.25% succinic acid and is actually succinite. Two specimens in the U.S. National Museum (Smithsonian Institution) have only traces of succinic acid and are proper gedanite. The other five specimens contain 0.42 to 2.87 % succinic acid and are gedano-succinite. The infrared spectra of these eight specimens and those of gedanite specimens in the Museum of the Earth (Poland) confirm the GC/MS results. The gedanite collection of the Museum of the Earth (Kosmowska-Ceranowicz, 1990) includes specimens of different regions and ages: Tertiary from the Baltic area and Saxony (Central Germany), and Cretaceous from Northern Siberia and France. IRS has identified all these as gedanite.

The spectra of gedano-succinite are very similar to those of succinite, beyond two overlapping carbonyl bands at 1695- 1735 cm^{-1}. Those of gedanite, however, have two absorptions in the ester region, at 1168 ± 6 cm^{-1}, where succinite has its only absorption, and at 1230 ± 5 cm^{-1}. There are also differences in the intensities of the carbonyl bands. The new results confirm that gedano-succinite is only a diagenetic form of succinite, but do not allow the same conclusion for gedanite.

References
Helm, O. (1896). *Schriften der naturforsch. Ges. in Danzig*, **9**(1),52-57.
Kosmowska-Ceranowicz, B. (1990). *Prace Muzeum Ziemi*, **41**, 141-144.
Mills, J.S. *et al.* (1985/85).*Chemical Geology*, **47**,15-39.
Savkevich, S.S. (1970). Jantar. Nedra, Leningrad, 192 pp.
Savkevich, S.S. (1983). *Izw. ANCCCP ser.geol.***12**,96-106.

COMPRASION STUDIES OF BISMUTH MINERALIZATION OF THREE RARE METALLS DEPOSITS

Strakhovenko V.D. (Geology Institute of SD RAS, Russia)

Comparison studies of three rare metalls deposits in Kazakhstan were performed for bismuth mineralization. All three deposits are presented the same sets of ore's elements, but they are distinguished by correlations between these elements (W,Mo,Cu,Bi) and by peculiarities of the genesis type. The Verhnee Kairakty is a tungsten deposit and belongs to quartzvein type. The Severny Katpar is a molybdenum-tungsten-cupper deposit assigning to the skarn-greisen type. The northern part of the Koktenkol deposit is a molybdenum deposit assigning to greisen - quartzvein type; the southern part is of the same type being a tungsten-molybdenum-cupper deposit. The Intermediate part of the Koktenkol deposit is a cupper-tungsten deposit of skarn-greisen type. Bismuth is presented in ores of all the deposits mentioned.

The minerals were diagnosed by the mineralgraphic method. The compositions of minerals were determined by X-ray microanalysis. To determine the spatial distribution of elements in minerals, the profile probe and the spatial scanning methods were used.

In all deposits, the bismuth minerals are presented as a fine grained mass closing gaps between grains of earlier minerals. Now and then stick-like crystals were found as well as clusters of idiomorphic graines.

The performed analysis of the data obtained shows that:
a) At the Verkhnee Kairakty deposit bismuth is associated with tungsten and separated from polymetals (Cu-Pb-Ag) during the process of ores generation. That is why the bismuth mineralization is presented only by three minerals (native bismuth, bismuthinite, hedleyite).
b) At Koktenkol and Severny Katpar depositions a wide spectrum of bismuth minerals is owing to simultaneous formation of Bi,Cu, Ag and Pb from fluids. At Severny Katpar native bismuth, tsumoite, tetradymite, joseite B, joseite A, hedleyite, hessite, all numbers of solid solution aikinite-bismuthinite, wittichenite, emplectite, cuprobismutite, cosalite, galenobismutite are determinted. Koktenkol's bismuth's mineralization is comprised of native bismuth, tetradymite, hedleyite, hessite, all numbers of solid solution aikinite-bismuthinite, cosalite, galenobismutite, emplectite, sulfobismuthidy Ag,Cu,Pb. It should be noted that an enclosing environment where bismuth sulfosalts are deposited, in fact does not influence their composition. It is clearly seen at different parts of the Koktenkol deposit and also at the composition of Katpar and Koktenkol bismuth mineralizations, which turn out to be very similar. A predominance of cupper-bismuth sulfosalts at Katpar and at the southern part of the Koktenkol deposit is the distruction in

bismuth mineralizations which can be explained by the dominant amount of cupper in these ores.
c) For all indicated deposits, the sequence in which bismuth minerals are deposited turns out o be the same: native bismuth, tellurids and sulfotellurids bismuth, hessite, galenite, then Pb sulfosalts of bismuth and the numbers of solid solution aikinite-bismuthinite, and finally sulfosalts of bismuth. Particular variations in the sequence of bismuth minerals crystallization, e.g., the sequence of number of solid solution, depend on the specific features of ore's solution evolution at each deposit.

MINERAL CLASSIFICATIONS, A REVIEW

Strunz H. (Inst. Min. Cryst., Techn. Univ. Berlin)

I. Chemical	II. Chemical-structural	III. Structural	IV. Genetic-structural
Berzelius 1819 Gustav Rose 1852 Dana 1854-1892 Groth 1874-1921 followed by: Hintze 1897-1968 Dana 1944,1951* (nonsilicates, 50 classes) Ferraiolo 1982* (50 classes) Hey 1950, 1975* (35 sections) Clark 1993* (Hey's Mineral Index,32 sections)	Strunz 1941-1982 (9 classes) followed by: Klockmann 1967-1980 Hölzel 1989, 1992 Nickel & Nichols 1990, 1991 Weiß & Hochleitner 1990 Makovicky 1981-1993 (sulfosalts) Strunz 1993* (sulfides and sulfosalts)	Bragg 1930 (silicates) Povarennykh 1962 Lima-de-Faria & Figueiredo 1978 Moore 1984 (phosphates and arsenates) Sabelli & Trosti-Ferroni 1985 (sulfates) Liebau 1985 (silicates) Gottardi & Galli 1985 (natural zeolites)	(Breithaupt 1849, paragenesis) Machatschki 1953 Kostov & Minceva-Stefanova 1981 (sulfides) Kostov & Breskovska 1989 (phosphates, arsenates, vanadates)
*Arabic numbers for mineral species without gaps	*Arabic numbers + Latin capitals for mineral groups, gaps 05. 10. 15. etc	Cation Size, Coordination Polyhedra, Polymerization Types: Neso-, Soro-, Cyclo-, Ino-, Phyllo-Tecto-Types. Homopolyhedral, heteropolyhedral	

Chemical-structural Mineral Classification (1941-1993)
Chemical, Cation Size, Coordination Polyhedra, Polymerization Type

Bond type:			Desmotropy:
Metallic and covalent	Siderophile Elements	1. Elements 1.A. Metals 1.B. Carbides etc. 1.C. Semimetals 1.D. Nonmetals	
	Sulfophile Elements	2. Sulfides Sulfosalts	
Ionic and covalent	Oxyphile Elements	3. Halides	Mostly isodesmic
		4. Oxides Hydroxides Sulfites Selenites Tellurites Arsenites [5]-Vanadates Iodates	
		5. $[RO_3]$-compounds 5a. Nitrates 5.A,B,C,etc Carbonates 5*.A,B,C,etc Borates	Aniso-desmic
		+ $[BO_4]$	
		$[RO_4]$-compounds 6. Sulfates 7. Phosphates 8. Silicates	Meso-desmic
Covalent and Van der Waals	9. Organic Compounds		

References: I.) Hintze (1897-1968). Handbuch d. Min., 6+3 vol. Berlin-Leipzig. - Palache et al.(1944,51). Dana's System of Mineralogy, 2 vol., New York.-Ferraiolo (1982). A sys. classification of nonsilicate minerals, Am. Mus. Nat. Hist., New York. - Clark (1993). Hey's Mineral Index, Nat. Hist. Mus., London.
II.) H.S. (1941, 7th ed. 1978, reprint 1982). Mineral. Tabellen. Leipzig. - Klockmann (1892, 15th/16th ed. 1967/78, repr. 1980). Lehrbuch d. Mineralogie. Stuttgart. - Hölzel (1989). Syst. of minerals; (1992) Crystal Data. - Nickel&Nichols (1990). Mineral database. (1991) Mineral reference manual. - Weiß&Hochleitner (1990). LAPIS Mineralienverzeichnis. - Makovicky. Building principles a. classification of sulphosalts. Fortsch. Min.1981, 137; 1985, 45; 1989, 269; Europ. Journ. Min. 1993, 545. - Strunz (1993): Sulfide classification. LAPIS.
III.) Bragg (1930). The structure of silicates, Z. Krist. (74), 237. - Povarennykh (1962). Crystal-chemical classifikation of minerals, Kiev, 1972 in english, New York. - Lima-de-Faria&Figueiredo (1978), Gen. chart of inorganic units and struct. units. G.d. Orta, Geol., Lisboa. - Moore (1984), Crystallochemical aspects of the phosphate minerals, in Nriagu & Moore, Phosphate Minerals, Berlin. - Sabelli&Trosti-Ferroni (1985), A structural classification of sulfate minerals, Per. Mineral., Firenze. - Liebau (1985), Struct. Chemistry of Silicates, Berlin. - Gottardi&Galli (1985), Natural Zeolites, Berlin.
IV.) Machatschki (1953), Spez. Mineralogie auf geochem. Grundlage, Wien. - Kostov & Minceva-Stefanova (1981), Sulphide Minerals, Bulgar. Acad. Sci., Sofia. - Kostov& Breskovska (1989), Phosphate, Arsenate and Vanadate Minerals, Bulgar. Acad. Sci, Sofia.
Selected publications in periodicals: Pabst (1950), Am. Min., 149 (Fluoaluminates) - Zoltai (1960), Am. Min., 960 (Silicates) - Keller (1972), N. Jb. Min. Abh., 217 (Phosphates, Arsenates). - Hellner (1984), Int. Congr. Cryst., C-214 (Frameworks and a classification scheme f. inorganic and intermetallic structure types. - Hawthorne (1983), Acta. Cryst., A.724 (Graphical enumeration of polyhedral structure types); (1985), Am. Min. , 455 (Towards a structural classification of minerals).

THE ADVANTAGE OF PLOTTING ALL OF THE CRYSTALLOGRAPHIC AND OPTICAL ELEMENTS ON A SINGLE PROJECTION.

Sturman B.D. *(Dept. of Mineralogy, Royal Ontario Museum)*

The positions of the crystallographic and optical elements determined on the optical goniometer, spindle stage, Weissenberg camera and Precession camera should be all plotted on a single stereographic projection. This allows easy determination of the spatial relationship between crystal faces, cleavage planes, principal vibration directions, reciprocal unit cell and crystallographic axes.

The plane of the stereographic projection is set perpendicular to dial axes of instruments. This is a change from the usual horizontal position used in the work with spindle stage. However, all constructions and methods for the spindle stage can be easily adjusted to the new vertical position of the stereographic projection.

The plotting of measurements should simulate the movements on the axes of instruments. The positions of the large and small arc of the goniometer head are also plotted as lines on the stereographic projection. After this, any movement on the arc and comparable movements of the crystallographic and optical elements, can be easily traced on the stereographic projection as crystal on the goniometer head is moved from one instrument to another. The arc on which the movement was made is set parallel to the equator of the stereographic projection and all elements are accordingly moved.

This method is indispensable in the study of triclinic minerals and can be very useful with monoclinic minerals. It allows easy presentation of all crystallographic and optical elements of twinned or intergrown crystals and is of great help in identification of twin laws or epitaxial relationship.

MODAL AND REACTION HEAT INFORMATION ON PSEUDOSECTIONS. USE AND APPLICATION IN THE STUDY OF METAMORPHIC *PT* PATHS

Stüwe K. (*Dept. of Geology, Univ. of Adelaide*) and Powell R. (*School of Earth Sci. , Univ. of Melbourne*)

Classical thermobarometry uses the qualitative appearance of phases and their compositional changes due to discontinuous and continuous reactions to place constraints on the formation conditions and the *PT* paths of metamorphic rocks. However, at least two additional changes

occur in mineralogical systems during metamorphic reaction that have received much less attention. Firstly, modal proportions of minerals change in direct connection with the compositional changes; this can therefore be used as an additional constraint to the form of a *PT* path. Secondly, the enthalpy of a system changes so that heat is liberated or consumed during metamorphic reactions and there may a feedback mechanism between the externally imposed temperature field and the reaction heat of the system. Both changes have long been recognized as important parts of reaction in metamorphic rocks but they have found comparably little application in metamorphic field studies. Indeed, modal information has found only limited application for the interpretation of some bulk compositions and in solid solution-free systems. Similarly, studies concerned with the influence of reaction heat on the heat budget of *PT* paths have used very generalised assumptions on the distribution of reaction heat with temperature.
Modal output is now available in the software package THERMOCALC and we are currently implementing reaction heat information as an additional output. Therefore pseudosections for many common bulk compositions may now be contoured for modal mineral proportions and for heat changes with a widely available software.
Two examples are discussed which demonstrate how the use of such information may provide insights into details of *PTt* paths that are difficult to obtain by conventional means.

Recent progress and perspectives of the high energy mineral science

Sueno S. (*Inst. of Geoscience, Univ. of Tsukuba*)

Mineralogy and the related sciences have made stepwise progress corresponded with the introduction of new probe and observational techniques on the material research, such as the founding of X-ray, invention of electron microscopes, EPMA etc. In recent years, several useful analytical techniques are newly developed in conjunction with the advances of the high energy physics and nuclear physics. One well-known example is the synchrotron orbit radiation (SR). This new photon beam brings on most remarkable progress not only on the crystal structure analysis but the SR-fluorescent X-ray micro analysis (SRXMA) which is powerful on the analysis of trace element in minerals. A continuing evolution in the field of the high energy physics and the nuclear physics made possible to provide a higher energy ion-beam as a new probe for the mineral sciences. PIXE (Particle Induced X-ray Emission) is similar to EPMA but extend its sensitivity to trace elements with the use of the light ion beam or heavier ion beam such as oxygen (1-5 MeV per nucleon) as the probe. PIXE experiment can be carried out using small particle accelerator around 3 MeV. NRA (nuclear reaction analysis), RBS (Rutherford backscattering spectrometry), ERDA (elastic recoil detection analysis) are other examples of newly derived analytical techniques based on the high energetic (MeV) ion beams mostly developed in the past decade. In this talk, I would like to call the mineral researches which made good use of the high energy particle beam as High Energy Mineral Science likened to High Energy Physics.

NRA, RBS and ERDA are still developing techniques and there are many limitations although they hold great promise for the quantitative analysis of mineral samples. The advantage of these analyses is that (1) non-destructive, (2) quantitative analysis, (3) depth profile of elements with high resolution (10-50nm) without destruction of the specimen surface by the sputtering erosion as on SIMS, (4) no matrix effect, (5) easy handling of insulating minerals with minimum charge up effect of the specimen surface, (6) light element analysis especialy for hydrogen and oxygen and (7) ppm-order sensibility. However, lateral resolution of these techniques is poor (0.1-1mm^2) comparing with EPMA and SIMS analyses because common accelerator is not designed for the aim of the chemical analysis therefore difficult to obtaining the finer and intense ion-beams. This will be a obstruction on the analysis of rock specimens. PIXE and these three techniques require appropriate standard materials for the quantitative analysis. Standard glass materials were prepared by melting the standard rock specimens published from the Geological Survey of Japan which are tested by the SIMS analysis. Standard materials for the trace hydrogen analysis were prepared using the ion-implantation method and standard glass materials synthesized by Toshiba Ceramic Co. The largest difficulty of these techniques for mineralogists is the use of accelerator facilities. It is important to recognize that good network among specialists from different disciplines is essential. However, in Physics community, the use of small accelerator become decreasing year by year and physicists looking for a challenging application for the surplus machine time.

In recent years, accelerator mass spectrometry is developed for the ultra high sensitivity analysis (10^{-15}). Last year, analysis of ^{14}C and ^{26}Al is succeeded in the University of Tsukuba using 12UD tandem. These curcumstances may imply that the high energy mineral science is steped into a new stage of it progress.

Reference:
Petit, J.C., Dran, J.C., Della Mea, G. (1990) *Nature*, **344**, 621-626.

SOME PETROLOGICAL AND GEOCHEMICAL ASPECTS OF RAPAKIVI OVOID ORIGIN

Sukhorukov Yu. T. (Institute of the Lithosphere, Russian Academy of Sciences, Moscow, Russia)

Potassium feldspar ovoids rimmed by oligoclase represent a remarkable feature of ovoid rapakivi granites, which belong to the Lower Proterozoic anorogenic anorthosite-rapakivi granite association. Relevant facts obtained by study of ovoids in many rapakivi massifs in the Baltic and Ukrainian shields are as follows:
(1) Granitoids of a rapakivi massif (for example, the Salmi and Korosten massifs) are made up of several varieties, which represent the following differentiation sequence: quartz monzonite - ovoid and nonovoid porphyritic hornblende-biotite granite - biotite granite - albite-protolithionite granite. Ovoids occur only in the hornblende-biotite granites.
(2) Size, morphology, quantity and spatial distribution of ovoid and nonovoid potassium feldspar phenocrysts are extremely irregular. Granulometric analysis allowed to distinguish from 3 to 5 types of such phenocrysts in different rapakivi massifs.
(3) Ovoids can make up to 65% of a rapakivi granite body volume (Vyborg massif). The Baltic rapakivis are more abundant in ovoids as compared to the Ukrainian rapakivis that suggests they were less deeply eroded.
(4) Rimmed and nonrimmed ovoids can be often observed in one hand-size specimen.
(5) Oligoclase rims around ovoids contain inclusions of hornblende, biotite, and quartz.
(6) Ovoid rapakivi granites are characterized by the following petrogeochemical parameters, which distinctly differ from other granite members of the above sequence: SiO = 69 - 72%, F = 0.09 - 0.13%, K/Na = 1.9 - 2.3, K/Rb = 243 - 263, Ba/Rb = 2.8 - 7.7, Rb/Sr = 1.5 - 2.8, Eu/Sm = 0.8 - 0.13, Ce/Yb = 5.0 - 5.9.

The above facts and application of experimental results on viscosity of granitic melts, thermobarometric and microprobe data allow to arrive at the following conclusions:
(1) Rapakivi ovoids were formed at a specific stage of magmatic differentiation (only during the crystallization of biotite-hornblende granites) characterized by specific petrogeochemical constraints providing sufficiently high viscosity of the melt for the formation of ovoids.
(2) Oligoclase rims are related to the latest events of the

crystallization of ovoid granite melt (at least, later than the crystallization of hornblende and biotite).
(3) With general temperature decrease, the crystallization of the ovoid granites took place under unequilibrium conditions and local variations in contents of alkalies, volatile , and other components as well as viscosity. That explains joint occurrence of rimmed and nonrimmed ovoids and irregular pattern of their distribution.

References:
(1) Li, L., Tsukamoto, K. & Sunagawa, I. (1990): J. Crystal Growth, 99, 150-155
(2) Watanabe, K. & Sunagawa, I. (1983): J. Crystal Growth, 65, 568-575
(3) Kanda, H., Ohsawa, T., Fukunaga, O. & Sunagawa, I. (1989): J. Crystal Growth, 94, 115-124
(4) Onuma, K., Tsukamoto, K. & Sunagawa, I. (1990): J. Crystal Growth, 100, 125-132
(5) Kanda, H., Ohsawa, T., Fukunaga, O. & Sunagawa, I.(1989): In "Morphology and Growth Unit of Crystals, Terrapub, Tokyo" 531-542

EFFECT OF IMPURITY COMPONENTS UPON GROWTH MORPHOLOGY OF CRYSTALS

Sunagawa, I. (Kasiwa-cho, Tachikawa, Tokyo)

It has been well known since the time of Rome de l'Isle that minor amounts of impurity components gave a drastic effect upon growth forms of crystals. This phenomenon has been infered to selective adsorption of impurity components at various levels on growing interfaces. The purpose of this presentation is to critically survey the observations on the effects of impurity components upon growth morphologies of crystals at various levels and to find out a general guidline on the problem. Not only variations of growth forms of polyhedral crystals (variation in crystal habits), but also of internal morphology (growth sectors and vicinal sectoriality) and surface microtopography (morphology of growth spirals and step patterns) will be analysed. Our observations on both natural and laboratory grown crystals will be used for this purpose.

Since the impurity effect operates at a growing interface, our discussion starts from this point. First of all, impurity effect upon the growth of a smooth and a rough interface will be compared, taking NaCl growing from aqueous solution containing Pb as an example (1). Rough {100} interface may transform to a much smoother interface on which layer and spiral growth becomes operative. Along similar line, observation on habit variation of flux grown corundum crystals due to rare earth elements (2), and of synthetic diamond grown from different metal solvents under HPHT conditions (3) are analysed. These analyses will be followed by the analysis of the effect of impurities upon the advancing rates of mono-molecular spiral layers on a smooth interface, using the results of in-situ investigation on K-alum crystals growing from the aqueous solution containing impurities of ppm order (4). How impurities affect the advancing of mono-molecular spiral layers and modify the morphology will be demonstrated in relation to the driving force at the interface (surface supersaturation).

Since the advancing rate of growth layers on a smooth interface is much higher than the normal growth rate of a rough interface, it is generally expected that the smoother interface is more affected by impurity component than the rougher interface. As a result, element partitioning shows an orientational dependency, leading to the formation of growth sectors and vicinal sectoriality (growth sectors depending on vicinal side faces of a growth hillock). Elements with effective distribution coefficient smaller than unity concentrate more in growth and vicinal sectors with smoother interface structure than in rougher interface.

Since disolvation process is essential in crystal growth from solution phase, impurities may give a drastic effect if the presence of impurity component modifies the solute-solvent interaction energy. As such an example, drastic morphology changes observed on synthetic diamond crystals grown in the presence of water in metal solution (5) and in different metal solutions (3) will be explained.

THERMONATRITE FORMATION IN TURKEY

Suner M.F. (*Dept. of Geology, Univ. of Istanbul Technique)*

Thermonatrite, $Na_2CO_3 H_2O$,is a rare forming evaporative mineral and it was discovered in Beypazarı, the province of Ankara, within Neogene volcanosedimentary sequences which have contained the second largest trona deposits in the world, alternating with claystones, mudstones, shales, bituminuous shales, carbonates and tuffits (Suner,1991). This mineral has been generally formed as a result of transformation mechanism from Tronas as well as from solutions primarely by direct precipitation and its deposition largely depends on the physicochemical parameters such as $^a CO_2$, ^aH_2O , a_{Na} and temperature. The changes in the effects of these parameters have resulted in the crystallisation of various minerals and also the transformation of early crystallized minerals.

As a result of detailed studies, in the Beypazarı basin, Thermonatrites were determined generally in the form of a thin cover on Trona nodules. In addition to these minerals, Natron, Pirrsonites (Bürküt & Suner, 1992), Gaylussites, Shortites, (Suner, 1992) are the other observed Na-bearing carbonates which were discovered using XRD, DTA and SEM techniques . Macro and micro investigations of Thermonatrite have revealed that it has covered Trona crystals in vibrous forms and mostly accumulated in cracks and that burried conditions together with high temperature and CO_3/HCO_3 were favourable factors in formation. The DTA studies have show that dehydration and decomposition of this mineral have resulted in two steps; 22 and 72°C for the former ; 93 and 116 C° for the latter. Chemical analyses have performed by spectrophotometrical methods and it was concluded that there was a significant similarity between Trona and Thermonatrite in the view trace elements contents, which has indicated the relationship in the formation also.

Furthermore, geostatistical studies have concluded that the standart deviation and skewness coefficients of observed elements were very low. These conclusions must be related to the stability and homogenious conditions of Thermonatrite deposition environments. SEM studies have also indicated that a transformation procedure might be performed.

Taking into account the observed properties and results from experimental data it was concluded that Thermonatrite, in Beypazarı, was formed secondarily, as result of transformation mechanism from Trona. In the basin ,during two seperate periods Trona were crystallized from solutions under mostly atmospheric conditions in the form of nine or ten1 sublevels in two main seams together with volcanosedimentary materials. Furthermore, after sediments have totaly covered the basin, circulated solutions within sediments were also responsible for Trona deposition. After that, solutions carrying high Na and

CO_3/HCO_3 have caused Thermonatrite crystallisation either by direct formation in atmospheric conditions; or by transformation from Tronas, that was generally observed. For this reason, in Turkey, Thermonatrites were formed in surfacial conditions and / or from circulated solutions within burried sediments in the form of a thin disconnected and irregular covers on early deposited Tronas at generally high temperatures.

References :

Suner,M.F.(1991).*The Porceedings of EUROCLAY '91,1035-1038.*

Suner,M.F.(1992).*The Abstracts of First South Asia Geological Congress, 42.*

Bürküt,Y & Suner,M.F.(1992).*Geosound, 20, 192-200.*

THE DISPERSION OF REFRACTION INDEXES IN GEMMOLOGY

Superchi M., Gambini E., Muzzioli D. and Donini A. (*CISGEM of Chamber of Commerce of Milano*)

The distinction between natural and synthetic gems as well as the distinction between natural specimens deriving from different genetic environments are among the leading problems in gemmology procedures.

In some cases is possible to identify these differences by observing inclusions and growth characteristics besides identifying classic basic data such as the refraction index, density, optically-detected visible absorption spectrum, and UV luminescence effects.

At times more sophisticated techniques are used but these are always strictly non-destructive such as the detection of trace elements (through low-energy spectrometers) or the detection of the absorption spectrum through spectrophotometers with wavelength ranges from ultraviolet to infrared. Numerous studies have been made to verify the validity of termoluminescence and cathodoluminescence methods, for solving these problems that are far from being resolved.

The aim of this study is to verify the possibilities offered by the dispersion of refraction indexes in the distinction between different gem origins.

This method has the advantage of being practical and inexpensive, but the most important characteristic registered in this case is the diagnostic capacity.

Results obtained for various mineralogical species will be presented and discussed: the comparison between the dispersion curves of natural samples (from different geographical regions) and synthetic gems obtained with different methods will be given.

MINABS - A MINERAL DATABASE 1920 - 1993

Susse, P. *(Institute of Mineralogy & Crystallography, University of Göttingen, Germany)*.

MINABS is a mineral data and reference file based on the *Mineralogical Abstracts*. Originally installed on a mainframe computer about 20 years ago, it was converted into a PC version in 1987, covering the *Abstracts* back to 1969. Since 1987 it was updated several times and gradually extended backwards.

The fifth edition, 1994, now covers the *Mineralogical Abstracts* from Vol. **1**(1920) up to Vol. **44**(1993). It contains about 16,000 mineral entries. One entry consists of name, chemism, cell parameters, crystal system and literatur reference.

MINABS comes with a specially written, easy to use retrieving software and may be installed on any IBM compatible PC. For the sake of wide portability, hardware requirements were set as low as possible: DOS version 2.1 or up and 500 K RAM. A hard disk drive, a color monitor and a math co-processor are recommended but not required, neither is a mouse.

MINABS is available on one HD disk of 5.25" or of one DD or HD disk of 3.5".

Reference:

Susse, P. (1988). *N. Jb. Miner. Mh.*, **1988**, 344 - 346.

INTEGRATED MINERALOGY, PETROLOGY AND GEMMOLOGY RESEARCH, AUSTRALIAN MUSEUM

Sutherland F.L., Pogson R.E. and Webb, G. (Mineral Section, The Australian Museum)

Mineralogy and allied petrological and gemmological studies are integrated in a long term research project at The Australian Museum. This project investigates a major geological feature, the East Australian Volcanic Belt, an intraplate belt 4000 km in length and active over 90 Ma. The Australian Museum study is also integrated with research by other institutions and companies on this large geological 'reservoir'.

Host mineralogy and petrology of the volcanic suites range from highly undersaturated (olivine melilitites, nephelinites and leucitites) to strongly silicic (trachytes, rhyolites) assemblages, with many fractionated variants. Miariolitic segregations include sodalite-bearing alkaline assemblages. Secondary minerals are common, particularly zeolites, clays, carbonates, silica and hydrated calcium silicates. High temperature-high pressure xenocrysts and xenoliths are abundant and include gem minerals (sapphire, ruby, zircon, diamond, feldspars, garnet, olivine, pyroxenes). Heavy mineral concentrates from alluvial deposits are studied to identify sources and evolution of palaeodrainages in volcanic terrains. Magnetic surveys are used to distinguish isolated flow-remnants from intrusive bodies.

Geochronology on volcanic sequences, using whole rock K-Ar dating, is augmented by K-Ar dating of xenocrysts (anorthoclase, amphibole, mica) and fission track and Pb-U isotope dating of zircon (xenocrysts and groundmass grains). This gives a more complex volcanic pattern than previously found and suggests several age-progressive strands. Commercially valuable sapphire fields (New England, New South Wales) and earthquake hazard zones (Newcastle, New South Wales) may be linked to such age-progressive activity.

Xenolith mineralogy provides a tool for reconstructing lithospheric sections and thermal states under eastern Australia. Garnet-two pyroxene assemblages (lower crust and mantle granulites, pyroxenites and peridotites) help define the spinel to garnet lherzolite transition and geothermal gradients at specific times and places. Established geotherms are used to locate Moho assemblages, where mineral phases only provide temperatures of equilibration. East Australia exhibits heat flows as high as young continental rifts, but in non-rift situations.

Among xenolith suites, rare assemblages shed light on

origins of gemstones e.g. sapphire-anorthoclase, sapphire-zircon and ruby-sapphire-sapphirine-spinel assemblages. Eastern Australian diamonds are notable for containing distinctive coesite and gossular-rich garnet inclusion suites and for showing heavy carbon isotopes. Studies are in train to establish the origin of these diamonds and their indicator minerals. Gem zircons are widespread and Rare Earth Elements analyses on different colours, morphologies and ages show a wide range in values, but similar patterns. Absence of Eu anomalies suggest a source lacking feldspar fractionation.

The studies extend to offshore volcanic islands (Bass Strait, NW Tasmania) and volcanic rocks drilled within offshore basins (Bass Basin). They include oceanic islands (Lord Howe, Balleny Islands), sea mounts (Tasmantid seamounts, Cascades plateau) and Antarctic volcanoes (Mt Erebus, Mt Melbourne), which are linked with Australian volcanic fields.

This integrated study not only serves academic and mining exploration interests, but is a rich resource for public education. The associations of volcanoes, earthquakes, landforms, attractive secondary minerals, gemstones, lapidary materials, entombed faunas and floras and plate tectonics all have popular appeal. The themes have much scope for talks, articles, media presentations, displays and excursions. A book being prepared by the Museum on Australian volcanic features will use many of these aspects.

THERMODYNAMIC PROPERTIES AND EQUATIONS OF STATE OF PHASES IN THE CaO-MgO-SiO_2 SYSTEM

Swamy V. (*Inst. Earth Sciences, Uppsala University*)

An internally consistent set of thermodynamic properties and equations of state for crystalline and liquid phases is important in modelling petrological processes thermodynamically. We have reported assessed data on the MgO-SiO_2 system elsewhere (Swamy & Saxena, 1993; Swamy *et al.*, 1994) which was an extension of Saxena *et al.*'s (1993) data base. Here we present an assessment of the CaO-MgO-SiO_2 system, including a number of crystalline and liquid phases that were not covered by Saxena *et al.* (1993).

The thermodynamic evaluation has been carried out using a computerized procedure included in the THERMO-CALC data bank system. Carefully selected experimental data on thermochemical, phase equilibrium, and thermophysical measurements were inlcuded in the assessment. Mixing in the liquid phase was modelled using the two-sublattice ionic liquid model of Hillert *et al.* (1985), and the pressure-dependence was described using a Murnaghan equation of state. Phase relations in the unary, binary and ternary systems will be presented.

References:

Hillert, M., Jansson, B., Sundman, B., Agren, J. (1985) *Met. Trans.*, **16A**, 261-266.

Saxena, S.K., Chatterjee, N., Fei, Y., Shen, G. (1993) *Thermodynamic Data on Oxides and Silicates*, Springer, 428pp.

Swamy, V. & Saxena, S.K. (1993) *Eos Trans. AGU*, 74(43), 555.

Swamy, V., Saxena, S.K., Sundman, B. (1994) *Calphad* (in press).

RAPAKIVI TEXTURE AS A RESULT OF THE SPECIFIC FLUID REGIME AND CRYSTALLIZATION KINETICS OF ANOROGENIC GRANITE MELT.

Sviridenko L. P. *(Institute of Geology Karelian Research Centre Russian Academy of Science)*

The rapakivi granites of three textural types of the Salmi pluton in Karelia represent K-rich supersolvus anorogenic granites. Its melt was formed by the low partial melting of the preheated lower crust under low water activity conditions. The rapakivi granite emplacement is characterized by the explosive intrusion of overheated melt and its crystallization at shallow to moderate depth. The explosive effect is favoured by the high concentration of carbon group gases (CO_2, CO and CH_4) in the melt and the oxidation of a reduced fluid as it is transported to the shallow zone.The high speed of granite melt movement contributes to high temperature K-feldspar and quartz crystallization over a narrow temperature range (950-900C) and at low water pressure when $P_{fl} < P_{tot}$. According to experimental data (Swanson, 1977, Simakin & Chevychelov, 1989), the high growth rate of K-feldspar ovoids is provided by the low undercooling of the melt and the low nucleation density. Wide crytals (ovoids) may be also produced by crystallization at low undercooling and low P_{H_2O} conditions. An increase in P_{H_2O} in near-contact facies gives rise to fine-grained texture , whereas the chemical composition of the granite remains the same.

Ovoid rapakivi granites were crystallized under quartz -magnetite-fayalite buffer, and the succession of the paragenesis magnetite+orthoclase by biotite+plagioclase is natural in the course of equilibrium crystallization with a decline in T and P_{O_2}. Numerous biotite and plagioclase inclusions in K-feldspar ovoids are presumably due to the local disturbance of equilibrium crystallization.

References:

Simakin, A. & Chevichelov, V. (1989). Geohimiya N1, 10-19 (in Russian) ,

Swanson, S. (1977). Am. Mineral., **62**, 966-978.

SULFIDE INCLUSIONS IN Cr-DIOPSIDE XENOLITHS FROM ALKALI BASALTS AND BASANITES, NÓGRÁD-GÖMÖR VOLCANIC FIELD (NORTH HUNGARY-SOUTH SLOVAKIA)

SZABÓ CS. [1,2] and BODNAR R. J.[1], *(1. Fluids Research Laboratory, Virginia Tech); 2. Department of Petrology and Geochemistry, Eötvös University)*

Tertiary-Quaternary alkali basalts and basanites from the Nógrád-Gömör Volcanic Field (NGVF) in North Hungary/South Slovakia contain deformed (porphyroclastic and equigranular) upper mantle xenoliths ranging in composition from spinel lherzolites to websterites (Group 1) and recrystallized upper mantle xenoliths ranging in composition from spinel lherzolites to dunites (Group 2). Based on a detailed geochemical study of these xenoliths, several mantle events (e.g., metasomatism, mantle veining) were identified which could have modified the lithospheric mantle beneath the NGVF by either extraction or introduction of melts of different chemical compositions.

A principal goal of this study was to characterize the sulfide inclusions in both xenolith groups and to identify possible genetic relationships between the sulfide mineralization and mantle events. Sulfide minerals occur in two distinct settings: (1) individual isolated, large (50 to 200 μm in diameter) irregular crystals (Type-1-i) or small (10 to 40 μm in diameter) spherical blebs (Type-1-e), and (2) small (1 to 15 μm in diameter) inclusion clusters connected either to healed intra- and intergranular fractures (Type-2-f) or to borders of mantle minerals (Type-2-b). In general, inclusions of Type-1-i are interstitial; however, a few are enclosed in olivine, orthopyroxene, and rarely clinopyroxene. Inclusions of Type-1-e are usually composed of two phases which are always enclosed in olivine and rarely orthopyroxene. Inclusions of Type-2 (either at fractures or grain borders) are pure sulfide minerals; however, they are rarely associated with silicate melt ± CO_2 inclusions.

Inclusions of Type-1-i consist mostly of chalcopyrite, Ni-rich monosulfide solid solution (MSS), and extremely Ni-rich MSS (NiO content is up to 50 wt%) ± Ni-Co-rich phase (CoO is up to 8.8 wt%) ± pyrrhotite. Inclusions of Type-1-e comprise MSS ± extremely Ni-rich MSS ± chalcopyrite. Inclusions of Type-2 also show compositions of MSS, sometimes with measurable Co content and rarely with chalcopyrite. The enrichment in Ni, Co, and Cu of sulfide inclusions in upper mantle xenoliths from the NGVF is very unusual for alkali basalt born xenoliths.

Based on the textural fabrics and chemical characteristics, inclusions of Type-1-e occurring particularly in secondary recrystallized xenoliths (Group 2) are interpreted to be immiscible sulfide melt blebs trapped

during a partial melting event in the mantle. A similar origin is possible for inclusions of Type-1-i. However, a metasomatic genesis cannot be excluded because these sulfide crystals occur only in metasomatized amphibole-bearing porphyroclastic xenoliths (Group 1). Inclusions of Type-2 formed during the ascent of the host basaltic lavas or after emplacement of the basaltic lavas at or near the Earth's surface. Remobilized melt contained in inclusions of Type-1 migrated along fractures and grain boundaries within the xenoliths and were trapped as secondary inclusions during cooling.

ECLOGITIC ROCKS FROM OPHIOLITIC MELANGE IN THE HOLGUÍN AREA (ORIENTE, EASTERN-CUBA)

Szakmány Gy., Andó J. and Kubovics I. (*Department of Petrology and Geochemistry, Eötvös Loránd University, Budapest*)

The main part of the fold belt in North-Cuba consists of an ophiolite melange overthrusted on the late Mesozoic Northern-American continental slope containing Cretaceous sediments. The overthrusting terminated by a collision during the Early to Middle Eocene, which formed the present belt structure of the island of Cuba. This structure is characterized by the following lithological units:

- Cretaceous carbonate platform & continental slope formations (north).
- Ophiolite melange and remnants of Cretaceous island arc (south).

Within the northern part of the ophiolite melange there is a highly dismembered narrow (about 5 km) belt parallel with the line of the former continental foreland. It has chaotic structure and consists of ophiolitic clasts embedded in a matrix of serpentinite or greywacke, and contains few diaphtorised eclogitic blocks with a size ranging from some decimeters to ten meters.

The primary minerals of the eclogite are garnet, omphacite (omph) (jd = 30-40 % dominantly) and subordinately rutile. Besides these components some zoisite and phengite have formed during the eclogitic metamorphism. During the retrograde metamorphism different types of amphibole (amph), albite (ab), phengite (phe), zoisite (zo), clinozoisite-epidote (czo-ep), titanite, chlorite and minor biotite were crystallized. Petrographic investigations indicate that the main retrograde reaction is: omph→amph+ab+phe+zo(czo-ep). The garnet was also involved in this reaction, sometimes it is replaced by albite. In addition garnet was altered to chlorite and clinozoisite. Amphibole-albite simplectite replacing former clinopyroxene.

Bulk rock chemistry of the eclogites implies that they were basic magmatic rocks.

Electron microprobe analyses of the pyroxenes and garnets refer to the ophiolitic ones (O-type) origin of the eclogites according to Smulikowski's classification (1972). Zoning of the garnets and geothermobarometric calculations from the garnet and pyroxene data indicate that the progressive metamorphism occurred under gradual increase of T. The temperature during the eclogitic phase could have been between 350 and 500°C under 9-13 kbar pressure. These estimates indicate that the eclogite is the low-T type (related to subduction) according to Carswell's classification (1990). Most of the pyroxene crystals were homogeneous, and became inhomogeneous only during the retrogression (decrease of the Na content). The composition of amphibole and the presence of albite suggest that the retrogression may have taken place two different ways:

1. Under greenschist facies conditions; P-T: 2-5 kbar at about 400-500°C.
2. Under blueschist- to greenschist facies conditions; P-T: from 7 kbar at 375-400°C to 2-5 kbar at 450-500°C respectively.

A metasomatic overprint with large edenitic amphiboles occurred during the latest retrograde phase.

Abundance of hydrous minerals in the diaphtorised eclogites indicates that retrogression took place under high P_{H_2O}. This could be interpreted in terms of high water activity in a rising, tectonically disturbed obduction zone.

References:

Carswell, D.A. (1990). *In* Carswell, D.A. (ed.), Eclogite facies rocks, 1-13; Blackie, Glasgow.

Smulikowski, K. (1972). *Krystalinikum*, **9**, 107-130.

PYROXENE PHASE RELATION AND COOLING HISTORY CHARACTERISTIC OF DIFFERENTIATED METEORITES AND UNCOMMON ON EARTH

Takeda H., Baba T., Chikami J. and Mori H.
(*Mineralogical Inst., Univ. of Tokyo*)

Because of their unhydrous and reducing condition of small planetary bodies, some meteorites provide us with welth of information on the pyroxene phase relation particularly close to the enstatite end member. In addition, destruction of the small parent bodies of meteorites by collision or impacts supply us equlibrated specimens quenched from high temperature. We investigated such pyroxenes found during our studies of partly differentiated meteorites such as ureilites, pallasites, primitive achondrites and a unique meteorite, Bencubbin by mineralogical techniques.

First example of coexisting orthopyroxene(Opx)-pigeonite was confirmed in the Y791538 ureilite (Takeda, 1989). An additional example has been found in the LEW88201 ureilite, in which Opx is the major phase. A pigeonite crystal has direct contact with Opx surrounded by the carbonaceous matrix characteristic of the ureilites. By combining coexisting pairs of all four ureilites with nearly identical Fs contents (8), we can constract a hypothetical phase relation of this section parallel to the enstatite-diopside join. The constant composition of Opx $Ca_{4.9}Mg_{88-87}Fe_{7-8}$ coexisting with pigeonite of variable compositions ($Ca_{7.2}Mg_{84.8}Fe_{8.0}$, $Ca_{9.0}Mg_{83.6}Fe_{7.3}$, $Ca_{9.2}Mg_{82.9}Fe_{7.9}$) and augite ($Ca_{36}Mg_{59}Fe_5$) is consistent with the presence of Opx between protoenstatite (Pro) and pigeonite at the Mg-rich region of the phase diagram (Longhi & Boudreau, 1980). The pigeonites in ureilites are uniform in composition, but are neither exsolved nor inverted to Opx by the rapid cooling due to destruction of the small planets. The coexisting inverted Pro ($Ca_{0.6}Mg_{90.7}Fe_{8.7}$) and Opx ($Ca_{2.1}Mg_{88.9}Fe_{9.0}$) were found in a pyroxene-bearing pallasite, Y8451 (Hiroi *et al.*, 1993). The low-Ca content of Opx suggests that the Opx field comes close to the En-Fs join. The coexisting Pro-Opx pair was found previously in Steinbach (Reid *et al.*, 1974). Inverted Pros are common in ordinary chondrites, but they are not well characterized mineralogically. A good example of Pro coexisting with olivine and melt (glass) has been found in large silicate inclusions of Bencubbin. The Pro composition is $Ca_{0.5}Mg_{97.2}Fe_{2.3}$ and that of olivine is $Fo_{97.1}$. The glass coexisting with Pro contains Al_2O_3 18.8 and CaO 11.4 wt %. The TEM study of this Pro shows that it consists of twinned slabs of different widths in the nm scale. The electron diffraction spots show streaks along a^*, but Opx reflections were not found, indicating rapid cooling.

The examples of the pyroxene characteristic of the differentiated meteorites recovered recently from Antarctica show us products difficult to obtain on Earth and in the experimental run of a short period. The condition achieved for these meteorites is reducing unhydrous condition coexisting with metallic Fe in an atmosphere-free small body. The temperature of melting is high due to the unhydrous source materials, and the mineral assemblages reached to the equilibrium condition in the interior of the parent body, subsequently quenched by destruction of the body.

We thank NIPR and Meteorite Working Group of the U. S. for samples.

References:

Hiroi, M. *et al.* (1993) Proc. NIPR Symp. Antarct. Meteorites, **6**, 234-245.

Longhi, J & Boudreau A. E. (1980) Am. Mineral ,**65**, 563-573.

Reid A. M. *et al.* (1974) Earth Planet. Sci. Lett., **22**, 67-74.

Takeda, H. (1989) Earth Planet. Sci Lett., **93**, 181-194.

LARGE CHEMICAL VARIATIONS IN MUSCOVITE-PARAGONITE AND MUSCOVITE-CELADONITE SYSTEMS OF WHITE MICAS FROM THE PIEMONTE BLUESCHIST-FACIES CALCSCHISTS IN ITALIAN WESTERN ALPS

Takeshita H. and Itaya T. (*Hiruzen Res. Inst., Okayama Univ. of Science*)

The Piemonte zone in the internal western Alps consists of the metamorphosed ophiolite and its Triassic-Cretaceous sedimentary cover which converted to "calcschists" by the Alpine metamorphism. The petrological study including XRD analysis of carbonaceous materials revealed that the calcschists have suffered blueschist-facies metamorphism in the subduction zone at a convergent margin between Apulian continental and Tethyan oceanic plates and that the metamorphic sequence is divided into three mineral zones, the chlorite (lower than 300°C), the chloritoid and the rutile (higher than 450°C).

Unusual large chemical variation in muscovite-paragonite system is observed in detrital white micas existing in the calcschists mainly from the chlorite zone. Muscovite (Mu) - paragonite (Pa) solid solution has been ever considered to have a miscibility gap from 40% to 80% in paragonite content from field evidence even in the high temperature condition (Guidotti & Sassi, 1976; Guidotti, 1984). However, it is noted that the detrital white micas have continuous compositional variations from pure Mu to $Mu_{0.2}Pa_{0.8}$ by EPMA analysis. There are two possibilities to explain this EPMA analytical results: 1) the white micas have submicroscopic paragonite exsolution lamellae and the part having various mixtures of submicroscopic muscovite and paragonite lamellae were analyzed by EPMA, the basis being by the miscibility gap in the system; 2) this system has a continuous solid solution in very high pressure and temperature condition in which the white mica has significant amount of celadonite composition, and the detrital micas were derived from the metamorphic terrain having the very high pressure and temperature condition.

Large chemical variation in muscovite-celadonite system is also observed in the metamorphic white micas from the Piemonte calcschists. The total range becomes wider with increasing of metamorphic grade; 3.20-3.38 pfu in Si (on the basis of 11 oxygens) for the chlorite zone, 3.18-3.42 pfu for the chloritoid zone and 3.04-3.55 pfu for the rutile zone. This clearly indicates that the mica grains have disequilibrium chemistry with other metamorphic phases, suggesting that the micas have experienced significant retrogressive chemical reactions in exhumation and cooling of the host schists. In the muscovite-celadonite system, the mica has higher celadonite components in the lower temperature and higher pressure as deduced from the experimental and field evidence. It is known well that the subduction related high-P/T metamorphic rocks have experienced clockwise features of the P-T-t history in a P-T diagram. Thus, in the present metamorphic sequence, the rocks had more celadonitic white mica at the peak metamorphism and less celadonitic one by the retrograde chemical reactions in exhumation and cooling of the host rocks, and the higher grade rocks had more celadonitic white mica than the lower grade one at the peak metamorphism, suggesting that the metamorphic P/T gradient was significantly higher than that of the isochemical lines of the muscovite-celadonite system.

References:
Guidotti, C.V. (1984). *Min. Soc. Am.*, **13**, 357-467.
Guidotti, C.V. & Sassi, F.P. (1976). *N. Jahrb. Abh.*, **127**, 97-142.

UNUSUAL MINERAL ASSOCIATION IN A CUBIC DIAMOND

Tal'nikova S.B. (*Lab. of Diamond Crystallogr. and Mineral., Yakut. Inst. Geol. Scienes)*

Recent study of cubic diamonds showed interesting results. Macroinclusions of ultrabasic and eclogitic parageneses are typical of octahedral rather than cubic diamonds. Cubes are saturated in tiny (a few tens of microns), K-rich particles of complex, varying composition (Navon et al., 1988).

It appears that these microinclusions represent a partially crystallized melt with dissolved volatiles or a fine mixture of several mineral phases (Tal'nikova & Pavlova, 1993).

Of interest is a find of a large intergrowth - an association of kimberlite minerals - in a cube diamond from Udachnaya pipe (sample of Spetsius Z.V.)

The diamond is a 2x3 mm fragment of a light yellow clear crystal of the 2nd mineralogical variety. The dark, opaque, irregular inclusion was found upon grinding the sculptured surface of the host. Crack connection to the surface of the host was not revealed, i.e. the inclusion was entirely insulated by diamond matrix. Other inclusions were absent in the diamond. Each of the successively exposed sections of the inclusion was analyzed on a microprobe. X-ray spectral analysis of the inclusion showed the presence of the mineral association serpentine+calcite+chromite+sulphides of Fe-Ni-Cu-S system. Sulphides decrease from margin toward center, i.e. with depth of exposure of the inclusion. Serpentine is distributed all over the inclusion in close contact with sulphides. Calcite is found in an apex of a cross-section, whereas chromite is mainly concentrated in the cenral part of the section.

Thus, the studied inclusion in cubic diamond is probably protogenetic, being entrapped during crystallization from kimberlite magma.

References:.

Navon, O., Hutcheon, I.D., Rossman, G.R. & Wasserburg, G.J. (1988). Nature.,**335**, 784-789..

Tal'nikova, S.B. & Pavlova, L.A. (1993). Geologiya and Geofizika., **6**, 111-119.

HYDROTHERMAL SYNTHESIS AND CRYSTAL STRUCTURE OF A VANADIUM OXIDE : $Ba_{0.4}V_3O_8(VO)_{0.4}.nH_2O$

Tamada O. and Yamamoto N. (*Graduate School of Human and Environmental Studies, Kyoto University*), Oka Y. (*Faculty of Integrated Human Studies, Kyoto University*) and Yao T. (*Graduate School of Engineering, Kyoto University*)

A new barium vanadium oxide $Ba_{0.4}V_3O_8(VO)_{0.4}.nH_2O$ (n~0.6) has been synthesized hydrothermally from a $VOCl_2$-$BaCl_2$ solution under the condition of 240°C for 24 hours. The green black single crystal in the shape of elongated thin plate, exhibits a monoclinic system : $P2_1/m$, a=10.153(3)Å, b=3.6329(9)Å, c=9.435(2)Å and β=102.10(2)°. A small thin crystal in the size of 0.33x0.05x0.01 mm^3 was used for the data collected (2θ<70°) by a Rigaku AFC-5S diffractometer. The data were corrected by the empirical Furnas method for absorption.

The strucutre was determined by the Patterson method using 951 independent reflections, but the descrepancy factor R remained in a high value (~0.30) due to the partial occupancy of unexpected existence of V and O sites and the deviated positioning of Ba ion. The structure was finally refined to R=0.063 and R_w=0.076. The chemical composition analyzed by an electron probe microanalyzer yields a good agreement with one determined by the X-ray structure refinement.

The structure is basically of a layered type made up from V_3O_8 layers with interstitial Ba^{2+} ions and water molecules. The main feature is that the V_3O_8 layers are bridged imperfectly by partially-lacking VO_5 trigonal bipyramids to form a tunnel-like opening as shown in Fig.1. The structure

is thus regarded as an intermediate type between layered and tunnel ones. Interstitial Ba^{2+} ions and water molecules exhibit an eleongated electron density distribution to give displaced occupancies from the special 2e position on the mirror plane, which is a common feature for interstitial cations like K, Rb and Ba in tunnel structures.

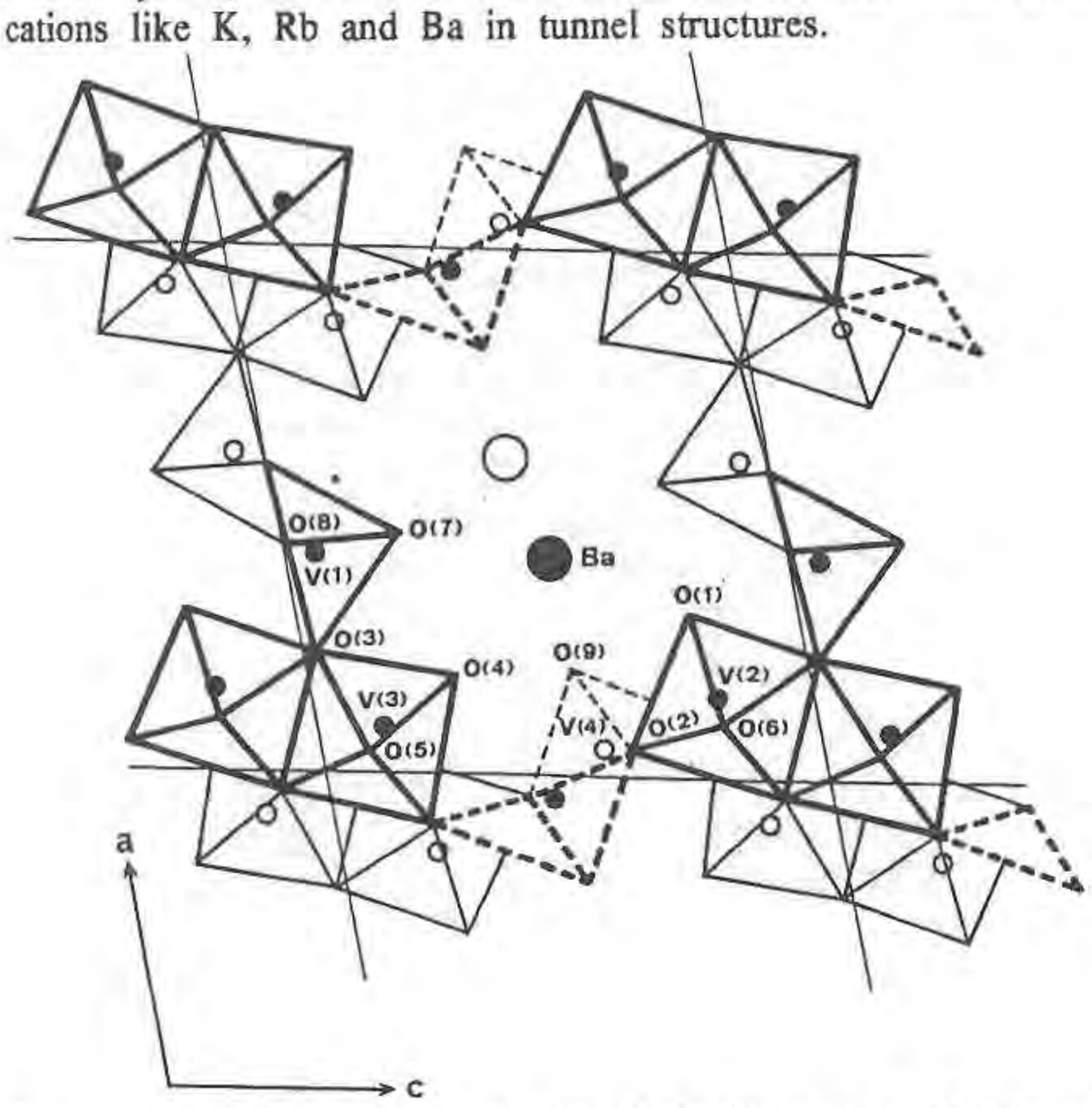

Fig. 1. Crystal structure of $Ba_{0.4}V_3O_8(VO)_{0.4}.nH_2O$ viewed along the b-axis. Large and small circles denote Ba and V atoms, respectively, at y=1/4 (open circles) and 3/4 (closed circles). The framework of V_3O_8 layer is drawn by solid lines and that of partially-lacking VO_5 bipyramid by broken lines.

Structural studies of $MgSiO_3$, $CaMgSi_2O_6$, $CaSiO_3$, and $CaBaSi_2O_6$ glasses by MD simulation

Taniguchi T., Okuno M., and Matsumoto T.
(*Dept. of Earth Sciences, Kanazawa Univ.*)

The structures of $MgSiO_3$, $CaMgSi_2O_6$, $CaSiO_3$, and $CaBaSi_2O_6$ glasses were studied by molecular dynamics (MD) simulation technique. These glass structures derived from MD calculations are shown in Fig.1. The potential energy of our model consists of pairwise additive Coulomb and repulsive terms between atoms, and van der Waals attraction terms for oxygen-oxygen interactions. The empirical energy parameters were used in this study. The results of these simulations agree well with those obtained from X-ray diffraction method. The partial distribution functions obtained by MD calculations show a clear maximum in the distributions of metal-oxygen and Si-Si pairs, while those of metal-metal (except Si-Si) pairs have no clear maxima. MD calculation results also show that local structures are similar one another for these glasses. Comparing these local structures with those of the corresponding crystals, we find out the remarkable difference of the polyhedra of modifier cations. This difference becomes small in the order of Mg, Ca, and Ba. The distributions of the numbers of bridging oxygen in SiO_4 tetrahedron are similar one another, and predominant numbers are 2 and 3. The distributions of the number of n-membered SiO_4 ring are different among these glasses. Large rings decrease and small rings (especially, three- or four-membered ring) increase in the order of $MgSiO_3$, $CaMgSi_2O_6$, $CaSiO_3$, and $CaBaSi_2O_6$ glasses. This tendency means that large modifier cations prevent the formation of SiO_4 network in glass.

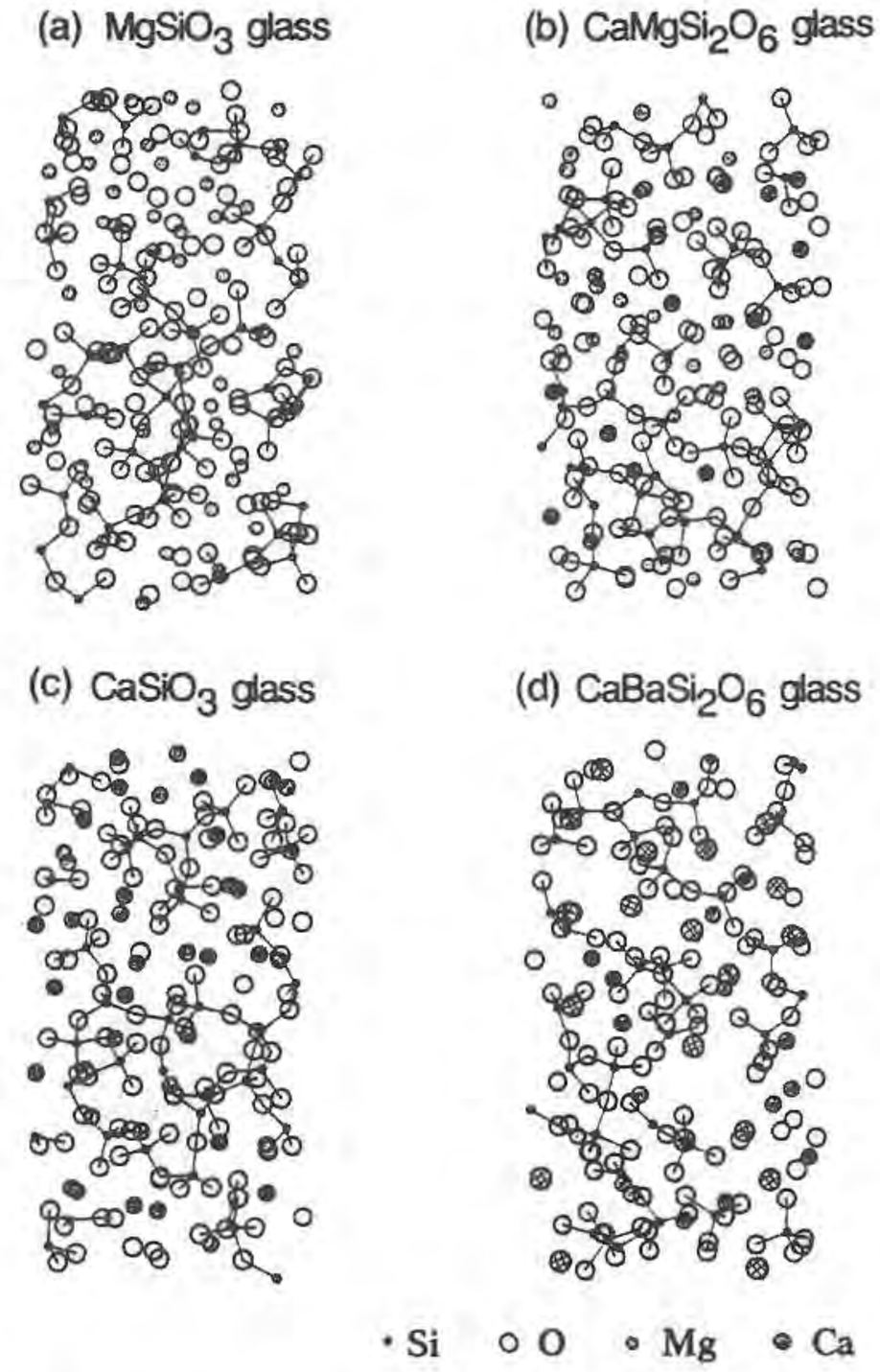

Fig. 1 MD-derived instantaneous glass structures.

HIGH-PRESSURE AND HIGH-TEMPERATURE OPTICAL ABSORPTION SPECTROSCOPY OF TRANSITION METAL IONS BEARING MINERALS

Taran M. N. *(Dept. of Spectral Methods of Investigation of Minerals, Inst. of Geo-chemistry, Mineralogy and Ore Formation, Acad. Sci. of Ukraine, Kiev)*

Andrut M. *(Inst. f. Mineralogie und Kristallographie, TU Berlin, Germany)*

Electronic spectra of minerals caused by most abundant in earth crust and upper mantle Cr^{3+}, Fe^{2+}, Fe^{3+} and Ti^{4+} transition metal ions have been investigated at pressure (P) up to 8 GPa and temperature (T) from 77 K to 750 K. It is stated that T mostly causes an expansion of $3d^N$-ions coordination polyhedra changing their distortion though in spinel and almandine FeO_4 and FeO_8 polyhedra seem to show a slight compressing at heating. P compresses and makes $3d^N$-ion polyhedra more regular. Mean thermal expansion coefficient of Cr^{3+}-octahedra, calculated from the spectra (α_{optic}), are different for different minerals and larger than those of host Al or Mg ions available from X-ray diffraction α_{diffr}. The largest differences between α_{optic} and α_{diffr} are

stated for garnets. In pyrope and grossulare α_{optic} = 1.5 and 2.0 while α_{diffr} = 0.7 and 1.0 (10^{-5} K^{-1}) (Hazen and Finger, 1982), respectively. Polyhedral moduli of CrO_6-octahedra are also different for different minerals and always larger than bulk moduli.

Crystal field stabilization energies of Cr^{3+} and Fe^{2+} are changed with T and P that should be taken into account for thermodynamics. For example, a significant difference in change of 3*d*-electrons levels split of Fe^{2+} in M1 and M2 sites at heating in olivine structure can be a cause of ordering of Fe^{2+} in M1 sites at elevated T. T and P dependencies of M-M charge-transfer, exchange-coupled pairs and *dd*-bands of $3d^N$-ions exhibit wide variations that can be used for interpretation of the spectra.

References:

Hazen, R.M., Finger, L.W. (1982) *Comparative Crystal Chemistry.(Wiley-Interscience, New York)*, 321 p.

LUMINESCENCE OF REE AND 3d-TRANSITION METAL IONS IN PHYLLOSILICATES

Tarashchan A.N. and Kuznetsov G.V. (*Inst. of Geochem. Mineral. and Ore Formation, Kiev*)

Fe^{3+} and Mn^{2+} ions were found to be the main luminescence activators for nature phyllosilicates. Spectra of some minerals of chlorite minerals display the characteristic sharp-line emission of corresponding REE: Ce^{3+}, Nd^{3+}, Sm^{3+},Gd^{3+},Tb^{3+}, Dy^{3+} (cookeite, ripidolite, pennine, brunsvigite) and Cr^{3+}ions (amesite, Cr-chlorite) besides theirs spectral bands. In order to explain the nature of this emission, the whole number of synthetic monocrystals (phlogopite) doped with REE and 3d-ions have been studied. Photoluminescence (PL) and X-ray luminescence (XL) spectra were analyzed from 200 to 1000 nm at 77K and 300K and compared to those of natural minerals.

Optimal concentration for the most of TR^{3+} is among limits 0.05 - 0.5%. Energy level diagrams for TR-ions were made on the base of XL spectra . Spectral band of these ions are ununiformly widen because of large number of centers unequivalent in structure. Isomorphic nature of TR-ions in interlayer cation position have been established under experiment.

Luminescence spectra of crystals activated by Fe are represented by wide band of 700nm. The broadening of the emission and its displacement to the long-vawe side while increasing activator concentration were observed. Excitation spectrum (main bands are 370, 383, 413,429,460 and 505 nm) are typical of Fe^{3+} in tetrahedral coordination. Mn^{2+} ion emission occurs in 530 nm band which are excitated at 347, 368, 441, and 458 nm spectral band. Common activations of micas with Fe and Mn was established to result in formation of pair Fe^{3+}- Mn^{2+} centers apart from single ones. Relaxation characteristics of centers are changed and excitation spectra become complicated due to sensibilization effect. Cr^{3+} ions photoluminescence (PL) spectra for chlorites are characterized by excessively large splitting.

Applied aspects of X-ray luminescence have been discussing.

GOLD FROM PREPOLAR URAL DEPOSITS OF DIFFERENT FORMATION TYPES

Tarbaev M.B. (Insnitute of Geology, Komi Science Centre,Ural Division, Russian Academy of Sciences, Syktyvkar, Russia)

Prepolar Ural is a region, which is a part of northern Ural segment. In struktural aspect this territory is a fragment of Central Ural uplift of Ural axial zone and its restrict. It is composed by ortho- and parametamorphic rocks of Ripheic ages with numerous intrusions of acid and basic compositions exposured in the core of the uplift. Its flanks are composed by slight metamorphised sedimentary rock masses of Paleozoic age. Alluvial placers of Quaternary age are widely distributed here. Known native gold deposits are presented by next types:

- lode, gold-quartz-sulphid objects
- zones of sulphid mineralisation, connected with metasomatites
- gold conglomerates

Typomorphic features of gold from these deposits are studied for a determination of their differences, conditions of their formation, and a revealing of possible sources of "nutrition" of placers.

Gold from lode ore deposits varies on grain sizes from the first tens of micrometers to small nuggets. The grain of 0.25-0.5 mkm prevail, a content of large gold grain (>1 mm) is equal to 1-3 %. This gold grain distribution on sizes is conditioned by phased gold precipitation.The late generation differs by larger gold grain.

The gold contains the next elements-impurities: Ag, Cu, Fe, Pb, Ti, As, Mn, Si, Al, Mg, Ca,. Ag (3.1-13.8 mass.%) and Cu (0.01-0.3 mass.%) are characterized by highest content among them. The gold fineness varies from 880 to 970 ppm. More pure gold deposited during late stages of ore process.

In zones of vein-sulphid mineralization, connected with metasomatosis, the gold assotiates closely with sulphids. It differs by small sizes (the first tens-hundreds of mkm) and high degree of isometricity. A number of crystals reaches 20-30 %. The fineness varies from 760 to 930 ppm. Ag (6.3-20.1 mass.%), Cu (0.1-0.5 mass.%) dominate among main elements-impurities. The rest impurities are presented by Fe, Pb, As, Ti, Zn, Mn, Mg, Si, Al.

Native gold of the conglomerates is characterized by a presence of two morphogenetic types. The first type is presented by grains of "hydrothermal" habitus. They are of isometric sometimes flattened shape, often with hidrooxydes Fe, mica, chlorite and quartz. The gold fineness of this type varies from 890 to 980 ppm. The content of Ag admixtures isn't significant, but that of Cu is high (0.08-2.53 mass. %).

The second type is presented by grains of "sedimentary" habitus with features of occurence in water stream. Roudness of grains reaches 40 %, the crumping of edges of grains is observed.

The composed toroidal grains are characteristics of this type. The gold of this type is characterized by very high fineness (960-990 ppm) and almost absence of impurities.

HEULANDITE, OPALE CT AND MORDENITE FORMING A VERY FINE GRAINED SEDIMENT IN A MIOCENIC MARINE SEQUENCE OF CENTRAL ITALY

Tateo F., Morandi N., Minguzzi V. and Felice G. (Dept. of Scienze Mineralogiche, Univ. of Bologna, Italy)

The mineralogical and geochemical study of a very fine grained sediment (≈ 30 cm thick) belonging to an early miocene marine sequence in the Marche Region (central Italy) is reported. The sediment appears light-coloured, ranging from white yellow to

brownish, with splintery breaking and primary laminar layers, interrupted by decimetric bioturbations. The examined sequence shows marls alternate with siliceous marls, interbedded to thick volcanoclastic sediments like cinerites and/or smectitic cinerites.The considered sediment appear like a volcanogenic deposit, but for the lighter color and the texture that is more homogeneous. Different portions of the deposit were sampled according to the variation of colour and position respect the base and top of the bed.

Different analyses were runned: chemical (major and minor elements), XRD (natural conditions and after thermal treatments at increasing temperature), thermal (TG, DTG and DTA), optical and SEM-EDS. The chemical results show that the white-yellow portion (an. 1) are rather similar to the brown one (an. 2); the SiO_2 and H_2O contents are high, whereas Fe_2O_3, MgO, Na_2O and K_2O are lower, compared to other altered volcanogenic sediments. Trace elements are not expressive of particolar enrichments.

	SiO_2	Al_2O_3	Fe_2O_3	MgO	CaO	SrO	BaO	Na_2O	K_2O	H_2O
1	68.83	9.66	0.22	0.37	3.81	0.16	0.51	0.41	0.86	14.41
2	72.56	9.16	0.22	0.30	3.61	0.18	0.29	0.46	0.86	12.42

The XRD spectra display few reflections with low intensity and high broadness. Two zeolites (heulandite and mordenite) and opal-CT are present in all samples. The occurrence of mordenite was never detected in oligo-miocene deposit of the northern and central Apennines. The distinction between heulandite and mordenite is hard if based on untreated samples only. The heating of powders enebled to overcome this problem (Fig.1): the reflections due to mordenite rest unaltered after heating at 700°C overnight, but the reflections due to heulandite start to decrease in intensity and sharpness after 300°C. The heulandite structure collapse over 450°C. The opal-CT reflection remains broad and unchanged (at about 4.05 Å). The thermal analyses record 2 dehydration reactions with sharp DTG variations at about 120° and 200°C and a slow weight loss between 200°C and 700°C.

Based on the whole data set, a reasonable guess about quatitative estimation can be proposed: the opal-CT range between 30% and 35%, zeolites between 65% and 70% (heulandite / mordenite ratio near 3:1).

The microscopical observations point out the occurrence of volcanic shard morphologies, replaced by crystalline components, and of altered feldspars crystals. SEM-EDS analyses revealed that zeolites and opal-CT are finely mixed and that their grain size is <2 μm. The occurence of fan-lamellar aggregate is widespread.

The heulandite and mordenite formation can be supposed to originate from the reaction between volcanic material (glass shards) and sea water. The reaction shold develop in hydrothermal conditions involving brief times because of the reduced crystallinity of zeolites. Moreover the most soluble ions (Mg, Na, K) are removed. The occurrence of opal-CT can be thought as the effect of a catastrophic event (volcanic) that caused the accumulation of siliceous shell (opal-A) later transformed in opal-CT under burial conditions.

Fig. 1

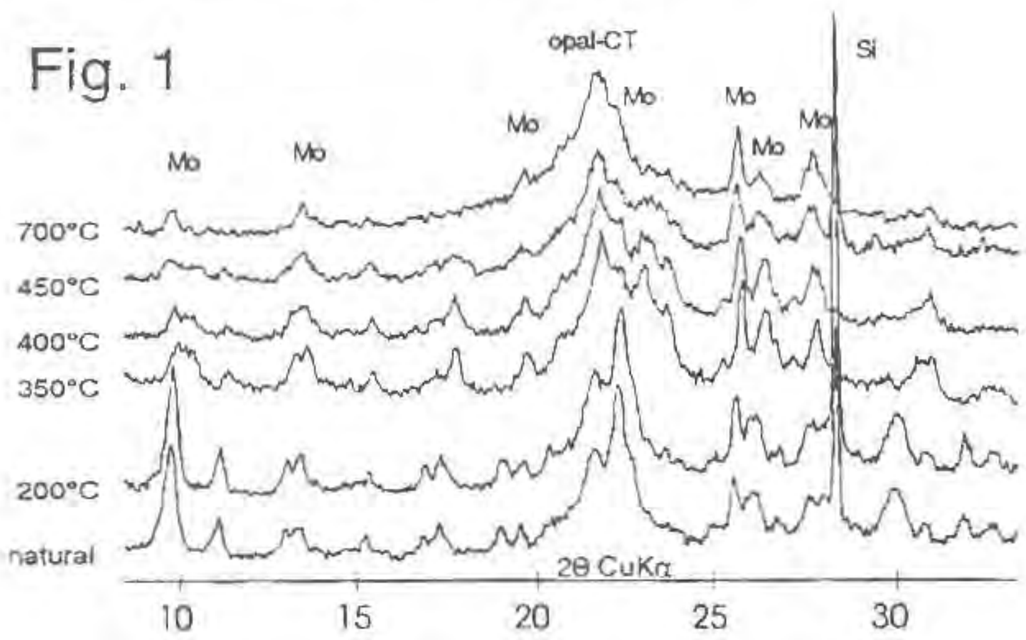

THE RAPAKIVI TEXTURES IN THE TISMANA GRANITOIDS , ROMANIA

Tatu M. and Berza T. (*Inst.of Geology and Geophysics, Bucharest*)

The presence of a lot large granitoids massifs is the most important features of the metamorphic basement of the Danubian units (South Carpathians). One of them, the Tismana massifs, appears as a concordant body in the Precambrian metamorphics of the Lainici Păiuş Group. In this paper we present for the first time in the Carpathian area the rapakivi textures as products of coeval magmatism which have generated the Tismana body.

The petrographic assemblage of the Tismana massif consists of porphyroid granites (about 80 percent of the massif) and of equigranular diorites, quartz-diorites, monzodiorites, granodiorites, tonalites. In the western part of the massif there appears the giant mafic magmatic enclaves (MME) of prevailing dioritic and quartz-dioritic composition. Eastwards, the size and the frequency of the MME is decreasing. According to the mineralogical and geochemical data, the Tismana massif has a calk-alkaline character for the equigranular rocks, but pronounced K-alkaline tendency for the porphyroid granites.

In the central part of the massif there occur several hectometric blobs of peridotitic composition. There is a compositional zoning from the ultrabasic blobs to the host acidic rocks (peridotite-mixed peridotite-mixed porphyroid granite-porhyroid granite). All around the blobs, the porhyroid granites present many disequilibrium textures typical for the rapakivi granitoids. Resorption and mantling of microcline megacrysts by plagioclase, the presence of quartz drops with fine grained mafic mantle composed of amphibole, biotite, apatite and ilmenite are interpreted as being resulted by mixing processes. Epitaxial nucleation of the plagioclase on microcline followed by dissolution of the latter with growth of a new generation of plagioclase as rims with cellular and fine cellular structures, claims changes in the composition and temperature during the mafic-felsic magma interaction. All these aspects point to the presence of rapakivi granites (wiborgite type) as a hectometric rim around the peridotite megaintrusions.

On the other hand, the presence in the mixed peridotite of the quartz drops and K-feldspar crystals with identical reaction rims as in surrounding mixed porhyroid granites reflects also the mixing processes between the mafic magma and the host granitic magma.

Mixing processes are preceded by the mingling at various stages of the massif's history, contemporary with ascent and emplacement of magmas.

VAPOR-PHASE BORIC ACID IN QUARTZ-HOSTED FLUID INCLUSIONS FROM A MIAROLITIC ELBAITE SUBTYPE, COMPLEX RARE-ELEMENT PEGMATITE, SOUTHERN CALIFORNIA

Taylor M.C., Williams A.E., and McKibben M.A. (*Dept. of Earth Sciences, Univ. of California, Riverside*)

Fluid inclusions in pegmatitic quartz were analyzed semi-quantitatively utilizing the RATFINC (Rapid Analyzer of Total Fluid INclusion Content) which consists of a heated crushing chamber close-coupled to a VG/Fisons SXP300 quadrupole mass spectrometer (*cf.* Williams *et al.*, 1992). Samples were heated to *ca.* 50°C before crushing. Data from the analysis was integrated off-line to establish relative abundances of major volatile components. The decrepitation-mass spectrometric analysis indicates that late-stage exsolved fluids trapped within miarolitic quartz-hosted pseudosecondary-secondary S+L+V inclusions were rich in CO_2, along with significant F (as HF), N_2, B (as H_3BO_3), H_2S, Ar, He, and minor HCl, SO_2 and hydrocarbons. These gases coexist with predominantly carbonate daughter crystals and aqueous liquid. Vapor-phase H_3BO_3 has not been previously observed in nature, though synthetic vapor-phase H_3BO_3 has been observed by Ogden and Young (1988) and Attinà *et al.* (1991). The mass spectra show $[B(OH)_2]^+$ and $[B(OH)_3]^+$ at *m/z* 44 & 45 and 61 & 62, respectively, corresponding to a mixture of *ca.* 20 atom% ^{10}B and 80 atom% ^{11}B.

The miarolitic elbaite subtype rare-element pegmatite

(Taylor *et al.*, 1993; Novák & Povondra, 1994) hosting the inclusion-bearing quartz was derived from a highly evolved hydrous granitic melt that was characterized by high B and low F and P activities. Boron mineralization culminated in the crystallization of danburite, hambergite, manganoan hellandite, schorl-elbaite-olenite, and tusionite without phosphates or primary micas within the pocket zone. Locally, moderate S activity promoted the precipitation of danalite.

Alkaline conditions during the formation of miarolitic cavities are indicated by the presence of the borate minerals hambergite and tusionite and the absence of primary muscovite (London, 1982; Němec, 1988; Foord *et al.*, 1991). Late muscovite locally replaces K-feldspar within preconsolidated zones and danalite is locally abundant within the pocket zone, signifying increasing acidity during the latest stages of crystallization (Burt, 1981; Fursenko, 1982).

References:

Attinà, M., Cacace, F., Ricci, A., Grandinetti, F., Occhiucci, G. (1991). *J. Chem. Soc., Chem. Commun.*, 66-68.

Burt, D.M. (1981). *Econ. Geol.*, **76**, 832-843.

Foord, E.E., London, D., Kampf, A.R., Shigley, J.E., and Snee, L.W. (1991). *Geol. Soc. Am. Ann. Mtg. Guidebk.*, 128-146.

Fursenko, D.A. (1982). *Fiz.-khim. issled. Mineralobraz. sist.*, 104-107 (in Russian, not seen; abstr. in Chemical Abstr., **98**, 219084n).

London, D. (1982). *Carnegie Inst. Wash. Yr. Bk.*, **81**, 331-334.

Němec, D. (1988). *Z. geol. Wiss.*, **16**, 245-251.

Novák, M. & Povondra, P. (1994). *Mineral. and Petrol.*, (in press).

Ogden, J.S. & Young, N.A. (1988). *J. Chem. Soc. Dalton Trans.*, 1645-1652.

Taylor, M.C., Williams A.E., McKibben M.A., Kimbrough, D.L., Novák, M. (1993). *Geol. Soc. Am. Abstr. Progr.*, **25**, 6, A321.

Williams, A.E., McKibben, M.A., Sloan, R.C., Jr. (1992). *Geothermal Resources Council Trans.*, **16**, 199-204.

THE CRYSTAL CHEMISTRY, STRUCTURE AND EVOLUTION OF POLLUCITE

Teertstra, D.K., Černý, P., Sherriff, B.L. and Hawthorne, F.C. (Department of Geological Sciences, University of Manitoba, Canada)

Pollucite is a Cs,Na-bearing zeolite isostructural with analcime, wairakite, leucite and ammonioleucite. Its occurrence is restricted to highly fractionated rare-element granitic pegmatites in association with Rb-rich K-feldspar, albite, quartz, lepidolite, tourmaline, amblygonite, spodumene and petalite. The formula is $(Cs>Na>Rb,Li)_xAl_xSi_{3-x}O_6 \cdot nH_2O$ with Z = 16. X apfu of extraframework cations are distributed between smaller 24c sites and the larger 16b sites by $Cs^+_{(16b)} + []_{(24c)} = Na^+_{(24c)} + (H_2O,[])_{(16b)}$.

Since 1988 we have examined 166 hand specimens of pollucite (representing about 70% of the known localities) and gathered 1625 analyses by electron microprobe on 173 thin sections + 14 grain mounts. Our main findings:

1) Histogram of CRK = 100(Cs+Rb+K)/Σ cations range from 69 to 89 (mean 81.1). Si/Al ratios in homogeneous primary magmatic pollucite range from 2.31 to 2.57 (mean 2.48, with a normal distribution).

2) There is no solid solution towards leucite or wairakite. K,Ca,Fe and Mg contents are near detection limits. High contents of these elements in wet chemical analyses indicate contamination by micas and feldspars. Wet, bulk analyses overestimate Al_2O_3.

3) The maximum H_2O contents may be calculated assuming no vacancy [] in 16b, and H_2O increases with Si/Al ratio. Li_2O may be present to 0.4 wt.%. Rb_2O is present to 2.97 wt.% and P_2O_5 to 1.5 wt.%. P enters the framework by $Al^{3+} + P^{5+} = 2Si^{4+}$.

4) Most pollucite is cubic and isotropic but is not completely disordered, as indicated by ^{27}Al and ^{29}Si MAS and DOR NMR. ^{23}Na NMR revealed two distinct Na environments, probably related to the number of H_2O nearest neighbors. Some samples show local birefringence, but single-crystal X-ray diffraction shows these to be metrically cubic with tetragonal symmetry; the anisotropy is therefore related to ordering.

5) Single-phase, primary pollucite reequilibrates with decreasing temperature. In these processes, (i) Na,Si-enriched and Cs,Al-enriched domains form, (ii) quartz may exsolve leading to Si-poor but (cation,Al)-rich pollucite, and (iii) solution-reprecipitation generates end-member $CsAlSi_2O_6$ in equilibrium with a relatively Na-rich fluid. At lower temperature, extensive analcimization occurs by cation exchange.

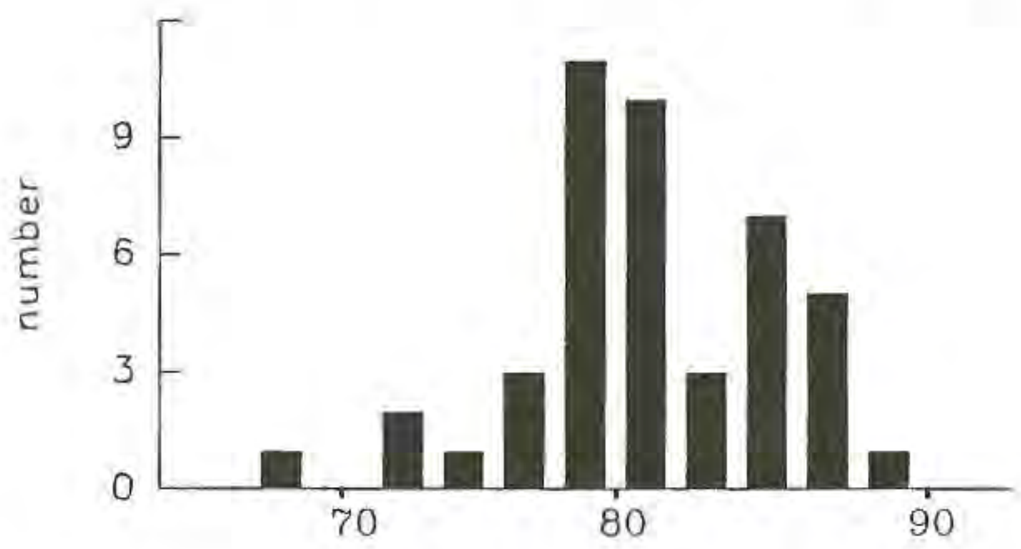

A NEW DYNAMIC MODEL OF HIGH PRESSURE GENERATION IN THE EARTH'S CRUST

Ten A. (Institute Mineralogy and Petrography, Novosibirsk, 630090, Russia)

One of the interesting problems of modern petrology is findings of ultrahigh pressure mineral associations [Chopin, 1984] and diamonds [Sobolev, Shatsky, 1990], [Xu et al, 1992] of metamorphic origin in the earth's crust. This paper presents the result of numerical investigations on rock shearing which demonstrates significant pressure rise due to inhomogeteiteis. This phenomenon could explain appearance of high pressure zones in the earth's crust.

Last decade experiments show very complex behaviour of rocks under the strength. But the fact that average tectonic strain rates fall into the interval 10^{-13}-10^{-15} sec^{-1} allows to use Newtonian rheology for rock deformation investigation [Ito, 1979]. Another important fact is that geologic objects are strongly inhomogeneous. It may be expressed in blocks of different rocks, different structures, temperature anomalies, and so on. All these peculiarities lead to significant changing of the rock properties from point to point, including viscosity - a principle property for creep. So it's not correct to neglect the inhomogeneities from model consideration. Thus the rheologic model is reflected by next equation: $\tau = \mu^* \dot{\varepsilon}$, where τ- stress tensor, $\dot{\varepsilon}$- strain rate tensor, μ - viscosity. This relation allows us to estimate pressure generated by rock deformations. Pressure is invariant of stress tensor so the estimation that the pressure proportional $\mu^* \dot{\varepsilon}$ is quite reasonable. Then the order of the

pressure generated by shearing is tens of Kbar. To consider these facts the dynamic numerical 2D model of Newtonian inhomogeneous viscous fluid was constructed [Ten,1993]. It takes into account both of earlier sited characteristics. The number of numerical experiments was curried out. As experimental situation the cylindrical inhomogetities in simple shear was used. The viscosity and strain rate were accepted 10^{24} P and 10^{-14} sec^{-1} accordingly. A single cylinder, which viscosity is two times higher than that of the country media, generates pressure about 5 Kbar. So low viscosity contrast was accepted for all numerical experiments to estimate a bottom pressure limit. Certain types of inhomogenety structures lead to essential rise of pressure up to value of 35-50 Kbar. For example the pressure reaches value of 35 Kbar in the interstitial space of two viscous cylinders. Under shear of inhomogeneous medium the pressure isn't been spread on large area but localised near the inhomogeneities and size of anomaly zone is comparable with that of viscous anomalies. Moreover some places of the "negative" pressures were observed. Similar structures (pressure shadow) were found in ductile sheared rocks. Thus the point of rock during deformation period passes zones of high and "negative" pressures. But if characteristic time of deformation is small enough the "spotted" pressure field could be fixed in the rocks. This fact coincides with field investigation in Kazakhstan diamondferous massif [Ten, Lepetiukha, 1994], where geobarometers indicate a significant pressure gradient which is higher than lithostatic one. Similar effect should be appear in collision zones and other places with active tectonic. But as it was mentioned the pressure is proportional to strain rate so its value may be varied significantly depending on maximal strain rate.

1. Chopin C., Contr. Miner. Petrol 86, 107-118, (1984)
2. Ito H., Tectonophysics 52, 629-641, (1979)
3. Sobolev N.V., Shatsky V.S., Nature 343, 742-746, (1990)
4 Ten A , Dokl. Akad. Nauk 328, 322-324, (1993)
5. Ten A., Lepetiukha V.V., Bk of conf. abstr. "Tectonics and Metamorphism", Moscow,22-25, (1994)
6. Xu S., Okay A.I, Ji S., et al, Science 256, 80-82, (1992)

• GENERATION OF SUBALKALIC GRANITES IN THE LAPLAND GRANULITE NAPPES AS A MODEL FOR THE ORIGIN OF RAPAKIVI-TYPE MAGMAS

Terekhov E.N. and Levitski V.I. (*Inst. of the Lithosphere, Moscow and Inst. of Geochemistry, Irkutsk, Russian Academy of Sciences, Russia*).

Medium- to coarse-grained microcline granites occur widely in the base of the Lapland granulite nappes. The granulite protolite seems to be of Archean age; in the Early Proteroizoic it was squeezed out from the deep horizons of the Earth's crust and thrust over the less metamorphosed rocks of differrent age. Garnet amphibolites developed at the base of the nappes during this thrusting. There are many thin, sill-like bodies of granites within amphibolites. Granites are generally foliated, though massive types are locally found.

These granites are subalkalic and characterized by high K, K/Na and Fe/Mg ratio, Ga, Rb, Zr, Y and REE. All these characteristics evidence that the granites of the Lapland nappes are very close to the rapakivi-type granites and especially to calculated composition of magma parental for rapakivi granites (Ramo, 1991). The Lapland belt granites are A-type granites in diagrams of Whalen et al. (1987); accordingly they could originate as a result of partial melting of the lower crust affected by hot deep-rooted fluids during thrusting. If such magma could move to extension environment, it crystallized giving origin to typical rapakivi massifs, which are confined to the rear portion of granulite nappes or upper structural level of the crust. Thus the origin of the rapakivi granites could be related to the final stages of evolution of the granulite belts.

High-pressure metamorphism in Verrucano metasediments of the Monte Argentario, Northern Apennines - A new occurrence of magnesiocarpholite

Theye, Th. (Univ. Braunschweig, Germany) and Reinhardt, J. (Univ. Darmstadt, Germany)

The promontory of Monte Argentario, Southern Tuscany, is one of the few localities in the Northern Apennines from where high-pressure metamorphic mineral assemblages have been reported (e.g., Ricci, 1972).The Monte Argentario tectonic complex comprises two major units which are separated from each other by a cataclastic fault zone of polymict breccia. The eastern part largely consists of Verrucano metasediments resting on a Variscan basement, whereas the overlying western part is a tectonic mélange containing ophiolitic fragments (metagabbro, metabasalt, serpentinite, pelagic metasediments), metapelites, metapsammites, carbonate rocks and gypsum of Triassic age, as well as greywacke blocks of uncertain provenance (Reinhardt, 1982; Strünitz, 1982).

Franceschelli *et al.* (1986) estimated the metamorphic P-T conditions for the Verrucano metasediments at about 300°C and 3-5 kbar, based on white mica compositions and assemblages containing chloritoid, pyrophyllite, and kaolinite. Conversely, mineral assemblages and reaction textures in the metabasites of the overlying unit indicate P-T conditions of the lawsonite-blueschist facies (Reinhardt, 1982; Strünitz, 1982). These observations suggested a pressure gap between the upper unit and the lower unit (or at least those parts of the upper unit that undoubtedly experienced high-P metamorphism).

On the basis of new mineralogical evidence and petrological analysis, we re-examined the P-T data for the Monte Argentario rocks. Mineral assemblages in metabasite rocks of the upper unit suitable to estimate P and T include quartz, albite, lawsonite, chlorite, pumpellyite, Na-amphibole, and rare occurrences of sodic pyroxene. Detailed microprobe work showed that Na-amphibole and Na-pyroxene are zoned. Both occur as reaction rims around augite and hornblende in metagabbro. From the most Al-rich blue amphibole (crossite) and the most jadeitic pyroxene ($Jd_{26}Ac_{49}Di_{22}$) P-T conditions of 340°C and 7 kbar have been calculated.

Likewise, high-P conditions in the Verrucano of the lower unit are indicated by the discovery of magnesiocarpholite of the composition $Mg_{.61}Fe_{.36}Mn_{.02}Al_{1.97}[Si_{2.01}O_6](OH_{3.86}F_{.14})$ that occurs in quartz segregations. Thermodynamic calculations result in a minimum pressure of about 7 kbar (at 350-400°C) and maximum temperature of about 370°C (at 7 kbar) for magnesiocarpholite formation. Magnesiocarpholite is partly replaced by sudoite of the composition $Mg_{1.70}Fe_{.52}Al_{2.83}[Al_{.96}Si_{3.04}O_{10}](OH)_8$. This retrograde reaction magnesiocarpholite --> sudoite + quartz must have occurred at lower pressure. Sudoite of the same composition also occurs in metapelites of the lower unit as rock-forming mineral, associated with quartz, muscovite, paragonite, pyrophyllite, chloritoid, hematite (Franceschelli *et al.* 1989), and, in some instances, chlorite. A retrograde formation of this type of sudoite have also to be envisaged. The high-P assemblage most likely comprised chloritoid, chlorite, pyrophyllite and relatively coarse-grained white mica. Calculation of chemical equilibria involving the components of white K-mica (data and activity models of Massonne, 1993) yields pressures of about 10 kbar (at 350-400°C). Therefore, evidence for high-P conditions is found in both the lower and upper parts of the Monte Argentario, contrary to previous views. Further petrological studies are required to establish whether there are still significant P-T differences between both units or not.

Franceschelli, M. Leoni, L., Memmi, I. & Puxeddu, M. (1986): *J. metamorphic Geol.*, **4**, 309-321.
Franceschelli, M., Mellini, M., Memmi, I. & Ricci, C.A. (1989): *Contrib. Mineral. Petrol.*, **101**, 274-279.
Massonne, H.-J. (1992): In: Water-Rock Interaction, Y.S. Kharaka & A.S. Maest (eds.) , p. 1523-1526. Balkema: Rotterdam.
Reinhardt, J. (1982): Diplomarbeit, Universität Göttingen, 172 p.
Ricci, C.A. (1972): *Atti Soc. Tosc. Sci. Nat., Mem. Ser. A*, **79**, 267-279.
Stünitz, H. (1982): Diplomarbeit, Universität Göttingen, 186 p.

THERMODYNAMIC PROPERTIES OF ENSTATITES

Thiéblot L., Richet P. (*Laboratoire des Géomatériaux, Institut de Physique du Globe, Paris*) and Gillet Ph (Géologie, E.N.S. Lyon)

Although the $MgSiO_3$ composition is particularly important in mineralogy, the thermodynamic properties of the various polymorphs are not so well known. This applies even to the low-pressure enstatite forms, for which available thermodynamic data are incomplete and often refer to uncharacterized samples.

As a starting point for a reliable data base for $MgSiO_3$ polymorphs, we have determined by drop-calorimetry the heat capacity of ortho- and protoenstatite from room temperature up to the upper stability limits of these phases. We have also measured the thermal expansion coefficient of protoenstatite from high-temperature X-ray diffraction experiments performed in an energy dispersive configuration on the wiggler line of the DCI storage ring of LURE (Orsay).

These results will be presented and discussed in terms of vibrational density of states determined from new Raman spectroscopy measurements. Particular attention will be paid to the difference in the properties of the low-pressure polymorphs.

A GOLD DEPOSIT RELATED TO SUB — ALKALINE ROCKS AND SOME POSSIBLE NEW MINERALS (UNNAMED) IN THEM, IN DONGPING, HEBEI PROVINCE, CHINA

Tian Shuzhang (*Gold Geo. Res. Inst., Langfang, Hebei, China*)

The Dongping gold deposit is a new type discovered for the first time in China. It is located in the endocontact zone of Shuiquangou sub—alkaline complex batholith (K—Ar isotopic age: 226 — 177.2 Ma). The rock types consist of amphibole monzonite, amphibole quartz monzonite, aegirine — augite monzonite, aegirine — augite syenite, syenite, quartz syenite, monzonite and quartz monzonite. the last two types are the host rock.

The Dongping gold deposit is a remelting — metasomatic, and meso to high timperature hydrothermal type. The ores are sub — divided into quartz vein and altered K — feldspar types. Mineralogical composition is complex. Primary ore minerals are: pyrite, pyrrhotite, magnetite, galena, sphalerite, chalcopyrite, native gold, calaverite, altaite, specularite, tetrahedrite, stibnite, proustite, pyrargyrite, lead — bearing tellurium and unnamed $Au_2Te_3S_2$, & Au_2Te. Secondary minerals are: limonite, bornite, chalcocite, digenite, covellite, anglesite and cerussite. The tellurides are not stable in oxidized zone. They are oxidized into some possible new minerals: Au_2TeO_3, $Au_2TeO_6 \cdot 2H_2O$, $Au_6[TeO_4][PbO_3]_2$, $Au_6Pb_2[TeO_4]_3[PbO_3]_2 \cdot 6H_2O$, $Au_2(Bi,Te)O_3$ and $(Zn,Pb,Cu)_3TeO_6 \cdot 2H_2O$.

Unnamed $Au_2Te_3S_2$

The average of four electron microprobe analyses of the single grain, 0.24 by 0.34mm, gave: Au 47.74, Te 44.84, S 7.10, Ag 0.98, Pb 0.29, sum 100.95 wt%, corresponding to $(Au_{2.05}, Ag_{0.08}, Pb_{0.01})_{2.14}Te_{2.88}S_{1.88}$, ideally $Au_2Te_3S_2$. The strongest powder diffraction lines [d in Å (I)] are: 5.24(82), 4.36(60), 4.10(58), 3.405(52), 2.850(100), 2.182(54), 2.085 (71), 2.059 (77). It is brown — yellow, with conchoidal fracture, and resin—like luster. In reflected light, it is grayish white with brown — yellowish tint. Bireflectant, reflection pleochroism and anisotropy are weak. Reflectance percentages in air for R1 and R2 are 486(nm)34.5, 31.3, 551 32.3, 29.8, 589 37.5, 34.8, 656 38.7, 36.5.

Unnamed Au_2Te

The average of two electron microprobe analyses gave: Au 72.16, Te 27.04, sum 99.20 wt%, corresponding to $Au_{1.90}Te_{1.10}$, ideally Au_2Te. The strongest lines of the X — ray powder—diffraction pattern [d in Å (I)] are: 2.22(47), 2.085 (100), 1.961(52) 1.787(51), 1.765(52), 1.479(64), 1.322 (59), 1.208(56). In reflected light, rose colour. Bireflectant, reflection pleochroism and anisotropy are very weak. Reflectance pecentages in air for R1 and R2 are: 486 (nm) 47.7, 45.6, 551 58.3, 55.6, 589 55.4, 53.6, 656 59.3, 54.7.

Oxygen — gold — bearing minerals: Au_2TeO_3, $Au_2TeO_6 \cdot 2H_2O$, $Au_6[TeO_4][PbO_3]_2$, $Au_6Pb_2[TeO_4]_3[PbO_3]_2 \cdot 6H_2O$ and $Au_2(Bi,Te)O_3$

The average of 3 — 7 electron microprobe analyses (with qualitative analyses and method of difference—substraction for oxygen) gave (wt%) as follows:

		Au	Te	Pb	Bi	Cu	Zn	Ag	O
Au_2TeO_3	(av. of7)	71.45	21.68						6.87
$Au_2TeO_6 \cdot 2H_2O$	(av. of4)	57.44	23.37						19.20
$Au_6[TeO_4][PbO_3]_2$	(av. of4)	61.54	7.78	23.58					7.11
$Au_6Pb_2[TeO_4]_3[PbO_3]_2 \cdot 6H_2O$	(av. of5)	42.51	13.26	29.56		0.07	0.05	0.47	13.98
$Au_2(Bi,Te)O_3$	(av. of3)	59.13	8.40	2.05	20.46	0.69	1.32	1.88	6.04

ESCA gave electron binding energy (ev) as follows:

	Au4f7/2	Te3d5/2	Pb4f7/2	
Au_2TeO_3	84.9	575.4		
$Au_2TeO_6 \cdot 2H_2O$	89.3	577.6		
$Au_6[TeO_4][PbO_3]_2$	86.0	577.7	139.9	
$Au_6Pb_2[TeO_4]_3[PbO_3]_2 \cdot 6H_2O$	84.9	577.0	139.4	138.4

In reflected light, brown with many different kinds of tint. Bireflectant, reflection pleochroism and anisotropy are strong. Reflectance is low (9.8—39.2%). Strong lines of the X — ray powder — diffraction pattern correspond to those of native gold, but with extra — weak lines, which don't correspond to any known minerals.

INTRACRYSTALLINE EXCHANGE REACTION IN A CLINOPYROXENE FROM MANTLE NODULE.

Tirone M. (1), Lucchesi S. (2), Principalle F. (1) ((1)*Ist. di Mineralogia e Petrografia, Univ. di Trieste;* (2)*Dip. di Scienze della Terra, Univ. di Roma*).

A single Cpx crystal enclosed in a spinel peridotite nodule from NE Brazil, was studied in order to verify the intracrystalline exchange reaction of Mg-Fe^{2+} between M1 and M2 sites. The sample PC135 (Salviulo et al., 1992; Principalle et al., 1994) shows a low Ca content (0.645 a.f.u.) and high Mg and Fe^{2+} content (0.957 and 0.099 a.f.u. respectively). R^{3+} (Al+Fe^{3+}+Cr+Ti) content is 0.203 a.f.u.. Using the Saxena formulation (Dal Negro et al., 1982), Principalle et al. (1994) obtained a intracrystalline temperature of 833°C. We made several heating experiments, followed by quench, at 1000 and 800°C, for increasing times until reaching Mg-Fe^{2+} equilibrium in M1 and M2 sites for both temperatures. The exchange of Mg-Fe^{2+} between M1 and M2 sites was controlled observing the variation of the ratio between the electrons of M1 and M2. The kinetic at 1000°C indicates a disordering process that reaches equilibrium for a $e^-_{(M1/M2)}$ ratio of 0.699 in 78h. The kinetic at 800°C indicates an ordering process that reaches equilibrium for a $e^-_{(M1/M2)}$ ratio of 0.671 in 177h. The exchange of electrons between M1 and M2 from 800 to 1000°C is of 0.28 that corresponds to an exchange of 0.02 atoms. The natural sample shows a $e^-_{(M1/M2)}$ ratio of 0.683 and this may indicate a closure temperature of intracrystalline M1-M2 exchange near to 850°C. This result is very closed with that obtained using Saxena formulation.

References:
Dal Negro A. et al., 1982: In Saxena Ed. Advances in physical geochemistry. Vol. 2.
Principalle F. et al., 1994: Contrib. to Mineral. Petrol. 116, 1-6.
Salviulo G. et al., 1992: Phys and Chem. Minerals 19, 213-219.

ORGANIC MINERALS AND ORGANIC COMPOUNDS OF CARBON IN BULGARIA: A REVIEW

Todorov T.A. (Geol. Inst., 1113 Sofia

The mineralogical discussion whether the natural organic compounds of carbon (OCC) can be considered minerals has not come to

an end yet. The present work is dedicated to the occurrences and the kind of the organic minerals (OM) and OCC in Bulgaria. Such formations can frequently be found in different geological environment but they do not form considerable deposits as a whole. To this time are discribed:

Weddellite was found in the Vitosha mountain near Sofia in the type of lichen-like powdered crusts. Under an electronmicroscope are seen his bipyramidal crystals.

The deposits of the fossil resins are in different parts of Bulgaria: in the Central Srednogorie, in the Eastern Balkan Mountains in the Western Bulgaria, in the Central Northern part of Bulgaria znd in the Western Balkan Mountains. The fossil resins from all of the deposits differ in their age and physical and chemical characteristics from the succinite and that is why the term "retinite" is used for them.

Osocerite and the natural paraffines are found in the shape of wax-like or hard dark brown crusts in the Lower Tithonian limstones in the Northeast of Bulgaria. Almost pure monoclinic crystals and aggregates have been found.

Hard hydrocarbons assumed to be paraffines (ceresine), isoparaffines, and alkilcyclanes have been found in the area of the Bobovdol coal deposit (Southwest Bulgaria). They are represented by slaty and needle-like orthorombic crystals with light yellow to max colour; sometimes they are mat and colourless.

The malt, the asphalts and the asphaltites are found in different places of South Bulgaria. The elastic malt is found in some Paleogene jointed sandstones of the Bobovdol coal deposit and in the same rocks and in the tuffs near Smoljan in the Central Rhodopes. In the Bobovdol coal deposit can also be found asphalt and asphaltite (grahamite and grahamite-gilsonite), in hard state. Hard bitumens of the asphalt type, the asphaltite (gilsonite) and the kerites (albertite) in association with pyrite, chalcopyrite, calcite and zeolites are found in Oligocene sediments, volcanites and their tuffs in the Easter Rhodopes. Similar is the genesis and the geological environment of the hard kerites from the albertite group in the region of Smoljan (Central Rhodopes).

From the hard organic compounds of the carbon also anthraxolites have been found in three occurrences: among the black shales of the Palaeozoic diabase-phyllitoid complex in the Western Balkan Mountain, and in the polymetallic deposits Sedmochislenitsi (Western Balkan Mountain) and Ptcheloiad (Eastern Rhodopes). It seems that in the last deposit anthraxolite is a product of the hydrothermal activity.

Along the Black sea coast southern from Burgas solid and semisolid substences of malt and asphalt types are found but they are industrial products.

"Organic minerals" have been also found in the kidneys and the bladder of people (whewellite, weddellite, uric acide, urinates, etc.) and their sudy is very important for the medicine.

Preparing the review the author used the data of many Bulgarian geologists which names will be given in the full text of the paper.

AURIFEROUS FLUIDS OF THE SOVETSKOE GOLD-QUARTZ DEPOSIT IN BLACK SHALES (YENISEY RIDGE, SIBERIA)

Tomilenko A.A. and Gibsher N.A. (*United Institute of Geology, Geophysics and Mineralogy, Novosibirsk, Russia*)

The deposit lies in the Precambrian gold-and carbon-bearing sedimentary metamorphic schales within the Central gold-bearing band on the eastern slope of the Yenisey ridge. The quartz veins and veined zones of the deposit were formed during repeated openings of vein-enclosing fractures in tectonically weak zones.

Vein-stringer zones are a group of contiguous, merging and newly branching veins, stringers and ore "columns". The veins and stringers are by 97% and more composed of quartz. Ore minerals are represented by pyrite, arsenopyrite, less often by pyrrhotite, galenite, sphalerite, chalcopyrite and marcasite. Gold occurs mainly in the native form, its distribution in ore bodies is irregular.

Based on phase proportions in the fluid inclusions at room temperature, three principal types may be recognized in quartz samples from the Sovetskoye deposit. Type 1 ($L_{H2O}+V_{H2O}$), gas/liquid ratios range from essentially gaseous to essentially liquid inclusions. Type 2 ($L_{H2O}+L_{CO2}$; $L_{H2O}+L_{CO2}+V_{CO2}$), CO_2 content varies from 15 to 90%. Type 3 (L_{CO2}; V_{CO2}; L_{CH4}; V_{CH4}). Negligible amounts of H_2O are found on the inclusion walls.

In the quartz of the deposit ore zones all three types of fluid inclusions were found. Homogenization is observed both into liquid and gaseous phases. Salt concentration, according to freezing investigations, reaches 15-25 wt.% NaCl equivalents. Abundance of CO_2-rich inclusions in the ore zone sometimes amounts to 50% and more of all fluid inclusions. Gas chromatography showed that main components of the fluid inclusions in quartz are H_2O (40-80 mole %), CO_2 (15-56 mole %), CH_4 (0.6-7.6 mole %) and N_2 (0.3-0.9 mole %); in native gold are CO_2 (29-64 mole %), H_2O (31-68 mole %), CH_4 (0.0-2.4 mole %) and N_2 (2.6-5.3 mole %).

Study of fluid inclusions in quartz and native gold of the deposit showed that gold-deposition occurred from heated, concentrated and CO_2-rich fluids. Fluids of ore quartz are characterized by homogeneous and heterogeneous state as well separation of fluid into brine and CO_2 components.

FEATURES OF DISTRIBUTION OF IMPURITIES IN SYNTHETIC PERICLASE

Tomilenko A.A. and Krylova V.V. (*United Institute of Geology, Geophysics and Mineralogy, Novosibirsk, Russia*)

The associations and amounts of more than 30 impurity-elements found in synthetic periclase are governed both by the initial raw material and crystallization conditions of periclase. Iron is known to be the most harmful impurity in periclase, which appreciably influences the electric resistance of periclase. Despite the great deal of works concerning periclase, the problem of the existence of iron and other impurities in this mineral remains debatable.

Microscopic investigations showed that periclase crystals produced by arc-fusion of natural magnesite contain abundant microinclusions of silicate melts (from almost entirely crystallized to glassy varieties). The compositions of melt inclusions mainly lie within the system $CaO-MgO-Al_2O_3-SiO_2$. Crystalline phases of inclusions according to data of microprobe analysis are represented by monticellite, two-calcium silicate, spinel, CaO, etc. The major components in the composition of glassy and crystallized inclusions are CaO (38-46 wt.%) and SiO_2 (36-42 wt.%), less often Al_2O_3 (2-11 wt.%). The content of MgO does not normally exceed 15-20 wt.%, while FeO ranges between 0.02-2.6 wt.%. FeO-rich melt inclusions are of particular interest. Besides glass and crystalline phases, they often contain ore phase (Fe - 90-96 wt.%, Si - 0.25-5.2 wt.%, P - 1.2-2.6 wt.%).

Concentration profiles of distribution of MgO, SiO_2, CaO, FeO and P_2O_5 in periclase and SEM-images of melt inclusions in characteristic emissions of Mg, Si, Ca, P and Fe showed that the elements considered are concentrated mainly in melt inclusions and are not involved in crystalline lattice of periclase in the form of isomorphous impurities as assumed before. By means of neutron-activation radiography, it was found that such trace elements as Sc, Sm, La, Eu and others are also concentrated mainly in melt inclusions.

FLUOR-EDENITE; ITS OCCURRENCE AND CRYSTAL CHEMISTRY

Tomita K. (*Dept. of Geol. & Min., Kyoto Univ.*) Makino K. and Yamaguchi Y. (*Dept. of Geol., Shinsyu Univ.*)

Fluor-edenite (F=1.5 pfu) was found in cavities of the pyroxene-hornblende andesite from Ishigamiyama, Kumamoto Pref., Japan. The edenite is characterized chemically and crystallographically.

The andesite was extruded to form a lava dome. Phenocrysts, of hornblende, hypersthene , augite, plagioclase, magnetite and apatite, are embedded in a groundmass of submicrocrystals and glass.

The cavities with fluor-edenite, tridymite and magnetite is 5-200cm in diameter and 1-5cm in thickness. The feature of the cavities suggests that they were produced to concentrate volatile elements in the later stage of solidification of the andesite .

The fluor-edenite is needle shaped crystals (1-10mm in length) and shows beautiful growthforms.

It's chemical formulae is
$K_{0.190}\ Na_{0.776}\ Ca_{1.704}\ Mg_{4.121}\ Fe^{2+}_{0.866}\ Ti_{0.143}\ Mn_{0.022}\ Al_{0.924}\ Si_{7.066}\ O_{22}\ F_{1.455}\ OH_{0.545}$.

It's unite cell parameters are
a=9.861(4)A, b=18.05(1)A, c=5.282(1)A, β=104.841(1) and V=908.9(6)A^3 with space group $C2/m$.

A structure refinement shows crystallographical features of the fluor-edenite replacing OH by F at the O3 site, as follows.

The O3 site contains 0.75F and 0.25OH, and the O3-position is refined. The interatomic distance between a O3 site and the adjacent O3 site is 2.633(9)A. This distance agrees with mean ionic radius 2.64A of the O3 site, which is calculated from effective ionic radii of F(1.30) and O(1.38). Therefore, anions in the O3 site may be contact each other.

The following chemical constraints are employed in the refinement. Small amount of Ti fixed at the M2 site conventionally, and a little of Mn is neglected. Mg and Fe^{2+} are particularly distributed among the octahedral sites in the fluor-edenite.

The site refinement shows that the M(2) site is enriched in Fe^{2+} over the M(1) and M(3) sites, and Mg is concentrated in the M(1) and M(3) sites against the M(2) site. The Mg-Fe^{2+} distribution in octahedral sites of the fluor-edenite is completely contrary to the Mg-Fe^{2+} distribution in "low-temperature" hydroxyl hornblendes (Makino and Tomita, 1989) . Thus, the incorporation of fluorine in the Ca-amphibole structure may requires the concentration of Mg in the M(1) and M(3), since fluorine in the O(3) bonds only cations in the M(1) and M(3) sites. The Mg-Fe^{2+} partitioning in the Cl rich hastingsite shows a strong preference of Fe^{2+} for the M(1) and M(3) sites rather than the M(2) site (Makino et al., 1993). Therefore, it is considered that the Fe-F avoidance rule appears to hold in intracrystalline Mg-Fe^{2+} exchange reactions in the fluor-edenite.

The observed mean M(2)-O length of the fluor-edenite is in good agreement with the length calculated from the mean ionic radius using Hawthorne's equation (Hawthorne, 1983). On the other hand, the observed mean M(1)-O and M(3)-O lengths disagree with calculated ones using the equations for OH amphibole, because the fluor-edenite is different from OH-amphiboles in the mean ionic radii of the O3 site.

In the fluor-edenite, the map of electron density of the A site shows the maximum region more elongated along about a^* than OH amphiboles. The strong elongation causes by substitution of F for OH. This elongation suggests that F in the O(3) site influences considerably Na and K in the A site.

References:

Hawthorne, F.C. (1983). *Can. Mineral.*,**21**, 173-480.
Makino, K. & Tomita, K. (1989). *Am. Mineral.*, **74**, 1097-1105.
Makino, K., Tomita, K., Suwa, K. (1993). *Mineral. Mag.*, **57**, 677-685

THE EASTERN SICILY LITHOSPHERE: Sr-Nd ISOTOPIC DATA FROM HYBLEAN XENOLITHS AND PRIMITIVE LAVAS

Tonarini S. (*IGGI, CNR, Pisa*), D'Orazio M. (*DST-Univ. of Pisa*), Armienti P. (*DST-Univ. of Pisa*), Innocenti F. (*DST-Univ. of Pisa*), Petrini R. (*IMP-Univ. of Trieste*), Scribano V. (*IST-Univ. of Catania*)

A widespread magmatic activity, with a dominant Na-alkaline signature, has been characterising eastern Sicily since Upper Trias up to Present (Mt. Etna), accompanying the rifting and thinning of the margin of the African Plate. In Plio-Pleistocene, volcanic activity concentrated in the northern Hyblean Plateau producing distinct near primary magmas ranging in composition from tholeiites to melanephelinites. In the same area, Upper Miocene volcanic activity generated several diatremic pipes that sampled upper mantle and lower crust rocks. We have determined the isotopic features of mantle and lower crust materials hosted by Hyblean volcanics of Miocene age, then comparing their isotopic signature with that of the most primitive Plio-Pleistocene Hyblean lavas. Ultramafic xenoliths (three harzburgites, one lherzolite and two pyroxenites) are LREE enriched in spite of the depleted nature of their major element composition; moreover the Sm/Nd ratios (<CHUR) are decoupled from the Nd isotopic ratios (0.51289 ÷ 0.51299), proving the occurrence of LREE enrichment events in relatively recent times. In these mantle samples the linear correlation observed between $^{147}Sm/^{144}Nd$ and $^{143}Nd/^{144}Nd$ is proportional to an age of 170 ± 90 Ma (MSWD=2.2); this suggests a maximum Permo-Trias age for the metasomatic event. Initial ε_{Nd} witnesses an asthenospheric source for the metasomatic agent that is also able to completely obscure the pristine isotopic signature of the pre-existing lithosphere.

Two of the deep crust xenoliths are mafic granulites that suffered ancient depletion processes, while a plagioclase-rich granulite is likely to belong to a lower crust segment which differentiated from a depleted mantle in Eo-Ercynic time. In this last sample, whole rock-plagioclase "isochron" age coincides with Nd model ages, thus pointing to a closed system behaviour.

The variability of Nd and Sr isotopic compositions of Plio-Pleistocene lavas, can be attributed to the interaction between a depleted MORB-like source, revealed by tholeiite lavas, and a relatively enriched source, akin to mantle xenoliths, dominating in the genesis of alkali basalts and melanephelinites.

MOLECULAR DYNAMICS SYNTHESIS OF DISLOCATIONS IN MgO

Mitsuhiro TORIUMI # and Masayuki KAWAMURA*
Geological Institute, Graduate School of Science, University of Tokyo
* Department of Earth and Planetary Sciences, Faculty of Science, Tokyo Intsitute of Technology

The molecular dynamics simulations of dislocation in MgO can reproduce two kinds of dislocations by insert of vacant layer and vacant crystal half plane in the basic cell which is composed initially with 2880 and 3240 ions. The edge dislocation having a Burgers' vector of 1/2<110> has relative small core of dislocation but the screw dislocation of 1/2<001> Burgers' vector is rather large core. The displacement field around edge dislocation display relative larger strain field than that around screw dislocation. The <110> dislocation of which glide plane is identical to be (110) shows perfectly the same structure as TEM observations in MgO, but <001> screw dislocation cannot be found in deformed MgO by means of TEM until now. The screw dislocation seems not to be formed in low stress and high temperature creep experiments because of its high self energy.

The edge dislocation introduced by above method moves in the

manner of glide along on the (110) plane due to the internal stress from another dislocation and surface induced in the MD simulation. In contrast, we can observe no dislocation glide of the screw dislocation during several picoseconds of MD experiments.

CRUSTAL XENOLITHS FROM THE PLIOCENE ALKALINE BASALTS FROM THE BALATON HIGHLAND (W-HUNGARY)

Török, K. *(Dept. of Petrology and Geochemistry, Eötvös Loránd University, Budapest)*

Crustal xenoliths in Pliocene alkaline basalts from some xenolith bearing localities of the Balaton Highland comprise garnet bearing and garnet free granulites, quartzites, plagioclase-biotite-potash feldspar fels and plagioclase-diopside-scapolite fels. Amongst the garnet free granulites there are orthopyroxene-clinopyroxene-plagioclase granulites, clinopyroxene-plagioclase granulites and clinopyroxene-plagioclase-quartz granulites.

Each of the xenoliths experienced some kind of melting during the way up in the basaltic melt. The most advanced melting phenomena can be observed in the quartzites where the interaction with the basaltic melt resulted in formation of rocks similar to the buchites in some cases. These rocks consist of relics of quartz, colourless or pale brown glass, fibrous sillimanite and idioblastic green spinel.

Some geothermometric measurements show 985-990°C for the orthopyroxene-clinopyroxene bearing granulites on the basis of two pyroxene thermometer of Wood and Banno (1973).

Fluid inclusion measurements were conducted on inclusions in clinopyroxene, plagioclase and quartz in garnet free granulites and quartzites. All inclusions seem to be of secondary origin occurring along healed fractures.

Fluid inclusions were measured from clinopyroxene, plagioclase and quartz. Fluid inclusions in granulites and quartzites contain predominantly CO_2, which is shown by the slight depression of melting points (-56.6/-58.5°C). However in those cases - in an orthopyroxene-clinopyroxene-plagioclase granulite - where the decrease was the most significant, initial melting was also observed between -64 and -62°C. These two facts imply the presence of an additional component (possibly N_2, CH_4 or CO).

All CO_2 inclusions homogenized to liquid phase between -0.8 and +27.5°C in the granulites. The tree mineralogically different granulite types have different T_h range. The lowest T_h range (-0.8/+9.4°C) was measured in the two pyroxene granulite and the highest one (+22.4/+26.4°C) in the quartz bearing sample. The clinopyroxene-plagioclase granulite gave the widest T_h range (+14.4/+27.5°C). Calculating with 980°C temperature which was obtained from the two pyroxene thermometry trapping of fluids occurred under pressure range from 6.2 to 3 kbar between 23.6 and 11.4 km and between 19.3 and 9.4 km assuming density of 2.7 g/cm^3 and 3.3 g/cm^3 respectively for the overlying rock column. The calculated pressure and depth from the most dense inclusions show that they may have sealed in the lower crust. Embey-Isztin et al. (1990) suggest higher pressures, above 7.5-8 for the two pyroxene granulites and about 9-10 kbar for the garnet granulites.

Quartzites contain some relict CO_2 inclusions which may have survived the partial melting of the rock in some relict quartz grains. Homogenization temperature of the inclusions is between +26.5 and +29.4°C.

Fluid inclusion data suggest that the two pyroxene granulites originate from the biggest depth (23.6 km or even deeper). Moving upwards in the rock column orthopyroxene disappears from the assemblage and quartz appears afterwards. Other metamorphics such as plagioclase-biotite-potash feldspar fels and plagioclase-diopside-scapolite fels are interbedded. Quartzites may represent the upper part of the metamorphic rock column.

References:

Embey-Isztin, A., Scharbert, H.G., Dietrich, H., Poultidis, H. (1990) *Miner. Mag.* **54/3**, 463-483.

Wood, B.J. & Banno S. (1973) *Contrib. Miner. Petr.* **42/2**, 109-125.

THE GABORONE GRANITE COMPLEX, BOTSWANA An archean(?) Rapakiwi granite-massive anorthosite suite

Touret J.L.R.*(Fac. Aardwetenschappen, Vrije Universiteit, De Boelelaan 1085, 1081 HV Amsterdam, The Netherlands)*

Covering a surface of more than 5000km2, the Gaborone granite complex, Botswana (Sibiya,1988), is one of the most important occurrence of typical Rapakiwi granite in the world. With an estimated age of intrusion at 2.8Ga, it is significantly older than most Proterozoic Rapakiwi granites, with which it bears a number of similarities, but also significant differences.

Similarities refer to the textures (mantled feldspars), chemical composition (major and trace elements), notably the REE patterns (highly differenciated light REE, strong Eu anomaly, flat heavy REE profiles). The major difference is that the granite emplacement was followed by massive outpouring of mafic to acid volcanics in a rifted basin. The emplacement of the complex occurred in a zone of repeated deformation, evolving from a active, subduction related continental margin to a rifted stable shield. The classical Rapakiwi texture (K-feldspar ovoids rimmed by plagioclase) is frequent, but very complex in detail. Strong variations in the mineral assemblage within the plagioclase rim suggest that plagioclase did first crystallize (skeletal crystals, related to strong undercooling in the crystallizing magma), then the inside was filled by K-feldspar and other minerals. Final shape was probably achieved by local diffusion between coexisting minerals.

Basic precursors of the granites have been found in some areas (Kubung granite), including gabbros, norites and few occurrences of massive anorthosites.The series is compared to the Proterozoic Rapakiwi granite-anorthosite kindred occurring in the Baltic Shield, from Southern Finland to Southern Norway.This last region, where anorthosites and augen gneisses with Rapakiwi affinities occur in an orogenic setting, bears a number of similarities with Botswana, but is much younger (1 to 1.2Ga). It is attempted to define some of the unique geodynamic conditions which have led to the formation of the massive anorthosite-Rapakiwi granite suite during a specific period of the Earth's history (between about 3 and 1Ga)

Sibiya, V. (1988). The Gaborone granite complex, Botswana, Southern Africa, Ph D Thesis, Free University Amsterdam, 449p.

• RENE JUST HAÜY (1743–1822), UNE OEUVRE SCIENTIFIQUE OUBLIÉE. U–Matic–video color film, 26 mn, realization Eric Gonthier

Touret L. and Serment R. *(Musée de l'ENSMP, Paris)*

René Just Haüy, founder of the science of crystallography, was born in Saint Just en Chaussée, a small town near Paris, precisely 250 years ago (1743). In order to celebrate this event, the Ecole des Mines de Paris, with the cooperation of the Musée National d'Histoire Naturelle, has organized an exhibition devoted to the scholar's life and work.

The name of Haüy is largely unknown by the "grand public". The intention was to present to a large audience Haüy's discoveries on the structure of crystal as well as his role as a teacher, organizer of major collections and a foremost public figure throughout the Revolution and Napoleonic Empire.

The exhibition shows now a number of rare items: original crystal–models sets, instruments, manuscripts, explaining the means by which a great scientist has developed one of the simplest observation into a real science.

In support of the display a U–Matic video color film of 26 mn, entitled: René Just Haüy, une vie scientifique oubliée, brings Haüy back in his time. This sonorous document replaces the modest abbé in the political and scientific context at the end of the enlightenment century. Thanks to the striking resemblance of Nicolas Simon in the role of Haüy, the spectator is really involved in the action, becoming Haüy's pupil who follows the master in his discoveries in the same way as many of his students did (Lucas, Tremery, ...).

This cinematographic experience is to be seen as a new step in the science vulgarization techniques according to the present audio–visual demand. This life document can be disconnected from the show and the scenario published in the catalogue of the exhibition (1) should be considered as an archive at the issue of the commemoration.

(1) "René Just Haüy, l'Ame des cristaux", tourct L., Exhibition Catalogue, 86 p., Dec. 1993, n° ISBN 2–9508065–0–3.

TRACE ELEMENT REDISTRIBUTION UNDER HIGH PRESSURE/LOW TEMPERATURE METAMORPHISM OF OPHIOLITIC Fe-Ti-GABBROS (LIGURIAN ALPS, NORTH WESTERN ITALY)

Tribuzio R., Messiga B., Vannucci R. and Bottazzi P. (*Dip. Scienze della Terra, Univ. di Pavia; CNR - CS Cristallochimica e Cristallografia, Pavia*)

The redistribution of trace elements under high pressure/low temperature conditions is of fundamental importance in modeling the metasomatic effects of a subducting slab on magma genesis at destructive plate margins. The ophiolitic Fe-Ti-gabbros of Ligurian Alps (north western Italy) were subjected to pervasive re-equilibration under high pressure/low temperature metamorphic conditions as a result of a subduction event probably of Cretaceous-Eocene age. Blueschist Fe-Ti-gabbros display an assemblage of lawsonite, Na-amphibole, Na-clinopyroxene and sphene, whereas eclogitized Fe-Ti-gabbros developed the bimineralic assemblage of omphacite and garnet, with accessory rutile. Eclogitized Fe-Ti-gabbros display coronitic to mylonitic textures, caused by stress gradient during synmetamorphic deformation; the local occurrence of garnet (± omphacite ± rutile) veins evidences for a hydraulic syneclogitic fracturing. Blueschist and eclogite facies events were probably controlled by water-preserving and water-evolving reactions, respectively. The involvement of H_2O in high pressure reactions is presumably related to the breakdown of hydrous minerals developed during the preceding ocean-floor metamorphism. In order to unravel the possible mobility of trace elements, REE and other selected trace elements (Y, Sc, V, Zr, Ti, Sr) of minerals were analyzed *in situ*, using a Cameca IMS 4F ion microprobe.

In blueschists and coronitic eclogites, high pressure clinopyroxenes have different compositions in relation to their development in the different microdomains inherited from the igneous protolith, e.g. growing after igneous plagioclase or diopside. The trace element variations among clinopyroxenes from the different microdomains are larger in the blueschists than in the eclogites. This suggests that blueschist facies reactions were characterized by smaller-range element diffusion than eclogite facies reactions. Finally, the clinopyroxenes from mylonitic eclogites show homogeneous trace element compositions, due to the enlargement of reaction domains into the shear zones.

Microanalyses on relics of igneous diopsides highlight a similar protolith for both eclogites and blueschists, i.e. gabbros from differentiated MORB-type magmas. Blueschist clinopyroxenes have subordinate lanthanide contents, due to the development of sphene and lawsonite which concentrate almost all the REE and Y of the protolith. Eclogitic clinopyroxenes are strongly depleted in LREE, due the coexistence with accessory allanite. The crystallization of allanite, which is absent in the blueschists, could result from the presence of a syneclogitic hydrous fluid phase, in which LREE are preferably partitioned relative to clinopyroxene.

In eclogites, garnets display strong evidence for disequilibrium trace element distribution at the hand sample scale, such as grain-by-grain inhomogeneity and marked zonings. The nucleation of garnet veins along primary grain boundaries suggests that the eclogite facies reactions were controlled by intergranular diffusion of a mobile fluid phase. However, field relations and whole-rock compositions indicate that, apart from H_2O, the metasomatism related to hydraulic fracturing was subordinate. A larger mobilization scale could derive from fluid infiltration into the syneclogitic shear zones.

HIGH-TEMPERATURE, fO2 CONTROLLED VOLTAMMETRY OF BINARY AND TERNARY LIQUID SILICATES.

Trigila R. (*Dip. di Scienze della Terra, Univ. di Roma - La Sapienza*) and Gozzi D. (*Dip. di Chimica, Univ. di Roma - La Sapienza*)

The influence of temperature and oxygen fugacity on the reactions involving bridging- not bridging- and free- oxygen bonds at the anode of a voltammetric cell has been investigated for the following binary (Na_2SiO_3, $Na_2Si_2O_5$, $Na_2Si_3O_7$) and ternary ($NaAlSi_2O_6$, $NaAlSi_3O_8$, $NaFeSi_2O_6$, $NaFeSi_3O_8$) oxides liquid silicates.

Based on the voltammetric behaviour of Na-silicates, Karlsson and Froberg (1986) proposed a structural polyanionic model of liquid silicates, in which the anodic reaction observed in the voltammetric cell has been interpreted as the closure of the gap between two adjacent not bridging oxides ions as follows:

$$2\,O^- = O^0 + 1/2\,O_2 + 2e^-$$

therefore when the composition and the boundary conditions are fixed there is a definite overvoltage (η) range at which the above reaction occurs.

In principle, the current density through a voltammetric cell is the conseguence of the charge transfer, and diffusive or capacitive processes. In the case of reversible reactions, the current density due to the charge transfer is constant through time and obeys to the Tafel relation (Bockris and Reddy, 1974), i.e. the overvoltage is linearly related to the natural logarithm of the current density.

Using this approach we aimed at investigating the charge transfer variations as a function of η for different compositions, temperatures, and oxygen fugacities and eventually looking for the implications brought by other supplementary anodic reactions. From the results of our voltammetric experiments under O_2 atmosphere, it appears:

i) Na_2SiO_3, at 1164 °C, is characterized by charge transfers of 4 and 2 electrons at increasing η; at 1251 °C it shows three linearly correlated ranges corresponding respectively to 6, 3, 2 electrons;

ii) $Na_2Si_2O_5$, at 985 °C, shows 2 and 1 electron charge transfer at respectively increasing η; at 1085 °C it has instead 2 and 4 electrons transferred;

iii) $Na_2Si_3O_7$, has a single η range which gives varying charge transfers for temperatures respectively increasing from 1160°C to 1290°C.

Working under UPPT Argon atmosphere a similar charge transfer is observed. As a general rule the set of z values is shifted towards lower η values indicating a more instable structure.

The voltammograms showing 2, 4, 6 transferred electrons at different temperatures fit the proposed model putting in evidence the existence of 1, 2, and 3 rings polyanions.

Charge transfer of 1 and 3 electrons seems due to a different mechanism probably involving the modification of the polyanionic structure. The current experiments on ternary compositions appear to stabilize the polyanionic structure favouring larger complexes. On the other side the more polymerized compositions show irreversible features of anodic reactions that make more difficult the evaluation of the number of the transferred electrons.

More experiments are in progress to optimize the experimental setting for all the studied compositions in order to show the effect of T and fO_2 on type and quantities of oxygen bonds.

References:
Karlssoll K.H., Froberg K., Perander M. (1986). *J.of Non-Cryst.Solids*, **84**, 183-185.
Bockris J.O'.M., Reddy A.K.N. (1974). Modern Electrochemistry. *Plenum Press N.Y.*

I.R. TRANSMISSION SPECTRA OF SOME ITALIAN METEORITES

Triscari M.(*) and Rosace G.(**) (* *Ist. Scienze della Terra, ** Dpt. Chimica Gen. e Inorg., University of Messina*)

Infrared trasmission spectra have been collected in the region 2.5 to 30 μm for some italian meteorites.

Investigated samples were BORGO S. DONNINO an LL 6 olivine-hypersthene chondrite (fell 19.4.1808), MESSINA an L 5 olivine-hypersthene chondrite (fell 16.7.1955), NOVENTA VICENTINA an H 4 olivine-bronzite chondrite (fell 12.5.1971) and CERESETO an H 5 olivine-bronzite chondrite (fell 17.7.1840).

Spectra were taken using a Perkin-Elmer FT I.R. 1720 spectrometer. All samples were mounted using the standard KBr pellet technique: 1.8 mg of meteorite taken from ground samples were added to 400 KBr, and attention was paid in not crushing the fusion crust.

Absorption in the middle infrared region is primarily due to the excitation of interatomic vibrations. These vibrations produce bands in several common minerals. The silicate bands in the region 800 - 1000 cm^{-1} and 300-600 cm^{-1} acquired at a resolution better than 4 cm^{-1} have been used to distinguish mineral phases in investigated meteorites.

As ordinary chondrites are also classified on the basis of their total iron content and the distribution of this iron between metal phases and silicates, recorded spectra have been plotted in the order LL 6, L 5, H 4, H 5, since total iron content increases as does the ratio of metallic iron to total iron.

Furthermore seems that the pyroxene to olivine ratio trend increases from LL subgroup to H subgroups.

To pyroxenes have been attributed band peaks measured at about 1057, 974, 940, 725, 688, 638, 538, 497, 356 cm^{-1}, while to olivines were referred band peaks at 883, 840, 603, 593, 522, 501, 410 cm^{-1}.

Recorded spectra have thus been compared with the ones reported in literature by Karr (1975) and Sanford (1984). Peaks in the region 300 - 400 cm^{-1} are of particular interest since in orthopyroxenes are related to the iron M1 - M2 site distribution.

Investigated spectra of these italian meteorites are fully consistent with the petrological data known from references.

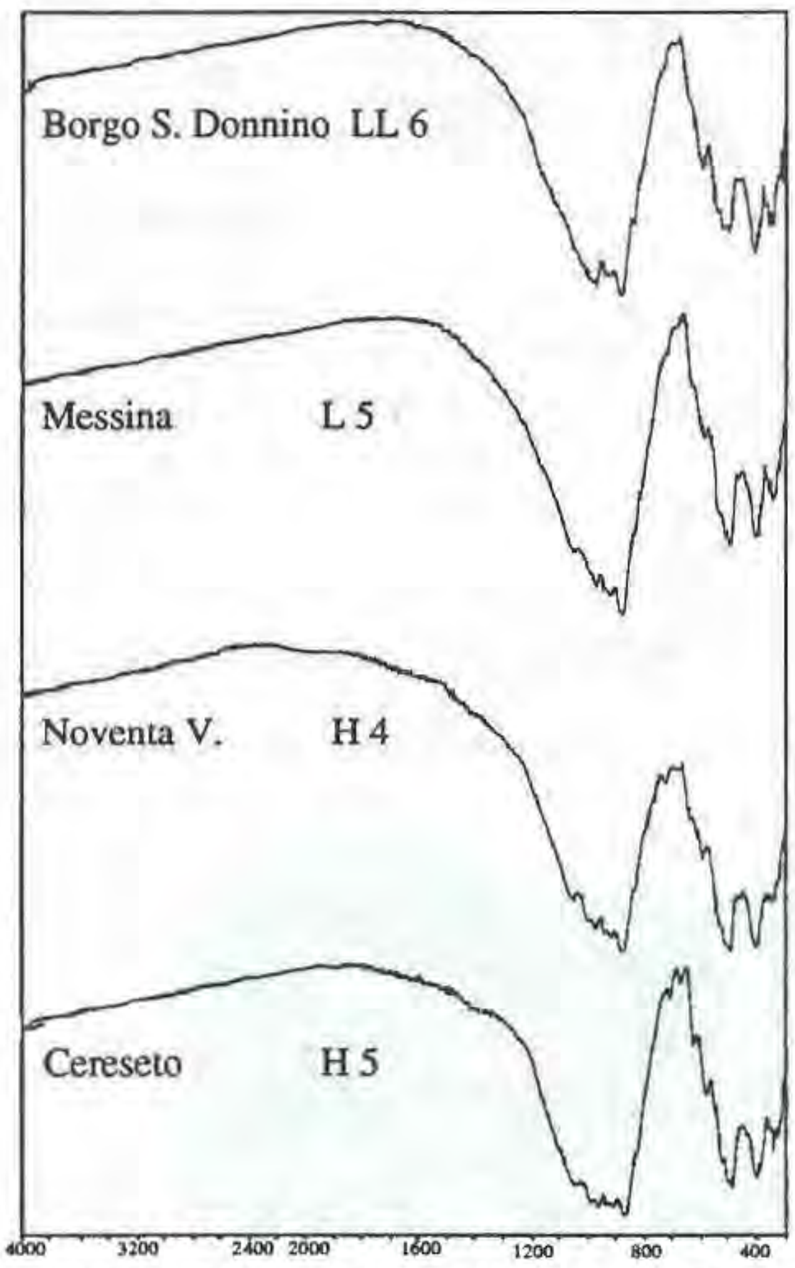

Fig. 1 - Spectra of some italian meteorites plotted in increasing order of metallic iron to total iron ratio.

References:
Farmer V.C. (Ed.) (1974) - The infrared spectra of minerals. Miner. Soc., London.
Graham A.L., Bevan A.W.R., Hutchinson R. (1985) - Catalogue of meteorites. B.M.N.H., London.
Sandford S.A. (1984) - *Icarus*, 60, 115-126.
Karr C. (1975) - Infrared and raman spectroscopy of lunar and terrestrial minerals. Academic Press, New York, 375.

FORMING OF THE GREAT MASS OF THE ACID MAGMA UNDER SUBVOLCANIC CONDITIONS

Tsarev D. I. (*Buryat Inst. of Geology, Siberian Division The Acad. of Sciences. Russia*)

A sequential transition from the volcanic rocks of a basic and middle composition to the banded silicic-alkaline metasomatites and to the stratiform acid magmatic rocks is recognised in the volcanic vents laid bare by an erosion. The banded metasomatites are distinguished from the banded (stratiform) magmatic rocks by that a structure in the latest is glassy with the filiform crystallites in one phase and felsitic or spherulitic in other one. The glassy structure and the crystallites do not form in the ribboned metasomatites. The streaky and lens-shaped phases of the magmatic rocks are distinguished from each other by a content of the rockforming oxides. Those and others correspond on the composition to a cotectic for a granite-alkaline-granite formation with P=2 kbars (Fig.). The stratiform acid volcanic rocks contain a mass of the unmelted relics of substratum.

The Cenozoic ignimbrites of Kamchatka and the Caucasus discover the similar textures, structures and differentiation of the substance in the foliation phases. The chemical compositions of a fiamme and the glass of the graundmass of the ignimbrites qualitatively regularly are different from each other by ones and the same independently of a region. The ignimbrites contain the relics of the unmelted substratum in the form of the fragments of the rocks of more basic composition, grains of plagioclases and pyroxenes with the traces of melting. Unlike a widespread opinion, that the ignimbrites are a melt is created by the high temperature, fluid saturation and stratification stipulating a fracture of the polymeric compositions. A presence in the relics of the effusive and subvolcanic rocks depriving of a regional metamorphism evidences about that an acid magma was originating in the subvolcanic facies of a depth of the volcanic centres. The petrographical investigations prove that a melt volume increase was originating at the expense of the substratum melting and not at the expense of a supply of it from the depthes. Forming laminated melt become more acid by action silicic alkaline transmagmatic fluids. All the process of the acid magma formation in the volcanic centres can be subdivided into three conjugated stages: metasomatism, melting, metamagmatism that corresponds on the whole to the magmatic replacement by D. S. Korzhinskii.

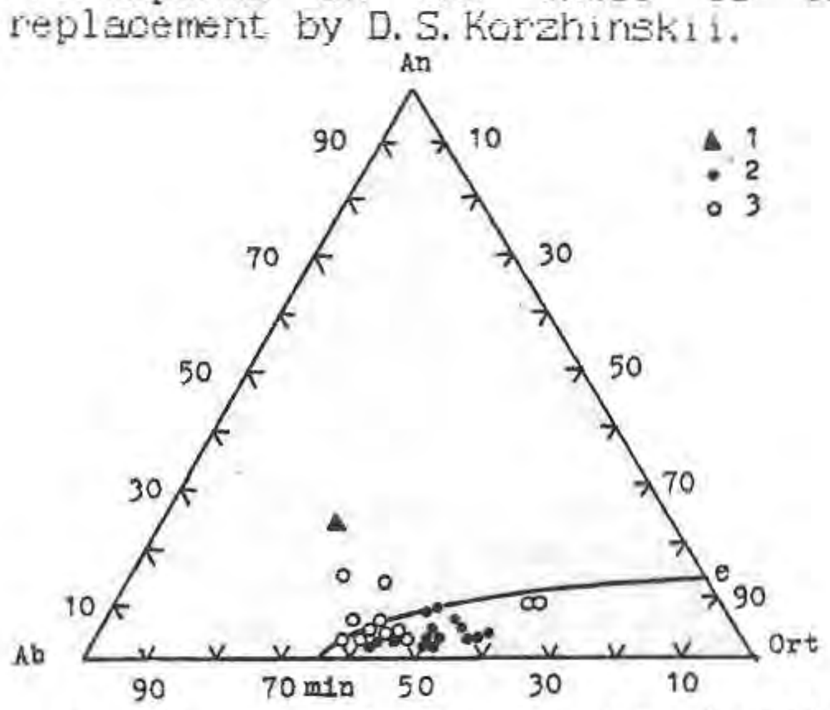

1 - the original andesite-basaltic porphyrites; 2 - the dark phase (fiamme, the lines); 3 - the light phase (the basic mass) e-min - the line of cotectic

EVAPORATION KINETICS OF MINERALS, AND THEIR SIGNIFICANCE FOR FRACTIONATIONS IN THE PRIMARY SOLAR NEBULA.

Tsuchiyama A, Takahashi T., Fujimoto K. and Uyeda C. *(Inst. Earth Planet. Sci., Coll. General Educ., Osaka Univ.)*

Recent model simulations for the planetary system

formation (*e.g.*, Nakagawa & Watanabe, 1993) together with observations of star formation regions suggest that the temperatures of the primary solar nebula were so low that (partial) evaporation of presolar dust could play an important role in elemental fractionations observed in chondrites and the planets. If the major elements for the terrestrial planets are concerned, we can divide the system into two reaction systems, Mg-Si-O-H and Fe-S-H, which are in eutectic relation at high temperatures in the solar nebula. Enstatite and FeS are in reaction relations, and evaporate incongruently with residues of forsterite and metallic iron, respectively. Mg/Si and Fe/S fractionations were expected depending on the degrees of the reactions in the systems.

There are two kinds of rate laws expected for the evaporation; the width of a mineral evaporated or formed as an evaporation residue or accompanied weight loss is proportional to time (a linear rate law) or to the square root of time (a parabolic rate law). The linear rate is controlled by reaction at the surface of an evaporated mineral, while the parabolic rate is controlled by diffusion of element(s) in a residual mineral layer formed on an evaporated crystal. The evaporation data are compiled in Table 1 based on experimental studies and calculations based on the Hertz-Knudsen equation (*e.g.*, Hirth & Pound, 1963) with the evaporation coefficient of unity. If the evaporation is controlled by diffusion, the rate data for evaporation into vacuum can be used for evaporation into H_2 atmospheres, such as in the solar nebula.

Based on the above data, evaporation behaviors of the minerals in the solar nebula were discussed. Amounts of the minerals evaporated or formed as evaporation residues were calculated in the active disk stage of the nebula in the model of Nakagawa & Watanabe (1993). The calculations indicate that (1) evaporation kinetics is important, and (2) congruent evaporation of enstatite and FeS might occur due to kinetic effects resulting from slow diffusivity in residual forsterite layers and slow incongruent evaporation rate of FeS controlled by surface reaction. If such kinetic congruent evaporation took place in the nebula, little Mg/Si and Fe/S fractionations were expected by evaporation processes.

Table 1. Evaporation of minerals in the solar nebula.

Mineral /residue	Rate Law	A	B	C	D (/Pa)	Ref.
Fo(vac.)	L	8.127	-27100	-0.5	0	Calculation
Fo(vac.)	L	7.00	-30100	0	0	[1]
Fo(H_2)	L	2.116	-13820	-0.5	0.5	Calculation
Fo(nebula)	L	12.495	-27640	-0.5	0	Calculation
En/Fo*(vac.)	P	-0.286	-26800	0	0	[2]
Fe(vac.)	L	7.025	-21380	-0.5	0	Calculation
FeS/Fe*(H_2)	L	-4.320	-3465	-0.5	1.0	Calculation
FeS/Fe*(H_2)	L	-7.693	-6010	0	1.0	[3]

Rate constant, k [ms^{-1}] for linear rate laws (X=kt; X= width of evaporation), or [m^2s^{-1}] for parabolic rate laws ($X=(kt)^{1/2}$); $\log k = A + B/T + C \log T + D \log p(H_2)$.
Fo=forsterite, En=enstatite, *=evaporation residue
vac.=vacuum, L = linear rate law, P = parabolic rate law.
[1] Hashimoto (1990), [2] Sata *et al.* (1978),
[3] Tsuchiyama *et al.* (1993).

References:

Hashimoto A. (1990) *Nature*, **347**, 53-55.
Hirth, J.P. and Pound, G.M. (1963) "*Condensation and evaporation, nucleation and growth kinetics*", 191pp., Pergamon Press.
Nakagawa, Y. & Watanabe, S. (19893) In "*Sciences for the planets*" ed. Shimizu, M., 185-219, Asakura Pub. Co.
Sata, T., Sasamoto, T., Lee, H.L., Maeda, E. (1978) *Rev. int. Hautes Temp. Refract. Fr.*, **15**, 237-248.
Tsuchiyama, A., Uyeda, C., Makoshi, U. (1993) *18th Symp. Antarctic Meteorites (abstract)*, 121-124.

CRYSTALLIZATION IN MICROGRAVITY

Tsukamoto K. (Faculty of Science, Tohoku University)

Nucleation and growth of crystals have been investigated by *in situ* methods in microgravity using a rocket, an aircraft and a drop facility, in order not only to verify the crystal growth theories but also to find peculiarity of crystallization in microgravity. Microgravity environments were kept from 10s to 6m. Among varieties of interesting results, a few topics that might be important for mineralogy have been selected.

While experiments are performed on earth, experimental results are more or less influenced by gravity. Fig.1 shows one the examples which shows a gravitational effect on nucleation. Two solutions were mixed to crystallize calcite crystals for the measurement of the size distribution of clusters in time by means of dynamic light scattering that can detect the diameters of a few nm. Although gradual increase of the size can be seen up to 600nm in diameter, the size appears not to increase furthermore. This is due to the gravitational segregation of larger crystals when the size reaches the critical. This effect prevents us to investigate the nucleation in more details.

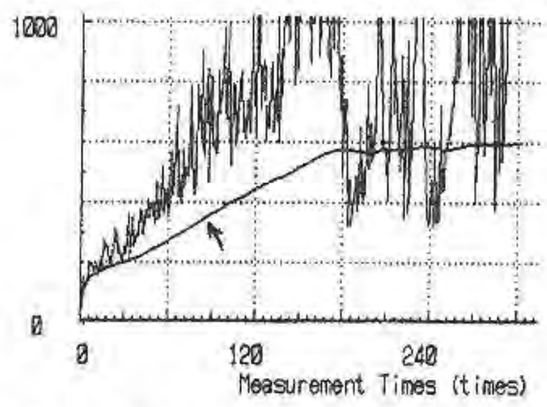

fig.1 Post nucleation of calcite, diameter (nm) *vs* time by dynamic light scattering. Arrow shows the analyzed diameter.

By cooling the melt of $LiBO_2$ employing the high temperature *in situ* observation system [1], special distribution of nucleated crystals was seen around a seed crystal (fig.2), in which one can see that nucleation takes place along the radial concentric temperature field, whereas nucleation in gravity takes place in the manner of avalanche. Much larger supercooling was needed in microgravity for nucleation, which suggests the presence of more metastable phases in space which are probably locally distributed.

fig.2 Ordered radial distribution of LiBO2 crystals, crystalized around the seed, *in situ* in microgravity.

The increase of melt temperature soon after the change of gravity from normal to microgravity is also interesting. When the melt temperature and the air temperature just near the met surface (~5mm) were measured *in situ*, the temperatures suddenly increased by 200°C and by 400°C, respectively, soon after microgravity was achieved. This was found to dissolve the seed crystal for the coming growth experiment in a very short time (<1s). The sharp increase of temperature was found to be due to the cease of air convection around the melt surface. This measurement indicates much slower cooling rate of melt in space than expected in gravity.

We would also like to mention that the suppression of convections in microgravity would lead the exact measurements of crystal growth rate and physical properties of crystals or of various melts such as thermal conductivities and mass diffusivities.

References

[1] T. Abe, K. Tsukamoto and I. Sunagawa, Mineralogical J. 13 (1987) 479–489.

• MINERALOGY AND THERMOMETRY OF GRANULITE–CHARNOCKITE COMPLEX OF NORTH PREBAIKALJE, EAST SIBERIA

Tsygankov A.A., Konnikov E.G. and Vrublevskaya T.T. *(Buryat Geol.Ins., Ulan–Ude,Russia)* Tomilenko A.A. *(Un. Ins. Geol. Geoph. Miner., Novosibirsk, Russia)*

Metamorphic rocks in granulitic facies – epibasic granulites (oPx+cPx+Pl+Hb+Ol+Ilm) and charnockite–enderbites (Q+oPx+cPx+Hb+Pl+ Fsp+Ilm) – have been found in the south–western part of the Baikalo–Mujsk volcano–plutonic belt. They are included in the field of developing amphibolites of the Nurundukan suite, attributed by a number of researchers to the volcanogenic complex of Riphean ophiolites. Granulites are intruded by gabbroids of magnesian and titanian types with age of 600 Ma years. The age of granulites is problematic: a series of data suggest a PR1 age, while, according to other approaches, they can be assigned, as the gabbroids, to the upper Riphean period. All the determined ages, including those of granulites, group near the age of about 600 Ma years. In the present paper we try to clarify this fact on the basis of mineralogical data.

The rocks under consideration are made of oPx, cPx, Pl and Hb; sometimes olivine (35% of Fa) is found in the granulites. The Fe/(Fe+Mg) (f) ratio of orthopyroxene varies from 0.3 to 0.5 in the epibasic granulites; the Al(IV) content is anticorrelated with f (r=–0.92). The highest tschermakite content in orthopyroxene is characteristic for olivine granulites (to 3.0 weight % of Al_2O_3), while the lowest content is found in the enderbites with the maximum f value (to 0.55), which reflects the conditions of pressure decrease when they form. Clinopyroxenes range from diopside–augite to subcalcic augite depending on Al(IV) content; their f value is lower than in the co–existing oPx. The ratio of Al(IV) and f in monoclinic pyroxenes is similar to that of orthopyroxenes. The calcium content ($Ca'=100*(CaO/Al_2O_3)$) of granulite clinopyroxenes increases with f, reaching the maximum in enderbites, which also reflects the conditions of pressure decrease. The coefficients of Fe and Mg distribution between coexisting oPx and cPx indicate their equilibration.

Temperature calculations of forming rocks on oPx–cPx geothermometers by Wells (1977) and Wood and Banno (1973) show that two associations are marked out in granulites: a low temperature association (about 800 °C) corresponding to Amf–oPx–cPx paragenesis and one of about 970 °C for oPx–cPx and Ol–oPx–cPx granulites. Intermediate values of 880 °C are obtained for enderbites. These data agree with the results of the analysis of fluid inclusions in charnockite quartz. Inclusions are filled with CO_2 having slight nitrogen admixture, which is characteristic for granulitic facies of metamorphism. The temperatures of 800–900 °C, determined for gabbroids, coincide with those of granulite metamorphism. Probably these values cannot meet the conditions of crystallization for gabbroids. Therefore, they both have experienced one and the same period of thermal influence that resulted in the observed mineral equilibration. This thermal influence has, probably, reset the isotopic systems.

TWO OLIVINES ASSEMBLAGES IN THE Fe-Mn DEPOSIT AT RĂZOARE, PRELUCA MTS., ROMANIA

Udubaşa G., Hârtopanu P. (*Institute of Geology and Geophysics, Bucharest, Romania*), Constantinescu S. (*Institute of Nuclear Physics, Bucharest, Romania*).

The regionally metamorphosed Fe-Mn deposit at Răzoare is contained by medium grade metamorphics and exhibits a very rich and complex mineral association (over 60 mineral species). The most typical features are: (i) the uncommon abundance of manganese humites, forming lenses and beds up to 2m thick, in which sonolite, leucophenicite, probably also alleghanyite and jerrygibbsite are closely associated with tephroite and jacobsite; (ii) the large development of manganoan fayalite both as regards its grain size, *i.e.* elongated crystals up to 7 cm, and the thickness of the lenses or beds, reaching 1 m. The manganoan fayalite is associated with rhodochrosite and apatite and is largely replaced by dannemorite and magnetite.

The two olivines assemblages do not contact each other, although they alternate within the "matrix" consisting of rhodochrosite (lower part of the ore sequence) or of dannemorite (upper part). It is likely that the two assemblages evolved separately as quasiclosed microsystems that remained as such during a very complex, polyphasic metamorphic evolution. The M2 metamorphic phase had mostly a static character, allowing the development of pegmatoid-like aggregates of pyroxmangite, manganoan fayalite, garnet and dannemorite to occur. In the host micaschists and gneisses the same metamorphic phase has produced large bodies of tourmaline- and apatite-bearing pegmatites.

The manganese olivine represents a nearly pure end-member tephroite, containing no iron and about one percent magnesium. Unlike this, the manganoan fayalite exhibits a larger compositional field, averaging 60 percent fayalite component. Further on, two generations of manganoan fayalite have been depicted, *i.e.* (1) the older fayalite, that appears associated with a scarcely developed orthopyroxene and (2) a late fayalite in association with dannemorite, fluor-apatite and pyroxmangite. The Mn:Fe ratio increases from (1) to (2) in accordance to the general trend of the whole mineral association of the deposit to be enriched in manganese in later generations.

Mössbauer spectra (^{57}Co:Rh source, at room temperature) of polycrystalline samples of manganoan fayalite show two inequivalent positions of bivalent iron in the octahedral sites corresponding to M1, M2. The weights of bivalent iron in the two sites, the covalency of the Fe-O bond and the distortion of the octahedral neighbourhoods given by the spectral parameters are discussed in terms of the abundance of the bivalent iron and manganese ions and their electronegativities in the studied samples of manganoan fayalite showing varying Fe:Mn ratios.

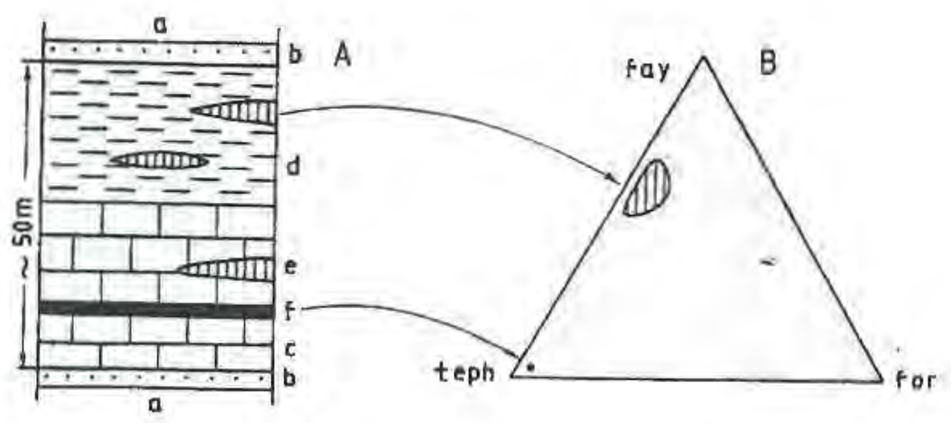

Position of the two olivines in the ore succession (A) and the ternary diagram (B): a - host micaschists and gneisses; b - black quartzites; c - rhodochrosite + jacobsite; d - dannemorite + magnetite ± pyrrhotite; e - manganoan fayalite; f - tephroite + manganese humites

NEEDLE-LIKE SULFOSALTS IN HYDROTHERMAL ORES IN ROMANIA

Udubaşa S.S. (*University of Bucharest*), Udubaşa G. (*Institute of Geology and Geophysics, Bucharest*), Ghiurcă V. (*University of Cluj-Napoca*)

The lead-antimony sulfosalts are quite widespread in different types of ore deposits in Romania. They occur either as microgranular aggregates associated with Ni-bearing pyrite and arsenopyrite (*e.g* Cioclovina ore occurrence), with tetrahedrite, bournonite and galena (Coranda-Hondol Pb-Zn ore deposit, Sasca Montană skarn deposit *etc.*) or as felt-like aggregates of fibrous crystals less than 0.1 mm thick (many hydrothermal ore deposits in the Baia Mare ore district and in the surrounding areas).

Most of the needle-like sulfosalts generally called "plumosite" occur either in geodes or appear intergrown with calcite crystals that become thus blackish in colour (typical occurrences: Dealu Crucii, in the Baia Mare ore district, Stânceni, in the South Călimani Mts., and Hărţăgani, in the Metaliferi Mts.). The geode "plumosites" commonly contain minute crystals of transparent

quartz (mainly in the gold ores) or of brownish siderite and/or sphalerite microcrystals (in base metal ores).

XRD analyses showed that most of the "plumosite" consists of jamesonite, some few others represent boulangerite and only a very limited number of samples gave the X-ray diffraction pattern of robinsonite, the latter being very typical of the gold-quartz ores.

Emission spectrography analyses gave interesting contents of some minor elements, characterising thus Bi-rich varieties of jamesonite (*e.g.* 3,000 ppm in Toroiaga ores) or Mn- and Tl-rich varieties (*e.g.* up to 3,000 ppm Mn at Baia Sprie and up to 200 ppm Tl at Herja).

The cell parameters, especially the cell volume and the c parameter decrease with decreasing Mn-content or with non-uniformly increasing Ag-content (see Table). Other minor elements so far determined (up to 950 ppm As, 200 ppm Ti *etc.*) seem not to have a significant influence on the cell parameters. In addition, the latter are randomly occurring in the analysed samples.

Table
Selected values of minor elements (ppm) in jamesonite in relation to the cell parameters

Sample	Mn	Ag	V, A^3	c, A
U - 1563 Săsar	3000	2300	1217.19	4.0518
U - 1559 Baia Sprie	2500	1200	1207.06	4.0210
U - 1534 Herja	650	4100	1206.96	4.0271
U - 844 Herja	50	1550	1206.34	4.0209
U - 1528 Toroiaga	15	1100	1204.80	4.0199
U - 1526 Herja	35	5000	1203.31	4.0143

A very typical yet uncommon feature of many felt-like jamesonite aggregates is the presence of some ring-shaped jamesonite crystals up to 1 mm in diameter or even spirals or hairpin-like forms, that never occurred in the similarly featured boulangerite or robinsonite aggregates. The Baia Sprie and the Herja jamesonites as well as some samples from Toroiaga show the most abundantly developed curved crystals.

Although late in the paragenetic succession, the jamesonite from the Herja and Baia Sprie ores shows sulfur isotopic compositions of 5 to 6 ‰ $\delta^{34}S$, not very different as compared to the earlier crystallised common sulfides.

ELECTRON DENSITY STUDY ON MnS_2 WITH SYNCHROTRON RADIATION

Ueki M., Ishizawa N. (*Tokyo Inst. of .Tech*),
Tabira Y.(*Ricoh Co. Ltd.*) and Marumo F. (*Nihon Univ.*)

A magnetic semiconductor MnS_2 (hauerite) crystallizes in the pyrite structure. The compound consists of S_2^{2-} dumbbells and Mn^{2+} ions in a high spin $3d^5$ state. The present study deals with the electron density distribution around the Mn atom obtained by the single crystal X-ray diffraction technique using synchrotron radiation.

Samples were octahedrally-shaped natural crystals from Osorezan, Aomori, Japan. A fragment of the sample was formed into a sphere of 36 μm in diameter by the Bond method. The space group was confirmed to be Pa3 with the cell dimension of a=6.1070(4) Å. The reflection data were collected with the horizontal-type high-speed four-circle diffractometer (Satow & Iitaka, 1989) at the beam line 14A, Photon Factory, National Laboratory for High Energy Physics, Japan. A focused beam with the wavelength of 0.75 Å was used. In all, 14921 reflections were measured in the entire sphere of $2\theta<138°$.

The reflection data were put on an equal scale based on the monitor count of the incident beam. The least-squares refinement gave the *R* and *Rw* values of 0.0119 and 0.0122, respectively for 539 independent reflections, when the isotropic extinction correction (Bekker & Coppens, 1974) was employed. The final atomic parameters and the bond distances obtained are essentially the same as those given by Chattopadhyay et al (1992). The effect of the extinction correction was small and only the strongest 200 and several other reflections were affected.

Difference Fourier map on (001) near the Mn atom at the origin is shown in the figure. Contours are drawn at 0.1 $eÅ^{-3}$ intervals. Excess electrons form six peaks with the height of 0.5 $eÅ^{-3}$ at positions 0.5 Å apart from the central Mn atom. These peaks are located close to the lines connecting the Mn and the ligand S atoms and considered to be due to the $d\gamma$ electrons of the Mn atom. No other significant peaks were observed in any region near Mn, indicating a high population in the $d\gamma$ orbitals. These features make a clear contrast to the electron density around Ni (d^8) in NiS_2 in our previous study, where the eight lobes due to excess electrons in the $d\varepsilon$ orbitals develop in directions near <111> to avoid the electrostatic repulsion of the ligand S atoms.

Professor Akira Kato, National Science Museum, Tokyo is appreciated for supplying the specimen.

References:

Bekker, P.J. & Coppens, P. (1974). Acta Cryst. **A30** 129.
Chattopadhyay, T., Schnering, H. G., Stansfield, R.F.D., McIntyre, G.J. (1992). Z. Kristallogr., **119**, 13-24
Satow, Y. & Iitaka, Y. (1989). Rev. Sci. Instrum., **60**, 2390

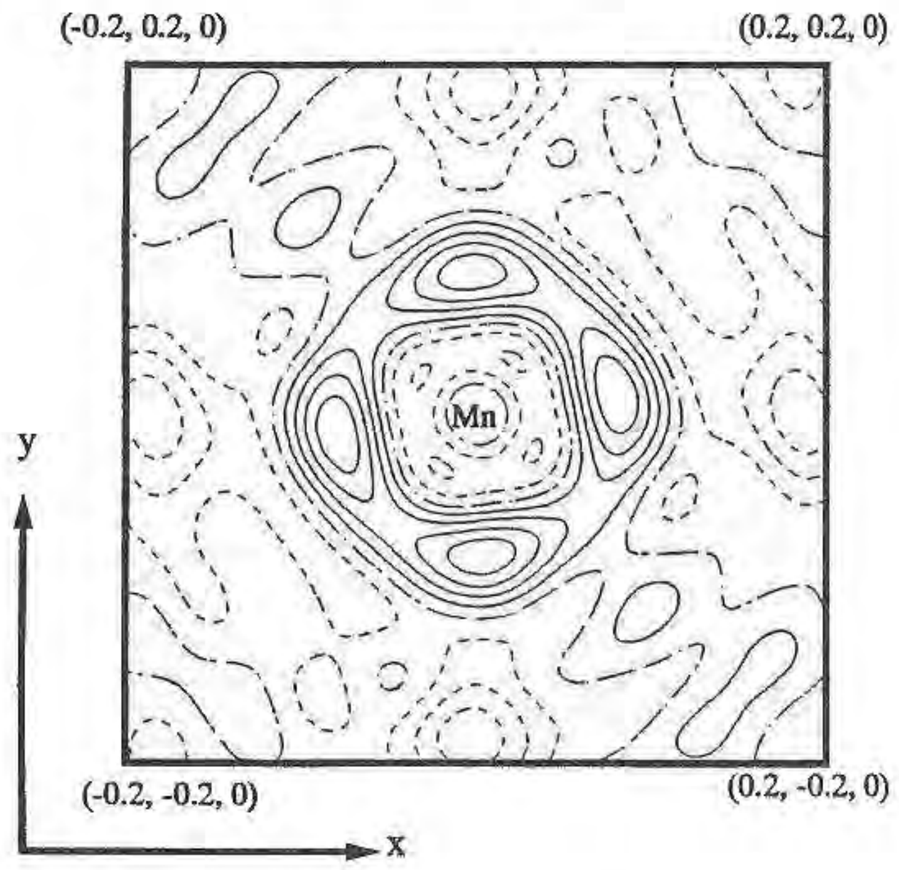

Difference Fourier map on (001). The origin is at the center.

PHASE RELATIONS ALONG THE JOIN ZnS-FeS-GaS AT 900°C AND 800°C

Ueno T.(*Dept. of Earth Sciences, Fukuoka Univ. of Education*) and Scott S.D.(*Dept. of Geology, Earth Sciences Centre, Univ. of Toronto*)

Phase relations along the join ZnS-FeS-GaS were investigated by 53 dry synthesis experiments at 900°C and 800°C. Knowledge of this join is important to furthering over understanding of the concentration of Ga in sulfide ores and in meteorites, and for developing various solid state electro-optical devices. The Zn-Fe-S system has previously been well studied from 200°C to 900°C (Barton & Toulmin 1966, Scott & Barnes 1971). In this system sphalerite solid solution, pyrrhotite solid solution, α-phase, γ-phase, liquid zinc and liquid sulfur exist at 900°C and 800°C. Phase relations in the system Ga-Fe-S at 900°C and 800°C were studied by Ueno & Scott (1994) and phase Z, phase W, phase X, alloy Y and $(Ga,Fe)_2S_3$ solid solution were found. The system Zn-Ga-S, investigated at 900°C and 800°C by Ueno & Scott (1994), has $(Zn,Ga)_{1-x}S$ solid solution, phase V, phase U, and $(Ga,Zn)_2S_3$ solid solution in its central portion. Experiments along the join ZnS-FeS-GaS at 900°C and 800°C produced $(Zn,Fe,Ga)_{1-x}S$ solid solution, phase V, phase X, phase Z, troilite, GaS, and alloy Y. However, only troilite, (Zn,Fe)S and GaS actually lie on this join,

other sulfur-rich phases (more than 50 at. % sulfur) are projected onto it. The $(Zn,Fe,Ga)_{1-x}S$ solid solution covers a large area, extending from ZnS to $(ZnS)_{15.7}(FeS)_{40.5}(GaS)_{43.8}$ at 900°C and to $(ZnS)_{14.8}(FeS)_{44.7}(GaS)_{40.5}$ at 800°C. The crystal structure of this solid solution is sphalerite-type, wurtzite-type or a mixture of these two types, depending on temperature and chemical composition. Wurtzite is the high temperature type, but the inversion from sphalerite to wurtzite is very sluggish. Thus, in the mixture of the two phases, sphalerite is probably metastable. Phases V and X are tetragonal, and phase Z is cubic. All three have small solid solution fields. Alloy Y is tetragonal and has an extensive solid solution area along the Fe-Ga join.

NON-IDEAL SOLID-SOLUTIONS IN GARNET: CRYSTAL-STRUCTURE EVIDENCE AND MODELLING.

Ungaretti L. *(CNR-CS Cristallochimica e Cristallografia, Pavia)*

Garnets are multicomponent solid-solutions able to retain the same crystallographic symmetry ($Ia\bar{3}d$) over very large ranges of chemical composition and unit-cell volume. Because of the symmetry, atomic coordinates of the three cationic sites ($^{[8]}X$, $^{[6]}Y$, $^{[4]}Z$) are fixed throughout the series; only the oxygen can slightly modify its position in order to adapt the structure to the chemical variations. Thus, a rather complex chemistry corresponds in garnet to a rather simple crystallographic situation, the unit-cell edge and the oxygen coordinates being the only geometric variables in any isomorphous substitution. It has to be stressed that the garnet structure is geometrically dominated by the X sites which form a continuous network of distorted cubes, each sharing four edges with other X polyhedra; further X edges are also shared with Y octahedra and Z tetrahedra. Therefore, any chemical change at X inevitably affects the whole structure both in terms of geometry and of vibrational parameters. Due to the large polyhedral edge-sharing, the garnet structure tends: i) to favour multiple solid-solutions having similar geometric effects on the three cationic polyhedra (e.g. there will be significant Z substitution only in Ca,Fe^{3+}-rich compositions); ii) to limit isomorphous substitutions which produce large geometric variations in only one site (this explains why Fe^{3+},Cr substitutions for Al at Y are usually low in pyralspites); iii) to avoid chemical changes producing contrasting geometric effects on the edge-sharing sites (e.g. significant Mg at X associated to significant substitution at Z). This means that the compositional space really occupied by natural garnets is much smaller than that stoichiometrically possible. In fact, if two garnet end-members, differing in composition and size of only one site, are both stable, they should have intrinsically different oxygen arrangements; consequently, their intermediate solid-solutions should be difficult to form or, if they do occur, should not result from a linear combination of the corresponding end-members.

Good evidence for non-ideal solid-solutions has been obtained during an X-ray single-crystal diffraction study of nearly 300 natural garnets representative of the main geologic environments, carried out in order to provide the crystal-chemical data to be used in a crystal-structure modelling process.

In particular, it turned out that the pyralspite-ugrandite solid-solutions (which occur in nature but show some compositional gap) are all characterized by a non-ideal behaviour, as it can be seen in the enclosed plots; any substitution at the X site moves the oxygen along a trend which progressively deviates from the join pyr-gro; this means that any Ca substituting for (Mg, Fe, Mn) on the pyrope side conform to a pyralspitic oxygen arrangement; viceversa, any (Mg,Fe,Mn) at the X site on the grossular side conforms an ugranditic oxygen arrangement. The maximum deviation from the pyr-gro join corresponds to the left limit of the compositional gap recognized in the analyzed samples and to the maximum ΔV of mixing (Merli *et al.*, this meeting) calculated by assuming subregular mixing for any cation pair in the system Mg-Fe-Ca. The existence and the limits of this compositional gap (1.4-2.1 Ca apfu) are fully confirmed by the analysis of the atomic displacement parameters. Other non-linear and linear correlations in garnet solid-solutions will be shown and discussed.

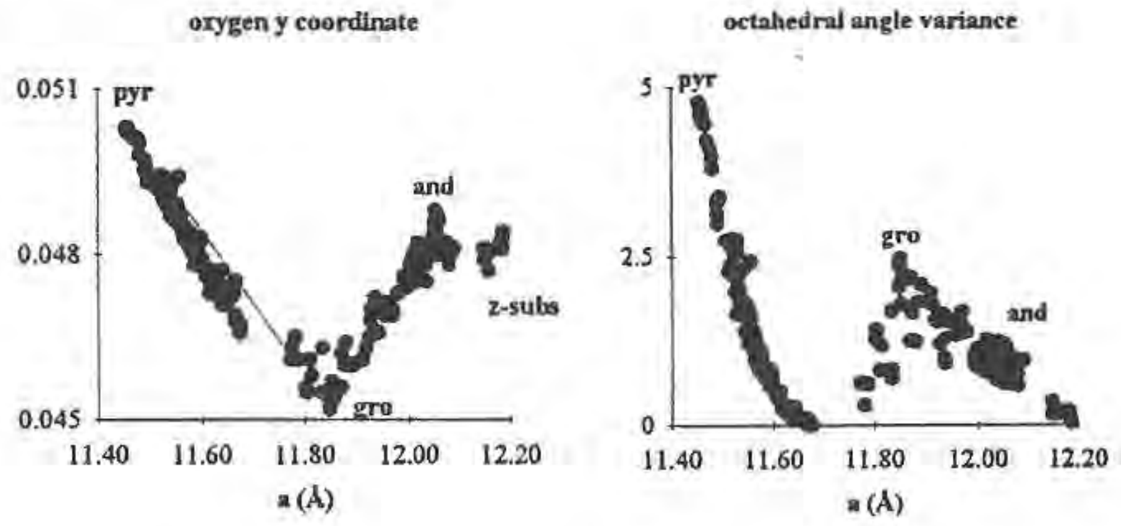

ENERGY MINIMUM CRITERIA IN MODELING STRUCTURES AND PROPERTIES OF MINERALS

Urusov V.S. and Eremin N.N. *(Institute of Geochemistry and Analytical Chemistry, Russian Acad. of Sci., Moscow)*

The leading principle in modeling procedure is minimization of a structure energy (SE). It is assumed that the calculated minimal energy has to be compared with the experimental estimate of cohesion energy of a crystal. The reference state for SE depends on bonding type: the lattice energy (LE) for purely ionic crystals consisting of cations and anions, the atomization energy (AE) for the covalent and metallic crystals consisting of atoms, the sublimation energy for molecular crystals consisting of molecules etc.

As well-known, a majority of minerals can not be correctly described as purely ionic crystals. Moreover, for these crystals LE cannot be determined empirically because free anions, such as O^{2-},S^{2-},As^{3-}, etc., do not exist. In order to describe crystal structures and properties in a better approximation it is usually proposed that bonding-character for such crystals is intermediate between ionic and covalent, so that effective charges and the covalent contribution are involved in energy calculations (e.g. Price & Parker (1984), Catti (1986), Matsui (1986)). However, the corresponding calculated SE are not comparable to any experimental values. Moreover, they decrease with increasing effective charges and a purely ionic structure seems, as before, to be most stable from energetic point of view.

To avoid this "energetic catastrophe" the so-called "charge transfer energy" (CTE) has to be taken into account (Urusov & Dubrovinsky, 1989). Estimations of CTE energies were sometimes faced with difficulties because of limitation of knowledge about valence-state energies.

Now it is possible to refine this approach using new data on the average one-electron energies of the valence-shell electrons in ground-state free atoms (Allen,1989). It is demonstrated for example of Si and O atoms. The successive ionization of mixed *s*, *p* valence-shell of silicon atom from Si^0 to Si^{4+} states is reconstructed and a new extrapolation procedure to obtain the electron affinity of O^{2-} is applied.

The SE of stishovite SiO_2 as a function of the ionicity degree parameter *f* is calculated with the aid of pair potential consisting of the effective ionic, the

covalent Morse type contributions and the charge transfer correction. The SE energy change from -5.17 eV for the ionic structure (f=1) to -8.59 eV for the covalent structure (f=0) with minimum value of -17.15 eV for f=0.68. The latter can be compared to the experimental value of AE (-18,9 eV). The corresponding oxygen atomic coordinate x varies from 0.308 (f=1) to 0.298 (f=0) being equal to the true value of 0.306 at f=0.62. At this f the sufficient improving of the simulated elastic and dielectric constants, when compared to the ionic model, is evident.

References:

Allen, L.C.(1989) *J.Am.Chem.Soc.*,**111**, 9003-14
Catti, M.(1986) *Adv.in Phys.Geochem.* **6**, 224-50
Price, G.G. & Parker, S.C. (1984) *Phys.Chem. Miner.* **10**, 209-216.
Matsui, M.(1986) *J.Miner.Soc.Jap.* **17**, 169-179
Urusov, V.S. & Dubrovinsky, L.S. (1986) *"Computer modelling of mineral structures and properties"* Moscow Univ. press.

MINERAL TRANSFORMATIONS IN SURFACE AND BURIAL FERROMANGANESE NODULES FROM GUATEMALA BASIN

Uspenskaya T.Yu. (*P.P. Shirshov Inst. of Oceanology, Moscow, Russia*) and Gorshkov A.I. (*IGEM RAS, Moscow, Russia*)

Ferromanganese nodules from Guatemala Basin have unique chemical composition, formed under the influence of specific sedimentary environments in this area. These nodules are enriched by Mn (39.9-59.2 %) and contain very low contents of Fe (1.05-4.46 %), Ni, Cu and Co.

The nodule mineral composition was determined using reflecting microscopy, analytical transmission electron microscopy (the combined use of electron microscopy, selected area electron diffraction, electron probe microanalysis) and X-ray powder diffraction analysis on untreated and heated samples at 100°C for 1 hour. Investigation of internal structure and detailed sampling of individual layers with known textures for mineralogical analysis were carried out in polished section, using an optical microscope.

The nodules from sediment surface and buried in sediments at different levels have similar internal structure and consist of two zones: an internal zone comprasing alternating massive-dendritic (MD) layers with well-crystallized manganese minerals and thinly laminated-dendritic (LD) layers with alternating laminae of isotropic ferromanganese, unisotropic manganese, and black (in reflecting light) clay minerals and thicker (especially from the bottom side of nodules) outher cover with alternation of massive-laminated (ML) and MD-layers with well-crystallized manganese minerals. The youngest bottom surface layers with ML- and MD-structure consist of buserite-I with admixture of unordered mix-channel todorokite. At the middle part of outher cover concentration of buserite-I decreases, content of todorokite increased, and buserite-II appears. In the internal zone, MD-layers mainly consist of more ordered todorokite (with a_o = 9.75 A) and LD-layers contain asbolan-buserite and vernadite. Such mineral composition is very unusual for surface nodules, because high content of todorokite not occure in widespread pelagic diagenetic nodules. The mineralogy of surface and buried nodules differs. In buried nodules, buserite-I dissappeares, ordering of todorokite increases. Discovered changes of mineral composition in the direction from the youngest layers to older ones of surface nodules and to the layers of burial nodules show in decreasing of buserite-I and its dissappearing after nodule buring; appearing of buserite-II and increasing of todorokite and its ordering. Such regularities in mineral composition seem to be related to ageing processes, which led to transformation of buserite-I to buserite-II and todorokite, that may be considered as the results of an ordering of vacancies in octahedral Mn-layers and transition of layered structure to tunnel one.

• A NEW KIND OF X-RAY LUMINESCENCE METHOD FOR STUDIES ON REE DISTRIBUTIONS IN NATIVE SCHEELITE

Uspensky E.I. *(IGEM, RAS, Moscow, Russia)*

Scheelite (SCH) is widespread in ore deposits of different metal/genetic types. It does not present significant selectivity in uptaking REE from fluids, as it appears at the early stages of ore-forming processes (fluids present relatively primary composition in REE at these stages). The method of luminescence spectroscopy makes it possible to study the substitutions of REE (in threevalent state) which occur in particular sites of SCH crystal structure. Thus SCH may be used as a good "tool" for the studies of REE behaviour in ore-forming processes and REE compositions of ore-forming fluids. The investigations of REE distributions in native SCH by luminescence methods are limited and in most cases are restricted to those specimens which present high level of REE substitutions. At the same time the large group of widespread SCH from skarns, metasomatic rocks and ores has not been studied (by usual X-ray and photo-luminescence techniques), due to the very small contents of REE substitutions in those cases. The SCHs from such rocks and ores usually have very high level of "self-luminescence" (visual SCH-luminescence, which is related to various defects in SCH structure); it creates serious difficulties for the registration of REE luminescence spectra by usual techniques.

A new kind of X-ray luminescence analysis of native SCH was worked up. This technique was created on the basis of a well known physical effect, which consists in different dependences on temperature of the of two main types of SCH-luminescence: 1) the so-called "self-luminescence" (broad band in blue spectral area; this one is related to complex aggregates of reduced Mo and W and oxygen vacancies); 2) luminescence of various REE-substoitutions (threevalent form) in calcium sites of SCH structure. The "self-luminescence" decreases very quickly when temperature increases; at the same time the intensities of the lines of REE multiplets increase slowly or remain constant when temperature increases.

Such analysis was named "Thermal X-ray luminescence method" (XLT). XLT-method gives the possibility to obtain the intensities of characteristic lines of threevalent REE (Pr, Sm, Eu, Tb, Dy, Er, Tm) in SCH in trace contents (up to 0.01 ppm and possibly less) and to obtain "clear" lines of Pr and Er luminescence multiplets, which is highly significant for sample classification, mathematical processing of the spectroscopic data, genetic and geochemical conclusions. In the usual X-ray luminescence spectra of SCHs, Er-lines are extremely rare and Pr-line is not convenient for measurements.

A collection of SCH (about 1000 samples from more than 200 ore deposits and occurrences) was studied by XLT-method. The different types of obtained REE distribution were used to analyse the special behaviour of single REE and REE-groups in ore-forming processes, for discovering various relations of REE-distributions with types of host rocks and their transformations (sometimes the peculiarities of SCH REE-distributions may be related to the types of transformations of host rocks, i.e. amphibolisation, greisenisation and so on), with minerals of SCH paragenesis (sometimes the SCH can "record" the influences of its paragenesis on REE-pattern - garnets, pyroxenes, amphiboles, etc), with metal-genetic types of ores, etc. Some data may be useful to discuss problems of ore-matter sources.

DIAMAGNETIC ANISOTROPIES OF NON-MAGNETIC OXIDE MINERALS

Uyeda C., Tsuchiyama A. and Yamanaka T.(Dept. Space & Earth Science, Faculty of Science, Osaka Univ.)

The systematic study on diamagnetic anisotropy of inorganic minerals started in the 1930's for several non-magnetic minerals. The results attracted little intrest since the values were considerably small compared to those of organic materials. The anisotropy reported in the oxide minerals cannot be explained by the well known mechanism of organic materials such as that of the benzene molecule.

Recently the anisotropy of oxide minerals has been explained in terms of a new model, in which the anisotropy is assigned to the individual chemical bond in the [MO_6] octahedral unit of the crystal(Uyeda 1993a). Here the diamagnetic principal axis of the individual bond is in the direction of the bond. The calculated anisotropy based on this model shows a good correlation with the measured diamagnetic anisotropy, $\Delta\chi$, for various minerals as is sen in Table 1.

The bond anisotropy, $\Delta\chi_{bd}$, is explained by the spatial anisotropy of electron probability in each bond. In the case of M-O bond at the octahedral site, the bond orbitals M-O bonds in the [MO_6] site are composed of the sp_3-orbitals of the O^{2-} ions. The distribution of each sp_3-orbital is extended in the direction of the bond forming a quasi-ellipsoid shape. When the [MO_6] unit holds the regular octahedral symmetry, the sum of the anisotropy of the six bond will cancel out and the the total susceptibility will be isotropic. However when the symmetry is distorted, the anisotropy for the six bonds will not cancel out.

The $\Delta\chi$ values of many diamagnetic minerals are still un-known because of various difficulties in its observations. The diamagnetic grain orientation in suspensions(Uyeda et al 1992) is effective for estimating the order of $\Delta\chi$ value, when the single crystal of the mineral cannot be obtained, as is the case of various sheetsilicates. The measurement of field-induced rotation and oscillation of large single crystals in the high magnetic fields can be applied for measuring the minerals with small $\Delta\chi$ values of less than 5×10^{-10} emu/cc(Uyeda et al 1993a). The chemical bond model on the diamagnetic anisotropy will be confirmed, when the compiling of $\Delta\chi$ data on various mineral is made by means of these new methods.

Table 1 Comparison between experimental and calculated values of diamagnetic anisotropy (UYEDA 1993a).

Mineral	anisotropy per molecular formula $\Delta\chi_{cal}$	$\Delta\chi_{mea}$
Talc	$1.62\ \Delta\chi_{bd}$	$0.21D_B$
Kaolin	$0.92\Delta\chi_{bd}$	$0.54D_B$
Sericite	$1.62\Delta\chi_{bd}$	$0.50D_B$
Corundum	$0.14\ \Delta\chi_{bd}$	$0.0018D_B$
[z'-x']	$0.20\Delta\chi_{bd}$	$0.0087D_B$
Forsterite[z'-y']	$0.16\Delta\chi_{bd}$	$0.0081D_B$
[y'-x']	$0.04\Delta\chi_{bd}$	$0.0011D_B$

$\Delta\chi_{bd}$: Diamagnetic anisotropy of a M-O chemical bond.
D_B: Diamagnetic anisotropy per benzene molecule.

References
UYEDA C et al. (1992) Physica B. 177 519-.
UYEDA C, TSUCHIYAMA A, YAMANAKA T and M.DATE(1993a) Phys. Chem. Minerals.20 77-81.
UYEDA C,(1993b) Jpn.J.Appl.Phys.32. 153-155.

ATOMIC FORCE MICROSCOPY OF MICA GROUP MINERALS

Valdrè G. (Dept of Mineralogical Sciences, University of Bologna)

The study of the static and dynamic atomic arrangement of crystal surfaces is of fundamental importance in geochemistry, crystal-chemistry and for elucidating the physical properties of minerals. This paper deals with investigations carried out on mica group minerals by means of the recently introduced atomic force microscopy, AFM, (Binnig et al., 1986). AFM is a breakthrough methodology that allows 3D imaging and measurement of surface structures from atomic to micron scale. It is based on the attractive or repulsive forces between a sharp tip, held on a cantilever, and the surface of the sample which can be a conductor or an insulator held in air, or in a liquid or in vacuum. The force is so sensitive to the tip-specimen distance that atomic resolution of the surface can be achieved if the tip is scanned in a regular pattern over the sample.

The observations made on a specimen consisting of a perfectly cleaved crystal of muscovite of well-known crystal-chemistry are here reported in order to show the potential of this new technique. The images were taken in standard T, P conditions, with about 50% humidity, using a Digital Nanoscope III Multimode AFM. The intensity of the force applied by the Si_3N_4 tip of the cantilever to the crystal surface was about $5\ 10^{-8}$ N.

Fig.1 is an AFM image of the muscovite surface with the [001] orientation coinciding with the direction of view. The corresponding Fourier transform is reported in Fig.2a. A slightly distorted "honeycomb" structure of bright contrast is clearly visible; each hexagon presents a dark centre. These dark dots (see Fig.2b for a clearer pattern) correspond to the location of the crystal sites of potassium atoms which are missing in the AFM image for two reasons. Firstly, the cleavage distributes the K-atoms between the two surfaces of the cleaved crystal and secondly, the force applied by the AFM tip is strong enough to drag the potassium over the surface, since its binding force is estimated, from electrostatic calculations, to be only $\sim10^{-8}$ N. The "honeycomb" is the structure formed by downward corner-sharing (Si,Al) O_4 tetrahedra (Fig.3a). Oxygen atoms and real lattice distortions can be detected. These data are in agreement with crystal-chemistry (Griffen, 1992). Fig.3b shows an AFM image simulation, obtained from the structural model showed in Fig.3a. To be noted the agreement between the simulated and the experimental images. In conclusion AFM introduces the possibility to gain information on the surface crystal-chemistry of minerals, which includes ordering, lattice distorsion and point, line and surface defects, not observable with conventional averaging techniques and without any particular specimen preparation (along at least the easy-cleavage surfaces). In addition, it is possible to study surface processes in minerals, like crystal growth and dissolution, by exploiting the short AFM data acquisition time (~tens of seconds) and the possibility of working with the specimen immersed in a fluid. Further experiments are in progress on other minerals.

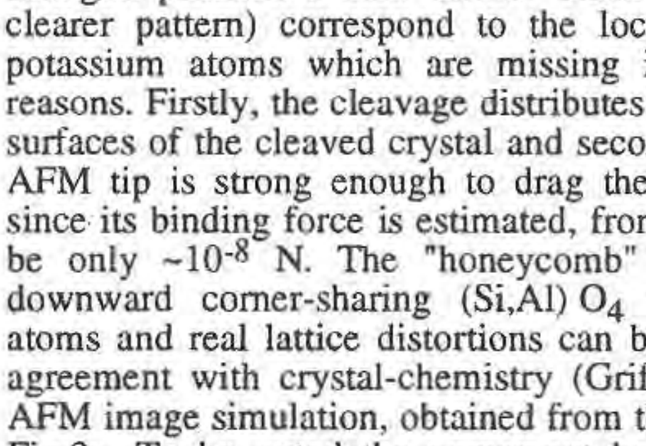

Fig.1 AFM image of muscovite seen along [001]. Lateral scales up to 5 nm; height up to 1 nm.

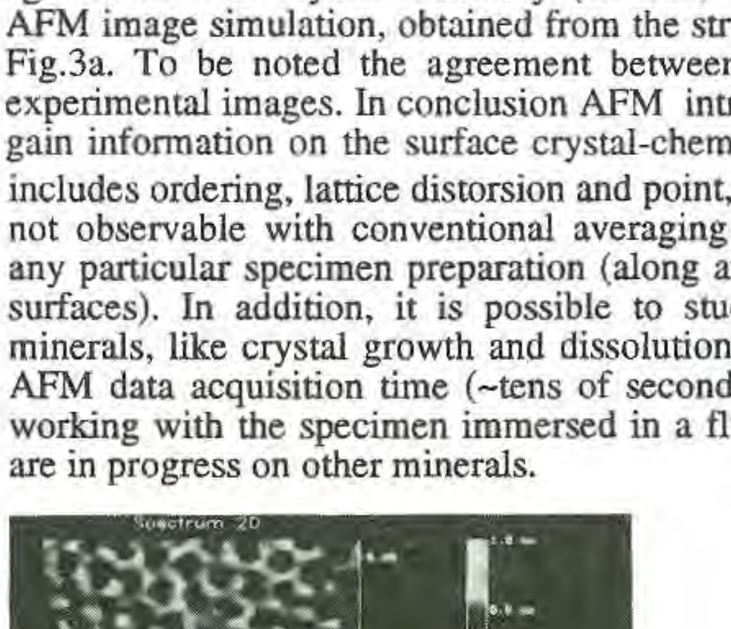

Fig.2 a) Fast Fourier Transform (FFT) of Fig.1; b) AFM reconstructed image using low order FFT reflections. Full scale: 5 nm.

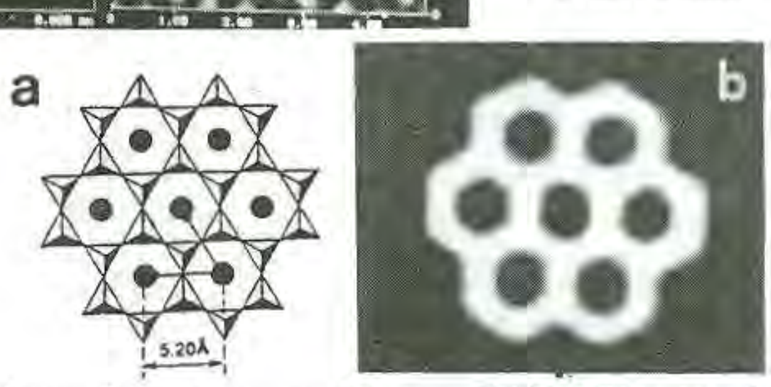

Fig.3 a) Top view of the hexagonal layer of (Si,Al)O_4 tetrahedra of muscovite,●=K; b) AFM image simulation of a) assuming van der Waals repulsive forces and a lateral resolution of 0.3 nm.

References:
Binnig, G., Quate C.F., Gerber C.,(1986). Phys. Rev. Lett. 56, 930.
Griffen, D.T., (1992). Silicate Crystal Chemistry, Oxford University Press, 101.

IMPACT DIAMONDS: ITS SIGNIFICANCE IN MINERALOGY

Valter A.A.[1], Eremenko G.K.[2] and Polkanov Yu.A.[2]
(1- Institut of Geochemistry, Mineralogy and Ore Formation, Acad.Sci.of Ukraine, Kiev; 2- Ukrainian State Institut of Mineral Resourses, Simferopol, Crimea, Ukraine)

Peculiarities of impact diamond grains (IDG) reflect extremely high for planet conditions PT- parameters and rates of mineral transformations.

The authors have studied IDG from astroblemes of Russia and Ukraine. IDG sizes vary from 1 mcm to 3 cm and is determined by grain sizes of initial graphite crystals and their aggregates, by methods of separation and by conditions of graphite-diamond transitions.

IDG structure is polycrystalline and, as a rule, multiphase one with crystallite sizes from nm to mcm. By phase composition five main varieties are to be distinguished among IDG: (1) lonsdaleite (L)-diamond (L<30%, sometimes with trace amounts of graphite (G)); (2) diamond-lonsdaleite,usually with graphite (L>30%; G>3%); (3) diamond, relatively coarse-grained; (4) diamond-graphite (G>>5%); (5) diamond-graphite with amorphous carbon.

Varieties of IDG(1-4) form paramorphoses on initial graphite grains(IGG). External morphology of IDG has regular distortions in comparison to IGG, adapting to structural transformation graphite (G)-lonsdaleite (L)-diamond (D). Internal structure of IDG reflects the same adaptation by formation of fine intergrowth of crystallites of diamond and lonsdaleite, regulary oriented as to initial graphite: $(10\bar{1}0)L//(111)\ D//(0001)\ G$; $[10\bar{1}0]\ L//[111]\ D//[0001]\ G$; $[0001]L//[112]D//[10\bar{1}0]G$ (Gorogotskaya et al., 1989; Valter et al.,1990).

Ratio lonsdaleite-diamond in grains is deter mined by regime of compression and varies from L about 100% to L=0. Substitution L-D takes place during the growth of crystals and is determined by duration of pressure action. Complete substitution of lonsdaleite by diamond (var.4) takes place, evidently only in very big structures.

IDG preservation is determined by quick cooling of silicate environment. As possible causes of this phenomenon evaporation, local cooling of melts by solid inclusions,cooling of melts forming thin injection veins in crater base are discussed.

Spesial features of structure and composition of IDG and their distribution in rocks of astro—blemes makes possible to jude aboute gaseous composition of fluids,rates of cooling of melts and variability of these factors within one astrobleme and in various structures.

References:
Gororogotskaya L.I., Kvasnitsa V.N., Nadezhdina E.D. (1989) Mineral.journal (in Russian), 11, N1, 26-33.
Valter A.A., Kvastnitsa V.N., Eremenco G.K. (1990) Ibid.,12, N 3,,3-16.

TEMPERATURE DEPENDENCE OF THE ^{57}FE MÖSSBAUER PARAMETERS IN RIEBECKITES

Van Alboom A. (*Industrial Highschool BME, Gent*) and De Grave E. (*Department of Subatomic and Radiation Physics, University of Gent*)

Riebeckite is a Na-amphibole with ideal chemical formula $Na_2Fe^{2+}{}_3Fe^{3+}{}_2Si_8O_{22}(OH)_2$. The amphibole structure contains four different cation sites, M1, M2, M3 and M4 respectively, with relative abundances of 2:2:1:2. The first three are octahedrally coordinated whereas the last one shows a strongly deformed six to eightfold coordination and is occupied by Na^+. These sites form ribbons of alternately three (M2-M3-M2) and four (M4-M1-M1-M4) polyhedra wide. These ribbons are sandwiched by double Si_4O_{11} chains which run parallel to the crystallographic c axis. The so-called A sites have a 10-12 fold coordination and can accomodate large monovalent cations, but are often unoccupied.

A survey of the literature concerning the Mössbauer effect in riebeckites and crocidolites has learned that a detailed study covering a broad temperature interval has not yet been conducted. In order to widen our knowledge about the microscopic properties of these minerals and in an attempt to gain information on the ^{5}D electronic level scheme of the various ferrous species, the Mössbauer spectra for two riebeckites (RBK1 and RBK2) with magnetic order-disorder transition temperatures of respectively 33± 1 K and 31±1 K, have been measured and critically analysed for temperatures in the range 4.2 to 500 K at steps of ≈25 K.

It was found that fitting the paramagnetic spectra (T > 40K) with a discrete number of doublets (three or four) did not lead to consistent parameter values. Instead, a superposition of an Fe^{3+}(M2) doublet and one distributed ferrous component was found to yield adequate fits with reasonable parameter values. For both samples, a minor quantity of Fe^{2+} was found to be present at the M4 sites and for RBK1 at the M2 sites as well. The major part of the Fe^{2+} was divided among the M1 and M3 sites, with no clear preference for either one.

The temperature variations of the ferrous center shifts were well reproduced using the Debije model of the lattice vibrational spectrum to evaluate the second-order Doppler shift. In line with the results for various other Fe^{2+}- and Fe^{3+}-containing compounds, the characteristic Mössbauer temperatures were found to be in the range 340-390 K for Fe^{2+}, and 520 K for Fe^{3+}.

The temperature dependences of the various ferrous quadrupole splittings could not be explained in terms of the point-charge model using a constant ^{5}D energy-level scheme. Instead, the observed $\Delta E_Q(T)$ curves suggest a gradual change with temperature of the orbital-level splittings. All calculations lead to a positive sign for the principal component of the *EFG*.

The spectrum recorded at 4.2 K for RBK1 was fitted with a superposition of an Fe^{3+} and an Fe^{2+} hyperfine-field distribution, the latter one primarily characterizing the Fe^{2+}(M1) cations (H_{hf}=161 kOe, ΔE_Q=3.11 mm/s, V_{zz} < 0 referring to the maximum-probability values). For RBK2 at 4.2 K, a second distributed component could independently be resolved. The Fe^{2+} hyperfine fields are 189 and 98 kOe, the ΔE_Q values are 3.10 and 2.67 mm/s respectively (V_{zz} < 0) and are attributed to M1 and M3 respectively. The negative V_{zz}'s are inconsistent with the point-

charge calculations, although their magnitudes are in line with the results from paramagnetic spectra. The Fe^{3+} hyperfine fields are 548±2 kOe for both riebeckites. The different value of the Fe^{3+} quadrupole shift $2\varepsilon_Q$ for the two samples is attributed to a different angle between the hyperfine field and the *EFG*'s principal axis. The magnetic spectra recorded at 15 K and higher, could not be reproduced adequately with reasonable parameter values.

CATHODOLUMINESCENCE OF QUARTZ AS A TOOL FOR THE CHARACTERIZATION OF RETROGRADE TRANSPOSITION OF FLUID INCLUSIONS

van den Kerkhof A.M. and Behr H.-J. *(IGDL Univ. of Göttingen FRG)*

The cathodoluminescence (CL) of quartz shows a wide variation in colour (blue, red, IR) and intensity caused by the complex relationship with trace elements (Al, Ti, Fe etc.), crystal lattice defects and the state of water (silanol, molecular). The extreme sensitivity of quartz CL for changes of the physico-chemical parameters makes it very useful for the interpretation of fluid-rock interaction processes like the transposition of fluid inclusions. Pioneering CL studies of microtextures (Frentzel-Beyme 1989; Behr 1989) showed the potential power of the method. Samples from selected high-grade metamorphic rocks and granite have been studied by SEM and optical CL and compared with fluid inclusion data (density, composition, shape) and retrograde uplift paths.

Decrepitation (explosion and implosion-decrepitation) resulting in volumetric and compositional changes is one of the basic problems for the interpretation of fluid inclusions. The physical conditions of decrepitation (fluid-confining pressure difference etc.) in quartz have been extensively studied by experimental methods (a.o. Bodnar *et al.*, 1989; Bakker & Jansen, 1991). However, the fluid-mineral interaction on micro-scale during fluid inclusion transposition is still poorly understood. The recognition of decrepitation in *natural*, notably metamorphic rocks is still problematic and cathodoluminescence studies of quartz may give important information about secondary changes of fluid inclusions. Particularly, explosion and implosion-decrepitation of fluid inclusions during rock evolution can be distinguished as different CL textures in rocks.

Textures which are related with the explosion/ implosion-decrepitation of fluid inclusions are refered to as "crackling textures". Besides, textures can be recognized, which are related with fluid infiltration and migration, and rock deformation: e.g. healed microfractures, channelways, micro and cryprocataclasis. A special case are radiogenic defects induced by radioactive elements dissolved in inclusion fluids or along cracks and grain boundaries.

Different types of crackling patterns can be distinguished. Irregular (star-shaped, amoeboid, rounded) forms are most typical, but regular (planar, hexagonal, or rhombohedral) forms are also found and related with the crystal symmetry like slip planes. "Crackling" is supposed to be the result of quartz recrystallization and diffusion on changing temperature and stress conditions, resulting in fluid over/underpressure, during retrogression.

Electron bombardment of quartz during the measurements generally causes CL colour changes (O-CL) from blue to violet and red, visible as intensity changes or even reversal of black/white contrasts (SEM-CL). These changes are minor in granulites and volcanic quartz, but strong in granite and hydrothermally altered rocks.

The results of metamorphic rocks have been compared with CL textures observed in granite, which are typically isobarically cooled. Fluids trapped in fluid inclusions are expected to be underpressurized during the cooling stage. CL textures in these samples show in echelon patches, interpreted as the result of implosion-decrepitation.

References:

Bakker, R.J. & Jansen, J.B.H. (1991). *Geochim. Cosmochim. Acta*, **55**, 2215-2230.
Behr, H.J. (1989). *Nds. Akad. Geowiss. Veröfftl.*, **1**, 7-41.
Bodnar, R.J., Binns, P.R. & Hall, D.L. (1989). *J. Metamorphic Geol.*, **7**, 229-242.
Frentzel-Beyme, K. (1989). *Ph.D. Dissertation University of Göttingen.*

Chromian Spinel mineralogy of the Staré Ransko gabbro-peridotite, Czech Republic, and its implications on sulfide mineralization

Adriaan H. van der Veen (1), and
Pieter Maaskant (2)

(1) formerly Billiton Research b.v., Arnhem, The Netherlands;
Faculty of Earth Sciences
Department of Geology, University of Utrecht.

(2) Institute of Earth Sciences, Vrije Universiteit, Amsterdam,
The Netherlands

ABSTRACT

Chromian spinels from the Staré Ransko gabbro-peridotite, Czech republic, display a distinct development trend: from primary Cr-rich spinels towards ferro-ferri (Ti-enriched magnetite) and magnesio-alumina (spinel sensu stricto) spinels. Zoning in the spinels is thought to be the result of a combination of exsolution, postdepositional diffusion and replacement processes.

Multiphase, globular silicate inclusions - mainly biotite and amphibole, also orthopyroxene, serpentine and chlorite - are present in euhedral, largely homogeneous chromian spinels which occur in a matrix of poikilitic amphibole. The enclosed minerals have similar compositions to the minerals in the host rock. These silicate inclusions are interpreted as being due to a late magmatic introduction of a hydrous K-Ca-rich melt phase, contaminated by wall-rock interaction, into a semi-solidified olivine (+/- pyroxene) cumulate.

The composition of the chromian spinel may be used as an indicator for sulfide mineralization conditions (Johan, 1979). The data reported in this paper are compatable with Johan's model.

References:

Johan, Z., (1979). In: M. Besson (ed.) Facteurs controlant les mineralisations sulfurees de nickel. Memoire de BRGM 97, Chpt. 3, Part II: 203 - 218.

CHEMICAL COMPOSITION OF MICROCRYSTALLINE QUARTZ FROM BEACONSFIELD, NORTHERN TASMANIA.

van Moort, J.C. and Russell, D.W. (Geology Department, University of Tasmania)

One hundred and twenty quartz samples from microcrystalline quartz reefs and associated veins from the Beaconsfield hypothermal goldfield in northern Tasmania were chemically analysed by simultaneous particle induced gamma ray emission (PIGME) and particle induced x-ray emission (PIXE). Possible sulphide and carbonate impurities were removed by acid treatment and inspection by electron microprobe did not reveal presence of sericite or potash feldspar. The quartz contained on average:

F	Li	Na	Al	Mg	Ge	As	Cl	K	Ca	Li	Mn	Fe	Rb	Sr	Zr	
2	5	56	746	13	1	4	55	546	34	66	26	117	1	1	1	ppm

Statistical analysis at 99.999 level of confidence of the relations between the elements is shown in the table below. The data indicate that most of the Al, Fe and Ti analysed substitute for Si in the quartz structure. The Zr, F and Mn in these statistics suggests that they too, may have a substitution role.

ΣAt% (compensating ions)	ΣAt% (substituting atoms)	R_S
K	Ti	0.799
K	Al	0.850
K	Al+Fe	0.855
K	Al+Ti	0.860
K	Fe+Ti+Fe	0.865
K	Fe+Ti+Zr+Mn+Al	0.866
K+Na	Fe+Ti+Zr+Mn	0.750
K+Na	Al+Ti+Fe	0.860
K+Na	Fe+Ti+Zr+Mn+Al	0.861
K+Na+Li	Fe+Ti+Zr+Mn+Al	0.856

Correlations between compensating ions and subsitituting atoms (N=120 and ρ=0.320)

One hundred and eight of these spot samples were selected from 1m core intervals without gold detectable by fire assay. The remaining fifty two spot samples came from goldbearing core. Only few of the former samples contained PIXE detectable gold and a large proportion of the latter group contained PIXE detectable gold. The samples from the goldbearing group are on average characterised by higher Li, Al, Ge, As, Cl, K, Ca, Mn and Zr contents, but considerable variations occur. The samples from the goldbearing core contain however 3±2 ppm Ge and the samples from the barren set contain usually less than 0.1 ppm Ge. The presence of Ge in quartz is of practical importance in exploration for hypothermal and mesothermal gold deposits.

References:

Russell, D.W. & van Moort, J.C. (1992). *Bull. geol. Surv. Tasm.* **70**, 208-226.
van Moort, J.C. & Hotchkis, M. (1993). *ICAM '93 Proceedings*, 217-221.

ARCHEAN LODE GOLD HOSTED BY CARBONATIZED SERPENTINITE: INCOMPATIBLE FLUID COMPOSITIONS ?

Van Schalkwyk JF (Dept. of Geology, Rand Afrikaans University, Johannesburg)

Archean lode gold deposits have been studied in great detail during the last decade and their general features are well-known. Results from a great number of fluid inclusion and stable isotope studies suggest that Archean auriferous fluids are characterized by:
i. Low salinity, < 2 wt% NaCl equivalent (Ho, 1987).
ii. An aqueous but CO_2-bearing composition $X_{CO_2} \approx 0.2 - 0.3$.
iii. Temperature of deposition (T_h) that ranges from 200°C to 400°C and clusters around 350°C (Ho, 1987).
iv. Moderate to high density from 0.7 to > 1.0 g/cm^3.
v. $\delta^{13}C$ of -7‰ to 0‰ with a median of -3.5‰.

When considering these general characteristics it is important to note that these results were derived predominantly exclusively from mineralized veins and not the altered/carbonatized host rock (e.g., Ho, 1987; De Ronde *et al.*, 1992).

Few of these studies attempted to reconcile the fluid inclusion and stable isotope data with the metamorphic or phase petrologic information that can be obtained from assemblages of the carbonatized host rock (Kishida and Kerrich, 1987).

Colvine *et al.*, (1988) demonstrated that Archean lode gold deposits are not hosted preferentially by a specific greenstone lithology but all the occurrences hosted by (altered) serpentinite display the well-known sequence of; serpentinite → talc-carbonate schist → quartz-carbonate ± fuchsite ± chlorite ± muscovite ± albite. The alteration sequence reflects a decrease in the a_{CO_2} of the fluid away from the mineralization contained exclusively by the quartz-carbonate zone.

A serpentinite-hosted gold occurrence from the Pietersburg greenstone belt in South Africa was studied in detail. The assemblages are related to isobaric univariant reactions and two populations of magnesite were produced; one (type 1) through the breakdown of antigorite at low X_{CO_2} (± 0.2), and the other (type 2), together with quartz, at high X_{CO_2} (> 0.7 at 350°C, 1Kbar) due to the breakdown of talc . The two different populatioms of magnesite can be distinguished texturally.

Type1 magnesite contains three-phase liquid dominated inclusions containing $H_2O_{(l)}$, $CO_{2(l)}$ and $CO_{2(v)}$ are characterized by:
Constant CO_2 volume of 15% to 30%, vapor bubbles ± 5 vol%. $T_{m_{CO_2}}$ between -57.9°C and -56.2°C, mean of -57.1°C. Low salinity, between 0.02 and 3.3 wt% NaCl a mean of 0.87 wt%. $T_{h(l)}$ range from ~ 320C to 375°C. Average density is 0.78 g/cm^3.
Fluid inclusions in quartz grains, produced simultaneously with type 2 magnesite are two phase CO_2-rich inclusions consisting of $CO_{2(l)}$ and $CO_{2(v)}$. $T_{m_{CO_2}}$ between -57.8°C and -55.8°C, mean of -56.7°C. $T_{h(l)}$ average value of 362°C. Average density of 0.82 g/cm^3.

The fluid inclusion results from the alteration assemblages agree remarkably with estimates of fluid composition from the isobaric diagram and show dramatic variations through the alteration sequence which suggest a complex interaction between alteration and mineralizing fluids.

References:

Colvine, A.C., Fyon, J.A., Heather, K.B., Martmont, S ., Smith, P.M. and Troop, D.G. (1988). *Ontario Geological Survey Miscellaneous Paper* **139**, 136pp.
De Ronde, C.E.J., Spooner, E.T.C., de Wit, M.J., and Bray, C.J. *Econom. Geol.*, **87(2)**, 366-402.
Ho, S.E. (1987). *Geology Department and University Extension. The University of Western Australia, Publication* **No.11**, 239-264.
Kishida, A. and Kerrich, R. (1987). *Econom. Geol.*, **82(3)**, 649-690.

• EVIDENCE FOR WATER-ROCK INTERACTION PROCESSES IN NORTHERN AEGEAN SEA

Varnavas S.P. (*Dept of Geology, University of Patras, Greece*)

The chemical analysis of marine sediments form a submarine hydrothermal field off Lesvos island, Greece, revealed that their geochemical features were very similar to those of hydrothermal metalliferous sediments encountered on the Hellenic Volcanic Arc. The concentration levels of Fe are comparable with those of Yali

hydrothermal sediments on the eastern sector of the Hellenic Volcanic Arc and the outer exhalative zone of Santorini hydrothermal field central Hellenic Volcanic Arc.

Mn values are higher than those of Santorini inner exhalative zone and the hydrothermal field but they are comparable with those of Milos hydrothermal fields and Santorini Channel. Cu, Pb and Zn are generally enriched relatively to the Hellenic Volcanic Arc hydrothermal sediments.

The Fe–Cu–Zn–Pb enrichments coincide with a sink in Mg both in the sediments and in the seawater and an increase in the water temperature. The variations in the chemical composition of the sediments and of the seawater fit very well in a geochemical processes model, involving seawater rock interaction reactions, subsurface hydrothermal circulation and leaching of basement rocks. These process are investigated in combination with the petrologic and tectonic setting of the area and implications in regard with the formation of mineral deposits are deduced.

References:
Varnavas, S.P., Cronan, D.S. (1988). *Chem. Geol.*, **67**, 295–305.
Varnavas, S.P. (1989). *Geochim. Cosmochim. Acta*, **53**, 1–15.
Varnavas, S.P., Cronan, D.S. (1991). *Marine Geology*, **99**, 109–133.

ELECTROCHEMICAL AND SPECTROSCOPIC (XPS, AES, REFLEXAFS) STUDIES OF THE OXIDATION OF CHALCOPYRITE AND RELATED COPPER-IRON SULPHIDES

Vaughan, D.J., England, K.E.R., Charnock, J.M. (*Dept. of Geology, Univ. of Manchester, England*), Yin, Q. and Kelsall, G.H. (*Dept. of Mineral Resources Engineering, Imperial College, London, England*).

Natural and synthetic chalcopyrite ($CuFeS_2$) and the related metal-enriched copper-iron sulphides haycockite ($Cu_4Fe_5S_8$), mooihoekite ($Cu_9Fe_9S_{16}$) and talnakhite ($Cu_9Fe_8S_{16}$) have been studied to determine the mechanisms and rates of oxidation in strongly acid and weakly alkaline aqueous solutions. Electrochemical techniques have been used to control the electrode potential and monitor reaction rates. Products formed at the surface during aqueous oxidation have been characterized using X-ray Photoelectron Spectroscopy (XPS), Auger Electron Spectroscopy (AES) and microscopy (AEM), and Reflection Extended X-ray Absorption Fine Structure Spectroscopy (REFLEXAFS).

The oxidation of chalcopyrite in strongly acidic solutions (pH<2) at lower potentials results in the formation of a passive film that consists of an iron-depleted chalcopyrite-like material of approximately 1Cu:2S stoichiometry (CuS_2^*), and at higher potentials in the formation of elemental sulphur. In weakly alkaline solution (pH>9), the oxidation of chalcopyrite creates a passive film of CuS_2^* plus Fe_2O_3 at lower potentials, via the reactions:

$$2CuFeS_2 + 6OH^- \Rightarrow 2CuS_2^* + Fe_2O_3 + 3H_2O + 6e^-$$

$$CuFeS_2 + 3OH^- \Rightarrow CuS_2^* + Fe(OH)_3 + 3e^-$$

At higher potentials in weakly alkaline solution the products consist of CuO, Fe_2O_3 and elemental sulphur, via the reactions:

$$CuS_2^* + 2OH^- \Rightarrow CuO + 2S + H_2O + 2e^-$$

$$CuS_2^* + 2OH^- \Rightarrow Cu(OH)_2 + 2S + 2e^-$$

The nature of these oxidation processes has been established using spectroscopic techniques. Those techniques (such as AEM) yielding information on spatial variations in oxidation phenomena across a surface demonstrate the importance of surface defects in controlling oxidation. The rates of oxidation for these copper-iron sulphides appear largely to be controlled by solid state mass transport. Thus, haycockite mooihoekite and talnakhite oxidize much more rapidly than stoichiometric chalcopyrite over a range of potentials, suggesting that the additional (interstitial) metal atoms can diffuse more rapidly, leading to more rapid reaction. In alkaline solutions (pH>9) haycockite, mooihoekite and talnakhite also oxidize more rapidly than chalcopyrite at lower potentials although the opposite is observed at higher potentials. This appears to be due to the formation of a passive film (largely Fe_2O_3) on the surface, and its retention retarding further oxidation.

• IDENTIFICATION OF LOW MOLECULAR WEIGHT ORGANIC COMPOUNDS FROM AUSTRIA'S FOSSIL RESINS BY MASS SPECTROSCOPY

Vávra N. (*Institut für Paläontologie, Universität Wien, Universitätsstraße 7/II, A-1010 Wien/Vienna Austria*)

Fossil resins from Austrian localities are usually available in small amounts only; being of different geological age and from different tectonical units they deserve some interest nevertheless. The oldest fossil resin reported from Austria is of Triassic age (Carnian), the most conspicuous finds of fossil resins within the last ten years or so have been detected in the Lower Cretaceous (Neocomian, Salzburg); rather frequent finds had been reported from the Gosau formation (Upper Cretaceous) and from the Flysch Zone (Upper Cretaceous to Paleogene). For some of these resins and for a few other organic minerals (e.g. Hartite, Ixolyte, Jaulingite, Koflachite, Rosthornite) type localities are situated in Austria.

Chemical studies of such minerals are usually performed for at least one of the following three goals: (1) characterization of a mineral species (2) study of diagenesis of organic substances and (3) determination of botanical sources. A rather great variety of different methods of physical chemistry has been used up till now for such studies: infrared spectroscopy being the most common for the characterization of such mineral samples especially in cases where only minute amounts of material are available. For soluble fractions a few research workers have used for seperation and identification of low molecular weight compounds combined gas liquid chromatography/mass spectroscopy. This method has been applied to the study of some of the organic minerals from Austria now.

In the course of such studies this method prooved useful as an additional tool for the characterization of mineral species as well as for the study of diagenetic processes concerning single terpene compounds. Moreover first results in respect to a "chemotaxonomy" (determination of botanical sources) have been yielded.

For Rosthornite (Eocene, Carinthia) the occurrence of two different isomeres of amyrine could be established, thus giving not only a rather reliable method to differentiate this resin from all other Austrian finds but being indicative also for a very special angiosperm origin (Burseraceae). In Koflachite quite a variety of hydrocarbons could be identified: sandarocopimarane, eudesmane, norpimarane, dehydroabietane, simonellite, retene and phyllocladane thus giving opportunities for more detailed studies of diagenetic pathways of terpenes. Phyllocladane is occurring in Austria also in the form of a well-defined mineral: "Hartite" - having its type locality in Lower Austria. Finds of Hartite from Styria have been restudied and could be confirmed to be extremely pure phyllocladane. An unsaturated hydrocarbon with the same carbon skeleton occurs in different plants of the Coniferopsida: Taxodiaceae as well as Podocarpaceae may be discussed as botanical sources for these remarkable mineral finds.

CHEMICAL REACTIONS IN MODULAR STRUCTURES

Veblen, D.R. (*Dept. of Earth & Planetary Sci., Johns Hopkins Univ.*)

Reactions from one modular structure to another may proceed either with or without a change in chemical composition. A purely polytypic reaction would be an example of the first type, but there exist few data on possible compositional changes accompanying a change of layer stacking sequence in real minerals. It is clear, however, that the transformation from $1M_d$ to $1M$ muscovite during prograde metamorphism can involve substantial compositional

change during structural reorganization (Lee *et al.*, 1986). Analytical electron microscopy (AEM) coupled with diffraction data and images from the same areas are essential for understanding the chemical changes accompanying change in polytype.

Reactions involving a change in polysomatic structure (Thompson, 1978) generally involve a change in stoichiometry, although this change may not be apparent unless structural formulae are written in terms of structurally dissimilar crystallographic sites (*e.g.*, the pyroxene-pyroxenoid polysomatic series). Stoichiometric change is a linear function of modular ratio in a polysomatic reaction, but the change in chemical composition may be either linear or nonlinear, within the accuracy of the analytical method (Livi and Veblen, 1992).

Topotactic polysomatic reactions commonly proceed by nucleation and growth of narrow lamellae that may be only one slab wide. Regardless of how the linear defect at the lamellar termination is described, this termination is inherently a zone of disrupted structure. Understanding the diffusion mechanisms and rates at these defects and their relationships to grain-boundary diffusion should be a high priority for future research on polysomatic minerals. Geological constraints suggest that the diffusion necessary for polysomatic reactions is concentrated at or restricted to these defects (Veblen, 1991), but a combination experimental, imaging, analytical, and diffusion modeling approach is required for a complete picture of chemical transport during reactions involving modular structures.

References:
Lee, J.H., Peacor, D.R., Lewis, D.D., Wintsch, R.P. (1986). *J. Struct. Geol.*, **8**, 767-780.
Livi, K.J.T., Veblen, D.R. (1992). *Am. Mineral.*, **77**, 380-390.
Thompson, J.B., Jr. (1978). *Am. Mineral.*, **63**, 239-249.
Veblen, D.R. (1991). *Am. Mineral.*, **76**, 801-826.

FRACTIONATION OF MICAS AND CARBONATES IN ULTRAMAFIC-ALKALINE INTRUSIONS: NEW EVIDENCE AND PETROLOGICAL IMPORTANCE

Veksler I.V., (*Vernadsky Inst. of Geochemistry)* and Nielsen T.F.D. (*Geol. Survey of Greenland*)

Micas, especially varieties of phlogopite, are common in silicate and carbonatitic rocks of ultramafic-alkaline intrusive complexes. However, it is not clear to what extent mica accumulations result from post-magmatic processes. Primary chemical composition and genesis of carbonatites are also subjects of debates. Here we present new evidence for the place and the role of micas and carbonates in the course of low-pressure magmatic evolution of ultramafic-alkaline plutons. The data is derived from (a) our study of melt inclusions in liquidus minerals and (b) experiments in synthetic simplified systems. The work is still in progress, but some preliminary results have been already obtained.

Tiny crystals of micas and carbonates found within melt inclusions could be more valuable for genetic speculations than huge masses of similar rocks. Primary melt inclusions trapped by chemically stable host minerals are not exposed to metasomatic alterations; their bulk composition remains constant. Inclusions crystallize (while rock cools down) like a closed isobaric system. Our electron microprobe study of melt inclusions in early liquidus olivine and perovskite from Kugda (Polar Siberia) and Kovdor (Kola Peninsula) intrusions shows that mica (biotite) and carbonates (calcite and shortite) are typical for their phase associations. We have evaluated the bulk compositions of trapped liquids in Kugda perovskites by heating experiments and probe analyses of homogenized inclusions. The liquids were found to be silicate-carbonate peralkaline melts (about 15 wt.% of normative calcite). Average composition of the most primitive liquids is: SiO_2- 34.6, TiO_2- 5.8, Al_2O_3- 3.95, FeO- 8.1, MgO- 10.4, CaO- 22.3, Na_2O- 3.8, K_2O- 3.1, P_2O_5- 0.63 (in wt.%). Mineral compositions of not heated inclusions suggest that such melt crystallizing in closed conditions at low pressure yields substantial amounts of phlogopite-biotite mica and Ca and Na-Ca carbonates.

Basing on chemical considerations we expect that fractionation of mica from ultramafic-alkaline parental liquid may change essentially the trend of melt evolution driving residual liquids to highly larnite-normative compositions. We have studied the effect of mica crystallization using simplified synthetic model system: $CaMgSi_2O_6$- Mg_2SiO_4-$KAlSiO_3F_2$ pseudo-ternary join. The join has been studied at 1 atm in sealed platinum capsules. Forsterite, diopside, F-phlogopite, leucite liquidus fields and silicate-fluoride liquid immiscibility are observed on liquidus surface (see the figure). Liquids evolve towards larnite-normative compositions and Akermanite appears in run products at near-solidus temperatures.

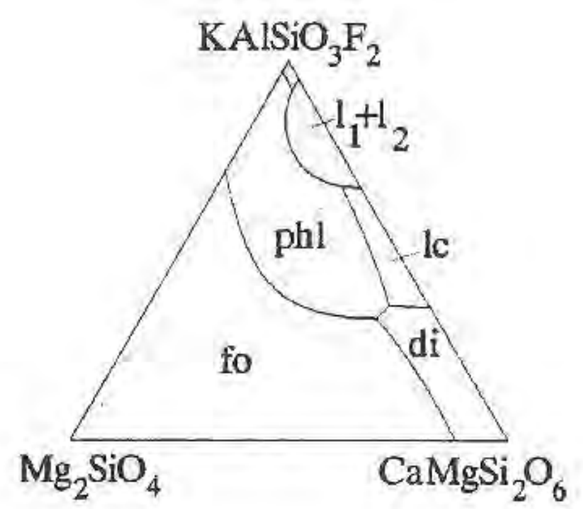

We can conclude, that fractionation of mica-bearing phase assemblages from primitive liquids observed as inclusions in Kugda perovskites could finally produce melilitolites and associated carbonatites. In melilites from melilitolitic dyke of Gardiner intrusion (East Greenland) we have found carbonatitic inclusions trapped at about 950-1050°C. Their bulk compositions range from high-calcium to high-sodium. Together with experimental data on the fluorine-doped model system this strongly suggests a genetic link from ultramafic-alkaline liquids to melilitic and carbonatitic melts. Natrocarbonatites (observed as inclusions in Gardiner melilites) could be produced by calcite fractionation from immiscible carbonatitic liquids.

AMPHIBOLE 1.0 : A SOFTWARE EMPLOYING GEOMETRIC AND ALGEBRIC APPROACH TO STUDY REACTIONS INVOLVING AMPHIBOLES

Verma P.K. and Purukayastha S.(Dept. of Geology, Univ. of Delhi, India) and Vyas R.K. (Delhi Univ. Computer Centre, India)

Amphibole 1.0, a programme written for IBM compatible PC in C++, carries out a series of linear algebric techniques for exploring the nature of univariant equilibria and invariant points in systems involving common amphiboles (Thompson et.al. 1982). The output is both numerical values and various plots.

The programme is executed in two parts. The first part consists of two databases. The first is the thermodynamic database. All available data on macroscopic properties of end-members of various participating phases are listed. The second database contains amphibole analyses from the literature. The data is well classified and may be selectively retrieved.

Part two of the programme calculates the end-member proportions of the minerals and then proceeds to estimate mixing properties according to a choice of mixing models. The input is in wt% oxides and can be drawn from the analyses database built-in in the software and also from the keyboard. The programme writes linearly independent reactions and identifies exchange reactions and net transfer reactions in P-T-μ_{fluid} space. The latter allows

i
us to define a reaction space in which other reactions may be considered as vectors. For n number of independent reactions, the vector space R^n is utilized to predict exchange reactions. The consideration of cation ordering also forms a part of the present treatment (Powell and Holland, 1993)

The software is user friendly and execute output by producing tables and phase diagrams. For the present, only calcic amphiboles are considered and the H_2O the only fluid species. However, the next version will have enlarged facility for more variations. The programme is useful for classroom exercises as well as research.

References:

Powell, R. & Holland, T.(1993) Am.Min., 78, 1174-1180.

Thompson, J.B. Jr., Laird, J., Thompson, A.B. (1982). J. Petrol., 23, 1-27.

FLUID COMPOSITION AND GEOCHEMICAL ZONATION OF ELDORADO GOLD DEPOSIT, ENISEI RIDGE

Vernikovskaya A.E. (United Insti. of Geol., Geophys. and Mineral., Novosibirsk, RUSSIA)

Eldorado ore deposit is localized within Riphean schist complex of epidote-amphibolite facies. Study of composition peculiarities of fluids from quartz veins and host schists was fulfilled using the detail investigation of gold and trace element distributions. Zonation of geochemical associations which characterize the ore and ore-free (background) geochemical zones was described. Samples were analyzed using atomic absorption, spectrochemistry, thermobarochemistry including gaseous chromotography, Raman-spectroscopy, etc. The increased concentrations of most trace elements (especially As and Ag) are typical of ore geochemical associations. The main fluid components are H_2O and CO_2, less CH_4 and CO. Due to Raman-spectroscopy the presence of N_2 and H_2S in the gaseous fluid component from individual inclusions was established. Quartz average fluid saturation, H2O and CO2 increases from pre-ore (140.5 mg/kg), to ore (200.9 mg/kg) and post-ore quartz (252.6 mg/kg). There is no predominant accumulation of one of the main fluid component. Their contents are close unlike those from greenschist facies deposits where H_2O significantly exceeds CO_2. In the zones of ore geochemical association the distribution of gaseous components becomes more regular resulting in increased correlative links between CO_2 and H_2O, N_2 and CH_4. Gold has no correlations with other components, because in ore quartz it occurs independently and does not relates to sulphides. Visible under microscope gold grains relate to micro fractures in quartz surrounded by areals of fluid inclusions. There are many types of these inclusions including most high-temperature water-salt inclusions.

Mostly, quartz veins represent the metamorphogenic recrystallization veins. The fluid metamorphogenic nature is confirmed by early pre-ore quartz (widespread in the veins from zones of ore-free geochemical associations) enrichment in high-dense CO_2-bearing inclusions. Homogenization temperature of these solutions is 300-570°C, density of solutions is 0.05-1.04 g/cm^3 and pressure (according to liquid CO_2) is 1.7-4 kbar. In ore quartz there are relict grains have not undergone significant recrystallization which carry the described above metamorphogenic types of inclusions (1% of all the inclusions). The temperature of complete homogenization of primary inclusions with CO_2 varies from 220 to 490°C. Ore quartz crystallization was followed by the boiling of solutions and their density change from 0.07 to 0.91 g/cm3. The highest CO_2 pressure is 2.2 kbar. Secondary single-phase inclusions with gaseous CO_2 contain low-dense solutions (0.04 g/cm^3). There are no CO_2-bearing inclusions in post-ore quartz. According to cryometry the composition of water-salt chloride solutions in CO_2-bearing inclusions changed insignificantly. Eutectic temperatures reveal the occurrence of Na and Ca cations. Concentration of solution varies from 8.2 to 16 wt% (equivalent to NaCl). Only the groups of secondary water-salt inclusions related to the fractures in quartz grains were found. The widest interval of homogenization temperatures was fixed for ore quartz: from 120 to 310°C. The lower values are typical of pre-ore (160-180°C) and post-ore (100-120°C) quartz. Concentration of chloride solutions in the secondary gas-liquid inclusions without solid phase ranges from 4 to 15.1 wt.% (equivalent to NaCl).

Thus, the process of quartz vein formation had multi-stage character and proceeded under decreasing temperature, pressure and density of solutions, in the regressive stage of metamorphism under frequently changing physical-chemical parameters.

PECULIARITIES OF MINERAL COMPOSITION AND CONDITIONS OF METAMORPHISM FOR VARIOUS GEODYNAMIC COMPLEXES, NORTHERN TAIMYR

Vernikovsky V.A. (United Inst. of Geol., Geophys. & Mineral., Novosibirsk, RUSSIA)

Precambrian metamorphic and magmatic rocks of the Northern Taimyr occur within two greatest structures of the region: Central Taimyr accretionary belt and Karsk terrain. They are divided by a system of thrusts and strike-slip faults and traced in a belt of north-eastern strike on over 750 km, total width 70-150 km. Formation of accretionary belt had occurred in the Late Riphean, i.g. 700-740 Ma ago, but its obduction over the passive margin of Siberian continent has proceeded from 620 to 600 Ma (after U-Pb, Sm-Nd and Rb-Sr study of island arc plagiogranites, collisional granites and garnet amphibolites). Obduction of the Karsk terrain over the continental margin has occurred 280-300 Ma ago, in the Late Paleozoic (U-Pb, Rb-Sr and K-Ar study for collisional granites, amphibolites and Karsk gneisses dating).

The stages of structural reconstruction of the Northern Taimyr are fixed both due to magmatic activity and a definite type of metamorphic transformations. Composition of minerals-indicators and their change were studied for every metamorphic complex. Geothermobarometric and geochronological research of the conditions of metamorphic transformations were carried out.

Within the accretionary belt the most complicated metamorphic alterations relate to the rocks of Mamonto=Shrenkovsk and Fadeev terrains. Here, the minerals assemblages corresponding to the amphibolite facies of regional metamorphism are present. The temperature and pressure of metamorphism reached 650-700°C and 5-6 kbar, respectively. Within the marginal zones of these terrains and the soles of thrusts the pressure was estimated as 7-9 kbar, and the sporadic occurrences of high-pressure stress-minerals (kyanite, sodium amphiboles and pyroxenes) were found. Compositionally, the garnet from metapelites is characterized by a very complicated zonation, the marginal zones of crystals being enriched in grossular minal. The change of mineral composition and widespread diaphthoresis zones accord with a suggestion about multi-stage metamorphism of these terrains.

Island arc, forearc and ophiolite complexes of accretionary belt terrains are characterized with greenschist changes of oceanic type (T<=500°C, P<=4-5 kbar). Only in the soles of thrusts there are garnet-bearing varieties in metabasites and kyanite in amphibolite crystalline schists which indicate on the pressure growth. Within these parts the pressure of metamorphism is estimated as 6-8 kbar.

Absolutely another type of metamorphism was described for Karsk terrain. There, flysch-like deposits have been regionally metamorphosed from the lowest grade of greenschist facies to the upper grade of amphibolite facies and are characterized by a successive change of isograde of index-minerals and their compositional change (Chl-Bt-Gr-St-Sill, T=650-700°C, P=4-6 kbar). Under the increase of pyrope component in garnet from 10-12 to 20-22 mol.% the content of spessartine component decreases from 12-17 to 2-3mol.%.

The intrusion of collisional granites (PZ_3) resulted in the formation of contact-metamorphic zonation with clearly emphasized isograde (Bt-And-Cord-Kfs) which is superimposed on the earlier regional-metamorphic zonation. The study of regional and contact metamorphism relations revealed two varieties of garnet which differ in dimension, degree of

replacement with secondary minerals and composition. Garnet from contact areals have higher Fe-Mg ratio, outside contact areals being the varieties with increased MnO.

COOPERITE, BRAGGITE, AND VYSOTSKITE FROM THE MERENSKY REEF AND THE UG-2 OF THE BUSHVELD COMPLEX

Verryn S.M.C., Merkle R.K.W. and Winkels-Herding, S. (*Dept. of Geology, Univ. of Pretoria)*

Cooperite (ideally PtS), braggite (ideally(Pt,Pd)S), and vysotskite (ideally PdS) are some of the economically most important platinum-group minerals. In nature, however, these three minerals are best represented by the system Pt-Pd-Ni-S. The compositions of coexisting and individual cooperite and braggite grains from the Merensky Reef, as well as cooperite, braggite, and vysotskite from the UG-2 were investigated.

A clearly defined miscibility gap, as previously described by Cabri *et al.* (1978) exists between cooperite and braggite due to their different crystal structures. No evident gap between braggite and vysotskite can be detected.

Coupled substitutions of Pd+Ni for Pt are indicated (Verryn & Merkle, 1994). Within the cooperite, the Pd:Ni ratio for this substitution is approximately 9:11. This substitution may also include Rh and Co.

In braggite the same coupled substitution is evident. It has been shown that the Pd:Ni ratio can be changed by postmagmatic processes, which are reflected in the base-metal sulphide (BMS) assemblage. If the Ni-bearing phase in association with the braggite is pentlandite, the Pd:Ni ratio is about 7:3 (Merensky Reef). If, however, the dominant Ni-bearing phase is millerite (UG-2), the Pd:Ni ratio changes to about 3:1 and the analysis plot on the Ni-poor side of the trend established for the pentlandite association. These trends extend right down to vysotskite. This observed dependance of the Pd:Ni ratio on BMS assemblages indicates that the temperature of formation or re-equilibration rather than the availability of NiS plays the dominant role in the Ni-content of braggite and vysotskite.

Partition coefficients between cooperite and braggite are approximated through coexisting phases from the Merensky Reef. The $K_D^{braggite/cooperite}$ in atomic proportions were estimated to be 0.54 for Pt, 15.81 for Pd and 5.93 for Ni. Rh and Co seem to show a higher affinity for cooperite and the $K_D^{cooperite/braggite}$ in atomic proportions are >1.40 for Rh and >1.46 for Co. No systematic behaviour was detected for Fe and Cu.

The extend of the miscibility gap between cooperite and braggite/vysotskite is temperature dependant, the gap widening with declining temperature. Braggite, which has formed at high temperatures can therefore be expected to exsolve surplus cooperite component (PtS) on cooling. Braggite grains from the Merensky Reef show only minor intra-granular compositional fluctuations in comparison with braggite grains occurring in the vicinity of potholes and in "pockets" of the UG-2. Braggite grains from "normal" UG-2 are too small to allow comments on their heterogeneity. In the Merensky Reef, the braggite grains are often found to coexist with cooperite grains. SEM investigations on the braggite grains from the UG-2 in the vicinity of potholes or in pockets, however, revealed the presence of submicroscopic intergrowth of phases with different Pt/Pd ratios. These differences in intergrowths between braggite and cooperite (granular and submicroscopic) can be attributed to different postmagmatic histories of the two occurrences.

References:

Cabri, L.J., Laflamme, J.H.G., Steward, J.M., Turner, K., Skinner, B.J. (1978). *Amer. Mineral.*, **63**, 832-839.

Verryn, S.M.C. & Merkle R.K.W. (1994). *Min. Mag.*, **58**, 223-234.

SOLUTION CHEMISTRY CONTROL ON THE GROWTH KINETICS OF ARTIFICIAL AND NATURAL WULFENITE CRYSTALS

Vesselinov I. (Geol. Inst., Sofia, Bulgaria)

Wulfenite (point group 4/m) is a typical supergene mineral growing from aqueous solutions. It is widely known for its variety of growth forms and contrasting habits which indicate high sensitivity of its crystallization kinetics to environmental conditions. Two-circle reflection goniometry, optical and scanning-electron microscopy, chemical etching, x-ray and microprobe techniques have been used in this study to reveal some solution chemistry effects on the stationary growth morphology and surface structure of this mineral.

Crystals (size 0.1÷0.2 mm, $c/a = 2.233 \pm 0.013$) grown in the laboratory under ambient conditions from nitric acid solutions at mean growth rates of about 10^{-8} cm/s exhibit two contrasting habits depending on the Pb to MoO_4 ratio in solution (Vesselinov, 1980), and two form combinations depending on the nitric acid concentration. Lead-to-molybdate ratios lower than unity always produce tabular {001} habits, whereas ratios higher than unity result in dipyramidal crystals. At the same time, low-acid forms (pH 6 ÷ 2) are always bounded by flat {001} and {112} with minor and less common {011} whereas high acid forms (pH 2÷1) develop curved, convex {001} and {211} (or {121}) with minor flat {112}. Although curved, the faces of the habit forms in general position {211} and {121} are very smooth, showing no surface structure even at high SEM magnifications. Measured on the goniometer, they are characterized by variable curvatures, yet their signals remain grouped around the poles of {211} or {121} and the whole reflection pattern of a given crystal generally obeys the point group symmetry of wulfenite. For the purpose of this study they are called "curvihedra" to distinguish them from the "planihedral" simple forms like {112} with smooth flat faces.

Natural crystals (1 ÷ 5 mm in size) in a hand specimen from Mežice, Slovenia, grown in alkaline (carbonate) environment, show similar morphological features. Across a distance of less than 4 cm they change from thin {001} plates to steep {211} and {121} dipyramids. The latter are again convex, their faces, however, being no longer smooth but covered by growth hillocks.

All habit forms observed, both on the artificial and natural crystals, are shown to be stationary forms (Chernov, 1984), the crystals remaining geometrically similar to themselves throughout growth.

The morphological changes observed have been traced back to interface kinetics effects controlled by crystal structure//solution chemistry interactions in the boundary layer adhering to the crystals. A mechanism involving decomposition of polymolybdate complexes is proposed for explaining the habit changes due to the varying Pb-to-MoO_4 ratio. The appearance of the "curvihedral" habit forms is referred to increased oxygen in solutions; both in nitric acid (which is an oxidant) and in some alkaline environments it may stabilize growth forms defined by the oxygen framework in the crystal structure of wulfenite. The proposed picture of wulfenite growth has a number of verifiable implications concerning the coloration of its crystals, the polarity of some natural specimens (point group 4), the uptake of certain impurities, the equilibrium forms in different environments, and the atomic structure of "curvihedral" surfaces. Implications of more general nature will be also discussed.

References:

Vesselinov,I. (1980). 6th Intern. Conf.on Crystal Growth, Moscow. Ext.Abstr., IV, 198-199.
Chernov,A.A. (1984). Modern Crystallography, III, Crystal Growth. Springer, Heidelberg, 517 pp.

THE LOWER CRUST OF THE KOLA PENINSULA: THE METAMORPHISM AGE AND PROTOLITH COMPOSITION

Vetrin V.R. (Geol. Inst. Kola Sci. Centre, Apatity, Russia)

The rocks of the lower crust are studied in xenoliths from breccia pipes and explosive dikes of the southern part of the Kola Peninsula.

Xenoliths are composed of eclogites, garnet granulites, eclogite-like rocks, websterites, clinopyroxenites and chemically are referred to basalts of the tholeiites series. The intrusive rocks of gabbro- and gabbroanorthosite composition are conceived to be a protolith for these xenoliths. They metamorphosed under eclogite and granulite-facies conditions and undergone deep potassium metasomatism 1.74-1.70 Ga ago. The maximum values of the P-T parameters for the eclogite and pyroxenite are 870-930° C and 10-16 Kbar, whereas the temperature of the garnet granulite and eclogite-like rock formation does not exceed 800-830° C and 6-10 Kbar. Sm-Nd and Pb-Pb study of isotope systems has yielded predominantly on Upper Archaean and to a lesser degree an Early Proterozoic age for protoliths of the lower crust (T^{Nd}_{DM} from 2,39 to 2,94 Ga) with the stages of mineral metamorphogenic parageneses formation at 2,6;1,8 and <1 Ga ago. A correlation in the age of the oldest protoliths and also in the periodicity of major thermal events in the upper and lower crust is observed, while magmatic and metamorphic processes in the lower crust occurred 100-150 Ma later. It is believed that the time shift of similar geological events is caused by a low rate of the heat front transfer from the upper to lower crust in regressive stages of endogenic activation with a later "closure" of isotope systems in the lower crust rocks.

CONTROL OF Si, Al AND Na MASS TRANSFER BY THE VARIATION OF TEMPERATURE WITH TIME OR DISTANCE

O. Vidal, Dpt Géologie, Ecole Normale Supérieure, Paris

Goffé et al. (1987) experimentally showed that the transfert/transport of Si, Al and Mg is effective and driven by the temperature variations in a closed system. In order to extend the results to alkaline bearing systems, new experiments have been conducted in the system SiO_2-Al_2O_3-Na_2O/K_2O, with mixtures composed of pyrophyllite (prl), mica (pg; 70% paragonite) and quartz (qtz). Experiments have been conducted in order to investigate the eventual control of mass transfer by variations of temperature or pressure with time or distance (thermal gradient). Mixtures of reactants in various proportions were sealed in perforated gold capsules to enable exchanges of solution. The gold capsules were enclosed in a gold tube along with pure water, and disposed in a cold seal pressure vessel. After quenching, the walls of the tube were observed with a SEM, in order to identify which phases precipitated outside the capsule from the solution.

1) *variation of temperature and pressure with time:* Before changing temperature and/or pressure, the starting conditions were maintained constant for one week. Temperature or pressure was then increased from 300 to 500°C at 2 kbar and 400 to 500°C at 4 kbar or decreased from 480 to 300°C at 4 kbar and 500 to 250°C at 2.5 kbar by step of 5°C/day. When qtz did not crystallized, Na-clays, probably beidellite, crystallized. The growth of prl (± beid) was enhanced by a decrease of temperature, while the growth of mica was enhanced by an increase of temperature or a decrease of pressure.

2) *variation of temperature with space (thermal gradient: 370-460°C over 15cm, pressure = 3 kbar):* Amorphous SiO_2 precipitated in all experiments at the hot extremity of the tube. When the capsule was located at the **hot extremity** of the tube, for 1:1:2 mica:prl:qtz starting molar proportions, mica + qtz ± clays crystallized in the middle part of tube, and clays + qtz at the cold extremity. For 1:0.2:2 starting proportions, prl + diaspore (dsp) crystallized toward the cold extremity, followed by clays + qtz. For 1:1:1 starting proportions, we observed the succession: prl + dsp + mica, prl + dsp + clays, clays. When the capsule was located at the **cold extremity**, prl + dsp + clays, followed by prl + mica + dsp, then by mica + dsp crystallized toward the hot extremity for 1:1:1 starting proportions. The succession qtz, prl + qtz and prl + pg has been observed for 1:1:2 starting compositions from the cold to the hot extremity.

These results give evidencies for mass transfer of Si, Al, and Na, exclusively controlled by changes of temperature in a closed system. Moreover, the spatial distribution of the phases is consistent with local equilibrium among aqueous and solid phases, so that the interpretation of the experimental results in term of activity diagrams appears warranted. The various sequences of crystallization are in agreement with the thermal evolution of the phase relations between mica, prl, beid, qtz or dsp, depicted in Log(H4SiO4)aq vs aNa+/H+s diagrams. Another important point is that the sequences of crystallization give informations about the respective thermal stability of the phases which occur, and the possible breakdown reactions in an isobaric section of the P-T field: This is particularly well illustrated by the progressive replacement, with decreasing temperature, of amorphous SiO_2 by quartz (in presence of mica), which is then overgrown by clays. This is also demonstrated by additional experiences realized in presence of prl + qtz at the hot extremity, leading to the crystallization of prl (transport of Si and Al) which is replaced by kaolinite toward the cold end of the tube.

The crystallization of Na-clays up to 460°C is in agreement with the observations of Chatterjee (1973). The fact that it formed in silica undersaturated conditions is in agreement with the approach of Giggenbach (1984), who described beidellite as an intermediate term of a theoretical solid solution between mica and pyrophyllite.

Goffé et al. (1987) Contrib. Mineral. Petrol., 97, 438-450
Chatterjee (1973) Contrib. Mineral. Petrol., 42, 259-271
Giggenbach (1984) Geochim. Cosmochim. Acta, 48, 2693-2711

CHEMICAL EVOLUTION FROM DETRITAL HYDRATED MICAS TO Mg-SMECTITES ORIGINATED IN THE DIAGENESIS OF NEOGENE LACUSTRINE SEDIMENTS IN THE MADRID BASIN

Vigil de la Villa, R., Cuevas, J., Garralón, A. and Leguey, S.
Dept. Química Agrícola, Geología y Geoquímica. Facultad de Ciencias, Univ. Autónoma de Madrid.

The neogene sedimentary basin of Madrid is characterized by several lacustrine episodes located in the miocene intemediate unit where Mg-smectites and sepiolite constitute the main mineralogical assemblages. The scope of this study is to analyze the chemical composition of hydrated micas present as the more common accessory minerals in the argilaceous sediments and their relation to Mg-smectites.

Some samples have been selected from the lacustrine episode

of Vicalvaro (Madrid) where sepiolite deposits are mined. The agillaceous sediments exhibit mineralogical zonal patterns that are related with different diagenetical processes . Deeper zones shows dark clays with salts and organic matter, being the sediment of arkosic origin. This is characterized by the predominance of illite and Al-smectites from the botton to the edge facies. In the intermediate zones, green clays of saponitic composition followed by whitish and ,occasionally, destratified materials of stevensitic or sepiolitic composition are the main mineralogical associations observed. The origin of this clays has been interpreted either as superficial processes where paleosoils have been developed in the presence of carbonated materials or linked to the evolution of deep regional groundwater flows influencing the lacustrine sediments.

Four clayey fractions (2-5μm, 1-2μm, 0.5-1μm and $<0.5\mu$m) has been separated by repeated dispersion and centrifuging of sediment suspensions involving illitic dark clays, saponitic and stevensitic assemblages. SEM-EDX punctual analyses have been performed. In the first two coarser fractions individual mica shaped platelets have been analyzed. The range of composition in the smaller fractions is obtained by performing several punctual analyses on a precompacted sample. Figures A and B shows a MR3-3R2-2R3 chemiographic plot of the composition obtained from the saponitic and the stevensitic assemblages. The saponitic assemblage contains almost exclusively micaceous minerals in the 0.5-5μm range being the coarser fractions a virtually unaltered mixture of dioctahedral mica , biotite and celadonitic compositions whereas $<0.5\mu$m composition are segregated to a saponitic pole. In contrast, mica shaped platelets analyzed in the stevensitic assemblage ressembled rich Mg altered micas including some stevensitic compositions, being the range of 1-$<0.5\mu$m shifted to the stevensitic pole. This difference has been interpreted as a more severe diagenetic alteration process, probably by means of the existence of more alkaline Mg-rich waters producing the stevensitic assemblages.

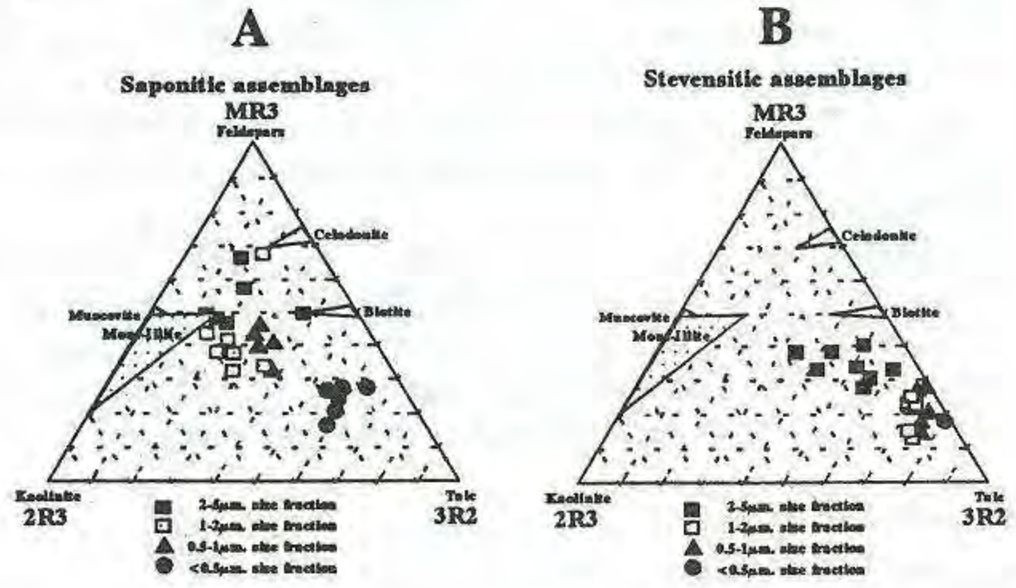

FLUORINE-BEARING METAMORPHIC MINERALS OF MASSIVE SULFIDE DEPOSITS

Vikentyev I.V., Laputina I.P. *(Institute of Geology of Ore Deposits, Petrography, Mineralogy and Geochemistry, Russian Academy of Sciences).*

Presence of fluorine has been found in ores and wall rocks of some massive sulfide deposits of FSU - on Cu deposits of the Caucasus (Gavriljuk et al., 1991), Cu-Zn deposits of the Urals (e.g. Pshenichny, 1982), Pb-Cu-Zn deposits of the Roudny Altai (Prokofyev et al., 1988). Nonetheless the F-bearing minerals have been unknown with the exception of the deposits of the Shemur ore field, the North Urals, where F and Cl were found in apatite (Holodnov et al, 1990). Authors using microprobe analyses studied mineral assemblages of rocks and ores of the biggest object of the Roudny Altai - Tishinskoye deposit (East Kazakhstan).

Mineral assemblages of the enclosing Middle Devonian volcanic rocks (dominant quartz, sericite, chlorite) correspond to the upper prehnite-pumpellyite and the greenschist facies of regional metamorphism (T=150-400^{o}C, P=0,5-3 kbar).

Metamorphic association of elevated alkalinity occurs along some late subvertical fractures and represents by quartz, sericite, carbonates and albite. Apatite, pyrite, rutile, sphene, muscovite, epidote, zoisite and biotite are less common. Previously unknown at the deposit garnet, fluorite and xenotime have been established in this association. These metamorphic rocks are marked by increased contents of the volatiles - F, P and B and some rare and TR elements.

F-OH-apatite (F=1.90-2.50%) contains trace elements - Sr, Y, Zn, sometimes Ba and Ce. F-content increases with the depth. The presence of F, occasionally Cl and Y has been discovered at carbonates. The composition of the carbonates changes in the vertical section (more than 1 km). At the upper horizons ankerite (F=0.07-0.10%) is wide-spread. F-bearing Fe-dolomite, F-Cl-bearing calcite (F to 1.14%, Y to 0.31%) and Cl-bearing Mn-breunnerite are common at the lower levels.

Garnet belongs to the pyrope-almandine-spessartite series with a predominance (62%) of the almandine component. Formation of this association occurred in the tectonic-metamorphic peak at T=600-250^{o}C.

References:

Gavriljuk, P.S., Magribi, A.A., Rusinov, V.L, Nosik, L.P. (1991). *Geologiya rudnih mestorojdeny (Geology of Ore Deposits)*, No 1, 56-68 (In Russ.).

Prokofyev, V.Ju., Vedjaeva, I.V., Koritov, F.Ja., Stepanova, T.P. (1988). *Geochemistry*, No 6, 834-842, (In Russ.).

Pshenichny, G.N. (1982) In *Mineral geochemical features of ore-bearing formations of the South Urals*, Ufa, 3-12, (In Russ.).

Holodnov, V.V., Artemenko, N.A., Vilisov, V.A. (1990). In *Mineralogy of the Urals deposits*, Sverdlovsk, 88-90, (In Russ.).

Do geochronometers ever lose radiogenic daughters by Fickian diffusion?

Igor M. Villa (Isotopengeologie, Erlachstrasse 9a, 3012 Bern, CH)

Understanding the timing of the p-T history of a rock involves many problems, of which the following two are central:
1. By what mechanism are geochronometers rejuvenated in nature?
2. Can we mimic natural diffusion by laboratory experiments?
The two questions are usually addressed by non-communicating groups which assume that the answer to the other question is simple (1 - Fickian diffusion, 2 - yes).
Indeed there may be exceptional cases where natural exchange is understood and laboratory data are internally and externally consistent. Divalent cation transport in gem garnets appears to follow a single mechanism (albeit non-Fickian due to its non-zero cross terms [3]). Micron-resolution electron microprobe profiles can be inverted and form the basis of geospeedometry [8].
Unfortunately geochronological techniques, unlike petrological ones, require use of bulk samples and spatial resolution is usually much worse than 100 μm. At this scale, natural samples show a palette of microstructures [2]. Gems are geological freaks whereas mineral geochronometers generally used to reconstruct p-T-t have

mineralogies that range from very complex to extremely complex [10]. Thus, if diffusion were occurring, it would not be Fickian diffusion but multipath diffusion [9].
The problem is, the very few field studies that examined regional age distributions as a function of chemical composition in bitites [1] and amphiboles [4] failed to detect any influence of the lattice field on cooling ages, implying that recrystallisation (or other phenomena that do NOT depend on the lattice field) predominates over lattice diffusion by orders of magnitude.
Finally, laboratory data on diffusivity in geochronometers are mostly confined to Ar or O (e.g [5,6]) with very scant Sr data [7]. But the hydrothermal experiments entail water oversaturation which is quite rare in nature, so a number of artefacts are likely to occur, at least one of which, dissolution/reprecipitation, has been documented [12]. Another technique, in-vacuo degassing of K-feldspars to obtain simultaneously a 39Ar/40Ar age and a Fickian diffusion coefficient, has been shown [11] to be based on an incorrect experimental protocol. Even zircons gems do not follow Fickian diffusion when Kr and Xe are degassed in vacuo [13].
Conclusion. It does not appear that a single case of bona fide Fickian diffusion of radiogenic isotopes has been reported so far in mineral geochronology. Geochronometers use many ways to look younger than they are, and there is no reason to believe that laboratory treatments follow physical mechanisms resembling these.

[1] Blanckenburg & Villa, Contrib Min Pet 100 (1988) 1
[2] Burgess et al, Earth Plan Sci Lett 109 (1991) 147
[3] Chakraborty & Ganguly, Adv Phys Geoch 3 (1983) 120
[4] Cosca & O´Nions, Chem Geol 112 (1994) 39
[5] Fortier & Giletti, Geoc Cosm Acta 55 (1991) 1319
[6] Giletti, Carnegie Spec Pub 634 (1974) 107
[7] Giletti, EOS 62 (1991) 428
[8] Lasaga, Adv Phys Geoch 3 (1983) 81
[9] Lee & Aldama, Comput Geosci 18 (1992) 531
[10] Veblen, Kyoto workshop, 1992
[11] Villa, Earth Plan Sci Lett, April 1994
[12] Villa & Puxeddu, Contrib Min Pet 115 (1994) 415
[13] Villa, Eikenberg, Lehmann, Schweiz Min Pet Mitt, 1994

Calculation of the configurational entropy of a solid solution with short range order restrictions based on computer simulation.

Vinograd V.L. *(Theoretical Geochemistry, Institute of Earth Sciences, Uppsala University)*

New constructive statistical method was used to simulate mineral lattices with short range order (SRO) restrictions. Examples are given for framework silicates (albite, anorthite, cordierite), micas (phlogopite-eastonite) with strict Al-avoidance on tetrahedral sites and spinel $(Mg_{1-x}Al_x)(Mg_xAl_{2-x})O_4$ with Mg-avoidance on octahedral sites. The method enables one not only to simulate a lattice and a solution with a particular SRO restriction but also to calculate the configurational entropy of this solution. The method gives better result compared to the well known quasi-chemical model, because only physically real configurations are taken into account. The lattice can be constructed from building units (atoms, pairs, triangles, tetrahedra etc.) which are successively placed in lattice site. The probability of placing a particular type of building unit is obtained with the help of an original computer algorithm described in Vinograd & Perchuk (1992). The probabilities obtained as a result of computer simulation are used to calculate configurational entropy through simple statistical thermodynamic relations. Using different types of building units and different directions of lattice growth one can introduce different kinds of long range order (LRO) into the model. The result of calculation of the configurational entropy depends on the presence of LRO. It was found that in certain cases solution with LRO can possess larger value of the configurational entropy compared to a solution in which LRO can not arise due to particular growth mechanism and formation of out-of-step boundaries. Second Pauling rule as a guide for SRO restrictions in solid solutions is discussed.

References:
Vinograd, V.L., Perchuk, L.L. (1992): Vestnik Moskovskogo Universiteta, ser.4, N 3, 45-59.

SPODUMENE, PETALITE AND CASSITERITE, NEW OCCURRENCE IN HIMALAYAN LEUCOGRANITE PEGMATITES: PETROLOGICAL IMPLICATIONS.

Visonà D. and Zantedeschi C. (*Dept. of Mineralogy and Petrology, Univ. of Padova, Italy*)

The high Himalayan crystalline (HHC) thust sheet is injected by numerous crust-derived leucogranites, generated after the Eocene collision of India with Eurasia.

In the Chomolungma (Everest)-Cho Oyu area, the basement contains a network of dykes, sheet-like bodies and diapires of Miocene leucogranite (Lombardo *et al.*, 1993). These two-mica tourmaline-bearing often contain aluminous minerals like garnet, andalusite, sillimanite and cordierite. and are characterized by a typical geochemical pattern of enrichment in light elements (Scaillet *et al.*, 1990).

Spodumene, petalite and cassiterite have been found in two pegmatites of a leucogranite pluton cropping out NW of Cho Oyu. These pegmatites are composed of Qtz + Ab + Spd + Kfs, with minor petalite, tourmaline, garnet and cassiterite. Spodumene forms euhedral, light yellow-green (hiddenite) crystals (up to 10 cm), while petalite and cassiterite are represented by microscopic crystals. Petalite has been found only in one of the two sampled outcrops and forms a discontinuous composite shell around spodumene. In this case, spodumene shows a myrmekitic rim with Qtz and Kfs drops; the inner part of the shell contains Kfs + Ab + Qtz + petalite while, the outer part is composed only of fine-grained crystals of petalite.

As the lithium alumosilicate phase diagram constitutes a petrogenetic grid (London, 1984), petalite + Qtz and Spd + Qtz assemblages can be used for geothermo-barometric considerations. In detail, petalite + Qtz after Spd + Qtz assemblages indicate crystallization at $T < 670$ °C and $P < 0.45$ GPa. As the two outcrops are very close to each other, it may be stated that the Li-rich pegmatitic melt was around the triple point of the lithium alumosilicate at $T \approx 670$ °C and $P \approx 0.45$ GPa.

References:
Lombardo, B., Pertusati, P., Borghi, S. (1993). *Geol. Society Special Paper Pubblication*, **74**, 341-355.
London, D. (1984). *Am. Miner.*, **69**, 995-1004.
Scaillet, B., France-Lanord, C., Le Fort, P. (1990). *J. Volc. Geoth. Res.*, **44**, 163-188.

Antigorites from Elba Island, Italy

Viti C. and Mellini M. (Dip. di Scienze della Terra, Universita' di Siena, Italy)

Contamination, deformation, crystal sizes and defects hamper knowledge of serpentine. A few drawbacks may be overcome by studying veins: just one phase often occurs, with no deformation and favourable crystal growth. So, we sampled the splintery veins from the Elba Island serpentinites, with the aim of deriving reliable data for antigorite.

Polysomatism: The structure modulation, with variable a periodicity and variable composition (the shortest the parameter the highest the brucite loss), was determined by electron diffraction: the range extends from 33 to 49 Å, with no prevailing value. At difference from rock-forming antigorite, no relation between polysomatism and outer conditions has been found.

Chemical and physical properties: TEM-EDS analyses bracket the compositional range
$M_{2.77}T_2$ and $M_{2.84}T_2$,
with M typically 0.92Mg+0.07Fe+0.01Al. Wet chemical analyses indicate iron completely present as Fe^{2+}. Loss of ignition is 12 wt.%, significantly lower than for other serpentines (12.6 for vein lizardite). Specific gravity plots in the 2.60-2.62 range.

Spectroscopic data: I.R. distinctive features are the bands at 3677, 1083, 986, 970 (shoulder), 635(shoulder), 618, 568, 544, and 444, 399, 392 cm^{-1}. NMR-MAS shows a wide band (-88 ppm), broadened by paramagnetic iron.

Hopefully, these chemical, physical and spectroscopic data may help in constraining the structure model. However, we are left with one problem more, which is to explain the different polysomatic behaviours of vein and rock-forming antigorite.

THE EFFECT OF TEMPERATURE ON FLUID INCLUSION RE-EQUILIBRATION BEHAVIOR UNDER CONDITIONS OF COMPRESSIVE LOADING

Vityk, M.O., and Bodnar, R. J., *(Fluids Research Laboratory, Department of Geological Sciences, Virginia Tech, U.S.A.)*

The effect of temperature on the re-equilibration behavior of fluid inclusions is poorly understood. Conceptually, one would expect the re-equilibration process at low temperatures, where minerals behave brittly, to be fundamentally different from processes acting at higher temperatures where ductile deformation becomes more important. Accordingly, different styles of fluid inclusion re-equilibration should be expected for different temperature environments. Most earlier published experimental studies of re-equilibration at elevated temperature were conducted under isothermal conditions and did not consider the effect of temperature on the style and ease of re-equilibration. We have initiated short term (7 days) experiments to examine re-equilibration of natural fluid inclusions in quartz under conditions simulating compression at 300°, 500° and 700°C and 1, 2, 3, 4 and 5 kbar in an isotropic stress field. The inclusions were formed at 350°C and 0.12 kbar - the re-equilibration conditions were thus 50° lower and 150° and 350°C higher than the formation temperature.

After re-equilibration at 300°C and 4 and 5 kbar of confining pressure (approximately 3.9 and 4.9 kbar effective pressure, defined as the difference between the confining pressure and the internal pressure in the inclusion), the fluid inclusions showed evidence of brittle deformation, producing a star-like fracture pattern. Much lower effective pressure (approximately 2.8 kbar) produced morphologically similar inclusion textures at 500°C. In both cases, at 300° and 500°C, the first evidence of re-equilibration was observed for small inclusions. Decrepitation of fluid inclusions under conditions of compressive loading up to 5 kbar of confining pressure (about 4.8 kbar of effective pressure) is controlled by corrosive action of water on the inclusion walls (subcritical crack growth) and is consistent with the known relationship between solubility, size and surface free energy predicted by the Kelvin equation.

After re-equilibration at 700°C and 3 and 4 kbar of confining pressure (about 2.7 and 3.7 kbar of effective pressure), all of the fluid inclusions (regardless of size) were deformed in a ductile manner as recrystallization and diffusion flow and other thermally activated processes begin to affect the strength of the host phase. After re-equilibration, the fluid inclusions showed specific deformation features manifested as dissolution of the inclusion walls to produce a scalloped or wave-like texture. The intensity of deformation features showed a positive correlation with amount of internal underpressure. After re-equilibration at 5 kbar and 700°C (about 4.7 kbar of effective pressure), which corresponds approximately to the α/β transition for quartz, the inclusion exhibited a cataclastic behavior.

It is clear that otherwise similar fluid inclusions at similar internal underpressure conditions show different re-equilibration behavior depending on the temperature at which re-equilibration occurs. Specifically, under conditions of hydrostatic compression at temperatures up to 500°C, deformation of the inclusion walls occurs in a brittle manner. During compression at higher temperature (700°C), re-equilibration of fluid inclusions is accommodated by plastic flow of the inclusion walls. At high temperature all inclusions, regardless of size show textures of similar intensity, distinct from the negative correlation between intensity of re-equilibration features and inclusion size at lower temperatures.

THE URAL KYANITE ORES AS THE RAW MATERIAL FOR THE PRODUCTION OF HIGH-QUALITY REFRACTORIES AND SPECIAL CERAMICS.

Vladimirov V.G., Zhirakovsky V.Ju., Lepezin G.G., Perepelitsin P.A., Sokol E.V. (*Institute of Mineralogy & Petrology, Novosibirsk; East Institute of Refractories, Ekaterinburg, Russia*)

At the present time the sillimanite minerals are industrially important in developed countries and are in demand wherever high temperatures and chemically-aggressive processes such as the smelting of metals and making of glass are carried on.

The most important producing countries are the Republic of South Africa, the United States and India. Russia having many large-scale deposits does not exploit it. Authors have investigated the most part of provinces of this raw materials on the territory of FSU and got to the conclusion that Russia have the reliable base for the production high-quality refractories and special ceramics. Among the Russian kyanite deposites the Ural ones have a great commercial importance, because of they are situated in the developed industrial region, including ferrous and non-ferrous metallurgy, glass, refractions, ceramics productions. The typical analysis of kyanite ores, concentrates and kyanites are summarized in tabl.1. Physical properties of calcined products and commercial finished productions are given in tables 2 and 3.

Tabl. 1

Chemical compositions of kyanite ores, concentrates and kyanites from the Ural.

SiO_2	TiO_2	Al_2O_3	Fe_2O_3	MnO	MgO	CaO	Na_2O	K_2O
Ores (n = 113)								
79.02	0.55	17.93	1.70	0.03	0.10	0.05	0.34	0.29
Concentrates (n = 5)								
38.38	0.35	60.64	0.40	0.03	0.00	0.03	0.00	0.06
Kyanites (n = 20)								
36.64	-	62.38	0.20	0.01	0.00	-	0.00	-

Tabl. 2

Refractoris characteristics of kyanite concentrates	Temperature (°C)				
	1200	1300	1400	1500	1600
Linear changes (%))	2.79	5.67	16.3	9.6	6.1
Specific gravite (g.p.c.c.)	3.55	3.24	2.80	2.95	2.98
Bulk density (g.p.c.c.)	1.98	1.72	1.47	1.70	1.72

Mullite products from Ural kyanite may be widely used in iron steel industry and in non-ferrous metallurgy. It should be particularly emphasized that the morphological features of kyanite crystals and its high chemical purity has made possible to produce same special sorts of ceramics.

Tabl. 3

Characteristics of the refractory products		
Refractoriness (°C)		1800
Latent porosity (%)		14.2
Compression strength (Nuton per sg.mm)		210
Refractoriness-under-load 0,2 (Nuton per sg.mm) rising:		
Temperature test (°C):	initial deformation	1560
	4% - deformation	1610
	40% - deformation	1650

Geochemical model processes of the differentiation of K-alkaline rocks from Aldan, Russia.

Vladykin N.V. (Institute of Geochem. Irkutsk)

The geochemistry, petrology and mineralogy of K-alkaline rocks of the Aldan province of K-alkaline rocks have been comprehensively studied. A new scheme of magmatism for the entire Aldan province of alkaline rocks has been developed. The geochemistry of reference massifs of the province was studied in detail. In the Murun and Bilibinsky massif there was for the first time discovered a complete series of K-alkaline rock differentiates: from alkaline-ultrabasic (Bt-pyroxenites) through basic (shonkinites), average (pseudoleucite syenites) to acid (alkaline granites). Lamproites - new type of diamond-bearing deposits were discovered in many massifs of the province and for the first time in Russia. The mineralogy of unique charoite rocks was studied in detail. The temperature of formation of the entire series of differentiates of the Murun massif and their final members charoite-carbonatite complex and a total range of temperatures from 1500′ to 750′ have been obtained. The charoite-carbonatite complex was proved to be formed from a residual melt-fluid with temperature of crystallization from 750′ to 550′. The distribution of petrogenic rare elements and spectra of rare-earth elements substantiates the fact that rocks refer to the same genetic series. Geochemistry of Sr-, Nd- and Pb-isotopes indicates a deep mantle source of formation of K-alkaline magma.

THE COMPOSITION AND TEMPERATURE OF THE EARTH'S CORE

L N Vočadlo, G D Price and J-P Poirier (Research School of Geological and Geophysical Sciences, University College London and Birkbeck College, London, and Institut de Physique de Globe de Paris)

The composition and temperature of the Earth's inner and outer core are currently ill-constrained. Although it is believed that the inner core is close to pure Fe, and the outer core is predominantly liquid iron alloyed with one or more lighter elements to account for the observed reduced density, there are currently no over-riding reasons to favour any one of the candidate elements (viz. C, O, S, or Si). Current estimates of the melting point of pure Fe at inner core pressures range between 4000K and 7000K. If the inner core is crystallizing from the liquid outer core, it will be necessary to assess the suppression of the liquidus temperature cause by the lighter elements if estimates of the inner core temperature are to be estimated. It is desirable therefore to establish the properties of the multicomponent system Fe-C-O-S-Si. Although much is known of the subsolidus phases in this system, the behaviour of the liquid system at high T and P is less well understood. To enhance our understanding of this system, we are developing an ionic mixing model between the potential components in the liquids that can develop in Fe-C-O-S-Si system, and are using the thermodynamic database, MTDATA, to calculate ternary phase diagrams for the Fe-C-S and Fe-S-Si systems as a function of temperature and pressure. We will present the results of our calculations and make some predictions on the pressure dependence of the liquidus temperature and eutectic composition of these two systems, and the possible implications for core temperature and composition.

CRYSTAL STRUCTURE OF SYNTHETIC ZIPPEITE

Vochten R., Van Haverbeke L. (Dept. of Chemistry, Univ. of Antwerpen), Blaton N., Peeters O. (Dept. Pharmaceutical Sci., Univ. of Leuven) and De Grave E. (Dept. of Subatomic and Radiation Physics, Univ. of Gent).

Zippeite is a basic potassium uranyl sulphate, easily formed in nature. It occurs as a yellow earthy efflorescences so that single crystal studies are impossible.
Synthetic crystals of zippeite were obtained in a pressure bomb at 150 °C and a corresponding pressure of ± 25 atm. by the reaction of UO_2SO_4 at pH 3.6 in the presence of an excess of KCl.
The well formed crystals, ranging from 0.1 up to 0.2 mm are best suited for single crystal studies.
From chemical analysis and crystallographic data the formula $K(UO_2)_2(SO_4)(OH)_3.H_2O$ is proposed.
Furthermore, the synthetic material is characterized by its infrared-luminescence spectrum and its solubility product.
The synthetic zippeite is biaxial negative with $\alpha = 1.625 \pm 0{,}001$; $\beta = 1.710 \pm 0.002$; $\gamma = 1.740 \pm 0.002$; $2V \approx 59°$.

The lattice paramters are:
space group C 2/c

a= 8.7554 (30)Å	b= 13.9866 (70)Å
c= 17.7298 (67)Å	β= 104.127 (34)°
Z= 8	ϱ= 4.7 g/cm^{-3}

The structure consists of very condensed uranyl-sulphate layers, between which potassium ions and water molecules are persent.
The structure will be proposed and discussed.

ON THE ROCK IN TEACHING MINERAL SCIENCES

Voitekhovsky Yu.L. (Geol.Inst.,Kola Sc.Centre, Russian Academy of Sciences)

Modern mineral sciences consider and classify rocks with respect to their relation to rock-forming geological processes, as a rule. But it must be admitted that the backbone of

this nature phenomenon must be understood,firstly,in pure structural (nongenetic) aspect. Just such kind of understanding should lay in the basis of teaching what is rock.

Some mathematical ideas can help us to put forward this problem,namely:
- the Set Theory axiomatics by E.Zermelo gives the possibilities to imagine rock as a nonhierarchic set of its own elements (mineral grains,subaggregates etc.),
- the Structure Theory allows to imagine this set as an algebraic structure in respect of the order relation to be determined,
- in a special case of rock being imagined as a so-called algebra of elements one may determine a quantitative measure of rock ordering,
- the variety of rock ordering types may be described and classified in terms of the Quadratic Form Theory.

So,we have a chance to build in this way a pure structural background of the knowledge about rocks and to give a new formulation of a number of questions about their classification and structural evolution in geological processes.

CONCERNING THE INCORPORATION OF ANIONS IN THE HYDROXYL SITE OF SILICATES

Volfinger M. – *CNRS-CRSCM Orléans.*

The knowledge of the crystallochemical control of the partitioning of elements between aqueous solutions and minerals is needed to make correct interpretations of fluid-rock interactions. Only from the crystalline point of view, during the incorporation of an ion into the mineral structure in hydrothermal equilibria, the fluid is a source which serves as reference media to express the partition coefficient. In the case of monovalent substitutions of metal cations, the partititon coefficient k_X (silicate / fluid) is a function of the absolute value of the difference $\delta_C = |r_C - r_+|$ between the effective coordination radius r_C of the crystalline site and the ionic radius r_+: k_X increases with δ_C [1]. Here, the speciation in solution, as cations or associated species, has only a weak effect on the value of the partition coefficient k_X because the ratios X^+/M^+ and $XCl°/MCl°$ are quite similar.

In case of substitution of the anion chlorine in hydroxyl site of a silicate from a hydrothermal fluid [2], it is not the same because the aqueous solvent must be considered in the exchange reaction. The partition coefficient k_{Cl} is measured with very different values depending on how the species in fluid are reported, e.g. $HCl°/H_2O$, Cl^-/OH^- or $MCl°/MOH°$. On the other hand, the dipole OH^- can adapt to coordinence dissymetries, cationic variations and structural deformations inside each individual crystalline sites because of possible O-H stretching [3], whereas it seems that the spherical larger Cl^- anion should less easily substitute in this site. It is then important to know if the anions obey the same crystallochemical rules of partition as the cations. In other words, does the above sterical model of cations subtitution also apply to anions in contact with the oxygens of the crystal lattice ?

An answer is provided by calculating the best adaptation of the k_X equilibrium constants of the Cl exchange to the "V" curve [1] of the cation model. Thus, two sets of crystalline parameters δ_C and two other of parameters in aqueous solution X/M are used to calculate four possible positions of the right side of the "V" curve $\log k_X = f(\delta_C)$. In solution, the ratios of dissociated to associated species are linked by the concerned molal disssociation constants k_D which have a large departure from HCl to H_2O: $(Cl^-/OH^-)/(HCl°/H_2O) = k_D(HCl)/k_D(H_2O)$. In the solid phases the two kinds of ionic distances considered are M^{2+}(or M^{3+}) – OH^- and the shortest O^{2-} – OH^- distances in the sites where Cl^- is incorporated. Phlogopite, annite, muscovite, paragonite, pyrophyllite, talc, tremolite, actinolite are the phases which were hydrothermaly synthetized (500 or 600°C; 1, 2 or 3 kbar) to perform experiments concerning the anion exchange.

The results show that only the cation-anion distances around the $OH^-(Cl^-)$ position in the crystal structure and the ratio of ionic species Cl^-/OH^- in the aqueous solution have to be considered to determine a consistant k_X function versus δ_C whatever the sign of the ion. Consequently it is possible to estimate the incorporation rate of the anion (or cation) in a given crystal lattice knowing its structural parameters, which is very useful when the contents are too low to have confidence in normal quantitative determinations.

References:
[1] Volfinger M. and Robert J-L. – *GCA, 44, 1980.*
[2] Volfinger M., Robert J-L., Vielzeuf D. and Neiva A.M.R. – *GCA, 49, 1985.*
[3] Robert J-L., Bény J-M., Della Ventura G. and Hardy M. – *EJM, 5, 1993.*

THE EVOLUTION OF CRYSTAL STRUCTURE MOTIFS OF THE COMPLEX NB-TA OXIDES IN THE NATURAL PROCESSES OF MINERAL REPLACEMENT

Voloshin A.V. (*Geol.Inst. Kola Sci.Centre RAS, Russia*)

New specific natural systems of Nb-Ta mineral forming processes evolve in rare metal granitic pegmatites at the later stages of their development to cause crystallization of new mineral species and mineral phases resulting from metasomatic alteration of primary Nb-Ta mineral forms. In the general evolution of Nb-Ta mineral forming processes, the oriented change of crystal structure motifs follows paths, the motif elements of structure being preserved: island-chain, island-framework-layered. The direction of the processes is controlled by minimization of the energy losses during transformations of crystal structures from early to new mineral phases.

The same two trends in motif formation, layered and framework, are distinguished in the development of minerals of the a-PbO_2 (ixiolite) structural type. Both motifs are not final. In fact, the framework motif of ixiolite is considerably lower in organization than that of layered tantalite as well as the latter is lower than the framework motif of wodginite. In this case, the above succession already reflects the relationships of the minerals in terms of the time of their formation, i.e. later minerals are characterized by more organized arrangement in one structural type with high degree of

differentiation of the cations on position, or different structural types (Table).

The instability of crystal structures of stibiotantalite group minerals and thoreaulite-foordite is caused by the presence of combined ion-covalent bonds. A topologic affinity of the stibiotantalite structure to pyrochlore and perovskite structural types determinates the exclusive capability of stibiotantalite to be replaced by microlite and other minerals with pyro-

Table. Structural types of newly formed minerals in the zones alteration and replacement of primary tantalo-niobates

Structural type	Simpsonite	Group Stibiotantalite	Thoreualite Foordite
a-PbO_2 (Ixiolite)	Ixiolite Tantalite Wodginite	Tantalite Fersmite	Ixiolite Lithiotantite Lithiowodginite Fersmite
ReO_3 (Perovskite)	Stibiotantalite Alumotantite	Rynersonite	
Pyrochlore	Microlite Cesstibtantite	Microlite Cesstibtantite Natrobistantite Stibiomicrolite Bismutomicrolite	Microlite Cesplumtantite
Rutile	Cassiterite Tapiolite		Cassiterite
$CaTa_4O_{11}$ (Calciotantite)		Calciotantite $CaTa_6O_{16}$	Calciotantite Irtyshite
TTB (Tetragonal Tungsten Bronze)	Rankamaite Sosedkoite Natrotantite $NaTa_5O_{13}$	Sosedkoite	Rankamaite

chlore structural type.

The ways of formation of tetratantalates as a result of replacement of microlite and in other associations are based on the topological and crystal chemical affinity of elements of pyrochlore structure with elements of structures where a sevenfold coordination for Ta in the shape of pentagonal bipyramid is realized.

High-Ta mineral phases commonly crystallize in the structural types with the sevenfold coordination of Ta, and the models crystal structures of these compounds are to a great extent similar to the structure of the most stable Ta_2O_5 modification.

MAFIC MINERALS WITH UNUSUALLY HIGH Mn-CONTENTS IN THE PERALKALINE ACID LAVAS FROM BELOGOLOVSKY VOLCANO, CENTRAL KAMCHATKA

Volynets O.N.(Inst. of Volcanic Geology and Geochemistry Academy of Sciences, Russia)

The lavas from the Late Pliocene - Early Pleistocene Belogolovsky volcano, Central Kamchatka, belong to meadly peralkaline differentiated rock series: transitional basalt-benmoreite-trachyte-trachyrhyolite-comendite.All rocks are leucocratic with low contents of mafic minerals. MnO concentrations in the bulk rock compositions decrease from basalts (0.16-0.18 wt.%) to comendites (0.05-0.06 wt.%), however, MnO contents in mafic minerals and their Mn-distribution coefficients (K_D^{Mn}) increase in this direction. The K_D^{Mn} for mafic - mineral phenocrysts from alkaline trachytes and trachyrhyolites (22-24 for olivines, 25-30 for clinopyroxenes,34-48 for magnetites, 55-80 for ilmenites) are close to values that were found in some high-silica peralkaline and metaluminous lavas (Guerin et al.,1980;Mahood & Hildreth 1983; Mahood, 1981; Nash, 1985). However, MnO contents in mafic minerals from acid lavas in our case are higher 2.0-3.5 wt.% in clinopyroxenes, 2.7-4.2 wt.% in magnetites, 4.4-6.7 wt.% in ilmenites, but for fayalites where MnO content is similar (3.4-3.5 wt.%). The maximum MnO concentrations (just as the maximum K_D^{Mn}) were defined in microlites of mafic minerals from comendite: 4.7-7.4 wt.% in sodic pyroxenes, 5.0-7.8 wt.% in alkaline amphiboles, 7.9-9.6 wt.% in magnetites, and even 15.6-22.7 wt % in ilmenites. Earlier mafic minerals with such high MnO-contents had been found only in some pegmatites and metamorphic rocks (Deer et al., 1963). It was found for many rare elements that K_D mineral-melt strongly increase when rare element concentrations decrease (Antipin et al., 1984). This phenomena are explained by the increasing difference between effective and equilibrium values of K_D.

Support for this research was provided by Russian Foundation of Fundamental Investigations (Grant 93-05-8521).

References:

Antipin, V.S., Kovalenko, V.I., Ryabchikov, I.D.(1984). Distribution coefficients of rare elements in magmatic rocks. Moscow, Nauka, 252 pp.(in Russian).

Deer W.A., Howie,R.A., Zussman,J. (1963). Rock-forming minerals, 2, 406 pp.

Guerin, H., Blanchard, F., Nativel, P.(1980). C.R.Acad. Sci., D229, 24, 1509-1512.

Mahood, G.A. (1981). Contrib. Mineral.Petrol., 77, 2, 129-149.

Mahood, G. & Hildreth, W. (1983). Geochim. et Cosmochim. Acta, 47, 1, 11-30.

Nash, W.P.(1985). Geochim. et Cosmochim. Acta, 49, 11, 2309-2322.

CRYSTAL GROWTH AND TRAPPING OF INCLUSIONS BY MINERALS

Yu.K.Vorobyov
Laboratory of Genetic Mineralogy, IGEM of the Russian Academy of Science

The natural crystal forming media are almost always very polluted, they include a great number of impurities. An experimental study of the crystallization in the specially polluted media has shown that the growth of a crystal is always a cyclic process, which is determined by periodic accumulation of the impurities. In every cycle the following phenophases of growth are distinguished:

Phase I - rapid growth of the pure crystallizing substance. As the impurity accumulates in the boundary layer the growth becomes slower and turns into the next phase -

Phase II - the rate of growth reduces to a complete stop: the impurities completely block the crystallization.

Phase III - relaxation of the impurity barrier: during the pause in growing the impurity concentration is decreased slowly by diffusion to a certain threshold level at which the crystallization is again possible. Because of the supersaturation of the main crystallizing component increases simultaneously, the last phase of the cycle begins -

Phase IV - a stormy growth is accompanied by trapping of a lot of medium inclusions. The growth rate increases about as compared to the growth rate in the end of the phenophase I. Due to this the most polluted part of crystallization halo is trapped by a crystal, forming a medium inclusion zone in the crystal.

Syngenetic inclusions are always either impurity phases (solid, liquid or gaseous) or an exhausted and impure medium. Mineralothermometry is particularly interested in the frequent phenomenon of local heterogenization and

exsolution of a gas, as the released bubbles are trapped by a crystal at a random ratio with the liquid. This is the reason why primary syngenetic inclusions cannot serve as a basis for the geothermometric measurements. These inclusions may be close in composition to the average composition of the crystal-forming medium only when the process of inclusion filling is separated from the growth process.

Because of the variety of relaxation variants of the impurity barrier the polluted zones may be as follows: 1) the zones of inclusions of the polluted medium and impurity phases (for instance in quartz, calcite, diopside); 2) the periodical sedimentation of impurity phase layers on the growth' front (quartz, ilmenite-spinel bicrystals, agates, fluorite); 3) the periodical trapping of high concentrations of homogeneous impurities (wolframite, granate, cassiterite, fluorite).

Typomorphic features of quartz of different genesis (from Uralian granitoids, ore deposits etc.) has been determined. The study of several hundreds of quartz samples from more than 20 Uralian commercial deposits revealed considerable variations of defects content between vein fields, among veins, within separate veins and in different zones of single crystals. The defects variations reflect their high sensitivity to the changes of mineral-forming conditions and postcrystallization evolution. Quartz samples of different genesis are characterised by individual response to the same kind of treatments. The criteria of raw-quartz quality estimation were determined.

References:

Halperin, A.& Sucov,E.(1993). J.Phys.Chem. Solids, 54,43-50.

Votyakov,S., Krasnobaev,A., Krokhalev,V. (1993): Problem of Applied Spectroscopy of Minerals. Nauka, Ekaterinburg, 236p. (in Russian).

Votyakov,S.,Krokhalev,V., Krasnobaev,A., Purtov,V. (1993) : Luminescence of Structural Imperfections in Quartz. Nauka, Ekaterinburg,70p. (in Russian).

LUMINESCENCE OF POINT DEFECTS IN NATURAL QUARTZ: DYNAMICS OF BEHAVIOR UNDER LABORATORY TREATMENTS, GEOLOGICAL AND TECHNOLOGICAL APPLICATIONS

Votyakov S.,Krokhalev V.,Krasnobaev A. (Institute of Geology and Geochemistry, Uralian Branch of RAS,Ekaterinburg,Russia)

Quartz is known as an important, widespread mineral-indicator of various geological processes. Present work continues luminescent investigations of synthetic (Halperin & Sucov,1993) and natural (Votyakov et al.,1993) quartz and is devoted to: a) analysis of natural quartz luminescent characteristics and dynamics of their changes under irradiations, high-pressure and high-temperature laboratory treatments; b) discussion of structural models of luminescent centers, hole and electron traps; c) classification of quartz of different genesis and analysis of its typomorphic features; d) application of luminescent parameters for estimation of raw quartz technological quality.

On the basis of X-ray induced luminescence in the range 77-600 K,electron spin resonance and thermoluminescence (TL) after X-irradiations at different conditions (at 77K - experimental scheme A; during cooling from 300 to 77K -B; at 300 K and than at 77 K - C) the analysis of point structural defects in quartz has been fulfilled. Such defects of quartz matrix as $[TiO_4]$, $[SiO_4/Li]$ and $[SiO_4/Na]$ were interpreted as electron traps connected with TL peaks at 165, 188 and 202 K (the last two peaks can be observed only in B or C schemes of X-irradiation). Dynamics of traps creation and destruction under various (X-, γ-, e-beam) irradiations was studied. Comparison of traps parameter with those for synthetic samples has been fulfilled. Al-impurity defects, in particular, associated with various alkaline ions as compensators, play the role of luminescence centers emitting in bands with maxima: 370, 390, 430, 490 and 530 nm, corresponding halfwidths of which are: 0.55-0.60, 0.90-1.0, 0.5-0.70, 0.40-0.50 and 0.45-0.55 eV. Optimal experimental conditions for observation of various luminescent centers has been suggested. Effects of annealings at temperatures up to 1500 °C under normal and high-pressure (up to 600 bar) parameters in H_2O, HCl, HF media and after - and e-beam irradiations has been studied. Influence of the treatments is connected with diffusion processes of impurity cations from interstitials into the structure; of Na, Li and H -ions along the c-canals; with destruction of gas and liquid inclusions and increase of matrix crystallinity. In particular, the intensity of 202 K TL peak increases after annealings at 300-500 °C simultaniously with the destruction of Na-containing inclusions.

BENTONITE CLAY FROM CHERKASSY DEPOSIT (UKRAINE) EXPOSED TO GAMMA RADIATION

Vovk I.F., Litovchenko A.S., Plastinina M.A., Zlobenko B.P. and Mazikin V.V. *(Inst. of Geochemistry, Mineralogy and Form.of Ores, Ukrainian Ac. of Sci.)*

Clay geological formations and application of clay minerals in clay technologies for the purposes of environmental protection is a subject of a special scientific attention nowadays. A number of national research projects have been carried out to study radiation effects in clays which are regarded as potential host formations or engineered barriers for high level radioactive waste repositories (Henrion *et al.*, 1988;Puch *et al.*, 1992). In Ukraine after the accident at the Chornobyl NPP an important part of research has been dedicated to clay minerals and clay compositions as effective and resourceful natural reserve for mitigation and prevention of radioactive contamination of the environment (Vovk *et. al.*,1993). Clay material was recommended as a liner for pits where radioactive wastes were placed after the accident and is now under further study as a barrier material to be used in the repository for final disposal of high level radioactive waste. In this connection, mineralogical and chemical changes in clays resulting from irradiation are a cause of concern.

Bentonite (its local natural form consists of up to 80% of Ca-montmorillonite) from Cherkassy deposit (300 km to the south of Chornobyl) is a basic clay material which has been used in the studies along with a number of other clay and non-clay silicates. The total absorbed doses of gamma irradiation integrated over the samples were 10^4, 10^6 and 10^8 Gy.

Chemical and mineralogical analysis as well as physical testing showed that no major changes in montmorillonite properties had taken place under effect of irradiation to the above doses (at the temperature of 300 K). Its sorption capacity also remained practically unchanged.

As evidenced by results of X-ray diffractometry, infra-red spectrosscopy, electron spin resonance data and accompanied chemical and mineralogical studies the

bentonite clay is not very homogeneous and its various constituents behave differently in the radiation physical and chemical processes. Besides the major constituent montmorillonite, bentonite includes quartz and feldspars, mica, gypsum, calcite, hematite and other clay and accessory minerals. In the experiments, radiation caused more crystal lattice defects in quartz and trioctahedral layered mineral structures containing elements of changable valence (Fe), such as tetraferrobiotite and biotite, notably less in dioctahedral structures such as that of glaukonite and celadonite.

Therefore, it is difficult to make a conclusive statement concerning the mineral and chemical changes that take place under effect of irradiation in bentonite. However, as far as montmorillonite is concerned, this clay minearal does not accumulate any notable amount of crystal lattice defects and seems stable in the irradiation process.

References:
Henrion P.N., Fonteyne A., Yan Jiade and Van Compel M.(1988). *Rad. Waste Manag. and Nuc.Fuel Cycle, 11(1), 41-60.*
Push R., Karnland O., Lajudie A., Decarreau A. (1992). *SKB TR 93-03, Stockholm, 47p.*
Vovk I.F., Blagoyev V.V., Lyashenko A.N. and KovalevI.S.(1993). *The Sci. of the Total Environ., 137, 49-63.*

X-RAY POWDER DIFFRACTION CHARACTERIZATION OF SPINEL

Wang Guanxin (*Institute of Geochemistry (Guangzhou Branch), Academia Sinica)*

The spinel group is a series of complex solid solutions caused by wide isomorphous substitution. Its general chemical formula can be expressed as AB_2O_4, where A refers to Mg, Zn, Fe^{2+}, or Mn and B to Al, Cr or Fe^{3+}.

Based on X-ray structure analysis, I_{220} / L_{400}, the intensity ratio of powder diffraction, can be taken as a criterion to identify the cations and their site occupancy in spinel.

The spinel group belongs to cubic system with space group Fd3m, Z=8. The structure was determined: 8 A in (a) 0, 0, 0; 16 B in (d) 5/8, 5/8, 5/8; 32 O in (e) x, x, x (x = 0.375 ~ 0.387). The general formula of structure factor can be written as:

$$F_{hkl} = 8f_a\cos\pi(h+k+l)/4 + 4f_d[\cos\pi(h+k+l) + \cos\pi(2h+k+l)/2 + \cos\pi(h+2k+l)/2 + \cos\pi(h+k+2l)/2] + 8f_o\{\cos2\pi x'(h+k+l) + \cos2\pi[(h+k)/4-(h+k-l)x'] + \cos2\pi[(h+l)/4 - (h-k+l)x'] + \cos2\pi[(k+l)/4 - (-h+k+l)x']\}$$

where f_a, f_d and f_o are the scattering factors of atom in (a), (d) and (e) respectively; $x'(x' = x - 1/8)$ is the coordinate of oxygen when the origin is moved to the centre(1/8, 1/8, 1/8). Some of the structure factors can be calculated as follows:

$$F_{111} = -5.657f_a + 8f_d + \zeta_{111}f_o$$
$$F_{220} = -f_a - \zeta_{220}f_o$$
$$F_{311} = -5.657f_a - 8f_d + \zeta_{311}f_o$$
$$F_{222} = 16f_d - \zeta_{222}f_o$$
$$F_{400} = -8f_a + 16f_d + \zeta_{400}f_o$$

Where ζ_{hkl} is a coefficent depending on oxygen's co-ordinate and hkl. For normal spinel structure the di-valant and trivalant cations are ordered in (a) and (d), so that the intensity ratio I_{220} / L_{400} calculated from F_{220} and F_{400} is highly sensitive to variation of composition in spinel. For example, the ratio I_{220}/L_{400} = 0.62 for spinel ($MgAl_2O_4$) while I_{220}/I_{400} = 10.5 for gahnite ($ZnAl_2O_4$) because of the difference great between f_{Mg} and f_{Zn}. For inverse spinel structure all of the cations are disordered, so that the contents of inverse and normal spinel structure can be calculated from I_{220} / L_{400}. For example, I_{220} / L_{400} = 1.4 for magnesioferrite ($MgFe_2O_4$) with 67% inverse.

Temperature-pressure Investigation of The Southern Part of The Southwest Swedish Granulite Region.

Wang X.D. and Lindh A. (*Dept. of Mineralogy and Petrology Univ. of Lund*)

The Southwest Swedish Granulite Region (SGR) is located in the southern part of the Southwest Swedish Gneiss Region. It is bordered by two large shear zones, the Mylonite Zone in the west and the Protogine Zone in the east. The SGR is dominated by high-grade rocks affected by the Sveconorwegian-Grenvillian orogeny.

The area under study is situated in the southern part of the SGR. The metamorphic history is poorly constrained. A few temperature and pressure estimates and age determinations have been published (Johansson et al., 1991). In this poster, 22 pairs of new temperature and pressure determinations on mafic rocks from the southern part of the SGR are displayed. Temperatures vary between 660 and 800°C (Grt-Cpx temperatures, Ellis & Green, 1979 and Grt-Hbl temperatures Graham & Powell, 1984). The pressures range between 8.5 and 11.8 kbar based on Grt-Cpx-Plg-Qz (Moecher et al., 1988) and Grt-Hbl-Plg-Qz (Kohn & Spear, 1990) barometers. The data we have obtained compare well with those obtained by Johansson et al. (1991). Published Sm-Nd isotope data on minerals from the mafic granulitic rocks give a late Sveconorwegian (Grenvillian) age for the high grade metamorphism (Johansson et al. 1991; Johansson & Kullerud, 1993).

The mafic rocks from the area have metamorphic assemblages consisting of Grt-Cpx-Hbl-Plg-Qz; Grt-Cpx-Opx-Plg-Qz; Grt-Cpx-Opx-Hbl-Plg-Qz; Grt-Hbl-Plg-Qz. These minerals have uniform chemical compositions and are essentially without any chemical zonation. Temperatures and pressures from these coexisting and equilibrated minerals are interpreted to represent nearly peak conditions. Temperatures and pressures appear to be higher in the eastern part of the SGR, close to the Protogine Zone.

Temperatures and pressures obtained from different thermometers and barometers consistently give somewhat different results. Temperatures obtained from the Grt-Cpx

thermometer of Ellis & Green (1979) are 70-145°C higher than those estimated from the Grt-Cpx thermometer of Pattison & Newton (1989), and 15-55°C higher than those from the Grt-Hbl thermometer of Graham & Powell (1984). Pressures based on the Mg-endmember of Grt-Cpx-Plg-Qz calibration of Moecher et al. (1988) are about 1.5-2.5 kbar higher than those from the Mg-endmember of Grt-Cpx-Plg-Qz calibration of Newton & Perkins (1982), and 0-1.6 kbar higher than those from the Mg-endmember of the Grt-Hbl-Plg-Qz calibration by Kohn & Spear (1990). The pressures obtained from the Mg-endmember of the Grt-Cpx-Plg-Qz barometer is 1.2-5.5 kbar higher than from the Fe- endmember (calibration by Moecher et al., 1988)

References:

Ellis, D. J. & Green, D. H. (1979). *Contrib. Mineral. Petrol.*, **71**, 13-22.

Graham, C. M. & Powell, R. (1984). *J. Metamorphic Petrol.*, **2**, 13-21.

Johansson, L., Lindh, A., Möller, C. (1991). *J. Metamorphic Petrol.*, **9**, 283-292.

Johansson, L. & Kullerud, L. (1993). *Precambrian Res.*, **64**, 347-360.

Kohn, M. J. & Spear, F. S. (1989). *American Mineralogist*, **74**, 77-84.

Kohn, M. J. & Spear, F. S. (1990). *American Mineralogist*, **75**, 89-96.

Moecher, D. P., Essene, E. J., Anovitz, L. M. (1988). *Contrib. Mineral. Petrol.*, **100**, 92-106.

Newton, R. C. & Perkins, D. III (1982). *American Mineralogist*, **67**, 203-222.

Pattison, D.R.M. & Newton, R.C. (1989). *Contrib. Mineral. Petrol.*, **101**, 87-103.

ANISOTROPIC THERMAL PROPERTIES OF QUARTZ AND RUTILE AT LOW TEMPERATURES

Watanabe H. (*General Education, Osaka Sangyo Univ.*)

Thermal diffusivities in the parallel and perpendicular directions to the c-axis of quartz, SiO_2, and rutile, TiO_2, thermal diffusivity of SiO_2 glass and specific heat capacities of quartz, rutile and SiO_2 glass were measured in the temperature range 120 K and 480 K in a vacuum condition, 10^{-3} Torr, using a laser flash calorimeter.

Linear thermal expansions in the parallel and perpendicular directions to the c-axis of quartz and rutile and linear thermal expansion of SiO_2 glass were measured in the temperature range 120 K and 480 K under the atmospheric pressure using a push-rod dilatometer.

Values of thermal conductivities, K, of the above five specimens were calculated from the measured values of thermal diffusivity, k, specific heat capacity, C_p, and density, ρ, from an equation, $K=kC_p\rho$. The thickness of the specimen was corrected from the measured values of linear thermal expansion.

All new data on the thermal diffusivities, specific heat capacities, linear thermal expansions, and thermal conductivities will be presented for quartz, rutile and SiO_2 glass at low temperatures.

The anisotropies on thermal diffusivity, linear thermal expansion and thermal conductivity at low temperatures will be discussed for quartz, and rutile.

EXAFS AND XANES STUDY OF ELEMENT SITE PARTITIONING IN Mg_2GeO_4-$MgGa_2O_4$ SPINELS

Waychunas G.A. (Center for Materials Research, Stanford University) and Leinenweber K. (CHiPR, State University of New York at StonyBrook)

Synthetic spinels along the join Mg_2GeO_4-$MgGa_2O_4$, as well as Mg_2GeO_4 olivine and β-phase ($Mg_3GeGa_2O_8$) have been characterized with Ga and Ge K-edge XANES and EXAFS spectroscopy. Because the x-ray scattering power of Ga and Ge are nearly identical, and the neutron scattering lengths not significantly different, site partitioning for this system is difficult to obtain by typical scattering experiments. However, the element specificity provided by x-ray absorption spectroscopy can readily separate Ga, Ge and Mg contributions in the pair-correlation function.

As shown in the Fourier-transformed Ge EXAFS shown below, there is little difference in the pair-correlation functions in going from pure Mg_2GeO_4 spinel to the composition 0.29 Mg_2GeO_4. The pattern is indicative of only tetrahedral Ge. However there is a dramatic change in the pair-correlation function for compositions with less Mg_2GeO_4 component. The first peak due to Ge-O is observed to have a shoulder and then a well-defined smaller peak at larger Ge-O distances, indicative of octahedral Ge. Concurrent with this change, the second shell of neighbor distances about the probe Ge, at about 3 Å (without phase-shift correction), splits into two well-defined peaks. Of these, the peak at the smaller interatomic distance is due to octahedral cation neighbors about the average octahedral cation. Hence it only appears if the probe ion is partially resident in the octahedral sites. Preliminary analysis, based only on the Ge-O shell analysis, yields 100% tetrahedral Ge for the composition 0.29 Mg_2GeO_4, 57% tetrahedral Ge for 0.20 Mg_2GeO_4, and 55% tetrahedral Ge for 0.11 Mg_2GeO_4. Analysis based on all shells, and including the Ga data, is in progress.

The XANES spectra observed for these materials demonstrate how multiple-scattering features are extremely sensitive to cation disorder associated with solid solutions. The Ge XANES spectrum of Mg_2GeO_4 olivine and spinel, and quartz-structure GeO_2, have a well-defined feature that is seemingly indicative of tetrahedral coordination for Ge. However, the 0.29 Mg_2GeO_4 composition solid solution sample, with essentially all Ge present in tetrahedral coordination, has a XANES spectrum which does not show the supposedly

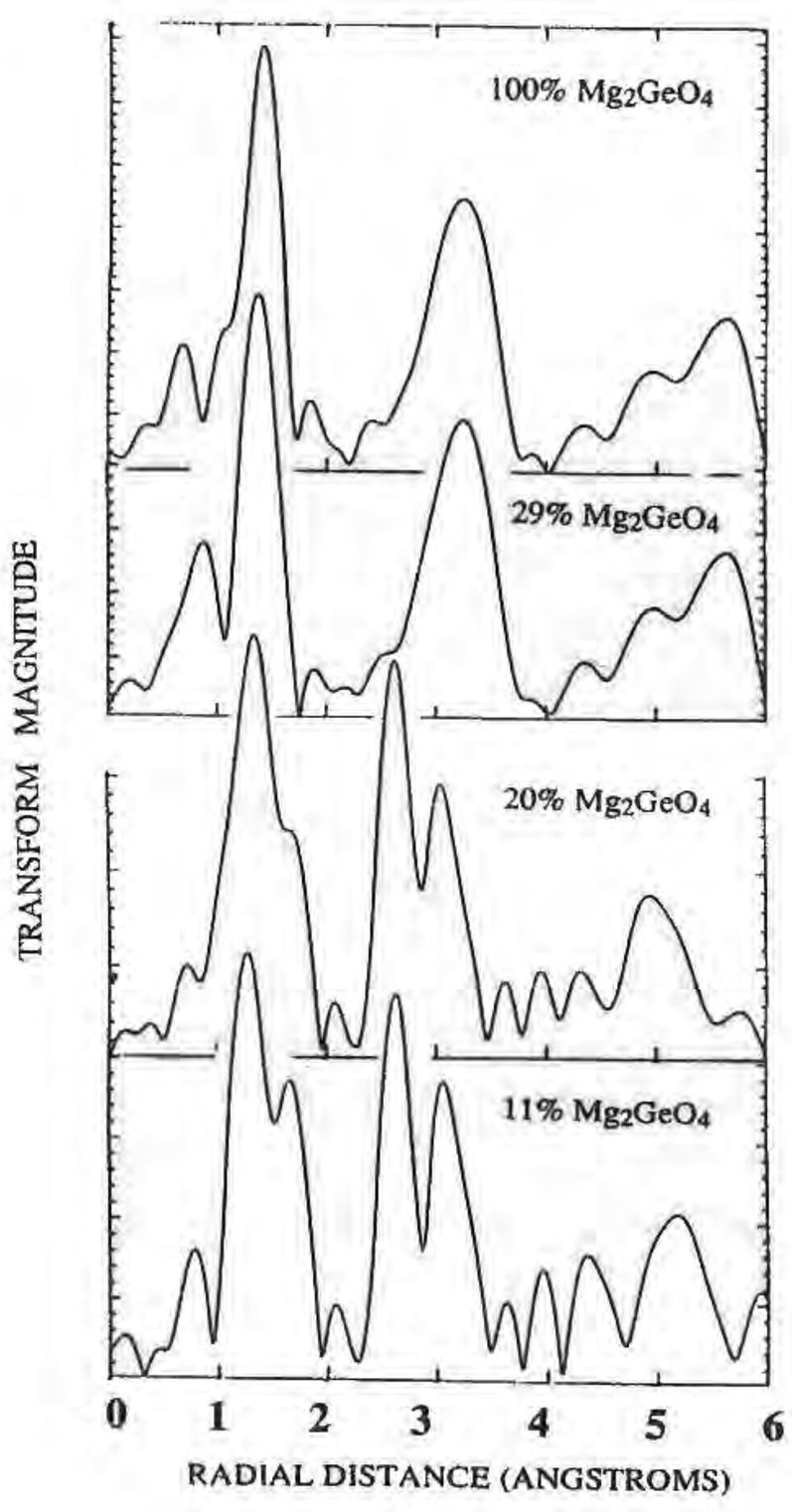

"tetrahedral" feature. Calculations of both EXAFS and XANES amplitudes using the *ab initio* program FEFF-6 are now being done to understand these observations, and place some constraints on how XANES structure can be used for structural characterization.

COMPOSITION DEPENDENT STRUCTURE OF SILICATE MELTS

Webb S.L. (*Bayerisches Geoinstitut, University of Bayreuth*)

Linear extrapolations in composition-space of melt properties do not always result in realistic approximations to the physical properties of the melt in question due to composition-dependent changes in the melt structure. This is the case for titanium-bearing melts where it is known that the density of the TiO_2 component of alkali-titanosilicate melts varies by 15% and linear fits to the bulk modulus do not converge to a common compressibility of the TiO_2 component. The presence or absence of aluminium in phosphosilicate melts is known to increase or decrease the viscosity of the melt as a function of the alkali to aluminium ratio. The anomalous physical properties of these melts points to structural changes occurring as a function of composition. A useful indicator of the co-ordination of atoms and the strength of bonds between atoms is the compressibility of a material. The compressibility of a series of titanium-bearing alkali- and alkaline-earth silicate melts and a series of aluminium-bearing and aluminium-free phosphosilicate melts has been determined in order to address the problem of structural changes as a function of composition in these melts.

The compressibility data for the alkali-titanosilicate melts indicates increasingly compressible Ti co-ordination polyhedra going from Cs- to Li-bearing titanosilicate melts: *i.e.* the average co-ordination number of Ti increases with decreasing cation size in the alkali-titanosilicate melts. Addition of Ti to the alkaline-earth metasilicate compositions would appear to result in the Ti co-ordination remaining constant independent of cation identity. The addition of phosphorus to Na_2SiO_3 melt results in a decrease in density. The addition of phosphorus to both the aluminium-free and aluminium-bearing melt results in a decrease in compressional wave velocity through the melt. In each of these examples the structure of the melt changes radically as a function of composition and it not possible to use linear systematic treatments to estimate either the melt density or the melt compressibility for other compositions in the XO- or X_2O-TiO_2-SiO_2 or X_2O-P_2O_5-Al_2O_3-SiO_2 systems.

SHORT TERM CHEMICAL AND MINERALOGICAL FRACTIONATION OF THE CERRO NEGRO, NICARAGUA MAGMA CHAMBER: EVIDENCE FROM THE APRIL 1992 ERUPTION

Webber K.L., Falster A.U. and Simmons Wm.B. (Department of Geology and Geophysics, University of New Orleans)

Our group witnessed the April, 1992 eruption of Cerro Negro, a cinder cone located 70 km northwest of Managua, Nicaragua, which last erupted in 1971. The 5-day April, 1992 eruption consisted of a series of closely spaced explosions of ash, cinders and blocks from a central vent. The trajectory of ballistic material was particularly evident at night. No lava flows were produced during this eruption. The ash column reached a height of over 5 km and ash inundated the town of Leon 20 km southwest of Cerro Negro. At the cessation of eruption, Cerro Negro was left with an asymmetric crater rim, which was lowest along the southeastern edge. We were able to collect ejected block samples from the slopes of the cinder cone and from several locations at distances up to 1/2 km away from the cinder cone from impact craters that measured up to 1 meter in diameter. The blocks sampled were gray in color which made them quite distinctive from previously erupted darker color material. We also collected glassy samples from the cinder cone slopes and ash from several locations in and around Leon. We collected additional samples from the crater rim in January 1994.

Based on XRF whole-rock analyses, block samples can be classified as low-Ti, high-Al basalts. The predominant phenocrysts are plagioclase (often corroded), oxidized olivine (some rimmed by pyroxene) and augite. Compared to samples from previous eruptions of Cerro Negro (Walker & Carr, 1986 & this study), 1992 eruptive samples are slightly more enriched in SiO_2 (51wt%), total alkalis (3.2 wt%) and P_2O_5 and have lower TiO_2, FeO*, MgO, CaO, Zr and Y. REE abundances for 1992 ash samples and ejected blocks and pre-1992 basalts are similar. Dark glassy samples collected from the slopes and rim of Cerro Negro are chemically very different. These samples are dacites with 67 wt% SiO_2, 5 wt% total alkalis and REE abundances much higher than other Cerro Negro samples.

Plagioclase phenocrysts show a wide range in chemistry with core compositions from 1992 eruptive samples ranging from An_{55-81} and rim compositions of An_{46-73}. Walker & Carr (1986) report pre-1992 core compositions of An_{85-96}. Pre-1992 pyroxene rim compositions average $Wo_{40}En_{45}Fs_{15}$ whereas 1992 rim compositions show enrichments in CaO and FeO and depletions in MgO and average $Wo_{44}En_{31}Fs_{25}$. Olivine phenocrysts show a core to rim increase in FeO and a decrease in MgO between pre-1992 eruptive samples and 1992 samples. Thus, based on our preliminary chemical and mineralogical data, it appears that fractionation has taken place at Cerro Negro during the twenty years since its last eruption. The glassy dacitic material which is chemically much different from either 1992 ash or ejected blocks suggests that this material may represent a differentiated cap that was present at Cerro Negro prior to eruption and fragmented during eruption.

References:
Walker, J.A. & Carr, M.J. (1986). *Geol. Soc. Amer. Bull.*, **97**, 1156-1162.

LARGE-VOLUME HIGH-PRESSURE APPARATUS WITH SYNCHROTRON RADIATION

Weidner, D.J. (CHiPR and Department of Earth and Space Sciences, University at Stony Brook)

In situ x-ray diffraction studies with SAM85, a large volume DIA type apparatus, using the superconducting wiggler source at the NSLS are used to study the P-V-T equation of state of many minerals, the phase boundaries of silicates, and yield strength at elevated pressure and temperature. The system has been used with sintered diamond anvils to provide pressure in excess of 15 GPa and temperatures up to 1800C. While temperature is monitored with a thermocouple, pressure, temperature gradient, and state of stress are determined from the x-ray diffraction pattern. Both energy dispersive and angle dispersive data have been collected.

X-ray diffraction of samples at high pressure and temperature provide information not only on the unit cell dimensions, but also on the deviatoric stress in the sample. Macroscopic stress is defined by the relative strains inferred from the different diffraction lines in an elastically anisotropic sample. Cubic materials are particularly useful for determining the macroscopic stress since, under hydrostatic stress, all diffraction lines will display the same strain. Measurements have been inverted for deviatoric stress as a function of pressure and temperature for NaCl and gold. The presence of deviatoric stress significantly effects the pressure calibration based on a diffraction standard. This error is reduced by heating the sample and reducing the yield strength which limits the amount of deviatoric stress that the sample can sustain.

Microscopic deviatoric stress, which varies from grain to grain is inferred from peak broadening. These stresses can be as large as twice the hydrostatic stress for powdered aggregates with significant pore space. Well sintered polycrystals exhibit very little peak broadening indicating that the deviatoric stresses are not appreciable in such samples. The magnitude of the microscopic deviatoric stress

is limited by the yield strength of the sample. Thus, yield strength can be deduced from the variation of peak width as a function of pressure and temperature. Measurements on diamond at temperatures up to 1500°C at 10 GPa in SAM85 illustrate the capability of this technique to determine yield strength. The deviatoric stress increases linearly with pressure throughout the 10 GPa pressure range. Yielding is observed by peak narrowing as temperature is raised above 1200°C. Yield strengths for MgO and NaCl deduced from peak broadening agree quite well with those determined in other studies.

MINERAL PHYSICS CONSTRAINTS ON THE LOWER MANTLE

Weidner, D.J. and Wang, Y. (CHiPR and Department of Earth and Space Sciences, University at Stony Brook)

One of the outstanding questions in Earth science is the composition of the lower mantle and its relationship with that of the upper mantle. This question has important bearing on the thermochemical state, the dynamic processes, and the evolution of the Earth. We utilize a DIA-type cubic-anvil apparatus (SAM-85) that is interfaced with synchrotron X-ray sources to study the P-V-T relations of $(Mg,Fe)SiO_3$ and $CaSiO_3$ perovskites up to 14 GPa and 1300°C. With existing data on (Mg,Fe)O, the three-component system covers about 95% of most composition models of the mantle. Although equation-of-state data of $(Mg,Fe)SiO_3$ (Mg-) perovskite are obtained under metastable conditions, special care has been taken to assure that the measured properties are reversible and are thermodynamically valid state parameters that can be extrapolated to lower mantle conditions. The P-V-T data for $CaSiO_3$ (Ca-) perovskite are obtained within the stability field. The temperature derivative of the isothermal bulk modulus for Mg-perovskite is determined to be $(\partial K_T/\partial T)_P$ = -0.023(11) GPa/K; the volumetric thermal expansion is estimated to be about 1.6×10^{-5} K^{-1} at 1071 km depth in the lower mantle. Thermal expansion of the Ca-perovskite is about 30 - 40% higher than that of Mg-perovskite.

Thermal expansion α and $(\partial K_T/\partial T)_P$ are the most important parameters in constraining composition of the lower mantle. α is the most sensitive to density and therefore controls the Fe/Mg ratio, $(\partial K_T/\partial T)_P$ dictates the bulk modulus at high temperature and thus determines the (Mg+Fe)/Si ratio of the lower mantle. Our data suggest Fe/(Mg+Fe) = 0.12(1) and (Mg+Fe+Ca)/Si = 1.7 for the lower mantle. These results are consistent with a pyrolitic lower mantle and suggests a chemically homogeneous mantle.

Assuming a pyrolitic lower mantle, we further examine the predicted physical properties and compare them with various geophysical observations. Our purposes are (1) to examine interconsistency of the model with available geophysical data, and (2) to provide a complete set of geophysical parameters for geodynamic analyses.

The values of $(\partial K_T/\partial T)_P$ for the perovskite and (Mg,Fe)O indicate that for the pyrolitic lower mantle, $(\partial K_S/\partial T)_P$ ranges from -0.005 to -0.015 GPa/K. A tighter constraint of -0.012(3) GPa/K is obtained by comparing the K_S profile of PREM at the adiabatic foot temperature (1800±200 K at 1 bar) with the ambient K_S of the model mineral assemblage of the lower mantle. More importantly, a similar constraint of $(\partial\mu/\partial T)_P$ = -0.029(6) GPa is obtained for the shear modulus. Assuming these values represent average temperature derivatives of the elastic moduli in the lower mantle, we calculate lateral variations in physical properties and compare directly with seismic tomography observations. For a typical δV_P of 0.5% and a δV_S of 1% from seismic tomography, the estimated lateral temperature variation, ΔT, is about 230 — 240 K for a thermal expansion α of 1.6×10^{-5} K^{-1}. Table below lists the results on selected parameters calculated at 1071 km. The successfulness of the model is shown by comparing the predicted parameters with available geophysical data.

Lateral Variations in Properties at 1071 km Depth

Parameter	Model Value	"Observed" Value
$\partial\ln V_S/\partial\ln V_P$ (Tomography)	1.7 — 1.9	1.75 — 2
ΔT	200 — 300 K	—
$\partial\ln\rho/\partial\ln V_S$ (tomogr./geodyn.)	0.25 — 0.36	0.2±0.1

HYDRATION EFFECTS ON OPTICAL PROPERTIES OF HEULANDITE-GROUP ZEOLITES

Weiszburg T. G. *(Department of Mineralogy, Eötvös L. University, Budapest)* and Gunter M. E. *(Department of Geology and Geological Engineering, University of Idaho, Moscow, Idaho)*

The optical properties of the heulandite-group zeolites, with end-members clinoptilolite, $(Na,K)_6(Al_6Si_{30}O_{72})\cdot20H_2O$, and heulandite, $(Na,K)Ca_4(Al_9Si_{27}O_{72})\cdot24H_2O$ are poorly known. Several reasons exist for this: there is little available optical data for clinoptilolite, different choices of crystallographic axes have been used (Gottardi & Galli, 1985), the optical properties are affected by hydration state (Boles, 1972), and zeolites in general have low birefringence, leading to changes in optical class and optical orientation with only slight structural or chemical variations (Gunter & Ribbe, 1993). General trends do exist however, for instance, there is an increase in the refractive indices from clinoptilolite to heulandite due either to changes in the channel cations (i.e., Ca replacing Na, as Al replaces Si in the framework) and/or increases in channel water. The optical orientation also changes for b=Y to b=Z, respectively.

Our project had two goals: 1) to collect optical data on a chemically intermediate heulandite-group zeolites and 2) to measure the effect of hydration on the optical properties. A sample from Succor Creek, Oregon, USA (Armbruster & Gunter, 1991) was chosen ($Ca_{2.1}Mg_{0.3}Na_{2.5}K_{0.28}Al_{8.0}Si_{28.2}O_{72}\cdot25.5H_2O$). The sample has intermediate chemistry. Its structure was determined in the fully hydrated state and four partially hydrated states. Originally, we planned to measure the optical properties (refractive indices, 2V and optical orientation) for the fully hydrated sample and the four partially hydrated states. However, we soon discovered the optical properties changed when the partially hydrated samples were placed in liquids used to measure refractive indices. Thus, dehydrated heulandite-group zeolites absorbed certain of the organic molecules present in the liquids used to measure refractive indices. This makes refractive index measurements invalid, because the refractive index of the zeolite changes with time as it absorbs molecules into its channels. Another experiment showed that fully-hydrated heulandite-group zeolites do not absorb any of the liquid and their optical properties are stable with time.

The clinoptilolite used by Armbruster & Gunter (1991) was placed in H_2O at room temperature for 24 hours. This sample was then mounted on a spindle stage and its α refractive index was measured to be 1.4900(3) by the double variation method (Bloss, 1981 and Gunter *et al.*, 1989). The crystal was left in the oil for 24 hours, and, after placing fresh liquid in the oil cell, the crystal's α value remained unchanged. Next, this same sample was dehydrated by the method described in Armbruster & Gunter (1991) to form their dehyd2. The sample was then immediately placed in the oil cell and its γ value found to be 1.4915(3). Timed data collected yielded the following: 3 hours = 1.4924, 5 hours = 1.4929, 20 hours = 1.4945, 24 hours = 1.4947 and 16 days = 1.4947. A new liquid was used for the last two measurements in case the refractive index of the liquid changed. Thus, γ increased by 0.0032 over 24 hours and then remained stable.

To see how 2V was affected, a second test was made on the Na-exchanged Poona, India, sample (Gunter *et al.*, 1994). Its value

of 2V was measured to be +82.4(4) by routine spindle stage methods (Bloss, 1981 and Gunter *et al.*, 1989) and left in the liquid for 5 days, at which time 2V was again determined and found to be +82.5(4), or unchanged. Samples of heulandite zeolites can dehydrate "on the shelf." A non-exchanged Poona, India, sample's 2V was found to be +56.0(5). After placing the sample in H_2O for 24 hours, its 2V changed to +48.8(4). These data are very disturbing and indicate that any optical data collected on zeolites may be in question unless the samples are first fully hydrated.

Acknowledgement: This work was partly supported by the Peregrinatio II Foundation (Budapest).

References:

Armbruster, T. & Gunter, M.E. (1991). Am. Miner., 76, 1872-1883.
Boles, J.R. (1972) Am. Miner., 57, 1452-1493.
Bloss, F.D. (1981) The Spindle Stage: Principles and Practice.
Gottardi, G. & Galli, D. (1985) Natural Zeolites.
Gunter, M.E. & Ribbe, P.H. (1993) Zeolites, 13, 435-440.
Gunter, M.E., Bloss, F.D., Su, S.C. (1989) The Microscope, 37, 167-171.
Gunter, M.E., Armbruster, T., Kohler, T., Knowles, C.R. (1994). Am. Miner., in press.

FOURIER-TRANSFORM INFRARED SPECTRAL INVESTIGATION OF THE $(Mg,Cr^{3+})(Si,Cr^{3+})O_3$-PEROVSKITE AT HIGH PRESSURES TO 21.9 GPa *

Weng K.N., Peng W.S., Xiao W.S. and Zhang Q.(*Guangzhou Institute of Geochemistry, Academia Sinica*)

The starting material($95MgSiO_3 \cdot 5Cr_2O_3$ glass) used in our experiment was prepared from gel to make it to be homogeneous. Then a new orthorhombic perovskite phase has been synthesized in a diamond anvil cell (DAC) at high pressure above 40 GPa and high temperature about 1200 -1500℃. According to the X-ray powder diffraction analysis, the lattice parameters of the $(Mg_{95}, Cr_5^{3+})(Si_{95}, Cr_5^{3+})O_3$-perovskite were obtained: a=0.4795(2) nm, b=0.4962(2) nm, c=0.6915(2) nm and v=0.1645(2) nm^3.

The Fourier-transform infrared spectral investigation of the perovskite was carried out by a DAC with type IIA diamonds at high pressures from 0 to 21.9 GPa. This study shows that the FTIR spectrum of $(Mg_{95},Cr_5^{3+})(Si_{95},Cr_5^{3+})O_3$-perovskite is similar in shape to the that of pure $MgSiO_3$-perovskite(Weng,K., 1983) having four absorption bands, and the Si-O stretching frequency in $(Mg_{95},Cr_5^{3+})(Si_{95},Cr_5^{3+})O_3$-perovskite has shifted by about 250 cm^{-1} to lower energy in comparison with starting material. The obvious increase of Si-O bond length appears that silicon is VI-fold coordinated in the silicate-perovskite structure.

With the increasing of pressure the absorption bands of $(Mg_{95},Cr_5^{3+})(Si_{95},Cr_5^{3+})O_3$—Perovskite shift to the higher energy lineally. The frequencies of these bands according to the sequence can be obtained from following equations:

$$\upsilon_1(cm^{-1}) = 783 + 4.51P \text{ (GPa)} \quad (r=0.916);$$
$$\upsilon_2(cm^{-1}) = 621 + 1.62P \text{ (GPa)} \quad (r=0.725);$$
$$\upsilon_3(cm^{-1}) = 488 + 4.18P \text{ (GPa)} \quad (r=0.953);$$
$$\upsilon_4(cm^{-1}) = 437 + 1.39P \text{ (GPa)} \quad (r=0.944).$$

Reference

Weng,K., Xu,J., Mao,H.K., Bell,P.M.(1983). *CIW Year Book, 82*, 355–356.

* The project supported by National Natural Science Foundation of China.

FLUID INCLUSION STUDIES OF ANHYDRITES FROM THE PERMO-SCYTHIAN BEDS OF THE HASELGEBIRGE FORMATION (NORTHERN CALCAREOUS ALPS, AUSTRIA/ GERMANY)

Wiesheu, R. & Grundmann, G. (Applied Mineralogy, TU München, Germany)

The Permo-Scythian beds of the so called Haselgebirge form a chaotic tectonic melange of halite, shale, silt, carbonate, anhydrite and gypsum at the base of the Northern Calcareous Alps (Schauberger, 1986). The most important anhydrite/gypsum/salt deposits within this Haselgebirge-Formation are: Berchtesgaden, (Germany); Alt Aussee, Bad Ischl, Golling, Grundlsee, Hall and Hallein (Austria). According to the illite crystallinity data and isotopic ages from Kralik et al. (1987) this area has been affected by very low to low grade metamorphic events.

From the anhydrite/gypsum/salt deposits fluid inclusions in anhydrite have been studied by microthermometry combined with microstructural analysis and stable isotope data of carbonates to clarify the diagenetic and/or metamorphic evolution.

Primary, type 1, at room temperature mono- or two-phased inclusions are found in areas relatively free of tectonic effects and characteristically have a high salinity up to 30 wt% NaCl, reflecting pre-metamorphic sealing. The secondary, mainly polyphased type 2, inclusions with generally large amounts of CO_2 show a wide range of compositions due to accumulation of tectonic effects, and subsequent fluctuation of trapping conditions. Minimum homogenization temperatures (starting at about 300° C) of type 2 inclusions e.g. from Golling and Bad Ischl are in accordance with the temperature of the very low grade metamorphism in the Permo-Scythian at the base of the Northern Calcareous Alps (compare: Kirchner, 1980; Kralik et al., 1987).

Stable isotope data for native sulfur in association with calcite and anhydrite suggest that the native sulfur and calcite are the result of bacterial activity ($\delta\ ^{13}C$ values ranging from -20 to -22‰).

References:

Kirchner, E.Ch. (1980). *Verh. Geol. B.-A.*, **3**, 249-279.
Kralik, M., Krumm, H. & Schramm, J.M. (1987). *in* "Geodynamic of the Eastern Alps", P. Faupl & H.W. Flügel, ed. Deuticke, Wien, 164-178.
Schauberger, O. (1986). *Archiv f. Lagerst.forsch. Geol. B.-A.*, 7, 217-254.

CRYSTAL STRUCTURES OF ERYTHRITE AND OF THE ISOTYPIC SYNTHETIC COMPOUNDS $Me_3(AsO_4)_2 \cdot 8H_2O$ (Me=Mg,Co,Ni)

Wildner M., Lengauer C.L. and Giester G.
(*Institut für Mineralogie und Kristallographie, Universität Wien, Austria*)

In the course of investigations on vivianite-type compounds $Me_3(AsO_4)_2 \cdot 8H_2O$, the crystal structures of erythrite from Schneeberg, Sachsen, as well as of three synthetic end-members (Me^{2+}=Mg, Co, Ni) were determined by X-ray single crystal and powder methods (Rietveld refinements), respectively. The synthetic compounds were precipitated at 350K from the reaction of an aqueous solution of $Na_2HAsO_4 \cdot 7H_2O$ with solutions of the respective nitrates of Me^{2+}. EDX analyses of the erythrite sample led to the empirical formula $(Co_{2.01}Fe_{0.74}Ni_{0.25})(AsO_4)_2 \cdot 8H_2O$.

The refinements were done in space group C2/m and confirmed the isotypy with vivianite (Mori & Ito, 1950). The refined lattice parameters and final R-values are as follows:

	a	b	c	β	V	
erythrite	10.251	13.447	4.764	104.98	634.4	R=2.8
$Co_3(AsO_4)_2 \cdot 8H_2O$	10.252	13.432	4.761	105.07	633.0	R_{wp}=5.3
$Mg_3(AsO_4)_2 \cdot 8H_2O$	10.288	13.462	4.755	105.11	635.6	R_{wp}=5.9
$Ni_3(AsO_4)_2 \cdot 8H_2O$	10.170	13.296	4.716	104.89	616.3	R_{wp}=4.4

The geometry of the AsO_4 tetrahedron is similar in all four compounds, mean As-O distances range from 1.694 (erythrite) to 1.703 Å (Mg). The $Me(2)O_6$ octahedra are moderately distorted and exhibit no obvious trend in the sequence of the individual Me(2)-O bond lengths, whereas the Me(1) atoms are distinctly [2+4] coordinated with longer mean Me-O distances. The Co(1)-O distances are practically equal in natural and synthetic erythrite, the Co(2)-O bond lengths, however, are significantly longer in the natural sample, indicating a preferred Me(2) site occupation by Fe^{2+} in erythrite. A corresponding Me(2) site preference of Mg in annabergite ("cabrerite") was already reported by Giuseppetti & Tadini (1982). It is also worth noticing that the lattice parameters of the Mg-compound are larger than expected considering the ionic radii of Mg^{2+} and of the divalent first row transition elements. This fact was also reported *e.g.* for kieserite-type compounds $Me(SO_4) \cdot H_2O$ (Wildner & Giester, 1991).

References:

Mori, H. & Ito, T. (1950) *Acta Cryst.*, **3**, 1-6
Giuseppetti, G. & Tadini, C. (1982) *Bull. Min.*, **105**, 333-337
Wildner, M. & Giester, G. (1991) *N. Jb. Min. Mh.*, **1991**, 296-306

ARCHEAN ECLOGITE AND HIGH-PRESSURE GRANULITE FACIES METAMORPHISM, WESTERN LAURENTIA.

Williams M.L. and Snoeyenbos D.R. *(Dept. of Geology and Geography, Univ. of Massachusetts, USA)*; Hanmer, S.K. *(Lithosphere and Canadian Shield Division, Geol. Surv. Canada)*

In extreme northern Saskatchewan, Canada, the 2000km long Snowbird Tectonic Zone widens into a triangular domain of heterogeneous Middle to Late Archean granulite facies and eclogite facies mylonites, where 2400 km^2 of remarkably fresh and well-exposed rock afford unprecedented views of petrologic and petrogenetic processes at the underside of an Archean continent. Two examples are here presented.

Generation of tonalitic melt in the lower crust. Regional metamorphic conditions of ca. 10 kb, 850°C are found in the 2000 km^2 of subvertically-foliated and subhorizontally-lineated mylonites of the 3.2 and 2.6 Ga 'Lower Deck' of the triangle. In the eastern half of the shear zone a swarm of >3.2 Ga mafic dikes intrudes the mylonitized tonalitic Chipman batholith. Dikes can be tens of meters wide and dominate zones kilometers across. Chemically the dikes are tholeiitic basalts, similar to N-MORB. The dikes span the deformational history; older dikes are intensely folded and sheared while younger dikes are undeformed. Syndeformational metamorphism progressively transforms Hbl+Pl-dominated dikes into Cpx-rich dikes with Grt megacrysts and cognate pools of segregated tonalitic melt. Where small, the melts occupy 'strain shadows' or 'tails' on every garnet crystal, dramatically defining the axial planes of folded dikes and the S-surfaces in S-C mylonites. Where garnets are large (up to 10 cm), melts form an interconnected network that extends into the host tonalite. Near the largest melt pools, garnet crystals are replaced by hornblende and plagioclase, suggesting release of water from the crystallizing melts back into the dikes. The presence of new garnets with melt tails within the pseudomorphs indicates polycyclic partial melting and rehydration. Grt-Cpx and Grt-Hbl thermobarometry indicate conditions of 800-900°C and 10 kbar. The Chipman Dikes were apparently emplaced, solidified, and immediately partially melted during a single sinistral ductile shearing event, near the base of the Archean crust. They may offer a classic view of felsic magma genesis where underplated mantle-derived mafic magmas provide not only heat but a component of the source material for new magmas. Deformation plays a key role in the process, allowing access of mafic magma into the lower crust, and facilitating the segregation of the new felsic melts from their source rocks.

An Archean eclogite facies terrane. Resting atop the granulite facies mylonites is the 2.6 Ga 'Upper Deck', 400 km^2 in outcrop area and 9 km in thickness. This terrane consists of mylonitic to ultramylonitic quartzofeldspathic gneisses of supracrustal derivation, and mafic rocks of undetermined affinity. Locally the gneisses host crustal eclogites that are the oldest known, worldwide.

The eclogites and their host gneisses alike record metamorphic conditions of at least 20 kb and 1000°C. Temperature is constrained by garnet-clinopyroxene geothermometry (970°C) in the eclogites and by retrograde ternary-feldspar homogenization (>1000°C) in the gneisses. Minimum pressure is established in the gneisses by pervasive polyphase kyanite-one alkali feldspar-quartz inclusions in calcic garnet. Ca-zonation patterns in the host garnet and late plagioclase rims developed between and among these phases show retrograde decompression into plagioclase stability (>20 kb) at high temperature. At highest grade, there was evidently regional development of the assemblage, garnet-kyanite-alkali feldspar-SiO_2-rutile. Many phases show significant departures from normal compositions: garnets have abundant rutile exsolution, rutile contains exsolved zircon needles, and rare white mica is highly titaniferous. The Upper Deck appears to be a sample of extremely dry, felsic material of supracrustal origin, stored at lithospheric depths before union in the lower crust with the granulite facies mylonites of the Lower Deck, apparently within an intracontinental transcurrent shear zone.

EFFECTS OF ACID PRECIPITATION UPON SOIL CLAY MINERALOGY AS ASSESSED BY THE ROTHAMSTED CLASSICAL FIELD EXPERIMENTS

Wilson, M.J. (Macaulay Land Use Research Institute, Aberdeen), Blake, L. and Goulding, K. (Rothamsted Experimental Station, Harpenden)

Soil acidification occurs through natural processes and is also considered to be exacerbated by anthropogenic acidic inputs. A consequence of such acidification is the increased mobilization of aluminium and other metals as soil pH declines. This aluminium can be released from structural sites to the soil solution in a range of monomeric or polymeric forms. It may then again become associated with clays, either displacing other cations from exchange sites, where it remains plant-available, or precipitating as a polymerized non-exchangeable form particularly in the interlamellar spaces of expansible minerals. Clay minerals therefore act as both sources and sinks for aluminium in soils according to pH conditions.

Studies of podzolic soils of acidified catchments in Scotland suggested that an expansible mineral, which was abundant in the clay fraction, was aluminium interlayered in B horizons (pH 4.3 to 4.8) but not in the E horizon (pH 3.8 to 4.1) where aluminium was present in an exchangeable form. It was impossible to know, however, whether these transformations had been accomplished entirely by natural acidification processes or whether anthropogenic acid inputs had played a significant role. Such a question can be addressed only if there is some kind of temporal control.

The Rothamsted Classical Field Experiments, initiated in 1843, include plots that have received only inputs from atmospheric deposition, afford such temporal control. A comparison was made of the clay mineralogy of soils from the Geescroft Wilderness (deciduous woodland) and Park Grass experiments, which date from 1883 and 1856, respectively. In both soils the major clay mineral is randomly interstratified illite-smectite (I/S) with subsidiary amounts of illite and kaolinite. Attention was focused on the expansible mineral.

The Geescroft Wilderness site was fenced-off in 1883 and simply left. The woodland has regenerated naturally. Soil samples were collected in 1883, 1904, 1964 and 1991. The surface horizon of the soil has acidified dramatically, falling from pH 6.2 (in 0.01M $CaCl_2$) in 1883 to pH 3.7 in 1991, most of this acidification occurring between 1890 and 1960. The XRD pattern of the I/S clay shows little change, but in the surface horizon of the 1964 and 1990 samples I/S expands less readily with ethylene glycol and contracts less readily with K-saturation. This can be accounted for by the introduction of a small amount of non-exchangeable aluminium into the interlayer space.

More significant changes were observed in the behaviour of the expansible mineral in the Park Grass soil. This site has probably been in grass for several hundred years and the soil studied (Plot 3d, unmanured, unlimed) has received only atmospheric inputs since 1856. Although the Park Grass soil was originally more acidic than the Geescroft Wilderness soil, the reverse is now the case, the surface horizon of Plot 3d on Park Grass having a pH value of 4.0 in 0.01M $CaCl_2$. A comparison of the I/S clay separated from soils sampled at different times shows that, in the 1991 sample, the mineral does not swell with ethylene glycol or contract on heating at 300°C to the same extent as the mineral in the 1876 sample. It is concluded that aluminium interlayering in the I/S mineral has increased significantly in relatively recent times.

These mineralogical observations are consistent with the chemical characteristics of the soils and particularly the amounts of the various forms of extractable aluminium which they contain. The findings are also consistent with the solubility of hydroxy aluminium compounds and their role in the buffering of protons at different pH values.

THE DYNAMICS OF H_2O IN MINERALS INVESTIGATED WITH INELASTIC AND QUASIELASTIC NEUTRON SPECTROSCOPY

Winkler B. (*Mineral. Inst. Univ. Kiel, FRG*), Hennion B. (*Lab. Leon Brillouin, CEN Saclay, France*)

Incoherent quasielastic and inelastic neutron scattering can be used to determine the dynamics of molecular H_2O in minerals, which is important for the understanding of their structures and thermodynamic properties. We present results obtained on an inverted time-of-flight spectrometer located at a spallation source. This spectrometer has a good energy resolution ($\Delta E/E = 2 - 3\%$) up to large (500 meV) energy transfers. It is ideally suited to study the intramolecular motions of H_2O. Also, quasieleastic neutron scattering experiments on a high resolution direct time-of-flight spectrometer have been performed to study the motion of molecular H_2O on a very short time scale (10^{-11} s).

The dynamics of molecular H_2O has been studied in gypsum, bassanite and cordierite, as in these three structures the H_2O is incorporated in three different ways. In gypsum, the H_2O is bound and the protons can be located in diffraction studies. Here, we have observed inter- and intramolecular motions of the H_2O and SO_4 groups. In bassanite, a spectrum recorded at 150 K implies that the H_2O is dynamically disordered. The spectrum is very similar to that observed in analcime, and is characterized by two broad bands. At very low temperature (3 K) we observed a large number of sharp bands, and at this temperature the bassanite spectrum resembles that of gypsum. This change is most probably due to an ordering of the H_2O molecules. In synthetic, alkali-free hydrous cordierite the H_2O molecules are dynamically disordered. This has been shown by earlier NMR and room temperature quasielastic neutron scattering studies, and has been confirmed here by low temperature (50 K) quasielastic neutron scattering. The inelastic cordierite spectra consist of two sharp and one broad band, which are assigned to translational and librational motions, respectively. A decrease of the temperature down to 3 K causes a gradual decrease of the width of the broad band. The dynamic disorder seems to persist even at 3 K, similar to findings for the closely related beryl structure, where NMR measurements have found a dynamic disorder down to at least 4 K. High resolution time of flight spectra obtained at 3 K exclude a tunneling motion.

AB INITIO TOTAL ENERGY STUDY OF MINERALS WITH HYDROGEN BONDS

Winkler B. (*Mineral. Inst. Univ. Kiel, FRG*), Milman V. (*Solid State Division, ORNL, USA*), Payne M.C. (*Cavendish Lab., Univ. of Cambridge, UK*) Lin, J.S (*Royal Inst., London, UK*)

Ab initio total energy calculations based on the local density approximation have been performed on brucite, $Mg(OH)_2$, and diaspore, AlOOH and cordierite, $Mg_2Al4_{Si_5}O_{18} \cdot (H_2O)$. The angle of the non-linear hydrogen bond in diaspore is reproduced well. The Raman active OH stretching frequency in brucite has been calculated using the frozen phonon approach and the calculated stretching frequency is in very good agreement with the observed value. The calculations unambigiously demonstrate that a kinetic energy cut-off of 600 eV is sufficient, and that the too small lattice parameters calculated here are not due to incomplete convergence.

The location, orientation and the total energy of hydration of molecular H_2O has been calculated. In the calculations up to 180 degrees of freedom have been relaxed. In contrast to diffraction studies, but consonant with the interpretation of infrared experiments, the calculations demonstrate that the energetically most stable orientation of the H_2O molecule in alkali-free Mg-cordierite is with the proton-proton vector parallel to [001]. The H_2O molecule in cordierite is calculated to be undistorted. It is only very weakly hydrogen bonded to the framework. The total energy of hydration for cordierite with 1 H_2O per primitive unit-cell, with fixed unit-cell parameters, has been calculated to be $\approx$0.4 eV. Local distortions in the framework caused by the incorporation of the H_2O molecule are very small, which indicates ideal mixing between H_2O and anhydrous Mg-cordierite.

PHOSPHORUS IN PEGMATITIC GARNETS - EXAMPLES FROM MAINE

Wise, M.A., (*Dept. of Mineral Sciences, Smithsonian Institution*)

The Oxford and Brunswick pegmatite fields of western Maine host rare-element granitic pegmatites enriched in Li,Rb,Cs,Be,Nb,Ta,B and F. The pegmatites are generally low in phosphorus, although local enrichment is observed. A study of garnet from the Maine pegmatites shows that phosphorus may be a significant component of the garnet chemistry in both P-rich and P-poor pegmatites.

Garnet occurs as small euhedral to subhedral crystals scattered throughout pegmatites, sodic aplites, and pegmatitic leucogranites. Garnet-rich bands (*garnet seam*), 1 to 5 cm thick, rarely occur in some pegmatites and granites. Garnet compositions examined from 50 localities are typically almandine with a few localities containing spessartine. Pyrope and andradite components are minor; combined MgO and CaO contents are generally less than 2 wt. %. Phosphorus concentrations determined by electron microprobe analysis vary from below detection limit to approximately 0.75 wt.% P_2O_5. Nearly 25% of the phosphorus data is greater than 0.2 wt.%. The distribution of phosphorus within indivdual garnet crystals and individual pegmatite bodies is variable. Although most crystals are zoned with respect to iron and manganese, phosphorus zonation was not evident.

Pegmatites hosting multi-generations of garnet show systematic variations in phosphorus content with progressive pegmatite crystallization. Early generations of garnet tend to have lower mean phosphorus contents than those found in later generations. Phosphorus contents increase with decreasing MgO and increasing Mn/(Mn + Fe). No trends were observed with CaO. Except for slightly higher phosphorus content of garnet from pegmatitic granites, no systematic differences are evident among the different subtypes of pegmatites. The mechanism most likely responsible for the substitution of phosphorus in garnet is $P^{5+} + Al^{3+} = 2Si^{4+}$.

RARE EARTH ELEMENTS OCCURRENCE MODES IN TROPICAL-SUBTROPICAL WEATHERING CRUST, SOUTH CHINA

Wu Chengyu, Lu Hailong and Xu Leiming (Institute of Mineral Deposits, Chinese Academy of Geological Sciences, 26 Baiwanzhuang Road, Beijing 100037, P.R. China)

Tropical-subtropical weathering crust of monosiallitization type

(Samama, 1986) are widely distributed in the Nanling Mountains area and the Hainan Island, south China. The weathered profile can be divided into three horizontal zones from top to bottom: (1) surface soil zone (soil-cap), 0.5-2 m in thickness, consisting of kaolinite, halloysite-(7Å), gibbsite, goethite and organic materials as the main composition; (2) wholly-weathered zone which is about 3 to 20 m thick and composed of mainly halloysite-(7Å) and kaolinite, with variable amounts of quartz and feldspar fragments; (3) sub-weathered zone, up to 5 m, having significant amounts of residual quartz and feldspar, along with halloysite-(7Å), kaolinite, some montmorillonite and vermiculite. Several tens of clay samples were collected from more than ten locations in the area, with their parent rocks including diorite, diabase, basalt, and various granitic rocks.

REE contents in the clays range from 180 to 2000 ppm which are 2 to 5 times enriched than those of their precursors, with variable LREE/HREE, Y/REE and Eu*/Eu ratios of 0.2-10, 0.05-0.6 and 0.007-0.5, respectively. Positive Ce*/Ce anomalies (1.5-4.7) are generally observed in layer (1) and negative anomalies (0.13-0.6) in layer (2). Five types of REE occurrence mode have been identified as follows:

(1) REE occur in an exchangeable state in clays, which are adsorbed by kaolinite, halloysite-(7Å) and smectite, and are readily extracted by acid and neutral electrolyte solutions. They account for 30 to 90% of the total REE amounts in the clays.

(2) REE enriched in various forms of ferromanganese oxides containing up to 1.3% REE with enrichment coefficients ranging from 5 to 80 relative to the surrounding clays.

(3) Various secondary REE minerals, or likewise, REE-rich colloidal particles. These micro-grained particles (0.1-4 μm) are observed under TEM, and analyzed by EDAX. They occur as spheroid, chain-like and irregular polygon forms with variable chemical compositions. Some of them are high in La (2-11), Ce (26-83%), Y (13-80%), Th (3-13%) and Ba (11-15%). Cerianite, thorite, rhabdophane and iimoriite (?) are also recognized.

(4) Residual rare earth-bearing minerals including monazite, xenotime, allanite, fergusonite, sphene and zircon.

(5) Very few amounts of REE are accommodated by residual rock-forming minerals of feldspar, micas and hornblende.

Based upon the above results, the main chemical controls on REE release, remobile, adsorption and precipitation in weathering environment of south China are discussed.

EXPERIMENTS ON THE ADSORPTION OF METAL IONS ONTO SULPHIDES(I): TYPES AND DYNAMIC MODEL

Wu Daqing,Peng Jinlian and Chen Guoxi (*Inst.of Geochem.Acad .Sinica, Guangzhou*)

Many experiments on the adsorption of the metal ions have been conducted by using natural minerals as absorbents,but no by the precipitated sulphides PbS and ZnS,which may play an important role of the genesis of trace elements in those sulphides in polymetal ore deposit. The adsorption isotherm curves of metal ions Cu^{2+},Ag^{+},Fe^{2+},Mn^{2+},Mg^{2+},Zn^{2+},Cd^{2+},Sb^{3+} and Bi^{3+} by newly precipitated sulphides PbS and ZnS with grain size about 1 m were determined in this study at 50 C. PH=3 and I=0.1(NaCl or Na_2SO4).Based on the curves, there are three types of the adsorption : A,the linear adsorption, e.g. adsorption density increases linearily with increasing of the absorbate initial concentration.No saturation phenomena were observed even the density as high as 0.59 mole/kg. This type includes the adsorption of metal ions Cu^{2+} and Ag^{+} by PbS,and Cu^{2+},Ag^{+} and Cd^{2+} by ZnS; B, the Langmuir adsorption, which includes the adsorptions of the metal ions Fe^{2+},Sb^{3+} and Bi^{3+} by PbS,and Fe^{2+} ,Mn^{2+} and $Mg^{2+}$by ZnS. Their densities at 50 C are that: $0.48x10^{-8}$ mol/kg for the adsorption of ion Fe^{2+} by PbS, $3.5x10^{-8}$—Sb^{3+} by PbS, $1.8x10^{-8}$—Fe^{2+} by ZnS, $2.4x10^{-8}$—Mn^{2+} by ZnS and $5.4\ x10^{-8}$—$Mg^{2+}$by ZnS, respectively. C, the reversal Langmuir adsorption,only the adsorption of the ion Zn^{2+} by PbS.

In comparision of those densities with the maximum contents of those elements in natural sulphide galena and sphalerite, we found as that: for A-type of the adsorption the densities are larger than the maximum contents of those elements in natural sulphides, and for the most of the B- and C-type of adsorptions the maximum contents are almost same with the densities ,except of the adsorption of ions Fe^{2+} and Mn^{2+} by ZnS. The densities of latter are much less than the maximum contents of those elements in natural sphalerite. However, in most of natural sphalerite the mangnese contents are no more than the density of $2.4x\ 10x^{-8}$ mol/kg.

As temperature raises from 30 C to 80 C, the 100 percent of adsorption is always observed and the concentration of the adsorbate ion in solution after equilibrum is less than 0.01 ppm that is out of the detectable limit of the flame atomic absorption spectrophotometer(FAA) for A- type of adsorption. The ionic exchange model is expected in this type of adsorption because the solubilities of the sulphides ofthe absorbate ions are less than that of the absorbent,so the equilibrium constants of the reactions are depended on the ratio of the solubilities of two sulphides.And the theoretical values are good agreement with the experimental results. As temperature raises, the higher adsorption density is expected in this type of adsorptions for more violent reaction. This was supported by the experiments on the adsorption of ion Ag^{+} by natural galena and sphalerite with the grain size about 58 -82 m.

For B- and C-types of adsorptions,the solubilities of the sulphides of the absorbets ions are larger than that of the absorbent, and the densities decrease exponently with temperature increasing. A collision actived model is adapted to those adsoptions with good agreement to the experimental results. The energies of the adsorption activation were calculated from the experimental results as following: 49. 4 KJ/mol for the sorption of the ion Fe^{2+} by PbS, 25.3 KJ/mol—Fe^{2+} by ZnS, 24.9 KJ/mol—Mn^{2+} by ZnS, 17.6 KJ/mol—Zn^{2+} by PbS—13.9 KJ/mol—Mg^{2+} by ZnS, 2.89 KJ/mol—Sb^{3+} by PbS and -0.08 KJ/mol—Bi^{3+} by PbS, respectively. For the adsorption of the ion Bi^{3+} by PbS,the negative activation energy means that the density slightly increases as temperature raises ,though it belongs to the B-type of adsorption. This is because of that the diffusion ability of the absorbed ion Bi^{3+} into the crystal lattice of the PbS increases when the temperature elevates for the similarity of the ionic rdii of Bi^{3+} and Pb^{2+}

EXPERIMENTS ON THE ADSORPTION OF METAL IONS ONTO SULPHIDES(II):INFLUENCE OF MEDIUM CONDITIONS

Wu Daqing,Peng Jinlian and Chen Guoxi (*Inst. of Geochem. Acad .Sinica,Guangzhou*)

The influence of the medium conditions(PH and ionic strength I) on the adsorption densities of the ion Cu^{2+},Ag^{+}, Fe^{2+},Zn^{2+},$Sb^{3+}$and Bi^{3+} by PbS,and ion Cu^{2+},Ag^{+},Cd^{2+},Fe^{2+},Mn^{2+} and $Mg^{2+}$by ZnS were observed at 50 C. For the A- type of adsorptions, e.g.ionic exchange-type, no remarkble variation of the densities was observed as PH ranges from 2 to 6 and ionic strength varies from 0.01 to 0.5(NaCl or Na_2SO_4) in the solution,especially for the adsorptions of the ions Cu^{2+} and Ag^{+} by PbS and ZnS with the equilibrium constants more than 10^{4}. However, the density with 0.5-0.6% fall was observed when the PH raises from 2 to 6 and the ionic strength increases from 0.01 to 0.5 for the adsorption of ion Cd^{2+} by ZnS.

For B- and C-types,e.g. the Languir and reversal Langmuir types, the influence of medium conditiuos on the densities is more complexe. As PH in the solution increases within 2-6, the density changes in different way depending on the Langmuir constants K of the adsorptions. When the K is more than 60 (l/mol) , for example of the adsorptions of the ions Fe^{2+} by PbS and Mg^{2+} by ZnS,the density increases with the PH raising. While the K is less than 40(l/mol), such as the adsorptions of the ions Fe^{2+}, Mn^{2+} by ZnS, and the ion Sb^{3+} by PbS, the densities decrease with the PH increasing. And the density is without variation when the PH variation for the K is between 40 and 60 (l/mol),such as ions Bi^{3+} and Zn^{2+} by PbS.

Initially, when the synthetic PbS and ZnS are brought

into an aqueous solution, the sulphur donor ligands of the sulphides will strongly attract the hydrogen ion H^+ to the surface with negative charges by forming the complexes MS–H or MSS_–H.The adion sorbed onto the surface of the absorbent may have following reactions as shown by R.O. James and M. G.MacNaughton(1977):

$$MS–H+A^{a+}=MSA^{+}+H^{+} \quad (1)$$
$$2MS–H+A^{a+}=(MS)_2A+2H^{+} \quad (2)$$

This is mostly true for the absorbent PbS in which the density increases with the PH increasing except of that the ions Bi^{a+} and Sb^{a+} have so strongly hydrolyze to that the tendency of the density variation has no change or fall down. On other hand, the synthetic ZnS has a PH sensitive surface charges(M.S. Moignard et al., 1977), and the very low density at PH>3 may suggest that the surface charges be turn into the positive. The exception was only found for the adion Mg^{a+} , of which sorbed by ZnS the density increasing with the PH raising is scarely detecble.

The ionic strength exerts an influence on the density by forming complexes. The variation trend of the density is depended on the competetion of the diffusion ability of the adion into the crystal lattice of the absorbent and the forming ability of the metal cation–chloride anion complexes in the solution, as well as the values of the constants C or K

For A–type of adsorption, e.g. the ionic exchange–type , the very large constants inhibit the falling down of the density detecable when the ionic strength increases. As the ionic strength raises the density decreasings were found in the ions Sb^{a+} and Fe^{a+} sorbed by PbS because of the low values of K, 70 and 38(l/mol), respectively.Meanwhile the dnsities of the ions Fe^{a+} and Mn^{a+} sorbed by ZnS increase with ionic strength raising. The reason is that the overall stability constants of the zinc chloride complexes are larger than that of the iron and mangnese, as well as the all of three ions can exchange each other in sphalerite lattice. In contrast, the stability constants of the zinc chloride complexes are smaller than that of the lead chloride, and the zinc atoms can not replace lead in galena(PbS). Hence the density has no variation for the adsorption of the Zn^{a+} by PbS. Same phenomena found at the adsorption of the ion Mg^{a+} by ZnS. Again, it was scarely detectable.

KINETIC STUDIES ON PHASE TRANSITIONS OF Mg_2SiO_4 AND Fe_2SiO_4 POLYMORPHS IN DIAMOND ANVIL CELLS

Wu, T.-C. and Bassett, W. A.
(Dept. of Geological Sciences, Cornell University, USA)

The olivine (α) to modified spinel (β) to spinel (γ) phase transitions in Mg_2SiO_4 and α to γ phase transition in Fe_2SiO_4 at high temperature and pressure under various stress environments are studied in diamond anvil cells. The types of stress environments include ungasketed powder sample, gasketed powder and hot-pressed aggregate sample with argon or nitrogen as pressure medium. For high deviatoric stress environment, the temperature range studied is chosen so that deformation has a distinctive effect on the phase transition (Wu et al., 1993). Phase transitions are studied in-situ under optical microscope or by synchrotron radiation. In the synchrotron radiation experiments, macroscopic and microscopic stress can be estimated from the anisotropic elastic strain and peak broadening of gold, which is used as pressure indicator. The growth rate of bulk sample can be measured by in-situ or post mortem X-ray diffraction. Under optical microscope, the growth rate of each spinel crystal is based on measurements of digital images captured during the experiments.

References:
T.-C. Wu, W. A. Bassett, P. C. Burnley and M. S. Weathers (1993). *J. Geophys. Res.*, **98**, 19767-19776

DEHYDRATION-MELTING OF AMPHIBOLITE AND H20-UNDERSATURATED LIQUIDUS SURFACES OF GRANITOID MAGMAS: ARCHEAN CRUST FORMATION

Wyllie P.J. (*Cal. Inst. Technology, U.S.A.*), Wolf M.B. (*Univ. Oklahoma, U.S.A.*) and van de Laan, S.R. (*Univ. Göttingen, Germany*)

It is commonly proposed that the tonalites, trondhjemites and granites of the Archean grey gneisses (TTG series), characterized by highly fractionated rare earth elements, were derived by partial melting of amphibolite, or the high pressure equivalent, hornblende-eclogite.

Five 1991 experimental studies on the solidus for dehydration-melting of amphibolites yield somewhat divergent results. Wyllie & Wolf (1993) explained these in the context of a new phase diagram showing the vapor-absent solidus for closed-system simple amphibolite (Hb + Pl) in two parts, the beginnings of multivariant reactions: (1) a near-vertical curve (steep positive dP/dT) where augite is formed, and (2) a near-horizontal curve BC at higher pressures (< 10 kb; shallow positive dP/dT) where garnet is formed (this curve and the associated solidus backbend to lower temperatures and pressures were previously unacknowledged). There is a wide, pressure-sensitive reaction interval for amphibole. The solidus curves shift with bulk composition. The field for liquid generation with garnet-amphibolite residues extends to much lower temperatures and pressures compared with the other recent experimental results. This feature has significance for REE and other trace element concentrations in partial melts from amphibolite.

The liquidus surfaces for H_2O-undersaturated TTG magmas can be mapped with contours for % H_2O and field boundaries separating fields of primary minerals. From such diagrams, one can read the depths, temperatures and H_2O contents of primary magmas that left specific residual minerals in the source rocks (van der Laan & Wyllie, 1992). We have determined liquidus surfaces and field boundaries for four TTG magmas (tonalite, trondhjemite, granite) with different SiO_2 contents. The field boundaries for amphibole and garnet in tonalites and trondhjemite occur in similar positions, but the granite has neither mineral on its liquidus.

Conclusions from the forward (amphibolite) and reverse (TTG magmas) experimental approaches include: (1) If TTG's leave residual amphibole, this requires moderate temperatures (800-1000°C) but H_2O contents (about 10-15%) which are higher than those in melts produced from dry amphibolite. (2) Residual garnet requires depths greater than ~50 km, temperatures higher than ~1,000°C and lower H_2O than for residual amphibole; greater depths and temperatures are required for magmas with lesser H_2O contents. (3) The limited area for coexisting garnet and amphibole on the liquidi (with relatively high H_2O contents) -- contrasting with the large, relatively low-temperature PT area for amphibolite where the residual minerals coexist with H_2O-undersaturated liquid -- suggests that although experimental liquids from amphibolites plot in the fields for trondhjemite and tonalite in feldspar classification diagrams, they do not necessarily have the compositions of real TTG's; they appear to need additional dissolved mafic mineral components to correspond to the natural magmas.

The concept of primary magmas for the Archean grey gneisses is an oversimplification, but the equilibrium phase relationships provide the framework for unravelling the complications of multiple melting and fractionation episodes. Experimental data are consistent with proposals that trondhjemites may be derived from secondary partial melting of tonalites which were derived by melting of amphibolite or eclogite. Further refinement of the experimental field maps for melting amphibolites and crystallizing TTG magmas will place tighter constraints on the conditions of generation and emplacement of the magmas in terms of depth, temperature and H_2O contents, yielding

insights into the tectonic environments for the formation of early continental crust.

References:
van der Laan, S.R. & Wyllie, P.J. (1992). *J. Geol.*, **100**, 57-68.
Wyllie, P.J. & Wolf, M.B. (1993). *Geol. Soc. (London) Spec. Paper* **76**, 405-416.

NONEQUILIBRIUM — STATE MICROSTRUCTURES IN THE HEAVILY SHOCKED ROCK — FORMING AND METALLIC MINERALS

XIE Xiande and CHEN Ming (*Institute of Geochemistry, Guangzhou Branch, Academia Sinica, Guangzhou* 510640, *P. R. China*)

The information of the deformation and phase transformation of minerals under impact of different intensities can be obtained from some meteorites and from shocked rocks of impact craters. Our SEM, TEM and Raman spectroscopic studies on the severely shocked (>100GPa and >2000℃) Yanzhuang H6 Chondrite and on the heavily shocked (>25GPa) quartz of Ries Crater, Germany, have revealed the following phase combinations of nonequilibrium—state microstructures in the very small grains of minerals.

For Olivine: (1) thetomorphic glass + ringwoodite + recrystallize olivine
(2) spinel (γ phase) + modified spinel (β phase)

For Pyroxene: (1) thetomorphic glass + highly disordered pyroxene
(2) Majorite + recrystallized pyroxene
(3) Combination of complicated Si—O tetrahedra groups, including the tetrahedra with one or four non—bridging oxygen and fully polymerized Si—O tetrahedra in addition to the two—bridging Si—O tetrahedra chain structure.

For (FeNi) metal: (1) α phase + (α Phase + martensite) + γ phase
(2) martensite + γ phase

For Quartz: (1) α phase + thetomorphic silica glass
(2) α phase + thetomorphic silica glass + coesite
(3) α phase + thetomorphic silica glass + coesite + stishovite

All the above mentioned phase phase combinations of nonequilibrium — state microstructures are the results of rapid cooling after shoch events.

THE AMPHIBOLES AND PYROXENES OF ALKALI-RICH INTRUSIONS IN QING-ZANG PLATEAU AND ITS ADJACENT AREA OF SOUTHWESTERN CHINA

Xie Y.W. and Zhang Y.Q. (*Guangzhou Institute of Geochemistry Academia Sinica, Guangzhou, P.R.C.*)

The alkali-rich intrusive rocks in Qing-Zang plateau and its adjacent area are divided into two zones: a) the sodium-rich intrusive rocks formed during the Late Hercynian-Indo Chinese epoch include the syenites and alkaline granites with $Na_2O > K_2O$ and low Ca, Sr, Ba and REE in Kang-Dian old land. b) the kalium-rich intrusive rocks named Ailaoshan-Jinshajiang zone formed during Himalayan epoch are constituted by syenites, syenite porphyries and diopside granites with $K_2O > Na_2O$ and high Ca, Sr, Ba and REE.

The associations and chemical compositions of melano-minerals are different in two zones. In sodium-rich series of rocks, the melano-minerals accounted for 4-8 per cent in rock are aegirines(Ac 80-87%) and minor aegirine-augites(Ac 32-47%) in alkaline granite. On the other hand, the syenites in kalium-rich series of rocks are composited by diopsides and amphiboles including edenite and magnesio-hastingsitic hornblendes, while the diopside granites are constituted by diopsides, hedenbergites, edenites and edenitic hornblendes.

In the genetic diagram of chemical classification of amphibole, they are ploted in the regions of intermediate-acidic rocks. The points of diopsides are located on the area of alkali- and superalkali-rocks in (Ca+Na+K)-Mg-(Fe+Mn) diagram. It means that the host rocks of the diopsides, especially the diopside granite, belong to the alkali and super alkali-series of rocks.

Both the melano-minerals and the host rocks in two zones possess the chemical evolutions of Fe richness. In the kalium-rich rocks, the values of F/M are changed from 1.98-3.76 in early alkaline rocks to 8.9-24.4 in later diopside granites, while the amphiboles with the F/M values of 0.77-1.99, and the diopsides with the Fs contents of 13-26%. The same patterns are appeared in the sodium-rich series of rocks.

PLATINUM GROUP MINERALS IN THE NUANQUANZI AND TULING-SHIHU GOLD DEPOSIT, NORTH CHINA: THEIR SIGNIFICANCE FOR SOURCES OF GOLD

Xu H. and Peng Q.M. (Dept. of Geoch., Changchun Uni. of Earth Sciences, 130026, Changchun, P.R.China)

The Nuanquanzi and Tuling-Shihu gold deposit are hosted in the Archaean greenstone belt and high grade terrane, respectively. The Nuanquanzi gold deposit is believed to be associated with ductile shearing, and the ore-hosting mafic- ultramafic rocks are regarded as the source rocks of gold (Xu, 1991). The Tuling-Shihu gold deposit is interpreted as a magmatic hydrothermal deposit, but the source of gold is still problematic (Li et al., 1987).

The affinity of platinum group elements (PGE) with mafic and ultramafic rocks have been well known. In those rocks PGE exist as platinum group minerals (PGM), exsolutions in sulfides or are hosted in rock-forming minerals (Cabri, 1992). Therefore, the presence of PGM can serve as path-finders for gold sources.

Native ruthenium has been found in the Nuanquanzi and Tuling-Shihu gold deposit. Meanwhile, Pt was identified in the native ruthenium and hedlyite from the Nuanquanzi deposit. These minerals are coeval with the gold mineralizations in the two areas. Coexisting iron-chrome mineral was also detected in the Nuanquanzi deposit, which coocures with the above minerals. Pt is heterogeneous in the native ruthenium and hedlyite, probably as exsolutions or inclusions. The presence of these minerals suggests that the ore-forming hydrothermal systems could be PGE-bearing.

Chemistry of native ruthenium from the two gold deposits exhabits high level of W, Fe and Co, with respect to those

from the oxidation zones of ultramafic rocks (Lin and Chen, 1980). This may be due to the ore-forming hydrothermal systems that are marked by W and Co anomalies.

The presence of native ruthenium and Pt-bearing hedlyite in the two gold deposits, along with S, O and H isotope data, suggest that Ru and Pt come from mantle-derived rocks, most likely the mafic and ultramafic rocks in the ore-hosting sequences. The higher Pt enrichment in the Nuanquanzi gold deposit is consistent with the fact that the deposit has a more direct link with the ultramafic rocks (komattites) in the Archaean greenstone belts.

References:
Alapieti, T.T., Halkoho, T.T.A., Iljina, M.J., and Tormanen, T.O., (1992) the 29 th IGC. Absract V.3, 721.
Cabri, L.J., (1992) The Mineralogical Magazine, 56, 289-308.
Li, G.S., Jia, K.S. and Yang, D.F. (1987), Unpublished research report, Changchun Uni. of Earth Sciences (in Chinese).
Lin, Y.C. and Chen, K.Q. (1980), Geological Review, 26, 74-76 (in Chinese)
Xu, H (1991), Unpublished research report, Changchun Uni. of Earth Sciences (in Chinese).

FLUID INCLUSION STUDY ON ALTERED ROCKS OF GOLD DEPOSITS IN THE XIAOQINLING MT. AREA, WEST HENAN, CHINA

XU Jiuhua (Dept. of geology, Univ. of Sci. and Tech. Beijing, China)

The Xiaoqinling Mt. area, located in the west Henan and extend to Shanxi, is one of the most famous gold production districts in China. The gold—bearing quartz veins, controlled by east—west strike shear zones and related to late Yanshanian granite, occur in the Archean Taihua group. The major metallic minerals in ore are native gold, electrum, pyrite, galena, chalcopyrite and sphalerite. The gangue minerals are dominated by quartz, sericite, ankerite and calcite. Five alteration zones can be recognized from wall rock to veins; unaltered rock (zone 0), weakly altered amphibolite or gneiss (zone I), intensive altered rock (zone Ⅱ), beresite and beresitic mylonite (zone Ⅲ), and veins (zone Ⅳ) (XU, 1993).

Four generations of quartz can be distinguished under microscope and their fluid inclusion characteristics have been studied recently. The earliest generation of quartz (Q_1), replacing plagioclase and hornblende, contains fluid inclusions with halite crystals (type N). The homogenization temperatures (T_h) of them are from 268 to 470℃, and melting temperatures (T_m) of halite crystals range from 225° to 465℃ which are lower or higher than T_hs. The salinities of type N inclusions are from 31.7 to 48wt%, and the mininum trapping pressure (P_t) may be about 170 MPa according to Roedder's method (1984). The second generation of quartz (Q_2), occuring as fine—grained aggregate and associated with sericite and replacing plagioclase and orthoclase, contains two phase (L+V) tiny fluid inclusions. The third generation of quartz (Q_3), replacing most of the earlier minerals, usually occurs in mylonites, intensive altered rocks, and especially beresite near the veins. Large amounts of fluid inclusions rich in CO_2 (high—density of CO_2 or containing liquid phase of CO_2, type C) are frequently found in Q_3. Their T_hs range from 210 to 295℃ and CO_2 contents are from 27.6 to 40 wt%. The mininum P_t of type C inclusions may be from 57 to 190 MPa, based on critical inclusions which have 250—310℃ of T_h. The fluid inclusion characteristics of Q_3 are so similar to those of quartz in veins that we can conclude that both of them formed from the same fluid during mineralization and alteration. Finally, the latest generation, Q_4, occurs as fine—grained aggregate in tiny fractures of Q_3, especially in mylonite. It is considered to be the product of dynamic recrystallization.

Q_1 can be usually seen in zone Ⅰ, and sometimes in zone Ⅱ. Q_3 may appear in zone Ⅱ, but they are more developed in zone Ⅲ. In some samples from zone Ⅱ, four phase fluid inclusions ($L_{H_2O}+L_{CO_2}+V_{CO_2}+S_{NaCl}$) can be found. It is indicated that the salinity of a hydrothemal fluid decreases from zone Ⅰ to Ⅲ, while CO_2 in fluid increases. Further study on physicochemical evolution in hydrothermal system during alteration now is carrying on.

SOME MINERALOGICAL CHARACTERISTICS OF SINTER-SYNTHETIC MULLITE

Xu Jianguo, Wang Guanxin and Peng Wenshi *(Institute of Geochemistry (Guangzhou Branch), Academia Sinica, PRC)*

As the main composition in aluminum-refractory material, mullite is the one of the predominant mineral phases in sintering clay minerals and bauxite. The experiment results of sintering bauxite show that the composition of mullite chages within in a rather large range. The ratio of Al to Si varies from 1.78 to 3.34, corresponding to molecular formula from $Al_2O_3.SiO_2$ to $2Al_2O_3.SiO_2$. This study also shows that the ratio depends to a great extent on the sintering temprature, and to a less extent on the composition of bauxite. Mullite starts crystallization at 1400 ℃ in a low ratio of Al/Si. It increases with increasing sintering temprature from 1400 to 1650 ℃. The maximum ratio is arrived at 1650 ℃ while the mullite crystallizes in a great quantity. The ratio will not change when the sintering temprature is over 1650 ℃. The spectra of NMR shows that there are two types of coordination polyhedron [AlO_4] and [AlO_6] in mullite structure. A small amount of Ti and Fe is determined and their contents do not relate to the sintering temprature. From the EPR it is suggested that Ti^{+4} and Fe^{+3} substitute for Al in [AlO_6].

• ULTRA-HIGH-PRESSURE MINERAL ASSEMBLAGE OF DABIE SHAN METAMORPHIC ROCKS, EASTERN CHINA

Xu Shutong *(Anhui Inst. of Geol., Hefei 230001, China)*

Dabie Mts. form the eastern part of Qingling orogen in central China and is a collision belt between Yangtze and Sino-Korea continental plate. The most interesting tectono-petrologic unit is the ultra-high-pressure belt composed of eclogite, garnet-pyroxenite, garnet-peridotite, jadeite-quartzite, ultramafics and some metasedimentary rock lenses rounded by sheared matrix or mylonite bands. Ultra-high-pressure mineral assemblages are: Gt + Omph + Ru + Zr + Cs + Dia + Ky + Zo + Ti in eclogite, and there is diopside instead of omphacite in garnet-pyroxenite, Gt + Cpx + Opx + Olv + Ru + Cs in garnet-peridotite and Jd + Q + Gt +

Ru + Cs + Dia(?) in jadeite–quartzite. There are also the assemblages Gt + Omph + Q + Phen + Zr + Zo + Ti and Q + Phen + Ky + Co + Tp + Gt + Ctd + Zo in schists, and Gt + Cpx + Phen + Pl + Kfs + Q + Ru + Zo in gneiss. The most important minerals in these assemblages are Gt, Omph, Jd, Phen, Ky, Co, Tp and especially Cs and Dia.

Garnet in tectonic lenses and matrices are almandine–rich, grossular–rich or pyrope–rich, some of which contain inclusions of Dia, Cs, Ru, Zr and Ti, and sometimes barroisite, and some of which are altered to symplectite composed of plagioclase and amphibole.

Omphacite is characterized by moderate Al_2O_3 and Na_2O. Some omphacite is altered to diopside by differentiation of jadeite component, thus the host rock comes to garnet–pyroxenite. Deep alteration always makes some of these rocks to be amphibolite.

Jadeite is always the major mineral of jadeite–quartzite with a composition of more than 85% $NaAlSi_2O_6$ associated with Q, Ru and Gt. Most jadeite grains are altered to plagioclase and minor amphibole.

Phengite occurred in both tectonic lenses and country rocks with the distinct feature of high Si (3.46–3.68 p.f.u.).

Corundum mainly occurs in phengite–quartz–schist and is sometimes associated with Ky, Gt, Tp and Ctd. 11.30–12.10 F_2 content was tested in topaz. According to experiments, the assemblage Q + Cs + Ky + Tp and Ky + Co + Tp is stable at P = 3.11 Gpa, T = 1214°C and P = 3.42 Gpa, T = 1074°C respectively.

Coesite found in Dabie Shan metamorphic rocks is the third occurrence of the world. It occurs as inclusions in garnet and sometimes in kyanite and omphacite. Typically, it is easily recognized with its high relief rounded by quartz pseudomorph after coesite in a host garnet with radial cracks. Coesite inclusions were found mainly in tectonic lenses, occasionally in gneiss.

Diamond crystals were found mainly in eclogite, garnet–pyroxenite and jadeite–quartzite(?). They were found at first in some polished thin sections from eclogite and garnet–pyroxenite and occurred as inclusions in host garnets. Most diamond crystals are euhedral octahedron, tetrahedron, and sometimes cube and dodecahedron. Features such as rounded, imbricated, laminar or curved striated crystal faces are visible. Identification of diamond was made by microscopy at first, then by X–ray diffraction and Raman spectroscopy on a 0.1–0.3 mm thick polished thin section. Extracted diamond crystals from rock samples were identified by X–ray diffraction with triaxial Gandolfi camera (designed by Dr. Zhang Hanqin). The principal peaks were observed at 2.06 Å(100), 1.26 Å (60), 1.075 Å (50), 0.892 Å (50) and 0.819 Å (60). Size of diamond grains found in thin section is 20–60 μm across but some larger ones up to 240 μm were also found. Extracted diamonds have diameter around 150 μm, though one is 700 μm. The presence of diamond inclusions indicates that the P/T condition during the peak metamorphism of eclogite should be approximately T > 900°C and P ≈ 4.0 Gpa. Thus, the ultra–high–pressure belt which is believed to be a tectonic melange and is continental origin during Mesozoic era by isotopic (Sm/Nd) analysis must be subducted to much greater depth than previously thought, and can subsequently return to the surface with its high–pressure signature intact.

Transmission Electron Microscopy of Stacking Disorder in Magnesian Amphibole

Xue Jiyue *(Department of Earth Sciences ,Nanjing University, PRC.)*

A magnesian amphibole (Mg/Fe+Mg=0.79—0.81) collected from a fault melange zone of Zhejiang Province , China was studied by means of TEM . CTEM study shows that certain areas of this amphibole are a kind of intergrowth of cummingtonite with anthophyllite. The cummingtonite has the space group C2/m, and anthophyllite is of Pnma symmetry. From the lattice fringe image (Fig.1) , it can be seen that the interfaces of two intergrowth phases are straight.

The coarse fringes with 1.8nm periodicity are the lattice fringes of anthophyllite, and the fine fringes are of cummingtonite. It is clear that the width of two phases varies randomly in several unit cell scale (measurement along a* direction). As it is known ,the difference between the crystal structures of cummingtonite and anthophyllite mainly lies in

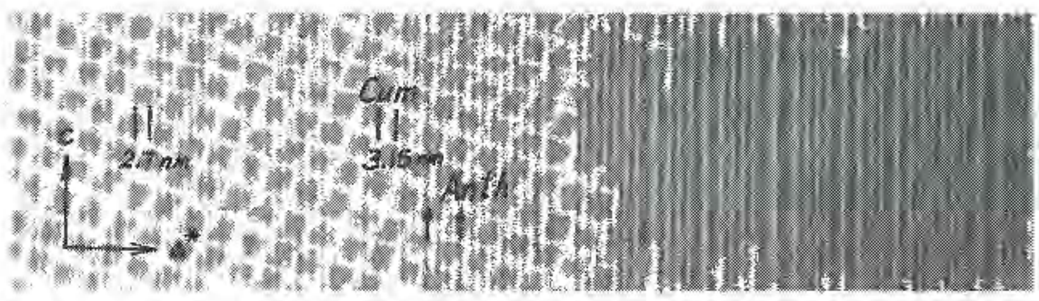

Fig.1 *Lattice image of magnesian amphibole showing the stacking disorder*

the stacking sequence along a*–axis . In other words, the width variance of two magnesian amphiboles in a very narrow range present a kind of stacking disorder . This kind of disorder should indicate a special forming condition of this amphibole. Anthophyllite and cummingtonite have the same composition, but the different crystal structure. Thus, their intergrowth reflect a kind of unthorough phase transformation. Having examined the width of monoclinic field of the lattice fringe image , it is found that their width is either in odd time of 0.45nm or in even time. In addition, there are the slabs with width in odd time of 0.45nm, which ar indicated by arrows in Fig1, in the anthophyllite field. These facts sho the orthorhombic fields in this amphibole transformed from monoclini amphibole, not reverse case, because there are four 0.45nm slabs for a orthoamphibole unit cell in a-axis direction .

TEM study also shows there are exsolution lamellae of calci amphibole (actinolite) within this magnesian amphibole. Therefore author believe that the initial crystals were homogeneous bearing wit calcium. The stable crystal structure of calcic amphibole has C2/m spac group. The exsolution of calcic amphibole caused the decreasing of C content, so that the host amphibole free of calcium transformed to a mor stable crystal structure. This structure should be in Pnma symmetry. Du to the mineral formed in a rapidly cooling condition, the transformation towards Pnma amphibole with C2/m-amphibole relic was frozen.

THERMOELASTIC PROPERTIES OF SILICATE PEROVSKITE UNDER LOWER MANTLE CONDITIONS

Yagi T., Funamori N.,Uchida M., Kondo T. and * Utsumi W. (*Inst for Solid State Physics, Univ. of Tokyo*, * now at *Dept. of Earth and Space Science, State Univ. of New York at Stony Brook*)

The orthorhombic (Fe, Mg)SiO_3 perovskite is considered to be the most dominant mineral in the Earth's lower mantle. Therefore, its thermoelastic properties (e.g., bulk modulus and thermal expansivity) play an essential role for understanding the physics and chemistry of the lower mantle. There is now a good agreement among several groups employing different techniques in yielding the value of bulk modulus and its pressure derivative (see Jeanloz and Hemley, 1994). However, it is quite difficult to determine the thermal expansion coefficient α, under lower mantle conditions (P>24 GPa, T>1900 K), because the effect of temperature on volume is much smaller than that of pressure.

Thermal expansion measurements under pressure were reported, so far, using four different types of apparatuses; externally heated diamond cell (Mao et al., 1991), DIA-type cubic-anvil apparatus (Wang et al., 1991), Drickamer-type opposed-anvil apparatus (Funamori and Yagi, 1993), and MA8-type double stage multi-anvil apparatus (Morishima et al., 1994). In all the experiments, a powder x-ray diffraction technique using a synchrotron radiation as an x-ray source was employed. The only measurement under lower mantle condition (Funamori and Yagi, 1993) clearly indicates that the orthorhombic perovskite-type $MgSiO_3$ is stable at least at the top part of the lower mantle. However, the thermal expansion coefficient so far reported are largely scattered and the problems of each measurements are discussed.

References:

Jeanloz R. and Hemley R. J. (1994) *EOS*, in press.

Mao H. K., Hemley R.J., Fei Y.,Shu J.F., Chen L.C., Jephcoat A.P., Wu Y. and Bassett W.A.(1991) *J. Geophys. Res.*, **96**, 8069-8079.

Wang Y.,Weidner D.J., Liebermann R.C., Liu X., Ko J., Vaughan M.T., Zhao Y., Yaeganeh-Haeri A., and Pacalo R.E.G.(1991) *Science*, **251**, 410-413.

Fumamori N. and Yagi T. (1993) *Geophys. Res. Lett.*, **20**, 387-390.
Morishima H., Ohtani E., Kato T., Shimomura O., Kikegawa T. (1994) *Geophys. Res. Lett.*, in press.

MINERAL SUBSTRATUM AND MICROORGANISMS: THEORETICAL PROBLEMS/TECNOLOGICAL APPLICATIONS

Yakhontova L. K. (Dept. of Geology, Moscow State Univ.) and Grudev A. P. (All-Russian Scientific-Research Institute of Mineral Resources, Moscow)

By maintaining (donor/acceptor) mechanism of interaction of microorganisms with mineral substratum, the mineral as a whole is subjected to oxidizing degradation. This process realizes by fermentative reactions, appreciably reducing corresponding activation energy.

Entropy effect for that evolution in a large measure is determinated by degree of mineral destruction, i. e. "external part" of the effect. Donoral (maintaining) property of any mineral by its interaction with microorganism is controlled by crystallochemical (atomization energy, effective parameters of structure), electrophysical (semiconductial) and topological (texture, microzonality, dislocations, blockness, fractal measureness, features of intercalating etc.) characteristics.

Investigation of mineral substratum firmness permits to estimate general perspectives of biotechnology for mineral raw materials. This problem strongly is studied by the authors by specialized investigation of various sulphides, silicates & carbonates in aspect of their interaction with industrial microorganisms. As a result authors propose any initial variant of being to standartization System of Mineralogical Providing of Biogeotechnology:

* Specialized revealing of mineralogical criteria of biogeotechnology effectiveness;
* Special mineralogical/technological mapping of the deposit by numerical simulating(PC).

References:
Yakhontova, L. K., Grudev, A. P. et al.(1991); Dokl. Acad. Sci. USSR 320, 1459-1462.

CARBONATE MINERALIZATION OF THE KHIBINY ALKALINE MASSIF

V Yakovenchuk, Ya Pakhomovskiy and A Bogdanova *(Geological Institute of the Kola Science Centre of the Russian Academy of Sciences)*

The Khibiny alkaline massif is one of the traditional objects for investigation of hydrothermal mineral-forming evolution. The massif is strongly differentiated and consists of rocks with normal Na-concentration as well as specific pegmatite-like rocks saturated by alkaline metals and REE. Carbonate - and zeolite - bearing veins cross-cut the rocks being wide-spread throughout ijolite-urtite arc and carbonatite core of the massif. It is possible to distinguish the following stages of carbonate crystallization:

1. Calcite, aragonite, rhodochrosite, siderite, ankerite, witherite, barytocalcite, strontianite;
2. Burbankite, carbocernaite, ancylite-(Ce), zhonghuacerite-(Ce) donnayite-(Y), ewaldite-(Y), mckelveite-(Y);
3. Pirssonite, shortite, tuliokite, sidorenkite, bonshtedtite;
4. Natrite, thermonatrite, natron, trona;
5. $Na_2C_2O_4$

A juxtaposition of mineral assemblage and their chemical compositions from the ijolite-urtites and from carbonatites allows us to conclude that it is the forming of carbonatite core that caused the carbonate-bearing veins crystallization in the outlying parts of the massif.

SUPRA-SUBDUCTION ZONE OPHIOLITES IN CENTRAL ANATOLIA: GEOCHEMICAL EVIDENCE FROM THE BASALTS OF THE SARIKARAMAN OPHIOLITE, AKSARAY, TURKEY

Yaliniz M. K. (*Dept. of Geol. Eng., METU*), Floyd P.A. (*Dept. of Geol., Univ. of Keele*) and Göncüoğlu M.C. (*Dept. of Geol. Eng., METU*)

Basaltic pillow lavas of Late Cretaceous age from the Sarikaraman Ophiolite (OP) have been systematically sampled and analysed geochemically to interpret the tectonic environment in which they formed. All the basaltic rocks are slightly metamorphosed, variably vesicular and differentially altered to mixtures of chlorite, epidote, iron-oxides, zeolite and carbonates. Petrographic and geochemical data on the least altered pillow lavas indicate that they were originally olivine-poor, plagioclase+clinopyroxene phyric tholeiites. In terms of immobile trace element data, they have the geochemical characteristics of island arc tholeiites. The distinctive feature of their N-MORB normalized spiderdiagram is the enrichment of LIL elements (Sr, K, Cs, Rb, Th ± U) and a relative depletion of HFS elements (Nb, Ta, Hf, Zr, Ti, Y, and Yb). In part the enrichment of some LIL elements is a reflection of the degree of low-grade alteration. However, overall the basalts display chemical features characteristic of supra-subduction zone ophiolites (Pearce,1984).

The geological and geochemical characteristics of late Cretaceous SO reveals a complex history interpreted as mainly the result of a progressive supra-subduction zone spreading process. The geochemical characteristics of these basalts are similar to the other late Cretaceous Tethyan ophiolitic basalts (Troodos, Pindos and Oman) and indicates a pre-collisional extension during the convergence of the Neo-Tethyan ocean.

IMAGING OF SERPENTINE SURFACES WITH THE AFM

YAMAGUCHI,K.,KAKITANI,S.,MIYAKE,H.(*Faculty of Science, Okayama University of Science*), KOHYAMA,N.(*National Institute of Industrial Health*) and SATO T. (*Okayama Ceramics Research foundation*)

We have used an atomic force microscope(AFM) Nanoscope II(Digital Instrument Inc.) to study the surface structures of serpentine, especially antigorite and chrysotile from Kumamoto in Japan.

The first, from the observation of the antigorite, the AFM image of it on a cleavage plane shows a regular stripe pattern corresponding to its tetrahedral and octahedral sheet appeared alternatively and periodically in the superstructure. The average width of high parts on the stripe is 2.40±0.25nm and that of low parts is 1.87± 0.37nm. Consequently the A value of antigorite superstructure is estimated to about 4.27nm.

Compared with the above-method, the same A value

obtained by the method of the HRTEM image ranges from 3.7 to 4.7nm and this method of the HRTEM image is not almost as equal as the result of the AFM image. The result of the AFM is similar to the data by Kunze(1956) and Uehara and Shirozu(1985).

According to the method of the AFM, the super-structure , both lateral and vertical is observed in higher accuracy and in more details on nano metre scale than any other methods.

The Second, the crysotile tube-shaped fibrous forms are imaged by the AFM. As its result, the outer diameter of crysotile fiber ranges from 50 to 100nm. With scanning further closely on the outer surface of the crysotile tube. the pattern in the AFM image of it is similar to the octahedral sheet of brucite obtained before.

It was found that the outside surface of the crysotile fiber not is composed of the tetrahedral sheet but it octahedral sheet only.

Reference

Kunze, G.(1956). Z. Krist.,108,82-107.

Uehara, S. & Shirozu, H.(1985). Mineral. J.,12,299-318.

POLARIZED MID INFRARED SPECTRA (2.5-14.3μm) OF CALCITE

Yamamoto A, Nakashima S, (*Graduate school of Science, Univ.of Tokyo*), Takahiro Shibatake (*Dept. Chem. Hokkaido Univ.*) ,and Kawamura K (*Tokyo Inst. of Tech.*)

Carbonate rocks, mainly composed of calcite, show a worldwide distribution and form important reservoirs for carbon dioxide, petroleum and ore deposits. We collect polarized infrared transmittance and reflectance spectra of calcite to study infrared polarization behavior of calcite. One of the reasons for employing polarized light in our study is that the reflectance spectra data of surface of the Solar planets, including the earth, by remote-sensing are obtained from reflected light of Solar luminescence which is not isotropic. (Mizutani *et al.*, 1984) Another reason is that calcite has a very clear cleavage along (10T1) and calcite is anisotropic between crossed nicoles under the visible microscope.

The sample used in this study was a single crystal of calcite of Sweetwater mine, Missouri, U.S.A. The calcite was sliced and the piece of 30μm thick and that of 3mm thick were used in this study. Then the samples were examined by micro FT-IR (JASCO Janssen). The sample was placed on the stage so that optical axis of micro FT-IR was normal to (10T1) plain of calcite, and polarized infrared spectra of calcite was collected every 30 degrees. We collected two types of spectra, reflected and transmitted. The obtained reflectance spectra were transformed by Kramers-Kronig method.

Reflectance spectra: Whether the IR polarizer was in or out of the optical axis, the relative intensities of the absorption bands of calcite in infrared changed with rotating the stage, but those positions did not shift. The absorption intensities at about 1450cm^{-1} due to C-O stretching vibrations and their overtone and combination mode, and at about 715cm^{-1}, 870cm^{-1} due to C-O bending vibrations and their overtones and combination mode seem to change every 180 degrees. The extent of the change of the intensities of absorption due to C-O stretching vibrations is more remarkable than that due to C-O bending vibrations. The thickness of samples did not influence the fact stated above.

Transmittance spectra: The main absorption band of calcite about at 1450cm^{-1} due to C-O stretching vibrations are not observed clearly with the 30μm thick calcite. The intensities of the absorption bands at about overtones of 1450cm^{-1} due to C-O stretching vibrations and at about 715cm^{-1}, 880cm^{-1} due to C-O bending vibrations and their overtone and combination modes change with rotating the stage, whether using IR polarizer or not. The trend of the extent of the change of intensities is same as that of reflectance spectra.

When we obtain the spectra data by remote-sensing, the data is in reflectance mode. Therefore the results of this study indicate that some cautions should be considered for the polarized IR intensities in the interpretation of infrared remote-sensing data.

Reference:
Mizutani, T., Maihara, T., Hiromoto, N., Takami, H., and Hasegawa, H. (1984), *Nature*, **312**, 134

DYNAMICAL PROCESS OF THE PRESSURE-INDUCED AMORPHIZATION AND DEHYDRATION OF HYDROUS MINERALS UNDER PRESSURE AND ITS GEOPHYSICAL MEANING

Yamanaka, T., Yano, K., Dejima, M. and Nagai, T. (*Dept. of Earth and Space Science, Faculty of Science, Osaka University*)

Kinetic studies concerning transition, recrystallization, decomposition and melting of hydrous minerals and mafic minerals in the subduction zone have become more significant projects to comprehend the dynamical subjects concerning to deep focus earthquake or global tectonics. We have reported pressure-induced amorphizations of quite a few substances, (Mg_2GeO_4 olivine, quartz-type compounds, hydroxide minerals and sulfates) and proposed their mechanisms from crystal chemical and physical aspects by time-resolved X-ray diffractometry, EXAFS, Raman spectroscopy and elastic measurement (Yamanaka et al., 1991a). Molecular dynamics calculation was also conducted for the amorphization of forsterite.

Pressure-induced amorphization of hydroxide minerals

Water content in mantle have been informed from analysis of minerals, (olivine, pyroxene and garnet) in the mafic rocks of harzburgite or lherzolite. A pressure-induced amorphization of serpentine was discussed to understand deep-focus earthquake (Meade & Jeanloz, 1991). To understand the recirculation of marine water to the deep interiors through subduction of hydroxide minerals, we investigated the mechanism of the amorphization and dehydration of $Ca(OH)_2$ and $Mg(OH)_2$ under compression using synchrotron radiation and Raman spectra.

Apparent activation energies of Ca and Mg hydroxide at ambient pressure indicates almost the same value, 209 and 197kJ/mole, respectively, though dehydration temperatures are quite different, 853K of the former and 623K of the latter (Yamanaka et al, 1991b). Under compression at room temperature $Ca(OH)_2$ shows the amorphization at about 11GPa by single crystal X-ray diffraction. The crystal is anisotropically more compressed in the direction perpendicular to the oxygen layer, as c/a ratio decreases with pressure. However, O-H interatomic distance increases with pressure probably due to enhancement of the hydrogen bond resulting from a lower energy shift of Raman band of OH stretching.

$Ca(OH)_2$ shows a recrystallization from the amorphous phase under decompression, which indicates the amorphization is caused by plastic disordering oxygen array. A transition to a new crystalline phase has been also found at 300°C at 18GPa and is reversibly transformed to the amorphous phase with decreasing pressure. The amorphization is characterized by a metastable and precursor phenomenon to the high pressure stable form.

At room temperature $Mg(OH)_2$ is directly decomposed to MgO and Ice VII at 5GPa without amorphization process, which accords with Fei and Mao (1993). Dehydration energy of both hydroxide mentioned above is provided only from compression energy $P\Delta V$ at ambient temperature. Their compressibilities determine which is energetically stable, dehydration or amorphization. A total volume of Ice-VII and CaO at high pressure does not exceed that of the amorphous phase of $Ca(OH)_2$, while $Mg(OH)_2$ is decomposed to MgO and Ice-VII.

The amophization in the cool and high stress subduction plays a role to recycle water in the mantle and to make a ductile flow of the slab.

Pressure-induced amorfization forsterite by MD calculation

From the view point of seismic mechanism, coordination change in metasilicates and transformation of olivine phase have been paid a large attention. The pressure-induced amorphization of olivine may also provide useful insights for the motivation of deep-focus

earthquake. Molecular dynamic calculation of Mg_2SiO_4 forsterite exhibits the amorphization at 40GPa at room temperature. The amorphization is resulted from swaying the hexagonal close packed oxygen layers just before the transition at 95GPa. Si atoms in the amorphous have not only fourfold but also fivefold, even sixfold coordination by displacement of oxygen. However, cation atoms of Si and Mg are retained at their atomic positions in olivine structure.

Amorfization of Mg_2GeO_4 olivine has been confirmed at 35GPa by X-ray diffraction study at Photon Factory.

REFERENCES:

C. Meade and R. Jeanloz *Science* 252, 68-72, 1991

Y. E. Fei and H.K. Mao *Jour. Geophys. Res.* 98, 11, 875-884, 1993

T. Yamanaka, T. Shibata, S. Kawasaki and S. Kume *High Press. Res. in Mineral Phys.* 3, 493-501, 1991

T. Yamanaka, S.Kawasaki and T. Shibata *Advance in X-ray Analysis* 35, 415-423 1991

IN-SITU Fe-Mg ORDER-DISORDER STUDIES AND THERMODYNAMIC PROPERTIES OF ORTHOPYROXENES, $(Mg,Fe)_2Si_2O_6$

Yang, H., and Ghose, S. (*Dept. of Geological Sciences, AJ-20, University of Washington, Seattle, WA 98195*)

A systematic in-situ high temperature study of Fe^{2+}-Mg distribution over the two octahedral sites M1 and M2 in synthetic orthopyroxenes ($En_{75}Fs_{25}$, $En_{61}Fs_{39}$, $En_{49}Fs_{51}$, $En_{25}Fs_{75}$ and $En_{17}Fs_{83}$) was undertaken at 1000, 1100, 1200 and 1300 K by the single-crystal x-ray diffraction method. The reversal measurements of cation ordering states were made on samples $En_{75}Fs_{25}$, $En_{61}Fs_{39}$, $En_{49}Fs_{51}$ and $En_{17}Fs_{83}$. Because of the ortho-clino phase transition observed at ~1255K for $En_{17}Fs_{83}$, no site occupancy determinations at 1300 K were made for $En_{25}Fs_{75}$ and $En_{17}Fs_{83}$. The site occupancies in the Mg-rich sample ($Fs_{25}En_{75}$) at 1300 K are anomalous due to the existence of a transitional structural state prior to a phase transition from ortho to proto phase. The asymmetry in the distribution of Fe and Mg over M1 and M2 sites is confirmed in the 1000-1200 K range (Fig. 1) although it is much less pronounced than that determined from quenched natural samples at lower temperatures (873-1073K). An analysis of the site occupancy data based on the regular solution model of Saxena and Ghose (1971) yields: ΔG_{exch} = 7751+3.000T (±246) (J/mol), W^{M1} = 10230–2.065T (±164) (J/mol) and W^{M2} = 14775–7.575T (±624) (J/mol), where T is in Kelvin. All three parameters are temperature-dependent with ΔG_{exch} increasing and W^{M1} and W^{M2} decreasing with increasing temperature (Fig. 2). The (W^{M1}–W^{M2}) term increases with increasing temperature, in accord with the result of Shi et al. (1992), but in contrast to most previous studies. This result suggests that the atomic configurations around the cations in M1 and M2 sites become more dissimilar and the asymmetry of the orthopyroxene solid solution increases at elevated temperatures (1000-1200 K). The sublattice (Shi et al., 1992) and the regular solution models (Saxena and Ghose, 1971), respectively, were used to derive the microscopic and macroscopic excess thermodynamic parameters (ΔG^{ex}, ΔH^{ex} and ΔS^{ex}) and the activity-composition relations. The macroscopic excess parameters show positive deviations from ideal mixing. The ΔG^{ex} and ΔH^{ex} values agree reasonably well with those determined experimentally.

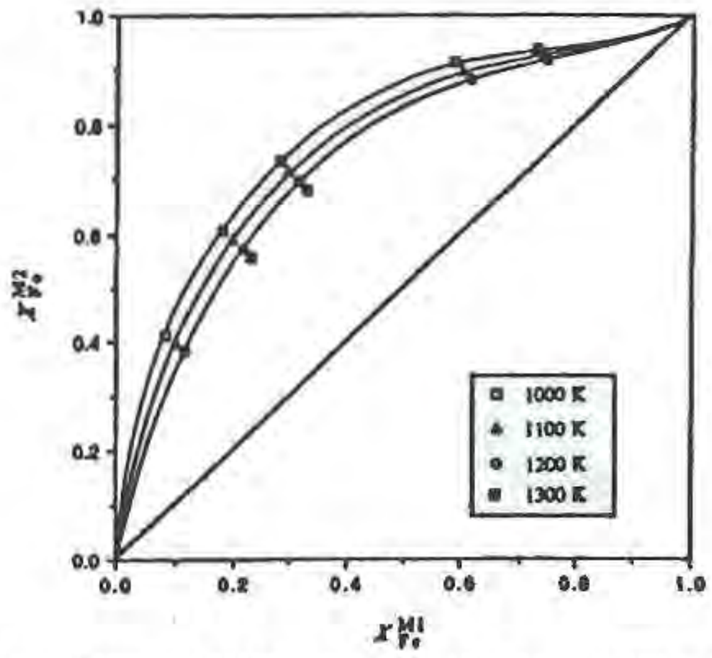

Fig. 1 Rooseboom plot of site occupancies of Fe between M1 and M2 sites in orthopyroxenes.

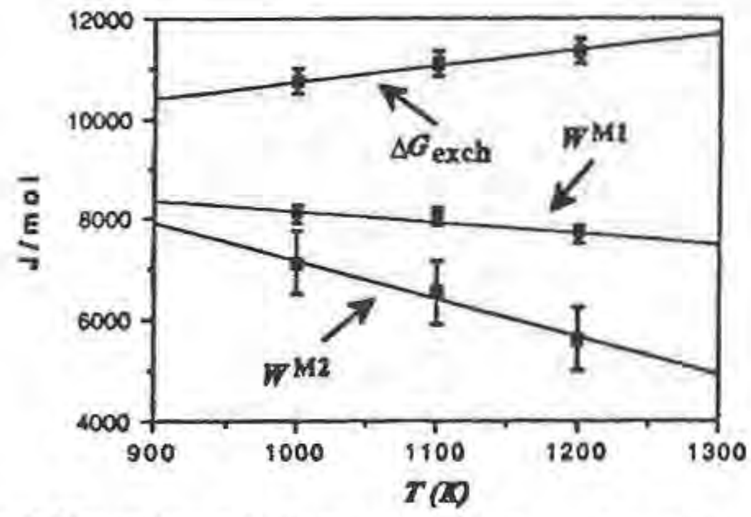

Fig. 2 The exchange Gibbs free energy (ΔG_{exch}) and interaction parameters (W^{M1} and W^{M2}) for M1 and M2 sites in orthopyroxenes as a function of temperature represented by ±1σ brackets.

References:

Sexana, S.K. & Ghose, S. (1971). *Amer. Mineral.*, **56**, 532-559.

Shi, P., Sexana, S. K. & Sundman, B. (1992). *Phys. Chem. Minrerals*, **18**, 393-405.

ALTERED TITANOMAGNETITES IN THE BASALTIC ROCKS OF NORTHERN TAIWAN

Yang, H.-Y. and Kao L.-S. (*Dept. of Earth Sciences, National Cheng Kung University*)

Basaltic rocks occur as dikes, sills, lava flows, and pyroclastics in association with the Miocene sedimentary rocks in northern Taiwan and have been spilitized to various extents. Titanomagnetite, one of the accessory minerals in these basaltic rocks, has been variably oxidized at high temperatures and hydrothermally replaced at low temperatures during the spilitization. The microstructures, constituent minerals, and topotaxial relationship among these coexisting, genetically-related minerals in these altered titanomagnetites were studied with petrographic microscopy, scanning electron microscopy, energy-dispersive microanalysis, and transmission electron microscopy. The results are used to interpret the behavior of titanomagnetites during the progressive oxidation processes as follows.

In the early stage of oxidation, titanomagnetites oxyexsolve three sets of well-oriented ilmenite lamellae shown as trellis texture in the weakly-oxidized titanomagnetites. Upon continuous oxidation in the stage of moderate oxidation, these lamellar ilmenites partly decompose to rutile and hematite, while the matrix low-Ti magnetites exsolve well-oriented euhedral grains of maghemites, as evident from the microstructures and mineral assemblages of moderately-oxidized titanomagnetites. In the stage of strong oxidation, the breakdown of lamellar ilmenites to rutile and hematite has almost gone to completion and the matrix low-Ti magnetites have been extensively oxidized to maghemites and hematites. Besides, the microstructures of the strongly-oxidized titanomagnetites also indicate that pseudobrookite did appear in patches but have already completely inverted to rutiles and hematites in finely-sheeted, intimate intergrowth. Finally, the residual ilmenites and titanomagnetites were hydrothermally replaced by anatase at low-temperatures during the spilitization.

Ilmenites, hematites, rutiles, spinels, maghemites, and anatase are the products of oxidation or hydrothermal replacement of titanomagnetites. They are genetically-related in the sense that the product minerals all have derived their structures directly or indirectly from the structure of titanomagnetites. All these minerals are close-packed or nearly so in their oxygen frameworks. Therefore, when these product minerals are transformed from titanomagnetites, a simple topotaxial relationship can reasonably be anticipated. Electron diffraction studies of these altered titanomagnetites show that the topotaxial relations among these coexisting, genetically-related minerals can be defined as follows

$a^*_{ilm}//a^*_{hm}//c_t//[\bar{1}10]_{mt}//[\bar{1}10]_{mh}//[\bar{1}10]_{ana}//[\bar{1}10]_{sp}$
$c_{ilm}//c_{hm}//a_t//[111]_{mt}//[111]_{mh}//[552]_{ana}//[111]_{sp}$

Because mineral transformations are required to be carried out least energetically, crystallographic orientation between the parent and product minerals must be strictly controlled by their structures. Additional studies on the titanomagnetites in the andesitic rocks from the Coastal Range of eastern Taiwan, which have also been oxidized at high temperatures and hydrothermally replaced at low-temperatures, have found that the above topotaxial relations are indeed strictly obeyed.

GEOCHEMISTRY OF CONTINENTAL BASALTS IN SOUTHWEST CHINA: IMPLICATIONS FOR THE LITHOSPHERIC BOUNDARY BETWEEN EURASIA AND GONDWANALAND

Yang Kaihui (Dept. of Geology, Univ. of Toronto and Inst. of Geology, Chinese Acad. of Geol. Sci.)

Investigation has been made on the continental basalts of Permo-Carboniferous ages from the eastern Tethyan orogen in southwestern China, a collisional belt between Eurasia and Gondwanaland. The continental basalts croping out in the area include alkalic basalts and tholeiites. Marked chemical differences are shown in the tholeiites from the regions bounded by the Lancangjiang suture, a stratigraphic and paleontological boundary between Gondwana and Eurasia facies. In the region northeast to the Lancangjiang suture are widely exposed Ol-normative tholeiites with relative high concentrations of incompatible elements and high La/Ybn (5.43-11.24), La/Smn (2.05-3.01) and $^{87}Sr/^{86}Sr$ (0.7074 on average) ratios, as well as low Al_2O_3/TiO_2 (3.42-5.84) and CaO/TiO_2 (2.1-3.94). Whileas, Q-nomative tholeiites with relative low La/Ybn (1.90-4.63), La/Smn (1.33-1.98) and $^{87}Sr/^{86}Sr$ (0.7054 on average) ratios as well as relative high Al_2O_3/TiO_2 (7.75-10.73) and CaO/TiO_2 (4.63-5.26) ratios, crop out in the region southwest to the suture, and are chemically comparable with Deccan basalt. These distinct features are also well demenstrated in plots between incompatible elements, as well as REE patterns and normalized incompatible element profiles. Such regional differences, which are impossible to be explained with crystal fractionation and contamination models, may have been largely inherited from the mantle sources of the tholeiitic magmas in both regions, implying that the subcontinental mantle east to the Lancangjiang suture may be more fertile than that west to the suture. It is thus suggested that the Lancangjiang suture could be a lithospheric boundary of the two supercontinents.

OPTICAL MEASUREMENT OF CATION DIFFUSION KINETICS AND STRUCTURAL REFINEMENT OF EXCHANGED HEULANDITE SINGLE CRYSTALS

Yang P. and Armbruster Th. (*Univ. Bern, Switzerland*)

Cation exchange experiments were conducted using a Ca-rich heulandite from the Nasik area, Deccan Traps of India. The coarse crystals were ground and sieved to a grain size between 0.1 and 0.5 mm and subsequently treated at different temperatures in 2 M NaCl solution either in a reflux apparatus (T < 110 °C) or in Teflon coated steel bombs (T > 110 °C). After various reaction times at different temperatures, the single crystals were studied under a polarizing microscope in oil immersion and the diffusion zone was determined by the extinction angle under crossed polarizers. Heulandite (space group C2/m) forms platy crystals parallel (010) and all structural channels (parallel *a*, *c*, and [102]) run perpendicular to the *b*-axis (optical Z-axis) thus the diffusion is two-dimensional which allows direct optical observation (Tiselius, 1934). The extinction angle X:*c* may vary significantly depending on the kind of channel cations. After obtaining Na-exchanged heulandites, the corresponding samples were treated as above in 2 M KCl, 2 M RbCl, and 2 M CsCl solution. Diffusion constants at various temperatures for Na -> Ca, Rb -> Na, and K -> Na were calculated by Fick's second law and activation energies were determined by the Arrhenius equation. When the crystals showed homogeneous optical properties, thus an exchange equilibrium was assumed, selected crystals were transferred for structural solution to a CAD4 single-crystal X-ray diffractometer operated at 100 K.

Reference:
Tiselius, A. (1934). *Zeitschr. Phys. Chem.*, **169A**, 435-458.

OBSERVATION OF ANTI-PHASE DOMAIN STRUCTURE IN CHLORAPATITE

Yang X. (*Dept. of Geology, China Univ. of Geosciences*)

The structure of chlorapatite has been determined and refined, assunming the space group $P2_1/b$ for stoichiometric chloraprtite, other than $P6_3/m$ of fluorapatite,which is caused by Cl ions shift

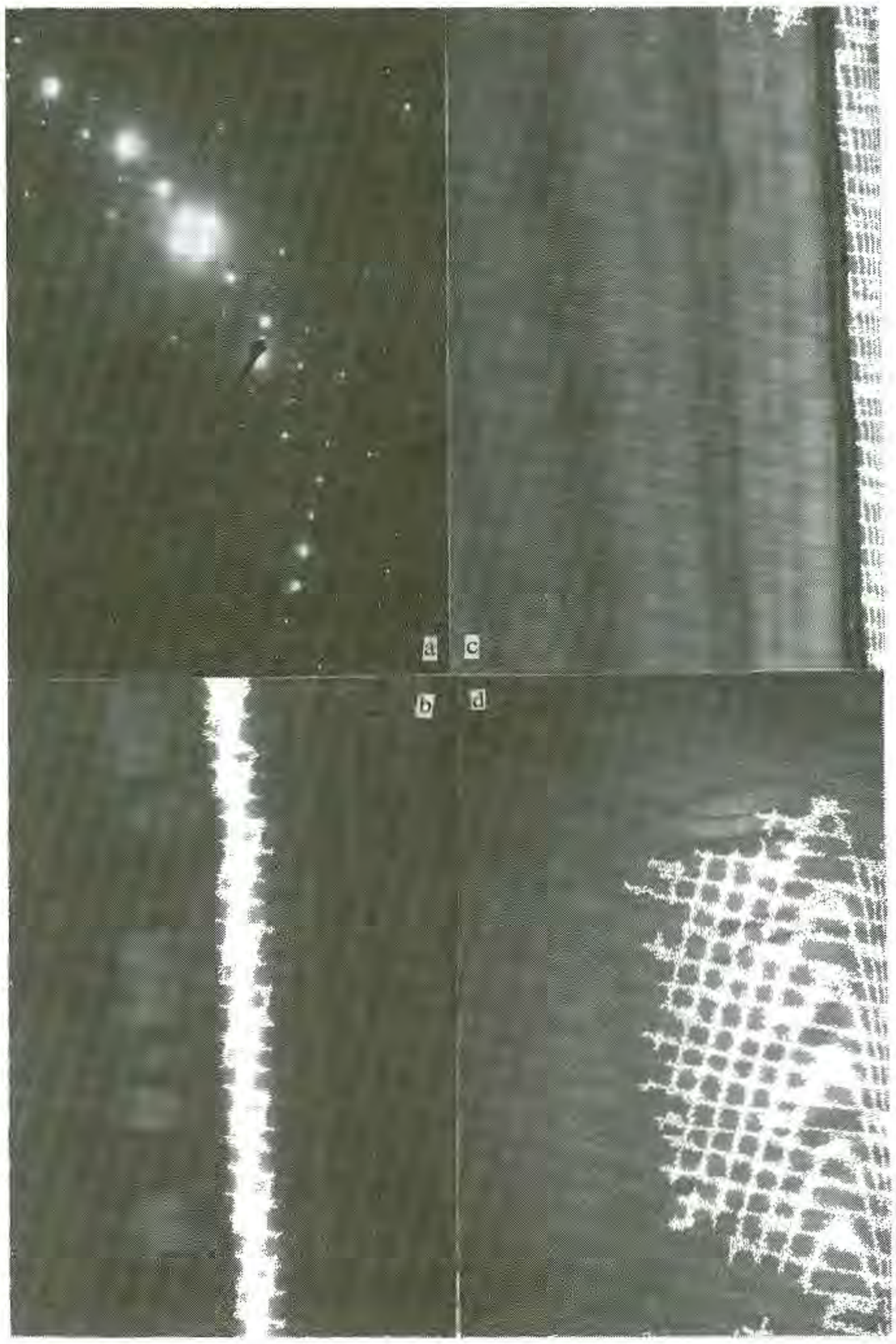

along c-axis .However,there were extensive studies showed that some stoichiometric chlorapatite had space group $P6_3/m$, other than $P2_1/b$.

Ultra thin sections suitable for transimission electron microscopy were made from synthetic chlorapatite single crystal (Yang et al, 1990) , polished on both sides, by argon beam ion bombardment.The reflexions from the chlorapatite may be classified into two groups; type a with 0kl k even are allowed for $P2_1/b$ space group and type b with 0kl k odd are forbidden for this group. There were extensive areas that appeared featureless under normal bright-field diffraction condition and in the dark field using type a reflexions. But the types of domain structure illustrated in fig.1b, 1d were observed by using type b reflexions for dark field viewing. There is no variation of contrast across the boundaries between these domains,and associated selected area diffraction patterns have a single crystal pattern; this indicates no change in the orientation of the diffracting planes. The thickness fringes observed are always continuous across the boundaries; thus the absolute values of the structure factors in the domains are identical. These properties and the fact that the domains can only be imaged with super structure(type b) reflexions mean that these domains are anti-phase domain structure. The displacement vector R is calculated and is equal to 1/2[010]. This displacement vector explains the origin of the domain in terms of ordering of chlorine ion position in the channel of chlorapatite.

Reference:
Yang Xiuming, Rachinger,W.A., Phakey,P.P., Palamara, J. (1990) 15th IMA, 1, 417-418

fig.1a Electron diffraction pattern of chlorapatite showing alternating strong rows of type a(0kl, k=even)and weak rows of type b(0kl, k=odd) reflections. 1b Antiphase domain in the chlorapatite, DF, g=052. 1c Same area of Fig.1b,BF. 1d Antiphase domain,DF,g=032.

TRANSIMISSION ELECTRON MICROSCOPY OF STACKING IRREGULARIES IN SYNCHISITE-(CE)

Yang Z. & Zhang P.(*Institute od Geology, Academia Sinica*)

Synchisite-(Ce), $CeCa(CO_3)_2F$, is one of the endmember of the polysomatic series (Donnay & Donnay, 1953, Van Landuyt & Amelinckx, 1975) and was suggested as well ordered stacking. Synchisite-(Ce) occurred in Kola peninsula, Russia, was observed by electron diffraction and lattice images taken along $[11\bar{2}0]$ direction. Three distinctive cases have been investigated: 1) Relatively ordered. The diffraction pattern shown in Fig.1 has well defined spots with k=3n and only minor streaking of rows with k≠3n. The weak spots $(20\bar{2}2)$ and $(10\bar{1}2)$ correspond to space group extinction: -h+k+l=3n l=2n and h-k+l=3n l=2n, respectively, and indicate a microtwin. The individuals contact each other on (0001) and are related by a 60° -rotation about the c axis. Fig.2 shows the lattice image of the same crystal. The alternating heavy and weak lines can be interpreted as being related to the Ce-F layer and Ca layer respectively. 2) Semirandom stacking. Fig.3 shows a diffraction pattern with sharps k=3n reflection and streaking of K≠3n reflections. The lattice image (Fig.4) of the area reveals lower density of stacking disorder. The streaking indicates stacking faults or displacements of CO_3 in the adjacent layers. 3) Disordered stacking. The diffraction pattern of Fig.5 shows that the reflections with K=3n and K≠3n all have streakings. The corresponding lattice image in Fig.6 reveals the stacking disorder of Ce-F layers and Ca layers, and Ca layers adjacent to each other. The composition of the crystal has been determined by electron microprobe analyses. The mean values are SrO 0.57, CaO 16.10, RE_2O_3 53.84(wt%), close to theoretical values (CaO 17.62, Ce_2O_3 51.25 wt%). It implies that the disorder stacking belongs to the short-range polysamatic disorder. The irregular stacking means that synchisite-(Ce) is a polysomatic mineral, not an endmember. The chemical composition of the endmembers in polysomatic series can be expressed as $CeCO_3F$---$CaCO_3$.

References:
Donnay,G & Donnay,J.D.H.,(1953). Am. Min., 38:932-963.
Van Landuyt,J. & Amelinckx,S.,(1975). Am. Min.,60:351-358.

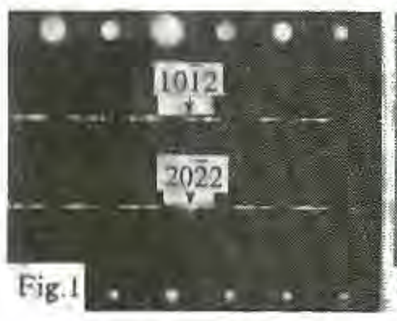

Fig.1

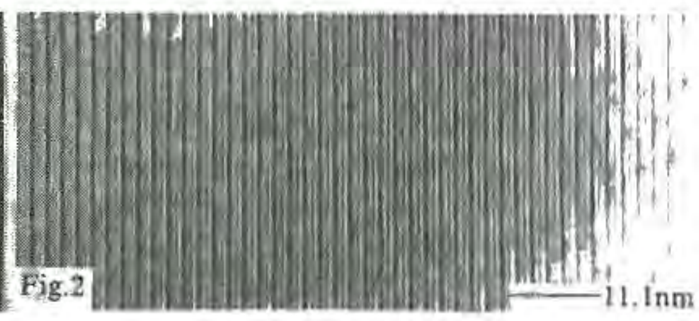

Fig.2

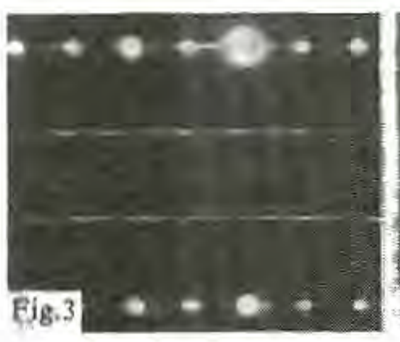
Fig.3

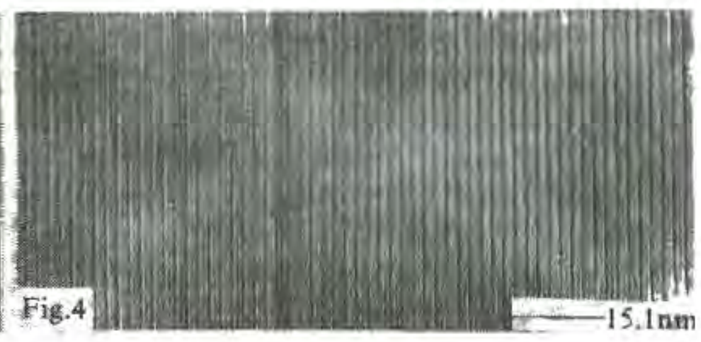

Fig.4

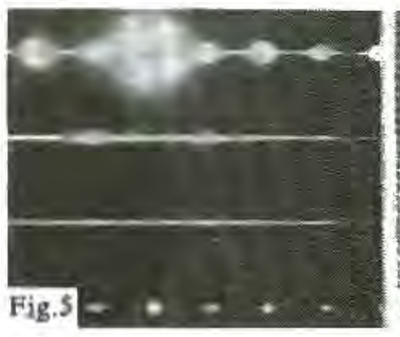
Fig.5

Fig.6

PETROLOGICAL AND GEOCHEMICAL CHARACTERISTICS OF DOFAN VOLCANO, MAIN ETHIOPIAN RIFT

Yirgu G.

Dofan is a volcanic centre in the northern sector of the Main Ethiopian Rift where a suite of products dominated by peralkaline silicic lavas have been erupted in Quaternary time. An initial phase of volcanic activity produced lava flows of intermediate and acid composition while a second and major phase was responsible for the effusive emplacement of large volumes of viscous lava flows, domes and scarce pyroclastics. The youngest volcanic products, postdating central activity, are represented by basaltic lavas and associated scoria.

Analytical data show a continuum in the variation of many major and trace elements. With increasing silica, MgO, CaO, TiO2, Total Iron, Ni, Cr and V decrease, while K2O, Na2O and the incompatible elements La, Ce, Zr, Y, Rb and Nb display the opposite tendency. Significant positive correlations are defined by incompatible elements on inter-elemental variation diagrams. Trace element enrichment-depletion patterns in the most evolved pantellerite are similar to several high-silica suites studied worldwide.

Volcanologic and petrographic observations combined with geochemical data indicate a cogenetic relationship between the evolved products and the mafic lavas. The regular geochemical trends are best explained by a model in which a primitive mildly alkaline transitional basalt magma evolved by crystal-liquid fractionation in a small, superficial magma chamber to give a series of variously differentiated liquids. The petrological features also suggest minor wall-rock assimilation. Compositional variations in the silica-oversaturated suite are consistent with fractionation controlled by alkali feldspar of changing composition.

VOLCANOLOGY AND GEOCHEMISTRY OF THE PERMIAN VOLCANIC COMPLEX OF THE KHENIFRA BASIN (MOROCCO).

Youbi N.* and Cabanis B.**

**Cadi Ayyad Univ., Dept. of Geology, P.O. Box S15, Marrakesh, Morocco;*

***Univ.PMC 6, Laboratoire de Géochimie C & S, Paris Cedex 05, France.*

The Autunian basin of Khenifra is situated at the south-eastern border of Central Morocco (a large paleozoic basement located at the north of the High-Atlas mountains), where basic, intermediate and acid magmatic rocks are well exposed, representing one of the best permian volcanic complexes for the study of succesive volcanic episodes and their relationships...

The volcanological history of Khenifra volcanic complex is subdivided into three very contrasted periods. The first period is characterized by an extrusive and effusive andesitic volcanic activity. It is represented, in the west of the volcanic complex, by pyroclastic breccias deposits with predominating rhyodacitic composition followed by formation of composite dome with hybrid lavas and the effusion of flows with olivine and pyroxene andesite composition. The second period is essentially explosive and rhyolitic. It began by air fall pyroclastic deposits followed by rhyolitic explosion alloclastic breccias and/or dacitic flows and associated pyroclastitc rocks. The third period is marked by the late intrusion of some pyroxene doleritic dykes.

Morb normalization spidergrams shows that all magmatic rocks except the doleritic dykes have a similar trace element signature, characterized by an important enrichment of LILE accompagnied by depletion of Nb (or Ta), Ti and P. These characters and high Th/Ta ratio are typical of orogenic series, with an important crustal component participation. In addition, the high light REE enrichment and fractionation with respect to heavy REE indicate a calc-alkaline affinity. The mineral chemistry also confirms these results.

The distribution of major and minor elements suggest that the petrogenesis of volcanics is controlled by an interplay of magma mixing, assimilation of crustal components, and crystal fractionation. The last period is a magmatic event with an anorogenic and hybrid (alkaline / calc-alkaline) character. The geochemical data suggest that magmas parental of these rocks have been produced by partial melting of mantle source which is influenced by a previous tectonic event (orogenic component).

The analysis of fracturation and its relationships with volcanic activity, shows that the distribution of large number of volcanic emission centers is tectonically controlled. Their localization, parallel to the senestral strike-slip faults oriented NE-SW suggests that the volcanic emissions occurred along tension gashes developed by sumeridian compession which is responsible for the opening of the Autunian Khenifra basin . This fact, associated with others such as evidence of autunian silicified wood and interstratified red sedimentary rocks in the volcanic pile, confim the permian age of the complex. The volcanological characteristics of the Khenifra permian volcanism are similar to the continental strato-volcanoe model facies with mutiple fissural vents.

The geodynamic context of the permian volcanism of the study area and, by extension, of the hercynian late-orogenic volcanism of Northern Morocco, will be discussed. A relationship with an active or fossile oceanic subduction (type B) is not possible; the hypothesis of an intracontinental subduction (type A) is offered. The permian magmatism of Morocco seems to be related to the functioning of shear zone.

STUDY ON STRUCTURE OF AN UNNAMED MINERAL $CuPb(Ir,Pt)_4S_7$[ref.1] WITH ELECTRON MICROSCOPY*

Yu Zuxiang, Institute of Geology, Chinese Academy of Geological Sciences, Beijing, 100037, People's Republic of China

The mineral $CuPb(Ir,Pt)_4S_7$ occurs in chromium-bearing dunite. It is a superstructure phase, composed of the $Cu(Ir,Pt)_2S_4$:$Pb(Ir,Pt)_2S_3$ = 1:1. Judging from its X-ray powder diffraction data, the primary isometric system of the mineral $CuIr_2S_4$(Fd3m, a 9.95 Å) has been transformed to trigonal or tetragonal system, with trigonal unit cell a = 7.01 Å, c = 11.3 Å or its multiple. The orientation of crystal $<001>_{SL} // <111>_{PL}$, $(006)_{SL}$, $(110)_{SL}$ and $(220)_{SL}$ corrsponds with $(111)_{PL}$, $(220)_{PL}$ and $(440)_{PL}$. The further studies of single-crystal X-ray were carried out using oscillation and weissenberg method by Peng Zhizhong. He suggested that the $CuPb(Ir,Pt)_4S_7$ is of trigonal system with its space group $R\bar{3}m$, a = 6.961(2) Å, c = 31.81(2) Å, $(012)_{SL}$, $(202)_{SL}$ and $(309)_{SL}$ corresponding with $(111)_{PL}$, $(113)_{PL}$ and $(440)_{PL}$.

Compared with the author's observation on the X-ray powder, Peng's result is puzzling, so analysis was made by the author for verification with transmission electron microscope. A schematic diagram of all the observed diffraction patterns from individual domains in (111), (110) and (101) foils are presented on fig.1. The superlattice spots in pattern $(111)_d$ exhibit six-fold symmetry, which indicates the presence of either a three or six-fold axis in the unit cell, belonging to either the hexagonal or cubic crystal class, because only these possess symmetry of this type. However, the demonstration for the cubic system could not be obtained from X-ray powder diffraction data.

The dimensions of the unit cell can be obtained from the d-spacings which are associated with various superlattice reflections given in fig.1. In the (111) foil, the orientation of the

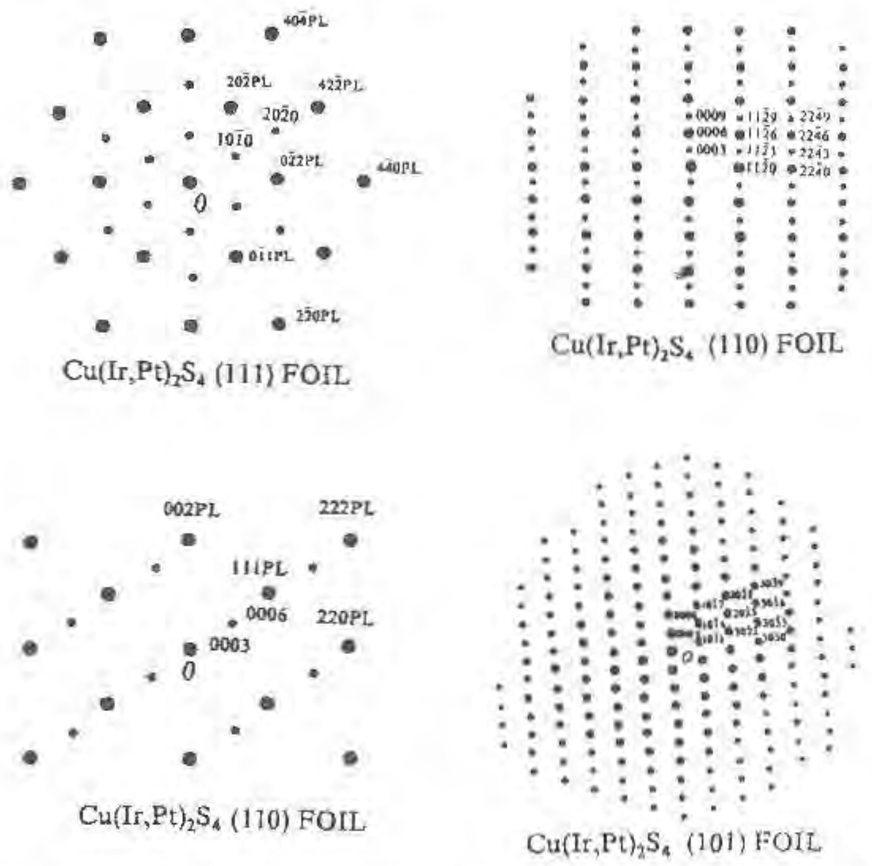

Fig.1 Electron diffraction patterns for $CuPb(Ir,Pt)_4S_7$

superlattice unit cell with respect to the primary unit cell is as follows: $<001>_{SL} // <111>_{PL}$, $<100>_{SL} // <42\bar{2}>_{PL}$. In the (111) primay foil, the $(10\bar{1}0)_{SL}$ spot is situated in 1 / 3 $(422)_{PL}$ distance, $g(10\bar{1}0) = (\sqrt{24} / 9.95) / 3 = 2 / \sqrt{3}\,a$, a = 7.03 Å.

The length of c axis corresponds to six complete {111} layers of atoms in the cubic lattice, which can be seen in the (101) foil, such as $(10\bar{1}1)$, $(10\bar{1}4)$, $(20\bar{2}2)$, $(20\bar{2}5)$, $(30\bar{3}3)$ and $(30\bar{3}6)$. In the (110) foils, the superlattice spot (0001) is situated in the $1 / 2(111)_{PL}$ distance, $c = (\sqrt{3} / 9.95) / 2 = 3 / c$, i.e. c = 34.46 Å. So, c is three fold $P3_1$ or $P3_2$. But $-h+k+l \neq 3n$, such as $(10\bar{1}0)$, the S.G. must be $P3_112$, $P3_121$, $P3_212$, $P3_221$, $P3_1$ or $P3_2$ identical with CBED investigation.

* Project Funded by the China National Foundation of Nature Sciences.

Reference: Yu Zuxiang (1990) Abstracts 15th IMA 287--288

THE CRYSTAL SPLITTING OF Fe^{2+} ION IN DIOPSIDE

YUAN Yunmei and QUI Xianjun (Dept. of Engineering Education, Guizhou Institute of Technology)

White & Keester (1966) measured the spectrum of a diopside and observed absorption bands at 13600cm^{-1}, 9730cm^{-1} and 4420cm^{-1}. Burns (1965, 1977) measured the spectrum of a diopside and observed absorption bands at 12200cm^{-1}, 9600cm^{-1}, 8400cm^{-1}.

They considered that two bands to belong to the d-d transition of Fe^{2+} at M(1).

Yuan etc.(1986) measured the spectrum of a diopside and observed absorption bands at 10309cm^{-1}, 9600cm^{-1}, 9333cm^{-1}.

The e_g, t_{2g} orbits of Fe^{2+} ion at M(1) in octahedron with C_{2v} symmetry occur splitting by the influence of crystal field. According to the theory of crystal field and point-charge model, the crystal field potential with C_{2v} symmetry may be written as:

$$V(r) = [\gamma^c_{20} Z_{20}(\theta,\varphi) + \gamma^c_{22} Z^c_{22}(\theta,\varphi)]\, r^2 + [\gamma_{40} Z_{40}(\theta,\varphi) + \gamma^c_{42} Z^c_{42}(\theta,\varphi) + \gamma^c_{44} Z^c_{44}(\theta,\varphi)]\, r^4 \qquad (1)$$

where

$$\gamma^{(a)}_{km} = \frac{4\pi e q}{2k+1} \sum_\tau \frac{1}{R_\tau^{k+1}} Z^{(a)}_{km}(\Theta_\tau, \Phi_\tau)$$

$Z^{(a)}_{km}$ denote real spherical harmonic functions; r, θ, φ are the coordinates of the d-electron in Fe^{2+}; R_τ, Θ_τ, Φ_τ are the coordinates of the τ—th ligand; e is the electron charge; q is the electric charge of the ligand. The crystal field coefficients, γ^c_{km}, can be calcullated from the crystal structure data (Warren & Bragg 1929) and the value of q (q = 2e for the O^{2-} ion).

According to Zhao's (1983) d-orbit theory of Fe^{2+},

$$R_d(r) = 0.5692 \left(\frac{11.03806^7}{6!}\right)^{1/2} r^2 \exp(-5.51903r) + 0.6500 \left(\frac{3.54794^7}{6!}\right)^{1/2} r^2 \exp(-1.77397r)$$

the expectation value of $\langle r^2 \rangle$ and $\langle r^4 \rangle$ are

$\langle r^2 \rangle = 2.2949$ a.u. $\quad \langle r^4 \rangle = 14$ a.u.

the 3d aproximate zero-level real wave functions are

$$|3d_{xy}\rangle = R_{3d}(r) Z^s_{22} \quad |3d_{xz}\rangle = R_{3d}(r) Z^s_{21} \quad |3d_{yz}\rangle = R_{yz}(r) Z^s_{21}$$
$$|3d_{x^2-y^2}\rangle = R_{3d}(r) Z^c_{22} \quad |3d_{z^2}\rangle = R_{3d}(r) Z_{20} \qquad (2)$$

according to (1) and (2), we arrived one level values of energy as follows:

$E(x^2 - y^2) = 7178\text{cm}^{-1}$ $\quad E(z^2) = 4971\text{cm}^{-1}$ $\quad E(xy) = -3461\text{cm}^{-1}$

$E(xz) = -4344\text{cm}^{-1}$ $\quad E(yz) = -4344\text{cm}^{-1}$

This are relative energy levels from the influence of crystal field spilitting, see Fig. (1)

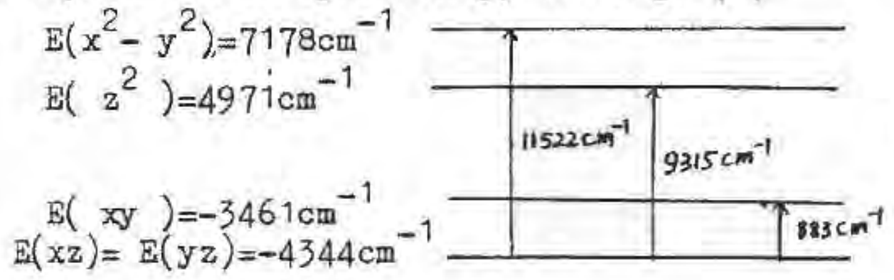

Fig.(1)

(1). The theoretical calculations and experiment are quiet agreement, we have proved the correct of white, Burns etc.'s prediction from theory that the absorption bonds occurred are caused from the splitting of e_g, t_{2g} obitals or the d-d transition, in M(1).

(2). There is no any fitting parameters in the calculation; therefore, we have avoided the difficulties in experimental fitting of many parameters and the arbitrary charcter of fitting.

(3). Thery predict existence of d-d transition 883cm^{-1} absorption band.

(4). It should express that there exists accidental degeneracy in the levels E(xz) and E(yz) originated from the specil structure data of diopside.

references: 1. Yuan Yun-mei etc. Abstructs with Program, 14 IMA, STANFORD UNIV., 1986, P.276-277. 2. Warren,B.E. and Bragg,W.L., Zeits. Krist., Vol. 69, 1929, P.168-193. 3. Zhao Minguang, Phys. Rev., B., Vol. 28. 1983, P.6481-6484.

• HP GLAUCOPHANE-BEARING SILICITES OF KARA ALLOCHTHONE, PAI -KHOY MOUNTAIN RIDGE, NORTH-EAST OF EUROPEAN RUSSIA

Yudovich Ya. E, Belyaev A.A., Ievlev A.A. (*Inst. Geology, Komi Sci. Centre, Ural Division, Russian Academy Sci.*)

Thin (10-20cm) layers bearing needle-like amphibole of glaucophane-arfvedsonite series were found in ferriferous and manganic carbonate-bearing silicites (jasperoids) of Famennian age on Yugorsky peninsula (North-East of European Russia). Jasperoid horizons with amphibole are observed for 50-80 km. Obviously they trace the zone of south Pai-Khoy overthrust in frontal part of Kara allochthone.

Under the microscope amphibole-bearing shales display porphyroblastic texture. Long prismatic prrphyroblasts of amphibole are zoned and strongly pleochroic from blue to dark blue. Probably amphibole shales primarily were the layers of alkaline tuffs in carbonate-siliceous sediments. Normative calculation of chemical composition of two, monofractions of amphibole gives following formulas:

$(NaCa_{.12}K_{.065}Ba_{.01})_{1.99}(Fe^{3+}_{2.67}Fe^{2+}_{.67}Mg_{1.28}Mn_{.13}Al_{.16}Ti_{.03})_{4.94}$

$[Si_{7.80}Al_{.20}O_{22}](OH_{1.22}(O,F)_{.78})_{2.00}$

and

$(Na_{1.91}Ca_{.12}K_{.03})_{2.06}(Fe^{3+}_{2.67}Fe^{2+}_{.87}Mg_{1.60}Al_{.22})_{5.43}$

$[Si_{7.88}Al_{.12}O_{22}](OH_{1.02}(O,F)_{.98})_{2.00}$

X-ray analysis of several amphibole crystals showed the prevalence of crossite and riebekite among them, ozannite was single. The find of glaucophane-bearing metasilicites allows to consider that temperatures at Kara allochthone formation were 350-500°C and pressure raised up to 8-10 kbar. Isotopic age of anphibole determined by K-Ar method gives the age diapason from Early Permian to Middle Jurassic. It may indicate the two stages of deformation - Ural (P2-T1) and Pai-Khoy (T1-J2) ones.

PETROGENETIC PROCESSES IN THE DEVELOPMENT OF THE NORTHEAST NIGDE VOLCANICS

Yurtmen S. (*Dept. of Geology, Çukurova Üniv.*) and Rowbotham G. (*Dept. of Geology, Univ. of Keele*)

The volcanics exposed to the northeast Niğde area are characterized by pumiceous pyroclastic rocks present as ash flows and falls. These pyroclastics are represented by the compositions ranging from basaltic andesite to rhyolite. These rocks exhibit linear chemical variations between end-member compositions and a continuity of trace element behaviour exists through the basaltic andesite-andesite-dacite-rhyolite compositional range, which is consistent with the fractionation of ferromagnesian minerals and plagioclase from parental basalts. They are peraluminous and show typical high-K calc-alkaline differentiation trends with total iron content decreasing progressively with increasing silica content. Also decreasing Na_2O/K_2O ratio with increasing silica, low MgO and TiO_2 contents, high Sr and high K/Rb, Rb/Sr, Ba/Rb, Ba/Sr and Ce_N/Yb_N ratios increase with increasing crystal fractionation.

Bulk rock and mineral compositional trends and petrographic phenomena suggest that crustal material was added to the mantle either by subducted oceanic crust or during the ascent of the magmas through the continental lithosphere and is likely contaminant of the source zone of the Niğde magmas.

The chemical variations in these volcanics indicate that crystal liquid fractionation has been a dominant process in controlling the chemistry of the northeast Niğde volcanics. This process includes crystal fractionation, restite separation and partial

melting of source rocks and chamber walls under conditions of low halogen activity. It is also clear that from the petrographic and chemical features, that magma mixing or disequilibrium also played a significant role in the evolution of the Niğde volcanic rocks. This is shown by normal and reverse zoning in plagioclase and chemical resorption of practically all the observed minerals.

Estimated solidus temperatures (675-695°C) determined from plagioclase-glass compositions demonstrate the water-saturated nature of the magma. The P_{H2O} for the ignimbrites (1.0-1.2 kbar P_{H2O}) and the mafic inclusions (1.2-2.5 kbar P_{H2O}) suggest a very shallow magma chamber (3.6-5 km) for the Niğde volcanics.

STARTING ROLE OF NATURAL CRYSTALS OF SOLID HYDROCARBONS IN ORIGIN OF LIFE

Yushkin N.P. *(Institute of Geology, Komi Sci. Centre, Ural Division, Russian Academy of Sci. Syktyvkar, Russia)*

Obviously, one of the most interesting and perspective problems of mineralogy in the end of XXth - the begining of XXIst centuries will be the problem of minerals role in origin, evolution and maintenance of life (Yushkin, 1993). By this time the conseption of biostarting role of minerals, i.e. minerals as information matrixs, protogenes and regulators of ordered synthesis of aminoacids in protoprotein, is developed quite effectivelly (Bernal, 1951, Cairns-Smith, 1982, etc).

The wide range of minerals - montmorillonite, kaolinite, apatite, calcite, zeolites, graphite and others - is considered to be the possible information matrixs. But these minerals which structures are really complimentary with organic components of living systems - DNA, collagenes and aminoacids differ from living systems by their composition very strongly. So, in appropriate models of life origin it is necessary to create unjustified long chain of intermediate stages in developing the "mineral -> life" process. Our investigations of structure and evolution of natural concentrated non-crystalline systems (mineraloids) convince us in idea that the most probable pre-biological systems in abiogenesis were not the inorganic mineral crystals but polymer crystals of solid hydrocarbons crystallized in pneumatolithic and hydrothermal systems.

Fibrocrystals of kerite from pegmatite deposits are considered to be the model of such initial system. They are complimentary by structure with living matter, dynamic to outer factor influence, they actively react with water and gases. Kerite fibrocrystals have the composition similar to one of living substance (%):

	Kerite	living substance	man body
H	5-7	10.5	62.8
O	9-23	70.0	25.4
C	60-77	18.0	9.4
N	9	0.3	1.4

They contain the all main structural elements of life (C, H, N, O, P, S, Na, K, F, Mg, Si, Ca), catalizators (Fe, Cu), microelements.

Kerite fibrocrystals and similar polymer hydrocarbon crystals growing in the conditions of aminoacid, sugar, porfirine and other organic compounds synthesis can evolve into nucleoproteid and gain the ability to consolidate the genetic information. Epithaxial spiral growth mechanism can provide the hyral selection of left aminoacids and right sugars.

Volcanos, sub-surface and submarine hydrothermal systems, espessialy the gas-steam bearing, cavities in pegmatites can be the places of life origin.

References:
Bernal J. (1951). *On physical basis of life.*- London, 48 p.
Cairns-Smith A.G. (1982). *Genetic takeover and the mineral origins of life.*- London, 477 p.
Yushkin N.P. (1993). *Mineralogy and life.*- Syktyvkar, 5-7
Yushkin N.P. (1992). *Abstracts of 29th IGC*, Kyoto, Japan, 3, 685

TRIBOCHEMICAL MODIFICATION OF CLINOPTILOLITE TUFFS BY PHOSPHORUS

Yusupov T. S., Shumskaya L. G., Belitsky I. A., and Kovaleva L. T. (*United Institute of Geology, Geophysics, and Mineralogy, Novosibirsk, Russia*)

Modification of clinoptilolite tuffs by phosphorus has mineralogic and practical interest due to the ability of phosphorus to enter the zeolite structure during interaction with phosphatic solutions (1).

Under discussion is modification of clinoptilolite by phosphorus during tribochemical effect in mills with the aim to study possibilities of producing prolonged phosphate fertilizers.

The investigation is concerned with clinoptilolite tuffs of the Shivyrtui deposit, which underwent benefication by gravitational-magnetic scheme (2, 3). The enriched clinoptilolite product had the following chemical composition (%): SiO_2 – 63.11; Al_2O_3 – 13.46; Fe_2O_3 – 1.78; CaO – 3.00; Na_2O – 0.84; K_2O – 2.38; loss on ignition – 13.24. The clinoptilolite content made up 80%, montmorillonite 10%, while feldspar, quartz, and hydromica were present in small amounts.

The solid phase interaction of clinoptilolite with superphosphate has been investigated. Previously it was shown that tribochemical reactions, when using gravitational mills, are revealed only on synthetic zeolites, while natural zeolites do not suffer any changes (4). For this reason centrifugal mills of elevated energetic power were used, which to a greater degree corresponded to the course of tribochemical reactions.

With the help of X-ray, IR, EPR, DTA studies it was found that during mechanical treatment partial disintegration and progressing amorphization of the zeolite structure and accompanying minerals takes place with transition into X-ray amorphous state. At the same time broken chemical bonds, active centers, and radicals appear, which also increase the reaction ability of minerals.

Solid phase modification of zeolites by phosphorus is shown by tribochemical treatment of clinoptilolite and superphosphate in the air. Tribochemically stimulated penetration of PO_4 into the structure of zeolite is established, which is indicated by the shift of the band of antisymmetric valence variations of the T–O bonds into the region of high frequencies – from 1060 cm^{-1} for starting mixture and to 1075 cm^{-1} from samples treated in the mill. This appears to be a result of fixing of phosphate-ions in active centers which appeared due to tribochemical treatment.

The studies of the kinetics of the solubility of phosphorus present in modified clinoptilolite tuffs showed a considerable decrease in its extraction into water (Table 1).

Effect of mechanical activation on the content of water soluble P_2O_5 in the mixture

Composition of mixture, % weight		Period of activation, min.	Transition of P_2O_5 into water, %
Clinoptilolite	Superphosphate		
–	100	–	40.3
–	100	5	34.0
80	20	5	6.0
70	30	5	7.2
50	50	5	9.1

Thus, the principle possibility of regulation of the content of water-soluble form is justified experimentally, which is important for solving agrochemical problems of feeding plants by phosphorus.

References:
1. Arens, V.Zh. (1984). *Application of natural zeolites in cattle production and plant growing* [in Russian], Tbilisi, 128-132.
2. Belitsky, I.A., *et al.* (1973). *Soviet Geology and Geophysics*, 7, 107-110.
3. Yusupov, T.S., *et al.* (1992). *Natural zeolites of Russia* [in Russian], I, Novosibirsk, 72-74.
4. Rogue-Moenerbe, R., *et al.* (1991), *Solid State Ionics*, **46**, 193-196.

INVESTIGATION OF CRYSTALLOCHEMICAL FEATURES OF MICROCLINE IN THE PROCESSES OF ITS SEPARATION FROM SYNNYRITE

Yusupov T.S, Shumskaya L.G., and Pantyukova L.P.

The main salic minerals of synnyrite – a new type of ultrapotassic rocks discovered in Russia, are microcline (50–60%) and kalsilite (10–30%). Nepheline, biotite, garnet, magnetite, and hematite are present in small quantities.

The distribution character of the main impurity elements, especially Fe, in the structure of the dominant minerals was studied with the aim of mineralogic investigation and evaluation of the possibility to separate microcline concentrates with minimum content of F and other impurities.

Synnyrite was separated into fractions by gravitation method in special organic liquids by a step change of the density with gradient d = 0.005 g/cm^3. The occurrence forms of Fe^{+3} in minerals under study was determined by EPR which allows the isomorphous impurity and micro inclusions of Fe-containing phases to be separated (distinguished)(1).

By means of X-ray and IRS it was established that in fractions with d = 2.555–2.595 g/cm^3 microcline is dominant. The increase of the density of these fractions leads to an increase of Fe_2O_3 from 0.03 to 0.37%, but the weight percent (output) of products containing 0.03–0.06% of Fe_2O_3 does not exceed 2–5%. Fractions with the highest content of kalsilite are separated in the d = 2.600–2.615 g/m^3. It was shown that microcline fractions contain more Sr and Ba, while kalsilite – more Fe.

Electromagnetic separation provides a possibility to obtain synnyrite products containing 0.2–0.3% of Fe_2O_3. It is difficult to attain further decrease in this property by physical methods, whereas chemical benefication is more efficient (2). The treatment by mineral acids results in dissolution of kalsilite with transition into a liquid phase K and Al, while the solid residue contains microcline with 0.10–0.12% of Fe_2O_3. The potassium modulus of this product reaches 12 and more (ratio of K_2O:Na_2O).

According to data of EPR, microcline products obtained by electromagnetic and gravitational separation are characterized by an intense wide line with g = 2.0 from aggregations of Fe^{+3} complexes and line with g = 4.3 which may be referred to micro inclusions of hematite.

The EPR spectra of microcline concentrates after being treated with acid show the presence of Fe oxides with lower concentrations of Fe+3 ions (the field with H = 0.1-0.4 T). The narrow line (H + 0.156 T and g = 4.3), is apparently associated with isomorphous occurrence of Fe^{+3} in positions of Al and Si.

The production of microcline with less than 0.1% of Fe_2O_3 is possible by mechanical destruction of micro inclusions in highly power-intensive mills with further chemical dissolution of Fe. If the character of reflexes resulting from isomorphous occurrence of Fe^{+3} does not change after the treatment, then the intensity of the lines responsible for the content of Fe-containing micro inclusions decreases approximately 5 times.

References:
1. Yusupov, T.S., et al. (199). *Physico-chemical problems of exploitation of commercial minerals* [inRussian], **6**, 89–92.
2. Yusupov, T.S. & Shumskaya, L.G. (1990), *Scientific bases for the development of optimum schemes of mineral products* [in Russian], Moscow, 195–198.

SPECTROSCOPIC EVIDENCE OF ORDERING IN THE VESUVIANITE STRUCTURE

Żabiński W., Paluszkiewicz Cz., Sojka Z. /Academy of Mining and Metallurgy, Cracow, Poland/

On the basis of high precision single crystal X-ray diffraction and high resolution TEM Allen and Burnham /1992/ have distinguished two structural forms of vesuvianite: 1° high-symmetry vesuvianites with long-range disordered structure, of P4/nnc average symmetry, formed as a component of calc-silicate metamorphic rocks at relatively high temperatures /400-800°C/, 2° low-symmetry vesuvianites containing ordered domains of lower than P4/nnc symmetry, formed in rodingites at lower temperatures /<300°C/.

The present authors have investigated several vesuvianite samples from rodingite-like rocks /low/ as well as coming from high-temperature calc-silicate rocks /high/ using IR and EPR spectroscopic methods. Though the powdered samples have been used, distinct differences could be observed on the spectra. In the OH-stretching region sharp bands ca. 3170 and 3530 cm^{-1} are characteristic of low vesuvianites, whereas in the case of high ones the corresponding bands appear at ca. 3200 and 3560 cm^{-1}. In the EPR spectra of Fe^{3+} a strong g = 6 line and a weaker one at g = 2 are characteristic of low vesuvianites, while in the case of high ones the line at g = 2 dominates in the spectrum and additionally a weak signal at g = 4.3 appears. It has been shown by both spectroscopic methods, that heating the sample can transform low into high vesuvianite. This research was supported by KBN grant 6 P201 018.

Reference:
Allen, F.M. & Burnham, Ch.W. /1992/. Canad. Miner. 30, 1, 1-18.

TOURMALINES FROM RARE-METAL AND MIAROLITIC PEGMATITES OF TRANSBAIKALIA, RUSSIA, AND PAMIRS, TADJIKISTAN

Zagorsky V.Ye. and Peretyazhko I.S. (Vinogradov Institute of Geochemistry, Siberian Branch of Russian Academy of Science), Irkutsk, 664033, P.O. Box 4019

Tourmaline is a mineral common to most of granitic pegmatites and is often used as an informative indicator of evolution of granite-pegmatite systems, pegmatite units and separate pegmatite bodies. Mineral associations, structural features, compositional evolution of tourmalines from Li, Ta-Be, complex rare-metal pegmatites (Zavitaya, Kanga, Kulinda, Durulguy, Menza) and numerous gem-bearing miarolitic pegmatites have been studied. Typomorphic features of tourmalines due to formational belonging, character of min-

eralization and type of pegmatites, regional features of pegmatite fields and peculiarities of separate pegmatites were revealed against a background of compositional evolution from Fe-Mg - tourmalines to Li-Al varieties, which is common to all pegmatites studied.

The most complete evolutionary sequences of tourmalines are typical of the actual gem tourmaline deposits. So, tourmaline samples from the Malkhan field, Transbaikalia, contain up to 7 colour zones. There the evolutionary sequence of tourmalines is as follows: black schorl (ol., buer.)*→brown, yellow or light-green elbaite-tsilaisite (ol.)→colourless, rose elbaite (ol.)→dark-green, brown elbaite (ts., sch., sometimes dr.). Ca contents increase in this sequence until formation of liddicoatites, which are found in the veins where oligoclase prevails over K-feldspar to a great extent. Quantities of olenite and tsilaisite minals reach 42 and 38% respectively. The regional feature of Malkhan tourmalines is their enrichment in Bi (up to 0,5%), which replaces Na and Ca in X site. Ordering of tourmalines, which reflects the degree of conformity of the samples to an ideal structure, where redistribution of cations between Y and Z sites is absent, was determined by special methods (Afonina et al.,1990). It increases from 0,65-0,75 in schorls to 0,95-1,0 in colourless and rose elbaites, decreasing slightly in later generations.

Formation of dark-coloured late generations is connected with inversion of compositional evolution of tourmalines when the tendency of mineral enrichment in Li and Al reverses and the role of R^{2+}-cations increases. One of the most original results of this process is the occurence of zonal Al-dravite crystals in Zapadnaya-1 mine. During the growth of these crystals charge compensation under substitution of Al^{3+} for Mg^{2+} was realized at the expence of Na^{+}, Ca^{2+} with participation of OH^{-} and quite possibly H_3O^{+} groups. The sequence dravite-Al-dravite is distinquished on cell parameters.

Evolutionary sequences of tourmalines in miarolitic pegmatites of SW Pamirs (Leskhozovskoye, Vez-Dara) and many tourmaline deposits in the Borschovochny ridge, (Gremyachinskoye, Savvateevskoye, Mokhovoye), Transbaikalia, are close to those in the Malkhan field but differ by a greater role of tsilaisite, olenite and the absence of late postinversional generations. On the contrary the role of tsilaisite is depressed in the samples from poorer in Li pegmatite veins of the Leskovskoye deposit (Borshovochny ridge) and olenite (but not elbaite) prevails in the late dark-blue generation.

A specific evolutionary sequence of tourmalines is established in the Kukurt pegmatite gemstone unit (Pamirs): enriched in ferricomponent black dravite (sch.) or schorl (dr.)→black schorl-buergerite (dr.)→black schorl (buer., ol., ts.)→dark-yellow, dark-green elbaite-olenite (sch., buer.)→white, rose elbaite (ol.). The Fe^{3+}quantity in Z site reaches 1,75 formula unit in the initial members of this sequence. Increased Ti^{4+} (up to 0,17 formula unit), maximum cell parameters and disordering are typical of such tourmalines. The tourmaline enrichment in Mg is due to the fact that pegmatites occur among a terrigenic-carbonaceous rocks.

Only schorls, differing in the ordering degree and alignment of secondary minals are typical of pegmatites with gem topazes and beryls (Adun-Chelon, Transbaikalia; Mokrusha, Semenikha, Ural; and others) and rare-metal Ta-Be pegmatites. Tourmaline varies in composition from schorl to elbaite and contain the olenite admixture as a rule in the fields of actually Li (spodumene) and complex rare-metal pegmatites. Note the presence of olenite component in the overwhelming majority of Fe-Mg - tourmalines as well as Li-Al - ones from rare-metal and miarolitic pegmatites.

Reference :
Afonina G.G. et al. (1990). Doklady Akademii Nauk SSSR, 313, No 5, 1207-1211.

* Here and below tourmalines are named after the prevaling minals; the secondary minals (higher than 5%) are in brackets; sch.-schorl, dr.-dravite, buer.-buergerite, el.-elbaite, ol.- olenite, ts.-tsilaisite; minals are given in descending order of their contents.

APATITE, CALCITE AND DOLOMITE AS INDICATORS OF Sr-Nd EVOLUTION OF PHOSCORITES AND CARBONATITES FROM THE KOVDOR MASSIF, KOLA , RUSSIA

Zaitsev A. (*Dept. of Mineralogy, St.-Petersburg Univ., Russia*) and Bell K. (*Dept. of Earth Sciences, Carleton Univ., Canada*)

A detailed Sr-Nd isotopic study of apatite, calcite and dolomite from the phoscorites and carbonatites of the Kovdor massif (380 Ma) reveal a complicated evolutionary history for these rocks. At least 5 types of phoscorites have been identified on the basis of their relative ages and mineralogy (Krasnova & Kopylova, 1988). They include (from oldest to youngest) 1) apatite-forsterite, 2) apatite-forsterite-magnetite, 3) calcite-forsterite-magnetite with phlogopite, 4) calcite-forsterite-magnetite with tetraferriphlogopite and 5) dolomite-magnetite. Carbonatites can be divided into three types: 1) calcite with forsterite and phlogopite, 2) calcite with tetraferriphlogopite and 3) dolomite. They have similar mineralogy to the phoscorites types 3, 4 and 5 respectively, end each carbonatite type formed later than their corresponding phoscorite.

Chemical data from apatite show the existence of, at least, two distinct groups. One is characterised by relatively low $^{87}Sr/^{86}Sr$ (0.70330-0.70349) and $^{143}Nd/^{144}Nd$ initial ratios (0.51230-0.51240) with F=2.01-2.22 wt%, Sr=2185-2975 ppm, Nd=275-434 ppm, Sm=31.7-67.7 ppm and corresponds to the earliest phoscorites (type 1, 2 and 3) and carbonatite (type 1). Apatite from the second group has higher $^{87}Sr/^{86}Sr$ (0.70350-0.70363) and $^{143}Nd/^{144}Nd$ initial ratios (0.51240-0.51247) and higher F (2.60-3.16 wt%), Sr (4790-7500 ppm), Nd (457-1074 ppm), Sm (68.7-147.6 ppm) contents. This second group corresponds to the younger phoscorites (type 4 and 5) and younger carbonatites (type 2 and 3). One apatite sample from carbonatite type 1 fits into neither of the two groups and is characterised by the highest initial $^{87}Sr/^{86}Sr$ (0.70385) and lowest $^{143}Nd/^{144}Nd$ (0.51229) of any of the apatites. Within each group initial rations of $^{87}Sr/^{86}Sr$ and $^{143}Nd/^{144}Nd$ show negative correlations. Sr isotope data from coexisting calcite and dolomite support the findings from the apatite study. The Sr and lNd isotopic similarities between carbonatites and phoscorites indicate a genetic relationship between the two. Wide variations in Sr and Nd isotopic composition within the type 1 carbonatites, show that these carbonatites are not uniform and probably contain several distinct intrusive phases. Data from O isotopic composition of calcite and dolomite ($\delta^{18}O$=+7.2 to 7.7 $^{o}/_{oo}$ SMOW) indicate the absence of any low-temperature secondary processes in phoscorites and carbonatites.

Apatite from both groups plot in the depleted quadrant of an ε Nd vs ε Sr diagram. Data for the first older group clearly lie along Kola carbonatite line (KCL) (Kramm, 1993), and data for the second younger group plot above the KCL.

The evolution of the phoscorites and carbonatites cannot be explained by simple magmatic differentiation assuming closed system conditions. The Sr-Nd data is best explained by the mixing of three components. Two of these are similar to the end members of the early phoscorites (type 1, 2 and 3) and carbonatites (type 1). A third component is needed to explain the isotopic characteristics of the younger group.

Our study shows that apatite is ideal for placing constraints on mantle sources and for monitoring the Sr-Nd evolution of carbonatites.

References:

Kramm, U. (1993). *Eur. J. Mineral.*, **5**, 985-989.
Krasnova, N.I. & Kopylova, L.N. (1988). *Int. Geol. Rev.*, **30**, 307-319.

SYNTHESIS OF FINE-DISPERSIVE CORUNDUM

Zakirov I.V., Sretenskaya N.G., *(Ins.of Exper.Min.Rus.Acad.Sci)*

Aluminium oxide with corundum strusture has been synthesized using an experimental apparatus was constracted for hydrothermal investigations at temperatures up to 773K and pressure up to 50 MPa. The apparatus allows to take samples of the coexisting phases "in situ" without disturbing the experimental conditions and with the pressure being precisely measured. Investigation of the material by methods of powder diffractometry and and electron microscopy has shown that:

1) Synthesized corundum is homogeneos and well-cristallized.

2) The unit cell parameters of the synthesized corundum are smaller than standart ones (ASTM) by approximately 0.5% are a higher density of synthesized cristallites.

3) Amorphus fraction is absent.

4) No quenching products in the form of hydroxides are formed.

5) The size of particles measured with an electon microscope is 1-1.5 mkm; particles are isometric crystals.

The method employed allows to synthesize material with a given size.

Thus the obtained material is characterized by a high homogeneity of particles and unusually high density of packing of atoms in crystals. A combination of these two properties allow one to affirm that the material suggested is unique abrasive with hardness exceeding all earlier known abrasives on the basis of corundum.

SIGNIFICANCE OF ORE TEXTURES AND MINERALOGY FOR CORRELATION PROBLEMS IN Fe-Ti DEPOSIT OF LIGANGA, TANZANIA

Zakrzewski M.A. *(Dept. of Earth Sciences, Vrije Univ., Amsterdam)*

Major problems considering the evaluation of the reserves of iron ore at Liganga, Tanzania are the correlation of outcropping, massive ore bodies and the recognition of the nature of loose ore blocks. The blocks may represent a surface expression of a hidden massive iron ore body or form an accumulation of ore blocks transported by hill creep from outcrops. Pessimistic *vs* optimistic interpretation have lead to estimates varying from 50 mln ton to more than 1000 mln ton ore.

The correlation problem is solved by means of ore petrology. Microscopic investigations on 200 sections have shown significant variations in mineral content and ore textures in different seams. The following criteria were considered:

1. Mineralogy of gangue; the presence of spinel, högbomite and chlorite.
2. Mineralogy of ores; relative amount of ilmenite, martitization grade of magnetite.
3. Mineral intergrowths.

The observations on ore textures may be essential in planning of mineral processing and metallurgy. Both textural and mineralogical properties of the Liganga ores were considered in construction of a new map. It shows the distribution of the 11 km long central ore body, some smaller seams and accumulations of blocks.

CRYSTAL-CHEMICAL CHANGES IN AMPHIBOLES FROM ZABARGAD PERIDOTITE: THE RECONSTRUCTION OF A COMPLEX SUB-SOLIDUS EVOLUTION

Zanetti A., Sardone N., Oberti R., Vannucci R., Ottolini L., Bottazzi P. *(Dip. Scienze della Terra, Univ. di Pavia; CNR-CS Cristallochimica e Cristallografia, Pavia)*

The Island of Zabargad (northern Red Sea) exposes very fresh mantle peridotites belonging to the Nubian-Arabian sub-continental lithospheric mantle. Present knowledges indicate that they underwent a multistage metasomatic process since their accretion to the lithosphere. The first event produced widespread crystallization of Ti-pargasite and kaersutite in textural and chemical equilibrium with the LILE-depleted spinel-bearing assemblage; subsequent metasomatic events are associated to the Cenozoic continental rifting and to the development of an oceanic hydrothermal system in the Red Sea, after continental breakup.

A SREF (single-crystal X-ray structure-refinement) + EMP + SIMS study of Ti-pargasite and kaersutite was performed in order to completely characterize crystal-chemical changes (in terms of major and trace elements) produced by sub-solidus re-equilibration during the decompressional evolution under conditions postdating the early metasomatism. Amphiboles were selected from spinel-bearing lherzolites which show evidence of partial to complete recrystallization to plagioclase-bearing assemblages.

Ti-pargasites show LILE-depleted compositions with high $^{[4]}Al$, ^{A}Na, and $^{[6]}Ti$ contents. The transition from Ti-pargasite to kaersutite is characterized by a strong increase in $^{[6]}Ti$, Cr and decrease in $^{[6]}Al$, $^{[6]}Fe^{3+}$ and H contents. Concerning trace elements, increasing Zr, V, Sc and decreasing Sr contents are observed.

These compositional changes strongly affect the geometry of the amphibole structure. Within the octahedral strip, the decrease in M1 site dimensions (due to $^{M1}Ti^{4+} + 2\ O^{2-} \rightarrow {}^{M1}Mg^{2+} + 2\ OH^{-}$ substitution) is overcome by the increase in M2 and M3 site dimensions (due to decreasing $^{[6]}Al$ contents). The entrance of ^{M1}Ti balancing dehydrogenation increases the amphibole thermal stability. Within the tetrahedral double-chain, the inverse behaviour of the dimensions of the two indipendent sites indicate progressive $^{[4]}Al$ disorder, which is also coherent with increasing T or with almost constant (high) T at decreasing P. The unit-cell volume increases.

The subsequent transition from kaersutite to pargasitic- and edenitic-hornblendes, which are the common amphiboles in the most re-equilibrated plagioclase lherzolite, is characterized by the significant decrease in $^{[6]}Ti$ and in $^{[4]}Al$ contents. Hornblendes also show higher REE abundances, accompanied by Sr and Eu negative anomalies. The consequent structural modifications are coherent with lower T and P of recrystallization.

An attemp was made in order to relate also trace element abundances to structural parameters. Trace element distributions observed in amphiboles and their partitioning among the coexisting phases in spinel-bearing assemblages during the spinel-facies sub-solidus evolution have been shown to depend on structural constraints: a positive relationship has in fact been found in amphiboles both between Sr and the volume of the M4 site, and between Zr and that of the M2 site. Therefore, the dimensions of the sites *involved in the substitutions* are important also at the trace element level. The transition from spinel- to plagioclase-facies stability strongly modifies trace element behaviour and provokes progressive departures from these trends. Thus, competition among the coexisting phases is an important factor to be taken into account when modelling trace element partitioning.

In conclusion, the observed crystal-chemical changes allowed the sequence of amphibole recrystallization to be reconstructed in the frame of the decompressional evolution of Zabargad peridotites from spinel- to plagioclase-bearing assemblages under relatively high T conditions.

6—31G* MO CALCULATION OF VIBRATIONAL FREQUENCIES OF BORATE POLYHEDRA

ZHA Fubiao XIE Xiande LIN Chuanyi (*Institue of Geochemistry, Guangzhou Branch, Academia Sinica, Guangzhou* 510640, *P. R. China*)
WANG Yibo (*Department of Chemistry, Guizhou University, Guiyang* 550025, *P. R. China*)

Many features of the structure and spectral properties include vibrational spectra can be explained using molecular orbital (MO) theory. The basic structural units of borate minerals are $[BO_3]$ and $[BO_4]$, and the main properties of this group of minerals are determined by $[BO_3]$, $[BO_4]$ and the way they linked. Consequently, the study of chemical bonding in isolated $[BO_3]$, $[BO_4]$ polyhedra as well as in the various polyanions they form is essential for a better understanding of the properties of borate minerals. In borate minerals, oxygen atoms can be coordinate with one, two, or three borons. In this paper, the selected clusters are $[B(OH)_3]$, $[B(OH)_4]^-$ and $[OB_2H_4]$.

First, the optimized geometries were calculated by the extensive *ab initio* MO theory using robust 6—31G*.

Then, because in the neighbourhood of the bottom of the potential energy curve, the total energy can be expanded as Taylor Series with respect to bond length and bond angle, and as a good approximation, the terms higher than quadratic can be neglected, the force constants can be calculated, and vibrational frequencies of the clusters can be obtained by using normal coordinate analysis. The results are listed in Table 1.

Table 1 Vibrational Frequencies of Borate Polyhedra

		Vibrational Model	Calculated (6—31G*)	Observed
[BO3]	ν_1	A´	927	950
	ν_2	A´	736	750
	ν_3	E´	1110,1110	1250
	ν_4	E´	458,458	600
$[BO_4]$	ν_1	A1	770	800—950
	ν_2	E	550,550	600
	ν_3	E+B2	1250,1250,1332	1000—1300
	ν_4	E+B2	870,1006,1006	<600
$[OB_2]$	ν_1	A1	352	—
	ν_2	A1	1178	930
	ν_3	B2	1462	1490

• THE NATURAL RESOURCES OF GEMSTONES, SICHUAN, CHINA

Zhang Ru bo, Zhang Yu Yu (*Dept. of Geology, Chengdu College of Geology*)

Sichuan is one of the largest province in China. Two nearly SN and EW trending alignments of gemstone minerogenetic zones were sited west of it. For this reason this province is rich in various natural precious resources: sapphire, aquamarine, chrysoberyl, amethyst, moonstone, amazonite, topaz, tourmaline (green, red, blue), uvavorite, opal, agate (red, dark), cassiterite, turquoise, jade stone, etc.

The research of gemstones in Sichuan has just begun its first stage, but along with the development of gem industry in China, we believe that Sichuan province will surely become one of the focal points of gemstone mineral deposits in China.

In this paper we give a minute description of all gemstone characteristics and enclose colour photographs.

Application of abrasive stripping voltammetry for identification and characterization of some sulfides and sulfosalts

Zhang S., Meyer B. and Scholz F. (Institut für Angewandte Analytik und Umweltchemie Humboldt Universität zu Berlin, Germany)

Abrasive stripping voltammetry is described as a simple solid state microanalytical technique for the application in the field of mineralogy. In this procedure trace amounts of synthetical sulfide and sulfosalts are transferred by mechanical abrasion from the plane disc surface onto the surface of a paraffin-impregnated graphite electrode and electrochemical reduction or oxidation is followed by voltammetric techniques. Nanogram-amounts of a substance are sufficient to perform a series of measurements. After a preliminary electrolytic reduction of the sulfides or sulfosalts to the elementary metal on the electrode surface the anodic dissolution voltammograms are recorded to distinguish different mineral phases. The absolute charges consumed during reduction and oxidation are also measured for the quantitative determination of solid phases. In this way the electrochemical behaviour of minerals can be better understood.

MINERALS FROM DIAMOND - BEARING PERIDOTITE XENOLITHS AND KYANITE OF ECLOGITES: REDOX CONDITIONS OF THEIR FORMATION (KIMBERLITE PIPE "UDACHNAYA", YAKUTIA).

Zharkova E.V., Kadik A.A.(*Vernadsky Institute, Moscow*), Sobolev N.V.(*Institute of Mineralogy and Petrology, Novosibirsk*), Spesius Z.V. (*Yakutdiamond, Mirnii*).

The redox state of upper mantle has long been under discussion but recent experiment data obtained on high-temperature furnace with two solid elecrtochemical cells

(double-cell, M.Sato, et al., 1973, A.A.Kadik, et al.,1988) can approach the solution of this very important problem.

Determinations of intrinsic oxygen fugacity (f_{O2}) of diamond-bearing peridotite xenoliths and diamond-bearing kyanite eclogites from kimberlite pipe "Udachnaya", Yakutia, are given in this paper. Oxygen fugacity for olivines show that redox conditions for diamond-pyrope facies of upper mantle beneath continents are characterized by f_{O2} values which are close to IW (iron-wustite) buffer equilibria on T v.s. f_{O2} plot. Ilmenite- bearing and high-temperature sheared peridotites are formed in more oxidizing conditions comparing to the rocks of diamond- bearing peridotite facies. On T v.s. f_{O2} plot oxygen fugacities of mineral equilibria of these rocks are close to WM (wustite-magnetite) buffer while f_{O2} values themselves are close to those typical for redox regime of generation of depth-derived portions of kimberlite magmas.

Thermodynamic estimations permit to consider that fluid phase with high content of CH_4 is in equilibria with the least depleted rocks of the diamond-bearing peridotites. Along with oxygen fugacity is increase it composition changes towards water- methane fluids. Evolution of rocks of diamond/ chrome-pyrope facies is characterized by significant changes of fluid and redox regimes which nature is still under discussion.

Measurements of kyanites from eclogites permit to suppose, that redox conditions of formation of kyanite eclogites corresponds to the values of f_{O2}, which are close to the equilibria of IW and WM. The value of f_{O2} for crystalls of kyanites are close to redox state conditions of formation of diamond-bearing peridotite nodules from kimberlites. Therefore it is possible to suppose, that the formation of kyanite eclogites and their diamond-bearing differences connect with the differentiation of mantle lithosphere, but not with the subduction of crust substance in her depth (Sobolev N.V., 1977).

Sato M., Hickling N.L., and McLane J.E. (1973). *Proceeding of the 4 th Lunar Conf.*,1, 1061-1079.

Kadik A.A.,Zharkova E.V.,Kovalenko V.I. (1988). *Geochimia, No 6, 783-793.*

Sobolev N.V.(1977). *Am. Geophys. Union, 279.*

EXPERIMENTAL INVESTIGATION OF THE GOLD AND SILVER MOBILIZATION UNDER HIGHTEMPERATURE WATER-ROCK INTERACTION

Zhatnuev N.S. and Mironov A.G. (Buryat Geol. Ins., Ulan-Ude, Russia)

Some series of experiments of hightemperature water-rock interaction have been carried out using the radioactive tracer method. Radioisotopes Au-195 and Ag-110m+110 have been placed in basalt, riolite and andesite glasses with total concentration of gold 50 ppb, silver - 50-100 ppm. The samples of glasses were located in quortz or metallic ample with pure water or water solution (3,2 mas % NaCl, 10 mas% HCl, 1 mas% H_2S). The experiment conditions: T=200-500°C, P=200-1000bars, t=5-40 days, oxygen fugitive 10^{-8}-10^{-27} bar. The study of gold and silver distribution in glass samples was carried out using autoradiography on the nuclear emulsion platte and film MR, AF-3. Specific radioactivity of glasses - 0.5-1.5 MBc/g, exposition - 1-5 days.

In process of water-glass and solution-glass interaction the hydratation re-crystallization and leach zones were formed. The dimensions of this zones depend on glass composition, pressure and temperature of the fluide system. Gold and silver were leached from hydratation zone and were re-concentrated in re-crystallization zone. The high leach from riolite, basalt and andesite glasses is more tipical for silver (60-95%), whereas the gold was leached from glasses with increase of the oxigen fugitive only in system. The gold and silver leached are re-concentrated in the re-crystallization zone as a microinclusions of native gold and silver.

A conclusion was made that volcanic rocks can be a source of a precious metals under hydrothermal alteration. For all this, the gold can be mobilized together with silver, each taken separately, can be re-concentrated in the alterated rocks and can be caused for a preliminarily stage of ore deposits formation.

Mineralogical and geochemical peculiarities of the interaction of intersticial and basaltic melts with the minerals of mantle xenoliths (Baikal rift zone, Russia)

Zhmodik S.M. and Ashchepkov I.V. (Associated Institute of Geology, Geophysics and Mineralogy, SB RAS, Novosibirsk, Russia)

The trace-elements distribution while and peculiarity interacting of basaltic and intersticial melts with mantle xenoliths of Baikal rift zone has been studied using neutron-activation autoradiography method. Such method permits to obtain the spacial distribution images for Cr, Co, Sc, La and Sm and other elements. The concentration of separate elements in mineral grain boundary layer is observed, both, on a contact with basaltic melt, and inside xenoliths - on a boundary with intersticial glass films which composition differs from basaltic one. In first case the clear diffusive rims occur, their dimention being dependent on mineral type but does not exceed 0,1 mm. In second case the irregular zonation is not so distinct and is distributed. It should be related to interaction of a mineral with fluid-saturated melts still in the mantle.

Interaction kinetics for basaltic melt with xenolith minerals can be represented as process of absorbtion layer formation on melt/ mineral boundary, when the substance (element) supply goes both from mineral - at the expense of a forming diffusive layer - and from the melt. Concentration of an element in absorbtion layer depends on melt/mineral element distribution coefficient and velocity of mineral dissolution. Mineral melting occurs after its diffusion alteration within 0,5-1 mm zone. Thus, the distinctive displacement of absorbtion layer and of zone of diffusive alteration occurs while mineral melting. Simultaneously, "driving away", separation and concentration of the oxidized phase is observed in the front part of the interaction zone in a mineral. The fluid (water or carbon dioxide) should play a significant role in this process, because such type of interaction is fixed while melting of water-saturated basaltic melts.

The time of interaction of basaltic and intersticial melts xenolith minerals is established to differ on several orders. Moreover, in case of intersticial melt/ xenolith minerals interaction we can prove the time of equilibrium reaching due to closed type of the system: porous melt - mineral. This time significantly exceeds the time of mineral/basaltic melt boundary

interaction. In some cases mineral zonation was noted to be referred to the rapid changes of T P conditions may be really formed due to similar type of interaction.

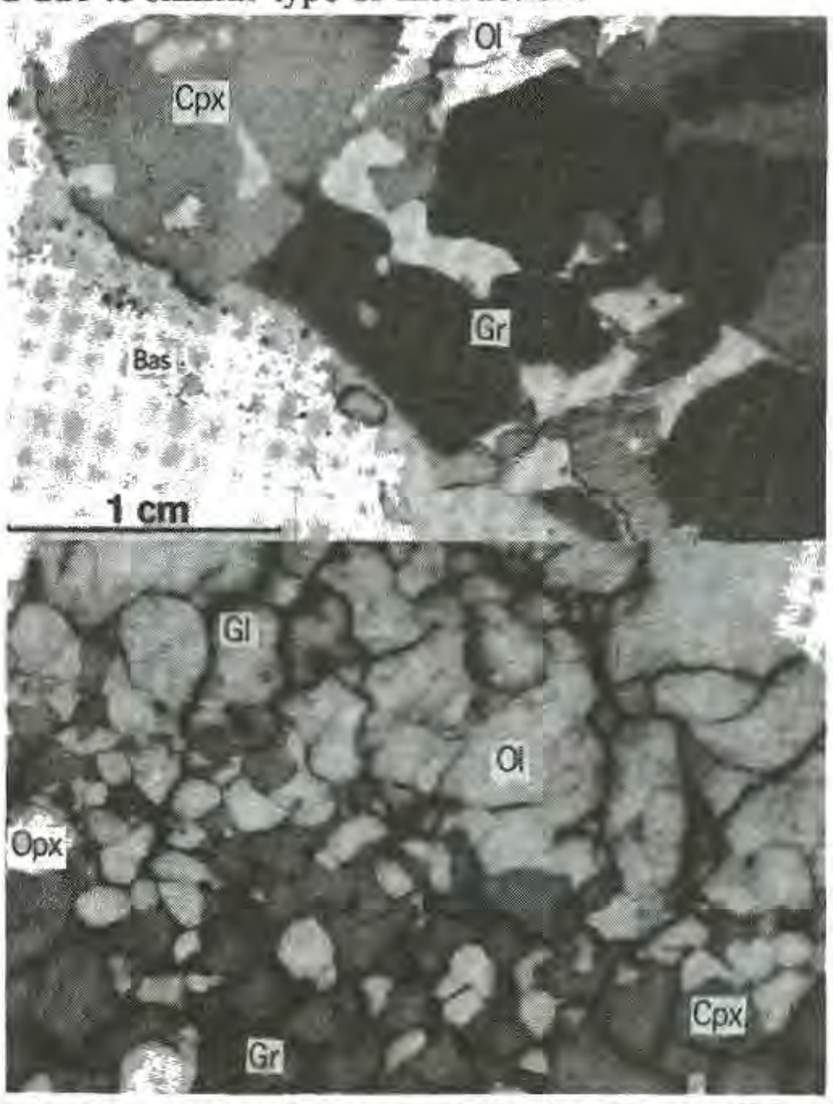

Cr distribution autoradiograms at the basalt-xenolith contact (1) and in intersticial melt (2) of the lherzolites

THE MINERALOGICAL INDICATORS FOR PREVAILING $Au(HS)_2^-$ IN PORPHYRY-TYPE HYDROTHERMAL FLUIDS

Zhou jianping
(Dept. of Earth Sciences, Nanjing Univ.)

It is a fact that there are some gold-rich ores which are more or less related to sulfidation in most porphyry type ore deposits. Lengshui silver ore deposit, one of the biggest porphyry silver ore deposits in China, has a series of significant mineralization of copper, zinc, lead to silver at different scale, and gold mineralization in some localities as well. The precipitation of all sulfides, silver and gold-bearing minerals except for native gold and electrum in oxidized ores are closely related with a sulfidation of the ascending hydrothermal fluid at varying physico-chemical conditions.

As illustrated in figure of evolution path of the hydrothermal fluid shown in $-\log fS_2$, —$-\log fO_2$ diagram, fS_2 increases gradually from extremely low at the early stage to much higher at the late stage under the prevailing ore-forming temperatures, so that sulfur-rich bornite and pyrite intergrowth may be expected to occur in the deposit, then it decreases gradually when the fluid passes through fractures or fissures near the surface, meanwhile fO_2 increases all the way from the commence to the end of mineralization. Occurrence of the minerals and their assemblages, variations in compositions of sulfides are therefore mineralogical indicators for the ore-forming surroundings, and in turn reflect a process of transportation and deposition of gold.

As to the complex species of gold in the porphyry type hydrothermal system, $Au(HS)_2^-$ is recommended for a predominant species carrying gold from deep to shallow based on a study on sulfide minerals, their paragenesis and the documented thermal dynamic data.

Gold precipitation in this hydrothermal system is most likely to take place in the upper part of the deposit, i e, in the late mineralization stage under lower temperatures, fS_2, and higher fO_2 conditions. So that gold may distinctly present in fissures affected by meteoric water and contact zone between rocks and high-porosity pyroclastic or carbonate rocks due to an oxidation, a sudden drop of temperature and drastic changes in pH, fS_2 and fO_2 etc.

Reference:

Craig J.R. and Vaughan D.J. (1981) Ore microscopy and ore petrography Holland, H.D., (1965) Econ. Geol. v.60 p.1101-1166
Jianping Z., & Wu, C., (1989) Journal of Nanjing University No.3 p.158-166
Wu, C., and Jianping, Z (1988) Minerals & Rocks, vol.8 No.2 p.84-91

^{29}Si MAS NMR SPECTROSCOPY OF SOME NA-K FELDSPARS

Zhou Lingdi, Guo Jiugao, Yuan Hanzhen and Li Liyun (*Wuhan Inst. of Phys., Acad. Sin.*)

We present in this paper ^{29}Si MAS NMR spectroscopic results for six kinds of natural Na- K feldspars which have been determined previously by XRD, IR and chemical analyses. Their NMR spectra were obtained using Bruker MSL-400 spectrometer. The representative ^{29}Si NMR spectra are showed in Fig. 1.

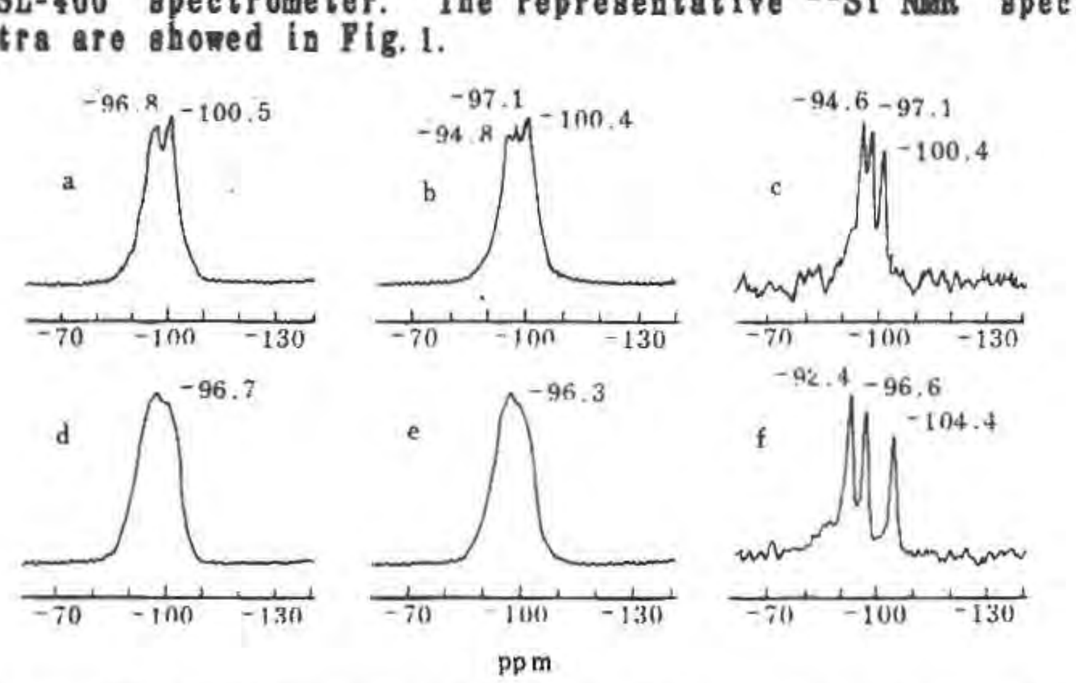

Fig. 1 ^{29}Si NMR spectra of the feldspars studied. (a) sanidine, (b) orthoclase, (c) microcline, (d) monalbite, (e) anorthoclase, (f) albite.

Fig. 1a, 1b and 1c are the ^{29}Si NMR spectra of K-feldspars with different degrees of Si/Al ordering. Of them, the highly disordered sanidine with $t_{1o}=t_{1m}=0.297$, showed a broad ^{29}Si doublet in Fig. 1a, indicative of disorder. The peaks at -96.8 and -100.5 ppm, as usual, were assigned to T_2 and T_1 respectively. The slightly larger intensity of the peak T_2 than that of T_1 indicates that Si prefers to occupy the T_2 site. Fig. 1c is a ^{29}Si NMR spectrum of the highly ordered microcline ($t_{1o}=0.898$). It consists of 3 narrow peaks at -94.6, -97.1 and -100.4 ppm, revealing that Si was restricted to site T_{2m}, T_{2o} and T_{1m}. According to Sherriff and Hartman (1985), Kirkpatrick *et. al.* (1985) and others, there are 2 sets of tetrahedral sites, T_1 and T_2, in orthoclase, giving rise to the two partially overlapping peaks due to T_1 and T_2. However, the orthoclase ($t_{1o}= t_{1m}= 0.358$) spectrum obtained by us exhibits three poorly resolved peaks at -94.8, -97.1 and -100.4 ppm (Fig. 1b) showing that Si distribute in T_{2m}, T_{2o} and T_{1m} randomly. The

five other orthoclases examed by us also gave similar NMR spectra. Obviously, there do exist three sits, T_{2m}, T_{2o} and T_{1m}, occupied by Si in those feldspars which were identified by XRD as orthoclases.

Fig. 1d, 1e and 1f are ^{29}Si NMR spectra of Na-feldspars of different degrees of ordering. Of them, the highly ordered albite shows a ^{29}Si NMR spectrum with 3 well resolved peaks at -92.4, -96.6 and -104.4 ppm assigned to T_{2m}, T_{2o} and T_{1m} (Fig. 1f), like the typical spectra of albites reported by many NMR laboratories. As to the other two Na- feldspars, monoclinic monalbite and triclinic anorthoclase, we have not got any NMR information about them previously. They both gave a broad ^{29}Si NMR signal with a maximum at -96.7 or -96.3 ppm (Fig. 1d, 1e) indicating high degree of Si/Al disorder and similar Si, Al distribution. The envelope of their peaks , extending from about -95 to -100 ppm, are in the range of K-feldspars, but quite different from that of albite (about -92 to -104 ppm) . The high structural state triclinic Na-feldspar and monoclinic K- feldspar have the same Si, Al distribution, as reported by Ribbe (1983) and others previously. The IR spectra of monalbite, anorthoclase and sanidine reported in this work are very similar, so that they can not be distinquished from each other by this technique. From above-mentioned, it is clear that the near- neighbour and next near-neighbour environments of ^{29}Si nuclei in high temperature monoclinic as well as triclinic Na-K feldspars are very similar.

Reference:
Kirkpatrick, R. J., et al. (1985) *Am. Miner.*, 7, 106-123.
Ribbe, R.H. ed (1983). Reviews in Mineralogy, Feldspar Mineralogy, Miner. Soc. Am.
Sherriff, B. L. & Hartman, J. S. (1986). *Can. Miner.*, 23, 205-212.

• MOBILE FORMS OF FLUORINE IN THE ENVIRONMENT (SOIL AND WATER)

Zhovinsky E.Ya. *(Inst. of Geochem., Miner. and Ore Form., Ac. Sci. Ukr., Kiev 252142, Ukraine)*

Under the term mobile forms of fluorine we mean the forms that are thermodynamically stable in pore solutions of soils, surface and underground waters under definite physical-chemical conditions of environment and that easily come to water solution from soils and rocks.

Content of mobile forms of fluorine as well as direction of natural processes in water-rock systems can be estimated according to programs especially worked out using the available results of chemical analysis and thermodynamic data (Zhovinsky, 1979).

Migrational ability of fluorine forms is determined through the experimental study of kinetics and dynamics of sorption and desorption process, as well as by use of several analytical methods.

The study of mobile forms of fluorine has great theoretical and practical value. The author has established that anomalous content of mobile forms of fluorine in soils and waters is an indicator for exploration of fluorite, polymetal, rare earth and other deposits (Zhovinsky, 1985).

Moreover a relation has been found between contents of various fluorine forms in waters and endemic diseases of man.

It makes possible to use widely the data on mobile forms of fluorine to forecast and explore mineral deposits and to work out environment protection measures.

Zhovinsky E. Ya. (1985): Fluorimetric methods of exploration. Sci. Kiev, 160 p.

REE DISTRIBUTION PATTERNS OF MONAZITE: CONSTRAINT ON MONAZITE ORIGIN IN METAMORPHIC ROCKS

Zhu X.-K., O'Nions R. K., Reed S.J.B. (*Dept. of Earth Sciences, University of Cambridge, UK.*)

Monazite is a common accessory mineral in intermediate-to high-grade metapelites. Recent studies have shown that monazite has the potential to provide chronological information on peak or even the prograde part of metamorphic thermal history. Furthermore monazite is also a valuable phase for *in situ* ion probe chronology of high-grade metamorphic rocks. Although documented inheritance of monazite is rare, it can not be assumed *a priori* to be absent. Therefore it is essential to identify the origin of monazite using chemical and petrological techniques as a prerequisite to age interpretation.

Monazite is a rare earth element (REE) phosphate. REE have been used as provenance indicators in many geological circumstances. Here we report REE distribution patterns for monazites with different origins and from different areas analysed by electron probe, in order to constrain the origin of monazite in metamorphic rocks.

Monazites analysed from Bayan Obo REE deposit, China, occur in a single thin section. They have a hydrothermal origin, and are assumed to have formed under identical geological conditions. All monazite grains have the same REE distribution pattern. Monazites in one thin section of tourmaline gneiss from Isua, Greenland, all have identical REE distribution patterns but are distinctly different from the Bayan Obo monazites. The similarity within each group and the difference between the two groups of monazite suggest that the REE distribution pattern of monazite is strongly influenced by the composition of the host rock (provenance) and/or physical-chemical (P, T, etc.) conditions at which monazite was formed.

Samples of granulites collected from the central Lewisian region, Scotland, which are assumed to have experienced the same high-grade metamorphic conditions have been analysed. Again, monazites in the same thin section have very similar REE distribution patterns, but they differ greatly from one sample to another. These observations suggest that the REE distribution pattern of monazite is influenced principally by the composition of the host rock (provenance). Thus if any grain or portion of monazite in a given sample was formed in a different provenance, it is most likely that that grain or portion will have a different REE distribution pattern from the others.

Zoned monazites in a single thin section of the Lewisian granulite have been studied, and the REE distribution patterns show remarkably little difference between different grains and between core and rim of the same grain. This demonstrates a constancy of REE supply to all the monazites at their various stages of growth and argues against any portion of these monazites being of very different provenance (i.e. inherited or detrital).

This study shows that REE distribution patterns of monazite provide a simple but useful constraint on monazite origin in metamorphic rocks. It may also be useful in the studies on REE provenances of REE deposits.

THE NETWORK THEORY AND THE MECHANISM OF MANTLE FLUID FORMATION

Zhu, Y. F. (*Department of Geology, Peking university*)

The heterogeneous mantle especially was shown by the

contents of volatiles. Some researchers even believed that in mantle exists or had existed alkali-rich and volatilerich lamination flow. In such fluid, the contents of SiO_2, K, and Na are very high. The process of many extra-big ore-deposit's formation related to it. Besides, by the study of Pb, Nd, Sr, Cs istopic in mineral oil, it was believed that in the process of mineral oil formation, mantle fluid also played an important role.

We studied the mechanism of mantle fluid formation in the light of network theory. Our point here is that the formation of mantle fluid is the result of mantle structure ordering process. prinitive mantle is composited by polymeres, centring around $[SiO_4]^{4-}$。Volatiles spread in space among polymeres, forming ionic and/or molecule bonding between K^+, Na^+, Fe^{2+}, Mg^{2+}, and $[SiO_4]^{4-}$. The polymeres bound together by ionic and molecule bonding formed network sturcture. This structure under primitive mantle condition is homogeneous, i. e. in all directions the strength was same, volatiles, K, Na, ore-forming elements spread in disorder state. When the situation changed (for example, nebular percussion, the cooling effect of Earth etc), primitive mantle would be driven far from thermal equilibrium, which can lead the mantle to undergo kinematic instabilities and symmetry breakings leading to the formation of coherent structures on the macroscopic scale, in our point it is mantle structure ordering process. Under this condition, in the network structure the weak bonding would break down, and net-work sturcture would have a change in order to respond the new condition. The bonding among K^+, Na^+, $[SiO_4]^{4-}$ and volatiles is weaker than the bonding between $[SiO_4]^{4-}$ and Fe^{2+}, Mg^{2+}. So, these bondings would be destroied at first. As a result, the volatiles, K, Na will exsolved from the net-work structure and concentrated. This process can be demonstrated by viscosity η.

$$\eta=\eta_m+((\eta_0+\eta_m)\tau/\beta)/\mathrm{Sinh}(\tau/\beta)$$

where η_m is the minimum viscosity ($\eta_m>0$) when mentle melt is acted by a maximum shear stress. η_0 represent the premitive viscosity of mantle melt, $\beta=2KT/\xi^3$, K-Boltzmann constant, T-temperature, ^0K. $\tau=\tau_0/\xi$, ξ is the acted region of shear stress τ_0, h represent the distance between chains in net-work stucture.

The lower η, the more the net-work structure changed, and the more chance of free mantle fluid formed.

However, the adjustment of network structure is reached by plastic deformation, which is a nonlinear dissipative process and ,can be described by the collective behavior of the dislocation popalations under stress. A physically based set of the reaction-diffusion type derived for the dislocation densities is able to qualitatively describe the various aspects of dislocation patterning during deformation processes and provides the framework where quantitative aspects may be obtained via specific analysis and numerical simulations.

NONCENTROSYMMETRIC MICAS 1M FROM THE EPITHERMAL POLYMETALLIC DEPOSIT BANSCKA STIAVNICA (SLOVAKIA)

Zhukhlistov A.P., Dragylesku E.M., Kovalenker B.A., Rusinov V.L. and Zvyagin B.B. (Inst. of Ore Mineralogy (IGEM) Rus. Ac. Sc., 109017 Moscow, Russia)

Contrary to usual centrosymmetric mica (CM), noncentrosymmetric micas (NCM) consist of dioctahedral 2:1 layers with vacant cis-octahedra. The tetrahedral sheets of the layers are related by two-fold axes and highest symmetry is C2, whereas in CM having vacant trans-octahedra and highest symmetry C2/m, they are related at least by pseudo-symmetry centres $\bar{1}$. Both mica polymorphs are distinguished by geometry and intensities in diffraction patterns (Zhukhlistov and Zvyagin, 1991).

The abundance of NCM is very low, and reasons for their formation are not yet clear. This defines the interest to the NCM identified in the samples of the epithermal polymetallic deposit studied by means of electron diffraction. This Pb-Zn-Ag-Au-Cu deposit in Banska Stiavnica (Slovakia) is enclosed in andesitic volcanics of Neogene age and contains several large and a lot of small subparallel ore veins. Near the veins the rocks underwent acidic metamorphism (quartz+sericite+carbonate+pyrite). One of the largest vein, Teresia, consists of quartz, somewhere with Mn-carbonate, and contains ore shoots rich in sulphides. The fluid inclusion data indicate that the ore forming solution nearly had T=250-300°C, P=100 b, salinity 8-10% equiv. NaCl.

Mica-containing samples were picked up from ore shoots in Teresia vein at 7 levels (vertical range about 500 m). All NCM-containing samples belong to hydrothermal breccia with quartz cementing rock fragments and with veinlets, slabs or nests of massive sulphides. NCM fills very small cavities mainly in massive sulphides or in quartz. It associates often with CM and seldom with kaolinite.

According to oblique-texture ED-patterns both NCM and CM are polytypes 1M, and the deviations from ideal relationship -ccosβ/a=1/3 were found to be 0.303-0.317 for the NCM studied and 0.380-0.393 for CM. Both mica polymorphs are also distinguished by intensities in single crystal SAED patterns and particle morphlogy in the EM images (elongate for CM and isometric for NCM).

The geological position, physico-chemical and mineralogical data suggest that NCM was deposited during the Pb-Zn stage of ore formation in connection with hydrotermal explosions by sedimentation from ore solutions in small cavities. All this favoured quick growth of metastable phases under unequilibrium conditions.

References:
Zhukhlistov, A.P. and Zvyagin, B.B. (1991). Proc. 7th Euroclay Conf. Dresden 91, 1211-1212.

SPINEL CLINOPYROXENITES WITH DIOPSIDE MEGACRYSTS FROM SW BULGARIA:PHASE COMPOSITION AND FORMATION CONDITIONS

Zidarov N.G., Nenova P.I. and Dimov V.I. *(Inst. of Applied Mineralogy, Sofia)*

Megacrystalline spinel pyroxenites together with peridotites, olivinic gabbronorites, gabbronorites and leucocratic pyroxenic gabbro, regionally metamorphosed to amphibolitic facies crop out in SW Bulgaria. All of them are a part of boudinated offiolitic massif placed in two-mica gneissies of Prerhodopian (Ograjdenian) Supergroup identical to Vertiskos Formation of Serbo-Macedonian Massif.

Gigantic diopside crystals up to 10cm as well as enstatite exsolution lamellaes and early enstatite poikilitic inclusions are observed in relicts of non-metamorphosed pyroxenites. Fine-crystalline aggregates of pan-

idiomorphic enstatite and diopside with enstatite lamellaes are formed interstitially among the gigantic crystals.

Diopside and enstatite compositions fall in to limits :

$Wo_{47-48}En_{39-42}Fs_{11}$ and $Wo_{1}En_{67-68}Fs_{31-32}$. Accessory minerals found are green spinel, ilmenite and magnetite.

According to the bulk chemical composition, the rock is clinopyroxenite chemically corresponding to prothoaugite $Wo_{34}En_{46}Fs_{20}$.

The determined unit cell parameters of diopside are: a=9.737 Å, b=8.887 Å, c= 5.282 Å, ß= 106.08°, V= 439.2 $Å^3$.

Coherent boundaries between diopside matrix and enstatite lamellaes with (110) of diopside and (210) of enstatite being parallel to each other are established by HRTEM.

The rock is evaluated to be formed at 10-15kbar and 1200-1150°C. The exsolution pyroxene is found to take place at 1000-930°C.

Gigantic diopside crystals are proposed to be result of very slow crystallization of melt in almost isothermic and isobaric conditions, which is typical for the upper mantle.

OPTICAL PROPERTIES OF DEFORMED CRYSTALS AND THE THERMOBAROMETRY

Zilbershtein A.Kh.(*All-Russia Res.-Geol.Inst., St.-Petersburg*)

The action of prestresses and crystallization conditions on optical properties of crystals was studied.

1. It was shown that different prestresses might induce the optical anomalies (changes of optical characteristics) for various crystals.

The anomalies permit to estimate the internal stresses induced by prestresses for the unloaded preliminary deformed crystals.

It was found that the magnitude of the stress is approximately proportional to the magnitude of the prestress. The proportion coefficient is the combination of constants of a material.

For all crystals under study, the united expression for the internal stress (or optical anomaly) as a function of the prestress was discovered.

The influence of prestresses parameters (as the exposition and temperature) on the anomalies was experimentally studied by use of garnet crystals as an example.

The general expression for the internal stress (or optical anomaly) as a function of all parameters of a prestress was obtained.

It was shown, that, using the measured optical anomalies, these expressions may be used for estimation of the prestress (paleostress) parameters for natural prestresses and crystals.

2. The influence of crystallization (formation) pressure and temperature on optical properties of inhomogeneous crystals was studied.

Optical anomalies may be observed in the vicinity of a boundary between homogeneous parts of inhomogeneous crystals.

These anomalies are induced by reciprocal deformation of the parts.

If the thermo-expansion tensor and compliances tensor for these neighbouring homogeneous parts are not equivalent, then the reciprocal deformation must exist due to a difference between the temperature and/or the pressure under observation conditions from those under formation conditions.

For optically transparent parts, the deformation induces the optical anomalies as induced birefringence.

It was found, that, using the measured magnitudes of these birefringences for two different pairs of neighbouring homogeneous parts of the inhomogeneous crystal, the deviation of the temperature and pressure under observation conditions from those under formation conditions may be determined.

Thus the temperature and pressure of a crystallization may be estimated by the new independent method.

THE NEW INTEGRAL OPTICAL METHODS FOR ESTIMATION OF ROCKS ANISOTROPY, DEFORMATION AND POROSITY

Zilbershtein A.Kh.(*All-Russia Res.-Geol.Inst., St.-Petersburg*) and Romm G.M. (*Inst.of Earth Physics, Russian Acad. Sci.*)

For analysis of integral optical characteristics of transparent and absorbing polycrystalline aggregates (as a whole) we designed the polarization laser macroscope-photometer.

This setup permits to study various integral optical properties of thin sections and polished sections made from the polycrysralline aggregates.

The macroscope-photometer permits us to measure the integral transmittance (T) for transparent thin sections placed between crossed or parallel polarizer and analyzer. Using different (in thin sections plane) orientations (a) of the thin section between relatively fixed polarizer and analyzer, one can obtain the angle function T(a). It may be shown, that this function is the sinusoidal function. The value Qt defined as $Qt = [maxT(a) - minT(a)] / [maxT(a) + minT(a)]$ is the quantitative parameter (measure) for integral optical anisotropy of transparent thin sections.

For strongly absorbing aggregates we can measure the integral reflectance (R) of polished sections. The reflectance has to be measured for polarized monochromatic (laser) light for different aggregates orientations (a) relatively polarization plane. R(a) is the sinusoidal function. In this case the quantitative parameter of integral optical anisotropy (Qr) may be expressed in the form $Qr = [maxR(a) - minR(a)] / [maxR(a) + minR(a)]$

Using thin sections of naturally deformed quartzites as an example,the linear correlation between integral optical anisotropy Qt and anisotropy of the deformation (Qd) was obtained at the first time. The correlation Qt(Qd) may be used for deformation anisotropy estimation.

Using the thin sections of natural dolomites as an example, the linear correlation between average light transmittance Ta (where $Ta = [max\ T(a) + min\ T(a)] / 2$) of thin section and dolomites porosity (P) was obtained at the first time. It is shown, that the transmittance Ta may be used for total porosity estimation.

Thus, integral optical characteristics of polycrystalline aggregates may be used for quantitative estimation of their anisotropy, deformation and porosity characteristics.

CONDITIONS FOR EQUILIBRIUM GROWTH OF LARGE TREMOLITIC AND RICHTERITIC AMPHIBOLES FROM EXCESS CA-, NA- AND K-CHLORIDE SOLUTION AS A FUNCTION OF FLUID COMPOSITION

Zimmermann R., Heinrich W., Pehlke I. *(Petrology, TU Berlin)* and Knop E. *(Mineralogy, Univ. of Innsbruck)*

Synthetic amphiboles are commonly very fine grained (< 5 to 10 μm), and the characterisation of experimental run products can only be done by XRD and spectroscopic methods. Neither composition (Raudsepp *et al.*, 1991), nor chemical homogeneity can be assured without reliable microprobe analyses. The investigation of exchange reactions, involving variable amphibole compositions is impossible without microprobe data, and it remains uncertain, whether chemical equilibrium has been achieved in experiments. Reliable analyses have scarcely been published. A further complication in amphibol synthesis is, that they are frequently structurally disordered (chain multiplicity faults, CMFs; Graham *et al.*, 1989).

Our exchange experiments in the system Na-richterite-K-richterite-tremolite-NaCl-KCl-$CaCl_2$ have initially been impaired by all these difficulties. Exchange reactions of synthetic Na-, K-richterite and tremolite with chloridic solutions did never approach equilibrium. The run products were chemically and structurally inhomogeneous. The composition of some of the partly reequilibrated amphiboles was degenerated.

A change of our experimental strategy yielded finally tremolite and richterite crystals several 100 μm long and up to 40 μm in cross section. Best results were obtained under the following conditions: Hydrothermal syntheses were performed at 700 to 800 °C and 2 kbar. Na, K and Ca was provided in stoichiometric amounts as hydroxide (solid $Ca(OH)_2$ or 2n NaOH resp. KOH solution). An excess chloridic exchange fluid (2n NaCl, KCl resp. $CaCl_2$ solution) was added, so that the (Ca+Na) solid/(Ca+Na)total-ratio resp. (K+Na)solid/(K+Na)total-ratio remained low (0.2 to 0.5). Microprobe analyses confirm that these crystals are chemically homogeneous and that they grew in chemical equilibrium with the chloridic exchange fluid. TEM investigations show that they are virtually free of CMFs.

Richterite syntheses from a chloridic fluid alone (without hydroxides) failed. Na and K remain mainly in the fluid, probably caused by the formation of 2 moles HCl per mole amphibole.

References:
Graham, C.M., Maresch, W.V., Welch, M.D., Pawley, A.R. (1989). *Eur. J. Mineral.*, **1**, 535-555.
Raudsepp, M., Turnock, A.C., Hawthorne, F.C. (1991). *Eur. J. Mineral.*, 3, 583-1004.

CLAY COMPOSITION FOR DECONTAMINATION OF THE URBAN ENVIRONMENT

Zlobenko B.P., Movchan N.P., Fedorenko Yu.G. and Spigun A.A. *(Dept. of Radiogeochemistry of Environment, IGMFO, Ukrainian Ac. of Sci.)*

After the accident at the Chernobyl Nuclear Power Plant a considerable part of research was devoted to study of clay minerals and clay based compositions as effective and having sufficient resources natural material used for radioactive decontamination of the environment. Clay minerals are known to be effective sorbents and these natural materials seem to be very promising for large-scale clean-up. A variety of compositions based on clay minerals has been developed and tested lately to be used as decontamination agents (Belfiore A.,1984; Movchan *et al.*,1990). Also, the clay decontaminative compositions were used for cleaning up a wide variety of materials (Panciatici *et al.*,1993).

Natural Ca-form of bentonite from Cherkassy deposit modified into Na-form and palygorskite were the basic clay materials selected for the studies. Research of the adsorption properties of these clays were carried out under various conditions. The distribution coefficient,usually denoted as Kd, of four radionuclides (Sr,Cs,Pu,Am) has been studied for the clay fraction of the clay materials. All the sorption-desorption experiments were performed in batch. The impact of time, ph, composition of sorbents has been examined. According to the experimental data, the distribution coefficient values range between: $(0.5\text{-}2.0)*10^2$ ml/g for Strontium; $(0.9\text{-}3.5)*10^3$ ml/g for Caesium; $(10^3\text{-}10^4)$ ml/g for Plutonium and Americium. The obtained results show that Na,Ca-bentonite and the natural mixture of bentonite and palygorskite are suitable materials to prepare decontaminative clay composition.

The combination of such properties as sorption capacity and swelling determines their behaviour when used as clening up materials for decontamination of houses and buildings on the urban environment.

Decontamination tests were made on the surface of a building six years after contamination. The field experiment consisted of treatment of wall surface with clay suspensions, drying and selfremoving of the clay covering. The decontamination factor was found to be 1.21, with a 95% confidence interval from 1.12 to 1.31.The loose contamination immobilized by clay is in the form ready to be disposed. The waste from the decontamination tests was collected by vacuum cleaning.

Decontamination using clay coating is ideally suitable for large scale decontaminative operations in the urban environment, since it is safe, practical and cost effective. However, in many cases the residual contamination remains rather high because of the porous nature and physico-chemical conditions of the surface of building materials as it was cleaned up several years after the contamination.

References
Belfiore A., (1984). *Neorg. Chim. Acta, 94, 159-160.*
Movchan N.P., Zlobenko B.P., Shpigun A.A., Fedorenko Yu.G., Govorun A.P.,Polskiy E.M. (1990). *SU Patent 18 17 935.*
Panciatici G.,Belfiore A.,Poggianti M.(1993). In: *Proceedings of the Int. Conf. on Nuclear Waste Management and Environmental Remediation.Prague,2,313-321.*

• THE MINERALS IN THE SYSTEM OF THE STRUCTURAL TYPES OF POLYMORPHS

Zvezdinskaya L.V. (*Institute of Geology of Ore Deposits, R.A.S., Moscow*)

The data obtained through the experimental investigations have substantiated the brilliant foresight of V.I. Vernadsky on the universality of polymorphism. Obviously we cannot agree on the quantity of polymorphs predicted by him (32 – according to the number of symmetry classes). The realization of all symmetry classes under phase transformation appears possible for the various compounds, especially for the high-symmetric ones. However in the case of the polytypism the number of polytypes may be large, but most of them will have the same space group symmetry.

Developing the principles of the general theory of polymorphism, N.V. Belov and N.L. Smirnova proposed to use the concept of te reationship of polymorphous structures with the same formula composition for the structural type (ST) classification of compounds. According to this concept the author has developed the systems of structural types (SST) of elements and binary and ternary compounds. Thus in studying polymorphous compounds with the formula composition ABX_2, ABX_3, ABX_4, AB_2X_4 it was found that more than 1000 polymorphs, whose structures can be described by 180 structural types, are known for 400 compounds presenting the mentioned compositions.

In accordance with the formula composition, the ST were pooled in the SST on the basis of the polymorphous transitions occuring in the particular substances, the ST being placed in the SST depending on the value of the volume per formula unit. The increase

of this volume occurs in the SST upwards and is determined by the conditions of the polymorphous transitions either under the increase of the temperature or under the decrease of the pressure, the two parameters rarely changing simultaneously. The mechanisms of the of the structural reconstruction, as well as the regularities of the change of coordination numbers of cations and their combination under polymorphism, were revealed. The general and particular regularities of the construction and development of different systems, as well as their genetic relationship ith the system of elements, were determined. The data obtained allow to use the SST to forecasting new polymorphous structures, in particular in obtaining semiconductors with pre-determined properties.

Since the majority of compounds discussed are minerals, the author proposes to use SST in studying mineral typomorphism and in modelling natural processes. The position of the structure of minerals in SST is exactly determined y the formation conditions and therefore reflects the typomorphic P-T parameters. Moreover, the SST allows to predict the structures of new polymorphs for the minerals with ternary composition, on the basis of the analogy with binary compounds, for which the same problem was successfully solved.

THE BEHAVIOUR OF NATURAL URANIUM OXIDE UNDER HEATING

Zvezdinskaya L.V., Timofeev A.V. (*Institute of Geology of Ore Deposits, R.A.S., Moscow*), Shtanov V.I. (*Moscow State University*)

The investigations were carried out on the pitchblende from the ores of one of the uranium deposits, North Kazakhstan. The pitchblende forms massive aggregates and thick disseminatons in the quartzite-like host rocks. The aggregates are composed by spheroliths with poorly manifested zonality. The pitchblende is characterized by highly cristallized structure; the square-shaped nuclei (uraninite?) in the centre of the individual spheroliths may be often detected under great magnification. The pitchblende is cubic, with a_0 = 5.452 (0.018) Å.

The changes of the morphology and phase composition of pitchblende, when heated from 25°C to 900°C, were analyzed in the dynamic regime (heating rate 10°C/min) by thermomicroscopy and X-ray diffraction. It was shown that:

a. The pitchblende is stable up to 300°C. The oxidation occurs in the range 390-700°C, being most intensive at 465-510°C. Over that values the pitchblende grains brighten up and then fractures appear on the surface and slowly spread over the whole grain area.

b. At 500°C rhombic U_3O_8 appears as oxidation product; under further temperature increase it partly transforms to hexagonal U_3O_8.

c. At temperatures higher than 730°C three distinct states of the grain surface were observed:

730-800°C - a small quantity of liquid escapes;

more than 810°C - the quantity of escaped liquid increases and the fracture obviously heals;

905-920°C - a sharp increase of the liquid formation occurs because of the regular mineral transformation.

The phase composition of the sample after the heating up to 900°C presents the following uranium oxides: UO_2, U_3O_8, U_2O_5, UO_3. The pitchblende cell parameter decreases, a_0 = 5.438 (0.028) Å, in comparison with the starting value.

d. After heating up to 800°C the mineral surface slowly raises over the bottom of the metal container and afterwards (in the range 885-900°C) sharply falls down, owing to the escape of the gases contained in the pitchblende (mainly radon).

DERIVATION AND PREDICTION OF MODULAR STRUCTURES

Zvyagin B.B. (Inst. of Ore Mineralogy (IGEM) Rus. Ac. Sc., 109017 Moscow, Russia)

Building modules (BM) usually represent fragments of simple compounds whose stability and formation economy are approved by the nature. Being combined under certain stacking rules, they compose sets of interrelated modular structures (MS) having both common and particular features and occupying definite positions in their systematics. The homogeneity condition being applied, sets of homogeneous MS may be derived and predicted according to procedures developed by Smith and Yoder (1956), Zvyagin (1967), Dornberger-Schiff (1982). Ingomogeneous structures are then interpreted as members of structural series between the homogeneous ones. Sometimes the inhomogeneous structures may be considered as homogeneous ones if some combinations of the initial BMs are fixed and accepted as enlarged BMs.

The analysis of MS is greatly facilitated by the use of symbols denoting single BMs, their arrangement and operations relating them. Latters of the type P (pyroxene), M (mica), S (spinel) emphasize the polysomatic aspect of MS; letters H, A, V, S, Z, N, И, b, d, p,q correspond to symmetry relationships; operations 1̄, 2, m, a, n ets. express homogeneity-inhomogeneity and proportions of homogeneous components in MS series.

In addition to the classical examples of 2H and 3C close-packed structures and 6 simple mica polypypes, a number of new MS has been considered during the last years, displaying the efficiency of the modular approach and forming a basis for modular crystallography as an specific scientific area. An especially rich material of a great instructive power has been delivered by the Italian scientific community (see e.g. Merlino, 1991). Other examples are presented by semiconducting layer chalcogenides (Zvyagin and Kyasimov, 1992), system Ca_2SiO_4-$Ca(OH)_2$-$Ca_4Si_3O_{10}$ (Zvyagin and Pushcharovsky, 1993) and Oxyborates (Zvyagin and Sydorenko, 1993).

References:
Dornberger-Schiff, K. (1982). Acta Cryst. A38, 483-491.
Merlino, S. (1990). Per. Mineral. 59, 69-92.
Smith, J.V. and Yoder, H.S. (1956). Mineral. Mag., 31, 209-235.
Zvyagin, B.B. (1967). Electron diffraction analysis of clay mineral structures. Plenum Press, N.-Y.
Zvyagin, B.B. and Kyazimov, M.G. (1992). Abstr. 14 th Eur. Crust. Meet., Enschede, 432.
Zvyagin, B.B. and Pushcharovsky, D.Yu. (1993). Z. f. Krist., 208, 1-10.
Zvyagin, B.B. and Sydorenko, G.A. (1993). Abstr. IUCr XVI, Beijng, 277.

EFFECT OF PRESSURE ON LAMPROITE MELT COMPOSITION

Zyryanov V.N. *(Institute of Experimental Mineralogy, Russian Academy of Sciences)*

The aim of these experiments was to investigate the effect of pressure on lamproite melt composition at interaction with the mantle material. A specific feature of the research was to create such experimental conditions, which ensure the maximal approach to the nature. The experiments were done using piston-cylinder apparatus in the pressure range 10 to 30 kbars at 1300°C. A starting material was a 50:50 fine-grain mixture of phlogopite-armarlcolite lamproite from the Smoky Butte (Montana, USA) and garnet lherzolite, xenolith from the Udachnaya pipe (Yakutia, Russia), with natural volatile content of 0.1 wt% CO_2 and 0.6 wt% H_2O).

Run products were glasses of variable composition in equilibrium with Ol at 10 kbars, Ol+Opx at 15-20 kbars and Opx at 30 kbars. Increase of pressure provided the basification of melts (glasses) due to crystallization and precipitation of the equilibrium mineral assemblage mentioned above. The generated melts corresponded in composition to Lc-lamproites and Ol-lamproites of Western Australia at 10-20 and 30 kbars, respectively. The results made it possible to estimate the role of pressure which defines generation of lamproites of different composition at other equal conditions. Crystallization differentiation of lamproite melt at interaction with mantle material may result in generation either Lc-lamproite at a depth up to 100km or Ol-lamproite at greater depths.

AUTHOR INDEX

Authors are listed alphabetically. The names of the communicating authors are typed in boldface. For each entry the following information is given:

- page of the corresponding abstract;
- session;
- day of presentation;
- hour of presentation (for oral communications only).

Therefore, the presence/absence of a time in the last column makes it easy to distinguish between oral and poster presentations (the latter are always scheduled for 14:30–17:30 on the indicated days).

Silvester, E.	261	7c	Fri 9	11:20
Simakin, A.G.	71	1b	Wed 7	
Simakin, A.G.	**378**	**1b**	**Wed 7**	**08:30**
Simakov, S.K.	**301**	**2a**	**Wed 7**	
Simkin, D.	25	9a	Wed 7	10:30
Simmons, Wm.B.	113	OS3	Mon 5	
Simmons, Wm.B.	**114**	**OS3**	**Mon 5**	
Simmons, Wm.B.	437	9d	Thu 8	10:45
Simon, G.	74	2c	Mon 5	11:00
Simon, G.	**379**	**OS4**	**Fri 9**	
Sinai, M.Yu.	146	1a	Mon 5	
Sinai, M.Yu.	**379**	**1a**	**Mon 5**	
Sinelnikov, Y.D.	243	3b	Mon 5	08:55
Sinitsyn, V.A.	201	6b	Fri 9	09:20
Sipavina, L.V.	305	8d	Fri 9	
Sivtsov, A.V.	36	OS1	Mon 5	
Sivtsov, A.V.	103	OS1	Mon 5	
Sivtsov, A.V.	150	7a	Fri 9	
Skarpelis, N.	**380**	**OS3**	**Mon 5**	
Skinner, H.C.W.	**380**	**6b**	**Fri 9**	**10:30**
Skobelev, V.M.	111	RS	Tue 6	16:00
Skobelev, V.M.	132	9b	Wed 7	
Skogby, H.	**380**	**8d**	**Fri 9**	
Skrok, V.	121	2c	Mon 5	08:30
Skuf'in, P.K.	**380**	**OS2**	**Mon 5**	
Skuf'in, P.K.	385	9b	Wed 7	
Skvirsky, A.L.	**381**	**3b**	**Mon 5**	
Słaby, E.	**381**	**OS2**	**Mon 5**	
Slivko, E.M.	260	9b	Wed 7	
Smelik, E.A.	**382**	**3a**	**Wed 7**	
Smelik, E.A.	**382**	**5b**	**Thu 8**	**10:30**
Smetannikova, O.G.	37	RS	Wed 7	
Smetannikova, O.G.	**341**	**OS1**	**Mon 5**	
Smirnov, S.Z.	**382**	**OS3**	**Mon 5**	
Smirnov, S.Z.	383	OS1	Mon 5	
Smirnov, Yu.P.	182	OS3	Mon 5	
Smirnova, O.K.	**383**	**1c**	**Wed 7**	
Smirnova, S.K.	**384**	**4a**	**Mon 5**	
Smith, D.G.W.	**384**	**4a**	**Mon 5**	**09:00**
Smith, D.K.	**385**	**4c**	**Thu 8**	**10:30**
Smolkin, V.F.	**385**	**9b**	**Wed 7**	
Smolskaya, L.S.	341	OS1	Mon 5	
Snigirev, A.	**385**	**8c**	**Fri 9**	**10:25**
Snoeyenbos, D.R.	**440**	**2c**	**Mon 5**	**11:45**
Sobolev, A.V.	334	OS2	Thu 8	15:00
Sobolev, N.V.	22	5c	Wed 7	
Sobolev, N.V.	210	2c	Mon 5	
Sobolev, N.V.	314	2a	Wed 7	
Sobolev, N.V.	**386**	**2c**	**Mon 5**	**09:00**
Sobolev, N.V.	458	9b	Wed 7	
Sobolev, R.N.	**386**	**1a**	**Mon 5**	
Soboleva, L.N.	**386**	**OS4**	**Fri 9**	
Soboleva, S.V.	46	6d	Wed 7	
Soboleva, S.V.	**117**	**OS1**	**Mon 5**	
Soboleva, S.V.	117	OS1	Tue 6	15:25
Sobrados, I.	364	OS1	Mon 5	
Sojka, Z.	455	8d	Fri 9	
Sokol, E.V.	240	1a	Mon 5	
Sokol, E.V.	**240**	**1a**	**Mon 5**	
Sokol, E.V.	430	6a	Mon 5	
Sokolov, S.V.	**387**	**OS2**	**Mon 5**	
Sokolova, E.V.	**387**	**8b**	**Tue 6**	**11:40**
Soldatos, T.	**387**	**9b**	**Wed 7**	
Solís-Pichardo, G.	209	OS3	Mon 5	
Solotchina, E.P.	**388**	**6d**	**Wed 7**	
Sonin, V.M.	70	2a	Wed 7	
Soták, J.	45	5c	Wed 7	
Soukharjevsky, S.M.	377	1a	Mon 5	
Spadini, L.	261	7c	Fri 9	11:20
Spadini, L.	**388**	**7c**	**Fri 9**	
Spangenberg, J.	**388**	**OS4**	**Fri 9**	
Spesius, Z.V.	458	9b	Wed 7	
Spetzler, H.	**389**	**2a**	**Tue 6**	**08:30**
Spiess, R.	**389**	**OS2**	**Mon 5**	
Spigarelli, S.	**390**	**8d**	**Fri 9**	
Spigun, A.A.	464	6d	Wed 7	
Spiridonov, E.M.	25	OS1	Mon 5	
Spiridonov, E.M.	**390**	**OS4**	**Fri 9**	
Spišiak, J.	45	5c	Wed 7	
Spišiak, J.	185	5c	Wed 7	
Spisiak, J.	**391**	**9b**	**Tue 6**	**10:50**
Spivak, D.Y.	**333**	**1c**	**Wed 7**	
Sretenskaya, N.G.	**457**	**6a**	**Mon 5**	**11:20**
Stalder, H.A.	**391**	**4b**	**Tue 6**	**11:20**
Stavrakeva, D.A.	**392**	**6a**	**Mon 5**	
Stebbins, J.F.	**392**	**9a**	**Wed 7**	
Stein, S.	357	1a	Mon 5	11:00
Steiner, J.D.	**392**	**OS3**	**Mon 5**	
Stekhin, A.I.	296	7a	Tue 6	15:40
Stelea, G.	167	OS1	Mon 5	
Stelea, G.	267	OS1	Mon 5	
Stelea, G.	**353**	**OS1**	**Mon 5**	
Stenina, N.G.	**392**	**1c**	**Wed 7**	
Stern, L.A.	205	1a	Mon 5	09:40
Stevenson, R.J.	**393**	**9a**	**Wed 7**	
Stimpfl, M.	**100**	**3c**	**Fri 9**	
Stipp, S.L.S.	**393**	**7c**	**Fri 9**	**09:40**
Stirling, J.A.R.	352	OS1	Mon 5	
Stixrude, L.	**393**	**3a**	**Wed 7**	**09:30**
Stixrude, L.	**394**	**2b**	**Wed 7**	**10:30**
Štohl, J.	356	OS4	Fri 9	
Stoian, T.	99	9b	Wed 7	
Stolpovskaja, V.N.	**394**	**5a**	**Wed 7**	
Storzer, D.	179	OS3	Mon 5	
Stout, E.C.	395	6e	Tue 6	08:50
Strakhovenko, V.D.	**395**	**OS4**	**Fri 9**	
Straschimirov, S.B.	217	4c	Fri 9	
Strizhov, S.V.	20	9c	Mon 5	
Strunz, H.	**396**	**4c**	**Thu 8**	**09:00**
Stupak, F.M.	371	9b	Wed 7	
Šturman, B.D.	41	5a	Wed 7	
Sturman, B.D.	**396**	**OS1**	**Mon 5**	
Stüßer, N.	2	8c	Fri 9	
Stüwe, K.	**396**	**3b**	**Mon 5**	
Sueno, S.	**397**	**PL**	**Thu 8**	**13:30**
Sukhorukov, Yu.T.	**397**	**RS**	**Thu 8**	**16:20**
Sun, D.	249	4c	Fri 9	
Sunagawa, I.	**398**	**1b**	**Wed 7**	
Suner, M.F.	**398**	**OS4**	**Fri 9**	
Superchi, M.	**399**	**6e**	**Wed 7**	
Susse, P.	**399**	**4c**	**Fri 9**	
Sutherland, F.L.	276	6c	Tue 6	11:30
Sutherland, F.L.	**399**	**4b**	**Tue 6**	**09:10**
Sutinen, M.	261	OS2	Mon 5	
Sutton, S.R.	47	8c	Fri 9	11:05
Sviridenko, L.P.	**400**	**RS**	**Wed 7**	
Svisero, D.	310	6e	Tue 6	10:50
Svisero, D.P.	194	6e	Wed 7	
Swamy, V.	**400**	**3b**	**Mon 5**	
Szabó, Cs.	**400**	**OS3**	**Mon 5**	
Szakmány, Gy.	**401**	**2c**	**Mon 5**	
Szymanski, A.	**301**	**6a**	**Mon 5**	
Szymanski, J.T.	231	OS1	Tue 6	16.10
Tabira, Y.	416	8c	Fri 9	
Tabit, A.	109	OS2	Mon 5	
Takahashi, T.	413	3c	Fri 9	
Takeda, H.	15	3c	Fri 9	11:00
Takeda, H.	277	3c	Fri 9	
Takeda, H.	**401**	**3c**	**Fri 9**	